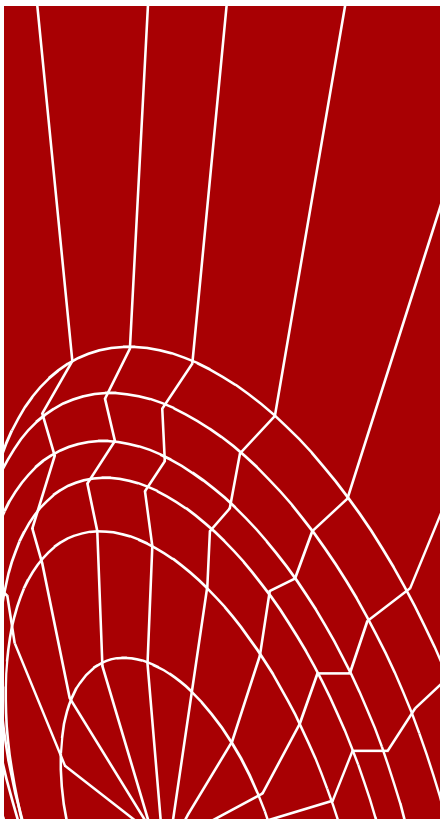

MARC Analysis Research Corporation

MARC®

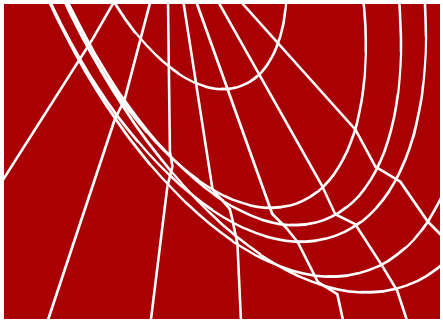

Volume E

Demonstration Problems

Version K7

Copyright © 1998 MARC Analysis Research Corporation
Printed in U. S. A.
This notice shall be marked on any reproduction of this data, in whole or in part.

MARC Analysis Research Corporation
260 Sheridan Avenue, Suite 309
Palo Alto, CA 94306 USA

Phone: (650) 329-6800
FAX: (650) 323-5892

Document Title: **MARC® Volume E: Demonstration Problems, Part I, Version K7**
Part Number: RF-3018-07.I
Revision Date: June, 1998

Proprietary Notice

MARC Analysis Research Corporation reserves the right to make changes in specifications and other information contained in this document without prior notice.

ALTHOUGH DUE CARE HAS BEEN TAKEN TO PRESENT ACCURATE INFORMATION, MARC ANALYSIS RESEARCH CORPORATION DISCLAIMS ALL WARRANTIES WITH RESPECT TO THE CONTENTS OF THIS DOCUMENT (INCLUDING, WITHOUT LIMITATION, WARRANTIES OR MERCHANTABILITY AND FITNESS FOR A PARTICULAR PURPOSE) EITHER EXPRESSED OR IMPLIED. MARC ANALYSIS RESEARCH CORPORATION SHALL NOT BE LIABLE FOR DAMAGES RESULTING FROM ANY ERROR CONTAINED HEREIN, INCLUDING, BUT NOT LIMITED TO, FOR ANY SPECIAL, INCIDENTAL OR CONSEQUENTIAL DAMAGES ARISING OUT OF, OR IN CONNECTION WITH, THE USE OF THIS DOCUMENT.

This software product and its documentation set are copyrighted and all rights are reserved by MARC Analysis Research Corporation. Usage of this product is only allowed under the terms set forth in the MARC Analysis Research Corporation License Agreement. Any reproduction or distribution of this document, in whole or in part, without the prior written consent of MARC Analysis Research Corporation is prohibited.

Restricted Rights Notice

This computer software is commercial computer software submitted with “restricted rights.” Use, duplication, or disclosure by the government is subject to restrictions as set forth in subparagraph (c)(i)(ii) or the Rights in technical Data and Computer Software clause at DFARS 252.227-7013, NASA FAR Supp. Clause 1852.227-86, or FAR 52.227-19. Unpublished rights reserved under the Copyright Laws of the United States.

Trademarks

All products mentioned are the trademarks, service marks, or registered trademarks of their respective holders.

Preface

MARC Volume E: Demonstration Problems demonstrates most of MARC's capabilities. MARC is a powerful, modern, general-purpose nonlinear finite element program for structural, thermal, and electromagnetic analyses.

In a typical finite element analysis, you need to define the:

mesh (which is an *approximate* model of the actual structure);

material properties (Young's modulus, Poisson's ration, etc.);

applied loads (static, dynamic temperature, inertial, etc.);

boundary conditions (geometric and kinematic constraints); and

type of analysis (linear static, nonlinear, buckling, thermal, etc.).

The steps leading up to the actual finite element analysis are generally termed preprocessing; currently, many users accomplish these steps by using an interactive color graphics pre- and postprocessing program such as the Mentat graphics program. After an analysis, the results evaluation phase (postprocessing) is where you check the adequacy of the design (and of the approximate finite analysis model) in terms of critical stresses, deflection, temperatures, and so forth.

MARC Volume E: Demonstration Problems is divided into five parts with each part containing two chapters. The manual has nine chapters grouped by the type of demonstration problems.

Part I

Chapter 1: *Introduction*

provides a general introduction to the problems demonstrated in all parts of *MARC Volume E: Demonstration Problems*. A set of cross-reference tables shows keywords for the following:

parameters
model definition options
mesh display options
history definition options
mesh rezoning options
element types
user subroutines

Each keyword is cross-referenced to the problem in which its use is demonstrated

Chapter 2: *Linear Analysis*

demonstrates most of the element types available to you. Many linear analysis features are illustrated. The use of adaptive meshing for linear analysis is demonstrated here.

Part II

Chapter 3: *Plasticity and Creep*

demonstrates the nonlinear material analysis capabilities. Both plasticity and creep phenomena are covered.

Chapter 4: *Large Displacement*

demonstrates MARC's ability to analyze both large displacement and small strain effects.

Part III

Chapter 5: *Heat Transfer* demonstrates both steady-state and transient heat transfer capabilities.

Chapter 6: *Dynamics* demonstrates many types of dynamic problems. These include analyses performed using both the modal and direct integration methods. The influences of fluid coupling and initial stresses on the calculated eigenvalues are shown.

Harmonic and spectrum response analysis is also demonstrated here.

Part IV

Chapter 7: *Contact* demonstrates some of the special program capabilities of MARC. This includes the ability to solve rubber (incompressible), foam, viscoelastic, contact, and composite problems as well as others.

Chapter 8: *Advanced Topics* demonstrates the capabilities most recently added to MARC. They include the ability to use substructures, in both linear and nonlinear analysis, to perform cracking analysis, analysis of contact problems, the ability to perform coupled thermal-mechanical analysis, electrostatic, magnetostatic and acoustic analysis. The use of adaptive meshing to solve nonlinear analysis is demonstrated here.

Part V

Chapter 9: *Fluid Analysis*	demonstrates the capabilities for performing fluid, fluid-thermal, and fluid-solid analyses.
Chapter 10: *Design Sensitivity and Optimization*	demonstrates the capabilities for calculating the sensitivities of the resultant based upon the design variables and optimizing the objective function for linear analysis.

MARC Volume E: Demonstration Problems summarizes the physics of each problem and describes the options required to define the problem. Figures are given of the mesh geometry and typical output results. The actual input and user subroutines are not included in the manual. They can be found on the distribution media associated with the MARC installation.

In addition to the overall Table of Contents for *MARC Volume E: Demonstration Problems*, each chapter has an individual Table of Contents, Figures, and Tables.

Each problem in *MARC Volume E, Demonstration Problems* has a **Parameters, Options, and Subroutines Summary**. Parameters, options, and user subroutines are called out in the text by the use of a different type font – such as parameter END, option CONTINUE, and user subroutine UFXORD.

Volume E Demonstration Problems

PART I

Chapter 1 Introduction
Chapter 2 Linear Analysis

PART II

Chapter 3 Plasticity And Creep
Chapter 4 Large Displacement

PART III

Chapter 5 Heat Transfer
Chapter 6 Dynamics

PART IV

Chapter 7 Contact
Chapter 8 Advanced Topics

PART V

Chapter 9 Fluids
Chapter 10 Design Sensivitity and Optimization

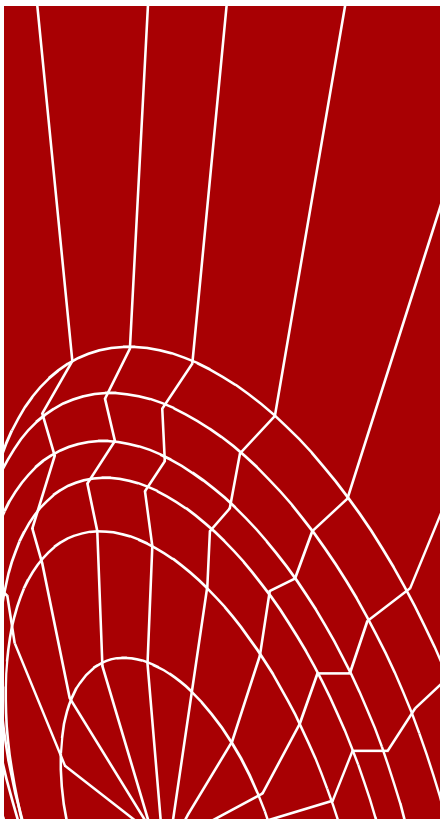

MARC Analysis Research Corporation

MARC®

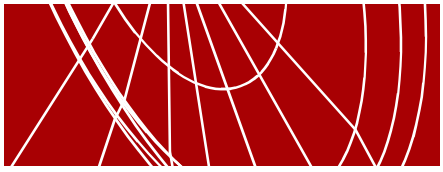

Volume E

Demonstration Problems

Version K7

Part I

- Introduction
- Linear Analysis

Part I

Volume E: Demonstration Problems

Chapter 1 **Introduction**

Chapter 2 **Linear Analysis**

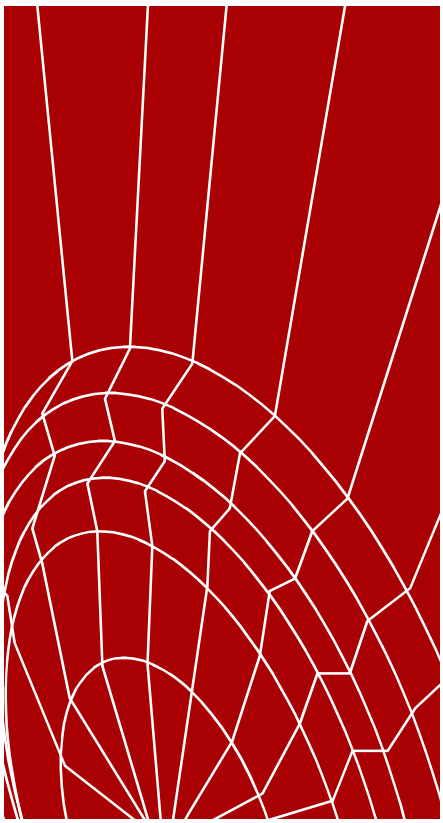

MARC Analysis Research Corporation

MARC®

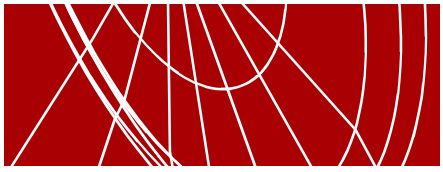

Volume E

Demonstration Problems

Version K7

Chapter 1
Introduction

1 Introduction Contents

Page

MARC Documentation 1-1
Mentat Documentation 1-2
Example Problems 1-2
Program Features 1-3
- Geometry 1-3
- Behavior 1-3
- Material 1-3
- Boundary Conditions 1-4
- Libraries 1-4
- Procedure Library 1-4
- Element Library 1-6
- Material Library 1-6
- Function Library 1-8

The Element Library 1-9
- Definitions 1-9
- Element Types 1-10
- Heat Transfer Elements 1-11
- Element Usage Hints 1-11

Input 1-12
- Input Units 1-12
- Input Sections 1-13
- Input Format 1-13
- Parameter Section 1-15
- Model Definition Section 1-15

Page

Output 1-18
Printed Output 1-18
Element Output 1-19
Modal Output 1-19
Selective Output 1-20
Post File 1-20
Graphical Output. 1-20
Discussion of MARC Input Format for New Users 1-21
Finite Element Modeling 1-21
Discussion of MARC Output for New Users 1-32
Cross-reference Tables. 1-47

1 Introduction List of Figures

Figure **Page**

1-1 Plate with Hole 1-22
1-2 Mesh Layout for Plate with Hole 1-27

Introduction List of Tables

Table		Page
1-1	Parameter Cross-reference	1-47
1-2	Model Definition Option Cross-reference	1-67
1-3	History Definition Option Cross-reference	1-107
1-4	Rezone Option Cross-reference	1-117
1-5	Element Type Cross-reference	1-120
1-6	User Subroutine Cross-reference	1-132

1 Introduction

This chapter provides a brief introduction to the MARC system. It serves as cursory background material for the demonstration problems; more detailed tables and descriptions are found in the MARC manuals. You should read this chapter and be familiar with its contents before going on to the examples. Each example is self-contained and illustrates certain MARC features and input requirements.

This manual is divided into nine main chapters. These chapters are summarized as follows:

Chapter 2	*Linear Analysis*
Chapter 3	*Plasticity and Creep*
Chapter 4	*Large Displacement*
Chapter 5	*Heat Transfer*
Chapter 6	*Dynamics*
Chapter 7	*Contact*
Chapter 8	*Advanced Topics*
Chapter 9	*Fluid Analyses*
Chapter 10	*Design Sensitivity and Optimization*

The following topics are covered in this chapter: a guide to MARC and Mentat documentation, MARC program features, element library, input description, output description, and a simple example of a hole-in-plate subjected to a distributed load.

MARC Documentation

In addition to this demonstration manual, several other MARC manuals are available. These are referential in nature and describe the features and applications of MARC in greater detail. Other manuals are as follows:

Primer	Tutorial
Volume A	*Theory and User Information* (technical basis of program and capabilities)
Volume B	*Element Library*
Volume C	*Program Input*
Volume D	*User Subroutines and Special Routines*
Volume F	*Background Papers* (Theoretical papers on MARC procedures)

For reference purposes, *MARC Volumes B: Element Library, C: Program Input*, and *D: User Subroutines* are used most often. *MARC Volume A: Theory and User Information* serves as an overview of MARC's capabilities and contains some theoretical background material. *MARC Volume F: Background Information* is a collection of journal papers which describe the algorithms and material characterizations in MARC.

Mentat Documentation

Mentat Command Reference
Mentat User's Guide (tutorial sessions on Mentat pre-/postprocessing)

Example Problems

The problems discussed in Chapters 2 through 10 are examples of the capabilities in MARC. They are designed to demonstrate the technical capability and usage using simple geometric configurations. Each description contains a statement of the problem, the element type chosen, the material properties, and the boundary conditions. The controls used are also discussed. The key features are discussed and the results are summarized. Where applicable, results are compared to analytical solutions. Figures are generated using the Mentat program to illustrate the solution.

The input data files are summarized, but not included, to reduce the volume of this manual. All input problems are included with the delivery media of the MARC system. They are found on the media in a subdirectory called "demo." Each problem is an individual file; for example, e2x1.dat for problem 2.1. A typical user subroutine is also an individual file; for example, u2x4.f for problem 2.4.

To execute an example on a UNIX system, copy the input file to your working directory and type:

```
marc -j e2x1
```

or if user subroutines are present type:

```
marc -j e2x4 -u u2x4
```

The name of the shell script can be different (such as marck72), so consult your local system administrator.

Program Features

MARC is a general purpose finite element (FE) program designed for both linear and nonlinear analyses of structural, thermal, electric, magnetic field problems. In addition, it can handle coupled thermal-mechanical, electric-thermal, and electromagnetic analyses. In nonlinear and transient problems, MARC makes your analysis easier by offering automatic load incrementation and time stepping capabilities.

Many types of analyses can be obtained by any combination of these basic MARC capabilities. The following is a cursory listing of MARC capabilities. Please refer to the appropriate MARC manual for more detailed descriptions.

Geometry

1-D: truss, beams (open or closed section)
2-D: plane stress, plane strain, generalized plane strain
2-D (axisymmetric):solid or shell (with nonaxisymmetric loading for linear problems)
3-D: solids, plates, shells, membranes

Behavior

linear/nonlinear for geometry or material
static/dynamic
steady-state/transient

Material

linear elastic
isotropic/orthotropic/anisotropic composites
elastic-plastic; work-hardening
isotropic, kinematic, and combined hardening
finite strain
cyclic loading
viscoplasticity
powder materials
rigid plastic flow
nonlinear elastic, elastomers, rubber
viscoelastic (Maxwell, Kelvin, combined)
cracking

Boundary Conditions

time/increment

temperature
displacements, velocities, accelerations
open/close contact

Libraries

- Procedure
- Element
- Material
- Function

You can combine almost any number of options from each of the four libraries and, consequently, solve virtually any structural mechanics or thermal problem.

Procedure Library

This includes all of the analysis types available in the MARC program:

Linear elastic
- standard linear finite element analysis
- superposition of multiple load cases
- Fourier (nonaxisymmetric) analysis of linear axisymmetric bodies
- design sensitivity
- design optimization

Substructuring
- multilevel, quasi-static

Nonlinear
- automatic load incrementation
- elastoplastic

  scaling to first yield
- large deformation/finite strain

  total and updated Lagrangian approaches
  buckling/collapse – linear/nonlinear
  creep buckling
  postbuckling – with adaptive load step
- rigid plastic flow – Eulerian, metal forming

	– creep – with adaptive load step
	– viscoelastic
	state equations (Kelvin model)
	hereditary integrals (generalized Maxwell or generalized Kelvin-Voigt model)
	thermo-rheologically simple behavior
	– viscoplastic – modified creep option to include plasticity effects
	– contact/friction – automatic convergence
Fracture mechanics	– linear/nonlinear
	– brittle/ductile
	– J-integral evaluation
	– dynamic J-integral
	– brittle cracking concrete model
Dynamics	– modal analysis/eigenvalue extraction
	inverse power sweep method Lanczos method
	– transient response
	modal superposition direct integration: Newmark-Beta method Houbolt method Central difference method
	– harmonic response
	– spectrum response
	– time stepping – linear/nonlinear
	– adaptive time stepping algorithm
Heat transfer	– steady-state and transient analysis
	conduction – linear/nonlinear convection/radiation boundary conditions internal heat generation latent heat phase changes adaptive time steps

Fluid analysis	– Navier Stokes (excluding turbulence
	– fluid-thermal
	– fluid-solid
Hydrodynamic bearings	– lubrication problems
	– pressure distribution and mass flow
Joule heating	– coupled electric flow with heat transfer
Electromagnetics	– electrostatics
	– magnetostatics
	– coupled electromagnetic analysis
	harmonics transient
Fluid/structure interaction	– incompressible and inviscid fluid
Thermo-mechanical	– quasi-coupled thermally driven stress analysis
	– fully coupled thermo-mechanical analysis solved by staggered scheme
	– large displacement effects on thermal boundary conditions
	– automated contact/friction capability
Change of state	– transient thermal analysis with change of phase and volume
	– associates stress analysis with plasticity and residual stresses

Element Library

MARC has a library of approximately 150 elements.

Material Library

This includes more than 40 different material models:

Linear elastic	– isotropic, orthotropic, and anisotropic (properties can be temperature dependent)
Composites	– laminated plates and shells
	– isotropic, orthotropic, or anisotropic layers
	– elastic or elastic-plastic behavior

Composites (continued)	– arbitrary material orientation definition with respect to any element edge with respect to global Cartesian axes with respect to a user-defined axis or through user subroutines
	– relative ply angle for each layer
	– multiple failure criteria maximum stress maximum strain Tsai-Wu Hill Hoffman, or user-defined
Hypoelastic	– nonlinear elastic (reversible)
Elastomers	– nonlinear elastic, incompressible
	– Mooney-Rivlin
	– Ogden
	– Elastomer damage model
Elastic-plastic	– Prandtl-Reuss flow rule
	– user-defined nonassociative flow law
	– von Mises yield criterion
	– Drucker-Prager yield criterion
	– isotropic, kinematic or combined hardening
	– strain hardening (or softening) as a function of strain rate and temperature
	– temperature dependence of yield stress and work hardening slopes
	– isotropic, orthotropic, and anisotropic
	– Hill’s anisotropic plasticity
	– Gurson damage model
Cyclic plasticity	– isotropic, kinematic, combined hardening

Creep	– deviatoric or volumetric (swelling) strains
	– piecewise linear or exponential forms for rate of equivalent creep strain
	– temperature dependence
	– Oak Ridge National Laboratory (ORNL) model – combine creep, plasticity, and cyclic loadings
Viscoelasticity	– Maxwell and Kelvin models
	– combined Kelvin-Voigt and Maxwell models
	– hereditary integrals of strain histories with both small and large strain formulations
	– thermo-rheologically simple behavior
	– isotropic or anisotropic material
Polymers	– thermo-rheologically simple behavior
Viscoplasticity	– combining plasticity and the Maxwell model of plasticity
	– general inelastic behavior
	– unified creep plasticity
Soils	– yield surfaces as a function of hydrostatic stress
	– linear or parabolic Mohr-Coulomb law
	– modified Cam-Clay model
Concrete	– low-tension cracking
	– crushing surfaces
	– rebars

Function Library

This includes the ability to define kinematic constraints, loads, bandwidth optimization, rezoning, in-core and out-of-core solution, user subroutines, restart, output on post file, selective print, error analysis, etc. Only loads and constraints are summarized below; refer to the MARC manuals for descriptions of the others.

Loads and constraints	– mechanical loads – concentrated, distributed, centrifugal, volumetric forces
	– thermal loads – initial temperatures read from a post file produced from a thermal analysis, or from data files
	– initial stresses and initial plastic strains

– kinematic constraints

transformation of degrees of freedom
elastic foundation
tying (multipoint constraints or MPCs)
boundary conditions in user-defined axes
springs and gaps – with and without friction contact surfaces

The Element Library

The heart of a finite element program lies in its element library which allows you to model a structure for analysis. MARC has a very comprehensive element library which lets you model virtually any conceivable 1-D, 2-D, or 3-D structure. This section gives some basic definitions, summarizes MARC element types, and describes the most commonly used elements of interest to the user.

Definitions

Isoparametric	is a single function used to define both the element geometry and the deformation.
Numerical integration	is a method used for evaluating integrals over an element. Element quantities – such as stresses, strains, and temperatures – are calculated at each integration point of the element.
Gauss points	is the optimal integration point locations for numerical accuracy.
Full integration (quadrature)	requires, for every element, 2^d integration points for linear interpolation and 3^d points for quadratic interpolation, where scalar “d” is the number of geometric dimensions of an element (that is, d = 2 for a quad; d = 3 for a hexahedron).
Reduced integration	uses a lower number of integration than necessary to integrate exactly. For example, for an 8-node quadrilateral, the number of integration points is reduced from 9 to 4 and, for a 20-node hexahedron, from 27 to 8. For some elements, an “hourglass” control method is used to insure an accurate solution.
Interpolation (shape) function	is an assumed function relating the displacements at a point inside an element to the displacements at the nodes of an element. In MARC, four types of shape functions are used: linear, quadratic, cubic, and Hermitian.

Degrees of freedom (DOF)	is the number of unknowns at a node. In the general case, there are six degrees of freedom (DOFs) at a node in structural analysis (three translations, three rotations), and one degree of freedom (DOF) in thermal analysis (nodal temperature). In special cases, the number of DOFs is two (translations) for plane stress, plane strain, and axisymmetric elements; three (translations) for 3D truss element; six (three translations, three rotations) for a 3D beam element).
Incompressible elements	is a special class of elements in MARC which can be used to analyze incompressible (zero volume change) and nearly incompressible materials such as elastomers and rubber. They are based on a modified Herrmann variational principle, and are sometimes referred to as “Herrmann elements.” Unlike the conventional finite element formulations, they can handle the case of Poisson’s ratio exactly equal to one-half. They are used for elastic analysis, but are capable of analyzing large displacement effects as well as thermal and creep strains. The incompressibility constraint is imposed by using Lagrange multipliers.
Assumed strain elements	is a special class of elements which are enriched such that they can accurately calculate the shear (bending) strain.

Element Types

MARC has an extensive element library with approximately 150 element types. They are basically of two categories: structural and thermal. They cover a wide variety of geometric domains and problems.

Truss	is a 3D rod with axial stiffness only (no bending).
Membrane	is a thin sheet with in-plane stiffness only (no bending resistance).
Beam	is a 3D bar with axial, bending, and torsional stiffness.
Plate	is a flat thin structure carrying in-plane and out-of-plane loads.
Shell	is a curved, thin or thick structure with membrane/bending capabilities.
Plane stress	is a thin plate with in-plane stresses only. All normal and shear stresses associated with the out-of-plane direction are assumed to be zero. (In MARC, all plane strain elements lie in the global x-y plane.)
Generalized plane strain	is the same as plane strain except that the normal z-strain can be a prescribed constant or function of x and y.

Axisymmetric	are elements lying in the z-r (x-y) plane in MARC.
3D solid	is a solid structure with only translational degrees of freedom for each node (linear or quadratic interpolation functions).
Special	are elements in MARC including a gap/friction element, a pipe-bend element, a shear panel element, rebar elements, and several “semi-infinite” elements (which are useful for modeling a domain unbounded in one direction).

Heat Transfer Elements

Heat transfer elements in MARC consists of 3D links, planar and axisymmetric elements, 3D solid elements, and shell elements. For each heat transfer element, there exists at least one corresponding stress element. Temperature is the only DOF for each node in these elements (except in the case of Joule heating analysis which is a coupled thermal-electrical analysis).

Element Usage Hints

The following hints on element usage are useful to most MARC users and especially the first-time user.

1. Element input data generally includes element connectivity; thickness for 2-D beam, plate, and shell elements; cross section for 3-D beam elements; coordinates of nodal points; and face identifications for distributed loadings.
2. You can select different element types to represent various parts of a model. If they are incompatible (meaning conflicting degrees of freedom), you have to provide appropriate tying constrains.
3. You can use most MARC elements for both linear and nonlinear analyses; exceptions are noted in *MARC Volume A: Theory and User Information*.
4. In linear analysis, you should consider using higher-order elements, especially in problems involving bending action. In nonlinear analysis, lower-order elements are preferred to reduce computational costs.
5. When using lower-order elements (whether the analysis is linear or nonlinear), 4-node quadrilaterals are preferred over 3-node triangles in 2D problems. Similarly, 8-node bricks perform significantly better than 4-node tetrahedra in 3D problems.

6. Stresses and strains of all continuum elements are defined in the global coordinate system. For truss, beam, plate, and shell elements, stresses and strains are output in the local system for the element and the output must be interpreted accordingly. You should pay special attention to the use of these elements if the material properties have preferred orientations.
7. The coordinates and degrees of freedom of all continuum elements are defined in the global coordinate system. Truss, beam, plate, and shell elements can be defined in a local coordinate system – and you must interpret the output accordingly.
8. Distributed loads can be applied along element edges, over element surface, or over the volume of the element. MARC automatically evaluates the consistent nodal forces using numerical integration. Concentrated forces can be applied at nodes.
9. For five bilinear elements (Types 7, 10, 11, 19, and 20), an optional integration scheme can be used which imposes a constant dilatational strain constraint on the element. This option is often useful in approximately incompressible, inelastic analyses such as large strain plasticity because conventional elements give results which are too stiff for nearly incompressible behavior.
10. For four elements (Types 3, 7, 11, and 19), optional interpolation functions can be used which improve the behavior of these elements in bending. The reduced integration elements, with hourglass control, also use an assumed strain formulation.
11. Five Fourier shell and solid elements (Types 62, 63, 73, 74, and 90) exist for the analysis of linear axisymmetric structures with nonaxisymmetric loads. The circumferential load and displacement is represented by a Fourier series, but the geometry and material properties cannot change in the circumferential direction. You can, therefore, reduce a 3D problem into a series of 2D problems. These elements can only be used for linear elastic analysis because the principle of superposition applies only to this type of analysis.

Input

This section highlights MARC input concepts. Concepts such as parameter, model definition, and load incrementation are briefly described as are input formats (fixed versus free field input of numerical data, lists) and input of loads and constraints. For details, please refer to *MARC Volume C: Program Input*.

Input Units

No units are actually entered in the input file by you. MARC simply assumes that all input is being provided in a consistent manner.

Input Sections

MARC is a batch program. This means that you define the input, and this input is not changed during the program execution. This input can be created using the Mentat graphics program or a text editor. The input can be modified upon restart for nonlinear or transient analysis.

MARC input consists of three major sections:

Parameters	define the title of the analysis, the storage allocation, analysis type, element type(s), etc. This section terminates with an END statement.
Model Definition Options	define coordinates, connectivity, materials, boundary conditions, initial loads, initial stresses, nonlinear analysis controls, output options, etc. This section terminates with an END OPTION statement.

Nonlinear and/or transient analyses are performed by increments (steps). The information required to define the load history requires the additional section:

History Definition Options	defines the increments in terms of load increments and/or boundary condition changes occurring during the history definition increment. This sections ends with a CONTINUE option. (At this stage, one or more increments are analyzed.)

The first two sections (parameter and model definition) are always present. You can stack as many load incrementation options as you want. They are analyzed by MARC in sequence until the last CONTINUE option is encountered.

Input Format

A MARC input file typically consists of many blocks or lines of input, each headed by a keyword. A keyword describes some attribute of the FE model of the structure (coordinates, materials, boundary conditions, etc.). A keyword can also describe a control function for the analysis (generation of printout, writing of a post file, numerical tolerances, etc.).

A block can contain three different types of input:

Alphabetic keyword	describes the contents of the block; placed on a single line.
Numerical data	quantifies the properties of the model; floating point or integer; placed on one or more lines.
Lists	denotes the nodes, elements, and DOFs to which the properties apply. Free format.

The numerical data can be in free or fixed format. Lines in free and fixed format can both exist in the input file, although a particular option can use only one format.

Free field	is easier, safer, and recommended for hand-generated input (Mentat graphics program casts input data in fixed field format). It is flagged by at least one comma existing in the input line The last item of the line must be a comma only if there is a single entry. Data items on a line are separated by commas, which can be preceded or followed by an arbitrary number of blanks. No imbedded blanks can appear within the data item itself. Each line must contain the same number of data items that it would have using the fixed format. Floating point numbers can be given with or without an exponent. The mantissa must contain a decimal point. If an exponent is given, it must be preceded by the letter E or D and must immediately follow the mantissa (no embedded blanks). An example is shown below: `5.4E6,0.3,11.,0.,18.`
Fixed field	is described in detail in MARC *Volume C: Program Input*. Standard FORTRAN conventions are observed. Integers must be right-justified in field. Floating point numbers can be given with or without exponent. The mantissa must contain a decimal point. If an exponent is given, it must be preceded by the letter E or D and must be right justified.

A list is a convenient way to identify a set of elements, nodes, DOFs, integration points, shell layers, etc. Lists come in three forms.

Sequence (`n1 n2 n3`)	list includes `n` numbers placed on one or more lines separated by blanks or commas. If a sequence continues onto another line, a `C` must be the last item on the line.
Range (`m TO n BY p`)	list includes all numbers from `m` to `n` with interval `p`. (Default `p = 1`)
Set name (`STEEL`)	list includes the numbers in the set named `STEEL` previously specified by the DEFINE option of the model definition options.

Furthermore, lists can be operated upon by the logical operations `AND`, `EXCEPT`, and `INTERSECT`. For example:

```
2 TO 38 BY 3 AND STEEL
```

Data can be either upper- or lowercase.

Parameter Section

Parameters control the scope and type of the analysis. Typically, the first parameter, TITLE, is the name of the problem. The SIZING parameter defines the problem size in words of the core buffer used by MARC. ELEMENTS indicates what MARC element types are used in the analysis. Other optional parameters include:

ALL POINTS	asks for stress output at all integration points of the elements.
BEAM SECT	defines the cross-sectional properties of a beam (that is, prismatic or thin-walled).
CENTROID	asks for stress output only at the centroids of the elements (not recommended for nonlinear analysis).
ELASTIC	flags linear elastic static analysis.
SHELL SECT	defines the number of integration points across the shell thickness ranging from 1 to 99.
STOP	tells MARC not to do the analysis (a check run of input only).
THERMAL	flags initial temperatures being input for stress analysis.

In this set of parameters, only the TITLE, SIZING, and END parameters are mandatory. The ELEMENTS parameter can, however, be used instead of (or in conjunction with) the SIZING parameter. All other parameters are optional.

The parameters can appear in any order. The only requirement is that they must terminate with an END parameter.

Model Definition Section

The model definition option describes the complete FE model for analysis:

- Mesh
- Materials
- Applied Loads
- Constraints
- Controls

The following paragraphs describe those options which you encounter most frequently. In a nonlinear analysis, you can alter most of this data during the later stages of the analysis. For a linear elastic analysis, the model is defined once using the model definition options. The model definition options also control the output. The selective output feature is described later in the **Output** section of this chapter.

Mesh

The shape and geometry of the FE mesh are specified using the following model definition options:

COORDINATES	of the nodes in the mesh
CONNECTIVITY	of the elements connecting the nodes
GEOMETRY	of the geometric properties of beam and shell elements (for example, beam cross section, shell thickness, etc.)
PROPERTY	of the material properties; for example: ISOTROPIC, ORTHOTROPIC, GAP DATA, MOONEY, OGDEN, WORK HARD, TEMPERATURE EFFECTS, STRAIN RATE, RATE EFFECTS, CREEP

The DOFs (loads, displacements) at a node depend on the element type connected to the node unless a triad of local axes is defined for a set of nodes using:

TRANSFORMATIONS	establishes the direction of the local nodal axes with respect to the global axes.

Mechanical Loads

Mechanical loads are of two types: concentrated and distributed.

POINT LOAD	concentrated load vector acting on a node.
DIST LOADS	volumetric (body forces such as gravity) or pressure loads (acting on surfaces or edges). The type is specified by defining the variable `IBODY`. It can be uniform or nonuniform.

Thermal Loads

The INITIAL STATE option can be used to define a nonhomogeneous initial temperature field in a stress analysis. This temperature does not produce any thermal strains. The temperatures can then be modified using the CHANGE STATE option. The change in temperature causes thermal strains, and possible changes in the material properties if TEMPERATURE EFFECTS are included.

Kinematic Constraints

You can prescribe values to individual DOFs using:

FIXED DISP	prescribed values for specified DOFs on a set of nodes.

Support Springs

Elastic springs can be defined between any two DOFs at any two nodes:

SPRINGS	assigned spring constant between two DOFs for two nodes.

CONTROL Option

Another important model definition option is the CONTROL option which lets you select input parameters governing convergence and accuracy in nonlinear analysis. Items in CONTROL are mostly integers (except for tolerances which are in floating point). The first two items are the most important. Note that the number of cycles includes the first cycle, and the number of increments likewise includes the first increment.

Item	Meaning	Default
step	maximum number of increments (loads) in this analysis	4
cycle	maximum number of iterations per increment	3

There are other items on the CONTROL option, but they are usually not needed by the first-time user. These items flag such options as convergence tests, iteration schemes, nonpositive definiteness checks, etc. (See *MARC Volume C: Program Input*.)

The first increment in an analysis is considered increment 0 and should be linear elastic. Thus, four increments imply increment 0, 1, 2, and 3. Similarly, three cycles imply the first cycle and two iterations.

OPTIMIZE Option

Finally, you need to be aware of the OPTIMZE option. This option lets you choose a bandwidth optimization algorithm. The default algorithm is Cuthill-McKee which is widely used in many FE codes and suffices for most cases. Minimizing the bandwidth in your problem reduces computational costs in medium to large-sized problems. Therefore, you should make a habit to invoke the OPTIMIZE option before performing an analysis. For a description of other available bandwidth optimization algorithms, see *MARC Volume C: Program Input*. Note that it is not necessary to use the OPTIMIZE option when the element-by-element iterative solver is used.

Output

This section summarizes the MARC output and postprocessing options. The MARC output can be obtained in four forms:

- Printed Output (standard)
- Selective Output
- Post File for Mentat postprocessing
- Restart file (for continuation of analysis)

Printed Output

A standard printed output from a MARC run contains three different parts:

- input echo and interpretation
- analysis messages
- output of analysis results

Input Echo and Interpretation

This portion repeats the input to allow you to verify its correctness. It includes various items such as position of the line columns, a line count for the blocks, set up of parameters for the run, and interpretation of the input (for example, connectivity, coordinates, properties, geometry, boundary conditions, loads, etc.).

Analysis Messages

During the analysis, MARC produces several diagnostic messages. Those of interest include the following:

Algebraic sum of the distributed and point loads over the whole model.

Singularity ratio of the matrix. This is a measure of the conditioning number (hence, the accuracy) in the solution of the linear equations. The ratio and its meanings are as follows:

between 10^{-4} and 1	acceptable
between 10^{-8} and 10^{-4}	possible numerical problems (...watch out)
on order of machine accuracy	singular equations
(10^{-14} to 10^{-8})	(unreliable solution)

During the analysis, MARC prints out the elapsed central processing unit (CPU) time at the following points:

State of increment
Start of assembly
Start of matrix solution
End of matrix solution
End of increment

Output of Analysis Results

At the end of the analysis, MARC prints out (for each increment) element data (stresses, strains, etc.) and nodal data (displacements, equivalent nodal forces, and reaction forces at fixed boundary conditions).

Element Output

At every Gaussian integration point, stresses (or forces) and strains are printed out, depending on the element type. (If you include a CENTROID parameter, only the centroidal results are reported.)

Continuum elements	are physical components (in global axes); principal values; mean normal values (hydrostatic); equivalent Tresca and von Mises values.
Shell elements	are generalized total stress and strain resultants (stretch, curvature) at midplane; total physical stresses at integration points through the thickness.
Beam elements	are resultant forces at Gauss points: axial force, bending moment (referred to local axes of beam element), and torque.

Modal Output

For every node, the vectors of these nodal quantities are printed out, depending on the analysis:

Static	incremental and total displacements; equivalent nodal loads; reaction forces (at boundary nodes); residual loads (at nodes without boundary conditions). (If convergence has occurred during the increment, the residual loads should be small compared with the reaction forces.)	
Dynamic	for modal analysis:	eigenvectors
	for transient analysis:	total displacements, velocities, and accelerations equivalent nodal loads reaction forces residual loads
	for heat transfer:	total temperatures and optional fluxes

Selective Output

You can selectively print out data for elements or nodes using these model definition options:

PRINT ELEMENT	selects elements, integration points, and layers (for plate and shell elements) to be printed in the output. **Note:** All stress components are printed out. The selected layers and integration points apply to all the selected elements in the model.
PRINT NODE	selects nodes and nodal quantities to be printed (e.g., displacements, input load vectors, output reactions/residuals).

Post File

You can use the POST command to flag the writing of a MARC post file, which can be processed later by the Mentat graphics program. The post file can be either binary or formatted. A *binary* file is machine-dependent, but is usually quite a bit smaller than a formatted file and cannot be edited. A *formatted* file is portable across different types of computers, but is usually larger than a binary file and can be edited.

The file output includes:

Complete mesh data (nodal coordinates, element connectivities)

All nodal variables (displacements, forces, etc.)

Element variables (strains, stresses, etc.) as selected in the POST option. You can select which stress component to write out for which layer. The output is produced for all integration points of all elements

A restart file can be made using the RESTART or RESTART LAST model definition option (See *MARC Volume C: Program Input*). This option is very convenient in nonlinear analysis.

Graphical Output

Almost all of the graphics in this manual have been generated using the Mentat graphics program. All input problems generate a post file which was then processed interactively. Please refer to the Mentat documentation for further details.

Discussion of MARC Input Format for New Users

The MARC input format is designed to allow the input of very complex problems. The new user is, however, faced with gaining familiarity with the system and its conventions. At the outset, therefore, the new user should adopt a systematic approach to the preparation of input data. One approach is to follow the construction of the program and adopt the procedure of preparing input for each of the parameters and options (model definition and history definition) in turn.

We shall illustrate our discussion by preparing input for the analysis of a thin plate with hole subjected to pressure loading. The problem shown in Figure 1-1 is well-known so the results can be compared to the exact solution (Timoshenko and Goodier, *Theory of Elasticity*). The hole/plate size ratio is chosen to approximate an infinite plate. A procedure for preparing the MARC input would take the following steps.

Finite Element Modeling

The plate has an outside dimension of 10” x 10” with a central hole of 1” radius. The thickness of the plate is assumed to be 0.1”. The material property is assumed to be isotropic and linear elastic. The Young’s modulus is 30 x 10^6 pounds per square inch (psi) with Poisson’s ratio of 0.3. These quantities are sufficient to define the behavior of an isotropic, linear-elastic material.

Figure 1-1 analyzes only a quarter of the plate due to symmetry conditions. Prescribed displacement boundary conditions exist along the lines of symmetry (that is, u = 0 at line x = 0; v = 0 at line y = 0) and traction (pressure) boundary condition exits at the top of the plate.

This quarter plate is approximated by a finite element mesh consisting of 20 eight-node plane stress elements with appropriate loading and boundary conditions. The element (MARC element type 26) is a second-order, isoparametric, two-dimensional element for plane stress. There are eight nodes with two translational degrees of freedom at each node. A description of element type 26 can be found in *MARC Volume B: Element Library.*

This example uses a coarse mesh for demonstration purposes only. The sharp stress gradients must be anticipated in this problem, and the mesh designed accordingly. This is achieved in this problem by using progressively smaller elements as the hole is approached. By adding elements to the mesh, further mesh refinement can be achieved.

The input data takes the following format:

```
FIXED DISP
2,
0.,
2,
34,37,42,45,25,22,5,8,13,16,21,
0.,
1,
71,73,77,79,64,62,49,51,55,57,61,
```

This concludes the minimum amount of data required to define the problem.

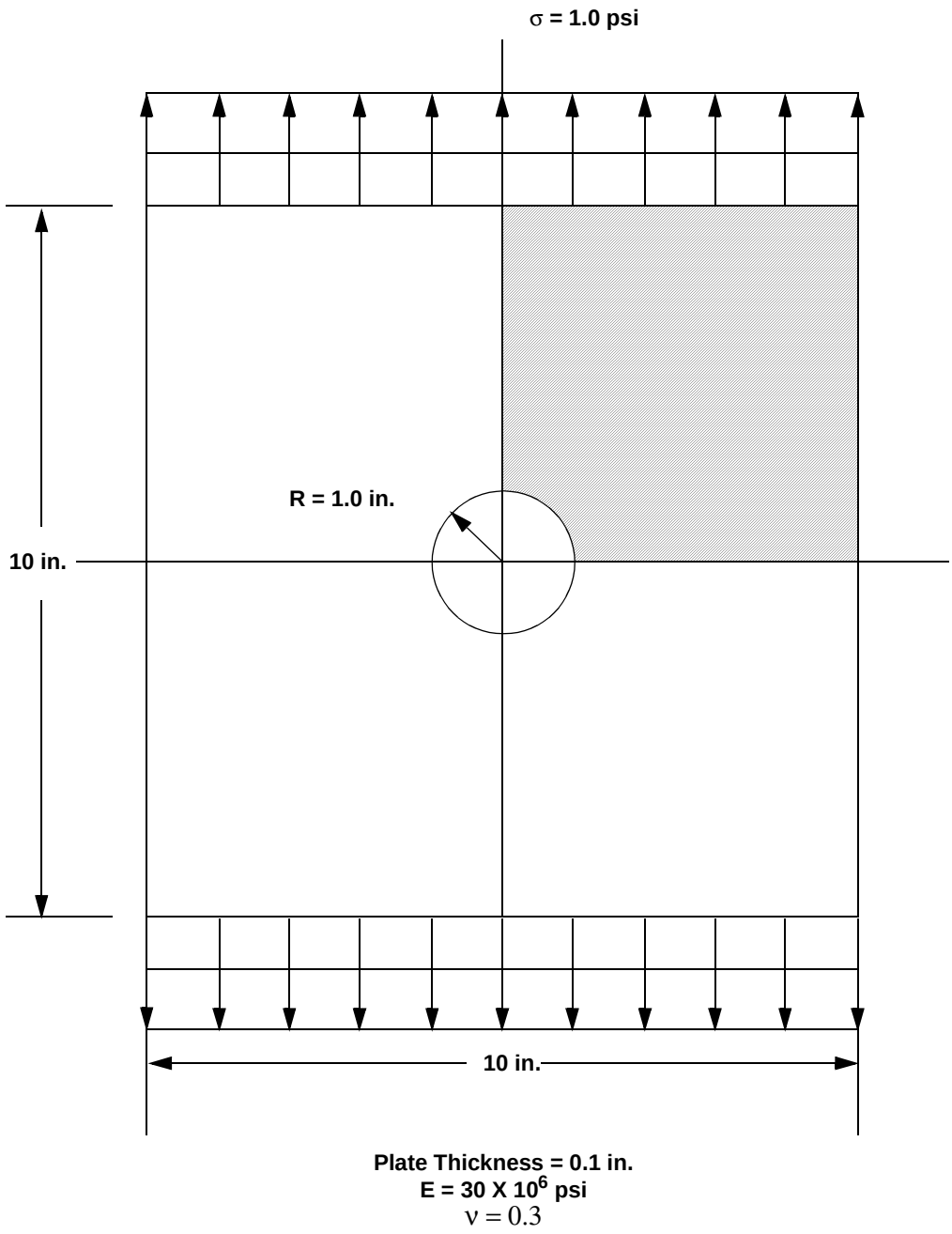

Figure 1-1 Plate with Hole

The preparation of parameter, model definition, and history definition data for this example is demonstrated below:

Parameters

The analysis to be carried out in this example is a linear elastic analysis. Consequently, only four parameters are needed for the input data:

TITLE
ELEMENTS
SIZING
END

In this example, the title *Elastic Analysis of a Thin Plate with Hole* is chosen for the problem and entered through the parameter TITLE.

The selected MARC element type 26 is entered through the parameter ELEMENTS.

The data on the parameter SIZING is selected as follows:

```
MAXALL = 100000 (core allocation)
```

Please note that the value of MAXALL should be checked with the in-house or data center system analyst for the maximum allowable core area on the system for running MARC. Refer to Table 2-1 and Table 2-2 in *MARC Volume C: Program Input* following the definition of the SIZING option in order to establish an estimate of the work space required in this problem. The estimate should only be approximate since the program adjusts the variables to use out-of-core storage if necessary. You do not need to input maximum values on SIZING.

Finally, the parameters are completed with END.

At this stage the input data is:

```
TITLE   ELASTIC ANALYSIS OF A THIN PLATE WITH HOLE
SIZING,100000,
ELEMENTS,26,
END
```

Model Definition Options

The model definition options contain the bulk data for the analysis. The data entered here concerns:

- Topology of the Model (finite element mesh in terms of element connectivity and nodal coordinates, as well as plate thickness)
- Material Property (Young’s modulus and Poisson’s ratio)
- Pressure Loading and Prescribed Displacement Boundary Conditions
- Controls for convergence and output selection.

Topology of the Model

The topology of the plate model is numerically defined by the following model definition options:

CONNECTIVITY
COORDINATES
GEOMETRY

In this example, the mesh consists of 20 elements and 79 nodes. The data required for element connectivity and nodal coordinates are:

```
CONNECTIVITY
                    20,
                     1   26    1    3   11    9    2    7   10    6
                     2   26    3    5   13   11    4    8   12    7
                     3   26    9   11   19   17   10   15   18   14
                     4   26   11   13   21   19   12   16   20   15
                     5   26    5    3   27   25    4   23   26   22
                     6   26    3    1   29   27    2   24   28   23
                     7   26   30   32   40   38   31   36   39   35
                     8   26   32   34   42   40   33   37   41   36
                     9   26   38   40   27   29   39   44   28   23
                    10   26   40   42   25   27   41   45   26   44
                    11   26    1    9   53   47    6   52   50   46
                    12   26   47   53   55   49   50   54   51   48
                    13   26    9   17   59   53   14   58   56   52
                    14   26   53   59   61   55   56   60   57   54
                    15   26   49   64   66   47   62   65   63   48
                    16   26   47   66   29    1   63   67   24   46
                    17   26   30   38   75   69   35   74   72   68
                    18   26   69   75   77   71   72   76   73   70
                    19   26   38   29   66   75   43   67   78   74
                    20   26   75   66   64   77   78   65   79   76
                COORDINATES
                     0    0
                     1    1.4000    1.4000
                     2    1.5500    1.0500
                     3    1.7000    0.7000
                     .
                     .
                     .
                    77    0.0000    1.2500
                    78    0.4931    1.1910
                    79    0.0000    1.3750
```

The data in the CONNECTIVITY block consists of element numbers (1,2,...,19,20); element type (26) and for each element, four corner node numbers and four mid-side node numbers.

The data in the coordinate block consists of the node number (1); and coordinates (x = 1.4, y = 1.4) of node 1 in the global coordinate system (x, y).

Finally, the plate thickness is entered through the GEOMETRY block as:

```
GEOMETRY
0,
0.1,
1 TO 20
```

A thickness of 0.1 inches is assumed for all twenty (1 to 20) elements.

Material Property

Material properties of the plate are entered through the ISOTROPIC block. For our problem, the only data required for a linear elastic analysis are Young's modulus and Poisson's ratio. The same material is used for the whole mesh (from Element No. 1 to Element No. 20). This is given a material id of 1. The data in the ISOTROPIC block is:

```
ISOTROPIC
1,
1
30.E6,0.3,
1 TO 20
```

Pressure Loading and Prescribed Displacement Boundary Conditions

As shown in Figure 1-2, the pressure loading is acted on two elements (elements 13 and 14), along the lines 61-60-59 and 59-58-17. From the CONNECTIVITY block, observe that these lines represent the 2-6-3 face of the elements. As a result, a distributed load type of 8 can be determined for the pressure loading from the **QUICK REFERENCE** of element 26 shown in *MARC Volume B: Element Library.*

```
"LOAD TYPE (IBODY)=8 FOR UNIFORM PRESSURE ON 2-6-3 FACE"
```

In addition, as shown in *MARC Volume B: Element Library*, the sign conversion of the pressure loading is that a negative magnitude represents a tensile distributed load. Consequently, the input for the 1 pound tensile distributed loading acting on elements 13 and 14 takes the following form:

```
DIST LOADS
0,
8,-1.,
13,14,
```

The FIXED DISP block is used for the input of prescribed displacement boundary conditions at the lines of symmetry (x = 0, y = 0). As indicated in the **QUICK REFERENCE** of element 26, the nodal degrees of freedom are:

```
dof 1 = u = global x-direction displacement
                dof 2 = v = global y-direction displacement.
```

In this example, the symmetry conditions require that:

```
dof 1 = u = 0 for nodes (71, 73, 77, 79, 64, 62, 49, 51, 55, 57, 61)
                along the line x=0.
```

and

```
dof 2 = v = 0 for nodes (34, 37, 42, 45, 25, 22, 5, 8, 13, 16, 21)
                along the line y=0.
```

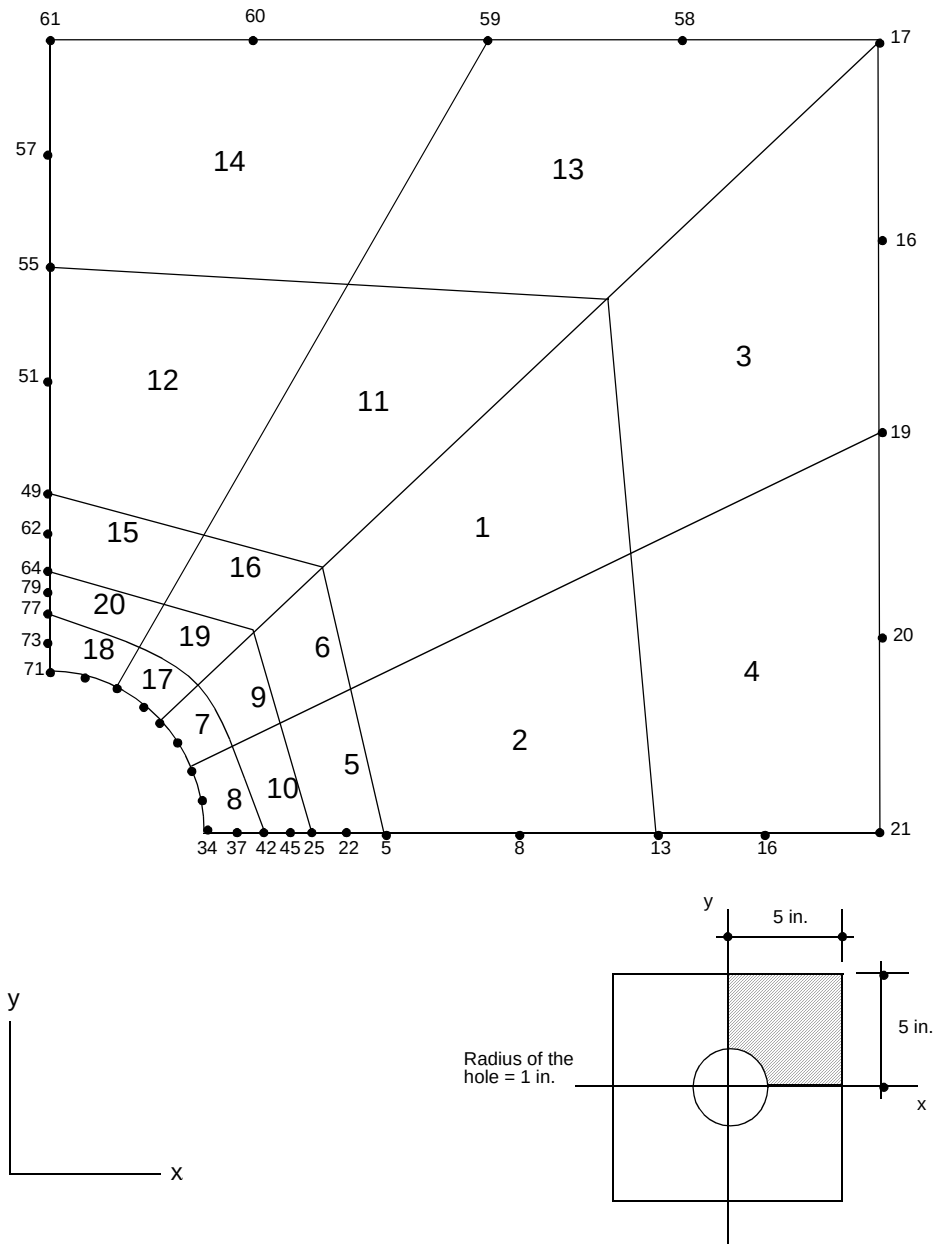

Figure 1-2 Mesh Layout for Plate with Hole

Controls

As discussed earlier, it is important to minimize the bandwidth to reduce the amount of computational time. In this problem, this is done using the Cuthill-McKee optimizer. Ten tries are used. The additional input is as follows:

```
OPTIMIZE,2,0,0,1
10,
```

As this is a linear analysis, it is unnecessary to have a CONTROL option in this problem.

The remainder of the input file is used to control the output. Only a portion of the stress and strain results are to be given in the listing file, elements 2, 4, 5, 8, and 10 at integration points 4 and 6. This is defined using the following:

```
PRINT ELEM
    1
    STRESS   STRAIN
    2    4    5    8   10
    4    6
```

MARC has the ability to report on the maximum and minimum values. This capability is invoked using the SUMMARY option.

Finally, the POST option is used to specify that an ASCII file be created on unit 19, and that it contain the components of stress and the equivalent stress. This is selected using the following:

```
POST
   0   16   17    1    0   19
  17
  11
  12
  13
```

The model definition section is concluded using the END OPTION.

A complete input data listing for the thin plate problem is given on the following page.

M A R C - C O N V E X

I N P U T D A T A

P A G E 1

```
                5   10   15   20   25   30   35   40   45   50   55   60   65   70   75   80
              ----------------------------------------------------------------------------
              TITLE     ELASTIC ANALYSIS OF A THIN PLATE WITH HOLE
              SIZING        100000
              ELEMENT       26
              END
CARD     5    CONNECTIVITY
                20
                 1   26    1    3   11    9    2    7   10    6
                 2   26    3    5   13   11    4    8   12    7
                 3   26    9   11   19   17   10   15   18   14
CARD    10       4   26   11   13   21   19   12   16   20   15
                 5   26    5    3   27   25    4   23   26   22
                 6   26    3    1   29   27    2   24   28   23
                 7   26   30   32   40   38   31   36   39   35
                 8   26   32   34   42   40   33   37   41   36
CARD    15       9   26   38   40   27   29   39   44   28   43
                10   26   40   42   25   27   41   45   26   44
                11   26    1    9   53   47    6   52   50   46
                12   26   47   53   55   49   50   54   51   48
                13   26    9   17   59   53   14   58   56   52
CARD    20      14   26   53   59   61   55   56   60   57   54
                15   26   49   64   66   47   62   65   63   48
                16   26   47   66   29    1   63   67   24   46
                17   26   30   38   75   69   35   74   72   68
                18   26   69   75   77   71   72   76   73   70
CARD    25      19   26   38   29   66   75   43   67   78   74
                20   26   75   66   64   77   78   65   79   76
              COORDINATES
                 2   79
                 1    1.4000    1.4000
CARD    30       2    1.5500    1.0500
                 3    1.7000    0.7000
                 4    1.8500    0.3500
                 5    2.0000    0.0000
                 6    2.3000    2.3000
CARD    35       7    2.5250    1.1500
                 8    2.7500    0.0000
                 9    3.2000    3.2000
                10    3.2750    2.4000
                11    3.3500    1.6000
CARD    40      12    3.4250    0.8000
                13    3.5000    0.0000
                14    4.1000    4.1000
                15    4.1750    2.0500
                16    4.2500    0.0000
CARD    45      17    5.0000    5.0000
              ----------------------------------------------------------------------------
                 5   10   15   20   25   30   35   40   45   50   55   60   65   70   75   80
```

```
                P A G E   2

                      5   10   15   20   25   30   35   40   45   50   55   60   65   70   75   80
                    ---------------------------------------------------------------------------------
                      18    5.0000    3.7500
                      19    5.0000    2.5000
                      20    5.0000    1.2500
                      21    5.0000    0.0000
CARD     50           22    1.7500    0.0000
                      23    1.4900    0.6150
                      24    1.2300    1.2300
                      25    1.5000    0.0000
                      26    1.3900    0.2650
CARD     55           27    1.2800    0.5300
                      28    1.1700    0.7950
                      29    1.0600    1.0600
                      30    0.7070    0.7070
                      31    0.8315    0.5557
CARD     60           32    0.9238    0.3825
                      33    0.9810    0.1948
                      34    1.0000    0.0000
                      35    0.7953    0.7953
                      36    1.0129    0.4194
CARD     65           37    1.1250    0.0000
                      38    0.8835    0.8835
                      39    1.0008    0.6753
                      40    1.1019    0.4562
                      41    1.1855    0.2299
CARD     70           42    1.2500    0.0000
                      43    0.9718    0.9718
                      44    1.1910    0.4931
                      45    1.3750    0.0000
                      46    1.0500    1.5500
CARD     75           47    0.7000    1.7000
                      48    0.3500    1.8500
                      49    0.0000    2.0000
                      50    1.1500    2.5250
                      51    0.0000    2.7500
CARD     80           52    2.4000    3.2750
                      53    1.6000    3.3500
                      54    0.8000    3.4250
                      55    0.0000    3.5000
                      56    2.0500    4.1750
CARD     85           57    0.0000    4.2500
                      58    3.7500    5.0000
                      59    2.5000    5.0000
                      60    1.2500    5.0000
                      61    0.0000    5.0000
CARD     90           62    0.0000    1.7500
                      63    0.6150    1.4900
                      64    0.0000    1.5000
                      65    0.2650    1.3900
                      66    0.5300    1.2800
CARD     95           67    0.7950    1.1700
                    ---------------------------------------------------------------------------------
                      5   10   15   20   25   30   35   40   45   50   55   60   65   70   75   80
```

```
          P A G E   3

                    5   10   15   20   25   30   35   40   45   50   55   60   65   70   75   80
                   --------------------------------------------------------------------------------
                      68    0.5557    0.8315
                      69    0.3825    0.9238
                      70    0.1948    0.9810
                      71    0.0000    1.0000
CARD    100           72    0.4194    1.0129
                      73    0.0000    1.1250
                      74    0.6753    1.0008
                      75    0.4562    1.1019
                      76    0.2299    1.1855
CARD    105           77    0.0000    1.2500
                      78    0.4931    1.1910
                      79    0.0000    1.3750
                   GEOMETRY
                       1
CARD    110          0.1
                     1 TO 20
                   ISOTROPIC
                       1
                       1
CARD    115         30000000.   .3
                     1 TO 20
                   DIST LOADS
                       1
                       8   -1.
CARD    120           13   14
                   FIXED DISPLACEMENT
                       2
                     0.0000E+00
                       2
CARD    125           34   37   42   45   25   22    5    8   13   16   21
                     0.0000E+00
                       1
                      71   73   77   79   64   62   49   51   55   57   61
                   OPTIMIZE,2,0,0,1,
CARD    130        10,
                   PRINT ELEMENT
                       1
                     STRESS STRAIN
                       2    4    5    8   10
CARD    135            4    6
                   SUMMARY
                   POST
                          16   17    1    0   19
                      17     EQUIVALENT VON MISES STRESS
CARD    140           11     1ST COMP OF TOTAL STRESS
                      12     2ND COMP OF TOTAL STRESS
                      13     3RD COMP OF TOTAL STRESS
                   END OPTION
                   --------------------------------------------------------------------------------
                       5   10   15   20   25   30   35   40   45   50   55   60   65   70   75   80
                   --------------------------------------------------------------------------------
```

Discussion of MARC Output for New Users

Selected portions of the output for this problem are shown below. The small type on the output is comments and gives a further explanation.

MARC first gives a “notes” section which identifies the version of MARC being used. This is followed by an echo of the input data and a summary of program sizing and options requested.

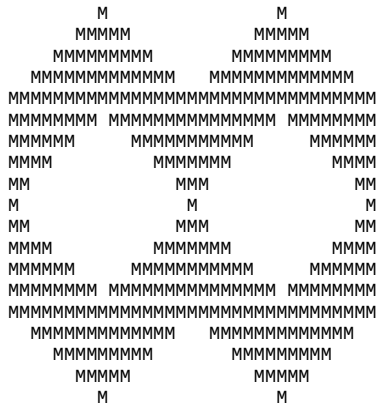

MARC- K7-2-L

MARC ANALYSIS RESEARCH CORPORATION

NORTH AMERICAN

CORPORATE HEADQUARTERS
MARC Analysis Research Corporation
260 Sheridan Avenue, Suite 309
Palo Alto, CA 94306-2089
Telephone: 650-329-6800
FAX : 650-323-5892

WEST COAST OFFICE
MARC Analysis Research Corporation
4330 LaJolla Village Dr.,Suite 320
San Diego, CA 92122-1244
Telephone: 619-658-9588
FAX : 619-587-8710

MIDWEST OFFICE
MARC Analysis Research Corporation
24 Frank Lloyd Wright drive
Ann Arbor, MI 48106-0523
Telephone: 734-998-0540
FAX : 734-998-0542

EAST COAST OFFICE
MARC Analysis Research Corporation
1224 Mill Street Bldg B
East Berlin, CT 06023
Telephone: 860-828-2055
FAX : 860-828-2031

EUROPE

EUROPEAN HEADQUARTERS
MARC-Europe
Dublinstraat 32
2713 HS Zoetermeer,The Netherlands
Telephone: 31-79-3510411
FAX : 31-79-3517560

GERMAN OFFICE
MARC Software Deutschland GmbH
Ismaninger Strasse 9
85609 Aschheim, Germany
Telephone: 49-89-9045033
FAX : 49-89-9030676

UNITED KINGDOM OFFICE
MARC (UK) Ltd.
11, Linford Forum
Rockingham Drive
Linford Wood
Milton Keynes MK14 6LY, UK
Telephone: 44-1908-606070
FAX : 44-1908-606633

ITALIAN OFFICE
Espri-MARC
16129 Viale Brigata Bisagno 2/10
16129 Genova, Italy
Telephone: 39-10-585949
FAX : 39-10-585949

FRENCH OFFICE
MARC France S.A.
Bercy Expo SR 6101A
40 Avenue des Terriors de France
75611 Paris Cedex 12
Telephone: 33-1-44741550
FAX : 33-1-44741554

CZECH OFFICE
MARC Overseas,Inc.
Podolska 50
14700 Prague 4
Telephone: 42-2-61214123
FAX : 42-2-61214123

PACIFIC RIM

FAR EAST HEADQUARTERS
Nippon MARC Co., Ltd.
P.O. Box 5056
Shinjuku Daiichi Seimei Bldg.
2-7-1 Nishi-Shinjuku 2-chome
Shinjuku-ku, Tokyo 163-07, Japan
Telephone: 81-3-3345-0181
FAX : 81-3-3345-1529

OSAKA OFFICE
Nippon MARC Co., Ltd.
4F, 2nd Kimi Building
2-11 Toyotucho Suita-shi
Osaka 564, Japan
Telephone: 81-6-385-1101
FAX : 81-6-385-4343

NAGOYA OFFICE
Nippon MARC Co., Ltd.
Nagoya Nishiki Daiichi Seimei Bldg
2F,6-5 Nishiki 1-chome
Naka-ku,Nagoya,Aichi 460
Telephone: 81-52-202-5661
FAX : 81-52-2-2-5665

CHINA OFFICE
MARC Overseas, Inc.
Bright Chang An Blgg, Suite 321
7#,Jian Guo Men Nei Strees
Beijing 100 005
Telephone: 86-10-6510-2056
FAX : 86-10-6510-2053

KOREAN OFFICE
MARC Overseas,Inc.
Dong Kyung Bldg 7Fl
824-19 Yuksam-Dong
Kangnam-Ku, Seoul,Korea
Telephone: 82-2-561-7543
FAX : 82-2-561-7767

(c) COPYRIGHT 1998 MARC ANALYSIS RESEARCH CORPORATION, all rights reserved

M A R C

I N P U T D A T A

P A G E 1

```
                 5   10   15   20   25   30   35   40   45   50   55   60   65   70   75   80
                ----------------------------------------------------------------------------
                TITLE     ELASTIC ANALYSIS OF A THIN PLATE WITH HOLE
                SIZING        100000
                ELEMENT       26
                END
CARD     5      CONNECTIVITY
                  20
                   1   26    1    3   11    9    2    7   10    6
                   2   26    3    5   13   11    4    8   12    7
                   3   26    9   11   19   17   10   15   18   14
CARD    10         4   26   11   13   21   19   12   16   20   15
                   5   26    5    3   27   25    4   23   26   22
                   6   26    3    1   29   27    2   24   28   23
                   7   26   30   32   40   38   31   36   39   35
                   8   26   32   34   42   40   33   37   41   36
CARD    15         9   26   38   40   27   29   39   44   28   43
                  10   26   40   42   25   27   41   45   26   44
                  11   26    1    9   53   47    6   52   50   46
                  12   26   47   53   55   49   50   54   51   48
                  13   26    9   17   59   53   14   58   56   52
CARD    20        14   26   53   59   61   55   56   60   57   54
                  15   26   49   64   66   47   62   65   63   48
                  16   26   47   66   29    1   63   67   24   46
                  17   26   30   38   75   69   35   74   72   68
                  18   26   69   75   77   71   72   76   73   70
CARD    25        19   26   38   29   66   75   43   67   78   74
                  20   26   75   66   64   77   78   65   79   76
                COORDINATES
                   2   79
                   1    1.4000    1.4000
CARD    30         2    1.5500    1.0500
                   3    1.7000    0.7000
                   4    1.8500    0.3500
                   5    2.0000    0.0000
                   6    2.3000    2.3000
CARD    35         7    2.5250    1.1500
                   8    2.7500    0.0000
                   9    3.2000    3.2000
                  10    3.2750    2.4000
                  11    3.3500    1.6000
CARD    40        12    3.4250    0.8000
                  13    3.5000    0.0000
                  14    4.1000    4.1000
                  15    4.1750    2.0500
                  16    4.2500    0.0000
CARD    45        17    5.0000    5.0000
                ----------------------------------------------------------------------------
                   5   10   15   20   25   30   35   40   45   50   55   60   65   70   75   80
```

```
                P A G E   2

                      5   10   15   20   25   30   35   40   45   50   55   60   65   70   75   80
                    ---------------------------------------------------------------------------------
                      18    5.0000    3.7500
                      19    5.0000    2.5000
                      20    5.0000    1.2500
                      21    5.0000    0.0000
CARD     50           22    1.7500    0.0000
                      23    1.4900    0.6150
                      24    1.2300    1.2300
                      25    1.5000    0.0000
                      26    1.3900    0.2650
CARD     55           27    1.2800    0.5300
                      28    1.1700    0.7950
                      29    1.0600    1.0600
                      30    0.7070    0.7070
                      31    0.8315    0.5557
CARD     60           32    0.9238    0.3825
                      33    0.9810    0.1948
                      34    1.0000    0.0000
                      35    0.7953    0.7953
                      36    1.0129    0.4194
CARD     65           37    1.1250    0.0000
                      38    0.8835    0.8835
                      39    1.0008    0.6753
                      40    1.1019    0.4562
                      41    1.1855    0.2299
CARD     70           42    1.2500    0.0000
                      43    0.9718    0.9718
                      44    1.1910    0.4931
                      45    1.3750    0.0000
                      46    1.0500    1.5500
CARD     75           47    0.7000    1.7000
                      48    0.3500    1.8500
                      49    0.0000    2.0000
                      50    1.1500    2.5250
                      51    0.0000    2.7500
CARD     80           52    2.4000    3.2750
                      53    1.6000    3.3500
                      54    0.8000    3.4250
                      55    0.0000    3.5000
                      56    2.0500    4.1750
CARD     85           57    0.0000    4.2500
                      58    3.7500    5.0000
                      59    2.5000    5.0000
                      60    1.2500    5.0000
                      61    0.0000    5.0000
CARD     90           62    0.0000    1.7500
                      63    0.6150    1.4900
                      64    0.0000    1.5000
                      65    0.2650    1.3900
                      66    0.5300    1.2800
CARD     95           67    0.7950    1.1700
                    ---------------------------------------------------------------------------------
                      5   10   15   20   25   30   35   40   45   50   55   60   65   70   75   80
```

```
          P A G E   3

                    5   10   15   20   25   30   35   40   45   50   55   60   65   70   75   80
                   ----------------------------------------------------------------------------
                      68    0.5557    0.8315
                      69    0.3825    0.9238
                      70    0.1948    0.9810
                      71    0.0000    1.0000
CARD   100            72    0.4194    1.0129
                      73    0.0000    1.1250
                      74    0.6753    1.0008
                      75    0.4562    1.1019
                      76    0.2299    1.1855
CARD   105            77    0.0000    1.2500
                      78    0.4931    1.1910
                      79    0.0000    1.3750
                   GEOMETRY
                       1
CARD   110           0.1
                     1 TO 20
                   ISOTROPIC
                       1
                       1
CARD   115          30000000.   .3
                     1 TO 20
                   DIST LOADS
                       1
                       8   -1.
CARD   120           13   14
                   FIXED DISPLACEMENT
                       2
                     0.0000E+00
                       2
CARD   125           34   37   42   45   25   22    5    8   13   16   21
                     0.0000E+00
                       1
                      71   73   77   79   64   62   49   51   55   57   61
                   OPTIMIZE,2,0,0,1,
CARD   130         10,
                   PRINT ELEMENT
                       1
                     STRESS STRAIN
                       2    4    5    8   10
CARD   135             4    6
                   SUMMARY
                   POST
                          16   17    1    0   19
                      17     EQUIVALENT VON MISES STRESS
CARD   140            11     1ST COMP OF TOTAL STRESS
                      12     2ND COMP OF TOTAL STRESS
                      13     3RD COMP OF TOTAL STRESS
                   END OPTION
                   ----------------------------------------------------------------------------
                       5   10   15   20   25   30   35   40   45   50   55   60   65   70   75   80
                   ----------------------------------------------------------------------------
```

```
************************************************
************************************************

 PROGRAM SIZING AND OPTIONS REQUESTED AS FOLLOWS


 ELEMENT TYPE REQUESTED*************************   26
 NUMBER OF ELEMENTS IN MESH*********************   20
 NUMBER OF NODES IN MESH************************   79
 MAX NUMBER OF ELEMENTS IN ANY DIST LOAD LIST***    2
 MAXIMUM NUMBER OF BOUNDARY CONDITIONS**********   22
 LOAD CORRECTION FLAGGED OR SET*****************
 NUMBER OF LISTS OF DISTRIBUTED LOADS***********    3
 STRESSES STORED AT ALL INTEGRATION POINTS******
 TAPE NO.FOR INPUT OF COORDINATES + CONNECTIVITY    5
 NO.OF DIFFERENT MATERIALS    1 MAX.NO OF SLOPES    5
 MAXIMUM ELEMENTS VARIABLES PER POINT ON POST TP   33
 NUMBER OF POINTS ON SHELL SECTION *************   11
 NEW STYLE INPUT FORMAT WILL BE USED************
 MAXIMUM NUMBER OF SET NAMES IS*****************   10
 NUMBER OF PROCESSORS USED **********************    1
 VECTOR LENGTH USED *****************************    1


 END OF PARAMETERS AND SIZING
************************************************
************************************************
```

At this stage, MARC attempts to allocate core for input of the model definition data and assembly of the element stiffness matrix. MARC first prints out the key to strain, stress, and displacement output for each element type chosen. Column numbers identifying output quantities are referenced to the appropriate components of stress, strain, or displacement. Then, the required number of words is printed out followed by a list of the internal core allocation parameters. They reflect the maximum requirements imposed by different elements. The internal element variables are different for each element type and are repeated for each element type used in a given analysis.

```
KEY TO STRESS, STRAIN AND DISPLACEMENT OUTPUT

          ELEMENT TYPE   26

8-NODE ISOPARAMETRIC PLANE STRESS QUADRILATERAL

STRESSES AND STRAINS IN GLOBAL DIRECTIONS
  1=XX
  2=YY
  3=XY

DISPLACEMENTS IN GLOBAL DIRECTIONS
  1=U GLOBAL X DIRECTION
  2=V GLOBAL Y DIRECTION


WORKSPACE NEEDED FOR INPUT AND STIFFNESS ASSEMBLY     48113
```

```
INTERNAL CORE ALLOCATION PARAMETERS
DEGREES OF FREEDOM PER NODE (NDEG)  2
COORDS PER NODE (NCRD)  2
STRAINS PER INTEGRATION POINT (NGENS)  3
MAX. NODES PER ELEMENT (NNODMX)  8
MAX.STRESS COMPONENTS PER INT. POINT (NSTRMX)   3
MAX. INVARIANTS PER INT. POINTS (NEQST)  1


FLAG FOR ELEMENT STORAGE (IELSTO)  0
ELEMENTS IN CORE, WORDS PER ELEMENT (NELSTO)      1840
                  TOTAL SPACE REQUIRED           36800
VECTORS IN CORE, TOTAL SPACE REQUIRED      2350


WORDS PER TRACK ON DISK SET TO 4096


INTERNAL ELEMENT VARIABLES


INTERNAL ELEMENT NUMBER  1  LIBRARY CODE TYPE 26
NUMBER OF NODES=  8
STRESSES STORED PER INTEGRATION POINT =  3
DIRECT CONTINUUM COMPONENTS STORED =  2
SHEAR CONTINUUM COMPONENTS STORED =  1
SHELL/BEAM FLAG = 0
CURVILINEAR  COORD. FLAG = 0
INT.POINTS FOR ELEM. STIFFNESS  9
NUMBER OF LOCAL INERTIA DIRECTIONS  2
INT.POINT FOR PRINT IF ALL POINTS NOT FLAGGED  5
INT. POINTS FOR DIST. SURFACE LOADS (PRESSURE)  3
LIBRARY CODE TYPE = 26
NO LOCAL ROTATION FLAG = 1
GENERALIZED DISPL. FLAG = 0
LARGE DISP. ROW COUNTS     4    4    7


RESIDUAL LOAD CORRECTION IS INVOKED
```

For nonlinear problems, it is important to note if the residual load correction was turned on. This is done automatically in the current version.

This is followed by the model definition data and how it is read and interpreted by MARC. MARC then calculates the bandwidth of the stiffness matrix and optimizes it if the OPTIMIZE model definition option is included. The original bandwidth (try 0) and the optimized bandwidth (try 10), as well as a correspondence table for nodes are then printed out.

```
MAXIMUM CONNECTIVITY IS   17  AT NODE   75


WORKSPACE NEEDED FOR OPTIMIZING =     46219
MAXIMUM SKY-LINE INCLUDING FILL-IN IS      1526 AT TRY    0 (FORWARD NUMBERING)
MAXIMUM SKY-LINE INCLUDING FILL-IN IS      1128 AT TRY    0 (BACKWARD NUMBERING)
MAXIMUM SKY-LINE INCLUDING FILL-IN IS      1679 AT TRY    1 (FORWARD NUMBERING)
MAXIMUM SKY-LINE INCLUDING FILL-IN IS      1070 AT TRY    1 (BACKWARD NUMBERING)
MAXIMUM SKY-LINE INCLUDING FILL-IN IS      1451 AT TRY    2 (FORWARD NUMBERING)
MAXIMUM SKY-LINE INCLUDING FILL-IN IS       966 AT TRY    2 (BACKWARD NUMBERING)
```

```
MAXIMUM SKY-LINE INCLUDING FILL-IN IS      1558 AT TRY    3 (FORWARD NUMBERING)
MAXIMUM SKY-LINE INCLUDING FILL-IN IS      1004 AT TRY    3 (BACKWARD NUMBERING)
MAXIMUM SKY-LINE INCLUDING FILL-IN IS      1451 AT TRY    4 (FORWARD NUMBERING)
MAXIMUM SKY-LINE INCLUDING FILL-IN IS       966 AT TRY    4 (BACKWARD NUMBERING)
MAXIMUM SKY-LINE INCLUDING FILL-IN IS      1451 AT TRY    5 (FORWARD NUMBERING)
MAXIMUM SKY-LINE INCLUDING FILL-IN IS       966 AT TRY    5 (BACKWARD NUMBERING)
MAXIMUM SKY-LINE INCLUDING FILL-IN IS      1800 AT TRY    6 (FORWARD NUMBERING)
MAXIMUM SKY-LINE INCLUDING FILL-IN IS      1133 AT TRY    6 (BACKWARD NUMBERING)
MAXIMUM SKY-LINE INCLUDING FILL-IN IS      1371 AT TRY    7 (FORWARD NUMBERING)
MAXIMUM SKY-LINE INCLUDING FILL-IN IS       936 AT TRY    7 (BACKWARD NUMBERING)
MAXIMUM SKY-LINE INCLUDING FILL-IN IS      1307 AT TRY    8 (FORWARD NUMBERING)
MAXIMUM SKY-LINE INCLUDING FILL-IN IS       900 AT TRY    8 (BACKWARD NUMBERING)
MAXIMUM SKY-LINE INCLUDING FILL-IN IS      1307 AT TRY    9 (FORWARD NUMBERING)
MAXIMUM SKY-LINE INCLUDING FILL-IN IS       900 AT TRY    9 (BACKWARD NUMBERING)
MAXIMUM SKY-LINE INCLUDING FILL-IN IS      1307 AT TRY   10 (FORWARD NUMBERING)
MAXIMUM SKY-LINE INCLUDING FILL-IN IS       900 AT TRY   10 (BACKWARD NUMBERING)


                    C O R R E S P O N D E N C E   T A B L E   F O R   N O D E S

USER, INTERNAL,   USER, INTERNAL, ETC

    1...   43     2...   45     3...   46     4...   49     5...   48     6...   23     7...   27     8...   28
    9...   21    10...   22    11...   24    12...   26    13...   25    14...    8    15...   11    16...   14
   17...    7    18...    9    19...   10    20...   13    21...   12    22...   50    23...   47    24...   44
   25...   65    26...   64    27...   62    28...   61    29...   59    30...   70    31...   71    32...   76
   33...   79    34...   78    35...   69    36...   75    37...   77    38...   67    39...   68    40...   72
   41...   74    42...   73    43...   60    44...   63    45...   66    46...   42    47...   40    48...   30
   49...   29    50...   20    51...   17    52...   19    53...   18    54...   16    55...   15    56...    5
   57...    3    58...    6    59...    4    60...    2    61...    1    62...   31    63...   41    64...   33
   65...   32    66...   51    67...   53    68...   58    69...   57    70...   39    71...   38    72...   56
   73...   37    74...   55    75...   54    76...   36    77...   35    78...   52    79...   34
```

After the bandwidth calculation (and optimization), MARC assigns the necessary workspace for the in-core solution of this matrix. If the workspace allocated in SIZING is insufficient, it dynamically allocates more memory. If it cannot allocate more memory, MARC attempts to allocate workspace for an out-of-core solution. Information on workspace requirement is printed out.

```
MAXIMUM CONNECTIVITY IS   14  AT NODE   40


MAXIMUM HALF-BANDWIDTH IS   26  BETWEEN NODES   21  AND   46

 NUMBER OF PROFILE ENTRIES INCLUDING FILL-IN IS        900

 NUMBER OF PROFILE ENTRIES EXCLUDING FILL-IN IS        546


TOTAL WORKSPACE NEEDED WITH IN-CORE MATRIX STORAGE =     56175
```

MARC then calculates the loading and sums the load applied to each degree of freedom for distributed loads and point loads. This information provides a valuable check on the total loads in the different degrees of freedom.

```
                    LOAD INCREMENTS ASSOCIATED WITH EACH DEGREE OF FREEDOM
                    SUMMED OVER THE WHOLE MODEL

                    DISTRIBUTED LOADS
1.233E-32 5.000E-01


                    POINT LOADS
0.000E+00 0.000E+00
```

It prints out the time (system billing units) at the start of assembly measured from the start of the job. It prints out the bandwidth which can have changed due to optimization of the nodal numbering (if specified by you). This is followed by a printout of the time at the start of the matrix solution.

```
START OF ASSEMBLY
 TIME =       0.93


START OF MATRIX SOLUTION
 TIME =       1.18
```

If the out-of-core solver is used, a figure representing the profile of the global stiffness matrix is shown.

It prints out the following message which gives an estimate of the conditioning of the matrix. If the singularity is of the order of the accuracy of the machine, (10^{-14} for 64 bits), the equations can be considered singular and the solution unreliable. For nonlinear problems, incremental changes in the singularity ratio reflects approaching instabilities. MARC prints the time at the end of the matrix solution. This is the time at the end of matrix triangularization.

```
SINGULARITY RATIO    1.8140E-01


END OF MATRIX SOLUTION
 TIME =       1.22
```

At this stage, MARC enters a back substitution for the displacements. This is followed by calculation of element stress values. Default yield stress is set by MARC for a linear elastic analysis.

```
                    OUTPUT FOR INCREMENT   0.   ELASTIC ANALYSIS OF A THIN PLATE WITH HOLE


                    ELEMENT WITH HIGHEST STRESS RELATIVE TO YIELD IS    8  WHERE EQUIVALENT STRESS IS 0.309E-
19  OF YIELD
```

A heading is printed next. The Tresca Intensity is output for application in ASME code applications. The von Mises Intensity is the equivalent yield stress. Principal stress and strain values are output. This is followed by individual stress and strain components. The number of each column is to be used with the key printed at the beginning of the analysis.

```
      TRESCA     MISES     MEAN   P R I N C I P A L   V A L U E S          P H Y S I C A L   C O M P O N E N T S
   INTENSITY INTENSITY  NORMAL   MINIMUM INTERMEDIATE MAXIMUM     1        2        3        4        5        6
                        INTENSITY


 ELEMENT    2  POINT   4       INTEGRATION PT. COORDINATE=     0.255E+01    0.102E+01
 SECTION THICKNESS = 0.100E+00
 STRESS  1.197E+00 1.189E+00 4.043E-01 0.000E+00 1.624E-02 1.197E+00 2.112E-02 1.192E+00 7.572E-02
 STRAIN  5.115E-08 3.375E-08 0.000E+00-1.142E-08 0.000E+00 3.972E-08-1.121E-08 3.951E-08 6.563E-09

 ELEMENT    2  POINT   6       INTEGRATION PT. COORDINATE=     0.272E+01    0.130E+00
 SECTION THICKNESS = 0.100E+00
 STRESS  1.133E+00 1.068E+00 4.260E-01 0.000E+00 1.452E-01 1.133E+00 1.458E-01 1.132E+00 2.424E-02
 STRAIN  4.280E-08 3.012E-08 0.000E+00-6.490E-09 0.000E+00 3.631E-08-6.464E-09 3.629E-08 2.101E-09
```

The stress and strain results follow the increment of displacements and the total displacements for all the nodes. If it is requested to print and store all stress points, a printout of the reaction forces follows the displacement output.

```
                    N O D A L   P O I N T   D A T A


                    I N C R E M E N T A L   D I S P L A C E M E N T S


       1 -2.17163E-08  7.15861E-08          2 -3.08177E-08  5.15029E-08          3 -4.07290E-08  3.20392E-08
       4 -4.76926E-08  1.49932E-08          5 -5.04297E-08        0.             6 -2.76616E-08  9.27126E-08
       7 -4.39062E-08  4.43055E-08          8 -5.45603E-08        0.             9 -3.22702E-08  1.16274E-07
      10 -4.01694E-08  8.65917E-08         11 -4.89835E-08  5.64992E-08         12 -5.65106E-08  2.76837E-08
      13 -6.02303E-08        0.            14 -3.35868E-08  1.37781E-07         15 -5.38023E-08  6.75310E-08
      16 -6.65910E-08           0.         17 -3.33965E-08  1.58494E-07         18 -4.60128E-08  1.17024E-07
      19 -5.78831E-08  7.56129E-08         20 -6.85415E-08  3.66168E-08         21 -7.32229E-08        0.
```

22	-4.96304E-08	0.	23	-4.01441E-08	3.13497E-08	24	-2.08547E-08	6.88011E-08
25	-4.87603E-08	0.	26	-4.63275E-08	1.48722E-08	27	-3.98008E-08	3.21380E-08
28	-3.05016E-08	5.02985E-08	29	-2.10768E-08	6.78244E-08	30	-3.00500E-08	7.88703E-08
31	-3.54531E-08	6.20915E-08	32	-3.95287E-08	4.28514E-08	33	-4.20973E-08	2.16157E-08
34	-4.27017E-08	0.	35	-2.56777E-08	7.31203E-08	6	-3.97634E-08	3.80063E-08
37	-4.58139E-08	0.	38	-2.31326E-08	6.98615E-08	39	-3.19519E-08	5.31707E-08
40	-3.97656E-08	3.50769E-08	41	-4.52082E-08	1.66544E-08	42	-4.73812E-08	0.
43	-2.17354E-08	6.82912E-08	44	-3.97941E-08	3.31902E-08	45	-4.82707E-08	0.
46	-1.27043E-08	8.80324E-08	47	-5.79619E-09	1.04377E-07	48	-1.99677E-09	1.15848E-07
49	0.	1.21338E-07	50	-9.95574E-09	1.19837E-07	51	0.	1.37765E-07
52	-2.22710E-08	1.27875E-07	53	-1.27136E-08	1.40913E-07	54	-5.45360E-09	1.52105E-07
55	0.	1.58308E-07	56	-1.33053E-08	1.63107E-07	57	0.	1.80704E-07
58	-2.09176E-08	1.71488E-07	59	-9.48572E-09	1.85090E-07	60	-2.76595E-09	1.98072E-07
61	0.	2.03816E-07	62	0.	1.17685E-07	63	-5.87403E-09	1.01890E-07
64	0.	1.15040E-07	65	-2.56043E-09	1.11113E-07	66	-6.94184E-09	1.00689E-07
67	-1.32932E-08	8.49588E-08	68	-2.37528E-08	9.27920E-08	69	-1.64856E-08	1.03335E-07
70	-8.24241E-09	1.09851E-07	71	0.	1.11859E-07	72	-1.22327E-08	1.02105E-07
73	0.	1.13032E-07	74	-1.60850E-08	8.68819E-08	5	-9.67773E-09	1.01195E-07
76	-4.07604E-09	1.10376E-07	77	0.	1.13596E-07	78	-7.96661E-09	1.00777E-07
79	0.	1.14257E-07						

T O T A L D I S P L A C E M E N T S

1	-2.17163E-08	7.15861E-08	2	-3.08177E-08	5.15029E-08	3	-4.07290E-08	3.20392E-08
4	-4.76926E-08	1.49932E-08	5	-5.04297E-08	0.	6	-2.76616E-08	9.27126E-08
7	-4.39062E-08	4.43055E-08	8	-5.45603E-08	0.	9	-3.22702E-08	1.16274E-07
10	-4.01694E-08	8.65917E-08	11	-4.89835E-08	5.64992E-08	12	-5.65106E-08	2.76837E-08
13	-6.02303E-08	0.	14	-3.35868E-08	1.37781E-07	15	-5.38023E-08	6.75310E-08
16	-6.65910E-08	0.	17	-3.33965E-08	1.58494E-07	18	-4.60128E-08	1.17024E-07
19	-5.78831E-08	7.56129E-08	20	-6.85415E-08	3.66168E-08	21	-7.32229E-08	0.
22	-4.96304E-08	0.	23	-4.01441E-08	3.13497E-08	24	-2.08547E-08	6.88011E-08
25	-4.87603E-08	0.	26	-4.63275E-08	1.48722E-08	27	-3.98008E-08	3.21380E-08
28	-3.05016E-08	5.02985E-08	29	-2.10768E-08	6.78244E-08	30	-3.00500E-08	7.88703E-08
31	-3.54531E-08	6.20915E-08	32	-3.95287E-08	4.28514E-08	33	-4.20973E-08	2.16157E-08
34	-4.27017E-08	0.	35	-2.56777E-08	7.31203E-08	36	-3.97634E-08	3.80063E-08
37	-4.58139E-08	0.	38	-2.31326E-08	6.98615E-08	39	-3.19519E-08	5.31707E-08
40	-3.97656E-08	3.50769E-08	41	-4.52082E-08	1.66544E-08	42	-4.73812E-08	0.
43	-2.17354E-08	6.82912E-08	44	-3.97941E-08	3.31902E-08	45	-4.82707E-08	0.
46	-1.27043E-08	8.80324E-08	47	-5.79619E-09	1.04377E-07	48	-1.99677E-09	1.15848E-07
49	0.	1.21338E-07	50	-9.95574E-09	1.19837E-07	51	0.	1.37765E-07
52	-2.22710E-08	1.27875E-07	53	-1.27136E-08	1.40913E-07	54	-5.45360E-09	1.52105E-07
55	0.	1.58308E-07	56	-1.33053E-08	1.63107E-07	57	0.	1.80704E-07
58	-2.09176E-08	1.71488E-07	59	-9.48572E-09	1.85090E-07	60	-2.76595E-09	1.98072E-07
61	0.	2.03816E-07	62	0.	1.17685E-07	63	-5.87403E-09	1.01890E-07
64	0.	1.15040E-07	65	-2.56043E-09	1.11113E-07	66	-6.94184E-09	1.00689E-07
67	-1.32932E-08	8.49588E-08	68	-2.37528E-08	9.27920E-08	69	-1.64856E-08	1.03335E-07
70	-8.24241E-09	1.09851E-07	71	0.	1.11859E-07	72	-1.22327E-08	1.02105E-07
73	0.	1.13032E-07	74	-1.60850E-08	8.68819E-08	75	-9.67773E-09	1.01195E-07
76	-4.07604E-09	1.10376E-07	77	0.	1.13596E-07	78	-7.96661E-09	1.00777E-07
79	0.	1.14257E-07						

TOTAL EQUIVALENT NODAL FORCES (DISTRIBUTED PLUS POINT LOADS)

1	0.	0.	2	0.	0.	3	0.	0.
4	0.	0.	5	0.	0.	6	0.	0.
7	0.	0.	8	0.	0.	9	0.	0.
10	0.	0.	11	0.	0.	12	0.	0.
13	0.	0.	14	0.	0.	15	0.	0.
16	0.	0.	17	3.82211E-17	4.16667E-02	18	0.	0.
19	0.	0.	20	0.	0.	21	0.	0.
22	0.	0.	23	0.	0.	24	0.	0.
25	0.	0.	26	0.	0.	27	0.	0.
28	0.	0.	29	0.	0.	30	0.	0.
31	0.	0.	32	0.	0.	33	0.	0.
34	0.	0.	35	0.	0.	36	0.	0.
37	0.	0.	38	0.	0.	39	0.	0.
40	0.	0.	41	0.	0.	42	0.	0.
43	0.	0.	44	0.	0.	45	0.	0.
46	0.	0.	47	0.	0.	48	0.	0.
49	0.	0.	50	0.	0.	51	0.	0.
52	0.	0.	53	0.	0.	54	0.	0.
55	0.	0.	56	0.	0.	57	0.	0.
58	0.	0.16667	59	0.	8.33333E-02	60	3.08149E-33	0.16667
61	-3.82211E-17	4.16667E-02	62	0.	0.	63	0.	0.
64	0.	0.	65	0.	0.	66	0.	0.
67	0.	0.	68	0.	0.	69	0.	0.
70	0.	0.	71	0.	0.	72	0.	0.
73	0.	0.	74	0.	0.	75	0.	0.
76	0.	0.	77	0.	0.	78	0.	0.
79	0.	0.						

REACTION FORCES AT FIXED BOUNDARY CONDITIONS, RESIDUAL LOAD CORRECTION ELSEWHERE

1	5.63785E-18	-2.80158E-16	2	-1.73472E-17	6.93889E-18	3	-1.42030E-17	-4.53197E-17
4	4.51028E-17	3.46945E-17	5	2.25514E-17	-4.27307E-02	6	2.42861E-17	-2.77556E-17
7	1.28370E-16	1.11022E-16	8	-1.10995E-16	-0.11445	9	5.73543E-17	-6.93889E-18
10	3.03577E-17	9.19403E-17	11	-6.11490E-17	-2.08167E-17	12	-1.21431E-16	8.67362E-17
13	3.33934E-17	-5.13267E-02	14	-5.33970E-17	8.32667E-17	15	5.37764E-17	8.32667E-17
16	1.20482E-17	-9.69000E-02	17	-7.04761E-17	-8.32667E-17	18	9.38513E-17	2.77759E-17
19	-1.38073E-16	6.93889E-17	20	-1.45283E-16	9.30381E-17	21	4.62954E-17	-2.06520E-02
22	7.18397E-17	-4.78099E-02	23	7.18148E-17	-6.93889E-18	24	1.49620E-17	-5.55112E-17
25	3.03577E-17	-2.05589E-02	26	3.46945E-17	8.67362E-17	27	4.66207E-17	6.93889E-17
28	4.77049E-17	2.08167E-17	29	-6.93889E-18	-1.69136E-16	30	5.20417E-18	3.87711E-16
31	-3.68629E-17	7.63278E-17	32	1.67834E-16	1.07553E-16	33	-1.67153E-17	-2.15756E-17
34	2.35526E-17	-1.38388E-02	35	-1.37911E-16	-9.02056E-17	36	8.32667E-17	-3.46945E-17
37	4.40051E-17	-4.31462E-02	38	-2.86229E-17	-9.88792E-17	39	6.89553E-17	-2.15106E-16
40	2.18141E-16	8.23994E-17	41	7.97973E-17	5.55112E-17	42	1.01915E-16	-1.78546E-02
43	1.34441E-17	-2.08167E-16	44	-3.36970E-16	-2.77556E-17	45	-2.16840E-17	-3.07317E-02
46	-5.20417E-17	-5.13478E-16	47	-1.83881E-16	1.90820E-16	48	1.11022E-16	-2.49800E-16
49	1.06549E-04	3.81639E-17	50	1.35308E-16	-1.11022E-16	51	-3.11517E-03	1.48536E-16
52	-1.21431E-17	6.93889E-17	53	-7.97973E-17	4.23273E-16	54	3.29597E-17	1.38778E-16
55	-4.59252E-03	-6.93889E-18	56	-3.81639E-17	-4.02456E-16	57	-1.38675E-02	1.65734E-16
58	-3.15164E-17	-3.88578E-16	59	6.63532E-17	-2.77556E-16	60	-5.46031E-17	2.49800E-16
61	-7.69689E-03	1.52656E-16	62	1.72880E-03	-2.53161E-17	63	-5.55112E-17	-8.32667E-17
64	1.83992E-03	1.04734E-16	65	8.32667E-17	-2.15973E-16	66	-5.63785E-17	2.24864E-16
67	3.12250E-17	-7.97973E-17	68	-4.87891E-18	-1.18073E-16	69	5.48606E-17	-2.27249E-16
70	2.41167E-17	-3.44268E-17	71	5.30290E-03	-6.60347E-17	72	8.93383E-17	-3.58220E-16

```
      73  1.22931E-02  6.55129E-17          74 -1.38778E-16 -1.76942E-16          75  2.10769E-16  2.35922E-16
      76  9.02056E-17  5.39933E-17          77  3.65933E-03 -2.60751E-17          78 -1.01915E-16  5.06539E-16
      79  4.34147E-03  2.59368E-16

                        SUMMARY OF EXTERNALLY APPLIED LOADS

 0.12326E-31    0.50000E+00

                        SUMMARY OF REACTION/RESIDUAL FORCES

-0.36479E-17   -0.50000E+00
```

The results are concluded with an indication of the magnitude of distributed loads.

```
                DISTRIBUTED LOAD    TYPE    CURRENT
                LIST NUMBER                 MAGNITUDE


                        1           8     -1.000          0.          0.
```

The SUMMARY model definition option asks MARC to print summary tables of stresses and strains as below:

```
*****************************************************************************
*****************************************************************************
*                                                                           *
*ELASTIC ANALYSIS OF A THIN PLATE WITH HOLE                                 *
*
*     INCREMENT     0                                        MARC K7      *
*                                                                           *
*****************************************************************************
*                                    *               *      *     *     *
*              QUANTITY              *    VALUE      * ELEM.* INT.*LAYER*
*                                    *               *NUMBER*POINT*     *
*                                    *               *      *     *     *
*****************************************************************************
*                                    *               *      *     *     *
* MAX FIRST  COMP. OF STRESS         *  0.52712E+00  *    7 *  2  *   1 *
* MIN FIRST  COMP. OF STRESS         * -0.11257E+01  *   18 *  7  *   1 *
*                                    *               *      *     *     *
*                                    *               *      *     *     *
* MAX SECOND COMP. OF STRESS         *  0.31370E+01  *    8 *  3  *   1 *
* MIN SECOND COMP. OF STRESS         * -0.75958E-01  *   18 *  4  *   1 *
*                                    *               *      *     *     *
*                                    *               *      *     *     *
* MAX THIRD  COMP. OF STRESS         *  0.15887E+00  *   18 *  1  *   1 *
* MIN THIRD  COMP. OF STRESS         * -0.84812E+00  *    7 *  3  *   1 *
*                                    *               *      *     *     *
*                                    *               *      *     *     *
* MAX   EQUIVALENT    STRESS         *  0.30910E+01  *    8 *  3  *   1 *
* MIN   EQUIVALENT    STRESS         *  0.26979E+00  *   17 *  4  *   1 *
*                                    *               *      *     *     *
*                                    *               *      *     *     *
* MAX      MEAN       STRESS         *  0.10821E+01  *    8 *  3  *   1 *
* MIN      MEAN       STRESS         * -0.38696E+00  *   18 *  7  *   1 *
*                                    *               *      *     *     *
```

```
*                                        *              *      *     *     *
* MAX     TRESCA      STRESS             *  0.31419E+01 *    8 *  3  *   1 *
* MIN     TRESCA      STRESS             *  0.29647E+00 *   17 *  4  *   1 *
*                                        *              *      *     *     *
*                                        *              *      *     *     *
* MAX FIRST  COMP. OF TOTAL STRAIN       *  0.58578E-08 *    7 *  1  *   1 *
* MIN FIRST  COMP. OF TOTAL STRAIN       * -0.37172E-07 *   18 *  7  *   1 *
*                                        *              *      *     *     *
*                                        *              *      *     *     *
* MAX SECOND COMP. OF TOTAL STRAIN       *  0.10347E-06 *    8 *  3  *   1 *
* MIN SECOND COMP. OF TOTAL STRAIN       *  0.34023E-08 *   17 *  7  *   1 *
*                                        *              *      *     *     *
*                                        *              *      *     *     *
* MAX THIRD  COMP. OF TOTAL STRAIN       *  0.13769E-07 *   18 *  1  *   1 *
* MIN THIRD  COMP. OF TOTAL STRAIN       * -0.73504E-07 *    7 *  3  *   1 *
*                                        *              *      *     *     *
*                                        *              *      *     *     *
* MAX   EQUIVALENT    TOTAL STRAIN       *  0.88382E-07 *    8 *  3  *   1 *
* MIN   EQUIVALENT    TOTAL STRAIN       *  0.88966E-08 *   17 *  4  *   1 *
*                                        *              *      *     *     *
*                                        *              *      *     *     *
* MAX      MEAN       TOTAL STRAIN       *  0.00000E+00 *    1 *  1  *   1 *
* MIN      MEAN       TOTAL STRAIN       *  0.00000E+00 *    1 *  1  *   1 *
*                                        *              *      *     *     *
**************************************************************************
```

The message “`END OF INCREMENT 0`” signifies the end of analysis for 0th increment.

```
 ************************************************************************
 ************************************************************************
 *                                                                      *
 *ELASTIC ANALYSIS OF A THIN PLATE WITH HOLE                            *
 *
 *     INCREMENT     0                                    MARC K7       *
 *                                                                      *
 ************************************************************************
 *                                  *              *      *     *      *
 *              QUANTITY            *    VALUE     * ELEM.* INT.*LAYER*
 *                                  *              *NUMBER*POINT*      *
 *                                  *              *      *     *      *
 ************************************************************************
 *                                  *              *      *     *      *
 * MAX     TRESCA      TOTAL STRAIN *  0.13162E-06 *    8 *  3  *   1 *
 * MIN     TRESCA      TOTAL STRAIN *  0.12847E-07 *   17 *  4  *   1 *
 *                                  *              *      *     *      *
 *                                  *              *      *     *      *
 * MAX TEMPERATURE                  *  0.00000E+00 *    1 *  1  *   1 *
 * MIN TEMPERATURE                  *  0.00000E+00 *    1 *  1  *   1 *
 *                                  *              *      *     *      *
 ************************************************************************
 ************************************************************************
1
```

```
*****************************************************************
*****************************************************************
*                                                               *
*ELASTIC ANALYSIS OF A THIN PLATE WITH HOLE                     *
*     INCREMENT     0                              MARC K7      *
*                                                               *
*****************************************************************
*                                    *                *        *
*               QUANTITY             *     VALUE      *  NODE  *
*                                    *                * NUMBER *
*                                    *                *        *
*****************************************************************
*                                    *                *        *
* MAX FIRST  COMP. OF INCREMENTAL DISP *  -0.19968E-08  *    48  *
* MIN FIRST  COMP. OF INCREMENTAL DISP *  -0.73223E-07  *    21  *
*                                    *                *        *
*                                    *                *        *
* MAX SECOND COMP. OF INCREMENTAL DISP *   0.20382E-06  *    61  *
* MIN SECOND COMP. OF INCREMENTAL DISP *   0.14872E-07  *    26  *
*                                    *                *        *
*                                    *                *        *
* MAX FIRST  COMP. OF TOTAL DISP.      *  -0.19968E-08  *    48  *
* MIN FIRST  COMP. OF TOTAL DISP.      *  -0.73223E-07  *    21  *
*                                    *                *        *
*                                    *                *        *
* MAX SECOND COMP. OF TOTAL DISP.      *   0.20382E-06  *    61  *
* MIN SECOND COMP. OF TOTAL DISP.      *   0.14872E-07  *    26  *
*                                    *                *        *
*                                    *                *        *
* MAX FIRST  COMP. OF REACTION FORCE   *   0.12293E-01  *    73  *
* MIN FIRST  COMP. OF REACTION FORCE   *  -0.13867E-01  *    57  *
*                                    *                *        *
*                                    *                *        *
* MAX SECOND COMP. OF REACTION FORCE   *  -0.13839E-01  *    34  *
* MIN SECOND COMP. OF REACTION FORCE   *  -0.11445E+00  *     8  *
*                                    *                *        *
*****************************************************************
*****************************************************************

                        E N D   O F   I N C R E M E N T   0
```

The MARC exit number 3004 indicates that all loading data has been successfully analyzed and the job is finished.

The above example explains the input and output for a simple elastic problem. It is our hope that these discussions give the new user a good introduction to the use of MARC.

Cross-reference Tables

The following tables give you an example(s) for parameters, model definition, history definition, or rezone options plus element types and user subroutines.

Table 1-1 Parameter Cross-reference

ACCUMULATE					
e3x15.dat					
ACOUSTIC					
e8x25.dat	e8x26.dat				
ADAPTIVE					
e2x10c.dat	e2x9d.dat	e3x21d.dat	e7x20c.dat	e8x12c.dat	e8x12e.dat
e8x40.dat	e8x41.dat	e8x42.dat	e8x43.dat	e8x43b.dat	e8x43c.dat
e8x44.dat	e8x44b.dat	e8x44c.dat	e8x57a.dat	e8x57b.dat	e8x57c.dat
e8x57d.dat	e8x58.dat				
ALIAS					
e2x10b.dat	e2x12d.dat	e2x25b.dat	e2x30.dat	e2x32.dat	e2x45.dat
e2x51a.dat	e2x51b.dat	e2x67b.dat	e2x70.dat	e3x19b.dat	e3x19c.dat
e3x21c.dat	e3x22a.dat	e3x28.dat	e3x30a.dat	e3x32c.dat	e3x33b.dat
e3x3b.dat	e5x12.dat	e5x16b.dat	e5x3e.dat	e5x4d.dat	e5x5a.dat
e6x20a.dat	e6x20b.dat	e7x20d.dat	e7x27.dat	e7x28a.dat	e7x28b.dat
e7x28c.dat	e7x28d.dat	e7x29b.dat	e7x31a.dat	e7x31b.dat	e8x13c.dat
e8x18c.dat	e8x25.dat	e8x36.dat	e8x38c.dat	e8x43.dat	e8x43b.dat
e8x43c.dat	e8x51a.dat	e8x57c.dat	e8x57d.dat	e8x60.dat	e9x13b.dat
ALL POINTS					
e2x40a.dat	e2x40b.dat	e2x41.dat	e2x68.dat	e2x75.dat	e2x76.dat
e2x77.dat	e3x34.dat	e3x35.dat	e3x36.dat	e3x6.dat	e4x11.dat
e4x14a.dat	e4x14b.dat	e4x15.dat	e4x2.dat	e4x2c.dat	e4x2d.dat
e4x2e.dat	e5x15b.dat	e5x17a.dat	e5x17b.dat	e5x18a.dat	e5x18b.dat
e7x23.dat	e7x30a.dat	e7x30b.dat	e7x31a.dat	e7x31b.dat	e7x32.dat

Table 1-1 Parameter Cross-reference (Continued)

ALL POINTS (Continued)					
e8x41.dat	e8x45.dat	e8x46.dat	e8x47.dat	e8x48.dat	e8x49.dat
e8x53a.dat	e8x53b.dat	e8x54.dat	e8x55a.dat	e8x55b.dat	e8x56a.dat
e8x56b.dat	e8x60.dat	e10x4a.dat	e10x4b.dat	e10x6a.dat	e10x6b.dat
APPBC					
e2x8.dat	e3x34.dat				
BEAM SECT					
e2x57a.dat	e2x57b.dat	e2x58a.dat	e2x58b.dat	e2x59b.dat	e2x6.dat
e2x66a.dat	e2x7.dat				
BEARING					
e7x15.dat	e7x16.dat				
BUCKLE					
e3x16.dat	e3x16b.dat	e4x10.dat	e4x10b.dat	e4x12a.dat	e4x12b.dat
e4x12c.dat	e4x12d.dat	e4x15.dat	e4x1a.dat	e4x1d.dat	e4x4.dat
e4x4b.dat	e4x9.dat	e4x9b.dat			
COMMENT					
e3x24a.dat	e3x24b.dat	e3x24c.dat	e5x17b.dat	e8x33a.dat	e8x33b.dat
e8x34.dat	e8x35.dat	e8x55a.dat	e8x55b.dat		
CONSTANT DILATATION					
e3x21f.dat					
COUPLE					
e3x26.dat	e7x1b.dat	e7x1c.dat	e8x13.dat	e8x13b.dat	e8x13c.dat
—	e8x7.dat				
CREEP					
e3x12.dat	e3x12b.dat	e3x13.dat	e3x14a.dat	e3x15.dat	e3x15b.dat
e3x22c.dat	e3x22d.dat	e3x24b.dat	e3x24c.dat	e3x29.dat	

Table 1-1 Parameter Cross-reference (Continued)

DESIGN OPTIMIZATION					
e10x1b.dat	e10x2b.dat	e10x3b.dat	e10x4b.dat	e10x5b.dat	e10x6b.dat
e10x7b.dat					
DESIGN SENSITIVITY					
e10x1a.dat	e10x2a.dat	e10x3a.dat	e10x4a.dat	e10x5a.dat	e10x6a.dat
e10x7a.dat					
DIST LOADS					
e2x40a.dat	e2x40b.dat	e2x41.dat	e2x64a.dat	e2x64b.dat	e2x68.dat
e2x72.dat	e2x73.dat	e2x74.dat	e3x32a.dat	e3x32b.dat	e3x32c.dat
e3x34.dat	e3x6.dat	e4x11.dat	e4x2.dat	e4x2c.dat	e4x2d.dat
e4x2e.dat	e5x17a.dat	e5x17b.dat	e5x18a.dat	e5x18b.dat	e6x1a.dat
e6x1b.dat	e6x1c.dat	e6x21.dat	e6x3a.dat	e6x3b.dat	e6x3c.dat
e6x3d.dat	e7x2.dat	e7x20.dat	e7x20b.dat	e7x20c.dat	e7x20d.dat
e8x33a.dat	e8x33b.dat	e8x36.dat	e8x42.dat	e8x43.dat	e8x43b.dat
e8x43c.dat	e8x46.dat	e8x47.dat	e8x48.dat	e8x49.dat	e8x53a.dat
e8x53b.dat	e9x11a.dat	e9x11b.dat	e9x12a.dat	e9x12b.dat	e9x12c.dat
e9x13a.dat	e9x13b.dat	e9x1a.dat	e9x1b.dat	e9x1c.dat	e9x1d.dat
e9x1e.dat	e9x7a.dat	e9x7b.dat	e9x7c.dat	e9x8.dat	
DYNAMIC					
e4x20.dat	e6x10.dat	e6x11.dat	e6x12.dat	e6x13.dat	e6x13b.dat
e6x14.dat	e6x15.dat	e6x15b.dat	e6x16a.dat	e6x16b.dat	e6x16c.dat
e6x17a.dat	e6x17b.dat	e6x18.dat	e6x19.dat	e6x1a.dat	e6x1b.dat
e6x1c.dat	e6x2.dat	e6x20b.dat	e6x21.dat	e6x3a.dat	e6x3b.dat
e6x3c.dat	e6x3d.dat	e6x4.dat	e6x5.dat	e6x6a.dat	e6x6b.dat
e6x9.dat	e10x1a.dat	e10x1b.dat	e10x3a.dat	e10x3b.dat	e10x4a.dat
e10x4b.dat	e10x7a.dat	e10x7b.dat			

Table 1-1 Parameter Cross-reference (Continued)

ELASTIC					
e2x10c.dat	e2x35.dat	e2x35a.dat	e2x51a.dat	e2x51b.dat	e2x64a.dat
e2x64b.dat	e2x9d.dat	e7x20.dat	e7x20b.dat	e7x20c.dat	e7x20d.dat
e7x27.dat	e7x28a.dat	e7x28b.dat	e7x28c.dat	e7x28d.dat	e7x30a.dat
e7x30b.dat	e7x31a.dat	e7x31b.dat	e8x1a.dat	e8x40.dat	e8x41.dat
e8x43.dat	e8x43b.dat	e8x43c.dat	e8x57a.dat	e8x57b.dat	e8x57c.dat
e8x57d.dat	e8x58.dat				
EL-MA					
e8x30.dat	e8x30b.dat	e8x31.dat	e8x32.dat	e8x33a.dat	e8x33b.dat
ELECTRO					
e8x20.dat	e8x21.dat	e8x28.dat			
ELEMENTS					
e2x1.dat	e2x10.dat	e2x10b.dat	e2x10c.dat	e2x11.dat	e2x12b.dat
e2x12c.dat	e2x12d.dat	e2x12e.dat	e2x13.dat	e2x14.dat	e2x14b.dat
e2x15.dat	e2x16.dat	e2x17.dat	e2x18.dat	e2x19.dat	e2x20.dat
e2x21.dat	e2x22.dat	e2x23.dat	e2x24.dat	e2x25.dat	e2x25b.dat
e2x26.dat	e2x26b.dat	e2x26c.dat	e2x26d.dat	e2x27.dat	e2x28.dat
e2x29.dat	e2x2b.dat	e2x2c.dat	e2x3.dat	e2x30.dat	e2x31a.dat
e2x31b.dat	e2x32.dat	e2x33.dat	e2x33b.dat	e2x34.dat	e2x35.dat
e2x35a.dat	e2x36.dat	e2x37.dat	e2x37b.dat	e2x38.dat	e2x39.dat
e2x4.dat	e2x40a.dat	e2x40b.dat	e2x41.dat	e2x42.dat	e2x43.dat
e2x44.dat	e2x45.dat	e2x46a.dat	e2x46b.dat	e2x46c.dat	e2x46d.dat
e2x47b.dat	e2x48.dat	e2x49.dat	e2x5.dat	e2x50.dat	e2x51a.dat
e2x51b.dat	e2x52.dat	e2x53.dat	e2x54.dat	e2x55.dat	e2x56.dat
e2x57a.dat	e2x57b.dat	e2x58a.dat	e2x58b.dat	e2x59a.dat	e2x59b.dat
e2x6.dat	e2x60a.dat	e2x60b.dat	e2x61a.dat	e2x61b.dat	e2x62.dat
e2x63a.dat	e2x63b.dat	e2x64a.dat	e2x64b.dat	e2x65.dat	e2x66a.dat
e2x66b.dat	e2x67a.dat	e2x67b.dat	e2x68.dat	e2x69.dat	e2x7.dat

Table 1-1 Parameter Cross-reference (Continued)

ELEMENTS (Continued)					
e2x70.dat	e2x71a.dat	e2x71b.dat	e2x72.dat	e2x73.dat	e2x74.dat
e2x75.dat	e2x76.dat	e2x77.dat	e2x8.dat	e2x9.dat	e2x9b.dat
e2x9c.dat	e2x9d.dat	e3x1.dat	e3x10.dat	e3x11.dat	e3x12.dat
e3x12b.dat	e3x13.dat	e3x15.dat	e3x15b.dat	e3x16.dat	e3x16b.dat
e3x17.dat	e3x18.dat	e3x19.dat	e3x19b.dat	e3x19c.dat	e3x19d.dat
e3x20.dat	e3x21a.dat	e3x21c.dat	e3x21d.dat	e3x21e.dat	e3x21f.dat
e3x22a.dat	e3x22c.dat	e3x22d.dat	e3x23.dat	e3x23b.dat	e3x24a.dat
e3x24b.dat	e3x24c.dat	e3x25.dat	e3x26.dat	e3x27.dat	e3x28.dat
e3x29.dat	e3x2a.dat	e3x2b.dat	e3x30a.dat	e3x30b.dat	e3x31.dat
e3x32a.dat	e3x32b.dat	e3x32c.dat	e3x33.dat	e3x33b.dat	e3x34.dat
e3x35.dat	e3x36.dat	e3x37a.dat	e3x37b.dat	e3x38a.dat	e3x38b.dat
e3x3b.dat	e3x4.dat	e3x5.dat	e3x6.dat	e3x8.dat	e3x9.dat
e4x10.dat	e4x10b.dat	e4x11.dat	e4x12a.dat	e4x12b.dat	e4x12c.dat
e4x12d.dat	e4x13a.dat	e4x13b.dat	e4x13c.dat	e4x14a.dat	e4x14b.dat
e4x15.dat	e4x1a.dat	e4x1b.dat	e4x1c.dat	e4x1d.dat	e4x2.dat
e4x20.dat	e4x2a.dat	e4x2b.dat	e4x2c.dat	e4x2d.dat	e4x2e.dat
e4x3.dat	e4x4.dat	e4x4b.dat	e4x5.dat	e4x6.dat	e4x7b.dat
e4x8.dat	e4x9.dat	e4x9b.dat	e5x1.dat	e5x11d.dat	e5x13a.dat
e5x13b.dat	e5x13c.dat	e5x13d.dat	e5x14.dat	e5x15.dat	e5x15b.dat
e5x16a.dat	e5x16b.dat	e5x16c.dat	e5x17a.dat	e5x17b.dat	e5x18a.dat
e5x18b.dat	e5x2a.dat	e5x2b.dat	e5x3a.dat	e5x3b.dat	e5x3c.dat
e5x3d.dat	e5x3e.dat	e5x3f.dat	e5x4a.dat	e5x4b.dat	e5x4c.dat
e5x4d.dat	e5x5a.dat	e5x5b.dat	e5x6.dat	e5x7a.dat	e5x7b.dat
e5x8a.dat	e5x8b.dat	e5x8c.dat	e5x8d.dat	e5x8e.dat	e5x9a.dat
e5x9d.dat	e5x9e.dat	e6x10.dat	e6x13.dat	e6x13b.dat	e6x14.dat
e6x15.dat	e6x15b.dat	e6x16a.dat	e6x16b.dat	e6x16c.dat	e6x17a.dat
e6x17b.dat	e6x18.dat	e6x19.dat	e6x1a.dat	e6x1b.dat	e6x1c.dat
e6x2.dat	e6x20a.dat	e6x20b.dat	e6x21.dat	e6x3a.dat	e6x3b.dat

Table 1-1 Parameter Cross-reference (Continued)

ELEMENTS (Continued)					
e6x3c.dat	e6x3d.dat	e6x4.dat	e6x5.dat	e6x6a.dat	e6x6b.dat
e6x9.dat	e7x1.dat	e7x10.dat	e7x11.dat	e7x12.dat	e7x13b.dat
e7x13c.dat	e7x13d.dat	e7x14.dat	e7x15.dat	e7x16.dat	e7x17a.dat
e7x17b.dat	e7x18.dat	e7x19.dat	e7x19b.dat	e7x1b.dat	e7x1c.dat
e7x2.dat	e7x20.dat	e7x20b.dat	e7x20c.dat	e7x20d.dat	e7x21.dat
e7x22a.dat	e7x22b.dat	e7x22c.dat	e7x23.dat	e7x24a.dat	e7x24b.dat
e7x24c.dat	e7x25.dat	e7x26.dat	e7x27.dat	e7x28a.dat	e7x28b.dat
e7x28c.dat	e7x28d.dat	e7x29a.dat	e7x29b.dat	e7x3.dat	e7x30a.dat
e7x30b.dat	e7x31a.dat	e7x31b.dat	e7x32.dat	e7x3b.dat	e7x4.dat
e7x4b.dat	e7x5.dat	e7x5b.dat	e7x5c.dat	e7x6.dat	e7x6b.dat
e7x7.dat	e7x8a.dat	e7x8b.dat	e7x8c.dat	e7x9a.dat	e7x9b.dat
e7x9c.dat	e8x10.dat	e8x11.dat	e8x12c.dat	e8x12d.dat	e8x12e.dat
e8x13.dat	e8x13b.dat	e8x13c.dat	e8x13k6.da	e8x14a.dat	e8x14b.dat
e8x14c.dat	e8x14d.dat	e8x14e.dat	e8x14f.dat	e8x15.dat	e8x15b.dat
e8x15c.dat	e8x15d.dat	e8x16.dat	e8x16b.dat	e8x17.dat	e8x17b.dat
e8x18.dat	e8x18b.dat	e8x18c.dat	e8x18d.dat	e8x19.dat	e8x19b.dat
e8x1a.dat	e8x2.dat	e8x20.dat	e8x21.dat	e8x22.dat	e8x23.dat
e8x23b.dat	e8x24a.dat	e8x24b.dat	e8x25.dat	e8x26.dat	e8x27.dat
e8x28.dat	e8x29.dat	e8x3.dat	e8x30.dat	e8x30b.dat	e8x31.dat
e8x32.dat	e8x33a.dat	e8x33b.dat	e8x34.dat	e8x35.dat	e8x36.dat
e8x37.dat	e8x38a.dat	e8x38b.dat	—	e8x38c.dat	e8x39.dat
e8x4.dat	e8x40.dat	e8x41.dat	e8x42.dat	e8x43.dat	e8x43b.dat
e8x43c.dat	e8x44.dat	e8x44b.dat	e8x44c.dat	e8x45.dat	e8x46.dat
e8x47.dat	e8x48.dat	e8x49.dat	e8x50.dat	e8x51a.dat	e8x51b.dat
e8x52.dat	e8x53a.dat	e8x53b.dat	e8x54.dat	e8x55a.dat	e8x55b.dat
e8x56a.dat	e8x56b.dat	e8x57a.dat	e8x57b.dat	e8x57c.dat	e8x57d.dat
e8x58.dat	e8x5a.dat	e8x5b.dat	e8x6.dat	e8x60.dat	e8x7.dat
e8x8a.dat	e8x8b.dat	e8x9.dat	e9x10a.dat	e9x10b.dat	e9x10c.dat

Table 1-1 Parameter Cross-reference (Continued)

ELEMENTS (Continued)					
e9x10d.dat	e9x11a.dat	e9x11b.dat	e9x12a.dat	e9x12b.dat	e9x12c.dat
e9x13a.dat	e9x13b.dat	e9x1a.dat	e9x1b.dat	e9x1c.dat	e9x1d.dat
e9x1e.dat	e9x2a.dat	e9x2b.dat	e9x2c.dat	e9x3a.dat	e9x3b.dat
e9x4.dat	e9x5a.dat	e9x5b.dat	e9x5c.dat	e9x5d.dat	e9x5e.dat
e9x6a.dat	e9x6b.dat	e9x7a.dat	e9x7b.dat	e9x7c.dat	e9x8.dat
e9x9a.dat	e9x9b.dat	e10x1a.dat	e10x1b.dat	e10x2a.dat	e10x2b.dat
e10x3a.dat	e10x3b.dat	e10x4a.dat	e10x4b.dat	e10x5a.dat	e10x5b.dat
e10x6a.dat	e10x6b.dat	e10x7a.dat	e10x7b.dat		
ELSTO					
e2x22.dat	e2x27.dat	e2x30.dat	e2x45.dat	e4x2a.dat	e4x2b.dat
e4x5.dat	e7x1.dat	e7x13b.dat	e7x13c.dat	e7x13d.dat	
END					
All MARC input files must have an END parameter line.					
EXTENDED					
e8x45.dat	e8x46.dat				
FINITE					
e3x18.dat	e3x19b.dat	e3x19c.dat	e3x20.dat	e3x21c.dat	e3x27.dat
e3x28.dat	e3x31.dat	e3x3b.dat	e7x17a.dat	e7x17b.dat	e8x12.dat
e8x12b.dat	e8x12c.dat	e8x12r.dat	e8x13.dat	e8x13b.dat	e8x13c.dat
—	e8x14a.dat	e8x14b.dat	e8x14c.dat	e8x14d.dat	e8x14e.dat
e8x14f.dat	e8x15.dat	e8x15b.dat	e8x15c.dat	e8x16.dat	e8x17.dat
e8x18.dat	e8x18b.dat	e8x18d.dat	e8x19.dat	e8x38a.dat	e8x38b.dat
—	e8x38c.dat	e8x44.dat	e8x44b.dat	e8x44c.dat	e8x50.dat
e8x51a.dat	e8x51b.dat	e8x52.dat	e8x55a.dat	e8x55b.dat	e8x56a.dat
e8x56b.dat	e8x7.dat				

Table 1-1 Parameter Cross-reference (Continued)

FLUID					
e9x10a.dat	e9x10b.dat	e9x10c.dat	e9x10d.dat	e9x11a.dat	e9x11b.dat
e9x12a.dat	e9x12b.dat	e9x12c.dat	e9x13a.dat	e9x13b.dat	e9x1a.dat
e9x1b.dat	e9x1c.dat	e9x1d.dat	e9x1e.dat	e9x2a.dat	9x2b.dat
e9x2c.dat	e9x3a.dat	e9x3b.dat	e9x4.dat	e9x5a.dat	e9x5b.dat
e9x5c.dat	e9x5d.dat	e9x5e.dat	e9x6a.dat	e9x6b.dat	e9x7a.dat
e9x7b.dat	e9x7c.dat	e9x8.dat	e9x9a.dat	e9x9b.dat	
FOLLOW FOR					
e3x20.dat	e3x25.dat	e3x26.dat	e3x32a.dat	e3x32b.dat	e3x32c.dat
e4x13a.dat	e4x13b.dat	e4x13c.dat	e4x14a.dat	e4x14b.dat	e4x8.dat
e6x21.dat	e6x4.dat	e7x20.dat	e7x20b.dat	e7x20c.dat	e7x20d.dat
e7x28a.dat	e7x28b.dat	e7x28c.dat	e7x28d.dat	e7x5.dat	e7x5b.dat
e7x5c.dat	e8x42.dat	e8x43.dat	e8x43b.dat	e8x43c.dat	
FOURIER					
e7x8a.dat	e7x8b.dat	e7x8c.dat	e7x9a.dat	e7x9b.dat	e7x9c.dat
HARMONIC					
e6x7.dat	e6x8.dat	e8x30.dat	e8x30b.dat	e8x32.dat	e8x33a.dat
HEAT					
e3x22a.dat	e3x24a.dat	e5x1.dat	e5x10.dat	e5x11a.dat	e5x12.dat
e5x14.dat	e5x15.dat	e5x15b.dat	e5x16a.dat	e5x16b.dat	e5x16c.dat
e5x18a.dat	e5x18b.dat	e5x2a.dat	e5x2b.dat	e5x3a.dat	e5x3b.dat
e5x3c.dat	e5x3d.dat	e5x3e.dat	e5x3f.dat	e5x4a.dat	e5x4b.dat
e5x4c.dat	e5x4d.dat	e5x5a.dat	e5x5b.dat	e5x6.dat	e5x7a.dat
e5x7b.dat	e5x8a.dat	e5x8b.dat	e5x8c.dat	e5x8d.dat	e5x8e.dat
e5x9a.dat	e5x9d.dat	e5x9e.dat			
ISTRESS					
e2x38.dat	e3x30a.dat	e3x32b.dat	e8x34.dat	e8x35.dat	

Table 1-1 Parameter Cross-reference (Continued)

JOULE					
e5x10.dat	e5x12.dat				
LARGE DISP					
e2x65.dat	e3x16.dat	e3x16b.dat	e3x17.dat	e3x18.dat	e3x19b.dat
e3x19c.dat	e3x19d.dat	e3x20.dat	e3x21c.dat	e3x21e.dat	e3x23.dat
e3x23b.dat	e3x25.dat	e3x26.dat	e3x27.dat	e3x28.dat	e3x31.dat
e3x33.dat	e3x33b.dat	e3x34.dat	e3x37a.dat	e3x37b.dat	e3x38a.dat
e3x38b.dat	e3x3b.dat	e4x11.dat	e4x12a.dat	e4x12b.dat	e4x12c.dat
e4x12d.dat	e4x13a.dat	e4x13b.dat	e4x13c.dat	e4x14a.dat	e4x14b.dat
e4x1a.dat	e4x1b.dat	e4x1c.dat	e4x1d.dat	e4x2.dat	e4x20.dat
e4x2a.dat	e4x2b.dat	e4x2c.dat	e4x2d.dat	e4x2e.dat	e4x3.dat
e4x4.dat	e4x4b.dat	e4x5.dat	e4x6.dat	e4x7.dat	e4x7b.dat
e4x7c.dat	e4x8.dat	e6x12.dat	e6x13b.dat	e6x16a.dat	e6x16b.dat
e6x16c.dat	e6x17a.dat	e6x17b.dat	e6x21.dat	e6x4.dat	e6x6a.dat
e6x7.dat	e6x8.dat	e7x17a.dat	e7x17b.dat	e7x18.dat	e7x19b.dat
e7x20d.dat	e7x21.dat	e7x22a.dat	e7x22b.dat	e7x22c.dat	e7x23.dat
e7x25.dat	e7x26.dat	e7x27.dat	e7x28a.dat	e7x28b.dat	e7x28c.dat
e7x28d.dat	e7x29a.dat	e7x30a.dat	e7x30b.dat	e7x31a.dat	e7x31b.dat
e7x4.dat	e7x4b.dat	e7x5.dat	e7x5b.dat	e7x5c.dat	e8x12.dat
e8x12b.dat	e8x12c.dat	e8x12r.dat	e8x13.dat	e8x13b.dat	e8x13c.dat
—	e8x14a.dat	e8x14b.dat	e8x14c.dat	e8x14d.dat	e8x14e.dat
e8x14f.dat	e8x15.dat	e8x15b.dat	e8x15c.dat	e8x16.dat	e8x16b.dat
e8x17.dat	e8x18.dat	e8x18b.dat	e8x18c.dat	e8x18d.dat	e8x19.dat
e8x38a.dat	e8x38b.dat	—	e8x38c.dat	e8x39.dat	e8x42.dat
e8x43b.dat	e8x43c.dat	e8x44.dat	e8x44b.dat	e8x44c.dat	e8x45.dat
e8x46.dat	e8x48.dat	e8x49.dat	e8x50.dat	e8x51a.dat	e8x51b.dat
e8x52.dat	e8x53a.dat	e8x53b.dat	e8x54.dat	e8x55a.dat	e8x55b.dat
e8x56a.dat	e8x56b.dat	e8x7.dat	e9x11b.dat	e9x13a.dat	e9x13b.dat

Table 1-1 Parameter Cross-reference (Continued)

LINEAR					
e6x11.dat					
LUMP					
e5x16a.dat	e5x16b.dat	e5x16c.dat	e5x18a.dat	e5x18b.dat	e6x15.dat
e6x15b.dat	e6x16a.dat	e6x16b.dat	e6x16c.dat	e6x17a.dat	e6x17b.dat
e6x19.dat	e6x9.dat				
MAGNETO					
e8x22.dat	e8x23.dat	e8x23b.dat	e8x24a.dat	e8x24b.dat	e8x29.dat
NEWDB					
e8x1a.dat	e8x2.dat	e8x3.dat			
PLASTICITY					
e3x19.dat	e3x19d.dat	e3x21a.dat	e3x21d.dat	e3x21e.dat	e3x21f.dat
e3x33.dat	e3x33b.dat	e3x34.dat	e3x35.dat	e3x36.dat	e3x37a.dat
e3x37b.dat	e3x38a.dat	e3x38b.dat	e8x12d.dat	e8x12e.dat	e8x15d.dat
e8x16b.dat	e8x17b.dat	e8x18c.dat	e8x19b.dat	e8x60.dat	
PRINT					
e2x14.dat	e2x14b.dat	e2x18.dat	e2x2.dat	e2x26.dat	e2x3.dat
e2x4.dat	e2x43.dat	e2x59a.dat	e2x62.dat	e2x70.dat	e2x9.dat
e3x11.dat	e3x21b.dat	e3x21f.dat	e3x23.dat	e3x23b.dat	e3x28.dat
e3x30a.dat	e3x30b.dat	e3x31.dat	e3x32a.dat	e3x32b.dat	e3x32c.dat
e3x33b.dat	e3x34.dat	e3x35.dat	e3x36.dat	e4x7.dat	e4x7b.dat
e4x7c.dat	e4x8.dat	e5x14.dat	e5x17a.dat	e5x17b.dat	e5x18a.dat
e6x15.dat	e6x16a.dat	e6x16b.dat	e6x16c.dat	e6x17a.dat	e6x17b.dat
e6x19.dat	e6x5.dat	e7x16.dat	e7x20.dat	e7x20b.dat	e7x20c.dat
e7x20d.dat	e7x23.dat	e7x26.dat	e7x31a.dat	e7x31b.dat	e8x12.dat
e8x12b.dat	e8x12c.dat	e8x12d.dat	e8x12e.dat	e8x12r.dat	e8x13.dat
e8x13b.dat	e8x13c.dat	—	e8x14a.dat	e8x14b.dat	e8x14c.dat
e8x14d.dat	e8x14e.dat	e8x14f.dat	e8x15.dat	e8x15b.dat	e8x15c.dat

Table 1-1 Parameter Cross-reference (Continued)

PRINT (Continued)					
e8x15d.dat	e8x16.dat	e8x16b.dat	e8x17.dat	e8x17b.dat	e8x18.dat
e8x18b.dat	e8x18c.dat	e8x18d.dat	e8x19.dat	e8x19b.dat	e8x1b.dat
e8x1c.dat	e8x25.dat	e8x26.dat	e8x28.dat	e8x30.dat	e8x30b.dat
e8x31.dat	e8x32.dat	e8x33b.dat	e8x36.dat	e8x37.dat	e8x38a.dat
e8x38b.dat	—	e8x38c.dat	e8x39.dat	e8x4.dat	e8x40.dat
e8x43.dat	e8x43b.dat	e8x43c.dat	e8x44.dat	e8x44b.dat	e8x44c.dat
e8x46.dat	e8x51a.dat	e8x51b.dat	e8x52.dat	e8x54.dat	e8x55a.dat
e8x55b.dat	e8x56a.dat	e8x56b.dat	e8x57a.dat	e8x57b.dat	e8x57c.dat
e8x57d.dat	e8x58.dat	e8x5a.dat	e8x5b.dat	e8x6.dat	e10x5a.dat
e10x5b.dat					
PROCESSOR					
e2x12c.dat	e2x12e.dat	e2x14.dat	e2x46d.dat	e2x9.dat	e3x21f.dat
e3x23b.dat	e3x32b.dat	e3x32c.dat	e3x38a.dat	e3x38b.dat	e7x29a.dat
e7x3.dat	e7x3b.dat	e8x19b.dat			
R-P FLOW					
e3x30a.dat	e3x30b.dat	e3x32a.dat	e3x32b.dat	e3x32c.dat	e7x1.dat
e7x1b.dat	e7x1c.dat				
RADIATION					
e5x15.dat	e5x15b.dat				
RESPONSE					
e6x18.dat	e6x6a.dat	e6x6b.dat			
REZONING					
e7x17a.dat	e7x17b.dat	e7x31a.dat	e7x31b.dat	e8x12.dat	e8x12b.dat
e8x12r.dat					

Table 1-1 Parameter Cross-reference (Continued)

SCALE					
e2x31a.dat	e2x31b.dat	e2x32.dat	e2x38.dat	e3x1.dat	e3x10.dat
e3x11.dat	e3x12.dat	e3x12b.dat	e3x2a.dat	e3x2b.dat	e3x4.dat
e3x7a.dat	e3x7b.dat	e3x7c.dat	e3x8.dat	e3x9.dat	e7x13b.dat
e7x13c.dat	e7x13d.dat				
SETNAME					
e2x40a.dat	e2x40b.dat	e2x41.dat	e2x46d.dat	e2x68.dat	e2x70.dat
e2x75.dat	e2x76.dat	e2x77.dat	e3x31.dat	e3x34.dat	e3x36.dat
e3x6.dat	e4x11.dat	e4x15.dat	e4x2.dat	e4x2c.dat	e4x2d.dat
e4x2e.dat	e5x15b.dat	e5x17a.dat	e5x17b.dat	e5x18a.dat	e5x18b.dat
e6x21.dat	e7x20c.dat	e7x23.dat	e7x29a.dat	e7x29b.dat	e7x30a.dat
e7x30b.dat	e7x31a.dat	e7x31b.dat	e7x32.dat	e8x15b.dat	e8x36.dat
e8x42.dat	e8x45.dat	e8x46.dat	e8x47.dat	e8x49.dat	e8x50.dat
e8x51a.dat	e8x51b.dat	e8x52.dat	e8x53a.dat	e8x53b.dat	e8x54.dat
e8x55a.dat	e8x55b.dat	e8x60.dat	e9x11a.dat	e9x11b.dat	e9x12a.dat
e9x12b.dat	e9x12c.dat	e9x13a.dat	e9x13b.dat	e9x1a.dat	e9x1b.dat
e9x1c.dat	e9x1d.dat	e9x1e.dat	e9x6a.dat	e9x6b.dat	e9x8.dat
e10x4a.dat	e10x4b.dat	e10x6a.dat	e10x6b.dat		
SHELL SECT					
e2x11.dat	e2x15.dat	e2x40a.dat	e2x40b.dat	e2x41.dat	e2x42.dat
e2x55.dat	e2x56.dat	e2x68.dat	e2x69.dat	e2x70.dat	e2x72.dat
e2x73.dat	e2x74.dat	e2x75.dat	e2x76.dat	e2x77.dat	e3x1.dat
e3x14a.dat	e3x16.dat	e3x16b.dat	e3x17.dat	e3x18.dat	e3x20.dat
e3x23.dat	e3x23b.dat	e3x32c.dat	e3x4.dat	e3x5.dat	e3x6.dat
e4x10.dat	e4x10b.dat	e4x11.dat	e4x1c.dat	e4x2.dat	e4x2c.dat
e4x2d.dat	e4x2e.dat	e4x7.dat	e4x7b.dat	e4x7c.dat	e4x9.dat
e4x9b.dat	e5x13a.dat	e5x13b.dat	e5x13c.dat	e5x13d.dat	e5x18a.dat
e5x18b.dat	e7x22a.dat	e7x22b.dat	e7x22c.dat	e7x24a.dat	e7x24b.dat

Table 1-1 Parameter Cross-reference (Continued)

SHELL SECT (Continued)					
e7x24c.dat	e7x25.dat	e7x26.dat	e7x3.dat	e7x3b.dat	e7x6.dat
e7x6b.dat	e7x7.dat	e8x18.dat	e8x18b.dat	e8x18d.dat	e8x38a.dat
e8x38b.dat	—	e8x38c.dat	e8x51a.dat	e8x51b.dat	e8x52.dat
e8x53a.dat	e8x53b.dat	e8x54.dat	e8x55a.dat	e8x55b.dat	e8x57a.dat
e8x57b.dat	e8x57c.dat	e8x57d.dat	e8x58.dat	e10x4a.dat	e10x4b.dat
SIZING					
e2x1.dat	e2x10.dat	e2x10b.dat	e2x10c.dat	e2x11.dat	e2x12b.dat
e2x12c.dat	e2x12d.dat	e2x12e.dat	e2x13.dat	e2x14.dat	e2x14b.dat
e2x15.dat	e2x16.dat	e2x17.dat	e2x18.dat	e2x19.dat	e2x2.dat
e2x20.dat	e2x21.dat	e2x22.dat	e2x23.dat	e2x24.dat	e2x25.dat
e2x25b.dat	e2x26.dat	e2x26b.dat	e2x26c.dat	e2x26d.dat	e2x27.dat
e2x28.dat	e2x29.dat	e2x2b.dat	e2x2c.dat	e2x3.dat	e2x30.dat
e2x31a.dat	e2x31b.dat	e2x32.dat	e2x33.dat	e2x33b.dat	e2x34.dat
e2x35.dat	e2x35a.dat	e2x36.dat	e2x37.dat	e2x37b.dat	e2x38.dat
e2x39.dat	e2x4.dat	e2x40a.dat	e2x40b.dat	e2x41.dat	e2x42.dat
e2x43.dat	e2x44.dat	e2x45.dat	e2x46a.dat	e2x46b.dat	e2x46c.dat
e2x46d.dat	e2x47b.dat	e2x48.dat	e2x49.dat	e2x5.dat	e2x50.dat
e2x51a.dat	e2x51b.dat	e2x52.dat	e2x53.dat	e2x54.dat	e2x55.dat
e2x56.dat	e2x57a.dat	e2x57b.dat	e2x58a.dat	e2x58b.dat	e2x59a.dat
e2x59b.dat	e2x6.dat	e2x60a.dat	e2x60b.dat	e2x61a.dat	e2x61b.dat
e2x62.dat	e2x63a.dat	e2x63b.dat	e2x64a.dat	e2x64b.dat	e2x65.dat
e2x66a.dat	e2x66b.dat	e2x67a.dat	e2x67b.dat	e2x68.dat	e2x69.dat
e2x7.dat	e2x70.dat	e2x71a.dat	e2x71b.dat	e2x72.dat	e2x73.dat
e2x74.dat	e2x75.dat	e2x76.dat	e2x77.dat	e2x8.dat	e2x9.dat
e2x9b.dat	e2x9c.dat	e2x9d.dat	e3x1.dat	e3x10.dat	e3x11.dat
e3x12.dat	e3x12b.dat	e3x13.dat	e3x14a.dat	e3x15.dat	e3x15b.dat
e3x16.dat	e3x16b.dat	e3x17.dat	e3x18.dat	e3x19.dat	e3x19b.dat

Table 1-1 Parameter Cross-reference (Continued)

SIZING (Continued)					
e3x19c.dat	e3x19d.dat	e3x20.dat	e3x21a.dat	e3x21c.dat	e3x21d.dat
e3x21e.dat	e3x21f.dat	e3x22a.dat	e3x22c.dat	e3x22d.dat	e3x23.dat
e3x23b.dat	e3x24a.dat	e3x24b.dat	e3x24c.dat	e3x25.dat	e3x26.dat
e3x27.dat	e3x28.dat	e3x29.dat	e3x2a.dat	e3x2b.dat	e3x3.dat
e3x30a.dat	e3x30b.dat	e3x31.dat	e3x32a.dat	e3x32b.dat	e3x32c.dat
e3x33.dat	e3x33b.dat	e3x34.dat	e3x35.dat	e3x36.dat	e3x37a.dat
e3x37b.dat	e3x38a.dat	e3x38b.dat	e3x3b.dat	e3x4.dat	e3x5.dat
e3x6.dat	e3x7a.dat	e3x7b.dat	e3x7c.dat	e3x8.dat	e3x9.dat
e4x10.dat	e4x10b.dat	e4x11.dat	e4x12a.dat	e4x12b.dat	e4x12c.dat
e4x12d.dat	e4x13a.dat	e4x13b.dat	e4x13c.dat	e4x14a.dat	e4x14b.dat
e4x15.dat	e4x1a.dat	e4x1b.dat	e4x1c.dat	e4x1d.dat	e4x2.dat
e4x20.dat	e4x2a.dat	e4x2b.dat	e4x2c.dat	e4x2d.dat	e4x2e.dat
e4x3.dat	e4x4.dat	e4x4b.dat	e4x5.dat	e4x6.dat	e4x7.dat
e4x7b.dat	e4x7c.dat	e4x8.dat	e4x9.dat	e4x9b.dat	e5x1.dat
e5x10.dat	e5x11a.dat	e5x11c.dat	e5x12.dat	e5x13a.dat	e5x13b.dat
e5x13c.dat	e5x13d.dat	e5x14.dat	e5x15.dat	e5x15b.dat	e5x16a.dat
e5x16b.dat	e5x16c.dat	e5x17a.dat	e5x17b.dat	e5x18a.dat	e5x18b.dat
e5x2a.dat	e5x2b.dat	e5x3a.dat	e5x3b.dat	e5x3c.dat	e5x3d.dat
e5x3e.dat	e5x3f.dat	e5x4a.dat	e5x4b.dat	e5x4c.dat	e5x4d.dat
e5x5a.dat	e5x5b.dat	e5x6.dat	e5x7a.dat	e5x7b.dat	e5x8a.dat
e5x8b.dat	e5x8c.dat	e5x8d.dat	e5x8e.dat	e5x9a.dat	e5x9b.dat
e5x9d.dat	e5x9e.dat	e6x10.dat	e6x11.dat	e6x12.dat	e6x13.dat
e6x13b.dat	e6x14.dat	e6x15.dat	e6x15b.dat	e6x16a.dat	e6x16b.dat
e6x16c.dat	e6x17a.dat	e6x17b.dat	e6x18.dat	e6x19.dat	e6x1a.dat
e6x1b.dat	e6x1c.dat	e6x2.dat	e6x20a.dat	e6x20b.dat	e6x21.dat
e6x3a.dat	e6x3b.dat	e6x3c.dat	e6x3d.dat	e6x4.dat	e6x5.dat
e6x6a.dat	e6x6b.dat	e6x7.dat	e6x8.dat	e6x9.dat	e7x1.dat
e7x10.dat	e7x11.dat	e7x12.dat	e7x13b.dat	e7x13c.dat	e7x13d.dat

Table 1-1 Parameter Cross-reference (Continued)

SIZING (Continued)					
e7x14.dat	e7x15.dat	e7x16.dat	e7x17a.dat	e7x17b.dat	e7x18.dat
e7x19.dat	e7x19b.dat	e7x1b.dat	e7x1c.dat	e7x2.dat	e7x20.dat
e7x20b.dat	e7x20c.dat	e7x20d.dat	e7x21.dat	e7x22a.dat	e7x22b.dat
e7x22c.dat	e7x23.dat	e7x24a.dat	e7x24b.dat	e7x24c.dat	e7x25.dat
e7x26.dat	e7x27.dat	e7x28a.dat	e7x28b.dat	e7x28c.dat	e7x28d.dat
e7x29a.dat	e7x29b.dat	e7x3.dat	e7x30a.dat	e7x30b.dat	e7x31a.dat
e7x31b.dat	e7x32.dat	e7x3b.dat	e7x4.dat	e7x4b.dat	e7x5.dat
e7x5b.dat	e7x5c.dat	e7x6.dat	e7x6b.dat	e7x7.dat	e7x8a.dat
e7x8b.dat	e7x8c.dat	e7x9a.dat	e7x9b.dat	e7x9c.dat	e8x10.dat
e8x11.dat	e8x12.dat	e8x12b.dat	e8x12c.dat	e8x12d.dat	e8x12e.dat
e8x12r.dat	e8x13.dat	e8x13b.dat	e8x13c.dat	—	e8x14a.dat
e8x14b.dat	e8x14c.dat	e8x14d.dat	e8x14e.dat	e8x14f.dat	e8x15.dat
e8x15b.dat	e8x15c.dat	e8x15d.dat	e8x16.dat	e8x16b.dat	e8x17.dat
e8x17b.dat	e8x18.dat	e8x18b.dat	e8x18c.dat	e8x18d.dat	e8x19.dat
e8x19b.dat	e8x1a.dat	e8x1b.dat	e8x1c.dat	e8x2.dat	e8x20.dat
e8x21.dat	e8x22.dat	e8x23.dat	e8x23b.dat	e8x24a.dat	e8x24b.dat
e8x25.dat	e8x26.dat	e8x27.dat	e8x28.dat	e8x29.dat	e8x3.dat
e8x30.dat	e8x30b.dat	e8x31.dat	e8x32.dat	e8x33a.dat	e8x33b.dat
e8x34.dat	e8x35.dat	e8x36.dat	e8x37.dat	e8x38a.dat	e8x38b.dat
—	e8x38c.dat	e8x39.dat	e8x4.dat	e8x40.dat	e8x41.dat
e8x42.dat	e8x43.dat	e8x43b.dat	e8x43c.dat	e8x44.dat	e8x44b.dat
e8x44c.dat	e8x45.dat	e8x46.dat	e8x47.dat	e8x48.dat	e8x49.dat
e8x50.dat	e8x51a.dat	e8x51b.dat	e8x52.dat	e8x53a.dat	e8x53b.dat
e8x54.dat	e8x55a.dat	e8x55b.dat	e8x56a.dat	e8x56b.dat	e8x57a.dat
e8x57b.dat	e8x57c.dat	e8x57d.dat	e8x58.dat	e8x5a.dat	e8x5b.dat
e8x6.dat	e8x60.dat	e8x7.dat	e8x8a.dat	e8x8b.dat	e8x9.dat
e9x10a.dat	e9x10b.dat	e9x10c.dat	e9x10d.dat	e9x11a.dat	e9x11b.dat
e9x12a.dat	e9x12b.dat	e9x12c.dat	e9x13a.dat	e9x13b.dat	e9x1a.dat

Table 1-1 Parameter Cross-reference (Continued)

SIZING (Continued)					
e9x1b.dat	e9x1c.dat	e9x1d.dat	e9x1e.dat	e9x2a.dat	e9x2b.dat
e9x2c.dat	e9x3a.dat	e9x3b.dat	e9x4.dat	e9x5a.dat	e9x5b.dat
e9x5c.dat	e9x5d.dat	e9x5e.dat	e9x6a.dat	e9x6b.dat	e9x7a.dat
e9x7b.dat	e9x7c.dat	e9x8.dat	e9x9a.dat	e9x9b.dat	e10x1a.dat
e10x1b.dat	e10x2a.dat	e10x2b.dat	e10x3a.dat	e10x3b.dat	e10x4a.dat
e10x4b.dat	e10x5a.dat	e10x5b.dat	e10x6a.dat	e10x6b.dat	e10x7a.dat
e10x7b.dat					
STATE VARS					
e3x13.dat	e7x32.dat				
SUBSTRUC					
e8x1a.dat	e8x2.dat	e8x3.dat			
SUPER					
e8x1b.dat	e8x1c.dat				
THERMAL					
e2x46a.dat	e2x46b.dat	e2x46d.dat	e2x49.dat	e2x51a.dat	e2x51b.dat
e3x11.dat	e3x13.dat	e3x22c.dat	e3x22d.dat	e3x5.dat	e5x11a.dat
e5x11c.dat					
TIE					
e2x47b.dat					
TITLE					
e2x1.dat	e2x10.dat	e2x10b.dat	e2x10c.dat	e2x11.dat	e2x12b.dat
e2x12c.dat	e2x12d.dat	e2x12e.dat	e2x13.dat	e2x14.dat	e2x14b.dat
e2x15.dat	e2x16.dat	e2x17.dat	e2x18.dat	e2x19.dat	e2x2.dat
e2x20.dat	e2x21.dat	e2x22.dat	e2x23.dat	e2x24.dat	e2x25.dat
e2x25b.dat	e2x26.dat	e2x26b.dat	e2x26c.dat	e2x26d.dat	e2x27.dat
e2x28.dat	e2x29.dat	e2x2b.dat	e2x2c.dat	e2x3.dat	e2x30.dat
e2x31a.dat	e2x31b.dat	e2x32.dat	e2x33.dat	e2x33b.dat	e2x34.dat
e2x35.dat	e2x35a.dat	e2x36.dat	e2x37.dat	e2x37b.dat	e2x38.dat

Table 1-1 Parameter Cross-reference (Continued)

TITLE (Continued)					
e2x39.dat	e2x4.dat	e2x40a.dat	e2x40b.dat	e2x41.dat	e2x42.dat
e2x43.dat	e2x44.dat	e2x45.dat	e2x46a.dat	e2x46b.dat	e2x46c.dat
e2x46d.dat	e2x47b.dat	e2x48.dat	e2x49.dat	e2x5.dat	e2x50.dat
e2x51a.dat	e2x51b.dat	e2x52.dat	e2x53.dat	e2x54.dat	e2x55.dat
e2x56.dat	e2x57a.dat	e2x57b.dat	e2x58a.dat	e2x58b.dat	e2x59a.dat
e2x59b.dat	e2x6.dat	e2x60a.dat	e2x60b.dat	e2x61a.dat	e2x61b.dat
e2x62.dat	e2x63a.dat	e2x63b.dat	e2x64a.dat	e2x64b.dat	e2x65.dat
e2x66a.dat	e2x66b.dat	e2x67a.dat	e2x67b.dat	e2x68.dat	e2x69.dat
e2x7.dat	e2x70.dat	e2x71a.dat	e2x71b.dat	e2x72.dat	e2x73.dat
e2x74.dat	e2x75.dat	e2x76.dat	e2x77.dat	e2x8.dat	e2x9.dat
e2x9b.dat	e2x9c.dat	e2x9d.dat	e3x1.dat	e3x10.dat	e3x11.dat
e3x12.dat	e3x12b.dat	e3x13.dat	e3x14a.dat	e3x14b.dat	e3x15.dat
e3x15b.dat	e3x16.dat	e3x16b.dat	e3x17.dat	e3x18.dat	e3x19.dat
e3x19b.dat	e3x19c.dat	e3x19d.dat	e3x20.dat	e3x21a.dat	e3x21b.dat
e3x21c.dat	e3x21d.dat	e3x21e.dat	e3x21f.dat	e3x22a.dat	e3x22b.dat
e3x22c.dat	e3x22d.dat	e3x23.dat	e3x23b.dat	e3x24a.dat	e3x24b.dat
e3x24c.dat	e3x25.dat	e3x26.dat	e3x27.dat	e3x28.dat	e3x29.dat
e3x2a.dat	e3x2b.dat	e3x3.dat	e3x30a.dat	e3x30b.dat	e3x31.dat
e3x32a.dat	e3x32b.dat	e3x32c.dat	e3x33.dat	e3x33b.dat	e3x34.dat
e3x35.dat	e3x36.dat	e3x37a.dat	e3x37b.dat	e3x38a.dat	e3x38b.dat
e3x3b.dat	e3x4.dat	e3x5.dat	e3x6.dat	e3x7a.dat	e3x7b.dat
e3x7c.dat	e3x8.dat	e3x9.dat	e4x10.dat	e4x10b.dat	e4x11.dat
e4x12a.dat	e4x12b.dat	e4x12c.dat	e4x12d.dat	e4x13a.dat	e4x13b.dat
e4x13c.dat	e4x14a.dat	e4x14b.dat	e4x15.dat	e4x1a.dat	e4x1b.dat
e4x1c.dat	e4x1d.dat	e4x2.dat	e4x20.dat	e4x2a.dat	e4x2b.dat
e4x2c.dat	e4x2d.dat	e4x2e.dat	e4x3.dat	e4x4.dat	e4x4b.dat
e4x5.dat	e4x6.dat	e4x7.dat	e4x7b.dat	e4x7c.dat	e4x8.dat
e4x9.dat	e4x9b.dat	e5x1.dat	e5x10.dat	e5x11a.dat	e5x11b.dat

Table 1-1 Parameter Cross-reference (Continued)

TITLE (Continued)					
e5x11c.dat	e5x11d.dat	e5x12.dat	e5x13a.dat	e5x13b.dat	e5x13c.dat
e5x13d.dat	e5x14.dat	e5x15.dat	e5x15b.dat	e5x16a.dat	e5x16b.dat
e5x16c.dat	e5x17a.dat	e5x17b.dat	e5x18a.dat	e5x18b.dat	e5x2a.dat
e5x2b.dat	e5x3a.dat	e5x3b.dat	e5x3c.dat	e5x3d.dat	e5x3e.dat
e5x3f.dat	e5x4a.dat	e5x4b.dat	e5x4c.dat	e5x4d.dat	e5x5a.dat
e5x5b.dat	e5x6.dat	e5x7a.dat	e5x7b.dat	e5x8a.dat	e5x8b.dat
e5x8c.dat	e5x8d.dat	e5x8e.dat	e5x9a.dat	e5x9b.dat	e5x9c.dat
e5x9d.dat	e5x9e.dat	e6x10.dat	e6x11.dat	e6x12.dat	e6x13.dat
e6x13b.dat	e6x14.dat	e6x15.dat	e6x15b.dat	e6x16a.dat	e6x16b.dat
e6x16c.dat	e6x17a.dat	e6x17b.dat	e6x18.dat	e6x19.dat	e6x1a.dat
e6x1b.dat	e6x1c.dat	e6x2.dat	e6x20a.dat	e6x20b.dat	e6x21.dat
e6x3a.dat	e6x3b.dat	e6x3c.dat	e6x3d.dat	e6x4.dat	e6x5.dat
e6x6a.dat	e6x6b.dat	e6x7.dat	e6x8.dat	e6x9.dat	e7x1.dat
e7x10.dat	e7x11.dat	e7x12.dat	e7x13b.dat	e7x13c.dat	e7x13d.dat
e7x14.dat	e7x15.dat	e7x16.dat	e7x17a.dat	e7x17b.dat	e7x18.dat
e7x19.dat	e7x19b.dat	e7x1b.dat	e7x1c.dat	e7x2.dat	e7x20.dat
e7x20b.dat	e7x20c.dat	e7x20d.dat	e7x21.dat	e7x22a.dat	e7x22b.dat
e7x22c.dat	e7x23.dat	e7x24a.dat	e7x24b.dat	e7x24c.dat	e7x25.dat
e7x26.dat	e7x27.dat	e7x28a.dat	e7x28b.dat	e7x28c.dat	e7x28d.dat
e7x29a.dat	e7x29b.dat	e7x3.dat	e7x30a.dat	e7x30b.dat	e7x31a.dat
e7x31b.dat	e7x32.dat	e7x3b.dat	e7x4.dat	e7x4b.dat	e7x5.dat
e7x5b.dat	e7x5c.dat	e7x6.dat	e7x6b.dat	e7x7.dat	e7x8a.dat
e7x8b.dat	e7x8c.dat	e7x9a.dat	e7x9b.dat	e7x9c.dat	e8x10.dat
e8x11.dat	e8x12.dat	e8x12b.dat	e8x12c.dat	e8x12d.dat	e8x12e.dat
e8x12r.dat	e8x13.dat	e8x13b.dat	e8x13c.dat	—	e8x14a.dat
e8x14b.dat	e8x14c.dat	e8x14d.dat	e8x14e.dat	e8x14f.dat	e8x15.dat
e8x15b.dat	e8x15c.dat	e8x15d.dat	e8x16.dat	e8x16b.dat	e8x17.dat
e8x17b.dat	e8x18.dat	e8x18b.dat	e8x18c.dat	e8x18d.dat	e8x19.dat

Table 1-1 Parameter Cross-reference (Continued)

TITLE (Continued)					
e8x19b.dat	e8x1a.dat	e8x1b.dat	e8x1c.dat	e8x2.dat	e8x20.dat
e8x21.dat	e8x22.dat	e8x23.dat	e8x23b.dat	e8x24a.dat	e8x24b.dat
e8x25.dat	e8x26.dat	e8x27.dat	e8x28.dat	e8x29.dat	e8x3.dat
e8x30.dat	e8x30b.dat	e8x31.dat	e8x32.dat	e8x33a.dat	e8x33b.dat
e8x34.dat	e8x35.dat	e8x36.dat	e8x37.dat	e8x38a.dat	e8x38b.dat
—	e8x38c.dat	e8x39.dat	e8x4.dat	e8x40.dat	e8x41.dat
e8x42.dat	e8x43.dat	e8x43b.dat	e8x43c.dat	e8x44.dat	e8x44b.dat
e8x44c.dat	e8x45.dat	e8x46.dat	e8x47.dat	e8x48.dat	e8x49.dat
e8x50.dat	e8x51a.dat	e8x51b.dat	e8x52.dat	e8x53a.dat	e8x53b.dat
e8x54.dat	e8x55a.dat	e8x55b.dat	e8x56a.dat	e8x56b.dat	e8x57a.dat
e8x57b.dat	e8x57c.dat	e8x57d.dat	e8x58.dat	e8x5a.dat	e8x5b.dat
e8x6.dat	e8x60.dat	e8x7.dat	e8x8a.dat	e8x8b.dat	e8x9.dat
e9x10a.dat	e9x10b.dat	e9x10c.dat	e9x10d.dat	e9x11a.dat	e9x11b.dat
e9x12a.dat	e9x12b.dat	e9x12c.dat	e9x13a.dat	e9x13b.dat	e9x1a.dat
e9x1b.dat	e9x1c.dat	e9x1d.dat	e9x1e.dat	e9x2a.dat	e9x2b.dat
e9x2c.dat	e9x3a.dat	e9x3b.dat	e9x4.dat	e9x5a.dat	e9x5b.dat
e9x5c.dat	e9x5d.dat	e9x5e.dat	e9x6a.dat	e9x6b.dat	e9x7a.dat
e9x7b.dat	e9x7c.dat	e9x8.dat	e9x9a.dat	e9x9b.dat	e10x1a.dat
e10x1b.dat	e10x2a.dat	e10x2b.dat	e10x3a.dat	e10x3b.dat	e10x4a.dat
e10x4b.dat	e10x5a.dat	e10x5b.dat	e10x6a.dat	e10x6b.dat	e10x7a.dat
e10x7b.dat					
T-T-T					
e5x11c.dat					

Table 1-1 Parameter Cross-reference (Continued)

UPDATE					
e3x18.dat	e3x19b.dat	e3x19c.dat	e3x20.dat	e3x21c.dat	e3x25.dat
e3x26.dat	e3x27.dat	e3x28.dat	e3x31.dat	e3x3b.dat	e4x3.dat
e4x7.dat	e4x7b.dat	e4x7c.dat	e6x12.dat	e7x17a.dat	e7x17b.dat
e7x25.dat	e7x29a.dat	e8x12.dat	e8x12b.dat	e8x12c.dat	e8x12r.dat
e8x13.dat	e8x13b.dat	e8x13c.dat	—	e8x14a.dat	e8x14b.dat
e8x14c.dat	e8x14d.dat	e8x14e.dat	e8x14f.dat	e8x15.dat	e8x15b.dat
e8x15c.dat	e8x16.dat	e8x17.dat	e8x18.dat	e8x18b.dat	e8x18d.dat
e8x19.dat	e8x34.dat	e8x38a.dat	e8x38b.dat	—	e8x38c.dat
e8x44.dat	e8x44b.dat	e8x44c.dat	e8x50.dat	e8x51a.dat	e8x51b.dat
e8x52.dat	e8x54.dat	e8x55a.dat	e8x55b.dat	e8x56a.dat	e8x56b.dat
e8x7.dat	e9x11b.dat	e9x13a.dat	e9x13b.dat		
USER					
e3x14b.dat	e3x21b.dat				

Table 1-2 Model Definition Option Cross-reference

ADAPTIVE					
e2x10c.dat	e2x9d.dat	e7x20c.dat	e8x12c.dat	e8x12e.dat	e8x40.dat
e8x41.dat	e8x42.dat	e8x43.dat	e8x43b.dat	e8x43c.dat	e8x44.dat
e8x44b.dat	e8x44c.dat	e8x57a.dat	e8x57b.dat	e8x57c.dat	e8x57d.dat
e8x58.dat					
ANISOTROPIC					
e5x7a.dat	e7x6b.dat				
ATTACH NODE					
e2x9d.dat	e7x20c.dat	e8x40.dat	e8x42.dat		
B-H RELATION					
e8x24b.dat					
BUCKLE INCREMENT					
e4x12c.dat	e4x12d.dat				
CASE COMBINATION					
e2x35a.dat	e2x51b.dat	e7x9c.dat			
CHANGE STATE					
e2x41.dat	e5x11c.dat	e7x32.dat	e7x7.dat	e8x45.dat	
CHANNEL					
e5x14.dat					
CHECK RESULTS					
e2x1.dat	e2x10.dat	e2x10b.dat	e2x10c.dat	e2x11.dat	e2x12b.dat
e2x12c.dat	e2x12d.dat	e2x12e.dat	e2x13.dat	e2x14.dat	e2x14b.dat
e2x15.dat	e2x16.dat	e2x17.dat	e2x18.dat	e2x19.dat	e2x2.dat
e2x20.dat	e2x21.dat	e2x22.dat	e2x23.dat	e2x24.dat	e2x25.dat
e2x25b.dat	e2x26.dat	e2x26b.dat	e2x26c.dat	e2x26d.dat	e2x27.dat
e2x28.dat	e2x29.dat	e2x2b.dat	e2x2c.dat	e2x3.dat	e2x30.dat
e2x31a.dat	e2x31b.dat	e2x32.dat	e2x33.dat	e2x33b.dat	e2x34.dat

Table 1-2 Model Definition Option Cross-reference (Continued)

CHECK RESULTS (Continued)					
e2x35.dat	e2x35a.dat	e2x36.dat	e2x37.dat	e2x37b.dat	e2x38.dat
e2x39.dat	e2x4.dat	e2x40a.dat	e2x40b.dat	e2x41.dat	e2x42.dat
e2x43.dat	e2x44.dat	e2x45.dat	e2x46a.dat	e2x46b.dat	e2x46c.dat
e2x46d.dat	e2x47b.dat	e2x48.dat	e2x49.dat	e2x5.dat	e2x50.dat
e2x51a.dat	e2x51b.dat	e2x52.dat	e2x53.dat	e2x54.dat	e2x55.dat
e2x56.dat	e2x57a.dat	e2x57b.dat	e2x58a.dat	e2x58b.dat	e2x59a.dat
e2x59b.dat	e2x6.dat	e2x60a.dat	e2x60b.dat	e2x61a.dat	e2x61b.dat
e2x62.dat	e2x63a.dat	e2x63b.dat	e2x64a.dat	e2x64b.dat	e2x65.dat
e2x66a.dat	e2x66b.dat	e2x67a.dat	e2x67b.dat	e2x68.dat	e2x69.dat
e2x7.dat	e2x70.dat	e2x71a.dat	e2x71b.dat	e2x72.dat	e2x73.dat
e2x74.dat	e2x75.dat	e2x76.dat	e2x77.dat	e2x8.dat	e2x9.dat
e2x9b.dat	e2x9c.dat	e2x9d.dat	e3x1.dat	e3x10.dat	e3x11.dat
e3x12.dat	e3x12b.dat	e3x13.dat	e3x14a.dat	e3x15.dat	e3x15b.dat
e3x16.dat	e3x16b.dat	e3x17.dat	e3x18.dat	e3x19.dat	e3x19b.dat
e3x19c.dat	e3x19d.dat	e3x20.dat	e3x21a.dat	e3x21c.dat	e3x21d.dat
e3x21e.dat	e3x21f.dat	e3x22a.dat	e3x22c.dat	e3x22d.dat	e3x23.dat
e3x23b.dat	e3x24a.dat	e3x24b.dat	e3x24c.dat	e3x25.dat	e3x26.dat
e3x27.dat	e3x28.dat	e3x29.dat	e3x2a.dat	e3x2b.dat	e3x3.dat
e3x30a.dat	e3x30b.dat	e3x31.dat	e3x32a.dat	e3x32b.dat	e3x32c.dat
e3x33.dat	e3x33b.dat	e3x34.dat	e3x35.dat	e3x36.dat	e3x37a.dat
e3x37b.dat	e3x38a.dat	e3x38b.dat	e3x3b.dat	e3x4.dat	e3x5.dat
e3x6.dat	e3x7a.dat	e3x7b.dat	e3x7c.dat	e3x8.dat	e3x9.dat
e4x10.dat	e4x10b.dat	e4x11.dat	e4x12a.dat	e4x12b.dat	e4x12c.dat
e4x12d.dat	e4x13a.dat	e4x13b.dat	e4x13c.dat	e4x14a.dat	e4x14b.dat
e4x15.dat	e4x1a.dat	e4x1b.dat	e4x1c.dat	e4x1d.dat	e4x2.dat
e4x20.dat	e4x2a.dat	e4x2b.dat	e4x2c.dat	e4x2d.dat	e4x2e.dat
e4x3.dat	e4x4.dat	e4x4b.dat	e4x5.dat	e4x6.dat	e4x7.dat
e4x7b.dat	e4x7c.dat	e4x8.dat	e4x9.dat	e4x9b.dat	e5x1.dat

Table 1-2 Model Definition Option Cross-reference (Continued)

CHECK RESULTS (Continued)					
e5x10.dat	e5x11a.dat	e5x11c.dat	e5x12.dat	e5x13a.dat	e5x13b.dat
e5x13c.dat	e5x13d.dat	e5x14.dat	e5x15.dat	e5x16a.dat	e5x16b.dat
e5x16c.dat	e5x17a.dat	e5x17b.dat	e5x18a.dat	e5x18b.dat	e5x2a.dat
e5x2b.dat	e5x3a.dat	e5x3b.dat	e5x3c.dat	e5x3d.dat	e5x3e.dat
e5x3f.dat	e5x4a.dat	e5x4b.dat	e5x4c.dat	e5x4d.dat	e5x5a.dat
e5x5b.dat	e5x6.dat	e5x7a.dat	e5x7b.dat	e5x8a.dat	e5x8b.dat
e5x8c.dat	e5x8d.dat	e5x8e.dat	e5x9a.dat	e5x9b.dat	e5x9d.dat
e5x9e.dat	e6x10.dat	e6x11.dat	e6x12.dat	e6x13.dat	e6x13b.dat
e6x14.dat	e6x15.dat	e6x15b.dat	e6x16a.dat	e6x16b.dat	e6x16c.dat
e6x17a.dat	e6x17b.dat	e6x18.dat	e6x19.dat	e6x1a.dat	e6x1b.dat
e6x1c.dat	e6x2.dat	e6x20a.dat	e6x20b.dat	e6x21.dat	e6x3a.dat
e6x3b.dat	e6x3c.dat	e6x3d.dat	e6x4.dat	e6x5.dat	e6x6a.dat
e6x6b.dat	e6x7.dat	e6x8.dat	e6x9.dat	e7x1.dat	e7x10.dat
e7x11.dat	e7x12.dat	e7x13b.dat	e7x13c.dat	e7x13d.dat	e7x14.dat
e7x15.dat	e7x16.dat	e7x17a.dat	e7x17b.dat	e7x18.dat	e7x19.dat
e7x19b.dat	e7x1b.dat	e7x1c.dat	e7x2.dat	e7x20.dat	e7x20b.dat
e7x20c.dat	e7x20d.dat	e7x21.dat	e7x22a.dat	e7x22b.dat	e7x22c.dat
e7x23.dat	e7x24a.dat	e7x24b.dat	e7x24c.dat	e7x25.dat	e7x26.dat
e7x27.dat	e7x28a.dat	e7x28b.dat	e7x28c.dat	e7x28d.dat	e7x29a.dat
e7x29b.dat	e7x3.dat	e7x30a.dat	e7x30b.dat	e7x31a.dat	e7x31b.dat
e7x32.dat	e7x3b.dat	e7x4.dat	e7x4b.dat	e7x5.dat	e7x5b.dat
e7x5c.dat	e7x6.dat	e7x6b.dat	e7x7.dat	e7x8a.dat	e7x8b.dat
e7x8c.dat	e7x9a.dat	e7x9b.dat	e7x9c.dat	e8x10.dat	e8x11.dat
e8x12.dat	e8x12b.dat	e8x12c.dat	e8x12d.dat	e8x12e.dat	e8x12r.dat
e8x13.dat	e8x13b.dat	e8x13c.dat	—	e8x14a.dat	e8x14b.dat
e8x14c.dat	e8x14d.dat	e8x14e.dat	e8x14f.dat	e8x15.dat	e8x15b.dat
e8x15c.dat	e8x15d.dat	e8x16.dat	e8x16b.dat	e8x17.dat	e8x17b.dat
e8x18.dat	e8x18b.dat	e8x18c.dat	e8x18d.dat	e8x19.dat	e8x19b.dat

Table 1-2 Model Definition Option Cross-reference (Continued)

CHECK RESULTS (Continued)					
e8x1a.dat	e8x1b.dat	e8x1c.dat	e8x2.dat	e8x20.dat	e8x21.dat
e8x22.dat	e8x23.dat	e8x23b.dat	e8x24a.dat	e8x24b.dat	e8x25.dat
e8x26.dat	e8x27.dat	e8x28.dat	e8x29.dat	e8x3.dat	e8x30.dat
e8x30b.dat	e8x31.dat	e8x32.dat	e8x33a.dat	e8x33b.dat	e8x34.dat
e8x35.dat	e8x36.dat	e8x37.dat	e8x38a.dat	e8x38b.dat	—
e8x38c.dat	e8x39.dat	e8x4.dat	e8x40.dat	e8x41.dat	e8x42.dat
e8x43.dat	e8x43b.dat	e8x43c.dat	e8x44.dat	e8x44b.dat	e8x44c.dat
e8x45.dat	e8x46.dat	e8x47.dat	e8x48.dat	e8x49.dat	e8x50.dat
e8x51a.dat	e8x51b.dat	e8x52.dat	e8x53a.dat	e8x53b.dat	e8x54.dat
e8x55a.dat	e8x55b.dat	e8x56a.dat	e8x56b.dat	e8x57a.dat	e8x57b.dat
e8x57c.dat	e8x57d.dat	e8x58.dat	e8x5a.dat	e8x5b.dat	e8x6.dat
e8x60.dat	e8x7.dat	e8x8a.dat	e8x8b.dat	e8x9.dat	e9x10a.dat
e9x10b.dat	e9x10c.dat	e9x10d.dat	e9x11a.dat	e9x11b.dat	e9x12a.dat
e9x12b.dat	e9x12c.dat	e9x13a.dat	e9x13b.dat	e9x1a.dat	e9x1b.dat
e9x1c.dat	e9x1d.dat	e9x1e.dat	e9x2a.dat	e9x2b.dat	e9x2c.dat
e9x3a.dat	e9x3b.dat	e9x4.dat	e9x5a.dat	e9x5b.dat	e9x5c.dat
e9x5d.dat	e9x5e.dat	e9x6a.dat	e9x6b.dat	e9x7a.dat	e9x7b.dat
e9x7c.dat	e9x8.dat	e9x9a.dat	e9x9b.dat	e10x1a.dat	e10x1b.dat
e10x2a.dat	e10x2b.dat	e10x3a.dat	e10x3b.dat	e10x4a.dat	e10x4b.dat
e10x5a.dat	e10x5b.dat	e10x6a.dat	e10x6b.dat	e10x7a.dat	e10x7b.dat
COMPOSITE					
e7x24a.dat	e7x24b.dat	e7x24c.dat	e7x25.dat	e7x6.dat	e7x6b.dat
e7x7.dat	e8x5a.dat	e8x5b.dat	e10x5a.dat	e10x5b.dat	
CONN FILL					
e2x34.dat					

Table 1-2 Model Definition Option Cross-reference (Continued)

CONN GENER					
e2x25.dat	e2x25b.dat	e2x33.dat	e2x33b.dat	e2x34.dat	e2x36.dat
e2x43.dat	e2x48.dat	e2x49.dat	e2x66a.dat	e3x20.dat	e4x4.dat
e4x4b.dat	e4x7.dat	e4x7c.dat	e6x18.dat	e7x16.dat	e8x5a.dat
e8x5b.dat	e8x6.dat	e10x5a.dat	e10x5b.dat		
CONNECTIVITY					
e2x1.dat	e2x10.dat	e2x10b.dat	e2x10c.dat	e2x11.dat	e2x12b.dat
e2x12c.dat	e2x12d.dat	e2x12e.dat	e2x13.dat	e2x14.dat	e2x14b.dat
e2x15.dat	e2x16.dat	e2x17.dat	e2x18.dat	e2x19.dat	e2x2.dat
e2x21.dat	e2x22.dat	e2x23.dat	e2x24.dat	e2x25.dat	e2x25b.dat
e2x26.dat	e2x26b.dat	e2x26c.dat	e2x26d.dat	e2x27.dat	e2x28.dat
e2x29.dat	e2x2b.dat	e2x2c.dat	e2x3.dat	e2x30.dat	e2x31a.dat
e2x31b.dat	e2x32.dat	e2x33.dat	e2x33b.dat	e2x34.dat	e2x35.dat
e2x35a.dat	e2x36.dat	e2x37.dat	e2x37b.dat	e2x38.dat	e2x39.dat
e2x4.dat	e2x40a.dat	e2x40b.dat	e2x41.dat	e2x42.dat	e2x43.dat
e2x44.dat	e2x45.dat	e2x46a.dat	e2x46b.dat	e2x46c.dat	e2x46d.dat
e2x47b.dat	e2x48.dat	e2x49.dat	e2x5.dat	e2x50.dat	e2x51a.dat
e2x51b.dat	e2x52.dat	e2x53.dat	e2x54.dat	e2x55.dat	e2x56.dat
e2x57a.dat	e2x57b.dat	e2x58a.dat	e2x58b.dat	e2x59a.dat	e2x59b.dat
e2x6.dat	e2x60a.dat	e2x60b.dat	e2x61a.dat	e2x61b.dat	e2x62.dat
e2x63a.dat	e2x63b.dat	e2x64a.dat	e2x64b.dat	e2x65.dat	e2x66a.dat
e2x66b.dat	e2x67a.dat	e2x67b.dat	e2x68.dat	e2x69.dat	e2x7.dat
e2x70.dat	e2x71a.dat	e2x71b.dat	e2x72.dat	e2x73.dat	e2x74.dat
e2x75.dat	e2x76.dat	e2x77.dat	e2x8.dat	e2x9.dat	e2x9b.dat
e2x9c.dat	e2x9d.dat	e3x1.dat	e3x10.dat	e3x11.dat	e3x12.dat
e3x12b.dat	e3x13.dat	e3x14a.dat	e3x15.dat	e3x15b.dat	e3x16.dat
e3x16b.dat	e3x17.dat	e3x18.dat	e3x19.dat	e3x19b.dat	e3x19c.dat
e3x19d.dat	e3x20.dat	e3x21a.dat	e3x21c.dat	e3x21d.dat	e3x21e.dat

Table 1-2 Model Definition Option Cross-reference (Continued)

CONNECTIVITY (Continued)					
e3x21f.dat	e3x22a.dat	e3x22c.dat	e3x22d.dat	e3x23.dat	e3x23b.dat
e3x24a.dat	e3x24b.dat	e3x24c.dat	e3x25.dat	e3x26.dat	e3x27.dat
e3x28.dat	e3x29.dat	e3x2a.dat	e3x2b.dat	e3x3.dat	e3x30a.dat
e3x30b.dat	e3x31.dat	e3x32a.dat	e3x32b.dat	e3x32c.dat	e3x33.dat
e3x33b.dat	e3x34.dat	e3x35.dat	e3x36.dat	e3x37a.dat	e3x37b.dat
e3x38a.dat	e3x38b.dat	e3x3b.dat	e3x4.dat	e3x5.dat	e3x6.dat
e3x7a.dat	e3x8.dat	e3x9.dat	e4x10.dat	e4x10b.dat	e4x11.dat
e4x12a.dat	e4x12b.dat	e4x12c.dat	e4x12d.dat	e4x13a.dat	e4x13b.dat
e4x13c.dat	e4x14a.dat	e4x14b.dat	e4x15.dat	e4x1a.dat	e4x1b.dat
e4x1c.dat	e4x1d.dat	e4x2.dat	e4x20.dat	e4x2a.dat	e4x2b.dat
e4x2c.dat	e4x2d.dat	e4x2e.dat	e4x3.dat	e4x4.dat	e4x4b.dat
e4x5.dat	e4x6.dat	e4x7.dat	e4x7b.dat	e4x7c.dat	e4x8.dat
e4x9.dat	e4x9b.dat	e5x1.dat	e5x10.dat	e5x11a.dat	e5x11c.dat
e5x12.dat	e5x13a.dat	e5x13b.dat	e5x13c.dat	e5x13d.dat	e5x14.dat
e5x15.dat	e5x15b.dat	e5x16a.dat	e5x16b.dat	e5x16c.dat	e5x17a.dat
e5x17b.dat	e5x18a.dat	e5x18b.dat	e5x2a.dat	e5x2b.dat	e5x3a.dat
e5x3b.dat	e5x3c.dat	e5x3d.dat	e5x3e.dat	e5x3f.dat	e5x4a.dat
e5x4b.dat	e5x4c.dat	e5x4d.dat	e5x5a.dat	e5x5b.dat	e5x6.dat
e5x7a.dat	e5x7b.dat	e5x8a.dat	e5x8c.dat	e5x8d.dat	e5x8e.dat
e5x9a.dat	e5x9b.dat	e5x9d.dat	e5x9e.dat	e6x10.dat	e6x11.dat
e6x12.dat	e6x13.dat	e6x13b.dat	e6x14.dat	e6x15.dat	e6x15b.dat
e6x16a.dat	e6x16b.dat	e6x16c.dat	e6x17a.dat	e6x17b.dat	e6x18.dat
e6x19.dat	e6x1a.dat	e6x1b.dat	e6x1c.dat	e6x2.dat	e6x20a.dat
e6x20b.dat	e6x21.dat	e6x3a.dat	e6x3b.dat	e6x3c.dat	e6x3d.dat
e6x4.dat	e6x5.dat	e6x6a.dat	e6x6b.dat	e6x7.dat	e6x8.dat
e6x9.dat	e7x1.dat	e7x10.dat	e7x11.dat	e7x12.dat	e7x13b.dat
e7x13c.dat	e7x14.dat	e7x15.dat	e7x16.dat	e7x17a.dat	e7x17b.dat
e7x18.dat	e7x19.dat	e7x19b.dat	e7x1b.dat	e7x1c.dat	e7x2.dat

Table 1-2 Model Definition Option Cross-reference (Continued)

CONNECTIVITY (Continued)					
e7x20.dat	e7x20b.dat	e7x20c.dat	e7x20d.dat	e7x21.dat	e7x22a.dat
e7x22b.dat	e7x22c.dat	e7x23.dat	e7x24a.dat	e7x24b.dat	e7x24c.dat
e7x25.dat	e7x26.dat	e7x27.dat	e7x28a.dat	e7x28b.dat	e7x28c.dat
e7x28d.dat	e7x29a.dat	e7x29b.dat	e7x3.dat	e7x30a.dat	e7x30b.dat
e7x31a.dat	e7x31b.dat	e7x32.dat	e7x3b.dat	e7x4.dat	e7x4b.dat
e7x5.dat	e7x5b.dat	e7x5c.dat	e7x6.dat	e7x6b.dat	e7x7.dat
e7x8a.dat	e7x8b.dat	e7x8c.dat	e7x9a.dat	e7x9b.dat	e8x10.dat
e8x11.dat	e8x12.dat	e8x12b.dat	e8x12c.dat	e8x12d.dat	e8x12e.dat
e8x12r.dat	e8x13.dat	e8x13b.dat	e8x13c.dat	—	e8x14a.dat
e8x14b.dat	e8x14c.dat	e8x14d.dat	e8x14e.dat	e8x14f.dat	e8x15.dat
e8x15b.dat	e8x15c.dat	e8x15d.dat	e8x16.dat	e8x16b.dat	e8x17.dat
e8x17b.dat	e8x18.dat	e8x18b.dat	e8x18c.dat	e8x18d.dat	e8x19.dat
e8x19b.dat	e8x1a.dat	e8x2.dat	e8x20.dat	e8x21.dat	e8x22.dat
e8x23.dat	e8x23b.dat	e8x24a.dat	e8x24b.dat	e8x25.dat	e8x26.dat
e8x27.dat	e8x28.dat	e8x29.dat	e8x3.dat	e8x30.dat	e8x30b.dat
e8x31.dat	e8x32.dat	e8x33a.dat	e8x33b.dat	e8x34.dat	e8x35.dat
e8x36.dat	e8x37.dat	e8x38a.dat	e8x38b.dat	—	e8x38c.dat
e8x39.dat	e8x4.dat	e8x40.dat	e8x41.dat	e8x42.dat	e8x43.dat
e8x43b.dat	e8x43c.dat	e8x44.dat	e8x44b.dat	e8x44c.dat	e8x45.dat
e8x46.dat	e8x47.dat	e8x48.dat	e8x49.dat	e8x50.dat	e8x51a.dat
e8x51b.dat	e8x52.dat	e8x53a.dat	e8x53b.dat	e8x54.dat	e8x55a.dat
e8x55b.dat	e8x56a.dat	e8x56b.dat	e8x57a.dat	e8x57b.dat	e8x57c.dat
e8x57d.dat	e8x58.dat	e8x5a.dat	e8x5b.dat	e8x6.dat	e8x60.dat
e8x7.dat	e8x8a.dat	e8x8b.dat	e8x9.dat	e9x10a.dat	e9x10b.dat
e9x10c.dat	e9x10d.dat	e9x11a.dat	e9x11b.dat	e9x12a.dat	e9x12b.dat
e9x12c.dat	e9x13a.dat	e9x13b.dat	e9x1a.dat	e9x1b.dat	e9x1c.dat
e9x1d.dat	e9x1e.dat	e9x2a.dat	e9x2b.dat	e9x2c.dat	e9x3a.dat
e9x3b.dat	e9x4.dat	e9x5a.dat	e9x5b.dat	e9x5c.dat	e9x5d.dat

Table 1-2 Model Definition Option Cross-reference (Continued)

CONNECTIVITY (Continued)					
e9x5e.dat	e9x6a.dat	e9x6b.dat	e9x7a.dat	e9x7b.dat	e9x7c.dat
e9x8.dat	e9x9a.dat	e9x9b.dat	e10x1a.dat	e10x1b.dat	e10x2a.dat
e10x2b.dat	e10x3a.dat	e10x3b.dat	e10x4a.dat	e10x4b.dat	e10x5a.dat
e10x5b.dat	e10x6a.dat	e10x6b.dat	e10x7a.dat	e10x7b.dat	
CONRAD GAP					
e5x14.dat					
CONTACT					
e3x30a.dat	e3x30b.dat	e3x31.dat	e3x32a.dat	e3x32b.dat	e3x32c.dat
e4x7b.dat	e6x16a.dat	e6x16b.dat	e6x16c.dat	e6x17a.dat	e6x17b.dat
e6x19.dat	e7x20.dat	e7x20b.dat	e7x20c.dat	e7x20d.dat	e7x23.dat
e7x31a.dat	e7x31b.dat	e8x12.dat	e8x12b.dat	e8x12c.dat	e8x12d.dat
e8x12e.dat	e8x12r.dat	e8x13.dat	e8x13b.dat	e8x13c.dat	—
e8x14a.dat	e8x14b.dat	e8x14c.dat	e8x14d.dat	e8x14e.dat	e8x14f.dat
e8x15.dat	e8x15b.dat	e8x15c.dat	e8x15d.dat	e8x16.dat	e8x16b.dat
e8x17.dat	e8x17b.dat	e8x18.dat	e8x18b.dat	e8x18c.dat	e8x18d.dat
e8x19.dat	e8x19b.dat	e8x36.dat	e8x37.dat	e8x38a.dat	e8x38b.dat
—	e8x38c.dat	e8x39.dat	e8x42.dat	e8x43.dat	e8x43b.dat
e8x43c.dat	e8x44.dat	e8x44b.dat	e8x44c.dat	e8x45.dat	e8x46.dat
e8x47.dat	e8x48.dat	e8x49.dat	e8x50.dat	e8x51a.dat	e8x51b.dat
e8x52.dat	e8x53a.dat	e8x53b.dat	e8x54.dat	e8x55a.dat	e8x55b.dat
e8x56a.dat	e8x56b.dat	e8x60.dat			
CONTACT NODE					
e8x15b.dat					

Table 1-2 Model Definition Option Cross-reference (Continued)

CONTACT TABLE					
e3x31.dat	e3x32b.dat	e3x32c.dat	e6x19.dat	e7x31a.dat	e7x31b.dat
e8x13c.dat	e8x15.dat	e8x15b.dat	e8x15c.dat	e8x15d.dat	e8x16b.dat
e8x38a.dat	e8x38b.dat	—	e8x38c.dat	e8x44.dat	e8x44b.dat
e8x44c.dat	e8x46.dat	e8x51a.dat	e8x51b.dat	e8x52.dat	e8x55b.dat
e8x56b.dat					
CONTROL					
e2x12b.dat	e2x65.dat	e2x67a.dat	e2x67b.dat	e2x70.dat	e2x9d.dat
e3x1.dat	e3x10.dat	e3x11.dat	e3x12.dat	e3x12b.dat	e3x13.dat
e3x14a.dat	e3x15.dat	e3x15b.dat	e3x16.dat	e3x16b.dat	e3x17.dat
e3x18.dat	e3x19.dat	e3x19b.dat	e3x19c.dat	e3x19d.dat	e3x20.dat
e3x21a.dat	e3x21c.dat	e3x21d.dat	e3x21e.dat	e3x21f.dat	e3x22a.dat
e3x22c.dat	e3x22d.dat	e3x23.dat	e3x23b.dat	e3x24a.dat	e3x24b.dat
e3x24c.dat	e3x25.dat	e3x26.dat	e3x27.dat	e3x28.dat	e3x29.dat
e3x2a.dat	e3x2b.dat	e3x3.dat	e3x30a.dat	e3x30b.dat	e3x31.dat
e3x32a.dat	e3x32b.dat	e3x32c.dat	e3x33.dat	e3x33b.dat	e3x35.dat
e3x36.dat	e3x37a.dat	e3x37b.dat	e3x38a.dat	e3x38b.dat	e3x3b.dat
e3x4.dat	e3x5.dat	e3x7a.dat	e3x7b.dat	e3x7c.dat	e3x8.dat
e3x9.dat	e4x12a.dat	e4x12b.dat	e4x12c.dat	e4x12d.dat	e4x13a.dat
e4x13b.dat	e4x13c.dat	e4x14a.dat	e4x14b.dat	e4x15.dat	e4x1a.dat
e4x1b.dat	e4x1c.dat	e4x1d.dat	e4x20.dat	e4x2a.dat	e4x2b.dat
e4x3.dat	e4x4.dat	e4x4b.dat	e4x5.dat	e4x6.dat	e4x7.dat
e4x7b.dat	e4x7c.dat	e4x8.dat	e5x11a.dat	e5x11c.dat	e5x13a.dat
e5x13b.dat	e5x13c.dat	e5x13d.dat	e5x14.dat	e5x15.dat	e5x16a.dat
e5x16b.dat	e5x16c.dat	e5x17a.dat	e5x17b.dat	e5x2a.dat	e5x2b.dat
e5x3a.dat	e5x3b.dat	e5x3c.dat	e5x3d.dat	e5x3e.dat	e5x3f.dat
e5x4a.dat	e5x4b.dat	e5x4c.dat	e5x4d.dat	e5x5a.dat	e5x5b.dat
e5x6.dat	e5x8a.dat	e5x8c.dat	e5x8d.dat	e5x8e.dat	e5x9a.dat

Table 1-2 Model Definition Option Cross-reference (Continued)

CONTROL (Continued)					
e5x9b.dat	e5x9d.dat	e5x9e.dat	e6x13.dat	e6x13b.dat	e6x14.dat
e6x16a.dat	e6x16b.dat	e6x16c.dat	e6x17a.dat	e6x17b.dat	e6x1a.dat
e6x1b.dat	e6x1c.dat	e6x21.dat	e6x3a.dat	e6x3b.dat	e6x3c.dat
e6x3d.dat	e6x4.dat	e6x7.dat	e6x8.dat	e6x9.dat	e7x1.dat
e7x11.dat	e7x12.dat	e7x13b.dat	e7x13c.dat	e7x13d.dat	e7x14.dat
e7x16.dat	e7x17a.dat	e7x17b.dat	e7x18.dat	e7x1b.dat	e7x1c.dat
e7x2.dat	e7x20.dat	e7x20b.dat	e7x20c.dat	e7x20d.dat	e7x21.dat
e7x22a.dat	e7x22b.dat	e7x22c.dat	e7x23.dat	e7x25.dat	e7x26.dat
e7x28a.dat	e7x28b.dat	e7x28c.dat	e7x28d.dat	e7x29a.dat	e7x29b.dat
e7x3.dat	e7x3b.dat	e7x4.dat	e7x4b.dat	e7x5.dat	e7x5b.dat
e7x5c.dat	e7x8a.dat	e7x8b.dat	e7x8c.dat	e7x9a.dat	e7x9b.dat
e7x9c.dat	e8x10.dat	e8x12.dat	e8x12b.dat	e8x12c.dat	e8x12d.dat
e8x12e.dat	e8x12r.dat	e8x13.dat	e8x13b.dat	e8x13c.dat	—
e8x14a.dat	e8x14b.dat	e8x14c.dat	e8x14d.dat	e8x14e.dat	e8x14f.dat
e8x15.dat	e8x15b.dat	e8x15c.dat	e8x15d.dat	e8x16.dat	e8x16b.dat
e8x17.dat	e8x17b.dat	e8x18.dat	e8x18b.dat	e8x18c.dat	e8x18d.dat
e8x19.dat	e8x19b.dat	e8x24b.dat	e8x26.dat	e8x27.dat	e8x31.dat
e8x33b.dat	e8x34.dat	e8x36.dat	e8x37.dat	e8x38a.dat	e8x38b.dat
—	e8x38c.dat	e8x39.dat	e8x4.dat	e8x41.dat	e8x42.dat
e8x44.dat	e8x44b.dat	e8x44c.dat	e8x51a.dat	e8x51b.dat	e8x55a.dat
e8x55b.dat	e8x56a.dat	e8x56b.dat	e8x5a.dat	e8x5b.dat	e8x6.dat
e8x7.dat	e9x10a.dat	e9x10b.dat	e9x10c.dat	e9x10d.dat	e9x11a.dat
e9x11b.dat	e9x12a.dat	e9x12b.dat	e9x12c.dat	e9x13a.dat	e9x13b.dat
e9x1a.dat	e9x1b.dat	e9x1c.dat	e9x1d.dat	e9x1e.dat	e9x2a.dat
e9x2b.dat	e9x2c.dat	e9x3a.dat	e9x3b.dat	e9x4.dat	e9x5a.dat
e9x5b.dat	e9x5c.dat	e9x5d.dat	e9x5e.dat	e9x6a.dat	e9x6b.dat
e9x7a.dat	e9x7b.dat	e9x7c.dat	e9x8.dat	e9x9a.dat	e9x9b.dat

Table 1-2 Model Definition Option Cross-reference (Continued)

CONVERT					
e8x13.dat	e8x13b.dat	e8x13c.dat	—	e8x7.dat	
COORDINATES					
e2x1.dat	e2x10.dat	e2x10b.dat	e2x10c.dat	e2x11.dat	e2x12b.dat
e2x12c.dat	e2x12d.dat	e2x12e.dat	e2x13.dat	e2x14.dat	e2x14b.dat
e2x15.dat	e2x16.dat	e2x17.dat	e2x18.dat	e2x19.dat	e2x2.dat
e2x21.dat	e2x22.dat	e2x23.dat	e2x24.dat	e2x25.dat	e2x25b.dat
e2x26.dat	e2x26b.dat	e2x26c.dat	e2x26d.dat	e2x27.dat	e2x28.dat
e2x29.dat	e2x2b.dat	e2x2c.dat	e2x3.dat	e2x30.dat	e2x31a.dat
e2x31b.dat	e2x32.dat	e2x33.dat	e2x33b.dat	e2x34.dat	e2x35.dat
e2x35a.dat	e2x36.dat	e2x37.dat	e2x37b.dat	e2x38.dat	e2x39.dat
e2x4.dat	e2x40a.dat	e2x40b.dat	e2x41.dat	e2x42.dat	e2x43.dat
e2x44.dat	e2x45.dat	e2x46a.dat	e2x46b.dat	e2x46c.dat	e2x46d.dat
e2x47b.dat	e2x48.dat	e2x49.dat	e2x5.dat	e2x50.dat	e2x51a.dat
e2x51b.dat	e2x52.dat	e2x53.dat	e2x54.dat	e2x55.dat	e2x56.dat
e2x57a.dat	e2x57b.dat	e2x58a.dat	e2x58b.dat	e2x59a.dat	e2x59b
e2x6.dat	e2x60a.dat	e2x60b.dat	e2x61a.dat	e2x61b.dat	e2x62.dat
e2x63a.dat	e2x63b.dat	e2x64a.dat	e2x64b.dat	e2x65.dat	e2x66a.dat
e2x66b.dat	e2x67a.dat	e2x67b.dat	e2x68.dat	e2x69.dat	e2x7.dat
e2x70.dat	e2x71a.dat	e2x71b.dat	e2x72.dat	e2x73.dat	e2x74.dat
e2x75.dat	e2x76.dat	e2x77.dat	e2x8.dat	e2x9.dat	e2x9b.dat
e2x9c.dat	e2x9d.dat	e3x1.dat	e3x10.dat	e3x11.dat	e3x12.dat
e3x12b.dat	e3x13.dat	e3x14a.dat	e3x15.dat	e3x15b.dat	e3x17.dat
e3x18.dat	e3x19.dat	e3x19b.dat	e3x19c.dat	e3x19d.dat	e3x20.dat
e3x21a.dat	e3x21c.dat	e3x21d.dat	e3x21e.dat	e3x21f.dat	e3x22a.dat
e3x22c.dat	e3x22d.dat	e3x23.dat	e3x23b.dat	e3x24a.dat	e3x24b.dat
e3x24c.dat	e3x25.dat	e3x26.dat	e3x27.dat	e3x28.dat	e3x29.dat
e3x2a.dat	e3x2b.dat	e3x3.dat	e3x30a.dat	e3x30b.dat	e3x31.dat

Table 1-2 Model Definition Option Cross-reference (Continued)

COORDINATES (Continued)					
e3x32a.dat	e3x32b.dat	e3x32c.dat	e3x33.dat	e3x33b.dat	e3x34.dat
e3x35.dat	e3x36.dat	e3x37a.dat	e3x37b.dat	e3x38a.dat	e3x38b.dat
e3x3b.dat	e3x4.dat	e3x6.dat	e3x7a.dat	e3x8.dat	e3x9.dat
e4x10.dat	e4x10b.dat	e4x11.dat	e4x12a.dat	e4x12b.dat	e4x12c.dat
e4x12d.dat	e4x13a.dat	e4x13b.dat	e4x13c.dat	e4x14a.dat	e4x14b.dat
e4x15.dat	e4x1c.dat	e4x2.dat	e4x20.dat	e4x2a.dat	e4x2b.dat
e4x2c.dat	e4x2d.dat	e4x2e.dat	e4x3.dat	e4x4.dat	e4x4b.dat
e4x5.dat	e4x6.dat	e4x7b.dat	e4x8.dat	e4x9.dat	e4x9b.dat
e5x1.dat	e5x10.dat	e5x11a.dat	e5x11c.dat	e5x12.dat	e5x13a.dat
e5x13b.dat	e5x13c.dat	e5x13d.dat	e5x14.dat	e5x15.dat	e5x15b.dat
e5x16a.dat	e5x16b.dat	e5x16c.dat	e5x17a.dat	e5x17b.dat	e5x18a.dat
e5x18b.dat	e5x2a.dat	e5x2b.dat	e5x3a.dat	e5x3b.dat	e5x3c.dat
e5x3d.dat	e5x3e.dat	e5x3f.dat	e5x4a.dat	e5x4b.dat	e5x4c.dat
e5x4d.dat	e5x5a.dat	e5x5b.dat	e5x6.dat	e5x7a.dat	e5x7b.dat
e5x8a.dat	e5x8c.dat	e5x8d.dat	e5x8e.dat	e5x9a.dat	e5x9b.dat
e5x9d.dat	e5x9e.dat	e6x10.dat	e6x11.dat	e6x12.dat	e6x13.dat
e6x13b.dat	e6x14.dat	e6x15.dat	e6x15b.dat	e6x16a.dat	e6x16b.dat
e6x16c.dat	e6x17a.dat	e6x17b.dat	e6x18.dat	e6x19.dat	e6x1a.dat
e6x1b.dat	e6x1c.dat	e6x2.dat	e6x20a.dat	e6x20b.dat	e6x21.dat
e6x3a.dat	e6x3b.dat	e6x3c.dat	e6x3d.dat	e6x4.dat	e6x5.dat
e6x6a.dat	e6x6b.dat	e6x7.dat	e6x8.dat	e6x9.dat	e7x1.dat
e7x10.dat	e7x11.dat	e7x12.dat	e7x13b.dat	e7x13c.dat	e7x14.dat
e7x15.dat	e7x16.dat	e7x17a.dat	e7x17b.dat	e7x18.dat	e7x19.dat
e7x19b.dat	e7x1b.dat	e7x1c.dat	e7x2.dat	e7x20.dat	e7x20b.dat
e7x20c.dat	e7x20d.dat	e7x21.dat	e7x22a.dat	e7x22b.dat	e7x22c.dat
e7x23.dat	e7x24a.dat	e7x24b.dat	e7x24c.dat	e7x25.dat	e7x26.dat
e7x27.dat	e7x28a.dat	e7x28b.dat	e7x28c.dat	e7x28d.dat	e7x29a.dat
e7x29b.dat	e7x3.dat	e7x30a.dat	e7x30b.dat	e7x31a.dat	e7x31b.dat

Table 1-2 Model Definition Option Cross-reference (Continued)

COORDINATES (Continued)					
e7x32.dat	e7x3b.dat	e7x4.dat	e7x4b.dat	e7x5.dat	e7x5b.dat
e7x5c.dat	e7x6.dat	e7x6b.dat	e7x7.dat	e7x8a.dat	e7x8b.dat
e7x8c.dat	e7x9a.dat	e7x9b.dat	e8x10.dat	e8x11.dat	e8x12.dat
e8x12b.dat	e8x12c.dat	e8x12d.dat	e8x12e.dat	e8x12r.dat	e8x13.dat
e8x13b.dat	e8x13c.dat	—	e8x14a.dat	e8x14b.dat	e8x14c.dat
e8x14d.dat	e8x14e.dat	e8x14f.dat	e8x15.dat	e8x15b.dat	e8x15c.dat
e8x15d.dat	e8x16.dat	e8x16b.dat	e8x17.dat	e8x17b.dat	e8x18.dat
e8x18b.dat	e8x18c.dat	e8x18d.dat	e8x19.dat	e8x19b.dat	e8x1a.dat
e8x2.dat	e8x20.dat	e8x21.dat	e8x22.dat	e8x23.dat	e8x23b.dat
e8x24a.dat	e8x24b.dat	e8x25.dat	e8x26.dat	e8x27.dat	e8x28.dat
e8x29.dat	e8x3.dat	e8x30.dat	e8x30b.dat	e8x31.dat	e8x32.dat
e8x33a.dat	e8x33b.dat	e8x34.dat	e8x35.dat	e8x36.dat	e8x37.dat
e8x38a.dat	e8x38b.dat	—	e8x38c.dat	e8x39.dat	e8x4.dat
e8x40.dat	e8x41.dat	e8x42.dat	e8x43.dat	e8x43b.dat	e8x43c.dat
e8x44.dat	e8x44b.dat	e8x44c.dat	e8x45.dat	e8x46.dat	e8x47.dat
e8x48.dat	e8x49.dat	e8x50.dat	e8x51a.dat	e8x51b.dat	e8x52.dat
e8x53a.dat	e8x53b.dat	e8x54.dat	e8x55a.dat	e8x55b.dat	e8x56a.dat
e8x56b.dat	e8x57a.dat	e8x57b.dat	e8x57c.dat	e8x57d.dat	e8x58.dat
e8x5a.dat	e8x5b.dat	e8x6.dat	e8x60.dat	e8x7.dat	e8x8a.dat
e8x8b.dat	e8x9.dat	e9x10a.dat	e9x10b.dat	e9x10c.dat	e9x10d.dat
e9x11a.dat	e9x11b.dat	e9x12a.dat	e9x12b.dat	e9x12c.dat	e9x13a.dat
e9x13b.dat	e9x1a.dat	e9x1b.dat	e9x1c.dat	e9x1d.dat	e9x1e.dat
e9x2a.dat	e9x2b.dat	e9x2c.dat	e9x3a.dat	e9x3b.dat	e9x4.dat
e9x5a.dat	e9x5b.dat	e9x5c.dat	e9x5d.dat	e9x5e.dat	e9x6a.dat
e9x6b.dat	e9x7a.dat	e9x7b.dat	e9x7c.dat	e9x8.dat	e9x9a.dat
e9x9b.dat	e10x1a.dat	e10x1b.dat	e10x2a.dat	e10x2b.dat	e10x3a.dat
e10x3b.dat	e10x4a.dat	e10x4b.dat	e10x5a.dat	e10x5b.dat	e10x6a.dat
e10x6b.dat	e10x7a.dat	e10x7b.dat			

Table 1-2 Model Definition Option Cross-reference (Continued)

CRACK DATA					
e7x11.dat	e7x3.dat	e7x3b.dat	e8x4.dat	e8x5a.dat	e8x5b.dat
e8x6.dat					
CREEP					
e3x12.dat	e3x12b.dat	e3x13.dat	e3x14a.dat	e3x15.dat	e3x15b.dat
e3x22c.dat	e3x22d.dat	e3x24b.dat	e3x24c.dat	e3x29.dat	
DAMAGE					
e3x27.dat	e3x28.dat	e7x22b.dat	e7x22c.dat	e7x30a.dat	e7x30b.dat
DAMPING					
e6x9.dat					
DEFINE					
e2x14b.dat	e2x37b.dat	e2x40a.dat	e2x40b.dat	e2x41.dat	e2x46d.dat
e2x60a.dat	e2x60b.dat	e2x61a.dat	e2x61b.dat	e2x68.dat	e2x70.dat
e3x12b.dat	e3x26.dat	e3x27.dat	e3x3.dat	e3x31.dat	e3x3b.dat
e3x4.dat	e3x5.dat	e3x6.dat	e4x11.dat	e4x12a.dat	e4x12b.dat
e4x12c.dat	e4x12d.dat	e4x2.dat	e5x14.dat	e5x17a.dat	e5x17b.dat
e5x18a.dat	e5x18b.dat	e5x9e.dat	e6x19.dat	e6x21.dat	e7x19.dat
e7x19b.dat	e7x20.dat	e7x20b.dat	e7x20c.dat	e7x20d.dat	e7x23.dat
e7x6.dat	e7x6b.dat	e7x7.dat	e8x15.dat	e8x15b.dat	e8x15c.dat
e8x15d.dat	e8x23b.dat	e8x26.dat	e8x28.dat	e8x29.dat	e8x30.dat
e8x30b.dat	e8x31.dat	e8x32.dat	e8x35.dat	e8x36.dat	e8x37.dat
e8x42.dat	e8x45.dat	e8x47.dat	e8x49.dat	e8x51a.dat	e8x51b.dat
e8x52.dat	e8x56a.dat	e8x56b.dat	e8x9.dat	e9x11a.dat	e9x11b.dat
e9x12a.dat	e9x12b.dat	e9x12c.dat	e9x13a.dat	e9x13b.dat	e9x5c.dat
e9x5d.dat	e9x6a.dat	e9x6b.dat	e9x7b.dat	e9x8.dat	
DENSITY EFFECTS					
e3x25.dat	e3x26.dat				

Table 1-2 Model Definition Option Cross-reference (Continued)

DESIGN DISPLACEMENT CONSTRAINTS					
e10x1a.dat	e10x1b.dat	e10x3a.dat	e10x3b.dat	e10x5a.dat	e10x5b.dat
e10x7a.dat	e10x7b.dat				
DESIGN FREQUENCY CONSTRAINTS					
e10x1a.dat	e10x1b.dat	e10x3a.dat	e10x3b.dat	e10x4a.dat	e10x4b.dat
e10x7a.dat	e10x7b.dat				
DESIGN OBJECTIVE					
e10x1a.dat	e10x1b.dat	e10x2a.dat	e10x2b.dat	e10x3a.dat	e10x3b.dat
e10x4a.dat	e10x4b.dat	e10x5a.dat	e10x5b.dat	e10x6a.dat	e10x6b.dat
e10x7a.dat	e10x7b.dat				
DESIGN STRAIN CONSTRAINTS					
e10x2a.dat	e10x2b.dat	e10x5a.dat	e10x5b.dat		
DESIGN STRESS CONSTRAINTS					
e10x1a.dat	e10x1b.dat	e10x3a.dat	e10x3b.dat	e10x4a.dat	e10x4b.dat
e10x5a.dat	e10x5b.dat	e10x6a.dat	e10x6b.dat	e10x7a.dat	e10x7b.dat
DESIGN VARIABLES					
e10x1a.dat	e10x1b.dat	e10x2a.dat	e10x2b.dat	e10x3a.dat	e10x3b.dat
e10x4a.dat	e10x4b.dat	e10x5a.dat	e10x5b.dat	e10x6a.dat	e10x6b.dat
e10x7a.dat	e10x7b.dat				
DIST CURRENT					
e5x10.dat					
DIST FLUXES					
e5x18a.dat	e5x18b.dat	e5x8a.dat	e5x8c.dat	e5x8d.dat	e5x8e.dat
e8x13.dat	e8x13b.dat	e8x13c.dat	—	e8x7.dat	e9x12b.dat
e9x12c.dat					

Table 1-2 Model Definition Option Cross-reference (Continued)

DIST LOADS					
e2x1.dat	e2x11.dat	e2x12b.dat	e2x12c.dat	e2x12d.dat	e2x12e.dat
e2x13.dat	e2x15.dat	e2x16.dat	e2x17.dat	e2x18.dat	e2x19.dat
e2x2.dat	e2x22.dat	e2x23.dat	e2x2b.dat	e2x2c.dat	e2x3.dat
e2x30.dat	e2x31a.dat	e2x31b.dat	e2x32.dat	e2x33.dat	e2x33b.dat
e2x35.dat	e2x35a.dat	e2x37.dat	e2x37b.dat	e2x39.dat	e2x4.dat
e2x40a.dat	e2x40b.dat	e2x43.dat	e2x44.dat	e2x45.dat	e2x46c.dat
e2x47b.dat	e2x49.dat	e2x5.dat	e2x51a.dat	e2x51b.dat	e2x53.dat
e2x55.dat	e2x56.dat	e2x58a.dat	e2x58b.dat	e2x6.dat	e2x60a.dat
e2x60b.dat	e2x62.dat	e2x63a.dat	e2x63b.dat	e2x64a.dat	e2x64b.dat
e2x66b.dat	e2x69.dat	e2x71a.dat	e2x71b.dat	e2x72.dat	e2x73.dat
e2x74.dat	e2x9.dat	e2x9b.dat	e2x9c.dat	e2x9d.dat	e3x10.dat
e3x12.dat	e3x12b.dat	e3x15.dat	e3x15b.dat	e3x16.dat	e3x16b.dat
e3x17.dat	e3x22c.dat	e3x22d.dat	e3x23.dat	e3x23b.dat	e3x25.dat
e3x26.dat	e3x29.dat	e3x31.dat	e3x32a.dat	e3x32b.dat	e3x32c.dat
e3x34.dat	e3x7a.dat	e3x7b.dat	e3x7c.dat	e3x8.dat	e3x9.dat
e4x13a.dat	e4x13b.dat	e4x13c.dat	e4x14a.dat	e4x14b.dat	e4x2a.dat
e4x2b.dat	e4x2c.dat	e4x2d.dat	e4x2e.dat	e4x8.dat	e4x9.dat
e4x9b.dat	e6x14.dat	e6x20a.dat	e6x20b.dat	e6x21.dat	e6x4.dat
e7x12.dat	e7x14.dat	e7x20.dat	e7x20b.dat	e7x20c.dat	e7x20d.dat
e7x22a.dat	e7x22b.dat	e7x22c.dat	e7x28a.dat	e7x28b.dat	e7x28c.dat
e7x28d.dat	e7x3.dat	e7x3b.dat	e7x5.dat	e7x5b.dat	e7x5c.dat
e7x6.dat	e7x6b.dat	e7x8a.dat	e7x8b.dat	e7x8c.dat	e7x9a.dat
e7x9b.dat	e7x9c.dat	e8x11.dat	e8x1a.dat	e8x2.dat	e8x27.dat
e8x34.dat	e8x35.dat	e8x38a.dat	e8x38b.dat	—	e8x38c.dat
e8x42.dat	e8x43.dat	e8x43b.dat	e8x43c.dat	e8x46.dat	e8x47.dat

Table 1-2 Model Definition Option Cross-reference (Continued)

DIST LOADS					
e8x53a.dat	e8x53b.dat	e8x58.dat	e8x8a.dat	e8x8b.dat	e9x1a.dat
e9x1b.dat	e9x1c.dat	e9x1d.dat	e9x1e.dat	e9x2a.dat	e9x2b.dat
e9x2c.dat	e9x7a.dat	e9x7b.dat	e9x7c.dat	e9x9a.dat	e9x9b.dat
e10x2a.dat	e10x2b.dat	e10x3a.dat	e10x3b.dat		
ELEM SORT					
e2x9b.dat					
END OPTION					
All MARC input files must have an END OPTION line.					
ERROR ESTIMATE					
e2x34.dat	e7x10.dat	e8x11.dat	e8x41.dat		
EXCLUDE					
e8x15d.dat	e8x46.dat				
EXIT					
e5x3c.dat	e5x3d.dat	e9x5c.dat	e9x5d.dat	e9x6a.dat	e9x6b.dat
e9x8.dat					
FAIL DATA					
e7x25.dat	e8x27.dat	e8x9.dat			
FILMS					
e3x22a.dat	e3x24a.dat	e5x10.dat	e5x11a.dat	e5x13a.dat	e5x13b.dat
e5x13c.dat	e5x13d.dat	e5x14.dat	e5x3a.dat	e5x3b.dat	e5x3c.dat
e5x3d.dat	e5x3e.dat	e5x3f.dat	e5x5a.dat	e5x5b.dat	e5x6.dat
e5x8a.dat	e5x8c.dat	e5x8d.dat	e5x8e.dat	e5x9a.dat	e5x9b.dat
e5x9d.dat	e5x9e.dat	e9x12b.dat	e9x12c.dat		

Table 1-2 Model Definition Option Cross-reference (Continued)

FIXED DISP					
e2x1.dat	e2x10.dat	e2x10b.dat	e2x10c.dat	e2x11.dat	e2x12b.dat
e2x12c.dat	e2x12d.dat	e2x12e.dat	e2x13.dat	e2x14.dat	e2x14b.dat
e2x15.dat	e2x16.dat	e2x17.dat	e2x18.dat	e2x19.dat	e2x2.dat
e2x20.dat	e2x21.dat	e2x22.dat	e2x23.dat	e2x24.dat	e2x25.dat
e2x25b.dat	e2x26.dat	e2x26b.dat	e2x26c.dat	e2x26d.dat	e2x27.dat
e2x28.dat	e2x29.dat	e2x2b.dat	e2x2c.dat	e2x3.dat	e2x30.dat
e2x31a.dat	e2x31b.dat	e2x32.dat	e2x33.dat	e2x33b.dat	e2x34.dat
e2x35.dat	e2x35a.dat	e2x36.dat	e2x37.dat	e2x37b.dat	e2x38.dat
e2x39.dat	e2x4.dat	e2x40a.dat	e2x40b.dat	e2x41.dat	e2x42.dat
e2x43.dat	e2x44.dat	e2x45.dat	e2x46a.dat	e2x46b.dat	e2x46c.dat
e2x46d.dat	e2x47b.dat	e2x48.dat	e2x49.dat	e2x5.dat	e2x50.dat
e2x51a.dat	e2x51b.dat	e2x52.dat	e2x53.dat	e2x54.dat	e2x55.dat
e2x56.dat	e2x57a.dat	e2x57b.dat	e2x58a.dat	e2x58b.dat	e2x59a.dat
e2x59b.dat	e2x6.dat	e2x60a.dat	e2x60b.dat	e2x61a.dat	e2x61b.dat
e2x62.dat	e2x63a.dat	e2x63b.dat	e2x64a.dat	e2x64b.dat	e2x65.dat
e2x66a.dat	e2x66b.dat	e2x67a.dat	e2x67b.dat	e2x68.dat	e2x69.dat
e2x7.dat	e2x70.dat	e2x71a.dat	e2x71b.dat	e2x72.dat	e2x73.dat
e2x74.dat	e2x75.dat	e2x76.dat	e2x77.dat	e2x8.dat	e2x9.dat
e2x9b.dat	e2x9c.dat	e2x9d.dat	e3x1.dat	e3x10.dat	e3x11.dat
e3x12.dat	e3x12b.dat	e3x13.dat	e3x14a.dat	e3x15.dat	e3x15b.dat
e3x16.dat	e3x16b.dat	e3x17.dat	e3x18.dat	e3x19.dat	e3x19b.dat
e3x19c.dat	e3x19d.dat	e3x20.dat	e3x21a.dat	e3x21c.dat	e3x21d.dat
e3x21e.dat	e3x21f.dat	e3x22c.dat	e3x22d.dat	e3x23.dat	e3x23b.dat
e3x24b.dat	e3x24c.dat	e3x25.dat	e3x26.dat	e3x27.dat	e3x28.dat
e3x29.dat	e3x2a.dat	e3x2b.dat	e3x3.dat	e3x30a.dat	e3x30b.dat
e3x31.dat	e3x32a.dat	e3x32b.dat	e3x32c.dat	e3x33.dat	e3x33b.dat
e3x34.dat	e3x35.dat	e3x36.dat	e3x37a.dat	e3x37b.dat	e3x38a.dat
e3x38b.dat	e3x3b.dat	e3x4.dat	e3x5.dat	e3x6.dat	e3x7a.dat

Table 1-2 Model Definition Option Cross-reference (Continued)

FIXED DISP (Continued)					
e3x7b.dat	e3x7c.dat	e3x8.dat	e3x9.dat	e4x10.dat	e4x10b.dat
e4x11.dat	e4x12a.dat	e4x12b.dat	e4x12c.dat	e4x12d.dat	e4x13a.dat
e4x13b.dat	e4x13c.dat	e4x14a.dat	e4x14b.dat	e4x15.dat	e4x1a.dat
e4x1b.dat	e4x1c.dat	e4x1d.dat	e4x2.dat	e4x20.dat	e4x2a.dat
e4x2b.dat	e4x2c.dat	e4x2d.dat	e4x2e.dat	e4x3.dat	e4x4.dat
e4x4b.dat	e4x5.dat	e4x6.dat	e4x7.dat	e4x7b.dat	e4x7c.dat
e4x8.dat	e4x9.dat	e4x9b.dat	e5x11c.dat	e6x10.dat	e6x11.dat
e6x12.dat	e6x13.dat	e6x13b.dat	e6x14.dat	e6x15.dat	e6x15b.dat
e6x16a.dat	e6x16b.dat	e6x16c.dat	e6x17a.dat	e6x17b.dat	e6x18.dat
e6x19.dat	e6x1a.dat	e6x1b.dat	e6x1c.dat	e6x2.dat	e6x20a.dat
e6x20b.dat	e6x3a.dat	e6x3b.dat	e6x3c.dat	e6x3d.dat	e6x4.dat
e6x5.dat	e6x6a.dat	e6x6b.dat	e6x7.dat	e6x8.dat	e6x9.dat
e7x1.dat	e7x10.dat	e7x11.dat	e7x12.dat	e7x13b.dat	e7x13c.dat
e7x13d.dat	e7x14.dat	e7x17a.dat	e7x17b.dat	e7x18.dat	e7x19.dat
e7x19b.dat	e7x1b.dat	e7x1c.dat	e7x2.dat	e7x21.dat	e7x22a.dat
e7x22b.dat	e7x22c.dat	e7x23.dat	e7x24a.dat	e7x24b.dat	e7x24c.dat
e7x25.dat	e7x26.dat	e7x27.dat	e7x28a.dat	e7x28b.dat	e7x28c.dat
e7x28d.dat	e7x29a.dat	e7x29b.dat	e7x3.dat	e7x32.dat	e7x3b.dat
e7x4.dat	e7x4b.dat	e7x5.dat	e7x5b.dat	e7x5c.dat	e7x6.dat
e7x6b.dat	e7x7.dat	e7x8a.dat	e7x8b.dat	e7x8c.dat	e7x9a.dat
e7x9b.dat	e7x9c.dat	e8x10.dat	e8x11.dat	e8x12.dat	e8x12b.dat
e8x12c.dat	e8x12d.dat	e8x12e.dat	e8x12r.dat	e8x13.dat	e8x13b.dat
e8x13c.dat	—	e8x14a.dat	e8x14b.dat	e8x14c.dat	e8x14d.dat
e8x14e.dat	e8x14f.dat	e8x15.dat	e8x15b.dat	e8x15c.dat	e8x15d.dat
e8x16.dat	e8x16b.dat	e8x17.dat	e8x17b.dat	e8x18.dat	e8x18b.dat
e8x18c.dat	e8x18d.dat	e8x19.dat	e8x19b.dat	e8x1a.dat	e8x2.dat
e8x27.dat	e8x3.dat	e8x34.dat	e8x35.dat	e8x38a.dat	e8x38b.dat
—	e8x38c.dat	e8x39.dat	e8x4.dat	e8x40.dat	e8x41.dat

Table 1-2 Model Definition Option Cross-reference (Continued)

FIXED DISP (Continued)					
e8x42.dat	e8x43.dat	e8x43b.dat	e8x43c.dat	e8x44.dat	e8x44b.dat
e8x44c.dat	e8x46.dat	e8x47.dat	e8x48.dat	e8x49.dat	e8x51a.dat
e8x51b.dat	e8x52.dat	e8x53a.dat	e8x53b.dat	e8x54.dat	e8x56a.dat
e8x56b.dat	e8x57a.dat	e8x57b.dat	e8x57c.dat	e8x57d.dat	e8x58.dat
e8x5a.dat	e8x5b.dat	e8x6.dat	e8x60.dat	e8x7.dat	e8x8a.dat
e8x8b.dat	e8x9.dat	e9x10a.dat	e9x10b.dat	e9x10c.dat	e9x10d.dat
e9x11a.dat	e9x11b.dat	e9x12c.dat	e9x13a.dat	e9x13b.dat	e9x9b.dat
e10x1a.dat	e10x1b.dat	e10x2a.dat	e10x2b.dat	e10x3a.dat	e10x3b.dat
e10x4a.dat	e10x4b.dat	e10x5a.dat	e10x5b.dat	e10x6a.dat	e10x6b.dat
e10x7a.dat	e10x7b.dat				
FIXED POTENTIAL					
e8x20.dat	e8x21.dat	e8x22.dat	e8x23.dat	e8x23b.dat	e8x24a.dat
e8x24b.dat	e8x28.dat	e8x29.dat	e8x30.dat	e8x30b.dat	e8x31.dat
e8x32.dat	e8x33a.dat	e8x33b.dat			
FIXED PRESSURE					
e7x15.dat	e7x16.dat	e8x26.dat			
FIXED TEMPERATURE					
e3x24a.dat	e3x26.dat	e5x1.dat	e5x12.dat	e5x15.dat	e5x15b.dat
e5x16a.dat	e5x16b.dat	e5x16c.dat	e5x17a.dat	e5x17b.dat	e5x18a.dat
e5x18b.dat	e5x2a.dat	e5x2b.dat	e5x3a.dat	e5x3b.dat	e5x3c.dat
e5x3d.dat	e5x3e.dat	e5x3f.dat	e5x4a.dat	e5x4b.dat	e5x4c.dat
e5x4d.dat	e5x7a.dat	e5x7b.dat	e5x8a.dat	e5x8c.dat	e5x8d.dat
e5x8e.dat	e7x1b.dat	e7x1c.dat	e8x13.dat	e8x13b.dat	e8x13c.dat
—	e8x7.dat				

Table 1-2 Model Definition Option Cross-reference (Continued)

FIXED VELOCITY					
e9x10a.dat	e9x10b.dat	e9x10c.dat	e9x10d.dat	e9x11a.dat	e9x11b.dat
e9x12a.dat	e9x12b.dat	e9x12c.dat	e9x13a.dat	e9x13b.dat	e9x1a.dat
e9x1b.dat	e9x1c.dat	e9x1d.dat	e9x1e.dat	e9x2a.dat	e9x2b.dat
e9x2c.dat	e9x3a.dat	e9x3b.dat	e9x4.dat	e9x5a.dat	e9x5b.dat
e9x5c.dat	e9x5d.dat	e9x5e.dat	e9x6a.dat	e9x6b.dat	e9x7a.dat
e9x7b.dat	e9x7c.dat	e9x8.dat	e9x9a.dat		
FLUID DRAG					
e6x20a.dat	e6x20b.dat				
FLUID SOLID					
e6x5.dat					
FOAM					
e7x19b.dat	e7x23.dat				
FORCDT					
e3x26.dat	e5x2b.dat	e7x17a.dat	e7x17b.dat	e8x26.dat	
FOUNDATION					
e2x29.dat	e2x36.dat	e2x42.dat			
FOURIER					
e7x8a.dat	e7x8b.dat	e7x8c.dat	e7x9a.dat	e7x9b.dat	e7x9c.dat
FXORD					
e2x11.dat	e2x15.dat	e3x1.dat	e6x3a.dat	e6x3c.dat	
GAP DATA					
e2x70.dat	e3x18.dat	e6x9.dat	e7x18.dat	e7x2.dat	e7x26.dat
e7x4.dat	e7x4b.dat	e8x7.dat			

Table 1-2 Model Definition Option Cross-reference (Continued)

GEOMETRY					
e2x1.dat	e2x10.dat	e2x10b.dat	e2x10c.dat	e2x11.dat	e2x14.dat
e2x14b.dat	e2x15.dat	e2x16.dat	e2x17.dat	e2x18.dat	e2x19.dat
e2x20.dat	e2x21.dat	e2x24.dat	e2x25.dat	e2x25b.dat	e2x26.dat
e2x26b.dat	e2x26c.dat	e2x26d.dat	e2x27.dat	e2x29.dat	e2x3.dat
e2x31a.dat	e2x31b.dat	e2x32.dat	e2x34.dat	e2x36.dat	e2x37.dat
e2x37b.dat	e2x38.dat	e2x39.dat	e2x4.dat	e2x40a.dat	e2x40b.dat
e2x41.dat	e2x42.dat	e2x43.dat	e2x44.dat	e2x46a.dat	e2x46b.dat
e2x46c.dat	e2x46d.dat	e2x5.dat	e2x54.dat	e2x55.dat	e2x56.dat
e2x57a.dat	e2x57b.dat	e2x58a.dat	e2x58b.dat	e2x59a.dat	e2x59b.dat
e2x6.dat	e2x62.dat	e2x64a.dat	e2x64b.dat	e2x65.dat	e2x66a.dat
e2x66b.dat	e2x68.dat	e2x7.dat	e2x71a.dat	e2x71b.dat	e2x72.dat
e2x73.dat	e2x74.dat	e2x75.dat	e2x76.dat	e2x77.dat	e2x8.dat
e2x9.dat	e2x9b.dat	e2x9c.dat	e2x9d.dat	e3x1.dat	e3x10.dat
e3x13.dat	e3x14a.dat	e3x15.dat	e3x15b.dat	e3x16.dat	e3x16b.dat
e3x17.dat	e3x18.dat	e3x19.dat	e3x19b.dat	e3x19c.dat	e3x19d.dat
e3x20.dat	e3x21a.dat	e3x21c.dat	e3x21d.dat	e3x21f.dat	e3x23.dat
e3x23b.dat	e3x24a.dat	e3x24b.dat	e3x24c.dat	e3x27.dat	e3x29.dat
e3x3.dat	e3x30a.dat	e3x30b.dat	e3x32a.dat	e3x32b.dat	e3x32c.dat
e3x33.dat	e3x33b.dat	e3x35.dat	e3x36.dat	e3x37a.dat	e3x37b.dat
e3x38a.dat	e3x38b.dat	e3x3b.dat	e3x4.dat	e3x5.dat	e3x6.dat
e4x10.dat	e4x10b.dat	e4x11.dat	e4x12a.dat	e4x12b.dat	e4x12c.dat
e4x12d.dat	e4x14a.dat	e4x14b.dat	e4x15.dat	e4x1a.dat	e4x1b.dat
e4x1c.dat	e4x1d.dat	e4x2.dat	e4x20.dat	e4x2a.dat	e4x2b.dat
e4x2c.dat	e4x2d.dat	e4x2e.dat	e4x3.dat	e4x4.dat	e4x4b.dat
e4x5.dat	e4x6.dat	e4x7.dat	e4x7b.dat	e4x7c.dat	e4x8.dat
e4x9.dat	e4x9b.dat	e5x13a.dat	e5x13b.dat	e5x13c.dat	e5x13d.dat
e5x14.dat	e5x18a.dat	e5x18b.dat	e5x3a.dat	e5x3b.dat	e5x3c.dat
e5x3d.dat	e5x3e.dat	e5x3f.dat	e6x10.dat	e6x11.dat	e6x12.dat

Table 1-2 Model Definition Option Cross-reference (Continued)

GEOMETRY (Continued)					
e6x13.dat	e6x13b.dat	e6x15.dat	e6x15b.dat	e6x18.dat	e6x1a.dat
e6x1b.dat	e6x1c.dat	e6x2.dat	e6x20a.dat	e6x20b.dat	e6x21.dat
e6x3a.dat	e6x3b.dat	e6x3c.dat	e6x3d.dat	e6x5.dat	e6x6a.dat
e6x6b.dat	e6x9.dat	e7x10.dat	e7x11.dat	e7x12.dat	e7x13b.dat
e7x13c.dat	e7x13d.dat	e7x17a.dat	e7x17b.dat	e7x19.dat	e7x19b.dat
e7x21.dat	e7x22a.dat	e7x22b.dat	e7x22c.dat	e7x29a.dat	e7x29b.dat
e7x3.dat	e7x3b.dat	e8x10.dat	e8x11.dat	e8x12.dat	e8x12b.dat
e8x12c.dat	e8x12d.dat	e8x12e.dat	e8x12r.dat	e8x13.dat	e8x13b.dat
e8x13c.dat	—	e8x14a.dat	e8x14b.dat	e8x14c.dat	e8x14d.dat
e8x14e.dat	e8x14f.dat	e8x15.dat	e8x15b.dat	e8x15c.dat	e8x16.dat
e8x16b.dat	e8x17.dat	e8x17b.dat	e8x18.dat	e8x18b.dat	e8x18c.dat
e8x18d.dat	e8x19.dat	e8x19b.dat	e8x1a.dat	e8x25.dat	e8x26.dat
e8x27.dat	e8x36.dat	e8x38a.dat	e8x38b.dat	—	e8x38c.dat
e8x39.dat	e8x4.dat	e8x41.dat	e8x44.dat	e8x44b.dat	e8x44c.dat
e8x48.dat	e8x49.dat	e8x50.dat	e8x51a.dat	e8x51b.dat	e8x52.dat
e8x53a.dat	e8x53b.dat	e8x54.dat	e8x55a.dat	e8x55b.dat	e8x56a.dat
e8x56b.dat	e8x57a.dat	e8x57b.dat	e8x57c.dat	e8x57d.dat	e8x58.dat
e8x6.dat	e8x7.dat	e10x1a.dat	e10x1b.dat	e10x2a.dat	e10x2b.dat
e10x4a.dat	e10x4b.dat	e10x6a.dat	e10x6b.dat	e10x7a.dat	e10x7b.dat
HYPOELASTIC					
e7x29a.dat	e8x10.dat				
INIT STRESS					
e3x34.dat	e8x34.dat	e8x35.dat			
INITIAL PC					
e8x34.dat	e8x35.dat				

Table 1-2 Model Definition Option Cross-reference (Continued)

INITIAL STATE					
e2x41.dat	e2x51a.dat	e2x51b.dat	e3x22c.dat	e3x22d.dat	e3x24b.dat
e3x24c.dat	e3x5.dat	e7x7.dat	e8x45.dat		
INITIAL TEMP					
e2x46d.dat	e3x22a.dat	e3x24a.dat	e5x11a.dat	e5x13a.dat	e5x13b.dat
e5x13c.dat	e5x13d.dat	e5x14.dat	e5x16a.dat	e5x16b.dat	e5x16c.dat
e5x17a.dat	e5x17b.dat	e5x18a.dat	e5x18b.dat	e5x2a.dat	e5x2b.dat
e5x3a.dat	e5x3b.dat	e5x3c.dat	e5x3d.dat	e5x3e.dat	e5x3f.dat
e5x4a.dat	e5x4b.dat	e5x4c.dat	e5x4d.dat	e5x5a.dat	e5x5b.dat
e5x6.dat	e5x8a.dat	e5x8c.dat	e5x8d.dat	e5x8e.dat	e5x9a.dat
e5x9b.dat	e5x9d.dat	e5x9e.dat	e7x1b.dat	e7x1c.dat	e8x13.dat
e8x13b.dat	e8x13c.dat	—	e8x7.dat		
INITIAL VEL					
e2x71b.dat	e6x13.dat	e6x13b.dat	e6x16a.dat	e6x16b.dat	e6x16c.dat
e6x17a.dat	e6x17b.dat	e6x19.dat	e6x9.dat	e9x10a.dat	e9x10b.dat
e9x10c.dat	e9x10d.dat	e9x11a.dat	e9x11b.dat	e9x12a.dat	e9x12b.dat
e9x12c.dat	e9x13a.dat	e9x13b.dat	e9x5a.dat	e9x5b.dat	e9x5c.dat
e9x5d.dat	e9x5e.dat	e9x6a.dat	e9x6b.dat	e9x7a.dat	e9x7b.dat
e9x7c.dat	e9x8.dat	e9x9a.dat	e9x9b.dat		
INITIAL VOID RATIO					
e8x34.dat	e8x35.dat				
ISOTROPIC					
e2x1.dat	e2x10.dat	e2x10b.dat	e2x10c.dat	e2x11.dat	e2x12b.dat
e2x12c.dat	e2x12d.dat	e2x12e.dat	e2x13.dat	e2x14.dat	e2x14b.dat
e2x15.dat	e2x16.dat	e2x17.dat	e2x18.dat	e2x19.dat	e2x2.dat
e2x20.dat	e2x21.dat	e2x22.dat	e2x23.dat	e2x24.dat	e2x25.dat
e2x25b.dat	e2x26.dat	e2x26b.dat	e2x26c.dat	e2x26d.dat	e2x27.dat
e2x28.dat	e2x29.dat	e2x2b.dat	e2x2c.dat	e2x3.dat	e2x30.dat

Table 1-2 Model Definition Option Cross-reference (Continued)

ISOTROPIC (Continued)					
e2x31a.dat	e2x31b.dat	e2x32.dat	e2x33.dat	e2x33b.dat	e2x34.dat
e2x35.dat	e2x35a.dat	e2x36.dat	e2x37.dat	e2x37b.dat	e2x38.dat
e2x39.dat	e2x4.dat	e2x40a.dat	e2x40b.dat	e2x41.dat	e2x42.dat
e2x43.dat	e2x44.dat	e2x45.dat	e2x46a.dat	e2x46b.dat	e2x46c.dat
e2x46d.dat	e2x47b.dat	e2x48.dat	e2x49.dat	e2x5.dat	e2x50.dat
e2x51a.dat	e2x51b.dat	e2x52.dat	e2x53.dat	e2x54.dat	e2x55.dat
e2x56.dat	e2x57a.dat	e2x57b.dat	e2x58a.dat	e2x58b.dat	e2x59a.dat
e2x59b.dat	e2x6.dat	e2x60a.dat	e2x60b.dat	e2x61a.dat	e2x61b.dat
e2x62.dat	e2x63a.dat	e2x63b.dat	e2x64a.dat	e2x64b.dat	e2x65.dat
e2x66a.dat	e2x66b.dat	e2x67a.dat	e2x67b.dat	e2x68.dat	e2x69.dat
e2x7.dat	e2x70.dat	e2x71a.dat	e2x71b.dat	e2x72.dat	e2x73.dat
e2x74.dat	e2x75.dat	e2x76.dat	e2x77.dat	e2x8.dat	e2x9.dat
e2x9b.dat	e2x9c.dat	e2x9d.dat	e3x1.dat	e3x10.dat	e3x11.dat
e3x12.dat	e3x12b.dat	e3x13.dat	e3x14a.dat	e3x15.dat	e3x15b.dat
e3x16.dat	e3x16b.dat	e3x17.dat	e3x18.dat	e3x19.dat	e3x19b.dat
e3x19c.dat	e3x19d.dat	e3x20.dat	e3x21a.dat	e3x21c.dat	e3x21d.dat
e3x21e.dat	e3x21f.dat	e3x22a.dat	e3x22c.dat	e3x22d.dat	e3x23.dat
e3x23b.dat	e3x24a.dat	e3x24b.dat	e3x24c.dat	e3x26.dat	e3x27.dat
e3x28.dat	e3x29.dat	e3x2a.dat	e3x2b.dat	e3x3.dat	e3x30a.dat
e3x30b.dat	e3x31.dat	e3x32a.dat	e3x32b.dat	e3x32c.dat	e3x33.dat
e3x33b.dat	e3x34.dat	e3x35.dat	e3x36.dat	e3x37a.dat	e3x37b.dat
e3x38a.dat	e3x38b.dat	e3x3b.dat	e3x4.dat	e3x5.dat	e3x6.dat
e3x7a.dat	e3x7b.dat	e3x7c.dat	e3x8.dat	e3x9.dat	e4x10.dat
e4x10b.dat	e4x11.dat	e4x12a.dat	e4x12b.dat	e4x12c.dat	e4x12d.dat
e4x13a.dat	e4x13b.dat	e4x13c.dat	e4x14a.dat	e4x14b.dat	e4x15.dat
e4x1a.dat	e4x1b.dat	e4x1c.dat	e4x1d.dat	e4x2.dat	e4x20.dat
e4x2a.dat	e4x2b.dat	e4x2c.dat	e4x2d.dat	e4x2e.dat	e4x3.dat
e4x4.dat	e4x4b.dat	e4x5.dat	e4x6.dat	e4x7.dat	e4x7b.dat

Table 1-2 Model Definition Option Cross-reference (Continued)

ISOTROPIC (Continued)					
e4x7c.dat	e4x8.dat	e4x9.dat	e4x9b.dat	e5x1.dat	e5x10.dat
e5x11a.dat	e5x12.dat	e5x13a.dat	e5x13b.dat	e5x13c.dat	e5x13d.dat
e5x14.dat	e5x15.dat	e5x15b.dat	e5x16a.dat	e5x16b.dat	e5x16c.dat
e5x17a.dat	e5x17b.dat	e5x2a.dat	e5x2b.dat	e5x3a.dat	e5x3b.dat
e5x3c.dat	e5x3d.dat	e5x3e.dat	e5x3f.dat	e5x4a.dat	e5x4b.dat
e5x4c.dat	e5x4d.dat	e5x5a.dat	e5x5b.dat	e5x6.dat	e5x7b.dat
e5x8a.dat	e5x8c.dat	e5x8d.dat	e5x8e.dat	e5x9a.dat	e5x9b.dat
e5x9d.dat	e5x9e.dat	e6x10.dat	e6x11.dat	e6x12.dat	e6x13.dat
e6x13b.dat	e6x14.dat	e6x15.dat	e6x15b.dat	e6x16a.dat	e6x16b.dat
e6x16c.dat	e6x17a.dat	e6x17b.dat	e6x18.dat	e6x19.dat	e6x1a.dat
e6x1b.dat	e6x1c.dat	e6x2.dat	e6x20a.dat	e6x20b.dat	e6x3a.dat
e6x3b.dat	e6x3c.dat	e6x3d.dat	e6x4.dat	e6x5.dat	e6x6a.dat
e6x6b.dat	e6x7.dat	e6x9.dat	e7x1.dat	e7x10.dat	e7x11.dat
e7x12.dat	e7x13b.dat	e7x13c.dat	e7x13d.dat	e7x14.dat	e7x15.dat
e7x16.dat	e7x17a.dat	e7x17b.dat	e7x1b.dat	e7x1c.dat	e7x2.dat
e7x26.dat	e7x3.dat	e7x32.dat	e7x3b.dat	e7x8a.dat	e7x8b.dat
e7x8c.dat	e7x9a.dat	e7x9b.dat	e7x9c.dat	e8x11.dat	e8x12.dat
e8x12b.dat	e8x12c.dat	e8x12d.dat	e8x12e.dat	e8x12r.dat	e8x13.dat
e8x13b.dat	e8x13c.dat	—	e8x14a.dat	e8x14b.dat	e8x14c.dat
e8x14d.dat	e8x14e.dat	e8x14f.dat	e8x15.dat	e8x15b.dat	e8x15c.dat
e8x15d.dat	e8x16.dat	e8x16b.dat	e8x17.dat	e8x17b.dat	e8x18.dat
e8x18b.dat	e8x18c.dat	e8x18d.dat	e8x19.dat	e8x19b.dat	e8x1a.dat
e8x2.dat	e8x20.dat	e8x21.dat	e8x22.dat	e8x23.dat	e8x23b.dat
e8x24a.dat	e8x25.dat	e8x26.dat	e8x28.dat	e8x29.dat	e8x3.dat
e8x30.dat	e8x30b.dat	e8x31.dat	e8x32.dat	e8x33a.dat	e8x33b.dat
e8x36.dat	e8x37.dat	e8x38a.da	e8x38b.dat	—	e8x38c.dat
e8x39.dat	e8x4.dat	e8x40.dat	e8x41.dat	e8x42.dat	e8x44.dat
e8x44b.dat	e8x44c.dat	e8x45.dat	e8x46.dat	e8x47.dat	e8x48.dat

Table 1-2 Model Definition Option Cross-reference (Continued)

ISOTROPIC (Continued)					
e8x50.dat	e8x51a.dat	e8x51b.dat	e8x52.dat	e8x53a.dat	e8x53b.dat
e8x54.dat	e8x55a.dat	e8x55b.dat	e8x56a.dat	e8x56b.dat	e8x57a.dat
e8x57b.dat	e8x57c.dat	e8x57d.dat	e8x58.dat	e8x5a.dat	e8x5b.dat
e8x6.dat	e8x60.dat	e8x7.dat	e9x10a.dat	e9x10b.dat	e9x10c.dat
e9x10d.dat	e9x11a.dat	e9x11b.dat	e9x12a.dat	e9x12b.dat	e9x12c.dat
e9x13a.dat	e9x13b.dat	e9x1a.dat	e9x1b.dat	e9x1c.dat	e9x1d.dat
e9x1e.dat	e9x2a.dat	e9x2b.dat	e9x2c.dat	e9x3a.dat	e9x3b.dat
e9x4.dat	e9x5a.dat	e9x5b.dat	e9x5c.dat	e9x5d.dat	e9x5e.dat
e9x6a.dat	e9x6b.dat	e9x7a.dat	e9x7b.dat	e9x7c.dat	e9x8.dat
e9x9a.dat	e9x9b.dat	e10x1a.dat	e10x1b.dat	e10x2a.dat	e10x2b.dat
e10x3a.dat	e10x3b.dat	e10x4a.dat	e10x4b.dat	e10x5a.dat	e10x5b.dat
e10x6a.dat	e10x6b.dat	e10x7a.dat	e10x7b.dat		
J-INTEGRAL					
e2x22.dat	e2x30.dat	e2x45.dat	e3x8.dat		
JOULE					
e5x10.dat	e5x12.dat				
LORENZI					
e2x63a.dat	e2x63b.dat	e6x14.dat			
MASSES					
e6x10.dat	e6x9.dat	e10x1a.dat	e10x1b.dat	e10x7a.dat	e10x7b.dat
MOONEY					
e4x14a.dat	e4x14b.dat	e6x7.dat	e6x8.dat	e7x18.dat	e7x19.dat
e7x28b.dat	e7x4.dat	e7x4b.dat	e7x5.dat	e7x5b.dat	e7x5c.dat
e8x43.dat	e8x43b.dat	e8x43c.dat	e8x49.dat		

Table 1-2 Model Definition Option Cross-reference (Continued)

NO PRINT					
e2x40a.dat	e2x40b.dat	e2x41.dat	e2x68.dat	e2x72.dat	e2x73.dat
e2x74.dat	e2x75.dat	e2x76.dat	e2x77.dat	e2x9c.dat	e3x27.dat
e3x28.dat	e3x31.dat	e3x32a.dat	e3x32b.dat	e3x32c.dat	e3x35.dat
e3x6.dat	e4x11.dat	e4x2.dat	e4x2c.dat	e4x2d.dat	e4x2e.dat
e5x15b.dat	e5x16a.dat	e5x17a.dat	e5x17b.dat	e5x18a.dat	e5x18b.dat
e6x14.dat	e7x1b.dat	e7x1c.dat	e7x20.dat	e7x20b.dat	e7x20c.dat
e7x20d.dat	e7x21.dat	e7x23.dat	e7x30a.dat	e7x30b.dat	e7x31a.dat
e7x31b.dat	e8x13.dat	e8x13b.dat	e8x13c.dat	—	e8x14a.dat
e8x14b.dat	e8x14c.dat	e8x14d.dat	e8x14e.dat	e8x14f.dat	e8x15.dat
e8x15b.dat	e8x15c.dat	e8x15d.dat	e8x18b.dat	e8x18d.dat	e8x19b.dat
e8x37.dat	e8x38a.dat	e8x38b.dat	—	e8x38c.dat	e8x40.dat
e8x42.dat	e8x43.dat	e8x43b.dat	e8x43c.dat	e8x44.dat	e8x44b.dat
e8x44c.dat	e8x45.dat	e8x46.dat	e8x47.dat	e8x48.dat	e8x49.dat
e8x50.dat	e8x51a.dat	e8x51b.dat	e8x52.dat	e8x53a.dat	e8x53b.dat
e8x54.dat	e8x58.dat	e8x60.dat	e9x1a.dat	e9x1b.dat	e9x1c.dat
e9x1d.dat	e9x1e.dat	e10x6a.dat	e10x6b.dat		
NODAL THICKNESS					
e8x9.dat					
NODE CIRCLE					
e2x48.dat	e2x49.dat	e2x50.dat			
NODE FILL					
e2x25.dat	e2x25b.dat	e2x33.dat	e2x33b.dat	e2x34.dat	e2x43.dat
e2x66a.dat	e3x20.dat	e4x4.dat	e4x4b.dat	e6x18.dat	e7x16.dat
e7x28c.dat	e7x28d.dat	e7x5.dat	e8x5a.dat	e8x5b.dat	e8x6.dat
e10x5a.dat	e10x5b.dat				
NODE SORT					
e2x9b.dat					

Table 1-2 Model Definition Option Cross-reference (Continued)

OGDEN					
e7x20.dat	e7x20b.dat	e7x20c.dat	e7x20d.dat	e7x21.dat	e7x22a.dat
e7x22b.dat	e7x22c.dat	e7x27.dat	e7x28a.dat	e7x28c.dat	e7x28d.dat
e7x29b.dat	e7x30a.dat	e7x30b.dat	e7x31a.dat	e7x31b.dat	
OPTIMIZE					
e2x10b.dat	e2x10c.dat	e2x26c.dat	e2x26d.dat	e2x2b.dat	e2x31a.dat
e2x31b.dat	e2x34.dat	e2x35.dat	e2x35a.dat	e2x37.dat	e2x38.dat
e2x40a.dat	e2x40b.dat	e2x41.dat	e2x45.dat	e2x46d.dat	e2x51a.dat
e2x51b.dat	e2x67a.dat	e2x67b.dat	e2x68.dat	e2x70.dat	e2x72.dat
e2x73.dat	e2x74.dat	e2x75.dat	e2x76.dat	e2x77.dat	e2x9c.dat
e3x32a.dat	e3x32b.dat	e3x32c.dat	e3x34.dat	e3x35.dat	e3x6.dat
e3x9.dat	e4x11.dat	e4x12a.dat	e4x12b.dat	e4x12c.dat	e4x12d.dat
e4x15.dat	e4x2.dat	e4x2c.dat	e4x2d.dat	e4x2e.dat	e4x5.dat
e5x15b.dat	e5x16c.dat	e5x18a.dat	e5x18b.dat	e5x8a.dat	e5x8c.dat
e5x8d.dat	e5x8e.dat	e6x21.dat	e7x2.dat	e7x20.dat	e7x20b.dat
e7x20d.dat	e7x22a.dat	e7x22b.dat	e7x22c.dat	e7x23.dat	e7x26.dat
e7x30a.dat	e7x30b.dat	e7x32.dat	e8x15b.dat	e8x30.dat	e8x30b.dat
e8x31.dat	e8x32.dat	e8x36.dat	e8x37.dat	e8x45.dat	e8x46.dat
e8x47.dat	e8x49.dat	e8x53a.dat	e8x53b.dat	e8x54.dat	e10x4a.dat
e10x4b.dat	e10x6a.dat	e10x6b.dat			
ORIENTATION					
e2x41.dat	e5x18a.dat	e5x18b.dat	e7x24a.dat	e7x24b.dat	e7x24c.dat
e7x25.dat	e7x6.dat	e7x6b.dat	e7x7.dat	e8x27.dat	e8x5a.dat
e8x5b.dat	e8x9.dat	e10x5a.dat	e10x5b.dat		
ORTHOTROPIC					
e2x70.dat	e5x18a.dat	e5x18b.dat	e7x24a.dat	e7x24b.dat	e7x24c.dat
e7x25.dat	e7x6.dat	e7x7.dat	e8x24b.dat	e8x27.dat	e8x5a.dat
e8x5b.dat	e8x8a.dat	e8x8b.dat	e8x9.dat	e10x5a.dat	e10x5b.dat

Table 1-2 Model Definition Option Cross-reference (Continued)

PARAMETERS					
e2x18.dat	e3x14a.dat	e3x23.dat	e3x23b.dat	e4x5.dat	e7x3.dat
e7x32.dat	e8x18.dat	e8x18d.dat	e9x7a.dat	e9x7b.dat	e9x7c.dat
PHI-COEFFICIENTS					
e6x7.dat	e6x8.dat				
POINT CHARGE					
e8x20.dat	e8x21.dat	e8x28.dat			
POINT CURRENT					
e8x22.dat	e8x23.dat	e8x23b.dat	e8x24a.dat	e8x24b.dat	e8x29.dat
POINT LOAD					
e2x10.dat	e2x10b.dat	e2x10c.dat	e2x14.dat	e2x14b.dat	e2x20.dat
e2x21.dat	e2x24.dat	e2x27.dat	e2x28.dat	e2x29.dat	e2x36.dat
e2x42.dat	e2x48.dat	e2x50.dat	e2x52.dat	e2x54.dat	e2x57a.dat
e2x57b.dat	e2x59a.dat	e2x59b.dat	e2x61a.dat	e2x61b.dat	e2x65.dat
e2x66a.dat	e2x66b.dat	e2x67a.dat	e2x67b.dat	e2x68.dat	e2x7.dat
e2x70.dat	e2x75.dat	e2x76.dat	e2x77.dat	e2x8.dat	e3x1.dat
e3x11.dat	e3x22c.dat	e3x22d.dat	e3x2a.dat	e3x2b.dat	e3x35.dat
e3x4.dat	e4x10.dat	e4x10b.dat	e4x11.dat	e4x12a.dat	e4x12b.dat
e4x12c.dat	e4x12d.dat	e4x15.dat	e4x1a.dat	e4x1c.dat	e4x1d.dat
e4x20.dat	e4x3.dat	e4x4.dat	e4x4b.dat	e4x5.dat	e4x6.dat
e4x7.dat	e4x7b.dat	e4x7c.dat	e6x11.dat	e6x12.dat	e6x3c.dat
e6x6a.dat	e6x6b.dat	e7x10.dat	e7x11.dat	e7x13b.dat	e7x13c.dat
e7x13d.dat	e7x2.dat	e7x27.dat	e8x39.dat	e8x40.dat	e8x55a.dat
e8x55b.dat	e8x56b.dat	e8x57a.dat	e8x57b.dat	e8x57c.dat	e8x57d.dat
e8x5a.dat	e8x5b.dat	e8x6.dat	e8x9.dat	e10x1a.dat	e10x1b.dat
e10x2a.dat	e10x2b.dat	e10x4a.dat	e10x4b.dat	e10x7a.dat	e10x7b.dat
POINT SOURCE					
e8x25.dat					

Table 1-2 Model Definition Option Cross-reference (Continued)

POINT TEMP					
e2x46d.dat					
POST					
e2x1.dat	e2x10.da	e2x10b.dat	e2x10c.dat	e2x11.dat	e2x12b.dat
e2x12c.dat	e2x12d.dat	e2x12e.dat	e2x13.dat	e2x14.dat	e2x14b.dat
e2x15.dat	e2x16.dat	e2x17.dat	e2x18.dat	e2x19.dat	e2x2.dat
e2x21.dat	e2x22.dat	e2x23.dat	e2x24.dat	e2x25.dat	e2x25b.dat
e2x26.dat	e2x26b.dat	e2x26c.dat	e2x26d.dat	e2x27.dat	e2x28.dat
e2x29.dat	e2x2b.dat	e2x2c.dat	e2x3.dat	e2x30.dat	e2x31a.dat
e2x31b.dat	e2x32.dat	e2x33.dat	e2x34.dat	e2x35.dat	e2x36.dat
e2x37.dat	e2x38.dat	e2x39.dat	e2x4.dat	e2x40a.dat	e2x40b.dat
e2x41.dat	e2x42.dat	e2x43.dat	e2x44.dat	e2x45.dat	e2x46a.dat
e2x46b.dat	e2x46c.dat	e2x46d.dat	e2x47b.dat	e2x48.dat	e2x49.dat
e2x5.dat	e2x50.dat	e2x51a.dat	e2x51b.dat	e2x52.dat	e2x53.dat
e2x54.dat	e2x55.dat	e2x56.dat	e2x57a.dat	e2x57b.dat	e2x58a.dat
e2x58b.dat	e2x59a.dat	e2x59b.dat	e2x6.dat	e2x60a.dat	e2x60b.dat
e2x61a.dat	e2x61b.dat	e2x62.dat	e2x63a.dat	e2x63b.dat	e2x64a.dat
e2x64b.dat	e2x65.dat	e2x66a.dat	e2x66b.da	e2x67a.dat	e2x67b.dat
e2x68.dat	e2x69.dat	e2x7.dat	e2x70.dat	e2x71a.dat	e2x71b.dat
e2x72.dat	e2x73.dat	e2x74.dat	e2x75.dat	e2x76.dat	e2x77.dat
e2x8.dat	e2x9.dat	e2x9c.dat	e2x9d.dat	e3x1.dat	e3x10.dat
e3x12b.dat	e3x13.dat	e3x14a.dat	e3x15.dat	e3x15b.dat	e3x16.dat
e3x16b.dat	e3x17.dat	e3x18.dat	e3x19.dat	e3x19b.dat	e3x19c.dat
e3x19d.dat	e3x20.dat	e3x21a.dat	e3x21c.dat	e3x21d.dat	e3x21e.dat
e3x21f.dat	e3x22a.dat	e3x23.dat	e3x23b.dat	e3x24a.dat	e3x25.dat
e3x26.dat	e3x27.dat	e3x28.dat	e3x29.dat	e3x2a.dat	e3x3.dat
e3x30a.dat	e3x30b.dat	e3x31.dat	e3x32a.dat	e3x32b.dat	e3x32c.dat
e3x33.dat	e3x33b.dat	e3x34.dat	e3x35.dat	e3x36.dat	e3x37a.dat

Table 1-2 Model Definition Option Cross-reference (Continued)

POST (Continued)					
e3x37b.dat	e3x38a.dat	e3x38b.dat	e3x3b.dat	e3x4.dat	e3x5.dat
e3x6.dat	e3x8.dat	e3x9.dat	e4x10.dat	e4x10b.dat	e4x11.dat
e4x12a.dat	e4x12b.dat	e4x12c.dat	e4x12d.dat	e4x13a.dat	e4x13b.dat
e4x13c.dat	e4x14a.dat	e4x14b.dat	e4x15.dat	e4x1a.dat	e4x1b.dat
e4x1c.dat	e4x1d.dat	e4x2.dat	e4x2a.dat	e4x2b.dat	e4x2c.dat
e4x2d.dat	e4x2e.dat	e4x3.dat	e4x4.dat	e4x4b.dat	e4x5.dat
e4x6.dat	e4x7.dat	e4x7b.dat	e4x7c.dat	e4x8.dat	e4x9.dat
e4x9b.dat	e5x11a.dat	e5x11c.dat	e5x12.dat	e5x13a.dat	e5x13b.dat
e5x13c.dat	e5x13d.dat	e5x14.dat	e5x15.dat	e5x15b.dat	e5x16a.dat
e5x16b.dat	e5x16c.dat	e5x17a.dat	e5x17b.dat	e5x18a.dat	e5x18b.dat
e5x2a.dat	e5x2b.dat	e5x3a.dat	e5x3b.dat	e5x3c.dat	e5x3d.dat
e5x3e.dat	e5x3f.dat	e5x4a.dat	e5x4b.dat	e5x4c.dat	e5x4d.dat
e5x5a.dat	e5x5b.dat	e5x6.dat	e5x8a.dat	e5x8c.dat	e5x8d.dat
e5x8e.dat	e5x9a.dat	e5x9b.dat	e5x9d.dat	e5x9e.dat	e6x10.dat
e6x11.dat	e6x12.dat	e6x13.dat	e6x13b.dat	e6x15.dat	e6x16a.dat
e6x16b.dat	e6x16c.dat	e6x17a.dat	e6x17b.dat	e6x18.dat	e6x19.dat
e6x1a.dat	e6x2.dat	e6x20a.dat	e6x20b.dat	e6x21.dat	e6x3a.dat
e6x5.dat	e6x6a.dat	e6x7.dat	e6x9.dat	e7x1.dat	e7x10.dat
e7x11.dat	e7x12.dat	e7x13b.dat	e7x13c.dat	e7x14.dat	e7x15.dat
e7x16.dat	e7x17a.dat	e7x17b.dat	e7x18.dat	e7x19.dat	e7x19b.dat
e7x1b.dat	e7x1c.dat	e7x2.dat	e7x20.dat	e7x20b.dat	e7x20c.dat
e7x20d.dat	e7x21.dat	e7x22a.dat	e7x22b.dat	e7x22c.dat	e7x23.dat
e7x24a.dat	e7x24b.dat	e7x24c.dat	e7x25.dat	e7x26.dat	e7x27.dat
e7x28a.dat	e7x28b.dat	e7x28c.dat	e7x28d.dat	e7x29a.dat	e7x29b.dat
e7x3.dat	e7x30a.dat	e7x30b.dat	e7x31a.dat	e7x31b.dat	e7x32.dat
e7x3b.dat	e7x4.dat	e7x4b.dat	e7x5.dat	e7x5b.dat	e7x5c.dat
e7x6.dat	e7x6b.dat	e7x7.dat	e7x8a.dat	e8x11.dat	e8x12.dat
e8x12b.dat	e8x12c.dat	e8x12d.dat	e8x12e.dat	e8x12r.dat	e8x13.dat

Table 1-2 Model Definition Option Cross-reference (Continued)

POST (Continued)					
e8x13b.dat	e8x13c.dat	—	e8x14a.dat	e8x14b.dat	e8x14c.dat
e8x14d.dat	e8x14e.dat	e8x14f.dat	e8x15.dat	e8x15b.dat	e8x15c.dat
e8x15d.dat	e8x16.dat	e8x16b.dat	e8x17.dat	e8x17b.dat	e8x18.dat
e8x18b.dat	e8x18c.dat	e8x18d.dat	e8x19.dat	e8x19b.dat	e8x20.dat
e8x21.dat	e8x22.dat	e8x23.dat	e8x23b.dat	e8x24a.dat	e8x24b.dat
e8x25.dat	e8x26.dat	e8x27.dat	e8x28.dat	e8x29.dat	e8x30.dat
e8x30b.dat	e8x31.dat	e8x32.dat	e8x33a.dat	e8x33b.dat	e8x34.dat
e8x35.dat	e8x36.dat	e8x37.dat	e8x38a.dat	e8x38b.dat	—
e8x38c.dat	e8x39.dat	e8x4.dat	e8x40.dat	e8x41.dat	e8x42.dat
e8x43.dat	e8x43b.dat	e8x43c.dat	e8x44.dat	e8x44b.dat	e8x44c.dat
e8x45.dat	e8x46.dat	e8x47.dat	e8x48.dat	e8x49.dat	e8x50.dat
e8x51a.dat	e8x51b.dat	e8x52.dat	e8x53a.dat	e8x53b.dat	e8x54.dat
e8x55a.dat	e8x55b.dat	e8x56a.dat	e8x56b.dat	e8x57a.dat	e8x57b.dat
e8x57c.dat	e8x57d.dat	e8x58.dat	e8x5a.dat	e8x5b.dat	e8x6.dat
e8x60.dat	e8x7.dat	e8x8a.dat	e8x8b.dat	e8x9.dat	e9x10a.dat
e9x10b.dat	e9x10c.dat	e9x10d.dat	e9x11a.dat	e9x11b.dat	e9x12a.dat
e9x12b.dat	e9x12c.dat	e9x13a.dat	e9x13b.dat	e9x1a.dat	e9x1b.dat
e9x1c.dat	e9x1d.dat	e9x1e.dat	e9x2a.dat	e9x2b.dat	e9x2c.dat
e9x3a.dat	e9x3b.dat	e9x4.dat	e9x5a.dat	e9x5b.dat	e9x5c.dat
e9x5d.dat	e9x5e.dat	e9x6a.dat	e9x6b.dat	e9x7a.da	e9x7b.dat
e9x7c.dat	e9x8.dat	e9x9a.dat	e9x9b.dat	e10x1a.dat	e10x1b.dat
e10x2a.dat	e10x2b.dat	e10x3a.dat	e10x3b.dat	e10x4a.dat	e10x4b.dat
e10x5a.dat	e10x5b.dat	e10x6a.dat	e10x6b.dat	e10x7a.dat	e10x7b.dat
POWDER					
e3x25.dat	e3x26.dat				

Table 1-2 Model Definition Option Cross-reference (Continued)

PRINT CHOICE					
e2x22.dat	e2x38.dat	e2x42.dat	e2x43.dat	e2x60a.dat	e2x60b.dat
e2x61a.dat	e2x61b.dat	e2x62.dat	e2x63a.dat	e2x63b.dat	e2x9b.dat
e3x1.dat	e3x10.dat	e3x11.dat	e3x12.dat	e3x12b.dat	e3x13.dat
e3x15.dat	e3x15b.dat	e3x16.dat	e3x16b.dat	e3x17.dat	e3x18.dat
e3x20.dat	e3x21a.dat	e3x21c.dat	e3x21d.dat	e3x21e.dat	e3x21f.dat
e3x22c.dat	e3x22d.dat	e3x23.dat	e3x23b.dat	e3x24a.dat	e3x24b.dat
e3x24c.dat	e3x2a.dat	e3x2b.dat	e3x3.dat	e3x30a.dat	e3x30b.dat
e3x33.dat	e3x33b.dat	e3x3b.dat	e3x4.dat	e3x5.dat	e3x7a.dat
e3x7b.dat	e3x7c.dat	e3x8.dat	e4x15.dat	e4x1b.dat	e4x1c.dat
e4x2a.dat	e4x2b.dat	e4x4.dat	e4x4b.dat	e4x7.dat	e4x7b.dat
e4x7c.dat	e5x11a.dat	e5x11c.dat	e5x13a.dat	e5x13b.dat	e5x13c.dat
e5x13d.dat	e5x4a.dat	e5x4b.dat	e5x4c.dat	e5x4d.dat	e5x9b.dat
e6x13.dat	e6x13b.dat	e6x1a.dat	e6x1b.dat	e6x1c.dat	e6x7.dat
e6x8.dat	e6x9.dat	e7x11.dat	e7x12.dat	e7x14.dat	e7x17a.dat
e7x17b.dat	e7x18.dat	e7x19.dat	e7x19b.dat	e7x3.dat	e7x3b.dat
e8x12.dat	e8x12b.dat	e8x12c.dat	e8x12e.dat	e8x12r.dat	e8x16.dat
e8x16b.dat	e8x17.dat	e8x17b.dat	e8x18.dat	e8x18c.dat	e8x19.dat
e8x31.dat	e8x4.dat	e8x57a.dat	e8x57c.dat	e8x57d.dat	e8x5a.dat
e8x5b.dat	e8x7.dat				
PRINT ELEMENT					
e2x46d.dat	e2x69.dat	e2x70.dat	e3x26.dat	e6x16a.dat	e6x16b.dat
e6x16c.dat	e6x17a.dat	e6x17b.dat	e6x19.dat	e7x24a.dat	e7x24b.dat
e7x24c.dat	e7x6.dat	e7x6b.dat	e7x7.dat	e8x24a.dat	e8x25.dat
e8x26.dat	e8x27.dat	e8x28.dat	e8x29.dat	e8x33a.dat	e8x33b.dat
e8x35.dat	e8x39.dat	e8x55a.dat	e8x55b.dat	e8x56a.dat	e8x56b.dat
e8x9.dat	e9x11a.dat	e9x11b.dat	e9x12a.dat	e9x12b.dat	e9x12c.dat
e9x13a.dat	e9x13b.dat	e9x2a.dat	e9x2b.dat	e9x2c.dat	e9x3a.dat

Table 1-2 Model Definition Option Cross-reference (Continued)

PRINT ELEMENT (Continued)					
e9x3b.dat	e9x4.dat	e9x5a.dat	e9x5b.dat	e9x5c.dat	e9x5d.dat
e9x5e.dat	e9x6a.dat	e9x6b.dat	e9x7a.dat	e9x7b.dat	e9x7c.dat
e9x9a.dat	e9x9b.dat				
PRINT NODE					
e2x2b.dat	e2x2c.dat	e2x46d.dat	e2x70.dat	e6x19.dat	e8x11.dat
e8x25.dat	e8x26.dat	e8x35.dat	e8x39.dat	e8x55a.dat	e8x55b.dat
RADIATING CAVITY					
e5x15.dat					
REAUTO					
e7x17b.dat	e7x31b.dat	e8x12r.dat			
REBAR					
e2x14b.dat	e2x37b.dat	e4x13a.dat	e4x13b.dat	e4x13c.dat	e4x14a.dat
e4x14b.dat					
REGION					
e9x10a.dat	e9x10b.dat	e9x10c.dat	e9x10d.dat	e9x11a.dat	e9x11b.dat
e9x12c.dat	e9x13a.dat	e9x13b.dat			
RELATIVE DENSITY					
e3x25.dat	e3x26.dat				
RESPONSE SPECTRUM					
e6x6a.dat	e6x6b.dat				
RESTART					
e2x35.dat	e2x35a.dat	e2x51a.dat	e2x51b.dat	e3x11.dat	e3x13.dat
e3x18.dat	e3x19.dat	e3x19b.dat	e3x19c.dat	e3x19d.dat	e3x20.dat
e3x21c.dat	e3x22c.dat	e3x22d.dat	e3x23.dat	e3x23b.dat	e3x26.dat
e3x27.dat	e3x28.dat	e3x2a.dat	e3x2b.dat	e3x7a.dat	e3x7b.dat
e3x7c.dat	e3x8.dat	e4x3.dat	e4x5.dat	e4x7.dat	e5x11c.dat

Table 1-2 Model Definition Option Cross-reference (Continued)

RESTART (Continued)					
e5x8a.dat	e5x8b.dat	e5x8c.dat	e5x8d.dat	e5x8e.dat	e6x13.dat
e6x13b.dat	e6x16a.dat	e6x16b.dat	e6x16c.dat	e6x17a.dat	e6x17b.dat
e6x6a.dat	e6x6b.dat	e6x8.dat	e7x11.dat	e7x13b.dat	e7x13c.dat
e7x13d.dat	e7x17a.dat	e7x17b.dat	e7x18.dat	e7x3.dat	e7x31a.dat
e7x31b.dat	e7x3b.dat	e7x4.dat	e7x4b.dat	e7x8a.dat	e7x8b.dat
e7x8c.dat	e7x9a.dat	e7x9b.dat	e7x9c.dat	e8x12.dat	e8x12b.dat
e8x12r.dat	e8x1b.dat	e8x1c.dat	e8x35.dat	e8x36.dat	e8x42.dat
e8x44.dat	e8x44b.dat	e8x44c.dat	e8x5a.dat	e8x5b.dat	e8x6.dat
e8x60.dat	e8x7.dat				
RESTART LAST					
e3x31.dat	e8x15.dat	e8x15b.dat	e8x15c.dat	e8x15d.dat	e8x17.dat
e8x17b.dat					
ROTATION A					
e2x33.dat	e2x33b.dat	e2x49.dat	e2x71a.dat	e2x71b.dat	e6x4.dat
SHELL TRANSFORMATION					
e3x1.dat	e3x20.dat				
SHIFT FUNCTION					
e7x32.dat					
SOIL					
e8x34.dat	e8x35.dat				
SOLVER					
e2x12c.dat	e2x12e.dat	e2x40a.dat	e2x40b.dat	e2x41.dat	e2x46d.dat
e2x68.dat	e2x72.dat	e2x73.dat	e2x74.dat	e2x75.dat	e2x76.dat
e2x77.dat	e3x32a.dat	e3x32b.dat	e3x32c.dat	e3x34.dat	e3x35.dat
e3x6.dat	e4x11.dat	e4x12a.dat	e4x12b.dat	e4x12c.dat	e4x12d.dat
e4x15.dat	e4x2.dat	e4x2c.dat	e4x2d.dat	e4x2e.dat	e5x15b.dat

Table 1-2 Model Definition Option Cross-reference (Continued)

SOLVER (Continued)					
e5x18a.dat	e5x18b.dat	e6x21.dat	e7x23.dat	e7x30a.dat	e7x30b.dat
e7x31a.dat	e7x31b.dat	e7x32.dat	e8x35.dat	e8x38b.dat	—
e8x38c.dat	e8x40.dat	e8x42.dat	e8x45.dat	e8x46.dat	e8x47.dat
e8x48.dat	e8x49.dat	e8x50.dat	e8x51a.dat	e8x51b.dat	e8x52.dat
e8x53a.dat	e8x53b.dat	e8x54.dat	e8x56a.dat	e8x56b.dat	e8x57a.dat
e8x57b.dat	e8x57c.dat	e8x57d.dat	e8x60.dat	e10x4a.dat	e10x4b.dat
e10x6a.dat	e10x6b.dat				
SPLINE					
e8x45.dat					
SPRINGS					
e2x54.dat	e3x13.dat	e4x6.dat	e8x16.dat	e8x16b.dat	e8x36.dat
e8x37.dat	e8x47.dat	e8x48.dat			
STIFSCALE					
e2x33b.dat					
STRAIN RATE					
e9x9a.dat	e9x9b.dat				
SUBSTRUCTURE					
e8x1a.dat	e8x2.dat	e8x3.dat			
SUMMARY					
e2x9b.dat					
SUPERINPUT					
e8x1b.dat	e8x1c.dat				
SURFACE					
e2x9d.dat	e7x20c.dat	e8x40.dat	e8x42.dat		

Table 1-2 Model Definition Option Cross-reference (Continued)

TEMPERATURE EFFECTS					
e3x26.dat	e3x5.dat	e5x11a.dat	e5x14.dat	e5x15.dat	e5x8a.dat
e5x8c.dat	e5x8d.dat	e5x8e.dat	e5x9a.dat	e5x9b.dat	e5x9d.dat
e5x9e.dat	e8x13.dat	e8x13b.dat	e8x13c.dat	—	e8x7.dat
THERMAL LOADS					
e2x46a.dat	e2x46b.dat	e2x49.dat	e3x13.dat	e3x5.dat	
THICKNESS					
e7x15.dat	e7x16.dat				
TIME-TEMP					
e5x11c.dat					
TRANSFORMATION					
e2x2.dat	e2x23.dat	e2x2b.dat	e2x2c.dat	e2x3.dat	e2x4.dat
e2x47b.dat	e3x16.dat	e3x16b.dat	e3x5.dat	e4x1a.dat	e4x1b.dat
e4x1c.dat	e4x1d.dat	e4x7.dat	e4x7c.dat		
TYING					
e2x15.dat	e2x28.dat	e2x3.dat	e2x4.dat	e2x43.dat	e2x44.dat
e2x47b.dat	e2x52.dat	e2x53.dat	e2x65.dat	e2x70.dat	e3x1.dat
e3x18.dat	e3x22c.dat	e3x22d.dat	e4x15.dat	e6x10.dat	e6x7.dat
e7x12.dat	e7x13b.dat	e7x13c.dat	e7x15.dat	e7x16.dat	e7x18.dat
e7x19.dat	e7x19b.dat	e7x25.dat	e7x27.dat	e7x4.dat	e7x4b.dat
e8x4.dat	e10x1a.dat	e10x1b.dat	e10x7a.dat	e10x7b.dat	
UDUMP					
e3x19.dat	e3x19b.dat	e3x19c.dat	e3x21a.dat	e3x21d.dat	e3x21e.dat
e3x21f.dat	e3x3.dat	e3x3b.dat	e4x7.dat	e5x3a.dat	e5x4a.dat
e5x9a.dat	e6x5.dat	e8x19.dat	e8x19b.dat		
UFCONN					
e2x20.dat	e2x27.dat	e2x34.dat	e2x46a.dat	e2x46b.dat	e7x15.dat

Table 1-2 Model Definition Option Cross-reference (Continued)

UFXORD					
e2x16.dat	e2x17.dat	e2x18.dat	e2x19.dat	e2x20.dat	e2x55.dat
e2x56.dat	e3x16.dat	e3x16b.dat	e3x17.dat	e3x23.dat	e3x23b.dat
e3x27.dat	e3x5.dat	e4x1a.dat	e4x1b.dat	e4x1d.dat	e4x5.dat
e4x7.dat	e4x7c.dat	e6x3b.dat	e6x3d.dat	e7x15.dat	e7x3.dat
e7x3b.dat					
UMOTION					
e8x19.dat	e8x19b.dat				
UTRANFORM					
e2x62.dat	e4x14a.dat	e4x14b.dat			
VELOCITY					
e5x17a.dat	e5x17b.dat	e7x15.dat	e7x16.dat		
VIEW FACTOR					
e5x15b.dat					
VISCEL EXP					
e7x32.dat					
VISCELMOON					
e7x18.dat					
VISCELOGDEN					
e7x22c.dat					
VISCELPROP					
e7x12.dat	e7x14.dat	e7x32.dat			
VOLTAGE					
e5x10.dat	e5x12.dat				

Table 1-2 Model Definition Option Cross-reference (Continued)

WORK HARD					
e3x1.dat	e3x10.dat	e3x11.dat	e3x16.dat	e3x16b.dat	e3x18.dat
e3x19.dat	e3x19b.dat	e3x19c.dat	e3x19d.dat	e3x20.dat	e3x21a.dat
e3x21c.dat	e3x21d.dat	e3x21e.dat	e3x21f.dat	e3x26.dat	e3x27.dat
e3x28.dat	e3x2a.dat	e3x2b.dat	e3x30a.dat	e3x30b.dat	e3x33.dat
e3x33b.dat	e3x34.dat	e3x35.dat	e3x36.dat	e3x38a.dat	e3x38b.dat
e3x4.dat	e3x5.dat	e3x8.dat	e7x17a.dat	e7x17b.dat	e8x12d.dat
e8x13.dat	e8x13b.dat	e8x13c.dat	—	e8x15.dat	e8x15b.dat
e8x15c.dat	e8x15d.dat	e8x16.dat	e8x16b.dat	e8x18.dat	e8x18b.dat
e8x18c.dat	e8x18d.dat	e8x38a.dat	e8x38b.dat	—	e8x38c.dat
e8x44.dat	e8x44b.dat	e8x44c.dat	e8x50.dat	e8x51a.dat	e8x51b.dat
e8x52.dat	e8x55a.dat	e8x55b.dat	e8x56a.dat	e8x56b.dat	e8x60.dat
e8x7.dat	e9x13a.dat				

Table 1-3 History Definition Option Cross-reference

ACCUMULATE					
e3x15.dat					
ACTIVATE					
e8x11.dat					
AUTO CREEP					
e3x12.dat	e3x13.dat	e3x14a.dat	e3x15.dat	e3x22c.dat	e3x22d.dat
e3x29.dat					
AUTO INCREMENT					
e3x23.dat	e3x23b.dat	e3x6.dat	e4x1c.dat	e4x7.dat	e4x7b.dat
e7x3.dat	e7x30a.dat	e7x30b.dat	e8x39.dat	e8x5a.dat	e8x5b.dat
e8x6.dat					
AUTO LOAD					
e2x65.dat	e2x70.dat	e3x1.dat	e3x10.dat	e3x15b.dat	e3x16.dat
e3x16b.dat	e3x17.dat	e3x18.dat	e3x19.dat	e3x19b.dat	e3x19c.dat
e3x19d.dat	e3x20.dat	e3x21a.dat	e3x21c.dat	e3x21d.dat	e3x21e.dat
e3x25.dat	e3x27.dat	e3x28.dat	e3x2a.dat	e3x2b.dat	e3x3.dat
e3x30a.dat	e3x30b.dat	e3x31.dat	e3x32a.dat	e3x32b.dat	e3x32c.dat
e3x33b.dat	e3x34.dat	e3x35.dat	e3x36.dat	e3x37a.dat	e3x37b.dat
e3x38a.dat	e3x38b.dat	e3x3b.dat	e3x4.dat	e3x7a.dat	e3x7b.dat
e3x8.dat	e3x9.dat	e4x11.dat	e4x12a.dat	e4x12b.dat	e4x12c.dat
e4x12d.dat	e4x13a.dat	e4x13b.dat	e4x13c.dat	e4x14a.dat	e4x14b.dat
e4x1b.dat	e4x2.dat	e4x2a.dat	e4x2b.dat	e4x2c.dat	e4x2d.dat
e4x2e.dat	e4x3.dat	e4x4.dat	e4x4b.dat	e4x5.dat	e4x6.dat
e4x8.dat	e6x21.dat	e6x3c.dat	e7x1.dat	e7x11.dat	e7x12.dat
e7x13b.dat	e7x13c.dat	e7x14.dat	e7x17a.dat	e7x17b.dat	e7x18.dat
e7x19.dat	e7x19b.dat	e7x1b.dat	e7x1c.dat	e7x2.dat	e7x20.dat
e7x20b.dat	e7x20c.dat	e7x20d.dat	e7x21.dat	e7x22a.dat	e7x22b.dat

Table 1-3 History Definition Option Cross-reference

AUTO LOAD (Continued)					
e7x22c.dat	e7x23.dat	e7x25.dat	e7x27.dat	e7x29a.dat	e7x29b.dat
e7x31a.dat	e7x31b.dat	e7x32.dat	e7x4.dat	e8x12.dat	e8x12c.dat
e8x12r.dat	e8x14a.dat	e8x14b.dat	e8x14c.dat	e8x14d.dat	e8x14e.dat
e8x14f.dat	e8x15.dat	e8x15b.dat	e8x15c.dat	e8x16.dat	e8x16b.dat
e8x17.dat	e8x18.dat	e8x18b.dat	e8x18c.dat	e8x19.dat	e8x19b.dat
e8x2.dat	e8x27.dat	e8x3.dat	e8x34.dat	e8x35.dat	e8x36.dat
e8x37.dat	e8x38a.dat	e8x38b.dat	—	e8x38c.dat	e8x4.dat
e8x42.dat	e8x43.dat	e8x43b.dat	e8x43c.dat	e8x44.dat	e8x44b.dat
e8x44c.dat	e8x45.dat	e8x46.dat	e8x47.dat	e8x48.dat	e8x49.dat
e8x50.dat	e8x51a.dat	e8x51b.dat	e8x52.dat	e8x53a.dat	e8x53b.dat
e8x54.dat	e8x55a.dat	e8x55b.dat	e8x56a.dat	e8x56b.dat	e8x60.dat
e9x13a.dat	e9x13b.dat				
AUTO STEP					
e3x12b.dat	e3x21f.dat	e3x33.dat	e4x7c.dat	e5x8e.dat	e7x3b.dat
e7x4b.dat	e8x12d.dat	e8x12e.dat	e8x13b.dat	e8x15d.dat	e8x16b.dat
e8x17b.dat	e8x18d.dat				
AUTO THERM					
e3x11.dat	e3x22c.dat	e3x24b.dat	e3x24c.dat	e3x5.dat	e5x11c.dat
AUTO TIME					
e6x13.dat	e6x13b.dat	e6x1c.dat	e8x12b.dat		
BACKTOSUBS					
e8x1c.dat	e8x3.dat				
BUCKLE					
e3x16.dat	e3x16b.dat	e4x10.dat	e4x10b.dat	e4x12a.dat	e4x12b.dat
e4x15.dat	e4x1a.dat	e4x1d.dat	e4x4.dat	e4x4b.dat	e4x9.dat
e4x9b.dat					

Table 1-3 History Definition Option Cross-reference

CHANGE STATE					
e2x70.dat	e3x11.dat	e3x22c.dat	e3x22d.dat	e3x24b.dat	e3x24c.dat
e3x5.dat	e5x11c.dat	e7x32.dat	e8x45.dat		
COMMENT					
e8x12.dat	e8x12r.dat	e8x52.dat			
CONTACT TABLE					
e7x31b.dat	e8x16b.dat	e8x36.dat	e8x37.dat	e8x44.dat	e8x44b.dat
e8x44c.dat	e8x46.dat				
CONTINUE					
e2x35.dat	e2x38.dat	e2x51a.dat	e2x64a.dat	e2x64b.dat	e2x65.dat
e2x66b.dat	e2x70.dat	3x1.dat	e3x10.dat	e3x11.dat	e3x12.dat
e3x12b.dat	e3x13.dat	e3x14a.dat	e3x15.dat	e3x15b.dat	e3x16.dat
e3x16b.dat	e3x17.dat	e3x18.dat	e3x19.dat	e3x19b.dat	e3x19c.dat
e3x19d.dat	e3x20.dat	e3x21a.dat	e3x21c.dat	e3x21d.dat	e3x21e.dat
e3x21f.dat	e3x22a.dat	e3x22c.dat	e3x22d.dat	e3x23.dat	e3x23b.dat
e3x24a.dat	e3x24b.dat	e3x24c.dat	e3x25.dat	e3x26.dat	e3x27.dat
e3x28.dat	e3x29.dat	e3x2a.dat	e3x2b.dat	e3x3.dat	e3x30a.dat
e3x30b.dat	e3x31.dat	e3x32a.dat	e3x32b.dat	e3x32c.dat	e3x33.dat
e3x33b.dat	e3x34.dat	e3x35.dat	e3x36.dat	e3x37a.dat	e3x37b.dat
e3x38a.dat	e3x38b.dat	e3x3b.dat	e3x4.dat	e3x5.dat	e3x6.dat
e3x7a.dat	e3x7b.dat	e3x7c.dat	e3x8.dat	e3x9.dat	e4x10.dat
e4x10b.dat	e4x11.dat	e4x12a.dat	e4x12b.dat	e4x12c.dat	e4x12d.dat
e4x13a.dat	e4x13b.dat	e4x13c.dat	e4x14a.dat	e4x14b.dat	e4x15.dat
e4x1a.dat	e4x1b.dat	e4x1c.dat	e4x1d.dat	e4x2.dat	e4x20.dat
e4x2a.dat	e4x2b.dat	e4x2c.dat	e4x2d.dat	e4x2e.dat	e4x3.dat
e4x4.dat	e4x4b.dat	e4x5.dat	e4x6.dat	e4x7.dat	e4x7b.dat
e4x7c.dat	e4x8.dat	e4x9.dat	e4x9b.dat	e5x1.dat	e5x10.dat
e5x11a.dat	e5x11c.dat	e5x12.dat	e5x13a.dat	e5x13b.dat	e5x13c.dat

Table 1-3 History Definition Option Cross-reference

CONTINUE (Continued)					
e5x13d.dat	e5x14.dat	e5x15.dat	e5x15b.dat	e5x16a.dat	e5x16b.dat
e5x16c.dat	e5x17a.dat	e5x17b.dat	e5x18a.dat	e5x18b.dat	e5x2a.dat
e5x2b.dat	e5x3a.dat	e5x3b.dat	e5x3c.dat	e5x3d.dat	e5x3e.dat
e5x3f.dat	e5x4a.dat	e5x4b.dat	e5x4c.dat	e5x4d.dat	e5x5a.dat
e5x5b.dat	e5x6.dat	e5x7a.dat	e5x7b.dat	e5x8a.dat	e5x8b.dat
e5x8c.dat	e5x8d.dat	e5x8e.dat	e5x9a.dat	e5x9b.dat	e5x9d.dat
e5x9e.dat	e6x10.dat	e6x11.dat	e6x12.dat	e6x13.dat	e6x13b.dat
e6x14.dat	e6x15.dat	e6x15b.dat	e6x16a.dat	e6x16b.dat	e6x16c.dat
e6x17a.dat	e6x17b.dat	e6x18.dat	e6x19.dat	e6x1a.dat	e6x1b.dat
e6x1c.dat	e6x2.dat	e6x20b.dat	e6x21.dat	e6x3a.dat	e6x3b.dat
e6x3c.dat	e6x3d.dat	e6x4.dat	e6x5.dat	e6x6a.dat	e6x6b.dat
e6x7.dat	e6x8.dat	e6x9.dat	e7x1.dat	e7x11.dat	e7x12.dat
e7x13b.dat	e7x13c.dat	e7x13d.dat	e7x14.dat	e7x16.dat	e7x17a.dat
e7x17b.dat	e7x18.dat	e7x19.dat	e7x19b.dat	e7x1b.dat	e7x1c.dat
e7x2.dat	e7x20.dat	e7x20b.dat	e7x20c.dat	e7x20d.dat	e7x21.dat
e7x22a.dat	e7x22b.dat	e7x22c.dat	e7x23.dat	e7x25.dat	e7x26.dat
e7x27.dat	e7x28a.dat	e7x28b.dat	e7x28c.dat	e7x28d.dat	e7x29a.dat
e7x29b.dat	e7x3.dat	e7x30a.dat	e7x30b.dat	e7x31a.dat	e7x31b.dat
e7x32.dat	e7x3b.dat	e7x4.dat	e7x4b.dat	e7x5.dat	e7x5b.dat
e7x5c.dat	e8x10.dat	e8x11.dat	e8x12.dat	e8x12b.dat	e8x12c.dat
e8x12d.dat	e8x12e.dat	e8x12r.dat	e8x13.dat	e8x13b.dat	e8x13c.dat
—	e8x14a.dat	e8x14b.dat	e8x14c.dat	e8x14d.dat	e8x14e.dat
e8x14f.dat	e8x15.dat	e8x15b.dat	e8x15c.dat	e8x15d.dat	e8x16.dat
e8x16b.dat	e8x17.dat	e8x17b.dat	e8x18.dat	e8x18b.dat	e8x18c.dat
e8x18d.dat	e8x19.dat	e8x19b.dat	e8x1c.dat	e8x2.dat	e8x20.dat
e8x21.dat	e8x22.dat	e8x23.dat	e8x23b.dat	e8x24a.dat	e8x24b.dat
e8x25.dat	e8x26.dat	e8x27.dat	e8x28.dat	e8x29.dat	e8x3.dat
e8x30.dat	e8x30b.dat	e8x31.dat	e8x32.dat	e8x33a.dat	e8x33b.dat

Table 1-3 History Definition Option Cross-reference

CONTINUE (Continued)					
e8x34.dat	e8x35.dat	e8x36.dat	e8x37.dat	e8x38a.dat	e8x38b.dat
—	e8x38c.dat	e8x39.dat	e8x4.dat	e8x42.dat	e8x43.dat
e8x43b.dat	e8x43c.dat	e8x44.dat	e8x44b.dat	e8x44c.dat	e8x45.dat
e8x46.dat	e8x47.dat	e8x48.dat	e8x49.dat	e8x50.dat	e8x51a.dat
e8x51b.dat	e8x52.dat	e8x53a.dat	e8x53b.dat	e8x54.dat	e8x55a.dat
e8x55b.dat	e8x56a.dat	e8x56b.dat	e8x5a.dat	e8x5b.dat	e8x6.dat
e8x60.dat	e8x7.dat	e9x10a.dat	e9x10b.dat	e9x10c.dat	e9x10d.dat
e9x11a.dat	e9x11b.dat	e9x12a.dat	e9x12b.dat	e9x12c.dat	e9x13a.dat
e9x13b.dat	e9x1a.dat	e9x1b.dat	e9x1c.dat	e9x1d.dat	e9x1e.dat
e9x2a.dat	e9x2b.dat	e9x2c.dat	e9x3a.dat	e9x3b.dat	e9x4.dat
e9x5a.dat	e9x5b.dat	e9x5c.dat	e9x5d.dat	e9x5e.dat	e9x6a.dat
e9x6b.dat	e9x7a.dat	e9x7b.dat	e9x7c.dat	e9x8.dat	e9x9a.dat
e9x9b.dat	e10x1a.dat	e10x1b.dat	e10x2a.dat	e10x2b.dat	e10x3a.dat
e10x3b.dat	e10x4a.dat	e10x4b.dat	e10x5a.dat	e10x5b.dat	e10x6a.dat
e10x6b.dat	e10x7a.dat	e10x7b.dat			
CONTROL					
e3x26.dat	e3x29.dat	e3x34.dat	e3x6.dat	e4x11.dat	e4x14b.dat
e4x2.dat	e4x2c.dat	e4x2d.dat	e4x2e.dat	e5x15b.dat	e5x18a.dat
e5x18b.dat	e6x21.dat	e7x22a.dat	e7x22b.dat	e7x22c.dat	e7x27.dat
e7x28a.dat	e7x28b.dat	e7x28c.dat	e7x28d.dat	e7x30a.dat	e7x30b.dat
e7x31a.dat	e7x31b.dat	e7x32.dat	e7x5.dat	e7x5b.dat	e7x5c.dat
e8x16b.dat	e8x3.dat	e8x35.dat	e8x43.dat	e8x43b.dat	e8x43c.dat
e8x44.dat	e8x44b.dat	e8x44c.dat	e8x45.dat	e8x46.dat	e8x47.dat
e8x48.dat	e8x49.dat	e8x50.dat	e8x51a.dat	e8x51b.dat	e8x52.dat
e8x53a.dat	e8x53b.dat	e8x54.dat	e8x60.dat		
CREEP INCREMENT					
e3x15.dat	e3x15b.dat				

Table 1-3 History Definition Option Cross-reference

DAMPING COMPONENTS					
e7x16.dat					
DEACTIVATE					
e8x11.dat					
DISP CHANGE					
e3x14a.dat	e3x18.dat	e3x20.dat	e3x21f.dat	e3x27.dat	e3x28.dat
e3x31.dat	e3x33.dat	e3x33b.dat	e3x36.dat	e3x37a.dat	e3x37b.dat
e3x38a.dat	e3x38b.dat	e4x10.dat	e4x10b.dat	e4x14a.dat	e4x14b.dat
e4x9.dat	e4x9b.dat	e6x21.dat	e6x7.dat	e6x8.dat	e7x18.dat
e7x19.dat	e7x19b.dat	e7x21.dat	e7x29a.dat	e7x29b.dat	e7x30a.dat
e7x30b.dat	e7x4b.dat	e8x10.dat	e8x12.dat	e8x12r.dat	e8x13.dat
e8x13b.dat	e8x13c.dat	—	e8x15d.dat	e8x16b.dat	e8x34.dat
e8x43.dat	e8x43b.dat	e8x43c.dat	e8x46.dat	e8x48.dat	e8x49.dat
e8x52.dat	e8x53b.dat	e8x54.dat	e8x56a.dat		
DIST CURRENT					
e8x30.dat	e8x32.dat				
DIST FLUXES					
e5x18a.dat	e5x18b.dat				
DIST LOADS					
e2x35.dat	e2x66b.dat	e3x12.dat	e3x12b.dat	e3x15.dat	e3x15b.dat
e3x23.dat	e3x23b.dat	e3x25.dat	e3x26.dat	e3x29.dat	e3x31.dat
e3x32a.dat	e3x32b.dat	e3x32c.dat	e3x34.dat	e3x6.dat	e4x13a.dat
e4x13b.dat	e4x13c.dat	e4x14a.dat	e4x14b.dat	e4x2.dat	e4x2a.dat
e4x2b.dat	e4x2c.dat	e4x2d.dat	e4x2e.dat	e4x8.dat	e6x14.dat
e6x1a.dat	e6x1b.dat	e6x1c.dat	e6x20b.dat	e6x21.dat	e6x3a.dat
e6x3b.dat	e6x3c.dat	e6x3d.dat	e6x4.dat	e7x12.dat	e7x14.dat
e7x2.dat	e7x20.dat	e7x20b.dat	e7x20c.dat	e7x20d.dat	e7x22a.dat
e7x22b.dat	e7x22c.dat	e7x26.dat	e7x28a.dat	e7x28b.dat	e7x28c.dat

Table 1-3 History Definition Option Cross-reference

DIST LOADS (Continued)					
e7x28d.dat	e7x3.dat	e7x3b.dat	e7x5.dat	e7x5b.dat	e7x5c.dat
e8x1a.dat	e8x34.dat	e8x35.dat	e8x42.dat	e8x43.dat	e8x43b.dat
e8x43c.dat	e8x46.dat	e8x47.dat	e8x48.dat	e8x53a.dat	e8x53b.dat
e10x2a.dat	e10x2b.dat	e10x3a.dat	e10x3b.dat		
DYNAMIC CHANGE					
e4x20.dat	e6x14.dat	e6x16a.dat	e6x16b.dat	e6x16c.dat	e6x17a.dat
e6x17b.dat	e6x19.dat	e6x1a.dat	e6x1b.dat	e6x1c.dat	e6x20b.dat
e6x3a.dat	e6x3b.dat	e6x3c.dat	e6x3d.dat	e6x9.dat	e8x25.dat
e8x26.dat	e8x31.dat	e8x33b.dat			
EXTRAPOLATE					
e3x15.dat					
HARMONIC					
e6x7.dat	e6x8.dat	e8x30.dat	e8x30b.dat	e8x32.dat	e8x33a.dat
MODAL SHAPE					
e6x10.dat	e6x11.dat	e6x12.dat	e6x15.dat	e6x15b.dat	e6x18.dat
e6x2.dat	e6x21.dat	e6x3a.dat	e6x3b.dat	e6x3c.dat	e6x3d.dat
e6x4.dat	e6x5.dat	e6x6a.dat	e6x6b.dat	e8x25.dat	e8x26.dat
e10x1a.dat	e10x1b.dat	e10x3a.dat	e10x3b.dat	e10x4a.dat	e10x4b.dat
e10x7a.dat	e10x7b.dat				
MOTION CHANGE					
e3x30a.dat	e3x30b.dat	e3x32a.dat	e3x32b.dat	e3x32c.dat	e7x20.dat
e7x20b.dat	e7x20c.dat	e7x20d.dat	e7x31a.dat	e7x31b.dat	e8x16.dat
e8x16b.dat	e8x18.dat	e8x18b.dat	e8x18c.dat	e8x18d.dat	e8x42.dat
e8x44.dat	e8x44b.dat	e8x44c.dat	e8x45.dat	e8x49.dat	e8x50.dat
e8x51a.dat	e8x51b.dat	e8x60.dat			

Table 1-3 History Definition Option Cross-reference

NO PRINT					
e3x31.dat	e7x25.dat				
POINT CURRENT					
e8x30b.dat	e8x33a.dat	e8x33b.dat			
POINT LOAD					
e2x64a.dat	e2x64b.dat	e2x65.dat	e2x66b.dat	e2x70.dat	e3x1.dat
e3x2b.dat	e3x35.dat	e3x38b.dat	e4x11.dat	e4x12a.dat	e4x12b.dat
e4x12c.dat	e4x12d.dat	e4x1c.dat	e4x20.dat	e4x3.dat	e4x6.dat
e4x7.dat	e4x7b.dat	e4x7c.dat	e7x11.dat	e7x2.dat	e7x25.dat
e7x27.dat	e8x3.dat	e8x39.dat	e8x55a.dat	e8x55b.dat	e8x56b.dat
e8x5a.dat	e8x5b.dat	e8x6.dat	e10x1a.dat	e10x1b.dat	e10x2a.dat
e10x2b.dat	e10x4a.dat	e10x4b.dat	e10x5a.dat	e10x5b.dat	e10x6a.dat
e10x6b.dat	e10x7a.dat	e10x7b.dat			
POINT SOURCE					
e8x25.dat					
POST INCREMENT					
e3x31.dat	e7x25.dat	e8x16.dat			
POTENTIAL CHANGE					
e8x31.dat					
PRINT CHOICE					
e3x14a.dat	e3x20.dat				
PRINT ELEMENT					
e7x25.dat					
PROPORTIONAL INCREMENT					
e2x38.dat	e2x70.dat	e3x1.dat	e3x10.dat	e3x11.dat	e3x16.dat
e3x16b.dat	e3x17.dat	e3x19.dat	e3x19b.dat	e3x19c.dat	e3x19d.dat
e3x20.dat	e3x21a.dat	e3x21c.dat	e3x21d.dat	e3x21e.dat	e3x22c.dat

Table 1-3 History Definition Option Cross-reference

PROPORTIONAL INCREMENT (Continued)					
e3x22d.dat	e3x2a.dat	e3x2b.dat	e3x3.dat	e3x34.dat	e3x35.dat
e3x3b.dat	e3x4.dat	e3x7a.dat	e3x7b.dat	e3x8.dat	e3x9.dat
e4x1a.dat	e4x1d.dat	e4x8.dat	e6x12.dat	e6x1c.dat	e6x3c.dat
e6x6a.dat	e6x7.dat	e6x8.dat	e7x11.dat	e7x13b.dat	e7x13c.dat
e7x25.dat	e7x4.dat	e8x2.dat	e8x27.dat	e8x4.dat	
RECOVER					
e3x16.dat	e3x16b.dat	e4x15.dat	e4x4.dat	e4x4b.dat	e6x10.dat
e6x15.dat	e6x18.dat	e6x2.dat	e6x21.dat	e6x5.dat	e6x6a.dat
e8x25.dat					
RELEASE					
e8x16.dat	e8x44.dat	e8x44b.dat	e8x44c.dat		
SPECTRUM					
e6x18.dat	e6x6a.dat	e6x6b.dat			
STEADY STATE					
e5x15.dat	e5x15b.dat	e5x18a.dat	e5x3a.dat	e8x20.dat	e8x21.dat
e8x22.dat	e8x23.dat	e8x23b.dat	e8x24a.dat	e8x24b.dat	e8x28.dat
e8x29.dat	e9x10a.dat	e9x10b.dat	e9x10c.dat	e9x10d.dat	e9x11a.dat
e9x12a.dat	e9x12b.dat	e9x12c.dat	e9x1a.dat	e9x1b.dat	e9x1c.dat
e9x1d.dat	e9x1e.dat	e9x2a.dat	e9x2b.dat	e9x2c.dat	e9x3a.dat
e9x3b.dat	e9x4.dat	e9x5a.dat	e9x5b.dat	e9x5c.dat	e9x5d.dat
e9x6a.dat	e9x6b.dat	e9x7a.dat	e9x7b.dat	e9x7c.dat	e9x8.dat
e9x9a.dat	e9x9b.dat				
STIFFNS COMPONENTS					
e7x16.dat					
TEMP CHANGE					
e5x15b.dat	e5x18a.dat	e5x18b.dat			

Table 1-3 History Definition Option Cross-reference

THERMAL LOADS					
e2x51a.dat	e3x13.dat				
THICKNS CHANGE					
e7x16.dat					
TIME STEP					
e3x25.dat	e3x30a.dat	e3x30b.dat	e3x31.dat	e3x32a.dat	e3x32b.dat
e3x32c.dat	e3x34.dat	e3x36.dat	e4x11.dat	e4x2.dat	e4x2c.dat
e4x2d.dat	e4x2e.dat	e6x21.dat	e7x12.dat	e7x14.dat	e7x18.dat
e7x1b.dat	e7x1c.dat	e7x20.dat	e7x20b.dat	e7x20c.dat	e7x20d.dat
e7x22c.dat	e7x23.dat	e7x31a.dat	e7x31b.dat	e7x32.dat	e8x12.dat
e8x12c.dat	e8x12r.dat	e8x14a.dat	e8x14b.dat	e8x14c.dat	e8x14d.dat
e8x14e.dat	e8x14f.dat	e8x15.dat	e8x15b.dat	e8x15c.dat	e8x16.dat
e8x16b.dat	e8x17.dat	e8x18.dat	e8x18b.dat	e8x18c.dat	e8x19.dat
e8x19b.dat	e8x34.dat	e8x35.dat	e8x36.dat	e8x37.dat	e8x38a.dat
e8x38b.dat	—-	e8x38c.dat	e8x42.dat	e8x43.dat	e8x43b.dat
e8x43c.dat	e8x44.dat	e8x44b.dat	e8x44c.dat	e8x45.dat	e8x46.dat
e8x47.dat	e8x48.dat	e8x49.dat	e8x50.dat	e8x51a.dat	e8x51b.dat
e8x52.dat	e8x53a.dat	e8x53b.dat	e8x54.dat	e8x55a.dat	e8x55b.dat
e8x56a.dat	e8x56b.dat	e8x60.dat	e9x13a.dat	e9x13b.dat	
TRANSIENT					
e3x22a.dat	e3x24a.dat	e5x1.dat	e5x10.dat	e5x11a.dat	e5x12.dat
e5x13a.dat	e5x13b.dat	e5x13c.dat	e5x13d.dat	e5x14.dat	e5x16a.dat
e5x16b.dat	e5x16c.dat	e5x17a.dat	e5x17b.dat	e5x18b.dat	e5x2a.dat
e5x2b.dat	e5x3a.dat	e5x3b.dat	e5x3c.dat	e5x3d.dat	e5x3e.dat
e5x3f.dat	e5x4a.dat	e5x4b.dat	e5x4c.dat	e5x4d.dat	e5x5a.dat
e5x5b.dat	e5x6.dat	e5x7a.dat	e5x7b.dat	e5x8a.dat	e5x8c.dat
e5x8d.dat	e5x9a.dat	e5x9b.dat	e5x9d.dat	e5x9e.dat	e8x13.dat
e8x13c.dat	—	e8x7.dat	e9x11b.dat	e9x5e.dat	

Table 1-4 Rezone Option Cross-reference

COMMENT					
e8x12.dat	e8x12r.dat	e8x52.dat			
CONNECTIVITY CHANGE					
e7x31b.dat	e8x12.dat	e8x12r.dat	e8x2.dat	e8x3.dat	
CONTACT CHANGE					
e7x31b.dat	e8x12.dat	e8x12r.dat			
CONTINUE					
e2x35.dat	e2x38.dat	e2x51a.dat	e2x64a.dat	e2x64b.dat	e2x65.dat
e2x66b.dat	e2x70.dat	e3x1.dat	e3x10.dat	e3x11.dat	e3x12.dat
e3x12b.dat	e3x13.dat	e3x14a.dat	e3x15.dat	e3x15b.dat	e3x16.dat
e3x16b.dat	e3x17.dat	e3x18.dat	e3x19.dat	e3x19b.dat	e3x19c.dat
e3x19d.dat	e3x20.dat	e3x21a.dat	e3x21c.dat	e3x21d.dat	e3x21e.dat
e3x21f.dat	e3x22a.dat	e3x22c.dat	e3x22d.dat	e3x23.dat	e3x23b.dat
e3x24a.dat	e3x24b.dat	e3x24c.dat	e3x25.dat	e3x26.dat	e3x27.dat
e3x28.dat	e3x29.dat	e3x2a.dat	e3x2b.dat	e3x3.dat	e3x30a.dat
e3x30b.dat	e3x31.dat	e3x32a.dat	e3x32b.dat	e3x32c.dat	e3x33.dat
e3x33b.dat	e3x34.dat	e3x35.dat	e3x36.dat	e3x37a.dat	e3x37b.dat
e3x38a.dat	e3x38b.dat	e3x3b.dat	e3x4.dat	e3x5.dat	e3x6.dat
e3x7a.dat	e3x7b.dat	e3x7c.dat	e3x8.dat	e3x9.dat	e4x10.dat
e4x10b.dat	e4x11.dat	e4x12a.dat	e4x12b.dat	e4x12c.dat	e4x12d.dat
e4x13a.dat	e4x13b.dat	e4x13c.dat	e4x14a.dat	e4x14b.dat	e4x15.dat
e4x1a.dat	e4x1b.dat	e4x1c.dat	e4x1d.dat	e4x2.dat	e4x20.dat
e4x2a.dat	e4x2b.dat	e4x2c.dat	e4x2d.dat	e4x2e.dat	e4x3.dat
e4x4.dat	e4x4b.dat	e4x5.dat	e4x6.dat	e4x7.dat	e4x7b.dat
e4x7c.dat	e4x8.dat	e4x9.dat	e4x9b.dat	e5x1.dat	e5x10.dat
e5x11a.dat	e5x11c.dat	e5x12.dat	e5x13a.dat	e5x13b.dat	e5x13c.dat
e5x13d.dat	e5x14.dat	e5x15.dat	e5x15b.dat	e5x16a.dat	e5x16b.dat
e5x16c.dat	e5x17a.dat	e5x17b.dat	e5x18a.dat	e5x18b.dat	e5x2a.dat

Table 1-4 Rezone Option Cross-reference (Continued)

CONTINUE (Continued)					
e5x2b.dat	e5x3a.dat	e5x3b.dat	e5x3c.dat	e5x3d.dat	e5x3e.dat
e5x3f.dat	e5x4a.dat	e5x4b.dat	e5x4c.dat	e5x4d.dat	e5x5a.dat
e5x5b.dat	e5x6.dat	e5x7a.dat	e5x7b.dat	e5x8a.dat	e5x8b.dat
e5x8c.dat	e5x8d.dat	e5x8e.dat	e5x9a.dat	e5x9b.dat	e5x9d.dat
e5x9e.dat	e6x10.dat	e6x11.dat	e6x12.dat	e6x13.dat	e6x13b.dat
e6x14.dat	e6x15.dat	e6x15b.dat	e6x16a.dat	e6x16b.dat	e6x16c.dat
e6x17a.dat	e6x17b.dat	e6x18.dat	e6x19.dat	e6x1a.dat	e6x1b.dat
e6x1c.dat	e6x2.dat	e6x20b.dat	e6x21.dat	e6x3a.dat	e6x3b.dat
e6x3c.dat	e6x3d.dat	e6x4.dat	e6x5.dat	e6x6a.dat	e6x6b.dat
e6x7.dat	e6x8.dat	e6x9.dat	e7x1.dat	e7x11.dat	e7x12.dat
e7x13b.dat	e7x13c.dat	e7x13d.dat	e7x14.dat	e7x16.dat	e7x17a.dat
e7x17b.dat	e7x18.dat	e7x19.dat	e7x19b.dat	e7x1b.dat	e7x1c.dat
e7x2.dat	e7x20.dat	e7x20b.dat	e7x20c.dat	e7x20d.dat	e7x21.dat
e7x22a.dat	e7x22b.dat	e7x22c.dat	e7x23.dat	e7x25.dat	e7x26.dat
e7x27.dat	e7x28a.dat	e7x28b.dat	e7x28c.dat	e7x28d.dat	e7x29a.dat
e7x29b.dat	e7x3.dat	e7x30a.dat	e7x30b.dat	e7x31a.dat	e7x31b.dat
e7x32.dat	e7x3b.dat	e7x4.dat	e7x4b.dat	e7x5.dat	e7x5b.dat
e7x5c.dat	e8x10.dat	e8x11.dat	e8x12.dat	e8x12b.dat	e8x12c.dat
e8x12d.dat	e8x12e.dat	e8x12r.dat	e8x13.dat	e8x13b.dat	e8x13c.dat
—	e8x14a.da	e8x14b.dat	e8x14c.dat	e8x14d.dat	e8x14e.dat
e8x14f.dat	e8x15.dat	e8x15b.dat	e8x15c.dat	e8x15d.dat	e8x16.dat
e8x16b.dat	e8x17.dat	e8x17b.dat	e8x18.dat	e8x18b.dat	e8x18c.dat
e8x18d.dat	e8x19.dat	e8x19b.dat	e8x1c.dat	e8x2.dat	e8x20.dat
e8x21.dat	e8x22.dat	e8x23.dat	e8x23b.dat	e8x24a.dat	e8x24b.dat
e8x25.dat	e8x26.dat	e8x27.dat	e8x28.dat	e8x29.dat	e8x3.dat
e8x30.dat	e8x30b.dat	e8x31.dat	e8x32.dat	e8x33a.dat	e8x33b.dat
e8x34.dat	e8x35.dat	e8x36.dat	e8x37.dat	e8x38a.dat	e8x38b.dat
—	e8x38c.dat	e8x39.dat	e8x4.dat	e8x42.dat	e8x43.dat

Table 1-4 Rezone Option Cross-reference (Continued)

CONTINUE (Continued)					
e8x43b.dat	e8x43c.dat	e8x44.dat	e8x44b.dat	e8x44c.dat	e8x45.dat
e8x46.dat	e8x47.dat	e8x48.dat	e8x49.dat	e8x50.dat	e8x51a.dat
e8x51b.dat	e8x52.dat	e8x53a.dat	e8x53b.dat	e8x54.dat	e8x55a.dat
e8x55b.dat	e8x56a.dat	e8x56b.dat	e8x5a.dat	e8x5b.dat	e8x6.dat
e8x60.dat	e8x7.dat	e9x10a.dat	e9x10b.dat	e9x10c.dat	e9x10d.dat
e9x11a.dat	e9x11b.dat	e9x12a.dat	e9x12b.dat	e9x12c.dat	e9x13a.dat
e9x13b.dat	e9x1a.dat	e9x1b.dat	e9x1c.dat	e9x1d.dat	e9x1e.dat
e9x2a.dat	e9x2b.dat	e9x2c.dat	e9x3a.dat	e9x3b.dat	e9x4.dat
e9x5a.dat	e9x5b.dat	e9x5c.dat	e9x5d.dat	e9x5e.dat	e9x6a.dat
e9x6b.dat	e9x7a.dat	e9x7b.dat	e9x7c.dat	e9x8.dat	e9x9a.dat
e9x9b.dat	e10x1a.dat	e10x1b.dat	e10x2a.dat	e10x2b.dat	e10x3a.dat
e10x3b.dat	e10x4a.dat	e10x4b.dat	e10x5a.dat	e10x5b.dat	e10x6a.dat
e10x6b.dat	e10x7a.dat	e10x7b.dat			
COORDINATE CHANGE					
e7x17b.dat	e7x31b.dat	e8x12.dat	e8x12r.dat	e8x2.dat	e8x3.dat
END REZONE					
e7x17b.dat	e7x31b.dat	e8x12.dat	e8x12r.dat		
ISOTROPIC CHANGE					
e8x12.dat	e8x12r.dat	e8x2.dat			
PRINT CHOICE					
e3x14a.dat	e3x20.dat				
REZONE					
e7x17b.dat	e8x12.dat	e8x12r.dat			
SECTIONING					
e7x13d.dat					

Table 1-5 Element Type Cross-reference

Element 1					
e2x1.dat	e2x3.dat				
Element 2					
e2x2.dat	e2x3.dat				
Element 3					
e2x10.dat	e2x27.dat	e3x38a.dat	e7x11.dat	e8x46.dat	e8x47.dat
e8x48.dat	e8x9.dat				
Element 4					
e2x17.dat	e3x1.dat	e6x3a.dat	e6x3c.dat		
Element 5					
e2x5.dat	e4x20.dat	e6x1a.dat			
Element 6					
e2x23.dat	e9x1d.dat	e9x3b.dat			
Element 7					
e2x12b.dat	e2x12c.dat	e2x14b.dat	e2x64a.dat	e2x64b.dat	e2x65.dat
e3x36.dat	e6x15.dat	e6x15b.dat	e6x16a.dat	e6x16b.dat	e6x17a.dat
e6x17b.dat	e7x29a.dat	e7x30a.dat	e7x30b.dat	e7x32.dat	e8x14a.dat
e8x14b.dat	e8x14c.dat	e8x14d.dat	e8x14e.dat	e8x17.dat	e8x17b.dat
e8x19.dat	e8x19b.dat				
Element 8					
e2x11.dat	e2x15.dat	e2x16.dat	e6x3b.dat	e6x3d.dat	
Element 9					
e2x24.dat	e2x54.dat	e4x6.dat	e6x12.dat	e6x6a.dat	e6x6b.dat
e6x9.dat	e7x11.dat	e10x6a.dat	e10x6b.dat		

Table 1-5 Element Type Cross-reference (Continued)

Element 10					
e2x4.dat	e2x61a.dat	e3x12.dat	e3x12b.dat	e3x19.dat	e3x19d.dat
e3x21a.dat	e3x21e.dat	e3x21f.dat	e3x29.dat	e3x35.dat	e3x37a.dat
e3x37b.dat	e3x38b.dat	e3x7a.dat	e3x7b.dat	e3x7c.dat	e4x13b.dat
e6x4.dat	e7x17a.dat	e7x17b.dat	e7x2.dat	e7x20d.dat	e7x28a.dat
e8x12.dat	e8x12b.dat	e8x12d.dat	e8x12e.dat	e8x12r.dat	e8x13.dat
e8x13b.dat	e8x3.dat	e8x43b.dat	e8x50.dat	e8x56a.dat	e8x56b.dat
e9x13a.dat	e9x2a.dat	e9x2b.dat			
Element 11					
e2x25.dat	e2x26.dat	e2x34.dat	e2x37b.dat	e2x60a.dat	e3x25.dat
e3x3.dat	e3x9.dat	e7x31a.dat	e7x31b.dat	e8x15.dat	e8x15c.dat
e8x15d.dat	e8x16.dat	e8x16b.dat	e8x37.dat	e8x44b.dat	e8x44c.dat
e8x45.dat	e8x60.dat	e8x7.dat	e9x1a.dat	e9x3a.dat	e9x4.dat
e9x5a.dat	e9x5b.dat	e9x5e.dat	e9x6a.dat	e9x6b.dat	e9x7a.dat
e9x7b.dat	e9x7c.dat	e9x8.dat	e9x9a.dat	e9x9b.dat	e9x10a.dat
e9x10b.dat	e9x10c.dat	e9x10d.dat	e9x11a.dat	e9x11b.dat	e9x12a.dat
e9x12b.dat	e9x12c.dat	e9x13b.dat			
Element 12					
e3x18.dat	e6x9.dat	e7x18.dat	e7x2.dat	e7x4.dat	e7x4b.dat
e8x3.dat	e8x7.dat				
Element 13					
e2x6.dat					
Element 14					
e2x7.dat	e7x13b.dat	e7x13c.dat	e7x13d.dat	e10x7a.dat	e10x7b.dat
Element 15					
e2x4.dat	e3x16.dat	e3x16b.dat	e3x18.dat	e3x5.dat	e4x1a.dat
e4x1b.dat	e4x1c.dat	e4x1d.dat	e4x4.dat	e4x4b.dat	

Table 1-5 Element Type Cross-reference (Continued)

Element 16					
e2x8.dat	e3x14a.dat	e3x20.dat	e3x4.dat	e4x7.dat	e4x7c.dat
e6x13.dat	e6x13b.dat				
Element 17					
e2x20.dat	e7x13b.dat	e7x13c.dat	e7x13d.dat		
Element 18					
e2x62.dat	e3x34.dat	e4x14a.dat	e8x18c.dat		
Element 19					
e2x27.dat					
Element 20					
e2x28.dat	e4x13c.dat				
Element 21					
e2x13.dat	e2x14.dat	e8x8a.dat	e8x8b.dat	e10x3a.dat	e10x3b.dat
Element 22					
e2x18.dat	e2x42.dat	e4x5.dat			
Element 23					
e2x14.dat					
Element 24					
e2x19.dat					
Element 25					
e2x29.dat	e3x13.dat	e4x3.dat			
Element 26					
e2x9.dat	e2x9b.dat	e3x10.dat	e3x15.dat	e3x15b.dat	e3x24b.dat
e3x24c.dat	e3x33.dat	e7x19.dat	e7x21.dat	e8x11.dat	e8x1a.dat
e8x27.dat	e8x4.dat	e10x2a.dat	e10x2b.dat		

Table 1-5 Element Type Cross-reference (Continued)

Element 27					
e2x22.dat	e2x37.dat	e2x60b.dat	e2x63a.dat	e2x63b.dat	e3x33b.dat
e3x8.dat	e6x14.dat	e6x5.dat	e7x10.dat	e7x12.dat	e8x15b.dat
e8x2.dat	e8x6.dat	e9x1b.dat	e9x1c.dat	e9x5c.dat	e9x5d.dat
Element 28					
e2x30.dat	e2x39.dat	e2x61b.dat	e3x11.dat	e3x22c.dat	e3x22d.dat
e3x26.dat	e7x14.dat	e7x28c.dat	e9x2c.dat		
Element 29					
e2x31a.dat	e2x38.dat	e2x46b.dat	e2x46c.dat		
Element 30					
e4x14b.dat	e6x11.dat				
Element 31					
e2x66a.dat	e2x66b.dat				
Element 32					
e2x32.dat	e7x1.dat	e7x18.dat	e7x4.dat	e7x4b.dat	e8x35.dat
Element 33					
e2x33.dat	e2x33b.dat	e6x7.dat	e7x5.dat		
Element 34					
e2x34.dat					
Element 35					
e2x35.dat	e2x35a.dat	e6x8.dat			
Element 36					
e5x1.dat					
Element 37					
e5x3d.dat	e7x15.dat				

Table 1-5 Element Type Cross-reference (Continued)

Element 39					
e5x12.dat	e5x14.dat	e5x3c.dat	e5x7a.dat	e5x7b.dat	e7x16.dat
e8x20.dat	e8x22.dat	e8x24a.dat	e8x24b.dat	e8x25.dat	e8x26.dat
e8x7.dat					
Element 40					
e5x10.dat	e5x9a.dat	e5x9b.dat			
Element 41					
e3x24a.dat	e5x3a.dat	e5x6.dat	e5x8a.dat	e5x8b.dat	e5x8c.dat
e5x8d.dat	e5x8e.dat	e6x5.dat	e8x28.dat	e8x29.dat	
Element 42					
e3x22a.dat	e5x11a.dat	e5x15.dat	e5x15b.dat	e5x5a.dat	
Element 43					
e5x4a.dat	e8x21.dat				
Element 44					
e5x4b.dat					
Element 45					
e2x36.dat	e6x1b.dat	e6x1c.dat	e6x2.dat		
Element 46					
e2x37.dat	e8x6.dat				
Element 47					
e2x38.dat					
Element 48					
e2x39.dat					
Element 49					
e2x40a.dat	e2x40b.dat	e4x2a.dat	e8x53b.dat		

Table 1-5 Element Type Cross-reference (Continued)

Element 50					
e2x41.dat	e3x6.dat	e4x2b.dat			
Element 51					
e4x8.dat					
Element 52					
e2x21.dat	e6x10.dat	e8x10.dat	e10x1a.dat	e10x1b.dat	
Element 53					
e2x43.dat					
Element 54					
e2x44.dat	e3x27.dat				
Element 55					
e2x45.dat	e3x28.dat	e7x28d.dat			
Element 56					
e2x31b.dat	e2x46a.dat				
Element 57					
e2x47b.dat					
Element 58					
e2x48.dat					
Element 59					
e2x49.dat					
Element 60					
e2x50.dat					
Element 61					
e2x51a.dat	e2x51b.dat				
Element 62					
e7x8a.dat	e7x8b.dat	e7x8c.dat	e7x9a.dat	e7x9b.dat	e7x9c.dat

Table 1-5 Element Type Cross-reference (Continued)

Element 64					
e2x43.dat					
Element 65					
e5x2a.dat	e5x2b.dat				
Element 66					
e2x52.dat					
Element 67					
e2x53.dat	e3x2a.dat	e3x2b.dat	e4x13a.dat	e7x27.dat	
Element 68					
e2x54.dat					
Element 69					
e5x3b.dat					
Element 70					
e5x5b.dat					
Element 71					
e5x4c.dat					
Element 72					
e2x55.dat	e2x56.dat	e3x17.dat			
Element 75					
e2x65.dat	e3x23.dat	e3x23b.dat	e4x15.dat	e7x22a.dat	e7x22b.dat
e7x22c.dat	e7x3.dat	e7x3b.dat	e7x6.dat	e7x7.dat	e8x18.dat
e8x18d.dat	e8x5a.dat	e8x5b.dat	e8x51b.dat	e8x52.dat	e8x53a.dat
e8x54.dat	e8x55a.dat	e8x55b.dat	e8x57a.dat	e8x58.dat	e8x6.dat
e10x4a.dat	e10x4b.dat	e10x5a.dat	e10x5b.dat		
Element 76					
e2x57a.dat					

Table 1-5 Element Type Cross-reference (Continued)

Element 77
e2x58a.dat
Element 78
e2x57b.dat
Element 79
e2x58b.dat
Element 80
e8x49.dat
Element 82
e7x20.dat e7x5b.dat
Element 85
e5x13a.dat
Element 86
e5x13b.dat
Element 87
e5x13c.dat
Element 88
e5x13d.dat
Element 90
e4x9.dat e4x9b.dat e4x10.dat e4x10b.dat
Element 91
e2x60a.dat
Element 92
e2x61a.dat
Element 93
e2x60b.dat

Table 1-5 Element Type Cross-reference (Continued)

Element 94	
e2x61b.dat	
Element 98	
e2x59a.dat e2x59b.dat	
Element 103	
e8x28.dat e8x29.dat	
Element 109	
e8x23.dat e8x23b.dat	
Element 111	
e8x30.dat e8x30b.dat e8x33a.dat e8x33b.dat	
Element 112	
e8x31.dat	
Element 113	
e8x32.dat	
Element 114	
e2x10b.dat	
Element 115	
e2x25b.dat e3x3b.dat	
Element 116	
e3x19b.dat e3x19c.dat e3x21c.dat e7x28b.dat e8x13c.dat e8x36.dat e8x43c.dat	
Element 117	
e2x12d.dat e7x29b.dat	
Element 118	
e2x26b.dat	

Table 1-5 Element Type Cross-reference (Continued)

Element 119	
e7x5c.dat	
Element 120	
e6x16c.dat	
Element 121	
e5x3e.dat	
Element 122	
e5x9d.dat	
Element 123	
e5x16a.dat	e5x4d.dat
Element 124	
e2x9c.dat	
Element 125	
e2x26c.dat	e9x1e.dat
Element 126	
e2x2b.dat	
Element 127	
e2x67a.dat	
Element 128	
e2x26d.dat	
Element 129	
e2x2c.dat	
Element 130	
e2x67b.dat	
Element 131	
e5x3f.dat	

Table 1-5 Element Type Cross-reference (Continued)

Element 132				
e5x9e.dat				
Element 133				
e5x16b.dat				
Element 134				
e2x67c.dat				
Element 135				
e5x16c.dat				
Element 138				
e2x72.dat	e2x75.dat	e4x2c.dat	e8x57b.dat	
Element 139				
e2x73.dat	e2x76.dat	e4x2d.dat	e8x51a.dat	e8x57c.dat
Element 140				
e2x74.dat	e2x77.dat	e4x2e.dat	e8x57d.dat	
Element 142				
e4x13a.dat				
Element 143				
e2x37b.dat				
Element 144				
e4x13b.dat				
Element 145				
e4x13c.dat				

Table 1-5 Element Type Cross-reference (Continued)

Element 146
e2x14b.dat
Element 147
e4x14a.dat
Element 148
e4x14b.dat

Table 1-6 User Subroutine Cross-reference

ANELAS					
u2x45.f	u2x50.f	u2x53.f	u3x8.f	u8x8.f	
ANKOND					
u5x7a.f					
ANPLAS					
u3x6.f					
CREDE					
u2x46a.f	u2x46b.f	u2x46c.f	u2x51a.f	u3x13f	
CRPLAW					
u3x12.f	u3x22c.f	u3x24.f			
FILM					
u3x22a.f	u5x5.f	u5x6.f	u5x8.f	u5x13.f	u5x14.f
FLOW					
u5x14.f					
FLUX					
u5x8.f					
FORCDT					
u3x26.f	u5x2.f	u7x17.f	u8x26.f		
FORCEM					
u2x35.f	u2x43.f	u2x46.f			
GAPU					
u2x70					
HOOKLW					
u8x8.f					
HYPELA2					
u7x29a.f					

Table 1-6 User Subroutine Cross-reference (Continued)

IMPD					
u3x3.f	u3x3b.f	u3x19.f	u3x19b.f	u3x19c.f	u3x21a.f
u3x21c.f	u2x21d.f	u4x7.f	u8x15b.f		
MOTION					
u8x16.f	u8x19.f	u8x19b.f			
ORIENT					
u2x50.f	u2x50b.f	u2.53.f			
PLOTV					
u2x26.f	u2x26b.f	u2x26c.f	u2x26d.f		
REBAR					
u2x14.f	u2x37.f	u2x38.f	u2x39.f	u8x6.f	
SSTRAN					
u8x1.f					
UBEAM					
u8x10.f					
UBEAR					
u7x16.f					
UFCONN					
u2x20.f	u2x27.f	u2x34.f	u2x46a.f	u2x46b.f	u7x15.f
UFORMS					
u2x4.f	u2x43.f				
UFOUR					
u7x8c.f	u7x9b.f				

Table 1-6 User Subroutine Cross-reference (Continued)

UFXORD					
u2x16.f	u2x17.f	u2x18.f	u2x19.f	u2x20.f	u2x55.f
u2x56.f	u3x5.f	u3x16.f	u3x17.f	u3x23.f	u3x27.f
u4x1.f	u4x5.f	u4x7.f	u6x3.f	u7x3.f	u7x15.f
UGROOV					
u7x15.f					
UINSTR					
u2x38.f	u3x30a.f				
USHELL					
u2x40b.f					
USSD					
u6x18.f					
UTHICK					
u7x15.f	u7x16.f				
UTRANS					
u2x62.f	u4x14.f				
UVELOC					
u7.15.f					
VSWELL					
u3x13.f					
WKSLP					
u3x5.f	u3x8.f	u3x30a.f	u3x30b.f	u3x38a.f	u8x2.f
u8x18.f					

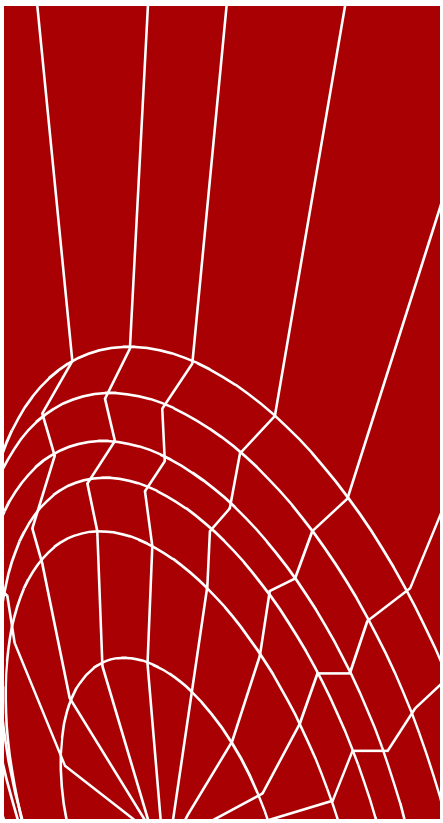

MARC Analysis Research Corporation

MARC®

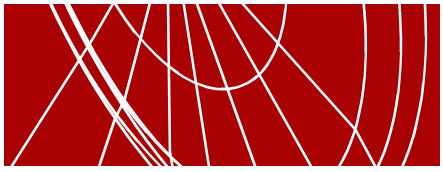

Volume E

Demonstration Problems

Version K7

Chapter 2
Linear Analysis

2 Linear Analysis Contents

Description	Problem
Hemispherical Shell Under Internal Pressure	2.1
Thick Sphere Under Internal Pressure	2.2
Axisymmetric Solid-Shell Intersection	2.3
Axisymmetric Solid-Shell Intersection	2.4
Doubly Cantilevered Beam Loaded Uniformly	2.5
Open Section, Double Cantilever Beam Loaded Uniformly	2.6
Closed Section Beam Subjected to a Point Load	2.7
Curved Beam Under a Point Load	2.8
Plate with Hole	2.9
Plane Stress Disk	2.10
Simply-Supported Square Plate Modeled by Shell Elements	2.11
Simply-Supported Thick Plate, using Three-Dimensional Elements	2.12
Simply-Supported Thick Plate, using Higher-order Three-Dimensional Elements	2.13
Reinforced Concrete Beam Analysis	2.14
Cylinder-sphere Intersection	2.15
Shell Roof using Element 8	2.16
Shell Roof using Element 4	2.17
Shell Roof using Element 22	2.18
Shell Roof using Element 24	2.19
Pipe Bend Analysis	2.20
Doubly Cantilevered Beam using Element 52	2.21
J-Integral Evaluation Example	2.22

Description	Problem
Thick Cylinder Under Internal Pressure	2.23
Three-Dimensional Frame Analysis	2.24
Two-Dimensional Strip Compressed by Rigid Plates	2.25
Two-Dimensional Strip Compressed by Rigid Plates	2.26
Generalized Plane-strain Disk, Point Loading	2.27
Circular Shaft of Variable Radius Under Tension and Twist	2.28
Thin-walled Beam on an Elastic Foundation	2.29
Notched Circular Bar, J-Integral Evaluation	2.30
Square Section with Central Hole using Generalized Plane Strain Element	2.31
Square Plate with Central Hole using Incompressible Element	2.32
Flat Spinning Disk	2.33
Strip with Bonded Edges, Error Estimates	2.34
Cube Under Pressure Loads	2.35
Timoshenko Beam on an Elastic Foundation	2.36
Reinforced Concrete Beam	2.37
Reinforced Concrete Plate with Central Hole	2.38
Cylinder with Rebars Under Internal Pressure	2.39
Simply Supported Square Plate of Variable Thickness	2.40
Thermal Stresses in a Simply Supported Triangular Plate	2.41
Square Plate on an Elastic Foundation	2.42
Cantilever Beam Subjected to Concentrated Tip Moment	2.43
Local Load on Half-Space	2.44
Notched Circular Bar with Anisotropy, J-Integral Evaluation	2.45
Square Plate with Central Hole, Thermal Stresses	2.46
Thick Cylinder with Internal Pressure; Three-Dimensional Model	2.47
Circular Cylinder Subjected to Point Loads	2.48

Description	Problem
Hollow Spinning Sphere	2.49
Anisotropic Ring Under Point Loads	2.50
Square Block Subjected to Pressure and Thermal Loads	2.51
Twist and Extension of Circular Bar of Variable Thickness	2.52
Cylinder with Helical Anisotropy Under Internal Pressure	2.53
Stiffened Shear Panels Supported by Springs	2.54
Shell Roof by Element 72	2.55
Cylinder-sphere Intersection by Element 72	2.56
Closed Section Beam Subjected to a Point Load	2.57
Open Section, Double Cantilever Beam Loaded Uniformly	2.58
Simply Supported Elastic Beam Under Point Load	2.59
Uniform Pressure on Cylindrical Cavity of an Infinite Body (The Lamé Solution)	2.60
The Boussinesq Problem (Point Load on Boundary of a Semi-infinite Body)	2.61
Truncated Spherical (Membrane) Shell Under Internal Pressure	2.62
J-Integral Evaluation Example using Delorenzi's Method	2.63
A Clamped Plate Modeled with Brick Elements	2.64
Use of Tying to Model a Rigid Region	2.65
Using Pipe Bend Element to Model Straight Beam or Elbow	2.66
Cantilever Beam Analyzed using Solid Elements	2.67
Linear Analysis of a Hemispherical Cap Loaded by Point Loads	2.68
Pipe Bend with Axisymmetric Element 95	2.69
Flange Joint Between Pressurized Pipes	2.70
Spinning Cantilever Beam	2.71
Shell Roof by Element 138	2.72
Shell Roof by Element 139	2.73
Shell Roof by Element 140	2.74

Description	Problem
Cylinder Subjected to a Point Load - Element Type 138	2.75
Cylinder Subjected to a Point Load - Element Type 139	2.76
Cylinder Subjected to a Point Load - Element Type 140	2.77

2 Linear Analysis List of Figures

Figure		Page
2.1-1	Geometry and Mesh Layout for Axisymmetric Shell	2.1-3
2.2-1	Thick Sphere Mesh for Element 2	2.2-4
2.2-2	Vector Plot of Reactions Element 2	2.2-5
2.2-3	Radial Stress Versus Radius Elements 2, 126, 129, and Exact	2.2-6
2.2-4	Hoop Stress Versus Radius Elements 2, 126, 129, and Exact	2.2-7
2.3-1	Mesh and Geometry for Axisymmetric Solid-Shell Intersection	2.3-3
2.3-2	Tying Description	2.3-4
2.4-1	Solid-Shell Intersection Model	2.4-4
2.4-2	Tying and Transformations	2.4-5
2.5-1	Beam Model	2.5-3
2.5-2	Deformations	2.5-4
2.6-1	Open Section Beam Model	2.6-3
2.6-2	Beam Section and Sequence of Branch Traversal	2.6-4
2.6-3	Moment Diagram	2.6-4
2.6-4	Deformations	2.6-5
2.7-1	Closed Section Beam Model	2.7-3
2.7-2	Hollow, Square-Section Beam	2.7-3
2.7-3	Deformed Beam	2.7-4
2.8-1	Curved Beam Model	2.8-3
2.9-1	Mesh Layout for Plate with Hole (Element 26)	2.9-5
2.9-2	Original Mesh for Plate with Hole When Using Adaptive Meshing	2.9-6
2.9-3	Contours of σ22 Element 26	2.9-7
2.9-4	Contours of σ22 Element 124	2.9-8

Figure **Page**

2.9-5 σ22 Along y = 0, Elements 26,124, and Exact 2.9-9
2.9-6 Mesh After First Refinement 2.9-10
2.9-7 Mesh After Second Refinement 2.9-11
2.9-8 Mesh After Third Refinement. 2.9-12
2.9-9 Mesh After Fourth Refinement. 2.9-13
2.9-10 Mesh After Fifth Refinement 2.9-14

2.10-1 Model 2.10-4
2.10-2 Sigma22 Along y = 0 Versus Radius 2.10-5
2.10-3 Stress Component Along Nodal Path 2.10-6
2.10-4 Close-up of Adapted Mesh 2.10-7

2.11-1 Geometry and Mesh for Square Plate Using Shell Elements 2.11-4
2.11-2 Comparison of Results for Shell and Three-Dimensional Models. 2.11-4

2.12-1 Model 2.12-5
2.12-2 Plot of von Mises Stress Element 7 . . . . . 2.12-6
2.12-3 Plot of von Mises Stress Element 117 . . . . . 2.12-7

2.13-1 Thick Plate Mesh 2.13-3
2.13-2 Pressure Loaded Simply-Supported Flat Plate Displacement Comparison 2.13-4
2.13-3 J2 Stress Contour 2.13-5

2.14-1 Reinforced Concrete Beam. 2.14-3
2.14-2 Concrete and Steel Stress With Beam Theory 2.14-4

2.15-1 Mesh and Geometry for Cylinder-Sphere Intersection Problem 2.15-3

2.16-1 Cylinder Shell Roof Configuration, Element 8 . . . . . 2.16-4
2.16-2 Shell Surface Coordinate System 2.16-5

2.17-1 Cylinder Shell Configuration, Element 4 . . . . . 2.17-3

2.18-1 Cylindrical Shell Roof Configuration, Element 22 . . . . . 2.18-3

2.19-1 Cylindrical Shell Roof Configuration, Element 24 . . . . . 2.19-4
2.19-2 Maximum Z Deflection Versus Total Active Degrees of Freedom 2.19-5

Figure **Page**

2.19-3 Vertical Deflection of the Y = 300 Symmetry Boundary vs. Distance From X = 0 Symmetry Boundary 2.19-6
2.19-4 Vertical Displacement at the Center of the Free Edge 2.19-7

2.20-1 Geometry and Mesh-Pipe Bending Problem 2.20-3
2.20-2 Distribution of Circumferential Stress λ = 0.0924 . . . . . 2.20-4
2.20-3 Distribution of Meridional Stress λ = 0.0924 . . . . . 2.20-4

2.21-1 Closed Section Beam Model. 2.21-3
2.21-2 Hollow, Square-Section Beam 2.21-3
2.21-3 Defections 2.21-4

2.22-1 Double-Edge Notch Specimen, Showing Blocks for Mesh Generation 2.22-4
2.22-2 Mesh for Double-Edge Notch Specimen 2.22-5
2.22-3 Mesh Detail of Double-Edge Notch Specimen. 2.22-6

2.23-1 Thick Cylinder and Mesh 2.23-2
2.23-2 Stresses vs. Radial Distance 2.23-3

2.24-1 Three-Dimensional Frame and Mesh 2.24-3
2.24-2 Deformed Mesh Plot of Three-Dimensional Frame 2.24-4

2.25-1 Deformed Mesh 2.25-3
2.25-2 Contours of σ22 Element 11. . . . . 2.25-4
2.25-3 Contours of σ22 Element 115. . . . . 2.25-5

2.26-1 Finite Element Mesh. 2.26-4
2.26-2 Contours of F = σ33 - ν(σ11 + σ22) Element 11 . . . . . 2.26-5
2.26-3 Contours of F = σ33 - ν(σ11 + σ22) Element 125 . . . . . 2.26-6
2.26-4 Contours of F = σ33 - ν(σ11 + σ22) Element 118 . . . . . 2.26-7
2.26-5 Contours of F = σ33 - ν(σ11 + σ22) Element 128 . . . . . 2.26-8

2.27-1 Disk and Mesh 2.27-3
2.27-2 Deformed Mesh Plot. 2.27-4

2.28-1 Circular Rod and Mesh. 2.28-3
2.28-2 Deformed Mesh Plot. 2.28-4

Figure **Page**

2.28-3 Stress Contours for σ_{zz} 2.28-5
2.28-4 Stress Contours for σ_{zq} 2.28-6
2.28-5 Stress Contours for σ_{rq} 2.28-7

2.29-1 Thin Walled Beam and Mesh 2.29-3
2.29-2 Deformed Mesh Plot 2.29-4

2.30-1 Notched Circular Bar and Mesh 2.30-4
2.30-2 Mesh for Double Edge Notch Specimen 2.30-5
2.30-3 Deformed Mesh 2.30-6
2.30-4 Stress Contours 2.30-7

2.31-1 Square Plate and Mesh 2.31-4
2.31-2 Deformed Mesh Plot 2.31-5
2.31-3 Stress Contours 2.31-6

2.32-1 Square Plate and Mesh 2.32-3
2.32-2 Stress Contours for σ_{xx} 2.32-4
2.32-3 Stress Contours for σ_{yy} 2.32-5
2.32-4 Stress Contours for σ_{zz} 2.32-6
2.32-5 Stress Contours for Equivalent Stress 2.32-7

2.33-1 Flat Disk and Mesh 2.33-3

2.34-1 Two-Dimensional Strip and Mesh 2.34-3
2.34-2 Deformed Mesh Plot 2.34-4
2.34-3 σ_{yy} Contours 2.34-5

2.35-1 Square Block and Mesh 2.35-3
2.35-2 Pressure Distribution 2.35-4
2.35-3 Deformed Mesh Plot 2.35-5
2.35-4 Stress Contours for σ_{zz} 2.35-6

2.36-1 Timoshenko Beam and Mesh 2.36-3
2.36-2 Deformed Mesh Plot 2.36-4

Figure **Page**

2.37-1 Reinforced Concrete Beam and Mesh 2.37-3
2.37-2 Deformed Mesh Plot 2.37-4
2.37-3 σxx Along Bottom Surface Along Nodes 1 to 17 . . . . . 2.37-5

2.38-1 Reinforced Concrete Plate and Mesh 2.38-3
2.38-2 Rebar Layers and Elements 2.38-4
2.38-3 Deformed Mesh Plot 2.38-5

2.39-1 Cylinder and Mesh 2.39-3
2.39-2 Rebar Layers and Elements 2.39-4
2.39-3 Deformed Mesh Plot 2.39-5
2.39-4 Hoop Stress Distribution Through Radius 2.39-6

2.40-1 Square Plate and Mesh 2.40-4
2.40-2 Stress Contours (Constant Thickness) 2.40-5
2.40-3 Stress Contours (Variable Thickness) 2.40-6

2.41-1 Triangular Plate and Finite Element Mesh 2.41-3
2.41-2 Stress Contours (x-component) 2.41-4
2.41-3 Stress Contours (y-component) 2.41-5

2.42-1 Square Plate and Mesh 2.42-3
2.42-2 Equivalent Stress Contours (Layer 1) 2.42-4

2.43-1 Cantilever Beam and Mesh 2.43-3

2.44-1 Half Space and Mesh 2.44-3
2.44-2 Deformed Mesh Plot 2.44-4
2.44-3 von Mises Stress Contours 2.44-5

2.45-1 (a) Notched Circular Bar and Mesh 2.45-4
2.45-1 (b) Detail of Notched Circular Bar and Mesh 2.45-5
2.45-2 Deformed Mesh Plot 2.45-6
2.45-3 Stress Contours for σ11 . . . . . 2.45-7

Figure **Page**

2.46-1 Square Plate with Central Hole and Mesh 2.46-5
2.46-2 Fine Element Mesh Using Element Type 19 . . . . . 2.46-6
2.46-3 Deformed Mesh Plot 2.46-7
2.46-4 Stress Contours for σ11 . . . . . 2.46-8
2.46-5 Contours of Thermal Strain 2.46-9

2.47-1 Cylinder and Mesh 2.47-3
2.47-2 Deformed Mesh Plot 2.47-4
2.47-3 Equivalent von Mises Stress Contours 2.47-5

2.48-1 Circular Ring and Mesh of Half-model 2.48-3
2.48-2 Deformed Mesh Plot 2.48-4
2.48-3 Equivalent von Mises Stress Contours 2.48-5

2.49-1 Hollow Sphere and Mesh 2.49-3
2.49-2 Deformed Mesh Plot 2.49-4
2.49-3 Equivalent von Mises Stress Contours 2.49-5

2.50-1 Anisotropic Ring and Mesh 2.50-4
2.50-2 Deformed Mesh Plot 2.50-5
2.50-3 Equivalent von Mises Stress Contours 2.50-6

2.51-1 Square Block and Mesh 2.51-4
2.51-2 Deformed Mesh Plot 2.51-5
2.51-3 Equivalent Stress Contours 2.51-6

2.52-1 Circular Bar and Mesh 2.52-3
2.52-2 Deformed Mesh Plot 2.52-4
2.52-3 Stresses Along Path Between Nodes 3 and 51 . . . . . 2.52-5

2.53-1 Cylinder and Mesh 2.53-3
2.53-2 Helical Anisotropy 2.53-4
2.53-3 Deformed Mesh Plot 2.53-5
2.53-4 Hoop Stress Through Radius 2.53-6

Figure **Page**

2.54-1 Stiffened Cubic Box and Mesh 2.54-3
2.54-2 Deformed Mesh Plot 2.54-4

2.55-1 Shell Roof and Mesh 2.55-3
2.55-2 Deformed Mesh Plot 2.55-4

2.56-1 Shell Structure and Mesh 2.56-3
2.56-2 Deformed Mesh Plot 2.56-4
2.56-3 Equivalent von Mises Stress Contours 2.56-5

2.57-1 Closed Section Beam Model 2.57-4
2.57-2 Hollow, Square-Section Beam 2.57-5

2.58-1 Open Section Beam Model 2.58-4
2.58-2 Beam Section and Sequence of Branch Traversal 2.58-5

2.59-1 Simply Supported Beam Under Point Load 2.59-4

2.60-1 Uniform Pressure on Cylindrical Cavity of an Infinite Body (The Lamé Solution) 2.60-4
2.60-2 Finite Element Mesh (Model A) (Elements 11 and 91) 2.60-5
2.60-3 Finite Element Mesh (Model B) (Elements 27 and 93) 2.60-6
2.60-4 Deformed Mesh (Model A) 2.60-7
2.60-5 Stress Distribution Along Radial Path 2.60-8
2.60-6 Deformed Mesh (Model B) 2.60-9
2.60-7 Stress Distribution Along Radial Path 2.60-10

2.61-1 Boussinesq Problem (POINT LOAD on Boundary of a Semi-infinite Body) 2.61-4
2.61-2 Finite Element Mesh (Model A) (Elements 10 and 92) 2.61-5
2.61-3 Finite Element Mesh (Model B) (Elements 28 and 94) 2.61-6
2.61-4 Stress Contours (Model A) 2.61-7
2.61-5 Stress Contours (Model B) 2.61-8

2.62-1 Membrane Structure 2.62-3
2.62-2 Deformed Mesh 2.62-4

2.64-1 Clamped Plate Mesh 2.64-3

Figure **Page**

2.65-1 Mesh Showing Rigid Regions 2.65-3
2.65-2 Deformations 2.65-4

2.66-1 Straight Beam Using Element 31 . . . . . 2.66-3
2.66-2 Pipe Bend Using Element 31 . . . . . 2.66-4
2.66-3 Deformed Beam 2.66-5

2.67-1 Model 2.67-4
2.67-2 Bending Stress Element 127 . . . . . 2.67-5
2.67-3 Bending Stress Element 130 . . . . . 2.67-6

2.68-1 Hemispherical Cap, Geometry, Loading, and Finite Element Mesh 2.68-3
2.68-2 Stress Contours Layer 2 (Equivalent von Mises Stress) 2.68-4

2.69-1 Element 95 Layer Points 2.69-3
2.69-2 Longitudinal Section of the Pipe 2.69-3
2.69-3 FEM Model of the Longitudinal Section of the Pipe 2.69-4
2.69-4 Distribution of the Longitudinal Pressure 2.69-4
2.69-5 Deflection of the Longitudinal Section of the Pipe 2.69-5

2.70-1 Element 95 Layer Points 2.70-5
2.70-2 Loads on the Flange Joint 2.70-5
2.70-3 Tying in the Flange Joint 2.70-6
2.70-4 von Mises Stress Induced by Preload 2.70-7
2.70-5 von Mises Stress Induced by Moment 2.70-8

2.71-1 Finite Element Model 2.71-3

2.72-1 Shell Roof and Mesh 2.72-3
2.72-2 Deformed Mesh Plot 2.72-4

2.73-1 Shell Roof and Mesh 2.73-3
2.73-2 Deformed Mesh Plot 2.73-4

2.74-1 Shell Roof and Mesh 2.74-3
2.74-2 Deformed Mesh Plot 2.74-4

Figure **Page**

2.75-1 Shell Roof and Mesh. 2.75-3
2.75-2 Deformed Mesh Plot. 2.75-4
2.75-3 Y Deformation Along X = 0. . . . . 2.75-5

2.76-1 Shell Roof and Mesh. 2.76-3
2.76-2 Deformed Mesh Plot. 2.76-4
2.76-3 Y Deformation Along X = 0. . . . . 2.76-5

2.77-1 Shell Roof and Mesh. 2.77-3
2.77-2 Deformed Mesh Plot. 2.77-4
2.77-3 Y Deformation Along X = 0. . . . . 2.77-5

2 Linear Analysis List of Tables

Table		Page
2-1	Linear Analysis Demonstration Problems	2-3
2.5-1	Results	2.5-2
2.6-1	Results	2.6-2
2.7-1	Y Deflection (in.)	2.7-2
2.7-2	Moments and Reaction Forces (lb.)	2.7-2
2.8-1	Displacement and Stress Results	2.8-2
2.21-1	Y Deflection (in.)	2.21-2
2.21-2	Moments (in.-lb.) and Reaction Forces (lb.)	2.21-2
2.22-1	J-Integral Evaluation Results	2.22-3
2.30-1	Comparison of J-Integral Evaluations	2.30-2
2.33-1	Comparison of Results	2.33-2
2.57-1	Y Deflection (inches)	2.57-2
2.57-2	Moments (inches-pounds) and Reaction Forces (pounds	2.57-3
2.58-1	Y Deflection (inches)	2.58-2
2.59-1	Comparison of Beam Deflections (in.)	2.59-2
2.60-1	Radial Displacements	2.60-2
2.61-1	Z-Displacements at R = 0	2.61-2

Table **Page**

2.63-1 J-Integral Evaluation Results for DEN-Specimen Under Axial Tension 2.63-3
2.63-2 J-Integral Evaluation Results for DEN-Specimen with Pressurized Cracks . . . 2.63-3

2.69-1 Analytical Solution 2.69-2

2.70-1 Balance of Moments 2.70-4

2.71-1 Beam Deflection (Inches) 2.71-2

2 Linear Analysis

MARC allows you to perform an elastic analysis using any element in the program. Problems in this chapter deal only with linear elastic stress analysis and are designed to guide you through various input options. The problems demonstrate the use of different elements such as plane stress, plane strain, generalized plane strain, axisymmetric, truss, beam, membrane, plate, shell and three-dimensional solids. They also illustrate the selection of isotropic or anisotropic elastic behavior. The options demonstrated are outlined below. For further details, see *MARC Volume C: Program Input*.

Mesh generation

- MESH2D
- Incremental
- FXORD
- User subroutine UFXORD
- User subroutine UFCONN

Kinematic constraints

- Fixed Displacement
- Tying
- Servolinks
- Springs
- Elastic foundations
- Transformations

Loads

- Point loads
- Distributed loads
- Centrifugal loads
- Thermal loads
- Initial stress

Controls

- J-Integral
- Sorting
- Print choices
- Restart
- Case combination

Table 2-1 shows MARC elements and options used in these demonstration problems. It should be pointed out that any example shown here can be considered as the first step in the solution of a nonlinear problem. Extensions to more complex solutions are accomplished by addition of further options using the keyword selection for those options as illustrated in the examples in later chapters.

Table 2-1 Linear Analysis Demonstration Problems

Problem Number	Element Type(s)	Parameters	Model Definition	History Definition	User Subroutines	Problem Description
2.1	1	—	—	—	—	Hemisphere under internal pressure.
2.2	2 126 129	—	TRANSFORMATION	—	—	Thick sphere under internal pressure.
2.3	1 2	TRANSFORM	TRANSFORMATION TYING	—	—	Axisymmetric solid/ axisymmetric shell intersection.
2.4	10 15	—	TRANSFORMATION TYING	—	UFORMS	Axisymmetric solid/ axisymmetric shell intersection.
2.5	5	—	—	—	—	Doubly cantilevered beam.
2.6	13	BEAM SECT	—	—	—	Doubly cantilevered beam, open section.
2.7	14	BEAM SECT	—	—	—	Doubly cantilevered beam, closed section.
2.8	16	—	—	—	—	Curved beam, point load.
2.9	26 124	—	OPTIMIZE	—	—	Plate with circular hole.
2.10	3 114	—	—	—	—	Plane stress disk, diametrically opposing point loads.
2.11	8	SHELL SECT	FXORD	—	—	Square plate by shell elements.
2.12	7 117	PROCESSOR	SOLVER	—	—	3-dimensional plate by 8-node brick elements.
2.13	21	—	—	—	—	3-dimensional plate by 20-node brick elements.
2.14	21 23	PROCESSOR	—	—	REBAR	3-dimensional cantilever beam, reinforced with rebar, brick elements.

Table 2-1 Linear Analysis Demonstration Problems (Continued)

Problem Number	Element Type(s)	Parameters	Model Definition	History Definition	User Subroutines	Problem Description
2.15	8	SHELL SECT	TYING FXORD	—	—	Cylinder-sphere intersection, tying type 18.
2.16	8	—	OPTIMIZE	—	UFXORD	Shell roof, element type 8.
2.17	4	—	—	—	UFXORD	Shell roof, element type 4.
2.18	22	—	—	—	UFXORD	Shell roof, element type 22.
2.19	24	—	—	—	UFXORD	Shell roof, element type 24.
2.20	17	—	—	—	—	Pipe band, in-plane, half section.
2.21	52	—	—	—	—	Doubly cantilevered beam, elastic.
2.22	27	J-INT	J-INT	—	—	Double edge notched specimen linear elastic fracture mechanics.
2.23	6	—	TRANSFORMATION	—	—	Thick cylinder under internal pressure.
2.24	9	—	——	—	—	20-bar, 3-dimensional truss.
2.25	11 115	—	CONN GENER NODE FILL	—	—	Strip, bonded edges, υ = .3.
2.26	11 118 125 128	—	—	—	PLOTV	Strip, bonded edges, υ = .4999, constant dilatation.
2.27	19	ELSTO	—	—	UFCONN	Generalized plane strain disk, diametrically opposing point loads.
2.28	20	—	TYING	—	—	Twist and tension circular bar with varying thickness.

Table 2-1 Linear Analysis Demonstration Problems (Continued)

Problem Number	Element Type(s)	Parameters	Model Definition	History Definition	User Subroutines	Problem Description
2.29	25	—	FOUNDATION	—	—	Beam in linear elastic foundation with point load.
2.30	28	ELSTO ALIAS	J-INTEGRAL	—	—	Cylindrical notched bar in tension.
2.31	29	SCALE	OPTIMIZE	—	UFCONN	Square plate with round hole, internal pressure, generalized plane strain.
2.32	32	SCALE ALIAS	OPTIMIZE	—	—	Square plate with round hole, internal pressure, generalized plane strain, υ = .5. Mesh as in E 2.31.
2.33	33	CENT LOAD	CONN GENER NODE FILL ROTATION A STIFF SCALE	—	—	Flat spinning disk, υ = .4999.
2.34	34	—	CONN FILL NODE FILL CONN GENER QUALIFY OPTIMIZE	—	—	Bar compressed sideways generalized plane strain.
2.35	35	ELASTIC RESTART	CASE COMBIN	—	FORCEM	Square block, 1/8 model 8 elements, υ = .4999 load case 1: compression; load case 2: bending, combined.
2.36	45	—	FOUNDATION	—	—	Timoshenko beam on elastic foundation.
2.37	27 46	—	—	—	REBAR	Reinforced cantilever beam.
2.38	29 47	SCALE ISTRESS	OPTIMIZE UFCONN	PROPORTIONAL	REBAR UFCONN UINSTR	Reinforced square plate with round hole, generalized plane strain. Prestressed reinforcement.
2.39	28 48	—	—	—	REBAR	Circular cylinder with reinforcement.

Table 2-1 Linear Analysis Demonstration Problems (Continued)

Problem Number	Element Type(s)	Parameters	Model Definition	History Definition	User Subroutines	Problem Description
2.40	49	SHELL SECT	—	—	—	Flat square plate, varying thickness, simply supported pressure load.
2.41	50	SHELL SECT	CONN GENER TYING NODE FILL	—	—	Tubular beam with square cross-section cantilevered self weight.
2.42	22	SHELL SECT	FOUNDATION	—	—	Square plate on elastic foundation point load, free edges 1/4 model.
2.43	53 64	—	TYING CONN GENER NODE FILL	—	FORCEM UFORMS	I-beam modeled with plane stress and line elements cantilever, moment load.
2.44	54	—	TYING	—	—	Local load on half-space. Mesh refinement tying.
2.45	55	ANISOTROPIC J-INT	OPTIMIZE J-INTEGRAL	—	ANELAS	Axisymmetric notched bar, anisotropic in longitudinal direction.
2.46	29 56	THERMAL	THERMAL LOADS UFCONN	—	CREDE UFCONN	Square plate with hole, thermal gradient towards outer edge.
2.47	57	TRANSFORMTIE	TRANSFORMATION TYING MESH 3D	—	—	Section of cylinder with uniform internal pressure. TYING to enforce axisymmetric solution.
2.48	58	—	NODE CIRCLE CONN GENER ROTATION A	—	—	Plane straining with diametrically opposing load (1/2 model).
2.49	59	THERMAL	NODE CIRCLE CONN GENER	—	CREDE	Hollow sphere, spinning gradient across wall thickness.

Table 2-1 Linear Analysis Demonstration Problems (Continued)

Problem Number	Element Type(s)	Parameters	Model Definition	History Definition	User Subroutines	Problem Description
2.50	60	ANISOTROPIC	NODE CIRCLE	—	ANELAS ORIENT	Generalized plane strain ring with diametrically opposing point loads, circular anisotropy.
2.51	61	THERMAL ELASTIC RESTART	CASE COMBIN	—	CREDE	Square block 1/8 model 8 elements υ = .4999 load case 1: thermal gradient; load case 2: compression, combined.
2.52	66	—	TYING OPTIMIZE	—	—	Twist and tension of a circular bar with varying cross-section, υ = .4999
2.53	67	—	TYING	—	ANELAS ORIENT	Cylinder with helical anisotropy under internal pressure.
2.54	9 68	—	SPRINGS	—	—	Truss cube with shear panels, supported by springs.
2.55	72	SHELL SECT	UFXORD	—	UFXORD	Shell roof, element type 72.
2.56	72	SHELL SECT	UFXORD	—	UFXORD	Cylinder-sphere intersection, element type 72, no tying.
2.57	76 78	BEAM SECT	POINT LOAD	—	—	Cantilever beam, under point load.
2.58	77 79	BEAM SECT	POINT LOAD	—	—	Double cantilever beam under point load.
2.59	98	BEAM SECT	POINT LOAD	—	—	Cantilever beam under point load.
2.60	11 91 27 93	—	MESH2D MANY TYPES	DIST LOADS	—	Uniform load in a cavity using semi-infinite elements.
2.61	10 92 28 94	—	MESH2D	POINT LOAD POST	—	Point load on a semi-infinite body.

Table 2-1 Linear Analysis Demonstration Problems (Continued)

Problem Number	Element Type(s)	Parameters	Model Definition	History Definition	User Subroutines	Problem Description
2.62	18	—	UTRANFORM DIST LOADS POST	—	UTRANS	Truncated spherical shell.
2.63	27	—	LORENZI DIST LOADS	CONTINUE POINT LOADS	—	Double edge notch specimen, DeLorenzi method used.
2.64	7	ELASTIC	FIXED DISP DIST LOADS	POINT LOADS	—	Bending on a plate, assumed strain elements used.
2.65	7 75	LARGE DISP	FIXED DISP	AUTO LOAD POINT LOAD	—	Rigid tying test.
2.66	31	BEAM SECT	CONN GENER POINT LOAD NODE FILL	—	—	Bending of a beam.
	31	—	ISOTROPIC	POINT LOAD DIST LOAD	—	Bending of an elbow.
2.67	127 130 21	—	POINT LOAD	—	—	Cantilever beam.
2.68	49	—	POINT LOAD	—	—	Spherical shell under Point Loads.
2.69	95	SHELL SECT	DIST LOADS	—	—	Pipe subjected to bending.
2.70	95 97	—	—	—	—	Flange joint between pressurized pipes.
2.71	98	—	DIST LOADS ROTATION AXIS	—	—	Spinning beam with and without Corrolis effect.
2.72	138	—	—	—	—	Shell roof element type 138
2.73	139	—	—	—	—	Shell roof element type 139
2.74	140	—	—	—	—	Shell roof element type 140
2.75	138	—	—	—	—	Pinched cylinder
2.76	139	—	—	—	—	Pinched cylinder
2.77	140	—	—	—	—	Pinched cylinder

2.1 Hemispherical Shell Under Internal Pressure

A thin hemispherical shell is analyzed subjected to uniform internal pressure. The material behavior is considered elastic. The accuracy of element type 1 is verified.

Element

Library element type 1 is used. Element 1 is a 2-node axisymmetric thin shell with three degrees of freedom per node.

For this element, as for any 2-node element, it is necessary to adopt some unambiguous direction convention in order to provide the correct sign to the pressure loads. The convention adopted for this element is to define a right-handed set of local coordinates (x,y) for each element, with the positive x-direction from node 1 to node 2 of the element (see CONNECTIVITY). This gives a unique positive y-direction (90° counterclockwise to local x), and with this definition the following conventions hold:

> Positive pressure always gives negative nodal load components in the positive local y-direction.

The sign convention that is adopted for the global axes should be noted. A positive rotation of 90° is assumed to transform the axis of symmetry Z to the radial axis R. Nodal points have three global displacement degrees of freedom:

1. Axial (parallel to the symmetry axis)
2. Radial (normal to symmetry axis)
3. Cross-sectional rotation (right-handed)

Model

The geometry of the middle surface of the hemisphere and the mesh are shown in Figure 2.1-1. A 90-degree section is referenced to the Z-R global coordinate system. The shell is divided into nine elements with 10 nodes, each element subtending an angle of 10 degrees.

Geometry

The wall thickness of the shell is 0.01 in. and the radius of curvature is 1.0 in. The thickness is entered as EGEOM1 in the GEOMETRY option. EGEOM2 and EGEOM3 are not used for this element type.

Material Properties

All elements are assumed to have the same properties. Values used for Young's modulus and Poisson's ratio are 5 x 10^6 psi and 0.3, respectively, and are entered in the ISOTROPIC option. The material is given a high yield stress so that it will not go plastic.

Loading

A uniform internal pressure of 1.0 psi is applied to all elements.

Boundary Conditions

Node 1 is constrained to move axially, with no rotation and no translation in the R-direction. Node 10 is constrained to move radially, with no rotation and no translation in the Z-direction.

Note

Element 15 or Element 89 could also be used to model this type of problem. This higher-order element would allow a coarser mesh to be used; two element type 15 would give equivalent results in this case. Element 15 or Element 89, in addition, allows the application of nonuniform loads through the use of user subroutine FORCEM.

Results

For a thin spherical shell, the solution is that the circumferential stress is equal to pr/2t, which, for this particular problem, is 50 psi. The MARC solution is given at layer 1 on the inner surface and layer 11 at the outer surface. One observes that the MARC solution is within .02% of the exact solution. A discussion of the analytic solution can be found in many elementary books on elasticity, such as *Theory of Elasticity* by Timoshenko and Goodier.

Parameters, Options, and Subroutines Summary

Example e2x1.dat:

Parameters	Model Definition Options
ELEMENTS	CONNECTIVITY
END	COORDINATES
SIZING	DIST LOADS
TITLE	END OPTION
	FIXED DISP
	GEOMETRY
	ISOTROPIC

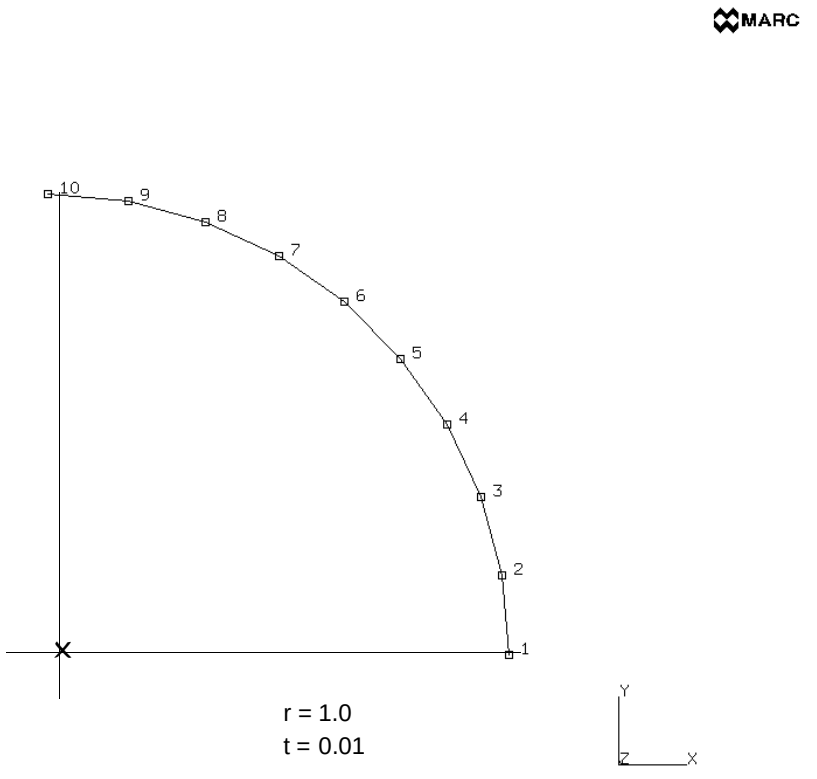

Figure 2.1-1 Geometry and Mesh Layout for Axisymmetric Shell

2.2 Thick Sphere Under Internal Pressure

A thick-walled sphere is subjected to a uniform internal pressure. The material behavior is considered elastic. The numerical solution is compared to the analytical solution. This problem demonstrates the use of element types 2, 126, and 129, and the TRANSFORMATION option.

This problem is modeled using the three techniques summarized below.

Data Set	Element Type(s)	Number of Elements	Number of Nodes
e2x2	2	16	18
e2x2b	126	26	51
e2x2c	129	16	51

Elements

Element type 2 and 126 are first and second-order isoparametric elements, respectively, with triangular cross-sections revolved around an axis of symmetry. Element type 129 is the same as type 126 with a Herrmann formulation.

Model

Only a small segment of the sphere is analyzed, with symmetry being enforced through the TRANSFORMATION option of the program. The inner radius of the sphere is 1.0 inch and the sphere thickness is 2.0 inches. A small wedge of ring elements span a 0.085 radian slice as shown in Figure 2.2-1 with 16 axisymmetric ring elements.

Material Properties

The material for all elements is treated as an elastic material, with Young’s modulus of 30.0E+06 psi, Poisson’s ratio of 0.0, and a yield stress of 35,000 psi entered in the ISOTROPIC option.

Geometry

The GEOMETRY option is not necessary for these elements because all integrations are performed about the axis of revolution.

Loads and Boundary Conditions

A uniform distributed load of 1.0 psi is applied to the inner surface of the sphere. The boundary conditions are determined by the symmetry conditions and require the nodes along x = 0 axis, and the theta = .085 radians axis to have no displacements normal to these surfaces.

Results

The innermost element, for each of the element types used, has the largest value of equivalent stress as expected. Scaling the load to first yield would lead to an internal pressure of 29,093 psi, 24,509 psi, and 24,578 psi for element types 2, 126, and 129, respectively. The coarse mesh, with fewer degrees of freedom, gives less conservative results. Figure 2.2-2 shows the vector plot of the reaction forces which are normal to the planes of symmetry.

The exact solution may be expressed as:

$$\text{Radial Stress} = \quad p r_i^3 (1 - r_o^3 / r^3) / (r_o^3 - r_i^3)$$

$$\text{Hoop Stress} = \quad p r_i^3 (1 + r_o^3 / 2r^3) / (r_o^3 - r_i^3)$$

For this particular problem this yields:

$$\text{Radial Stress} = \quad (1 - 27 / r^3) / 26$$

$$\text{Hoop Stress} = \quad (1 + 27 / 2r^3) / 26$$

Figure 2.2-3 plots the radial stress for element type 2, 126, 129 and the exact value versus the radius. Note how the stress boundary conditions at the inner and outer radii are approximately satisfied by the two element types. Figure 2.2-4 plots the hoop stress for element type 2, 126, 129, and the exact value versus the radius. Here again, the 6-noded element is more accurate at the price of more nodes.

Parameters, Options, and Subroutines Summary

Example e2x2.dat:

Parameters	Model Definition Options
END	CONNECTIVITY
SIZING	COORDINATES
TITLE	DIST LOADS
	END OPTION
	FIXED DISP
	ISOTROPIC
	POST
	TRANSFORMATIONS

Example e2x2b.dat:

Parameters	Model Definition Options
ELEMENTS	CONNECTIVITY
END	COORDINATES
SIZING	DIST LOADS
TITLE	END OPTION
	FIXED DISP
	ISOTROPIC
	OPTIMIZE
	POST
	PRINT NODE
	TRANSFORMATIONS

Example e2x2c.dat:

Parameters	Model Definition Options
ELEMENTS	CONNECTIVITY
END	COORDINATES
SIZING	DIST LOADS
TITLE	END OPTION
	FIXED DISP
	ISOTROPIC
	POST
	PRINT NODE
	TRANSFORMATIONS

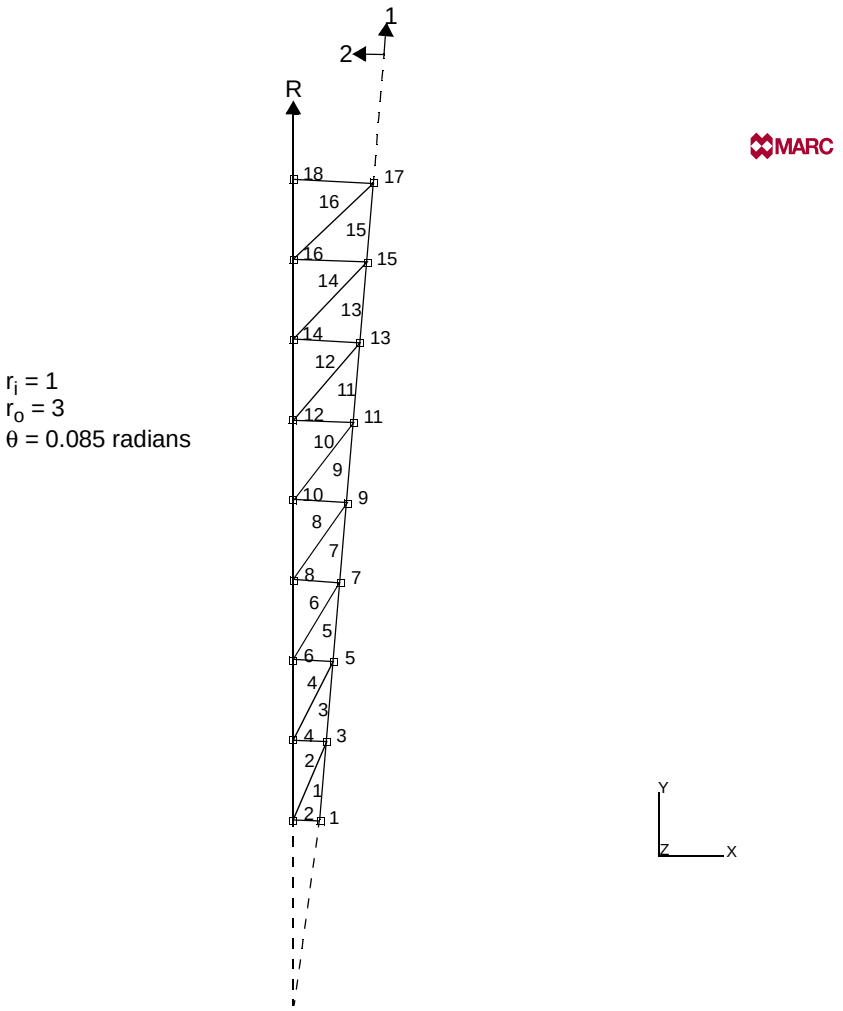

Figure 2.2-1 Thick Sphere Mesh for Element 2

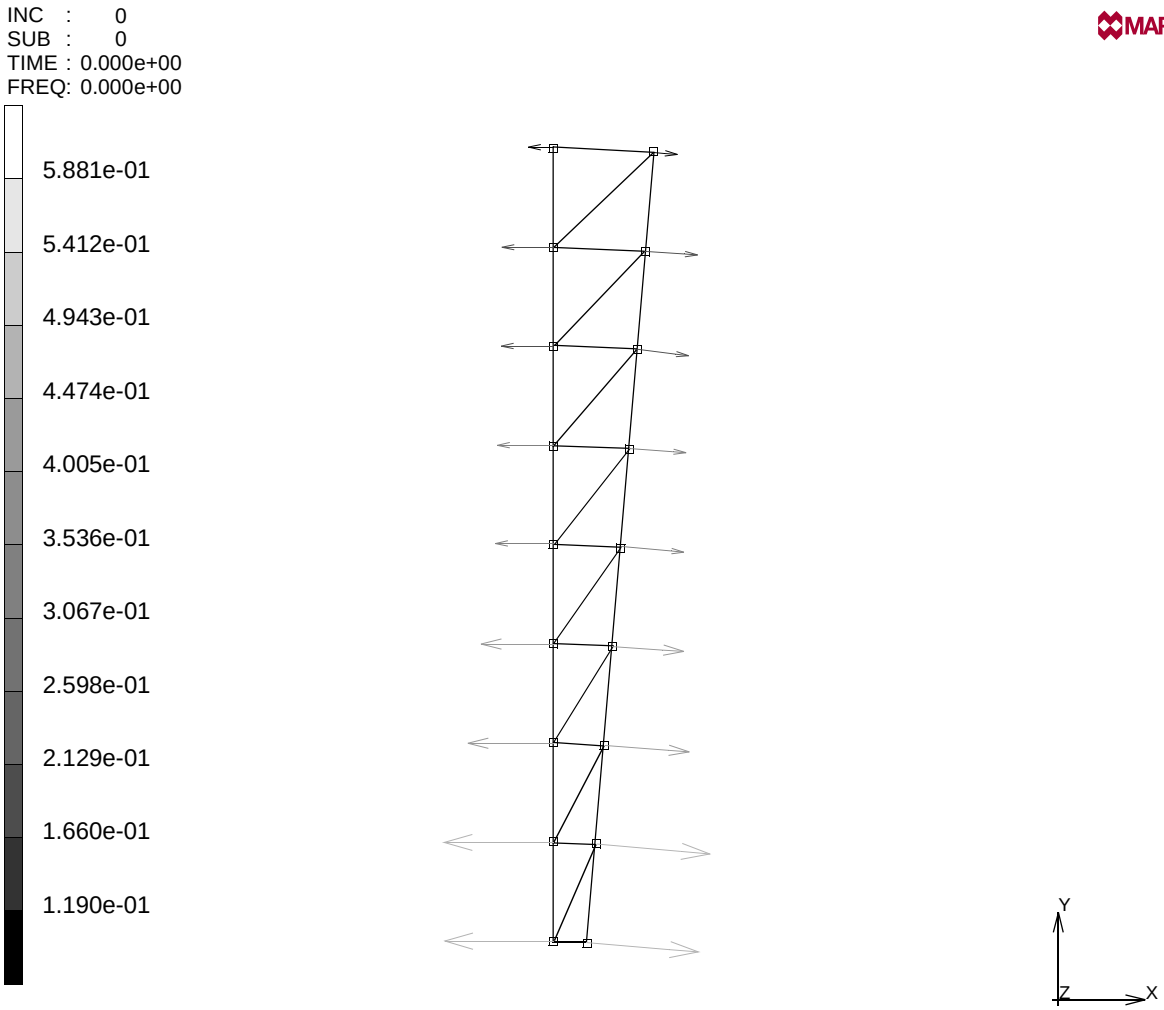

Figure 2.2-2 Vector Plot of Reactions Element 2

Radius	Type 2	Type 126	Type 129	Exact
1.	-0.65939E+00	-0.95125E+00	-0.8715844E+00	-1.0000
1.25	-0.47083E+00	-0.47338E+00	-0.4665929E+00	-0.4932
1.5	-0.26017E+00	-0.26165E+00	-0.2567940E+00	-0.2692
1.75	-0.14958E+00	-0.15189E+00	-0.1487170E+00	-0.1553
2.	-0.87530E-01	-0.89656E-01	-0.8752283E-01	-0.09135
2.25	-0.50137E-01	-0.51800E-01	-0.5034145E-01	-0.05271
2.5	-0.26241E-01	-0.27487E-01	-0.2645840E-01	-0.02800
2.75	-0.10161E-01	-0.11172E-01	-0.1042592E-01	-0.01147
3.	-0.52244E-02	0.18073E-03	-0.1021735E-02	0.0

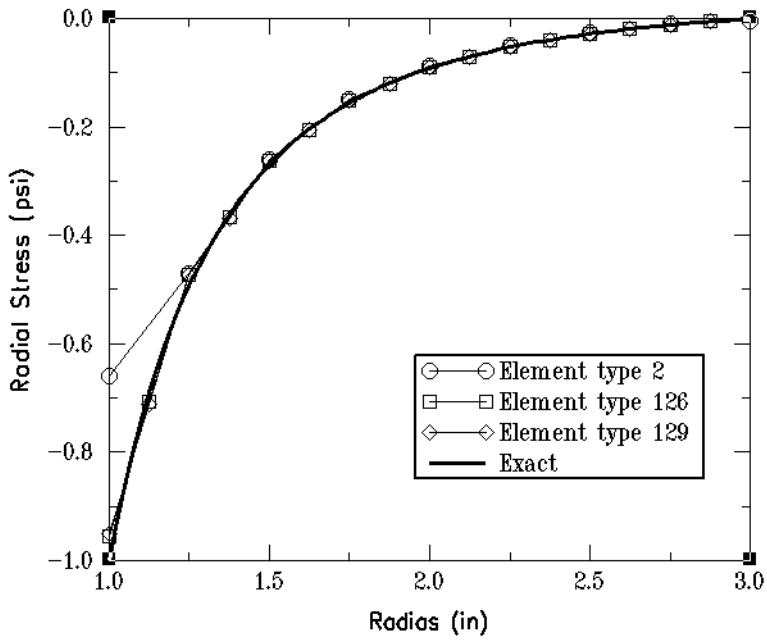

Figure 2.2-3 Radial Stress Versus Radius Elements 2, 126, 129, and Exact

Radius	Type 2	Type 126	Type 129	Exact
1.	0.42237E+00	0.53225E+00	0.4913680E+00	0.55769
1.25	0.25709E+00	0.29693E+00	0.2921591E+00	0.30431
1.5	0.16556E+00	0.18906E+00	0.1862493E+00	0.19231
1.75	0.11959E+00	0.13376E+00	0.1321118E+00	0.13534
2.	0.93388E-01	0.10251E+01	0.1014724E+01	0.10337
2.25	0.77296E-01	0.83555E-01	0.8286265E-01	0.08405
2.5	0.66863E-01	0.71393E-01	0.7091602E-01	0.07169
2.75	0.59815E-01	0.63233E-01	0.6289676E-01	0.06343
3.	0.56498E-01	0.57593E-01	0.5820292E-01	0.05769

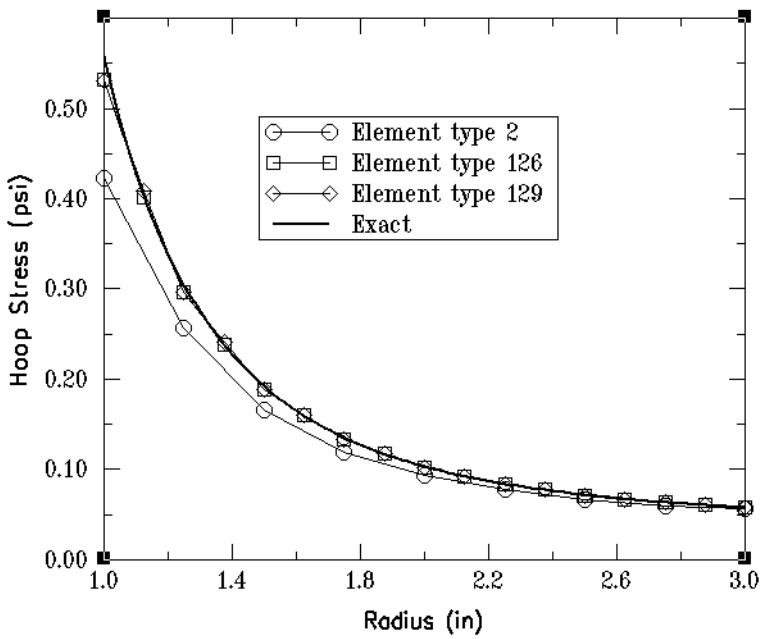

Figure 2.2-4 Hoop Stress Versus Radius Elements 2, 126, 129, and Exact

2.3 Axisymmetric Solid-Shell Intersection

This problem demonstrates the use of tying to impose the kinematic constraint at a solid-to-shell intersection. A thin axisymmetric cylinder is intersected with a thick cylinder. The combined structure is subjected to internal pressure. The cylinder is constrained such that there is no axial displacement.

Elements

Library element types 1 and 2 are used. Element type 1 is a two-node axisymmetric thin shell with three degrees of freedom per node. Element type 2 is an axisymmetric triangular ring with two degrees of freedom per node.

Model

Four shell elements are used to model the thin shell part of the structure. The solid end is modeled with 32 ring elements using 29 nodes. The finite element model is illustrated in Figure 2.3-1.

Geometry

For the shell element, EGEOM1 is used for thickness. No geometry input is required for the ring element.

Material Properties

All elements are assumed to have uniform properties. Values for Young's modulus, Poisson's ratio and yield stress used are 30 x 10^6 psi, 0.3 and 35000 psi, respectively, and are entered in the ISOTROPIC option.

Loading

Internal pressure of 1.0 psi is applied to elements 1, 2, 3, 4, 12, 20, 28, 36 (the connectivity for ring elements 12, 20, 28, 36 indicates the pressure is applied on the 1-3 element face.)

Tying

The single type of tying required between the two elements is imposed through nodal constraints on the plane of transition (z = 4.75") between the element types. Figure 2.3-2 shows the transition plane through node s (shell node) and t (ring node) normal to the RZ plane. Local coordinates are also shown. In this coordinate system the constraints are:

$v_t = v_s + z\phi_s$ (t = node numbers 5, 6, 7, 8, 9)

where z is the distance from the ring node to the shell node along local z-axis, and

$u_t = u_s$ for t = node 7

These compatibility constraints are implemented in the program as tying type 23. They are programmed in local coordinates as defined above.

Transformation

In this example, degrees of freedom at nodes 5 to 9 must be rotated clockwise 90 degrees (using the TRANSFORMATION option) to match this type of coordinate system. Then tying type 23 is used to tie the two degrees of freedom of each ring node to the three degrees of freedom of the shell node (u_s, v_s, δ_s). The constrained node is the particular off center node of the transition plane; the retained node is the middle surface node of the shell. A general discussion of tying degrees of freedom is in *Volume A: Theory and User Information*.

Boundary Conditions

Other constraints applied to the structure are fixed-end conditions for both degrees of freedom on nodal point 25 to 29 and a rotational constraint for shell node 1. The boundary conditions shown for the third degree of freedom of the ring elements are not necessary and can be deleted if desired.

Results

The structure was elastically analyzed and element 2 was found to have the largest equivalent stress and the largest membrane stress.

If one can consider the shell to be long, then in element 1 away from the thick cylinder, the hoop stress would be:

$$\frac{pr}{t} = 150 \text{ psi}$$

The calculated MARC solution is 149.4 psi. for element 1, integration pt. 1.

Parameters, Options, and Subroutines Summary

Example e2x3.dat:

Parameters	Model Definition Options
ELEMENTS	CONNECTIVITY
END	COORDINATES
PRINT	DIST LOADS
SIZING	END OPTION
TITLE	FIXED DISP
	GEOMETRY
	ISOTROPIC
	TRANSFORMATION
	TYING

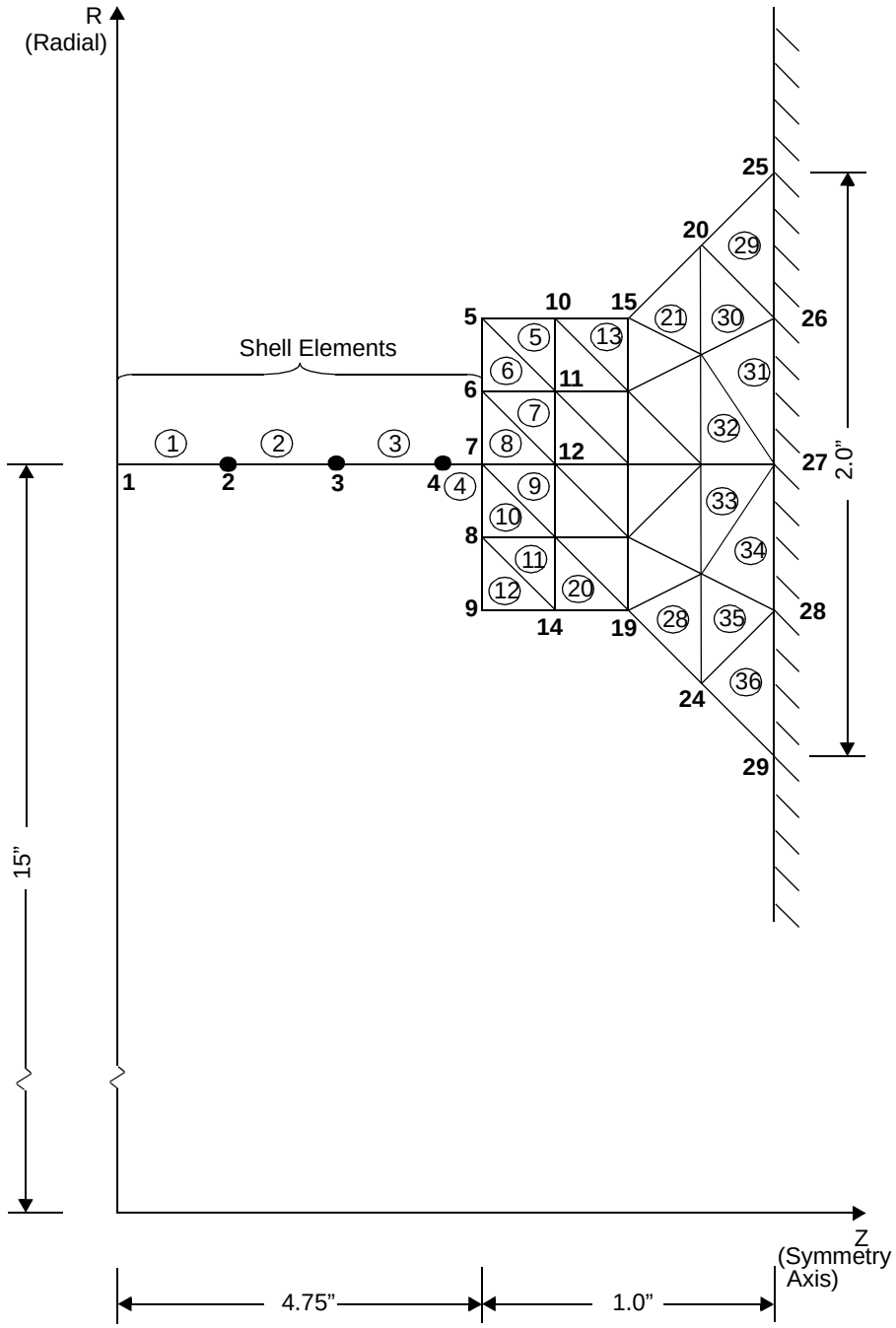

Figure 2.3-1 Mesh and Geometry for Axisymmetric Solid-Shell Intersection

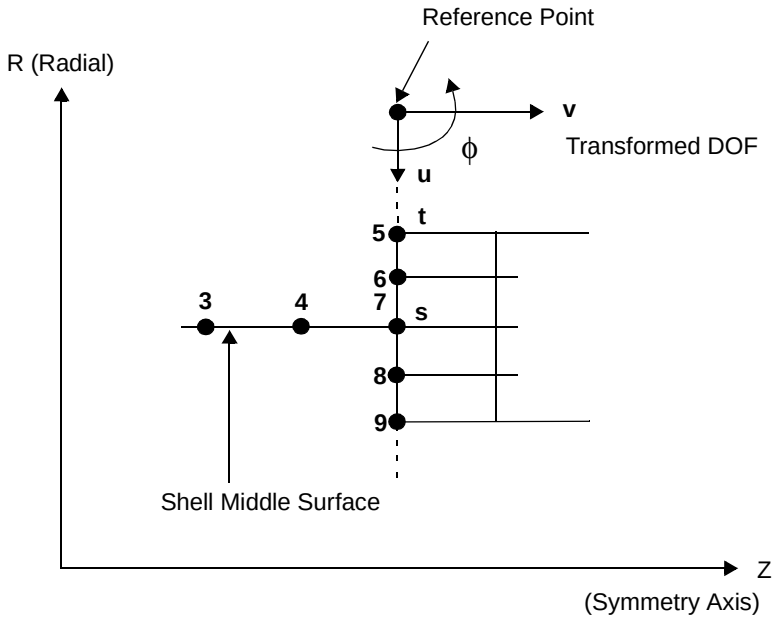

Figure 2.3-2 Tying Description

2.4 Axisymmetric Solid-Shell Intersection

This problem demonstrates the use of user subroutine UFORMS to model a solid-to-shell intersection. A thin axisymmetric cylinder is intersected with a thick cylinder. The combined structure is subjected to uniform internal pressure. This problem is identical to the one analyzed in problem 2.3, and the solution of the two can be compared.

Elements

Element types 15 and 10 are used. Element type 15 is a 2-node axisymmetric thin-shell element. Element type 10 is an axisymmetric ring element with arbitrary quadrilateral cross-section.

Model

Four shell elements, 16 ring elements, 29 nodes, and 68 degrees of freedom total are used (see Figure 2.4-1).

Geometry

Thickness (0.1 in.) for elements 1 to 4 (shell elements) is stored in EGEOM1. No geometry specification is required for the ring element.

Loading

Internal pressure of 1.0 psi is applied to elements 1, 2, 3, 4, 8, 12, 16, and 20. Please note the connectivity specifications for these elements; pressures on the 1-2 face of element type 10 (IBODY = 0), and uniform pressure (IBODY = 0) on element type 15.

Transformation

Nodes 5, 6, 8, and 9 have their degrees of freedom transformed to facilitate the use of tying.

Tying (UFORMS)

The compatibility constraint at the junction of the solid and shell elements is imposed by tying degrees of freedom between node 7 (shell degrees of freedom) and nodes 5, 6, 8, 9 (solid degrees of freedom). The tying is accomplished with a UFORMS user subroutine. First, the two degrees of freedom at nodes 5, 6, 8, 9 are rotated clockwise 90 degrees (see Figure 2.4-2). The constraint matrix equation for a node is as follows:

$$\begin{bmatrix} u_t \\ v_t \end{bmatrix} = \begin{bmatrix} 0 & 0 & 0 & 0 \\ 1 & 0 & 0 & z_1 \end{bmatrix} \begin{bmatrix} u_s \\ v_s \\ du/ds \\ dv/ds \end{bmatrix}$$

(constrained quadrilateral node)(middle shell surface node 7)

$v_t = u_s + z_1\, dv/ds$

z_1 is the directed distance parallel to the global R-axis and positive toward the symmetry axis between the retained node and the tied node. Thus,

$v_t = u_s$ at node 7.

The tying could alternatively have been done using tying type 25.

Boundary Conditions

Nodes 25 to 29 are fixed in both degrees of freedom, and shell node 1 is fixed against rotation, dv/ds = 0.

Results

The structure was elastically analyzed. Element 1 was found to have the largest equivalent stress and the largest membrane stress.

The results compare closely to problem 2.3. The following results are for integration point 2.

Element	Example 2.3		Example 2.4	
	σ_1 (psi)	σ_2 (psi)	σ_1 (psi)	σ_2 (psi)
1	-.1549	151.1	-.0508	151.1
2	.9264	160.5	.0067	160.6
3	1.8610	110.9	.0598	110.6
4	.03161	19.79	.01398	19.80

The differences in the membrane stress σ_1 are attributable to the fact that element type 1 as used in problem 2.3 has a constant membrane strain variation whereas element type 15 as used in this problem allows a linear variation in membrane strain.

Parameters, Options, and Subroutines Summary

Example e2x4.dat:

Parameters	Model Definition Options
ELEMENTS	CONNECTIVITY
END	COORDINATES
PRINT	DIST LOADS
SIZING	END OPTION
TITLE	FIXED DISP
	GEOMETRY
	ISOTROPIC
	TRANSFORMATION
	TYING

User subroutine in u2x4.f:

UFORMS

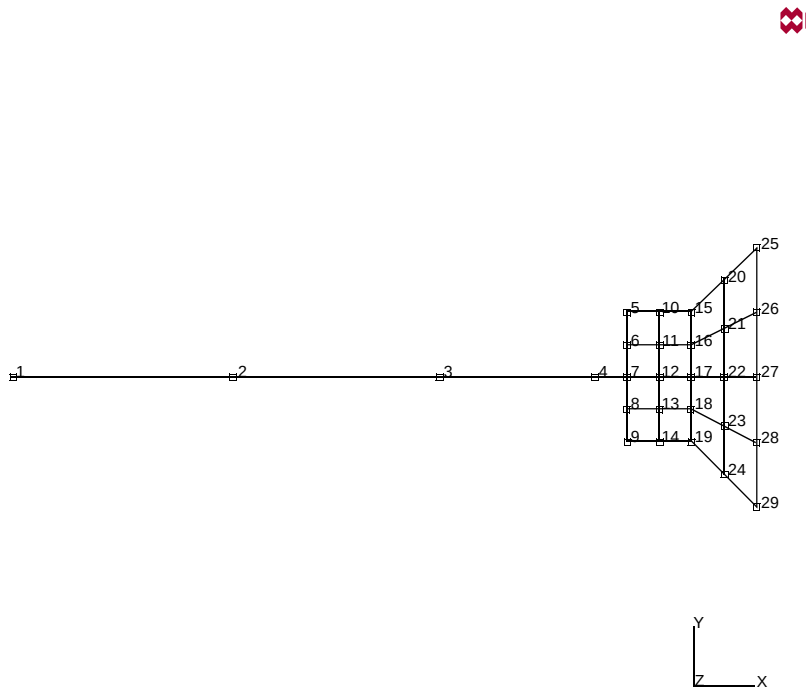

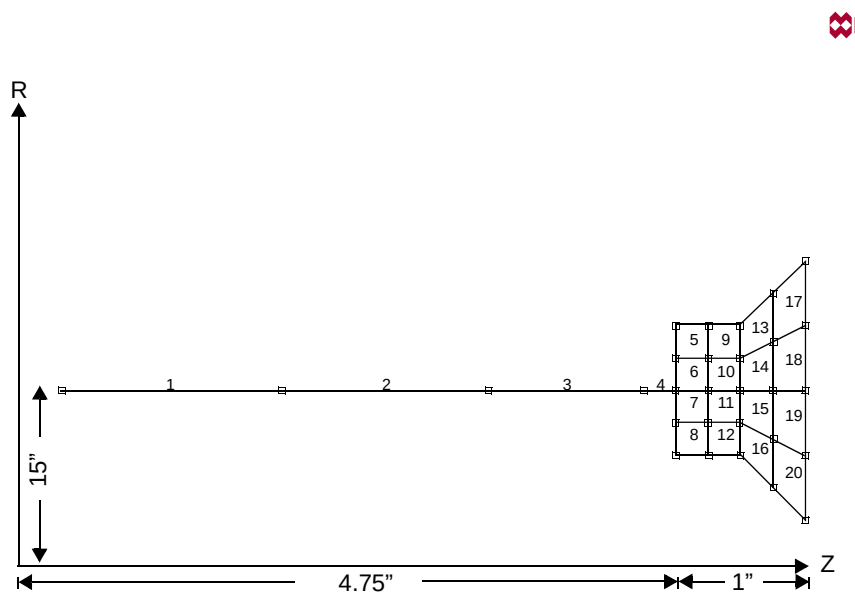

Figure 2.4-1 Solid-Shell Intersection Model

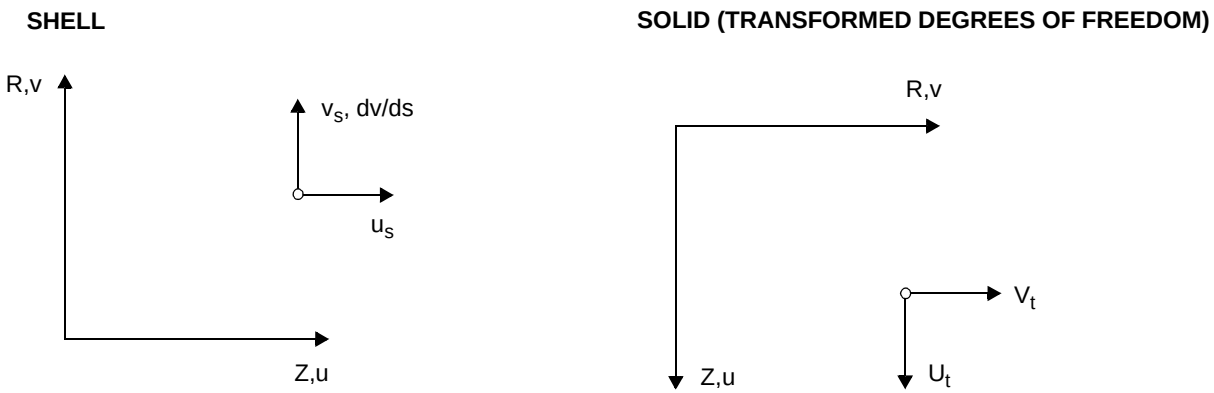

Figure 2.4-2 Tying and Transformations

2.5 Doubly Cantilevered Beam Loaded Uniformly

The solution of a cantilevered beam with a rectangular cross section subjected to a uniform load is obtained. This problem demonstrates the accuracy of the simple two-dimensional beam element.

Element

As this is a two-dimensional problem, it is possible to use element type 5, a straight, 2-node, rectangular-section, beam column. The displacement assumption is linear along the length (L) of the beam and a cubic displacement assumption in the direction normal to the beam. The numerical integration is 3-point Gaussian quadrature along the length of the element and 11-point Simpson's rule through the thickness. The two nodes of each element have three degrees of freedom each: u, v, and right-hand rotation.

Model

Symmetry allows a model of one-half the beam to be used. Five elements and six nodes are used for a total of 18 degrees of freedom (see Figure 2.5-1).

Geometry

The height of 1.0 (in-plane) is specified in the first data field, EGEOM1. The cross-sectional area of 1.0 is specified in the second data field, EGEOM2.

Loading

All five elements are loaded with a uniform distributed load of magnitude 10. This load is specified in the DIST LOADS option as type 0 (IBODY = 0).

Boundary Conditions

One end of the beam is rigidly fixed; $u = v = \theta = 0$ for node 1. The midbeam node (6) is fixed against axial expansion ($u = 0$) and against right-hand rotation ($\theta = 0$); this ensures the correct symmetry conditions.

Results

Deflections at nodal points shown in Figure 2.5-2 are tabulated in Table 2.5-1 and compared with exact answers. Correlation is very good. However, for a problem where the beam bending aspect of the model is critical, element type 16 should be used. With its higher-order integration and additional degrees of freedom per node, it will yield better answers.

Table 2.5-1 Results

Node	MARC Computed Deflection	Analytically Calculated Deflection
1	0	0
2	2.03×10^{-5}	2.03×10^{-5}
3	6.40×10^{-5}	6.40×10^{-5}
4	1.103×10^{-4}	1.103×10^{-4}
5	1.440×10^{-4}	1.440×10^{-4}
6	1.563×10^{-4}	1.563×10^{-4}

The solution can be expressed as:

$$\sigma = \frac{My}{I}$$

$$\text{Shear force } V = p\left(\frac{L}{2} - x\right)$$

$$\text{Moment } M = \frac{pL^2}{12}\left(1 - \frac{6x}{L} + \frac{6x^2}{L^2}\right)$$

$$\text{Rotation} = \frac{PL^3}{12EI}\left(\frac{2x}{L} - \frac{3x^2}{L^2} + \frac{2x^3}{L^3}\right)$$

$$\text{Displacement} = \frac{pL^4}{24EI}\left(\frac{x^2}{L^2} - \frac{2x^3}{L^3} + \frac{x^4}{L^4}\right)$$

Parameters, Options, and Subroutines Summary

Example e2x5.dat:

Parameters	Model Definition Options
ELEMENTS	CONNECTIVITY
END	COORDINATES
SIZING	DIST LOADS
TITLE	END OPTION
	FIXED DISP
	GEOMETRY
	ISOTROPIC

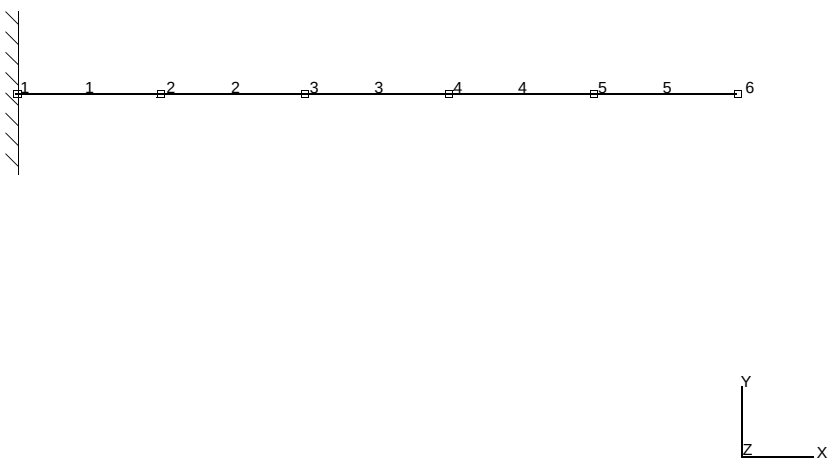

Figure 2.5-1 Beam Model

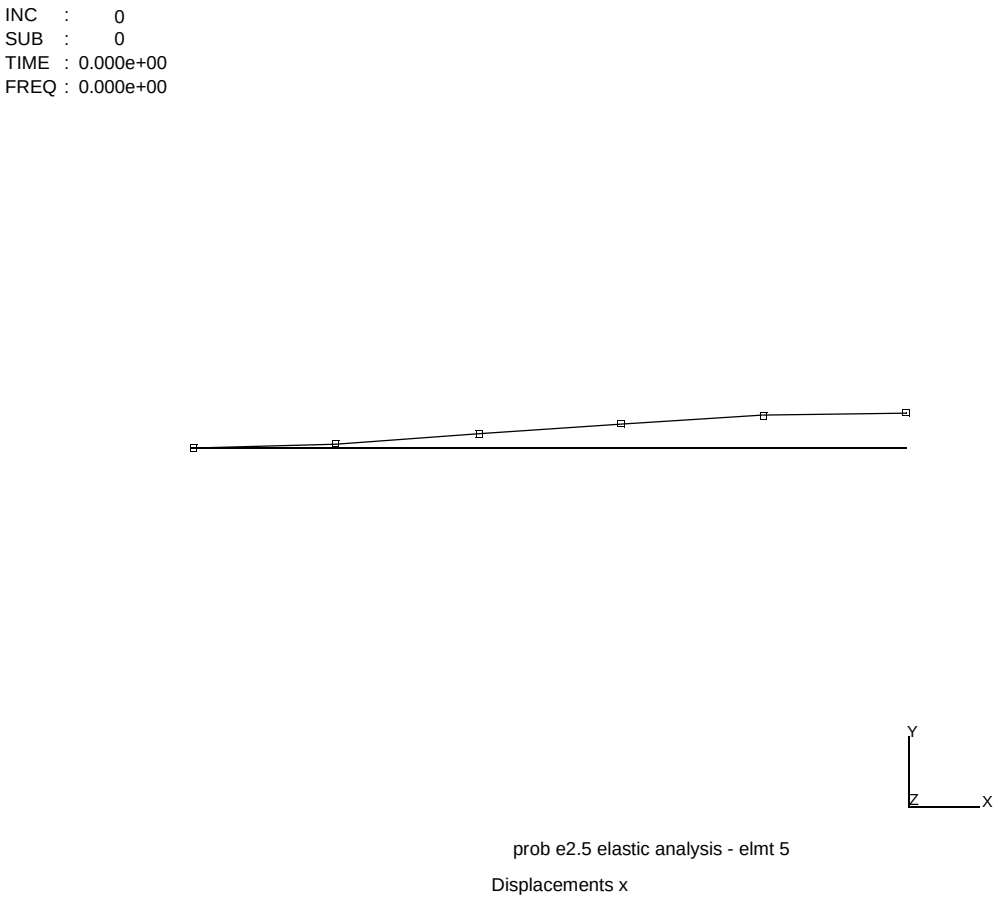

Figure 2.5-2 Deformations

2.6 Open Section, Double Cantilever Beam Loaded Uniformly

An I-section beam is loaded uniformly, parallel to the plane of the web. The beam is fixed against rotation and displacement at each end. This problem demonstrates the use of the BEAM SECT parameter to define the cross section of a beam. The results are compared to the analytic solution.

Element

Library element type 13 is used. This element is an open-section, curved, thin-walled beam of arbitrary section. It is based on classical theory of thin-walled beams with primary warping effects. The beam axis and cross-section orientation are interpolated cubically from 13 coordinates per node. This element has eight degrees of freedom per node.

Model

The beam of length 10 is modeled with 10 elements and 11 nodes for a total of 88 degrees of freedom (see Figure 2.6-1).

Geometry

EGEOM2 is used as a floating point value to cross reference the section number. EGEOM2 = 1 as only one section type is given here.

Material Properties

The Young's modulus is specified as 20×10^6 psi. Consistency with the analytical solution requires Poisson's ratio to be 0.

Loading

Uniform pressure of 10 pounds per length in the negative global Y direction.

Boundary Conditions

The beam is fixed against rotation and displacement at each end; that is:

$u = 0$	$dv/ds = 0$	$d\theta/ds = 0$
$v = 0$	$dw/ds = 0$	
$w = 0$	$\phi = 0$	

Special Considerations (Beam Section)

Element 13 has a cross-section specification that is entered in the parameter card section, after the header BEAM SECT. Details are given in *MARC Volume A: Theory and User Information*. In the present case, five branches are used to define the beam section (see Figure 2.6-2).

The first branch is one flange of beam, read in at constant thickness (0.18 inch) and with no curvature. The second branch is a zero thickness branch that doubles back to the flange center. The third branch is the web, straight and with constant thickness (0.31 inch). The fourth branch is half the remaining flange, with zero thickness. The fifth branch is straight and with constant thickness (0.18 inch) which doubles back over the fourth branch.

This element also requires 13 coordinates. In a more complex configuration, it would be advantageous to use subroutine UFXORD as a coordinate generator. Here, generation by hand is simpler. dx/ds and dy/ds in the section specification are not the same as dx/ds and dy/ds in the coordinate specification. The latter s is distance along the beam; the former is distance along a branch of the section. Also note the director specification, coordinates seven through nine, which orients the first axis of the local xy section plane in global xyz coordinates.

Results

An elastic analysis was performed. Five generalized strains and axial stress at integration points are printed out. The results are compared with calculated results from *Formulas for Stress and Strain*, R. J. Roark. These are summarized in Table 2.6-1. Figure 2.6-3 shows the moment diagram which was obtained by using the LINEAR parameter. Figure 2.6-4 shows the deformations.

Table 2.6-1 Results

Node	MARC Computer Deflection	Analytically Calculated Deflection
1	0	0
2	1.82×10^{-5}	1.82×10^{-5}
3	5.79×10^{-5}	5.75×10^{-5}
4	9.99×10^{-5}	9.91×10^{-5}
5	1.307×10^{-4}	1.295×10^{-4}
6	1.419×10^{-4}	1.404×10^{-4}

Parameters, Options, and Subroutines Summary

Example e2x6.dat:

Parameters	Model Definition Options
BEAM SECT	CONNECTIVITY
ELEMENTS	COORDINATES
END	DIST LOADS
SIZING	END OPTION
TITLE	FIXED DISP
	GEOMETRY
	ISOTROPIC

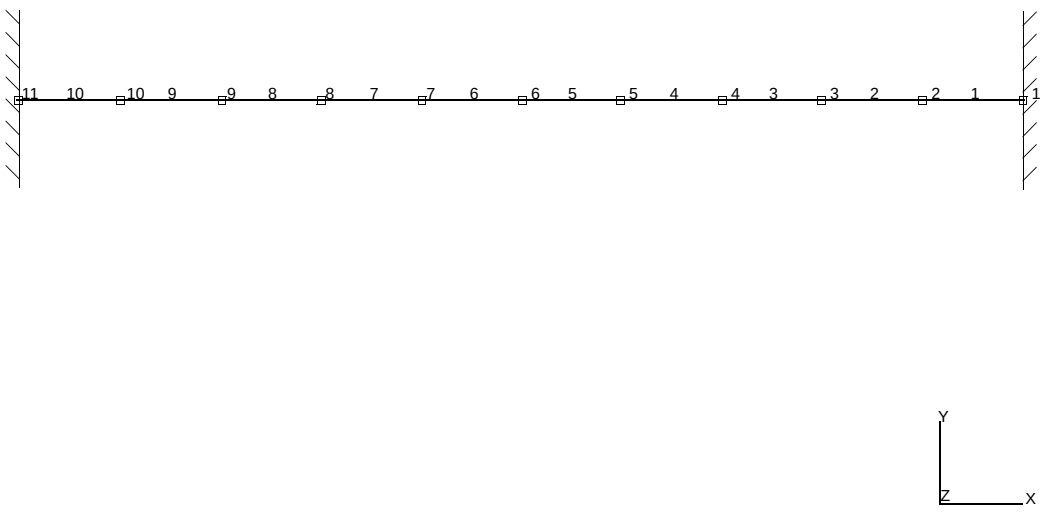

Figure 2.6-1 Open Section Beam Model

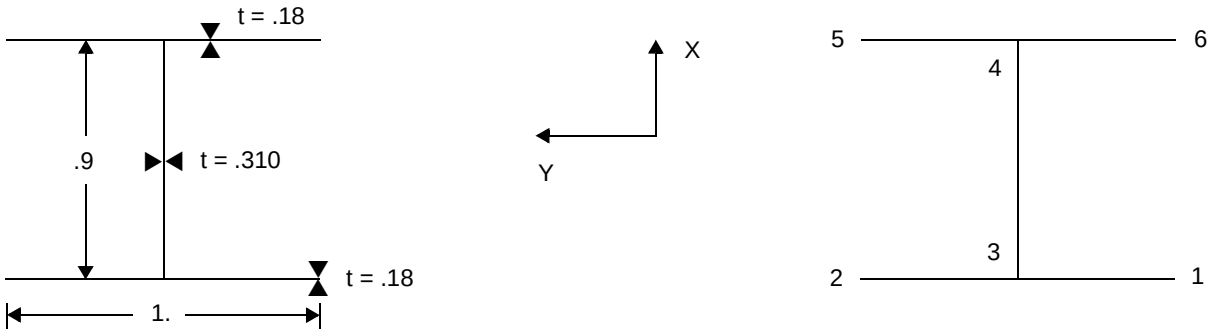

Figure 2.6-2 Beam Section and Sequence of Branch Traversal

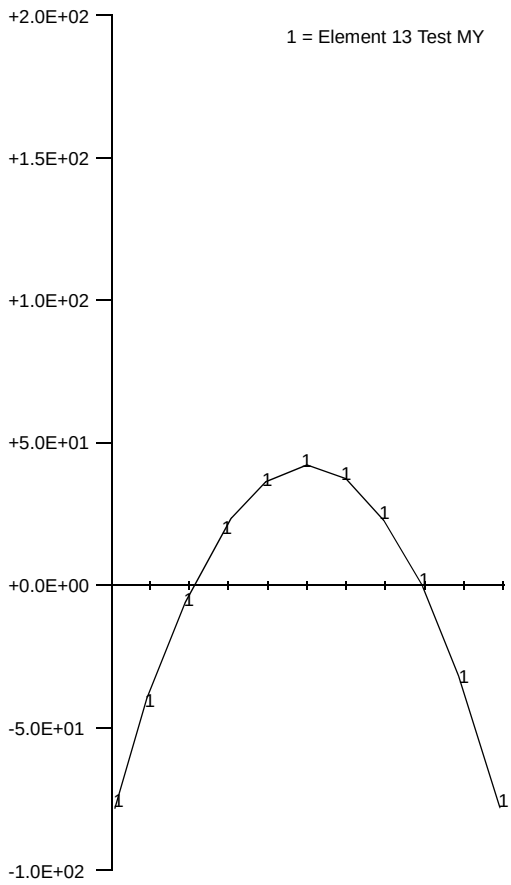

Figure 2.6-3 Moment Diagram

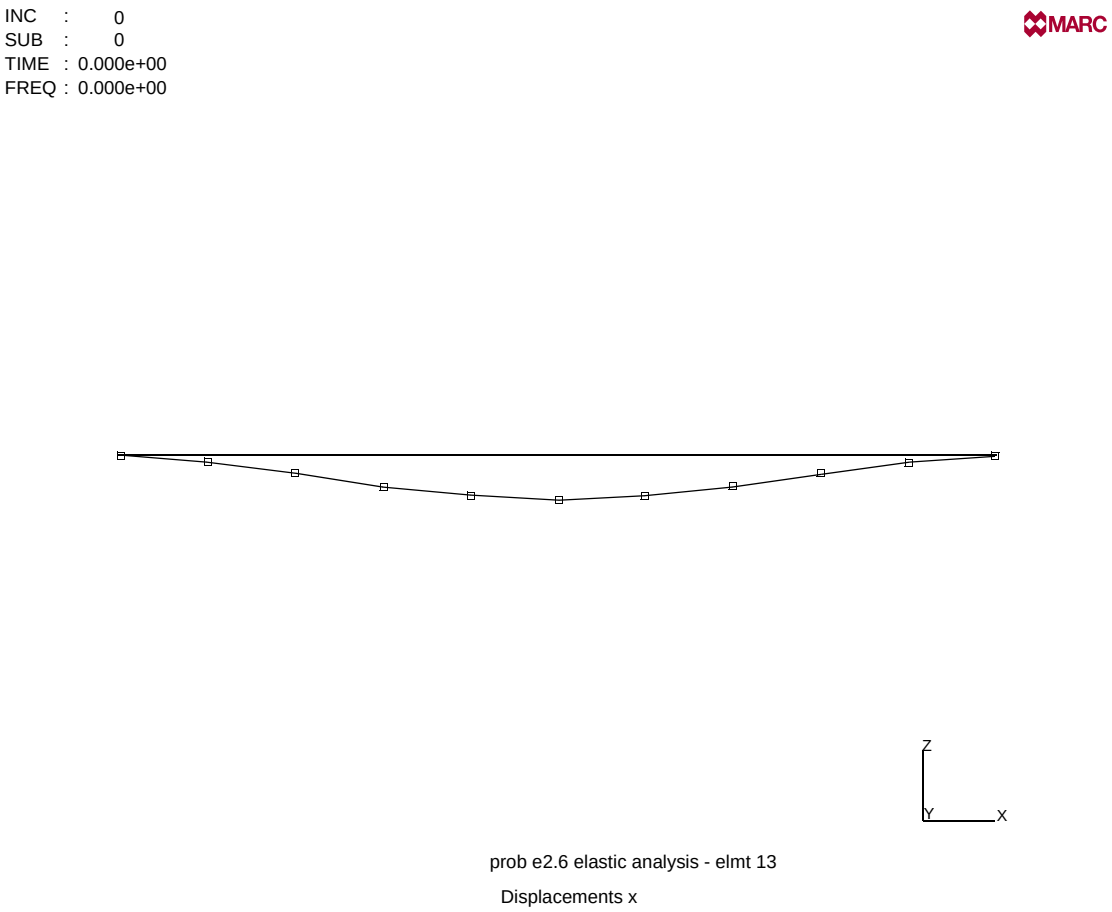

Figure 2.6-4 Deformations

2.7 Closed Section Beam Subjected to a Point Load

This problem demonstrates the use of the closed-section beam element. A hollow, square-section beam, which is clamped at both ends, has a single-point load applied at the center. The results are compared to the analytical solution.

Element

Library element type 14 is used. Element 14 is a closed-section, straight-beam element with no warping of the section, but including twist. This element has six degrees of freedom per node – three displacements and three rotations in the global coordinate system.

Model

Only half of the beam, whose total length is 10 inches, is modeled, taking advantage of the beam's symmetry. Five elements and six nodes are used for a total of 36 degrees of freedom. (See Figure 2.7-1.)

Geometry

The model uses the BEAM SECT parameter to define its cross-sectional geometry. EGEOM1 = 0 indicates a noncircular cross section. EGEOM2 gives the section number as a floating point value, here equal to 1.

Material Properties

The beam is considered elastic with a Young's modulus of 20.0×10^6 psi.

Loading

A single-point load of 50 lbs. is applied in the negative y-direction at the center node of the beam.

Boundary Conditions

In the model, the beam-end node (node 1) is fixed against displacement and rotation, simulating a fully built-in condition. Thus, $u = v = w = \theta_x = \theta_y = \theta_z = 0$. The midpoint node, node 6, is fixed against axial displacement and rotation; $u = \theta_x = \theta_y = \theta_z = 0$, thus ensuring symmetry boundary conditions.

Special Considerations

Element 14 has its cross section specified by the BEAM SECT parameter which is given in the parameter section. Details are given in *MARC Volume A: Theory and User Information*. In this case, four branches are used to define the hollow, square section. (see Figure 2.7-2)

Each branch is of constant thickness (.01 in.) with no curvature and is .99 in. in length. The branches are defined at the midpoint of the thickness of the cross section. The first branch begins at local coordinates, x = 0.495, y = -0.495 and each following branch begins its length

at the end coordinates of the previous branch. Thus, except for the first branch, only the coordinates at the end of the branch need to be defined. Each branch has four divisions which provide the four stress points for the branch.

Results

A simple elastic analysis was run with one load increment of negative 50 lb. applied to node 6 in the zeroth increment. The computed results are compared with an exact solution in Tables 2.7-1 and 2.7-2.The deflections are shown in Figure 2.7-3.

Table 2.7-1 Y Deflection (in.)

Node	Element 14	MARC Calculated
1	0.	0.
2	.000419	.000422
3	.001417	.001428
4	.002609	.002628
5	.003607	.003634
6	.004026	.004056

Table 2.7-2 Moments and Reaction Forces (lb.)

Element 14	MARC Calculated
M = 125.	M = 125.
R = 50.	R = 50.

Parameters, Options, and Subroutines Summary

Example e2x7.dat:

Parameters	Model Definition Options
BEAM SECT	CONNECTIVITY
ELEMENTS	COORDINATES
END	END OPTION
SIZING	FIXED DISP
TITLE	GEOMETRY
	ISOTROPIC
	POINT LOAD

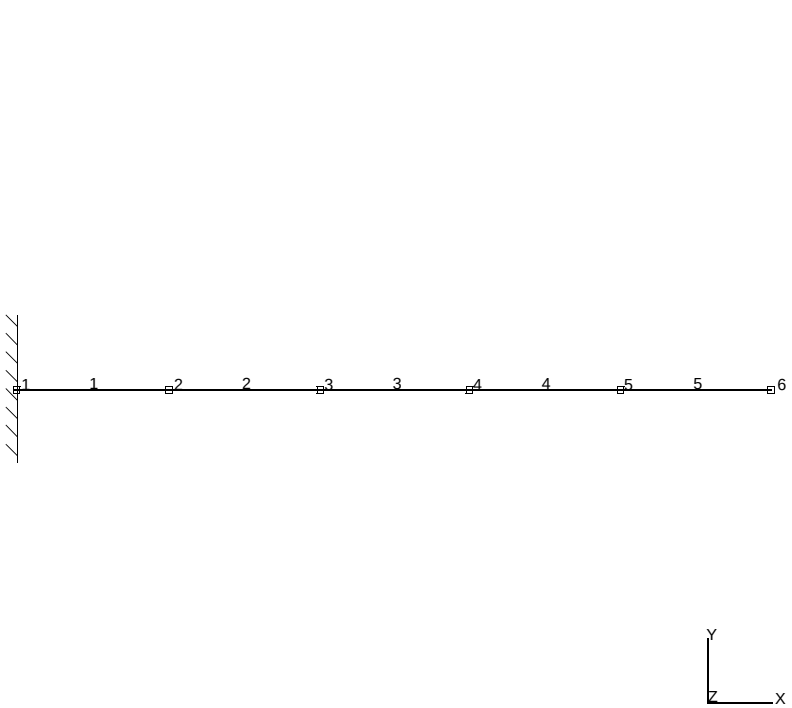

Figure 2.7-1 Closed Section Beam Model

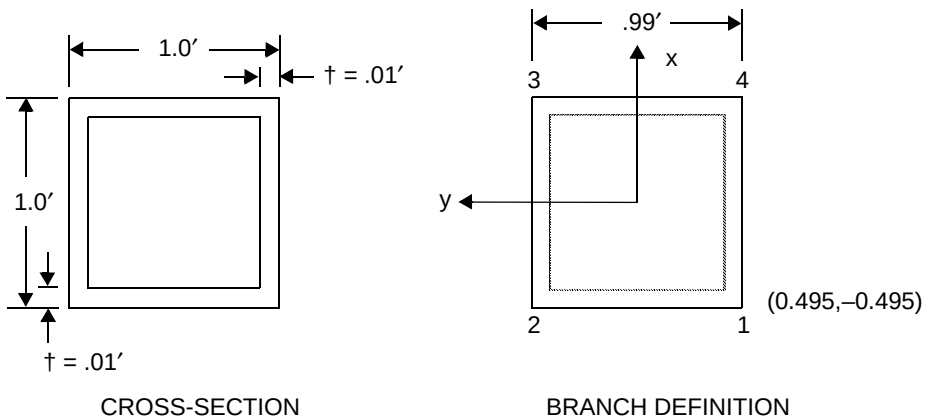

Figure 2.7-2 Hollow, Square-Section Beam

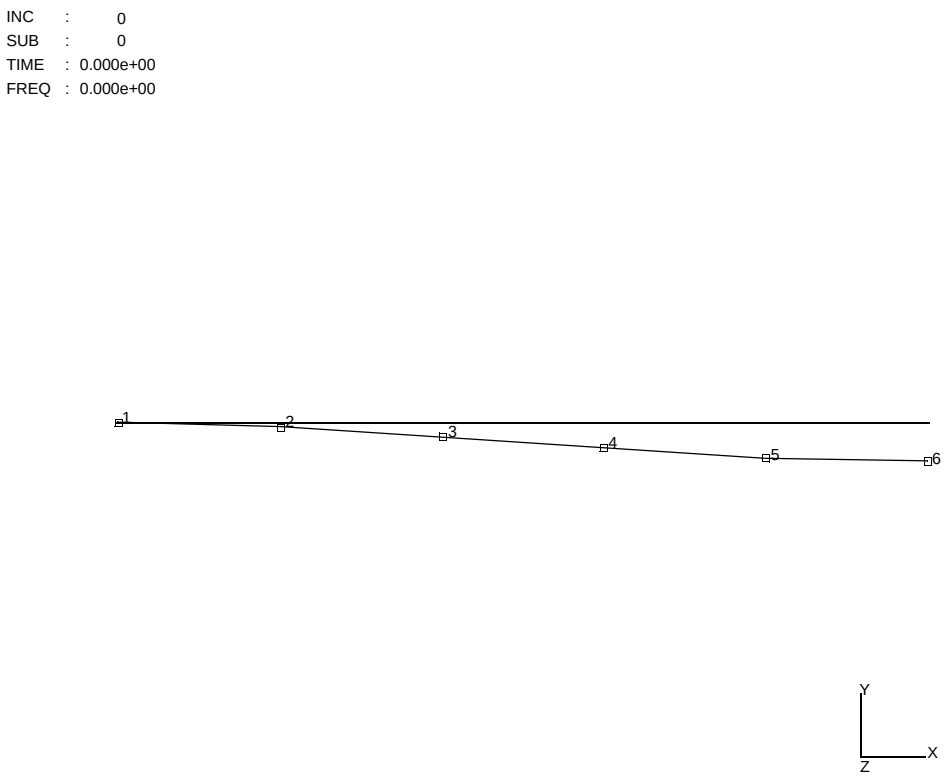

Figure 2.7-3 Deformed Beam

2.8 Curved Beam Under a Point Load

This problem demonstrates the use of the curved-beam element to model a 90-degree section of a circular beam. The beam is loaded in its plane in a radial direction on its free end. The solution is compared to the analytic solution.

Element

Since this is a two-dimensional problem, library element type 16 can be used. It is a curved, two-dimensional beam. The displacements are interpolated cubically and the element formulation is isoparametric. The four degrees of freedom are two in-plane displacements and two derivatives with respect to s, the length of the beam. See *MARC Volume B: Element Library* for a complete description.

Model

One end of the beam is fixed; the other end is loaded. There are four elements and five nodes for a total of 20 degrees of freedom (see Figure 2.8-1).

Geometry

The first data field, EGEOM1 specifies thickness at the first node of an element as 1.6 inches. Linear thickness variation is allowed along the length of the element. The third data field default, EGEOM3 = 0., assumes constant thickness. If linear thickness variation is needed, the ALL POINTS parameter should be included. The second data field EGEOM2, is used to specify the beam width; the default width is unity; here it has been set to .1 inch. Thickness is in-plane and width is normal to the plane of the beam.

Material Properties

The Young's modulus is 26 x 10^6 psi, and Poisson's ratio is 0.3.

Loading

A single point load of 100 lbs. in the x-direction is applied to free-end node 5.

Boundary Conditions (APPBC)

One end of the beam is fixed against displacement and rotation (dv/ds = 0). The APPBC parameter is included, which allows for a more accurate calculation of the boundary condition constraints. The APPBC parameter uses row and column elimination of the stiffness matrix for the constrained degree of freedom, resulting in a slight increased accuracy of solution.

Results

The deflection of the end node and the stresses at the end of the beam are compared with calculated values in Table 2.8-1. The analytic solution may be found in Timoshenko and Goodier, *Theory of Elasticity.*

Table 2.8-1 Displacement and Stress Results

	Analytically Calculated	MARC Computed
u displacement (in.) node 5	.04536	.04543
v displacement (in.) node 5	-.02888	-.02874
σ_o max (psi)	17625.	18620.
σ_i max (psi)	-20060.	-17270.
σ_o is stress in extreme fiber on the convex side. σ_i is stress in extreme fiber on the concave side.		

Parameters, Options, and Subroutines Summary

Example e2x8.dat:

Parameters	Model Definition Options
APPBC	CONNECTIVITY
ELEMENTS	COORDINATES
END	END OPTION
PRINT	FIXED DISP
SIZING	GEOMETRY
TITLE	ISOTROPIC
	POINT LOAD

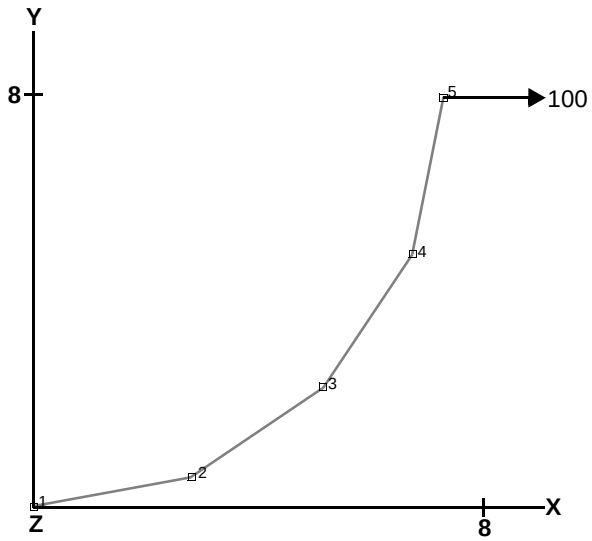

Figure 2.8-1 Curved Beam Model

2.9 Plate with Hole

This problem demonstrates several ways to solve the problem of a circular hole in plate which has a known solution (Timoshenko and Goodier, *Theory of Elasticity*). The hole radius to plate size ratio is chosen to be 5, approximating an infinite plate. The second order isoparametric elements (types 26 and 124) are used first, followed by the use of the linear order type 3 using adaptive meshing.

This problem is modeled using the four techniques summarized below.

Data Set	Element Type(s)	Number of Elements	Number of Nodes	Differentiating Features
e2x9	26	20	79	
e2x9b	26	20	79	ELEM SORT, NODE SORT
e2x9c	124	40	99	
e2x9d	3	2	6	ADAPTIVE

Elements

Element type 26 and 124 are second-order isoparametric elements for plane stress. Type 26 is an 8-node quadrilateral, and type 126 is a 6-node triangle. Element type 3 is a 4-node first-order isoparametric element.

Model

The dimensions of the plate are 5 inches square with a 1 inch radius. Only one quarter of the plate is modeled due to symmetry conditions. The finite element mesh for element type 26 is shown in Figure 2.9-1, and the elements near the hole are made smaller. There are 20 elements in the quadrilateral meshes and 40 elements in the triangular meshes. The triangular mesh is made from the quadrilateral mesh by adding a node in the center of each element; then, the quadrilaterals are broken up into triangles. In problem e2x9d, the mesh initially consists of two elements as shown in Figure 2.9-2. As the mesh adapts, the number of elements increase until there are 65 elements in the mesh.

Material Properties

The material for all elements is treated as an elastic material with Young’s modulus of 30.0E+06 psi and Poisson’s ratio (ν) of .3.

Geometry

The plate has a thickness of 1 inch given in the first field.

Loads and Boundary Conditions

A distributed load of -1.0 psi is applied to the top edge of the mesh. The boundary conditions are determined by the symmetry conditions and require that the nodes along y = 0 axis have no vertical displacement, and the nodes along the x = 0 axis have no horizontal displacement. The origin of the model is at the center of the hole.

Adaptive Meshing

Problem e2x9d demonstrates the use of adaptive meshing. The ADAPTIVE parameter defines an upper bound to the number of elements and nodes. The ADAPTIVE model definition option is used to indicate that the adaptive criteria is based upon the stress in an element which is not to exceed 75% of the maximum stress. As this would clearly refine forever, a limit of five levels is requested. This procedure is a way to add elements where a stress concentration exists. The SURFACE option defines a circle with a radius of one. When used with the ATTACH NODE option, this insures that the newly created nodes are places on the circle. The ATTACH NODE option indicates that nodes 1, 2, and 3 are on the circle, and any newly created nodes also lie on the circle. Boundary conditions are generated automatically for the nodes created along y = 0.

Results

Figure 2.9-3 and Figure 2.9-4 contour the second component of stress (σ_{22}) over the mesh. Figure 2.9-5 tabulates and plots values of σ_{22} for Element types 26, 124 and the exact solution along the y = 0 axis. The finite element solution is approximated by a plate of finite dimensions; there is some difference in predicting the exact solution. The results would improve if more elements were used. Figure 2.9-7 through Figure 2.9-10 show the progression of the mesh during the adaptive meshing process. After adaptive meshing, the stress concentration predicted is 2.86.

Parameters, Options, and Subroutines Summary

Example e2x9.dat:

Parameters	Model Definition Options
ELEMENTS	CONNECTIVITY
END	COORDINATES
SIZING	DIST LOADS
TITLE	END OPTION
	FIXED DISP
	GEOMETRY
	ISOTROPIC
	POST

Example e2x9b.dat:

Parameters	Model Definition Options
ELEMENTS	CONNECTIVITY
END	COORDINATES
SIZING	DIST LOADS
TITLE	ELEM SORT
	END OPTION
	FIXED DISP
	GEOMETRY
	ISOTROPIC
	NODE SORT
	PRINT CHOICE
	SUMMARY

Example e2x9c.dat:

Parameters	Model Definition Options
ELEMENTS	CONNECTIVITY
END	COORDINATES
SIZING	DIST LOADS
TITLE	END OPTION
	FIXED DISP
	GEOMETRY
	ISOTROPIC
	NO PRINT
	OPTIMIZE
	POST

Example e2x9d.dat:

Parameters

ADAPT
ELASTIC
ELEMENTS
END
SIZING
TITLE

Model Definition Options

ADAPTIVE
ATTACH NODE
CONNECTIVITY
COORDINATES
DIST LOADS
END OPTION
FIXED DISP
GEOMETRY
ISOTROPIC
OPTIMIZE
POST
SURFACE

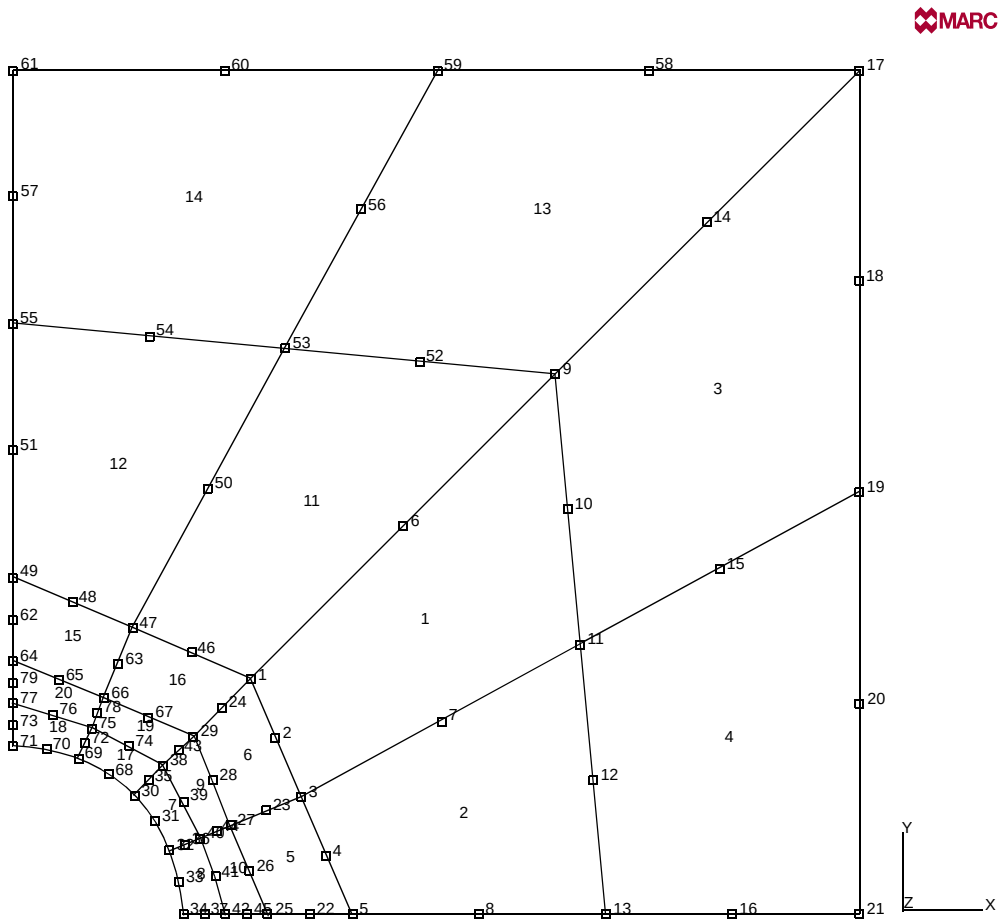

Figure 2.9-1 Mesh Layout for Plate with Hole (Element 26)

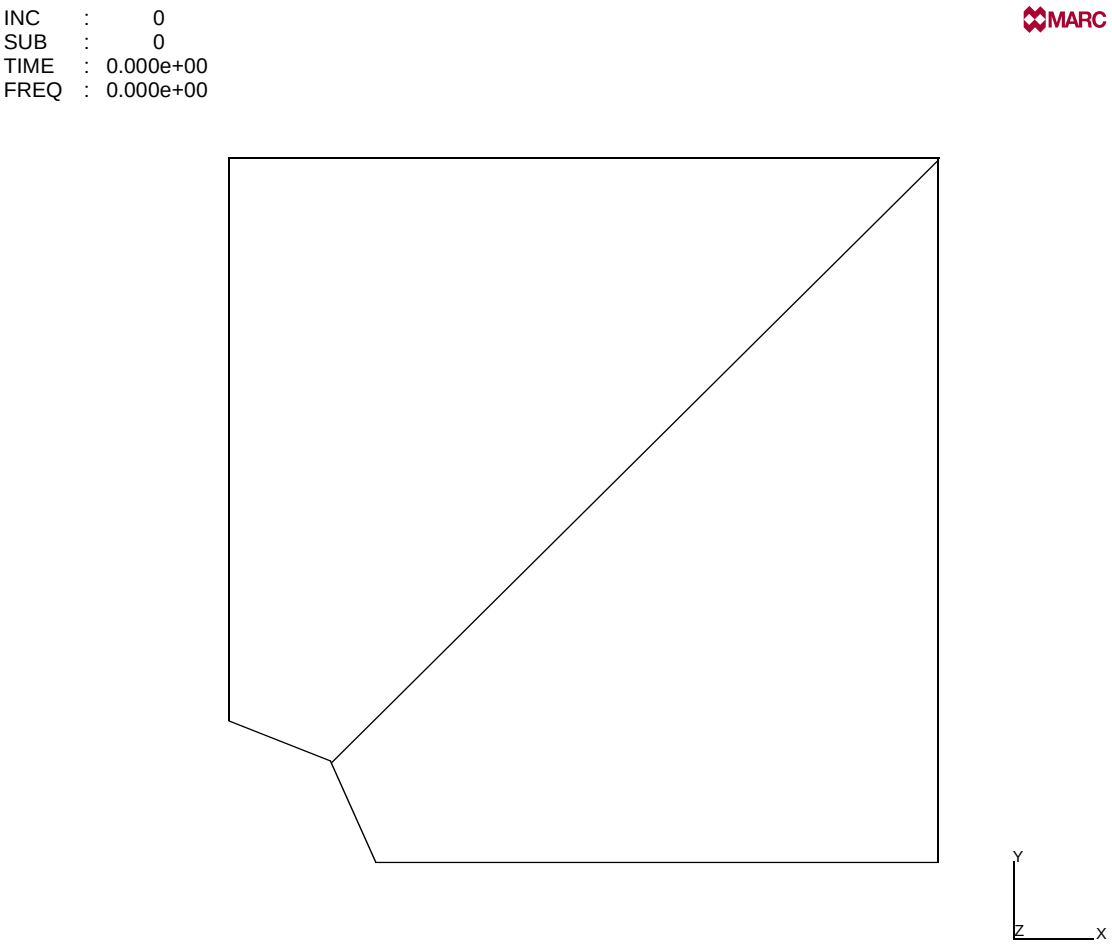

Figure 2.9-2 Original Mesh for Plate with Hole When Using Adaptive Meshing

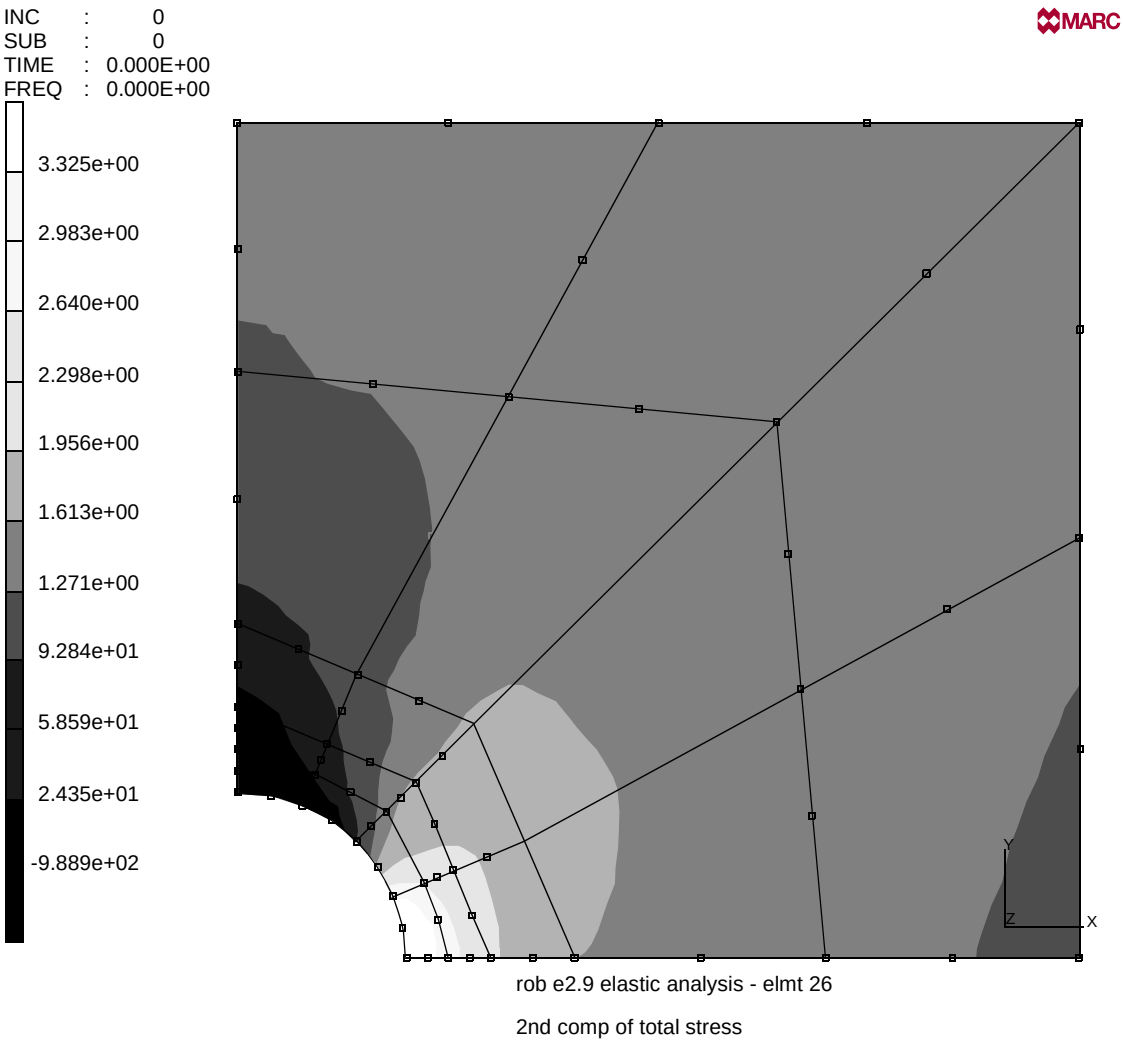

Figure 2.9-3 Contours of σ_{22} Element 26

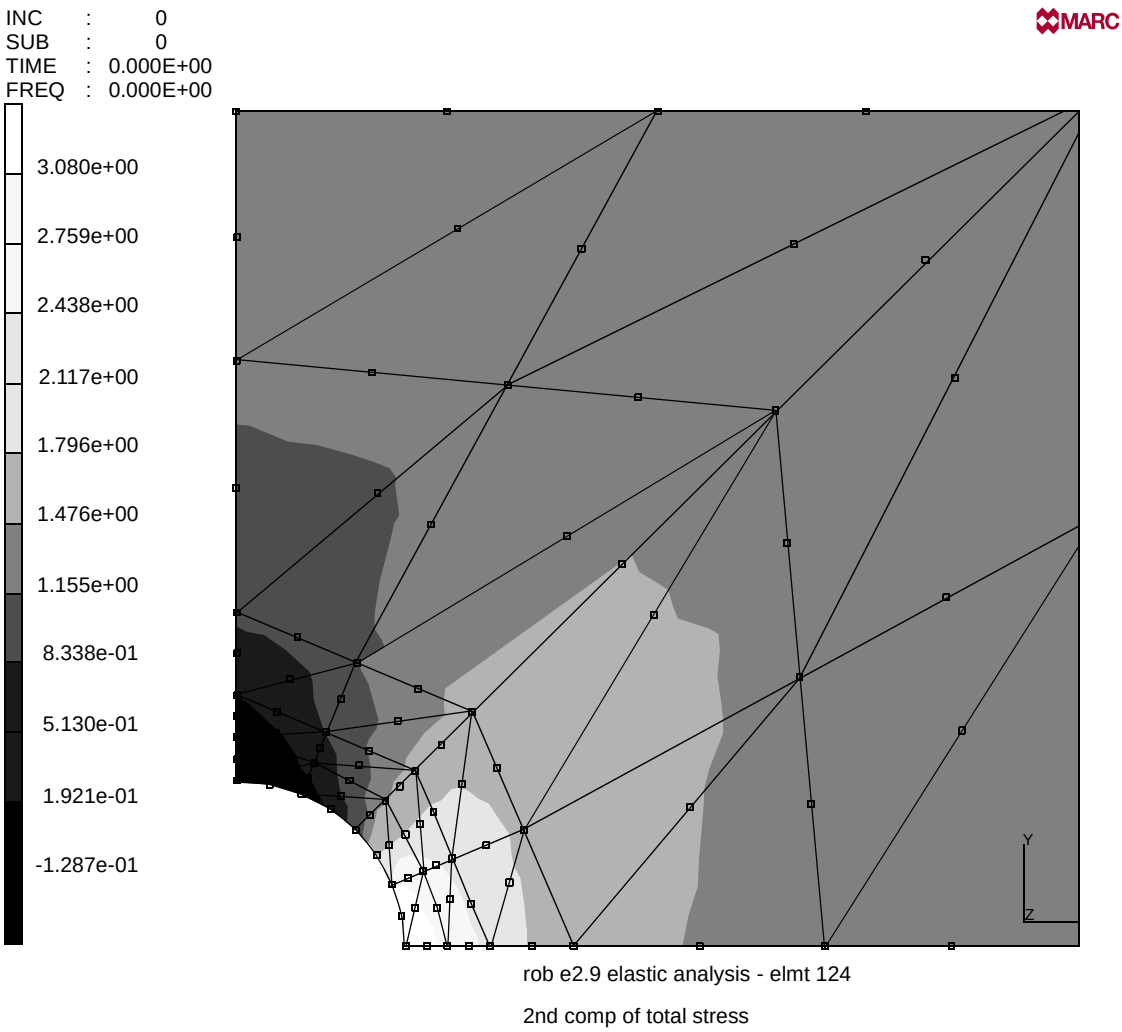

Figure 2.9-4 Contours of σ_{22} Element 124

Radius	Type 26	Type 124	Exact
1.00000	3.325290E+00	3.079772E+00	3.0000
1.12500	2.656915E+00	2.643165E+00	2.3315
1.25000	2.181081E+00	2.152462E+00	1.9344
1.37500	1.885873E+00	1.895210E+00	1.6841
1.50000	1.670818E+00	1.650798E+00	1.5185
1.75000	1.416509E+00	1.446365E+00	1.3232
2.00000	1.276260E+00	1.264376E+00	1.2188
2.75000	1.117434E+00	1.127211E+00	1.0923
3.50000	1.028915E+00	1.032025E+00	1.0508
4.25000	9.466122E-01	9.452355E-01	1.0323
5.00000	8.523712E-01	8.844259E-01	1.0224

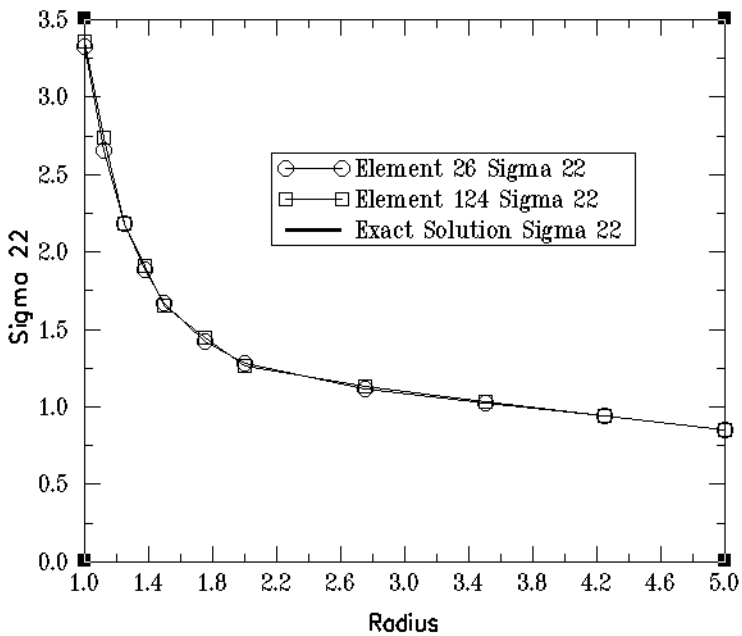

Figure 2.9-5 σ_{22} Along y = 0, Elements 26,124, and Exact

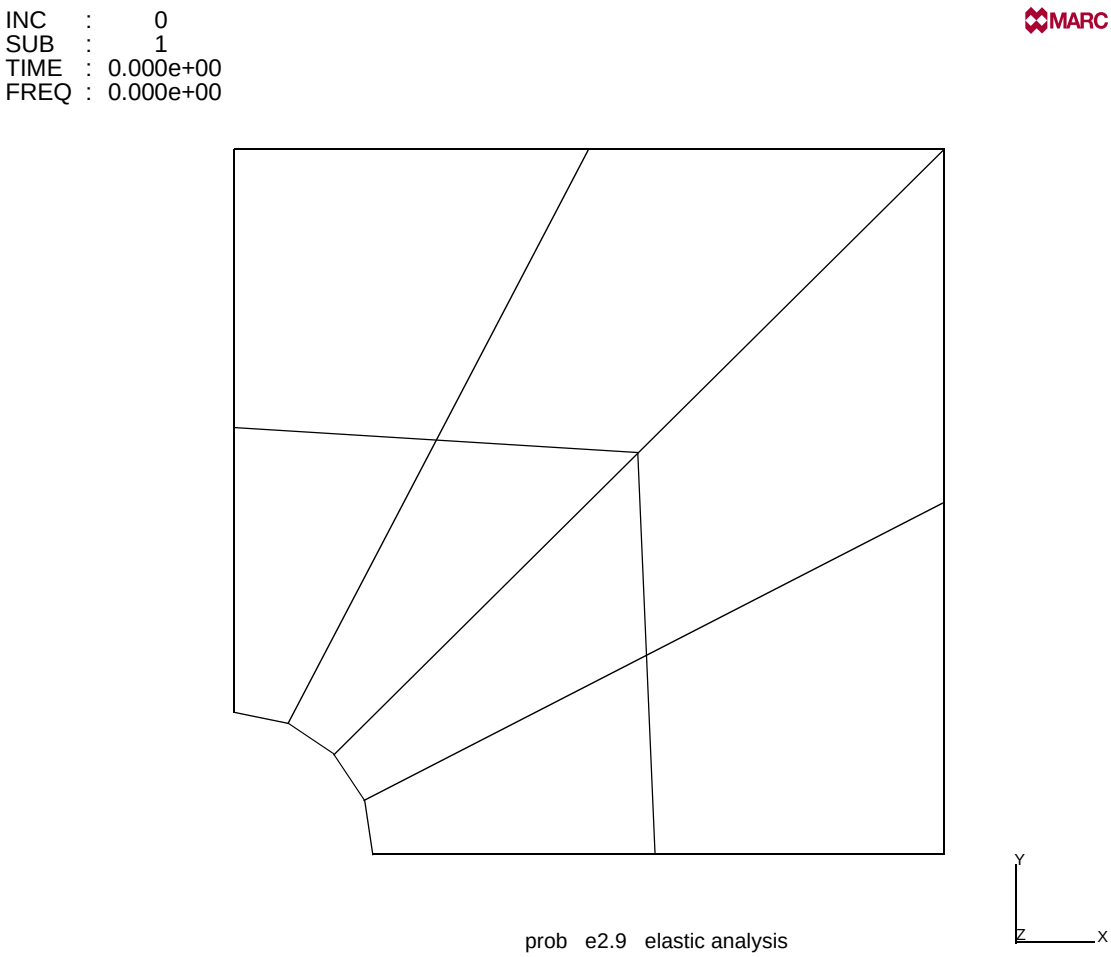

Figure 2.9-6 Mesh After First Refinement

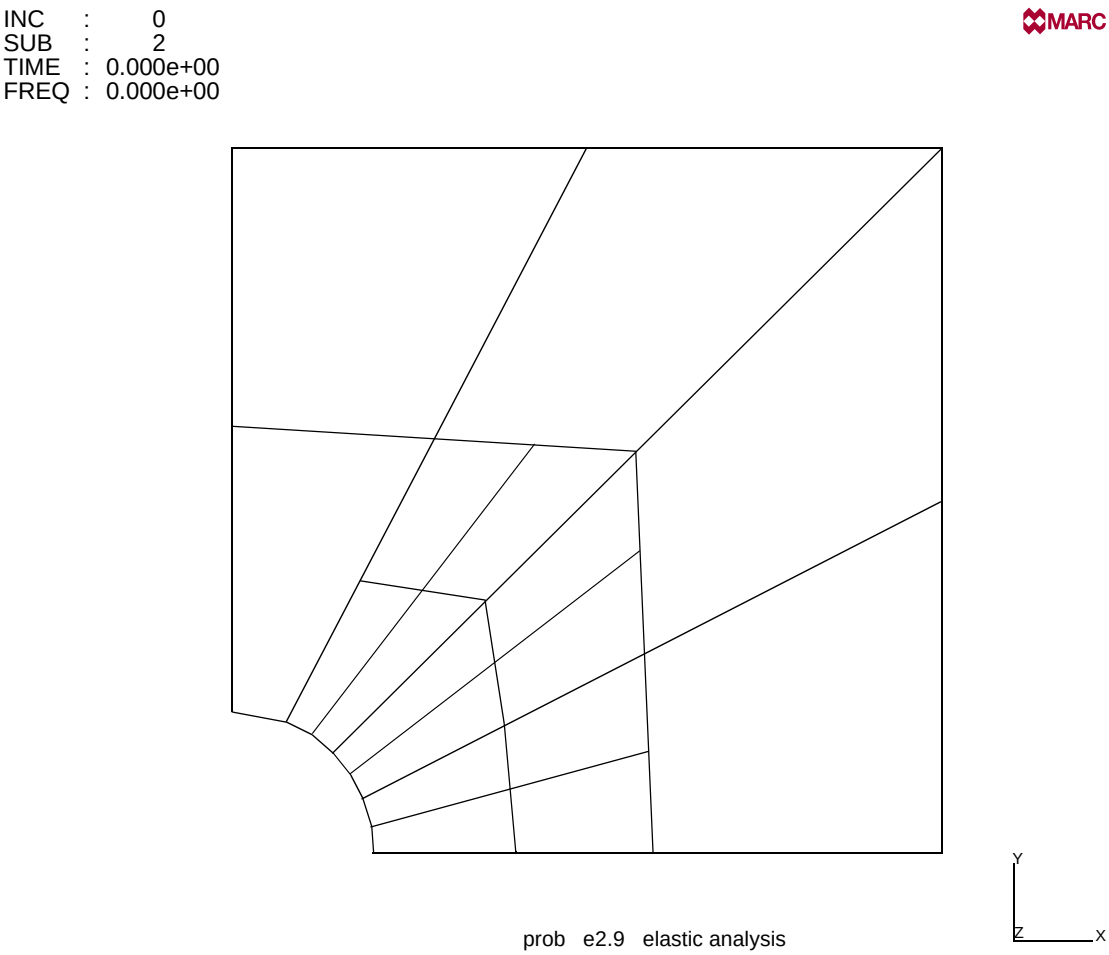

Figure 2.9-7 Mesh After Second Refinement

INC : 0
SUB : 3
TIME : 0.000e+00
FREQ : 0.000e+00

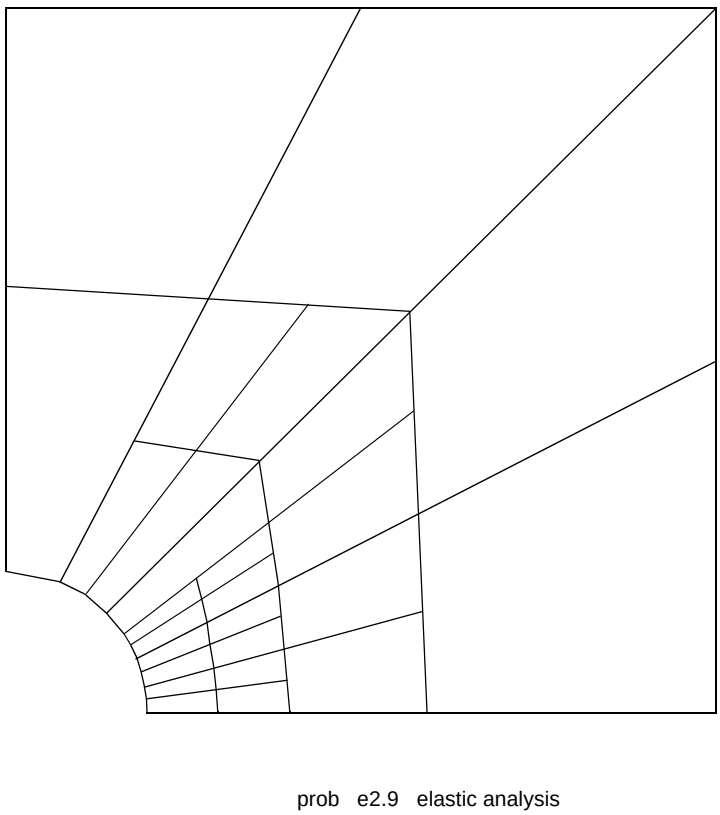

Figure 2.9-8 Mesh After Third Refinement

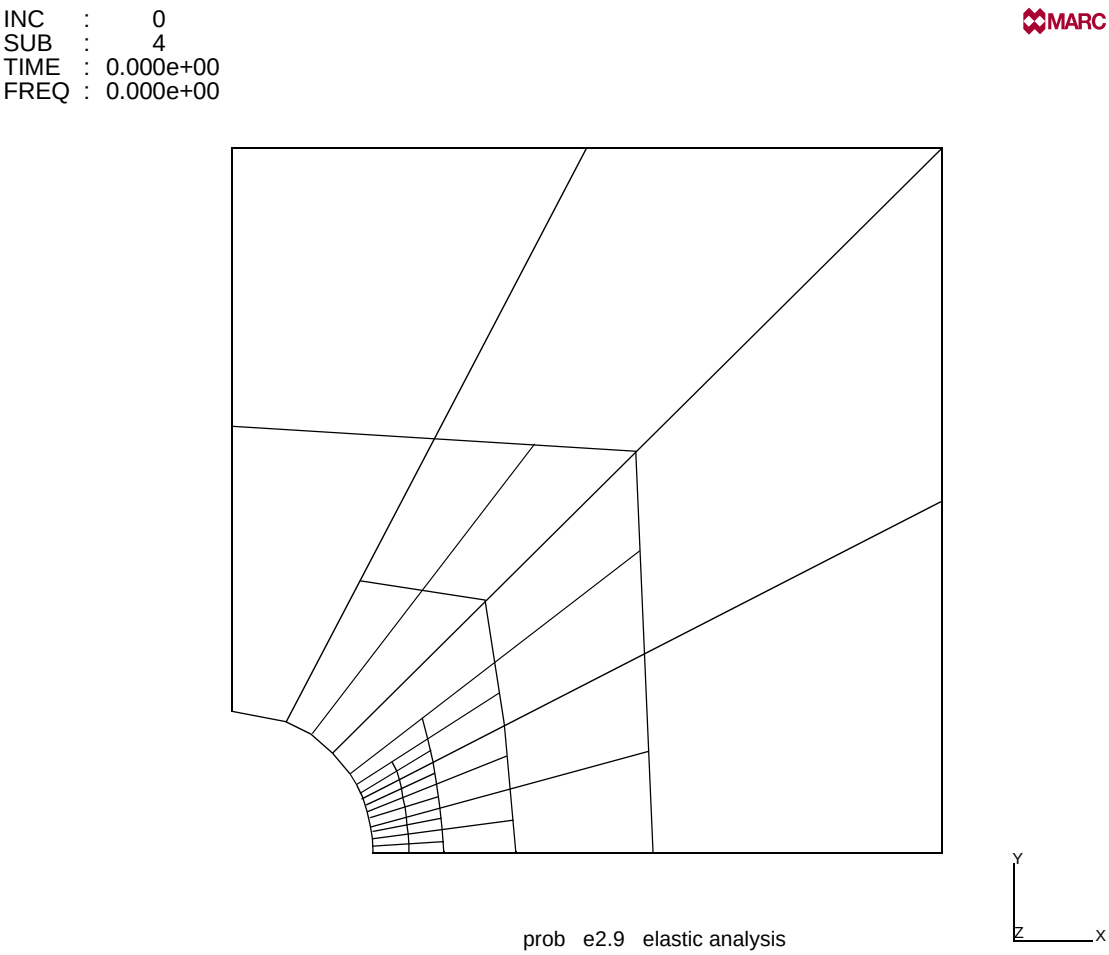

Figure 2.9-9 Mesh After Fourth Refinement

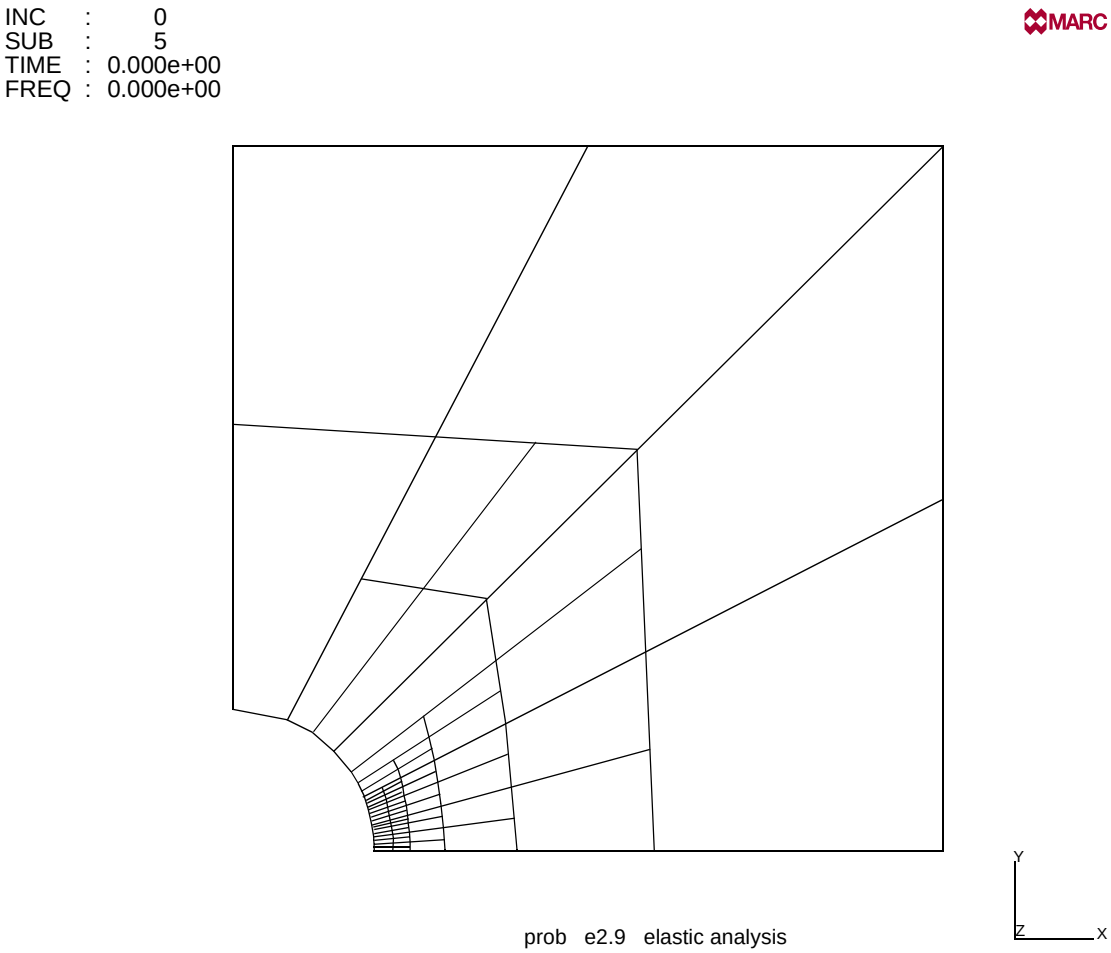

Figure 2.9-10 Mesh After Fifth Refinement

2.10 Plane Stress Disk

A thin circular disk with a diameter of 12 inches is subjected to diametrically-opposed concentrated loads of 100 lbf. The disk is modeled as an elastic material using two different types of plane stress elements. The results are compared to the analytic solution demonstrating the accuracy of the finite element model.

This problem is also modeled using the adaptive meshing procedure.

This problem is modeled using the three techniques summarized below.

Data Set	Element Type(s)	Number of Elements	Number of Nodes	Differentiating Features
e2x10	3	64	82	
e2x10b	114	64	82	
e2x10c	3	64	82	adaptive meshing

Elements

The solution is obtained using first order isoparametric quadrilateral elements for plane stress, element types 3 and 114, respectively. Type 114 is similar to type 3; however, it uses reduced integration with hourglass control. The ALIAS parameter is used to switch elements between the two models.

Model

The diameter of the disk is 12 inches and only one half of the disk is modeled due to symmetry conditions. The finite element mesh used for both element types is shown in Figure 2.10-1. Initially, there are 64 elements and 82 nodes. The model origin is at the center of the disk.

Material Properties

The material for all elements is treated as an elastic material, with Young's modulus of 30.0E+04 psi, Poisson's ratio (v) of .3, and a yield strength of 40,000 psi.

Geometry

The disk has a thickness of 1 inch given in the first field.

Loads and Boundary Conditions

A point load of -50 lbf (half of the total load) is placed on node 1 in the vertical direction. This point load is reacted by constraining the vertical displacement of the diametrically-opposed node (number 79) to zero. All nodes along the y-axis at x = 0 have their horizontal displacements constrained to zero.

Optimization

The Cuthill-McKee optimizer is used to reduce the bandwidth and hence the computational costs. Also notice that the computational costs of using element type 114 with reduced integration with hourglass control is lower than that of element type 3.

Adaptive Meshing

In problem e2x10c, the Zienkiewicz-Zhu stress error criteria is used with a tolerance of 0.05 in the third example. A maximum of three levels is allowed. The ELASTIC parameter is added to insure reanalysis until the error criteria is satisfied.

Results

The accuracy of the solution to this problem is shown in Figure 2.10-2, where the direct stress component in the vertical direction along the y = 0 axis is plotted against its exact value given in *Theory of Elasticity*, Timoshenko and Goodier, McGraw Hill, 1970, pp 122-123 as:

$$\sigma_{yy}(x,0) = 2P\,[1 - 4d^4 / (d^2 + 4x^2)^2] / \pi d$$

Both σ_{xx} and σ_{yy} are shown in Figure 2.10-3.

The value of stress predicted by element type 114 is closer to the theoretical solution than element type 3. Also, the finite element solution cannot capture the singular behavior under the concentrated loads, and special elements and/or meshes are usually needed in order to obtain accurate solutions near such singularities. The adaptive meshing procedure is useful for these problems.

After the first solution in the third analysis, elements 1, 2, 4, 5, 58, 59, 62, and 63 are refined to satisfy the error criteria. After the second trial, original elements 8 and 53 are subdivided along with eight of the new elements. After the third trial, eight elements are subdivided. This procedure is continued until all of the elements either satisfy the error criteria or have been refined three times. A close-up of the final mesh is shown in Figure 2.10-4.

Parameters, Options, and Subroutines Summary

Example e2x10.dat:

Parameters	Model Definition Options
ELEMENTS	CONNECTIVITY
END	COORDINATES
SIZING	END OPTION
TITLE	FIXED DISP
	GEOMETRY
	ISOTROPIC
	OPTIMIZE
	POINT LOAD
	POST

Example e2x10b.dat:

Parameters	Model Definition Options
ALIAS	CONNECTIVITY
ELEMENTS	COORDINATES
END	END OPTION
SIZING	FIXED DISP
TITLE	GEOMETRY
	ISOTROPIC
	OPTIMIZE
	POINT LOAD
	POST

Example e2x10c.dat:

Parameters	Model Definition Options
ADAPTIVE	ADAPTIVE
ELASTIC	CONNECTIVITY
ELEMENTS	COORDINATES
END	END OPTION
SIZING	FIXED DISP
TITLE	GEOMETRY
	ISOTROPIC
	OPTIMIZE
	POINT LOAD
	POST

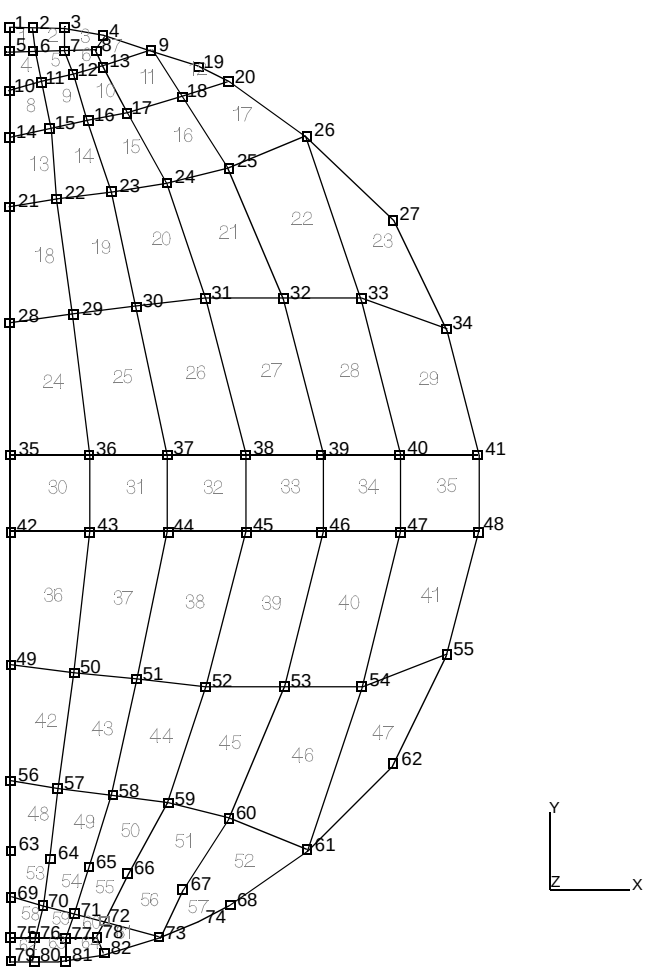

Figure 2.10-1 Model

Radius	Type 3	Type 114	Exact
0	-1.681E+01	-1.616E+01	-1.592E+01
1	-1.571E+01	-1.508E+01	-1.478E+01
2	-1.288E+01	-1.222E+01	-1.188E+01
3	-9.108E+00	-8.615E+00	-8.276E+00
4	-5.441E+00	-5.185E+00	-4.866E+00
5	-2.489E+00	-2.174E+00	-2.086E+00
6	4.879E-01	-7.582E-01	0.000E+00

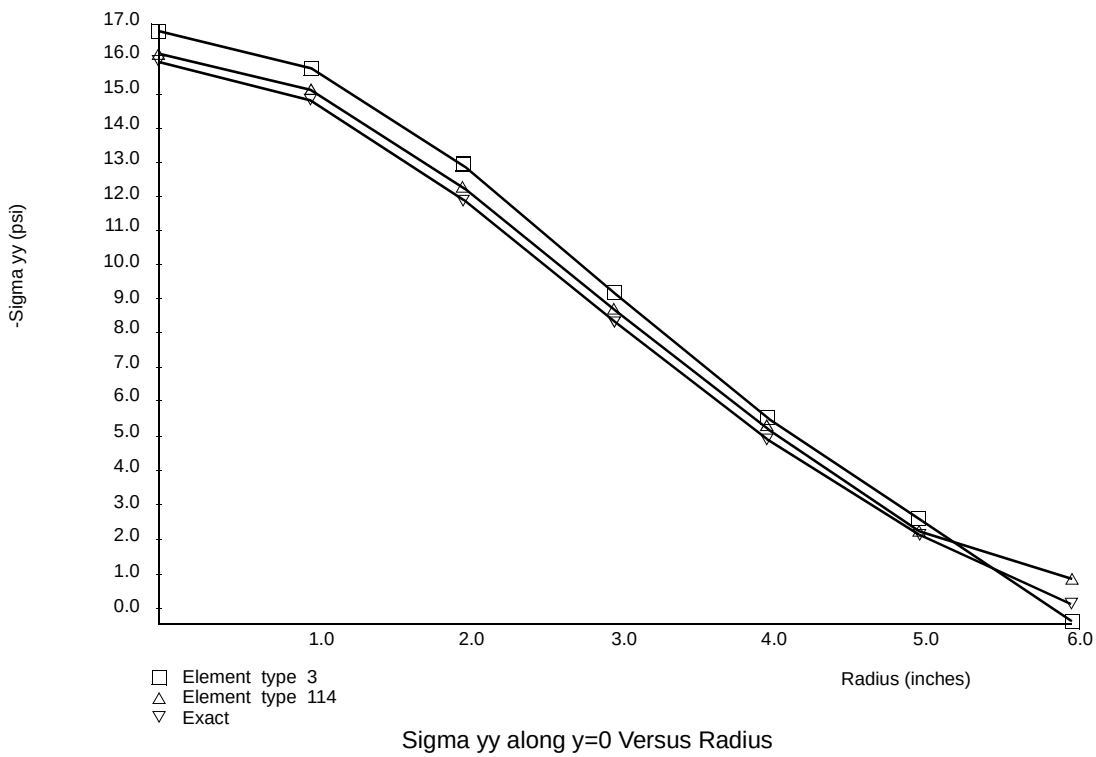

Figure 2.10-2 $Sigma_{22}$ Along y = 0 Versus Radius

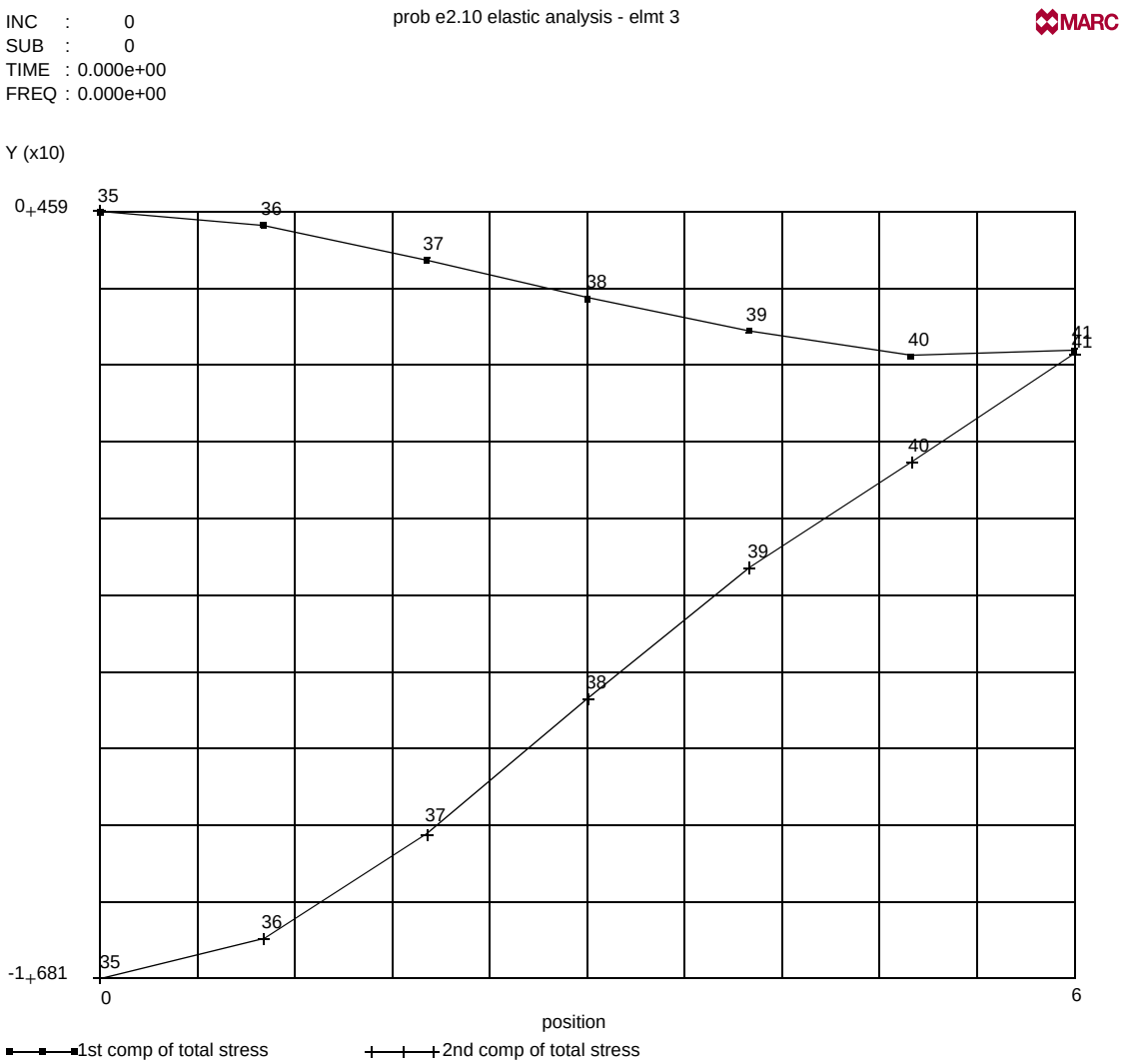

Figure 2.10-3 Stress Component Along Nodal Path

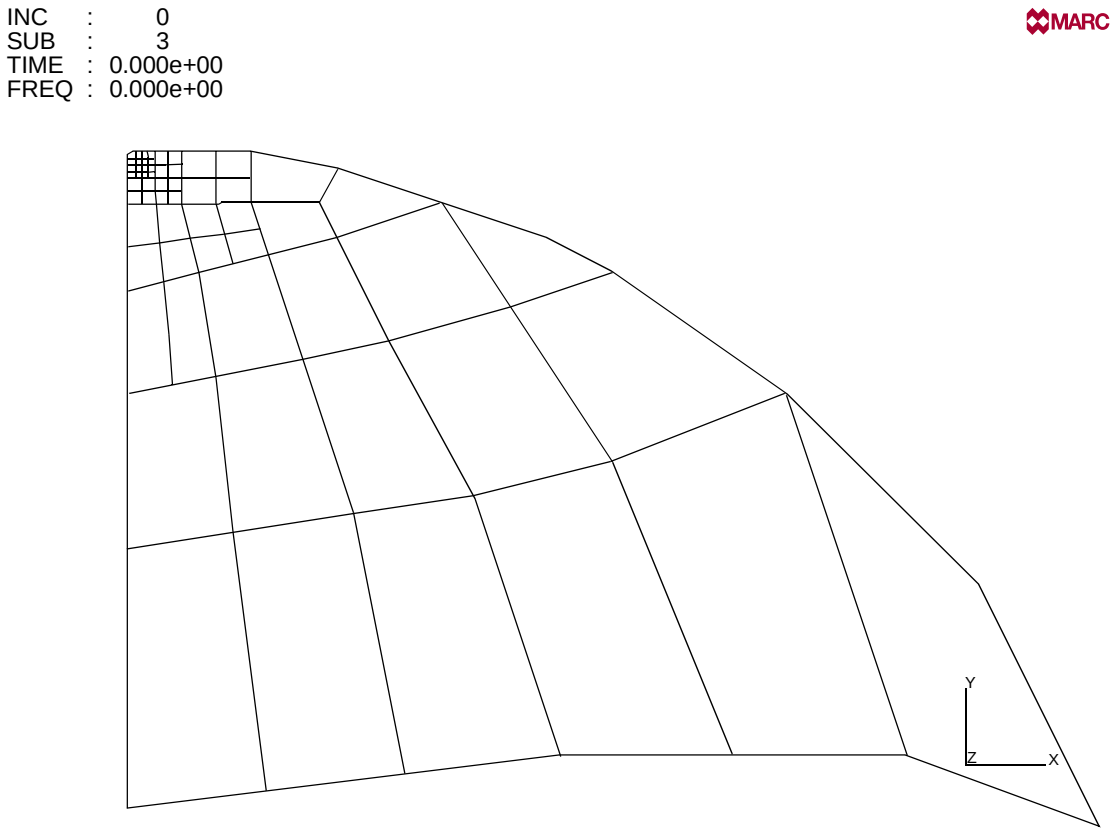

Figure 2.10-4 Close-up of Adapted Mesh

2.11 Simply-Supported Square Plate Modeled by Shell Elements

A simply-supported flat plate under uniform transverse pressure is elastically analyzed. The same problem is solved in later sections using the 8-node and 20-node bricks. This problem demonstrates the use of shell elements to solve a plate problem, and imposing the correct boundary conditions on these higher-order elements.

Element

It is often convenient to analyze plate and shell structures with a single element type; that is, by treatment of the plate problem as a degenerate shell problem. To illustrate this approach, library element type 8 is used. (Details regarding this element can be found in *MARC Volume B: Element Library.*) It is a fully conforming, triangular element that includes both bending and stretching deformation, and has nine degrees of freedom at each vertex.

The coordinates of the nodes are referred to a global Cartesian system. These coordinates can be supplied in several different ways depending on your choice. The FXORD option allows the coordinates to be generated for a choice of several simple shapes. A user subroutine, UFXORD, is also available to allow you to write your own special coordinate generation routine.

Model

One-quarter of the plate is modeled since there are two planes of symmetry in this problem. The geometry and mesh are shown in Figure 2.11-1. It contains 35 nodes and 50 triangular elements. The coordinate data which must be supplied depends on the option selection. In this case, use was made of the FXORD option and type 5 was selected. This allows specification of the x-y coordinates of each node point in the COORDINATE option, which are then converted to the required 11 coordinates through the FXORD option using the specified identity transformation between the global coordinates and the plate coordinates of that option. It should be noted that FXORD assumes that the middle plane of the plate is the x-y plane.

It should also be pointed out that the MESH2D option could be used to generate the original COORDINATE data in this case, followed by the same FXORD selection or a user-written UFXORD subroutine.

Geometry

The three-inch plate thickness is specified as EGEOM1.

Material Properties

All elements are assumed to be made of the same isotropic material. Values for Young’s modulus, Poisson’s ratio, and yield stress are 20 x 10^6 psi, 0.3, and 20,000 psi, respectively.

Loading

All 50 elements are loaded by a pressure of 1.0 psi. The resulting total load transverse to the plane of the plate is thus 900 lb.

Boundary Conditions

The specification of kinematic boundary conditions is somewhat more involved for an element with nine degrees of freedom per node. For transverse bending, such boundary conditions can be written only for the transverse displacement and its normal derivative, while the extensional boundary conditions can be prescribed only for the in-plane displacements. However, higher order derivatives must be made to conform to these constraints; for example, along the edges $x = 0$ and $y = 0$, the simple support condition requires that $w = 0$, which implies that $\frac{\partial w}{\partial Y} = 0$ along $x = 0$ and $\frac{\partial w}{\partial X} = 0$ along $y = 0$. Also, symmetry along the line $x = 30$ requires that $\frac{\partial w}{\partial X} = 0$, $u = 0$, and that v reach a stationary value, as a function of x. The implication are that $\frac{\partial u}{\partial Y} = 0$ and that $\frac{\partial v}{\partial X} = 0$, as well. Similar arguments indicate that $v = \frac{\partial v}{\partial X} = \frac{\partial u}{\partial Y} = \frac{\partial w}{\partial Y} = 0$ along $y = 30$.

Results

The output for this example includes the local-global transformation matrix for FXORD. The transformation matrix is an identity matrix (apart from some roundoff error). The coordinates, by columns, are:

$$X, Y, x, \frac{\partial x}{\partial X}, \frac{\partial x}{\partial Y}, y, \frac{\partial y}{\partial X}, \frac{\partial y}{\partial Y}, z, \frac{\partial z}{\partial X}, \frac{\partial z}{\partial Y}.$$

Element data that is printed out includes the six generalized stretching and bending strains:

$$\varepsilon_{xx}, \varepsilon_{yy}, \varepsilon_{xy}, \rho_{xx}, \rho_{yy}, \rho_{xy}$$

given at the element centroid, and the stresses:

$$\sigma_{xx}, \sigma_{yy}, \text{ and } \tau_{xy}$$

given at 11 equally-spaced points through the plate cross section at the centroid. Nodal data that is printed consists of incremental and total values of the nodal variables, referred to the local coordinate system.

Figure 2.11-2 compares the transverse displacements across a plane of the plate, as obtained by the three-dimensional example of a later example, and by this degenerate shell example. The significantly greater flexibility (and, therefore, accuracy) of the latter formulation is evident. As a thin-shell element was used, there is no transverse shear (τ_{xy}, τ_{yz}) effects. As the model involves a reasonably thick shell, this results in a larger midsurface deflection than observed using the brick elements. Element type 22 or 75 would have been more appropriate.

Parameters, Options, and Subroutines Summary

Example e2x11.dat:

Parameters	Model Definition Options
ELEMENTS	CONNECTIVITY
END	COORDINATES
SHELL SECT	DIST LOADS
SIZING	END OPTION
TITLE	FIXED DISP
	FXORD
	GEOMETRY
	ISOTROPIC

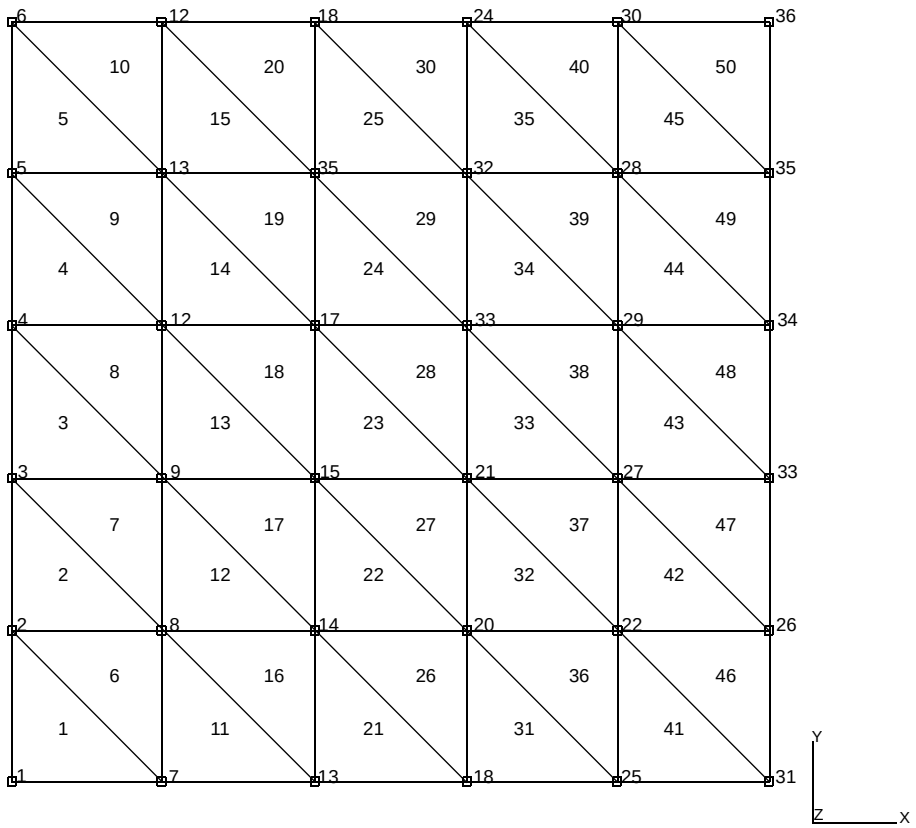

Figure 2.11-1 Geometry and Mesh for Square Plate Using Shell Elements

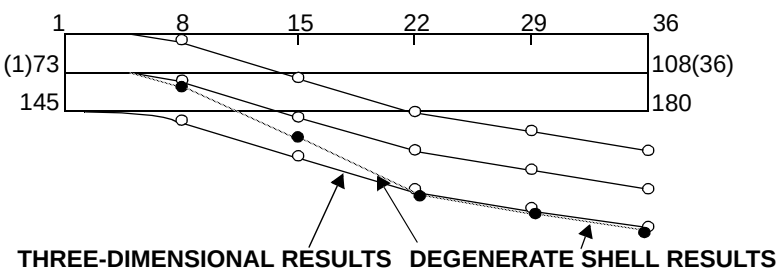

Figure 2.11-2 Comparison of Results for Shell and Three-Dimensional Models

2.12 Simply-Supported Thick Plate, using Three-Dimensional Elements

A simply-supported thick plate under uniform transverse pressure is elastically analyzed. This problem is the same as problems 2.11 and 2.13; hence, the solutions can be compared showing the discrepancies due to the choice of element types. This problem is also used to demonstrate the different choices of solution procedures.

This problem is modeled using the four techniques summarized below.

Data Set	Element Type(s)	Number of Elements	Number of Nodes	Differentiating Features
e2x12b	7	100	180	
e2x12c	7	100	180	Processor, EBE solver
e2x12d	117	100	180	
e2x12e	7	100	180	Processor, sparse solver

Elements

This example illustrates the use of element types 7 and 117, the three-dimensional isoparametric elements, details of which are given in *MARC Volume B: Element Library.* There are three degrees of freedom per node point for these elements:

u displacement (parallel to the x-axis)
v displacement (parallel to the y-axis)
w displacement (parallel to the z-axis)

Model

One-quarter of the plate (60 x 60 x 3 inches) is modeled since there are two planes of symmetry in this problem. The generated mesh is shown in Figure 2.12-1. The thickness of the plate was divided into four tiers of elements. Each tier was subdivided into a five-by-five element pattern, resulting in a mesh containing 180 nodes and 100 elements.

Geometry

A nonzero number is entered in the third Geometry field to indicate that the assumed strain formulation will be activated.

Material Properties

All elements are assumed to be uniform here. Values for Young's modulus, Poisson's ratio, and yield stress used are 20 x 10^6 psi, 0.3 and 20,000 psi, respectively.

Loading

The 25 elements with faces in the upper plane (z = 3 in.) are loaded by a pressure of 1.0 psi; the total load is 900 lb. in the negative z direction. Loading of this face of the elements is obtained by setting IBODY = 0 in the DIST LOAD input.

Boundary Conditions

Homogeneous boundary conditions are imposed on u for all nodes in the plane x = 30 and on v for all nodes in the plane y = 30 to account for the symmetry conditions. Simple support conditions are imposed on w for those points in the plane z = 1.5 inches that lie along the edges x = 0 and y = 0. A total of 71 degrees of freedom, out of the total of 540, are restrained.

Solvers

Problem e2x12b uses the default MARC profile solver. The SOLVER option is not included. Problem e2x12c uses the element-by-element iterative solver. A convergence criteria of $1x10^{-16}$ is specified. Problem e2x12e uses the sparse direct solver.

Results

The six components of strain and stress for each element are referred to the global coordinate system and are computed at the element's integration points. Element type 7 has 8 integration points. Element type 117 has 1 integration point. A comparison of the maximum transverse deflection at the center of the plate shows good agreement between elements type 7, 117 and, from problem 2.11, element type 8. These are summarized below:

Type 7	1.09293E-03 inch	node	180
Type 117	1.09193E-03 inch	node	180
Type 8	1.06190E-03 inch	node	36

In addition, contour plots of von Mises stresses are shown for element types 7 and 117 on the deformed shape in Figure 2.12-2 and Figure 2.12-3. Maximum von Mises stresses are:

Type 7	1.035E+02 psi	Element 100	point 8
Type 117	8.553E+01 psi	Element 100	point 1
Type 8	1.300E+01 psi	Element 1	point 1

In problem e2x12b, you can observe that the half bandwidth is 44 and the:

number of profile entries including fill-in is	6414
number of profile entries excluding fill-in is	1754
total Workspace needed with in-core matrix storage is	320745 words

As this is a small problem, the ebe iterative solver actually requires more memory requiring 356875 words. To achieve the convergence requested, 175 iterations were required. Normally, a larger tolerance, such as 0.001, would have been chosen. In e2x12e, when using the sparse direct solver, the Workspace requirement is only 30,3619 words. For this problem, the computational speed is 2 to 3 times faster.

Parameters, Options, and Subroutines Summary

The input for MESH3D is e2x12a.dat.

Example e2x12b.dat:

Parameters	Model Definition Options
ELEMENTS	CONNECTIVITY
END	CONTROL
SIZING	COORDINATES
TITLE	DIST LOADS
	END OPTION
	FIXED DISP
	ISOTROPIC
	POST

Example e2x12c.dat:

Parameters	Model Definition Options
ELEMENTS	CONNECTIVITY
END	CONTROL
PROCESS	COORDINATES
SIZING	DIST LOADS
TITLE	END OPTION
	FIXED DISP
	ISOTROPIC
	POST
	SOLVER

Example e2x12d.dat:

Parameters	Model Definition Options
ELEMENTS	CONNECTIVITY
END	CONTROL
SIZING	COORDINATES
TITLE	DIST LOADS
	END OPTION
	FIXED DISP
	ISOTROPI C
	POST

Example e2x12e.dat:

Parameters	Model Definition Options
ELEMENTS	CONNECTIVITY
END	CONTROL
SIZING	COORDINATES
TITLE	DIST LOADS
	END OPTION
	FIXED DISP
	ISOTROPIC
	POST
	SOLVER

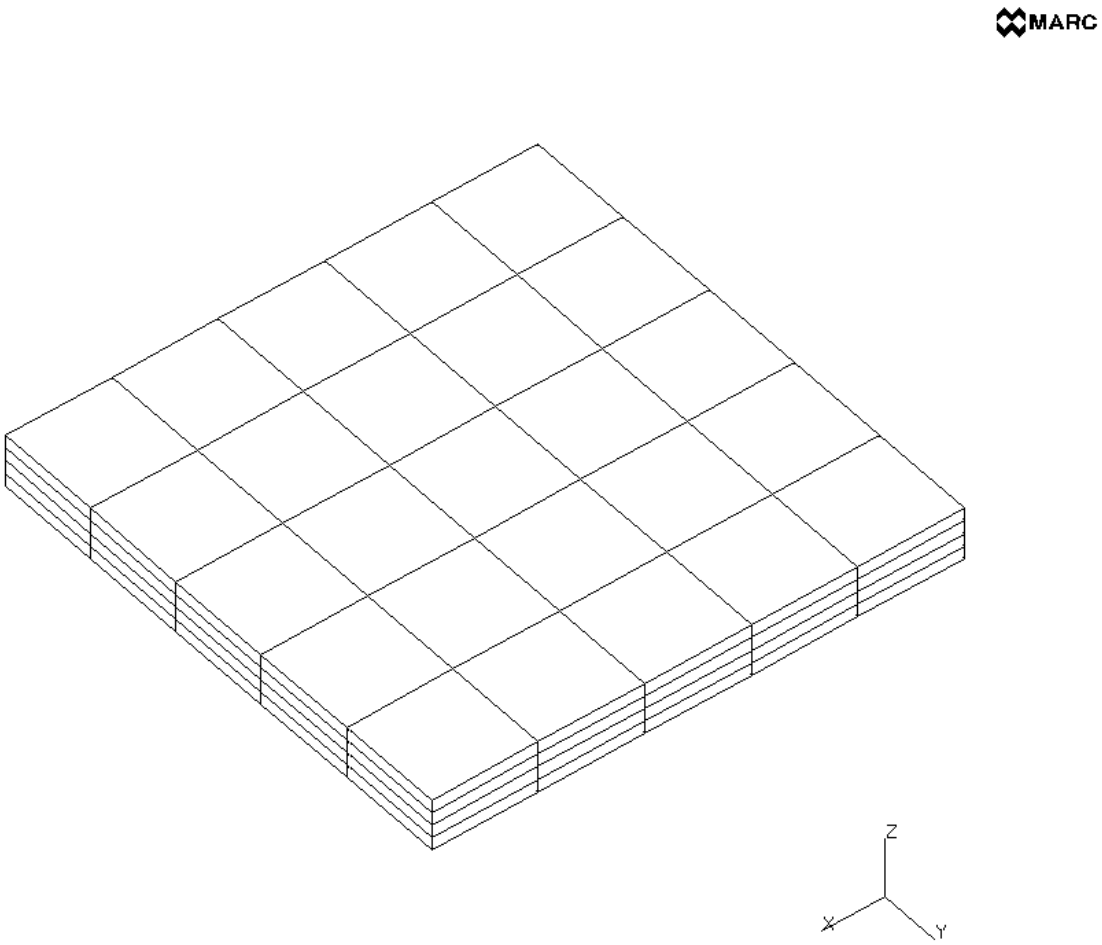

Figure 2.12-1 Model

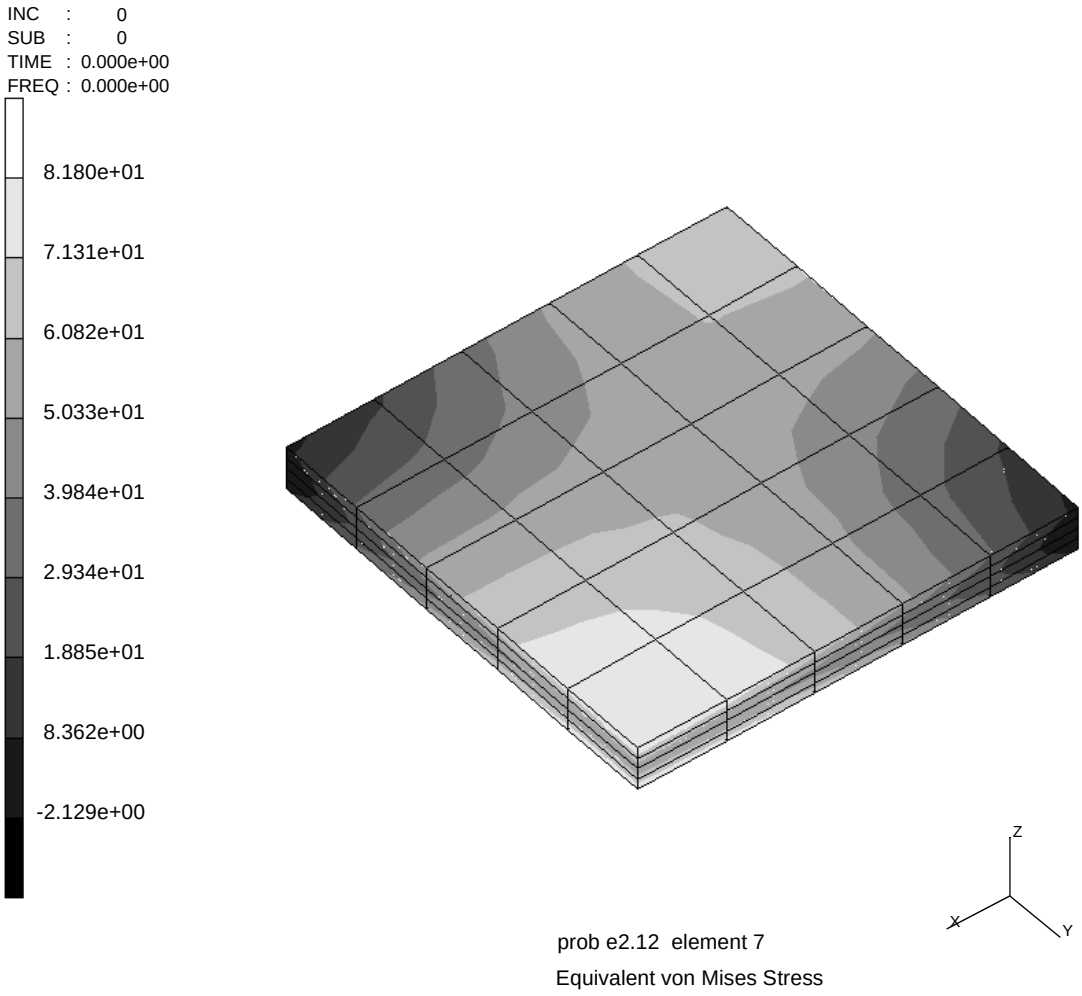

Figure 2.12-2 Plot of von Mises Stress Element 7

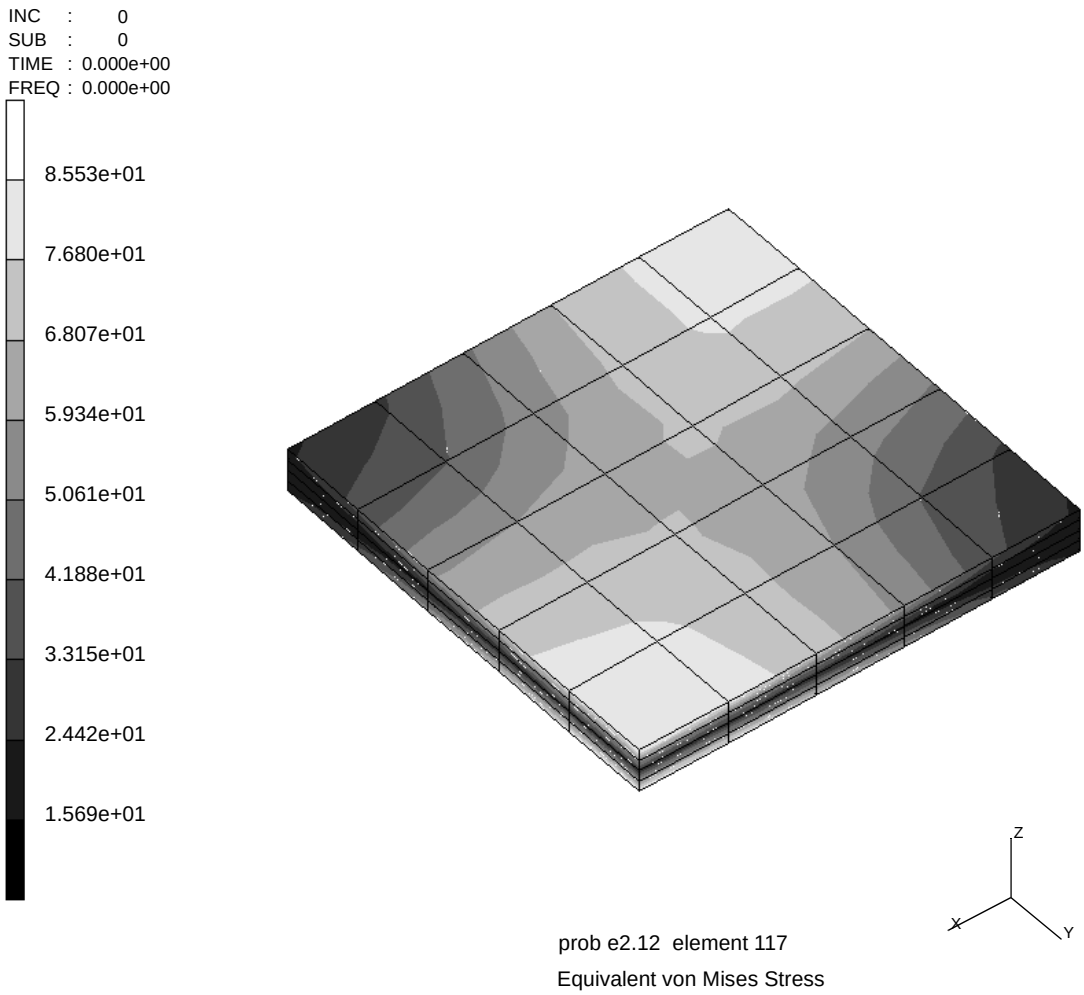

Figure 2.12-3 Plot of von Mises Stress Element 117

2.13 Simply-Supported Thick Plate, using Higher-order Three-Dimensional Elements

A thick plate, simply supported around its perimeter, is analyzed with a pressure load normal to the plate surface. This problem is the same as problems 2.11 and 2.12; hence, the solutions can be compared. This problem demonstrates the higher-order three-dimensional element.

Element

Element type 21 is a 20-node isoparametric brick. There are three displacement degrees of freedom at each node; eight are corner nodes, 12 midside. Each edge of the brick can be parabolic; a curve is fitted through the midside node. Numerical integration is accomplished with 27 points using Gaussian quadrature. See *MARC Volume B: Element Library* for further details.

Model

Because of symmetry, only one-quarter of the plate is modeled. One element is used through the thickness, two in each direction in the plane of the plate. There are 51 nodes for a total of 153 degrees of freedom. See Figure 2.13-1.

Geometry

No geometry specification is used.

Loading

A uniform pressure of 1.00 psi is applied in the DIST LOADS block. Load type 4 is specified for uniform pressure on the 6-5-8-7 face of all four elements.

Boundary Conditions

On the symmetry planes, x = 30 and y = 30, in-plane movement is constrained. On the x = 30 plane, u = 0, and on the y = 30 plane, v = 0. On the plate edges, x = 0 and y = 0; the plate is simply supported, w = 0.

Results

The solution of an elastic analysis is compared in Figure 2.13-2 with the solution of problem 2.12. A contour plot of the equivalent stress is shown in Figure 2.13-3. The exact solution is from Roark's *Formulas For Stress and Strain*.

Parameters, Options, and Subroutines Summary

Example e2x13.dat:

Parameters	Model Definition Options
ELEMENTS	CONNECTIVITY
END	COORDINATES
SIZING	DIST LOADS
TITLE	END OPTION
	FIXED DISP
	ISOTROPIC

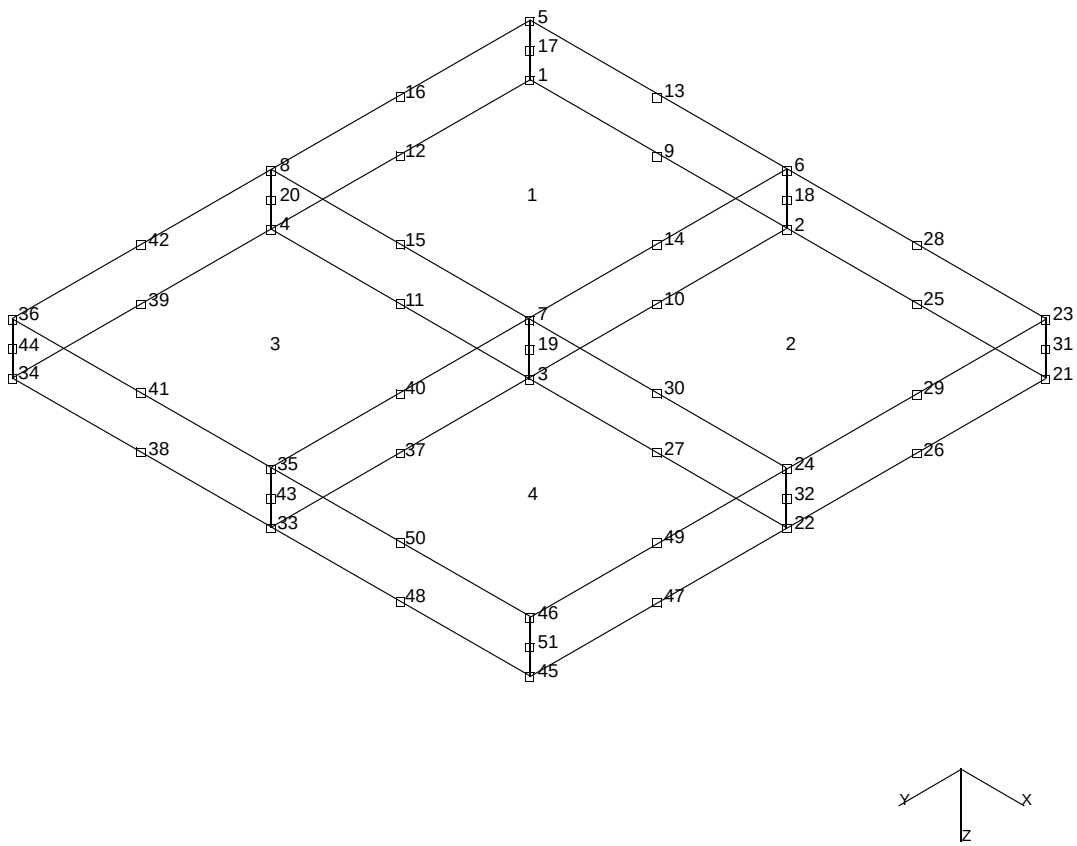

Figure 2.13-1 Thick Plate Mesh

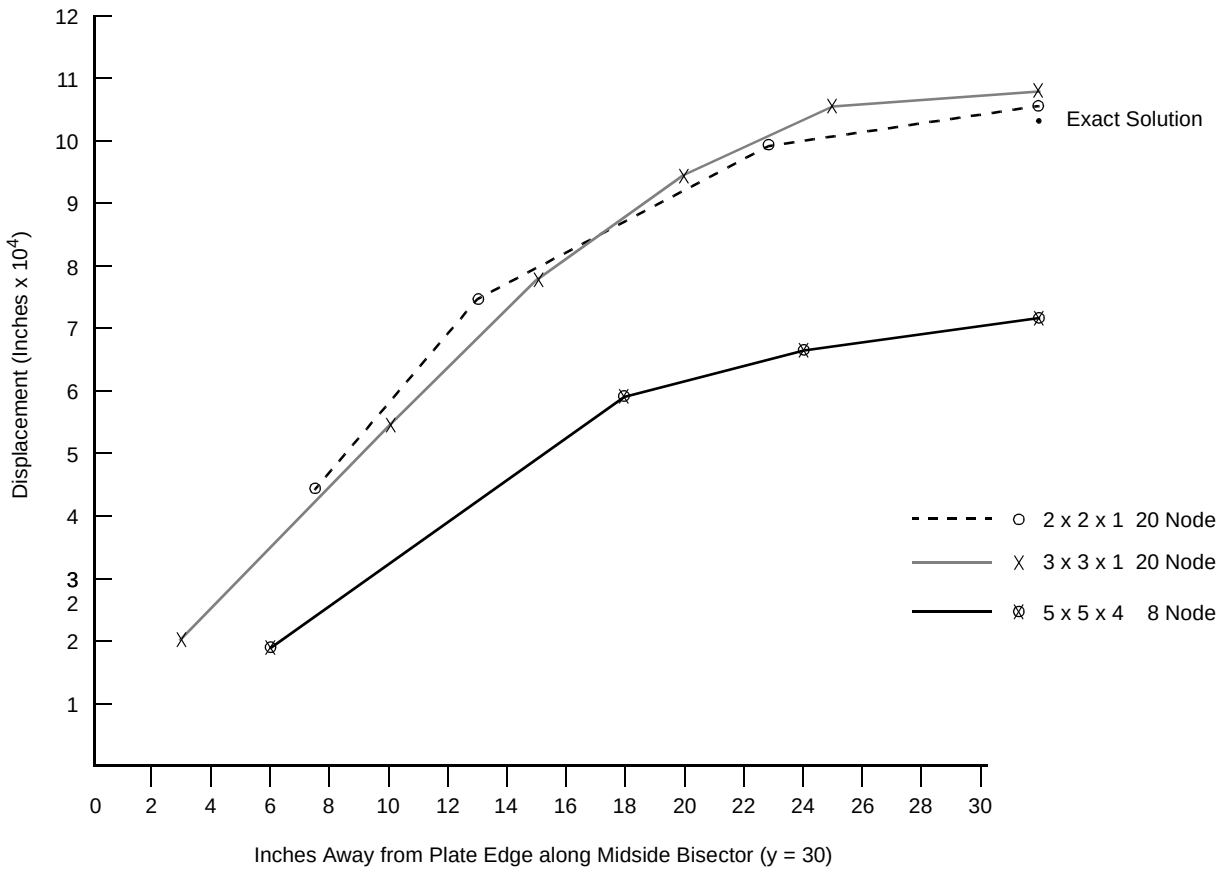

Figure 2.13-2 Pressure Loaded Simply-Supported Flat Plate Displacement Comparison

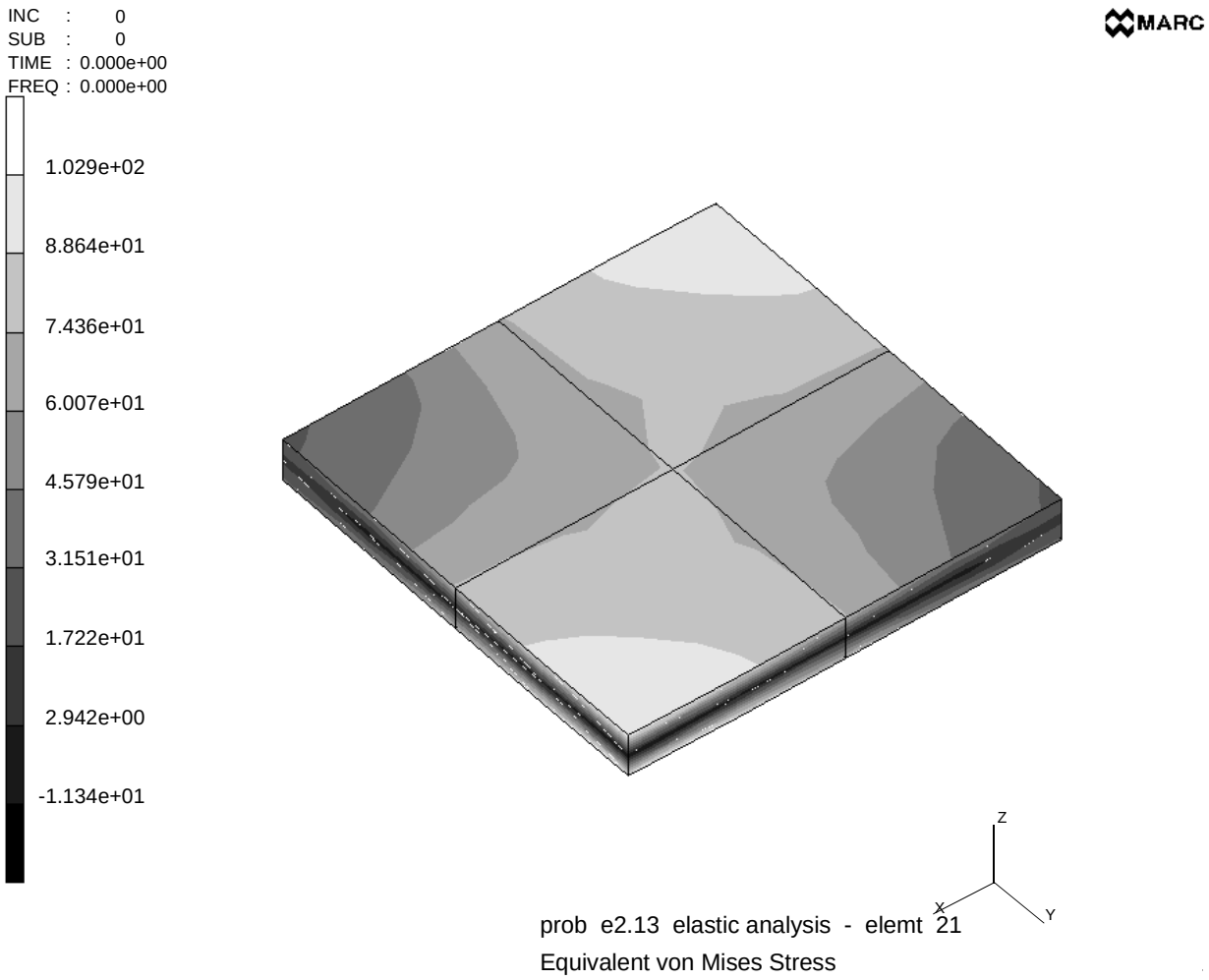

Figure 2.13-3 J2 Stress Contour

2.14 Reinforced Concrete Beam Analysis

A reinforced concrete cantilever beam is elastically analyzed. A point load at the free end of the beam is applied. This problem demonstrates the use of the rebar elements in three-dimensional analysis.

This problem is modeled using the two techniques summarized below.

Data Set	Fill Element	Rebar Element	Element Type(s)	Number of Elements	Number of Nodes	Differentiating Features
e2x14	21	23	26	20	79	rebar subroutine
e2x14b	7	146	320	405	79	REBAR option

Elements

Either element types 21 and 23 (20-node bricks) or 7 and 146 (8-node bricks) are used in the analysis. Element 21 and 7 represent the concrete. Element 23 and 146, which are specifically designed to simulate reinforcing layers in three-dimensional problems, represent the steel reinforcements in the concrete.

Model

The beam is idealized either by using 4 20-node concrete brick elements and 4 20-node rebar elements as shown in Figure 2.14-1 or by using 256 8-node concrete brick elements and 65 8-node rebar elements. One layer of steel rebars is embedded in the concrete.

Geometry

The third field defines the orientation of rebar layers with respect to the element faces (see *MARC Volume B: Element Library*). If user subroutine REBAR is used for input of rebar properties, the number of rebar layers is entered in the second field. In this example, only one layer of rebars exists.

Material Properties

The concrete has a Young's modulus of 3.0×10^6 psi and a Poisson's ratio of 0.2. The steel reinforcing bars have a Young's modulus of 2.9×10^7 psi, a cross-sectional area of 2.65 square inch, and an equivalent thickness of 0.0883 inch.

Loading

A total load of 6000 pounds is applied at the free end of the beam. This load is represented by 2000 pound loads at three of the top free-end nodes.

Boundary Conditions

The nodes at the wall are fixed in the three global degrees of freedom to simulate a built-in or clamped condition.

Rebar Data

By virtue of the simplicity of the problem, either the user subroutine REBAR or the REBAR option can be used to specify the orientation and the equivalent thickness of the reinforcing layers. The repetition is admissible by virtue of the problem simplicity. In this example, the rebars are parallel to the y-axis.

Results

A comparison of concrete and steel stress with beam theory (uncracked section) is shown in Figure 2.14-2. The concrete stress is compared at the upper and lower integration point layers. (All comparisons are at the inner layers of integration points across the width.)

Parameters, Options, and Subroutines Summary

Example e2x14.dat:

Parameters	Model Definition Options
ELEMENTS	CONNECTIVITY
END	COORDINATES
PRINT	END OPTION
SIZING	FIXED DISP
TITLE	GEOMETRY
	ISOTROPIC
	POINT LOAD

Example e2x14b.dat:

Parameters	Model Definition Options
ELEMENTS	CONNECTIVITY
END	COORDINATES
SIZING	END OPTION
TITLE	FIXED DISP
	GEOMETRY
	ISOTROPIC
	POINT LOAD
	REBAR

User subroutine in u2x14.f:

REBAR

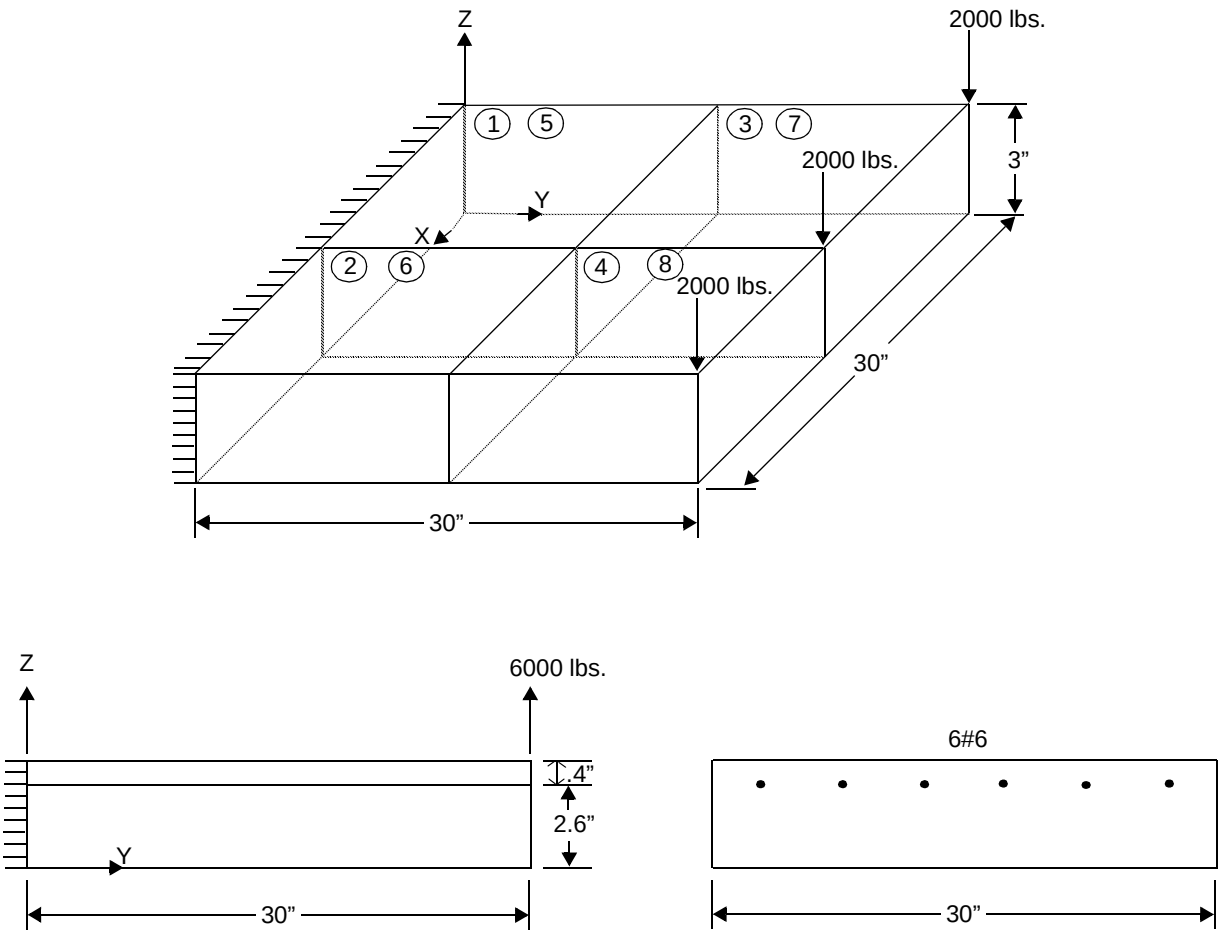

Figure 2.14-1 Reinforced Concrete Beam

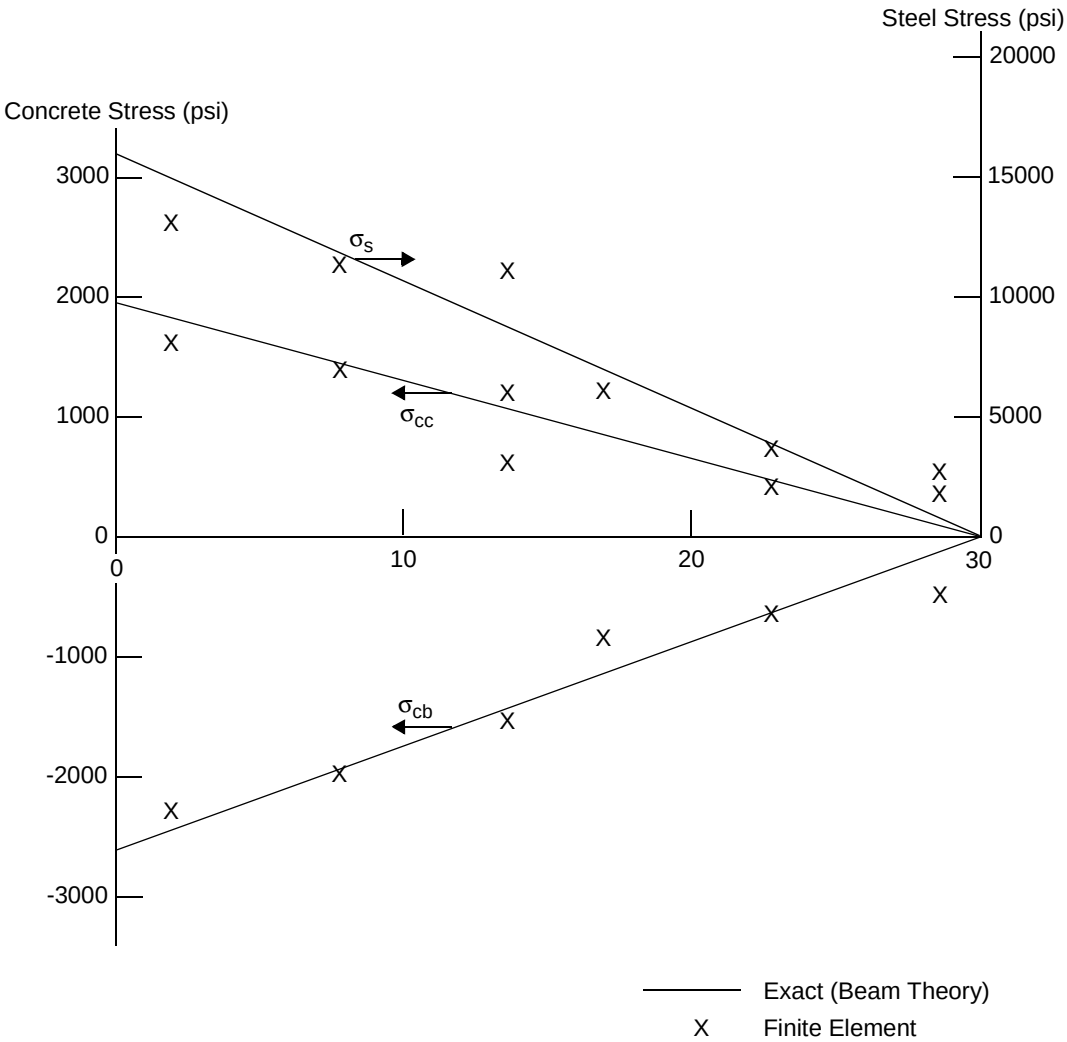

Figure 2.14-2 Concrete and Steel Stress With Beam Theory

2.15 Cylinder-sphere Intersection

A cylinder-sphere intersection under the action of uniform internal pressure is analyzed. The material is linear-elastic throughout the analysis. This problem demonstrates the program's ability to model a typical shell intersection. The FXORD and TYING capabilities are utilized in this analysis.

Element

The cylinder and sphere in this problem are both thin shells and can be modeled using element type 8. Element 8 is a doubly-curved, triangular-shell element. The details on this element are given in *MARC Volume B: Element Library.*

Model

The geometry and mesh are shown in Figure 2.15-1. The symmetry of this problem requires that only one-quarter of the shell (the x-z plane and the y-z plane are both planes of symmetry) need be modeled.

For motions other than axial shift, both shells use the same global coordinate system. The local Gaussian coordinate systems are shown on the shell surfaces for reference. The FXORD option is utilized. There are two different types of surfaces which must be developed. The TYING options in MARC are used to join the two surfaces.

The structure is modeled with four cylindrical elements (FXORD: type 4) and four spherical elements (FXORD: type 2). The SHELL SECT parameter is used to set the number of integration points through the thickness to 3. Reducing the number of integration points through the thickness does not diminish the solution accuracy for linear-elastic problems, yet it enhances the program efficiency.

Geometry

The shell thickness is taken to be 1.0 inch and is specified as EGEOM1 of this option.

Material Properties

All elements have the same elastic properties. Values for Young's modulus and yield stress are 1000 psi and 100 psi, respectively.

Loading

The uniform external pressure is applied to both shells by specifying a positive pressure of 1.0 psi of type 2 (IBODY = 2) to the θ^1, θ^2 surface. This implies a pressure in the negative outward normal direction.

Boundary Conditions

Symmetry conditions are imposed at nodes 1, 4, 7 and 10 in the x-z plane, and nodes 3, 6, 9 and 12 in the y-z plane. Support conditions are imposed on nodes 10, 11 and 12.

Tying

At the intersection of the two shells, nodes 4, 5 and 6 are joined to nodes 7, 8 and 9 through the use of the TYING option, type 18. The tying is such that each tied node is also a retained node; for example, certain degrees of freedom of the tied node are linear functions of other degrees of freedom of the tied node. In addition, they depend on degrees of freedom of the retained node. Due to the manner in which the tying is effected, the tied node that is also retained must be placed last in the tying data field.

Results

Following the tying option output (the tied nodes are also retained nodes), the sum of the consistently lumped nodal forces in each coordinate direction is printed. A check of the values shows symmetry with respect to x and y loads (first and fourth columns). The load in the z-direction is somewhat less as a result of the opening in the spherical shell. Scaling was not requested for this example, although the scale factor to cause first yielding is printed (in this case, first yielding would have occurred in element 8).

Generalized bending and stretching strains at the shell middle surface are printed (for each element) referred to the θ^1, θ^2 system. Following the strains, the physical stress components at three points through the thickness are output. In this case, θ^1 and θ^2 are orthogonal; thus, these stresses are the direct and shear stresses in the meridional and hoop directions, respectively. In a more general case involving skewed coordinates (θ^1,θ^2), the physical stress components should be interpreted with care. The equivalent stress (printed in the first column) then becomes a more convenient measure of the stress state.

The element output is followed by the incremental and total nodal point displacements, referred to the global coordinate system.

The POST option is used to write the stresses onto the auxiliary post file. This information can be processed by either the plot program or the Mentat graphics program.

Parameters, Options, and Subroutines Summary

Example e2x15.dat:

Parameters	Model Definition Options
ELEMENTS	CONNECTIVITY
END	COORDINATES
SHELL SECT	DIST LOADS
SIZING	END OPTION
TITLE	FXORD
	GEOMETRY
	ISOTROPIC
	POST
	TYING

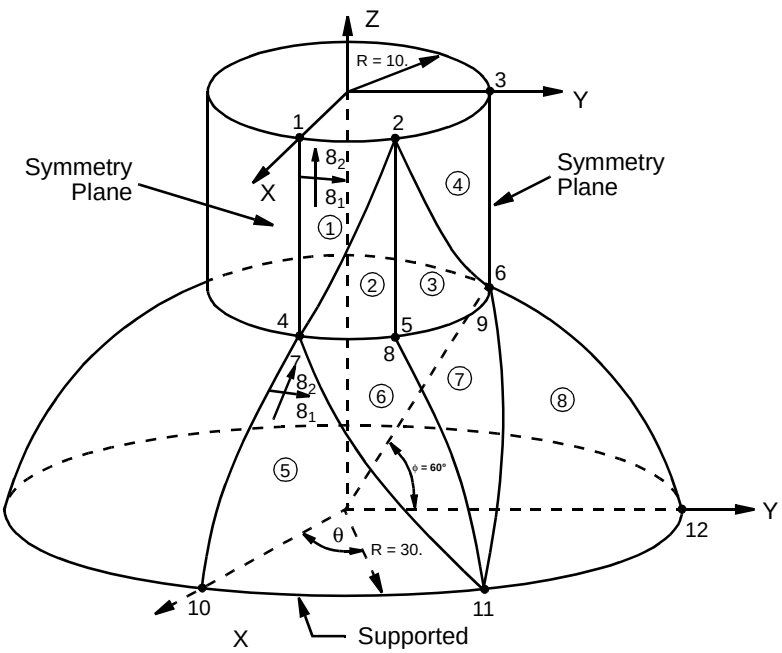

Figure 2.15-1 Mesh and Geometry for Cylinder-Sphere Intersection Problem

2.16 Shell Roof using Element 8

This problem is one of several in which a barrel-vault shell roof is loaded under its own weight. The results of these analyses are compared in problem 2.19. This example demonstrates the use of user subroutine UFXORD to generate the coordinates for element type 8.

Element

Library element type 8, an isoparametric curved triangular shell, is used. The element is based on Koiter-Sanders shell theory. The displacement interpolation functions are defined such that displacements and their first derivatives are compatible between elements. The nine degrees of freedom are three displacements in the global axes directions and six first derivatives of these displacements with respect to the surface coordinates. See *MARC Volume B: Element Library.*

Model

Forty elements are used to model one-quarter of the shell taking advantage of symmetry. The ends of the structure are supported by diaphragms and there are two free edges. The model has 30 nodes and 270 degrees of freedom (see Figure 2.16-1).

Mesh Generation

The coordinates are first entered in the x-y plane. These two coordinates are used by subroutine UFXORD to generate the full set.

Geometry

Linear thickness variation is allowed; the three nodal values are input in the first three data fields of the third block of the GEOMETRY option. Here the default of constant thickness is used with EGEOM2 = EGEOM3 = 0 and EGEOM1, the first data field, is set to the thickness of 3.

Material Properties

Young’s modulus is 3.0 x 10^6 psi; Poisson’s ratio is taken as 0.

Loading

All 40 elements are loaded with self weight of 90 lb/square foot or .625 lb/square inch in the negative z-direction. This is the load type (IBODY = 1) specified in the DIST LOADS option.

Boundary Conditions

Three sets of boundary conditions are required. Displacement in the plane normal to the shell is continuously zero at the supported end $\left(u = w = \frac{\partial u}{\partial \theta^1} = \frac{\partial w}{\partial \theta^1} = 0\right)$. On the y = 300 symmetry boundary, axial displacement is fixed and is continuously zero $\left(v = \frac{\partial v}{\partial \theta^1} = 0\right)$. From symmetry considerations, $\frac{\partial u}{\partial \theta^2}$ and $\frac{\partial w}{\partial \theta^2}$ must be fixed, or inadmissible warping is allowed. On the x = 0 symmetry boundary, movement tangential to the shell surface is continuously zero $\left(u = \frac{\partial u}{\partial \theta^2} = 0\right)$. From symmetry considerations, to fix the model against inadmissible rotations, $\frac{\partial w}{\partial \theta^1}$ and $\frac{\partial v}{\partial \theta^1}$ must be zero (see Figure 2.16-2).

User Subroutine

Subroutine UFXORD is used to generate the requisite 11 coordinates. The first coordinate read from the COORDINATE block is an angle that is used to generate θ^1, x, $\frac{\partial x}{\partial \theta^1}$, z, and $\frac{\partial z}{\partial \theta^1}$, the second coordinate is, in this case, y and θ^2. Remember to set NCRD = 2 in the first data field of the second line of the COORDINATE block.

Results

A comparison of the results of this problem and problems 2.17, 2.18, and 2.19 is found at the end of problem 2.19.

Parameters, Options, and Subroutines Summary

Example e2x16.dat:

Parameters	Model Definition Options
ELEMENTS	CONNECTIVITY
END	COORDINATES
SIZING	DIST LOADS
TITLE	END OPTION
	FIXED DISP
	GEOMETRY
	ISOTROPIC
	OPTIMIZE
	UFXORD

User subroutine in u2x16.f:

UFXORD

INC : 0
SUB : 0
TIME : 0.000e+00
FREQ : 0.000e+00

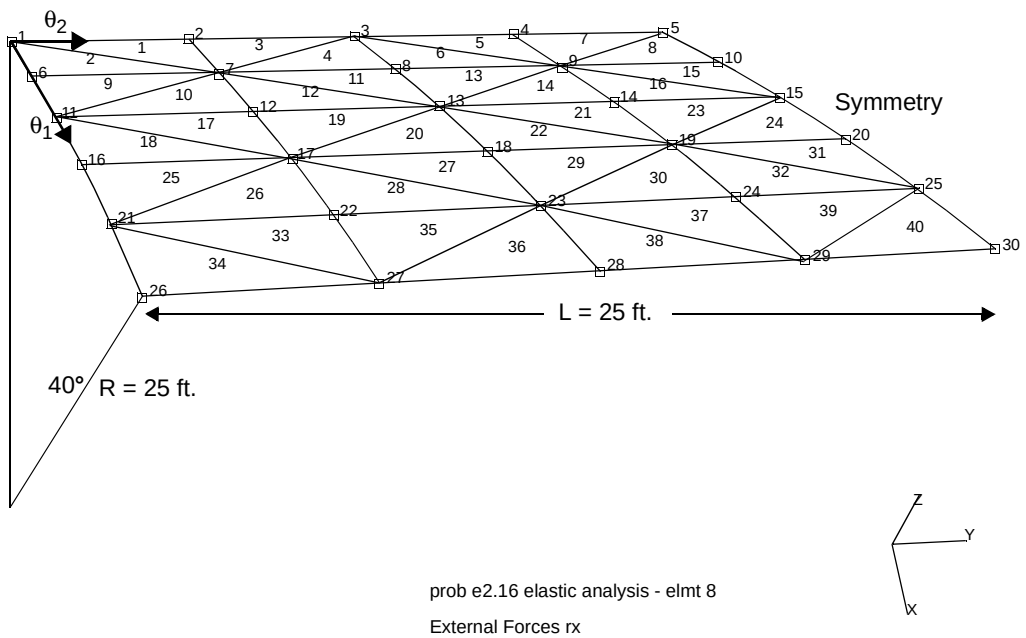

Figure 2.16-1 Cylinder Shell Roof Configuration, Element 8

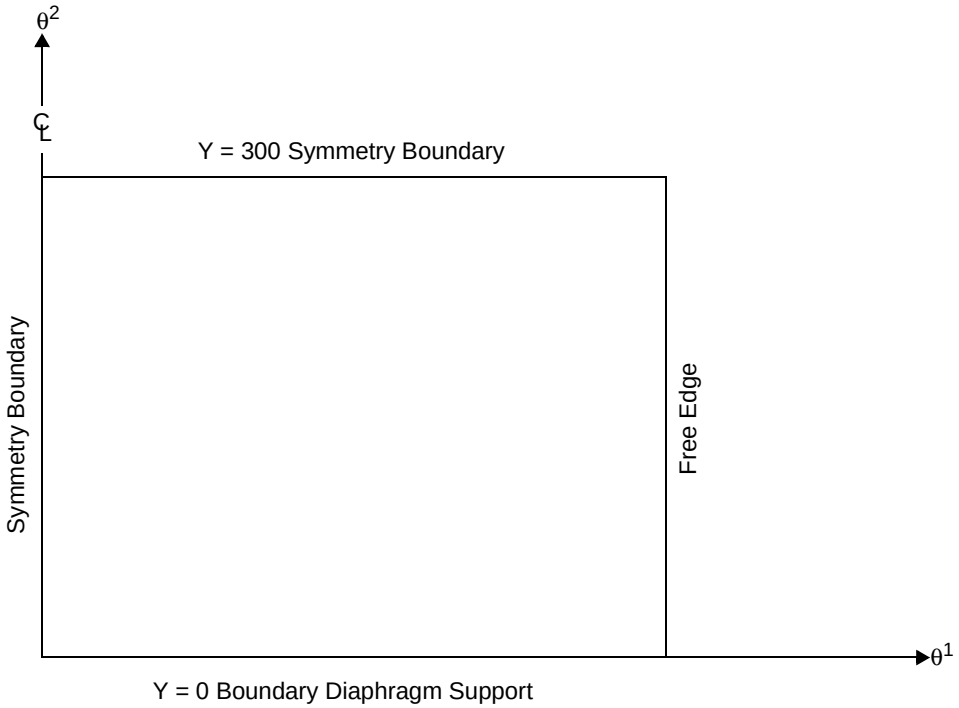

Figure 2.16-2 Shell Surface Coordinate System

2.17 Shell Roof using Element 4

This problem is one of several in which a barrel-vault shell roof is loaded under its own weight. The results of these analyses are compared in problem 2.19. This example demonstrates the use of user subroutine UFXORD to generate the coordinates for element type 4.

Element

Library element type 4 is used. It is an isoparametric, doubly-curved thin shell that is based on Koiter-Sanders shell theory. Bicubic interpolation functions are used and the numerical integration is 9-point Gaussian quadrature. Rigid body modes are represented exactly. The mesh must be rectangular in the θ^1,θ^2 plane, but any mapping can be used onto the surface.

Model

The four-element model is of a one-quarter section of the structure taking advantage of symmetry. Support conditions are as in the other shell roof examples; diaphragm supports on axial ends. There are nine nodes for a total of 108 degrees of freedom. See Figure 2.17-1.

Geometry

The thickness of the shell is 3 inches, which is specified in the first data field of the third block of the GEOMETRY option, EGEOM1 = 3.

Material Properties

Young's modulus is 3.0 x 10^6 psi; Poisson's ratio is taken as 0.

Loading

The four elements are loaded with self-weight, positive in the negative z direction. The magnitude is 90 lb./sq.ft. or .625 lb./square inch, and is specified as a distributed load (IBODY = 1) in the DIST LOAD option.

Boundary Conditions

Three sets of boundary conditions are necessary. (See Figure 2.16-2 and Figure 2.17-1). On the diaphragm supported end, movement in the plane normal to the shell is continuously zero $\left(u = w = \frac{\partial u}{\partial \theta^1} = \frac{\partial w}{\partial \theta^1} = 0\right)$. None of the cross-derivative terms, which represent rates of change of shear and direct strains, are zero. Care must be taken in specifying these terms. On the y = 300 symmetry boundary, axial displacement is continuously zero $\left(v = \frac{\partial v}{\partial \theta^1} = 0\right)$.

Rotation and shear are fixed $\left(\frac{\partial u}{\partial \theta^2} = \frac{\partial w}{\partial \theta^2} = 0\right)$. Also, two of the cross-derivatives are fixed by symmetry considerations $\left(\frac{\partial^2 u}{\partial \theta^1 \partial \theta^2} = \frac{\partial^2 w}{\partial \theta^1 \partial \theta^2} = 0\right)$. A nonzero rate of change of normal strain, $\frac{\partial^2 v}{\partial \theta^1 \partial \theta^2}$, is allowable. On the x = 0 symmetry boundary, movement tangential to the shell surface is continuously zero $\left(u = \frac{\partial u}{\partial \theta^2} = 0\right)$. Rotation and shear are fixed $\left(\frac{\partial v}{\partial \theta^1} = \frac{\partial w}{\partial \theta^1} = 0\right)$. Two of the three cross-derivatives, $\frac{\partial^2 v}{\partial \theta^1 \partial \theta^2}$ and $\frac{\partial^2 w}{\partial \theta^1 \partial \theta^2}$ are zero. Unfixed, these could allow warping across the symmetry boundary.

User Subroutines

Subroutine UFXORD is used to generate a full set of coordinates from two inputs from the COORDINATE block. The first coordinate is equal to both θ^2 and y; the second is used to generate x and y.

Results

The results of the model are compared with other results using shell elements type 8, 22, 24. The comparison is found following problem 2.19.

Parameters, Options, and Subroutines Summary

Example e2x17.dat:

Parameters	Model Definition Options
ELEMENTS	CONNECTIVITY
END	COORDINATES
SIZING	DIST LOADS
TITLE	END OPTION
	FIXED DISP
	GEOMETRY
	ISOTROPIC
	UFXORD

User subroutine in u2x17.f:

UFXORD

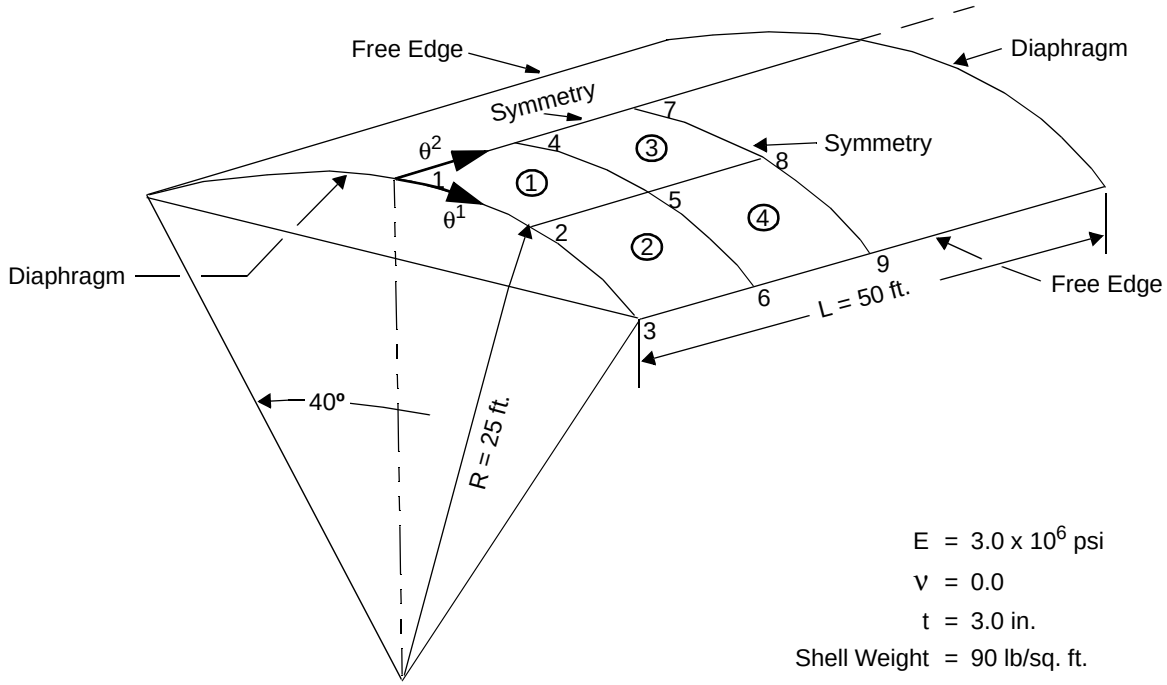

Figure 2.17-1 Cylinder Shell Configuration, Element 4

2.18 Shell Roof using Element 22

This problem is one of several in which a barrel-vault shell roof is loaded under its own weight. The results of these analyses are compared in problem 2.19. This example demonstrates the use of user subroutine UFXORD to generate the coordinates for element type 22.

Element

Element type 22, a curved quadrilateral thick-shell element, is used. The displacements are interpolated from the values of the eight nodes on the middle shell surface. The four corner nodes and four midside nodes each have six degrees of freedom, three displacements, and three rotations.

Model

The four element model takes advantage of symmetry conditions for a one-quarter section of the shell. The ends of the structure are supported by diaphragms with two free edges. The model has a support end, two symmetry boundaries, and one free edge. There are 21 nodes for a total of 126 degrees of freedom. See Figure 2.18-1.

Geometry

The thickness is 3.0 inches.

Material Properties

Young's modulus is 3.0×10^6 psi; Poisson's ratio is taken as 0.

Loading

All four elements are loaded under self-weight, positive in the negative z-direction. This corresponds to IBODY = 1 in the DIST LOADS option.

Boundary Conditions

Three sets of boundary conditions are necessary; one on each of the symmetry edges and one on the supported edge. At the supported end, we have u = w = 0. On the y = 300 symmetry boundary, axial displacement is fixed ($v = \theta_x = 0$). On the x = 0 symmetry boundary, movement tangential to the shell surface is fixed ($u = \theta_y = 0$). The constraint on rotation normal to the shell is imposed only at node 15. See Figure 2.16-2 and Figure 2.18-1.

User Subroutines

Subroutine UFXORD is used to generate the three coordinates. The first coordinate read from the COORDINATE block is used to generate two of the three global coordinates. Notice that NCRD = 2 on the second block of the COORDINATE block, rather than the default of 3 for this element.

Results

The results from problems 2.16, 2.17, 2.18, and 2.19 are compared in problem 2.19.

Parameters, Options, and Subroutines Summary

Example e2x18.dat:

Parameters	Model Definition Options
ELEMENTS	CONNECTIVITY
END	COORDINATES
SIZING	DIST LOADS
TITLE	END OPTION
	FIXED DISP
	GEOMETRY
	ISOTROPIC
	UFXORD

User subroutine in u2x18.f:

UFXORD

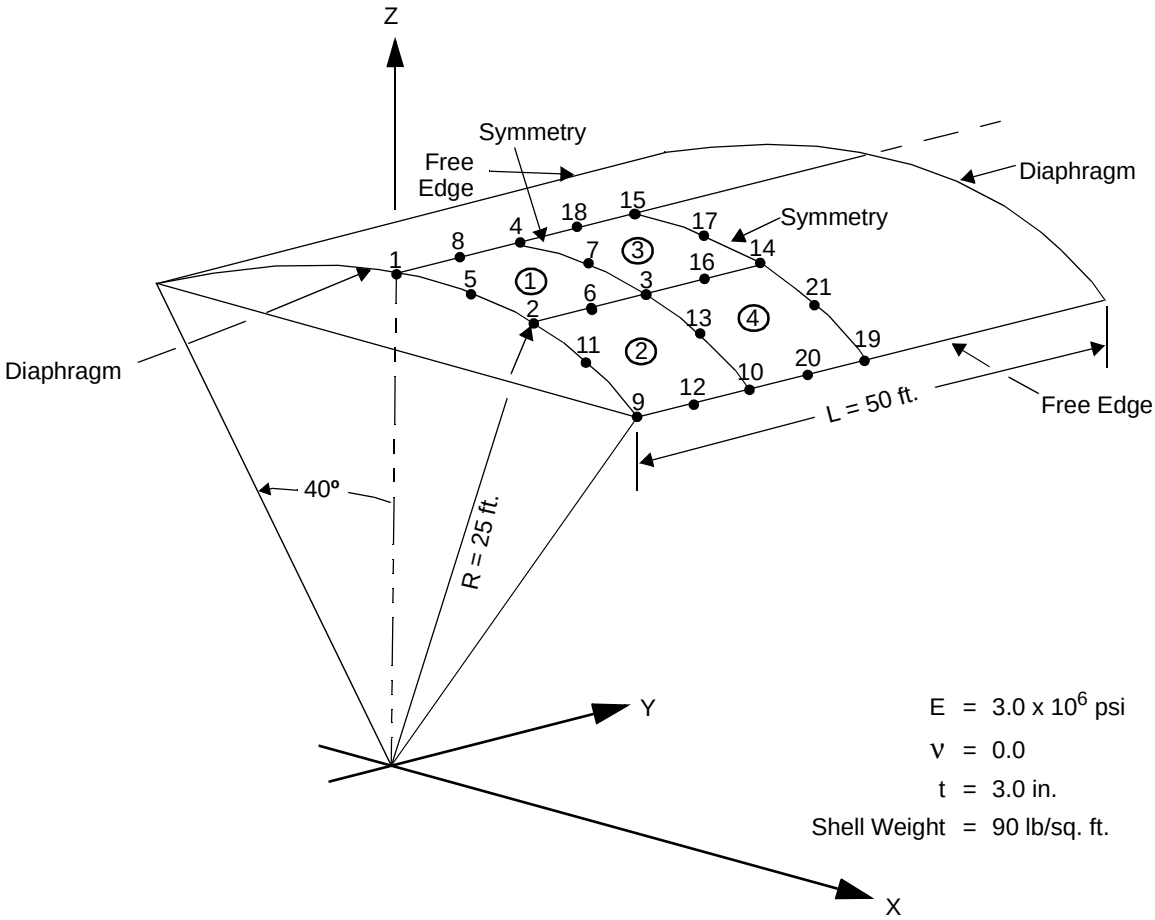

Figure 2.18-1 Cylindrical Shell Roof Configuration, Element 22

2.19 Shell Roof using Element 24

This problem is one of several in which a barrel-vault shell roof is loaded under its own weight. The results of these analyses are compared in this example. This example demonstrates the use of user subroutine UXFORD to generate the coordinates for element type 24.

Elements

Element type 24, a doubly-curved isoparametric quadrilateral shell element, is used. It is based on Koiter-Sanders shell theory and uses a De Veubeke interpolation function. It represents rigid body modes exactly and is suited to large displacement analysis. In the mapped plane, the quadrilateral shape can be arbitrary. The four corner nodes of each element have nine degrees of freedom; three are displacements in the global axes' directions, and the remaining six are first derivatives of these displacements with respect to the surface coordinates. The four midside nodes of each element have three degrees of freedom each. These are derivatives of the three displacements at the node with respect to the vector normal to the element edge in the (θ^1, θ^2) plane.

Model

Four elements are used to model one-quarter of the shell, taking advantage of symmetry. The ends of the structure are supported by diaphragm walls and there are two free edges. The model has 21 nodes and 117 degrees of freedom (see Figure 2.19-1).

Geometry

The shell thickness is specified in the first data field of the third block of the GEOMETRY option (EGEOM1 = 3).

Material Properties

A Young's modulus of 3.0 x 10^6 psi is specified.

Loading

All four elements are loaded under self-weight, positive in the negative z-direction. This is load type 1 (IBODY = 1), specified in the DIST LOAD option.

Boundary Conditions

Three sets of boundary conditions are necessary, for element vertex nodes (Figure 2.19-2). Displacement in the plane normal to the shell is continuously zero at y = 0

$\left(u = w = \frac{\partial u}{\partial \theta^1} = \frac{\partial w}{\partial \theta^1} = 0\right)$. On the y = 300 symmetry boundary, axial displacement is fixed

and is continuously zero $\left(v = \frac{\partial v}{\partial \theta^1} = 0\right)$. From symmetry considerations, $\frac{\partial u}{\partial \theta^2}$ and $\frac{\partial w}{\partial \theta^2}$ must be fixed. On the x = 10 symmetry boundary, movement tangential to the shell surface is continuously zero $\left(u = \frac{\partial u}{\partial \theta^2} = 0\right)$. From symmetry considerations, to fix the model against rotations, $\frac{\partial w}{\partial \theta^1}$ and $\frac{\partial v}{\partial \theta^1}$ must be zero.

Two sets of boundary conditions are necessary for the midside nodes. From symmetry considerations, $\frac{\partial v}{\partial n} = \frac{\partial w}{\partial n} = 0$ on x = 0 and $\frac{\partial u}{\partial n}$ and $\frac{\partial w}{\partial n} = 0$ on y = 300.

User Subroutine

Subroutine UFXORD is used to generate the necessary 11 coordinates. The first coordinate read from the COORDINATE block is the θ^2 and y coordinate. The second coordinate is the angle, in degrees, of the normal to the shell surface, with 0 degrees being a normal parallel to the z-axis. It is used to generate θ^1, x, $\frac{\partial x}{\partial \theta^1}$, w, and $\frac{\partial w}{\partial \theta^1}$. NCRD must be set to 2 in the first data field of the second line of the COORDINATE block, and UFXORD must come after, not before, the COORDINATE block.

Results

The results of this problem are compared with the results of problems 2.16, 2.17, and 2.18.

Figure 2.19-2 and Figure 2.19-3 indicate that excellent results can be obtained by using doubly-curved isoparametric shell elements. Element type 8, the only triangular element used, is the lowest-order complete shell element that can be used.

The results from the quadrilateral shell elements are clearly superior. Element type 22, a thick shell element, shows reasonable results even in a thin shell problem. However, it tends to give a solution which is too stiff and it is known to be sensitive to the shape of the mapped mesh. (The angle between the surface coordinate axes should be orthogonal, if possible.) All of the other elements are well suited to large displacement analysis. Element type 4 yields extremely good results at a reasonable cost, but since the element has no patching functions, the mesh in the (θ^1 -θ^2) plane must be rectangular. Use of element type 24 yields the most accurate results, but it is somewhat more expensive to use than element 4. However, the

specification of boundary conditions is easier for this element and it is less sensitive to the boundary conditions. Since it uses complete basis functions, it is well-known to be insensitive to distortion of the mesh.

A comparison of results against the closed-form Scordelis-Lo solution is found in Figure 2.19-4. All of the MARC doubly-curved shell elements converge very rapidly compared to flat plate elements and curved elements such as Strickland's. These elements do not fulfill either compatibility conditions or rigid body requirements.

Parameters, Options, and Subroutines Summary

Example e2x19.dat:

Parameters	Model Definition Options
ELEMENTS	CONNECTIVITY
END	COORDINATES
SIZING	DIST LOADS
TITLE	END OPTION
	FIXED DISP
	GEOMETRY
	ISOTROPIC
	UFXORD

User subroutine in u2x19.f:

UFXORD

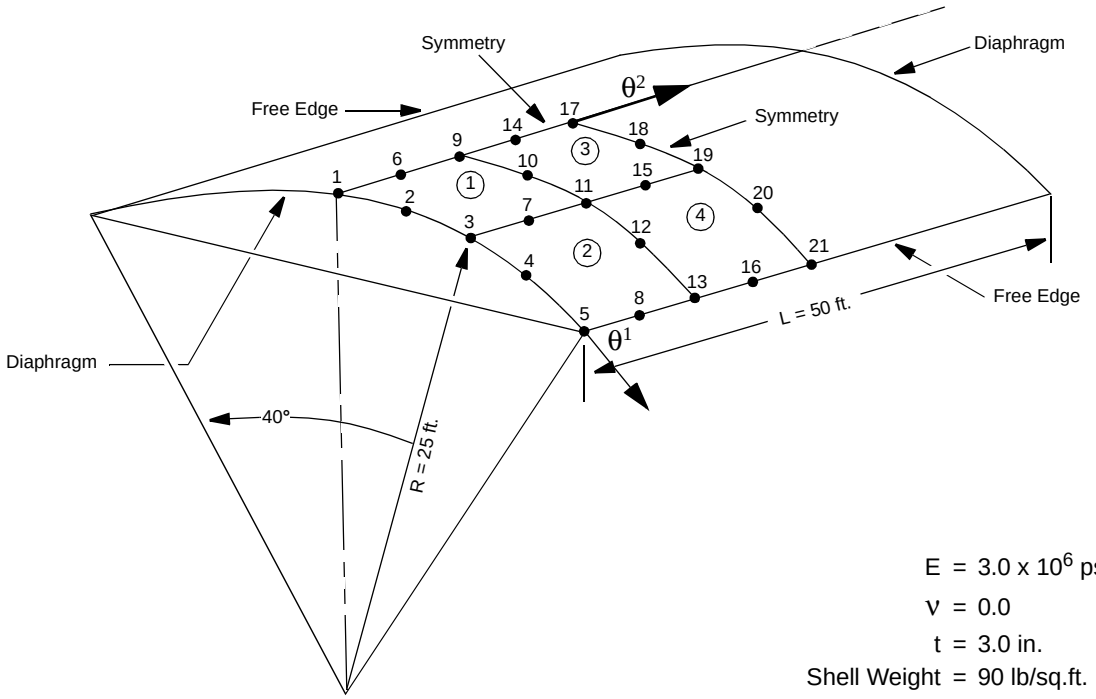

Figure 2.19-1 Cylindrical Shell Roof Configuration, Element 24

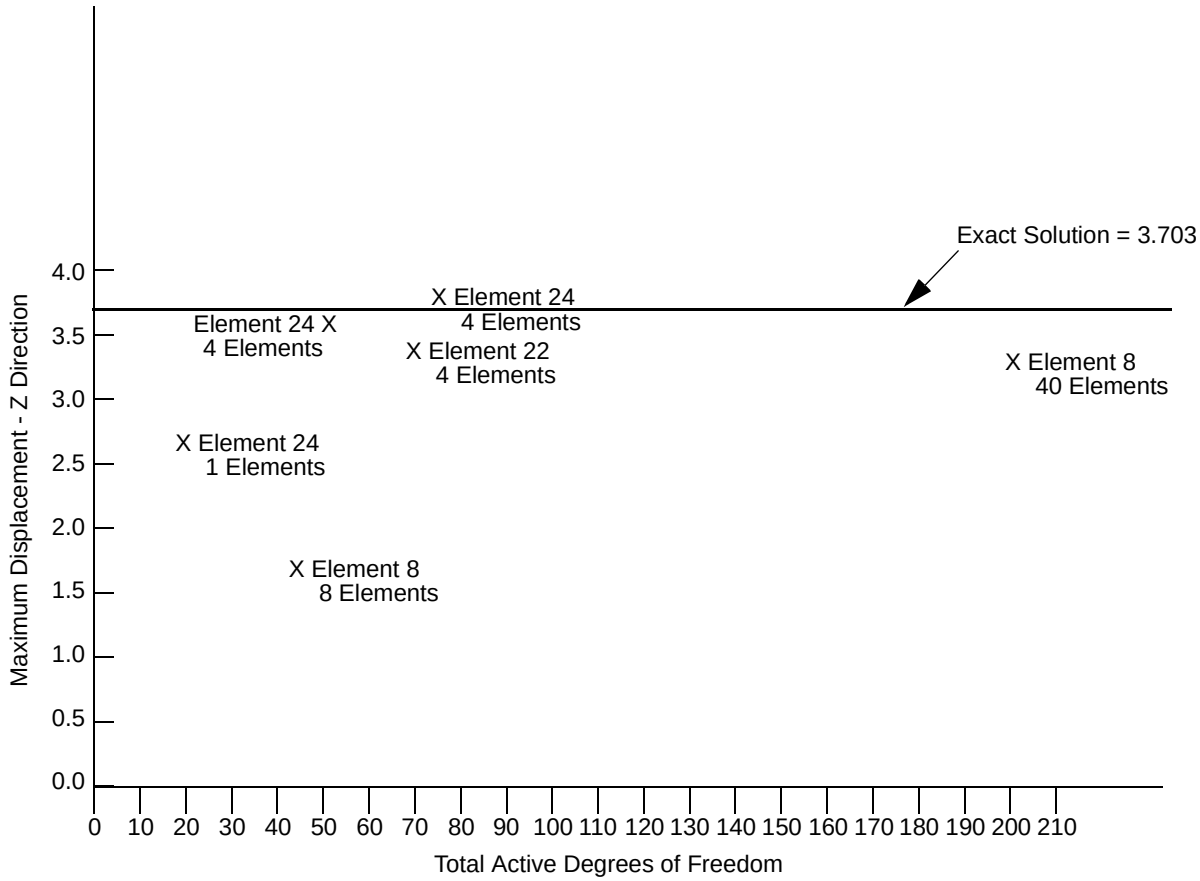

Figure 2.19-2 Maximum Z Deflection Versus Total Active Degrees of Freedom

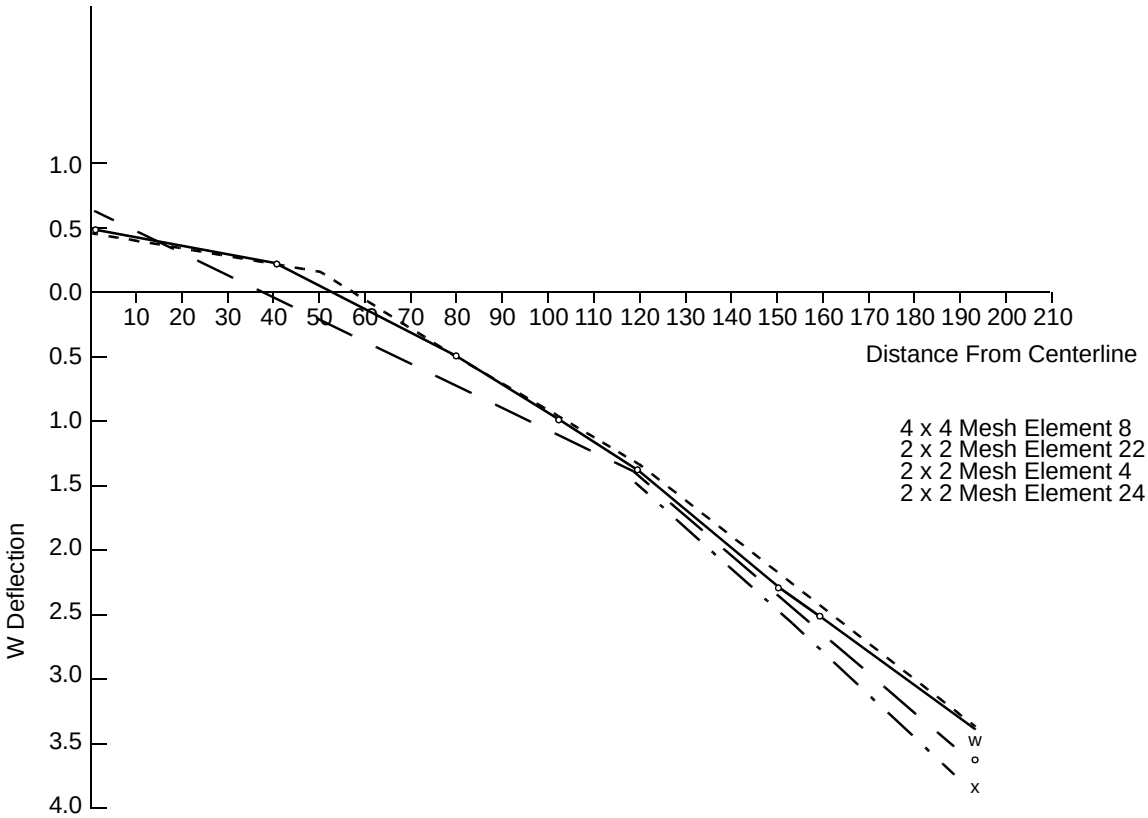

Figure 2.19-3 Vertical Deflection of the Y = 300 Symmetry Boundary vs. Distance From X = 0 Symmetry Boundary

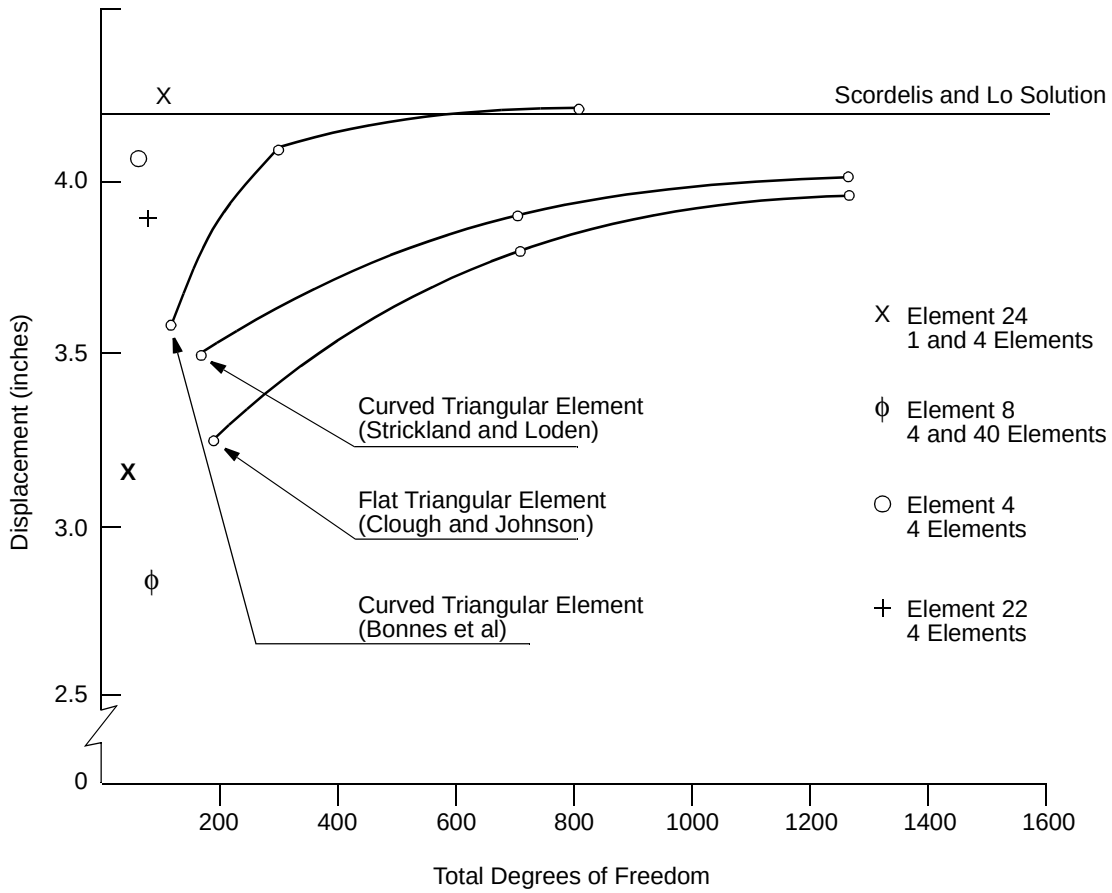

Figure 2.19-4 Vertical Displacement at the Center of the Free Edge

2.20 Pipe Bend Analysis

A 90-degree pipe bend under a concentrated 1-lb. load is elastically analyzed. This problem demonstrates the use of the special pipe bend element. For a more elaborate example, the reader is referred to problem 7.13.

Element

Element type 17 is used, which is a modification of element type 15, the two-node axisymmetric shell with four global degrees of freedom. The modification into a pipe bend approximation consists of introducing additional degrees of freedom at the centroid of the pipe in the r-z plane. The three degrees of freedom at this additional node are:

1 = Δu – normal motion of one end plane with the other plane fixed
2 = $\Delta \phi$ – in-plane rotation of one end plane with the other end plane fixed
3 = $\Delta \psi$ – out-of-plane rotation of one end plane with the other end plane fixed

Details concerning this element are found in *MARC Volume B: Element Library.*

Model

One-half of the r-z plane cross section has been modeled with 10 elements and 12 nodes. The mesh and geometry are shown in Figure 2.20-1. The centroid node has been chosen as number 12. For convenience, user subroutines UFCONN and UFXORD are used to compute the CONNECTIVITY and COORDINATE input data and is shown in the input file.

Geometry

For this element, EGEOM1, EGEOM2 and EGEOM3 are pipe wall thickness, angular extent of the pipe bend, and radius of curvature, respectively.

Material Properties

All elements are assumed to be uniform here. Values for Young's modulus, Poisson's ratio, and yield stress used here are 30 x 10^6 psi, 0.3, and 30,000 psi, respectively.

Loading

A concentrated load of 1.0 lb. is applied in the r-direction at the common node, 12.

Boundary Conditions

Nodes 1 and 11 have been restrained in the one and four displacement degrees of freedom in order to prescribe symmetry about the r-axis. The common node, 12, is restrained against out-of-plane bending.

Results

Figure 2.20-2 and Figure 2.20-3 give a comparison of the stresses predicted by this analysis with experimental results of Gross, N., and Ford, H., “Flexibility of Short-Radius Pipe Bends”, *Proc. Inst. Mech. Engr.*, Vol. 1B, p. 480, 1952. The stress predictions are in reasonable agreement with this experiment. It should be noted, that use of just five elements around the half pipe would yield satisfactory results in this case. For further discussion of this type of pipe bending theory for elastic-plastic analysis, see Marcal, P. V., “Elastic-Plastic Behavior of Pipe Bends With In-Plane Bending”, *J. Strain Analysis*, Vol. 2, p. 84, 1967.

Parameters, Options, and Subroutines Summary

Example e2x20.dat:

Parameters	Model Definition Options
ELEMENTS	END OPTION
END	FIXED DISP
SIZING	GEOMETRY
TITLE	ISOTROPIC
	POINT LOAD
	UFCONN
	UFXORD

User subroutines in u2x20.f:

UFXORD
UFCONN

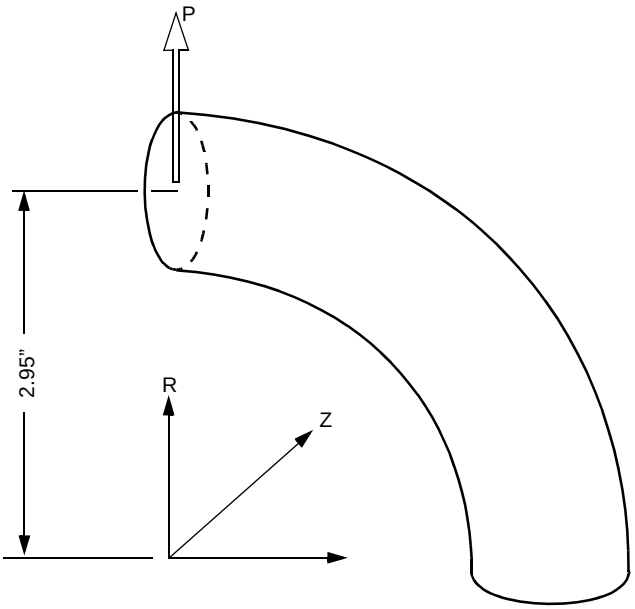

(a) Geometry

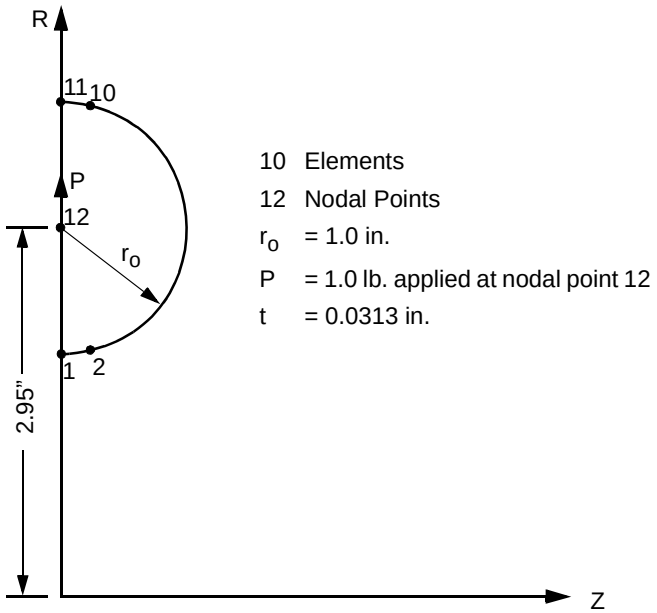

10 Elements
12 Nodal Points
r_o = 1.0 in.
P = 1.0 lb. applied at nodal point 12
t = 0.0313 in.

(b) Mesh

Figure 2.20-1 Geometry and Mesh-Pipe Bending Problem

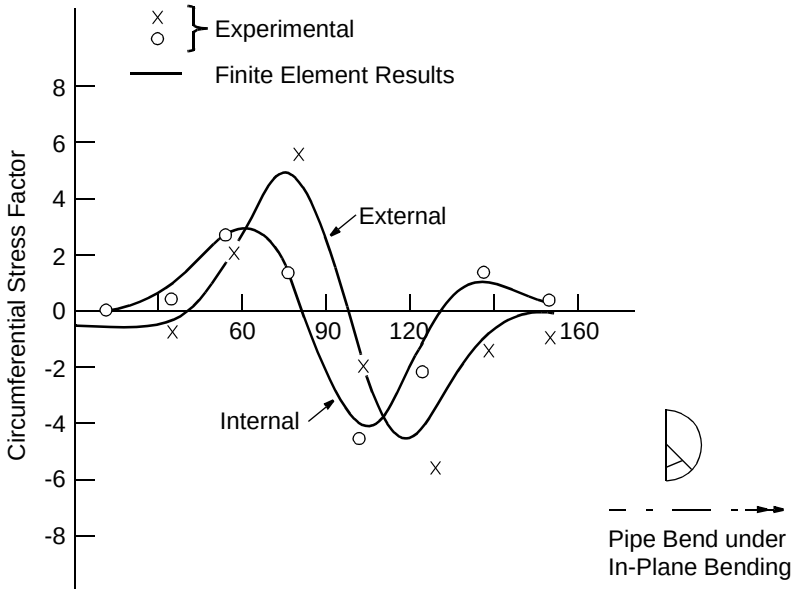

Figure 2.20-2 Distribution of Circumferential Stress $\lambda = 0.0924$

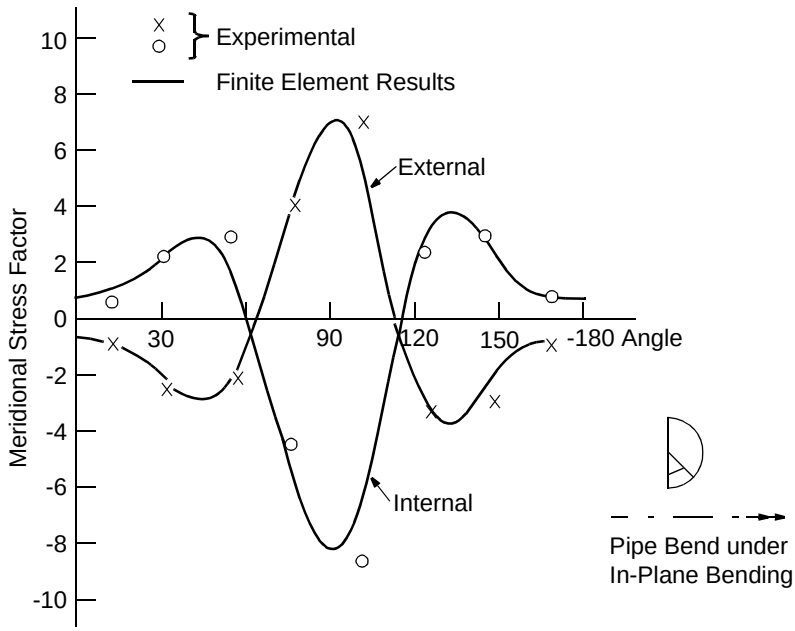

Figure 2.20-3 Distribution of Meridional Stress $\lambda = 0.0924$

2.21 Doubly Cantilevered Beam using Element 52

A hollow, square-section beam clamped at both ends is subjected to a single-point load applied at its center. This is the same problem as problem 2.7, but using element type 52. The results are compared to the analytic solution.

Element

Element type 52 is used, a straight Euler-Bernoulli beam in space. It has six degrees of freedom per node – three global Cartesian displacement coordinates and three global components of rotation. This element only allows linear elastic behavior, or nonlinear elastic behavior if user subroutine UBEAM is used in conjunction with HYPOELAS.

Model

Due to symmetry conditions, only half the beam is modeled. Five elements and six nodes are used for a total of 36 degrees of freedom. (See Figure 2.21-1). A cross-section of the beam is shown in Figure 2.21-2.

Geometry

To use element 52, the moments of inertia of the section about the local x- and y-axes and area are needed. The area is 0.0396 in^2. I_{xx} and I_{yy} are 0.0064693 in^4. Because this is an elastic element, no integration around the beam section is necessary.

Material Properties

Young's modulus is 30 x 10^6 psi; Poisson's ratio is taken as 0.

Loading

A single point load of 50 pounds is applied in the negative y-direction at the center node of the beam.

Boundary Conditions

In the model, the beam end node (node 1) is fixed against displacement and rotation. Thus, $u = v = w = \theta_x = \theta_y = \theta_z = 0$. The midpoint node, node 6, is fixed against axial displacement and rotation; $u = \theta_x = \theta_y = \theta_z = 0$ to ensure that symmetry is satisfied.

Results

A simple elastic analysis was run with one load increment of 50 pounds applied to node 6 in the zeroth increment. The computed results are compared with an exact solution in Table 2.21-1 and Table 2.21-2. Correlation is good for element type 52. The analytic solution may be found in R. J. Roark, *Formulas for Stress and Strain*. The deflected shape is shown in Figure 2.21-3.

Table 2.21-1 Y Deflection (in.)

Node	MARC Element 52	Analytically Calculated
1	0.	0.
2	.000419	.000422
3	.001417	.001428
4	.002609	.002628
5	.003607	.003634
6	.004026	.004056

Table 2.21-2 Moments (in.-lb.) and Reaction Forces (lb.)

MARC Element 52	Analytically Calculated
M = 125.	M = 125.
R = 50.	R = 50.

Parameters, Options, and Subroutines Summary

Example e2x21.dat:

Parameters

ELEMENTS
END
SIZING
TITLE

Model Definition Options

CONNECTIVITY
COORDINATES
END OPTION
FIXED DISP
GEOMETRY
ISOTROPIC
POINT LOAD

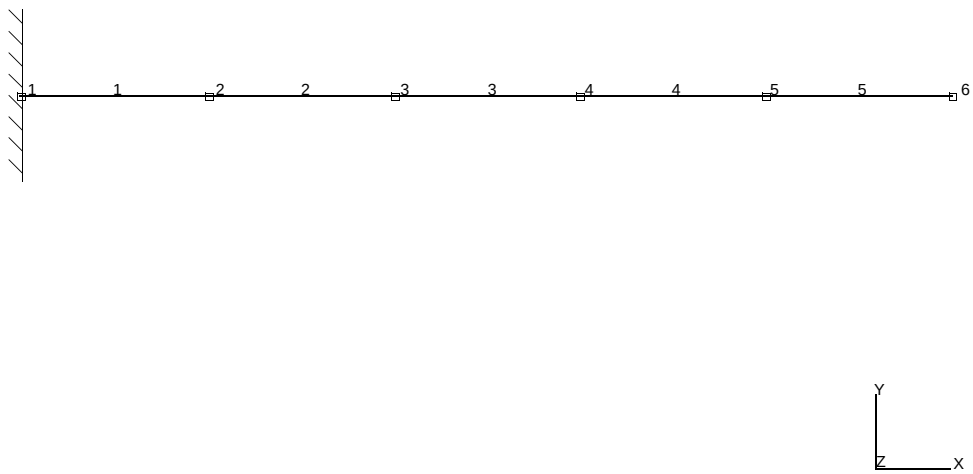

Figure 2.21-1 Closed Section Beam Model

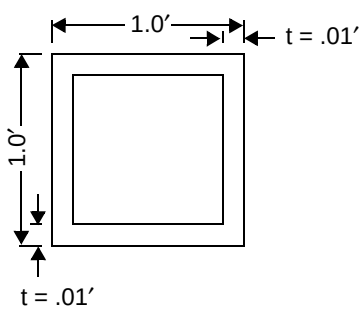

Cross-Section

Figure 2.21-2 Hollow, Square-Section Beam

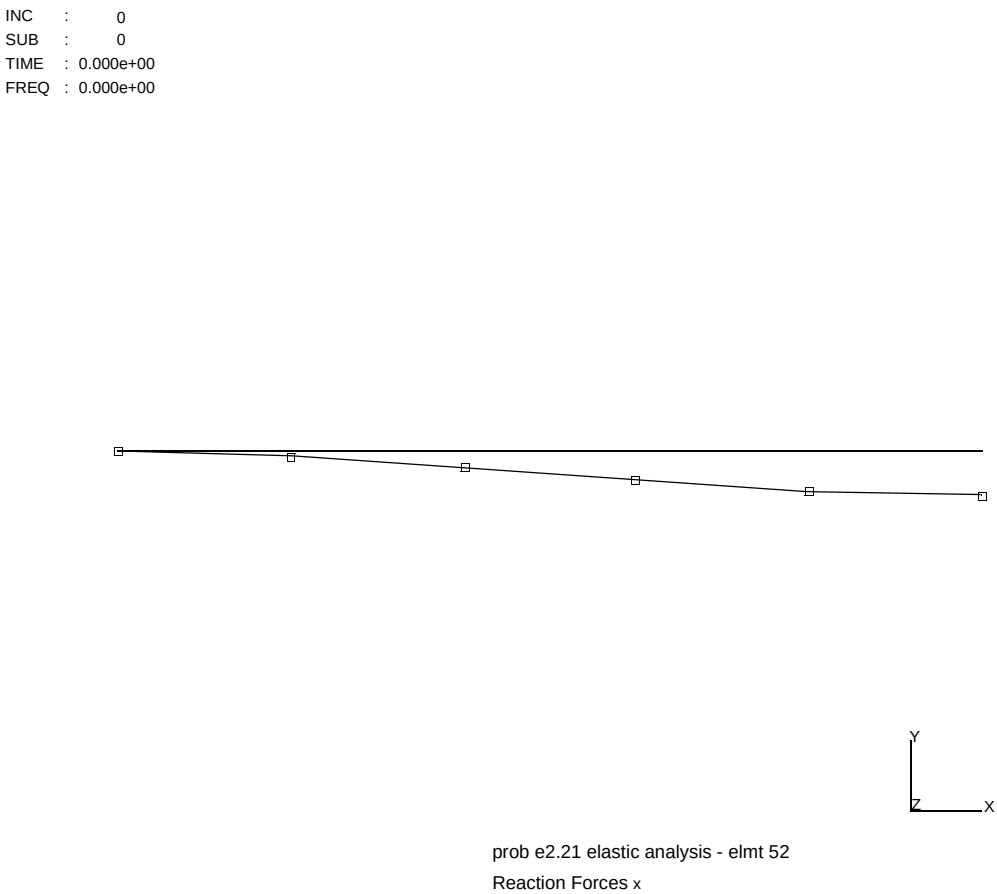

Figure 2.21-3 Defections

2.22 J-Integral Evaluation Example

This example illustrates the use of the J-Integral evaluation procedure in MARC, as well as the 1/4-point element geometry at the crack tip. The example is that of a double-edge notch (DEN) specimen under axial tension (Mode I) (Figure 2.22-1). This example is chosen because of the availability of an accepted value for K_I for comparison. The fundamental problem in a crack problem is the singularity in the strain field at the crack tip. For elastic response the singularity is of order $1/\sqrt{r}$, where r measures distance away from the crack tip. It can be shown that the second order isoparametric elements reproduce this singularity when the side nodes are placed at the 1/4-points instead of at the midsides. This condition is achieved by merging two nodes in each element at the crack tip. Based on this consideration, a rather coarse mesh for the problem is shown in Figure 2.22-2 and Figure 2.22-3. The coarseness of the mesh is acceptable because the only output required is the J-integral value, and it has been shown [1] that the differential stiffness technique, as is used in MARC, provides good estimates of J with relatively coarse models.

Element

Element type 27 is a plane-strain quadrilateral element. There are eight nodes and two degrees of freedom at each node.

Model

Only a quadrant of the model is used because of obvious symmetries. A second COORDINATES block was used to move the side nodes of the crack tip elements to the 1/4 points (1/4 of the way along the sides from the crack tip to the opposite face of the element).

Geometry

No geometry is specified.

Material Properties

The Young's modulus is 30 x 10^6 psi and Poisson's ratio is 0.3.

Loading

The loading is shown in Figure 2.22-1. The load is applied as a uniform negative pressure of 100 psi on the appropriate faces of the end elements.

Boundary Conditions

The boundary conditions for the model quadrant are determined by symmetry conditions. The edge along the y-direction is constrained in both degrees of freedom. The edge along the x-direction is constrained to displacement along the x-axis. Boundary conditions are illustrated in Figure 2.22-1.

J-Integral

The J-integral is evaluated numerically by moving nodes within a certain ring of elements around the crack tip to represent a differential crack advance and measuring the change in strain energy. The J is the negative differential of strain energy with respect to crack advance. This mesh has three obvious “rings” of elements around the crack tip, so that three evaluations of J are available. Since the J-integral should be path independent for elastic problems, the variation in J between the three values gives some idea of the accuracy of the solution. A differential movement has to be supplied to evaluate J. Numerical experiments have indicated that setting this movement to less than 1/50 times the size of the smallest crack tip element gives a convergent solution (convergence in the sense of the numerical difference providing the differential). The use of too small a movement causes roundoff difficulties.

In this case, a value of 10^{-2} was used. The smallest element dimension is 1, so that this represents 1/100, a satisfactory value. The midside nodes are moved proportionally for each evaluation.

Results

MARC provides an output of the strain energy difference. This must be normalized by the crack opening area to obtain the value of J. Since this specimen is of unit thickness, the crack opening area is $\Omega 1$, where $\Omega 1$ is the differential crack motion. The mesh used symmetry about the crack line, so that that strain energy change in the actual specimen would be twice that printed out. Finally, since this is a plane strain, Mode I problem, the J-integral can immediately be converted to K_I, the stress intensity factor, by the relation:

$$K_I = \sqrt{\frac{E}{1-\nu^2}}\ J$$

These results are summarized in Table 2.22-1.

It is clear from these results that the path independence is well reproduced, and that the error in the solution for K_I is quite small. The user should note that such a coarse mesh does not give an accurate model of the stress field close to the cracktip. However, because the 1/4-point technique used here includes the $1/\sqrt{r}$ singularity, a reasonable refinement of the same mesh

would give excellent predictions of the near-tip elastic stress field. As a general guideline, it appears that second-order elements with the 1/4-point technique give good results for J-integral evaluation when the crack tip elements are sized about 20% of the crack depth or ligament width, whichever is smaller. For near-tip stress field prediction, the size should be reduced to about 5% of crack depth or ligament width.

Table 2.22-1 J-Integral Evaluation Results

	Move Tip Only	**Move First Ring of Elements**	**Move Second Ring of Elements**
Strain energy change given in program (Δu)	6.7313×10^{-5}	6.693×10^{-5}	6.689×10^{-5}
J-Integral	1.324×10^{-2}	1.3386×10^{-2}	1.3378×10^{-2}
$K_I = \sqrt{\frac{E}{1-\nu^2}}\ J$	666.	664.	664.
$K_I/\sigma_{net}\sqrt{1}$	1.052	1.050	1.050
cf 1.028 [2]	+2.4%	+2.2%	+2.2%

References

1. Parks, D. M., “A Stiffness Derivative Finite Element Technique for Determination of Elastic Crack Tip Stress Intensity Factors,” *Int. J. Fracture*, Vol. 10, No. 4, December 1974, pp. 487-502.
2. Bowie, I. L., “Rectangular Tensile Sheet With Symmetric Edge Cracks,” *J. Applied Mechanics*, Vol. 31, 1964, pp. 208-212.

Parameters, Options, and Subroutines Summary

Example e2x22.dat:

Parameters	Model Definition Options
ELEMENTS	CONNECTIVITY
ELSTO	COORDINATES
END	DIST LOADS
J-INT	END OPTION
SIZING	FIXED DISP
TITLE	ISOTROPIC
	J-INTEGRAL
	PRINT CHOICE

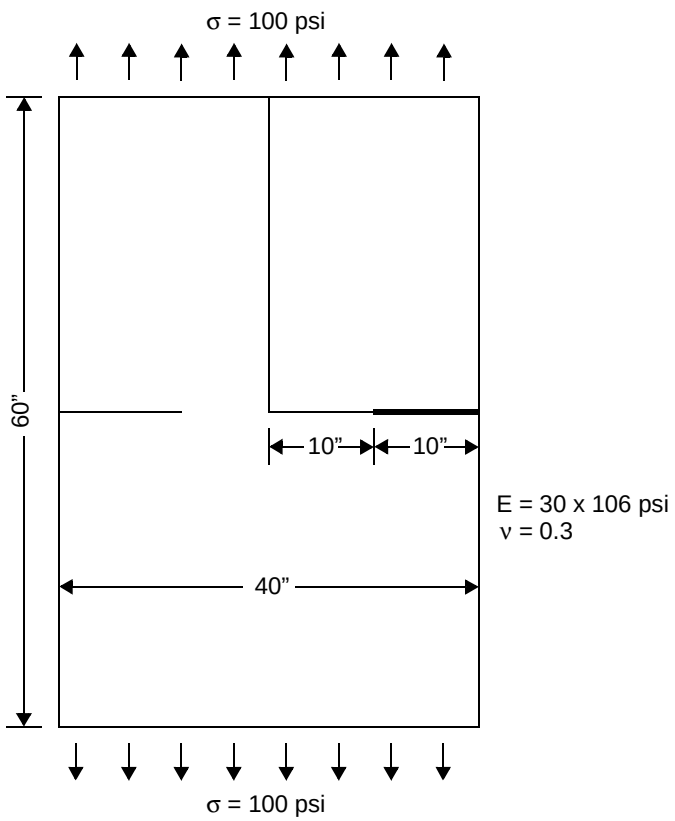

Figure 2.22-1 Double-Edge Notch Specimen, Showing Blocks for Mesh Generation

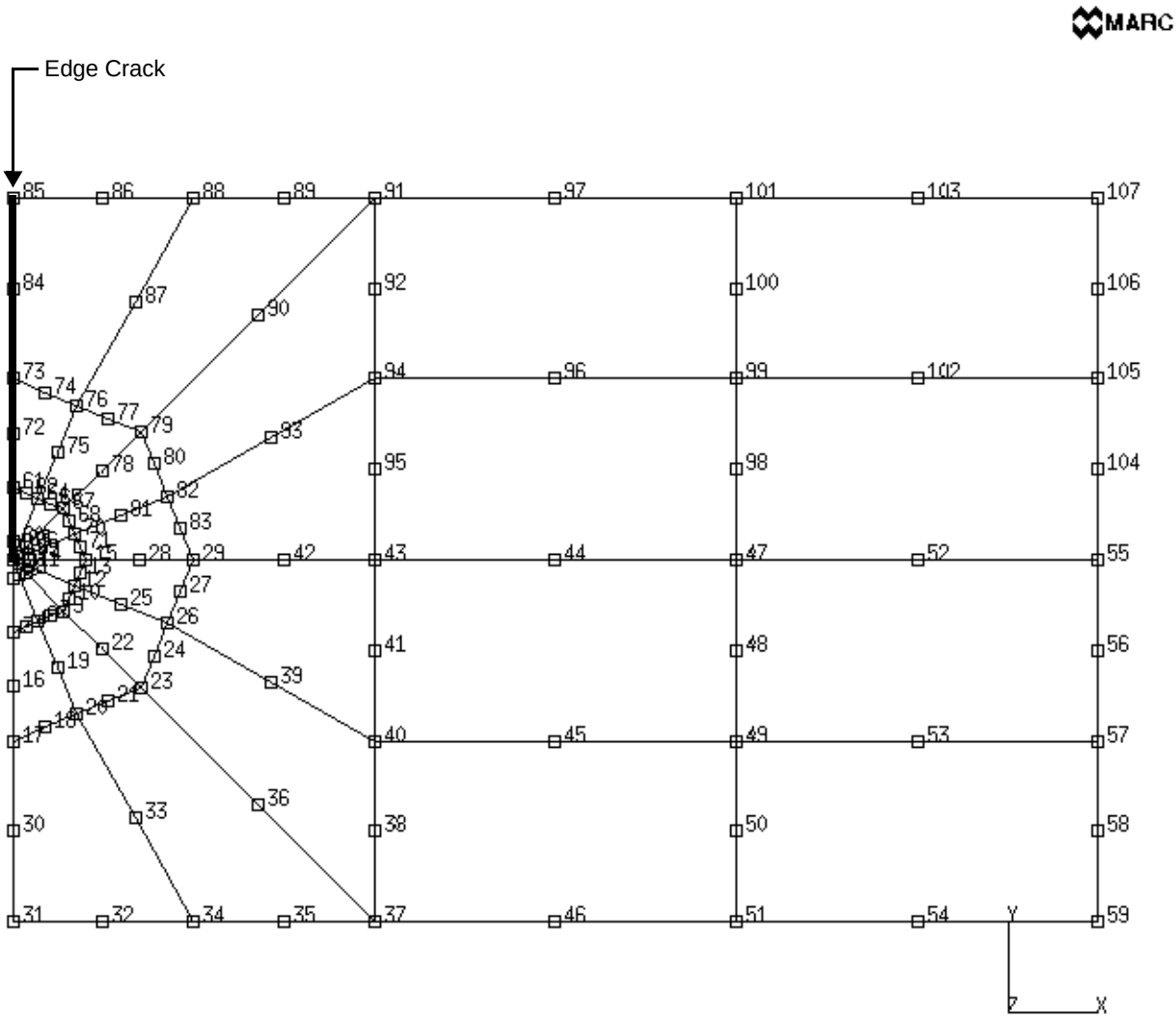

Figure 2.22-2 Mesh for Double-Edge Notch Specimen

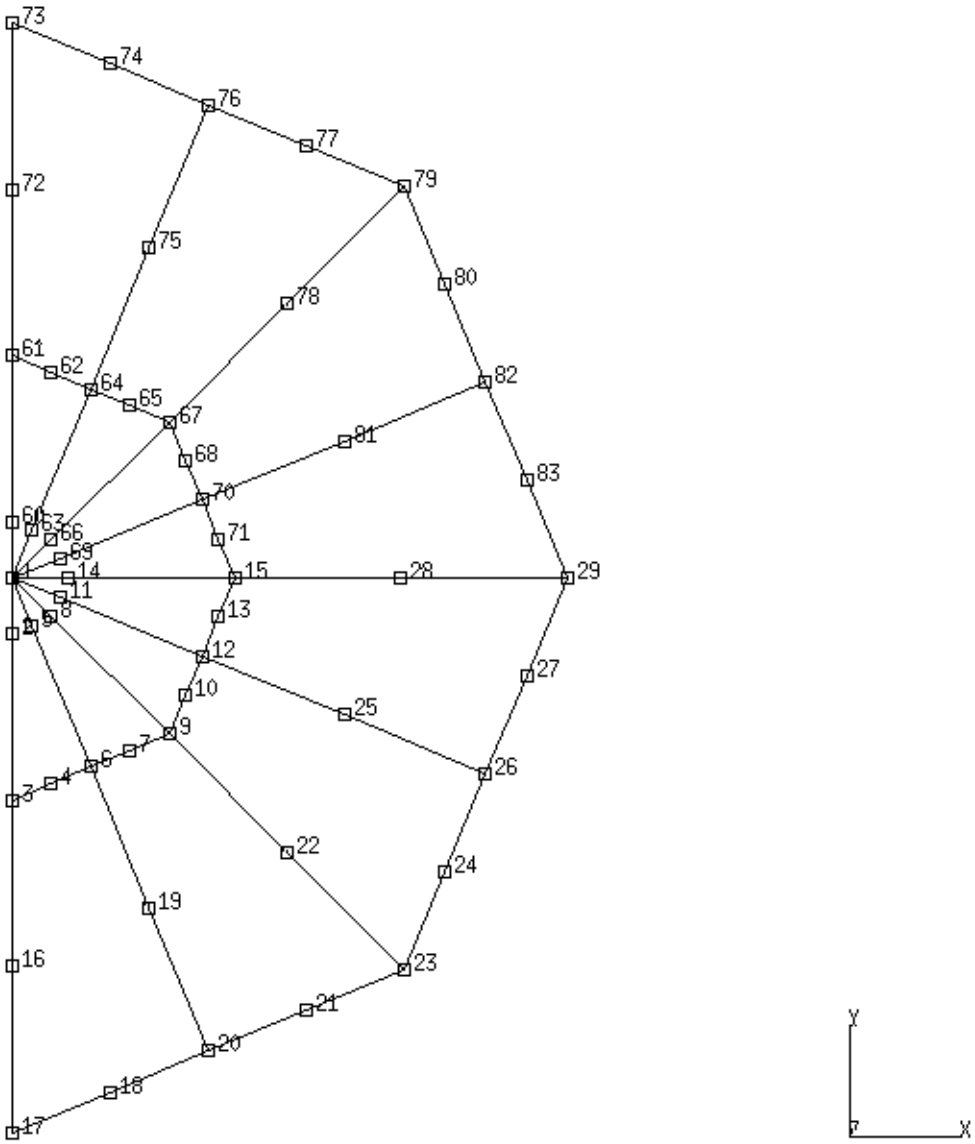

Figure 2.22-3 Mesh Detail of Double-Edge Notch Specimen

2.23 Thick Cylinder Under Internal Pressure

This problem illustrates the use of MARC element type 6 and the TRANSFORMATION option for an elastic analysis of a thick cylinder using planar elements. The cylinder is subjected to internal pressure. The results can be compared with the analytical prediction.

Element

Element type 6, the triangular plane-strain element, is used to model a section of the thick cylinder.

Model

Because of the symmetrical behavior, only a portion of the cylinder needs to be analyzed. The dimensions of the cylinder and the finite element mesh are shown in Figure 2.23-1. Sixteen elements with 18 nodes are used in the mesh.

Material Properties

The material is a typical steel with Young's modulus of 30 x 10^6 psi and Poisson's ratio of 0.3. The data is entered using the ISOTROPIC option.

Geometry

The thickness is equal to unity, the default value; hence, the GEOMETRY option is not used.

Loading

The cylinder is under an internal pressure of 1 psi. This is applied to the 2-1 face of element 1 using traction type 8 using the DIST LOADS option.

Boundary Conditions

Symmetry conditions are assumed at radial lines OY and OX. Degrees of freedom at nodal points 1, 3, 5, 7, 9, 11, 13, 15 and 17 are transformed into local coordinate system (x,y).

Results

Stresses in the thick cylinder are (as given in Timoshenko and Goodier, *Theory of Elasticity*):

$$\sigma_r = \frac{pR_1^2}{R_2^2 - R_1^2}\left(1 - \frac{R_2^2}{r^2}\right), \qquad \sigma_\theta = \frac{pR_1^2}{R_2^2 - R_1^2}\left(1 + \frac{R_2^2}{r^2}\right)$$

The stresses are plotted as a function of radial distance in Figure 2.23-2.

Parameters, Options, and Subroutines Summary

Example e2x23.dat:

Parameters	Model Definition Options
ELEMENTS	CONNECTIVITY
END	COORDINATES
SIZING	DIST LOADS
TITLE	END OPTION
	FIXED DISP
	ISOTROPIC
	TRANSFORMATION

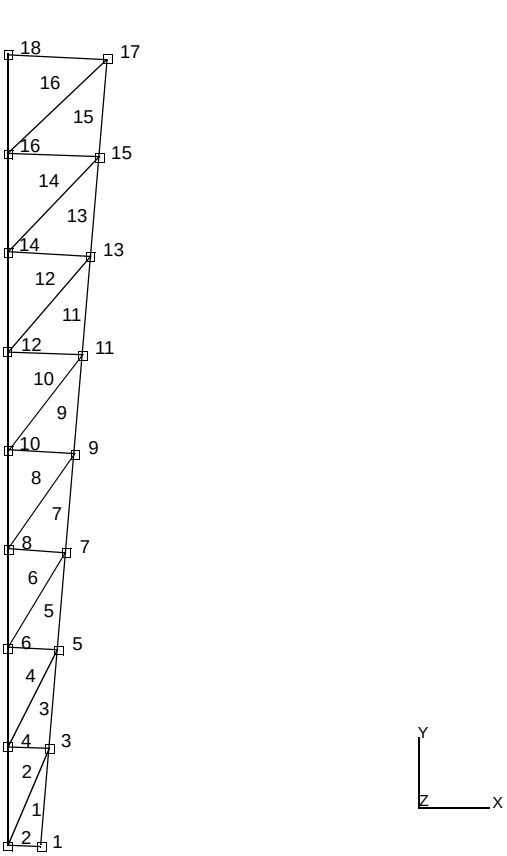

Figure 2.23-1 Thick Cylinder and Mesh

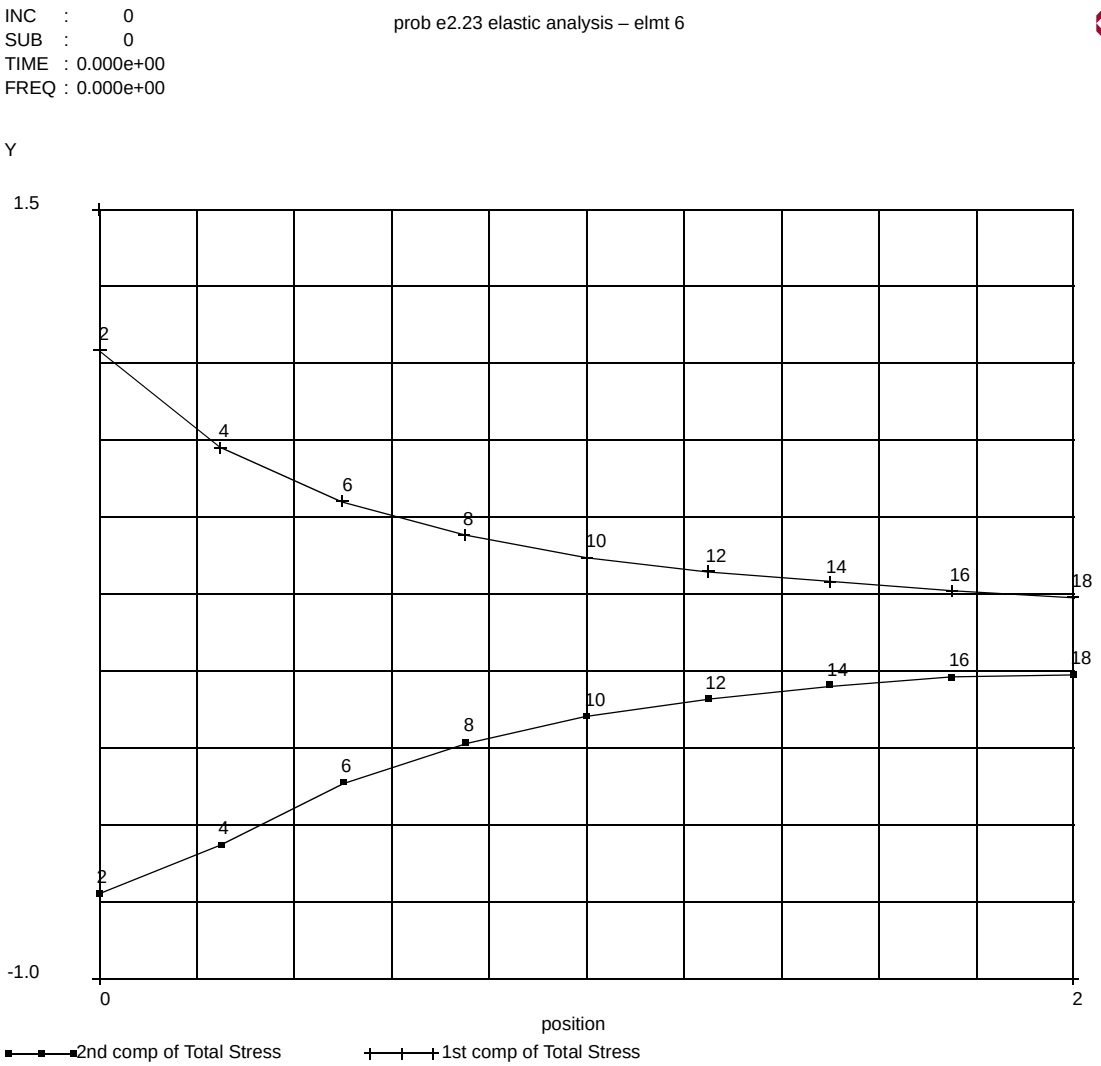

Figure 2.23-2 Stresses vs. Radial Distance

2.24 Three-Dimensional Frame Analysis

This problem illustrates the use of MARC element type 9 for an elastic analysis of a three-dimensional frame structure (a guyed wire tower). The frame is subjected to a concentrated load at the top.

Element

This frame analysis is performed with three-dimensional truss elements type 9. This element has two nodes with three degrees of freedom at each node.

Model

The dimensions of the frame structure and the finite element mesh are shown in Figure 2.24-1. There are 20 elements and 9 nodes in the mesh.

Material Properties

Elastic behavior is investigated with Young's modulus of 30 x 10^6 psi; the value is entered through the ISOTROPIC option.

Geometry

Two element cross sections are stored in two block pairs in variable EGEOM1. The cross-sectional area is 1.0 square inch for the primary members, elements 1 to 12.

The cross-section area is 0.25 square inch for the secondary members, elements 13 to 20.

Loading

A 10,000 pound concentrated load at the top (node 1) is applied in the horizontal direction (x-direction) using the POINT LOAD option.

Boundary Conditions

The FIXED DISP option is used to constrain the nodal points at the base (3, 5, 7 and 9).

Results

A deformed mesh plot is shown in Figure 2.24-2. To verify that the structure is in equilibrium, we add the reaction forces at nodes 3, 5, 7, 9 and observe that the total reactions are:

R_x = -10,000 pounds
R_y = 0 pounds
R_z = 0 pounds

balancing the applied load of 10,000 pounds.

Parameters, Options, and Subroutines Summary

Example e2x24.dat:

Parameters	Model Definition Options
ELEMENTS	CONNECTIVITY
END	COORDINATES
SIZING	END OPTION
TITLE	FIXED DISP
	GEOMETRY
	ISOTROPIC
	POINT LOAD

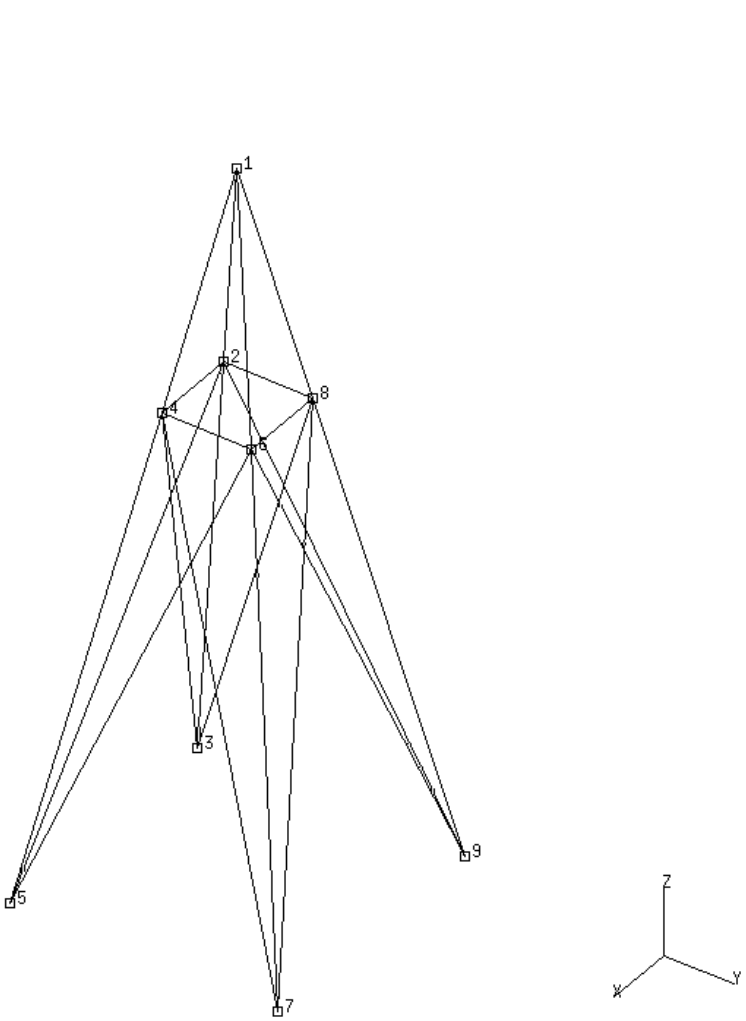

Figure 2.24-1 Three-Dimensional Frame and Mesh

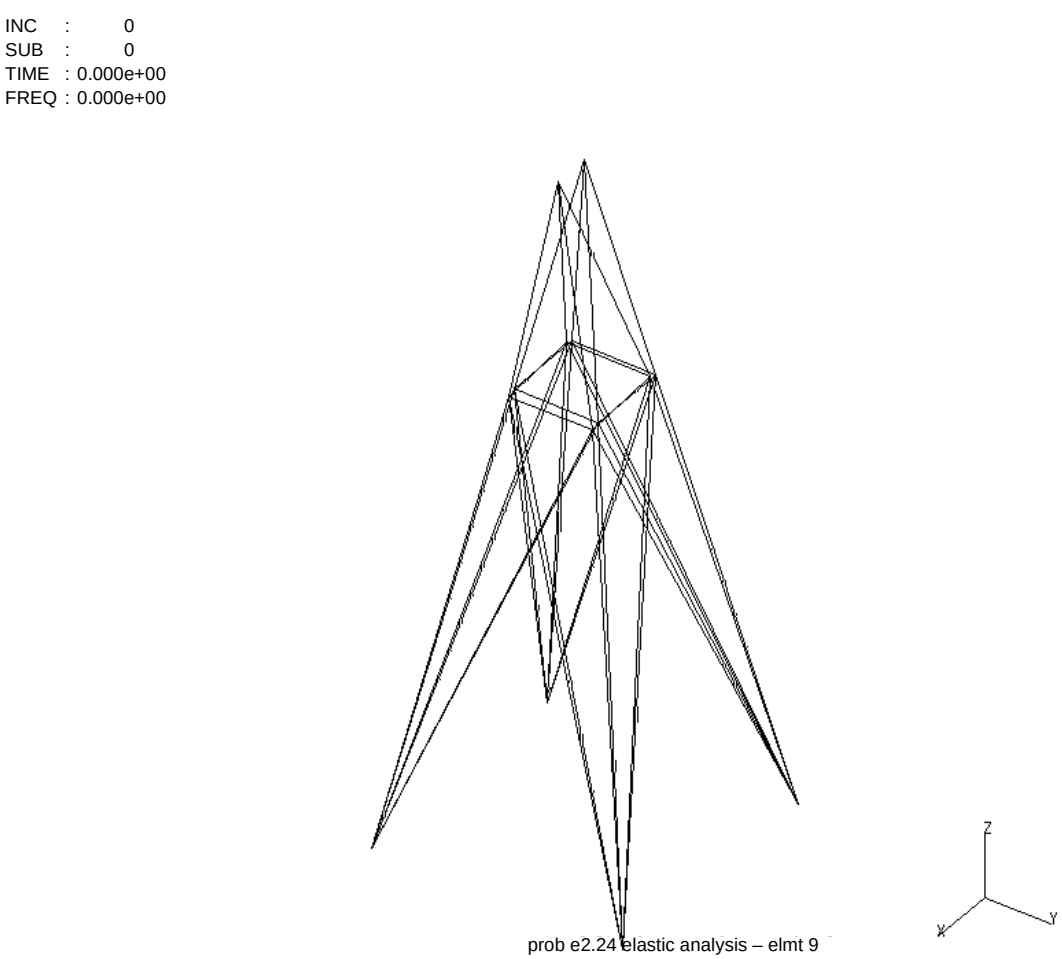

Figure 2.24-2 Deformed Mesh Plot of Three-Dimensional Frame

2.25 Two-Dimensional Strip Compressed by Rigid Plates

This problem demonstrates the use of MARC element types 11 and 115 for an elastic analysis of a two-dimensional strip subjected to known displacements at a boundary line.

This problem is modeled using the two techniques summarized below.

Data Set	Element Type(s)	Number of Elements	Number of Nodes
e2x25	11	24	35
e2x25b	115	24	35

Elements

Element types 11 and 115 are 4 node plane-strain quadrilaterals. Element 115 uses reduced integration with hourglass control.

Model

One quarter of a 2 by 3 inch plate is modeled with 24 elements and 35 nodes, as shown in Figure 2.25-1 on the deformed mesh. The displacements are magnified by 1200.

Material Properties

The material for all elements is treated as an elastic material with Young's modulus of 30.0E+06 psi and Poisson's ratio of 0.3.

Geometry

The strip has a thickness of 1 inch given in the first field.

Loads and Boundary Conditions

Symmetry conditions require that the vertical displacements along the bottom surface (y = 0), and the horizontal displacements along the left surface (x = 0), are constrained to zero. The applied displacement on the top surface (y = 1 inch) is -0.0001 inch in the vertical direction and zero in the horizontal direction.

Results

Figure 2.25-2 and Figure 2.25-3 show the variation of the second component of stress (σ_{22}) over the mesh for element types 11 and 115, respectively. Examining these figures, we see that the second component of stress is nearly uniform, except near the free surface. The stresses are typically within 10% of a homogeneous compression problem. This is an expected variation, due to edge effects. The far-field analytical solution becomes:

ε_{22} = 1.0E-04 in/in, and σ_{22} = 3510 psi.

The values of σ_{22} (0,0) for element types 11 and 115 from element 1 are 3791 psi and 3665 psi, respectively. The bonded top surface does not allow the material to deform in a homogeneous manner.

Parameters, Options, and Subroutines Summary

Example e2x25.dat:

Parameters	Model Definition Options
ELEMENTS	CONN GENER
END	CONNECTIVITY
SIZING	COORDINATES
TITLE	END OPTION
	FIXED DISP
	GEOMETRY
	ISOTROPIC
	NODE FILL
	POST

Example e2x25b.dat:

Parameters	Model Definition Options
ALIAS	CONN GENER
ELEMENTS	CONNECTIVITY
END	COORDINATES
SIZING	END OPTION
TITLE	FIXED DISP
	GEOMETRY
	ISOTROPIC
	NODE FILL
	POST

INC : 0
SUB : 0
TIME : 0.000e+00
FREQ : 0.000e+00

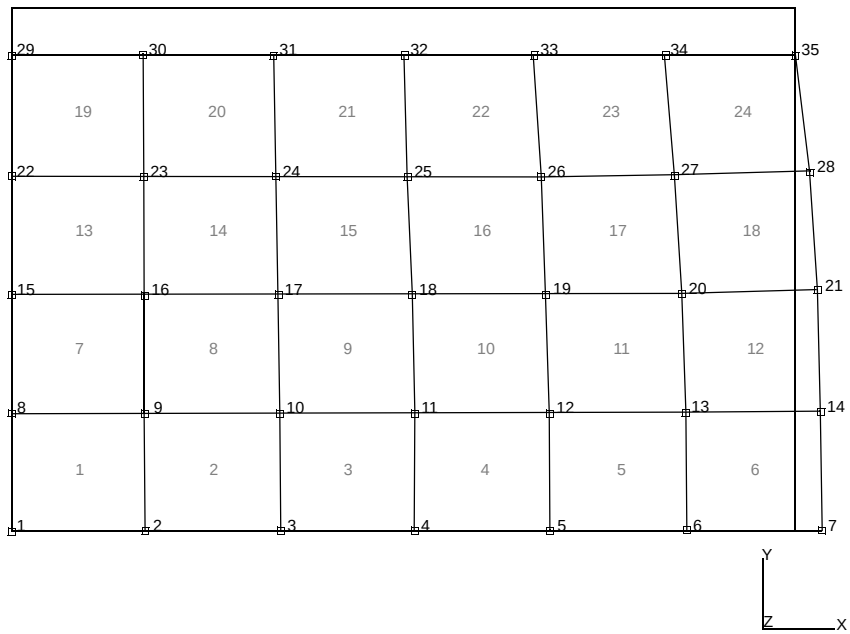

prob e2.25 elastic analysis - elmt 11

Displacements x

Figure 2.25-1 Deformed Mesh

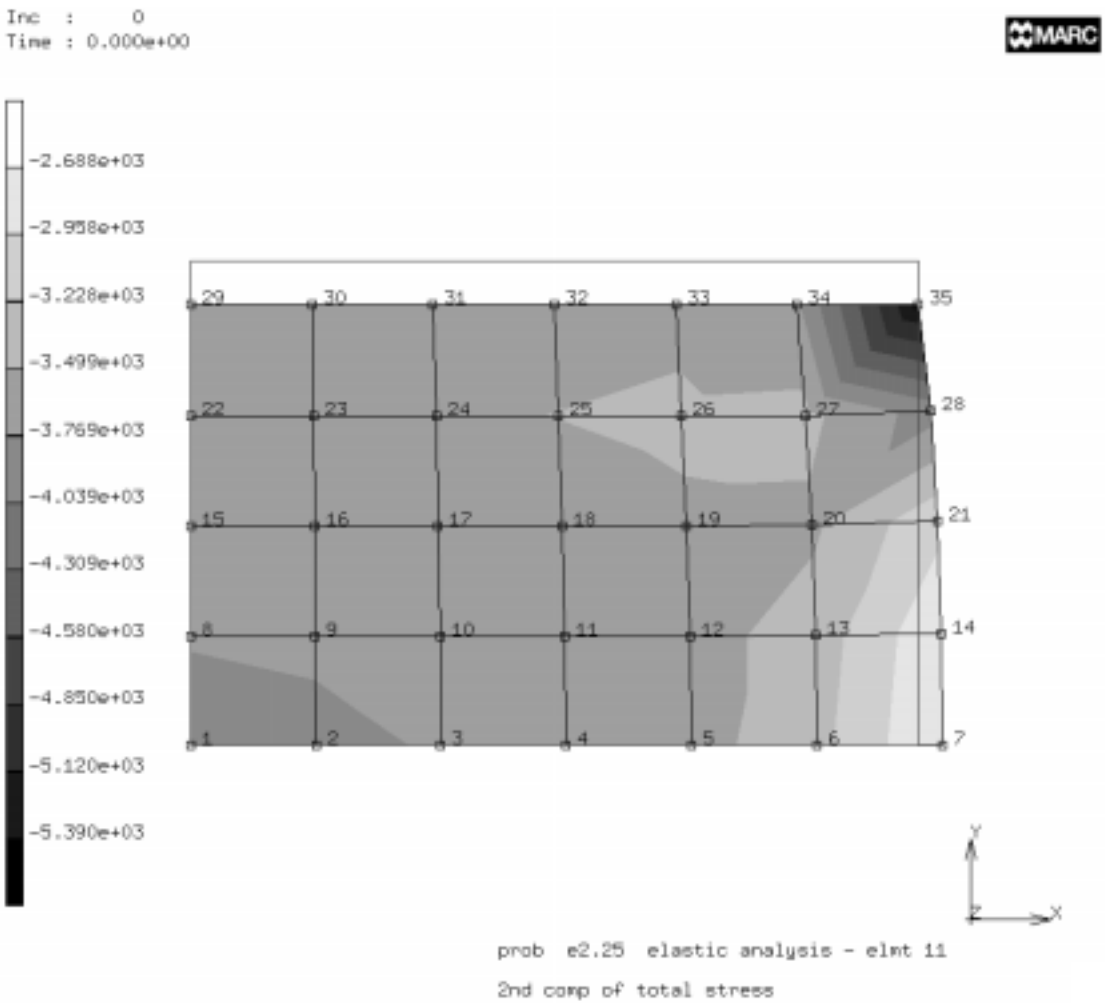

Figure 2.25-2 Contours of σ_{22} Element 11

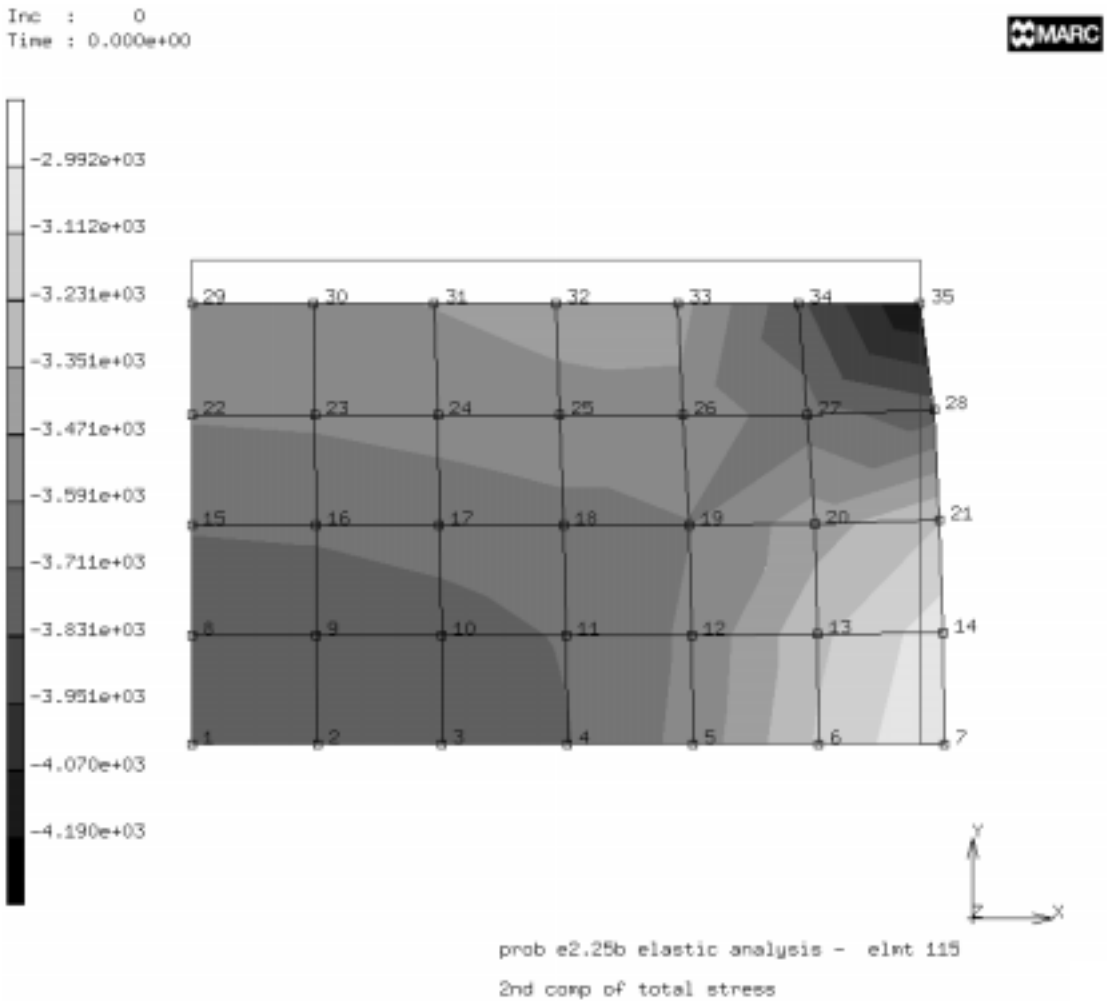

Figure 2.25-3 Contours of σ_{22} Element 115

2.26 Two-Dimensional Strip Compressed by Rigid Plates

This problem demonstrates the use of MARC element types 11, 118, 125, and 128. The nearly incompressible material (Poisson's ratio = .4999) of a strip is subjected to compression by prescribed displacements. The constant dilatation option is also used.

This problem is modeled using the four techniques summarized below.

Data Set	Element Type(s)	Number of Elements	Number of Nodes
e2x26	11	24	35
e2x26b	118	24	35
e2x26c	125	48	117
e2x26d	128	48	117

Elements

Element type 11 is an 4-node, incompressible, plane-strain element. Element type 118 is a 5-node plane strain element with reduced integration and has a Herrmann formulation. Element types 125 and 128 are 6 node plane strain triangles with type 128 having a Herrmann formulation.

Model

The dimensions of the strip and the finite element meshes are shown in Figure 2.26-1. There are 24 elements in the quadrilateral meshes and 48 elements in the triangular meshes.

Material Properties

The material for all elements is treated as an elastic material with Young's modulus of 3.0E+06 psi and Poisson's ratio (ν) of .4999.

Geometry

The strip has a thickness of 1 inch given in the first field. A nonzero value is input in the second field of this option to impose a constant dilatation constraint. Improved accuracy is obtained with this technique for nearly incompressible and incompressible behavior when using element type 11.

Results

The condition of plane strain requires the third direct component of stress to become:

$$F = \sigma_{33} - \nu(\sigma_{11} + \sigma_{22}) = 0$$

Element type 11 and 125 satisfies this condition, namely F = 0, exactly. User subroutine PLOTV is used to calculate the above value of F at all integration points. Figure 2.26-2 and Figure 2.26-3 show the contours of F on the deformed shape where the displacements are magnified by 2000. Because of the Lagrange multipliers used in the Herrmann formulation for element types 118 and 128, the plane strain condition is only satisfied on the average and not at each integration point. Figure 2.26-5 and Figure 2.26-5 show the contours of F on the deformed mesh for element types 118 and 128, respectively. The maximum absolute value of F is about 63 psi compared to a maximum von Mises intensity of about 700 psi.

Parameters, Options, and Subroutines Summary

Example e2x26.dat:

Parameters	Model Definition Options
ELEMENTS	CONNECTIVITY
END	COORDINATES
SIZING	END OPTION
TITLE	FIXED DISP
	GEOMETRY
	ISOTROPIC
	POST

User subroutine in u2x26.f:

PLOTV

Example e2x26b.dat:

Parameters	Model Definition Options
ELEMENTS	CONNECTIVITY
END	COORDINATES
SIZING	END OPTION
TITLE	FIXED DISP
	GEOMETRY
	ISOTROPIC
	POST

User subroutine in u2x26b.f:

PLOTV

Example e2x26c.dat:

Parameters	Model Definition Options
ELEMENTS	CONNECTIVITY
END	COORDINATES
SIZING	END OPTION
TITLE	FIXED DISP
	GEOMETRY
	ISOTROPIC
	OPTIMIZE
	POST

User subroutine in u2x26c.f:

PLOTV

Example e2x26d.dat:

Parameters	Model Definition Options
ELEMENTS	CONNECTIVITY
END	COORDINATES
SIZING	END OPTION
TITLE	FIXED DISP
	GEOMETRY
	ISOTROPIC
	OPTIMIZE
	POST

User subroutine in u2x26d.f:

PLOTV

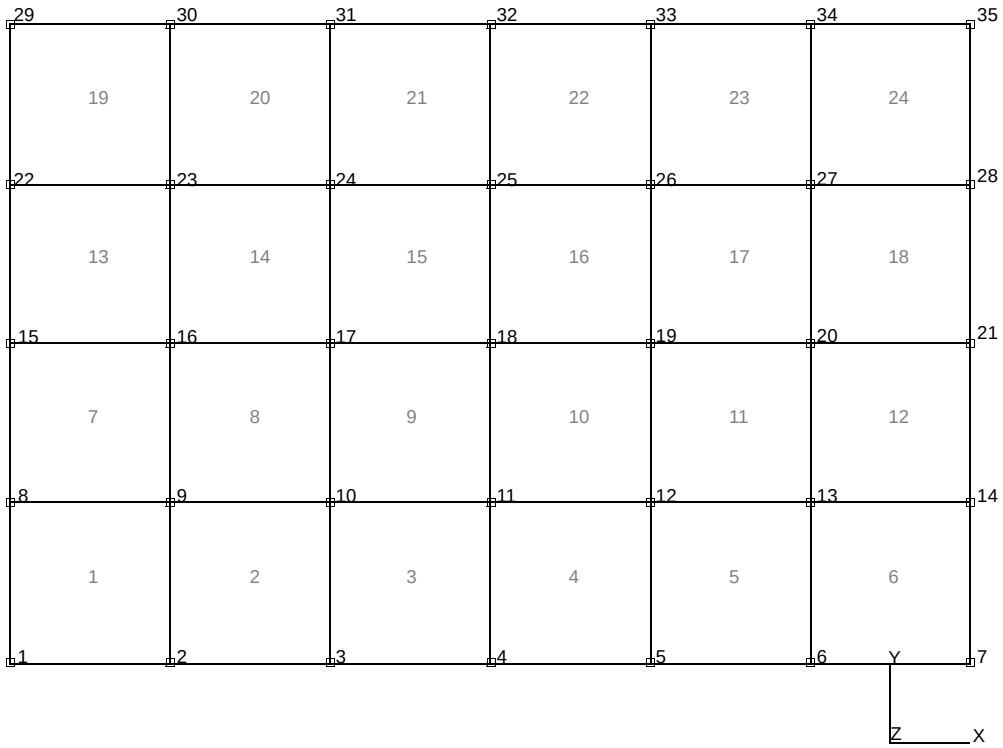

Figure 2.26-1 Finite Element Mesh

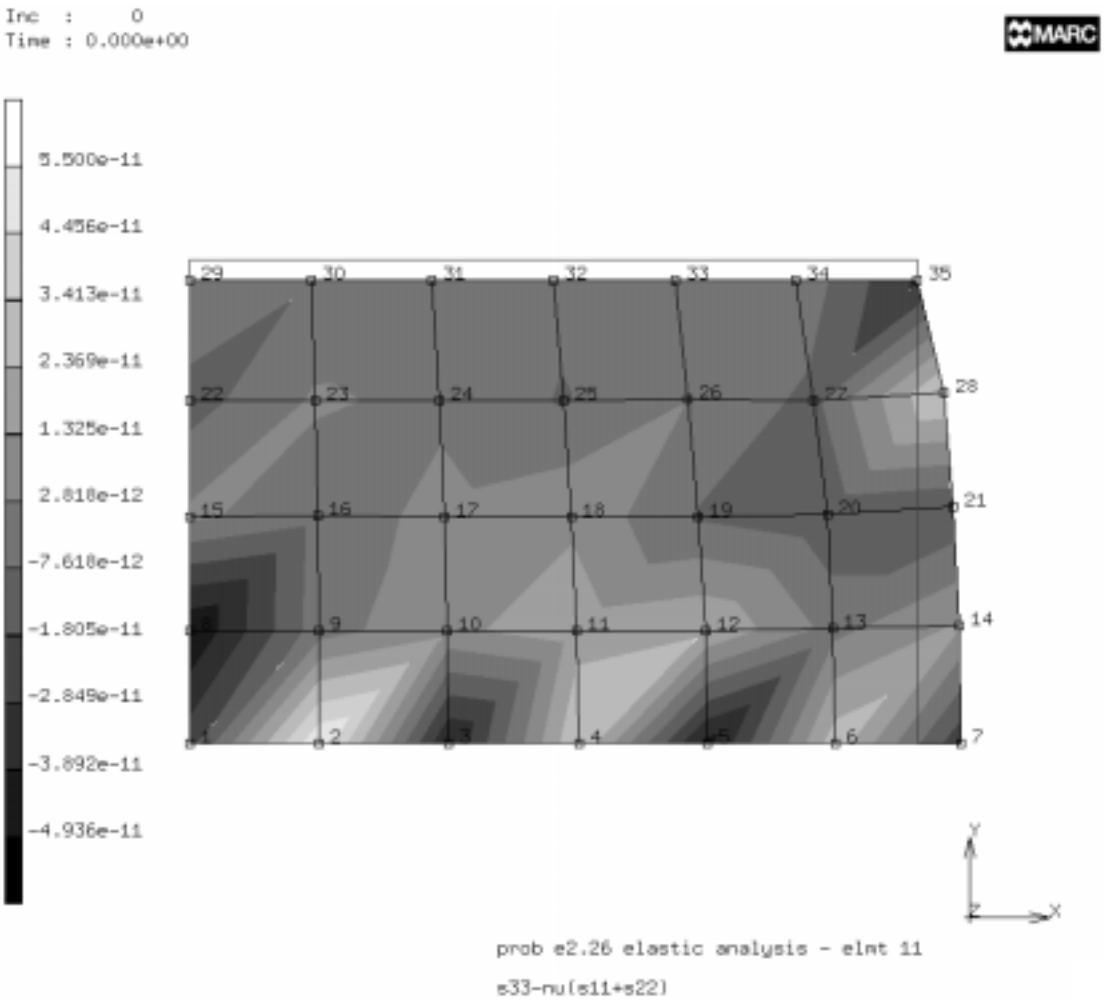

Figure 2.26-2 Contours of F = σ_{33} - $\nu(\sigma_{11} + \sigma_{22})$ Element 11

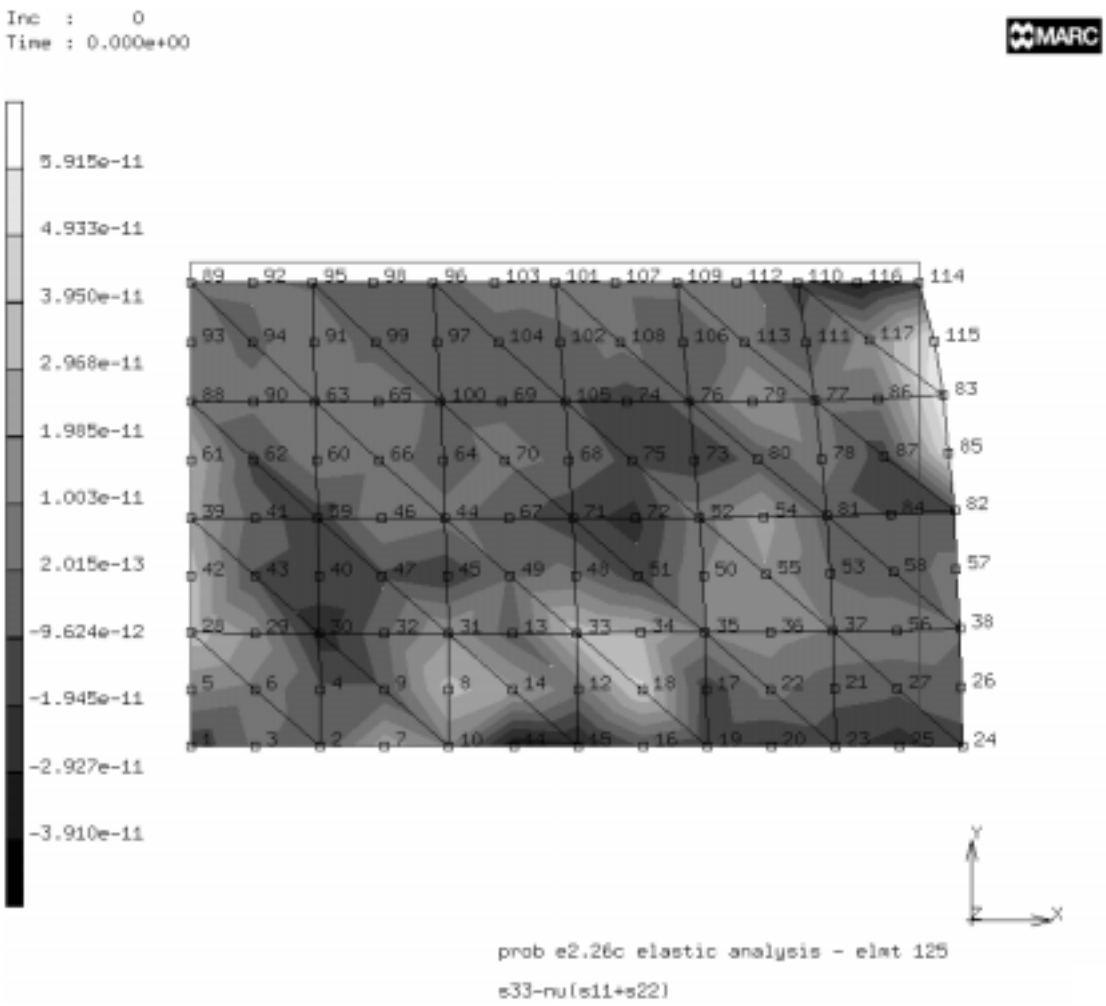

Figure 2.26-3 Contours of F = σ_{33} - $\nu(\sigma_{11} + \sigma_{22})$ Element 125

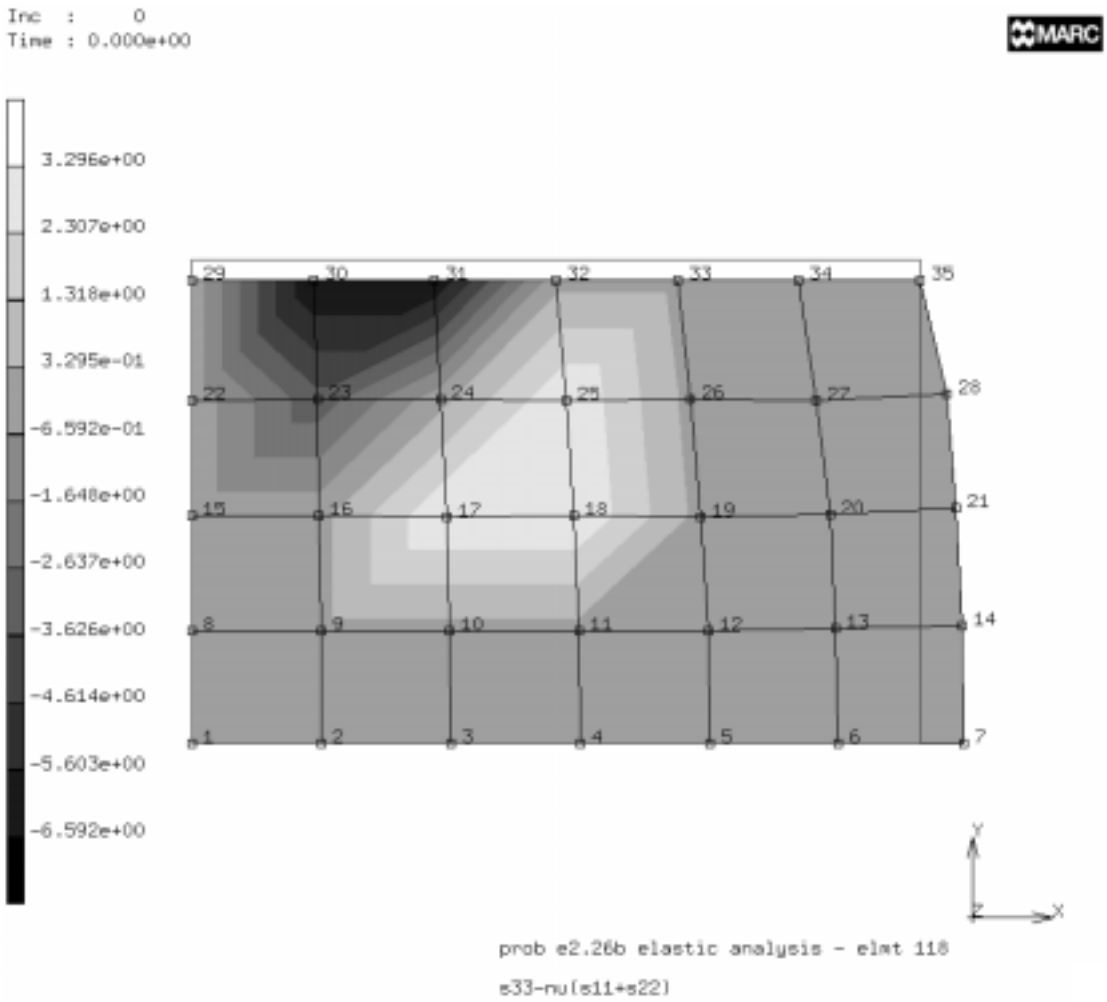

Figure 2.26-4 Contours of F = σ_{33} - $\nu(\sigma_{11} + \sigma_{22})$ Element 118

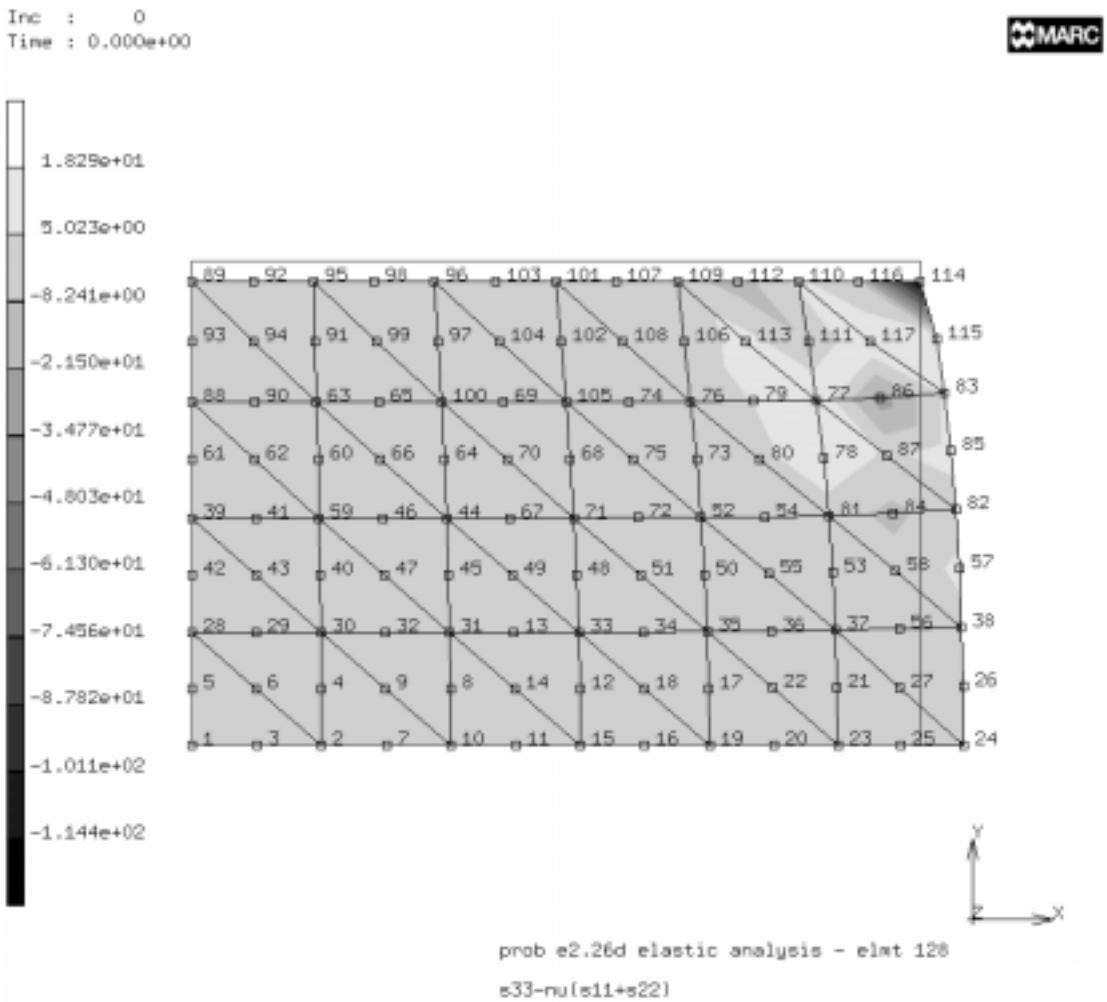

Figure 2.26-5 Contours of F = σ_{33} - $\nu(\sigma_{11} + \sigma_{22})$ Element 128

2.27 Generalized Plane-strain Disk, Point Loading

This problem illustrates the use of MARC element type 19 and user subroutine UFCONN for an elastic analysis of a two-dimensional circular disk. The disk is subjected to diametrically-opposite point loads. The user subroutine UFCONN is used for the modification fo element types 3 to 19, and the addition of the two shared nodes (nodal numbers 83 and 84) for each element in the CONNECTIVITY data block. This is the same problem as 2.10 except the generalized plane strain condition is imposed.

Element

Element type 19 is an extension of element type 11 (plane-strain isoparametric quadrilateral). Two extra nodes are included in each element to create the generalized plane-strain condition.

Model

The dimensions of the disk and a finite element mesh are shown in Figure 2.27-1. The extra two nodes for generalized plane-strain elements are located at the center of the disk. The degrees of freedom associated with these extra nodes represent the relative displacement and rotation of the front and back surfaces. These nodes are shared by all elements in the disk. There are 64 elements and 84 nodes in the mesh.

Material Properties

All elements are elastic with a Young's modulus of 30×10^6 psi and Poisson's ratio equal to 0.3.

Boundary Conditions

Both degrees of freedom are constrained for the second extra node (node 84). First degree of freedom of all nodal points are constrained ($u = 0$) along symmetry line ($x = 0$). The bottom of the disk is constrained to eliminate the rigid body mode.

Geometry

The thickness of the disk is specified as unity in EGEOM1 of this option.

Loading

A concentrated load at the top (node 1) of 100.0 lb. in the negative y-direction is applied.

ELSTO

Out-of-core storage of element data (ELSTO) is used for this problem.

Results

A displaced mesh plot is shown in Figure 2.27-2. The answers agree with those using the plane stress element (problem 2.10) for the stresses.

	Element 1 Problem 2.10 (psi)	Element 1 Problem 2.27 (psi)	Element 30 Problem 2.10 (psi)	Element 30 Problem 2.27 (psi)
σ_{xx}	1.632E2	1.655E2	1.003E1	1.001E1
σ_{yy}	-3.343E2	-3.356E2	-3.092E1	-3.089E1

Parameters, Options, and Subroutines Summary

Example e2x27.dat:

Parameters	Model Definition Options
ELEMENTS	CONNECTIVITY
ELSTO	COORDINATES
END	END OPTION
SIZING	FIXED DISP
TITLE	GEOMETRY
	ISOTROPIC
	POINT LOAD
	UFCONN

User subroutine found in u2x27.f:

UFCONN

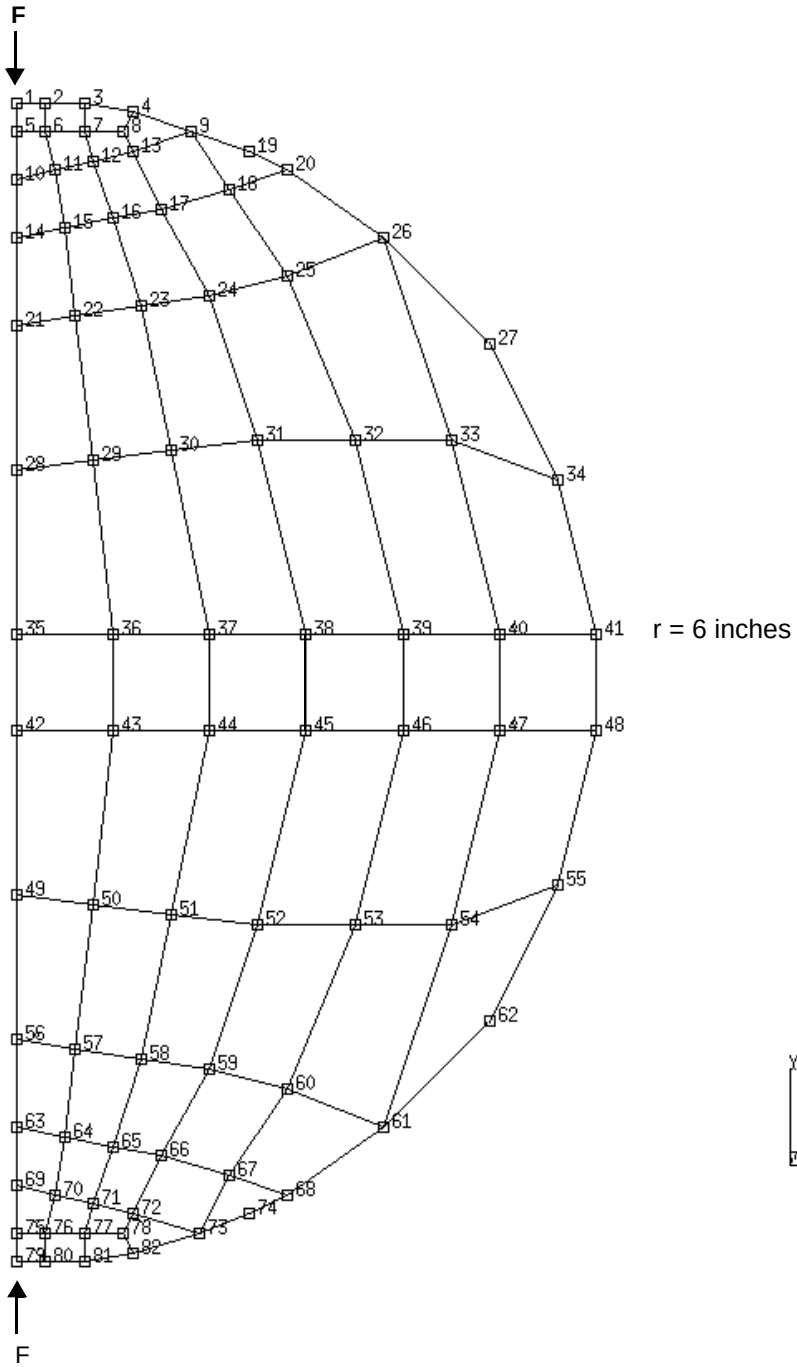

Figure 2.27-1 Disk and Mesh

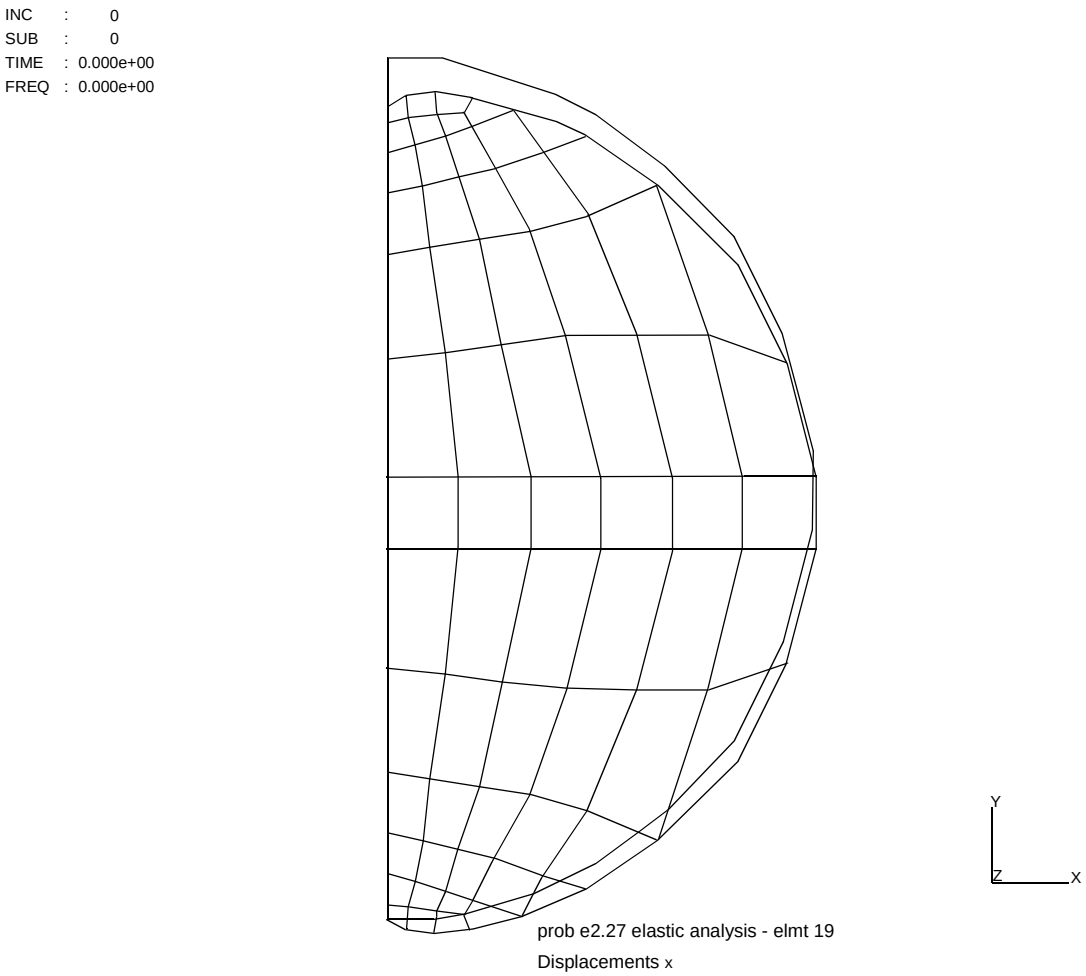

Figure 2.27-2 Deformed Mesh Plot

2.28 Circular Shaft of Variable Radius Under Tension and Twist

This problem illustrates the use of MARC element type 20 and tying constraint options for an elastic analysis of a circular rod of variable radius. The rod is subjected to a combined loading of tension and twist.

Element

Element type 20 is an isoparametric axisymmetric ring with a quadrilateral cross section. This element is identical to element type 10, modified to allow twist about the axis of symmetry. There are four nodes per element.

Model

The dimensions of the circular rod and the finite element mesh are shown in Figure 2.28-1. The ratio of radii is 2.5:1 or a ratio in area of 6.25:1. The mesh consists of 33 elements of type 20. There are a total of 8 nodes.

Material Properties

The material is considered elastic with a Young's modulus of 2.08×10^6 psi and a Poisson's ratio of 0.3.

Geometry

Not required for axisymmetric elements.

Loading

A point load ($P = 10^5$ lb.) and a torque ($T = 2 \times 10^5$ in-lb.) are applied at node 48.

Boundary Conditions

All degrees of freedom of nodes at y = 0 are constrained to simulate a built-in end. Radial displacements (second degree of freedom) along the symmetric axis (r = 0) are fixed (v = 0).

Tying Constraints

There are two tying types in this problem.

Tying Type	Retained Node	Tied Nodes
1	48	36, 40, 44
3	48	36, 40, 44

The total number of tying equations is six and the maximum number of retained nodes in all tying types is one. These ties are used to simulate a generalized plane-strain condition. Thus, the loaded face nodes are forced to move together.

Results

A deformed mesh plot is shown in Figure 2.28-2 and stress contours are depicted in Figure 2.28-3 through Figure 2.28-5. σ_{zz} is at x=21, approximately 6.25 times σ_{zz} at x=0.

An analytical solution for a similar problem is found in I. S. Solkolnikoff, *Mathematical Theory of Elasticity.* The displacement and stresses are compared for the MARC solution and the analytical solution:

Displacement*		**Stress σ_{zq}**	
MARC Computed	**Analytically Computed**	**MARC Computed****	**Analytically Computed*****
4.5057×10^{-2}	4.5223×10^{-2}	8.770×10^{3}	$\sigma_{z\theta}^{max} = 9.120 \times 10^{3}$
* Angular displacement about symmetric axis at point 48. ** σ_{zq} at point 3 in element 30. *** σ_{zq} at R=2.4.			

Parameters, Options, and Subroutines Summary

Example e2x28.dat:

Parameters	**Model Definition Options**
ELEMENTS	CONNECTIVITY
END	COORDINATES
SIZING	END OPTION
TITLE	FIXED DISP
	ISOTROPIC
	POINT LOAD
	TYING

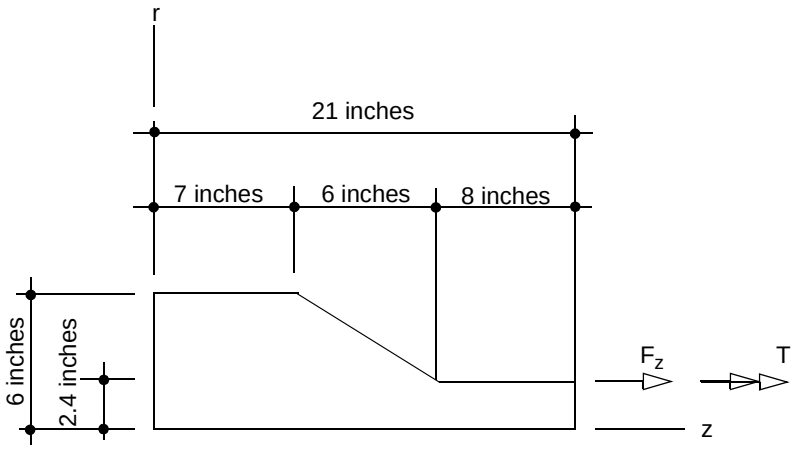

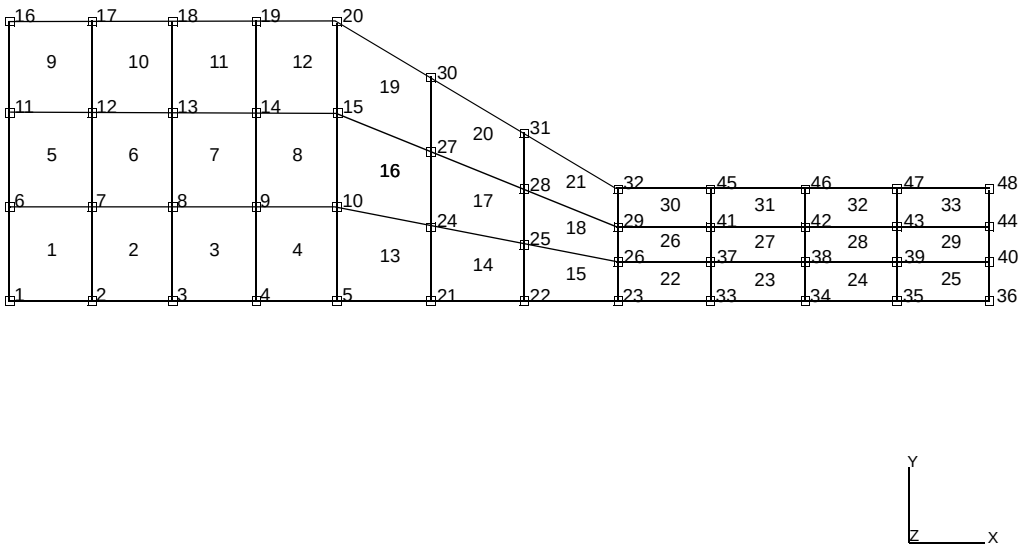

Figure 2.28-1 Circular Rod and Mesh

INC : 0
SUB : 0
TIME : 0.000e+00
FREQ : 0.000e+00

MARC

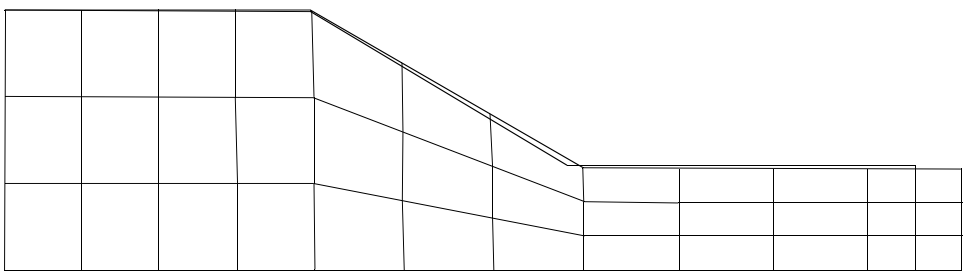

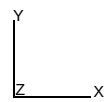

prob e2.28 elastic analysis – elmt 20
Displacements x

Figure 2.28-2 Deformed Mesh Plot

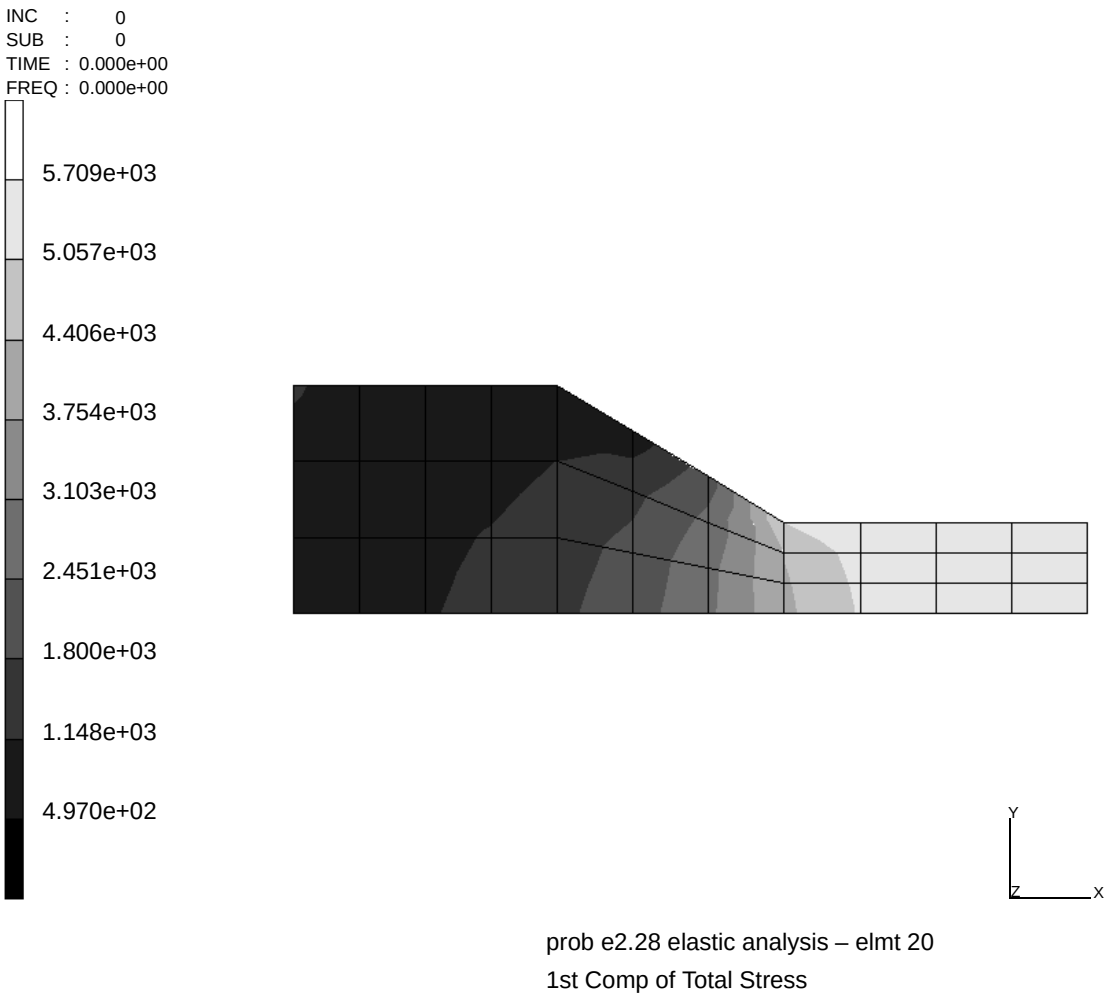

Figure 2.28-3 Stress Contours for σ_{zz}

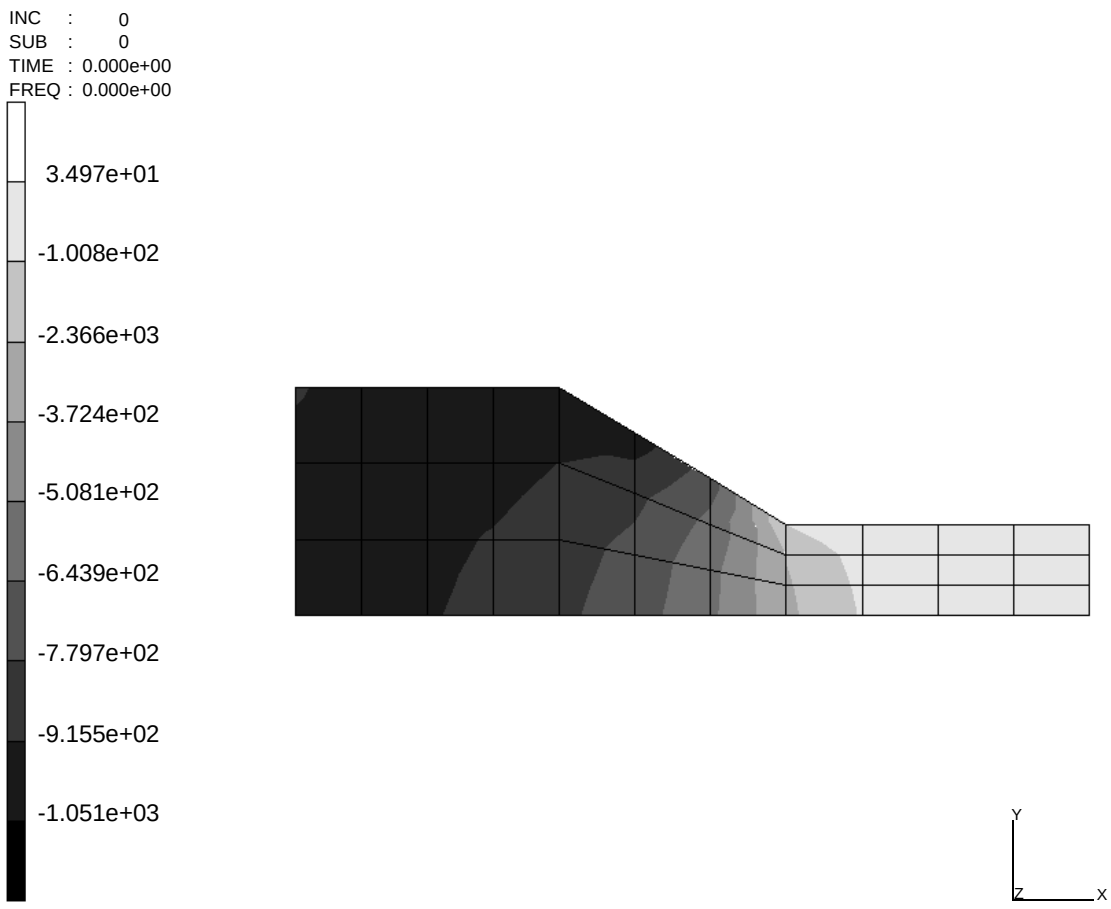

Figure 2.28-4 Stress Contours for σ_{zq}

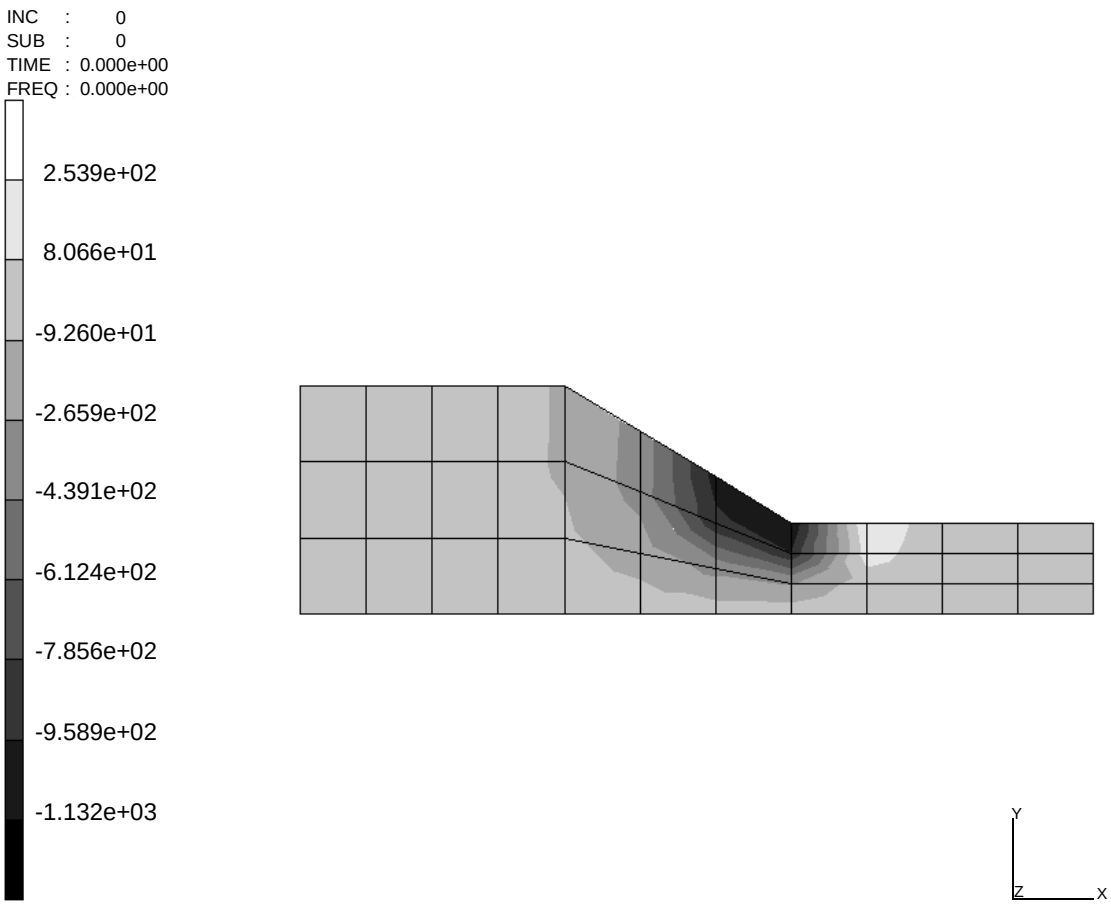

Figure 2.28-5 Stress Contours for σ_{rq}

2.29 Thin-walled Beam on an Elastic Foundation

This problem illustrates the use of MARC element type 25 and the FOUNDATION options for elastic analysis of a thin-walled beam subjected to a concentrated load at the center of the beam. The beam rests on an elastic foundation.

Element

Element type 25 is a thin-walled beam with no section warp, but with twist. The beam is a closed section hollow cylinder when EGEOM1 = 0. This is similar to element type 14, but the accuracy is greater for behavior parallel to the beam axis. The element is particularly useful for problems involving thermal gradients or large displacements.

The beam is considered to be elastic with a Young's modulus of 2×10^5 psi and a modulus of foundation of 10 lb/inch.

Model

The dimensions of the beam and a finite element mesh are shown in Figure 2.29-1. The finite element mesh consists of 20 elements of type 25; there are 21 nodes in the mesh. Only half of the beam is modeled due to symmetry.

Geometry

The beam consists of a pipe with wall thickness of 0.2 inch (EGEOM1) and mean radius (EGEOM2) of 3 inches.

Loading

A concentrated load of P/2 = 1000 pounds is applied at the center of the beam.

Boundary Conditions

Symmetry conditions are imposed at X = 0; Y = 0, Z = 0 (i.e. u = 0, $\theta_x = 0$, $\theta_y = 0$, $\theta_z = 0$, du/ds = 0). All degrees of freedom in the Y-direction are assumed to be fixed in space; hence, the analysis may be considered two-dimensional.

Elastic Foundation

The whole beam is assumed to rest on an elastic foundation. The description of the elastic foundation is given in model definition option FOUNDATION:

- Element numbers = 1 through 20
- Spring stiffness per unit length of the beam = 10. pounds/inch
- Element face I.D. = 3
- The element face identification indicates which face the beam is resting on the foundation.

Results

A deformed mesh plot is shown in Figure 2.29-2 and a comparison of deflection and moment at node 1 is given below:

Displacement:

MARC-Computed Solution δ_1 = -2.93 inches
Analytic Solution δ_1 = -2.926 inches

Moment:

MARC Solution M_1 = 17066. in-lb.
Analytic Solution M_1 = 17065. in-lb.

The analytic solution is obtained from R.J. Roark, *Formulas for Stress and Strain*, assuming that the beam is of infinite length. For beams of a finite length, the analytic solutions for an elastic beam may be found in *Handbook of Engineering Mechanics*, ed. W. Flugge.

Parameters, Options, and Subroutines Summary

Example e2x29.dat:

Parameters	Model Definition Options
ELEMENTS	CONNECTIVITY
END	COORDINATES
SIZING	END OPTION
TITLE	FIXED DISP
	FOUNDATION
	GEOMETRY
	ISOTROPIC
	POINT LOAD

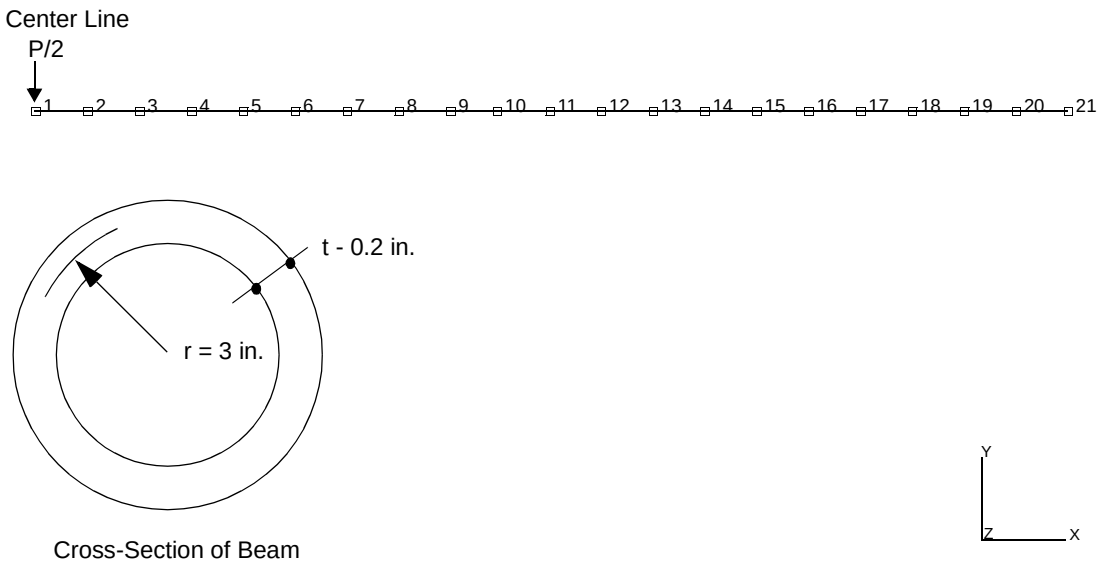

Figure 2.29-1 Thin Walled Beam and Mesh

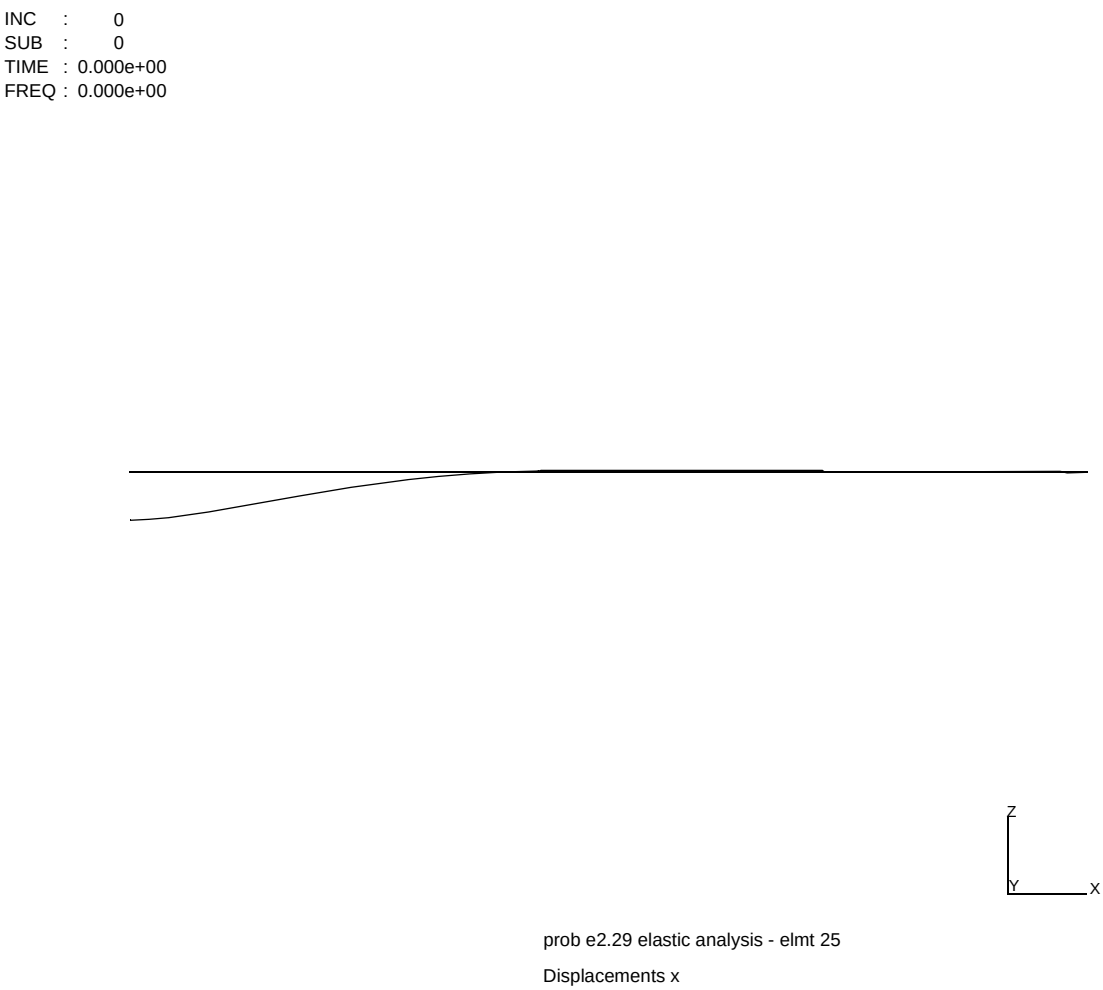

Figure 2.29-2 Deformed Mesh Plot

2.30 Notched Circular Bar, J-Integral Evaluation

This problem illustrates the use of MARC element type 28 and the J-INT option for an elastic analysis of a notched circular bar, subjected to uniformly distributed axial forces. The J-integral evaluation is intended for the study of the stress concentration at the notch of the bar. The use of parameters ELSTO and ALIAS is also illustrated.

Element

Element type 28 is a second order distorted quadrilateral with eight nodes. Each node has two degrees of freedom. For J-integral calculations, a high-order element is required; hence, the selection of element type 28.

Model

The dimensions of the bar and the finite element mesh are shown in Figure 2.30-1. This is the same mesh used in problem 2.22. The mesh consists of 32 elements and 107 nodes. The ALIAS parameter is used to convert element type 27 to 28.

Material Properties

The material is elastic with a Young's modulus of 30.E6 psi and Poisson's ratio of 0.3.

Geometry

Not required for axisymmetric elements.

Boundary Conditions

The following boundary conditions are imposed: v = 0 at r = 0 (axis of symmetry) and u = 0 at uncracked portion of line z = 0.

Loading

A distributed load of 100 psi is applied on the outer edge of elements 15, 16, 31 and 32.

The midside nodes 2, 5, 8, 11, 14, 69, 66, 63 and 60 have been moved to quarter-point position for the J-integral evaluations. The quarter-point nodes more accurately reflect the singularity at the crack tip. Their coordinates are modified by inputting a new COORDINATES model definition block. The mesh is generated as if it was made of element type 27, and the ALIAS parameter was used so that MARC would consider them to be type 28.

J-INTEGRAL

In the current analysis three rings of elements are chosen for the J-integral evaluations.

J-Integral Evaluations	Number of Nodes Moved in List Number		Nodal Movements of List Number in r Direction	
	1	2	1	2
1	1	9	-0.01	-0.0075
2	27	9	-0.01	-0.0050
3	53	9	-0.01	-0.0050

Node numbers are shown in the J-INTEGRAL model definition block.

Results

A comparison of the J-integral evaluation is tabulated in Table 2.30-1. A deformed mesh plot and stress contours are shown in Figure 2.30-3 and Figure 2.30-4, respectively.

Table 2.30-1 Comparison of J-Integral Evaluations

MARC	SED Output	J	K	Difference (K/K_I)
1	0.01131	0.0360189	1089.7	2.28%
2	0.01127	0.0358915	1087.8	2.01%
3	0.01125	0.0358278	1086.8	2.01%

Note: Stress intensity factor estimation for mode I cracking

The stress intensity factor K_I for an axisymmetric bar is:

$$K_I = \sigma_n \sqrt{\pi b} \quad F_2\left(\frac{b}{R}\right)$$

$$\sigma_n = \frac{P}{\pi b} \quad ,$$

$$F_2(\xi) = \frac{1}{2}\left(1 + \frac{1}{2}\ \xi + \frac{3}{8}\ \xi^2 - 0.363\ \xi^3 + 0.731\ \xi^4\right)\sqrt{1-\xi}$$

(error < 1%)

therefore, $K_I = 1065.39$

For an axisymmetric model, plane strain assumption is assumed to exist locally, and the relation between J and K_I is:

$$K_I = \sqrt{\frac{E}{1-\nu^2}J} = \sqrt{32967033*J}$$

MARC output is the strain energy density (SED) of the area of crack tip movement. The expression of J-integral is:

$$J = \frac{SED*2}{\pi b^2 - \pi(b-\delta b)z^2} = \frac{SED*2}{\pi(10^2 - 9.99^2)} = \frac{SED}{0.3140022}$$

Parameters, Options, and Subroutines Summary

Example e2x30.dat:

Parameters	Model Definition Options
ALIAS	CONNECTIVITY
ELEMENTS	COORDINATES
ELSTO	DIST LOADS
END	END OPTION
J-INT	FIXED DISP
SIZING	ISOTROPIC
TITLE	J-INTEGRAL

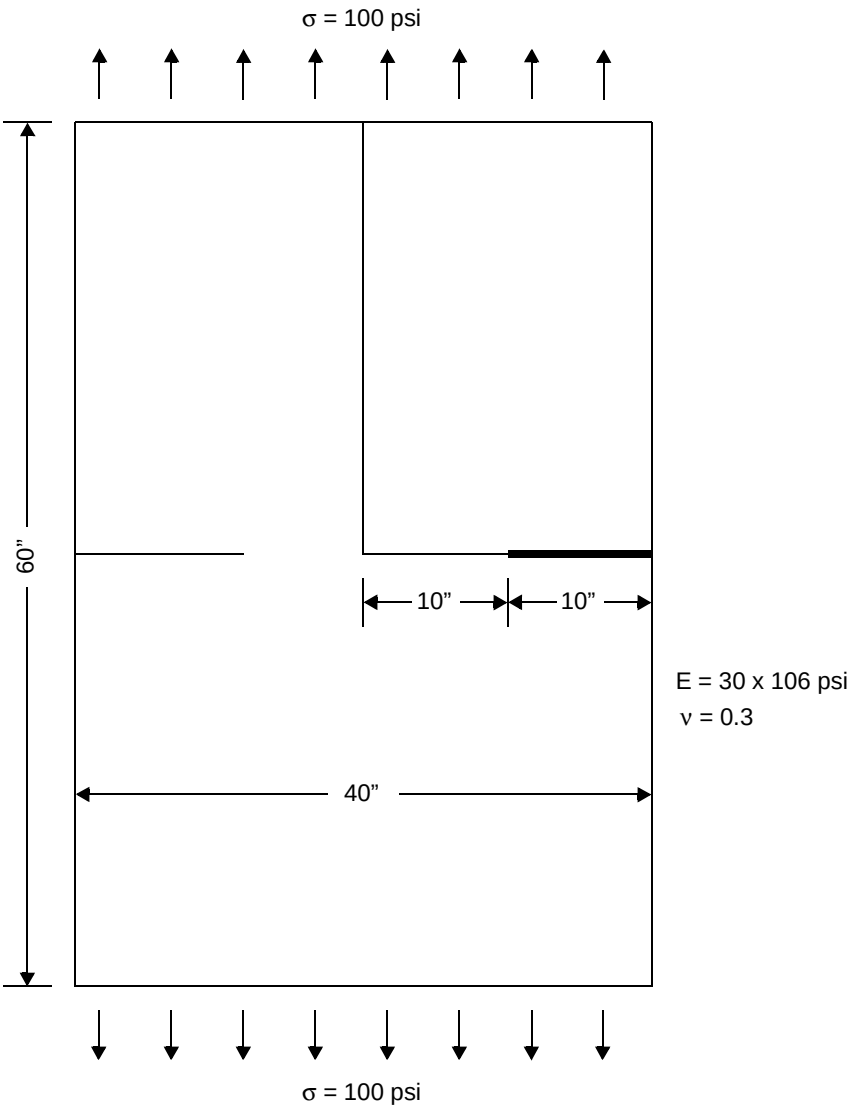

Figure 2.30-1 Notched Circular Bar and Mesh

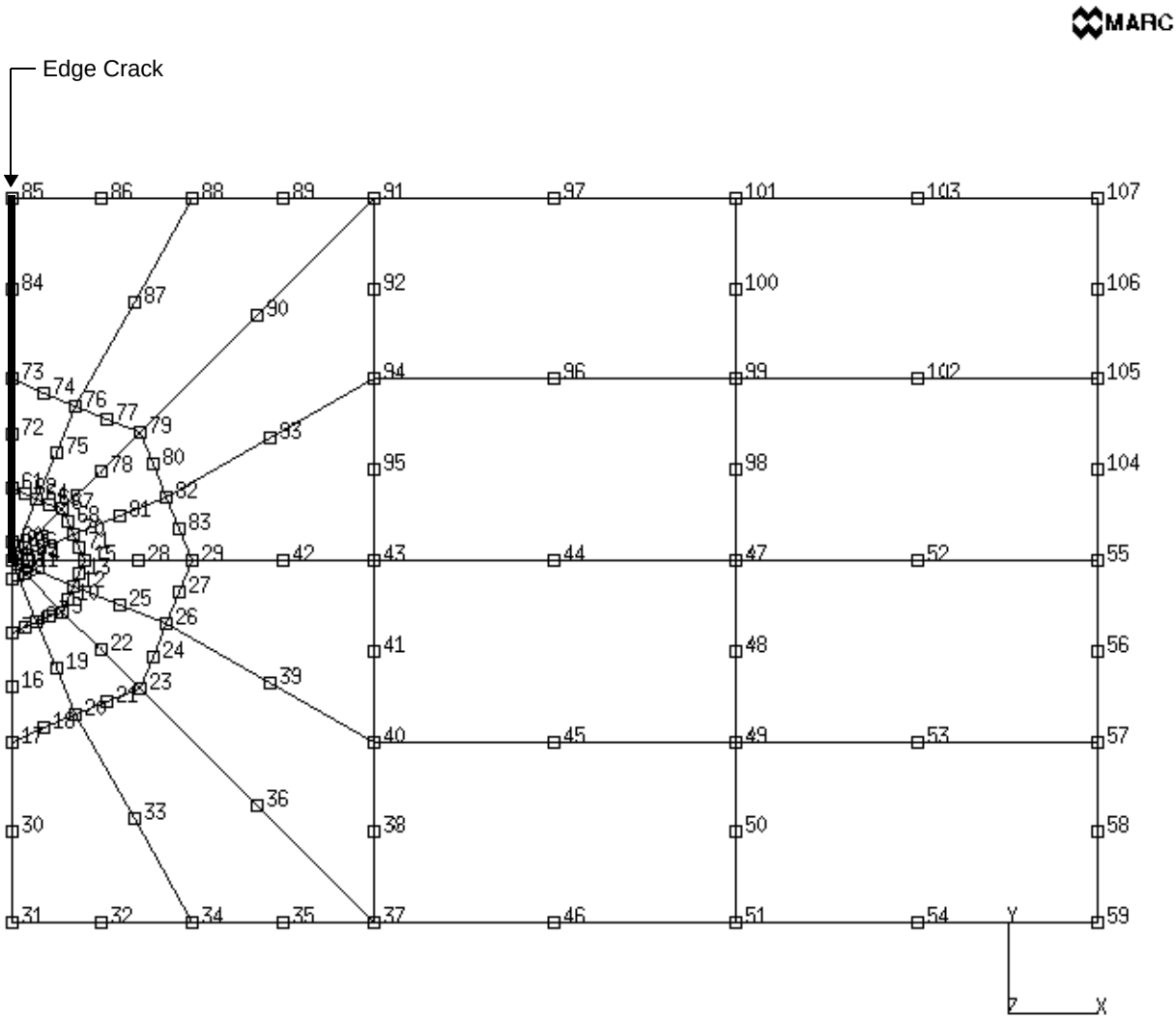

Figure 2.30-2 Mesh for Double Edge Notch Specimen

INC : 0
SUB : 0
TIME : 0.000e+00
FREQ: 0.000e+00

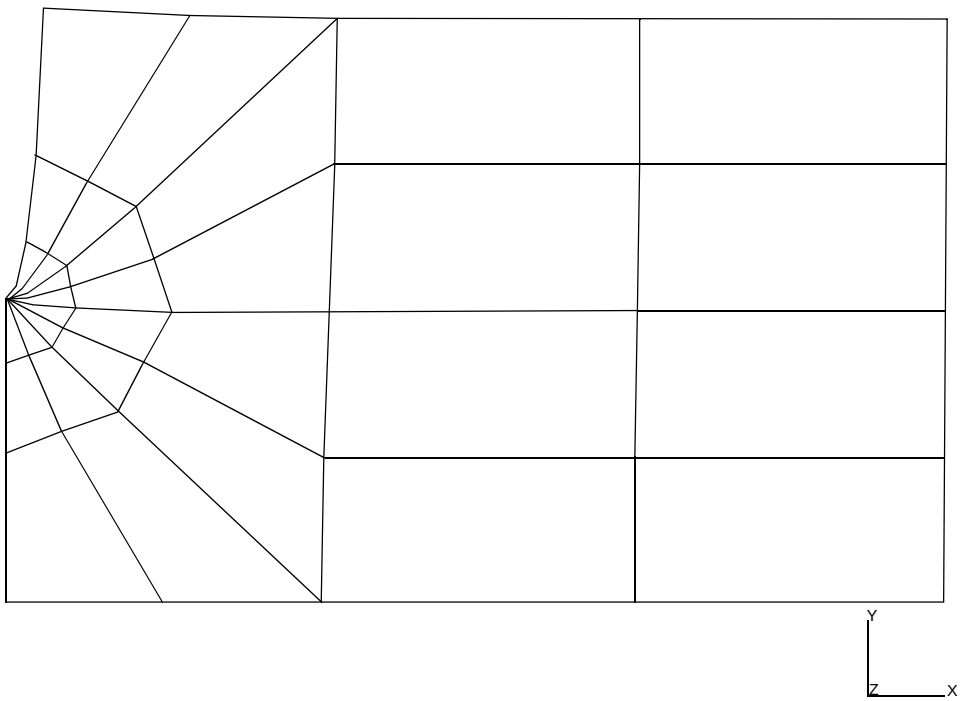

Figure 2.30-3 Deformed Mesh

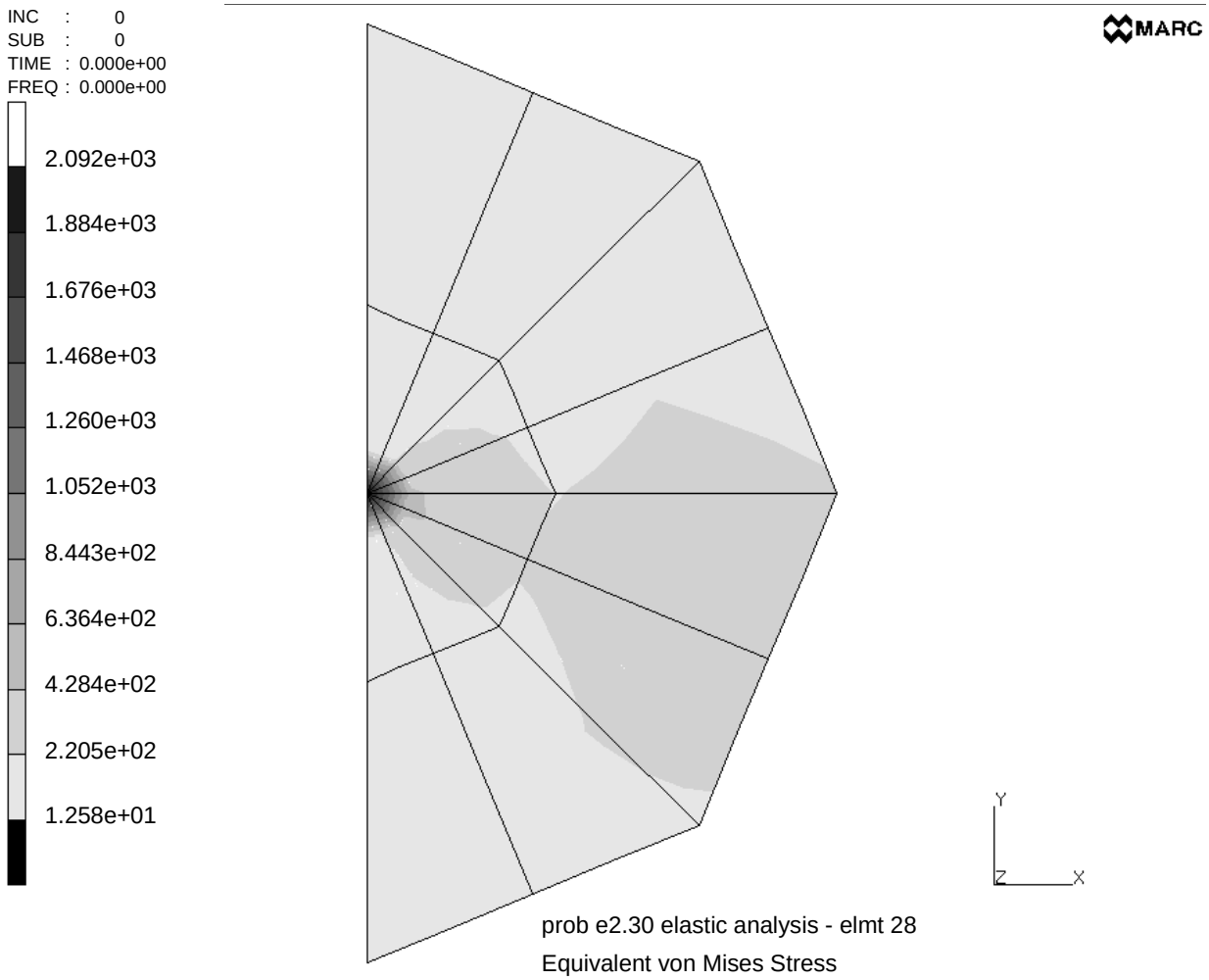

Figure 2.30-4 Stress Contours

2.31 Square Section with Central Hole using Generalized Plane Strain Element

This problem illustrates the use of MARC element types 29 and 56 (generalized plane strain, distorted quadrilateral), OPTIMIZE option, and SCALE parameter for an elastic analysis of a square plate subjected to a uniform pressure. The pressure is applied to the surface of a circular hole located at the center of the section.

This problem is modeled using the two techniques summarized below.

Data Set	Element Type(s)	Number of Elements	Number of Nodes
e2x31a	29	20	79
e2x31b	56	20	79

Elements

The analysis is performed twice: first with element type 29, which uses 9-point integration, and then with element type 56, which uses 4-point integration.

Model

The dimensions of the plate and a finite element mesh are shown in Figure 2.31-1. The model consists of 20 elements and 81 nodes. Only one-quarter of the section is modeled due to symmetry.

Material Properties

The material behaves elastically with a Young's modulus of 50 x 10^4 psi and the Poisson's ratio of 0.2. The solution is scaled such that one integration point has reached the yield stress of 200 psi.

Geometry

The thickness of the section is 1.0 inch, which is given in EGEOM1.

Loading

A uniform pressure of 1000 psi is applied to the inner surface of the hole. The pressure load is scaled to the condition of first yield.

Boundary Conditions

Zero displacements are assumed to exist on the lines of symmetry: u = 0 at x = 0, and v = 0 at y = 0.

Optimization

The Sloan optimizer is used. As this is a generalized plane strain model, the bandwidth does not decrease, but the number of profile entries, including fill-in, is reduced from 1687 to 1198.

Results

A deformed mesh plot is shown in Figure 2.31-2 and the stress contours are depicted in Figure 2.31-3. First, one observes that the results are symmetrical about the 45-degree line. The scale factor using element type 29 (full integration) is 0.116, and the scale factor using element type 56 is 0.120 more than the factor computed for element 29. Element type 29 has integration points closer to the hole where the stress is larger, resulting in a lower scaling factor.

The results are compared with the analytically calculated (Timoshenko and Goodier, *Theory of Elasticity*) results of a hollow cylinder submitted to uniform pressure on the inner surface and are summarized below.

Displacement* (in.)		Stress Components (psi)	
Computed	**Calculated**	**Computed****	**Calculated*****
2.97×10^{-4}	2.80×10^{-4}	$\sigma_x = -1.08 \times 10^{-2}$	$\sigma_x = -1.16 \times 10^{-2}$ (σ_r)
		$\sigma_y = 1.18 \times 10^{-2}$	$\sigma_y = -1.16 \times 10^{-2}$ ($\sigma\theta$)
*At node point 34.		**At node point 3 in element 8	***On the inner surface

Parameters, Options, and Subroutines Summary

Example e2x31a.dat:

Parameters	Model Definition Options
ELEMENTS	CONNECTIVITY
END	COORDINATES
SCALE	DIST LOADS
SIZING	END OPTION
TITLE	FIXED DISP
	GEOMETRY
	ISOTROPIC
	OPTIMIZE

Example e2x31b.dat:

Parameters	Model Definition Options
ELEMENTS	CONNECTIVITY
END	COORDINATES
SCALE	DIST LOADS
SIZING	END OPTION
TITLE	FIXED DISP
	GEOMETRY
	ISOTROPIC
	OPTIMIZE

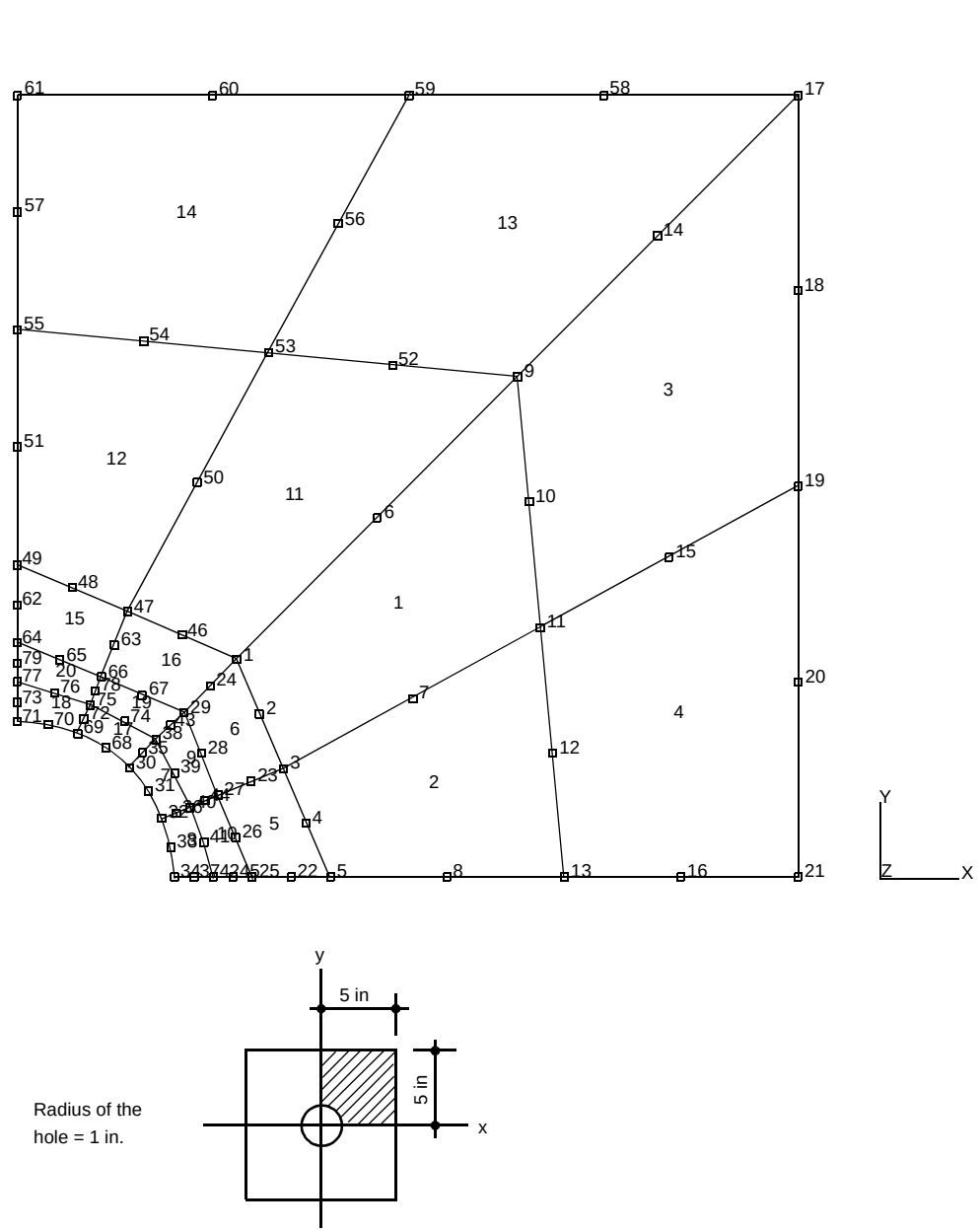

Figure 2.31-1 Square Plate and Mesh

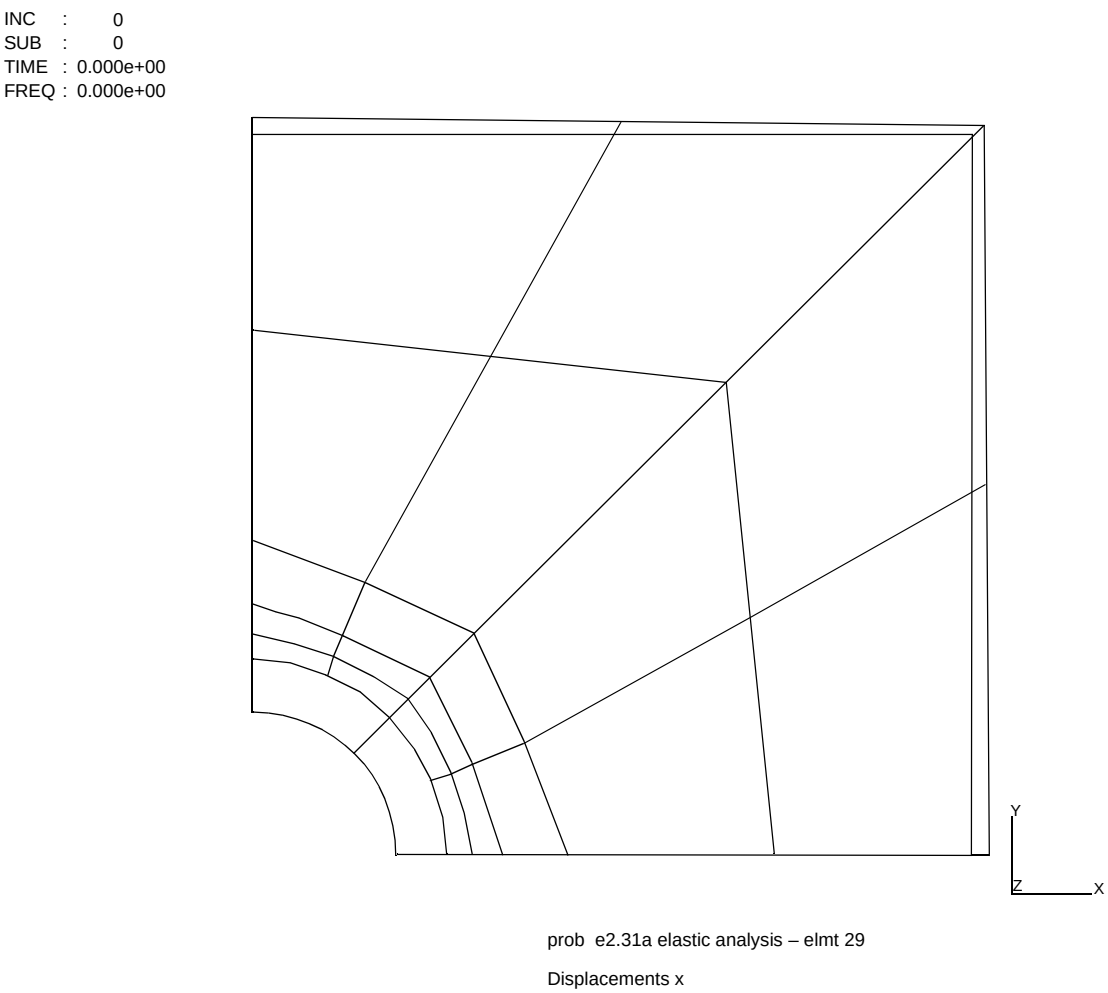

Figure 2.31-2 Deformed Mesh Plot

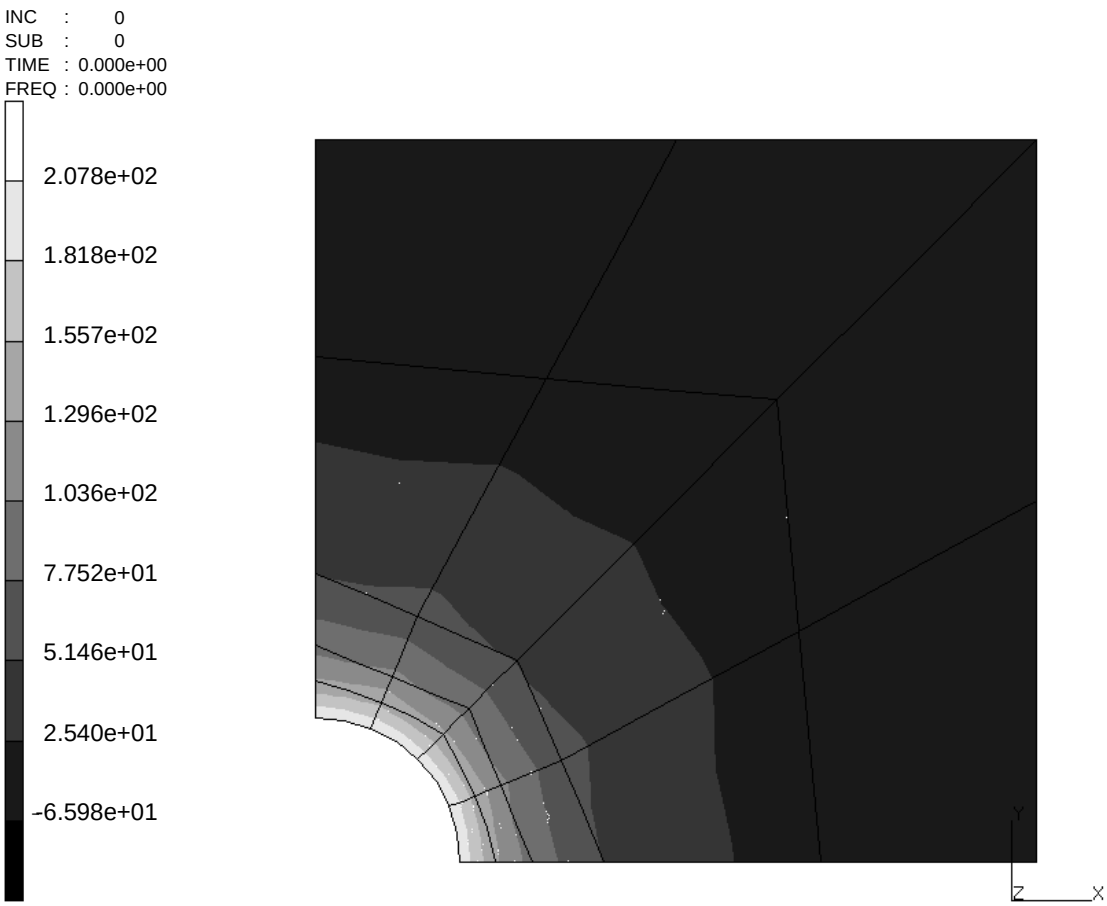

Figure 2.31-3 Stress Contours

2.32 Square Plate with Central Hole using Incompressible Element

This problem illustrates the use of MARC element type 32, the OPTIMIZE option, and the ALIAS and SCALE parameters for an elastic analysis of a square plate. The plate is subjected to a uniform pressure. The pressure is applied to the surface of a circular hole located at the center of the plate.

Element

Element type 32, which is similar to element type 27 but modified for the Herrmann variational principle, has been developed for incompressible and nearly incompressible analysis.

Model

The dimensions of the plate and a finite element mesh are shown in Figure 2.32-1. The mesh is the same as that used in problem 2.31. There are 20 elements with 79 nodes in the mesh.

Material Properties

The properties are as follows: Young's modulus of 50×10^4 psi, Poisson's ratio of 0.5, and yield stress of 200 psi.

Geometry

The thickness of the plate is 1.0 inch.

Loading

A uniform pressure of 1000 psi is applied to the inner surface of the hole. The pressure load is scaled to the condition of first yield.

Boundary Conditions

Zero displacements are assumed to exist on the lines of symmetry: $u = 0$ at $x = 0$, and $v = 0$ at $y = 0$.

Optimize

The Sloan optimizer is used to reduce the bandwidth from 67 to 35.

Results

Stress contours are shown in Figure 2.32-2 through Figure 2.32-5.

Parameters, Options, and Subroutines Summary

Example e2x32.dat:

Parameters	Model Definition Options
ALIAS	CONNECTIVITY
ELEMENTS	COORDINATES
END	DIST LOADS
SCALE	END OPTION
SIZING	FIXED DISP
TITLE	GEOMETRY
	ISOTROPIC

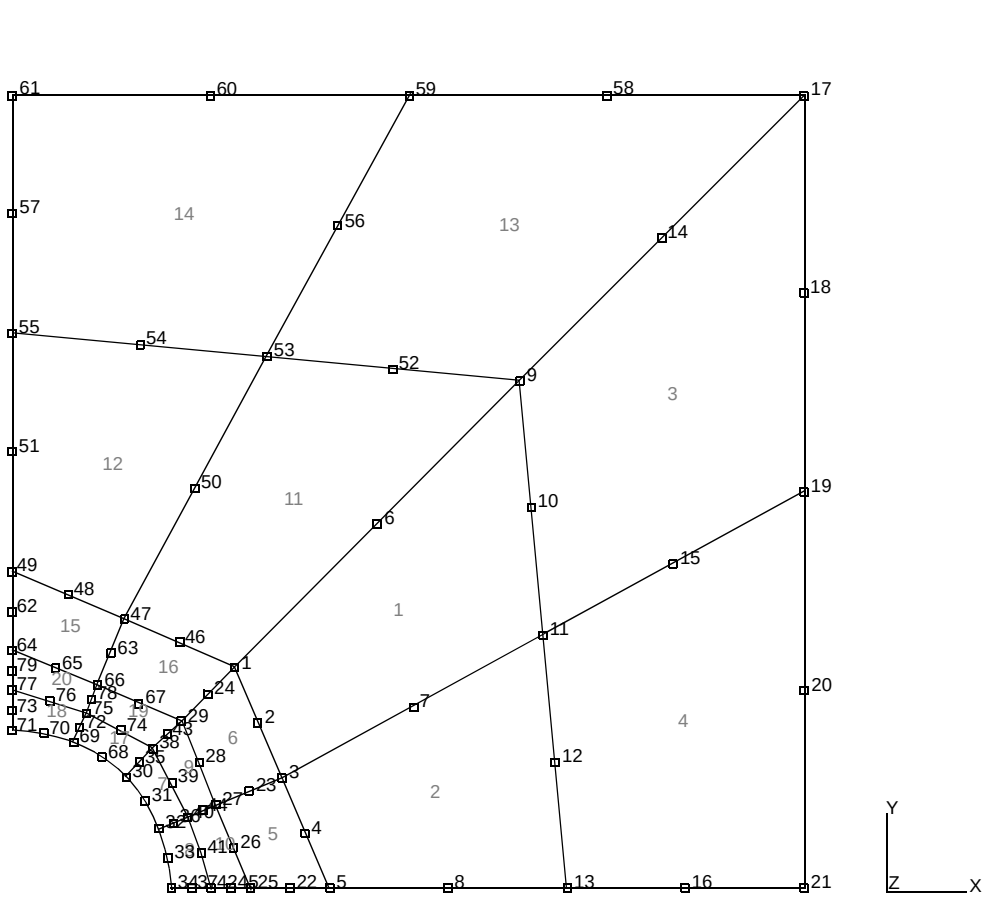

Figure 2.32-1 Square Plate and Mesh

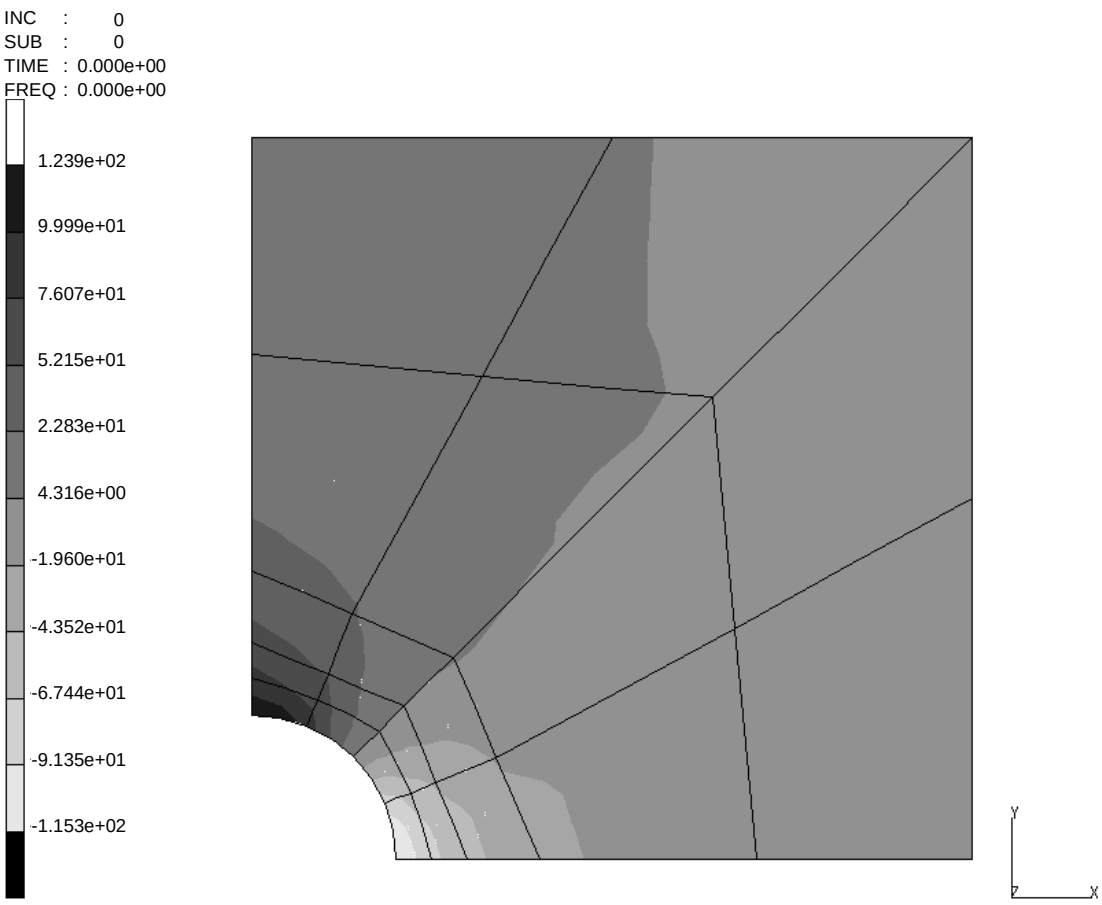

Figure 2.32-2 Stress Contours for σ_{xx}

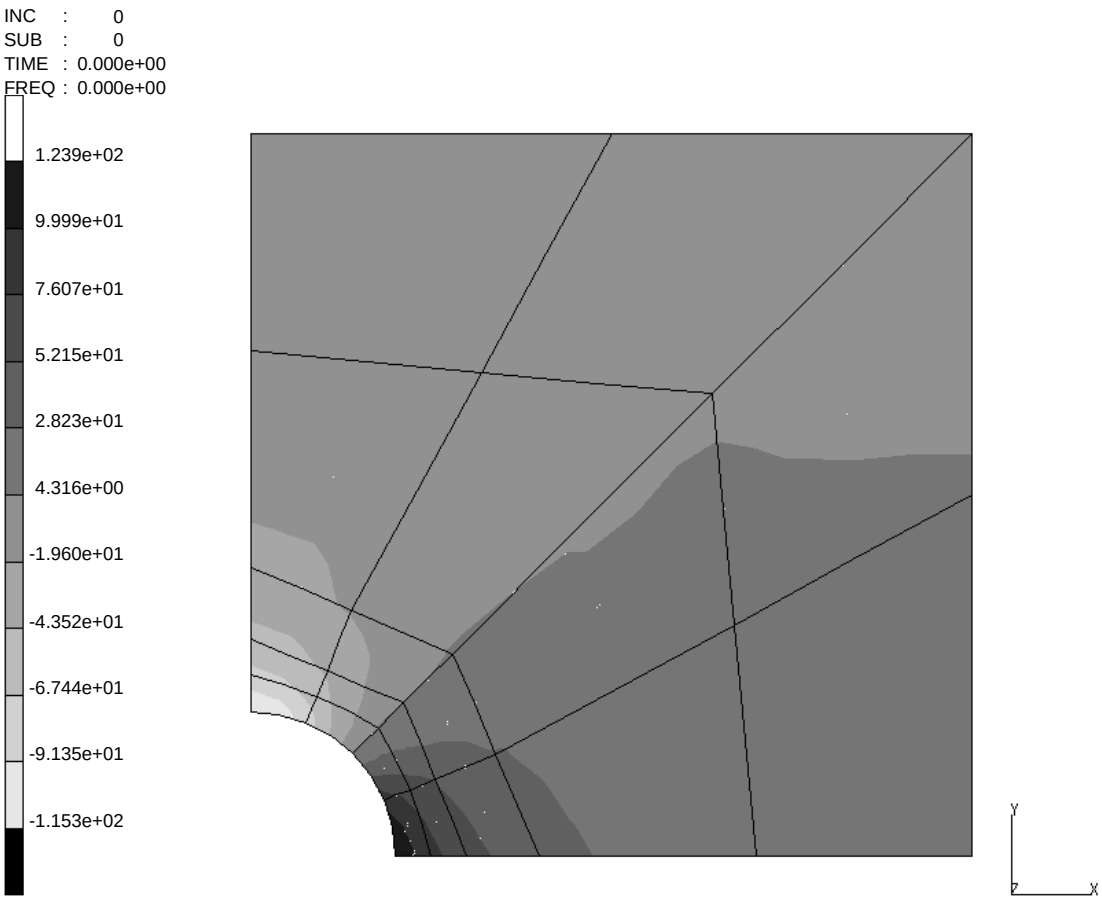

Figure 2.32-3 Stress Contours for σ_{yy}

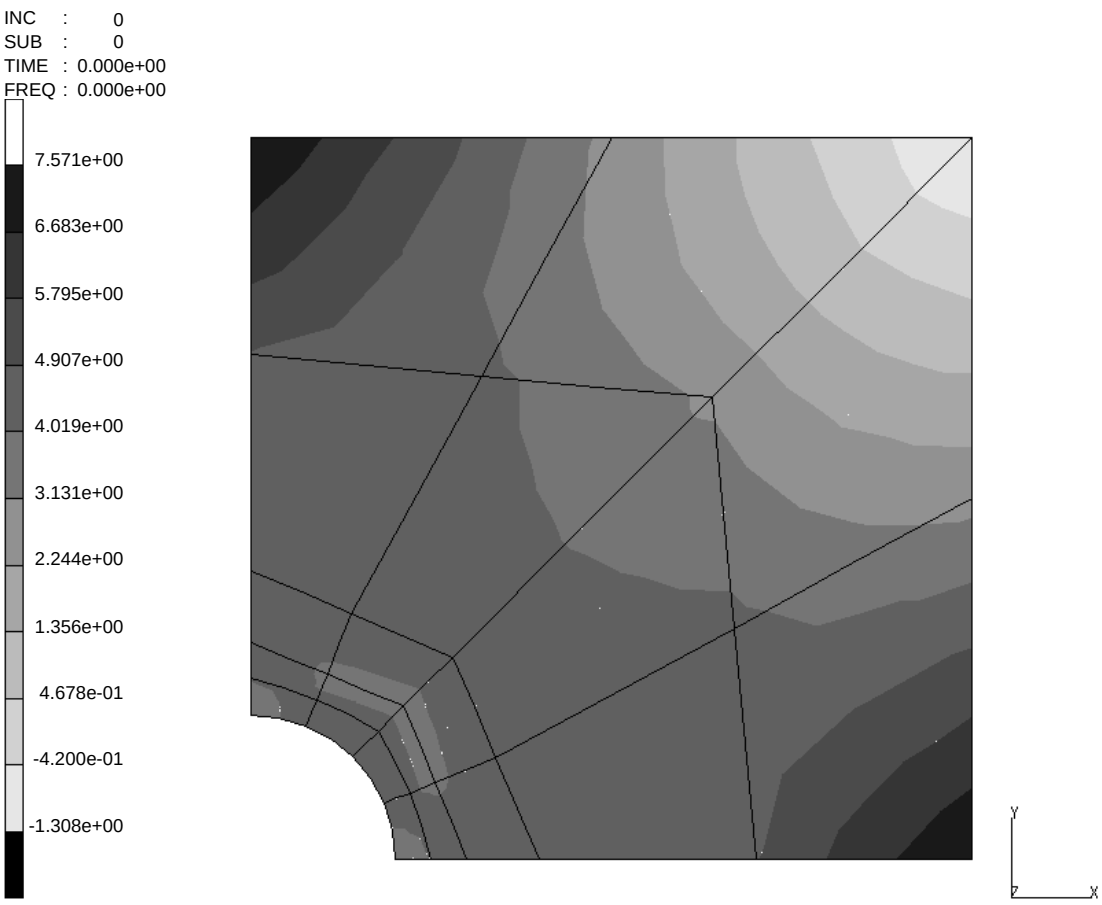

Figure 2.32-4 Stress Contours for σ_{zz}

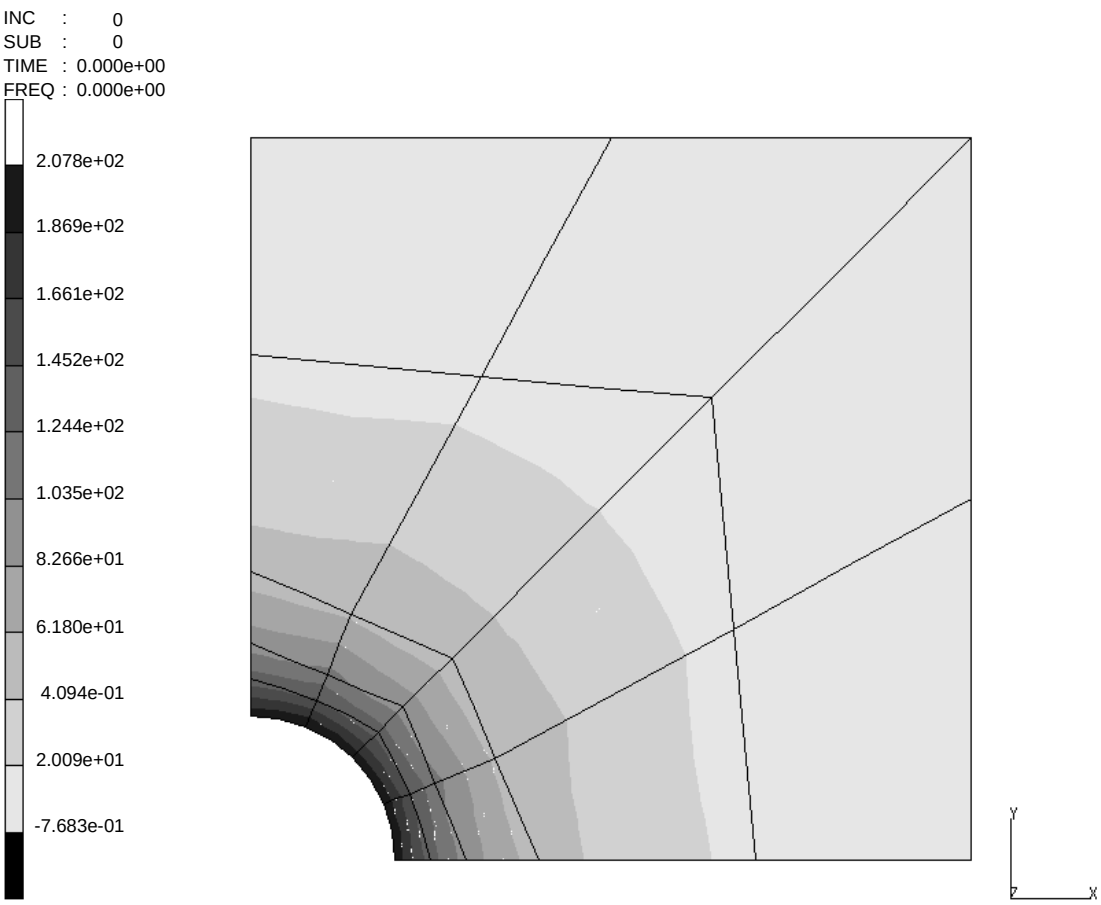

Figure 2.32-5 Stress Contours for Equivalent Stress

2.33 Flat Spinning Disk

This problem illustrates the use of MARC element type 33 for the solution of a circular disk. The disk rotates about the axis of symmetry at a constant angular velocity. The options ROTATION A and DIST LOADS are used for the input of centrifugal load. Options NODE FILL and CONN GENER are used to generate the mesh.

This problem is modeled using the two techniques summarized below.

Data Set	Element Type(s)	Number of Elements	Number of Nodes	Differentiating Features
e2x33	33	15	78	
e2x33b	33	15	78	STIFFSCALE

Element

Element type 33 is used in this analysis. This is an 8-node isoparametric element similar to element 28 but modified for the Herrmann variational principle. This element has been developed for incompressible and nearly incompressible analysis.

Model

The dimensions of the disk and a finite element mesh are shown in Figure 2.33-1. The mesh consists of 15 elements and 78 nodes. The mesh is formed by one element given as an example through the CONNECTIVITY option and then CONN GENER is used to generate the rest of the elements. The coordinates of the nodes at the inner and outer radius are given, and then NODE FILL is used to generate the rest of the coordinates.

Material Properties

The properties are: Young's modulus is 30×10^6 psi, Poisson's ratio is 0.4999, and mass density is 0.2808 lb-sec /in^4.

Loading

Face identification for centrifugal force (IBODY = 100). The angular velocity (ω) is 20 radian/sec ($\omega^2 = 400$), and the axis of rotation is the symmetry axis (z-axis).

Boundary Conditions

The boundary conditions are u = 0 at z = 0 and v = 0 at r = 0 (line of symmetry).

Results

A comparison of the results and the analytic solution are given in Table 2.33-1. The analytical solution may be found in Timoshenko and Goodier, *Theory of Elasticity.*

Table 2.33-1 Comparison of Results

Item	Calculated	MARC
Equivalent Nodal Force (lbs)	7.93433×10^{5}	7.939×10^{5}
Nodal Displacement at r = 15 (in.)	1.5792×10^{-3}	1.586×10^{-3}
Radial Stress at r = 0 (psi)	11056	11050
Hoop Stress at r = 15 (psi)	3159	3260

Parameters, Options, and Subroutines Summary

Example e2x33.dat:

Parameters	Model Definition Options
ELEMENTS	CONN GENER
END	CONNECTIVITY
SIZING	COORDINATES
TITLE	DIST LOADS
	END OPTIO
	FIXED DISP
	ISOTROPIC
	NODE FILL
	ROTATION AXIS

Example e2x33b.dat:

Parameters	Model Definition Options
ELEMENTS	CONN GENER
END	CONNECTIVITY
SIZING	COORDINATES
TITLE	DIST LOADS
	END OPTION
	FIXED DISP
	ISOTROPIC
	NODE FILL
	ROTATION AXIS
	STIFSCALE

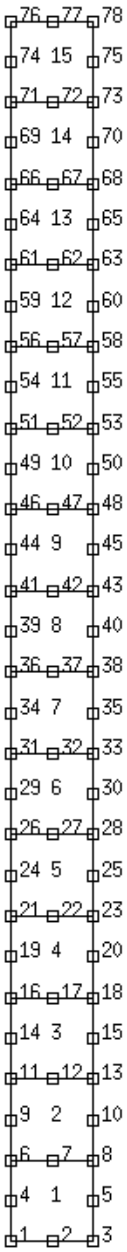

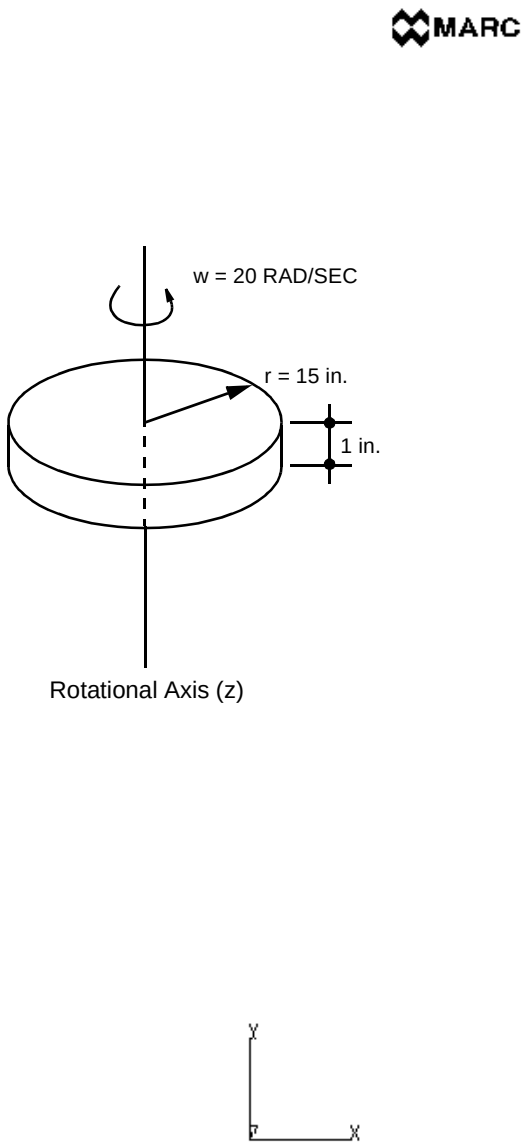

Figure 2.33-1 Flat Disk and Mesh

2.34 Strip with Bonded Edges, Error Estimates

This problem illustrates the use of MARC element type 34, option CONN FILL, OPTIMIZE, and the user subroutine UFCONN for an elastic analysis of a strip. The strip is subjected to compression. This is the same problem as 2.26, but modeled with a different element. The ERROR ESTIMATE option is used to determine mesh quality.

Element

Element type 34 is an 8-node, incompressible, generalized plane-strain element, Herrmann formulation. There are 10 nodes per element.

Model

The dimensions of the strip and a finite element mesh are shown in Figure 2.34-1. There are 24 elements and 95 nodes in the mesh.

Material Properties

The elastic properties are: Young's modulus is 3×10^6 psi and Poisson's ratio is 0.4999.

Geometry

The strip has a thickness of 1 inch.

Boundary Conditions

Symmetry conditions are imposed such that u = 0 at x = 0 and v = 0 at y = 0. At the top, nonzero displacement boundary condition v = -0.001 inch in the y-direction. For the second extra node of elements (node 95), both degrees of freedom are constrained (no relative rotation between planes).

Optimize

The Sloan optimizer is used here. Because generalized plane strain elements are used, the bandwidth does not change, but the number of profile entries including fill-in is reduced.

Results

A deformed mesh plot is shown in Figure 2.34-2 and a contour plot of the second component of stress is shown in Figure 2.34-3. To increase the accuracy of the analysis, additional mesh refinement should be applied to the elements associated with the node where the largest normalized stress discontinuity occurs. In this analysis, this would be elements 23 and 24. The stress singularity exists because on one edge of element 24 shear stresses are allowed to occur, but the perpendicular side is a free edge.

Parameters, Options, and Subroutines Summary

Example e2x34.dat:

Parameters	Model Definition Options
ELEMENTS	CONN FILL
END	CONN GENER
QUALIFY	CONNECTIVITY
SIZING	COORDINATES
TITLE	END OPTION
	FIXED DISP
	GEOMETRY
	ISOTROPIC
	NODE FILL
	OPTIMIZE
	UFCONN

User subroutine in u2x24.f:

UFCONN

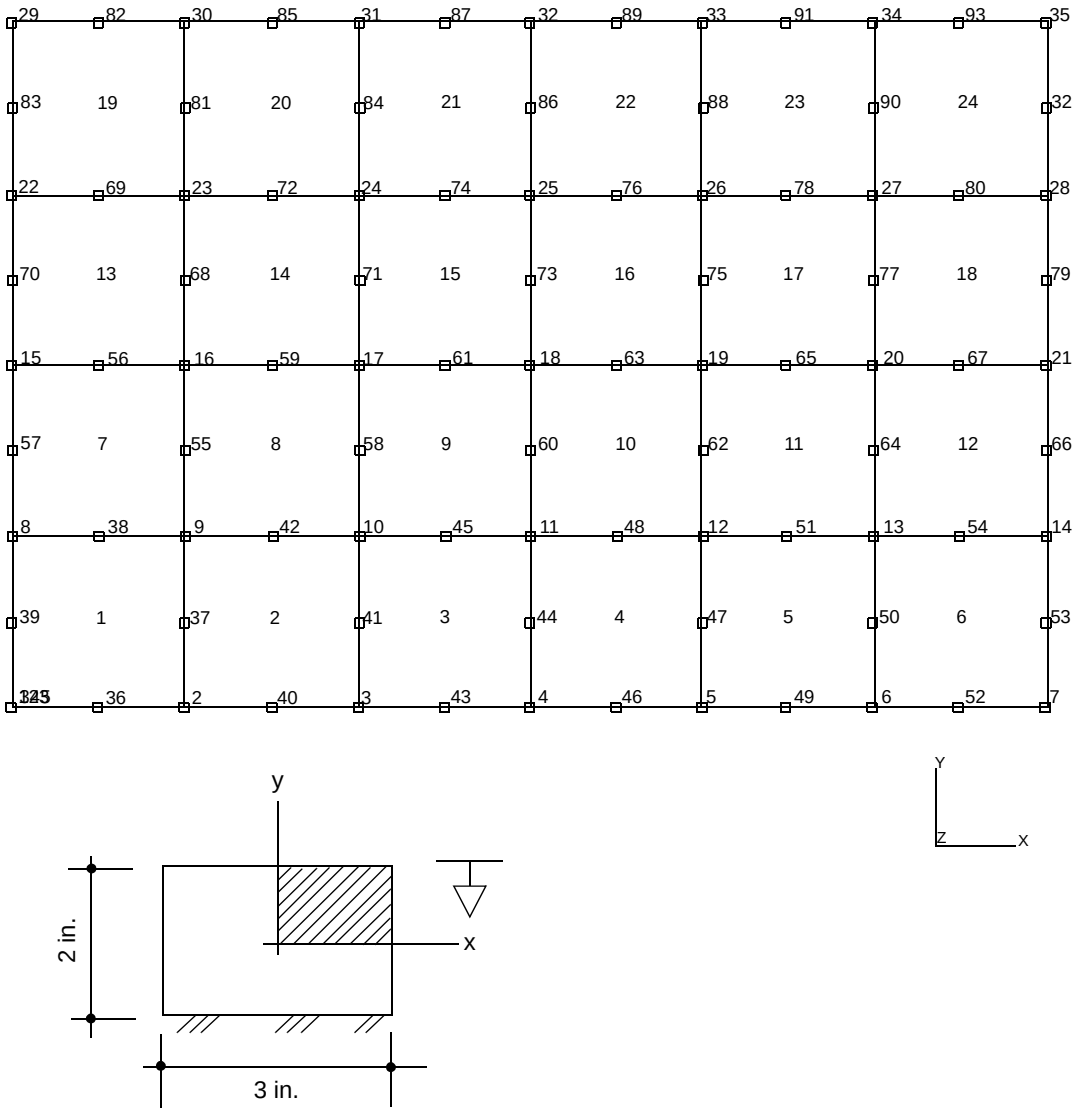

Figure 2.34-1 Two-Dimensional Strip and Mesh

INC : 0
SUB : 0
TIME : 0.000e+00
FREQ : 0.000e+00

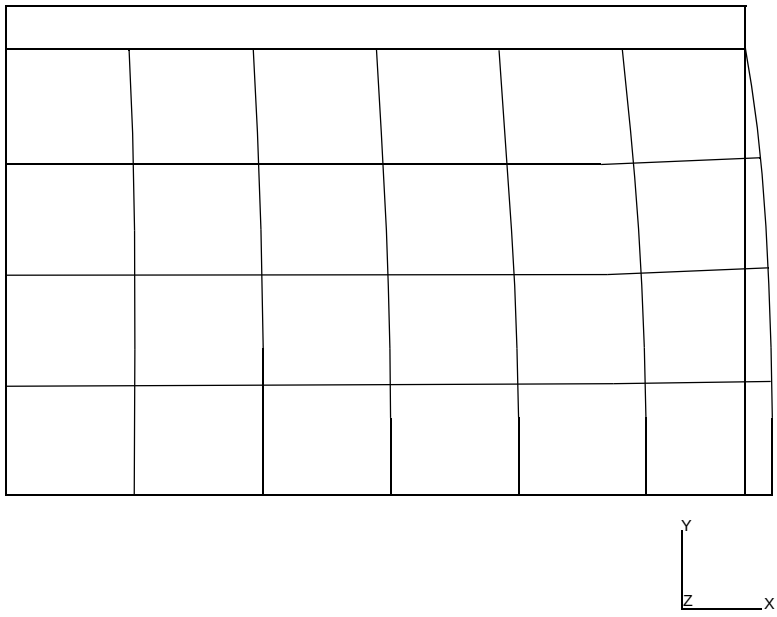

prob e2.34 elastic analysis - elmt 34

Displacements x

Figure 2.34-2 Deformed Mesh Plot

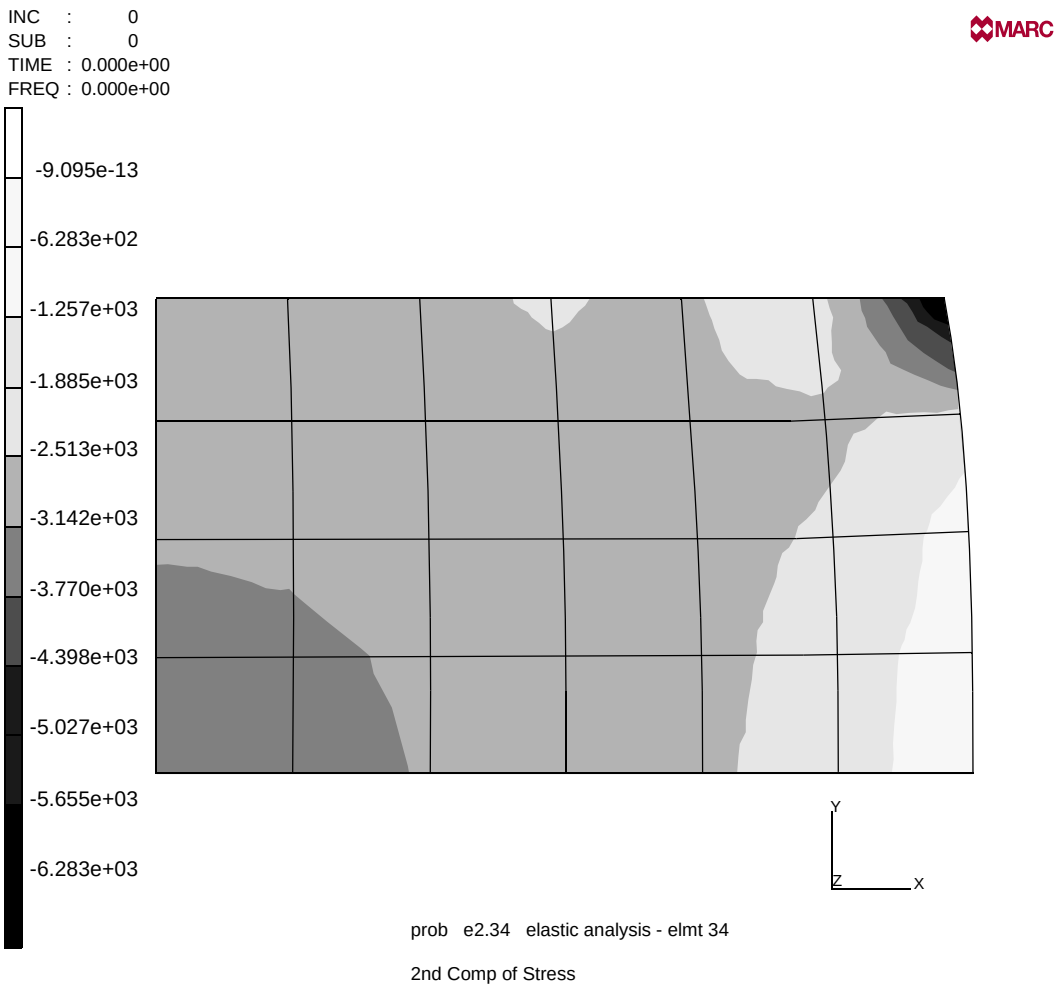

Figure 2.34-3 σ_{yy} Contours

2.35 Cube Under Pressure Loads

This problem illustrates the use of MARC element type 35, the ELASTIC parameter, the CASE COMBIN and RESTART options, and the FORCEM user subroutine for an elastic analysis of a cube. The cube is subjected to uniform and nonuniform distributed pressure.

Element

Element type 35 is written for incompressible and nearly incompressible behavior. The element is a three-dimensional brick with 20 nodes.

Model

The dimensions of the cube and a finite element mesh are shown in Figure 2.35-1. The cube is divided into eight cubes with a total of 81 nodes.

Material Properties

The elastic properties are Young's modulus is 30.E5 psi and Poisson's ratio is 0.4999.

Loading

The pressure is applied to the top surface of the block (elements 5, 6, 7 and 8). Both the uniform (IBODY = 4) and nonuniform (IBODY = 5) distributed pressure are shown in Figure 2.35-2. The uniform pressure is applied in increment 0, the nonuniform load in increment 1. Subroutine FORCEM is used to input the nonuniform distributed load. Because the ELASTIC parameter is used, the loads applied in increment 1 are total loads and not incremental loads.

Boundary Conditions

Symmetry conditions are imposed such that: u = 0 on plane x = 0, v = 0 on plane y = 0, and w = 0 on plane z = 0. The second input demonstrates the CASE COMBIN feature to superimpose the two solutions obtained in the first analysis. This is acceptable in an elastic analysis.

Results

In the first analysis the results were saved by using the RESTART option, writing to unit 8. In the second analysis, the CASE COMBINATION option was used to retrieve these results off unit 9 and combine them. This option can only be used if an ELASTIC parameter is included. In the second analysis, the two cases performed before were combined, each with a default weighting factor of 1.0. The deformed mesh for the first load case is shown in Figure 2.35-3. The third stress contours for the second load case are shown in Figure 2.35-4.

Parameters, Options, and Subroutines Summary

Example e2x35.dat:

Parameters	Model Definition Options	History Definition Options
ELASTIC	CONNECTIVITY	CONTINUE
ELEMENTS	COORDINATES	DIST LOADS
END	DIST LOADS	
SIZING	END OPTION	
TITLE	FIXED DISP	
	ISOTROPIC	
	OPTIMIZE	
	RESTART	

User subroutine in u2x35.f:

FORCEM

Example e2x35a.dat:

Parameters	Model Definition Options
ELASTIC	CASE COMBINATION
ELEMENTS	CONNECTIVITY
END	COORDINATES
SIZING	DIST LOADS
TITLE	END OPTION
	FIXED DISP
	ISOTROPIC
	OPTIMIZE
	RESTART

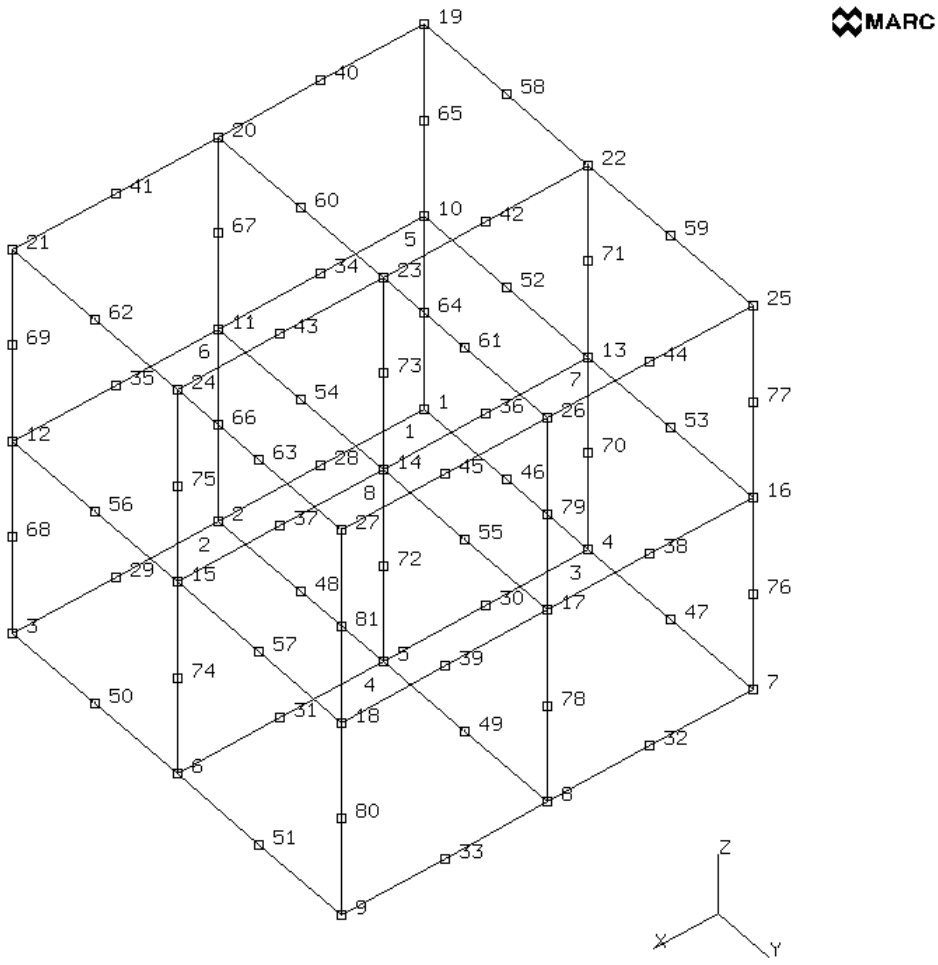

Figure 2.35-1 Square Block and Mesh

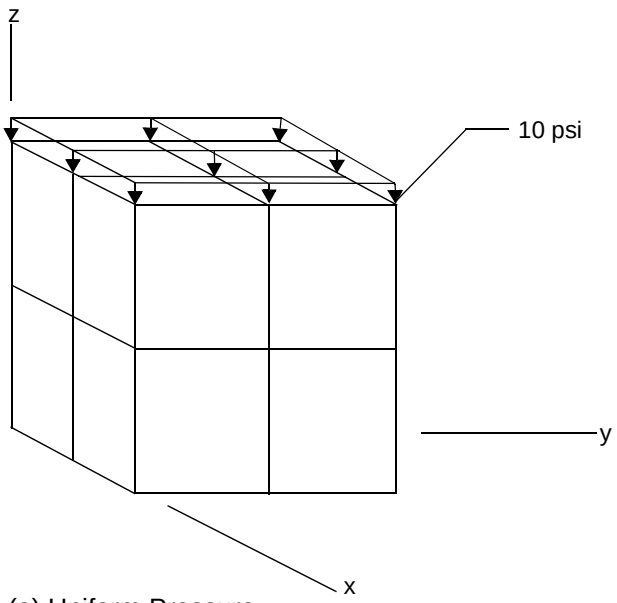

(a) Uniform Pressure

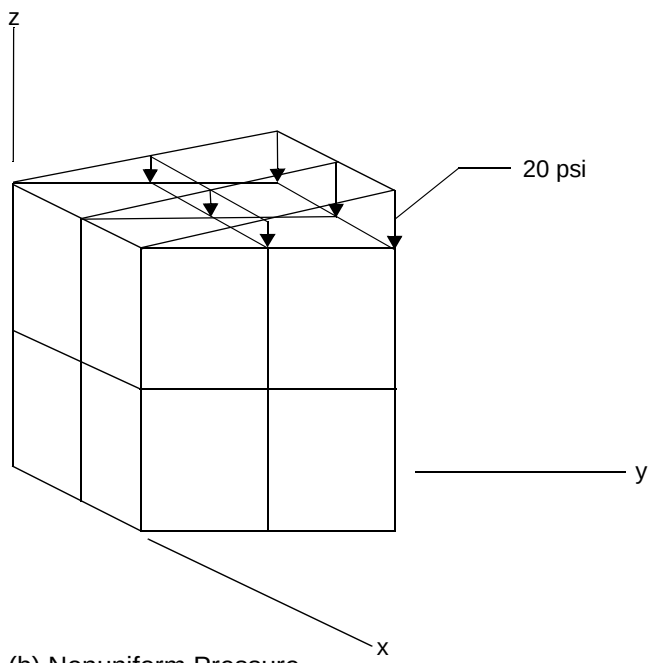

(b) Nonuniform Pressure

Figure 2.35-2 Pressure Distribution

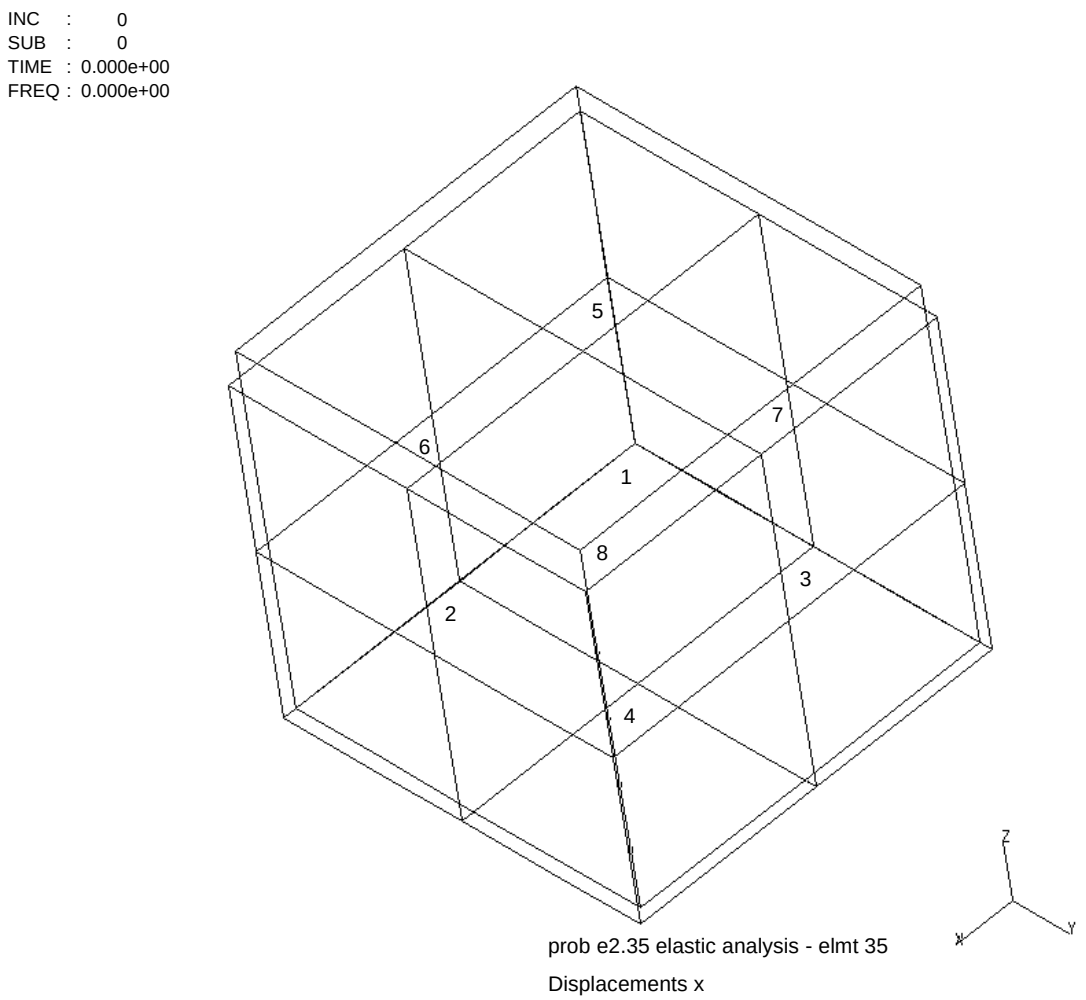

Figure 2.35-3 Deformed Mesh Plot

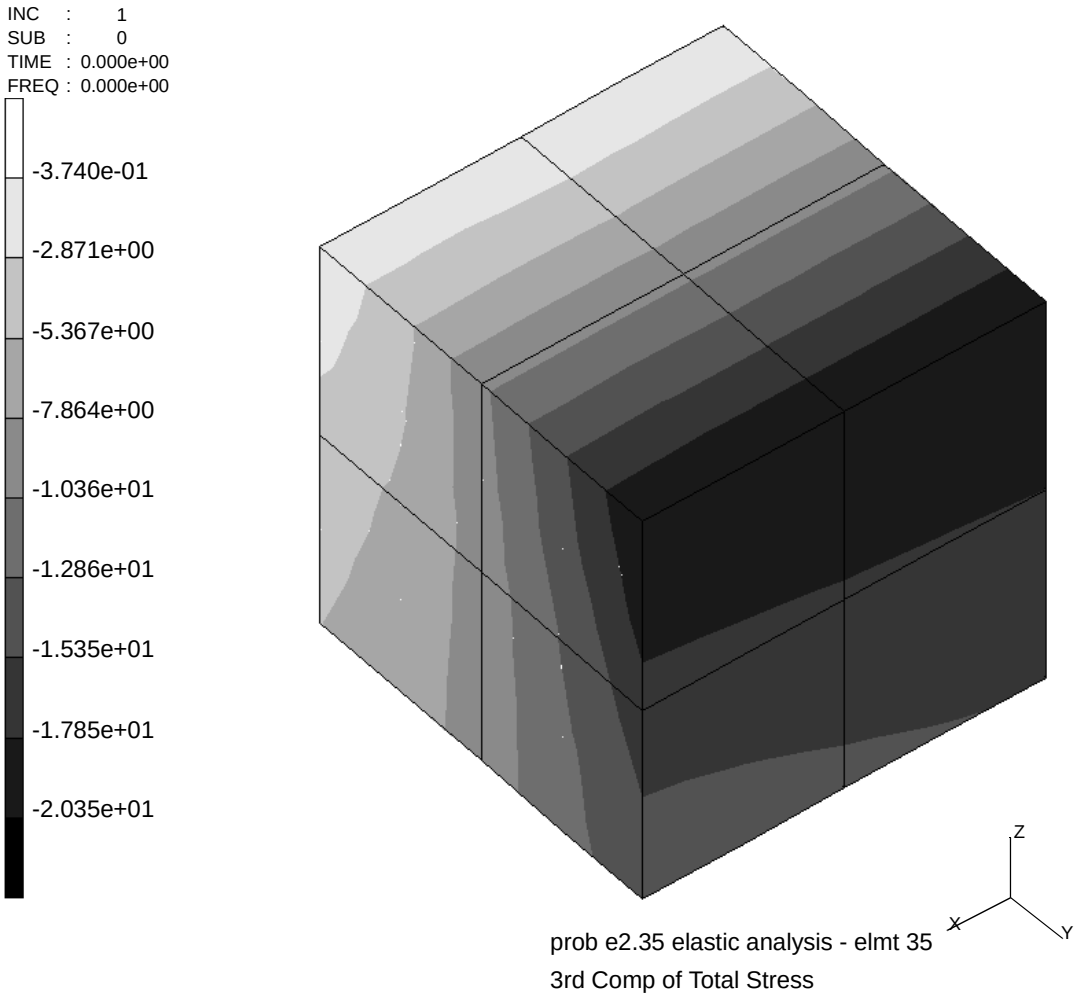

Figure 2.35-4 Stress Contours for σ_{zz}

2.36 Timoshenko Beam on an Elastic Foundation

This problem illustrates the use of MARC element type 45 and the FOUNDATION option for an elastic analysis of a Timoshenko beam resting on an elastic foundation. The beam is subjected to a concentrated load at the center of the beam. This problem is the same as 2.29, except that a different cross section is used.

Element

Element 45, a planar three-noded Timoshenko curved beam, is used for the analysis. This beam allows transverse shear strains, which improves the accuracy, especially for deep-beam analysis. The beam only has in-plane behavior.

Model

The dimensions of the beam and a finite element mesh are shown in Figure 2.36-1. The finite element mesh consists of 20 elements of type 45, with 41 nodes. Only half of the beam is modeled due to symmetry.

Material Properties

The Young's modulus is 2.0×10^5 psi. The Poisson's ratio υ is 0.3.

Geometry

The beam thickness is 5.885 inches with width of 1.0 inch. A cross section of the beam is shown in Figure 2.36-1.

Loading

A concentrated load (P/2) of 1000 pounds is applied at the center of the beam.

Boundary Conditions

Symmetry conditions are imposed at x = 0, y = 0; i.e., u = 0, and $\phi_a = 0$.

Elastic Foundation

The whole beam is assumed to rest on an elastic foundation. The description of the elastic foundation is given in model definition option FOUNDATION:

Element numbers = 1 through 20
Spring stiffness per unit length of the beam = 10. lb./inch
Element face I.D. = 0

Results

A deformed mesh plot is shown in Figure 2.36-2. The solution for maximum displacement agrees well with the analytic solution of classical beam theory. The calculated moment is less when using this element which allows transverse shear strain.

	Analytically Computed	MARC Computed
Y_{max} (x = 0)	2.929	2.963
σ_{max} (x = 2.11)	2603	2592

$$\beta = \sqrt[4]{k/4EI}$$

$$Y(x) = (P/8\beta^3 EI)e^{-\beta x}(\sin(\beta x) + \cos(\beta x))$$

$$M(x) = (P/4\beta)e^{-\beta x}(\sin(\beta x) - \cos(\beta x))$$

$$\sigma = Mc/I$$

Reference

Roark, R. J., *Formulas for Stress and Strain*

Parameters, Options, and Subroutines Summary

Example e2x36.dat:

Parameters	Model Definition Options
ELEMENTS	CONN GENER
END	CONNECTIVITY
SIZING	COORDINATES
TITLE	END OPTION
	FIXED DISP
	FOUNDATION
	GEOMETRY
	ISOTROPIC
	POINT LOAD

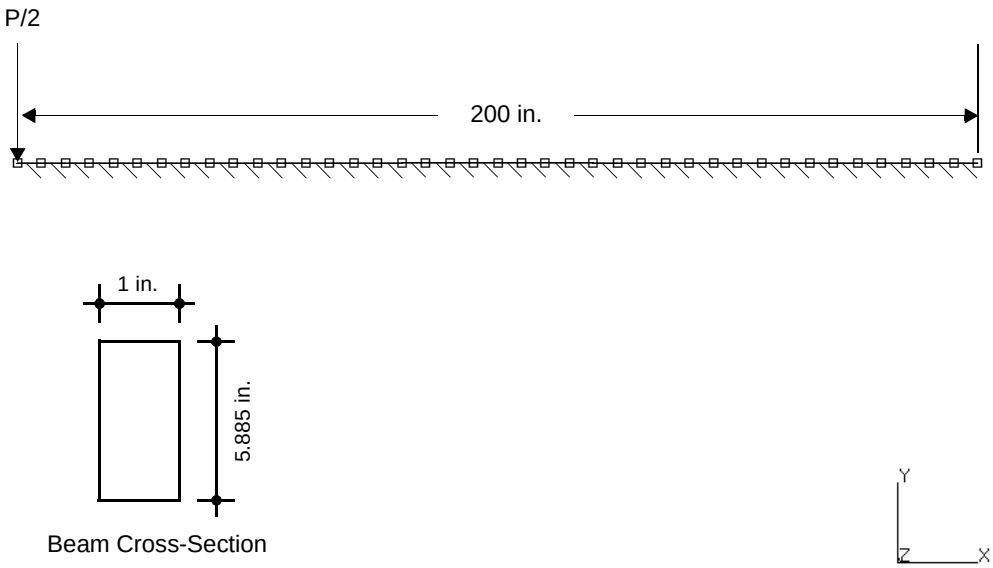

Figure 2.36-1 Timoshenko Beam and Mesh

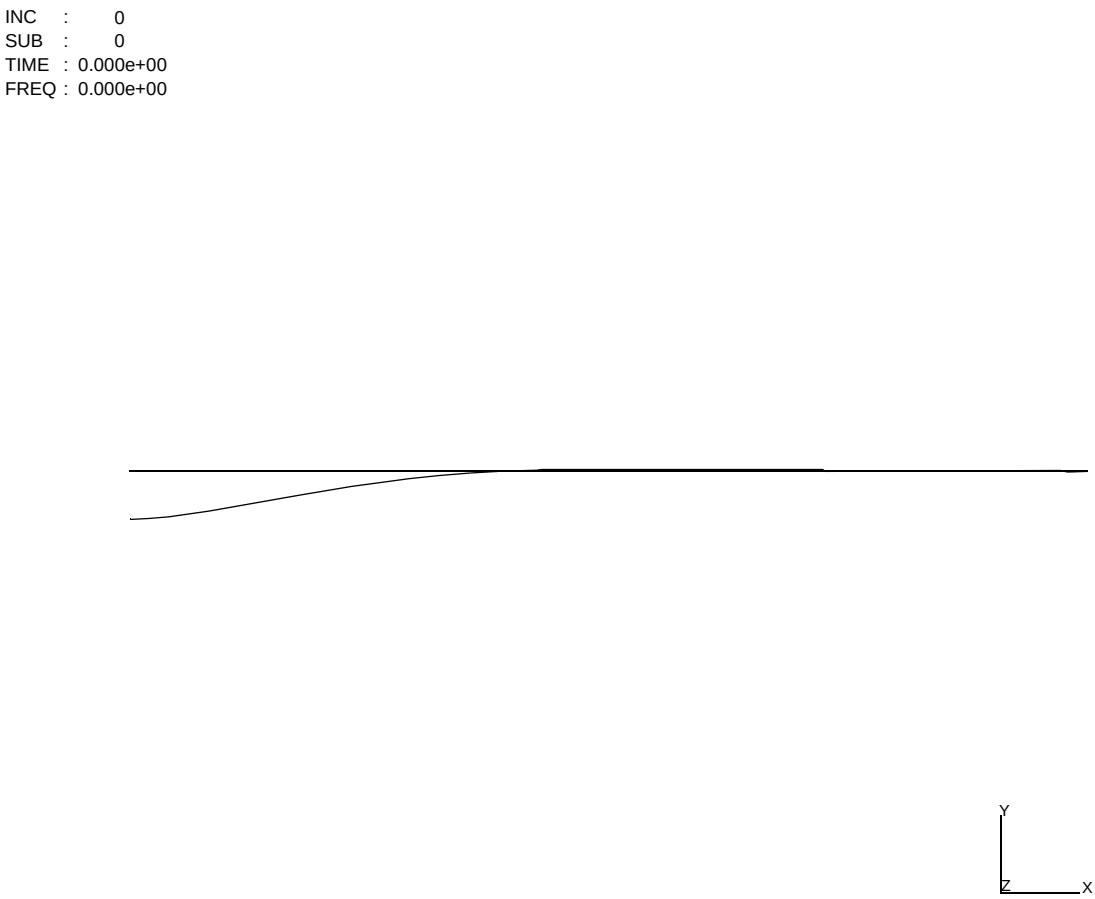

Figure 2.36-2 Deformed Mesh Plot

2.37 Reinforced Concrete Beam

This problem illustrates the use of MARC element types 27 and 46 (or 11 and 143) for an elastic analysis of a cantilevered concrete beam. The beam is subjected to a uniformly distributed load. The REBAR user subroutine or REBAR option for the input of rebar data is also demonstrated.

This problem is modeled using the two techniques summarized below.

Data Set	Element Type(s)	Number of Elements	Number of Nodes	Differentiating Features
e2x37	27 & 46	24	69	rebar subroutine
e2x37b	11 & 143	192	195	REBAR option

Elements

Either element types 27 or 46 (8-node plane strain) or 11 and 143 (4-node plane strain) are used in the analysis. Element 27 and 11 represent the concrete. Element 46 and 143, which are specifically designed to simulate reinforcing layers in plane strain problems, represent the stell reinforcements in the concrete.

Model

The beam is modeled either by using 16 8-node plane strain concrete elements and 8 8-node plane strain rebar elements (data set e2x37) or by using 128 4-node plane strain concrete elements and 64 4-node plane strain rebar elements (data set e2x37b).

Material Properties

The Young’s modulus is 140,000 psi for the concrete elements (elements 1-16), and 2,100,000 psi for the rebar elements (elements 17-24). The Poisson’s ratio is 0.2 for the concrete elements and 0.30 for the steel elements.

Geometry

The beam thickness is 1.0 inch (see Figure 2.37-1). For the rebar elements, one layer of rebars is used.

Loading

A uniform distributed load (q) of 0.025 psi in the y-direction is applied to the beam.

Boundary Conditions

All degrees of freedom of nodes at x = 0 are constrained to model the built-in condition. The other end of the beam is free.

Optimization

The Cuthill-McKee optimizer is used.

Rebar Data

The steel cross-sectional area A_s = 0.23 in. The rebars lie along the length of the beam; that is, the x-direction. Equivalent thickness $TR = A_s / B = \frac{0.23}{1} = 0.23$ in. See Figure 2.37-1.

The data is either read in via user subroutine REBAR or by using the REBAR option.

Results

A deformed mesh plot for example e2x37.dat is shown in Figure 2.37-2 and stresses are depicted in Figure 2.37-3. The rebar elements are coincident with the 7,8,9 integration points of elements 1-8. When examining the stresses of the rebar element 17 with respect to element 1, it is found that the rebar element supports 15 times the stress of the concrete element, which can be anticipated by examination of the ratios of the respective Young's moduli.

Parameters, Options, and Subroutines Summary

Example e2x37.dat:

Parameters	Model Definition Options
ELEMENTS	CONNECTIVITY
END	COORDINATES
SIZING	DIST LOADS
TITLE	END OPTION
	FIXED DISP
	GEOMETRY
	ISOTROPIC
	OPTIMIZE

User subroutine in u2x37.f:

REBAR

Example e2x37b.dat:

Parameters	Model Definition Options
ELEMENTS	CONNECTIVITY
END	COORDINATES
SIZING	DIST LOADS
TITLE	END OPTION
	FIXED DISP
	GEOMETRY
	ISOTROPIC
	OPTIMIZE
	REBAR

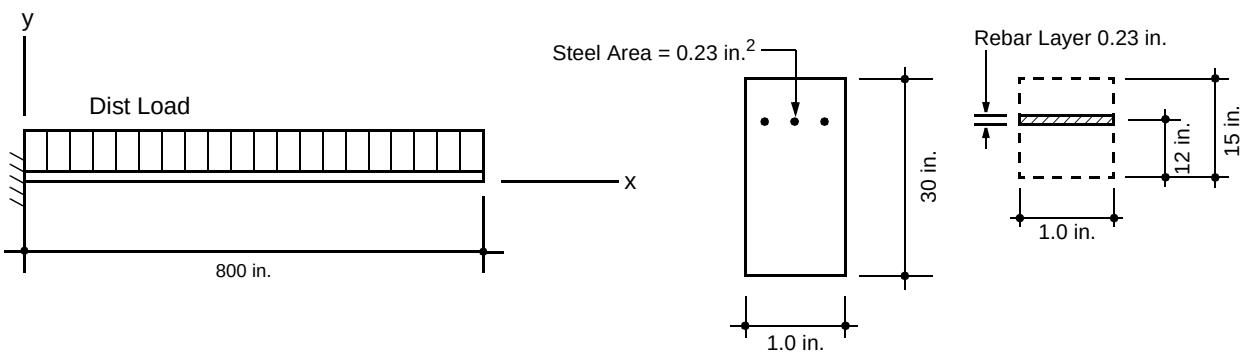

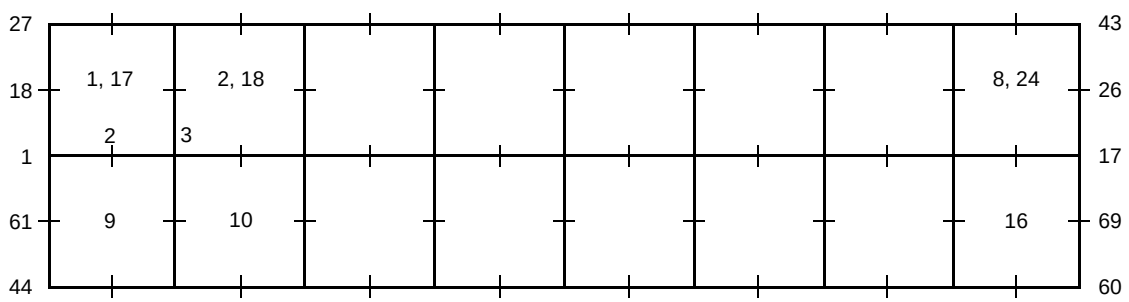

Figure 2.37-1 Reinforced Concrete Beam and Mesh

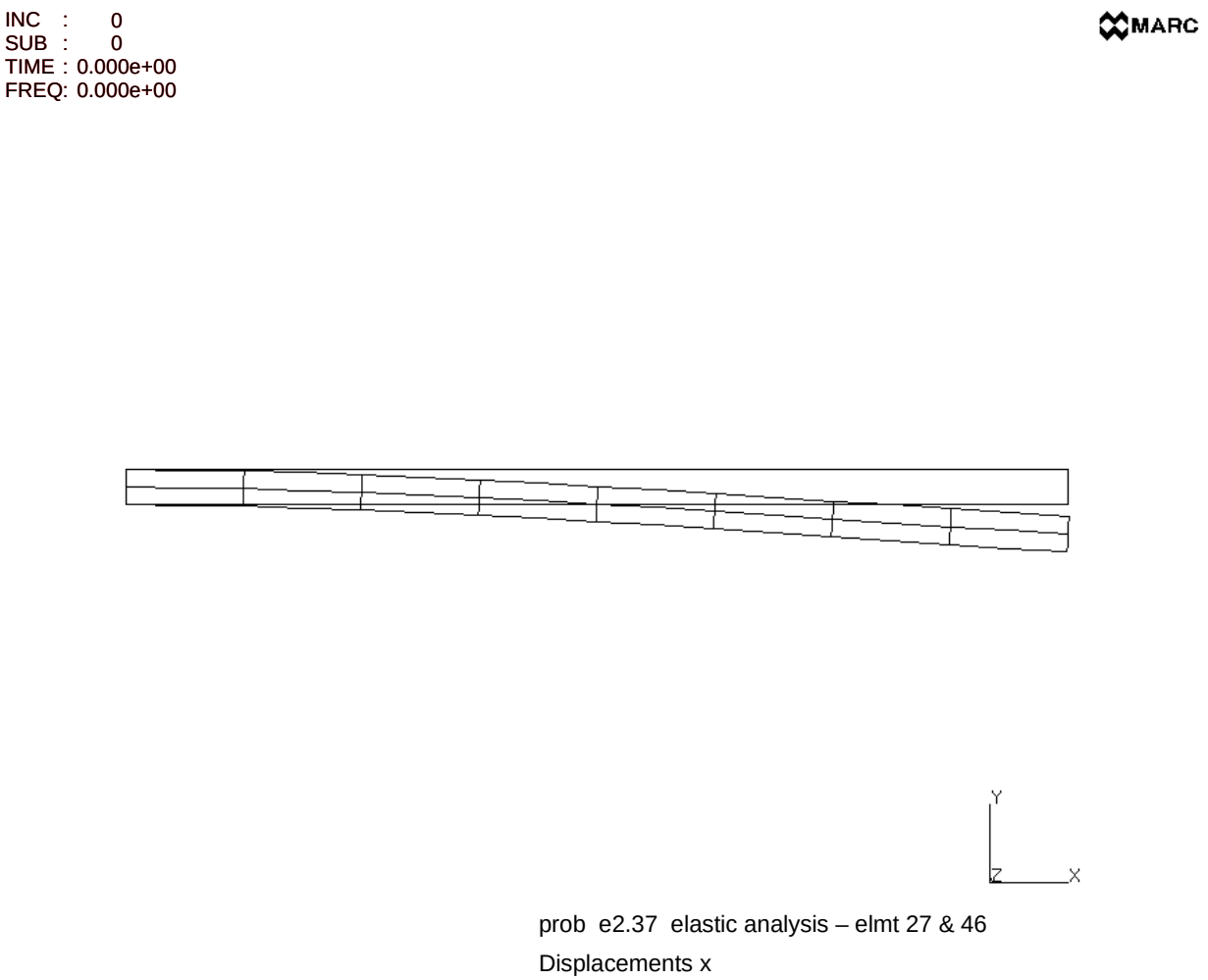

Figure 2.37-2 Deformed Mesh Plot

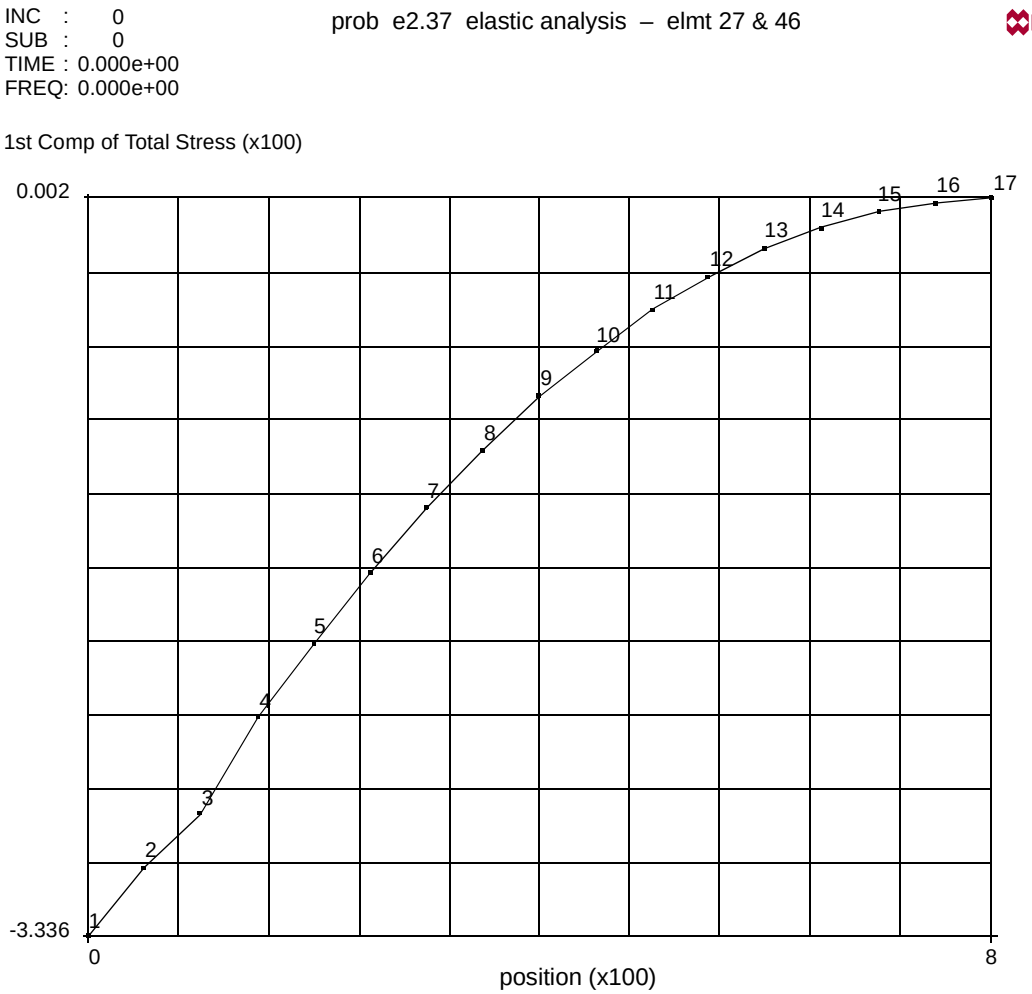

Figure 2.37-3 σ_{xx} Along Bottom Surface Along Nodes 1 to 17

2.38 Reinforced Concrete Plate with Central Hole

This problem illustrates the use of MARC elements type 29 and type 47 and user subroutines UINSTR and REBAR for an elastic analysis of a reinforced concrete plate. The plate is subject to an initial stress in the rebars. The use of the parameters ELSTO and SCALE is also demonstrated.

Model

The dimensions of the plate and a finite element mesh are shown in Figure 2.38-1. The plate is modeled under conditions of generalized plane strain. The geometry is similar to problem 2.31 with the addition that reinforcements have been placed concentrically with respect to the hole. There are 28 elements and 81 nodes in the mesh. Eight of the elements are rebar elements type 47.

Material Properties

The properties of the concrete are Young's modulus is 30×10^5 psi and Poisson's ratio is 0.2.

The properties of the steel are Young's modulus is 30×10^6 psi, and Poisson's ratio is 0.3 with a yield stress of 30×10^3 psi.

Boundary Conditions

Symmetry conditions exist on the lines x = 0 and y = 0 (u = 0 at x = 0; v = 0 at y = 0). Both degrees of freedom of the second extra node of generalized plane-strain elements (element 29) are constrained, restraining the relative rotation of the top and bottom surfaces.

Rebar

Three layers of rebars are assumed to be in the plate, the cross-sectional area of which is 0.25. The direction and position of the rebar layers are shown in Figure 2.38-2. The rebar data is defined in the user subroutine REBAR.

ELSTO allows the use of out-of-core element storage option; this reduces the amount of workspace necessary for the analysis.

ISTRESS allows you to input initial stresses in the rebars through the user subroutines UINSTR. The rebars are given a prestress of 100 psi, which is then scaled to the yield stress of 30000 psi.

SCALE allows the stresses in the plate to be scaled to the condition of first yield.

Optimization

The bandwidth optimization is performed by using the Sloan method.

Results

In increment zero, the initial stresses are applied and scaled to the yield stress. In increment one, the structure is allowed to return to equilibrium. The resulting deformed mesh plot is shown in Figure 2.38-3. As anticipated, the reinforcements force the plate into compression.

Parameters, Options, and Subroutines Summary

Example e2x38.dat:

Parameters	Model Definition Options
ELEMENTS	CONNECTIVITY
END	COORDINATES
ISTRESS	END OPTION
SCALE	FIXED DISP
SIZING	GEOMETRY
TITLE	ISOTROPIC
	OPTIMIZE
	PRINT CHOICE

User subroutines found in u2x28.f:

REBAR
UINSTR

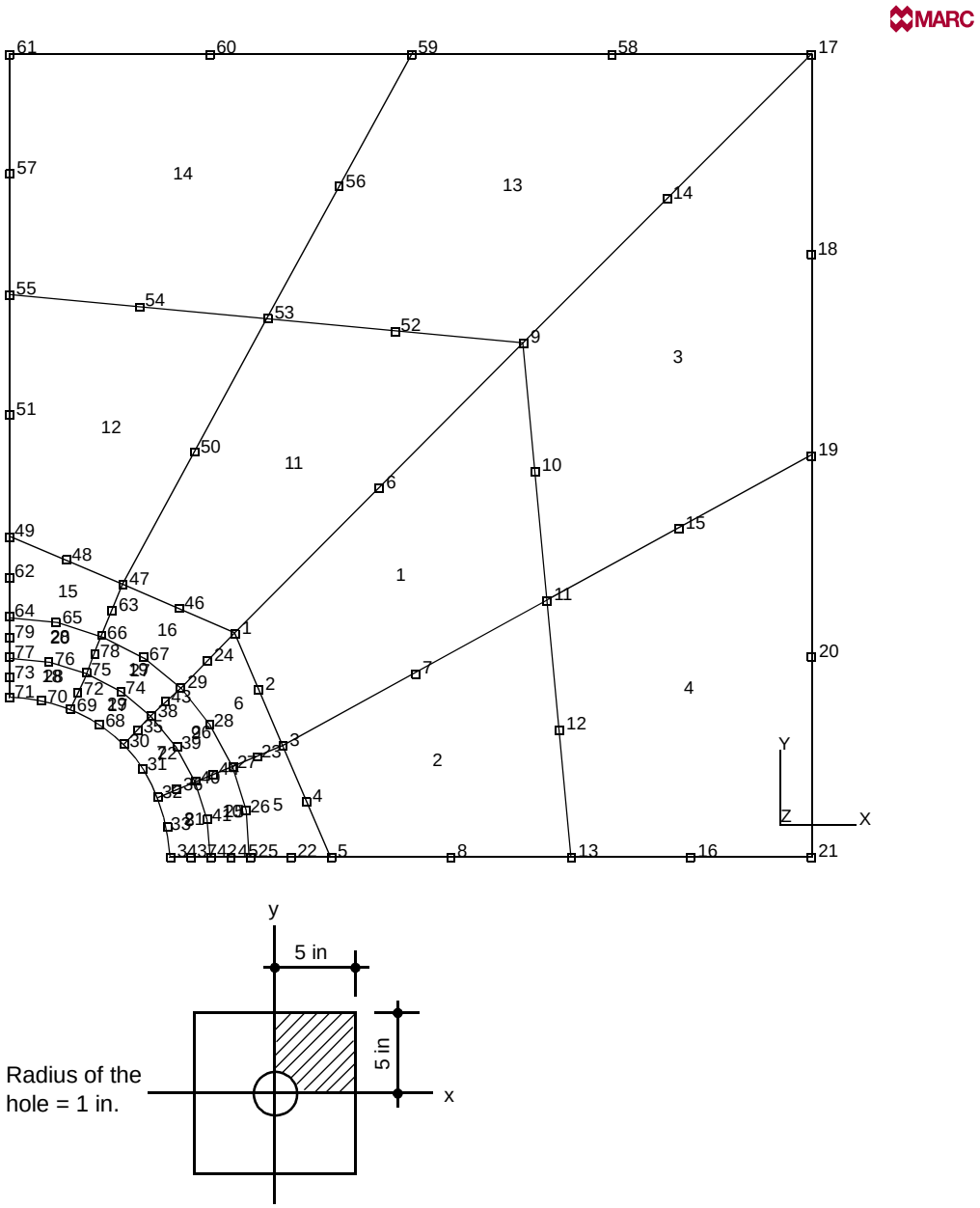

Figure 2.38-1 Reinforced Concrete Plate and Mesh

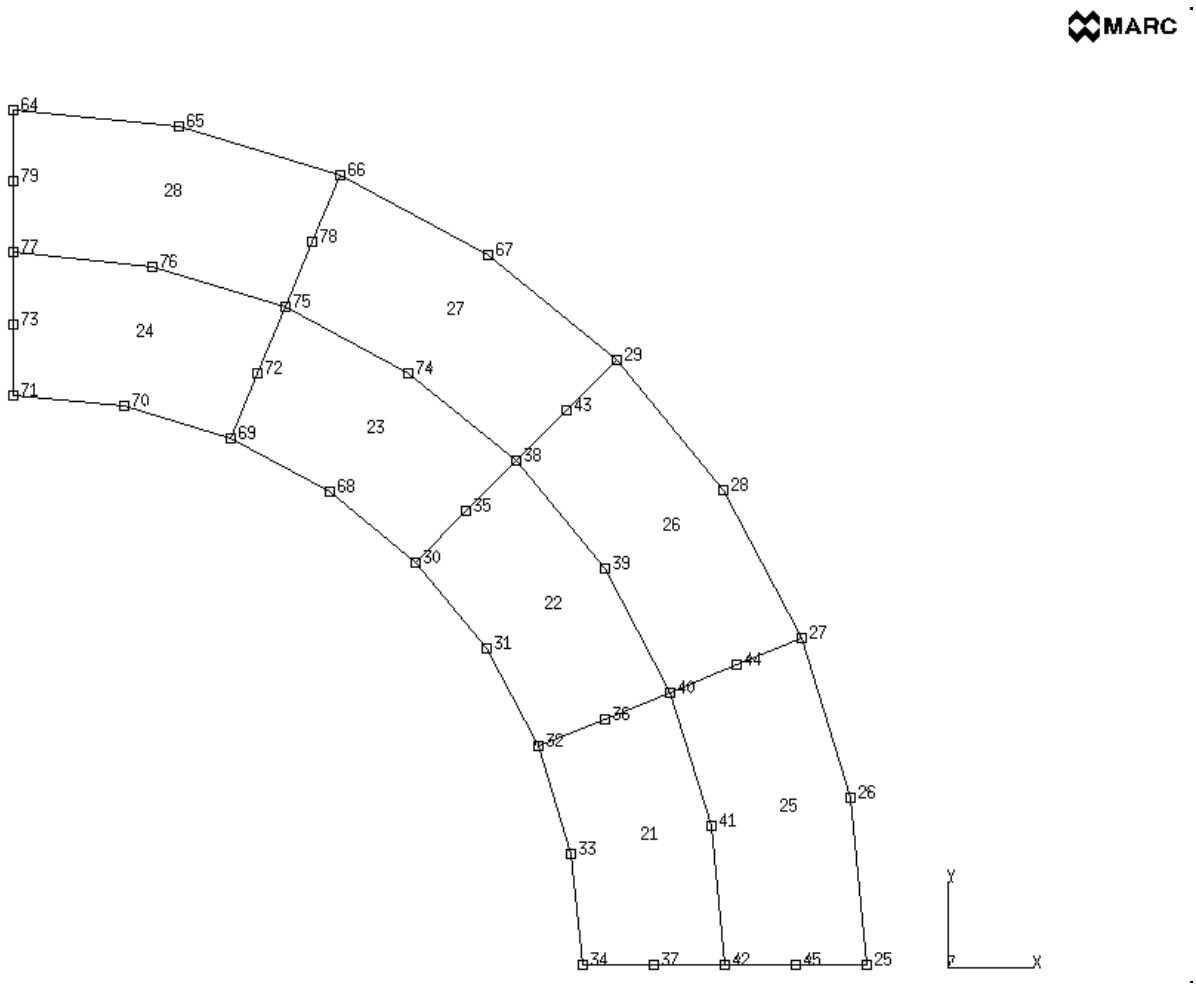

Figure 2.38-2 Rebar Layers and Elements

INC : 1
SUB : 0
TIME : 0.000e+00
FREQ: 0.000e+00

MARC

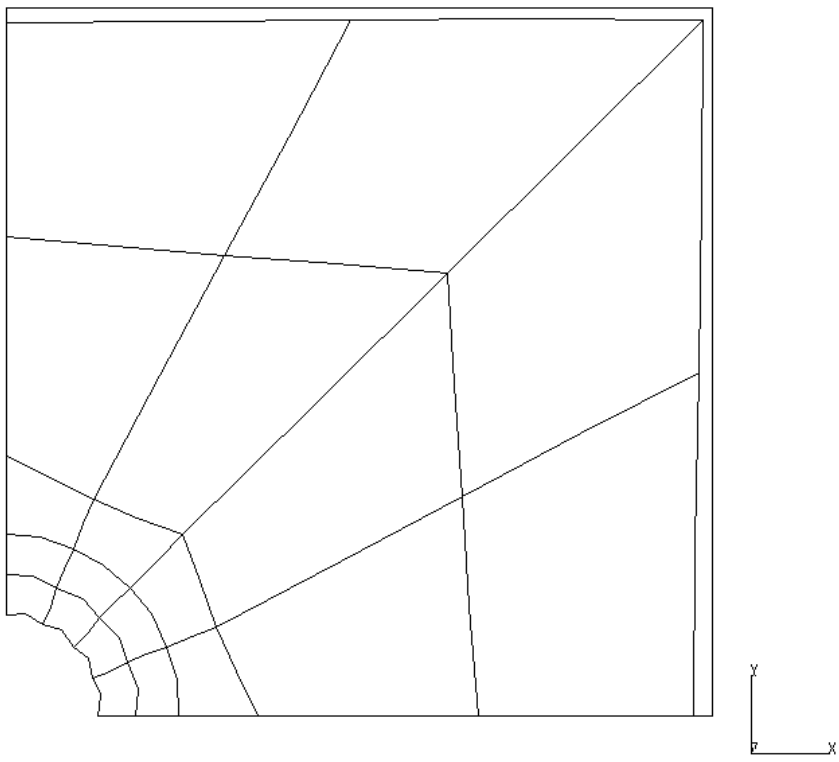

prob e2.38 elastic analysis – elmt 29 & 47
Displacements x

1

Figure 2.38-3 Deformed Mesh Plot

2.39 Cylinder with Rebars Under Internal Pressure

This problem illustrates the use of MARC elements types 28 and 48 for an elastic analysis of a hollow cylinder with rebars. The cylinder is subjected to internal pressure.

Elements

Element type 28 as a second-order distorted quadrilateral, with eight nodes. There are two degrees of freedom at each node.

Element type 48 is a hollow, 8-node quadrilateral in which you can place single strain members – in this case, reinforcing bars.

Model

The dimensions of the cylinder and the finite element mesh are shown in Figure 2.39-1. The cylinder is allowed to expand radially with no constraints; thus, there is no variation in the axial direction. The mesh is composed of 10 elements through the radius of type 28. Superimposed on this are two elements of type 48 that model the reinforcements. There are 53 nodes in the structure.

Material Properties

For Element Type 28: The Young's modulus is 30×10^5 psi and the Poisson's ratio is 0.2.

For Element Type 48: The Young's modulus is 30×10^6 and the Poisson's ratio is 0.3.

Boundary Conditions

The degrees of freedom in the z-direction (v = 0) are constrained at both ends (z = 0 and z = 1.0), which represents a plane-strain condition.

Loading

An internal pressure of magnitude = 500 psi acts on element 1. It is implemented by giving a DIST LOAD type = 0 (1-5-2 face)

Rebar

The number of rebar layers = 2 (1 for each element, see Figure 2.39-2). The rebar direction is in the hoop direction and the user subroutine REBAR is used for the input of rebar data.

Results

A deformed mesh plot is shown in Figure 2.39-3 and hoop stress distribution are depicted in Figure 2.39-4.

Parameters, Options, and Subroutines Summary

Example e2x39.dat:

Parameters	Model Definition Options
ELEMENTS	CONNECTIVITY
END	COORDINATES
SIZING	DIST LOADS
TITLE	END OPTION
	FIXED DISP
	GEOMETRY
	ISOTROPIC
	POST

User subroutine in u2x39.f:

REBAR

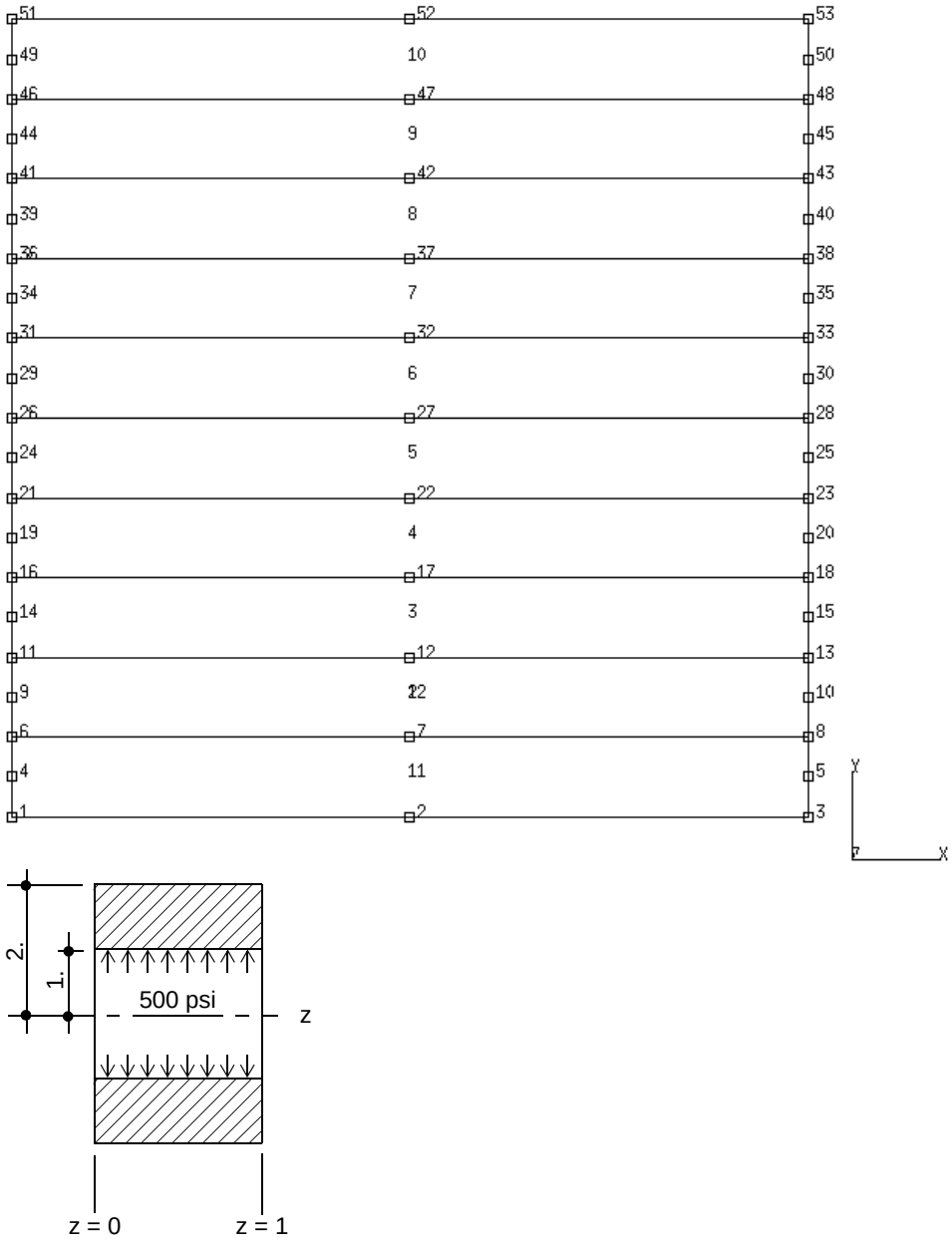

Figure 2.39-1 Cylinder and Mesh

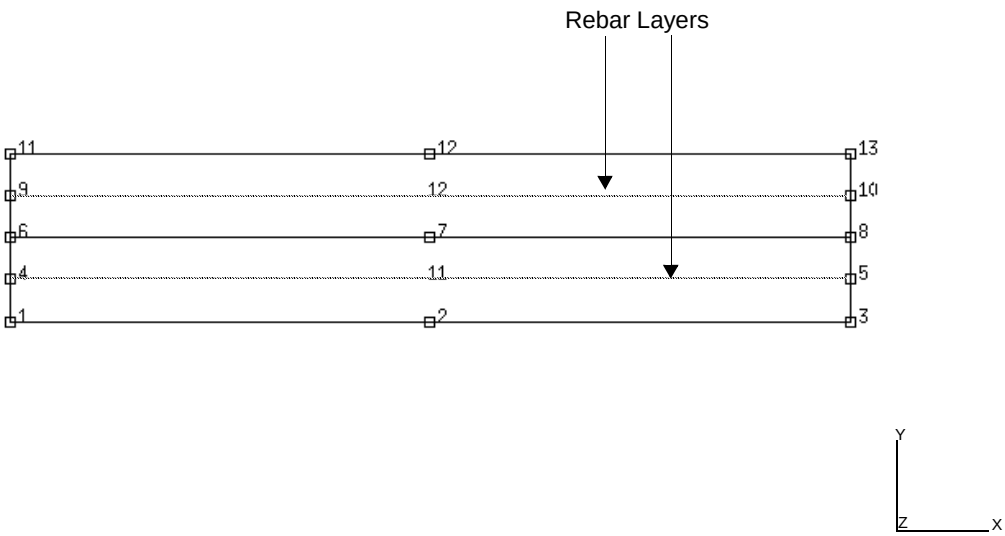

Figure 2.39-2 Rebar Layers and Elements

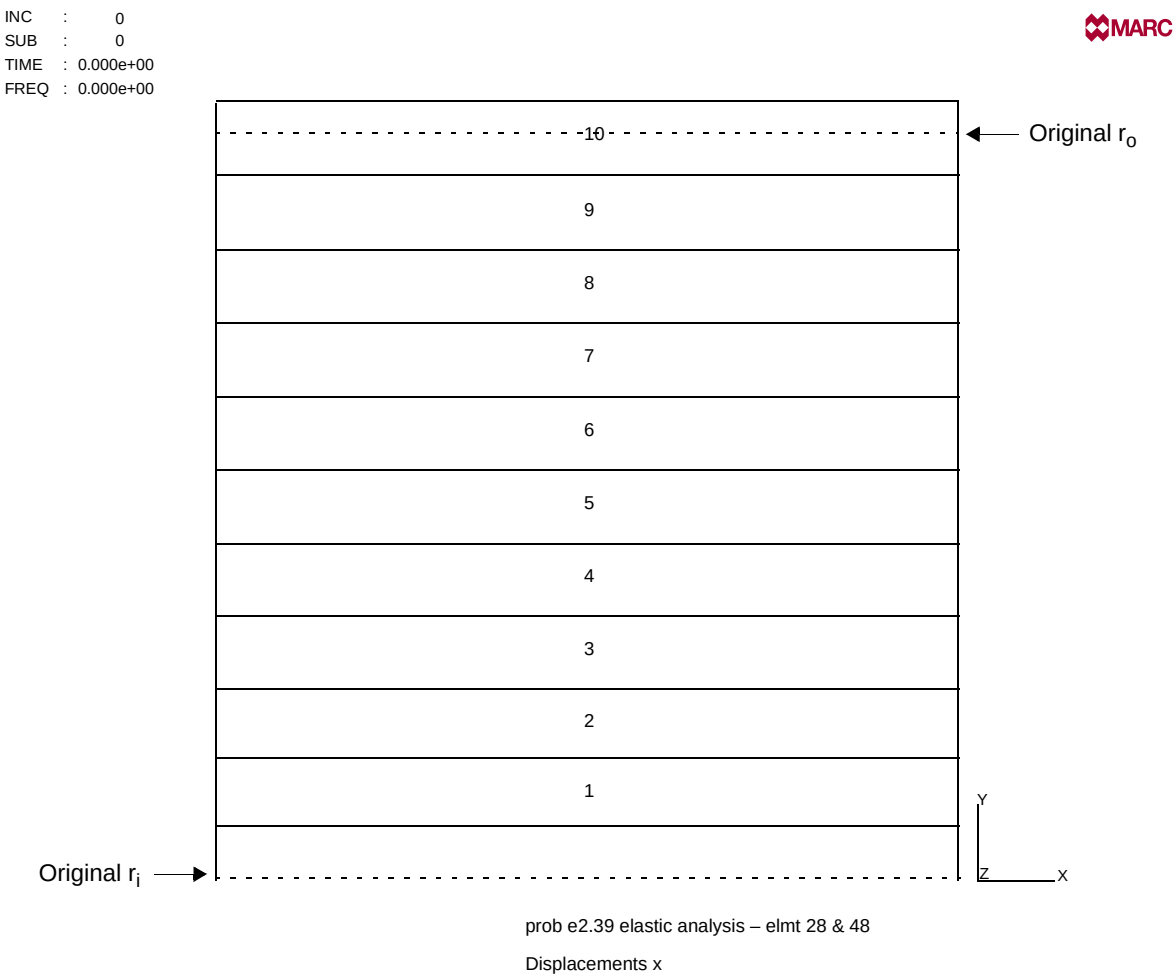

Figure 2.39-3 Deformed Mesh Plot

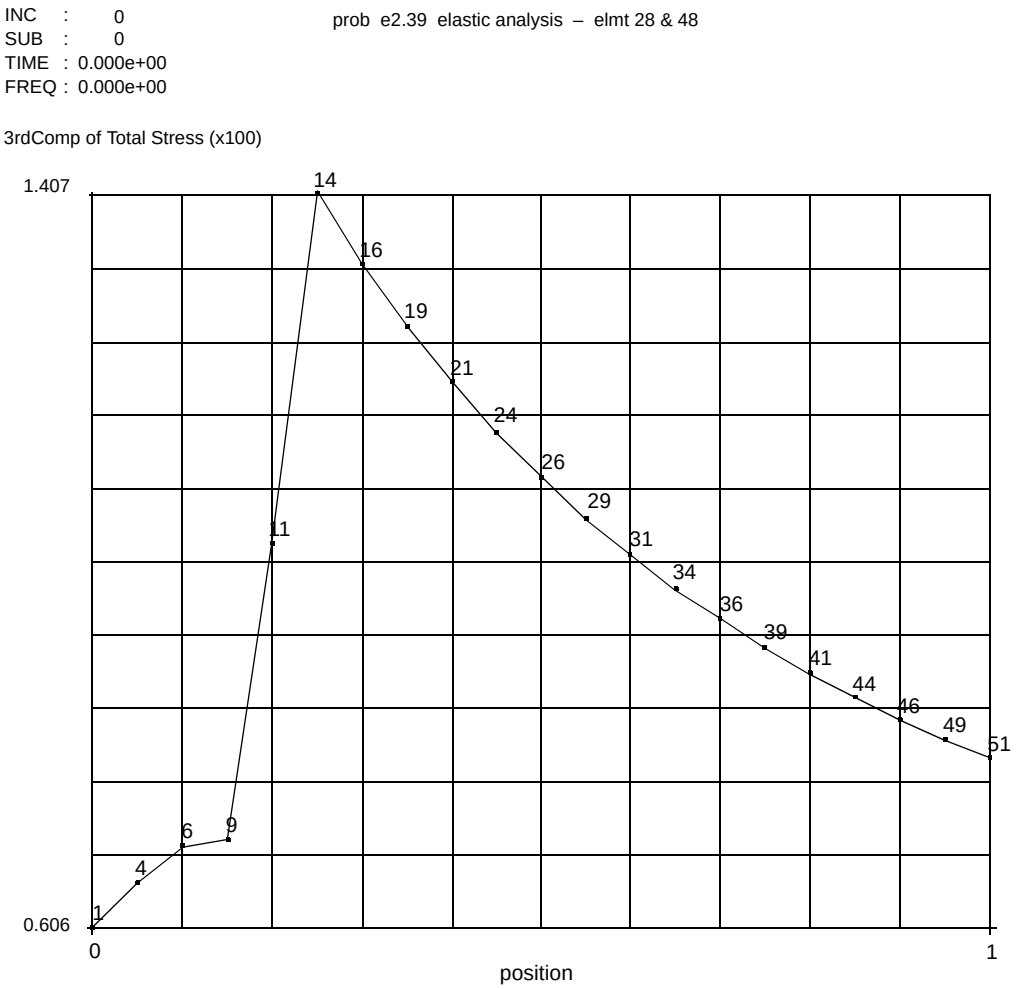

Figure 2.39-4 Hoop Stress Distribution Through Radius

2.40 Simply Supported Square Plate of Variable Thickness

This problem illustrates the use of MARC element type 49 for an elastic analysis of a simply supported square plate. The plate is subjected to uniformly distributed pressure. The analysis is performed first with a constant plate thickness and then with a linearly varying thickness. This varying thickness is entered by means of user subroutine USHELL. The SHELL SECT parameter is used for the reduction of the number of integration points through the thickness.

This problem is modeled using the two techniques summarized below.

Data Set	Element Type(s)	Number of Elements	Number of Nodes	Differentiating Features
e2x40a	49	50	121	
e2x40b	49	50	121	Variable thickness

Element

Element type 49 is a nonconforming triangular shell element with arbitrary spatial orientation. There are six nodes per element, with assignable thickness at each corner node. Actually, the average thickness is used which can also be entered by means of user subroutine USHELL.

Model

The dimensions of the plate and the finite element mesh are shown in Figure 2.40-1. The plate is analyzed using 50 elements and 121 nodes. One-quarter of the plate is modelled due to symmetry considerations.

Material Properties

The elastic analysis is performed with a Young's modulus of 2×10^5 N/mm^2 and a Poisson's ratio of 0.3.

Geometry

In the first analysis (A), the plate has a constant thickness of 3.0 mm. In the second analysis (B), the plate thickness varies in both the x- and y-directions (see Figure 2.40-1). The length of the plate edges is 60 mm. Since a linear plate problem is solved, the elements can be considered as flat which is indicated by a 1 on the fifth geometry field. In this way, computational time is reduced.

Loading

A uniform pressure of 0.01 N/mm^2 in the negative z-direction is applied.

Boundary Conditions

Symmetry conditions are imposed on edges x = 30 ($u_x = 0$, $\phi = 0$ and y = 30 ($u_y = 0$, $\phi = 0$). Notice that the rotation constraints only apply for the midside nodes.

Simply supported conditions are imposed on edges x = 0 and y = 0 ($u_z = 0$).

Results

Stress contours are depicted in Figure 2.40-2 and Figure 2.40-3 for constant and varying plate thicknesses, respectively. As anticipated, the stress increases in the second analysis. The maximum stresses and deflections are:

	Constant Thickness		Varied Thickness
	MARC Solution	**Analytical Solution**	**MARC Solution**
Deflection (mm)	1.093×10^{-3}	1.065×10^{-3}	2.677×10^{-3}
Stress (N/mm^2)	1.229	1.248	2.302

The exact solution may be found in S. P. Timoshenko and S. Woinowsky-Kreiger, *Theory of Plates and Shells*.

Parameters, Options, and Subroutines Summary

Example e2x40a.dat:

Parameters

ELEMENTS
END
SHELL SECT
SIZING
TITLE

Model Definition Options

CONNECTIVITY
COORDINATES
DEFINE
DIST LOADS
END OPTION
FIXED DISP
GEOMETRY
ISOTROPIC
POST
PRINT CHOICE

Example e2x40b.dat:

Parameters	Model Definition Options
ELEMENTS	CONNECTIVITY
END	COORDINATES
SHELL SECT	DEFINE
SIZING	DIST LOADS
TITLE	END OPTION
	FIXED DISP
	GEOMETRY
	ISOTROPIC
	POST
	PRINT CHOICE

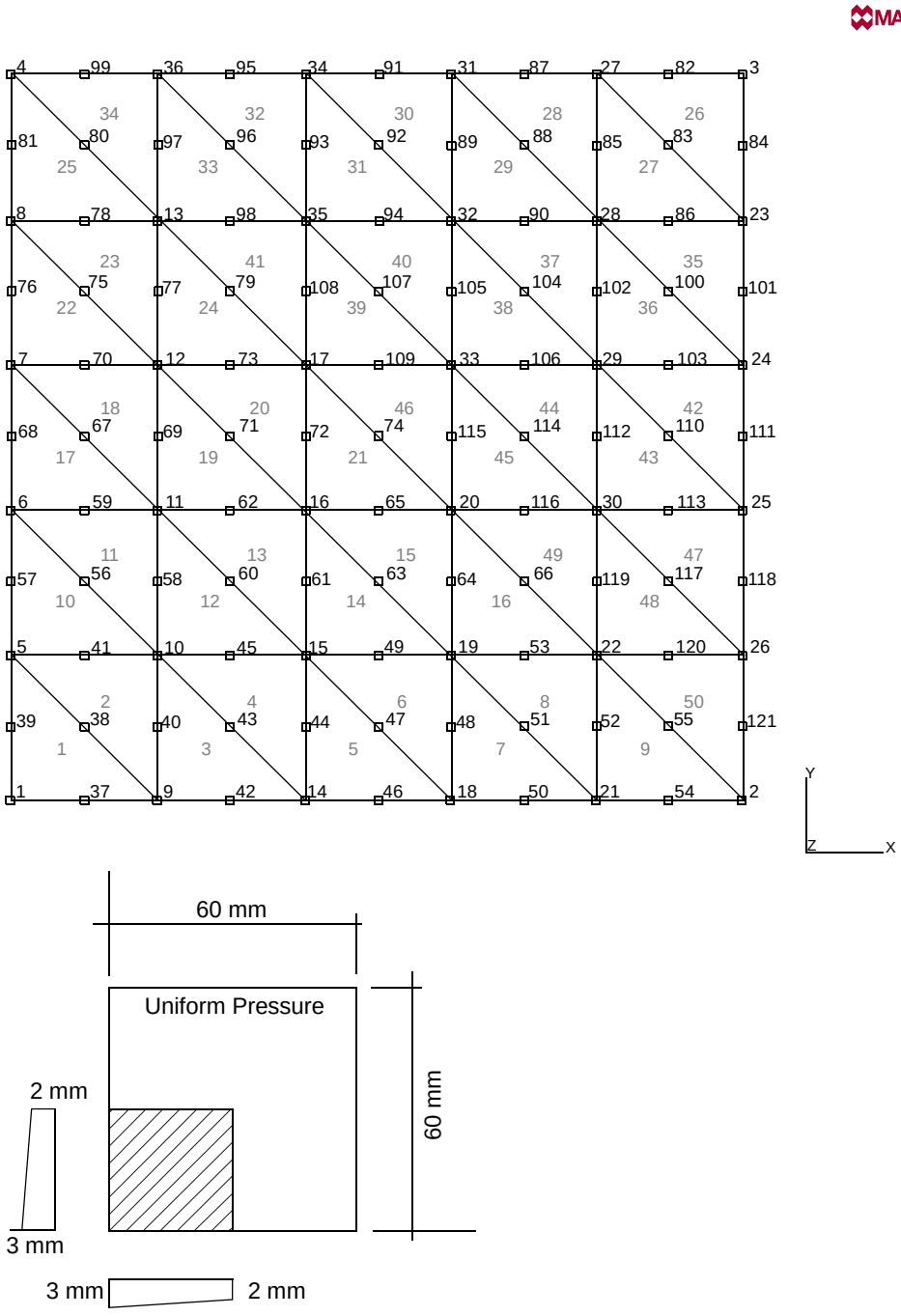

Figure 2.40-1 Square Plate and Mesh

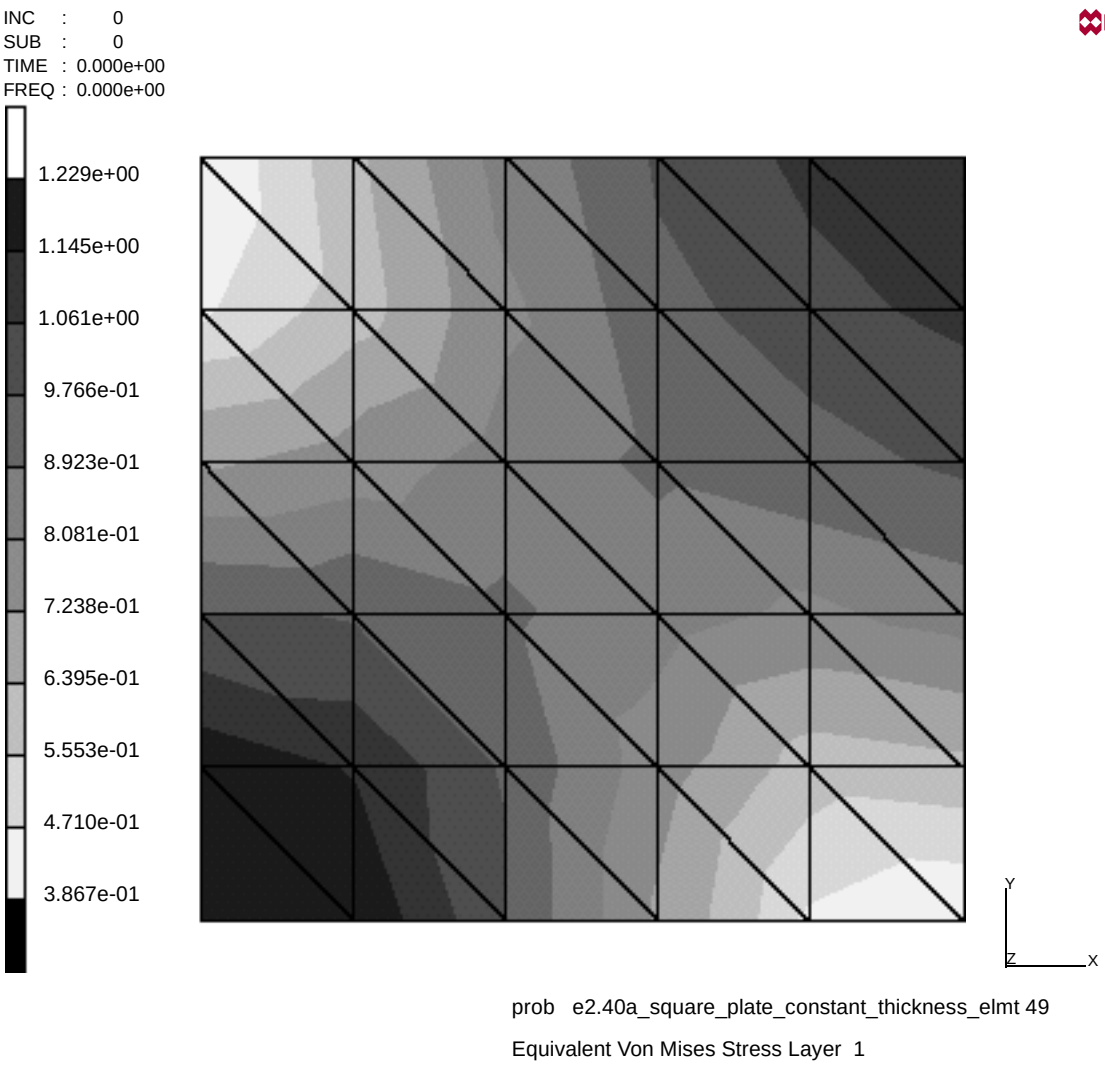

Figure 2.40-2 Stress Contours (Constant Thickness)

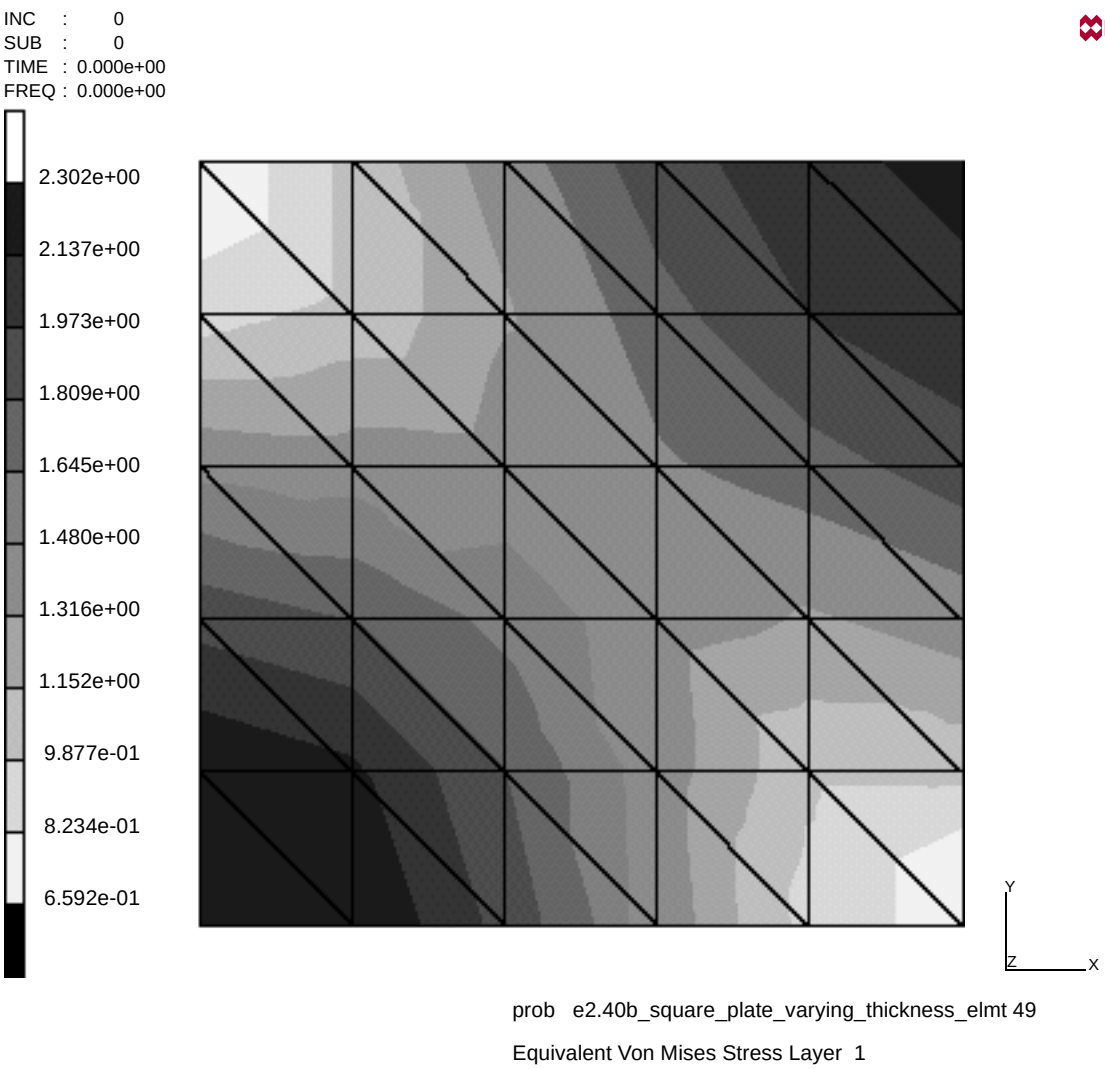

Figure 2.40-3 Stress Contours (Variable Thickness)

2.41 Thermal Stresses in a Simply Supported Triangular Plate

This problem illustrates the use of MARC element type 49 for an elastic analysis of a simply supported triangular plate subjected to nonuniform heating. The temperature variation through the thickness is entered using the INITIAL STATE and CHANGE STATE model definition options. The SHELL SECT parameter is used to reduce of the number of integration points through the thickness.

Element

Element 49 is a nonconforming triangular shell element with six nodes per element.

Model

The dimensions of the plate and the finite element mesh are shown in Figure 2.41-1. Based on symmetry considerations, only one half of the plate is modeled. The mesh is composed of 36 elements and 91 nodes.

Material Properties

The material is elastic with a Young's modulus of 2.1×10^5 N/mm^2, a Poisson's ratio of 0.3, and a coefficient of thermal expansion of 1×10^{-5}. In order to obtain layer stress components in the same direction for all elements, the ORIENTATION option is used to specify an offset of 0° with respect to the z,x-plane.

Geometry

The thickness of the equilateral triangular plate is 0.02 mm. Since a linear plate problem is solved, the elements can be considered as flat, which is indicated by a 1 on the fifth geometry field. In this way, computational time is reduced.

Loading

Initially, the temperature through the thickness is set to 10° The thermal load is applied by changing the temperature of layer 1 to 0° and of layer 3 to 20°.

Boundary Conditions

Symmetry conditions are imposed in the edge y = 0 ($u_y = 0$, $\phi = 0$). Notice that the rotation constraint is only applied on the midside nodes.

Simply supported conditions are imposed on the outer edges ($u_z = 0$). The remaining rigid body mode is suppressed by setting $u_x = 0$ for the node at x = 0, y = 0

Results

Stress contours of the first and second component in the preferred system for layer 1 are depicted in Figure 2.41-2 and Figure 2.41-3, respectively. The maximum stresses are:

	MARC Solution	Analytical Solution
Stress_x (N/mm^2)	24.98	26.67
Stress_y (N/mm^2)	17.85	20.00

The analytical solution can be found in *Theory of Plates and Shells* by S. P. Timoshenko and S. Woinowsky-Krieger. Since the generalized stresses per element are constant, the present finite element mesh is fairly coarse to accurately describe the stress variations.

Parameters, Options, and Subroutines Summary

Example e2x41.dat:

Parameters

ELEMENTS
END
SHELL SECT
SIZING
TITLE

Model Definition Options

CONN GENER
CONNECTIVITY
COORDINATES
DIST LOADS
END OPTION
FIXED DISP
GEOMETRY
ISOTROPIC
NODE FILL
POST
TYING

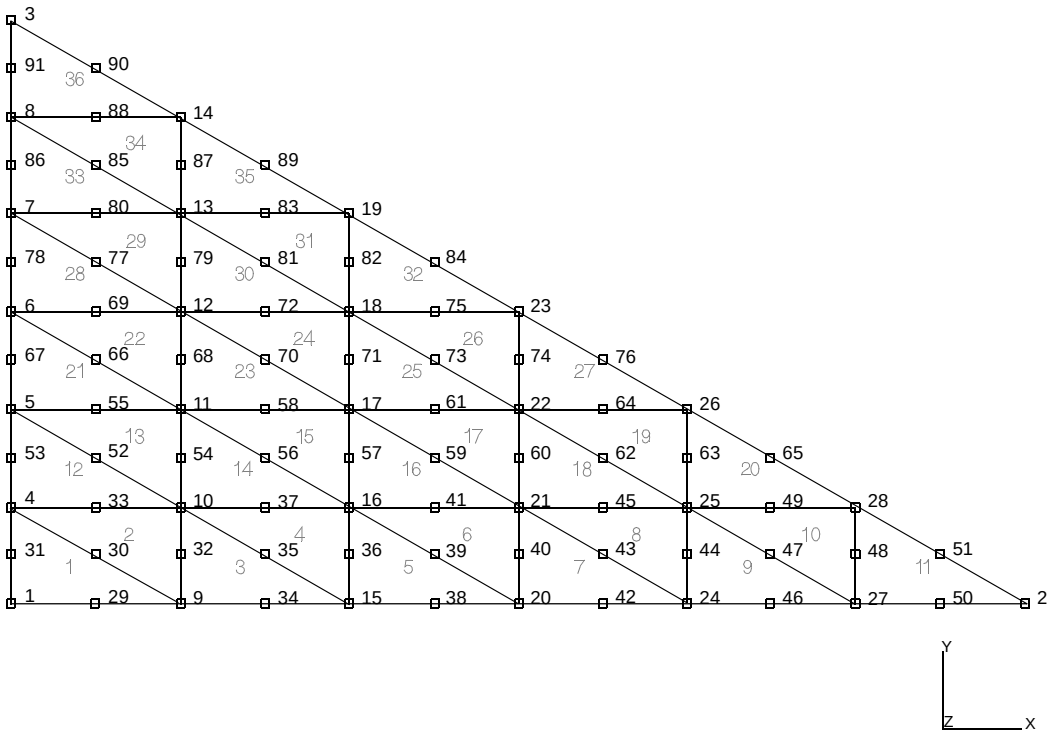

Figure 2.41-1 Triangular Plate and Finite Element Mesh

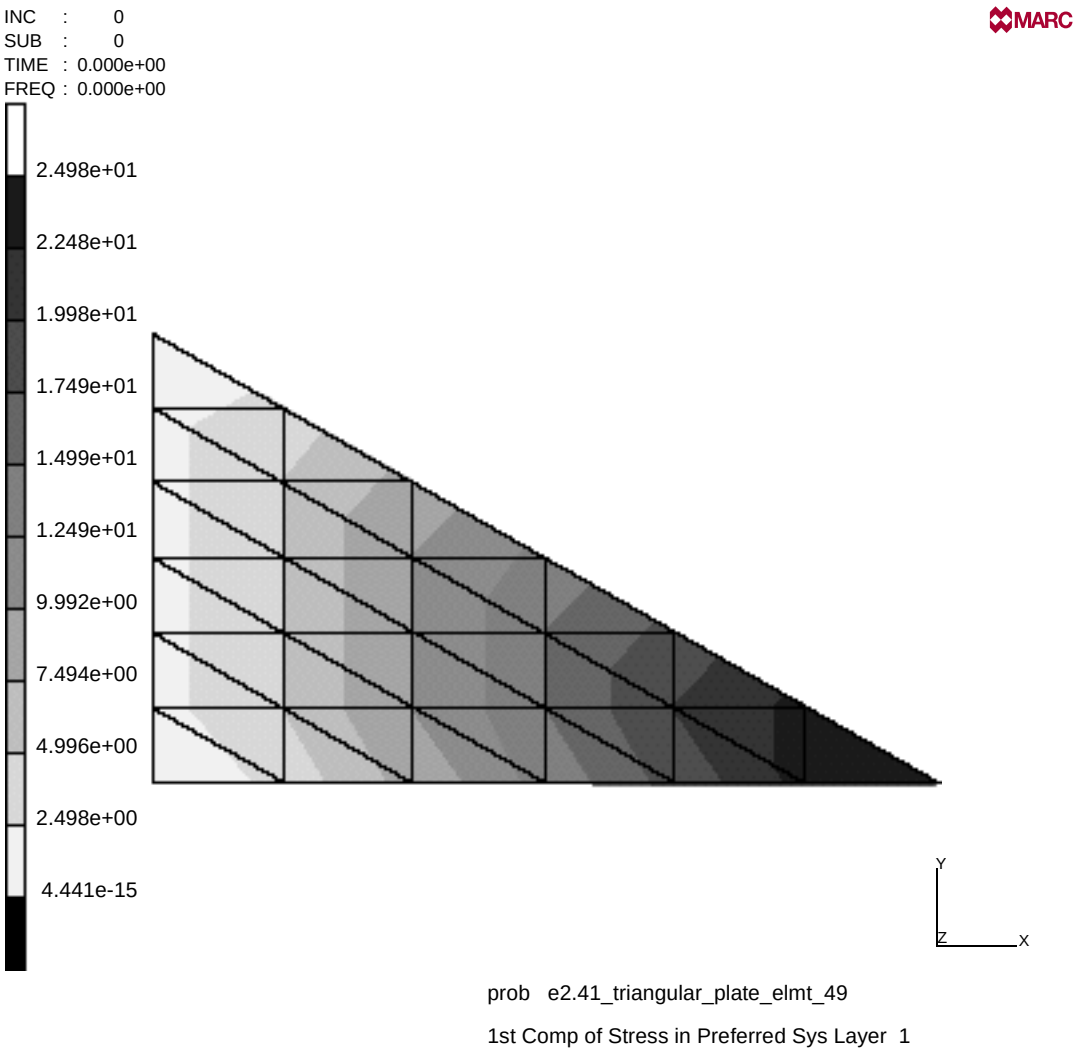

Figure 2.41-2 Stress Contours (x-component)

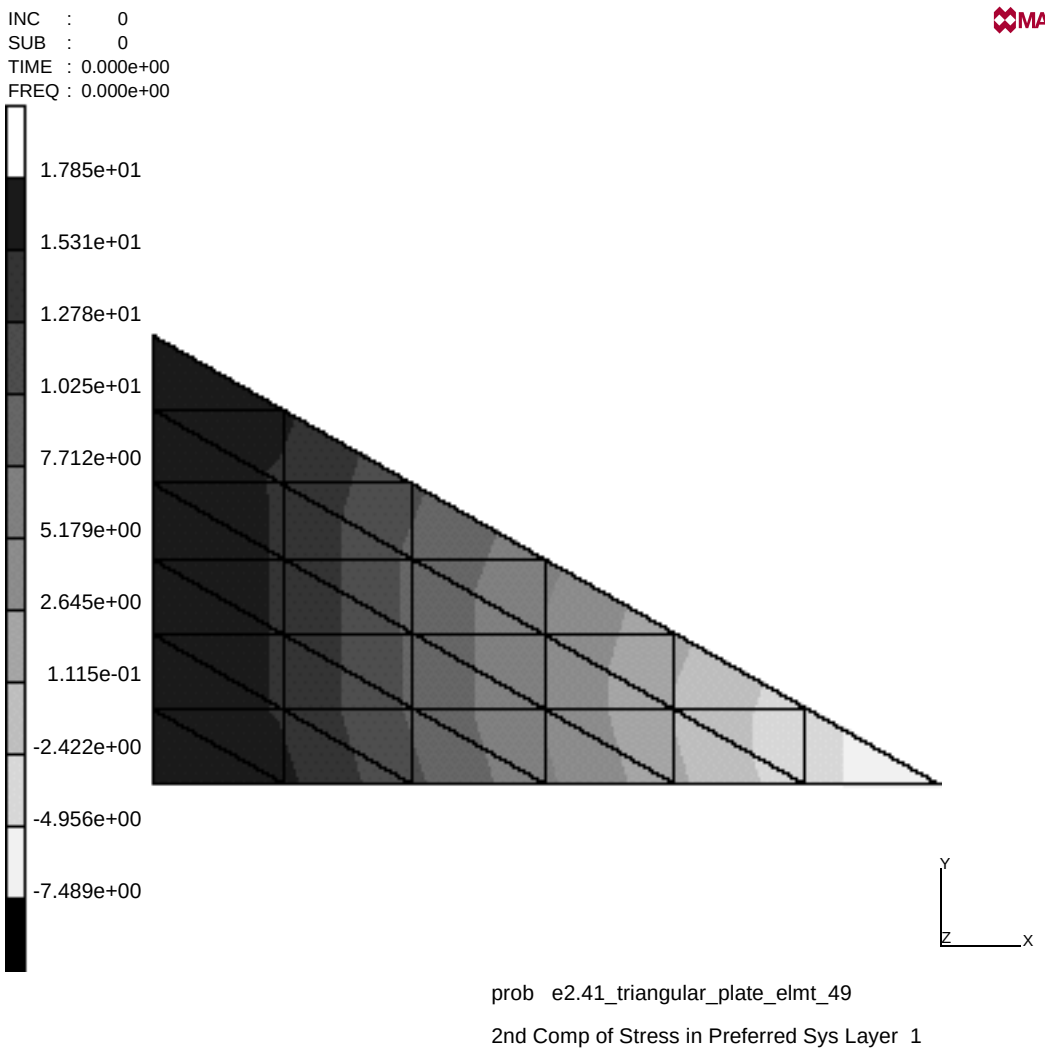

Figure 2.41-3 Stress Contours (y-component)

2.42 Square Plate on an Elastic Foundation

This problem illustrates the use of MARC element type 22 for an elastic analysis of a square plate. The plate is on an elastic foundation and subjected to a concentrated load at the center of the plate.

Element

Library element type 22, a curved quadrilateral thick-shell element, is used. The displacements are interpolated from the values at the eight nodes to the middle shell surface. The four corner nodes and four midside nodes each have six degrees of freedom, three displacements and three rotations.

Model

The dimensions of the plate and the finite element mesh are shown in Figure 2.42-1. Sixteen type 22 elements are used for this mesh. There are 65 nodes. Only one-quarter of the plate is modeled due to symmetry.

Material Properties

The material is elastic with a Young's modulus of 2.E5 psi and Poisson's ratio of 0.0.

Loading

A point load of 10.0 lb. (1/4 P) in the negative z-direction is applied at the center (node 1) of the plate.

Boundary Conditions

Displacements at the lines of symmetry are constrained, along $x = 0$, $u = 0$, $\theta_y = \theta_z = 0$, and along $y = 0$, $v = 0$, $\theta_x = \theta_z = 0$.

SHELL SECT

This option allows you to reduce the number of integration points from default value to a minimum value of three, in the plate thickness direction, for an elastic analysis.

Elastic Foundation

The whole plate is assumed to rest on an elastic foundation. The description of the elastic foundation is given in the model definition option FOUNDATION:

Element numbers = 1 through 16
Spring stiffness per unit area of the plate = 10.0 lb/in^2
Element face I.D. = 2

Results

Stress contours are shown in Figure 2.42-2. The PRINT CHOICE option is used to limit the output to element 1. The exact solution is found in Timoshenko and Woinowsky-Krieger, *Theory of Plates and Shells*.

Parameters, Options, and Subroutines Summary

Example e2x42.dat:

Parameters	Model Definition Options
ELEMENTS	CONNECTIVITY
END	COORDINATES
SHELL SECT	END OPTION
SIZING	FIXED DISP
TITLE	FOUNDATION
	GEOMETRY
	ISOTROPIC
	POINT LOAD
	PRINT CHOICE

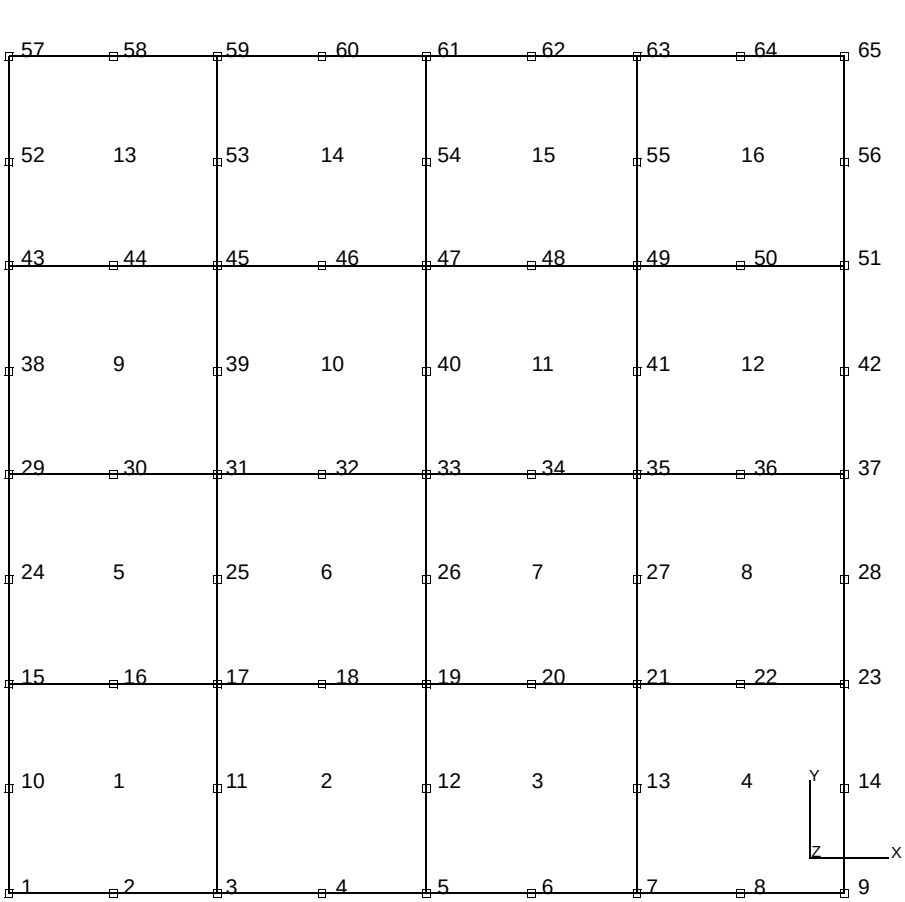

Figure 2.42-1 Square Plate and Mesh

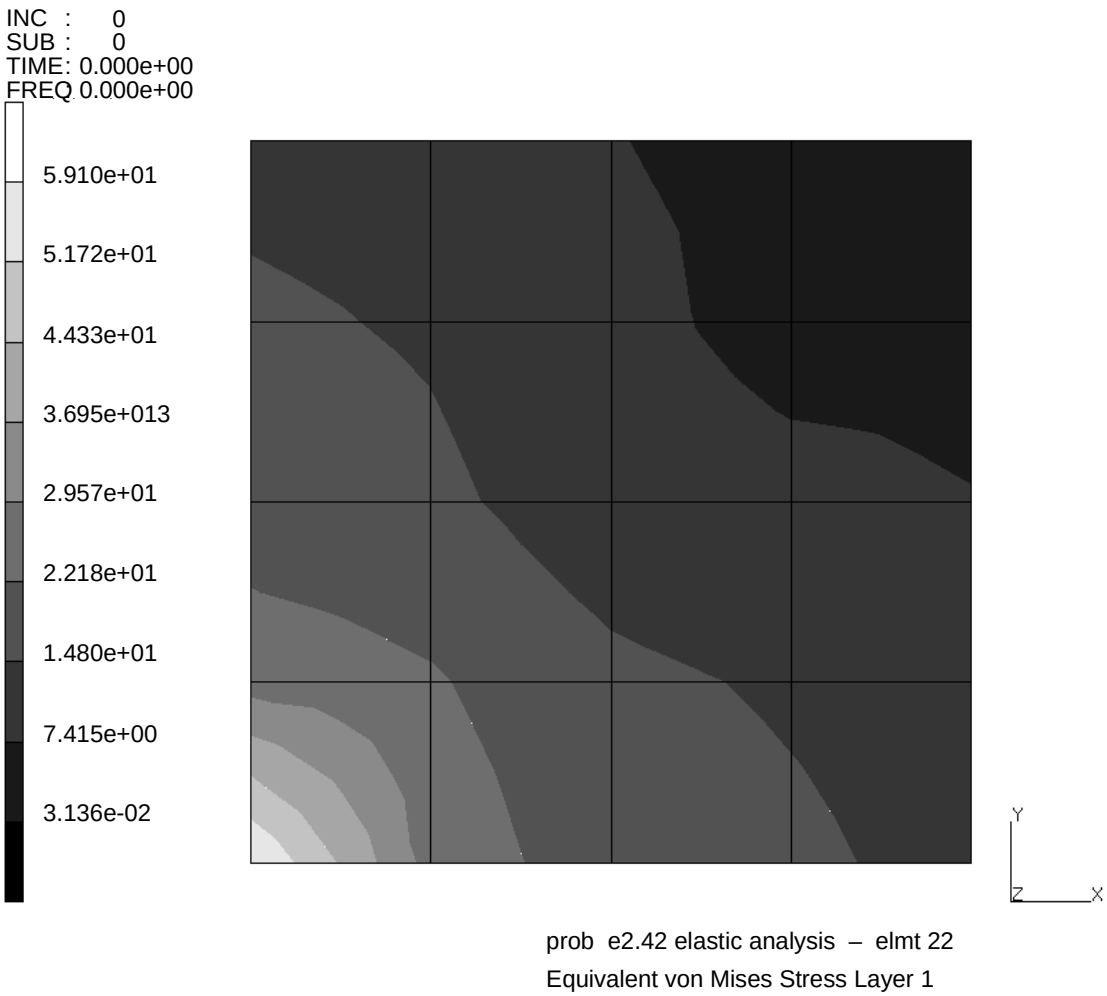

Figure 2.42-2 Equivalent Stress Contours (Layer 1)

2.43 Cantilever Beam Subjected to Concentrated Tip Moment

This problem illustrates the use of MARC element types 53 and 64 for an elastic analysis of a cantilever beam. The beam is subjected to a concentrated moment applied at the tip of the beam. The use of user subroutines UFORMS and FORCEM is also demonstrated. Subroutine UFORMS is used for the input of nodal degrees of freedom constraint relations, between truss and plane stress elements. Subroutine FORCEM allows the input of the end moment through a set of nonuniform distributed forces applied at the free end face of the beam.

Model

The dimensions of the beam and a finite element mesh are shown in Figure 2.43-1. The total number of elements is 30, with 95 nodes.

Elements

Element type 53 is a second-order, two-dimensional element with eight nodes. Each node has two degrees of freedom.

Element type 64 is an isoparametric 3-node truss. Each node has three degrees of freedom.

Material Properties

For Element 53: The Young's modulus is 2×10^5 psi and Poisson's ratio is 0.0.

For Element 64: The Young's modulus is 0.04 psi and Poisson's ratio is 0.0.

Loading

A linearly varying distributed load on nodes 21 to 53 simulates a moment applied to the beam. Nonuniform distributed forces are applied at the free end face of the beam (element 10). Subroutine FORCEM is used for the input of force magnitude.

The magnitude of the moment is equal to 0.0833333 in-lb, represented by a linearly varying distributed load with a maximum load intensity of 1.25 lb/square inch at nodes 21 and 53, respectively.

Boundary Conditions

A fixed-end condition is assumed to exist at x = 0. All degrees of freedom at nodes 1, 22 and 33 are constrained.

Geometry

Thickness of the plane stress element is 0.1 in. Area of the truss element is 1.0 inch.

Constraints

The nodal points of all the truss elements are constrained to have the same movements of that of the plane stress elements. Consequently, the total number of constraints is 42. The retained nodes are 1 through 21 and 33 through 53. The tied nodes are 54 through 74 and 75 through 95. This was entered using the list feature for defining the nodes. In order to illustrate the use of user subroutine UFORMS, the tying type is defined as -1.

In addition, options CONN GENER and NODE FILL are also used for the generation of a finite element mesh.

Results

The deflection at the tip of the beam is 1.251×10^{-3} in. ($\delta = Ml^2/2EI$, $I = 0.1 \times 2^3/12$) and the MARC result is 1.25136×10^{-3} in. The addition of the limp truss elements allows computation of the strains at the outer and innermost fibers.

Parameters, Options, and Subroutines Summary

Example e2x43.dat:

Parameters	Model Definition Options
ELEMENTS	CONN GENER
END	CONNECTIVITY
SIZING	COORDINATES
TITLE	DIST LOADS
	END OPTION
	FIXED DISP
	GEOMETRY
	ISOTROPIC
	NODE FILL
	PRINT CHOICE
	TYING

User subroutines in u2x43.f:

FORCEM
UFORMS

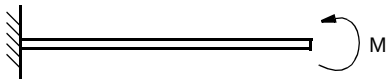

Cantilever Beam and Tip Moment

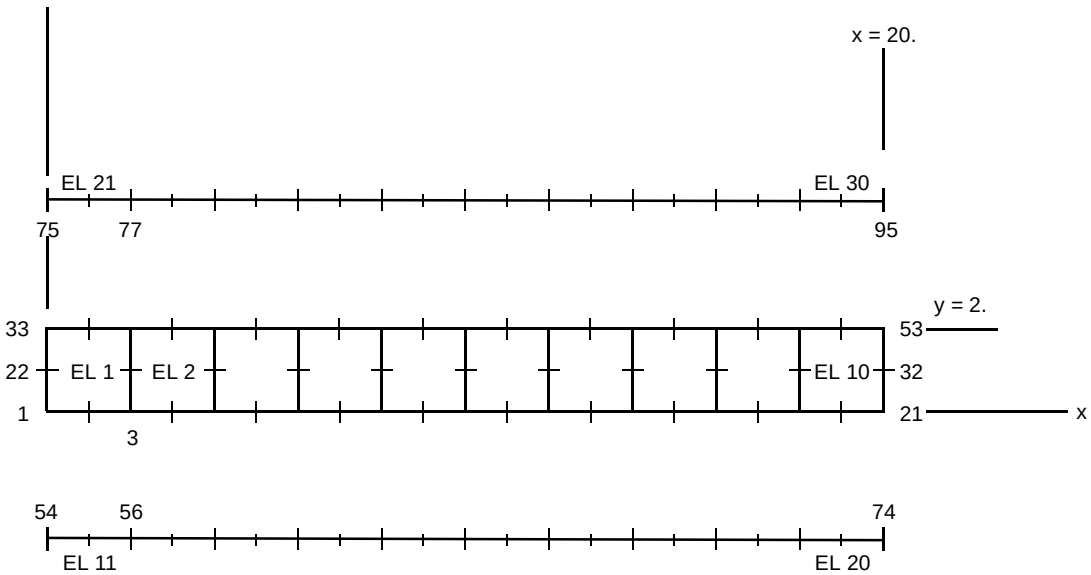

Figure 2.43-1 Cantilever Beam and Mesh

2.44 Local Load on Half-Space

This problem illustrates the use of MARC elements type 54 for an elastic analysis of a half-space subjected to a locally distributed load. The standard tying constraint option is selected for a compatible refinement of the mesh.

Element

Element type 54 is a distorted quadrilateral for plane strain. There are eight nodes and two degrees of freedom per node.

Model

The finite element mesh is shown in Figure 2.44-1. This mesh has been generated such that a more refined mesh would be near the distributed load. A total of 33 elements and 128 nodes are used in the analysis.

Material Properties

The material is elastic with a Young's modulus of 5×10^5 psi and Poisson's ratio of 0.2.

Geometry

The thickness of the model is assumed to be 1.0 inch.

Loading

A uniform pressure (w) of 150 psi is applied for a horizontal distance of 10 inches along the top surface.

Boundary Conditions

Symmetry conditions are imposed at x = 30.0, u = 0. Lines x = 0, y = 0, are assumed to be far away from the load; therefore, u = 0, v = 0.

Tying Constraint

Standard tying type 32 is used for locations where the mesh has been refined. This is necessary to ensure compatibility. A mesh plot was obtained before the tying relations could be formulated.

Results

A deformed mesh plot is shown in Figure 2.44-2. The von Mises stress intensity contours are shown in Figure 2.44-3. Mesh refinement is appropriate for a region with localized loading.

Displacement (inches)		Stress (psi)	
MARC Computed	**Analytically Computed**	**MARC Computed**	**Analytically Computed**
6.080×10^{-3}	5.724×10^{-3}	102.1	98.38

Reference

Timoshenko, S. P., and Goodier, J. N., *Theory of Elasticity*, McGraw-Hill, 1956, New York.

Parameters, Options, and Subroutines Summary

Example e2x44.dat:

Parameters

ELEMENTS
END
SIZING
TITLE

Model Definition Options

CONNECTIVITY
COORDINATES
DIST LOADS
END OPTION
FIXED DISP
GEOMETRY
ISOTROPIC
TYING

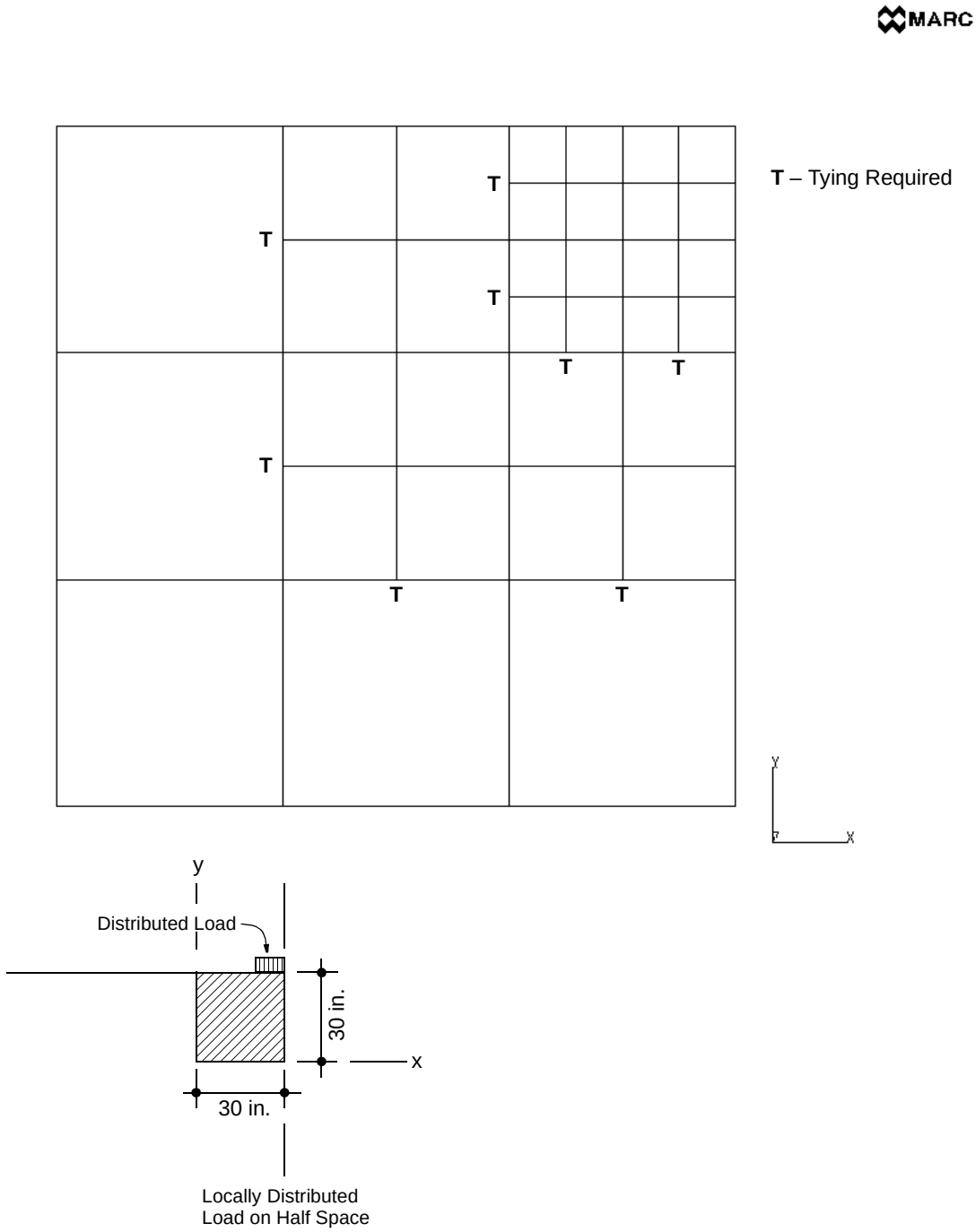

Figure 2.44-1 Half Space and Mesh

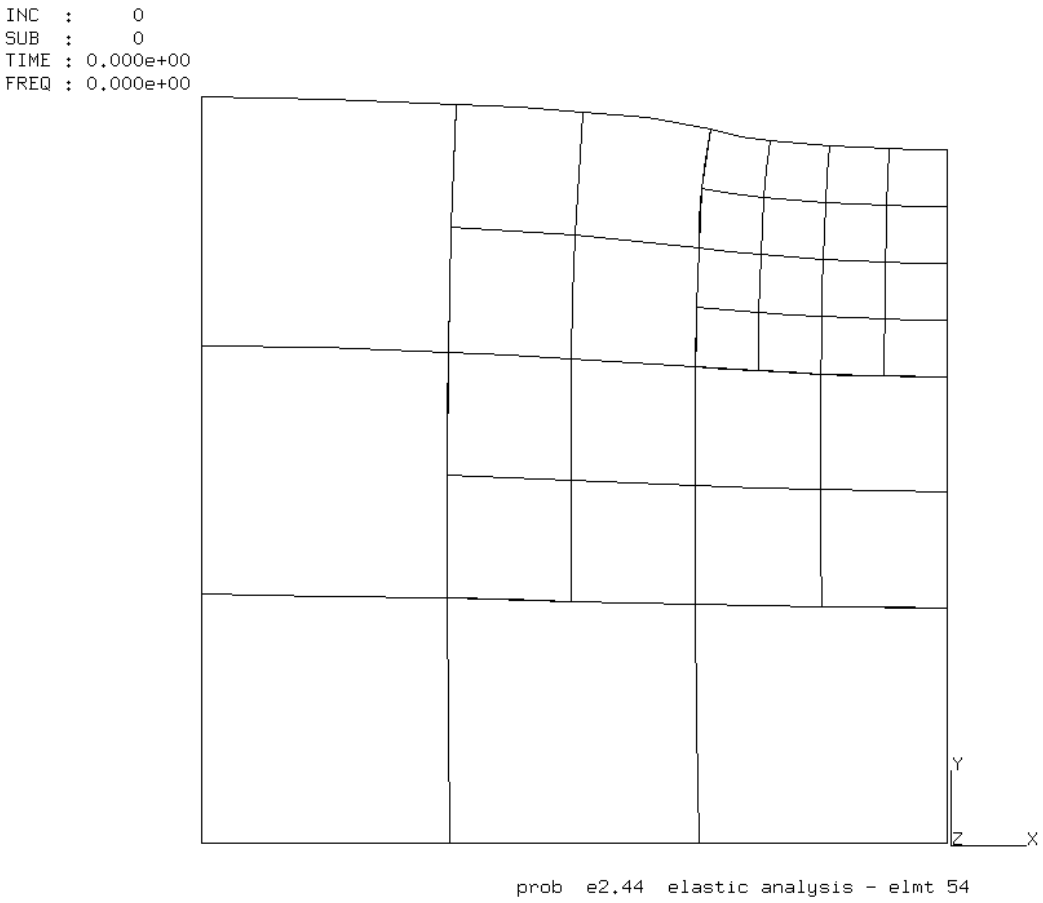

Figure 2.44-2 Deformed Mesh Plot

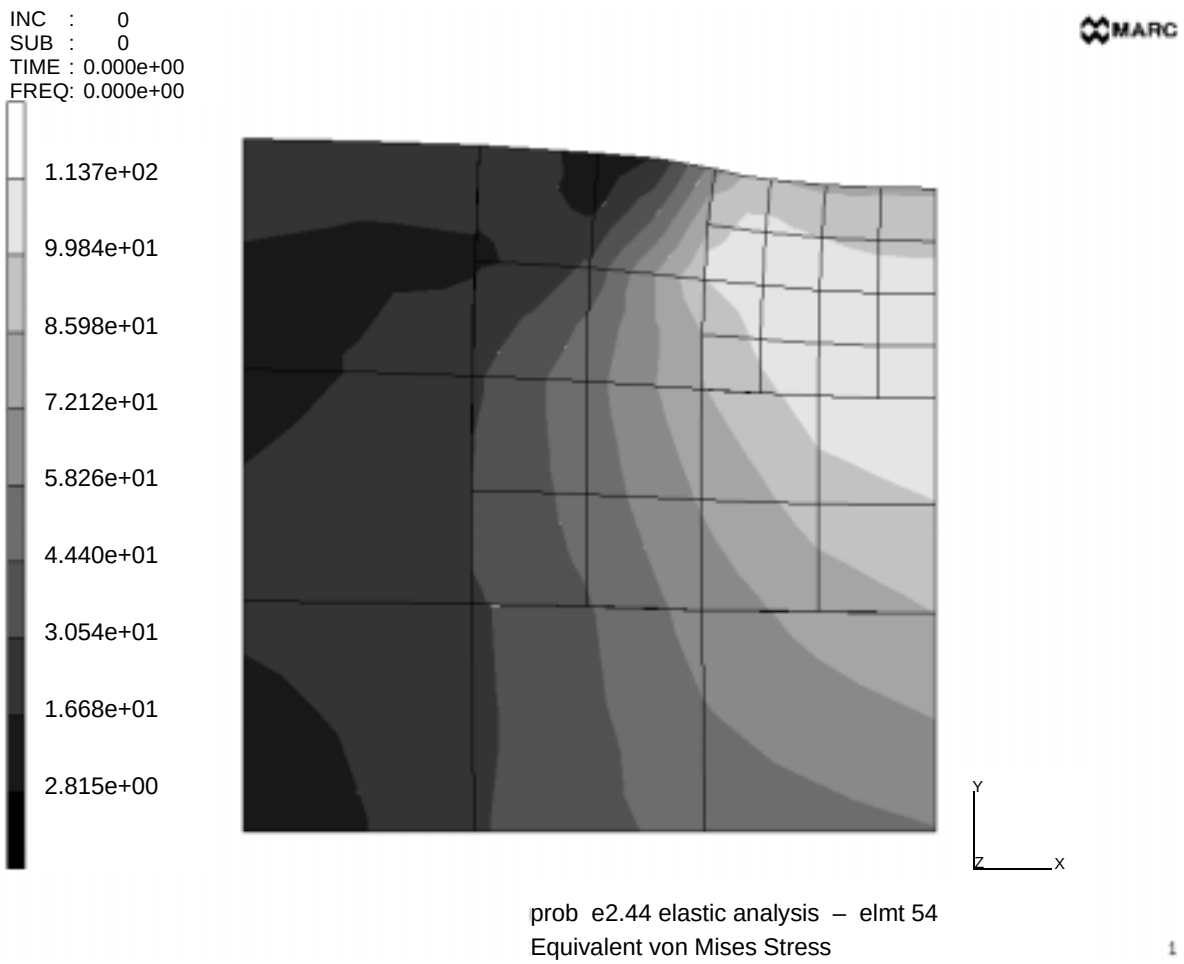

Figure 2.44-3 von Mises Stress Contours

2.45 Notched Circular Bar with Anisotropy, J-Integral Evaluation

This problem illustrates the use of MARC element type 55 and the J-INT option for an elastic analysis of an anisotropic notched bar. The bar is subjected to a distributed axial load. The MARC J-integral calculation is a measure of the strength of the subplasticity of the elastic stress field near the crack tip. The material is orthotropic with a 10 times higher modulus in the axial direction than in the other directions. The use of the ELSTO and ALIAS parameters is also illustrated.

Element

Element type 55 is an 8-node axisymmetric reduced integration element, with two degrees of freedom at each node.

Model

The element type is 55. There are 32 elements and a total of 107 nodes. The so-called "quarter-point node" technique is used for the elements adjacent to the crack tip. This involves redefinition of the coordinates of the midside nodes on the edges adjacent to the crack tip with use of a second COORDINATES block.

The dimensions of the bar and the finite element mesh are shown in Figure 2.45-1 (a and b).

Material Properties

The following properties are specified in this option: Young's modulus of 30×10^6, and Poisson's ratio of 0.3 These properties are subsequently modified with the user subroutine ANELAS.

Geometry

Not required for axisymmetric elements.

Boundary Conditions

The following symmetry conditions are applied:

v = 0 at r = 0 (axis of symmetry)
u = 0 at uncracked portion ligament on the line z = 0

Loading

A distributed tensile pressure of 100 psi is applied to the boundary line of elements 15, 16, 31 and 32.

J-INTEGRAL

In this analysis, the J-integral is evaluated for three different element rings.

J-Integral Evaluations	Number of Nodes Moved in List Number		Nodal Movements of List Number in r-Direction	
	1	2	1	2
1	1	9	-0.01	-0.0075
2	27	9	-0.01	-0.0050
3	53	9	-0.01	-0.0050

Node numbers are shown in the J-INTEGRAL Model Definition block. The midside nodes surrounding the moved part of the mesh move one-half of the distance, whereas the quarter-point nodes move three-fourths of the distance.

User Subroutine ANELAS

It is assumed that the material has “stratified” anisotropy. With the first direction the “stiff” direction, the constitutive equation has the form:

$$D = \alpha \begin{bmatrix} 1-\nu_2^2 & n\nu_1(1+\nu_2) & n\nu_1(1+\nu_2) \\ n\nu_1(1+\nu_2) & n(1-n\nu_1^2) & n(\nu_2+n\nu_1^2) \\ n\nu_1(1+\nu_2) & n(\nu_2+n\nu_1^2) & n(1-n\nu_1^2) \\ 0 & 0 & 0 \end{bmatrix} \begin{bmatrix} 0 \\ 0 \\ 0 \\ E_1/2\alpha(1+\nu_1) \end{bmatrix}$$

with $n = E_2/E_1$ and $\alpha = E_1/(1+\nu_2)(1-\nu_2-2n\nu_1^2)$, where $n \le 1$.

For material stress in the x-direction (1), this equation yields:

$$\sigma_x = E_1\varepsilon_x,\ \varepsilon_y = \varepsilon_z = -\nu_1\varepsilon_x$$

For uniaxial stress in the y-direction (2), one finds:

$$\sigma_y = E_2\varepsilon_y,\ \varepsilon_x = -n\nu_1\varepsilon_y,\ \varepsilon_z = -\nu_2\varepsilon_y,$$

and similar relations are found for uniaxial stress in the z-direction (3).

In the current problem the following values are selected:

$E_1 = 30 \bullet 10^6$, $E_2 = 30 \bullet 10^5$, $\nu_1 = \nu_2 = 0.3$

For isotropic materials, $E_1 = E_2 = E$ and $\nu_1 = \nu_2 = \nu$ and the above constitutive equation degenerates to the usual isotropic equation. In the subroutine ANELAS, the ratio between anisotropic and isotropic components needs to be specified.

Since the preferred directions of the anisotropic material are the same as that of the global coordinate system, the default subroutine ORIENT is used for this problem.

Results

The strain energy differences ΔW calculated by the MARC program are 0.01987, 0.01979 and 0.01975. In order to obtain the J-integral from ΔW, you have to divide ΔW by the crack length and the nodal movement distance, and multiply the results by 2 to take into account that only half of the bar is modeled:

$$J = 2\Delta W / 2\pi r \Delta l$$

In the current problem, r = 10 and Δl = .01, which yields the following values of J:

J(1) = 0.06325 (lbs/in)
J(2) = 0.06299
J(3) = 0.06287

A deformed mesh plot is shown in Figure 2.45-2, and stress contours are depicted in Figure 2.45-3.

Parameters, Options, and Subroutines Summary

Example e2x45.dat:

Parameters	Model Definition Options
ALIAS	CONNECTIVITY
ELEMENTS	COORDINATES
ELSTO	DIST LOADS
END	END OPTION
J-INT	FIXED DISP
SIZING	ISOTROPIC
TITLE	J-INTEGRAL
	OPTIMIZE

User subroutine in u2x45.f:

ANELAS

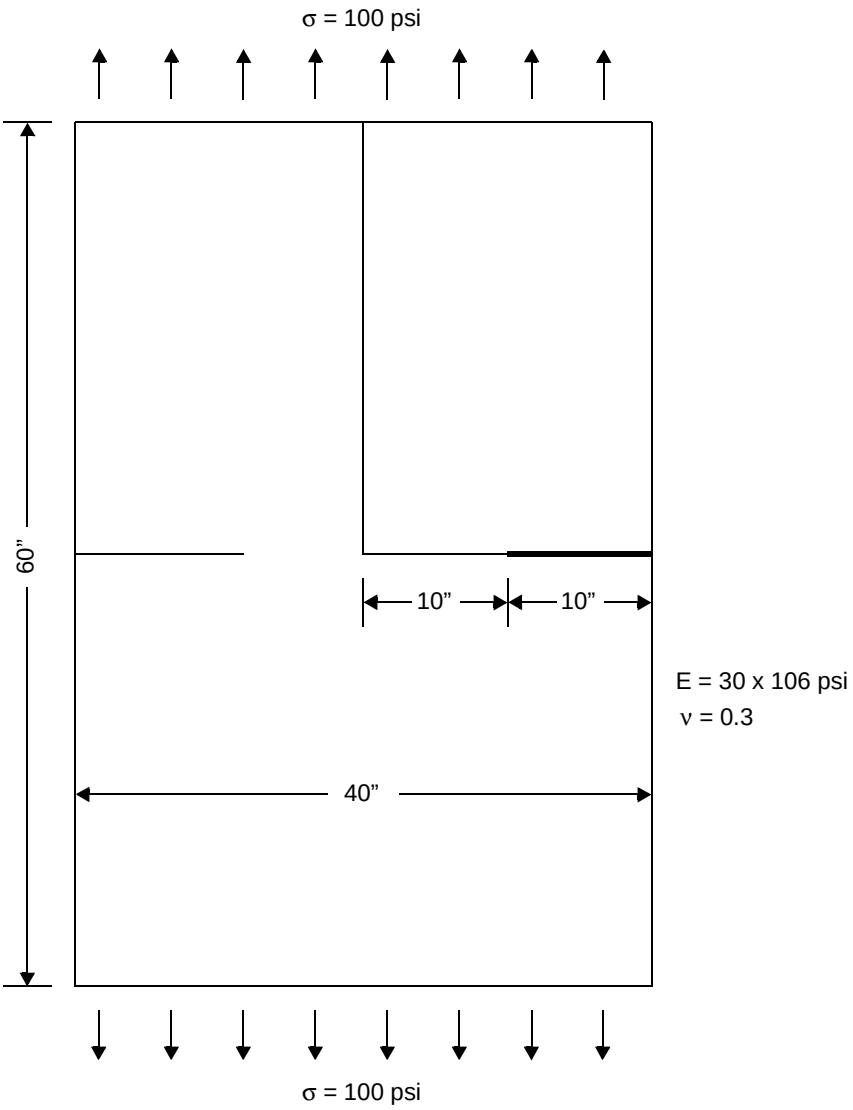

Figure 2.45-1 (a) Notched Circular Bar and Mesh

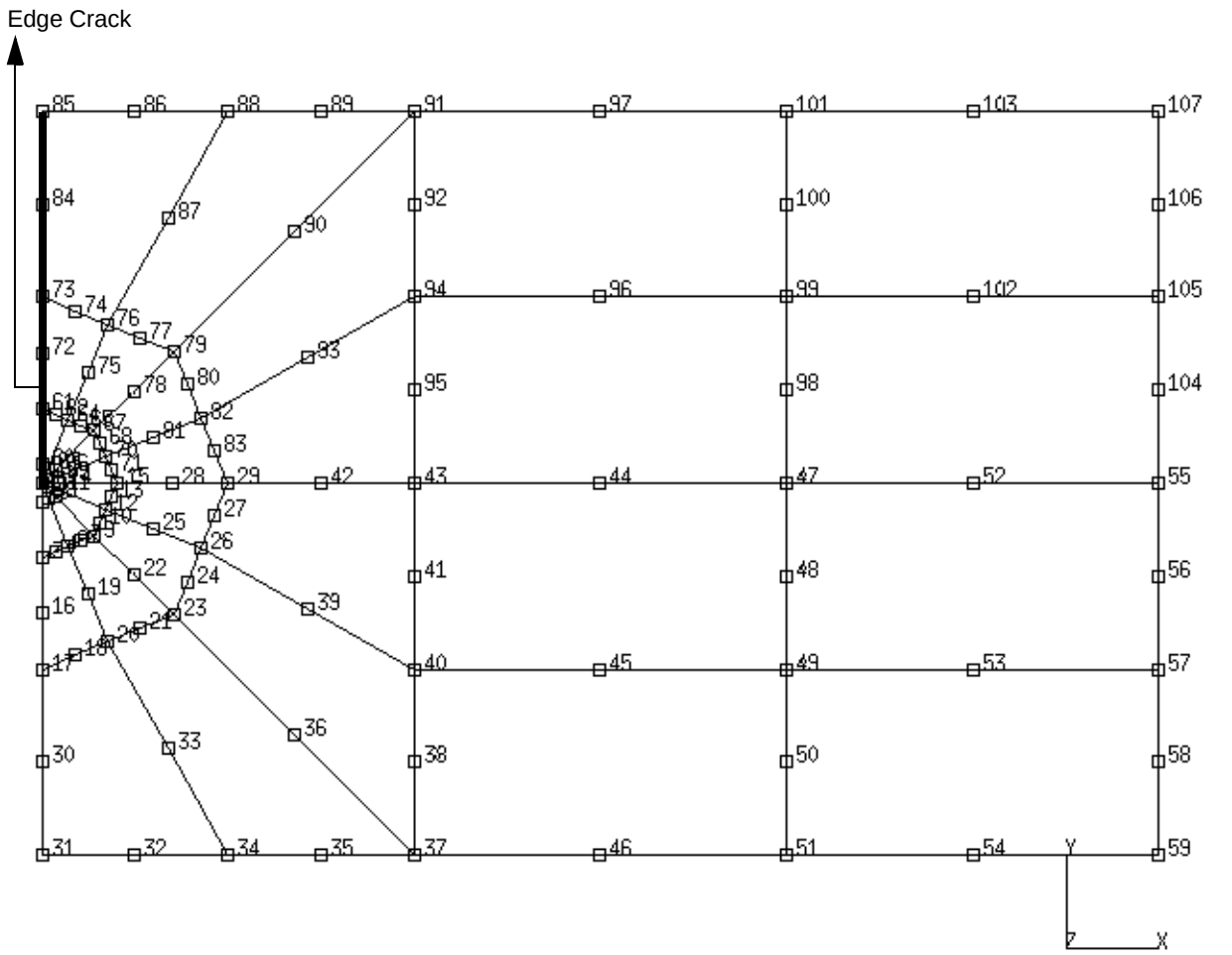

Figure 2.45-1 (b) Detail of Notched Circular Bar and Mesh

INC : 0
SUB : 0
TIME : 0.000e+00
FREQ : 0.000e+00

MARC

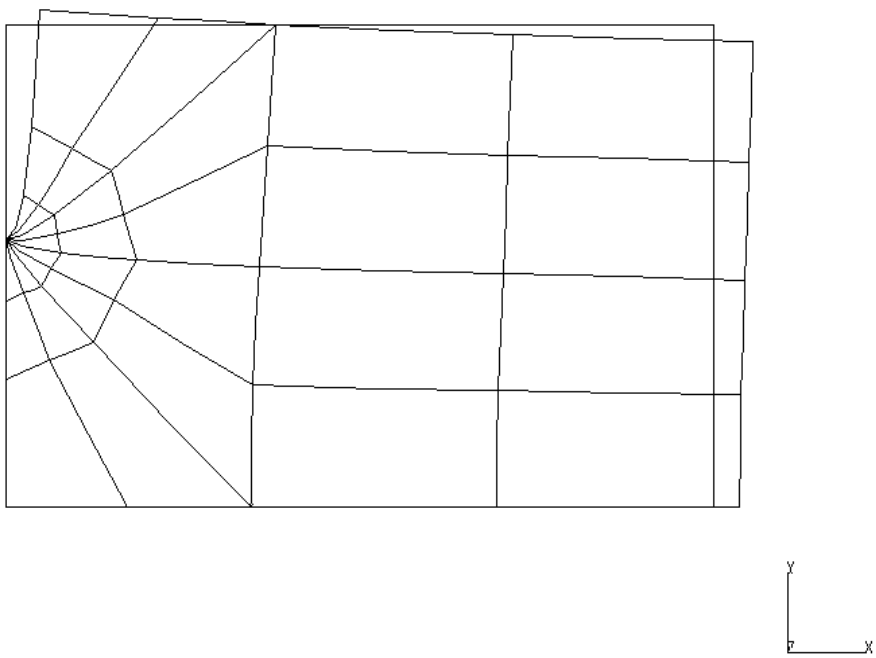

prob e2.45 elastic analysis - elmt 55
Displacements x

Figure 2.45-2 Deformed Mesh Plot

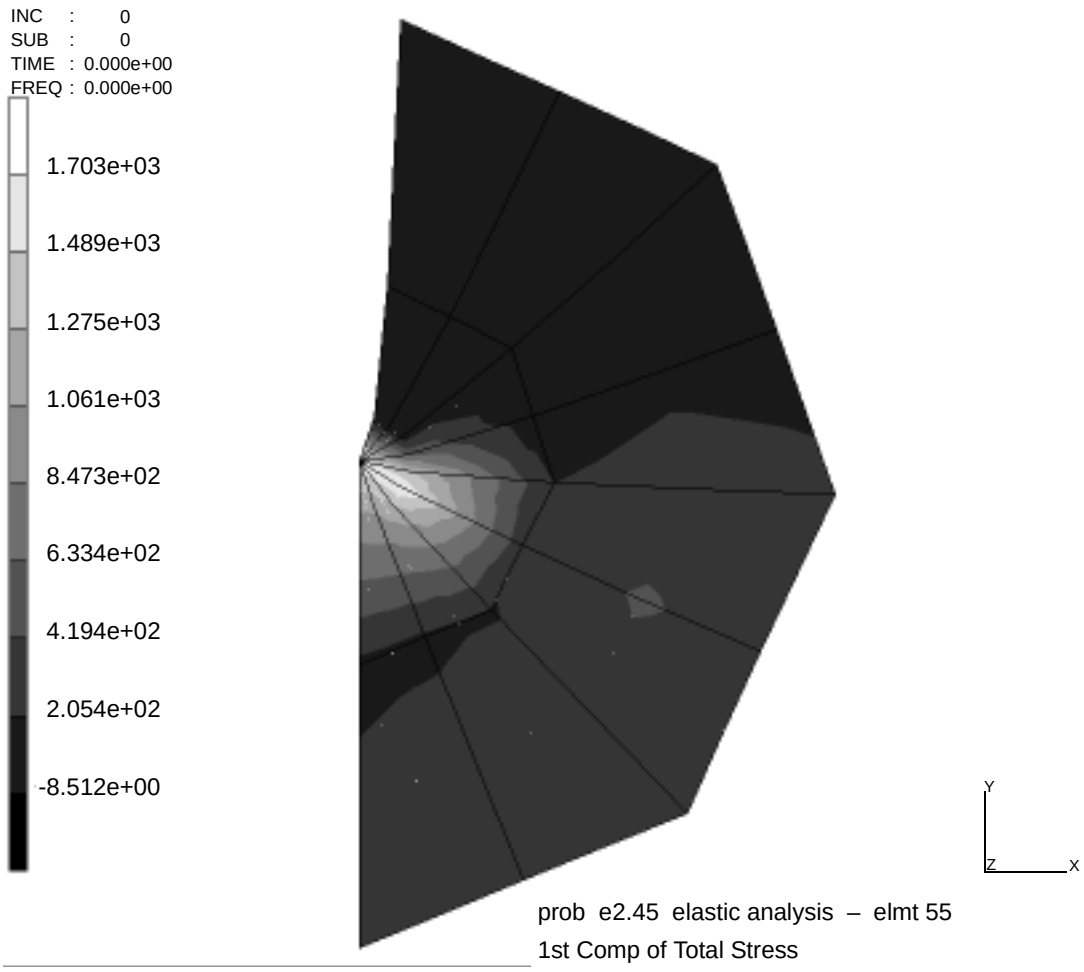

Figure 2.45-3 Stress Contours for σ_{11}

2.46 Square Plate with Central Hole, Thermal Stresses

This problem illustrates the use of MARC element types 19, 29, and 56 for an elastic analysis of a square plate with a central hole. The hole is subjected to a linearly varying thermal load in the radial direction. User subroutine CREDE is also demonstrated.

This problem is modeled using the four techniques summarized below.

Data Set	Element Type(s)	Number of Elements	Number of Nodes	Differentiating Features
e2x46a	56	20	79	Uses CREDE
e2x46b	29	20	79	Uses FORCEM
e2x46c	29	20	79	Uses FORCEM
e2x46d	19	80	99	

Elements

Element 19 is a 4-node, generalized plane-strain element. Element 29 is an 8-node, generalized plane-strain element, with two degrees of freedom at each node. Element type 56 has the same functionality as element 29 but uses reduced integration.

Model

The analysis is first performed using element types 29 and 56. There are 20 elements with a total of 81 nodes. The dimensions of the plate and the finite element mesh are shown in Figure 2.46-1. In the last model, element type 19 is used with a mesh consisting of 80 elements and 101 nodes. This mesh is shown in Figure 2.46-2.

Material Properties

The Young's modulus is 30×10^5 psi, with Poisson's ratio of 0.3. The coefficient of thermal expansion is 12.4×10^{-7} in/in/°F. The plate is stress-free at a temperature of 0°F.

Geometry

The thickness of the plate is 1.0 inch.

Boundary Conditions

The following boundary conditions are applied along the symmetry lines:

$u = 0$ at $x = 0$
$v = 0$ at $y = 0$

At the shared node 81, rotations about both x- and y-axes are constrained:

$\theta_x = \theta_y = 0$

Thermal Load

The thermal load is caused by a linearly varying temperature in the radial direction. The temperatures are interpolated/extrapolated with:

T = 20°F at r = 1.0 inches
T = 100°F at r = 5.0 inches

User subroutine CREDE is used for the input of thermal load at each integration point of each element. In problems e2x46c and e2x46d, the temperatures are input via user subroutine FORCEM. This procedure has some advantages when using adaptive time stepping procedures because forcem.f is called within the iteration loop and CREDE is not. Temperatures at integration points as interpolated from the given linear distribution are specified with a data statement.

In problem e2x46d, the thermal loads are prescribed by specifying the temperature at the nodal points using the INITIAL TEMPERATURE and POINT TEMPERATURE options.

Optimization

The Cuthill-McKee technique is used to minimize the bandwidth.

Results

A deformed mesh plot is shown in Figure 2.46-3 and stress contours are depicted in Figure 2.46-4. The thermal strains created are shown in Figure 2.46-5.

Parameters, Options, and Subroutines Summary

Example e2x46a.dat:

Parameters	Model Definition Options
ELEMENTS	CONNECTIVITY
END	COORDINATES
SIZING	END OPTION
THERMAL	FIXED DISP
TITLE	GEOMETRY
	ISOTROPIC
	THERMAL LOADS
	UFCONN

User subroutine in u2x46a.f:

CREDE

Example e2x46b.dat:

Parameters	Model Definition Options
ELEMENTS	CONNECTIVITY
END	COORDINATES
SIZING	END OPTION
THERMAL	FIXED DISP
TITLE	GEOMETRY
	ISOTROPIC
	THERMAL LOADS
	UFCONN

User subroutines in u2x46b.f:

CREDE
UFCONN

Example e2x46c.dat:

Parameters	Model Definition Options
ELEMENTS	CONNECTIVITY
END	COORDINATES
SIZING	DIST LOADS
TITLE	END OPTION
	FIXED DISP
	GEOMETRY
	ISOTROPIC

User subroutine in u2x46c.f:

FORCEM

Example e2x46d.dat:

Parameters

ELEMENTS
END
PROCESS
SETNAME
SIZING

Model Definition Options

CONNECTIVITY
COORDINATES
DEFINE
END OPTION
FIXED DISP
GEOMETRY
INITIAL TEMP
ISOTROPIC
OPTIMIZE
POINT TEMP
POST
PRINT ELEM
PRINT NODE
SOLVER

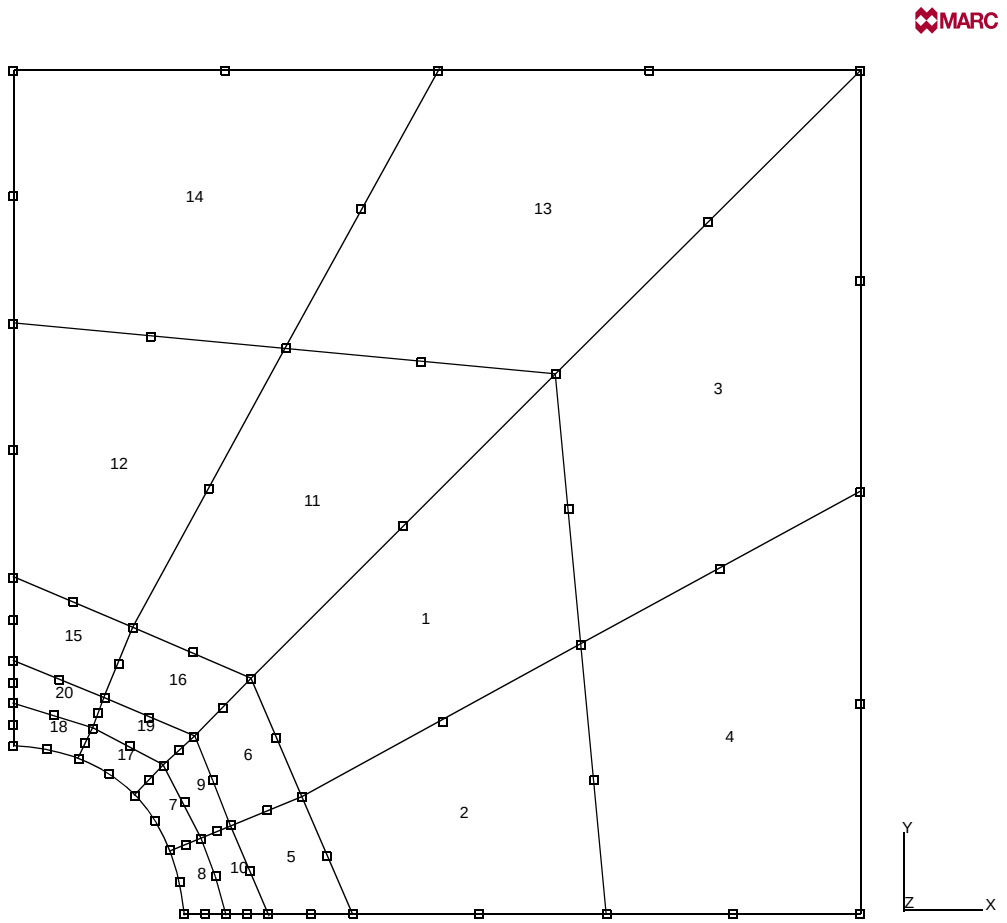

Figure 2.46-1 Square Plate with Central Hole and Mesh

INC : 0
SUB : 0
TIME : 0.000e+00
FREQ : 0.000e+00

MARC

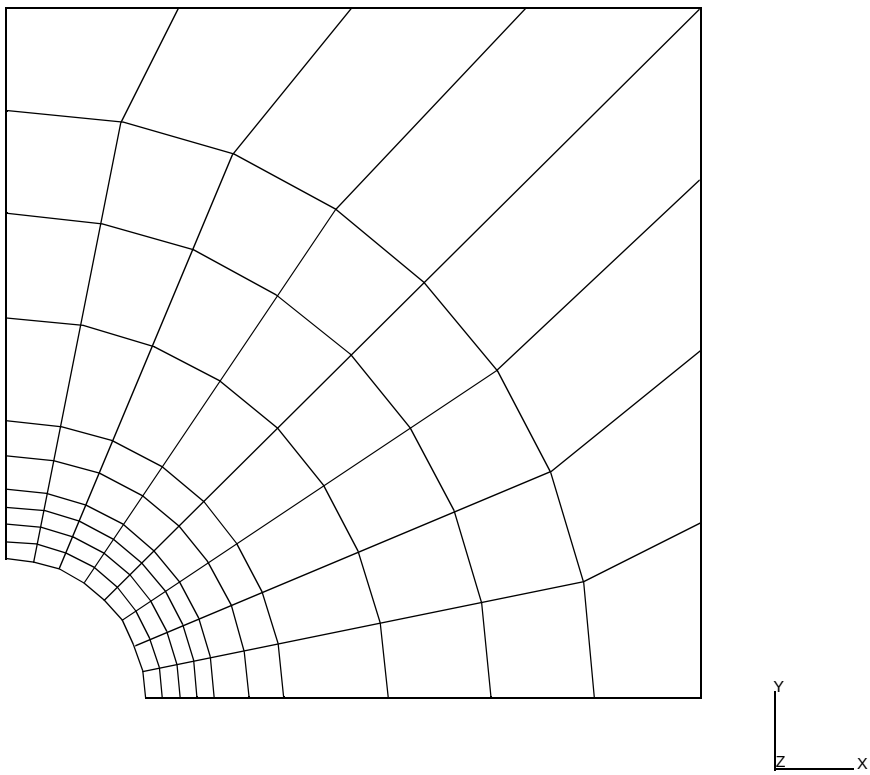

Figure 2.46-2 Fine Element Mesh Using Element Type 19

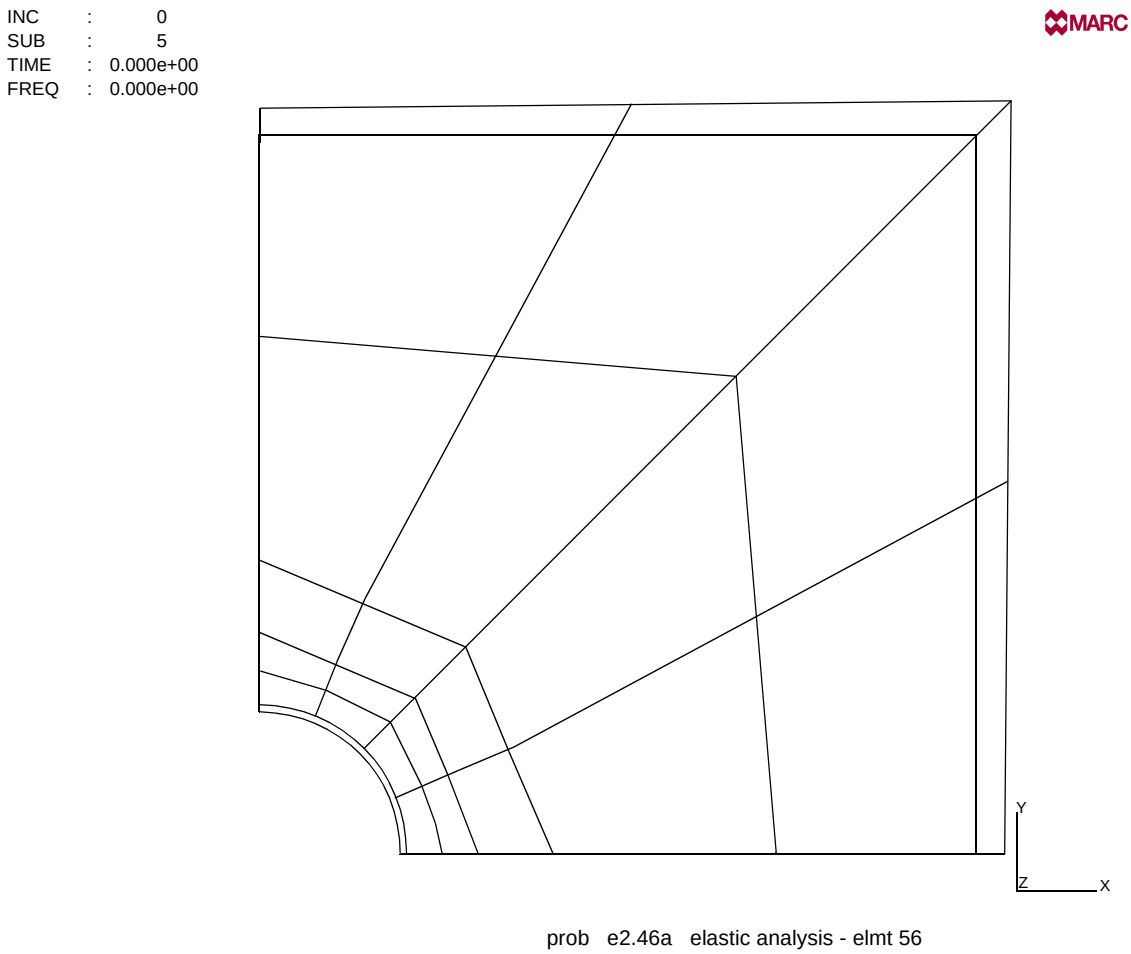

Figure 2.46-3 Deformed Mesh Plot

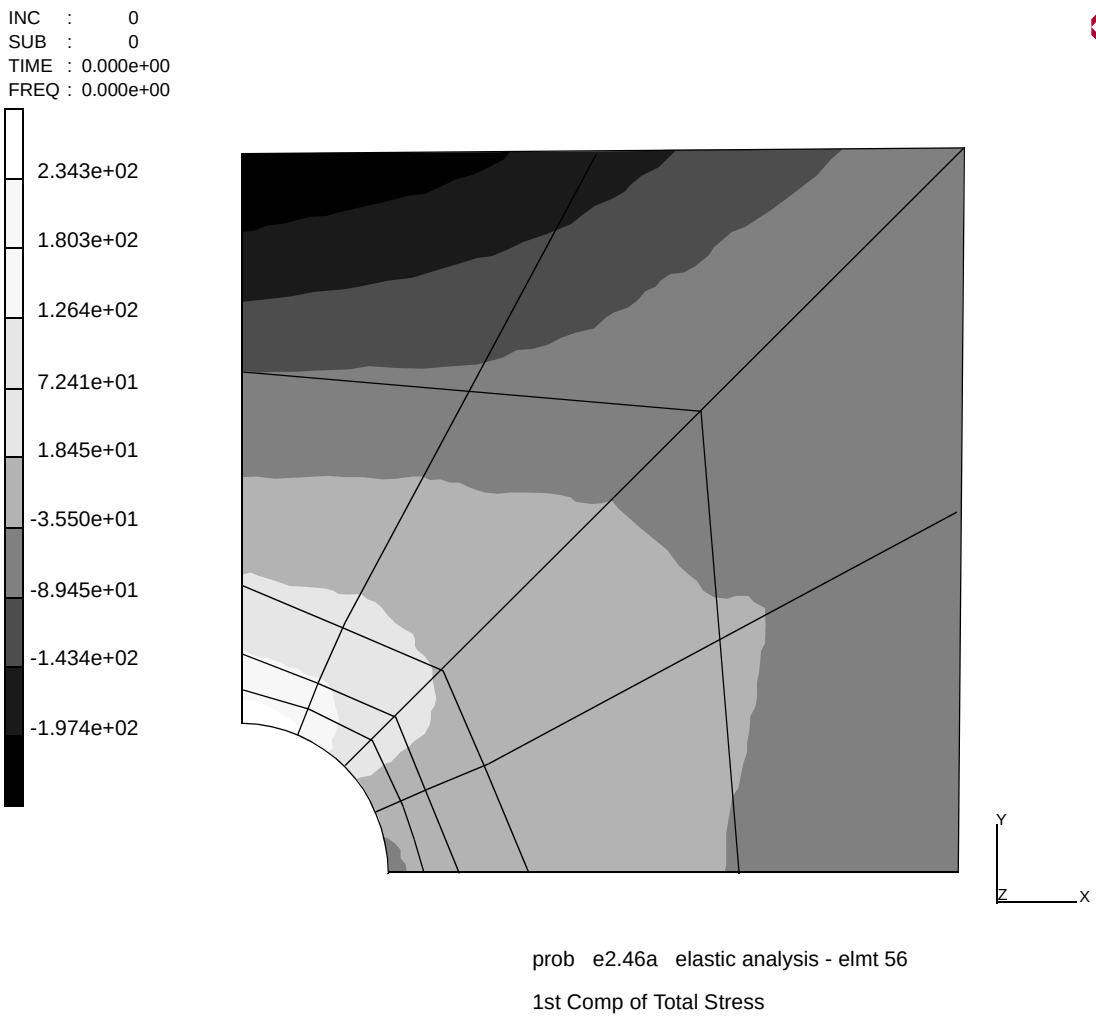

Figure 2.46-4 Stress Contours for σ_{11}

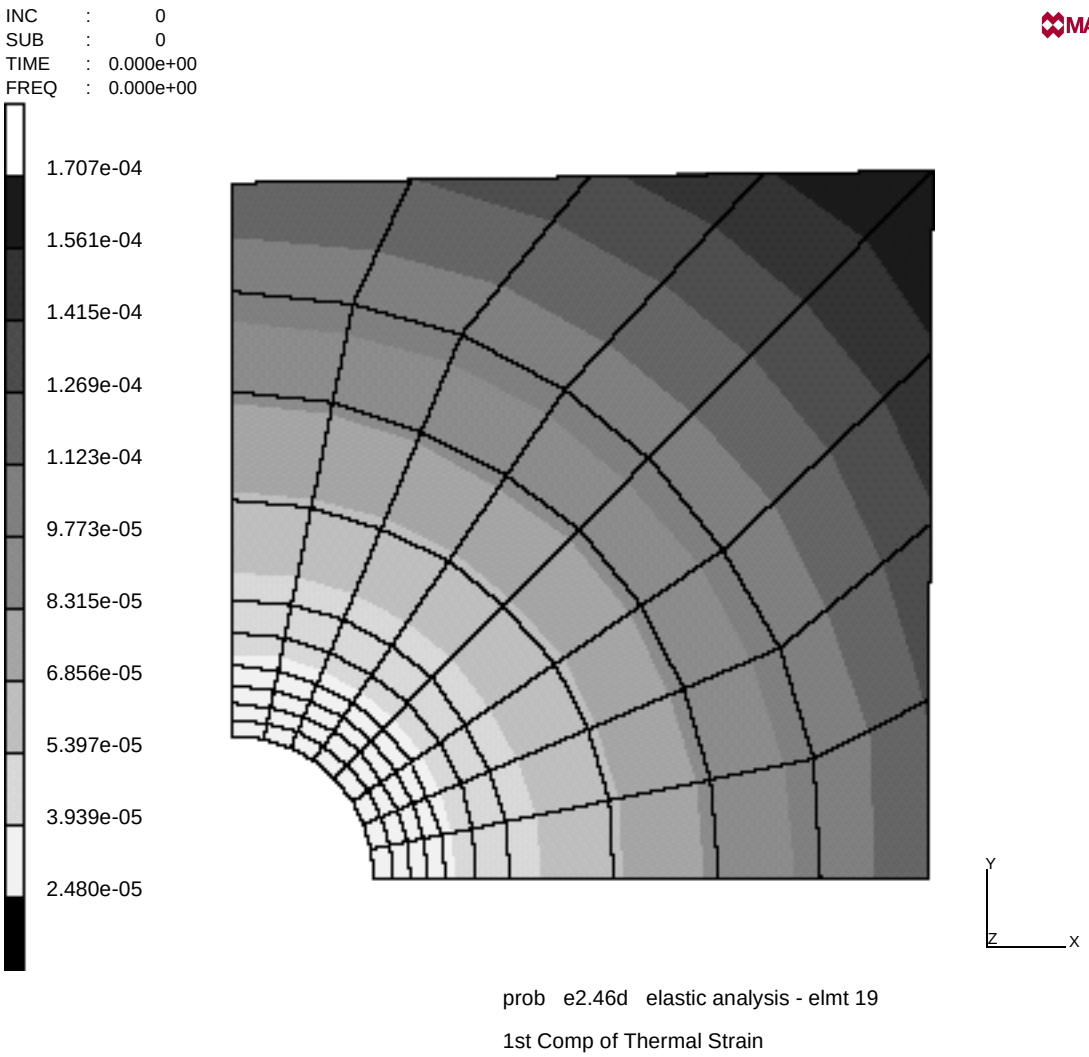

Figure 2.46-5 Contours of Thermal Strain

2.47 Thick Cylinder with Internal Pressure; Three-Dimensional Model

This problem illustrates the use of MARC element type 57 and the options TRANSFORMATION and TYING for an elastic analysis of a thick cylinder. The cylinder is subjected to a uniform internal pressure. The use of MESH3D for the generation of connectivity and coordinates blocks is also demonstrated.

Element

Element type 57 is a three-dimensional 20-node brick with reduced integration, with three global degrees of freedom.

Model

The element is type 57. There are 12 elements, with a total of 111 nodes. Dimensions of the cylinder and the finite element mesh are shown in Figure 2.47-1.

Material Properties

The Young's modulus is 2,100,000 kgf/cm^2 and Poisson's ratio is 0.3.

Loading

A uniform pressure (p) of 1000 kgf/cm^2, is applied in the radial direction at elements 2, 4, 6, 8, and 10.

Boundary Conditions

The third degree of freedom for nodes on the z = 0 plane is constrained (w = 0). Planes of symmetry: v = 0. (nodes 1 through 29, and 83 through 111)

Transformation

Degrees of freedom at nodal points 83 through 111 are transformed into local coordinate system for the convenience of defining boundary conditions (v = 0 for symmetry condition).

Tying Constraint

One type 3 tying constraint is imposed in this problem. Tying type 3 ties the degrees of freedom of all nodes on the top surface (z = 6) to node 25, which is constrained. This ensures plane strain conditions.

MESH3D

Connectivity and coordinate blocks are generated by using MESH3D.

Results

A deformed mesh plot is shown in Figure 2.47-2 and von Mises stress contours are depicted in Figure 2.47-3. This problem could have been solved using axisymmetric elements with less complications. A three-dimensional analysis would be necessary if there were any material or loading variations in the r-direction.

Parameters, Options, and Subroutines Summary

MESH3D is used in example e2x47a.dat:

Example e2x47b.dat:

Parameters	Model Definition Options
ELEMENTS	CONNECTIVITY
END	COORDINATES
SIZING	DIST LOADS
TIE	END OPTION
TITLE	FIXED DISP
	ISOTROPIC
	TRANSFORMATION
	TYING

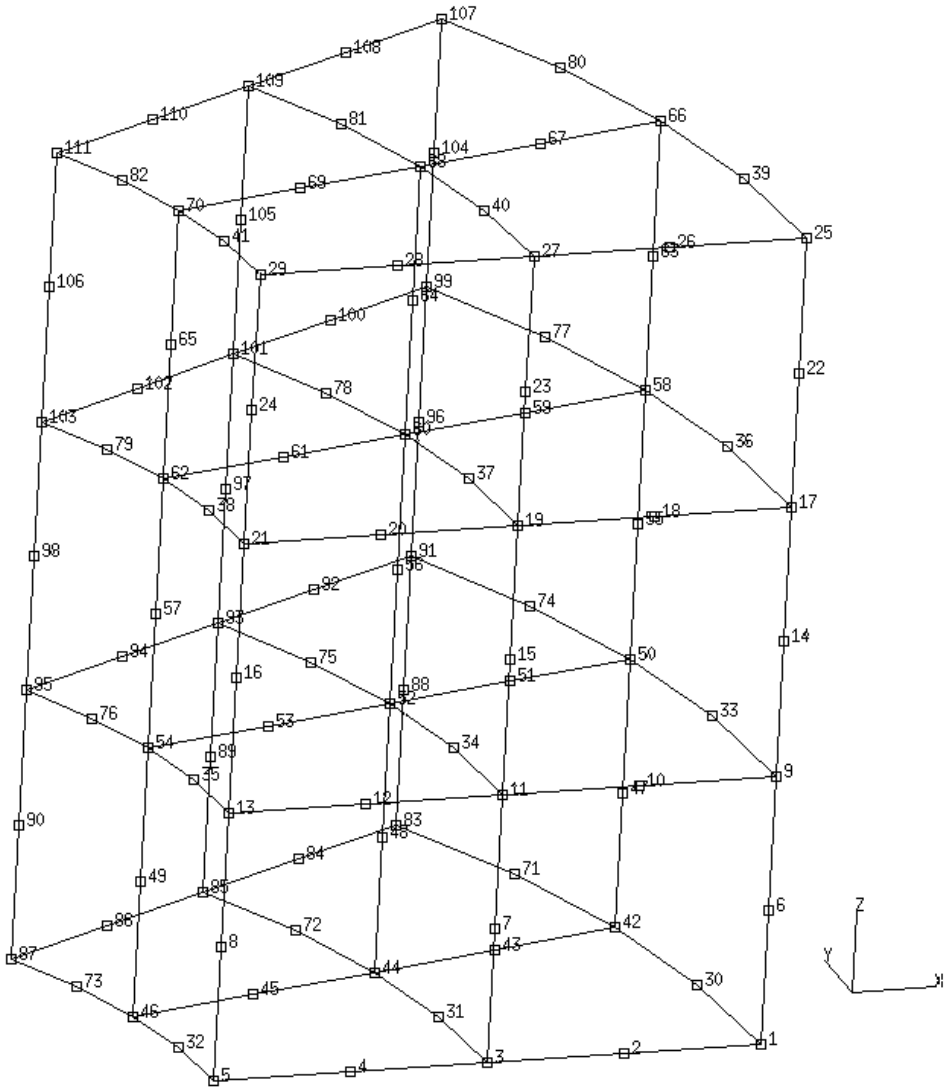

Figure 2.47-1 Cylinder and Mesh

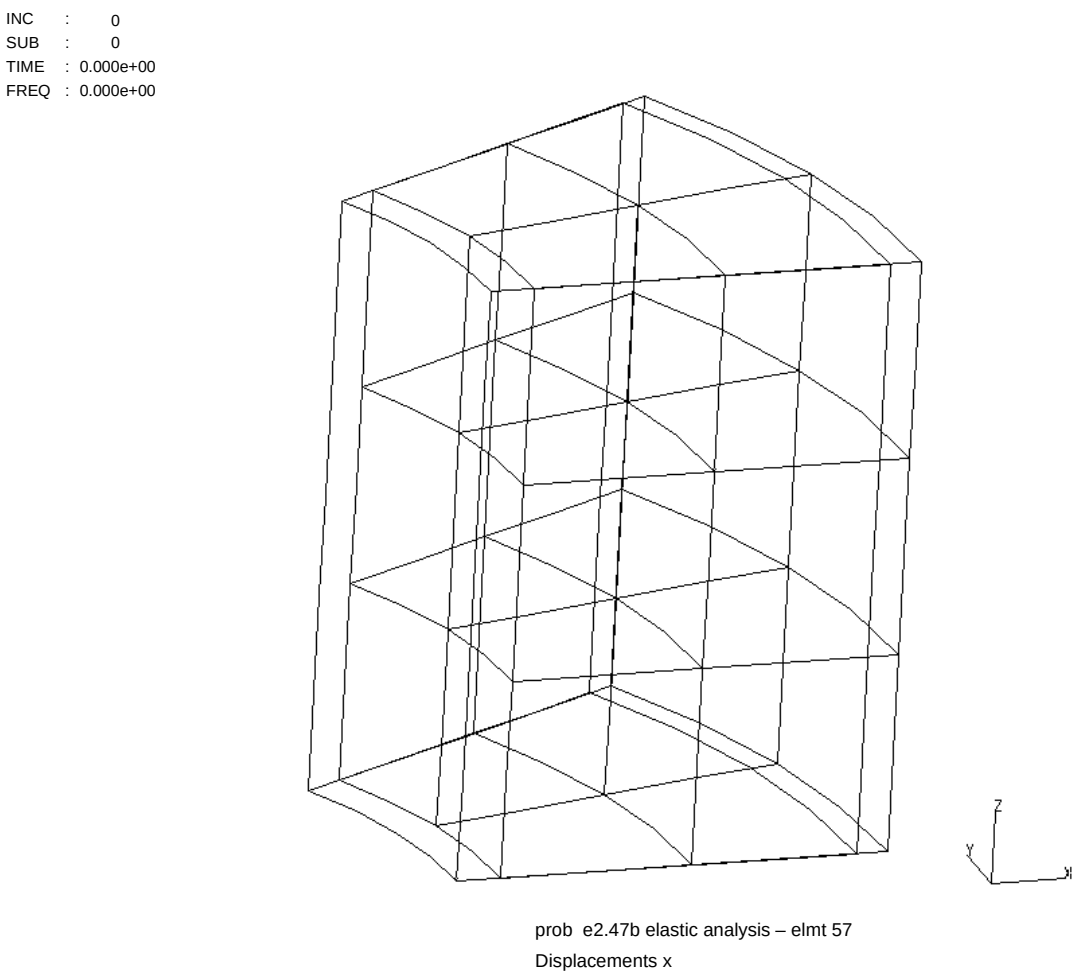

Figure 2.47-2 Deformed Mesh Plot

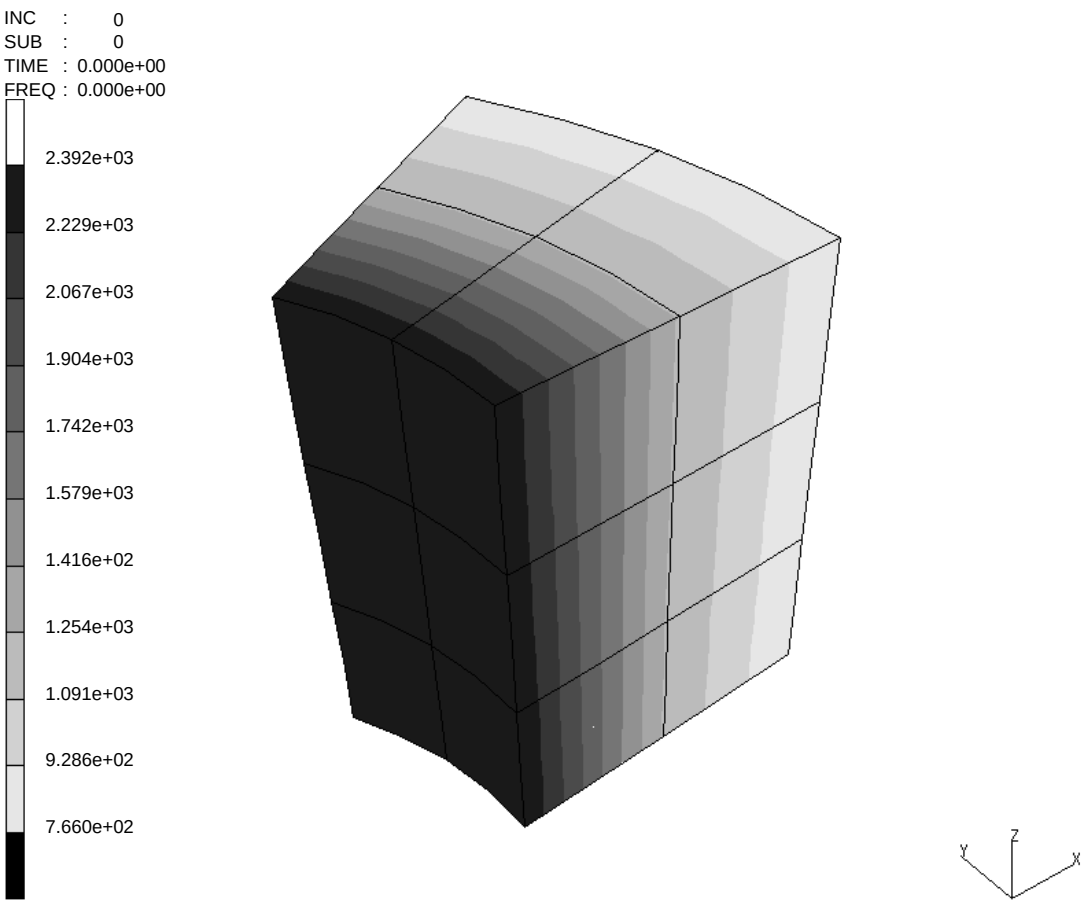

Figure 2.47-3 Equivalent von Mises Stress Contours

2.48 Circular Cylinder Subjected to Point Loads

This problem illustrates the use of MARC element type 58 and options CONN GENER and NODE CIRCLE for an elastic analysis of a hollow circular cylinder. The cylinder is subjected to diametrically opposite line loads.

Element

Element type 58 is an 8-node incompressible plane-strain element with reduced integration. There are three degrees of freedom at each corner node and two or three at each midside.

Model

The element is type 58. There are 16 elements with a total of 69 nodes. Dimensions of the cylinder and the finite element mesh are shown in Figure 2.48-1. The NODE CIRCLE option is used to generate the coordinates on the arcs.

Material Properties

Young's modulus is 30 x 10^3 psi with a Poisson's ratio of 0.4999.

Loading

A line load of 500 pounds is applied at node 69 in the positive x-direction. An equal load appears as reaction at node 5 in the negative x-direction.

Boundary Conditions

Symmetry conditions require that v = 0 at nodes 1 through 5 and 65 through 69. To eliminate rigid body motion, the displacement in the z-direction at node 33 is 0 (u = 0).

Results

A deformed mesh plot is shown in Figure 2.48-2 and stress contours are depicted in Figure 2.48-3.

Parameters, Options, and Subroutines Summary

Example e2x48.dat:

Parameters	Model Definition Options
ELEMENTS	CONN GENER
END	CONNECTIVITY
SIZING	COORDINATES
TITLE	END OPTION
	FIXED DISP
	ISOTROPIC
	NODE CIRCLE
	POINT LOAD

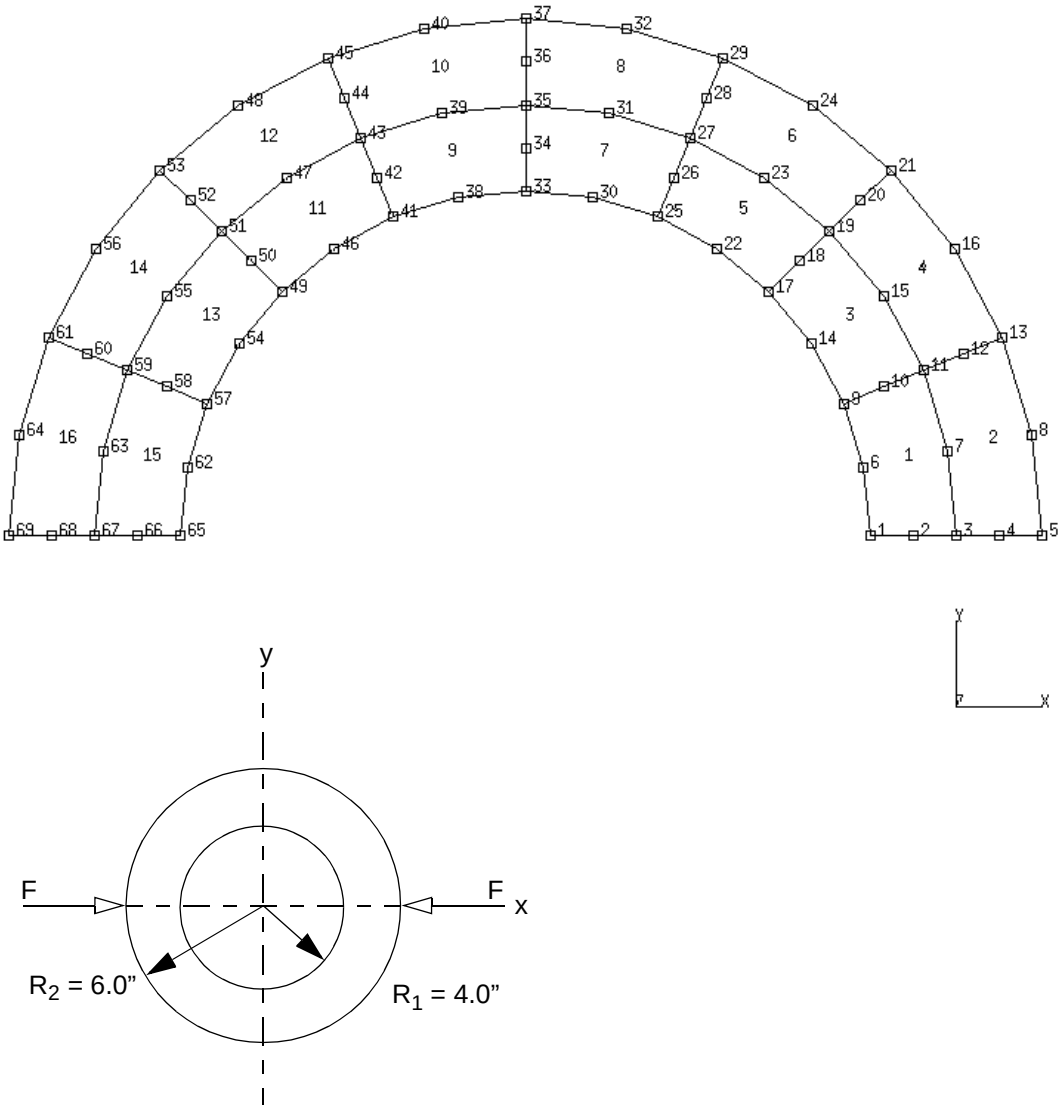

Figure 2.48-1 Circular Ring and Mesh of Half-model

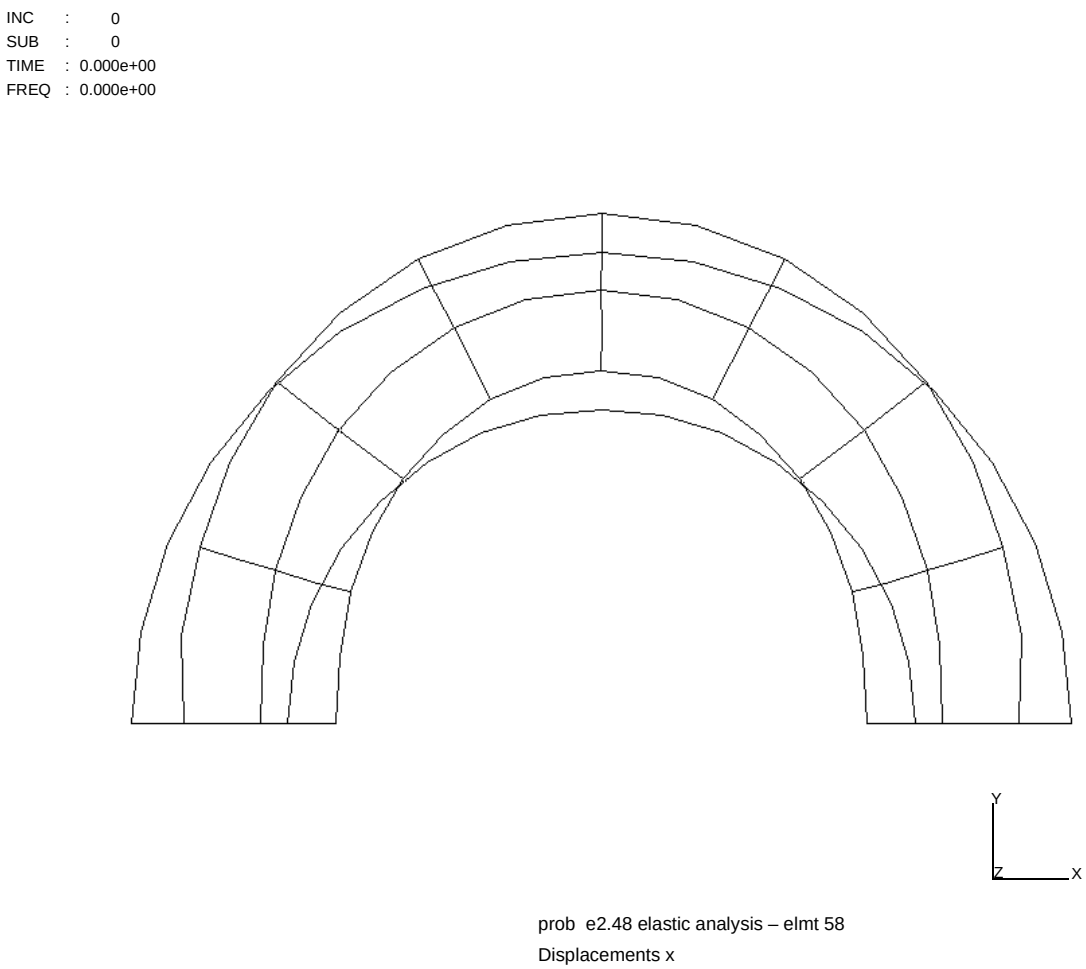

Figure 2.48-2 Deformed Mesh Plot

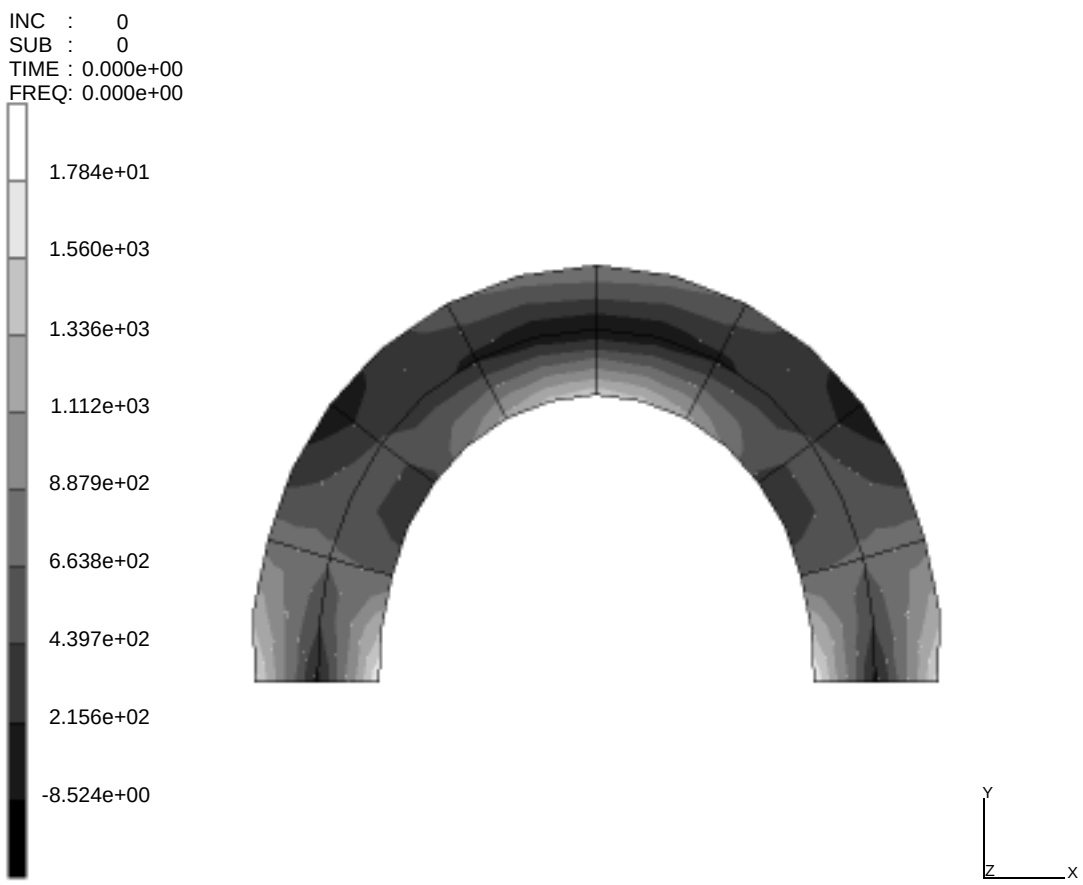

Figure 2.48-3 Equivalent von Mises Stress Contours

2.49 Hollow Spinning Sphere

This problem illustrates the use of MARC element type 59 and options CONN GENER, NODE CIRCLE, ROTATION A, and parameter CENTROID, for an elastic analysis of a hollow sphere. The sphere is subjected to both centrifugal load and nonuniform thermal load.

Element

Element type 59 is an 8-node, incompressible, axisymmetric element with reduced integration.

Model

The element is type 59. There are 16 elements, with a total of 69 nodes. The dimensions of the sphere and the finite element mesh are shown in Figure 2.49-1.

Material Properties

Young's modulus is 30 x 10^3 psi with a Poisson's ratio of 0.4999; the mass density is 0.2808 lb.sec^2/in.^{3}; the thermal expansion coefficient is 10 x 10^{-6} in/in/°F; and the initial stress-free temperature is 500°F.

Loading

A centrifugal load is applied through IBODY = 100. The angular velocity is 10 rad/sec (ω = 100) about the z-axis.

The thermal load is 500°F at the inside surface and 1000°F at the outside surface. A linear distribution of the temperatures is assumed to exist in the radial direction. The temperature is input through the user subroutine CREDE.

Boundary Conditions

Symmetry conditions are applied at r = 0 (v = 0 at nodes 1-5 and 65-69) and u = 0 at node 5 to suppress the (axial) rigid body mode.

Results

A deformed mesh plot is shown in Figure 2.49-2 and stress contours are depicted in Figure 2.49-3. The stress solution is symmetric with respect to the plane z = 0. In addition, the thermal strains and temperature are given in the output. The total centrifugal load as computed by MARC is 72,050 pounds versus the analytical solution of 72,056 pounds.

Parameters, Options, and Subroutines Summary

Example e2x49.dat:

Parameters	Model Definition Options
ELEMENTS	CONN GENER
END	CONNECTIVITY
SIZING	COORDINATES
THERMAL	DIST LOADS
TITLE	END OPTION
	FIXED DISP
	ISOTROPIC
	NODE CIRCLE
	ROTATION AXIS
	THERMAL LOADS

User subroutine in u2x49.f:

CREDE

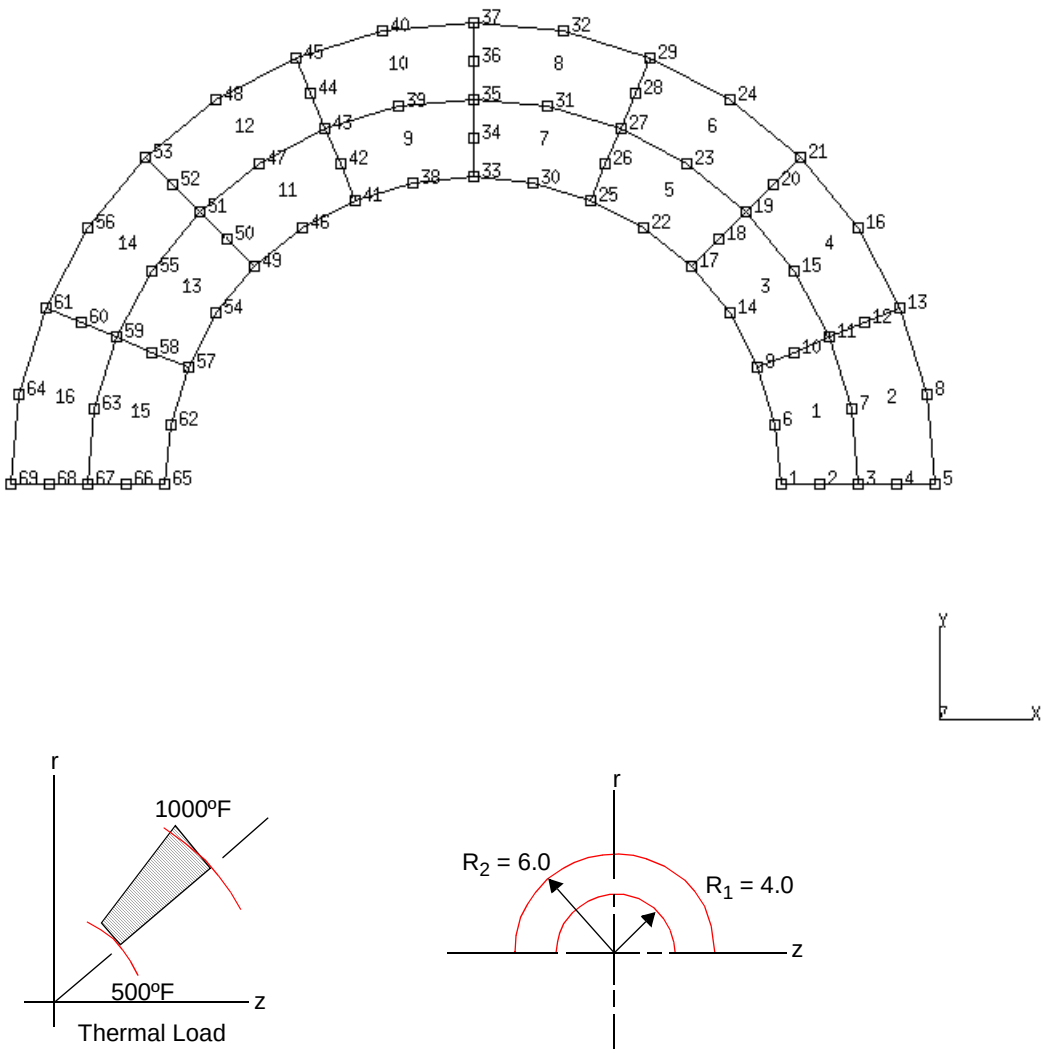

Figure 2.49-1 Hollow Sphere and Mesh

INC : 0
SUB : 0
TIME : 0.000e+00
FREQ : 0.000e+00

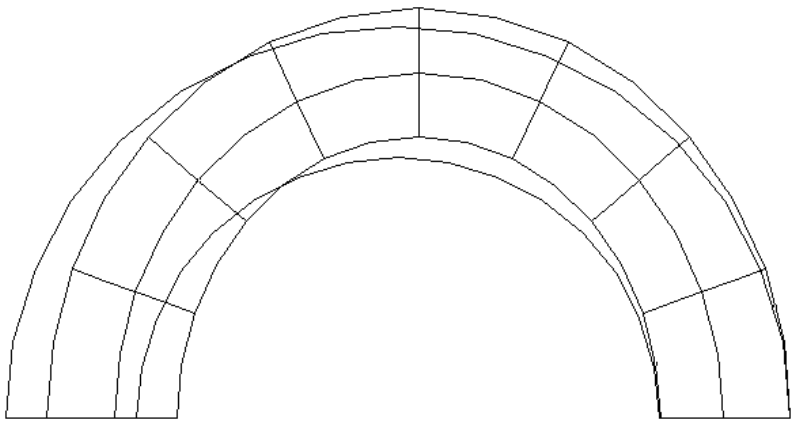

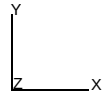

prob e2.49 elastic analysis – elmt 59
Equivalent von Mises Stress

Figure 2.49-2 Deformed Mesh Plot

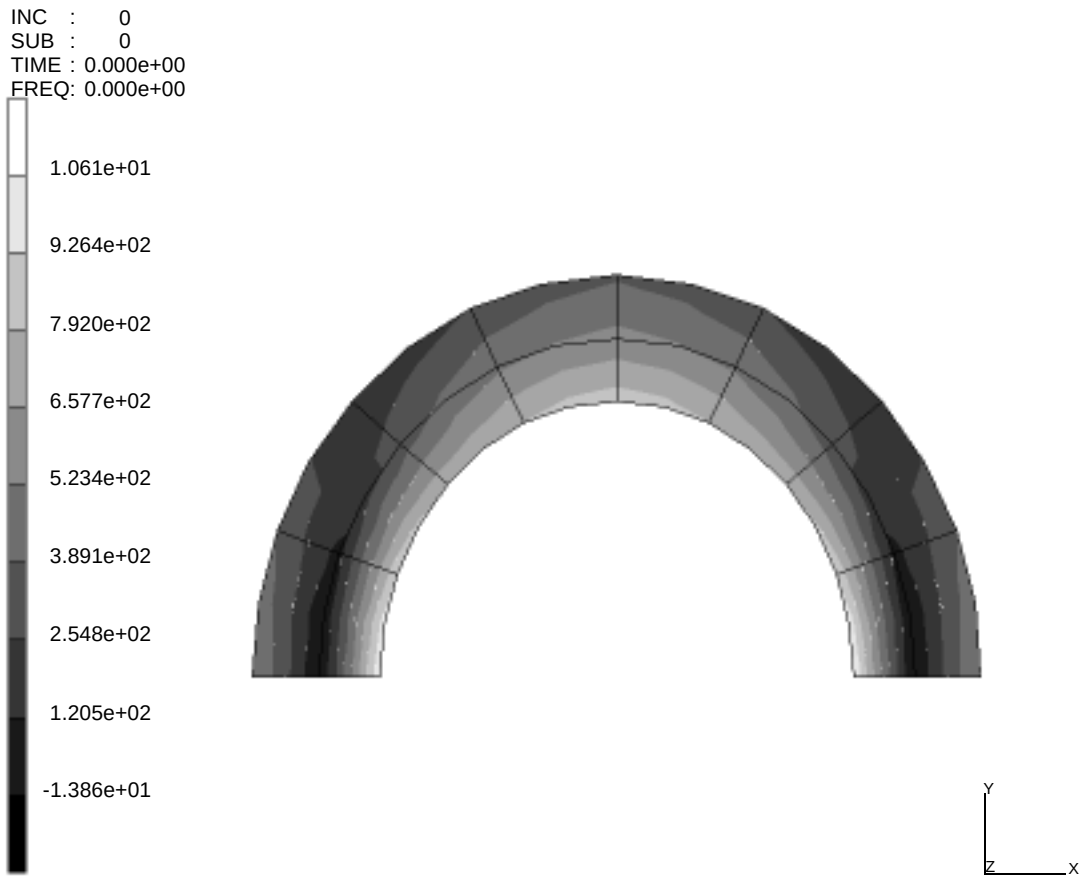

Figure 2.49-3 Equivalent von Mises Stress Contours

2.50 Anisotropic Ring Under Point Loads

This problem illustrates the use of MARC element type 60 for an elastic analysis of an anisotropic ring. The ring is subjected to equal and diametrically opposite point forces. One of the two forces is explicitly applied; the other appears as the medium force in the support. The use of option NODE CIRCLE and user subroutines ANELAS and ORIENT is also demonstrated.

Element

Element type 60 is an 8-node, incompressible, generalized plane-strain element with reduced integration.

Model

The element is type 60. There are 16 elements with a total of 71 nodes. There are 69 “regular” nodes and two nodes required for generalized plane strain. Dimensions of the ring and the finite element mesh are shown in Figure 2.50-1.

Material Properties

In the ISOTROPIC block, isotropic properties are specified. These properties are later completely overwritten with the user subroutines ANELAS and ORIENT. The fourth field is used to indicate that user subroutines are used.

Boundary Conditions

Symmetry conditions are applied at y = 0 (v = 0 at nodes 1-5 and 65-69) and u = 0 at node 5. The reaction force appears at this node. $\theta_x = \theta_y = 0$ at node 71. With these constraints, the strain in the direction normal to the ring is forced to be constant.

Loading

A 500 pound point load is applied at node 69 in the positive x-direction.

NODE CIRCLE

This option allows you to generate the coordinates of a series of nodes which lie on a circular arc.

Geometry

The default element thickness of 1.0 inch is selected for this analysis. No input data is required.

User Subroutine ORIENT

The ring is to be reinforced in the circumferential direction. The user subroutine ORIENT is used to define the local coordinate direction x^1, y^1, z^1 as follows (see Figure 2.50-1):

$$\frac{\partial x^1}{\partial x} = \cos\theta\ , \frac{\partial x^1}{\partial y} = \sin\theta\ , \frac{\partial x^1}{\partial z} = 0,$$

$$\frac{\partial y^1}{\partial x} = -\sin\theta, \frac{\partial y^1}{\partial y} = \cos\theta, \frac{\partial y^1}{\partial z} = 0,$$

$$\frac{\partial z^1}{\partial x} = 0 \quad , \frac{\partial z^1}{\partial y} = 0 \quad , \frac{\partial z^1}{\partial z} = 1.$$

y^1 is the circumferential direction in which the ring is reinforced.

User Subroutine ANELAS

For the incompressible elements in MARC, you have to specify the anisotropic compliance matrix of the material. Now we assume the ring is stiff in the tangential (y^1) direction. The (inverse) constitutive equation can then be approximated by:

$$\varepsilon_x^1 = \frac{1}{E_1}\sigma_x^1 - \frac{\nu}{E_2}\sigma_y^1 - \frac{\nu}{E_1}\sigma_z^1$$

$$\varepsilon_y^1 = \frac{\nu}{E_2}\sigma_x^1 - \frac{1}{E_2}\sigma_y^1 - \frac{\nu}{E_2}\sigma_z^1$$

$$\varepsilon_z^1 = \frac{\nu}{E_2}\sigma_x^1 - \frac{\nu}{E_2}\sigma_y^1 - \frac{1}{E_2}\sigma_z^1$$

$$\gamma_{xy}^1 = \frac{2(1+\nu)}{E_1}\sigma_{xy}^1$$

where $E_1 = 30 \times 10^3$, $E_2 = 30 \times 10^5$ and $\nu = .4999$. If the stress in the circumferential direction vanishes, the properties in the x^1-z^1 plane are isotropic. True modeling of uniaxial reinforcement in the circumferential direction would yield isotropic x^1-z^1 properties if $\varepsilon_y^1 = 0$ (plane strain). For such modeling, the constitutive equations are similar, but considerably more complicated.

Results

A deformed mesh plot is shown in Figure 2.50-2 and stress contours are depicted in Figure 2.50-3.

Parameters, Options, and Subroutines Summary

Example e2x50.dat:

Parameters	Model Definition Options
ELEMENTS	CONNECTIVITY
END	COORDINATES
SIZING	END OPTION
TITLE	FIXED DISP
	ISOTROPIC
	NODE CIRCLE
	POINT LOAD

User subroutine in u2x50.f:

ORIENT
ANELAS

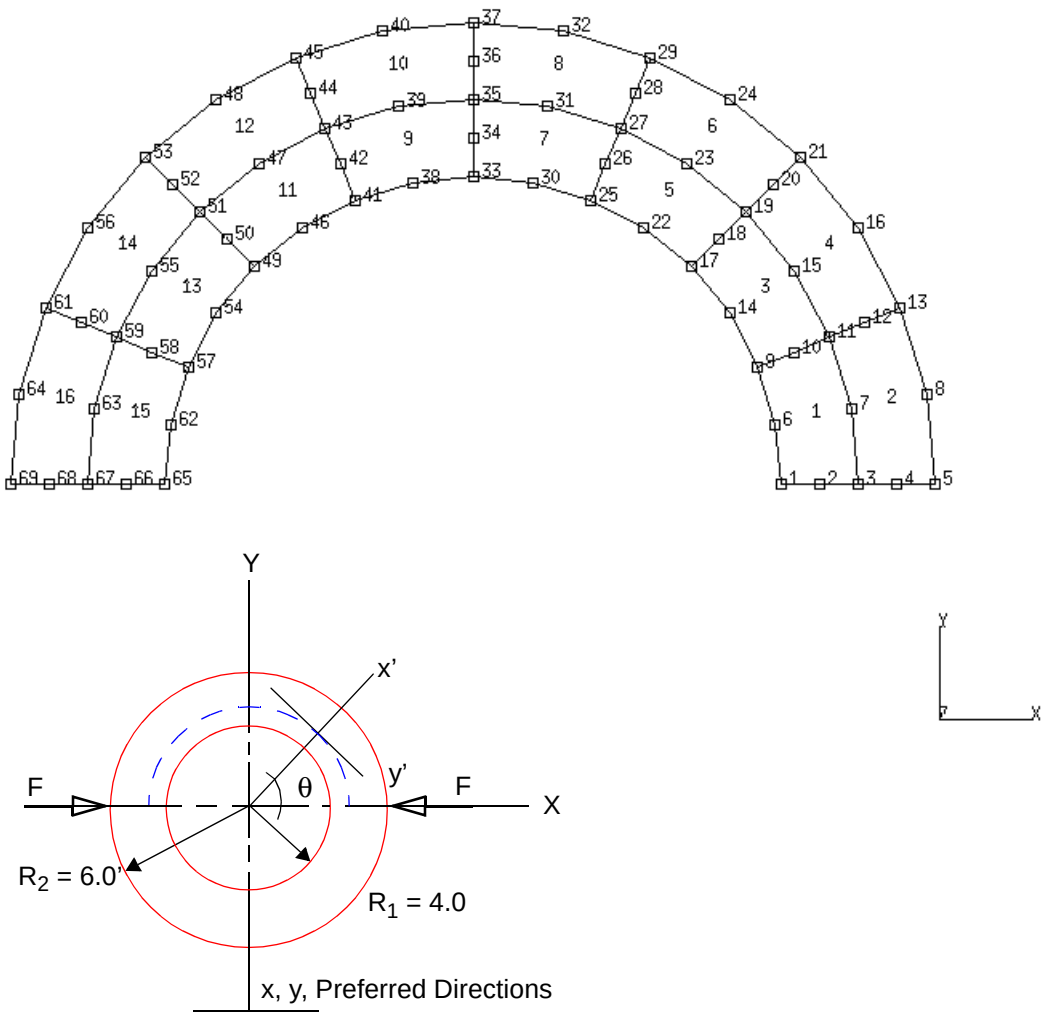

Figure 2.50-1 Anisotropic Ring and Mesh

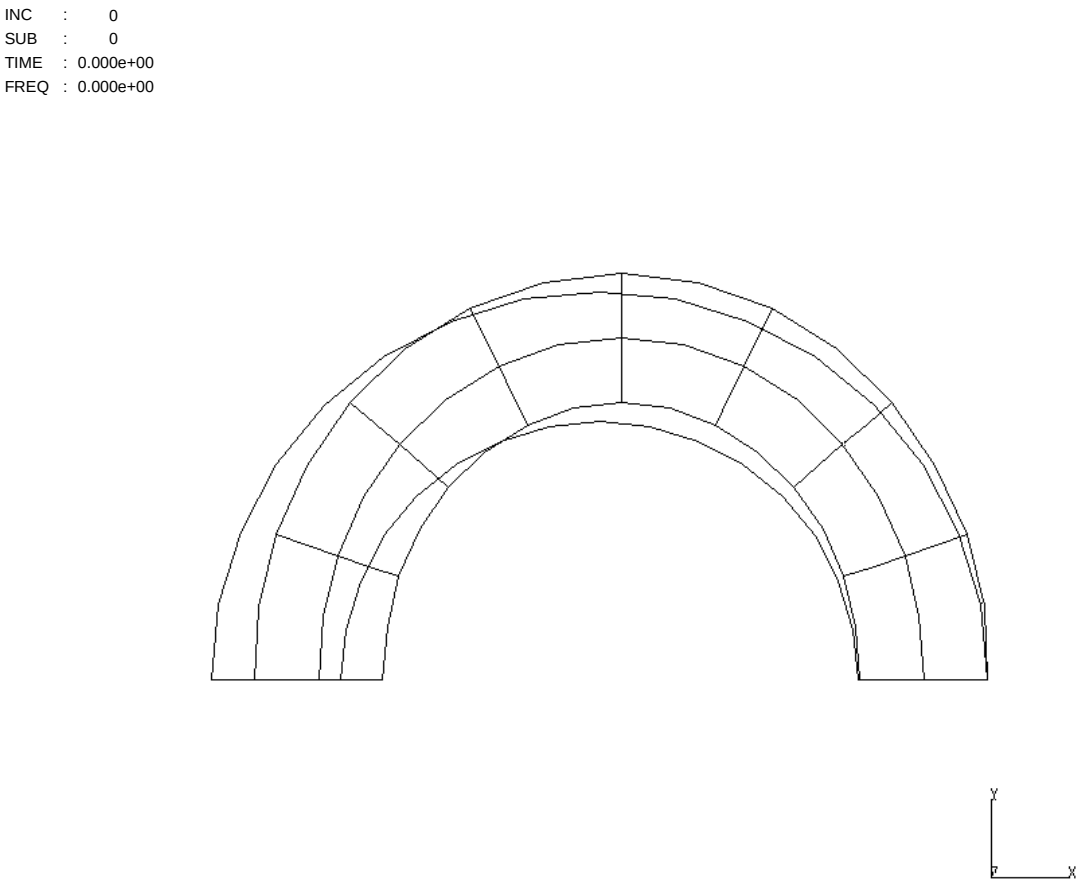

Figure 2.50-2 Deformed Mesh Plot

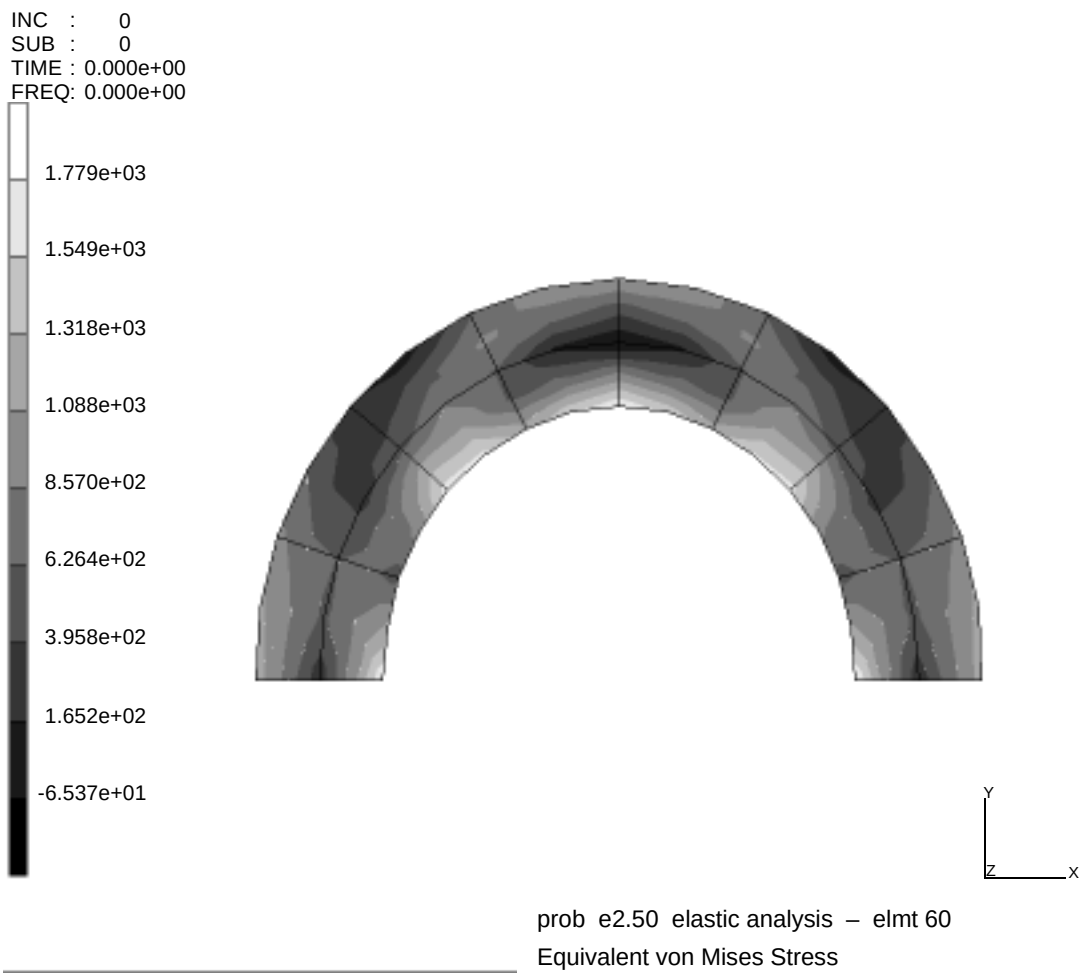

Figure 2.50-3 Equivalent von Mises Stress Contours

2.51 Square Block Subjected to Pressure and Thermal Loads

This problem illustrates the use of MARC element type 61 for an elastic analysis of a square block. The block is subjected to pressure and thermal loads. The use of the ELASTIC parameter, the CASE COMBIN and RESTART options, and the CREDE user subroutine is also demonstrated.

Element

Element 61 is a 20-node, incompressible, reduced integration solid element, with three global degrees of freedom per node.

Model

The element is type 61. There are eight elements with a total of 81 nodes. The dimensions of the square block and the finite element mesh are shown in Figure 2.51-1.

Material Properties

The Young's modulus is 30 x 10^5 psi with a Poisson's ratio of 0.4999; the thermal expansion coefficient is 10 x 10^{-7} in/in/°F; the initial stress-free temperature is 60.0°F.

Loading

Pressure load:

Uniform pressure of 100.0 psi (load type = 4) is applied at the top surface (z = 2.0) of the block.

Thermal load:

The temperature varies linearly from of 60°F at z = 0 (the plane of symmetry) to 130°F at z = 2.0 (the top surface).

User subroutine CREDE is used to input the temperature distribution. Typically, incremental temperatures are applied using the THERMAL LOAD option, but for this elastic analysis, the total temperatures are inserted.

Boundary Conditions

The following symmetry conditions are applied:

u = 0 in the plane x = 0;
v = 0 in the plane y = 0;
w = 0 in the plane z = 0.

ELASTIC

This option allows you to calculate stresses caused by the pressure and the thermal load separately. The stresses caused by the pressure load are calculated in increment 0 and the thermal stresses are calculated in increment 1.

Restart

In the first analysis, the RESTART option is used to store the solutions of the two cases obtained in increments 0 and 1.

CASE COMBIN

In a restart run, CASE COMBIN allows the results of analyses for various loading cases to be separately scaled, and then combined. In this example, the load case associated with the pressure load was scaled by a factor of 1.25. This was then added to the load case resulting from the thermal loading. The stresses and displacements under combined loading are obtained as a result.

User Subroutine CREDE

The CREDE user subroutine is used for the input of the linearly distributed temperature in the block. Usually, CREDE is used to read in the temperature distribution from a data file, such as a post file. In this problem, the temperature distribution is generated in CREDE.

Results

A deformed mesh plot for combined and thermal loads is shown in Figure 2.51-2. Stress contours are depicted in Figure 2.51-3.

Increment 0 - Uniform distributed load

	Analytically Computed	MARC Computed
σ_{zz} (psi)	–100	–100
ε_{zz}	-3.33×10^{-5}	-3.33×10^{-5}

Increment 1 - Thermal load at element 8, integration point 7

	Analytically Computed	MARC Computed
σ_{zz} (psi)	0	–3.50
ε_{zz}	6.23×10^{-5}	6.23×10^{-5}

Case combination

1.25 * inc 0 + 1.0 * inc 1

σ_{zz} = 1.25 * (–100) – 3.5 = –128.5 psi

ε_{zz} = 1.25 * ($-3.33 * 10^{-5}$) + $6.23 * 10^{-5}$

= 2.06 x 10^{-5}

Parameters, Options, and Subroutines Summary

Example e2x51a.dat:

Parameters	Model Definition Options
ALIAS	CONNECTIVITY
ELASTIC	COORDINATES
ELEMENTS	DIST LOADS
END	END OPTION
SIZING	FIXED DISP
THERMAL	ISOTROPIC
TITLE	OPTIMIZE
	RESTART

User subroutine in u2x51a.f:

CREDE

Example e2x51b.dat:

Parameters	Model Definition Options
ALIAS	CASE COMBINATION
ELASTIC	CONNECTIVITY
ELEMENTS	COORDINATES
END	DIST LOADS
SIZING	END OPTION
THERMAL	FIXED DISP
TITLE	INITIAL STATE
	ISOTROPIC
	OPTIMIZE
	RESTART

user subroutine in u2x51.f

CREDE

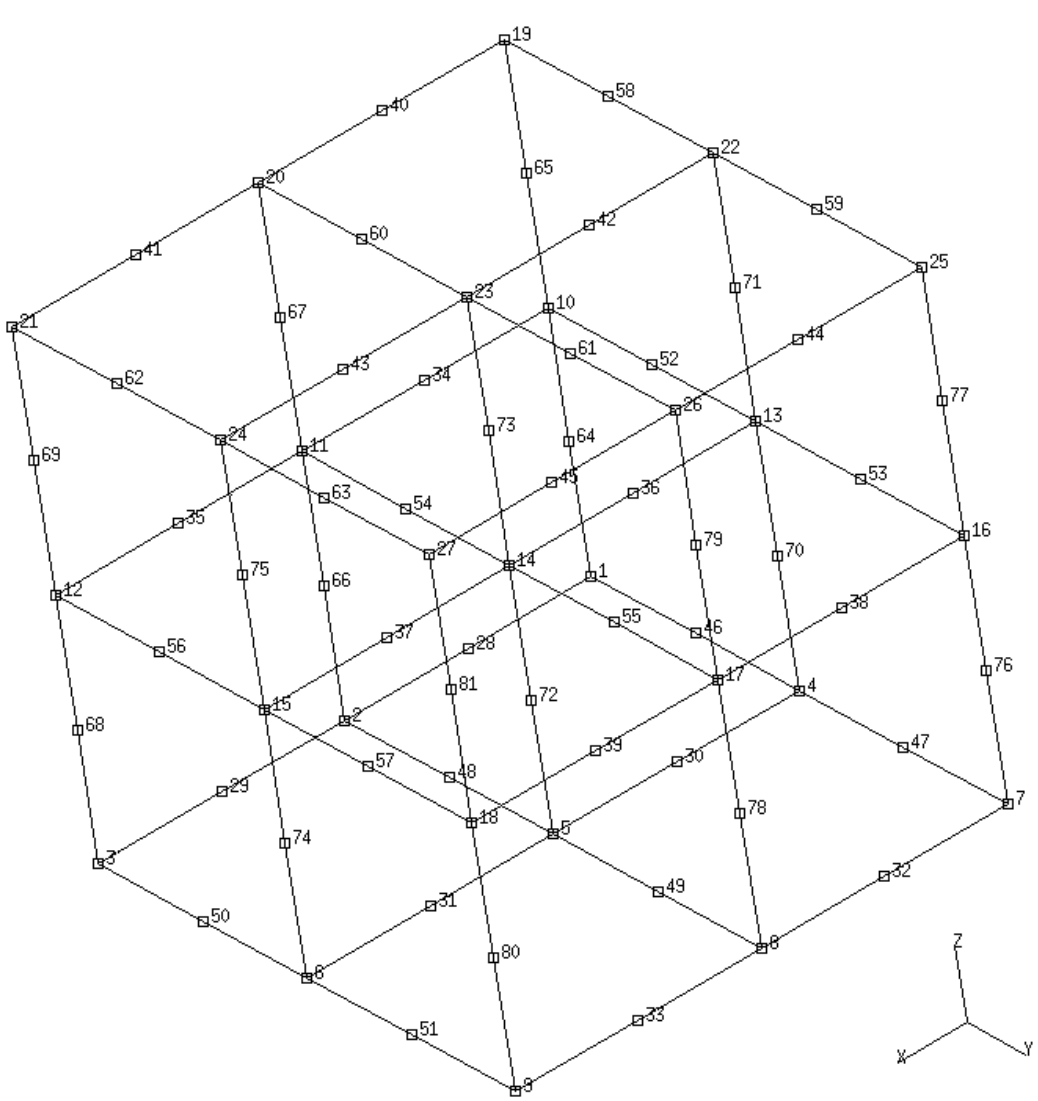

Figure 2.51-1 Square Block and Mesh

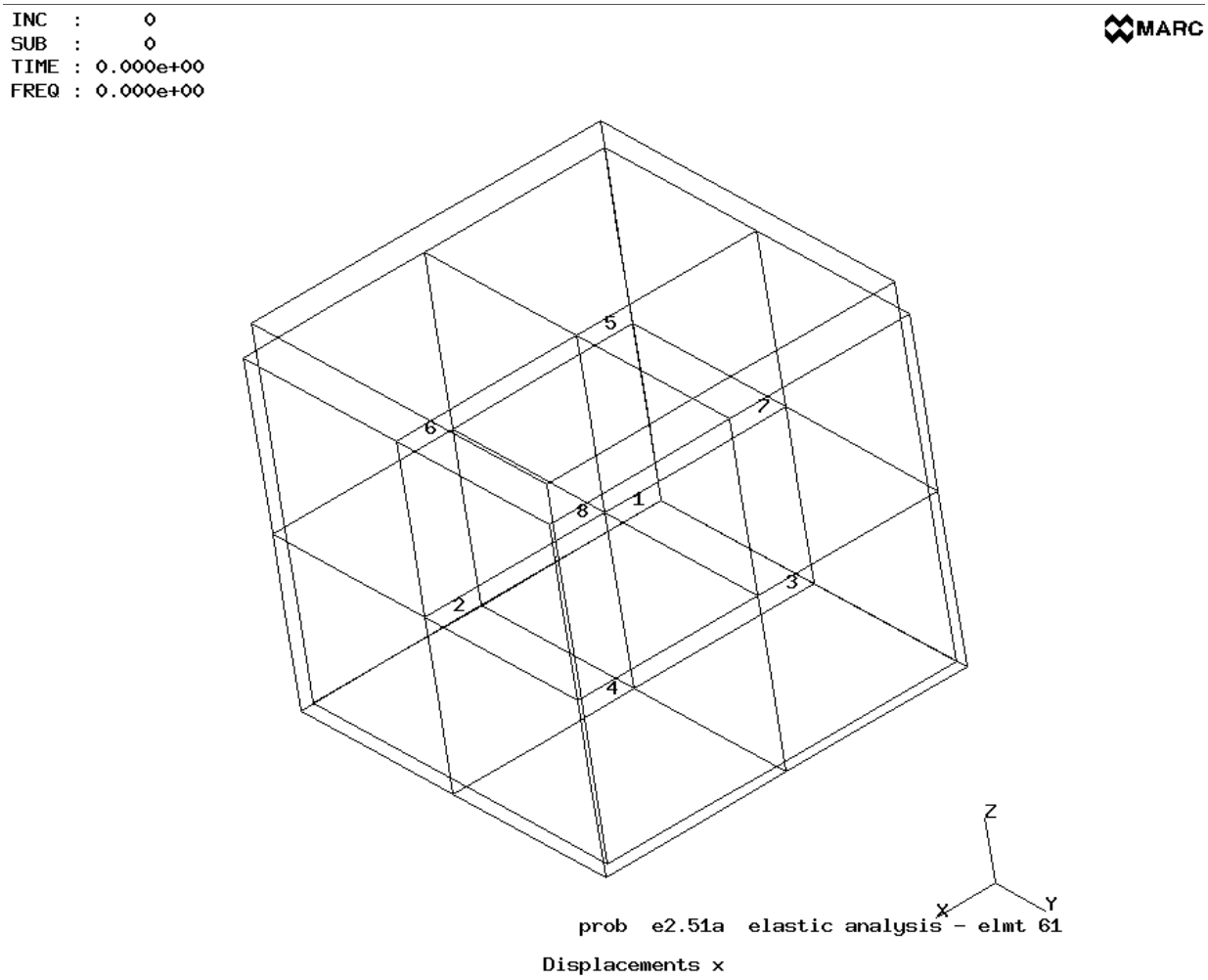

Figure 2.51-2 Deformed Mesh Plot

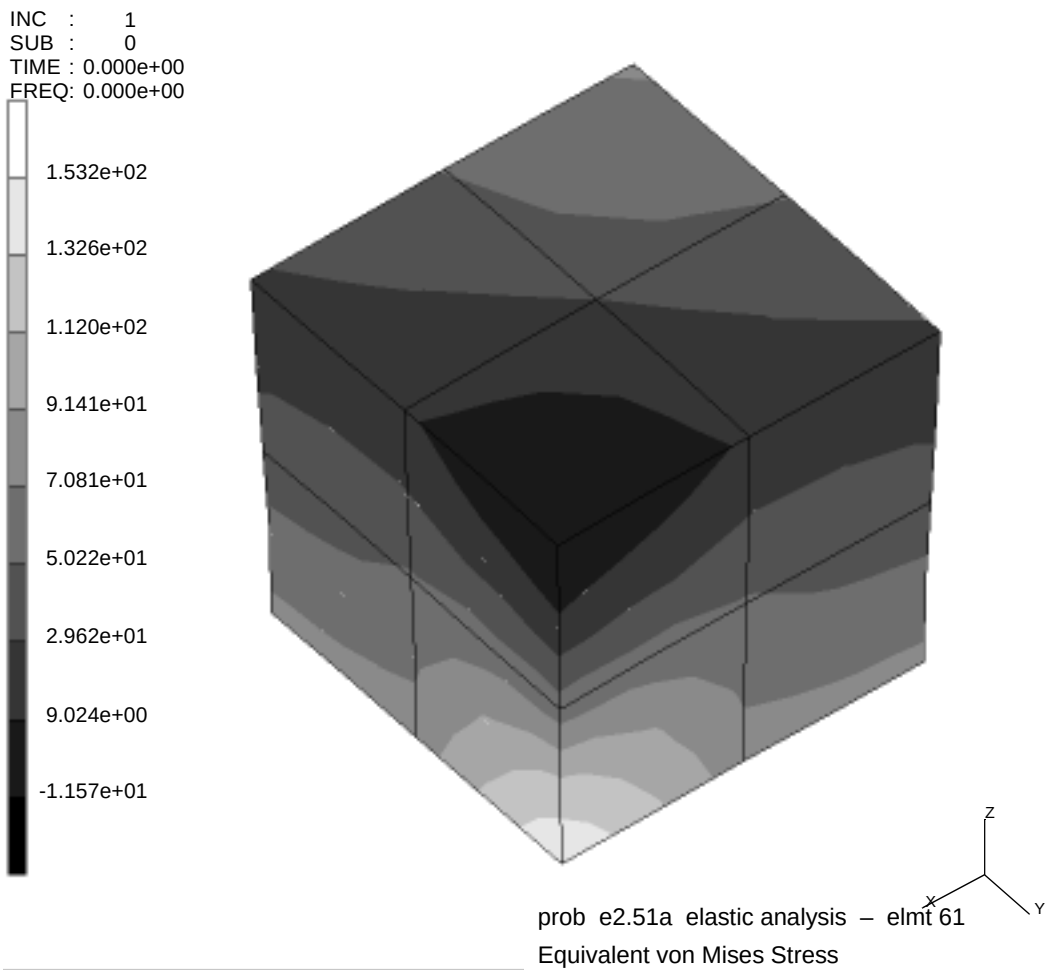

Figure 2.51-3 Equivalent Stress Contours

2.52 Twist and Extension of Circular Bar of Variable Thickness

This problem illustrates the use of MARC element 66 for an elastic analysis of a circular bar of variable thickness. The bar is subjected to both a twist moment and an axial force at the free end of the circular bar. The tying constraint option is used to insure that the cross section at the small end of the bar remains flat. This problem is identical to problem 2.28 except for the selection of element types.

Element

Element type 66 is an 8-node, incompressible, axisymmetric element with twist.

Model

The element type is 66. There are 12 elements, with a total of 53 nodes. Dimensions of the circular bar and the finite element mesh are shown in Figure 2.52-1.

Material Properties

The Young's modulus is 2,080,000 psi with a Poisson's ratio of 0.4999. A Poisson's ratio equal or close to 0.5 can be used with this element, which uses an augmented Herrmann type variational principle.

Boundary Conditions

Degrees of freedom u and w are 0 at the fixed end (nodes 1-5). Symmetry conditions are imposed at r = 0 (v = 0).

Loading

A 5000 pound point load in the positive z-direction and a 2000 inch per pound torque is applied at node 49. Due to the applied tying, the point load is distributed over the whole cross section.

Tying

Tying type 1 is used at the free end to simulate a generalized plane-strain condition in the axial (z) direction. The tied nodes are 50, 51, 52, and 53 and the retained node is 49.

Results

A deformed mesh plot is shown in Figure 2.52-2 and the stress distribution is depicted in Figure 2.52-3.

Parameters, Options, and Subroutines Summary

Example e2x52.dat:

Parameters	Model Definition Options
ELEMENTS	CONNECTIVITY
END	COORDINATES
SIZING	END OPTION
TITLE	FIXED DISP
	ISOTROPIC
	POINT LOAD
	TYING

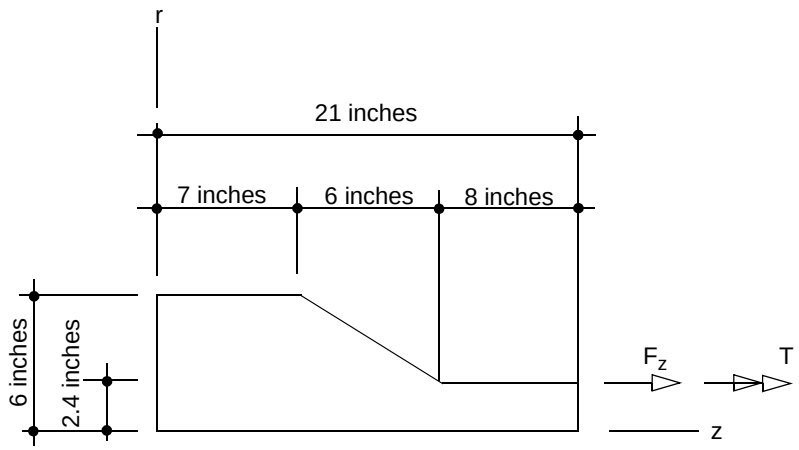

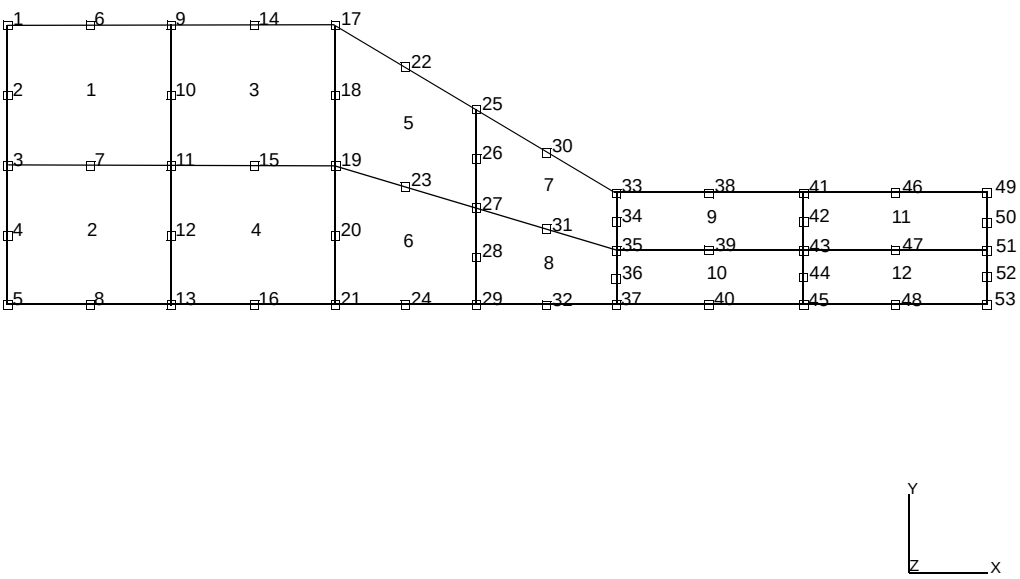

Figure 2.52-1 Circular Bar and Mesh

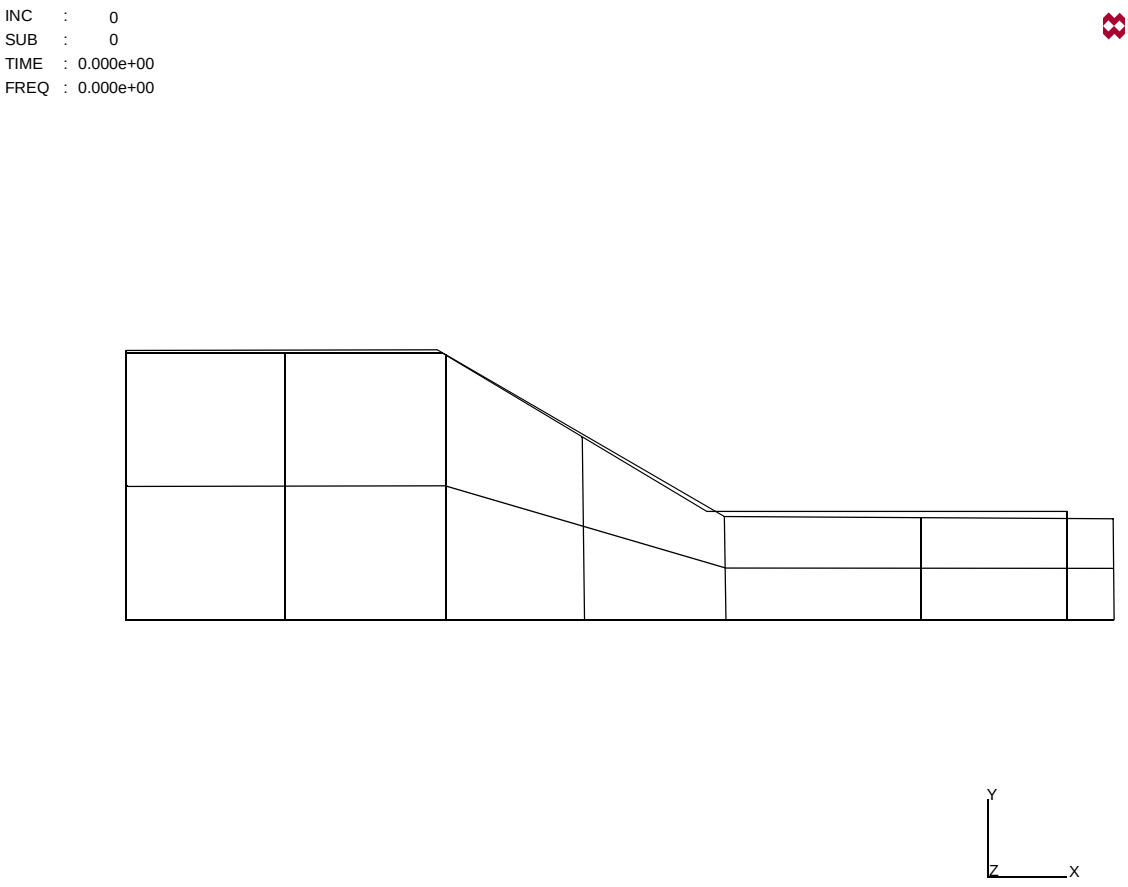

Figure 2.52-2 Deformed Mesh Plot

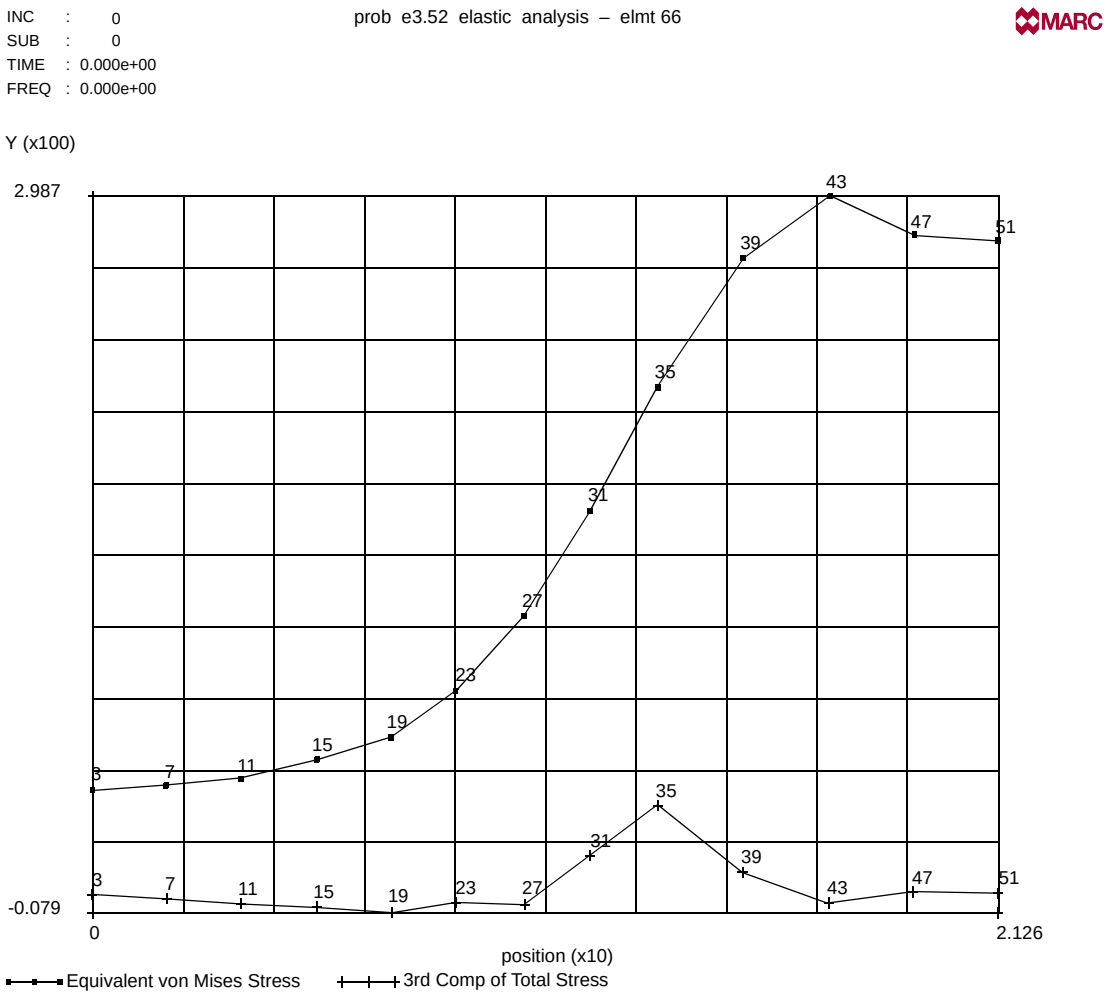

Figure 2.52-3 Stresses Along Path Between Nodes 3 and 51

2.53 Cylinder with Helical Anisotropy Under Internal Pressure

This problem illustrates the use of MARC element 67 for an elastic analysis of a thick cylinder with helical anisotropy. The cylinder is subjected to internal pressure. The use of the option TYING is also demonstrated. The tying constraint option simulates a generalized plane strain condition of the cylinder in the axial z-direction.

Element

Element type 67 is an 8-node, axisymmetric element with twist, with three degrees of freedom at each node.

Model

The element is type 67. There are 10 elements and a total of 53 nodes. The dimensions of the cylinder and the finite element mesh are shown in Figure 2.53-1.

Material Properties

In the ISOTROPIC option, isotropic properties are specified. These properties are later modified in the user subroutines ANELAS and ORIENT. The Young's modulus is 30 x 10^5 psi, with a Poisson's ratio of 0.3. The fourth field is set to one to indicate that the user subroutines are to be used.

Loading

Internal pressure of 500 psi is applied on the inside element 1.

Boundary Conditions

$u_z = u\theta = 0$ at nodes 1,4,6,...,51 (z = 0). u_z = constant at the plane 3,5,8,...,53 (z = 1.0).

User Subroutines ANELAS and ORIENT

As shown in Figure 2.53-2, the orientation of anisotropy is assumed to be helical. This helical anisotropy represents a filament-wound type structure covering an axial distance of one for every full revolution. Let x, y, z be the local coordinate system representing the preferred direction. The expression of the transformation matrix, from global (Z, R, S) to local, is as follows:

$$\begin{bmatrix} x \\ y \\ z \end{bmatrix} = \begin{bmatrix} \sin\alpha & 0 & \cos\alpha \\ 0 & 1 & 0 \\ -\cos\alpha & 0 & \sin\alpha \end{bmatrix} \begin{bmatrix} Z \\ R \\ \theta \end{bmatrix}$$

The angle $\alpha(r)$ is a function of r and can be computed from:

$\alpha = \text{ARCTAN}\ (1.0/2\pi r)$

Results

A deformed mesh plot is shown in Figure 2.53-3 and hoop stress through the radius is depicted in Figure 2.53-4. Due to the anisotropy, the ends of the cylinder rotate with respect to each other by -1.187×10^{-5} radians at the inside and -2.252×10^{-5} radians at the outside radii.

Parameters, Options, and Subroutines Summary

Example e2x53.dat:

Parameters	Model Definition Options
ELEMENTS	CONNECTIVITY
END	COORDINATES
SIZING	DIST LOADS
TITLE	END OPTION
	FIXED DISP
	ISOTROPIC
	TYING

User subroutines in u2x53.f:

ANELAS
ORIENT

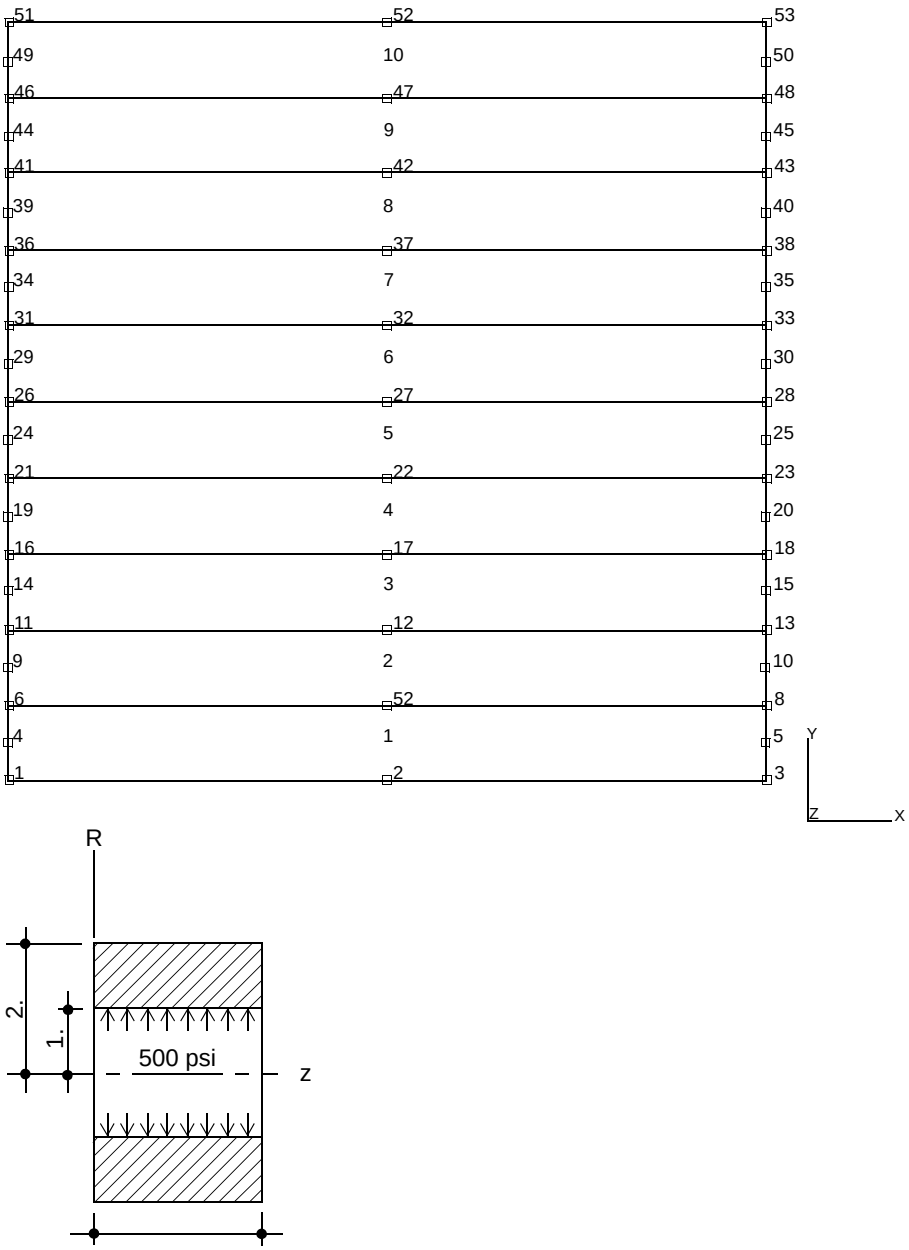

Figure 2.53-1 Cylinder and Mesh

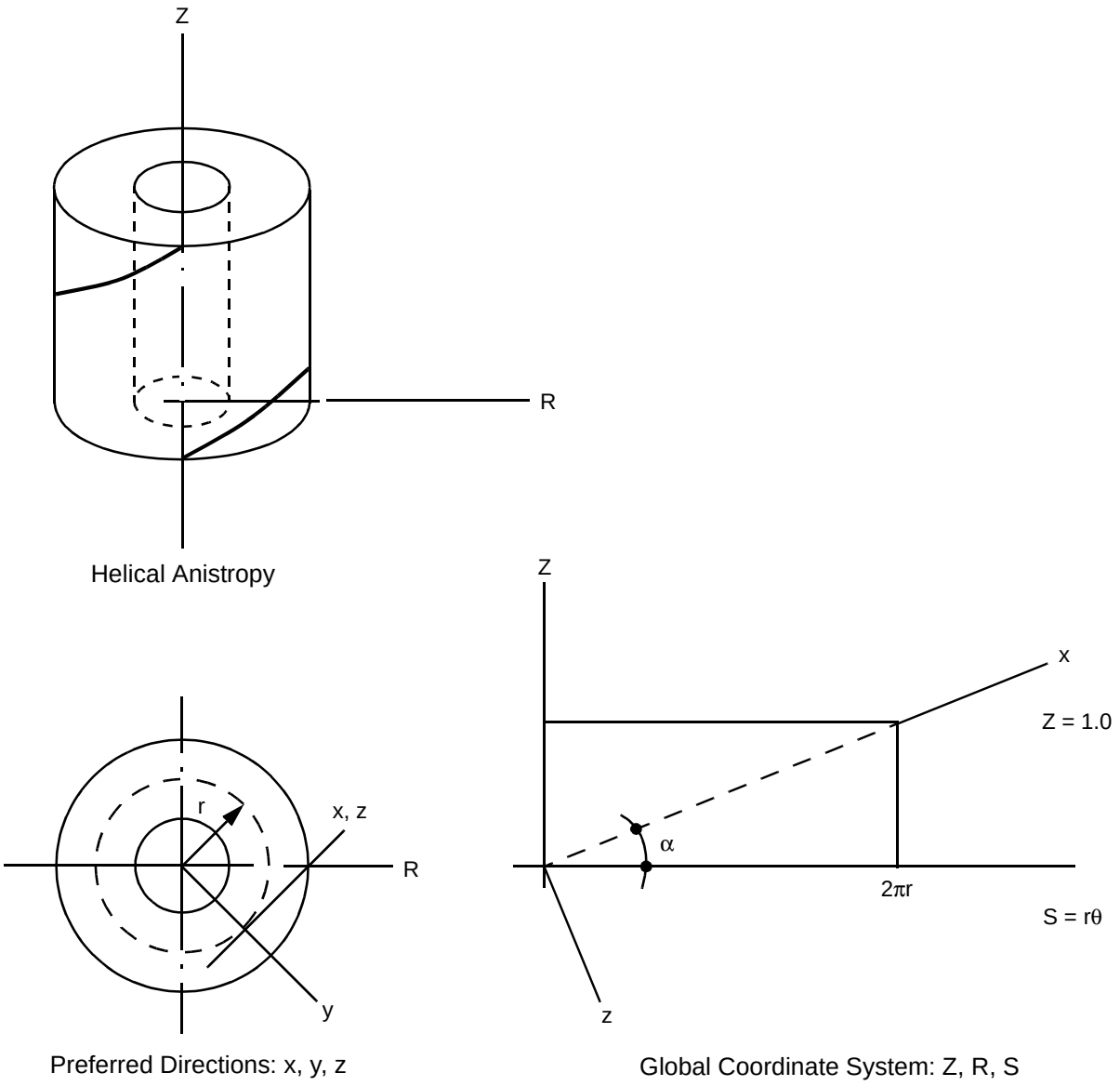

Figure 2.53-2 Helical Anisotropy

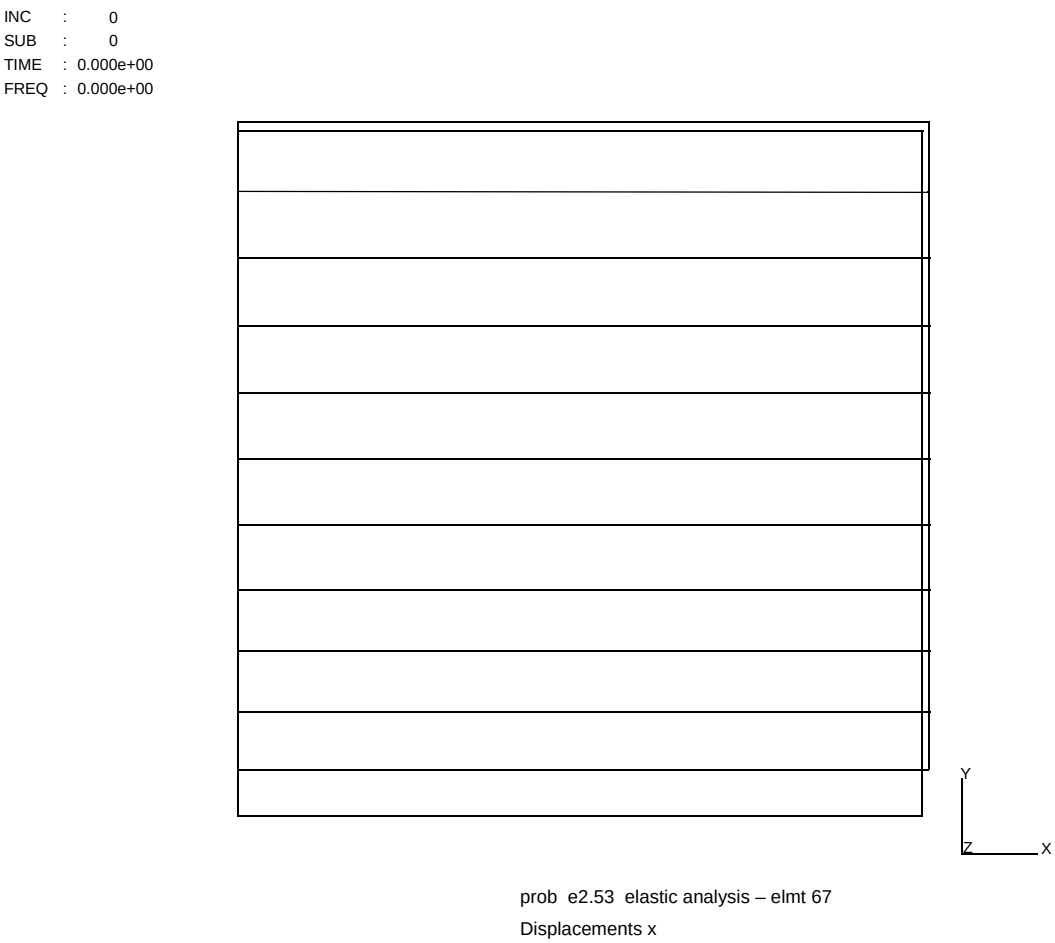

Figure 2.53-3 Deformed Mesh Plot

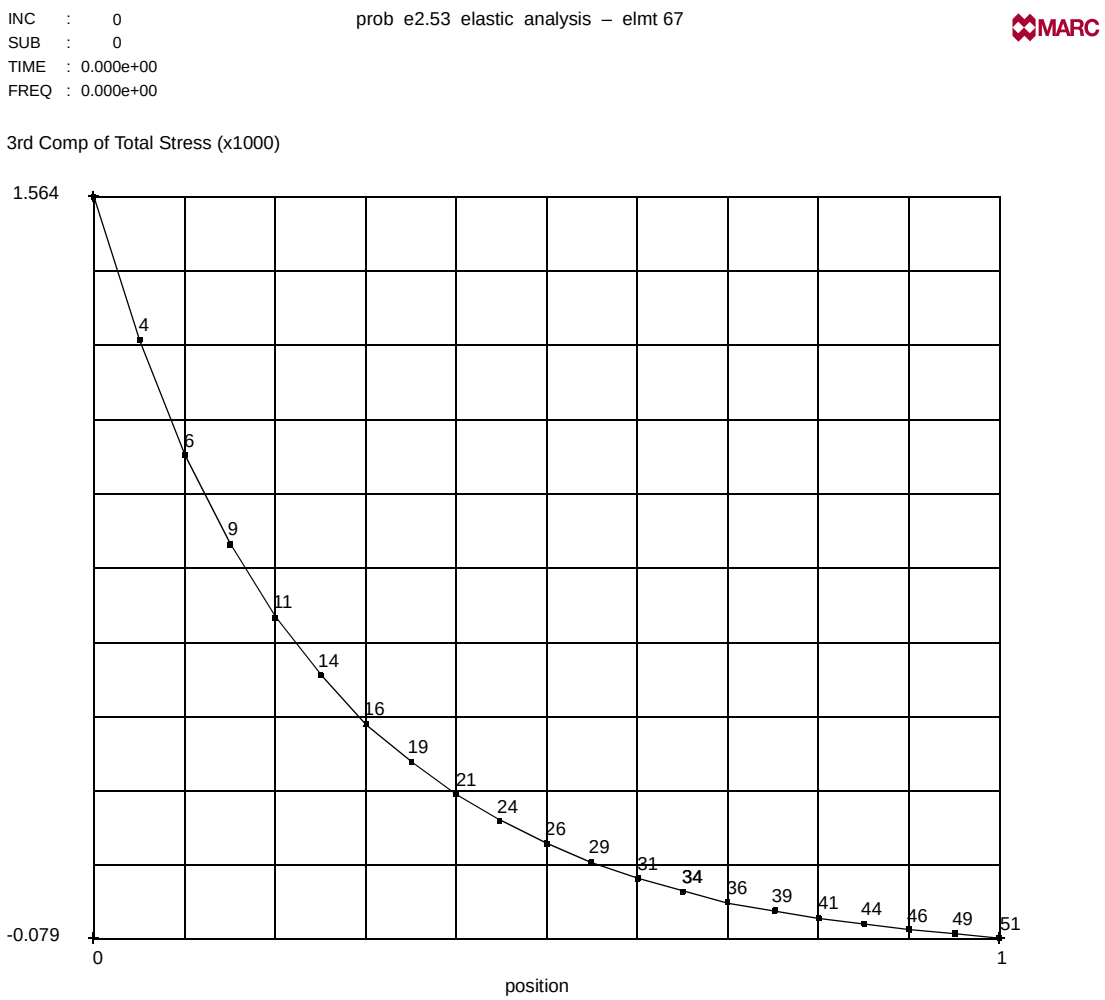

Figure 2.53-4 Hoop Stress Through Radius

2.54 Stiffened Shear Panels Supported by Springs

This problem illustrates the use of MARC element types 68 and 9, and the SPRINGS option for an elastic analysis of a stiffened cubical, supported by linear springs. The box is subjected to point forces (in-plane twisting loads). As the name indicates, the shear panel can only support shear loads. Hence, the element when used without stiffness is singular. The element can be used to stiffen frames, as in this demonstration problem.

Element

Element type 68 is a linear elastic shear panel of arbitrary shape. This element only resists shear forces. There are four nodes per element, with three degrees of freedom for each node.

Element type 9 is a three-dimensional truss element with constant cross section. There are three degrees of freedom for each node.

Model

The elements are types 68 and 9. There is a total of 18 elements – 6 elements type 68 and 12 elements type 9. There is a total of 12 nodes. Twelve springs act on the box as shown in Figure 2.54-1.

Material Properties

For element type 9, Young's modulus is 30×10^6 psi.

For element type 68, Young's modulus is 30×10^5 psi and Poisson's ratio is 0.2.

Geometry

The cross-sectional area of element type 9 is 0.6 square inch; the thickness of element type 68 is 0.05 inches.

Spring Constant

Nodes 5, 6, 7 and 8 are supported by springs in all three (x, y, z) directions. The spring constant is 18×10^4 pounds per inch. These springs simulate an elastic foundation in this example.

Loading

At the upper four corners, twisting loads are applied in the x-y plane. Magnitudes of the point loads are 100 pounds.

Boundary Conditions

Nodes 9, 10, 11 and 12 (the other end of the springs) are constrained in all directions (that is, $u = v = w = 0$).

Results

A deformed mesh plot is shown in Figure 2.54-2.

Parameters, Options, and Subroutines Summary

Example e2x54.dat:

Parameters	Model Definition Options
ELEMENTS	CONNECTIVITY
END	COORDINATES
SIZING	END OPTION
TITLE	FIXED DISP
	GEOMETRY
	ISOTROPIC
	POINT LOAD
	SPRINGS

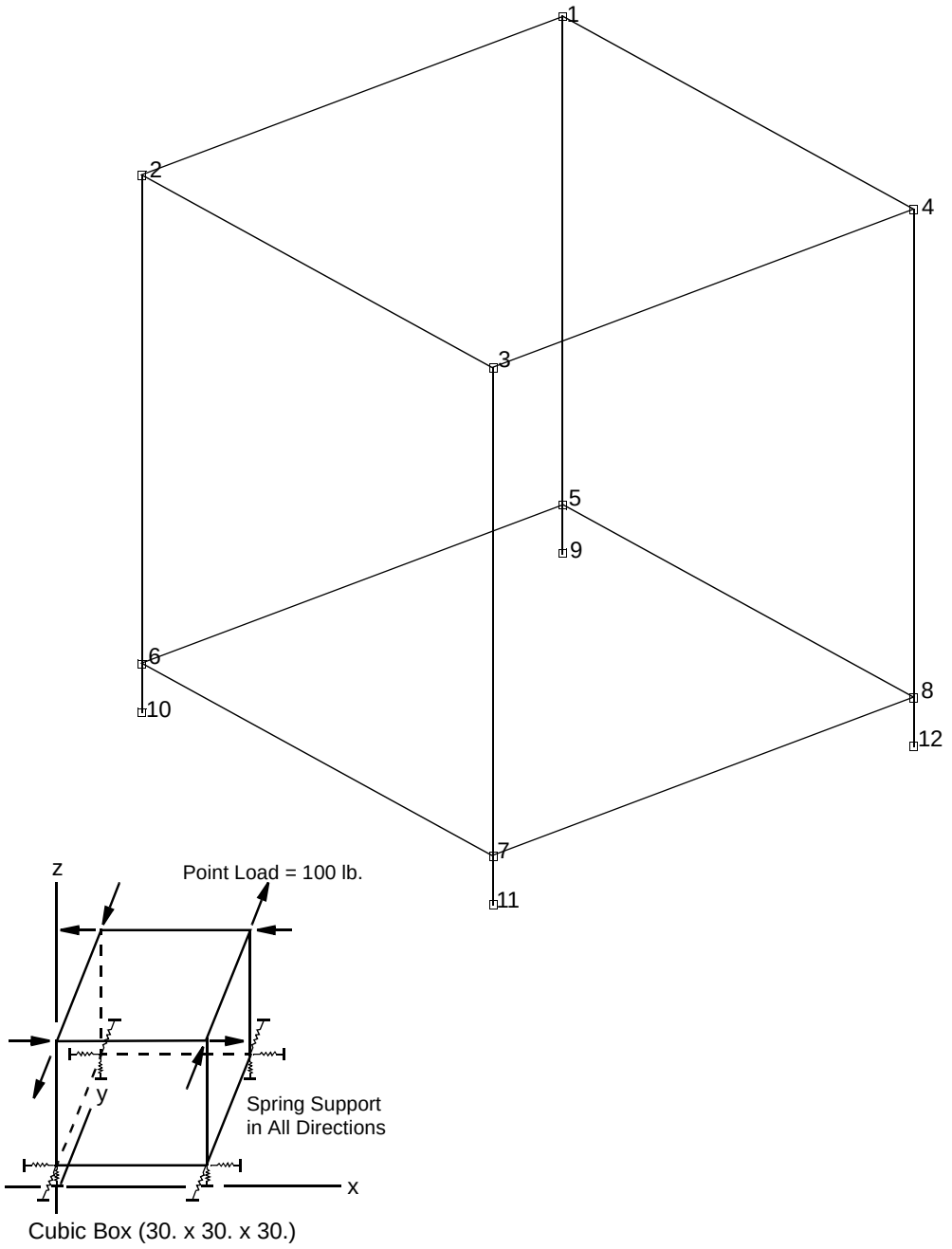

Figure 2.54-1 Stiffened Cubic Box and Mesh

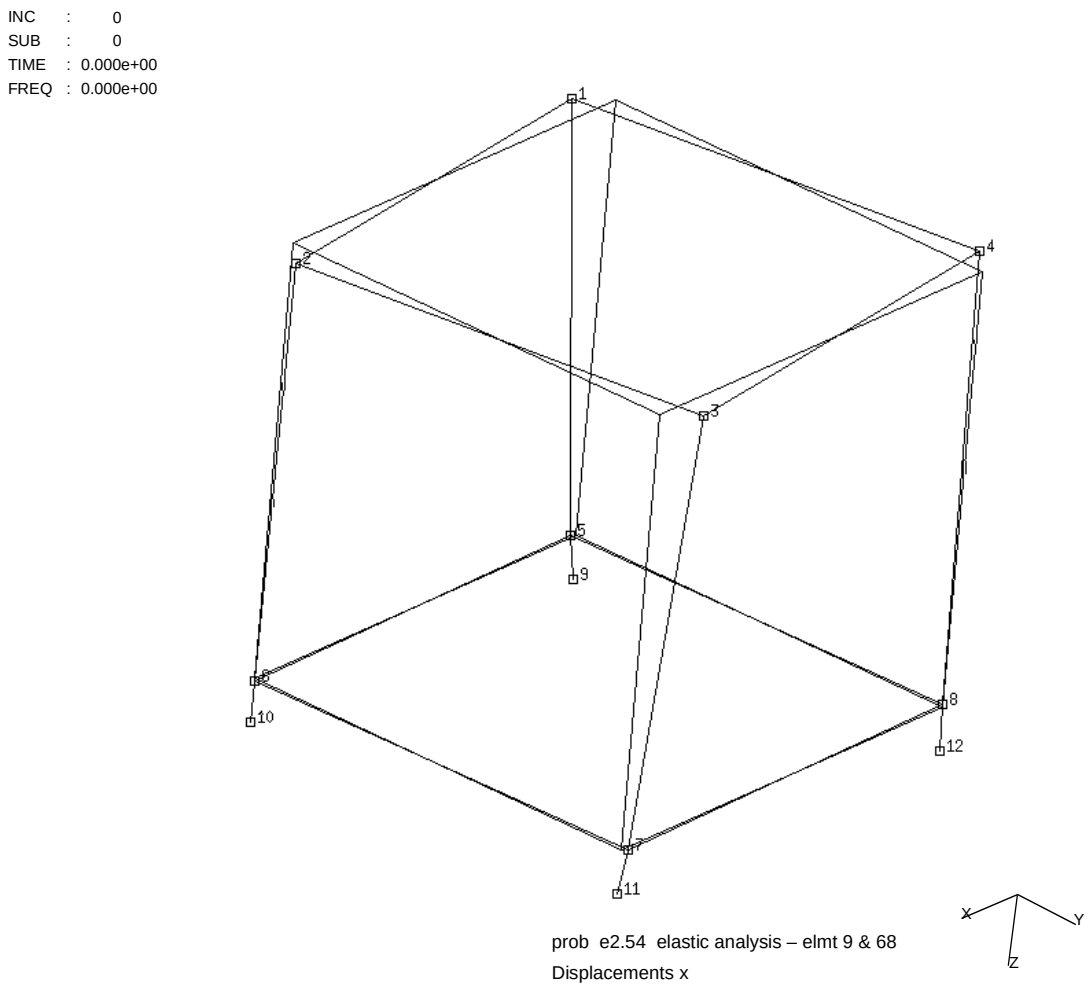

Figure 2.54-2 Deformed Mesh Plot

2.55 Shell Roof by Element 72

This problem illustrates the use of MARC element type 72 for an elastic analysis of a barrel vault shell roof. The roof is subjected to its own weight. This problem is similar to problems 2.16, 2.17, 2.18, and 2.19.

Element

Element type 72 is an 8-node thin-shell element with three degrees of freedom at each corner node, and an additional degree of freedom at the midside nodes (edge self-rotation).

Model

The element is type 72. There are 16 elements with a total of 65 nodes. The dimensions of the shell roof and the finite element mesh are shown in Figure 2.55-1.

Material Properties

Young's modulus is 30 x 10^5 psi. Poisson's ratio is taken to be 0.

Geometry

The shell thickness is 3.0 inches.

Loading

Uniform load in negative z-direction, specified with load type 1. The magnitude of the weight is 0.625 psi.

Boundary Conditions

Supported end:

A. u = 0, w = 0, at y = 0

The following degrees of freedom are constrained at the lines of symmetry:

B. u = 0 and ϕ = 0 at x = 0

C. v = 0 and ϕ = 0 at y = 300

SHELL SECT

The SHELL SECT option allows you to reduce the number of integration points from the default value of 11 to a minimum value of three in the shell thickness direction. This three-point integration scheme is exact as for a linear elastic problem.

Subroutine UFXORD

The coordinates are first defined in the x-y plane and are then modified by the use of the user subroutine UFXORD in order to obtain the three-dimensional model.

Results

A deformed mesh plot is shown in Figure 2.55-2. The results are in good agreement with problem 2.19. The element is much easier to use than elements type 4, 8, or 24 (used in previous problems).

Parameters, Options, and Subroutines Summary

Example e2x55.dat:

Parameters	Model Definition Options
ELEMENTS	CONNECTIVITY
END	COORDINATES
SHELL SECT	DIST LOADS
SIZING	END OPTION
TITLE	FIXED DISP
	GEOMETRY
	ISOTROPIC
	UFXORD

User subroutine in u2x55.f:

UFXORD

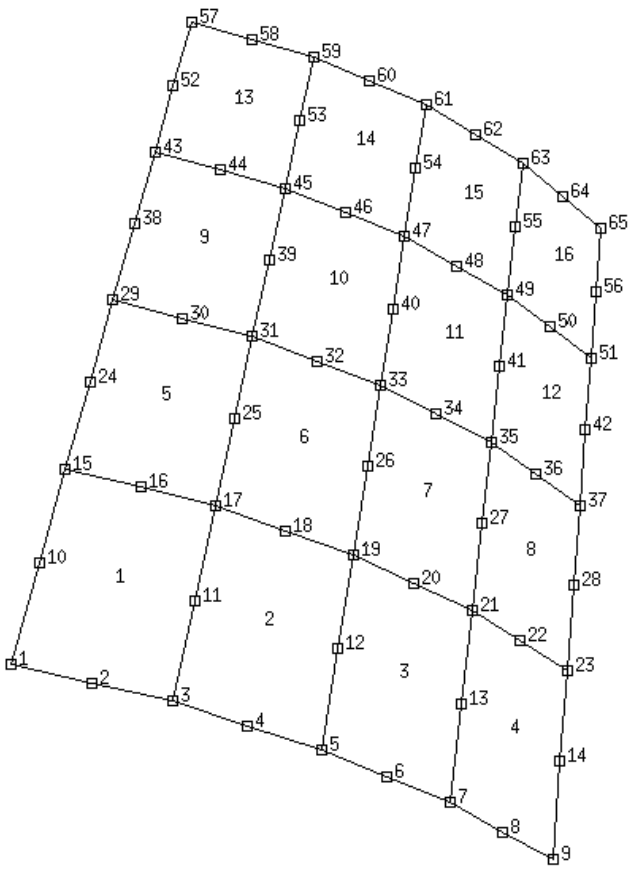

Figure 2.55-1 Shell Roof and Mesh

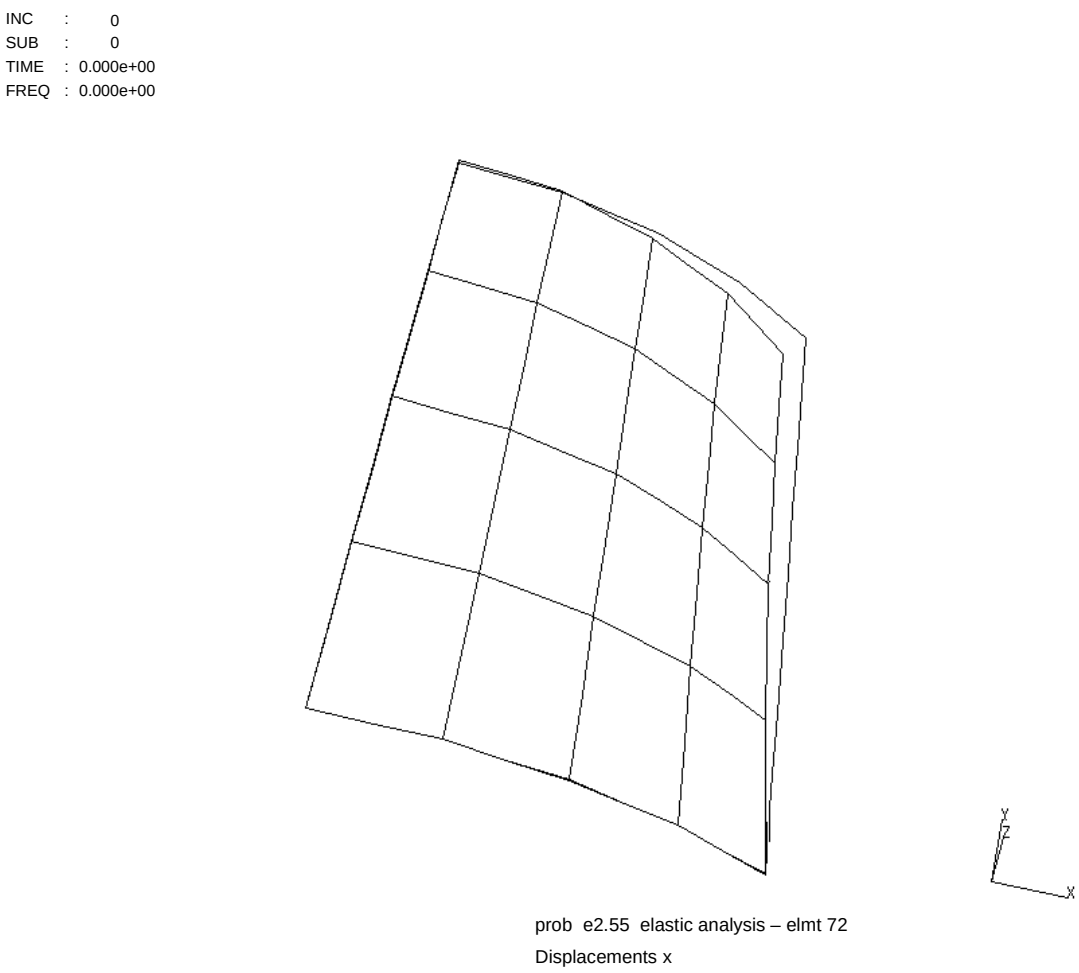

Figure 2.55-2 Deformed Mesh Plot

2.56 Cylinder-sphere Intersection by Element 72

This problem illustrates the use of MARC element type 72 for an elastic analysis of a cylinder-sphere intersection. The cylinder is subjected to internal pressure. The use of the SHELL SECT parameter and the user subroutine UFXORD is also illustrated. This problem is similar to 2.15.

Element

Element type 72 is a bilinear, constrained, 8-node shell element. With element type 72, no tying is necessary at the intersection.

Model

The element is type 72. There are 24 elements, with a total of 93 nodes. The dimensions of the shell structure and the finite element mesh used are shown in Figure 2.56-1.

Material Properties

Young's modulus is 1000.0 psi with a Poisson's ratio of 0.

Geometry

The shell thickness is 1.0 inch.

Loading

Internal pressure: this is specified with load type 2, with magnitude of 1.0 psi.

Boundary Conditions

The following degrees of freedom are constrained at the lines of symmetry:

A. $v = 0$ and $\phi = 0$ at $y = 0$,

B. $w = 0$ and $\phi = 0$ at $z = 0$,

C. $u = 0$ and $\phi = 0$ at $x = 0$,

where ϕ is the rotation around the edge.

SHELL SECT

The SHELL SECT allows you to reduce the number of integration points in the shell thickness direction from the default value of 11 to a minimum value of three. For elastic analysis, this three-point integration scheme is exact.

Subroutine UFXORD

The coordinates are first entered in the x-y plane. The coordinates are then modified by the use of user subroutine UFXORD in order to obtain the three-dimensional model.

Results

A deformed mesh plot is shown in Figure 2.56-2 and stress contours are depicted in Figure 2.56-3. The solution is axisymmetric as anticipated. The maximum stress of 1.27 occurs in the spherical shell close to the intersection. While this problem uses three times the number of elements as problem 2.15, the ratio of degrees of freedom is only 11:9.

Parameters, Options, and Subroutines Summary

Example e2x56.dat:

Parameters	Model Definition Options
ELEMENTS	CONNECTIVITY
END	COORDINATES
SHELL SECT	DIST LOADS
SIZING	END OPTION
TITLE	FIXED DISP
	GEOMETRY
	ISOTROPIC
	UFXORD

User subroutine in u2x56.f:

UFXORD

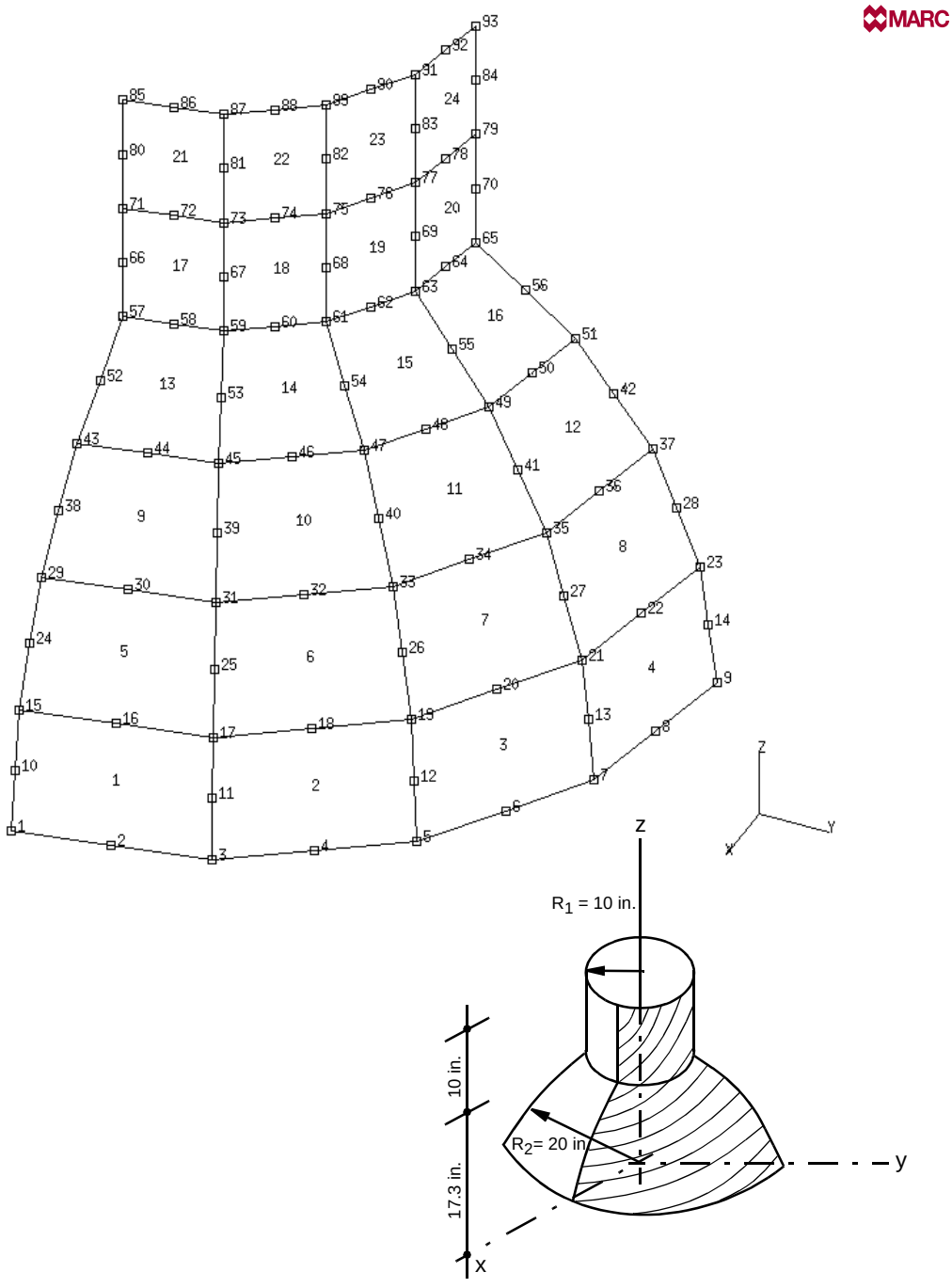

Figure 2.56-1 Shell Structure and Mesh

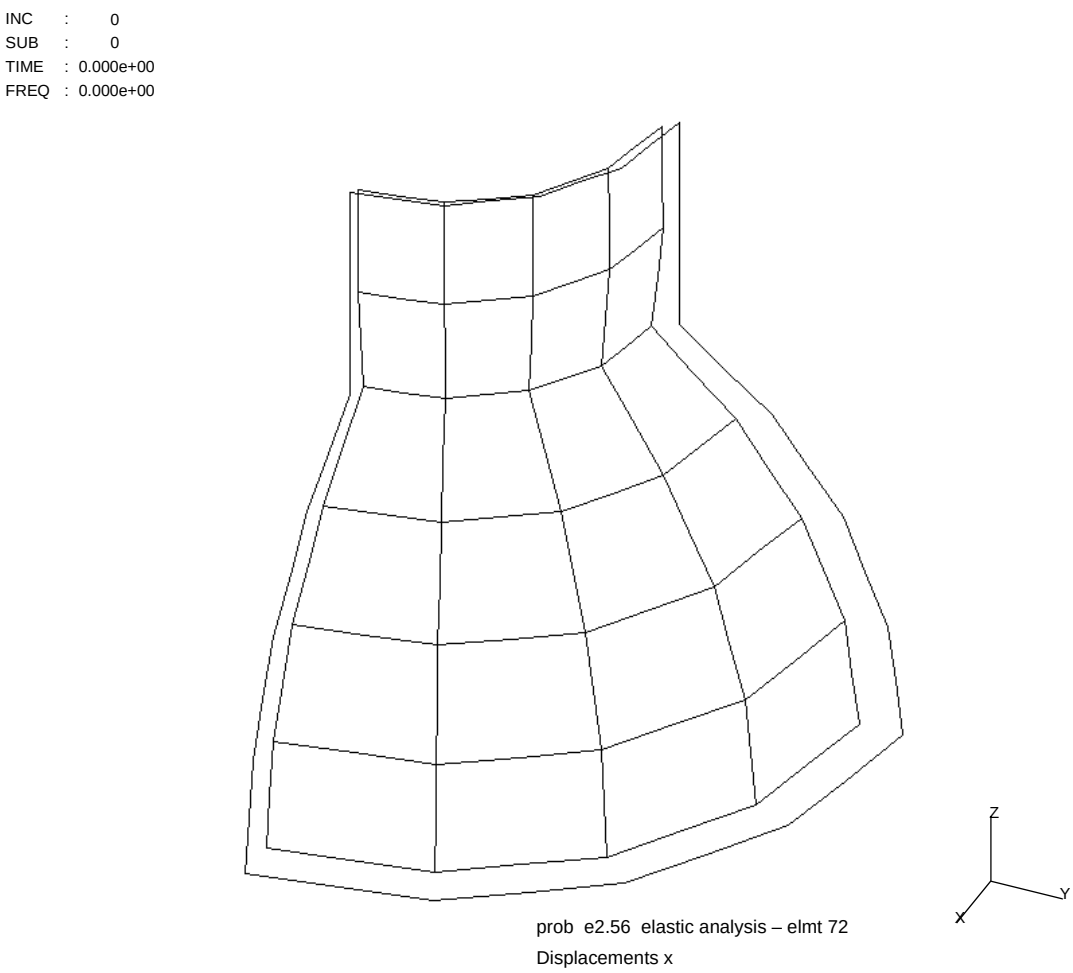

Figure 2.56-2 Deformed Mesh Plot

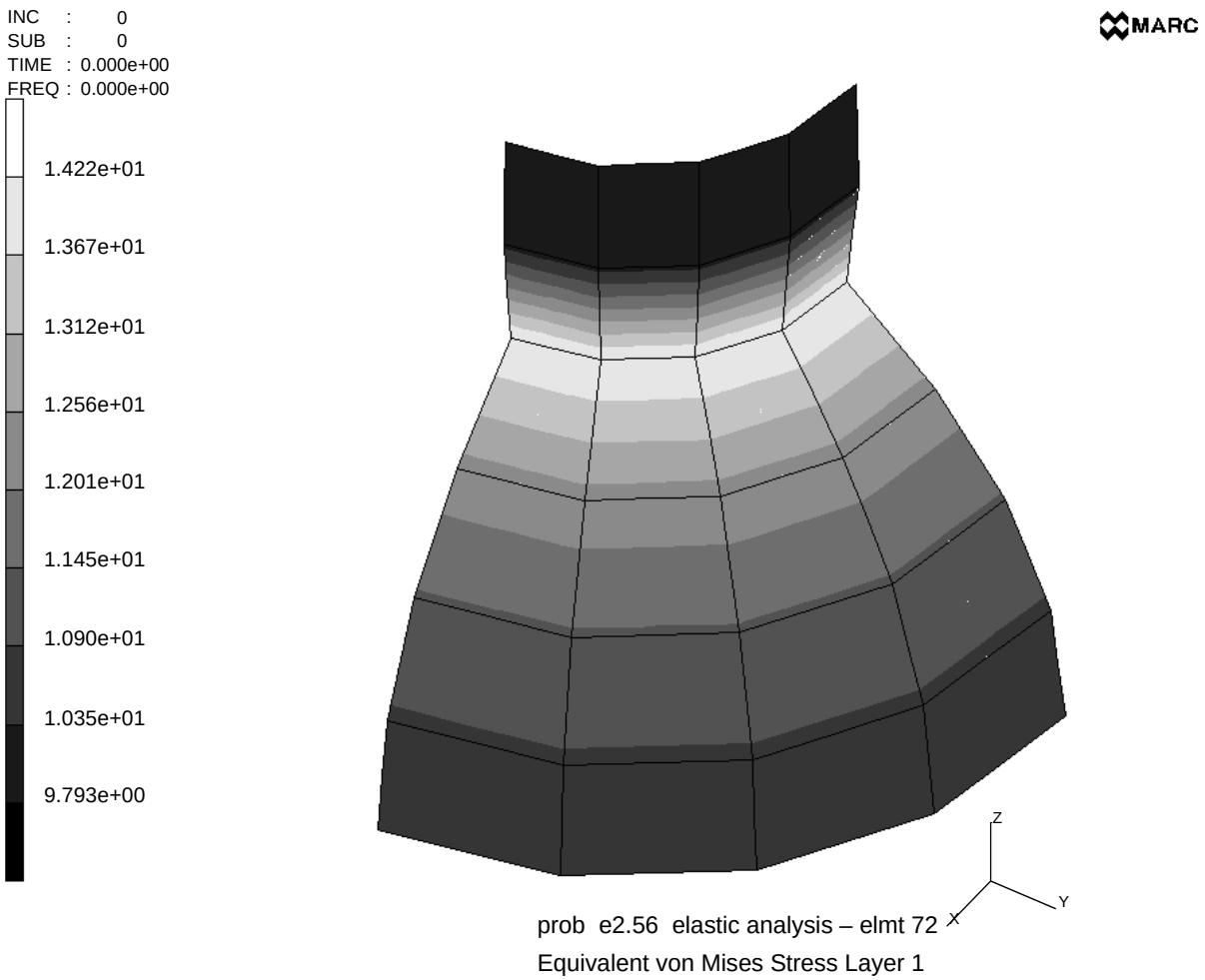

Figure 2.56-3 Equivalent von Mises Stress Contours

2.57 Closed Section Beam Subjected to a Point Load

This problem, same as problem 2.7, demonstrates the use of two closed-section beam elements (type 76, 3-node and type 78, 2-node). A hollow, square-section beam, clamped at both ends, has a single-point load applied at the center. The results are compared to the analytical solution.

This problem is modeled using the two techniques summarized below.

Data Set	Element Type(s)	Number of Elements	Number of Nodes
e2x57a	76	5	11
e2x57b	78	5	6

Elements

Library element types 76 and 78 are used. Both elements are closed-section, straight-beam elements with no warping of the section, but including twist. These elements have six degrees of freedom per node – three displacements and three rotations in the global coordinate system. For the 3-node beam element (type 76), the degrees of freedom at midside node is the rotation about the beam axis.

Model

Only half of the beam with a total length of 10 inches, is modeled, taking advantage of the beam's symmetry. Five elements are used for the beam. The total number of nodes is 11 for 3-node and 6 for 2-node beam elements, respectively. (see Figure 2.57-1).

Geometry

The model uses the BEAM SECT parameter to define its cross-sectional geometry. EGEOM1 = 0 indicates a noncircular cross section. EGEOM2 gives the section number as a floating point value, here equal to 1.

Material Properties

The beam is considered elastic with a Young's modulus of 20.0×10^6 psi.

Loading

A single-point load of 50 pounds is applied in the negative y-direction at the center node of the beam.

Boundary Conditions

In the model, the beam-end node (node 1) is fixed against displacement and rotation, simulating a fully built-in condition. Thus, $u = v = w = \theta_x = \theta_y = \theta_z = 0$. The midpoint node, node 6, is fixed against axial displacement and rotation; $u = \theta_x = \theta_y = \theta_z = 0$, thus ensuring symmetry boundary conditions. For the 3-node beam element (type 76), the rotation about the beam axis is also constrained, $\phi_t = 0$, for all mid-side nodes (nodes 7 to 11).

Special Considerations

Elements 76 and 78 have their cross sections specified by the BEAM SECT parameter, which is given in the parameters section. Details are given in *MARC Volume A: Theory and User Information*. In this case, four branches are used to define the hollow, square section (see Figure 2.57-2).

Each branch is of constant thickness (0.01 inch) with no curvature and is 0.99 inch in length. The branches are defined at the midpoint of the thickness of the cross section. The first branch begins at local coordinates, x = -0.495, y = -0.495 and each following branch begins its length at the end coordinates of the previous branch. Except for the first branch, only the coordinates at the end of the branch need to be defined. Each branch has four divisions which provide the four stress points for the branch.

Results

A simple elastic analysis was run with one load increment of negative 50 pounds applied to node 6 in the zeroth increment. The computed results are compared with an exact solution in Table 2.57-1 and Table 2.57-2.

Table 2.57-1 Y Deflection (inches)

Node	Element 14	Element 52	Elements 76 & 78	Calculated
1	0.	0.	0.	0.
2	.000419	.000419	.000419	.000422
3	.001417	.001417	.001417	.001428
4	.002609	.002609	.002609	.002628
5	.003607	.003607	.003607	.003634
6	.004026	.004025	.004026	.004056

Table 2.57-2 Moments (inches-pounds) and Reaction Forces (pounds

Element 14	Element 52	Elements 76 & 78	Calculated
M = 125.	M = 125.	M = 125.	M = 125.
R = 50.	R = 50.	R = 50.	R = 50.

Parameters, Options, and Subroutines Summary

Example e2x57a.dat:

Parameters	Model Definition Options
BEAM SECT	CONNECTIVITY
ELEMENTS	COORDINATES
END	END OPTION
SIZING	FIXED DISP
TITLE	GEOMETRY
	ISOTROPIC
	POINT LOAD

Example e2x57b.dat:

Parameters	Model Definition Options
BEAM SECT	CONNECTIVITY
ELEMENTS	COORDINATES
END	END OPTION
SIZING	FIXED DISP
TITLE	GEOMETRY
	ISOTROPIC
	POINT LOAD

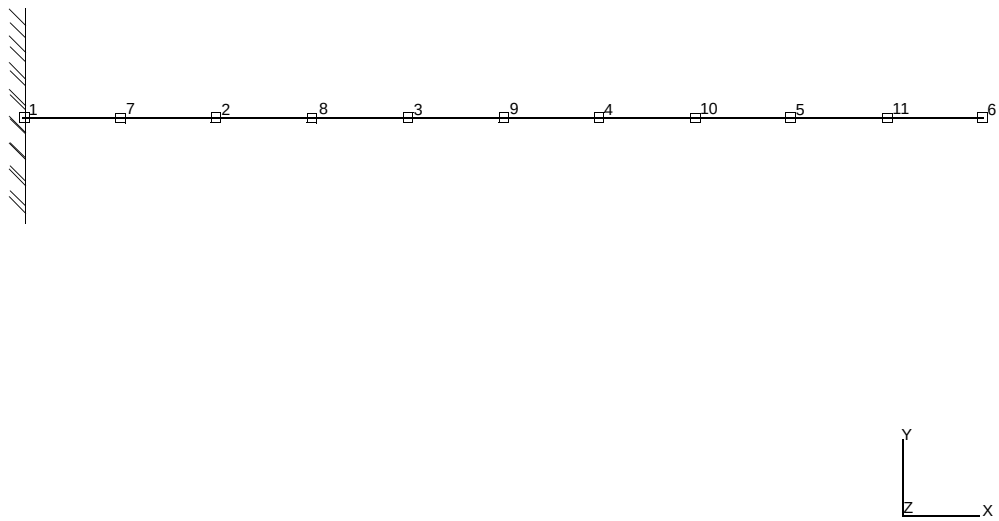

Figure 2.57-1 Closed Section Beam Model

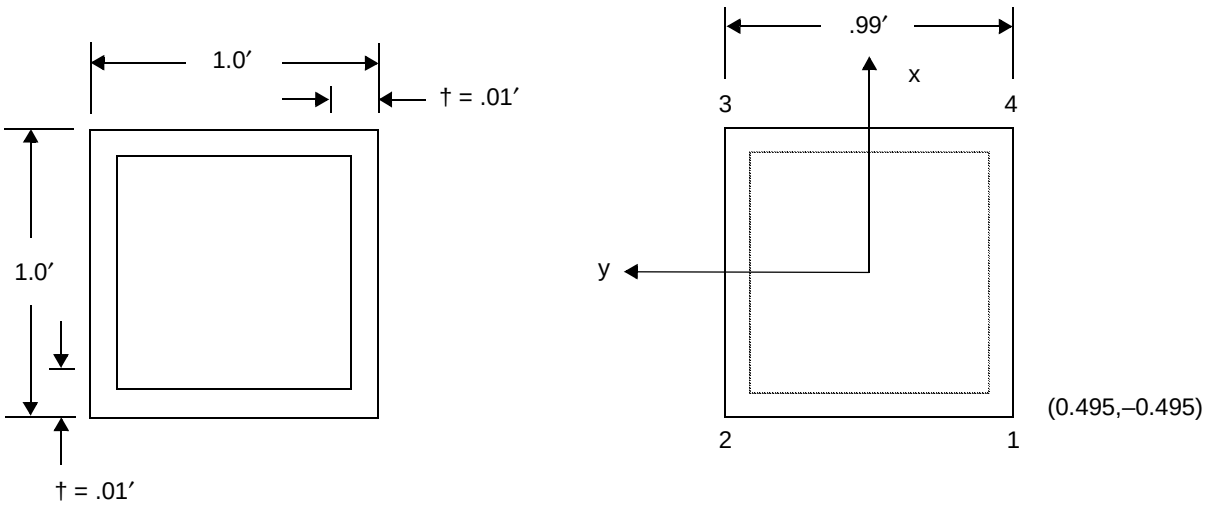

Cross-section

Branch Definition

Figure 2.57-2 Hollow, Square-Section Beam

2.58 Open Section, Double Cantilever Beam Loaded Uniformly

Same as problem 2.6, an I-section beam is loaded uniformly, parallel to the plane of the web. The beam is fixed against rotation and displacement at each end. This problem demonstrates the use of the BEAM SECT parameter to define the cross section of a beam and the use of two open section beam elements (type 77, 3-node and type 79, 2-node). The results are compared to the analytic solution.

This problem is modeled using the two techniques summarized below.

Data Set	Element Type(s)	Number of Elements	Number of Nodes
e2x58a	77	10	21
e2x58b	79	10	11

Elements

Library element types 77 and 79 are used. Both elements are open-section, straight, thin-walled beams including warping and twist of the section. These elements have six degrees of freedom per node – three displacements and three rotations in the global coordinate system. For the 3-node beam element (type 77), the degrees of freedom at the midside node is the rotation about the beam axis.

Model

The beam of length 10 inches is modeled with 10 elements (see Figure 2.58-1). The number of nodes is 21 for 3-node and 11 for 2-node beam elements, respectively.

Geometry

EGEOM2 is used as a floating point value to cross reference the section number; here EGEOM2 = 1. as only one section type is given.

Material Properties

Young's modulus is specified as 20×10^6 psi. Consistency with the analytical solution requires Poisson's ratio to be 0.

Loading

Uniform pressure of 10 pounds per length in the negative global Y direction.

Boundary Conditions

The beam is fixed against rotation and displacement at each end; that is:

$u = 0 \qquad \phi_x = 0$
$v = 0 \qquad \phi_y = 0$
$w = 0 \qquad \phi_z = 0$

Special Considerations

Element types 77 and 79 have a cross-section specification that is entered in the parameter block section, after the header BEAM SECT. Details are given in *MARC Volume A: Theory and User Information*. In the present case, five branches are used to define the beam section (see Figure 2.58-2).

The first branch is one flange of beam, read in at constant thickness (0.18 inch) and with no curvature. The second branch is a zero thickness branch that doubles back to the flange center. The third branch is the web, straight and with constant thickness (0.31 inch). The fourth branch is half the remaining flange, with zero thickness. The fifth branch is straight and with constant thickness (0.18 in.) which doubles back over the fourth branch.

Results

An elastic analysis was performed. Five generalized strains and axial stress at integration points are printed out. The results are compared with calculated results from *Formulas for Stress and Strain*, R. J. Roark. These are summarized in Table 2.58-1.

Table 2.58-1 Y Deflection (inches)

Node	Element 13	Elements 77 & 79	Calculated
1	0.	0.	0.
2	1.82×10^{-5}	1.83×10^{-5}	1.82×10^{-5}
3	5.79×10^{-5}	5.81×10^{-5}	5.75×10^{-5}
4	9.99×10^{-5}	10.0×10^{-5}	9.91×10^{-5}
5	1.307×10^{-4}	1.308×10^{-4}	1.295×10^{-4}
6	1.419×10^{-4}	1.419×10^{-4}	1.404×10^{-4}

Parameters, Options, and Subroutines Summary

Example e2x58a.dat:

Parameters	Model Definition Options
BEAM SECT	CONNECTIVITY
ELEMENTS	COORDINATES
END	DIST LOADS
SIZING	END OPTION
TITLE	FIXED DISP
	GEOMETRY
	ISOTROPIC

Example e2x58b.dat:

Parameters	Model Definition Options
BEAM SECT	CONNECTIVITY
ELEMENTS	COORDINATES
END	DIST LOADS
SIZING	END OPTION
TITLE	FIXED DISP
	GEOMETRY
	ISOTROPIC

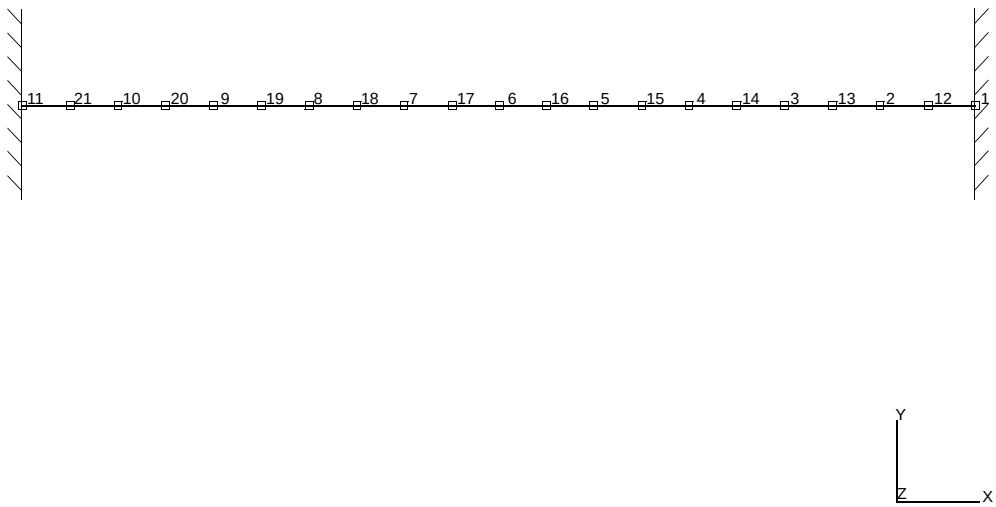

Figure 2.58-1 Open Section Beam Model

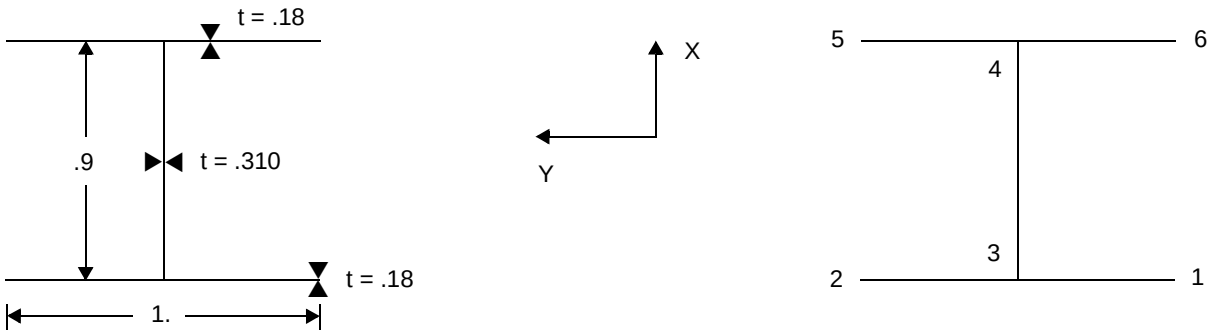

Figure 2.58-2 Beam Section and Sequence of Branch Traversal

2.59 Simply Supported Elastic Beam Under Point Load

This problem demonstrates the use of a two-node straight elastic beam for a simply supported beam structure subjected to a point load at midspan of the beam. The effects of transverse shear are included in the formulation of the beam element.

This problem is modeled using the two techniques summarized below.

Data Set	Element Type(s)	Number of Elements	Number of Nodes	Differentiating Features
e2x59a	98	5	6	
e2x59b	98	5	6	BEAM SECT

Element

Element type 98 is a two-node straight elastic beam in space and includes the transverse shear effects in its formulation. It uses a linear interpolation in displacement along the axis of the beam and a cubic interpolation in the direction normal to the beam axis. In addition to elastic behavior, the element can also be used for hypoelastic materials. The hypoelastic behavior must be defined in the UBEAM user subroutine.

Model

As shown in Figure 2.59-1, due to symmetry, only one-half of the simply supported beam is modeled. The finite element mesh consists of five elements and six nodes. The span of the beam is 10 inches and the cross-section of the beam is assumed to be a closed, thin, square section.

Geometry

The GEOMETRY block is used for entering the beam section properties. There are two options available to you for the use of the GEOMETRY block. The section properties area = 0.0396 inches^2, $I_x = I_y = 6.4693 \times 10^{-3}$ inches^4, can be directly entered through the GEOMETRY block or through the BEAM SECT parameter by defining area = 0.0, I_x = section number, in the GEOMETRY block. In the latter case, you must enter the beam section properties through the BEAM SECT parameter.

BEAM SECT

The BEAM SECT parameter is required only if you choose to enter area = 0.0 and I_x = section number, in the GEOMETRY block. The beam section properties to be entered through this option area: area, I_x, I_y, torsional stiffness factor, and effective transverse shear areas.

Material Properties

The material of the beam is assumed to have a Young's modulus of 20,000 psi and Poisson's ratio of 0.3.

Loading

The beam is assumed to be subjected to a point load of 20 pounds. Due to symmetry, a 10 pound point load is applied at node 6 in the positive x-direction.

Boundary Conditions

At node 1, all translational degrees of freedom are constrained ($u_x = u_y = u_z = 0$) for the simulation of simply-supported conditions. At midspan (node 6), all degrees of freedom except u_x are constrained for the simulation of symmetry condition.

Results

A comparison of beam deflections is shown in Table 2.59-1. The beam deflection at node 6 predicted by element 98 is 4% larger than that of element 52 (3.3523/3.2203 = 1.041). The additional beam deflection is clearly due to the effect of transverse shear allowed in element 98.

Table 2.59-1 Comparison of Beam Deflections (in.)

Node	Element 52	Element 98
1	0.0	0.0
2	0.9532	0.9796
3	1.8291	1.8819
4	2.5505	2.6297
5	3.0399	3.1455
6	3.2203	3.3523

Parameters, Options, and Subroutines Summary

Example e2x59a.dat:

Parameters	Model Definition Options
ELEMENTS	CONNECTIVITY
END	COORDINATES
SIZING	END OPTION
TITLE	FIXED DISP
	GEOMETRY
	ISOTROPIC
	POINT LOAD

Example e2x59b.dat:

Parameters	Model Definition Options
BEAM SECT	CONNECTIVITY
ELEMENTS	COORDINATES
END	END OPTION
SIZING	FIXED DISP
TITLE	GEOMETRY
	ISOTROPIC
	POINT LOAD

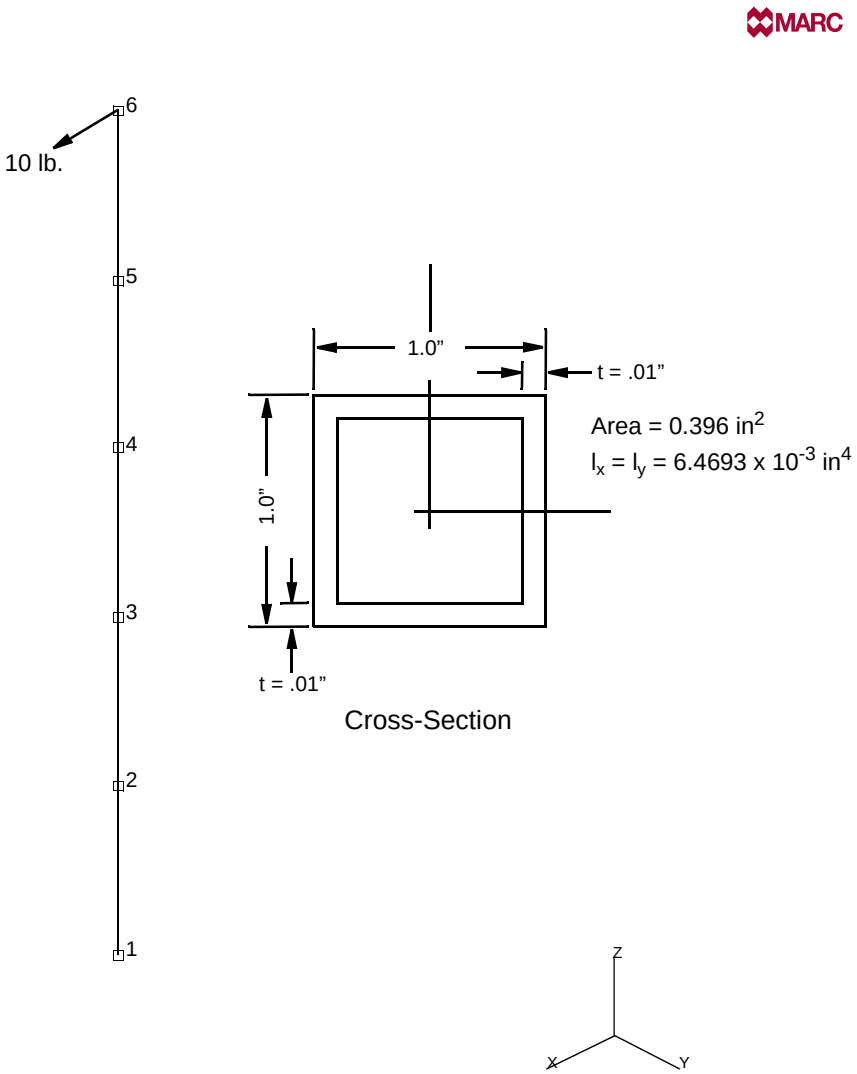

Figure 2.59-1 Simply Supported Beam Under Point Load

2.60 Uniform Pressure on Cylindrical Cavity of an Infinite Body (The Lamé Solution)

This problem demonstrates the use of plane strain and plane strain semi-infinite elements for the solution of a classical elasticity (Lamé) problem. As shown in Figure 2.60-1, the cylindrical cavity of radius a is located in the x-y plane and is extended to infinity in both the positive and negative z-directions. A uniformly distributed pressure p is assumed to be acted on the interior surface of the cavity. The finite element solution to this problem is evaluated in this example.

This problem is modeled using the two techniques summarized below.

Data Set	Element Type(s)	Number of Elements	Number of Nodes
e2x60a	11 & 91	16	30
e2x60b	27 & 93	16	69

Elements

Since the Lamé problem deals with two-dimensional infinite body, it is convenient to use two types of plane strain elements for the modeling of the near and far fields of the body. In this example, the regular plane strain element types 11 (4-node) and 27 (8-node) are used for the near field and the plane strain semi-infinite element types 91 (6-node) and 93 (9-node) are used for the far field of the two-dimensional infinite body. Element type 11 is compatible with element type 91, and element type 27 is compatible with element type 93. The interpolation functions of element types 91 and 93 are such that the elements expand to infinity and the displacements at infinity are implied to be zero.

Model

A plane strain model consisting of twelve regular plane strain elements and four plane strain semi-infinite elements are used for the Lamé problem. The total number of nodes in the model is 30 for Model A (element types 11 and 91), and 69 for Model B (element types 27 and 93). Finite element meshes are shown in Figure 2.60-2 and Figure 2.60-3, respectively.

Geometry

The GEOMETRY block is not selected for this problem. As a result, a default thickness of 1.0 is used for this example.

Material Properties

The material is assumed to have a Young’s modulus of 1.0 and a Poisson’s ratio of 0.1.

Loading

A uniformly distributed pressure (DIST LOADS) of 1.0 is applied along the interior surface of the cavity (Elements 1, 4, 7 and 10).

Boundary Conditions

The first degrees of freedom are constrained for nodes located along the line of x = 0; the second degrees of freedom are constrained for nodes located along the line of y = 0, for the simulation of symmetry conditions. No boundary conditions at infinity are required.

Results

Deformed meshes and von Mises stress distributions are shown in Figure 2.60-4 through Figure 2.60-7 for Models A and B. Radial displacements are tabulated in Table 2.60-1. The comparison of finite element results with calculated values is reasonably good.

Table 2.60-1 Radial Displacements

Analytical Solution*		Element 91		Element 93	
R =	Displacement	Node	Displacement	Node	Displacement
1.0	1.1000	2	1.0156	3	1.0685
1.5	0.7333			5	0.7128
2.0	0.5500	4	0.5189	8	0.5357
2.5	0.4400			10	0.4280
3.0	0.3667	6	0.3480	13	0.3565
3.5	0.3143			15	0.3055
4.0	0.2750	8	0.2618	18	0.2674
8.0	0.1375	21	0.1309	53	0.1337
12.0	0.0917	26	0.0873	56	0.0891

*The R-displacements are calculated from:

$$u = \frac{(1+\nu)}{Er} pa^2$$

Parameters, Options, and Subroutines Summary

Example e2x60a.dat:

Parameters	Model Definition Options
ELEMENTS	CONNECTIVITY
END	COORDINATES
SIZING	DEFINE
TITLE	DIST LOADS
	END OPTION
	FIXED DISP
	ISOTROPIC
	POST
	PRINT CHOICE

Example e2x60b.dat:

Parameters	Model Definition Options
ELEMENTS	CONNECTIVITY
END	COORDINATES
SIZING	DEFINE
TITLE	DIST LOADS
	END OPTION
	FIXED DISP
	ISOTROPIC
	POST
	PRINT CHOICE

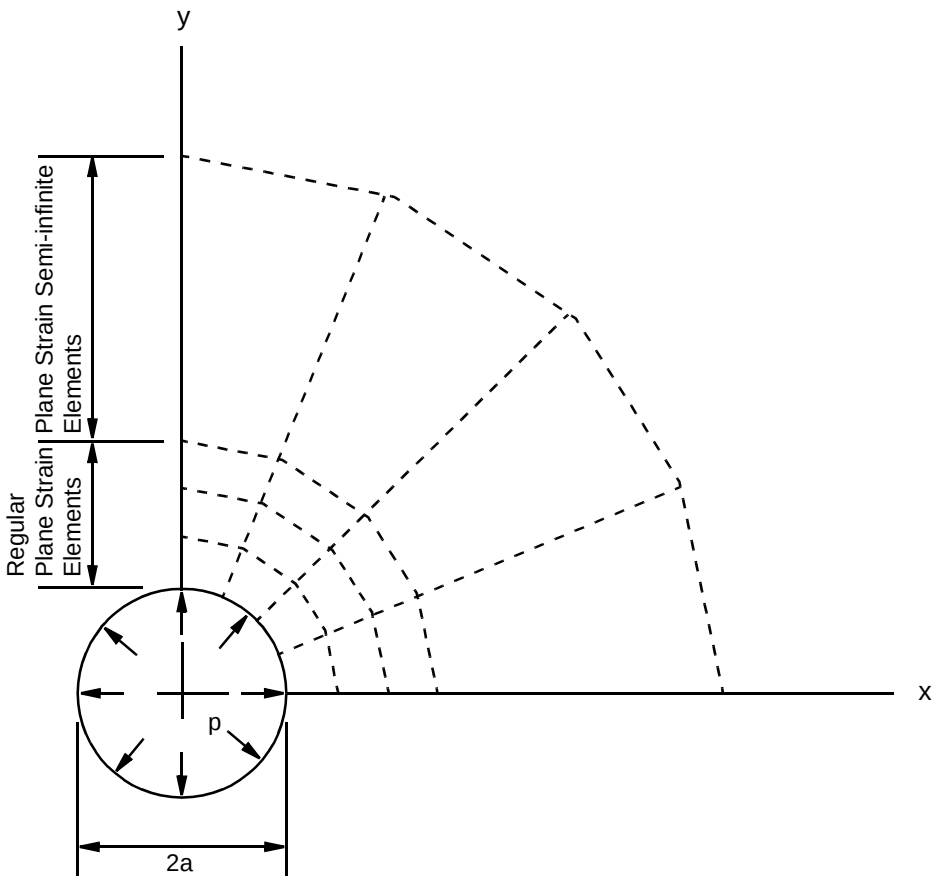

Figure 2.60-1 Uniform Pressure on Cylindrical Cavity of an Infinite Body (The Lamé Solution)

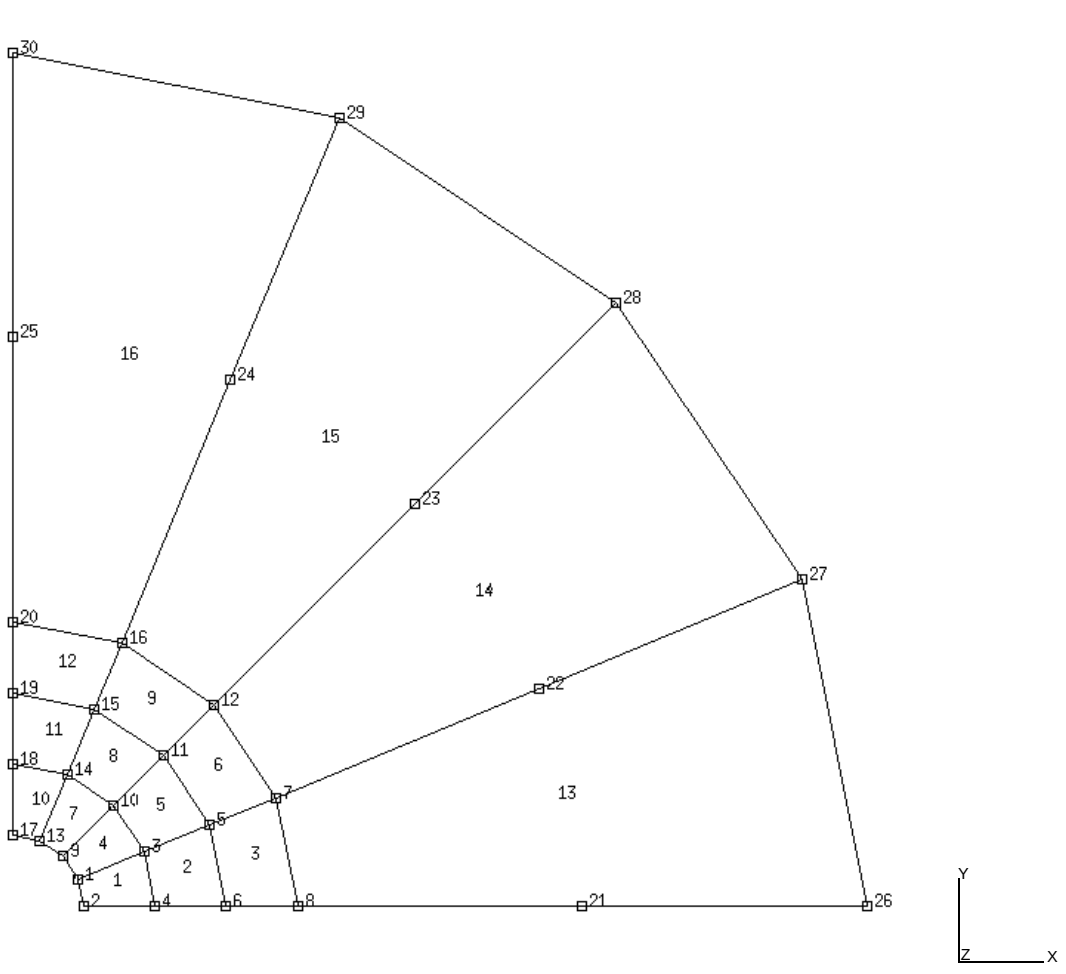

Figure 2.60-2 Finite Element Mesh (Model A) (Elements 11 and 91)

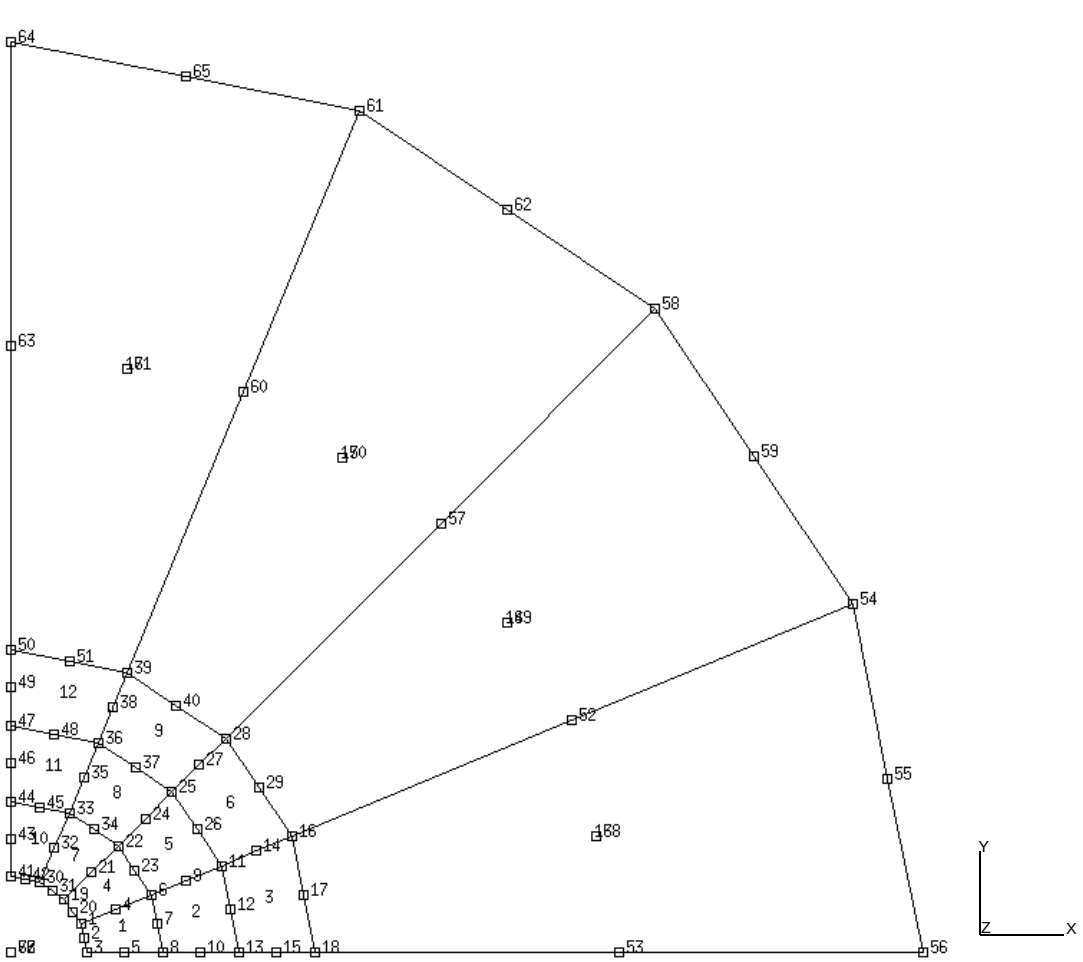

Figure 2.60-3 Finite Element Mesh (Model B) (Elements 27 and 93)

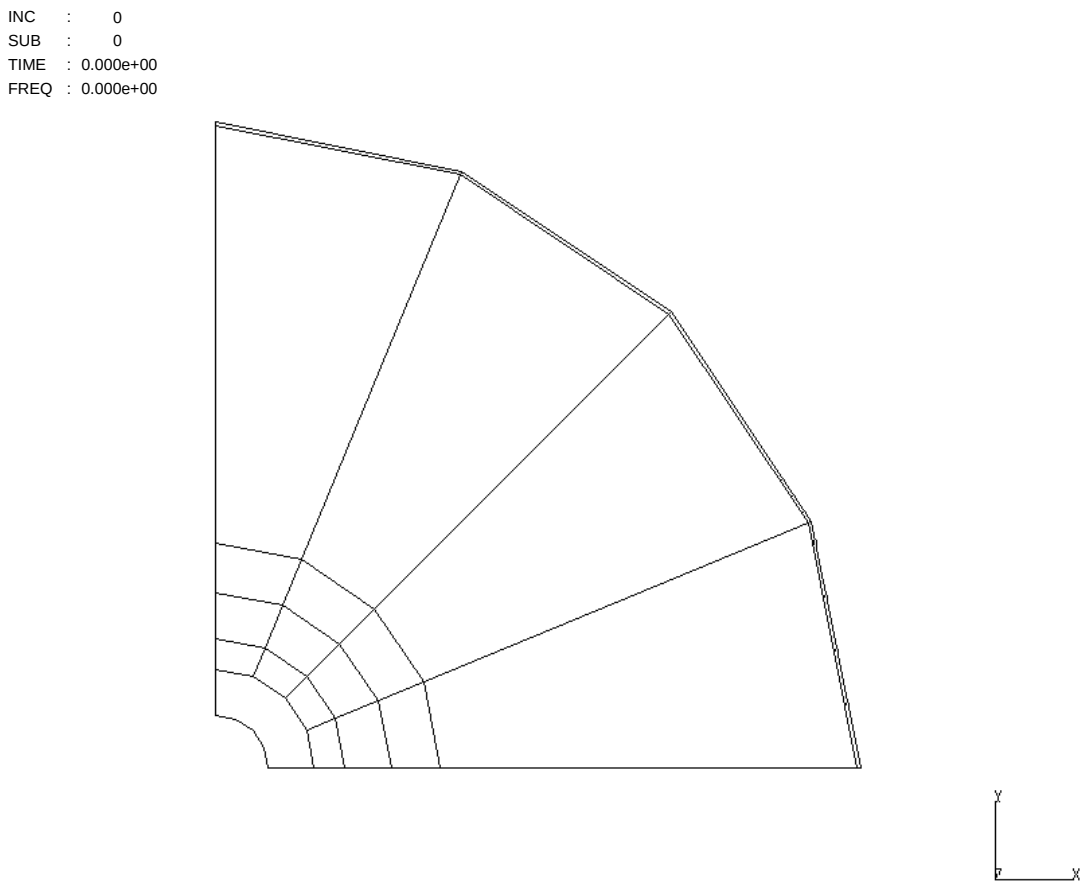

Figure 2.60-4 Deformed Mesh (Model A)

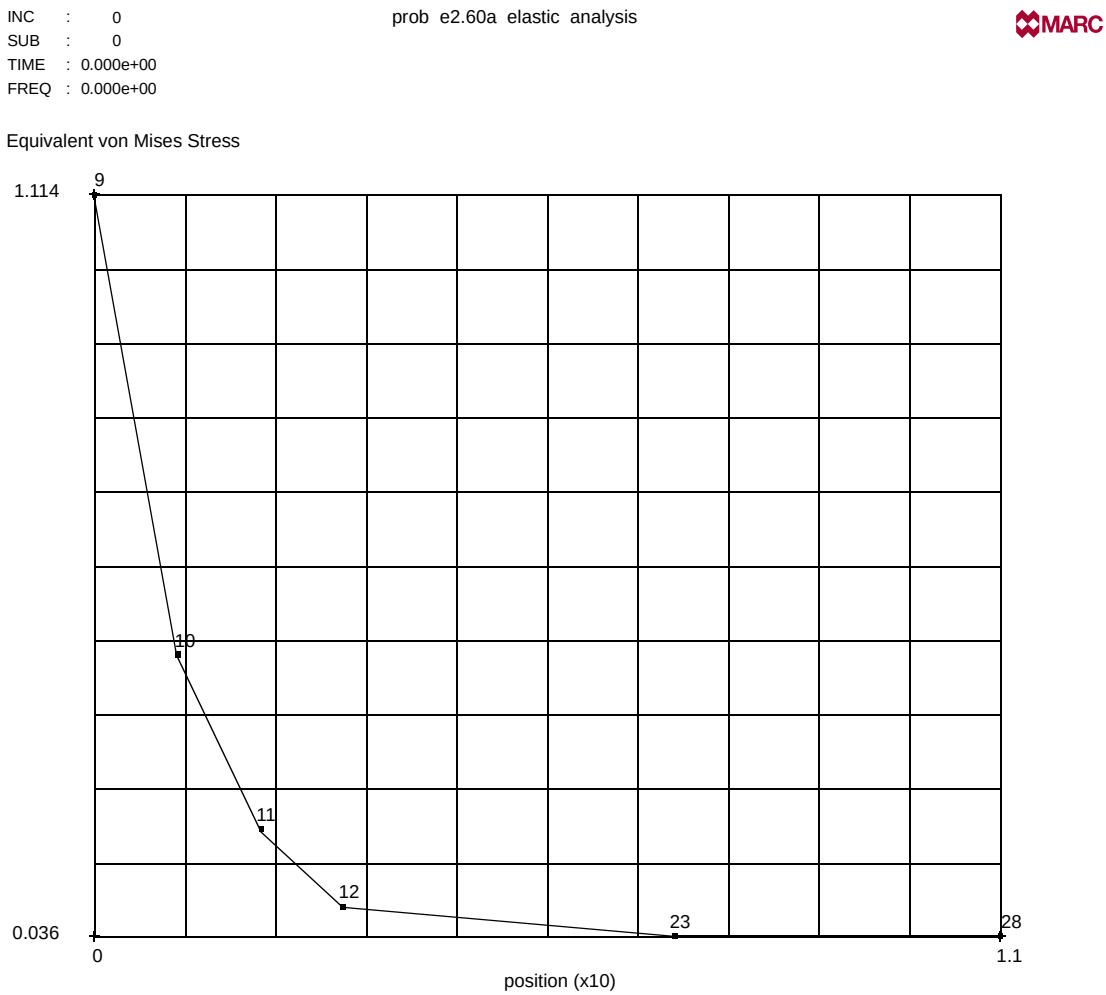

Figure 2.60-5 Stress Distribution Along Radial Path

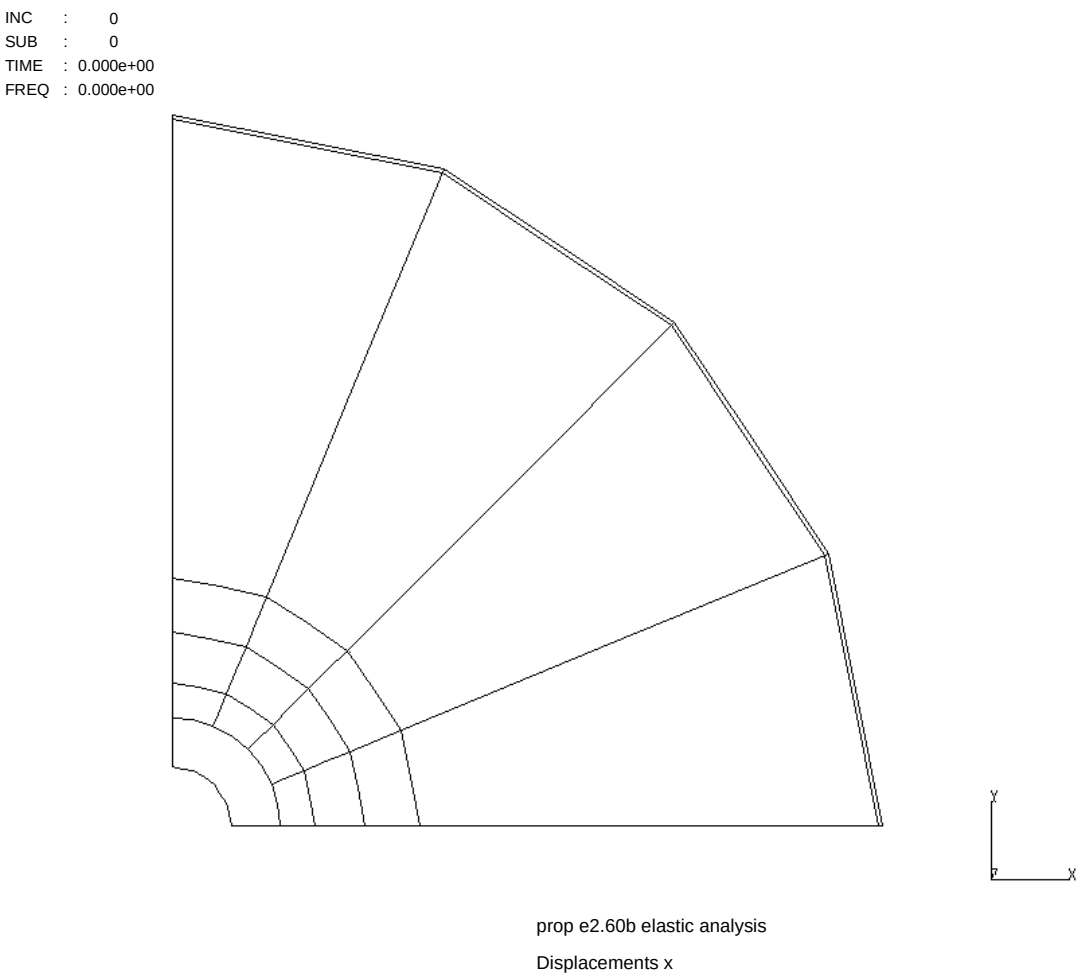

Figure 2.60-6 Deformed Mesh (Model B)

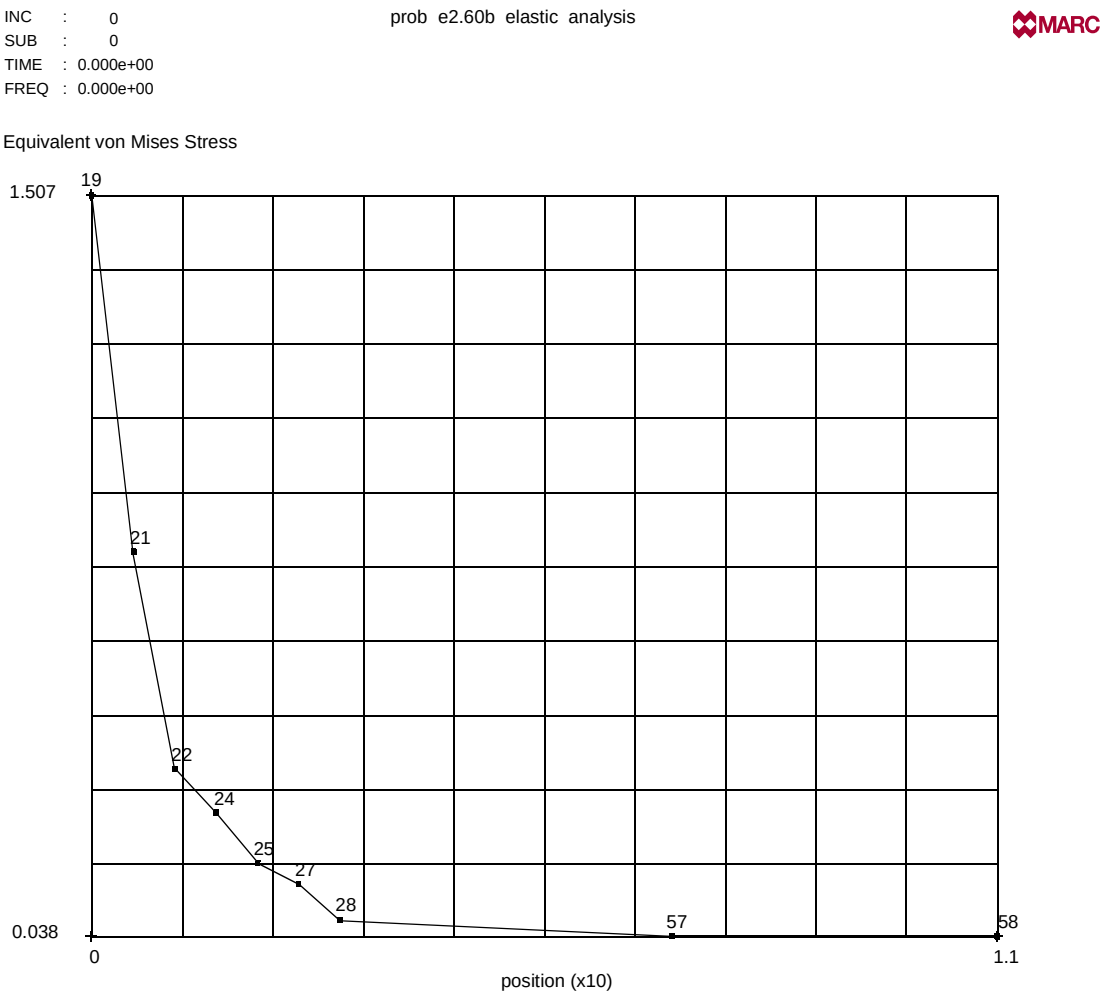

Figure 2.60-7 Stress Distribution Along Radial Path

2.61 The Boussinesq Problem (Point Load on Boundary of a Semi-infinite Body)

This problem demonstrates the use of axisymmetric ring and axisymmetric semi-infinite elements for the solution of a classical elasticity (Boussinesq) problem. As shown in Figure 2.61-1, the plane z = 0 is the boundary of a semi-infinite solid and a force P is acting on this plane along the z-axis. The solution of this problem was originally given by J. Boussinesq and a detailed discussion of the solution can be found in the reference *Theory of Elasticity*, by S. Timoshenko and J. N. Goodier, p. 362.

This problem is modeled using the two techniques summarized below.

Data Set	Element Type(s)	Number of Elements	Number of Nodes
e2x61a	10 & 92	20	31
e2x61b	28 & 94	20	75

Elements

Since the Boussinesq problem deals with semi-infinite body, it is convenient to choose two types of axisymmetric elements for the modeling of the near and far fields of the body. In this example, the regular axisymmetric ring element types 10 (4-node) and 28 (8-node) are used for the near field and the axisymmetric semi-infinite element types 92 (6-node) and 94 (9-node) are used for the far field of the semi-infinite body. Element type 10 is compatible with element type 92 and element type 28 is compatible with element type 94. The interpolation functions of element types 92 and 94 are such that the elements expand to infinity, and the displacements at infinity are implied to be zero.

Model

An axisymmetric model consisting of 16 regular axisymmetric ring elements and 4 axisymmetric semi-infinite elements is used for the Boussinesq problem. The total number of nodes in the model is 31 for Model A (Elements 10 and 92), and 75 for Model B (element types 28 and 94). Finite element meshes for both models are shown in Figure 2.61-2 and Figure 2.61-3, respectively.

Geometry

For axisymmetric models, the GEOMETRY block is not required.

Material Properties

The material is assumed to have a Young’s modulus of 1.0 and a Poisson’s ratio of 0.1.

Loading

A unit force (POINT LOAD) is applied at node 1 in the positive z (axial) direction.

Boundary Conditions

The radial displacements (second degrees of freedom) of all the nodes located along the z-axis (line of symmetry) are constrained. No boundary conditions at infinity are required.

Results

Stress contours on the deformed mesh are shown in Figure 2.61-4 and Figure 2.61-5 for Models A and B. Z-displacements at R = 0 are tabulated in Table 2.61-1. The comparison of finite element results with calculated values is reasonably good.

Table 2.61-1 Z-Displacements at R = 0

Analytical Solution*		Element 92		Element 94	
Z =	**Displacement**	**Node**	**Displacement**	**Node**	**Displacement**
0.	∞	1	1.2579	1	3.0197
0.5	0.9549			3	1.1476
1.0	0.4775	3	0.4655	6	0.4780
1.5	0.3183			8	0.3259
2.0	0.2387	5	0.2526	11	0.2506
2.5	0.1910			13	0.1991
3.0	0.1592	7	0.1717	16	0.1639
3.5	0.1364			18	0.1404
4.0	0.1194	9	0.1295	21	0.1231
8.0	0.0597	22	0.0640	59	0.0614
12.0	0.0398	27	0.0426	62	0.0409

*The Z-displacements are calculated from:

$$w = \frac{P}{2\pi E}\left[(1+\nu)z^2(r^2+z^2)^{-\frac{3}{2}} + 2(1-\nu^2)(r^2+z^2)^{-\frac{1}{2}}\right]$$

Parameters, Options, and Subroutines Summary

Example e2x61a.dat:

Parameters	Model Definition Options
ELEMENTS	CONNECTIVITY
END	COORDINATES
SIZING	DEFINE
TITLE	END OPTION
	FIXED DISP
	ISOTROPIC
	POINT LOAD
	POST
	PRINT CHOICE

Example e2x61b.dat:

Parameters	Model Definition Options
ELEMENTS	CONNECTIVITY
END	COORDINATES
SIZING	DEFINE
TITLE	END OPTION
	FIXED DISP
	ISOTROPIC
	POINT LOAD
	POST
	PRINT CHOICE

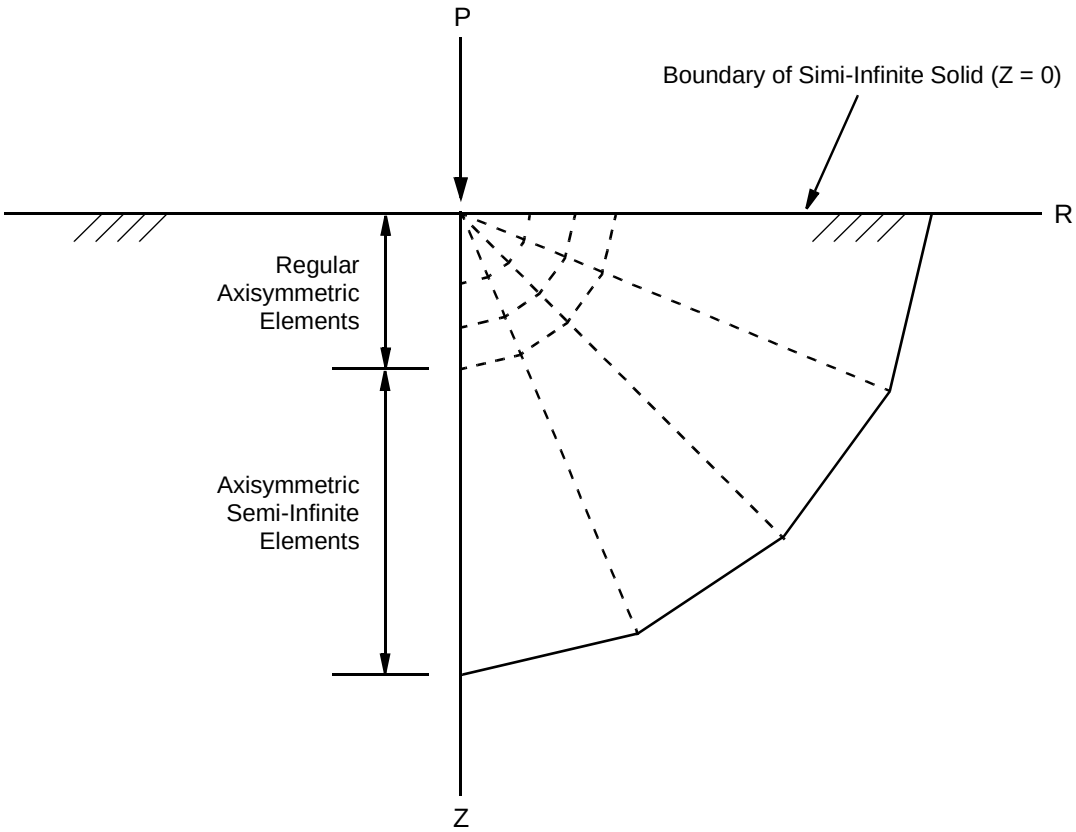

Figure 2.61-1 Boussinesq Problem (POINT LOAD on Boundary of a Semi-infinite Body)

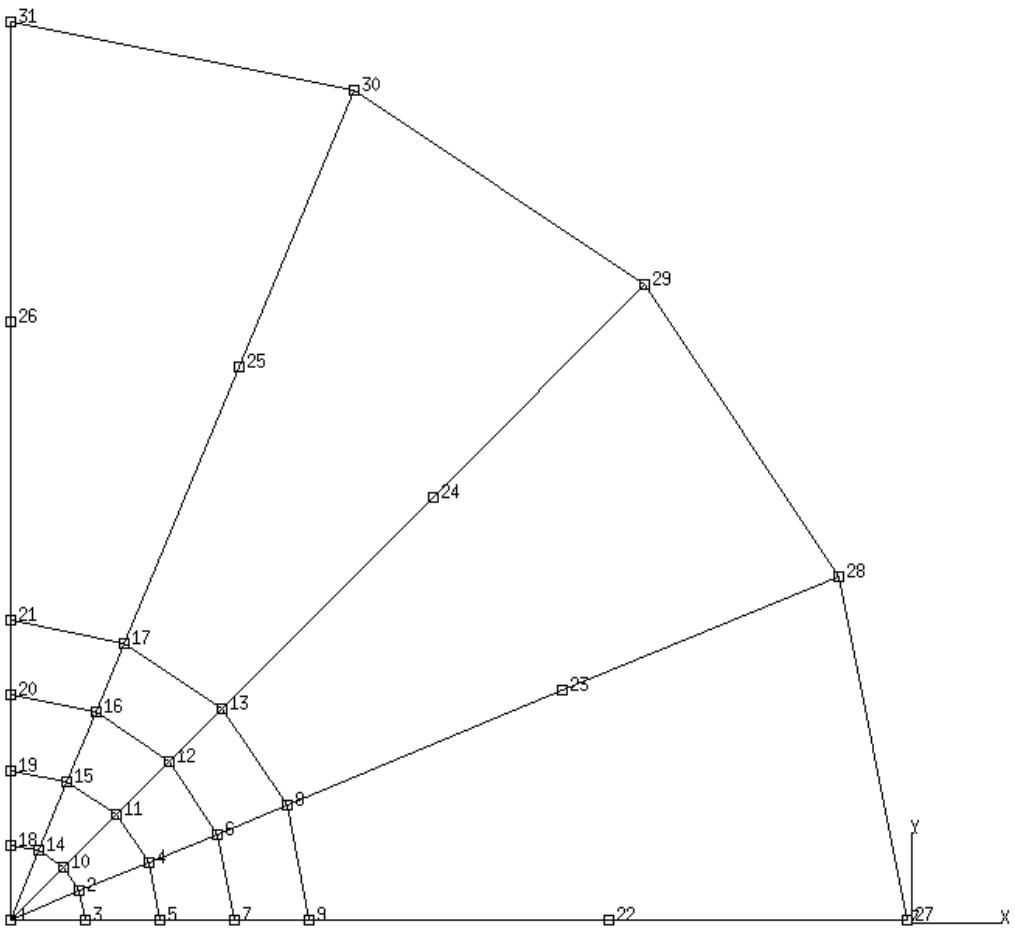

Figure 2.61-2 Finite Element Mesh (Model A) (Elements 10 and 92)

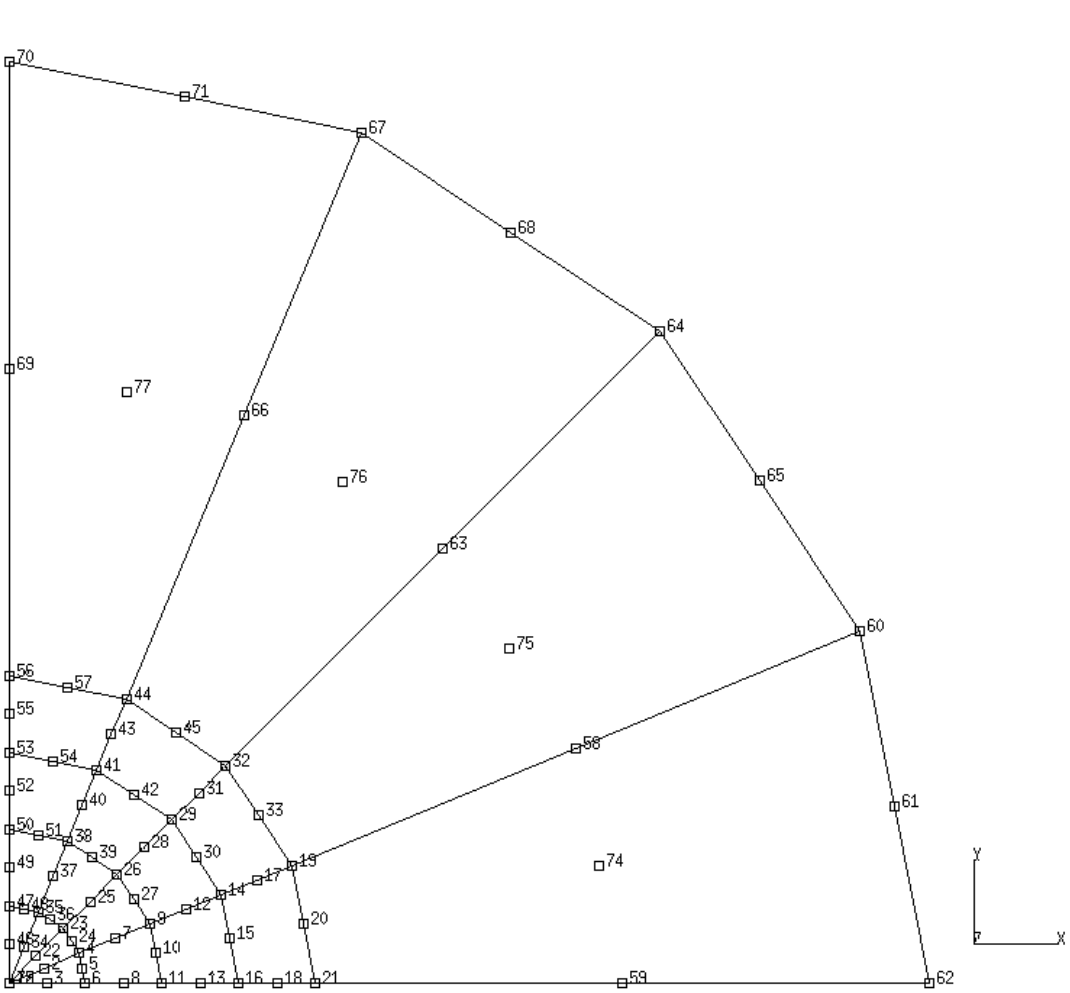

Figure 2.61-3 Finite Element Mesh (Model B) (Elements 28 and 94)

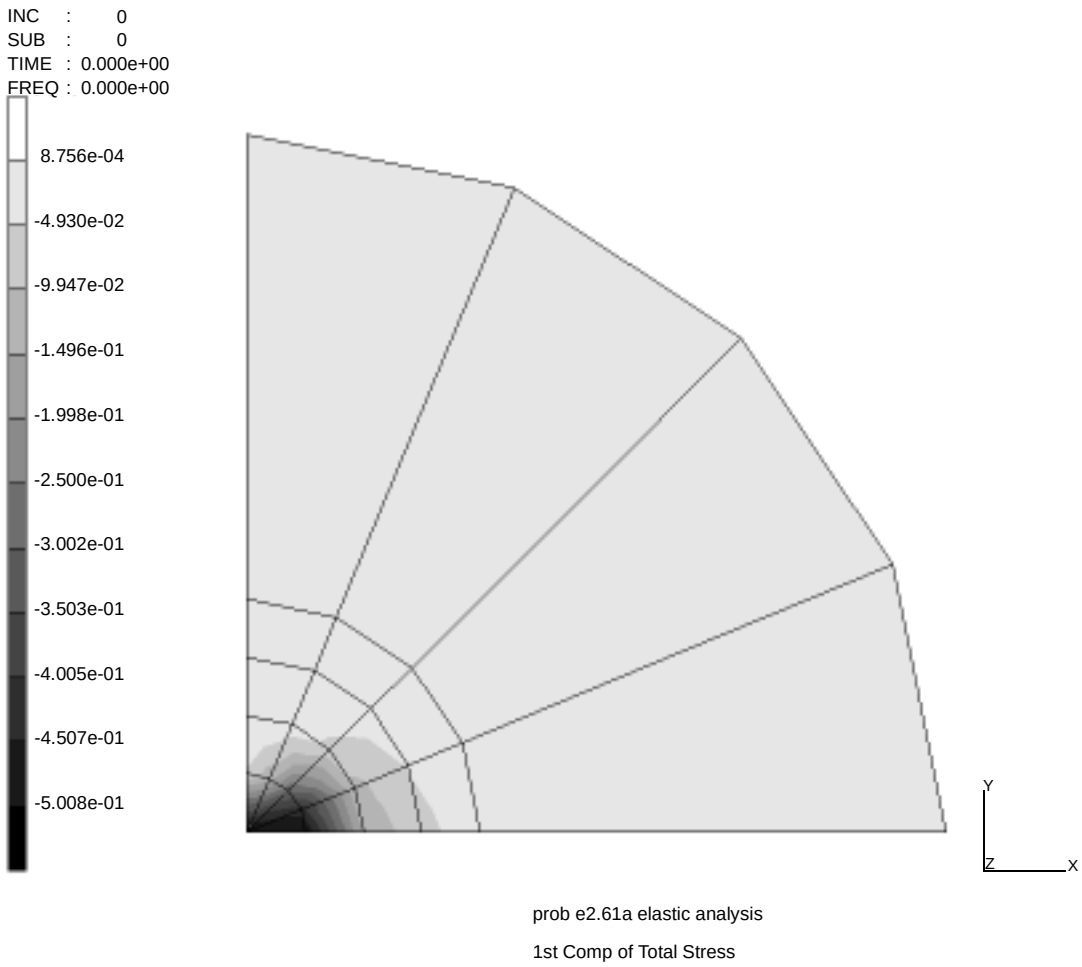

Figure 2.61-4 Stress Contours (Model A)

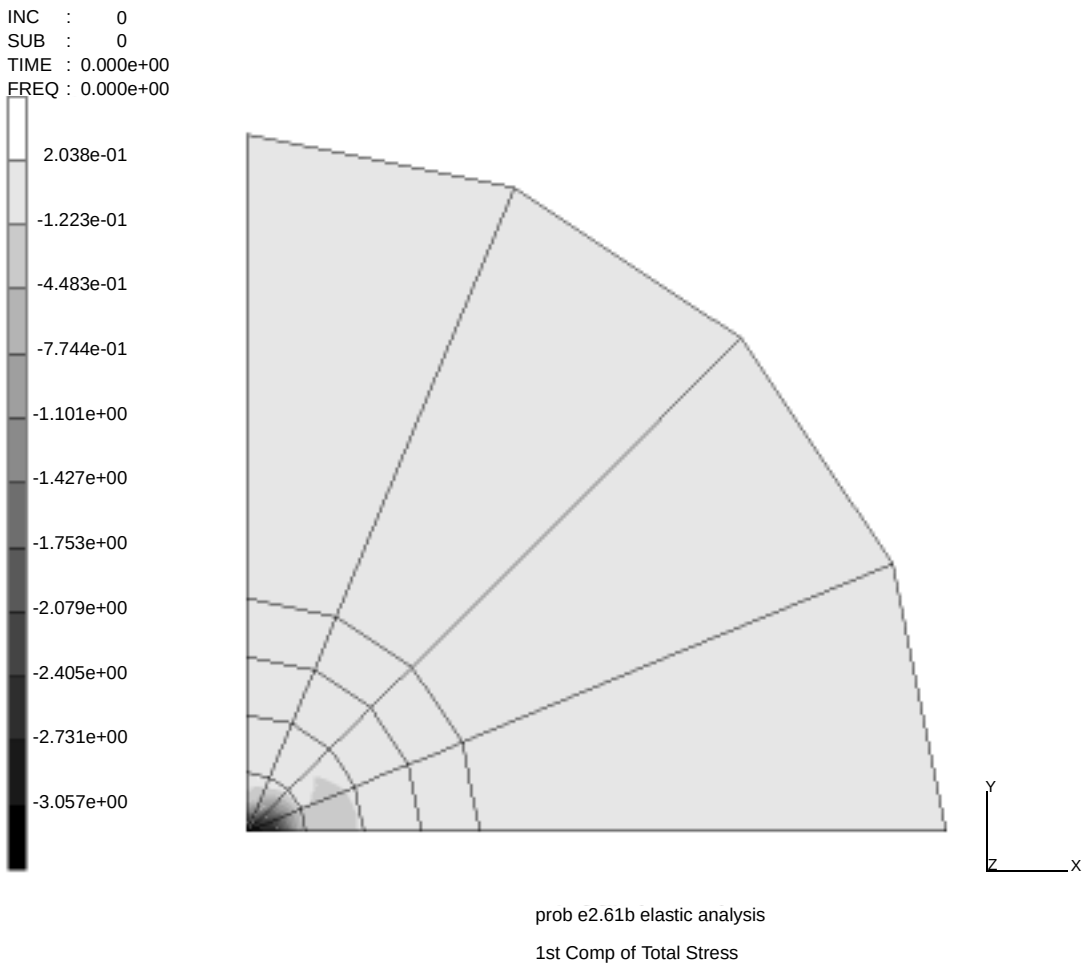

Figure 2.61-5 Stress Contours (Model B)

2.62 Truncated Spherical (Membrane) Shell Under Internal Pressure

A truncated spherical membrane shell subjected to internal pressure is analyzed using MARC membrane element type 18. The analysis is assumed to be linear elastic and demonstrates the use of MARC membrane elements.

Elements

Element type 18 is a 4-node linear, isoparametric membrane element, defined geometrically by the global Cartesian coordinates of the nodes associated with the elements. Stresses and strains are given in a local orthogonal surface coordinate system and a state of plane stress is assumed for these elements. These elements have no bending stiffness.

Model

As shown in Figure 2.62-1, due to symmetry, a 10 element mesh is used for modeling the truncated spherical membrane shell. These elements have no bending stiffness. The model is constrained along edges to ensure symmetry conditions.

Geometry

For the membrane elements, EGEOM1 is used to input the thickness of the element. A thickness of 2 inches is assumed in this analysis.

Material Properties

All elements are assumed to have constant properties. A Young's modulus of 21.8E6 psi and a Poisson's ratio of 0.32 are chosen for the model.

Loading

Internal pressure of 1.0 psi is applied to elements 1 to 10. The load type for uniform pressure is 2.

Boundary Conditions

Edges of the model are constrained (1) for the simulation of fixed support at top and bottom of the model and (2) for ensuring the symmetric conditions in the analysis.

Fixed support	:	u = v = w = 0	at nodes 1, 12, 11, 22
Symmetry	:	w = 0	at nodes 1 through 11
		v = 0	at nodes 12 through 22

Transformation

The UTRANS user subroutine is used to define a transformation matrix for nodes along the 30-degree line. The UTRANFORM model definition option is needed for input of the node numbers to be transformed. The node numbers are 12 to 22 for the model.

Results

The deformed mesh is shown in Figure 2.62-2.

Parameters, Options, and Subroutines Summary

Example e2x62.dat:

Parameters	Model Definition Options
ELEMENTS	CONNECTIVITY
END	COORDINATES
SIZING	DIST LOADS
TITLE	END OPTION
	FIXED DISP
	GEOMETRY
	ISOTROPIC
	POST
	PRINT CHOICE
	UTRANFORM

User subroutine in u2x62.f:

UTRANS

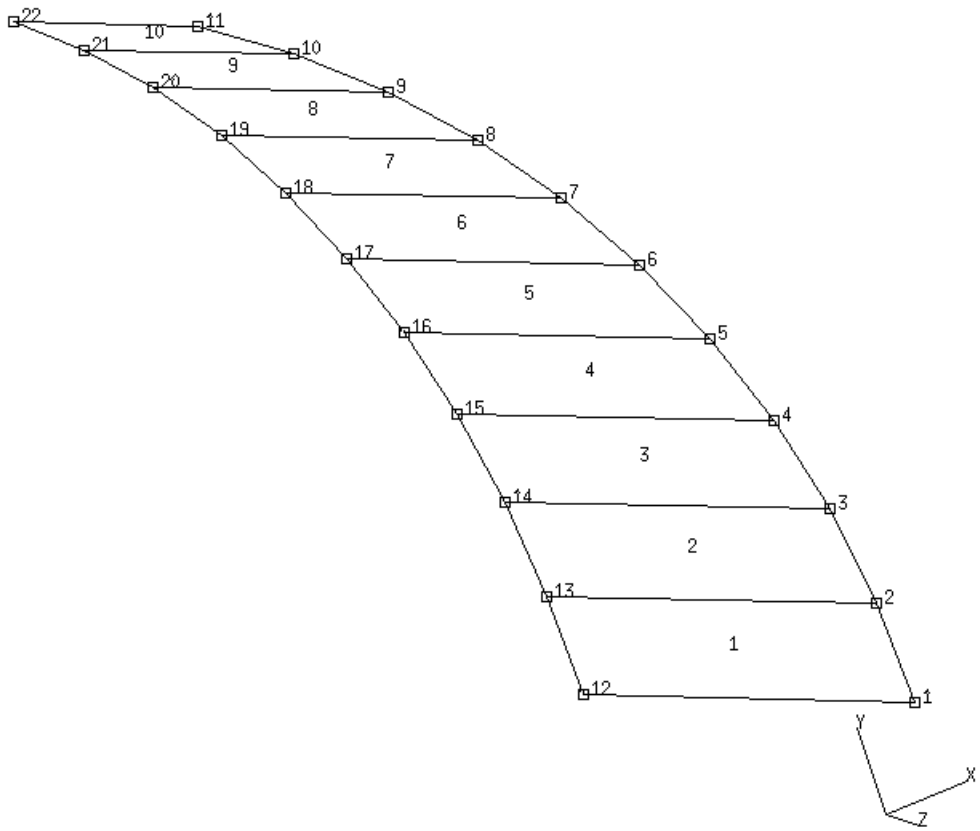

Figure 2.62-1 Membrane Structure

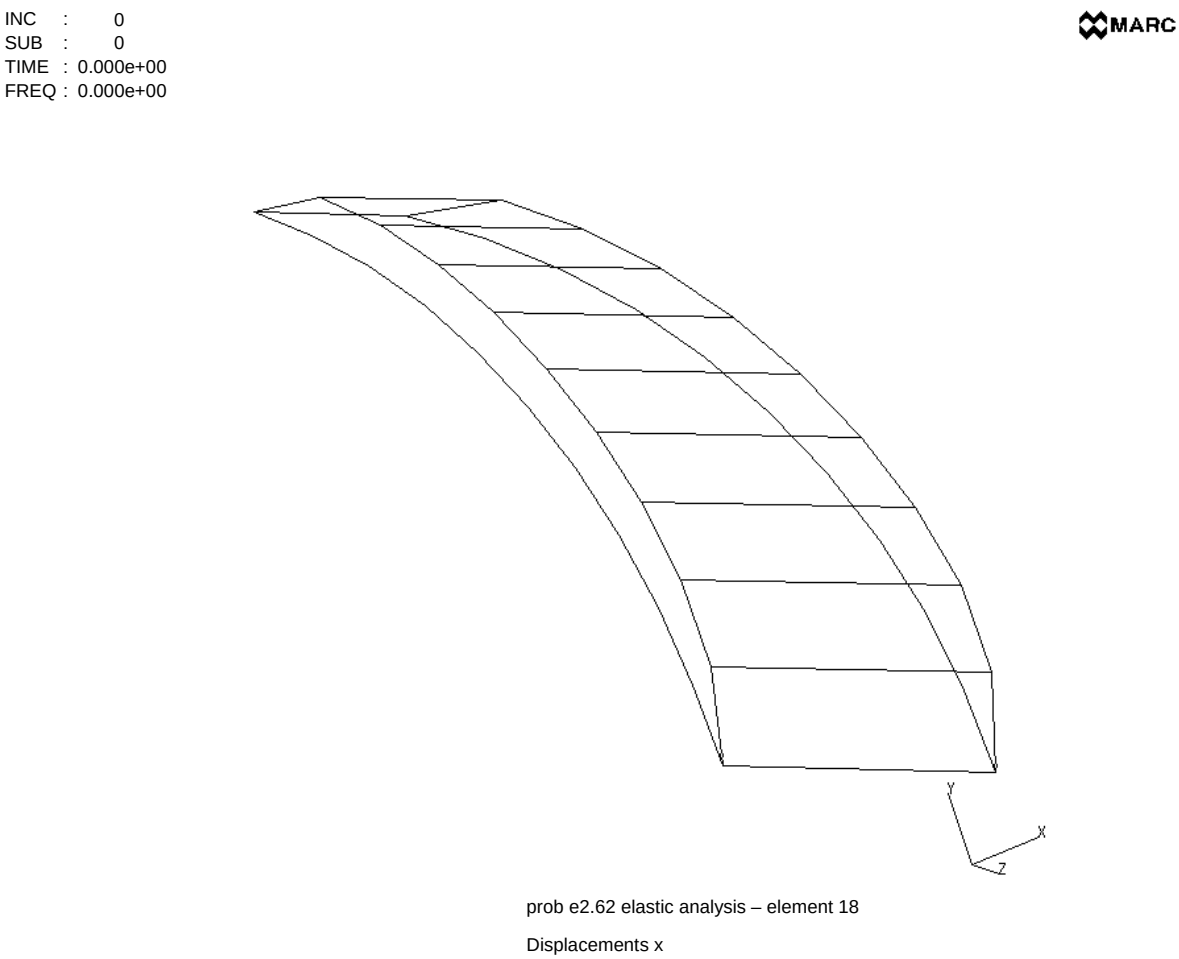

Figure 2.62-2 Deformed Mesh

2.63 J-Integral Evaluation Example using Delorenzi's Method

This example illustrates the use of the DeLorenzi method [1] to evaluate J-integral values in MARC for a double edge notched (DEN) specimen. In order to be able to compare the calculated J and K values with those obtained by means of the stiffness derivative technique [2] (J-INT option in MARC), the same problem as in 2.22 is analyzed.

This problem consists of a DEN specimen under axial tension loading. In addition, the problem of a DEN specimen with pressurized crack surfaces is analyzed to demonstrate the ability of the DeLorenzi method to obtain path-independent J-values for cracked structures subject to mechanical loads in the vicinity of the crack tip.

This problem is modeled using the two techniques summarized below.

Data Set	Element Type(s)	Number of Elements	Number of Nodes	Differentiating Features
e2x63a	27	32	107	
e2x63b	27	32	107	Pressure on crack surface

Element

Element type 27 is a plane-strain quadrilateral element. There are eight nodes and two degrees of freedom at each node.

Model

Only a quadrant of the model is used because of obvious symmetries. A second COORDINATES block is used to move the side nodes of the crack tip elements to the 1/4 points (1/4 of the way along the sides from the crack tip to the opposite face of the element).

Geometry

No geometry is specified.

Material Properties

Young's modulus is 30 x 10^6 psi and Poisson's ratio is 0.3.

Loading

The loading of the DEN specimen under axial tension is specified as a uniform negative pressure of 100 psi on the appropriate faces of the end elements. For the specimen with pressurized crack surfaces, a uniform pressure of 100 psi is applied on the crack surface.

Lorenzi

One of the main differences between the differential stiffness technique and the modified DeLorenzi approach [3] as implemented in MARC is that no numerical differentiation is performed to calculate the change in strain energy. This implies that the obtained J-values (that is, energy release per crack extension) are independent of the value of the crack extension that is specified. The crack extension is specified in a similar manner as is the case with the J-INTEGRAL option. However, it is not necessary to assure that the differential movements are sufficiently small without introducing round-off difficulties. For this reason, a crack tip movement of 1. was used.

Similar to the J-INTEGRAL option of problem 2.22, three different paths have been specified in order to analyze the path independently. It should be noted that in the DeLorenzi technique, an integral over the region of deformed elements as well as an integral over the region of translated rigid elements is numerically evaluated. In case no initial strain effects (for example, thermal and creep strains) nor inertia effects nor mechanical loads are present in the rigid region, only nonzero nodal movements of the deformed elements as well as the list of deformed elements needs to be specified. In case of the pressurized crack problem, the nodal movements of the rigid elements as well as the list of rigid elements are additionally specified in order to incorporate the contribution from the distributed pressure loads.

Results

MARC provides an output of the strain energy difference. This must be normalized by the crack opening area to obtain the value of J. Since this specimen is of unit thickness, the crack opening area is Wa, where Wa is the crack extension. The mesh uses symmetry about the crack line, so that the strain energy change in the actual specimen is twice that printed out. Finally, since this is a plane strain, mode I problem, the J-integral can be immediately converted to K, the stress intensity factor, by the relation:

$$K = \sqrt{\frac{EJ}{1-\nu^2}}$$

The results are summarized in Table 2.63-1.

It is clear from these results that the path independence is well reproduced, and that the error in the solution for K is quite small. It should be noted that the accuracy is identical as obtained with the J-INTEGRAL option with an appropriate crack movement.

The results for the problem of the DEN-specimen with pressurized crack surfaces are summarized in Table 2.63-1. Because of the superposition principle, the K value for an axially loaded DEN-specimen is identical to the K value of the same specimen with pressurized crack

surfaces, where the magnitude of this pressure loading equals the stress level in the noncracked structure at the position where the crack is located. From the results of Table 2.63-1, it is clear that the evaluated K values are nearly path independent and that they only differ marginally from the theoretical results.

Table 2.63-1 J-Integral Evaluation Results for DEN-Specimen Under Axial Tension

	Move Tip Only	**Move First Ring of Elements**	**Move Second Ring of Elements**
Strain energy change given in program (ΔU)	6.717×10^{-2}	6.695×10^{-2}	6.689×10^{-2}
J-Integral Δu/Δ1	1.343×10^{-1}	1.3390×10^{-1}	1.3378×10^{-1}
$K = \sqrt{\frac{EJ}{1-\nu^2}}$	665.5	664.4	664.1
$K_I/\sigma_{net}\sqrt{l}$	1.062	1.050	1.050
cf 1.028 [4]	+2.4%	+2.2%	+2.2%

Table 2.63-2 J-Integral Evaluation Results for DEN-Specimen with Pressurized Cracks

	Move Tip Only	**Move First Ring of Elements**	**Move Second Ring of Elements**
Strain energy change given in program (Δu)	5.9402×10^{-2}	5.8148×10^{-2}	5.8153×10^{-2}
J-Integral Δu/Δ1	1.1880×10^{-1}	1.1630×10^{-1}	1.1631×10^{-1}
$K = \sqrt{\frac{EJ}{1-\nu^2}}$	625.8	619.2	619.2
$K_I/\sigma_{net}\sqrt{l}$	1.979	1.958	1.958
cf 2.056 (=1.028)	-3.7%	-4.8%	-4.8%

References

1. DeLorenzi, H.G., "On the energy release rate and the J-integral for 3D crack configurations", *Inst. J. Fracture*, Vol. 19, 1982, pp.183-193.
2. Parks, D.M, "A Stiffness Derivative Finite Element Technique for Determination of Elastic Crack Tip Stress Intensity Factors", *Int. J. Fracture*, Vol. 10, no. 4, December 1974, pp. 487-502.
3. Peeters, F.J.H. and Koers, R.W.J., "Numerical Simulation of Dynamic Crack Propagation Phenomena by Means of the Finite Element Method", Proceedings of the 6th European Conference on Fracture, ECF6, Amsterdam, The Netherlands, June 15-20, 1986.
4. Bowie, I.L., "Rectangular Tensile Sheet With Symmetric Edge Cracks," *J. Applied Mechanics*, Vol. 31, 1964, pp. 208-212.

Parameters, Options, and Subroutines Summary

Example e2x63a.dat:

Parameters	Model Definition Options
ELEMENTS	CONNECTIVITY
END	COORDINATES
SIZING	DIST LOADS
TITLE	END OPTION
	FIXED DISP
	ISOTROPIC
	LORENZI
	PRINT CHOICE

Example e2x63b.dat:

Parameters	Model Definition Options
ELEMENTS	CONNECTIVITY
END	COORDINATES
SIZING	DIST LOADS
TITLE	END OPTION
	FIXED DISP
	ISOTROPIC
	LORENZI
	PRINT CHOICE

2.64 A Clamped Plate Modeled with Brick Elements

In this problem, a thin plate is modeled with brick elements to demonstrate the benefit of the assumed strain element formulation. In general, the lower-order elements do not behave well under bending because of their inability to fully represent linear variations in shear stress. The assumed strain elements reduce this error.

Model

Sixteen elements are used to model one quarter of the plate as shown in Figure 2.64-1. The square plate total dimensions are 2 inches and the thickness is 0.01 inch. Element type 7, the eight-node brick element, is used.

Geometry

In 2.64b, the third field of the GEOMETRY option is set to 1. This invokes the assumed strain option.

Material Properties

The material is elastic with a Young's modulus of 1.7472E7 lbf/in^2 and a Poisson ratio of .3.

Loading

Two independent analyses are performed by including the ELASTIC parameter. In increment zero, a uniformly distributed pressure of 1.E-4 is applied on the top surface. In increment one, a point load of magnitude $4x10^{-4}$ is applied at the center of the plate. Only one quarter of the load is applied due to symmetry.

Results

The analytic solution for the maximum displacement of the plate is given by:

Distributed load $y = 0.138\ da^4/Et^3$
Point Load $y = 0.0056\ Pa^2/D$
$D = Et^3/12(1-v)$

The results can be summarized as:

	Distributed Load	Point Load
Analytic	$1.234x10^{-4}$	$4.30x10^{-6}$
Conventional	$7.800x10^{-9}$	$3.59x10^{-8}$
Assumed Strain	$1.258x10^{-6}$	$5.44x10^{-6}$

The conventional element gives very poor behavior in bending, when only a single element is used through the thickness. You should also observe that while traditional isoparametric elements are always too stiff, this is not the case for the assumed strain elements.

Parameters, Options, and Subroutines Summary

Example e2x64a.dat:

Parameters	Model Definition Options	History Definition Options
ELASTIC	CONNECTIVITY	CONTINUE
ELEMENTS	COORDINATES	POINT LOAD
END	DIST LOADS	
SIZING	END OPTION	
TITLE	FIXED DISP	
	GEOMETRY	
	ISOTROPIC	
	POST	

Example e2x64b.dat:

Parameters	Model Definition Options	History Definision Options
ELASTIC	CONNECTIVITY	CONTINUE
ELEMENTS	COORDINATES	POINT LOAD
END	DIST LOADS	
SIZING	END OPTION	
TITLE	FIXED DISP	
	GEOMETRY	
	ISOTROPIC	
	POST	

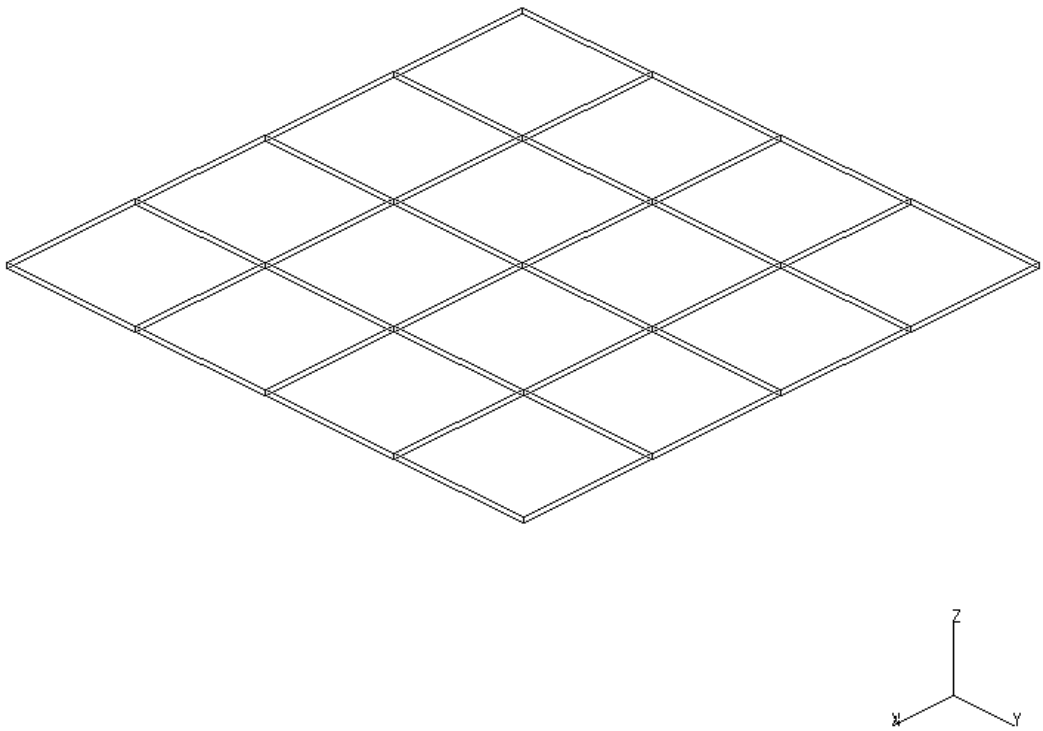

Figure 2.64-1 Clamped Plate Mesh

2.65 Use of Tying to Model a Rigid Region

This problem demonstrates the use of tying to model a rigid region. If large rotations/displacements occur, this is a nonlinear problem.

Model

The model is shown in Figure 2.65-1. Two rigid regions are included. The first represents a volume between the first and second block. The second is the surface enclosed by nodes 13, 14, 15, and 16. These are indicated by the cross-hatched regions. Element types 7 and 75 are used in this analysis.

Geometry

The shell is given a thickness of 0.01. This is element 3.

Material Properties

The material is elastic with a Young's modulus of 1000 and a Poisson's ratio of 0.3.

Loading

The bottom of the first cube is held fixed. A point load of 8 is applied to the top surface through the POINT LOAD and AUTO LOAD options.

Rigid Region

The two rigid regions are modeled using tying. An additional mode must be defined for each rigid region. The degrees of freedom associated with this node represent the rigid body rotations about this point. In the first rigid region, node 20 is used which has the same coordinate position as node 13. Tying type 80 is used to connect all of the other points associated with the rigid region to these two points.

Results

The displaced mesh is shown in Figure 2.65-2. The total displacements are on the order of 0.0. (Remember, the cubes have a length of one.)

Parameters, Options, and Subroutines Summary

Example e2x65.dat:

Parameters	Model Definition Options	History Definition Options
ELEMENTS	CONNECTIVITY	AUTO LOAD
END	CONTROL	CONTINUE
LARGE DISP	COORDINATES	POINT LOAD
SIZING	END OPTION	
TITLE	FIXED DISP	
	GEOMETRY	
	ISOTROPIC	
	POST	
	TYING	

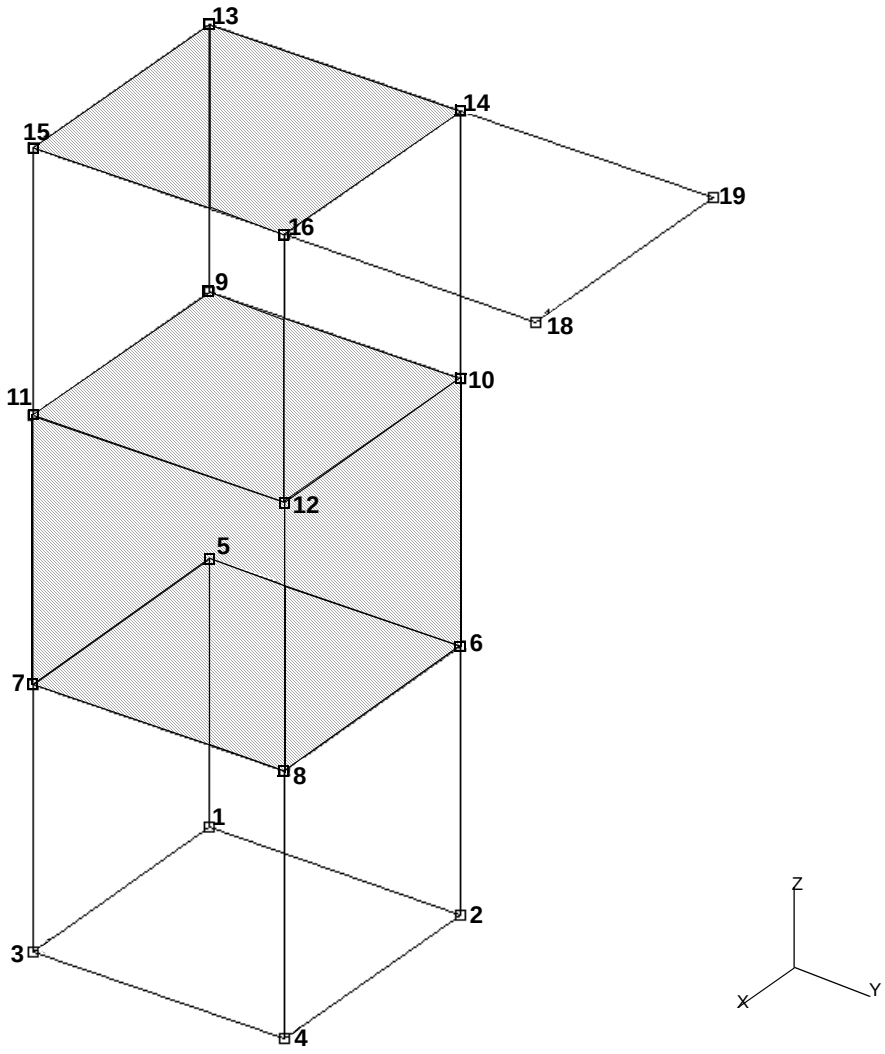

Figure 2.65-1 Mesh Showing Rigid Regions

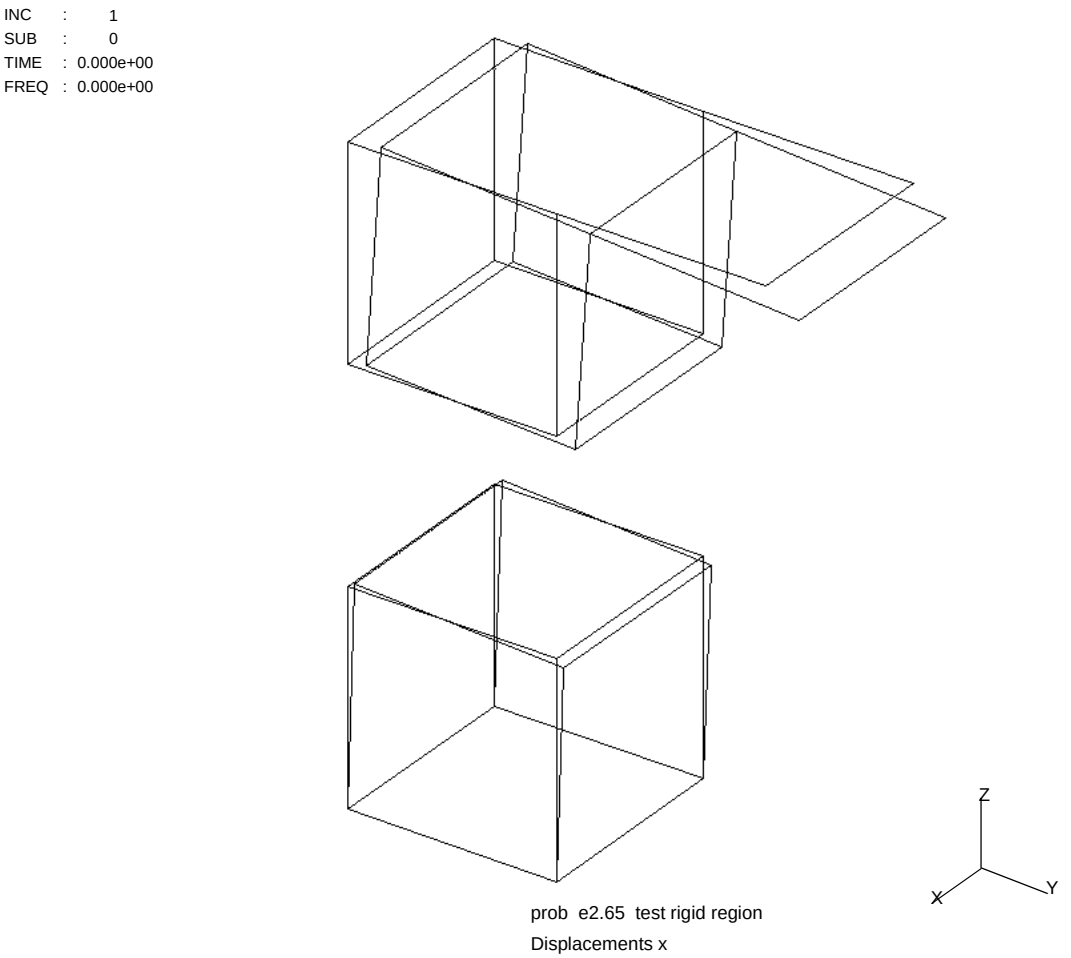

Figure 2.65-2 Deformations

2.66 Using Pipe Bend Element to Model Straight Beam or Elbow

This problem demonstrates the use of the elastic pipe bend element for modeling both a straight beam or an elbow.

Model

Two analyses are performed. Figure 2.66-1 shows a straight beam clamped at node 1 and a load placed at node 11. The beam is modeled using ten elements.

Figure 2.66-2 shows a 90° elbow section of radius 100 inches modeled using two elements. The elements are displayed as straight line segments. The elbow is clamped at node 1. Element type 31 is used in these models.

Geometry

In problem e2.66a, the BEAM SECT parameter is used to define a cross section of height 10 and width 1. The area = 10 in^2, I_{xx} = 83.33 in^4, I_{yy} = .8333 in^4, K = 84.1663 in^2. The local x direction is given through the GEOMETRY option as being in the global x direction.

In problem 2.66a, the pipe is given a radius of 10 inches and a thickness of 1 inch. The radius of curvature of the elbow is given in the third field as 100 inches.

Material Properties

The pipe is made of steel with a Young's modulus of 30.E6 psi and a Poisson ratio of .3.

Loading

In problem 2.66a, a tip load of magnitude $1000\sqrt{3}$ pounds is applied with components of 1000 pounds in each direction at node 11. In problem 2.66b, an out-of-plane load of 100 pounds is applied. In increment one, an internal pressure of 3,000,000 psi is applied.

Results

For problem 2.66a, the analytic solution for the tip deflection is:

$$y = \frac{1}{3}\ \frac{w1^3}{EI}$$

Hence:

	y	z
Analytic	13333.	133.33
Calculated	13330.	133.34

which is exact.

For problem 2.66b, the solution is compared to a model made up of 9 elements type 14:

	Increment zero	
element 31	2 elements	w = 1.89E-3
element 14	9 elements	w = 1.317E-3

You can observe that the element 31 is more flexible when no internal pressure exists.

In increment one, a large internal pressure is applied which stiffens the elbow. The solution then becomes:

element 31	2 elements	w = 1.363E-3

which agrees well with the element 14 results.

Parameters, Options, and Subroutines Summary

Example e2x66a.dat:

Parameters	Model Definition Options
BEAM SECT	CONN GENER
ELEMENTS	CONNECTIVITY
END	COORDINATES
SIZING	END OPTION
TITLE	FIXED DISP
	GEOMETRY
	ISOTROPIC
	NODE FILL
	POINT LOAD

Example e2x66b.dat:

Parameters	Model Definition Options	History Definition Options
ELEMENTS	CONNECTIVITY	CONTINUE
END	COORDINATES	DIST LOADS
SIZING	DIST LOADS	POINT LOAD
TITLE	END OPTION	
	FIXED DISP	
	GEOMETRY	
	ISOTROPIC	
	POINT LOAD	

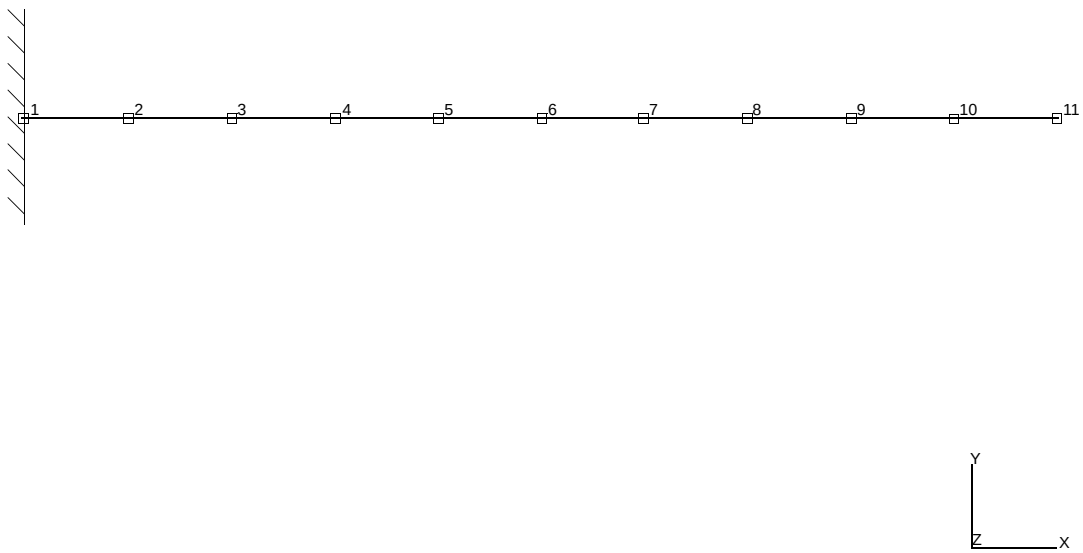

Figure 2.66-1 Straight Beam Using Element 31

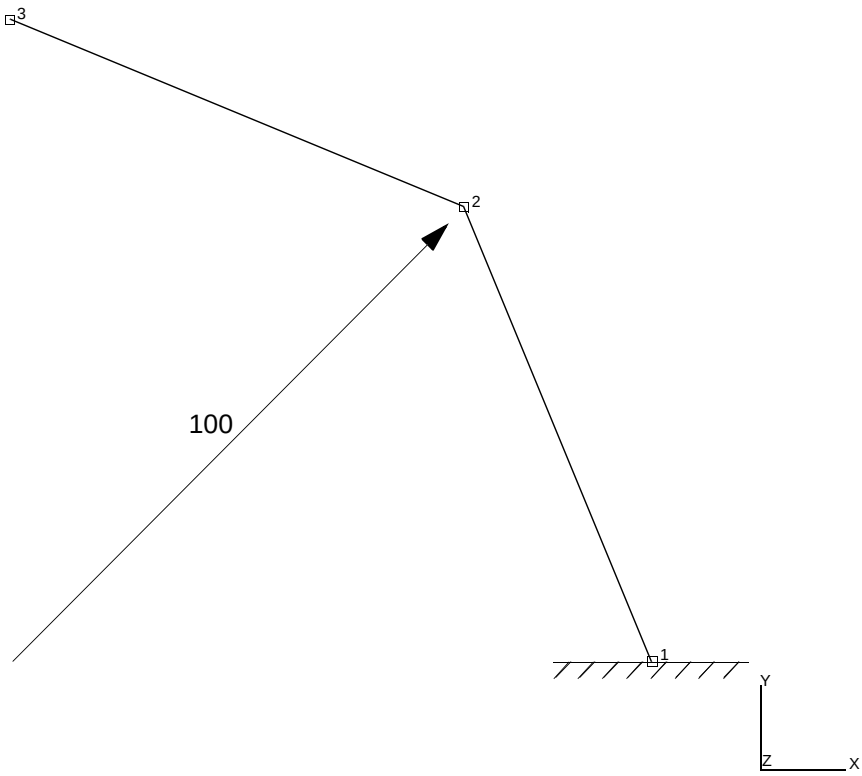

Figure 2.66-2 Pipe Bend Using Element 31

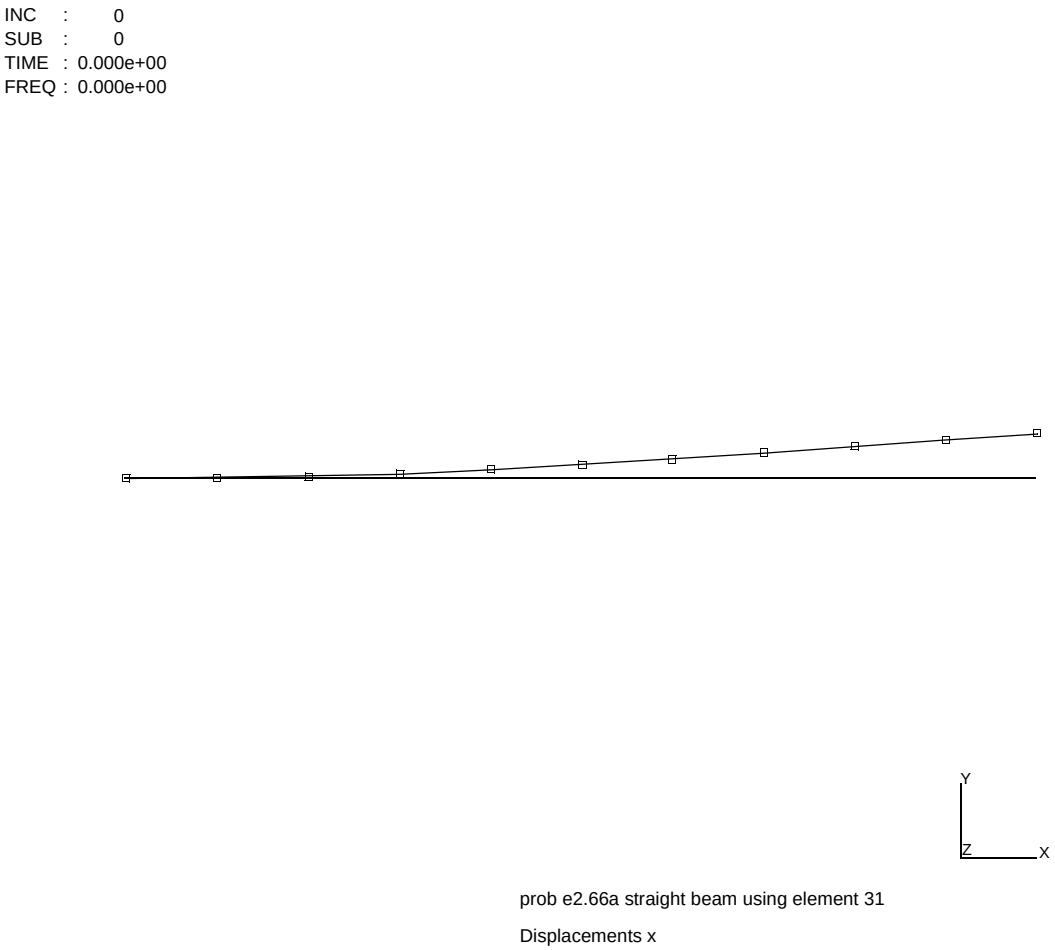

Figure 2.66-3 Deformed Beam

2.67 Cantilever Beam Analyzed using Solid Elements

A cantilever beam is analyzed subjected to a point load on the end. The material behavior is considered elastic. Three element types are used: a parabolic brick (type 21) and two tetrahedron element types 127 and 130, respectively.

This problem is modeled using the two techniques summarized below.

Data Set	Element Type(s)	Number of Elements	Number of Nodes
e2x67a	127	96	225
e2x67b	130	96	225

Elements

The brick and both tetrahedral elements are second-order isoparametric elements. The brick element type 21 has 20 nodes while the tetrahedral elements have 10 nodes. Element type 130 is similar to type 127 but with a Herrmann formulation.

Model

A two inch long beam with a 1 inch square cross section is modeled with 16 brick elements and 96 tetrahedrons. The mesh using the brick elements is shown in Figure 2.67-1. The origin of the axis is on the neutral axis of the beam with the z-axis in the longitudinal direction.

Material Properties

The material for all elements is treated as elastic with Young's modulus of 30.0E+06 psi and a Poisson's ratio of 0.0.

Loads and Boundary Conditions

Two point loads are applied at the free end of the cantilever beam with magnitudes of 1000 lbf directed in the positive x and y directions. At the fixed end (the z = 2 plane), all z displacements are fixed to 0.0, and the x and y displacements along the y = 0 and x = 0 axis are fixed to 0.0.

Results

The exact solution may be expressed as:

$$\sigma_{zz} = -\{[M_y I_x - M_x I_{xy}]x + [M_x I_y - M_x I_y]y\} / (I_x I_y - I_{xy}^2)$$

Due to the symmetry of the cross section, $I_x = I_y = I$ and $I_{xy} = 0$. The symmetry in load gives $M_x = - M_y = PL$. The maximum bending stress in the z = 2 plane becomes:

$$\sigma_{zz} = \frac{-PL(x + y)}{I}$$

and the maximum component of displacement becomes:

$$u = v = \frac{-PL^3}{3(EI))}$$

Hence the neutral surface is the x + y = 0, plane that passes through the centroid of the cross section. Comparing the results we have:

	max $\lvert\sigma_{zz}\rvert$	**u(0,0,0)**
Theory	24.00 ksi	1.067-03 in
Type 21	24.15 ksi	1.207-03 in
Type 127	19.36 ksi	1.250-03 in
Type 130	19.36 ksi	1.250-03 in

Parameters, Options, and Subroutines Summary

E2x67a.dat:

Parameters	**Model Definition Options**
ELEMENTS	CONNECTIVITY
END	CONTROL
SIZING	COORDINATES
TITLE	END OPTION
	FIXED DISP
	ISOTROPIC
	OPTIMIZE
	POINT LOAD
	POST

E2x67b.dat:

Parameters	Model Definition Options
ALIAS	CONNECTIVITY
ELEMENTS	CONTROL
END	COORDINATES
SIZING	END OPTION
TITLE	FIXED DISP
	ISOTROPIC
	OPTIMIZE
	POINT LOAD
	POST

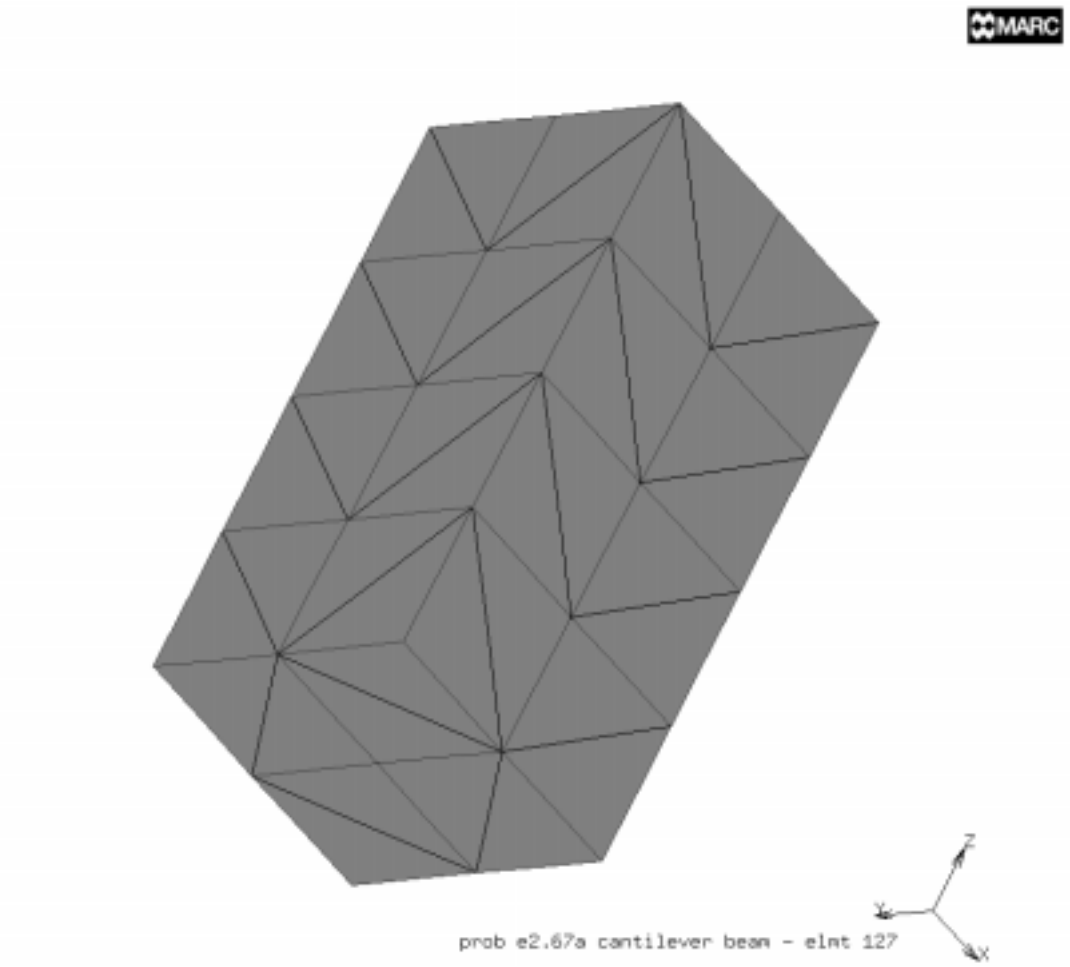

Figure 2.67-1 Model

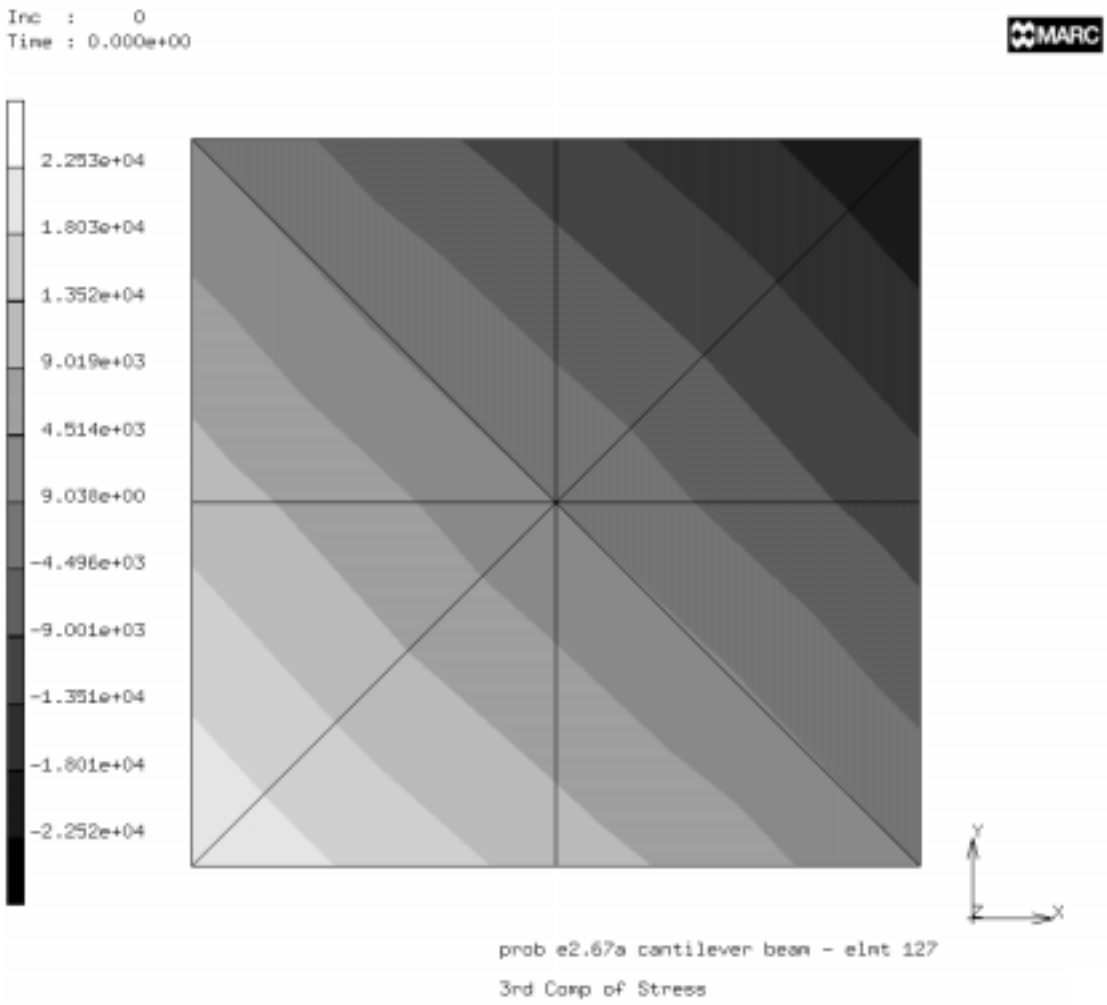

Figure 2.67-2 Bending Stress Element 127

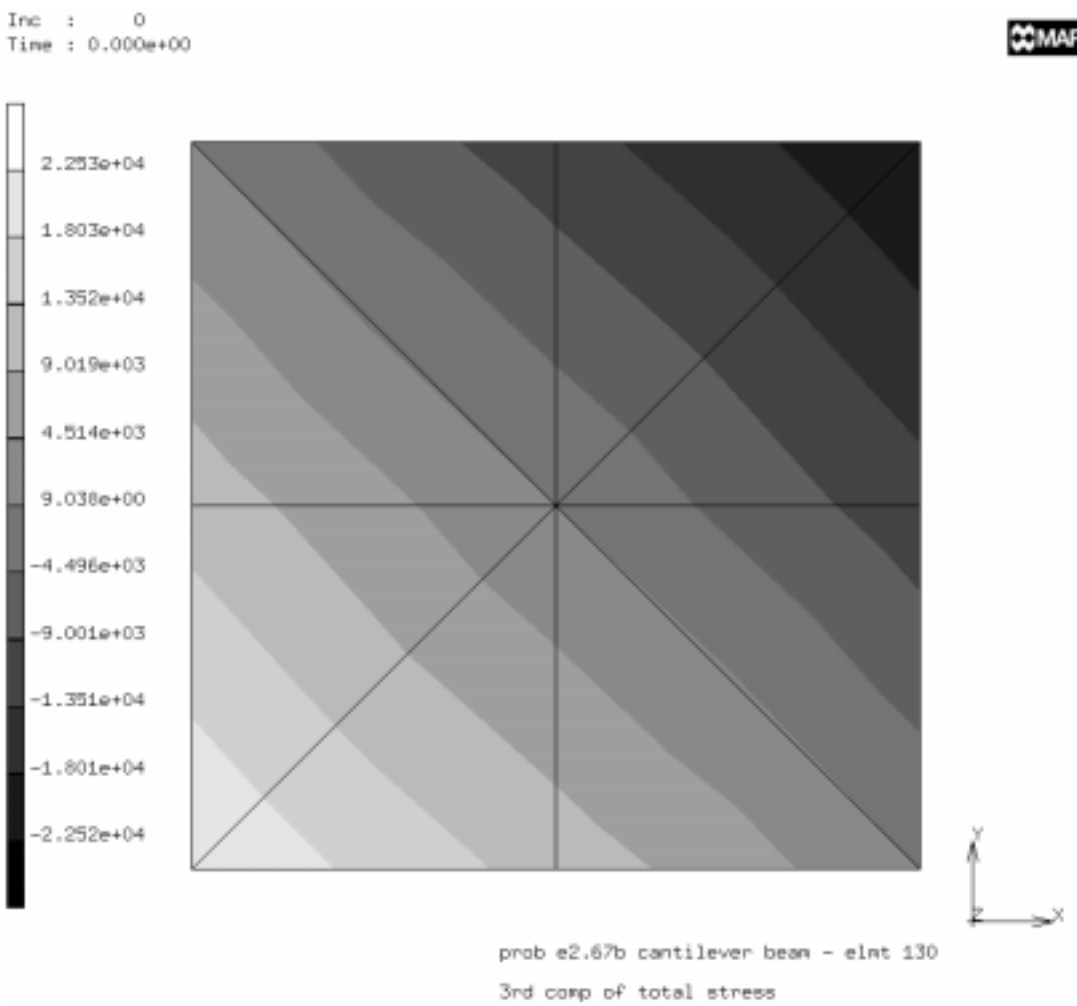

Figure 2.67-3 Bending Stress Element 130

2.68 Linear Analysis of a Hemispherical Cap Loaded by Point Loads

A hemispherical cap with an 18° hole is loaded by two inward and two outward forces (see Figure 2.68-1).

Element

Library element type 49, a 6-node triangular thin shell element, is used.

Model

The dimensions of the cap and the finite element mesh are shown in Figure 2.68-1. Based on symmetry considerations, only one quarter of the cap is modeled. The mesh is composed of 128 elements and 289 nodes.

Material Properties

The material is elastic with a Young' modulus of 6.835×10^{7} N/mm^2 and a Poisson's ratio of 0.3.

Geometry

A uniform thickness of 0.04 mm is assumed. In the thickness direction, three layers are chosen using the SHELL SECT parameter. Notice that for this problem, which is dominated by nearly inextensional bending, the initial curvature of the elements is important. This means that the default setting for the fifth geometry field must be used.

Loading

The loading consists of 2 inward and 2 outward point loads with a magnitude of 20 N.

Boundary Conditions

Symmetry conditions are imposed on the edges x = 0 ($u_x = 0$, $\varphi = 0$) and y = 0 ($u_y = 0$, $\varphi = 0$). Notice that the rotation constraints only apply for the midside nodes. To suppress the remaining rigid body motion for node 278, the z-displacement is fixed.

Results

The reference solution for the displacements of the points of application of the load is 0.93 (see, for example, J. C. Simo, D. D. Fox, and M. S. Rifai, "On a stress resultant geometrically exact shell model, Part II: The linear theory: computational aspects", *Comp. Meth. Appl. Mech. Eng.*, 79, 21-20, 1990). The results found by MARC (0.93027 for the inward displacement and 0.02708 for the outward displacement) are in close agreement with the reference solution. Finally Figure 2.68-2 shows the equivalent von Mises stress for layer 1.

Parameters, Options, and Subroutines Summary

Example e2x68.dat:

Parameters	Model Definition Options
ELEMENTS	CONNECTIVITY
END	COORDINATES
SHELL SECT	END OPTION
SIZING	FIXED DISP
TITLE	GEOMETRY
	ISOTROPIC
	NO PRINT
	OPTIMIZE
	POINT LOAD
	POST
	SOLVER

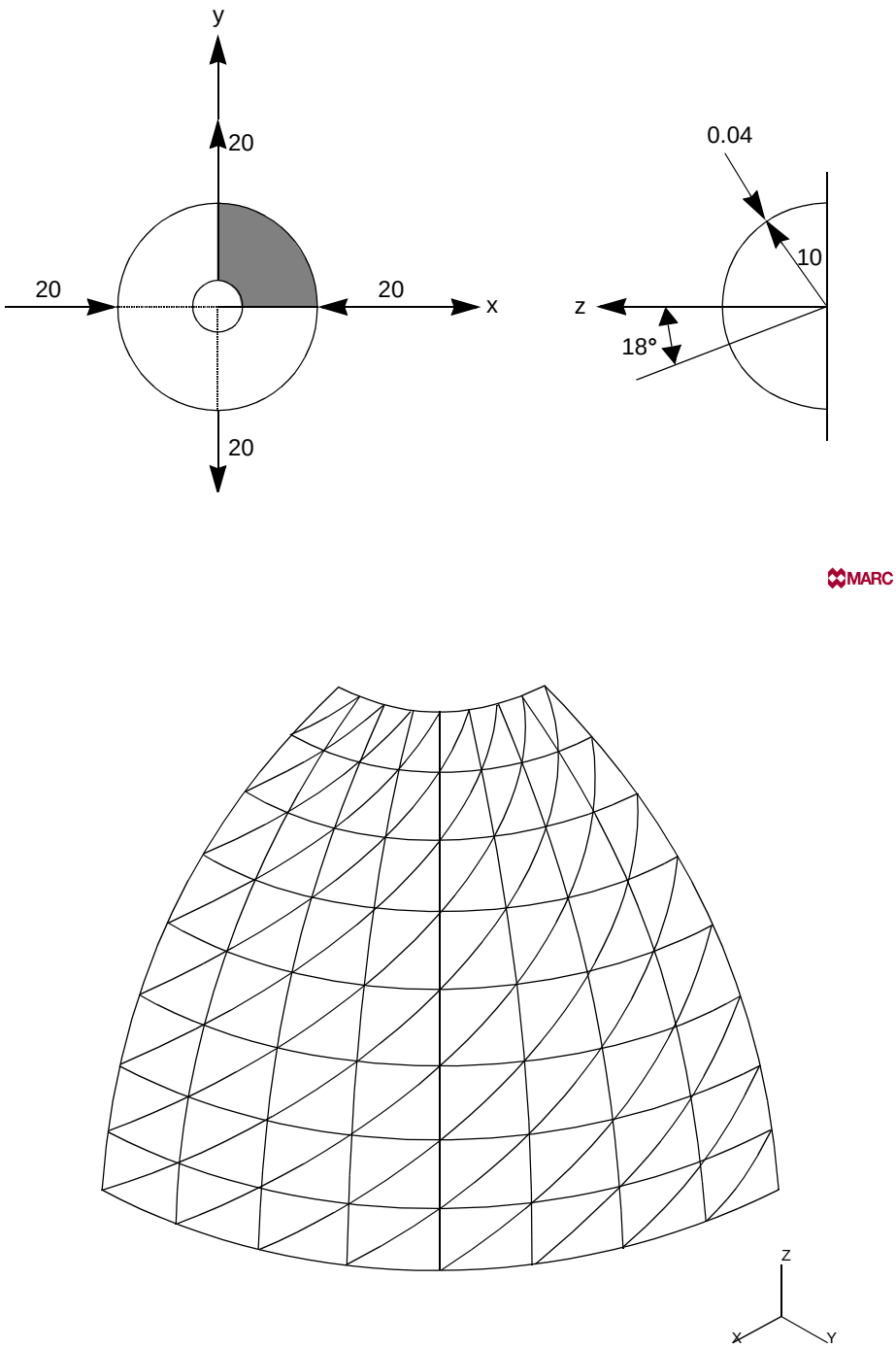

Figure 2.68-1 Hemispherical Cap, Geometry, Loading, and Finite Element Mesh

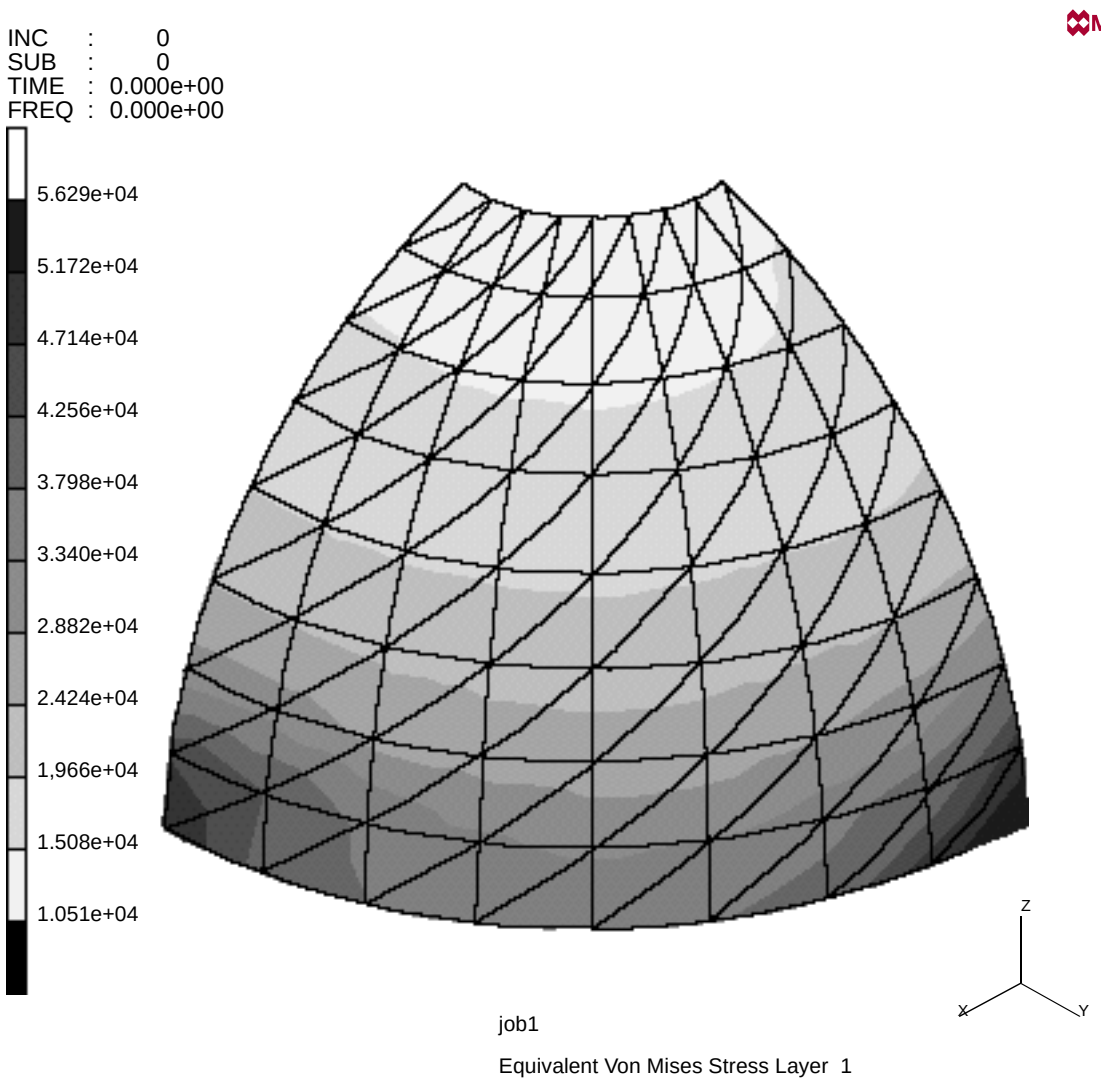

Figure 2.68-2 Stress Contours Layer 2 (Equivalent von Mises Stress)

2.69 Pipe Bend with Axisymmetric Element 95

This problem demonstrates the use of the axisymmetric element with bending (element 95) to model the flexure of a straight pipe. Units [N, mm].

The quadrilateral element 95 represents the cross-section of a ring in the r,z symmetry plane at $\theta = 0°$. A pure axisymmetric deformation induces displacements u,v in the z,r plane which remain constant for θ ranging from 0° to 360° degrees. A flexural deformation in the z,r plane induces different displacements u,v at the opposite sections; $\theta = 0°$ and $\theta = 180°$ along the ring. A twist in the ring induces a circumferential displacement w, equal at every θ, and assigned to the position $\theta = 90$.

Element

Thus, five degrees of freedom are associated to each node:

u,v displacements, at 0° and 180°, respectively
w circumferential displacement at 90° angle

Element 95 is integrated numerically in the circumferential direction. The number of integration points (odd number) is given on the SHELL SECT parameter. The points are equidistant on the half circumference. See Figure 2.69-1.

Models

The FEM model represents the longitudinal section of the pipe in the z,r plane (x,y plane for Mentat) is shown in Figure 2.69-2. The FEM mesh consists of 80 type 95 elements for a total of 123 nodes as shown in Figure 2.69-3.

Material Properties

The Young's modulus of the material is 2.0E5 N/mm^2; the Poisson's ratio is .3.

Loading

A distributed load, P = 100 N/mm^2, is assigned at increment 1, at elements 79 and 80. The load acts as a pressure in the longitudinal direction and is distributed with a sinusoidal variation along θ between 0° and 180° and producing a bending moment around z;

$M = \left(2 \cdot \left(P \cdot \frac{\pi}{2} \cdot t \cdot R\right) \cdot R\right) = 2 \cdot 1.57E5 \cdot 100 = 3.1416E7$ applied at the free edge of the beam. See Figure 2.69-4.

Results

The analytic solution is compared with the MARC, element 95, solution in Table 2.69-1.

Table 2.69-1 Analytical Solution

	Analytic	MARC
$Y_{max} = \frac{Ml^2}{2EJ}$	0.624 mm	0.636 mm (Node 122)
$\sigma_{xx} = \frac{Mz}{J}$ $J = \frac{\pi}{4}(R_e^4 - R_i^4) = 3.149E7\ mm^4$	99.73 N/mm^2	100.5 N/mm^2 (Element 80, Node 122)

At increment 0, the y displacement difference is of the order of 1.9% while the stress σ_{xx} value difference is of the order of 0.7%.

Figure 2.69-5 shows the distribution of the y deflection along the axis of the pipe and the deformed shape under flexural load.

Note: Only the deformed shape at 0° can be visualized with the Mentat graphics program even if all the elements variables can be visualized. The displacements and all the nodal quantities referring to 180° can be seen on the output file.

Parameters, Options, and Subroutines Summary

Example e2x69.dat:

Parameters

ELEMENTS
END
SHELL SECT
SIZING
TITLE

Model Definition Options

CONNECTIVITY
COORDINATES
DIST LOADS
END OPTION
FIXED DISP
ISOTROPIC
POST
PRINT ELEM

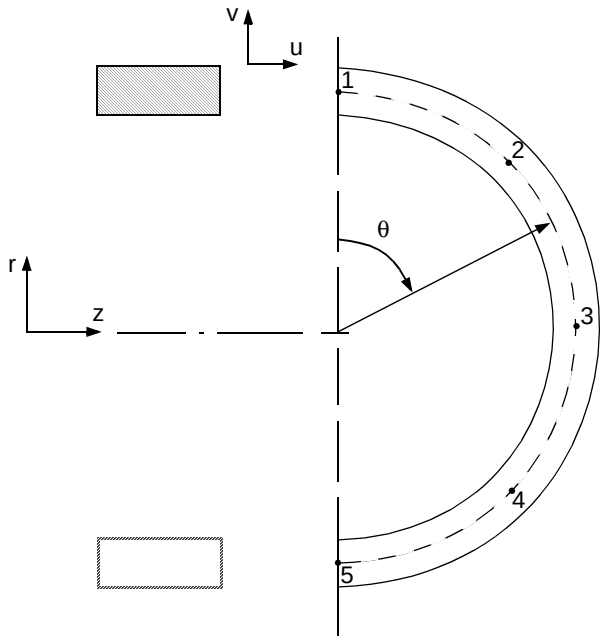

Figure 2.69-1 Element 95 Layer Points

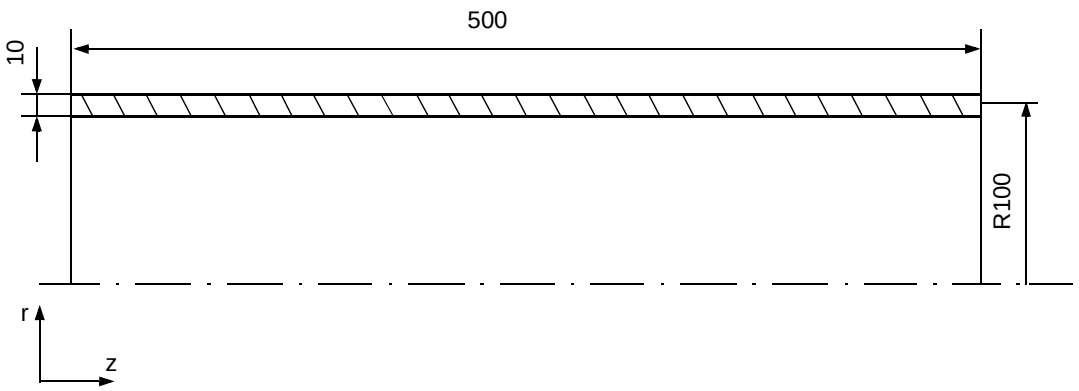

Figure 2.69-2 Longitudinal Section of the Pipe

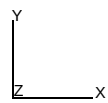

Figure 2.69-3 FEM Model of the Longitudinal Section of the Pipe

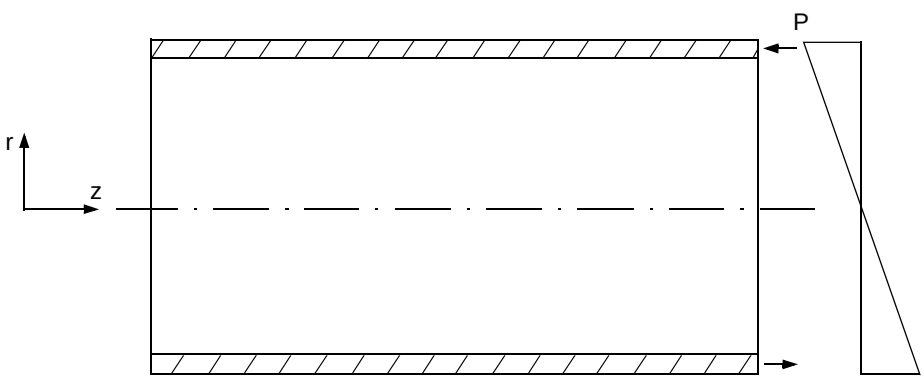

Figure 2.69-4 Distribution of the Longitudinal Pressure

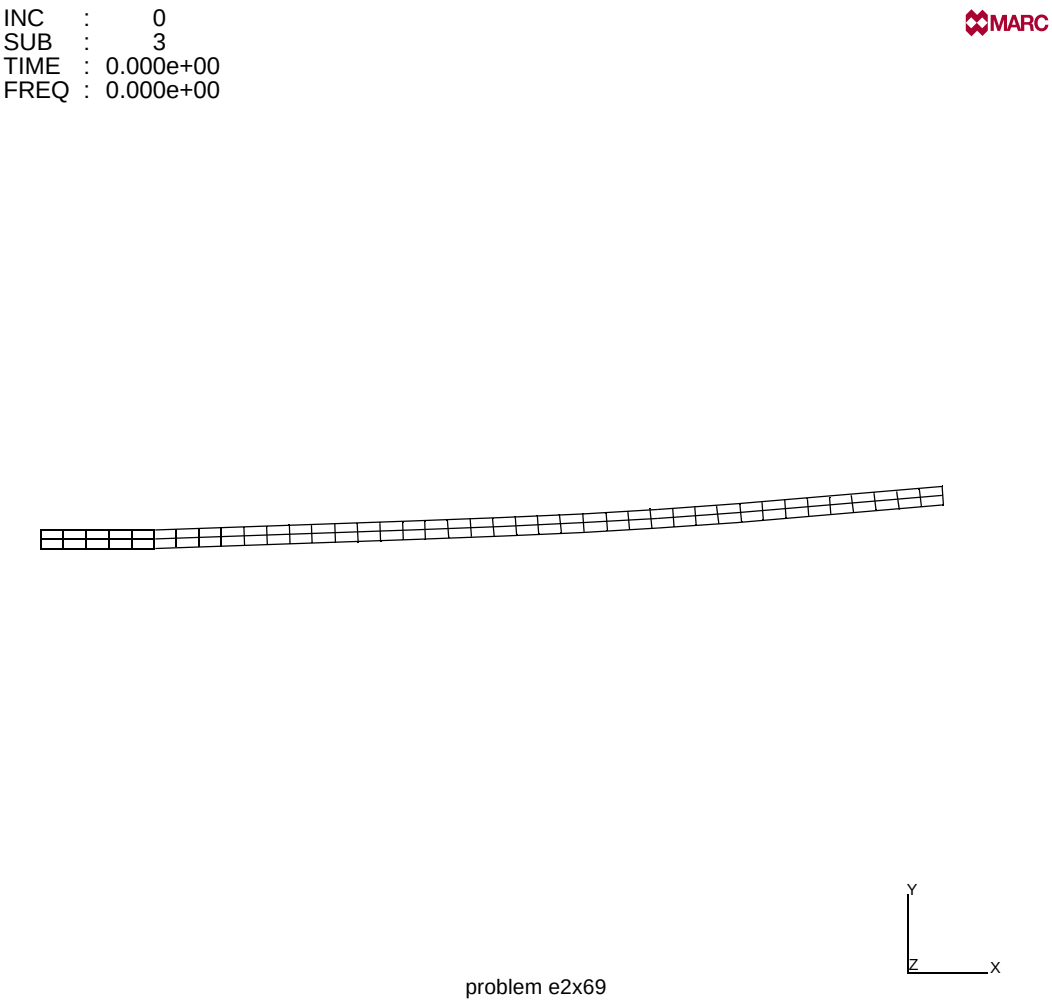

Figure 2.69-5 Deflection of the Longitudinal Section of the Pipe

2.70 Flange Joint Between Pressurized Pipes

This problem demonstrates the capability of the axisymmetric elements 95 together with the axisymmetric gap element 97 to model a flange joint between pressurized pipes including the gasket. These elements may be used even if the loads are nonaxisymmetric as in the case of bending moment and shear applied to the cross-section of one of the pipes.

The model represents an actual joint (see Figure 2.70-1). A square section cavity is filled with a thoroidal gasket. Under the gasket, a tooth of the right-hand flange penetrates into the left-hand flange. Units [N, m].

Object of the analysis is to compute:

Stresses on the flanges and pipes
Axial loads on each bolt
Value of the applied moment that opens the flanges (loss of pressure)

The quadrilateral element 95 represents the cross-section of a ring in the z,r symmetry plane at $\theta = 0°$. A pure axisymmetric deformation induces displacements u,v in the z,r plane. These remain constant for θ ranging from 0° to 360°. A flexural deformation in the z,r plane induces different displacements u,v at the opposite sections, $\theta = 0°$ and $\theta = 180°$, along the ring. A twist in the ring induces a circumferential displacement w, equal at every θ, and assigned to the position $\theta = 90°$.

The gap element 97 works in the flexural mode. Extra degrees of freedom have been added to account for independent contact and friction between the facing sides of element 95 (q = 0° - 180°).

Elements

Element 95 had five degrees of freedom associated to each node:

u,v displacements at 0° and 180°, respectively.
w circumferential displace at 90° angle

Element 95 is integrated numerically in the circumferential direction. The number of integration points (odd number) is given in the SHELL SECT parameter. The points are equidistant on the half circumference (see Figure 2.70-1). Here seven integration points along the half circumference are chosen via the SHELL SECT parameter.

Element 97 is a 4-node gap and friction link with double contact and friction (0° - 180°). It is designed to be used with element type 95.

Model

The FEM model represents the longitudinal section of the pipe joint in the z,r plane. The mesh consists of 613 elements type 95 and 18 elements type 97 for a total of 751 nodes. The mesh is shown in Figure 2.70-1.

The 12 bolts are “smeared” into a ring of equivalent stiffness that is represented by the central strip in the shadowed area in Figure 2.70-1. The remainder of the shaded area represents the “fill” in the section of the bolt.

Material Properties

The two pipes are made with the same material:

E (Young modulus) = 2.05 E11 N/m^2
ν (Poisson ratio) = 0.3

The 12 bolts are modeled with an equivalent axisymmetric ring having material properties:

E (Young modulus) = 2.702 E13 N/m^2
ν (Poisson ratio) = 0.3

The gasket material between bolts is modeled with a coarse mesh of elements type 95 having reduced properties:

E (Young modulus) = 9.04 E10 N/m^2
ν (Poisson ratio) = 0.3

For the bolts and the gasket, the moduli in the hoop direction are strongly reduced.

Loading

Bolts are pre-loaded with an axial force. This is modeled with a local reduction of temperature on the elements modeling the bolts. The bending moment applied to the pipe is assigned with a couple of point loads at the edge of the left pipe as shown in Figure 2.70-2.

Tying

The bolts are connected with the external faces of flange with a tying that links all the degrees of freedom of the joined nodes as shown in Figure 2.70-3.

Gap

The contact between the flanges is modeled with 18 gap elements placed as shown in Figure 2.70-3. Friction is not taken into account. All closure distances are nil; therefore, all gaps are closed until a force greater than 100. N acts on the gap (tensile force). A gap with assigned stiffness represents the gasket.

Boundary Condition

The edge of the right pipe is clamped. Therefore, all degrees of freedom are prescribed to be zero on this edge (see Figure 2.70-2).

Results

The results produced by MARC for the flange joint are shown in the following figures:

Figure 2.70-3 The von Mises stress at 0° at increment 1 (pre-load)
Figure 2.70-5 The von Mises stress at 0° at increment 19 (bending moment)

Note: Only the deformed shape at 0° can be visualized with the Mentat graphics program even if all the element variables can be visualized. The displacements and all the nodal quantities referring to 180 degrees can be read from the MARC output file.

In Table 2.70-1, the balance of the bending moment M_z about the symmetry axis is checked by comparing the sum of all moments due to increments of compressive force in the gaps plus the increment of force in the bolts with the moment of the applied load.

Parameters, Options, and Subroutines Summary

Example e2x70.dat:

Parameters	Model Definition Options	History Definition Options
ALIAS	CONNECTIVITY	AUTO LOAD
ELEMENTS	CONTROL	CHANGE STATE
END	COORDINATES	CONTINUE
PRINT	DEFINE	POINT LOAD
SETNAME	END OPTION	PROPORTIONAL INC
SHELL SECT	FIXED DISP	
SIZING	GAP DATA	
TITLE	ISOTROPIC	
	OPTIMIZE	
	ORTHOTROPIC	
	POINT LOAD	
	POST	
	PRINT ELEM	
	PRINT NODE	
	TYING	

Table 2.70-1 Balance of Moments

Gap	Node 1	Node 2	INC = 1 Force [N]	INC = 19 Force [N]	Δ [N]	Distance [m]	M_z [N · m]
359	359	735	3653.	3651.	-2.	0.0235	-0.0470
360	358	734	2671.	2674.	3.	0.023875	0.0716
361	357	737	2313.	2319.	6.	0.02425	0.1455
362	356	738	2158.	2167.	9.	0.024625	0.2216
363	355	740	2029.	2041.	12.	0.025	0.3000
364	354	739	1871.	1886.	15.	0.025375	0.3806
365	353	751	836.	845.	9.	0.02575	0.2318
366	368	749	1243.	1228.	-15.	0.016	-0.24
367	367	750	1768.	1743.	-25.	0.016375	-0.4094
368	366	741	1788.	1761.	-27.	0.01675	-0.4523
369	365	742	2059.	2028.	-31.	0.017125	-0.5309
370	364	748	2821.	2782.	-39.	0.0175	-0.6825
371	230	747	-74.	0.	74.	0.00825	0.6105
372	228	746	45.	-99.	-144.	0.009375	-1.3500
373	223	744	375.	275.	-100.	0.0105	-1.0500
374	222	736	840.	751.	-89.	0.011625	-1.0346
375	219	745	1047.	997.	-50.	0.01275	-0.6375
376	349	743	760.	713.	-47.	0.014766	-0.6940
$\sum$			2.82E4		-441.		-5.1665
Bolt Stress [N/m^2]			4.3778E8	4.495E8	1.17E7 (x-1.288E-4/2)		
Bolt Force [N]					-753.	0.0205	-15.45
							-20.62
Applied Moment [N. m]				900 x 2 = 1800.		0.013875	24.98
							Δ% = 17%

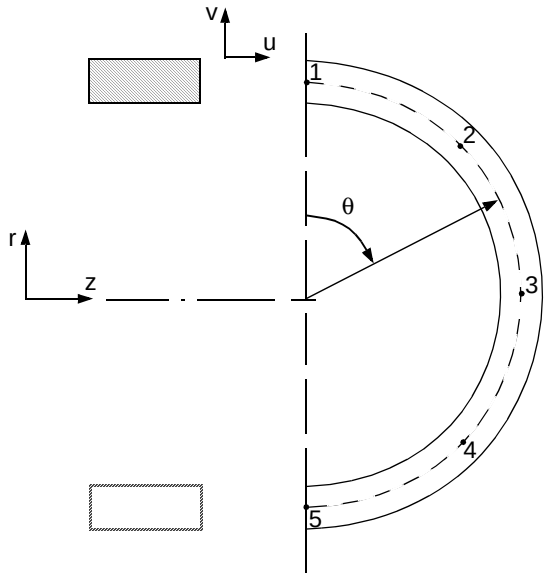

Figure 2.70-1 Element 95 Layer Points

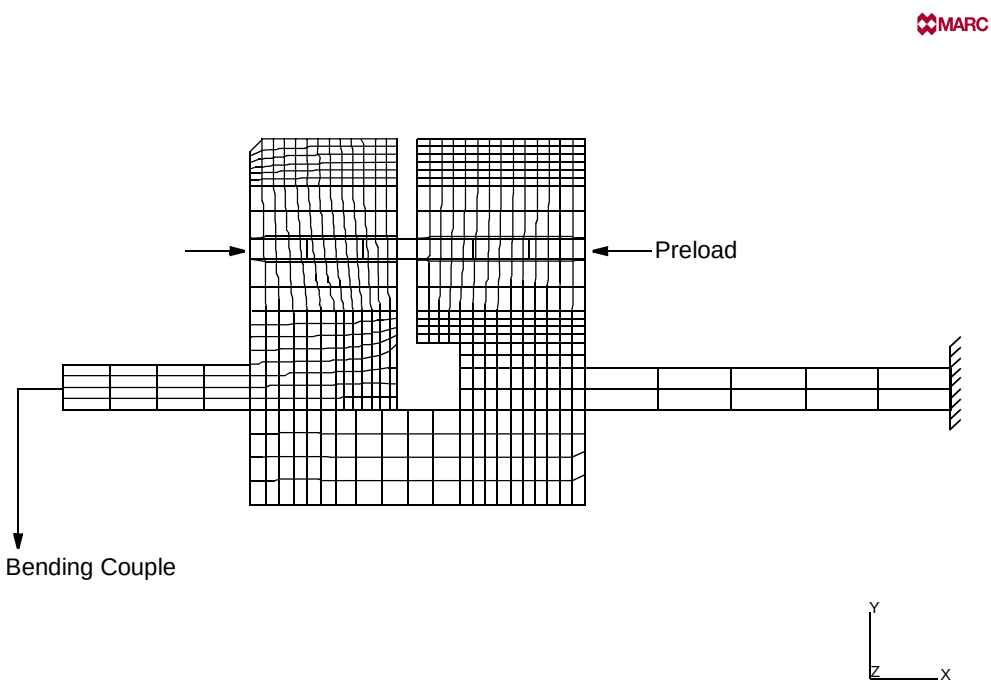

Figure 2.70-2 Loads on the Flange Joint

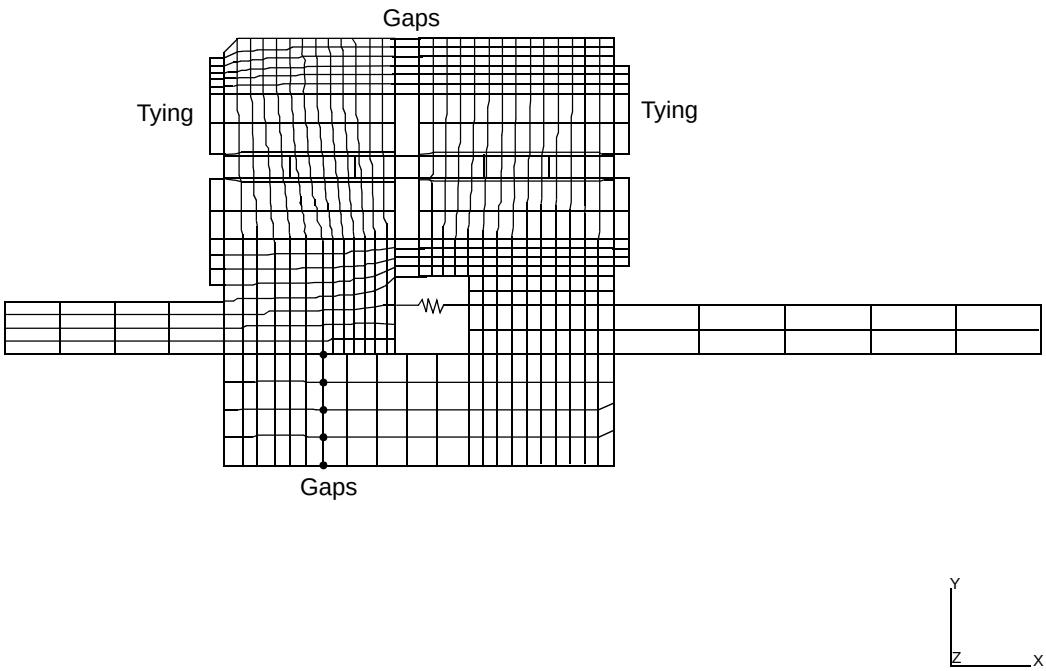

Figure 2.70-3 Tying in the Flange Joint

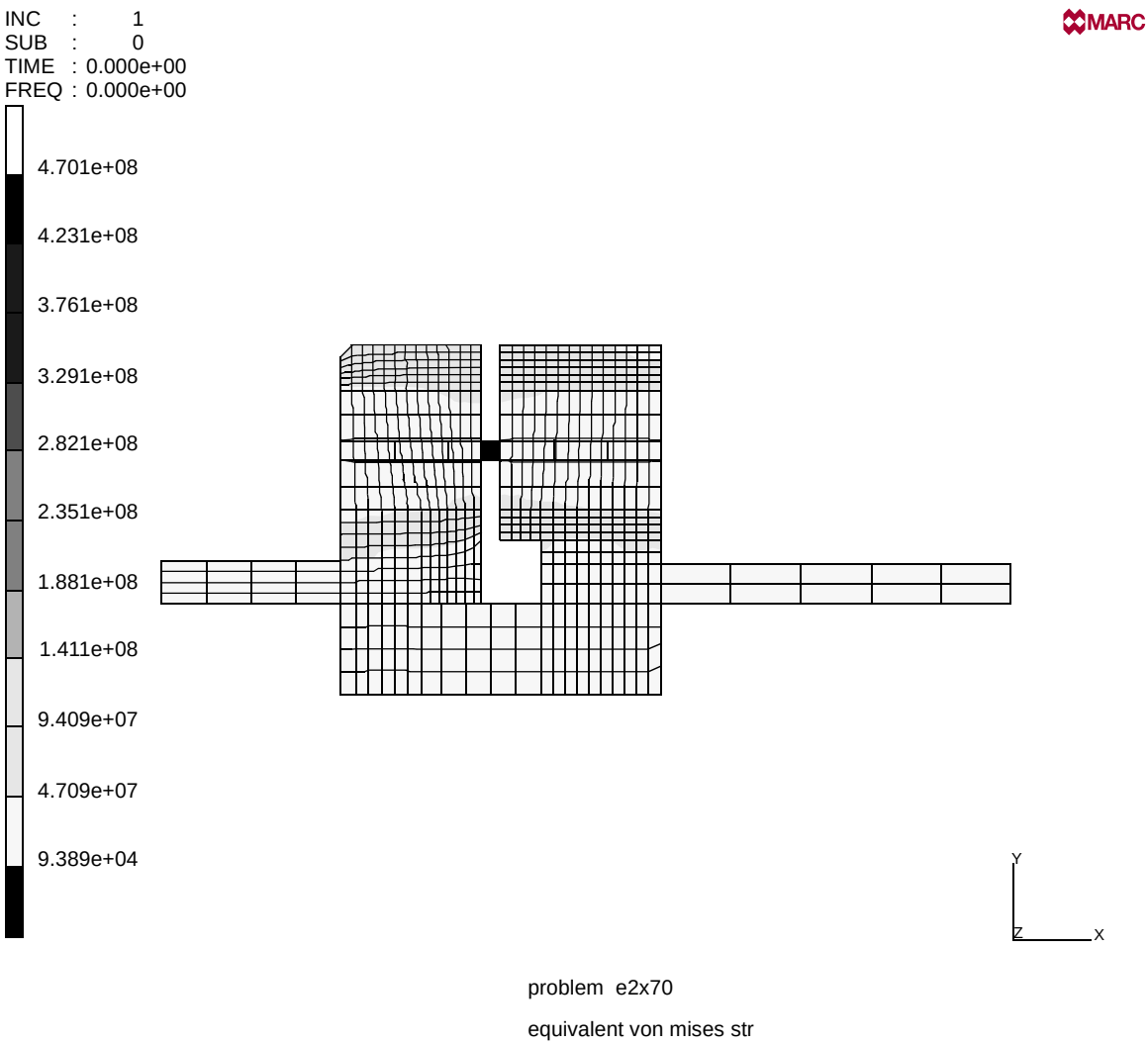

Figure 2.70-4 von Mises Stress Induced by Preload

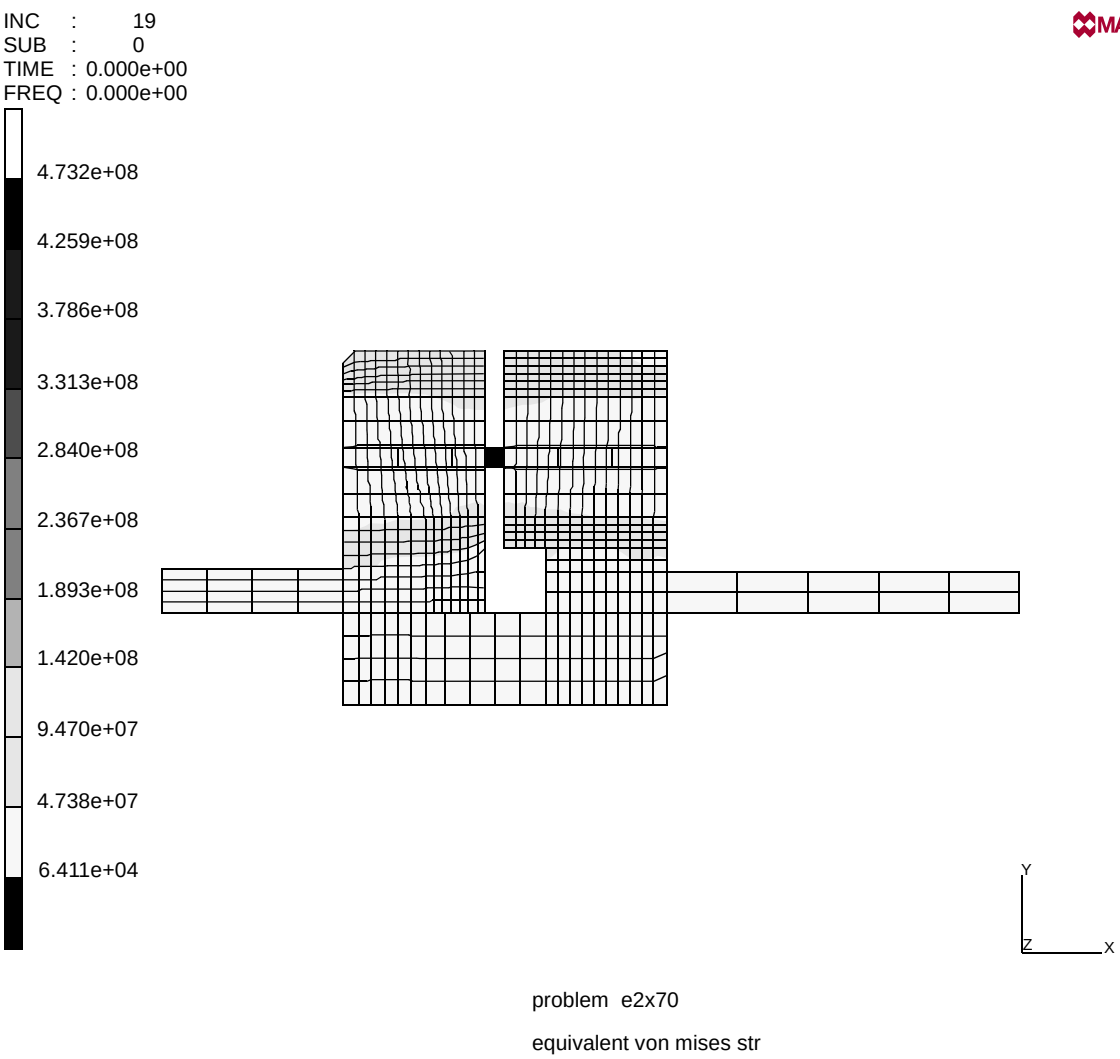

Figure 2.70-5 von Mises Stress Induced by Moment

2.71 Spinning Cantilever Beam

This problem demonstrates the use of MARC element type 98 for the solution of spinning cantilever beam. The beam rotates at a constant angular velocity. The beam also has an initial velocity which induces Coriolis effect. The ROTATION A and DIST LOADS options are used for the input of Centrifugal load. The INITIAL VEL option is used to input the initial velocity.

This problem is modeled using the two techniques summarized below.

Data Set	Element Type(s)	Number of Elements	Number of Nodes	Differentiating Features
e2x71a	98	5	6	Centrifugal loads
e2x71b	95	5	6	Centrifugal and Coriolis loads

Element

The element (Element 98) is a 2-node straight elastic beam in space and includes the transverse shear effects in its formulation.

Model

As shown in Figure 2.71-1, the finite element mesh consists of five elements and six nodes. The span on the beam is five inches and the cross-section of the beam is assumed to be a closed, thin, square section.

Geometry

The GEOMETRY block is used for entering the beam section properties. The section properties (area = 0.0369 inches^2, $I_x = I_y = 6.4693 \times 10^{-3}$ inches^4) are entered through the GEOMETRY block.

Material Properties

The material of the beam is assumed to have a Young's modulus of 3.0e+08 psi, Poisson's ratio of 0.3, and a mass density of 0.281 lb-seconds/inch^4.

Loading

The beam is subjected to Centrifugal loading (IBODY = 100) resulting from the rotation of the beam. With an angular velocity of 20 • radian/seconds ($\omega^2 = 400$) and the axis of rotation is the y axis. The beam has an initial velocity of 100 inches/second in the x-direction which induces Coriolis effect (IBODY = 103).

Boundary Condition

At node 1, all the degrees of freedom are constrained ($U_x = U_y = U_z = \theta_x = \theta_y = \theta_z = 0$).

Results

The deformation of the beam is given is Table 2.71-1.

Table 2.71-1 Beam Deflection (Inches)

Node	δ_x(x10^{-4}) (Due to Centrifugal Loading)	δ_y(x10^{-4}) (Due to Coriolis Effect)
1	0.	
2	1.305	1.61
3	2.385	5.022
4	3.203	9.422
5	3.722	14.241
6	3.903	19.135

Parameters, Options, and Subroutines Summary

Example e2x71a.dat:

Parameters

ELEMENTS
END
SIZING
TITLE

Model Definition Options

CONNECTIVITY
COORDINATES
DIST LOADS
END OPTION
FIXED DISP
GEOMETRY
ISOTROPIC
POST
ROTATION A

Example e2x71b.dat:

Parameters	Model Definition Options
ELEMENTS	CONNECTIVITY
END	COORDINATES
SIZING	DIST LOADS
TITLE	END OPTION
	FIXED DISP
	GEOMETRY
	INITIAL VEL
	ISOTROPIC
	POST
	ROTATION A

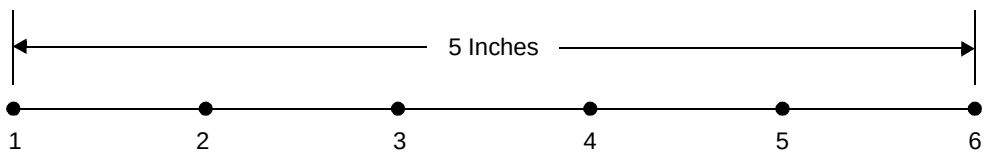

Figure 2.71-1 Finite Element Model

2.72 Shell Roof by Element 138

This problem illustrates the use of MARC element type 138 for an elastic analysis of a barrel vault shell roof. The roof is subjected to its own weight. This problem is similar to problems 2.16, 2.17, 2.18, 2.19, 2.55, 2.73, and 2.74.

Element

Element type 138 is a 3-node thin-shell element with six degrees of freedom at each corner node.

Model

The element is type 138. There are 128 elements with a total of 61 nodes. The shell roof and the finite element mesh are shown in Figure 2.72-1.

Material Properties

Young's modulus is 30 x 10^5 psi. Poisson's ratio is taken to be 0. The mass density is 1.0 lb-sec^2/in^4.

Geometry

The shell thickness is 3.0 inches.

Loading

Uniform gravity load in negative z-direction, specified with load type 102. The magnitude of the force per unit mass is 0.20833.

Boundary Conditions

Supported end:

A. u = 0, w = 0, at y = 0

The following degrees of freedom are constrained at the lines of symmetry:

B. u = 0 and θ_y = 0 at x = 0

C. v = 0 and θ_x = 0 at y = 300

SHELL SECT

The SHELL SECT option allows you to reduce the number of integration points from the default value of 11 to a minimum value of 3 in the shell thickness direction. This three-point integration scheme is exact as for a linear elastic problem.

Results

A deformed mesh plot is shown in Figure 2.72-2. The results are in good agreement with problem 2.19. The element is easy to use and inexpensive.

Parameters, Options, and Subroutines Summary

Example e2x72.dat:

Parameters	Model Definition Options
ELEMENTS	CONNECTIVITY
END	COORDINATES
SHELL SECT	DIST LOADS
SIZING	END OPTION
TITLE	FIXED DISP
	GEOMETRY
	ISOTROPIC
	NO PRINT
	POST

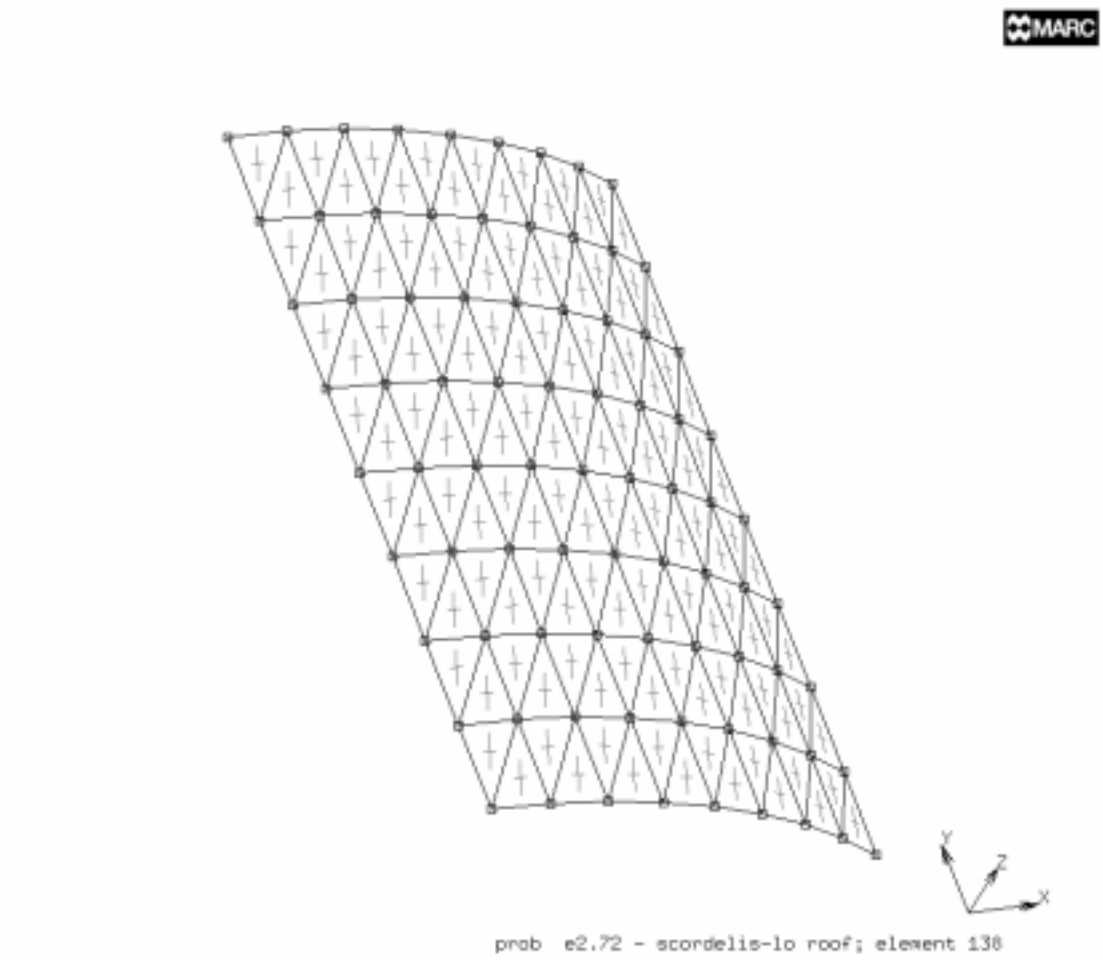

Figure 2.72-1 Shell Roof and Mesh

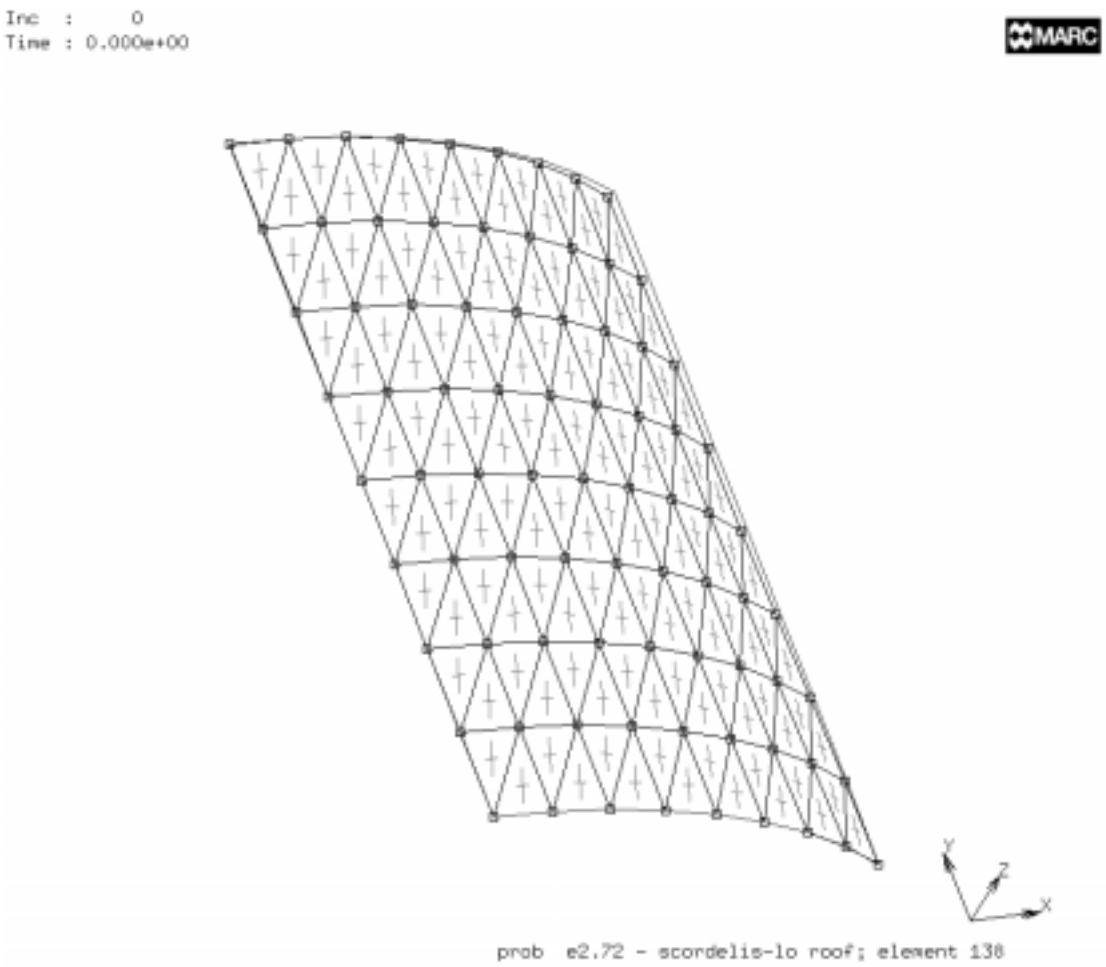

Figure 2.72-2 Deformed Mesh Plot

2.73 Shell Roof by Element 139

This problem illustrates the use of MARC element type 139 for an elastic analysis of a barrel vault shell roof. The roof is subjected to its own weight. This problem is similar to problems 2.16, 2.17, 2.18, 2.19, 2.55, 2.72, and 2.74.

Element

Element type 139 is a 4-node thin-shell element with six degrees of freedom at each corner node.

Model

The element is type 139. There are 64 elements with a total of 48 nodes. The shell roof and the finite element mesh are shown in Figure 2.73-1.

Material Properties

Young's modulus is 30 x 10^5 psi. Poisson's ratio is taken to be 0. The mass density is 1.0 lb-sec^2/in^4.

Geometry

The shell thickness is 3.0 inches.

Loading

Uniform gravity load in negative z-direction, specified with load type 102. The magnitude of the force per unit mass is 0.20833.

Boundary Conditions

Supported end:

A. u = 0, w = 0, at y = 0

The following degrees of freedom are constrained at the lines of symmetry:

B. u = 0 and θ_y = 0 at x = 0

C. v = 0 and θ_x = 0 at y = 300

SHELL SECT

The SHELL SECT option allows you to reduce the number of integration points from the default value of 11 to a minimum value of 3 in the shell thickness direction. This three-point integration scheme is exact as for a linear elastic problem.

Results

A deformed mesh plot is shown in Figure 2.73-2. The results are in good agreement with problem 2.19. The element is easy to use and less expensive than element type 25.

Parameters, Options, and Subroutines Summary

Example e2x73.dat:

Parameters	Model Definition Options
ELEMENTS	CONNECTIVITY
END	COORDINATES
SHELL SECT	DIST LOADS
SIZING	END OPTION
TITLE	FIXED DISP
	GEOMETRY
	ISOTROPIC
	NO PRINT
	POST

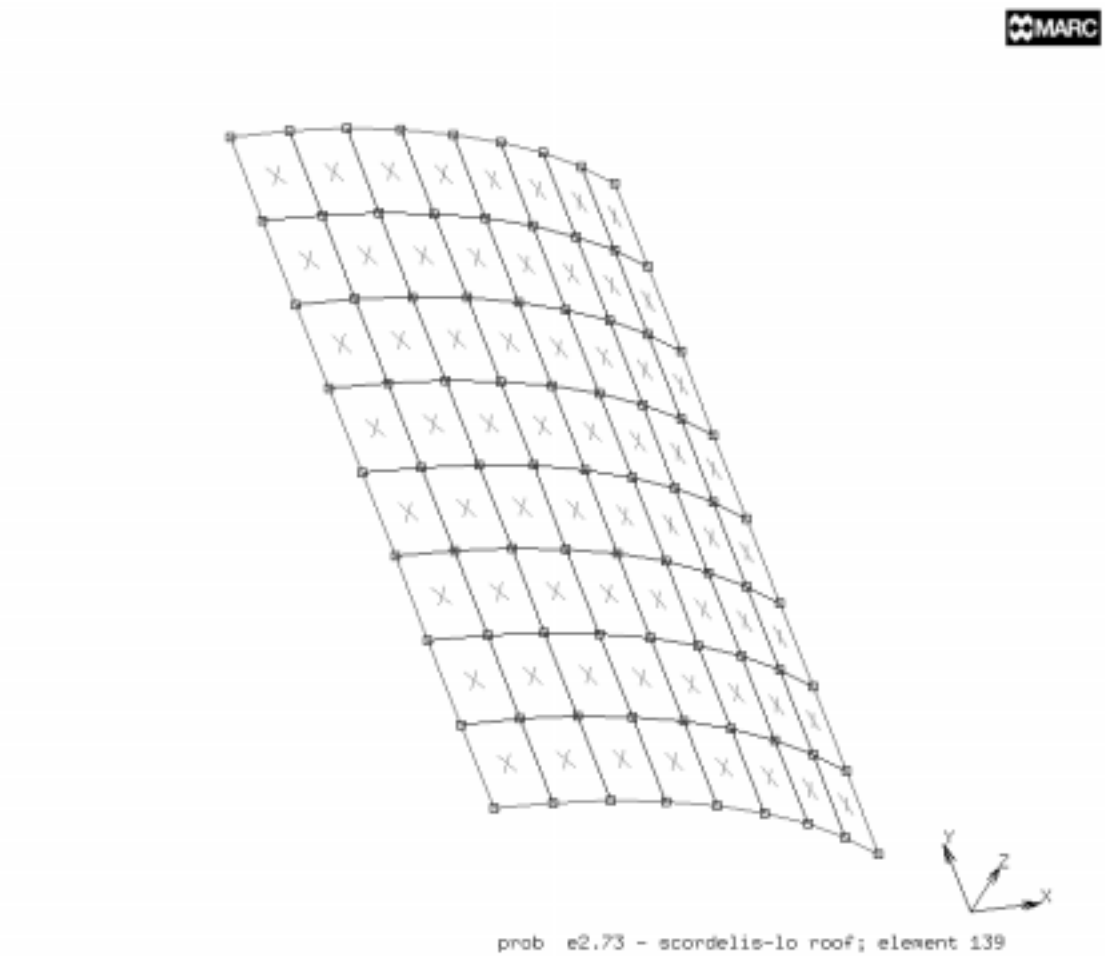

Figure 2.73-1 Shell Roof and Mesh

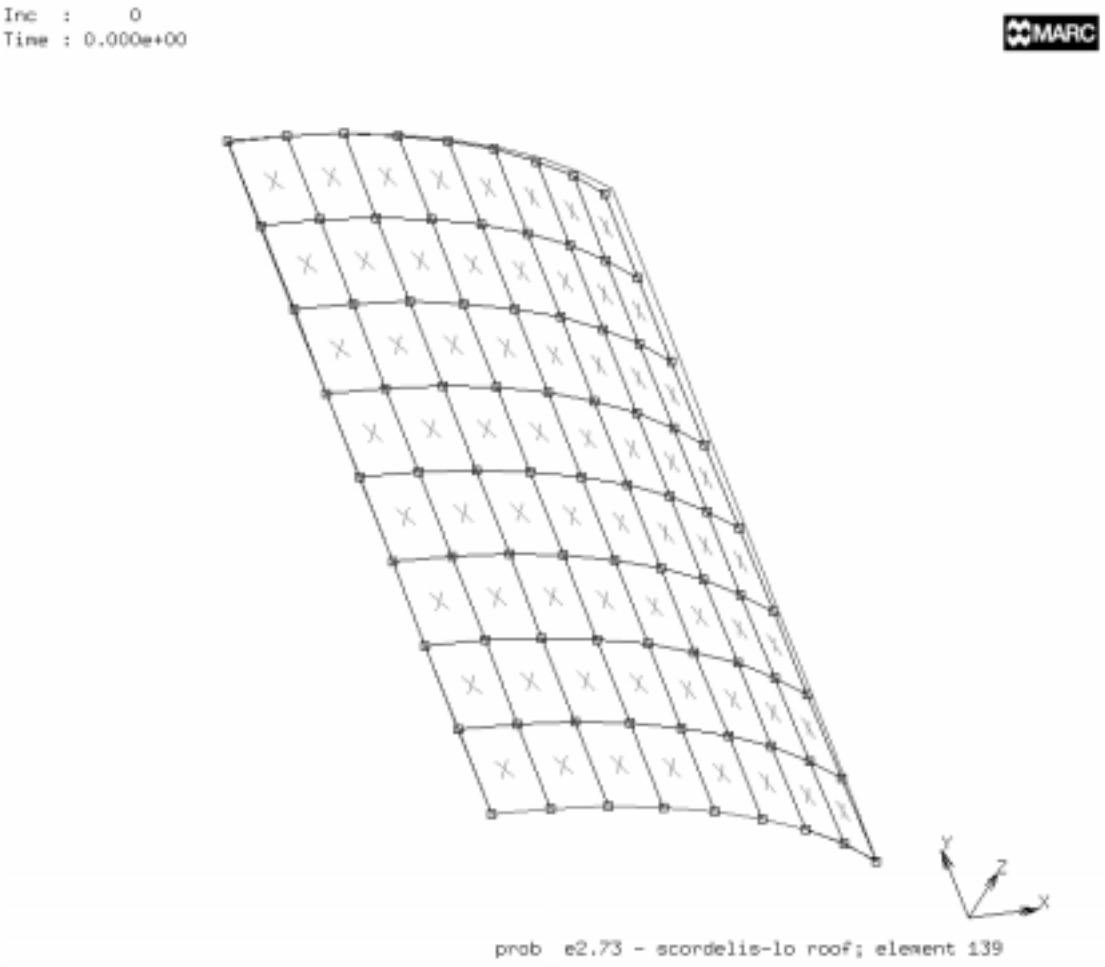

Figure 2.73-2 Deformed Mesh Plot

2.74 Shell Roof by Element 140

This problem illustrates the use of MARC element type 140 for an elastic analysis of a barrel vault shell roof. The roof is subjected to its own weight. This problem is similar to problems 2.16, 2.17, 2.18, 2.19, 2.55, 2.72, and 2.73.

Element

Element type 140 is a 4-node thin-shell element with six degrees of freedom at each corner node. This element is similar to element 75 but uses a single intergration point per element.

Model

The element is type 140. There are 64 elements, with a total of 81 nodes. The shell roof and the finite element mesh are shown in Figure 2.74-1.

Material Properties

Young's modulus is 30 x 10^5 psi. Poisson's ratio is taken to be 0. The mass density is 1.0 lb-sec^2/in^4.

Geometry

The shell thickness is 3.0 inches.

Loading

Uniform gravity load in negative z-direction, specified with load type 102. The magnitude of the force per unit mass is 0.20833.

Boundary Conditions

Supported end:

A. u = 0, w = 0, at y = 0

The following degrees of freedom are constrained at the lines of symmetry:

B. u = 0 and θ_y = 0 at x = 0

C. v = 0 and θ_x = 0 at y = 300

SHELL SECT

The SHELL SECT option allows you to reduce the number of integration points from the default value of 11 to a minimum value of 3 in the shell thickness direction. This three-point integration scheme is exact as for a linear elastic problem.

Results

A deformed mesh plot is shown in Figure 2.74-2. The results are in good agreement with problem 2.19. The element is easy to use and inexpensive.

Parameters, Options, and Subroutines Summary

Example e2x74.dat:

Parameters	Model Definition Options
ELEMENTS	CONNECTIVITY
END	COORDINATES
SHELL SECT	DIST LOADS
SIZING	END OPTION
TITLE	FIXED DISP
	GEOMETRY
	ISOTROPIC
	NO PRINT
	POST

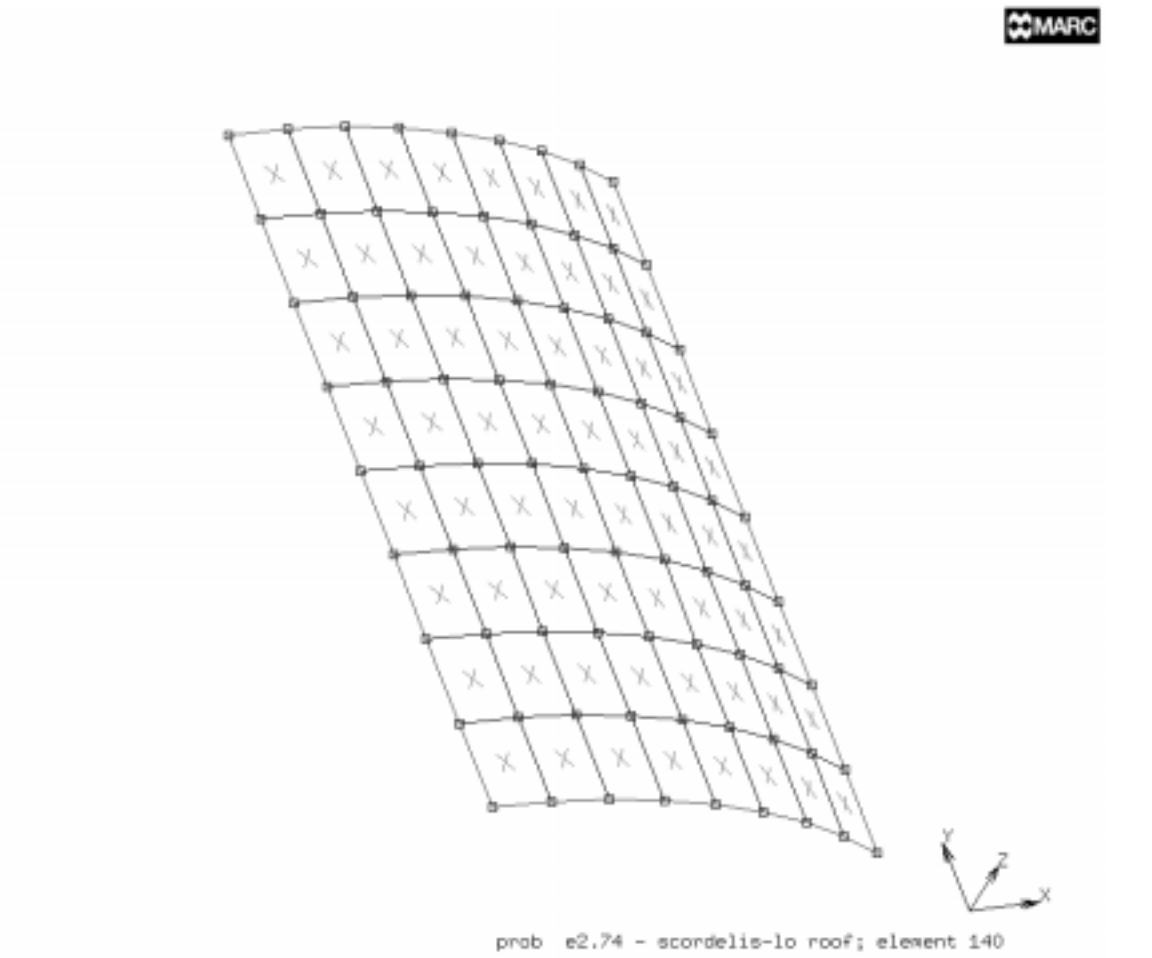

Figure 2.74-1 Shell Roof and Mesh

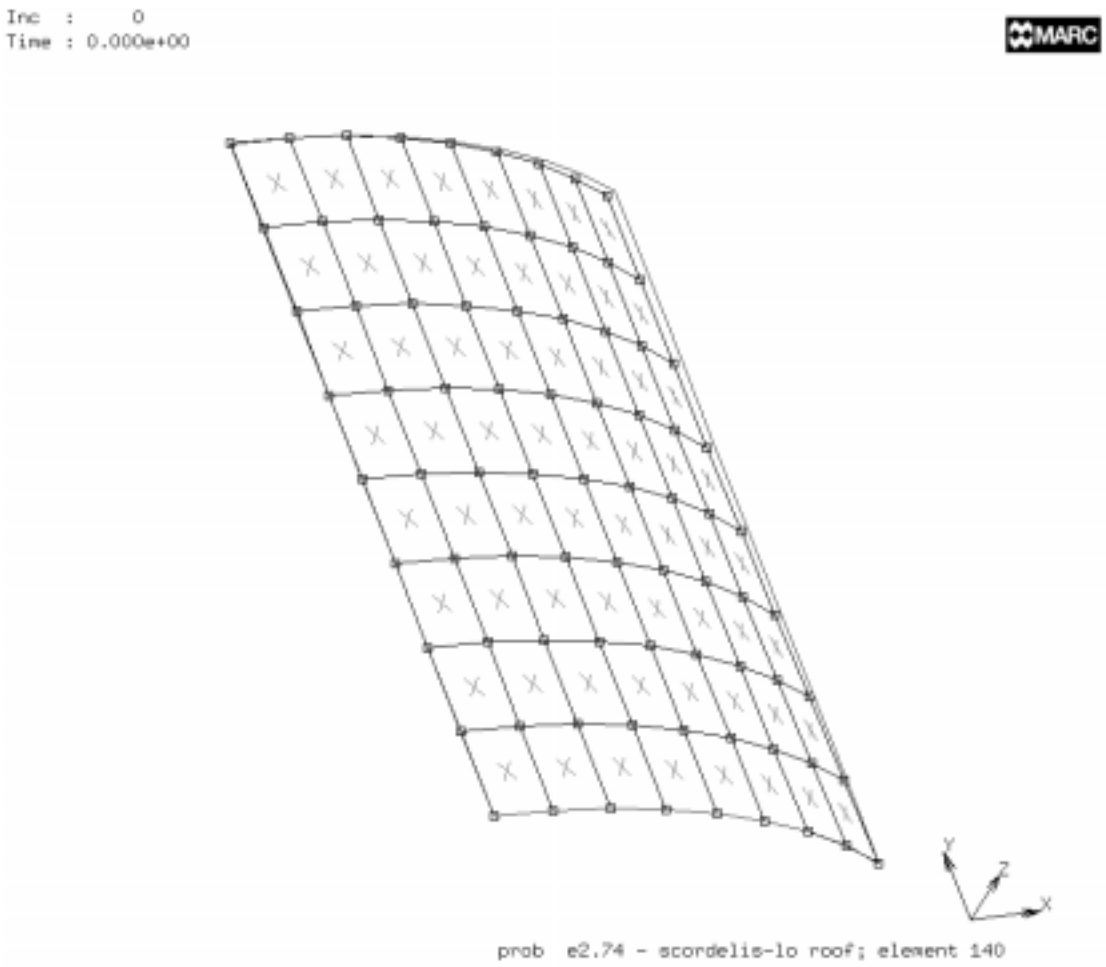

Figure 2.74-2 Deformed Mesh Plot

2.75 Cylinder Subjected to a Point Load - Element Type 138

This problem demonstrates the use of element type 138 for an elastic analysis of a cylindrical shell subjected to a point load. This example demonstrates the coupling between membrane and bending behavior.

Elements

The 3-node thin shell element is used. This element uses discrete Kirchhoff theory. There are three displacements and three rotations per node.

Model

The cylinder has a length of 60 inches, a radius of 30 inches, and a thickness of 3 inches. Because of symmetry, only 1/8 of the actual cylinder is modeled. The mesh has 288 elements and 169 nodes. The mesh is shown in Figure 2.75-1.

Material Properties

Young's modulus is 3×10^5 psi. Poisson's ratio is 0.3.

Geometry

The shell thickness is 3.0 inches and is entered through the GEOMETRY option. The radius/thickness (r/t) is 30/3 = 10 which suggests that this is a thick shell. The thick shell elements may be more appropriate (see Figure 2.75-2).

Loading

A point load of 0.50 pound is applied to the structure. Because of symmetry, 0.25 pound is applied to node 13.

Boundary Conditions

At z = 30 inches, the shell is held such that:

$U_x = 0$ $U_y = 0$

At z = 0, symmetry conditions are applied:

$u_z = 0$ $\theta_x = 0$ $\theta_y = 0$

At x = 0, y = 30, symmetry conditions are:

$U_x = 0$ $\theta_z = 0$

At x = 30, y = 0, symmetry conditions are:

$U_y = 0$ $\theta_z = 0$

Solution Procedure

The default profile solver is used with the Sloan bandwidth optimization procedure.

Results

A deformed mesh is shown in Figure 2.75-2. The y deformation at x = 0 is shown as a path plot in Figure 2.75-3.

Parameters, Options, and Subroutines Summary

Example e2x75.dat:

Parameters	Model Definition Options
ALL POINTS	CONNECTIVITY
ELEMENTS	COORDINATES
END	END OPTION
SETNAME	FIXED DISP
SHELL SECT	GEOMETRY
SIZING	ISOTROPIC
TITLE	NO PRINT
	POINT LOADS
	POST

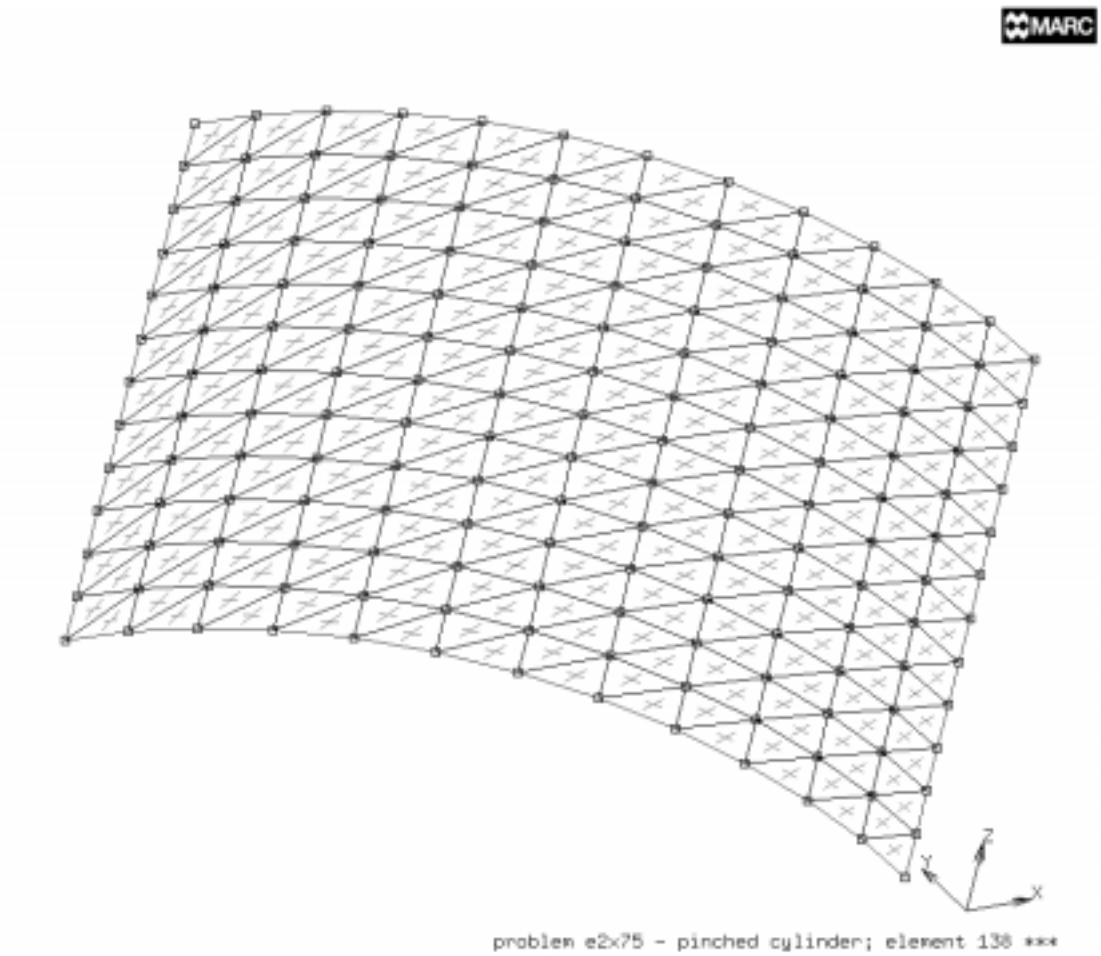

Figure 2.75-1 Shell Roof and Mesh

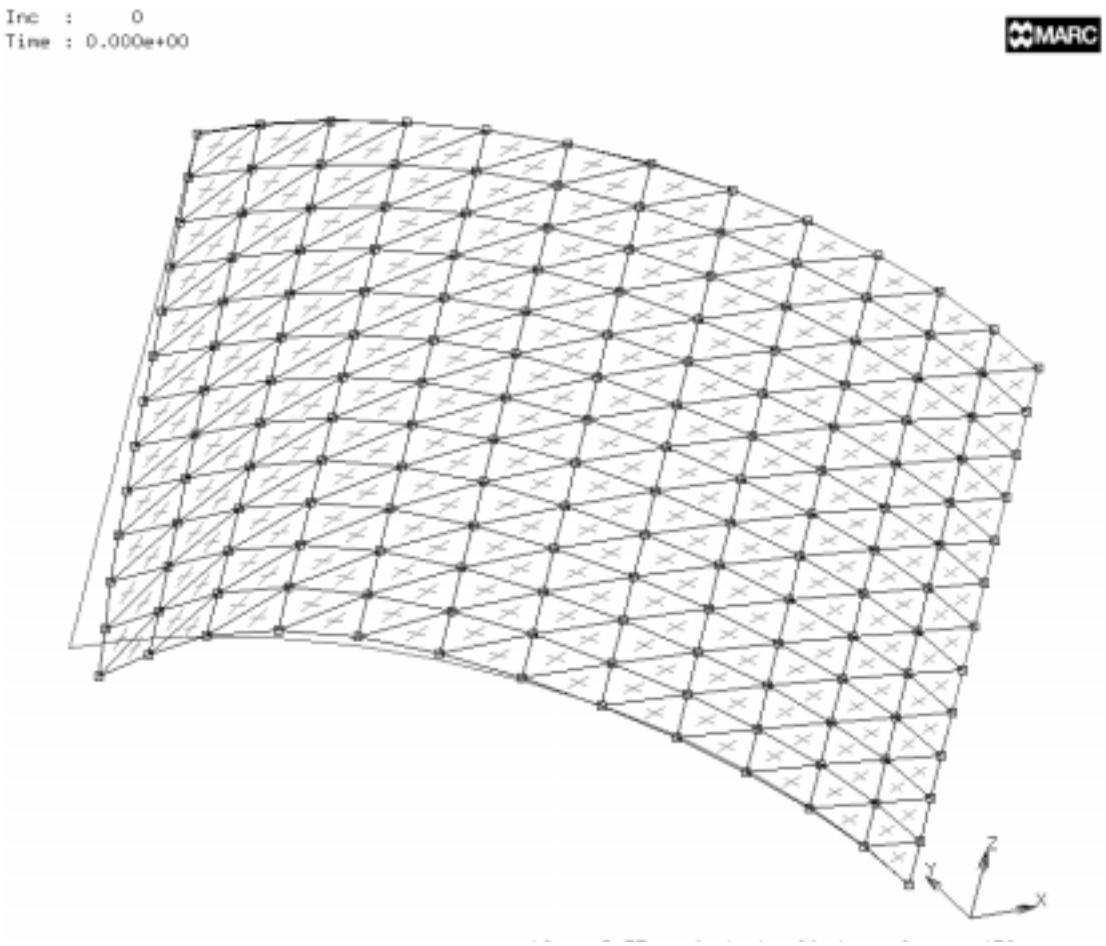

Figure 2.75-2 Deformed Mesh Plot

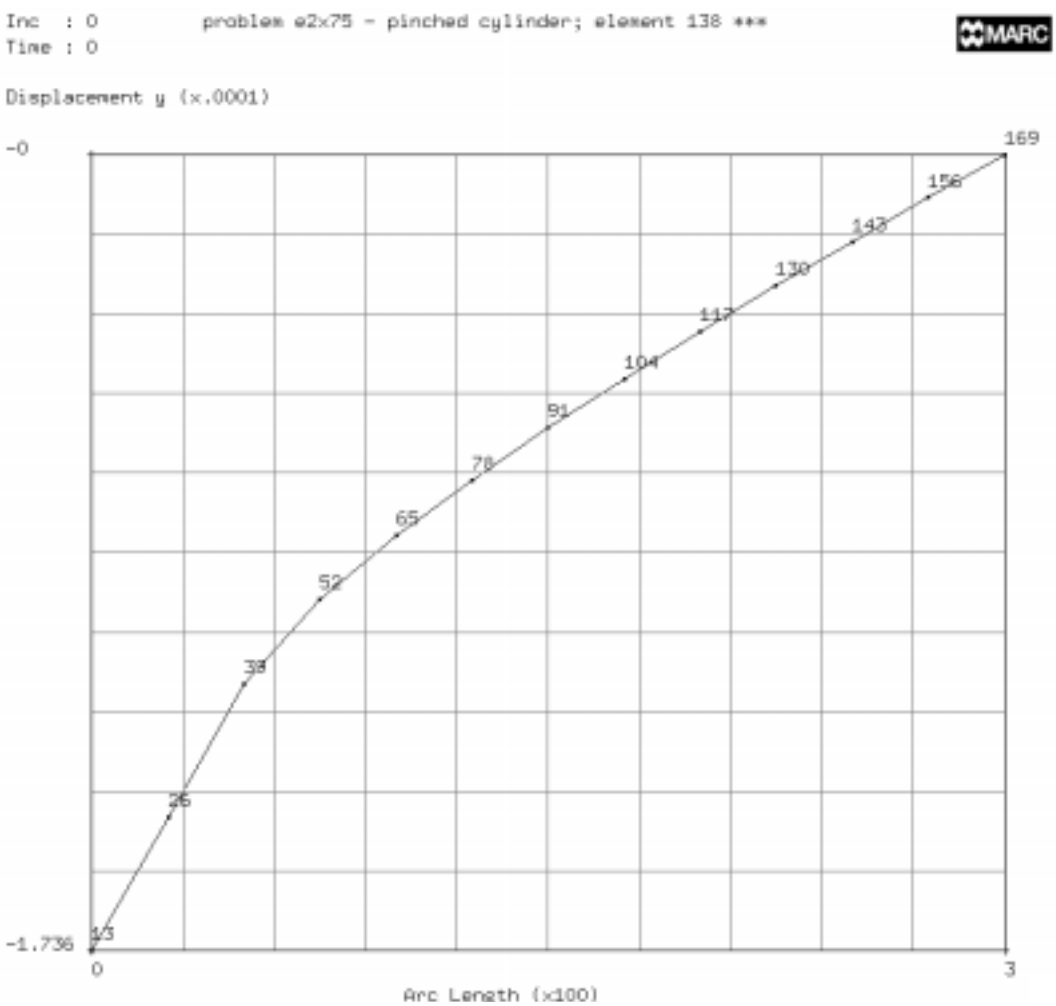

Figure 2.75-3 Y Deformation Along X = 0

2.76 Cylinder Subjected to a Point Load - Element Type 139

This problem demonstrates the use of element type 139 for an elastic analysis of a cylindrical shell subjected to a point load. This example demonstrates the coupling between membrane and bending behavior.

Elements

Element type 139 is a 4-node thin-shell element. This element uses discrete Kirchhoff theory. There are three displacements and three rotations per node.

Model

The cylinder has a length of 60 inches, a radius of 30 inches, and a thickness of 3 inches. Because of symmetry, only 1/8 of the actual cylinder is modeled. The mesh has 144 elements and 169 nodes. The mesh is shown in Figure 2.76-1.

Material Properties

Young's modulus is 3×10^5 psi. Poisson's ratio is 0.3.

Geometry

The shell thickness is 3.0 inches and is entered through the GEOMETRY option. The radius/thickness (r/t) is 30/3 = 10 which suggests that this is a thick shell. The thick shell elements may be more appropriate (see Figure 2.76-2).

Loading

A point load of 0.50 pound is applied to the structure. Because of symmetry, a load of 0.25 pound is applied to node 13.

Boundary Conditions

At z = 30 inches, the shell is held such that:

$U_x = 0$ $U_y = 0$

At z = 0, symmetry conditions are applied:

$u_z = 0$ $\theta_x = 0$ $\theta_y = 0$

At x = 0, y = 30, symmetry conditions are:

$U_x = 0$ $\theta_z = 0$

At x = 30, y = 0, symmetry conditions are:

$U_y = 0$ $\theta_z = 0$

Solution Procedure

The default profile solver is used with the Sloan bandwidth optimization procedure.

Results

A deformed mesh is shown in Figure 2.76-2. The y deformation at x = 0 is shown as a path plot in Figure 2.76-3.

Parameters, Options, and Subroutines Summary

Example e2x76.dat:

Parameters	Model Definition Options
ALL POINTS	CONNECTIVITY
ELEMENTS	COORDINATES
END	END OPTION
SETNAME	FIXED DISP
SHELL SECT	GEOMETRY
SIZING	ISOTROPIC
TITLE	NO PRINT
	POINT LOADS
	POST

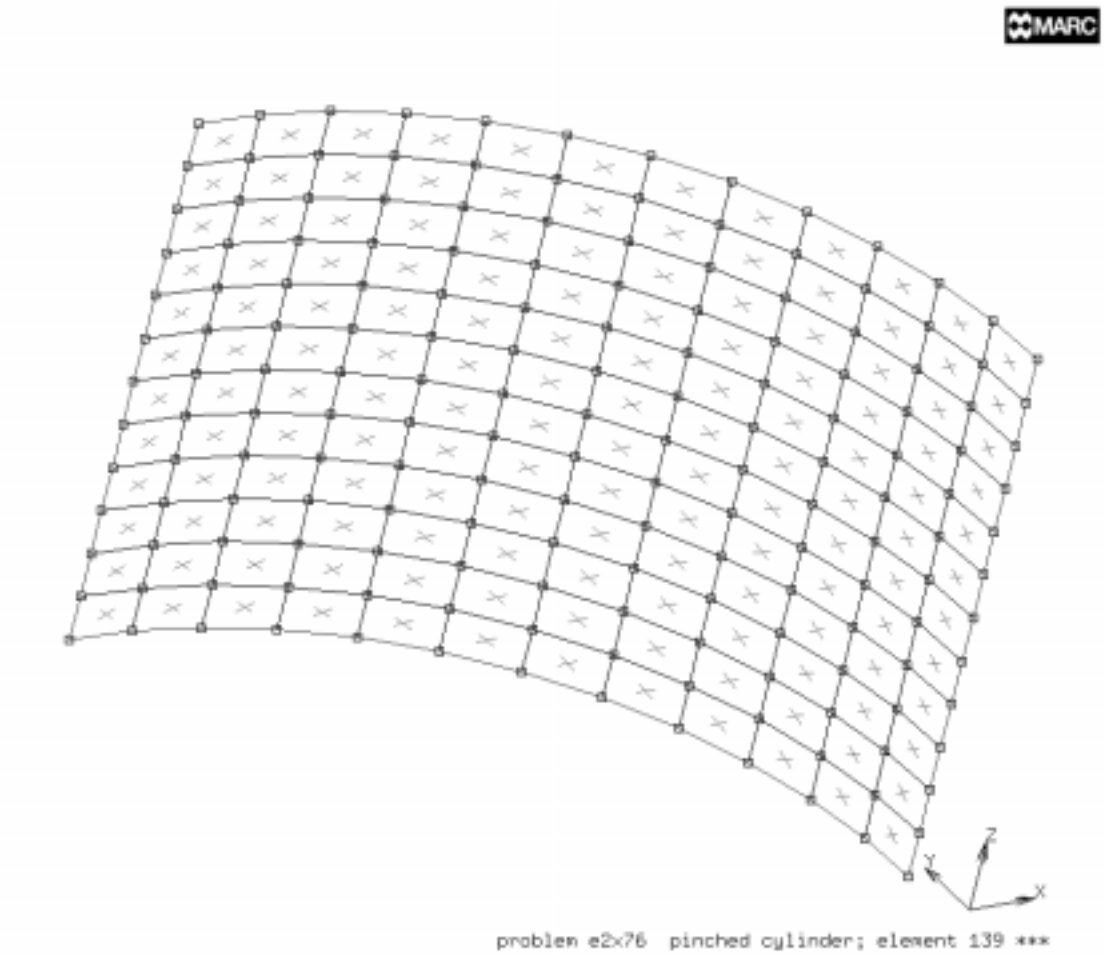

Figure 2.76-1 Shell Roof and Mesh

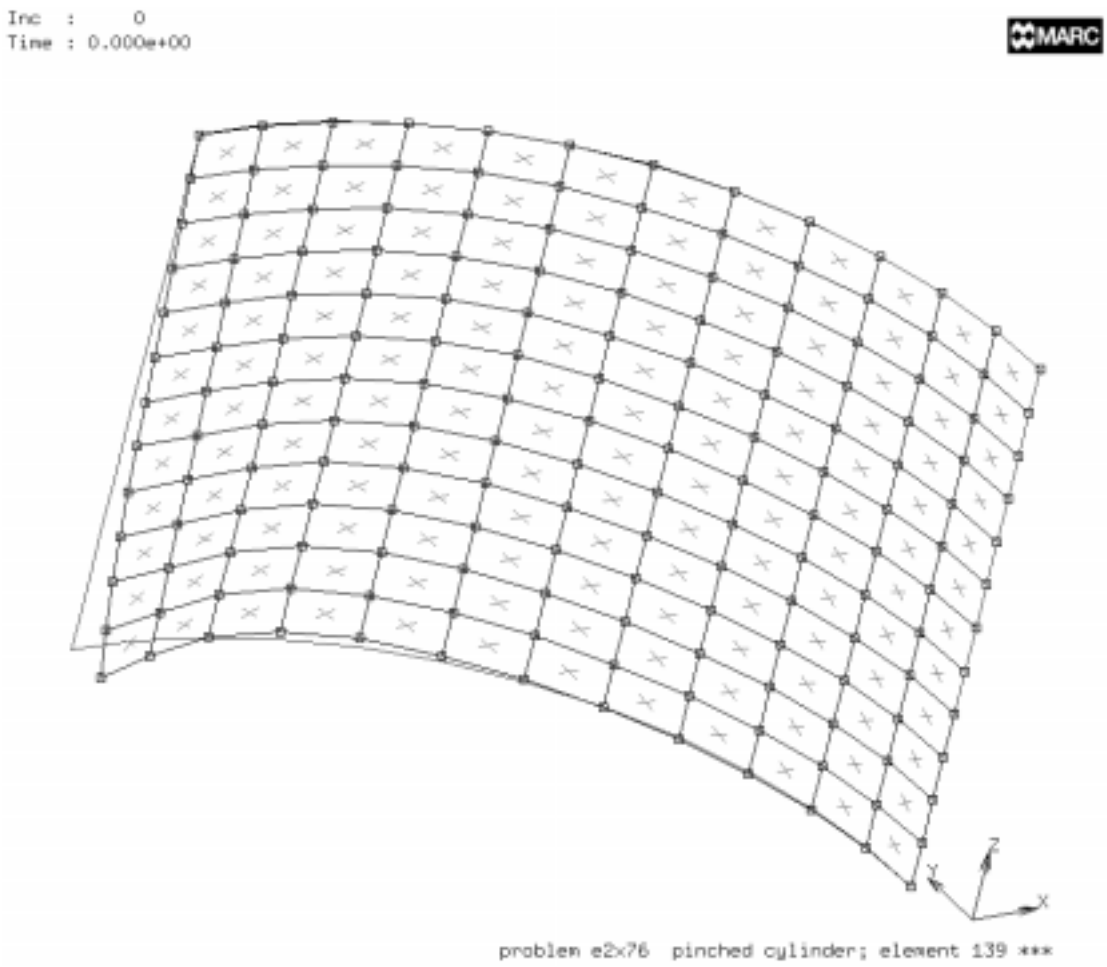

Figure 2.76-2 Deformed Mesh Plot

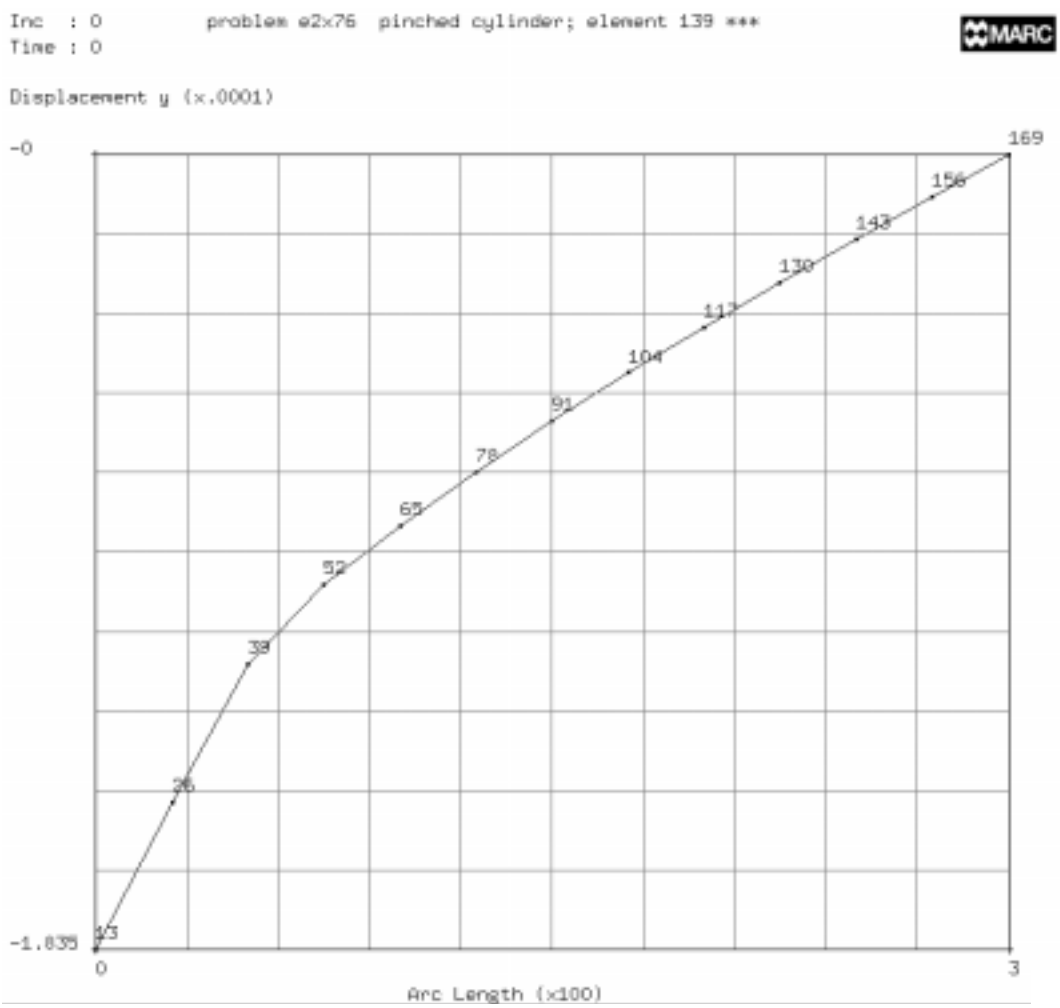

Figure 2.76-3 Y Deformation Along X = 0

2.77 Cylinder Subjected to a Point Load - Element Type 140

This problem demonstrates the use of element type 140 for an elastic analysis of a cylindrical shell subjected to a point load. It shows the coupling between membrane and bending behavior.

Elements

Element type 140 is a 4-node thick-shell element with six degrees of freedom at each corner node. This element is similar to element 75 but uses a single intergration point per element.

Model

The cylinder has a length of 60 inches, a radius of 30 inches, and a thickness of 3 inches. Because of symmetry, only 1/8 of the actual cylinder is modeled. The mesh has 144 elements and 169 nodes. The mesh is shown in Figure 2.77-1.

Material Properties

Young's modulus is 3×10^5 psi. Poisson's ratio is 0.3.

Geometry

The shell thickness is 3.0 inches and is entered through the GEOMETRY option. The radius/thickness (r/t) is 30/3 = 10 which suggests that this is a thick shell. The thick shell elements may be more appropriate (see Figure 2.77-2).

Loading

A point load of 0.50 pound is applied to the structure. Because of symmetry, a load of 0.25 pound is applied to node 13.

Boundary Conditions

At z = 30 inches, the shell is held such that:

$U_x = 0$ $U_y = 0$

At z = 0, symmetry conditions are applied:

$u_z = 0$ $\theta_x = 0$ $\theta_y = 0$

At x = 0, y = 30, symmetry conditions are:

$U_x = 0$ $\theta_z = 0$

At x = 30, y = 0, symmetry conditions are:

$U_y = 0$ $\theta_z = 0$

Solution Procedure

The default profile solver is used with the Sloan bandwidth optimization procedure.

Results

A deformed mesh is shown in Figure 2.77-2. The y deformation at x = 0 is shown as a path plot in Figure 2.77-3.

Parameters, Options, and Subroutines Summary

Example e2x77.dat:

Parameters	Model Definition Options
ALL POINTS	CONNECTIVITY
ELEMENTS	COORDINATES
END	END OPTION
SETNAME	FIXED DISP
SHELL SECT	GEOMETRY
SIZING	ISOTROPIC
TITLE	NO PRINT
	POINT LOADS
	POST

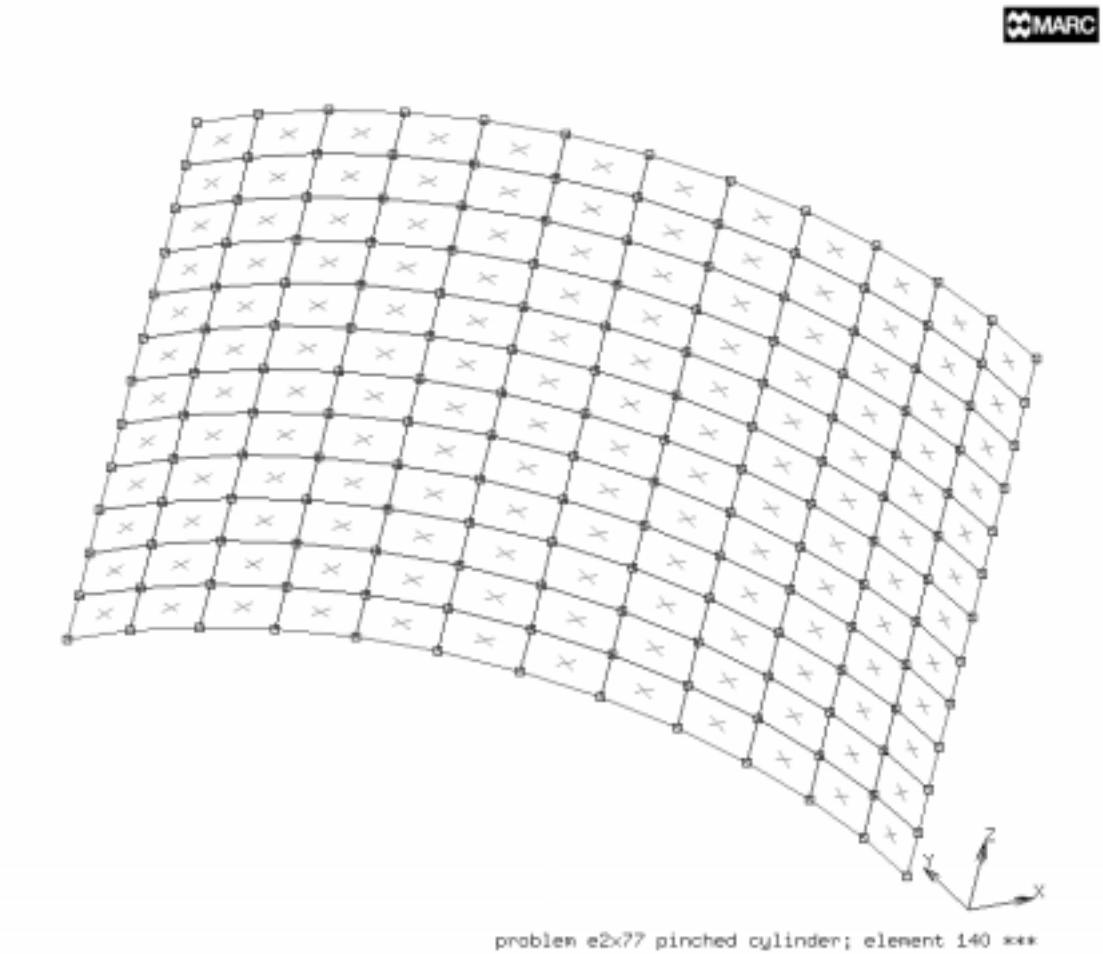

Figure 2.77-1 Shell Roof and Mesh

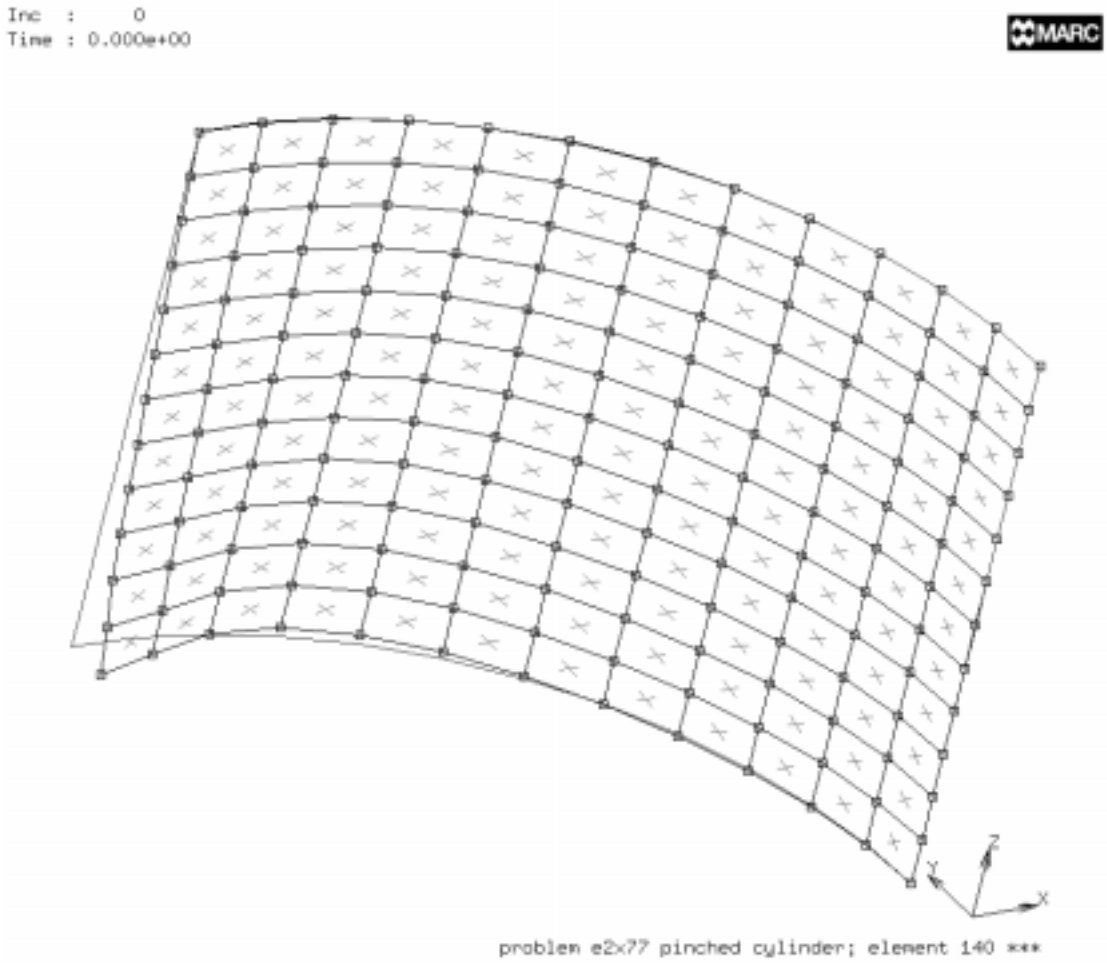

Figure 2.77-2 Deformed Mesh Plot

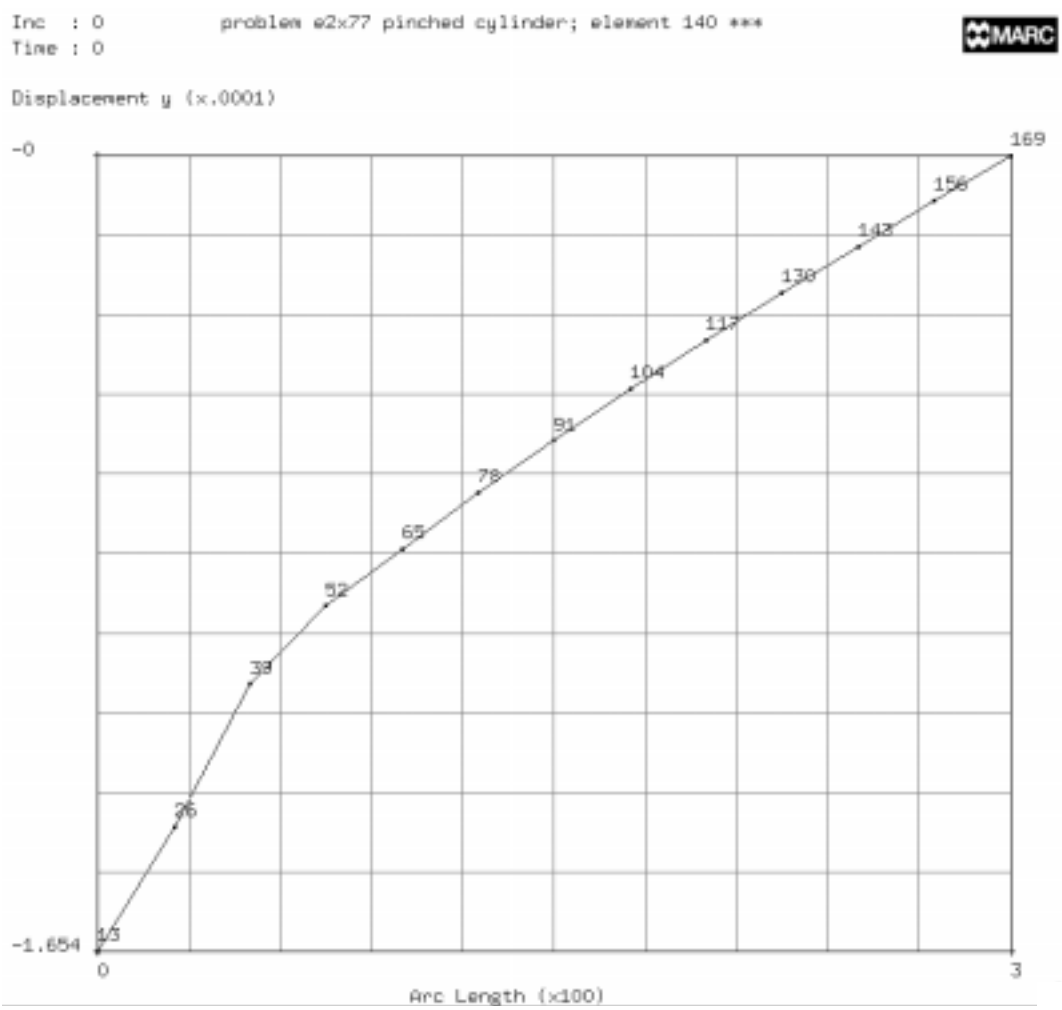

Figure 2.77-3 Y Deformation Along X = 0

Document Title: **MARC® Volume E: Demonstration Problems, Part I, K7**
Part Number: RF-3018-07.I
Revision Date: June, 1998

UNITED STATES

CALIFORNIA - Palo Alto
MARC Corporate Headquarters
260 Sheridan Avenue, Suite 309
Palo Alto, CA 94306, USA
Tel: 1 650 329 6800
Fax: 1 650 323 5892
Email: support@marc.com

CALIFORNIA - San Diego
MARC Analysis Research Corp.
4330 LaJolla Village Drive, Suite 320
San Diego, CA 92122
Tel: 1 619 658 9588
Fax: 1 619 758 8710

CONNECTICUT - E. Berlin
MARC Analysis Research Corp.
1224 Mill Street
E. Berlin, CT 06023
Tel: 1 860 828 2055
Fax: 1 860 828 2031

MICHIGAN - Ann Arbor
MARC Analysis Research Corp.
24 Frank Lloyd Wright Drive
Ann Arbor, MI 48106-0523
Tel: 1 734 998 0540
Fax: 1 734 998 0542

EUROPE

CZECH REPUBLIC
MARC Overseas, Inc.
Podolska 50
147 00 Praha 4
Czech Republic
Tel: 420 (2) 6121 4123
420 (2) 6121 4111 x252
Fax: 420 (2) 6121 4123
Email: support@marc.cz

FRANCE
MARC France S.A.
Bercy Expo SR 6101A
40 Avenue des Terroirs de France
75611 Paris Cedex 12, France
Tel: 33 (1) 4474 1550
Fax: 33 (1) 4474 1554
Email: support@marc.fr

GERMANY - Munich
MARC Software Deutschland GmbH
Ismaninger Str. 9
85609 Aschheim (bie Munich)
Germany
Tel: 49 (89) 904 50 33
Fax: 49 (89) 903 06 76
Email: support@marc.de

GERMANY - Hannover
MARC Software Deutschland GmbH
Alte Dohrener Str. 66
D 30173 Hannover, Germany
Tel: 49 (511) 980 5182
Fax: 49 (511) 980 5187

ITALY
Espri-MARC s.r.l.
Viale Brigata Bisagno 2 / 10
16129 Genova, Italy
Tel: 39 (10) 585 949
Fax: 39 (10) 585 949
Email: espri.marc@interbusiness.it

THE NETHERLANDS
MARC Analysis Research Corporation
Dublinstraat 32
2713 HS Zoetermeer
The Netherlands
Tel: 31 (79) 3510 411
Fax: 31 (79) 3517 560
Email: support@marc.nl

UNITED KINGDOM
MARC UK Ltd.
11 Linford Forum, Rockingham Drive
Linford Wood
Milton Keynes, MK14 6LY
Tel: 44 (1908) 606 070
Fax: 44 (1908) 606 633
Email: support@marc.co.uk

PACIFIC RIM

CHINA
MARC Overseas, Inc.
Bright Chang An Building, Suite 321
7# Jian Guo Men Nei Street
Beijing, China 100 005
Tel: 86 (10) 6510 2056
86 (10) 6510 2057
86 (10) 6510 2058
Fax: 86 (10) 6510 2053
Email: marcbj@public.bta.net.cn

JAPAN - Nagoya
Nippon MARC Co., Ltd.
Nagoya Nishiki Daiichi Seimei Bldg.
2F, 6-5 Nishiki 1-chome
Naka-ku, Nagoya, Aichi 460-0003
Tel: 81 (52) 202 5661
Fax: 81 (52) 202 5665

JAPAN - Osaka
Nippon MARC Co., Ltd.
4F 2nd Kimi Building
2-11 Toyotucho Suita-shi
Osaka 564-0051
Tel: 81 (6) 385 1101
Fax: 81 (6) 385 4343

JAPAN - Tokyo
(Asian Operations Headquarters)
Nippon MARC Co., Ltd.
Shinjuku Daiichi Seimei Building
P.O. Box 5056
2-7-1 Nishi-Shinjuku, Shinjuku-ku
Tokyo 163-0704
Tel: 81 (3) 3345 0181
Fax: 81 (3) 3345 1529
Email: support@marc.co.jp

KOREA
Dong Kyung Bldg. 7FL
824-19 Yuksam-Dong
Kangnam-Ku, Seoul, Korea
Tel: 82 (2) 561 7543
Fax: 82 (2) 561 7767
Email: marck@unitel.co.kr

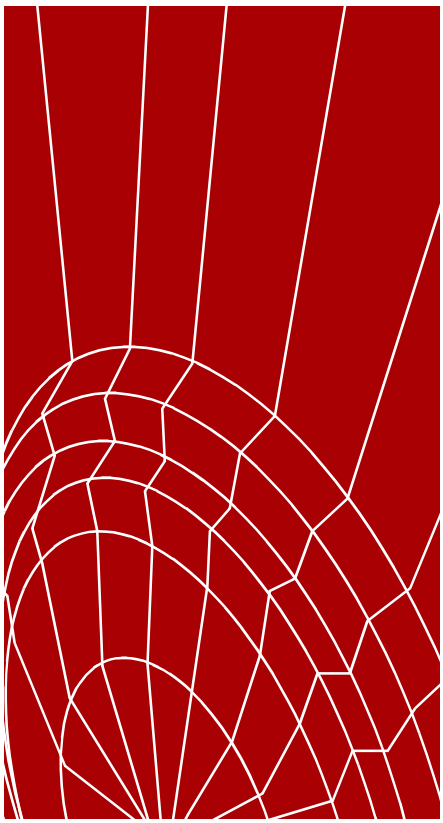

MARC Analysis Research Corporation

MARC®

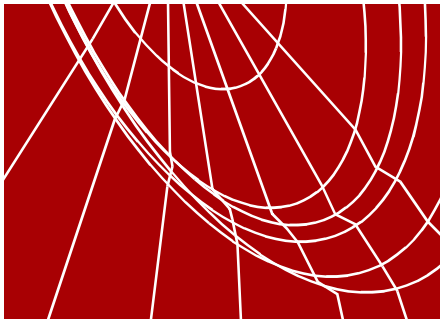

Volume E

Demonstration Problems

Version K7

Copyright © 1998 MARC Analysis Research Corporation
Printed in U. S. A.
This notice shall be marked on any reproduction of this data, in whole or in part.

MARC Analysis Research Corporation
260 Sheridan Avenue, Suite 309
Palo Alto, CA 94306 USA

Phone: (650) 329-6800
FAX: (650) 323-5892

Document Title: **MARC® Volume E: Demonstration Problems, Part II, Version K7**
Part Number: RF-3018-07.II
Revision Date: June, 1998

Proprietary Notice

MARC Analysis Research Corporation reserves the right to make changes in specifications and other information contained in this document without prior notice.

ALTHOUGH DUE CARE HAS BEEN TAKEN TO PRESENT ACCURATE INFORMATION, MARC ANALYSIS RESEARCH CORPORATION DISCLAIMS ALL WARRANTIES WITH RESPECT TO THE CONTENTS OF THIS DOCUMENT (INCLUDING, WITHOUT LIMITATION, WARRANTIES OR MERCHANTABILITY AND FITNESS FOR A PARTICULAR PURPOSE) EITHER EXPRESSED OR IMPLIED. MARC ANALYSIS RESEARCH CORPORATION SHALL NOT BE LIABLE FOR DAMAGES RESULTING FROM ANY ERROR CONTAINED HEREIN, INCLUDING, BUT NOT LIMITED TO, FOR ANY SPECIAL, INCIDENTAL OR CONSEQUENTIAL DAMAGES ARISING OUT OF, OR IN CONNECTION WITH, THE USE OF THIS DOCUMENT.

This software product and its documentation set are copyrighted and all rights are reserved by MARC Analysis Research Corporation. Usage of this product is only allowed under the terms set forth in the MARC Analysis Research Corporation License Agreement. Any reproduction or distribution of this document, in whole or in part, without the prior written consent of MARC Analysis Research Corporation is prohibited.

Restricted Rights Notice

This computer software is commercial computer software submitted with “restricted rights.” Use, duplication, or disclosure by the government is subject to restrictions as set forth in subparagraph (c)(i)(ii) or the Rights in technical Data and Computer Software clause at DFARS 252.227-7013, NASA FAR Supp. Clause 1852.227-86, or FAR 52.227-19. Unpublished rights reserved under the Copyright Laws of the United States.

Trademarks

All products mentioned are the trademarks, service marks, or registered trademarks of their respective holders.

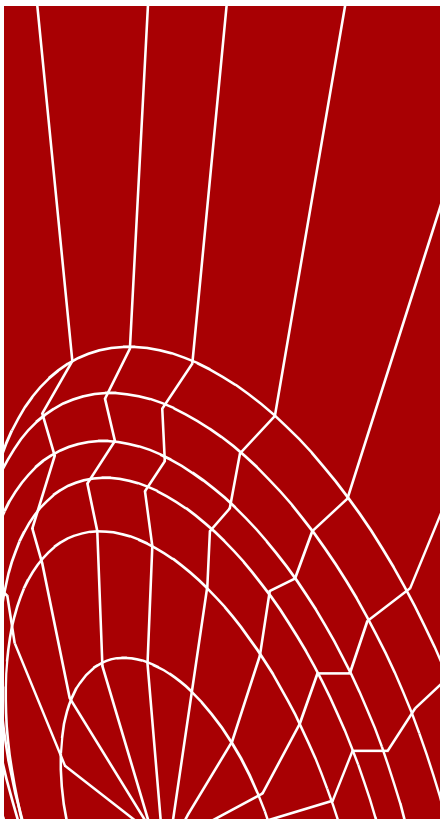

MARC Analysis Research Corporation

MARC®

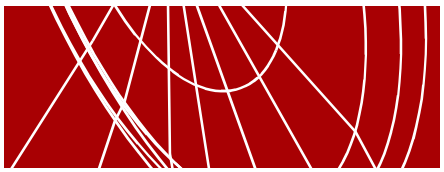

Volume E

Demonstration Problems

Version K7

Part II

- Plasticity and Creep
- Large Displacement

Part II

Volume E: Demonstration Problems

Chapter 3 **Plasticity And Creep**

Chapter 4 **Large Displacement**

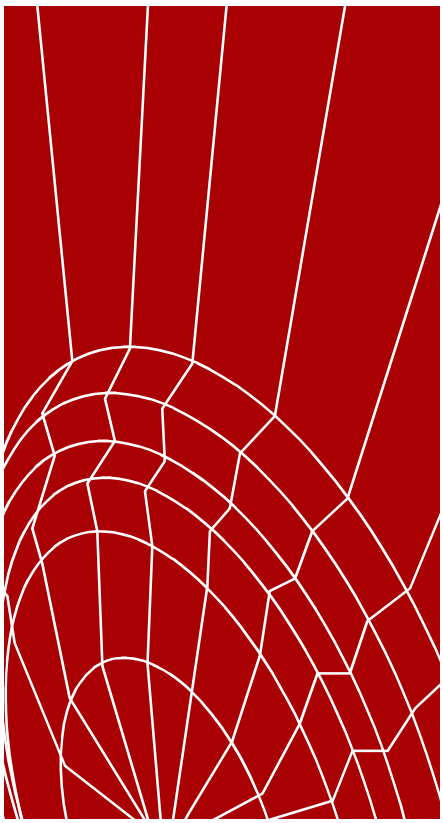

MARC Analysis Research Corporation

MARC®

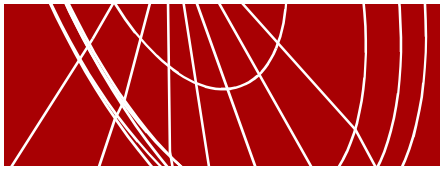

Volume E

Demonstration Problems

Version K7

Chapter 3 Plasticity and Creep

3 Plasticity And Creep Contents

Description	Problem
Combined Tension and Torsion of a Thin-walled Cylinder	3.1
Combined Tension and Torsion of a Thick-walled Cylinder	3.2
Limit Load Analysis	3.3
Bending of Prismatic Beam	3.4
Hemispherical Shell under Thermal Expansion	3.5
Collapse Load of a Simply Supported Square Plate	3.6
Elastic-Plastic Analysis of a Thick Cylinder	3.7
Double-Edge Notch Specimen under Axial Tension	3.8
Analysis of a Soil with a Cavity, Mohr-Coulomb Example	3.9
Plate with Hole Subjected to a Cyclic Load	3.10
Axisymmetric Bar in Combined Tension and Thermal Expansion	3.11
Creep of Thick Cylinder (Plane Strain)	3.12
Beam Under Axial Thermal Gradient and Radiation-induced Swelling	3.13
Creep Bending of Prismatic Beam with ORNL Constitutive Equation and Load Reversal	3.14
Creep of a Square Plate with a Central Hole using Creep Extrapolation	3.15
Plastic Buckling of an Externally Pressurized Hemispherical Dome	3.16
Shell Roof with Geometric and Material Nonlinearity	3.17
Analysis of the Modified Olson Cup Test	3.18
Axisymmetric Upsetting – Height Reduction 20%	3.19
Plastic Bending of a Straight Beam into a Semicircle	3.20
Necking of a Cylindrical Bar	3.21

Combined Thermal, Elastic-plastic, and Creep Analysis 3.22
Nonlinear Analysis of a Shell Roof, using Automatic Incrementation 3.23
Creep Analysis of a Plate with a Hole using AUTO-THERM-CREEP Option. 3.24
Pressing of a Powder Material 3.25
Hot Isostatic Pressing of a Powder Material. 3.26
Shear Band Development 3.27
Void Growth in a Notched Specimen 3.28
Creep of a Thick Walled Cylinder - Implicit Procedure 3.29
3D Forming of a Circular Blank using Rigid-Plastic Formulation 3.30
Formation of Geological Series 3.31
Superplastic Forming of a Strip 3.32
Large Strain Tensile Loading of a Plate with a Hole 3.33
Inflation of a Thin Cylinder 3.34
Cantilever Beam under Point Load 3.35
Tensile Loading of a Strip with a Cylindrical Hole 3.36
Elastic Deformation in a Closed Loop. 3.37
Tensile Loading and Rigid Body Rotation. 3.38

3 Plasticity and Creep List of Figures

Figure		Page
3.1-1	Thin Walled Cylinder and Mesh	3.1-4
3.2-1	Thick Walled Cylinder and Mesh	3.2-4
3.2-2	Stress-Strain Curve	3.2-5
3.2-3	Displacement History at Inner Radius	3.2-5
3.3-1	Finite Element Mesh	3.35
3.3-2	σxy Contour Element 11	3.36
3.3-3	σxy Contour Element 115	3.37
3.3-4	Load-Displacement Curve	3.38
3.4-1	Prismatic Beam Model and Mesh	3.4-3
3.4-2	Moment-Rotation Diagram	3.4-4
3.4-3	Residual Stress Distribution for Zero Moment	3.4-5
3.5-1	Hemispherical Shell and Mesh	3.5-4
3.5-2	Workhardening Curve	3.5-5
3.5-3	Displaced Mesh	3.5-6
3.6-1	Square Plate and Finite Element Mesh	3.6-3
3.6-2	Central Deflection Versus Nodal Load (MARC Solution)	3.6-4
3.6-3	Central Deflection Versus Nodal Load (Reference Solution)	3.6-5
3.7-1	Cylinder Wall	3.7-5
3.7-2	Cylinder Wall Generated Mesh	3.7-6
3.7-3	Pressure Versus Elastic-Plastic Boundary	3.7-6
3.7-4	Radial Stress Distribution	3.7-7
3.7-5	Circumferential Stress Distribution	3.7-7
3.7-6	Axial Stress Distribution	3.7-8

Figure **Page**

3.8-1 D.E.N. Specimen 3.8-5
3.8-2 Mesh for D.E.N. 3.8-6
3.8-3 Workhardening Slopes 3.8-7
3.8-4 Equivalent Plastic Strain for Increment 5 . . . . . 3.8-8

3.9-1 Simple Geometry Mesh. 3.9-4
3.9-2 Plane Strain Yield Surfaces. 3.9-5
3.9-3 Yield Surfaces in Plane 3.9-5
3.9-4 Global Load Displacement 3.9-6
3.9-5 Equivalent Stress at 307 psi. 3.9-7
3.9-6 Mean Normal Stress at 307 psi 3.9-8
3.9-7 Equivalent Plastic Strain at 307 psi. 3.9-9
3.9-8 Equivalent von Mises Stress at 475 psi. 3.9-10
3.9-9 Mean Normal Stress at 475 psi 3.9-11
3.9-10 Equivalent Plastic Strain at 475 psi. 3.9-12

3.10-1 Mesh Layout for Plate with Hole 3.10-3
3.10-2 Workhardening Curve. 3.10-4
3.10-3 von Mises Stress Results. 3.10-5
3.10-4 Displaced Mesh. 3.10-6

3.11-1 Axisymmetric Bar and Mesh. 3.11-3

3.12-1 Thick Cylinder Geometry and Mesh. 3.12-8
3.12-2 Creep of Thick Cylinder, Long Time Results. 3.12-8
3.12-3 Creep of Thick Cylinder – Numerical Comparisons. 3.12-9
3.12-4 Creep of Thick Cylinder – Numerical Comparisons. 3.12-9
3.12-5 Creep of Thick Cylinder – Numerical Comparisons. 3.12-10
3.12-6 Creep Ring. 3.12-10

3.13-1 Beam-Spring Model 3.13-5
3.13-2 Transient Extreme Fiber Stress 3.13-5

3.14-1 Geometry of Beam and Finite Element Mesh. 3.14-4
3.14-2 Creep Strain Coefficient as Function of Creep Strain. 3.14-5
3.14-3 Stress Distribution through the Thickness before Load Reversal. 3.14-6
3.14-4 Stress Distribution through the Thickness after Load Reversal 3.14-6
3.14-5 Relaxation Curve for Bending Moment 3.14-7

Figure **Page**

3.15-1 Mesh Layout for Plate with Hole 3.15-5
3.15-2 Stress Relaxation 3.15-6
3.15-3 Creep Strain History 3.15-7

3.16-1 Geometry and Mesh 3.16-6
3.16-2 Buckling Mode, Increment 0 . . . . . 3.16-7
3.16-3 Buckling Mode, Increment 2 . . . . . 3.16-8
3.16-4 Buckling Mode, Increment 4 . . . . . 3.16-9
3.16-5 Second Buckling Mode, Increment 6 . . . . . 3.16-10
3.16-6 Second Buckling Mode, Increment 8 . . . . . 3.16-11

3.17-1 Shell Roof 3.17-4
3.17-2 Mesh of Shell Roof 3.17-5
3.17-3 Load Displacement Curve, Node 96 . . . . . 3.17-6
3.17-4 Equivalent Plastic Strain in Layer 1 History for Selective Nodes 3.17-7

3.18-1 Modified Olsen Cup Test 3.18-4
3.18-2 Tensile Stress-Strain Curve 3.18-4
3.18-3 Load vs. Displacement 3.18-5

3.19-1 Model with Elements and Nodes Labeled 3.19-6
3.19-2 von Mises Stress Contours at Increment 20 Element Type 10 . . . . . 3.19-7
3.19-3 von Mises Stress Contours at Increment 20 Element Type 116 . . . . . 3.19-8
3.19-4 von Mises Stress Contours at Increment 20 Element Type 116 (Fine Mesh) 3.19-9
3.19-5 von Mises Stress Contours at Increment 20, Element Type 10, F^eF^p Formulation 3.19-10
3.19-6 Load Displacement Curve 3.19-11

3.20-1 Workhardening Curve 3.20-4
3.20-2 Deformed Beam after Release of End 3.20-5

3.21-1 Model with Elements Numbered 3.21-6
3.21-2 Model with Nodes Labeled 3.21-7
3.21-3 Load -Displacement Curve 3.21-8
3.21-4 Vector Plot of Reactions for Type 10 . . . . . 3.21-9
3.21-5 Contour Plot of Equivalent Strain for Type 10 . . . . . 3.21-10
3.21-6 Vector Plot of Reactions for Type 116 (Coarse Mesh) 3.21-11
3.21-7 Contour Plot of Equivalent Plastic Strain for Type 116 (Coarse Mesh) 3.21-12

Figure **Page**

3.21-8 Final Mesh After Adaptive Meshing. 3.21-13
3.21-9 Vector Plot of Reactions for Type 10 (F^eF^p) 3.21-14
3.21-10 Contour Plot of Equivalent Strain for Type 10 (F^eF^p) 3.21-15

3.22-1 Temperature-Time History 3.22-7
3.22-2 Pressure-Time History. 3.22-7
3.22-3 Geometry and Mesh for Combined Thermal, Elastic-Plastic, and Creep Problem. 3.22-8
3.22-4 Transient Temperature Time History (Auto Time Step). 3.22-9
3.22-5 Temperature Distribution in Cylinder Wall 3.22-10
3.22-6 Thermal Elastic Plastic Results 3.22-11
3.22-7 Creep Results. 3.22-12

3.23-1 Model with Elements and Nodes Labeled. 3.23-4
3.23-2 Equivalent Plastic Strain, Layer 1 . . . . . 3.23-5
3.23-3 Equivalent Plastic Strain, Layer 3 . . . . . 3.23-6
3.23-4 Equivalent Plastic Strain, Layer 5 . . . . . 3.23-7
3.23-5 Load Displacement Curve 3.23-8

3.24-1 Plate with a Hole 3.24-6
3.24-2 Nodal Temperature vs. Time (Node 9) 3.24-7
3.24-3 Effective Stresses at Element 4 . . . . . 3.24-8

3.25-1 Finite Element Mesh 3.25-3
3.25-2 Time History of Externally Applied Load 3.25-4
3.25-3 Time History of Relative Density 3.25-5
3.25-4 Time History of Strain Rate 3.25-6
3.25-5 Time History of Equivalent Plastic Strain. 3.25-7

3.26-1 Mesh 3.26-4
3.26-2 Time History 3.26-5
3.26-3 Final Relative Density. 3.26-6
3.26-4 Time History of Relative Density 3.26-7
3.26-5 Time History of Equivalent Strain Rate 3.26-8
3.26-6 Time History of Equivalent Plastic Strain. 3.26-9

3.27-1 Finite Element Mesh 3.27-3
3.27-2 Stress-Strain Law 3.27-4

Figure **Page**

3.27-3 Deformed Mesh at Increment 120. . . . . 3.27-5
3.27-4 Deformed Mesh at Increment 160. . . . . 3.27-6
3.27-5 Deformed Mesh at Increment 200. . . . . 3.27-7
3.27-6 Void Volume Fraction at Increment 120. . . . . 3.27-8
3.27-7 Void Volume Fraction at Increment 160. . . . . 3.27-9
3.27-8 Void Volume Fraction at Increment 200. . . . . 3.27-10
3.27-9 Void Volume Fraction at Increment 240. . . . . 3.27-11
3.27-10 Time History of Void Volume Fraction 3.27-12
3.27-11 Time History of Plastic Strain. 3.27-13

3.28-1 Notched Specimen. 3.28-3
3.28-2 Mesh 3.28-4
3.28-3 Stress-Strain Curve 3.28-5
3.28-4 Deformed Mesh. 3.28-6
3.28-5 Void Volume Fraction. 3.28-7
3.28-6 Equivalent Plastic Strain 3.28-8
3.28-7 Time History of Void Volume Fraction 3.28-9

3.29-1 Finite Element Mesh 3.29-3
3.29-2 Time History of Equivalent Creep Strain – Implicit Procedure 3.29-4
3.29-3 Time History of Equivalent Creep Strain – Explicit Procedure 3.29-5

3.30-1 Circular Blank Holder and Punch 3.30-5
3.30-2 Deformed Sheet at Increment 40. . . . . 3.30-6
3.30-3 Equivalent Plastic Strains in Membrane 3.30-7
3.30-4 Equivalent Stresses in Membrane 3.30-8
3.30-5 Equivalent Plastic Strains at Midlayer of Shell. 3.30-9
3.30-6 Equivalent Stresses at Midlayer of Shell. 3.30-10

3.31-1 FEM Model of the Geological Strata 3.31-3
3.31-2 Detailed Mesh at the Fault Plane. 3.31-4
3.31-3 Overlap of the Geological Strata. 3.31-5
3.31-4 Distribution of the σ_{xx} Stress Component (Global Axes) 3.31-6
3.31-5 Distribution of the σ_{yy} Stress Component (Global Axes) 3.31-7

3.32-1 Plane Strain SPF Model with Boundary Conditions. 3.32-4
3.32-2 Membrane and Shell SPF Model with Boundary Conditions. 3.32-5

Figure **Page**

3.32-3 Plane Strain SPF Model Final Shape 3.32-6
3.32-4 Pressure Schedule for all Models 3.32-7
3.32-5 Thickness Profile for all Models 3.32-8
3.32-6 Thickness Profile Membrane Friction Effects. 3.32-9

3.33-1 Initial Model for Hole-in-Plate 3.33-3
3.33-2 Equivalent Plastic Strain on the Deformed Model 3.33-4
3.33-3 History Plot of x Displacement versus Increment for Node 34 . . . . . 3.33-5

3.34-1 Initial Mesh for Cylinder Inflation 3.34-3
3.34-2 Initial and Final Configuration for Cylinder Inflation. 3.34-4

3.35-1 Cantilever Beam under Point Load 3.35-2
3.35-2 FE-Mesh 3.35-3
3.35-3 Deformed Mesh and Distribution of Equivalent Plastic Strain at Increment 30. . . 3.35-4
3.35-4 Deformed Mesh and Distribution of Equivalent Plastic Strain at Increment 90. . . 3.35-5

3.36-1 Plasticity Initiates at the Hole in Increment 2 . . . . . 3.36-3
3.36-2 Contours of Effective Plastic Strain after 20 Increments 3.36-4
3.36-3 Contours of Effective Plastic Strain after 37 Increments 3.36-5

3.37-1 Elastic Deformation in a Closed Loop 3.37-2
3.37-2 Nodal Reaction Forces after a Closed Loop of Elastic Deformation 3.37-3
3.37-3 History Plot of Equivalent von Mises Stress. 3.37-3

3.38-1 Initial Model 3.38-3
3.38-2 Deformed Model at the End of Increment 10 . . . . . 3.38-4
3.38-3 Deformed Model at the End of Increment 11 . . . . . 3.38-5
3.38-4 History Plot of Equivalent Stress versus Effective Plastic Strain for Nodes 1 and 9 . . . . . 3.38-6

3 Plasticity and Creep List of Tables

Table		Page
3-1	Nonlinear Material Demonstration Problems	3-2
3.8-1	J-Integral Evaluation Results	3.8-3
3.12-1	Creep of Thick Cylinder – Comparison of Results at 20 Hours	3.12-6
3.16-1	Eigenvalues	3.16-5
3.24-1	von Mises Stresses at Element 4	3.24-3
3.33-1	Hardening Behavior	3.33-2
3.34-1	Effective Plastic Strain.	3.34-2

3 Plasticity and Creep

MARC contains an extensive material library. A discussion on the use of these capabilities is found in *Volume A: User Information*. In this chapter, material nonlinearity often exhibited in metals is demonstrated. Material nonlinearity associated with rubber or polymer materials can be found in Chapter 7. The capabilities demonstrated here can be summarized as:

Variable load paths

- Proportional loads
- Nonproportional loads

Choice of yield functions

- von Mises
- Drucker-Prager, Mohr-Coulomb
- Gurson
- Shima

Strain magnitude

- Infinitesimal plasticity
- Finite strain plasticity

Strain hardening

- Limit Analysis
- Isotropic hardening
- Kinematic hardening

Rate effects

- Deviatoric creep
- Volumetric swelling
- ORNL

Compiled in this chapter are a number of solved problems. Table 3-1 summarizes the element type and options used in these demonstration problems.

Table 3-1 Nonlinear Material Demonstration Problems

Problem Number	Element Type(s)	Parameters	Model Definition	History Definition	User Subroutines	Problem Description
3.1	4	TIE SCALE SHELL TRAN SHELL SECT	WORK HARD CONTROL FXORD SHELL TRAN TYING, 2, 6, & 100	AUTO LOAD PROPORTIONAL	—	Combines tension and torsion of a thin-walled cylinder
3.2	67	SCALE	TYING, 1 & 3 WORK HARD CONTROL	AUTO LOAD PROPORTIONAL	—	Combines tension and torsion of a thick-walled cylinder.
3.3	11 115	SCALE	MESH2D CONTROL	AUTO LOAD PROPORTIONAL	IMPD	Limit load analysis of bar.
3.4	16	SCALE SHELL SECT	WORK HARD CONTROL	AUTO LOAD PROPORTIONAL	UFORMS	Bending of prismatic beam.
3.5	15	THERMAL SHELL SECT	UFXORD TRANSFORMATION THERMAL LOAD WORK HARD TEMPERATURE EFFECT CONTROL INITIAL STATE	AUTO THERM CHANGE STATE	WKSLP UFXORD	Hemispherical shell under thermal expansion.
3.6	50	SCALE SHELL SECT	DEFINE CONTROL	AUTO LOAD PROPORTIONAL	ANPLAS	Bending of square plate, simple supported, pressure load.
3.7	10	SCALE	CONTROL RESTART	AUTO LOAD PROPORTIONAL	—	Elastic-plastic analysis of a thick cylinder
3.8	27	SCALE J-INT	J INTEGRAL WORK HARD CONTROL	PROPORTIONAL	WKSLP	Double edge notch specimen under axial tension.
3.9	11	SCALE	OPTIMIZE, 2 CONTROL	AUTO LOAD PROPORTIONAL	—	Mises Mohr-Coulomb example.
3.10	26	SCALE	WORK HARD CONTROL OPTIMIZE, 2	AUTO LOAD PROPORTIONAL	—	Plate with hole.
3.11	28	SCALE THERMAL	TYING, 1 WORK HARD CONTROL RESTART	AUTO THERM CHANGE STATE PROPORTIONAL	—	Axisymmetric bar in combined tension and thermal expansion.

Table 3-1 Nonlinear Material Demonstration Problems (Continued)

Problem Number	Element Type(s)	Parameters	Model Definition	History Definition	User Subroutines	Problem Description
3.12	10	CREEP SCALE	CREEP CONTROL	AUTO CREEP	CRPLAW	Creep ring.
3.13	25	THERMAL STATE VARS CREEP	THERMAL LOADS SPRINGS CREEP CONTROL	AUTO CREEP	VSWELL CREDE	Beam under axial thermal gradient.
3.14	16	CREEP SHELL SECT	CONTROL CREEP	DISP CHANGE AUTO CREEP	—	Creep bending of prismatic beam.
3.15	26	POST CREEP ACCUM BUC	OPTIMIZE, 2 CONTROL CREEP	AUTO CREEP CREEP INCREMEN T EXTRAPOLATE	—	Creep of a square plate with central hole.
3.16	15	LARGE DISP SHELL SECT BUCKLE	UFXORD TRANSFORMATION WORK HARD CONTROL	AUTO LOAD PROPORTIONAL BUCKLE	UFXORD	Plastic buckling of externally pressurized hemispherical dome.
3.17	72	SHELL SECT LARGE DISP	UFXORD	AUTO LOAD PROPORTIONAL	UFXORD	Shell roof with nonlinearities.
3.18	15 12	LARGE DISP UPDATE FINITE SHELL SECT MATERIAL	WORK HARD TYING, 102 CONTROL GAP DATA	AUTO LOAD DISP CHANGE	—	Olson cup test.
3.19	10 116	LARGE DISP UPDATE FINITE	WORK HARD CONTROL UDUMP	AUTO LOAD PROPORTIONAL	IMPD	Compression of an axisymmetric member, height reduction 20%.
3.20	16	LARGE DISP FOLLOW FOR SHELL TRAN UPDATE FINITE	CONN GENER WORK HARD CONTROL NODE FILL SHELL TRAN	AUTO LOAD PROPORTIONAL	—	Bending of beam into semicircle.
3.21	10 116	UPDATE LARGE DISP FINITE	WORK HARD UDUMP	AUTO LOAD PROPORTIONAL	IMPD	Necking of a cylindrical bar.
3.22	42 28	ALIAS HEAT CREEP THERMAL	INITIAL TEMP CONTROL FILMS TYING, 1 CREEP INITIAL STATE	TRANSIENT AUTO THERM CHANGE STATE AUTO CREEP	FILM CRPLAW	Combined thermal, elastic-plastic, and creep analysis.

Table 3-1 Nonlinear Material Demonstration Problems (Continued)

Problem Number	Element Type(s)	Parameters	Model Definition	History Definition	User Subroutines	Problem Description
3.23	75	SHELL SECT LARGE DISP PROCESSOR	POST CONTROL	AUTO INCREMENT	UFXORD	Analysis of a shell roof with material and geometric nonlinearity. Demonstrate adaptive load control.
3.24	41 26	HEAT CREEP	INITIAL TEMP FIXED TEMP FILMS INITIAL STATE CREEP	TRANSIENT AUTO THERM CREEP CHANGE STATE	CRPLAW	Uncoupled thermal creep stress analysis of a pressure vessel.
3.25	11	LARGE DISP UPDATE FOLLOW FOR	POWDER RELATIVE DENSITY DENSITY EFFECTS	TIME STEP AUTO LOAD	—	Hot isostatic pressing of a can demonstrates powder model.
3.26	28	LARGE DISP UPDATE FOLLOW FOR COUPLE	DEFINE POWDER WORK HARD RELATIVE DENSITY TEMP EFFECTS DENSITY EFFECTS FIXED TEMP FORCDT	TRANSIENT	FORCDT	Hot isostatic pressing coupled analysis.
3.27	54	UPDATE FINITE LARGE DISP	DEFINE UFXORD WORK HARD DAMAGE	DISP CHANGE AUTO LOAD	UFXORD	Shear band development, Gurson damage model.
3.28	55	UPDATE FINITE LARGE DISP	DEFINE WORK HARD DAMAGE	DISP CHANGE AUTO LOAD	—	Notched Specimen, Gurson damage model.
3.29	10	CREEP	CREEP	AUTO CREEP	—	Creep ring – implicit procedure.
3.30	18 75	R-P FLOW ISTRESS	CONTACT WORK HARD	AUTO LOAD MOTION CHANGE	WKSLP UINSTR	Deep drawing by a spherical punch.
3.31	11	LARGE DISP UPDATE	CONTACT CONTACT TABLE	AUTO LOAD DISP CHANGE DIST LOADS	—	Formation of geological strata.
3.32	11 18 75	R-P FLOW FOLLOW FOR	CONTACT	AUTO LOAD	UINSTR URPFLO PLOTV	Superplastic forming of a strip.
3.33	26	PLASTICITY	WORK HARD	AUTO STEP DISP CHANGE	—	Large strain stretching of plate with hole.

Table 3-1 Nonlinear Material Demonstration Problems (Continued)

Problem Number	Element Type(s)	Parameters	Model Definition	History Definition	User Subroutines	Problem Description
3.34	18	PLASTICITY FOLLOW FOR	WORK HARD	AUTO LOAD DIST LOADS	—	Inflation of thin cylinder.
3.35	11	PLASTICITY	WORK HARD	AUTO LOAD POINT LOAD PROPORTIONAL	—	Large bending of a cantilever beam.
3.36	7	PLASTICITY	WORK HARD	AUTO LOAD DISP CHANGE	—	Large strain stretching of plate with hole.
3.37	11	PLASTICITY	—	AUTO LOAD DISP CHANGE	—	Elastic, closed loop deformation path.
3.38	3	PLASTICITY	WORK HARD	AUTO LOAD DISP CHANGE	—	Test rotational invarience.

3.1 Combined Tension and Torsion of a Thin-walled Cylinder

A thin-walled cylinder of 1 inch radius and 10 inches length is extended 1% of its original length ($\lambda = l/l_o = 1.01$) and then twisted so that the twist per unit original length ($\psi = \theta/l_o$) is 0.02. The material is elastic-plastic with isotropic hardening. This is the default option of MARC. This example demonstrates the ability of MARC to analyze small strain elastic-plastic problems.

Element

Element type 4, a curved quadrilateral thin shell, is used. This is a very accurate element for analyzing regular curved shells. Elements 22, 72, or 75 are easier to use.

Model

The cylinder is divided into four elements with ten nodes. As θ^1 and θ^2 must be continuous, the cylinder is modeled with a joint at angular coordinates (θ) 0 and 360 degrees. This joint is closed with use of TYING. The geometry and finite element mesh are shown in Figure 3.1-1. The nodal point input is θ, Z, and R. Since R is constant, it needs to be given only for the first nodal point. Type 4 of the FXORD option is then used to generate the complete coordinate set required by the elements in the program. One end of the cylinder is assumed fixed; the other end is under the combined action of tension and torsion.

Geometry

The cylinder thickness is 0.01 in. and is assigned in EGEOM1 of this option.

Shell Transformation

This option allows transformation of the even-numbered nodes from the global to a local direction. It facilitates the application of tension and torsion loading at the Z = 10 end in the POINT LOAD option. In particular, the degrees of freedom are transformed such that they are in the plane of the shell or normal to it at each node.

Tying

Three types of tying constraints are imposed in this example. The tying type 2 ties the second degree of freedom between node 2 and nodes 4, 6, and 8 for tensile load. The tying type 6 ties the sixth degree of freedom between node 2 and nodes 4, 6, and 8 for torsion load. The tying type 100 ties all degrees of freedom between node 1 and node 9, and between node 2 and node 10, joining together the shell boundaries at angular coordinates (θ) 0° and 360°.

Boundary Conditions

The cylinder is fixed against rotation and displacement at the Z = 0 end. Four sets of boundary conditions are necessary. Movement in the θ_2 direction is continuously zero $\left(\frac{\partial u}{\partial \theta_2} = \frac{\partial v}{\partial \theta_2} = w = 0\right)$. Also, movement tangent to the shell surface is zero $\left(\frac{\partial w}{\partial \theta_1} = 0\right)$ for nodes 1, 3, 5 and 7, $\frac{\partial u}{\partial \theta_1} = 0$ for nodes 1 and 5).

Material Properties

Values for Young's modulus, Poisson's ratio, and initial yield stress used here are 10.0×10^6 psi, 0.3 and 20,000 psi, respectively.

Work Hard

The single workhardening slope of 20.0×10^5 psi starts at zero plastic strain.

Loading

Axial tension is first applied to the second degree of freedom of node 2 in nine steps. At this increment, the maximum stress is 32,790 psi and the total plastic strain is 63.85×10^{-4}. The load is scaled to reach the yield surface in the first step. Subsequently, a torsion is applied to the sixth degree of freedom of node 2 in eight steps. The final maximum Mises' stress intensity is 51,300 psi with a plastic strain of 0.0168.

Results

The results show the cylinder is stretched axially to an extension of (λ) 1.00967 and the axial tension is 2044.4 pounds in nine steps. The cylinder is then twisted to ratio (ψ) 0.0204 and the torsion is 10 49.6 in-lb. in eight steps. The plastic strains are only 1.5% and the final stress is much less than the workhardening modulus; therefore, small strain theory is acceptable for this analysis. The PRINT CHOICE option is used to limit the printout to shell layers 2, 5, and 8.

Parameters, Options, and Subroutines Summary

Example e3x1.dat:

Parameter	Model Definition Options	History Definition Options
ELEMENTS	CONNECTIVITY	AUTO LOAD
END	CONTROL	CONTINUE
SCALE	COORDINATES	POINT LOAD
SHELL SECT	END OPTION	PROPORTIONAL INCREMENT
SIZING	FIXED DISP	
TITLE	FXORD	
	GEOMETRY	
	ISOTROPIC	
	POINT LOAD	
	PRINT CHOICE	
	SHELL TRANFORMATIONS	
	TYING	
	WORK HARD	

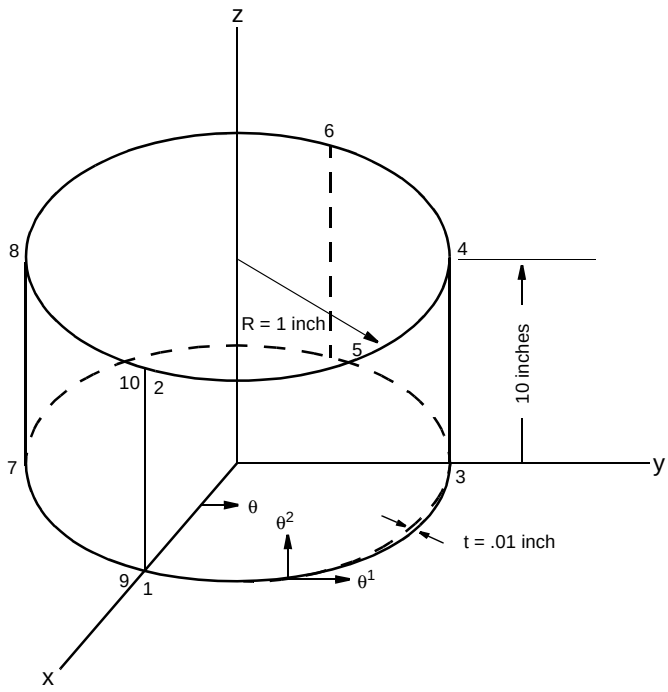

Figure 3.1-1 Thin Walled Cylinder and Mesh

3.2 Combined Tension and Torsion of a Thick-walled Cylinder

A thick-walled cylinder of 1 inch length, 2 inches outer radius, and 1 inch inner radius is extended 1% of its original length ($\lambda = l/l_o = 1.01$) and then twisted so that the twist per unit original length ($\psi = \theta/l_o$) is 1%. The material is elastic-plastic with kinematic hardening. This example demonstrates the ability of the program to analyze small strain elastic-plastic problems with kinematic hardening and change of loading conditions. The RESTART option is also demonstrated.

Element

Element type 67 is an axisymmetric 8-node distorted quadrilateral including a twist mode of deformation.

Model

The cylinder has been divided into five elements through the thickness with a total of 28 nodes. The mesh is shown in Figure 3.2-1.

Geometry

This option is not required for this element.

Tying

The displacements in Z and θ direction at the free (Z = 1) end are made the same by tying the first and third degrees of freedom of all nodes at this end to node 3. TYING types 1 and 3 are used for this purpose. This simulates a generalized plane-strain condition.

Boundary Conditions

The cylinder is fixed against rotation (θ) and displacement (Z) at the built-in end (Z = 0).

Material Properties

Values for Young's modulus, Poisson's ratio, and yield stress used here are 10.0×10^6 psi, 0.3 and 20,000 psi, respectively.

Workhard

The workhardening curve is specified with two primary workhardening slopes and breakpoints. The first workhardening slope is 2.0×10^6 psi. The second workhardening slope of 0.5×10^6 psi starts at a plastic strain of 1.0×10^{-2}. This is depicted in Figure 3.2-2.

Loading

An end load is applied axially to the cylinder through the first degree of freedom of node 3 in nine steps. Subsequently, an eight-step torsion load is applied in the third degree of freedom of node 3.

Restart

The analysis has been made in two runs using the RESTART option. The increment 0 loading is scaled to initiate yielding in the most highly stressed element. In the first run, the elastic-plastic solution due to tension is obtained in increments 0 through 8. The plastic strain is 30.64% at increment 8. Restart data is written to file 8 and is saved. The restart file is used for the second run, which starts at increment 8. In this run, torsion is applied in increments 9 through 17. The total plastic strain at increment 17 is 1.28%. The equivalent stress is 39,000 psi in this increment.

Results

The results show the cylinder is stretched axially to a strain of 0.68%, creating an axial load of 309,129 pounds. The cylinder is then twisted by an angular ratio (ψ) of 0.00779. The resultant twisting moment is 180,000 inches-pound. The displacement history is shown in Figure 3.2-3.

Parameters, Options, and Subroutines Summary

Example e3x2a.dat:

Parameter	Model Definition Options	History Definition Options
ELEMENTS	CONNECTIVITY	AUTO LOAD
END	CONTROL	CONTINUE
SCALE	COORDINATES	PROPORTIONAL INCREMENT
SIZING	END OPTION	
TITLE	FIXED DISP	
	ISOTROPIC	
	POINT LOAD	
	PRINT CHOICE	
	RESTART	
	WORK HARD	

Example e3x2b.dat:

Parameter Options	Model Definition Options	History Definition Options
ELEMENT	CONNECTIVITY	AUTO LOAD
END	CONTROL	CONTINUE
SCALE	COORDINATE	POINT LOAD
SIZING	END OPTION	PROPORTIONAL INCREMENT
TITLE	FIXED DISP	
	ISOTROPIC	
	POINT LOAD	
	PRINT CHOICE	
	RESTART	
	WORK HARD	

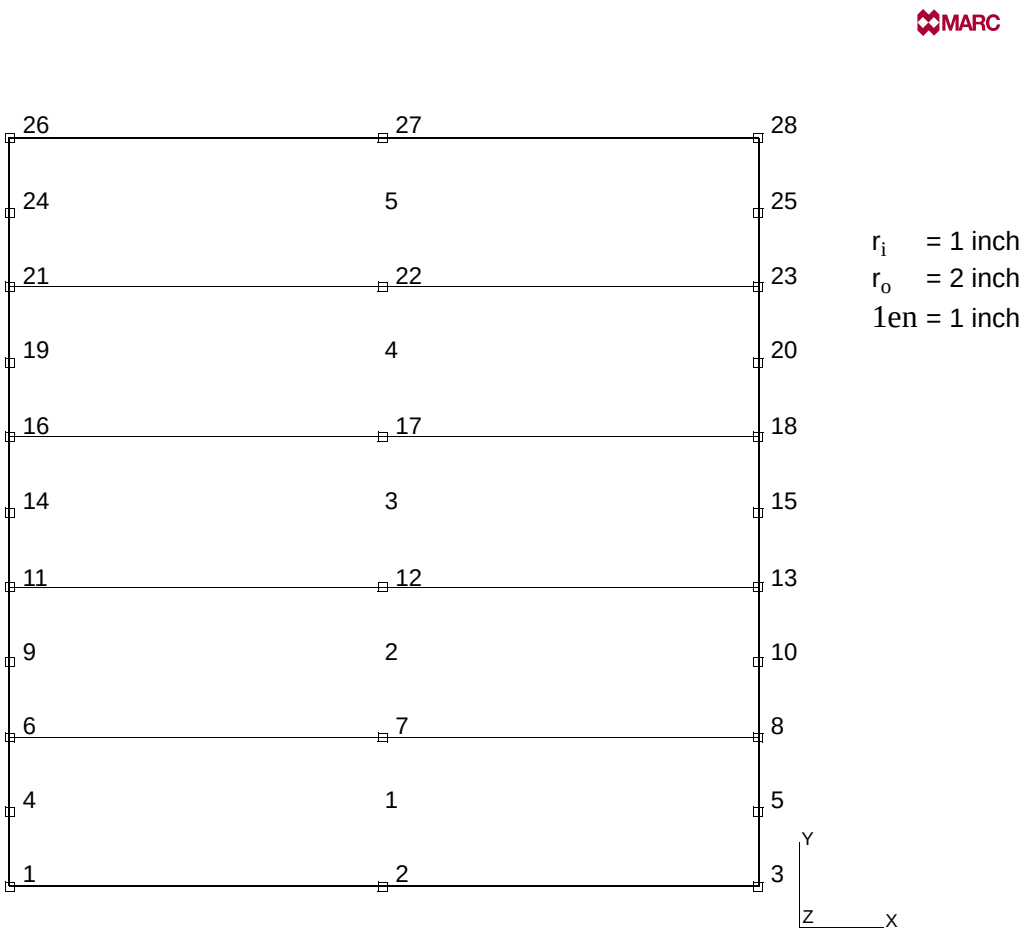

Figure 3.2-1 Thick Walled Cylinder and Mesh

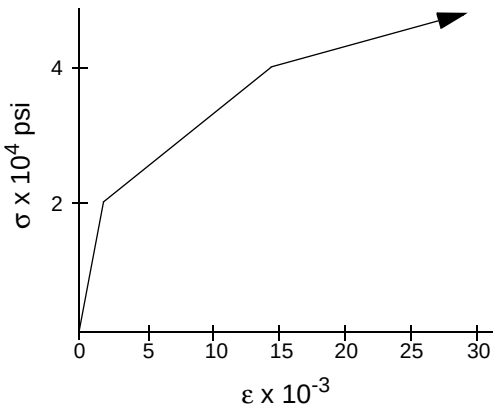

Figure 3.2-2 Stress-Strain Curve

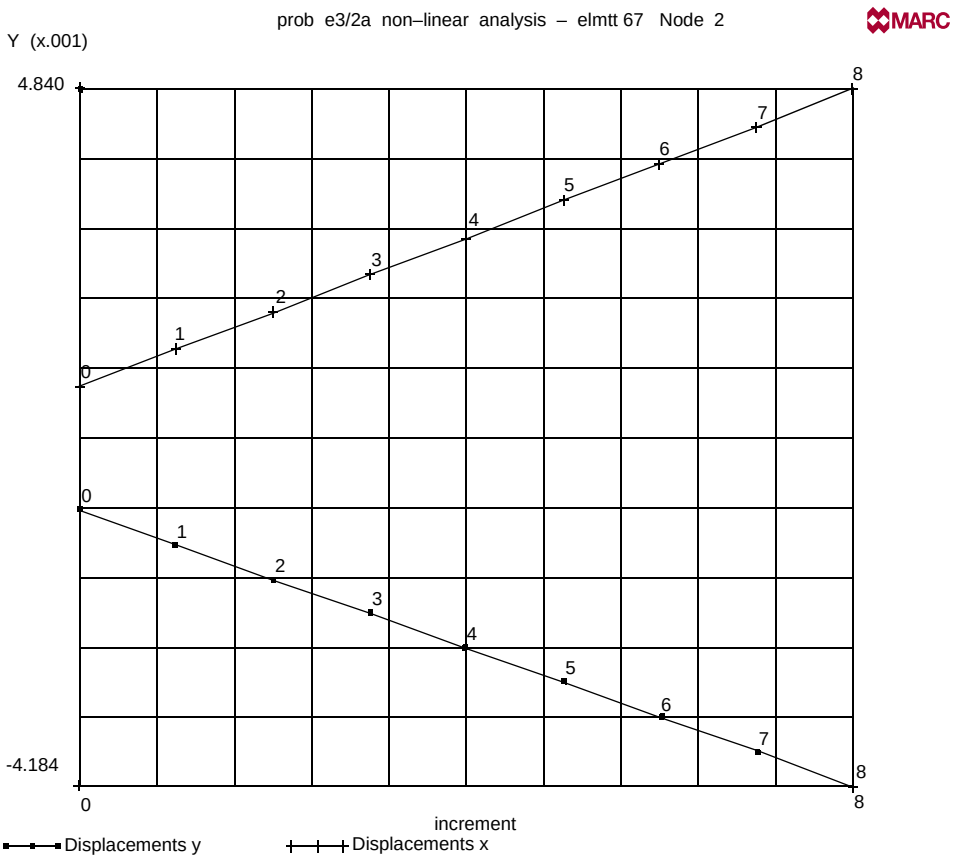

Figure 3.2-3 Displacement History at Inner Radius

3.3 Limit Load Analysis

The compression of a layer between two rigid plates is studied in this problem and compared to theoretical results.

This problem is modeled using the two techniques summarized below.

Data Set	Element Type(s)	Number of Elements	Number of Nodes
e3x3	11	24	35
e3x3b	115	24	35

Elements

The solution is obtained using first order isoparametric quadrilateral elements for plane strain, element types 11 and 115, respectively. Type 115 is similar to type 11; however, it uses reduced integration with hourglass control.

Model

The plate dimensions are 4 inches wide by 40 inches high, where ($-h < x < h$) and ($-l < y < l$), $h = 2$ and $l = 20$. Due to symmetry, only one-quarter of the layer is modeled, namely ($0 < x < h$ and $0 < y < l$). Figure 3.3-1 shows the mesh that is used for both element types.

Geometry

The strip has a thickness of 1 inch given in the first field (EGEOM1). To obtain the constant volumetric strain formulation, (EGEOM2) is set to unity. This is applied to all elements of type 11. This has no effect for element type 115 because the element does not lock.

Material Properties

The material for all elements is treated as an elastic perfectly-plastic material, with Young's modulus of 10.0 E+06 psi, Poisson's ratio (ν) of 0.3, and a yield strength of 20,000 psi.

Boundary Conditions

The symmetry conditions require that all nodes along the $x = 0$ axis have their horizontal displacements constrained to zero, and all nodes along the $y = 0$ axis have their vertical displacements constrained to zero.

Load History

The x-displacement enforced across the x = h surface during increment 0 is -0.003, and the y-displacement is enforced to be zero. Ten load steps with a PROPORTIONAL INCREMENT of 0.5 follow. Another sequence of ten load steps with a proportionality factor of 3 is added, for a total of 20 increments resulting in a total displacement of -0.063.

Results

The analytical slip-line solution was found by Prandtl for a rigid-plastic material and published in *Foundations of the Theory of Plasticity*, Kachanov, North Holland Publishing, Amsterdam, 1971. The stresses in a plate are expressed as follows:

$$- \sigma_{xx} (x,y) = p + k [y/h -2 (1 - x^2/h^2)^{1/2}]$$

$$- \sigma_{yy} (x,y) = p + k\ y/h$$

$$- \sigma_{xy} (x,y) = k\ x/h$$

and the limit load is found as:

$$P = -kl(l/h + \pi)$$

Where p is the surrounding pressure, and the yield condition is:

$$k^2 = 1/4\ (\sigma_{xx} - \sigma_{yy})^2 + \sigma_{xy}{}^2.$$

The relationship between k and the von Mises yield strength, Y, for plane strain conditions becomes:

$$3\ k^2 = Y^2.$$

Contour plots for the of stress are shown in Figure 3.3-2 and Figure 3.3-3. Comparing the predictions of maximum shear to the analytical values shows:

Component	Analytical	Type 11	Type 115
$- \sigma_{xy}$ =	11,541 psi	11,770 psi	11,540 psi

A user-written subroutine, IMPD, was written to sum the reactions at the nodes where the displacements are prescribed to determine the load-deflection curve shown in Figure 3.3-4. The curve clearly shows that a limit load has been reached. The last several increments show no increase in loading, indicating a steady state plastic flow condition. Comparison of the limit load becomes:

$- P$ = 1,512,000 lbf (Slip-line solution)
1,665,000 lbf (Element type 11)
1,754,000 lbf (Element type 115)

The value of the limit load predicted by element type 11 is closer to theoretical than element type 115.

Computationally, it is interesting to note that, during the analysis, the singularity ratio was reduced by a factor of five.

Parameters, Options, and Subroutines Summary

Example e3x3.dat:

Parameters	Model Definition Options	History Definition Options
END	CONNECTIVITY	AUTO LOAD
SIZING	CONTROL	CONTINUE
TITLE	COORDINATES	PROPORTIONAL INCREMENT
	DEFINE	
	END OPTION	
	FIXED DISP	
	GEOMETRY	
	ISOTROPIC	
	POST	
	PRINT CHOICE	
	UDUMP	

User subroutine in u3x3.f

IMPD

Example e3x3b.dat:

Parameters	Model Definition Options	History Definition Options
ALIAS	CONNECTIVITY	AUTO LOAD
ELEMENTS	CONTROL	CONTINUE
END	COORDINATES	PROPORTIONAL INCREMENT
FINITE	DEFINE	
LARGE DISP	END OPTION	
SIZING	FIXED DISP	
TITLE	GEOMETRY	
UPDATE	ISOTROPIC	
	POST	
	PRINT CHOICE	
	UDUMP	

User subroutine in u3x3b.f:

IMPD

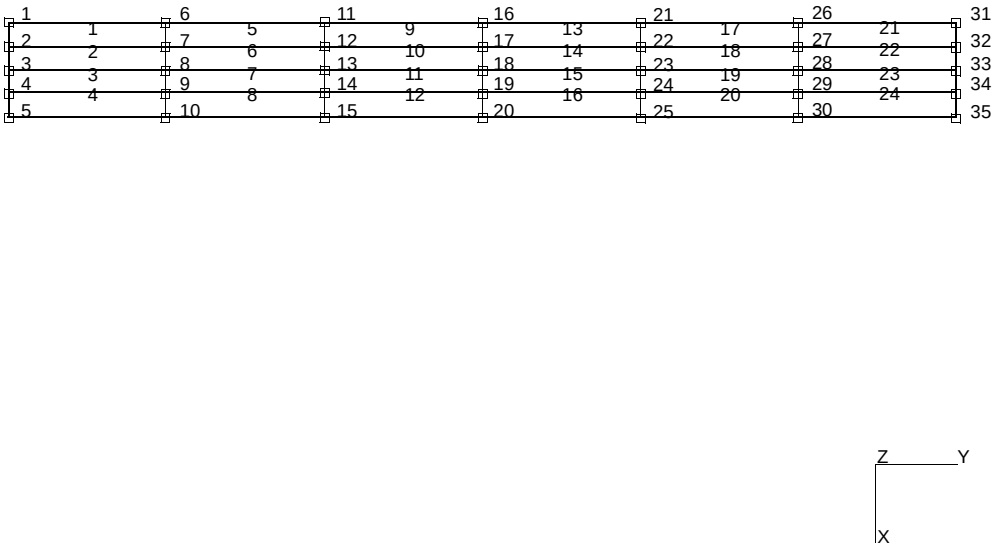

Figure 3.3-1 Finite Element Mesh

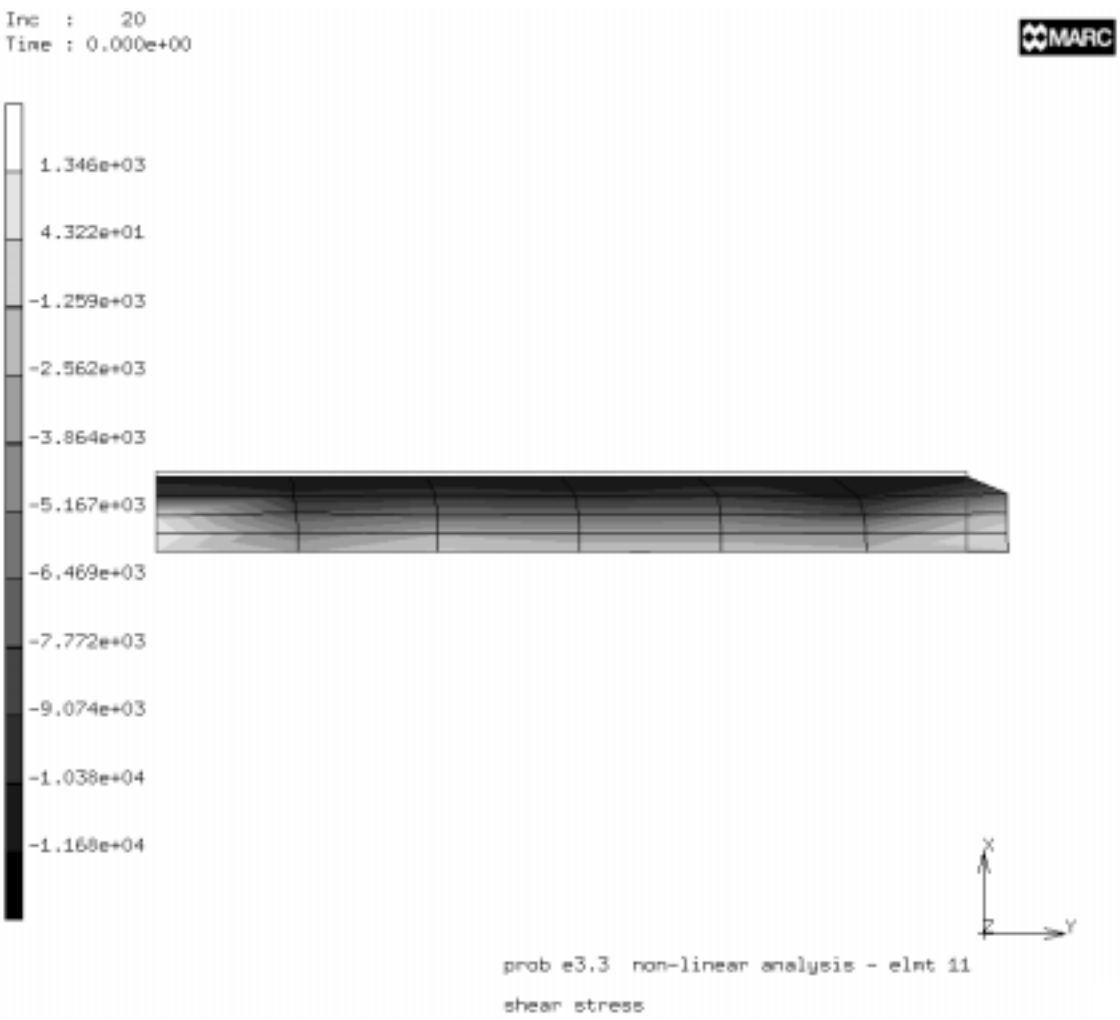

Figure 3.3-2 σ_{xy} Contour Element 11

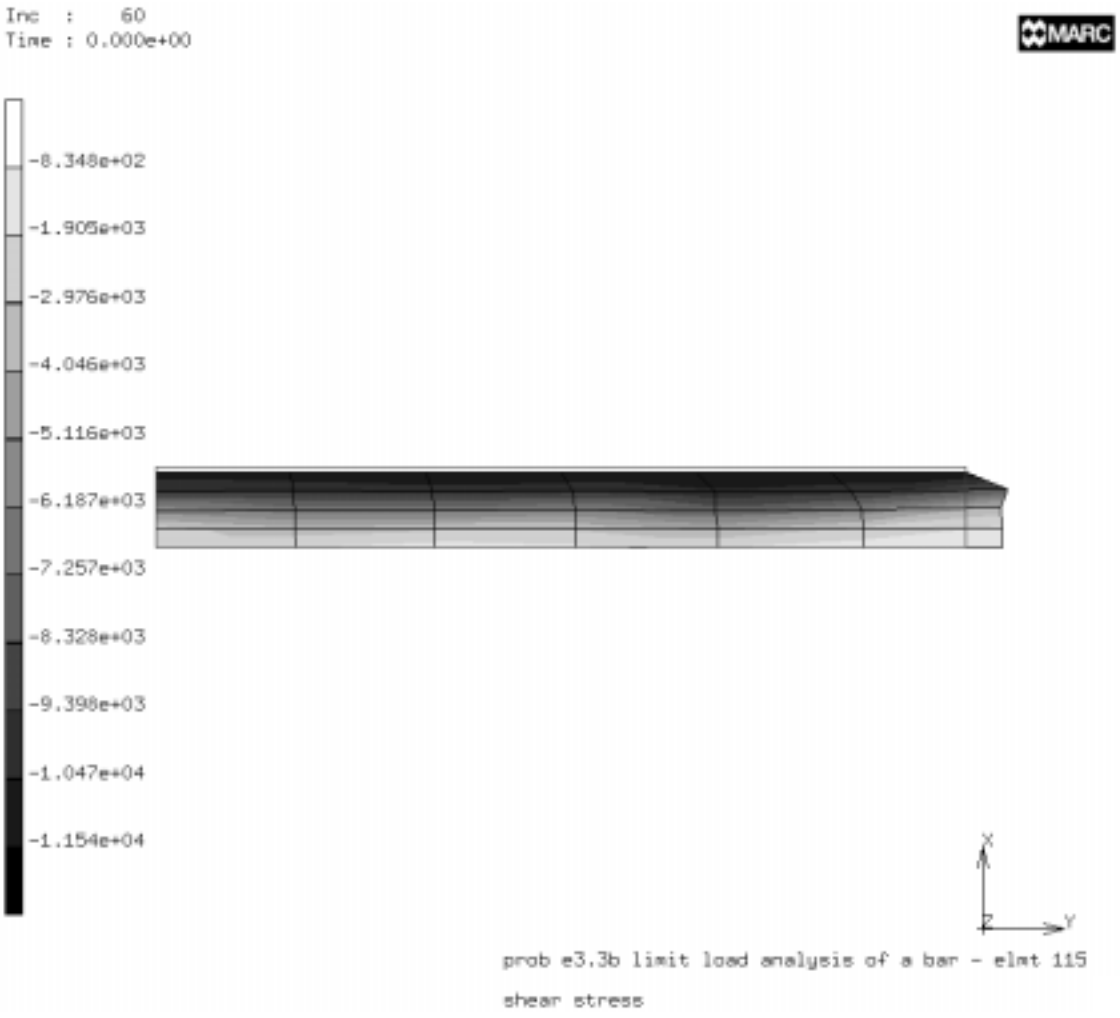

Figure 3.3-3 σ_{xy} Contour Element 115

Displacement (in.)	Element 11	Element 115
0.0	0.0	0.0
3.00E-03	3.96824E-01	3.96262E-01
6.00E-03	7.26945E-01	7.28464E-01
9.00E-03	9.22769E-01	9.25604E-01
1.20E-02	1.09504E+00	1.09972E+00
1.50E-02	1.24589E+00	1.25424E+00
1.80E-02	1.37297E+00	1.38484E+00
2.10E-02	1.47581E+00	1.49313E+00
2.40E-02	1.55544E+00	1.57812E+00
2.70E-02	1.61131E+00	1.63987E+00
3.00E-02	1.64520E+00	1.68006E+00
3.30E-02	1.65915E+00	1.70095E+00
3.90E-02	1.66661E+00	1.72789E+00
4.80E-02	1.66520E+00	1.74967E+00
4.98E-02	1.66517E+00	1.75428E+00

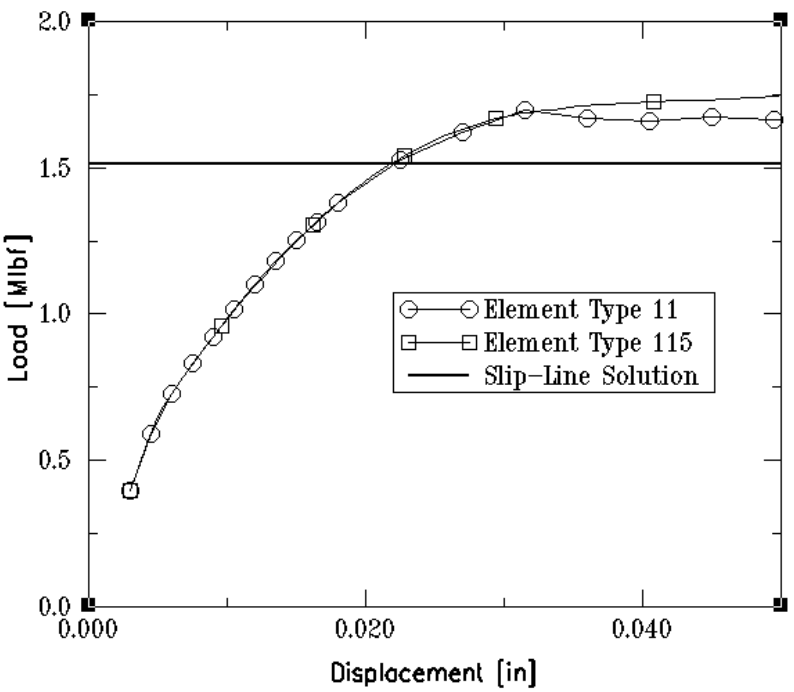

Figure 3.3-4 Load-Displacement Curve

3.4 Bending of Prismatic Beam

A prismatic beam is loaded into the elastic-plastic range by an end moment. Subsequently, the loading direction is reversed. The material follows the ORNL recommended constitutive theories. This problem demonstrates nonproportional loading for an elastic-plastic analysis.

Element

Element type 16 is a 2-node curved beam element.

Model

One end of the beam is fixed; the other end is subjected to a moment. There are four elements and five nodes for a total of 20 degrees of freedom (see Figure 3.4-1). The length of the beam is 100 inches.

Geometry

The beam height is taken to be 10.0 inches and is specified as EGEOM1. The beam width is 1.0 inches and is specified as EGEOM2. Seven layers are used for integration through the height of the beam (SHELL SECT option).

Boundary Conditions

One end of the beam is fixed against displacement (u = v = 0) and rotation ($\frac{dv}{ds} = 0$), simulating a cantilevered beam.

Material Properties

The material is elastic-plastic. The ORNL constitutive theory is used; consequently kinematic hardening is automatically invoked by the program. The ORNL theory is flagged through the ISOTROPIC option. Values for Young's modulus, Poisson's ratio, first and second yield stresses used here are 10.0×10^6 psi, 0.3, 20,000 psi, and 22,000 psi, respectively.

Work Hard

The primary workhardening slope is 3.0×10^5 psi. The initial secondary workhardening slope is $10. \times 10^5$ psi. The subsequent secondary workhardening slope of 3.0×10^5 psi starts at a plastic strain of 1%.

Loading

An end moment is applied in the fourth degree of freedom of node 5 in 13 steps. The moment is then reversed in direction and is incremented for 25 steps.

Results

The results show that the program is capable of treating problems involving loading paths with reversal of plastic deformation. The end moment is scaled to reach yield stress in element 4 and proportionally incremented to 160% of the moment to first yield in 12 steps. All seven layers of beam element 1 have developed plastic strain. The maximum effective plastic strain is around 1%. The end moment is then reversed with a small negative scaling factor (-0.05). Once elastic response is established, a large step can be taken using a scaling factor of 40. Twenty-four more steps are used to bring the reversed moment to about the same maximum in the opposite direction. The reversed maximum effective plastic strain is around 0.35%. The moment-rotation diagram is shown in Figure 3.4-2. The residual stress distribution for zero applied moment after first loading is shown in Figure 3.4-3. The reverse plastic flow starts at a moment of -0.1833×10^6 in-lb. This is 55% of the load to first yield in the original, undeformed beam. The PRINT CHOICE option is used to restrict the output to layer 2 of element 1 only.

Parameters, Options, and Subroutines Summary

Example e3x4.dat:

Parameters	Model Definition Options	History Definition Options
ELEMENTS	CONNECTIVITY	AUTO LOAD
END	CONTROL	CONTINUE
SCALE	COORDINATES	PROPORTIONAL INCREMENT
SHELL SECT	DEFINE	
SIZING	END OPTION	
TITLE	FIXED DISP	
	GEOMETRY	
	ISOTROPIC	
	POINT LOAD	
	POST	
	PRINT CHOICE	
	WORK HARD	

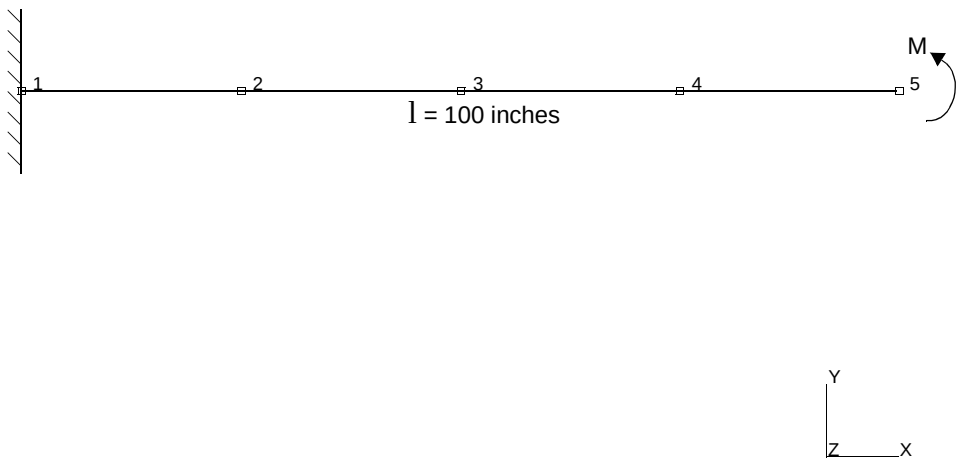

Figure 3.4-1 Prismatic Beam Model and Mesh

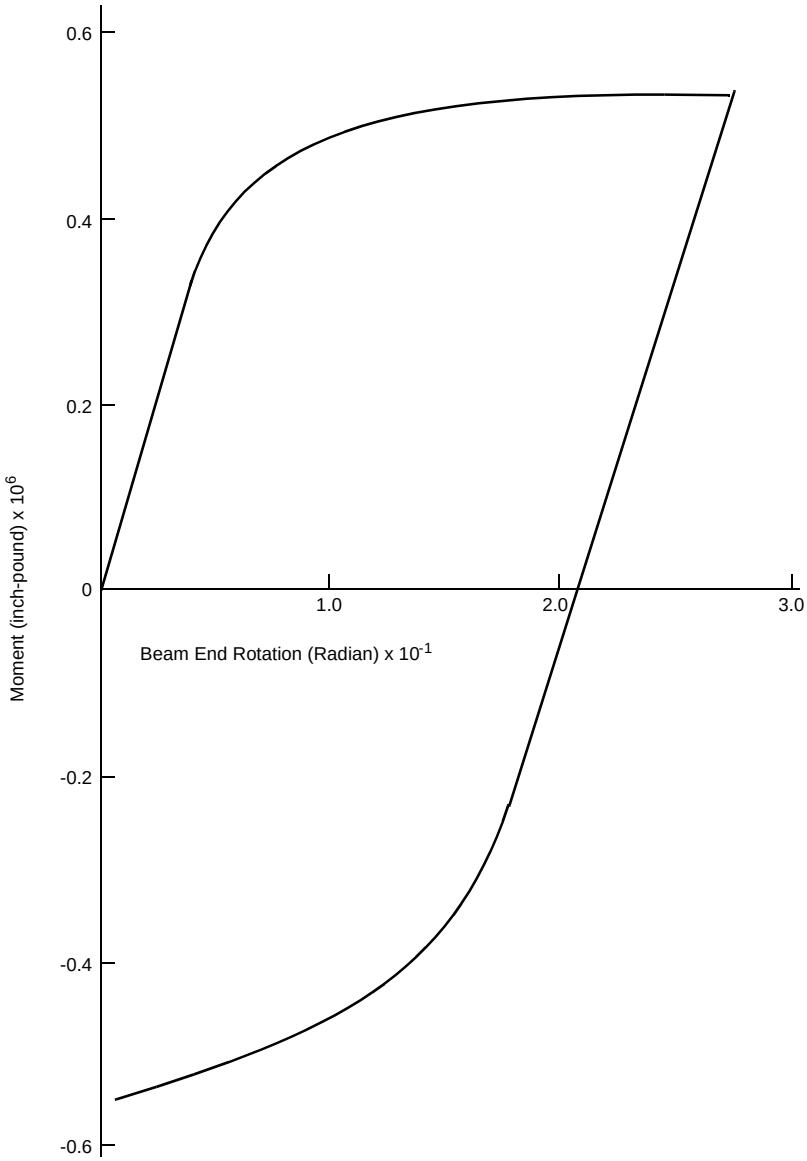

Figure 3.4-2 Moment-Rotation Diagram

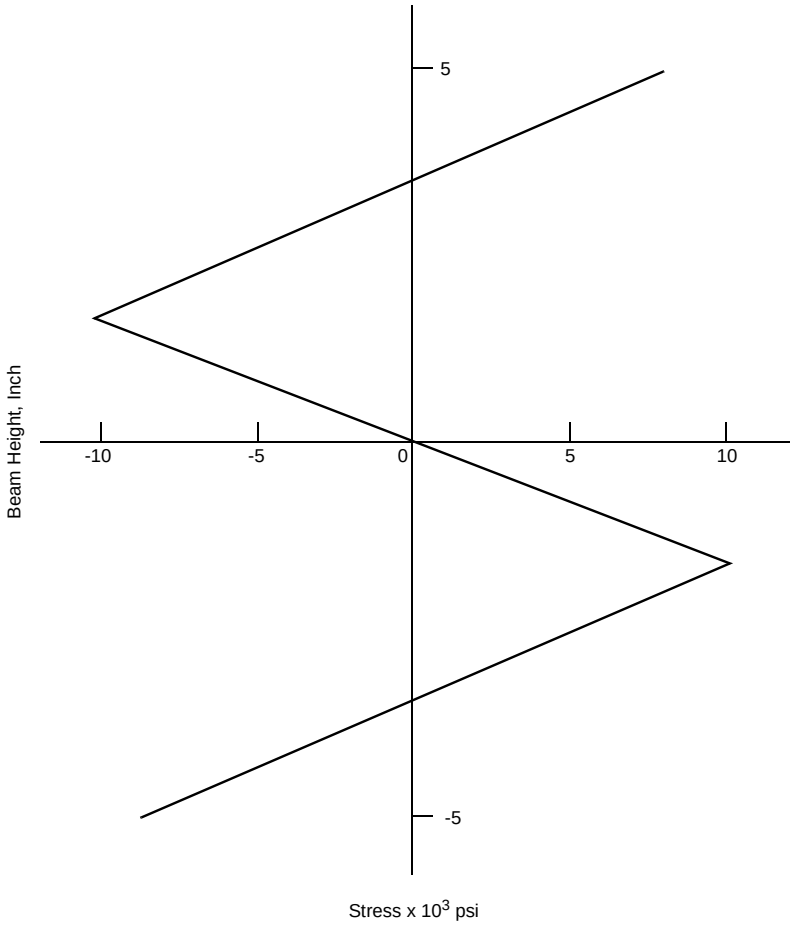

Figure 3.4-3 Residual Stress Distribution for Zero Moment

3.5 Hemispherical Shell under Thermal Expansion

A hemispherical shell under uniform thermal load is analyzed. The temperatures are prescribed and elastic-plastic stress and strain are computed.

Element

Element type 15, a 2-node axisymmetric thin shell, is used.

Model

The geometry of the hemisphere and the mesh is shown in Figure 3.5-1. A 90° cross section is referenced with respect to an R-Z global coordinate system. The shell has been divided into eight elements with nine nodes.

Geometry

The shell thickness is 2.0 inches and specified as EGEOM1 of this option. Five layers are used for integration through the shell cross section as prescribed in the SHELL SECT option.

Boundary Conditions

Fixed boundary conditions are specified at node 9 $\left(u = v = \frac{du}{ds} = 0\right)$. Symmetry boundary conditions are specified at node 1 $\left(v = \frac{du}{ds} = 0\right)$.

Transformation

Nodes 2 through 9 have been transformed to a new local coordinate system. Boundary conditions at node 9 are input in the transformed system such that at each node the displacements are given as radial and tangential.

Material Properties

The material is assumed to be elastic-plastic with strain hardening. The elastic properties are considered to be independent of temperature. The yield stress decreases with temperature to a value of zero at 2000°F. Values for Young's modulus, Poisson's ratio, coefficient of thermal expansion, initial temperature, and yield stress used here are 10.0 x 10^6 psi, 0.3, 1.0 x 10^{-6} in/in/°F, 70°F, and 20,000 psi, respectively.

UFXORD

User subroutine UFXORD is used to generate a full set of five coordinates required for element type 15.

Work Hard

The user subroutine WKSLP is used to generate the current yield stress and the corresponding workhardening slope. The workhardening curve is shown in Figure 3.5-2.

Loading

A uniform temperature of 800°F is applied to all elements. The temperature is then proportionally incremented 100°F for 11 steps.

Temperature Effects

The initial yield stress decreases 10 psi for each increase in temperature of 1°F above 70°F.

Results

Temperature is increased to 1970°F by increment 11; plastic strain at layer 1 of integration point 3 of element 8 is 0.29. The total displacement due to thermal expansion for node 1 is 0.224 inches. The resultant displacement is shown in Figure 3.5-3. The PRINT CHOICE option is used to restrict printout to layers 1 through 3.

The highest stressed element is element 8, which is at the fixed boundary. This boundary condition is quite severe and a more accurate solution would have been obtained if mesh refinement would have been used in this region. Initial yield can be predicted by assuming that a small region near this boundary is constrained. Then,

$$\sigma_{11} = \sigma_{22} = E\alpha\Delta T \qquad \sigma_{33} = 0$$

$$\bar{\sigma} = \sqrt{\frac{3}{2}S_{ij}S_{ij}} = E\alpha\Delta T$$

$Y(T) = \bar{\sigma}$ at yield, so

$$(20000 - 10\Delta T = 10.0 \times 10^{6} \times 1.0 \times 10^{-6}\Delta T)$$

$$\Delta T = 1000°F$$

Hence, yield should occur in increment 2, as it does.

Parameters, Options, and Subroutines Summary

Example e3x5.dat:

Parameters	Model Definition Options	History Definition Options
ELEMENTS	CONNECTIVITY	AUTO THERM
END	CONTROL	CHANGE STATE
NEW	DEFINE	CONTINUE
SHELL SECT	END OPTION	
SIZING	FIXED DISP	
THERMAL	GEOMETRY	
TITLE	INITIAL STATE	
	ISOTROPIC	
	PRINT CHOICE	
	TEMPERATURE EFFECTS	
	THERMAL LOADS	
	TRANSFORMATION	
	UFXORD	
	WORK HARD	

User subroutines in u3x5.f:

WKSLP
UFXORD

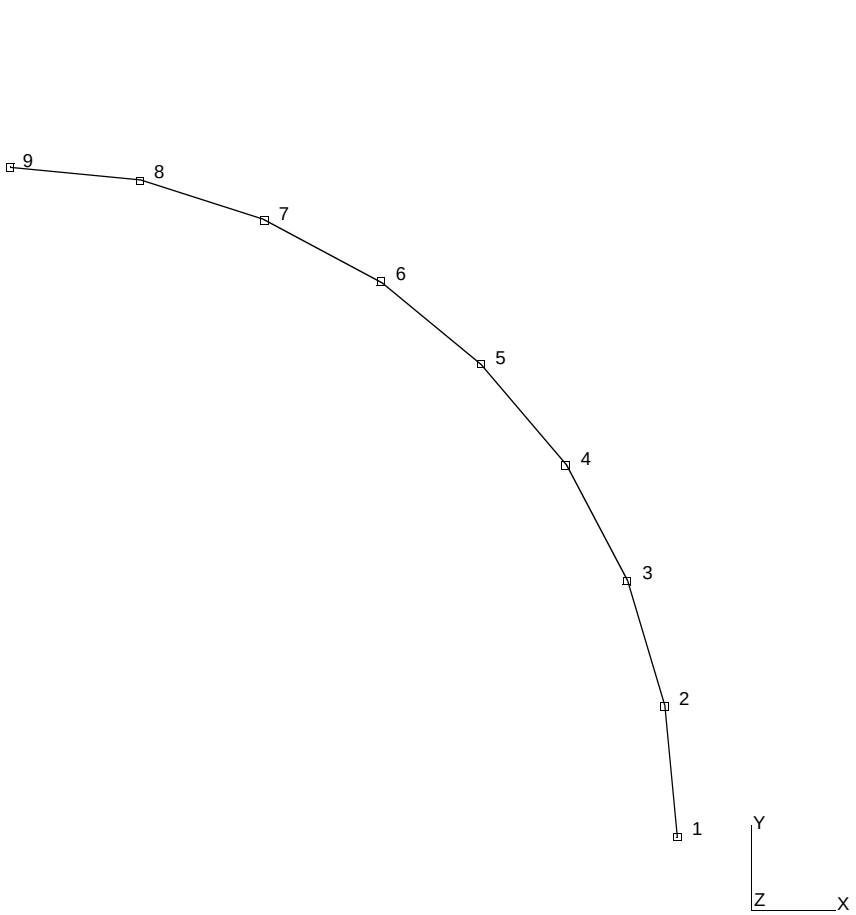

Figure 3.5-1 Hemispherical Shell and Mesh

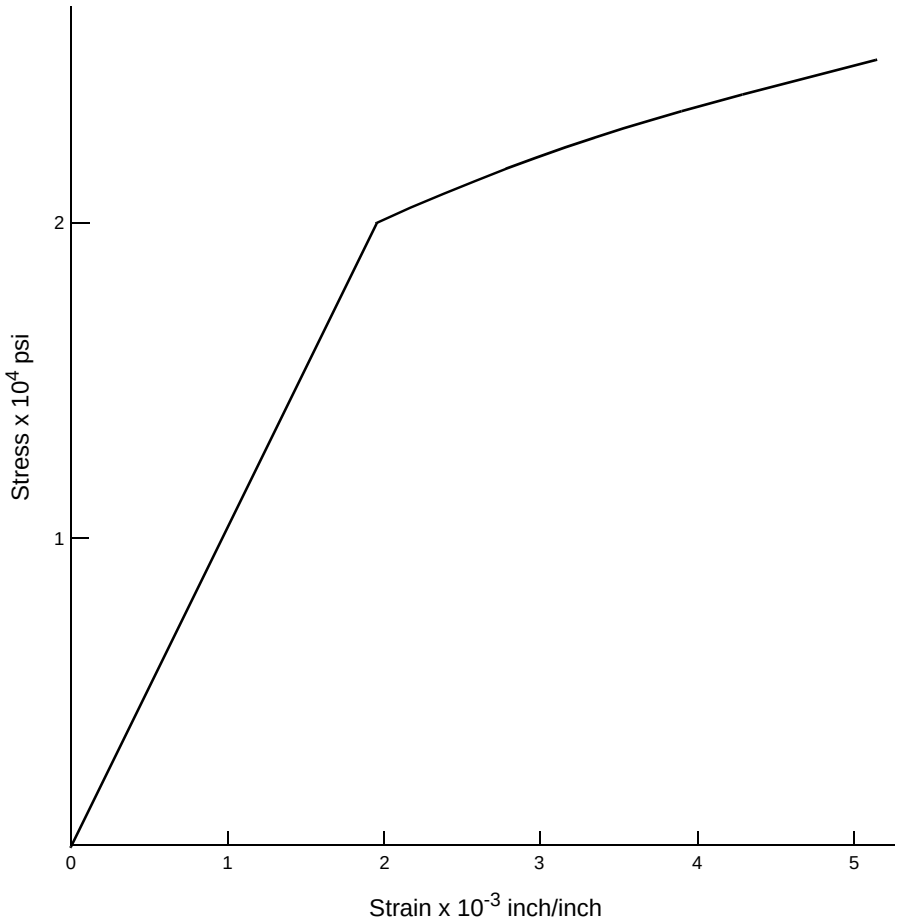

Figure 3.5-2 Workhardening Curve

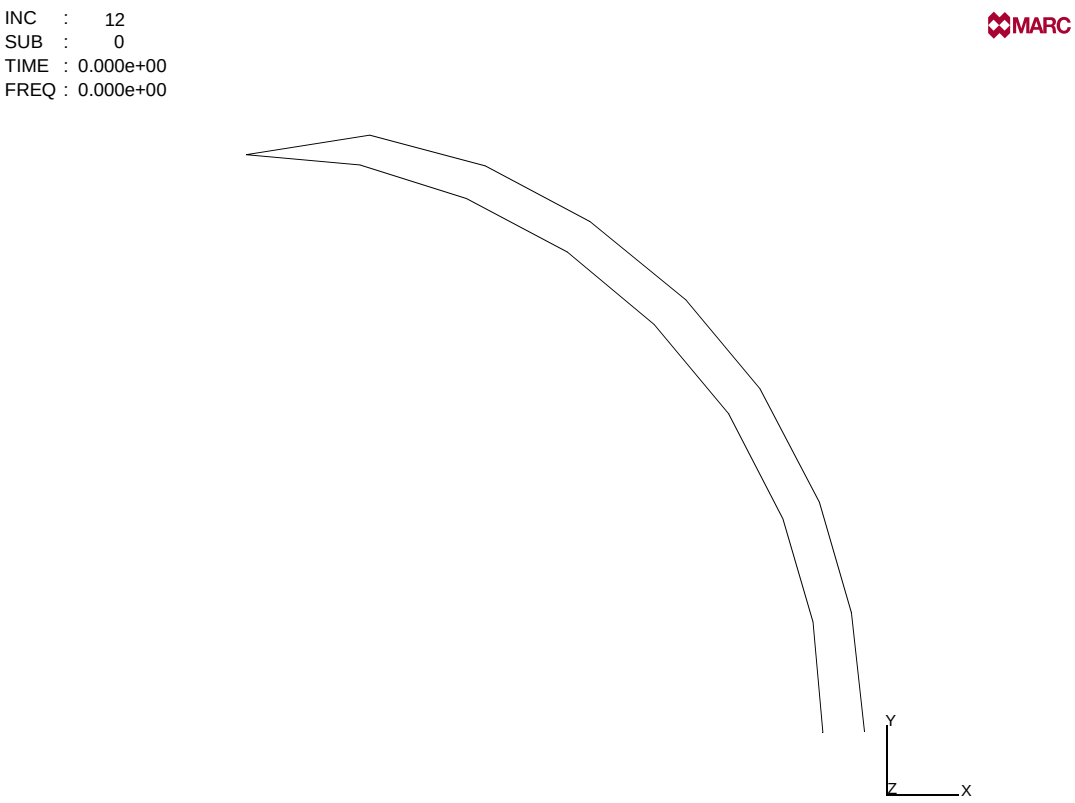

Figure 3.5-3 Displaced Mesh

3.6 Collapse Load of a Simply Supported Square Plate

In this problem, the maximum transverse load that a square plate of isotropic material can sustain is determined.

Element

Library element type 49 is a 6-node triangular thin shell element.

Model

The dimensions of the plate and the finite element mesh are shown in Figure 3.6-1. Based on symmetry considerations, only one-quarter of the plate is modeled. The mesh is composed of 32 elements and 81 nodes.

Material Properties

The material is elastic with a Young's modulus of 3.0×10^4 N/mm^2, a Poisson's ratio or 0.3, and a yield stress of 30 N/mm^2.

Geometry

The thickness of the plate is specified as 0.4 mm. Since a geometrically linear plate problem is solved, the elements can be considered as flat, which is indicated by a 1 on the fifth geometry field. In this way, computational time is reduced. In order to trigger the response in thickness directions, five layers are chosen using the SHELL SECT parameter.

Loading

A uniform pressure load of 0.02 N/mm^2 is applied. Since this load is larger than the actual collapse load, the auto increment option is used with a limited number of increments. In this way, the analysis stops if the maximum allowed number of increments is reached.

Boundary Conditions

Symmetry conditions are imposed on the edges x = 20 ($u_x = 0, \phi = 0$) and y = 20 ($u_y = 0, \phi = 0$). Notice that the rotation constraints only apply for the midside nodes. Simply supported conditions are imposed on the edges x = 0 and y = 0 ($u_z = 0$).

Results

Figure 3.6-2 shows the deflection of the central node as a function of the equivalent nodal load. The solution turns out to be in reasonable agreement with the reference solution taken from *Selected Benchmarks for Material Non-Linearity* by D. Linkens (published by NAFEMS, 1993). This reference solution, which is obtained using higher order elements is indicated in Figure 3.6-3.

Parameters, Options, and Subroutines Summary

Example e3x6.dat:

Parameters	Model Definition Options	History Definition Options
ALL POINTS	CONNECTIVITY	AUTO INCREMENT
DIST LOADS	COORDINATES	CONTINUE
ELEMENTS	DEFINE	CONTROL
END	END OPTION	DIST LOADS
SETNAME	FIXED DISP	
SIZING	GEOMETRY	
TITLE	ISOTROPIC	
	NO PRINT	
	OPTIMIZE	
	POST	
	SOLVER	

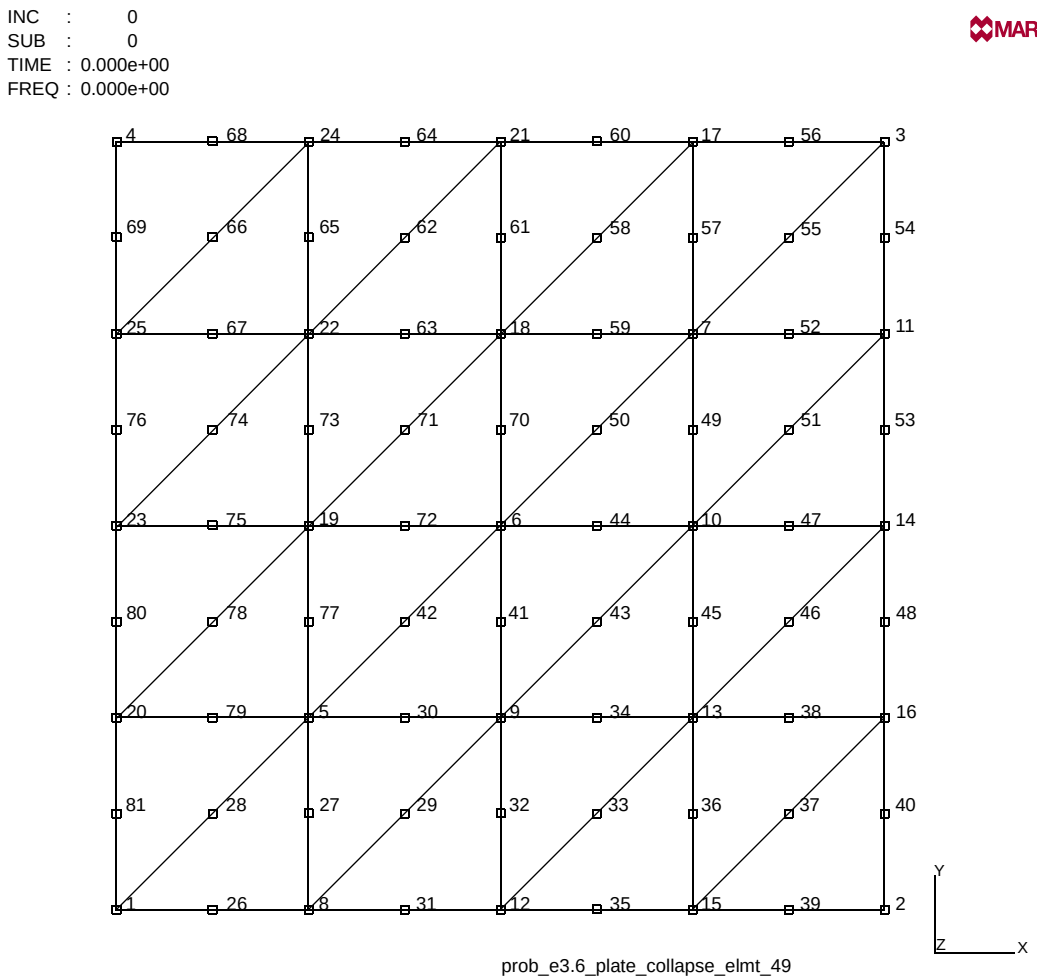

Figure 3.6-1 Square Plate and Finite Element Mesh

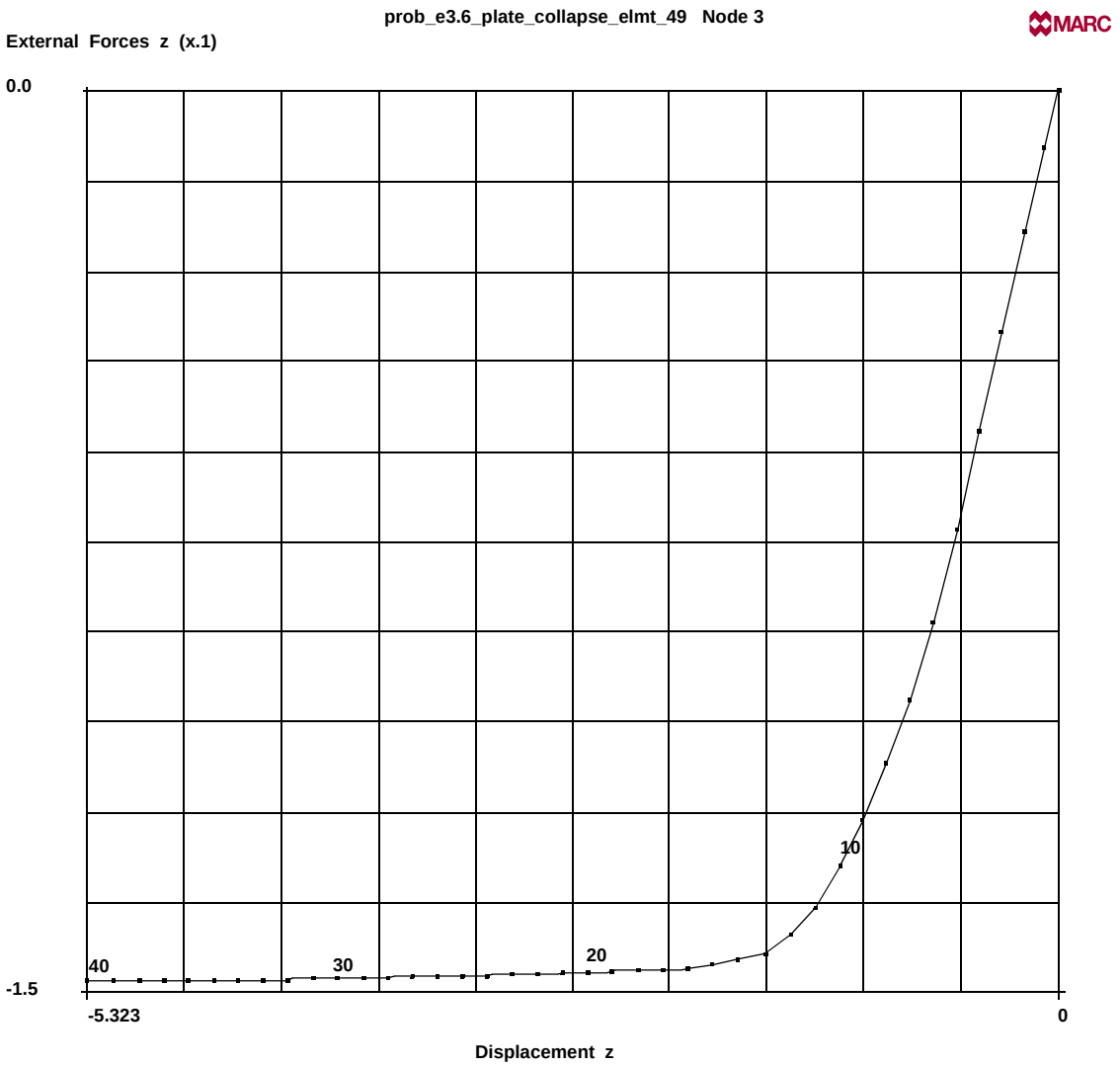

Figure 3.6-2 Central Deflection Versus Nodal Load (MARC Solution)

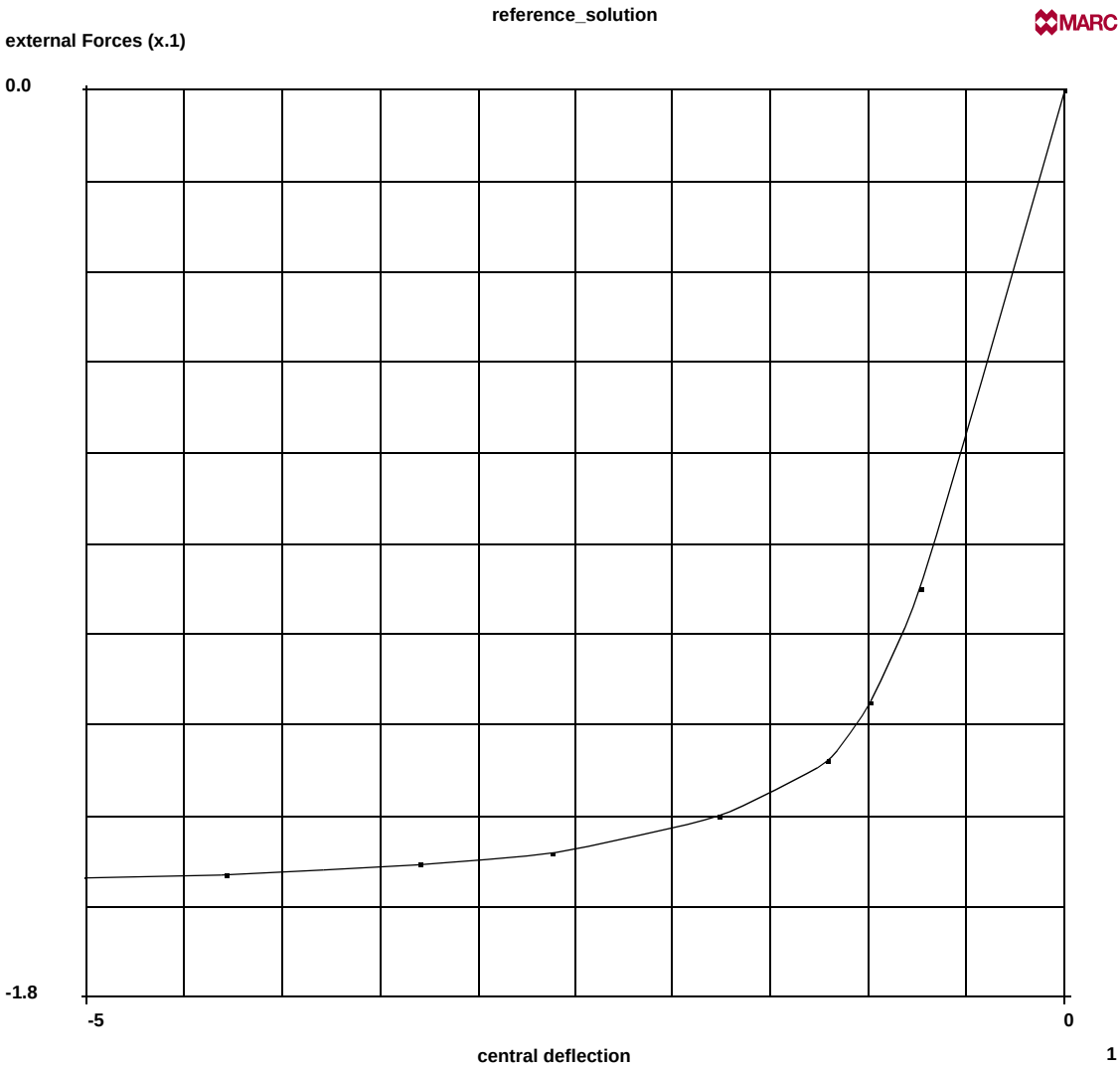

Figure 3.6-3 Central Deflection Versus Nodal Load (Reference Solution)

3.7 Elastic-Plastic Analysis of a Thick Cylinder

In this problem, a thick cylinder under the action of uniform internal pressure is loaded into the plastic region. A comparison with rigid plastic results is provided.

Element

The axisymmetric quadrilateral element, library element type 10, is used to model the wall of the cylinder. Details for this element are found in *MARC Volume B: Element Library.*

Model

Figure 3.7-1 shows the model geometry for this example. The cylinder wall has an inner radius of 1.0 inches and an outer radius of 2.0 inches.

The mesh is shown in Figure 3.7-2 and results in a model of the wall consisting of 20 elements, 42 nodes and 84 degrees of freedom.

Geometry

The geometry option is not required for this element.

Material Properties

The material data is: Young's modulus (E) of 30.0 x 10^6 psi, Poisson's ratio (ν) of 0.3, and von Mises yield stress (σ_y) of 45,000 psi. The material is assumed to behave elastic-perfectly plastic; that is, no strain hardening.

Boundary Conditions

Restraint boundary conditions are imposed in the axial direction on all nodes thus allowing only radial motion of the wall. This solution corresponds to a plane strain case.

Loading

An initial uniform pressure of 19,550 psi is applied using the DIST LOAD option. To investigate the plastic effects, SCALE is used to raise this pressure to a magnitude such that the highest stressed element (element 1) in the model has an equivalent yield stress (J2) which is equal to the specified yield stress of 45,000 psi. The resulting scale factor here is 1.045 which indicates the applied pressure for increment zero is 20,430 psi.

The data before END OPTION provides the elastic solution such that the highest stressed element is at first yield of 45,000 psi and any further loading is done incrementally into the plastic region.

Control

This option specifies a maximum of 15 increments in this example and a tolerance of 15% for convergence. (Only 11 increments are provided as the input data count for the zero increment.)

Incremental Loading

The data blocks following END OPTION are used to specify the incremental load step into the plastic region. The AUTO LOAD option is used to apply two load increments of equal size and the PROPORTIONAL INCREMENT option is used to provide a scaling factor of the load step size for each application of the AUTO LOAD option.

The PROPORTIONAL INCREMENT option as used here specifies a scaling factor to be applied to the previous load step size, and the minimum number of cycles through the prediction of plastic effects (NCYCM) was set to 2 to improve solution accuracy. The scaling factor is adjusted to give the necessary small load steps to keep the solution within the desired tolerance.

The incremental loads which are applied in this example are as follows:

Increment

0 $P_0 = sp = (1.03)(19550) = 20{,}136$ psi

1 $P_1 = P_0 + \Delta P_1$: $\Delta P_1 = fsp = (0.13)(1.03)(19{,}550)$

2 $P_2 = P_0 + \Delta P_1 + \Delta P_2$: $\Delta P_2 = \Delta P_1$

3 $P_3 = P_0 + \Delta P_1 + \Delta P_0 + \Delta P_3$: $\Delta P_3 = 0.8\Delta P_2$

5 $P_5 = P_0 + \Delta P_1 + ... + \Delta P_5$: $\Delta P_5 = 0.7\Delta P_4$

7 $P_7 = P_0 + \Delta P_1 + ... + \Delta P_7$: $\Delta P_7 = 0.667\Delta P_6$

10 $P_{10} = P_0 + \Delta P_1 + ... + \Delta P_{10}$

$\Delta P_{10} = \Delta P_9 = 0.5\Delta P_8 = 0.5\Delta P_7 = ... = 0.5(0.667)(0.7)(0.8)(0.13)\Delta p =$

$= 1.04052 \times 10^{-2}\ \Delta p = 488$ psi

If a reverse load is desired, a negative scale factor should be used only once to reverse the sign of the load step.

If a load step is applied which is too large to allow the energy change tolerance to be satisfied, MARC, in this case, cycles through the predicted displacement iteration five times. On the last try, a message indicating NO CONVERGENCE TO TOLERANCE is printed out. Then the strains and stresses corresponding to the last iteration are printed in the output, and MARC exits with an appropriate exit message.

Restart

To protect against failure to meet tolerances, use of the restart capability available in the program is recommended. The RESTART option has been used in this example. Two input decks which follow this discussion illustrate the use of RESTART. The first run creates a restart file (unit 8) and writes the necessary data to this file so that the analysis can be restarted at any increment.

The initial deck is set up to run completely through the analysis while the second is used to restart the problem at a point in the middle of the analysis. The analysis was restarted at increment 7.

In general, this specification requires the program to read the next set of load data following END OPTION to be applied as the increment 8 load set. In this case, the program already has the required load data for the increment 8 solution because of the use of the AUTO LOAD option, and it will complete the step of the option before reading the additional data after END OPTION. The data supplied after END OPTION is only enough to complete increments 9 and 10. In the third part, the restart file is read and positioned so that postprocessing plotting can be done.

Results

The results of this analysis are shown in Figure 3.7-3 through Figure 3.7-6. Comparison is made with the results of the finite difference solution given in Chapter 4 of *Theory of Perfectly Plastic Solids* by W. Prager and P. G. Hodge, Jr. (published by John Wiley and Sons, 1963).

Comparison is shown for two values of tolerance which varied from 0.5 to 0.1. The results did not vary appreciably as a function of the displacement tolerance.

The following terminology is used in Figure 3.7-4 through Figure 3.7-6:

a = inner radius

b = outer radius

ρ = radius of elastic-plastic boundary

σ_r = radial stress

$\sigma\theta$ = circumferential stress

σ_z = axial stress

Y = yield stress

$k = Y/\sqrt{3}$

The elastic-plastic boundary is shown as a function of the pressure, p, in Figure 3.7-3.

For the plane strain condition, a numerical solution obtained by finite difference methods was given in the reference. The radial stress distribution for two different positions of the elastic-plastic boundary ($\rho/a = 1.2$ and $\rho/a = 2.0$) are compared to the solution given in the reference in Figure 3.7-4. Excellent agreement is observed. The circumferential stress distribution in the partially plastic tube is similarly compared in Figure 3.7-5. A comparison of the axial stress distribution is given in Figure 3.7-6. The two solutions are seen to be in good agreement.

Parameters, Options, and Subroutines Summary

Example e3x7a.dat:

Parameters	Model Definition Options	History Definition Options
END	CONNECTIVITY	AUTO LOAD
SCALE	CONTROL	CONTINUE
SIZING	COORDINATES	PROPORTIONAL INCREMENT
TITLE	DIST LOADS	
	END OPTION	
	FIXED DISP	
	ISOTROPIC	
	PRINT CHOICE	
	RESTART	

Example e3x7b.dat:

Parameters	Model Definition Options	History Definition Options
END	CONTROL	AUTO LOAD
SCALE	DIST LOADS	CONTINUE
SIZING	END OPTION	PROPORTIONAL INCREMENT
TITLE	FIXED DISP	
	ISOTROPIC	
	PRINT CHOICE	

Example e3x7c.dat:

Parameters	Model Definition Options	History Definition Options
END	BOUNDARY CONDITIONS	CONTINUE
MESH PLOT	CONTROL	
SCALE	DIST LOADS	
SIZING	END OPTION	
	TITLE	
	ISOTROPIC	
	PRINT CHOICE	
	RESTART	

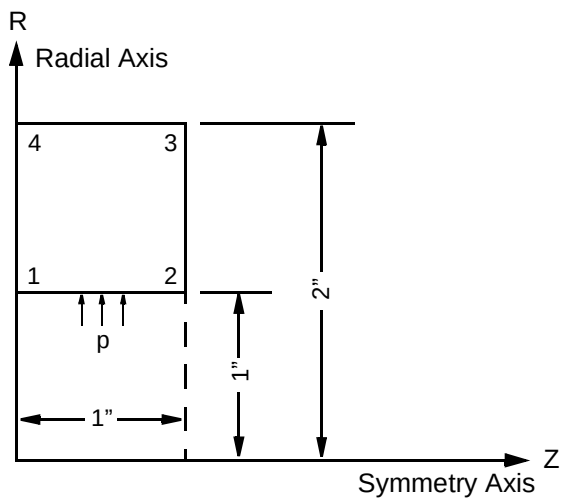

Figure 3.7-1 Cylinder Wall

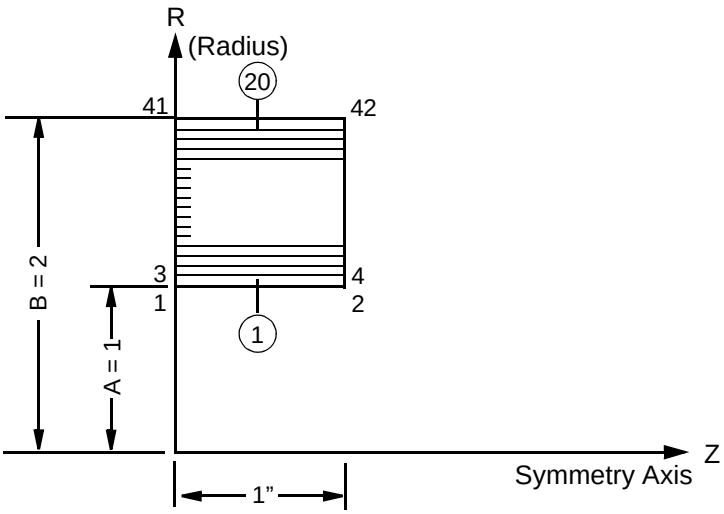

Figure 3.7-2 Cylinder Wall Generated Mesh

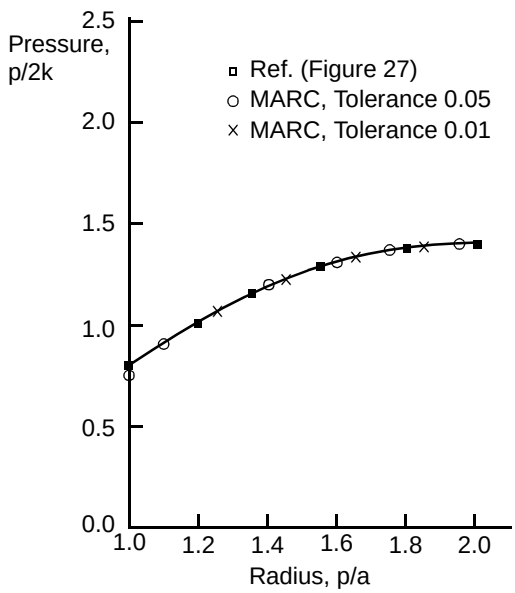

Figure 3.7-3 Pressure Versus Elastic-Plastic Boundary

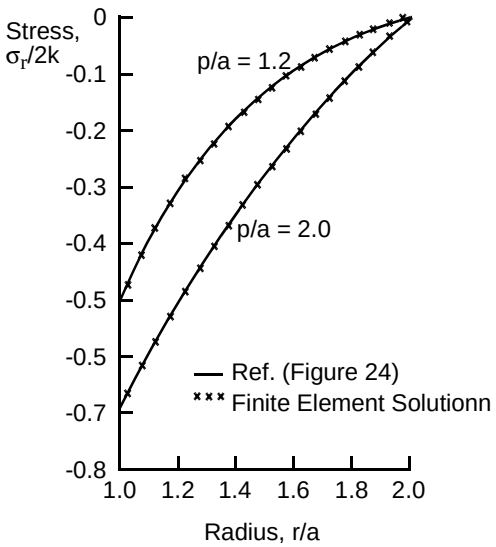

Figure 3.7-4 Radial Stress Distribution

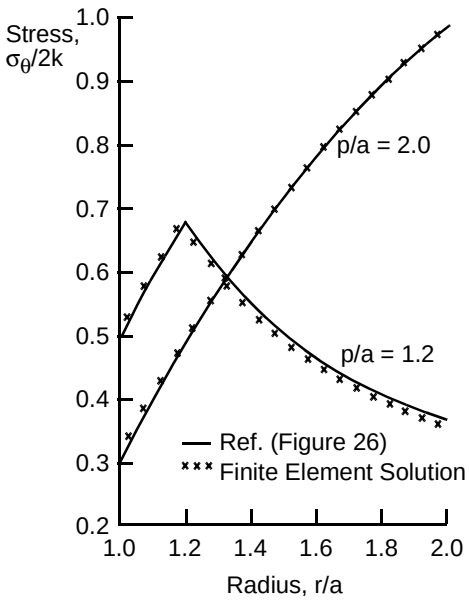

Figure 3.7-5 Circumferential Stress Distribution

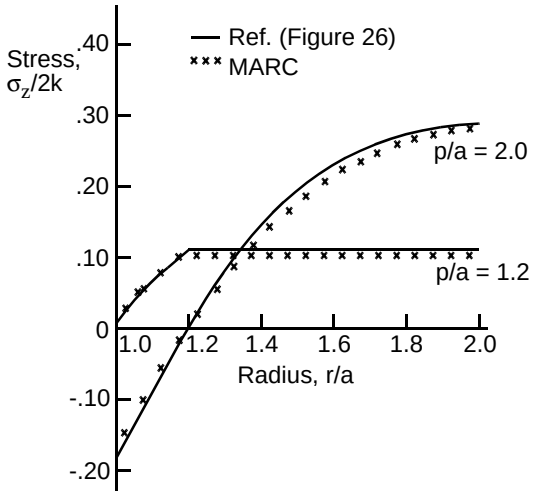

Figure 3.7-6 Axial Stress Distribution

3.8 Double-Edge Notch Specimen under Axial Tension

In this problem, the J-integral is evaluated for an elastic-plastic Double-Edge Notch (D.E.N.) specimen under axial tension. Three different paths are used for the J-integral evaluation. The variation in the value of J between the three paths indicates the accuracy of the solution.

Element

Element type 27 is an 8-node plane-strain quadrilateral.

Model

Figure 3.8-1 shows the geometry and the principal boundary nodes for the seven blocks used to define the quarter specimen. Figure 3.8-2 shows the mesh with 32 elements and 107 nodes. A second COORDINATES block is used to move the side nodes of the crack tip elements to the one-quarter points (one-quarter of the way along the sides from the crack tip to the opposite face of the element).

Geometry

The option is not required for this element as a unit thickness will be considered.

Boundary Conditions

Boundary conditions are used to enforce symmetry about the x- and y-axes.

Material Properties

The material is elastic-plastic with strain hardening. Values for Young's modulus, Poisson's ratio, and yield stress used here are 30 x 10^6 psi, 0.3 and 50.0 x 10^3 psi, respectively.

Workhard

User subroutine WKSLP is used to input the workhardening slope. The workhardening curve is shown in Figure 3.8-3. The yield surface can be expressed as:

$$\bar{\sigma}(\bar{\varepsilon}^p) = \sigma_o(1 + E\bar{\varepsilon}^p/\sigma_o)^{0.2}$$

$$\frac{\partial\bar{\sigma}}{\partial\bar{\varepsilon}^p} = 0.2\ E(1 + E\bar{\varepsilon}^p/\sigma_o)^{-0.8}$$

J-Integral

The J-integral is evaluated numerically by moving nodes within a certain ring of elements around the crack tip and measuring the change in strain energy. (This node movement represents a differential crack advance.) This mesh has three obvious “rings” of elements around the crack tip, so that three evaluations of J are provided. A differential movement of 10^{-2} is used in all three evaluations.

Loading

An initial uniform pressure of 100 psi is applied using the DIST LOAD option. The SCALE parameter is used to raise this pressure to a magnitude such that the highest stressed element (element 20 here) is at first yield. The pressure is scaled to 3,047 psi. The pressure is then incremented for five steps until the final pressure is 3,308 psi.

Results

The program provides an output of the strain energy differences. This must be normalized by the crack opening area to obtain the value of J. Since this specimen is of unit thickness, the crack opening area is Δl, where Δl is the differential crack motion. The mesh used symmetry about the crack line, so that the strain energy change in the actual specimen would be twice that printed out. These results are summarized in Table 3.8-1. It is clear that these results do demonstrate the path independence for the J-integral evaluation. A plot of the equivalent stress for increment 5 is shown in Figure 3.8-4. The plastic deformation is local to the crack tip only, occurring in elements 3, 4, 19, and 20. The PRINT CHOICE option is used to restrict the printout to those elements in the inner rings surrounding the crack tip.

Table 3.8-1 J-Integral Evaluation Results

	Move Tip Only	Move First Ring of Elements	Move Second Ring of Elements
Strain Energy Change for increment 0 (Δu)	6.220×10^{-2}	6.203×10^{-2}	6.199×10^{-2}
J-Integral $\left(\frac{2\Delta u}{\Delta l}\right)$	12.46	12.424	12.418
Strain Energy Change for increment 1 (Δu)	6.858×10^{-2}	6.839×10^{-2}	6.834×10^{-2}
J-Integral $\left(\frac{2\Delta u}{\Delta l}\right)$	13.738	13.698	13.69
Strain Energy Change for increment 2 (Δu)	7.528×10^{-2}	7.506×10^{-2}	7.501×10^{-2}
J-Integral $\left(\frac{2\Delta u}{\Delta l}\right)$	15.078	15.034	15.026
Strain Energy Change for increment 3 (Δu)	8.228×10^{-2}	8.205×10^{-2}	8.199×10^{-2}
J-Integral $\left(\frac{2\Delta u}{\Delta l}\right)$	16.482	16.434	16.424
Strain Energy Change for increment 4 (Δu)	8.960×10^{-2}	8.934×10^{-2}	8.929×10^{-2}
J-Integral $\left(\frac{2\Delta u}{\Delta l}\right)$	17.948	17.896	17.886
Strain Energy Change for increment 1 (Δu)	9.723×10^{-2}	9.695×10^{-2}	9.689×10^{-2}
J-Integral $\left(\frac{2\Delta u}{\Delta l}\right)$	19.476	19.422	19.41

Parameters, Options, and Subroutines Summary

Example e3x8.dat:

Parameters	Model Definition Options	History Definition Options
ELEMENTS	CONNECTIVITY	AUTO LOAD
END	CONTROL	CONTINUE
J-INT	COORDINATES	PROPORTIONAL INCREMENT
SCALE	DIST LOADS	
SIZING	END OPTION	
TITLE	FIXED DISP	
	ISOTROPIC	
	J-INTEGRAL	
	PRINT CHOICE	
	RESTART	
	WORK HARD	

User subroutine in u3x8.f:

WKSLP

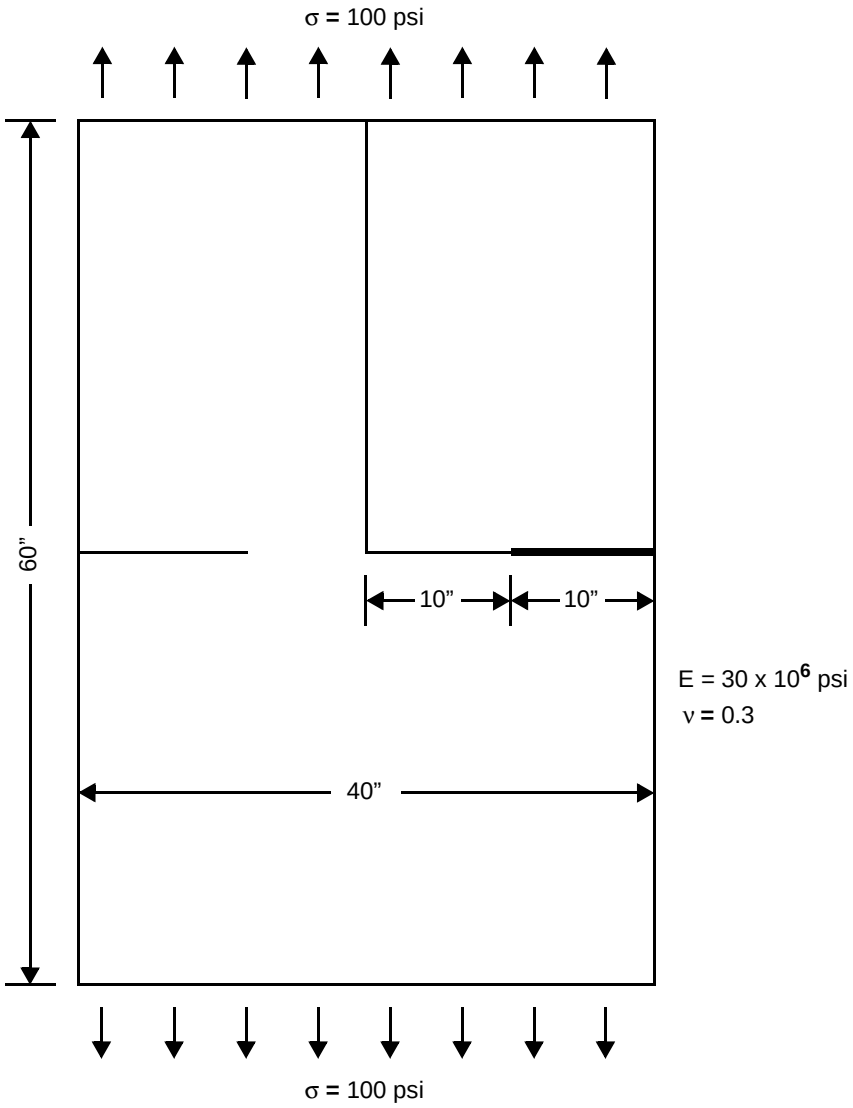

Figure 3.8-1 D.E.N. Specimen

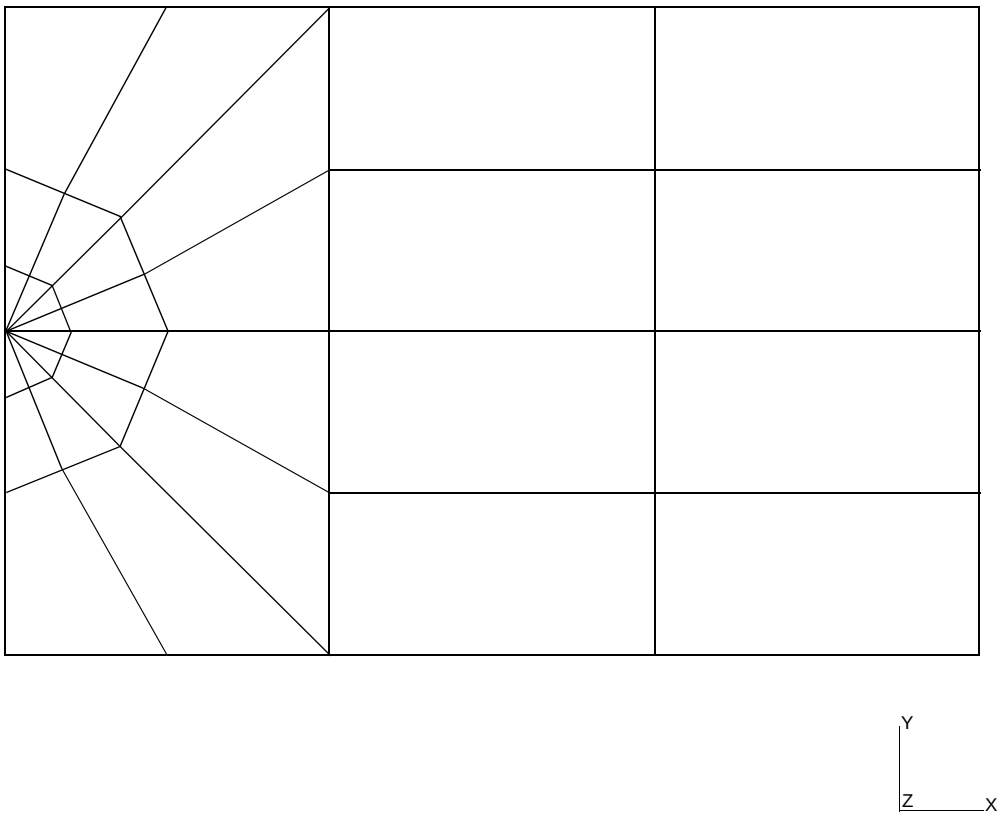

Figure 3.8-2 Mesh for D.E.N.

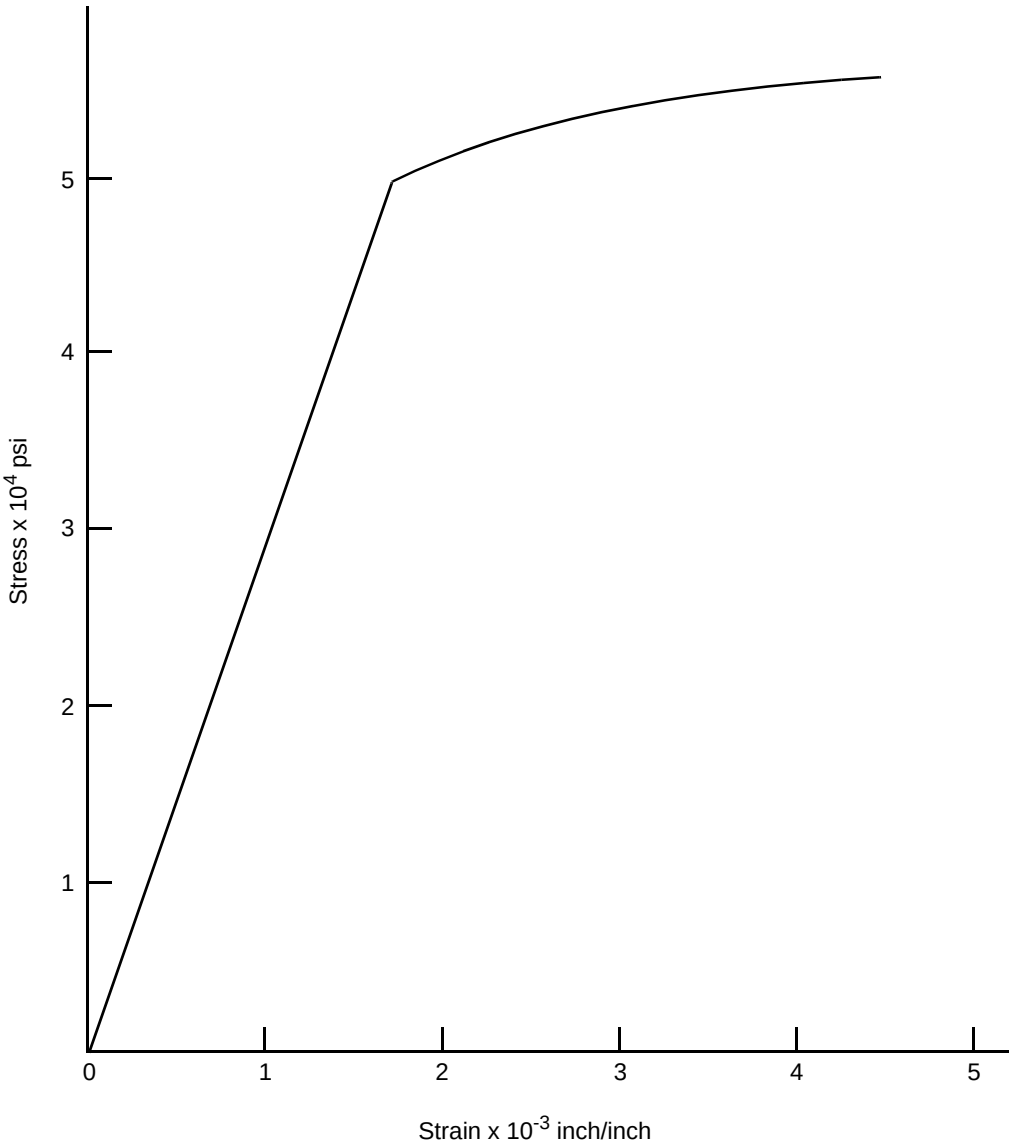

Figure 3.8-3 Workhardening Slopes

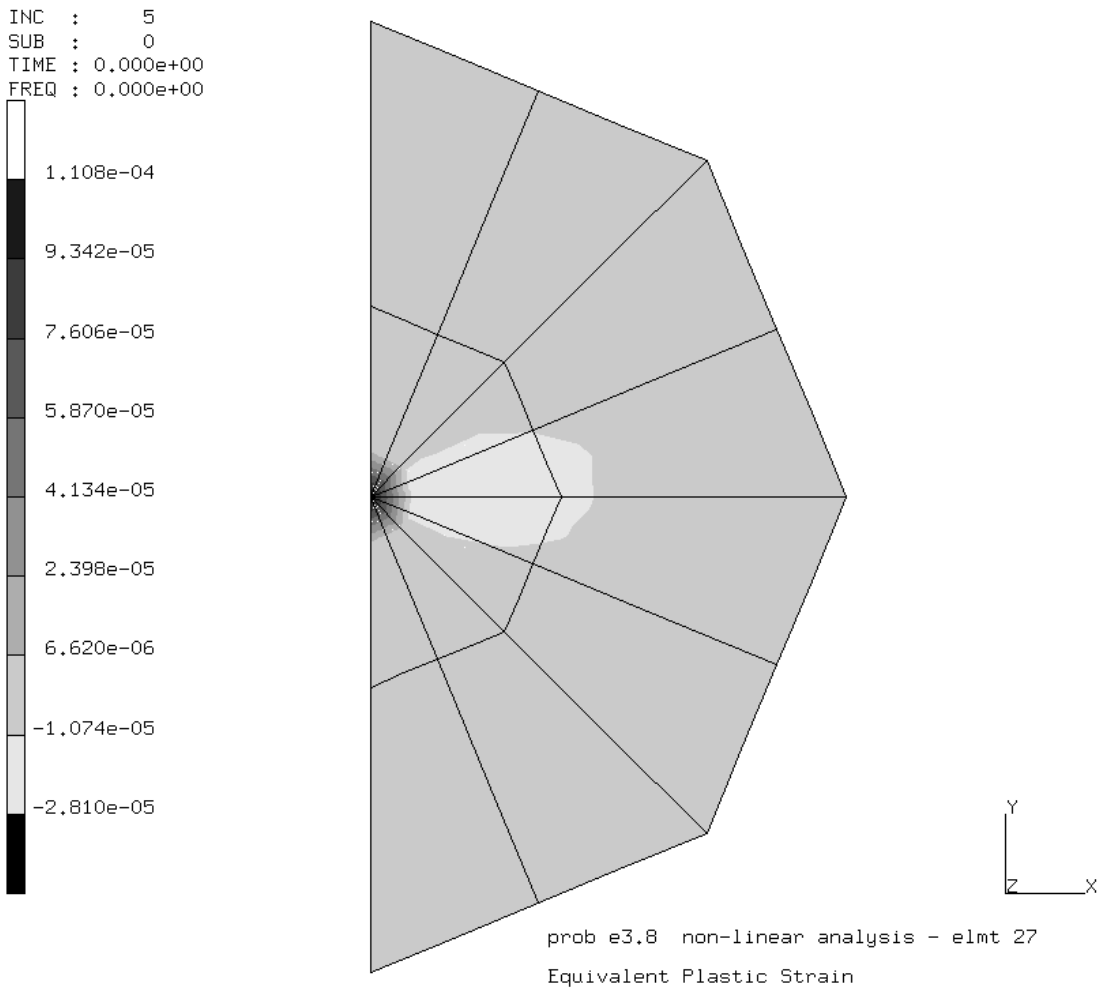

Figure 3.8-4 Equivalent Plastic Strain for Increment 5

3.9 Analysis of a Soil with a Cavity, Mohr-Coulomb Example

The availability of complex yield functions in the material library of MARC allows the modeling of many problems involving materials with hydrostatic yield dependence, such as ice, soil, and rock. A parabolic hydrostatic stress dependency is available as an alternative to the more usual linear model, so that the hydrostatic dependence of the yield function can be closely modeled over a wider range of stress. The dilatancy can be made a function of the hydrostatic stress using parabolic dependency; therefore, it is felt that this is a more straightforward approach than adopting a nonassociative flow rule (see "Theories of Plasticity and the Failure of Soil Masses" by E. H. David in *Soil Mechanics, Selected Topics*, I. K. Lee, ed., American Elsevier Publishing Co., 1968). As an example of the various yield functions, a simple structure was analyzed under small displacement assumptions and plane strain conditions.

Element

The plane-strain quadrilateral element type 11 is used in this example.

Model

The geometry of the generated mesh used is shown in Figure 3.9-1. The final model consists of 80 elements, 99 nodes, and 198 degrees of freedom.

Geometry

This option is not required for this element as a unit thickness is considered.

Boundary Conditions

A plane strain condition is assumed. The displacement boundary conditions are due to symmetry on the inner edges ($y = 0$ and $x = 0$). The zero displacement at all points on the rigid circular cutout ($x^2 + y^2 = 50$) is zero, representing a rigid inclusion.

Loading

The edge ($y = 300$) is loaded with a uniform pressure in an incremental fashion. The initial load is scaled to a condition of first yield and is proportionally incremented using the automatic load incrementation option for several steps. No other forms of load are applied.

Material Properties

The material is assumed to have elastic constants: $E = 5.0 \times 10^5$ psi and $\nu = 0.2$. Several yield surfaces were assumed:

1. von Mises material: $c = 140$ psi ($\sigma = 202$ psi).
2. Linear Mohr-Coulomb: $c = 140$ psi, $\phi = 30°$.

3. Parabolic Mohr-Coulomb: c = 140 psi, $\alpha = \frac{c}{\cos 30°}$.
4. Parabolic Mohr-Coulomb: c = 140 psi, $\alpha = c \tan 30°$.
5. Item (3) is such that the angle of friction at zero mean stress is the same as in the linear surface (2), while (4) has the same yield as (2) at zero shear. The plane-strain forms of those surfaces are shown in Figure 3.9-2. Their generalization into the (J_1 - J_2) plane is shown in Figure 3.9-3. For the present analysis only (1), (2) and (4) were used. The type of constitutive law is set in the ISOTROPIC option.

Results

Global load-displacement behavior is shown in Figure 3.9-4. Node 35 (at approximately x = 300) represents motion of the free surface in a negative x-direction.

The von Mises idealization shows first yielding at 167 psi pressure and reaches a limit load at about 230 psi pressure when all elements are in a state of plastic flow. The parabolic Mohr-Coulomb idealization yields first at 238 psi pressure. At 315 psi pressure, a sharp change in stiffness is observed. A limit load is not reached, though the stiffness is relatively low above the load.

The linear Mohr-Coulomb material shows a rather different behavior; after yielding initially at 264 psi pressure, a gradual change in stiffness occurs until, at about 400 psi pressure, all elements are flowing plastically. Above that load, the structure continues to respond with the same resistance, as the hydrostatic stress build up.

The stress fields at high load levels are shown for the various material idealizations in Figure 3.9-5 through Figure 3.9-10. Figure 3.9-5, Figure 3.9-6, and Figure 3.9-7 show σ_{yy} for von Mises, linear Mohr-Coulomb and parabolic Mohr-Coulomb respectively; the von Mises material is just below limit load at 220 psi pressure. The linear Mohr-Coulomb is in the fully plastic state at 475 psi pressure, and the parabolic is close to the fully plastic state at 327 psi pressure. These stress fields are similar for the three materials. In Figure 3.9-8 and Figure 3.9-9, the mean normal stress and deviatoric stress ($\sqrt{3J_2}$) are shown for the linear Mohr-Coulomb model in the fully plastic state (p = 475 psi). The linear relation between these stress measures is apparent. Notice the high compression just above the cutout and on the edge of the prism. The edge stress is probably due to the symmetry condition and the plain strain constant. Figure 3.9-10 shows two stress measures (mean normal and deviatoric, respectively) for the parabolic Mohr-Coulomb model close to the fully plastic state (at p = 327 psi). Here the ($\sqrt{3J_2}$) plot shows a more uniform field, since the parabola in the (J_1 - J_2) plane is considerably reduced in slope compared to the straight line at the hydro-static stress levels (see Figure 3.9-3).

Finally, in Figure 3.9-10, the contours of plastic strain are displayed. Interestingly, the peak value is somewhat above the cutout, at x = 0, y = 100.

Input Deck

The input deck is set up to do only the analysis for the parabolic Mohr-Coulomb case. Appropriate changes are necessary for the other forms discussed. The contour plots shown were obtained using Mentat.

Parameters, Options, and Subroutines Summary

Example e3x9.dat:

Parameters	Model Definition Options	History Definition Options
ELEMENTS	CONNECTIVITY	AUTO LOAD
END	CONTROL	CONTINUE
SCALE	COORDINATES	PROPORTIONAL INCREMENT
SIZING	DIST LOADS	
TITLE	END OPTION	
	FIXED DISP	
	ISOTROPIC	
	OPTIMIZE	

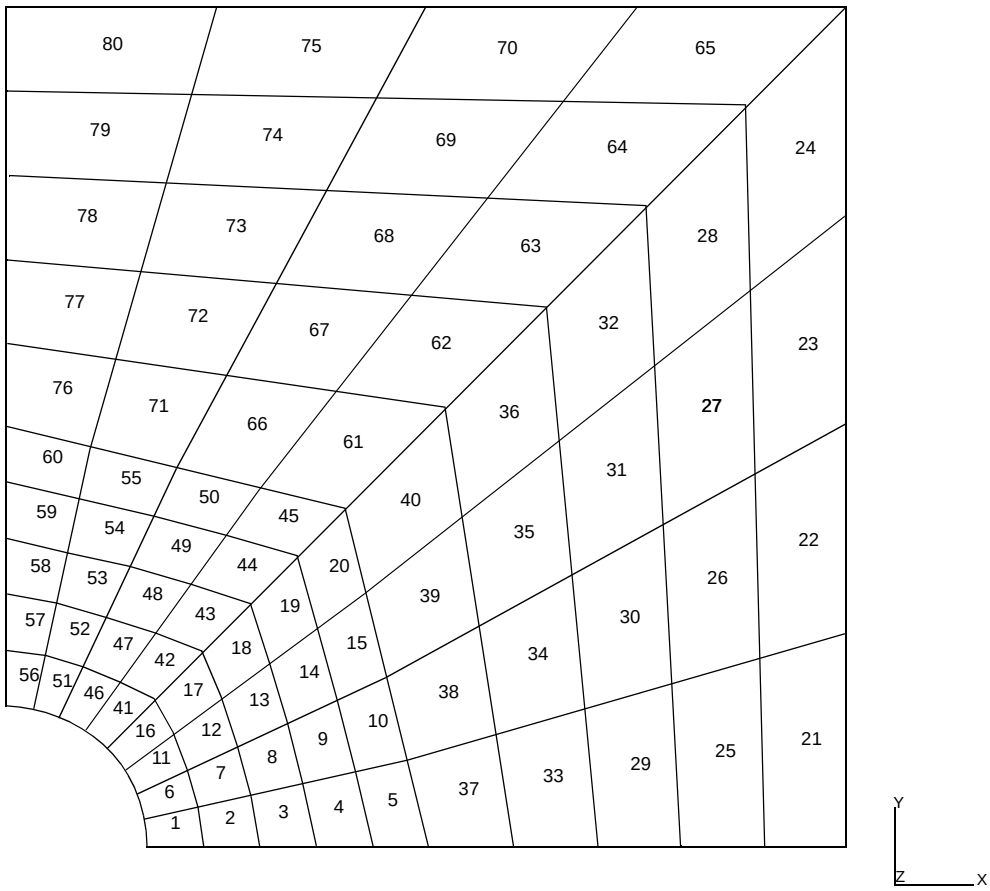

Figure 3.9-1 Simple Geometry Mesh

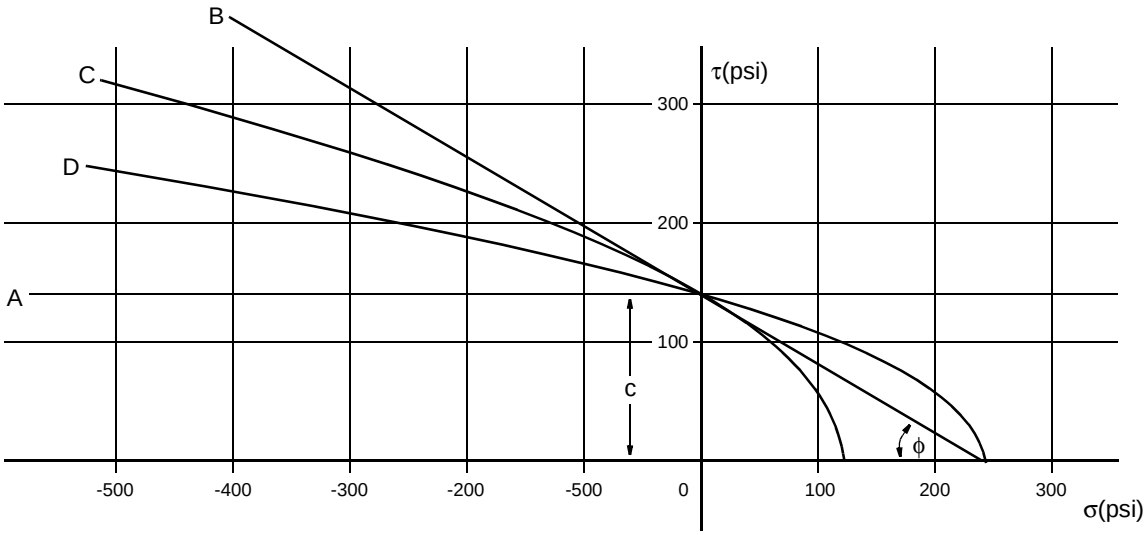

A – von Mises, c = 140 psi
B – Linear Mohr-Coulomb, c = 140 psi, f = 30°
C – Parabolic Mohr-Coulomb, c = 140 psi, $\alpha = \frac{c}{\cos 30°}$
D – Parabolic Mohr-Coulomb, c = 140 psi, $\alpha = c \tan 30°$

Figure 3.9-2 Plane Strain Yield Surfaces

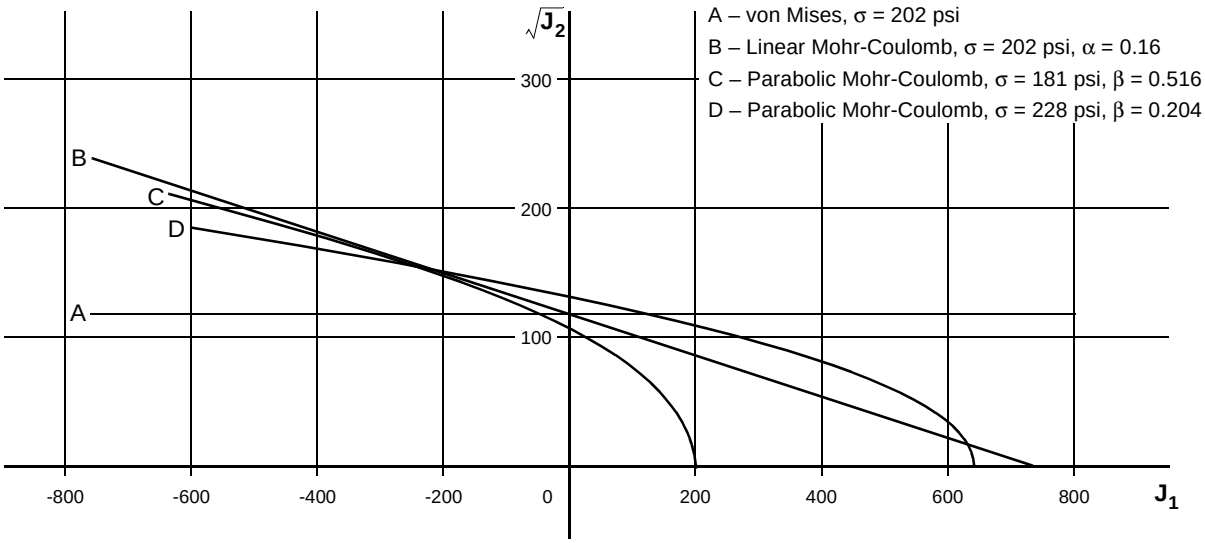

Figure 3.9-3 Yield Surfaces in $J_1 - \sqrt{J_2}$ Plane

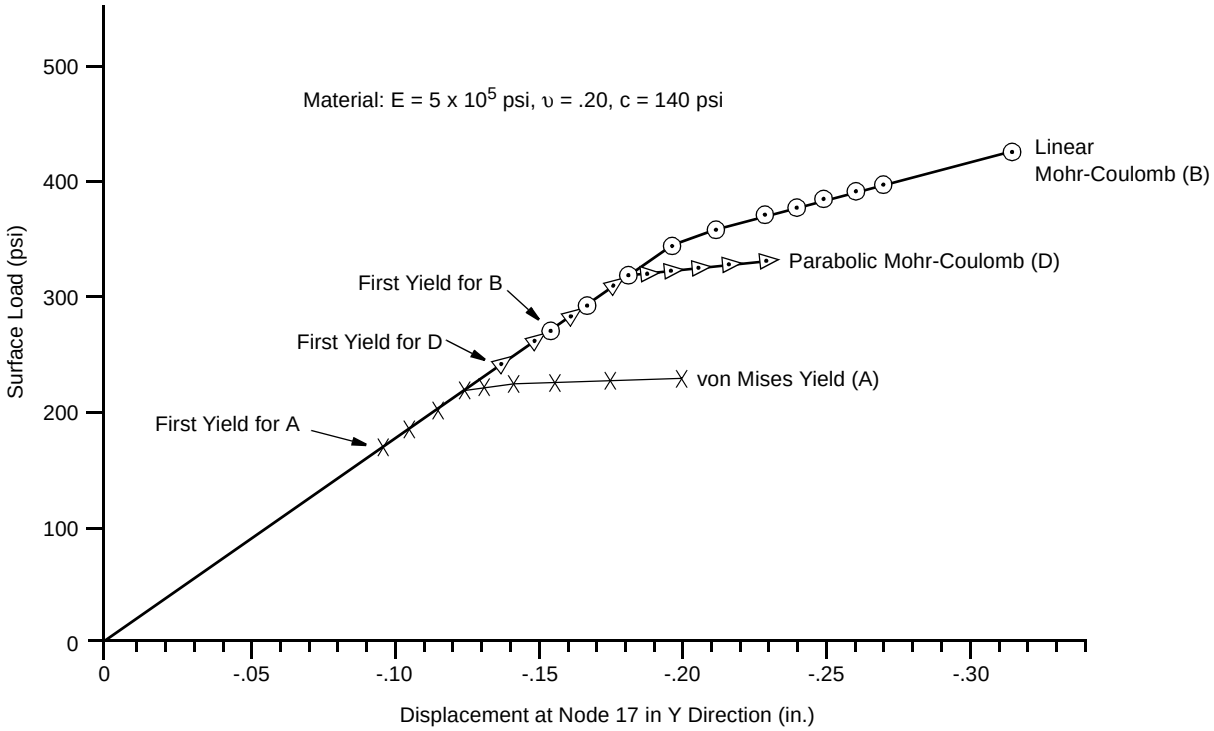

Figure 3.9-4 Global Load Displacement

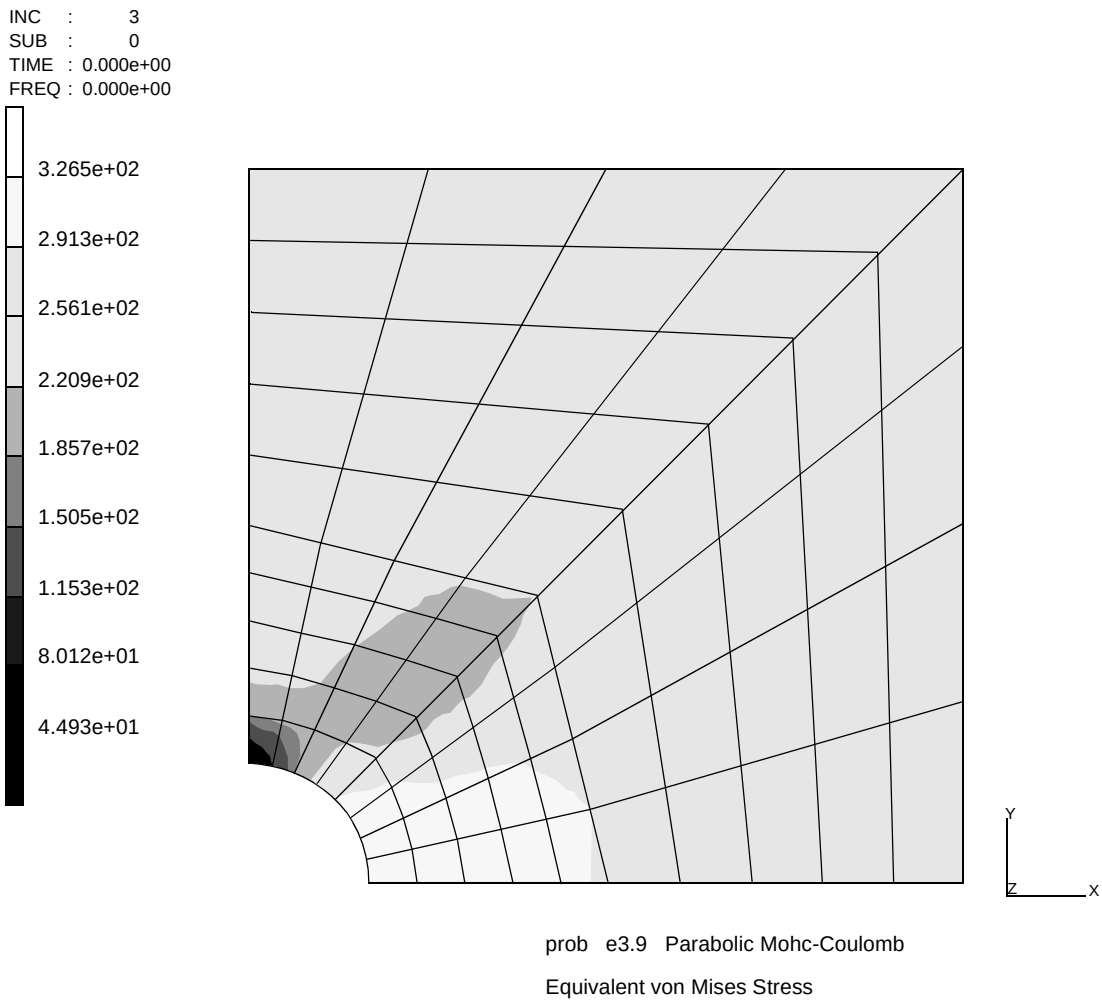

Figure 3.9-5 Equivalent Stress at 307 psi

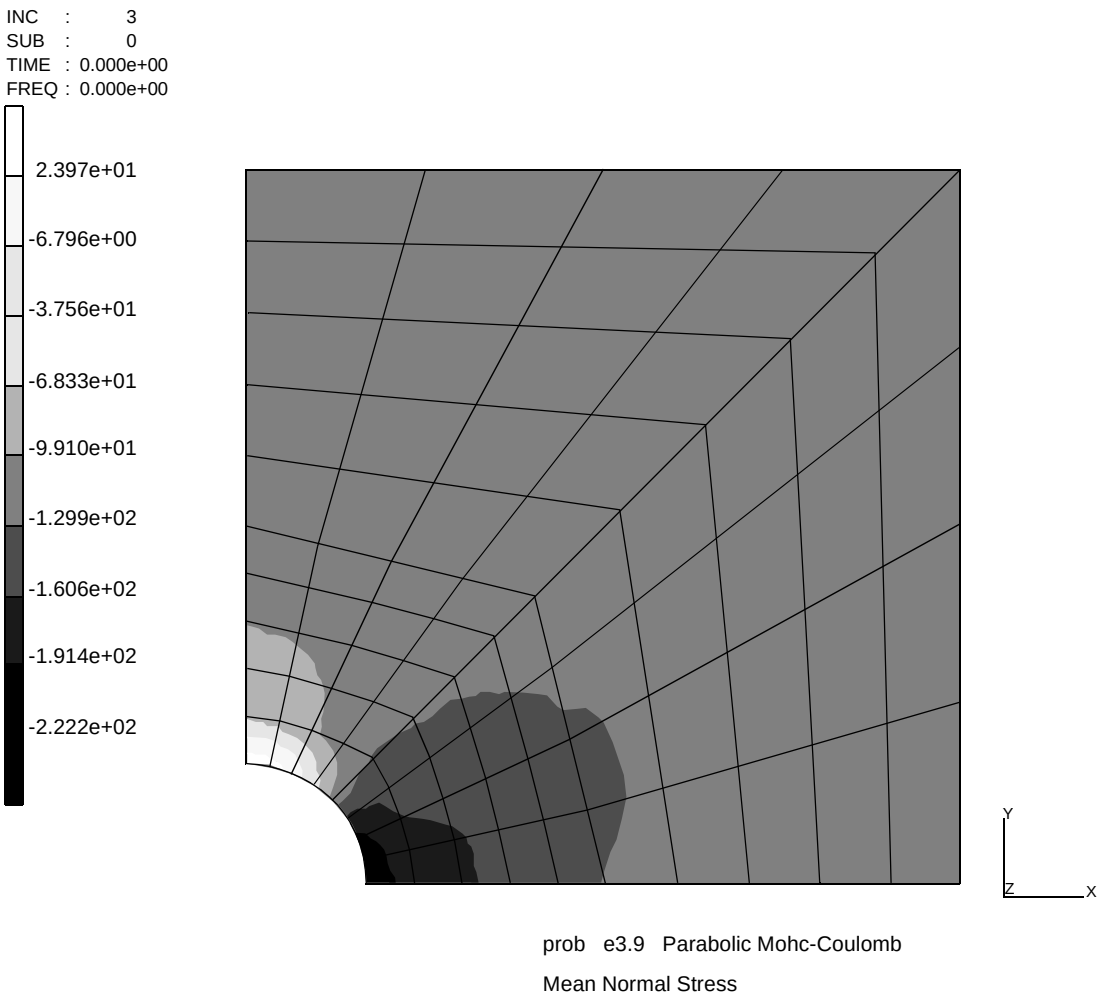

Figure 3.9-6 Mean Normal Stress at 307 psi

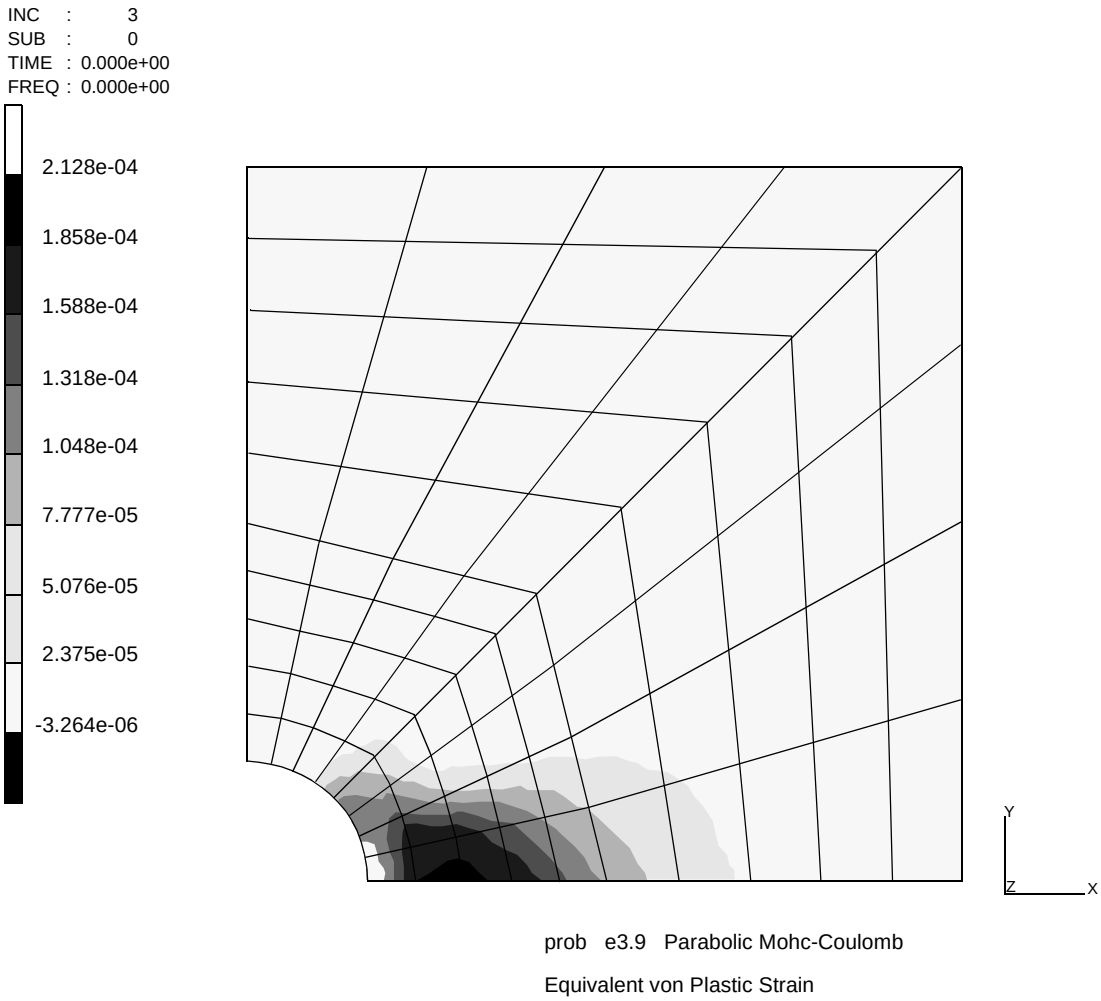

Figure 3.9-7 Equivalent Plastic Strain at 307 psi

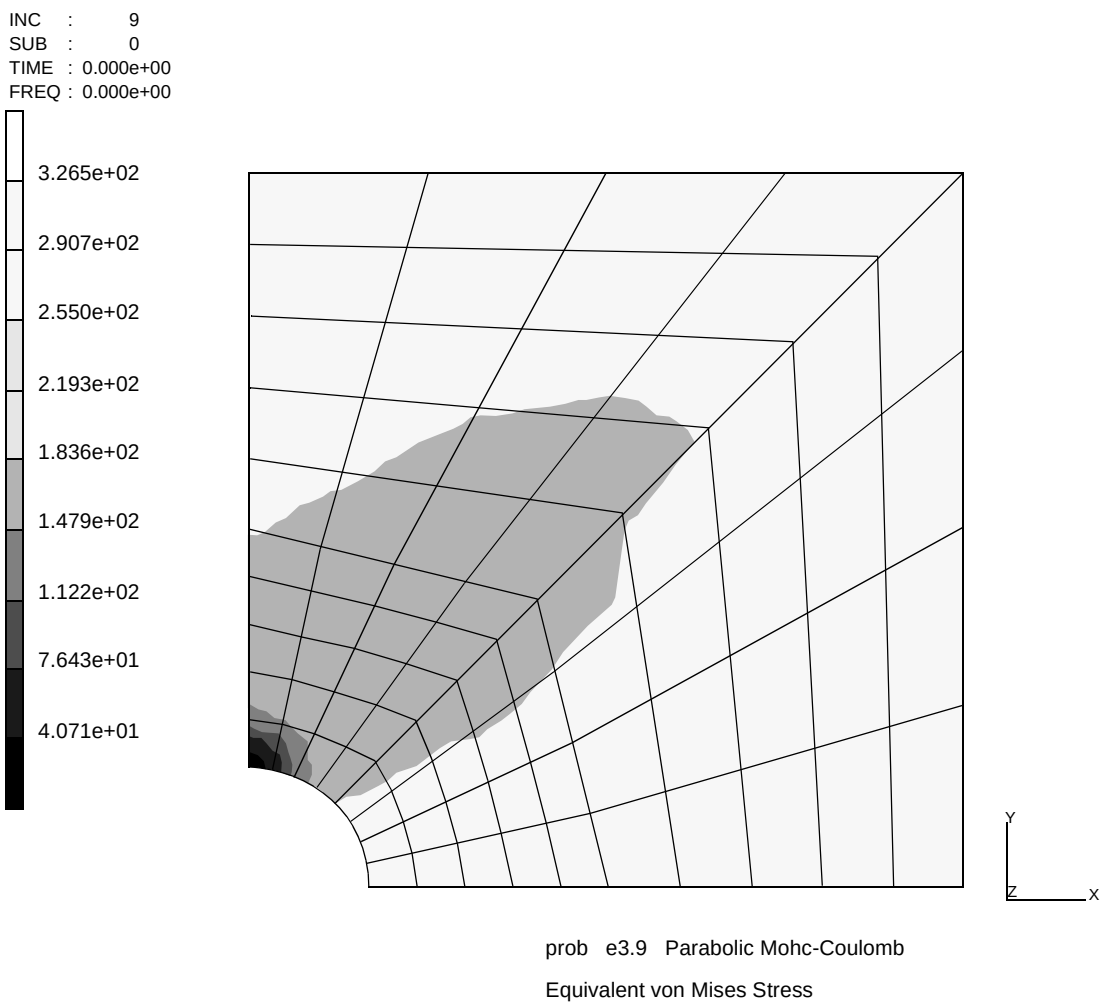

Figure 3.9-8 Equivalent von Mises Stress at 475 psi

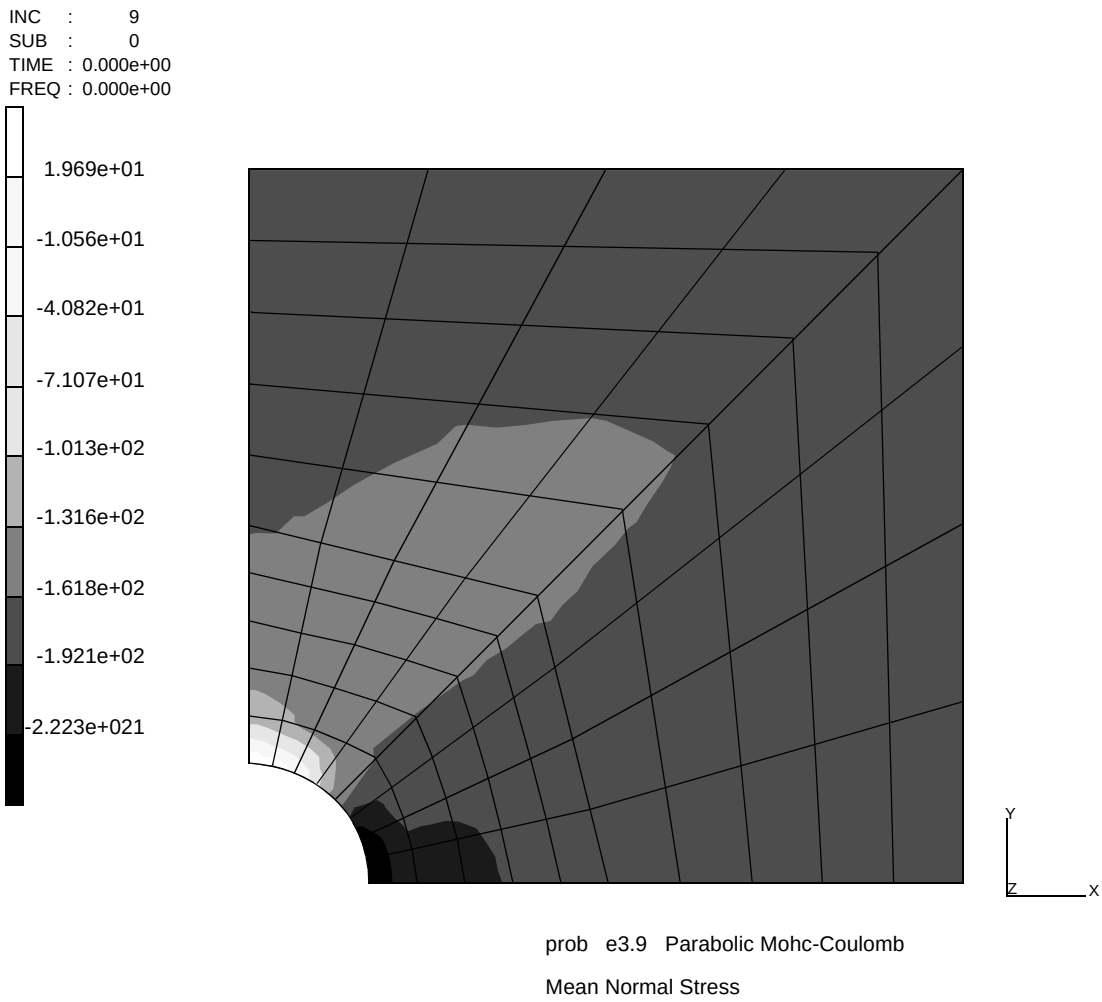

Figure 3.9-9 Mean Normal Stress at 475 psi

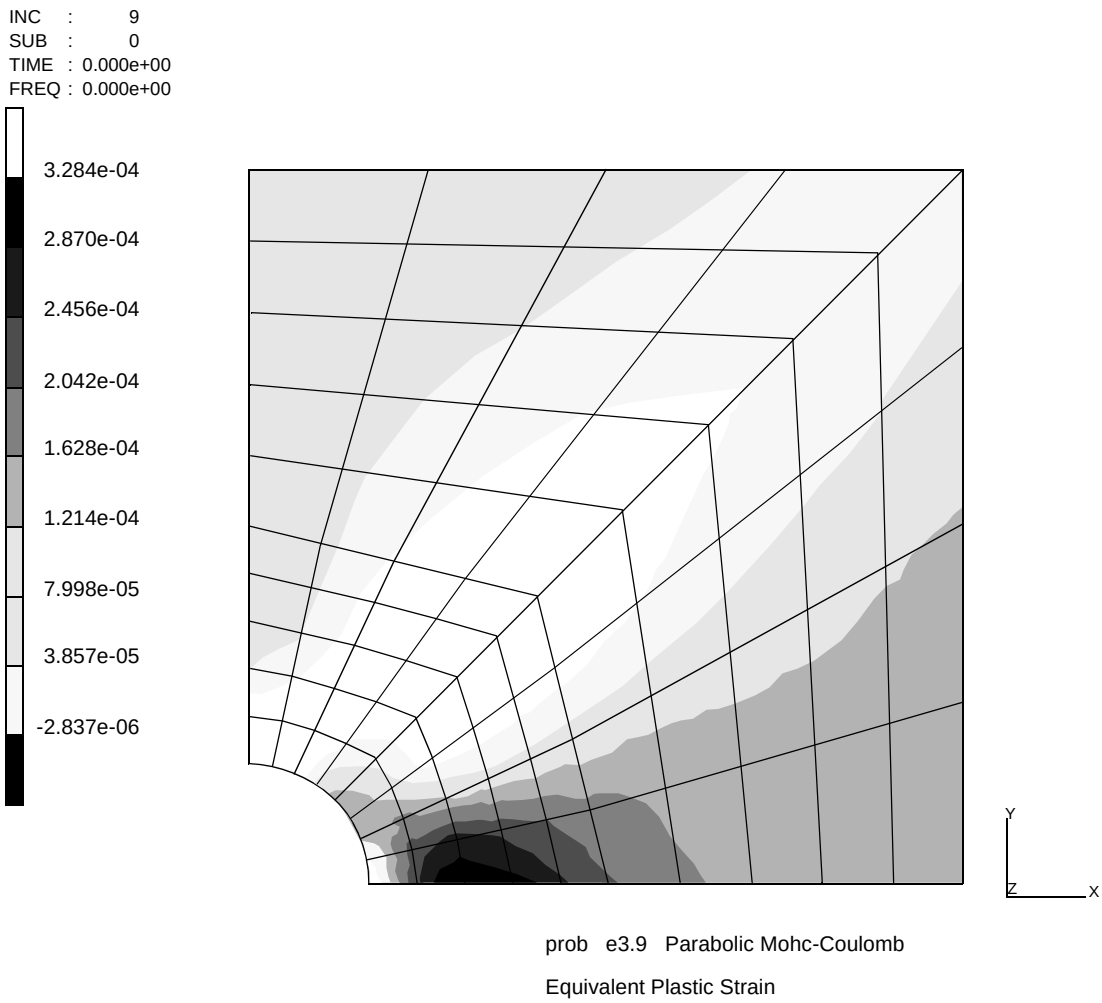

Figure 3.9-10 Equivalent Plastic Strain at 475 psi

3.10 Plate with Hole Subjected to a Cyclic Load

A plate with hole under the action of an in-plane force is loaded into an elastic-plastic range. The load is reversed until it reaches an absolute value which is the same as the initial load. The material is elastic-plastic with combined isotropic and kinematic hardening.

Element

Element 26 is an 8-node plane-stress quadrilateral.

Model

The mesh, consisting of 20 elements and 79 nodes, is shown in Figure 3.10-1.

Geometry

The thickness of the plate is specified as 1.0 in. in EGEOM1.

Boundary Condition

Boundary conditions are used to enforce symmetry about the x- and y-axes.

Material Properties

The material is elastic-plastic with combined isotropic and kinematic hardening. Values for Young's modulus, Poisson's ratio, and yield stress used here are 30×10^6 psi, 0.3, 50×10^3 psi, respectively.

Workhard

Five sets of workhardening slope and breakpoint are used to define the workhardening curve as shown in Figure 3.10-2:

First workhardening slope	$= 14.3 \times 10^6$,	breakpoint = 0.
Second workhardening slope	$= 3. \times 10^6$,	breakpoint = 0.7×10^{-3}
Third workhardening slope	$= 1.9 \times 10^6$,	breakpoint = 1.6×10^{-3}
Fourth workhardening slope	$= 0.67 \times 10^6$,	breakpoint = 2.55×10^{-3}
Fifth workhardening slope	$= 0.3 \times 10^6$,	breakpoint = 3.3×10^{-3}

The final slope is used for the kinematic hardening portion of the workhardening behavior.

Loading

An initial in-plane tension is applied on the top edge of the mesh. SCALE is used to raise this tension to a magnitude such that the highest stressed element (in this case element 8) is at first yield. The tension is then incremented to 130% of load to first yield in five steps. The in-plane load is then reversed in direction and is incremented to the same absolute magnitude in 19 steps.

Optimization

The Cuthill-McKee algorithm is used to obtain a nodal bandwidth of 26 after 10 trials. The correspondence table is written to unit 1.

Results

The plate with hole reaches yield stress at a tension of 1.62×10^4 pounds. As the tension increases to 130% of yield load (2.1×10^4 pounds) in 5 increments, yielding advances from integration point 2 to 5 of element 8. The maximum effective plastic strain is around 3.3×10^{-4}. After the in-plane load is reversed in direction and incremented to the same absolute maximum in 19 steps, the maximum effective plastic strain is 2.0×10^{-4}. A contour plot of von Mises stress for increment 23 is shown in Figure 3.10-3. The displacements are shown in Figure 3.10-4. The PRINT CHOICE option is used to restrict the output to layers 2, 5, and 8 of elements 7 and 8.

Parameters, Options, and Subroutines Summary

Example e3x10.dat:

Parameters	Model Definition Options	History Definition Options
ELEMENTS	CONNECTIVITY	AUTO LOAD
END	CONTROL	CONTINUE
SCALE	COORDINATES	PROPORTIONAL INCREMENT
SIZING	DIST LOADS	
TITLE	END OPTION	
	FIXED DISP	
	GEOMETRY	
	ISOTROPIC	
	PRINT CHOICE	
	WORK HARD	

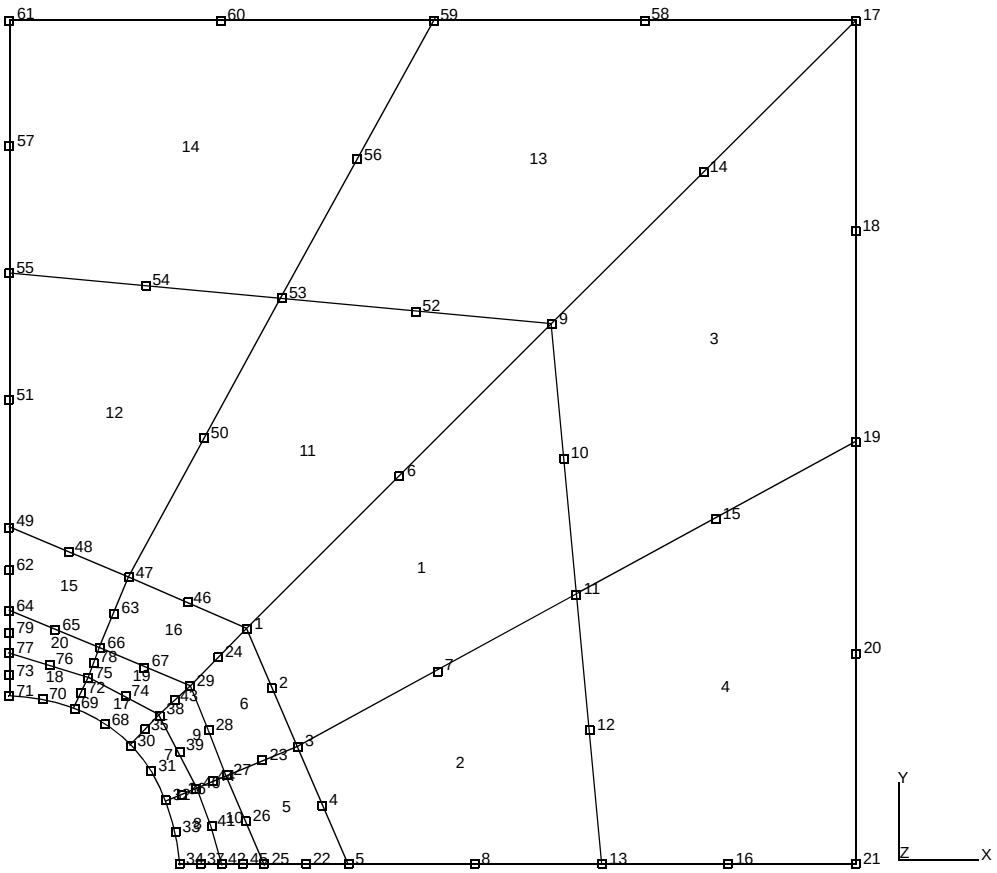

Figure 3.10-1 Mesh Layout for Plate with Hole

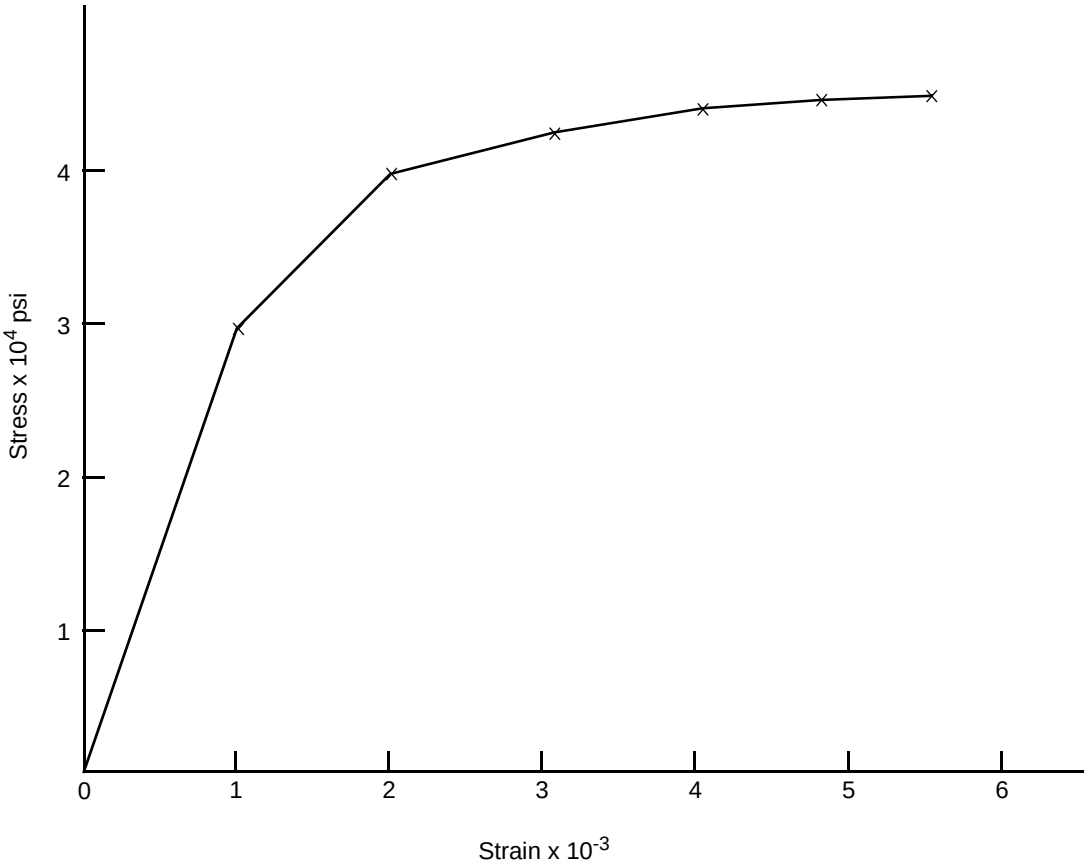

Figure 3.10-2 Workhardening Curve

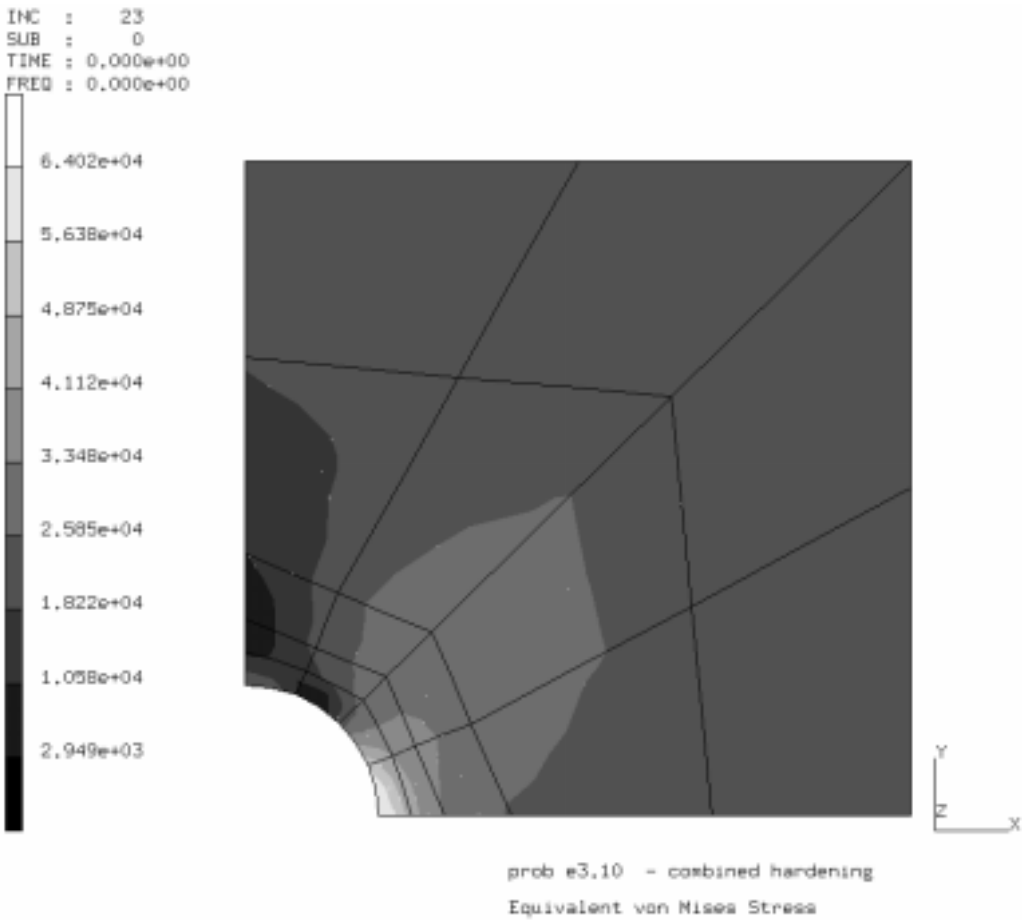

Figure 3.10-3 von Mises Stress Results

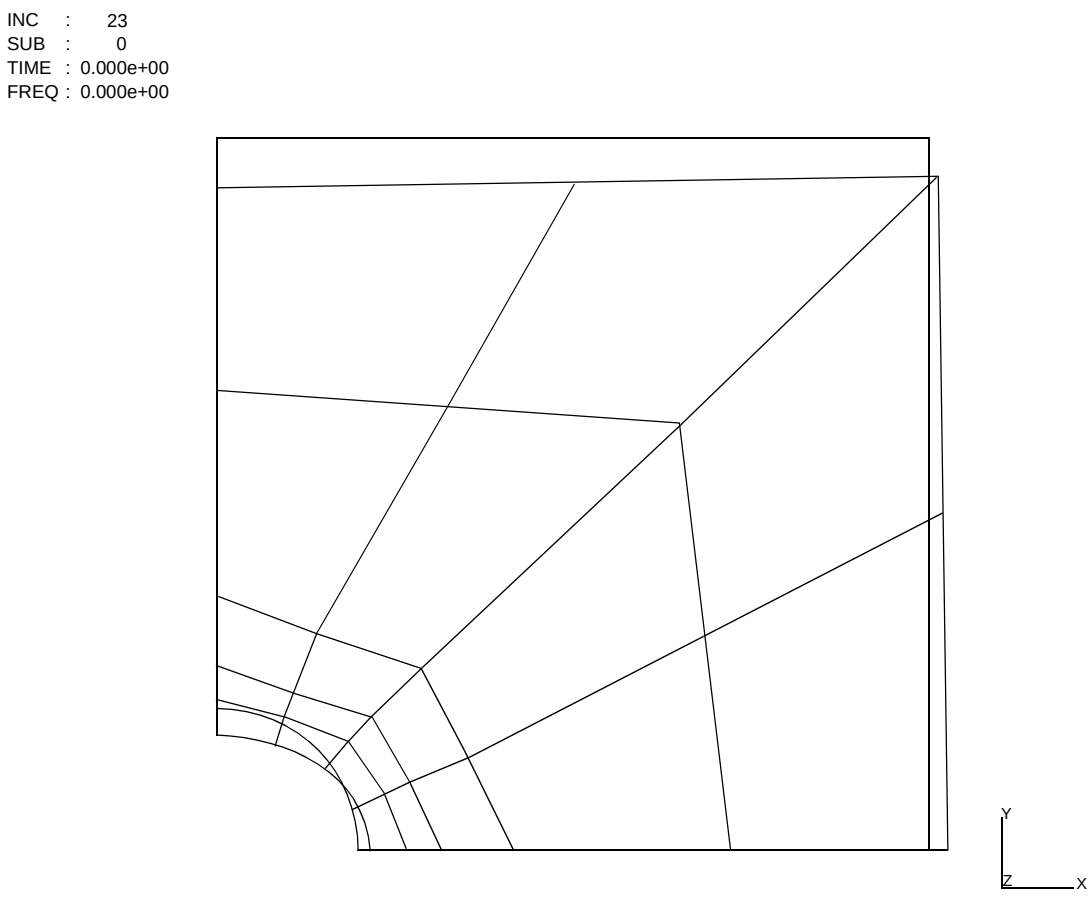

Figure 3.10-4 Displaced Mesh

3.11 Axisymmetric Bar in Combined Tension and Thermal Expansion

An axisymmetric bar under combined tension and thermal expansion is loaded into the elastic-plastic range. The bar is loaded in tension to yield, and the temperature and mechanical load are subsequently increased.

Element

Element type 28 is an 8-node distorted quadrilateral.

Model

The geometry of the bar and the mesh are shown in Figure 3.11-1. The bar is divided into five elements with 28 nodes.

Geometry

This option is not required for this element.

Tying

The same axial displacements are imposed by TYING the first degree of freedom of all nodes in the loaded face (Z = 1) to node 3, producing a generalized plane-strain condition.

Boundary Conditions

Fixed boundary conditions in the z-direction are specified at the built-in end (Z = 0).

Material Properties

The material is assumed to be elastic-plastic with isotropic strain hardening. Values for Young's modulus, Poisson's ratio, coefficient of thermal expansion and yield stress used here are 10.0×10^{6} psi, 0.3, 1.0×10^{-5} in/°F, and 20,000. psi, respectively.

Work Hard

A constant workhardening slope of 30.0×10^{4} psi is used.

Loading

An end load of 10,000 pounds is first applied to the bar in the direction of the first degree of freedom of node 3 using the POINT LOAD option. The load is scaled to a condition of first yield. The temperature is then increased by a total of 500° in five steps. The mechanical load is scaled by a factor of 0.15376.

Results

The bar reaches yield stress due to tension at a load of 1.57×10^5 pounds. At the maximum temperature, the plastic strain is about 0.5% and the total load is 1.68×10^6 pounds. The loading is proportional; therefore, no iteration is required for a convergent solution. The PRINT CHOICE option is used to restrict the output to shell layers 2, 5, and 8. A restart file was created at every increment. This can be used to extend the analysis or for postprocessing.

Parameters, Options, and Subroutines Summary

Example e3x11.dat:

Parameters	Model Definition Options	History Definition Options
ELEMENTS	CONNECTIVITY	AUTO THERM
END	CONTROL	CHANGE STATE
SCALE	COORDINATES	CONTINUE
SIZING	END OPTION	PROPORTIONAL INCREMENT
THERMAL	FIXED DISP	
TITLE	ISOTROPIC	
	POINT LOAD	
	PRINT CHOICE	
	RESTART	
	WORK HARD	

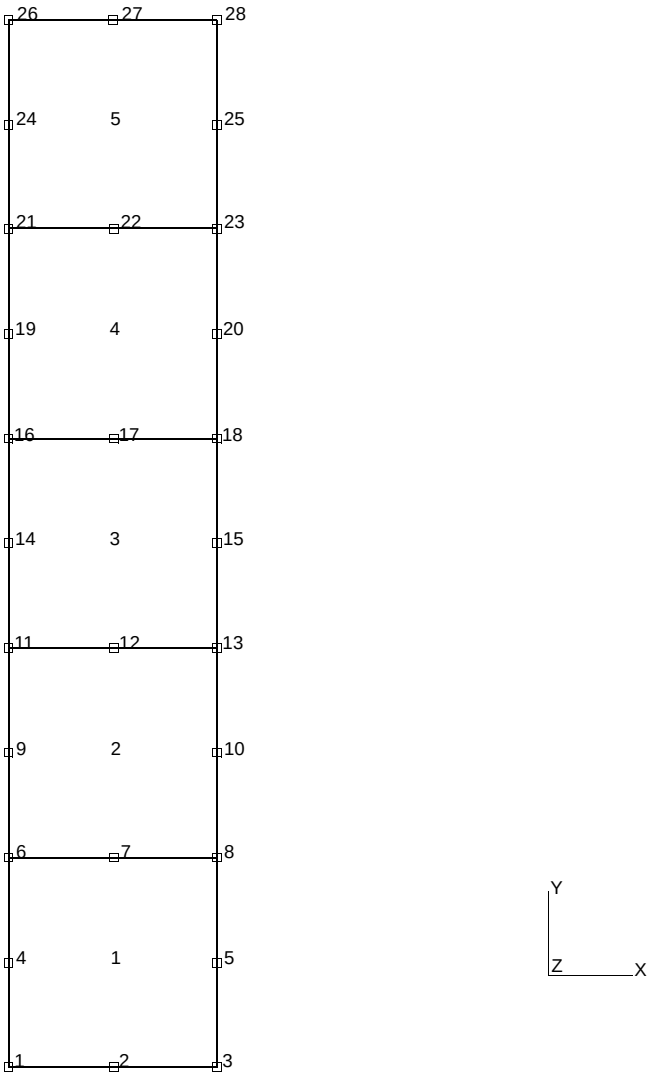

Figure 3.11-1 Axisymmetric Bar and Mesh

3.12 Creep of Thick Cylinder (Plane Strain)

A thick-walled cylinder loaded by internal pressure is analyzed using the creep analysis procedure available in MARC. This example provides you with guidelines for specifying stress and strain tolerances.

This problem is modeled using the two techniques summarized below.

Data Set	Element Type(s)	Number of Elements	Number of Nodes	Differentiating Features
e3x12	10	20	42	AUTO CREEP
e3x12b	10	20	42	AUTO STEP

Element

Element type 10, the axisymmetric quadrilateral, is used here.

Model

The geometry and mesh used are shown in Figure 3.12-1. The cylinder has an outer to inner radius ratio of 2 to 1. The mesh has 20 elements, 42 nodes and 84 degrees of freedom.

Geometry

This option is not required for this element.

Material Properties

The material data assumed for this example is: Young's modulus (E) is 30.0×10^6 psi, Poisson's ratio (ν) is 0.3, and yield stress (σ_y) is 20,000 psi.

Loading

A uniform internal pressure of 1000 psi is applied to the inner wall of the cylinder using the DIST LOAD option. The inclusion of the SCALE parameter causes this load to be automatically scaled upward to 9081.3 psi which is the pressure load which causes the highest stress element (number 1 here) to be at a J_2 stress of 20,000 psi.

Boundary Conditions

All nodes are constrained in the axial direction such that only radial motion is allowed.

Creep

Creep analysis is flagged by use of CREEP and the conditions are set using the CREEP model definition block. The creep law used here is:

$$\dot{\varepsilon} = A\sigma^n \quad \text{, in/in-hr.}$$

where:

A is 1.075×10^{-26}

and:

n = 5.5 (where the stress is given in psi).

The exact, steady-state solution for this problem is:

$$\sigma_{zz} = \frac{p}{d}\left[\left(\frac{1}{n} - 1\right)\left(\frac{b}{r}\right)^{2/n} + 1\right]$$

$$\sigma_{rr} = \frac{p}{d}\left[\left(\frac{b}{r}\right)^{2/n} - 1\right]$$

$$\sigma_{\theta\theta} = \frac{p}{d}\left[\left(\frac{2}{n} - 1\right)\left(\frac{b}{r}\right)^{2/n} + 1\right]$$

where:

p is the internal pressure

a is the inside radius

b is the outside radius

and:

$$d = \left(\frac{b}{a}\right)^{2/n} - 1$$

The CREEP model definition option has set the fifth field to zero; therefore, the creep law has been introduced via user subroutine CRPLAW (see *MARC Volume D: User Subroutines & Special Routines).*

Creep Control Tolerances – AUTO CREEP Option

MARC runs a creep solution (under constant load conditions) via the AUTO CREEP history definition option. This option chooses time steps automatically based on a set of tolerances and controls provided by you. These are as follows:

1. Stress Change Tolerance (AUTO CREEP Model Definition Set, Line 3, Columns 11-20). This tolerance controls the allowable stress change per time step during the creep solution, as a fraction of the total stress at a point. The stress changes during the transient creep, and the creep strain rate is usually very strongly dependent on stress (in this case, the dependence is $\sigma^{5.5}$); this tolerance governs the accuracy of the transient creep response. Due to accurate track of the transient, a tight tolerance (1% or 2% stress change per time step) should be specified. If only the steady-state solution is sought, a relatively loose tolerance (10-20%) can be assigned.

2. Creep Strain Increment Per Elastic Strain (AUTO CREEP Model Definition Set, Line 3, Columns 1-10).

   MARC explicitly integrates the creep rate equation, and hence requires a stability limit. This tolerance provides that stability limit. In almost all cases, the default of 50% represents that limit, and the user need not provide any entry for this value. Figure 3.12-6 illustrates the problems that can occur if the stability limit is violated.

3. Maximum Number of Recycles for Satisfaction of Tolerances (AUTO CREEP Model Definition Set, Line 2, Columns 36-40).

   MARC chooses its own time step during AUTO CREEP based on the algorithm described below. In some cases, MARC may recycle in order to choose a time step to satisfy tolerances, but it is rare for the recycling to occur more than once per step. If excessive recycling occurs, it may be because of physical problems (such as creep buckling), bad coding of user subroutine CRPLAW, or excessive residual load correction. Excessive residual load correction occurs when the creep solution begins from a state which is not in equilibrium. This entry prevents wasted machine time by limiting the number of cycles to a prescribed value. The default of 5 cycles is reasonable in most normal cases.

4. Low Stress Cut-Off (AUTO CREEP Model Definition Set, Line 3, Columns 21-30.)

   This control avoids excessive iteration and small time steps caused by tolerance checks on elements with small round-off stress states. A simple example is a beam column in pure bending – the stress on the neutral axis will be a very small number; it would make no sense to base time step choice on satisfying tolerances at such points. The default here of 5% is satisfactory for most cases – MARC does not check those points where the stress is less than 5% of the highest stress in the structure.

5. Choice of Element For Tolerance Checking (AUTO CREEP Model Definition Set, Line 7, Columns 31-35.)

   The default option for creep tolerance checking is having all integration points in all elements checked. To save time, tolerances are checked in one selected element – this field is then used to select that element. Usually, the most highly stressed element is chosen.

Notes

All stress and strain measures used in tolerance checks are second invariants of the deviatoric state (that is, equivalent von Mises uniaxial values).

All tolerances and controls can be reset upon restart.

When a tolerance or control can be entered in two places (for example, on the CREEP or CONTROL model definition set), the values or defaults provided by the last of these options in the input deck are used.

Auto Creep

This history definition set chooses time steps according to an automatic scheme based on the tolerances described above. AUTO CREEP is designed to take advantage of diffusive characteristics of most creep solutions – rapid initial gradients which settle down with time. The algorithm is as follows:

- For a given time step Δt, a solution is obtained.
- The largest value of stress change per stress $\left|\frac{\Delta\sigma}{\sigma}\right|$ and creep strain change per elastic strain, $\left|\frac{\underline{\varepsilon}^c}{\underline{\varepsilon}^e}\right|$ are found. These are compared to the tolerance values set by the user, T_σ and T_ε.

- Then the value p is calculated as the bigger of $\left|\frac{\Delta\sigma}{\sigma}\right| / T_\sigma$ or $\left|\frac{\Delta\varepsilon^c}{\varepsilon^e}\right| / T_\varepsilon$.

  a. Clearly if p > 1, the solution is violating one of your tolerances in some part of the structure. In this case, MARC resets the time step as:

  $\Delta t_{new} = \Delta t_{old} * .8/p$

  that is, as 80% of the time step which would just allow satisfaction of the tolerances. The time increment is then repeated. Such repetition continues until tolerances are successfully satisfied, or until the maximum recycle control is exceeded – in the latter case the run is ended. Clearly, the first repeat should satisfy tolerances – if it does not, the cause could be:

  excessive residual load correction
  creep buckling – creep collapse
  bad coding in subroutine CRPLAW or VSWELL

  and appropriate action should be taken before the solution is restarted.

  b. If p<1 the solution is satisfactory in the sense of the user supplied tolerances. In this case, the solution is stepped forward to t+Δt and the next time step begun. The time step used in the next increment is chosen as:

  $\Delta t_{new} = \Delta t_{old}$ if $0.8 \le p \le 1.0$

  $\Delta t_{new} = 1.25 * \Delta t_{old}$ if $0.65 \le p \le 0.8$

  $\Delta t_{new} = 1.5 * \Delta t_{old}$ if $p \ge 0.65$

The diffusive nature of the creep solution is utilized to generate a series of monotonically increasing time steps.

Results

Four solutions were found and compared to the steady-state solution as shown in Table 3.12-1 using the notation below.

1. Column A – 3% stress tolerance, 30% strain tolerance, with residual load correction.
2. Column B – 10% stress tolerance, 50% strain tolerance, with residual load correction.
3. Column C – 10% stress tolerance, 100% strain tolerance, with residual load correction.

These solutions are compared (at 20 hours) in Table 3.12-1. Graphical comparisons are drawn in Figure 3.12-2 through Figure 3.12-6.

Table 3.12-1 Creep of Thick Cylinder – Comparison of Results at 20 Hours

Stress	Location	EXACT Steady-State	A (85)†	B (48)	C (42)
σ_{zz}	inside (r=1.025)	-1372.2	-1369.2	-1375.4	-1332.8
	middle (r=1.475)	2725.1	2725.1	2725.6	2725.3
	outside (r=1.975)	5641.0	5635.9	5636.7	5638.2
σ_{rr}	inside	-8717.0	-8712.4	-8714.0	-8710.9
	middle	-3709.2	-3707.1	-3707.4	-3707.3
	outside	-145.24	-144.49	-144.56	-144.58
$\sigma_{\theta\theta}$	inside	5972.6	5974.0	5948.3	6072.8
	middle	9159.3	9158.0	9158.9	9156.4
	outside	11427.0	11424.0	11425.0	11426.0
σ	inside	12741.0	12719.0	12698.0	12803.0
	middle	11144.0	11141.0	11143.0	11140.0
	outside	10022.0	10019.0	10019.0	10020.0

†Number of steps required to reach 20 hours.

All solutions are satisfactory in the sense that monotonic convergence, with monotonic increase in time-step size, is achieved except for the strain-controlled part of the solution with 100% strain tolerance. Here the stresses oscillate. In fact, it may be shown that the strain change repeats a numerical stability criterion, and that 50% is the stability limit. The residual load correction controls the oscillation in the sense that the solution does not diverge completely. The residual load correction has little effect until a large number of steady-state increments (that is, strain-controlled increments) have been performed. At this point, it is essential for an accurate solution. The 10% stress control allows a slightly more rapid convergence to steady-state. This control is quite satisfactory, considering that it reduces the number of increments needed by 42%.

Parameters, Options, and Subroutines Summary

Example e3x12a.dat:

Parameters	Model Definition Options	History Definition Options
CREEP	CONNECTIVITY	AUTO CREEP
END	CONTROL	CONTINUE
SCALE	COORDINATES	DIST LOADS
SIZING	CREEP	
TITLE	DIST LOADS	
	ELEMENT	
	END OPTION	
	FIXED DISP	
	ISOTROPIC	
	PRINT CHOICE	

Example e3x12b.dat:

Parameters	Model Definition Options	History Definition Options
CREEP	CONNECTIVITY	AUTO STEP
END	CONTROL	CONTINUE
SCALE	COORDINATES	DIST LOADS
SIZING	CREEP	
TITLE	DIST LOADS	
	ELEMENT	
	END OPTION	
	FIXED DISP	
	ISOTROPIC	
	PRINT CHOICE	

User subroutine in u3x12.f:

CRPLAW

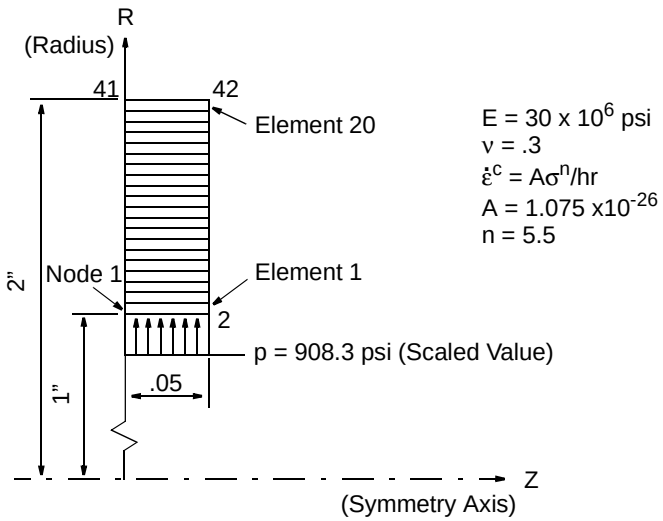

Figure 3.12-1 Thick Cylinder Geometry and Mesh

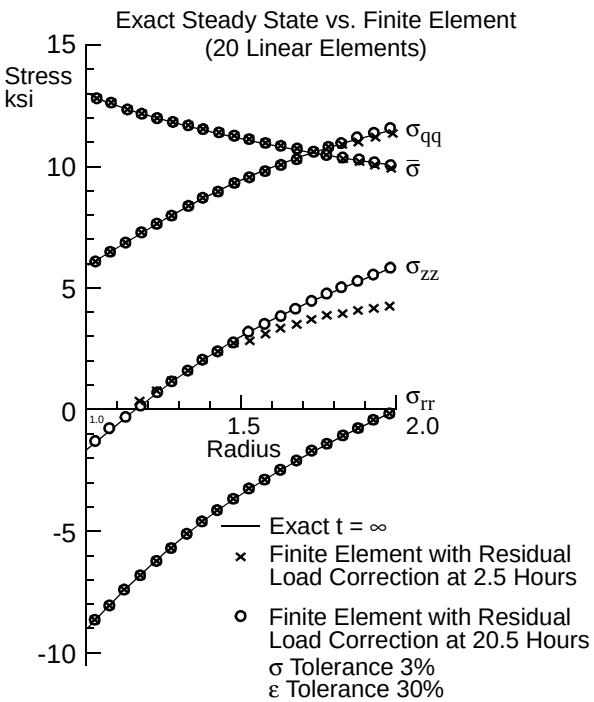

Figure 3.12-2 Creep of Thick Cylinder, Long Time Results

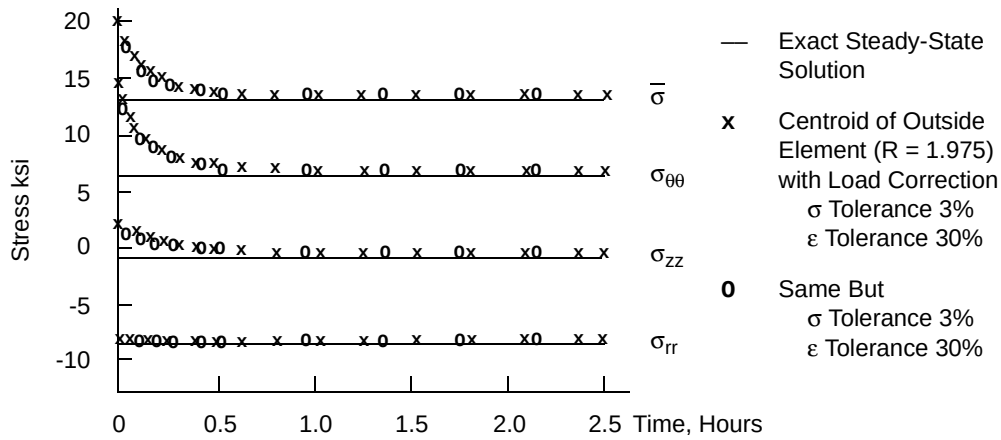

Figure 3.12-3 Creep of Thick Cylinder – Numerical Comparisons

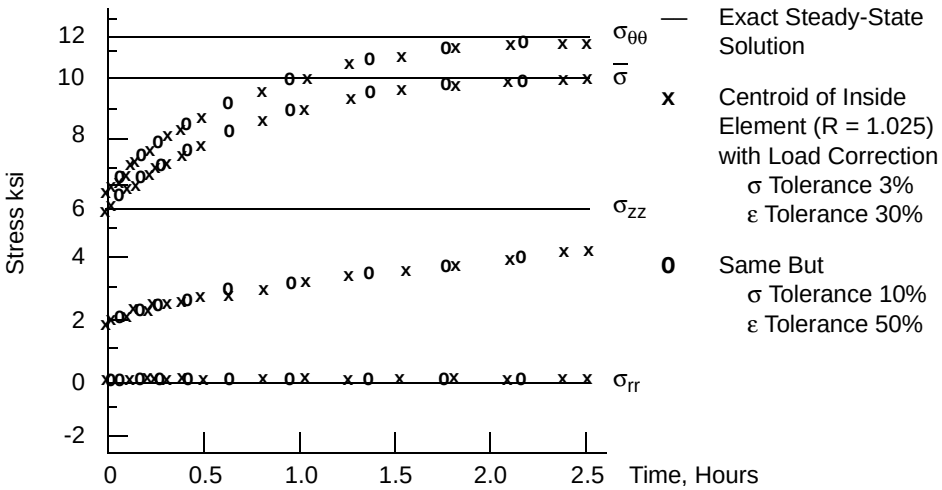

Figure 3.12-4 Creep of Thick Cylinder – Numerical Comparisons

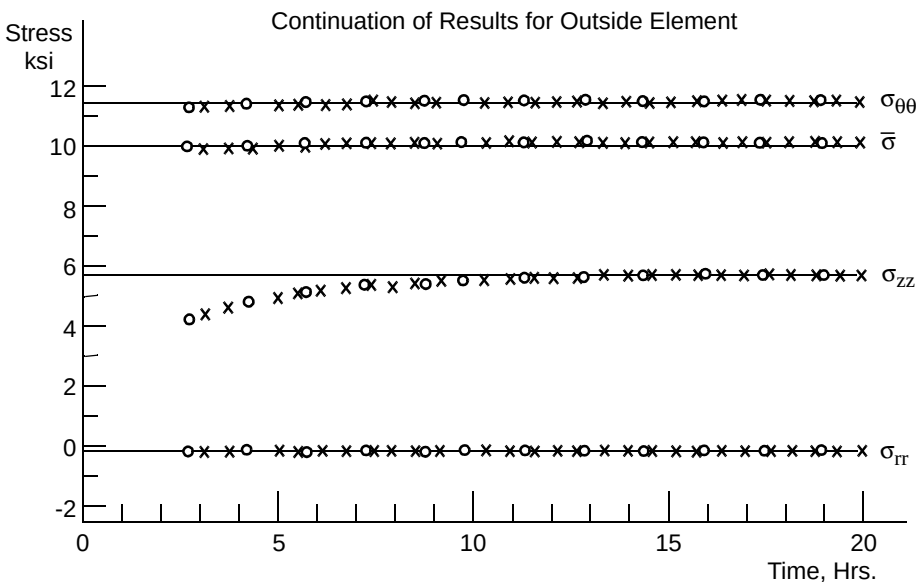

Figure 3.12-5 Creep of Thick Cylinder – Numerical Comparisons

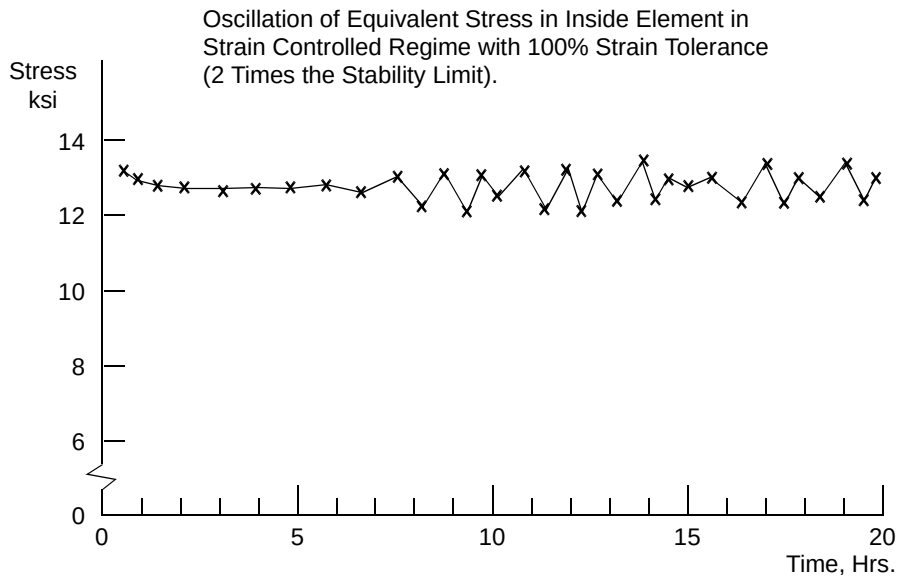

Figure 3.12-6 Creep Ring

3.13 Beam Under Axial Thermal Gradient and Radiation-induced Swelling

A hollow circular-section beam is analyzed under axial and transverse temperature gradients. It is also subject to a variable neutron flux field resulting in irradiation-induced creep swelling.

Element

In this problem, thermal gradients will result in an axial strain that varies along the length of the beam. Element type 14 only allows constant axial strain so it is not suitable here; element 25 is used instead. This is element type 14 with an additional local degree of freedom which allows nonuniform axial strain. Element type 25 is a closed-section straight beam element with no warping of the section, but including twist. The element has seven degrees of freedom per node; three displacements and three rotations in the global coordinate system and axial strain.

Model

The beam is constrained axially at its base; rotations are allowed. Reaction forces at the base and three collars are computed. Each reaction force is modeled by the use of a linear spring, one end of which is attached to the node at the base or collar point; the remaining end is attached to a fixed node. The springs are dimensionless and completely linear. There are 21 elements and 20 nodes for a total of 182 degrees of freedom (see Figure 3.13-1).

Geometry

The BEAM SECT can be used to specify a cross section other than the default (circular section) used here.

Material Properties

The material is elastic with a Young's modulus of 26.4×10^6 psi and Poisson's ratio of 0.3. The initial stress-free temperature is 400°F and the coefficient of thermal expansion is 0.96×10^{-5} in/in/°F.

Loading

Thermal gradients and neutron flux are the only loading imposed; no mechanical loads are applied.

Boundary Conditions

The beam end is fixed axially (u = o). In order to model reaction forces, the beam end and collar points are "fixed" by linear springs that are stiff enough to effectively zero the displacements.

User Subroutines

Long-term creep and swelling results are desired. Subroutine VSWELL is used. The creep law is written for 304 and 306 stainless steel. The swelling is written in accordance with ORNL recommendations.

The creep law can be expressed as:

$$\dot{\bar{\varepsilon}}^c = A\bar{E} \bullet \bar{\sigma}(1 - \exp(-\bar{E}\phi t/B)) + C\bar{E}\phi \bullet \bar{\sigma}t$$

Differentiating:

$$\dot{\bar{\varepsilon}}^c = A\bar{E}\phi\bar{\sigma} \bullet \bar{E}\phi/B \bullet \exp(-\bar{E}\phi \bullet t/B) + C\bar{E}\phi \bullet \bar{\sigma}\varepsilon$$

where:

$\bar{\varepsilon}^c$ is the equivalent creep strain
t is the time (sec.)
ϕ is the neutron density
$\bar{E}$ is the mean neutron energy in MeV
σ is the equivalent J_2 stress
T is the temperature
A = 1.7×10^{-23}
B = 2.0×10^{20}
C = 7.5×10^{-30}

The radiation-induced swelling strain model can be expressed as:

$$\frac{\Delta V\ \%}{V} = R\phi t + \frac{R}{\alpha}\ln\left[\frac{1 + \exp(\alpha(\tau - \phi t))}{1 + \exp\tau}\right]$$

where R, τ, α are functions of temperature. Differentiating:

$$100\dot{\varepsilon}_{ii} = R\phi - R\phi\left[\frac{\exp(\alpha(\tau - \phi t))}{(1 + \exp(\alpha(\tau - \phi t)))}\right]$$

$$R = \exp B$$

$$B = -88.5499 + 0.531072T - 1.24156 \times 10^{-3}T^2 + 1.37215 \times 10^{-6}T^3 - 6.14 \times 10^{-10}T^2$$

$$\tau = \exp[-16.7382 + 0.130532T - 3.81081 \times 10^{-4}T^4$$

To properly model the complex temperature and flux distributions for use by these subroutines, a subroutine CREDE has been written with two state variables. The first state variable is temperature; the second is the neutron flux density. Two linear gradients, in the coordinate

directions on the section, are assumed for both state variables. The four values of each variable at each node correspond to the values at the first, fifth, eighth, and thirteenth points on the section. The remaining values are determined by bilinear interpolation.

Special Considerations

The RESTART option is used, as the prediction of the number of increments that will be analyzed is difficult. The option also permits the input and output to be checked as often as each increment. When the problem is restarted, the parameters and loads can be changed. To modify the time increments specified in the AUTO CREEP option, the REAUTO model definition option would be necessary. The CONTROL option can be used to specify the number of increments in this analysis. To determine the creep increment input in the first field, second line of the AUTO CREEP option, the procedure outlined in *Volume A: Theory and User Information* was used. Briefly a "worst" case with highest stress and temperature (extracted from the elastic load case) is studied. The total strain rate is set to zero as in a relaxation test; then the initial creep strain rate and the tolerance for stress change (AUTO CREEP option, second field of the third line) are used to determine a conservative upper bound on the initial creep time step.

MARC used three Gaussian integration points per element rather than just the centroid for calculation and storage of element stresses.

The nonuniform temperature and flux information was input in the THERMAL LOADS option. A well-behaved temperature and flux variation could be generated within the CREDE subroutine, in which case the THERMAL LOAD series would consist of just the first two lines.

Results

After 4500 hours of creeping the plot of stress versus time changes from straightforward stress relaxation to an oscillation. This change is due to an increase in swelling contribution. Stress relaxation has been plotted in Figure 3.13-2.

Parameters, Options, and Subroutines Summary

Example e3x13.dat:

Parameters	Model Definition Options	History Definition Options
CREEP	CONNECTIVITY	AUTO CREEP
ELEMENTS	CONTROL	CONTINUE
END	COORDINATES	
SIZING	CREEP	
STATE VARS	END OPTION	
THERMAL	FIXED DISP	
TITLE	GEOMETRY	
	ISOTROPIC	
	PRINT CHOICE	
	RESTART	
	SPRINGS	
	THERMAL LOADS	

User subroutines in u3x13.f:

CREDE
VSWELL

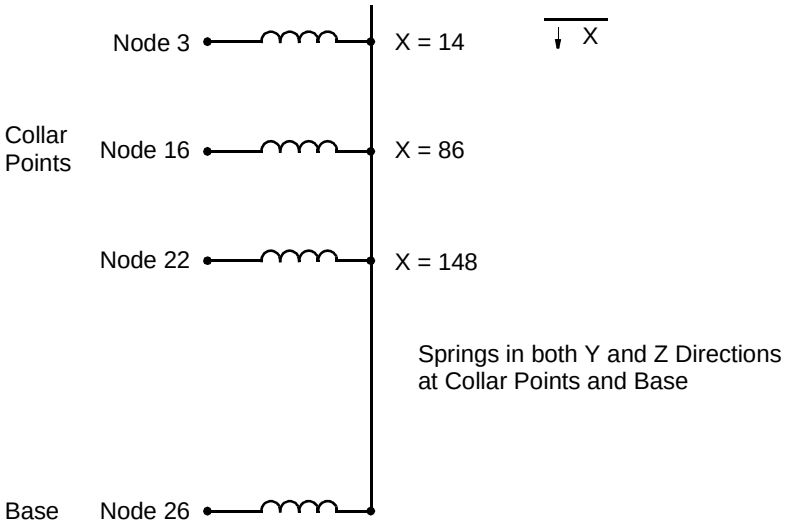

Figure 3.13-1 Beam-Spring Model

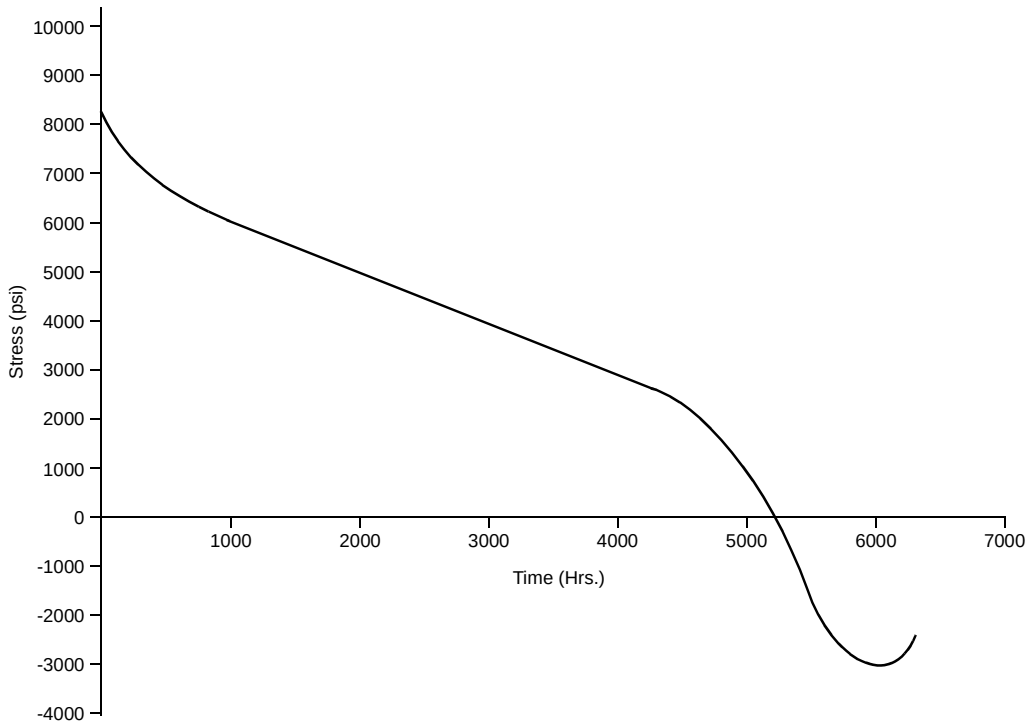

Figure 3.13-2 Transient Extreme Fiber Stress

3.14 Creep Bending of Prismatic Beam with ORNL Constitutive Equation and Load Reversal

A cantilever beam of 100 inches length, with a solid cross section of 4 inches height and 2 inches width, is subjected to a forced rotation of 1/20 radians at the free end at time zero (see Figure 3.14-1).

Due to creep, stress relaxation occurs. Subsequently, the prescribed rotation is reversed to -1/20 radians, and again stress relaxation is allowed to occur. The creep law is of the strain hardening type, and for load reversals follows the ORNL recommendation. Automatic time stepping is used in both creep periods.

Discussion of Constitutive Equation

The creep equation used in this example has the form:

$$\dot{\bar{\varepsilon}}^{c} = 10^{-24} f(\bar{\varepsilon}^{c}) \bar{\sigma}^{5}$$

where $f(\varepsilon^c)$ is specified through slope-breakpoint data. The MARC slope-breakpoint data assumes that at the first breakpoint the function f is equal to zero. However, for our constitutive equation it is required that f(0)=1. The first breakpoint is defined (in reality, this cannot occur) at an equivalent creep strain of -1.0, and a slope of 1.0 is entered. The function f will be 1.0 at the start of the analysis. The specified curve for positive equivalent creep strain is shown in Figure 3.14-2.

If a load reversal occurs, the ORNL rules take effect. In a uniaxial situation, these rules assume the existence of two values of the creep strain: ε^{c^+} and ε^{c^-}. For tension, ε^{c^+} is used in the calculation of $f(\varepsilon^c)$, and during tensile creep ε^{c^+} is updated. During compression, ε^{c^-} is used in the calculation of $f(\varepsilon^c)$, and ε^{c^-} is updated. After the first load reversal, ε^{c^-} is still zero and the material starts creeping as if no previous creep-strain hardening occurred. For the ORNL material relaxation of the stresses after load reversal, it starts more quickly than for a standard isotropically hardening material.

Element)

The two-dimensional cubic beam element, MARC type 16, is used in this analysis.

Model

Four elements are used in this example. The moment is constant throughout the beam; therefore, all elements will undergo the same deformation. The geometry of the mesh is shown in Figure 3.14-1.

Geometry

Beam height and width are specified in the first and second fields of the GEOMETRY option.

Material Properties

Linear elastic material behavior with Young's modulus (E) of 1 x 10^7 psi and Poisson's ratio (n) of 0.3 is specified on the ISOTROPIC option. Since no plasticity is assumed to occur, no yield stress is specified. The creep properties are specified on the CREEP model definition block. The CREEP properties were discussed before.

Boundary Conditions

Element 16 has as degrees of freedom: u, v, $\frac{du}{dv}$ and $\frac{dv}{ds}$. In this problem, the beam-axis corresponds with the x-axis, $\frac{dv}{ds}$ is equal to the rotation. Therefore, at node 1, both displacements and the rotation are suppressed, whereas at node 5 the rotation is prescribed as a nonzero value.

SHELL SECT

The SHELL SECT parameter is used to specify seven layers for integration through the thickness. Since the material does not have tangent-modulus nonlinearities, the elastic properties will be integrated exactly. The creep strain increment will be integrated with sufficient accuracy with the seven points specified.

PRINT CHOICE

In this option, output is requested at only one integration point (2) and one element (1), and nodal quantities are only printed at node 5. At the one integration point, all layers are printed, however.

Post File

A post file is written containing only the displacements and the reaction forces. This can be used by Mentat.

Creep Analysis Procedure

The AUTO CREEP option is used to analyze the first relaxation period of 200 hours. An initial time step of 100 hours is specified. MARC scales this down in order to obtain a starting value such that the tolerances are satisfied. All control parameters are set to their default values. The testing for the satisfaction of CREEP tolerances is done for element type 1 only. A zero rotation increment is specified for node 5 with the DISP CHANGE option. This is done in order to ensure

constant rotation during the creep period. A maximum number of increments in each AUTO CREEP block is 50; the total number of increments must be less than 80, as specified in the CONTROL option.

At the end of the first creep period, a rotation increment of negative-2 times the originally specified rotation is prescribed. This effectively reverses the loading. Then another creep period is started similar to the previous one.

Results

In increment zero, the elastic solution is obtained. The stress and strain in the extreme fiber of the beam are equal to 10^4 and 10^{-3} psi, respectively. With the specified creep law, this yields an initial creep strain rate of 10^{-4} hours^{-1}. If the stress change is to be less than 10% (the default on AUTO CREEP), the creep strain increment must be less than 10^{-4}. The initial time step must be less than 1. MARC selects an initial time step of 0.8. Due to the stress relaxation, the creep strain rate rapidly decreases, and MARC rapidly increases the time step. In 15 steps, the creep period of 200 hours is traversed. The last step prior to load reversal is equal to 42.7 hours. The stresses through the section before and after relaxation are shown in Figure 3.14-3. The creep strain in the extreme fibers has reached a value of 6.2×10^{-4}, and the creep strain rate has been reduced by a factor of more than 2 due to creep strain hardening.

Subsequently the load is reversed. The stresses in the extreme fibers now increase to a value of 1.622×10^4. Since the load is reversed, the ORNL creep equation predicts a creep rate as if no hardening had occurred: $\varepsilon^c = 11.23 \times 10^{-4}$ hours^1. In order to satisfy the creep tolerances, the initial time step must now be less than 0.1445 hours. MARC selects a time step of 0.1157 hours. Again, the time step rapidly increases during the creep period. Now, 20 steps are needed to cover the 200-hour period, with the time step in the last increment equal to 45 hours. The stress profiles at the beginning and the end of the increment are compared in Figure 3.14-4.

Also of interest is the variation of the bending moment in the beam during the two creep periods. For that purpose, a post file is written. Only displacement and reaction forces are written on this tape. The MARC PLOT program is then used to plot the bending moment (the reaction force at node 1, degree of freedom 4) against time. The result is shown in Figure 3.14-5. The input for the MARC PLOT can be found at the end of the input for the MARC STRESS program.

Parameters, Options, and Subroutines Summary

Example e3x14a.dat:

Parameters	Model Definition Options	History Definition Options
CREEP	CONNECTIVITY	AUTO CREEP
END	CONTROL	CONTINUE
NEW	COORDINATES	DISP CHANGE
SHELL SECT	CREEP	PRINT CHOICE
SIZING	END OPTION	
TITLE	FIXED DISP	
	GEOMETRY	
	ISOTROPIC	
	POST	

Example e3x14b.dat:

Parameters
END
TITLE
USER

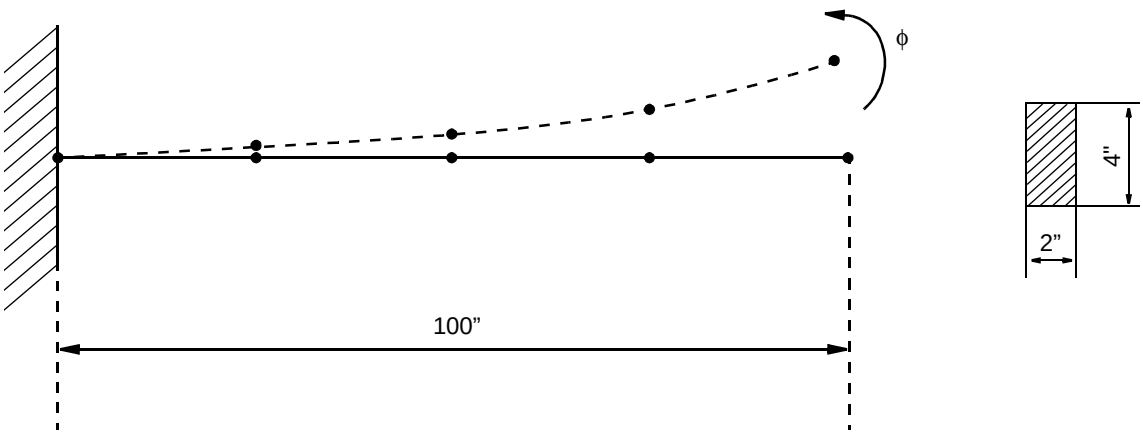

Figure 3.14-1 Geometry of Beam and Finite Element Mesh

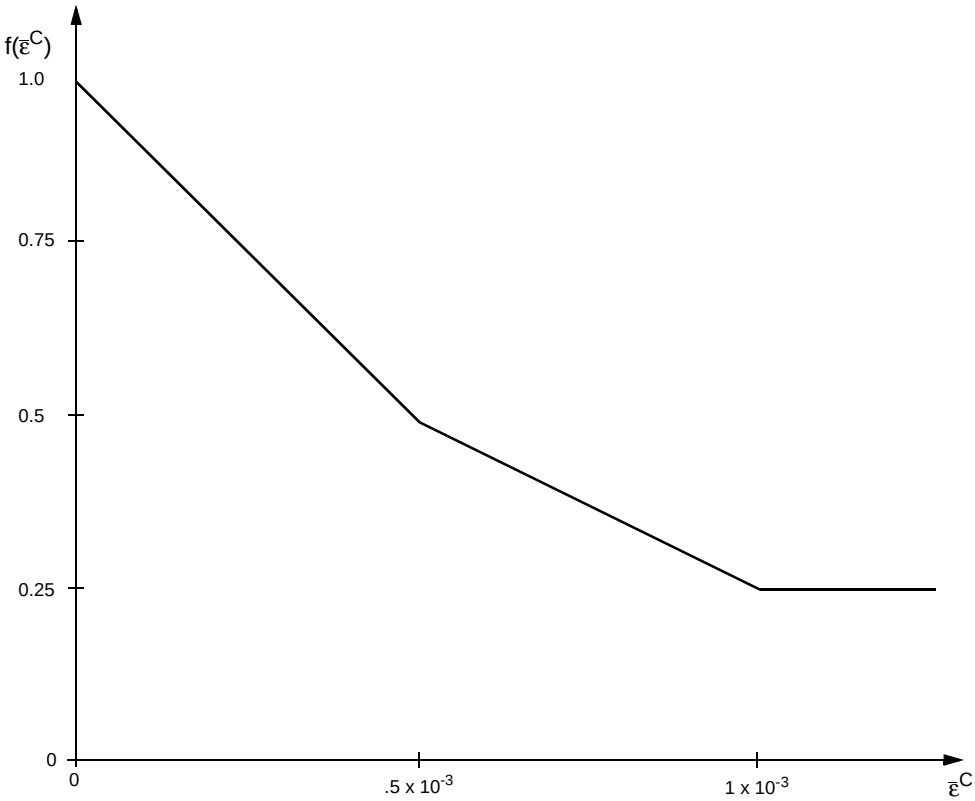

Figure 3.14-2 Creep Strain Coefficient as Function of Creep Strain

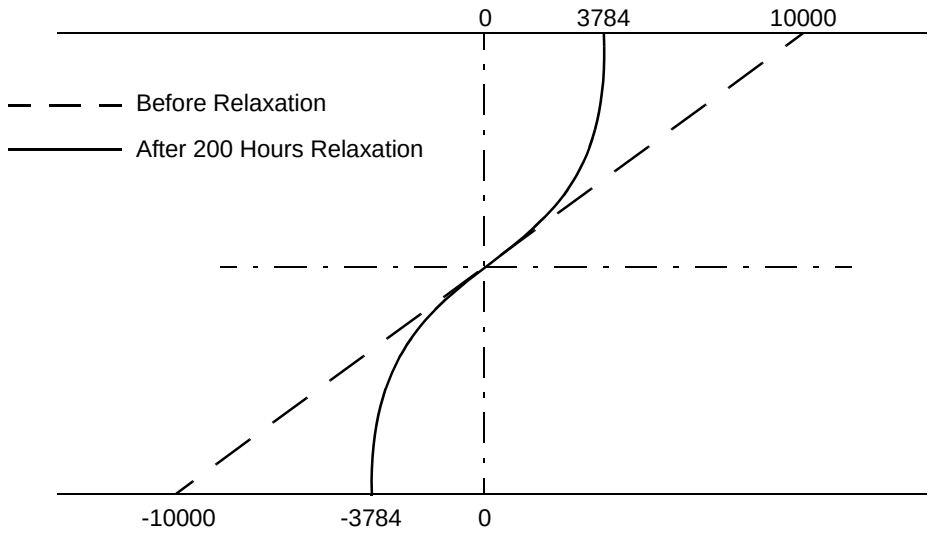

Figure 3.14-3 Stress Distribution through the Thickness before Load Reversal

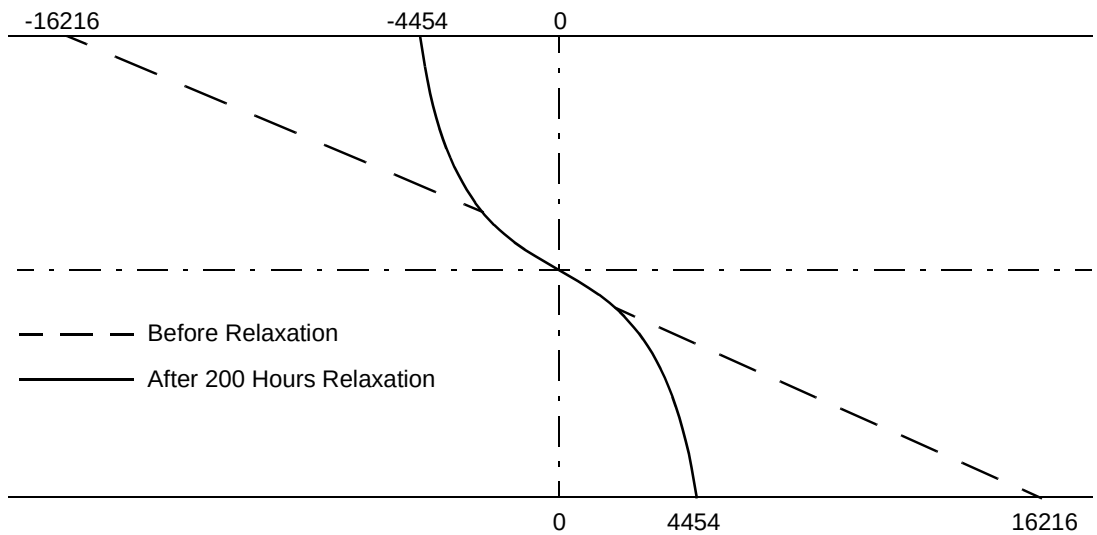

Figure 3.14-4 Stress Distribution through the Thickness after Load Reversal

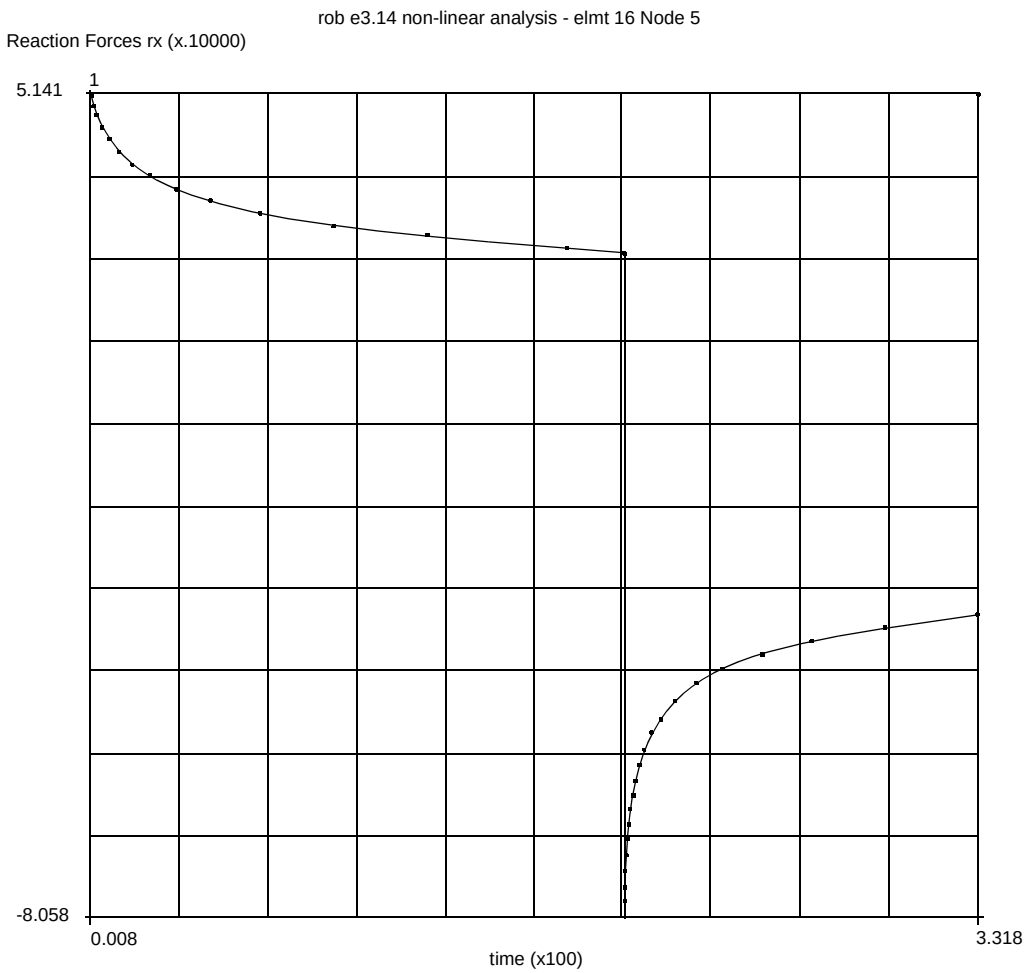

Figure 3.14-5 Relaxation Curve for Bending Moment

3.15 Creep of a Square Plate with a Central Hole using Creep Extrapolation

A square plate of 10 x 10 inches with a central hole of 1-in. radius is loaded in tension.

A state of plane stress is assumed in the plate, and the thickness of the plate is taken as 1 in.

A tensile load of 10,000 psi is applied. The plate is allowed to creep for a period of 10,000 hours. Followed by a single creep increment of 100 hours is taken, during which the strains and displacements are accumulated. Based on the accumulated strains and displacements, the solution is then extrapolated to a total creep time of 20,000 hours.

This problem is modeled using the two techniques summarized below.

Data Set	Element Type(s)	Number of Elements	Number of Nodes	Differentiating Features
e3x15	26	20	79	CREEP
e3x15b	26	20	79	Implicit Creep

Element

MARC element type 26, an 8-node quadrilateral plane stress element, is used in this analysis. Because of symmetry, only one-quarter of the plate is modeled. The mesh is shown in Figure 3.15-1.

Material Properties

The elastic properties of the material are a Young's modulus (E) of 30.E6 psi and Poisson's ratio (ν) of 0.3. The creep properties are characterized by the Power law equation: $\dot{\varepsilon}^c = 10^{-24}\sigma^4$. The elastic properties are entered through the ISOTROPIC option. The creep properties are entered through the CREEP option. Note that stress and strain changes, as used for the AUTO CREEP options, will only be monitored in element 8, where the maximum stress occurs. The CREEP parameter block flags use of the creep option.

Boundary Condition

Symmetry conditions are imposed on the two edges intersecting the central hole.

Loading

A distributed load of 10,000 psi is applied to the upper edge of the plate. For element type 26, the load type 8 is used to apply the load to the correct face of elements 13 and 14. Load type 8 is a pressure load; a negative value is entered to obtain a tensile load.

Optimization

Ten Cuthill-McKee iterations are allowed to reduce the bandwidth. The original bandwidth was equal to 67. In the third iteration, a minimum of 26 is reached. The correspondence table is written to file 1.

Post File Generation

The equivalent stress and creep strain are written on the post file. Both total displacements and reaction forces are written on the post file.

Analysis Control

All default controls are in effect. The CONTROL option is only used to increase the number of increments to more than the default of 4.

PRINT CHOICE

The PRINT CHOICE option is used to select output for element 8 and for nodes 30 through 34 and 68 through 71, which are the nodes on the edge of the hole.

Automatic Creep Analysis

The AUTO CREEP option is used for the first creep period of 10,000 hours. A time step of 1,000 hours is specified as the starting value. If necessary, MARC scales this value down to a time step which satisfies the specified stress and strain control criteria.

Strain and Displacement Accumulation

After the AUTO CREEP period is completed, accumulation of total strains, creep strains, and displacements is started with use of the ACCUMULATE option. Because storage of the accumulated values requires additional core allocation, the ACCUMULATE parameter must be included.

User Controlled Creep Analysis

The CREEP INCREMENT option is used to specify a single creep increment of 100 hours. If the CREEP INCREMENT option is invoked, the time step is not adjusted to satisfy the creep tolerances.

Strain and Displacement Extrapolation

Based on the incremental results obtained during the CREEP INCREMENT, the total strains, creep strains and displacements are extrapolated to estimate values at a total CREEP time of 20,000 hours. The EXTRAPOLATE option is used for this purpose. The extrapolation from a single increment is rather trivial; a more meaningful use of the EXTRAPOLATE option can be found in extrapolation of cyclic loading results.

Results

The results of increment 0 indicate that a maximum stress of 31,370 psi in the y-direction occurs in element 8. This corresponds to a stress concentration factor of 3.137, which is slightly higher than the factor of 3 occurring in an infinite plate. In increment 1, your selected time step of 1,000 hours yields a stress change which is almost five times higher than the maximum allowed in the CONTROL option. MARC then picks a time step of 161.2 hours, with which the tolerances are satisfied. The maximum stress change governs the time incrementation up to increment 7, where at a total creep time of 3,685 hours the strain control becomes effective. The time step rapidly stabilizes at a value of about 2,000 hours, until the end of the AUTO CREEP period is reached in increment 12. A single time step of 100 hours is taken, during which the displacements, total strains and creep strains are accumulated. The options used for this are CREEP INCREMENT and ACCUMULATE. In increment 13, the accumulated quantities are subsequently extrapolated to a time of 20,000 hours. The stress relaxation is shown in Figure 3.15-2. The creep strain history is shown in Figure 3.15-3. One can observe the creep strain at node 30 appears to be zero. As the creep strain goes as the fourth power of stress, we see that neighboring points can have substantially different amounts of creep.

Although the ACCUMULATE and EXTRAPOLATE options are primarily useful for extrapolation of cyclic loading results, they also offer some advantage in analysis of creep problems in which steady state is approached. If a long steady state phase must be analyzed, the standard explicit creep procedure still limits the maximum time step because of the existence of a stability limit. This stability limit corresponds with the default value of the strain change control set in the CONTROL option. This stability problem is absent in the EXTRAPOLATE options, however, since the stresses are not affected by extrapolation. Substantial savings in computer run time can be obtained. It should be noted, however, that extrapolation can lead to considerable errors in strains and displacements, particularly if extrapolation is done from an increment in which steady state creep had not yet been reached. Extreme care must be exercised when this option is used.

Parameters, Options, and Subroutines Summary

Example e3x15.dat:

Parameters	Model Definition Options	History Definition Options
ACCUMULATE	CONNECTIVITY	ACCUMULATE
CREEP	CONTROL	AUTO CREEP
ELEMENTS	COORDINATES	CONTINUE
END	CREEP	CREEP INCREMENT
SIZING	DIST LOADS	DIST LOADS
TITLE	END OPTION	EXTRAPOLATE
	FIXED DISP	
	GEOMETRY	
	ISOTROPIC	
	POST	
	PRINT CHOICE	

Example e3x15b.dat:

Parameters	Model Definition Options	History Definition Options
CREEP	CONNECTIVITY	AUTO LOAD
ELEMENTS	CONTROL	CONTINUE
END	COORDINATES	CREEP INCREMENT
SIZING	CREEP	DIST LOADS
TITLE	DIST LOADS	
	END OPTION	
	FIXED DISP	
	GEOMETRY	
	ISOTROPIC	
	POST	
	PRINT CHOICE	

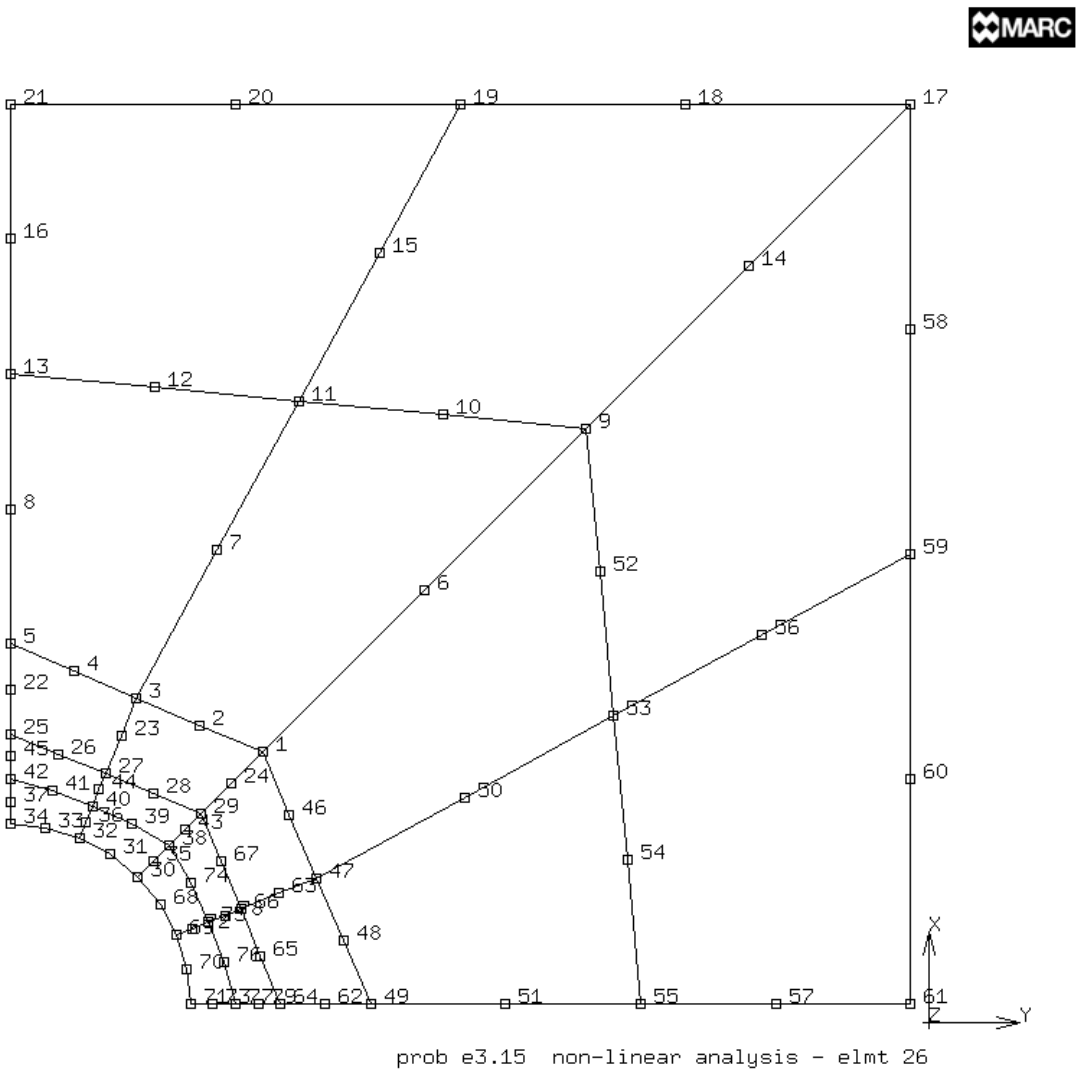

Figure 3.15-1 Mesh Layout for Plate with Hole

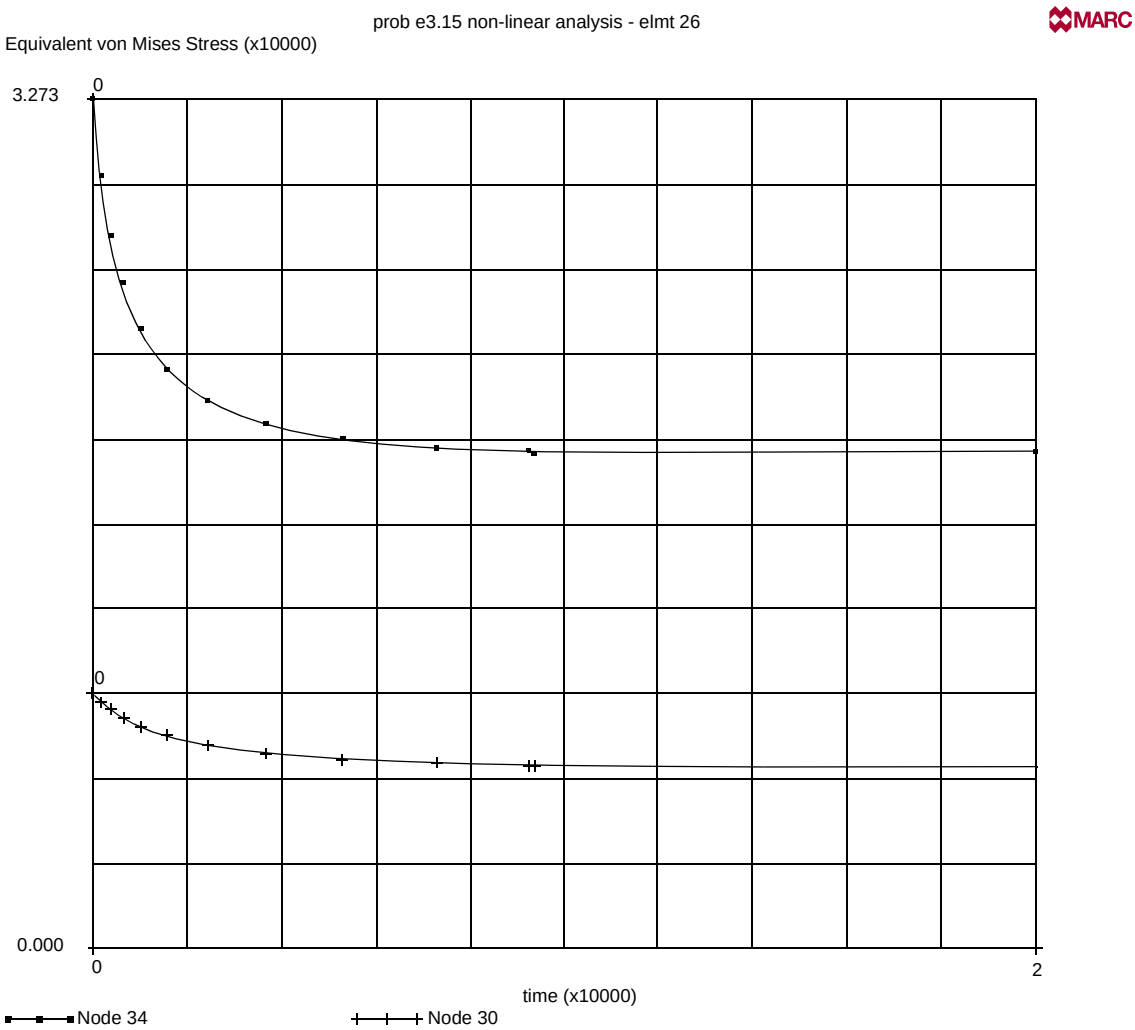

Figure 3.15-2 Stress Relaxation

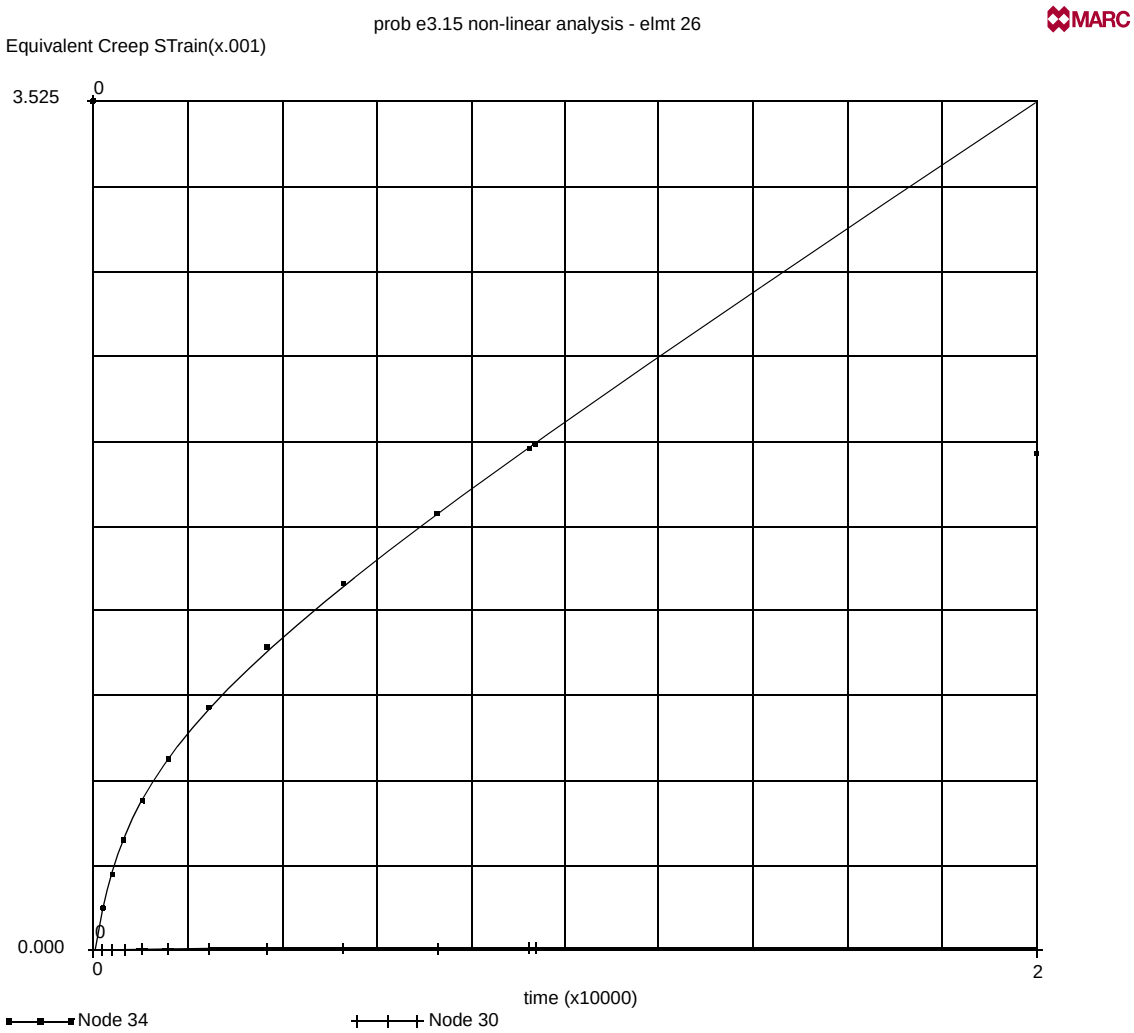

Figure 3.15-3 Creep Strain History

3.16 Plastic Buckling of an Externally Pressurized Hemispherical Dome

In this problem, MARC analyzes structures in which both geometric and material nonlinearities occur and cause collapse of the structure. The model used is a hemispherical dome with a radius of 100 inches and a thickness of 2 inches which is clamped at the edge (Figure 3.16-1). The material is elastic-plastic, with a Young's modulus of 21.8×10^6 psi, a Poisson's ratio of 0.32 and a yield stress of 20,000 psi.

This geometrically nonlinear problem is solved incrementally with Newton-Raphson style iteration. The analysis is continued until plastic collapse occurs. In MARC, such collapse becomes apparent either due to failure to converge in the iteration process (MARC exit 3002) or due to the stiffness matrix turning nonpositive definite (MARC exit 2004).

It is assumed that the collapse is axisymmetric, so that the problem can be analyzed with an axisymmetric finite element model. If it were likely that a nonsymmetric collapse mode would occur, the problem would have to be analyzed with a full three-dimensional shell model (using MARC element type 22, 72, or 75). Two analyses are performed. In the first analysis, the inverse power sweep method is used to extract the collapse load; while in the second analysis, the Lanczos method is used. This is controlled by the BUCKLE parameter. The properties of the dome change strongly as plasticity develops; and, hence, the results of the eigenvalue extraction vary substantially during the analysis.

This problem is modeled using the two techniques summarized below.

Data Set	Element Type(s)	Number of Elements	Number of Nodes	Differentiating Features
e3x16	15	8	9	Buckling by inverse power sweep
e3x16b	15	8	9	Buckling by Lanczos procedure

Element

Eight axisymmetric shell elements (MARC type 15) were used in this analysis. Element 15 is an element with fully cubic interpolation functions, quadratic membrane strain variation and linear curvature change variation along its length. This element yields rapid convergence and behaves very well in geometrically nonlinear situations.

Geometry

A thickness of 2.0 inches is specified in the first data field (EGEOM1) of the GEOMETRY option.

Coordinate Generation

Element type 15 requires input of higher order coordinates. For a simple shape like a dome, these coordinates are most easily generated automatically. The model definition option UFXORD and the user subroutine UFXORD are used for this purpose.

Material Properties

The elastic properties (Young's modulus, Poisson's ratio, yield stress) are specified in the ISOTROPIC option. The WORK HARD option is used to specify two slopes.

Transformations

Transformations are applied to all nodes except node 1. For all nodes, the transformed degrees of the freedom are the same:

1 = Radial displacement
2 = Tangential displacement
3 = Rotation
4 = Meridional membrane strain

This transformation is not necessary, but facilitates visual inspection of displacement vectors and buckling nodes.

Boundary Conditions

Symmetry conditions are specified for node 1, fully clamped conditions for node 9.

Loading

The DIST LOAD option is used to specify a distributed pressure load of 540 psi on all elements.

Control

Since the objective of the analysis is to calculate the collapse load, a large number of recycles (six) is allowed. Default convergence controls are used.

Stress Storage

The SHELL SECT parameter is used to specify a five-point integration through the thickness.

Geometric Nonlinearity

The LARGE DISP parameter indicates that geometrically nonlinear analysis will be performed.

Buckling

The BUCKLE parameter is included to indicate that a maximum of three buckling modes are to be extracted, with a minimum of one mode with a positive buckling load. The sixth parameter is used to activate the Lanczos method.

After increment 0 (the linear elastic increment) is carried out, the BUCKLE history definition option is used to extract the linear buckling mode. The BUCKLE option does not increment the analysis (increment number or loads). After the execution of the BUCKLE option, MARC proceeds as usual.

Load Incrementation

The AUTO LOAD and PROPORTIONAL INCREMENT options are used to increase the pressure during four increments with an increment of 10% of the applied pressure in increment 0. Subsequently, the same options are used to increase the pressure with an increment of 20% (2% of the original load) for two increments. With the PROPORTIONAL INCREMENT option, the load increment is then divided by 2, which brings the total pressure up to: 1.45 x 540 = 783 psi. A buckling mode extraction is performed to estimate the collapse mode and collapse pressure. Plots are made of deformation increment and the buckling mode. This last sequence is repeated twice, with the total pressure at the end of increment 9 equal to 793.8 psi.

Results

In increment 0, the linear elastic solution is obtained. The maximum stress of 19,720 psi occurs in element 8, integration point 3, layer 1, which is the point closest to the clamped edge. The displacement increment is shown in Figure 3.16-2. The linear elastic buckling analysis, which is subsequently carried out, yields a collapse pressure of: 19.74 x 540 = 10,660 psi. The buckling mode is shown in Figure 3.16-3, the calculated pressure is very close to the buckling pressure of a perfect sphere. For the perfect sphere, the buckling pressure (taken from Timoshenko's and Gere, *Theory of Elastic Stability*) is given by the equation:

$$P_c = \frac{2\ Et^2}{r^2\sqrt{3(1-\nu^2)}}$$

The data for this problem yields 10,628 psi from this equation. As the load is increased, the plastic flow begins to occur near the clamped edge. At the end of increment 6, plasticity occurs at all points in elements 7 and 8. The average membrane stress level is now only 2.7% under the yield stress.

In increment 6, the plasticity spreads out into element 6. The maximum plastic strain is about 0.12% and occurs at the inside of element 8. The average membrane stress is 2.1% under the yield stress.

The buckling analysis at this state yields a collapse pressure equal to the current pressure plus 158 times the pressure increment. This corresponds to a collapse pressure of 1,609 psi. The buckling mode has the same shape as the displacement increment, as follows from comparison of Figure 3.16-4 and Figure 3.16-5.

Increment 8 is applied. Plasticity spreads deeper into the model, and the average membrane stress is 1.5% under the yield stress. The buckling analysis yields a collapse pressure of current pressure plus 64 times the pressure increment, which is equal to 1,134 psi. Some differences now occur between buckling mode and displacement increment, as shown in Figure 3.16-6.

At increment 9, the pressure is 793 psi. If additional load is applied, the stiffness matrix becomes nonpositive definite.

As indicated by Table 3.16-1, the frequencies obtained by both, Inverse power sweep as well as the Lanczos method are identical.

Discussion of Results

It is clear that in this problem the dominant mode of failure is plastic collapse. Throughout most of the analysis, the geometric nonlinearities do not play a significant role. In fact, if the simple failure criterion is used that collapse occurred when the membrane stress reaches yield, a collapse pressure of

$$p_c = 2\frac{\sigma_y t}{r} = 800 \text{ psi}$$

is calculated, which is only 1% over the result obtained in the finite element analysis. It should be noted that in this demonstration problem, the step size is decreased gradually when the critical point is approached. In a practical situation, one does not know when this critical point occurs. The procedure would then be to analyze the problem first without step refinement and write a RESTART file. The analysis will still come to a point where no convergence occurs or where the matrix turns nonpositive definite. The analysis is then restarted with a smaller load step one or two increments before the critical point, and a solution with improved accuracy is obtained. This procedure can be refined as often as necessary to get the required accuracy. In the present example, two restarts would probably have been necessary in order to obtain the above results. The first run would have been with a constant pressure increment of 54 psi. The second run would have restarted at increment 4 with a pressure increment of 10.8 psi. The final run would involve a restart at increment 6 with a pressure increment of 5.4 psi. The PRINT CHOICE option is used to restrict the output to layers 1 through 3.

Table 3.16-1 Eigenvalues

	Inverse Power Sweep	Lanczos
0	19.99	19.99
2	188.7	188.2
4	122.7	122.7
6	2050.0	2050.0
7	1845.0	1845.0
8	1623.0	1623.0
9	1387.0	1387.0

Parameters, Options, and Subroutines Summary

Example e3x16a.dat and e3x16b.dat:

Parameters	Model Definition Options	History Definition Options
BUCKLE	CONTROL	AUTO LOAD
ELEMENTS	CONNECTIVITY	BUCKLE
END	DIST LOADS	CONTINUE
SHELL SECT	END OPTION	PROPORTIONAL INCREMENT
SIZING	GEOMETRY	
TRANSFORM	FIXED DISP	
	ISOTROPIC	
	PRINT CHOICE	
	TRANSFORMATION	
	WORK HARD	
	UFXORD	

User subroutine in u3x16.f:

UFXORD

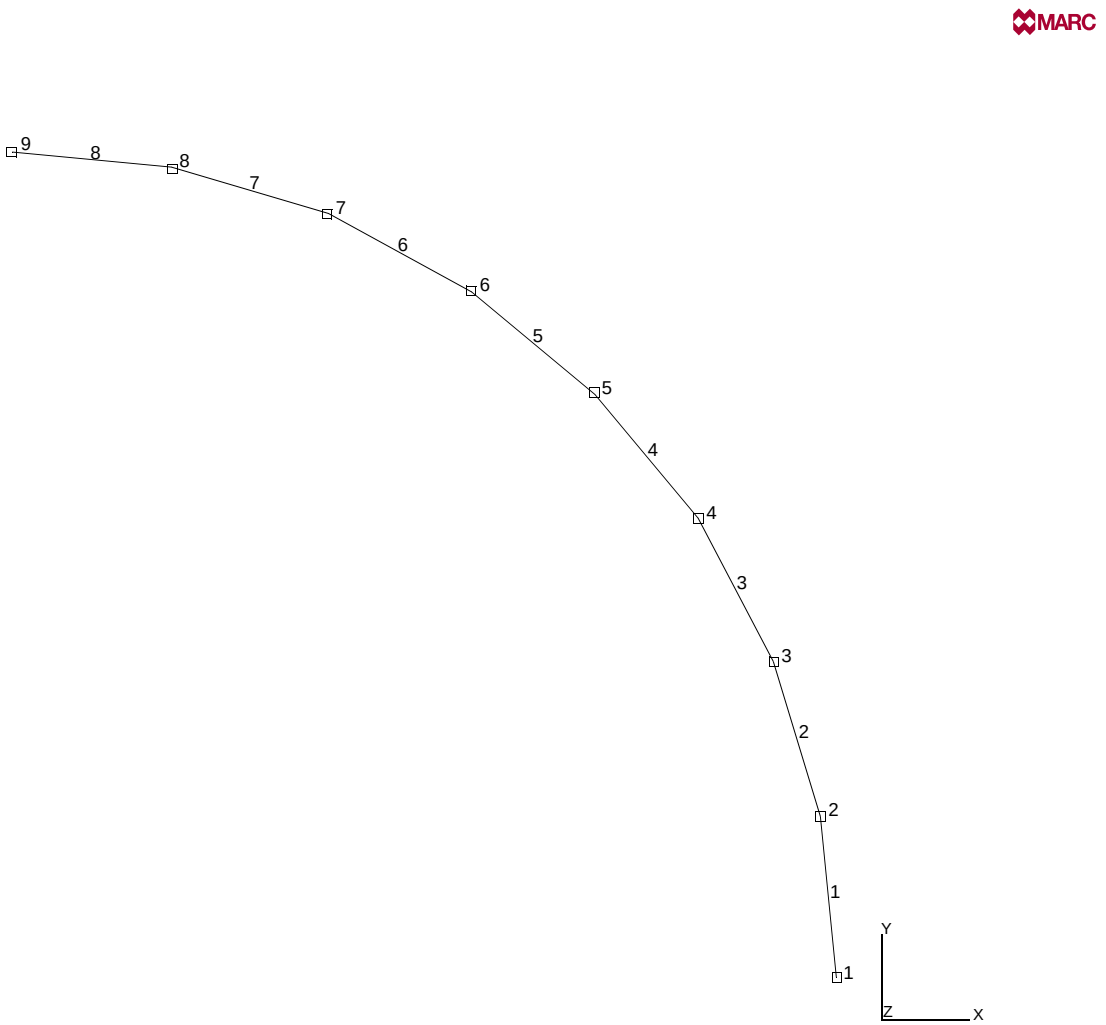

Figure 3.16-1 Geometry and Mesh

Figure 3.16-2 Buckling Mode, Increment 0

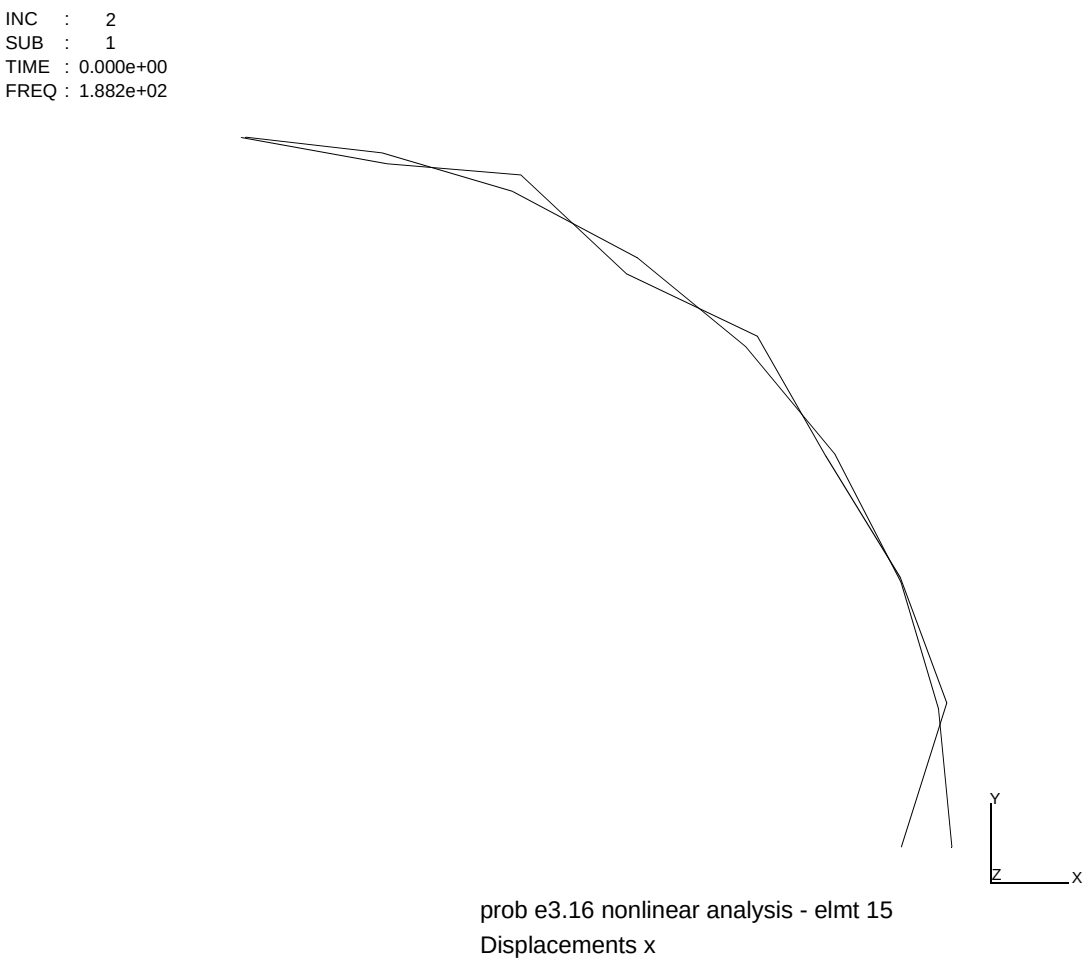

Figure 3.16-3 Buckling Mode, Increment 2

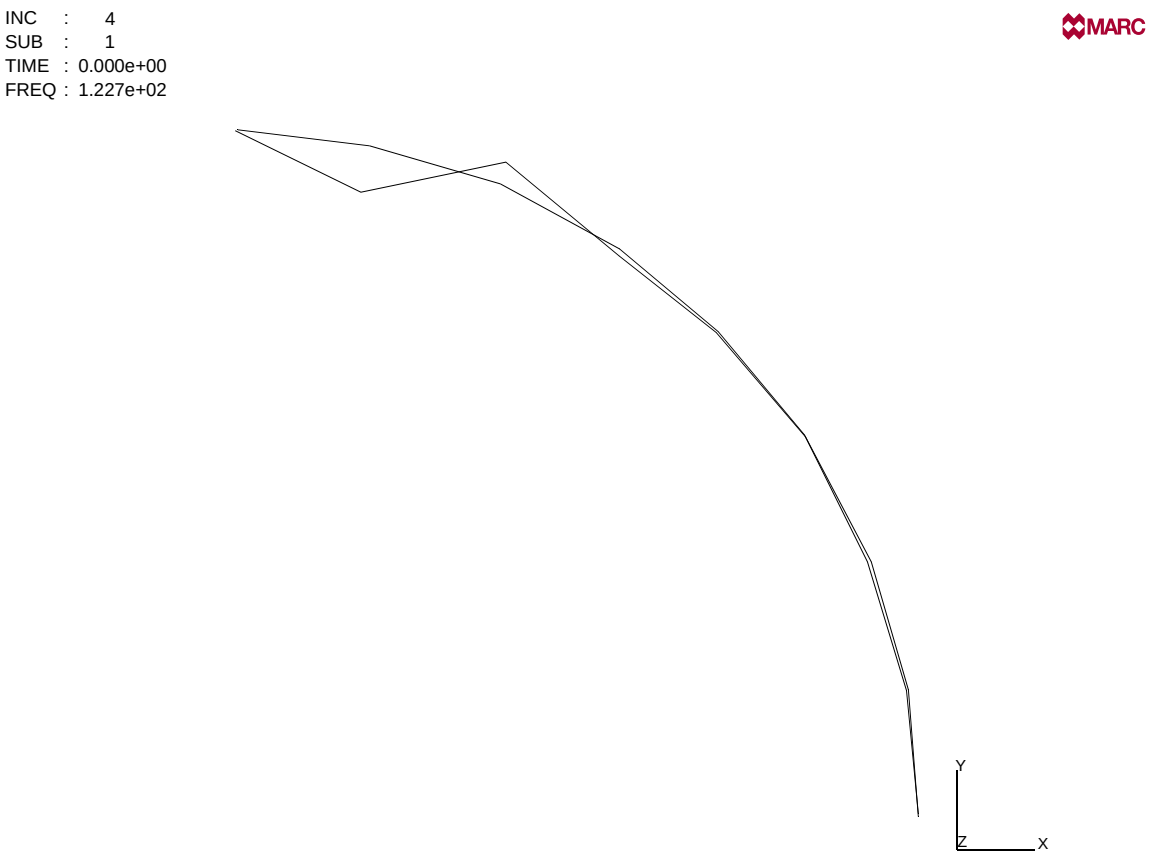

Figure 3.16-4 Buckling Mode, Increment 4

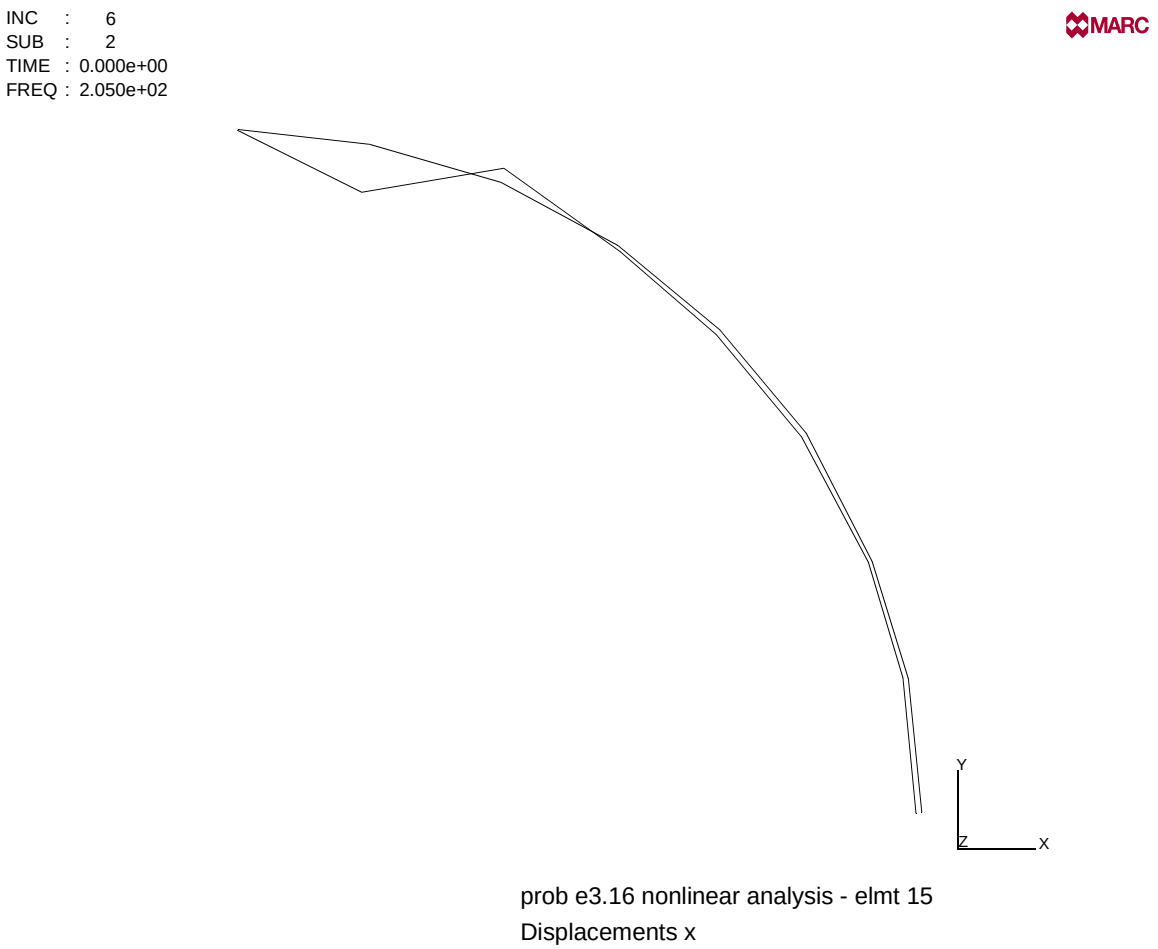

Figure 3.16-5 Second Buckling Mode, Increment 6

Figure 3.16-6 Second Buckling Mode, Increment 8

3.17 Shell Roof with Geometric and Material Nonlinearity

One of the standard problems for testing the performance of linear shell elements is the shell roof shown in Figure 3.17-1. The shell roof is supported at the curved edge by a rigid diaphragm. The linear solution for this problem can be compared with the analytical results obtained by Scordelis and Lo [1]. The solution for this nonlinear problem can be compared with the results of another finite element study, carried out by Kråkeland [2]. In this problem, combined geometric and material nonlinearities are considered. An elastic perfectly plastic material model is used. Young's modulus is equal to 2.1×10^4 N/mm^2 and Poisson's ratio is assumed to be zero. A gravity type load of 3.5×10^{-4} N/mm^2 (= 350 N/m^2) is applied in increment 0. In nine increments, this load is increased by a factor of 10 to a total value of 3,500 N/m^2. During this loading, geometric and material nonlinearities have a clear effect on the behavior of the structure.

Element

One quarter of the roof is modeled with 25 elements of MARC type 72. This is a noncompatible thin-shell element based on discrete Kirchhoff theory. With this element, the stiffness of a structure is not necessarily overestimated. After elimination of suppressed degrees of freedom, the finite element model has a total of 135 active degrees of freedom.

Model

The coordinates are first entered as a two-dimensional mesh, in which the first and second coordinates represent circumferential and axial coordinates of the shell roof. The UFXORD option is then used to transform these cylindrical coordinates to Cartesian coordinates.

Geometry

The thickness of 76 mm is specified with use of the GEOMETRY option.

Boundary Conditions

The diaphragm support conditions and appropriate symmetry conditions are specified with the use of the FIXED DISPLACEMENT option. With element type 72, the degrees of freedom have very clear physical significance, and the specification of boundary conditions is very simple and does not need further clarification.

Material Properties

Since no workhardening is included, all properties (Young's modulus, Poisson's ratio, and yield stress) can be specified with the ISOTROPIC option.

Loading

A distributed load of type 1 with a magnitude of 3.5×10^{-4} N/mm^2 is prescribed with the DIST LOAD option. This is a gravity type load, working in the negative z-direction.

Data Storage

The number of integration stations through the thickness of the shell is set to 5 with the SHELL SECT parameter. Because of the fact that nonlinear shell elements require storage of fairly large amounts of data, the ELSTO parameter is used to store this data out-of-core. With this procedure, more workspace is available for assembly and solution of the main system of equations.

Geometric Nonlinearity

The LARGE DISP option is included to invoke geometric nonlinear behavior. The Newton-Raphson iterative technique (default option in MARC) is used to solve the nonlinear equations.

Analysis Control

With the CONTROL option, the maximum number of load increments (including increment 0) is specified as 10. All other CONTROL parameters have the default value.

Post-Processing

In addition, a POST file is written. No element variables are written on this file. Both the total displacement and the reaction forces appear on the POST file.

Print Control

The PRINT CHOICE option is used to limit print output to one element (25) at one integration point (1) at two layers (1 and 5) and one node (96). More complete nodal data is stored on the POST file, whereas plotted information is obtained concerning the plastic strains.

Load Incrementation

Nine equal load increments are applied with the use of the AUTO LOAD option, to bring the total load up to 3.5×10^{-3} N/mm^2.

Results

The generated mesh is shown in Figure 3.17-2. The mesh generation process generates coordinates for corner nodes and midside nodes. For the midside nodes of element type 72, coordinates do not have to be specified, and the program does not utilize any coordinates generated. This is also clear from Figure 3.17-2, where the elements are plotted with straight edges.

The most interesting result of the analysis is the z-displacement of node 96; because, for this degree of freedom, results are available from the literature. In Figure 3.17-3, the results obtained in this analysis are compared with those of Kråkeland [2]. It is clear that good agreement is obtained.

The extent of plasticity is shown in Figure 3.17-4. From these plots, it is clear that plasticity in the extreme layers has spread out over a fairly large region. Nevertheless, the nonlinearity in this problem can still be considered mild. As a result, for most increments, minimal iterations are necessary to obtain a convergent solution.

References

1. A. C. Scordelis and K. S. Lo, "Computer analysis of cylindrical shells," *J. Am. Concrete Inst.*, Vol. 61 (May 1964).
2. B. Kråkeland, "Large displacement analysis of shells considering elasto-plastic and elasto-viscoplastic materials," Technical report no. 77-6, Division of Structural Mechanics, The Norwegian Institute of Technology, University of Trondheim, Norway, 1977.

Parameters, Options, and Subroutines Summary

Example e3x17.dat:

Parameters	Model Definition Options	History Definition Options
ELEMENTS	CONNECTIVITY	AUTO LOAD
END	CONTROL	CONTINUE
LARGE DISP	COORDINATES	PROPORTIONAL INCREMENT
SHELL SECT	DIST LOADS	
SIZING	END OPTION	
TITLE	FIXED DISP	
	GEOMETRY	
	ISOTROPIC	
	POST	
	PRINT CHOICE	
	UFXORD	

User subroutine in u3x17.f:

UFXORD

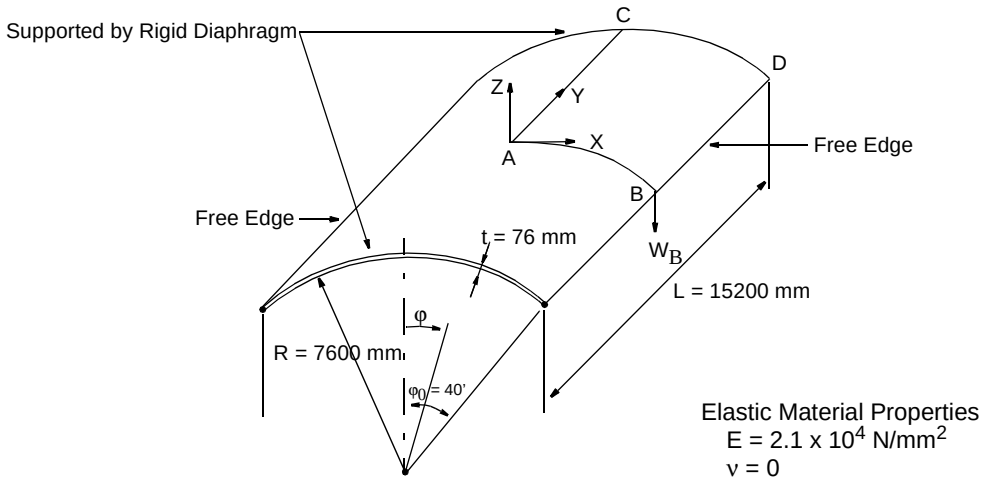

Figure 3.17-1 Shell Roof

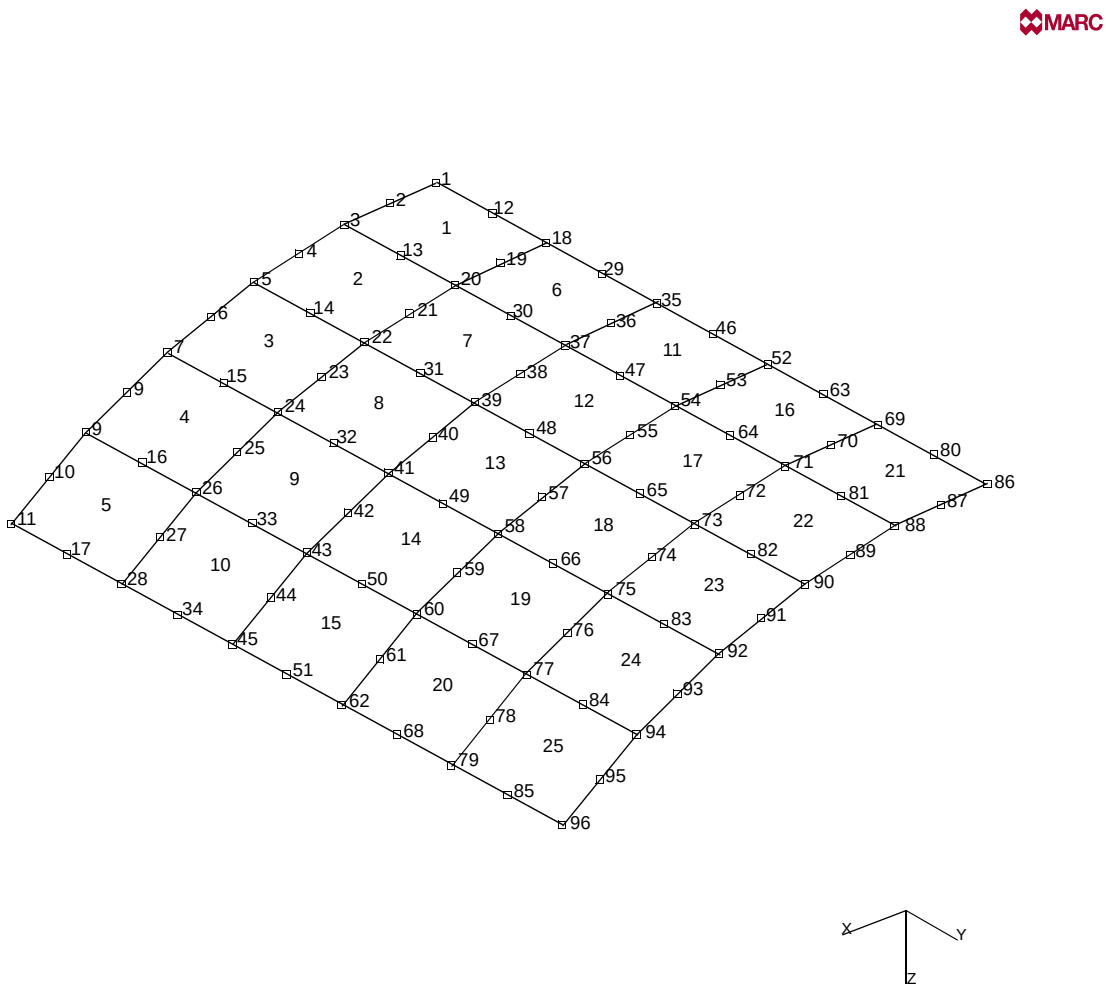

Figure 3.17-2 Mesh of Shell Roof

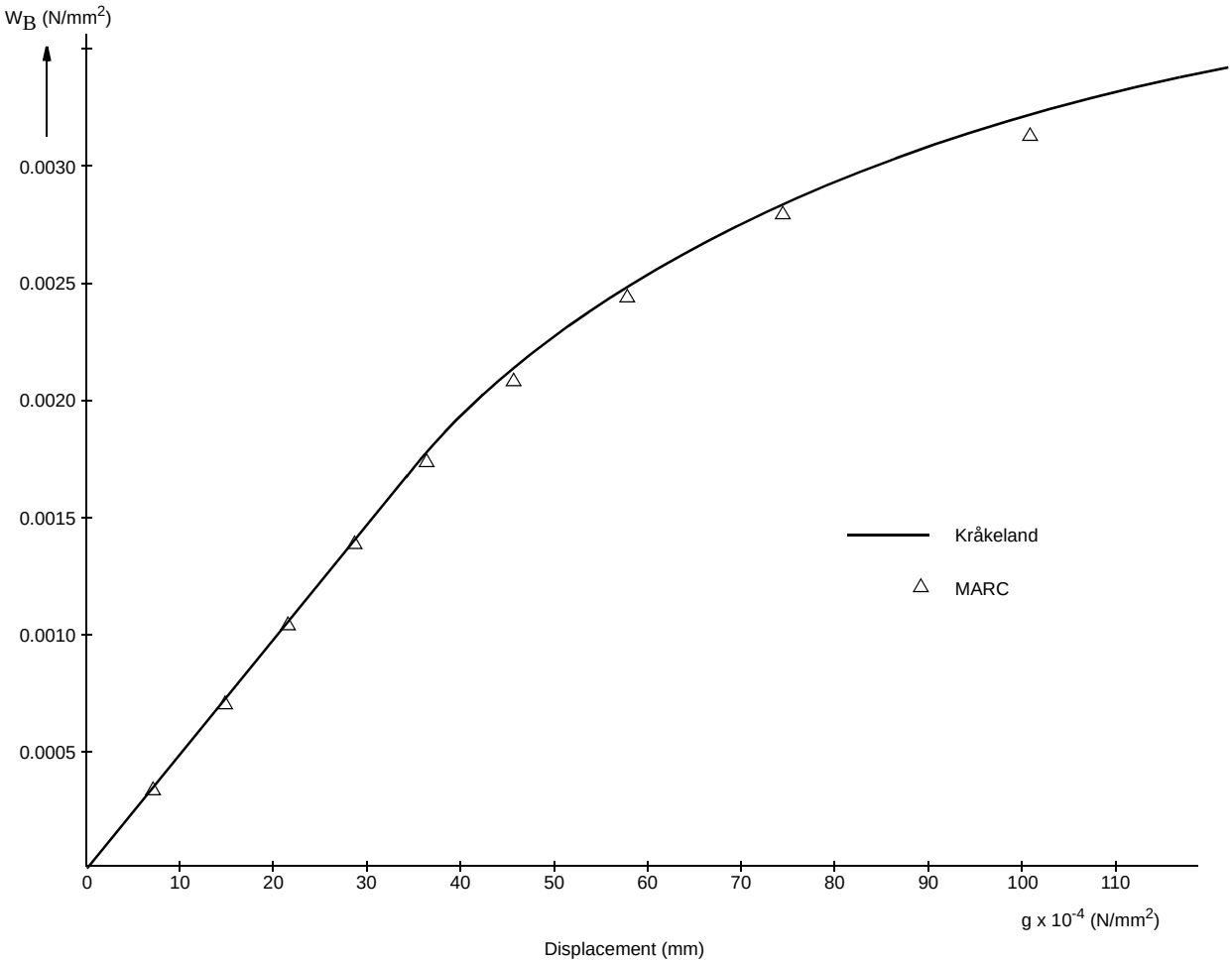

Figure 3.17-3 Load Displacement Curve, Node 96

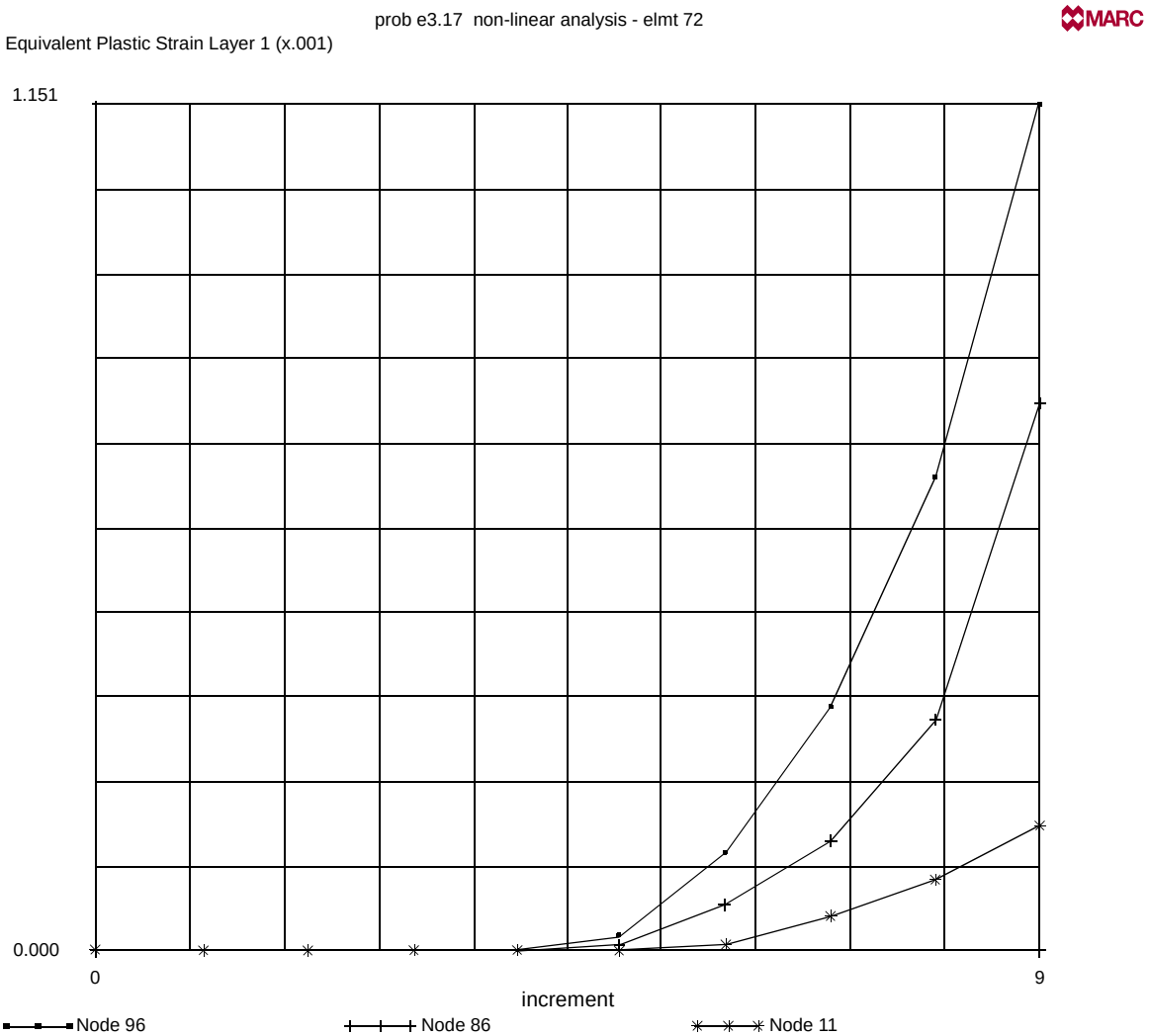

Figure 3.17-4 Equivalent Plastic Strain in Layer 1 History for Selective Nodes

3.18 Analysis of the Modified Olson Cup Test

The modified Olson Cup test is used to determine material properties of a metal for the purpose of stretch forming. In this test, a thin plate is clamped in a rigid circular die. The die has an inner radius of 1.2 inches, and the plate has a thickness of 0.04 inches. Subsequently, a rigid, hemispherical punch is forced into the plate, causing considerable plastic strain. This punch has a radius of 1 inch, and is assumed to be frictionless. A sketch of the process is shown in Figure 3.18-1.

This problem demonstrates the capability of MARC to analyze large plastic deformations in shell-like structures. It also demonstrates the use of the “true distance” gap element.

Element

The plate is modeled with 12 axisymmetric shell elements of MARC type 15. These elements all have the same length of 0.1 inch, and a thickness of 0.04 inch, which is specified with the GEOMETRY option. Gap elements of MARC type 12 are used to model the punch. One of the gap ends is attached to the shell nodes and the other end is attached to the center of the punch. Only the nodes of the shell are forced to be on the punch surface; and since the shell elements have cubic interpolation functions, it is possible that local penetration of the punch between nodes occurs. If the mesh is sufficiently refined, such local penetration will only be a source of small inaccuracies in the analysis.

Material Properties

The plate has elastic-plastic material behavior with isotropic workhardening. The Young’s modulus of 1.0×10^7 psi, the Poisson’s ratio of 0.3, and the initial yield stress of 3.0×10^4 psi are entered through the ISOTROPIC option. The workhardening data are entered in slope-breakpoint form with use of the WORK HARD option. The limiting yield stress of 6.13×10^4 is reached after 29.8% plastic strain. The workhardening curve is displayed in Figure 3.18-2.

Gap Data

The gaps used in this analysis use the optional true distance formulation. This is flagged in the seventh field of the GAP DATA input. The minimum separation distance between the two end nodes of the gap which represents the punch radius is 1.0 and is entered in the first field.

Boundary Conditions

Symmetry conditions are prescribed on node 1 on the axis of symmetry, whereas clamping conditions are prescribed for node 13 at the outer edge of the disk. The gap node at the center of the punch is also constrained, as well as the third degree of freedom for all end nodes of the gaps. The node at the center of the punch is later moved in the axial direction to simulate movement of the punch.

Tying

The shell nodes have four degrees of freedom: u, v, $\frac{du}{ds}$ and $\frac{dv}{ds}$. The first two agree with the u, v, w degrees of freedom of the gap element. The third degree of freedom is different, so it is not possible to use the shell nodes also as end nodes of the gap. Separate node sets are defined, and TYING type 102 is used to equate degrees of freedom 1 and 2 only.

Nonlinear Analysis Options

In order to perform a finite strain plasticity analysis, a number of parameter blocks are included. The LARGE DISP option indicates that a geometrically nonlinear analysis is to be done. The UPDATE option indicates that the stiffness formulation will be done in the updated (current) configuration. For shell elements, this makes the treatment of large rotation increments feasible. The FINITE option insures that the constitutive equations are used in appropriate invariant formulation. For shell elements, it also invokes a procedure to update the thickness of the elements due to plastic straining.

With use of the CONTROL model definition option, the maximum number of increments is set equal to 31, and the maximum number of recycles is set equal to 8. The iteration control is left on the default value of 0.1. The strain correction procedure is used to improve the convergence of this large displacement shell problem.

Data Storage Options

The SHELL SECT parameter is used to indicate that five layers will be used for integration through the shell thickness. The element data are stored out-of-core; this makes analysis with a fairly small workspace of 60,000 possible.

Output Files

The PRINT CHOICE option is used to create printed output for integration point 2, layer 1, 3, and 5 only. The POST option indicates that a post file will be written with nodal variables only. The RESTART option here indicates that at every increment the state is written to the RESTART file.

Incremental Load Specification

The DISP CHANGE option is used to prescribe a punch displacement increment of 0.025 inches. With the AUTO LOAD option, 30 of the above increments are applied. This brings the total displacement up to 0.75 inches, or three-fourths of the radius of the punch.

Results

The deformation process starts with only the center gap element closed in increment 1. In increment 2, the first two gaps are closed. In increment 3, the center gap element opens again. The center gap recloses in increment 6; the other gaps do not open up after first closure. The closing sequence is as follows:

the 3rd gap closes in increment 4;
the 4th gap closes in increment 6;
the 5th gap closes in increment 9;
the 6th gap closes in increment 13;
the 7th gap closes in increment 16;
the 8th gap closes in increment 20.

During most of the analysis one recycle is needed to obtain convergence, except in the first eight increments, when two recycles are needed. The largest number of recycles is six – needed in increment 1. Here, the overall deformation pattern is first established. The punch force versus punch displacement is shown in Figure 3.18-3. The punch force is obtained as the reaction force on node 50 in the center of the punch. The force steadily rises. The thickness in the center of element 1 reduces from 0.04 to 0.0165, whereas away from the center the thickness reduction is much smaller. In this example, the punch eventually penetrates the plate through rupture in the center of the plate.

Parameters, Options, and Subroutines Summary

Example e3x18.dat:

Parameters	Model Definition Options	History Definition Options
ELEMENTS	CONNECTIVITY	AUTO LOAD
END	CONTROL	CONTINUE
FINITE	COORDINATES	DISP CHANGE
LARGE DISP	END OPTION	
MATERIAL	FIXED DISP	
SHELL SECT	GAP DATA	
SIZING	GEOMETRY	
TITLE	ISOTROPIC	
UPDATE	POST	
	PRINT CHOICE	
	RESTART	
	TYING	
	WORK HARD	

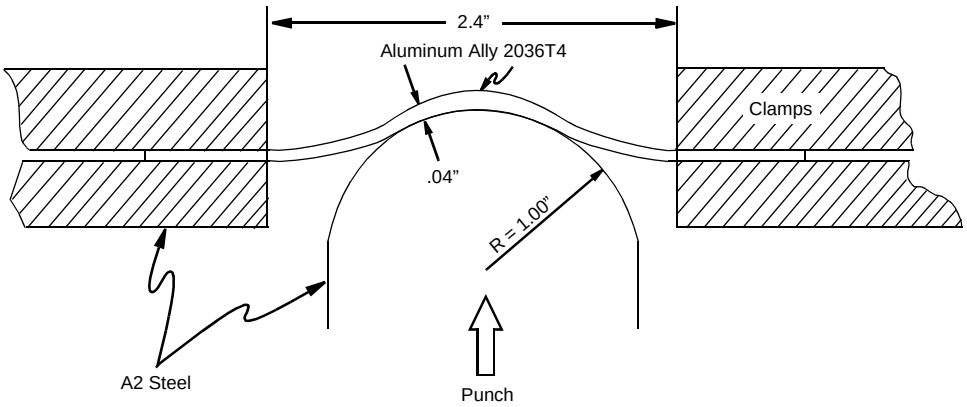

Figure 3.18-1 Modified Olsen Cup Test

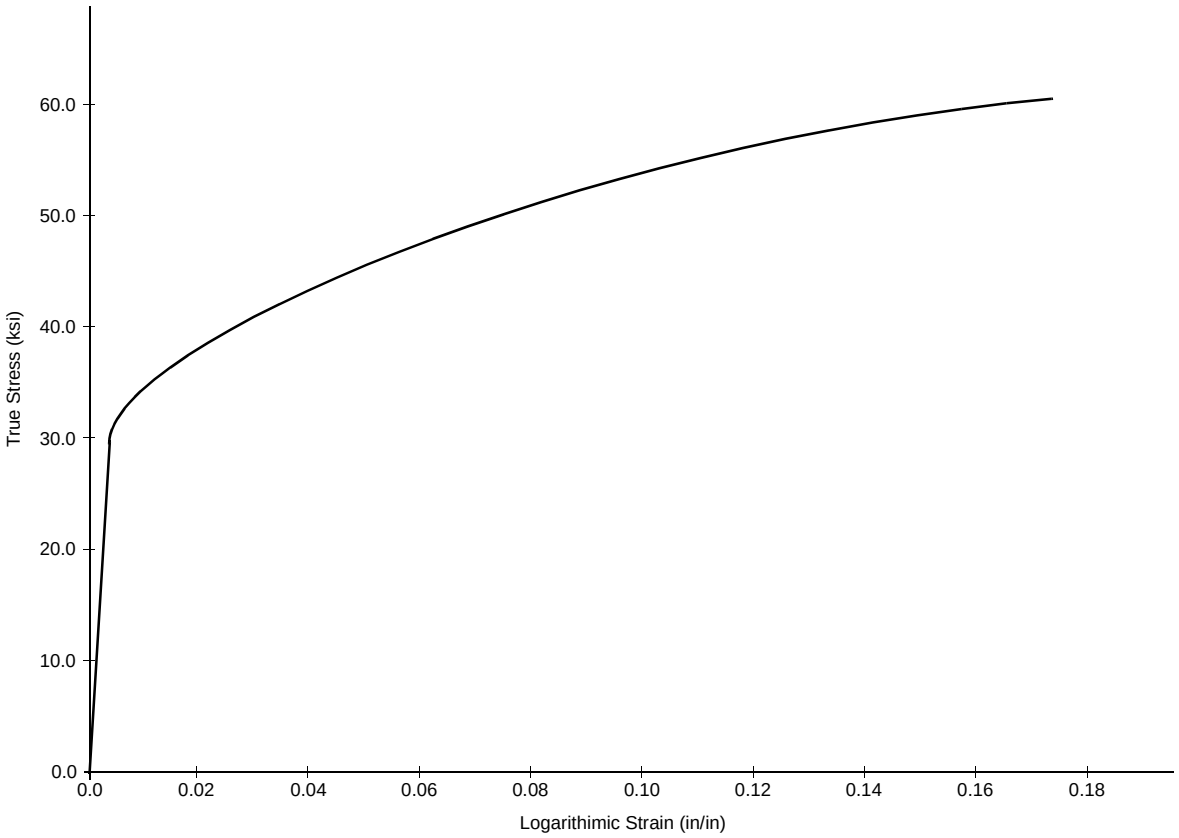

Figure 3.18-2 Tensile Stress-Strain Curve

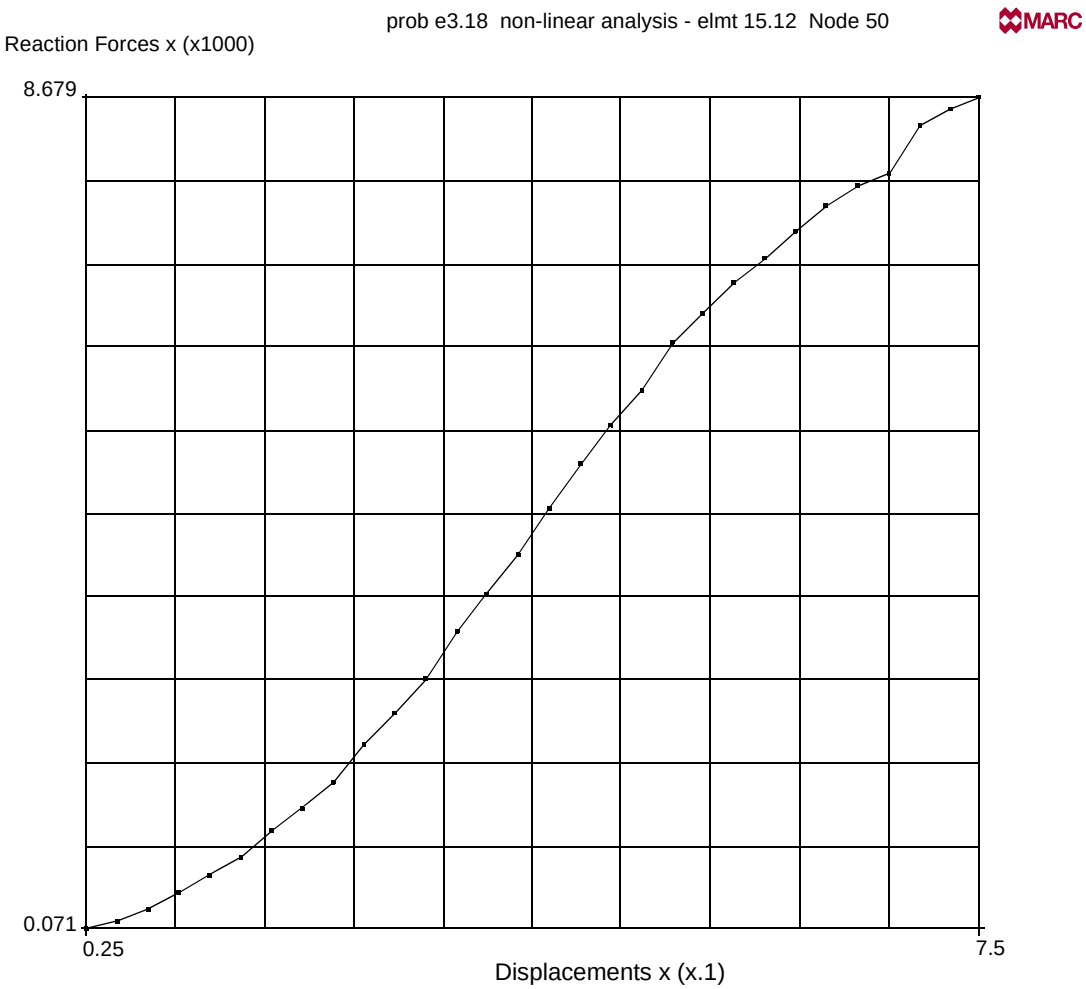

Figure 3.18-3 Load vs. Displacement

3.19 Axisymmetric Upsetting – Height Reduction 20%

An axisymmetric cylinder with a height of 8 inches and a diameter of 20 inches is compressed between two rough rigid plates. A total height reduction of 20% is obtained in 20 increments. The material is elastic-plastic with linear workhardening. The updated Lagrange and finite strain plasticity options in MARC are used to model the large-strain elastic-plastic material behavior.

This problem is modeled using the four techniques summarized below.

Data Set	Element Type(s)	Number of Elements	Number of Nodes	Differentiating Features
e3x19	10	24	35	Fully integrated element
e3x19b	116	24	35	Reduced integration hourglass element
e3x19c	116	384	425	Fine model with hourglass element
e3x19d	10	24	35	Multiplicative Decomposition (F^eF^p) Plasticity

Elements

These models are made with 4-node axisymmetric elements. Element type 10 uses full integration, while element type 116 uses reduced integration with hourglass stabilization. Because the conventional element type 10 normally locks, the constant dilatation procedure is used. This is not necessary for element type 116. When these elements are used with the F^eF^p procedure, an augmented variational principal is used, and MARC insures that the modeling of the incompressibility is accurate.

Finite Element Mesh

A mesh with 24 axisymmetric MARC type 10 and type 116 elements is used to model one-half of the cylinder. The mesh has six elements in the radial direction and four in the axial direction. Symmetry conditions are specified on the axis and the midplane of the cylinder. Sticking conditions and a prescribed compressive displacement are specified at the tool-workpiece interface. The mesh is displayed in Figure 3.19-1.

Geometry

A nonzero number is entered in the second GEOMETRY field to indicate that the elements are to be used with the constant dilatation formulation. For the F^eF^p formulation, this flag is not necessary since the incompressibility is imposed using a mixed formulation.

Property and Workhardening

The material has a Young's modulus of 10^7 psi, a Poisson's ratio of 0.3 and initial yield stress of 20,000 psi. The material is linearly workhardening with a hardening coefficient of 10^5 psi. At large strains, most materials reach a limiting stress; more sophisticated hardening behavior can be specified with either extended slope-breakpoint data or with the user subroutine WKSLP.

Geometric Nonlinearity

In the upsetting problem, large strains and rotations occur. Hence, the problem is geometrically nonlinear. The large rotations are taken care of with the LARGE DISP option; the large strain effects are taken into account with the FINITE option, which, in turn, necessitates the use of the updated Lagrange formulation (UPDATE option). In model e3x19d, the F^eF^p procedure is used which automatically activates all required options for geometric nonlinearity.

Control

A fairly coarse tolerance of 20% is specified for the iterative procedure. With only one iteration in each increment, this tolerance is easily satisfied. A restart file is written in case part of the analysis would have to be repeated with a different load step. In order to reduce the amount of printed output, only the element with the highest stress (element 24) is printed.

Load History

The displacement of the tool is prescribed. In increment 0, this displacement is 0.003 inches, which brings the stress to 46% of yield. As increment 0 is a linear elastic increment, the prescribed load was kept small. The PROPORTIONAL INCREMENT option is then used to increase the displacement increment such that the total displacement at the end of increment 1 is equal to 0.009 inches, corresponding to 0.225% height reduction. Subsequently, the displacement increment is increased to 0.034 inches. Twenty increments are applied to bring the total height reduction to 20%.

Results

The maximum stress in increment 0 (the elastic increment) occurs in element 24, integration point 3 and is equal to 9,311 psi. In the first increment, plasticity develops throughout the mesh. The von Mises stress contours after this increment (Figure 3.19-2) are in excess of the initial yield stress everywhere. No special care has to be taken to accurately follow the elastic-plastic transition. Subsequently, plastic deformation continues without giving rise to any particular problems.

The residual stress calculation indicates that the solution is somewhat in equilibrium. Compared to the reaction forces, the errors in nodal equilibrium are on the order of 1%. A total height reduction of 20% is obtained at the end of increment 22. Here, the Von Mises stress has risen to a value of 103,800 psi, as shown in the contour plot in Figure 3.19-2, for element type

10. The maximum integration point value occurs in element 24, integration point 4, and is 83,840 psi, which corresponds to a calculated plastic strain of 61.7%. This equivalent plastic strain is calculated from the strain components. The strain path is not straight, and so the calculated value differs slightly from the integrated equivalent plastic strain rate. The integrated equivalent plastic strain rate is 63.8%. The maximum stress for element type 116 is 67,090 psi (Figure 3.19-3) and is much lower because of the large element size and that this element has only one integration point per element. A new mesh is made that subdivides each of the 24 elements into 4 elements for a total of 96 elements. This model is subjected to the same loads and boundary conditions, and the stress contours are shown in Figure 3.19-4. The maximum stress for this model is 119,400 psi. Figure 3.19-6 shows the results using the F^eF^p (finite strain plasticity using multiplicative decomposition) formulation. The maximum von Mises stress is 89590 psi which is nearly midway between the full and reduced integration elements. For the axisymmetric case, the incompressibility is handled better by the mixed formulation used in the F^eF^p framework and hence it yields lower stresses. These stresses are however higher than the reduced integration, which use only one integration point for calculation of the stresses. Finally, the load deflection curve is constructed using user subroutine IMPD which determines the total load placed on the structure for each increment. The load deflection curve for this problem, as shown in Figure 3.19-5, is calculated from the total reaction forces in the plane of symmetry using subroutine IMPD. The total reaction force on the tool interface is the same. The finer mesh is slightly more flexible than the coarser models. This is reflected by a lower load required as shown in Figure 3.19-5.

The contours plotted on the deformed geometry show some perturbation in the internal mesh boundaries. This so-called hourglassing is a side effect of constant dilatation for the elements. The high bulk stiffness requires each element to retain approximately constant volume and so hourglassing type modes can develop. These modes only include deviatoric strains. This hourglassing has very little effect on the solution accuracy.

Also, the severe distortion that occurs in the fine mesh near the singularity should be remeshed using the REZONE option for more accuracy. This would prevent the mesh from becoming too distorted. Finally, the CONTACT option could be used to automatically enforce the contact constraints at the tool-workpiece interface.

Parameters, Options, and Subroutines Summary

Example e3x19.dat:

Parameters	Model Definition Options	History Definition Options
ELEMENTS	CONNECTIVITY	AUTO LOAD
END	CONTROL	CONTINUE
FINITE	COORDINATES	PROPORTIONAL INCREMENT
LARGE DISP	END OPTION	
SIZING	FIXED DISP	
TITLE	GEOMETRY	
UPDATE	ISOTROPIC	
	POST	
	RESTART	
	UDUMP	
	WORK HARD	

User subroutine in u3x19.f:

IMPD

Example e3x19b.dat:

Parameters	Model Definition Options	History Definition Options
ALIAS	CONNECTIVITY	AUTO LOAD
ELEMENTS	CONTROL	CONTINUE
END	COORDINATES	PROPORTIONAL INCREMENT
FINITE	END OPTION	
LARGE DISP	FIXED DISP	
SIZING	GEOMETRY	
TITLE	ISOTROPIC	
UPDATE	POST	
	RESTART	
	UDUMP	
	WORK HARD	

User subroutine in u3x19b.f:

IMPD

Example e3x19c.dat:

Parameters	Model Definition Options	History Definition Options
ALIAS	CONNECTIVITY	AUTO LOAD
ELEMENTS	CONTROL	CONTINUE
END	COORDINATES	PROPORTIONAL INCREMENT
FINITE	END OPTION	
LARGE DISP	FIXED DISP	
SIZING	GEOMETRY	
TITLE	POST	
UPDATE	PROPERTY	
	RESTART	
	UDUMP	
	WORK HARD	

User subroutine in u3x19c.f:

IMPD

Example e3x19.dat:

Parameters	Model Definition Options	History Definition Options
ELEMENTS	CONNECTIVITY	AUTO LOAD
END	CONTROL	CONTINUE
LARGE DISP	COORDINATES	PROPORTIONAL INCREMENT
PLASTICITY	END OPTION	
SIZING	FIXED DISP	
TITLE	GEOMETRY	
UPDATE	ISOTROPIC	
	POST	
	RESTART	
	UDUMP	
	WORK HARD	

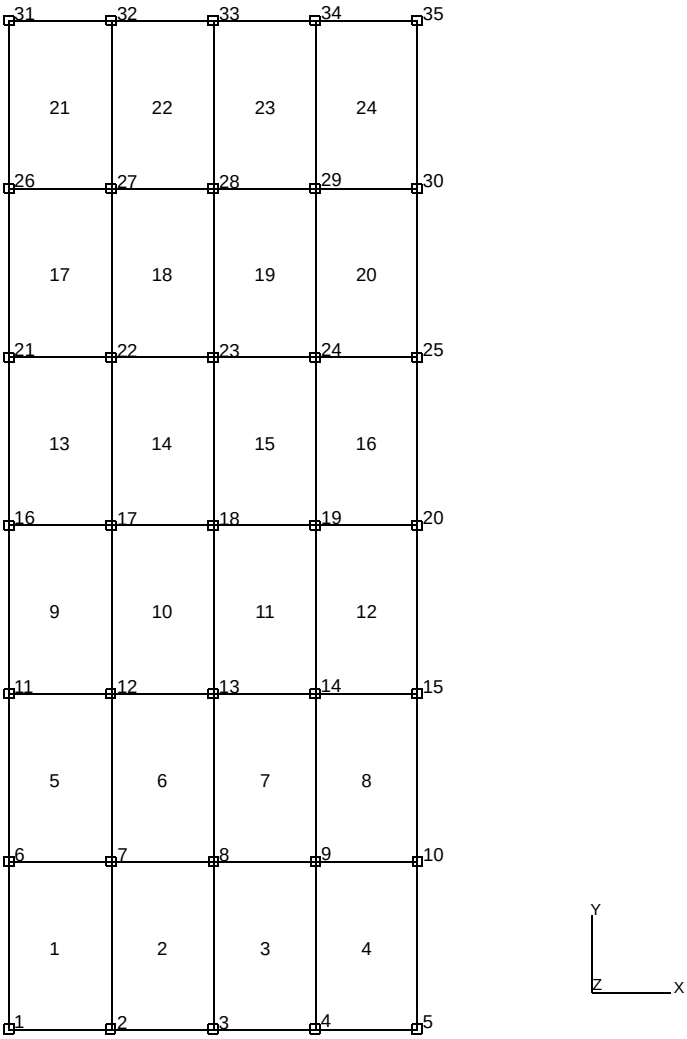

Figure 3.19-1 Model with Elements and Nodes Labeled

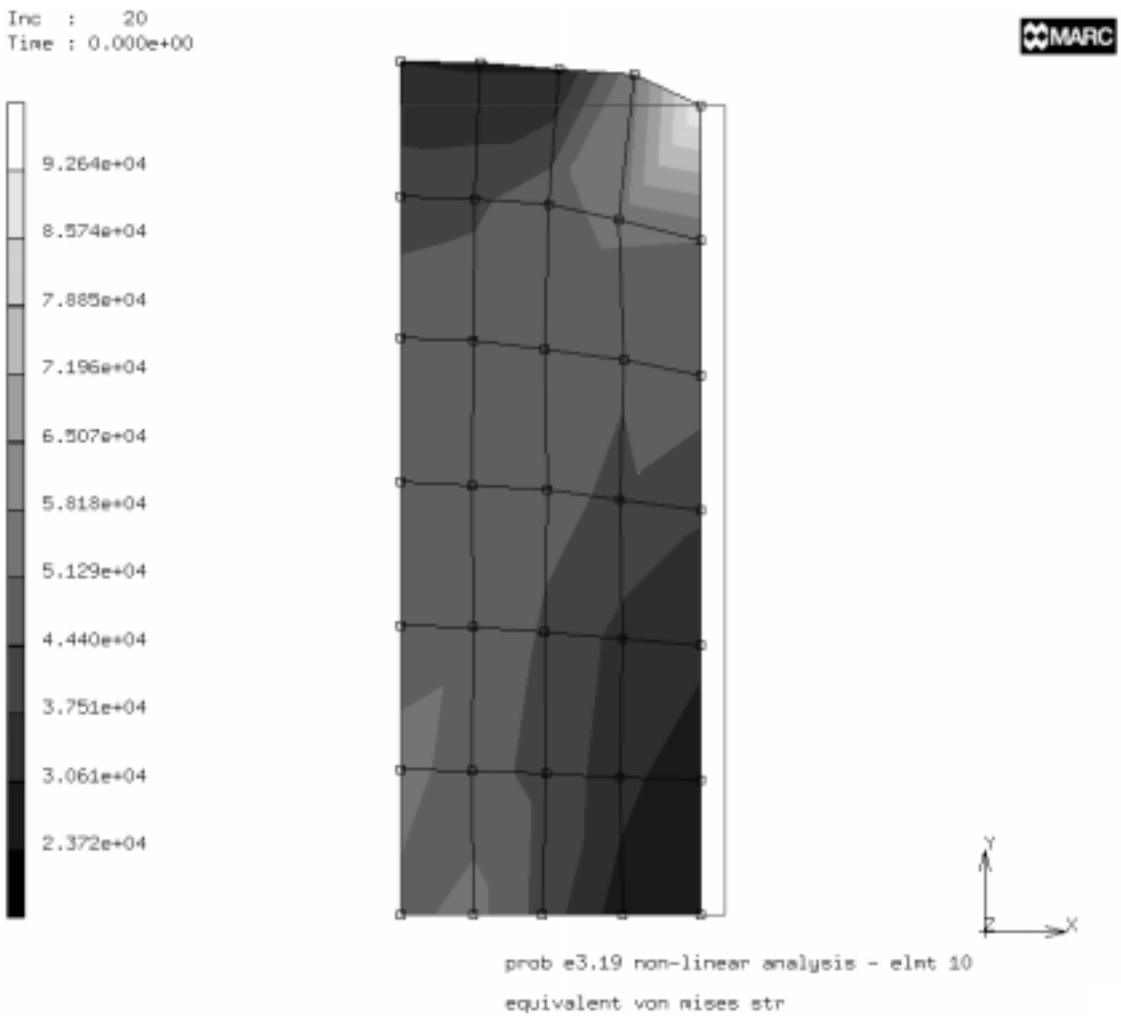

Figure 3.19-2 von Mises Stress Contours at Increment 20 Element Type 10

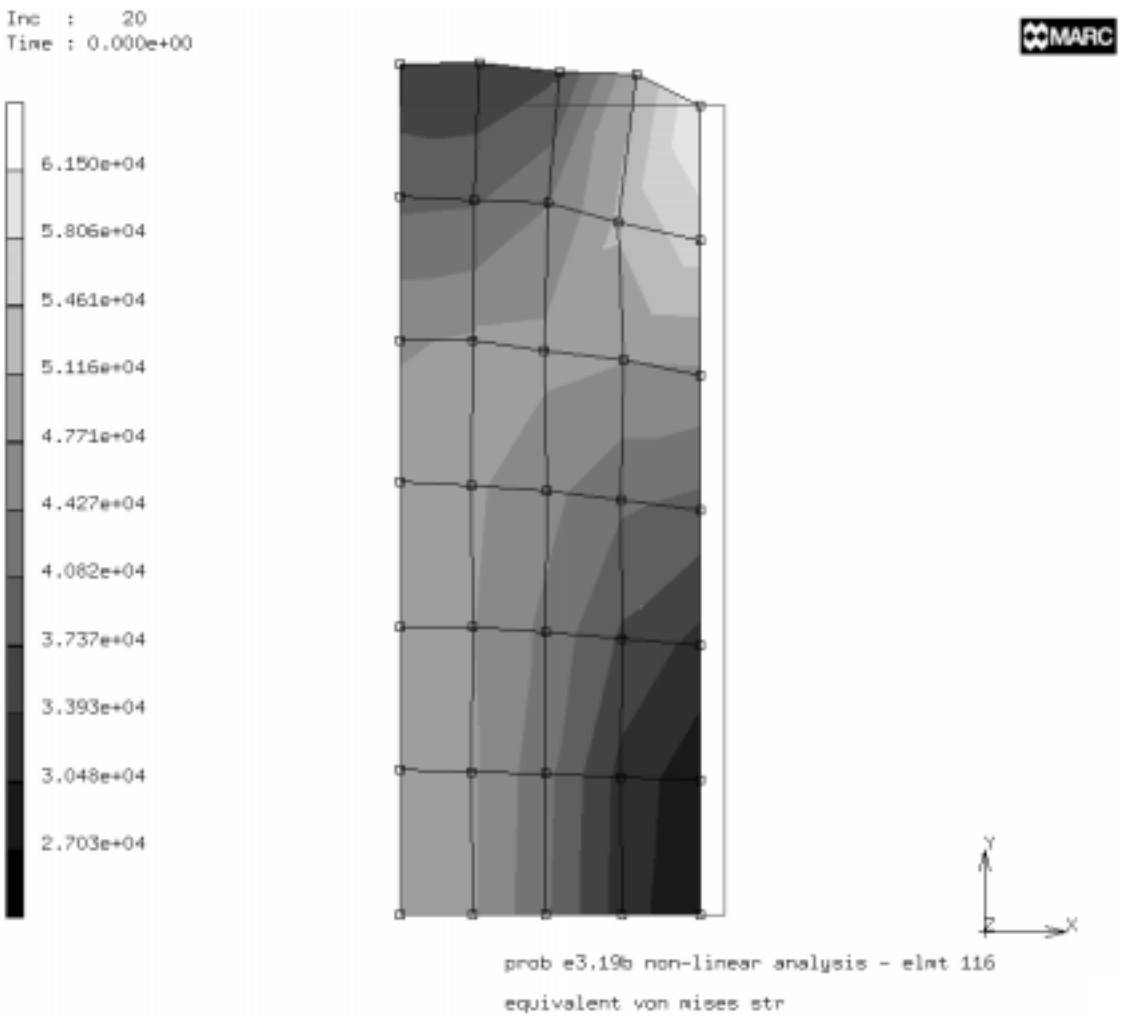

Figure 3.19-3 von Mises Stress Contours at Increment 20 Element Type 116

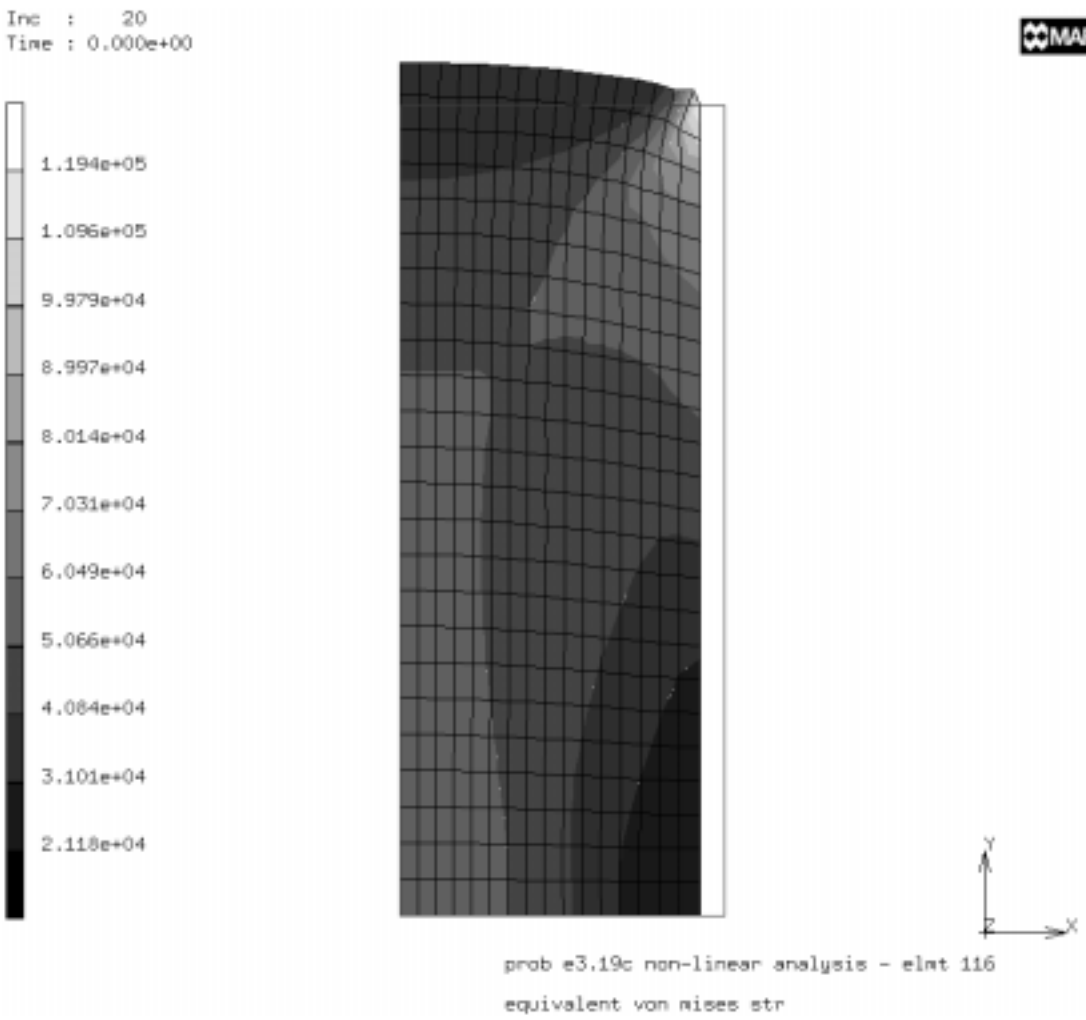

Figure 3.19-4 von Mises Stress Contours at Increment 20 Element Type 116 (Fine Mesh)

Displacement (x-1 inches)	Load (x-10**7 lbf)			
	Type 10	Type 116	Type 116 fine	Type 10, F^eF^p
0.0	0.0	0.0	0.0	
6.0E-03	5.44666E-01	5.44678E-01	5.42062E-01	
4.0E-02	9.09003E-01	9.51534E-01	8.73461E-01	
8.0E-02	9.53196E-01	9.86861E-01	9.39867E-01	
1.2E-01	1.05619E+00	1.05823E+00	1.02221E+00	
1.6E-01	1.14687E+00	1.14637E+00	1.10502E+00	
2.0E-01	1.21936E+00	1.23329E+00	1.18878E+00	
2.4E-01	1.31785E+00	1.32650E+00	1.28633E+00	
2.8E-01	1.38827E+00	1.40290E+00	1.37896E+00	
3.2E-01	1.49609E+00	1.50275E+00	1.46018E+00	
3.6E-01	1.56728E+00	1.62923E+00	1.54599E+00	
4.0E-01	1.68304E+00	1.68450E+00	1.63446E+00	
4.4E-01	1.82681E+00	1.77902E+00	1.72597E+00	
4.8E-01	1.86321E+00	1.92374E+00	1.82075E+00	
5.2E-01	1.97708E+00	1.99075E+00	1.91924E+00	
5.6E-01	2.14452E+00	2.09846E+00	2.02156E+00	
6.0E-01	2.28568E+00	2.26072E+00	2.12789E+00	
6.4E-01	2.40272E+00	2.41074E+00	2.23832E+00	
6.8E-01	2.52240E+00	2.53974E+00	2.35296E+00	
7.2E-01	2.65395E+00	2.66853E+00	2.47188E+00	
7.6E-01	2.79495E+00	2.80702E+00	2.59501E+00	
8.0E-01	2.94241E+00	2.95548E+00	2.72212E+00	

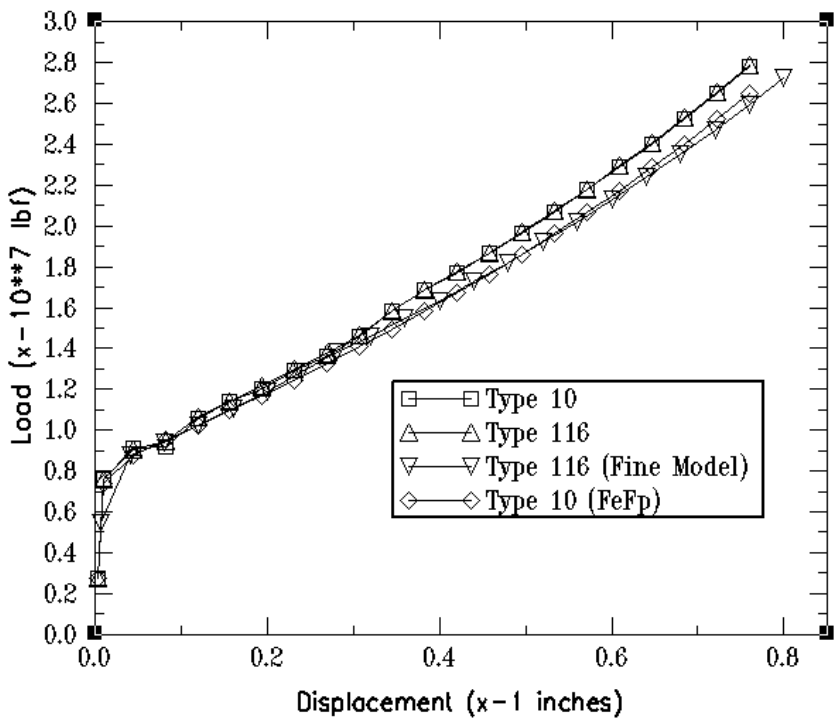

Figure 3.19-5 von Mises Stress Contours at Increment 20, Element Type 10, F^eF^p Formulation

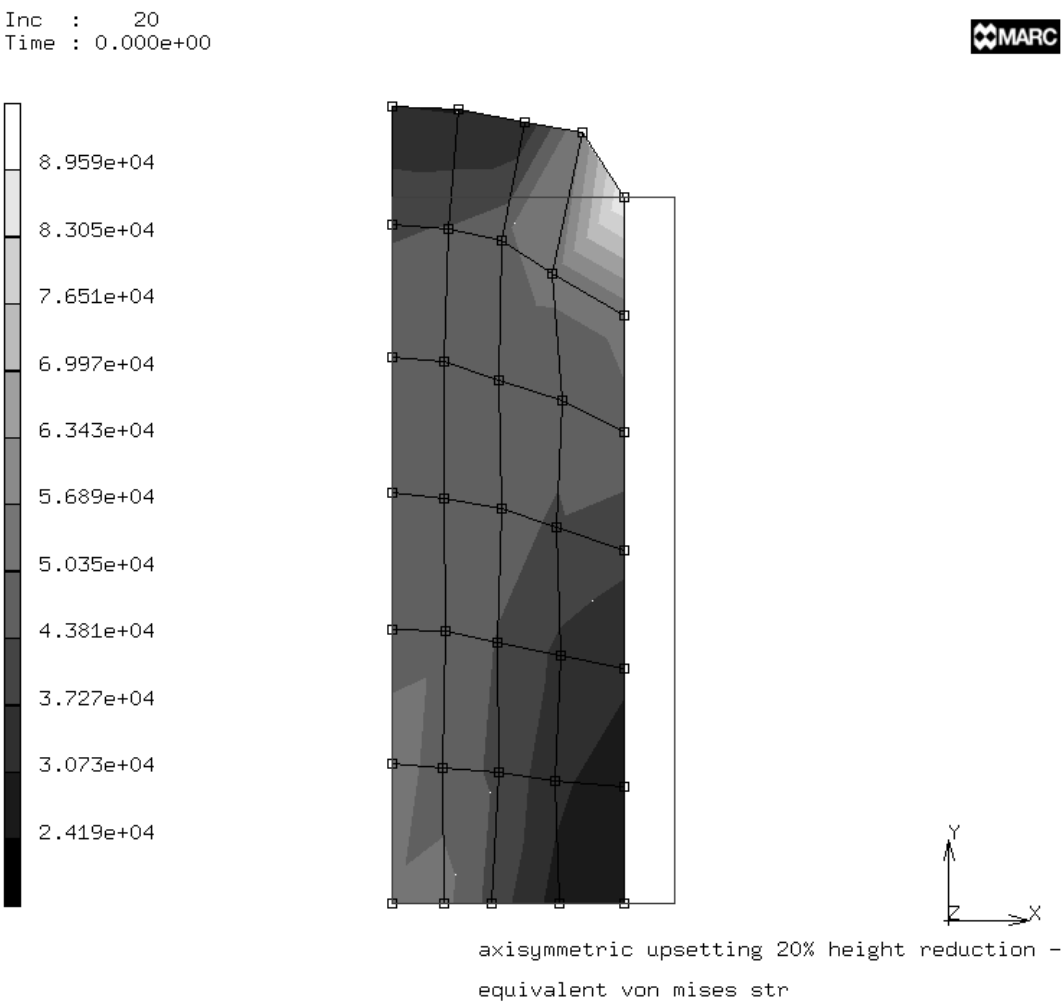

Figure 3.19-6 Load Displacement Curve

3.20 Plastic Bending of a Straight Beam into a Semicircle

A straight two-dimensional cantilever beam is subjected to a prescribed end rotation. The beam deforms plastically into a semicircle, and has a length of 20 inches and square cross section of 1 square inch. After a prescribed rotation of 90°, the end is released and the beam springs back elastically to a permanently deformed state.

Element

A 10-element mesh of MARC element type 16 models the beam. This is a two-dimensional beam element with fully cubic interpolation functions. This element type is particularly suited for problems in which geometrically nonlinear effects are important. Only one element (number 1) and two nodes (numbers 1 and 11) are specified directly. The connectivity and coordinates of the remaining elements and nodes are generated with the CONN GENER and NODE FILL options, respectively. The element type 16 has a rectangular cross section. In this problem, the GEOMETRY option is used to specify both height and width equal to 1 in. Seven-point integration through the height of the beam is specified with the SHELL SECT parameter.

Material Properties

The elastic properties are specified with the ISOTROPIC option. Young's modulus is equal to 10^7 psi and Poisson's ratio is equal to 0.33. The initial yield stress of 20,000 psi is also specified with the ISOTROPIC option. The remaining part of the stress-strain curve is specified with the WORK HARD option. The initial workhardening slope is equal to 238,029 psi, up to a plastic strain of 0.196%, which corresponds to a stress of 20,466 psi. Subsequently, the workhardening slope is equal to 97,515 psi, up to a plastic strain of 5.671%, or 25,805 psi. At this stress level, no further hardening occurs. The workhardening curve is shown in Figure 3.20-1.

Transformations and Boundary Conditions

MARC element type 16 has degrees of freedom at each node u, v, $\frac{du}{ds}$, $\frac{dv}{ds}$, where u and v are the global displacements, $\frac{du}{ds}$ and $\frac{dv}{ds}$ are the derivatives of these displacements along the length of the beam. These degrees of freedom are not suitable for application of bending moments and/or boundary conditions, particularly if the beam is to undergo large rotations. For the end nodes 1 and 11, the SHELL TRAN option type 1 is used. This transforms the degrees of freedom of these nodes into u, v, ϕ, and e.

The SHELL TRAN option is used here in conjunction with the FOLLOW FORCE option. This combination ensures that the transformations are carried out in the deformed configuration of the beam. To incrementally prescribe a finite rotation, one applies a nonzero incremental boundary condition to degree of freedom 3 of node 11. The clamped conditions at the other end of the beam are enforced by specifying degrees of freedom 1 to 3 at node 1 as zero.

Geometric Nonlinearity

Large rotations occur in this problem; therefore, the problem is definitely geometrically nonlinear. The nonlinearity in the axial strain terms is included with the LARGE DISP option. This is a problem in which the bending effects are dominant; therefore, the strain correction algorithm is used to handle the nonlinear terms. With this algorithm, large errors in the axial forces during iteration are avoided. Default tolerance is specified on the CONTROL option. The number of iterations is set to a high value in order to obtain results for the load reversal at the end of the analysis. In order to ensure correct calculation of the curvature change, the updated Lagrange formulation must be invoked with the UPDATE option. In that case, reasonably accurate results are obtained for incremental rotations of up to approximately 0.1 radians, which is greater than the incremental rotation in this problem. In this analysis, the strains will only be moderately large, namely about 8%, which follows from simple kinematic considerations. Large strain effects will not be considered in this problem.

Printing, Plotting, and Postprocessing

For nonlinear analysis, the default printout for beam elements yields a large amount of output. In particular, the stress and plastic strains in each layer in which plasticity occurs are printed. The PRINT CHOICE option is used to select printout at only one integration point in one element. Additional output is obtained graphically; in particular, the displaced mesh is shown at the end of the analysis. Finally, a formatted post file is written with a number of element variables included.

Loading

The initially prescribed rotation is 0.025 radians. With this rotation value, the stresses in the extreme fibers remain below yield. Subsequently, 62 equal increments of 0.25 radians are applied, which brings the total rotation to 1.57 radians, a little more than the desired rotation of 90 degrees. In increment 66, the boundary condition at node 11 is removed with the boundary change option, and two zero load increments obtain the unloaded deformed shape of the beam.

Results

The stress printout for increment 0 shows the stress equal to 15,870 psi, or 79.3% of yield. Subsequently, the beam gradually becomes plastic – two layers 1, 2, 6, and 7 in increment 1; all layers, except the central layer 6, in all other increments. In increment 46, maximum stress is reached in the extreme layers. The stress in the subsequent layers almost reaches yield in increment 48. The maximum tip rotation of 1.57 radians is reached in the same increment. The tip displacements at this point are -3.732 inches in the beam direction, and 6.42 inches in the direction perpendicular to the beam. This only slightly differs from the theoretical values of -3.634 inches and 6.366 inches expected for a rotation of exactly 90°. The bending moment at the clamped end at this stage in the analysis is 6054 lb-inch, which is 6.1% less than the moment needed to form a plastic hinge: $\sigma_{max}\, h^2/4 = 61{,}451$ lb-inch.

Up to this point, the secant modulus method does not need any recycling. This is because the first estimate of the stress-strain law is based on the extrapolation of the strain change in the last increment. In increment 66, the tip condition is released. This causes a considerable imbalance. During the first estimate, the constitutive routine assumes continued plastic loading. As a result of the initial imbalance and the assumed plastic loading, the elastic spring back is grossly overestimated.Three iterations are needed to correct this initial error, resulting in an elastic springback of 0.1447 radians. The strain correction method can still yield inaccurate results at this stage; therefore, one more zero increment is applied. This correction is minor, as demonstrated by the results. From the calculated bending moment of 5991.7 lb-inch, the theory predicts an elastic spring back of 0.1438 radians. The numerical results differ only marginally from the theoretically expected results. The displaced mesh representing the permanently deformed beam is shown in Figure 3.20-2.

Parameters, Options, and Subroutines Summary

Example e3x20.dat:

Parameters	Model Definition Options	History Definition Options
ELEMENTS	CONN GENER	AUTO LOAD
END	CONNECTIVITY	CONTINUE
FINITE	CONTROL	DISP CHANGE
FOLLOW FORCE	COORDINATES	PRINT CHOICE
LARGE DISP	END OPTION	PROPORTIONAL INCREMENT
SHELL SECT	FIXED DISP	
SIZING	GEOMETRY	
TITLE	ISOTROPIC	
UPDATE	NODE FILL	
	POST	
	PRINT CHOICE	
	RESTART	
	SHELL TRANFORMATIONS	
	WORK HARD	

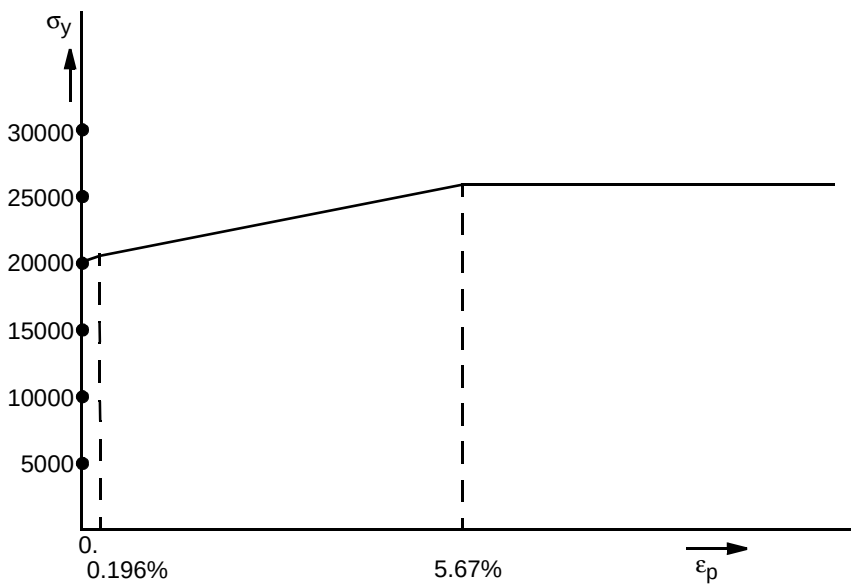

Figure 3.20-1 Workhardening Curve

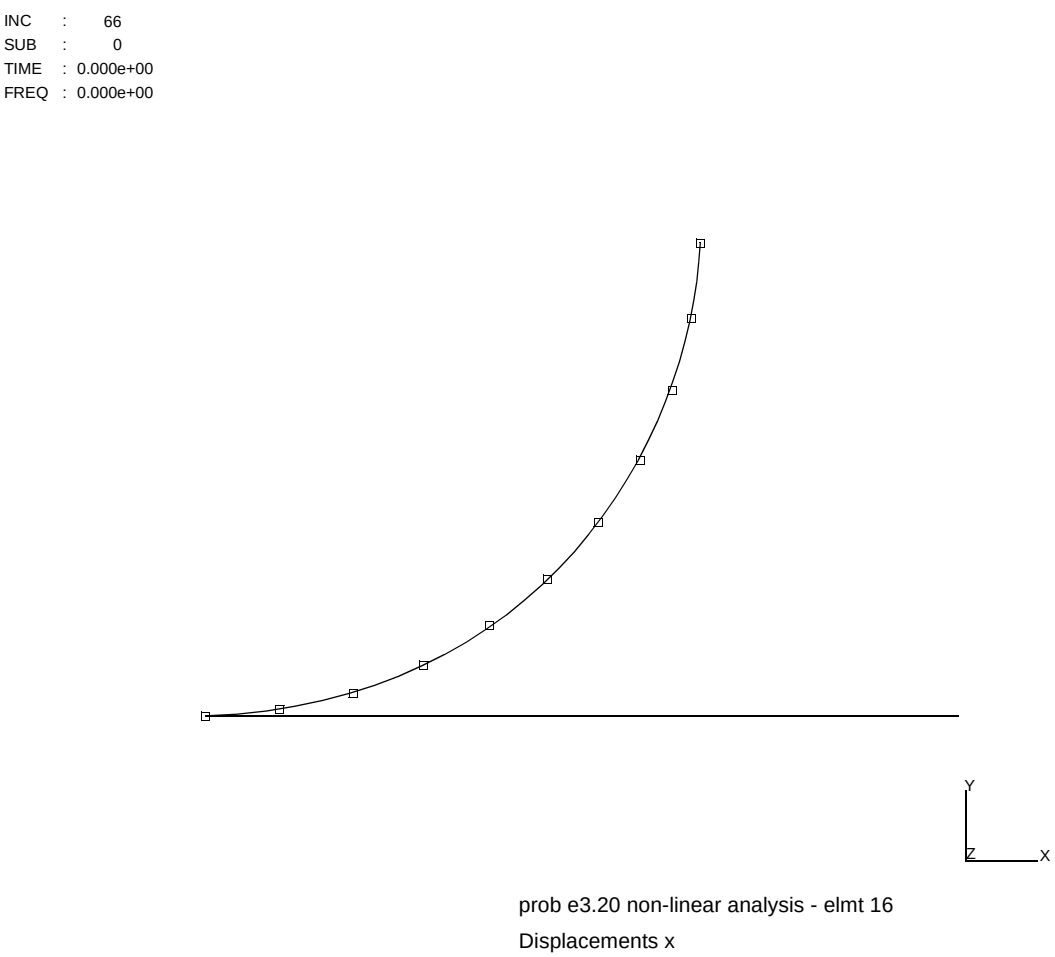

Figure 3.20-2 Deformed Beam after Release of End

3.21 Necking of a Cylindrical Bar

A cylindrical bar of 20 inches long and 6 inches in diameter is loaded in tension. The ends of the bar are clamped and radial motion is prevented. Away from the ends, the deformation is initially homogeneous. At a certain elongation, the deformation starts to localize. The onset of such localization occurs when the load in the bar reaches a maximum.

This problem is modeled using the five techniques summarized below.

Data Set	Element Type(s)	Number of Elements	Number of Nodes	Differentiating Features
e3x21	10	60	80	Fully integrated element
e3x21c	116	60	80	Reduced integration hourglass element
e3x21d	10	60	80	ADAPTIVE meshing
e3x21e	10	60	80	Multiplicative Decomposition (F^eF^p)
e3x21f	10	60	80	CONSTANT DILATATION

Elements

The solution is obtained using first-order isoparametric quadrilateral elements for axisymmetric analysis with element types 10 and 116, respectively. Type 116 is similar to type 10; however, it uses reduced integration with hourglass control.

Model

Because of symmetry, only one-half of the length of the bar is modeled where the axial coordinate x ranges from 0 to 10 inches and the radial coordinate y ranges from 0 to 3 inches. More elements are placed near the middle of the bar at x = 0 and fewer are placed at the end of the bar at x=10 inches. The mesh with numbered elements is shown in Figure 3.21-1 and Figure 3.21-2 shows the numbered nodes. In problem e3x21d, the adaptive meshing procedure is used.

Geometry

To obtain the constant volumetric strain formulation, (EGEOM2) is set to unity. This is applied to all elements of type 10 in models e2x21 and e3x21d. In model e3x21f, the CONSTANT DILATATION parameter is used. This has the same effect. For element type 116, it has no effect because the element does not lock. The incompressibility is automatically in the F^eF^p procedure.

Material Properties

The material for all elements is treated as an elastic perfectly-plastic material, with a Young's modulus of 10.0E+06 psi, Poisson's ratio of 0.3, and a yield strength of 20,000 psi. The LARGE DISP, UPDATE, and FINITE options are used in this analysis. The constant workhardening rate of 30,000 psi applies to the true stress versus logarithmic strain curve.

Boundary Conditions

The symmetry conditions require that all nodes along the x = 0 axis have their x-displacements constrained to zero; all nodes along the y = 0 axis have their y-displacements constrained to zero. All nodes along the x = 10 axis have their y-displacements constrained to zero and an initial x-displacement of .01 inches.

Load History

All nodes along the x = 10 axis will continue to have their x-displacements increased by .01 inches/increment for 9 increments; then increased by 0.1 inches for 59 increments for the bar to reach a total length of 32 inches.

Analysis Control

The CONTROL option is used to specify a maximum of 80 increments and a maximum of 10 iterations. This number of iterations is specified in order to deal with sudden changes in the deformation field. The convergence checking is done on residuals with a control tolerance of 0.01. Several element variables are written onto the post file and subroutine IMPD sums the load for the load-deflection curve.

Adaptive Meshing

The adaptive meshing procedure is used based upon the Zienkiewicz-Zhu error criteria. A maximum of three levels is allowed.

Results

The value of the maximum load is readily calculated. The force, F, in the bar can be expressed in terms of the true stress σ and current cross-sectional area, A, by:

$$F = A\sigma$$

Assuming incompressibility, the current area can be related to the initial area, A_o, and the elongation, λ, by:

$$F = A_o\sigma/\lambda$$

The load reaches a maximum if the force does not change for increasing elongation. This furnishes a condition for the onset of necking, whereby:

$$dF/d\lambda = A_o (d\sigma/d\lambda - \sigma/\lambda)/\lambda = 0$$

With the introduction of the logarithmic strain $e = \ln \lambda$, this condition can also be expressed as:

$$h = d\sigma/de = \sigma$$

The onset of necking occurs if the true stress is equal to hardening modulus in the true stress-logarithmic strain curve. For a material with constant hardening modulus, h, this relation can be worked out in greater detail. For such a material, the true stress can be expressed in terms of the elongation by:

$$\sigma = \sigma_y + he,$$

where σ_y is the initial yield stress. Substituting yields the logarithmic strain:

$$e = 1 - \sigma_y/h.$$

In the current problem, the initial yield stress, σ_y = 20,000 psi and the hardening modulus, h = 30,000 psi, yielding a logarithmic strain of 33.33%. The onset of necking occurs at an engineering strain (the length change divided by the original length) of 39.56% or an end point displacement of 3.956 inches.

The results from the model shown in Figure 3.21-3 predict the onset of necking occurring earlier at about 3.0 inches. However, the load displacement curve is very flat due to the low value of the hardening modulus and an accurate value is hard to achieve. Also, the load displacement curve shows the model with element type 10, necking more than the element type 116 after the maximum load is reached. The amount of necking is also shown in the deformed plots of Figure 3.21-4 through Figure 3.21-10. This is because element type 116 only has one integration point (element type 10 has four) used for stress recovery and requires more elements.

Figures 3.21-5, 3.21-7, and 3.21-10 show the equivalent plastic strains for the different case. It can be seen that the results obtained with element 10 using the two formulations, additive and multiplicative decompostion, within 2%. Similarly, the reaction forces for the two formulations are also within 2% as indicated by Figure 3.21-4 and Figure 3.21-9. The differences are due to the way incompressibility is imposed in the two formulations. The F^eF^p formulation uses a more accurate tangent with an exact treatment for large strain kinematics and elasticity. However, the reduced integration elements depict a much softer response and does not yield an accurate solution even with the finer mesh.

Parameters, Options, and Subroutines Summary

Example e3x21a.dat:

Parameters	Model Definition Options	History Definition Options
ELEMENTS	CONNECTIVITY	AUTO LOAD
END	CONTROL	CONTINUE
FINITE	COORDINATES	PROPORTIONAL INCREMENT
LARGE DISP	END OPTION	
SIZING	FIXED DISP	
TITLE	GEOMETRY	
UPDATE	ISOTROPIC	
	POST	
	PRINT CHOICE	
	UDUMP	
	WORK HARD	

Example e3x21b.dat:

Parameters
COMBINED
ELEMENTS
END
PRINT
TITLE
USER

Example e3x21c.dat:

Parameters	Model Definition Options	History Definition Options
ALIAS	CONNECTIVITY	AUTO LOAD
ELEMENTS	CONTROL	CONTINUE
END	COORDINATE	PROPORTIONAL INCREMENT
FINITE	END OPTION	
LARGE DISP	FIXED DISP	
SIZING	GEOMETRY	
TITLE	ISOTROPIC	
UPDATE	POST	
	PRINT CHOICE	
	RESTART	
	WORK HARD	

Example e3x21d.dat:

Parameters	Model Definition Options	History Definition Options
ADAPTIVE	ADAPTIVE	AUTO LOAD
ELEMENTS	CONNECTIVITY	CONTINUE
END	CONTROL	PROPORTIONAL INCREMENT
FINITE	COORDINATES	
LARGE DISP	END OPTION	
SIZING	FIXED DISP	
TITLE	GEOMETRY	
UPDATE	ISOTROPIC	
	POST	
	PRINT CHOICE	
	UDUMP	
	WORK HARD	

Example e3x21e.dat:

Parameters	Model Definition Options	History Definition Options
ELEMENTS	CONNECTIVITY	AUTO LOAD
END	CONTROL	CONTINUE
TITLE	COORDINATES	PROPORTIONAL INCREMENT
LARGE DISP	END OPTION	
SIZING	FIXED DISP	
PLASTICITY	WORK HARD	
	ISOTROPIC	
	POST	
	PRINT CHOICE	
	UDUMP	

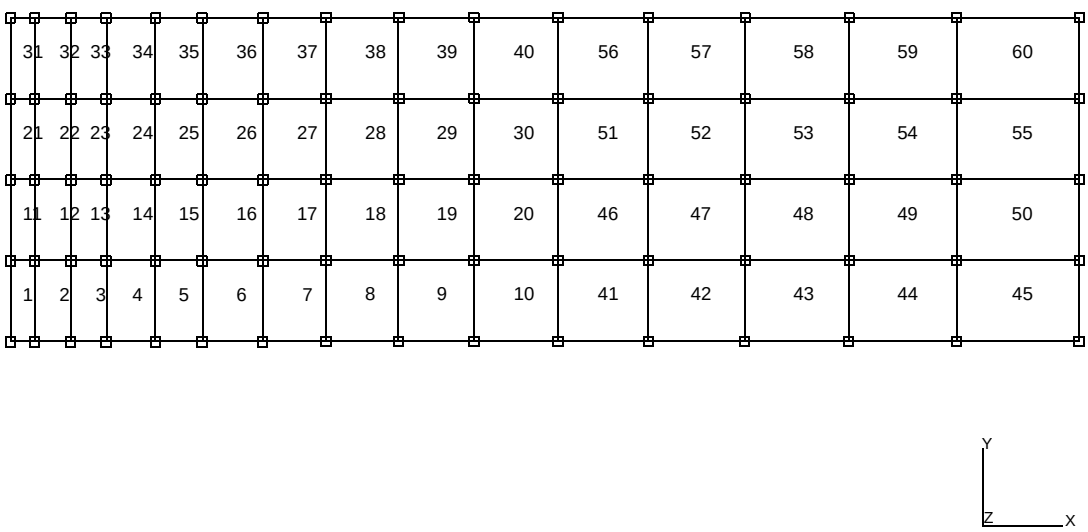

Figure 3.21-1 Model with Elements Numbered

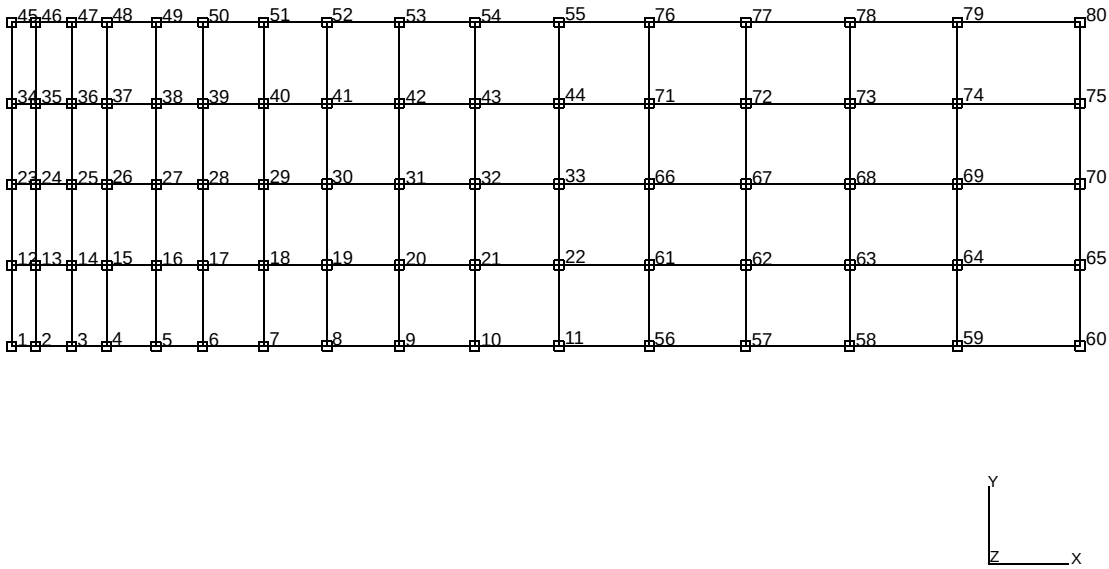

Figure 3.21-2 Model with Nodes Labeled

Displacement	Load (x10**5 lbf)		
	Type 10	Type 116	Type 116 fine
0.0	0.0	0.0	0.0
1.00000E-02	2.86645E+00	2.87316E+00	2.86198E+00
2.00000E-02	5.64279E+00	5.65044E+00	5.65154E+00
3.00000E-02	5.65075E+00	5.65181E+00	5.65312E+oo
2.70000E+00	6.08106E+00	6.08466E+00	6.08170E+oo
2.80000E+00	6.08219E+00	6.08442E+00	6.08266E+00
2.90000E+00	6.08235E+00	6.08293E+00	6.08259E+00
3.00000E+00	6.08144E+00	6.07998E+00	6.08137E+00
3.10000E+00	6.07933E+00	6.07538E+00	6.07879E+00
3.20000E+00	6.07580E+00	6.06831E+00	6.07457E+00
3.30000E+00	6.07060E+00	6.05820E+00	6.06833E+00
3.40000E+00	6.06339E+00	6.04646E+00	6.05973E+00
4.70000E+00	5.56913E+00	5.24714E+00	5.46007E+00
4.80000E+00	5.47695E+00	5.06798E+00	5.34126E+00
4.90000E+00	5.37292E+00	4.84365E+00	5.20284E+00
5.00000E+00	5.25596E+00	4.59166E+00	5.04048E+00

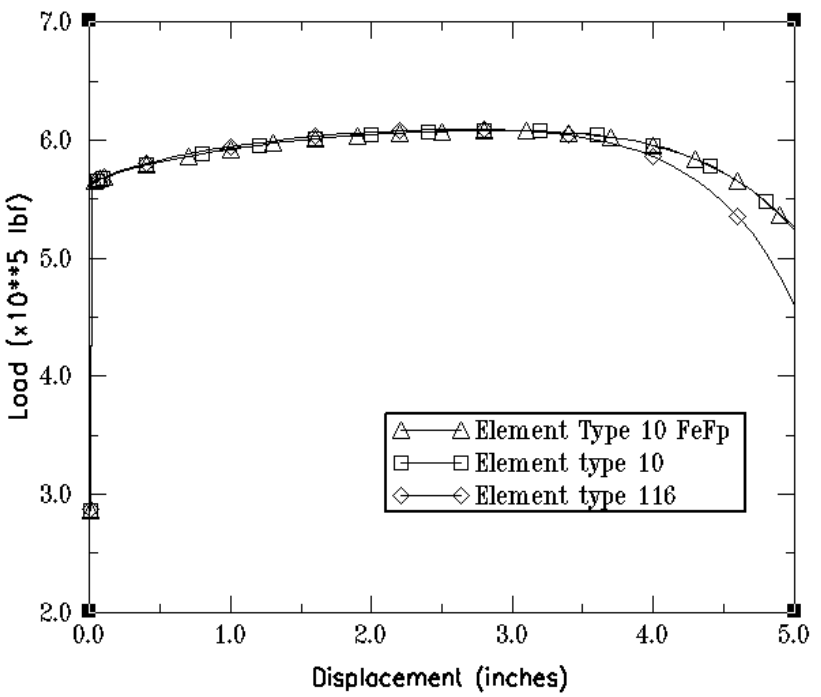

Figure 3.21-3 Load -Displacement Curve

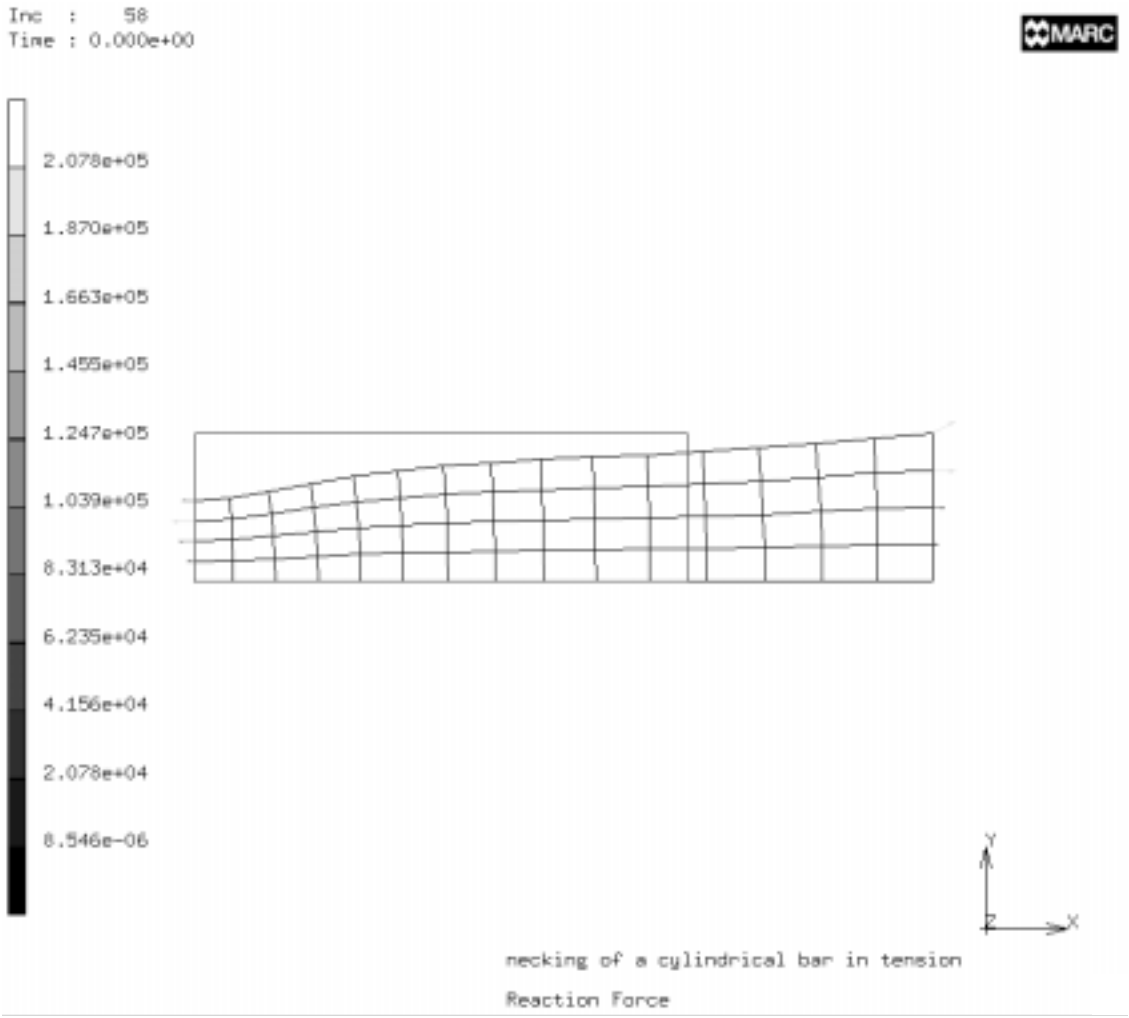

Figure 3.21-4 Vector Plot of Reactions for Type 10

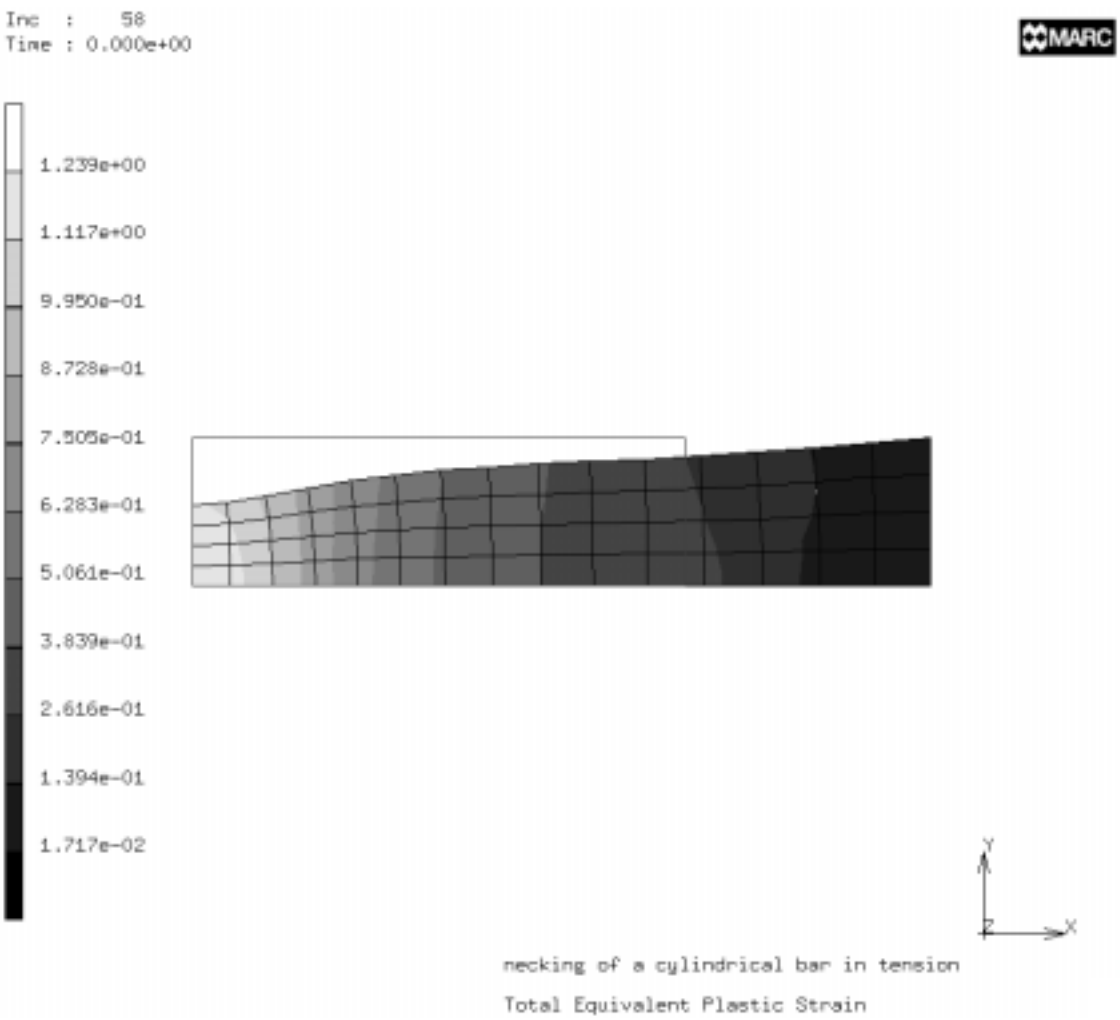

Figure 3.21-5 Contour Plot of Equivalent Strain for Type 10

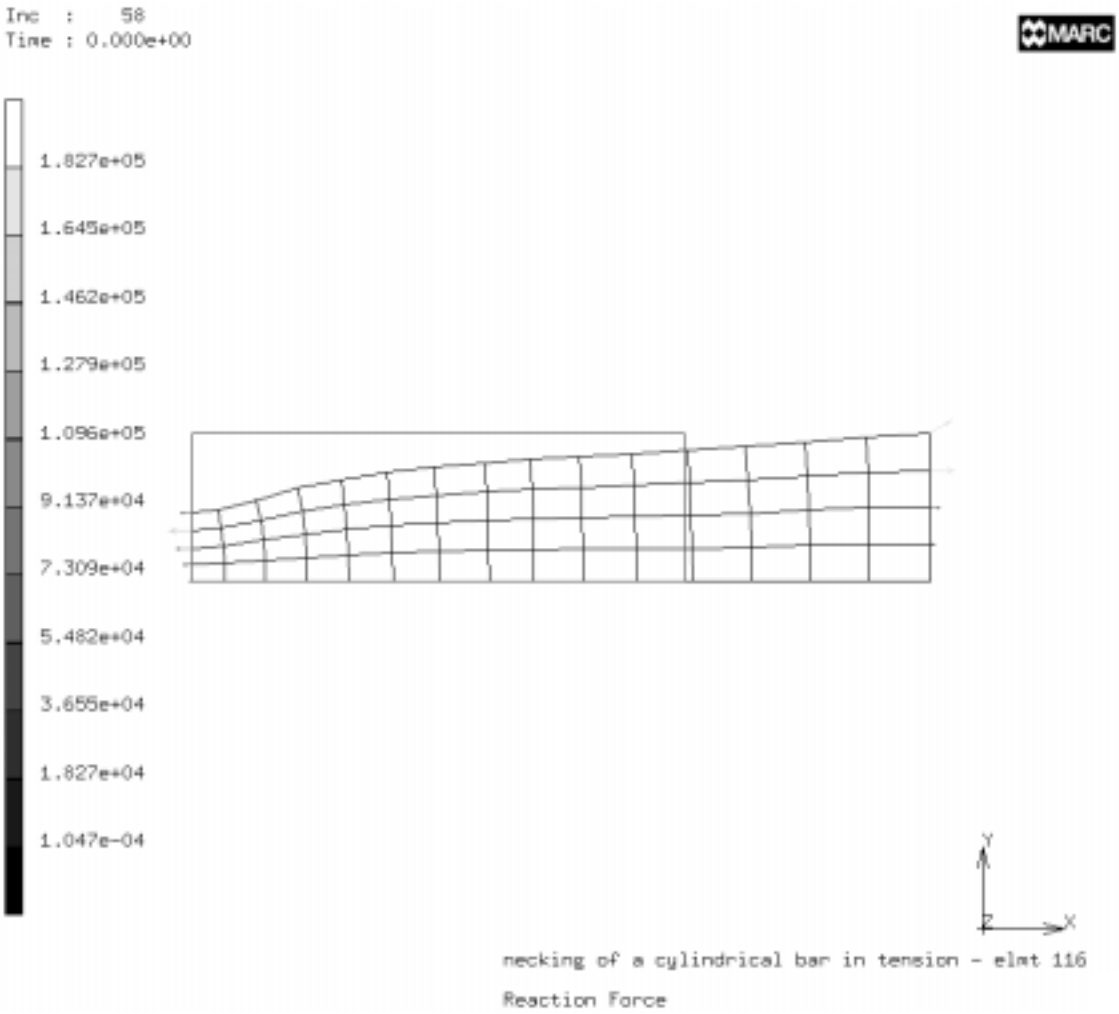

Figure 3.21-6 Vector Plot of Reactions for Type 116 (Coarse Mesh)

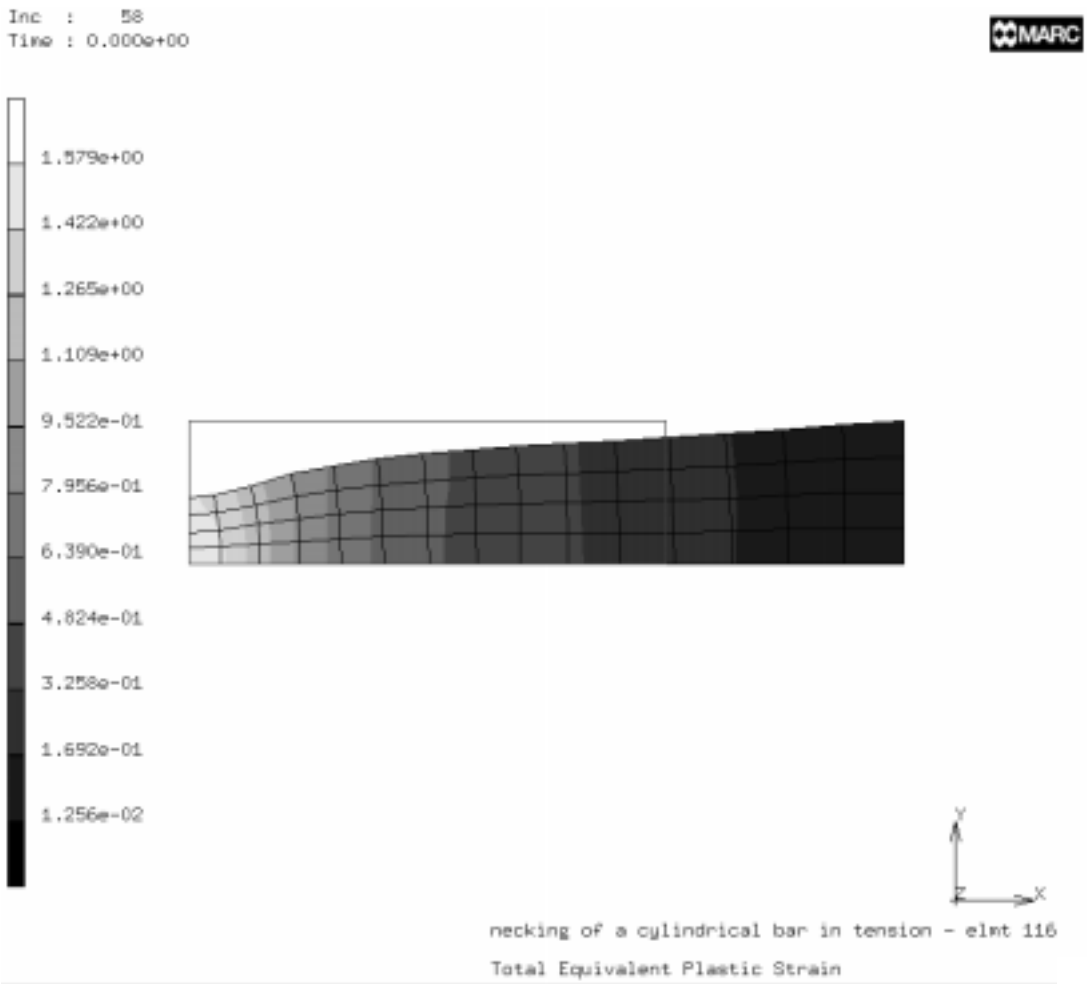

Figure 3.21-7 Contour Plot of Equivalent Plastic Strain for Type 116 (Coarse Mesh)

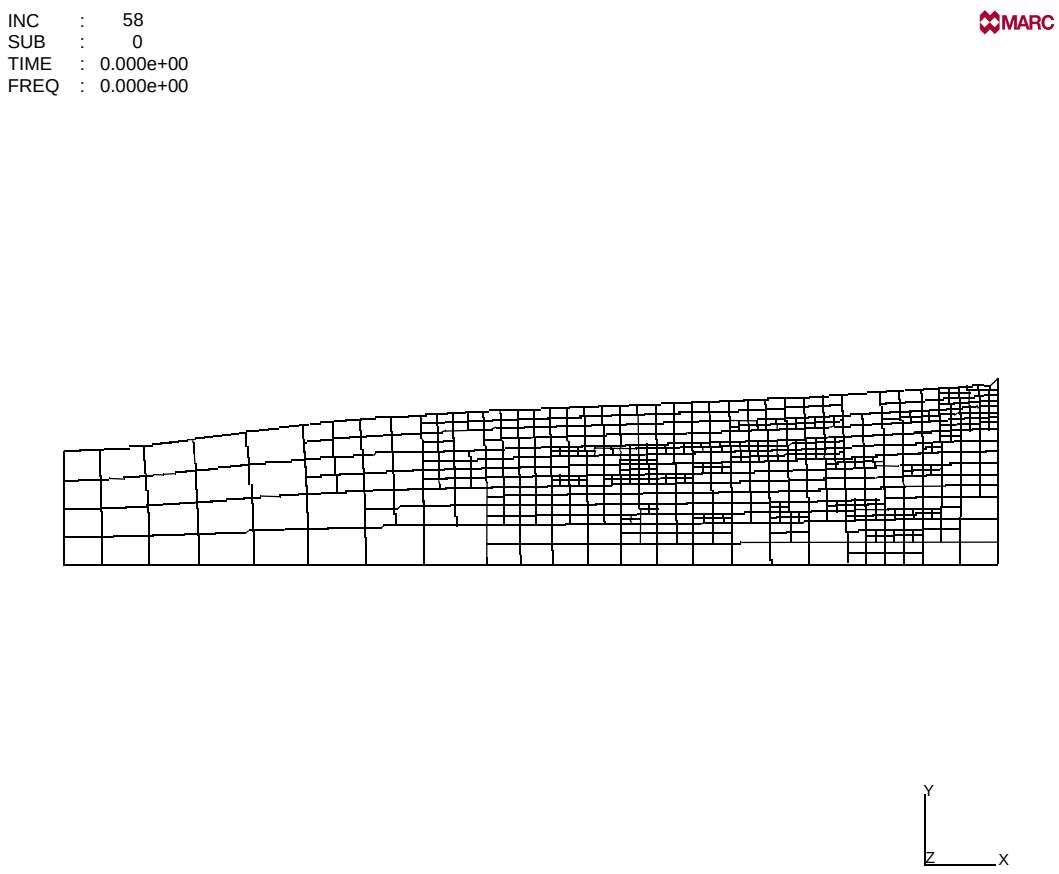

Figure 3.21-8 Final Mesh After Adaptive Meshing

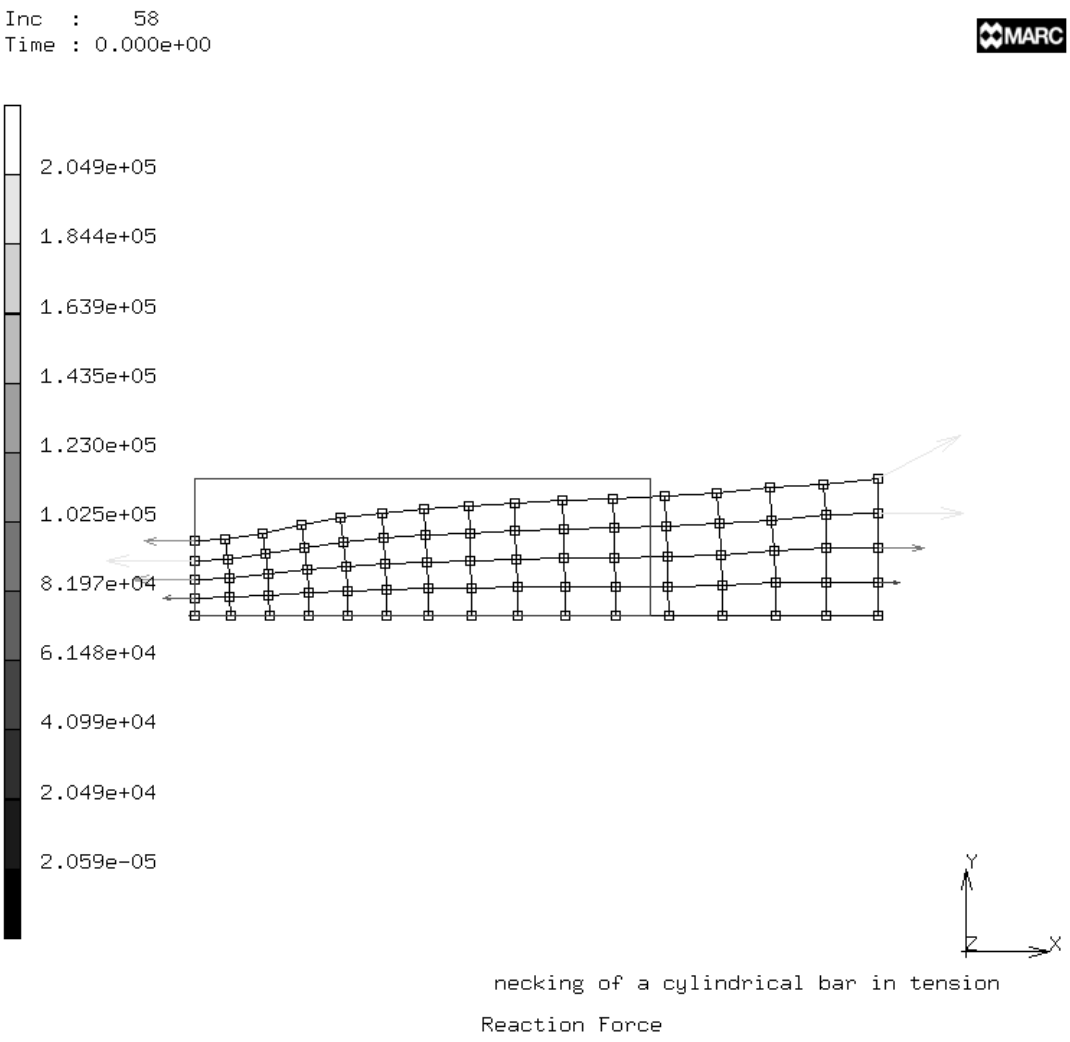

Figure 3.21-9 Vector Plot of Reactions for Type 10 (F^eF^p)

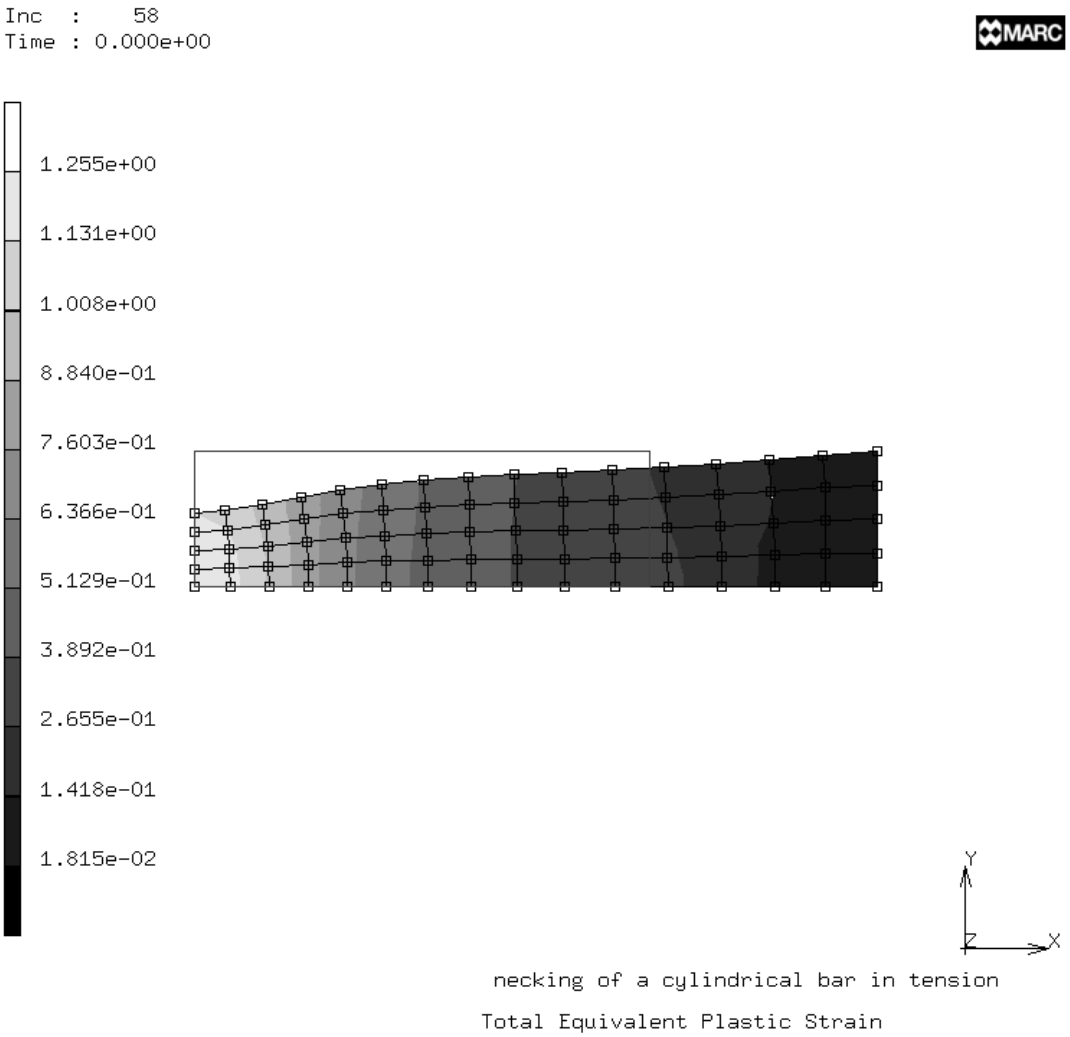

Figure 3.21-10 Contour Plot of Equivalent Strain for Type 10 (F^eF^p)

3.22 Combined Thermal, Elastic-plastic, and Creep Analysis

A realistic design problem, such as thermal ratcheting analysis, involves a working knowledge of a significant number of program features. This example illustrates how these features can be used to analyze a simplified form of a pressure vessel component which is subjected to a uniform pressure and thermal downshock. This type of problem typifies reactor component analysis. The general temperature-time history is shown in Figure 3.22-1 and the pressure history is shown in Figure 3.22-2.

An analysis of this type requires the use of heat transfer analysis to determine the transient temperature distribution in the wall of a cylindrical pressure vessel under cool-down conditions. This temperature distribution must be saved and presented to MARC through the CHANGE STATE option. The AUTO THERM option then creates its own incremental changes in temperature for use in the stress analysis. MARC then proceeds to find the elastic plastic state of stress in the cylinder due to the combined effects of internal pressure and thermal loading and the long time residual effects of creep.

Elements

The 8-node axisymmetric, quadrilateral element is used in this example. The heat transfer element type 42, is used in the determination of the transient temperature distribution while the 8-node distorted quadrilateral element type 28 is used in the stress analysis.

Model

The geometry and mesh for this example are shown in Figure 3.22-3. A cylindrical wall segment is evenly divided in six axisymmetric quadrilateral elements with a total of 33 nodes. The ALIAS parameter block allows you to generate your connectivity data with the stress analysis element and then to replace this element with the corresponding heat transfer element type.

Heat Transfer Properties

It is assumed here that the material properties do not depend on temperature; therefore, no slope-breakpoint data are input. The uniform properties used here are: specific heat (c) of 0.116 Btu/lb-°F, thermal conductivity (k) is 4.85×10^{-4} Btu/in-sec°F, and density (ρ) is 0.283 lb^3/inch.

Heat Transfer Boundary Conditions

The initial temperature across the wall and ambient temperature are 1100°F as specified in the initial conditions block. The outer ambient temperature is held constant at 1100°F. The inner ambient temperature decreases from 1100°F to 800°F in 10 secs and remains constant thereafter.

The FILMS option is used to input the film coefficients and associated sink temperatures for the inner and outer surface. A uniform film coefficient for the outside surface is specified for element 65 as 1.93×10^{-6} Btu/sq.in-sec.-°F providing a nearly insulated wall condition. The

inner surface has a film coefficient of 38.56 x 10^{-5} Btu/sq.in-sec-°F to simulate forced convection. The temperature down-ramp of 300°F for this inner wall is specified here as a nonuniform sink temperature and is applied using user subroutine FILM.

Subroutine FILM linearly interpolates the 300°F decrease in ambient temperature over 10 seconds and then holds the inner wall temperature constant at 800°F. It is called at each time step for each integration point on each element surface given in the FILMS option. This subroutine does nothing if it is called for element 65 to keep the outer surface at 1100°F. It applies the necessary ratio to reduce the inner wall temperature.

The TRANSIENT option controls the heat transfer analysis. MARC automatically calculates the time steps to be used based on the maximum nodal temperature change allowed as input in the CONTROL option. The solution begins with the suggested initial time step input and ends according to the time period specified. It will not exceed the maximum number of steps input in this option.

Finally, note in the heat transfer run the use of the POST option. This allows the creation of a postprocessor file containing element temperatures at each integration point and nodal point temperatures. The file is used later as input to the stress analysis run through the use of the CHANGE STATE and AUTO THERM options.

Heat Transfer Results

The transient thermal analysis is linear; the material properties do not depend on temperature, and the boundary conditions depend on the surface temperature linearly. The analysis is completed using the auto time step feature in the TRANSIENT option.

The TRANSIENT AUTO run reached completion in 33 increments with a specified starting time step of 0.5 seconds. A 15°F temperature change tolerance was input in the CONTROL option and controlled the auto time stepping scheme. The reduction to approximately 800°F throughout the wall was reached in increment 33 at a total time of 250 seconds.

The temperature-time histories of inner wall element (1) and outer wall element (6) for auto time stepping is shown in Figure 3.22-4. The data for plotting was saved using the POST option on a file.

The temperature distribution across the wall at various solution times is shown in Figure 3.22-5. These distributions correspond to incremental solution points in the stress analysis. Convergence to steady state is apparent here. The thermal gradient is characteristic of the downshock.

Stress Analysis

The stress analysis of the cylinder wall was accomplished in three separate runs. The first run proceeds from the elastic, increment 0, pressure load only, through the transient thermal analysis. The second run restarts at increment 27, sets all the elements to a uniform temperature of 800°F, and then proceeds to ramp the temperatures back up to 1100°F in six uniform temperature steps. The third run restarts at this original, stress-free temperature and allows the structure to creep for one hour.

Material Properties

All elements are isotropic. Young's modulus (E) is 21.8 x 10^6 psi; Poisson's ratio (ν) is 0.32; coefficient of thermal expansion (α) is 12.4 x 10^{-6} in/°F; initial stress-free temperature (T) is 1100°F; and yield stress (σ_y) is 20,000 psi. These values are assumed to be independent of temperature.

Loading

A uniform pressure of 900 psi is applied to the inner surface (1-2 face of element 1) of the cylinder and the appropriate end load of 210,344.5 pounds is applied axially to the cylinder through node 3 in increment 0. The mechanical load is held constant throughout the analysis. This is implemented using the PROPORTIONAL INC option.

Boundary Conditions

All nodal points in the left face (Z = 0) plane are restrained against motion in the axial direction. The TYING option is then used to ensure a generalized plane strain condition (all nodes in the Z = 0.1 plane are constrained to move identically to node 3 in the axial direction).

Restart

The analysis shown here was made in three runs using the RESTART option. The option allows you to control the analysis through several smaller runs with fewer increments at a time. Parameters, such as loading rates and tolerances, can be altered and increments then repeated if it is necessary.

The first stress analysis run shown provides the thermal elastic-plastic solution in increments 1 through 27. Restart data is written at every increment. This allows restarting at any point in the solution. The restart data is written to unit 8 and is saved as a file.

The second and third runs allow for reading and writing of restart data. The second run restarts at increment 27 and brings the wall temperature to 1100°F again at increment 34. The third run initiates the creep analysis by restarting at increment 37 and finishes at increment 55. Each of these runs writes the data to unit 8 at every increment to ensure continuation. This may be necessary if an extended creep solution is desired.

Control

The limit on the total number of increments must be properly set from one run to the next. Tolerances can be specified here for any restarted run.

State Variables Options

The INITIAL STATE and the CHANGE STATE options each provides three ways of initializing or changing the state variables specified. A range of elements, integration points and layers and a corresponding state variable values can be read in. Secondly, values can be read in through the corresponding user subroutine INITSV (for initialization) or NEWSV (for a change). Third, the state variable values can be read from a named step of the post file output from a previous heat transfer analysis with MARC. The number of state variable per point can be defined in the STATE VARS parameter block. In this analysis, the default of 1 is used for the temperature as the first state variable at a point.

In the first run, the INITIAL STATE option is used to define the initial stress-free temperature for all six elements and nine integration points at 1100°F. The CHANGE STATE option here uses the values from the post file created in the heat transfer analysis in conjunction with the AUTO THERM option. It is used in the second run to ramp the uniform wall temperature from 800°F to 1100°F in six equal increments.

Auto Therm

This option allows automatic, static, elastic-plastic, thermally loaded stress analysis based on a set of temperatures defined throughout the mesh as a function of time. The CHANGE STATE option must be used with the AUTO THERM option to present the temperatures in MARC. MARC then calculates its own temperature increment based on the temperature change tolerance provided.

A tolerance of 17º was used for the AUTO THERM analysis of the first run. It was calculated as 20% to 50% of the strain to cause yield, equal to $\frac{\bar{\sigma}}{E\alpha}$, where σ is the yield stress, E is the Young's modulus, and α is the coefficient of thermal expansion. This strain size gives an accurate elastic-plastic analysis. The temperature set is provided in the CHANGE STATE option from the heat transfer post file attached as unit 20. These temperatures are from steps 1 through 32 of that heat transfer analysis. A maximum of 35 increments was specified for this AUTO THERM. This provides a limit to avoid excessive computation in case of a data error.

Creep

The CREEP parameter block and CREEP model definition block are required to flag creep analysis and set the type of creep law and creep tolerances. Here the creep law is provided using user subroutine CRPLAW. The creep law used is:

$$\dot{\varepsilon}^{\circ C} = 1.075(10^{-26})\sigma^{5.5}$$

An initial time step size of 0.02 hours and an end time of 1.0 hour is specified in the AUTO CREEP option of the third stress run. The time step is automatically adjusted based on the stress and strain-change tolerance specified. Due to this adjustment, final time of 1.0 hour is obtained in 12 increments rather than the 50 increments that the initial time step would require. The initial time step can be determined using the methods outlined in *MARC Volume A: User Information*.

Print Choice

Because the temperatures and stresses across a layer of an element do not change, the PRINT CHOICE option can be used to reduce the output. Here, the solutions are output in each run for only three integration points per element; one in each layer, points, 2, 5, and 8.

Results

Figure 3.22-6 shows the equivalent stress distribution through the cylinder wall during the elastic-plastic solution. No yielding occurs due to mechanical loading. As the thermal loads are superimposed, yielding advances across the cylinder wall from the inside. The thermal gradients decrease and the inside wall element begins to unload. Here the region of yielding is in the midwall. The outside elements reverse their unloading trend at this time and show yielding stress levels. Finally, at the end of the elastic-plastic solution, the midwall has yielded. The outside elements are very close to yield and the inside wall element has unloaded. The creep solution, shown in Figure 3.22-7, finds the equivalent stress distribution relaxed back to very nearly the isothermal elastic state.

Parameters, Options, and Subroutines Summary

Example e3x22a.dat:

Parameters	Model Definition Options	History Definition Options
ALIAS	CONNECTIVITY	CONTINUE
ELEMENTS	CONTROL	TRANSIENT
END	COORDINATES	
HEAT	END OPTION	
SIZING	FILMS	
TITLE	INITIAL TEMPERATURE	
	ISOTROPIC	
	POST	

User subroutine in u3x22a.f:

FILM

Example e3x22b.dat:

Parameters

ELEMENTS
END
TITLE

Example e3x22c.dat:

Parameters	Model Definition Options	History Definition Options
CREEP	CONNECTIVITY	AUTO CREEP
ELEMENTS	CONTROL	AUTO THERM
END	COORDINATES	CHANGE STATE
SIZING	CREEP	CONTINUE
THERMAL	DIST LOADS	PROPORTIONAL INCREMENT
TITLE	END OPTION	
	FIXED DISP	
	INITIAL STATE	
	ISOTROPIC	
	POINT LOAD	
	PRINT CHOICE	
	RESTART	
	TYING	

User subroutine in u3x22c.f:

CRPLAW

Example e3x22d.dat:

Parameters	Model Definition Options	History Definition Options
ALL POINTS	CONNECTIVITY	AUTO CREEP
CREEP	CONTROL	CHANGE STATE
ELEMENTS	COORDINATES	CONTINUE
END	CREEP	
SIZING	DIST LOADS	
THERMAL	END OPTION	
TITLE	FIXED DISP	
	INITIAL STATE	
	ISOTROPIC	
	POINT LOAD	
	PRINT CHOICE	
	RESTART	
	TYING	

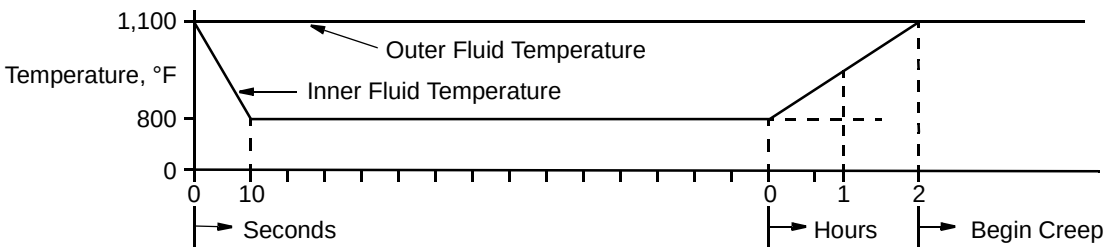

Figure 3.22-1 Temperature-Time History

Figure 3.22-2 Pressure-Time History

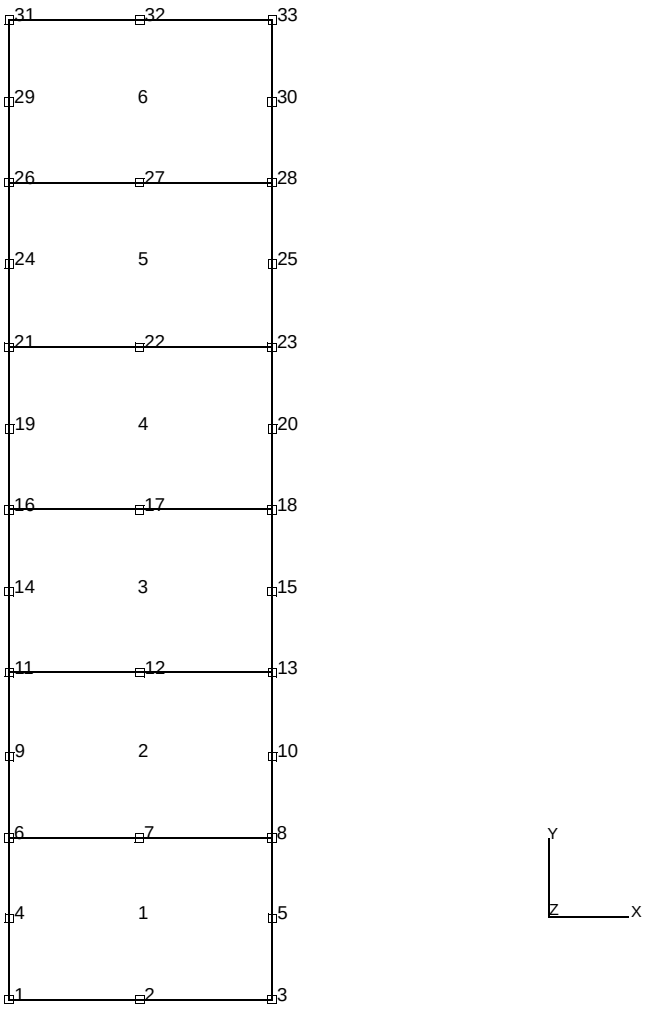

Figure 3.22-3 Geometry and Mesh for Combined Thermal, Elastic-Plastic, and Creep Problem

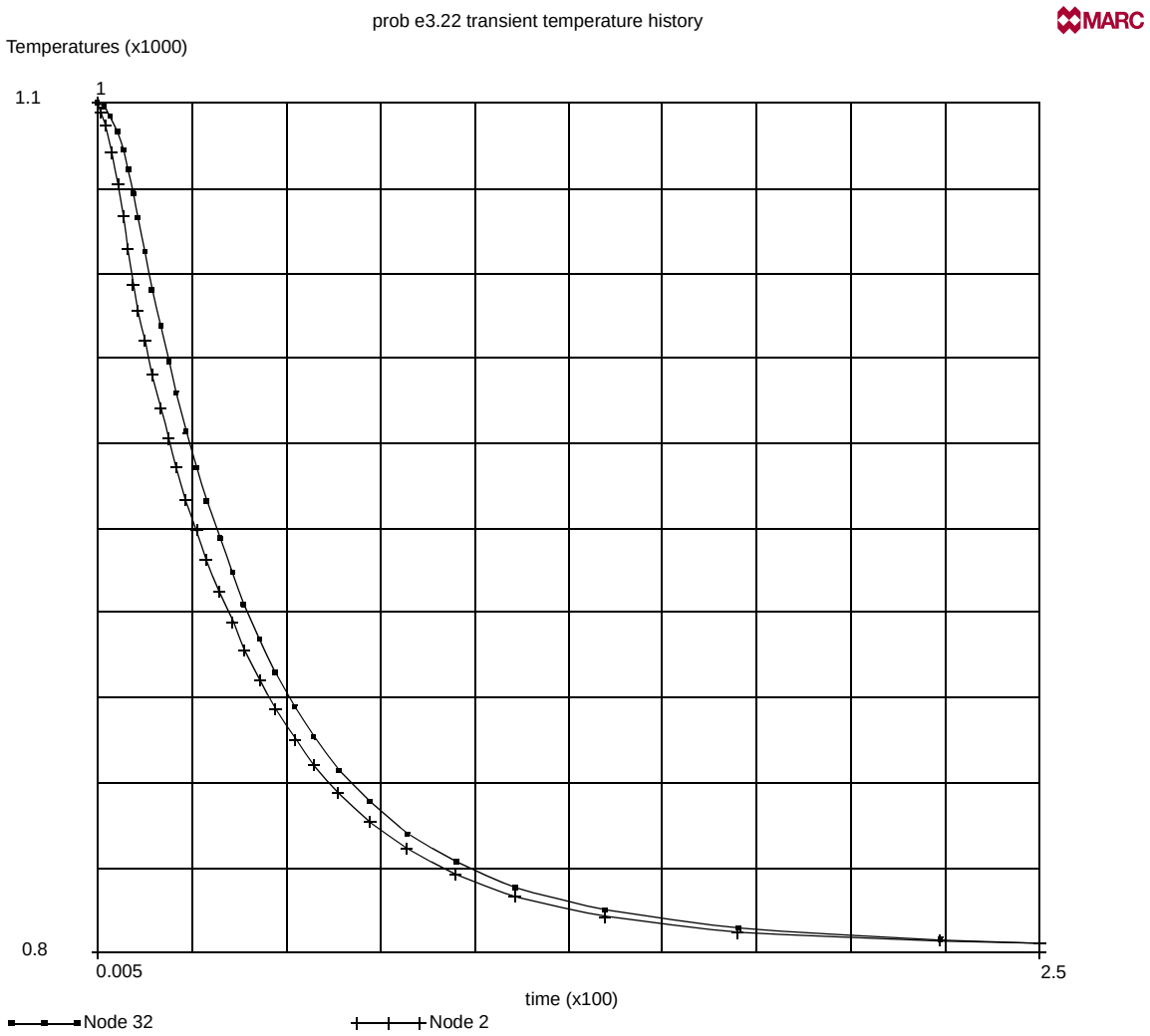

Figure 3.22-4 Transient Temperature Time History (Auto Time Step)

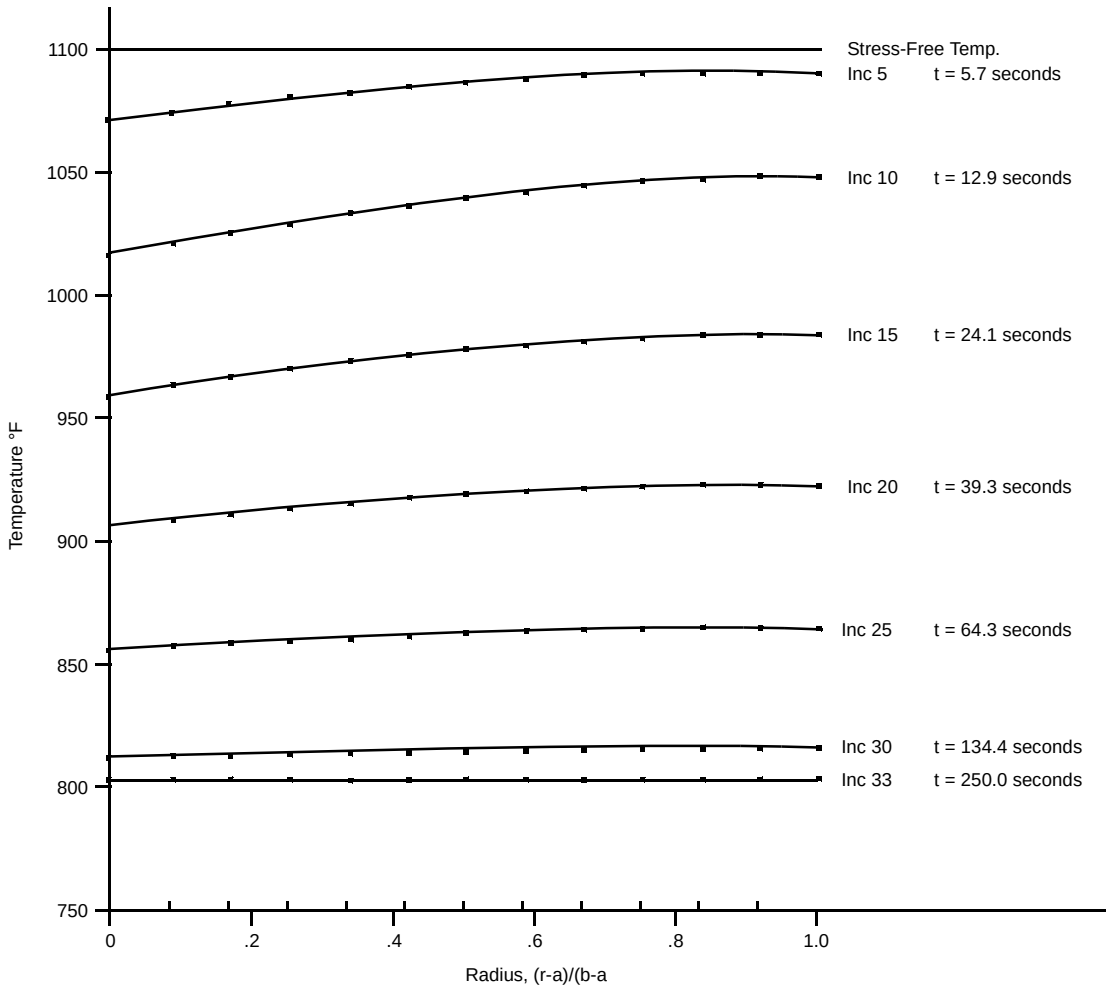

Figure 3.22-5 Temperature Distribution in Cylinder Wall

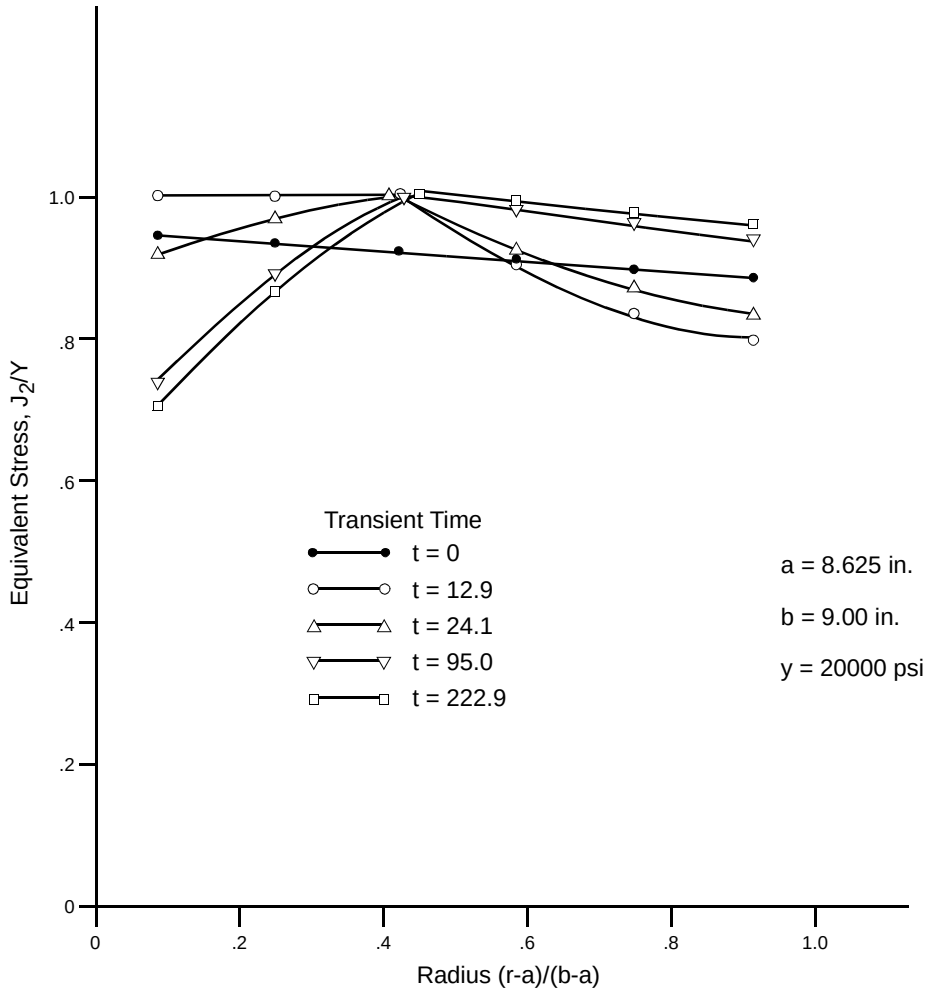

Figure 3.22-6 Thermal Elastic Plastic Results

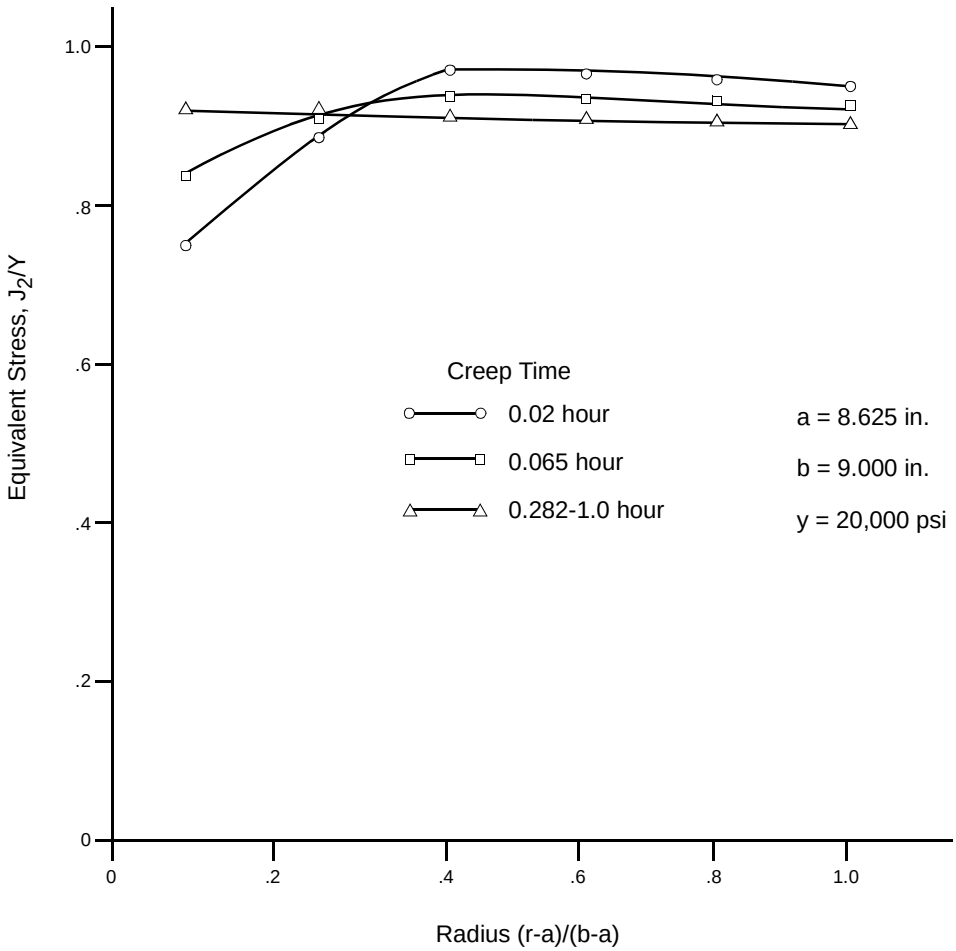

Figure 3.22-7 Creep Results

3.23 Nonlinear Analysis of a Shell Roof, using Automatic Incrementation

A shell roof is supported by a rigid diaphram at the curved edges. A snow load is uniformly applied to the roof. The shell material is modeled as elastic-perfectly plastic, and geometric nonlinearities are considered. An initial load of 3.5 x 10^{-4} N/mm^2 is applied; the load is automatically incremented until the structure is completely plastic. This problem is similar to problem 3.17. However, this problem uses element type 75 and adaptive load incrementation.

This problem is modeled using the two techniques summarized below.

Data Set	Element Type(s)	Number of Elements	Number of Nodes	Differentiating Features
e3x23	75	36	49	AUTO LOAD
e3x23b	75	36	49	AUTO INCREMENT

Elements

Element type 75 is a 4-node, thick-shell element with six global degrees of freedom per node.

Model

One-quarter of the roof is modeled with 36 type 75 elements, with a total of 49 nodes (Figure 3.23-1). The UFXORD option transforms these cylindrical coordinates into global Cartesian coordinates.

Geometry

A thickness of 76 mm is specified in the EGEOM1 field of the GEOMETRY option.

Material Properties

The material is modeled as elastic-perfectly plastic; no workhardening data is given. The elastic properties are specified by a Young's modulus of 2.1 x 10^4 N/mm^2. Plasticity occurs after a von Mises yield stress of 4.2 N/mm^2.

Loading

A gravity-type load models the weight of the snow on the roof. The initial load of 3.5 x 10^{-4} N/mm^2 is applied in increment 0. The AUTO INCREMENT option gradually increases the load to a specified total of 3.5 x 10^{-2} N/mm^2.

Boundary Conditions

Diaphram support conditions are given on the curved edges and appropriate symmetry conditions are given in the FIXED DISP option.

Data Storage

The number of integration stations through the thickness of the shell is set to five with the SHELL SECT option.

Geometric Nonlinearity

The LARGE DISP option is included to invoke geometric nonlinear behavior. The Newton-Raphson iterative technique (default option in MARC) is used to solve the nonlinear equations.

Analysis Control

With the CONTROL option, the maximum number of load increments (including increment 0) is specified as 40. All other CONTROL parameters have the default value. In addition, the elements are assembled in parallel using the PROCESSOR option.

Postprocessing

A post file is written. The PRINT CHOICE option is used to limit print output to one element (36) at one integration point (1), at two layers (1 and 5), and one node (49). More complete nodal data is stored on the post file, whereas plotted information is obtained concerning the plastic strains.

Auto Incrementation

Nine increments are applied with the use of the AUTO INCREMENT option. A final loading of 3.5×10^{-2} N/mm^2 is specified, although complete plasticity is reached well before this load.

Results

The analysis ends at a distributed snow load of 5.0×10^{-3} N/mm^2. At this load, the structure is plastic throughout. The equivalent plastic strains plotted for layers 1, 3, and 5 are shown in Figure 3.23-2, Figure 3.23-3 and Figure 3.23-4, respectively. The final snow loading is equivalent to a 13,040-mm (42.85-ft) layer of freshly fallen snow resting on the shell roof. The vertical displacement of node 49 is plotted against the reaction at the diaphram support in Figure 3.23-5. The displacements at lower loads correspond well with those calculated in Example 3.17. The performance of using the PROCESSOR option to assemble the elements in parallel showed an overall speed improvement of 22%.

Parameters, Options, and Subroutines Summary

Example e3x23.dat:

Parameters	Model Definition Options	History Definition Options
ELEMENTS	CONNECTIVITY	AUTO INCREMENT
END	CONTROL	CONTINUE
LARGE DISP	COORDINATES	DIST LOADS
PRINT	DIST LOADS	
SHELL SECT	END OPTION	
SIZING	FIXED DISP	
TITLE	GEOMETRY	
	ISOTROPIC	
	POST	
	PRINT CHOICE	
	RESTART	
	UFXORD	

Example e3x23b.dat:

Parameters	Model Definition Options	History Definition Options
ELEMENTS	CONNECTIVITY	AUTO INCREMENT
END	CONTROL	CONTINUE
LARGE DISP	COORDINATES	DIST LOADS
PRINT	DIST LOADS	
PROCESS	END OPTION	
SHELL SECT	FIXED DISP	
SIZING	GEOMETRY	
TITLE	ISOTROPIC	
	POST	
	PRINT CHOICE	
	RESTART	
	UFXORD	

User subroutine in u3x23.f:

UFXORD

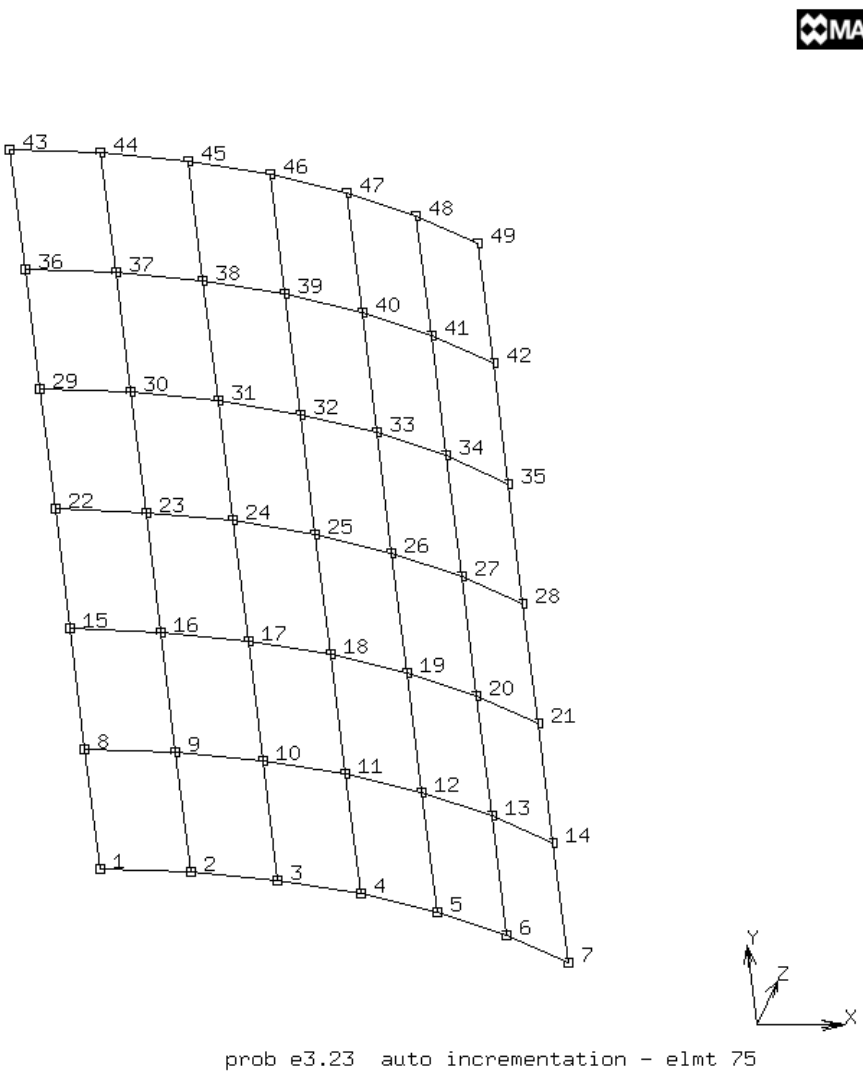

Figure 3.23-1 Model with Elements and Nodes Labeled

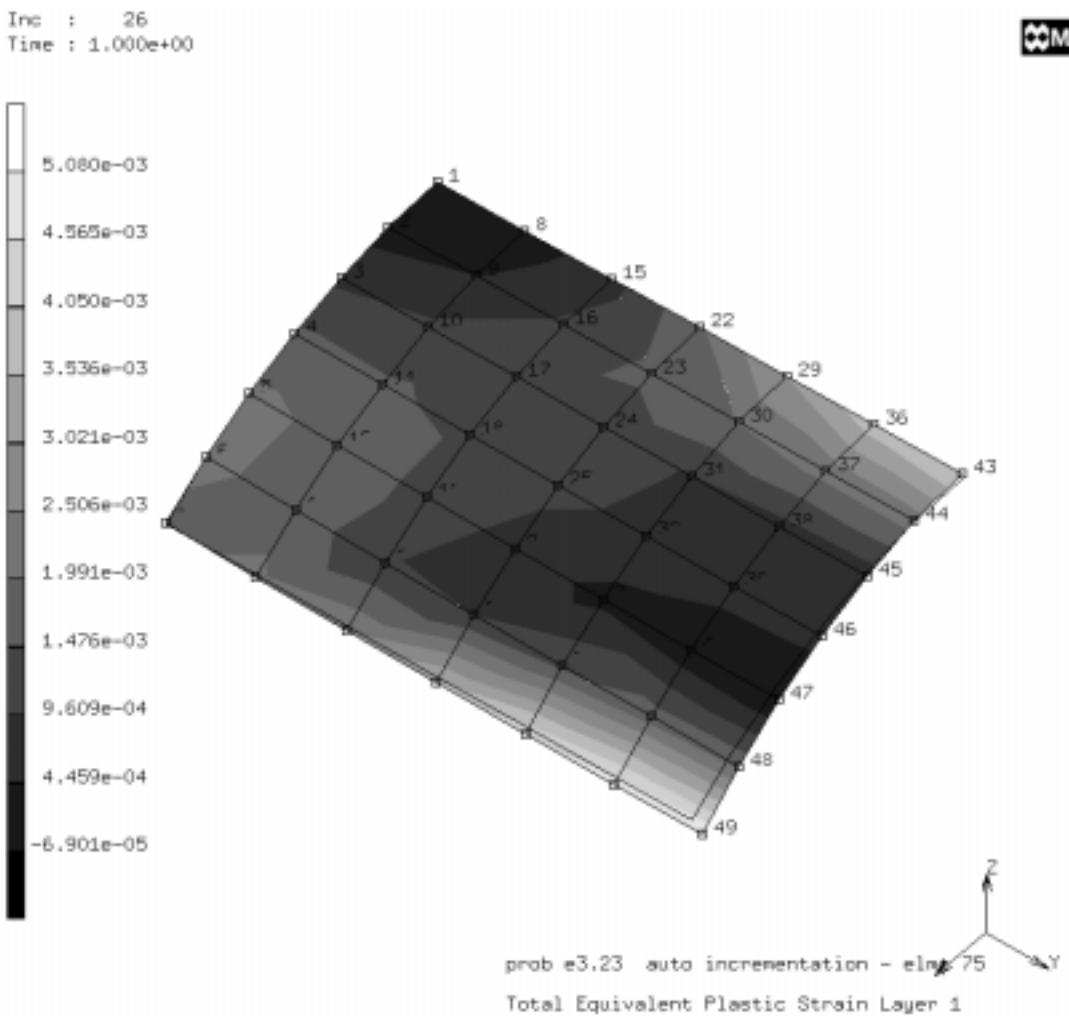

Figure 3.23-2 Equivalent Plastic Strain, Layer 1

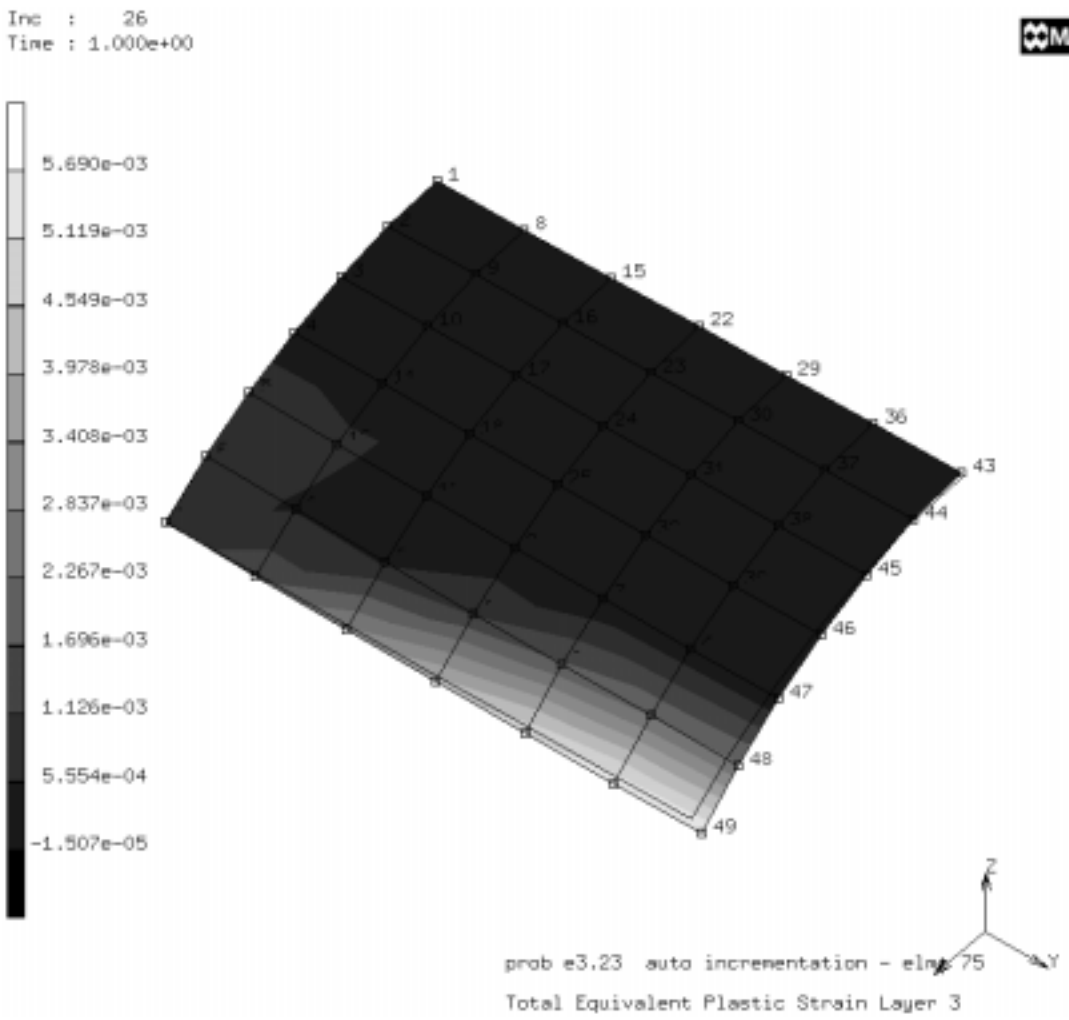

Figure 3.23-3 Equivalent Plastic Strain, Layer 3

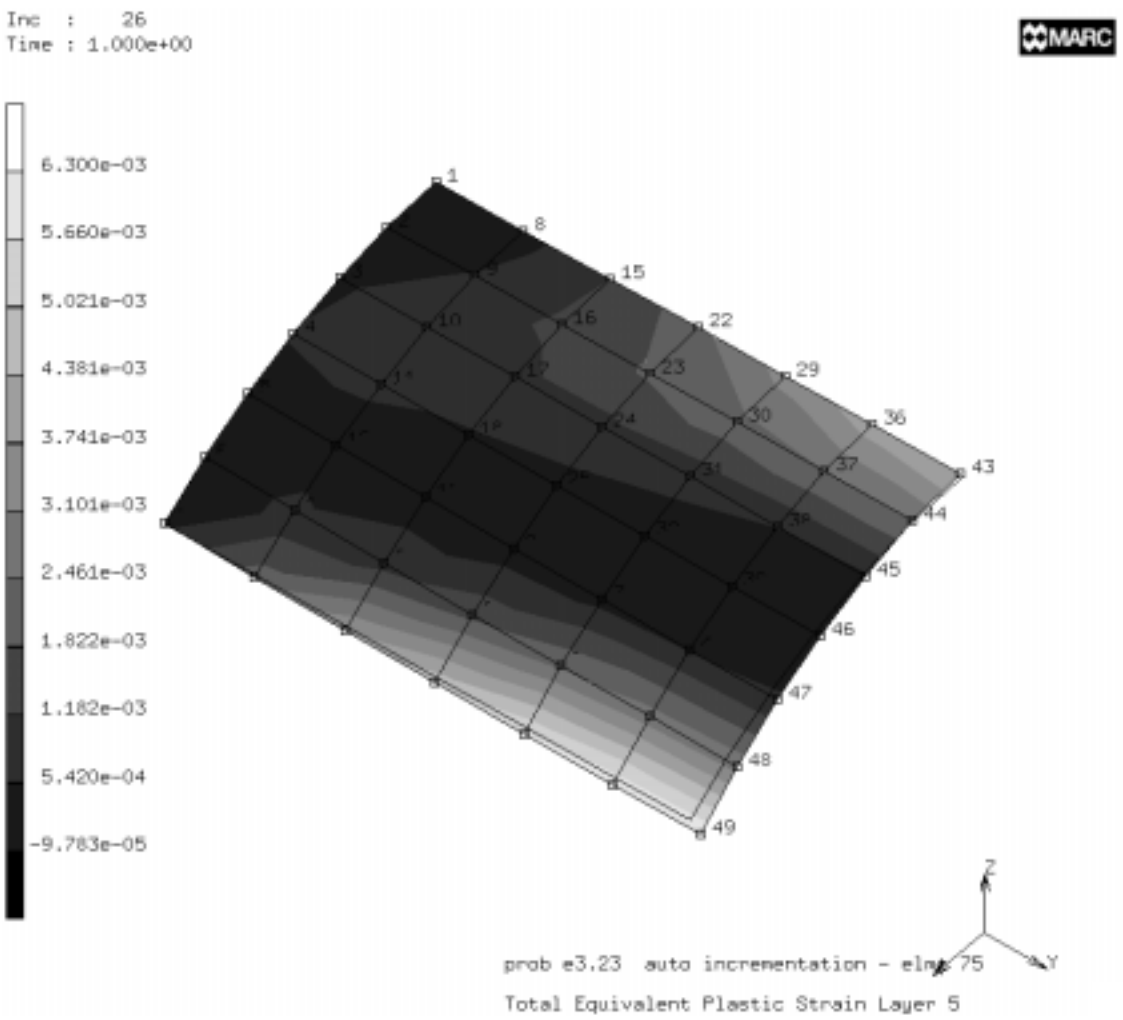

Figure 3.23-4 Equivalent Plastic Strain, Layer 5

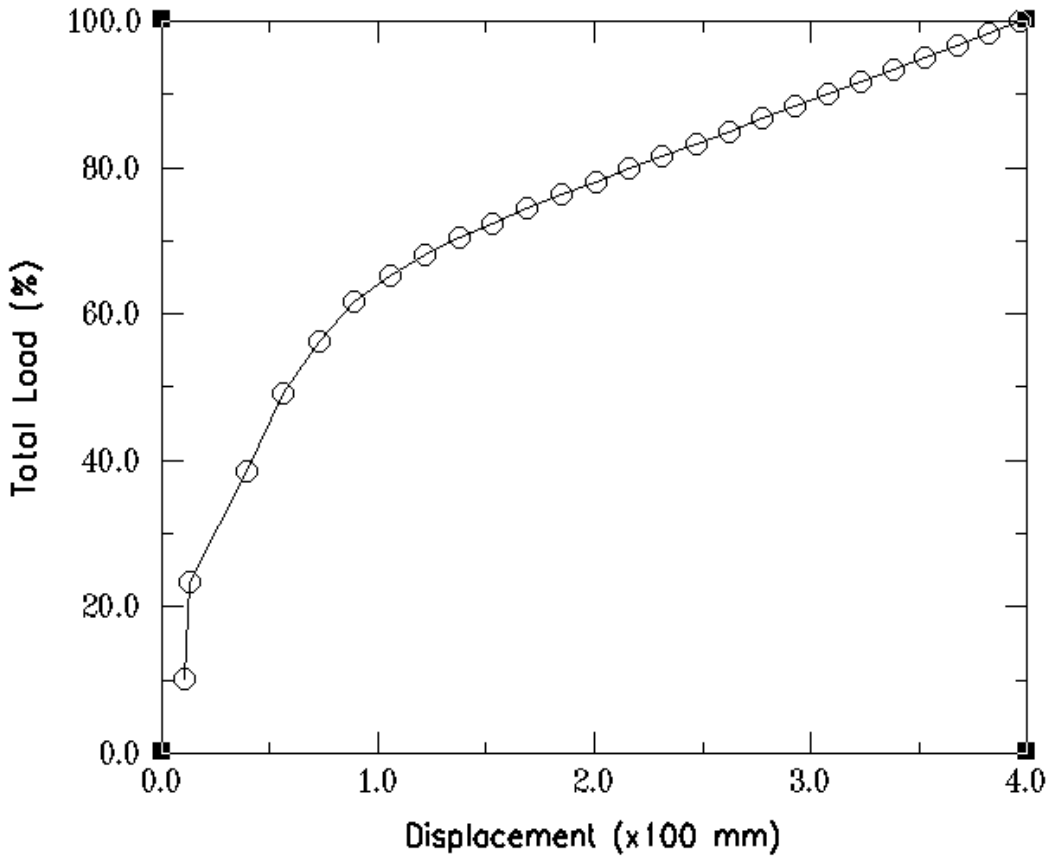

Figure 3.23-5 Load Displacement Curve

3.24 Creep Analysis of a Plate with a Hole using AUTO-THERM-CREEP Option

This problem demonstrates the use of AUTO-THERM-CREEP option for the creep analysis of a plate with a hole, subjected to transient thermal loading. The analysis consists of two parts: a transient heat conduction analysis and a creep analysis.

TRANSIENT HEAT CONDUCTION ANALYSIS

A two-dimensional transient heat conduction problem of a plate with a circular hole is analyzed by using MARC element type 41 (8-node planar elements). Fluid at temperature 1000°F fills the circular hole. The exterior edges of the plate are held at constant temperature (500°F).

Model

Due to symmetry, only a quarter of the plate (see Figure 3.24-1) is modeled for the analysis. See *MARC Volume B: Element Library* for detailed element descriptions.

Material Properties

The conductivity is 0.42117×10^5 Btu/sec-in.-°F. The specific heat is 0.3523×10^3 Btu/lb-°F, and the mass density is 0.7254×10^3 lb/cubic inch.

Geometry

The thickness of the plate is 0.1 inch.

Initial Condition

The initial nodal temperatures are homogeneous at 500°F.

Boundary Conditions

No input data is required at insulated boundary conditions located at lines of symmetry (x = 0 and y = 0). Constant temperatures of 500°F are specified at lines x = 10, and y = 12. Convective boundary conditions are assumed to exist at the inner surface of the circular hole. The fluid temperature is 1000°F, and the film coefficient is 0.46875×10^5 Btu/sec-sq.in.-°F.

Transient

The total transient time in the analysis is assumed to be 5.0 seconds and a constant time step of 0.5 seconds is chosen for the problem. Nonautomatic time stepping option is also invoked; hence, 10 increments will be performed.

Post File

A formatted post file (unit 19) is generated during the transient heat transfer analysis. Element temperatures stored on the post file are to be used for creep analysis. The code number for element temperatures is 9.

CREEP ANALYSIS

Model

The mesh used for creep analysis is the same as that in the heat conduction analysis with the exception that the element type in the mesh is 26 (8-node plane stress element). Due to symmetry, only a quarter of the plate is modeled.

Material Properties

The material is assumed to be linear elastic with a Young's modulus of 30 x 10^6psi; Poisson's ratio of 0.3; and a coefficient of thermal expansion of 1.0 x 10^{-5} in/in/°F.

Geometry

The thickness of the plate is 0.1 inch.

Initial State (Stress-Free Temperature)

The stress-free temperature is assumed to be 500°F for all elements.

Fixed Disp

Zero displacement boundary conditions are prescribed at lines x = 0 and y = 0, for the simulation of symmetry conditions.

d.o.f. 1 = u = 0 at (x = 0)	Nodes 22, 26, 28, 32, 34
d.o.f. 2 = v = 0 at (y = 0)	Nodes 5, 8, 13, 16, 21

Creep

The user subroutine CRPLAW is used for the input of a creep law of the following form:

$$\dot{\varepsilon}_c = 1.075^{-26}\sigma^{5.0}$$

AUTO-THERM-CREEP

The creep analysis is carried out using the AUTO-THERM-CREEP load incrementation option. A detailed discussion of this option can be found in *MARC Volume C: User Input*, "Chapter 5". Input data for this option associated with the current problem is as follows: a temperature change tolerance of 100°F is set for the creation of temperature steps (increments) by the program; the

total transient time in thermal analysis is equal to 5.0; the suggested time increment for creep analysis is 0.1; and the total creep time (time for the termination of this analysis) is 0.6. The total creep time cannot be greater than the total transient time in thermal analysis.

The data in the CHANGE STATE option indicates that the temperatures are stored in a formatted post file and there are four sets of temperatures on the file.

Results

Effective (von Mises) stresses at the centroid (integration point 5) of element 4 are tabulated in Table 3.24-1 and plotted in Figure 3.24-3. The stress increases due to thermal load at each increment, and the stress redistributions due to creep at subincrements, are clearly demonstrated.

Table 3.24-1 von Mises Stresses at Element 4

Inc.	Creep Time (seconds)	EL Temp (°F)	von Mises Stress (σ) (psi)
1	0.0	513.2	9.483×10^3
1.1	0.1	513.2	9.476×10^3
1.2	0.15876	513.2	9.471×10^3
2	0.15876	526.4	1.895×10^4
2.1	0.23536	526.4	1.877×10^4
2.2	0.31752	526.4	1.863×10^4
3	0.31752	539.7	2.811×10^4
3.1	0.33858	539.7	2.784×10^4
3.2	0.36490	539.7	2.759×10^4
3.3	0.39780	539.7	2.735×10^4
3.4	0.43893	539.7	2.711×10^4
3.5	0.47628	539.7	2.692×10^4
4	0.47628	565.2	3.468×10^4
4.1	0.52142	565.2	3.476×10^4
4.2	0.56655	565.2	3.455×10^4
4.3	0.6	565.2	3.433×10^4
5	0.6	565.2	3.433×10^4

Parameters, Options, and Subroutines Summary

Example e3x24a.dat:

Parameters	Model Definition Options	Options
COMMENT	CONNECTIVITY	CONTINUE
ELEMENTS	CONTROL	TRANSIENT
END	COORDINATES	
HEAT	END OPTION	
SIZING	FILMS	
TITLE	FIXED TEMPERATURE	
	GEOMETRY	
	INITIAL TEMPERATURE	
	ISOTROPIC	
	POST	
	PRINT CHOICE	

Example e3x24b.dat:

Parameters	Model Definition Options	History Definition Options
COMMENT	CONNECTIVITY	AUTO THERM
CREEP	CONTROL	CHANGE STATE
ELEMENTS	COORDINATES	CONTINUE
END	CREEP	
SIZING	END OPTION	
TITLE	FIXED DISP	
	GEOMETRY	
	INITIAL STATE	
	ISOTROPIC	
	PRINT CHOICE	

Example e3x24c.dat:

Parameters	Model Definition Options	History Definition Options
COMMENT	CONNECTIVITY	AUTO THERM
CREEP	CONTROL	CHANGE STATE
ELEMENTS	COORDINATES	CONTINUE
END	CREEP	
SIZING	END OPTION	
TITLE	FIXED DISP	
	GEOMETRY	
	INITIAL STATE	
	ISOTROPIC	
	PRINT CHOICE	

User subroutine in u3x24.f:

CRPLAW

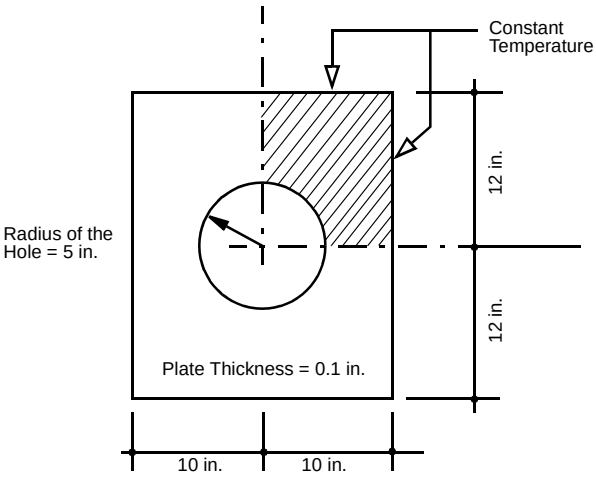

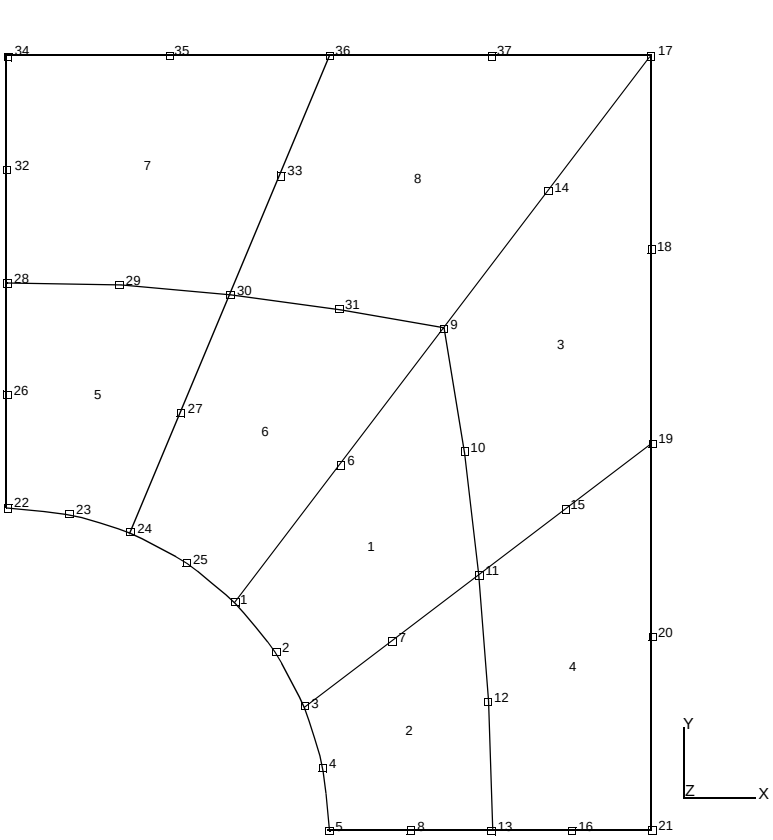

Figure 3.24-1 Plate with a Hole

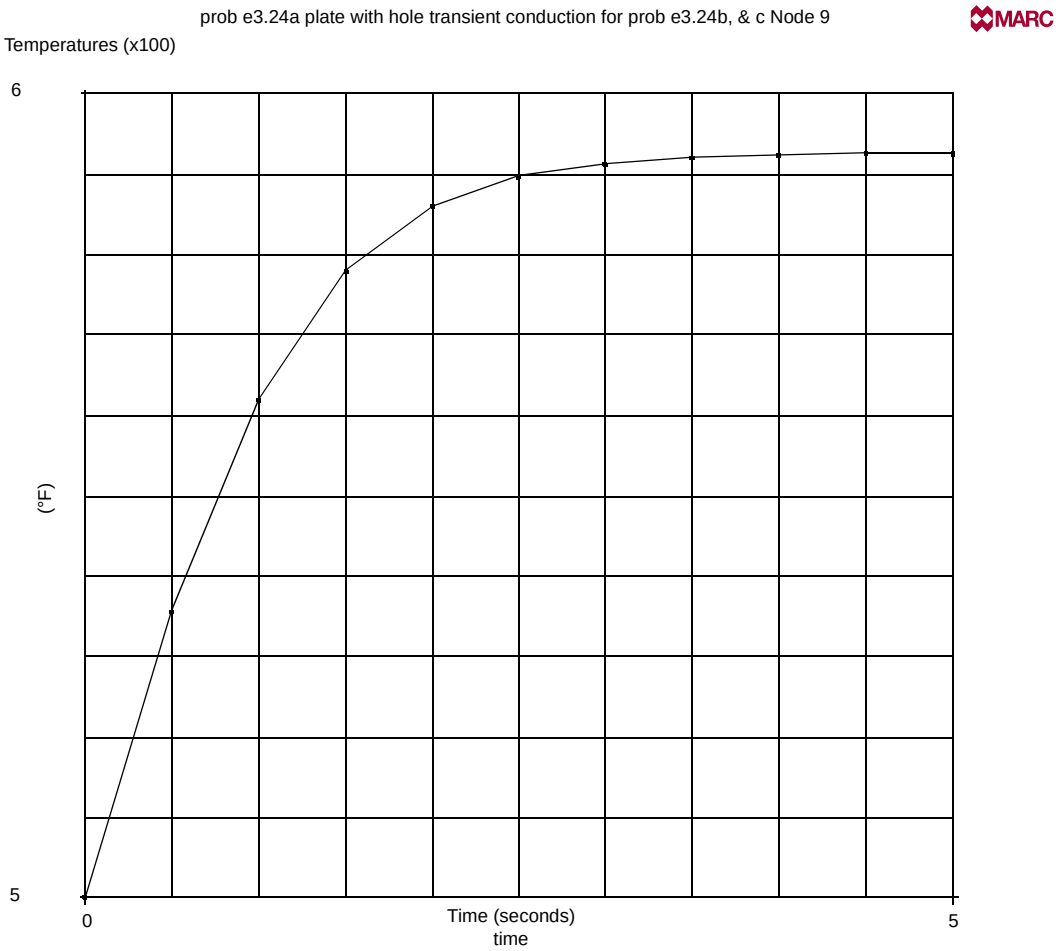

Figure 3.24-2 Nodal Temperature vs. Time (Node 9)

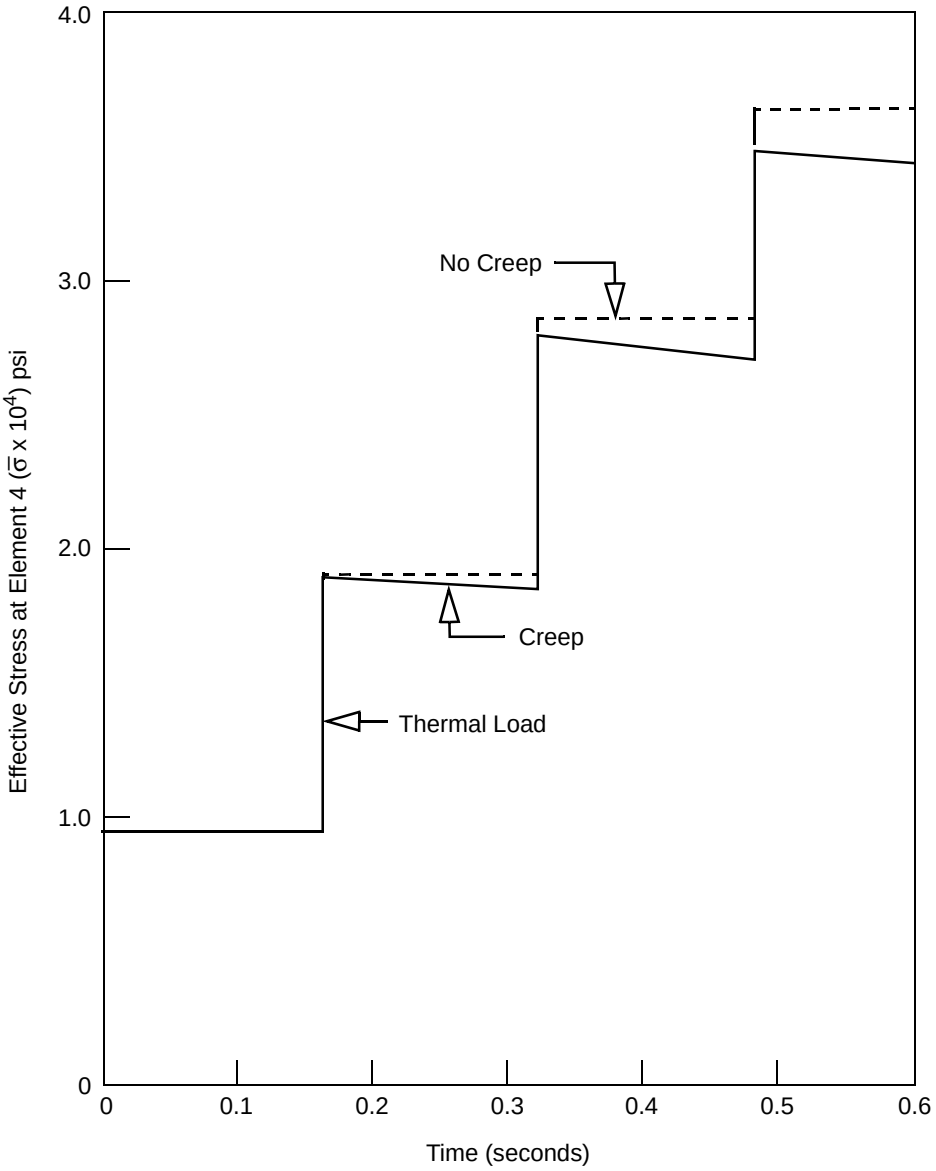

Figure 3.24-3 Effective Stresses at Element 4

3.25 Pressing of a Powder Material

This example illustrates the use of element type 11 and options LARGE DISP, UPDATE, and FOLLOW FORCE for the homogeneous compaction of a rectangular preform. A cyclic pressure is applied to one side of the preform.

Element

Element 11 is a 4-node plane strain element with two degrees of freedom per node used to model the powder. Fifty elements are used in this model. The initial dimensions are 10 by 5 mm as shown in Figure 3.25-1.

Loading

The pressure is first ramped up to 5500 MPa in a period of 2200 seconds. The load is then reduced to 100 MPa in 2160 seconds. The load is then increased to 7600 MPa in 300 seconds and finally reduced back to 100 MPa in 3000 seconds. The load is applied in the x-direction of the elements on the right side.

Material Properties

The powder material is represented by a modified Shima model. The Young's modulus and Poisson ratio are bilinear functions of the relative density and temperature. Because this is an uncoupled analysis, the temperature effects are not included here. See problem 3.26 for an example of a coupled analysis. E_o and ν_o are the initial Young's modulus and Poisson ratio equal to 20,000 MPa and 0.3, respectively.

The relative density effects on the elastic properties are given through the RELATIVE DENSITY option. They are entered as multiplicative factors to the values given on the POWDER option or the TEMPERATURE EFFECTS option if applicable. In this problem, the data obtained from an experiment indicates that:

ρ	**E (MPa)**	ν	**E/E_o**	ν/ν_o
0.7	20,000	0.3	1.0	1.0
1.0	30,000	0.33	1.5	1.1

The initial yield stress is 6000 MPa and the viscosity is 50,000 seconds. The values of γ and β, which are used to define the yield surface, have initial values of 0.1406174 and 1.375. These material data are functions of the relative density. This is expressed as:

$$\gamma = (1. + \bar{\rho})^{5.5} \text{ and}$$

$$\beta = 6.25\ (1 - \bar{\rho})^{-0.5}$$

Therefore, b_1, b_2, b_3, b_4 are entered as 1.0, 1.0, 1.0, 5.5 and q_1, q_2, q_3, q_4 are entered as 6.25, -6.25, 1.0, -0.5, respectively. The initial relative density is 0.7.

Boundary Conditions

The left end of the preform is prescribed to have no displacement in the x-direction. Node 23 is fixed in the y-direction to eliminate the rigid body mode.

Control

A control tolerance of 0.01 on residuals is requested. Because this problem involves homogeneous loading, almost no iterations are required.

Results

The results show that the billet is compressed from an initial length of 10 to a final height of 7.523 and a width of 5.731. Figure 3.25-2 shows the externally applied force history on node 33. Note that it is not exactly linear because of the follower force effects. Figure 3.25-3 shows the history of the relative density. We see that the peak density is the value of 0.92 and the final relative density is 0.81. Figure 3.25-4 shows the history of the inelastic strain rate. One observes that there are periods in the load cycle when no inelastic behavior occurs. Finally, Figure 3.25-5 shows the equivalent plastic strain history.

We can check the results for consistency by examining the conservation of mass.

$$\rho_o A_o = \rho A$$
$$0.7 \times 10 \times 5 = .81 \times 7.523 \times 5.731$$
$$35 = 34.92$$

this check is within 0.2%.

Parameters, Options, and Subroutines Summary

Example e3x25.dat:

Parameters	Model Definition Options	History Definition Options
ELEMENTS	CONNECTIVITY	AUTO LOAD
END	CONTROL	CONTINUE
FOLLOW FOR	COORDINATES	DIST LOADS
LARGE DISP	DENSITY EFFECTS	TIME STEP
SIZING	DIST LOADS	
TITLE	END OPTION	
UPDATE	POST	
	POWDER	
	RELATIVE DENSITY	

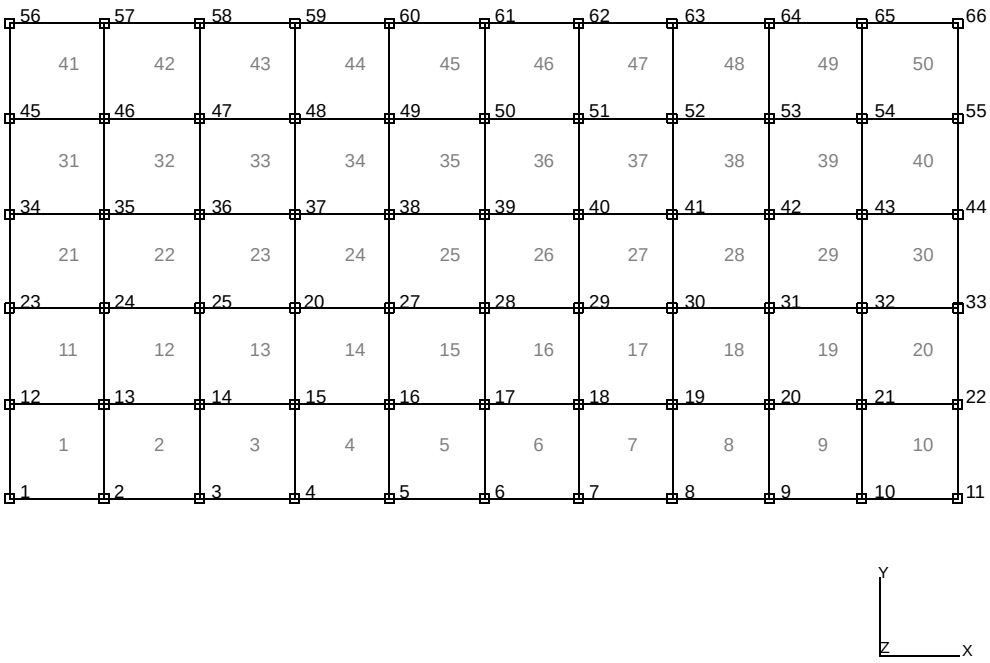

Figure 3.25-1 Finite Element Mesh

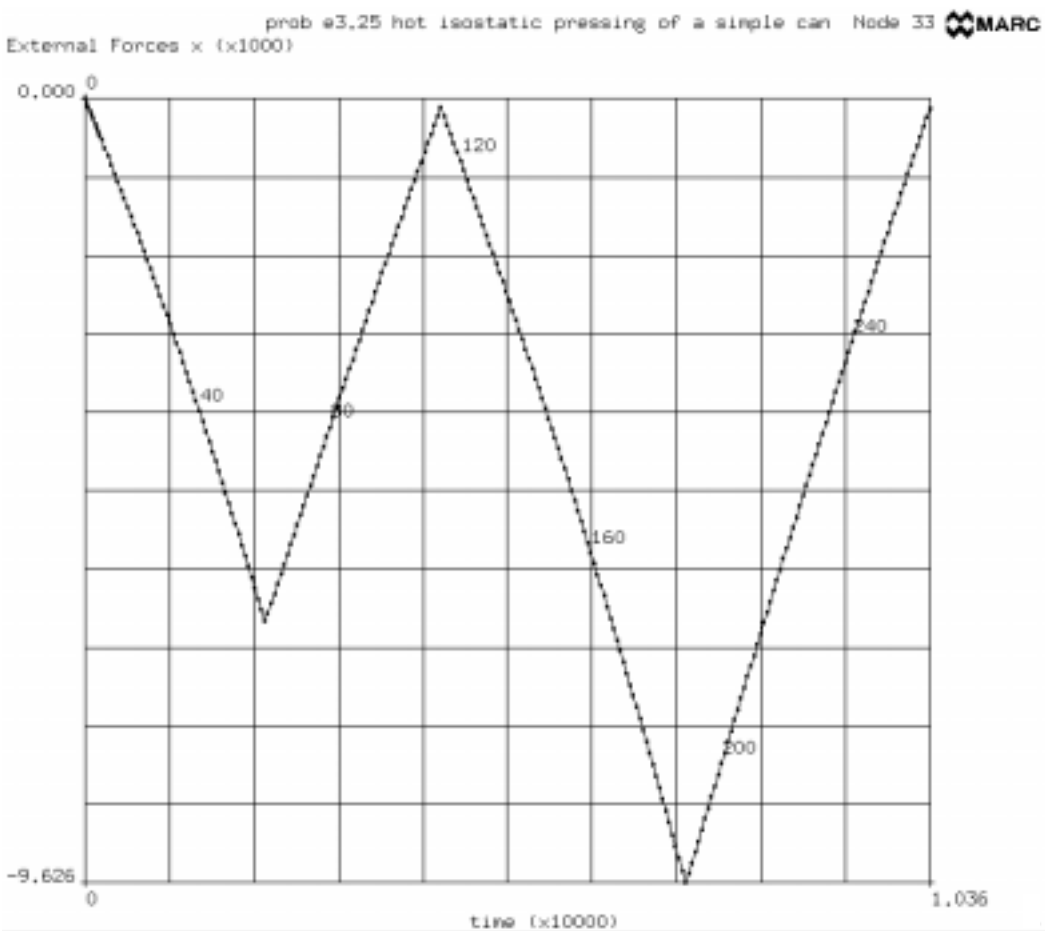

Figure 3.25-2 Time History of Externally Applied Load

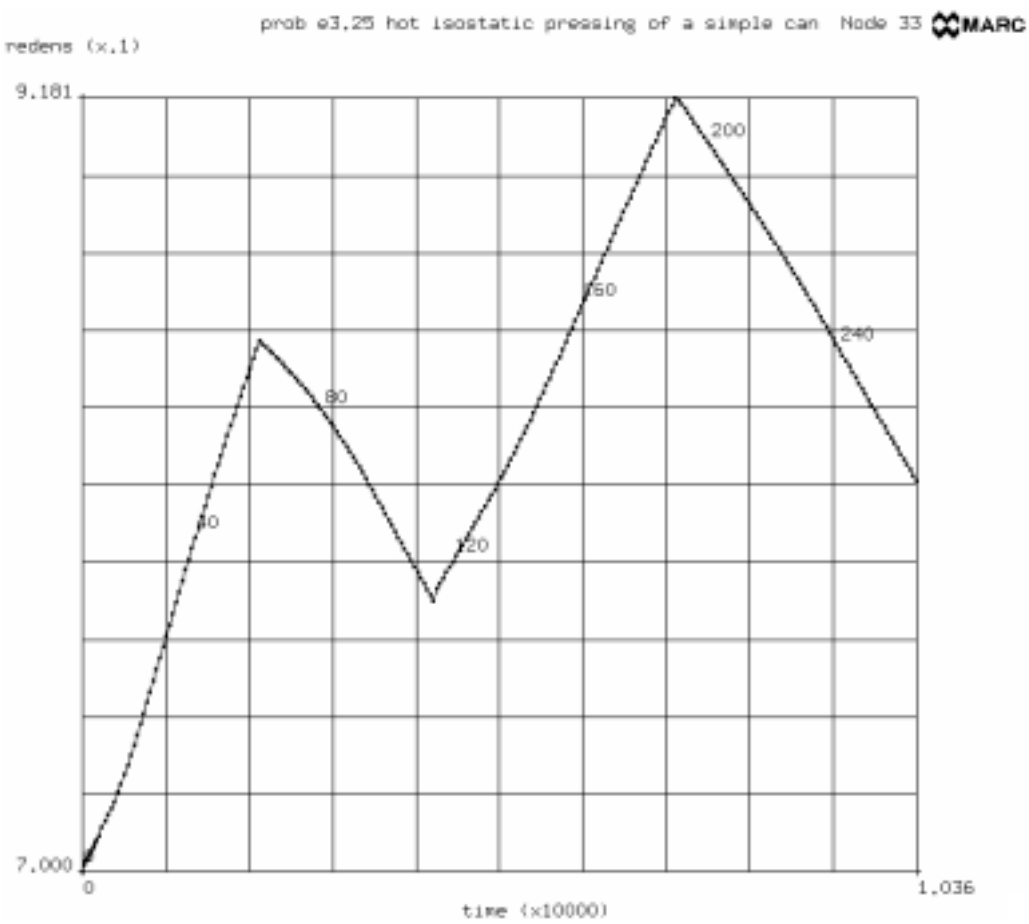

Figure 3.25-3 Time History of Relative Density

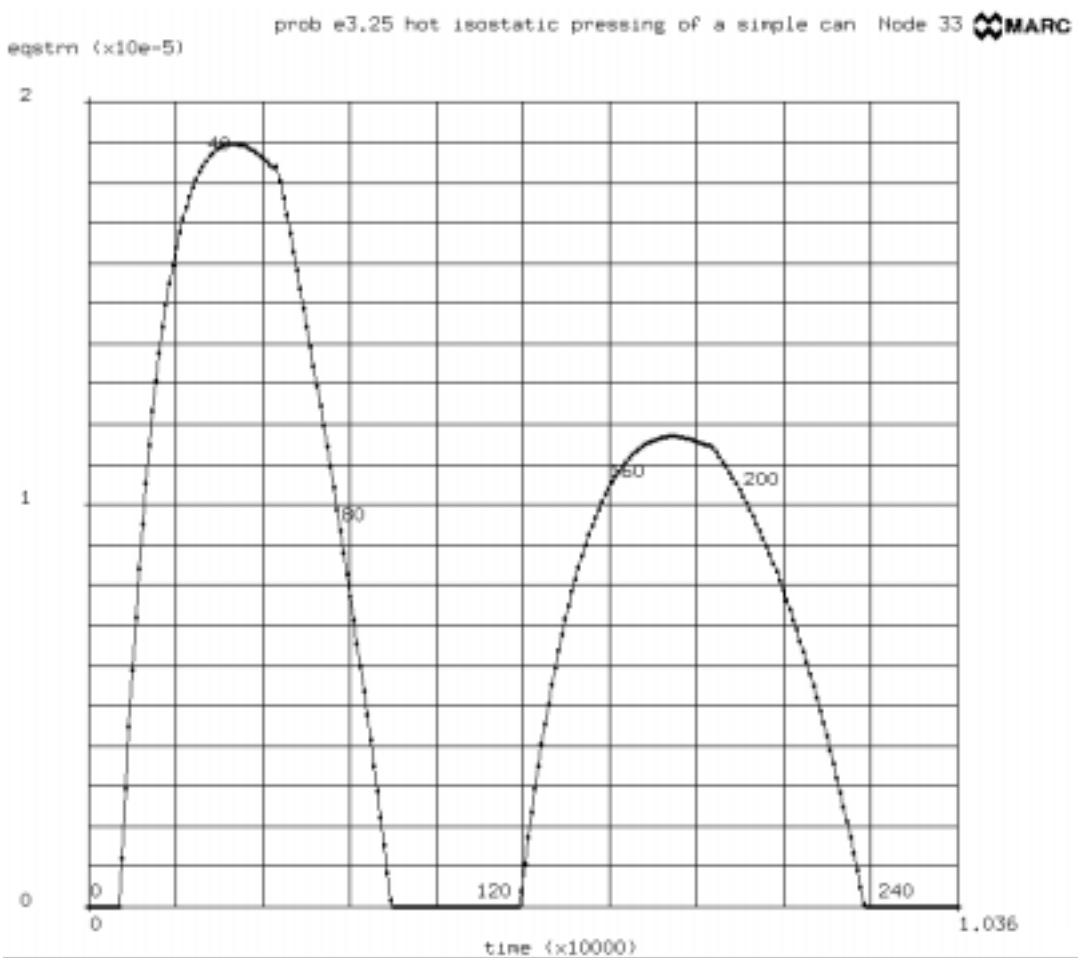

Figure 3.25-4 Time History of Strain Rate

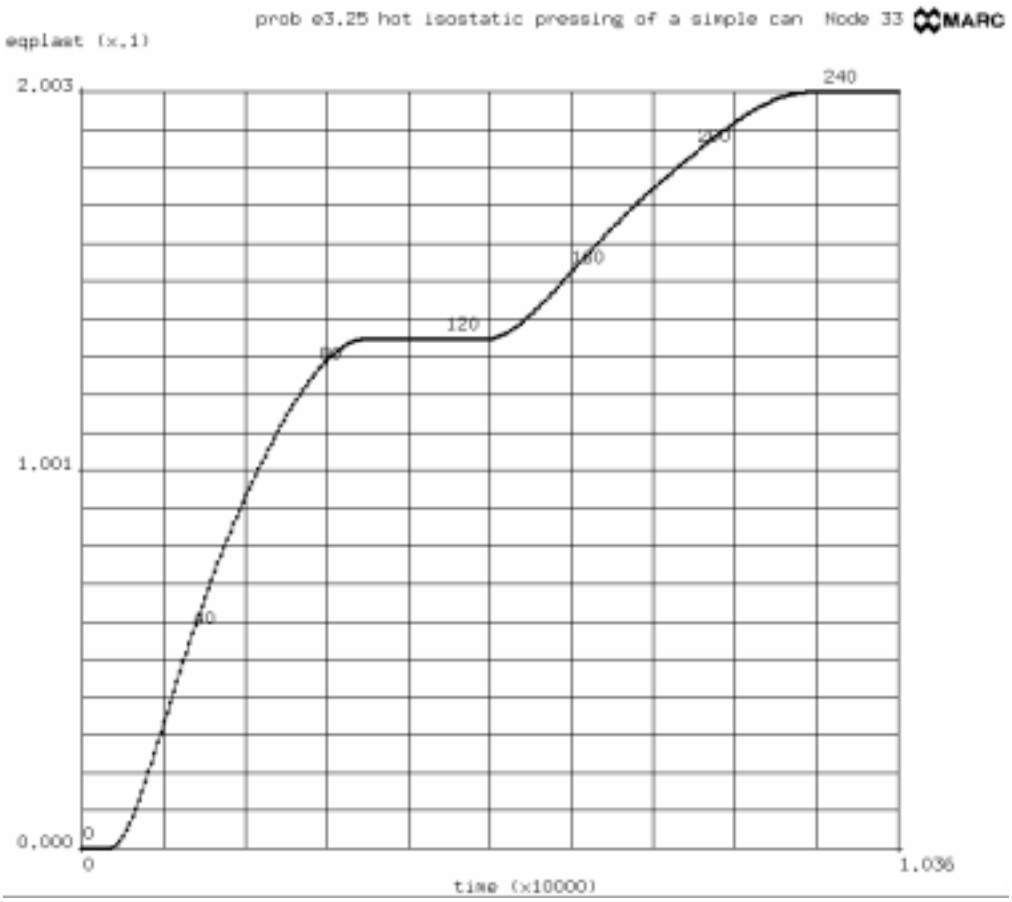

Figure 3.25-5 Time History of Equivalent Plastic Strain

3.26 Hot Isostatic Pressing of a Powder Material

This example illustrates the use of element 28 in a thermal mechanically coupled hot isostatic pressing problem. A powder material is placed into a stiffer cylindrical can which is then subjected to a pressure and thermal cycle.

Element

Element type 28 is an 8-node axisymmetric element used to model the powder and the can. Seventy elements are used to model the powder and 26 to represent the can. In a coupled analysis, element type 42 is the corresponding heat transfer element. The initial dimensions of the powder are 97 mm x 47.0 mm. The can thickness is 3 mm as shown in Figure 3.26-1.

Loading

The loading history is shown in Figure 3.26-3. The external pressure is ramped to 1500 MPa in 9000 seconds; it is then held constant for 10,800 seconds and then reduced to zero in 7200 seconds. The exterior temperature on the can is raised from 0° to 1440°C in the first 9000 seconds and also reduced to zero in 7200 seconds. The FORCDT option is used to prescribe the nodal temperatures. The DIST LOADS option is used to define the external pressure. Note that the FOLLOW FORCE option is used to prescribe the load on the deformed configuration.

Material Properties

As this is a coupled analysis, both mechanical and thermal properties must be prescribed. Furthermore, the material behavior is both temperature and relative density dependent. The powder is represented using the modified Shima model. The Young' modulus and Poisson's ratio are bilinear functions of the relative density and the temperature. E_o and ν_o are the initial values 20,000 MPa and 0.3, respectively. The initial yield stress is 1000 MPa.

The experimental data is:

T°(C)	ρ	E (MPa)	ν	σ	E/E_o	ν/ν_o
0.0	0.7	20,000	0.3	1000.0	1.0	1.0
2000.0	0.7	2,000	0.49	100.0	0.1	1.633
0.0	1.0	30,000	0.33	Shima	1.5	1.1

The temperature-dependent properties are entered via data field in the TEMPERATURE EFFECTS option. The relative density effects for Young's modulus and Poisson's ratio are given as multiplicative factors relative to this data via the REALTIVE DENSITY option.

The values of γ and β, which are used to define the yield surfaces dependence on relative density, have initial values of 0.1406174 and 1.375. These material data are functions of the relative density:

$\gamma = (1. + \bar{\rho})^{5.5}$ and
$\beta = 6.25\ (1 - \bar{\rho})^{-0.5}$

Therefore, q_1, q_2, q_3, q_4 are entered as 1.0, 1.0, 1.0, 5.5 and b_1, b_2, b_3, b_4 are entered as 6.25, -6.25, 1.0, -0.5, respectively. The initial relative density is 0.7.

The viscosity is also a function of the temperature with a value of 50,000 at 0°C and 25,000 at 200°C.

The coefficient of thermal expansion is -1×10^{-7} mm/mm°C. The mass density is 4×10^{-6} kg/mm^3.

The thermal conductivity and the specific heat are also bilinear functions of the temperature and relative density.

The experimental data is:

T°C	ρ	KW/m°C	KJ/Kg°C	K/K_o	C/Co
0	0.7	0.03	30.0	1.0	1.0
2000	0.7	0.04	50.0	1.333	1.666
0	1.0	0.042	45.0	1.4	0.9

The temperature dependent properties are entered via the data fields in the TEMPERATURE EFFECTS option. The relative density effects for the conductivity and specific head are defined as multiplicative factors relative to this data via the RELATIVE DENSITY option.

The can is represented as an elastic-plastic material. The properties are a function of temperature only:

T°C	E (MPa)	ν	$\sigma_{y\ (MPa)}$	K	C
0	200,000	0.3	1000	0.03	30
2000	100,000	0.4	500	0.04	50

The coefficient of thermal expansion is 1.0×10^{-6} m/m°C and the mass density is 8.0×10^{-6}. This data is defined in the ISOTROPIC and TEMPERATURE EFFECTS option. The initial relative density of 0.7 is entered through the RELATIVE DENSITY option.

Control

In this problem, the convergence requirement is 10% on relative displacements with a maximum number of 20 iterations. Typically, increments required one to three iterations. The TRANSIENT NON AUTO option was used to provide fixed time steps per increment. As the exterior temperature is completely prescribed, it is not likely that large changes in temperature will occur. The third line on the CONTROL option specifies a maximum allowable temperature difference of 1000 (not used anyway because of fixed time procedure) and an error in temperature of 0.1. This will result in an accurate temperature analysis.

The RESTART option controls the restart to be written every 10 increments. The POST option insures that all the strains, stresses, equivalent plastic strain, strain rate and the relative density may be postprocessed. The post file is written every 10 increments.

Results

The relative density at the end of the analysis is shown in Figure 3.26-3 on the deformed mesh. One can observe that the material has densified to a value of 0.98 in most of the region. The area near the corners shows a reduced level of densification. The time history of relative density, inelastic strain rate, and equivalent plastic strain are shown in Figure 3.26-4, Figure 3.26-5, and Figure 3.26-6, respectively.

Parameters, Options, and Subroutines Summary

Example e3x26.dat:

Parameters	Model Definition Options	History Definition Options
COUPLE	CONNECTIVITY	CONTINUE
ELEMENTS	CONTROL	DIST LOADS
END	COORDINATES	TRANSIENT
LARGE DISP	DEFINE	
SIZING	DENSITY EFFECTS	
TITLE	DIST LOADS	
UPDATE	END OPTION	
	FIXED DISP	
	FIXED TEMPERATURE	
	FORCDT	
	ISOTROPIC	
	POST	
	POWDER	
	RELATIVE DENSITY	
	RESTART	
	TEMPERATURE EFFECTS	
	WORK HARD	

User subroutine in u3x26.f:

FORCDT

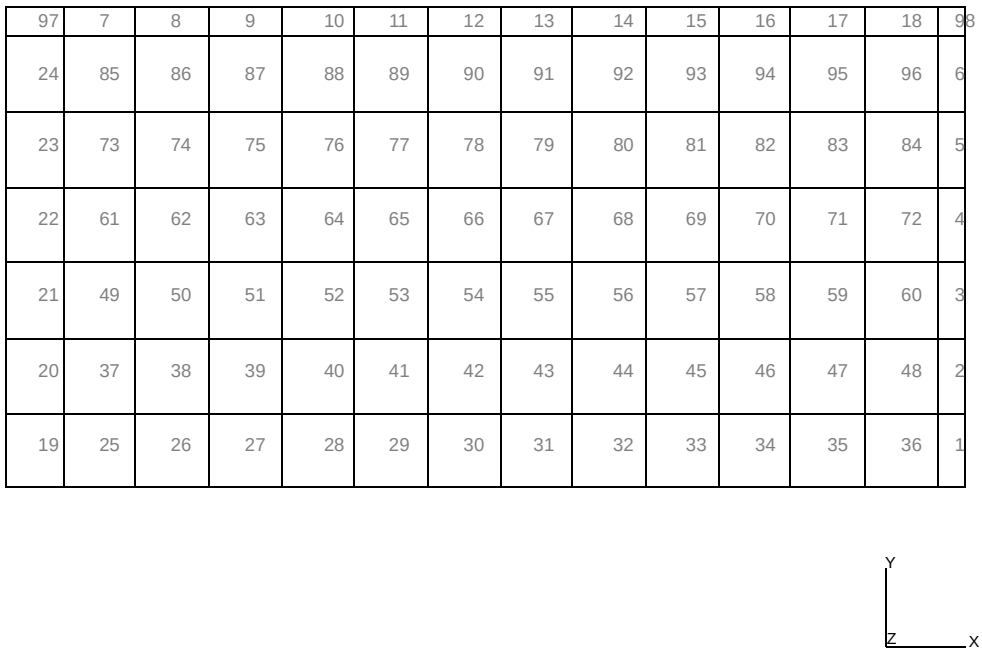

Figure 3.26-1 Mesh

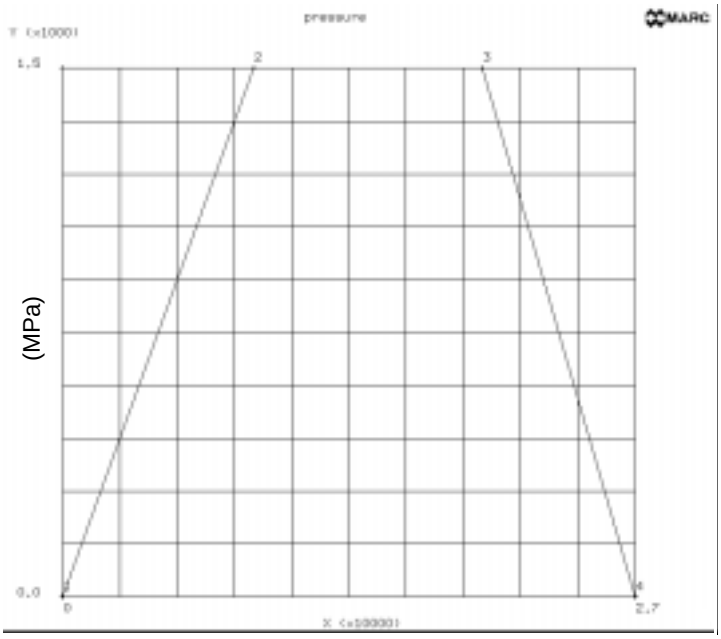

Externally Applied Pressure

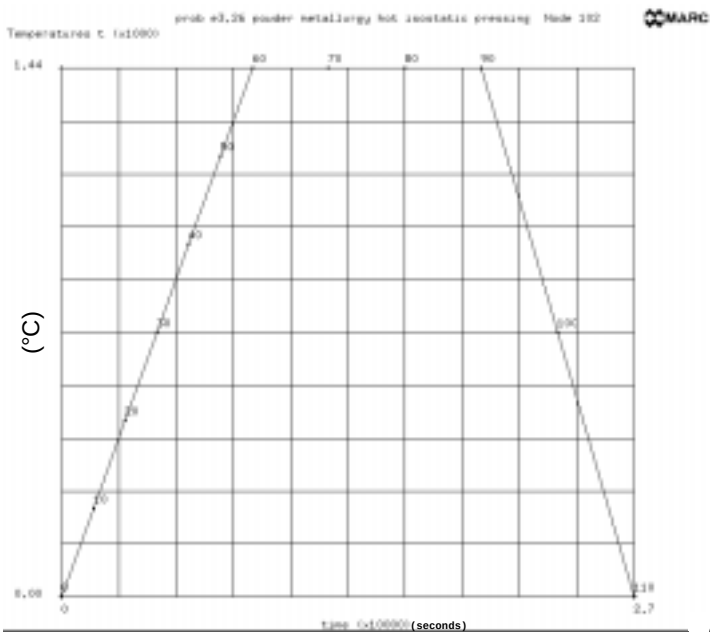

Externally Applied Temperature

Figure 3.26-2 Time History

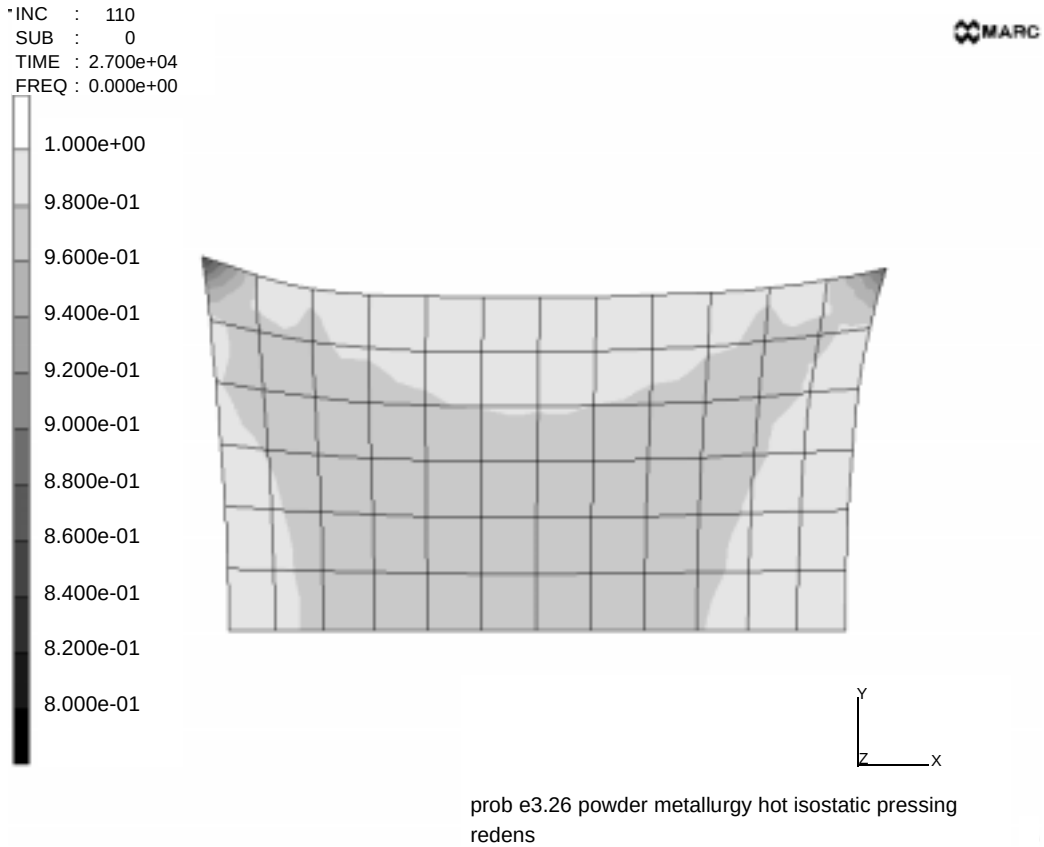

Figure 3.26-3 Final Relative Density

Figure 3.26-4 Time History of Relative Density

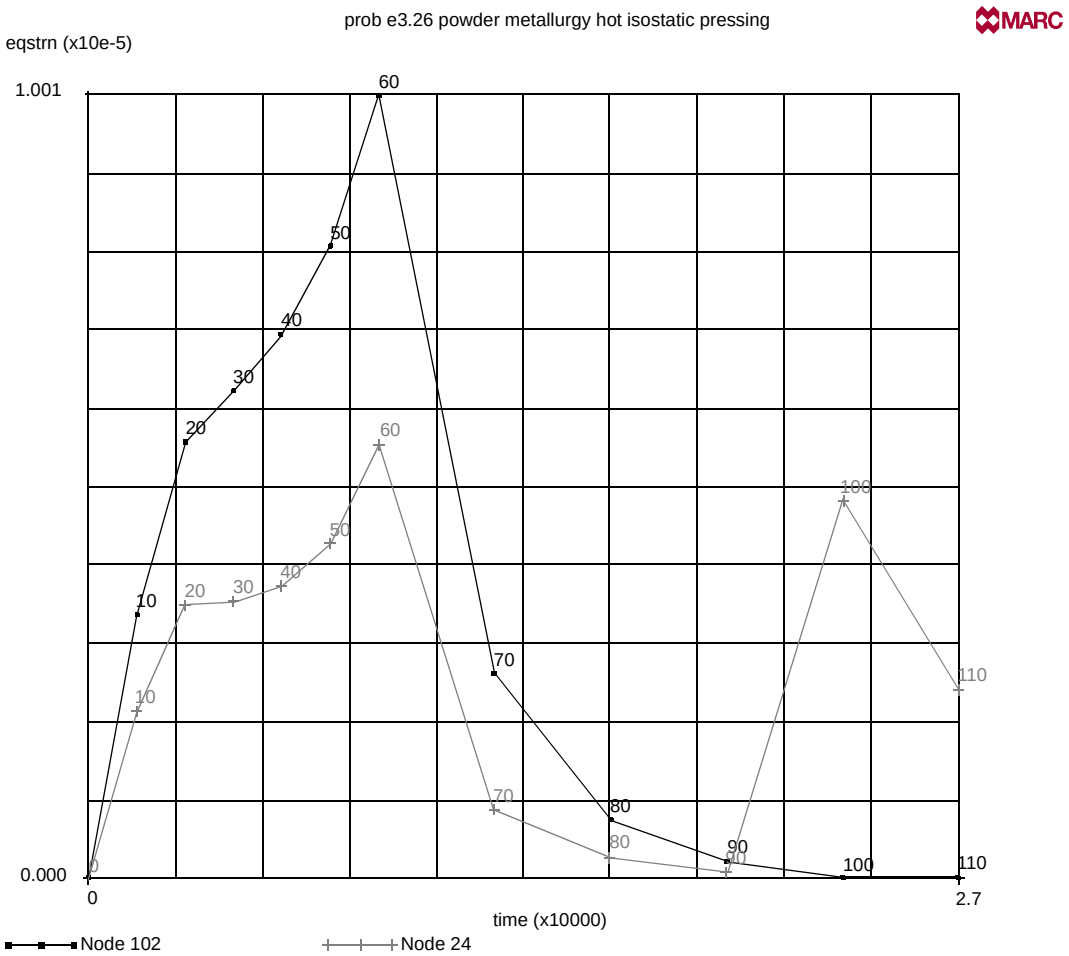

Figure 3.26-5 Time History of Equivalent Strain Rate

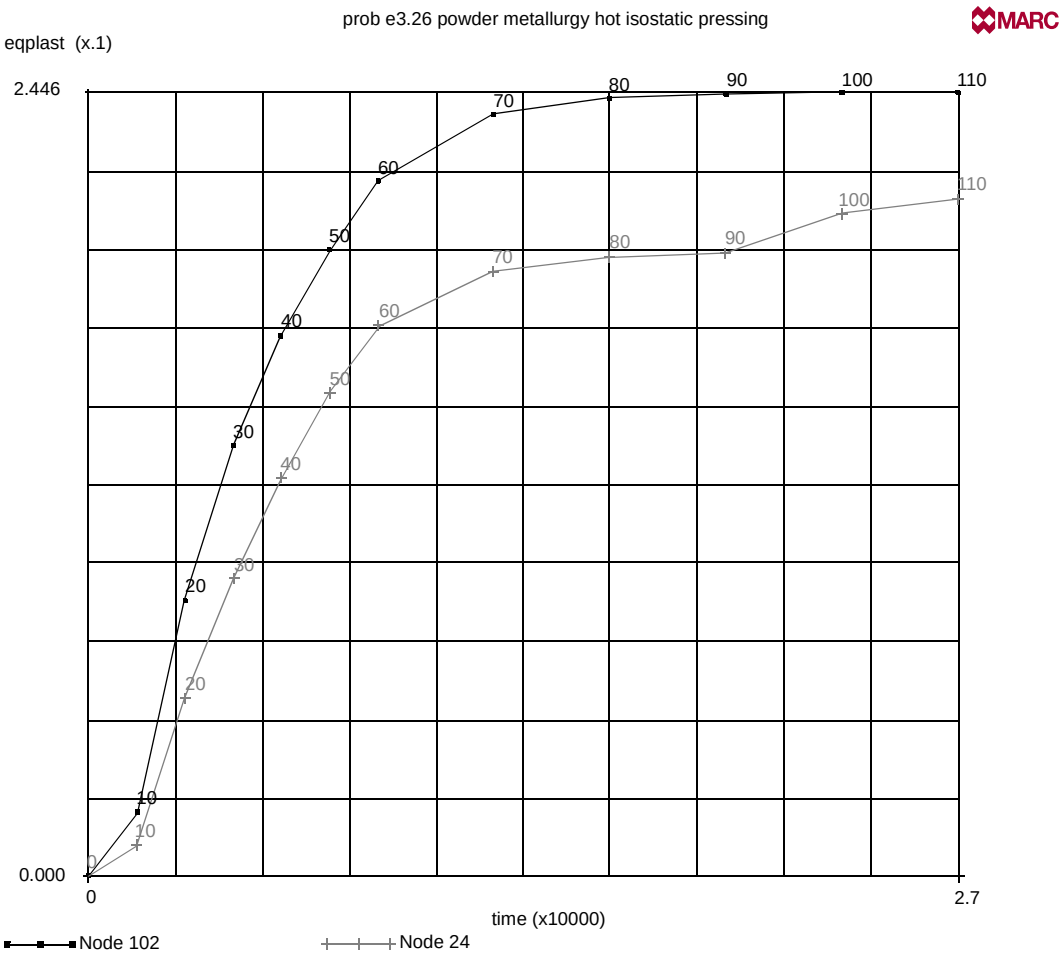

Figure 3.26-6 Time History of Equivalent Plastic Strain

3.27 Shear Band Development

This example illustrates the formation of shear bands in a strip being pulled. The Gurson damage model is used to predict void growth in the material.

Element

Element type 54, a plane strain reduced integration element, is used to model the strip. The strip, as shown in Figure 3.27-1, has dimensions of L = 10 and h = 68 with a slight imperfection at the free end y = h. $\Delta y = 0.0025\cos\left(\frac{\pi x}{L}\right)$. User subroutine UFXORD is used to define this imperfection.

The mesh consists of 8 x 32 eight noded elements.

Boundary Conditions

The boundary conditions are x = 0, v = 0, x = L, v is prescribed, y = 0, v = 0, and y = h is free. The maximum displacement is at increment 280 = 5.6 or log strain of .4447.

Material Properties

The material is an elastic plastic workhardening material with Young's modulus = 30,000 MPa, Poisson's ratio = 0.3 and initial yield of 100 MPa. The workhardening slope is shown in Figure 3.27-2. The Gurson damage model is used to invoke the plastic-strain controlled nucleation model. The parameters used are:

First yield surface multiplier, q_1	=	1.5
Second yield surface multiplier, q_2	=	1.0
Initial void fraction	=	0.0
Critical void fraction, f_c	=	0.15
Failure void fraction, f_f	=	0.25
Mean strain for nucleation	=	0.3
Standard deviation	=	0.1
Volume fraction of void nucleating particles	=	0.04

Control

The convergence ratio required is 2.5%. Because this is a highly nonlinear problem, the maximum number of iterations permitted is 20. The post file is written every 10 increments. The restart file is written every 40 increments.

Results

The deformed meshes at increments 120, 160, and 200 are shown in Figure 3.27-3 through Figure 3.27-5. One can clearly see the formation of the shear bands. The void volume fraction is then shown for the same increments. Again, the largest number of voids occurs where the shear bands form. Figure 3.27-10 shows the time history of the formation of voids for 3 points. One can see that for node 507, which is not in the shear band, the void volume matches that of nodes 607 and 745 until the shear band forms. At this point, “all” of the strain is localized and no additional void volume occurs. While for nodes 607 and 745, which are within the band, one sees an increase in the void volume with node 745 reaching close to the maximum-minus half the standard deviation. At this point, the equivalent plastic strain is 116%. The time history of the plastic strain is shown in Figure 3.27-11.

Parameters, Options, and Subroutines Summary

Example e3x27.dat:

Parameters	Model Definition Options	History Definition Options
ELEMENTS	CONNECTIVITY	AUTO LOAD
END	CONTROL	CONTINUE
FINITE	COORDINATES	DIST CHANGE
LARGE DISP	DAMAGE	
SIZING	DEFINE	
TITLE	END OPTION	
UPDATE	FIXED DISP	
	GEOMETRY	
	ISOTROPIC	
	NO PRINT	
	POST	
	RESTART	
	UFXORD	
	WORK HARD	

User subroutine in u3x27.f:

UFXORD

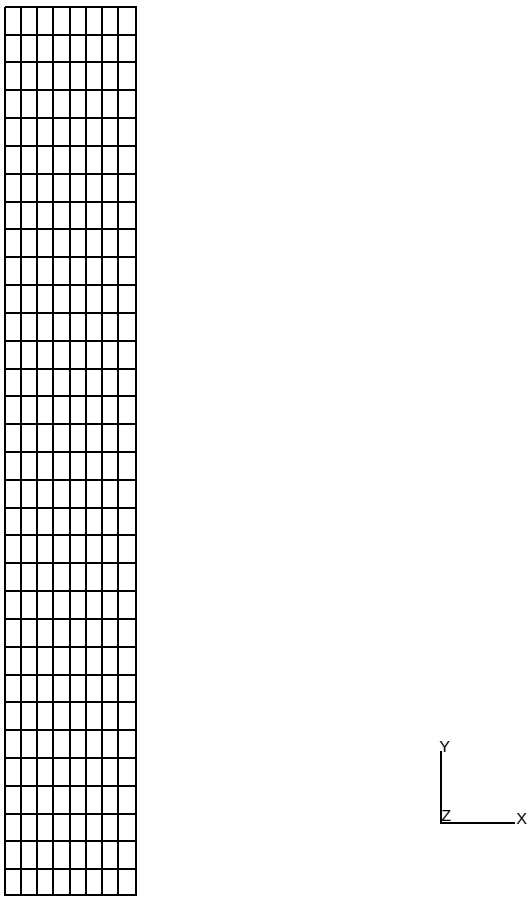

Figure 3.27-1 Finite Element Mesh

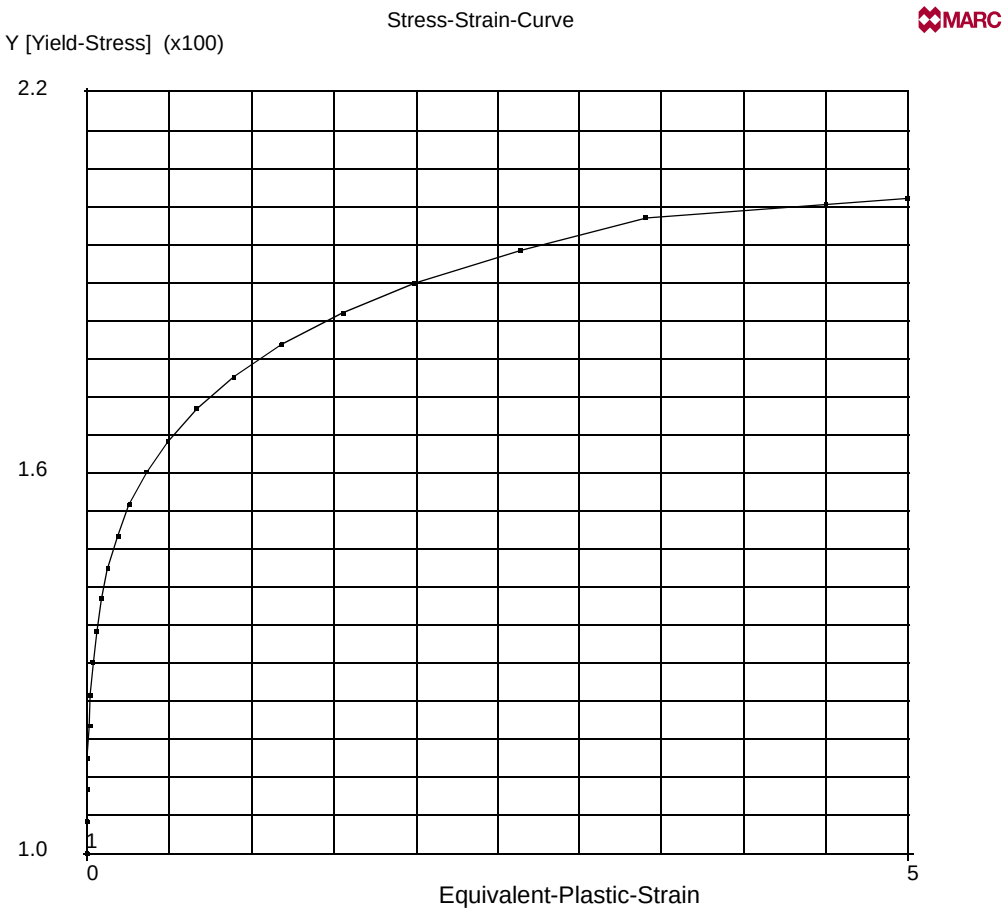

Figure 3.27-2 Stress-Strain Law

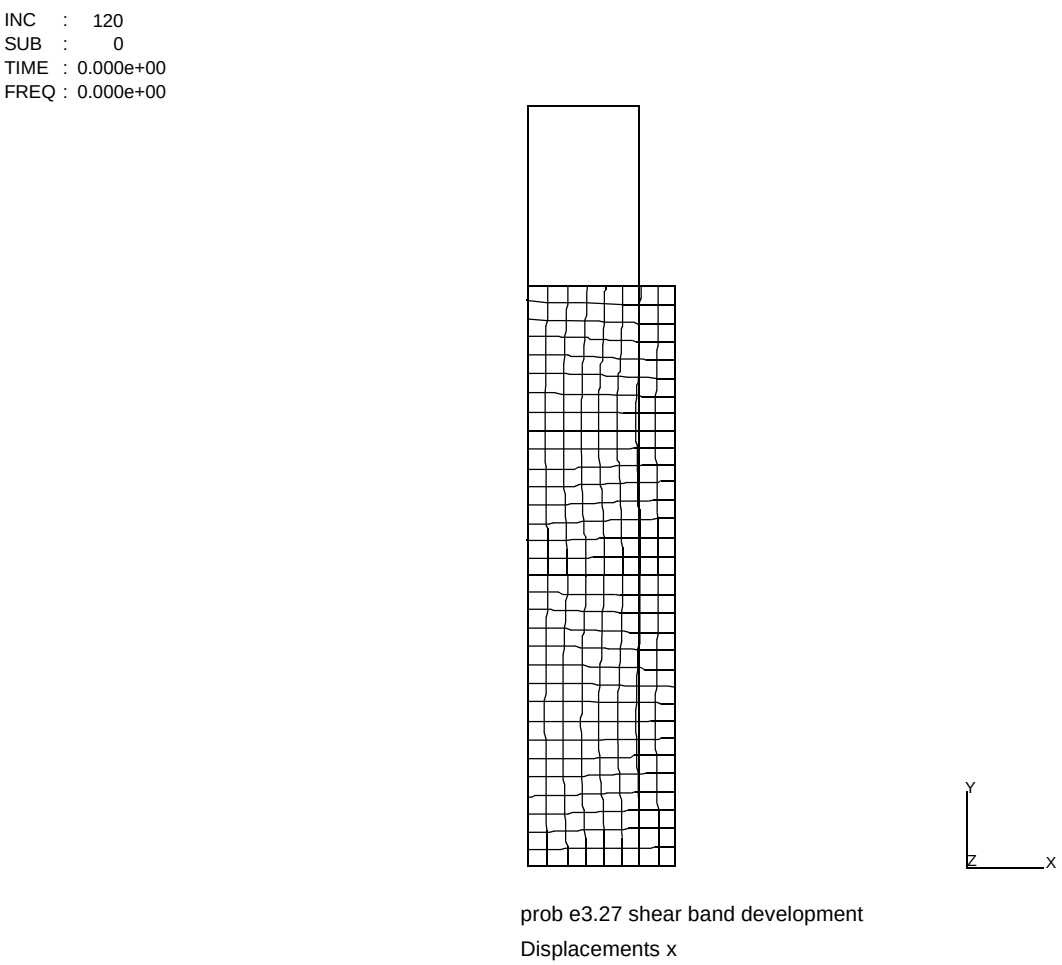

Figure 3.27-3 Deformed Mesh at Increment 120

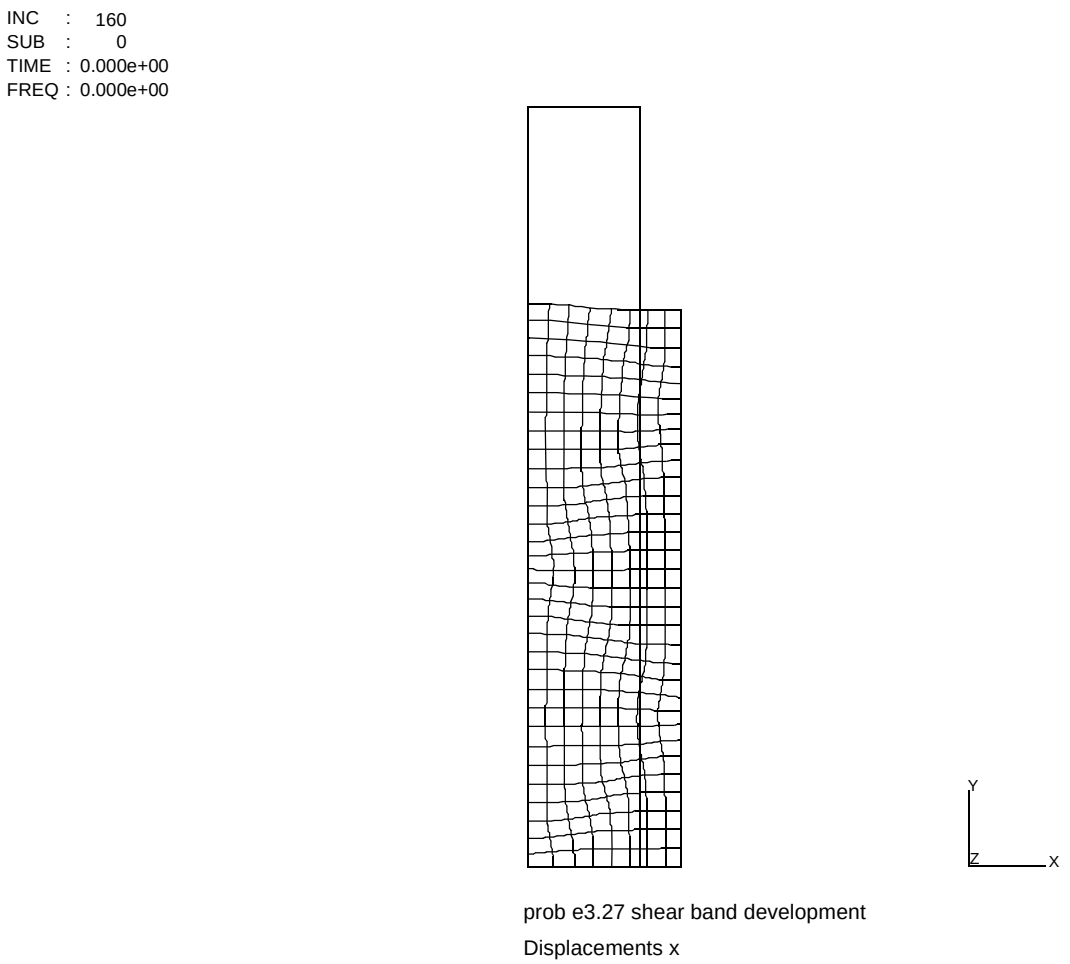

Figure 3.27-4 Deformed Mesh at Increment 160

Figure 3.27-5 Deformed Mesh at Increment 200

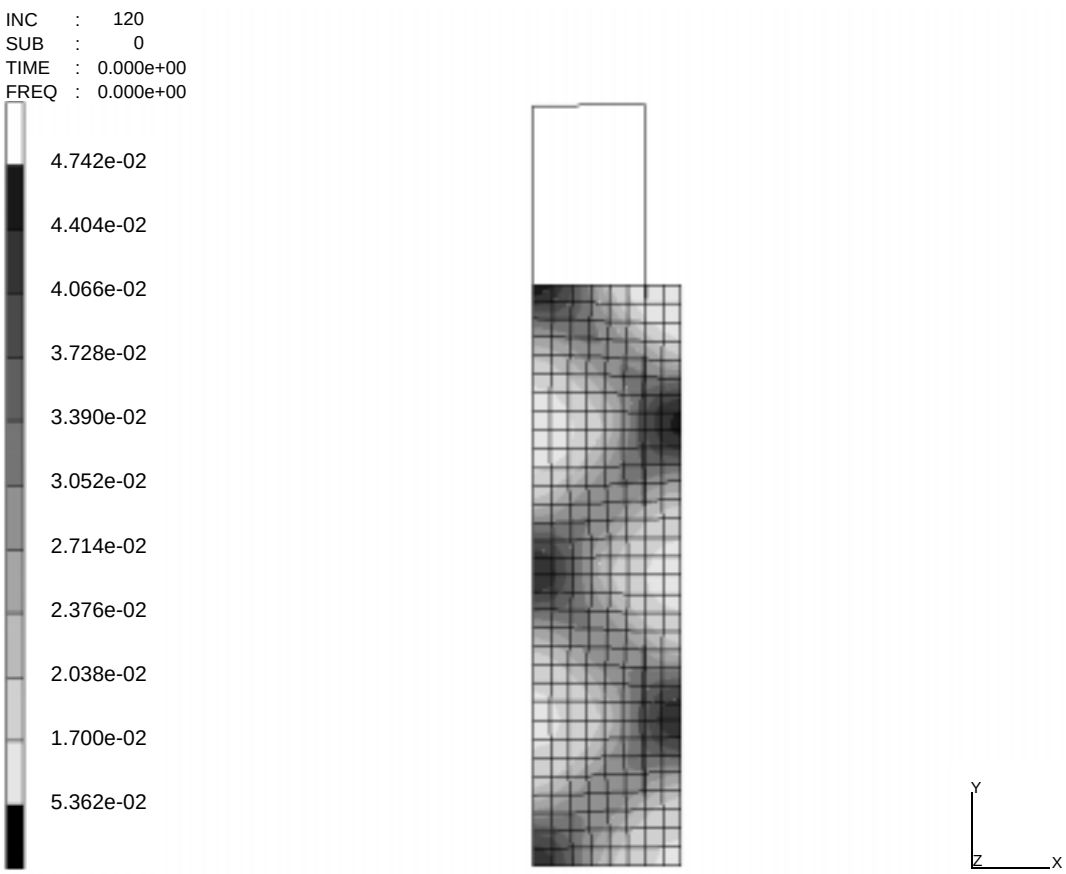

Figure 3.27-6 Void Volume Fraction at Increment 120

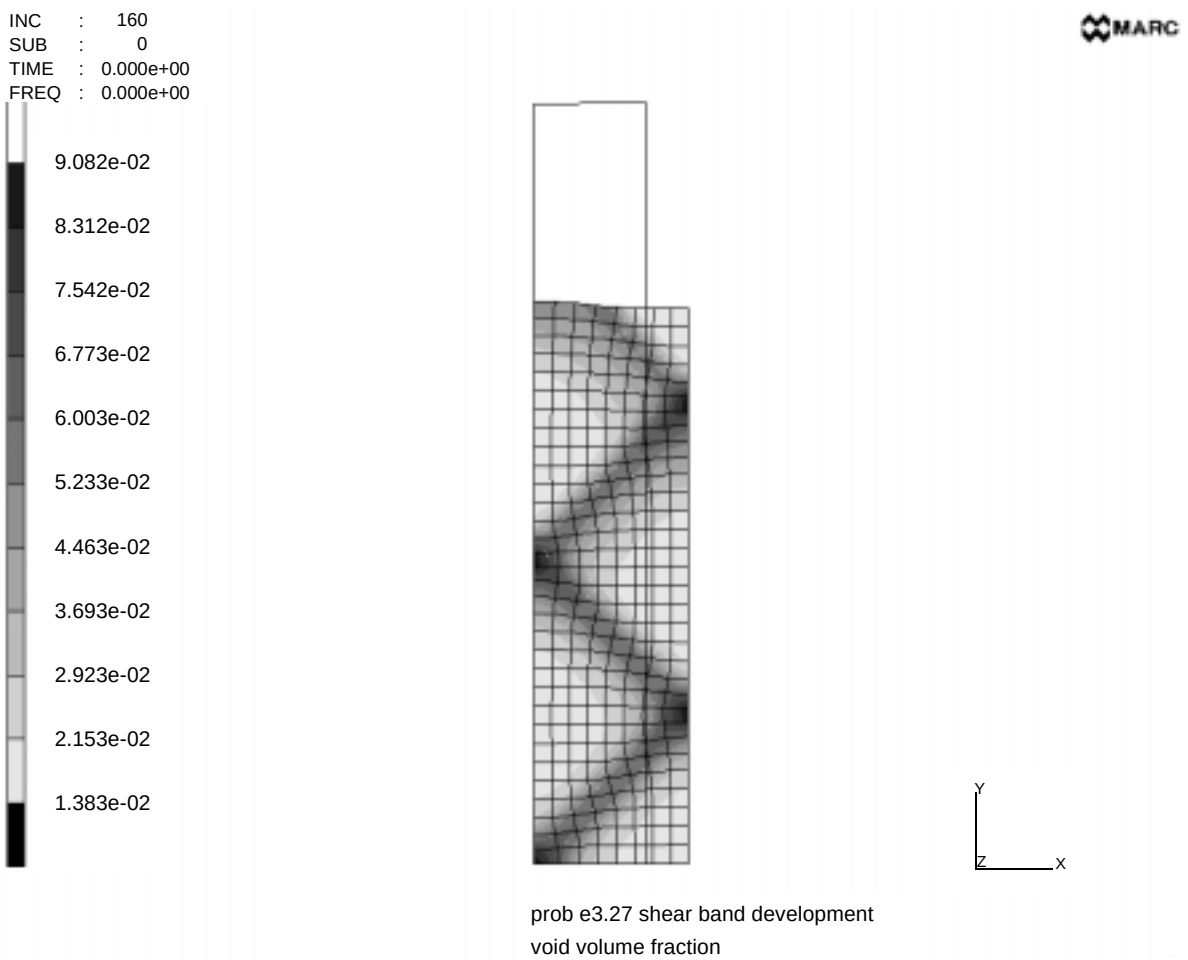

Figure 3.27-7 Void Volume Fraction at Increment 160

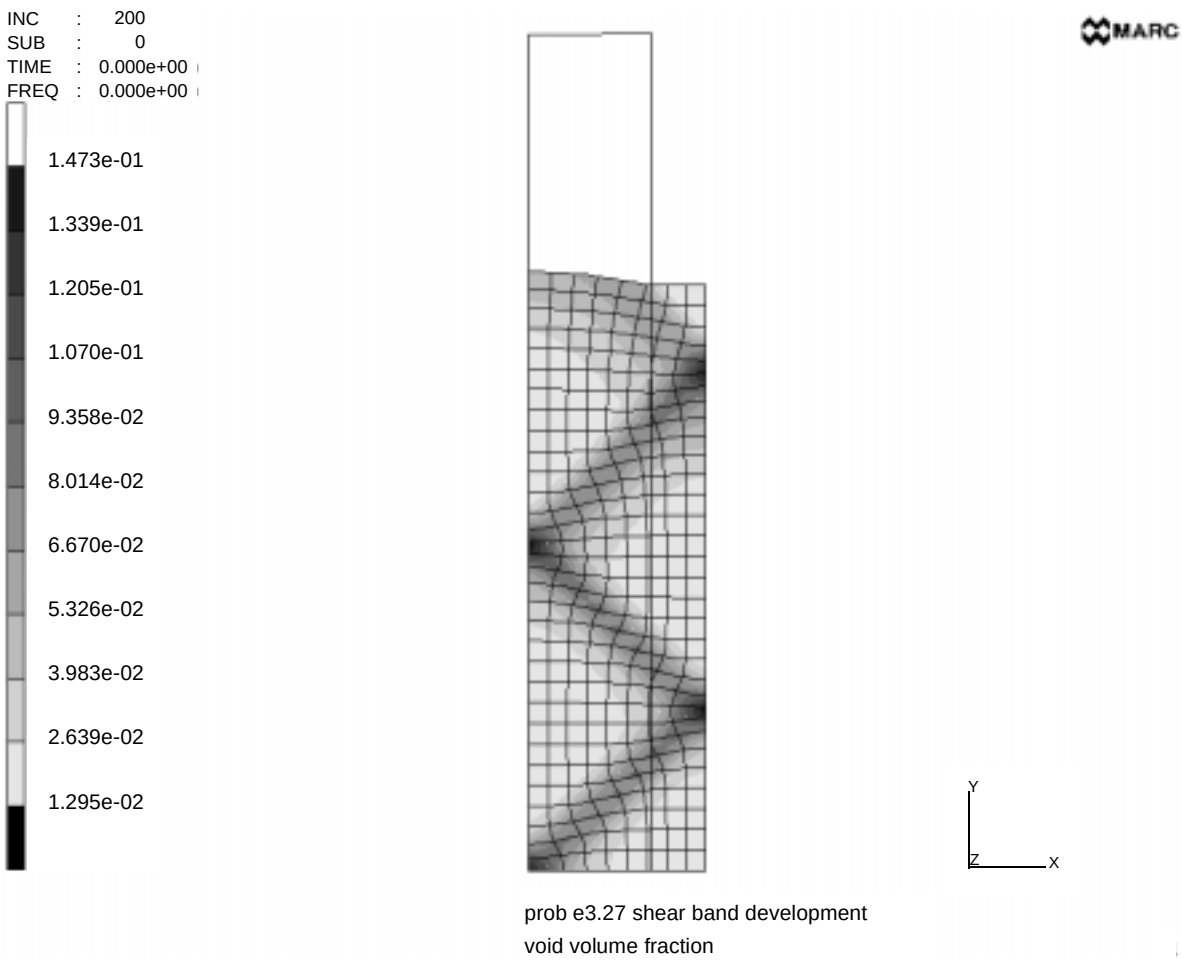

Figure 3.27-8 Void Volume Fraction at Increment 200

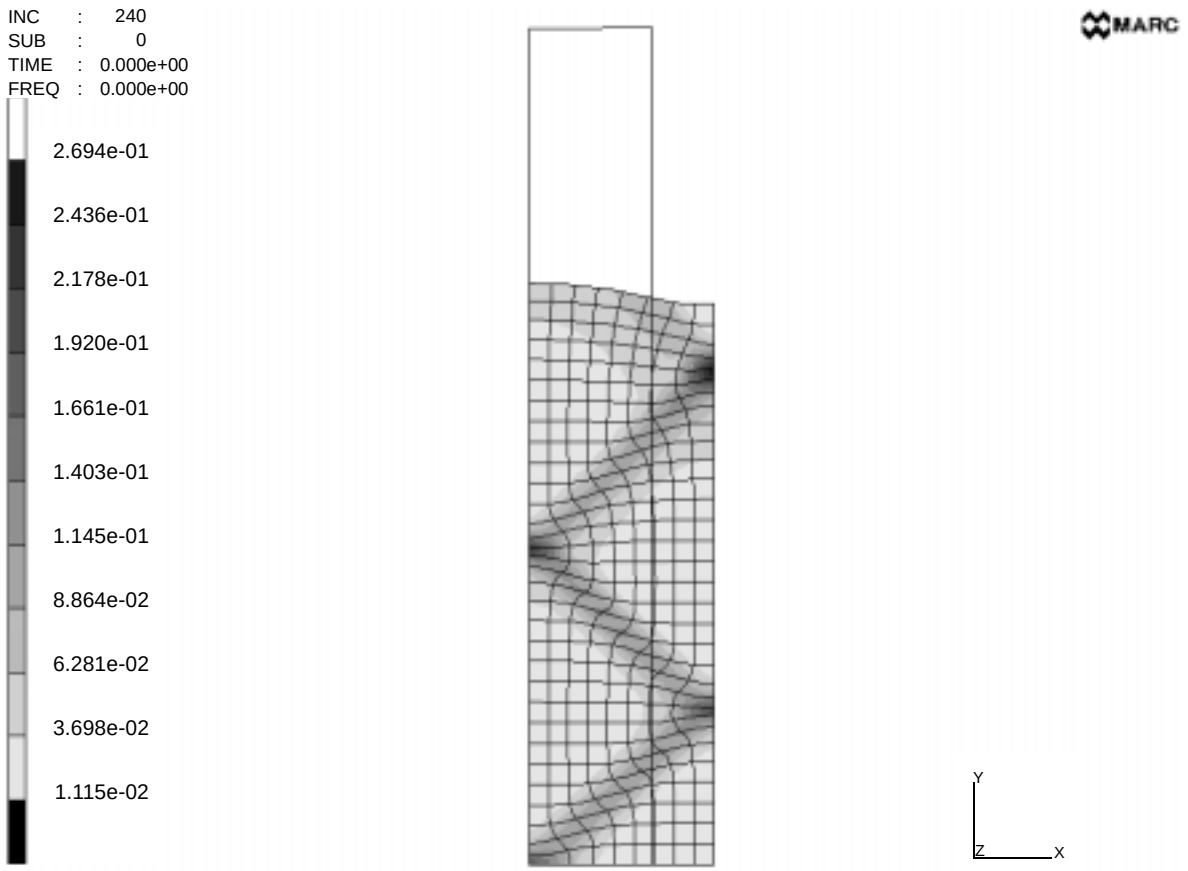

Figure 3.27-9 Void Volume Fraction at Increment 240

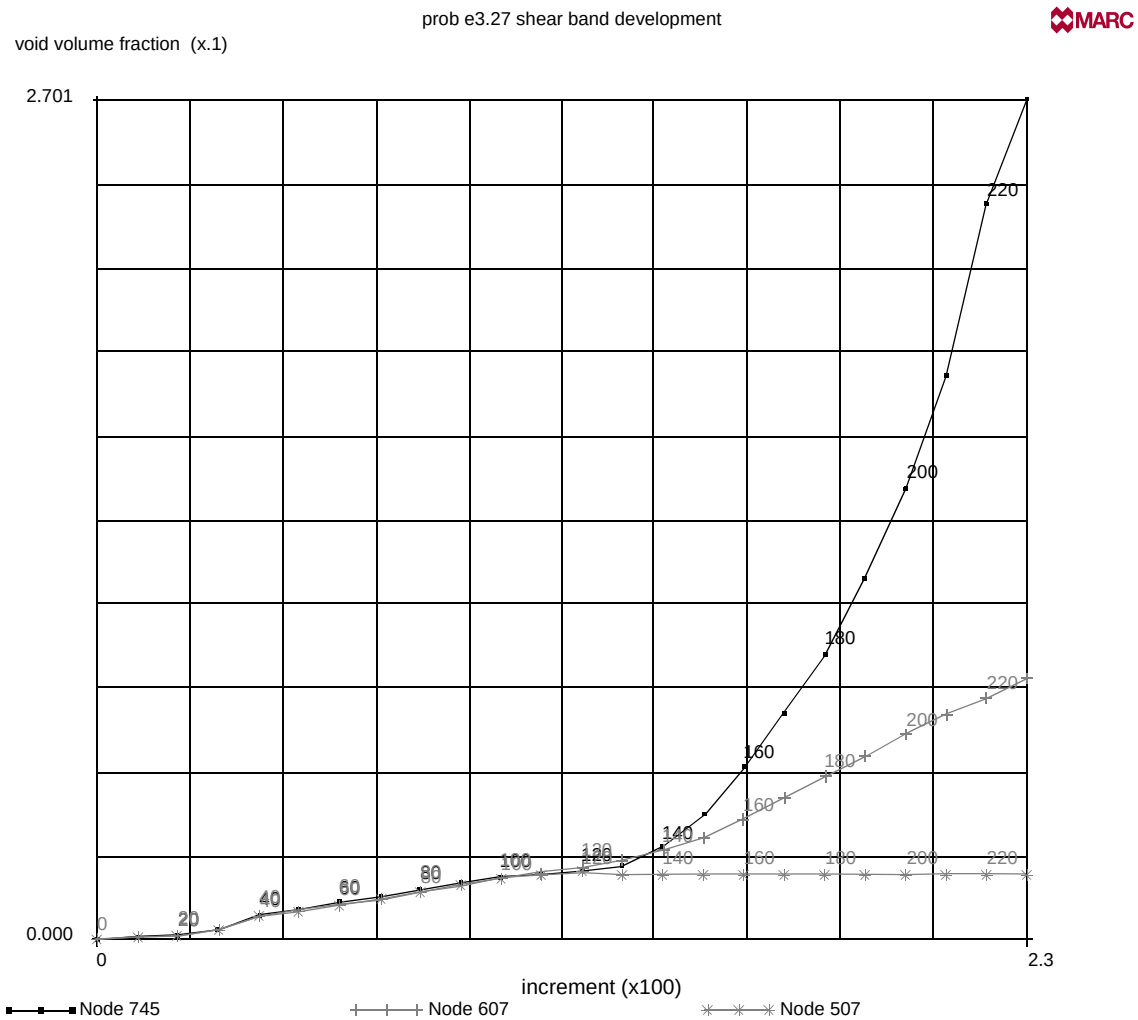

Figure 3.27-10 Time History of Void Volume Fraction

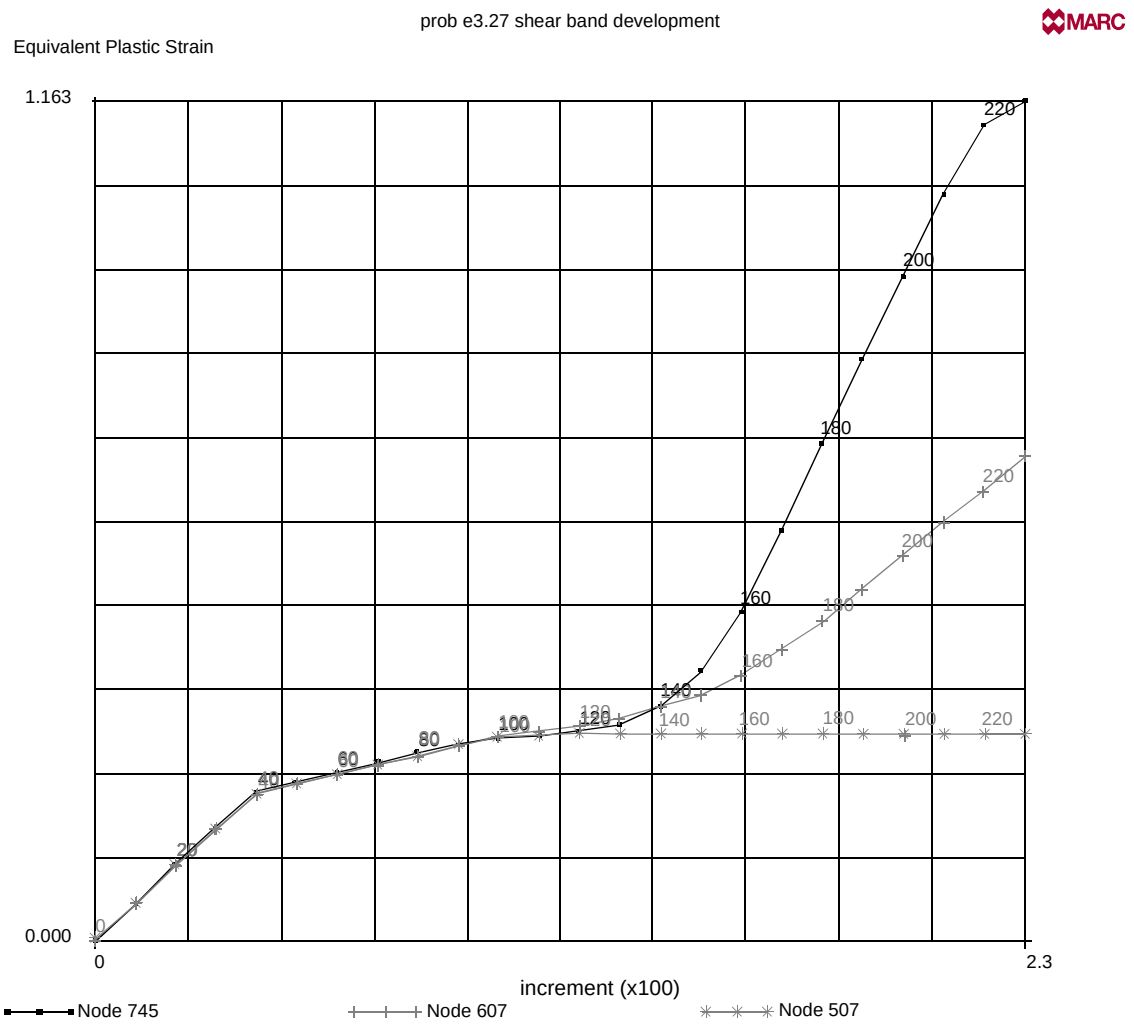

Figure 3.27-11 Time History of Plastic Strain

3.28 Void Growth in a Notched Specimen

This example illustrates the prediction of void growth in a notched specimen. This problem was first analyzed using a damage model by Sun.

Element

Element type 55 is an 8-node reduced integration axisymmetric element used in this analysis. The bar is 25 mm long with a radius of 7mm, and an elliptical notch (minor axis of 3, major of 3.873) is shown in Figure 3.28-1. The model consists of 500 elements and 1601 nodes and is shown in Figure 3.28-2.

Loading

Symmetry conditions are applied on the center line and the left side. The bar has an applied displacement of 1.775 applied in 230 increments using the DISP CHANGE and AUTO LOAD options.

Material Properties

The material is represented using a workhardening model. The Young's modulus is 21,000.0 N/mm^2. The workhardening data is shown in Figure 3.28-3.

The Gurson damage model is invoked using the strain-controlled nucleation model. The parameters used are:

First yield surface multiplier, q_1	=	1.5
Second yield surface multiplier, q_2	=	1.0
Initial void volume fraction, f_i	=	0.00057
Critical void volume fraction, f_c	=	0.3
Failure void volume fraction, f_f	=	0.15
Mean strain for nucleation	=	0.3
Standard deviation	=	0.1
Volume fraction of void nucleating particles	=	0.00408

Control

The required convergence tolerance is 5% on residuals. A maximum of 15 iterations per increment is allowed. The restart file is generated every 20 increments. The post file is generated every 10 increments. The bandwidth is minimized using the Cuthill-McKee optimizer. The AUTO LOAD option is invoked twice; the first time 80 increments of 0.1 mm are taken and then 150 more increments of 0.0025 mm are taken.

Results

The deformed geometry is shown in Figure 3.28-4. The distribution of the void is represented in Figure 3.28-5. Linear elastic analysis would reveal that the highest stress is at the outside radius. Due to the redistribution of the stresses and because of elastic plastic behavior, the highest triaxial stress occurs at the center and the crack initiation due to void coalescence begins here. The equivalent plastic strain is shown in Figure 3.28-6. On subsequent loading, the cracks grow radially along the symmetry line. Figure 3.28-7 shows the history of the void ratio at three nodes along this line.

Parameters, Options, and Subroutines Summary

Example e3x28.dat:

Parameters	Model Definition Options	History Definition Options
ALIAS	CONNECTIVITY	AUTO LOAD
ELEMENTS	CONTROL	CONTINUE
END	COORDINATES	DIST CHANGE
FINITE	DAMAGE	
LARGE DISP	DEFINE	
PRINT	END OPTION	
SIZING	FIXED DISP	
TITLE	ISOTROPIC	
UPDATE	NO PRINT	
	OPTIMIZE	
	POST	
	RESTART	
	WORK HARD	

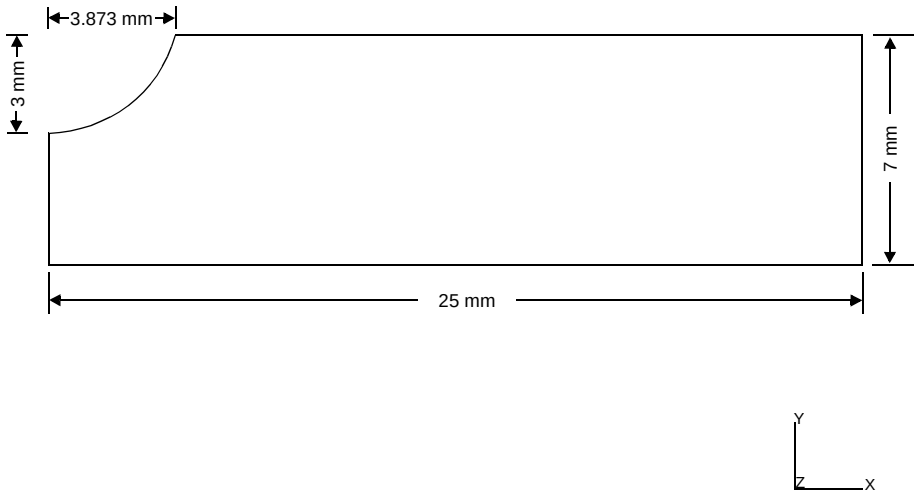

Figure 3.28-1 Notched Specimen

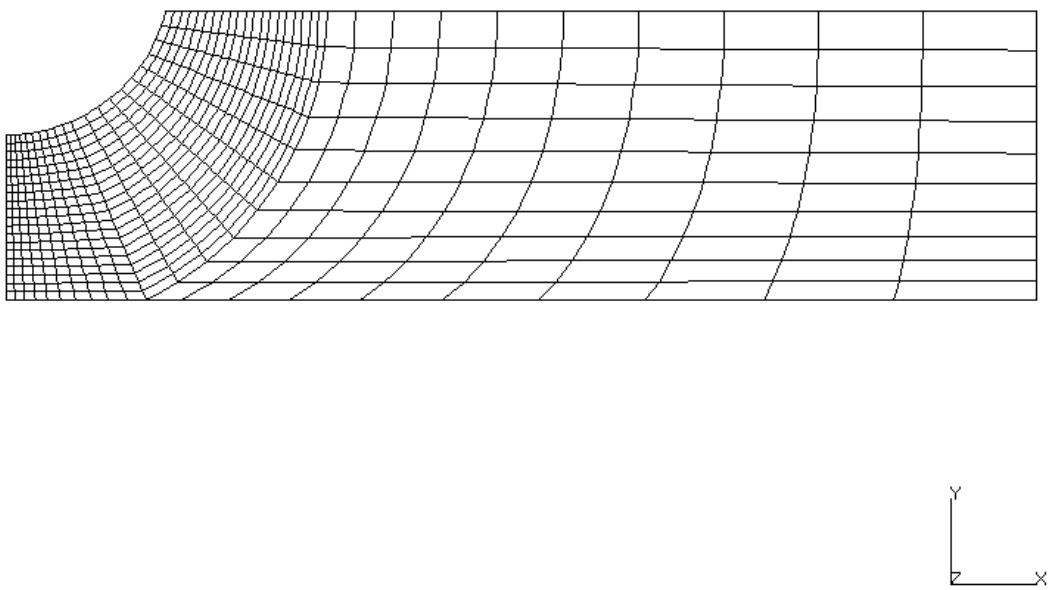

Figure 3.28-2 Mesh

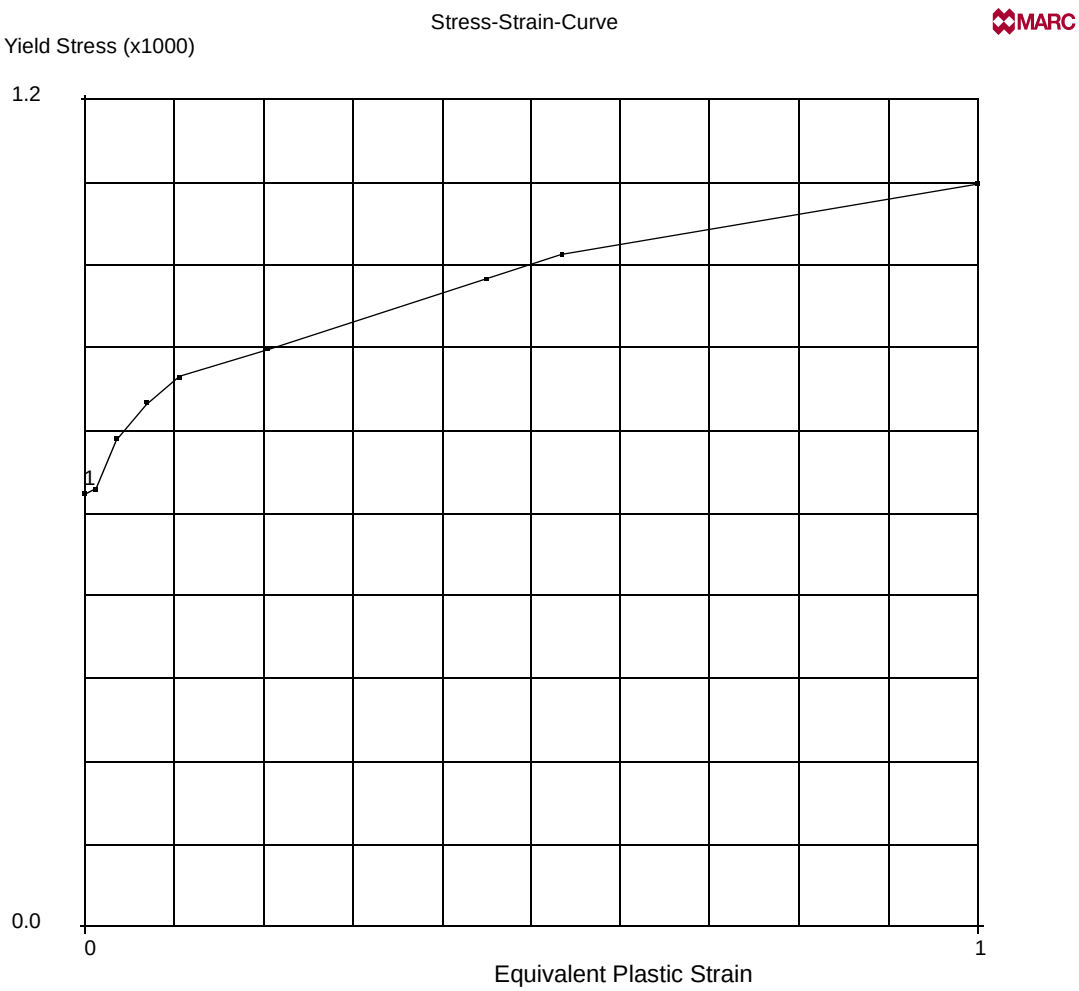

Figure 3.28-3 Stress-Strain Curve

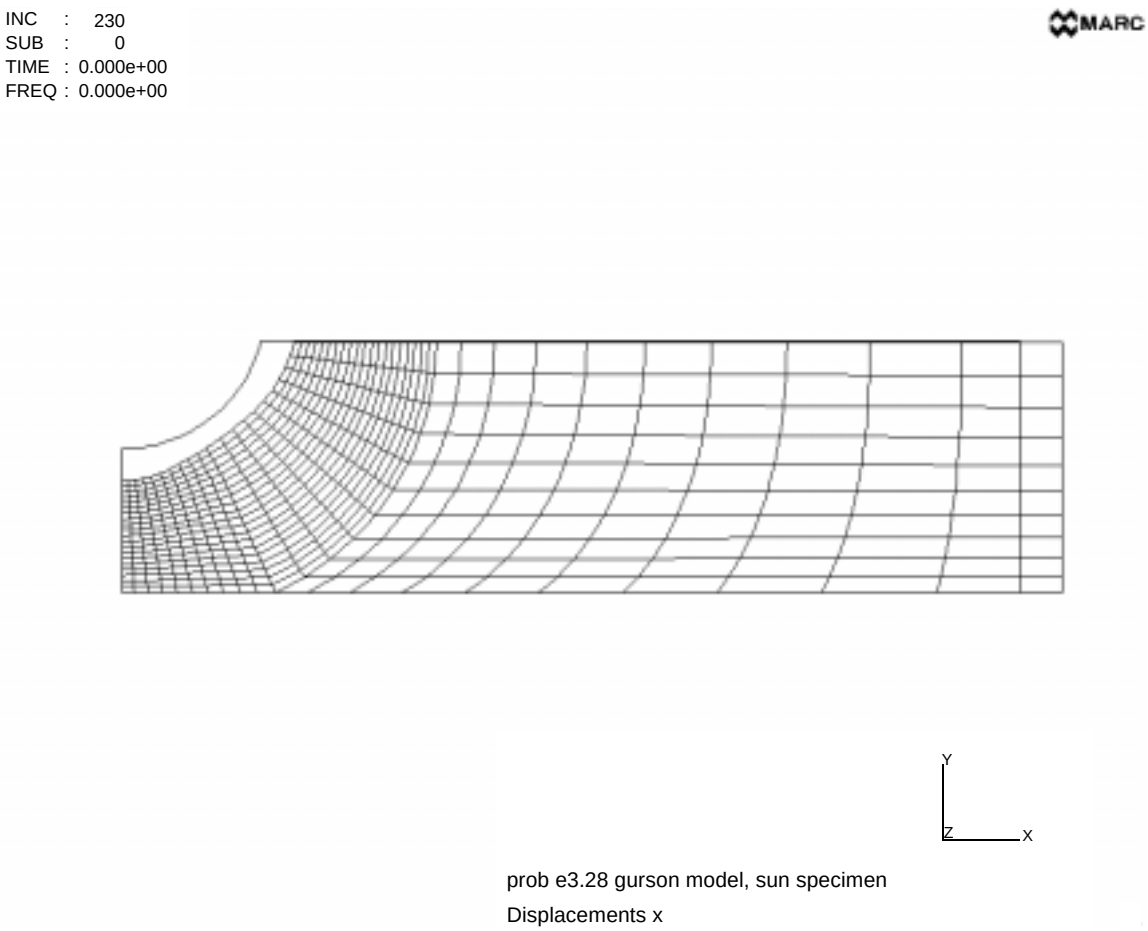

Figure 3.28-4 Deformed Mesh

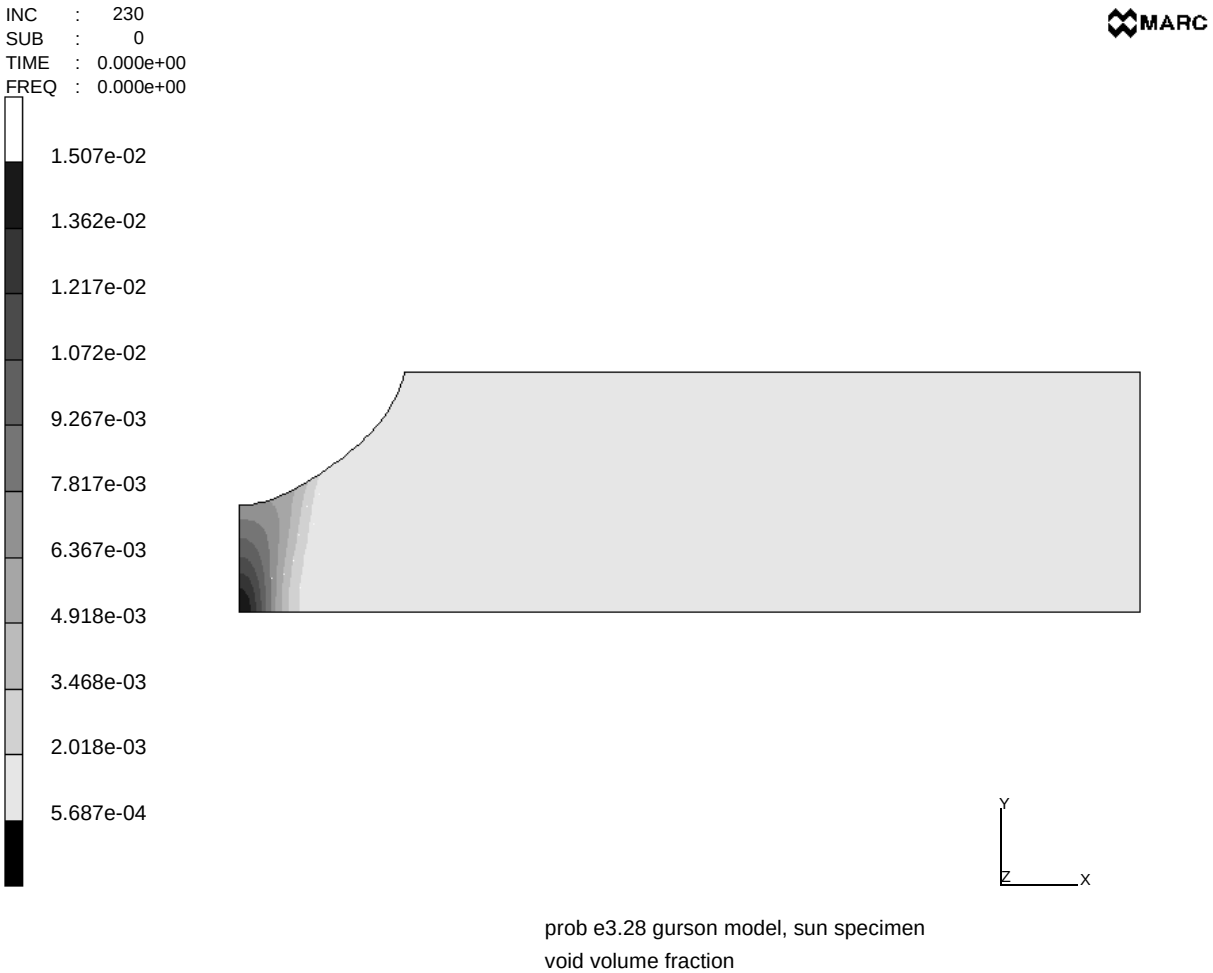

Figure 3.28-5 Void Volume Fraction

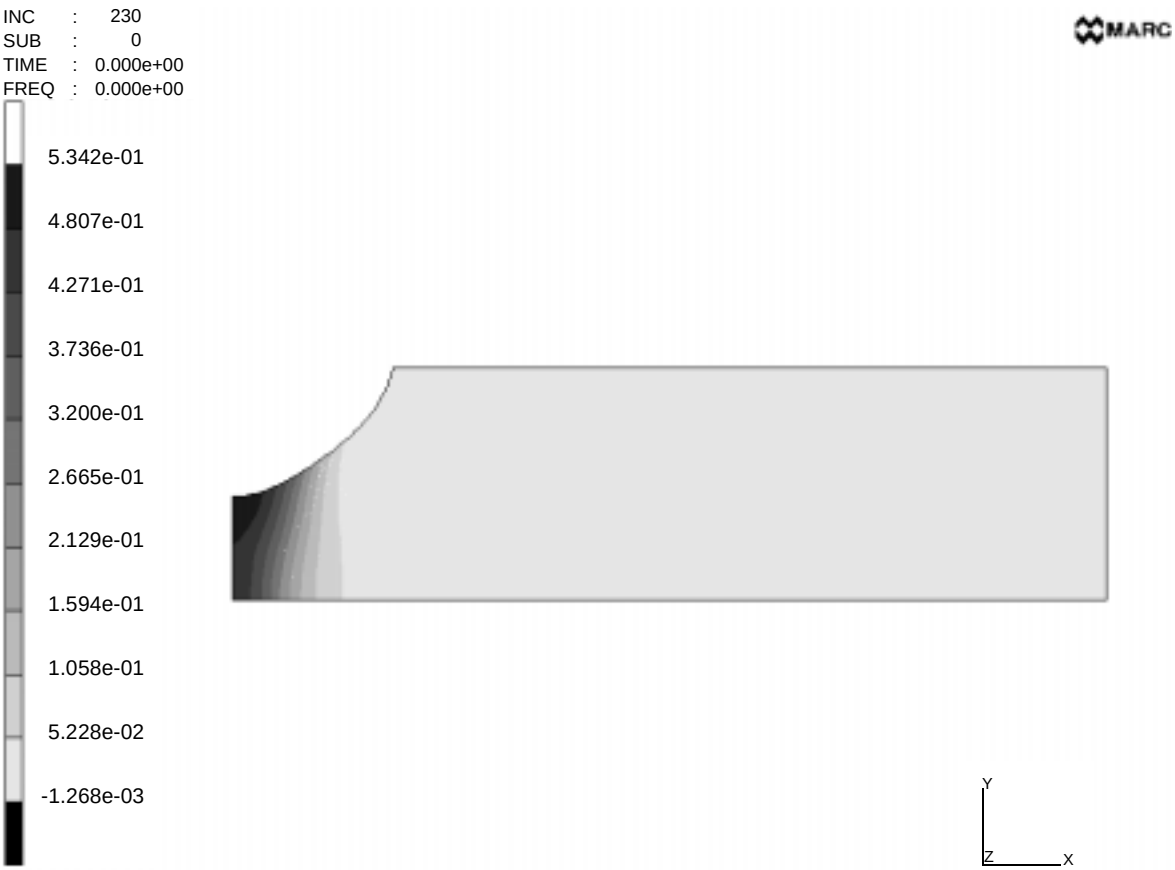

Figure 3.28-6 Equivalent Plastic Strain

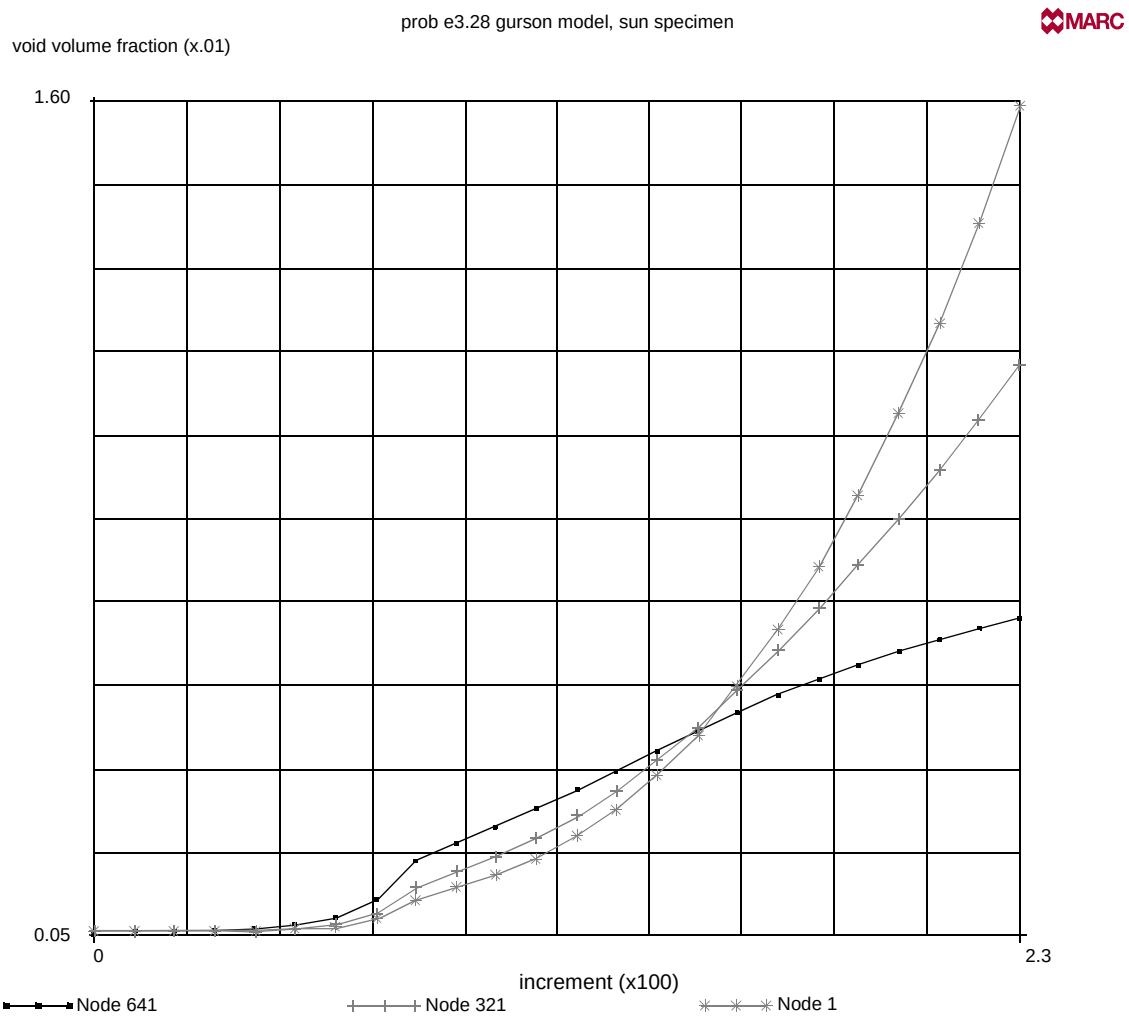

Figure 3.28-7 Time History of Void Volume Fraction

3.29 Creep of a Thick Walled Cylinder - Implicit Procedure

This example illustrates the implicit formulation for performing power-law creep analysis. A thick-walled cylinder is pressurized and then allowed to creep.

Element

Element type 10, the 4-node axisymmetric element is used. The constant dilatation option was used. Twenty elements are used through the cylinder which has an inner radius of one inch and an outer radius of two inches. The mesh is shown in Figure 3.29-1.

Loading

The cylinder is constrained axially along the left edge; the right edge is free to allow expansion. The internal pressure of 14,000 psi is applied in increment one and then held constant during the creep process.

Material Properties

The material is steel with a Young's modulus of 30 x 10^6 psi and a Poisson's ratio of 0.3. The creep strain rate is of the Norton type defined as:

$$\dot{\varepsilon}^c = 1 \times 10^{-19} \text{ in/in/hr} \bullet \bar{\sigma}^{3.5}$$

The constants are given in the CREEP model definition block.

Control

The CREEP parameter is used to indicate that this is a creep analysis. The default is that an explicit procedure is used. The third flag indicates that the implicit method will be used. When the implicit method is used, you have three choices on how the stiffness matrix is to be formed (elastic tangent, secant, or radial return). In this analysis, the secant method was chosen by setting the eighth field of the CONTROL option to one. The convergence required was 1% on residuals. The AUTO CREEP option was used to indicate that a total time period of 100 hours was to be covered and the first time step should be one hour.

Results

Using the implicit procedure, the analysis was completed in 28 increments while the explicit procedure required 39 increments. The time history of the resultant analyses are shown in Figure 3.29-2 and Figure 3.29-3, respectively. One should note that the implicit analysis does not exhibit the oscillations that occur when using the explicit method.

Parameters, Options, and Subroutines Summary

Example e3x29.dat:

Parameters	Model Definition Options	History Definition Options
CREEP	CONNECTIVITY	AUTO CREEP
ELEMENTS	CONTROL	CONTINUE
END	COORDINATES	CONTROL
SIZING	CREEP	DIST LOADS
TITLE	DISP LOADS	
	END OPTION	
	FIXED DISP	
	GEOMETRY	
	ISOTROPIC	
	POST	

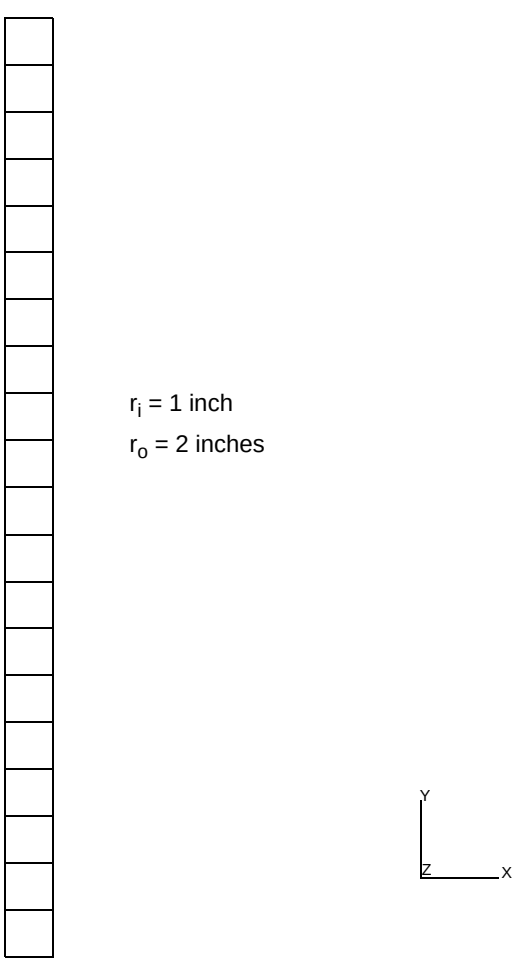

Figure 3.29-1 Finite Element Mesh

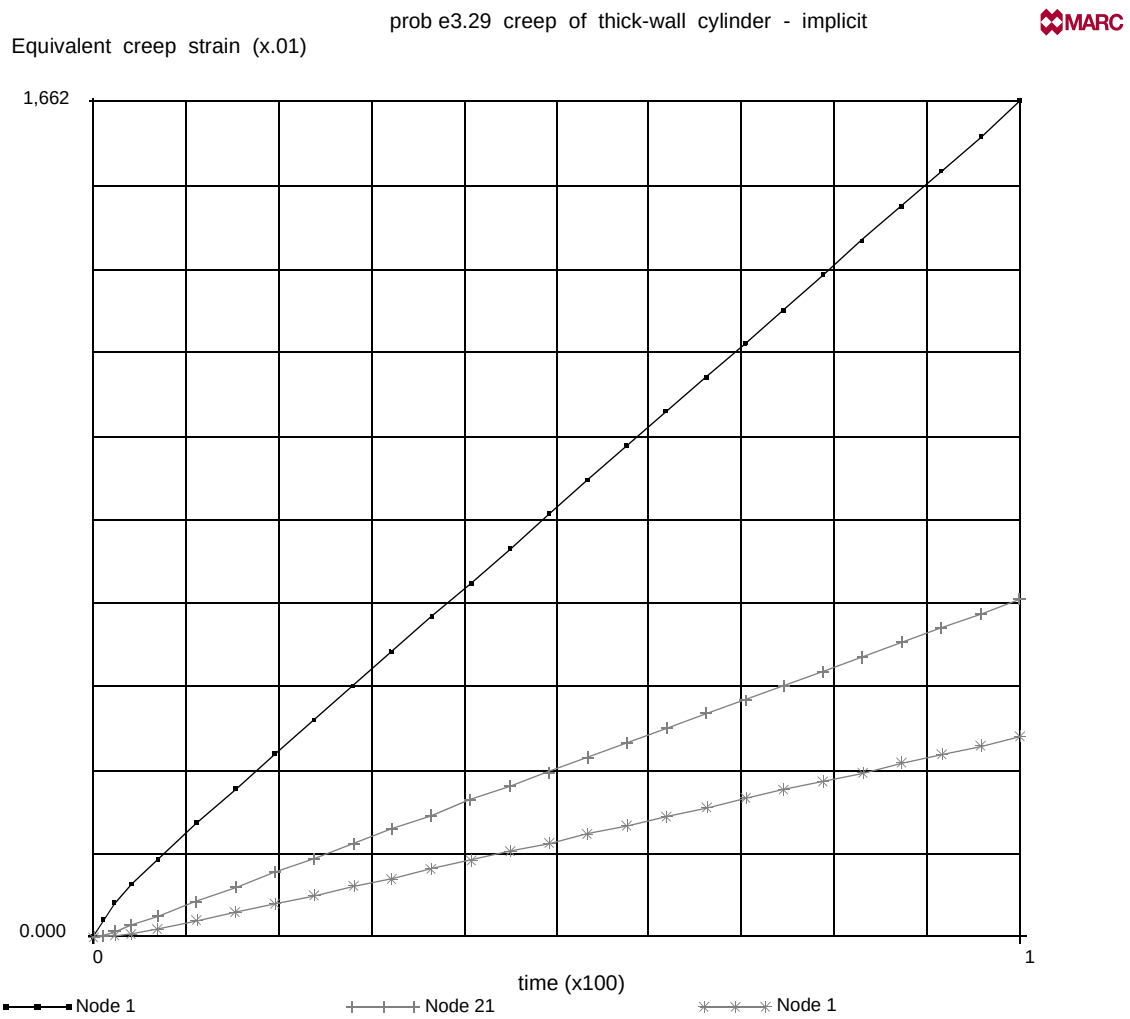

Figure 3.29-2 Time History of Equivalent Creep Strain – Implicit Procedure

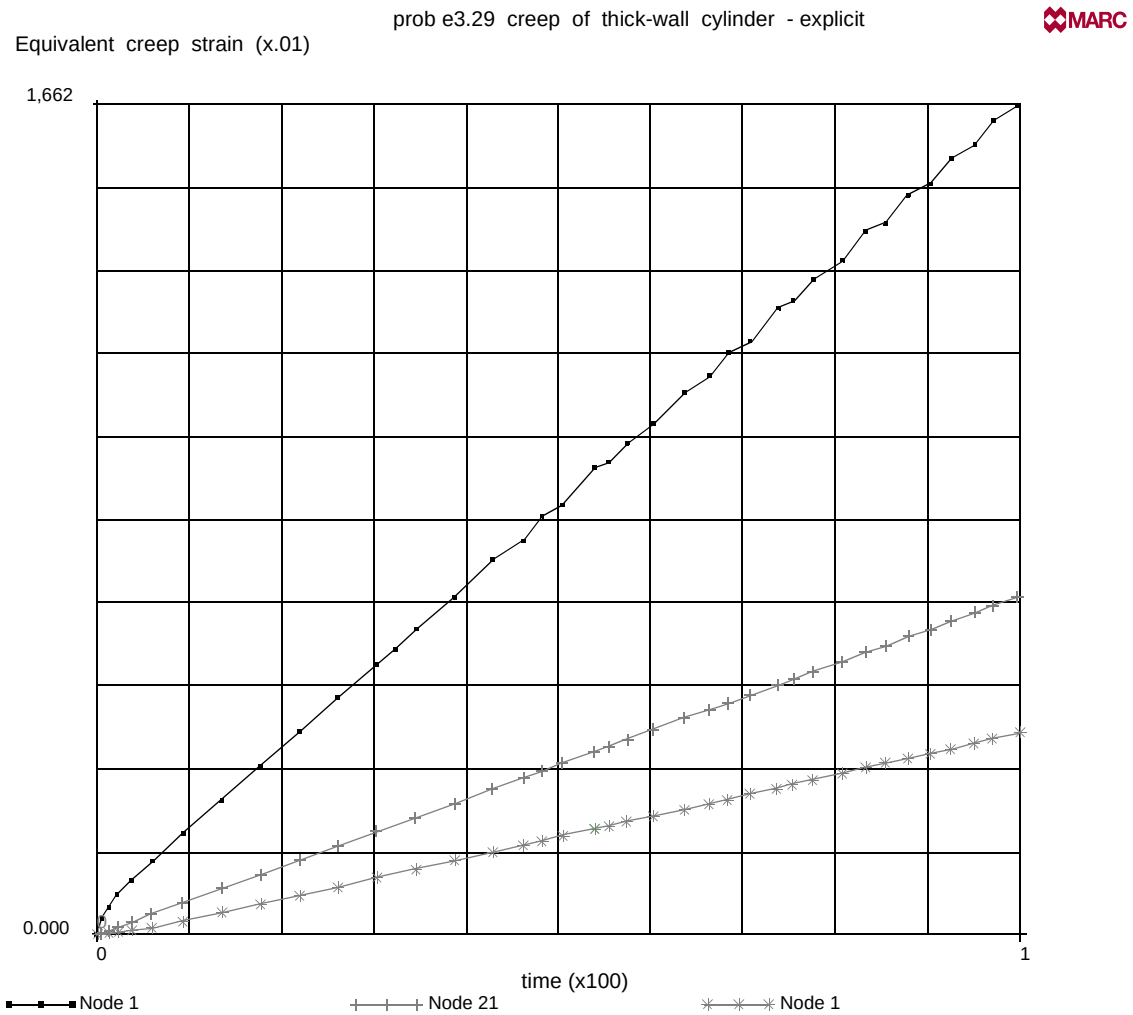

Figure 3.29-3 Time History of Equivalent Creep Strain – Explicit Procedure

3.30 3D Forming of a Circular Blank using Rigid-Plastic Formulation

This problem demonstrates the program's ability to perform stretchforming by a spherical punch using the CONTACT option and the rigid-plastic formulation. First, the problem will be analyzed using membrane elements, and then be analyzed with shell elements.

This problem is modeled using the two techniques summarized below.

Data Set	Element Type(s)	Number of Elements	Number of Nodes
e3x30a	18	112	127
e3x30b	75	112	127

Parameters

The R-P FLOW parameter is included to indicate that this is a rigid-plastic flow problem. The PRINT,8 option requests the output of incremental displacements in the local system. Element type 18 is a 4-node membrane element used in the first analysis. Element type 75 is a 4-node thick shell element used in the second analysis. Eleven layers are used through the thickness of the shell. The ISTRESS parameter is used to indicate that an initial stress is going to be imposed which stabilizes the membrane element solution. In the membrane analysis, the ALIAS option is used to change the element type.

Geometry

A shell thickness of 1 cm is specified through the GEOMETRY option in the first field (EGEOM1).

Boundary Conditions

The first boundary condition is used to model the binding in the stretch forming process. The second and third boundary conditions are used to represent the symmetry conditions.

Post

The following variables are written to a formatted post file:

7 } Equivalent plastic strain 17 } Equivalent von Mises stress

20 } Element thickness

Furthermore, the above three variables are also requested for all shell elements at layer number 4, which is the midsurface.

Control

A full Newton-Raphson iterative procedure is requested. Displacement control is used, with a relative error of 5%. Fifty load steps are prescribed, with a maximum of 30 recycles (iterations) per load step.

Material Properties

The material for all elements is treated as an rigid-plastic material an initial yield stress of 80.6 lbf/cm^2. The yield stress is given in the form of a power law and is defined through the WKSLP user subroutine.

Contact

This option declares that there are three bodies in contact with Coulomb friction between them. A coefficient of friction of 0.3 is associated with each rigid die. The first body represents the work piece. The second body is the lower die, defined as three surfaces of revolution. The first and third surfaces of revolution use a straight line as the generator, the second uses a circle as the generator. The third body (the punch) is defined as two surface of revolution. These surfaces are extended from -0.5 to 101.21 degrees.The rigid surfaces are shown in Figure 3.30-1. The relative slip velocity is specified as 0.01 cm/sec. The contact tolerance distance is 0.05 cm. When using the rigid-plastic option, nodal based friction should be used. This is because the solution of the stresses cannot be accurate.

Load Control

This problem is displacement controlled with a velocity of 1 cm/second applied in the negative Z direction with the AUTO LOAD option. The load increment is applied 40 times. The MOTION CHANGE option is illustrated to control the velocity of the rigid surfaces.

Results

Figure 3.30-2 shows the deformed body at the end of 40 increments with the deformation at the same scale as the coordinates. Due to the high level of friction, significant transverse deformation is shown along the contact surfaces.

Figure 3.30-3 shows the equivalent plastic strain contours on the deformed structure at increment 40, with the largest strain level at 60% using membrane elements.

Figure 3.30-4 shows the equivalent von Mises stress contours on the deformed structure at increment 40 with peak values at 527 lbf/cm^2 using membrane elements.

Figure 3.30-5 shows the equivalent plastic strain contours on the deformed structure at increment 40, with the largest strain level at 52% using shell elements.

Figure 3.30-6 shows the equivalent von Mises stress contours on the deformed structure at increment 40 with peak values at 512 lbf/cm^2 using shell elements.

You can observe very good correlation between the two element formulations. Comparing problem e3x30 with e8x18, there is also very good agreement. As long as springback is not required, the rigid-plastic formulation is viable for performing sheet forming simulations. The benefit of using the rigid-plastic formulation is that the computational times are less than those for a full elastic-plastic analysis.

Parameters, Options, and Subroutines Summary

Example e3x30a.dat:

Parameters	Model Definition Options	History Definition Options
ALIAS	CONNECTIVITY	AUTO LOAD
ELEMENTS	CONTACT	CONTINUE
END	CONTROL	MOTION CHANGE
ISTRESS	COORDINATES	TIME STEP
PRINT	END OPTION	
R-P FLOW	FIXED DISP	
SIZING	GEOMETRY	
TITLE	ISOTROPIC	
	OPTIMIZE	
	POST	
	PRINT CHOICE	
	WORK HARD	

User subroutines in example u3x30a.f:

WKSLP
UINSTR

Example e3x30b.dat:

Parameters	Model Definition Options	History Definition Options
ELEMENTS	CONNECTIVITY	AUTO LOAD
END	CONTACT	CONTINUE
PRINT	CONTROL	MOTION CHANGE
R-P FLOW	COORDINATES	TIME STEP
SIZING	END OPTION	
TITLE	FIXED DISP	
	GEOMETRY	
	ISOTROPIC	
	OPTIMIZE	
	POST	
	PRINT CHOICE	
	WORK HARD	

User subroutine in example u3x30b.f:

WKSLP

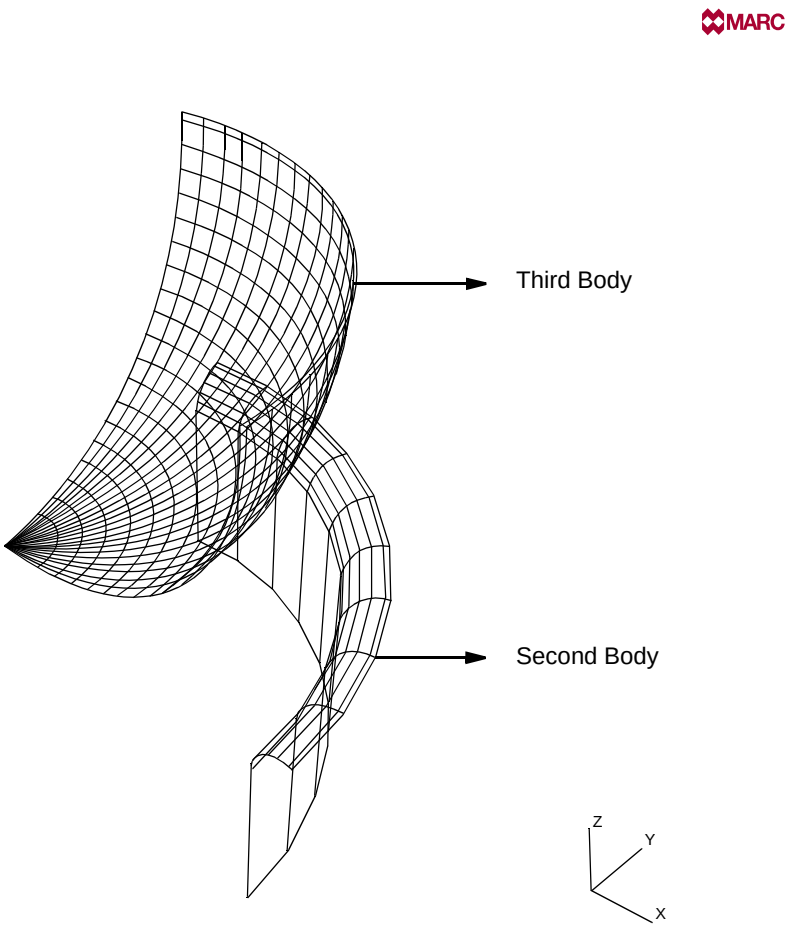

Figure 3.30-1 Circular Blank Holder and Punch

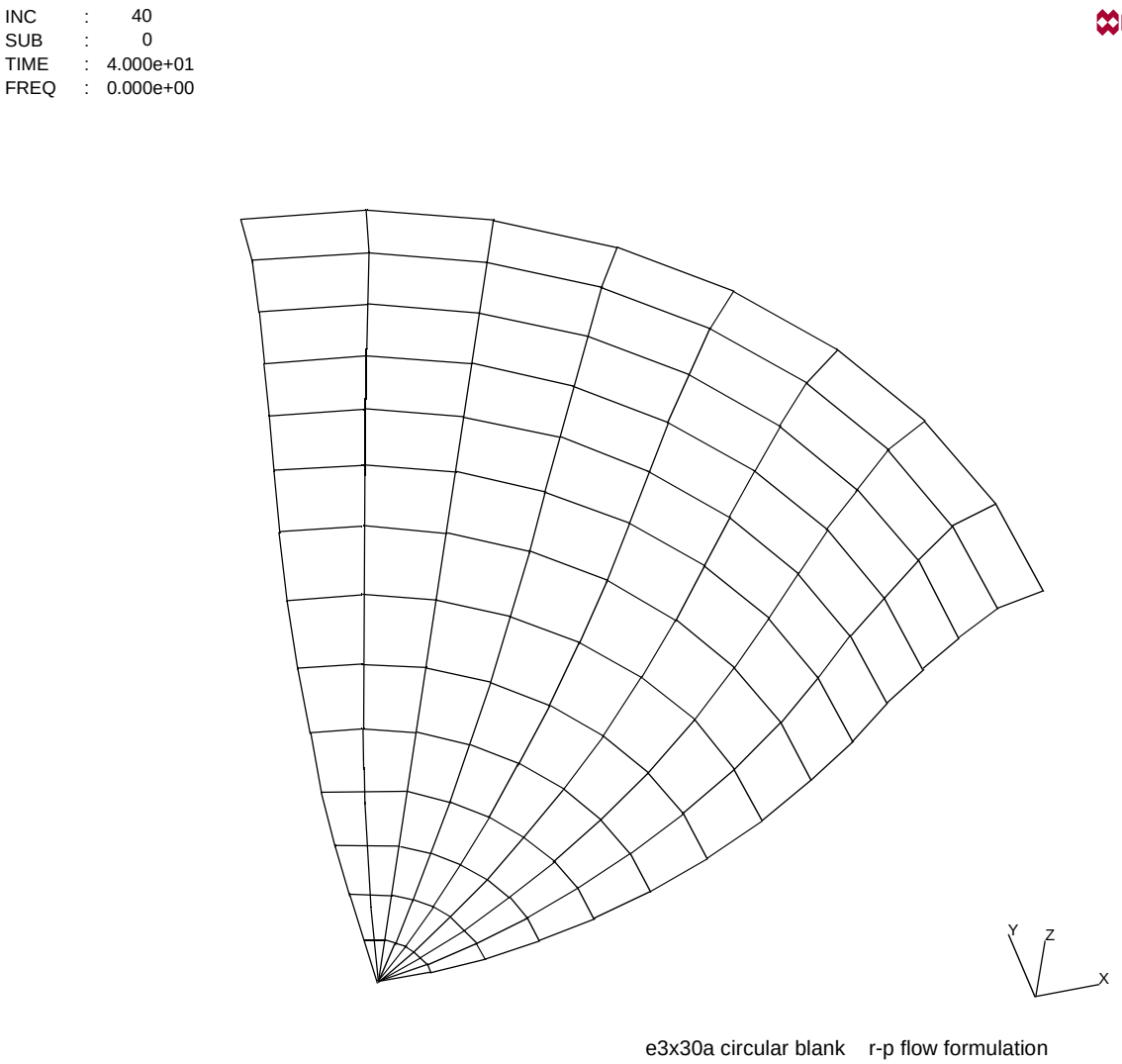

Figure 3.30-2 Deformed Sheet at Increment 40

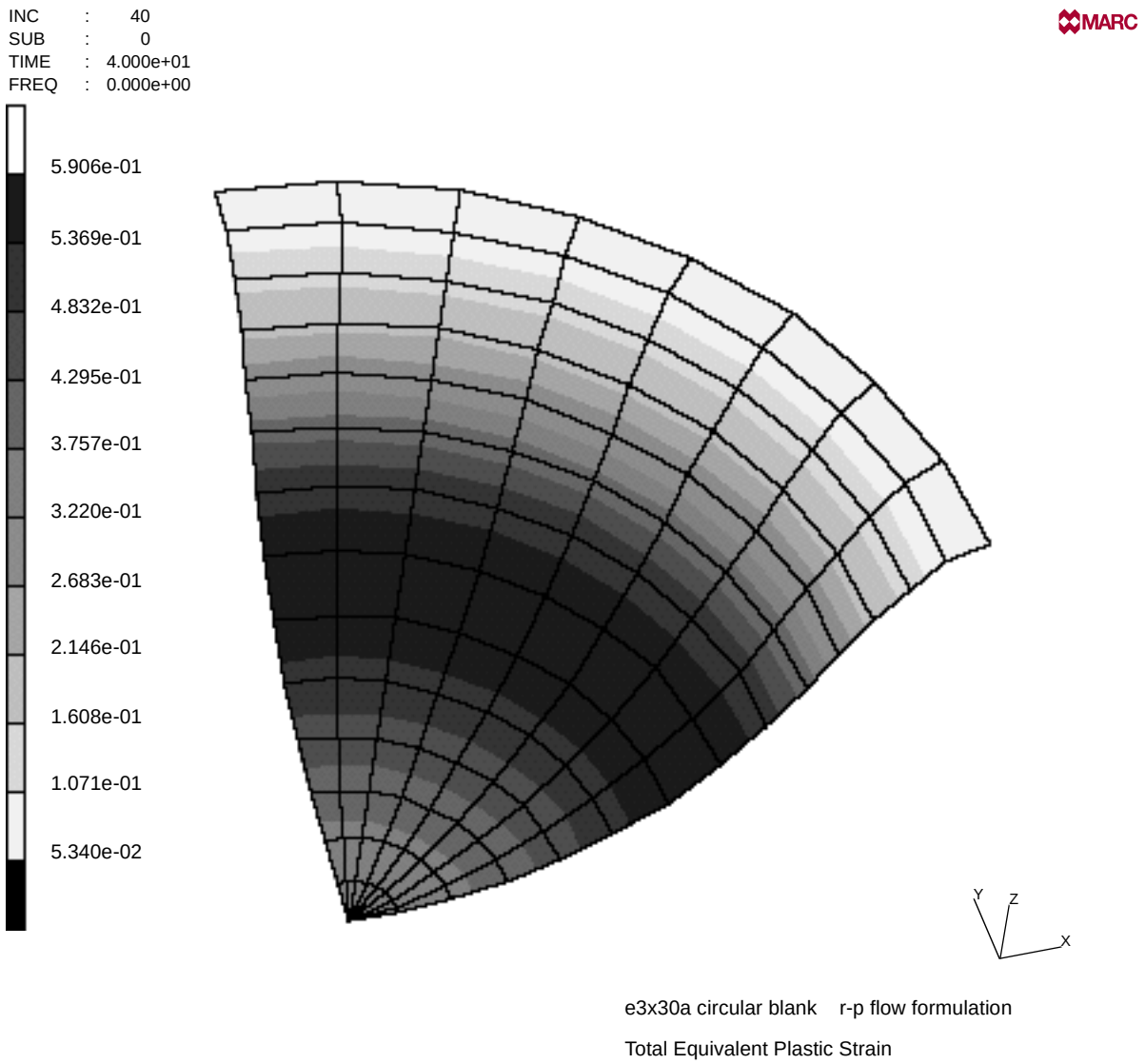

Figure 3.30-3 Equivalent Plastic Strains in Membrane

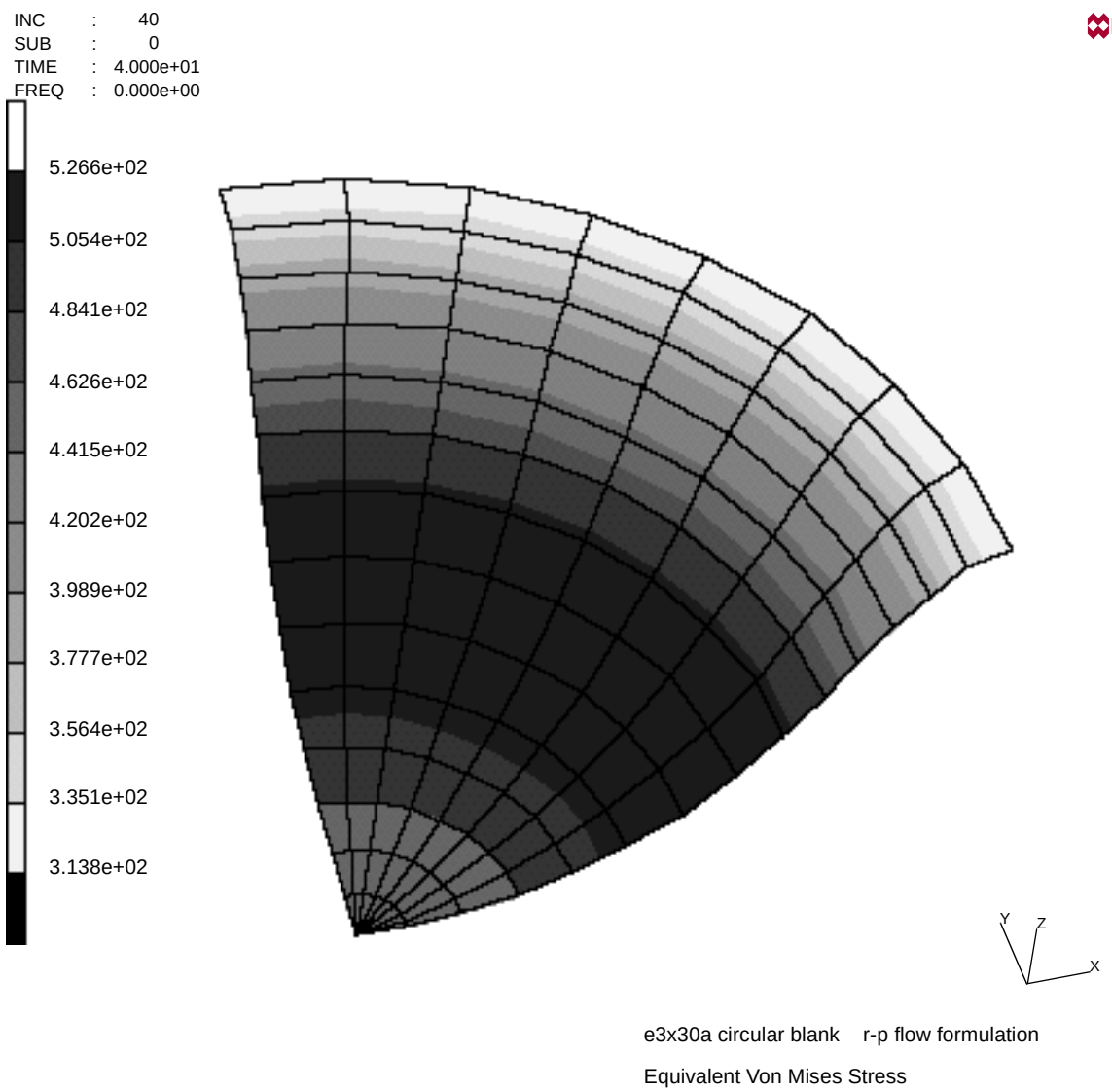

Figure 3.30-4 Equivalent Stresses in Membrane

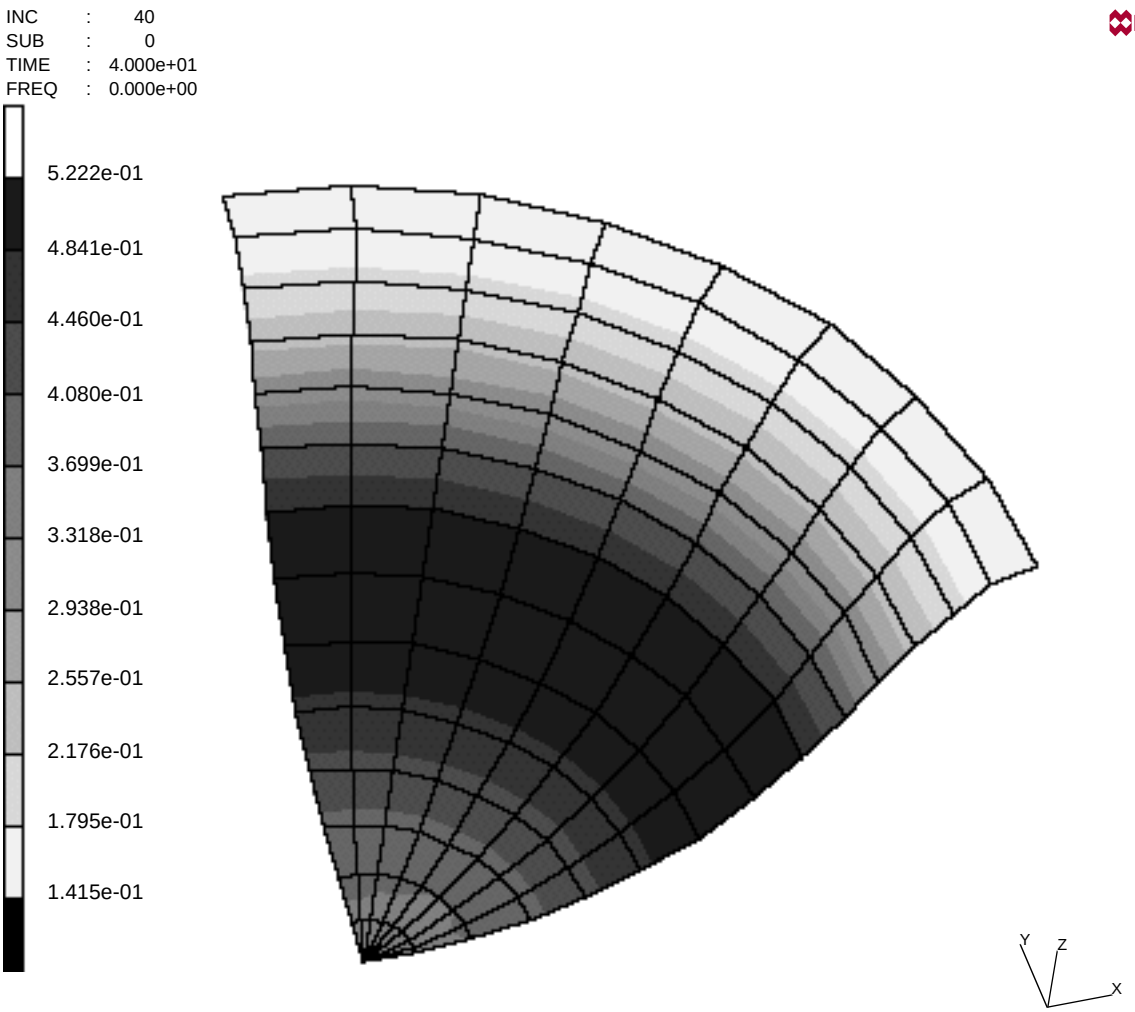

Figure 3.30-5 Equivalent Plastic Strains at Midlayer of Shell

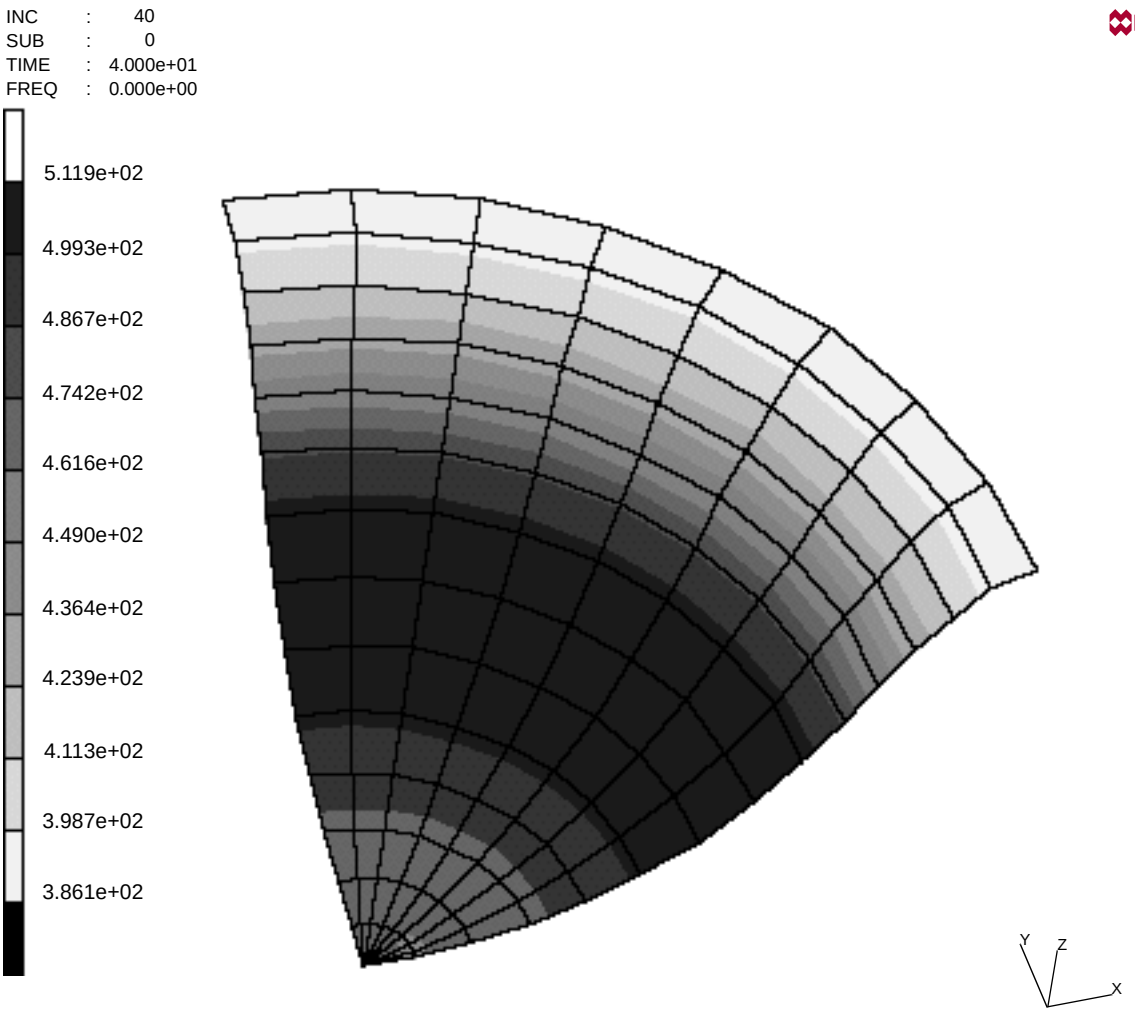

Figure 3.30-6 Equivalent Stresses at Midlayer of Shell

3.31 Formation of Geological Series

This problem demonstrates the capability of MARC to analyze the sliding of geological strata along fault planes until reaching a partial overlap.

In this case, there are two strata separated by an inclined fault. The upper stratum is pushed in the horizontal direction to move against the fault. It will slide along the fault overlapping the lower stratum. The stratum is 6 Km deep and 100 Km long. The computational model is plane strain. The cross section of the strata is represented. Units [N, m].

Element

Library element type 11 is a plane-strain 4-node isoparametric quadrilateral element.

Model

The geometry of the strata and their mesh is shown in Figure 3.31-1. The model consists of 696 plane-strain, type 11, element for a total of 856 nodes. Figure 3.31-3 shows the details of the mesh at the fault plane.

Geometry

This option is not required for a plane-strain element as a unit thickness is assumed.

Boundary Conditions

Symmetry conditions are applied at the edges 1, 2, and 3 (see Figure 3.31-1). Automated contact is applied at the interface of the fault. No friction is assumed between the two deformable strata.

Material Properties

The material of the strata is assumed to be isotropic (no variation along the thickness) with the properties:

Young modulus	E	= 34.15 E8 N/m^2
Poisson ratio	ν	= 0.23
Mass density	ρ	= 2200 kg/m^3

The linear Mohr-Coulomb criterion is assumed for the ideal yield surface with values of the two constants (refer to *MARC Volume A: User Information*):

σ = 22.25 E6 N/m^2
α = .15 N/m^2

Loading

The strata are loaded with the gravity load in ten increments. In the subsequent 25 increments, an incremental displacement of 250 m in the horizontal direction is assigned to the upper part of edge 3 (see Figure 3.31-1).

Results

The results produced by MARC are shown in the following figures:

Figure 3.31-3 The deformed shape of the strata after a slide of the upper stratum of 6250 m. Notice the growth of a hill of 1019 m in the neighboring of the fault.

Figure 3.31-4 The distribution across the strata of the σ_{xx} stress components (referred to the global axes) at the final step.

Figure 3.31-5 The distribution across the strata of the σ_{yy} stress components (referred to the global axes) at the final step.

Parameters, Options, and Subroutines Summary

Example e3x31.dat:

Parameters	Model Definition Options	History Definition Options
ELEMENTS	CONNECTIVITY	AUTO LOAD
END	CONTACT	CONTINUE
FINITE	CONTACT TABLE	DISP CHANGE
LARGE DISP	CONTROL	DIST LOADS
PRINT	COORDINATES	NO PRINT
SETNAME	DEFINE	POST INCREMENT
SIZING	DIST LOADS	TIME STEP
TITLE	END OPTION	
UPDATE	FIXED DISP	
	ISOTROPIC	
	NO PRINT	
	POST	
	RESTART LAST	

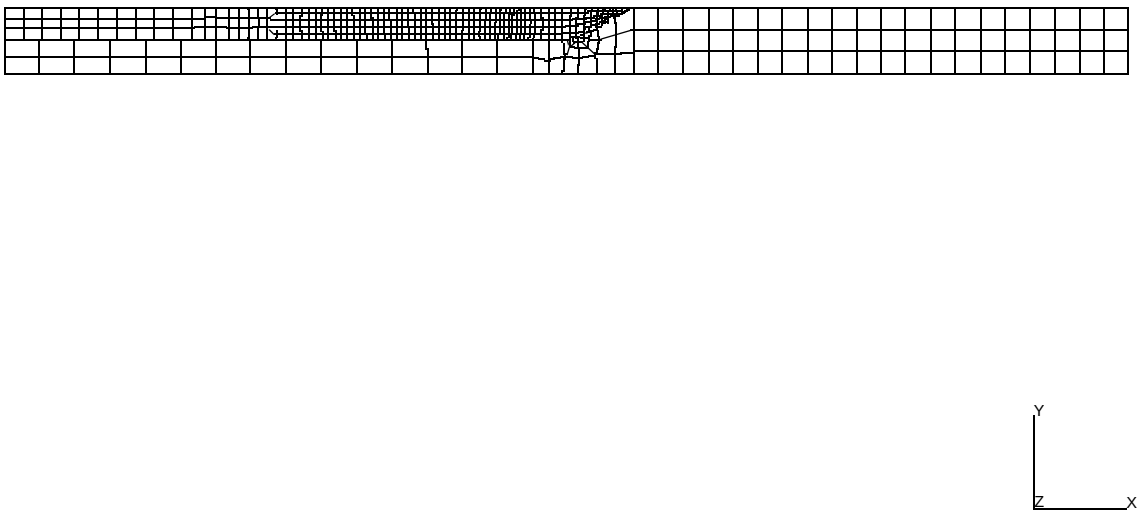

Figure 3.31-1 FEM Model of the Geological Strata

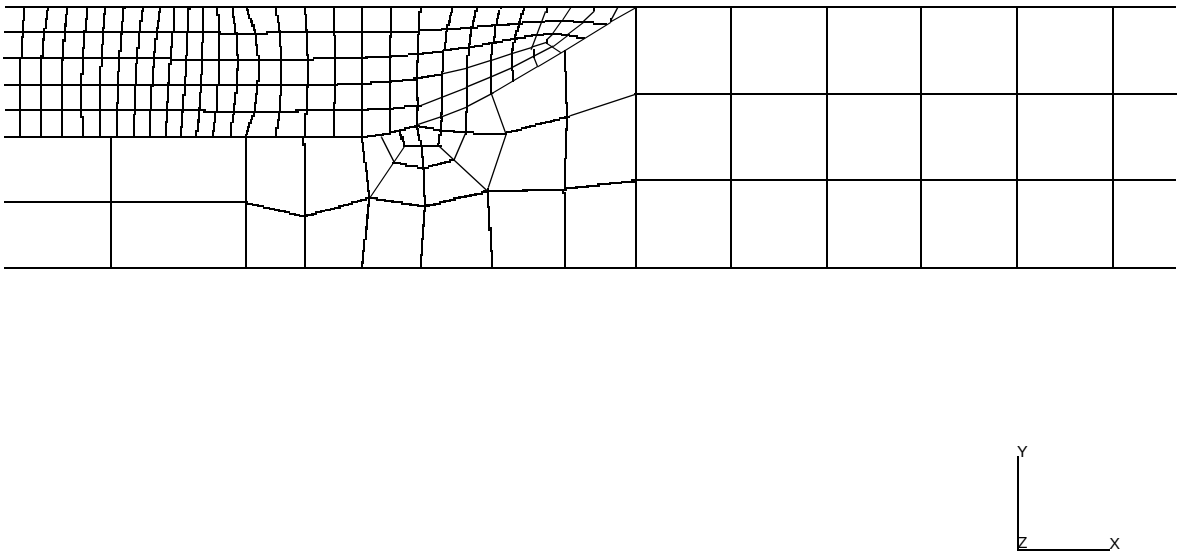

Figure 3.31-2 Detailed Mesh at the Fault Plane

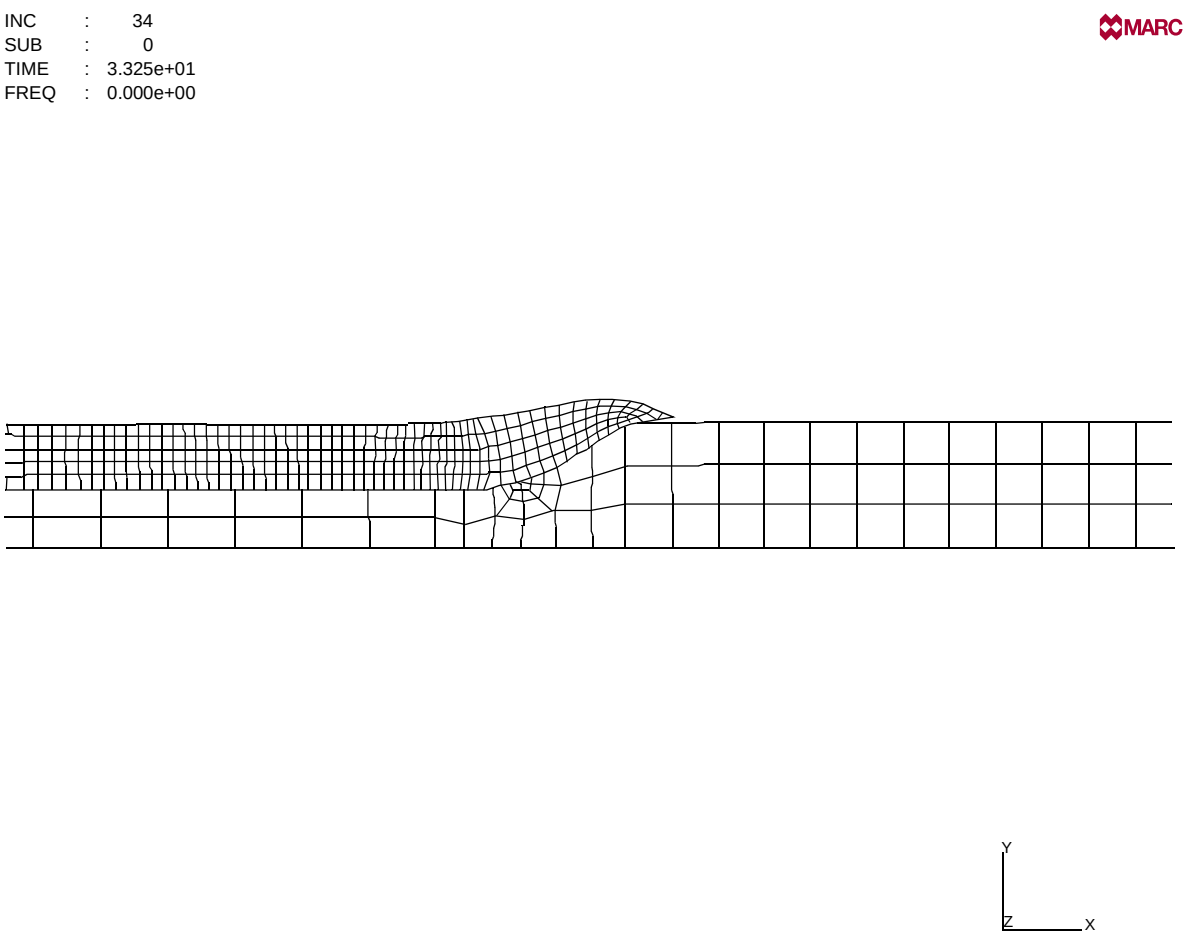

Figure 3.31-3 Overlap of the Geological Strata

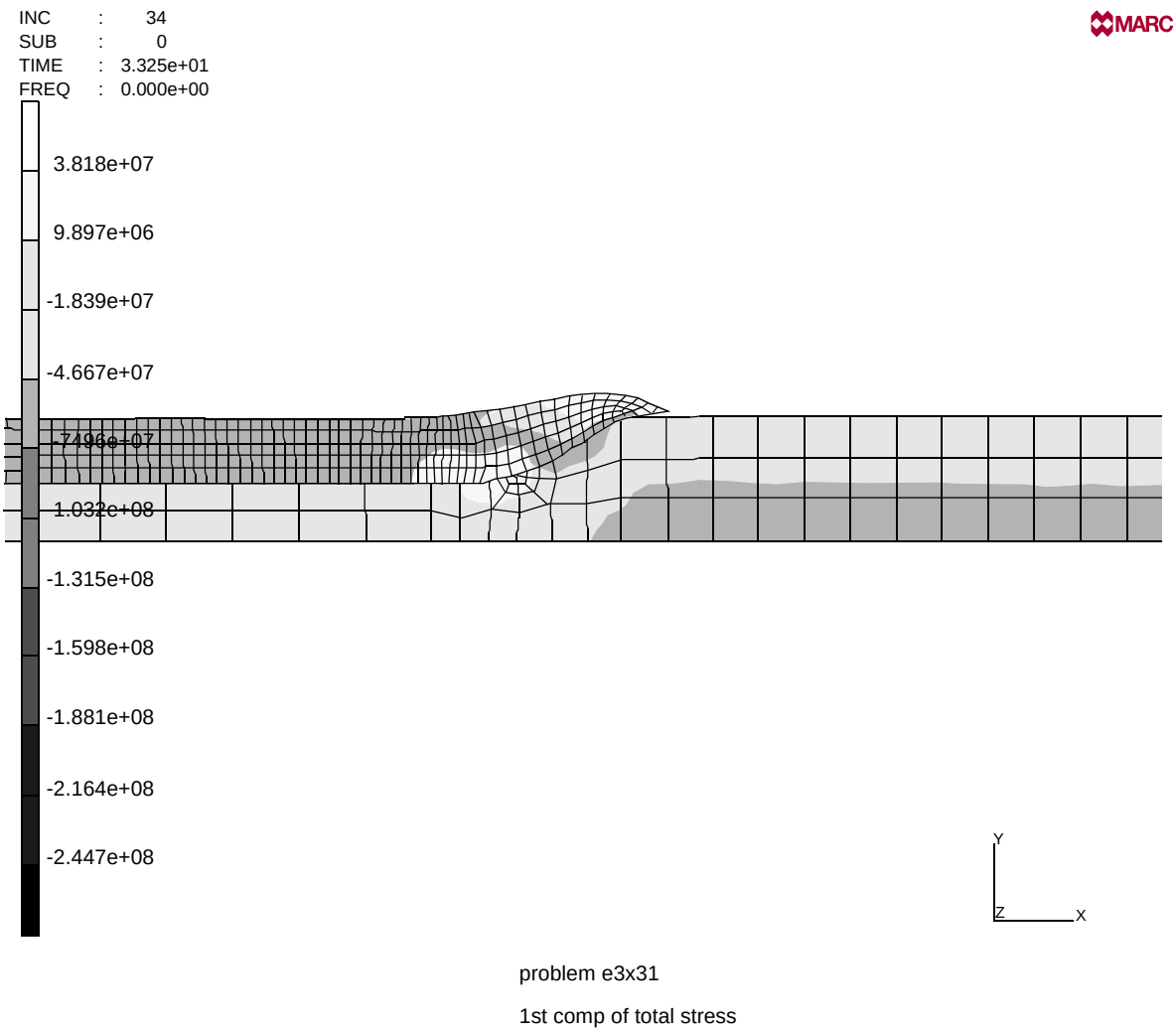

Figure 3.31-4 Distribution of the σ_{xx} Stress Component (Global Axes)

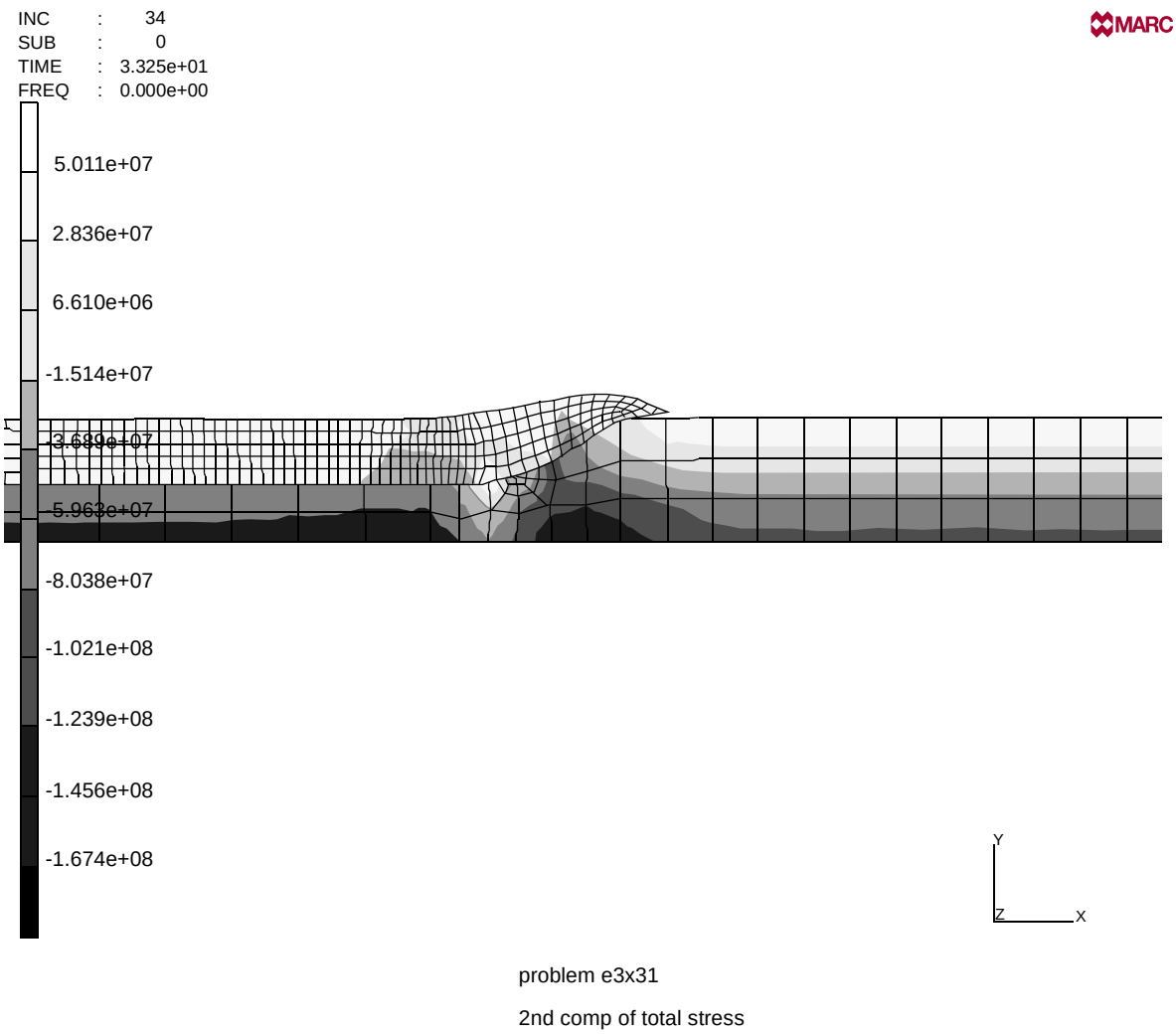

Figure 3.31-5 Distribution of the σ_{yy} Stress Component (Global Axes)

3.32 Superplastic Forming of a Strip

This problem demonstrates how to form a shape with a superplastic material. A two-dimensional flat workpiece is pressurized into a die of the desired final shape. Three different models are constructed using two-dimensional plane strain elements, three-dimensional membrane elements, and three-dimensional shell elements.

This problem is modeled using the three techniques summarized below.

Data Set	Element Type(s)	Number of Elements	Number of Nodes	Differentiating Features
e3x32a	11	340	430	F^eF^p
e3x32b	18	80	162	F^eF^p
e3x32c	75	80	162	Contact

Mesh Generation

These three models consist of 340 4-node isoparametric quadrilateral plane strain elements, 80 membrane elements, and 80 shell elements. The workpiece is 2.3 inches long with an in-plane thickness of 0.078 inches.

Boundary Conditions

The sheet is fixed at both ends in the x-direction and the left end is fixed in the y-direction where the workpiece contacts the die. The membrane and shell models have similar boundary conditions and their out-of-plane displacements are fixed to simulate plane strain. Furthermore, the membrane model will have an initial in-plane tensile stress of 50 psi for the first five increments to avoid any instabilities. This initial state of stress is supplied via user subroutine UINSTR. The workpiece is subjected to a uniform pressure whose magnitude is determined automatically in the user subroutine FORCEM to maintain a target strain rate of 0.0002. The model with these boundary condition is shown in Figure 3.32-1 and Figure 3.32-2 for the plane strain and membrane (shell) models, respectively.

Material Properties

The out-of-plane thickness is 1.0 inch for all models. The constant dilatation from of the plane strain elements is used. Superplastic materials can be viewed as exhibiting time-dependent inelastic behavior with the yield stress a function of time, temperature, strain rate, total stress, and total strain. In this case, the yield stress is only a function of the strain rate and id determined in user subroutine URPFLO. the equation used is $\sigma = \dot{\varepsilon}^b$ where $\dot{\varepsilon}$ = strain rate, σ = yield stress, a = 50,000 psi, b = 0.6

Contact

Each model has one rigid body and one deformable body. In increment 0, the rigid body is moved into first contact with the workpiece and held fixed thereafter.

Loading

The load schedule consists of a single rigid plastic loadcase with a total time period of 2500 seconds and 500 steps with convergence testing on displacements.

Rigid Plastic Analysis Class

Analysis options include the follow force options. The analysis dimension is either plane strain or three-dimensional. The results contain several variables including the pressure supplied through user subroutine PLOTV. In contact control, Coulomb friction with $\mu = 0.5$, a separation force of 1.0e6 lbf, and a sliding velocity of 1.0e-5 inches/seconds are used. For the membrane and shell models, the bias factor is set to .99 to reduce the touching distance because of the large thickness. Because nodal based friction forces must be used with membrane and shell elements, it is used for all models.

Results

Although the total time period is 2500 seconds, the part forms in a little over 2000 seconds (34 minutes). As expected, the bending of the workpiece is insignificant and the results of all models are in close agreement. The membrane elements are superior in conforming to the die shape and are substantially faster (2.5 times faster) than the plane strain or shell models.

Figure 3.32-3 shows the final deformed shape of the plane strain model. The final average thickness is 0.0554 and the sheet has elongated to 3.231 inches, showing virtually no change in volume. The final average thickness can be estimated prior to the finite element analysis since the original and final sheet length are known and the sheet is incompressible.

Figure 3.32-4 shows the pressure schedule for all models with very small differences. These small differences in the pressure schedule are caused when the sheet begins to fill the concave corner. As the sheet begins to fill the concave corner, the pressure must increase rapidly to maintain the target strain rate of 2.03-4/seconds. Note that the sliding velocity is 1/20 of the target strain rate which is a typical value (this is true for length units of inches and would need to be modified for other length units). The maximum pressure is physically limited and has a maximum value of 300 psi set in subroutine FORCEM. Furthermore, Figure 3.32-4 also plots the vertical reaction on the die divided by the sheet area versus time. This die pressure leads the sheet pressure because of friction acting on the vertical portion of the die. Here more

differences exist between the three models. The biggest difference is around 1800 seconds where the friction stops contributing to the die force because of the inability of the plane strain model to completely fill the concave corner.

Figure 3.32-5 shows the thickness profile over the deformed position along the sheet. The largest thinning in all models occurs at the 1.0 inch position or the concave corner. The significant area of difference occurs at the convex radius at the 1.9 inch position. This difference is because of transverse normal stresses caused by bearing on the radius, the plane strain elements thin more since the membrane and shell elements cannot support this deformation state. The membrane elements only thin because they are stretched and must maintain volume. The shell elements thin because they stretch and bend while maintaining volume. The plane strain elements thin because of stretching, bending, and transverse deformations while maintaining volume.

Since friction plays a large roll in the thinning of the sheet and the membrane model runs fastest, a frictionless case is run for the membrane elements. The thickness profiles of the friction and frictionless cases are shown in Figure 3.32-6. Without friction, the thinning is very uniform and the final thickness is almost the average thickness everywhere.

Summary of Parameters, Options, and Subroutines Used

Example e3x32a.dat, e3x32b, e3x32c:

Parameters	Model Definition Options	History Definition Options
ELEMENTS	CONNECTIVITY	AUTO LOAD
END	CONTROL	CONTINUE
FOLLOW FOR	COORDINATES	DIST LOADS
PRINT	DIST LOADS	MOTION CHANGE
R-P FLOW	FIXED DISP	TIME STEP
SIZING	GEOMETRY	
TITLE	ISOTROPIC	
	NO PRINT	
	OPTIMIZE	
	POST	
	SOLVER	

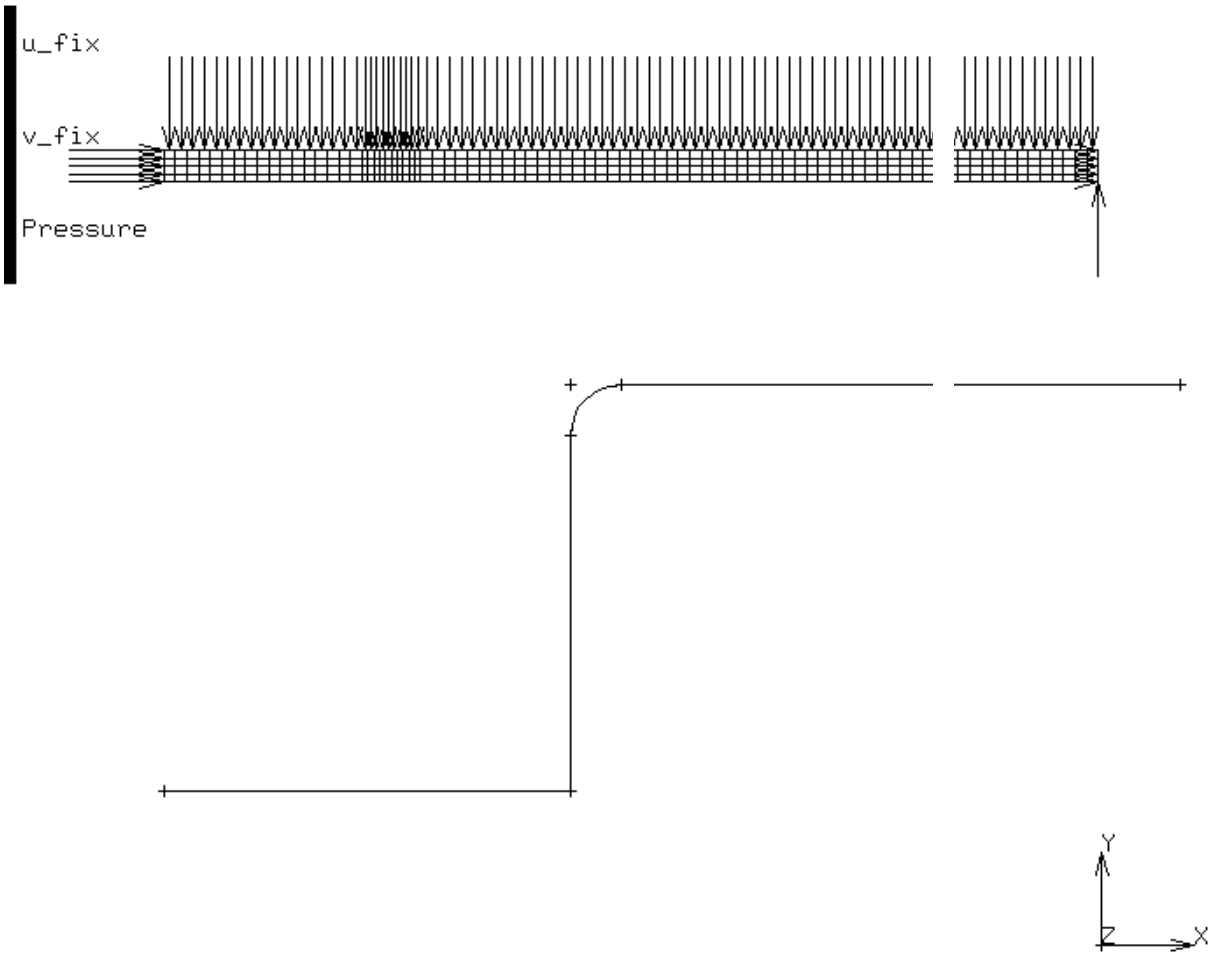

Figure 3.32-1 Plane Strain SPF Model with Boundary Conditions

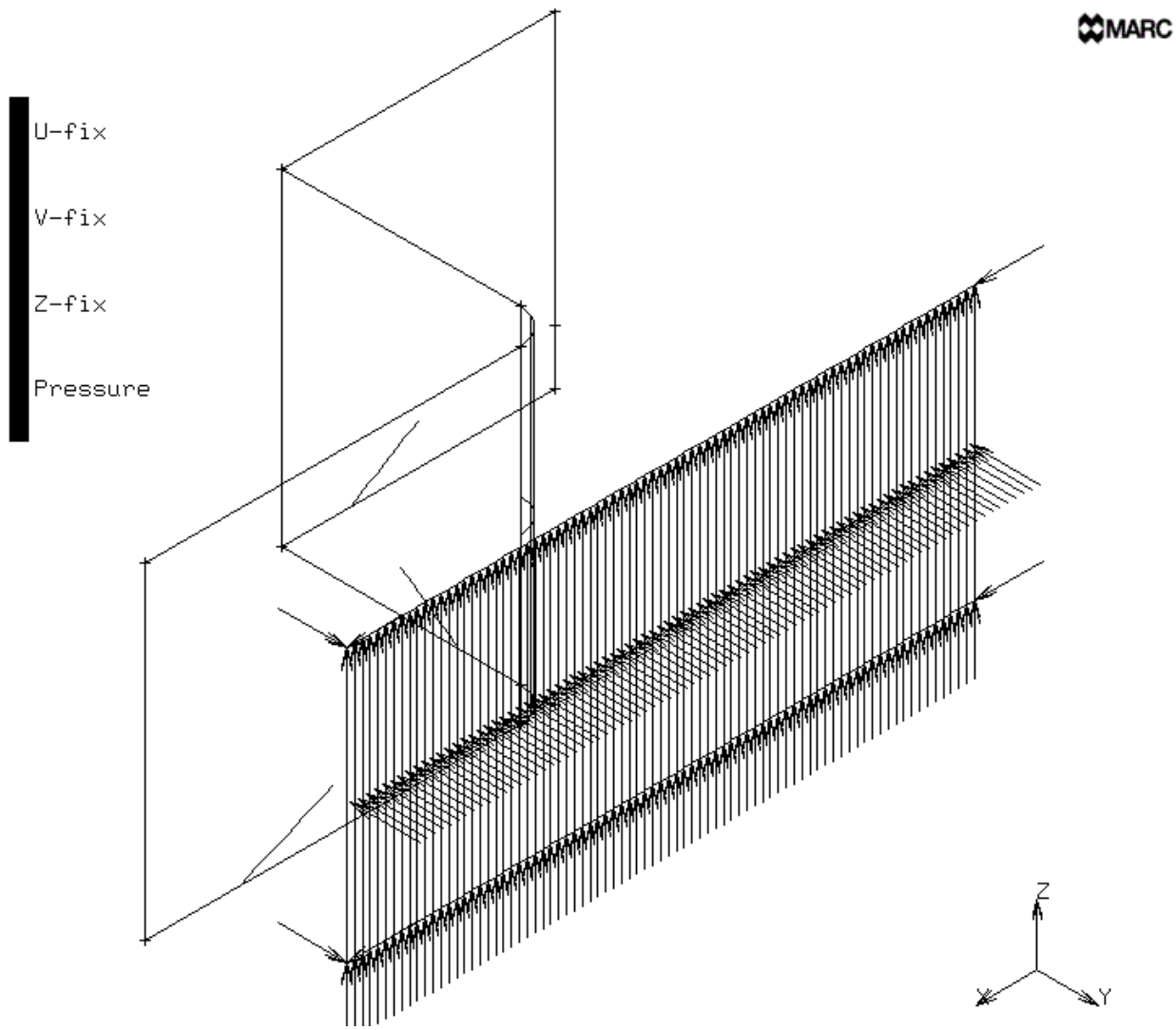

Figure 3.32-2 Membrane and Shell SPF Model with Boundary Conditions

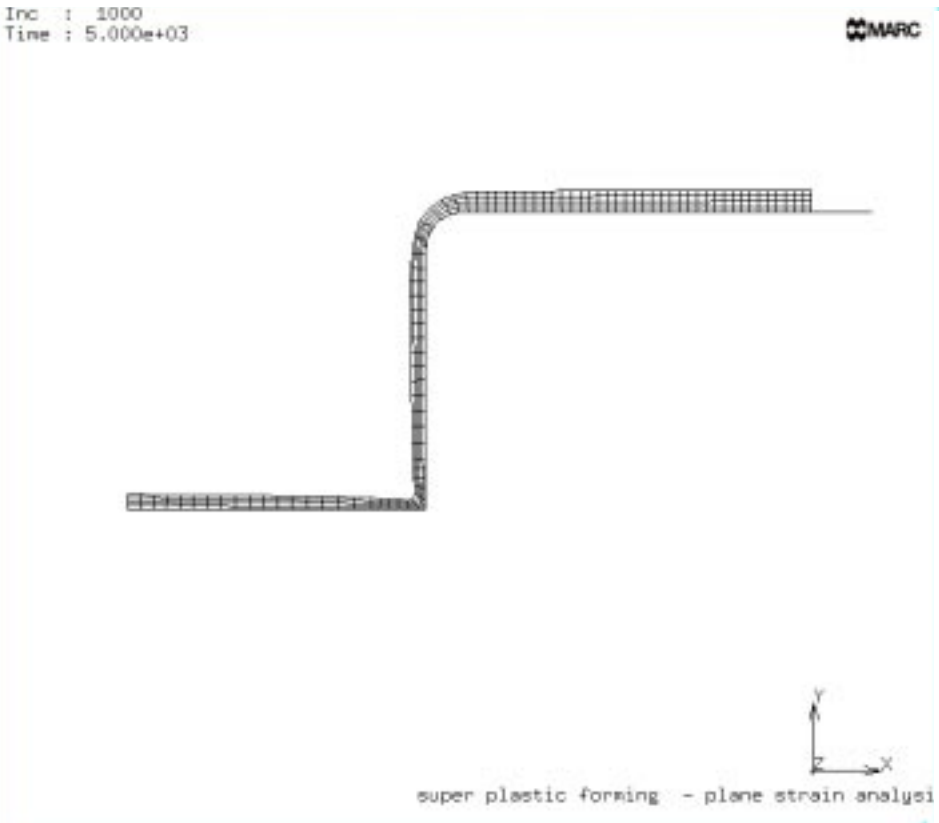

Figure 3.32-3 Plane Strain SPF Model Final Shape

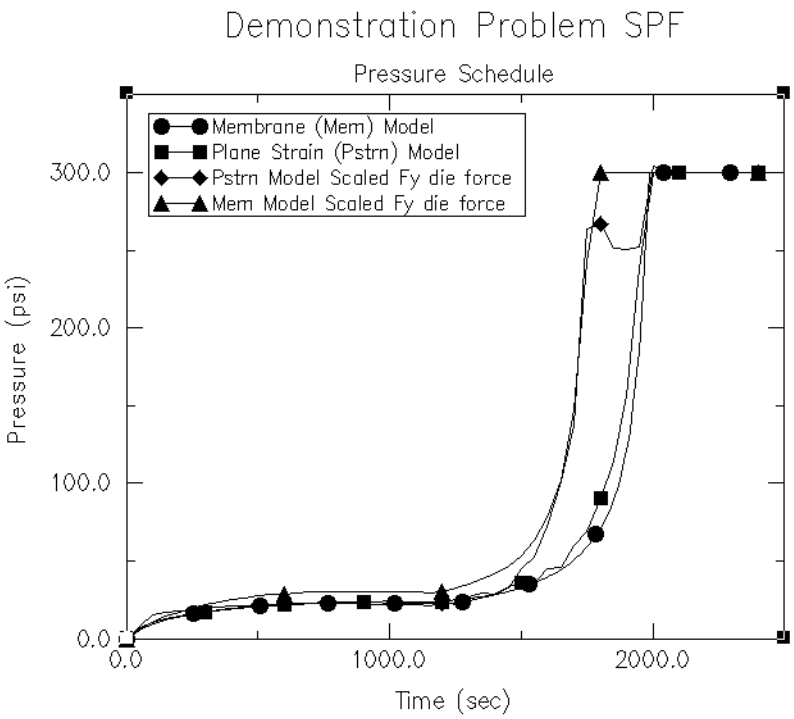

Figure 3.32-4 Pressure Schedule for all Models

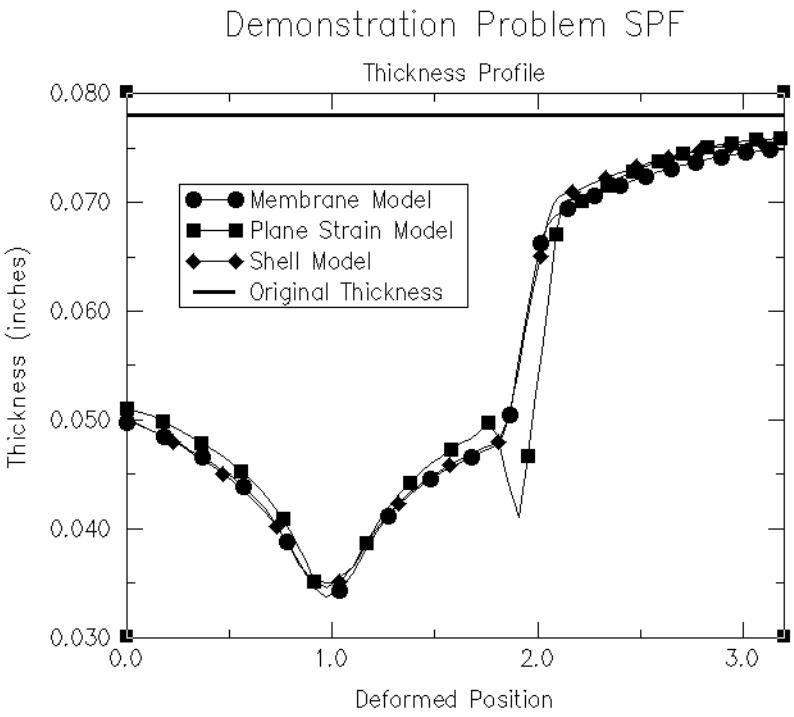

Figure 3.32-5 Thickness Profile for all Models

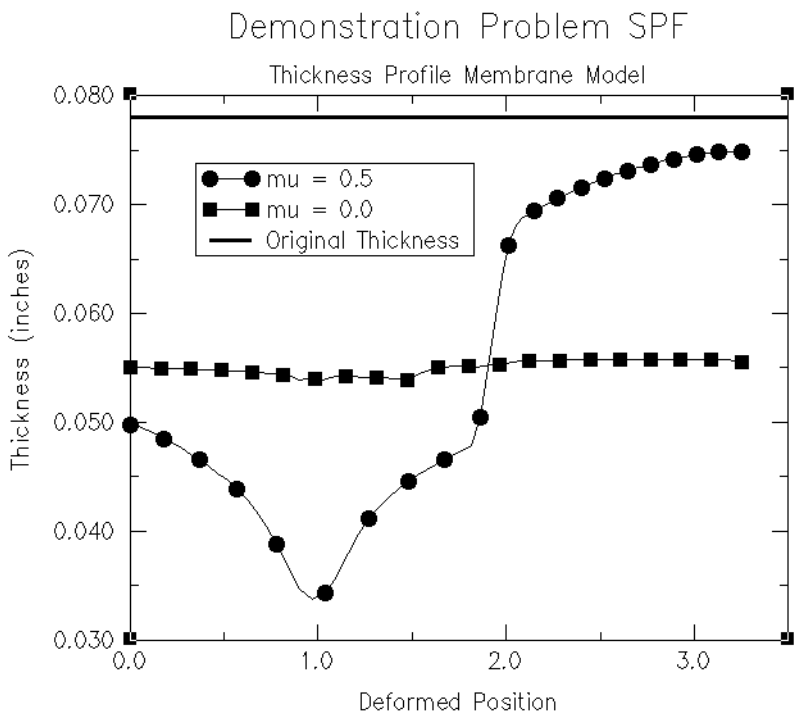

Figure 3.32-6 Thickness Profile Membrane Friction Effects

3.33 Large Strain Tensile Loading of a Plate with a Hole

This problem simulates the tensile loading of a plate with a hole to large strains. The example demonstrates the accuracy of the finite strain plasticity algorithm using F^eF^p formulation to simulate large strains. The multiplicative decomposition procedure is invoked using the PLASTICITY option.

This problem is modeled using two techniques summarized below.

Data Set	Element Type(s)	Number of Elements	Number of Nodes	Differentiating Features
e3x33	26	20	79	Plane Stress
e3x33b	27	20	79	Plane Strain

Element

This problem simulates two-dimensional plane stress and plane strain cases. For the plane stress case, an 8-node plane stress isoparametric element type 26 is used to construct a mesh while for the plane strain case, an 8-node plane stress isoparametric element type 27 is used. There are two degrees of freedom per node with a bi-quadratic interpolation and eight-point Gaussian quadrature for stiffness assembly.

Model

Due to symmetry of the geometry and loading, a quarter of the actual model is simulated. The finite element model is made up of 20 elements and 79 nodes. There is a total of 158 degrees of freedom. The model is shown in Figure 3.33-1.

Geometry

The model is assumed to be a square of side five units from which a quarter of a circle of radius one unit has been cut out. In the plane stress case, the initial thickness is one unit.

Material Properties

The material is assumed to be isotropic elastic plastic. The Young’s modulus is 3.0E+07 psi. Poisson’s ratio is 0.30. The initial yield stress is 5.0E+04 psi. The hardening behavior is given is Table 3.33-1.

Table 3.33-1 Hardening Behavior

Equivalent Plastic Strain	Workhardening Slope (psi)
0.00	14.30E+06
7.00E-04	3.00E+06
1.60E-03	1.90E+06
2.55E-03	6.70E+05
3.30E-03	3.00E+05
1.00	1.00E+05

Boundary Conditions

The loading is tensile. The lower edge of the model is restrained to have no y displacements, while the left edge the model is constrained to have no x displacements. The top edge is subjected to displacement increments in the y direction.

Results

The contours of effective plastic strain on the deformed model are shown in Figure 3.33-2. Plasticity initiates at the hole due to the stress concentration and accumulates with increasing strain. The maximum value is 186% at the end of the last increment. The history plot of x displacement at node 34 as a function of the increment is shown in Figure 3.33-3. Node 34 is the node on the hole edge and has specified zero y displacement. Figure 3.33-3 shows that the increments of x displacement at node 34 are initially negative, indicating that the hole is shrinking in dimension perpendicular to the loading direction. However, as plasticity accumulates, the x displacement increments become positive, indicating a growth in the hole dimension perpendicular to the loading direction. As the hole surface grows outward, the external surface continues to move inward. This reduces the ligament size available to carry load and necking results. This behavior is also seen for the plane strain case although with different numerical values.

Parameters, Options, and Subroutines Summary

Examples e3x33a.dat and e3x33b.dat :

Parameters	Model Definition Options	History Definition Options
TITLE	CONNECTIVITY	AUTO STEP
SIZING	COORDINATES	DISP CHANGE
ELEMENTS	ISOTROPIC	CONTINUE
LARGE DISP	GEOMETRY	
PLASTICITY	WORK HARD	
	FIXED DISP	

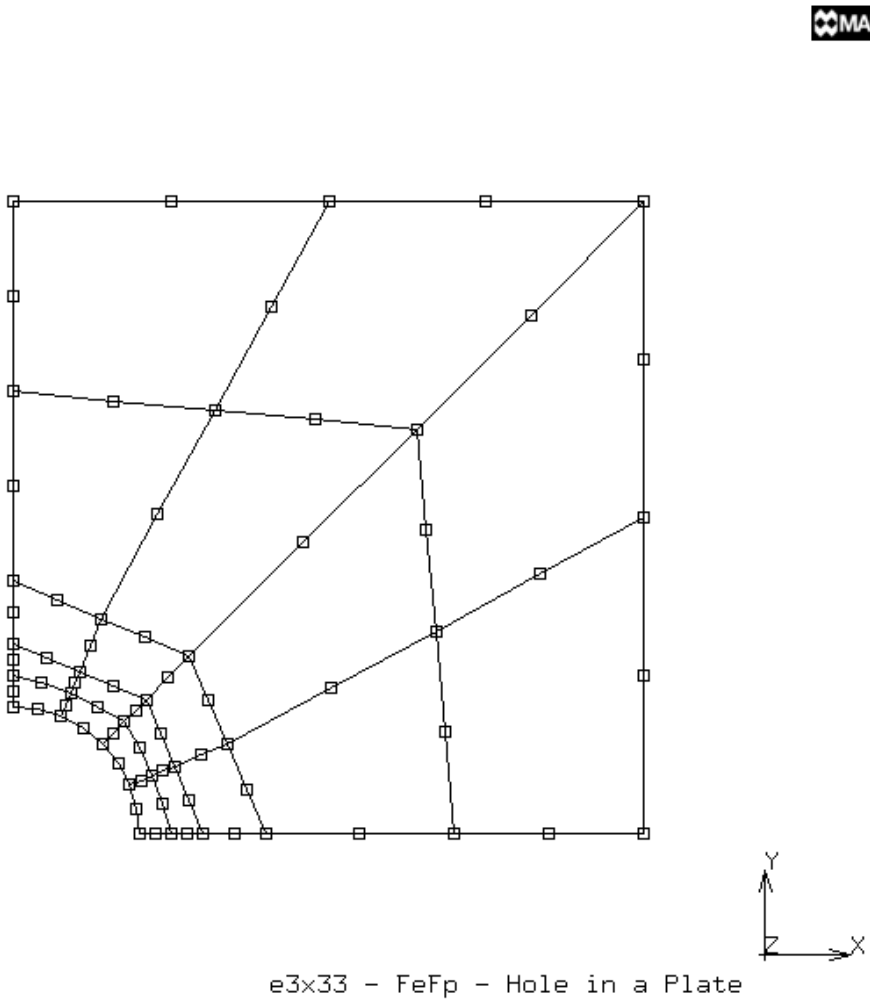

Figure 3.33-1 Initial Model for Hole-in-Plate

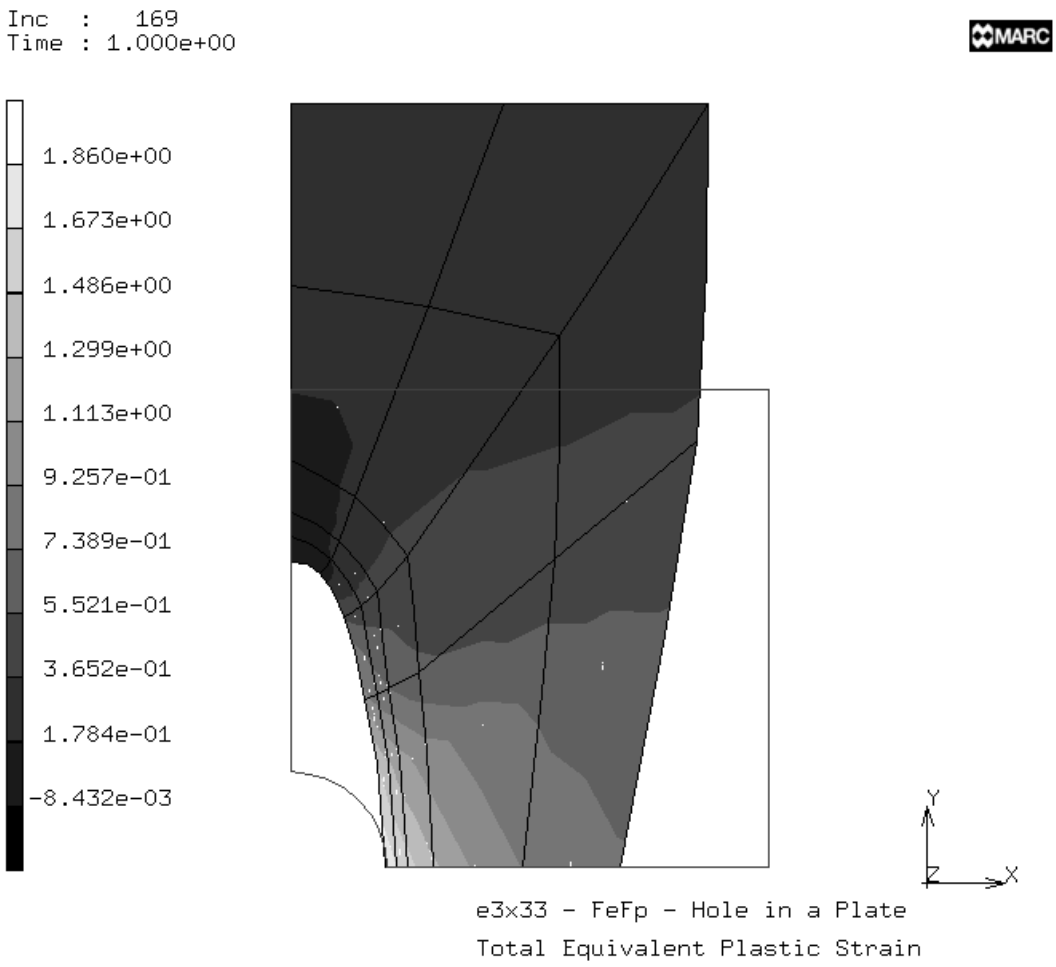

Figure 3.33-2 Equivalent Plastic Strain on the Deformed Model

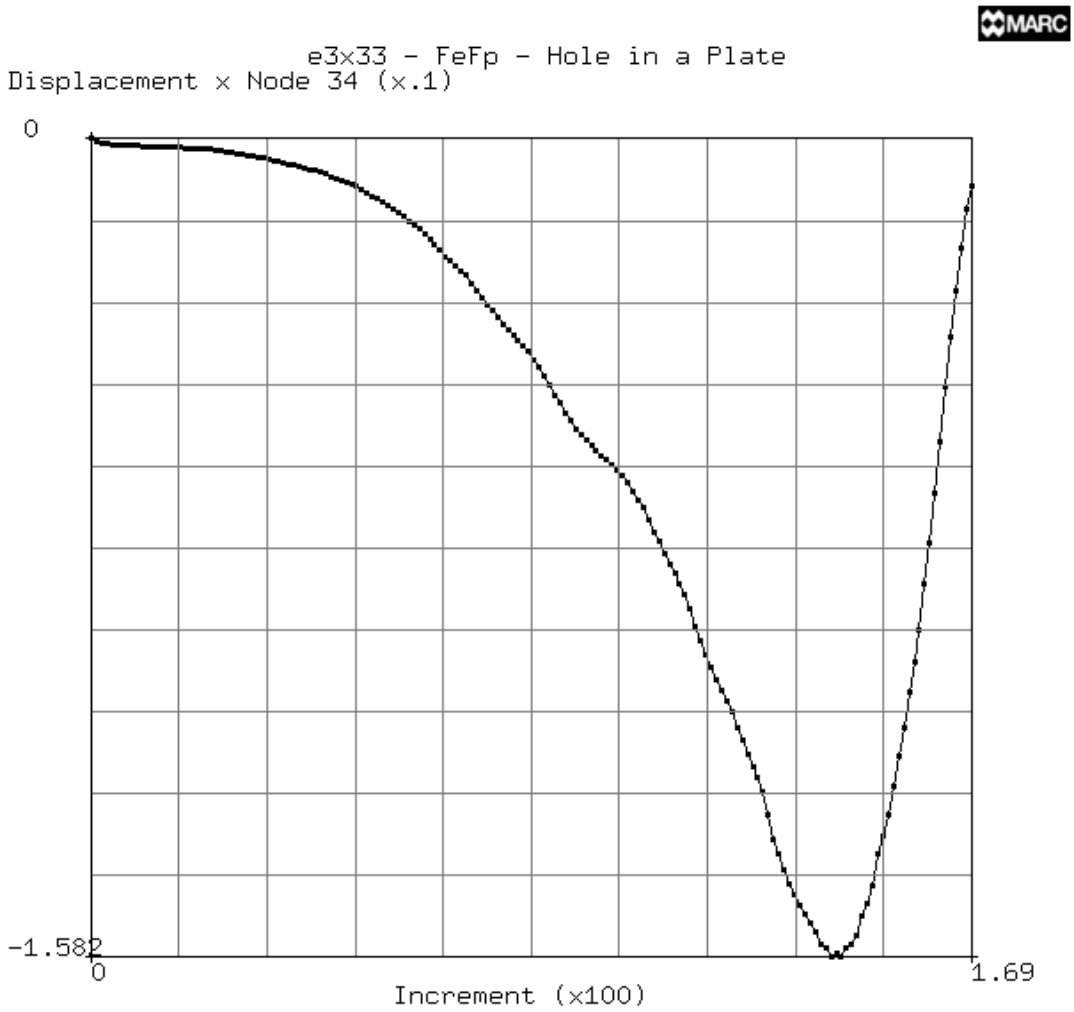

Figure 3.33-3 History Plot of x Displacement versus Increment for Node 34

3.34 Inflation of a Thin Cylinder

This problem simulates the elasto-plastic inflation of a thin cylinder.

Element

The 4-node membrane element type 18 is used. There are three degrees of freedom per node with bilinear interpolation and four-point Gaussian quadrature.

Model

Due to symmetry of the geometry and loading, a quarter of the cylinder is simulated. The finite element model is made up of 100 elements and 126 nodes. There is a total of 378 degrees of freedom. The initial mesh is shown in Figure 3.34-1.

Geometry

The cylinder is of unit radius and a length of 5 units.

Material Properties

The material is assumed to be isotropic elastic plastic. The Young's modulus is 3.0E+07 psi. Poisson's ratio is 0.30. The initial yield stress is 2.5E+04 psi. The slope of the plastic stress strain curve is assumed to be 3.E+05. The multiplicative decomposition radial return procedure is used for this large strain plasticity problem. This is invoked by the PLASTICITY parameter.

Boundary Conditions

The model is restrained to have no Y-displacements on nodes 1, 3, 5, 6, 7, and 8. X-displacements are zero on nodes 2, 4, 123, 124, 125, and 126. The Z-displacements are held to zero on nodes 1, 2, 9, 15, 21, 27, 33, 39, 45, 51, 57, 63, 69, 75, 81, 87, 93, 99, 105, 111, and 117. A distributed load of 200 psi is imposed on all elements to simulate the pressurization of the cylinder. This distributed load is applied consecutively for five increments.

Results

The final deformed mesh is shown in Figure 3.34-2. Due to the nature of the geometry and boundary conditions, the problem is homogeneous. The first increment is purely elastic and plasticity evolves from the second increment. The effective plastic strain is shown as a function of the increments in Table 3.34-1.

Table 3.34-1 Effective Plastic Strain

Increment Number	Total Effective Plastic Strain (%)
1	0.00000
2	5.79726
3	14.89630
4	26.47110
5	43.13700

Parameters, Options, and Subroutines Summary

Example e3x34.dat:

Parameters	Model Definition Options	History Definition Options
APPBC	CONNECTIVITY	AUTO LOAD
ELEMENTS	COORDINATES	CONTINUE
FOLLOW FOR	DIST LOADS	CONTROL
LARGE DISP	FIXED DISP	DIST LOAD
PLASTICITY	GEOMETRY	PROPORTIONAL INC
PRINT	ISOTROPIC	TIME STEP
SIZING	OPTIMIZE	
TITLE	SOLVER	
	WORK HARD	

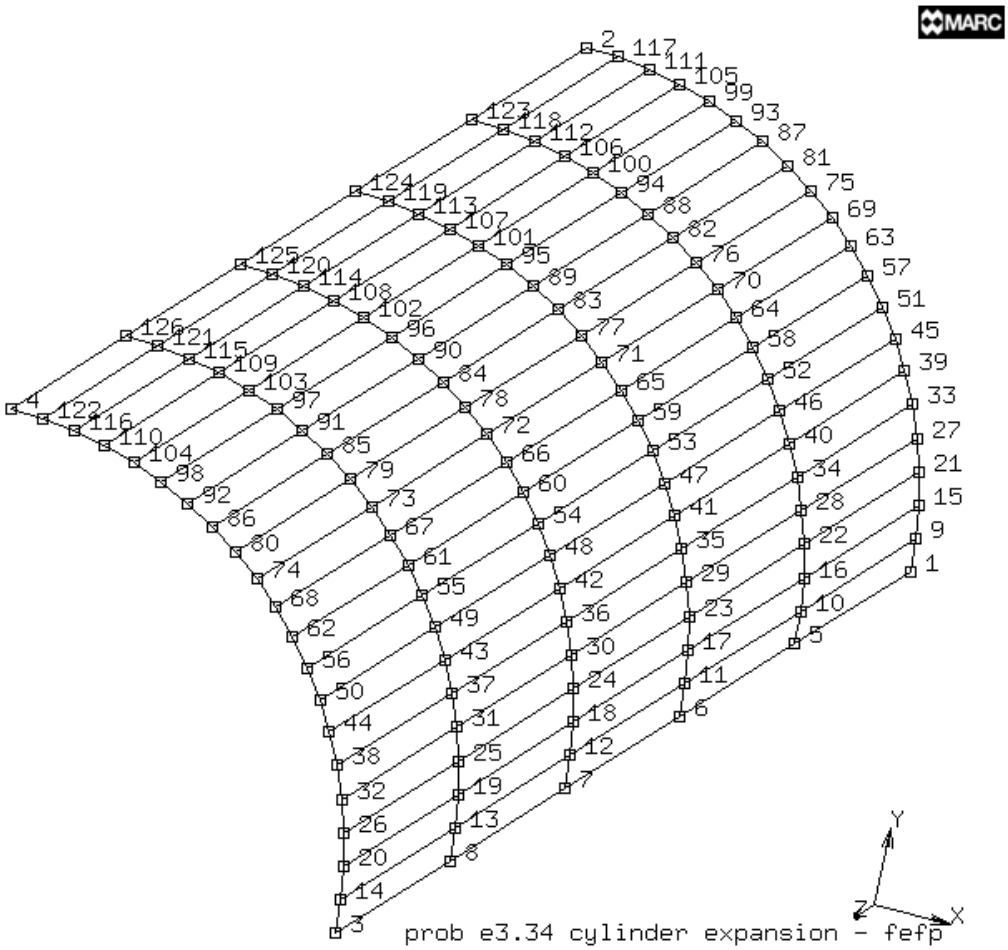

Figure 3.34-1 Initial Mesh for Cylinder Inflation

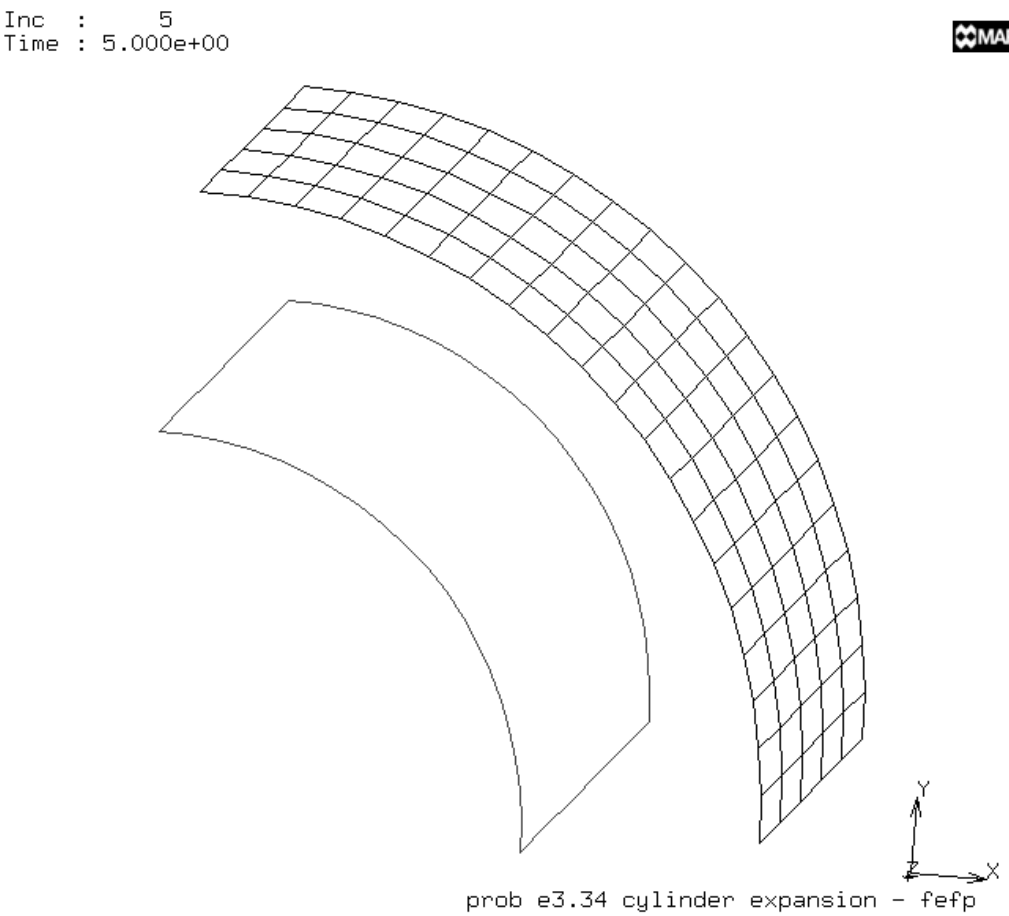

Figure 3.34-2 Initial and Final Configuration for Cylinder Inflation

3.35 Cantilever Beam under Point Load

An large strain elastoplastic analysis is carried out for cantilever beam subjected to point load. This problem demonstrates the use of MARC algorithm for large strain plasticity. The algorithm, activated by option PLASTICITY,5 is based on hyperelasticity and multiplicative decomposition of deformation gradient into a elastic part and a plastic part (F^eF^p). The problem is modeled using element type 11.

Element

Library element 11 is a 4-node bilinear plane strain element with displacements in x and y directions as degrees of freedom.

Model

The total length of the beam is 20 mm. The cross-section of the beam is a quadrilateral with a side length of 1 mm. Figure 3.35-1 illustrates the beam configuration. The beam is modeled using 60 4-node bilinear plane strain elements (see Figure 3.35-2).

Material Properties

All elements have the same properties: Young's modulus is 3.0E7 N/mm^2; Poisson's ratio is 0.3; the initial yield stress is 3.0E4 N/mm^2. A piecewise linear approximation is used to represent the workhardening behavior of the material.

Loading

A point load of -.74E3 N is applied to the tip node at the free end of the beam (see Figure 3.35-1) in 91 increments. It is done by using PROPORTIONAL INC option.

Boundary Conditions

The four nodes at one end of the beam are fixed (see Figure 3.35-1).

Results

The deformed configurations and the distributions of equivalent plastic strains for increments 30 and 90 are shown in Figure 3.35-3 and Figure 3.35-4 respectively.

Parameters, Options, and Subroutines Summary

Example e3x35.dat:

Parameters	Model Definition Options	History Definition Options
ALL POINTS	CONNECTIVITY	AUTO LOAD
ELEMENTS	CONTROL	CONTINUE
END	COORDINATES	POINT LOAD
PLASTICITY	END OPTION	PROPORTIONAL INC
PRINT	FIXED DISP	
SIZING	GEOMETRY	
TITLE	ISOTROPIC	
	NO PRINT	
	OPTIMIZE	
	POST	
	POINT LOAD	
	SOLVER	
	TYING	
	WORK HARD	

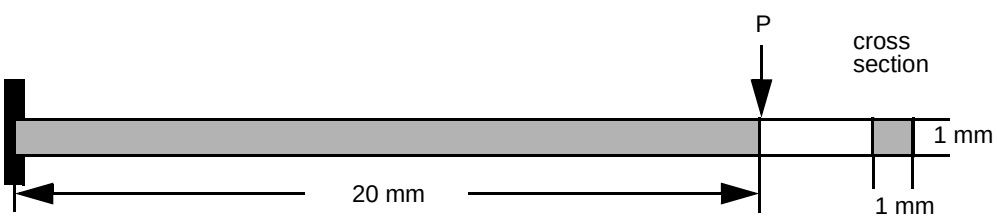

Figure 3.35-1 Cantilever Beam under Point Load

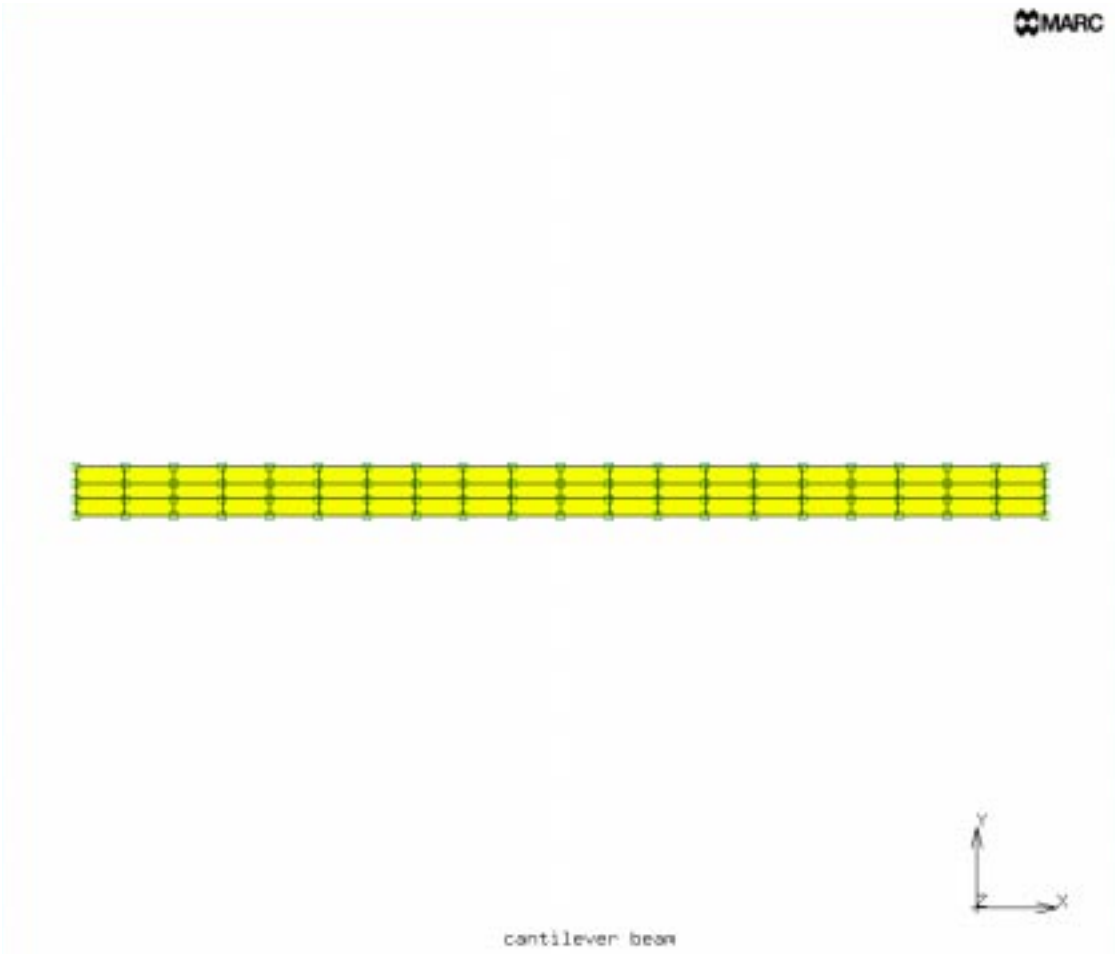

Figure 3.35-2 FE-Mesh

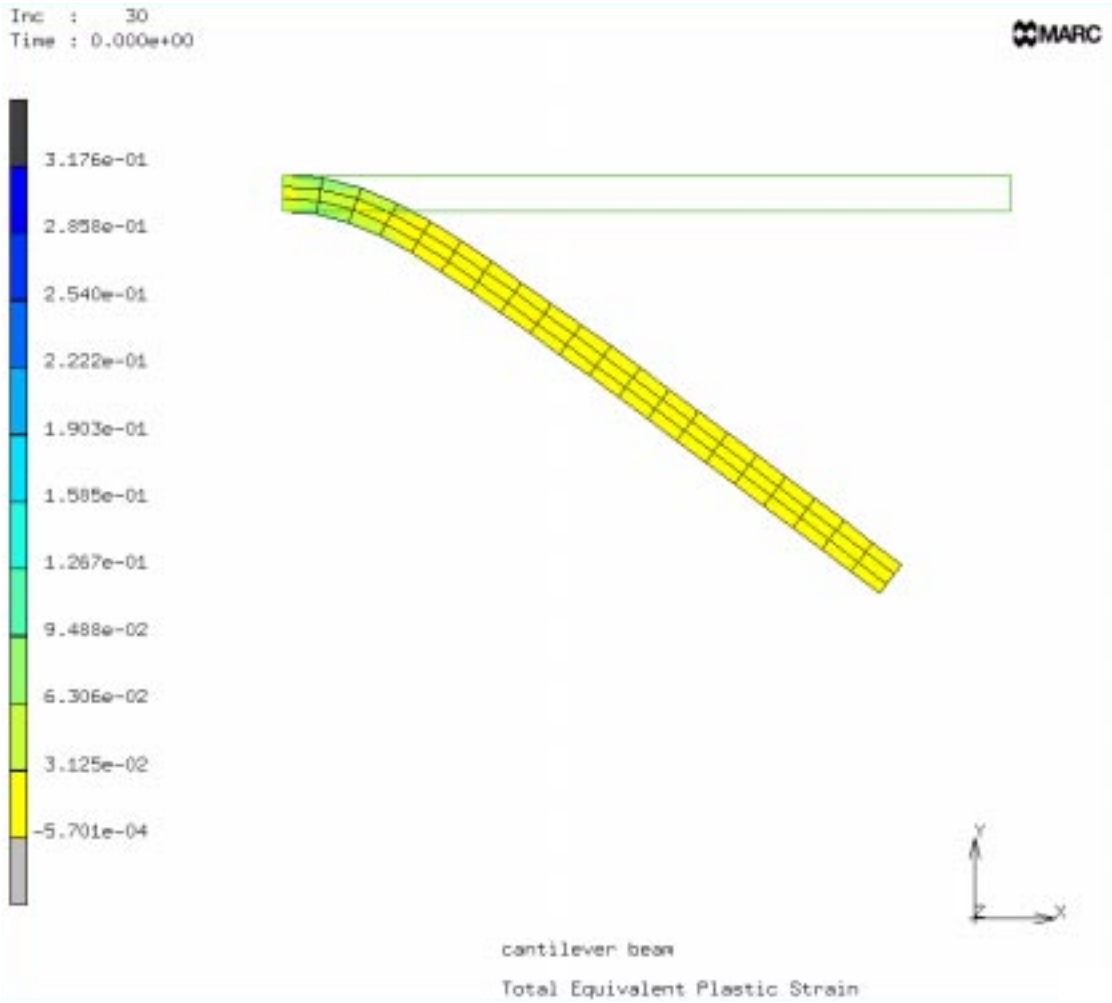

Figure 3.35-3 Deformed Mesh and Distribution of Equivalent Plastic Strain at Increment 30

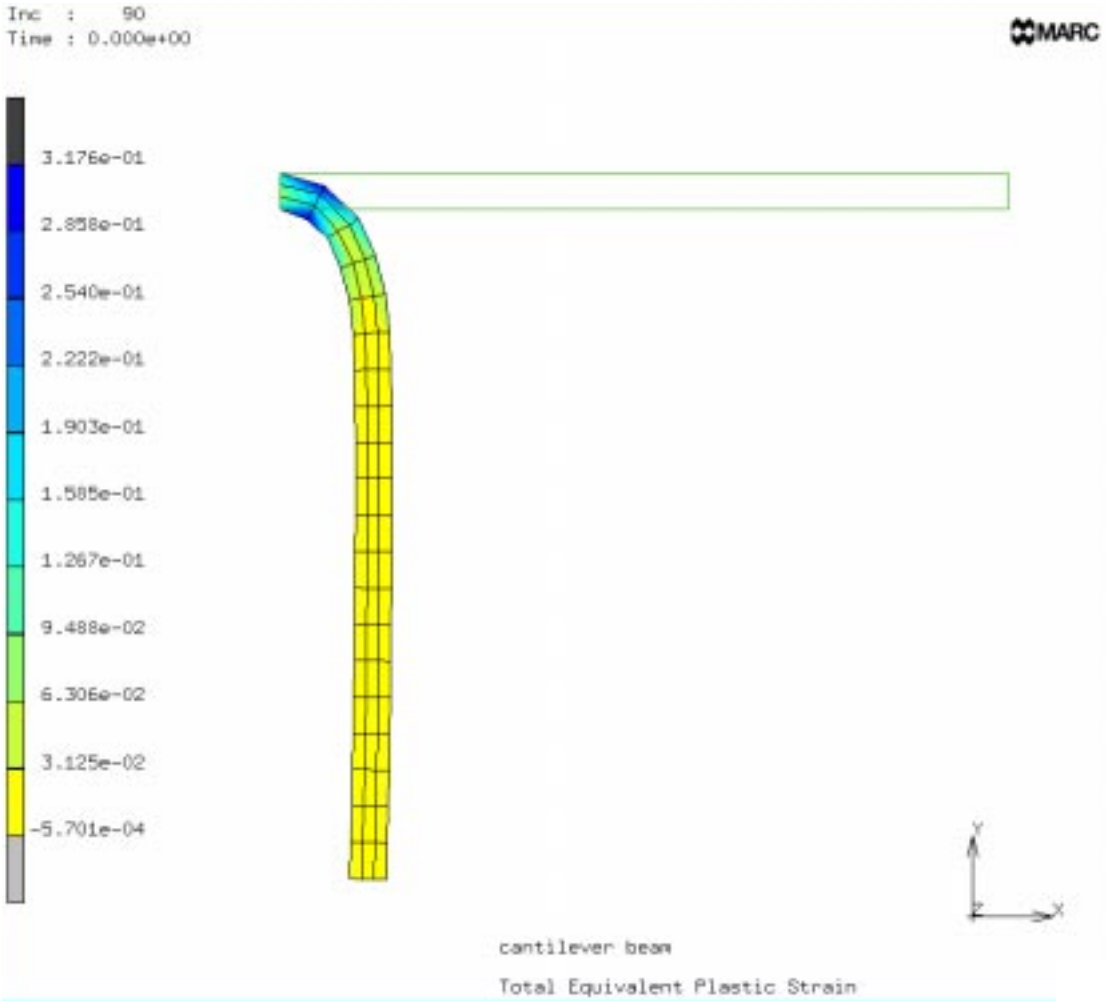

Figure 3.35-4 Deformed Mesh and Distribution of Equivalent Plastic Strain at Increment 90

3.36 Tensile Loading of a Strip with a Cylindrical Hole

This example uses the multiplicative decomposition radial return F^eF^p plasticity to model the tensile behavior of a three-dimensional strip with a through thickness cylindrical hole in the center.

Model

The strip is of square cross section of side 4 mm and a thickness of 0.4 mm. A cylindrical hole of radius 0.6 mm is at the center. Due to symmetry, an eighth of the geometry is modeled. Thus the model is a square of side 2 mm in the x-y plane and a thickness of 0.2 mm in the z-direction, with a cylindrical hole of radius 0.6 mm. The model is comprised of 92 elements and 218 nodes and is shown in Figure 3.36-1.

Element

The 8-node, 3D, brick element type 7 is used in this analysis.

Boundary Conditions

The boundary conditions used reflect the geometrical and loading symmetry in the model. The x- and y-displacements are constrained in the Z = 0.2 plane while the z-displacements are constrained to be zero in the Z = 0 plane.

Material Properties

All elements are treated as isotropic. The Young's modulus is 3×10^7 N/mm^2. The Poisson's ratio is 0.33 and the initial yield stress is 3.5×10^4 N/mm^2. The hardening behavior is specified using the WORK HARD model definition option.

History Definition

The loading of the three-dimensional strip is carried out using displacement increments specified on the top surface along the y-direction as given below:

Number of Increments	Y-displacement Increment (mm)
2	0.001
10	0.002
25	0.020

There are no loads in the x- or z-direction and the strip is free to move in, along these directions. The small thickness in the z-direction compared to the x and y dimensions approximates a case of plane stress along the z-direction. The displacement increments are imposed using the DISP CHANGE and AUTO LOAD history definition options. There are a total of 37 increments.

Results

Increment 1 is elastic. However, plasticity is incipient and increment 2 shows the initiation of plasticity at the stress concentration at the equator of the hole (Figure 3.36-1). At the end of increment 12, a radial swath of plasticity develop with a maximum value of the effective plastic strain is 8.14%. The displacement increments after increment 12 are large and the plastic strain continues to accumulate rapidly from increment 13. The contours of effective plastic strain at increments 20 and 37 are shown in Figure 3.36-2 and Figure 3.36-3 respectively. The shape of the hole develops into a progressively prolate shape. Necking behavior is evident from the deformation. From Figure 3.36-3, it can be seen that the material near the hole thins more rapidly in the z-direction than the material near the edges. Continued loading will lead to failure by loss of load carrying capacity in the X-Z plane.

Parameters, Options, and User Subroutines Summary

Parameters	Model Definition Options	History Definition Options
ALL POINTS	CONNECTIVITY	AUTO LOAD
ELEMENTS	COORDINATES	CONTINUE
END	END OPTION	DISP CHANGE
PLASTICITY	FIXED DISP	
PRINT	GEOMETRY	
SETNAME	ISOTROPIC	
SIZING	WORK HARD	
TITLE		

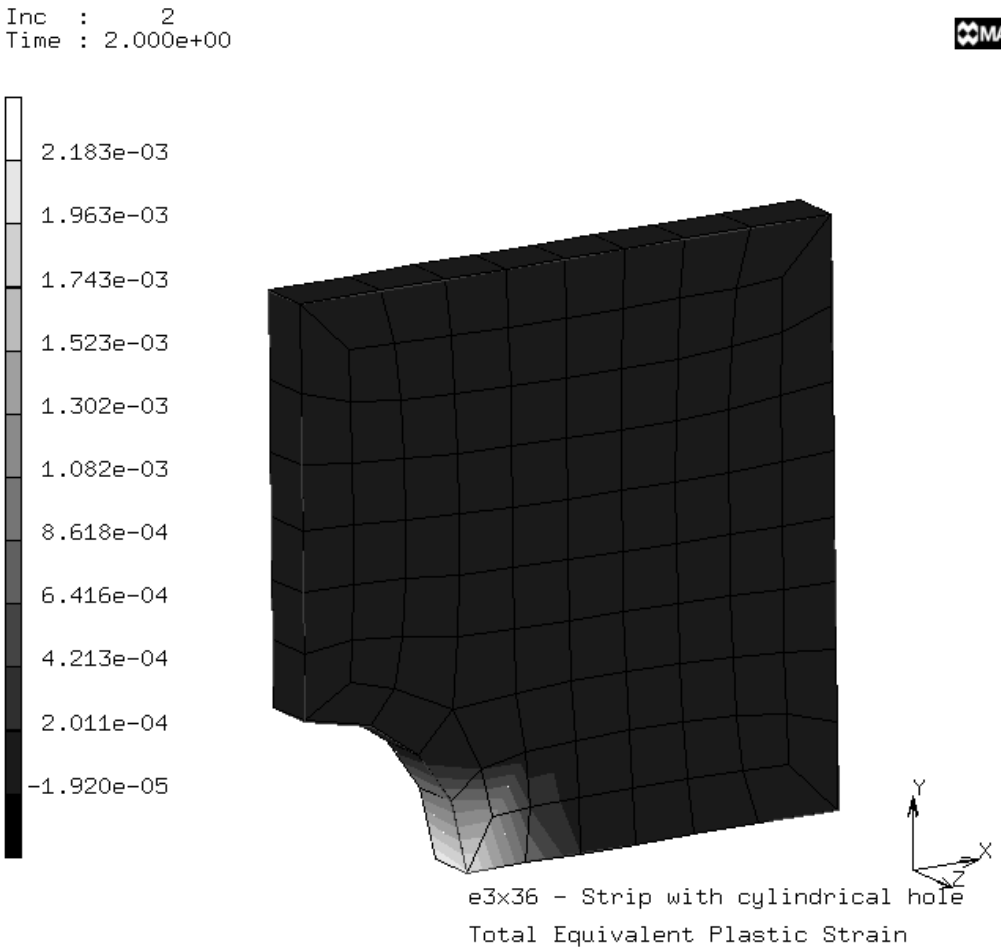

Figure 3.36-1 Plasticity Initiates at the Hole in Increment 2

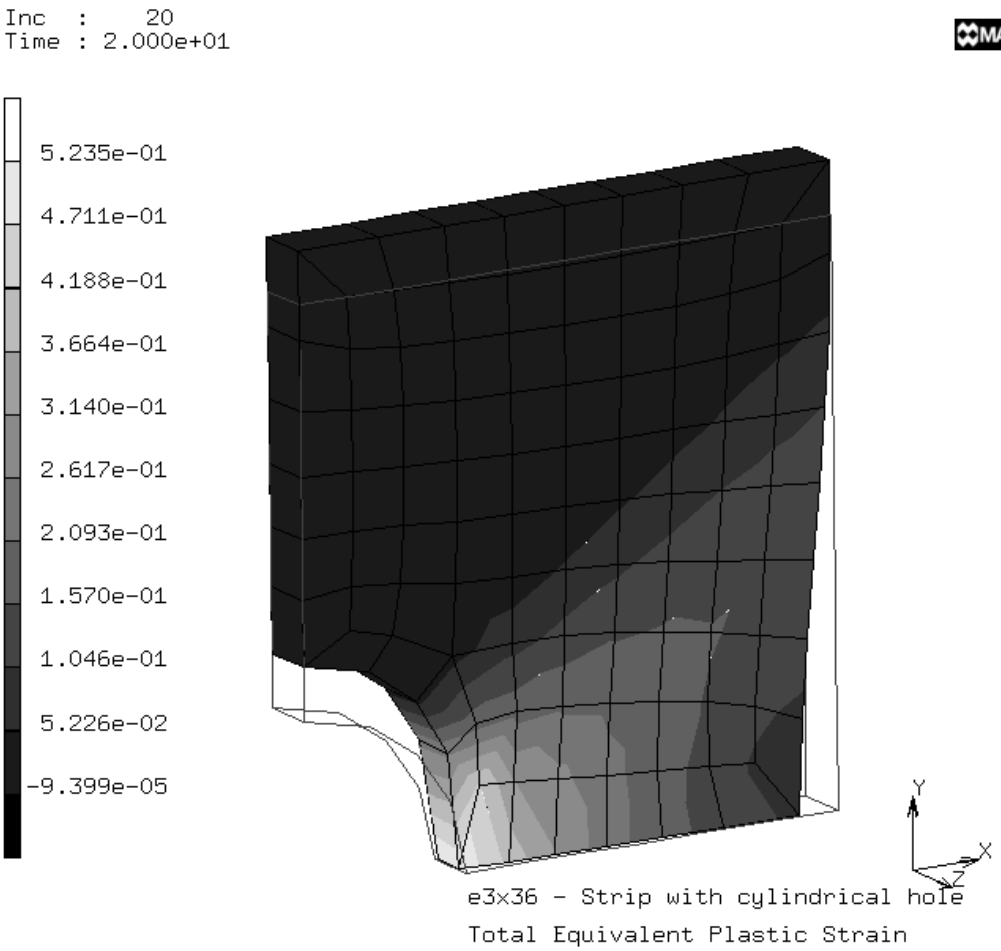

Figure 3.36-2 Contours of Effective Plastic Strain after 20 Increments

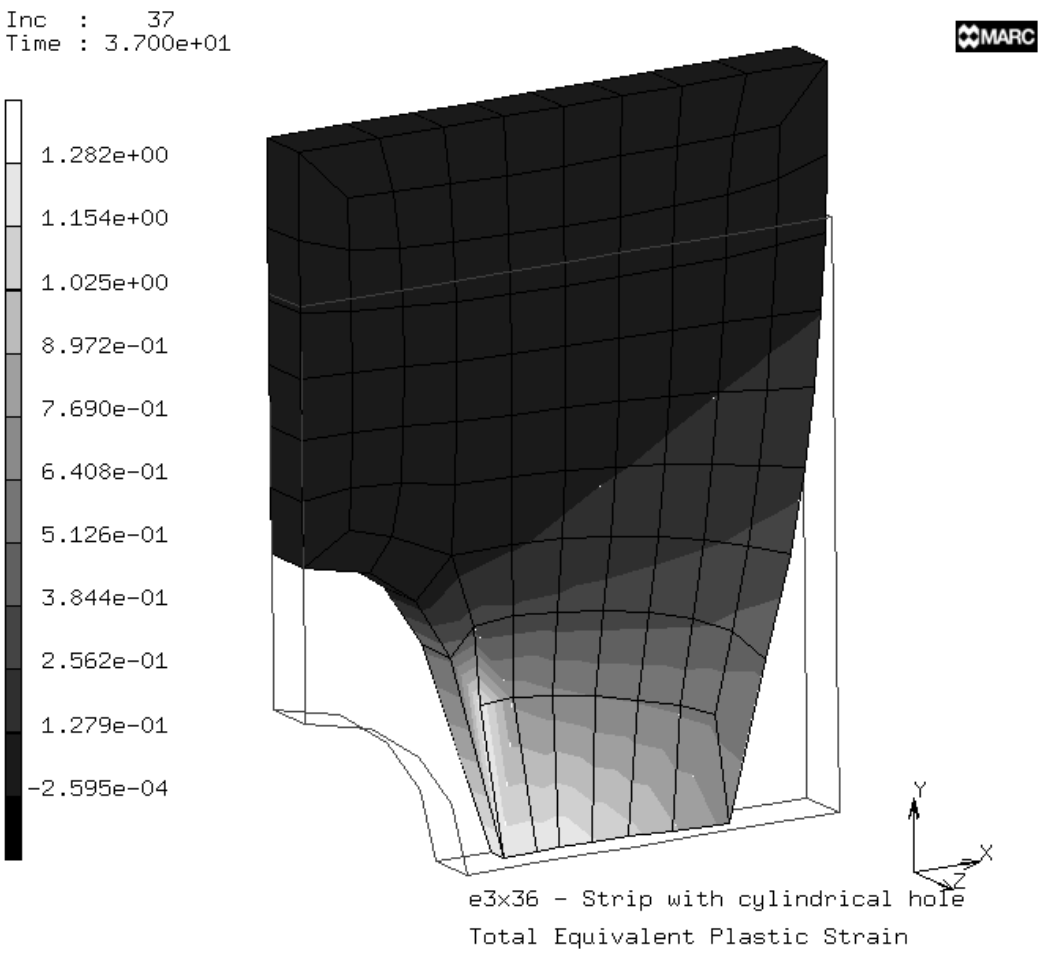

Figure 3.36-3 Contours of Effective Plastic Strain after 37 Increments

3.37 Elastic Deformation in a Closed Loop

This problem shows the fundamental difference between the use of hypoelasticity and hyperelasticity. One plane strain element subjected to a closed loop of large elastic deformation is considered. Element type 11 is employed. To activate hypoelastic constitutive equations, parameter PLASTICITY,3 is used in e3x37a.dat. The problem e3x37b.dat activates hyperelastic constitutive equations via PLASTICITY,5. A very large yield stress is given to guarantee the deformation remains elastic.

Element

Library element 11 is a 4-node bilinear plane strain element with displacements in x and y directions as degrees of freedom.

Model and Boundary Conditions

A quadrilateral element with the side length of 1 mm. The nodes 1 and 2 are fixed.

Material Properties

Material same properties are given as: Young's modulus is 20300.0 N/mm^2; Poisson's ratio is 0.33; Yield stress is 999999999.0 N/mm^2.

Loading

A closed loop of large elastic deformation is applied to the element by using prescribed displacements for the nodes 3 and 4. The sequence of the prescribed displacements for the nodes 3 and 4 are given as: (a) u = 5 mm, (b) v = 5 mm, (c) u = -5 mm, and (d) v = -5 mm. Each is applied with 5 equal increments and is shown in Figure 3.37-1.

Results

Figure 3.37-2 shows the nodal reaction forces obtained from both e3x37a.dat and e3x37b.dat, after the closed loop of large elastic deformation. It can be seen that the use of hypoelasticity in e3x37a.dat results in nonzero reaction forces even if the deformation becomes zero. The job e3x37b.dat which is based on hyperelasticity via PLASTICITY,5 leads to correct results. Figure 3.37-3 is the history plot of the equivalent von Mises stress. Nonzero stress is obtained after the closed loop of elastic deformation for hypoelasticity based solution.

Parameters, Options, and Subroutines Summary

Example e3x37.dat:

Parameters	Model Definition Options	History Definition Options
ELEMENTS	CONNECTIVITY	AUTO LOAD
END	CONTROL	CONTINUE
LARGE DISP	COORDINATES	DISP CHANGE
PLASTICITY	END OPTION	
SIZING	FIXED DISP	
TITLE	GEOMETRY	
	ISOTROPIC	
	POST	

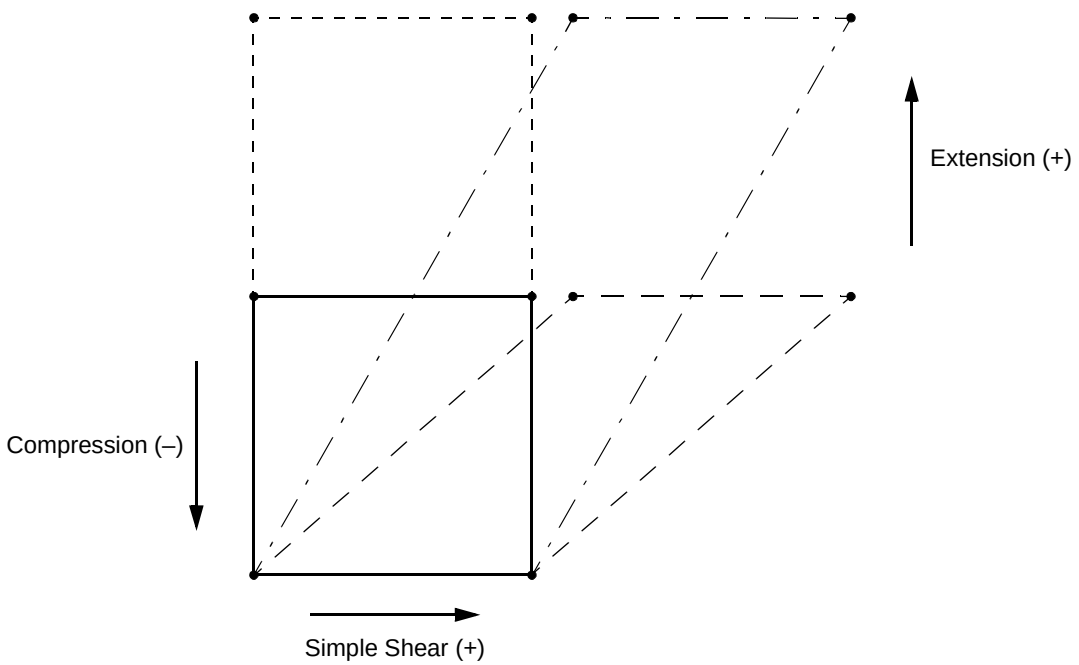

Figure 3.37-1 Elastic Deformation in a Closed Loop

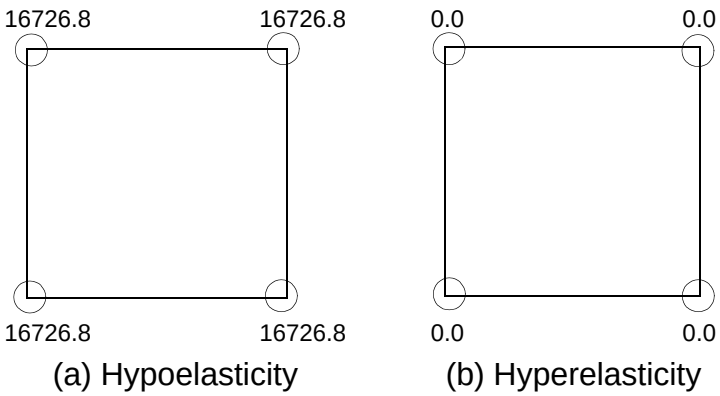

Figure 3.37-2 Nodal Reaction Forces after a Closed Loop of Elastic Deformation

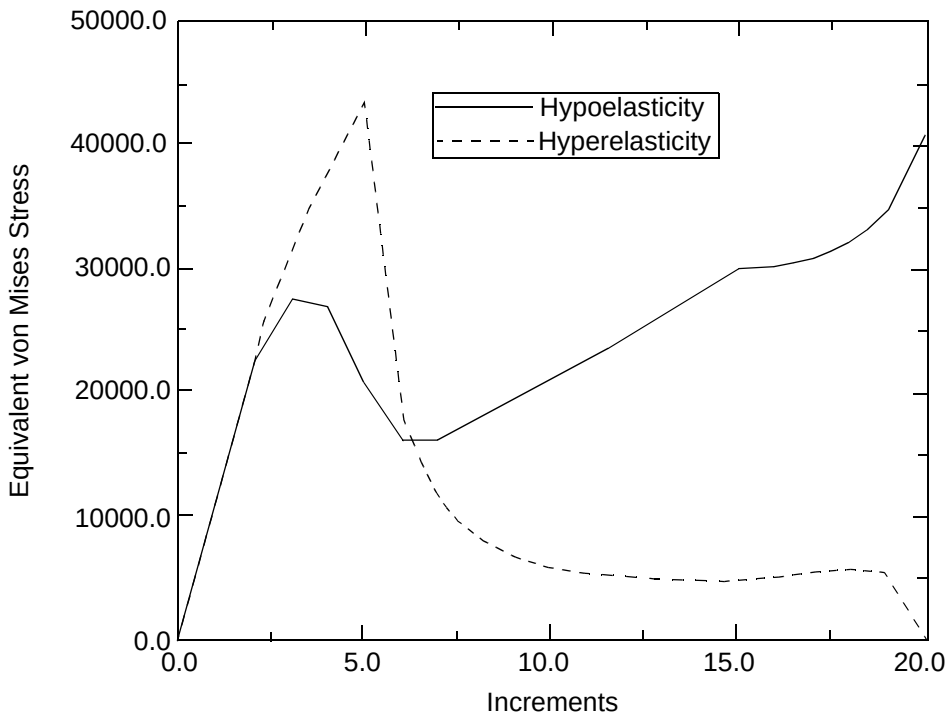

Figure 3.37-3 History Plot of Equivalent von Mises Stress

3.38 Tensile Loading and Rigid Body Rotation

This problem simulates the tensile loading of a sheet to large plastic strains, followed by a large rigid rotation. The solution demonstrates the accuracy of the plasticity model under large strains and rotations.

Element

This problem is simulated as a two-dimensional plane stress case. The 4-node plane stress element 3 is used to construct a mesh. There are two degrees of freedom per node with a bilinear interpolation and full four point Gaussian quadrature.

Model

Due to symmetry of the geometry and loading, a quarter of the actual model is simulated. The finite element model is made up of 9 elements and 16 nodes. There are a total of 32 degrees of freedom. The model is shown in Figure 3.38-1.

Geometry

The model is assumed to be a square of side 9 inches. The initial thickness is one inch.

Material Properties

The material is assumed to be isotropic elastic plastic. The Young's modulus is 1.E+06 psi, Poisson's ratio is 0.30 and the initial yield stress is 1000.0 psi. The hardening behavior is input using a user subroutine and is given by the equation:

$$\bar{\sigma} = \bar{\sigma}_o + \alpha(2-\alpha)(\bar{\sigma}_\infty - \bar{\sigma}_o); \alpha = \frac{\bar{\varepsilon}^p}{\bar{\varepsilon}^p_\infty}$$

$$\bar{\sigma}_o = 1000, \bar{\varepsilon}_\infty = 0.6; \bar{\sigma}_\infty = 1200$$

Boundary Conditions

The loading is initially tensile. The lower end of the model (nodes 1, 2, 3, and 10) is restrained to have no vertical motion. The top end (nodes 7, 8, 9, and 16) is subjected to displacement increments in the y direction. The left end (nodes 1, 4, 7, and 12) is held from displacing in the x direction. After 10 increments, the boundary nodes of the model are given specified displacement increments corresponding to a large finite rotation of 90 degrees. This entire rotation is applied in a single increment.

Results

The deformed model is shown after the 10th and 11th increments in Figures 3.38-2 and 3.38-3 respectively. Contours of total effective plastic strain are also superimposed. The deformation is homogeneous as expected. After the 10th increment, the effective plastic strain is 0.4730. The next increment is the rigid rotation of 90 degrees. At the end of this increment, no further plasticity has occurred. The von Mises effective stress at the end of the tenth increment is 1286.46 psi in all the elements. This value remains constant during the rigid body rotation of increment 11. A history plot of the von Mises effective stress as a function of plastic strain is shown in Figures 3.38-4 for nodes 1 and 9. It can be seen that the results are identical for both nodes for all increments. No change in either the von Mises stress or effective plastic strain is observed in increment 11. This shows the accuracy of the plasticity algorithms in MARC for large strains and rotations.

Parameters, Options, and Subroutines Summary

Parameters	Model Definition Options
ELEMENTS	CONNECTIVITY
LARGE DISP	COORDINATES
PLASTICITY	FIXED DISP
PRINT	GEOMETRY
PROCESSOR	ISOTROPIC
SIZING	WORK HARD DATA
TITLE	

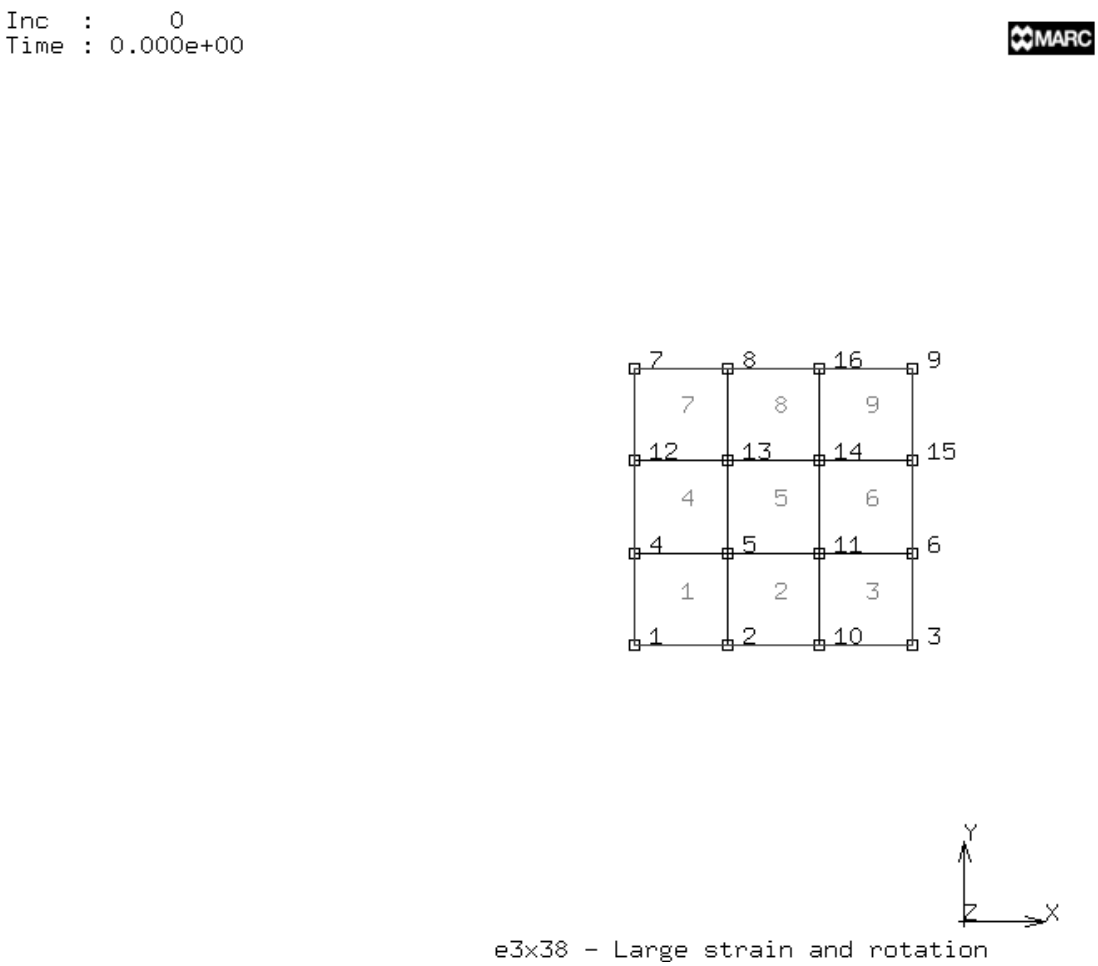

Figure 3.38-1 Initial Model

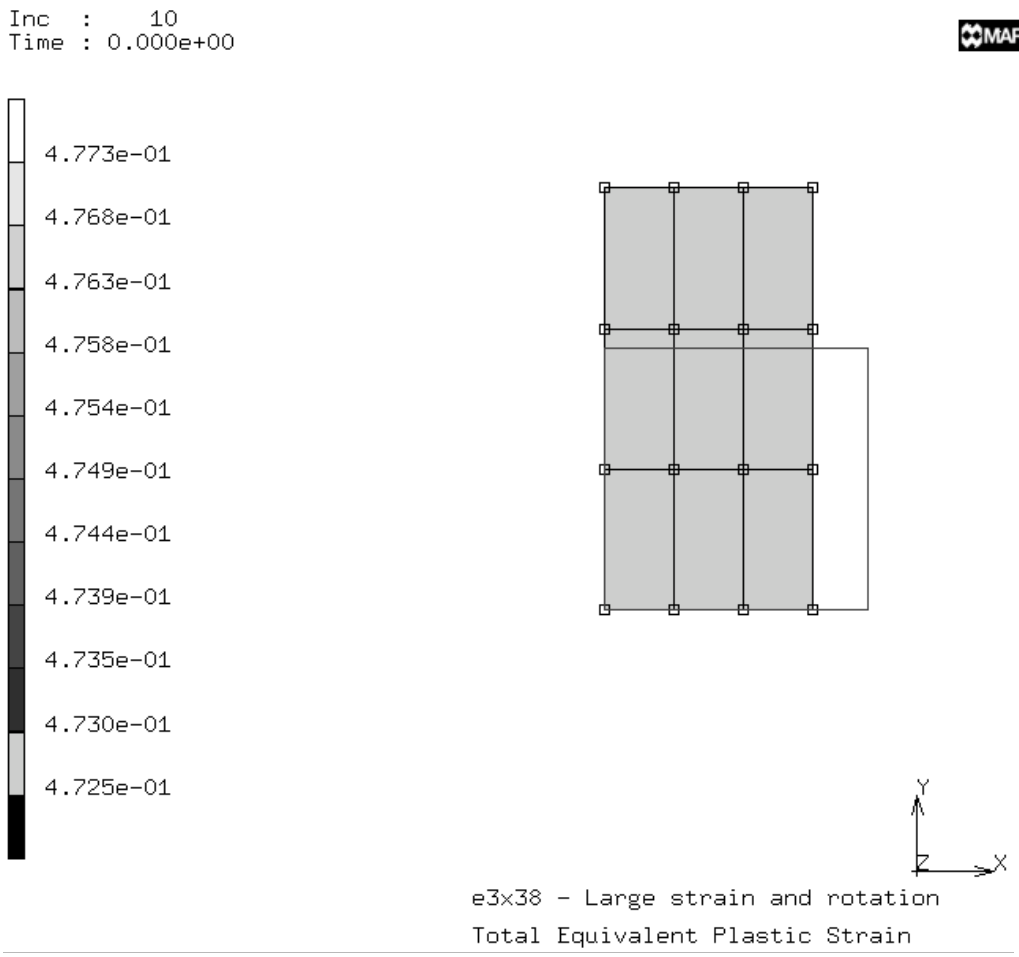

Figure 3.38-2 Deformed Model at the End of Increment 10

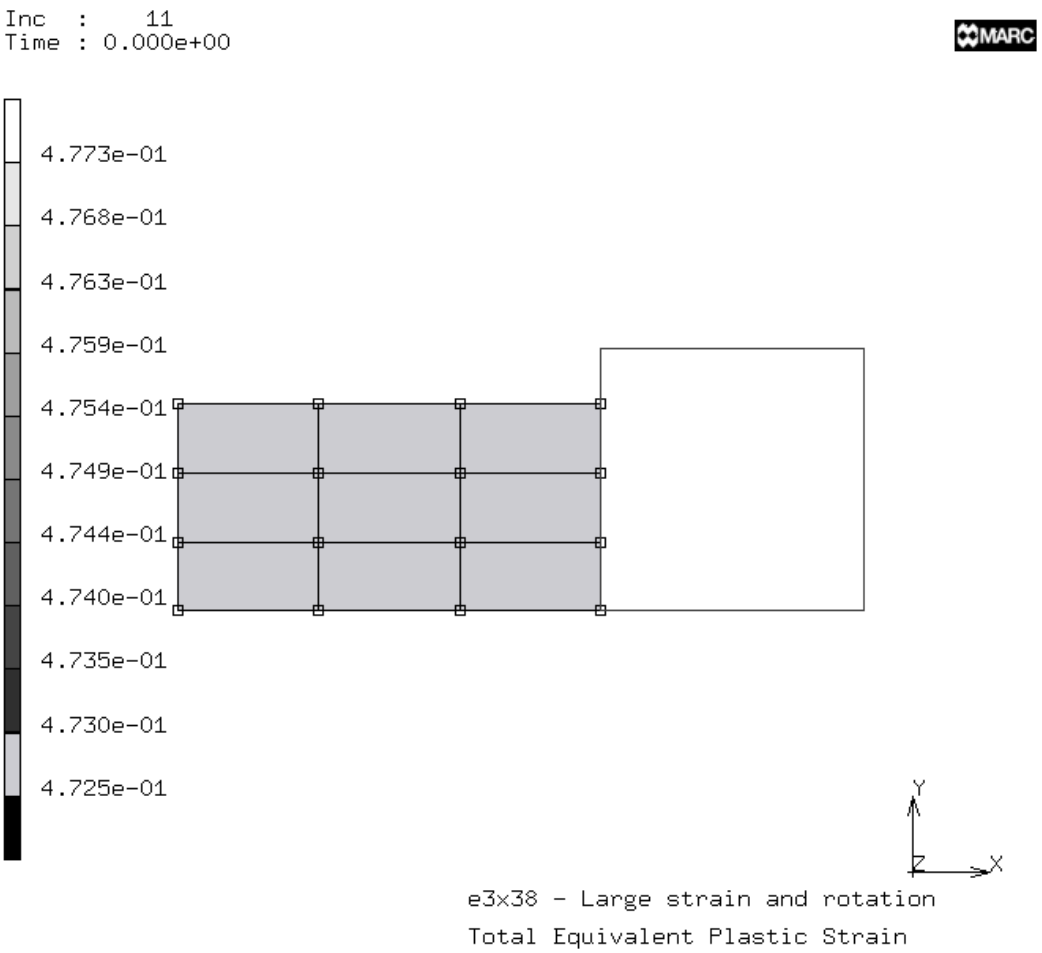

Figure 3.38-3 Deformed Model at the End of Increment 11

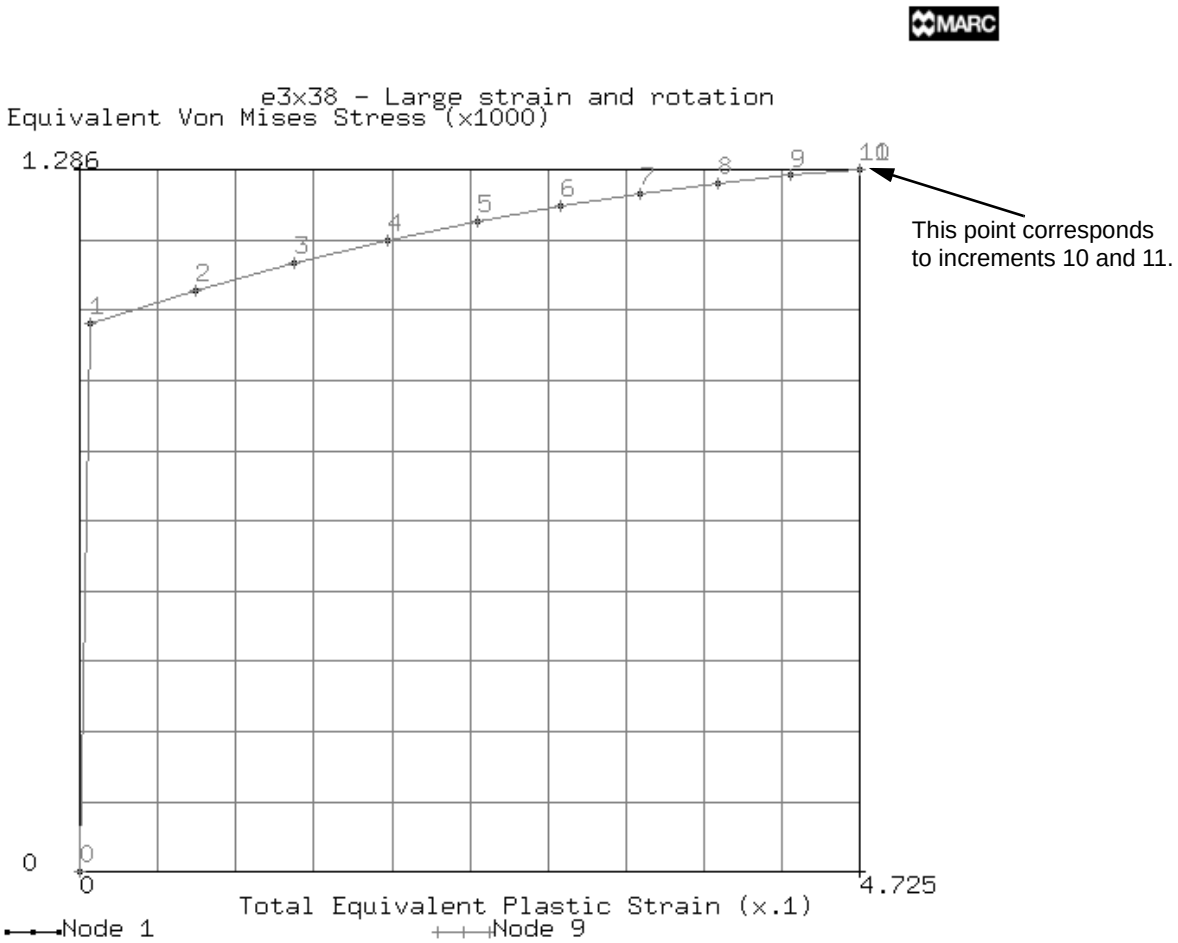

Figure 3.38-4 History Plot of Equivalent Stress versus Effective Plastic Strain for Nodes 1 and 9

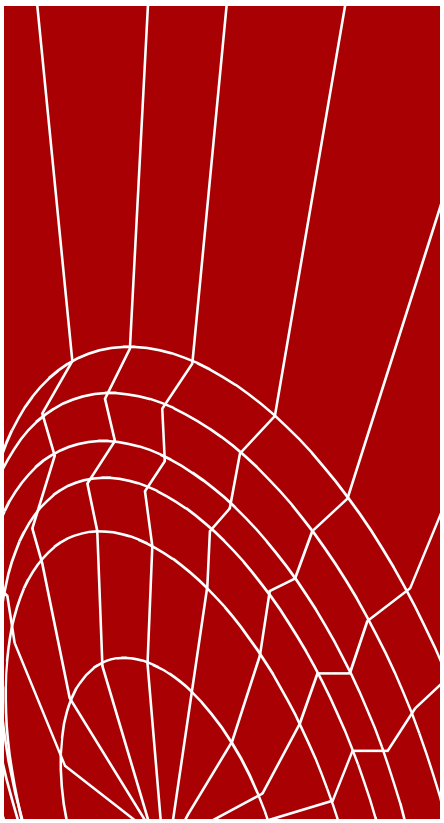

MARC Analysis Research Corporation

MARC®

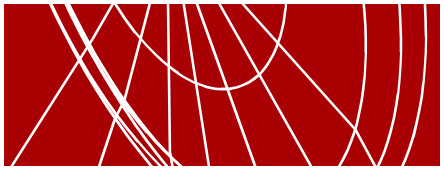

Volume E

Demonstration Problems

Version K7

Chapter 4
Large Displacement

4 Large Displacement Contents

Description	Problem
Elastic Large Displacement – Shell Buckling	4.1
Square Plate under Distributed Load	4.2
Cantilever Beam under Point Load	4.3
Axisymmetric Buckling of a Cylinder	4.4
Large Displacement Analysis of a Pinched Cylinder	4.5
One-Dimensional Elastic Truss-Spring System	4.6
Post-Buckling Analysis of a Deep Arch	4.7
Large Displacement Analysis of a Cable Network	4.8
Nonsymmetric Buckling of a Ring	4.9
Nonsymmetric Buckling of a Cylinder	4.10
Geometrically Nonlinear Analysis of a Tapered Plate	4.11
Perturbation Buckling of a Strut	4.12
Cord-reinforced Thin-wall Cylinder subjected to Inner Pressure using Axisymmetric Elements	4.13
Cord-reinforced Thin-wall Cylinder subjected to Inner Pressure using Membrane Elements	4.14
Buckling of a Cylinder Tube	4.15

4 Large Displacement List of Figures

Figure		Page
4.1-1	Geometry for Elastic Large Displacement Example	4.1-7
4.1-2	Point Loaded Shell Cap Force Loading	4.1-8
4.1-3	Point Loaded Shell Cap Displacement Loading	4.1-9
4.2-1	Square Plate, Finite Element Mesh, and Boundary Conditions	4.2-6
4.2-2	Node 1 Displacement History	4.2-7
4.2-3	Stress Contour of von Mises Stress in Layer 1 (Increment 10)	4.2-8
4.2-4	Stress Contour of von Mises Stress in Layer 3 (Increment 10)	4.2-9
4.3-1	Cantilever Beam and Mesh	4.3-3
4.3-2	Load vs. Deflection	4.3-4
4.3-3	Displaced Mesh	4.3-5
4.3-4	Moment Diagram	4.3-6
4.4-1	Cylinder Buckling	4.4-4
4.4-2	Mode Shapes	4.4-5
4.5-1	Pinched Cylinder and Mesh Blocks	4.5-3
4.5-2	Finite Element Mesh for a Pinched Cylinder	4.5-4
4.5-3	Displaced Mesh for a Pinched Cylinder	4.5-5
4.5-4	Stress Contours Equivalent Stress	4.5-6
4.6-1	Truss-Spring System	4.6-2
4.6-2	Load vs. Displacement at Node 2	4.6-3
4.7-1	Deep Arch	4.7-5
4.7-2	Displaced Mesh	4.7-6
4.7-3	Displaced Mesh (Continued)	4.7-7
4.7-4	Load vs. Displacement (Node 77) – No Contact	4.7-8
4.7-5	Displaced Mesh with Contact at Pin	4.7-9
4.7-6	Displaced Mesh with Contact at Pin	4.7-10

Figure **Page**

4.7-7 Displaced Mesh with Contact at Pin. 4.7-11
4.7-8 Load vs. Displacement (Node 77) with Contact at Pin. 4.7-12

4.8-1 Cable Network Mesh 4.8-3
4.8-2 Cable Network Deformed Mesh (Gravity Load) 4.8-4
4.8-3 Cable Network Deformed Mesh (Gravity + Wind Load). 4.8-5

4.9-1 Mesh 4.9-4

4.10-1 Mesh 4.10-4

4.11-1 Clamped Tapered Plate, Geometry, and Finite Element Mesh. 4.11-3
4.11-2 Undeformed and Final Deformed Configuration 4.11-4
4.11-3 Finite Element Solution Horizontal and Vertical Tip Displacement 4.11-5
4.11-4 Reference Solution Tip Deflection 4.11-6
4.11-5 Reference Solution Horizontal Tip Displacement 4.11-7

4.12-1 Mesh of Strut 4.12-4
4.12-2 Displacements Using First Mode 4.12-5
4.12-3 Displacements Using Second Mode 4.12-6

4.13-1 Cord-reinforced Thin-wall Cylinder subjected to Inner Pressure. 4.13-4
4.13-2 Finite Element Mesh for Analysis of Cord-reinforced Thin-wall Cylinder subjected to Inner Pressure using Axisymmetric Elements 4.13-5
4.13-3 Radius of the Cylinder subjected to Inner Pressure: Comparison of Numerical Results and Analytical Solutions 4.13-5
4.13-4 Second Piola-Kirchhoff Stress of the Cords in the Cylinder subjected to Inner Pressure: Comparison of Numerical Results and Analytical Solutions 4.13-6
4.14-1 Finite Element Mesh for Analysis of Cord-reinforced Thin-wall Cylinder subjected to Inner Pressure using Membrane Elements 4.14-3

4.15-1 Finite Element Mesh. 4.15-3

4 Large Displacement List of Tables

Table		Page
4-1	Nonlinear Material Demonstration Problems	4-2
4.1-1	Collapse Load Estimates	4.1-4
4.4-1	Cylinder Buckling (Eigenvalues and Collapse Load Estimations)	4.4-2

4

Large Displacement

MARC contains an extensive large displacement analysis capability. A discussion of the use of this capability can be found in *MARC Volume A: User Information*. A summary of the features is given below.

Selection of elements

- Available in all stress elements

Choice of operators

- Newton-Raphson
- Strain-Correction
- Modified Newton-Raphson

Estimation of buckling loads

- Elastic-, plastic-, static- and dynamic-buckling

Choice of procedures

- Total Lagrangian
- Updated Lagrangian
- Eulerian

Large strain elastic analysis

Hyperelastic material (Mooney) behavior

Large strain elastic-plastic analysis

Distributed loads calculated based on deformed structure

Compiled in this chapter are a number of solved problems. These problems illustrate the use of the LARGE DISP option for various types of analyses. Table 4-1 shows MARC elements and options used in these demonstration problems.

Table 4-1 Nonlinear Material Demonstration Problems

Problem Number	Element Type(s)	Parameters	Model Definition	History Definition	User Subroutines	Problem Description
4.1	15	LARGE DISP BUCKLE	UFXORD CONTROL TRANSFORMATION	BUCKLE PROPORTIONAL AUTO LOAD AUTO INCREMENT	UFXORD	Elastic, large displacement, buckling analysis of a thin shallow, spherical cap, point load, eigenvalue extraction and load incrementation.
4.2	49 50 22	LARGE DISP ELSTO	CONTROL PRINT CHOICE	AUTO LOAD DIST LOADS	—	Elastic-plastic, large displacement analysis of a square plate, simply supported, distributed load.
4.3	25	LARGE DISP ELSTO UPDATE	CONTROL	AUTO LOAD	—	Elastic, large displacement analysis of a cantilever beam subjected to a tip load.
4.4	15	LARGE DISP BUCKLE	CONN GENER NODE FILL	AUTO LOAD BUCKLE	—	Elastic buckling of a cylinder, axial compression, buckling loads and modal shapes.
4.5	22	LARGE DISP	UFXORD OPTIMIZE POST	AUTO LOAD	UFXORD	Large displacement analysis of a pinched cylinder.
4.6	9	LARGE DISP	SPRINGS CONTROL	AUTO LOAD	—	Large displacement of an elastic truss-spring.
4.7	16	PRINT, 3 UPDATE LARGE DISP SHELL SECT	TRANSFORMATION CONN GENER UDUMP UFXORD	AUTO INCREMENT	UFXORD	Postbuckling of a deep arch.
4.8	51	PRINT, 3 FOLLOW FORCE LARGE DISP	DIST LOADS	AUTO LOAD	—	Analysis of a cable network.
4.9	90	SHELL SECT BUCKLE	—	BUCKLE	—	Buckling of a radially loaded ring.

Table 4-1 Nonlinear Material Demonstration Problems (Continued)

Problem Number	Element Type(s)	Parameters	Model Definition	History Definition	User Subroutines	Problem Description
4.10	90	SHELL SECT BUCKLE	—	DISP CHANGE BUCKLE	—	Nonsymmetric buckling modes of a circular cylinder.
4.11	49	LARGE DISP	FIXED DISP POINT LOAD	AUTO LOAD POINT LOAD	—	Large displacement analysis of a tapered plate.
4.12	3	LARGE DISP BUCKLE	FIXED DISP POINT LOAD BUCKLE INCREMENT	BUCKLE	—	Buckling of a strut using perturbation method.
4.13	67 142 10 144 20 145	LARGE DISP FOLLOW FOR	REBAR	AUTO LOAD DIST LOADS	—	Analysis of a thin cylinder with helical plys.
4.14	18 147 30 148	LARGE DISP FOLLOW FOR	REBAR MOONEY UTRANFORM	AUTO LOAD DIST LOADS	UTRANS	Analysis of a thin cylinder with a helical ply.
4.15	75	BUCKLE	TYING SOLVER	BUCKLE RECOVER	—	Buckling of a cylinder tube

4.1 Elastic Large Displacement – Shell Buckling

In this example, we illustrate a typical large displacement analysis, and the effectiveness of the eigenvalue buckling estimate analysis. The objective is to estimate the elastic collapse load of a thin, shallow, spherical cap under an apex point load.

This problem is modeled using the four techniques summarized below.

Data Set	Element Type(s)	Number of Elements	Number of Nodes	Differentiating Features
e4x1a	15	5	6	Modified Newton
e4x1b	15	5	6	Strain correction
e4x1c	15	5	6	Full Newton
e4x1d	15	5	6	Lanczos Method, Modified Newton

Model/Element

The geometry of the shallow spherical cap is shown in Figure 4.1-1. The collapse is assumed to be axisymmetric. If asymmetric buckling were probable, the analysis would be performed using a complete doubly-curved shell formulation, such as element types 22, 49, 72, 75, 138, 139, or 140. The axisymmetric assumption indicates a choice of element type 15. Element 15 is preferred over element 1, since the latter uses shallow shell theory with linear and cubic interpolations along and normal to the secant. Element 15 uses a full cubic interpolation, and hence contains all the rigid-body modes needed for accurate large displacement analysis. Experience shows element 15 to be rapidly convergent. In this problem, the deformation is expected to be global (rather than a local snap-through), so only five elements are used. The UFXORD user subroutine is used to generate the coordinates for this model.

Geometry

The thickness of the shell is 0.01576 inches. This value is entered in EGEOM1.

Material Properties

The Young's modulus is 1.0×10^7 psi. Poisson's ratio is 0.3 for this material.

Loading

In a simple problem such as this, it is possible to proceed with displacement loading and thus control the solution more accurately as the collapse occurs, since the extent of collapse is prescribed in each increment. However, in a distributed load problem (the more common case) displacement control is not possible. Also, eigenvalue buckling estimates would not make sense if the apex has a vertical displacement boundary condition. In this demonstration, we begin with

load control. The difficulty with load control is the certainty of nonpositive-definiteness if the system collapses. If post-collapse behavior must be studied, the AUTO INCREMENT option should be used. In this example, the first data set uses a point load and eigenvalue analysis to anticipate the collapse load. The second data set uses displacement control. In this example, the structure never actually collapses, so that the entire response could be obtained by either loading method. The load begins at 2.0 lb for increment 0. In the third analysis, a point load is applied to the structure – the magnitude of which is controlled by the AUTO INCREMENT option. The fourth analysis is similar to the first analysis, but the Lanczos method is used to extract the eigenmodes.

Boundary Conditions

The boundary conditions in the input deck reflect the symmetry of the problem as well as the built-in edge of the cap.

BUCKLE

The size of the load step is important in order to satisfy the piecewise linear approximation of the tangent modulus technique. As a general rule, the analysis may first be approached by taking 5 to 15 steps to initial collapse estimate obtained from the BUCKLE option. The procedure suggested is:

1. Apply an arbitrary load step and ask for a BUCKLE collapse estimate.
2. The eigenvalue obtained indicates (roughly) the multiplier to collapse for the applied load. Based on this estimate, choose a load step of 1/5 to 1/15 of the collapse load and perform a nonlinear incremental analysis.
3. The estimated collapse load may also give an idea of whether material nonlinearities (for example, plasticity) can occur during the collapse since the eigenvalue can also be used as a multiplier on stress to estimate the stress at collapse.
4. It is very important to plot and study the eigenvector predicted in this way – the mesh must be of sufficient detail to describe the collapse mode accurately (for example, no curvature change reversals in a single element); otherwise, the collapse estimates can have large errors.

The BUCKLE option is based on second-order expansion of the total equilibrium equation (see *MARC Volume F: Background Information*, "Effective Use of the Incremental Stiffness Matrix"). The option allows eigenvalue estimates to be made by second-order expansion from an arbitrary point in the history. This is illustrated in this example.

ALL POINTS

The analysis involves large displacement and, hence, is nonlinear. Clearly, the residual load correction (total equilibrium check) is essential. This depends on integration of stress throughout the mesh, and, since element 15 is basically cubic, the stress must be $0(s^2)$; thus, the ALL POINTS option is necessary for accurate stress integration. This is the general case for nonlinear analysis with higher order elements. This is the default in MARC.

Results

The initial BUCKLE option gives a collapse estimate of 15 lb. Based on this, a load step of 2 pounds per increment is chosen. The collapse mode (eigenvector) appears quite smooth in this case (a global collapse) and seems adequately described by the 5-element mesh.

The incremental load blocks are arranged to apply increments of loads and obtain collapse estimates alternately. This is an extreme demonstration. In a more realistic analysis, the BUCKLE estimate would probably be obtained only during the first part of the history, and the analysis discontinued when the estimates converged. As an alternative, the BUCKLE INCREMENT model definition option could be used effectively. For this purpose, the RESTART option is of great value.

Following this analysis (Figure 4.1-3), a displacement-controlled analysis is also shown with more of the response. This technique is often not useful, since a true collapse often gives rise to a nonpositive definite system even with displacement loading (except in the trivial case of a one degree of freedom system). In this case, a step size of 0.005 inch is used, based on the observed response in the initial load-controlled analysis. Since the structure does not, in fact, buckle but always retains some positive stiffness, it is possible to follow the solution arbitrarily far through the inversion of the cap.

The results are summarized in Table 4.1-1 and in Figure 4.1-2 and Figure 4.1-3. Notice the nonlinear load-displacement behavior. The collapse load estimates converges on 15.0 pounds after four increments, and it is apparent that a definite lack of stiffness is present above this load level.

Based on this preliminary study, the analyst can have enough information for design purposes. He now knows that the structure is extremely weak (about 10% of its initial stiffness) above a 12 pound load. If more detail is required, a restart would be made at about 8 or 9 pound load (assuming that a restart file had been written) and smaller steps would be used. With displacement control instead, we pursue this possibility and find (Figure 4.1-3) that, although the structure becomes extremely weak, it does not “snap through”, but retains positive stiffness until it is folded back and continues to support load in an inverted cap mode essentially with membrane action, so that its stiffness then becomes quite high compared to the initial bending stiffness.

Table 4.1-1 Collapse Load Estimates

Inc. No.	Load No.	Previous Load	Eigenvalues λ (LARGE DISP Option)			Collapse Load P^c (LARGE DISP Option)		
			No. 0	No. 1	No. 2	No. 0	No. 1	No. 2
0	2	0	7.81	7.66	7.81	15.62	15.32	15.62
1	2	2	5.92	5.84	5.92	13.84	13.68	13.85
2	2	4	4.47	4.40	4.47	12.94	12.80	12.94
3	2	6	3.23	3.16	3.23	12.46	12.32	12.46
4	2	8	2.19	2.11	2.19	12.38	12.22	12.38
5	2	10	1.37	1.29	1.37	12.74	12.58	12.74
6	2	16	.78	.76	.78	13.56	13.40	13.56
7	2	14	.235	.33	.38	14.47	14.66	14.76
8	2	16	.184	.16	–	16.37	16.32	–

Note: $P^c = P + \lambda \Delta P$

The solution obtained here can be compared with the semianalytic solution presented by Timoshenko and Gere [1]. Using their notation:

$$b = 0.9,\ a = 4.76,\ h = 0.01576,\ E = 10^7$$

$$\lambda = b^4 / a^2 h^2 = 116.585$$

$$\mu = \sqrt{0.093 \times (\lambda + 115)} - 0.94 = 2.511$$

$$P_c = \mu E h^3 / a = 20.6$$

The collapse load obtained by MARC, which includes all geometry nonlinearity effects, is less than the classical buckling load.

Reference

Timoshenko, S. P., and Gere, J. M.,*Theory of Elastic Stability,* (McGraw-Hill, New York, 1961).

Parameters, Options, and Subroutines Summary

Example e4x1a.dat:

Parameters	Model Definition Options	History Definition Options
BUCKLE	CONNECTIVITY	BUCKLE
ELEMENT	CONTROL	CONTINUE
END	END OPTION	PROPORTIONAL INCREMENT
LARGE DISP	FIXED DISP	
SIZING	GEOMETRY	
TITLE	ISOTROPIC	
	POINT LOAD	
	TRANSFORMATIONS	
	UFXORD	

User subroutine in u4x1a.f:

UFXORD

Example e4x1b.dat:

Parameters	Model Definition Options	History Definition Options
ELEMENT	CONNECTIVITY	AUTO LOAD
END	CONTROL	CONTINUE
LARGE DISP	END OPTION	
SIZING	FIXED DISP	
TITLE	GEOMETRY	
	ISOTROPIC	
	PRINT CHOICE	
	TRANSFORMATIONS	
	UFXORD	

User subroutine in u4x1b.f:

UFXORD

Example e4x1c.dat:

Parameters	Model Definition Options	History Definition Options
ELEMENT	CONNECTIVITY	AUTO INCREMENT
END	CONTROL	CONTINUE
LARGE DISP	COORDINATE	POINT LOAD
SHELL SECT	END OPTION	
SIZING	FIXED DISP	
TITLE	GEOMETRY	
	ISOTROPIC	
	POINT LOAD	
	PRINT CHOICE	
	TRANSFORMATIONS	

Example e4x1d.dat:

Parameters	Model Definition Options	History Definition Options
BUCKLE	CONNECTIVITY	BUCKLE
ELEMENT	CONTROL	CONTINUE
END	END OPTION	PROPORTIONAL INCREMENT
LARGE DISP	FIXED DISP	
SIZING	GEOMETRY	
TITLE	ISOTROPIC	
	POINT LOAD	
	TRANSFORMATIONS	
	UFXORD	

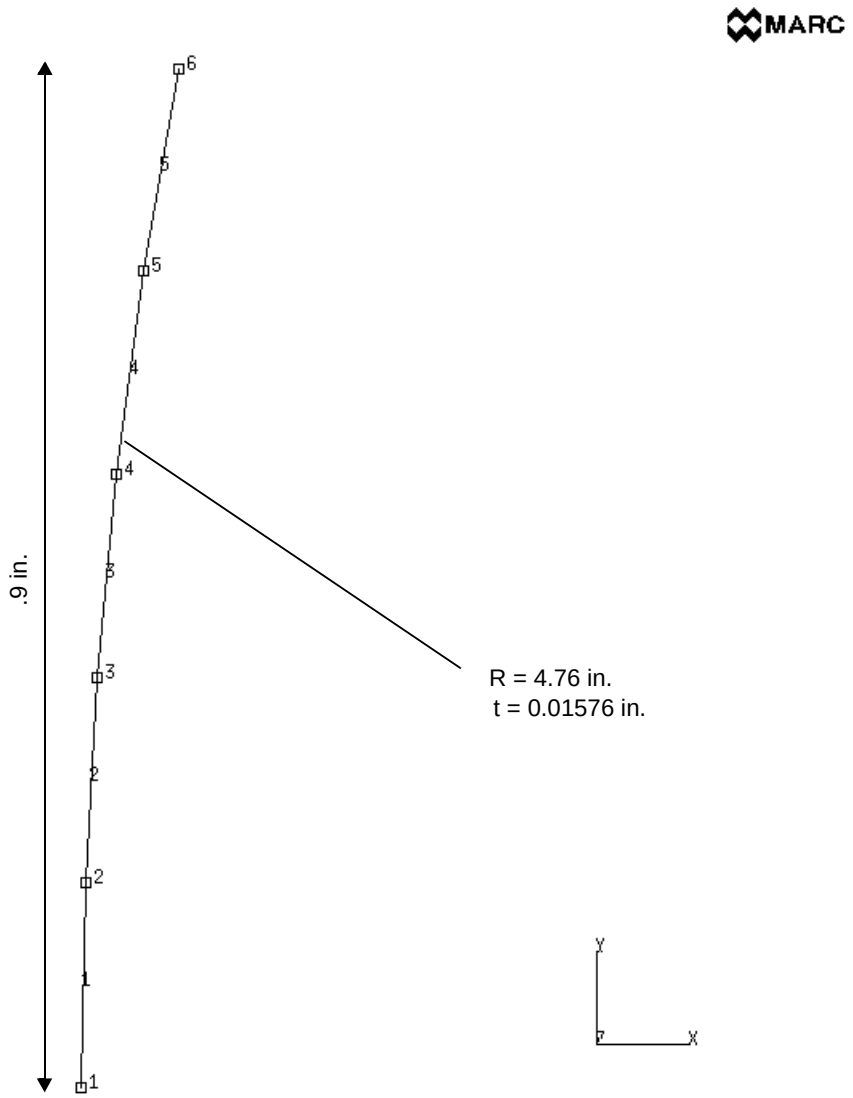

Figure 4.1-1 Geometry for Elastic Large Displacement Example

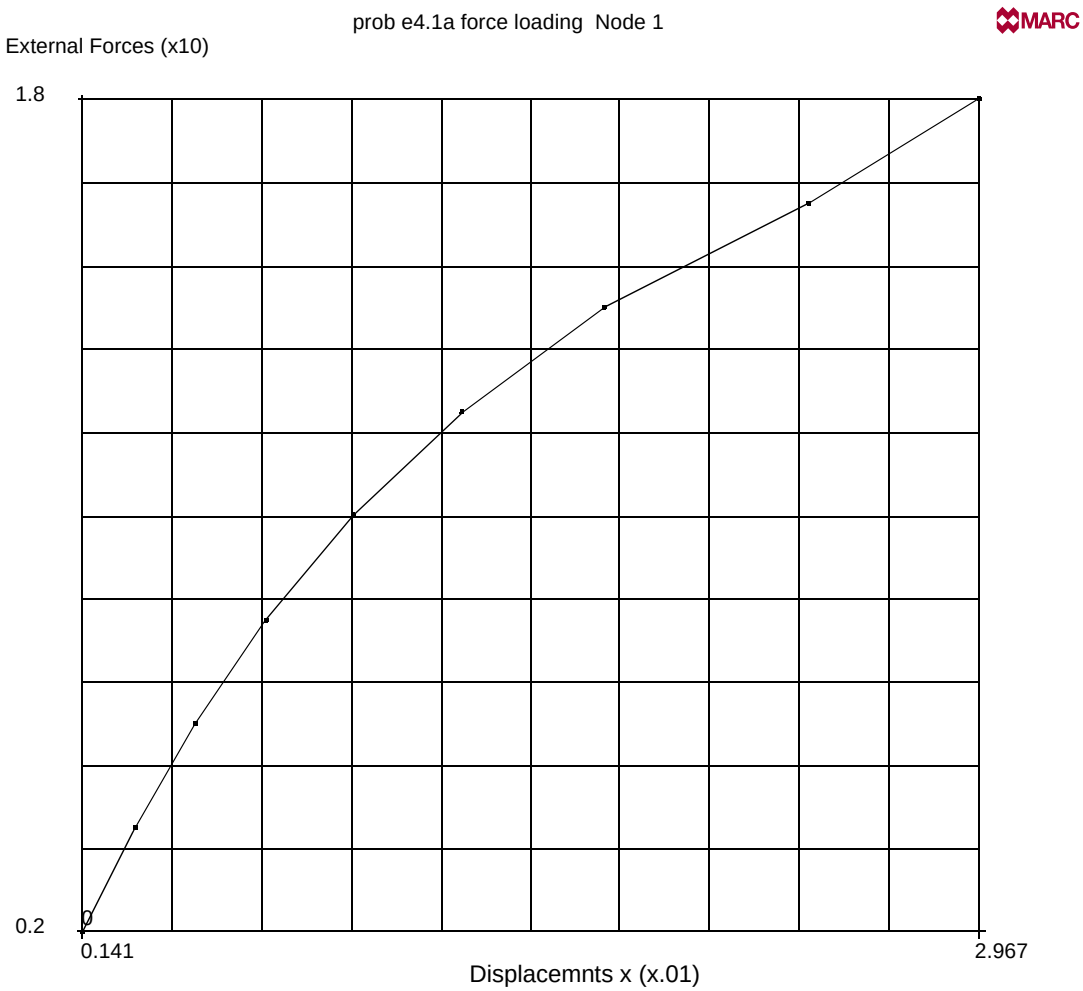

Figure 4.1-2 Point Loaded Shell Cap Force Loading

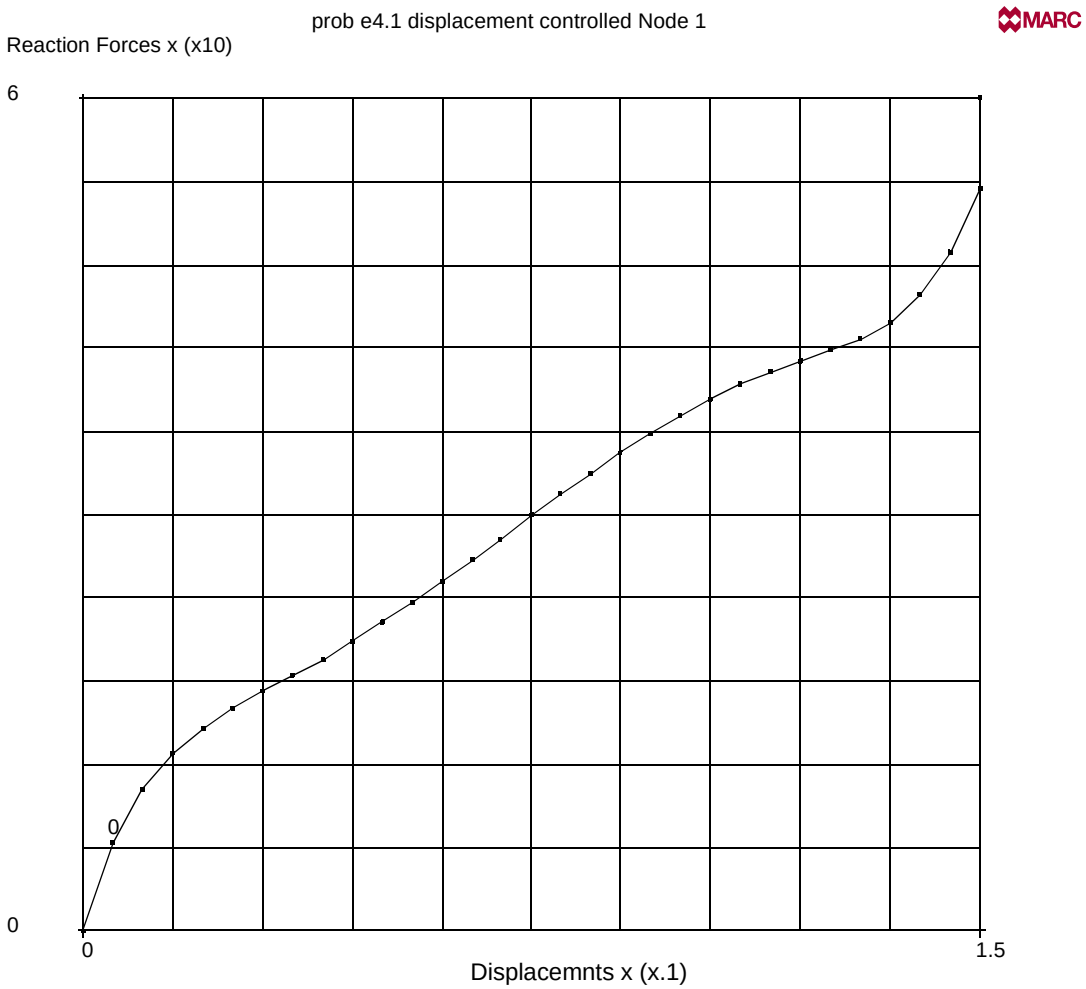

Figure 4.1-3 Point Loaded Shell Cap Displacement Loading

4.2 Square Plate under Distributed Load

A simply-supported square plate subjected to uniformly distributed pressure is analyzed. MARC element types 49, 75, 138, 139, and 140 are utilized. In the analysis, geometrically nonlinear effects are considered. The AUTO LOAD option is used for the load incrementation.

This problem is modeled using the four techniques summarized below.

Data Set	Element Type(s)	Number of Elements	Number of Nodes
e4x2	49	32	81
e4x2a	49	8	25
e4x2b	75	4	36
e4x2c	138	50	36
e4x2d	139	25	36
e4x2e	140	25	36

Element

Library element type 49 is a 6-node triangular thin shell element.

Library element type 75 is a 4-node quadrilateral thick shell element.

Library element type 138 is a 3-node triangular thin shell element.

Library element type 139 is a 4-node quadrilateral thin shell element.

Library element type 140 is a 4-node quadrilateral thick shell element.

The length to thickness ratio is 10/0.25 = 40, which suggests that the thin shell theory is appropriate for this problem.

Model

The dimensions of the plate and the finite element mesh are shown in Figure 4.2-1. Based on symmetry considerations, only one quarter of the plate is modeled.

Material Properties

The material is elastic with a Young's modulus of 10×10^6 N/mm^2 and a Poisson's ratio of 0.3.

Geometry

A uniform thickness of 0.25 mm is assumed. In thickness direction, three layers are chosen using the SHELL SECT parameter.

Boundary Conditions

Symmetry conditions are imposed on the edges x = 10 ($u_x = 0$, $\phi = 0$) and y = 10 ($u_y = 0$, $\phi = 0$). Notice that the rotation constraints only apply for the midside nodes. Simply supported conditions are imposed on the edges x = 0 and y = 0 ($u_x = u_y = u_z = 0$).

Loading

A uniform pressure load of 50 N/mm^2 is applied in ten equally sized increments. The default control settings are used. Convergence control is accomplished by a check on relative residuals with a tolerance of 0.1.

Results

The displacement history of node 1 is shown in Figure 4.2-2. For increment 10, stress contours of the von Mises stress in the outer layers are shown in Figure 4.2-3 and Figure 4.2-4. Due to the geometrically nonlinear effects, the stress distribution is clearly not symmetric with respect to the midplane of the plate. The deflections at the center of the plate are given by:

Pressure (N/mm^2)	Normalized Deflection w/h						
	e4x2	e4x2a	e4x2b	e4x2c	e4x2d	e4x2e	Reference
10	0.86	0.77	0.92	0.67	0.90	0.91	0.84
20	1.14	1.08	1.28	1.04	1.19	1.20	1.17
30	1.32	1.29	1.51	1.35	1.39	1.40	1.37
40	1.47	1.46	1.69	1.50	1.54	1.56	1.53
50	1.59	1.59	1.83	1.63	1.67	1.69	1.65

The reference solution can be found in “Bending of Rectangular Plates with Large Deflection” by S. Levy in the NACA Report 737, Washington, DC, 1942.

Parameters, Options, and Subroutines Summary

Example e4x2a.dat and e5x2a.dat:

Parameters	Model Definition Options	History Definition Options
ALL POINTS	CONNECTIVITY	AUTO LOAD
ELEMENTS	COORDINATES	CONTINUE
DIST LOADS	DEFINE	CONTROL
END	DIST LOADS	DIST LOAD
LARGE DISP	END OPTION	TIME STEP
SET NAME	FIXED DISP	
SHELL SECT	GEOMETRY	
SIZING	ISOTROPIC	
	NO PRINT	
	OPTIMIZE	
	PRINT	
	SOLVER	

Example e4x2b.dat:

Parameters	Model Definition Options	History Definition Options
ALL POINTS	CONNECTIVITY	AUTO LOAD
ELEMENTS	COORDINATES	CONTINUE
DIST LOADS	DEFINE	CONTROL
END	DIST LOADS	DIST LOAD
LARGE DISP	END OPTION	TIME STEP
SET NAME	FIXED DISP	
SHELL SECT	GEOMETRY	
SIZING	ISOTROPIC	
	NO PRINT	
	OPTIMIZE	
	PRINT	
	SOLVER	

Example e4x2c.dat:

Parameters	Model Definition Options	History Definition Options
ALL POINTS	CONNECTIVITY	AUTO LOAD
ELEMENTS	COORDINATES	CONTINUE
DIST LOADS	DEFINE	CONTROL
END	DIST LOADS	DIST LOAD
LARGE DISP	END OPTION	TIME STEP
SET NAME	FIXED DISP	
SHELL SECT	GEOMETRY	
SIZING	ISOTROPIC	
	NO PRINT	
	OPTIMIZE	
	PRINT	
	SOLVER	

Example e4x2d.dat:

Parameters	Model Definition Options	History Definition Options
ALL POINTS	CONNECTIVITY	AUTO LOAD
ELEMENTS	COORDINATES	CONTINUE
DIST LOADS	DEFINE	CONTROL
END	DIST LOADS	DIST LOAD
LARGE DISP	END OPTION	TIME STEP
SET NAME	FIXED DISP	
SHELL SECT	GEOMETRY	
SIZING	ISOTROPIC	
	NO PRINT	
	OPTIMIZE	
	PRINT	
	SOLVER	

Example e4x2e.dat:

Parameters	Model Definition Options	History Definition Options
ALL POINTS	CONNECTIVITY	AUTO LOAD
ELEMENTS	COORDINATES	CONTINUE
DIST LOADS	DIST LOADS	CONTROL
END	END OPTION	DIST LOAD
LARGE DISP	FIXED DISP	TIME STEP
SET NAME	GEOMETRY	
SHELL SECT	ISOTROPIC	
SIZING	NO PRINT	
	OPTIMIZE	
	POST	
	SOLVER	

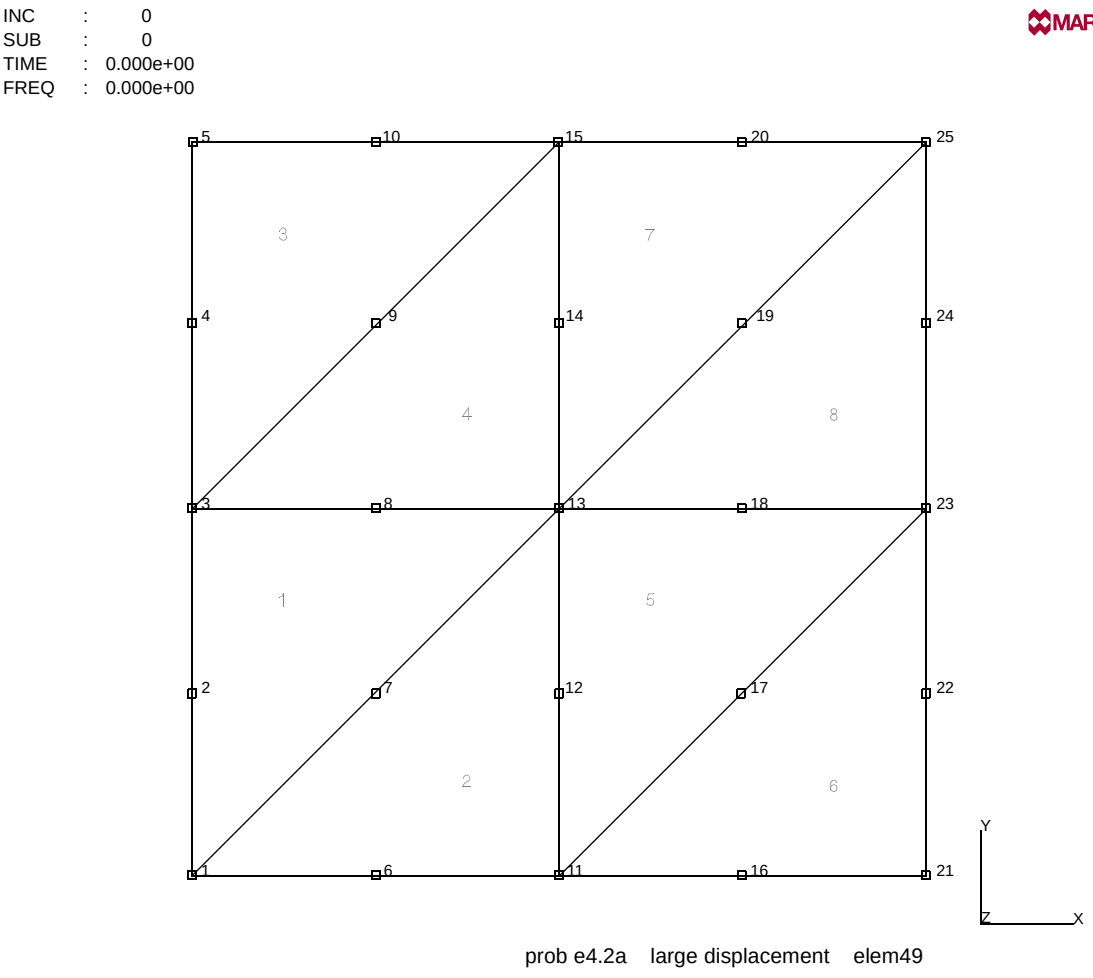

Figure 4.2-1 Square Plate, Finite Element Mesh, and Boundary Conditions

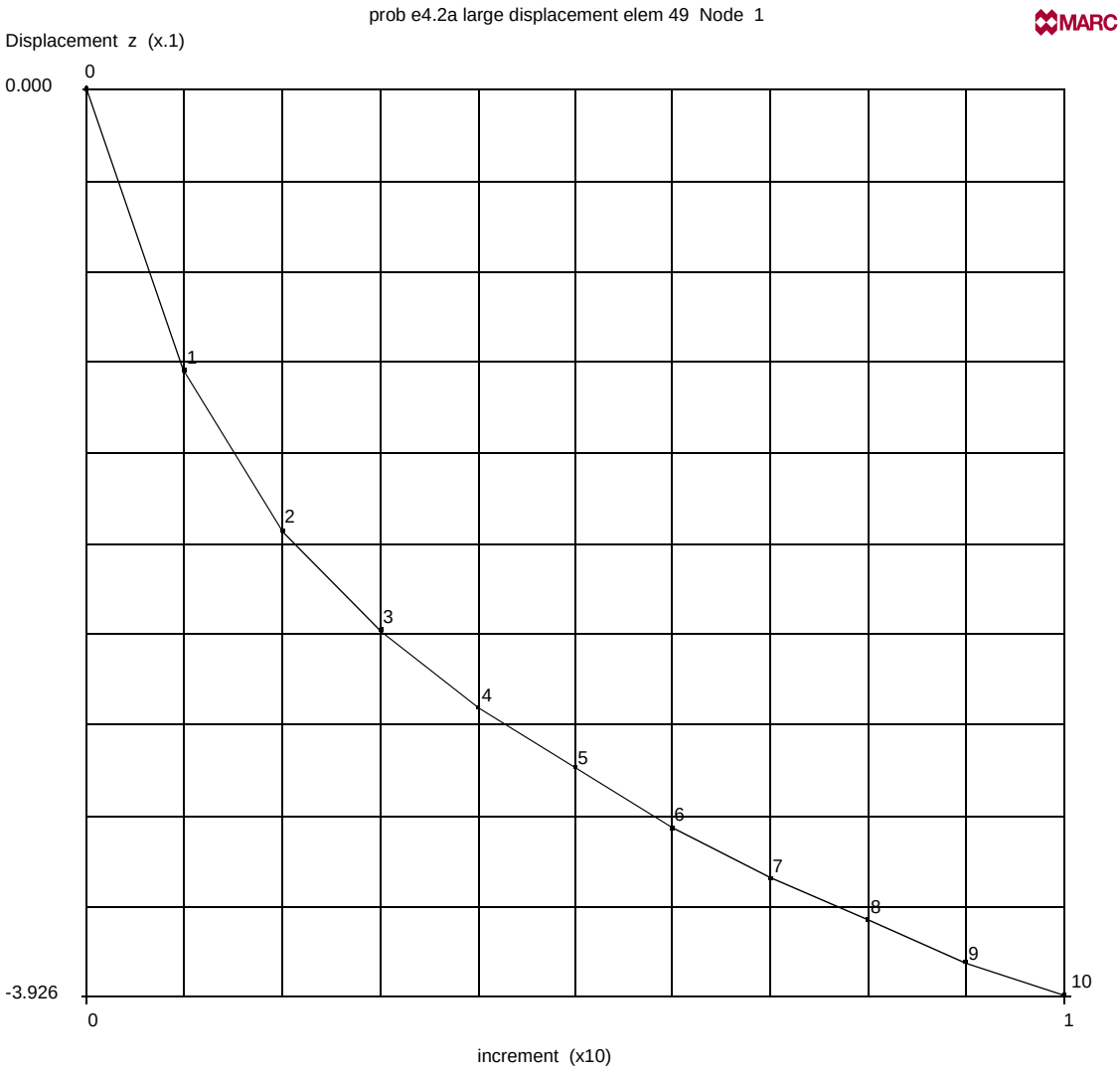

Figure 4.2-2 Node 1 Displacement History

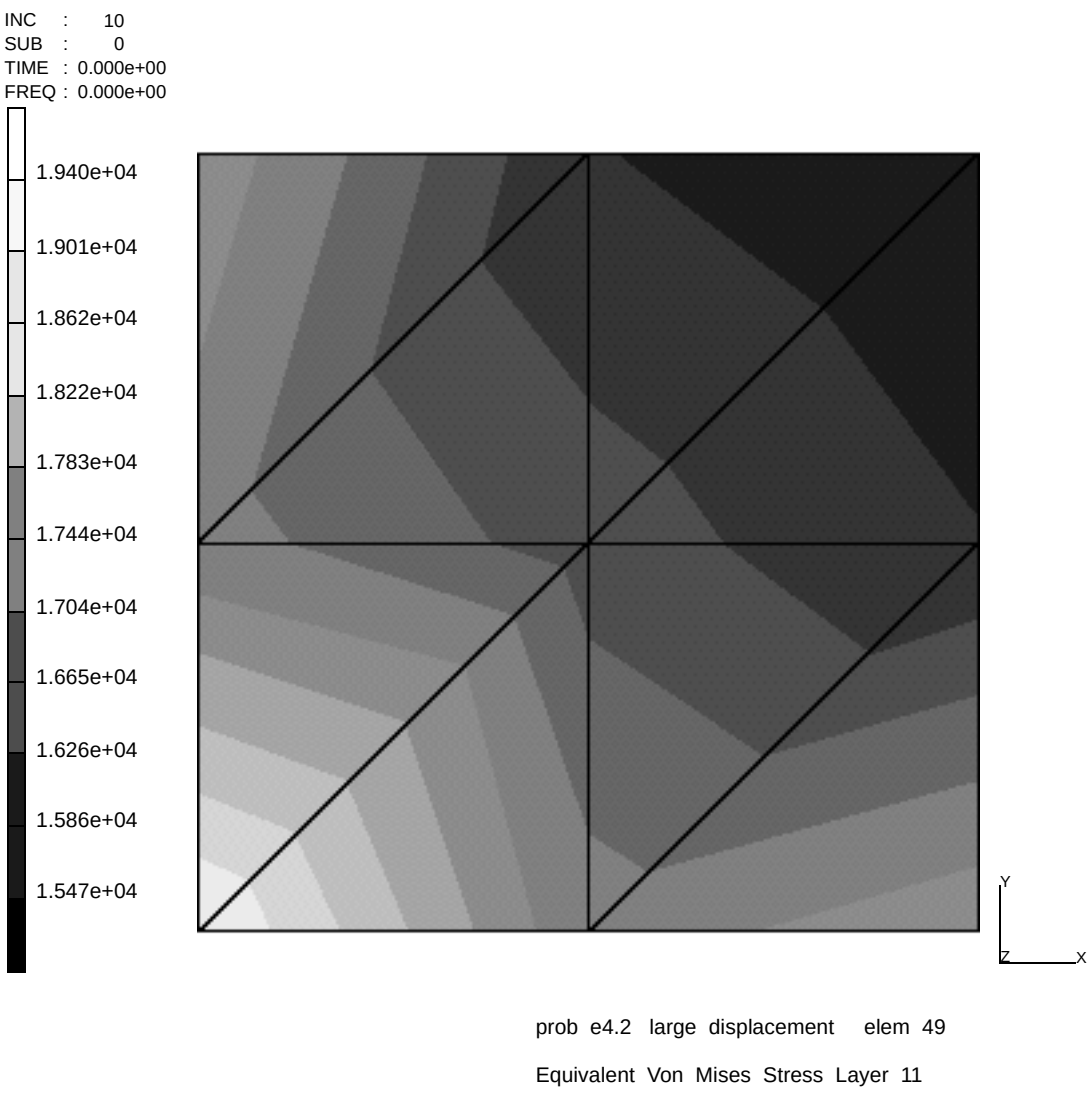

Figure 4.2-3 Stress Contour of von Mises Stress in Layer 1 (Increment 10)

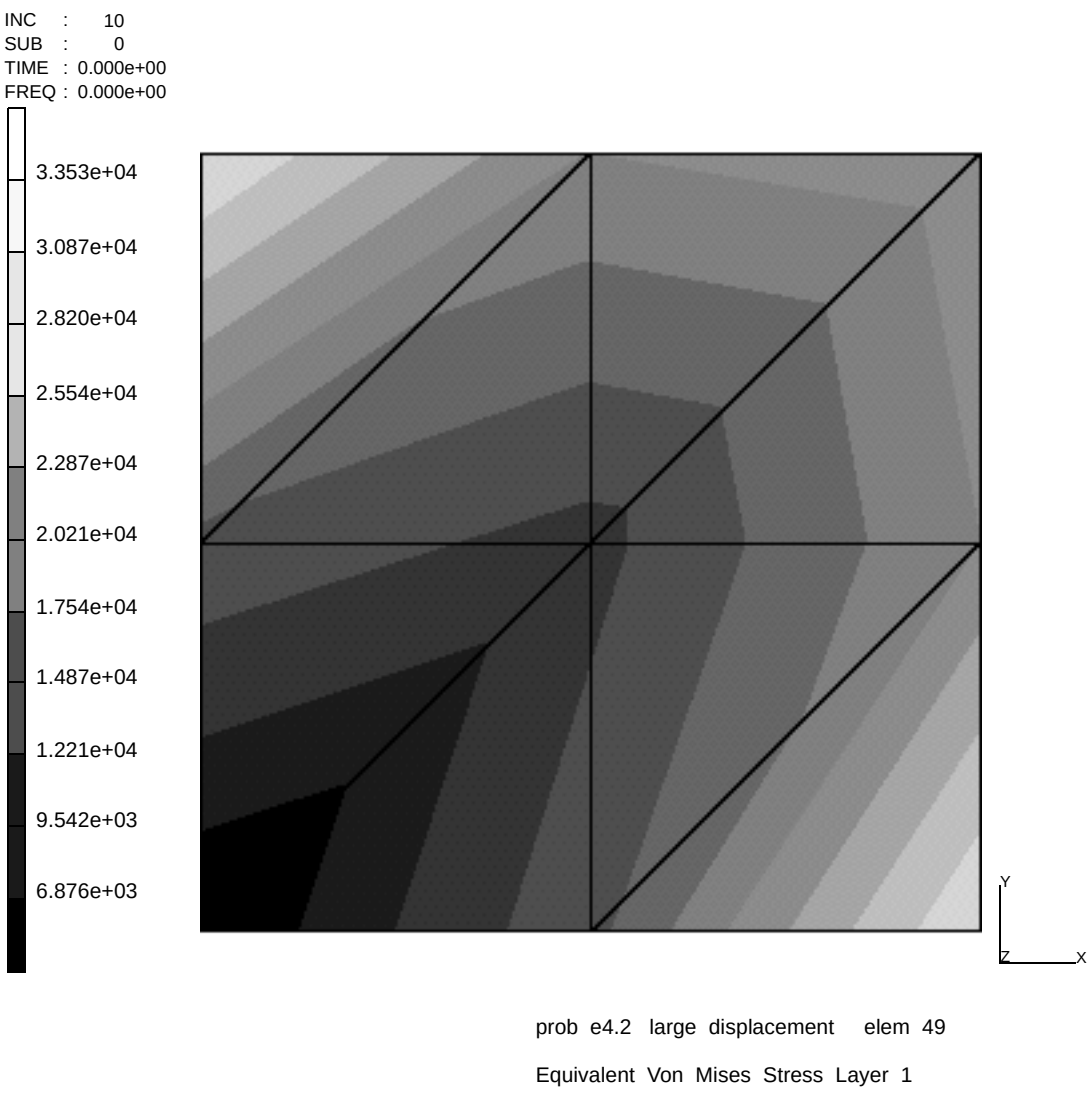

Figure 4.2-4 Stress Contour of von Mises Stress in Layer 3 (Increment 10)

4.3 Cantilever Beam under Point Load

An elastic, large displacement analysis is carried out for a cantilever straight pipe subjected to a tip load. This problem illustrates the use of MARC element type 25 (three-dimensional thin-walled beam) and options LARGE DISP, UPDATE, and ELSTO for large displacement analysis.

Model/Element

The beam, whose total length is 100 inches, is modeled using five elements and six nodal points. A plot of the beam and mesh is shown in Figure 4.3-1. Element 25 is a very accurate element to use for nonlinear beam analysis.

Material Properties

The material of the beam is assumed to be linear elastic with a Young's modulus of 31.63×10^6 psi and a Poisson's ratio of 0.3.

Geometry

The thickness of the circular beam cross section is 0.001 inch and the mean radius of the section is 3.00 inches.

Loading

A total point load of 2.7 pounds is applied at the tip of the beam in the negative y-direction. It is applied in ten equal load increments by using the AUTO LOAD option.

Boundary Conditions

All degrees of freedom at node 1 are constrained for the simulation of a fixed-end condition.

LARGE DISP

This option indicates that the problem is a large displacement analysis. The updated Lagrange technique is used in this analysis. The solution is obtained using the full Newton-Raphson method.

ELSTO

This option allows the use of out-of-core element storage for element data; this reduces the amount of workspace necessary.

Results

A load-deflection curve is shown in Figure 4.3-2. This is in excellent agreement with the solution given in Timoshenko. In increment one, several iterations were necessary, which indicates that the load applied in the zeroth linear increment was too large. Later increments required only one

iteration per increment. As this problem involves primarily rotational behavior, a high tolerance was placed on force residuals and a tight tolerance was placed on moment residuals. The displaced mesh is illustrated in Figure 4.3-3. Examination of the deformed structure indicates that very large rotations occurred. The output of the residual loads indicates that mesh refinement near the built-in end is necessary. Figure 4.3-4 shows the resultant moment diagram; this was obtained by using the LINEAR plot option.

Parameters, Options, and Subroutines Summary

Example e4x3.dat:

Parameters	Model Definition Options	History Definition Options
ELEMENT	CONNECTIVITY	AUTO LOAD
END	CONTROL	CONTINUE
LARGE DISP	COORDINATE	POINT LOAD
SIZING	END OPTION	
TITLE	FIXED DISP	
UPDATE	GEOMETRY	
	ISOTROPIC	
	POINT LOAD	
	RESTART	

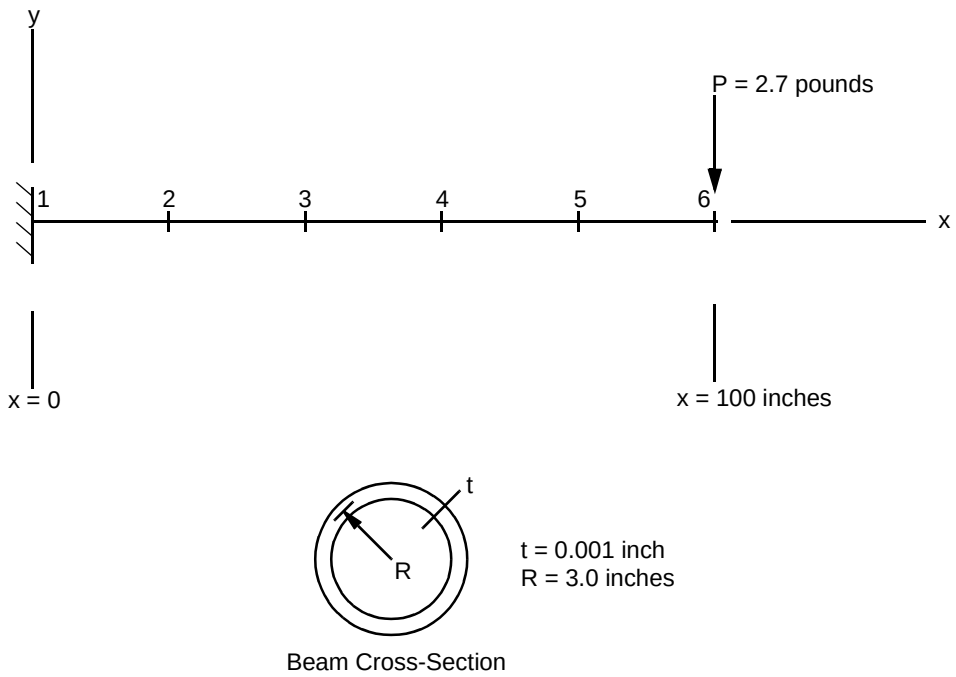

Figure 4.3-1 Cantilever Beam and Mesh

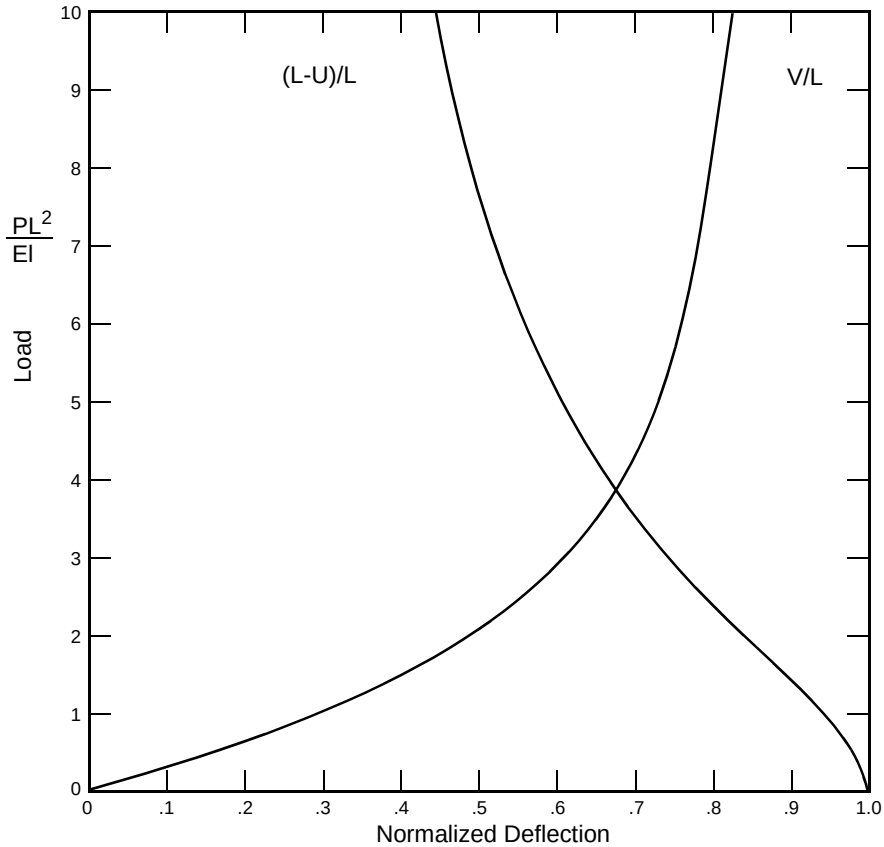

Figure 4.3-2 Load vs. Deflection

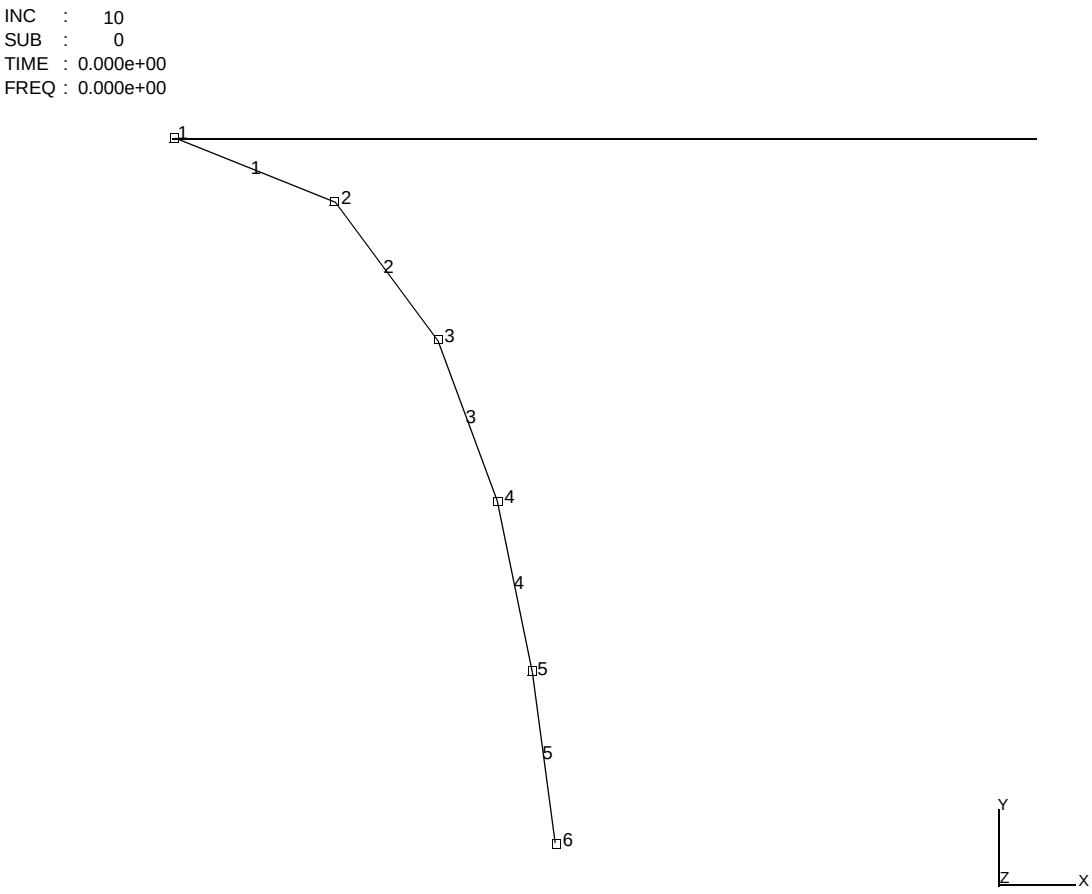

Figure 4.3-3 Displaced Mesh

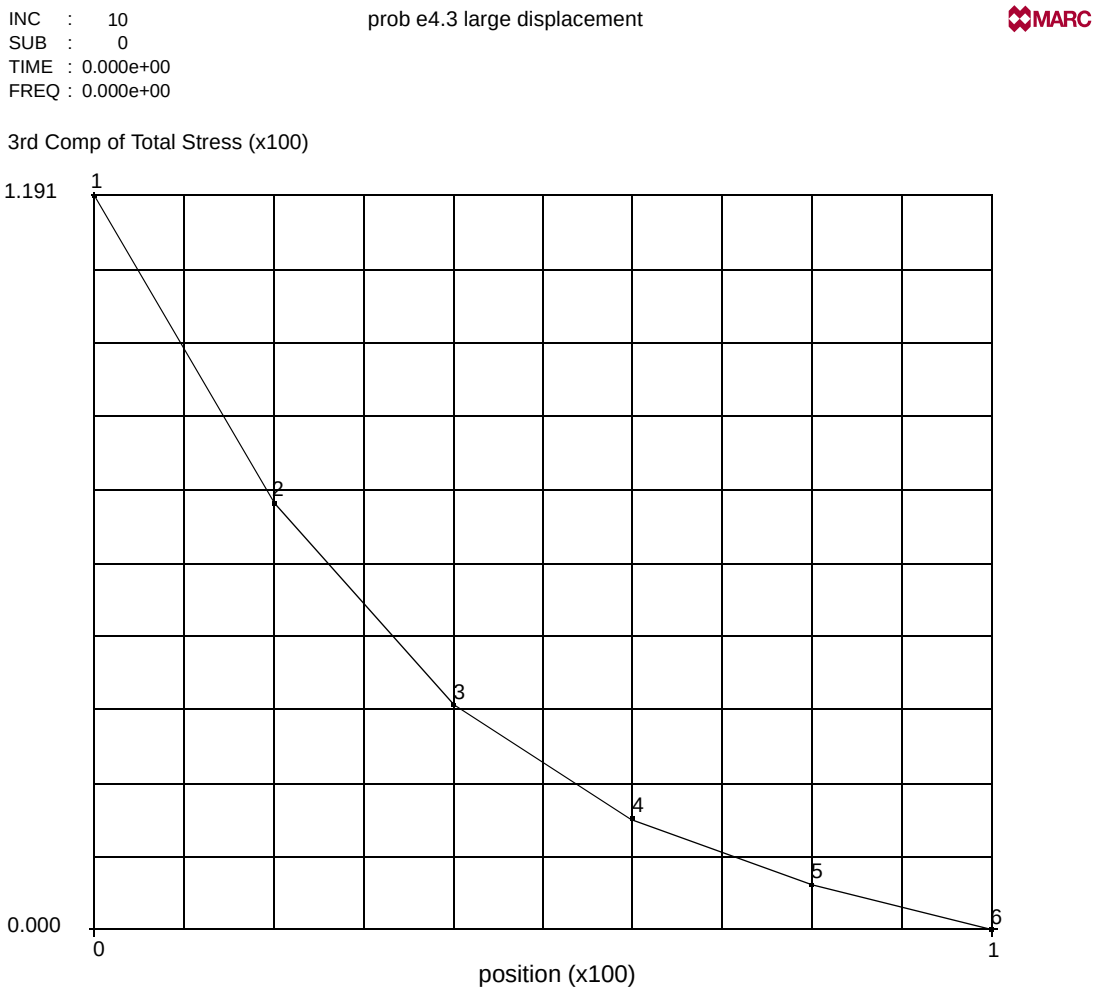

Figure 4.3-4 Moment Diagram

4.4 Axisymmetric Buckling of a Cylinder

An elastic buckling analysis is carried out for a short right cylinder subjected to axial compression. This problem illustrates the use of MARC element type 15 (axisymmetric shell element) and option LARGE DISP and BUCKLE for finding the first four buckling loads and mode shapes.

This problem is modeled using the two techniques summarized below.

Data Set	Element Type(s)	Number of Elements	Number of Nodes	Differentiating Features
e4x4	15	10	11	Inverse Power Sweep
e4x4b	15	10	11	Lanczos

Model/Element

They cylinder has a length of 100 inches and a radius of 80 inches. Because of symmetry, only one half of the cylinder is modeled.

The model consists of ten elements and 11 nodal points. Incremental mesh generation options CONN GENER and NODE FILL are used for the mesh generation. The cylinder and a finite element mesh are shown in Figure 4.4-1.

Material Properties

In this analysis, the Young's modulus and Poisson's ratio are assumed to be 1.0×10^4 psi and 0.3, respectively.

Geometry

The wall thickness of the cylinder is 2.5 inches (EGEOM1).

Loading

Two point loads, equal and opposite, are applied at nodal points 1 and 11. The magnitude of the load increment is 22,800 pounds. This load represents an integrated value along the circumference.

Boundary Conditions

Both ends of the cylinder are simply supported (v = 0, at nodes 1 and 11) and axial movement is constrained at the line of symmetry (u = 0 at node 6).

Buckle

The parameter BUCKLE indicates a buckling analysis is to be performed in this problem. It also asks for a maximum number of four buckling modes to be estimated. It is also used to indicate which method, the inverse power sweep or the Lanczos, is to be used.

In the load incrementation block, the BUCKLE option allows the use to input control values for eigenvalue extractions. The default values of 40 iterations and 0.0001 convergence tolerance are used for this analysis. The AUTO LOAD option allows you to apply additional load increment prior to the eigenvalue extraction.

Results

Eigenvalues and collapse load estimations are identical for e4x4 and e4x4b as expected and are shown in Table 4.4-1 and mode shapes are depicted in Figure 4.4-2. The PRINT CHOICE option was used to restrict the printout to integration point 2 of element 1.

The analytic solution for the critical load is 189 psi, as given in Timoshenko and Gere's *Theory of Elastic Stability.*

Table 4.4-1 Cylinder Buckling (Eigenvalues and Collapse Load Estimations)

Eigenvalues (λ)					
Mode	**Inc 0**	**Inc 1**	**Inc 2**	**Inc 3**	**Inc 4**
1		7.81	6.79	5.71	4.65
2		10.63	9.57	8.40	7.23
3		18.04	16.87	15.48	14.05
4		25.83	24.51	15.49	20.66
Previous Load: (N-Multiple of ΔP)					
Mode	**Inc 0**	**Inc 1**	**Inc 2**	**Inc 3**	**Inc 4**
1	1	2	3	4	5
2	1	2	3	4	5
3	1	2	3	4	5
4	1	2	3	4	5
Collapse Load Estimations: ($N_{i-1} + \lambda_i$, i = 1, 4, multiple of ΔP)					
Mode	**Inc 0**	**Inc 1**	**Inc 2**	**Inc 3**	**Inc 4**
1		9.81	9.79	9.71	9.65
2		12.63	12.57	12.40	12.23
3		20.04	19.87	19.48	19.05
4		27.83	27.51	19.49	25.66

Note: First Mode Collapse Load= 9.65 ΔP = 9.65 x 22,769 = 219,721

Critical Load= 219,721/(2π x 2.5 x 80) = 175 psi

Parameters, Options, and Subroutines Summary

Example e4x4.dat and e4x4b.dat:

Parameters	Model Definition Options	History Definition Options
BUCKLE	CONN GENER	AUTO LOAD
ELEMENT	CONNECTIVITY	BUCKLE
END	CONTROL	CONTINUE
LARGE DISP	COORDINATE	
SIZING	END OPTION	
TITLE	FIXED DISP	
	GEOMETRY	
	ISOTROPIC	
	NODE FILL	
	POINT LOAD	
	PRINT CHOICE	

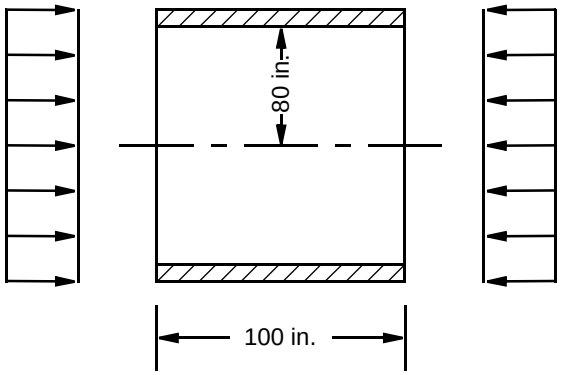

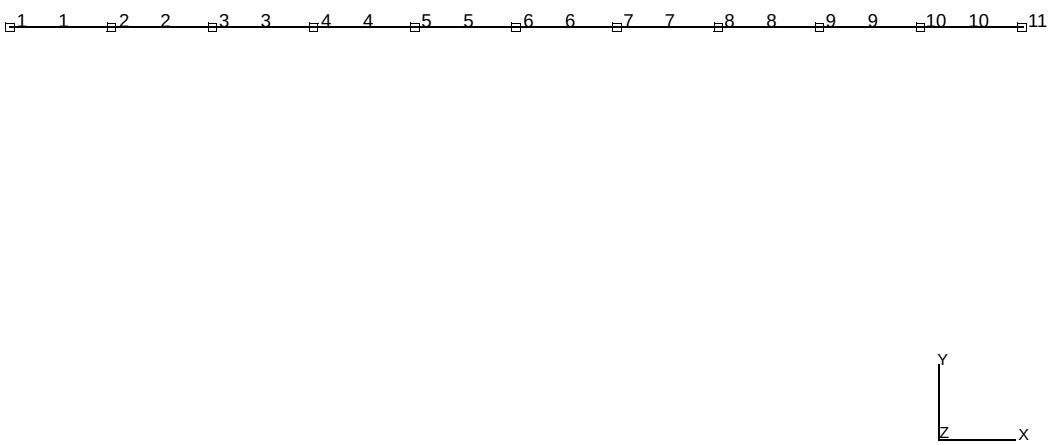

Figure 4.4-1 Cylinder Buckling

Mode 1
FREQ : 8.812

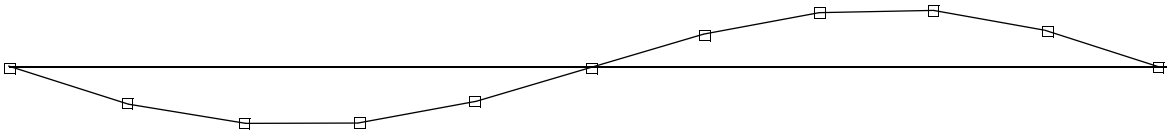

Mode 2
FREQ : 11.63

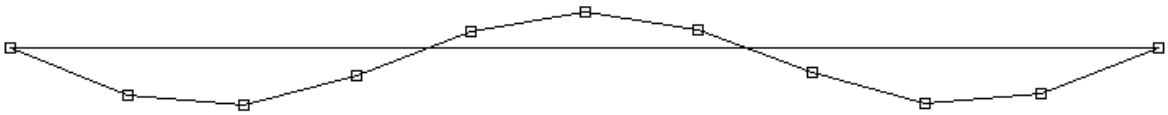

Mode 3
FREQ : 19.04

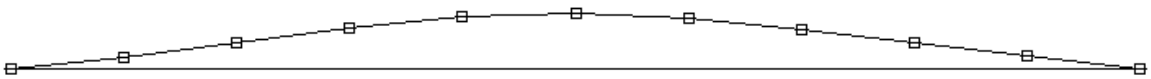

Mode 4
FREQ : 18.31

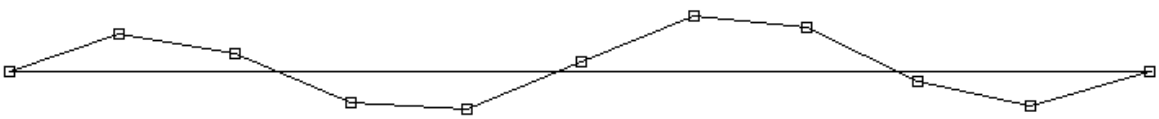

Figure 4.4-2 Mode Shapes

4.5 Large Displacement Analysis of a Pinched Cylinder

An elastic, large displacement analysis is carried out for a pinched cylinder subjected to a line load. This problem illustrates the use of MARC element type 22 (8-node thick shell element) and option LARGE DISP for a large displacement analysis.

Model/Element

The mesh consists of eight elements (type 22) and 37 nodal points. The dimensions of the cylinder and a finite element mesh are shown in Figure 4.5-1 and Figure 4.5-2. The coordinates are first generated in a plane. User subroutine UFXORD is then used for the modification of nodal coordinates. Bandwidth optimization option OPTIMIZE is also chosen for renumbering the mesh.

Material Properties

The Young's modulus and Poisson's ratio are assumed to be 30×10^6 psi and 0.3, respectively.

Loading

Total nodal forces of 100, 400, 200, 400, and 100 pounds are applied at nodal points 34, 35, 36, 37, and 17, respectively. The loads are applied in 10 equal increments through the AUTO LOAD option.

Boundary Conditions

Degrees of freedom are constrained at the lines of symmetry.

Results

A displaced mesh is shown in Figure 4.5-3 and stress contours are depicted in Figure 4.5-4. As anticipated, the largest stresses are near the cutout. This problem converges to typically 2% error in equilibrium in one to two iterations.

Parameters, Options, and Subroutines Summary

Example e4x5.dat:

Parameters	Model Definition Options	History Definition Options
ELEMENT	CONNECTIVITY	AUTO LOAD
ELSTO	CONTROL	CONTINUE
END	COORDINATE	
LARGE DISP	END OPTION	
SIZING	FIXED DISP	
TITLE	GEOMETRY	
	ISOTROPIC	
	OPTIMIZE	
	POINT LOAD	
	POST	
	RESTART	
	UFXORD	

User subroutine in u4x5.f:

UFXORD

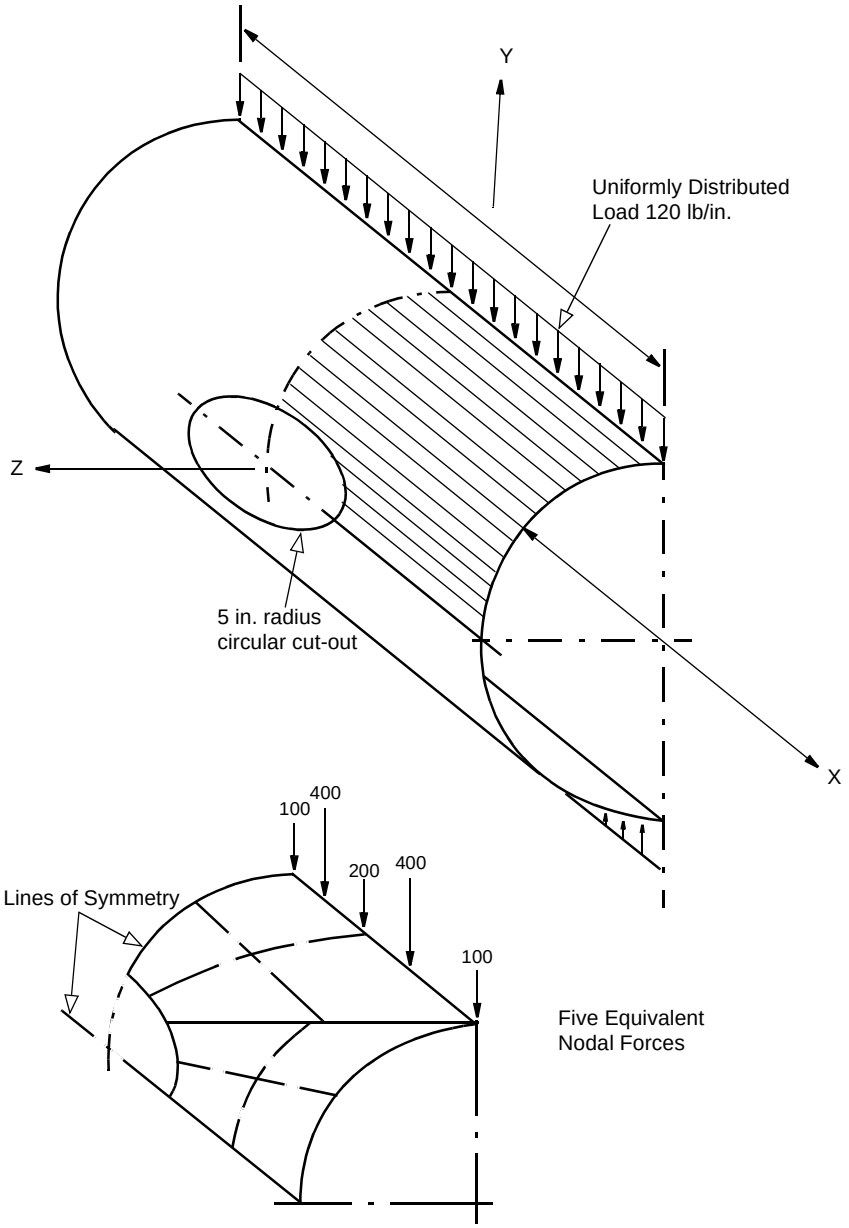

Figure 4.5-1 Pinched Cylinder and Mesh Blocks

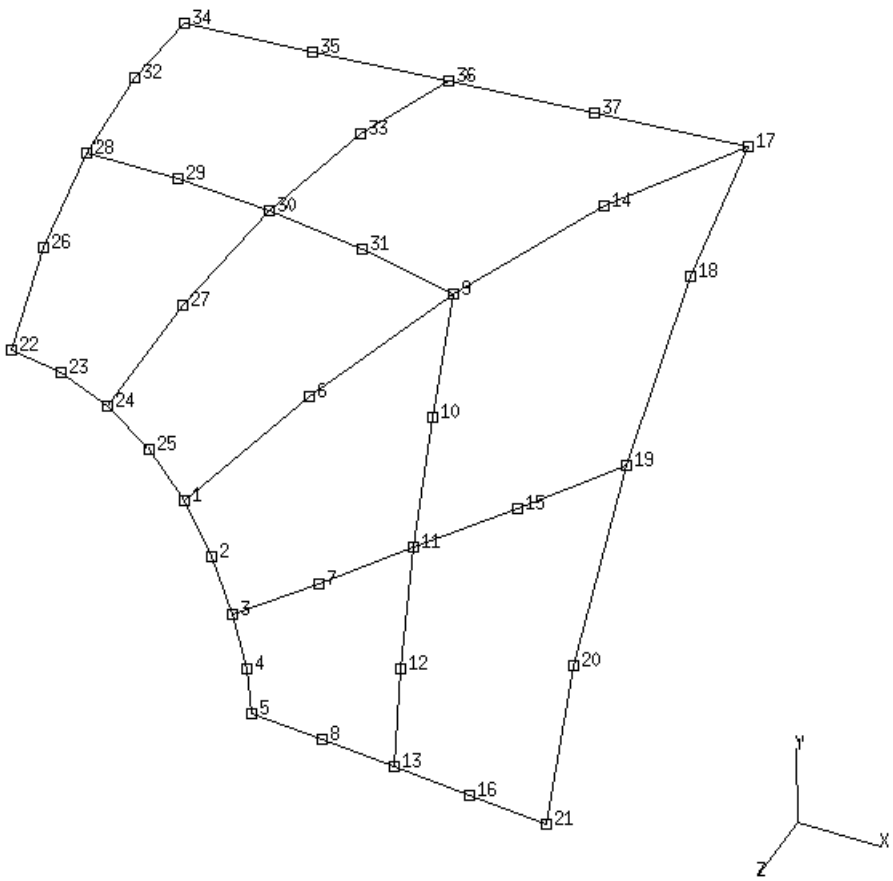

Figure 4.5-2 Finite Element Mesh for a Pinched Cylinder

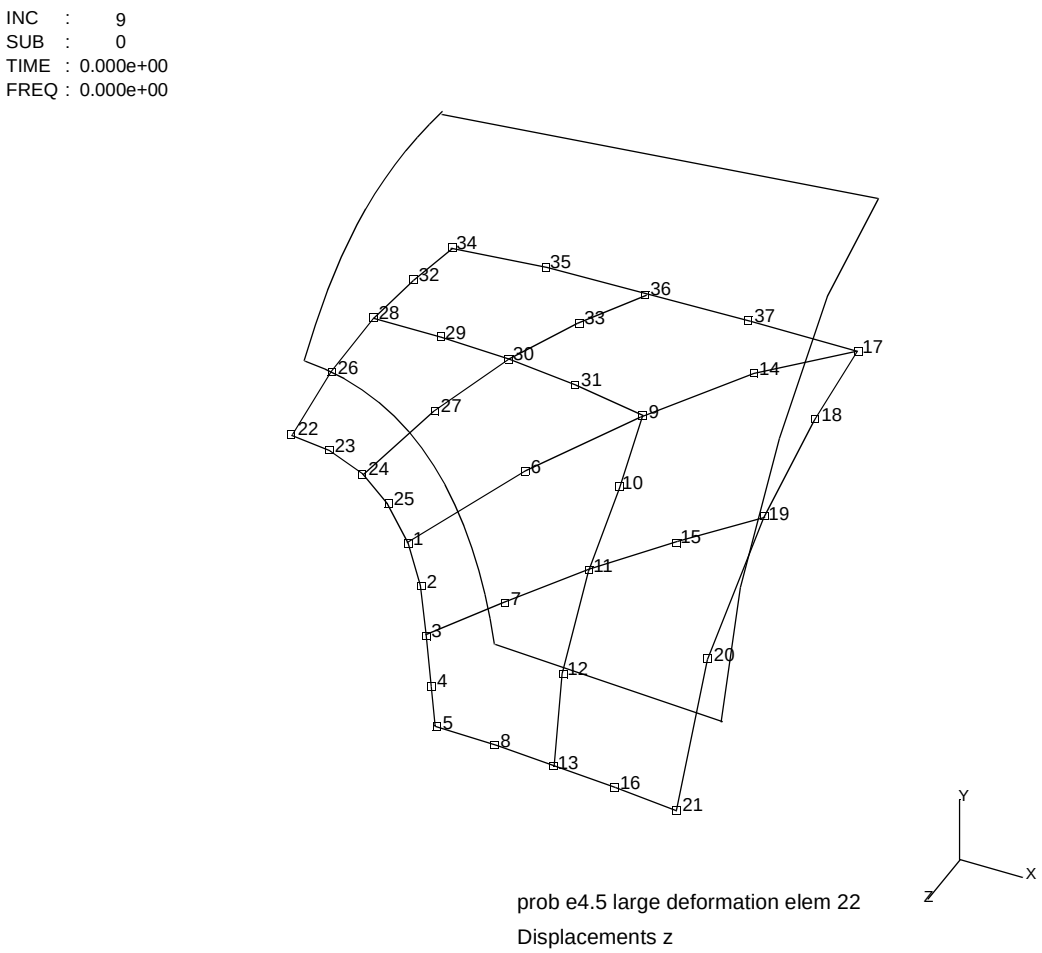

Figure 4.5-3 Displaced Mesh for a Pinched Cylinder

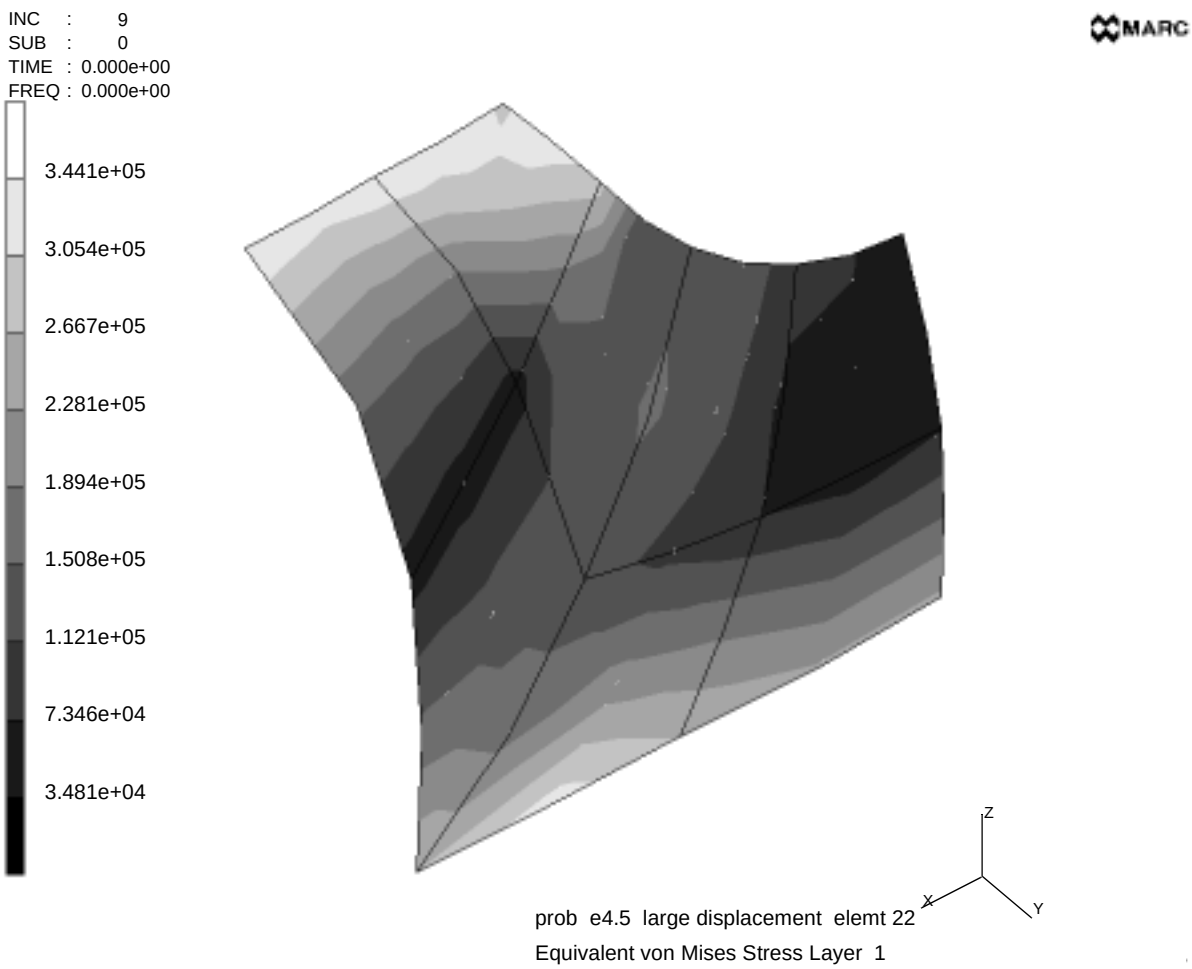

Figure 4.5-4 Stress Contours Equivalent Stress

4.6 One-Dimensional Elastic Truss-Spring System

A linear truss-spring system is analyzed by using the MARC element type 9 and the SPRINGS and LARGE DISP options.

Model

The model consists of one truss element and a linear spring. Dimensions of the model and a finite element mesh are shown in Figure 4.6-1.

Material Properties

The modulus of elasticity and Poisson's ratio of the truss element are assumed to be 1.0×10^7 and 0.3, respectively.

Boundary Conditions

One end of the truss element (node 1) is assumed to be fixed and the other end of the truss element is constrained to move only in the vertical direction.

Geometry

The truss has a unit cross-sectional area.

Loading

A concentrated force of 30 pounds is applied at node 2 in the negative y-direction. Various load increments (0.5, 0.1, and 1.0) were used in the analysis.

Springs

As shown in Figure 4.6-1, the moving end of the truss is supported by a linear spring. The spring constant is assumed to be 6 lb/in.

Auto Load

The total load of 30 pounds has been subdivided into four loading sequences. A different incremental load was used in each sequence. As an alternative, AUTO INCREMENT could have been used to adaptively adjust the load.

Results

The MARC finite element solution is shown in Figure 4.6-2. The exact solution (smooth curve) was obtained by numerical integration using a Runge-Kutta technique.

Parameters, Options, and Subroutines Summary

Example e4x6.dat:

Parameters	Model Definition Options	History Definition Options
ELEMENT	CONNECTIVITY	AUTO LOAD
END	CONTROL	CONTINUE
LARGE DISP	COORDINATE	POINT LOAD
SIZING	END OPTION	
TITLE	FIXED DISP	
	GEOMETRY	
	ISOTROPIC	
	POINT LOAD	
	SPRINGS	

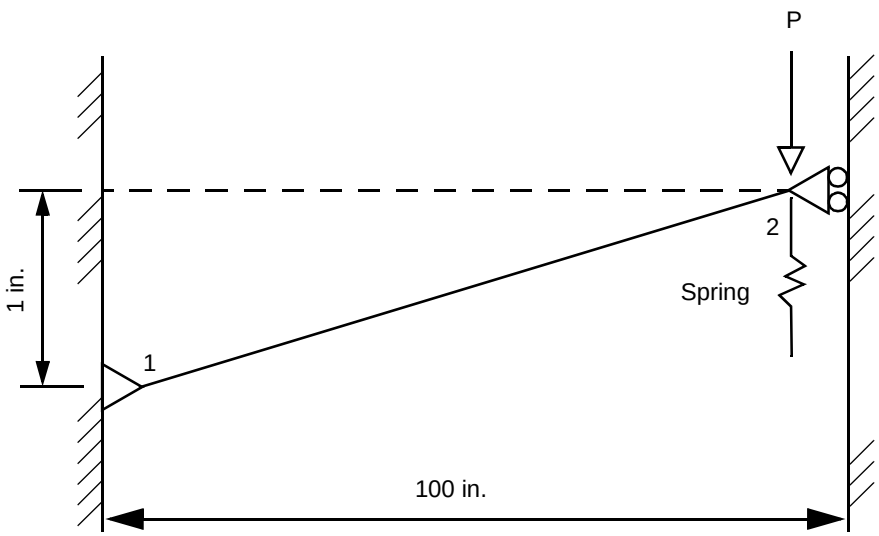

Figure 4.6-1 Truss-Spring System

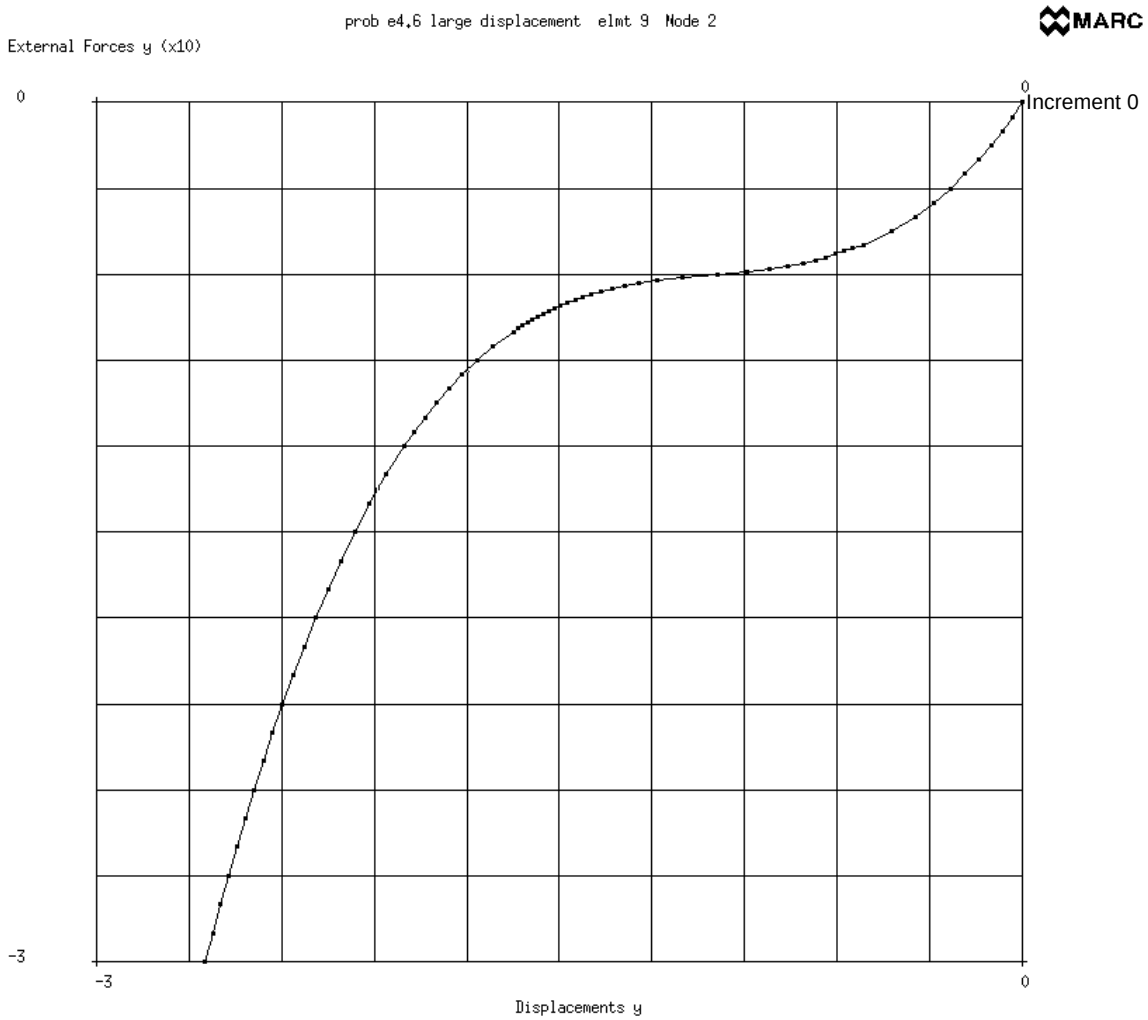

Figure 4.6-2 Load vs. Displacement at Node 2

4.7 Post-Buckling Analysis of a Deep Arch

A point load is applied to the apex of a semicircular arch. The arch gradually collapses as the applied load is incremented. The arch configuration after collapse is calculated and plotted. The load-displacement curve at the apex is plotted. This analysis utilizes the AUTO INCREMENT option to control the magnitude of the incremental solution and, hence, the magnitude of the load increment. The second analysis is the same as the first, but the arch is not allowed to penetrate itself. The analysis is performed elastically for both the pre- and post-buckling configurations.

This problem is modeled using the three techniques summarized below.

Data Set	Element Type(s)	Number of Elements	Number of Nodes	Differentiating Features
e4x7	16	20	21	AUTO INCREMENT
e4x7b	16	20	21	AUTO INCREMENT and CONTACT
e4x7c	16	20	21	AUTO STEP

Element

Element type 16 is a 2-node curved beam, with cubically interpolated global displacement and displacement derivatives. There are four degrees of freedom at each node. Membrane and curvature strains are output as well as axial stresses through the element thickness.

Model

The arch is modeled using 20 beam elements and 21 nodes. Only connectivity of element 1 is specified in the input. The connectivities for elements 2 through 21 are generated by option CONN GENER using element 1 as a model. The node coordinates are generated using user subroutine UFXORD. The coordinates are generated around a semicircle of radius 100 inches subtending an angle of 215 degrees. The finite element mesh is shown in Figure 4.7-1.

Material Properties

A Young's modulus of 12.0 x 10^6 psi and a Poisson's ratio of 0.2 are specified in the ISOTROPIC option.

Geometry

The beam thickness is 1 inch, as specified in EGEOM1. The width of the arch elements are specified as 1 inch in EGEOM2. Omission of the third field indicates a constant beam thickness.

Loading

The total applied load is specified in the POINT LOAD block, following the END OPTION. A total load of 1200 pounds is applied at node 11, over a maximum of 300 increments. The maximum load that can be applied in the first increment is 10% of the total load, or 120 pounds. These maxima are set in the AUTO INCREMENT option.

Boundary Conditions

The arch is pinned at one support and built in at the other. Thus, the degrees of freedom at node 1 (u and v) are constrained. At node 21, a coordinate transformation is carried out such that the boundary conditions here are simply specified. So, in the transformed coordinates at node 21, degrees of freedom u', v', and $\partial u'/\partial s$ are constrained.

Contact

The results of the first analysis indicate that the arch will pass through itself which is physically impossible. To prevent this, the second data set uses the CONTACT option.

This option declares that here is only one flexible body which is made up of 20 elements. In order to avoid unexpected separation, the high separation forces are entered as the arch hits the left support. Contact tolerance distance is 0.02 which is 2% of thickness of shell.

Notes

A 5% residual force relative error is specified in the CONTROL OPTION.

The option SHELL SECT reduces the number of integration points through the element thickness from a default value of 11 to the specified three points.This greatly reduces computation time with no loss of accuracy in an elastic analysis.

The PRINT parameter is set to 3. This option forces MARC to solve nonpositive definite matrices; this parameter is required for all post-buckling analyses.

The UPDATE parameter assembles the stiffness matrix of the current deformed configuration; as well, this parameter writes out the stresses and strains in terms of the current deformed geometry.

The UDUMP model definition option indicates by default that all nodes and all elements are made available for postprocessing by user subroutines IMPD and ELEVAR. In this example, the data is postprocessed to create a load-displacement curve for the arch.

Results Without CONTACT

The analysis ends in increment 75, at a load of 290.4 pounds. The total requested load is not reached due to an excessive number of recycles required for solution in the last increment. Resetting the maximum number of recycles and residual load tolerance allows the analysis to be continued using the RESTART file generated during the analysis. Displaced mesh plots are shown in Figure 4.7-2 (a) through Figure 4.7-3 (d). The displaced plots are obtained using the

second data set. The POSITION option is used to access the restart file at several different increments. The structure actually loops through the pinned support as there is no obstruction to this motion. A load-deflection curve is plotted for node 77 in Figure 4.7-4.

Results With CONTACT

In example e4x7b, as the CONTACT option is used, the left support prevents the arch from passing through and gives the reasonable deformation shape. Figure 4.7-5 through Figure 4.7-7 show a progression of the deformation. From the load deflection curve (Figure 4.7-8), you can observe the strong nonlinearities due to the contact which leads to a stiffening effect in the structure and a different snap-through behavior.

Parameters, Options, and Subroutines Summary

Example e4x7.dat:

Parameters	Model Definition Options	History Definition Options
END	CONN GENER	AUTO INCREMENT
LARGE DISP	CONNECTIVITY	CONTINUE
PRINT	CONTROL	POINT LOAD
SHELL SECT	END OPTION	
SIZING	FIXED DISP	
TITLE	GEOMETRY	
UPDATE	ISOTROPIC	
	PRINT CHOICE	
	RESTART	
	TRANSFORMATIONS	
	UDUMP	
	UFXORD	

User subroutine in u4x7.f:

UFXORD

Example e4x7b.dat:

Parameters	Model Definition Options	History Definition Options
END	CONNECTIVITY	AUTO INCREMENT
LARGE DISP	CONTACT	CONTINUE
PRINT	CONTROL	POINT LOAD
SHELL SECT	COORDINATE	
SIZING	END OPTION	
TITLE	FIXED DISP	
UPDATE	GEOMETRY	
	ISOTROPIC	
	PRINT CHOICE	
	POINT LOAD	
	POST	

Example e4x7c.dat:

Parameters	Model Definition Options	History Definition Options
END	CONN GENER	AUTO STEP
LARGE DISP	CONNECTIVITY	CONTINUE
PRINT	CONTROL	POINT LOAD
SHELL SECT	END OPTION	
SIZING	FIXED DISP	
TITLE	GEOMETRY	
UPDATE	ISOTROPIC	
	PRINT CHOICE	
	POINT LOAD	
	POST	
	TRANSFORMATIONS	
	UFXORD	

User subroutine in u4x7.f:

UFXORD

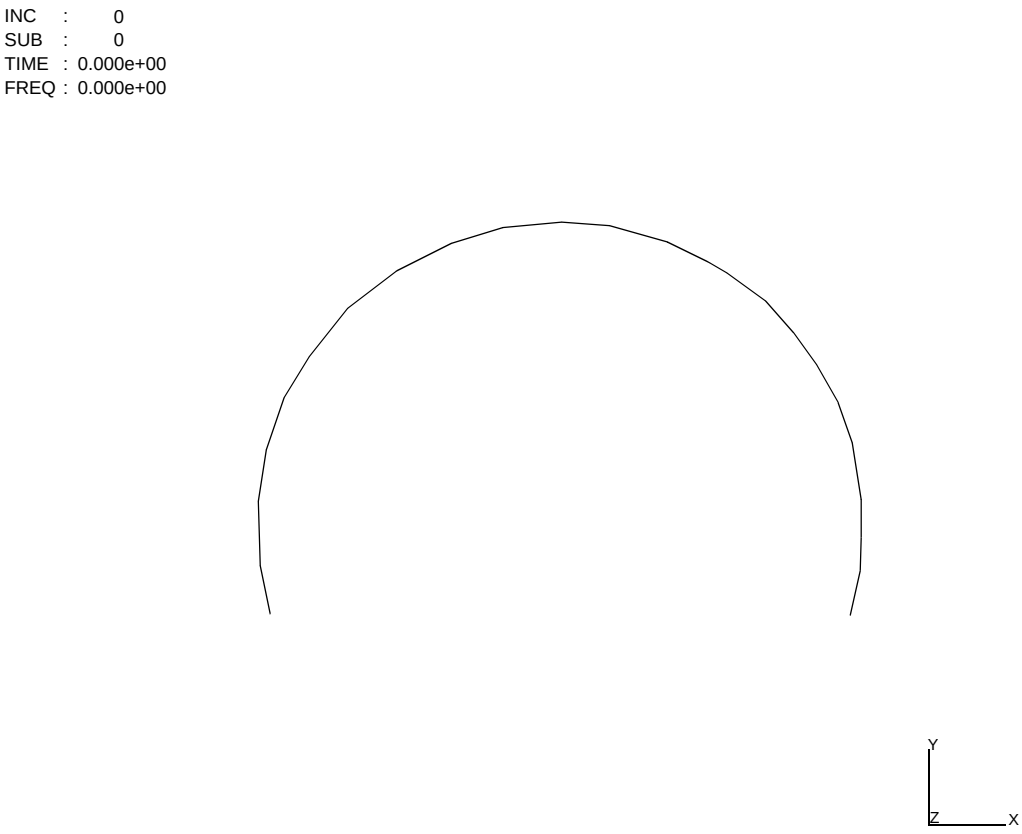

Figure 4.7-1 Deep Arch

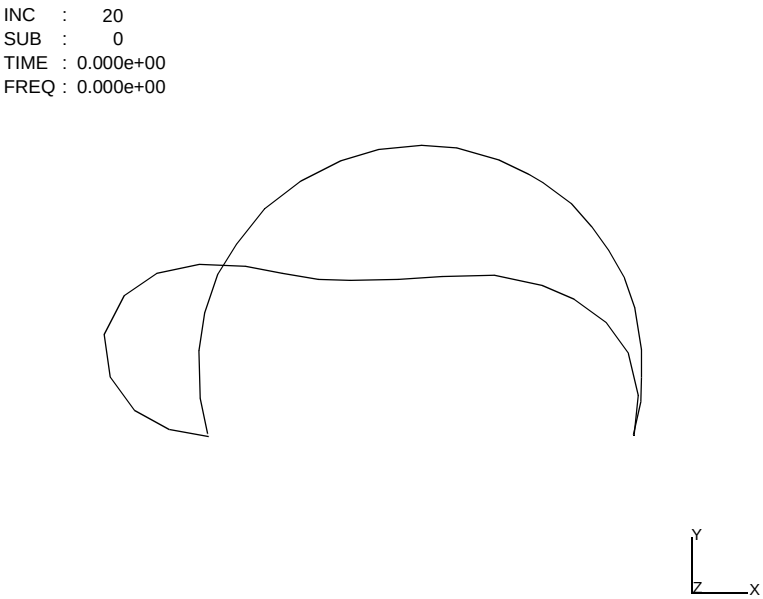

(a)

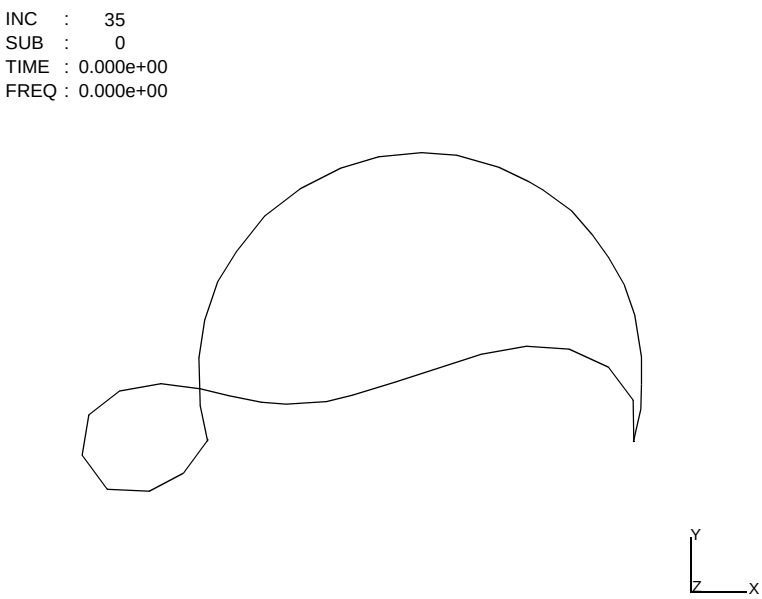

(b)

Figure 4.7-2 Displaced Mesh

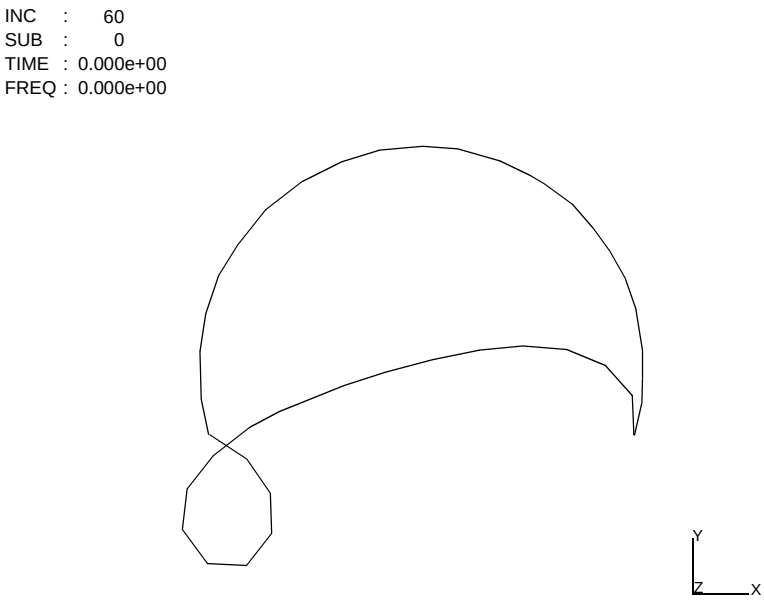

(c)

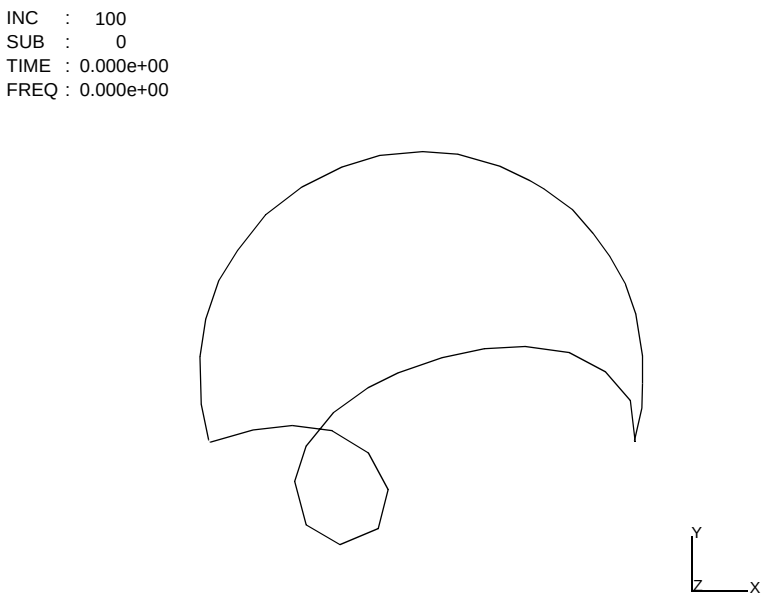

(d)

Figure 4.7-3 Displaced Mesh (Continued)

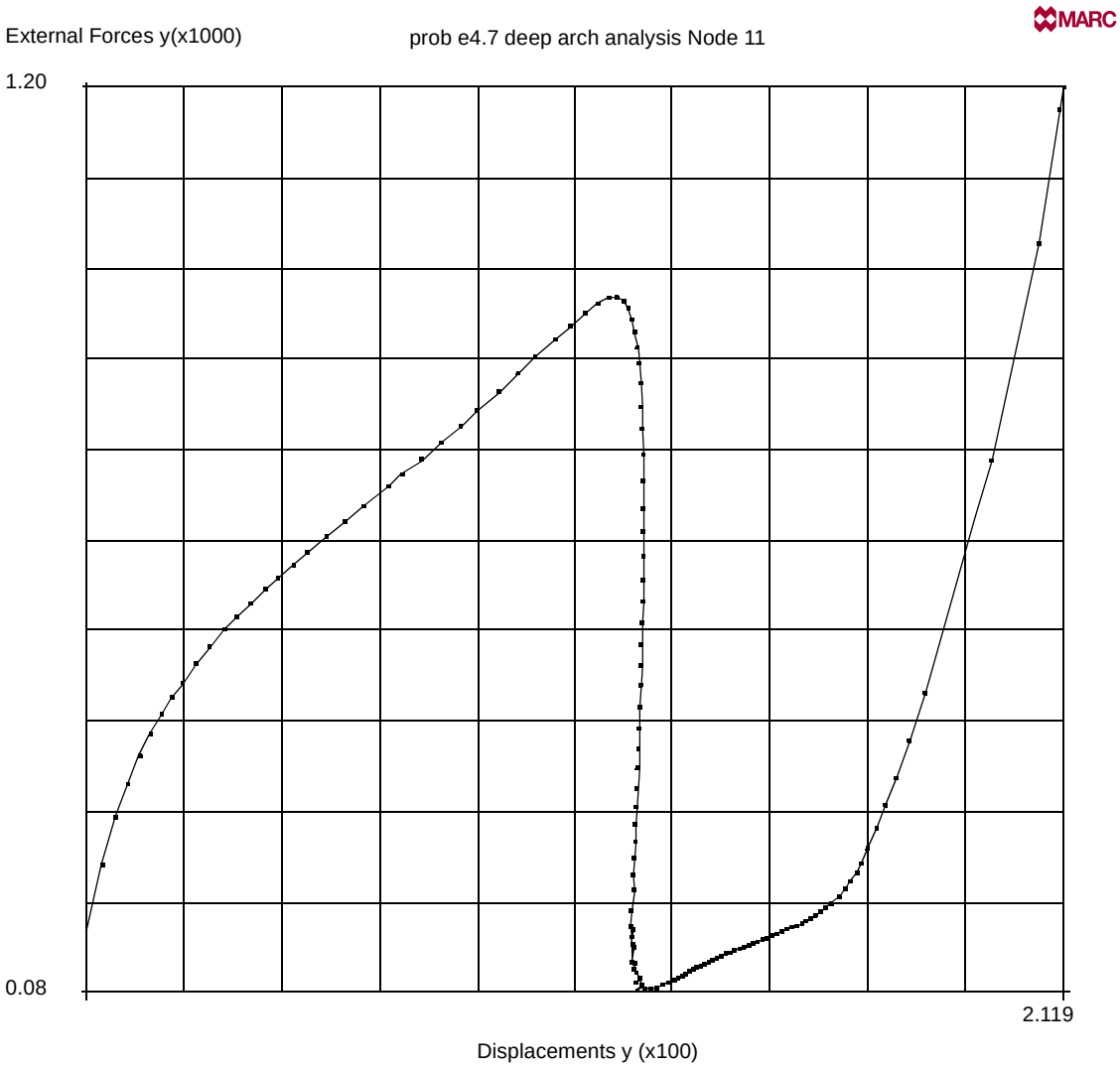

Figure 4.7-4 Load vs. Displacement (Node 77) – No Contact

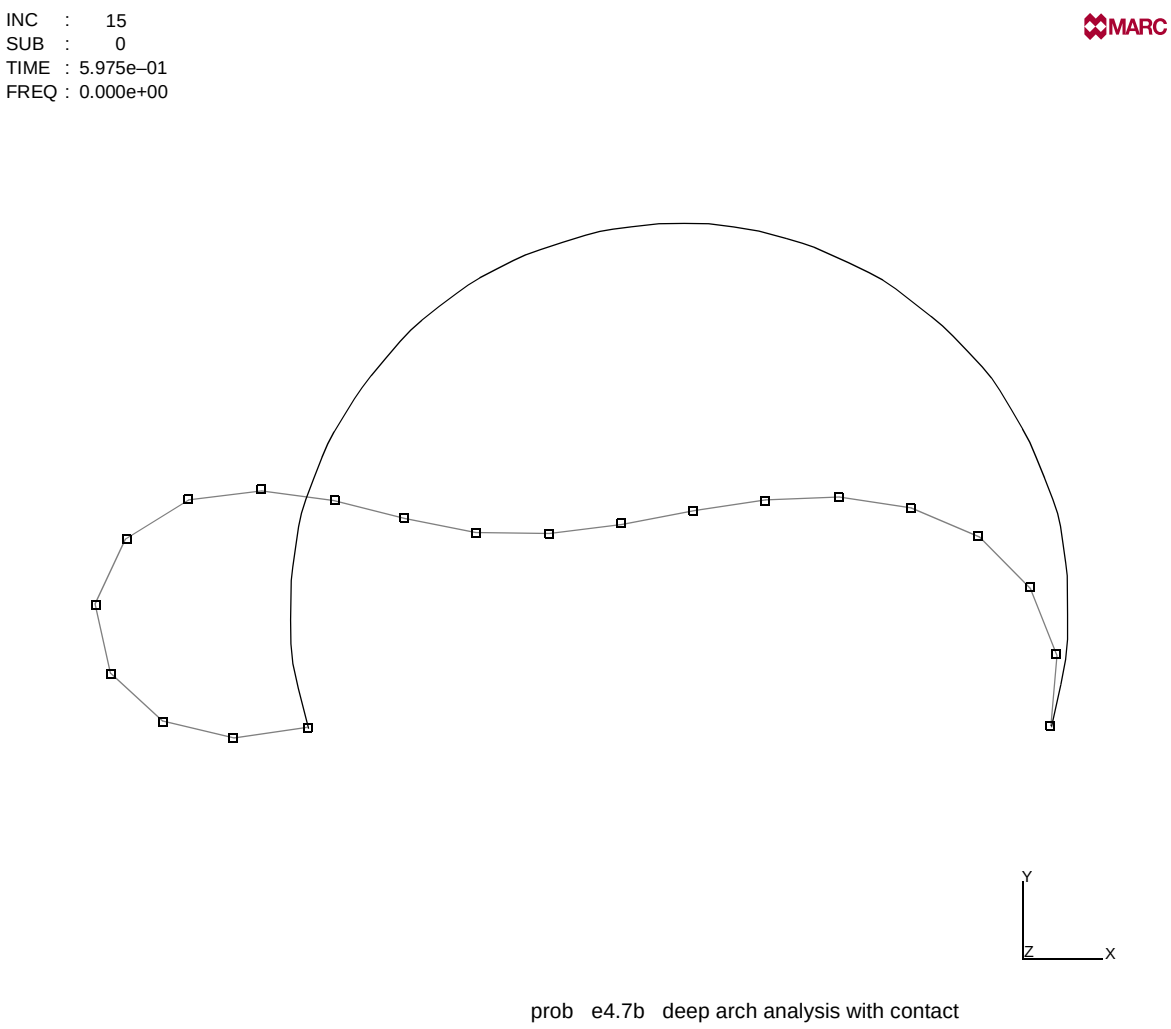

Figure 4.7-5 Displaced Mesh with Contact at Pin

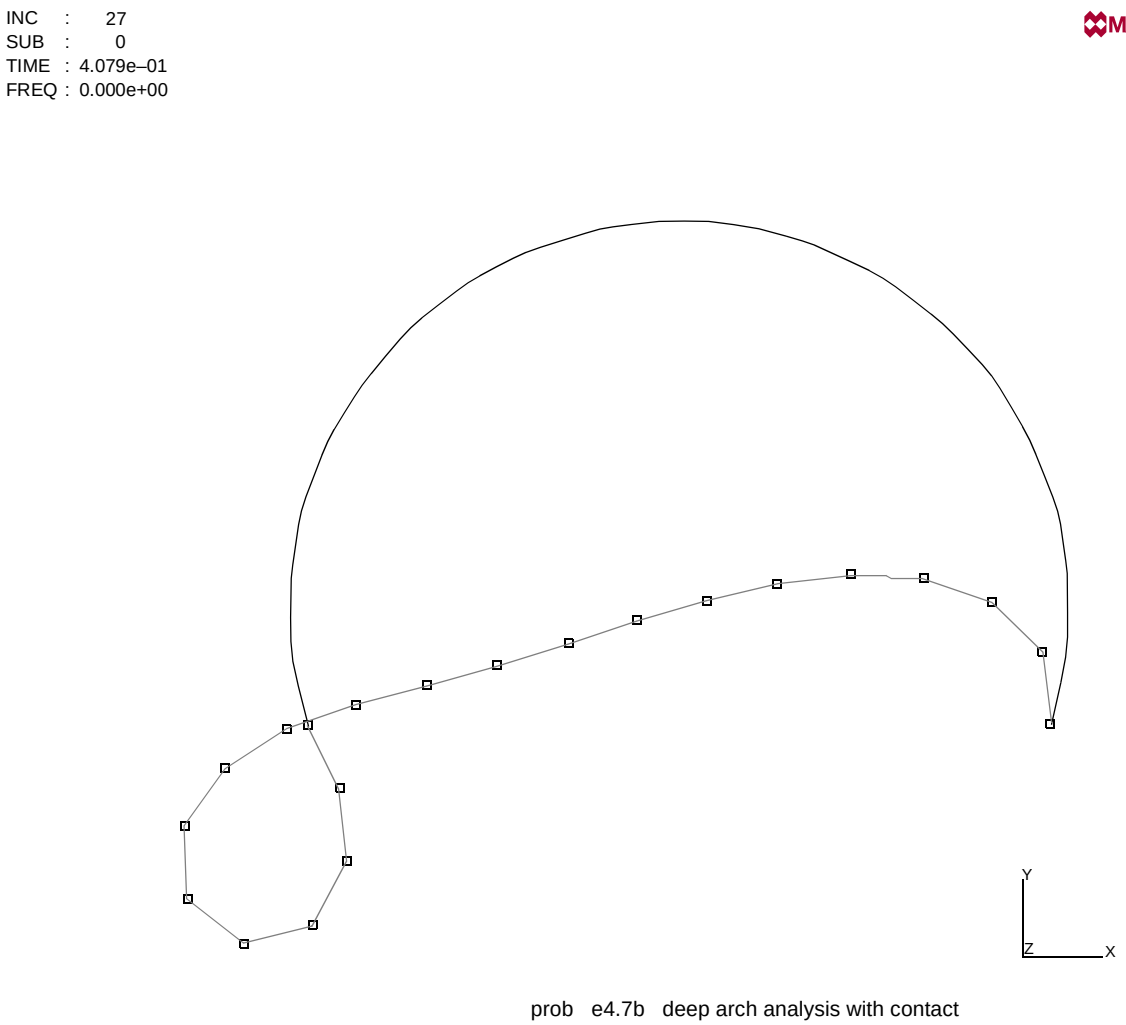

Figure 4.7-6 Displaced Mesh with Contact at Pin

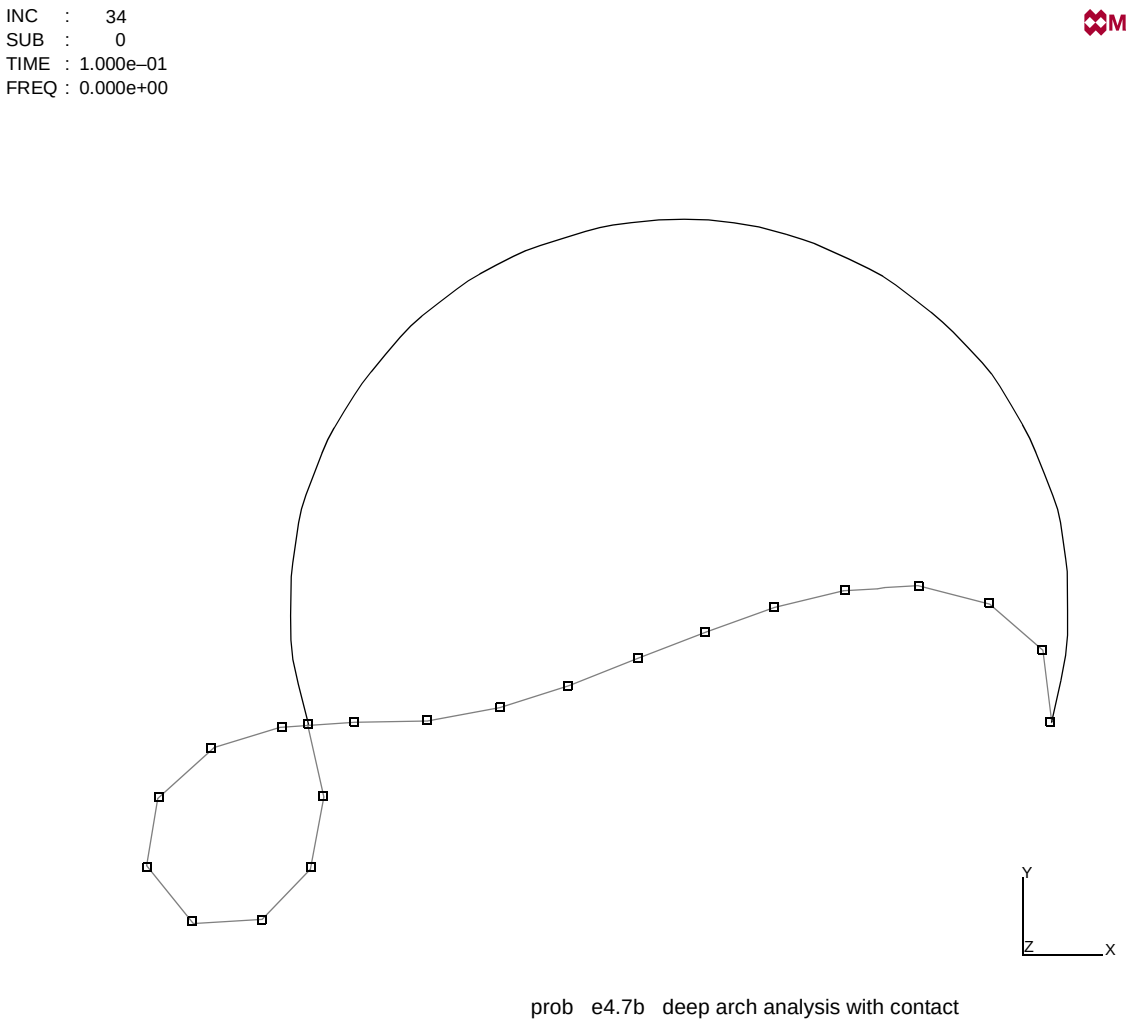

Figure 4.7-7 Displaced Mesh with Contact at Pin

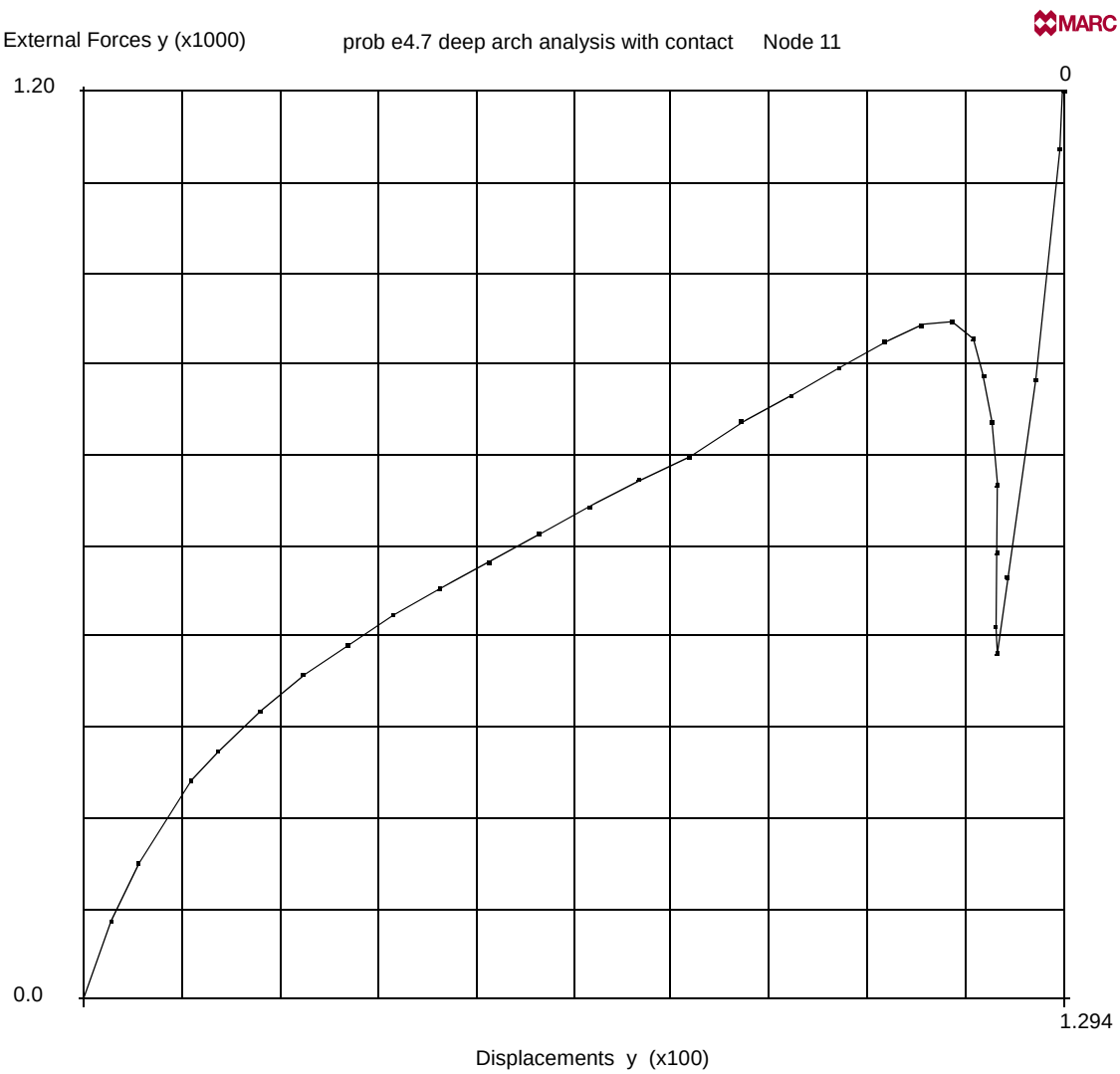

Figure 4.7-8 Load vs. Displacement (Node 77) with Contact at Pin

4.8 Large Displacement Analysis of a Cable Network

A cable network subjected to gravity and wind loads is analyzed using MARC cable element (element type 51). The analysis includes both large displacement and follower force effects.

Element

Element 51 is a 3D, 2-node cable element, defined in space by global coordinates (x,y,z) at two nodal points with three translational DOFs (u,v,w) at each node. The load-displacement relationship of this element is directly, numerically calculated and requires to be acted on by at least one type of distributed load (for example, weight of the cable) for the proper formulation of the stiffness matrix. Detailed discussion on this element can be found in *MARC Volume B: Element Library.*

Model

As shown in Figure 4.8-1, there are 45 cable elements in the mesh. The number of nodes in the mesh is 27 and the total degrees of freedom is 81. The network is assumed to be fully supported at end of the six legs.

Geometry

The first data field, EGEOM1, specifies the cross-sectional area. The second data field, EGEOM2, specifies the cable length. The third data field, EGEOM3, specifies the initial stress. In this example, the second data field is set to zero because the cable length is assumed to be equal to the cable distance. If the EGEOM2 data is entered as 0.0, the program calculates the distance between the two nodes and then automatically takes it as the cable length. Another situation is that we know the initial stress, but not the cable length. In this case, you can use the third data field (EGEOM3) to specify the initial stress and set to zero the second data field (EGEOM2).

Material Properties

The Young's modulus is 1.0×10^2 psi.

Displacement Loads

A gravity load of -1.0 pounds in the y-direction is applied to all elements in the zeroth increment. A zero incremental load is then applied for one increment to reduce the residual load. A wind load of -2.0 pounds in the z-direction is applied for the second, third and fourth increments as incremental load. As a result, a -1.0 pounds gravity load and -6.0 pounds wind load are applied to the cable network as the total distributed loads.

Fixed Displacement

Three degrees of freedom (u = v = w = 0) of six (6) end points (nodes 1, 3, 24, 27, 25, and 4) are fully fixed.

Large Displacement

The LARGE DISP option flags the program control for large displacement analysis. MARC calculates the geometric stiffness matrix and the initial stress stiffness matrix when the LARGE DISP option is flagged.

Follow Force

The FOLLOW FOR option allows MARC to form all distributed loads on the basis of current geometry. This is an important consideration in a large displacement analysis.

PRINT,3,

In the analysis of a cable network, the initial stiffness matrix of the network can possibly be singular for the lack of cable forces in the system. The PRINT,3, option allows for the completion of numerical computations of an initially singular system, and for the continuation of subsequent load increments.

Results

Deformed meshes of the cable network are plotted in Figure 4.8-2 and Figure 4.8-3.

Parameters, Options, and Subroutines Summary

Example e4x8.dat:

Parameters	Model Definition Options	History Definition Options
ELEMENT	CONNECTIVITY	AUTO LOAD
END	CONTROL	CONTINUE
FOLLOW FORCE	COORDINATE	DIST LOADS
LARGE DISP	DIST LOADS	PROPORTIONAL INCREMENT
PRINT	END OPTION	
SIZING	FIXED DISP	
TITLE	GEOMETRY	
	ISOTROPIC	
	POST	

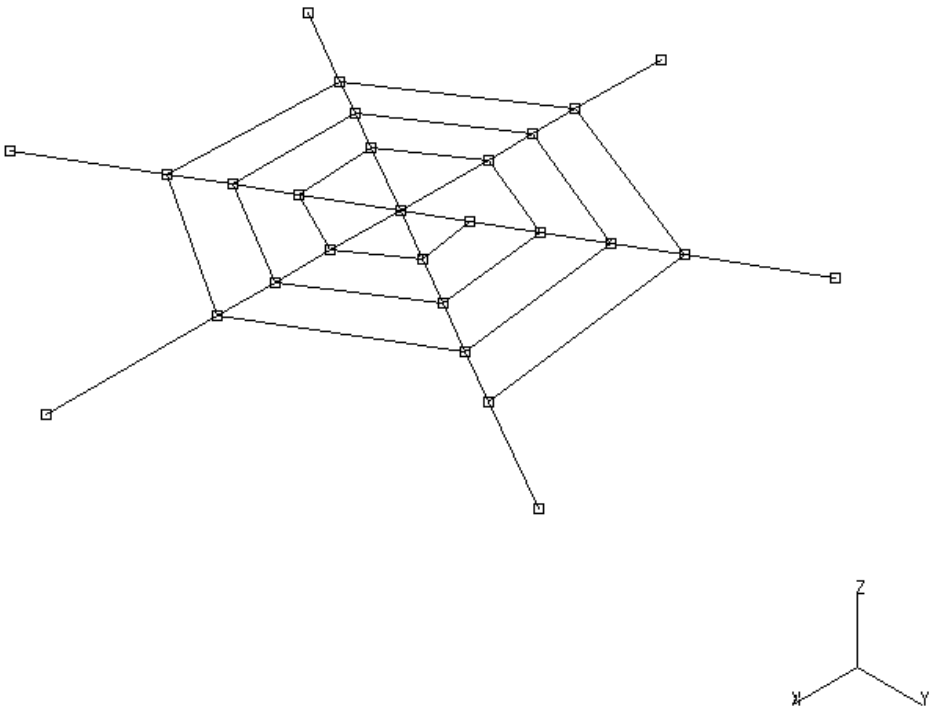

Figure 4.8-1 Cable Network Mesh

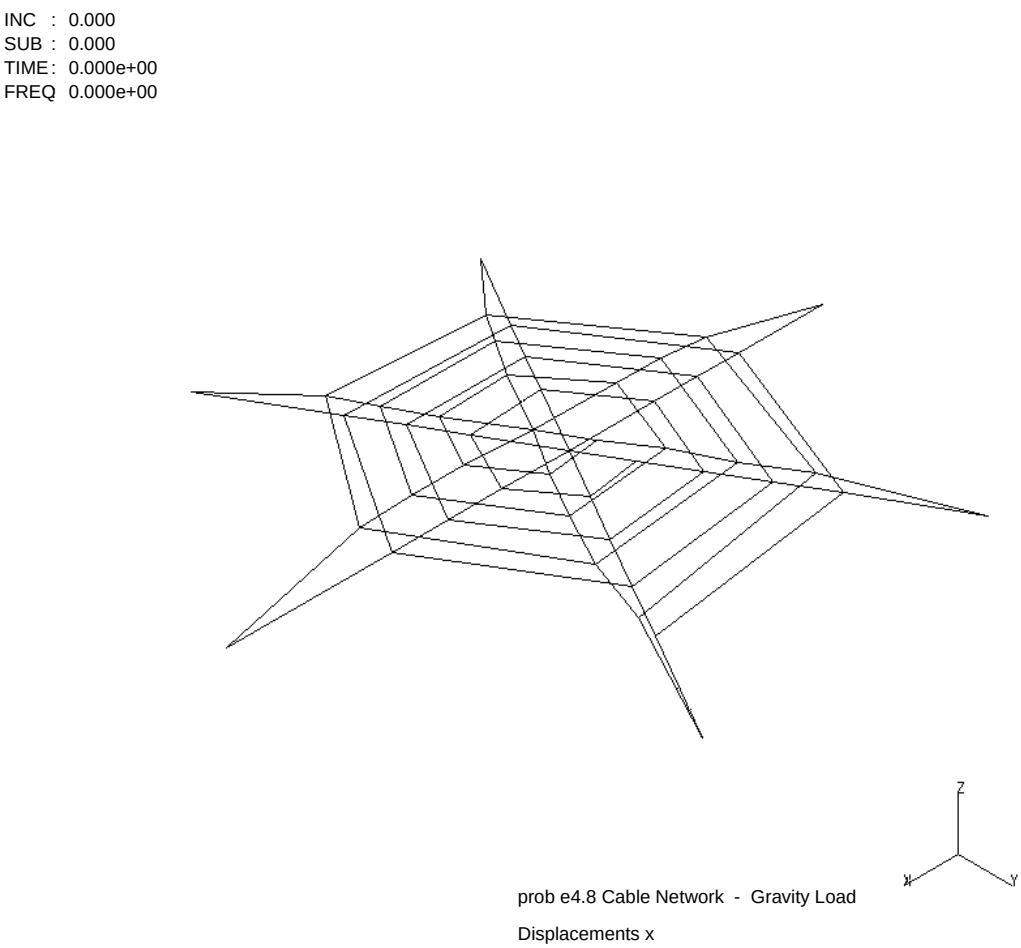

Figure 4.8-2 Cable Network Deformed Mesh (Gravity Load)

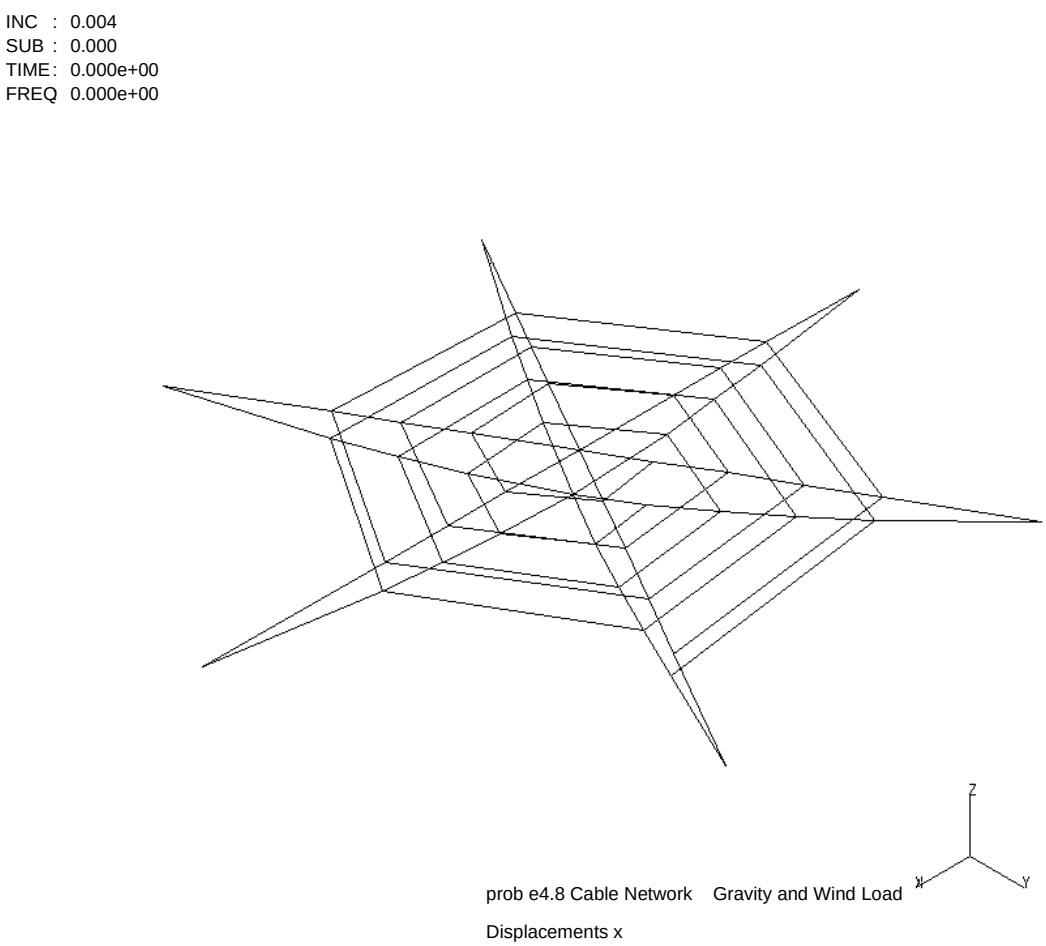

Figure 4.8-3 Cable Network Deformed Mesh (Gravity + Wind Load)

4.9 Nonsymmetric Buckling of a Ring

The buckling load of a radially loaded ring is determined using MARC element 90. It is important to notice that the load is radially directed, not only with respect to the initial geometry, but also with respect to the deformed one. Since MARC uses the stresses following from the linear pre-buckling state, this problem is easily analyzed. On the other hand, if the load would be of fluid-type, the buckling load could be approximated by means of an incremental nonlinear analysis using 3D shell elements, with the parameter blocks FOLLOW FOR and LARGE DISP.

This problem is modeled using the two techniques summarized below.

Data Set	Element Type(s)	Number of Elements	Number of Nodes	Differentiating Features
e4x9	90	1	3	Fourier Buckling Inverse Power Sweep
e4x9b	90	1	3	Fourier Buckling Laczos

Element

Element type 90 is a 3-node thick shell element for the analysis of arbitrary loading of axisymmetric shells. Each node has five degrees of freedom. Although for this problem, the (initial) geometry and the loading are axially symmetric, the buckling mode is not.

Model

The ring with a length of 2.0 inches is modeled using 1 element. This is sufficient since the problem is actually one-dimensional as shown in Figure 4.9-1.

Geometry

The radius and the wall thickness are 10.0 inches and 0.1 inch, respectively.

Material Properties

All elements have the same properties: Young’s modulus equals 1.2E7 psi, while Poisson’s ratio equals 0.0.

Loading

A uniform pressure (IBODY = 0) of 1.0 is applied to the element.

Boundary Conditions

The boundary conditions for the linear elastic calculation and the buckling analyses are not the same. As for the linear elastic calculation, the axial and circumferential displacement of nodal point 3 are suppressed in order to be sure that no rigid body motions are present. To obtain a homogeneous deformation in axial direction, the rotations in the Z-R plane are also suppressed. As for the buckling analyses, it is essential to release the circumferential displacement of nodal point 3; otherwise, the structure would behave too stiff.

Analysis

After a linear elastic calculation (increment 0), several buckling analyses are performed. The maximum number of iterations, the tolerance and the harmonic number are set equal to 100 and 0.00001, respectively. Since, in general, the harmonic number corresponding to the lowest buckling load is unknown a priori, the harmonic number is chosen to vary from 2 to 7. The meaning of the parameters SHELL SECT,3 and BUCKLE,5,1,0,3 can be explained as follows:

SHELL SECT,3 : 3: use 3 integration points in thickness direction of the elements.

BUCKLE,5,1,0,3,0,0: 5: in a buckling analysis, 5 modes are required;

1: 1 mode must correspond to a positive eigenvalue: once a mode with a positive eigenvalue is found, the program will stop, even if not all 5 previously mentioned modes are found;

0: the eigenvectors are not stored on the post file;

3: a Fourier buckling analysis is performed.

0: Inverse power sweep method

0: In the third analysis, this last parameter is set to 1 to indicate that the Lanczos method is used

The model definition option BUCKLE INCREMENT cannot be used since, in this problem, the buckling analyses are performed using the stress state corresponding to increment 0, but with modified boundary conditions. Using BUCKLE INCREMENT, you can either perform buckling analyses using the stress state corresponding to increment 0 with the boundary conditions of increment 0, or buckling analyses in increment 1 using modified boundary conditions, but also with a modified stress state (since an eigenvalue analysis is always performed using the incremental stresses).

Discussion

The analytical solution for the lowest buckling load is given by (for example, Don O. Bruce and Bo O. Almroth, *Buckling of Bars, Plates and Shells*, McGraw-Hill, 1975):

$$q_{analytical} = \frac{(n^2-1)^2}{(n^2-2)} \cdot \frac{EI}{r^3}, \text{ with } I = \frac{Lh^3}{12}$$

Here n represents the harmonic number. The lowest buckling load corresponds to n = 2. Substituting further E = 1.2e7, L = 2.0, r = 10.0 and h = 0.1.

$$q_{analytical} = 9.000$$

so the critical pressure is:

$$P_{analytical} = \frac{1}{L} q_{analytical} = 4.50$$

The MARC solutions for the buckling load for the various numbers of n are given below (where the corresponding analytical values are also presented):

n	Buckling Load		
	Inverse Power Sweep	Lanczos	Analytical
2	4.498	4.498	4.500
3	9.497	9.497	9.143
4	16.49	16.49	16.07
5	25.49	25.49	25.04
6	36.48	36.48	36.03
7	49.46	49.46	49.02

The MARC solution for the lowest buckling load turns out to be:

$$P_{MARC} = 4.428 \text{ for } n = 2.$$

The difference between this and the analytical solution is about 0.04%.

Parameters, Options, and Subroutines Summary

Example e4x9.dat and e4x9b.dat:

Parameters	Model Definition Options	History Definition Options
BUCKLE	CONNECTIVITY	BUCKLE
ELEMENT	COORDINATES	CONTINUE
END	DIST LOAD	DISP CHANGE
SHELL SECT	FIXED DISP	
SIZING	END OPTION	
TITLE	GEOMETRY	
	ISOTROPIC	
	POST	

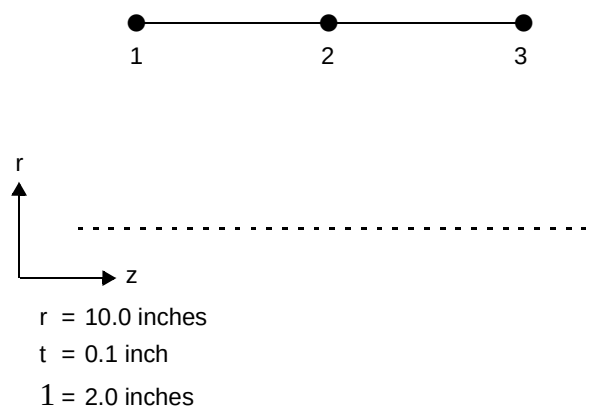

Figure 4.9-1 Mesh

4.10 Nonsymmetric Buckling of a Cylinder

The buckling load of an axially loaded cylinder is determined using MARC element 90.

This problem is modeled using the two techniques summarized below.

Data Set	Element Type(s)	Number of Elements	Number of Nodes	Differentiating Features
e4x10	90	20	41	Inverse power sweep
e4x10b	90	20	41	Lanczos method

Element

Library element 90 is a 3-node thick shell element for the analysis of arbitrary loading of axisymmetric shells. Each node has five degrees of freedom. Although for this problem, the (initial) geometry and the loading are axially symmetric, the buckling mode is not.

Model

The cylinder with a length of 20.0 inches is divided into 20 equally sized elements as shown in Figure 4.10-1.

Geometry

The radius and the wall thickness are 20.0 inches and 0.2 inches, respectively.

Material Properties

All elements have the same properties: Young’s modulus equals 10.0E6 psi, while Poisson’s ratio equals 0.3.

Loading

A point load of –1.0 pounds is applied to nodal point 41; thus, introducing an axial load.

Boundary Conditions

The boundary conditions for the linear elastic calculation and the buckling analyses will not be the same. This is necessary to make a comparison with the analytical solution possible. As for the linear elastic calculation, the radial displacements at the ends of the cylinder remain free in order to obtain a homogeneous pre-buckling state. The remaining degrees of freedom of node 1 and node 41, with exception of the axial displacement of node 41, are suppressed. In the buckling analyses, the radial displacements at the ends are suppressed as well.

Analysis

After a linear elastic calculation (increment 0), a number buckling analyses are performed. The maximum number of iterations and the tolerance are set equal to 100 and 0.001, respectively. Since, in general, the harmonic number corresponding to the lowest buckling load is unknown a priori, the harmonic number, is chosen to vary from 1 to 15. The meaning of the parameter options SHELL SECT,3 and BUCKLE,5,1,0,3 can be explained as follows:

SHELL SECT,3 : 3: use 3 integration points in thickness direction of the elements.

BUCKLE,5,1,0,3,0,0: 5: in a buckling analysis, 5 modes are required;

1: 1 mode must correspond to a positive eigenvalue: once a mode with a positive eigenvalue is found, the program will stop, even if not all 5 previously mentioned modes are found;

0: the eigenvectors are not stored on the post file;

3: a Fourier buckling analysis is performed.

0: Inverse power sweep method

For data set 4x10b, this last parameter is set to 1 to indicate that the Lanczos method is used

The model definition option BUCKLE INCREMENT cannot be used since, in this problem, the buckling analyses are performed using the stress state corresponding to increment 0, but with modified boundary conditions. Using BUCKLE INCREMENT, one can either perform buckling analyses using the stress state corresponding to increment 0 with the boundary conditions of increment 0, or buckling analyses in increment 1 using modified boundary conditions, but also with a modified stress state (since an eigenvalue analysis is always performed using the incremental stresses).

Discussion

For this problem, no closed form analytical solution for the lowest buckling load is available. The solution has to be deduced from (e.g, Don O Bruce and Bo O. Almroth, *Buckling of Bars, Plates and Shells*, McGraw-Hill, 1975):

$$F(anal)/(2*\pi*r) = \{mb*mb+n*n)*(mb*mb+n*n)/(mb*mb)\}*\{D/(r*r)\}+ \{(mb*mb)/\{(mb*mb+n*n)*mb*mb+n*n)]\}*(1-\nu*\nu)*C,$$

with $C = E*h/(1-\nu*\nu)$ and $D = E*h*h*h/\{12*(1-\nu*\nu)\}$

By means of a simple program, the minimum value of F(anal), depending on mb and n, can easily be determined. With E = 10.0E6, ν = 0.3, L = 20.0, r = 20.0 and h = 0.2, one finds:

F(anal) = 1.521E6, corresponding to n = 9 and m = 3, where m is given by $m = mb*L/(\pi*r)$.

The MARC solution for the lowest buckling load for the various numbers of n are given below:

n	Buckling Load (MARC)
1	1.607E6
2	1.605E6
3	1.602E6
4	1.595E6
5	1.586E6
6	1.573E6
7	1.573E6
8	1.522E6
9	1.532E6
10	1.547E6
11	1.666E6
12	1.806E6
13	1.968E6
14	2.176E6
15	2.396E6

The MARC solution for the lowest buckling load turns out to be:

F(MARC) = 1.522E6, for n = 8.

The difference between this and the analytical solution is about 0.07%. The corresponding harmonic numbers n are not the same. However, it can easily be verified that the difference between the solutions for n = 8 and n = 9 is small. The difference between the MARC solution for n = 9 and the analytical solution is about 0.7%.

Parameters, Options, and Subroutines Summary

Example e4x10.dat:

Parameters	Model Definition Options	History Definition Options
BUCKLE	CONNECTIVITY	BUCKLE
ELEMENTS	COORDINATES	CONTINUE
END	END OPTION	DISP CHANGE
SHELL SECT	FIXED DISP	
SIZING	GEOMETRY	
TITLE	ISOTROPIC	
	POINT LOADS	
	POST	

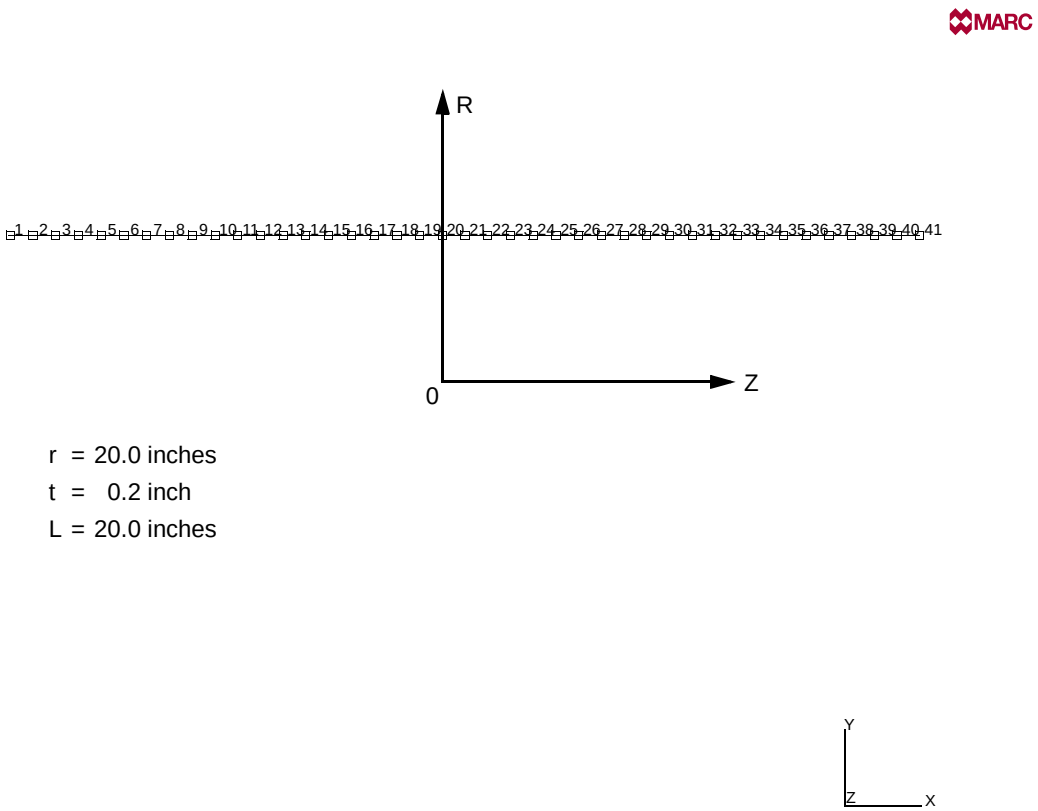

r = 20.0 inches
t = 0.2 inch
L = 20.0 inches

Figure 4.10-1 Mesh

4.11 Geometrically Nonlinear Analysis of a Tapered Plate

A tapered plate is clamped at one edge and loaded by a bending moment at the opposite edge (see Figure 4.11-1). By means of this problems, the capability of a finite element to represent inextensional bending in the geometrically nonlinear regime can be investigated.

Element

Library element type 4 is a 6-node triangular thin shell element. This element allows finite rotational increments so that large load steps can be chosen.

Model

The dimensions of the plate and the finite element mesh are shown in Figure 4.11-1. Based on symmetry considerations, only one-half of the plate is modeled. The mesh is composed of 80 elements and 243 nodes.

Geometry

A uniform thickness of 0.5 mm is assumed. In thickness direction, three layers are chosen using the SHELL SECT parameter. Although initially the mesh consists of flat elements, the coupling between the changes of curvature and the membrane deformations becomes important during the loading process. This means that the default setting for the fifth geometry field must be used.

Material Properties

The material is elastic with a Young's modulus of 2.1×10^5 N/mm^2 and a Poisson's ratio of 0.0.

Loading

The loading consists of a bending moment at the edge opposite to the clamped edge. The magnitude of this bending moment is written as f * 365.284 Nmm, where the maximum value of the scalar multiplier f equals 1.5. The total load is applied in 15 equally sized increments.

Boundary Conditions

Symmetry conditions are imposed on the edge y = 0 ($u_y = 0$, $\varphi = 0$). Clamped conditions are applied to the edge x = 0 ($u_x = 0$, $u_y = 0$, and $\varphi = 0$). Notice that the rotation constraints only apply for the midside nodes.

Results

The final deformed configuration is outlines in Figure 4.11-5. Since this state is reached in 15 equally sized increments, a finite rotation formulation is necessary. The horizontal and vertical tip displacements as a function of the load factor f (notice that this factor corresponds to the time) are given in Figure 4.11-3. An analytical solution for this problem can be found in Y. Ding, *Finite-Rotations-Elements zur geometrisch nichtlinearen Analyse algemeiner*

Flachentragwerke, Thesis Insititut für Statik und Dynamik, Ruhr-Univ Rochum, Germany (1989). The analytical solution for the above mentioned displacements components is given in Figure 4.11-4 and Figure 4.11-5. The finite element and the analytical solutions are in good agreement.

Parameters, Options, and Subroutines Summary

Example e4x11.dat:

Parameters	Model Definition Options	History Definition Options
ALL POINTS	CONNECTIVITY	ACTIVATE
DIST LOADS	COORDINATE	AUTO LOAD
ELEMENTS	DEFINE	CONTINUE
END	END OPTION	DISP CHANGE
LARGE DISP	FIXED DISP	POINT LOAD
SETNAME	GEOMETRY	TIME STEP
SHELL SECT	ISOTROPIC	
SIZING	NO PRINT	
TITLE	OPTIMIZE	
	POST	
	SOLVER	

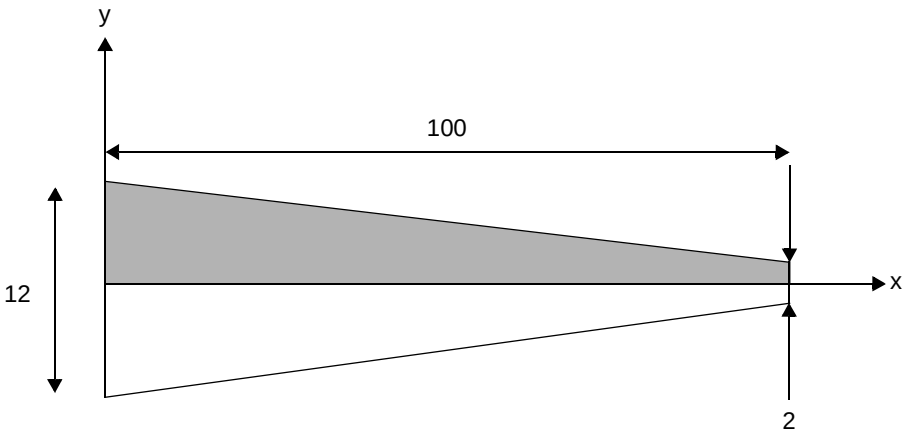

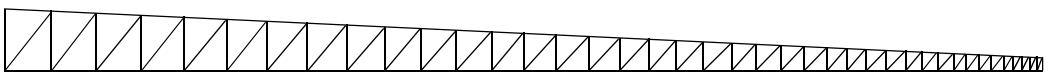

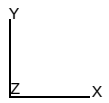

Figure 4.11-1 Clamped Tapered Plate, Geometry, and Finite Element Mesh

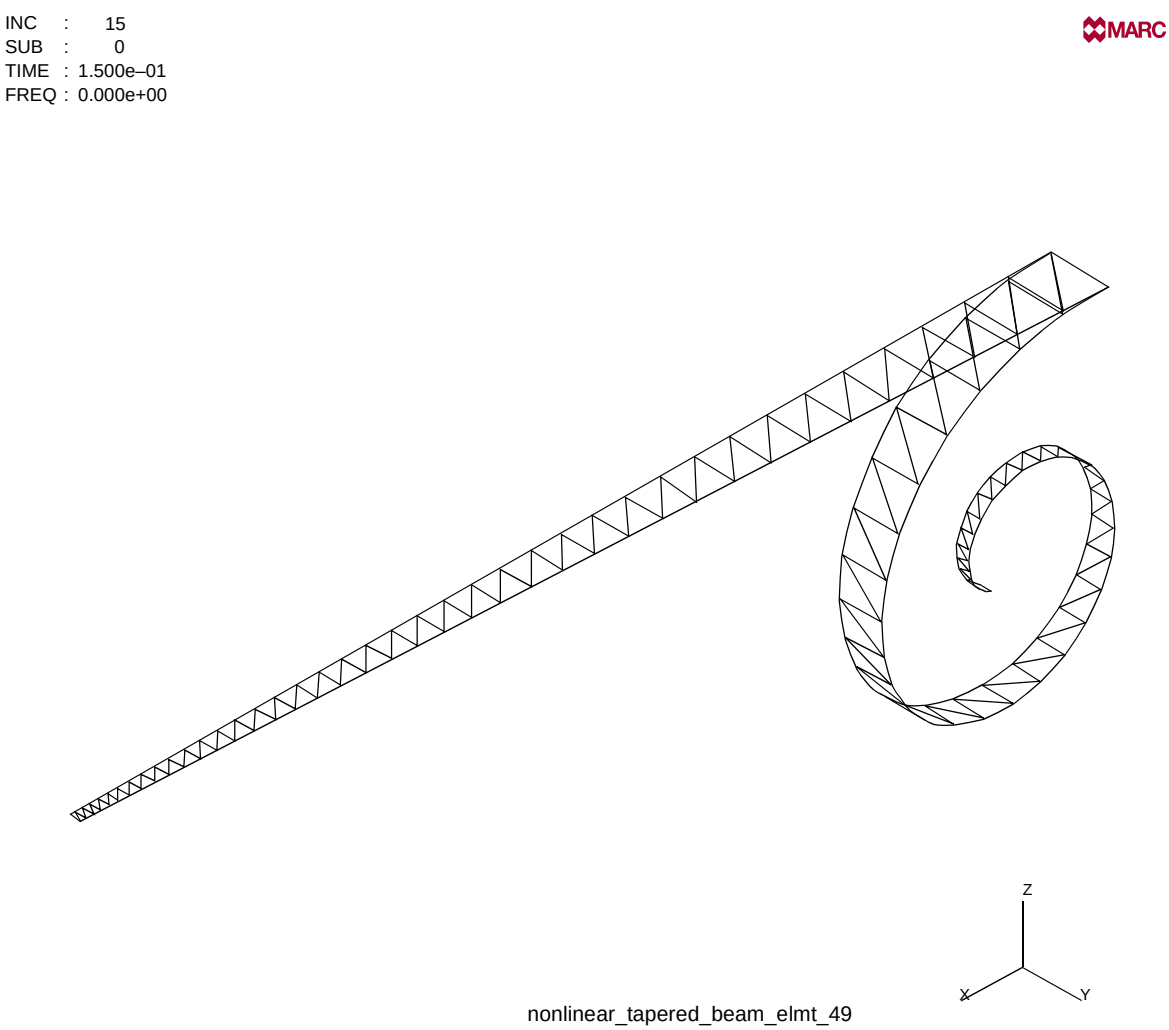

Figure 4.11-2 Undeformed and Final Deformed Configuration

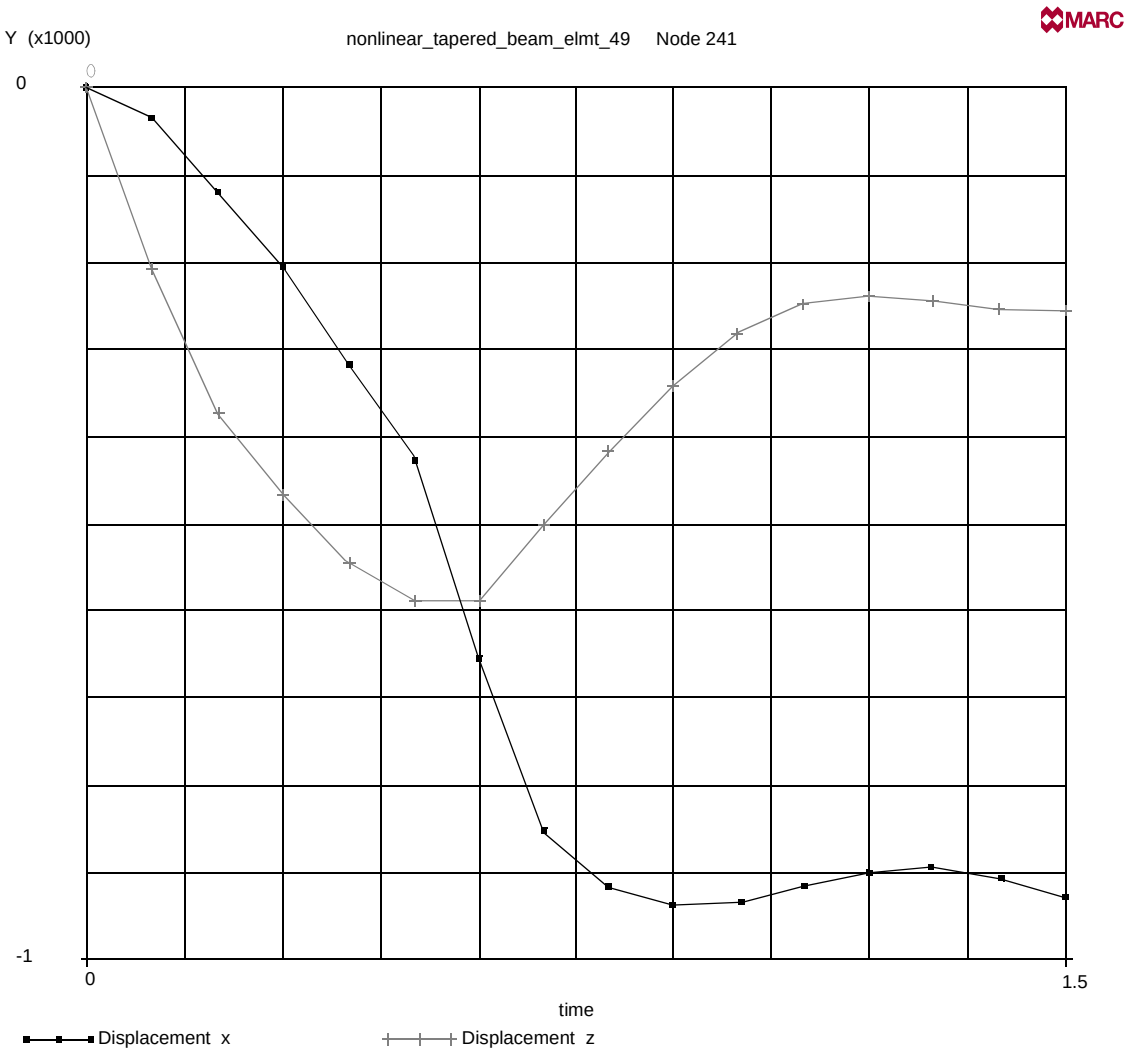

Figure 4.11-3 Finite Element Solution Horizontal and Vertical Tip Displacement

Figure 4.11-4 Reference Solution Tip Deflection

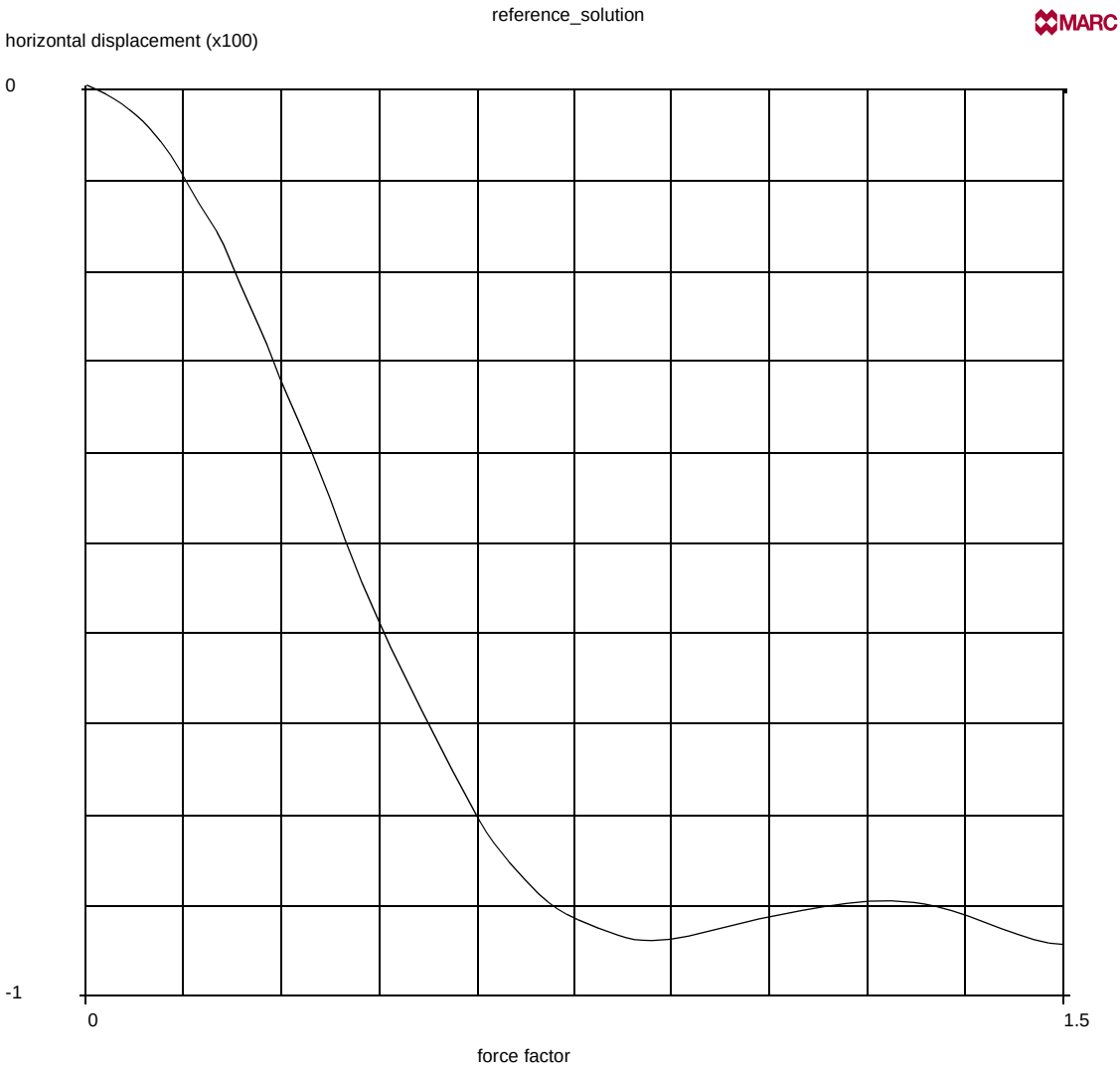

Figure 4.11-5 Reference Solution Horizontal Tip Displacement

4.12 Perturbation Buckling of a Strut

An elastic post buckling analysis is conducted on an initially straight strut. The perturbation buckling technique is demonstrated.

This problem is modeled using the four techniques summarized below.

Data Set	Element Type(s)	Number of Elements	Number of Nodes	Differentiating Features
e4x12a	3	20	42	Peturb to First Mode
e4x12b	3	20	42	Peturb to Second Mode
e4x12c	3	20	42	Buckle Increment
e4x12d	3	20	42	Full Automatic Perturbation

Model/Element

The model consists of 20 plane stress element, type 3, as shown in Figure 4.12-1. The length is 2.0 meters and the width is 0.1.

The LARGE DISP parameter is used to indicate that the total Lagrange large displacement formulation is used. The BUCKLE option indicates how many buckling modes are to be extracted.

Material Properties

The material has a Young's modulus of 1×10^9 N/m^2 and the Poisson's ratio is 0.3.

Geometry

The strut has a uniform thickness of 1 cm.

Boundary Conditions

The bottom of the strut is clamped, and, at the top, no motion is allowed in the x-direction.

Loading

This analysis is performed using four different procedures:

In the first analysis, a load is applied of magnitude 6000 (3000 at nodes 1 and 4) in increment 1, followed by 200. A buckle eigenmode is extracted and then a perturbation is applied, and then a load of 1800 is applied over nine increments. The first perturbation buckling mode is selected through the BUCKLE history definition option.

In the second analysis, a load is applied of magnitude 10,000 in increment 1, followed by 200. A buckle eigenmode is extracted and then a perturbation is applied, and then a load of

9000 is applied over nine increments. The second perturbation buckling mode is selected through the BUCKLE history definition option.

In the third analysis, a load is applied of magnitude 6000, followed by a load of 2000 over ten increments. Hence, the total load is the same as in the first analysis. In this analysis, the BUCKLE INCREMENT mode definition option is used to add the first buckle perturbation mode at the end of increment 2.

The fourth analysis is identical to the third analysis, except that the increment at which the perturbation is applied is automatically determined by the program. The perturbation is applied in the increment after the increment where a nonpositive definite system occurs.

In all problems, the perturbation has a scaled magnitude of 0.001.

Control

The CONTROL option is used to specify that displacement testing is to be performed with a tolerance of one percent. The solution of nonpositive definite systems is forced.

Results

The linear collapse load of this strut is 6050 N. Figure 4.12-2 shows the resultant deformation from the first analysis when the first mode is used. Figure 4.12-3 shows the resultant deformation from the second analysis when the second mode is used. The results of the third analysis are identical to the first analysis. When the fully automatic perturbation procedure is used in the fourth analysis, MARC senses the nonpositive definite system in increment 2, and then automatically extracts the buckle mode. This gives the same results as before. Note that after the perturbation is applied and there is some lateral deflection, you again have a stable physical system and no longer have a nonpositive definite numerical problem.

Parameters, Options, and Subroutines Summary

Examples e4x12a.dat and e4x12b.dat:

Parameters	Model Definition Options	History Definition Options
BUCKLE	CONTROL	AUTO LOAD
ELEMENTS	CONNECTIVITY	BUCKLE
END	COORDINATES	CONTINUE
LARGE DISP	DEFINE	POINT LOAD
SIZING	END OPTION	
	FIXED DISP	
	GEOMETRY	
	ISOTROPIC	
	OPTIMIZE	
	POINT LOAD	
	POST	
	SOLVER	

Examples e4x12c.dat and e4x11d.dat:

Parameters	Model Definition Options	History Definition Options
BUCKLE	BUCKLE INCREMENT	AUTO LOAD
ELEMENTS	CONTROL	CONTINUE
END	CONNECTIVITY	POINT LOAD
LARGE DISP	COORDINATES	
SIZING	DEFINE	
	END OPTION	
	FIXED DISP	
	GEOMETRY	
	ISOTROPIC	
	OPTIMIZE	
	POINT LOAD	
	POST	
	SOLVER	

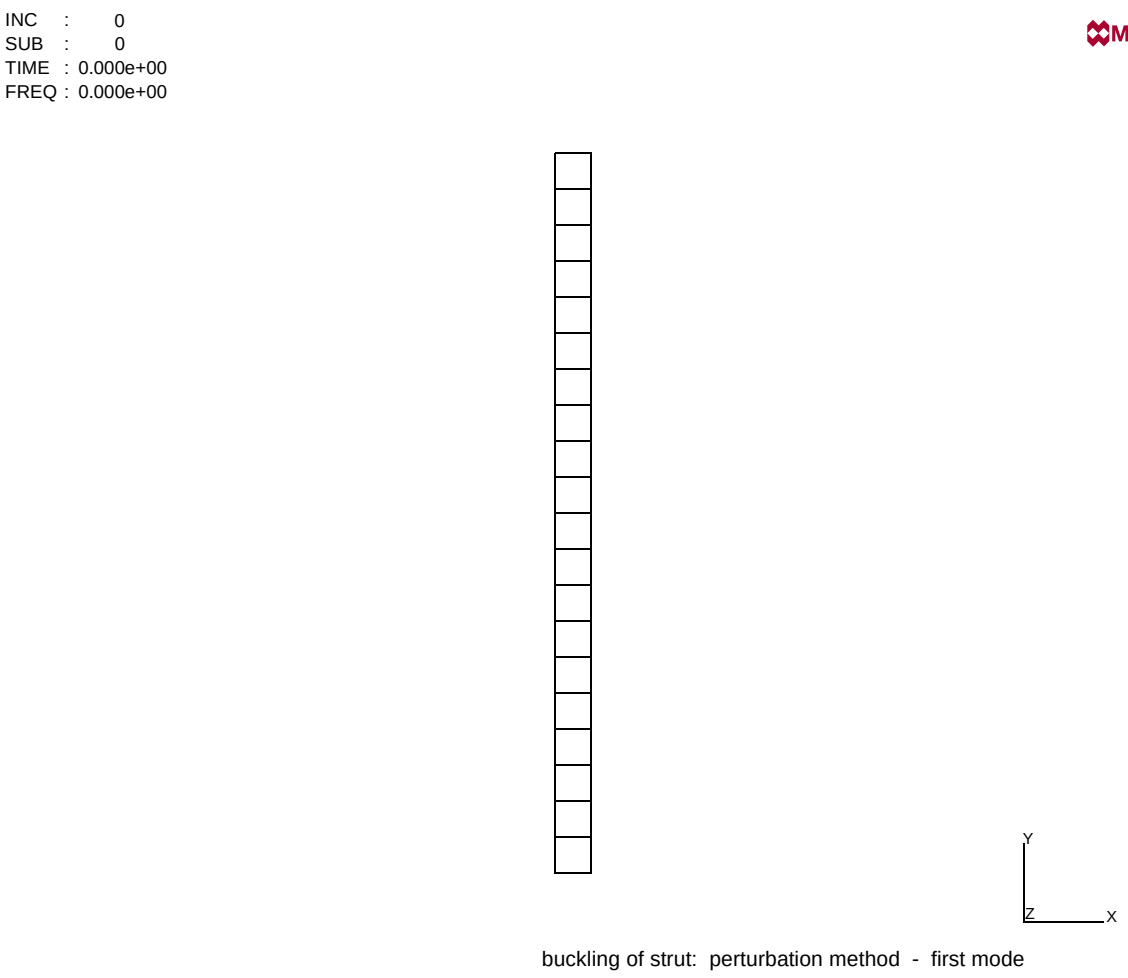

Figure 4.12-1 Mesh of Strut

Figure 4.12-2 Displacements Using First Mode

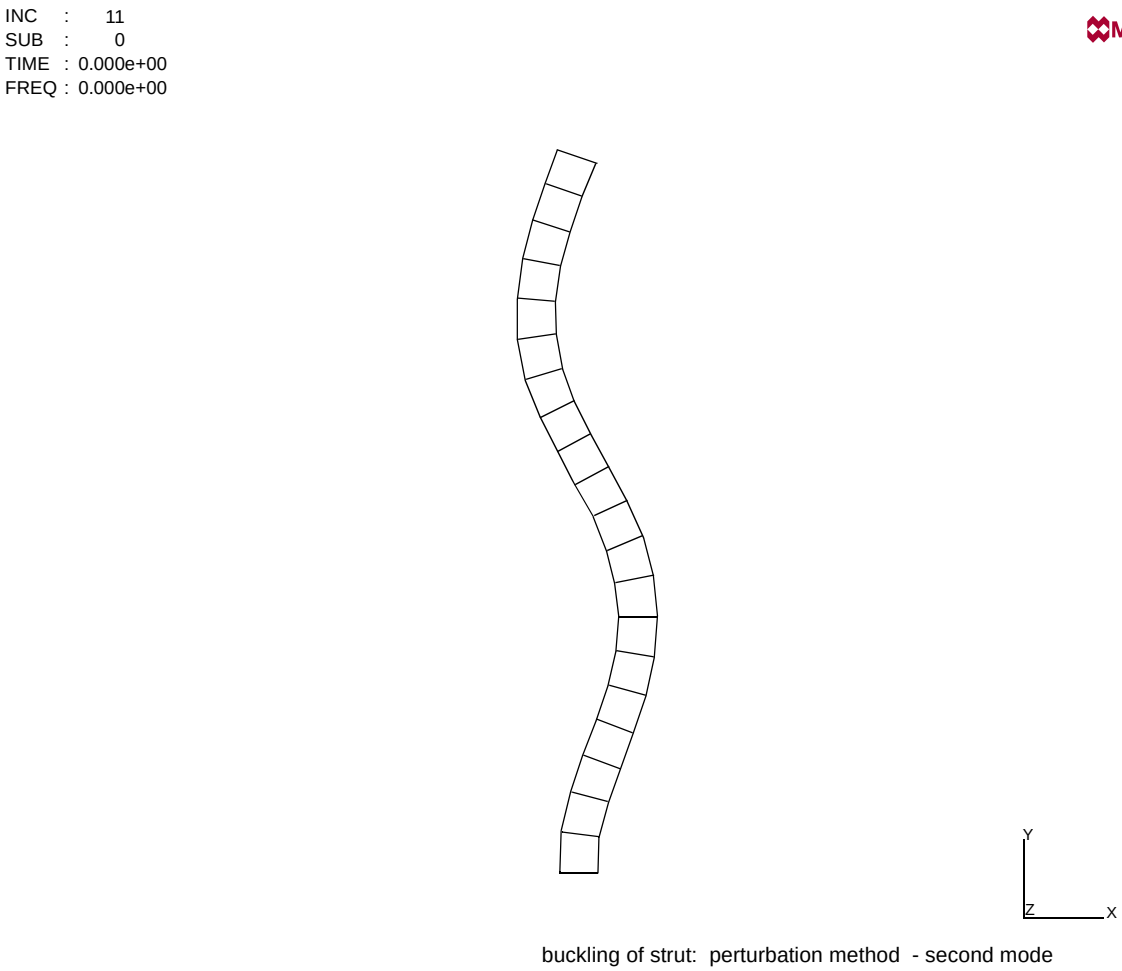

Figure 4.12-3 Displacements Using Second Mode

4.13 Cord-reinforced Thin-wall Cylinder subjected to Inner Pressure using Axisymmetric Elements

As shown in Figure 4.13-1, a thin-wall cylinder, reinforced by two cord layers is subjected to inner pressure. This problem demonstrates the application of axisymmetric rebar elements to cord-reinforced composites at large strains.

This problem is modeled using the three techniques summarized below.

Data Set	Element Type(s)	Number of Elements	Number of Nodes	Differentiating Features
e4x13a	67 & 142	2	8	REBAR
e4x13b	10 & 144	2	4	REBAR
e4x13c	20 & 145	2	4	REBAR

Element

Either element types 67 and 142 (8-node axisymmetric with twist), or element types 10 and 144 (4-node axisymmetric), or element types 20 and 145 (4-node axisymmetric with twist) are used. Elements 142, 144, and 145 are specifically designed to simulate reinforcements in axisymmetric problems. Elements 10, 20, and 67 are used to represent the matrix material in the cord-reinforced composite structure.

Model

The cylinder is modeled by one rebar element and one continuum element as shown in Figure 4.13-2.

Geometry

The radius of the cylinder is 10 inches and the thickness is 0.1 inch.

Material Properties

The Young’s modulus is 1500 psi and the Poisson’s ratio is 0.3 for the reinforcements. The Young’s modulus is 1.5 psi and the Poisson’s ratio is 0.3 for the matrix material.

Loading

A uniform distributed inner pressure is applied whose total magnitude is 6.0 psi.

Boundary Conditions

The top and the bottom and fixed in the axial direction.

Rebar Data

The cross-sectional area of each rebar is 0.08 inch^2. The spacing is 1 inch. Therefore, the equivalent thickness is 0.08 inch. The relative position of rebar layer is 0.5. The angle between the axial axis and rebar is ±30. The data is read in via the REBAR option.

Results

The evolution of the radius and the second Piola-Kirchhoff stress due to the inner pressure are given in Figure 4.13-3 and Figure 4.13-4. The agreement between the numerical results and analytical solutions is close. The analytical solution can be derived as:

$$r = r_0 \sqrt{1 + \frac{pr_0}{Et_0 \mathrm{Sin}^4 \alpha_0}}$$

$$S_R = \frac{pr_0}{2t_0 \mathrm{Sin}^2 \alpha_0}$$

where

r_0 : original cylinder radius

p : pressure

E : Young's modulus

t_0 : ply thickness

α_0 : original rebar angle

S_R : 2nd Piola-Kirchhoff stress

Parameters, Options, and Subroutines Summary

Example e4x13a.dat:

Parameters	Model Definition Options	History Definition Options
ELEMENTS	CONNECTIVITY	AUTO LOAD
END	CONTROL	CONTINUE
FOLLOW FOR	COORDINATES	DIST LOADS
LARGE DISP	DIST LOADS	
SIZING	END OPTION	
TITLE	ISOTROPIC	
	FIXED DISP	
	POST	
	REBAR	

Example e4x13b.dat:

Parameters	Model Definition Options	History Definition Options
ELEMENTS	CONNECTIVITY	AUTO LOAD
END	CONTROL	CONTINUE
FOLLOW FOR	COORDINATES	DIST LOADS
LARGE DISP	DIST LOADS	
SIZING	END OPTION	
TITLE	ISOTROPIC	
	FIXED DISP	
	POST	
	REBAR	

Example e4x13c.dat:

Parameters	Model Definition Options	History Definition Options
ELEMENTS	CONNECTIVITY	AUTO LOAD
END	CONTROL	CONTINUE
FOLLOW FOR	COORDINATES	DIST LOADS
LARGE DISP	DIST LOADS	
SIZING	END OPTION	
TITLE	ISOTROPIC	
	FIXED DISP	
	POST	
	REBAR	

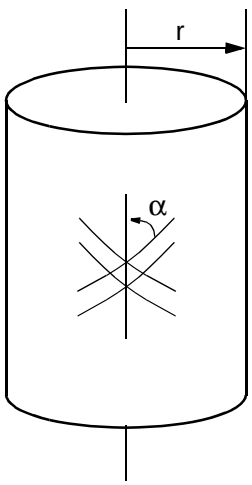

Figure 4.13-1 Cord-reinforced Thin-wall Cylinder subjected to Inner Pressure

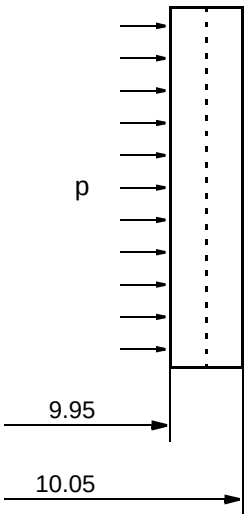

Figure 4.13-2 Finite Element Mesh for Analysis of Cord-reinforced Thin-wall Cylinder subjected to Inner Pressure using Axisymmetric Elements

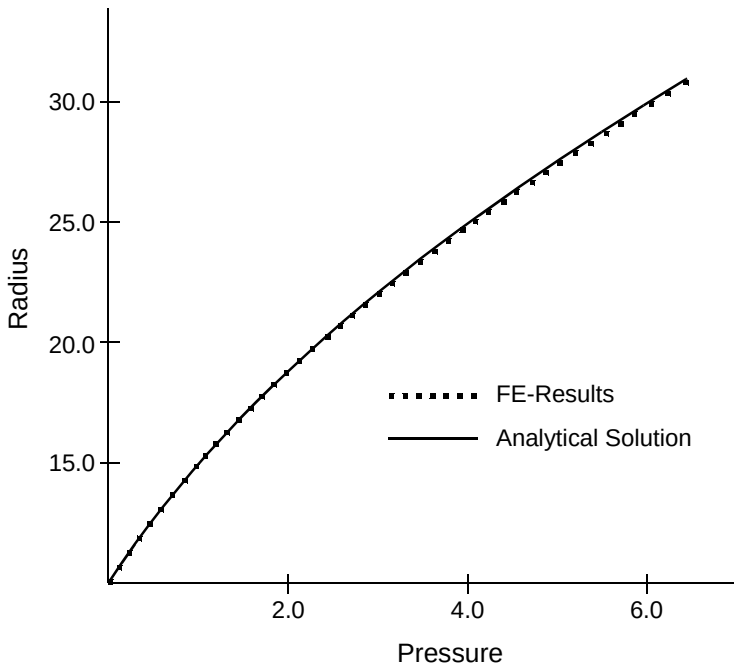

Figure 4.13-3 Radius of the Cylinder subjected to Inner Pressure: Comparison of Numerical Results and Analytical Solutions

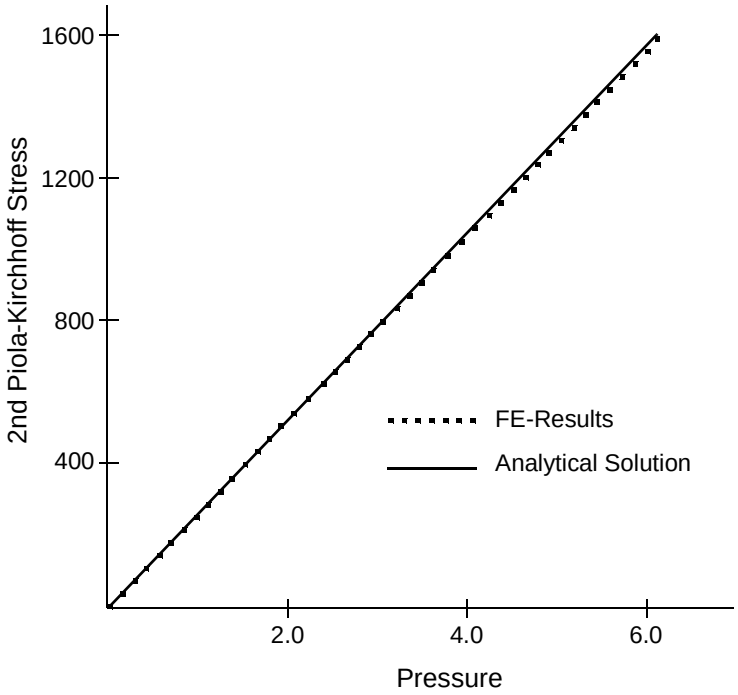

Figure 4.13-4 Second Piola-Kirchhoff Stress of the Cords in the Cylinder subjected to Inner Pressure: Comparison of Numerical Results and Analytical Solutions

4.14 Cord-reinforced Thin-wall Cylinder subjected to Inner Pressure using Membrane Elements

This example is similar to problem 4.13. As shown in Figure 4.13-1, a thin-wall cylinder, reinforced by two cord layers is subjected to inner pressure. The MOONEY option is used in this problem to model the matrix material. This problem demonstrates the application of membrane rebar elements to cord-reinforced rubber composites at large strains.

This problem is modeled using the two techniques summarized below.

Data Set	Element Type(s)	Number of Elements	Number of Nodes	Differentiating Features
e4x14a	18 & 147	20	22	REBAR and MOONEY
e4x14b	30 & 148	20	53	REBAR and MOONEY

Element

Either element types 18 and 147 (4-node membrane elements), or element types 30 and 148 (4-node membrane elements) are used. Elements 147 and 148 are specifically designed to simulate reinforcements in membrane problems. Elements 18 and 30 are used to represent the rubber matrix material in the cord-reinforced rubber composite structure.

Model

The cylinder is modeled by ten rebar elements and ten membrane elements as shown in Figure 4.14-1.

Geometry

For the membrane elements, EGEOM1 is used to input the thickness of the elements. The thickness in this analysis is 1 inch.

Material Properties

The Young’s modulus is 1500 psi and the Poisson’s ratio is 0.3 for the reinforcements. The Mooney parameters for the rubber matrix material are 1.0 psi and 0.5 psi.

Loading

A uniform distributed inner pressure is applied.

Boundary Conditions

The displacements of all nodes are restricted to radial direction.

Transformation

The user subroutine UTRANS is used to define transformation matrices for all nodes so that the boundary conditions can be easily specified. A model definition block, UTRANFORM, is needed for input of the node numbers to be transformed.

Rebar Data

The cross-sectional area of each rebar is 0.08 inch^2. The spacing is 1 inch. Therefore, the equivalent thickness is 0.08. The angle between the axial axis and rebar is ±30. The data is read in via the REBAR option.

Results

Since the boundary conditions are such that an axisymmetric problem is solved, the results are identical to those in problem 4.13. The evolution of the radius and the second Piola-Kirchhoff stress due to the inner pressure are given in Figure 4.13-3 and Figure 4.13-4. The agreement between the numerical results and analytical solutions is good.

Parameters, Options, and Subroutines Summary

Example e4x14a.dat and e4x14b.dat:

Parameters	Model Definition Options	History Definition Options
ELEMENTS	CONNECTIVITY	AUTO LOAD
END	CONTROL	CONTINUE
FOLLOW FOR	COORDINATES	DIST LOADS
LARGE DISP	DIST LOADS	
SIZING	END OPTION	
TITLE	ISOTROPIC	
	FIXED DISP	
	POST	
	REBAR	

User subroutine in u4x14.f

UTRANS

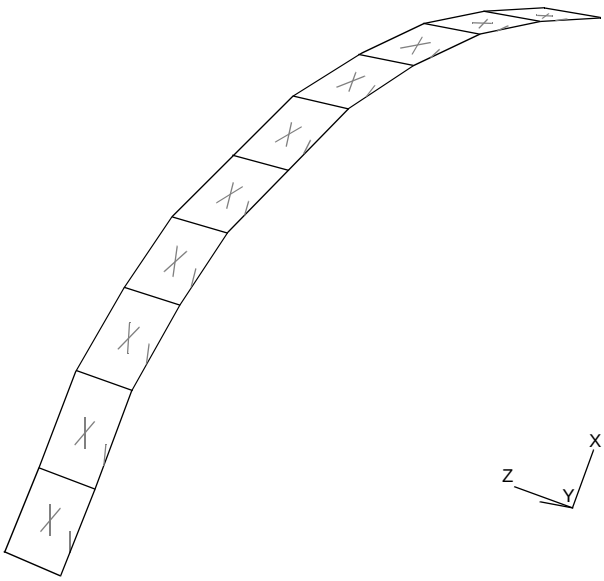

Figure 4.14-1 Finite Element Mesh for Analysis of Cord-reinforced Thin-wall Cylinder subjected to Inner Pressure using Membrane Elements

4.15 Buckling of a Cylinder Tube

The buckling load of a cylinder tube subjected to a lateral load at one end of the tube is calculated using Lanczos procedure. The problem is modeled using element type 75.

Element

Element type 75 is a 4-node bilinear thick shell element with global displacements and rotations as degrees of freedom.

Model

The cylinder tube is modeled using 432 elements and 468 nodes. The finite element meshes shown in Figure 4.15-1. To simulate the lateral load, two additional nodes (469 and 470) are introduced. The two nodes are tied with the nodes on the low end of the cylinder tube using rigid links.

Geometry

The radius and the wall thickness of the cylinder tube are 1 mm and 100 mm, respectively. The length of the tube is 600 mm.

Material Properties

All elements have the same properties. Young's modulus is 3.63E3 N/mm^2. Poisson's ratio is 0.3.

Loading

A point load of 100 N is applied to node 449.

Boundary Conditions

The nodes on the high end of the tube are fixed. The nodes on the low end of the tube are tied with nodes 469 and 470 using rigid links forming a rigid circle.

Results

The MARC solution for the buckling load is given below:

Mode Number	Buckling Load (N)
1	1.786E+01
2	-1.786E+01
3	1.787+01
4	-1.787E+01
5	1.855E+01
6	-1.855E+01

Parameters, Options, and Subroutines Summary

Example e4x15.dat:

Parameters	Model Definition Options	History Definition Options
ALL POINTS	CONNECTIVITY	BUCKLE
BUCKLE	CONTROL	CONTINUE
ELEMENTS	COORDINATES	RECOVER
END	END OPTION	
SETNAME	FIXED DISP	
SIZING	GEOMETRY	
TITLE	ISOTROPIC	
	OPTIMIZE	
	PRINT CHOICE	
	POST	
	POINT LOAD	
	SOLVER	
	TYING	

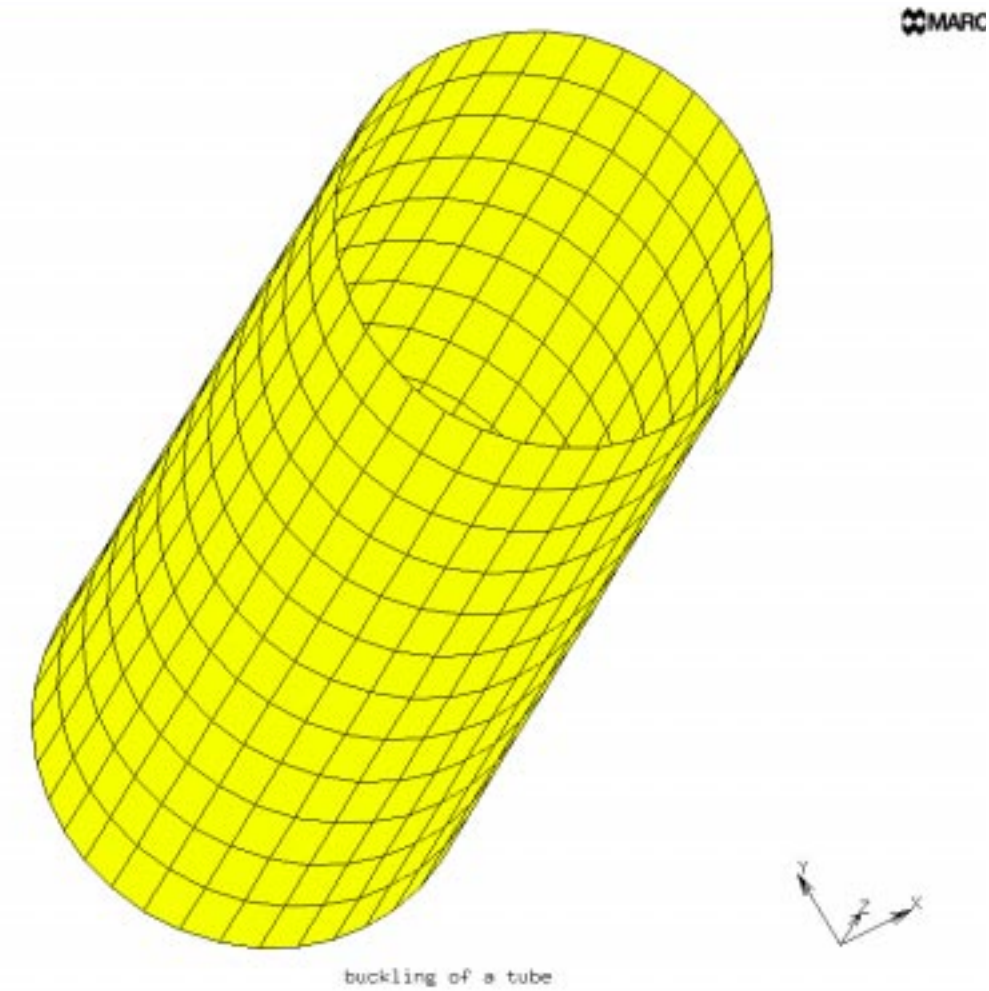

Figure 4.15-1 Finite Element Mesh

Document Title: **MARC® Volume E: Demonstration Problems, Part II, K7**
Part Number: RF-3018-07.II
Revision Date: June, 1998

UNITED STATES

CALIFORNIA - Palo Alto
MARC Corporate Headquarters
260 Sheridan Avenue, Suite 309
Palo Alto, CA 94306, USA
Tel: 1 650 329 6800
Fax: 1 650 323 5892
Email: support@marc.com

CALIFORNIA - San Diego
MARC Analysis Research Corp.
4330 LaJolla Village Drive, Suite 320
San Diego, CA 92122
Tel: 1 619 658 9588
Fax: 1 619 758 8710

CONNECTICUT - E. Berlin
MARC Analysis Research Corp.
1224 Mill Street
E. Berlin, CT 06023
Tel: 1 860 828 2055
Fax: 1 860 828 2031

MICHIGAN - Ann Arbor
MARC Analysis Research Corp.
24 Frank Lloyd Wright Drive
Ann Arbor, MI 48106-0523
Tel: 1 734 998 0540
Fax: 1 734 998 0542

EUROPE

CZECH REPUBLIC
MARC Overseas, Inc.
Podolska 50
147 00 Praha 4
Czech Republic
Tel: 420 (2) 6121 4123
420 (2) 6121 4111 x252
Fax: 420 (2) 6121 4123
Email: support@marc.cz

FRANCE
MARC France S.A.
Bercy Expo SR 6101A
40 Avenue des Terroirs de France
75611 Paris Cedex 12, France
Tel: 33 (1) 4474 1550
Fax: 33 (1) 4474 1554
Email: support@marc.fr

GERMANY - Munich
MARC Software Deutschland GmbH
Ismaninger Str. 9
85609 Aschheim (bie Munich)
Germany
Tel: 49 (89) 904 50 33
Fax: 49 (89) 903 06 76
Email: support@marc.de

GERMANY - Hannover
MARC Software Deutschland GmbH
Alte Dohrener Str. 66
D 30173 Hannover, Germany
Tel: 49 (511) 980 5182
Fax: 49 (511) 980 5187

ITALY
Espri-MARC s.r.l.
Viale Brigata Bisagno 2 / 10
16129 Genova, Italy
Tel: 39 (10) 585 949
Fax: 39 (10) 585 949
Email: espri.marc@interbusiness.it

THE NETHERLANDS
MARC Analysis Research Corporation
Dublinstraat 32
2713 HS Zoetermeer
The Netherlands
Tel: 31 (79) 3510 411
Fax: 31 (79) 3517 560
Email: support@marc.nl

UNITED KINGDOM
MARC UK Ltd.
11 Linford Forum, Rockingham Drive
Linford Wood
Milton Keynes, MK14 6LY
Tel: 44 (1908) 606 070
Fax: 44 (1908) 606 633
Email: support@marc.co.uk

PACIFIC RIM

CHINA
MARC Overseas, Inc.
Bright Chang An Building, Suite 321
7# Jian Guo Men Nei Street
Beijing, China 100 005
Tel: 86 (10) 6510 2056
86 (10) 6510 2057
86 (10) 6510 2058
Fax: 86 (10) 6510 2053
Email: marcbj@public.bta.net.cn

JAPAN - Nagoya
Nippon MARC Co., Ltd.
Nagoya Nishiki Daiichi Seimei Bldg.
2F, 6-5 Nishiki 1-chome
Naka-ku, Nagoya, Aichi 460-0003
Tel: 81 (52) 202 5661
Fax: 81 (52) 202 5665

JAPAN - Osaka
Nippon MARC Co., Ltd.
4F 2nd Kimi Building
2-11 Toyotucho Suita-shi
Osaka 564-0051
Tel: 81 (6) 385 1101
Fax: 81 (6) 385 4343

JAPAN - Tokyo
(Asian Operations Headquarters)
Nippon MARC Co., Ltd.
Shinjuku Daiichi Seimei Building
P.O. Box 5056
2-7-1 Nishi-Shinjuku, Shinjuku-ku
Tokyo 163-0704
Tel: 81 (3) 3345 0181
Fax: 81 (3) 3345 1529
Email: support@marc.co.jp

KOREA
Dong Kyung Bldg. 7FL
824-19 Yuksam-Dong
Kangnam-Ku, Seoul, Korea
Tel: 82 (2) 561 7543
Fax: 82 (2) 561 7767
Email: marck@unitel.co.kr

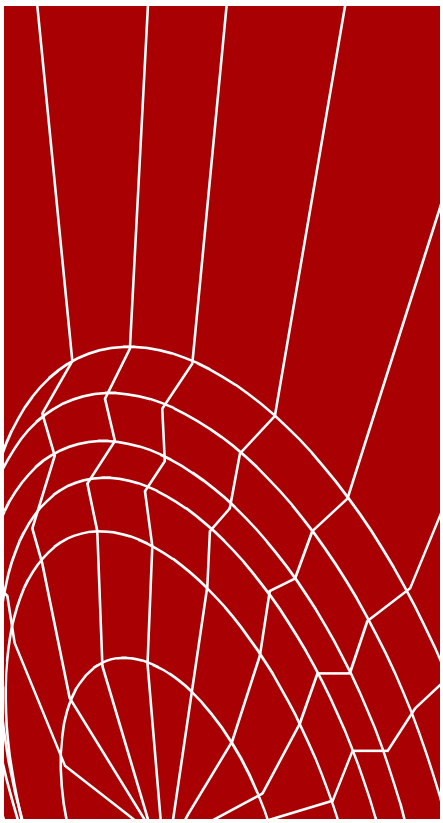

MARC Analysis Research Corporation

MARC®

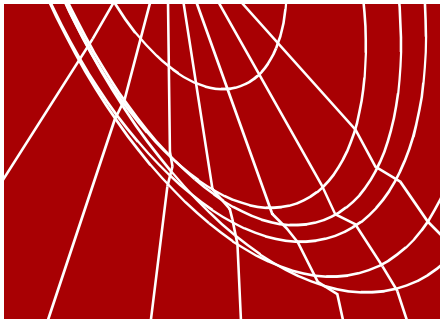

Volume E

Demonstration Problems

Version K7

Copyright © 1998 MARC Analysis Research Corporation
Printed in U. S. A.
This notice shall be marked on any reproduction of this data, in whole or in part.

MARC Analysis Research Corporation
260 Sheridan Avenue, Suite 309
Palo Alto, CA 94306 USA

Phone: (650) 329-6800
FAX: (650) 323-5892

Document Title: **MARC® Volume E: Demonstration Problems, Part III, Version K7**
Part Number: RF-3018-07.III
Revision Date: June, 1998

Proprietary Notice

MARC Analysis Research Corporation reserves the right to make changes in specifications and other information contained in this document without prior notice.

ALTHOUGH DUE CARE HAS BEEN TAKEN TO PRESENT ACCURATE INFORMATION, MARC ANALYSIS RESEARCH CORPORATION DISCLAIMS ALL WARRANTIES WITH RESPECT TO THE CONTENTS OF THIS DOCUMENT (INCLUDING, WITHOUT LIMITATION, WARRANTIES OR MERCHANTABILITY AND FITNESS FOR A PARTICULAR PURPOSE) EITHER EXPRESSED OR IMPLIED. MARC ANALYSIS RESEARCH CORPORATION SHALL NOT BE LIABLE FOR DAMAGES RESULTING FROM ANY ERROR CONTAINED HEREIN, INCLUDING, BUT NOT LIMITED TO, FOR ANY SPECIAL, INCIDENTAL OR CONSEQUENTIAL DAMAGES ARISING OUT OF, OR IN CONNECTION WITH, THE USE OF THIS DOCUMENT.

This software product and its documentation set are copyrighted and all rights are reserved by MARC Analysis Research Corporation. Usage of this product is only allowed under the terms set forth in the MARC Analysis Research Corporation License Agreement. Any reproduction or distribution of this document, in whole or in part, without the prior written consent of MARC Analysis Research Corporation is prohibited.

Restricted Rights Notice

This computer software is commercial computer software submitted with “restricted rights.” Use, duplication, or disclosure by the government is subject to restrictions as set forth in subparagraph (c)(i)(ii) or the Rights in technical Data and Computer Software clause at DFARS 252.227-7013, NASA FAR Supp. Clause 1852.227-86, or FAR 52.227-19. Unpublished rights reserved under the Copyright Laws of the United States.

Trademarks

All products mentioned are the trademarks, service marks, or registered trademarks of their respective holders.

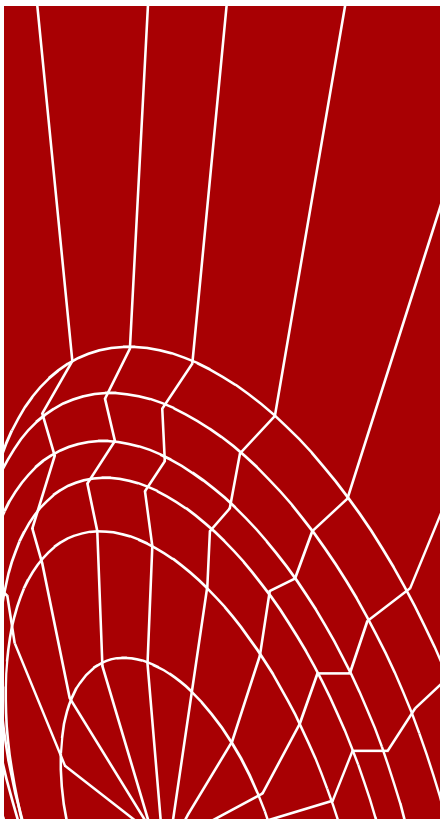

MARC Analysis Research Corporation

MARC®

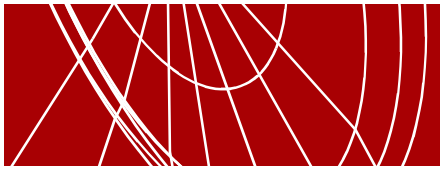

Volume E

Demonstration Problems

Version K7

Part III

- Heat Transfer
- Dynamics

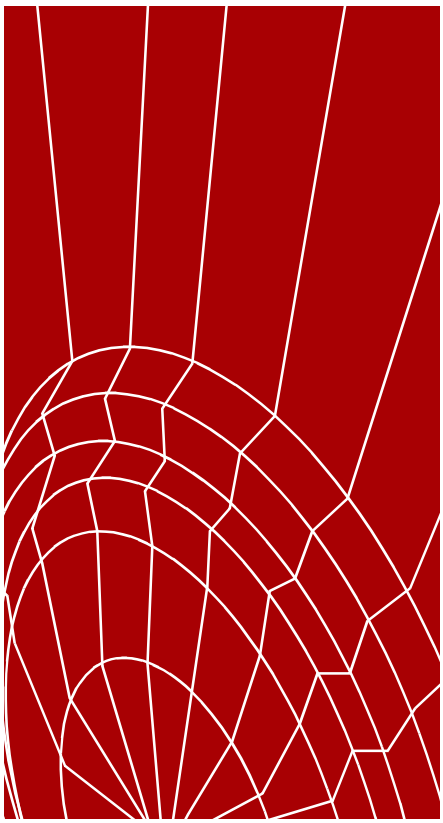

MARC Analysis Research Corporation

MARC®

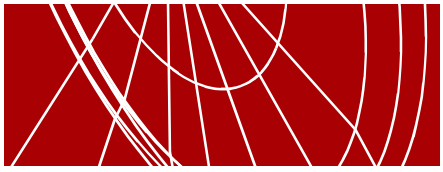

Volume E

Demonstration Problems

Version K7

Chapter 5
Heat Transfer

5 Heat Transfer Contents

Description	Problem
One-Dimensional Steady State Heat Conduction	5.1
One-Dimensional Transient Heat Conduction	5.2
Plate with a Fluid Passing through a Circular Hole	5.3
Three-Dimensional Transient Heat Conduction	5.4
Pressure Vessel Subjected to Thermal Downshock	5.5
Axisymmetric Transient Heat Conduction Simulated by Planar Elements	5.6
Steady State Analysis of an Anisotropic Plate	5.7
Nonlinear Heat Conduction of a Channel	5.8
Latent Heat Effect	5.9
Centerline Temperature of a Bare Steel Wire	5.10
Heat Transfer and Stress Analysis of a Jominy End Quench Test Specimen	5.11
Cylinder-plane Electrode	5.12
Axisymmetric Transient Heat Conduction Simulated by Heat Transfer Shell Elements	5.13
Steady-state Temperature Distribution of a Generic Fuel Nozzle	5.14
Radiation Between Concentric Spheres	5.15
Three-Dimensional Thermal Shock	5.16
Cooling of Electronic Chips	5.17
Square Plate Heated at a Center Portion	5.18

5 Heat Transfer List of Tables

Table		Page
5.1	Heat Transfer Analysis Demonstration Problems	5-2
5.2-1	Nodal Temperatures.	5.2-2
5.6-1	Comparison of Nodal Temperatures	5.6-2
5.10-1	Nodal Voltages and Temperatures	5.10-2
5.11-1	Thermal Conductivity vs. Temperature (AISI 4140 Steel)	5.11-2
5.11-2	Specific Heat vs. Temperature (AISI 4140)	5.11-3
5.11-3	Coefficient of Thermal Expansion (AISI 4140)	5.11-4
5.13-1	Comparison of Nodal Temperatures	5.13-3

5 Heat Transfer List of Figures

Figure		Page
5.1-1	One-Dimensional Link and Mesh	5.1-3
5.2-1	One-Dimensional Link and Mesh	5.2-3
5.2-2	Temperature Distributions, t = 4 seconds	5.2-4
5.2-3	Temperature Distributions, t = 10 seconds	5.2-5
5.2-4	Temperature Distribution, t = 20 seconds	5.2-6
5.3-1	Mesh for Element Type 41	5.3-6
5.3-2	Mesh for Element Type 69	5.3-7
5.3-3	Mesh for Element Type 39	5.3-8
5.3-4	Mesh for Element Type 37	5.3-9
5.3-5	Mesh for Element Type 121	5.3-10
5.3-6	Mesh for Element Type 131	5.3-11
5.3-7	Temperature History for Elements Types: 37, 39, 41, 69, 121, and 131	5.3-12
5.4-1	Mesh for the Unit Cube Linear Elements	5.4-4
5.4-2	Mesh for the Unit Cube Parabolic Elements	5.4-5
5.4-3	Cube Center Temperature History for Element Types: 43, 44, 71, and 123	5.4-6
5.5-1	Temperature Time History	5.5-4
5.5-2	Geometry and Mesh	5.5-4
5.5-3	Transient Temperature Time History (Auto Time Step)	5.5-5
5.5-4	Temperature Distribution in Cylinder Wall	5.5-6
5.6-1	Cylinder and Mesh	5.6-4
5.7-1	Plate and Mesh	5.7-3
5.8-1	Geometry for Nonlinear Heat Conduction	5.8-7
5.8-2	Heat Transfer Example Mesh	5.8-8
5.8-3	Isotherms at 100 Seconds	5.8-9

Figure **Page**

5.8-4 Isotherms at 400 Seconds 5.8-10
5.8-5 Isotherms at 1000 Seconds 5.8-11
5.8-6 Temperature History 5.8-12

5.9-1 Cylinder Meshes 5.9-5
5.9-2 Temperature Dependent Thermal Properties 5.9-6
5.9-3 Temperature History for Center and Outer Surface of Cylinder 5.9-7

5.10-1 Mesh of Steel Wire 5.10-3

5.11-1 Thermal Conductivity vs. Temperature 5.11-7
5.11-2 Specific Heat vs. Temperature 5.11-8
5.11-3 Jominy Bar – Axisymmetric Finite Element Model (Elements) 5.11-9
5.11-4 Jominy Bar – Axisymmetric Finite Element Model (Nodes) 5.11-10
5.11-5 Material Properties vs. Temperature 5.11-11
5.11-6 Yield Stress vs. Temperature 5.11-12
5.11-7 Workhardening vs. Temperature 5.11-13
5.11-8 Jominy End Quench Test – Temperature vs. Time 5.11-14
5.11-9 Jominy End Quench Test – Temperature vs. Increment 5.11-15
5.11-10 Jominy End Quench Test – Equivalent Stress vs. Increment 5.11-16
5.11-11 Jominy End Quench Test – Axial Stress vs. Increment 5.11-17
5.11-12 Jominy End Quench Test – Radial Stress vs. Increment 5.11-18
5.11-13 Jominy End Quench Text – Hoop Stress vs. Increment 5.11-19

5.12-1 Geometry of the Problem 5.12-2
5.12-2 Temperature Dependent Properties 5.12-2
5.12-3 Mesh 5.12-3
5.12-4 Temperature Distribution 5.12-4
5.12-5 Voltage Distribution 5.12-5
5.12-6 Current Distribution 5.12-6

5.13-1 Cylinder Model and Fluid Temperature History 5.13-6
5.13-2 Finite Element Model (Model A - Element 85) 5.13-7
5.13-3 Finite Element Model (Model B - Element 86) 5.13-8
5.13-4 Finite Element Model (Model C - Element 87) 5.13-9
5.13-5 Finite Element Model (Model D - Element 88) 5.13-9

Figure **Page**

5.14-1 Simplified Nozzle 5.14-5
5.14-2 Simplified Nozzle (Finite Element Mesh) 5.14-6
5.14-3 Simplified Nozzle Solid and Fluid Temperatures) 5.14-7

5.15-1 Radiating Concentric Spheres. 5.15-4
5.15-2 Mesh with Element Numbers 5.15-5
5.15-3 Mesh with Node Numbers 5.15-6

5.16-1 Temperature History for Free End Node 136 Element Type 44. . . . . 5.16-4
5.16-2 Temperature History for Free End Node 126 (Element Type 123) 5.16-5
5.16-3 Iso-thermal Surfaces at t = 0.0196 seconds (Element Type 123). 5.16-6
5.16-4 Temperature History for Free End Node 26 (Element Type 133) 5.16-7
5.16-5 Iso-thermal Surfaces at t = 0.0193 seconds (Element Type 133). 5.16-8

5.17-1 Complete Finite Element Mesh 5.17-3
5.17-2 Finite Element Mesh of Chips and Board. 5.17-4
5.17-3 Temperature Distribution Excluding Heat Convection 5.17-5
5.17-4 Temperature Distribution Including Heat Convection 5.17-6

5.18-1 Heated Square Plate, Geometry, and Finite Element Mesh 5.18-4
5.18-2 Temperature Distribution Steady-state Analysis 5.18-5
5.18-3 Path Plots for Upper and Lower Temperature at x = 0 (inc = 1) 5.18-6
5.18-4 Path Plots for Upper and Lower Temperature at x = 0 (inc = 15) 5.18-7

5 Heat Transfer

MARC contains a solid body heat transfer capability for one-, two- and three-dimensional, steady-state and transient analyses. A discussion of the use of this capability can be found in *MARC Volume A: Theory and User Information* and a summary of the features is given below.

Selection of elements:

- 1-D: Three-dimensional links (2-, 3-node)
- 2-D: Planar and axisymmetric elements (3-, 4-, 6-, and 8-node)
- 3-D: Brick elements (8- and 20-node)
- Reduced integration elements with hourglass control

Time integration operator:

- Backward difference –unconditionally stable for linear problems; automatic time-step choice; in-core and out-of-core solutions.

Temperature dependent materials (including latent heat effects); anisotropic thermal conductivity.

Extrapolated averaging for the evaluation of temperature-dependent properties.

Nonuniform initial conditions.

Temperature, time-dependent boundary conditions: prescribed temperature history, volumetric flux, surface flux, film coefficients, radiation; change of prescribed temperature boundary conditions during analysis.

Tying constraints on nodal temperatures.

Two- and three-dimensional mesh generation; bandwidth optimization.

Contour or temperature time history plots; mesh plots.

Ability to restart the analysis.

Selective print of nodal and/or element temperatures; consistent nodal fluxes.

Direct interface with stress analysis.

User subroutines.

A number of solved problems are compiled in this chapter. These problems illustrate the use of various MARC heat transfer elements and demonstrate the selection of different options. Table 5.1 shows MARC elements and options used in these demonstration problems.

Table 5.1 Heat Transfer Analysis Demonstration Problems

Problem Number (E)	Element Type	Parameters	Model Definition	History Definition	User Subroutines	Problem Description
5.1	36	HEAT	—	TRANSIENT NON AUTO	—	One-dimensional steady-state heat conduction, constant properties, prescribed temperature boundary conditions, 2-node link element.
5.2	65	HEAT FORCDT	FORCDT INITIAL TEMP	TRANSIENT NON AUTO	FORCDT	One-dimensional transient heat conduction, constant properties, prescribed temperature boundary conditions, 3-node link element.
5.3	41 69 39 37 121 131	HEAT FILMS ALIAS	INITIAL TEMP FILMS CONTROL OPTIMIZE	TRANSIENT NON AUTO	—	Two-dimensional transient heat conduction, constant properties, prescribed temperature and convective boundary conditions, 3-, 4-, and 8-node reduced integration planar elements.
5.4	43 44 71 123	HEAT	INITIAL TEMP CONTROL PRINT CHOICE UDUMP	TRANSIENT NON AUTO	—	Three-dimensional transient heat conduction, constant properties, prescribed temperature and insulated boundary conditions, 8-, 20-node and reduced integration elements.
5.5	42 70	HEAT FILMS ALIAS	INITIAL TEMP CONTROL FILMS	TRANSIENT	FILM	Axisymmetric transient heat conduction, constant properties, convective boundary conditions, 8-node axisymmetric and reduced integration elements.

Table 5.1 Heat Transfer Analysis Demonstration Problems (Continued)

Problem Number (E)	Element Type	Parameters	Model Definition	History Definition	User Subroutines	Problem Description
5.6	41	HEAT FILMS	INITIAL TEMP CONTROL FILMS	TRANSIENT	FILM	Same as problem 5.5, except using 8-node planar element.
5.7	39	HEAT	ANISOTROPIC	TRANSIENT NON AUTO	ANKOND	Two-dimensional heat conduction, constant properties, anisotropic conductivity, prescribed conditions, 4-node planar element.
5.8	41	HEAT MESH PLOT	FILMS FLUXES INITIAL TEMP CONTROL TEMP EFFECTS RESTART OPTIMIZE	TRANSIENT	FILM FLUX	Nonlinear heat conduction, temperature dependent properties, prescribed temperature, convective, and radiative boundary conditions, 8-node planar element.
5.9	40 122 132	HEAT	TEMP EFFECTS INITIAL TEMP CONTROL FILMS PRINT CHOICE UDUMP	TRANSIENT NON AUTO	—	Latent heat effect, temperature dependent properties, convective boundary condition 4-node axisymmetric element.
5.10	40	HEAT JOULE	JOULE DIST CURRENT VOLTAGE FILMS	TRANSIENT NON AUTO	—	Evaluate temperatures in a wire due to current.
5.11	42 28	HEAT MARC.PLOT THERMAL T-T-T	TEMP EFFECTS FILMS TIME-TEMP CHANGE STATE INITIAL TEMP	TRANSIENT AUTO THERM CHANGE STATE	—	Evaluate transient temperature response due quenching process. Evaluate thermally-induced stresses.
5.12	39	ALIAS JOULE HEAT	VOLTAGE POST JOULE	TRANSIENT	—	Electro static planar analysis.

Table 5.1 Heat Transfer Analysis Demonstration Problems (Continued)

Problem Number (E)	Element Type	Parameters	Model Definition	History Definition	User Subroutines	Problem Description
5.13	85 86 87 88	HEAT SHELL SECT	INITIAL TEMP FILMS POST	TRANSIENT	FILM	Thermal ratchetting using shell elements.
5.14	39	HEAT PRINT, 7	DEFINE TEMP EFFECTS CONRAD GAP CHANNEL FILMS	TRANSIENT	FILM FLOW	Steady state temperature distribution of a fuel nozzle.
5.15	42	HEAT RADIATION	RADIATING CAVITY TEMP EFFECTS FIXED TEMP	STEADY STATE	—	Radiating concentrical spherical bodies.
5.16	123 133 135	HEAT LUMP	INITIAL TEMP	TRANSIENT	—	Thermal shock.
5.17	39	HEAT	FIXED TEMP INITIAL TEMP VELOCITY	TRANSIENT NONAUTO	—	Cooling of electronic chips.
5.18	50	HEAT LUMP SHELL SECT	ORTHOTROPIC ORIENTATION INITIAL TEMP DIST FLUXES	STEADY STATE TRANSIENT	—	Thermal behavior in orthotropic shell.

5.1 One-Dimensional Steady State Heat Conduction

A bar has an initial temperature of 0°F. One end is subsequently subjected to 100°F; the other to 200°F. The temperature distribution along the bar is calculated for subsequent times.

Model/Element

This one-dimensional steady-state heat conduction problem is analyzed by using element type 36 (three-dimensional link). The model consists of six nodes and five elements, which allows a linear variation of temperature along its length. The dimensions of the model and a finite element mesh are shown in Figure 5.1-1.

Material Properties

The conductivity is 0.000213 Btu/sec-in.-°F. The specific heat is 0.105 BTU/lb-°F. The mass density is 0.283 lb/cu/inch.

Geometry

The default value of 1.0 square inch is used for the cross-sectional area of the link. No geometry input data is required.

Boundary Conditions

Constant nodal temperatures of 100°F and 200°F are prescribed at nodes 1 and 6, respectively.

Transient

A very large time step (Δt = 100,000 sec) is chosen for obtaining the steady-state solution and the total transient time is also assumed to be 100,000 seconds. Consequently, the steady state solution is reached in one time step. The nonautomatic TIME STEP option in MARC is invoked in the analysis. As an alternative, the STEADY STATE option could be used.

Results

A linear distribution of steady state temperatures is obtained, as expected. The nodal temperatures are:

Node Number	Temperature °F
1	100
2	120
3	140
4	160
5	180
6	200

Parameters, Options, and Subroutines Summary

Example e5x1.dat:

Parameters	Model Definition Options	History Definition Options
ELEMENT	CONNECTIVITY	CONTINUE
END	COORDINATE	TRANSIENT
HEAT	END OPTION	
SIZING	FIXED TEMPERATURE	
TITLE	ISOTROPIC	

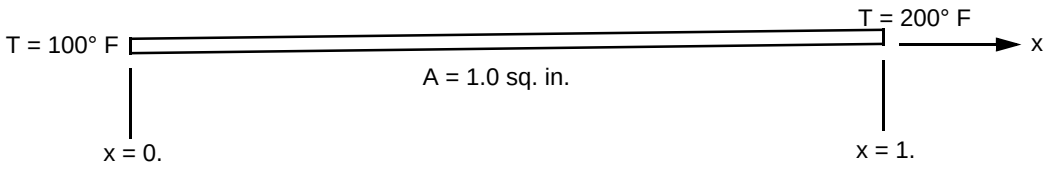

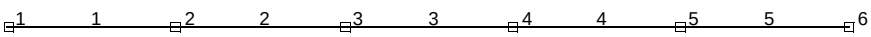

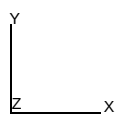

Figure 5.1-1 One-Dimensional Link and Mesh

5.2 One-Dimensional Transient Heat Conduction

A bar has an initial temperature of 0°F. One end is subsequently subjected to 100°F, the other to 200°F. The temperature distribution along the bar is calculated for subsequent times.

This problem is modeled using the two techniques summarized below.

Data Set	Element Type(s)	Number of Elements	Number of Nodes	Differentiating Features
e5x2a	65	5	11	
e5x2b	65	5	11	FORCDT

Model

This one-dimensional transient heat conduction problem is analyzed by using element type 65 (3-node truss). The model consists of eleven nodes and five elements. The element type 65 allows a quadratic variation of temperature along its length. The dimension of the model and a finite element mesh are shown in Figure 5.2-1.

Material Properties

Material properties of the model are:

Conductivity is 0.000213 Btu/sec-in.-°F
Specific heat is 0.105 Btu/lb-°F
Mass density is 0.283 lb/cubic inch

Geometry

The default value of 1.0 square inch is used for the cross-section area of the link. No geometry input data is required.

Boundary Conditions

Constant nodal temperatures of 100°F and 200°F are prescribed at nodes 1 and 11, respectively. This problem is evaluated twice: In the first input, the boundary temperature is specified using the FIXED TEMP option; in the second case, subroutine FORCDT is used to specify the temperatures.

Initial Condition

Initial nodal temperatures are assumed to be 0°F.

Transient

The transient time is assumed to be 20 seconds and a constant time step of 1.0 seconds selected for the analysis. The total number of time steps in the analysis is 20. The time step is kept constant by using the nonautomatic TIME STEP option in the program.

Results

Temperature distributions are tabulated in Table 5.2-1 and plotted in Figure 5.2-2, Figure 5.2-3 and Figure 5.2-4. At the end of 20 seconds, the steady-state conditions have not yet been achieved.

Because there are no temperature-dependent material properties and the time increment is fixed, the analysis is performed through a series of back substitutions. In increment 3, the total temperature change was greater than that given in the CONTROL option. In increment 4, MARC resassembled. This was not necessary for the accuracy of this particular problem.

Table 5.2-1 Nodal Temperatures

Time Sec.	Node 1	Node 2	Node 3	Node 4	Node 5	Node 6	Node 7	Node 8	Node 9	Node 10	Node 11
2.	100	49.0	20.3	8.3	3.9	3.3	6.5	16.2	40.4	98.0	200
4.	100	64.9	37.8	21.0	13.2	13.0	20.7	39.5	74.5	129.5	200
6.	100	72.4	49.3	33.2	25.4	26.5	37.3	59.8	95.5	143.7	200
8.	100	77.4	58.0	44.3	38.1	40.6	53.0	76.1	109.7	152.3	200
10.	100	81.4	65.4	54.3	50.1	54.0	67.0	89.4	120.4	158.3	200
S.S	100	110	120	130	140	150	160	170	180	190	200

Parameters, Options, and Subroutines Summary

Example e5x2a.dat:

Parameters	Model Definition Options	History Definition Options
ELEMENT	CONNECTIVITY	CONTINUE
END	CONTROL	TRANSIENT
HEAT	COORDINATE	
SIZING	END OPTION	
TITLE	FIXED TEMP	
	INITIAL TEMP	
	ISOTROPIC	

User subroutine in u5x2.f:

FORCDT

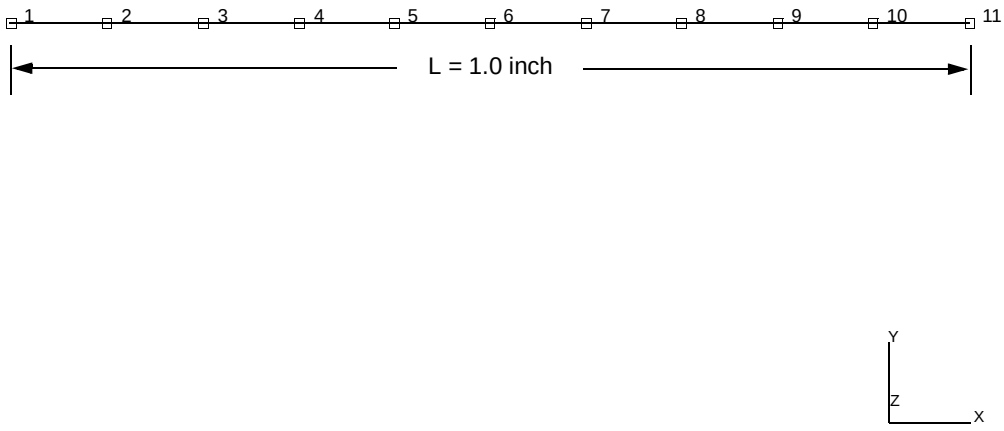

Figure 5.2-1 One-Dimensional Link and Mesh

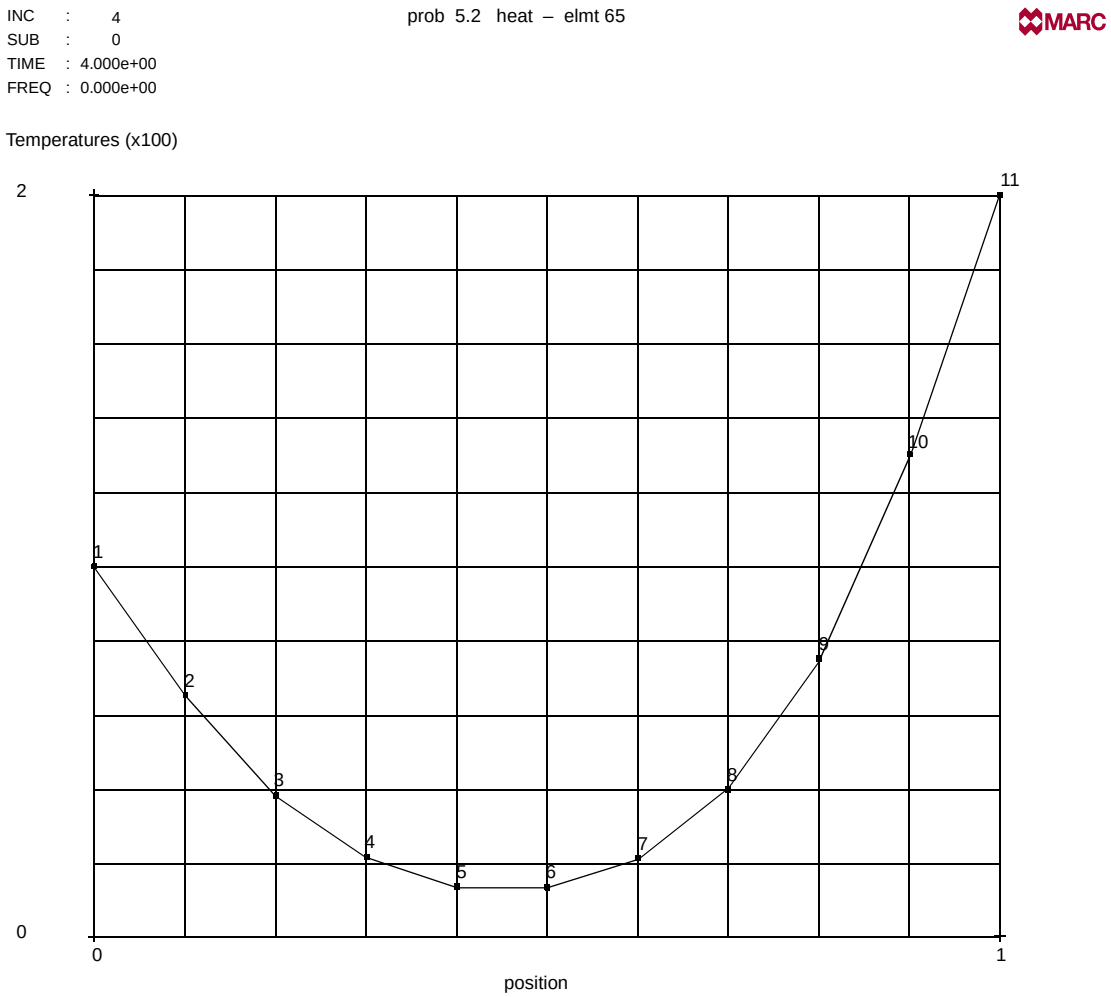

Figure 5.2-2 Temperature Distributions, t = 4 seconds

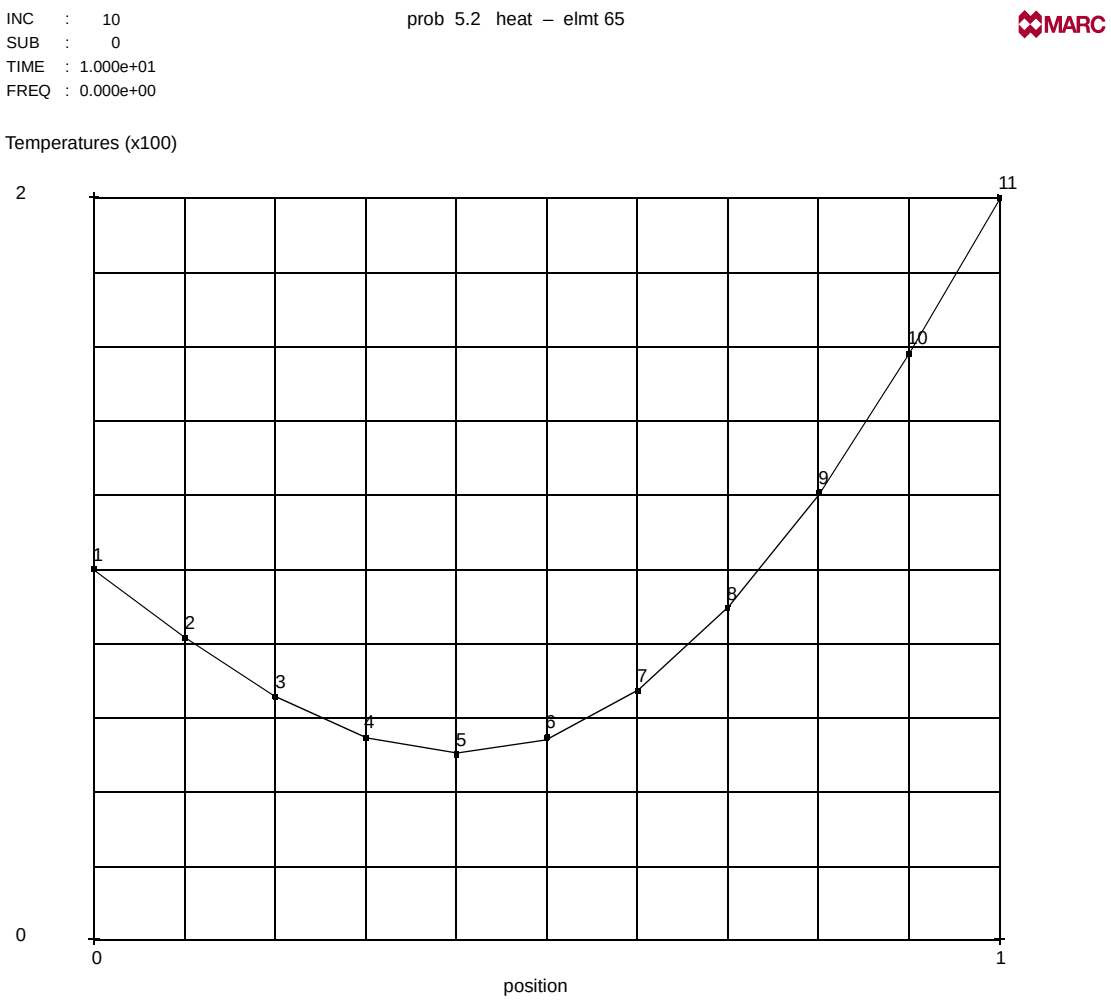

Figure 5.2-3 Temperature Distributions, t = 10 seconds

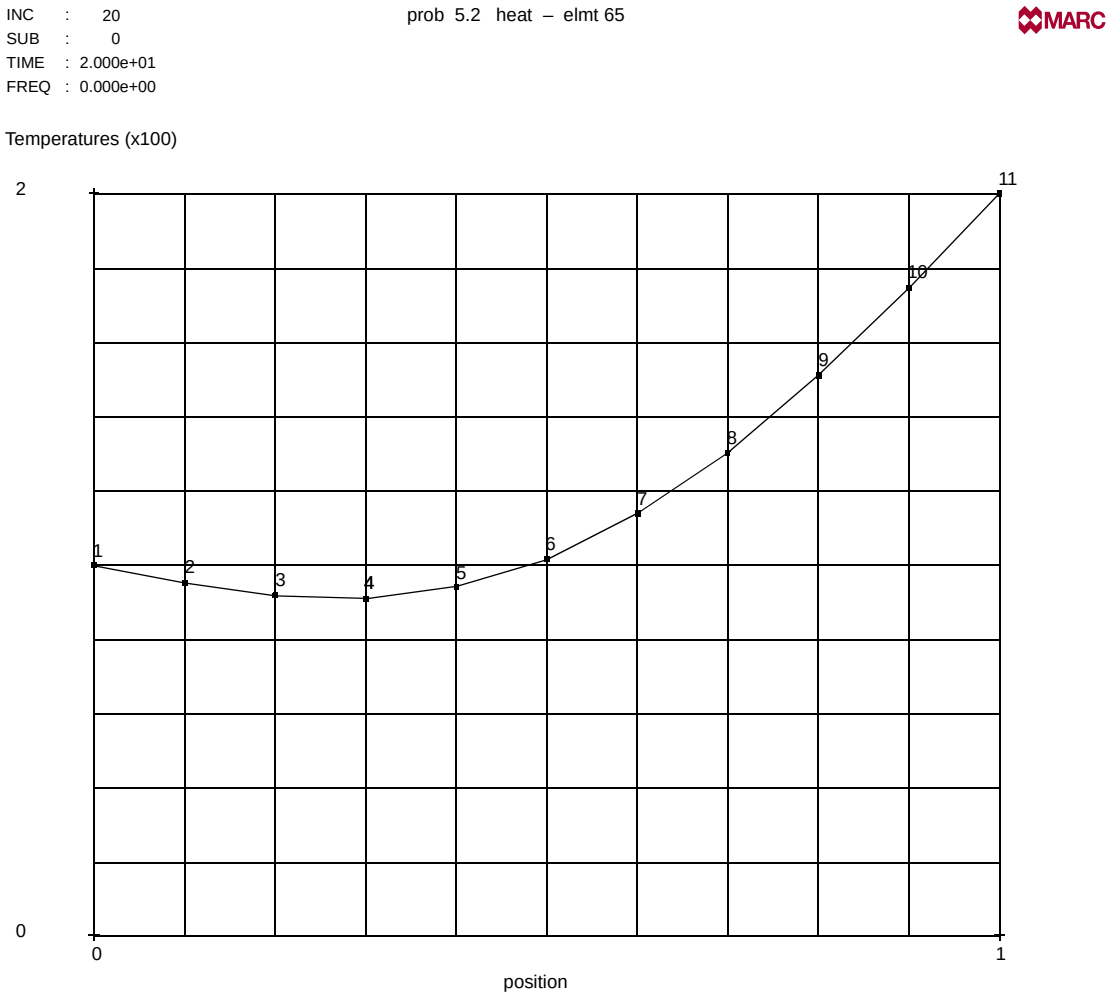

Figure 5.2-4 Temperature Distribution, t = 20 seconds

5.3 Plate with a Fluid Passing through a Circular Hole

A two-dimensional transient heat conduction problem of a plate with a circular hole is analyzed by using several MARC elements. The hole is filled with a fluid at a temperature 1000°F with the exterior square edges at a fixed temperature of 500°F. The plate is initially at 500°F and is allowed to heat up for 5 seconds.

This problem is modeled using the six techniques summarized below.

Data Set	Element Type(s)	Number of Elements	Number of Nodes
e5x3a	41	8	37
e5x3b	69	8	37
e5x3c	39	32	45
e5x3d	37	64	65
e5x3e	121	32	45
e5x3f	131	16	45

Elements

Element types 37, 39, 41, 69, 121, and 131 (3-, 4-, 8-, 8-, 4-, and 6-node planar elements). Type 69 is an 8-node quadrilateral element with reduced integration. Type 121 is a 4-node quadrilateral element with reduced integration with hourglass control. Type 131 is a 6-node triangular element.

Model

This problem demonstrates the use of a variety of elements and the FILM option for prescribing convective boundary conditions. A rectangular plate 20 inches by 29 inches with a hole of radius 5 inches placed in the center is modeled.

Due to symmetry only a quarter of the plate is modeled for the analysis as shown in Figure 5.3-1 through Figure 5.3-4.

Thermal Property

One set of thermal properties is specified in the PROPERTY block: the isotropic thermal conductivity value of 0.42117 E5 Btu/sec-in.-°F; the specific heat is 0.3523 E-3 Btu/lb-°F; and the mass density is 0.7254 E-3 lb/cubic inch.

Geometry

The thickness of the plate is 0.1 inches.

Thermal Boundary Conditions

The initial temperature distribution is that all nodes have a temperature of 500.0°F. The lines of symmetry (x = 0 and y = 0) are adiabatic and require no data input. A time, t = 0, the fluid is exposed to the circular hole with a sink temperature of 1000°F, and a film coefficient of 0.4678E-5 Btu/sec-sq.in.-°F. The outer edges (x = y = 12 inches) are held at a fixed temperature of 500°F.

Load HIstory

The maximum number of time points are fixed at 10 with a final time of 5 seconds. Nonautomatic time stepping is used with a constant time step of 0.5 seconds/increment.

Results

The temperature history at the center point between the radius of the hole and the corner of the plate (nodes 11, 23, 9, 9, 23, 9 for mesh composed of element type 37, 39, 41, 69, 121 and 131) is shown in Figure 5.3-4.

Parameters, Options, and Subroutines Summary

Example e5x3a.dat:

Parameters	Model Definition Options	History Definition Options
ELEMENT	CONNECTIVITY	CONTINUE
END	CONTROL	STEADY STATE
HEAT	COORDINATE	TRANSIENT
SIZING	END OPTION	
TITLE	FILMS	
	FIXED TEMP	
	GEOMETRY	
	INITIAL TEMP	
	ISOTROPIC	
	POST	
	UDUMP	

Example e5x3b.dat:

Parameters	Model Definition Options	History Definition Options
ELEMENT	CONNECTIVITY	CONTINUE
END	CONTROL	TRANSIENT
HEAT	COORDINATE	
SIZING	END OPTION	
TITLE	FILMS	
	FIXED TEMP	
	GEOMETRY	
	INITIAL TEMP	
	ISOTROPIC	
	POST	

Example e5x3c.dat:

Parameters	Model Definition Options	History Definition Options
ELEMENT	CONNECTIVITY	CONTINUE
END	CONTROL	TRANSIENT
HEAT	COORDINATE	
SIZING	END OPTION	
TITLE	EXIT	
	FILMS	
	FIXED TEMP	
	GEOMETRY	
	INITIAL TEMP	
	ISOTROPIC	
	POST	

Example e5x3d.dat:

Parameters	Model Definition Options	History Definition Options
ELEMENT	CONNECTIVITY	CONTINUE
END	CONTROL	TRANSIENT
HEAT	COORDINATE	
SIZING	END OPTION	
TITLE	EXIT	
	FILMS	
	FIXED TEMP	
	GEOMETRY	
	INITIAL TEMP	
	ISOTROPIC	
	POST	

Example e5x3e.dat:

Parameters	Model Definition Options	History Definition Options
ALIAS	CONNECTIVITY	CONTINUE
ELEMENT	CONTROL	TRANSIENT
END	COORDINATE	
HEAT	END OPTION	
SIZING	FILMS	
TITLE	FIXED TEMP	
	GEOMETRY	
	INITIAL TEMP	
	ISOTROPIC	
	POST	

Example e5x3f.dat:

Parameters	Model Definition Options	History Definition Options
ALL POINTS	CONNECTIVITY	CONTINUE
ELEMENT	CONTROL	TRANSIENT
END	COORDINATE	
HEAT	END OPTION	
SIZING	FILMS	
TITLE	FIXED TEMP	
	GEOMETRY	
	INITIAL TEMP	
	ISOTROPIC	
	POST	

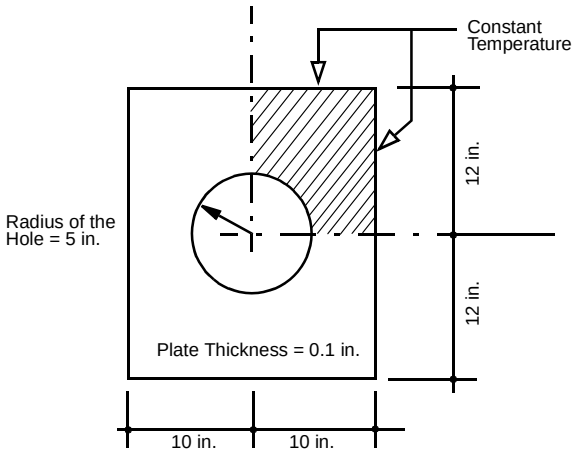

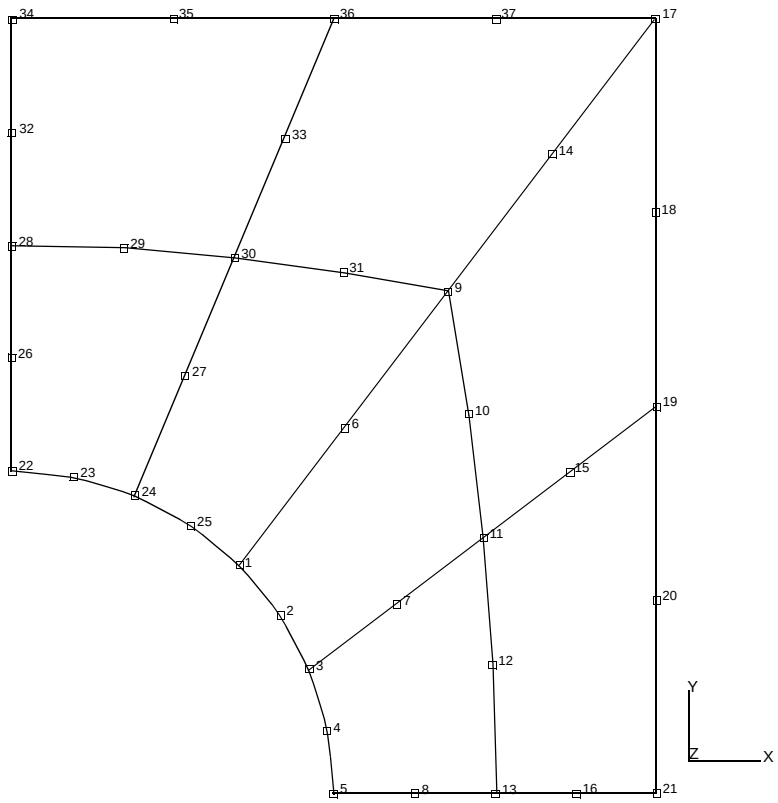

Figure 5.3-1 Mesh for Element Type 41

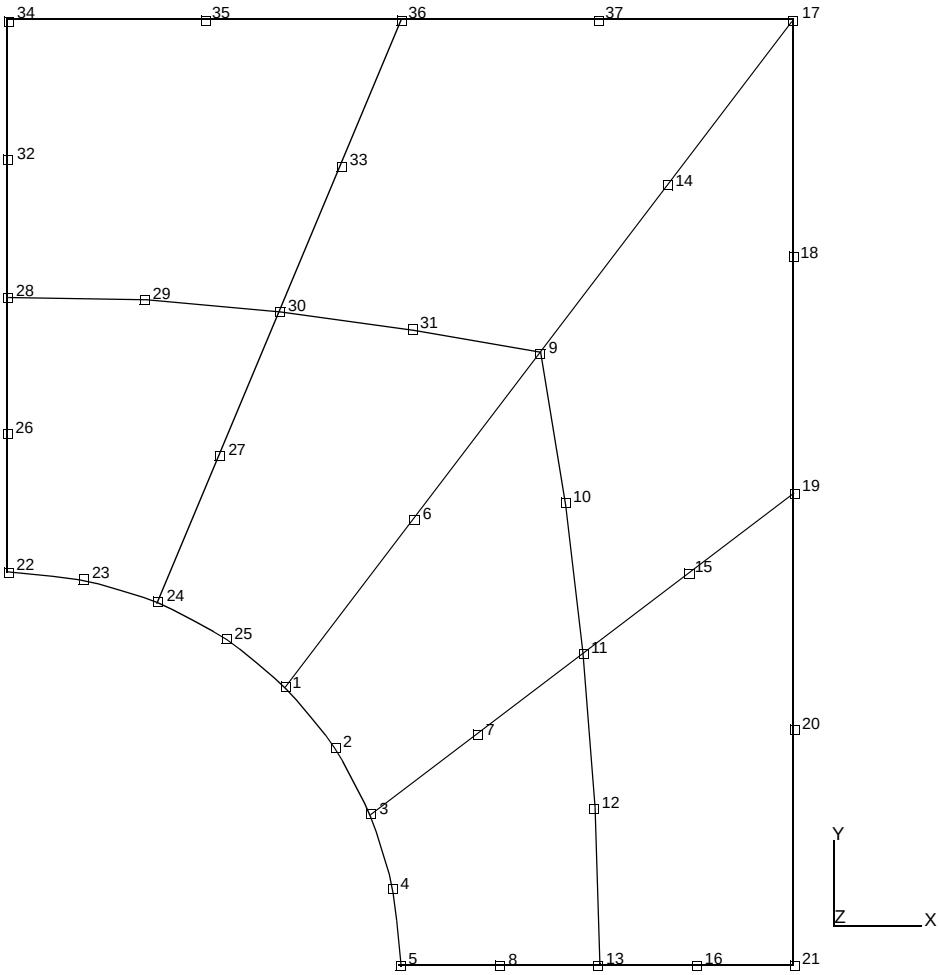

Figure 5.3-2 Mesh for Element Type 69

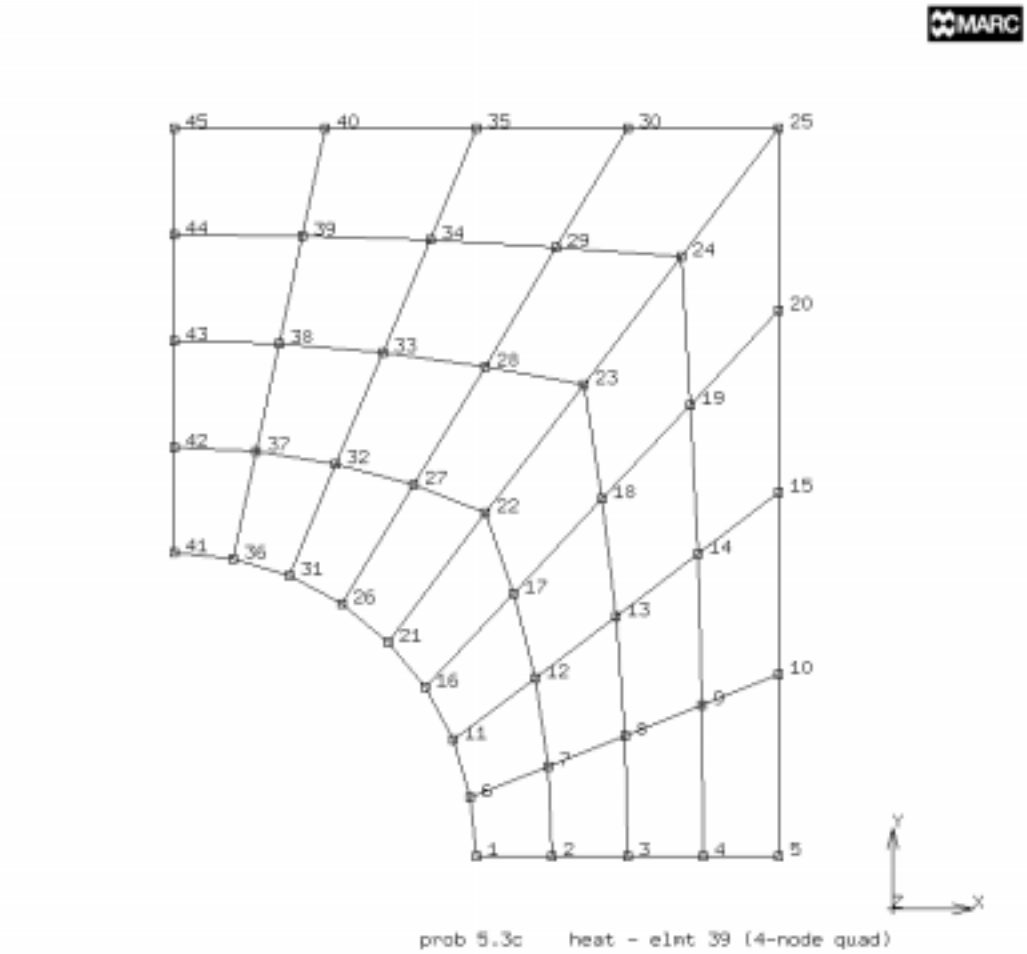

Figure 5.3-3 Mesh for Element Type 39

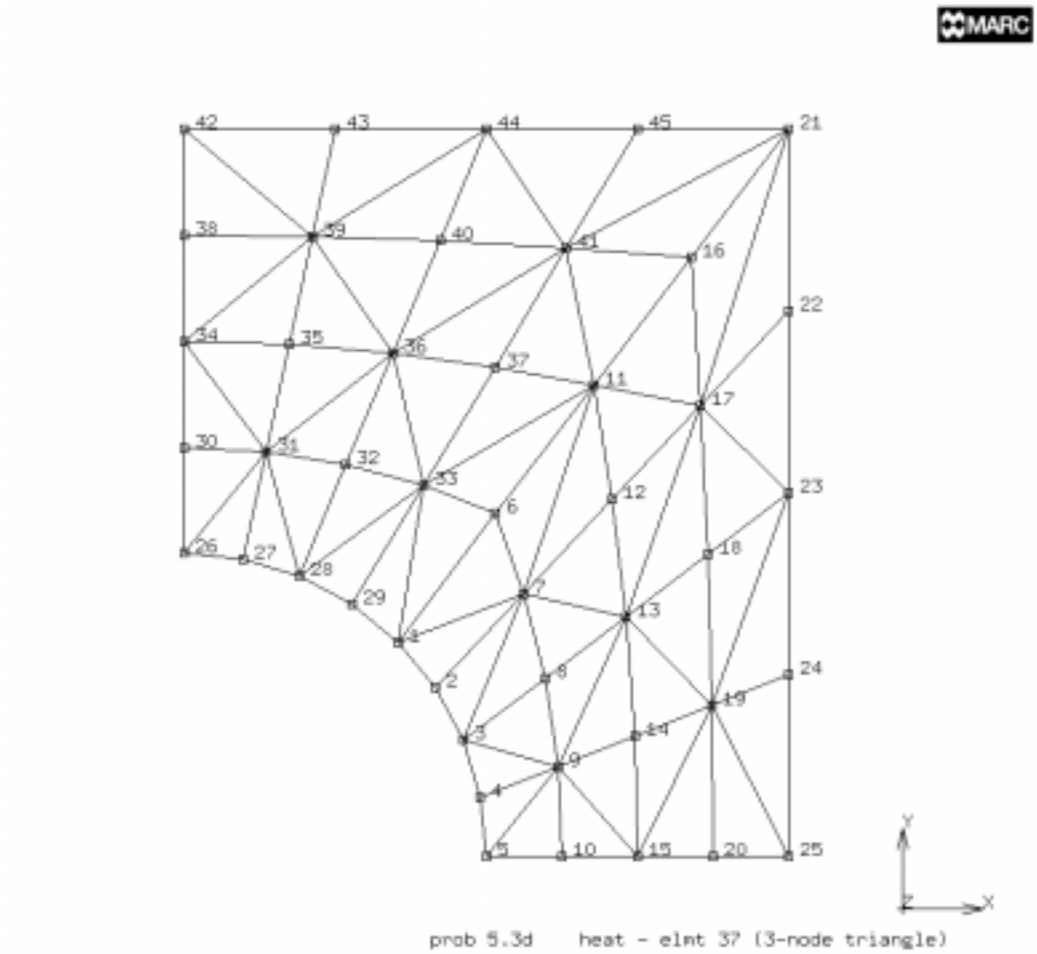

Figure 5.3-4 Mesh for Element Type 37

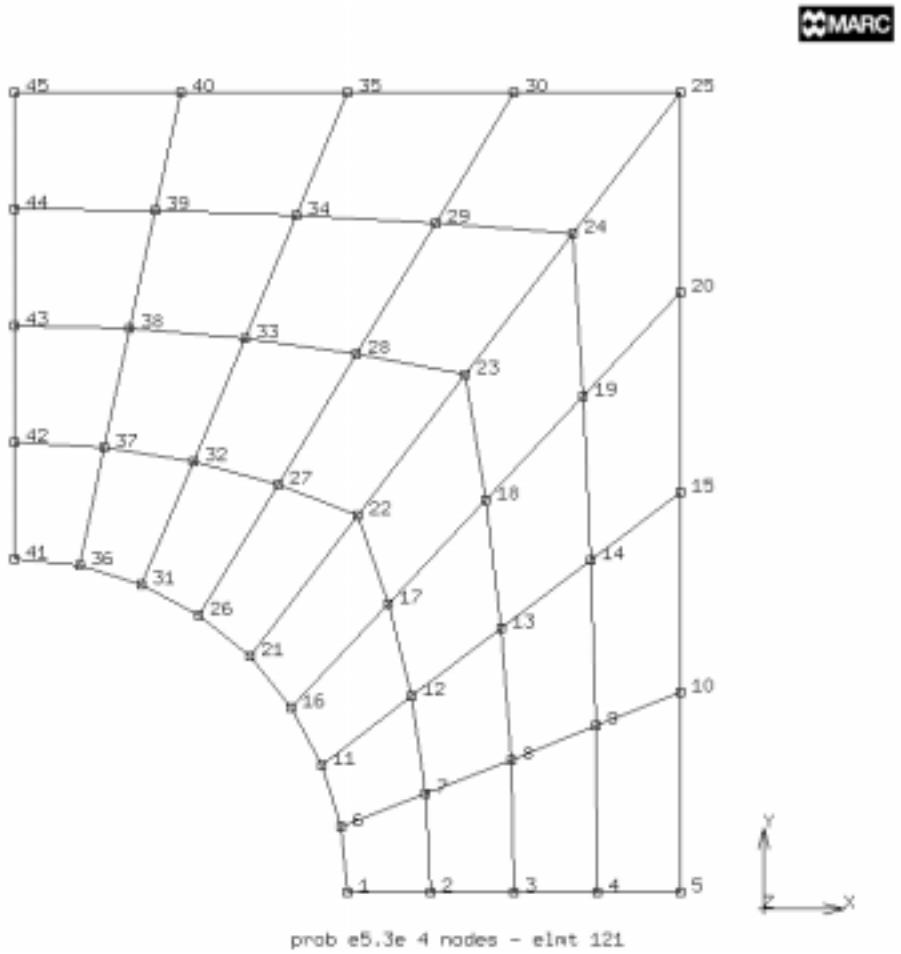

Figure 5.3-5 Mesh for Element Type 121

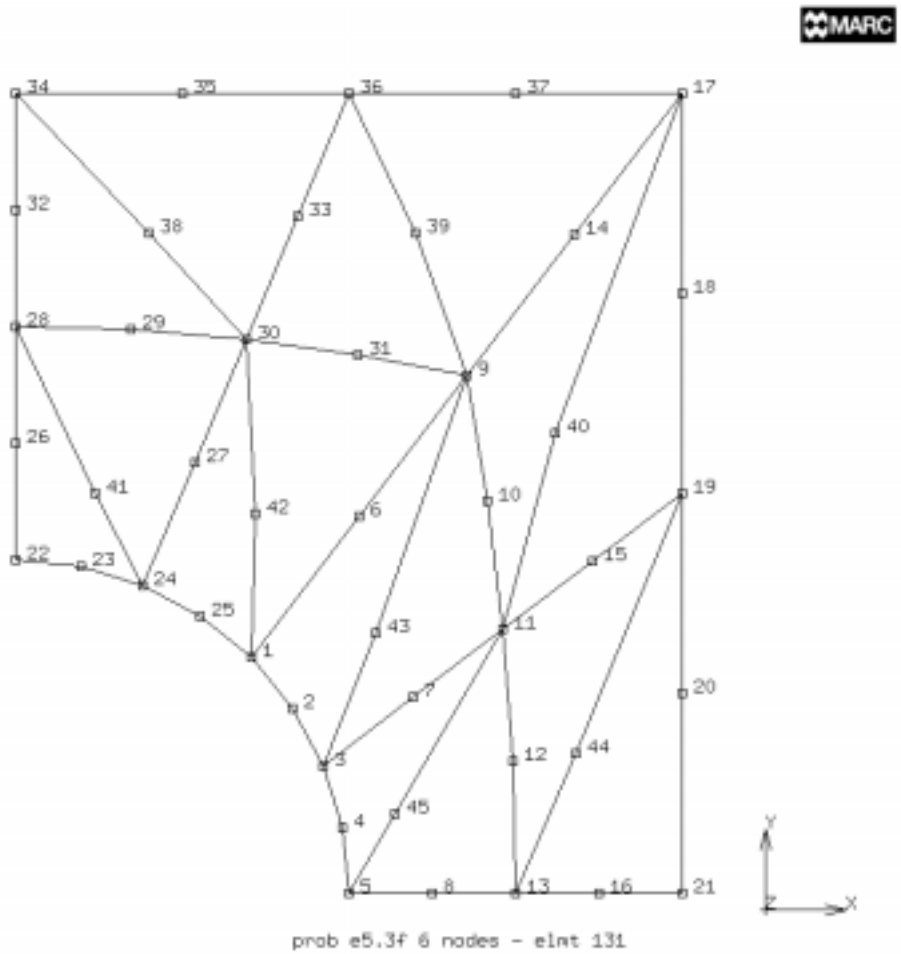

Figure 5.3-6 Mesh for Element Type 131

Time Sec	Temperatures (element type, node number)					
	41, n9	69, n9	39, n23	37, n11	121, n23	131, n9
.50	535.403	534.993	529.728	526.038	529.731	528.283
1.0	561.951	561.689	558.964	555.728	558.690	556.195
1.5	577.971	577.786	575.893	573.122	575.814	573.194
2.0	585.914	585.783	584.044	581.475	584.040	581.393
2.5	589.609	589.509	587.735	585.241	589.839	585.109
3.0	591.287	591.206	589.369	586.900	591.577	586.756
3.5	592.042	591.970	590.086	587.624	592.278	587.481
4.0	592.381	592.314	590.400	587.939	592.577	587.799
4.5	592.533	592.468	590.537	588.076	592.707	587.938
5.0	592.601	592.538	590.597	588.136	592.763	587.999

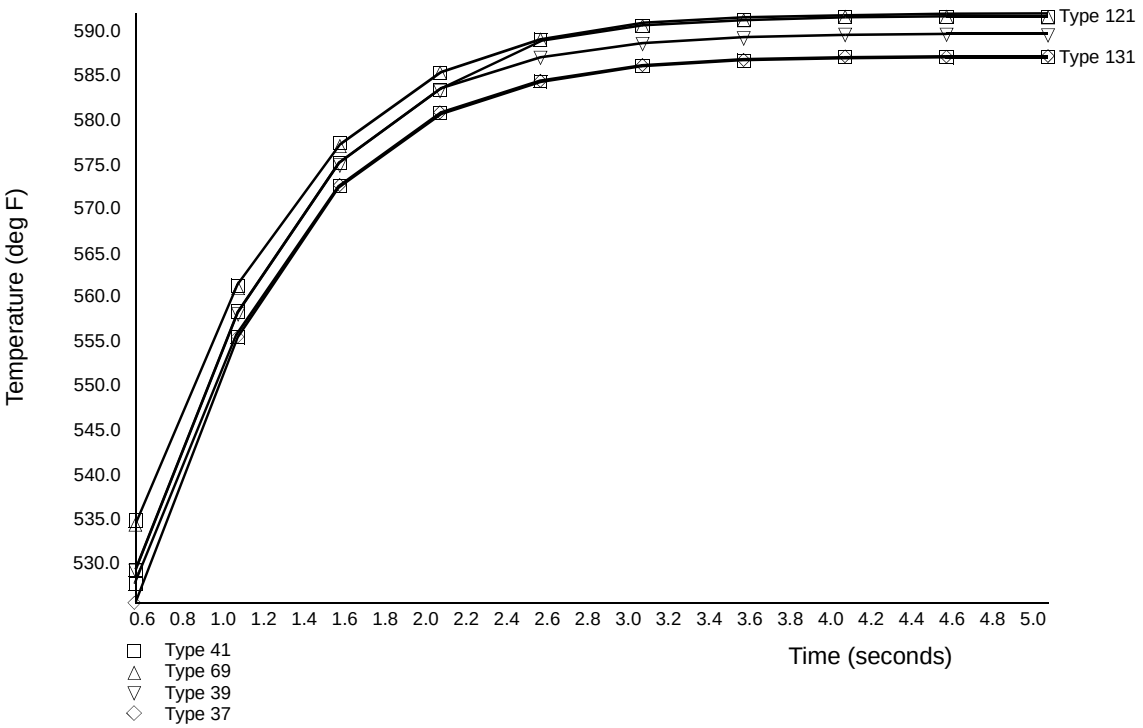

Figure 5.3-7 Temperature History for Elements Types: 37, 39, 41, 69, 121, and 131

5.4 Three-Dimensional Transient Heat Conduction

A unit cube is initially at a temperature of 100°F throughout. Two faces of the cube have a temperature of 0°F. The other faces are insulated. The temperature at the center of the cube is calculated for subsequent times (0 to 10 seconds).

This problem is modeled using the three techniques summarized below.

Data Set	Element Type(s)	Number of Elements	Number of Nodes
e5x4a	43	8	27
e5x4c	71	8	81
e5x4d	123	8	27

Elements

Element types 43 and 123 are 8-node linear brick elements where type 123 has reduced integration with hourglass control. Types 44 and 71 are 20-node parabolic brick elements where type 71 uses reduced integration. The cube has equal dimensions of 1 inch where x, y, and z range from 0 to 1 inch. The cube is modeled with 8 brick elements as shown in Figure 5.4-1 and Figure 5.4-3 for the linear and parabolic meshes.

Thermal Properties

One set of thermal properties is specified in the ISOTROPIC block: the isotropic thermal conductivity value is 1.0 Btu/sec-in-°F; the specific heat is 1.0 Btu/lb-°F; and the mass density is 1.0 lb/cubic inch.

Thermal Boundary Conditions

The initial temperature distribution is that all nodes have a temperature of 100.0°F. At time t = 0, x = 0 and z = 1 surfaces have a prescribed temperature of 0°F; all other surfaces are adiabatic and require no data input. A transient solution is performed with 10 uniform time steps of 0.1 seconds each for a total time of 1 second.

Results

The temperature at the center of the unit cube is plotted versus time for the various element types and is shown in Figure 5.4-3. The cube has almost cooled down completely after 1 second. The linear elements (types 43 and 123) initially cool down slower than the parabolic elements (types 44 and 71).

Parameters, Options, and Subroutines Summary

Example e5x4a.dat:

Parameters	Model Definition Options	History Definition Options
ELEMENT	CONNECTIVITY	CONTINUE
END	CONTROL	TRANSIENT
HEAT	COORDINATE	
SIZING	END OPTION	
TITLE	FIXED TEMP	
	INITIAL TEMP	
	ISOTROPIC	
	POST	
	PRINT CHOICE	
	UDUMP	

Example e5x4b.dat:

Parameters	Model Definition Options	History Definition Options
ELEMENT	CONNECTIVITY	
END	CONTROL	CONTINUE
HEAT	COORDINATE	TRANSIENT
SIZING	END OPTION	
TITLE	FIXED TEMP	
	INITIAL TEMP	
	ISOTROPIC	
	POST	
	PRINT CHOICE	

Example e5x4c.dat:

Parameters	Model Definition Options	History Definition Options
ELEMENT	CONNECTIVITY	CONTINUE
END	CONTROL	TRANSIENT
HEAT	COORDINATE	
SIZING	END OPTION	
TITLE	FIXED TEMP	
	INITIAL TEMP	
	ISOTROPIC	
	POST	
	PRINT CHOICE	

Example e5x4d.dat:

Parameters	Model Definition Options	History Definition Options
ALIAS	CONNECTIVITY	CONTINUE
ELEMENT	CONTROL	TRANSIENT
END	COORDINATE	
HEAT	END OPTION	
SIZING	FIXED TEMP	
TITLE	INITIAL TEMP	
	ISOTROPIC	
	POST	
	PRINT CHOICE	

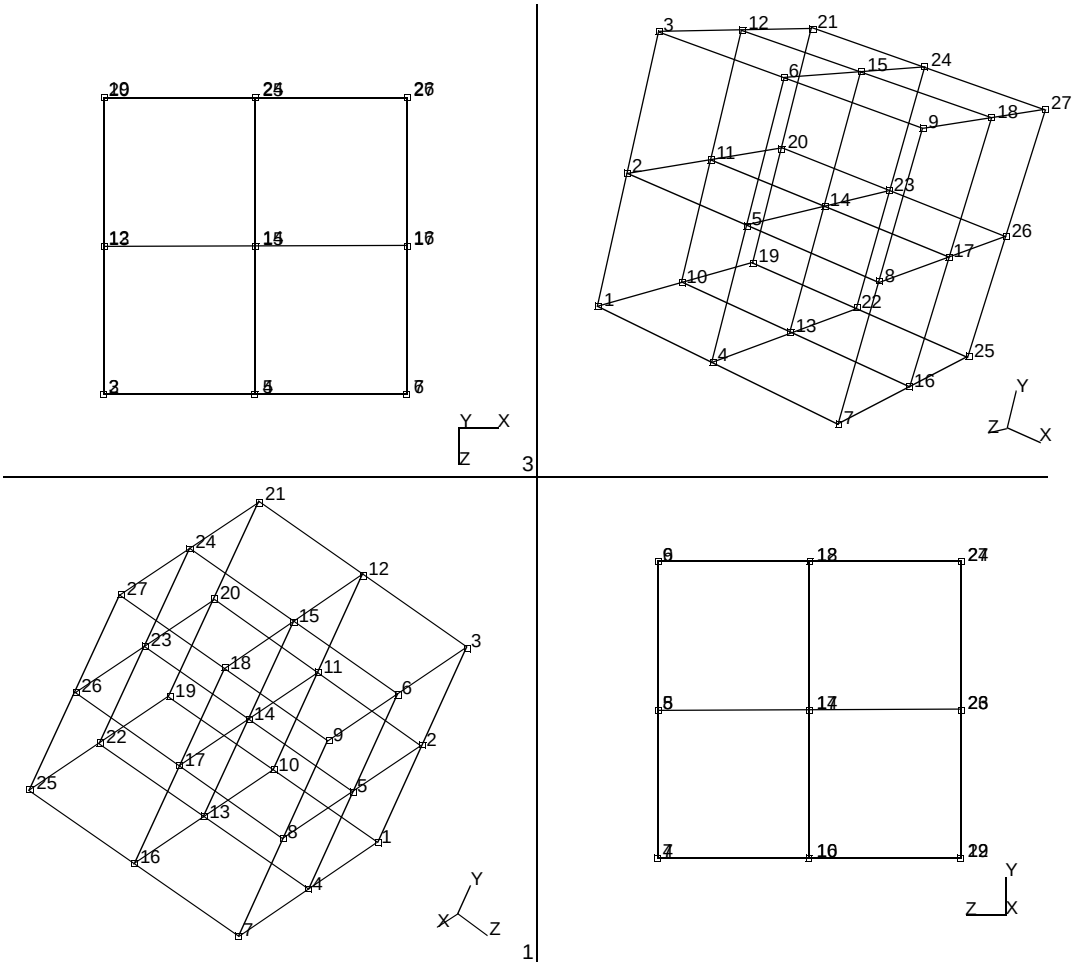

Figure 5.4-1 Mesh for the Unit Cube Linear Elements

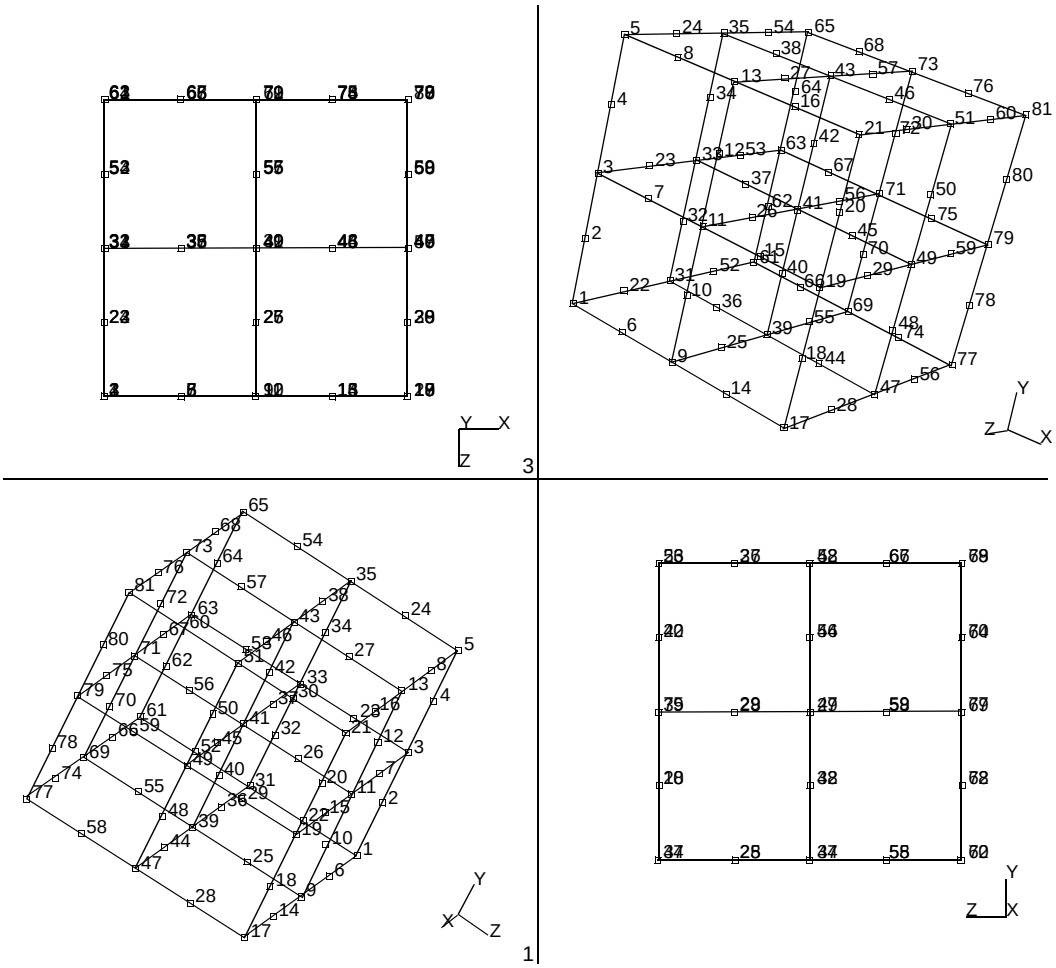

Figure 5.4-2 Mesh for the Unit Cube Parabolic Elements

Time (Seconds)	Temperatures (element type, node number)			
	Type 43, n14	Type 44, n41	Type 71, n41	Type 123, n41
0.0	1.00000E+02	1.00000E+02	1.00000E+02	1.00000E+02
1.00000E-01	7.49796E+01	6.36616E+01	6.33202E+01	7.49796E+01
2.00000E-01	4.22526E+01	4.03147E+01	4.02325E+01	4.22526E+01
3.00000E-01	2.62808E+01	2.55396E+01	2.55179E+01	2.62808E+01
4.00000E-01	1.69623E+01	1.66272E+01	1.66202E+01	1.69623E+01
5.00000E-01	1.10900E+01	1.09937E+01	1.09915E+01	1.10900E+01
6.00000E-01	7.28266E+00	7.32065E+00	7.32054E+00	7.28266E+00
7.00000E-01	4.78960E+00	4.88981E+00	4.89058E+00	4.78960E+00
8.00000E-01	3.15160E+00	3.27040E+00	3.27148E+00	3.15160E+00
9.00000E-01	2.07415E+00	2.18852E+00	2.18962E+00	2.07415E+00
1.00001E+00	1.36513E+00	1.46487E+00	1.46587E+00	1.36513E+00

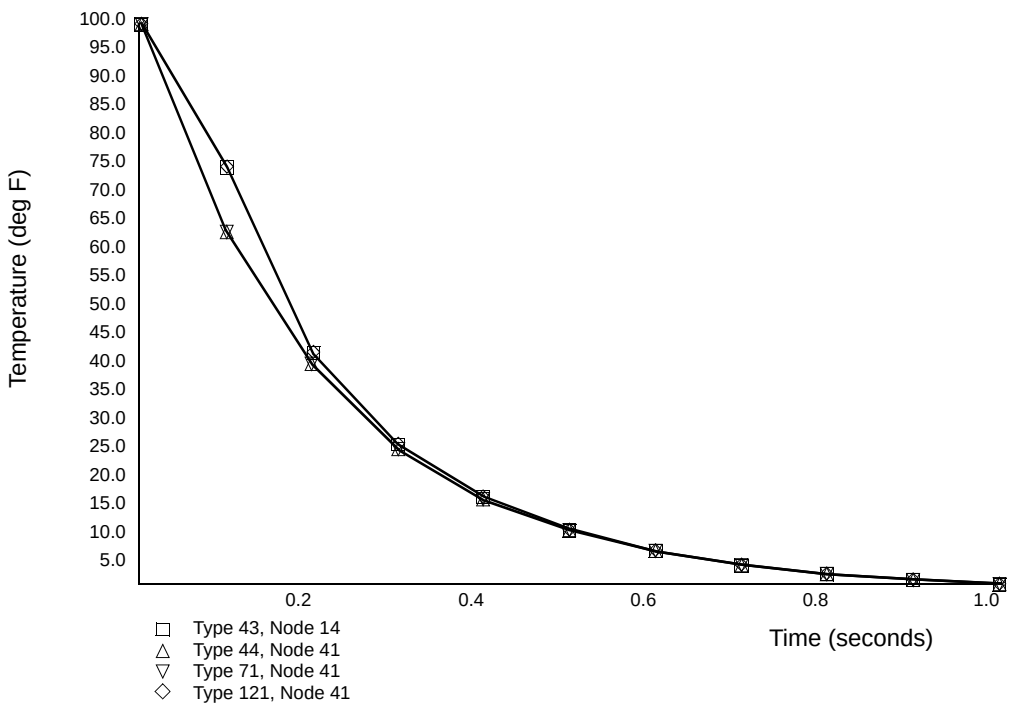

Figure 5.4-3 Cube Center Temperature History for Element Types: 43, 44, 71, and 123

5.5 Pressure Vessel Subjected to Thermal Downshock

A realistic design problem, such as thermal ratcheting analysis, involves a working knowledge of a significant number of MARC features. This example illustrates how these features are used to analyze a simplified form of a pressure vessel component which is subjected to a thermal downshock. This problem is typical of reactor component analysis. The general temperature-time history which is used is shown in Figure 5.5-1.

An analysis of this type requires heat transfer analysis to determine the transient temperature distribution. This distribution is calculated for the wall of a cylindrical pressure vessel under cool-down conditions. The resulting data must be saved for use in the stress analysis.

This problem is modeled using the two techniques summarized below.

Data Set	Element Type(s)	Number of Elements	Number of Nodes
e5x5a	42	6	33
e5x5b	70	6	33

Elements

The 8-node axisymmetric, quadrilateral elements are used in this example. The heat transfer elements 42 and 70, are used in the determination of the transient temperature distributions.

Model

The geometry and mesh for this example are shown in Figure 5.5-2. A cylindrical wall segment is evenly divided in six axisymmetric quadrilateral elements with a total of 33 nodes. The mesh data is entered as element type 28. The ALIAS parameter allows you to generate your connectivity data with the stress analysis element and then to replace this element with the corresponding heat transfer element type.

Heat Transfer Properties

It is assumed here that the material properties do not depend on temperature; no slope-breakpoint data is input. The uniform properties used here are:

specific heat (c) = 0.116 Btu/lb-°F
thermal conductivity (k) = 4.85 (10^{-4}) Btu/in-sec-°F
density (ρ) = 0.283 lb/cubic inch

Heat Transfer Boundary Conditions

The initial temperature across the wall and ambient temperature are 1100°F as specified in the initial conditions block. The outer ambient temperature is held constant at 1100°F while the inner ambient temperature decreases from 1100°F to 800°F in 10 secs and remains constant thereafter.

The FILMS option is used to input the film coefficients and associated sink temperatures for the inner and outer surface. A uniform film coefficient for the outside surface is specified for element 6 as 1.93×10^{-6} Btu/sq.in-sec-°F in order to provide a nearly insulated wall condition. The inner surface has a film coefficient of 38.56×10^{-5} Btu/sq.in-sec-°F to simulate forced convection. The temperature down-ramp of 300°F for this inner wall is specified here as a nonuniform sink temperature and is applied using user subroutine FILM.

Subroutine FILM linearly interpolates the 300°F decrease in ambient temperature over 10 secs and holds the inner wall temperature constant at 800°F. It is called at each time step for each integration point on each element surface given in the FILMS option. Thus, this subroutine does nothing if it is called for element 6 to keep the outer surface at 1100°F. It applies the necessary ratio to reduce the inner wall temperature.

The TRANSIENT option controls the heat transfer analysis. MARC automatically calculates the time steps to be used based on the maximum nodal temperature change allowed as input in the CONTROL option. The solution begins with the suggested initial time step of one-half second input and ends according to the time period of 250 secs specified. It will not exceed the maximum number of steps input as 120 in this option.

The CONTROL option requires that the maximum temperature change per increment is 15°F. If this is exceeded, MARC automatically scales down the time step. The second tolerance on the CONTROL option requires that the program reassembles the operator matrix if the temperature has changed by 1000°F since the last reassembly.

Finally, note in the heat transfer run the use of the POST option. This allows the creation of a postprocessor file containing element temperatures at each integration point and nodal point temperatures. The file is used later as input to the stress analysis run.

Heat Transfer Results

The transient thermal analysis is linear in that material properties do not depend on temperature and the boundary conditions depend on the surface temperature linearly. The analysis has been completed using the automatic time step feature in the TRANSIENT option.

The transient run reached completion in 33 increments with a specified starting time step of 0.5 seconds. A 15°F temperature change tolerance was input in the CONTROL option and controlled the auto time stepping scheme. The reduction to approximately 800°F throughout the wall was reached in increment 33 at a total time of 250 seconds.

The temperature-time histories of elements 1 (inner wall) and 6 (outer wall) for auto time stepping is shown in Figure 5.5-3.

The temperature distribution across the wall at various solution times is shown in Figure 5.5-4. Convergence to steady state is apparent here as is the thermal gradient characteristic of the downshock.

Parameters, Options, and Subroutines Summary

Example e5x5a.dat:

Parameters	Model Definition Options	History Definition Options
ALIAS	CONNECTIVITY	CONTINUE
ELEMENT	CONTROL	TRANSIENT
END	COORDINATE	
HEAT	END OPTION	
SIZING	FILMS	
TITLE	INITIAL TEMP	
	ISOTROPIC	
	POST	

User subroutine in u5x5.f:

FILM

Example e5x5b.dat:

Parameters	Model Definition Options	History Definition Options
ELEMENT	CONNECTIVITY	CONTINUE
END	CONTROL	TRANSIENT
HEAT	COORDINATE	
SIZING	END OPTION	
TITLE	FILMS	
	INITIAL TEMPERATURE	
	ISOTROPIC	
	POST	

User subroutine in u5x5.f:

FILM

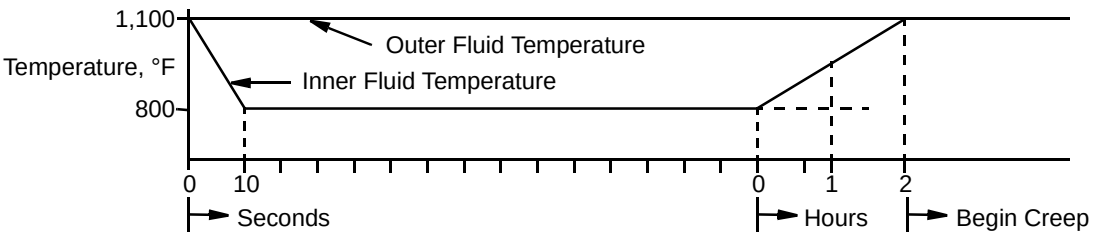

Figure 5.5-1 Temperature Time History

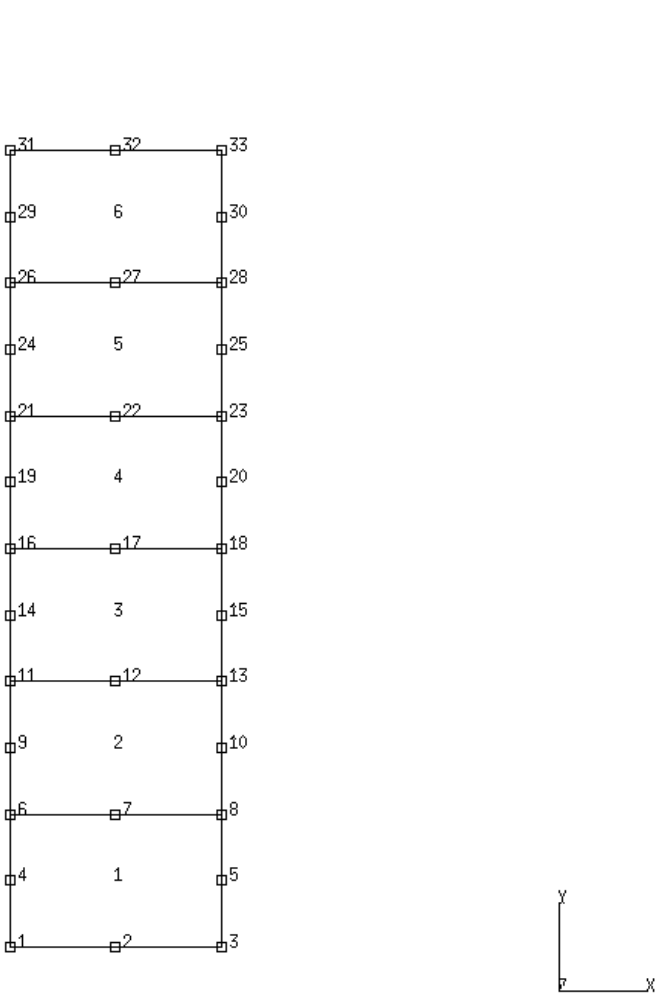

Figure 5.5-2 Geometry and Mesh

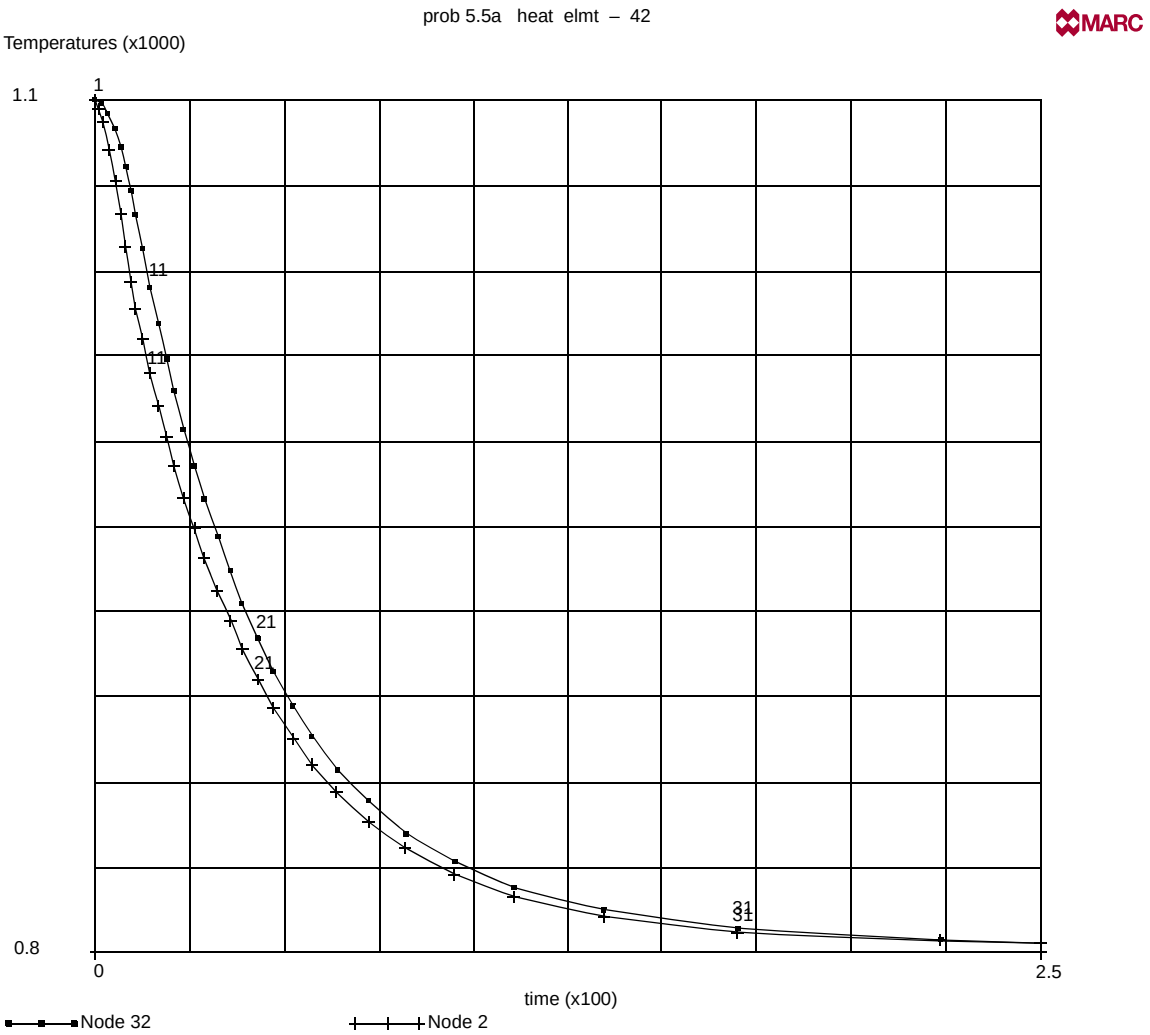

Figure 5.5-3 Transient Temperature Time History (Auto Time Step)

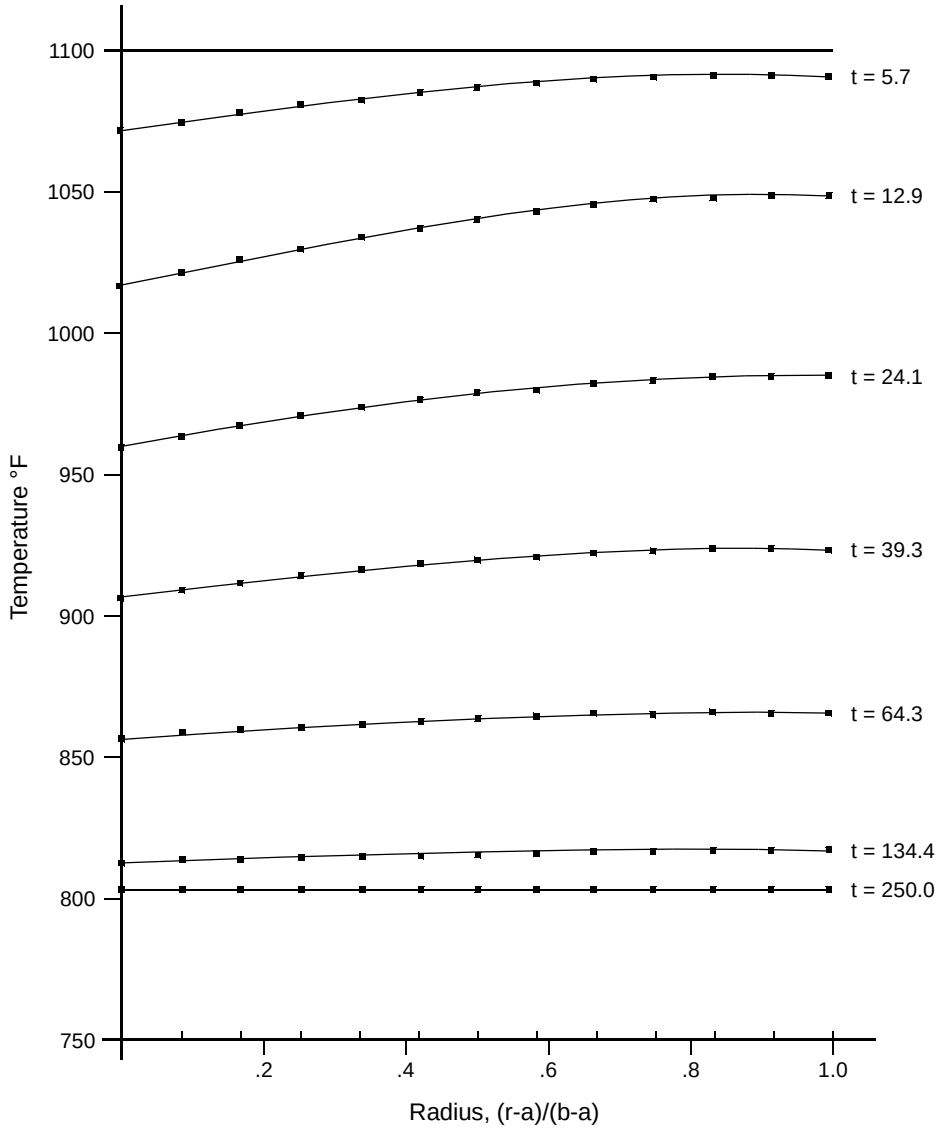

Figure 5.5-4 Temperature Distribution in Cylinder Wall

5.6 Axisymmetric Transient Heat Conduction Simulated by Planar Elements

The transient heat conduction of a thick cylinder, subjected to a thermal downshock, is analyzed by using MARC planar heat transfer element. This is the same as problem 5.5.

Model/Element

A 45-degree sector of the cylinder is modeled in the x-y plane as shown in Figure 5.6-1. The MARC heat transfer element type 41 (8-node planar quadrilateral) is selected for the analysis.

Material Properties

The conductivity is 4.85×10^{-4} Btu/sec-in- F. The specific heat is 0.116 Btu/lb-°F. The mass density is 0.283 lb/cu.inch.

Initial Condition

Initial nodal temperatures are assumed to be homogeneous at 1100°F.

Boundary Conditions

No input data is required for insulated boundary conditions along symmetry lines at y = 0 and y = x. Fluid temperatures and film coefficients for both inner and outer surfaces of the cylinder are:

Inner surface: H_i = 38.56×10^{-5} Btu/sec-sq.in-°F
T_i = 1100°F at t = 0. second
800°F at t = 10. second

Outer surface: H_0 = 1.93×10^{6} Btu/sec-sq.in-°F
(low value to simulate insulated boundary condition).
T_0 = 1100°F

The FILMS option is used to input the film coefficients and associated fluid temperatures for the inner and outer surfaces. Subroutine FILM linearly interpolates the 300°F decrease in ambient temperature over 10 seconds and holds the inner wall temperature constant at 800°F. It is called at each time step for each integration point on each element surface given in the FILMS option.

POST

In the heat transfer run, the use of the POST option allows the creation of a postprocessor file containing element temperatures at each integration point and nodal point temperatures. The file can be used later as input to the stress analysis run.

TRANSIENT

The TRANSIENT option controls the heat transfer analysis. MARC automatically calculates the time steps to be used based on the maximum nodal temperature change allowed as input in the CONTROL option. The solution begins with the suggested initial time step input of 0.5 seconds and ends according to the time period specified of 250 seconds. It does not exceed the maximum number of steps input in this option.

Results

A comparison of nodal temperatures with the results of an axisymmetric model (problem 5.5) are shown in Table 5.6-1.

Table 5.6-1 Comparison of Nodal Temperatures

Increment No.	Time (Seconds)	Nodal Temperature (°F)	
		Problem 5.5	Problem 5.6
2	1.25	1099.3	1099.3
4	4.06	1092.6	1092.6
6	7.22	1078.1	1078.1
8	9.94	1068.4	1060.4
10	12.96	1039.8	1039.8
12	17.21	1014.0	1014.0
14	21.44	990.8	990.8
16	26.72	965.7	965.7
18	32.65	941.7	941.5
20	39.2	919.0	918.8

Parameters, Options, and Subroutines Summary

Example e5x6.dat:

Parameters	Model Definition Options	History Definition Options
ELEMENT	CONNECTIVITY	CONTINUE
END	CONTROL	TRANSIENT
HEAT	COORDINATE	
SIZING	END OPTION	
TITLE	FILMS	
	INITIAL TEMP	
	ISOTROPIC	
	POST	

User subroutine in u5x6.f:

FILM

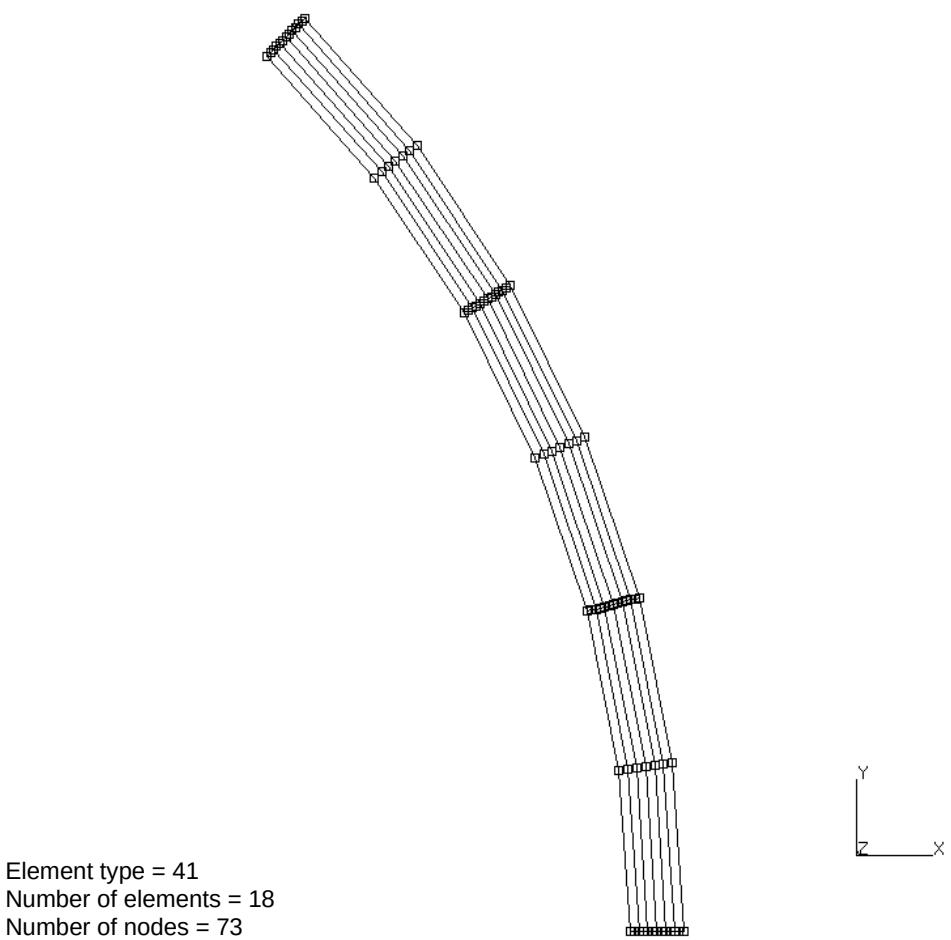

Figure 5.6-1 Cylinder and Mesh

5.7 Steady State Analysis of an Anisotropic Plate

Two plates are subjected to similar temperature conditions. One plate has thermally isotropic properties; the other is anisotropic. The temperatures of the plate centers are calculated. In this problem, the thermal conductivity of the material is assumed to be anisotropic.

This problem is modeled using the two techniques summarized below.

Data Set	Element Type(s)	Number of Elements	Number of Nodes	Differentiating Features
e5x7a	39	4	9	ANISOTROPIC
e5x7b	39	4	9	ISOTROPIC

Model/Element

This two-dimensional steady state heat conduction problem is analyzed using MARC heat transfer element type 39 (4-node planar quadrilateral). A plate is modeled by using four MARC planar heat transfer elements; the number of nodes in the mesh is nine. The size of the plate is 2.0 x 2.0 sq.in. for the anisotropic material and 0.2 x 2.0 sq.in. for the isotropic material.The plate and meshes are shown in Figure 5.7-1.

Material Properties

The conductivity is 1.0 Btu/sec-in-°F for the isotropic material. k_x is 100.0 and k_y is 1.0 for the anisotropic material. The specific heat is 1.0 Btu/lb.-°F for both plates. The mass density of 1.0 lb/cu.in. is the same for both cases.

Boundary Conditions

A constant temperature of 100°F is prescribed at nodes 1, 2, 3, 4, 6 and of 0°F at nodes 7, 8, and 9.

Transient

A transient time of 1000 seconds is assumed for the analysis and the selected time step is 250 seconds. Nonautomatic TIME STEP option is also invoked.

User Subroutine ANKOND

The COND array in the subroutine ANKOND is used for the modification of conductivity due to anisotropic behavior of the material.

Results

Node temperatures at node 5 are identical (25.743°F) for both plates. This is to be expected as the length of the anisotropic plate was adjusted so that the same behavior would be obtained.

Parameters, Options, and Subroutines Summary

Example e5x7a.dat:

Parameterns	Model Definition Options	History Definition Options
ELEMENT	ANISOTROPIC	CONTINUE
END	CONNECTIVITY	TRANSIENT
HEAT	COORDINATE	
SIZING	END OPTION	
TITLE	FIXED TEMP	

User subroutine in u5x7a.f:

ANKOND

Example e5x7b.dat:

Parameters	Model Definition Options	History Definition Options
ELEMENT	CONNECTIVITY	CONTINUE
END	COORDINATE	TRANSIENT
HEAT	END OPTION	
SIZING	FIXED TEMP	
TITLE	ISOTROPIC	

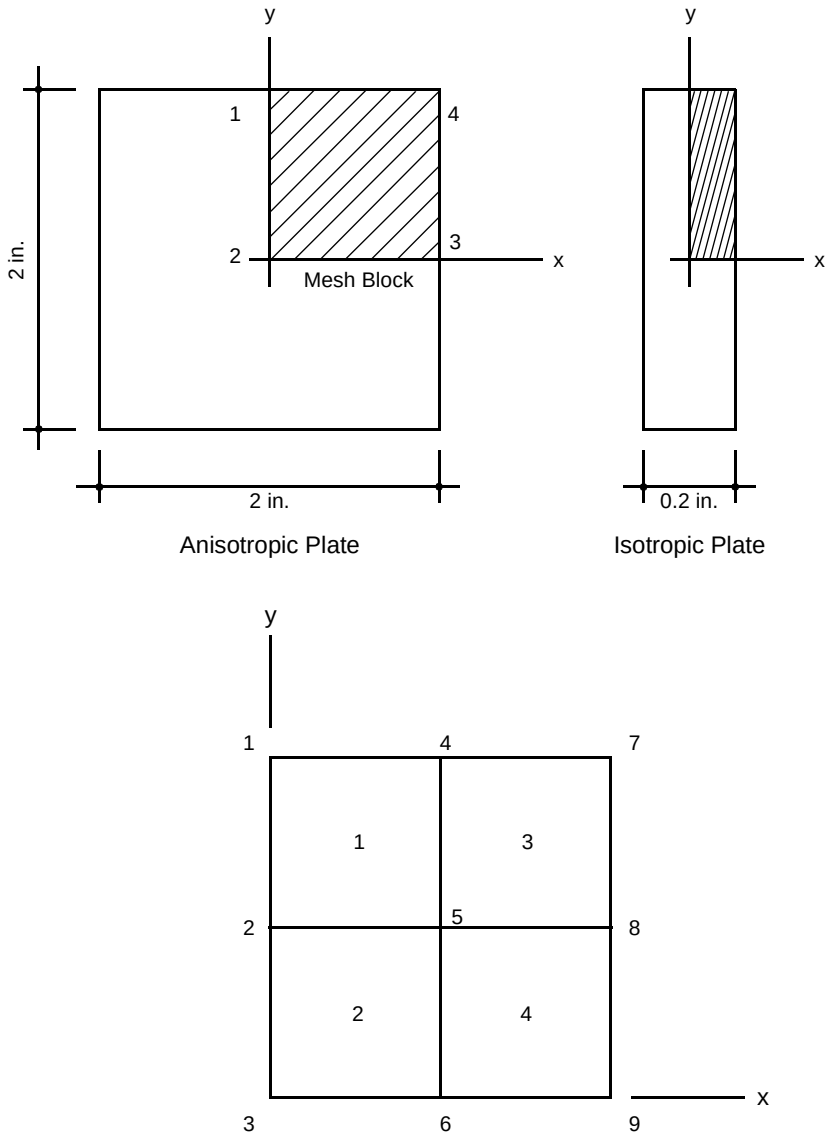

Figure 5.7-1 Plate and Mesh

5.8 Nonlinear Heat Conduction of a Channel

Many important problems in heat transfer involve the interaction between transient heat conduction in a solid body and convection and radiative heat transfer in surrounding media. These problems are inherently nonlinear (although a linearized model is often sufficient) due to the complex nature of this interaction. For instance, radiative heat transfer rates depend on the surface temperature raised to the fourth power, and the emissivity ε of a gray body can be a strong function of surface temperature, as well. Convective heat transfer rates depend linearly on the surface temperature explicitly, but the convective coefficients themselves may depend on the surface temperature (for example, in evaluating mean film properties), giving rise to an implicit nonlinear dependence.

This example illustrates the ability of MARC to treat this class of nonlinear problems, provided that some care is taken in modeling. A user-supplied subroutine is exhibited which computes the radiation and convection effects for the surface of the solid by using estimates of the surface temperatures, iterating if necessary.

The mesh used and tolerances set in this example are intended for demonstration purposes only – an accurate solution would require a more detailed mesh as well as tighter tolerances.

This problem is modeled using the four techniques summarized below.

Data Set	Element Type(s)	Number of Elements	Number of Nodes	Differentiating Features
e5x8a	41	40	149	TRANSIENT
e5x8b	41	40	149	TRANSIENT (RESTART)
e5x8c	41	40	149	TRANSIENT NONAUTO
e5x8d	41	40	149	TRANSIENT NONAUTO
e5x8e	41	40	149	AUTO STEP

Element

The element used here is the 8-node planar heat transfer element, element type 41. (See *MARC Volume B: Element Library* for details of this element.)

Model

The geometry for the heat transfer problem is shown in Figure 5.8-1. A liquid flows down a U-shaped channel at 10 in/second. The liquid temperature increases steadily from 70°F to 400°F and remains at 400°F for the rest of the analysis. A uniform heat flux of 10^{-4} Btu/sq.in-sec is being steadily applied along the extremities of the channel legs; free convective transfer and radiative transfer are specified on the inside and outside faces of the channel legs, respectively; and a

uniform temperature of 70°F is maintained on the base of the channel. The problem is not intended to represent any physical situation – it simply serves as an illustration of the modeling techniques used with heat transfer analysis.

The mesh is shown in Figure 5.8-2. For a more accurate geometric modeling, more blocks should be used at the corner.

Boundary Conditions

The boundary conditions for the analysis are shown in Figure 5.8-1. The simpler conditions (fixed temperature, flux) are input directly. The more complex radiation and convection conditions are input through subroutine FILM.

The FILMS model definition option causes the routine to be called at each surface integration point of each element listed in that model definition set. Then, based on the element number (which is passed in to the routine) the following sections are provided:

A. Forced, liquid metal convection on all elements adjacent to the metal stream. Here the routine calculates a film coefficient as follows:

The liquid metal properties – conductivity, Prandtl number, and kinematic viscosity – are assumed to be functions of the average boundary layer temperature (the average temperature is based on the mean of the free stream temperature and the estimated surface temperature). Then, the hydraulic diameter is computed from the formula:

$$D_H = \frac{4\ (\text{flow cross-sectional area})}{(\text{wetted perimeter})}$$

For this example, D_H = 10 inches approximately. The Reynolds number is given by the relation:

$$Re_D = \frac{D_H V}{\nu}$$

where:

V is the velocity of the flow
ν is the kinematic viscosity

The Peclet number, Pe, is given by the product of the Reynolds and Prandtl (Pr) numbers. Then the average Nusselt number, Nu, is found from the experimentally verified formula for fully developed turbulent flow of liquid metals (see Lubarsky, B, and Kaufman, S. J., “Review of Experimental Investigations of Liquid-Metal Heat Transfer”, NACA TN 3336, 1955.):

$\overline{Nu} = 0.625\ (Pe)^{0.4}$

The final step is to find the average heat transfer coefficient from:

$$\bar{h}_e = \frac{k\ \overline{Nu}}{D_H}$$

where k is the thermal conductivity of the liquid metal. The bulk fluid temperature increases linearly with time from 70°F to 400°F, then remains constant at 400ºF for the rest of the analysis. These values of $\bar{h}_e$ and the bulk fluid temperature are passed back from FILM in H and TINF, respectively. Note that the film coefficient is so high that the surface nodes effectively take on the bulk fluid temperature directly as a prescribed surface temperature boundary condition.

B. Free Convection:

Here the constant film coefficient and bulk temperature are entered directly in H and TINF.

C. Radiation:

The radiation law is: $q = \varepsilon\sigma(T^4 - T_\infty^4)$

where ε is the emissivity of the surface (here assumed to be 0.6), σ is the Stefan-Boltzmann constant, and temperatures are in absolute units. In this case, T_∞ is 460 + 70 = 530°R. In order to perform a linear time stepping scheme, the above equation is rewritten as:

$$q = \varepsilon\sigma(T^3 + T^2T_\infty + T\ T_\infty^2)(T - T_\infty)$$

and a temperature dependent film coefficient:

$$h = \varepsilon\sigma(T^3 + T^2T_\infty + T\ T_\infty^2 + T_\infty^3)$$

is calculated in the subroutine.

Subroutine FILM defines relative values; that is, multipliers of the data values for H and TINF entered on the FILMS model definition set. In this case, it is more convenient to program absolute values in FILM; therefore, values of 1. are entered in the model definition set.

Time Stepping

In this case, the automatic time stepping scheme is chosen based on a maximum temperature change per increment of 50°F. MARC adjusts time steps to conform to this criterion according to the scheme defined in *MARC Volume F: Background Information*. Tolerances are also placed

on the maximum temperature change before the program recalculates nonlinear effects; that is, temperature-dependent material properties and temperature-dependent boundary conditions, both of which are present in this example, and on the maximum temperature variation between the temperature used to evaluate properties and the resulting solution to allow iteration as necessary. It should be emphasized that for an accurate solution as well as a finer mesh, a tighter tolerance on temperature change per step should be provided.

Results

Isotherm plots are shown in Figure 5.8-3, Figure 5.8-4 and Figure 5.8-5 showing the temperature field after 100, 400 and 10,000 seconds. They illustrate the progress toward steady state conditions. At 10,000 seconds, the solution is not yet at steady state. The last step of about 1000 seconds shows a maximum nodal temperature change of 11°F. Therefore, steady state would be reached in a smaller number of additional steps. The program used 18 steps to produce this solution (based on the 50°F per step maximum temperature change tolerance) with an initial step of 100 seconds and a final step size of about 2000 seconds. This is a typical illustration of the effectiveness of the automatic stepping scheme. The transient temperature for selected nodes is shown in Figure 5.8-6.

Parameters, Options, and Subroutines Summary

Example e5x8a.dat:

Parameters	Model Definition Options	History Definiton Options
ELEMENT	CONNECTIVITY	CONTINUE
END	CONTROL	TRANSIENT
HEAT	COORDINATE	
MESH PLOT	DIST FLUXES	
SIZING	END OPTION	
TITLE	FILMS	
	FIXED TEMP	
	INITIAL TEMP	
	ISOTROPIC	
	OPTIMIZE	
	POST	
	RESTART	
	TEMPERATURE EFFECTS	

User subroutine found in u5x8.f:

FILM
FLUX

Example e5x8b.dat:

Parameters	Model Definition Options	History Definition Options
ELEMENT	END OPTION	CONTINUE
END	RESTART	
HEAT		
MESH PLOT		
SIZING		
TITLE		

Example e5x8c.dat:

Parameters	Model Definition Options	History Defintion Options
ELEMENT	CONTROL	CONTINUE
END	COORDINATE	TRANSIENT
HEAT	DIST FLUXES	
SIZING	END OPTION	
TITLE	FILMS	
	FIXED TEMP	
	INITIAL TEMP	
	ISOTROPIC	
	OPTIMIZE	
	POST	
	RESTART	
	TEMPERATURE EFFECTS	

Example e5x8d.dat:

Parameters	Model Definition Options	History Definition Options
ELEMENT	CONNECTIVITY	CONTINUE
END	CONTROL	TRANSIENT
HEAT	COORDINATE	
SIZING	DIST FLUXES	
TITLE	END OPTION	
	FILMS	
	FIXED TEMP	
	INITIAL TEMP	
	ISOTROPIC	
	OPTIMIZE	
	POST	
	RESTART	
	TEMPERATURE EFFECTS	

Example e5x8e.dat:

Parameters	Model Definition Options	History Definition Options
ELEMENT	CONNECTIVITY	CONTINUE
END	CONTROL	AUTO STEP
HEAT	COORDINATE	
SIZING	DIST FLUXES	
TITLE	END OPTION	
	FILMS	
	FIXED TEMP	
	INITIAL TEMP	
	ISOTROPIC	
	OPTIMIZE	
	POST	
	RESTART	
	TEMPERATURE EFFECTS	

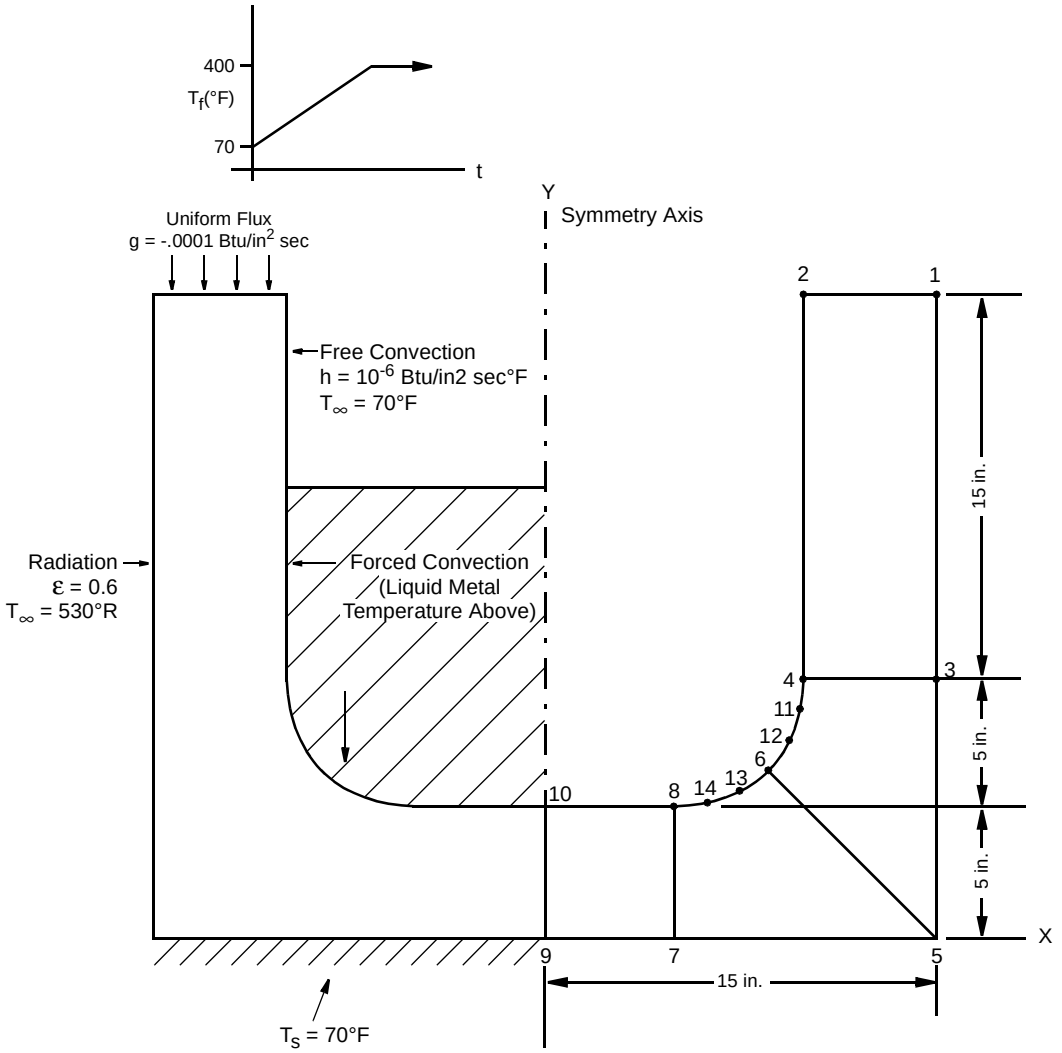

Figure 5.8-1 Geometry for Nonlinear Heat Conduction

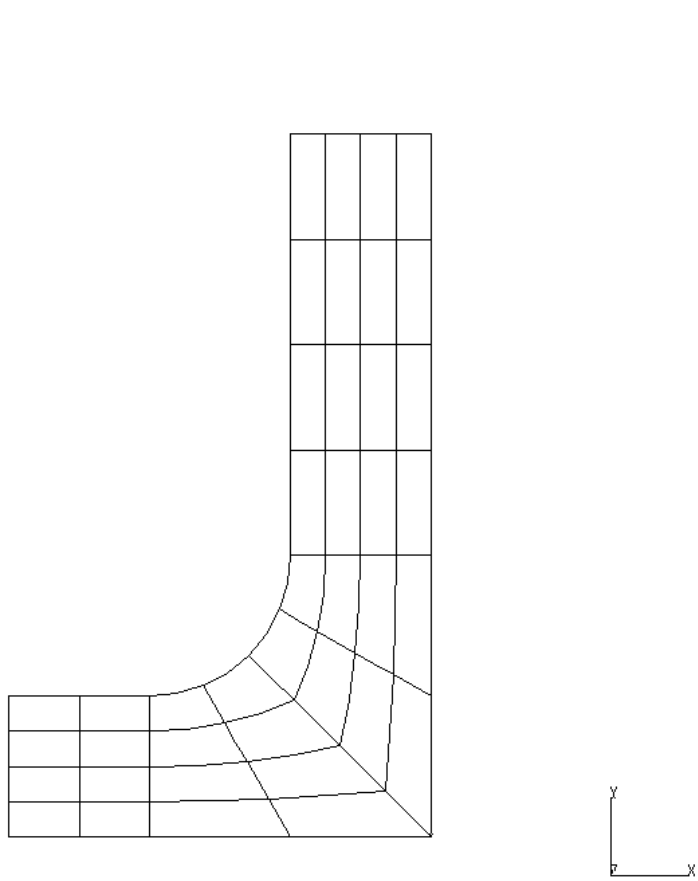

Figure 5.8-2 Heat Transfer Example Mesh

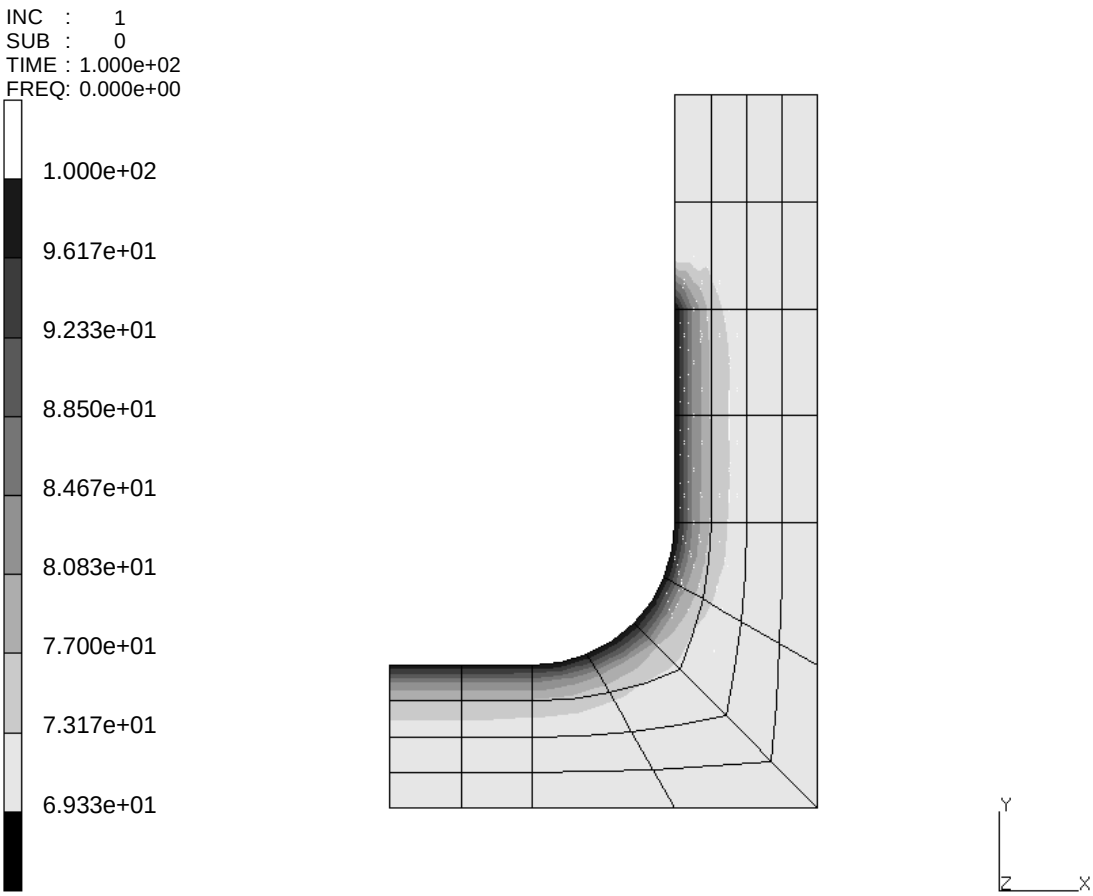

Figure 5.8-3 Isotherms at 100 Seconds

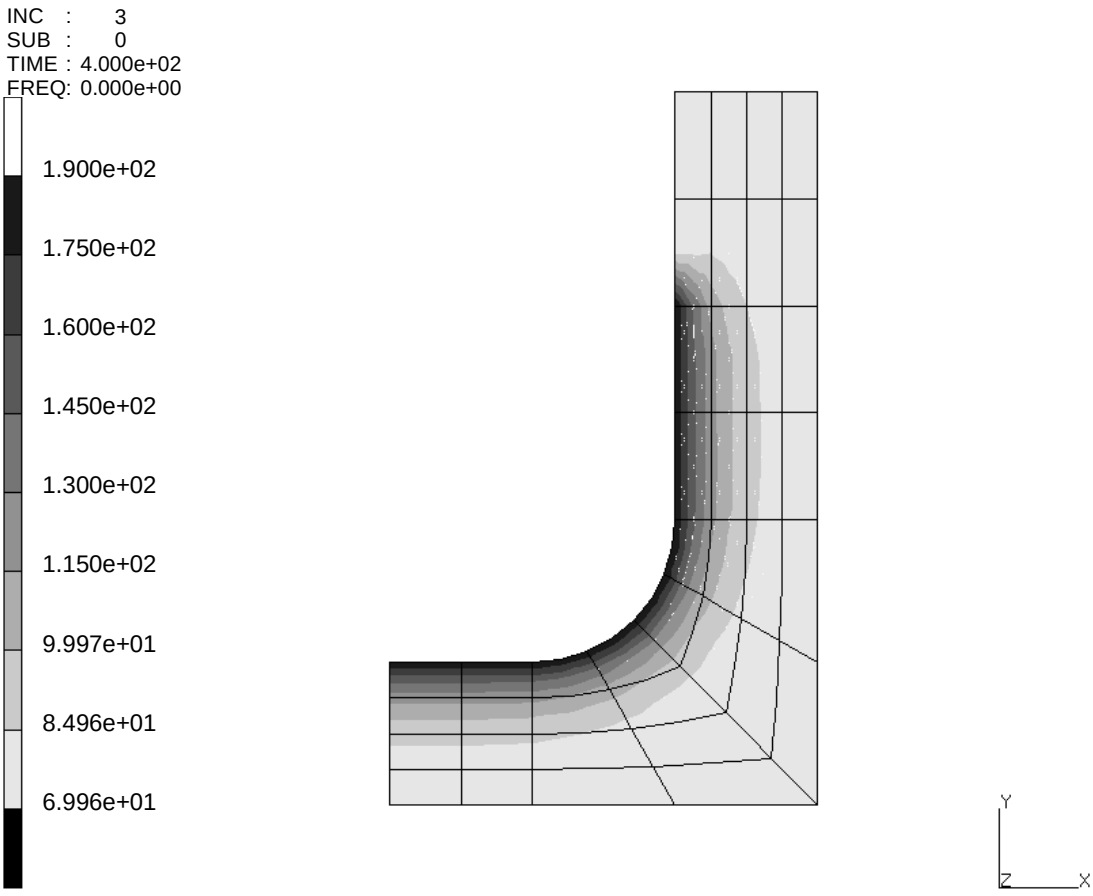

Figure 5.8-4 Isotherms at 400 Seconds

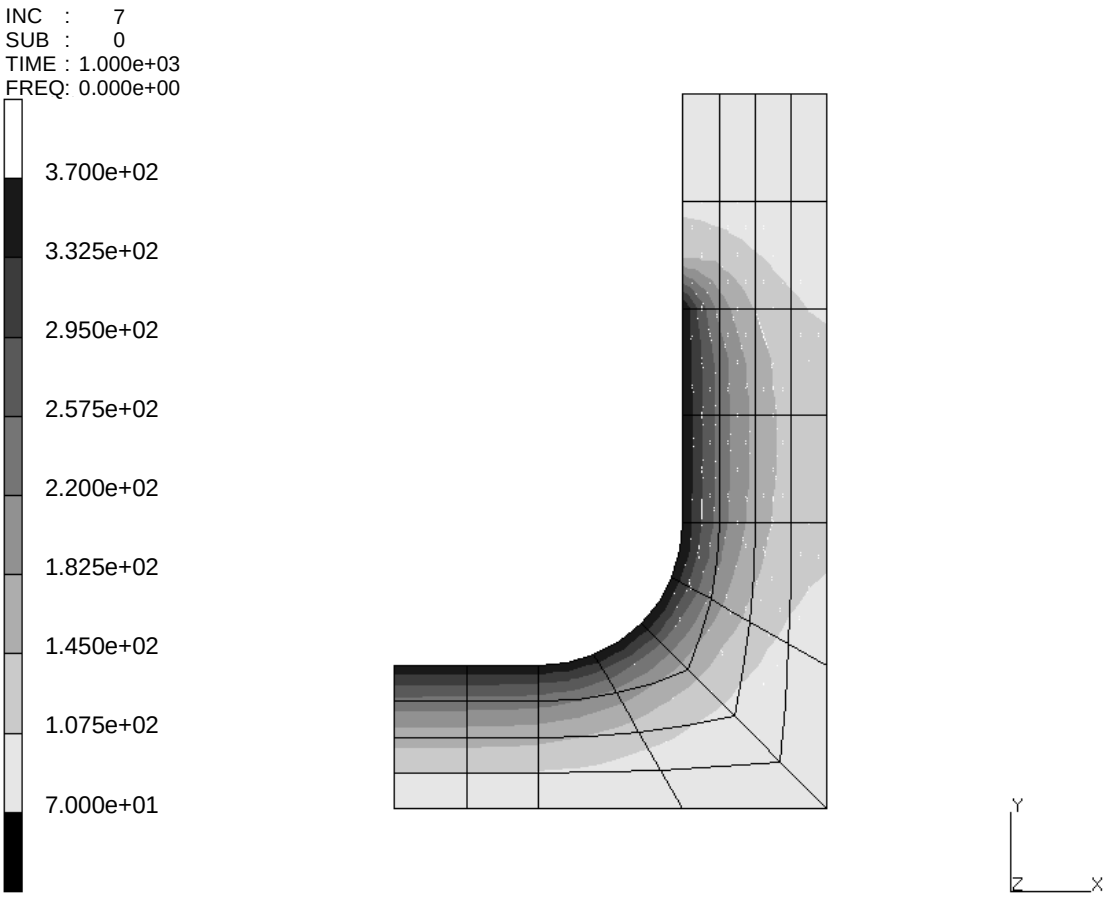

Figure 5.8-5 Isotherms at 1000 Seconds

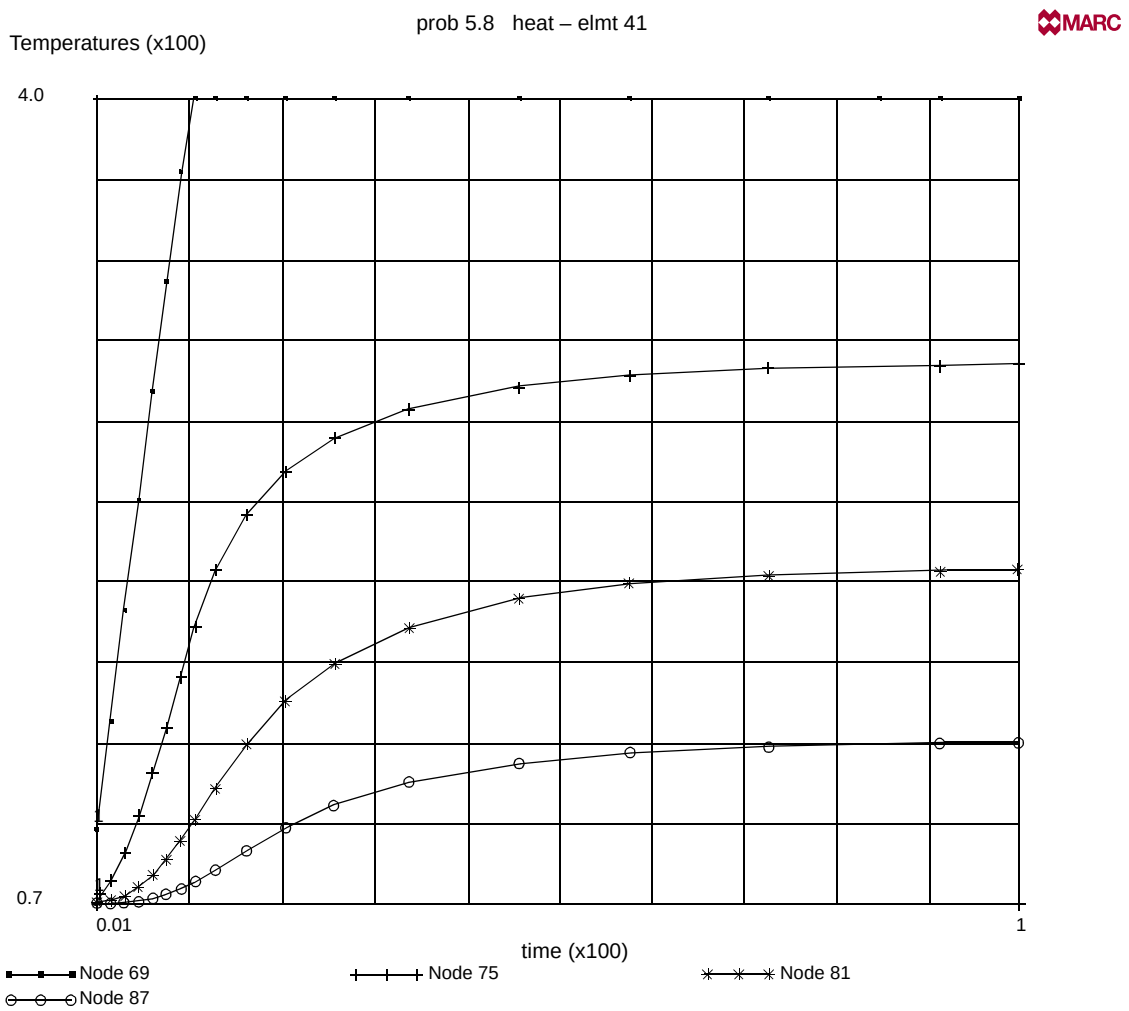

Figure 5.8-6 Temperature History

5.9 Latent Heat Effect

In heat conduction analysis, the material may exhibit phase change at certain temperature levels. This change of phase can be characterized by a sharp change in temperature dependent specific heat of the material or a latent heat associated with a given temperature range. A solid cylinder subjected to convective boundary condition and the effect of latent heat on the thermal response is studied.

This problem is modeled using the four techniques summarized below.

Data Set	Element Type(s)	Number of Elements	Number of Nodes	Differentiating Features
e5x9a	40	10	22	Include latent heat
e5x9b	40	10	22	ELEM SORT, NODE SORT
e5x9d	122	10	22	Include latent heat
e5x9e	132	20	63	Triangular 6-noded element 132 used

Model

The cylinder is of radius 0.594 inches and length 0.1 inches. For data sets e5x9a and e5x9b, the 4-noded axisymmetric quadrilateral element number 40 is used. For data set e5x9d, the 4-noded reduced integration element number 122 is used. For data set e5x9e, the 6-noded axisymmetric triangular element number 132 is used. The initial model is shown in Figure 5.9-1.

Thermal Properties

Material properties are as follows: isotropic thermal conductivity is 0.5712E-04 Btu/sec-in°F; specific heat is 0.11199 Btu/lb-°F; mass density is 0.281 lb/cu.in.; latent heat is 76.51 Btu/lb with a solidus temperature of 423°F and a liquidus temperature of 757°F.

The properties as a function of temperature are shown in Figure 5.9-2. A second temperature dependent specific heat curve with a latent heat is also shown in the same figure. The TEMPERATURE EFFECTS option is used to input these functions.

Thermal Boundary Conditions

The initial temperature distribution is that all nodes have a temperature of 1550.0°F. At time t = 0, the outer surface begins to convect to the surroundings with a sink temperature of 100°F and a film coefficient of 0.009412 Btu/sec.-sq.-in.-°F. Nonautomatic time-stepping is invoked where the total transient time is 100 seconds using eight different time steps. The time steps are:

Time Step (seconds)	Number of Steps	Transient Time (seconds)
0.001	10	0.01
0.005	8	0.04
0.01	15	0.15
0.05	16	0.80
0.1	20	2.00
0.5	44	22.00
1.0	15	15.00
5.0	12	60.00
Total =	140	100.00

Results

The thermal response is summarized by plotting the temperature history of the center and outer surface of the cylinder shown in Figure 5.9-3. Notice how the temperature at the center of the cylinder drops as the material solidifies.

Parameters, Options, and Subroutines Summary

Example e5x9a.dat:

Parameters	Model Definition Options	History Definition Options
ELEMENT	CONNECTIVITY	CONTINUE
END	CONTROL	CONTINUE
HEAT	COORDINATE	
SIZING	END OPTION	
TITLE	FILMS	
	INITIAL TEMP	
	ISOTROPIC	
	POST	
	TEMPERATURE EFFECTS	
	UDUMP	

Example e5x9b.dat:

Parameters	Model Definition Options	History Definition Options
END	CONNECTIVITY	CONTINUE
SIZING	CONTROL	TRANSIENT
TITLE	COORDINATE	
	END OPTION	
	FILMS	
	INITIAL TEMP	
	ISOTROPIC	
	POST	
	PRINT CHOICE	
	TEMPERATURE EFFECTS	

MARC-PLOT is used in example e5.9c.

Example e5x9d.dat:

Parameters	Model Definition Options	History Definition Options
ELEMENT	CONNECTIVITY	CONTINUE
END	CONTROL	TRANSIENT
HEAT	COORDINATE	
SIZING	END OPTION	
TITLE	FILMS	
	INITIAL TEMP	
	ISOTROPIC	
	POST	
	TEMPERATURE EFFECTS	

Example e5x9e.dat:

Parameters	Model Definition Options	History Definition Options
ELEMENT	CONNECTIVITY	CONTINUE
END	CONTROL	TRANSIENT
HEAT	COORDINATE	
SIZING	DEFINE	
TITLE	END OPTION	
	FILMS	
	INITIAL TEMP	
	ISOTROPIC	
	POST	
	TEMPERATURE EFFECTS	

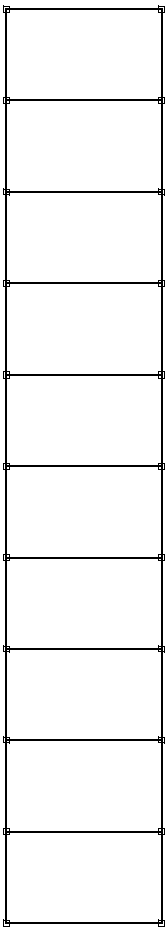

Mesh used for
element types 40 and 122

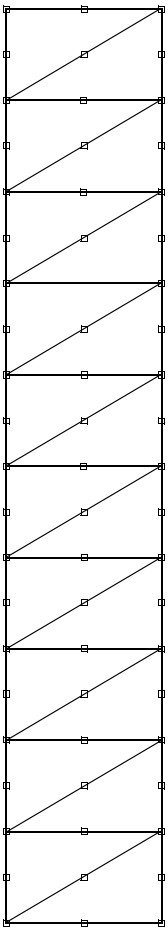

Mesh used for
element type 132

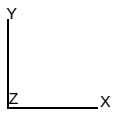

Figure 5.9-1 Cylinder Meshes

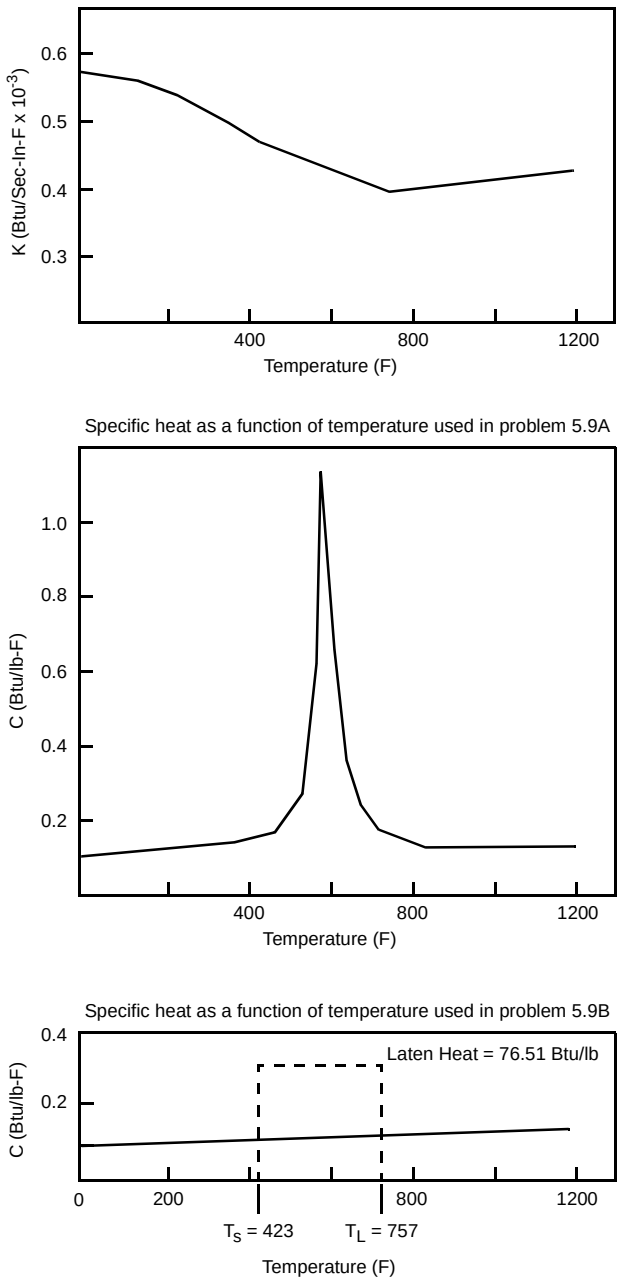

Figure 5.9-2 Temperature Dependent Thermal Properties

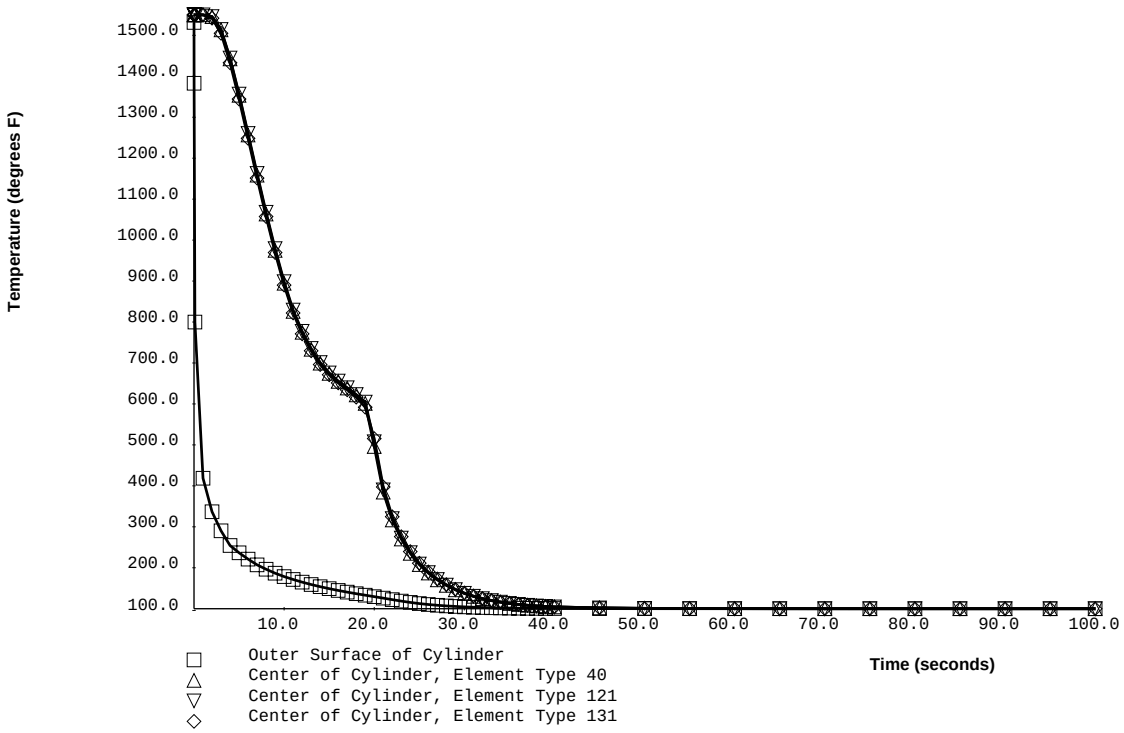

Figure 5.9-3 Temperature History for Center and Outer Surface of Cylinder

5.10 Centerline Temperature of a Bare Steel Wire

The problem is to determine the centerline temperature of a bare steel wire of constant diameter, carrying a constant current. This wire is 0.75 inches (0.0625 feet) in diameter with conductivity of 13 Btu/hr-ft-°F. A current of 0.325946×10^{6} amps is continuously run through the wire. The surface film coefficient is 5.0 Btu/hr-sq.ft-°F for the outer wire surface.The ambient air temperature is 70°F. The electric resistance of the wire is 30.68×10^{-8} ohm/feet. A centerline temperature of 420°F and a surface temperature of 418°F were predicted by Rohsenow and Choi [1]. This same problem is analyzed by using the Joule heating capability developed in MARC.

Model

A finite element model of five 4-node axisymmetric elements (MARC element type 40) and 12 nodal points was selected for this problem. Dimensions of the model and the mesh are depicted in Figure 5.10-1.

Material Properties

The electrical resistivity is given as 30.68×10^{-8} ohm-feet. The thermal conductivity is 13 Btu/hr-ft-°F.

Current

A distributed current of 0.325946×10^{6} amps/square foot is applied to the entire surface of the wire at z = 0.

Joule

A conversion factor of 3.4129 is chosen for the electricity-to-heat unit conversion (from Watts/ft to Btu/hr-ft). The model definition option JOULE is used for the input of this data.

Films

In the thermal analysis, a convective boundary condition is assumed to exist at the outer surface of the wire (element No. 1). The film coefficient and the ambient temperature are 5.0 Btu/hr-sq.ft-°F and 70°F, respectively.

Transient

In order to obtain a steady-state solution of the problem, a large time step (10,000 hrs) is used for a time period of 10,000 hours.

Results

Both the nodal voltages and the nodal temperatures are tabulated as shown in Table 5.10-1. The agreement between finite element and calculated results is excellent.

Table 5.10-1 Nodal Voltages and Temperatures

Node Number	Voltages	Temperatures
1	0.1	417.63
2	0.1	418.39
3	0.1	418.98
4	0.1	419.40
5	0.1	419.66
6	0.1	419.77
7	0.0	417.63
8	0.0	418.39
9	0.0	418.98
10	0.0	419.40
11	0.0	419.66
12	0.0	419.77

Reference

Rohsenow, W. M. and Choi, H. Y., *Heat, Mass and Momentum Transfer*, Prentice-Hall, Inc., 1961, p. 106.

Parameters, Options, and Subroutines Summary

Example e5x10.dat:

Parameters	Model Definition Options	History Definition Options
END	CONNECTIVITY	CONTINUE
HEAT	COORDINATE	TRANSIENT
JOULE	DIST CURRENT	
SIZING	END OPTION	
TITLE	FILMS	
	ISOTROPIC	
	JOULE	
	VOLTAGE	

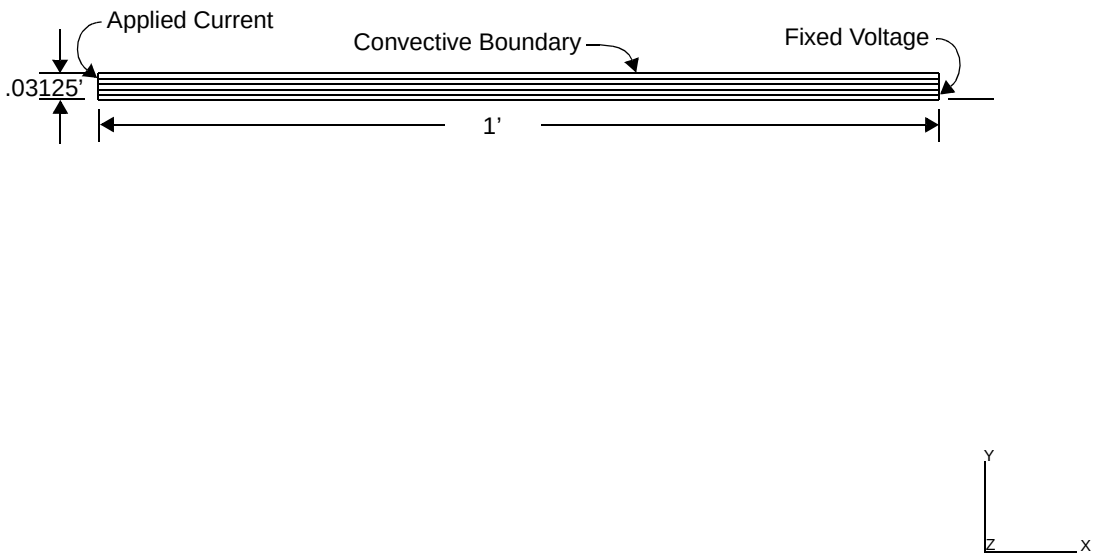

Figure 5.10-1 Mesh of Steel Wire

5.11 Heat Transfer and Stress Analysis of a Jominy End Quench Test Specimen

This example considers the transient heat transfer and thermal stress analyses of the Jominy End Quench Test. A right circular cylindrical bar of 1-inch diameter and 3-inch length, initially at a uniform temperature of 1550°F, is quenched to steady-state temperature. The quenching process consists of water impinging on one of the circular faces of the cylinder. The quench water temperature is 71°F. The bar is made from AISI 4140 steel. Its thermal (that is, heat transfer) properties are a function of temperature only. The thermal conductivity data is listed in Table 5.11-1 and plotted in Figure 5.11-1. The specific heat data is listed in Table 5.11-2 and plotted in Figure 5.11-2.

Cooling occurs by forced convection along the quench end and by free convection along the cylindrical surface. It is assumed that the cylindrical face opposite the quench end is fully insulated. The “forced” heat transfer coefficient for cooling of the material in water is 9.412×10^{-3} Btu/sec-°F-sq.in. The “free” heat transfer coefficient for cooling in air is 5.5941×10^{-6} Btu/sec-°F-sq.in.

Element

Element type 42 is used for the heat-transfer analysis of the specimen. This is an axisymmetric 8-node biquadratic element, with one degree of freedom (temperature). Element type 28 is used for the stress analysis portion of this example. This element is an 8-node distorted quadrilateral, with two degrees of freedom at each node.

Model

The nonuniform transient temperature field was computed in a preliminary heat transfer analysis.The finite element model is illustrated in Figure 5.11-3 and Figure 5.11-4. Due to symmetry, only one-half of the bar is modeled. This same model is used in the subsequent transient thermal stress analysis.

Geometry

No values need be given in this option.

Material Properties

The mechanical properties of AISI 4140 are a function of both time and temperature. The data pertaining to Young’s modulus, Poisson’s ratio, yield stress, and the workhardening rate are given in Figure 5.11-5, Figure 5.11-6, and Figure 5.11-7. The data is presented in the form of property values as a function of both temperature and the previously described fixed cooling rates. Data is provided for two rates. The durations of these two “Newton Cooling” processes (see Figure 5.11-3) are 6 and 20 seconds. The mass density of the material is 0.281 lb/cu.in.

Table 5.11-1 Thermal Conductivity vs. Temperature (AISI 4140 Steel)

Temperature (°C)	Conductivity (cal/cm-sec)	Temperature (°C)	Conductivity (cal/cm-sec)
0	.102	500	.052
19	.102	550	.054
39	.101	600	.055
58	.099	650	.056
78	.098	700	.058
97	.095	750	.059
116	.093	800	.060
136	.092	850	.062
155	.088	900	.063
174	.084	950	.064
193	.080	1000	.065
213	.073	1050	.067
233	.068	1100	.068
252	.063	1150	.069
271	.057	1200	.071
291	.051	1250	.072
310	.047	1300	.074
350	.048	1350	.075
400	.050	1400	.076

Table 5.11-2 Specific Heat vs. Temperature (AISI 4140)

Temperature (°C)	Specific Heat (cal/cm-sec)
50	.112
110	.117
120	.118
130	.121
140	.126
150	.132
160	.141
170	.153
180	.167
190	.184
200	.205
210	.238
220	.289
230	.615
240	1.482
250	.824
260	.530
270	.357
280	.290
290	.247
300	.214
310	.189
320	.168
330	.150
340	.136
350	.121
450	.122
550	.126
650	.131

The thermal conductivity vs. temperature curve (Figure 5.11-7) was approximated by three straight-line segments. The corresponding slope-breakpoint data was entered in the TEMPERATURE EFFECTS block. The data for the specific heat (Figure 5.11-2) was re-expressed in slope-breakpoint form and also entered in this block.

The thermal coefficient of expansion is also a function of time and temperature. In this instance, this property is derived from thermal strain data which is described in terms of fourth order polynomial expansions about different temperature levels. This is done for the above two mentioned cooling rates. The coefficients for each of the polynomials are listed in Table 5.11-3 along with the corresponding temperature levels.

Table 5.11-3 Coefficient of Thermal Expansion (AISI 4140)

A_1	A_2	A_3	A_4	A_5	T	Cooling Rate (seconds)
0.3439E-02	0.1063E-04	0.2847E-07	0.4245E-10	-0.2345E-13	32	6
0.1603E-01	0.3600E-04	0.2147E-07	0.0	0.0	753	
0.5852E-02	0.2047E-05	0.5401E-09	0.0	0.0	1148	
0.2204E-01	0.5857E-04	-0.5401E-09	0.4211E-09	-0.2792E-12	32	20
0.7145E-01	0.7366E-04	-0.5966E-07	-0.3517E-10	0.3747E-13	545	
0.2193-01	-0.7130E-06	0.5190E-08	-0.1872E-11	0.2479E-15	896	

Results

Thermal Analysis

A variable time step is used in the analysis and that 61 increments are required. MARC automatically recomputes the time step at each increment such that the maximum incremental change in temperature never exceeds 100°F. Also, the temperature-dependent heat transfer properties were recomputed whenever a maximum change of 100°F occurred anywhere within the model.

The quenching process was found to take approximately 1600 seconds. The temperatures at selective points along the axis are plotted as a function of time in Figure 5.11-8. Stress contours and deformed structure plots will be presented for the same four stages of the thermal stress analysis. The temperature history for each integration point in the model was stored on a post file for subsequent use in the stress run.

Stress Analysis

The time-temperature dependent material property data is described in the TIME-TEMP model definition option. The thermal loading is read from the heat transfer post file via the CHANGE STATE option. MARC controls are such that the maximum allowable temperature change in any increment did not exceed 100°F. In view of the controls which were set for the heat transfer analysis, this causes two or more heat increments to be merged into a single stress increment at occasional stages in the analysis. Eighty increments are required for this analysis. The resultant temperature, as a function of increment, is given in Figure 5.11-9.

It is interesting to note that in the early stages of cooling (that is, within approximately the first 50 seconds), the Jominy bar actually increases in volume. As the nominal steady-state room temperature is approached, the bar then shrinks to less than its initial dimensions. The initial increase in volume can be attributed to phase changes which occur at the higher temperatures. These are accounted for via the piecewise polynominal description of the thermal coefficient of expansion. (See Table 5.11-3.)

The effective, or von Mises, equivalent stress, the axial, radial and hoop components of stress are plotted against the increment number in Figure 5.11-10 to Figure 5.11-13. The most severely stressed region occurs at the intersection between the quench end face and the center cylindrical surface. It is interesting to note from the equivalent stress plots that the stress intensity in this region grows from a level of 32,930 psi at stage 1 to a final level of 130,400 psi. Nevertheless, throughout the cooling process the maximum intensity never exceeded the corresponding instantaneous yield stress level; that is, no plastic deformation was found to occur.

Despite this fact,as observed from the stress contour plots there is still a significant nonuniform and appreciable distribution of stress in the bar. However, it should be noted that the analysis was terminated before a uniform steady-state temperature was reached. At the final increment of the analysis, a temperature gradient still exists which ranges from 73°F at the quench end to approximately 90°F at the opposite end. It is believed that a portion of the essentially residual stress state is not due simply to thermal gradients, but rather to nonuniform volumetric changes which occurred in the early stages of cooling. The temperature at elements 1, 10, 13, and 16 are plotted against increment and temperature, respectively, in Figure 5.11-12 and Figure 5.11-13.

Coefficients for a polynomial fit of thermal strain, e(T), where:

$$e(T) = A_1 + A_2T + A_3T^2 + A_4T^3 + A_5T^4$$

Parameters, Options, and Subroutines Summary

Example e5x11a.dat:

Parameters	Model Definition Options	History Definition Options
END	CONNECTIVITY	CONTINUE
HEAT	CONTROL	TRANSIENT
MATERIAL	COORDINATE	
SIZING	END OPTION	
THERMAL	FILMS	
TITLE	INITIAL TEMP	
	ISOTROPIC	
	POST	
	PRINT CHOICE	
	TEMPERATURE EFFECTS	

Example e5x11b.dat:

Parameters
ELEMENT
END
TITLE

Example e5x11c.dat:

Parameters	Model Definition Options	History Definition Options
END	CHANGE STATE	AUTO THERM
SIZING	CONNECTIVITY	CHANGE STATE
T-T-T	CONTROL	CONTINUE
THERMAL	COORDINATE	
TITLE	END OPTION	
	FIXED DISP	
	POST	
	PRINT CHOICE	
	RESTART	
	TIME-TEMP	

Example e5x11d.dat:

Parameters

ELEMENT
END
TITLE

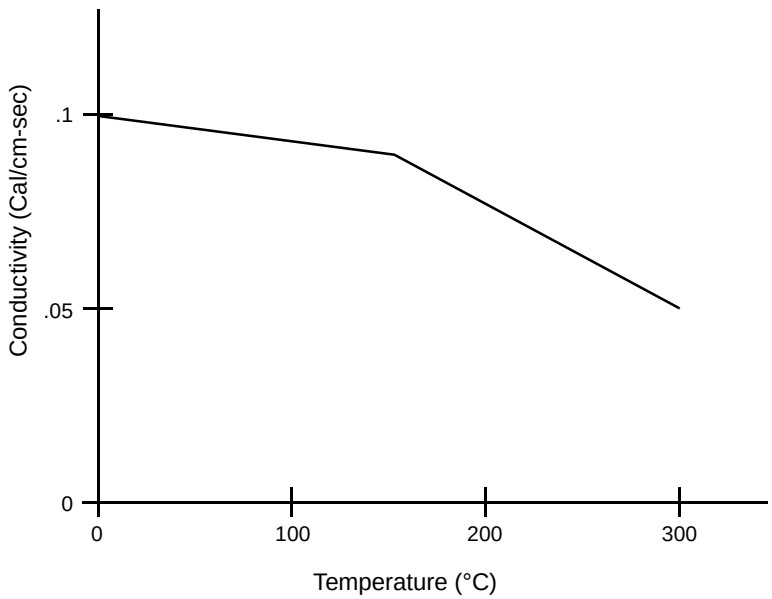

Figure 5.11-1 Thermal Conductivity vs. Temperature

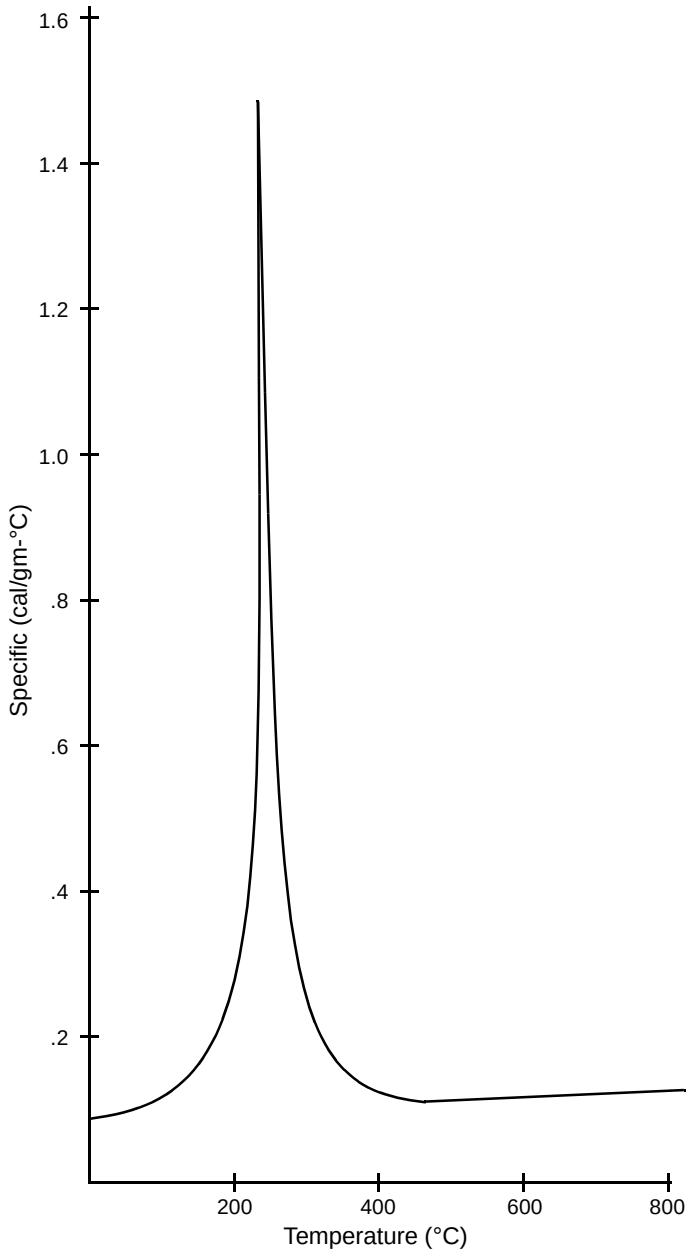

Figure 5.11-2 Specific Heat vs. Temperature

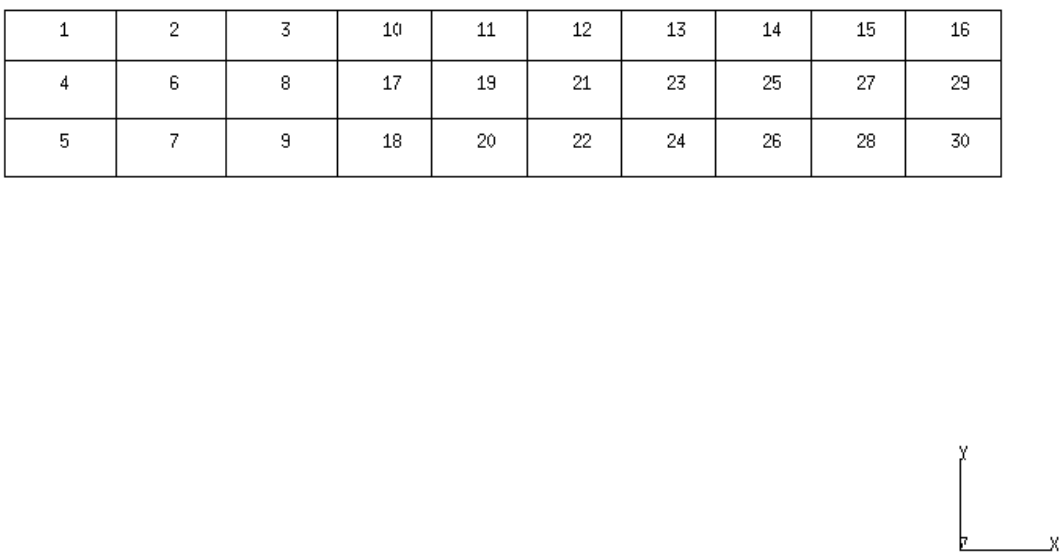

Figure 5.11-3 Jominy Bar – Axisymmetric Finite Element Model (Elements)

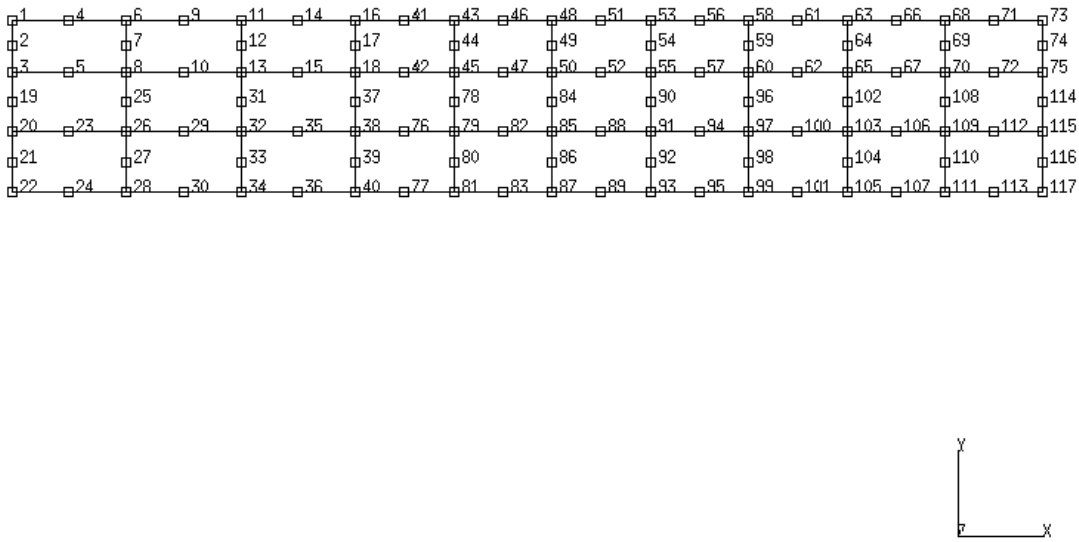

Figure 5.11-4 Jominy Bar – Axisymmetric Finite Element Model (Nodes)

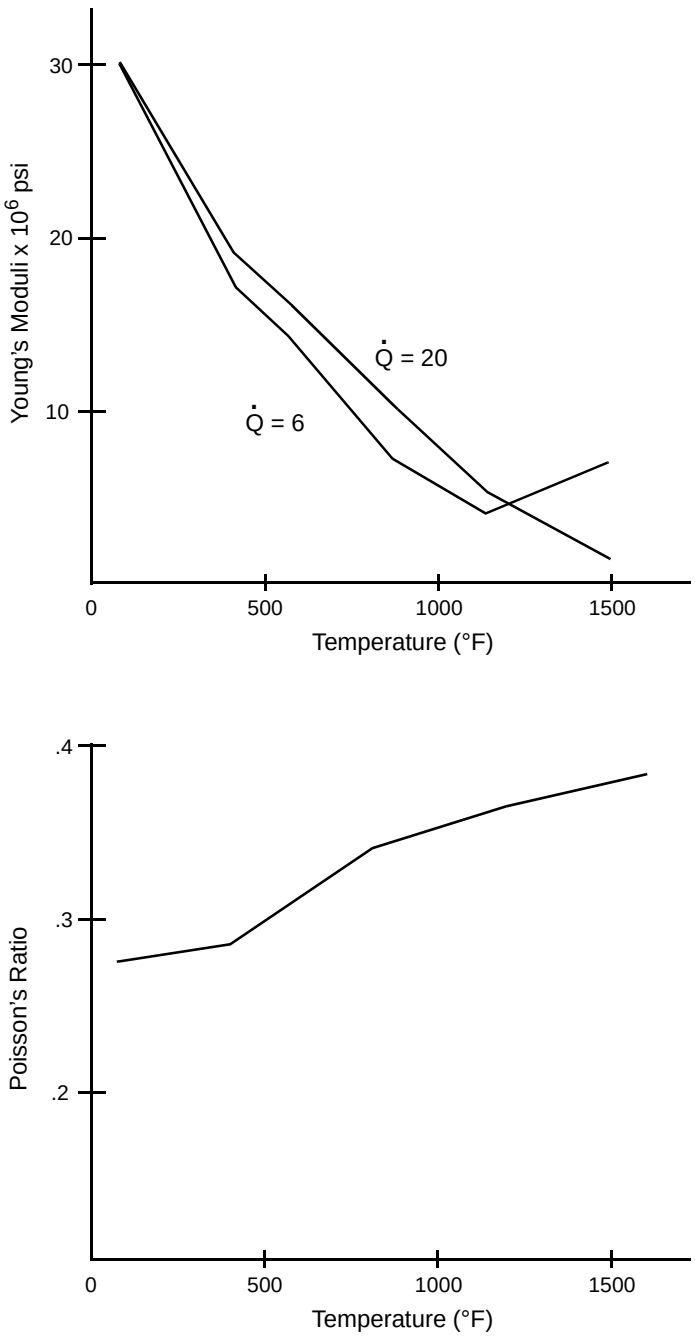

Figure 5.11-5 Material Properties vs. Temperature

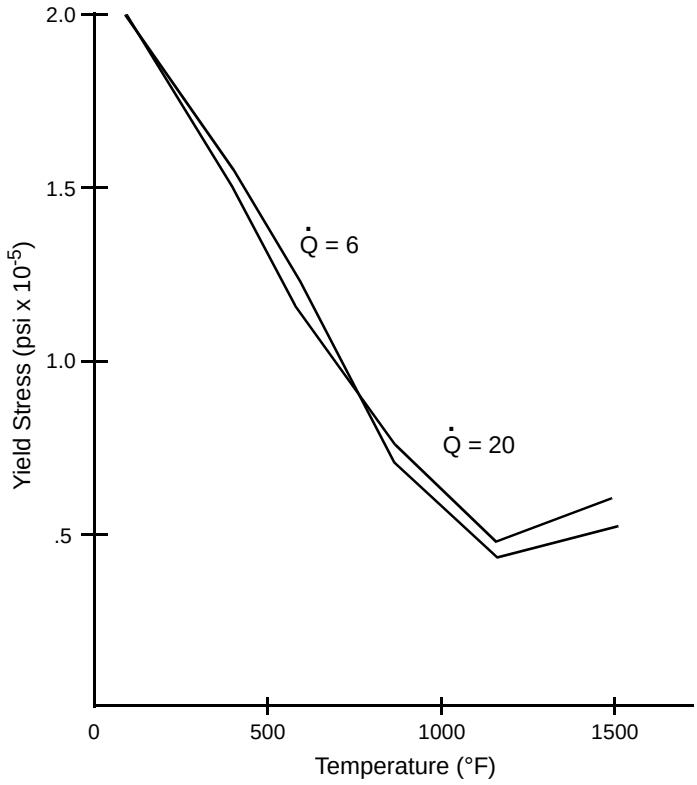

Figure 5.11-6 Yield Stress vs. Temperature

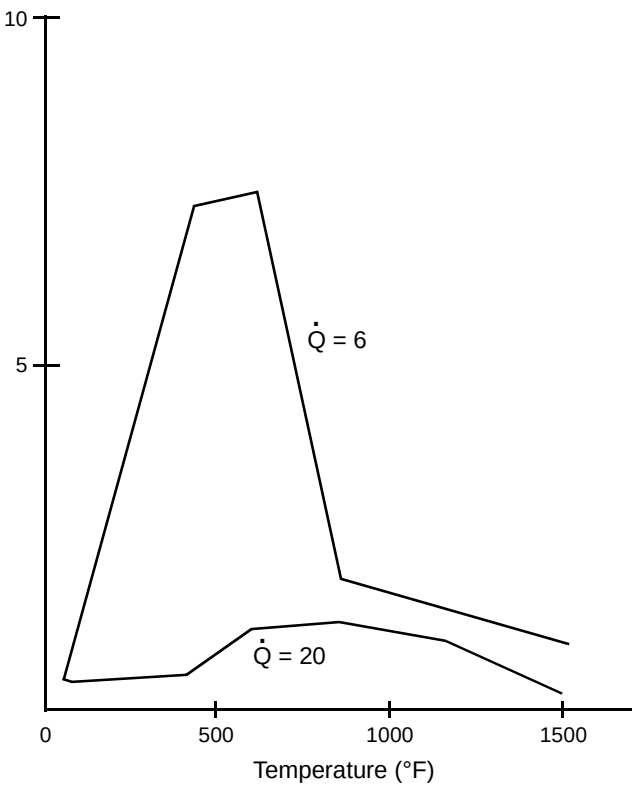

Figure 5.11-7 Workhardening vs. Temperature

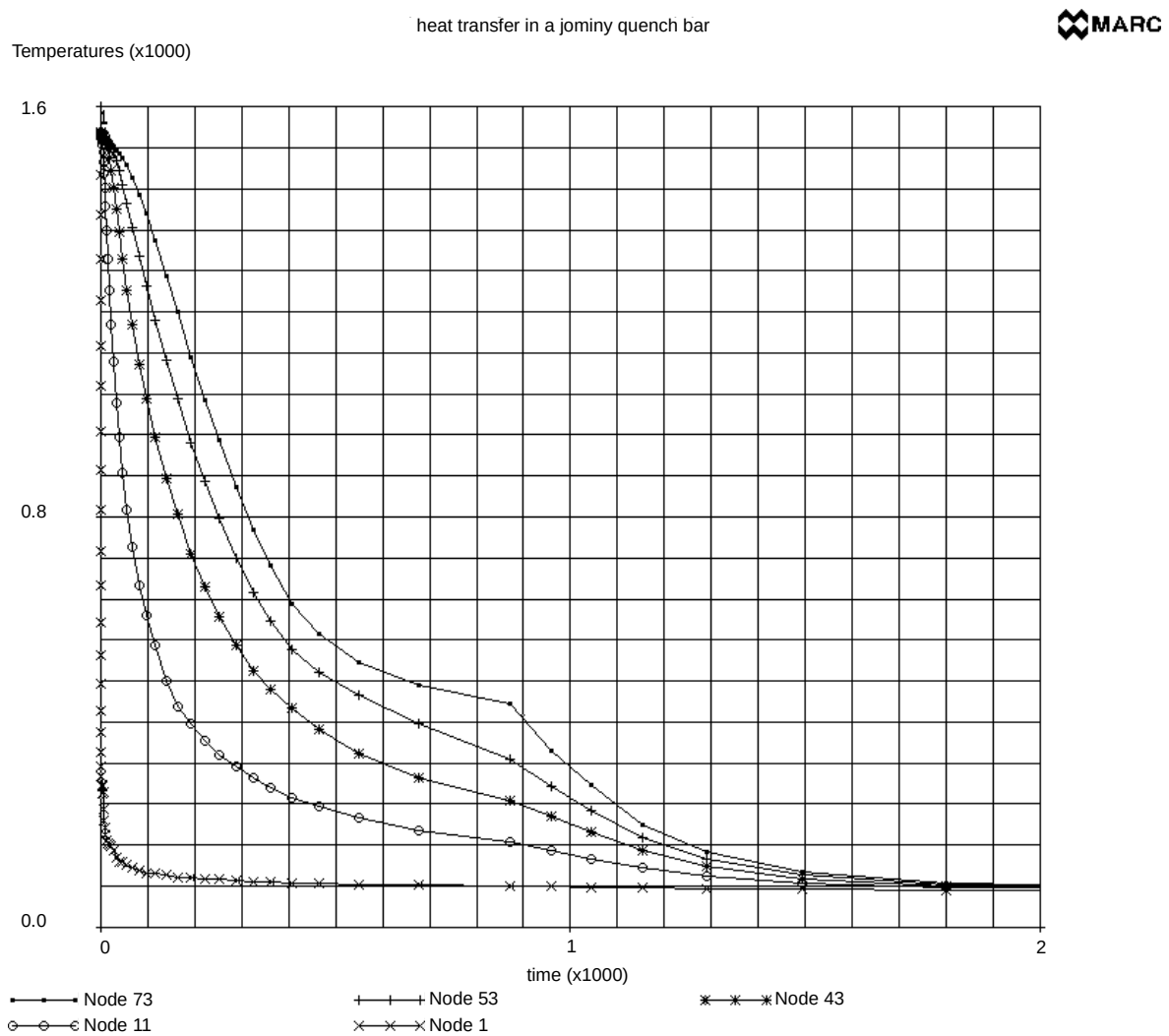

Figure 5.11-8 Jominy End Quench Test – Temperature vs. Time

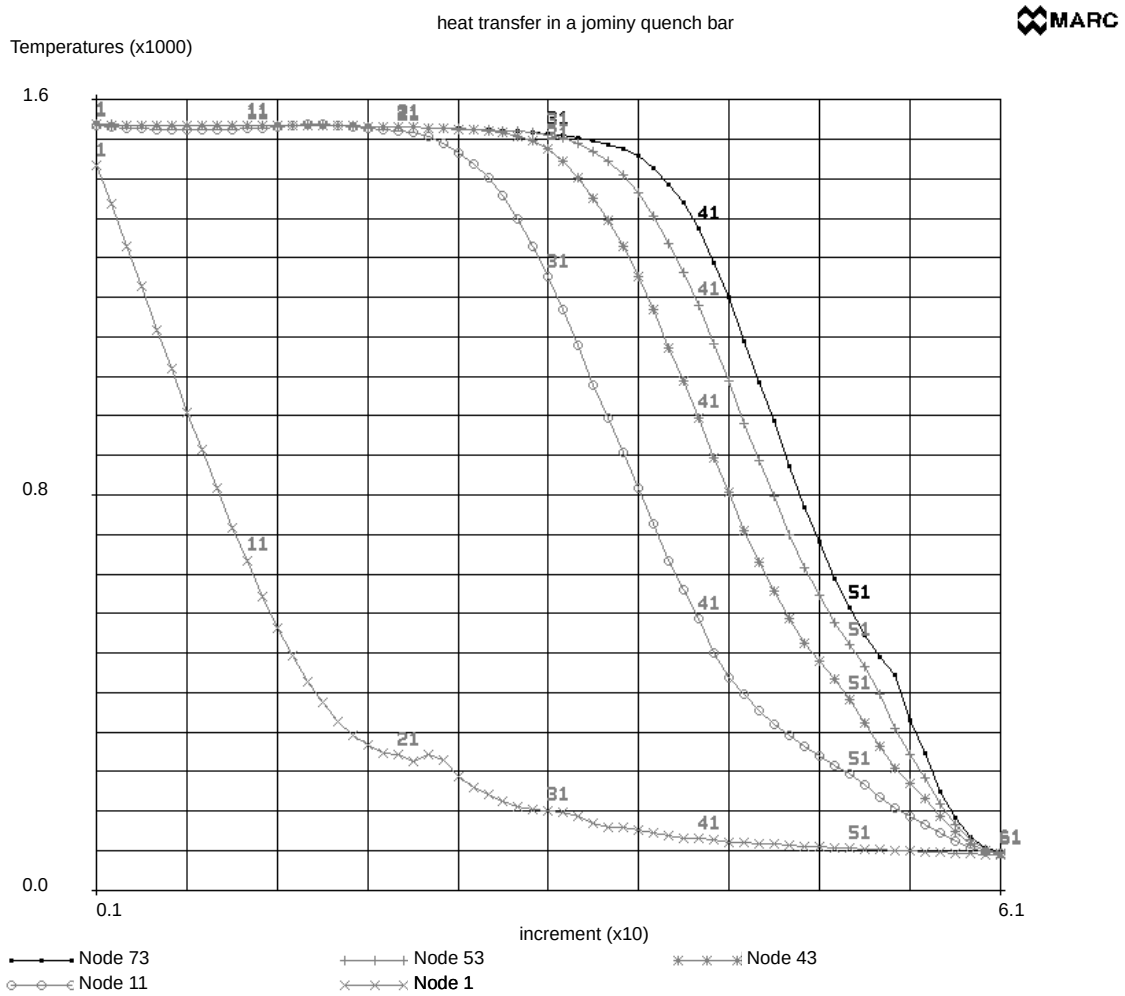

Figure 5.11-9 Jominy End Quench Test – Temperature vs. Increment

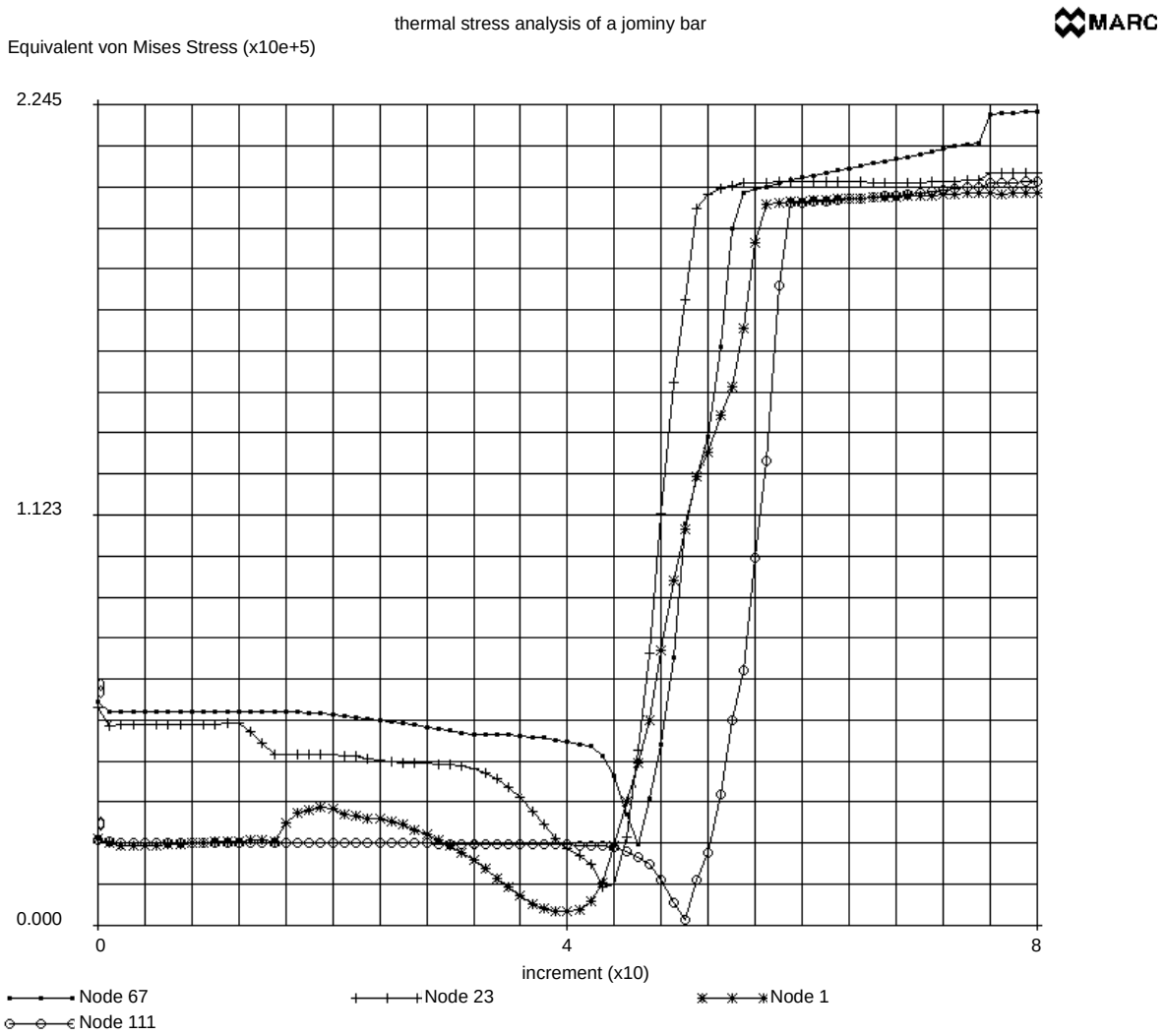

Figure 5.11-10 Jominy End Quench Test – Equivalent Stress vs. Increment

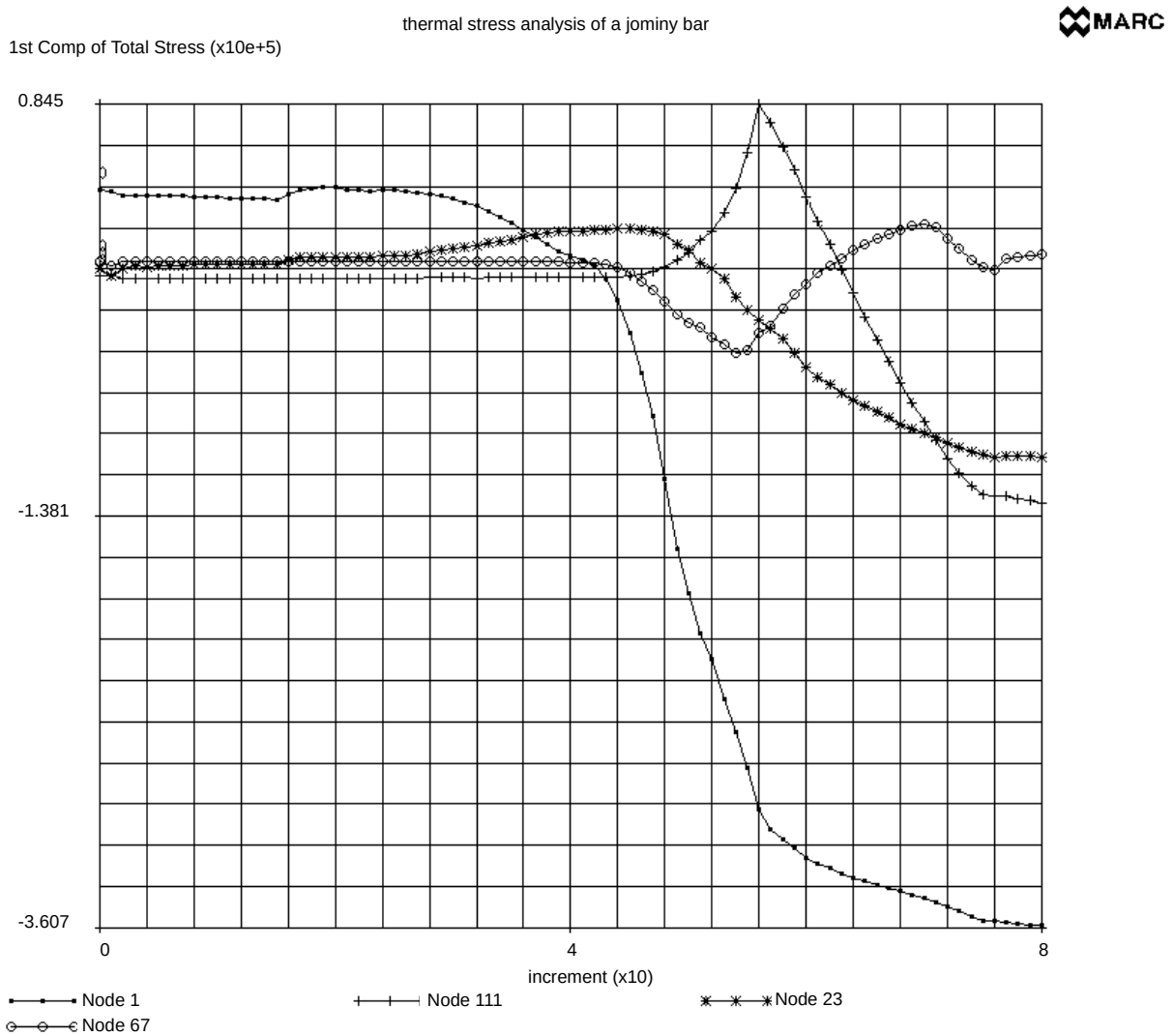

Figure 5.11-11 Jominy End Quench Test – Axial Stress vs. Increment

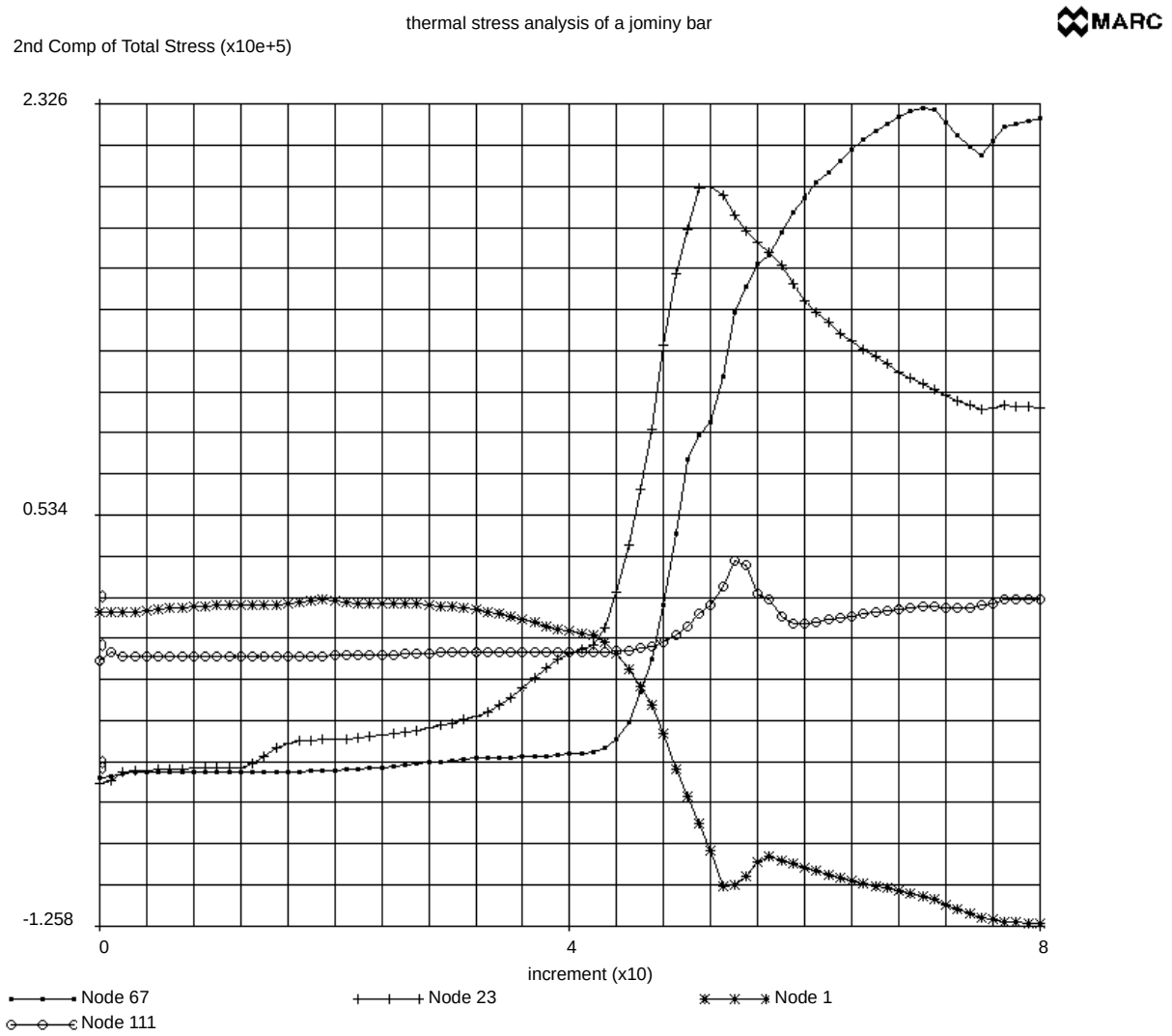

Figure 5.11-12 Jominy End Quench Test – Radial Stress vs. Increment

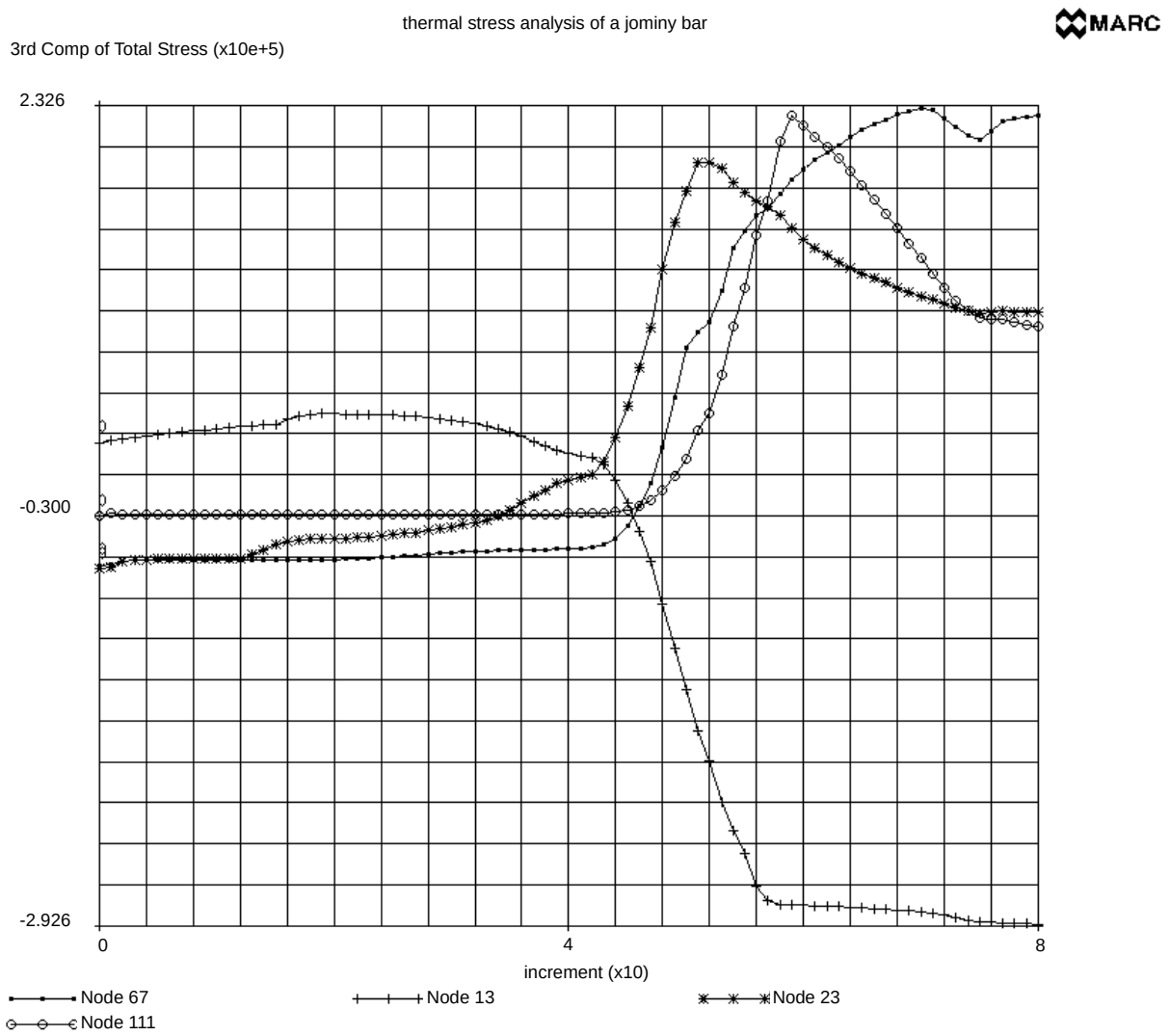

Figure 5.11-13 Jominy End Quench Text – Hoop Stress vs. Increment

5.12 Cylinder-plane Electrode

A cylinder-plane electrode has been analyzed using a coupled thermo-electric model. MARC element type 39 (4-node isoparametric quadrilateral element) has been used. Two electrodes are applied to the two faces shown in Figure 5.12-1, producing a uniform difference of electric potential between the upper and the lower face.

Model

This problem demonstrates the use of the JOULE option for Joule heating problems. (See *MARC Volume A: Theory and User Information* for a general discussion of the problem).

Material Properties

The specific heat and density of the material are 0.26 cal/gm-°C and 3.4 gm/cm^3, respectively. The surface film coefficient is 0.677-3 cal/sec-cm^2-°C. The temperature dependent thermal conductivity and resistivity are shown in Figure 5.12-2.

Initial Conditions

The initial nodal temperatures are 20°C throughout.

Boundary Conditions

The upper face has 1 V; V = 0 at the lower face. Convective boundary conditions are assumed to exist at the lower face.

Transient

Nonautomatic time stepping is used setting the initial step at 100 seconds. The transient solution lasts for 100 seconds.

Results

Voltage, current and temperature distributions are shown in Figure 5.12-4 through Figure 5.12-6.

Parameters, Options, and Subroutines Summary

Example e5x12.dat:

Parameters	Model Definition Options	History Definition Options
ALIAS	CONNECTIVITY	CONTINUE
END	COORDINATE	TRANSIENT
HEAT	END OPTION	
JOULE	FIXED TEMP	
SIZING	ISOTROPIC	
TITLE	JOULE	
	POST	
	VOLTAGE	

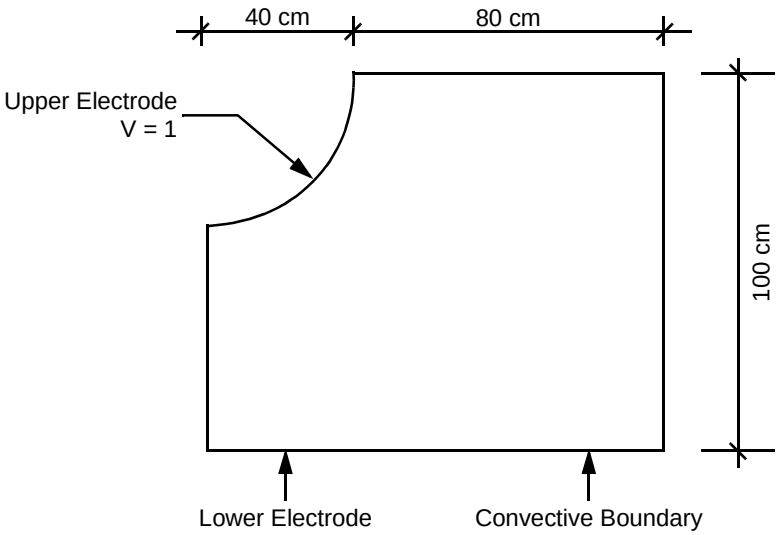

Figure 5.12-1 Geometry of the Problem

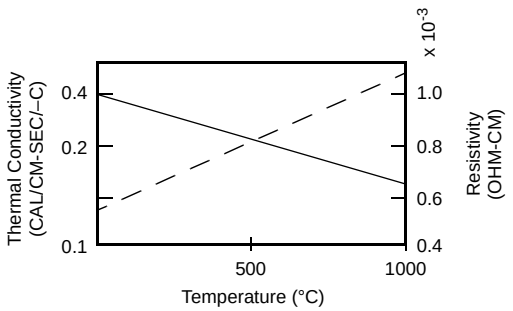

Figure 5.12-2 Temperature Dependent Properties

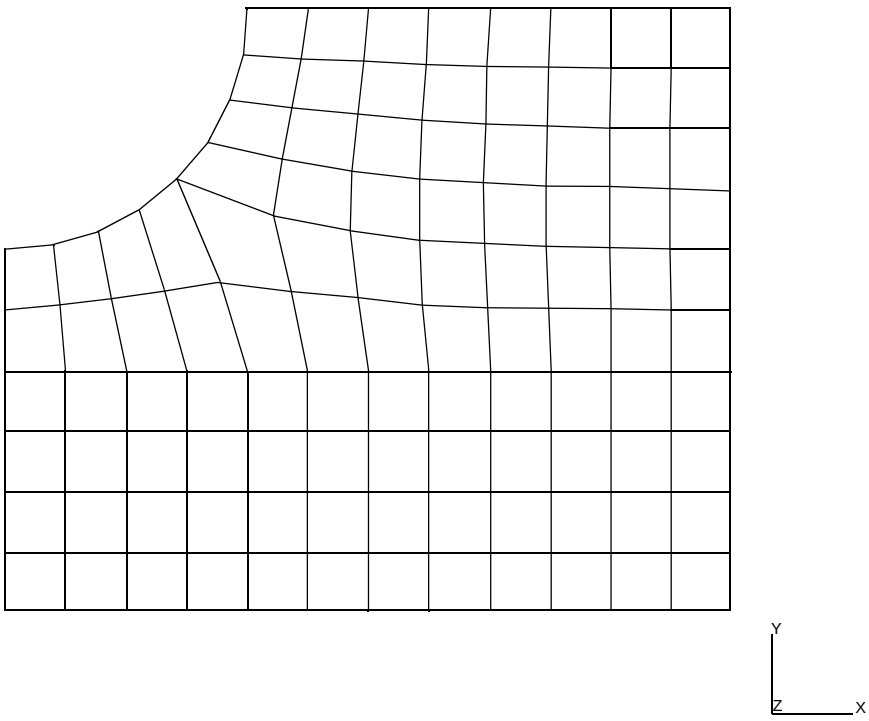

Figure 5.12-3 Mesh

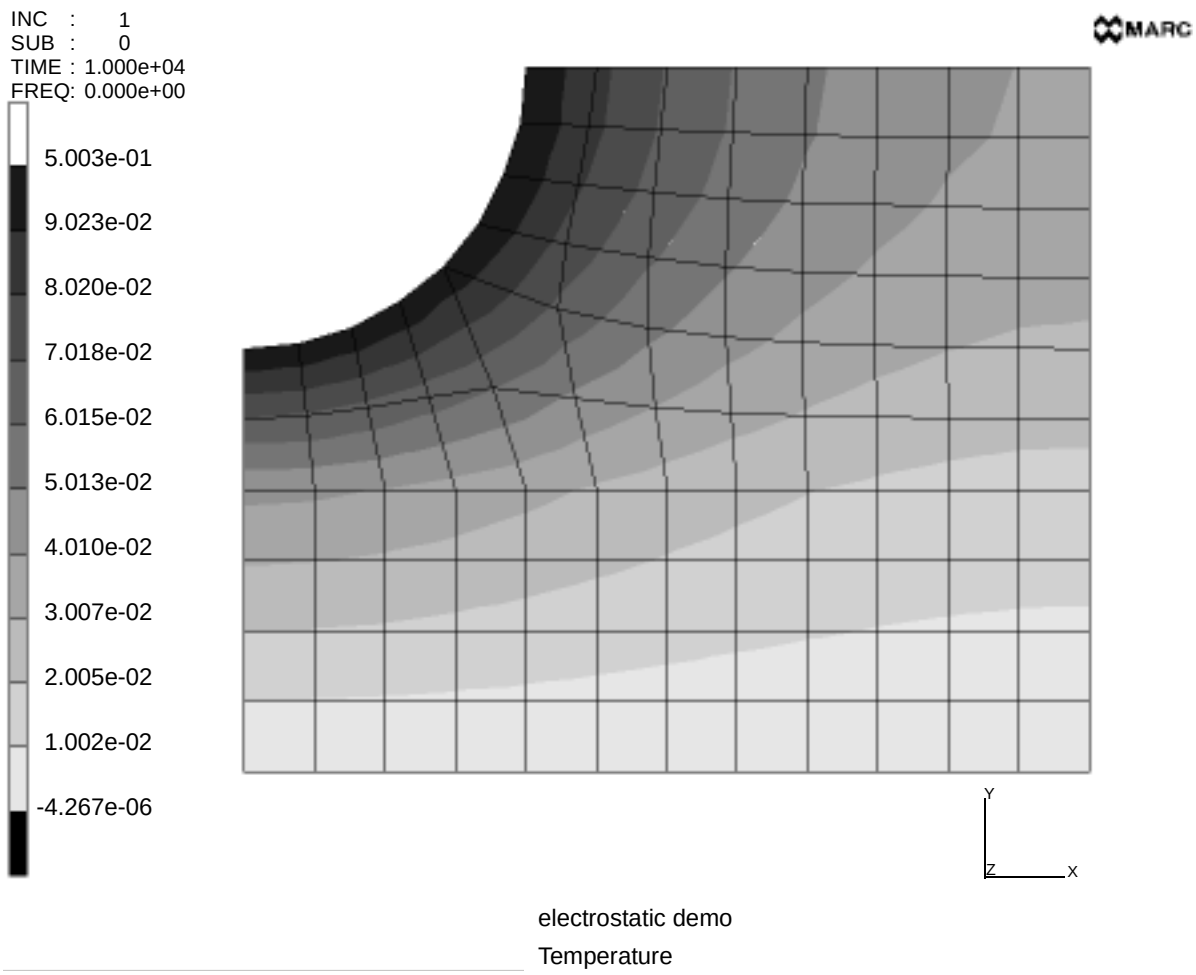

Figure 5.12-4 Temperature Distribution

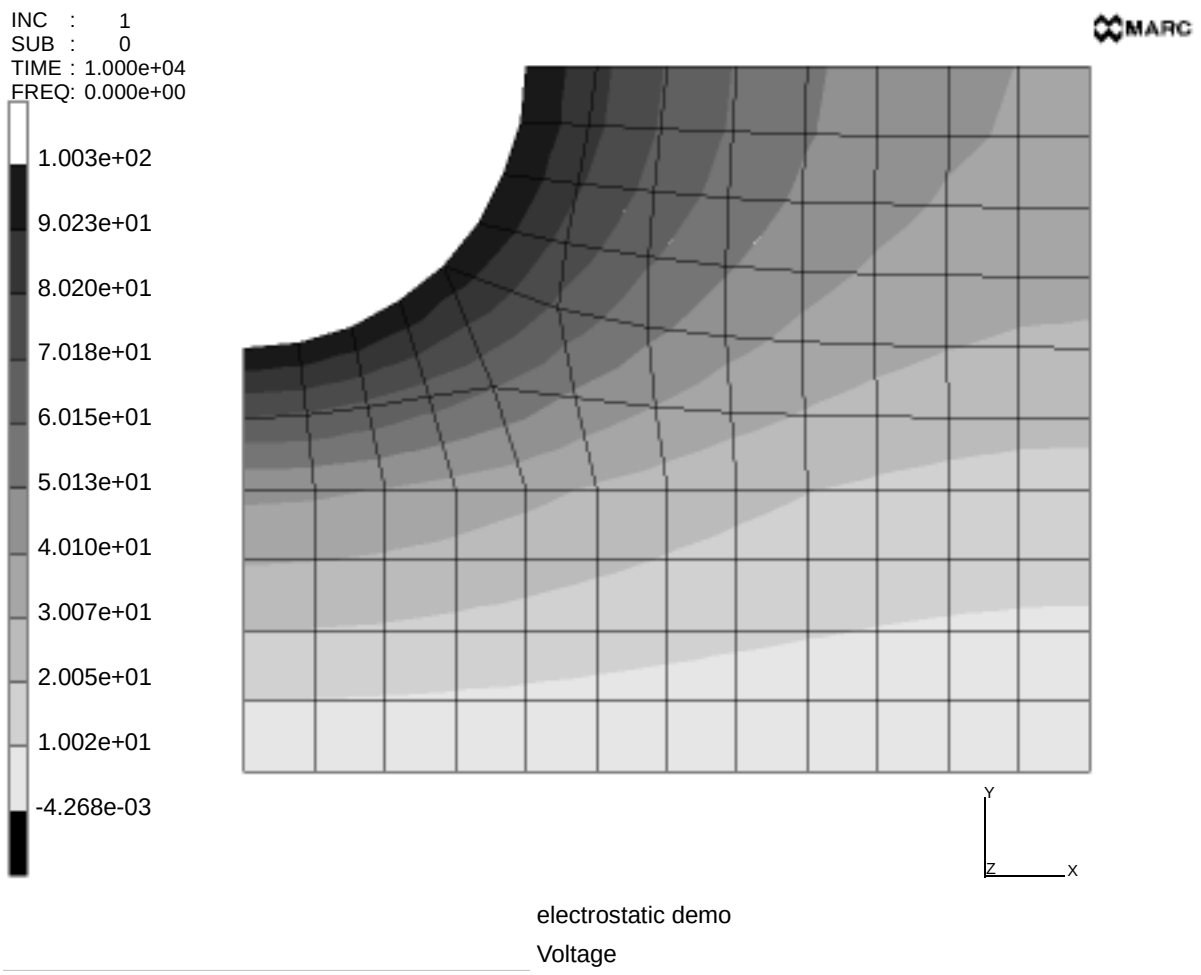

Figure 5.12-5 Voltage Distribution

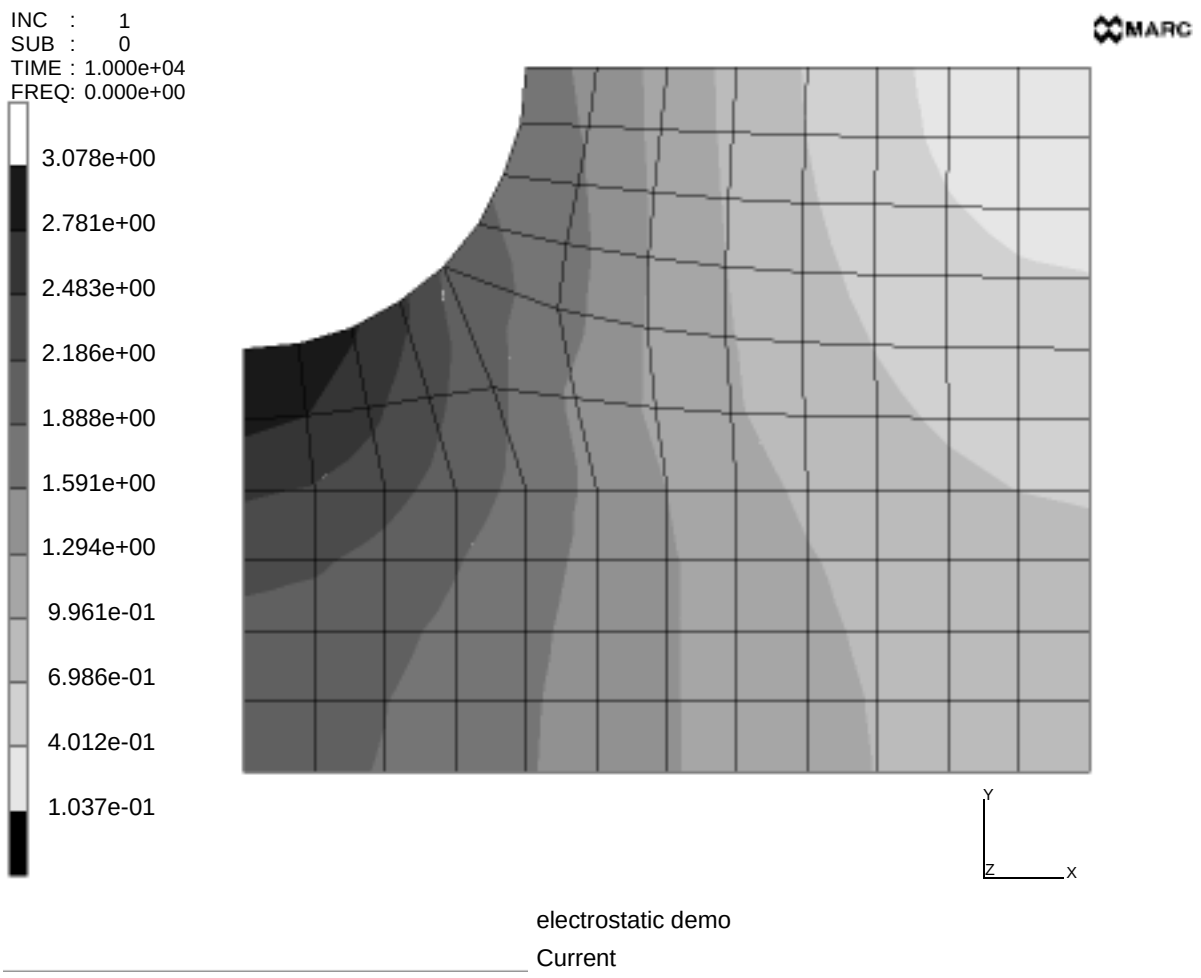

Figure 5.12-6 Current Distribution

5.13 Axisymmetric Transient Heat Conduction Simulated by Heat Transfer Shell Elements

The transient heat conduction of a cylinder, subjected to a thermal downshock, is analyzed by using MARC heat transfer shell elements. This is the same as problem 5.5. The model and input data of the problem are:

This problem is modeled using the four techniques summarized below.

Data Set	Element Type(s)	Number of Elements	Number of Nodes
e5x13a	85	6	12
e5x13b	86	6	29
e5x13c	87	2	5
e5x13d	88	2	3

Model/Elements

The MARC heat transfer shell elements consist of elements 85 (4-node), 86 (8-node), 87 (3-node axisymmetric) and 88 (2-node axisymmetric). Element temperatures are either linearly (elements 85 and 88) or quadratically interpolated in the plane of the shell and assumed to have a linear/quadratic distribution in the thickness direction of the shell. The nodal degrees of freedom is two if a linear distribution of temperatures is assumed in the shell thickness direction, and three if a quadratic distribution of temperatures is assumed in the thickness direction of the shell. This is set by you on the HEAT parameter. These heat transfer shell elements are compatible with stress shell elements (see below) for thermal stress analysis.

Heat Transfer Shell Elements	Stress Shell Elements
85	72, 75
86	22
87	89
88	1

Models

As shown in Figure 5.13-1, the cylinder has an inner radius of 8.625 inches and a wall thickness of 0.375 inches. It is subjected to a constant initial condition and different convective boundary conditions on the inner and outer surfaces of the cylinder. Finite meshes for heat transfer shell elements 85, 86, 87, and 88 and shown in Figure 5.13-2 through Figure 5.13-5, respectively. The number of elements and number of nodes in each mesh are:

Mesh	Element	Number of Elements	Number of Nodes
A	85	6	12
B	86	6	29
C	87	2	5
D	88	2	3

SHELL SECT

The SHELL SECT option allows you to specify the number of points to be used for numerical integration in the thickness direction of the shell. The number of integration points in the thickness direction of the shell is chosen to be seven in this example.

Geometry

The shell thickness of 0.375 inches is entered as EGEOM1 in the GEOMETRY block and a positive (nonzero) number is entered as EGEOM2 for the selection of a quadratic distribution of temperatures in the thickness direction.

Material Properties

The conductivity is 4.85E-4 BTU/sec-in-°F. The specific heat is 0.116 BTU/lb-°F. The mass density is 0.283 lb/cubic inch.

Initial Condition

Initial nodal temperatures are assumed to be homogeneus at 1100°F.

Boundary Conditions

No input data is required for insulated boundary conditions at z = 0 and z = 2.0. Fluid temperatures and film coefficients for both inner and outer surfaces of the cylinder are:

Inner surface:

H_i = 38.56E-5 BTU/second-square inch-°F
T_i = 1100°F at t = 0. second
800°F at t = 10. seconds

Outer surface:

H_0 = 1.93E-6 BTU/second-square inch-°F (low value to simulate insulated boundary condition).

T_0 = 1100°F

The low value of H_0 simulates an insulated boundary.

The FILMS option is used to input the film coefficients and associated fluid temperatures for the inner and outer surfaces. Subroutine FILM linearly interpolates the 300°F decrease in ambient temperature over 10 seconds and then holds the inner wall temperature constant at 800°F. It is called at each time step for each integration point on each element surface given in the FILMS option.

Post

In a heat transfer run, the use of the POST option allows the creation of a post file containing element temperatures at each integration point and nodal point temperatures. The file can be used later as input to the stress analysis run. The code number for element temperatures of heat transfer elements is 9 followed by a layer number (that is, 9,1, and 9,2, etc.). These code numbers must be entered sequentially.

Transient

The TRANSIENT option controls time steps in a transient heat transfer analysis. MARC automatically calculates the time steps to be used based on the maximum nodal temperature change allowed as input in the CONTROL option. The solution begins with the suggested initial time step input and ends according to the time period specified. It does not exceed the maximum number of steps input in this option.

Results

A comparison of nodal temperatures with the results of an axisymmetric model (problem 5.5) is shown in Table 5.13-1.

Table 5.13-1 Comparison of Nodal Temperatures

Time (Sec.)	Nodal Temperature (°F) (Node 17)	Element Temperatures (°F) – 4th Layer			
		Element 85	Element 86	Element 87	Element 88
	5.5	(Model A)	(Model B)	(Model C)	(Model D)
1.25	1099.3	1099.3	1099.3	1099.3	1099.3
4.06	1092.6	1092.4	1092.4	1092.4	1092.4
7.18	1078.3	1077.9	1077.9	1077.9	1077.9
9,.84	1061.2	1060.3	1060.3	1060.3	1060.3
12.79	1041.1	1039.7	1039.7	1039.7	1039.7
16.90	1015.7	1013.8	1013.8	1013.8	1013.8
21.00	993.1	990.7	990.7	990.7	990.7
26.13	968.3	965.5	965.5	965.5	965.5
31.90	944.3	941.3	941.3	941.3	941.3
38.31	921.8	918.5	918.5	918.5	918.5

Parameters, Options, and Subroutines Summary

Example e5x13a.dat:

Parameters	Model Definition Options	History Definition Options
ELEMENT	CONNECTIVITY	CONTINUE
END	CONTROL	TRANSIENT
SHELL SECT	COORDINATE	
SIZING	END OPTION	
TITLE	FILMS	
	GEOMETRY	
	INITIAL TEMP	
	ISOTROPIC	
	POST	
	PRINT CHOICE	

User subroutine in u5x13.f:

FILM

Example e5x13b.dat:

Parameters	Model Definition Options	History Definition Options
ELEMENT	CONNECTIVITY	CONTINUE
END	CONTROL	TRANSIENT
SHELL SECT	COORDINATE	
SIZING	END OPTION	
TITLE	FILMS	
	GEOMETRY	
	INITIAL TEMP	
	ISOTROPIC	
	POST	
	PRINT CHOICE	

User subroutine found in u5x13.f:

FILM

Example e5x13c.dat:

Parameters	Model Definition Options	History Definition Options
ELEMENT	CONNECTIVITY	CONTINUE
END	CONTROL	TRANSIENT
SHELL SECT	COORDINATE	
SIZING	END OPTION	
TITLE	FILMS	
	GEOMETRY	
	INITIAL TEMP	
	ISOTROPIC	
	POST	
	PRINT CHOICE	

User subroutine found in u5x13.f:

FILM

Example e5x13d.dat:

Parameters	Model Definition Options	History Definition Options
ELEMENT	CONNECTIVITY	CONTINUE
END	CONTROL	TRANSIENT
SHELL SECT	COORDINATE	
SIZING	END OPTION	
TITLE	FILMS	
	GEOMETRY	
	INITIAL TEMP	
	ISOTROPIC	
	POST	
	PRINT CHOICE	

User subroutine in u5x13.f:

FILM

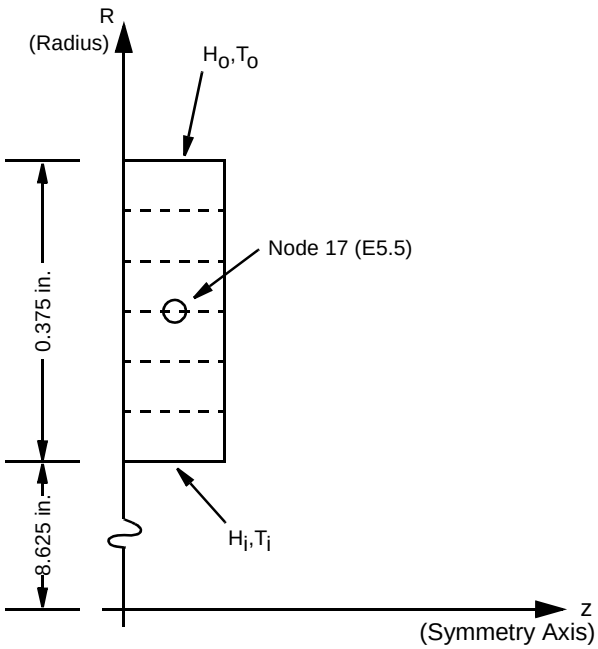

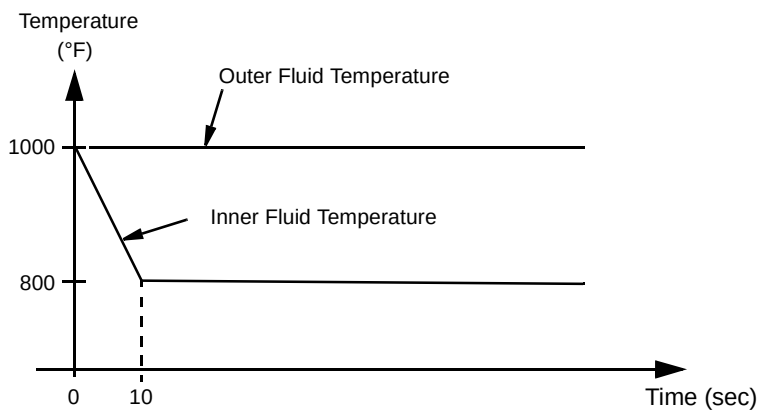

Figure 5.13-1 Cylinder Model and Fluid Temperature History

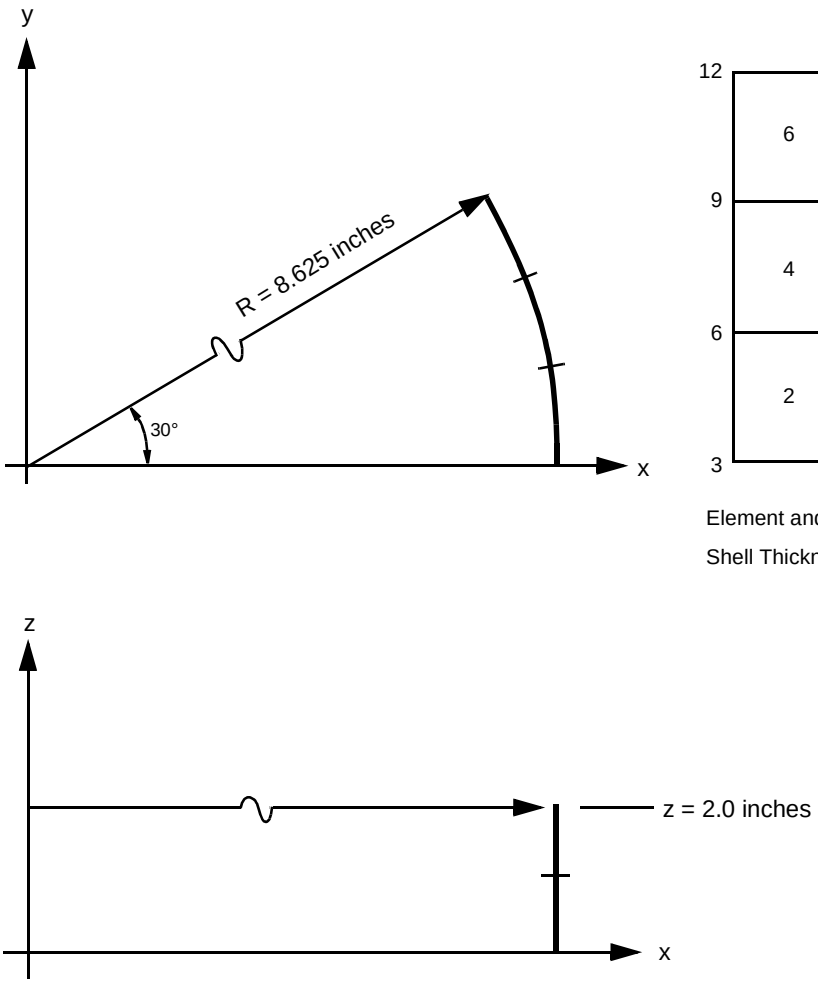

Figure 5.13-2 Finite Element Model (Model A - Element 85)

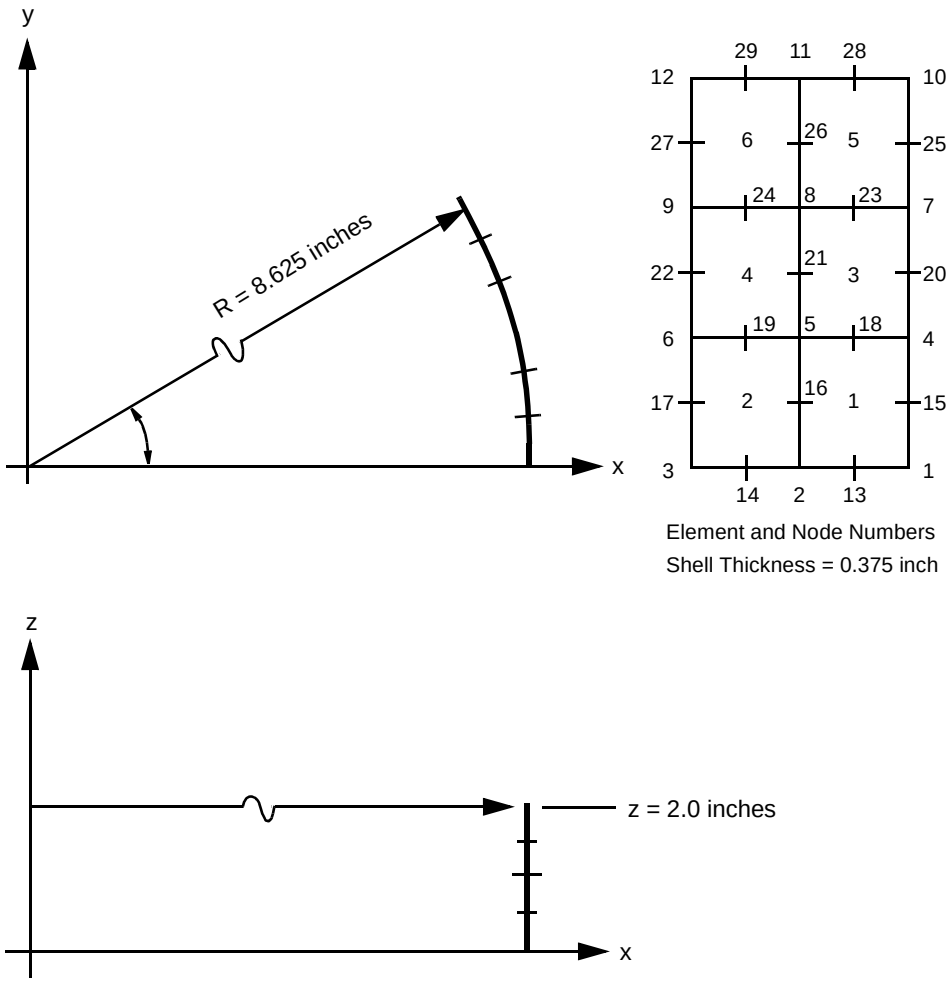

Figure 5.13-3 Finite Element Model (Model B - Element 86)

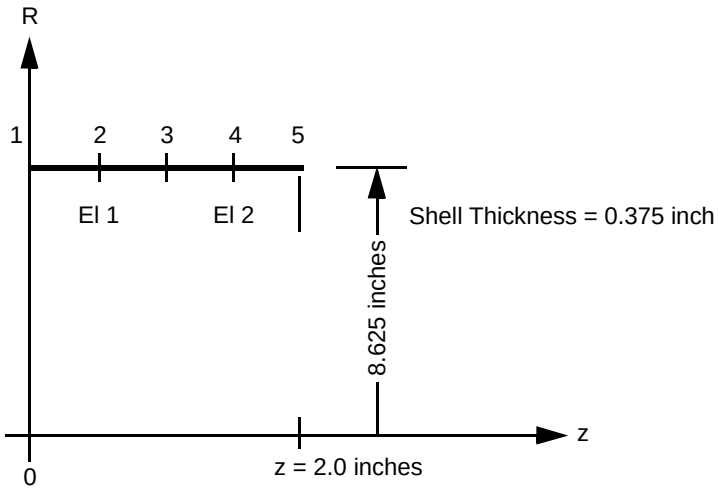

Figure 5.13-4 Finite Element Model (Model C - Element 87)

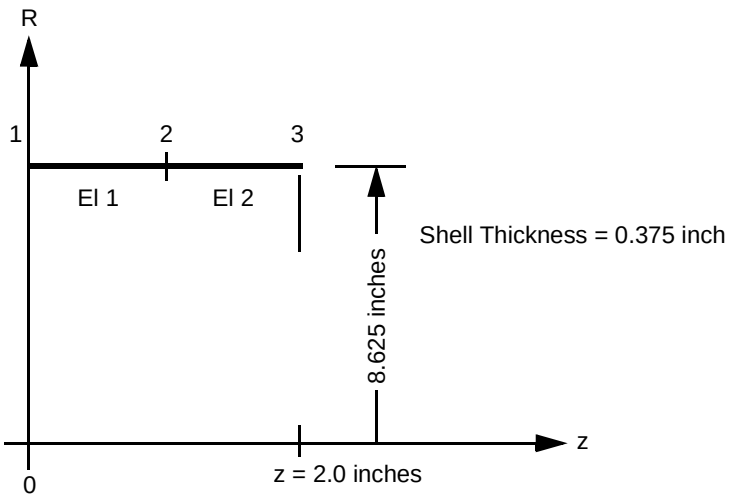

Figure 5.13-5 Finite Element Model (Model D - Element 88)

5.14 Steady-state Temperature Distribution of a Generic Fuel Nozzle

A steady-state heat transfer analysis is performed on a simplified two-dimensional model of a generic fuel nozzle for a turbine engine. The nozzle has both fluid heat-up and radiation across gaps which are simulated by fluid channel and thermal contact gap elements in the program. Model definition options CHANNEL and CONRAD GAP are used for fluid channel and radiation gaps, respectively. A 4-node-planar quad is chosen for modeling the entire nozzle.

Element

Library element type 39 is a 4-node planar isoparametric quadrilateral heat transfer element. Each nodal point is defined by two global coordinates (x,y) and has temperature as the nodal degrees of freedom. See *MARC Volume B: Element Library* for further details.

Model

As shown in Figure 5.14-1, the simplified nozzle model is a two-dimensional structure, made of steel, containing two radiational gaps and a fluid channel. The nozzle is heated up from room temperature by a 200°F fluid flow in the channel as well as convective heat transfers from the external boundaries with ambient temperatures at 400°F and 1600°F, respectively. Thermal properties of steel and fluid are assumed to be dependent on temperatures.

Figure 5.14-2 shows a finite element mesh for the MARC heat transfer analysis. The mesh contains 103 4-node quad elements and 142 nodes. A fluid channel consisting of elements 1, 30 through 37, 24 through 29, and two thermal contact gaps (GAP1: elements 38 through 45; GAP2: elements 82 through 89), are also depicted in Figure 5.14-2.

Define (Element Set)

In the MARC input, set names are used to represent various regions in the model. The set WHOLE contains all the elements in the model. The fluid channel and two thermal gaps are represented by set names CHANL, GAP1, and GAP2, respectively. A set operation, WHOLE EXCEPT GAP1 EXCEPT GAP2 EXCEPT CHANL, defines the steel elements.

Material Properties

Thermal properties for steel are: $K = 1.85 \times 10^{-4}$ BTU/sec-in-°F, C = 0.1 BTU/lb-°F, and $\rho = 0.285$ lb/in^3. The specific heat of the fluid is assumed to be 0.4625 BTU/lb-°F. Both the thermal conductivity (k) and the specific heat (C) are dependent on temperature. Slopes and break point data are entered through the TEMPERATURE EFFECTS model definition option. Material identifications 1, 2 and 3 are assigned to STEEL, CHANL (fluid), GAP1 and GAP2 (thermal gaps), respectively. Both the thermal conductivity and mass density of fluid, as well as the thermal properties of thermal gap elements, are set to zero.

Initial Temp

A constant initial temperature of 70°F is assumed for the entire model.

Geometry

The model thickness of 1.0 inch is entered through the GEOMETRY block.

Input for Thermal Contact Gap

In problems involving thermal contact gaps, the model definition option CONRAD GAP is used for the input of all gap properties. The data needed for each gap are: face identification, emissivity, Stefan-Boltzmann constant, absolute temperature conversion factor, film coefficient, gap closure temperature and a list of elements in the gap. Discussions on the gap face identification can be found in *MARC Volume B: Element Library.*

Since the thermal gap element serves as a radiation/convection link or, as tying constraints, thermal properties are not required for the element. Consequently, all the entries (conductivity, specific heat, density) in the ISOTROPIC option must be set to zero for all thermal contact elements.

In addition, because thermal contact and solid elements have same topology, the connectivity data format of thermal contact element is same as that of a solid element. As a result, mesh generators such as MESH2D or Mentat can be used for the generation of thermal contact gaps. All the thermal contact elements in one gap must be numbered in the same order.

Conrad Gap

The CONRAD GAP model definition option is used for entering thermal contact gap information. In the model, the number of thermal gaps is 2; and in each gap: the Stenfan-Boltzmann constant is 0.3306E-14 BTU/sec - in^2 -$°R^4$; the absolute temperature conversion factor from Fahrenheit to Rankine is 459.7; and the gap-closure temperature is assumed to be 2000°F (thermal gaps remain open throughout the analysis). The thermal gap elements are defined in sets GAP1 and GAP2, respectively.

Input for Fluid Channel

The data associated with fluids channels can be entered using the model definition option CHANNEL. The data needed for each channel are: channel face identification, lead element number, inlet temperature, mass flow rate, film coefficient and a list of fluid elements in the channel. Discussions on the channel face identification can be found in *MARC Volume B: Element Library.*

The topology of the fluid channel element is the same as that of solid element. Additional input is not needed for the mesh definition of fluid channels. All the fluid channel elements in one channel must be numbered in the same order.

Since the fluid flow in the channel is assumed to be convective, and based on the mass flow rate, in the ISOTROPIC block only the specific heat of the fluid is required. Both the conductivity and density of the fluid must be set to zero. The model definition option TEMPERATURE EFFECTS can be used for temperature dependent specific heat of the fluid.

For planar elements, the GEOMETRY block is needed for the input of channel thickness.

Channel

The CHANNEL model definition option is used for the input of fluid channel data. In the current model, the number of channels is 1; the channel face identification is 2; the lead element number is 1; the inlet temperature is 200°F; the mass flow rate is 0.02778 lb/sec (or 100 lb/hr); and the film coefficients in the channel are entered using user subroutine FLOW (set to 0. in the input deck). A list of the subroutine FLOW is shown on a latter page. Finally, the fluid elements is contained in the set CHANL.

Films

Finally, 16 sets of film data are used for the input of convective thermal boundary conditions in the model. The user subroutine FILM is used for entering film coefficient and sink temperature of each film boundary (H = 1.0, T_{inf} = 1.0 in the input). Both the film index and the fluid temp index are used for film boundary condition input.

Transient

Steady state temperatures in the generic fuel nozzle with temperature dependent thermal properties can be obtained from a MARC heat transfer analysis using: (1) several transient time-steps with large time increments or, (2) one time-step with a number of iterations within the time-step. Both approaches converge to the same steady-state solution.

Results

Both the channel and solid temperatures are depicted in Figure 5.14-3. Comparisons between finite element and finite difference results are favorable.

Parameters, Options, and Subroutines Summary

Example e5x14.dat:

Parameters	Model Definition Options	History Definition Options
ELEMENT	CHANNEL	TRANSIENT
END	CONNECTIVITY	CONTINUE
HEAT	CONRAD GAP	
PRINT	CONTROL	
SIZING	COORDINATE	
TITLE	DEFINE	
	END OPTION	
	FILMS	
	GEOMETRY	
	INITIAL TEMP	
	ISOTROPIC	
	TEMPERATURE EFFECTS	

User subroutine in u5x14.f:

FILM
FLOW

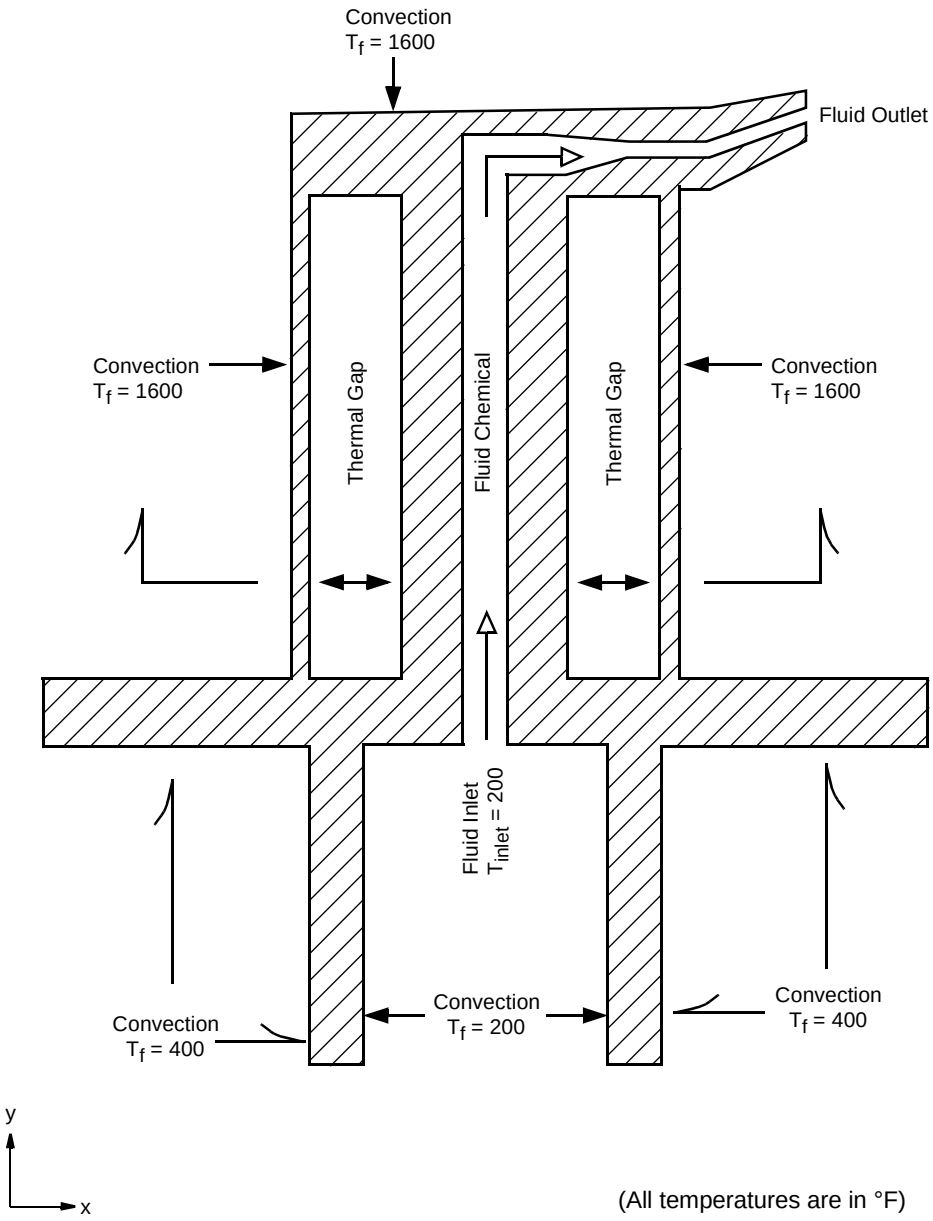

Figure 5.14-1 Simplified Nozzle

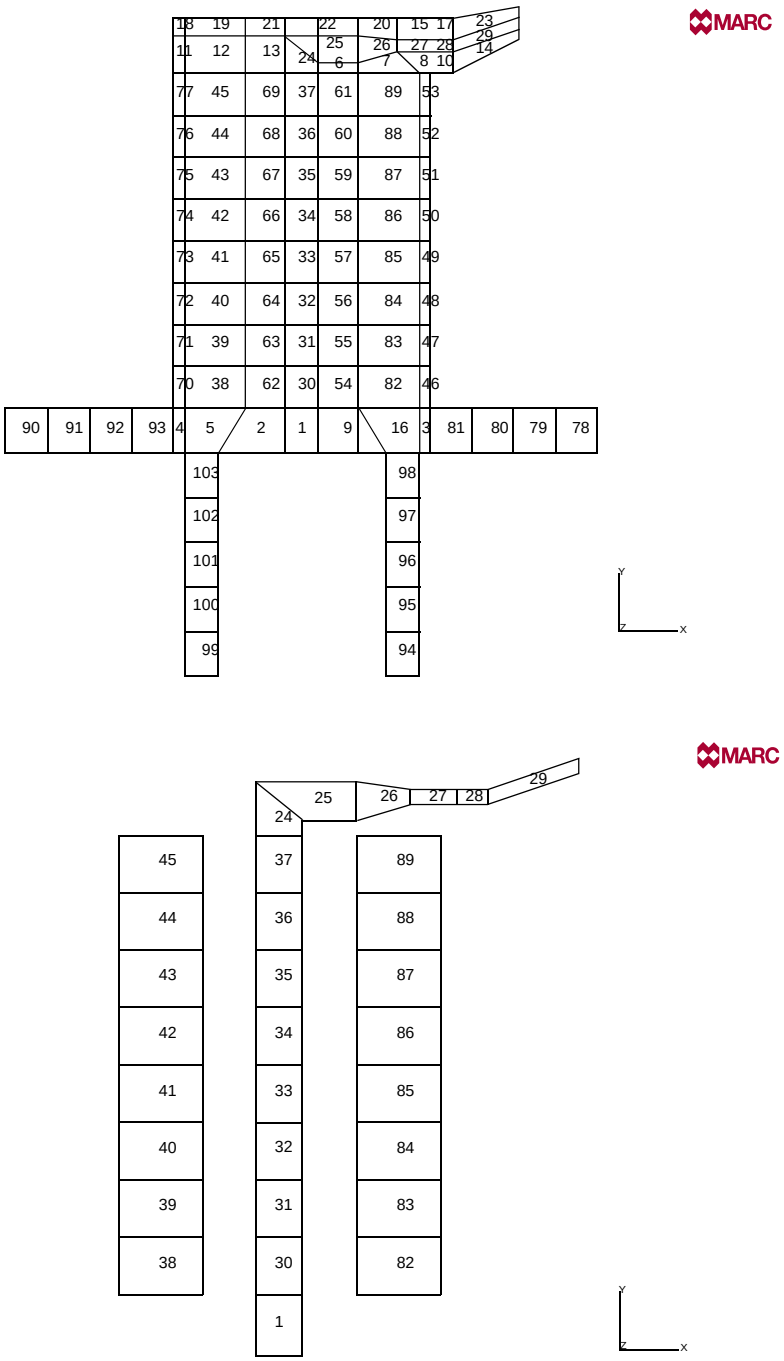

Figure 5.14-2 Simplified Nozzle (Finite Element Mesh)

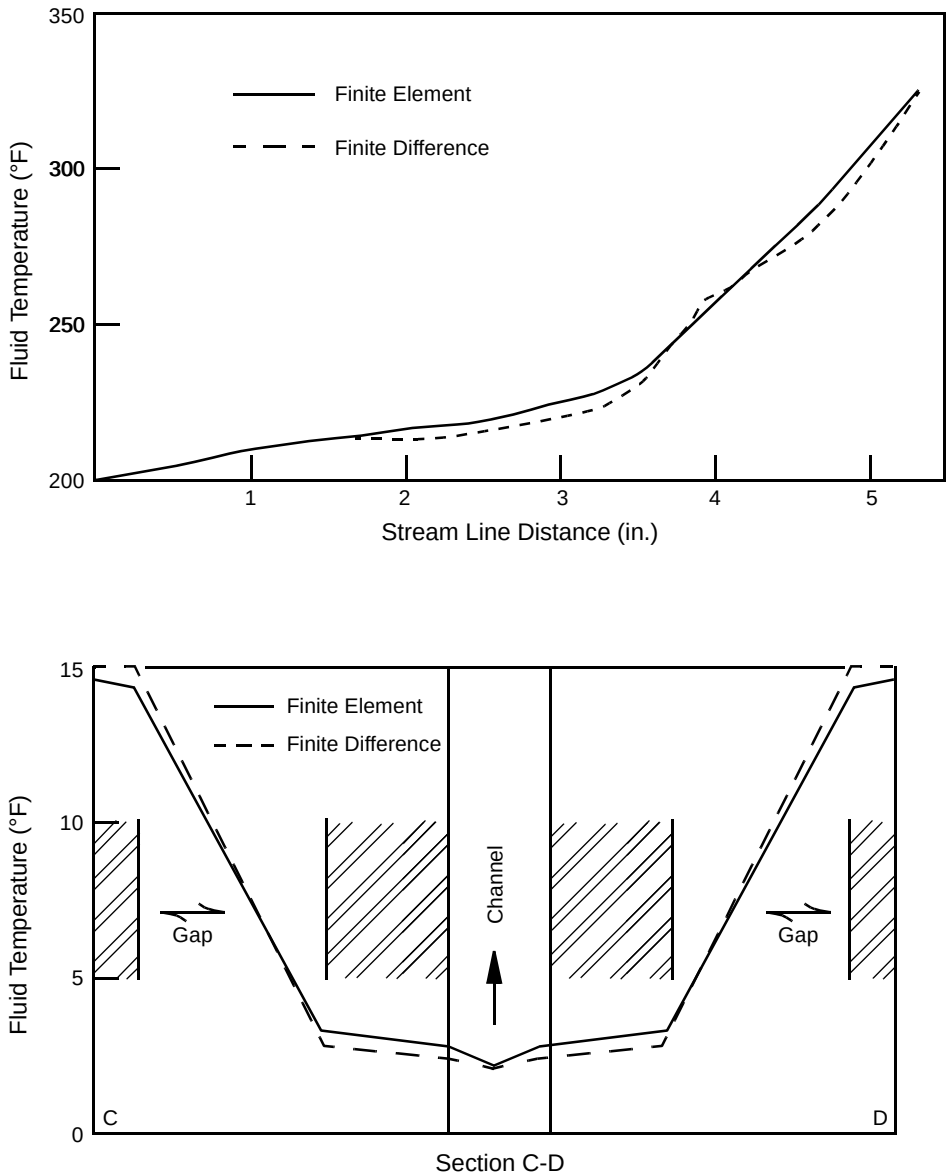

Figure 5.14-3 Simplified Nozzle Solid and Fluid Temperatures)

5.15 Radiation Between Concentric Spheres

A typical radiation heat-exchange problem between gray bodies is solved here in order to show the capabilities of MARC in dealing with the radiations boundary conditions in heat conduction problems. The radiation heat exchange is based on the computation of the “view factors” depending purely upon the geometrical shape of the radiating boundaries. The computed steady-state temperature distribution is shown and is compared with an analytical solution.

The geometry of the model is shown in Figure 5.15-1; two concentric spherical bodies and four spherical surfaces can be identified: surfaces 1 and 2 define the first body and surfaces 3 and 4 define the second spherical gray body. Surface 1 has a radius of r_1, surface 2 – radius of r_2, surface 3 – radius of r_3, and surface 4 – radius of r_4 (Figure 5.15-1). Temperatures on surfaces 1 and 4 are known; radiative heat transfer takes place between surfaces 2 and 3.

This example uses two data sets. Data set e5x15 involves radiation view factor calculation by MARC. Data set e5x15b uses the view factors generated by Mentat. the view factor file e5x15b.vfs stores the Mentat generated view factors.

Element

Element type 42, a second order distorted axisymmetric quadrilateral element for heat-transfer analysis, is used. There are eight nodes per element and one degree of freedom (temperature) per node. (See *MARC Volume B: Element Library* for further details.)

Model

The axisymmetric section and the finite element model shown in Figure 5.15-2; 24 elements, with two elements in the radial direction, describe each body for a total of 48 elements and 202 nodes.

Radiation

The RADIATION parameter is used to activate the heat transfer analysis with radiative heat exchange and to specify the view factors calculation (or for reading them from a file). In addition, the units are specified for length and for temperature. In problem e5x15, the view factors during analysis are calculated using RADIATING CAVITY input. Problem e5x15b uses MENTAT to calculate the view factors. They are read in from e5x15b.vfs.

Radiating Cavity

One radiating cavity is defined in this option: the cavity is bounded by the spherical surfaces nos. 2 and 3 in Figure 5.15-1. The anti-clockwise list of nodes defining the outline of the cavity is assigned.

Thermal Properties

One set of thermal properties is specified in the ISOTROPIC block; the isotropic thermal conductivity value of 1.E-4 W/mm °C is assigned in the first field and the temperature-dependent value of the emissivity is specified in the fourth field. (Special input for radiation problems.)

Thermal Boundary Conditions

The temperature value of the internal and external spherical surfaces in imposed in the FIXED TEMP option as follows:

Surface no. 1 T_1 = 332.561 °C Surface no. 4 T_4 = 532.114 °C

See Figure 5.15-1 for cross reference.

Control for Thermal Analysis

The maximum error in temperature estimate used for property evaluation is set to 0.1 °C. This control provides a recycling capability to improve accuracy in this highly non-linear heat transfer problem. See *MARC Volume C: User Input* model definition option CONTROL for further details.

Thermal History

A steady-state thermal analysis is specified via STEADY STATE history definition option.

Results

The computed distribution of the temperature at the steady-state condition is compared with the analytical solution and it is summarized below.

Surface Temperature	Analytic (°C)	e5x15.dat	e5x15b.dat
T1	332.561	332.561	332.561
T2	400.00	401.364	391.624
T3	500.00	500.475	504.185
T4	532.114	532.114	532.114

Reference

Frank Kreith, *Principles of Heat Transfer*, Donnelly Publishing Corp., N.Y.

Parameters, Options, and Subroutines Summary

Example e5x15.dat:

Parameters	Model Definition Options	History Definition Options
ELEMENT	BOUNDARY CONDITIONS	CONTINUE
END	CONNECTIVITY	STEADY STATE
HEAT	CONTROL	
RADIATION	COORDINATE	
SIZING	END OPTION	
TITLE	ISOTROPIC	
	RADIATING	
	TEMPERATURE EFFECTS	

Parameters, Options, and Subroutines Summary

Example e5x15b.dat:

Parameters	Model Definition Options	History Definition Options
ALL POINTS	CONNECTIVITY	CONTINUE
ELEMENT	COORDINATE	CONTROL
END	END OPTION	STEADY STATE
HEAT	FIXED TEMPERATURE	TEMP CHANGE
RADIATION	ISOTROPIC	
SET NAME	NON PRINT	
SIZING	OPTIMIZE	
TITLE	POST	
	SOLVER	
	VIEW FACTOR	

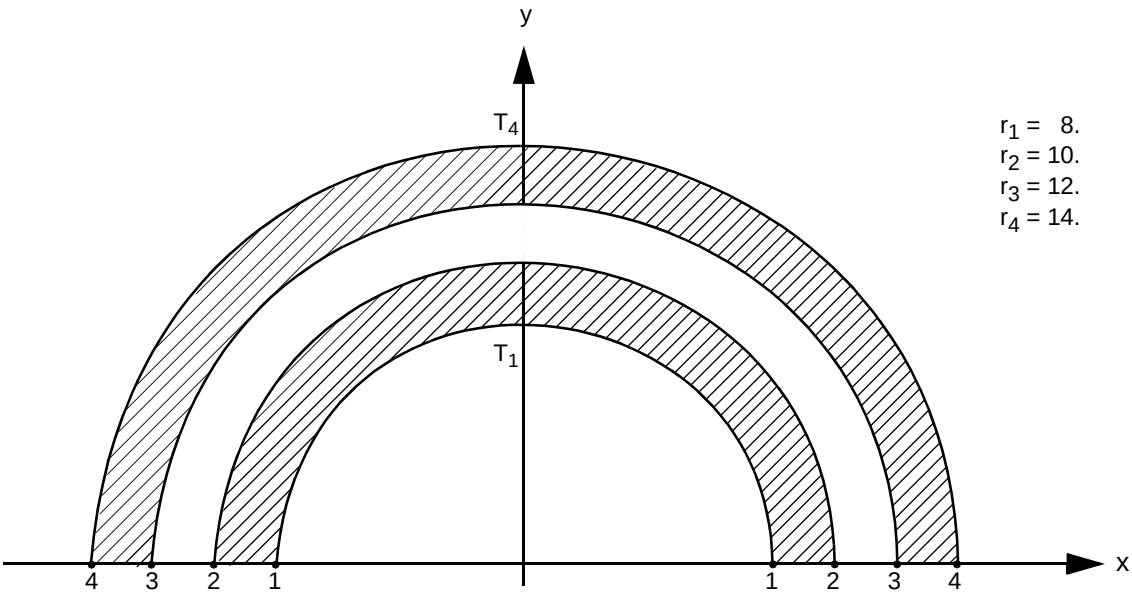

Figure 5.15-1 Radiating Concentric Spheres

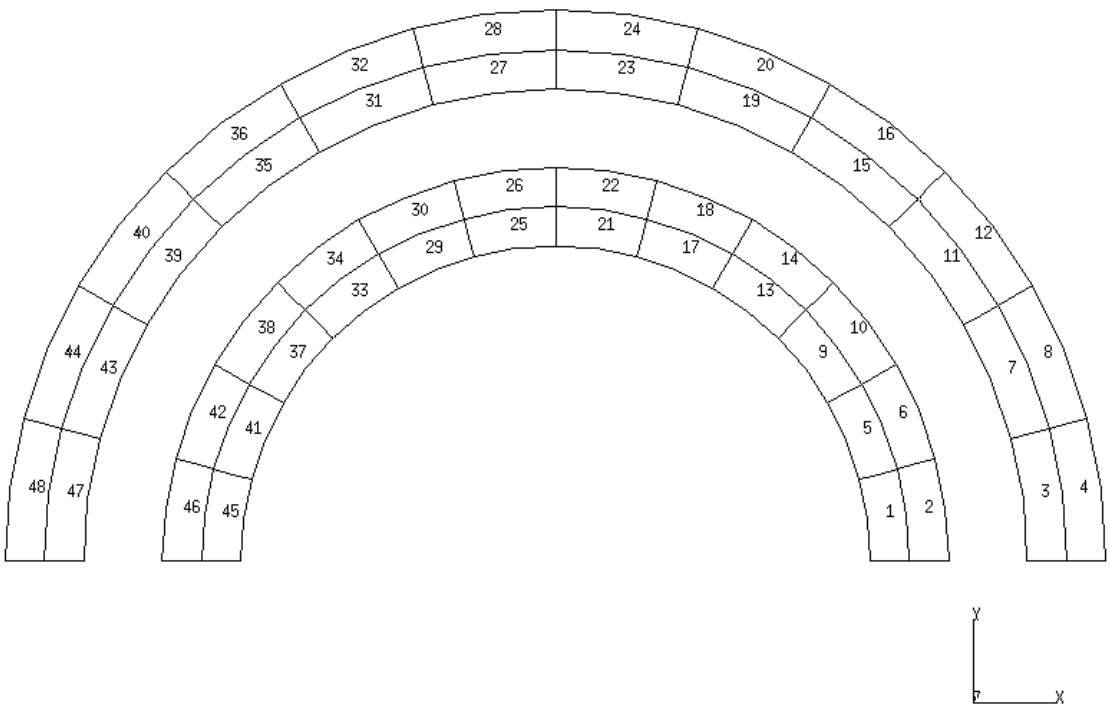

Figure 5.15-2 Mesh with Element Numbers

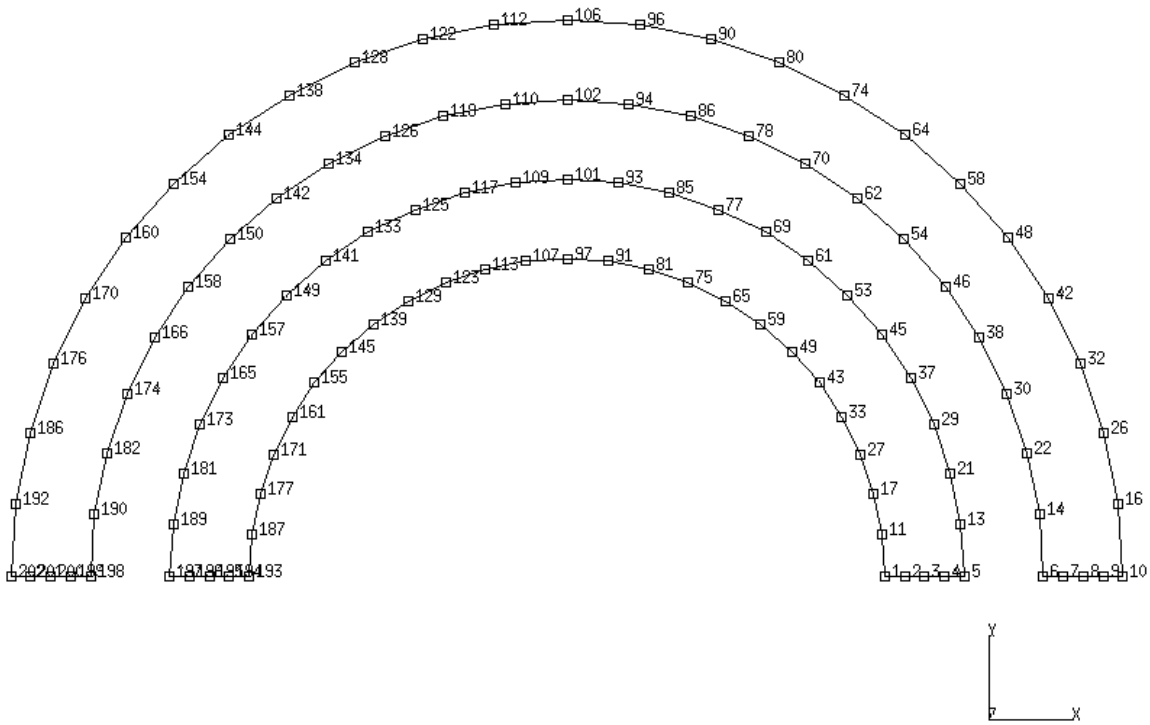

Figure 5.15-3 Mesh with Node Numbers

5.16 Three-Dimensional Thermal Shock

The bar of a rectangular cross section is initially at rest. At time t = 0, one end of the bar is held at a fixed temperature of 1000°F, and a transient conduction problem is solved.

This problem is modeled using the three techniques summarized below.

Data Set	Element Type(s)	Number of Elements	Number of Nodes
e5x16a	123	16	45
e5x16b	133	43	120
e5x16c	135	43	27

Element

Element types 44 and 133 are second-order isoparametric three-dimensional heat conduction elements. There are twenty nodes for brick element type 44 and 10 nodes for the tetrahedral element type 133. Element type 123 is an 8-node brick with reduced integration and hourglass control.

Model

The bar cross section is square with a thickness of one inch and a length of two inches. This transient conduction problem is performed for three meshes comprised of element types 44, 123, and 133.

Thermal Properties

The isotropic thermal conductivity value of 0.42117E-5 Btu/sec.-in.-°F. The specific heat is 0.3523E-3 Btu/lb°F. The mass density is 0.7254E-3 lb/cu.inch.

Thermal Boundary Conditions

The initial temperature distribution is that all nodes have a temperature of 0.0°F. At time, t = 0, the nodal temperatures of one end of the bar are fixed at 1000°F, and a transient conduction problem is solved to its completion at steady state, where all nodes will have a final temperature of 1000°F.

Control for Thermal Analysis

The maximum number of time points are fixed at 100. The maximum change in nodal temperature will be 100°F.

Thermal History

A transient thermal analysis is specified via the TRANSIENT option, with the automatic time stepping feature turned on. The initial time increment is 1.0E-2 seconds, with a final time period of 10 seconds.

Results

From the temperature history shown in Figure 5.16-1, Figure 5.16-2, and Figure 5.16-4 for element types 44, 123, and 133, respectively, the automatic time stepping feature shows ever increasing time steps as the solution approaches steady state. The temperature of the free end goes slightly negative by about a tenth of a degree for element types 123 and 133. This effect has been minimized by the inclusion of the LUMP parameter which instructs MARC to lump the capacitance matrix, instead of using the consistent capacitance matrix which is the default. There is virtually no difference in the thermal history of the free end between different element types. Figure 5.16-3, and Figure 5.16-5 are iso-thermal surfaces at a time when the free end starts to heat up significantly. These iso-thermal surfaces should be flat and perpendicular to the axis of the bar. The iso-thermal surfaces become flatter as the bar becomes hotter. Also, the iso-thermal surfaces are more irregular for the tetrahedron mesh than the brick mesh, because the brick element faces are either perpendicular or parallel to the head flow. This effect is minimized if more tetrahedron elements are used.

Parameters, Options, and Subroutines Summary

Example e5x16a.dat:

Parameters	Model Definition Options	History Definition Options
ELEMENT	CONNECTIVITY	CONTINUE
END	CONTROL	TRANSIENT
HEAT	COORDINATE	
LUMP	END OPTION	
SIZING	FIXED TEMP	
TITLE	INITIAL TEMP	
	ISOTROPIC	
	NO PRINT	
	POST	

Example e5x16b.dat:

Parameters	Model Definition Options	History Definition Options
ALIAS	CONNECTIVITY	CONTINUE
ELEMENT	CONTROL	TRANSIENT
END	COORDINATE	
HEAT	END OPTION	
LUMP	FIXED TEMP	
SIZING	INITIAL TEMP	
TITLE	ISOTROPIC	
	POST	

Time	Temperature (°F)	Time	Temperature (°F)
0.0	0.0		
1.82307E-04	7.62101E-02	8.46059E-02	4.34587E+02
3.64615E-04	2.46594E-01	1.00722E-01	5.12089E+02
5.92499E-04	5.48778E-01	1.20868E-01	5.93519E+02
8.77355E-04	9.32763E-01	1.41014E-01	6.61590E+02
1.30464E-03	1.32789E+00	1.66196E-01	7.29694E+02
1.83874E-03	1.53547E+00	1.97673E-01	7.94479E+02
2.63990E-03	1.53524E+00	2.44890E-01	8.60475E+02
3.84163E-03	1.49460E+00	3.03910E-01	9.12322E+02
5.64423E-03	2.05263E+00	3.92441E-01	9.53537E+02
7.89748E-03	4.10911E+00	5.25236E-01	9.80063E+02
1.07140E-02	9.03647E+00	7.24430E-01	9.93345E+02
1.42348E-02	1.88757E+01	1.02322E+00	9.98334E+02
1.86356E-02	3.63171E+01	1.47141E+00	9.99697E+02
2.41367E-02	6.43750E+01	2.14369E+00	9.99961E+02
3.23884E-02	1.14785E+02	3.15211E+00	9.99996E+02
4.27029E-02	1.82812E+02	4.66473E+00	1.00000E+03
5.55962E-02	2.67022E+02	6.93368E+00	1.00000E+03
6.84894E-02	3.46206E+02	1.00003E+01	1.00000E+03

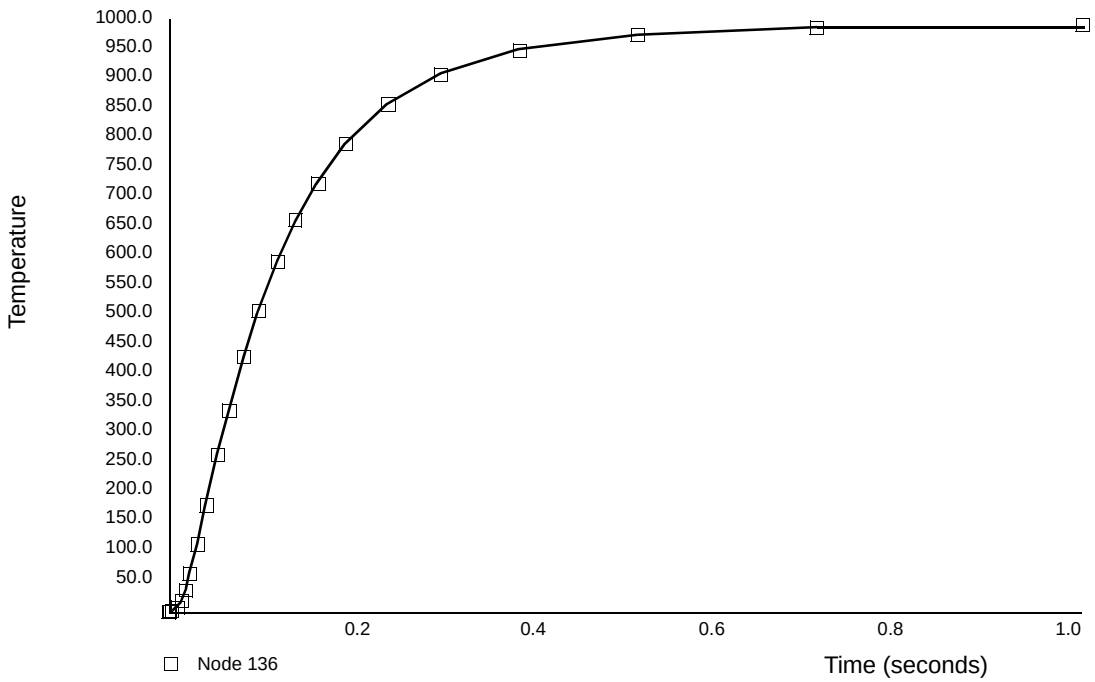

Figure 5.16-1 Temperature History for Free End Node 136 Element Type 44

Time	Temperature (°F)	Time	Temperature (°F)
0.0	0.0		
1.99113E-04	-3.03712E-03	1.04521E-01	4.03045E+02
3.98226E-04	1.81682E-04	1.24798E-01	4.74083E+02
6.47118E-04	8.32631E-03	1.50145E-01	5.50460E+02
1.02045E-03	3.44541E-02	1.81829E-01	6.29444E+02
1.58046E-03	1.14610E-01	2.13513E-01	6.94672E+02
2.42047E-03	3.42895E-01	2.53118E-01	7.59006E+02
3.68048E-03	9.54424E-01	3.02624E-01	8.19336E+02
5.57050E-03	2.52048E+00	3.76883E-01	8.79604E+02
7.93302E-03	5.50497E+00	4.88272E-01	9.31265E+02
1.08862E-02	1.08245E+01	6.55355E-01	9.67696E+02
1.45776E-02	1.97886E+01	9.05980E-01	9.88009E+02
1.91919E-02	3.40969E+01	1.28192E+00	9.96615E+02
2.61134E-02	6.06809E+01	1.84582E+00	9.99298E+02
3.47652E-02	9.86775E+01	2.69168E+00	9.99896E+02
4.77429E-02	1.59734E+02	3.96047E+00	9.99989E+02
6.39651E-02	2.35397E+02	5.86365E+00	9.99999E+02
8.42428E-02	3.23410E+02	8.71842E+00	1.00000E+03
		1.00001E+01	1.00000E+03

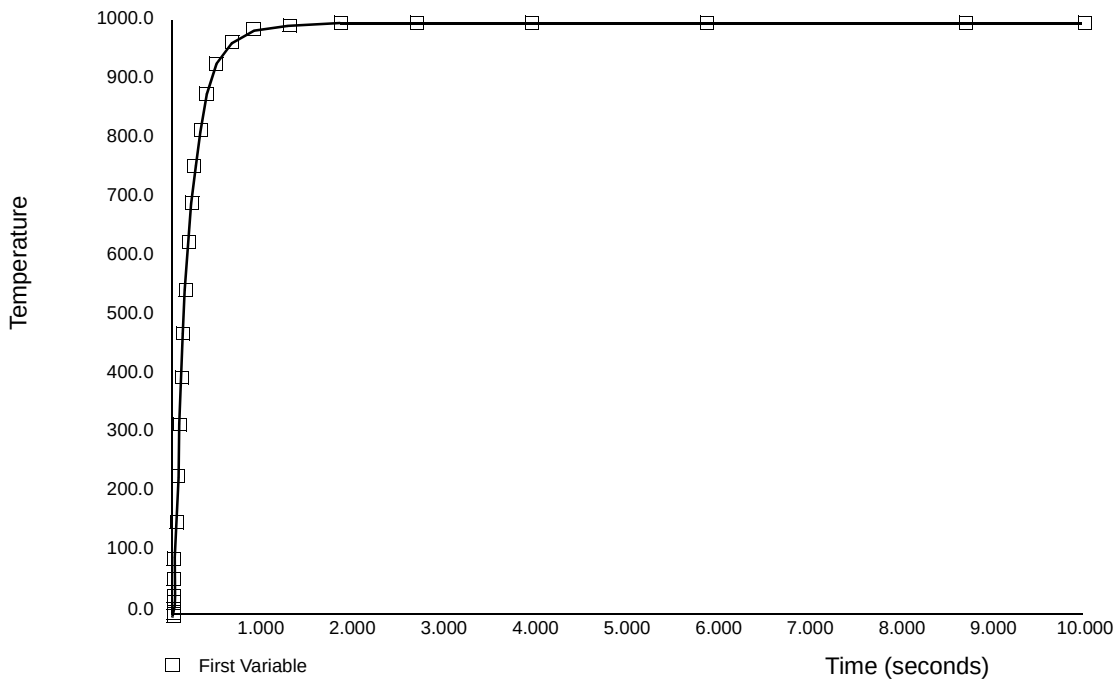

Figure 5.16-2 Temperature History for Free End Node 126 (Element Type 123)

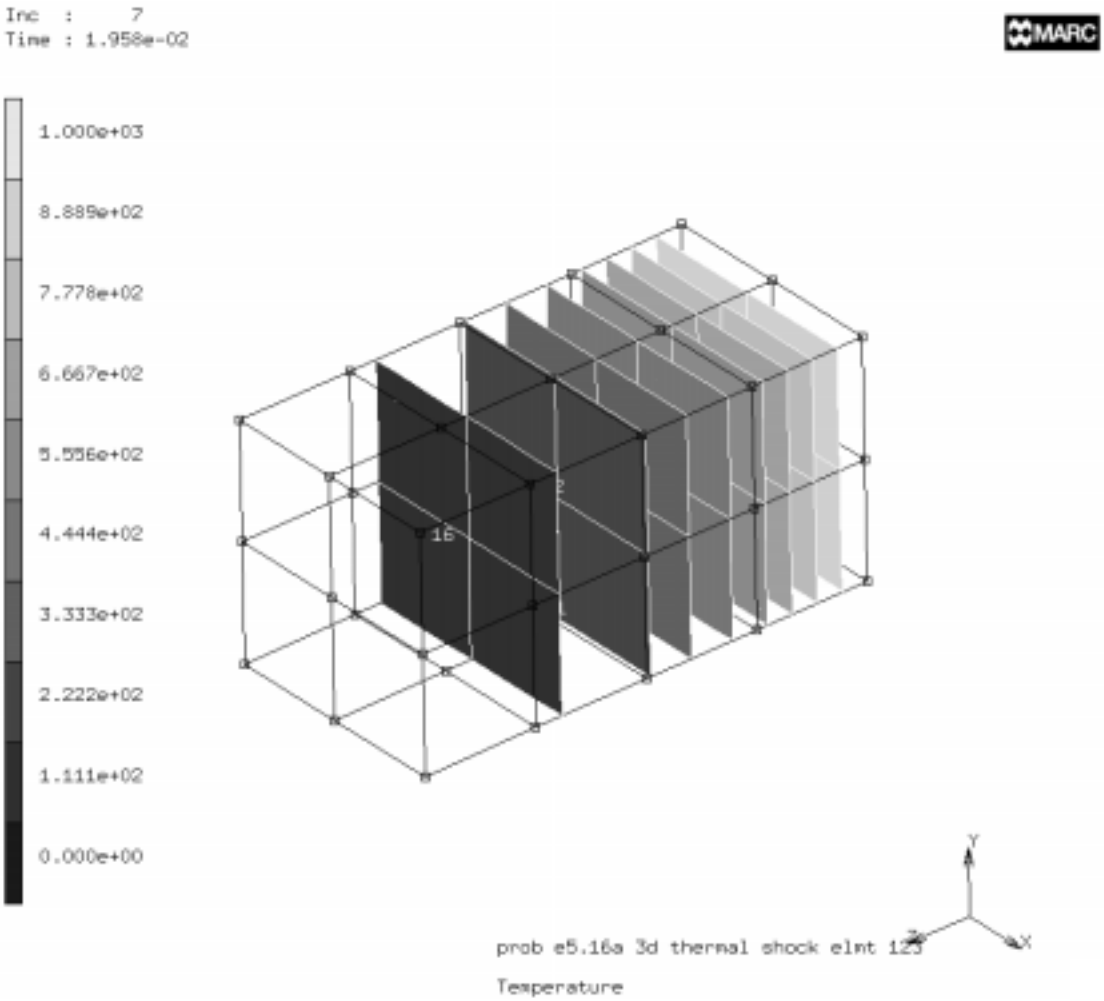

Figure 5.16-3 Iso-thermal Surfaces at t = 0.0196 seconds (Element Type 123)

Time	Temperature (°F)	Time	Temperature (°F)
0.0	0.0		
7.10402E-04	-1.63117E-01	1.14734E-01	5.64931E+02
1.42080E-03	-3.29948E-01	1.33342E-01	6.33486E+02
2.30881E-03	-4.95783E-01	1.56602E-01	7.03065E+02
3.64081E-03	-6.80945E-01	1.85677E-01	7.70386E+02
5.30582E-03	-7.92613E-01	2.22020E-01	8.31985E+02
7.38707E-03	-4.82283E-01	2.76536E-01	8.91606E+02
1.05090E-02	2.03853E+00	3.58309E-01	9.40608E+02
1.44113E-02	9.60317E+00	4.80968E-01	9.73458E+02
1.92893E-02	2.61956E+01	6.64957E-01	9.90708E+02
2.53867E-02	5.59788E+01	9.40940E-01	9.97545E+02
3.30085E-02	1.02089E+02	1.35492E+00	9.99526E+02
4.25357E-02	1.65698E+02	1.97588E+00	9.99935E+02
5.44447E-02	2.45701E+02	2.90732E+00	9.99994E+02
6.63538E-02	3.21802E+02	4.30449E+00	1.00000E+03
8.12401E-02	4.07738E+02	6.40024E+00	1.00000E+03
9.61264E-02	4.83906E+02	9.54387E+00	1.00000E+03
		1.0000E+01	1.00000E+03

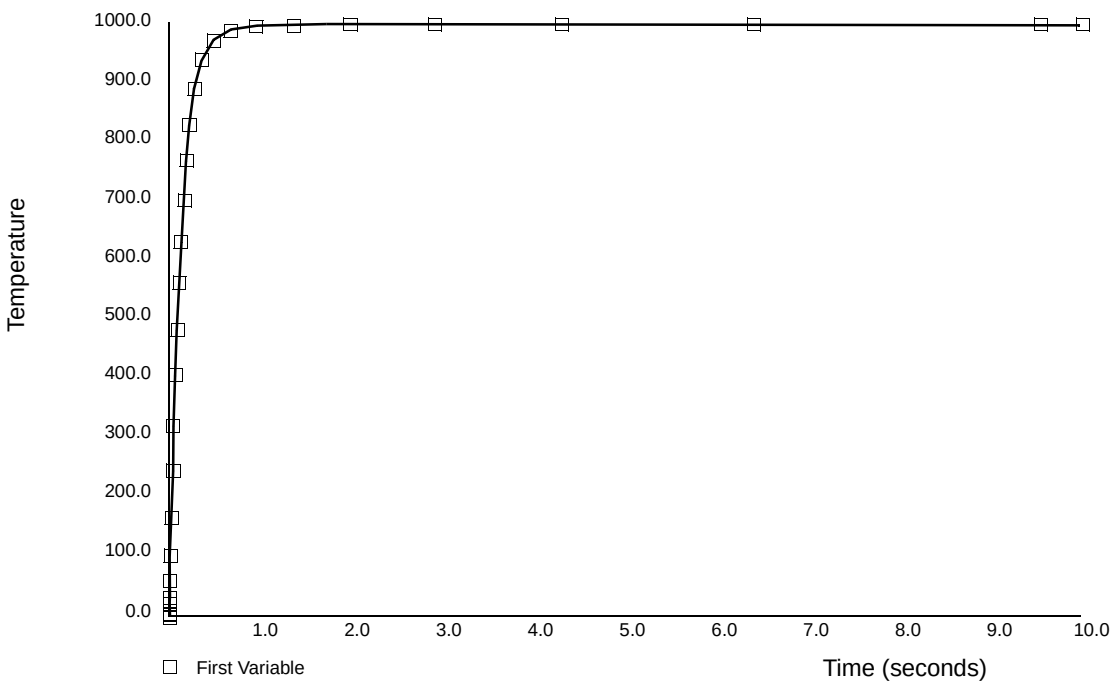

Figure 5.16-4 Temperature History for Free End Node 26 (Element Type 133)

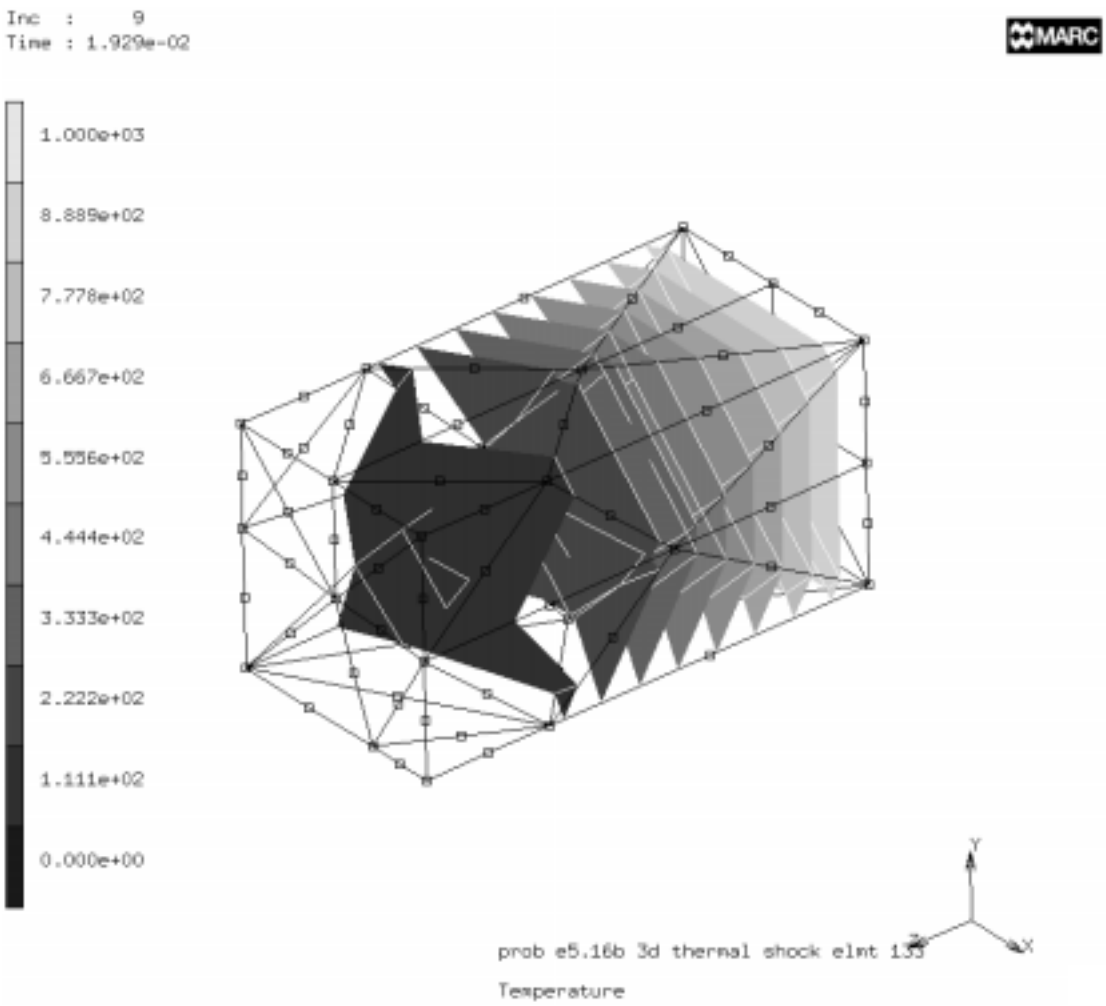

Figure 5.16-5 Iso-thermal Surfaces at t = 0.0193 seconds (Element Type 133)

5.17 Cooling of Electronic Chips

This problem demonstrates the air cooling of an electronic chip at room temperature. The comparison of the no-inclusion of heat convection, e5x17a.dat, and the inclusion of the contribution of heat convection, e5x17b.dat, by air is made. The nonsymmetric solver is turned on automatically when heat convection is included.

This problem is modeled using the two techniques summarized below.

Data Set	Element Type(s)	Number of Elements	Number of Nodes	Differentiating Features
e5x17a	39	360	399	Exclude convection
e5x17b	39	360	399	Include convection

Element

Element type 39 is used for both the air region and the chip body. The model is shown in Figure 5.17-1 and Figure 5.17-3.

Material properties

Room temperature thermal properties for air are used. The specific heat is 5.8e-5 kJ/kg.°C, the density is 0.24l kg/m^3, and thermal conductivity is 0.129e-2 W/m.°C. Thermal properties for pure copper are used for the chip. The specific heat is 0.93 kJ/kg.°C, the density is 0.0914 kg/m^3, and thermal conductivity is 8.94 W/m.°C. Assume the variation of properties with temperature is negligible.

Initial Conditions

The initial nodal temperature for chips is 40°C and for air is 10°C throughout.

Boundary Conditions

The temperature of the air far away from chips is fixed at 10°C and velocity of the air is kept at a constant 100 cm/second. The velocity of the chips is zero.

Transient Nonauto

A fixed, large time step is used to simulate the cooling process near steady-state condition.

Results

The temperature distributions shown in Figure 5.17-4 and Figure 5.17-2 indicate the effect of heat convection on the cooling of the chips. The chips have cooled down faster on the left side because, as heat convection of the air is included, more heat is carried away by the air. The

effect of the boundary layer between the air and the surface of the chips is neglected. Because the Courant number is too large, which indicates the time step is also too large, numerical dispersion occurs at the air region far away from the chips.

Parameters, Options, and Subroutines Summary

Example e5x17a.dat:

Parameters	Model Definition Options	History Definition Options
ALL POINTS	CONNECTIVITY	CONTINUE
COMMENT	CONTROL	TRANSIENT
DIST LOADS	COORDINATE	
END	DEFINE	
HEAT	END OPTION	
PRINT	FIXED TEMP	
SETNAME	INITIAL TEMP	
SIZING	ISOTROPIC	
TITLE	NO PRINT	
	POST	
	VELOCITY	

Example e5x17b.dat:

Parameters	Model Definition Options	History Definition Options
ALL POINTS	CONNECTIVITY	CONTINUE
COMMENT	CONTROL	
DIST LOADS	COORDINATE	
END	DEFINE	TRANSIENT
HEAT	END OPTION	
PRINT	FIXED TEMP	
SETNAME	INITIAL TEMP	
SIZING	ISOTROPIC	
TITLE	NO PRINT	
	POST	
	VELOCITY	

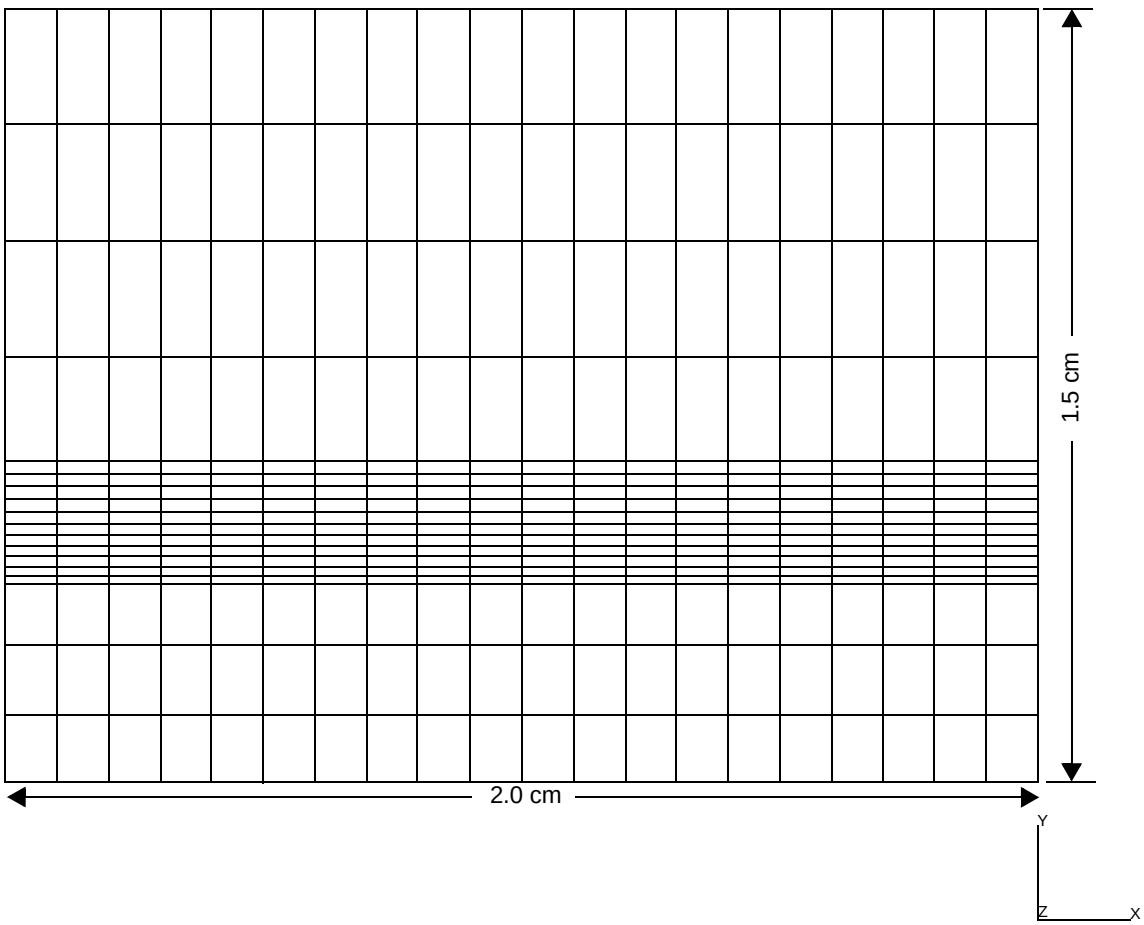

Figure 5.17-1 Complete Finite Element Mesh

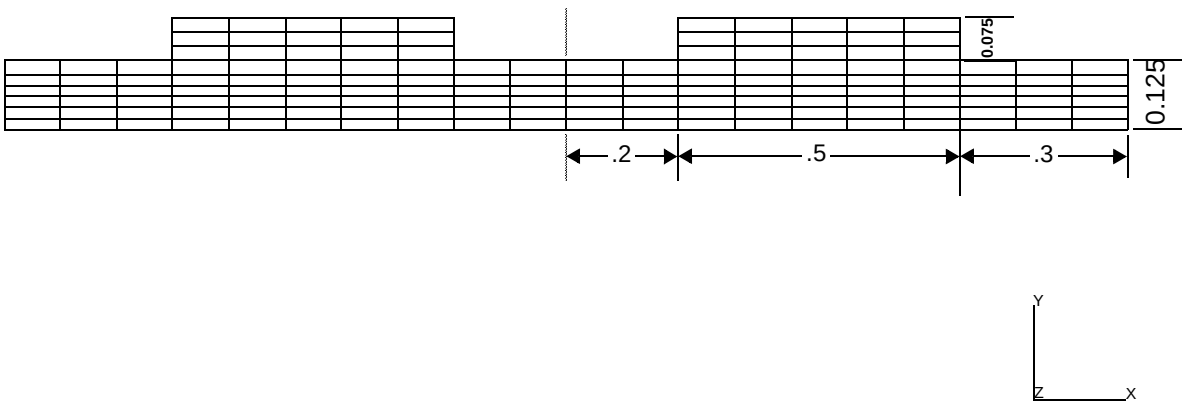

Figure 5.17-2 Finite Element Mesh of Chips and Board

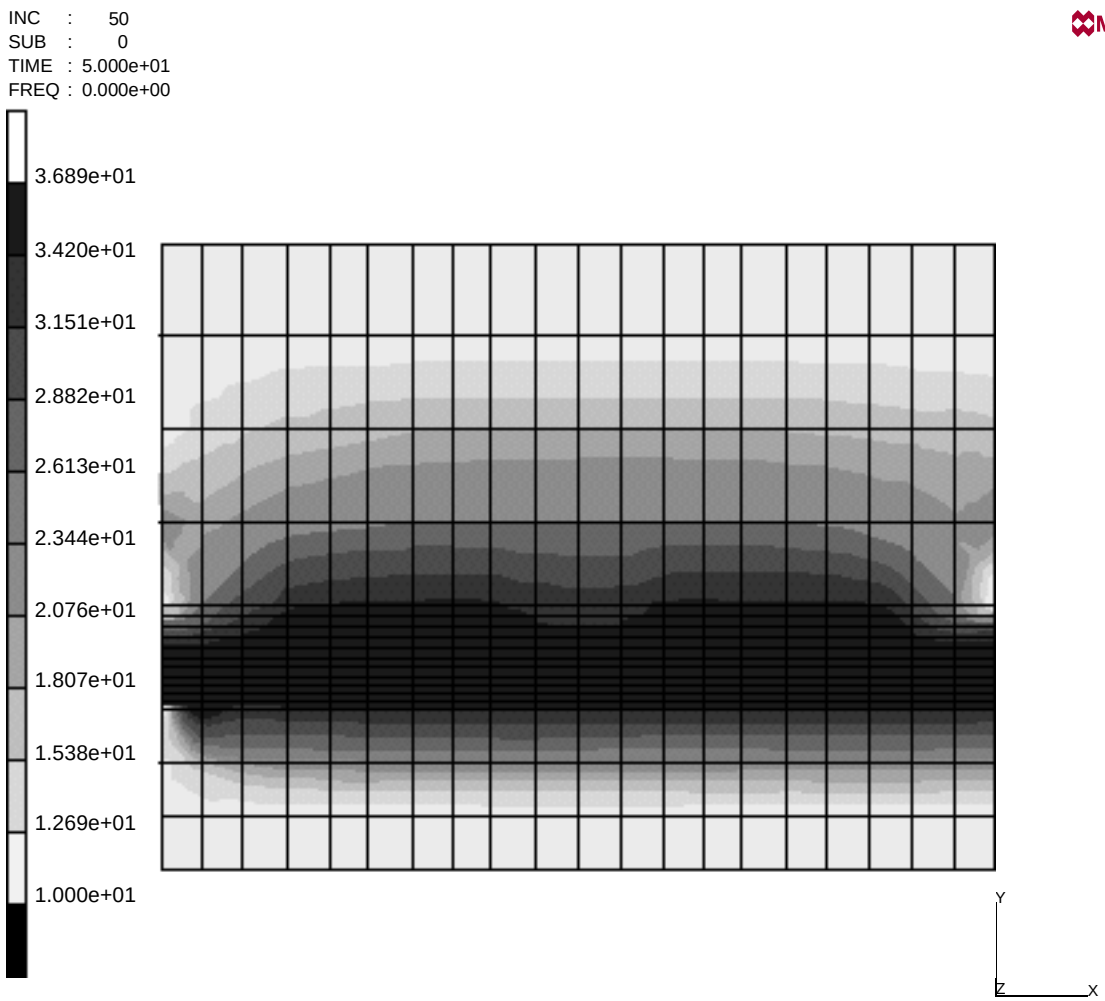

Figure 5.17-3 Temperature Distribution Excluding Heat Convection

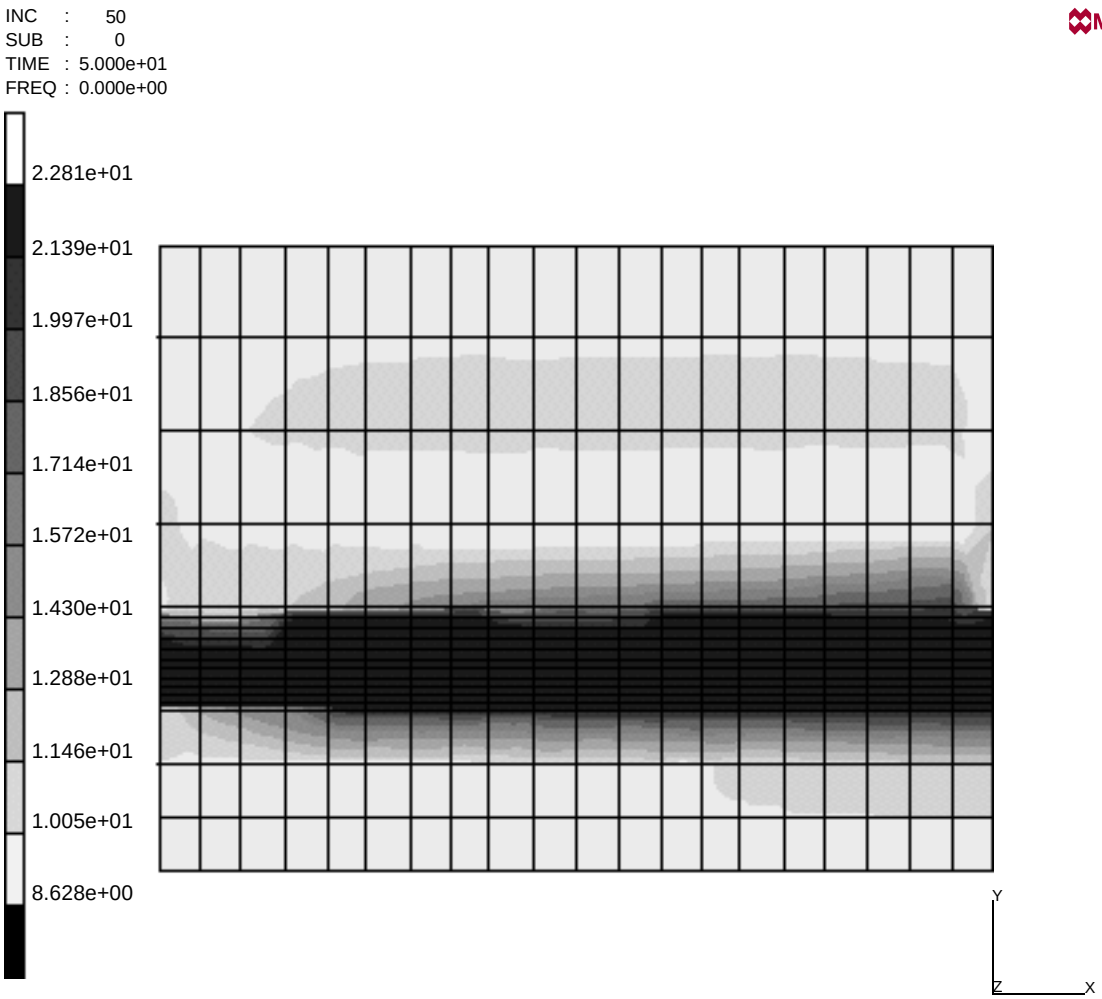

Figure 5.17-4 Temperature Distribution Including Heat Convection

5.18 Square Plate Heated at a Center Portion

A square plate with an initial temperature of 20°C is heated at the upper side of a square center portion (see Figure 5.18-1). The temperature at the outer edges is kept constant.

This problem is modeled using the two techniques summarized below.

Data Set	Element Type(s)	Number of Elements	Number of Nodes	Differentiating Features
e5x18a	50	128	81	STEADY STATE
e5x18b	50	128	81	TRANSIENT

Element

Library element type 50 is a 3-node triangular heat transfer shell element.

Model

The dimensions of the plate and the finite element mesh are shown in Figure 5.18-1. Based on symmetry considerations, only one quarter of the plate is modeled. The mesh is composed of 128 elements and 81 nodes.

Material Properties

The material is orthotropic with the following material constants:

Conductivity: λ_{11} = 50 W/m°C, λ_{22} = 5000 W/m°C, λ_{33} = 500 W/m°C

Density: $\rho = 7000\ kg/m^3$

Specific Heat: c = 450 J/kg°C

Since, by default, the properties are applied with respect to element directions, the orientation option is used to specify an offset of 0 to the zx-plane (see Figure 5.18-1).

Geometry

A uniform thickness of 0.5 m is assumed. In thickness direction, a parabolic temperature distribution is selected using the HEAT parameter. The number of layers is set equal to 3 using the SHELL SECT parameter.

Loading

The loading consists of a distributed flux of 800 W/m2 on the upper side of a square center portion. Two analyses are carried out. The first one (a) is a steady-state analysis; the second one (b) is a transient analysis.

Boundary Conditions

Symmetry conditions are imposed on the edges x = 0 and y = 0. Fixed temperatures are applied on the outer edges. Notice that this involves three degrees of freedom since, in thickness direction, a parabolic temperature distribution has been chosen.

Results

The steady-state temperature distribution of the top layer is shown in Figure 5.18-2. Due to the orthotropic material properties, the temperature distribution is nonsymmetric with respect to a diagonal of the plate. As a result of the transient analysis, the temperature distribution of the top and bottom layer along the line x = 0 are shown in Figure 5.18-3 and Figure 5.18-4, where Figure 5.18-3 refers to increment 1 and Figure 5.18-4 refers to increment 15. The situation of increment 15 corresponds to the steady-state solution.

Parameters, Options, and Subroutines Summary

Example e5x18a.dat:

Parameters	Model Definition Options	History Definition Options
ALL POINTS	CONNECTIVITY	ACTIVATE
DIST LOADS	COORDINATE	CONTINUE
ELEMENTS	DEFINE	CONTROL
END	DIST FLUXES	DIST FLUXES
HEAT	END OPTION	STEADY STATE
LUMP	FIXED TEMP	TEMP CHANGE
SETNAME	GEOMETRY	
SHELL SECT	INITIAL TEMP	
SIZING	NO PRINT	
TITLE	OPTIMIZE	
	ORIENTATION	
	ORTHOTROPIC	
	POST	
	SOLVER	

Example e5x18b.dat:

Parameters	Model Definition Options	History Definition Options
ALL POINTS	CONNECTIVITY	ACTIVATE
DIST LOADS	COORDINATE	CONTINUE
ELEMENTS	DEFINE	CONTROL
END	DIST FLUXES	DIST FLUXES
HEAT	END OPTION	STEADY STATE
LUMP	FIXED TEMP	TEMP CHANGE
SETNAME	GEOMETRY	
SHELL SECT	INITIAL TEMP	
SIZING	NO PRINT	
TITLE	OPTIMIZE	
	ORIENTATION	
	ORTHOTROPIC	
	POST	
	SOLVER	

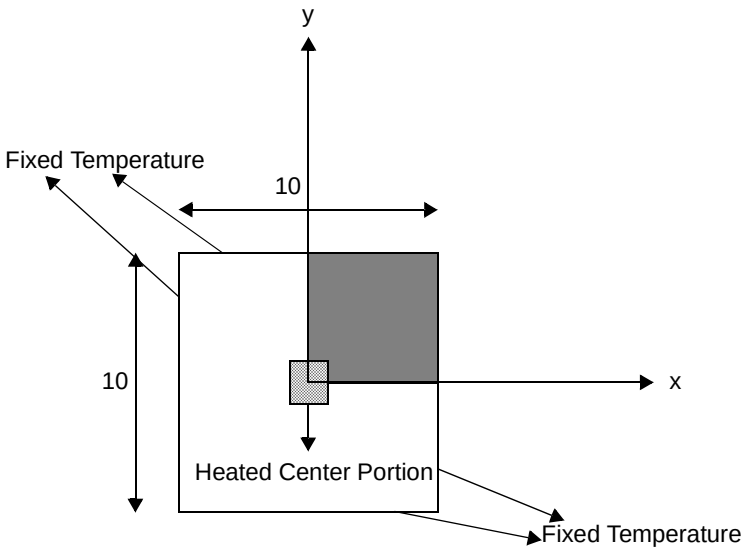

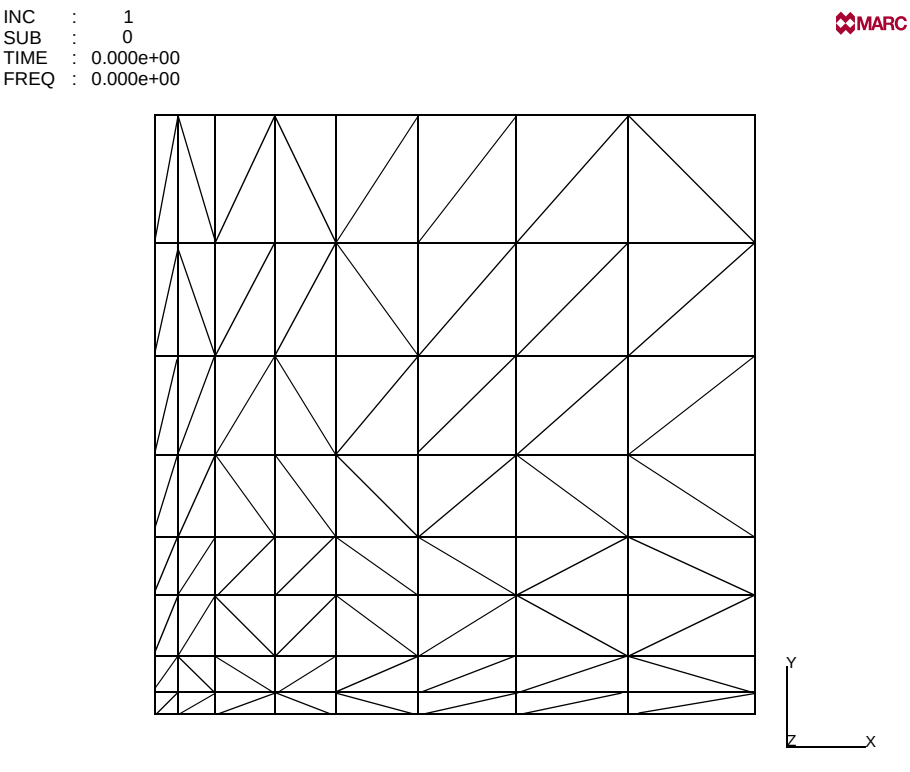

Figure 5.18-1 Heated Square Plate, Geometry, and Finite Element Mesh

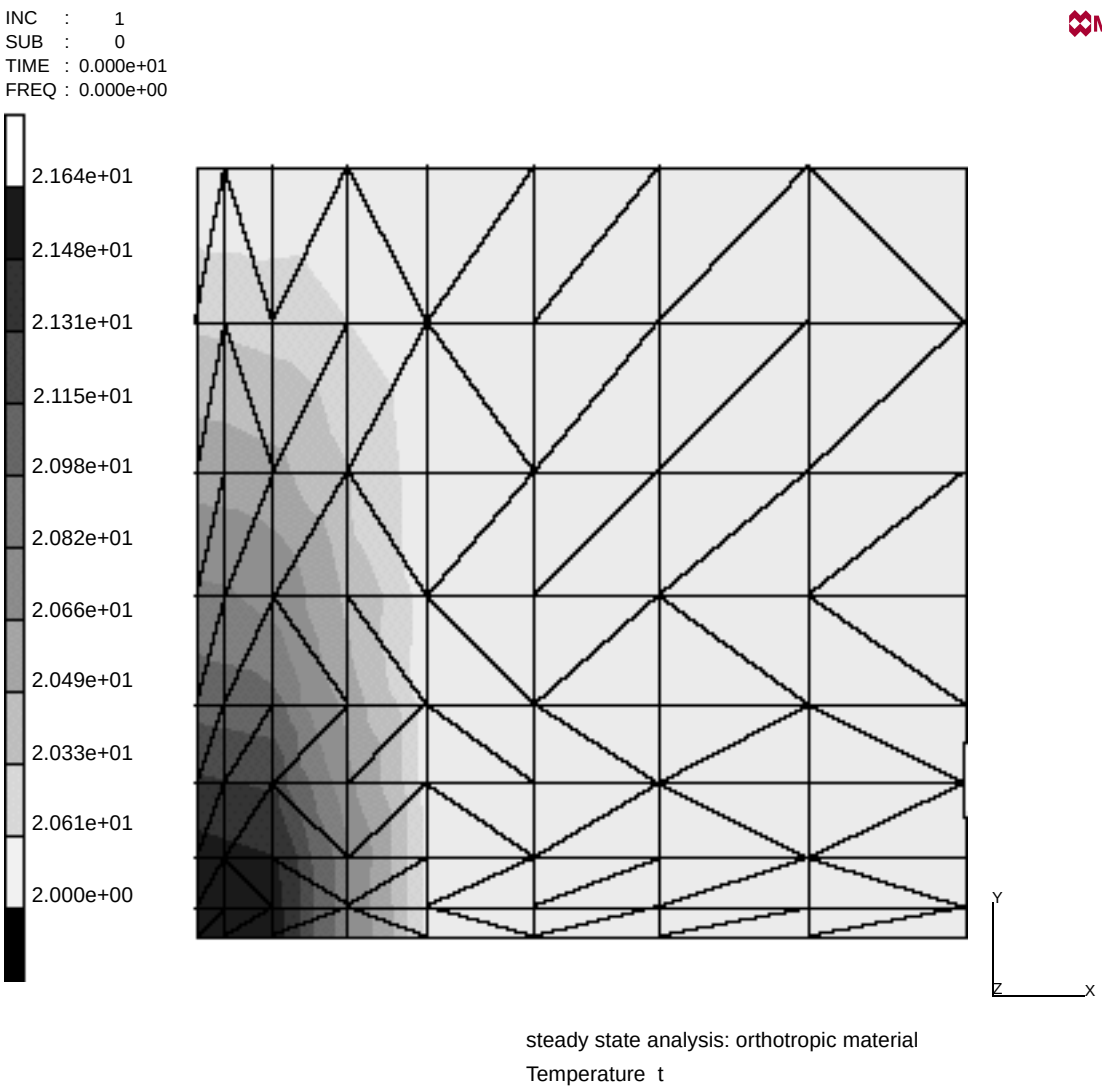

Figure 5.18-2 Temperature Distribution Steady-state Analysis

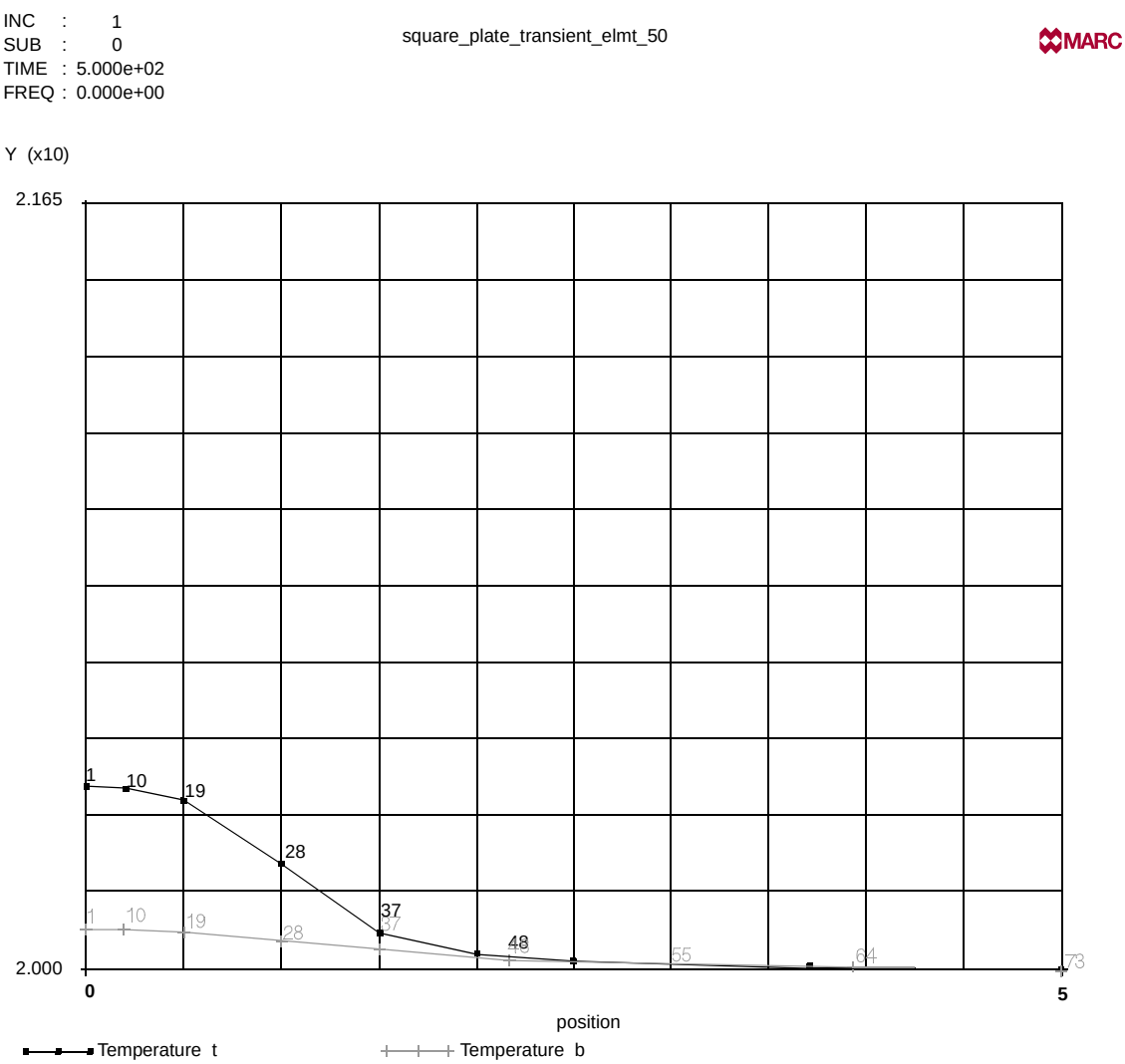

Figure 5.18-3 Path Plots for Upper and Lower Temperature at x = 0 (inc = 1)

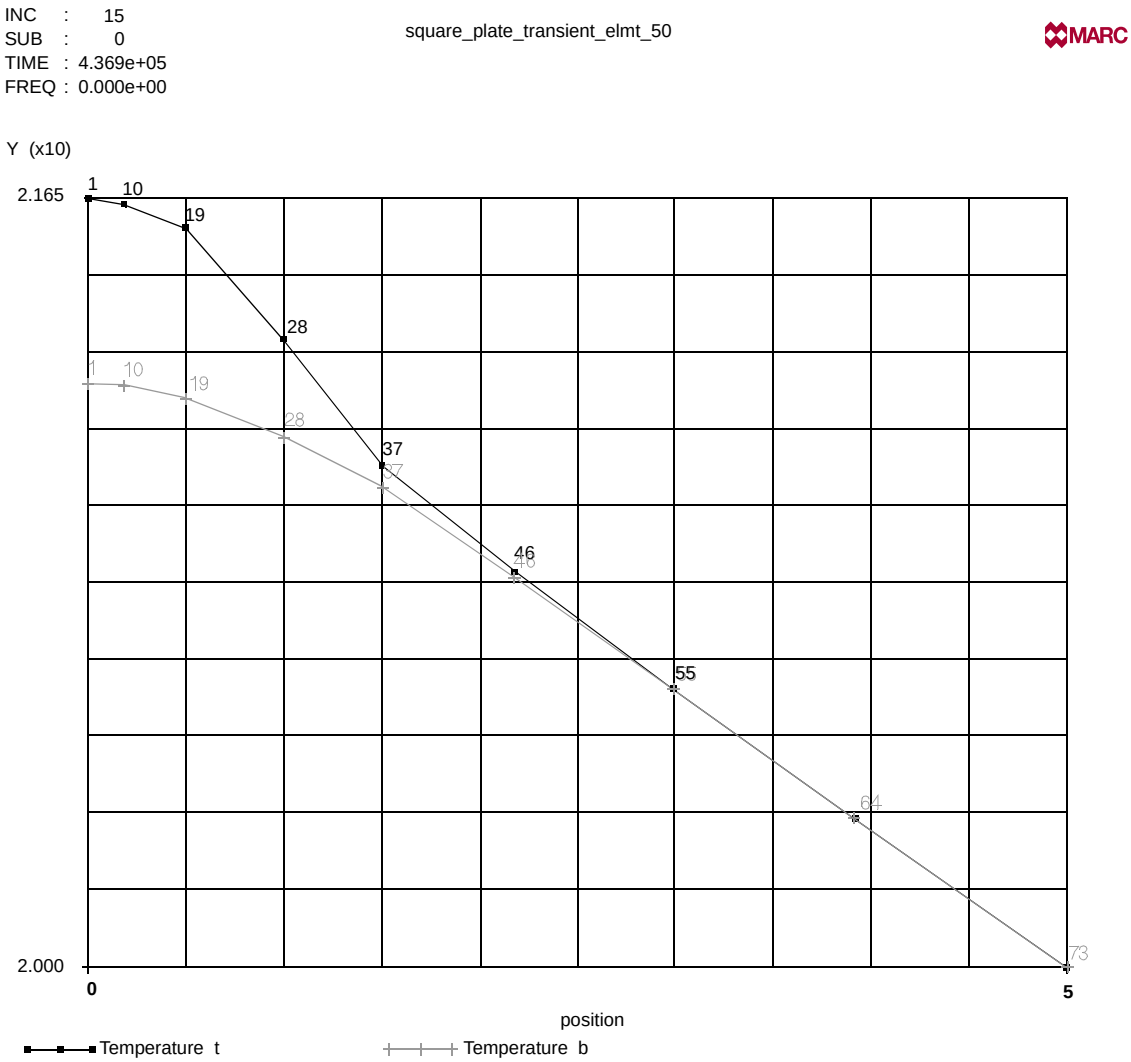

Figure 5.18-4 Path Plots for Upper and Lower Temperature at x = 0 (inc = 15)

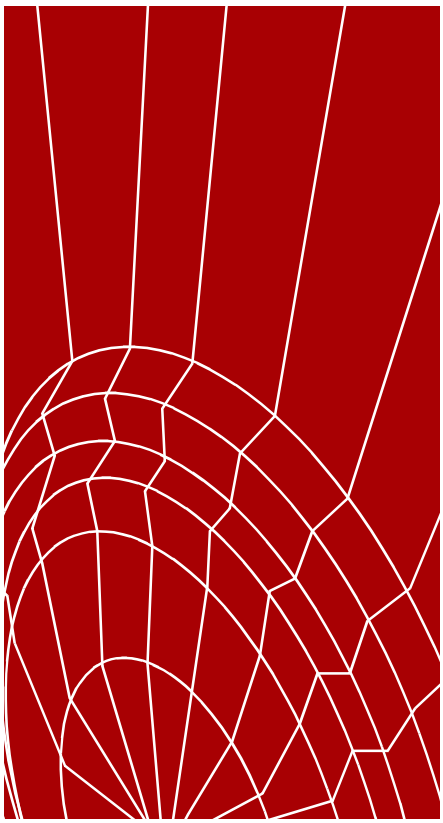

MARC Analysis Research Corporation

MARC®

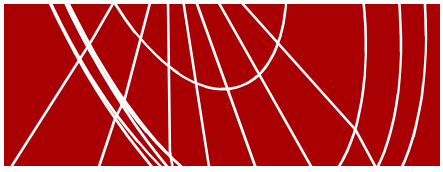

Volume E

Demonstration Problems

Version K7

Chapter 6
Dynamics

6 Dynamics Contents

Description	Problem
Dynamic Analysis of a Beam with Small Displacement Response	6.1
Beam Modes and Frequencies	6.2
Dynamic Analysis of a Plate with the Modal Procedure	6.3
Frequencies of a Rotating Disk	6.4
Frequencies of Fluid-solid Coupled System	6.5
Spectrum Response of a Space Frame	6.6
Harmonic Analysis of a Capped Mount	6.7
Harmonic Response of a Rubber Block	6.8
Elastic Impact of a Bar	6.9
Frequencies of an Alternator Mount	6.10
Modal Analysis of a Wing Caisson	6.11
Vibrations of a Cable	6.12
Perfectly Plastic Beam Explosively Loaded	6.13
Dynamic Fracture Mechanics	6.14
Eigenmodes of a Plate	6.15
Dynamic Contact Between a Projectile and a Rigid Barrier	6.16
Dynamic Contact Between Two Deformable Bodies	6.17
Spectral Response of a Pipe	6.18
Dynamic Impact of Two Bars	6.19
Elastic Beam Subjected to Fluid-Drag Loading	6.20
Eigenvalue Analysis of a Box	6.21

6 Dynamics List of Figures

Figure		Page
6.1-1	Element Type 5 Beam-Column Model	6.1-5
6.1-2	Ramp Pressure Forcing Function	6.1-6
6.1-3	Time Step = .001 Second	6.1-7
6.1-4	Time Step = .00025 Second	6.1-8
6.1-5	Timoshenko Beam, Time Step = .001 Second	6.1-9
6.2-1	Timoshenko Beam	6.2-3
6.2-2	Calculated Mode Shapes and Frequencies for a Timoshenko Cantilever Beam	6.2-3
6.3-1	Element 4 Plate Model	6.3-5
6.3-2	Element 8 Plate Model	6.3-6
6.3-3	Applied Pressure History	6.3-7
6.3-4	Displacements at Tip	6.3-7
6.4-1	Disk and Mesh	6.4-3
6.5-1	Dam/Water System and Mesh	6.5-4
6.6-1	Three-Dimensional Frame and Model	6.6-5
6.6-2	Spectral Density Function	6.6-6
6.6-3	Three-Dimensional Frame – Mode 1 (Extensional)	6.6-7
6.6-4	Three-Dimensional Frame – Mode 2 (Bending)	6.6-8
6.6-5	Three-Dimensional Frame – Mode 3 (Torsional)	6.6-9
6.7-1	Capped Rubber Mount	6.7-4
6.7-2	Displaced Mesh, Increment 1	6.7-5
6.7-3	von Mises Stress Distribution, Increment 1	6.7-6
6.7-4	Real Radial Stress 0.05 Cycle/Second	6.7-7
6.7-5	Imaginary Radial Stress 0.05 Cycle/Second	6.7-8
6.7-6	Real Radial Stress 0.5 Cycle/Second	6.7-9
6.7-7	Imaginary Radial Stress 0.5 Cycle/Second	6.7-10

Figure **Page**

6.8-1 Tensile Harmonic Analysis Mesh 6.8-3

6.9-1 Mesh of the Bar 6.9-3
6.9-2 Time History of Displacements 6.9-4
6.9-3 Time History of Velocity 6.9-5
6.9-4 Time History of the Reaction 6.9-6

6.10-1 Alternator Mount Model 6.10-5
6.10-2 First Mode 6.10-6
6.10-3 Second Mode 6.10-7
6.10-4 Third Mode 6.10-8

6.11-1 Mesh of a Wing Structure 6.11-3

6.13-1 Mesh with Initial Velocity 6.13-3
6.13-2 Small Displacement Analysis 6.13-4
6.13-3 Small Displacement Analysis 6.13-5
6.13-4 Small Displacement Analysis 6.13-6
6.13-5 Includes Geometric Nonlinearity 6.13-7
6.13-6 Includes Geometric Nonlinearity 6.13-8
6.13-7 Includes Geometric Nonlinearity 6.13-9

6.14-1 Dynamically Loaded Center-Cracked Rectangular Plate Problem 6.14-4
6.14-2 Dynamic Crack Problem Mesh 6.14-5
6.14-3 Crack Tip Region 6.14-6
6.14-4 Normalized Dynamic Stress Intensity Factors 6.14-7

6.15-1 Mesh 6.15-3
6.15-2 First Mode Shape of Cantilevered Plate 6.15-4
6.15-3 Third Mode Shape of Cantilevered Plate 6.15-5

6.16-1 Impactor and Rigid Wall 6.16-5
6.16-2 Impactor Geometry 6.16-6
6.16-3 Deformation at Initial Contact 6.16-7
6.16-4 Final Deformation 6.16-8
6.16-5 (A) Displacement History (Newmark-Beta Method) 6.16-9
6.16-5 (B) Displacement History (Central Difference Method) 6.16-10

Figure **Page**

6.16-6 (A) Velocity History (Newmark-Beta Method) 6.16-11
6.16-6 (B) Velocity History (Central Difference Method) 6.16-12
6.16-7 (A) Reaction/Impact Force History (Newmark-Beta Method). 6.16-13
6.16-7 (B) Reaction/Impact Force History (Central Difference Method) 6.16-14

6.17-1 Impactor and Deformable Barrier. 6.17-4
6.17-2 Geometries 6.17-5
6.17-3 Final Deformation. 6.17-6
6.17-4 (A) Displacement Histories (Newmark-beta Method) 6.17-7
6.17-4 (B) Displacement History (Central Difference Method) 6.17-8
6.17-5 (A) Velocity History (Newmark-beta Method) 6.17-9
6.17-5 (B) Velocity History (Central Difference Method) 6.17-10

6.18-1 Cantilever Pipe and its Cross Section. 6.18-3

6.19-1 Finite Element Mesh of Two Bars 6.19-3
6.19-2 Displacement History of Selected Nodes 6.19-4
6.19-3 Velocity History of Selected Nodes 6.19-5
6.19-4 Acceleration History of Selected Node 6.19-6
6.19-5 Reaction Force at Wall 6.19-7

6.20-1 Beam Partially Submerged in Fluid 6.20-4

6.21-1 Mesh of Box 6.21-3
6.21-2 Seventh Eigenmode 6.21-4
6.21-3 Ninth Eigenmode 6.21-5

6 Dynamics List of Tables

Table		Page
6.1	Dynamic Analysis Demonstration Problems	6-2
6.2-1	Beam Frequencies (cps)	6.2-2
6.3-1	Comparison of Frequencies in Cycles/Seconds	6.3-3
6.4-1	Frequencies of the Disk (cps)	6.4-2
6.5-1	Natural Frequencies of Dam/Water System (f = cps)	6.5-2
6.6-1	Eigenvalues (cps)	6.6-2
6.6-2	Spectrum Response at Node 2	6.6-3
6.8-1	Summary of Results: Real and Imaginary Displacements of Node 19	6.8-2
6.10-1	Geometric Properties of Beams Sections.	6.10-2
6.14-1	Normalized Dynamic Stress Intensity Factors	6.14-2
6.15-1	Frequencies in Hertz	6.15-2
6.18-1	Spectral Accelerations [m/sec2]	6.18-1
6.18-2	Displacements [m] in x and y Direction	6.18-2
6.18-3	Eigenvalues [Hz]	6.18-2
6.20-1	Displacements of the Beam (m)	6.20-2

6 Dynamics

MARC K.7 contains both the modal superposition and direct integration capabilities for the analysis of dynamic problems. A discussion on the use of these capabilities can be found in *MARC Volume A: Theory and User Information* and a summary of the feature is given below.

Modal Analysis (inverse power sweep or Lanczos)

Direct Integration
- Newmark-beta operator
- Houbolt operator
- Central difference operator
- Modal superposition

Consistent and lumped mass matrices

Damping
- Modal damping
- Stiffness and/or mass damping
- Numerical damping

Initial conditions
- Nodal displacement
- Nodal velocity

Boundary conditions
- Nodal displacement history
- Nodal velocity history
- Nodal acceleration history

Nonlinear effects
- Material nonlinearity (plasticity)
- Geometric nonlinearity (large displacement)
- Boundary nonlinearity (gap-friction)

Variable time steps
- Newmark-beta operator

Compiled in this chapter are a number of solved problems. These problems illustrate the use of dynamic analysis options in MARC. Table 6.1 shows the MARC elements and options used in these demonstration problems.

Table 6.1 Dynamic Analysis Demonstration Problems

Problem Number	Element Type	Parameters	Model Definition	History Definition	User Subroutines	Problem Description
6.1	5 45	DYNAMIC	CONTROL PRINT CHOICE	DYNAMIC CHANGE DIST LOADS	—	Dynamic response of a simply supported beam subjected to a uniformly distributed load.
6.2	45	DYNAMIC	—	MODAL SHAPE RECOVER	—	Frequencies and modal shapes of a Timoshenko beam.
6.3	4 8	DYNAMIC	CONTROL UFXORD FXORD INITIAL CONDITIONS	MODAL SHAPE DYNAMIC CHANGE DIST LOADS	UFXORD	Dynamic analysis of a cantilever plate using the modal procedure. Both inverse power sweep and Lanczos method.
6.4	10	DYNAMIC LARGE DISP FOLLOW FOR	ROTATION A CONTROL	MODAL SHAPE DIST LOADS	—	Frequencies of a rotating disk (centrifugal loading effect).
6.5	27 41	DYNAMIC FLU LOAD	FLUID SOLID	MODAL SHAPE	—	Frequencies of fluid-solid coupled (dam/water) system.
6.6	9	LARGE DISP DYNAMIC RESPONSE	RESPONSE SPECTRUM	MODAL SHAPE SPECTRUM	—	Evaluate eigenvalues for a space frame and perform spectrum response calculation.
6.7	28 33	LARGE DISP HARMONIC	TYING PHI-COEFI MOONEY	HARMONIC DISP CHANGE	—	Evaluate the response of a rubber mount subjected to several frequencies.
6.8	35	LARGE DISP HARMONIC	PHI-COEFI MOONEY	HARMONIC DISP CHANGE	—	Evaluate the response of a rubber block subjected to several frequencies at different amounts of deformation.
6.9	9	PRINT DAMPING LUMP DYNAMIC	POST INITIAL VEL DAMPING MASSES GAP DATA	DYNAMIC CHANGE	—	Elastic impact of a bar.

Table 6.1 Dynamic Analysis Demonstration Problems (Continued)

Problem Number	Element Type	Parameters	Model Definition	History Definition	User Subroutines	Problem Description
6.10	52	DYNAMIC	POST TYING MASSES	MODAL SHAPE RECOVER	—	Frequencies of an alternator mount.
6.11	30	DYNAMIC LINEAR	POINT LOADS	MODAL SHAPE	—	Modal analysis of a wing caisson.
6.12	9	DYNAMIC UPDATE LARGE DISP	POINT LOADS	PROPORTIONAL MODAL SHAPE	—	Vibration of a cable.
6.13	16	DYNAMIC LARGE DISP	INITIAL VELOCITY RESTART	AUTO TIME	—	Elastic-perfectly plastic beam explosively loaded.
6.14	27	DYNAMIC	DEFINE LORENZI	DYNAMIC CHANGE DIST LOADS	—	Impact loading of a center cracked rectangular plate. DeLorenzi method used to evaluate K.
6.15	7	LUMP DYNAMIC PRINT, 3	FIXED DISP	MODAL SHAPE RECOVER	—	Modal shape calculations using assumed strain element.
6.16	7	PRINT, 5 LARGE DISP DYNAMIC LUMP	INITIAL VELOCITY FIXED DISP DAMPING CONTACT	DYNAMIC CHANGE	—	Dynamic impact between deformable body and a rigid surface.
6.17	7	PRINT, 5 DYNAMIC LUMP LARGE DISP	DAMPING FIXED DISP INITIAL VELOCITY CONTACT	DYNAMIC CHANGE	—	Dynamic contact between two deformable bodies.
6.18	52	DYNAMIC RESPONSE	CONN GENER NODE FILL	MODAL SHAPE RECOVER SPECTRUM	—	Spectral response of a pipe.
6.19	11	DYNAMIC LUMP	INITIAL VELOCITY CONTACT CONTACT TABLE	DYNAMIC CHANGE	—	Dynamic impact using explicit dynamics.
6.20	98	DYNAMIC	DIST LOADS FLUID DRAG	DYNAMIC CHANGE	—	Beam subjected to fluid loads.
6.21	72	DYNAMIC FOLLOW FOR LARGE DISP	DIST LOADS	DIST LOADS DISP CHANGE MODAL SHAPE RECOVER	—	Eigenvalues of structure with rigid body modes.

6.1 Dynamic Analysis of a Beam with Small Displacement Response

The dynamic response of a simply supported rectangular beam is analyzed. The beam is subjected to a uniformly distributed load over its length. Three different methods of analysis are employed and their results are compared. These methods are the Newmark-beta and the Houbolt method of direct integration and the method of modal extraction and superposition.

This problem is modeled using the three techniques summarized below.

Data Set	Element Type(s)	Number of Elements	Number of Nodes	Differentiating Features
e6x1a	5	3	4	Houbolt
e6x1b	45	3	7	Newmark-beta
e6x1c	45	3	7	Newmark-beta, AUTO TIME

Element

Element type 5 is a simple, two-dimensional, rectangular section beam-column. It has three degrees of freedom per node: u, v, and right-handed rotation.

Model

The intent of the example is to illustrate the comparable accuracies of different dynamic operators. Therefore, a very simple model is used. Only half the beam is modeled and only the symmetrical response is sought. It is modeled with three type 5 elements. Because this example involves the small displacement and pure bending of a beam, this type of element is adequate. It should be noted that any beam type element in MARC could be chosen for this problem and would produce the same results.

Geometry

The beam is as shown in Figure 6.1-1 with height 23.13 in. (EGEOM1), cross-sectional area of 14.70 sq.in. and length of 144.0 inches.

Material Properties

The material properties input are Young's modulus of 30×10^6 psi, Poisson's ratio of 0.3, and mass density of $7.6754 \times l0^{-4}$ lb-sec^2/in^4.

Loading

The beam is loaded with the ramp pressure forcing function shown in Figure 6.1-2. The pressure load is ramped in the first increment to -655.65 psi and then brought down with constant slope to zero at time of .01 second. It remains at zero from then on as the beam's displacement oscillates around zero. Two different time steps are used for comparison with the implicit integration schemes, .001 second and .00025 second. For comparison, the natural frequencies are shown below:

Mode	Frequency (cycles per sec)
1	$.100 \times 10^3$
2	$.904 \times 10^3$
3	$.257 \times 10^4$
4	$.540 \times 10^4$
5	$.100 \times 10^5$

Boundary Conditions

The boundary conditions specify that all four nodes are constrained from movement in the u direction, the cantilevered end (node 1) is also fixed in the v direction and the midpoint (node 4) is constrained from any right-hand rotation.

Dynamic

The options are chosen on the DYNAMIC parameter by IDYN = 1 for modal extraction, IDYN = 2 for Newmark-beta, IDYN = 3 for Houbolt direct integration, and IDYN = 4 for the central difference operator. For the modal extraction scheme, the MODAL SHAPE option must be used. Although the beam response has six modes, only the first five modes are extracted in the solution. The assumption is made that the highest mode makes little contribution to the total response.

Results

The results are summarized in the two plots (see Figure 6.1-3 and Figure 6.1-4) of the beam's midpoint (node 4) displacement, v, versus time for time steps of .001 and .0025 seconds. We know that for any sine, cosine, or constant ramping with time forcing function, the modal solution gives an exact integration independent of time step size based on the modes extracted [1]. Since we have assumed that the highest mode made no significant contribution to the response, we can also assume that our modal solution defines an exact solution for the beam's response.

The plot of the larger time step = .001 second (Figure 6.1-3) illustrates the inherent errors introduced by the implicit integration schemes. The Newmark operator introduces some periodicity error and so its response is slightly out of phase with the exact modal solution. The Houbolt operator shows larger differences both in the amplitude and the period of the response. This larger phase error is due to the artificial damping introduced by the Houbolt operator. Although this damping causes inaccuracies for this large time step, small displacement problem, it is sometimes a useful feature in large nonlinear dynamic analyses. There it serves to damp out any high-frequency responses which may cause instabilities in the solution [2].

The plot of the small time step = .00025 second (Figure 6.1-4) shows good agreement between the Newmark-beta and the Houbolt direct integration operator solutions and the exact or modal solution.

The central difference operator proves to be unsuitable for this problem. The stability limit for the time increment of this explicit integration operator is $.172 \times 10^{-4}$, which is far too small to show enough of the beam's response in a reasonable number of increments.

When the problem was run with beam element type 45, the curved Timoshenko beam in a plane, the comparative results between the methods were the same. Again, the Newmark operator introduced some error in both the period and amplitude of the response as shown by the exact modal solution (see Figure 6.1-5).

The Timoshenko beam element is a 3-node planar beam element which allows transverse shear. It has three nodes per element with three degrees of freedom per node. As shown in Figure 6.1-5, the greater flexibility of the Timoshenko beam model gives its displacement function a greater amplitude and a slightly longer period than the response of the type 5 element model.

References

1. Dunham, R. S., Nickell, R. E., Stickler, D. S., "Integration Operators for Transient Structural Response", *Computers and Structures*, Vol. 2, pp. 1-15 (Pergamon Press, 1972).
2. Marcal, P. V., McNamara, J., "Incremental Stiffness Method for Finite Element Analysis of Nonlinear Dynamic Problem," *Numerical & Computer Methods in Structural Mechanics*, Symposium, Urbana, Illinois, September, 1971.

Parameters, Options, and Subroutines Summary

Example e6x1a.dat:

Parameters	Model Definition Options	History Definition Options
DIST LOADS	CONNECTIVITY	CONTINUE
DYNAMIC	CONTROL	DIST LOADS
ELEMENT	COORDINATES	DYNAMIC CHANGE
END	END OPTION	
SIZING	FIXED DISP	
TITLE	GEOMETRY	
	ISOTROPIC	
	POST	
	PRINT CHOICE	

Example e6x1b.dat:

Parameters	Model Definition Options	History Definition Options
DIST LOADS	CONNECTIVITY	CONTINUE
DYNAMIC	CONTROL	DIST LOADS
ELEMENT	COORDINATE	DYNAMIC CHANGE
END	END OPTION	
SIZING	FIXED DISP	
TITLE	GEOMETRY	
	ISOTROPIC	
	PRINT CHOICE	

Example e6x1c.dat:

Parameters	Model Definition Options	History Definition Options
DIST LOADS	CONNECTIVITY	AUTO TIME
DYNAMIC	CONTROL	CONTINUE
ELEMENT	COORDINATE	DIST LOADS
END	END OPTION	DYNAMIC CHANGE
SIZING	FIXED DISP	PROPORTIONAL INCREMENT
TITLE	GEOMETRY	
	ISOTROPIC	
	PRINT CHOICE	

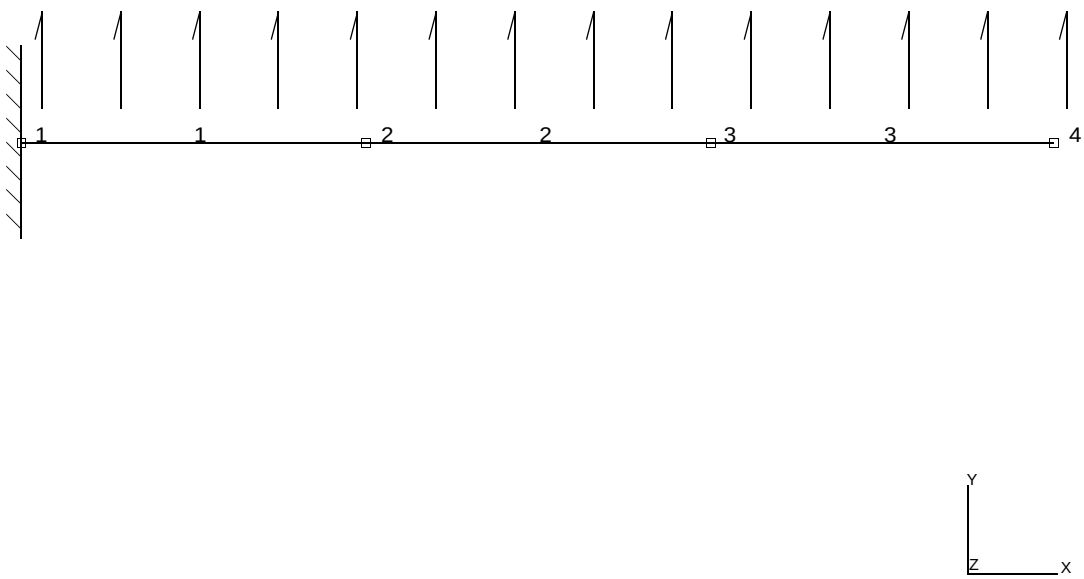

Figure 6.1-1 Element Type 5 Beam-Column Model

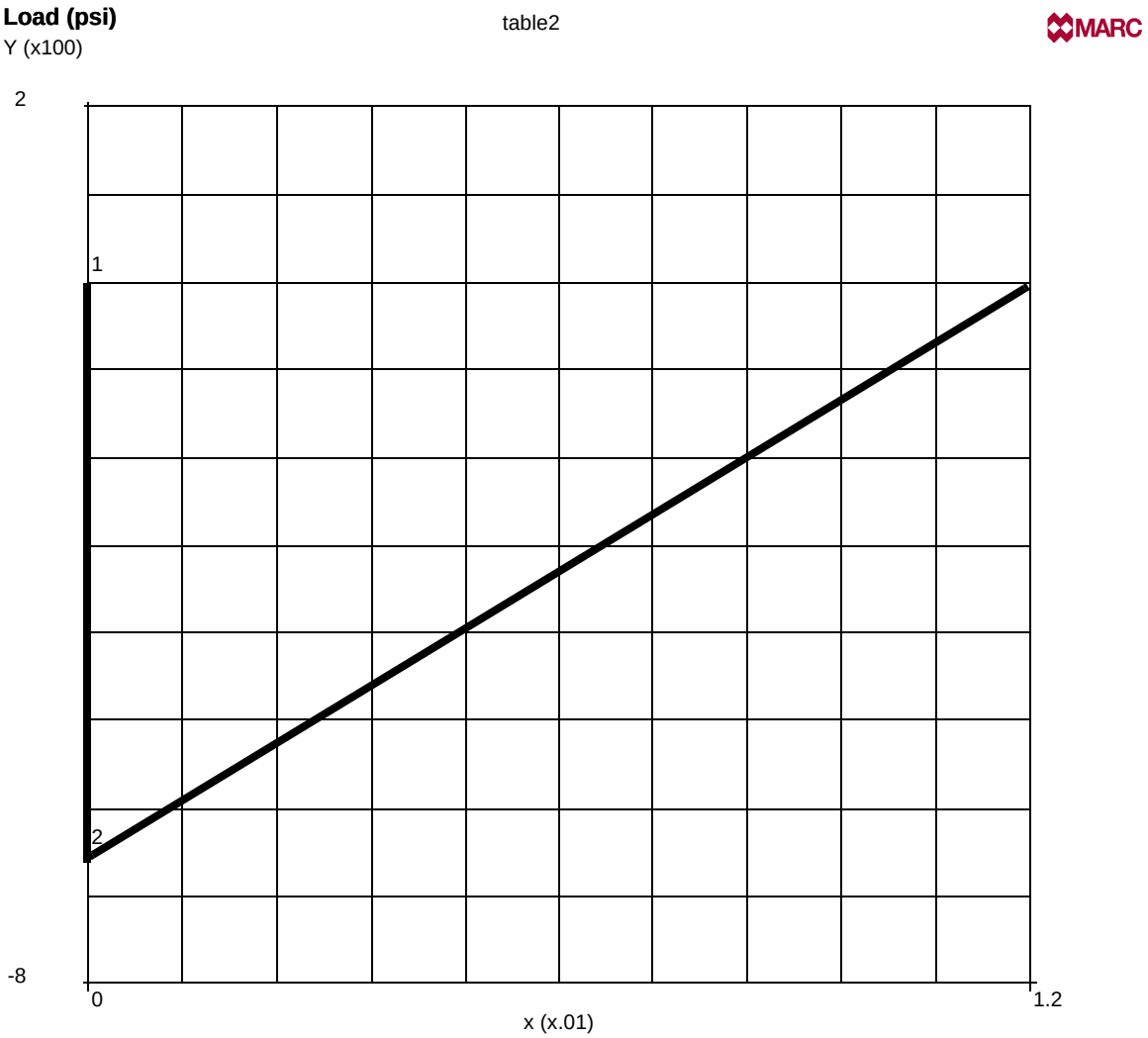

Figure 6.1-2 Ramp Pressure Forcing Function

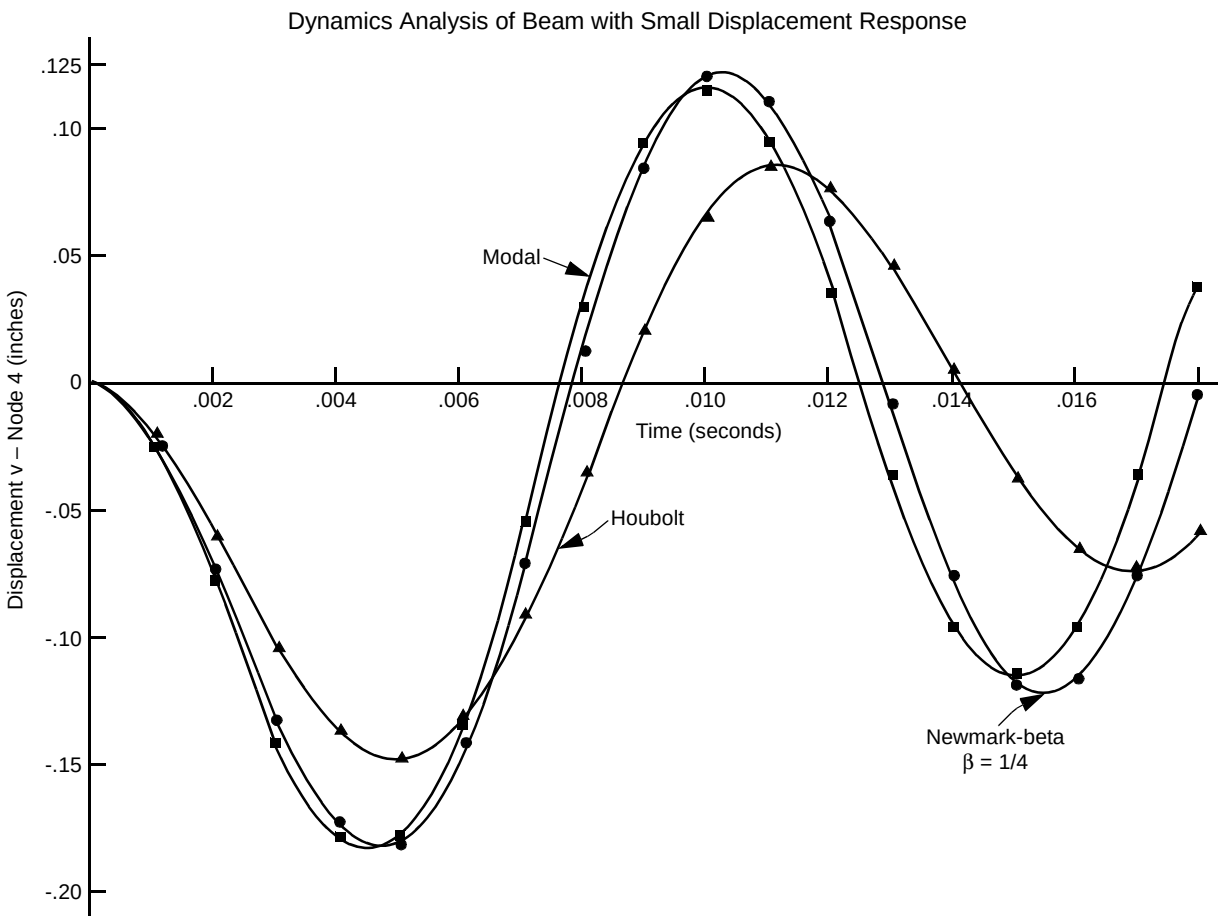

Figure 6.1-3 Time Step = .001 Second

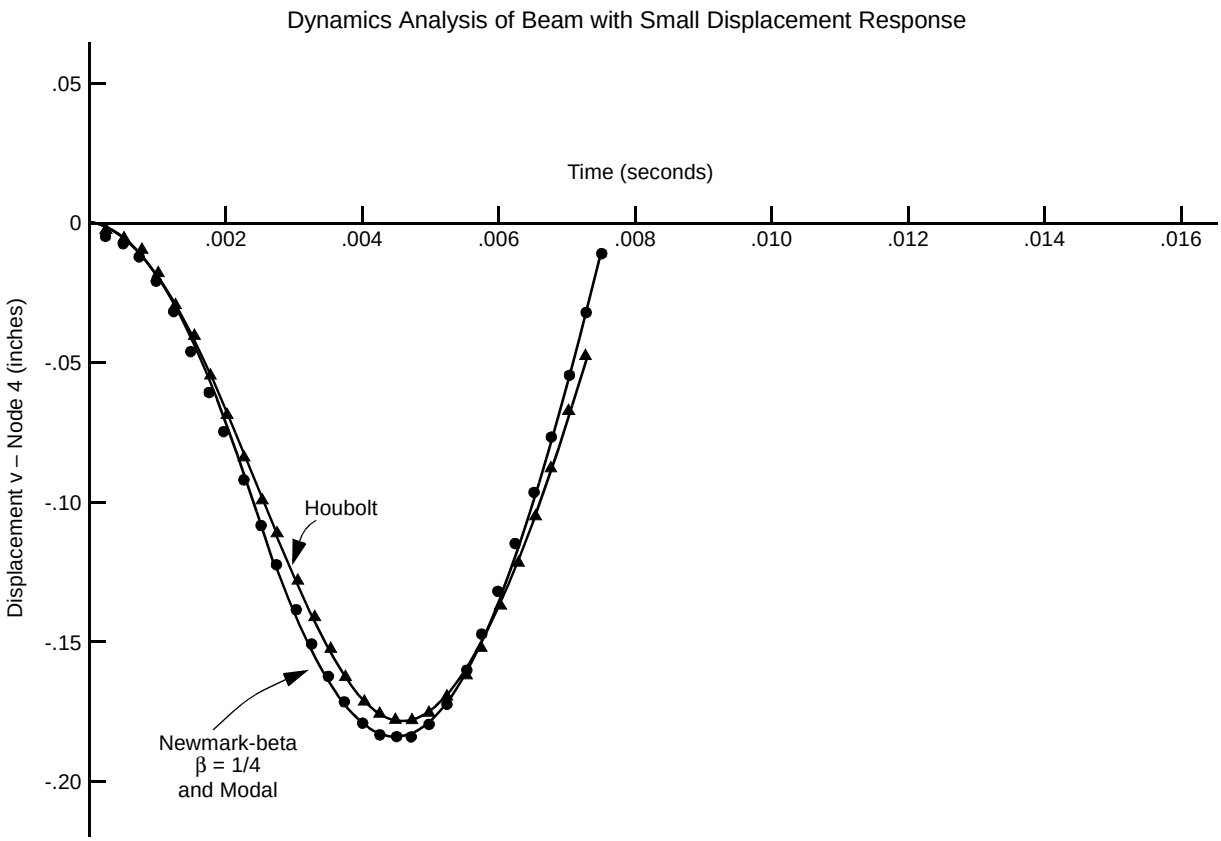

Figure 6.1-4 Time Step = .00025 Second

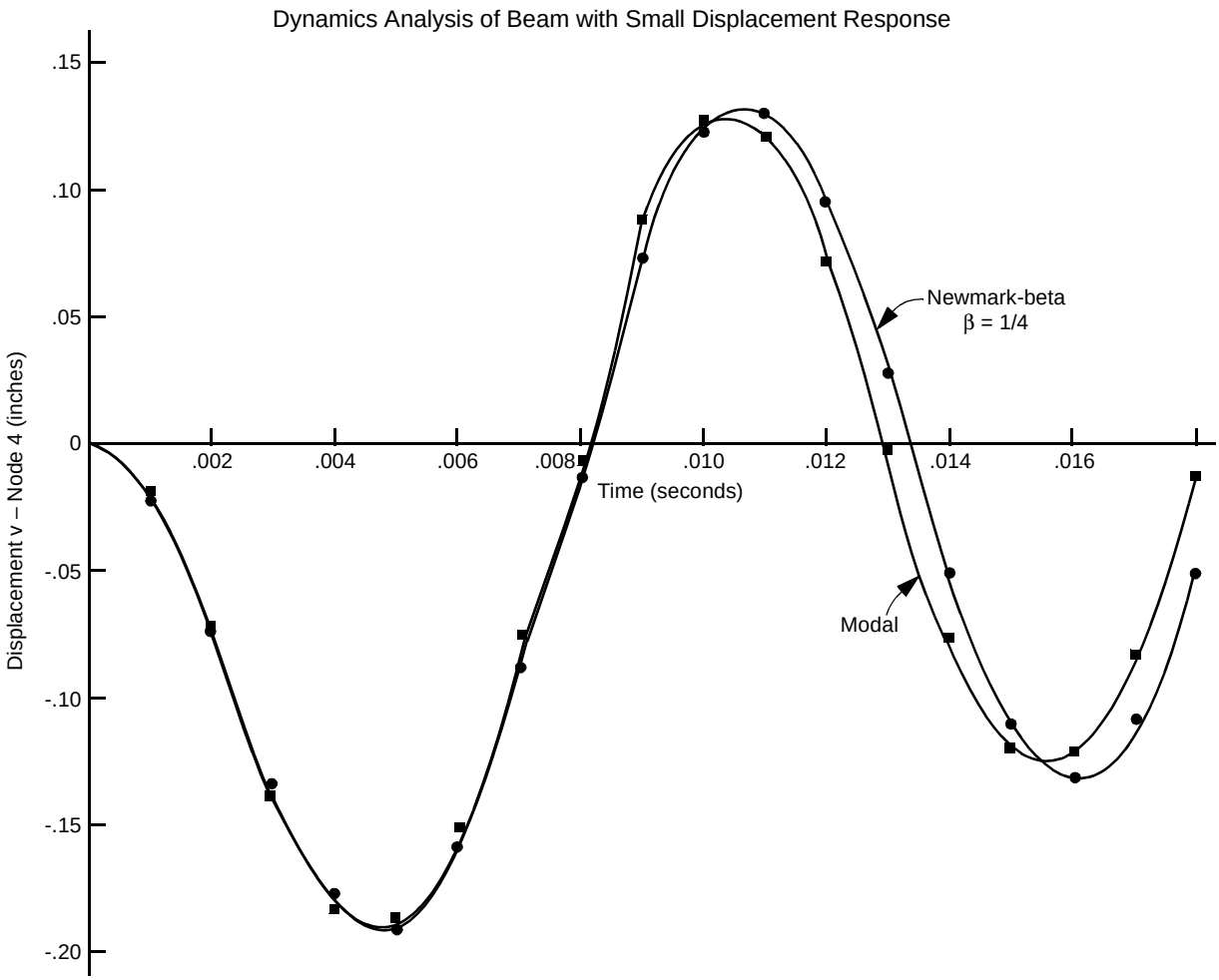

Figure 6.1-5 Timoshenko Beam, Time Step = .001 Second

6.2 Beam Modes and Frequencies

This problem is an illustration of the use of the Timoshenko beam element. The first three modes of a square-section, cantilever beam are extracted.

Element

Element type 45 is a two-dimensional Timoshenko beam with three nodes. Each node has two displacements and one rotational degree of freedom. The element uses a three-point Gaussian integration for mass and a two-point integration for stiffness. This is a consistently derived Timoshenko beam element.

Such elements are most commonly used in dynamic problems, because of the importance of shear and rotatory inertia effects in high-frequency beam response. The particular example is chosen because an exact Timoshenko beam solution is available.

Model

The geometry and dimensions are shown in Figure 6.2-1.

Material Properties

MARC only allows input of Poisson's ratio and Young's modulus as elastic material properties. The shear modulus is calculated from these. The Young's modulus is 30×10^6 psi and the Poisson's ratio is 1/3. The density is 7.25257×10^{-4} lb-sec^2/in^4.

Loading

No load is imposed, since only modes and frequencies are calculated.

Boundary Conditions

One end of the beam is built-in. All displacements and rotations are fixed. Thus, $u = v = \phi_a = 0$ for the built-in end node.

Results

The results in Table 6.2-1 are obtained for the first three modes. This mesh has 16 active degrees of freedom; a more refined mesh would show the calculated values converging on the exact values.

The first three mode shapes are shown in Figure 6.2-2.

Table 6.2-1 Beam Frequencies (cps)

Node	Exact*	Calculated
1	995.2	992.3
2	6065.0	6098.0
3	16469.0	16594.0

*Huang, T. C., “The Effect of Rotary Inertia and Shear Deformation on the Frequency and Normal Modes of Uniform Beams with Simple End Conditions,” *J. Applied Mechanics.*, Vol. 28, pp. 279-584 (December 1961).

Parameters, Options, and Subroutines Summary

Example e6x2.dat:

Parameters	Model Definition Options	History Definition Options
DYNAMIC	CONNECTIVITY	CONTINUE
ELEMENT	COORDINATE	MODAL SHAPE
END	END OPTION	
SIZING	FIXED DISP	
TITLE	GEOMETRY	
	ISOTROPIC	

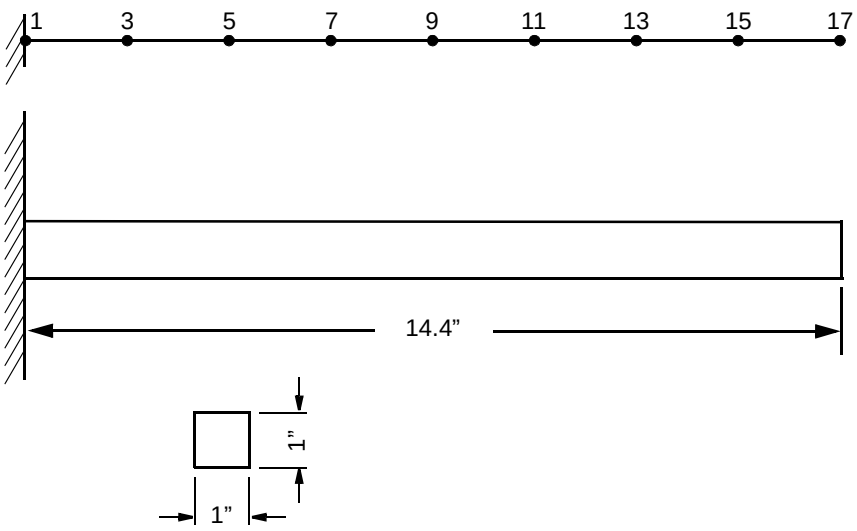

Figure 6.2-1 Timoshenko Beam

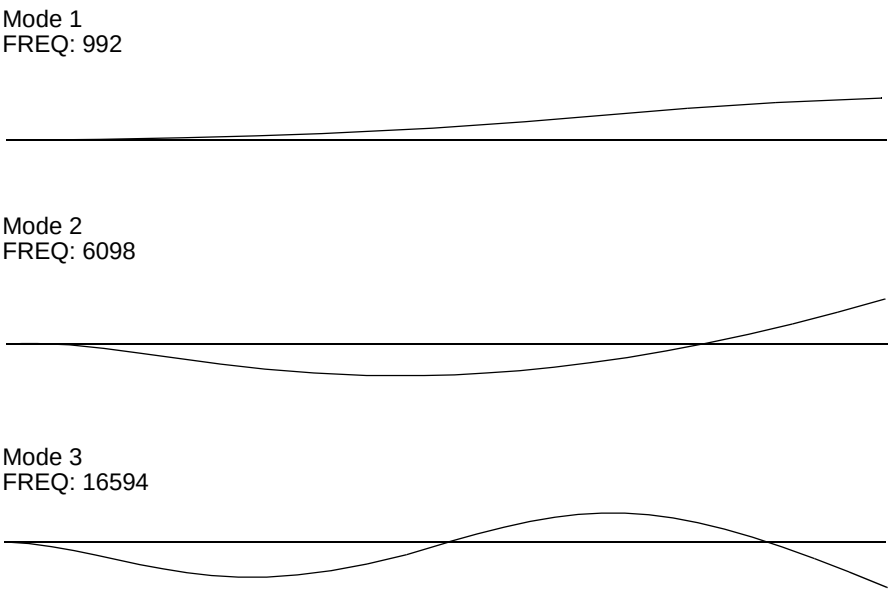

Figure 6.2-2 Calculated Mode Shapes and Frequencies for a Timoshenko Cantilever Beam

6.3 Dynamic Analysis of a Plate with the Modal Procedure

The vibration analysis of a cantilevered plate is considered here. The use of the modal analysis procedure available in the program is demonstrated. The normal modes are subsequently used for a transient analysis of the same plate subjected to a suddenly applied pressure. This analysis is repeated four times for comparison of different techniques. The plate is modeled using element type 4 and element type 8. Each finite element model is analyzed once using the power sweep method (four modes are extracted), and again utilizing the Lanczos technique (20 modes are calculated).

This problem is modeled using the four techniques summarized below.

Data Set	Element Type(s)	Number of Elements	Number of Nodes	Differentiating Features
e6x3a	4	2	6	Inverse Power Sweep
e6x3b	8	4	6	Inverse Power Sweep
e6x3c	4	2	6	Lanczos
e6x3d	8	4	6	Lanczos

Elements

This problem illustrates the use of both element 4 and element 8, the doubly-curved quadrilateral and triangular shell elements.

Model

The mesh for the element 4 model is shown in Figure 6.3-1. It consists of 2 elements and 6 nodes with 66 degrees of freedom. The element 8 model is given in Figure 6.3-2 and consists of 4 elements, 6 nodes and 54 degrees of freedom.

For the element 4 model, use was made of the internal FXORD option for generation of the required 14 coordinates per node. The flat plate (type 5) option requires only the specification of two coordinates (global x and y) in this case.

The element 8 model makes use of the user subroutine UFXORD option and illustrates the ease with which various complex coordinate systems may be programmed by the user. This routine provides the 11 nodal coordinates required for element 8 at each of the nodes specified in the UFXORD option. The subroutine is written to allow for inclusion of various twist angles such as would be evident in a turbine blade for example.

Geometry

For both models the plate is assumed to have a uniform thickness of 0.1 in. and is specified as EGEOM1.

Material Properties

The following material data was assumed for both models: Young's modulus (E) is 30.0×10^6 psi, Poisson's ratio (ν) is 0.3, weight density (w) is 0.283 lb/in^3, and mass density (ρ) is 7.324×10^{-4} lb-sec^2/in^4. The use of the default value for yield stress precludes any material nonlinear effects.

Boundary Conditions

In both cases, a clamped end condition is specified for nodes 1 and 2.

Dynamics

The modal method is selected by setting IDYN as 1 in the DYNAMIC parameter; the number of modes to be extracted (4 in this case) is also specified.

For input to E6.3A and E6.3B, the four designated modes and eigenvalues are extracted with the inverse power sweep method. This is accomplished by use of the MODAL SHAPE option immediately following the END OPTION option. A tolerance of 0.00001 was specified in this option as well as a limit on the number of sweeps of 40. MARC iterates until the change in eigenvalue is below the specified tolerance or the maximum number of iterations is reached.

Twenty modes are requested in E6.3C and E6.3D; and you request that the Lanczos technique of eigenvalue extraction be used.

Loading

The calculated modes and corresponding eigenvectors are then used to generate the transient solution induced by a suddenly applied uniform pressure transverse to the plate. The pressure time history is shown in Figure 6.3-3.

This loading is accomplished by use of a DYNAMIC CHANGE and DIST LOADS option. As can be seen in the input, the pressure (100 psi) is applied over a short time interval (0.00002 seconds) by the first of these options and removed by a second set with the same time interval but a reversed pressure loading. The final set of these options continues the transient analysis with the pressure held at zero for a total time of 0.001 seconds.

Control

The number of increments has been limited to six in the input decks; more complete output can be obtained by increasing the total number of increments allowed.

Output

The output provides first the increment zero results, which serve only to show the resulting initial accelerations. The output then provides four modal eigenvalues and eigenvectors as requested. This is followed by the transient analysis results.

Results

Referring to Table 6.3-1, the frequencies obtained for the first three modes compare quite well with the results found in Zienkiewicz, O. C., *The Finite Element Method in Engineering Science*, McGraw-Hill, 1971.

Table 6.3-1 Comparison of Frequencies in Cycles/Seconds

	Element 4		Element 8		
Modes	**Inverse Power Sweep**	**Lanczos**	**Inverse Power Sweep**	**Lanczos**	**Zienkiewicz**
1	845	845	858	858	846
2	3,651	3,651	4,190	4,190	3,638
3	5,280	5,280	6,348	6,348	5,266
4	7,137	7,137	7,371	7,371	11,870
5		12,100		15,130	
6		17,830		19,370	
7		25,630		25,750	
8		26,000		29,190	
9		27,060		30,890	
10		28,150		35,200	
11		34,930		42,770	
12		49,980		64,360	
13		55,160		65,150	
14		60,540		75,480	
15		60,720		78,280	
16		74,830		81,830	
17		76,060		96,710	
18		90,760		107,000	

Table 6.3-1 Comparison of Frequencies in Cycles/Seconds (Continued)

	Element 4		Element 8		
Modes	**Inverse Power Sweep**	**Lanczos**	**Inverse Power Sweep**	**Lanczos**	**Zienkiewicz**
19		92,070		111,600	
20		97,170		119,500	

The element type 4 results show agreement in this case, although results at the higher modes do not agree with those found in Zienkiewicz for element type 8. The fifth mode calculated by MARC agrees with the fourth mode of the reference; therefore, it is presumed that the Zienkiewicz solution omitted the fourth mode.

The modes and eigenvalues are used to follow the transient solution for a suddenly applied pressure on the top face of the beam. Figure 6.3-4 shows the variation with time of the displacement of two nodes at the end of the cantilever. A maximum of 0.145 in. was reached during the first excursion. This displacement may be compared with the static displacement of 0.08 inches for the same beam and loading. The dominance of the first mode is indicated as the maximum displacement was reached at about half the longest period.

Parameters, Options, and Subroutines Summary

Examples e6x3a.dat, e6x3b.dat, e6x3c.dat, and e6x3d.dat:

Parameters	**Model Definition Options**	**History Definition Options**
DIST LOADS	CONNECTIVITY	DIST LOADS
DYNAMIC	CONTROL	DYNAMIC CHANGE
ELMENT	COORDINATES	CONTINUE
END	END OPTION	MODAL SHAPE
SIZING	FIXED DISP	
TITLE	GEOMETRY	
	ISOTROPIC	
	POST	

User subroutine in u6x3b.f and u6x3d.f:

UFXORD

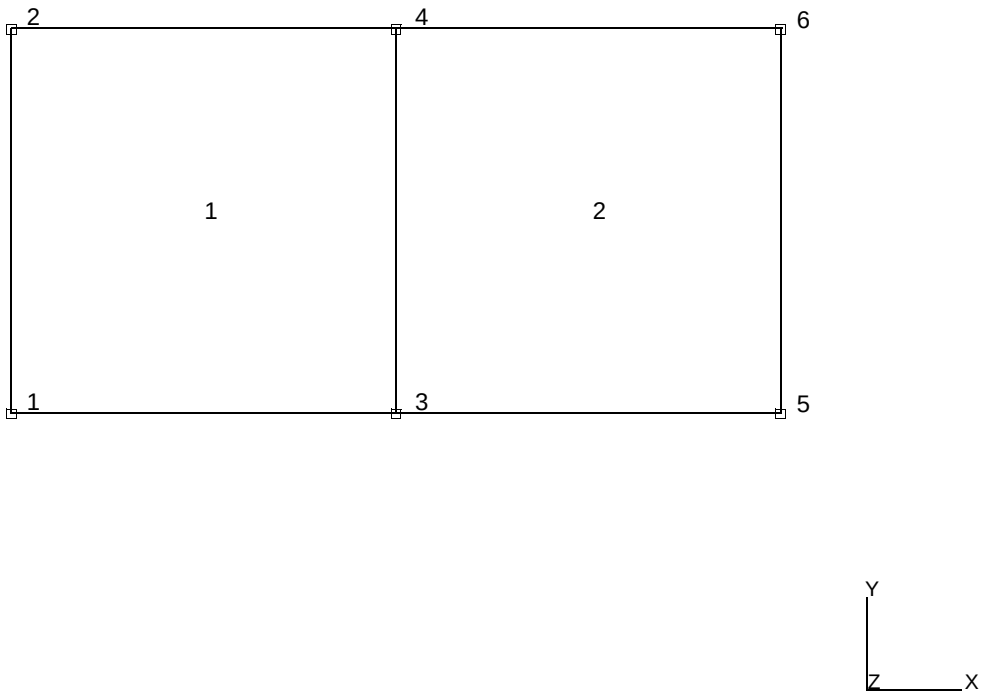

Figure 6.3-1 Element 4 Plate Model

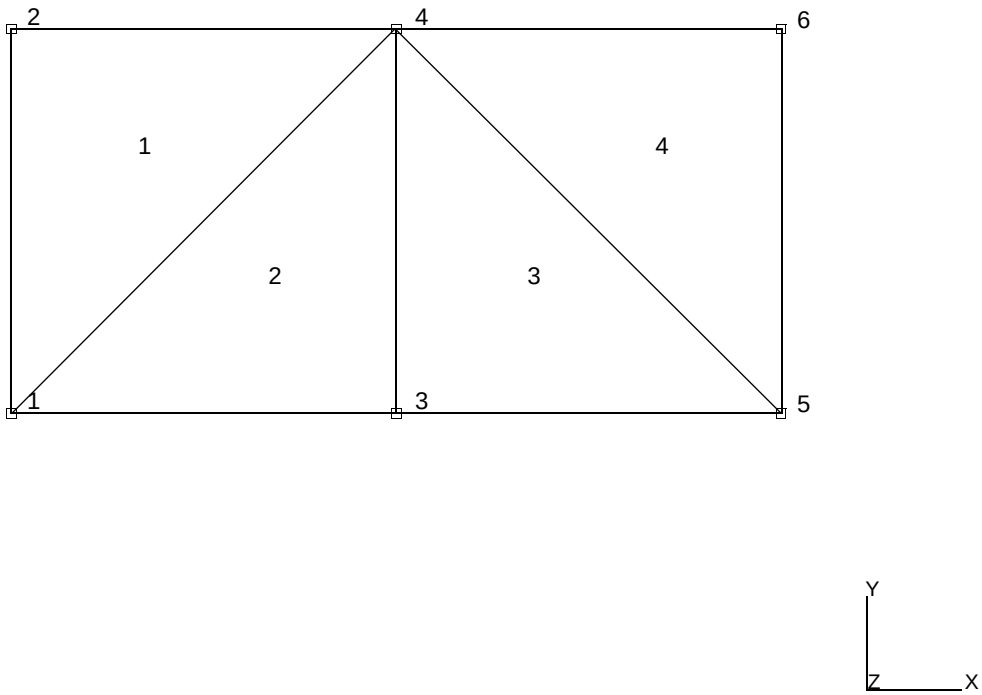

Figure 6.3-2 Element 8 Plate Model

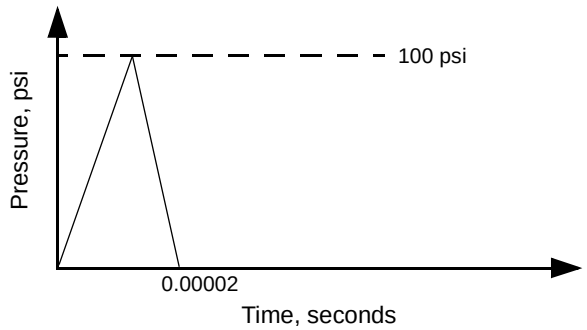

Figure 6.3-3 Applied Pressure History

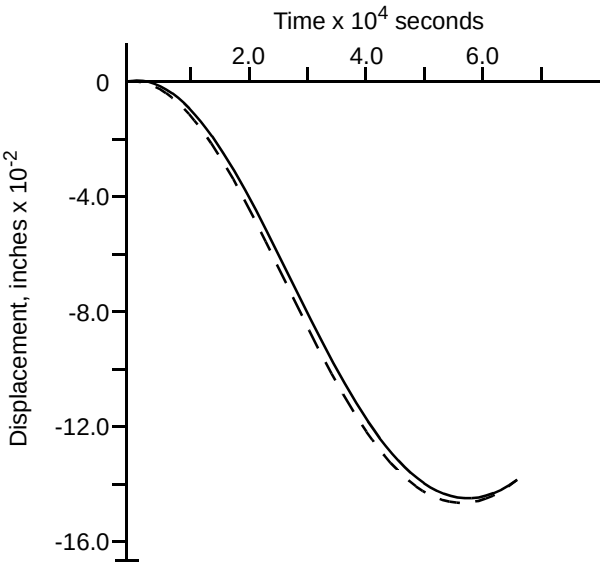

Figure 6.3-4 Displacements at Tip

6.4 Frequencies of a Rotating Disk

This problem illustrates the use of the LARGE DISP and Centrifugal Loading options for the study of natural frequencies of a rotating disk.

Model

Element type 10 is used in this analysis. There are 5 elements and 12 nodes. Disk dimensions and a finite element mesh are shown in Figure 6.4-1.

Material Properties

The material properties of the disk are: Young's modulus is 30×10^6 psi, and Poisson's ratio is 0.3. Mass density is 7.338×10^{-4} lb-sec/in^4.

Boundary Conditions

The z-displacements are constrained at the disk faces (z = 0 and z = 0.5). The radial-displacements are constrained at the line of symmetry (r = 0).

Centrifugal Loading

The input data for centrifugal loading is supplied by using the model definition option ROTATION A, the direction of the axis of rotation, and a point on that axis. The actual load is then invoked in the DIST LOADS option by specifying an IBODY load type = 100 and entering the quantity square of rotation speed in radians per time (ω^2), for the magnitude of the distributed load.

In the current problem the angular speed is:

$$\omega = 1000 \text{ rad/sec} = 500/\pi \text{ cycles/second}$$

and the axis of rotation is the symmetry axis.

LARGE DISPLACEMENT Option

The load stiffness matrix is a large displacement effect; therefore, it is only formed after increment 0. To obtain the modes and frequencies including all the large displacement terms, the user inputs the centrifugal load in the DIST LOADS block in increment 0. Following increment 0, use one or two steps of zero increments of load. This will update the stiffness matrix so that the user can then invoke the MODAL SHAPE option in the next increment. The FOLLOW FOR option should also be invoked since centrifugal loading is a follower force effect.

Results

Natural frequencies of the disk with and without rotation are shown in Table 6.4-1. The effect of centrifugal force on natural frequencies of the disk is evident. A body which is in tension will have its natural frequencies increased due to the initial stress stiffness effects; the opposite will be true for a body in compression.

Table 6.4-1 Frequencies of the Disk (cps)

No Rotation: $\omega^2 = 0$ (Small Displacement)	**$\omega^2 = 1.E8$ (Large Displacement)**	**% Increase**
$\omega_1 = 1.593 \times 10^4$	1.620×10^4	1.6
$\omega_2 = 4.172 \times 10^4$	4.236×10^4	1.4
$\omega_3 = 6.978 \times 10^4$	7.118×10^4	1.4
$\omega_4 = 1.008 \times 10^5$	1.040×10^5	1.5

Parameters, Options, and Subroutines Summary

Example e6x4.dat:

Parameters	**Model Definition Options**	**History Definition Options**
DYNAMIC	CONNECTIVITY	CONTINUE
ELEMENT	CONTROL	DIST LOADS
END	COORDINATE	MODAL SHAPE
FOLLOW FOR	DIST LOADS	
LARGE DISP	END OPTION	
SIZING	FIXED DISP	
TITLE	ISOTROPIC	
	ROTATION AXIS	

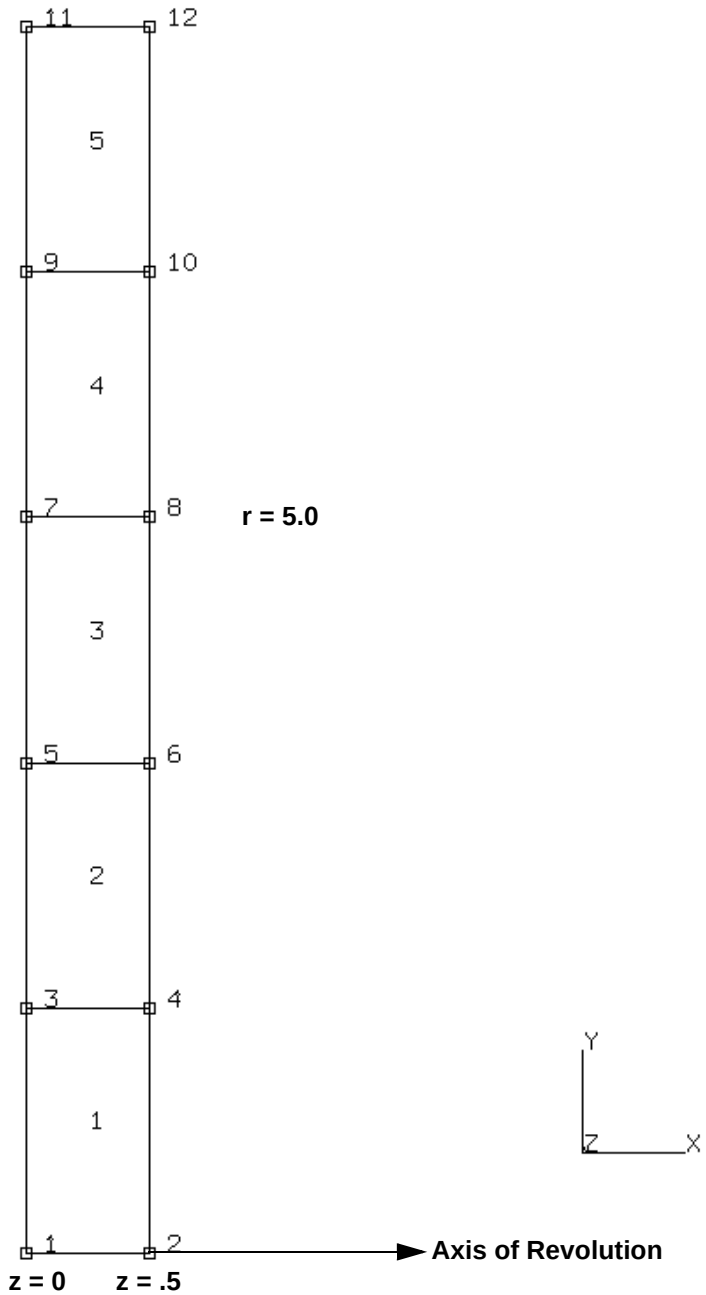

Figure 6.4-1 Disk and Mesh

6.5 Frequencies of Fluid-solid Coupled System

Utilizing the low viscosity and incompressibility of water, a fluid-solid interaction model has been developed and included in MARC. This capability allows the study of natural frequencies of structures immersed in or containing a fluid which is assumed to be inviscid and incompressible. The fluid model allows infinitesimal vibrations only, so that a pressure potential description of the fluid is assumed. The model allows for the effect of pressure waves in the fluid. It is only relevant to dynamic analysis, since the only effect of the fluid is to augment the mass matrix of the structure.

The fluid is modeled with heat transfer elements (potential theory) and the structure modeled with normal stress-displacement elements. The element choice should ensure the interface between the structural and fluid models has compatible interpolation; that is, first order solid and fluid elements, or both second order. If necessary, the tying option can be used to achieve compatibility.

A dam vibration problem was solved using the solid/fluid interaction option. As shown in Figure 6.5-1, the problem consists of a concrete dam section with water on one side, all on a rigid foundation.

Model

Number of elements = 6 (water: four element 41's; concrete: two element 27's)
Number of nodes = 31
Dimensions of the model and a finite element mesh are shown in Figure 6.5-1.

Material Properties

For concrete elements:

$E = 288 \times 10^6$ psf

$\nu = 0$

$\rho = 4.66$ lb-sec/ft^4

For fluid (water) elements:

$\rho = 1.94$ lb-sec/ft^4

Boundary Conditions

u = 0 at nodes 1, 6, 9, 14, 17

u = v = 0 at nodes 23, 26, 31

Fluid-Solid Interaction

The inputs for this are:

On the parameter FLUID LOAD and the number of solid/fluid interface element surfaces (2) must be entered.

Using the model definition FLUID SOLID option, the element number and element face number for solid and fluid elements must be entered. The element numbers and face numbers are, respectively:

Solid Element Number	Solid Element Face Number	Fluid Element Number	Fluid Element Face Number
5	1	3	10
6	1	4	10

Geometry

The thickness of the dam/water system is 1.0 foot.

Modal Shape

Default control values are used for the eigenvalue extraction.

Results

Frequencies of the dam/water system are given in Table 6.5-1. As anticipated, the inclusion of the water increases the effective mass and reduces the natural frequency of the dam.

Table 6.5-1 Natural Frequencies of Dam/Water System (f = cps)

Mode	Dam Without Water	Dam With Water
1	4.74	2.46
2	13.6	9.09

Parameters, Options, and Subroutines Summary

Example e6x5.dat:

Parameters	Model Definition Options	History Definition Options
DYNAMIC	CONNECTIVITY	CONTINUE
ELEMENT	COORDINATE	MODAL SHAPE
END	END OPTION	RECOVER
FLU LOAD	FIXED DISP	
SIZING	FLUID SOLID	
TITLE	GEOMETRY	
	ISOTROPIC	
	POST	
	UDUMP	

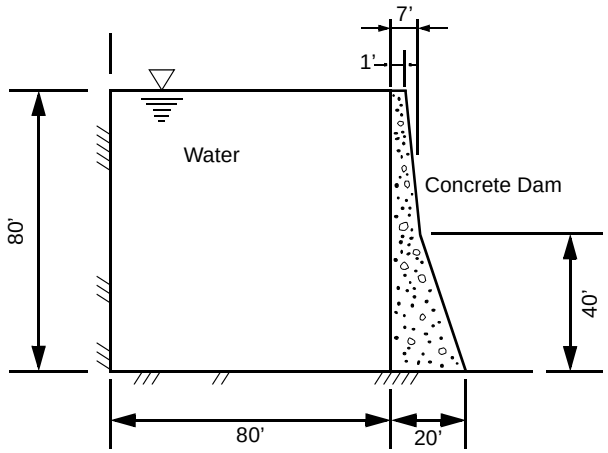

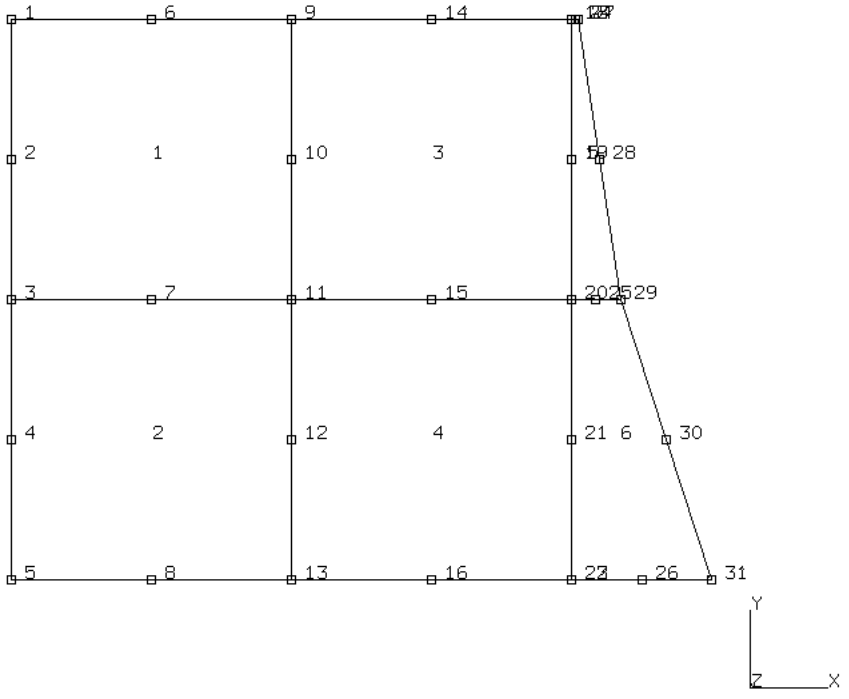

Figure 6.5-1 Dam/Water System and Mesh

6.6 Spectrum Response of a Space Frame

This problem illustrates the spectrum response capabilities of the program to determine the behavior of a three-dimensional frame. In addition, the influence of a compressive load on the eigenvalues of the system is demonstrated. This in turn affects the spectrum response analysis.

This problem is modeled using the two techniques summarized below.

Data Set	Element Type(s)	Number of Elements	Number of Nodes	Differentiating Features
e6x6a	9	20	9	Include LARGE DISP
e6x6b	9	20	9	

Model

The model is identical to that used in problem 2.24, consisting of 20 truss elements (type 9) and 9 nodes. The dimensions of the frame structure and a finite element model are shown in Figure 6.6-1.

Material Properties

The Young's modulus is 10×10^6 psi. The mass density is 0.1 lb-sec^2/in^4.

Geometry

The primary members (elements 1-12) have a cross-sectional area of 1 square inch. The secondary members (elements 13-20) have a cross-sectional area of 0.25 square inch.

Loads

A concentrated load at the apex (node 1) of 200,000 pounds is applied in the negative z-direction. This load is used to apply a compressive stress in the frame, as would be produced by guy wires.

Boundary Conditions

The base (nodes 3, 5, 7, and 9) is assumed to be fixed in space.

Displacement Spectral Density

A typical displacement spectral density function is entered. This could have optionally been specified through user subroutine USSD. The frequency is given in cycles per time unit (second). This function is shown in Figure 6.6-2.

Eigenvalue Response

This problem was run twice to observe the eigenvalue with and without the influence of the applied load. In the first case, the modal shape was placed immediately after the END OPTION; the stiffness matrix used includes only the elastic stiffness. In the second case, the modal shape was placed following a zero load step; the stiffness matrix also includes the initial stress stiffness contribution. In both problems, ten modes were extracted using the inverse power sweep method. The program performs a shift after the fifth mode. Table 6.6-1 gives the eigenvalues for the two cases. The “double modes” are clearly due to the symmetry with respect to the x,y axes.

Table 6.6-1 Eigenvalues (cps)

	No Initial Stress	With Initial Stress
1	13.205*	12.520*
2	14.999	13.442
3	16.386	14.944
4	13.204*	18.867*
5	25.172*	12.520*
6	25.172*	18.745*
7	60.196	59.840
8	121.12*	120.29*
9	123.11	122.42
10	121.11*	120.29*
*Indicates “double mode” pairs (closely-spaced modes).		

As anticipated, the inclusion of the initial compressive stress resulted in a reduction in the magnitude of the eigenvalues. The mode shapes for the first, second, and third modes are shown in Figure 6.6-3 through Figure 6.6-5. It is important to ensure the body is in equilibrium before extracting mode if the initial stress stiffness is included.

Spectrum Response

After the eigenmodes were extracted, a spectrum response calculation was performed. This response was calculated using only the lowest eight modes. This was done in an arbitrary manner. It is also possible to give a range of frequencies for which the response is based. The program computes the root mean square of the displacement (RMS), velocity, and acceleration. Table 6.6-2 gives the response at node 2 of the structure.

Table 6.6-2 Spectrum Response at Node 2

	No Initial Stress	With Initial Stress
RMS – Displacement	0.405 in	0.47 in
RMS – Velocity	33.600 in/sec	37.00 in/sec
RMS – Acceleration	2793.000 in/sec^2	2923.00 n/sec^2

Parameters, Options, and Subroutines Summary

Example e6x6a.dat:

Parameters	Model Definition Options	History Definition Options
DYNAMIC	CONNECTIVITY	CONTINUE
ELEMENT	COORDINATE	MODAL SHAPE
END	END OPTION	PROPORTIONAL INCREMENT
LARGE DISP	FIXED DISP	SPECTRUM
MESH PLOT	GEOMETRY	
SIZING	ISOTROPIC	
TITLE	POINT LOAD	
	RESPONSE SPECTRUM	
	RESTART	

Example e6x6b.dat:

Parameters	Model Definition Options	History Definition Options
DYNAMIC	CONNECTIVITY	CONTINUE
ELEMENT	COORDINATE	MODAL SHAPE
END	END OPTION	SPECTRUM
MESH PLOT	FIXED DISP	
SIZING	GEOMETRY	
TITLE	ISOTROPIC	
	POINT LOAD	
	RESPONSE SPECTRUM	
	RESTART	

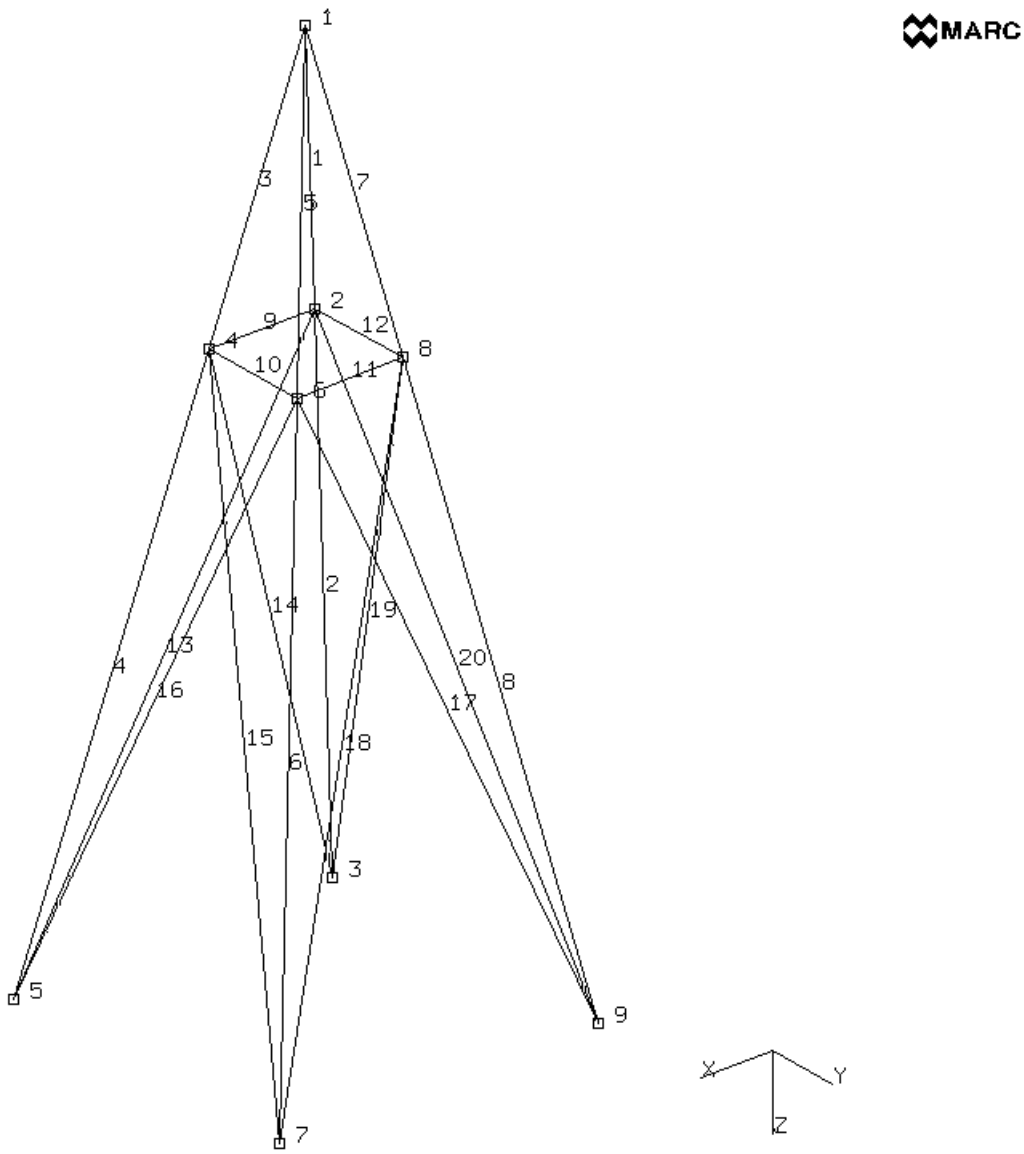

Figure 6.6-1 Three-Dimensional Frame and Model

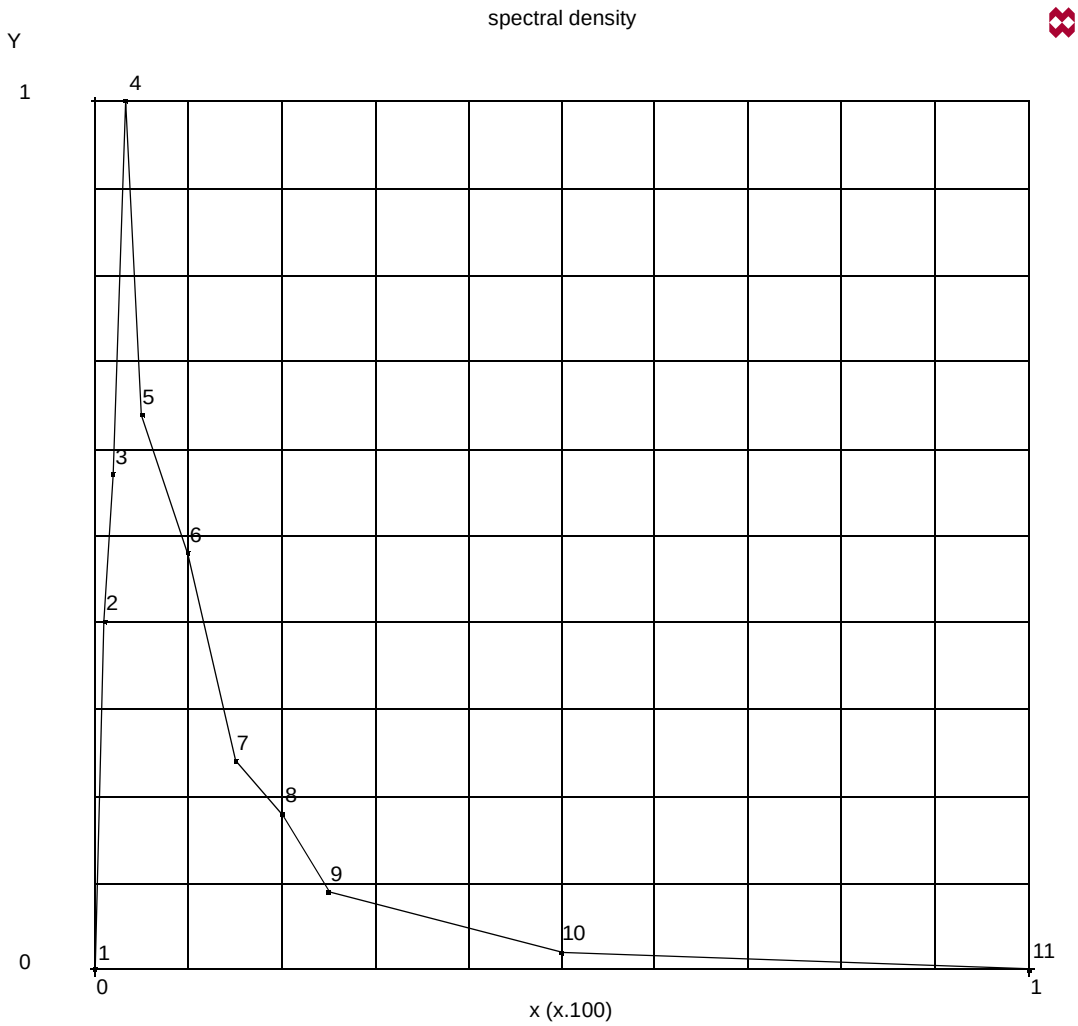

Figure 6.6-2 Spectral Density Function

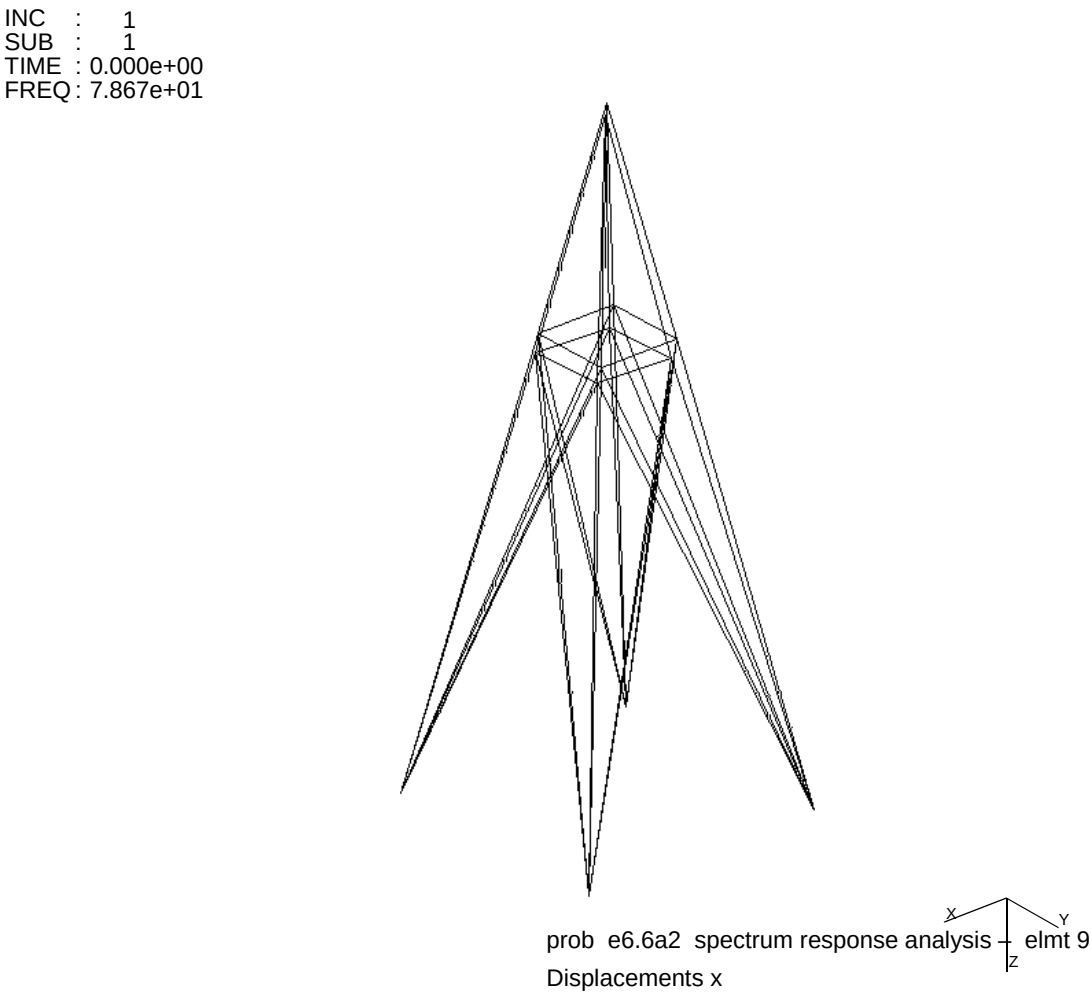

Figure 6.6-3 Three-Dimensional Frame – Mode 1 (Extensional)

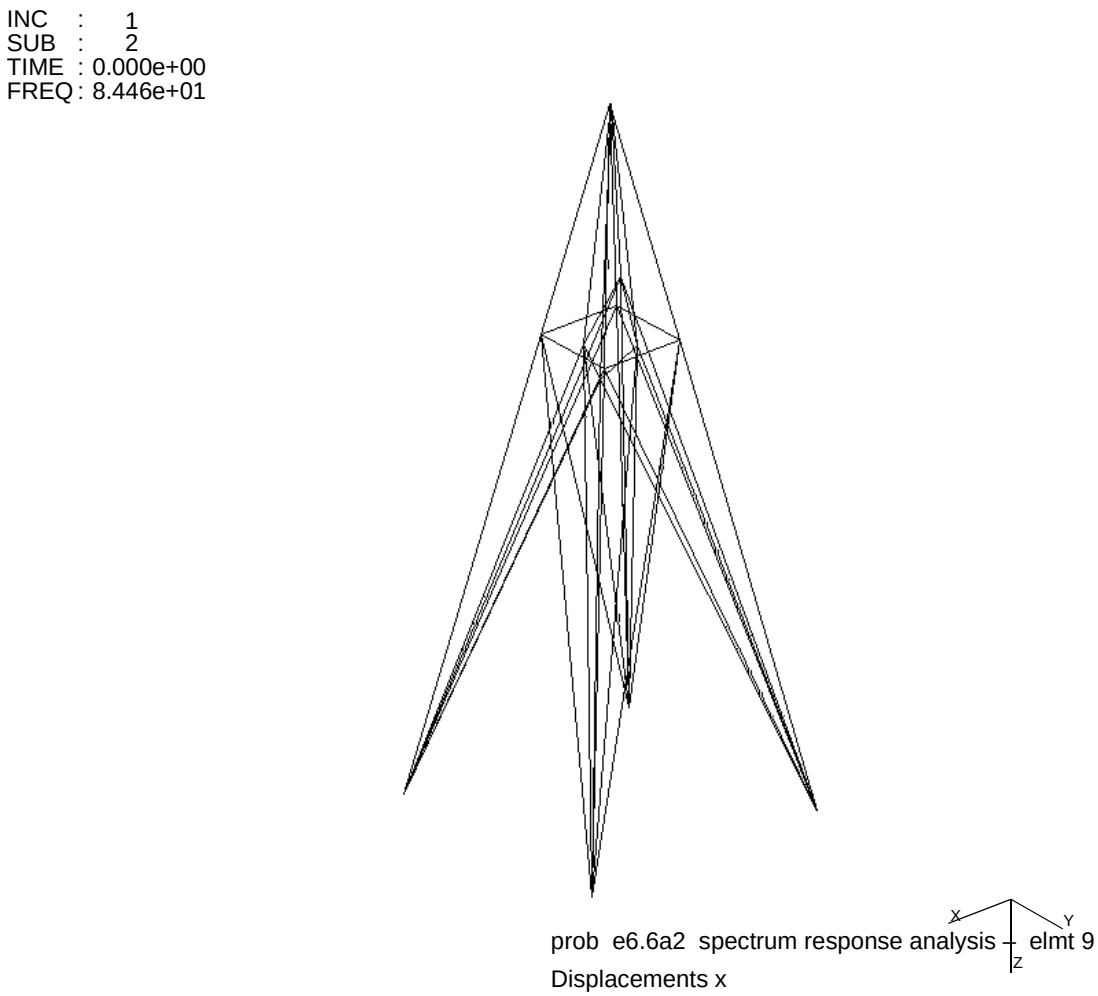

Figure 6.6-4 Three-Dimensional Frame – Mode 2 (Bending)

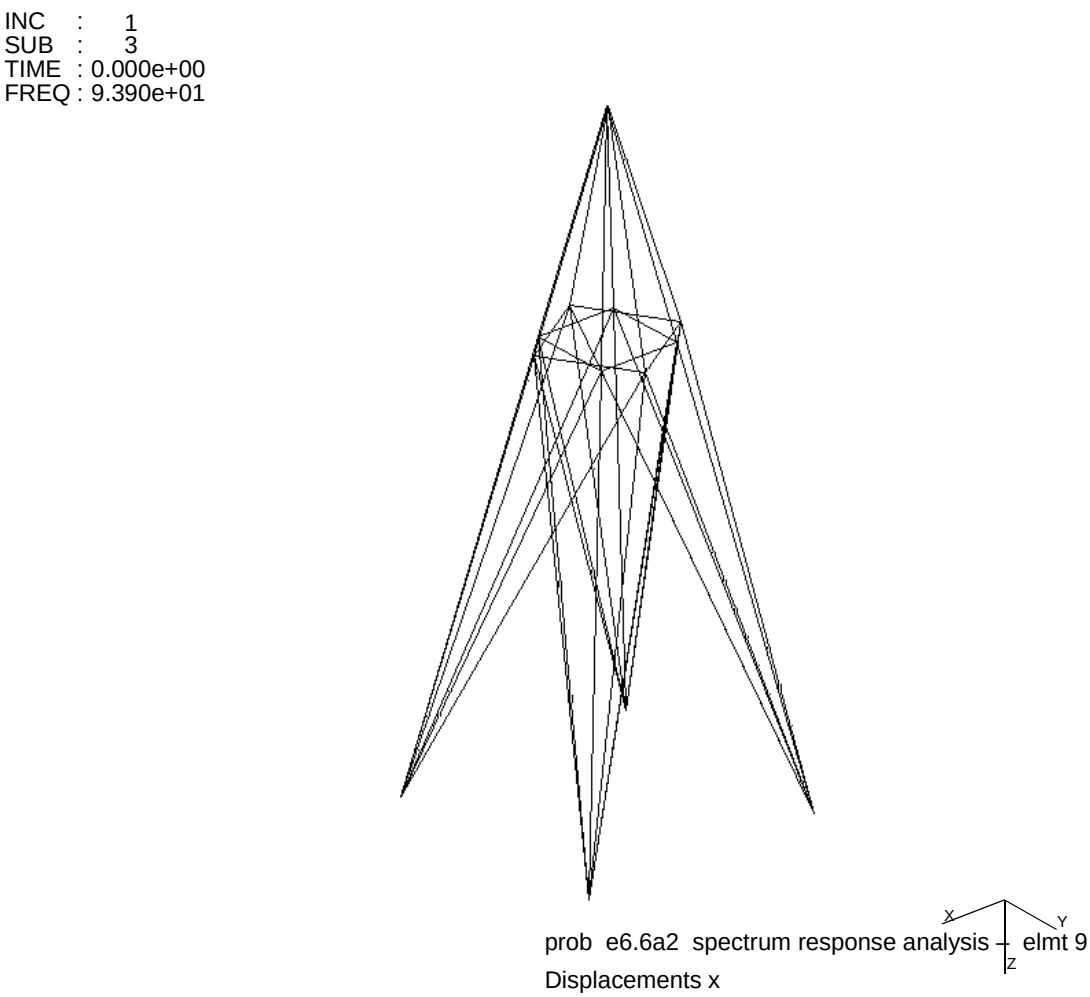

Figure 6.6-5 Three-Dimensional Frame – Mode 3 (Torsional)

6.7 Harmonic Analysis of a Capped Mount

A cylindrical rubber mount is bonded to two metal end caps and compressed to an in-service configuration. This assembly is subsequently subjected to harmonic excitation and the resultant harmonic response computed. This example demonstrates the use of the HARMONIC option of MARC.

Element

Only one-quarter of the mount assembly is represented due to symmetry. A total of 20 elements and 88 nodes define the mount model.

Two different element types are selected. Element type 28 models the metal behavior and element type 33 the rubber behavior. These are both 8-node axisymmetric quadrilateral elements. Element type 33 is the hybrid formulation equivalent of type 28. This finite element mesh is shown in Figure 6.7-1.

Model

The cylindrical rubber insert has a radius of 0.55 inch and a length of 0.5 inch. The metal end plates are 0.187 inch thick. A Mooney material model is used to describe the rubber behavior.

Geometry

No geometry inputs are required for element types 28 and 33.

Material Properties

The material constants for the third order invariant form C_{10}, C_{01}, C_{11}, C_{20}, and C_{30} are specified as 36.012, 6.061, 1.443, -1.504, and 1.690 psi, respectively. The mass density for the rubber is 9.53×10^{-5} lbm/in^3.

The metal has a Young's modulus of 3×10^7 psi and Poisson's ratio of 0.3. The von Mises yield point is specified as 1×10^{21} psi. The rubber data is input through the MOONEY option, while the steel data is entered through the ISOTROPIC option.

Boundary Conditions

Symmetry conditions are specified on the interior surfaces of the model. An initial displacement is applied to the metal caps of 0.022 in. total (0.011 in. for each cap).

An excitation magnitude of 0.05 in. is specified in the history definition DISP CHANGE option. This harmonic excitation is applied to the end caps.

PHI-COEFF

The real and imaginary components of the relaxation function coefficients for the rubber material are defined in this option as functions of frequency.

Optimize

The Cuthill-McKee bandwidth optimization algorithm is requested. This reduces the half-bandwidth for this problem to 27 from 68 in 19 iterations resulting in improved efficiency.

Restart

The RESTART option is included such that the analysis can be continued at some later time. This can be used to perform either additional quasi-static deformation, perform a harmonic response calculation at an additional frequency, or for postprocessing.

Harmonic

The HARMONIC history definition option defines an excitation frequency of 0.05 cycles/second for the first analysis, and 0.5 cycles/second during the second.

Tying

In this option, the cap/rubber interface is defined by tying the first two degrees of freedom of nodes representing the rubber material to corresponding metal cap model nodes. The third degree of freedom of corner nodes in this first layer of elements (4, 8, 12, 16) are tied. Here, the reduction of Herrmann variables in the intefacing elements improves the solution quality.

Proportional Increment

A proportional increment of 0.0. enforces equilibrium after the initial deformation. This was necessary because the total displacement was applied in the zeroth increment, where linear behavior is assumed. Thus, the subsequent harmonic analysis is performed on an equilibrated configuration of the mount model.

Results

The displacement after the initial displacement is shown in Figure 6.7-2. The von Mises stresses for this configuration are plotted in Figure 6.7-3. The real and imaginary stress components are plotted for excitation frequencies 0.05 cycles/second and 0.5 cycles/second in Figure 6.7-4 through Figure 6.7-7.

Parameters, Options, and Subroutines Summary

Example e6x7.dat:

Parameters	Model Definition Options	History Definition Options
END	CONNECTIVITY	CONTINUE
HARMONICS	CONTROL	DISP CHANGE
LARGE DISP	COORDINATE	HARMONIC
SIZING	END OPTION	PROPORTIONAL INCREMENT
TITLE	FIXED DISP	
	ISOTROPIC	
	MOONEY	
	PRINT CHOICE	
	TYING	

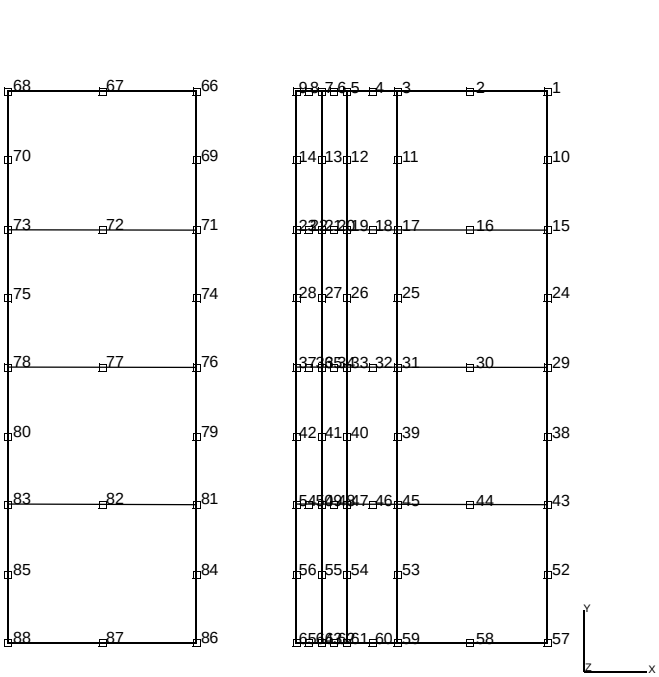

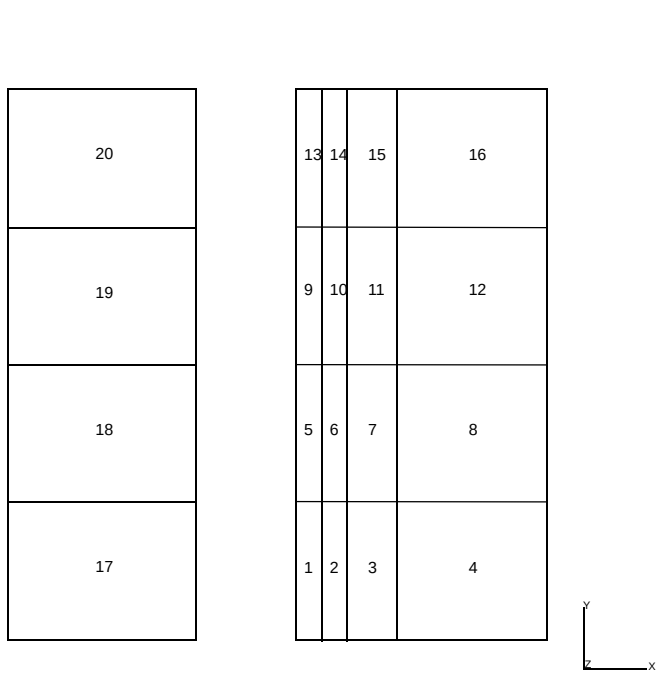

Figure 6.7-1 Capped Rubber Mount

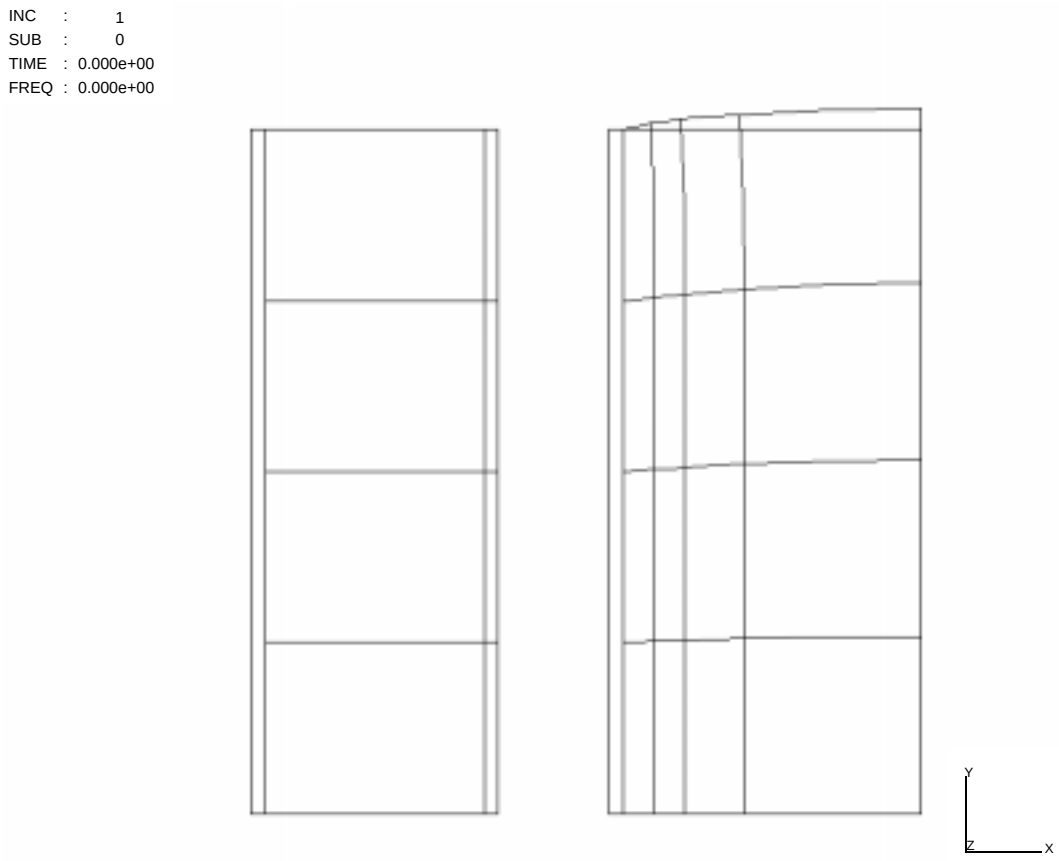

Figure 6.7-2 Displaced Mesh, Increment 1

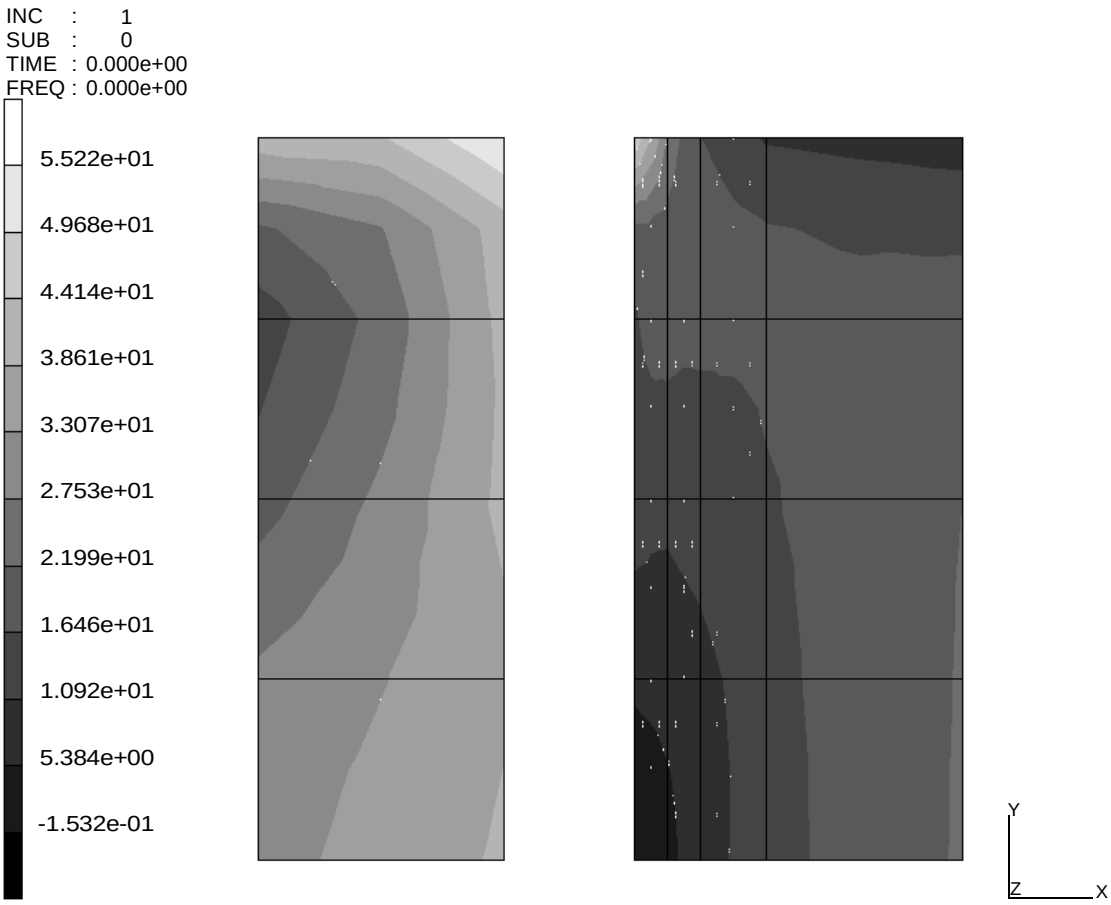

Figure 6.7-3 von Mises Stress Distribution, Increment 1

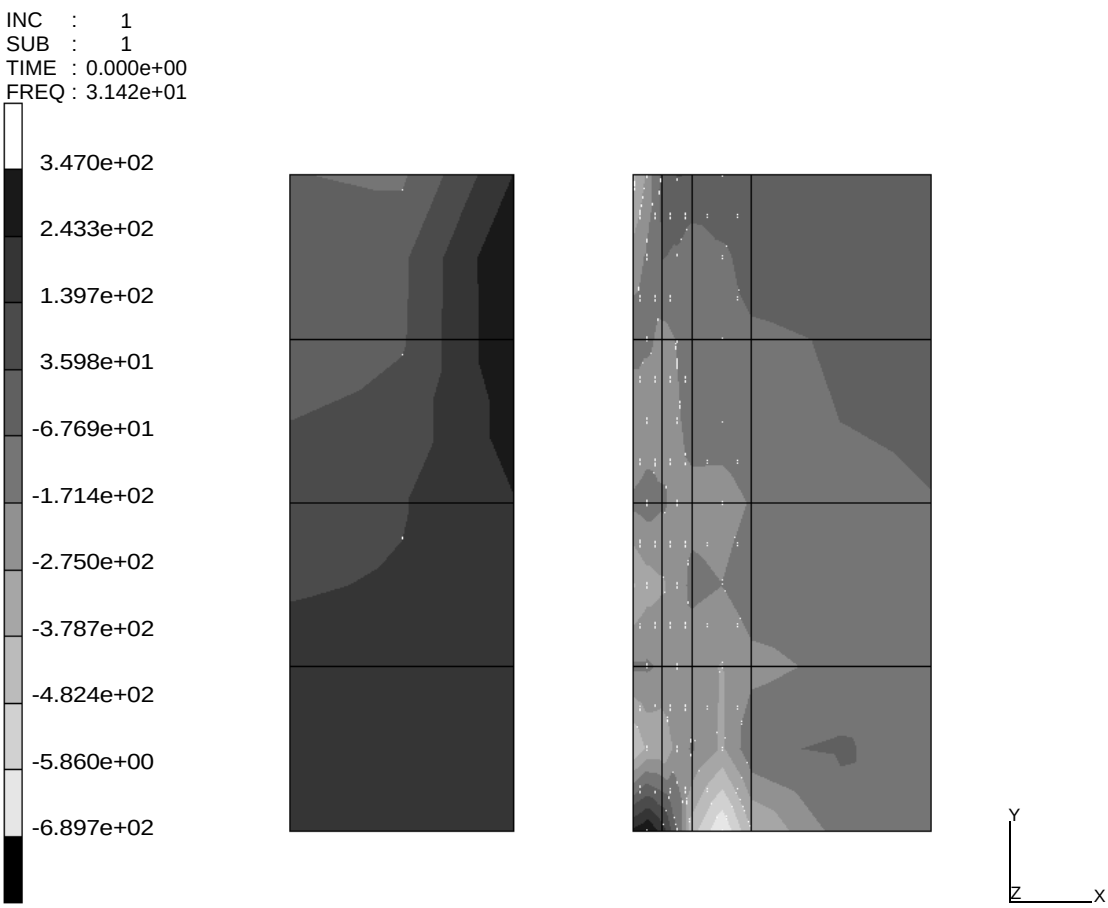

Figure 6.7-4 Real Radial Stress 0.05 Cycle/Second

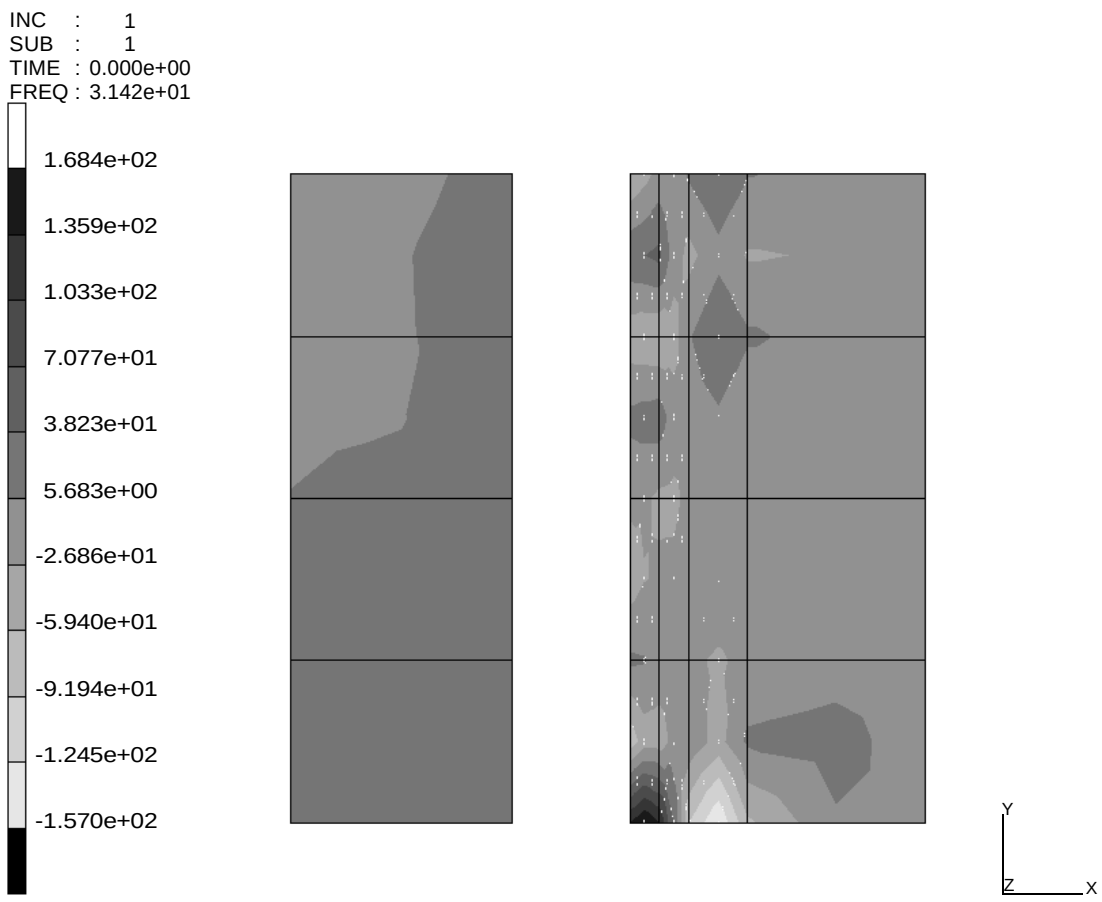

Figure 6.7-5 Imaginary Radial Stress 0.05 Cycle/Second

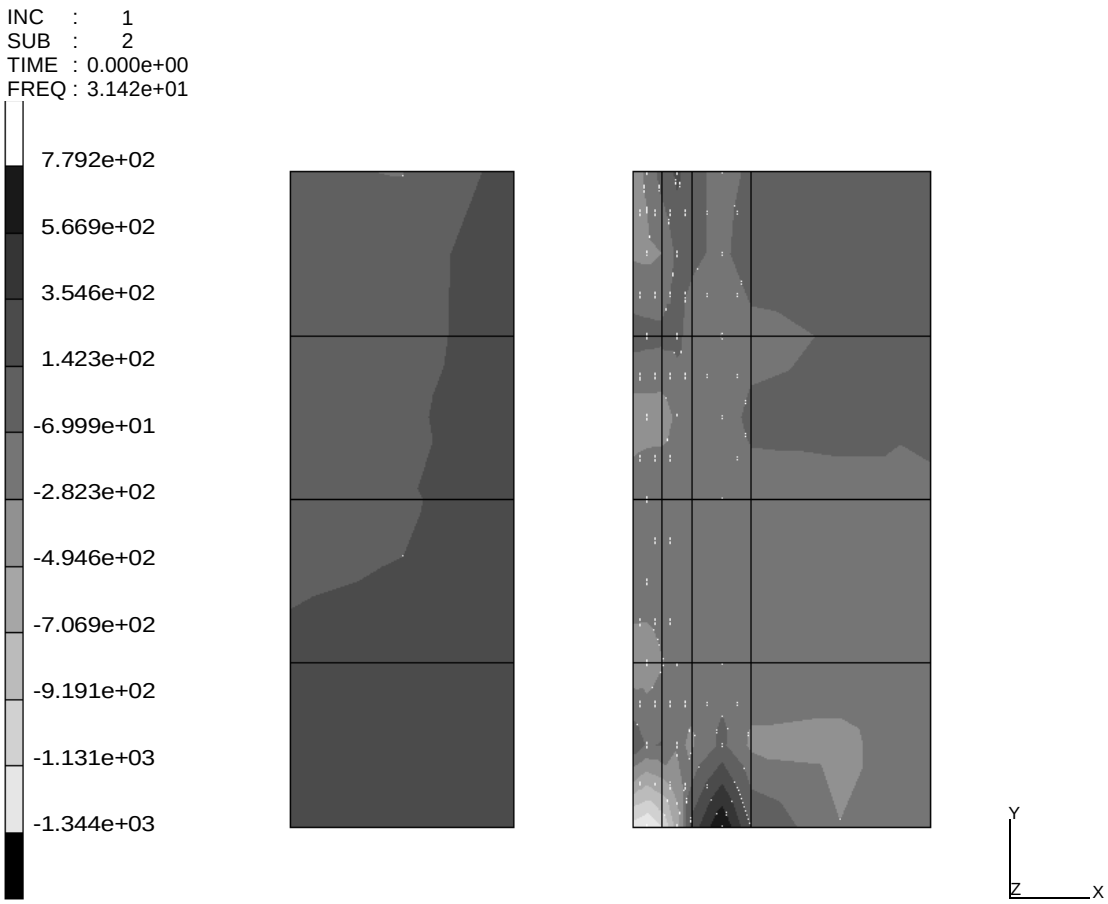

Figure 6.7-6 Real Radial Stress 0.5 Cycle/Second

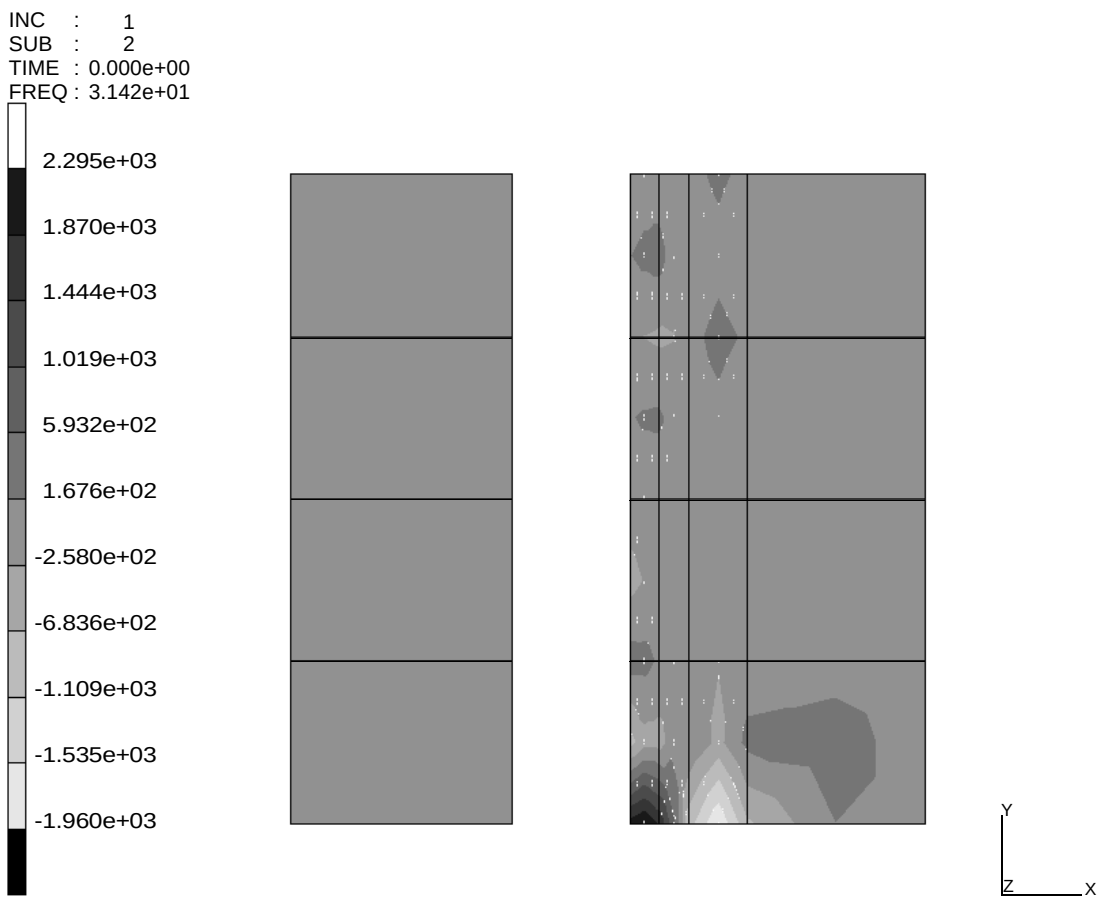

Figure 6.7-7 Imaginary Radial Stress 0.5 Cycle/Second

6.8 Harmonic Response of a Rubber Block

Using the HARMONIC option, the response of a solid block of elastometric material is calculated. The block is stretched in a quasi-static manner. The harmonic response of the block at three distinct frequencies are evaluated for three stretch ratios.

Element

Element type 35 is used to model the block.This is a 20-node isoparametric brick element using the Herrmann formulation for Mooney or Ogden material models.

Model

The finite element model of the block is shown in Figure 6.8-1. Only one element is used to model the block. Applying symmetry boundary conditions allows this single element to represent the whole block. The block dimensions are 50.8 x 9.754 x 9.754 inches.

Geometry

No geometry is specified.

Mooney

The material constants for the third order invariant form C_{10}, C_{01}, C_{11}, C_{20}, and C_{30} are specified as 36.012, 6.061, 1.443, -1.504, and 1.690 psi, respectively. The mass density is given as 9.53×10^{-5} lbm/in^3.

Boundary Conditions

The base of the block is constrained axially. The x = 0 and y = 0 faces have symmetry conditions applied. Initially, the block is stretched 2.54 in. or 10% of the block height. Subsequently, the DISP CHANGE option increases the stretch to 4.791 inches, and then to 7.086 inches.

The DISP CHANGE option with a flag 1 in the second field of card 2 is used to specify the harmonic excitation magnitude of 1 inch.

PHI-COEFF

The relaxation function coefficients are specified as a function of frequency in this option.

Harmonic

Excitation frequencies of 0.1, 1.0 and 5.0 cycles/seconds are specified for each deformed configuration.

Results

A summary of the harmonic displacements at node 19 for three stretch ratios are given in Table 6.8-1.

Table 6.8-1 Summary of Results: Real and Imaginary Displacements of Node 19

Frequency (cycles/sec)		Stretch Ratios		
		1.2	**1.338**	**1.558**
0.1	U_R	.4966	.4773	.4872
0.1	U_I	.00028	.00040	.00339
1.0	U_R	.4966	.4764	.4792
1.0	U_I	.00022	.00025	.00145
5.0	U_R	.4949	.4721	.4876
5.0	U_I	.00015	.00012	.0004

Parameters, Options, and Subroutines Summary

Example e6x8.dat:

Parameters	**Model Definition Options**	**History Definition Options**
END	CONNECTIVITY	CONTINUE
HARMONICS	CONTROL	DISP CHANGE
LARGE DISP	COORDINATE	HARMONIC
SIZING	END OPTION	PROPORTIONAL INCREMENT
TITLE	FIXED DISP	
	MOONEY	
	PRINT CHOICE	
	RESTART	

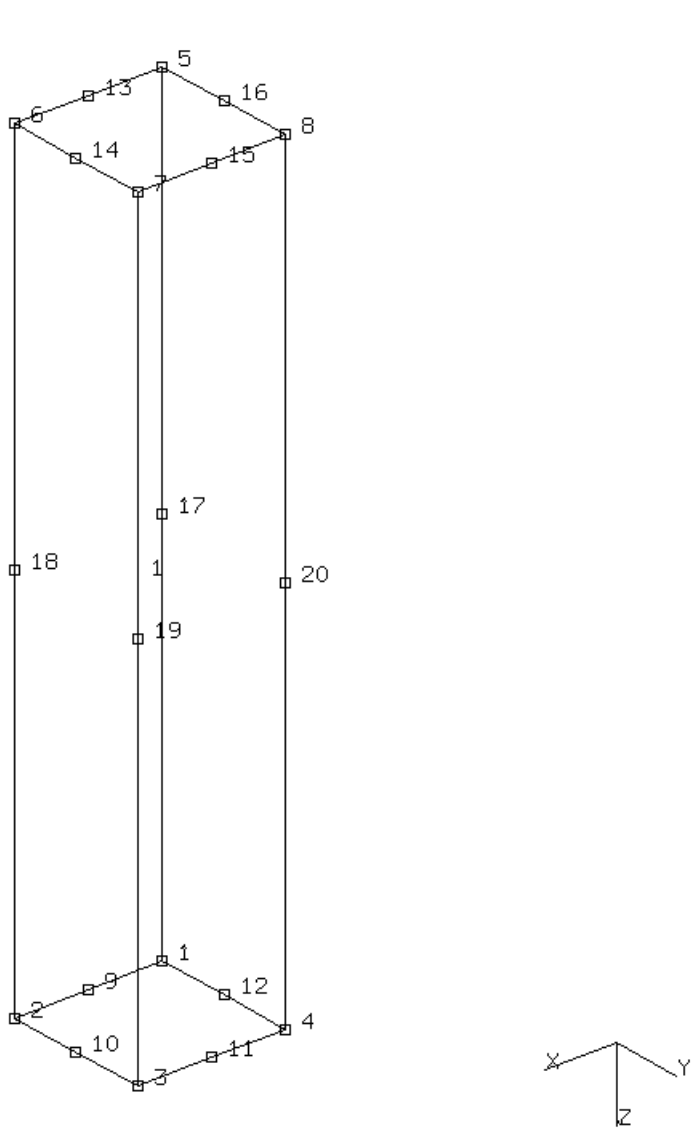

Figure 6.8-1 Tensile Harmonic Analysis Mesh

6.9 Elastic Impact of a Bar

The dynamic impact of a bar hitting against a rigid wall has been computed using the Newmark-beta direct integration algorithm. The contact has been represented by a gap element. The material is assumed to remain elastic.

Element

Element type 9, a simple linear straight truss with constant cross-section, has been used to represent the bar. It has three coordinates per node in the global x, y, z directions and uniaxial stress and strain. A gap element type 12 has been used to impose the contact condition.

Model

A simple model is assumed to represent the problem of a bar hitting against a wall. The mesh consists of 15 elements of type 9 and 1 gap element – a total of 19 nodes. The mesh is more refined where the contact will occur.

Geometry

The bar is shown in Figure 6.9-1. It is 100 mm long and has a uniform cross section of 314.15 mm^2.

Material Properties

The material properties of the bar are:

Young's modulus is E = 1.96E+5 N/mm^2,
Poisson's ratio is ν = 3,
mass density is ρ = 7.85E-6Kg/mm^3, and
yield point is σ_y = 235.2 N/mm^2.

Boundary Conditions

Only the axial displacements are free. The end node of the gap element associated with the wall has every degree of freedom constrained.

Dynamics

The body has an initial velocity of 50 m/seconds.

The case has been studied for 200 seconds using 200 time-steps of 1 second in the DYNAMIC CHANGE option.

Results

The displacement of the last node is shown in Figure 6.9-2. The velocity is shown in Figure 6.9-3. The elastic wave is moving with a velocity:

$$c = \left[\frac{E}{\rho}\right]^{1/2} = 5 \times 10^{3} \text{m/sec.}$$

The bar rebounds after a time:

$$t = \frac{21}{c} = 40 \times 10^{-6} \text{sec.}$$

In Figure 6.9-4, the reaction in the gap is equal to zero in the fourth increment, implying that separation has occurred.

Parameters, Options, and Subroutines Summary

Example e6x9.dat:

Parameters	Model Definition Options	History Definition Options
DAMPING	CONNECTIVITY	CONTINUE
DYNAMIC	CONTROL	DYNAMIC CHANGE
END	COORDINATE	
LUMP	DAMPING	
SIZING	END OPTION	
TITLE	FIXED DISP	
	GAP DATA	
	GEOMETRY	
	INITIAL VELOCITY	
	ISOTROPIC	
	MASSES	
	POST	
	PRINT CHOICE	

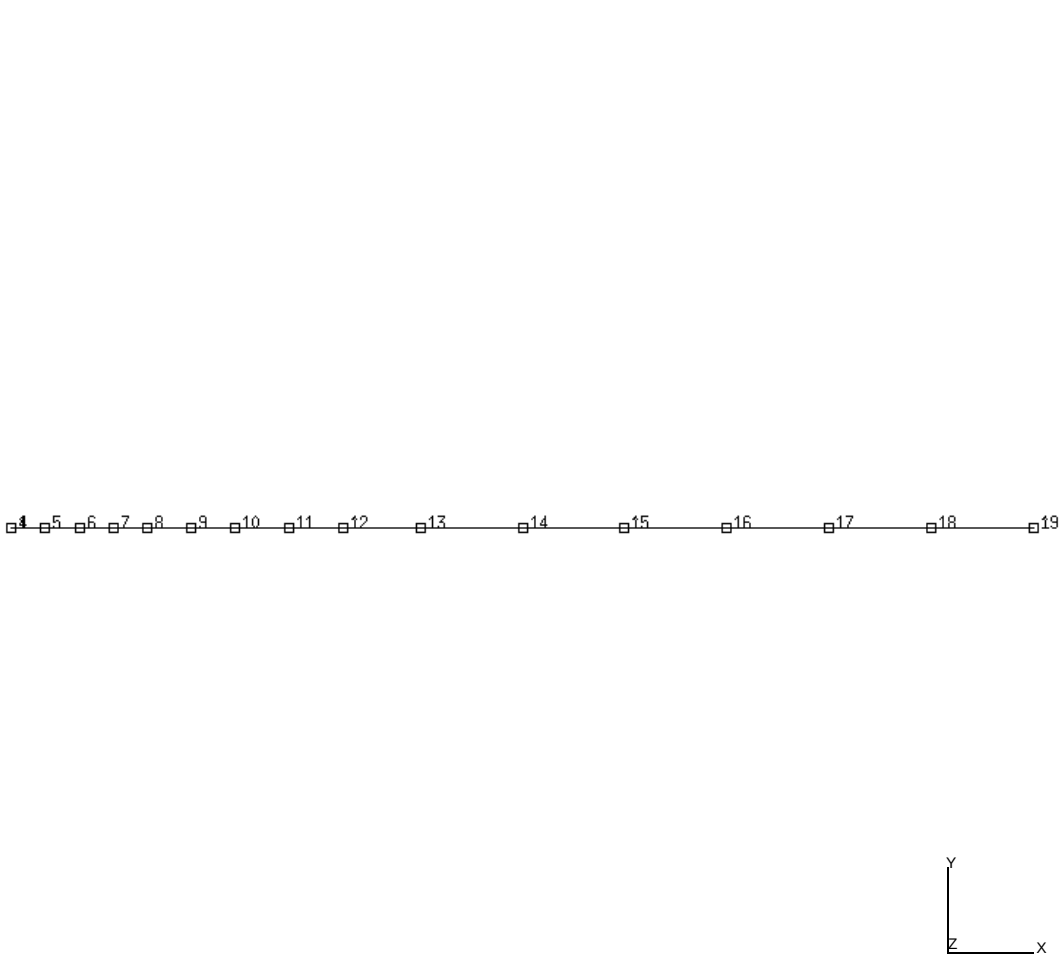

Figure 6.9-1 Mesh of the Bar

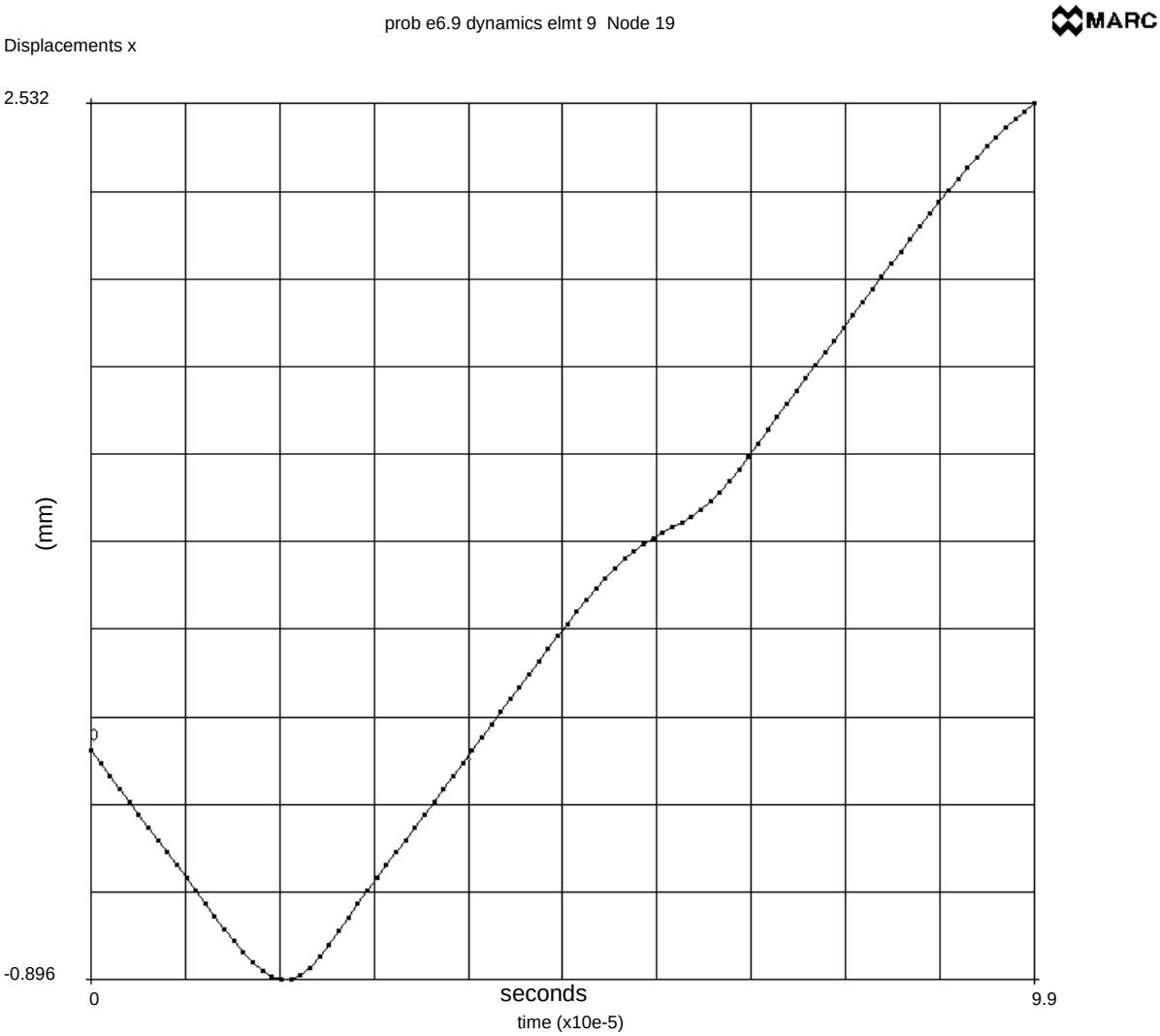

Figure 6.9-2 Time History of Displacements

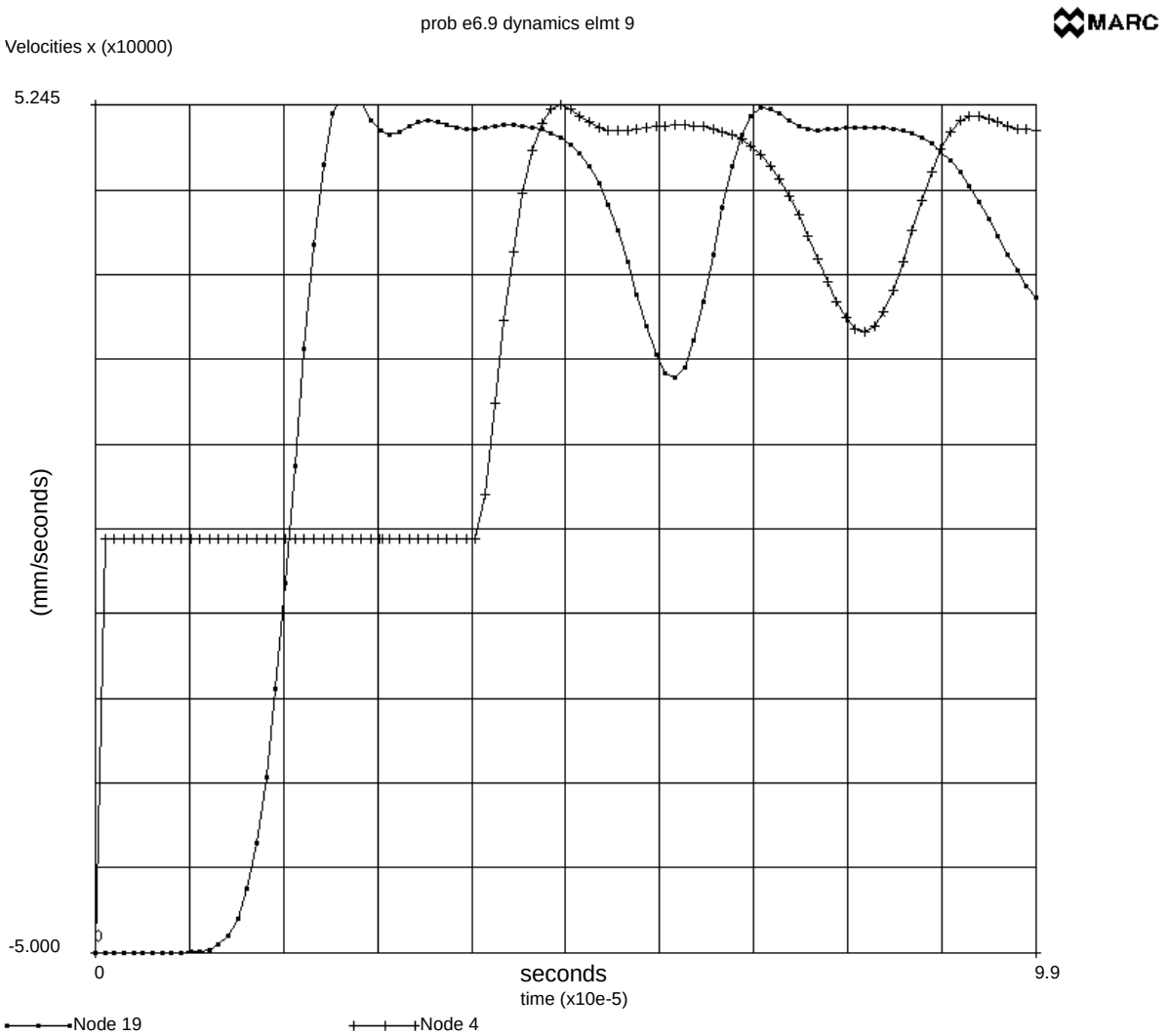

Figure 6.9-3 Time History of Velocity

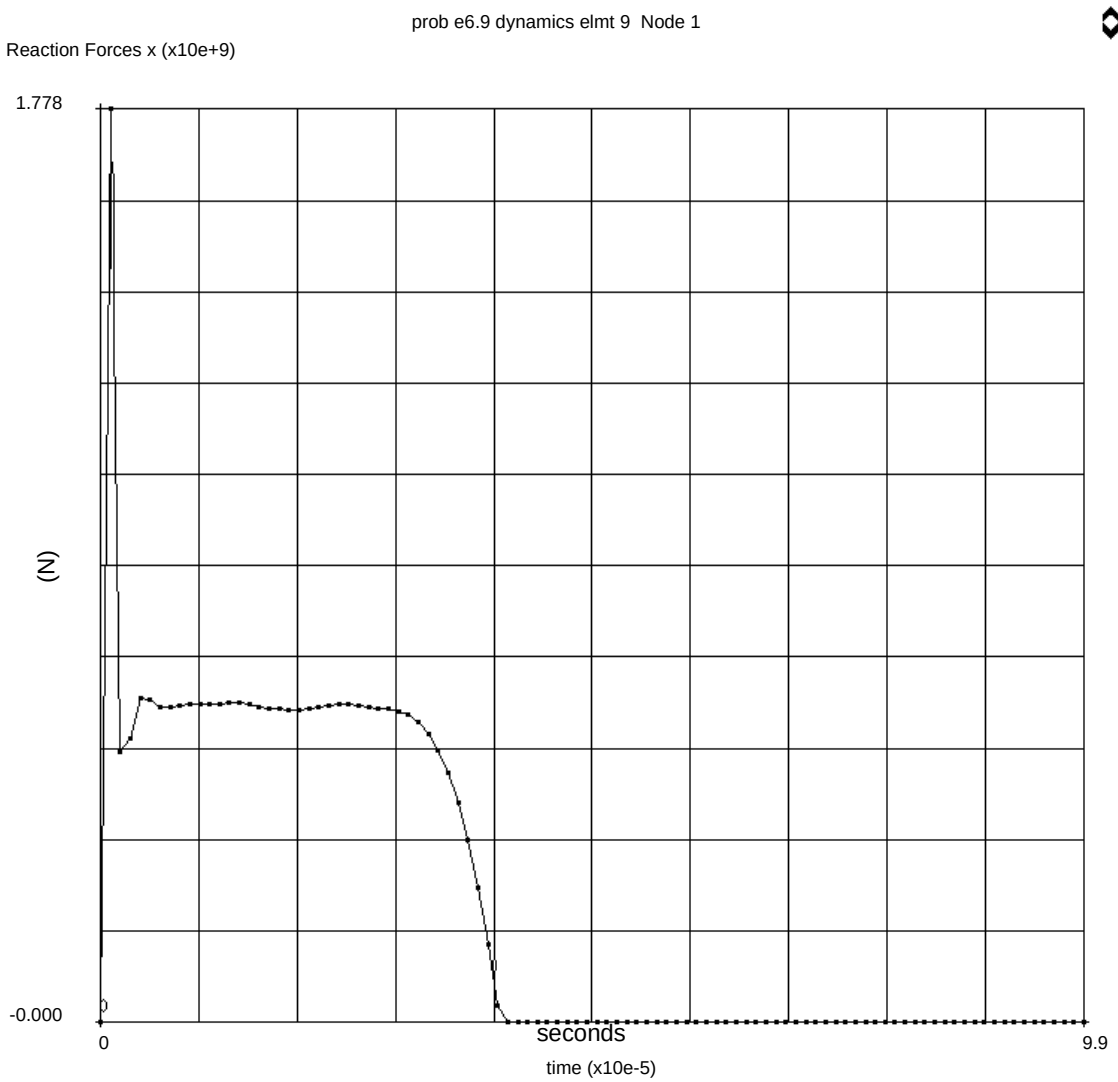

Figure 6.9-4 Time History of the Reaction

6.10 Frequencies of an Alternator Mount

The first six modal frequencies are computed for a spatial frame representing the support of an alternator. Two masses are lumped in the middle of two horizontal beams, at nodes 14 and 18 (Figure 6.10-1). The use of history definition option RECOVER for modal stress calculations is also demonstrated in this problem.

Element

Element 52, a straight Euler-Bernoulli beam in space with linear elastic response, has been used. It has six coordinates per node: the first three are (x,y,z) global coordinates of the system, the other three are the global coordinates of a point in space which locates the local x-axis of the cross section.

Model

The spatial frame has been modeled using 16 elements and 20 nodes. The columns are clamped at the base.

Geometry

The columns are 250 cm high; the beams in the x-direction are 192.5 cm long and 157.5 cm in the z-direction. The geometric properties of the sections are given in Table 6.10-1.

The torsional stiffness for the rectangular section is as follows:

$$K_t = \frac{E}{2(1+\nu)} I_t$$

$$I_t = hb^3 \left[\frac{1}{3} - \frac{3.35}{16} \frac{b}{h} \left(1 - \frac{b^4}{12h^4} \right) \right]$$

Element 52 computes the torsional stiffness of the section as:

$$K_t = \frac{E}{2(1+\nu)} (I_{xx} + I_{yy})$$

Then, in order to use the correct stiffness, an artificial Poisson's ratio ν^* is chosen so that:

$$\frac{E}{2(1+\nu)} I_t = \frac{E}{2(1+\nu^*)} (I_{xx} + I_{yy})$$

$$\nu^* = \frac{(I_{xx} + I_{yy}) \cdot (1+\nu)}{I_t} - 1$$

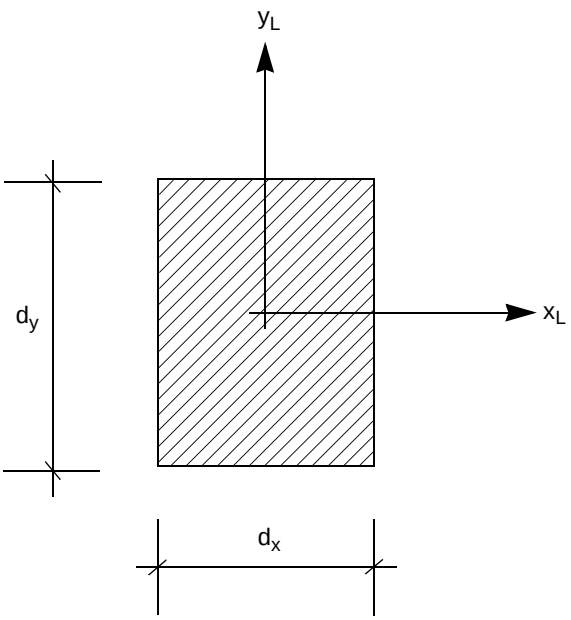

Table 6.10-1 Geometric Properties of Beams Sections

Set n	Elements n	d_x [cm]	d_y [cm]	A [cm]	J_x [cm^4]	J_y [cm^4]
1	1, 2, 7, 8	75	115	8,625	9,500,000	4,000,000
2	3, 4, 5, 6	85	115	10,925	12,000,000	8,200,000
3	9, 10, 13, 14	196	74	4,810	2,194,000	1,693,000
4	1, 12	196	74	14,504	6,618,000	46,430,000
5	15 16	133	74	9,842	4,491,000	14,500,000

Material Properties

The frame is made of reinforced concrete. Young's modulus is $E = 2.5 \times 10^8 kg/cm\ sec^2$ and the density is $\rho = 2.55\ 10^{-3}\ kg/cm^3$. Poisson's ratio is 0.3. The lumped masses are M = 19000 kg.

Analytical Solution

An approximate analytical solution is used to compare analytic results with the MARC output. The volume of concrete, the total mass and the moment of inertia are as follows:

$V = 30.923 \times 10^6 \text{ cm}^3$

$M = 1.09 \times 10^5 \text{ kg}$

$I = 5.4 \times 10^9 \text{ kg. cm}^2$

Let us write the following:

$$K_x \approx \frac{12\ E\ \Sigma\ (J_y)col}{h^3} = 5.86 \times 10^8 \text{kg/sec}^2$$

$$K_y \approx \frac{12\ E\ \Sigma\ (J_x)col}{h^3} = 1.03 \times 19^9 \text{kg/sec}^2$$

The first three modal frequencies are as follows

$$T_x = \frac{1}{2\pi} \qquad \frac{K_x}{M} = 11.7 \text{ Hz}$$

$$T_z = \frac{1}{2\pi} \qquad \frac{K_z}{M} = 15.5 \text{ Hz}$$

$$T_\theta = \frac{1}{2\pi} \qquad \frac{K_\theta}{I} = 21.7 \text{ Hz}$$

Recover

The RECOVER option is used to first place the six eigenvectors on the post file.

The load incrementation option RECOVER is then used for the modal stress calculations for the first and second modes. The modal stresses are computed from the modal displacement vector ϕ (eigenvector without normalization), and the nodal reactions are calculated from $F = K\phi - \omega^2 M\phi$.

Results

The comparison between the approximate analytical solution and the numerical results is shown below:

Eigenvalue	MARC Solution	Approximate Solution	Difference
1	10.3 Hz	11.7 Hz	12%
2	14.0 Hz	15.5 Hz	10%
3	19. 2 Hz	21.7 Hz	10%

It can be seen that the MARC solution is different from the analytical one by no more than 12%; the analytical solution is approximate. The three different modes are shown in Figure 6.10-2.

Parameters, Options, and Subroutines Summary

Example e6x10.dat:

Parameters	Model Definition Options	History Definition Options
DYNAMIC	CONNECTIVITY	CONTINUE
ELEMENT	COORDINATE	MODAL SHAPE
END	END OPTION	RECOVER
SIZING	FIXED DISP	
TITLE	GEOMETRY	
	ISOTROPIC	
	MASSES	
	POST	
	TYING	

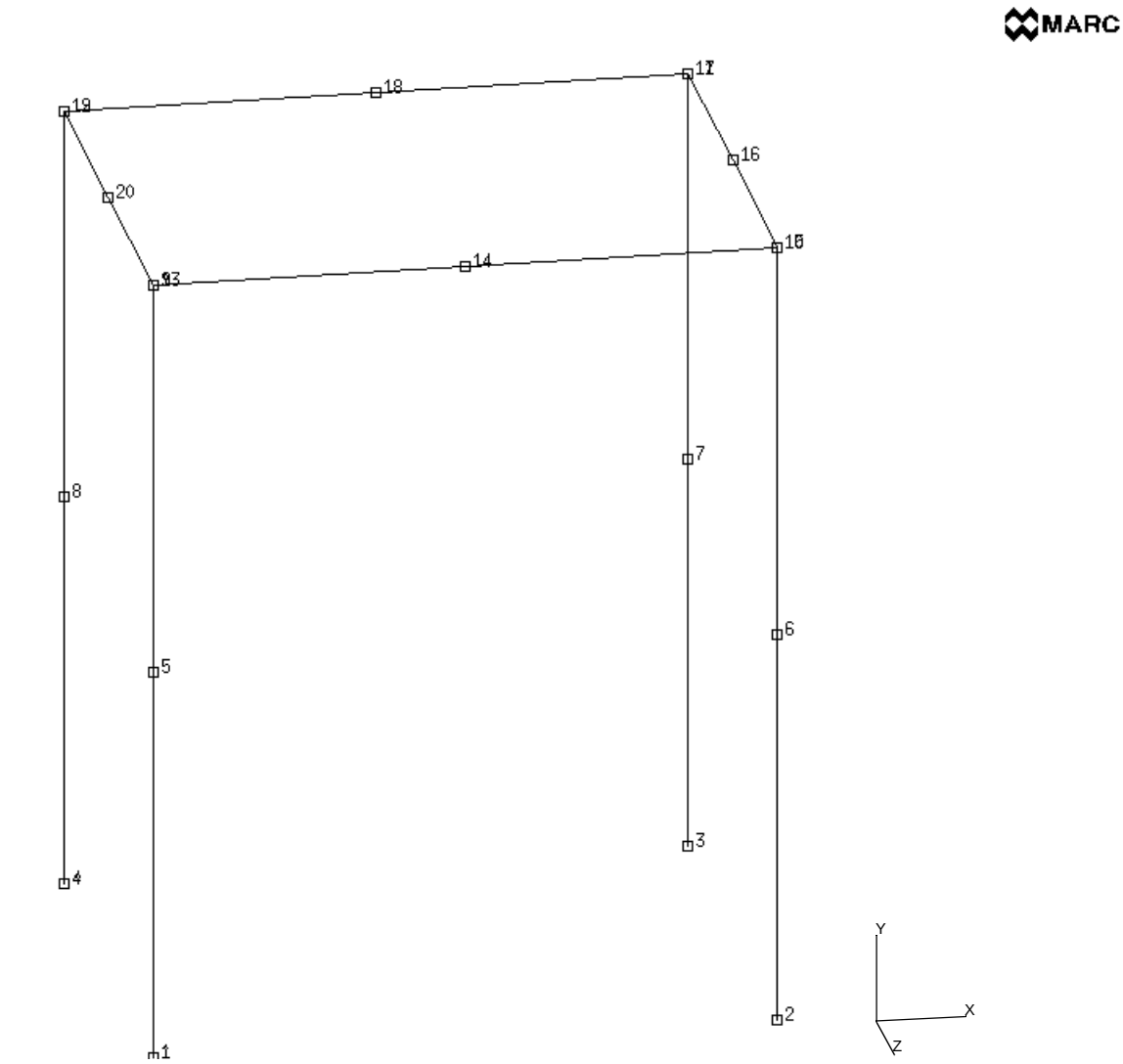

Figure 6.10-1 Alternator Mount Model

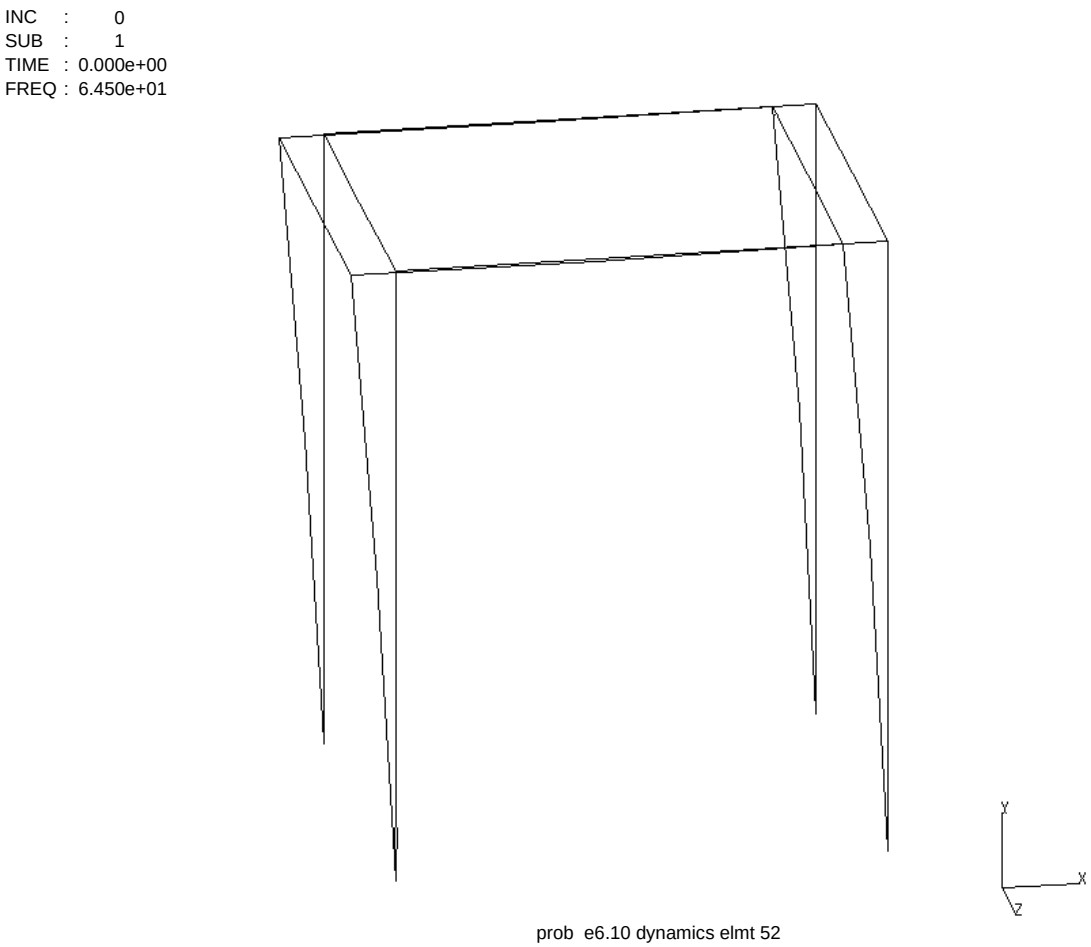

Figure 6.10-2 First Mode

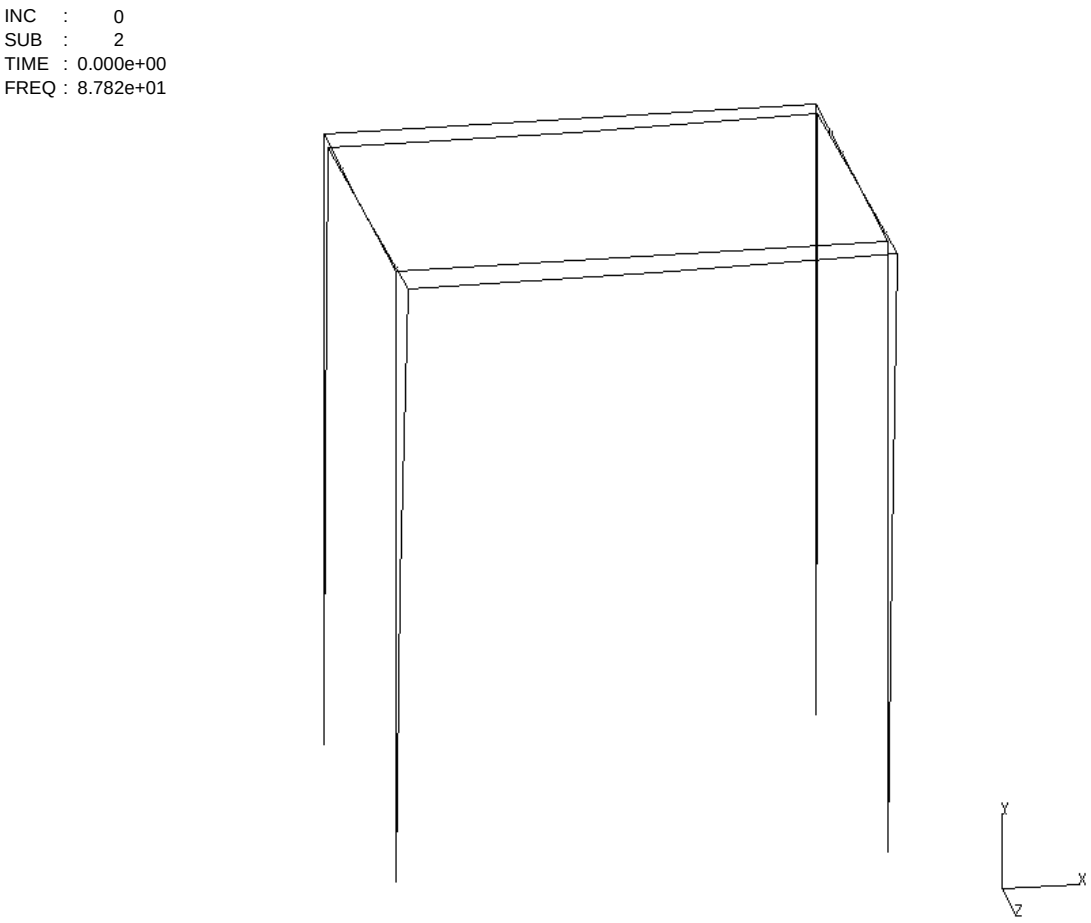

Figure 6.10-3 Second Mode

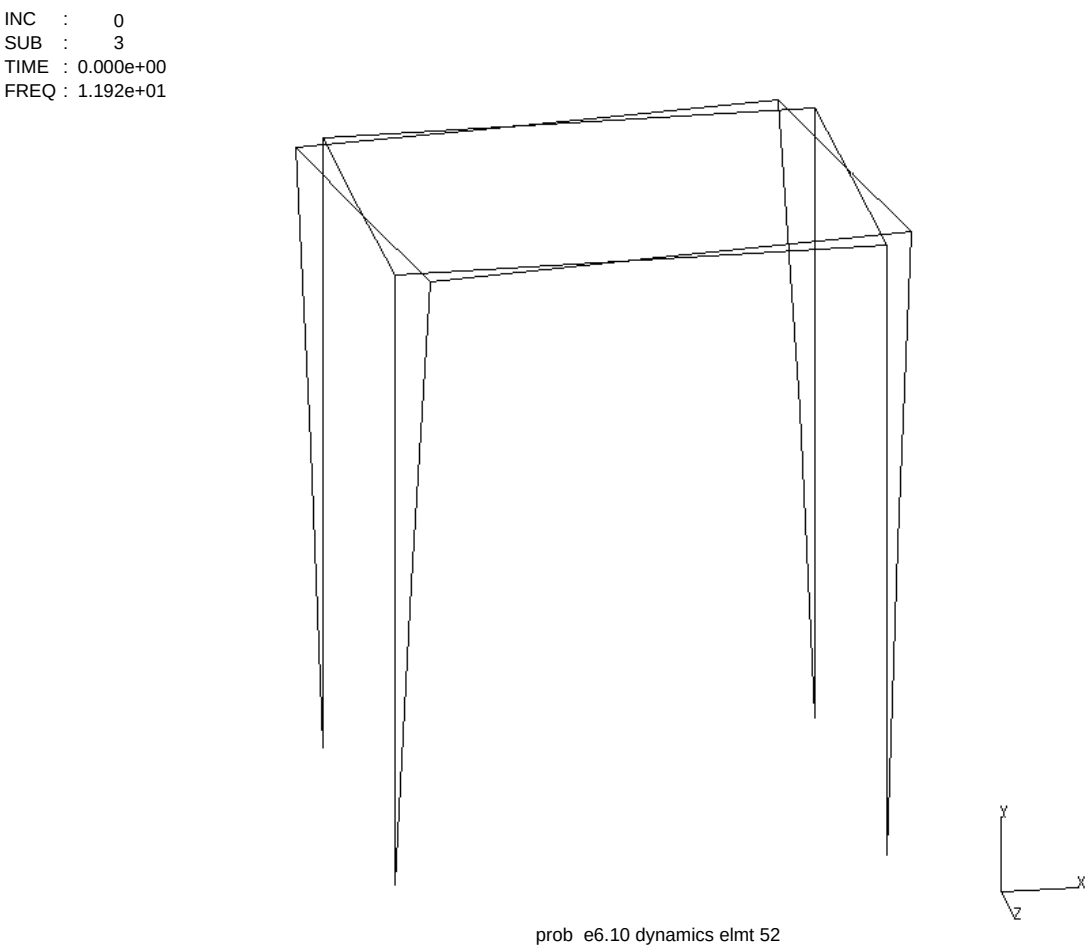

Figure 6.10-4 Third Mode

6.11 Modal Analysis of a Wing Caisson

The modal analysis is performed of a thin-walled caisson in a wing structure. The problem is simplified by assuming the cross-section of the wing to remain constant.

In this case, the MARC results are compared with approximate analytical results.

Element

Elements type 30 are used in the mesh. They are 8-node, second order isoparametric membrane elements, and have three global coordinates (x,y,z) at each node. The stress state of element 30 is that of a flat membrane.

Model

The generated mesh is shown in Figure 6.11-1. It has 174 elements and 353 coordinates.

Geometry

The caisson in 6000 mm long and the section is 1200 mm x 200 mm. The following geometric properties of the structure are computed, to be used in the analytical solution:

bending moment of inertia	$I_x = 2.6984 \times 10^7$ mm^4
bending moment of inertia	$I_y = 4.6764 \times 10^8$ mm^4
polar moment of inertia	$I_r = 4.9473 \times 10^8$ mm^4

Material Properties

The element properties are uniform; the material is elastic. Values for Young's modulus and Poisson's ratio are respectively E = 7750 kg/mm^2 and $\nu = 0.3$; density is $\rho = 2.75$ kg/mm^3.

Boundary Conditions

The model is clamped in the first 22 nodes, along the edge at y = 0.

Approximate Analytic Solution

The structure has been analyzed as a thin-walled closed section beam. The first two bending modes are:

$$\omega_n = K_n^2 \frac{\pi^2}{1^2} \sqrt{\frac{EI}{M}}$$

where $K_1 = 0.597$ and $K_2 = 1.49$. Thus,

$\omega_1 =$ 46.3 rad/sec
$\omega_2 =$ 169.2 rad/sec

The torsional frequency is:

$$\omega_4 = n \frac{\pi}{21} \sqrt{\frac{GJ}{I_o}} = 353.29 \text{ rad/sec}$$

Results

The approximate solutions provided by beam theory are compared with the results from MARC as shown below. The largest difference among the first three modes is 6%.

Eigenvalue	MARC Output	Approximate Solution	Difference
1	43.3	46.3	6%
2	172.1	169.2	2%
3	342.3	353.3	3%

Parameters, Options, and Subroutines Summary

Example e6x11.dat:

Parameters	Model Definition Options	History Definition Options
DYNAMIC	CONNECTIVITY	CONTINUE
END	COORDINATE	MODAL SHAPE
LINEAR	END OPTION	
SIZING	FIXED DISP	
TITLE	ISOTROPIC	
	POINT LOAD	
	POST	

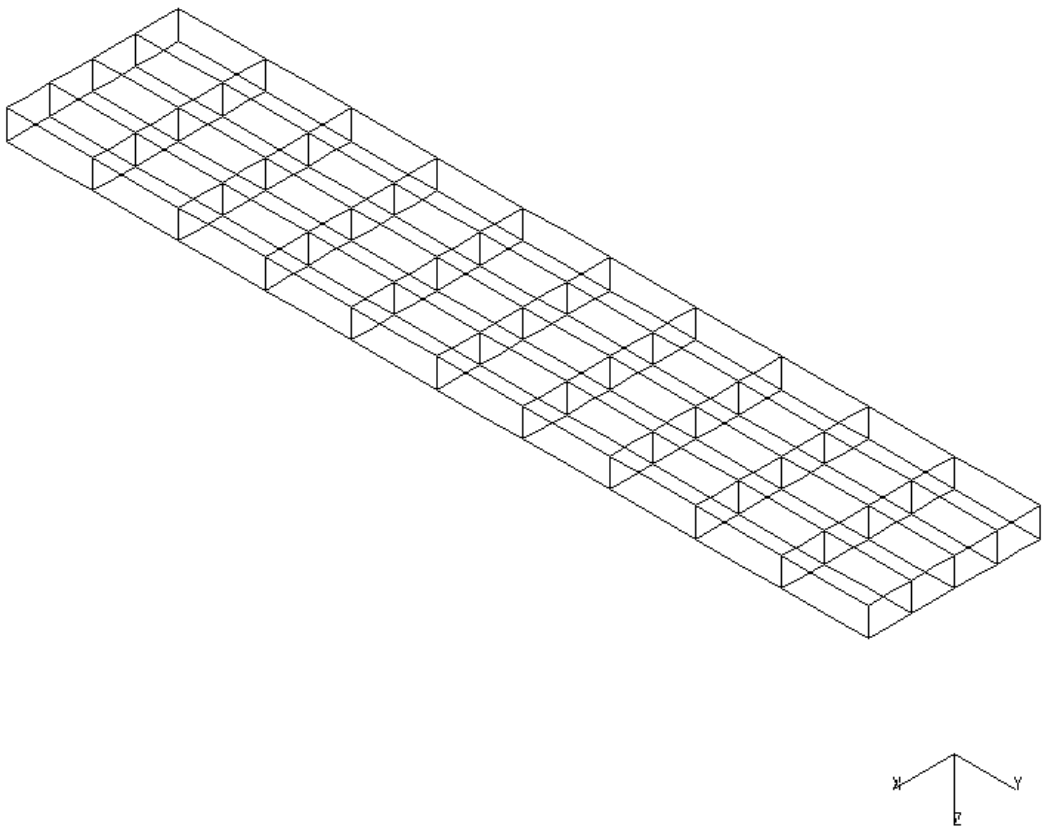

Figure 6.11-1 Mesh of a Wing Structure

6.12 Vibrations of a Cable

The first two modal frequencies are computed for a straight flexible cable. The MARC results are checked against the analytical solution.

Element

Element type 9, a three-dimensional two-node straight truss, is used. It has three coordinates per node in the global x, y, and z directions and an uniaxial state of stress.

Model

The mesh is generated using the CONN GENER option. It has 11 elements and 12 nodes. One end is fixed; the other is free.

Material Properties

The density is uniform throughout the cable and it is $\rho = 84.969$ t/m^3. The Young's modulus varies along the length of the cable:

$0 < L < 4.31$ m	$E = 1.4715 \times 10^8$ kN/m^2
$4.31 < L < 96.5$ m	$E = 6.658 \times 10^6$ kN/m^2

Geometry

The cable has length $L = 96.5$ m and $A = 2.54 \times 10^{-4}$ m^2.

Loading

A normal force is applied at the free end and its value is $p = 49.05$ kN.

Analytical Solution

The analytical formula for the modal frequencies of a prestressed cable is:

$$f_n = \frac{n}{2}\sqrt{\frac{p}{\rho A L^2}}$$

In this case, we obtain $f_1 = 0.247$ Hz and $f_2 = 0.494$ Hz.

Results

The structure is not statically stable. Thus it has been necessary to use a nonlinear step of PROPORTIONAL INCREMENT, to apply the load before asking for the modes. This option forces the assembly of the incremental stiffness matrix.

The results are as follows:

Eigenvalue	MARC Output	Analytical Solution
1	0.2477 Hz	0.247 Hz
2	0.5010 Hz	0.494 Hz

It can be seen that the MARC results are very close to the analytical results. In fact, the larger difference is only 1.3%.

Parameters, Options, and Subroutines Summary

Example e6x12.dat:

Parameters	Model Definition Options	History Definition Options
DYNAMIC	CONNECTIVITY	CONTINUE
END	COORDINATE	MODAL SHAPE
LARGE DISP	END OPTION	PROPORTIONAL INCREMENT
SIZING	FIXED DISP	
TITLE	GEOMETRY	
UPDATE	ISOTROPIC	
	POINT LOAD	
	POST	

6.13 Perfectly Plastic Beam Explosively Loaded

This demonstration problem illustrates the use of the adaptive time-stepping procedure for the analysis of a beam subjected to an impulsive load. The beam is elastic, perfectly plastic. The analysis is performed twice, first with no geometric nonlinearities included, and then doing a finite strain plasticity, updated Lagrange analysis.

A simple beam with built-in ends is modeled using element type 16. Only one half of the beam is used because of symmetry. The model consists of five elements with six nodes. The beam is five inches long.

This problem is modeled using the two techniques summarized below.

Data Set	Element Type(s)	Number of Elements	Number of Nodes	Differentiating Features
e6x13	16	5	6	AUTO TIME
e6x13b	16	5	6	

Geometry

The beam has a height of 0.125 inches and a depth of 1.2 inches.

Material Properties

Young's modulus is 10.4 x 10^6 psi, and Poisson's ratio is 0.3. The mass density is 2.5 x 10^{-4} lb/in^3. The yield stress is 41,400 psi and there is no work hardening in the material.

Boundary Conditions

The first node is given the boundary conditions of built in u = v = $\frac{\partial v}{\partial s}$ = 0.

The last node is given the symmetry boundary conditions u = $\frac{\partial v}{\partial s}$ = 0.

Loading

The problem is driven by the initial conditions, which are a large initial velocity at the center of the beam. An initial condition of 5020 in/second is applied at nodes 5 and 6.

Control

The AUTO TIME option is used to control the time step size. The procedure is such that if the residuals are large compared to the reactions, the time step is reduced. If the convergence is well satisfied, the time step is increased in the next increment. The initial time step is chosen as 5 x

10^{-6} s. This time step was chosen such that $[\Delta t \cdot V_o]$ was small compared to the other geometric dimensions. The total time to be modeled is 1.5 x 10^{-3}s. A maximum of 100 steps is allowed.

Results

Figure 6.13-2 through Figure 6.13-4 show the displacements, velocities, and accelerations for the small displacement analysis. Figure 6.13-5 through Figure 6.13-7 show the results for the large displacement analysis. Each mark on the graph indicates a new increment; hence, you can observe the change in the time step. In the problem including geometric nonlinearities, many more time steps are used to remain in equilibrium. You can observe that there is a large acceleration initially, which reverses the sign for the center node and then begins to approach zero.

Parameters, Options, and Subroutines Summary

Example e6x13.dat:

Parameters	Model Definition Options
DYNAMIC	CONNECTIVITY
ELEMENT	CONTROL
END	COORDINATE
SIZING	END OPTION
TITLE	FIXED DISP
	GEOMETRY
	INITIAL VELOCITY
	ISOTROPIC
	POST
	PRINT CHOICE
	RESTART

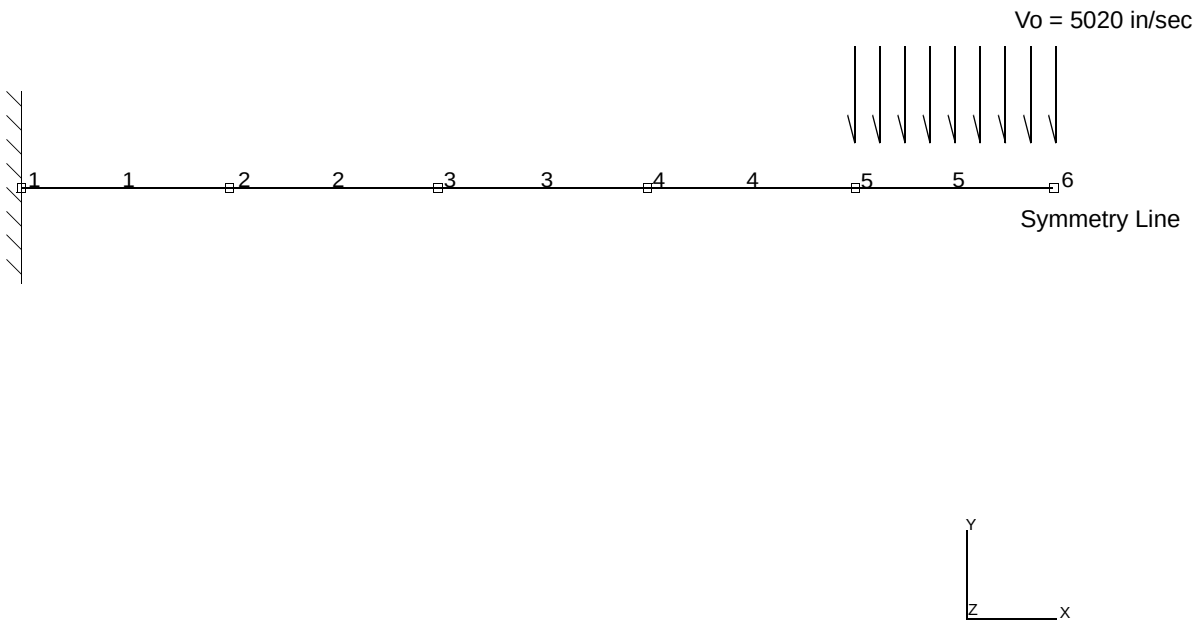

Figure 6.13-1 Mesh with Initial Velocity

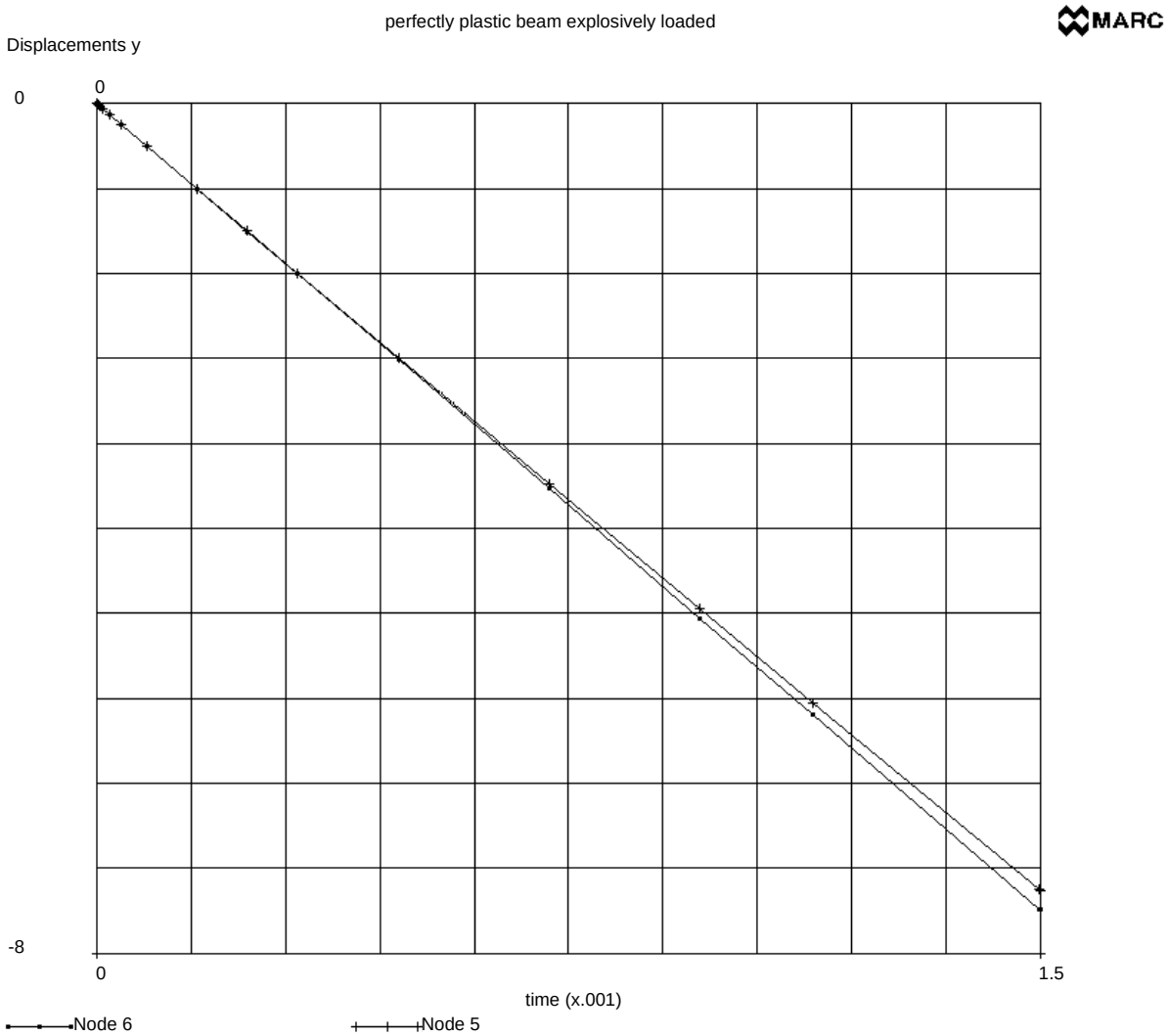

Figure 6.13-2 Small Displacement Analysis

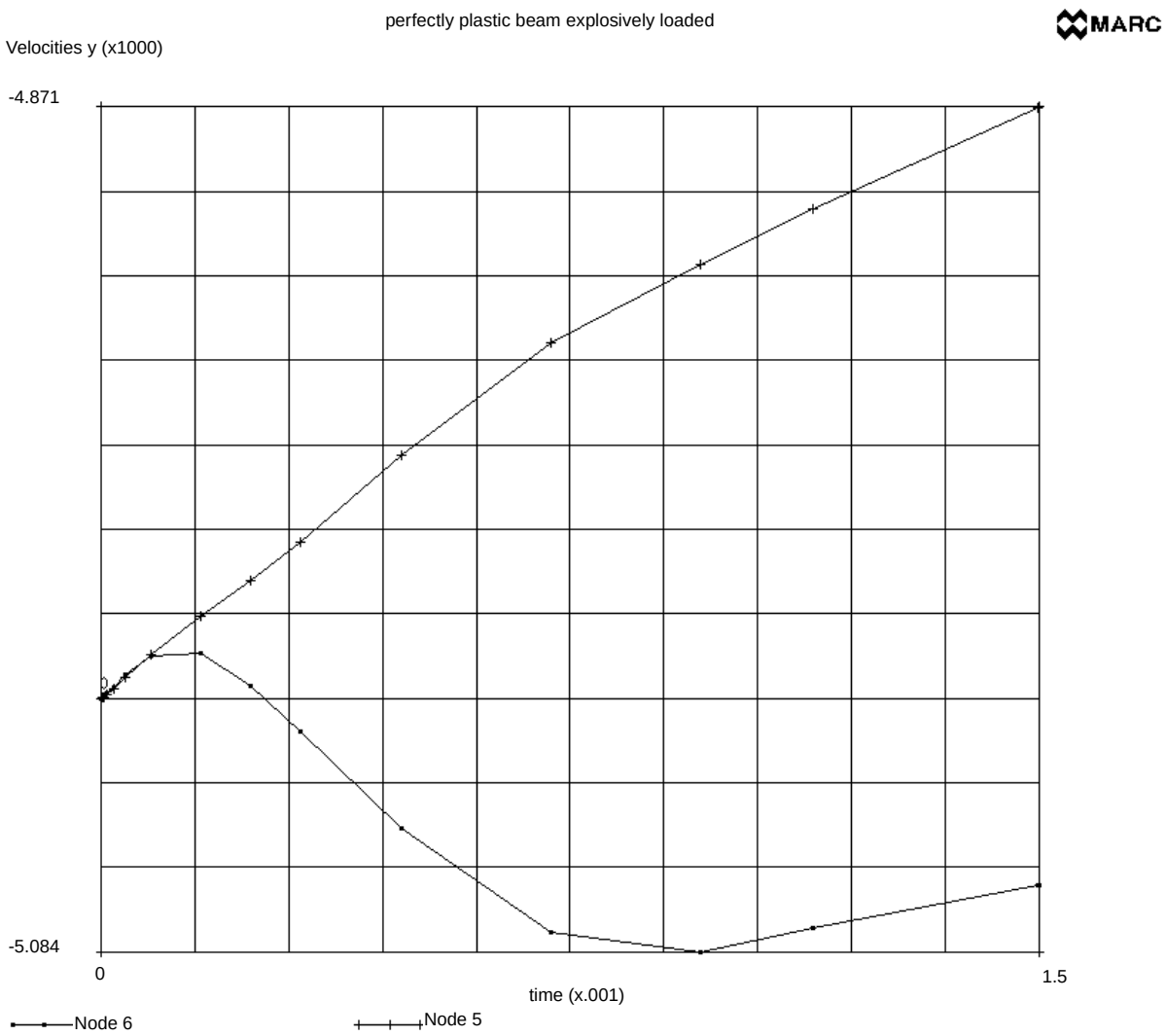

Figure 6.13-3 Small Displacement Analysis

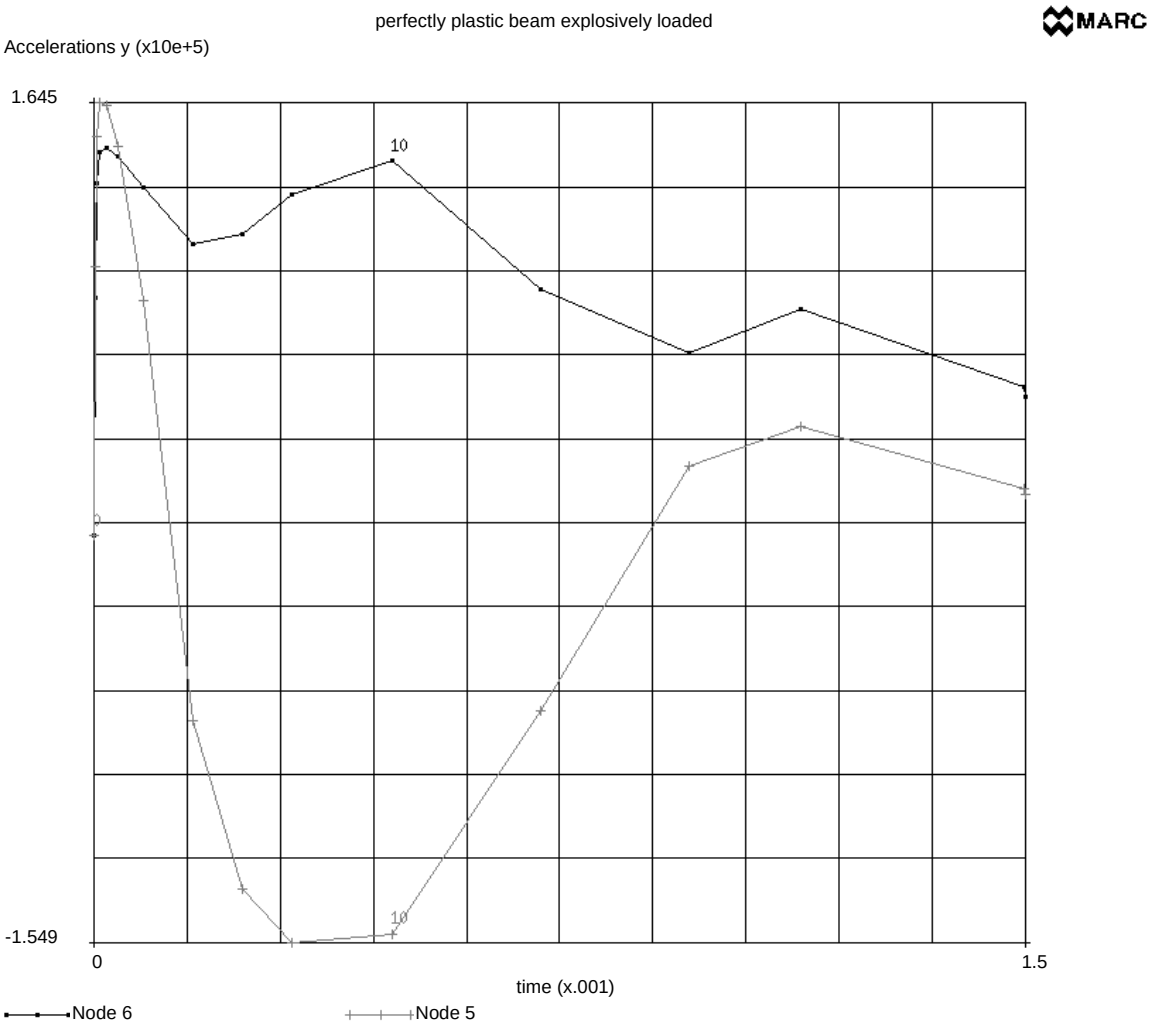

Figure 6.13-4 Small Displacement Analysis

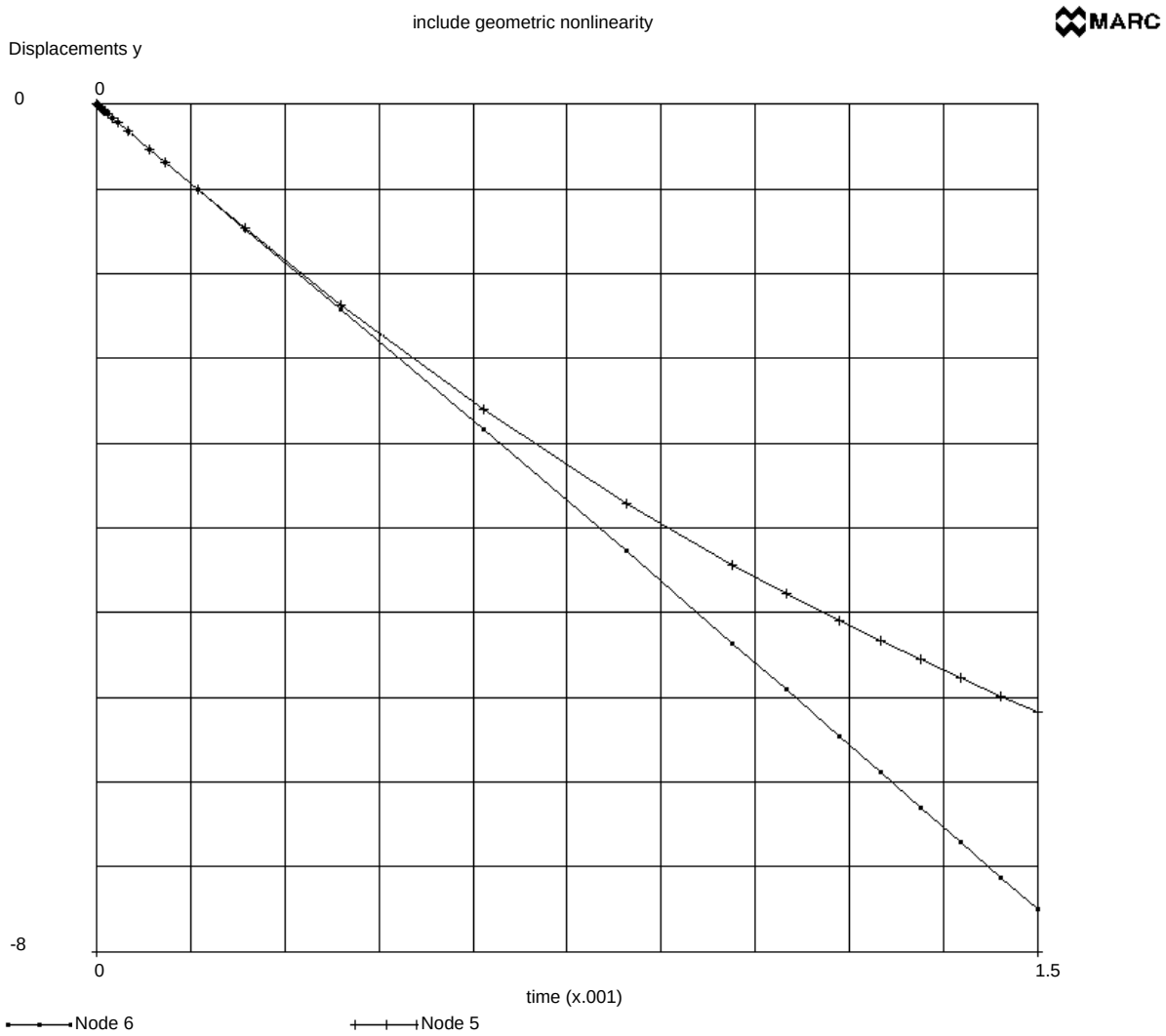

Figure 6.13-5 Includes Geometric Nonlinearity

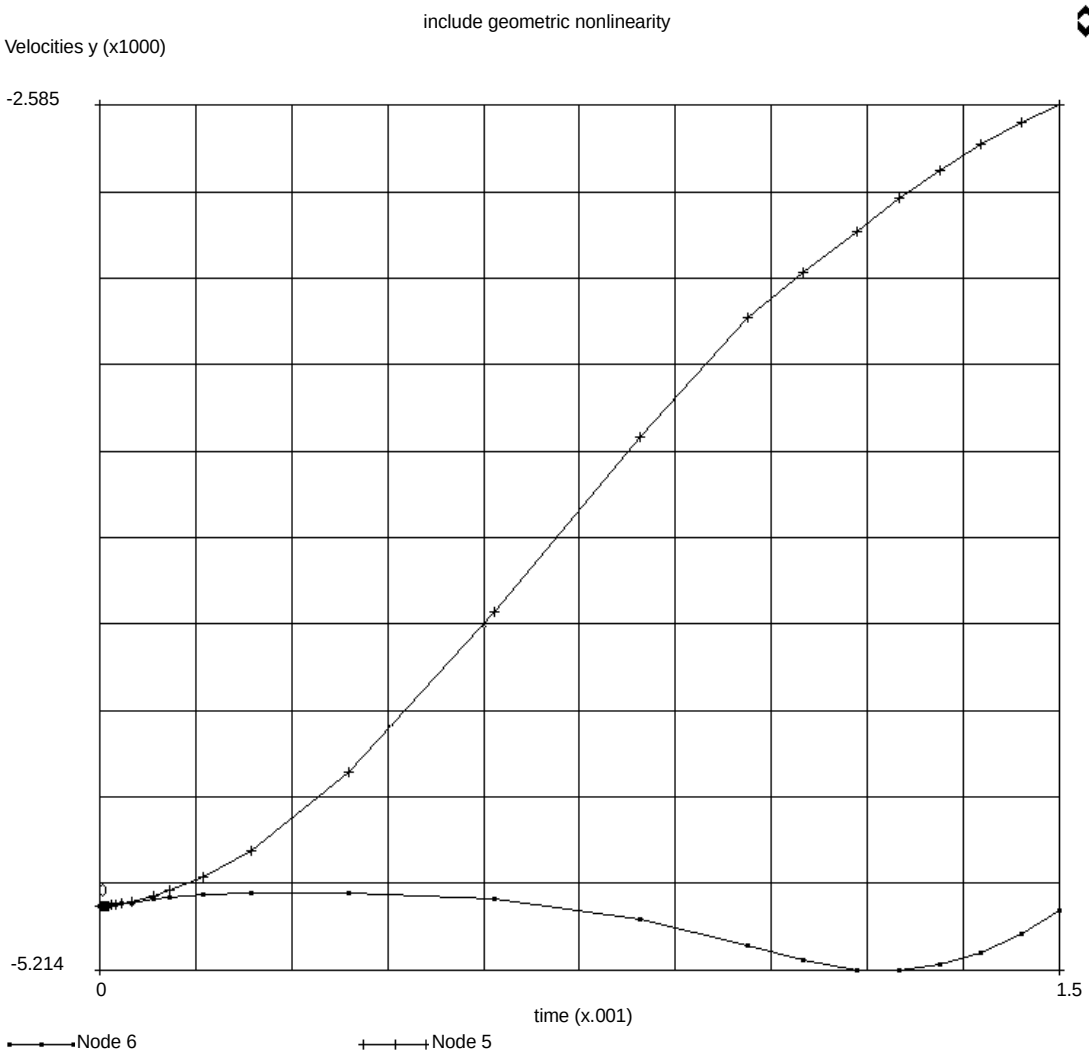

Figure 6.13-6 Includes Geometric Nonlinearity

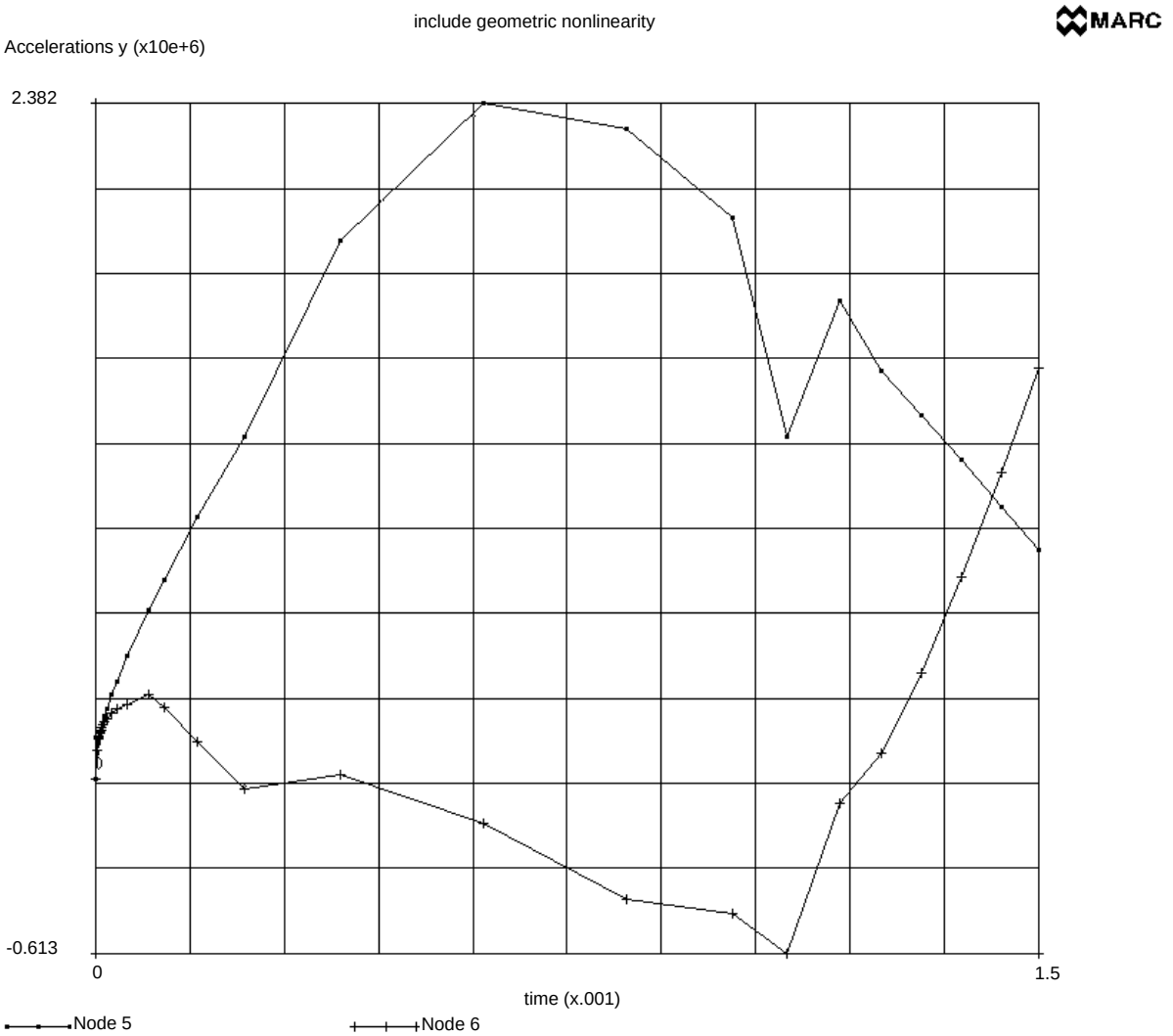

Figure 6.13-7 Includes Geometric Nonlinearity

6.14 Dynamic Fracture Mechanics

This example illustrates the use of the DeLorenzi method [1] to evaluate J-integral values in MARC for dynamically responding structures. The problem consists of a center-cracked plate which is initially at rest, and which is subjected to a uniform tensile load that is suddenly applied and then maintained for t > 0. This problem was originally analyzed by Chen [2] who used a finite difference method. Over the past years, it has become more or less a benchmark problem for demonstrating the applicability of various alternative procedures to calculate dynamic stress intensity factors. See Brickstad [3] and Jung [4].

Details on the dimensions, material properties, and loading conditions are given in Figure 6.14-1.

Element

Element type 27 is an 8-noded plane strain quadrilateral.

Model

Because of symmetry, only one quarter of the plate is modeled. A graded mesh subdivision is chosen, identical to the mesh used in [4]. No quarter-point elements are used. Figure 6.14-2 shows the finite element model.

Geometry

No geometry is specified and thus a unit thickness is assumed by MARC.

Material Properties

The Young's modulus is set to 2000 N/cm^2 and Poisson's ratio is 0.3. The mass density amounts to 5 g/cm^3. In order to obtain consistent units, a value of 5.0×10^{-5} has to be entered in the mass density field of the ISOTROPIC block.

Boundary Conditions

Because of symmetry conditions all nodal DOF's in the first coordinate direction are suppressed along x = 0. All nodal DOF's in the second coordinate direction are suppressed along the uncracked part of y = 0.

Loading

The step function in the tensile load is specified as follows:

increment 0 : $\sigma = 0$

increment 1 : $\Delta\sigma = 40000\ N/cm^2$

increment > 1 : $\Delta\sigma = 0$

The full tensile load is applied in a single short time step of 1 x 10^{-4} μsec. The implicit Newmark-beta method with a constant time step of 0.15 μsec. is employed for the direct time integration up to a time of 12 μsec. The time step is chosen such that the longitudinal wave reaches the crack-plane in approximately 10 increments. Because of the linear nature of the problem the control value for residual checking has been set to a large value (that is, 10).

Lorenzi

A unit crack extension of 1 cm. has been specified for three different paths. The first J-value is based on a unit movement of the crack tip only. Elements 3 and 4 will be the only deforming elements. The second J-value is based on a rigid movement of the first ring of elements (3 and 4). The third J-value is based on a rigid movement of the first and second ring of elements. In order to incorporate all inertia effects, all movements of the nodes in the regions with "rigid" movements must be specified. Figure 6.14-3 shows the relevant element and node numbers in the crack-tip region.

Results

MARC provides for the output of the strain energy changes per crack movement for each increment. These values have to be normalized by the crack opening area to obtain the J-values. Because of symmetry, the actual strain energy that can be released at every crack tip is twice the value that is printed out. In addition, the J-values can be converted to K_I values using the relation:

$$K_I = \sqrt{\frac{E}{1-\nu^2}}\ J$$

Table 6.14-1 summarizes the J-values that are obtained for the first path as well as the normalized K_I values $\left(\text{that is, } K_I/\sigma\sqrt{\pi a}\right)$ for every 10th increment. More details about the results and a comparison with other numerical solutions can be found in [5]. Figure 6.14-4 shows the dynamic stress intensity factors normalized with respect to a static stress intensity factor of an infinite plate as a function of time for the complete analysis.

Table 6.14-1 Normalized Dynamic Stress Intensity Factors

Increment Number	Time (μsec)	J/2	$K_{dynamic}/\sigma\sqrt{\pi a}$
11	1.5	0.103E-4	0.0061
21	3.0	29.92	1.0442
31	4.5	82.26	1.7313

Table 6.14-1 Normalized Dynamic Stress Intensity Factors (Continued)

Increment Number	Time (μsec)	J/2	$K_{dynamic}/\sigma\sqrt{\pi a}$
41	6.0	171.50	2.4998
51	7.5	146.62	2.3114
61	9.0	45.58	1.2887
71	10.5	11.91	0.6588

References

1. DeLorenzi, H.G., “On the Energy Release Rate and the J-integral for 3D Crack Configurations”, *Inst. J. Fracture*, Vol. 19, 1982, pp. 183-193.
2. Chen, Y.M, “Numerical Computation of Dynamic Stress Intensity Factors” by a Lagrangian Finite Difference Method (the HEMP Code)”, *Eng. Fract. Mech.*, Vol. 7, 1975, pp. 653-660.
3. Brickstad, B., “A FEM Analysis of Crack Arrest Experiments”, *Int. J. Fract.*, Vol. 21, 1983, pp. 177-194.
4. Jung, J., Ahmad, J., Kanninen, M.F. and Popelar, C.H., “Finite Element Analysis of Dynamic Crack Propagation”, presented at the 1981 ASEM Failure Prevention and Reliability Conference, September 23-26, 1981, Hartford, Conn., U.S.A.
5. Peeters, F.J.H. and Koers, R.W.J., “Numerical Simulation of Dynamic Crack Propagation Phenomena by Means of the Finite Element Method”, *Proceedings of the 6th European Conference on Fracture*, ECF6, Amsterdam, The Netherlands, June 15-20, 1986.

Parameters, Options, and Subroutines Summary

Example e6x14.dat:

Parameters	Model Definition Options	History Definition Options
DYNAMIC	CONNECTIVITY	CONTINUE
ELEMENT	CONTROL	DIST LOADS
END	COORDINATE	DYNAMIC CHANGE
SIZING	DIST LOADS	
TITLE	END OPTION	
	FIXED DISP	
	ISOTROPIC	
	LORENZI	
	NO PRINT	

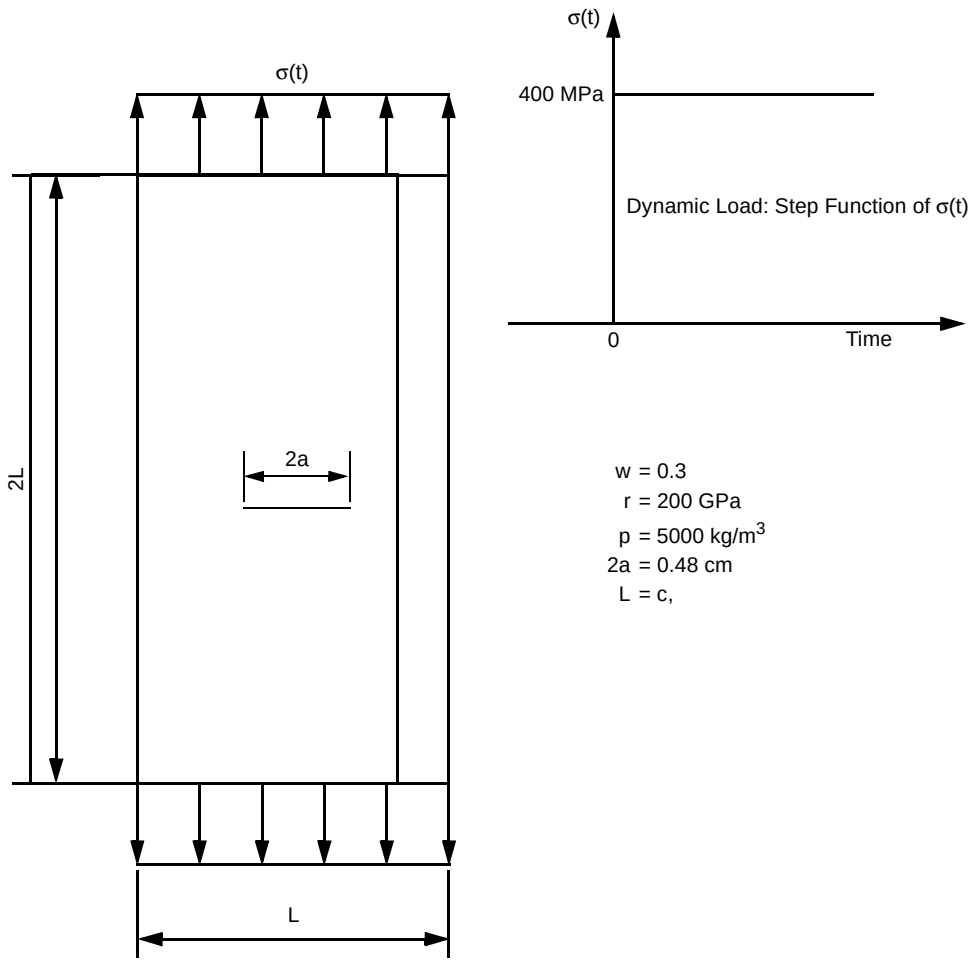

Figure 6.14-1 Dynamically Loaded Center-Cracked Rectangular Plate Problem

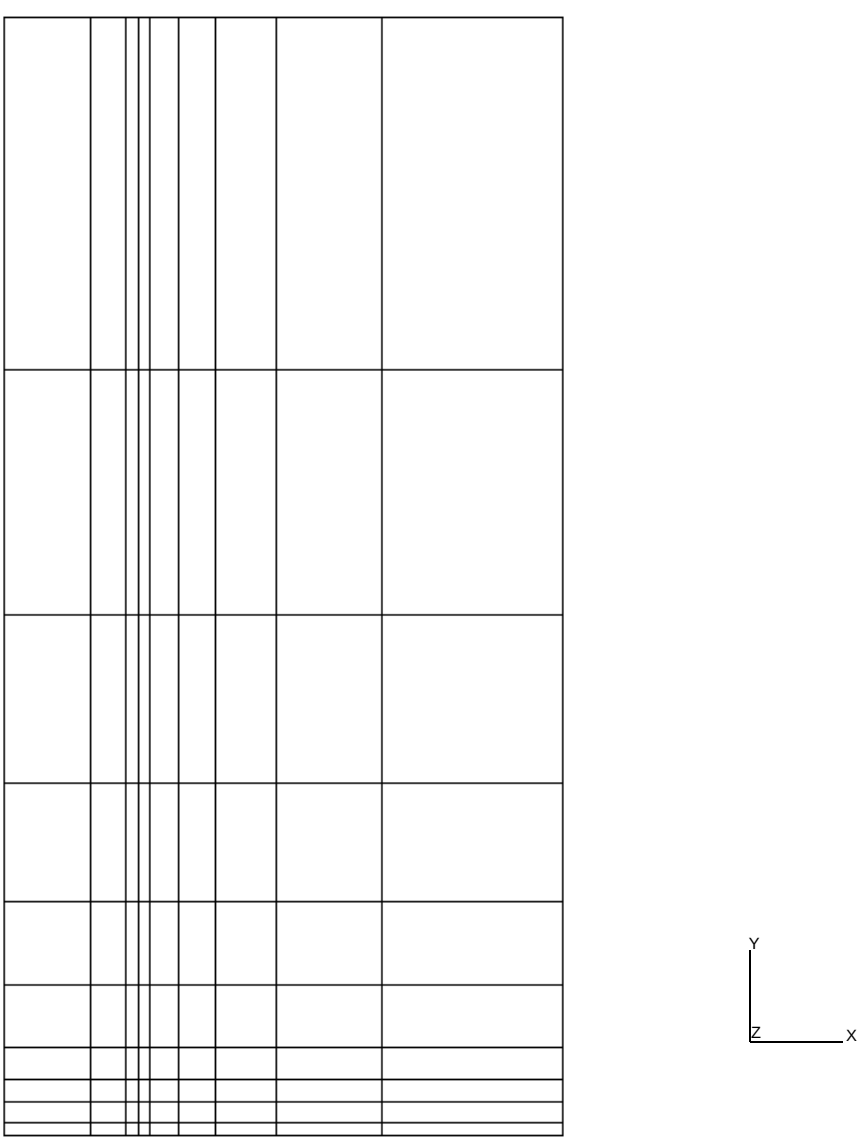

Figure 6.14-2 Dynamic Crack Problem Mesh

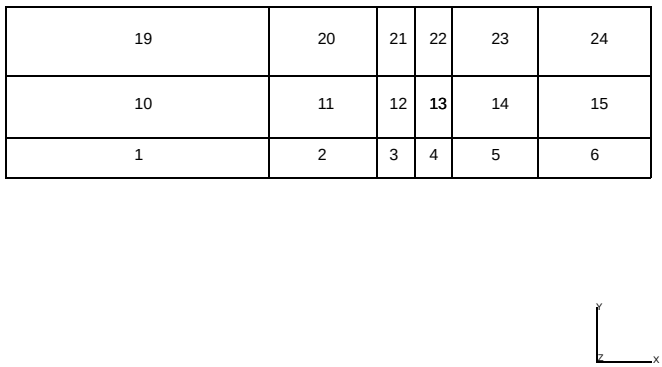

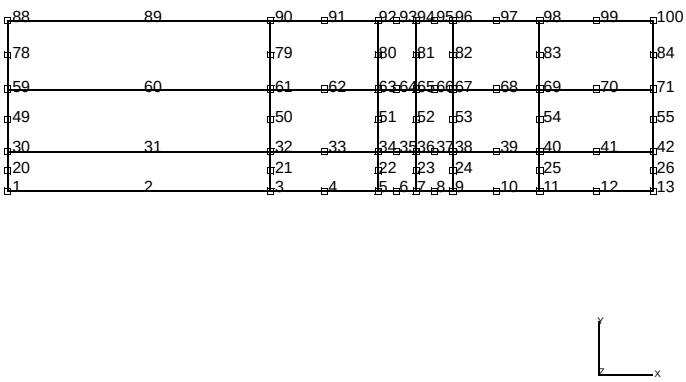

Figure 6.14-3 Crack Tip Region

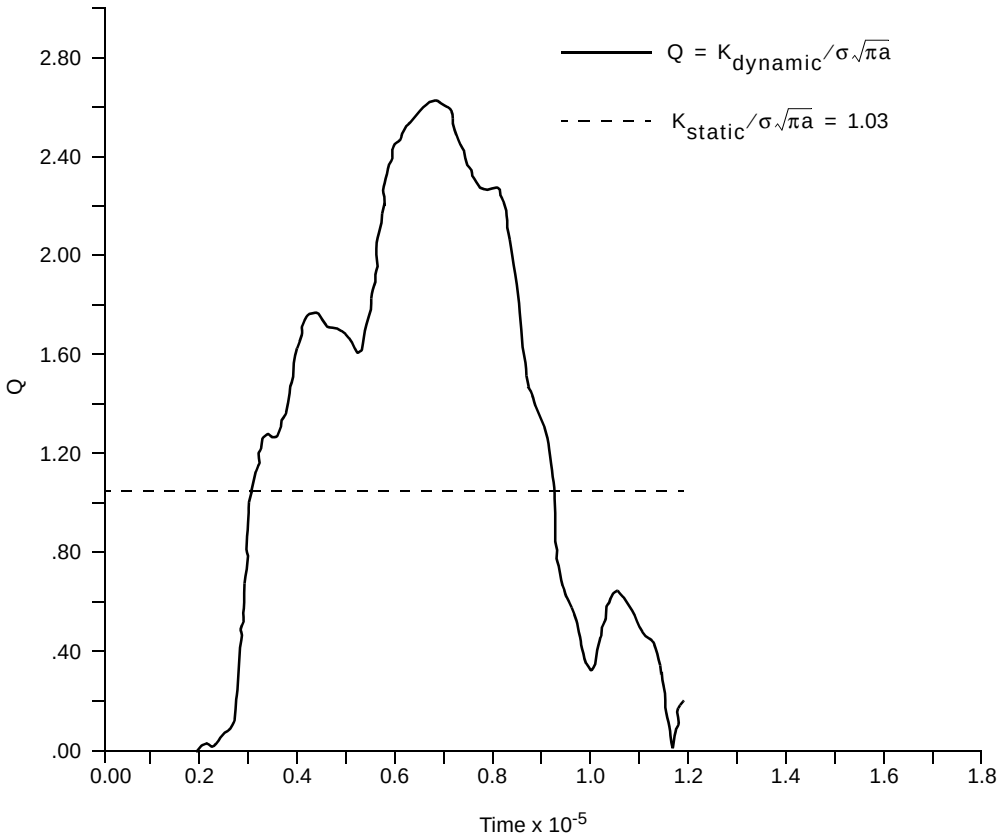

Figure 6.14-4 Normalized Dynamic Stress Intensity Factors

6.15 Eigenmodes of a Plate

In this problem, the eigenvalues are calculated for a cantilevered, rectangular plate, using element type 7. In the first case, the assumed strain formulation is used. In the second case, the conventional isoparametric element is used. This eigenproblem illustrates the superiority of the assumed strain element over the conventional isoparametric element in the plate or shell analyses.

This problem is modeled using the two techniques summarized below.

Data Set	Element Type(s)	Number of Elements	Number of Nodes	Differentiating Features
e6x15	7	392	870	Assumed strain
e6x15b	7	392	870	Without assumed strain

Model

The plate is of length 0.6 inch and width 0.25 inch and thickness of 0.003 inch. It is modeled using a 28x14 mesh of element type 7, eight-node brick as shown in Figure 6.15-1. Four eigenvalues are extracted using the inverse power sweep method. The lumped mass matrix is formed.

Geometry

In the first case, a “1” is placed in the third field to indicate that the assumed strain formulation is to be used.

Material Properties

The material has a Young’s modulus of 26 x 10^6 psi, and a Poisson’s ratio of 0.32. The mass density is 0.000755 lb/in^3.

Boundary Conditions

The one end is completely constrained to represent the cantilevered boundary conditions. The other end is simply supported at its midpoint.

Results

The frequencies calculated are summarized in Table 6.15-1. For comparison, the results using element 75 are also included.

Table 6.15-1 Frequencies in Hertz

Mode	Assumed Strain Element	Conventional Isoparametric Element	Element 75
1	1140	1929	1140
2	1323	5024	1324
3	3551	8469	3553
4	4235	14713	4239

One observes that using the conventional elements, the frequencies are significantly higher and incorrect. This is because the element is too stiff in bending. The agreement between the assumed strain element and the shell element is very good.

Figure 6.15-2 and Figure 6.15-3 show the first and third mode shapes.

Parameters, Options, and Subroutines Summary

Example e6x15.dat:

Parameters	Model Definition Options	History Definition Options
DYNAMIC	CONNECTIVITY	CONTINUE
ELEMENT	COORDINATE	MODAL SHAPE
END	END OPTION	
LUMP	FIXED DISP	
PRINT	GEOMETRY	
SIZING	ISOTROPIC	
TITLE		

Example e6x15b.dat:

Parameters	Model Definition Options	History Definition Options
DYNAMIC	CONNECTIVITY	CONTINUE
ELEMENT	COORDINATE	MODAL SHAPE
END	END OPTION	
LUMP	FIXED DISP	
SIZING	GEOMETRY	
TITLE	ISOTROPIC	

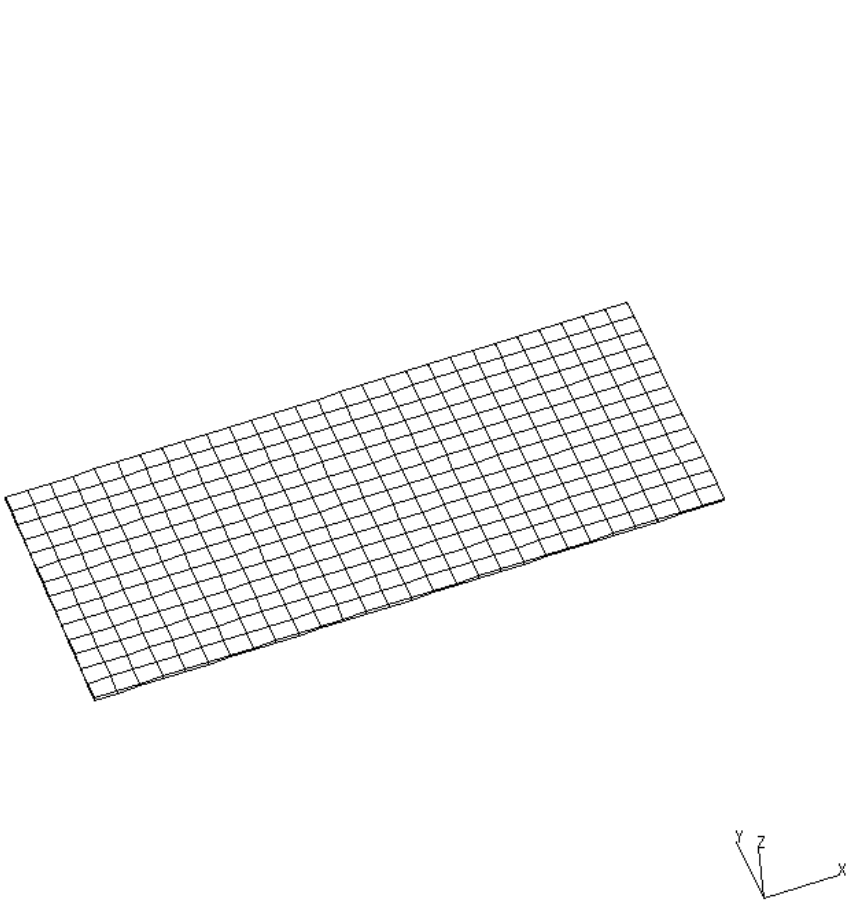

Figure 6.15-1 Mesh

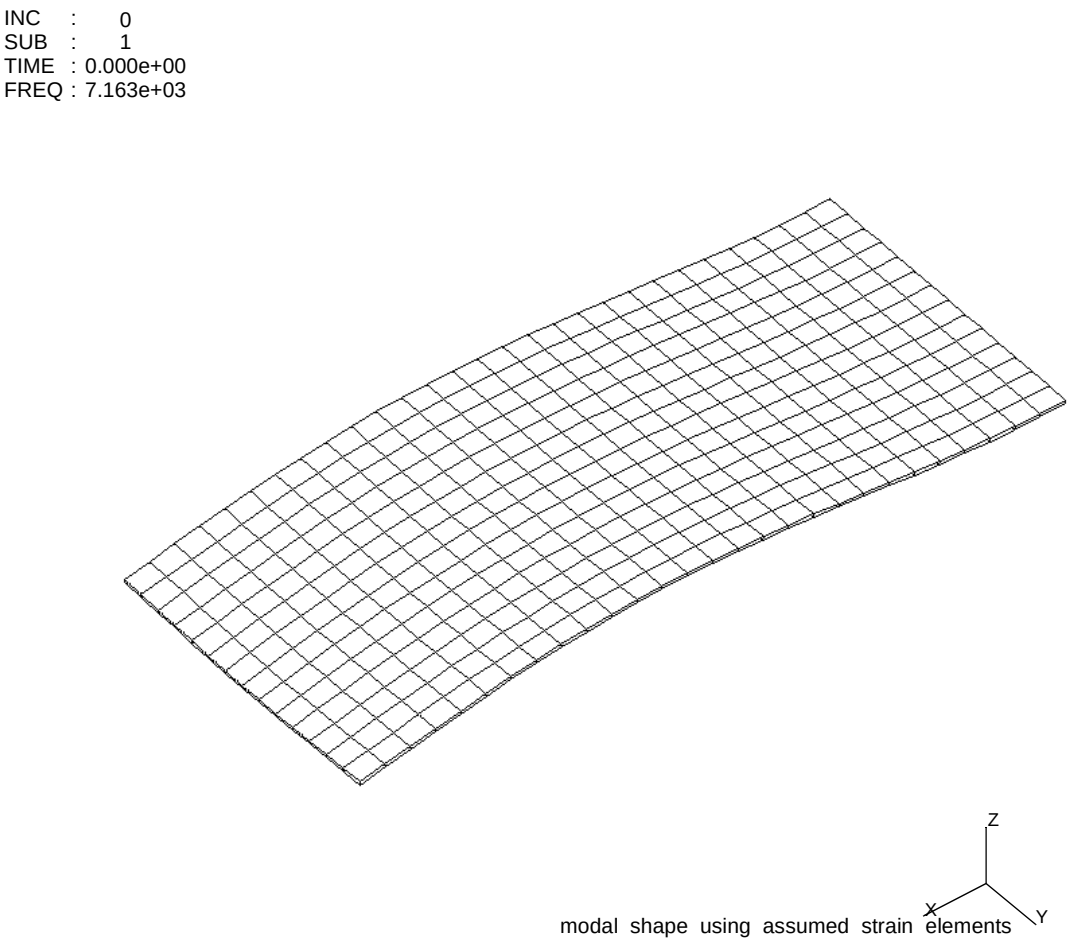

Figure 6.15-2 First Mode Shape of Cantilevered Plate

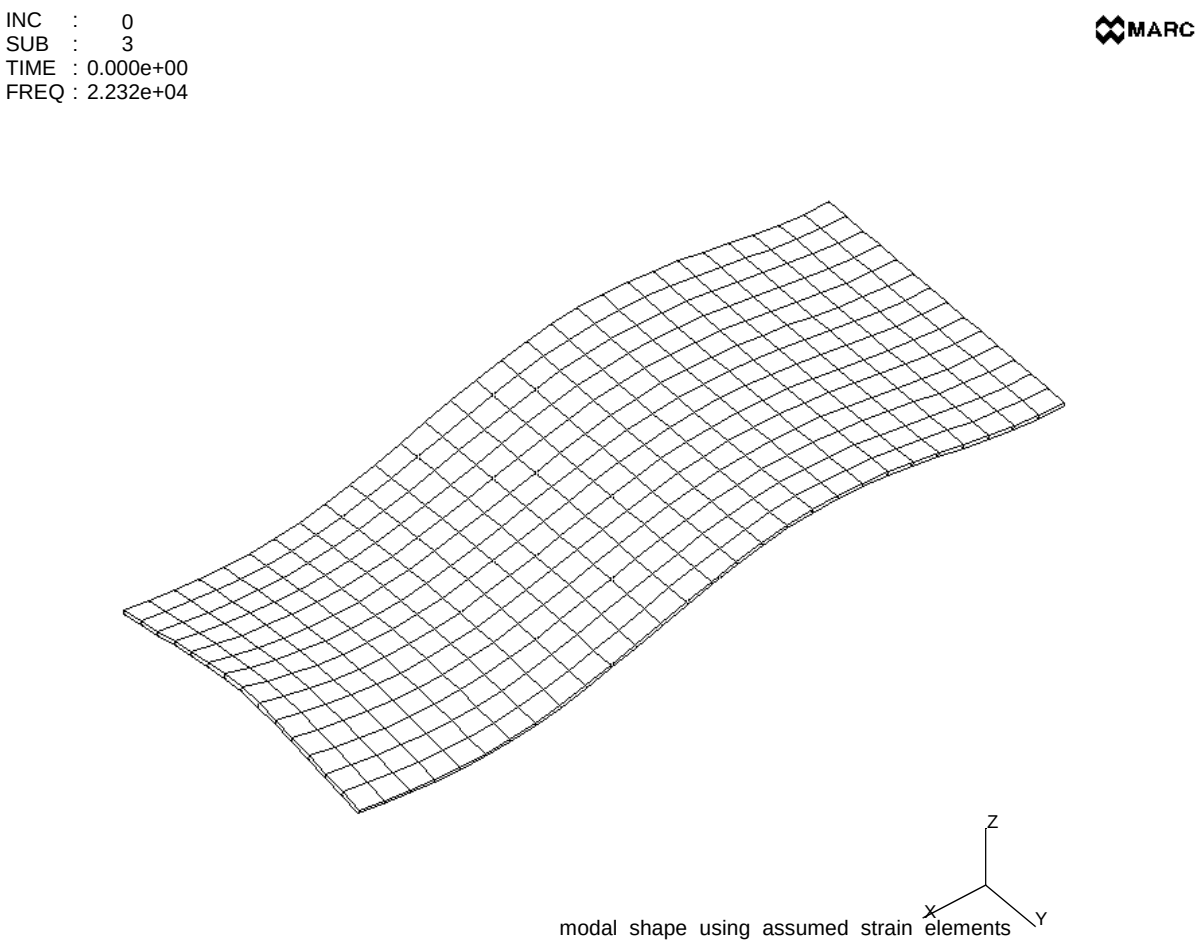

Figure 6.15-3 Third Mode Shape of Cantilevered Plate

6.16 Dynamic Contact Between a Projectile and a Rigid Barrier

This problem demonstrates the dynamic impact between a deformable body and a rigid surface. The problem is executed using both an implicit Newmark-beta operator and the explicit central difference operator.

This problem is modeled using the four techniques summarized below.

Data Set	Element Type(s)	Number of Elements	Number of Nodes	Differentiating Features
e6x16a	7	9	32	DYNAMIC,2 DEF-RIGID
e6x16b	7	9	32	DYNAMIC,4 DEF-RIGID
e6x16c	7	9	32	DYNAMIC,5 DEF-RIGID

Model

A deformable projectile consists of nine element type 7, eight-node bricks as shown in Figure 6.16-1. As an alternative, the analysis is also performed with element type 120 which is the reduced integration formulation. The projectile is initially 0.1 units away from the rigid surface. The DYNAMIC parameter specifies which operator is to be chosen: a “2” indicates Newmark-beta and a “4” indicates central difference. The projectile may undergo large deformations, so a LARGE DISP parameter is included. The projectile is considered elastic and a total Lagrange analysis is performed.

Material Properties

An artificial material was created, such that the stability limit for central difference was a large number. The Young’s modulus is 10,000 psi and the mass density is 0.1 lbf-sec^2/in^4. A lumped mass matrix is created based upon the LUMP parameter. The projectile is given a numerical damping of 0.4. Numerical dampening is preferred over stiffness damping, because the time step can change in contact analyses, resulting in stiffness damping overdamping the system.

Given the material parameters, the elastic wave speed is $c = \sqrt{E/\rho} = 316$ in./s.

Boundary Conditions

The nodes on the xz-plane have been constrained in the y-direction. The nodes on the xy-plane have been constrained in the z-direction. The projectile has an initial velocity of -100 in/second in the x-direction.

Controls

The maximum number of increments is 100 with the maximum number of iterations being three. Relative displacement error control is used with a tolerance value of 10%. Note that when using the explicit dynamic method, iteration does not occur. A formatted post file is written which contains only nodal information. The restart file is written at every increment.

Contact

There are two bodies in this analysis. The first is the deformable projectile. The second is the rigid barrier. There is no friction between these two surfaces.

The other parameters on the second block are upper bounds to the number of surface entities and surface nodes.

The contact tolerance is 0.03 inch which is small compared to an element dimension. A very large separation force is given which effectively ensures that the projectile sticks to the barrier.

The first body is the deformable one consisting of nine elements. The second body consists of one patch. The order of the numbering ensures the correct normal direction is associated with the rigid surface.

Time Step

The time step chosen is 0.0005 second which is below the stability limit of 0.002 second. In this period, the elastic wave travels 0.158 inch which is smaller than a typical element dimension. The total period is 0.01 second, so 20 increments are performed.

Results

Figure 6.16-3 and Figure 6.16-4 show the projectile at increment two after contact first occurs, and at increment 20 at the end of the analysis. Figure 6.16-5, Figure 6.16-6, and Figure 6.16-7 show the displacement, velocity, and reaction forces at selected nodes for the Newmark-beta analysis and central difference analysis. You can observe that the results are almost indistinguishable. Node 26 first comes into contact at increment 2, the displacement is .1 and remains fixed for the remainder of the analysis; velocity is zero. Node 25 comes into contact during increment 10 and remains fixed the remainder of the analysis. Nodes 31 and 32 simply decelerate during the analysis. The reactions show that spikes occur at the increments where contact occurs. The results using the reduced integration element are not substantially different.

The implicit Newmark-beta ran three times longer. This is an anomaly due to the fact that an artificial material was created such that the time steps in the two procedures were allowed to be the same.

Parameters, Options, and Subroutines Summary

Example e6x16a.dat:

Parameters	Model Definition Options	History Definition Options
DYNAMIC	CONNECTIVITY	CONTINUE
ELEMENT	CONTACT	DYNAMIC CHANGE
END	CONTROL	
LARGE DISP	COORDINATE	
LUMP	END OPTION	
PRINT	FIXED DISP	
SIZING	INITIAL VELOCITY	
TITLE	ISOTROPIC	
	POST	
	PRINT ELEM	
	RESTART	

Example e6x16b.dat:

Parameters	Model Definition Options	History Definition Options
DYNAMIC	CONNECTIVITY	CONTINUE
ELEMENT	CONTACT	DYNAMIC CHANGE
END	CONTROL	
LARGE DISP	COORDINATE	
LUMP	END OPTION	
PRINT	FIXED DISP	
SIZING	INITIAL VELOCITY	
TITLE	ISOTROPIC	
	POST	
	PRINT ELEM	
	RESTART	

Example e6x16c.dat:

Parameters	Model Definition Options	History Definition Options
ALIAS	CONNECTIVITY	CONTINUE
DYNAMIC	CONTACT	DYNAMIC CHANGE
ELEMENT	CONTROL	
END	COORDINATE	
LARGE DISP	END OPTION	
LUMP	FIXED DISP	
PRINT	INITIAL VELOCITY	
SIZING	ISOTROPIC	
TITLE	POST	
	RESTART	

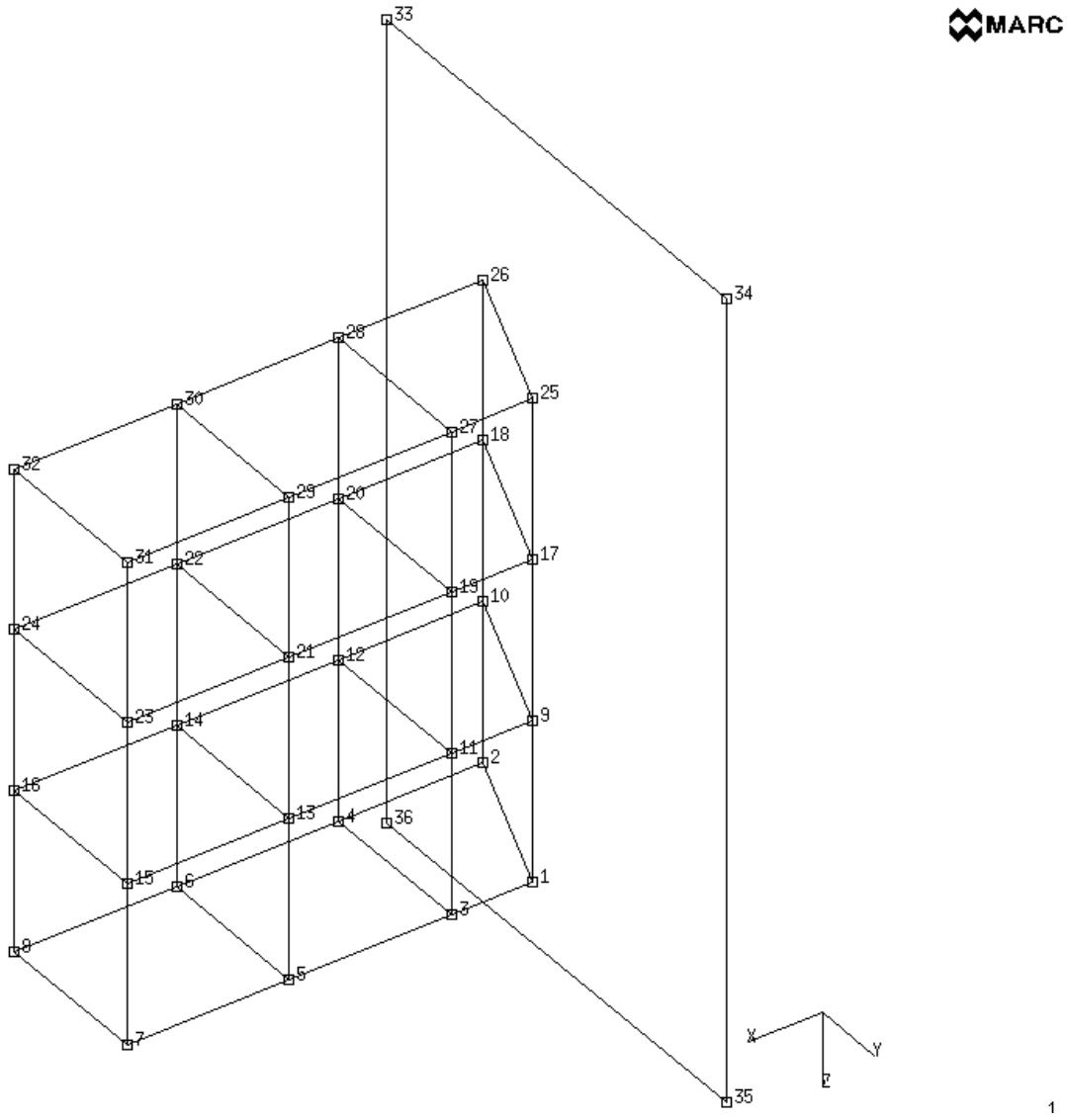

Figure 6.16-1 Impactor and Rigid Wall

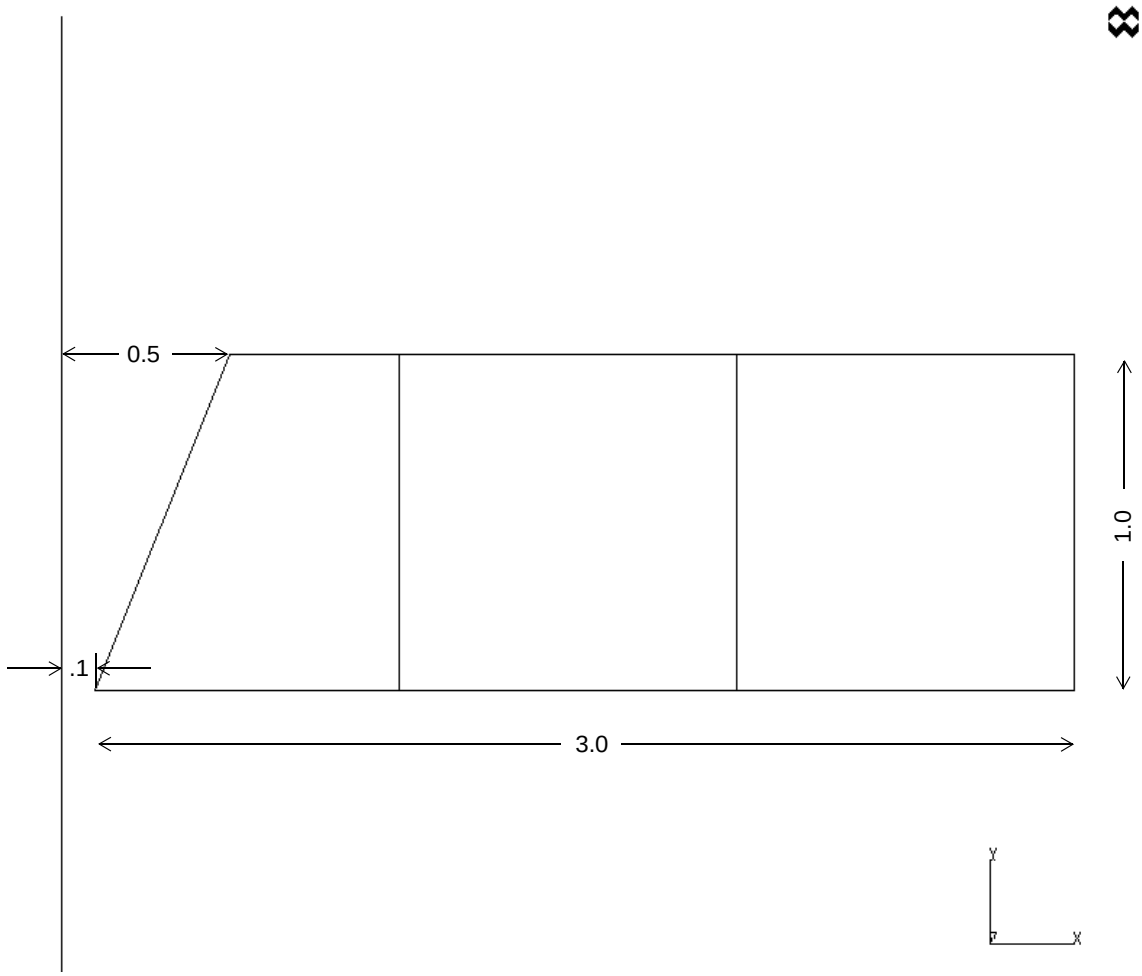

Figure 6.16-2 Impactor Geometry

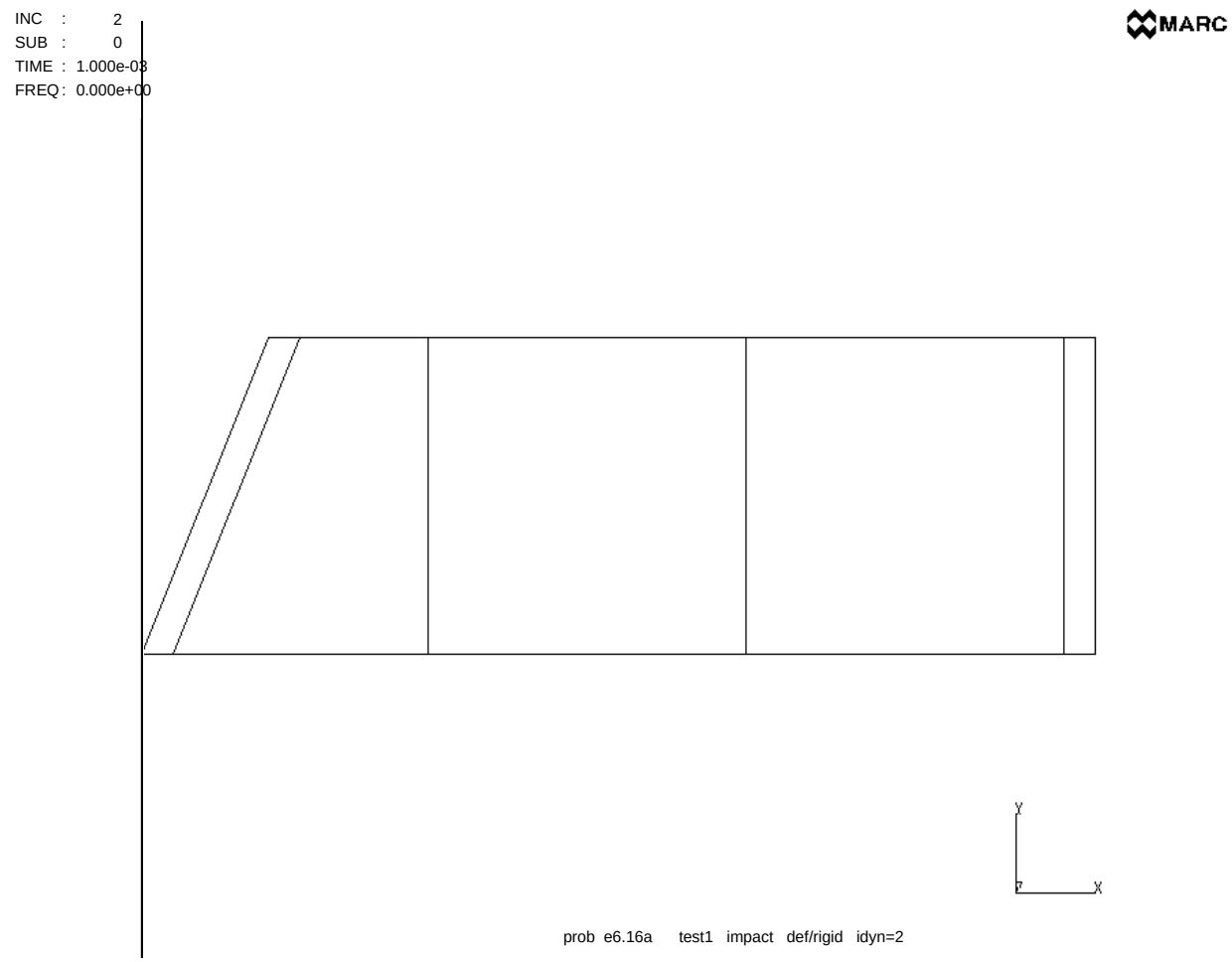

Figure 6.16-3 Deformation at Initial Contact

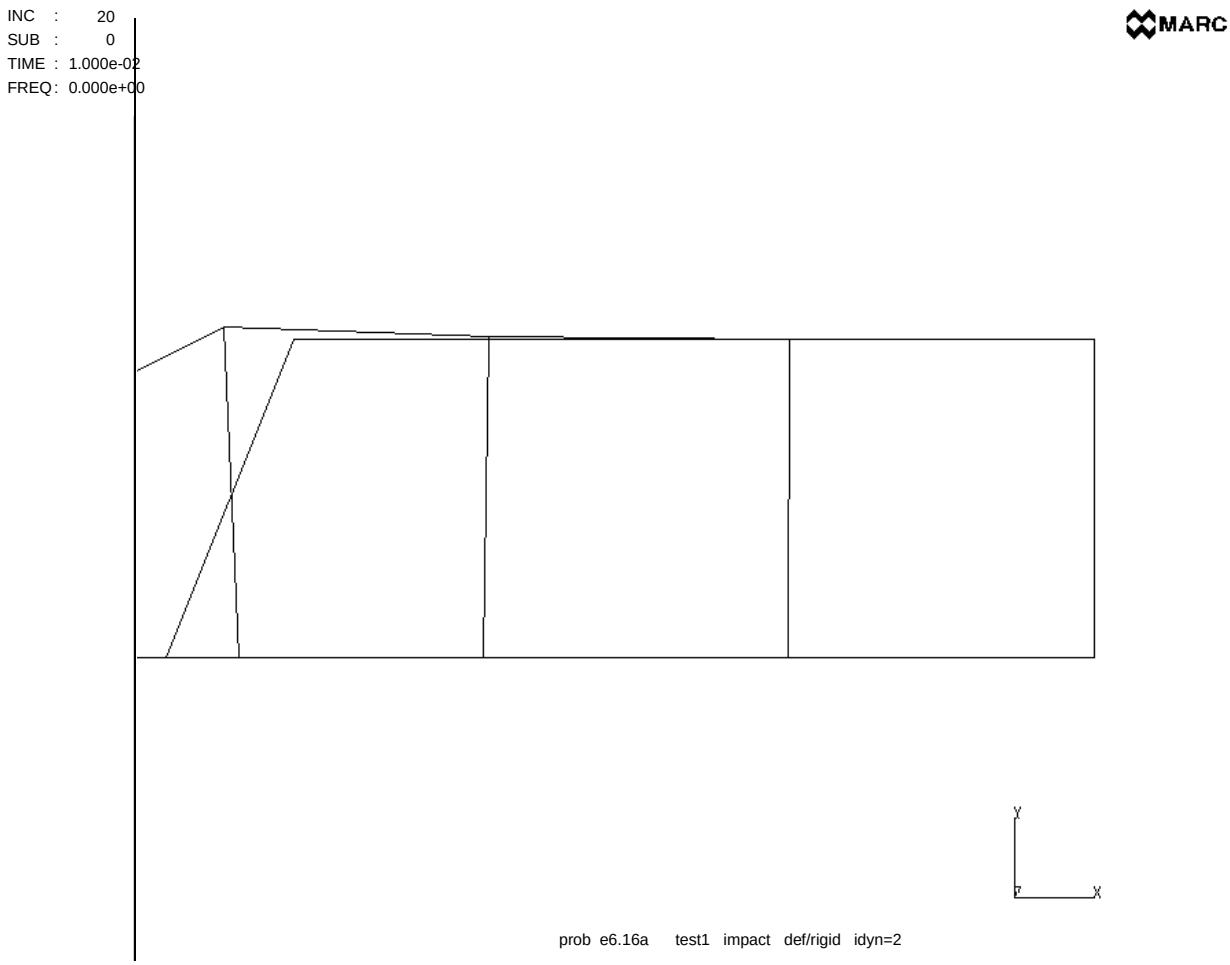

Figure 6.16-4 Final Deformation

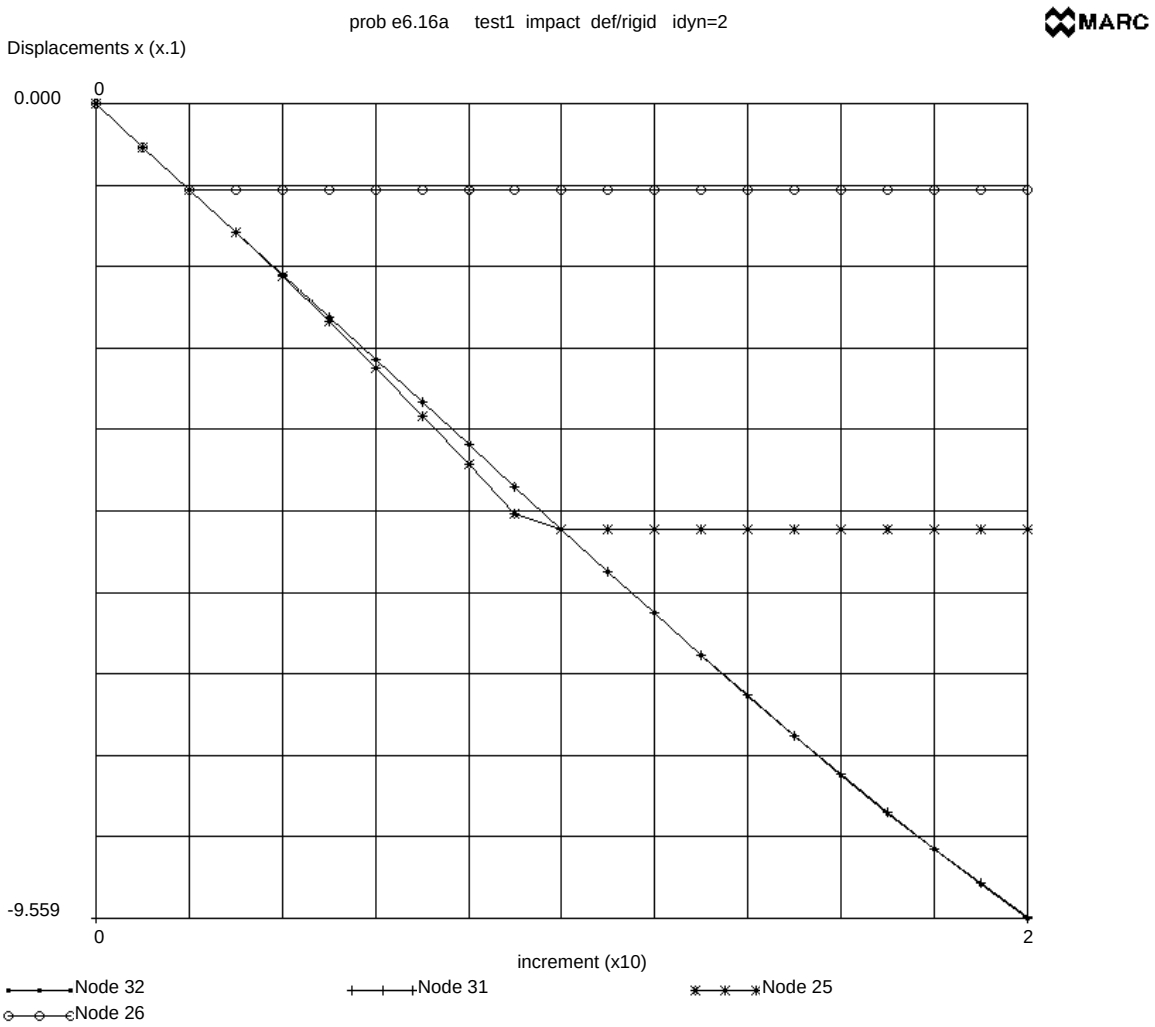

Figure 6.16-5 (A) Displacement History (Newmark-Beta Method)

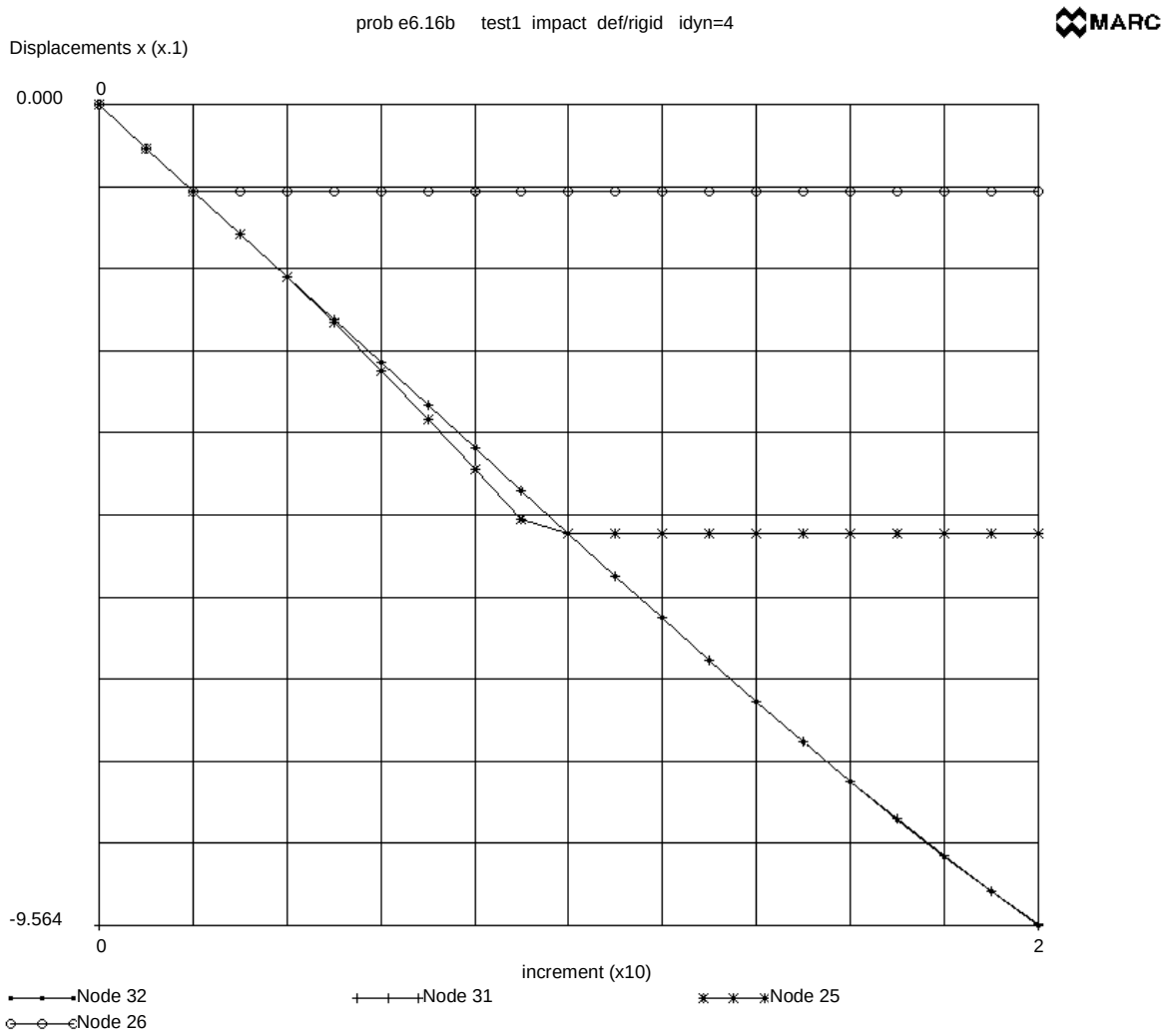

Figure 6.16-5 (B) Displacement History (Central Difference Method)

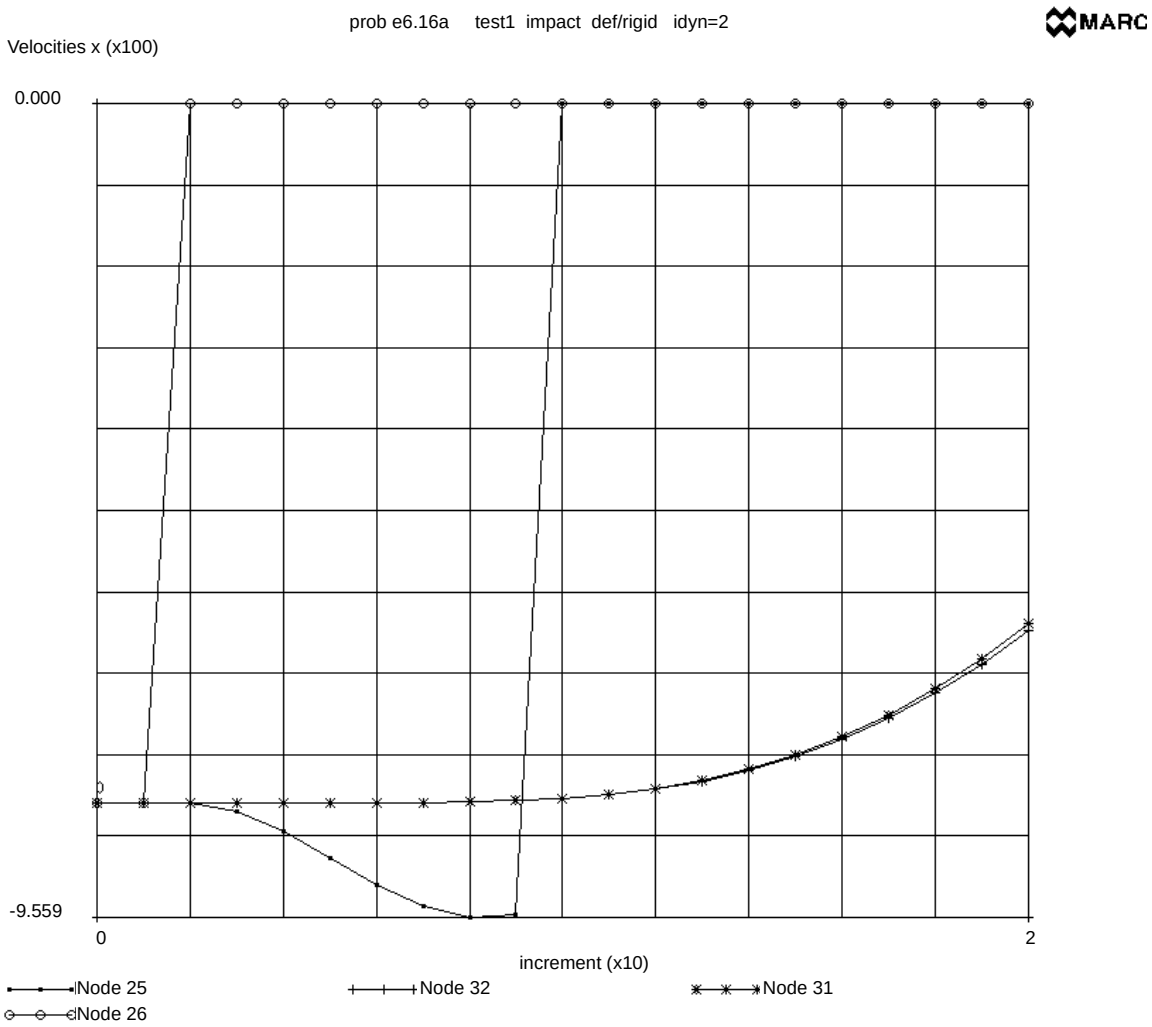

Figure 6.16-6 (A) Velocity History (Newmark-Beta Method)

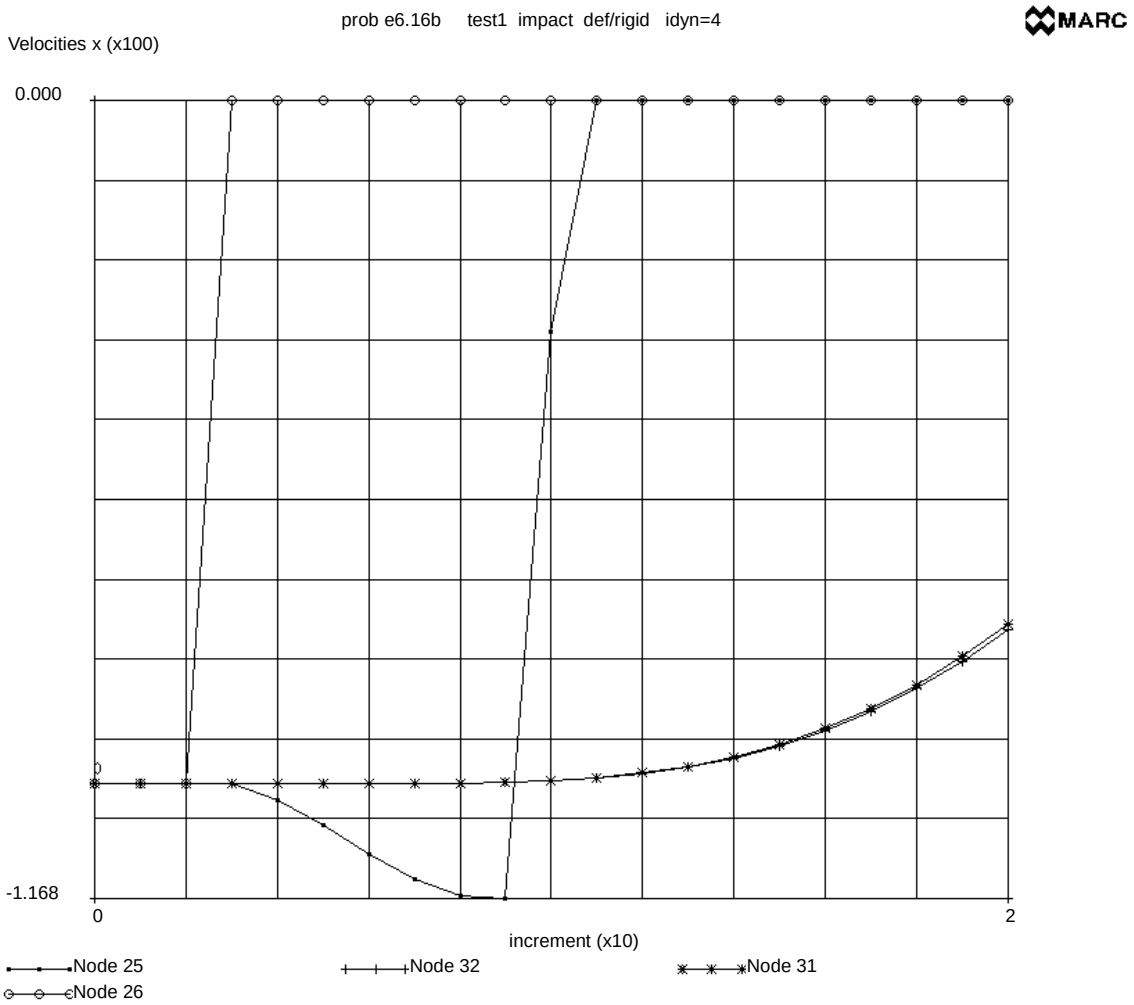

Figure 6.16-6 (B) Velocity History (Central Difference Method)

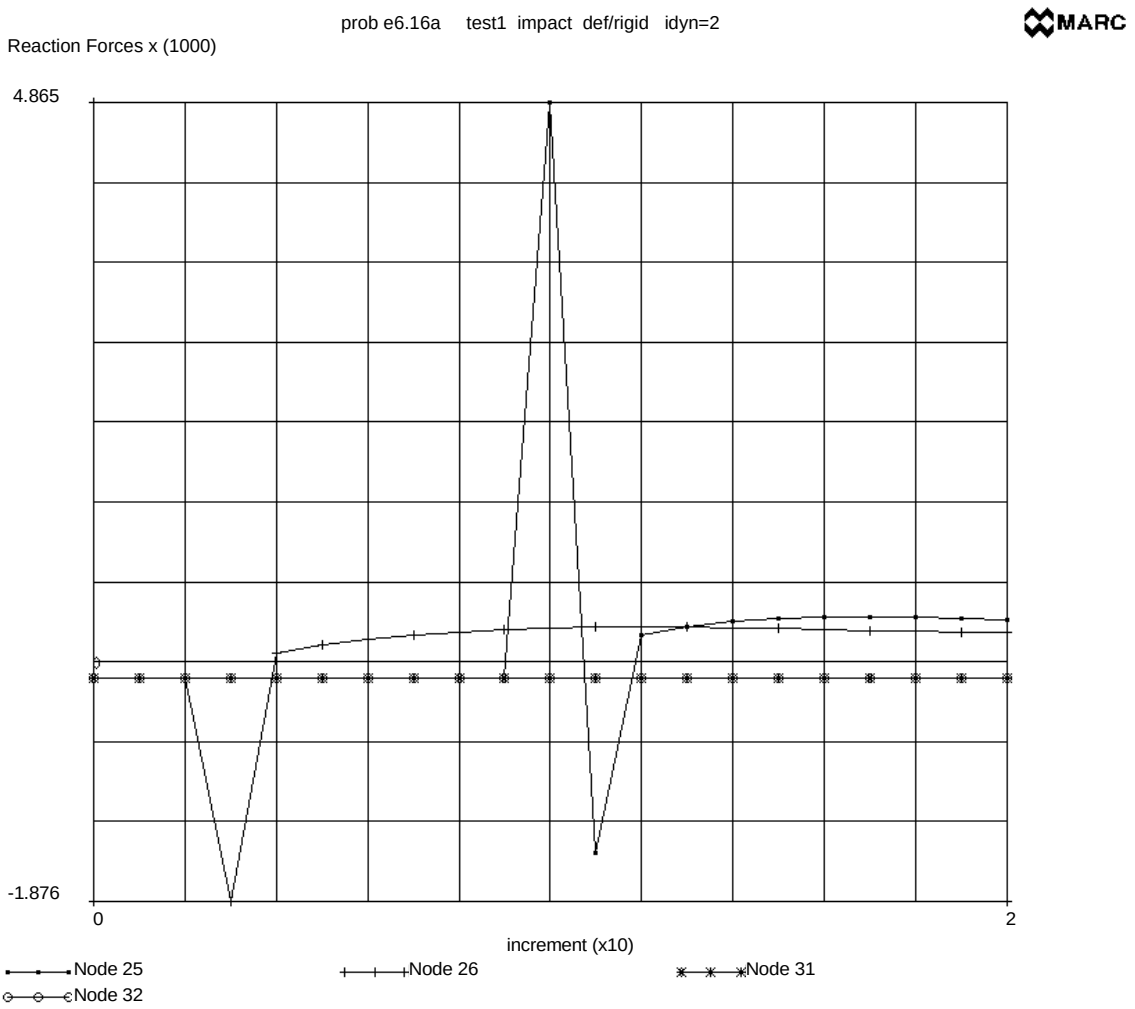

Figure 6.16-7 (A) Reaction/Impact Force History (Newmark-Beta Method)

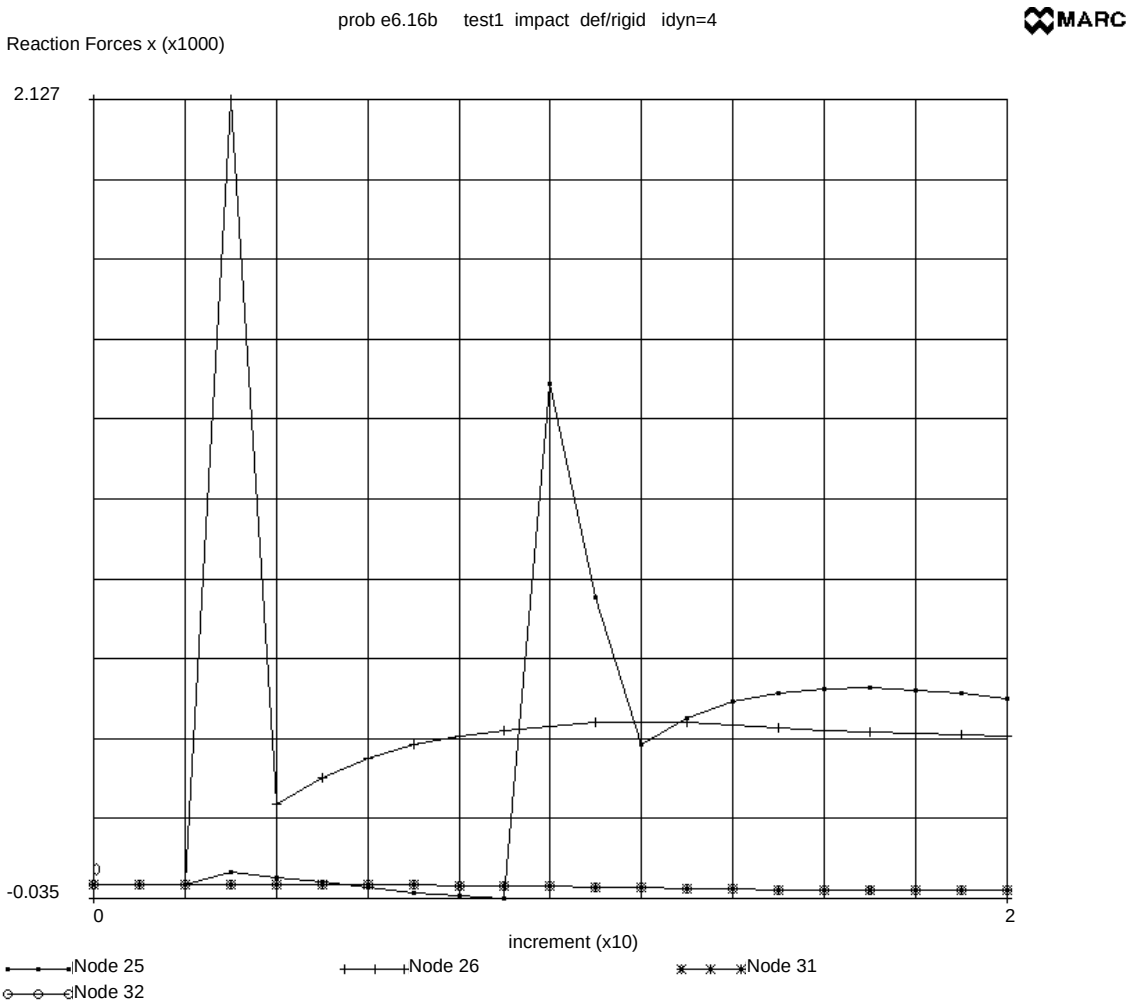

Figure 6.16-7 (B) Reaction/Impact Force History (Central Difference Method)

6.17 Dynamic Contact Between Two Deformable Bodies

This problem demonstrates the dynamic impact between two deformable bodies. It is very similar to problem 6.16, except the rigid barrier has been replaced by a deformable, yet stiff, body. Both the implicit Newmark-beta and explicit central difference procedures are demonstrated.

This problem is modeled using the two techniques summarized below.

Data Set	Element Type(s)	Number of Elements	Number of Nodes	Differentiating Features
e6x17a	7	49	122	DYNAMIC,2 Newmark-beta
e6x17b	7	49	122	DYNAMIC,4 Central Difference

Model

The model is shown in Figure 6.17-1 and Figure 6.17-2. The project is made up of 9 brick elements type 7, where the barrier is composed of 40 brick elements. The DYNAMIC parameter specifies which operator is to be chosen: a “2” indicates Newmark-beta and a “4” indicates central difference. The projectile may undergo elastic deformation, so the LARGE DISP parameter is included.

Material Properties

An artificial material was created, such that the stability limit for central difference was a large number. For the projectile (elements 1 – 9), the Young’s modulus is 10,000 psi and the mass density is 0.1 lbf-sec^2/in^4. The barrier is ten times stiffer with a Young’s modulus of 100,000 psi. A lumped mass matrix is created based upon the LUMP parameter. The model is given a numerical damping of 0.4. Given the material parameters, the elastic wave speed in the projectile is $c = \sqrt{E/p} = 316$ in/sec. In the barrier, it is 1000 in/second.

Boundary Conditions

The nodes on the xz-plane have been constrained in the y-direction. The nodes on the xy-plane have been constrained in the z-direction for the projectile. The projectile has an initial velocity of -100 in/second in the x-direction.

Controls

The maximum number of increments is 100 with the maximum number of iterations as 25. Relative displacement error control is used with a tolerance value of 10%. A formatted post file is written which contains only nodal information. Both the restart and post file are written every increment.

Contact

There are two bodies in this analysis. The first is the deformable projectile. The second is the deformable barrier. There is no friction between these two surfaces.

The other parameters on the second block are upper bounds to the number of surface entities and surface nodes.

The contact tolerance is 0.032 inch which is small compared to an element dimension. A very large separation force is given which effectively ensures that the projectile sticks to the barrier.

Time Step

The time step chosen is 0.0005 second which is below the stability limit of 0.0012 second. The stability limit is smaller in this problem than in 6.16 because of the stiff barrier. The total period is 0.01 second, so 20 increments are performed.

Results

Figure 6.17-3 shows the deformation at increment 20. The barrier is significantly stiffer and undergoes very little deformation. The projectile is originally 0.2 inches from the barrier. You can observe in Figure 6.17-4 that node 26 contacts the barrier in increment 3 using the implicit procedure, and increment 4 in the explicit procedure. This is due to the nature of these two different methods. There is more deformation of the barrier using the implicit procedure. Figure 6.17-5 shows the velocity histories using the new methods. The basic correlation is good. The Newmark-beta method shows some oscillations at later increments. This could be eliminated by using more damping or decreasing the time step.

Parameters, Options, and Subroutines Summary

Example e6x17a.dat:

Parameters	Model Definition Options	History Definition Options
DYNAMIC	CONNECTIVITY	CONTINUE
ELEMENT	CONTACT	DYNAMIC CHANGE
END	CONTROL	
LARGE DISP	COORDINATE	
LUMP	END OPTION	
PRINT	FIXED DISP	
SIZING	INITIAL VELOCITY	
TITLE	ISOTROPIC	
	POST	
	PRINT ELEM	
	RESTART	

Example e6x17b.dat:

Parameters	Model Definition Options	History Definition Options
DYNAMIC	CONNECTIVITY	CONTINUE
ELEMENT	CONTACT	DYNAMIC CHANGE
END	CONTROL	
LARGE DISP	COORDINATE	
LUMP	END OPTION	
PRINT	FIXED DISP	
SIZING	INITIAL VELOCITY	
TITLE	ISOTROPIC	
	POST	
	PRINT ELEM	
	RESTART	

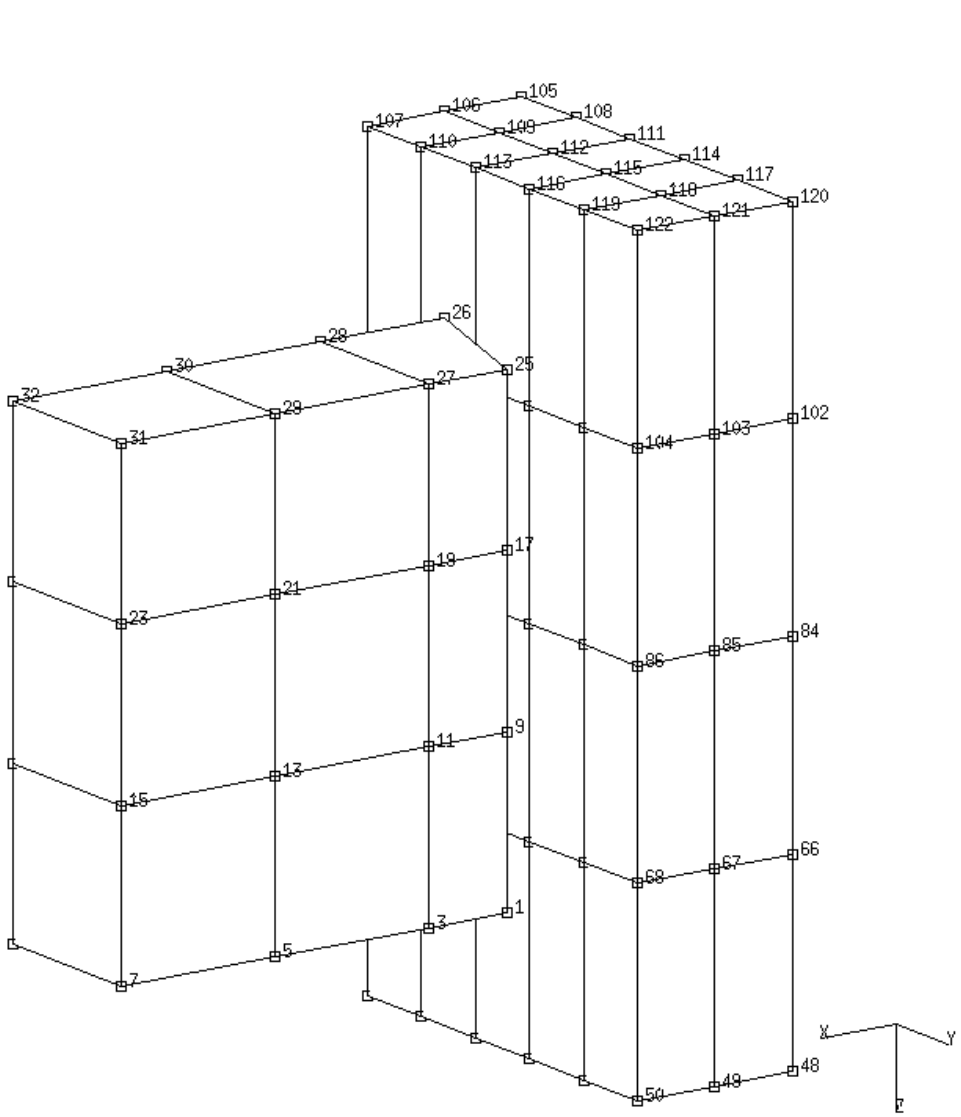

Figure 6.17-1 Impactor and Deformable Barrier

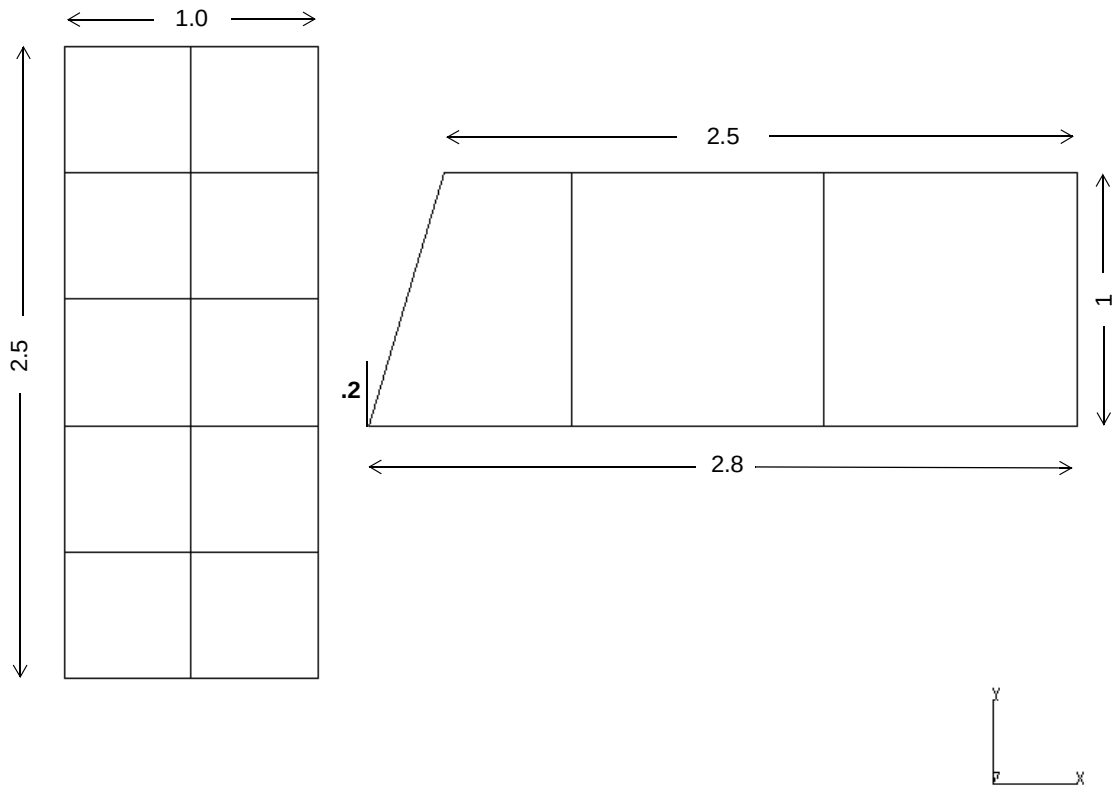

Figure 6.17-2 Geometries

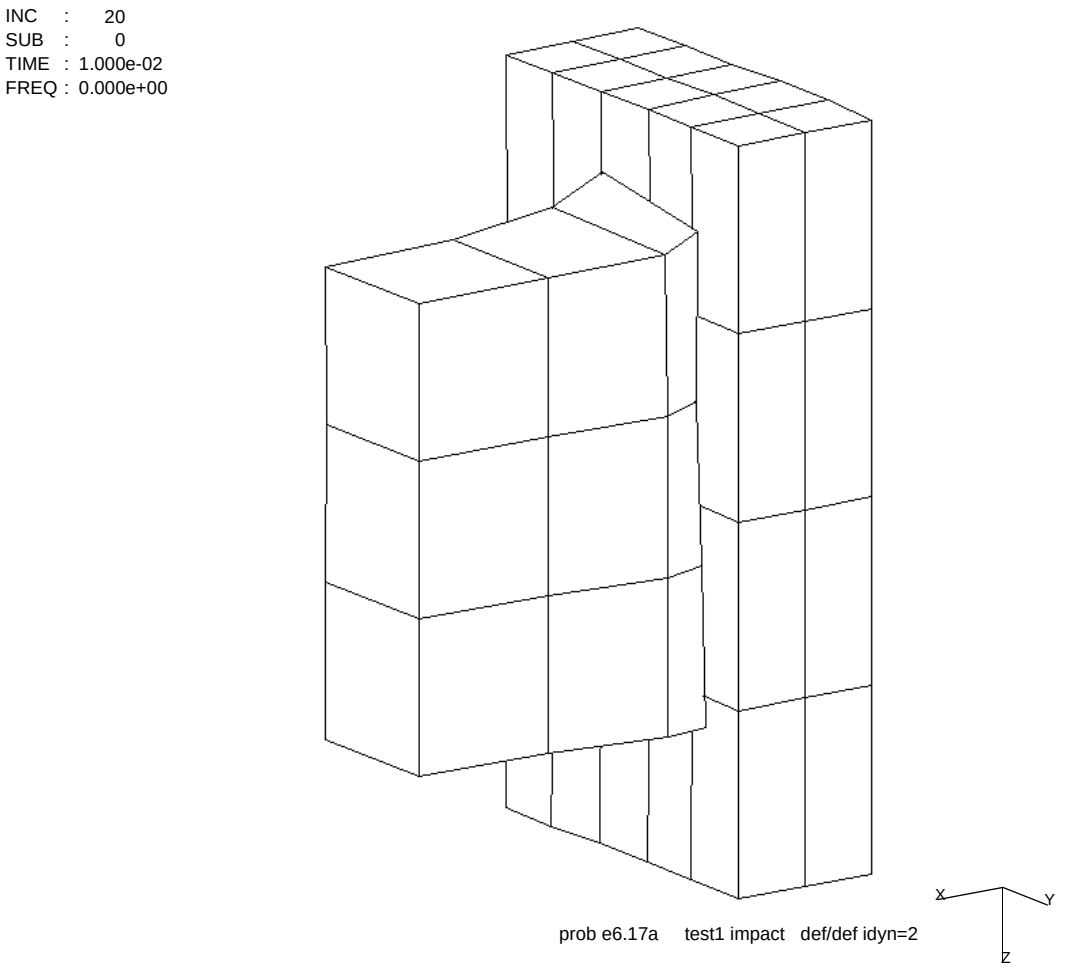

Figure 6.17-3 Final Deformation

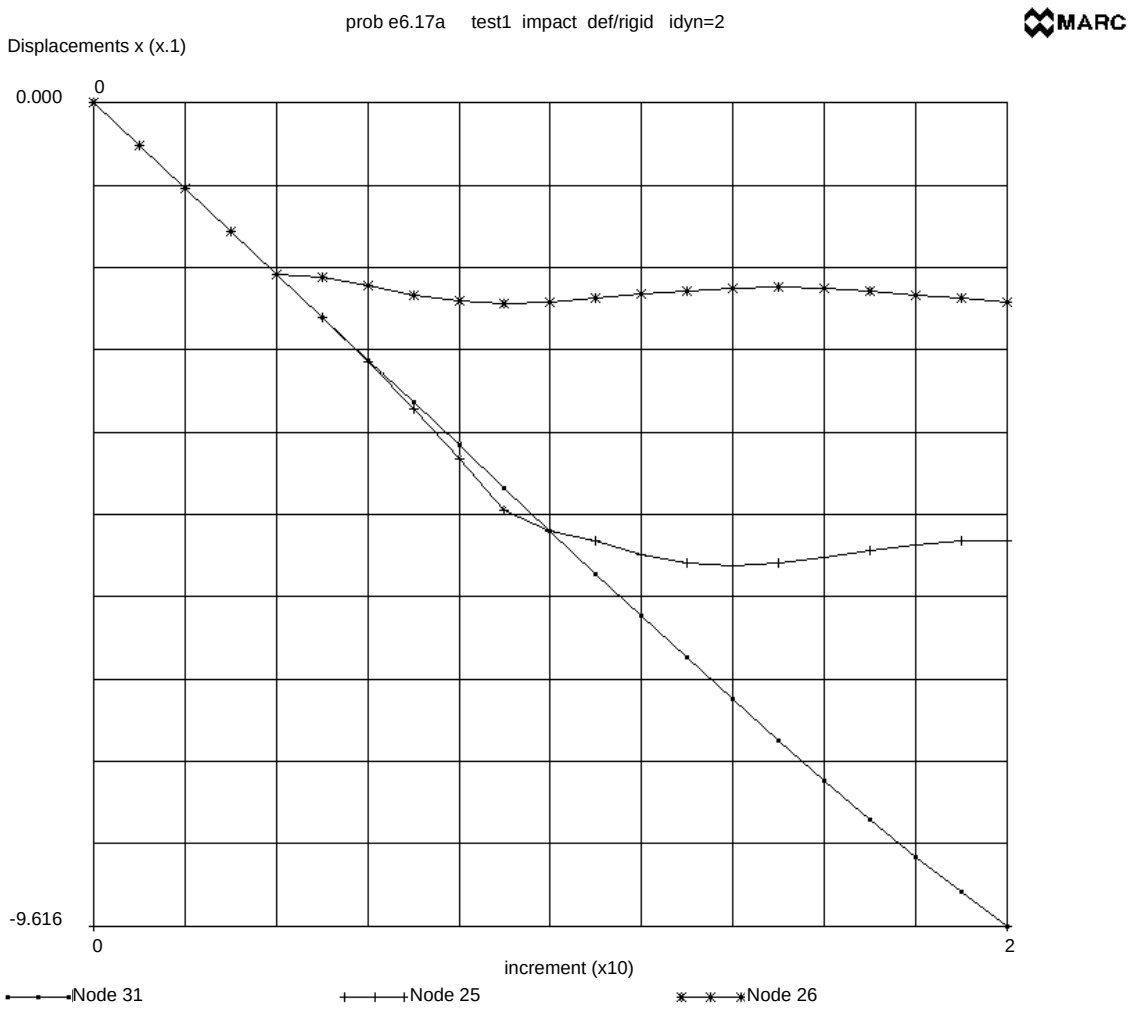

Figure 6.17-4 (A) Displacement Histories (Newmark-beta Method)

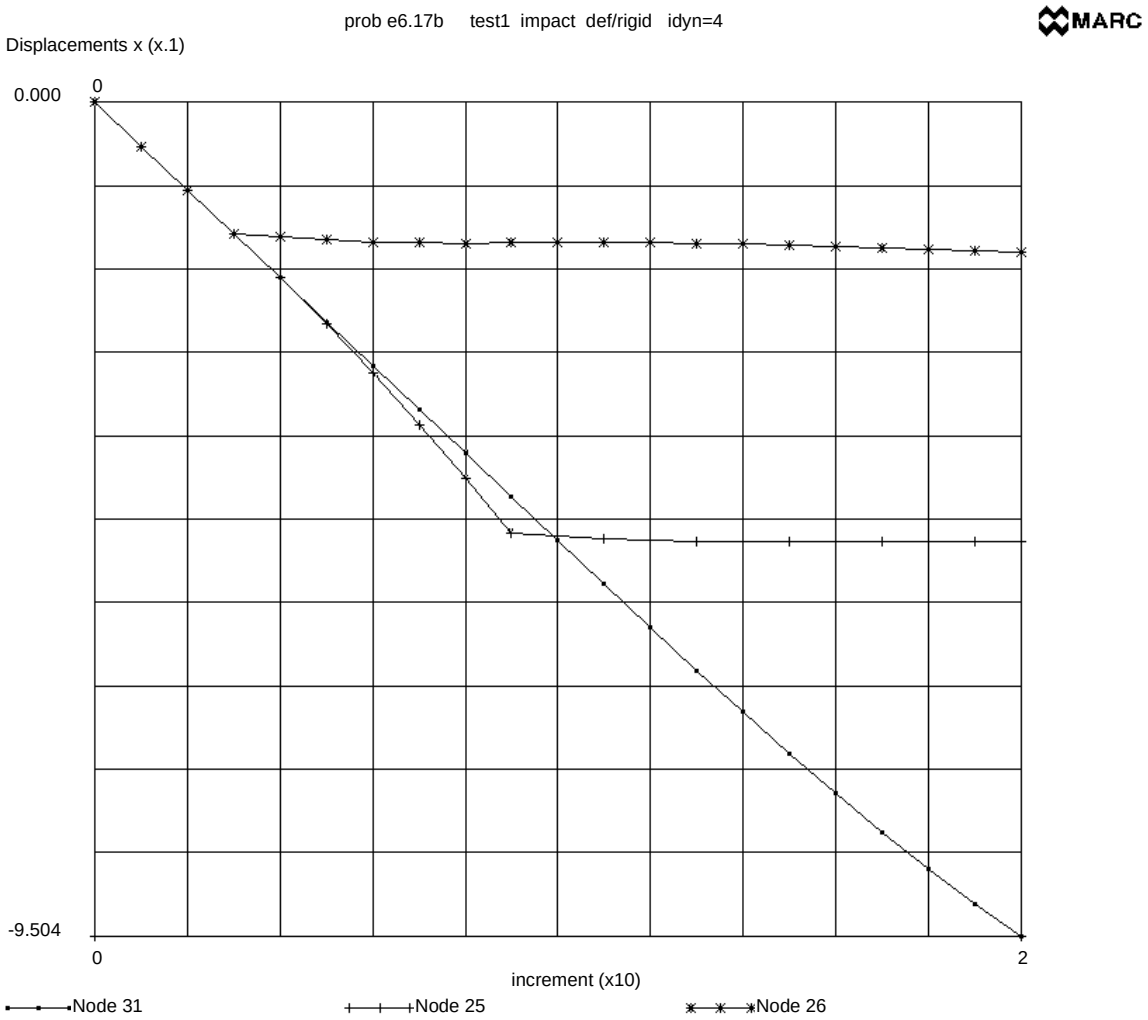

Figure 6.17-4 (B) Displacement History (Central Difference Method)

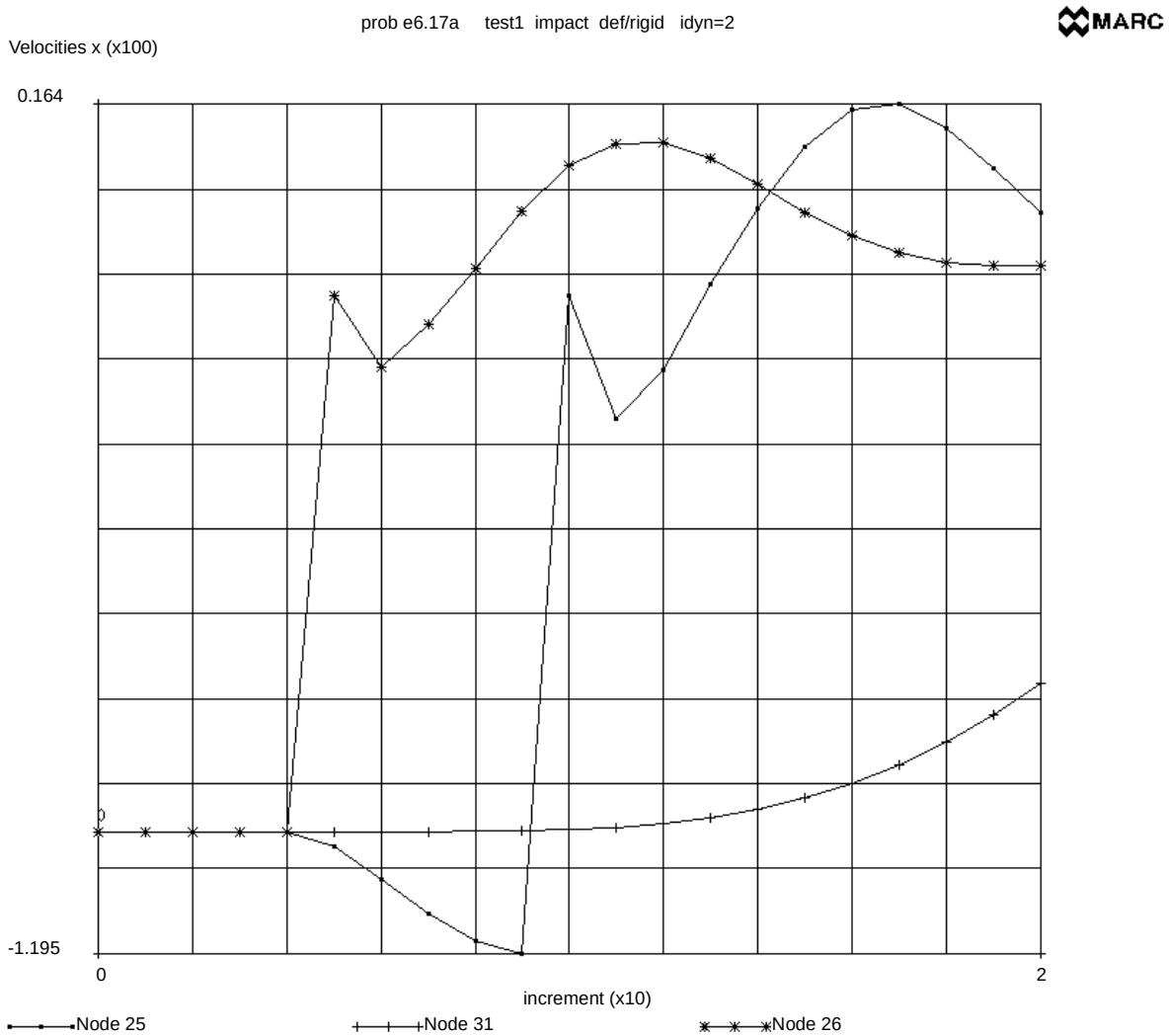

Figure 6.17-5 (A) Velocity History (Newmark-beta Method)

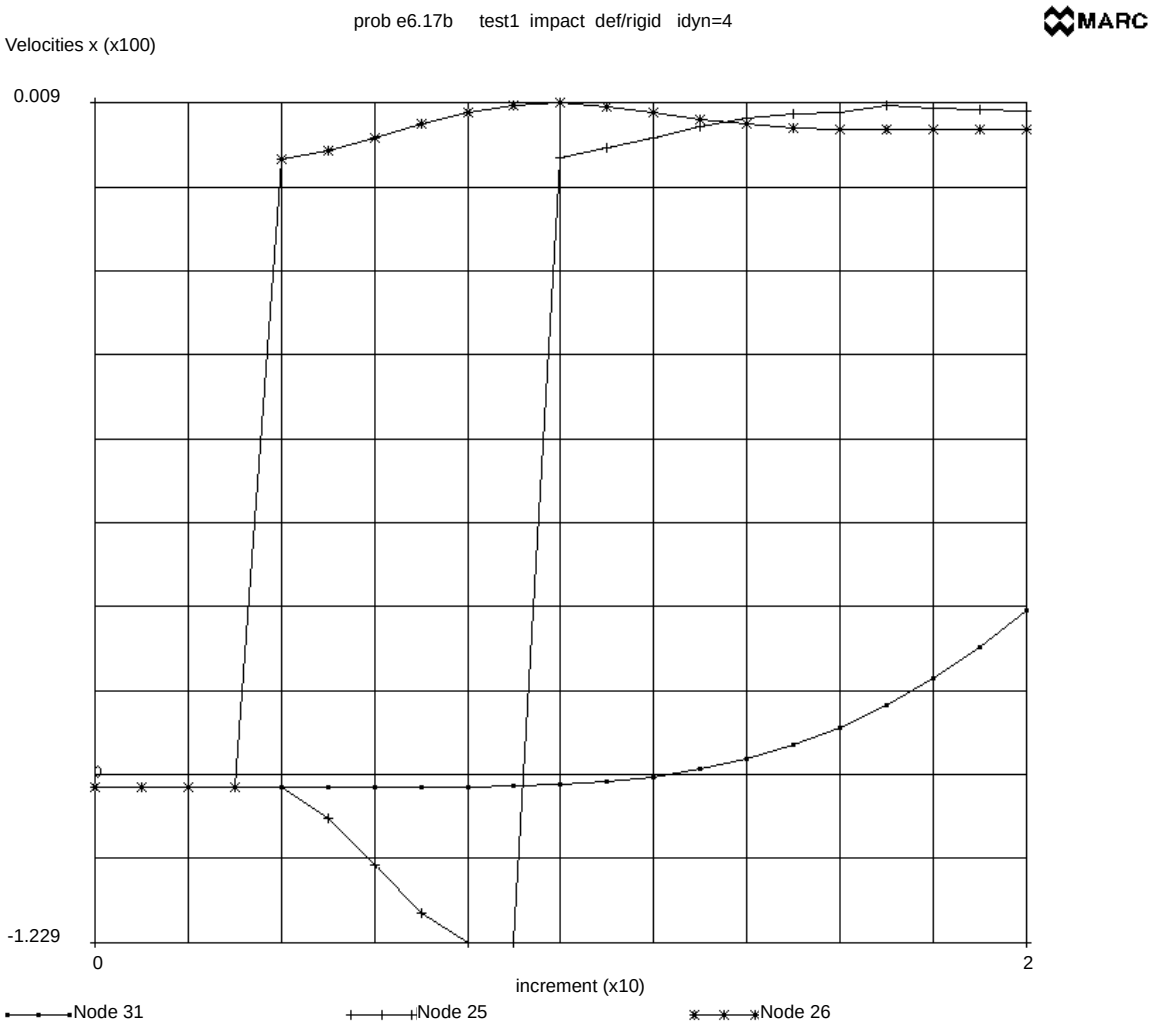

Figure 6.17-5 (B) Velocity History (Central Difference Method)

6.18 Spectral Response of a Pipe

This problem illustrates the spectrum response capabilities of MARC. The spectral displacements of a cantilever are computed and compared with analytical results.

Model

The structure is shown in Figure 6.18-1. The mesh consists of 21 type 52 elements and 22 nodes.

Geometry

The pipe has a cross-sectional area of 5.34 E-3 square meters. The moments of inertia of the section are 1.936 E-5m^4 about the local x-axis and 1.936 E-5 m^4 about the local y-axis.

Boundary Conditions

The pipe is clamped at the left end. Node 1 is assumed to be fixed.

Material Properties

Young's modulus is 1.58 E11 Newton/m^2. The mass density is 21138 kg/m^3.

Displacement Spectral Density

A displacement spectral density function is entered through user subroutine USSD and is assigned in both the x- and y-directions. The spectral values are obtained from the spectral accelerations shown in Table 6.18-1 via linear interpolation in a semilogarithmic plane.

Spectral Response

Four eigenvalues and the related eigenmodes were extracted using the inverse power sweep method. The response was calculated based on the extracted modes. The spectral displacements, both analytical and computed by MARC, are given in Table 6.18-2. The eigenvalues are given in Table 6.18-3.

Notice that the analytical values do not include the rotational inertia effects.

Table 6.18-1 Spectral Accelerations [m/sec^2]

Frequencies (Hz)	Accelerations (g)
0.0001	0.03
0.1	0.03
0.85	0.98
1.15	0.98
3.21	0.35
3.83	0.44
5.18	0.44
13.	0.24
1000.	0.24

Table 6.18-2 Displacements [m] in x and y Direction

z	Analytical	MARC
0.8	3.77 E-4	3.78 E-4
1.2	8.08 E-4	8.10 E-4
1.8	1.68 E-3	1.69 E-3
2.2	2.39 E-3	2.39 E-3
2.8	3.56 E-3	3.56 E-3
3.4	4.81 E-3	4.82 E-3
4.0	6.10 E-3	6.11 E-3
4.265	6.67 E-3	6.68 E-3

Table 6.18-3 Eigenvalues [Hz]

N	Analytical	MARC
1	5.066	5.059
2	5.066	5.059
3	31.986	31.61
4	31.986	31.61

Parameters, Options, and Subroutines Summary

Example e6x18.dat:

Parameters	Model Definition Options	History Definition Options
DYNAMIC	CON GENER	CONTINUE
ELEMENTS	CONNECTIVITY	MODAL SHAPE
END	COORDINATE	RECOVER
RESPONSE	END OPTION	SPECTRUM
SIZING	FIXED DISP	
TITLE	GEOMETRY	
	ISOTROPIC	
	NODE FILL	
	POST	

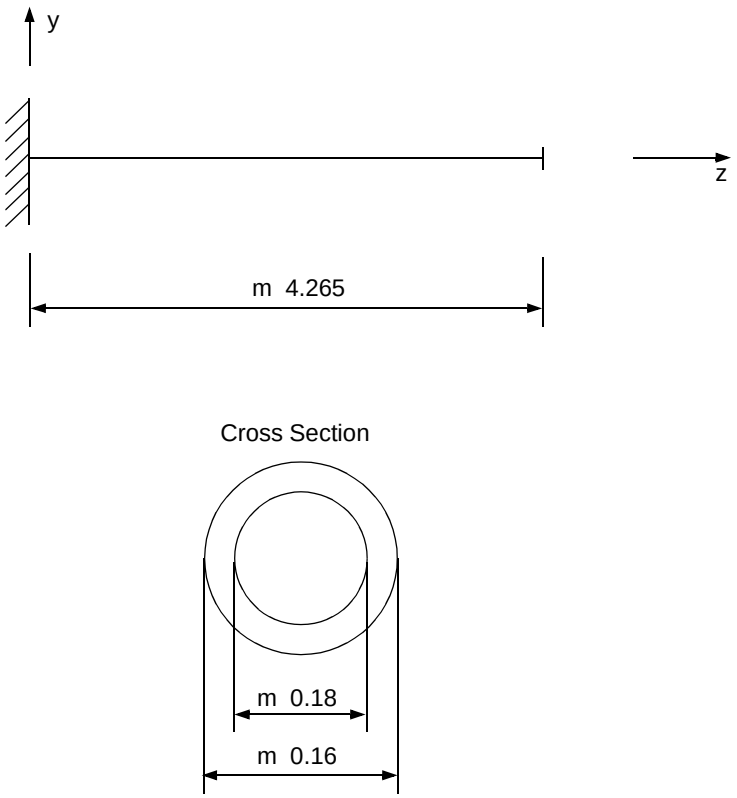

Figure 6.18-1 Cantilever Pipe and its Cross Section

6.19 Dynamic Impact of Two Bars

This problem demonstrates the dynamic impact of a bar hitting against another bar fixed in space using the explicit method. The DYNAMIC, 5 option is used in this example.

Element

Element type 11 is a plane-strain element used to model both bars. Both bars are 10 cm x 1 cm and are modeled by 10 beam elements, respectively. There is a 0.5 cm gap between the two bars as shown in Figure 6.19-1.

Model

The structure is shown in Figure 6.19-1. The mesh consists of 20 type 10 elements and 44 nodes.

Material Properties

The material properties of both bars are:

Young's modulus is $E = 1000.0\ N/cm^2$

Poisson's ratio is $\nu = 0.0$

Mass density is $\rho = 1.0\ kg/cm^3$

Boundary Conditions

Only the displacement along x-direction is free. The bar at the right is fixed at the right end.

Dynamics

The body has an initial velocity of 1.0 cm/second. The case has been studied for 12.0 seconds using a time step of 0.04 second through the DYNAMIC CHANGE option.

Results

Figure 6.19-2 illustrates contact occurring at increment 13 and separation occurring approximately at increment 125. Figure 6.19-3 and Figure 6.19-4 show the velocity and acceleration histories. The reaction force at the wall is shown in Figure 6.19-5.

Parameters, Options, and Subroutines Summary

Example 6x19.dat:

Parameters	Model Definition Options	History Definition Options
SIZING	CONNECTIVITY	DYNAMIC CHANGE
ELEMENTS	OPTIMIZE	CONTINUE
DYNAMIC	COORDINATES	
PRINT	ISOTROPIC	
LUMP	INITIAL VELOCITY	
	CONTACT	
	CONTACT TABLE	
	FIXED DISPLACEMENT	
	POST	
	PRINT ELEMENT	
	PRINT NODE	
	END OPTION	

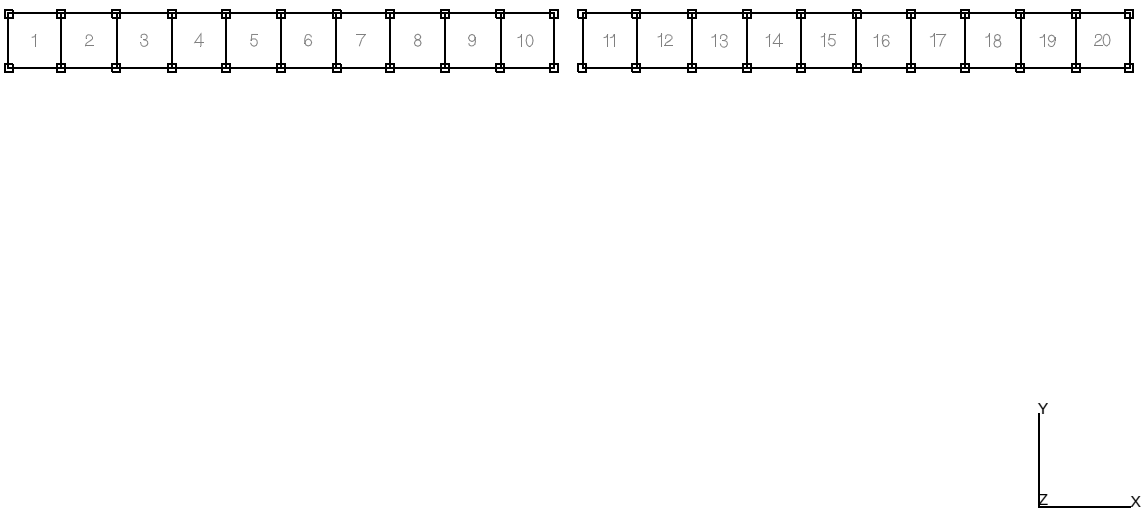

Figure 6.19-1 Finite Element Mesh of Two Bars

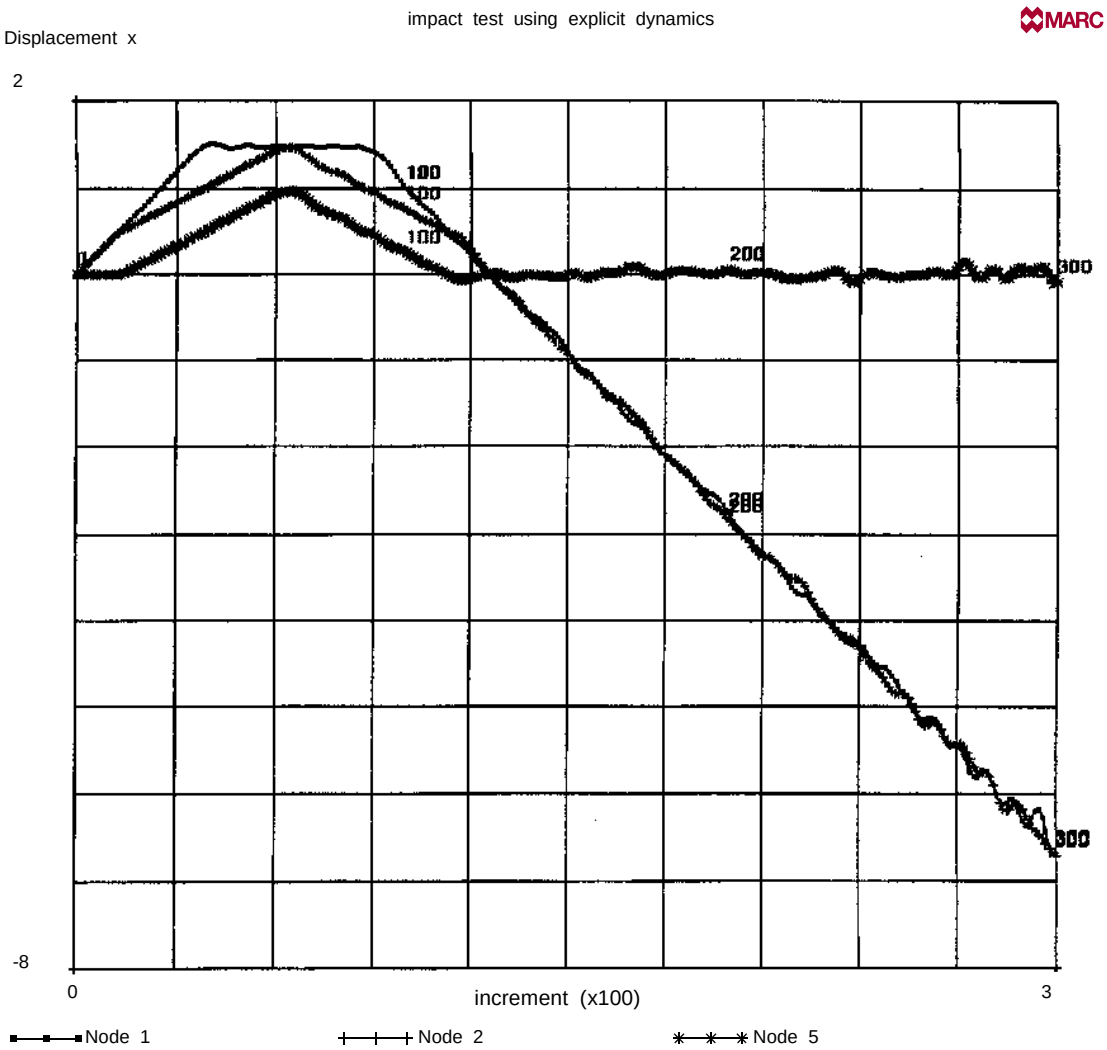

Figure 6.19-2 Displacement History of Selected Nodes

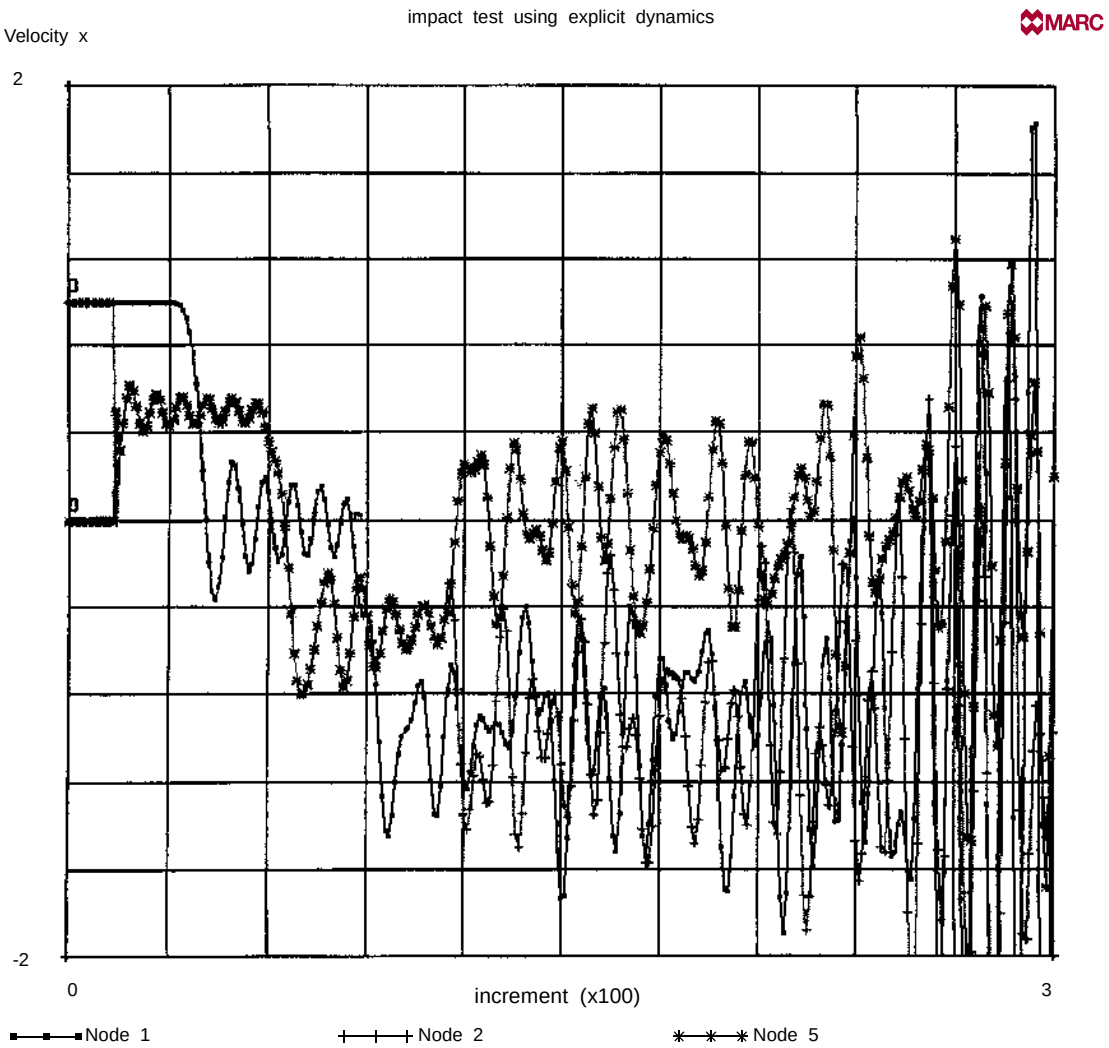

Figure 6.19-3 Velocity History of Selected Nodes

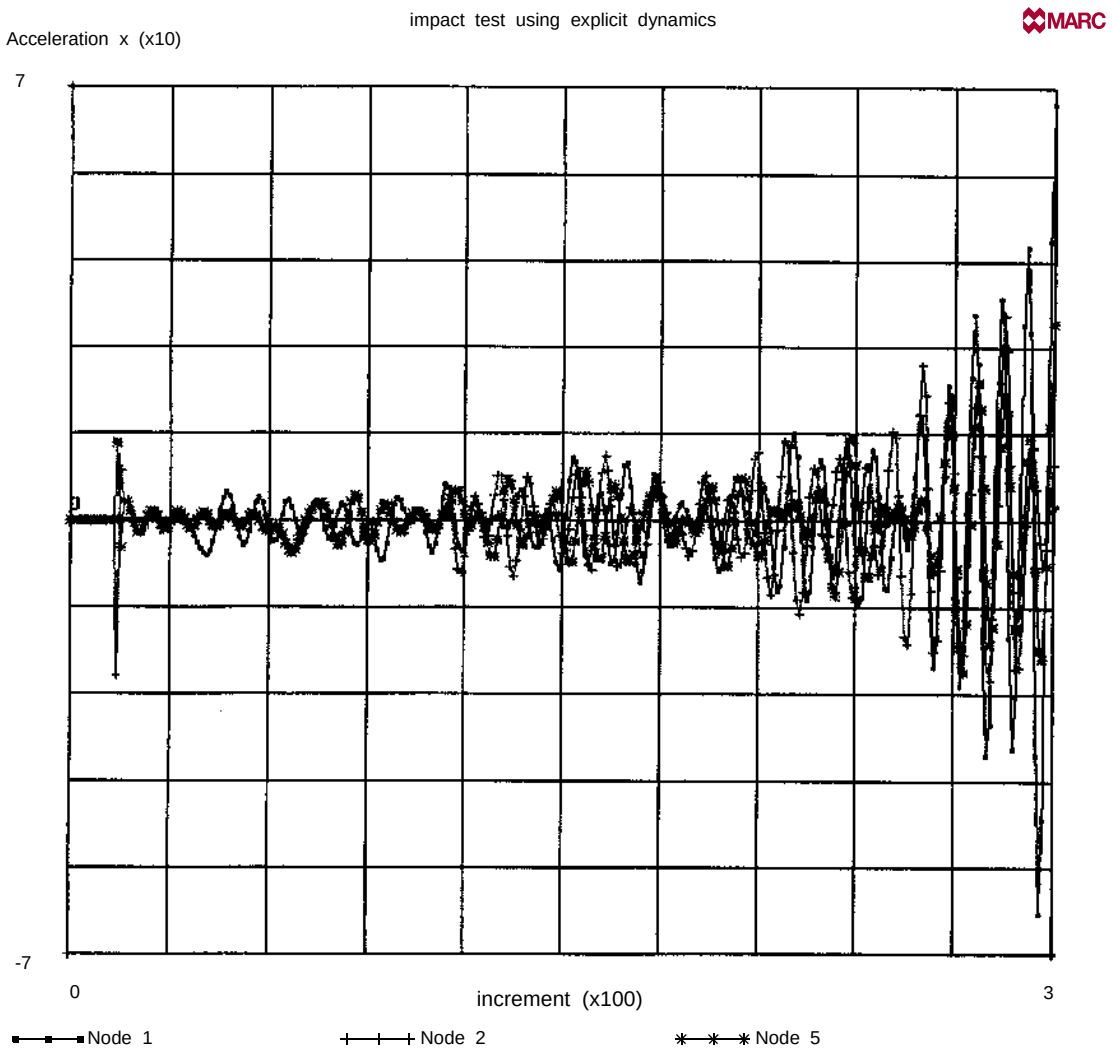

Figure 6.19-4 Acceleration History of Selected Node

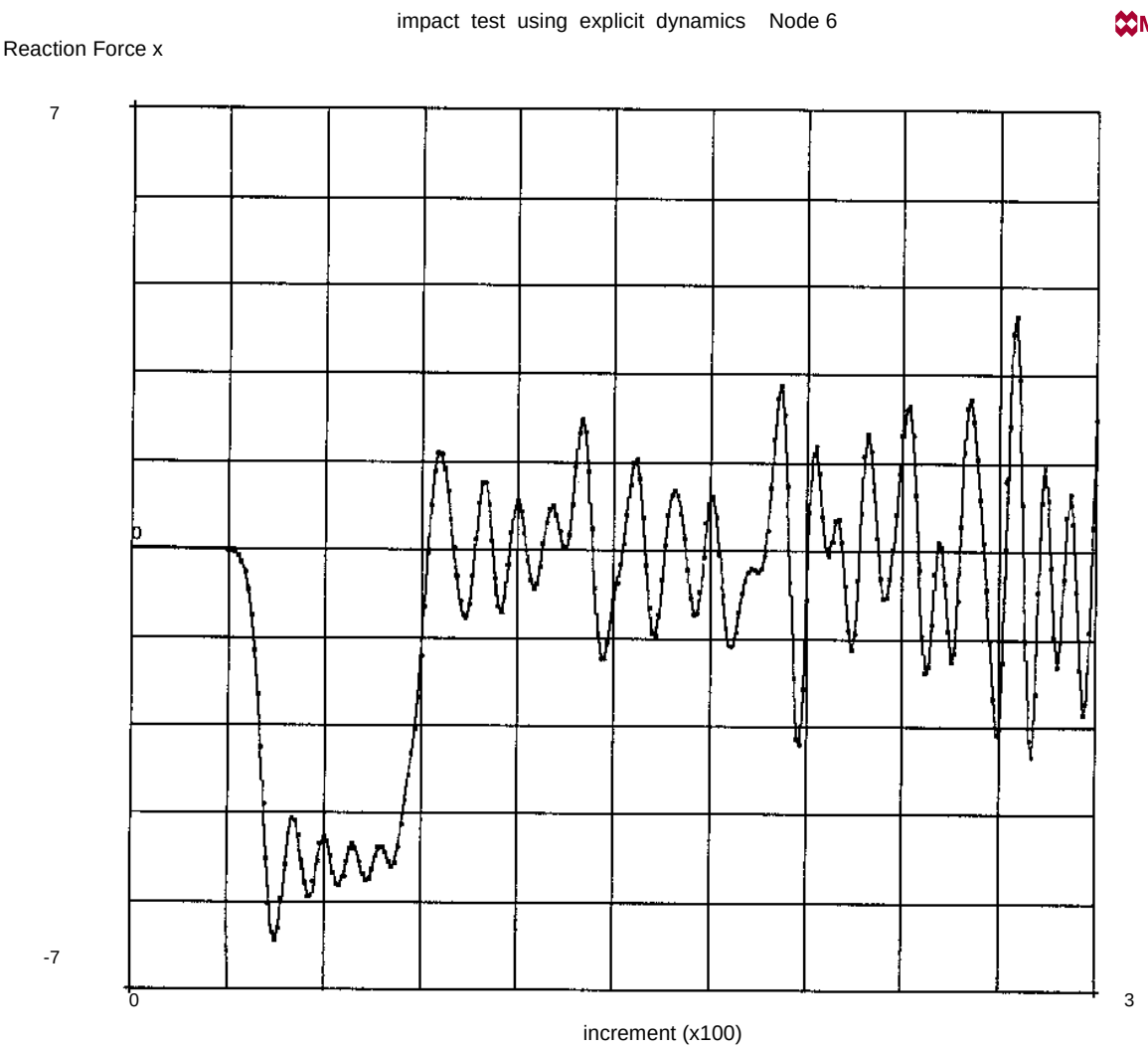

Figure 6.19-5 Reaction Force at Wall

6.20 Elastic Beam Subjected to Fluid-Drag Loading

This problem demonstrates an elastic beam partially submerged under a flowing fluid being analyzed for static analysis. In addition, a dynamic analysis is performed in which wave loading is also considered.

This problem is modeled using the two techniques summarized below.

Data Set	Element Type(s)	Number of Elements	Number of Nodes	Differentiating Features
e6x20a	98	10	11	Fluid Drag - Static
e6x20b	98	10	11	Fluid Drag - Dynamic

Element

Element type 98 is a 2-node straight elastic beam with the transverse shear effect in its formulation.

Model

An elastic beam of length 115.47 m which lies at an angle of 60° is partially submerged under some fluid (Figure 6.20-1). The depth of the fluid of 50 m. The beam is modeled using 10 elements and 11 nodes.

Geometry

The GEOMETRY block is used for inputting beam section properties. The beam has a cross-section area of 0.1935 m^2 and moments of inertia (I_{xx} and I_{yy}) equaling 0.00321 m^4.

Material Properties

The material of the beam is assumed to have a Young's modulus of 2.6e+07 $N/m^2$and a Possion's ratio of 0.3. The beam has a mass density of 8.0e+4 Kg/m^3.

Loading

Elements 1 to 5 are subjected to fluid drag loading. The mass density of the fluid inside the pipe is assumed to be 0.8 Kg/m^3 and the fluid outside of the pipe is assumed to be 1 Kg/m^3. The gravity constant is assumed to be 10 m/sec^2. The drag coefficient is assumed to be 0.05, and the inertia coefficient is assumed to be 0.05. The fluid outside of the pipe is flowing with a velocity of 1 m/sec in the x-direction. It has a velocity gradient of 0.04 per second. For the dynamic analysis case, the beam is subjected to wave loading in addition to the fluid-drag loading. The wave height is assumed to be 2 and the wave period is assumed to be 5. The wave phase is taken to be 0. The wave front is assumed to be moving in the x-direction.

Boundary Conditions

Nodes 1 and 11 are assumed to be hinged ($u_x = u_y = u_z = \theta_x = \theta_z = 0$).

Results

The displacements of the beam due to fluid drag loading are given in Table 6.20-1.

Table 6.20-1 Displacements of the Beam (m)

Node	u_x (m)	u_z (m)	θ_y (rad)
1	0	0	-7.96×10^{-2}
2	-0.767	0.443	-7.40×10^{-2}
3	-1.432	0.827	-5.89×10^{-2}
4	-1.916	1.106	-3.78×10^{-2}
5	-2.176	1.256	-1.41×10^{-2}
6	-2.204	1.272	8.60×10^{-3}
7	-2.021	1.167	2.79×10^{-2}
8	-1.666	0.962	4.3×10^{-2}
9	-1.183	0.683	5.37×10^{-2}
10	-0.613	0.354	6.02×10^{-2}
11	0	0	6.23×10^{-2}

Parameters, Options, and Subroutines Summary

Example 6x20a.dat:

Parameters	Model Definition Options	History Definition Options
ALIAS	CONTINUE	DYNAMIC CHANGE
ELEMENT	CONNECTIVITY	CONTINUE
END	COORDINATES	
SIZING	DIST LOADS	
TITLE	END OPTIONS	
	FIXED DISP	
	FLUID DRAG	
	GEOMETRY	
	ISOTROPIC	

Example 6x20b.dat:

Parameters	Model Definition Options	History Definition Options
ALIAS	CONNECTIVITY	CONTINUE
DYNAMIC	COORDINATES	DIST LOADS
ELEMENT	DIST LOADS	DYNAMIC CHANGE
END	END OPTION	
SIZING	FIXED DISP	
TITLE	FLUID DRAG	
	GEOMETRY	
	ISOTROPIC	

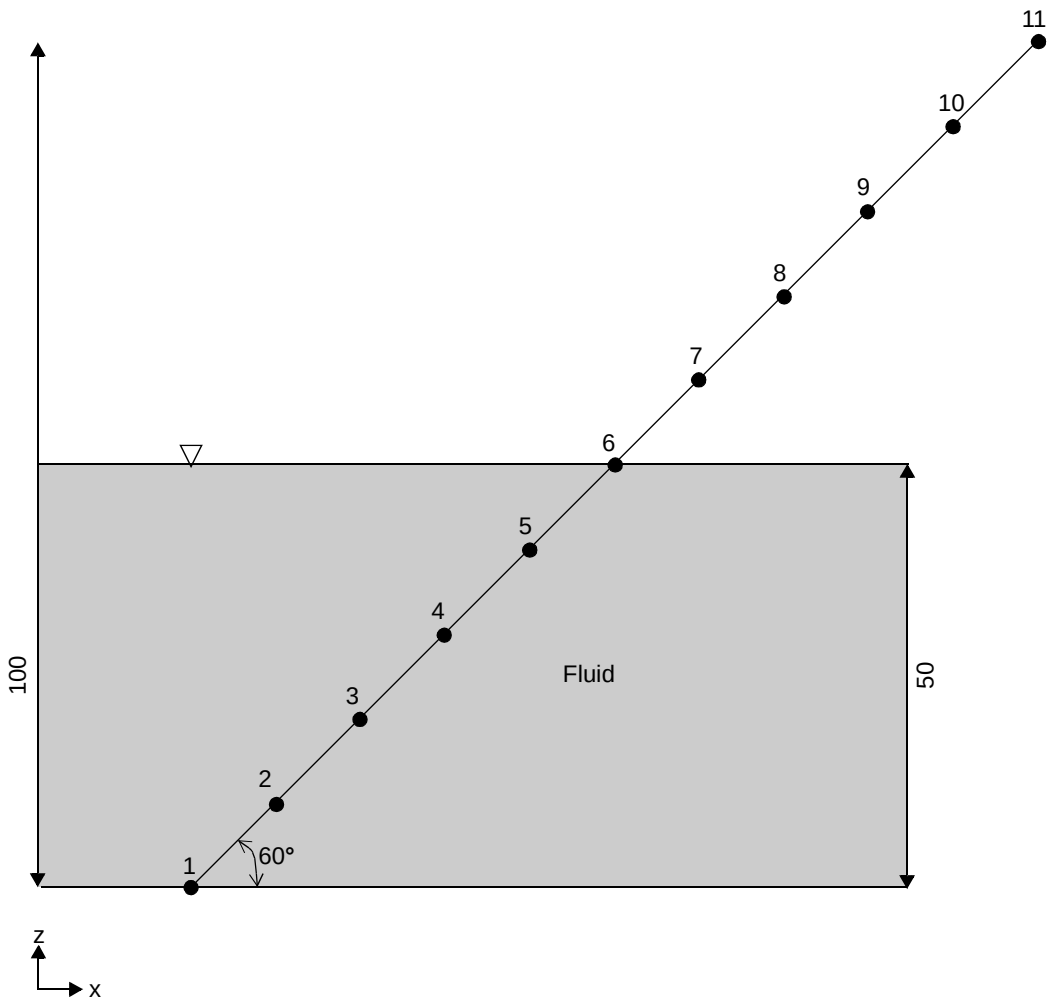

Figure 6.20-1 Beam Partially Submerged in Fluid

6.21 Eigenvalue Analysis of a Box

This example demonstrates the use of follower force stiffness for the eigenvalue analysis of a preloaded box.

Element

Library element type 72 is a thin shell used for this analysis. There are 96 elements and 290 nodes in the model as shown in Figure 6.21-1. The box, 10 cm x 10 cm x 10 cm, is fixed in space to prevent rigid body motion and preloaded with uniform pressure of 10.0 N/cm^2. The rigid body constraint is then released and the eigenvalue analysis is preformed. The FOLLOW FOR option is used to insure that the load is applied on the deformed geometry.

Material Properties

The material is elastic and its properties are:

Young's modulus is $E = 10000.0\ N/cm^2$

Poisson's ratio is $\nu = 0.45$

Mass density is $\rho = 7.0e\text{-}5\ kg/cm^3$

Geometry

The thickness of the shell is 0.5 cm.

Boundary Conditions

The model is fixed at three corners of the box. The constraints are then released to demonstrate the extraction of rigid body modes.

Control

The full Newton-Raphson iterative method is used with a convergence tolerance of 0.0001% on residuals requested.

Results

The modal shapes are shown in Figure 6.21-2 andFigure 6.21-2. The six eigenvalues for rigid body are:

Eigenvalue	With Follower Force Stiffness (Cycles/s)	Without Follower Force Stiffness (Cycles/s)
1	1.29857e-4	3.38527e-6
2	9.55539e-6	5.83730e-6
3	1.75523e-5	1.94645e-4

Eigenvalue	With Follower Force Stiffness (Cycles/s)	Without Follower Force Stiffness (Cycles/s)
4	5.2039e+0	30.1477e+0
5	5.20390e+0	30.1573e+0
6	5.20390e+0	30.1478e+0

You can observe that the inclusion of the follower force stiffness results in a more accurate representation.

Parameters, Options, and Subroutines Summary

Example e6x21.dat:

Parameters	Model Definition Options	History Definition Options
ELEMENT	CONNECTIVITY	DIST LOADS
DYNAMIC	CONTROL	AUTO LOAD
FOLLOW FOR	COORDINATES	CONTINUE
END	GEOMETRYTIME STEP	
LARGE DISP	ISOTROPIC	DISP CHANGE
SIZING	FIXED DISP	MODAL SHAPE
TITLE	DEFINE	RECOVER
	DIST LOADS	
	END OPTION	
	OPTIMIZE	
	POST	

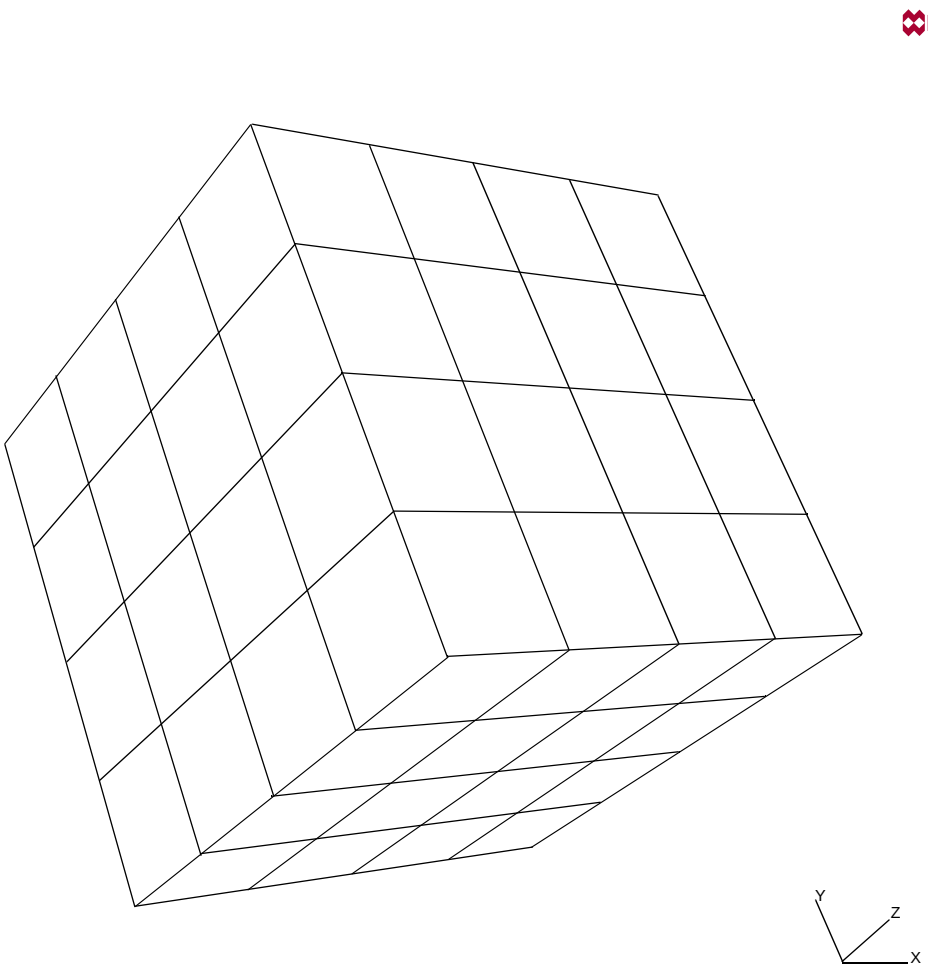

Figure 6.21-1 Mesh of Box

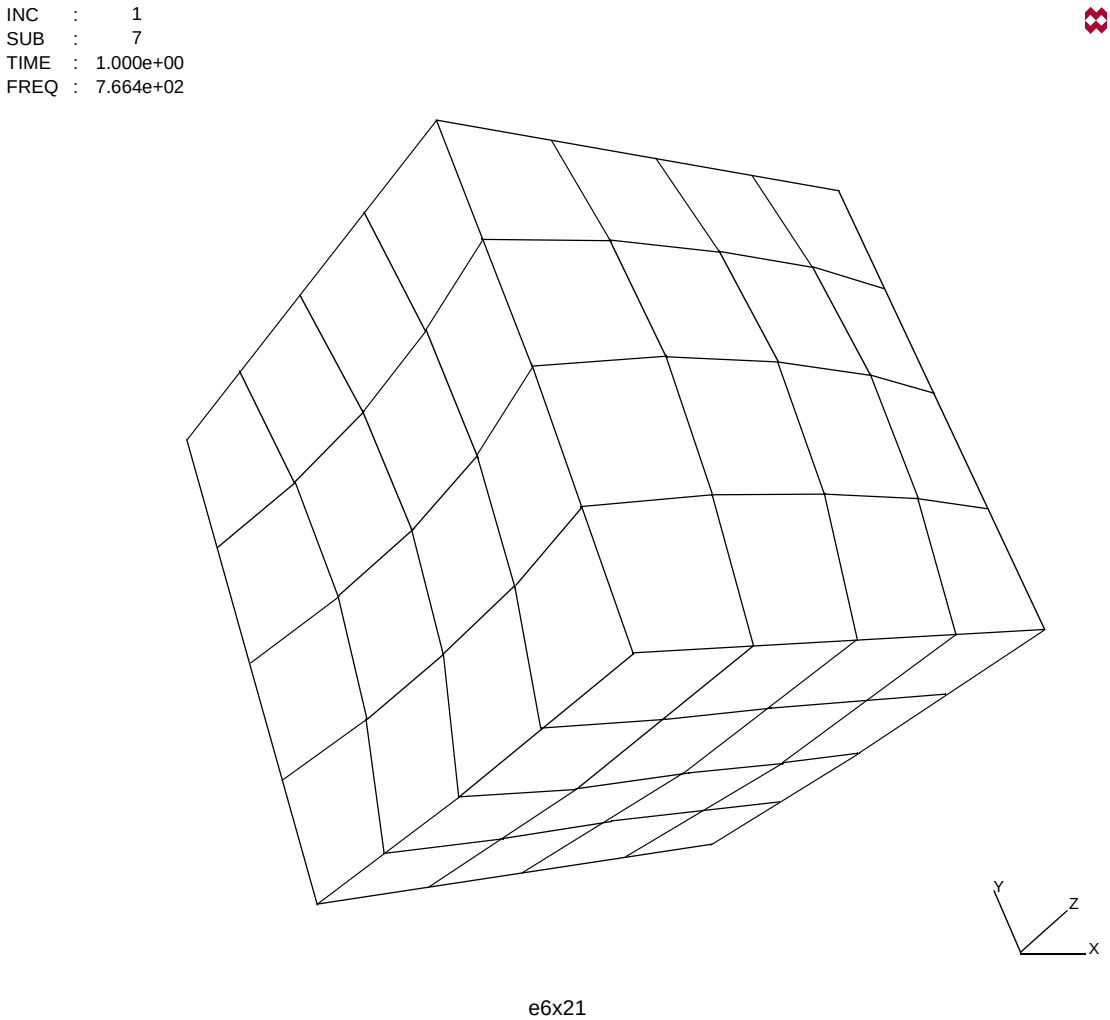

Figure 6.21-2 Seventh Eigenmode

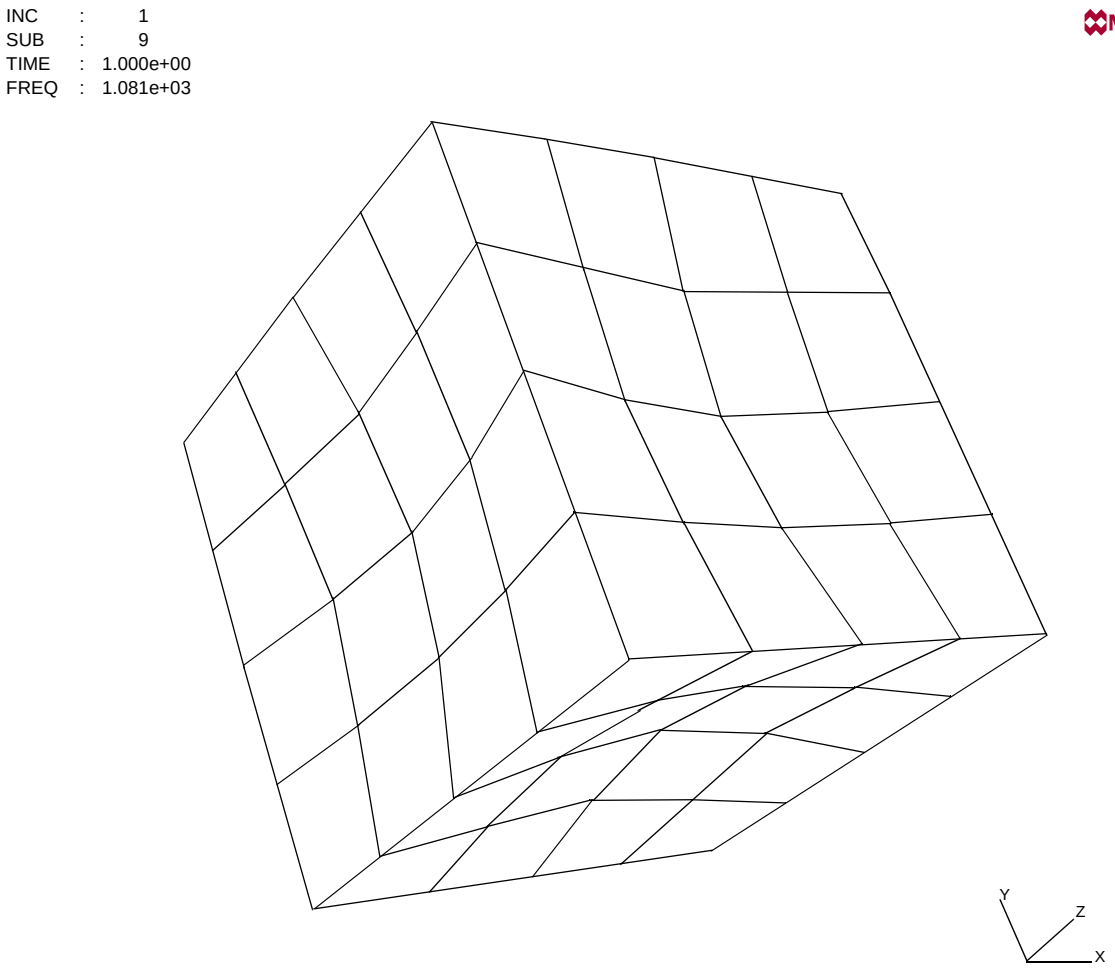

Figure 6.21-3 Ninth Eigenmode

Document Title: **MARC® Volume E: Demonstration Problems, Part III, K7**
Part Number: RF-3018-07.III
Revision Date: June, 1998

UNITED STATES

CALIFORNIA - Palo Alto
MARC Corporate Headquarters
260 Sheridan Avenue, Suite 309
Palo Alto, CA 94306, USA
Tel: 1 650 329 6800
Fax: 1 650 323 5892
Email: support@marc.com

CALIFORNIA - San Diego
MARC Analysis Research Corp.
4330 LaJolla Village Drive, Suite 320
San Diego, CA 92122
Tel: 1 619 658 9588
Fax: 1 619 758 8710

CONNECTICUT - E. Berlin
MARC Analysis Research Corp.
1224 Mill Street
E. Berlin, CT 06023
Tel: 1 860 828 2055
Fax: 1 860 828 2031

MICHIGAN - Ann Arbor
MARC Analysis Research Corp.
24 Frank Lloyd Wright Drive
Ann Arbor, MI 48106-0523
Tel: 1 734 998 0540
Fax: 1 734 998 0542

EUROPE

CZECH REPUBLIC
MARC Overseas, Inc.
Podolska 50
147 00 Praha 4
Czech Republic
Tel: 420 (2) 6121 4123
420 (2) 6121 4111 x252
Fax: 420 (2) 6121 4123
Email: support@marc.cz

FRANCE
MARC France S.A.
Bercy Expo SR 6101A
40 Avenue des Terroirs de France
75611 Paris Cedex 12, France
Tel: 33 (1) 4474 1550
Fax: 33 (1) 4474 1554
Email: support@marc.fr

GERMANY - Munich
MARC Software Deutschland GmbH
Ismaninger Str. 9
85609 Aschheim (bie Munich)
Germany
Tel: 49 (89) 904 50 33
Fax: 49 (89) 903 06 76
Email: support@marc.de

GERMANY - Hannover
MARC Software Deutschland GmbH
Alte Dohrener Str. 66
D 30173 Hannover, Germany
Tel: 49 (511) 980 5182
Fax: 49 (511) 980 5187

ITALY
Espri-MARC s.r.l.
Viale Brigata Bisagno 2 / 10
16129 Genova, Italy
Tel: 39 (10) 585 949
Fax: 39 (10) 585 949
Email: espri.marc@interbusiness.it

THE NETHERLANDS
MARC Analysis Research Corporation
Dublinstraat 32
2713 HS Zoetermeer
The Netherlands
Tel: 31 (79) 3510 411
Fax: 31 (79) 3517 560
Email: support@marc.nl

UNITED KINGDOM
MARC UK Ltd.
11 Linford Forum, Rockingham Drive
Linford Wood
Milton Keynes, MK14 6LY
Tel: 44 (1908) 606 070
Fax: 44 (1908) 606 633
Email: support@marc.co.uk

PACIFIC RIM

CHINA
MARC Overseas, Inc.
Bright Chang An Building, Suite 321
7# Jian Guo Men Nei Street
Beijing, China 100 005
Tel: 86 (10) 6510 2056
86 (10) 6510 2057
86 (10) 6510 2058
Fax: 86 (10) 6510 2053
Email: marcbj@public.bta.net.cn

JAPAN - Nagoya
Nippon MARC Co., Ltd.
Nagoya Nishiki Daiichi Seimei Bldg.
2F, 6-5 Nishiki 1-chome
Naka-ku, Nagoya, Aichi 460-0003
Tel: 81 (52) 202 5661
Fax: 81 (52) 202 5665

JAPAN - Osaka
Nippon MARC Co., Ltd.
4F 2nd Kimi Building
2-11 Toyotucho Suita-shi
Osaka 564-0051
Tel: 81 (6) 385 1101
Fax: 81 (6) 385 4343

JAPAN - Tokyo
(Asian Operations Headquarters)
Nippon MARC Co., Ltd.
Shinjuku Daiichi Seimei Building
P.O. Box 5056
2-7-1 Nishi-Shinjuku, Shinjuku-ku
Tokyo 163-0704
Tel: 81 (3) 3345 0181
Fax: 81 (3) 3345 1529
Email: support@marc.co.jp

KOREA
Dong Kyung Bldg. 7FL
824-19 Yuksam-Dong
Kangnam-Ku, Seoul, Korea
Tel: 82 (2) 561 7543
Fax: 82 (2) 561 7767
Email: marck@unitel.co.kr

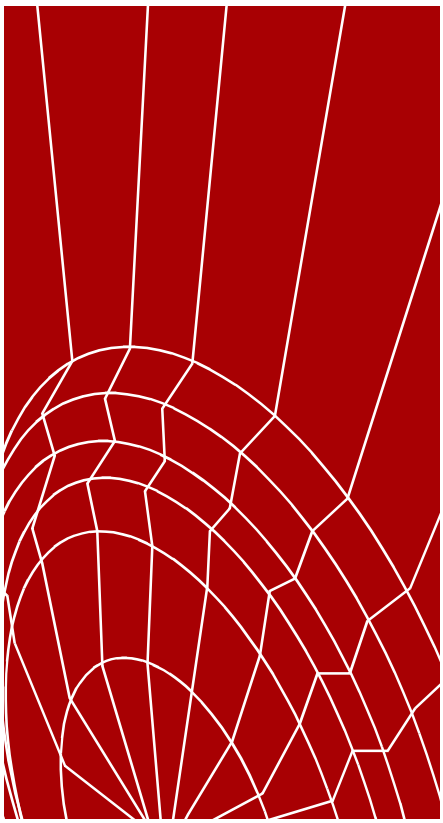

MARC Analysis Research Corporation

MARC®

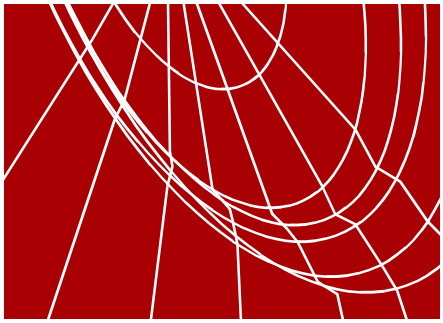

Volume E

Demonstration Problems

Version K7

Copyright © 1998 MARC Analysis Research Corporation
Printed in U. S. A.
This notice shall be marked on any reproduction of this data, in whole or in part.

MARC Analysis Research Corporation
260 Sheridan Avenue, Suite 309
Palo Alto, CA 94306 USA

Phone: (650) 329-6800
FAX: (650) 323-5892

Document Title: **MARC® Volume E: Demonstration Problems, Part IV, Version K7**
Part Number: RF-3018-07.IV
Revision Date: June, 1998

Proprietary Notice

MARC Analysis Research Corporation reserves the right to make changes in specifications and other information contained in this document without prior notice.

ALTHOUGH DUE CARE HAS BEEN TAKEN TO PRESENT ACCURATE INFORMATION, MARC ANALYSIS RESEARCH CORPORATION DISCLAIMS ALL WARRANTIES WITH RESPECT TO THE CONTENTS OF THIS DOCUMENT (INCLUDING, WITHOUT LIMITATION, WARRANTIES OR MERCHANTABILITY AND FITNESS FOR A PARTICULAR PURPOSE) EITHER EXPRESSED OR IMPLIED. MARC ANALYSIS RESEARCH CORPORATION SHALL NOT BE LIABLE FOR DAMAGES RESULTING FROM ANY ERROR CONTAINED HEREIN, INCLUDING, BUT NOT LIMITED TO, FOR ANY SPECIAL, INCIDENTAL OR CONSEQUENTIAL DAMAGES ARISING OUT OF, OR IN CONNECTION WITH, THE USE OF THIS DOCUMENT.

This software product and its documentation set are copyrighted and all rights are reserved by MARC Analysis Research Corporation. Usage of this product is only allowed under the terms set forth in the MARC Analysis Research Corporation License Agreement. Any reproduction or distribution of this document, in whole or in part, without the prior written consent of MARC Analysis Research Corporation is prohibited.

Restricted Rights Notice

This computer software is commercial computer software submitted with “restricted rights.” Use, duplication, or disclosure by the government is subject to restrictions as set forth in subparagraph (c)(i)(ii) or the Rights in technical Data and Computer Software clause at DFARS 252.227-7013, NASA FAR Supp. Clause 1852.227-86, or FAR 52.227-19. Unpublished rights reserved under the Copyright Laws of the United States.

Trademarks

All products mentioned are the trademarks, service marks, or registered trademarks of their respective holders.

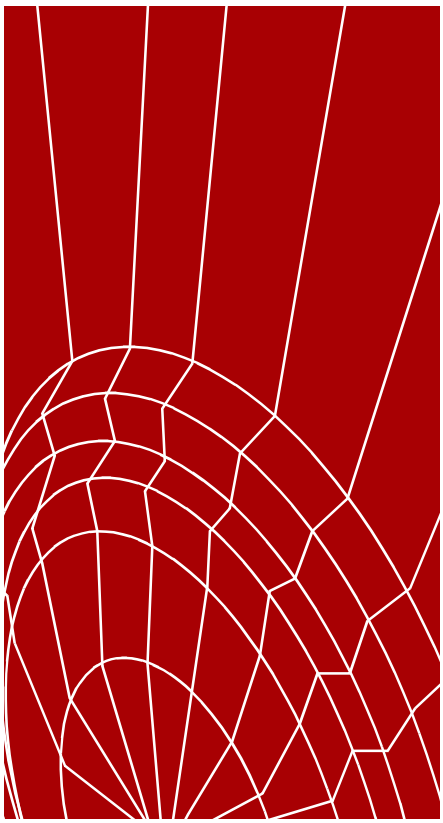

MARC Analysis Research Corporation

MARC®

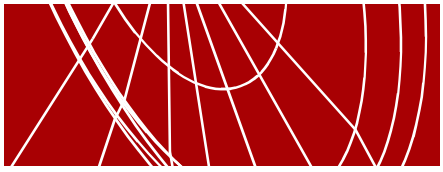

Volume E

Demonstration Problems

Version K7

Part IV

- Contact
- Advanced Topics

Part III

Volume E: Demonstration Problems

Chapter 7 **Contact**

Chapter 8 **Advanced Topics**

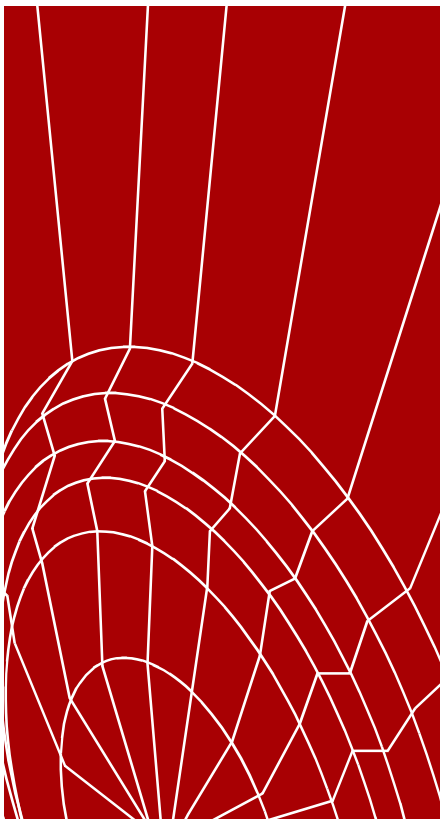

MARC Analysis Research Corporation

MARC®

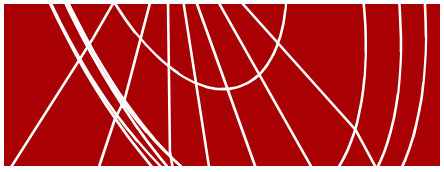

Volume E

Demonstration Problems

Version K7

Chapter 7
Contact

7 Contact Contents

Description	Problem
Rigid Perfectly Plastic Extrusion Isothermal and Coupled Analysis	7.1
End-Plate-Aperture Breakaway	7.2
Barrel Vault Shell under Self-weight (Shell Cracking)	7.3
Side Pressing of a Hollow Rubber Cylinder (Mooney Material)	7.4
Analysis of a Thick Rubber Cylinder under Internal Pressure	7.5
Biaxial Stress in a Composite Plate	7.6
Composite Plate Subjected to Thermal Load	7.7
Cylinder under External Pressure (Fourier Analysis)	7.8
Cylinder under Line Load (Fourier Analysis)	7.9
Mesh Qualification	7.10
Concrete Beam under Point Loads	7.11
Constant Uniaxial Stress Applied to Plate in Plane Strain (Viscoelasticity)	7.12
Analysis of Pipeline Structure	7.13
Viscoelastic Analysis of an Externally Reinforced Thick-Walled Cylinder under Internal Pressure	7.14
Spiral Groove Thrust Bearing with Tilt	7.15
Hydrodynamic Journal Bearing of Finite Width	7.16
Elastic-Plastic Finite Deformation of a Thick-Walled Cylinder	7.17
Side Pressing of a Hollow Rubber Cylinder	7.18
Stretching of a Rubber Sheet with a Hole	7.19
Compression of an O-Ring using Ogden Model	7.20
Stretching of a Rubber Plate with Hole	7.21

Description	Problem
Loading of a Rubber Plate	7.22
Compression of a Foam Tube	7.23
Constitutive Law for a Composite Plate	7.24
Progressive Failure of a Composite Strip	7.25
Pipe Collars in Contact	7.26
Twist and Extension of Circular Bar of Variable Thickness at Large Strains	7.27
Analysis of a Thick Rubber Cylinder under Internal Pressure	7.28
3D Analyses of a Plate with a Hole at Large Strains	7.29
Damage in Elastomeric Materials	7.30
Rezoning in an Elastomeric Seal	7.31
Structural Relaxation of a Glass Cube	7.32

7 Contact List of Figures

Figure		Page
7.1-1	50% Reduction Die Problem	7.1-5
7.1-2	Mesh and Boundary Conditions for 50% Reduction Example	7.1-6
7.1-3	50% Reduction Extrusion Velocity Field	7.1-7
7.1-4	Temperature Distribution in the Billet Neglecting Thermal Convection	7.1-8
7.1-5	Temperature Distribution in the Billet including Convection	7.1-9
7.1-6	Equivalent Plastic Strains in Billet Neglecting Thermal Convection	7.1-10
7.2-1	Geometry and Mesh of End Plate-Aperture	7.2-4
7.2-2	Transient Normal Forces in Bolts	7.2-5
7.2-3	Transient Shear Force in Bolts	7.2-6
7.2-4	Radial Displacement at Outside Top (Node 46)	7.2-7
7.3-1	Mesh for the Shell Roof	7.3-4
7.3-2	Load-Vertical Deflection Curve at Node 3	7.3-5
7.4-1	Rubber Cylinder and Mesh	7.4-4
7.4-2	Deformed Mesh Plot	7.4-5
7.5-1	Cylinder Mesh (8-Node Model)	7.5-4
7.5-2	Radial Stress Through Radius	7.5-5
7.6-1	Composite Plate	7.6-5
7.6-2	Finite Element Mesh	7.6-6
7.6-3	Deformed Mesh Plot	7.6-7
7.7-1	Plate Geometry and Mesh	7.7-3
7.7-2	Displaced Mesh	7.7-4
7.8-1	Cylinder and Mesh	7.8-5
7.8-2	First Mode Solid Cylinder Plane Strain	7.8-6
7.8-3	Second Mode Solid Cylinder Plane Strain	7.8-7

Figure **Page**

7.9-1 Cylinder and Mesh 7.9-4
7.9-2 Concentrated Load on a Solid Cylinder 7.9-5

7.10-1 Membrane and Mesh. 7.10-3
7.10-2 Strain Energy Difference 7.10-4

7.11-1 Concrete Beam and Mesh 7.11-4
7.11-2 Deformed Mesh Plot 7.11-5
7.11-3 Regions of Cracking 7.11-6

7.12-1 Geometry. 7.12-4
7.12-2 Finite Element Model 7.12-4
7.12-3 Normalized Displacement vs. Time 7.12-5
7.12-4 Normalized Out-of-Plane Stress, σ_{zz} vs. Time 7.12-5

7.13-1 Pipe Line Geometry and Model 7.13-5
7.13-2 Load vs. Displacement 7.13-6
7.13-3 Ovalization Behavior Due to Out-of-Plane and In-Plane Moments 7.13-7

7.14-1 Long Thick-Walled Cylinder 7.14-6
7.14-2 Simple Maxwell Model. 7.14-6
7.14-3 Finite Element Model 7.14-7
7.14-4 Radial Stress vs. Time. 7.14-8
7.14-5 Hoop Stress vs. Time 7.14-9

7.15-1 Spiral Groove Thrust Bearing with Tilt 7.15-4
7.15-2 Vector Plot of Mass Flow 7.15-5

7.16-1 Journal Bearing of Finite Width 7.16-5
7.16-2 Path Plot of Pressure Distribution. 7.16-6

7.17-1 Thick-Walled Cylinder 7.17-3
7.17-2 Applied Load History 7.17-4
7.17-3 Deformed Meshes at Increments 6, 10, and 20. . . . . 7.17-4
7.17-4 Internal Pressure vs. Inner Radius. 7.17-5

Figure **Page**

7.18-1 Rubber Cylinder and Mesh 7.18-3
7.18-2 Deformed Mesh Plot 7.18-4
7.18-3 Displacement History of Node 53. . . . . 7.18-5
7.18-4 Stress Relaxation. 7.18-6

7.19-1 Finite Element Mesh 7.19-4
7.19-2 Incompressible Model Deformed Mesh 7.19-5
7.19-3 Incompressible Model Load Deflection Curve at Node 277 . . . . . 7.19-6
7.19-4 Foam Model Deformed Mesh. 7.19-7
7.19-5 Foam Model Load Deflection Curve at Node 277 . . . . . 7.19-8

7.20-1 O-Ring Mesh. 7.20-4
7.20-2 Coarse O-Ring Initial Mesh for Data Set e7x20c 7.20-5
7.20-3 Stress-Strain Curve 7.20-6
7.20-4 Deformed Mesh, Increment 10 . . . . . 7.20-7
7.20-5 Deformed Mesh, Increment 30 . . . . . 7.20-8
7.20-6 Deformed Mesh, Increment 50 . . . . . 7.20-9
7.20-7 Mean Stress Distribution. 7.20-10
7.20-8 Contact Forces. 7.20-11
7.20-9 Adaptive Mesh at Increment 10 . . . . . 7.20-12
7.20-10 Adaptive Mesh at Increment 20 . . . . . 7.20-13
7.20-11 Adaptive Mesh at Increment 40 . . . . . 7.20-14
7.20-12 Adaptive Mesh at Increment 67 . . . . . 7.20-15
7.20-13 Contact Forces for the Updated Lagrange Formulation 7.20-16

7.21-1 Finite Element Mesh 7.21-3
7.21-2 Stress-Strain Curve 7.21-4
7.21-3 Deformed Mesh. 7.21-5
7.21-4 Stress Distribution. 7.21-6
7.21-5 Strain Distribution. 7.21-7

7.22-1 Finite Element Mesh 7.22-5
7.22-2 Stress-Strain Curve 7.22-6
7.22-3 Displacement History of Center Node – Elastic Effects Only 7.22-7
7.22-4 Displacement History of Center Node – Including Damage Effects 7.22-8

Figure **Page**

7.22-5 Displacement History of Center Node – Including Damage and Viscoelastic Effects 7.22-9
7.22-6 Displacement History as a Function of Time – Including Damage and Viscoelastic Effects 7.22-10

7.23-1 Finite Element Mesh of Tube 7.23-3
7.23-2 Deformed Mesh at Increment 10 . . . . . 7.23-4
7.23-3 Deformed Mesh at Increment 16 . . . . . 7.23-5
7.23-4 Deformed Mesh at Increment 29 . . . . . 7.23-6
7.23-5 Shear Strain in Compressed Tube 7.23-7

7.24-1 Geometry and Lamination of a Composite Plate 7.24-4

7.25-1 Finite Element Mesh of Strip 7.25-3
7.25-2 History of Deflection of the Tip 7.25-4
7.25-3 History of First Component of Stress in Layer 1 . . . . . 7.25-5
7.25-4 History of First Component of Stress in Layer 5 . . . . . 7.25-6
7.25-5 History of the Reaction Force at Clamped End 7.25-7

7.26-1 Geometric Dimension and Bending Loads 7.26-3
7.26-2 FEM Model 7.26-4
7.26-3 Deformed Shape at 0° 7.26-4
7.26-4 von Mises Stress Contour at 0°, Layer 1 . . . . . 7.26-5
7.26-5 von Mises Stress Contour at 180°, Layer 9 . . . . . 7.26-6
7.26-6 Plastic Strain Contour at 0°, Layer 1 . . . . . 7.26-7

7.27-1 Circular Bar and Mesh 7.27-3
7.27-2 Deformed Mesh and Distribution of Equivalent von Mises Stress 7.27-4

7.28-1 Cylinder Mesh (8-Node Model) 7.28-5

7.29-1 Initial Mesh 7.29-4
7.29-2 Deformed Model and Distribution of Equivalent von Mises Stress for e7x29a . . . 7.29-5
7.29-3 Deformed Model and Distribution of Equivalent von Mises Stress for e7x29b . . . 7.29-6

7.30-1 Discontinuous Damage 7.30-4
7.30-2 Continuous Damage 7.30-5

Figure **Page**

7.31-1 Deformed Mesh at Increment 0 . . . . . 7.31-4
7.31-2 Deformed Mesh at Increment 7 . . . . . 7.31-5
7.31-3 Deformed Mesh at Increment 14 . . . . . 7.31-6
7.31-4 Deformed Mesh at Increment 15 . . . . . 7.31-7
7.31-5 Deformed Mesh at Increment 29 . . . . . 7.31-8
7.31-6 Contact Force Distribution 7.31-9

7.32-1 Structural Relaxation Phenomenon. 7.32-3
7.32-2 Property (Volume) – Temperature Plot 7.32-3
7.32-3 Volume Change during Cyclic Temperature History 7.32-5

7 Contact List of Tables

Table		Page
7-1	Special Topics Demonstration Problems	7-2

7 Contact

In addition to the various analysis capabilities discussed in previous chapters concerned with problems of linear elasticity, plasticity and creep, large displacement, heat transfer as well as dynamics, this chapter contains demonstration problems for the illustration of additional analysis capabilities in MARC. Detailed discussions of these capabilities can be found in *MARC Volume A: Theory and User Information* and a summary of the various capabilities illustrated is given below.

- Steady, creeping flow of rigid, perfectly plastic material (R-P FLOW).
- The use of gap-friction element (Element Type 12 and Type 97).
- Analysis of concrete (CRACK DATA) structures.
- Analysis of rubber structures (MOONEY, OGDEN, and FOAM).
- Simulation of composite material (COMPOSITE).
- Simulation of viscoelastic material.
- Axisymmetric structure under nonsymmetric loading (Fourier Analysis).
- Study of mesh refinement (QUALIFY).
- Analysis of hydrodynamic bearings.
- Use of the rezoning technique for large deformation analysis.

Compiled in this chapter are a number of solved problems. Table 7-1 shows the MARC elements and options used in these demonstration problems.

Table 7-1 Special Topics Demonstration Problems

Problem Number	Element Type(s)	Parameters	Model Definition	History Definition	User Subroutines	Problem Description
7.1	32	ELSTO R-P FLOW	CONTROL	AUTO LOAD	—	Steady, creeping flow of rigid, perfectly plastic material (R-P Flow).
7.2	10 12	—	OPTIMIZE CONTROL ISOTROPIC GAP DATA	POINT LOADS DIST LOADS AUTO LOAD	—	The use of gap-friction element in the analysis of a manhole cover in a pressure vessel.
7.3	75	SHELL SECT	UFXORD CONTROL CRACK DATA ISOTROPIC	AUTO INCREMENT	UFXORD	Analysis of a concrete barrel vault shell subjected to self-weight.
7.4	12 32	LARGE DISP	RESTART CONTROL MOONEY GAP DATA	PROPORTIONAL AUTO LOAD	—	Side pressing of a hollow rubber cylinder.
7.5	33 82 119	LARGE DISP FOLLOW FOR	NODE FILL CONTROL MOONEY	DIST LOADS	—	Analysis of a thick rubber cylinder.
7.6	75	SHELL SECT	DEFINE COMPOSITE ORIENTATION ORTHOTROPIC PRINT ELEM	—	—	Elastic analysis of a multilayered square plate under uniform pressure (composite material).
7.7	75	SHELL SECT	DEFINE COMPOSITE ORTHOTROPIC PRINT ELEM ORIENTATION INITIAL STATE CHANGE STATE	—	—	Elastic analysis of a multilayered square plate subjected to uniform pressure and thermal loading (composite material).
7.8	62	FOURIER	CONTROL FOURIER RESTART	—	UFOUR	Fourier analysis of a cylinder under external pressure.
7.9	62	FOURIER	CONTROL FOURIER RESTART CASE COMBIN	—	UFOUR	Fourier analysis of a cylinder in plane strain subjected to a line load.

Table 7-1 Special Topics Demonstration Problems (Continued)

Problem Number	Element Type(s)	Parameters	Model Definition	History Definition	User Subroutines	Problem Description
7.10	27	MESH PLOT QUALIFY	POST	—	—	Use of the QUALIFY option for the study of mesh refinement.
7.11	3 9	—	CONTROL CRACK DATA ISOTROPIC RESTART	POINT LOAD	—	Analysis of a simply supported concrete beam subjected to concentrated loads.
7.12	27	—	TYING PRINT CHOICE ISOTROPIC VISCELPROP	AUTO LOAD TIME STEP	—	Analysis of a simply supported concrete beam subjected to concentrated loads.
7.13	14 17	SCALE ELSTO	TYING	AUTO LOAD PROPORTIONAL INC	—	Analysis of pipeline structure using element type 14 and 17, and the pipeline mesh generator MARCPIPE.
7.14	28	—	ISOTROPIC VISCELPROP PRINT CHOICE	AUTO LOAD TIME STEP	—	Internal pressurization of an externally reinforced long, thick walled, viscoelastic cylinder.
7.15	37	BEARING	THICKNESS VELOCITY TYING	—	UFXORD UFCONN UTHICK UVELOC UGROOV	Calculation of the pressure distribution in a spiral groove thrust bearing including grooves.
7.16	39	BEARING	CONN GENER NODE FILL THICKNESS VELOCITY	DAMPING COMPONENTS STIFFNESS COMPONENTS THICKNESS CHANGE	UTHICK UBEAR	Analysis of a journal bearing. Determine the load carrying capacity of the bearing.
7.17	10	UPDATE FINITE LARGE DISP REZONE	FORCDT WORK HARD	AUTO LOAD COORDINATE CHANGE REZONE	FORCDT	Analysis of a thick-walled cylinder under internal pressure. Demonstration of rezoning capability.
7.18	32 12	LARGE DISP	MOONEY GAP DATA VISCELMOONEY	AUTO LOAD TIME STEP	—	Side pressing of a hollow viscoelastic rubber cylinder.

Table 7-1 Special Topics Demonstration Problems (Continued)

Problem Number	Element Type(s)	Parameters	Model Definition	History Definition	User Subroutines	Problem Description
7.19	26	—	MOONEY TYING	AUTO LOAD	—	Plane stress stretching of a rubber sheet with a hole.
7.20	82	FOLLOW FOR PRINT, 5	DEFINE CONTACT CONTROL OGDEN	MOTION CHANGE AUTO LOAD DIST LOADS TIME STEP	—	Compression of an O-ring.
7.21	26	—	OGDEN	DISP CHANGE AUTO LOAD		Plane stress stretching of a rubber sheet with a hole.
7.22	75	LARGE DISP SHELL SECT	OGDEN DIST LOADS DAMAGE VISCELOGDEN	AUTO LOAD DIST LOADS TIME STEP	—	Loading of a rubber plate including damage and rate effects.
7.23	11	LARGE DISP	FOAM CONTACT	AUTO LOAD TIME STEP	—	Compression of a foam tube.
7.24	75	—	ORIENTATION ORTHOTROPIC COMPOSITE	—	—	Demonstrate composites.
7.25	22	LARGE DISP	ORIENTATION ORTHOTROPIC FAIL DATA COMPOSITE	POINT LOAD POST INCREMENT AUTO LOAD PROPORTIONAL INC	—	Progressive failure of fiber reinforced composite.
7.26	95 97	—	GAP DATA WORK HARD DIST LOAD	DIST LOADS	—	Pipe collars in contact.
7.27	67	ELASTICITY ALIAS	DIST LOAD TYING	AUTO LOAD POINT LOAD	—	Twist and extension of a circular bar of variable thickness at large strains.
7.28	10 116 28 55	FOLLOW FOR ELASTICITY	DIST LOAD OGDEN NODE FILL	DIST LOAD	—	Analysis of a thick rubber cylinder under internal pressure.
7.29	7 117	User Defaults ELASTICITY PROCESS	OGDEN OPTIMIZE	AUTO LOAD DISP CHANGE	HYPELA2	3D analysis of a plate with a hole at large strains.
7.30	7	ELASTICITY	DEFINE DAMAGE OGDEN‘	AUTO INC DISP CHANGE	—	Damage in elastomeric materials.

Table 7-1 Special Topics Demonstration Problems (Continued)

Problem Number	Element Type(s)	Parameters	Model Definition	History Definition	User Subroutines	Problem Description
7.31	11	ELASTICITY REZONE ALIAS	CONTACT CONTACT TABLE OGDEN RESTART CONNECTIVITY CHANGE COORDINATE CHANGE CONTACT CHANGE END REZONE	AUTO LOAD TIME STEP	—	Rezoning in an elastomeric seal.
7.32	7	STATE VARS	SHIFT FUNCTION VISCEL EXP VISCLEPROP CHANGE STATE	AUTO LOAD CHANGE STATE TIME STEP	—	Structural relaxation of a glass cube.

7.1 Rigid Perfectly Plastic Extrusion Isothermal and Coupled Analysis

This example illustrates the use of the R-P FLOW option in a classic plastic flow problem – the extrusion of metal in-plane strain through a 50% reduction, frictionless die. The problem is shown in Figure 7.1-1; a uniform velocity is applied at the left-hand side. The required solution is the velocity field and extrusion force. The slip-line solution to this problem is well known [1, 2].

The rigid-plastic flow option uses Herrmann incompressible elements to solve for the velocity field. The material is modeled as a non-Newtonian fluid and MARC iterates for the viscosity, which is $\frac{2}{3}\frac{\bar{\sigma}}{\dot{\bar{\varepsilon}}}$, where σ is the yield stress and $\dot{\bar{\varepsilon}}$ is the equivalent plastic strain rate.

The second part of this example demonstrates the coupled analysis for steady-state rigid-plastic flow. The comparison between effect of no heat convection contribution and heat convection contribution is made in e7x1b and e7x1c. Uniform velocity and fixed temperature is applied at the left-hand side. The contribution of convection heat is made after the solution of velocity is obtained. The nonsymmetric solver is turned on automatically when heat convection is included. The parameter COUPLE is used to flag the coupling procedures.

This problem is modeled using the three techniques summarized below.

Data Set	Element Type(s)	Number of Elements	Number of Nodes	Differentiating Features
e7x1	32	32	121	Isothermal
e7x1b	32	32	121	Coupled without Convection
e7x1c	32	32	121	Coupled with Convection

Element

In this example, the plane-strain Herrmann element (element 32) is used. This element is a second-order, distorted quadrilateral (plane-strain). There are 32 elements and a total of 121 nodes.

Material Properties

The equivalent von Mises yield stress is entered as 30 x 10^3 psi in this option. The thermal properties are:

specific heat	4.2117E-2
density	0.3523E-3
thermal conductivity	0.7254E-3

The property is specified for elements 1 through 32.

Geometry

No geometry is specified.

Loading

No loading is specified.

Boundary Conditions

The material entering the die is assigned a velocity of 1 in/sec in the x-direction. The material velocities normal to the die walls are fixed as zero. In the thermal mechanically coupled analysis, the inlet temperature of the material is fixed at 800°F. The wall temperature is fixed at 500°F.

Control

A 10% tolerance on the relative residual force was chosen to determine if convergence was achieved. In a rigid plastic analysis, the computational time would have been reduced if the convergence based upon velocities was requested.

Auto Load

Because the contribution of heat convection is accounted after the solution of velocity distribution is obtained, two fixed time steps are used to simulate the coupling process. In the first increment, the heat transfer analysis is done first and subsequent stress analysis uses this new temperature distribution for material properties to obtain the solution of velocity distribution. In the next increment, the temperature distribution is obtained based on the velocity distribution result of the previous increment.

Results

The solution for the 50% reduction case chosen here is a centered fan – outside the fan the material moves as a rigid body or is stationary. The mesh is confined to the neighborhood of the fan region (Figure 7.1-2).

Note a special consideration for the fully incompressible Herrmann formulation: since the system is semidefinite, it is only possible to solve by Gauss elimination if the first active degree of freedom is a stiffness degree of freedom and not a pressure variable (Lagrange multiplier). Thus, node 1 must have at least one unconstrained velocity component. In this case, one and two are swapped to achieve this by adding additional CONNECTIVITY and COORDINATES set by hand. The value of the input velocity is arbitrary in this case, since the yield is assumed to be rate independent. The accuracy of the solution is determined by the convergency requirements. In this analysis, nine iterations were required.

Extrusion force in 50% reduction, frictionless die. (Normalized by the tensile yield stress and input width).

Calculated at input stream	1.347
Calculated from reaction on die face	1.393
Exact (slip line) solution, $.5(1 + \pi/2)$	1.285

The predicted flow field is illustrated in Figure 7.1-3. Velocity vectors are shown in this figure. The slip-line fan has been superimposed on this picture. The “dead” region in the corner of the die is well predicted by the finite element model, before it reaches the fan. The downstream solution also shows a little rotation of the velocity field just below the corner of the die. This is more accurate than the upstream solution. The strain gradients on entry to the fan are very high. At this point, the slip solution shows a discontinuity in tangential velocity. A finer mesh in this region would improve this part of the solution.

The temperature distributions shown in Figure 7.1-4 and Figure 7.1-6 indicate the effect of heat convection on the plastic extrusion. As the contribution of heat convection is included, the heat transferred into exit from the inlet is faster and the temperature gradient between the wall and the central region is higher. The equivalent plastic strain is shown in Figure 7.1-5. The shear bands are clearly visible.

References

1. Hill, R., *Mathematical Theory of Plasticity,* Chapter 4, (Oxford University Press, 1950.).
2. Prager, W., and Hodge, P. G., *Theory of Perfectly Plastic Solids,* Section 298 (John Wiley, 1951).

Parameters, Options, and Subroutines Summary

Example e7x1.dat:

Parameters	Model Definition Options	History Definition Options
ELEMENT	CONNECTIVITY	AUTO LOAD
ELSTO	CONTROL	CONTINUE
END	COORDINATE	
R-P FLOW	END OPTION	
SIZING	FIXED DISP	
TITLE	ISOTROPIC	

Example e7x1b.dat:

Parameters	Model Definition Options	History Definition Options
COUPLE	CONNECTIVITY	AUTO LOAD
END	CONTROL	CONTINUE
ELEMENTS	COORDINATE	TIME STEP
HEAT	END OPTION	
R-P FLOW	FIXED DISPLACEMENT	
SIZING	FIXED TEMPERATURE	
TITLE	INITIAL TEMPERATURE	
	ISOTROPIC	
	NO PRINT	
	POST	

Example e7x1c.dat:

Parameters	Model Definition Options	History Definition Options
COUPLE	CONNECTIVITY	AUTO LOAD
END	CONTROL	CONTINUE
ELEMENTS	COORDINATE	TIME STEP
HEAT	END OPTION	
R-P FLOW	FIXED DISPLACEMENT	
SIZING	FIXED TEMPERATURE	
TITLE	INITIAL TEMPERATURE	
	ISOTROPIC	
	NO PRINT	
	POST	

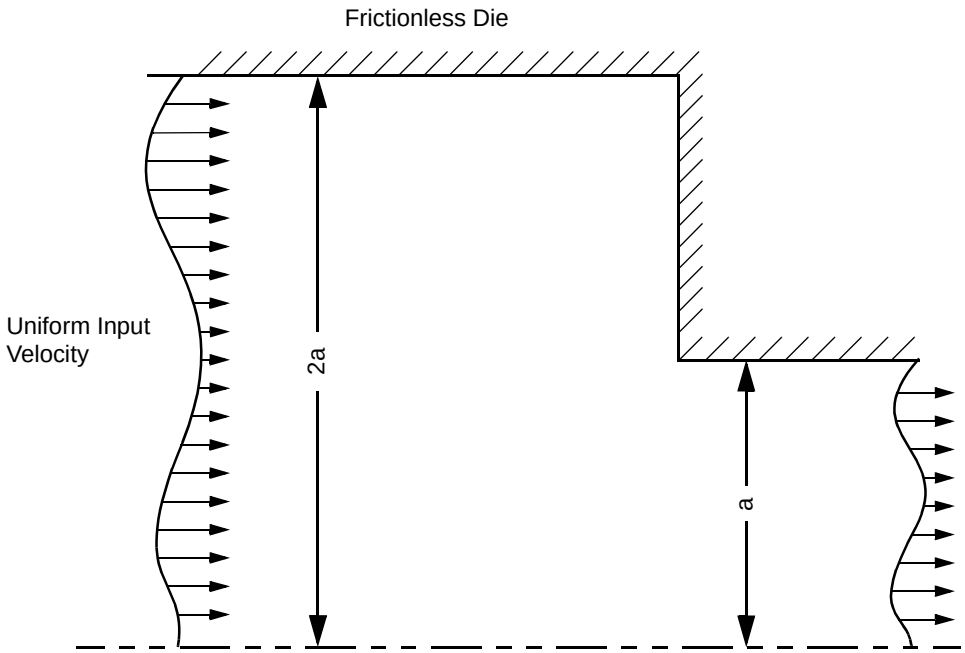

Figure 7.1-1 50% Reduction Die Problem

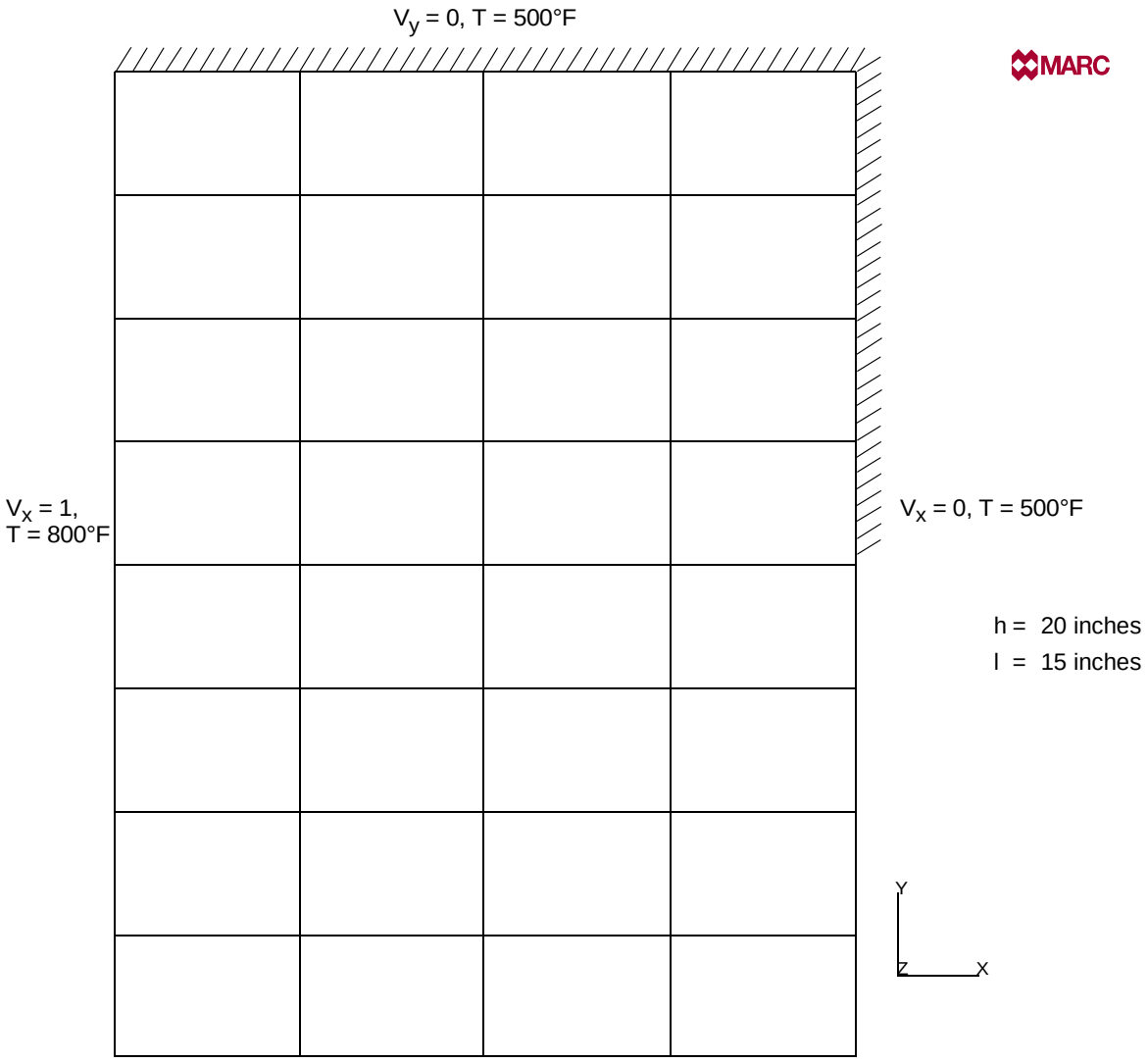

Figure 7.1-2 Mesh and Boundary Conditions for 50% Reduction Example

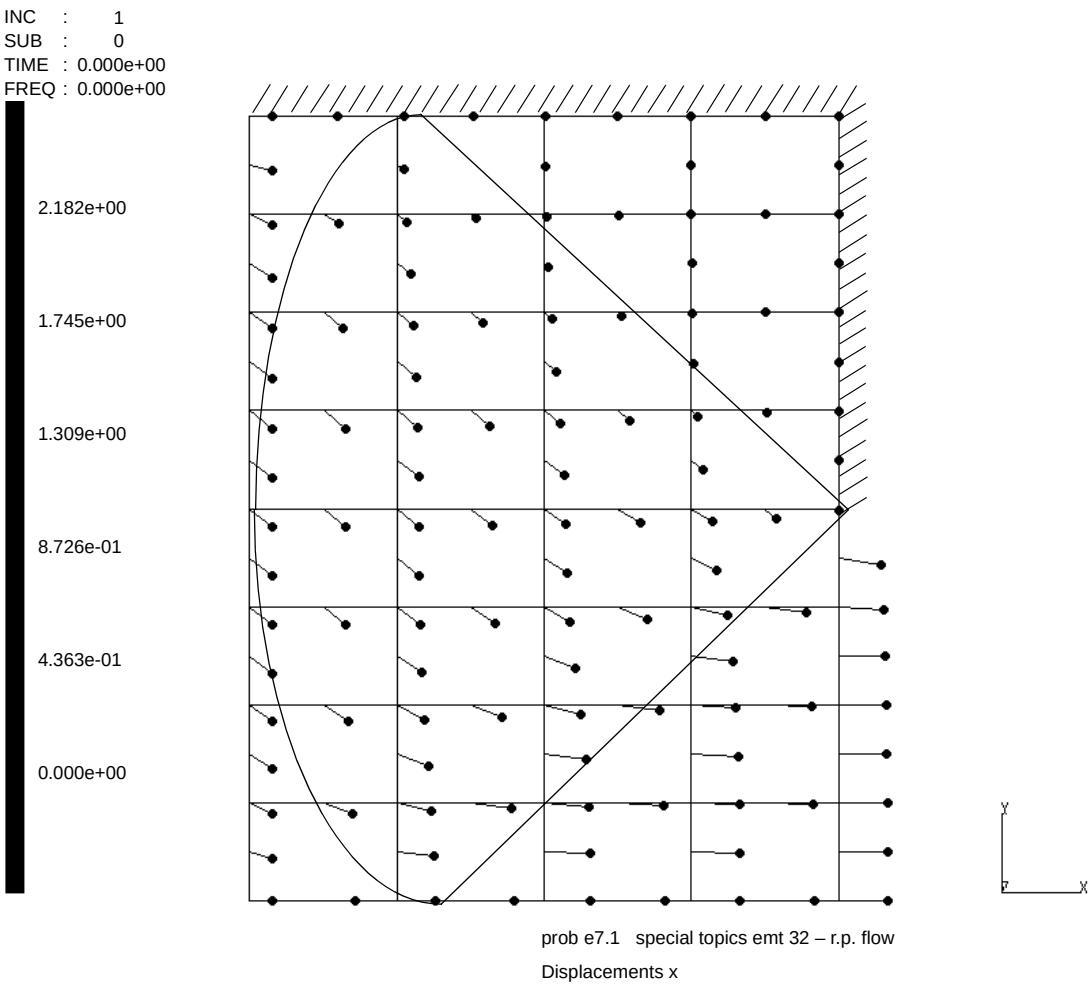

Figure 7.1-3 50% Reduction Extrusion Velocity Field

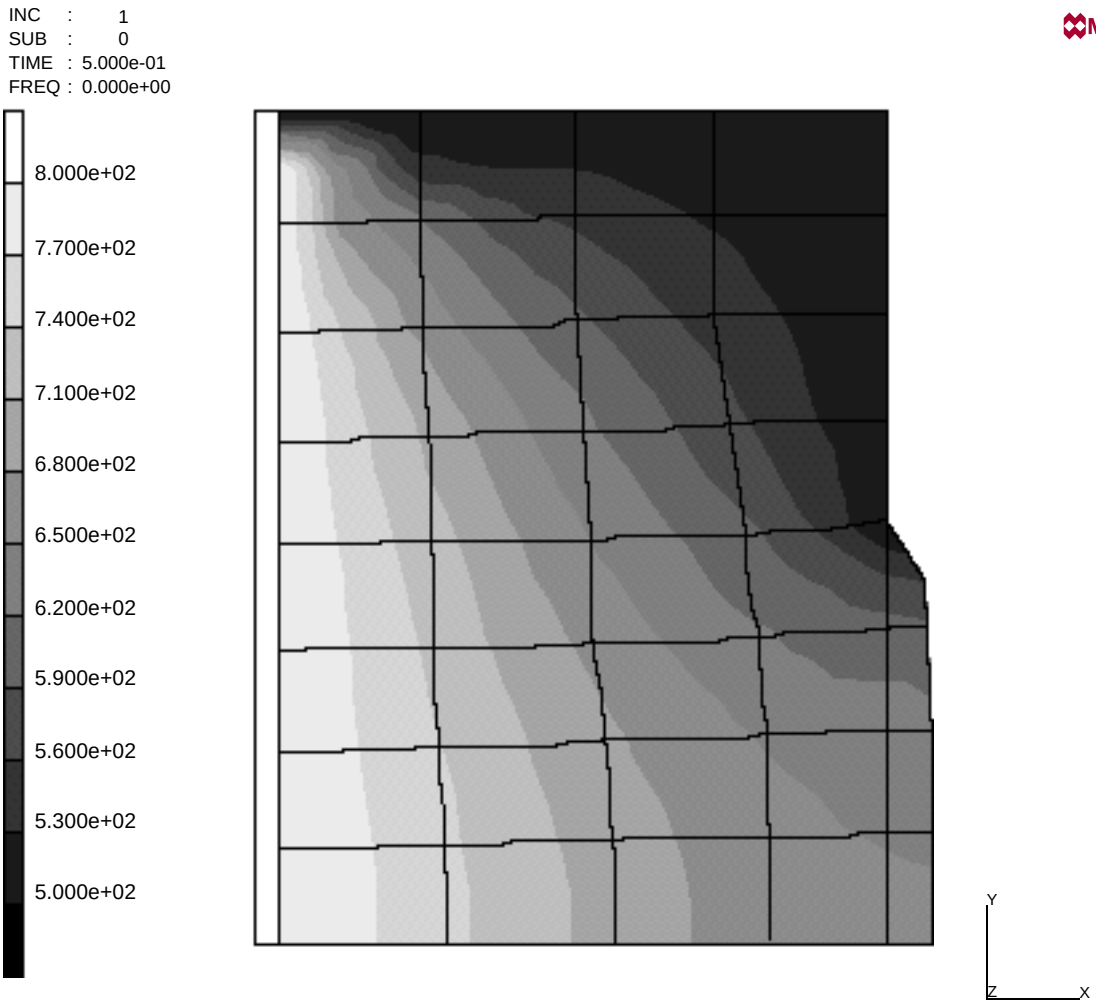

Figure 7.1-4 Temperature Distribution in the Billet Neglecting Thermal Convection

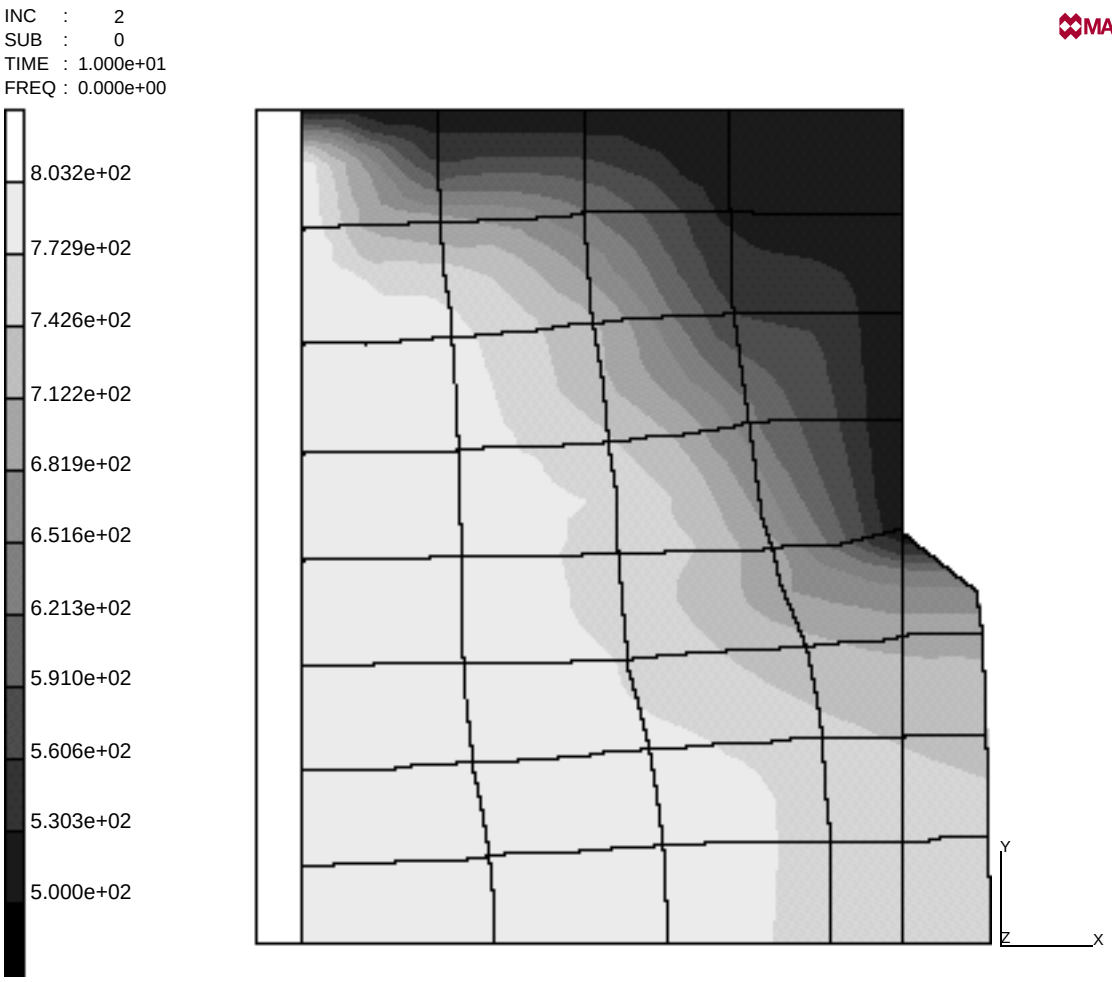

Figure 7.1-5 Temperature Distribution in the Billet including Convection

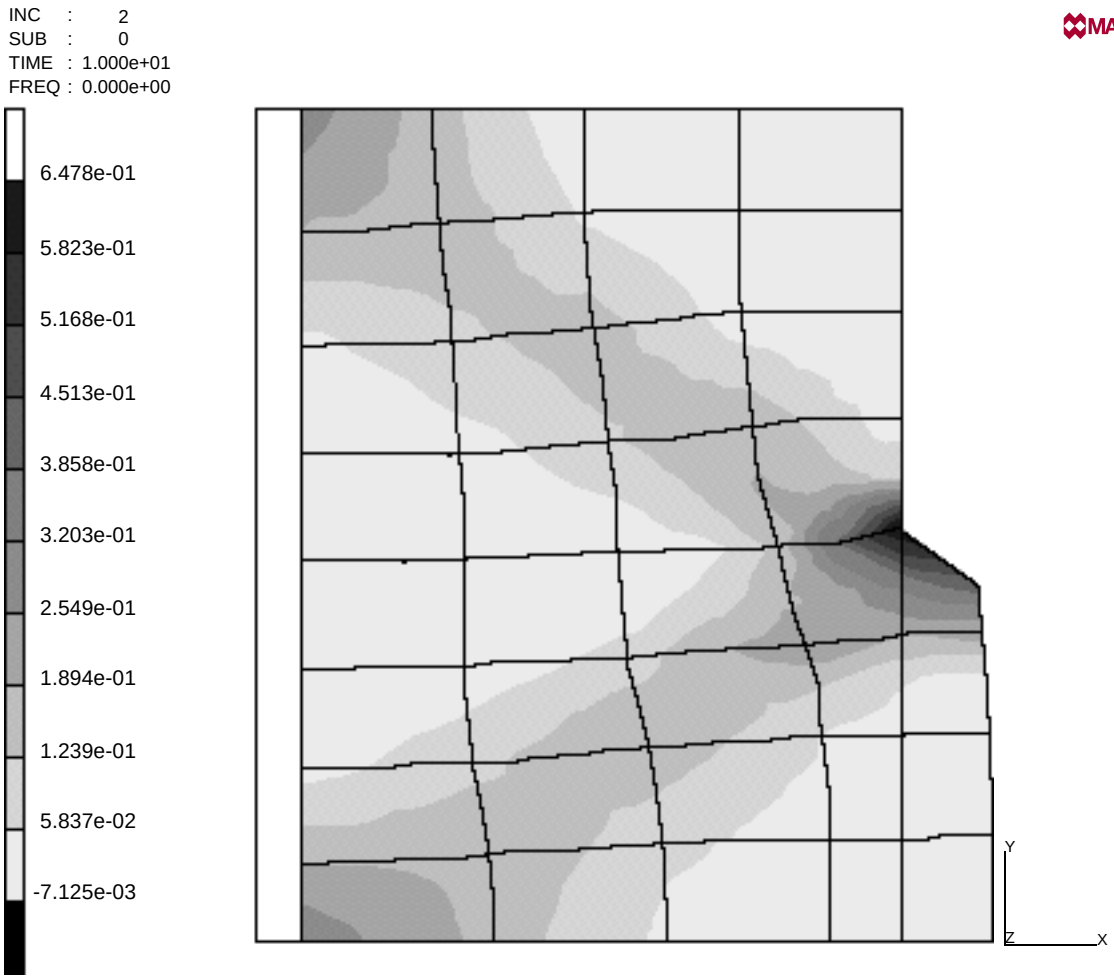

Figure 7.1-6 Equivalent Plastic Strains in Billet Neglecting Thermal Convection

7.2 End-Plate-Aperture Breakaway

This example illustrates the use of the gap and friction link, element type 12. This element allows surface friction effects to be modeled. This example is a simple model of a man-hole cover in a pressure vessel. The axisymmetric mesh is shown in Figure 7.2-1. The object of this analysis is to establish the response of the bolted joint between the manhole cover (elements 1-12) and the vessel (elements 13-27). The bolts are first tightened, and then the main vessel expands radially (as might occur due to thermal or internal pressure effects). You should be aware that this problem is presented only as a demonstration. The mesh is too coarse for accurate results.

Elements

Element 12 is a friction and gap element. It is based on the imposition of a gap closure constraint and/or a frictional constraint via Lagrange multipliers. The element has four nodes: nodes 1 and 4 are the end nodes of the link and each has two degrees of freedom (u, v,) in the global coordinate direction; node 2 gives the gap direction cosines (n_x, n_y) and has λ_n, the force in the gap direction, as its one degree of freedom; node 3 gives the friction direction cosines (t_{1_x}, t_{1_y}) and has γ_1, the frictional shear forces, and p, the net frictional slip, as its two degrees of freedom.

Model

Twenty-seven type 10 elements are used for the two discrete structures, the end cap and the aperture. These are then joined by four type 12 elements. There are 54 nodes and a total of 108 degrees of freedom in the mesh.

Loading

The load history consists of applying bolt loads (that is, tightening down the bolts), then pulling out the outer perimeter of the main vessel model. Bolt loads are modeled here as point loads applied in opposite directions (self-equilibrating) on node pairs 4 and 32, 5 and 33. Since there is a possibility of gaps developing between the facing surfaces of the cover and vessel, the bolt load is initially applied as a small magnitude, then incremented up to the total value of 2000 pounds per bolt ring. This usually requires two runs of the problem: an initial run with a “small” load to see the pattern developing, from which some judgement can be made about the load steps which can be used to apply the total bolt force. In this case, it was determined by this method that no surface separation occurred, so that, in the actual run, the full bolt loads are applied in one increment.

The radial expansion of the main vessel is modeled as a uniform negative pressure on the outer surfaces of the outer elements (15, 21, 27). (Note this is given as load type 8 to apply it to the correct face of the elements.) Again, the purpose of the analysis is to watch the development of slippage between the main vessel and the cover plate, and the analyst cannot easily estimate the appropriate load increments to apply to model this nonlinearity. For this purpose, the RESTART

option can be used effectively. A restart is written at the point where full bolt load is applied, and then a trial increment of pull-out force is applied. Based on the response to this (in the friction links), a reasonable size for the sequence of loading increments can be determined. This procedure is frequently necessary in such problems. For brevity, this example shows only the final load sequence obtained as a result of such trials.

Boundary Conditions

The nodes on the axis of symmetry are constrained radially, and the rigid body mode in the axial direction is removed at node 46.

Isotropic

The ISOTROPIC option is used to enter the mechanical properties of the manhole cover.

Gap Data

In this example, a small negative closure distance of -0.001 is given for the gaps. This indicates that the gaps are initially closed and solve for an interference fit in increment 0. The coefficient of friction μ is 0.8.

Results

The results of the analysis are shown in Figure 7.2-2 through Figure 7.2-4. First of all, it is observed in Figure 7.2-2 that the force at node 53, associated with gap element 31 goes to zero, indicating that the gap has opened. The interested user can investigate here possible model changes and their effect – for example, the effect of inaccurate bolt tightening, so that the two bolt rings have different loadings.

In this case, the initial bolt load is carried quite uniformly (A in Figure 7.2-2), but as the pull-out increases, the inner two links take more of the stress and the outer link (element 31) sheds stress. The shear stress development is followed in Figure 7.2-3 – initially (bold load only), all shear stresses are essentially zero. The two outer links slip first, but then the additional forces required to resist the pull develops in the inner two elements until the shear stress pattern follows the normal stress pattern, when the shear in the pair of links also slip ($\tau = \mu\sigma$). Figure 7.2-4 shows a plot of radial displacement of the outer perimeter against pull-out force. Notice the small loss of stiffness caused by slip developing as the vessel model has to resist the extra force along without any further force transfer to the cover.

Parameters, Options, and Subroutines Summary

Example e7x2.dat:

Parameters	Model Definition Options	History Definition Options
DIST LOADS	CONNECTIVITY	AUTO LOAD
ELEMENT	CONTROL	CONTINUE
END	COORDINATE	DIST LOADS
SIZING	END OPTION	POINT LOAD
TITLE	FIXED DISP	
	GAP DATA	
	ISOTROPIC	
	OPTIMIZE	
	POINT LOAD	

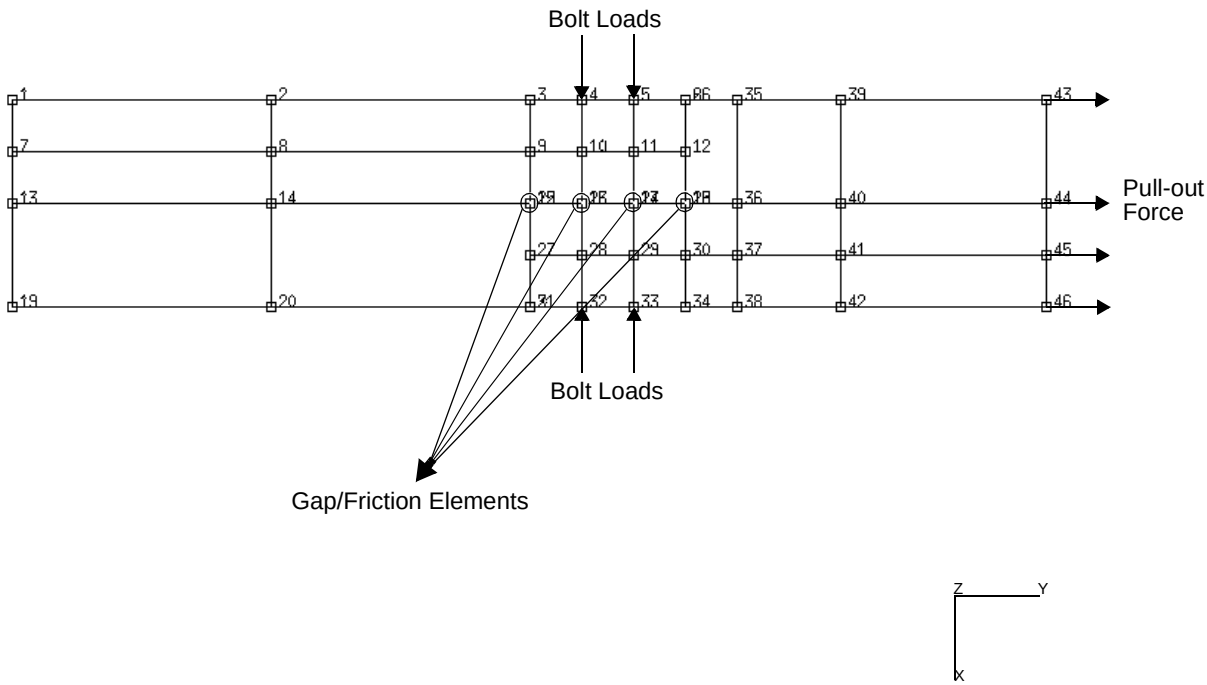

Figure 7.2-1 Geometry and Mesh of End Plate-Aperture

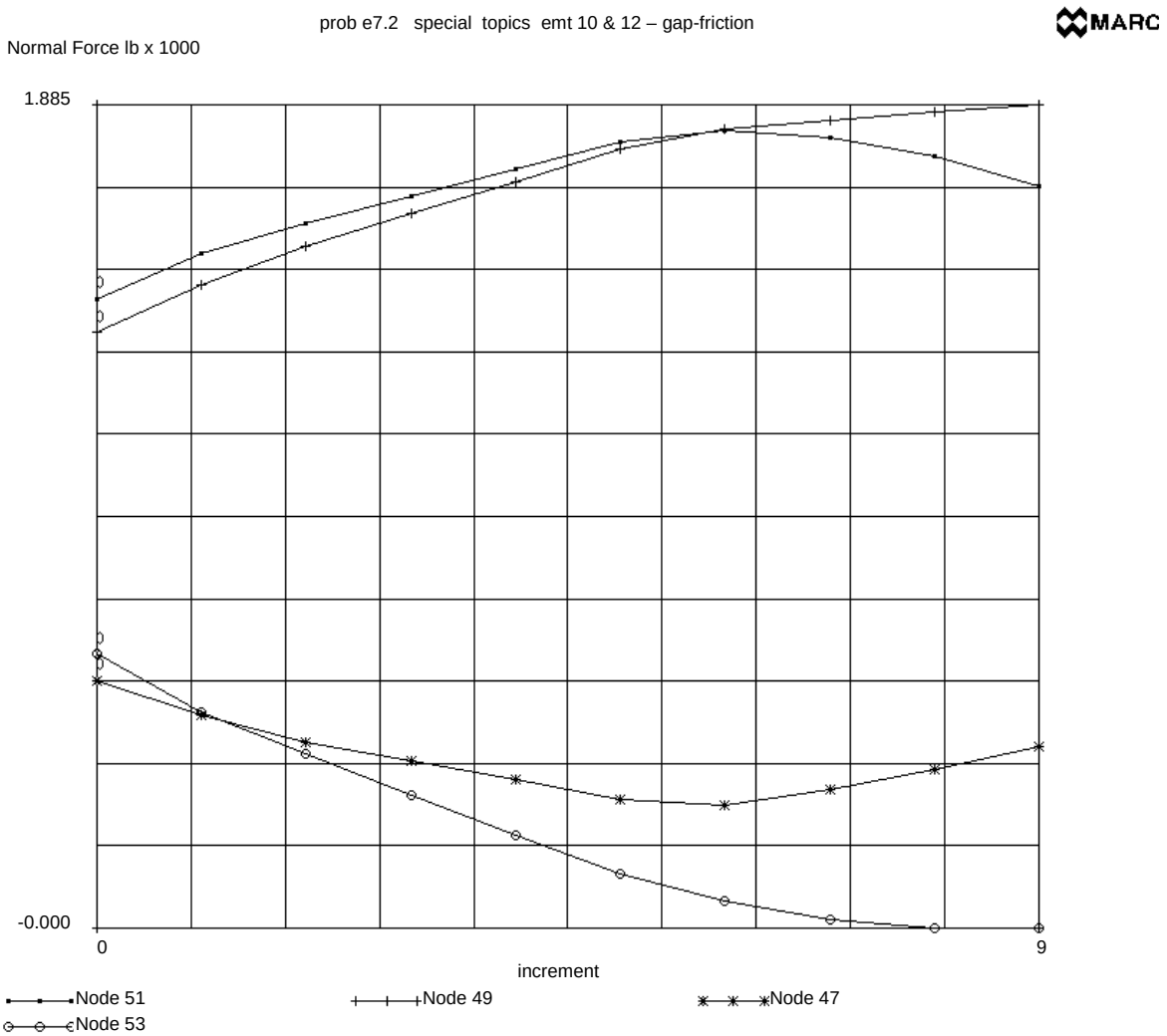

Figure 7.2-2 Transient Normal Forces in Bolts

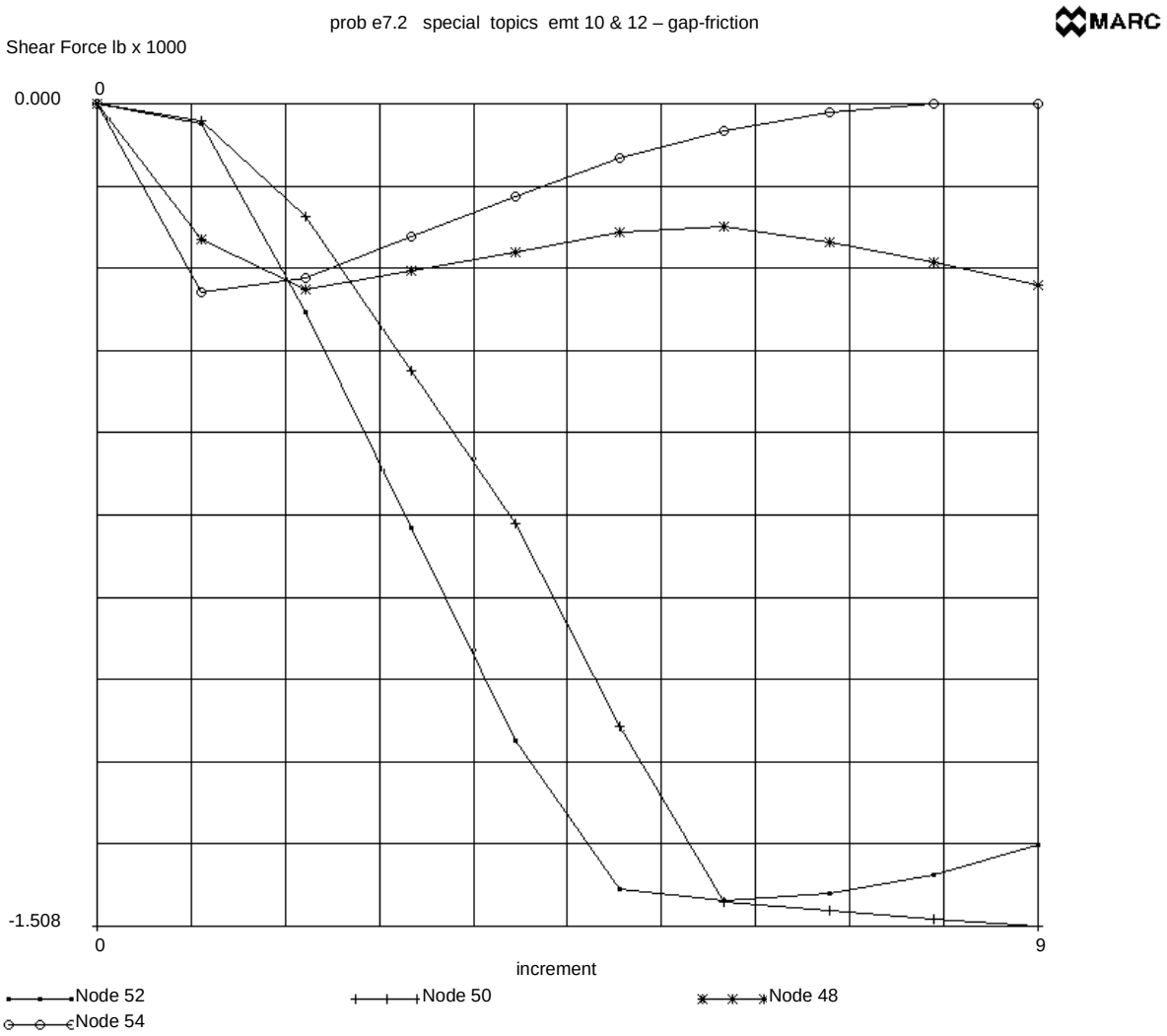

Figure 7.2-3 Transient Shear Force in Bolts

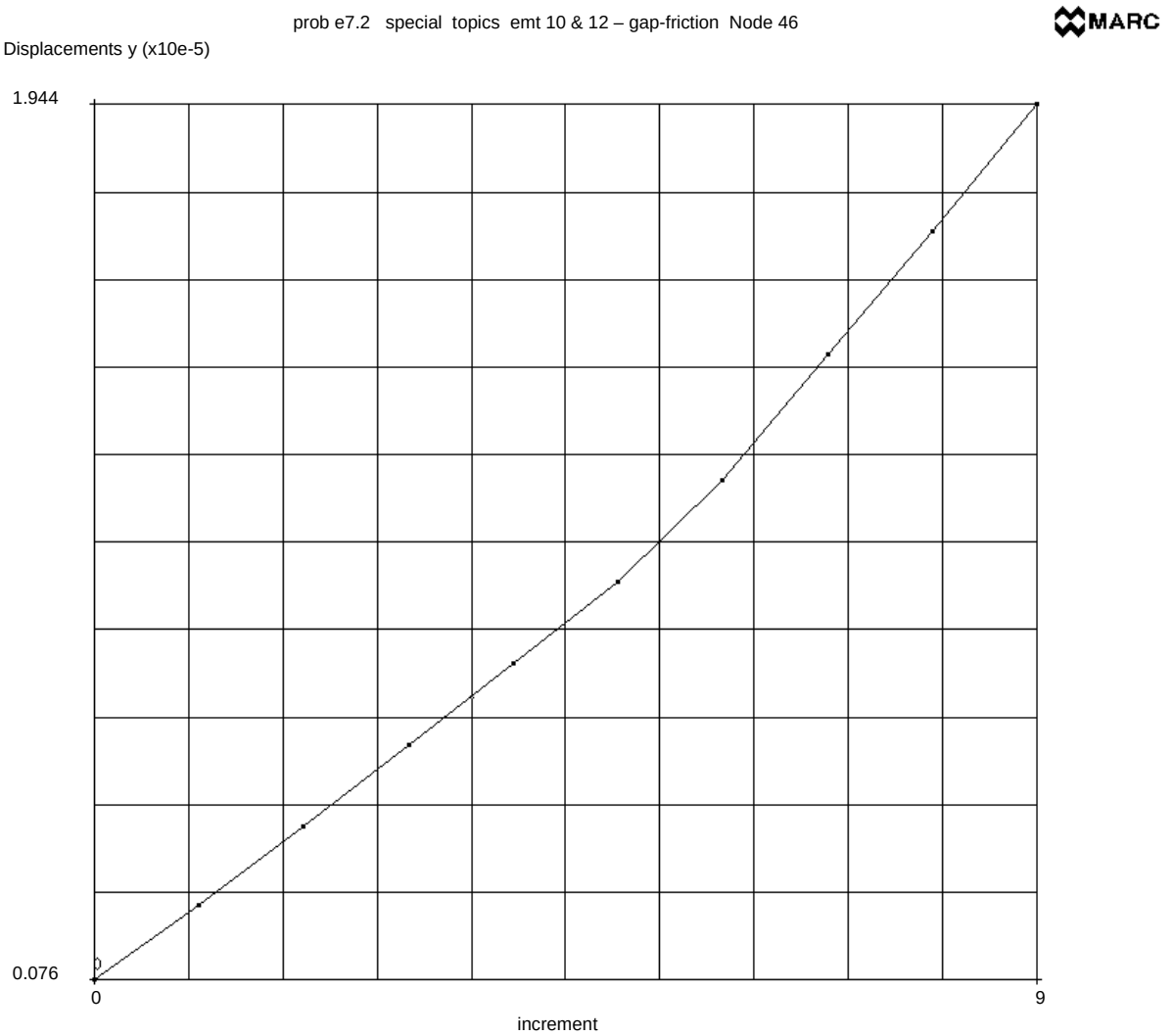

Figure 7.2-4 Radial Displacement at Outside Top (Node 46)

7.3 Barrel Vault Shell under Self-weight (Shell Cracking)

A concrete barrel vault shell is loaded under increasing snow load until cracking is developed. This is the same as problem 3.23 with the addition of nonlinear behavior.

This problem is modeled using the two techniques summarized below.

Data Set	Element Type(s)	Number of Elements	Number of Nodes	Differentiating Features
e7x3	75	36	49	AUTO INCREMENT
e7x3b	75	36	49	AUTO STEP

Element

Element type 75 is a 4 node thick shell element. The cylinder has a half length of 100 inches and a constant thickness of 3 inches. The radius is 300 inches.

Model

Thirty-six elements are used to model one-quarter of the shell taking advantage of symmetry. The model has 49 nodes. The mesh is shown in Figure 7.3-1. Subroutine UFXORD is used to generate the full set of coordinates.

Material Properties

The Young's modulus is 3×10^6 psi, the ultimate compressive strain is 0.002 in/inch. Failure in tension is assumed to occur at 1000 psi. The material is given a strain softening modulus of 3×10^5 psi. A shear retention coefficient of 0.5 is used for the concrete. The ISOTROPIC option is used to indicate that cracking is to be used.

Loading

In e7x3.dat, a total load of 2.0 psi is applied using the AUTO INCREMENT option. The load in the first increment is 10% of the total load.

In the second analysis, the total load of 2.0 psi is applied using the AUTO STEP procedure. The loading criteria is, based upon a maximum change in displacement of 0.5 inch and a maximum change in stress of 200 psi per increment.

Boundary Conditions

The ends of the structure are supported by diaphragms. There are two free edges.

Results

The first cracks occur at the bottom layers of element numbers 24 and 36 during increment 5. Subsequent loading results in formation of new cracks. Increasing loads propagate the cracks through the thickness of the shell.

The load deflection results for the midpoint of the edge of the shell (node 3), as shown in Figure 7.3-2. The effect of cracking is highly pronounced. This results in significant nonlinearity and leads to a reduction in the effective stiffness of the structure. The concrete's failure in tension dominates the response of this structure. In addition, a few points also fail due to crushing.

A rather large tolerance was necessary to obtain convergence in this analysis. This is not unusual for problems involving cracking.

Parameters, Options, and Subroutines Summary

Example e7x3.dat:

Parameters	Model Definition Options	History Definition Options
ELEMENT	CONNECTIVITY	AUTO INCREMENT
END	CONTROL	CONTINUE
SHELL SECT	COORDINATE	DIST LOADS
SIZING	CRACK DATA	
TITLE	DIST LOADS	
	END OPTION	
	FIXED DISP	
	GEOMETRY	
	ISOTROPIC	
	POST	
	PRINT CHOICE	
	RESTART	
	UFXORD	

Example e7x3b.dat:

Parameters	Model Definition Options	History Definition Options
ELEMENT	CONNECTIVITY	AUTO STEP
END	CONTROL	CONTINUE
SHELL SECT	COORDINATE	DIST LOADS
SIZING	CRACK DATA	
TITLE	DIST LOADS	
	END OPTION	
	FIXED DISP	
	GEOMETRY	
	ISOTROPIC	
	POST	
	PRINT CHOICE	
	RESTART	
	UFXORD	

User subroutine in u7x3.f:

UFXORD

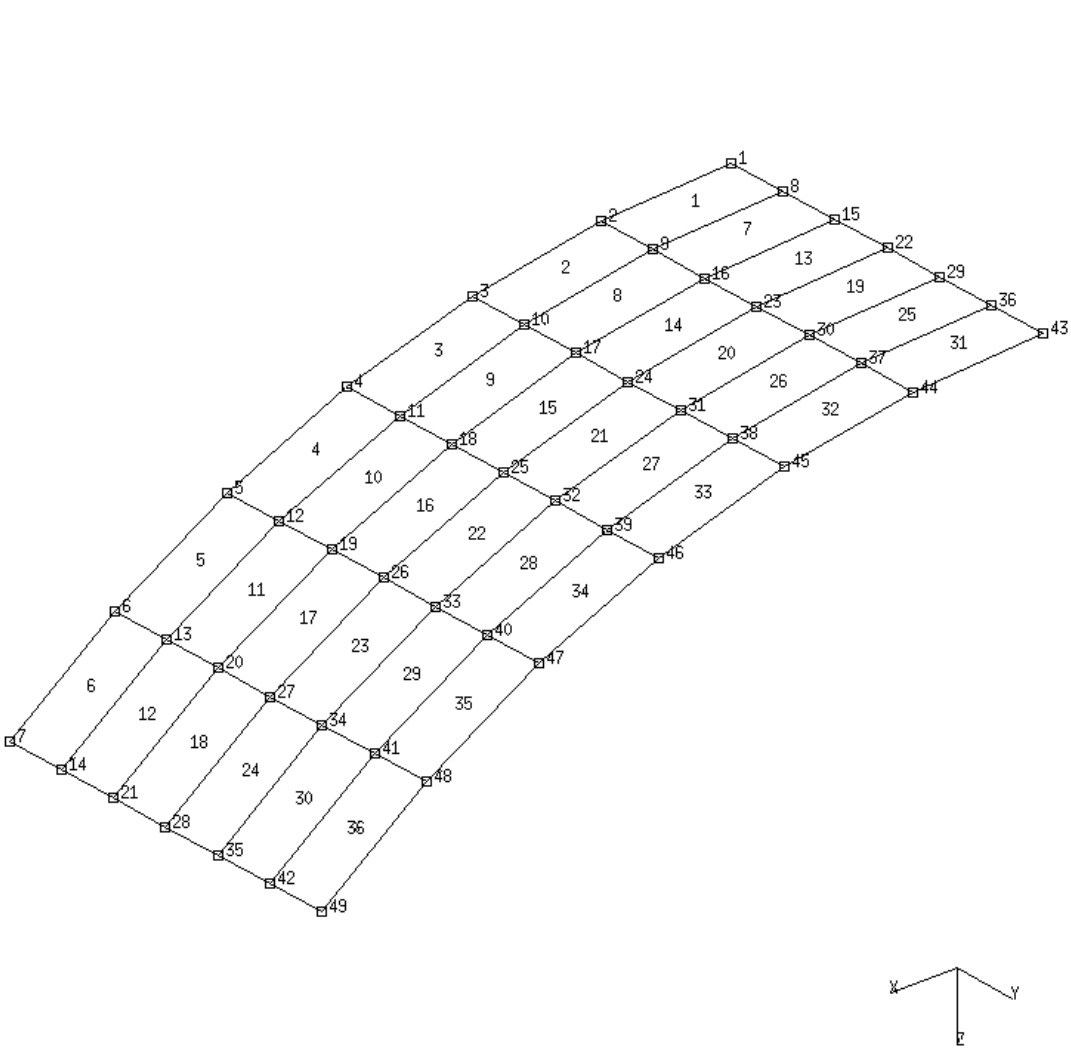

Figure 7.3-1 Mesh for the Shell Roof

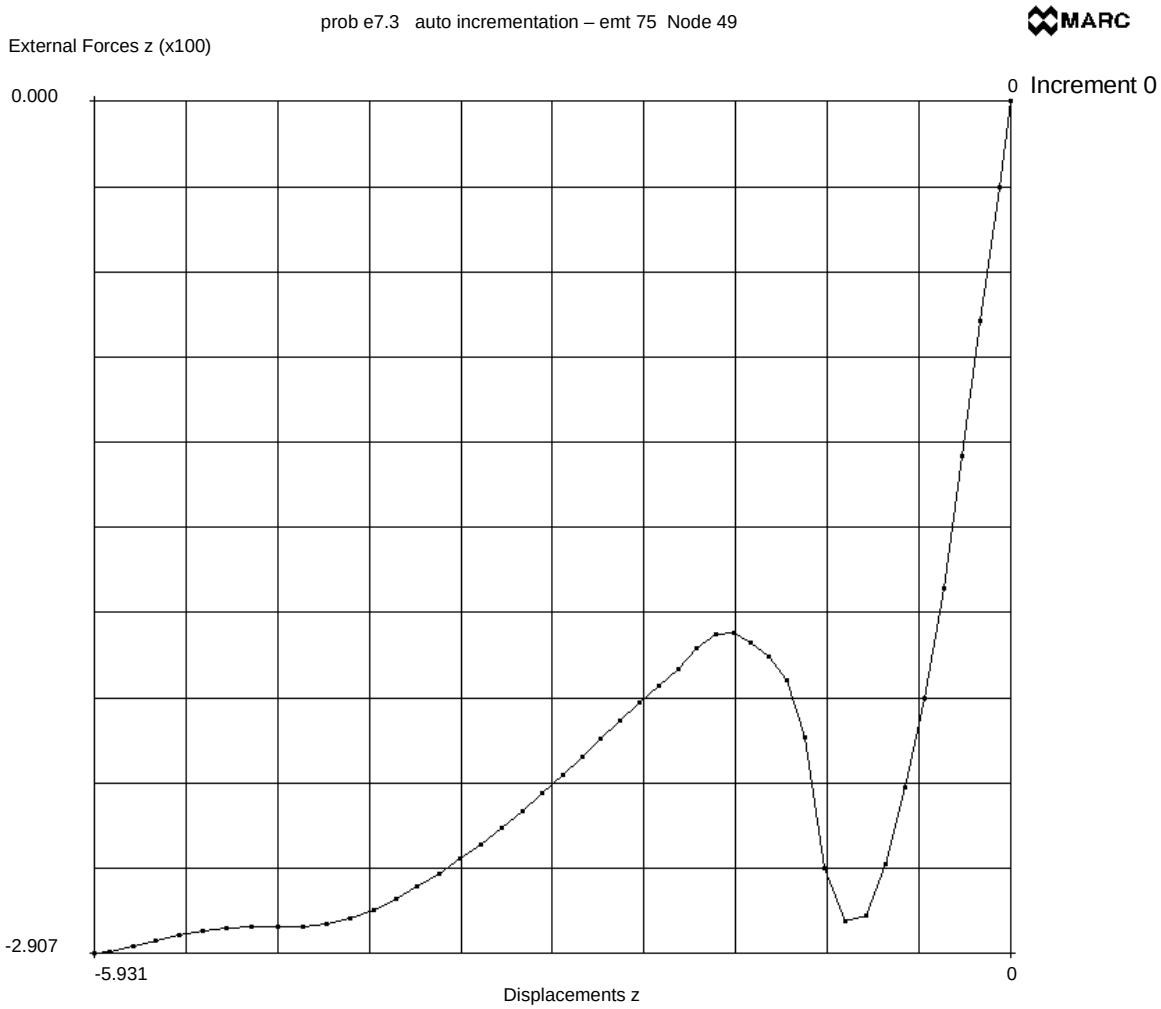

Figure 7.3-2 Load-Vertical Deflection Curve at Node 3

7.4 Side Pressing of a Hollow Rubber Cylinder (Mooney Material)

The behavior of a thick hollow rubber cylinder, compressed between two rigid plates, is analyzed. The cylinder is long; hence, a condition of plane strain in the cross section will be assumed. For reasons of symmetry, only one-quarter of the cylinder needs to be modeled. No friction will be assumed between cylinder and plates. A MOONEY material behavior is used to represent the rubber. The LARGE DISPLACEMENT option is used.

This problem is modeled using the two techniques summarized below.

Data Set	Element Type(s)	Number of Elements	Number of Nodes	Differentiating Features
e7x4	32 & 12	19	53	AUTO LOAD
e7x4b	32 & 12	19	53	AUTO STEP

Element

The quarter cylinder is modeled by using 8-node hybrid plane strain elements (MARC element type 32). This element can be used in conjunction with Mooney material. The corner nodes have an additional degree of freedom to represent the hydrostatic pressure. Seven gap elements are used to model the potential contact.

Model

The outer radius of the cylinder is 3 mm and the inner radius of the cylinder is 2 mm. Twelve elements are used for the cylinder, with two elements specified over the thickness. The geometry of the cylinder and the mesh are shown in Figure 7.4-1.

MOONEY

The MOONEY option is used to specify the rubber properties. The rubber material can be modeled as a Mooney-Rivlin material with C_{10} = 8 N/mm^2, C_{01} = 2 N/mm^2.

GAP DATA

The gap closure distance is defined as the initial nodal distance between the cylinder and the plate and is entered via the GAP DATA option.

Loading

In the first analysis, the AUTO LOAD option is used to apply five displacement increments to the plate. The increment is equal to the one applied in increment 0. After load application, one iteration is carried out by using PROPORTIONAL INCREMENT option with zero load increment to insure that the solution is in equilibrium. This is not necessary if the tolerance specified on the CONTROL option is sufficiently small.

In the second analysis, a total displacement of 1 inch is applied using AUTO STEP. The load is controlled by requiring that the incremental strain be less than 10% per increment.

Connectivity

The CONNECTIVITY option is used twice. It is used the first time to read the data of the mesh of the cylinder. The option is then used again to read gap data.

Tying

TYING establishes the connections between the nodal degrees of freedom of the cylinder and that of the gaps. This is necessary because the degrees of freedom of these two elements are not the same.

Results

The cylinder outer diameter is reduced from 6 inches to 4 inches in five increments. The cylinder is in contact with the plate at four nodes (four gaps have been closed). The incremental displacements become very small and equilibrium is satisfied with high accuracy. The incremental full Newton-Raphson method was used to solve the nonlinear system. The total force on the plate may either be calculated by summing up the gap forces, or directly obtained from the reaction force on node 75. For both the data sets, this leads to a total force F = 1.91 N. A plot of the deformed cylinder is shown in Figure 7.4-2.

Parameters, Options, and Subroutines Summary

Example e7x4.dat:

Parameters	Model Definition Options	History Definition Options
ELEMENT	CONNECTIVITY	AUTO LOAD
END	CONTROL	CONTINUE
LARGE DISP	COORDINATE	PROPORTIONAL INCREMENT
SIZING	END OPTION	
TITLE	FIXED DISP	
	GAP DATA	
	MOONEY	
	RESTART	
	TYING	

Example e7x4b.dat:

Parameters	Model Definition Options	History Definition Options
ELEMENT	CONNECTIVITY	AUTO STEP
END	CONTROL	CONTINUE
LARGE DISP	COORDINATE	PROPORTIONAL INCREMENT
SIZING	END OPTION	
TITLE	FIXED DISP	
	GAP DATA	
	MOONEY	
	RESTART	
	TYING	

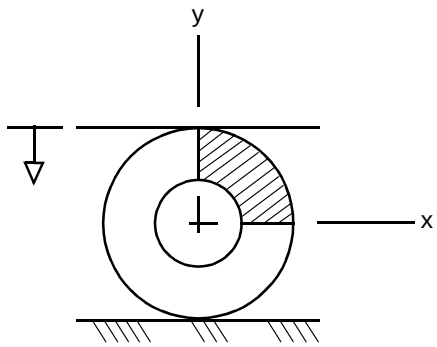

$C_1 = 8$
$C_2 = 2$
$r_i = 2$
$r_o = 3$

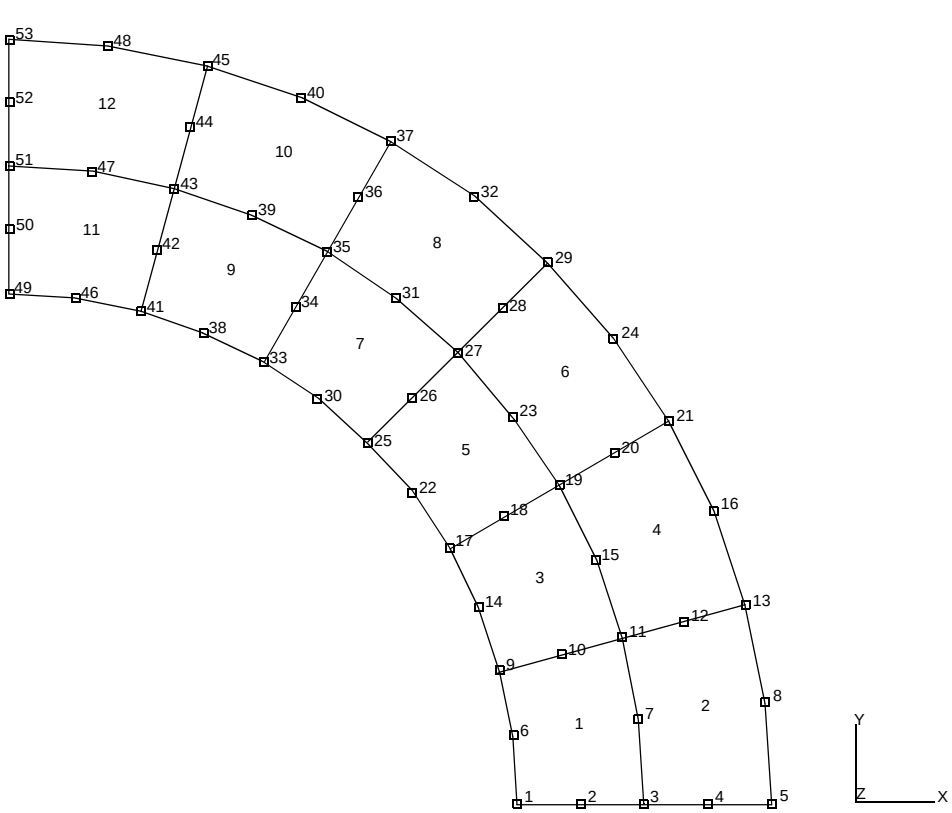

Figure 7.4-1 Rubber Cylinder and Mesh

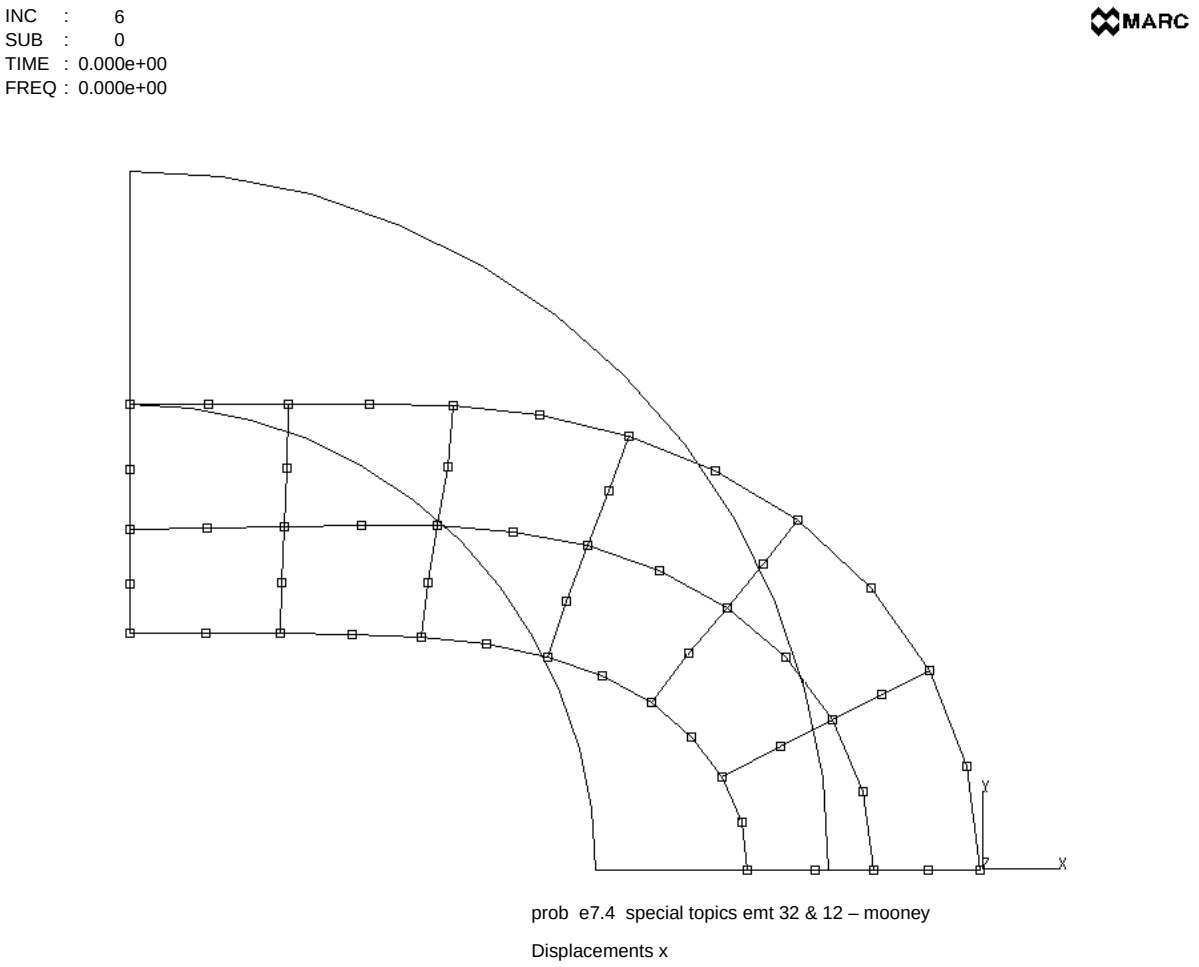

Figure 7.4-2 Deformed Mesh Plot

7.5 Analysis of a Thick Rubber Cylinder under Internal Pressure

This problem illustrates the use of MARC elements types 33, 82, and 120 (8- and 4-node incompressible, axisymmetric elements) and options, LARGE DISP, FOLLOW FOR, and MOONEY for an elastic, large strain analysis of a rubber cylinder subjected to a uniformly distributed internal pressure. The pressure load is applied in a single step, and the Newton-Raphson iteration procedure is used to obtain an equilibrium state.

This problem is modeled using the three techniques summarized below.

Data Set	Element Type(s)	Number of Elements	Number of Nodes
e7x5	33	4	23
e7x5b	82	4	14
e7x5c	119	4	14

Model

The dimensions of the rubber cylinder and finite element meshes are shown in Figure 7.5-1. The 8-node model consists of four elements of type 33 and 23 nodes, and the 4-node model consists of four elements of type 82 or type 120, and 14 nodes.

Material Properties

The material of the rubber cylinder is assumed to be MOONEY material with material constants:

$$C_{10} = 8 \text{ N/mm}^2$$
$$C_{01} = 2 \text{ N/mm}^2$$

Loading

Uniformly distributed internal pressure = 11.5 N/mm^2 is applied on element number 1. This load is applied in increment zero. In MARC, increment 0 is treated as linear so an additional increment, with no additional load, is used to bring the solution to the correct nonlinear state.

Boundary Conditions

u = 0 on the planes z = 0 and z = 1.0 to simulate a plane strain condition.

Note

LARGE DISP is included to obtain the geometric nonlinear effects; the full Newton-Raphson technique is used.

FOLLOW FOR indicates that pressures will be applied on the current geometry of the cylinder.

CONTROL block is used to specify the number of increments in the analysis. In this analysis, two increments are specified with a maximum of 15 Newton-Raphson iterations to obtain equilibrium.

Newton-Raphson iterations are obtained with PROPORTIONAL INCREMENT. This indicates that the previous load increment has to be multiplied by a certain user specified factor and has to be added to the current loads. The loads can be pressures, nodal loads, or nonzero kinematic boundary conditions. If the multiplication factor is set to be zero (0), then no load is added. Iterations are performed until the maximum residual force is less than 10% of the maximum reaction force.

Results

A. 8-Node Model (Element Type 33)

After the linear elastic step (increment 0), the radial displacements of the inside nodes (nodes 1, 10 and 15) are:

Node	Radial Displacement (mm) (MARC)
1	0.38351
10	0.38351
15	0.38350

They are in good agreement with analytical solution which predicts a radial displacement of 0.38333.

After ten iterations, the radial displacement at the inside node is 1.0026, and the corresponding pressure can be computed from the following expression:

$$P = (C_1 + C_2)\left[\log\left(\frac{B^2a^2}{A^2(B^2 - A^2 + a^2)}\right) + \frac{(a^2 - A^2)(B^2 - A^2)}{a^2(B^2 - A^2 + a^2)}\right]$$

where A and B are the inner and outer radius of the cylinder in the undeformed state, and “a” is the inner radius in the deformed state, and C_1 and C_2 are material constants.

The computed pressure (11.49) is in very good agreement with the prescribed value of 11.5.

B. 4-Node Model (Element Type 82, 120)

After the linear elastic step (increment 0), the radial displacements of the inside nodes (nodes 1 and 6) are:

Node	Radial Displacement (MARC) type 82	Radial Displacement (MARC) type 120
1	0.38174	0.38335
6	0.38174	0.38335

Agreement with analytical solution of 0.38333 is good. After ten iterations, the radial displacement at inside node is 1.0061, and the corresponding pressure is 10.35 for element 82. For element 120, the displacement at the inside node is 1.0063 and the corresponding pressure is 11.5. Agreement with prescribed value or 11.5 is excellent.

Parameters, Options, and Subroutines Summary

Example e7x5.dat:

Parameters	Model Definition Options	History Definition Options
ELEMENT	CONNECTIVITY	CONTINUE
END	CONTROL	CONTROL
FOLLOW FORCE	COORDINATE	DIST LOADS
LARGE DISP	DIST LOADS	
SIZING	END OPTION	
TITLE	FIXED DISP	
	MOONEY	
	NODE FILL	
	POST	

Example e7x5b.dat or e7x5c.dat:

Parameters	Model Definition Options	History Definition Options
ELEMENT	CONNECTIVITY	CONTINUE
END	CONTROL	CONTROL
FOLLOW FORCE	COORDINATE	DIST LOADS
LARGE DISP	DIST LOADS	
SIZING	END OPTION	
TITLE	FIXED DISP	
	MOONEY	
	POST	

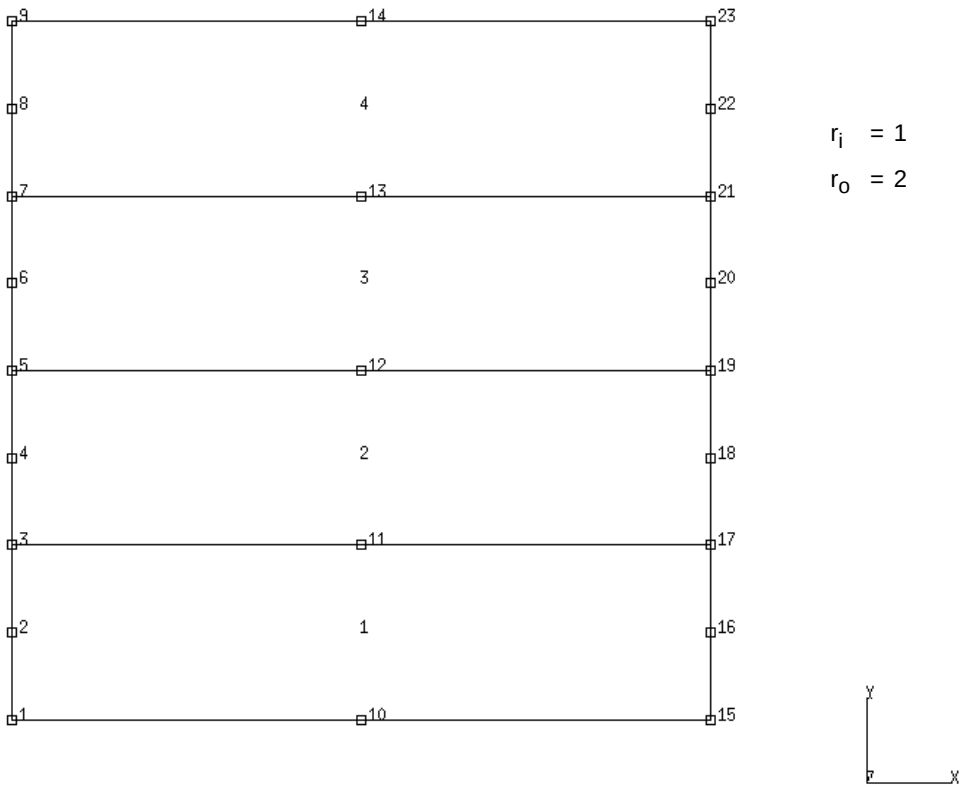

Figure 7.5-1 Cylinder Mesh (8-Node Model)

INC : 0
SUB : 0
TIME : 0.000e+00
FREQ: 0.000e+00

prob e7.5 special topics emt 33 – mooney

MARC

2nd comp of cauchy stres (x10)

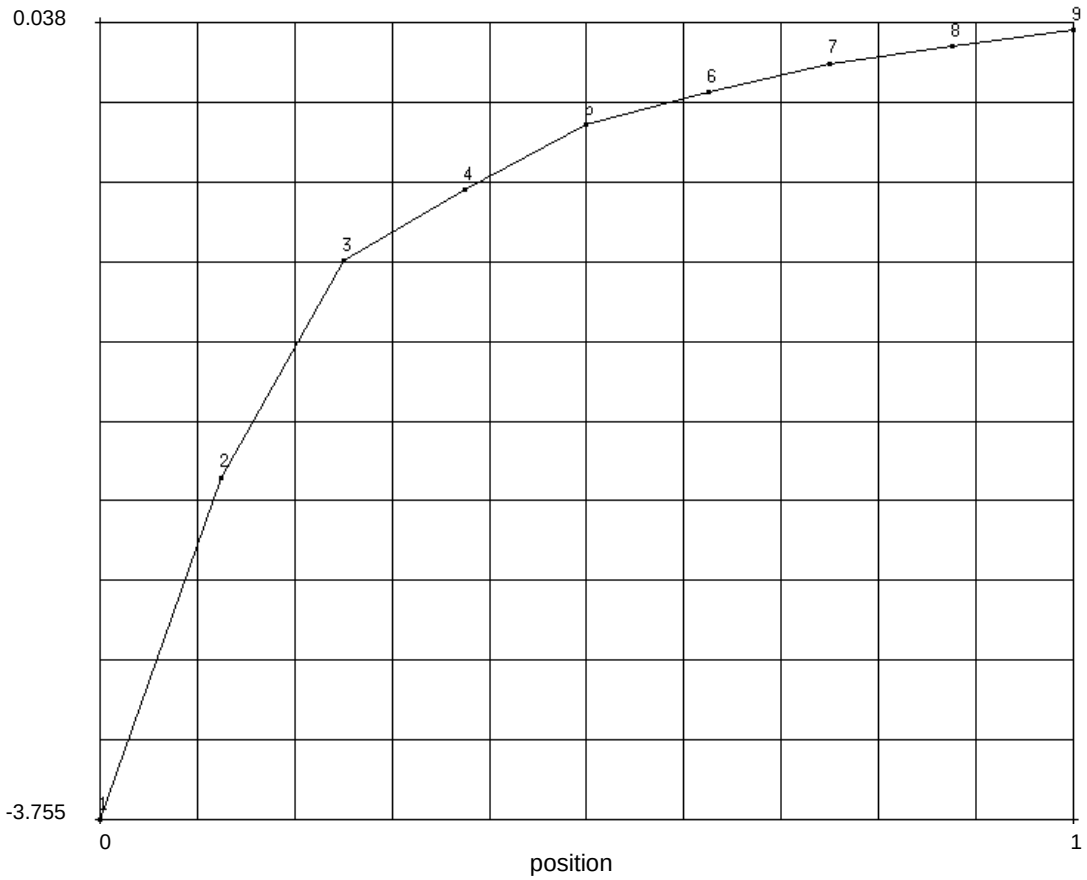

Figure 7.5-2 Radial Stress Through Radius

7.6 Biaxial Stress in a Composite Plate

This problem illustrates the analysis of a plate made of layered composite material as shown in Figure 7.6-1. A biaxial stress field is applied and the results are compared with a textbook solution (Reference 1).

This problem is modeled using the two techniques summarized below.

Data Set	Element Type(s)	Number of Elements	Number of Nodes	Differentiating Features
e7x6	75	20	25	User subroutine ANISOTROPIC
e7x6b	75	20	25	

Element

Shell element 75 is used to model the plate. It is a four-node bilinear thick shell element capable of modeling the behavior of layered composite materials.

Model

A 4 x 4 mesh of shells is used for a total of 16 elements, 25 nodes, and 150 degrees of freedom. (See Figure 7.6-2.)

Material Properties

The plate consists of three layers of an orthotropic material. The top layer is 3 mm thick and is offset 45° from the middle layer. The middle layer is 4 mm thick. The bottom layer is also 3 mm thick and is offset 45° from the middle layer. This data is entered in the COMPOSITE option.

The orthotropic material properties are first entered in the ORTHOTROPIC option. The data entered here are the engineering constants E_{11}, E_{22}, E_{33}, ν_{12}, ν_{23}, ν_{31}, G_{12}, G_{22}, and G_{33} with respect to the three planes of elastic symmetry. In problem e7x6b, the anisotropic stress-strain law is entered directly through the ANISOTROPIC option. When entering the data using the ANISOTROPIC option, you must specify the values (21 values) in the symmetric triangle for a compressed form 6x6 matrix. The ply angle for the various layers is given in the COMPOSITE option.

Element type 75 has only two direct strains. Using the PRINT,11 option, you would observe the following printout:

```
layer stress-strain law in layer coords for elem 5.
```

Row \ Column	1	2	3	4	5
1	.200456E11	.70159E9	0	0	0
2	.70159E9	.200456E11	0	0	0
3	0	0	.7E9	0	0
4	0	0	0	.7E9	0
5	0	0	0	0	.7E9

The input required when using the ANISOTROPIC option is:

Row \ Column	1	2	3	4	5	6
1	.200456E11	.70159E9	0	0	0	0
2	.70159E9	.200456E11	0	0	0	0
3	0	0	.7E9	0	0	0
4	0	0	0	.7E9	0	0
5	0	0	0	0	.7E9	0
6	0	0	0	0	0	0

Loading

The biaxial stresses applied to the plate are $\sigma_x = 1. \times 10^6$ N/m^2, $\sigma_y = 2. \times 10^5$ N/m^2 and $\tau_{xy} = 0.$ These distributed loads are specified in the DIST LOADS option (the units in this problem are m-kg-s). The applied load magnitudes are negative so that the applied loading is directed out of the element.

Boundary Conditions

In order to fully restrain the rigid body modes without introducing any elastic constraints, a special set of boundary conditions is used. Degrees of freedom 1 to 5 are suppressed at node 1 and degree of freedom 1 is suppressed along the entire left-hand edge. Since the layup is symmetric, only in-plane deformations are expected. The specification of additional rotational constraints at the left-hand edge is irrelevant.

Print Control

The use of the suboption PREF under PRINT ELEM allows you to obtain printout of the layer stresses in the preferred (ply) coordinate system. The generalized shell resultant quantities are always expressed in the local shell $\tilde{\nu}^1$, $\tilde{\nu}^2$ system. Here, these coordinates are parallel to global x and y, respectively.

Results

Results for this problem are given on page 169 in the reference below. They are summarized below:

		Reference	MARC
ε_x^o		.00685	.006875
ε_y^o		.00332	.003324
ε_{xy}^o		-.00784	-.007845
Layers 1,3 x 10^6N/m^2	σ_1	29.6	29.85
	σ_2	18.8	18.87
	σ_{12}	-2.5	-2.49
Layer 2 x 10^6N/m^2	σ_1	139.3	139.8
	σ_2	11.4	11.46
	σ_{12}	-5.5	-5.49

Figure 7.6-3 shows the deformed shape of the structure. The displacements are all planar, and there is no coupling between bending and axial extension due to the symmetry of the layup. There is, however, coupling between axial extension and in–plane shear. The results are identical, independent of the way the material is input.

Reference

Agarwal, B.D., Broutman, L., *Analysis and Performance of Fiber Composites*, Wiley, 1980.

Parameters, Options, and Subroutines Summary

Example e7x6.dat:

Parameters	Model Definition Options
ELEMENT	COMPOSITE
END	CONNECTIVITY
SHELL SECT	COORDINATE
SIZING	DEFINE
TITLE	DIST LOADS
	END OPTION
	FIXED DISP
	ORIENTATION
	ORTHOTROPIC
	POST
	PRINT ELEM

Example e7x6b.dat:

Parameters	Model Definition Options
ELEMENT	ANISOTROPIC
END	COMPOSITE
SHELL SECT	COORDINATE
SIZING	DEFINE
TITLE	DIST LOADS
	END OPTION
	FIXED DISP
	ORIENTATION
	POST
	PRINT ELEM

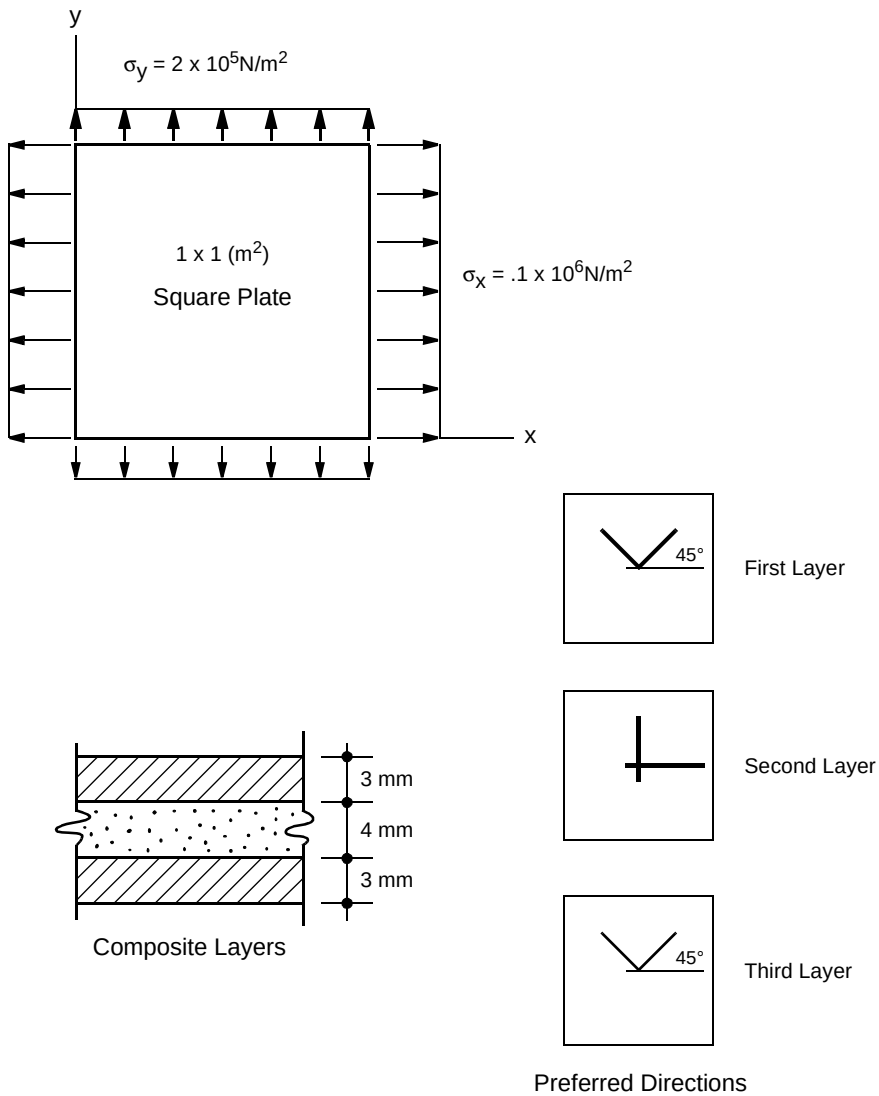

Figure 7.6-1 Composite Plate

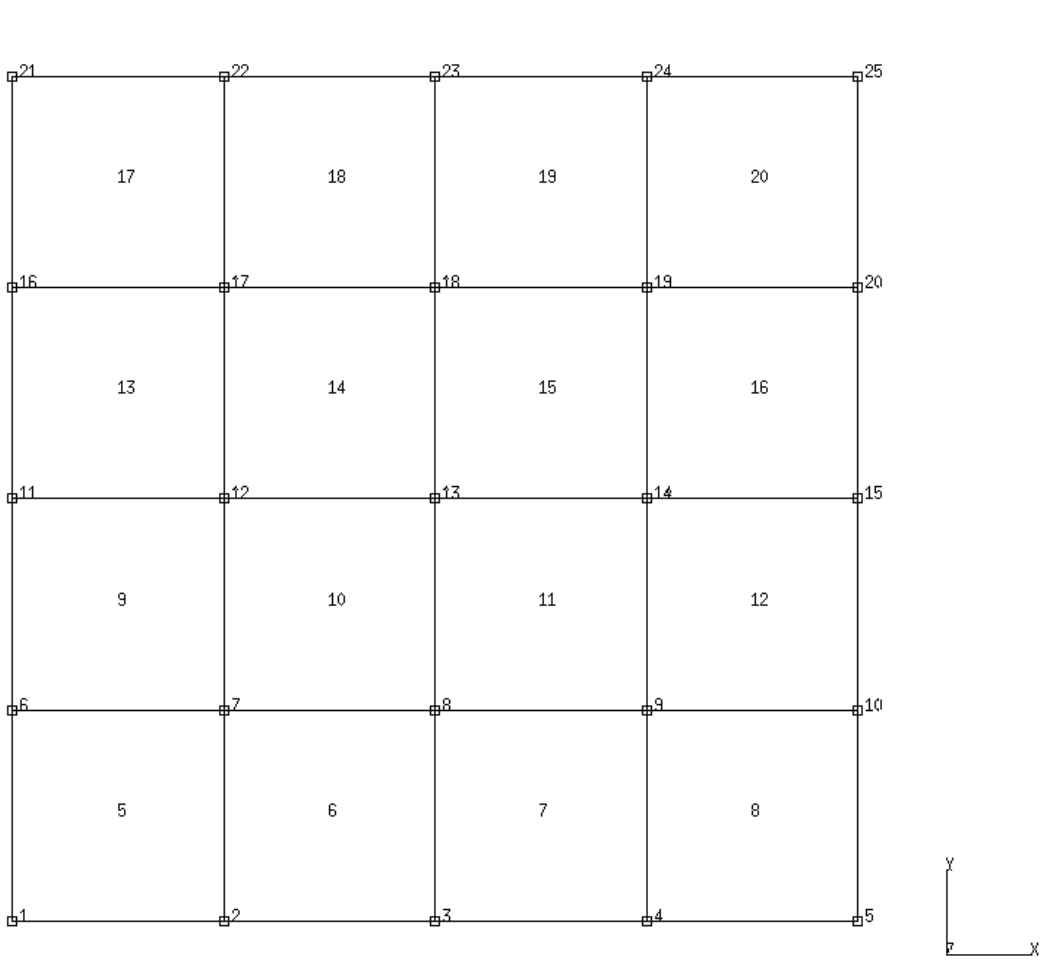

Figure 7.6-2 Finite Element Mesh

INC : 0
SUB : 0
TIME : 0.000e+00
FREQ : 0.000e+00

MARC

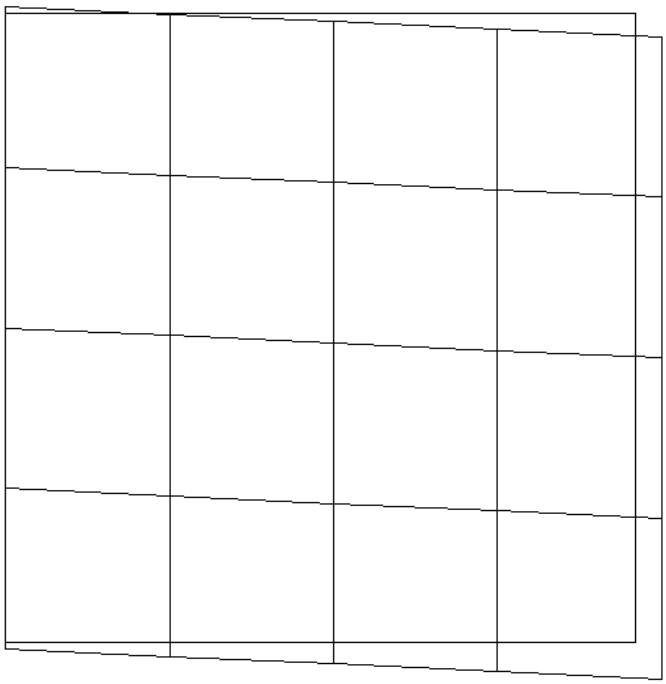

prob e7.6 special topics – elmt 75

Displacements x

Figure 7.6-3 Deformed Mesh Plot

7.7 Composite Plate Subjected to Thermal Load

A composite plate is subjected to a uniform thermal load.

Element

Element 75, the four-node bilinear thick shell element, is used. In this analysis, three layers will be used through the thickness.

Model

The square plate of 1 inch length has been divided into 16 elements with 25 nodes as shown in Figure 7.7-1. To demonstrate that the element numbers do not need to begin with 1, they are given id's of 5 to 20.

Geometry

No geometry specification is used. The plate thickness on a layer-by-layer basis is specified with the COMPOSITE option. Then the thickness of layers 1 to 3 are 0.003, 0.0025, 0.0025 respectively, giving a total thickness of 0.008 inch.

Loading

The initial temperature for all the layers is 125°F, and the plate is cooled to 25°F in increment 0. All elements, integration points and layers are given the same temperature. The INITIAL STATE and CHANGE STATE options are used to define this data.

Boundary Conditions

The edge x = 0, with nodes 1, 6, 11, 16, 21 are prescribed to have no x-displacement. Additionally, node 11 is constrained such that $u_y = u_z = \phi_x = \phi_y = 0$. This eliminates any rigid body motion. Note that if the material was isotropic, there would be free thermal expansion given these boundary conditions, and the stresses would be zero.

Material Properties

The plate is made of a single orthotropic material which is oriented differently between layers 1 and 2 and 3. First the ORTHOTROPIC option is used to define the material properties:

WWW

$E_{11} = 19.8 \times 10^9$	$\upsilon_{12} = .35$	$G_{12} = 70 \times 10^7$	$\alpha_{11} = .7 \times 10^{-5}$ in/in°F
$E_{22} = 19.8 \times 10^8$	$\upsilon_{23} = 0.0$	$G_{13} = 70 \times 10^7$	$\alpha_{22} = .23 \times 10^{-5}$ in/in°F
$E_{33} = 0$	$\upsilon_{31} = 0.0$	$G_{31} = 70 \times 10^7$	$\alpha_{33} = 0.0$

As element 75 has only two direct components of stress (NDI = 2), it is not necessary to define E_{33} and α_{33}. Since the element has three components of shear (in-plane and transverse), all values of G were entered. As $\upsilon_{23} = \upsilon_{31} = 0$, this is an odd material.

The base material orientation is given in the ORIENTATION block as being at 0° with respect to the 1-2 edge which will place it along the x-axis. The actual orientation is given in the COMPOSITE option as ply angles with respect to this base orientation.

The COMPOSITE option is used to define three layers, each of the same material but with thickness of 0.003, 0.0025 and 0.0025 inch. The stacking sequence is +45./0./0.

There are no temperature dependent effects in this example. If necessary, the ORTHO TEMP option would be used to enter this data.

Controls

The PRINT ELEM option is used to request that the stresses are output in both the conventional elements system and the local preferred system.

Results

The results indicate that the non-isotropic nature of the composite plate results in a generation of out-of-plane displacements as large as 0.05 inch and equivalent stresses as high as 1×10^6 psi.

Parameters, Options, and Subroutines Summary

Example e7x7.dat:

Parameters	Model Definition Options
ELEMENT	CHANGE STATE
END	COMPOSITE
SHELL SECT	CONNECTIVITY
SIZING	COORDINATE
TITLE	DEFINE
	END OPTION
	FIXED DISP
	INITIAL STATE
	ORIENTATION
	ORTHOTROPIC
	POST
	PRINT ELEM

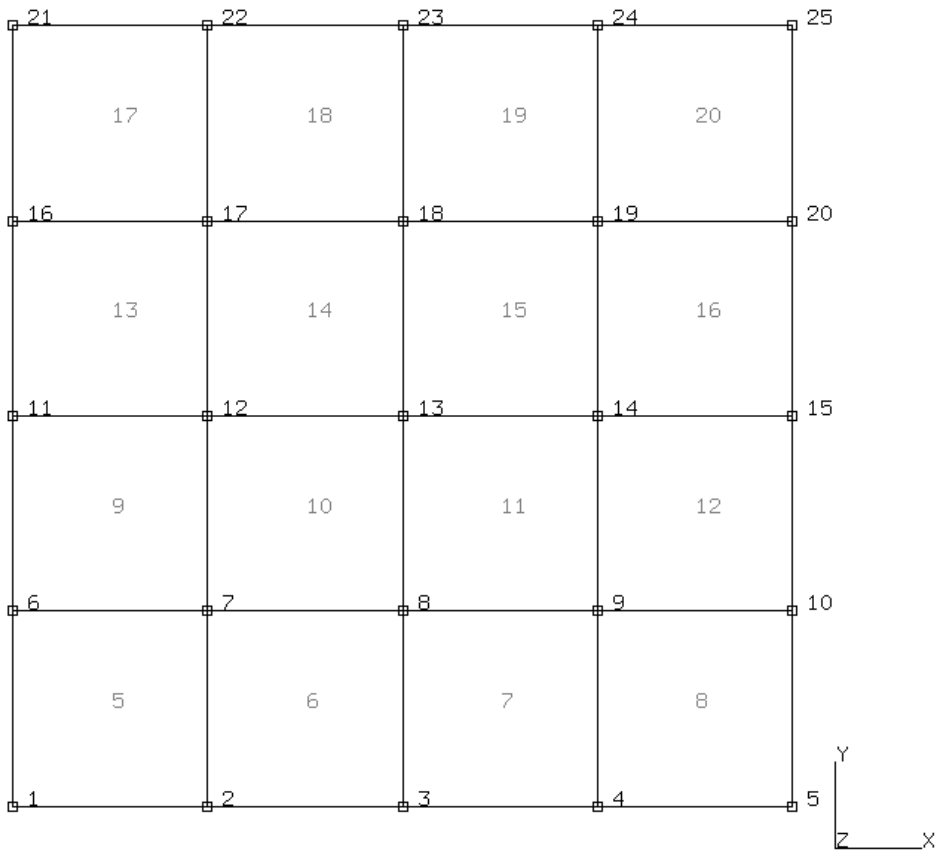

Figure 7.7-1 Plate Geometry and Mesh

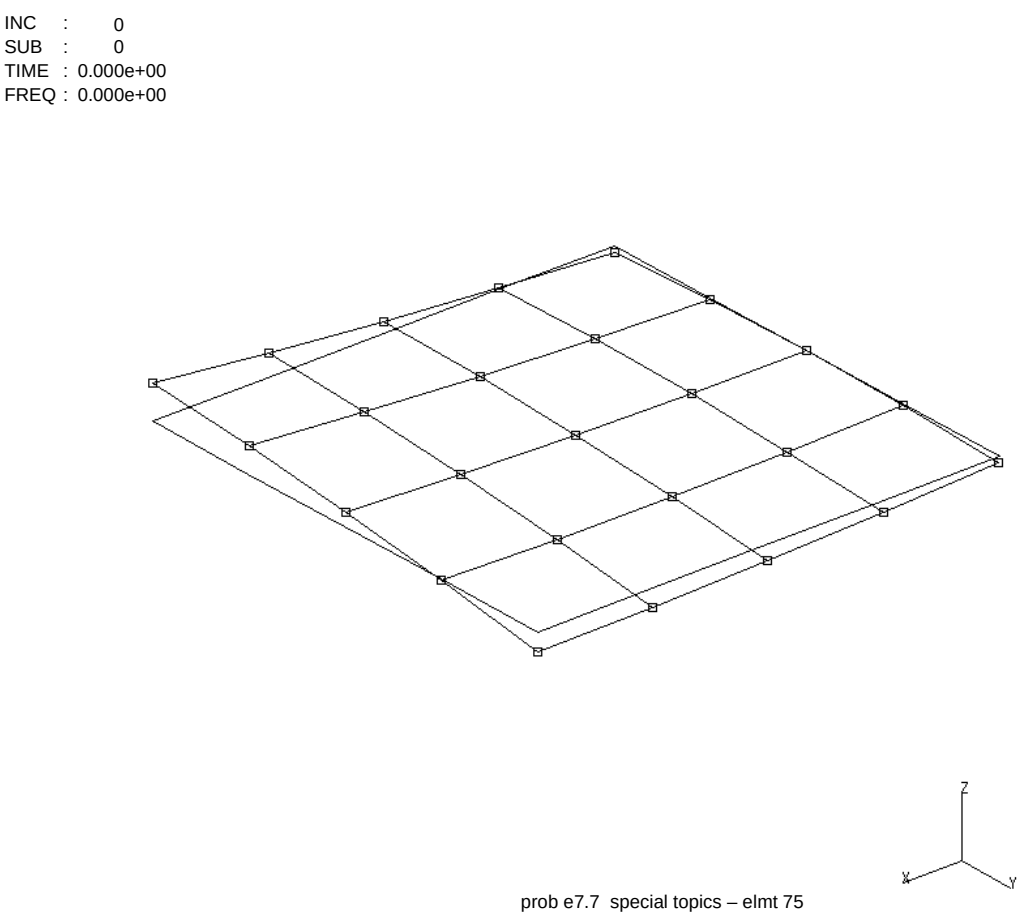

Figure 7.7-2 Displaced Mesh

7.8 Cylinder under External Pressure (Fourier Analysis)

A solid cylinder in plane strain with radius (a) and external pressure (p_o) is elastically analyzed. Love [1] gives the solutions to the first and second modes of this problem as follows:

$\sigma_{rr} = p_o\, r \cos\theta$

$\sigma\theta\theta = 3p_o\, r \cos\theta$

$\sigma_r\theta = p_o\, r \sin\theta$

for the first mode, and

$\sigma_{rr} = p_o \cos 2\theta$

$$\sigma_{\theta\theta} = p_o\left(\frac{2r^2 - a^2}{a^2}\right)\cos 2\theta$$

$$\sigma_{r\theta} = p_o\left(\frac{r^2 - a^2}{a^2}\right)\sin 2\theta$$

for the second mode. It should be noted that for the first mode, the condition $\sigma_{rr}(a) = p_o \cos\theta$ requires that $\sigma_r\theta(a) = p_0 \sin\theta$, where “a” is 1 inch. Two Fourier series are used for expansion of the 100 psi pressure loading. One series is for the cosine terms and the other for the sine terms. Three different methods, as shown in Problems e7-8a, e7.8b and e7.8c are demonstrated in describing the series. Comparison of the results with Love’s [1] exact solution is presented.

This problem is modeled using the three techniques summarized below.

Data Set	Element Type(s)	Number of Elements	Number of Nodes	Differentiating Features
e7x8a	62	10	53	Fourier coefficients input
e7x8b	62	10	53	Define nonsymmetric
e7x8c	52	10	53	User subroutine UFOUR

Element

Element type 62, the axisymmetric quadrilateral element for arbitrary loading, is used here. Details on this element are found in *MARC Volume B: User Input*.

Model

The geometry and mesh used are shown in Figure 7.8-1. The solid cylinder has a height of 0.1 inch and a radius of 1.0 inch. The mesh has 10 elements and 53 nodes.

Geometry

This option is not required for this problem.

Material Properties

The elastic material data assumed for this example is Young's modulus (E) is 30. x 10^6 psi and Poisson's ratio (ν) is 0.25.

Loading

The 100 psi external pressure is specified as a distributed load (IBODY=0) and associated with Fourier series number 1. The -100 psi shear is specified as a uniform load in the circumferential direction (IBODY=14) and associated with Fourier series number 2. Only element 10 is specified with the above loads using the DIST LOAD option.

Boundary Conditions

All nodes on the plane Z = 0. and Z = 0.1 are constrained in the axial direction such that only radial motion is permitted. Nodes 1, 2, and 3 on the plane R = 0 are also constrained in the radial direction due to symmetry.

Fourier

Three different ways are used to describe the series:

1. Specify the first two nonzero terms for series number 1 by evaluating the following integral:

$$a_n = \frac{1}{\pi}\int_o^{2\pi} \begin{pmatrix} \cos\theta \\ \cos 2\theta \end{pmatrix} \cos\, n\theta\, d\theta = \begin{cases} 0, \text{ all n except} \\ 1, \text{ n = 1, and 2} \end{cases}$$

   and the first nonzero term for series number 2 by evaluating the following integral:

$$b_n = \frac{1}{\pi}\int_o^{2\pi} \sin\,\theta\, \sin\, n\theta\, d\theta = \begin{cases} 0, \text{ all n except} \\ 1, \text{ n = 1} \end{cases}$$

2. Describe the function $F(\theta)$ which is to be expanded into a Fourier series by an arbitrary number (say 5) of $[\theta, F(\theta)]$ pairs of data.
3. Use user subroutine UFOUR to generate an arbitrary number of $[\theta,F(\theta)]$ pairs and let MARC calculate the Fourier series coefficients. Five pairs of $[\theta,F(\theta)]$ are defined in this example.

It should be pointed out that five pairs of [θ,F(θ)] have been chosen for demonstration only. It is easy to add more by changing the number 5 in the user subroutine UFOUR. An increased number of [θ,F(θ)] pairs would yield better results in comparison with the exact coefficient evaluations.

Results

The results for the radial and circumferential stresses of Problem e7.8a and Love's exact solution are plotted in Figure 7.8-2 and Figure 7.8-3. They indicate that the finite element solutions are in good agreement with the exact solutions.

Reference

Love, A.E.H., *A Treatise on the Mathematical Theory of Elasticity*, Dover, New York.

Parameters, Options, and Subroutines Summary

Example e7x8a.dat:

Parameters	Model Definition Options
ELEMENT	CONNECTIVITY
END	CONTROL
FOURIER	COORDINATE
SIZING	DIST LOADS
TITLE	END OPTION
	FIXED DISP
	FOURIER
	ISOTROPIC
	RESTART

Example e7x8b.dat:

Parameters	Model Definition Options
ELEMENT	CONNECTIVITY
END	CONTROL
FOURIER	COORDINATE
SIZING	DIST LOADS
TITLE	END OPTION
	FIXED DISP
	FOURIER
	ISOTROPIC
	RESTART

Example e7x8c.dat:

Parameters	Model Definition Options
ELEMENT	CONNECTIVITY
END	CONTROL
FOURIER	COORDINATE
SIZING	DIST LOADS
TITLE	END OPTION
	FIXED DISP
	FOURIER
	ISOTROPIC
	RESTART

User subroutine in u7x8c.f:

UFOUR

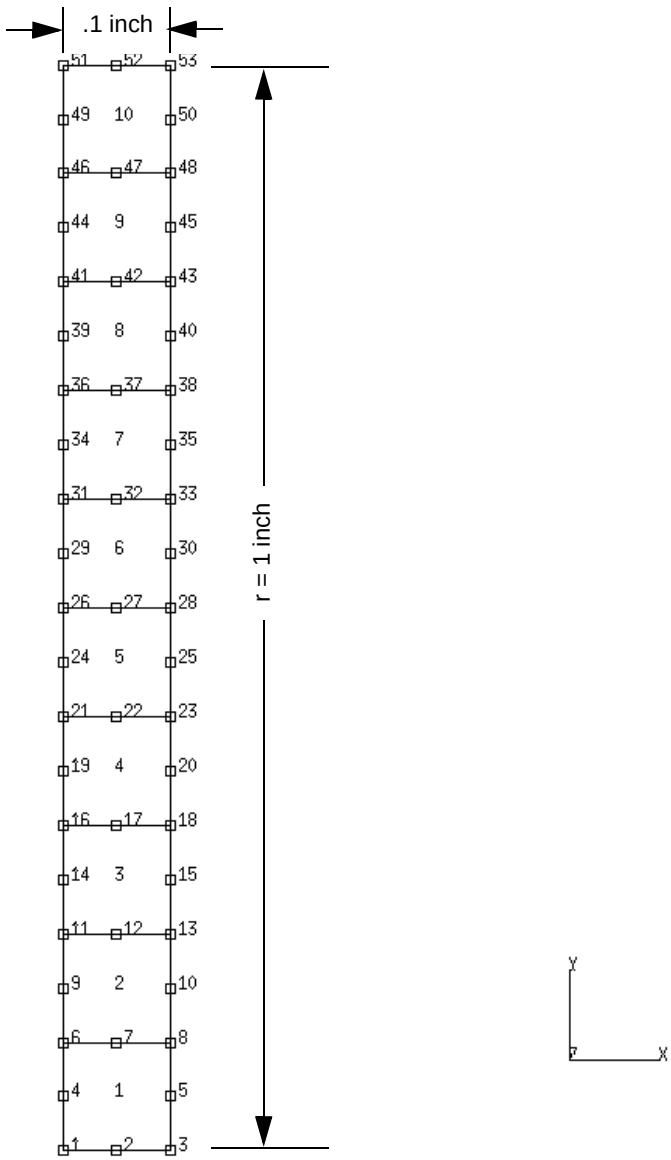

Figure 7.8-1 Cylinder and Mesh

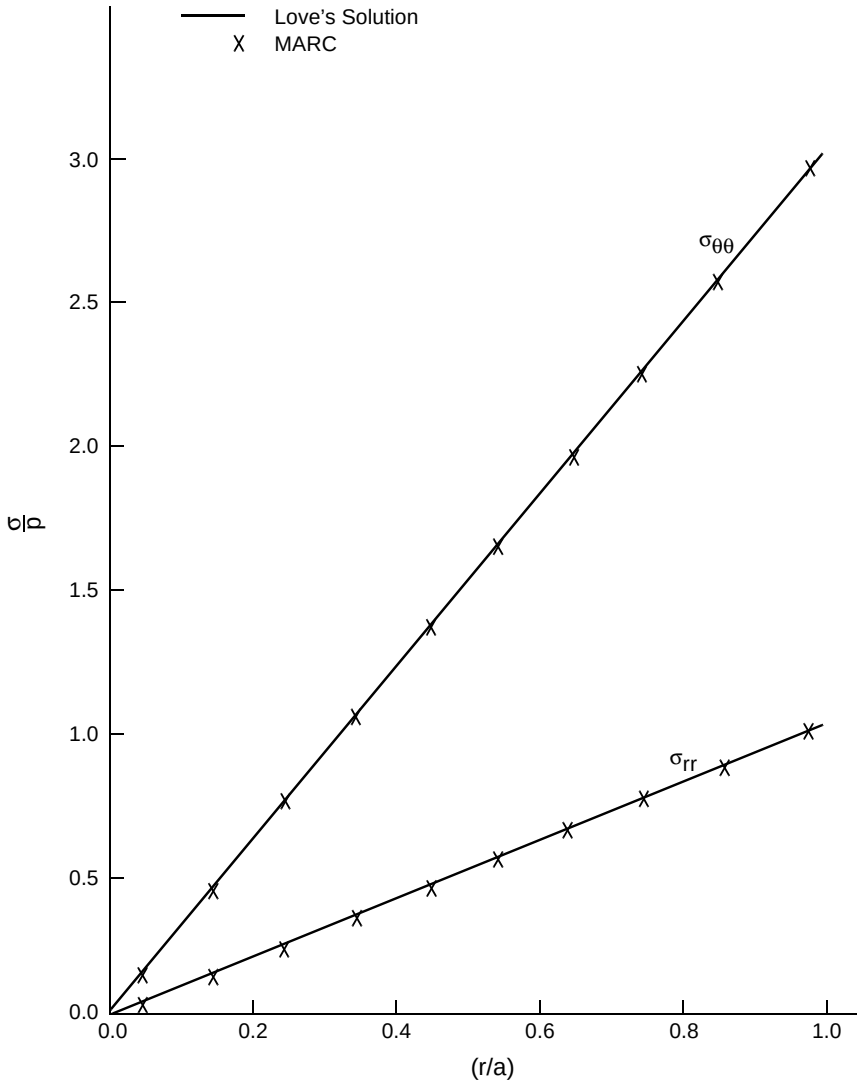

Figure 7.8-2 First Mode Solid Cylinder Plane Strain

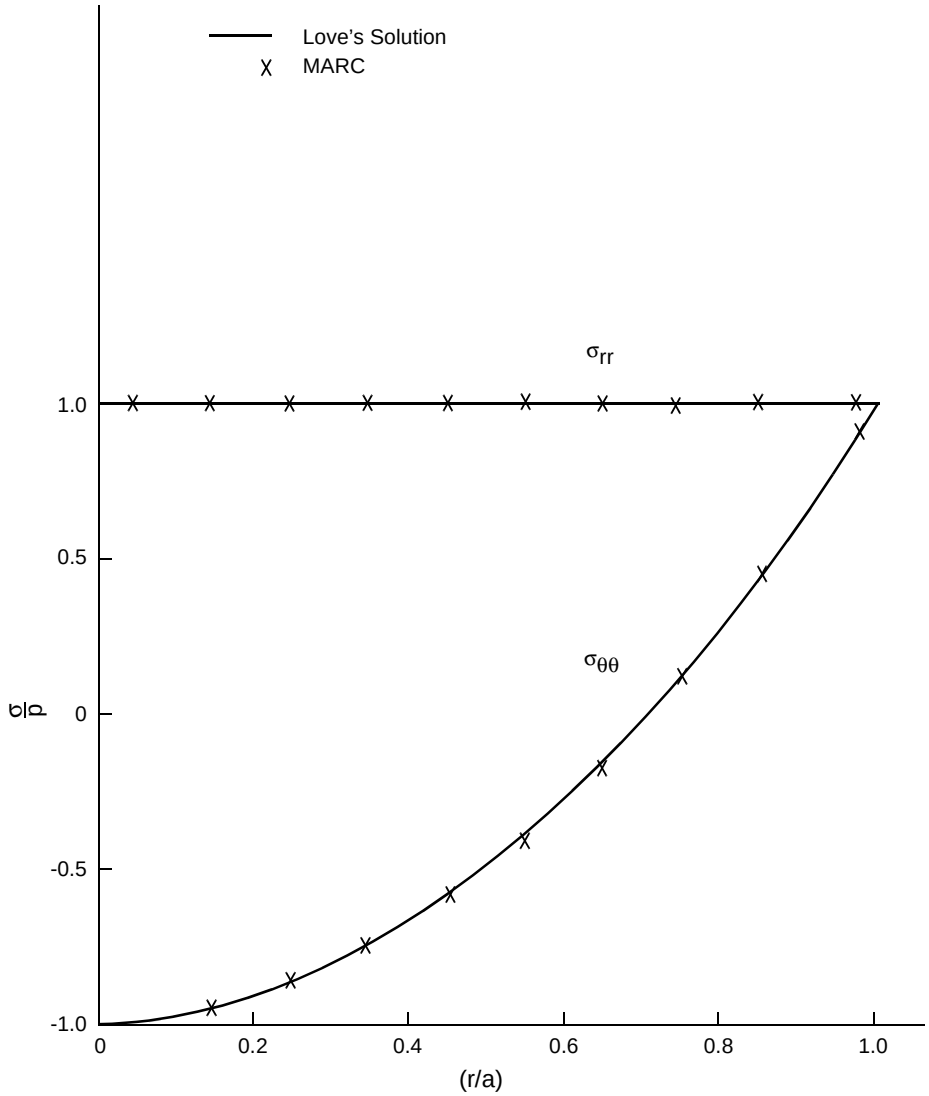

Figure 7.8-3 Second Mode Solid Cylinder Plane Strain

7.9 Cylinder under Line Load (Fourier Analysis)

A solid cylinder in plane strain with a concentrated line load acting across the diameter is elastically analyzed. One FOURIER series with only symmetric terms is used to characterize the circumferential variation of the loading. Two different methods are demonstrated in describing the FOURIER series (problems e7.9a and e7.9b). The CASE COMBIN option is used to obtain the final results by superposition at four equally spaced stations around the circumference in problem e7.9c.

This problem is modeled using the two techniques summarized below.

Data Set	Element Type(s)	Number of Elements	Number of Nodes	Differentiating Features
e7x9a	62	10	53	Specify Fourier Coefficients
e7x9b	62	10	53	User Subroutine UFOUR

Element

Element 62, the axisymmetric quadrilateral for arbitrary loading, is used here. Details on this element are found in *MARC Volume B: User Input*.

Model

The geometry and mesh are shown in Figure 7.9-1. The solid cylinder has a height of 0.1 inch and a radius of 1.0 inch. The mesh consists of 10 elements and 53 nodes.

Geometry

This option is not required for this problem.

Material Properties

The elastic material data assumed for this example is Young's modulus (E) of 30. x 10^6 psi and Poisson's ratio (ν) of 0.25.

Loading

The 100 pound line load acting across the diameter is specified as a distributed load (IBODY=0) on element 10 and associated with Fourier series number 1. The force magnitude given in the DIST LOAD block is equal to $100/\pi$.

Boundary Conditions

All nodes on the planes Z = 0. and Z = 0.1 are constrained in the axial direction such that only radial motion is permitted. Nodes 1, 2 and 3 on the plane R = 0 are also constrained in the radial direction due to symmetry.

Fourier

Two different methods are used to describe the series:

1. Specifying the first eight nonzero terms to approximate the infinite series representing the actual loading:

$$a_o = \frac{1}{2\pi}\int_0^{2\pi} P(\theta)\,d\theta = \frac{1}{\pi}$$

$$a_n = \frac{1}{\pi}\int_o^{2\pi} P(\theta)\cos n\theta\, d\theta = \begin{cases} 0, \text{ n-odd} \\ \frac{2}{\pi}, \text{ n-even} \end{cases}$$

2. Using user subroutine UFOUR generates an arbitrary number (say 361) of [θ,F(θ)] pairs and the program calculates the series coefficients. The results should compare closely with the above exact calculations. In this example, 6 function pairs are generated by the subroutine.

Results

Figure 7.9-2 gives a comparison of the radial displacements at θ = 0° predicted by this analysis with the exact solution of Muskhelishvili. For θ = 0°, a = 1.0 and ν = 0.25, the solution is:

$$u_r(\theta=0°) = \frac{1}{2\pi}\left[3\ln\frac{\left(1+\frac{r}{a}\right)}{\left(1-\frac{r}{a}\right)} - \frac{r}{a}\right]\frac{P(1+\nu)}{E}$$

The comparison is very good except at r ’ a. Here, the finite element solution cannot capture the singular behavior of the problem and falls below the unbounded exact solution.

Reference

Muskhelishvili, N. I., *Some Basic Problems of the Mathematical Theory of Elasticity*, translated by J.R.M. Radok, Erven P. Noordhoff, The Netherlands, 1963.

Parameters, Options, and Subroutines Summary

Example e7x9a.dat:

Parameters	Model Definition Options
ELEMENT	CONNECTIVITY
END	CONTROL
FOURIER	COORDINATE
SIZING	DIST LOADS
TITLE	END OPTION
	FIXED DISP
	FOURIER
	ISOTROPIC
	RESTART

Example e7x9b.dat:

Parameters	Model Definition Options
ELEMENT	CONNECTIVITY
END	CONTROL
FOURIER	COORDINATE
SIZING	DIST LOADS
TITLE	END OPTION
	FIXED DISP
	FOURIER
	ISOTROPIC
	RESTART

User subroutine in u7x9b.f:

UFOUR

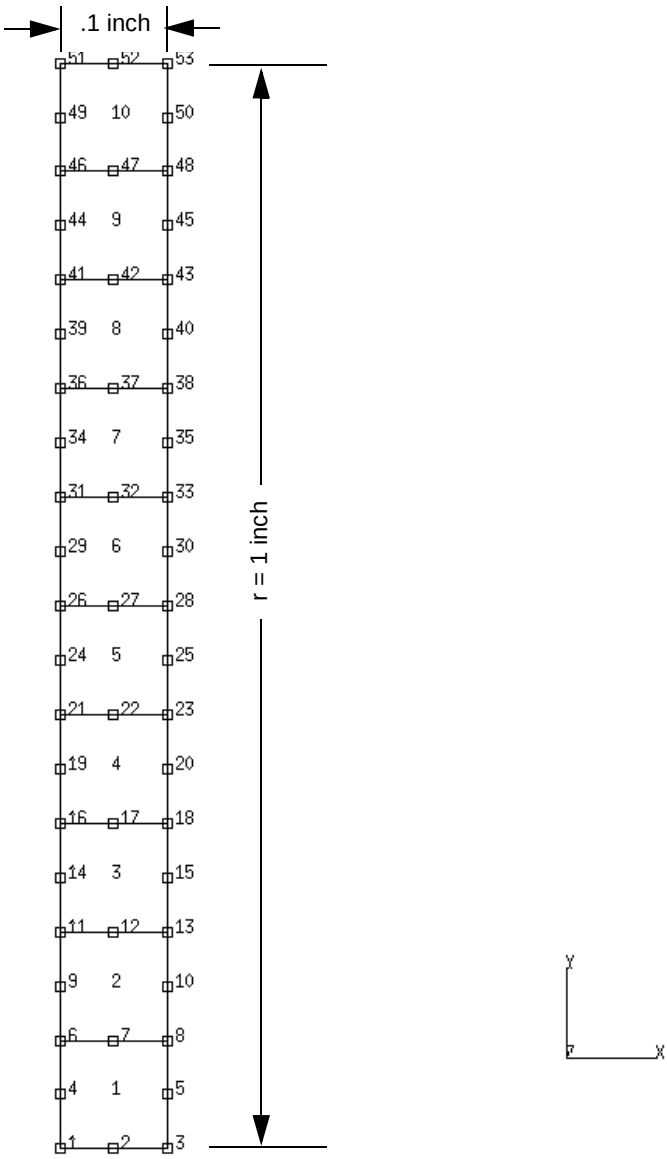

Figure 7.9-1 Cylinder and Mesh

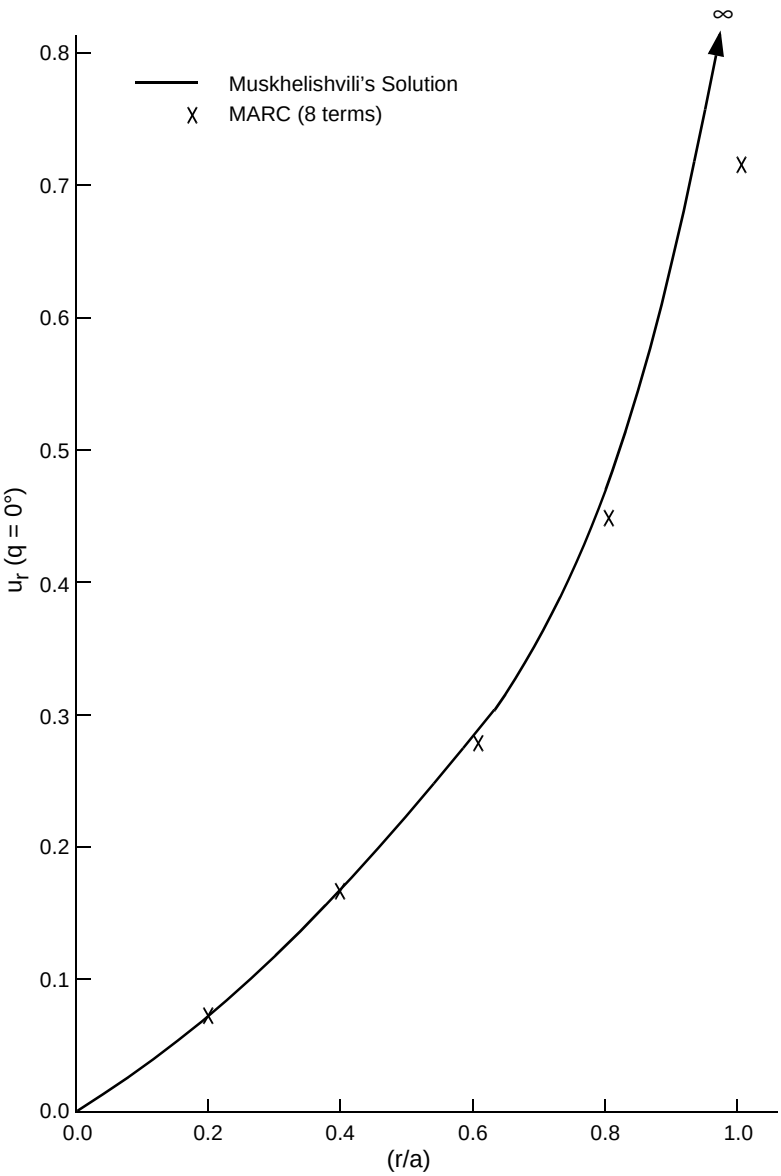

Figure 7.9-2 Concentrated Load on a Solid Cylinder

7.10 Mesh Qualification

This problem uses the QUALIFY option for mesh refinement studies. This option is invoked by adding the QUALIFY parameter. It is only applicable for the higher order isoparametric elements. The model and input data of the problem follow.

Model

A quarter of a square membrane structure is modeled using four 8-node quadrilateral elements type 27 (8-node plane-strain element). Dimensions of the model and a finite element mesh are shown in Figure 7.10-1.

Material Properties

The Young's modulus and Poisson's ratio of the membrane are assumed to be 10E6 psi and 0.3, respectively.

Loading

Two concentrated forces of equal magnitude are applied at the corner of the membrane (node 21). The forces are $F_x = F_y = 7.07$ pounds.

Boundary Conditions

Displacement at lines of symmetry are constrained (u = 0 at x = 0 and v = 0 at y = 0).

Geometry

The membrane thickness is 0.1 inch.

Results

Strain Energy Difference (SED) contours are shown in Figure 7.10-2. The large value in the corner implies that for this loading condition the mesh refinement should take place in the corner region of element number 4.

Parameters, Options, and Subroutines Summary

Example e7x10.dat:

Parameters	Model Definition Options
ELEMENT	CONNECTIVITY
END	COORDINATE
MESH PLOT	END OPTION
QUALIFY	FIXED DISP
SIZING	GEOMETRY
TITLE	ISOTROPIC
	POINT LOAD

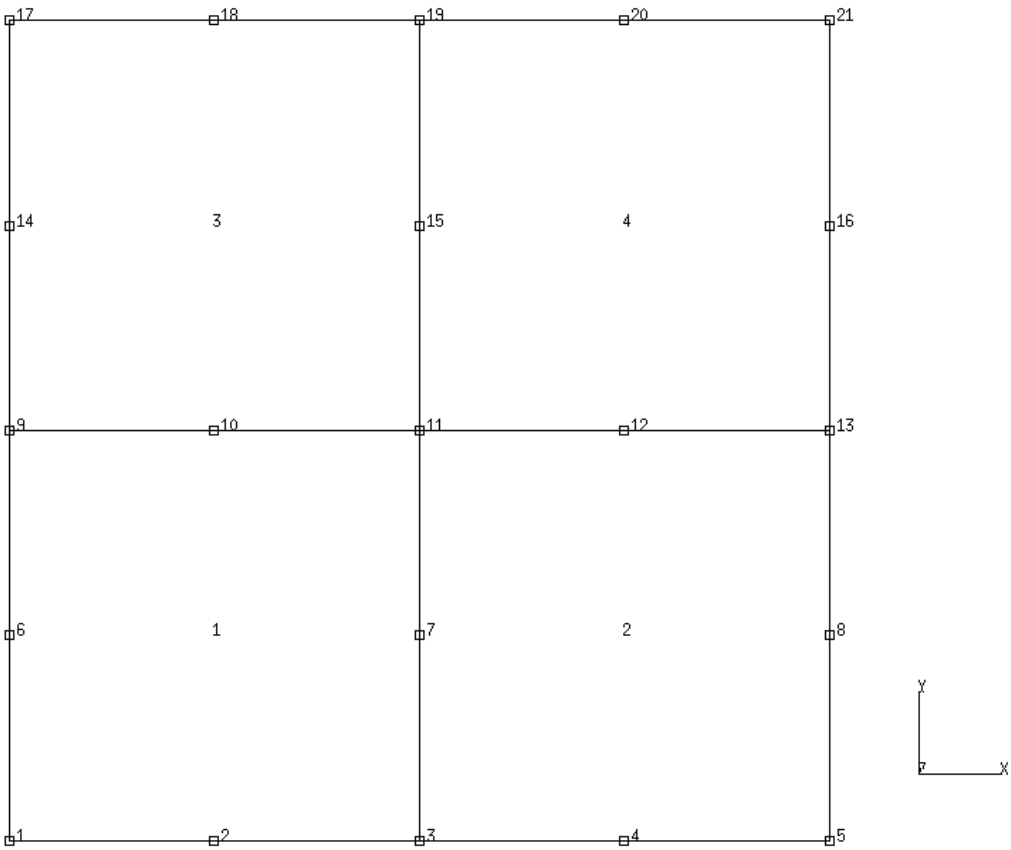

Figure 7.10-1 Membrane and Mesh

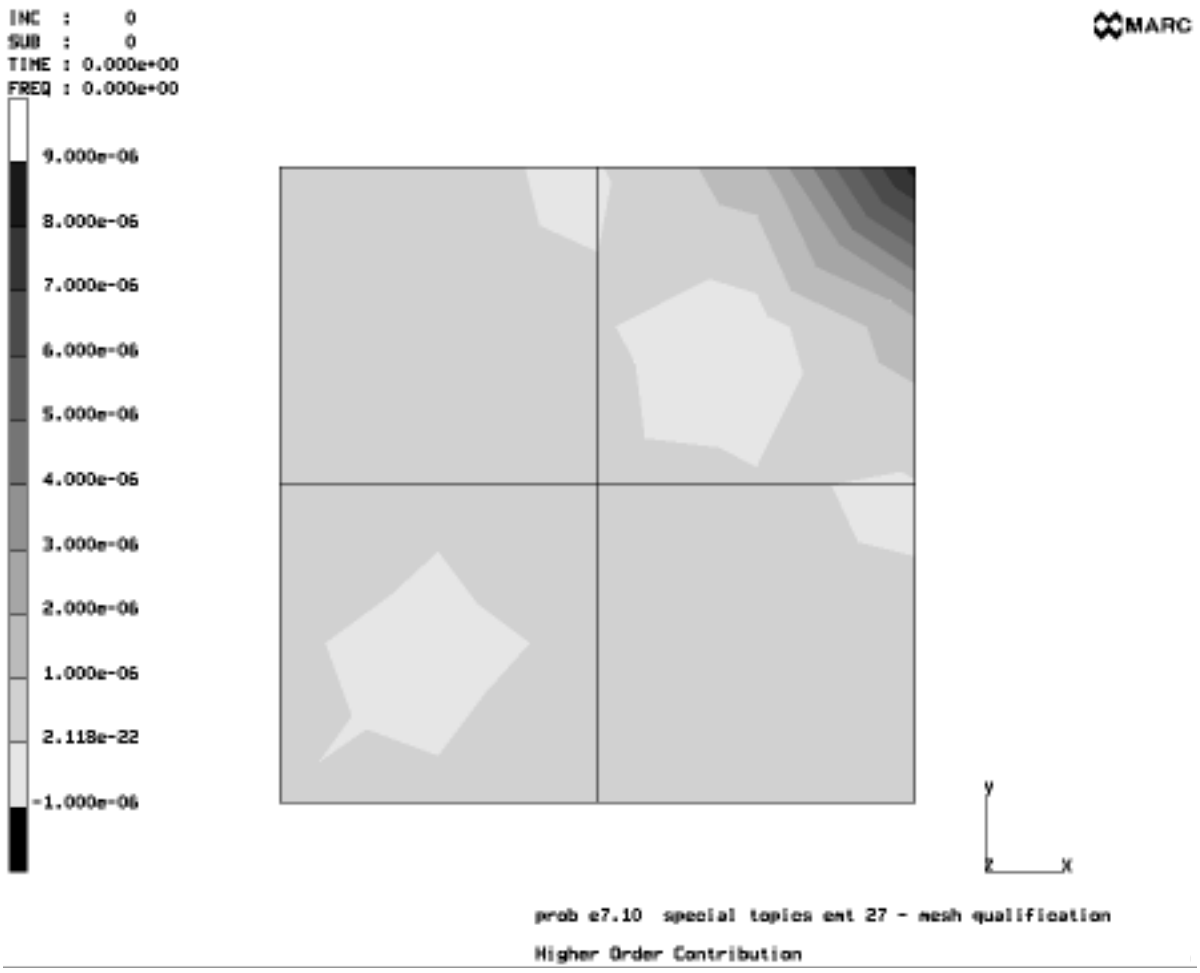

Figure 7.10-2 Strain Energy Difference

7.11 Concrete Beam under Point Loads

A simply supported concrete beam is subjected to two concentrated loads. The beam is analyzed using the concrete cracking option in MARC. Plane stress element (element type 3) is used for modeling the concrete and truss element (element type 9) is chosen for the simulation of steel reinforcement. The cracking option allows cracks to initiate in the concrete elements.

Model

The dimensions of the beam and the finite element mesh are shown in Figure 7.11-1. The model consists of 80 elements representing the concrete and 10 elements representing the steel.

Material Properties

The elastic-plastic material data is given through the ISOTROPIC option.

For concrete (Elements 1-80), material id of 1

E_c = 3.E6 psi

ν_c = 0.15

σ_{yc} = 1250 psi

For steel reinforcement (Elements 81-90), material id of 2

E_s = 3.E7 psi

ν_s = 0.3

σ_{ys} = 40,000 psi

For both the concrete and the rebars, an isotropic plasticity model is used. For the concrete elements the cracking flag is initiated.

Crack Data

The concrete (material id of 1) has an ultimate tensile stress of 700 psi. The shear retention factor is 0.5. The strain softening modulus is 365 psi.

Geometry

Thickness of the concrete beam 1.0 inch; area of the steel reinforcement = 0.1 square inch.

Loading

Two concentrated loads are symmetrically placed near the centerline of the beam. A total of 1175 pounds (2 x 587.5 pounds) is applied to the beam in 10 increments. Variable load increments, through the use of options POINT LOAD, PROPORTIONAL INCREMENT, and AUTO LOAD are:

Inc. No.	Load Increment
0	2 x 250
1	2 x 62.5
2	2 x 62.5
3	2 x 62.5
4	0.
5	2 x 50.
6	0.
7	2 x 50.
8	0.
9	2 x 50.

Boundary Conditions

Out-of-plane degrees of freedom are constrained for all nodal points (w = 0 for all nodes). Symmetry conditions are imposed along line x = 68 (u = 0 for nodes 29, 31, 33, 89, 91, 93, 95, 97, and 99). Simply-supported conditions are placed at node 1 (v = 0).

Results

A deformed mesh plot is shown in Figure 7.11-2. Cracking begins in increment 4 and the program begins to iterate. By increment 9, seven elements have developed cracks and the largest crack strain is about 0.034%. Figure 7.11-3 shows the final cracked region consisting of 14 elements near the bottom center portion of the beam.

Parameters, Options, and Subroutines Summary

Example e7x11.dat:

Parameters	Model Definition Options	History Definition Options
ELEMENT	CONNECTIVITY	AUTO LOAD
END	CONTROL	CONTINUE
SIZING	COORDINATE	POINT LOAD
TITLE	CRACK DATA	PROPORTIONAL INCREMENT
	END OPTION	
	FIXED DISP	
	GEOMETRY	
	ISOTROPIC	
	POINT LOAD	
	PRINT CHOICE	
	RESTART	

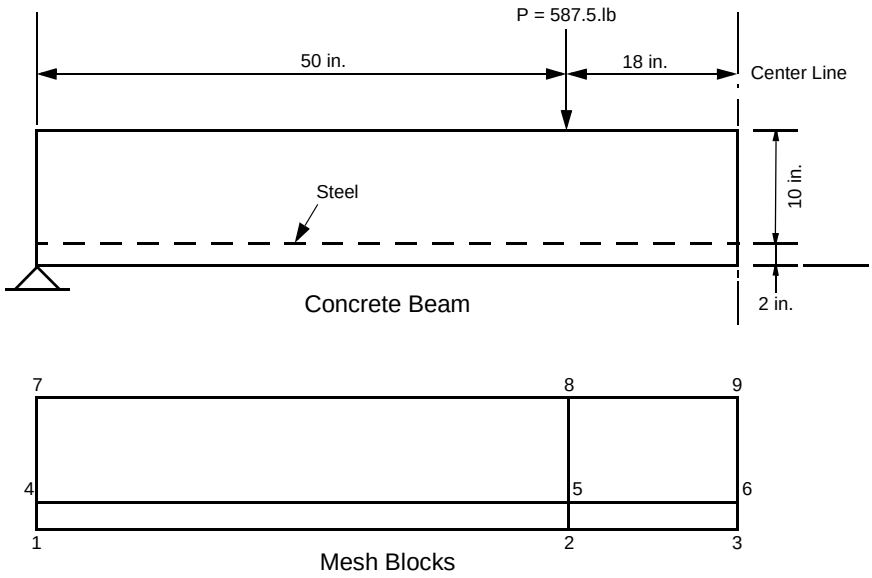

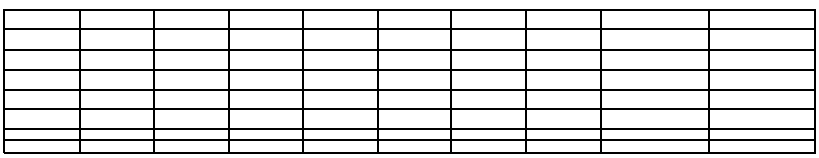

Figure 7.11-1 Concrete Beam and Mesh

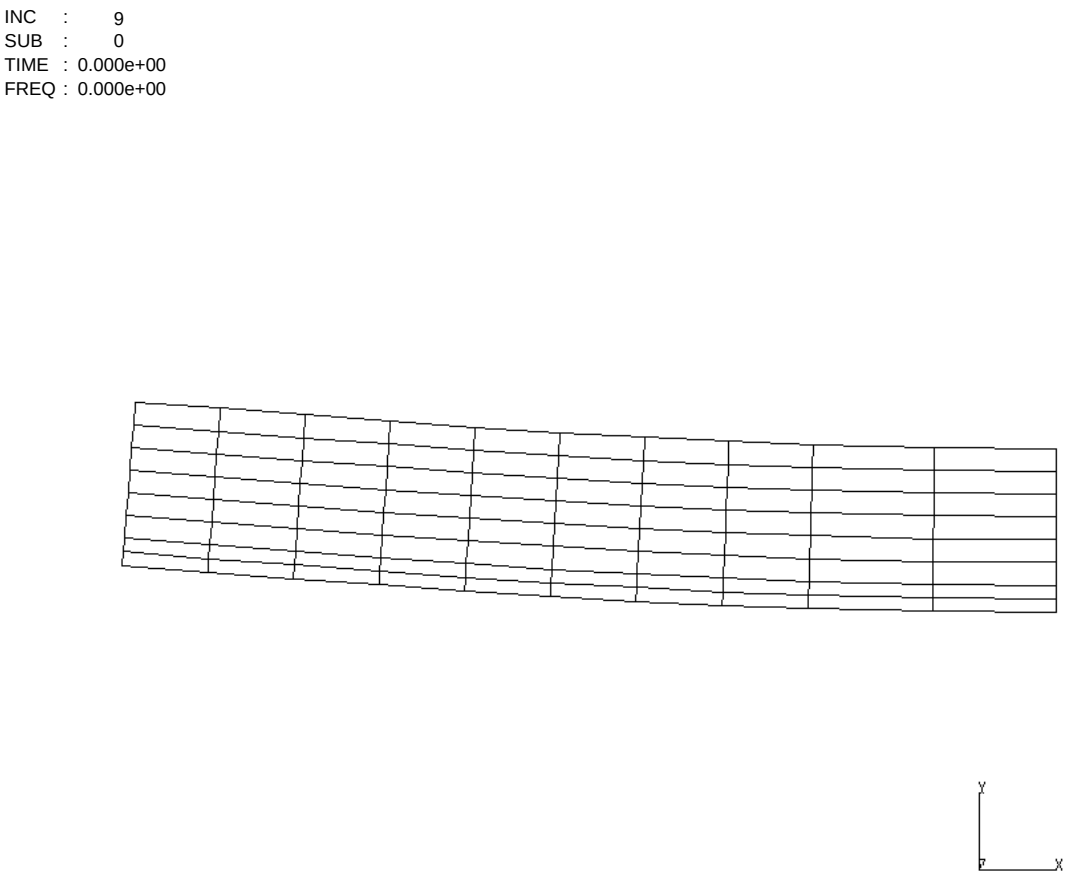

Figure 7.11-2 Deformed Mesh Plot

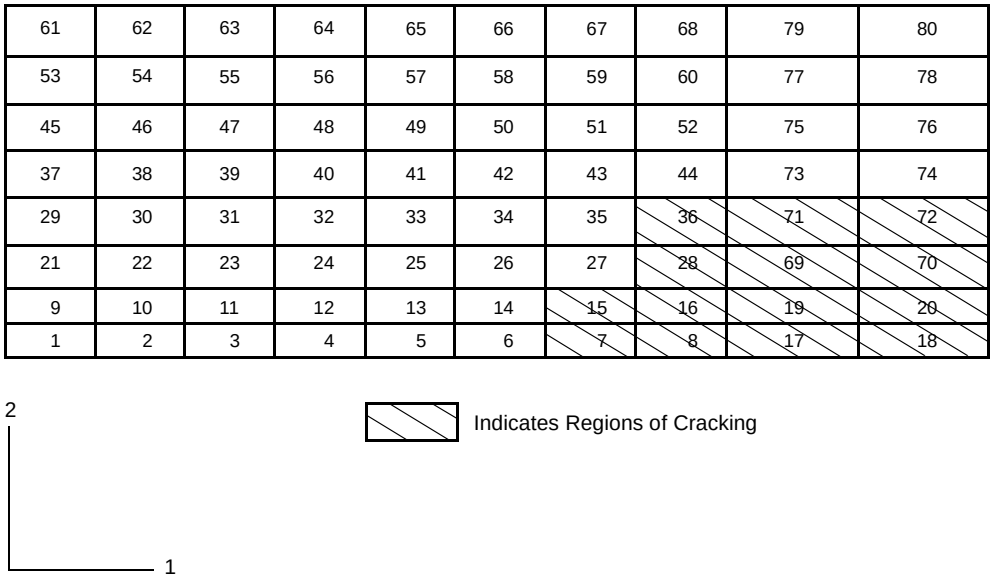

Figure 7.11-3 Regions of Cracking

7.12 Constant Uniaxial Stress Applied to Plate in Plane Strain (Viscoelasticity)

A viscoelastic rectangular plate (Figure 7.12-1) is subjected to a constant and uniform tensile stress of 10 psi in the x-direction. The deformation conforms to the plane strain idealization. The material is isotropic and strictly elastic in dilatational response. The bulk modulus is 20,000 psi. The time-dependent shear relaxation modulus is given as:

$$G(t) = 100 + 9900\, e^{-2.3979t} \quad \text{(psi)}$$

where the units of time are seconds. The displacements $u_i\,(x_i,t)$ are required as well as the out-of-plane stress, $\sigma_{zz}(t)$. The numerical results are compared to the closed form solution.

By converting the stress relaxation function defined above to a creep function, you obtain the creep function for isotropic shear behavior. The corresponding stress relaxation is:

$$J(t) = \left(1 \times 10^{-4}\right) + 9.9 \times 10^{-3}\,[1-\exp(-t/41.703)] \quad \text{sq.in/lb.}$$

The constant elastic dilatational response (bulk modulus, K) is now expressed in reciprocal form compatible with the creep function formulation.

This is:

$$B = \frac{1}{K} = 0.5 \times 10^{-4} \quad \text{sq.in/lb.}$$

Element

Element type 27 is used. This is an isoparametric distorted quadrilateral element for plane strain. There are two degrees of freedom at each node and four nodes per element.

Model

There are four elements and a total of 23 nodes as shown in Figure 7.12-2.

Geometry

The thickness is specified in EGEOM1 as 0.2 inch.

ISOTROPIC/VISCELPROP

The details of any viscoelastic material model are given in the model definition section. For an isotropic material, strictly elastic in dilatational response, the material characteristics can be completely represented by the model definition options ISOTROPIC and VISCELPROP.

Both the Young's modulus (E) and Poisson's Ratio (ν) are entered through the ISOTROPIC option. Recall that the expressions of shear modulus (G) and the bulk modulus (K) are:

$$G = \frac{E}{2(1+\nu)} \quad ; \quad K = \frac{E}{3(1-2\nu)}$$

By eliminating E, we obtain the expression of ν in terms of G and K as:

$$3\,(1-2\nu)\,K = 2\,(1+\nu)\,G$$

In the current problem, the bulk modulus K is equal to 20,000. The shear modulus G is equal to 10,000 [G(0) = 100 + 9900]. So, you obtain the values of ν = 0.2857 and E = 25714.

Rewrite the expression of time dependent shear relaxation modulus as:

$$G(t) = 100 + 9900\, e^{-(t/0.4170316)}$$
$$= G_0 + G_1 * e^{-(t/t_1)}$$

We have $G_1 = 9900$ and $\tau_1 = 0.4170316$ that are entered through the VISCELPROP option.

Loading

The execution of this analysis consisted of three parts. The application of the tensile 10 psi load was accomplished with the DIST LOADS block. The instantaneous elastic response was then determined in increment 0. This load was held constant for the duration of the analysis using a second DIST LOADS block after END OPTION with zero incremental load.

Subsequent to this, two creep stages were applied by means of the TIME STEP and AUTO LOAD history definition options. Knowledge of the closed form solution shows that most of the deformation and stress relaxation occurs in the first five seconds. Consequently, the suggested time step in the first TIME STEP block was specified as 0.1 second for a time span of 5.0 seconds. The number of increments was set at 50 and the time step was to remain fixed for all increments at the suggested value.

In the second TIME STEP load incrementation block, the constant time step size was increased to 4.0 seconds and 50 increments were requested to cover a span of 200 seconds.

It will be noted that the step size in the second creep stage is approximately one-tenth of the retardation time. This is more typical of the appropriate size which should be used in an analysis where no other characteristic times are present. Such other factors that might influence the choice of a time step are:

1. diffusional times for transient thermal analysis;
2. characteristic times associated with the application of external loads; or
3. the existence of a significant shift factor in the analysis of materials classified as being thermo-rheologically simple.

A series of different time step sizes might be used for different stages of an analysis where materials exhibit several characteristic relaxation or retardation times.

It was predetermined, with consideration of the closed form solution, that 100 increments would be sufficient to reach approximately to the steady state condition. A maximum value of 200 was entered in the CONTROL block. Tolerances and control limits for the analysis assume default values.

FIXED DISP

The unloaded face of the plate (x = 0) is fixed against displacement in the x-direction. The plane strain assumptions limit all displacements of the plate to the x-y plane.

Results

The exact solution for displacement of the end face, u_x (2,t), is plotted in Figure 7.12-3. The out-of-plane stress, σ_{zz}(t), is shown in Figure 7.12-4. The corresponding numerical results, obtained with MARC, are also plotted in these figures. The numerical results were found to be identical to the exact solution even at the point in the numerical analysis where the time step was changed from 0.1 seconds to 4.0 second.

Parameters, Options, and Subroutines Summary

Example e7x12.dat:

Parameters	Model Definition Options	History Definition Options
ELEMENT	CONNECTIVITY	AUTO LOAD
END	CONTROL	CONTINUE
SIZING	COORDINATE	DIST LOADS
TITLE	DIST LOADS	TIME STEP
	END OPTION	
	FIXED DISP	
	GEOMETRY	
	ISOTROPIC	
	PRINT CHOICE	
	TYING	
	VISCELPROP	

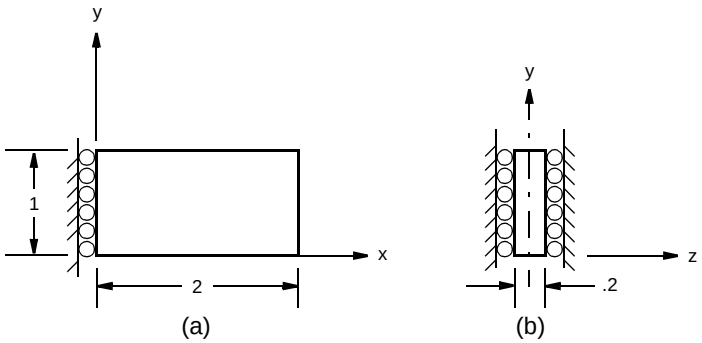

Figure 7.12-1 Geometry

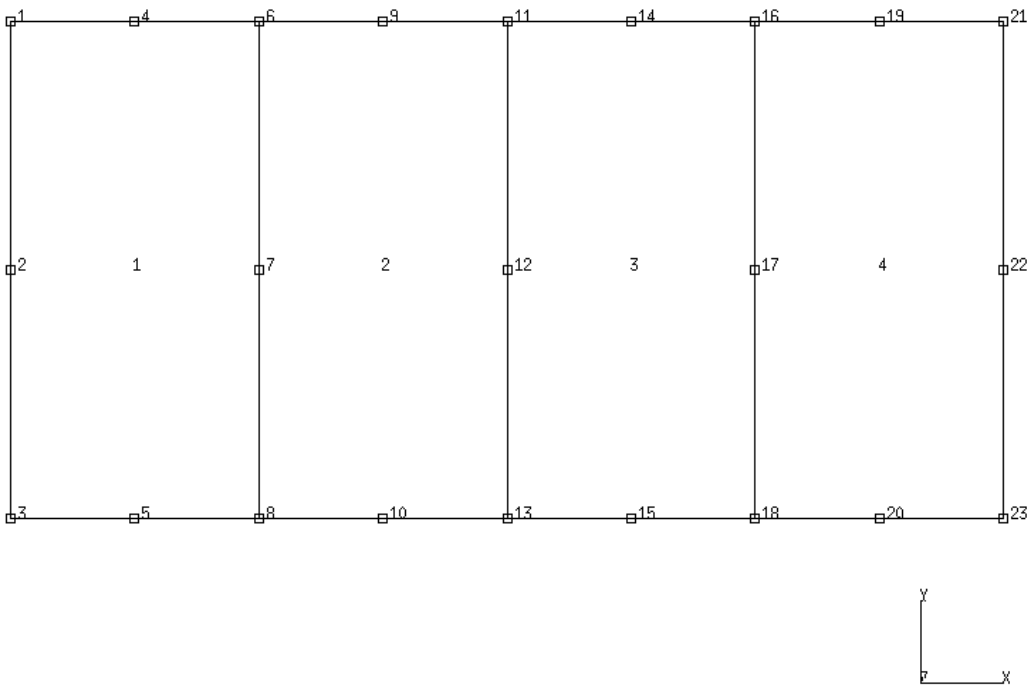

Figure 7.12-2 Finite Element Model

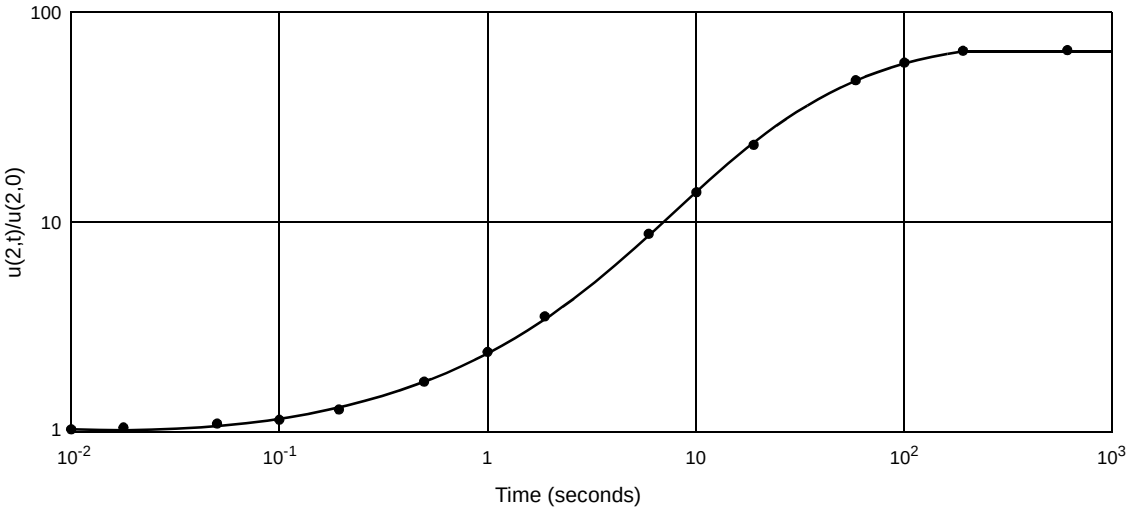

Figure 7.12-3 Normalized Displacement vs. Time

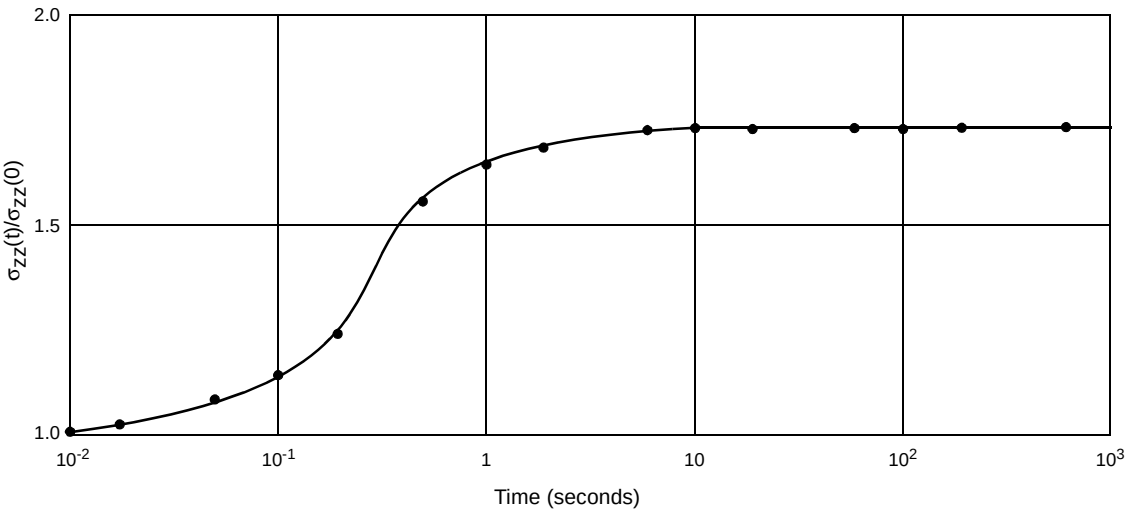

Figure 7.12-4 Normalized Out-of-Plane Stress, σ_{zz} vs. Time

7.13 Analysis of Pipeline Structure

MARC beam element type 14 and pipe-bend element type 17 are utilized for the elastic analysis of a pipeline structure subjected to either in-plane or out-of-plane bending. The structure is loaded until the limit load is reached. The pipeline mesh generation MARC-PIPE is used for the generation of CONNECTIVITY and COORDINATES data blocks as well as the tying data required for the use of element types 14 and 17.

Model

There are a total of 20 elements in the model, of which 6 are type 14 and 14 are type 17. A total of 26 nodes are used. The dimension of the pipeline structure and a finite element mesh are shown in Figure 7.13-1. MARC-PIPE is used for the mesh generation and the tying information.

Material Properties

The Young's modulus and Poisson's ratio of the pipeline material are 155.53×10^3 (ksi) and 0.3, respectively.

Tractions

An out-of-plane moment of 2.06×10^7 (in-kips) is applied at node 1 in the first analysis. As shown in Figure 7.13-1, the applied load is a moment about the y-axis (the fifth degree of freedom of node 1). The load is increased to a final load of 3.71×10^7 (in-kips) by increment 8. In the second analysis, an in-plane moment of 1.37×10^7 (in-kips) is applied at node 1. The applied load is about the z-axis (the sixth degree of freedom of node 1). The load is increased to a final load of 2.87×10^7 (in-kips) by increment 11.

Boundary Conditions

All degrees of freedom of node 26 are constrained for the fixed-end condition.

Geometry

The wall thickness and mean radius of the beam elements (element type 14) are:

For Elements 1, 2, 19, and 20:

Wall Thickness= 8.8 inches
Mean Radius = 275 inches

For Elements 3 and 18:

Wall Thickness= 10.4 inches
Mean Radius = 274.5 inches

For the pipe-bend elements (element type 17) the geometry data are:

Pipe thickness, t = 10.4 inches
The angular extent of the pipe-bend section, $\phi = 90°$
The radius to the center of the pipe in the r-z plane, R= 838.2 inches

MARC-PIPE

As shown in Figure 7.13-1 and in the MARC-PIPE input listing, the pipeline structure is subdivided into two straight and one curved segments for mesh generation. As a result, the number of joints and the number of sections on first card series are 4 and 3, respectively. Next, the two straight sections identified by nodal points 1-2 and 3-4, are further divided into three finite elements each, along the pipe direction. The input data for these two straight sections are:

				Subdivision
Section Number	Section Number	Node Numbers		Along the Pipe Direction
1	0	1	2	3
3	0	3	4	3

The curved portion of the pipeline structure, identified by nodes 2-3, is subdivided into 14 elements around the pipe cross section. There is no further subdivision along the pipe direction.

				Subdivision	
Section Number	Section Number	Node Numbers		Pipe Direction	Around Pipe Cross Section
2	1	2	3	1	14

Coordinates of Center of Curvature of the Curved Portion			
x	y	z	Pipe Radius
1500.0	838.2	0	274.2

Finally, the coordinates of the four joints are given below:

Joint Number	x	y	z
1	0	0	0
2	1500	0	0
3	2338.2	838.2	0
4	2338.2	2338.2	0

Connectivity, Coordinates and Tying Type

Since all three blocks of data are generated from MARC-PIPE, only the key word and the file number on which the data have been stored are required for the input.

Results

In both analyses, the load is scaled such that incipient yield occurs at increment 1. The loading was increased until the limit load was reached. This was due to an inability to obtain a convergent solution. At the limit load, plasticity had occurred through all 11 layers through the thickness of the elbow section. Figure 7.13-2 shows the load-displacement results of this analysis. The special pipe bend element (type 17) allows the analyst to examine the ovalization of the cross section of the pipe. Using the SECTIONING option in the plot description section, we can examine this effect. Figure 7.13-3 shows the ovalization due to the two types of loading conditions.

Parameters, Options, and Subroutines Summary

The data file used for MARC-PLOT is e7x13a.dat:

Example e7x13b.dat:

Parameters	Model Definition Options	History Definition Options
ELEMENT	CONNECTIVITY	AUTO LOAD
ELSTO	CONTROL	CONTINUE
END	COORDINATE	PROPORTIONAL INCREMENT
SCALE	END OPTION	
SIZING	FIXED DISP	
TITLE	GEOMETRY	
	ISOTROPIC	
	POINT LOAD	
	RESTART	
	TYING	

Example e7x13c.dat:

Parameters	Model Definition Options	History Definition Options
ELEMENT	CONNECTIVITY	AUTO LOAD
ELSTO	CONTROL	CONTINUE
END	COORDINATE	PROPORTIONAL INCREMENT
SCALE	END OPTION	
SIZING	FIXED DISP	
TITLE	GEOMETRY	
	ISOTROPIC	
	POINT LOAD	
	RESTART	
	TYING	

Example e7x13d.dat:

Parameters	Model Definition Options	History Definition Options
ELEMENT	BOUNDARY COUNDITIONS	CONTINUE
ELSTO	CONTROL	
END	END OPTION	
MESH PLOT	GEOMETRY	
SCALE	ISOTROPIC	
SIZING	POINT LOAD	
TITLE	RESTART	

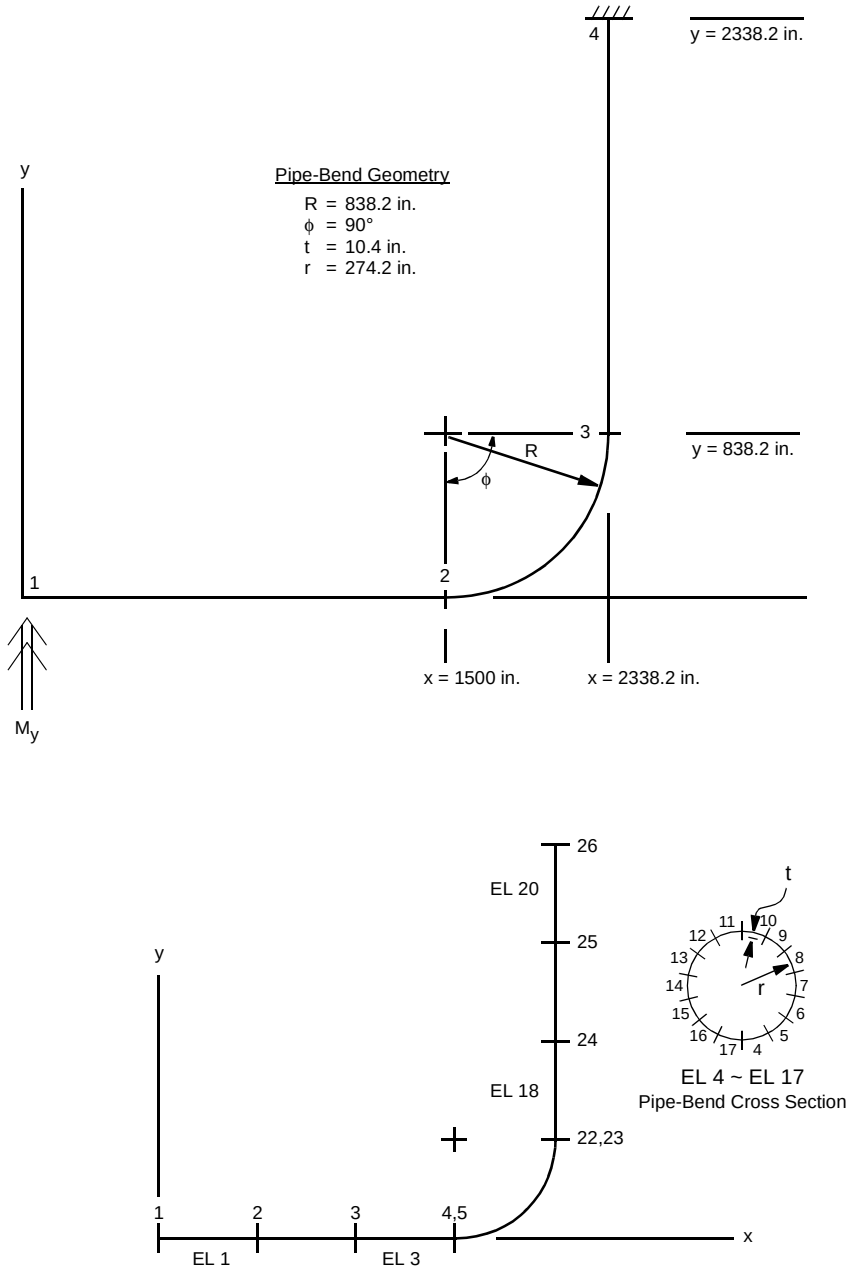

Figure 7.13-1 Pipe Line Geometry and Model

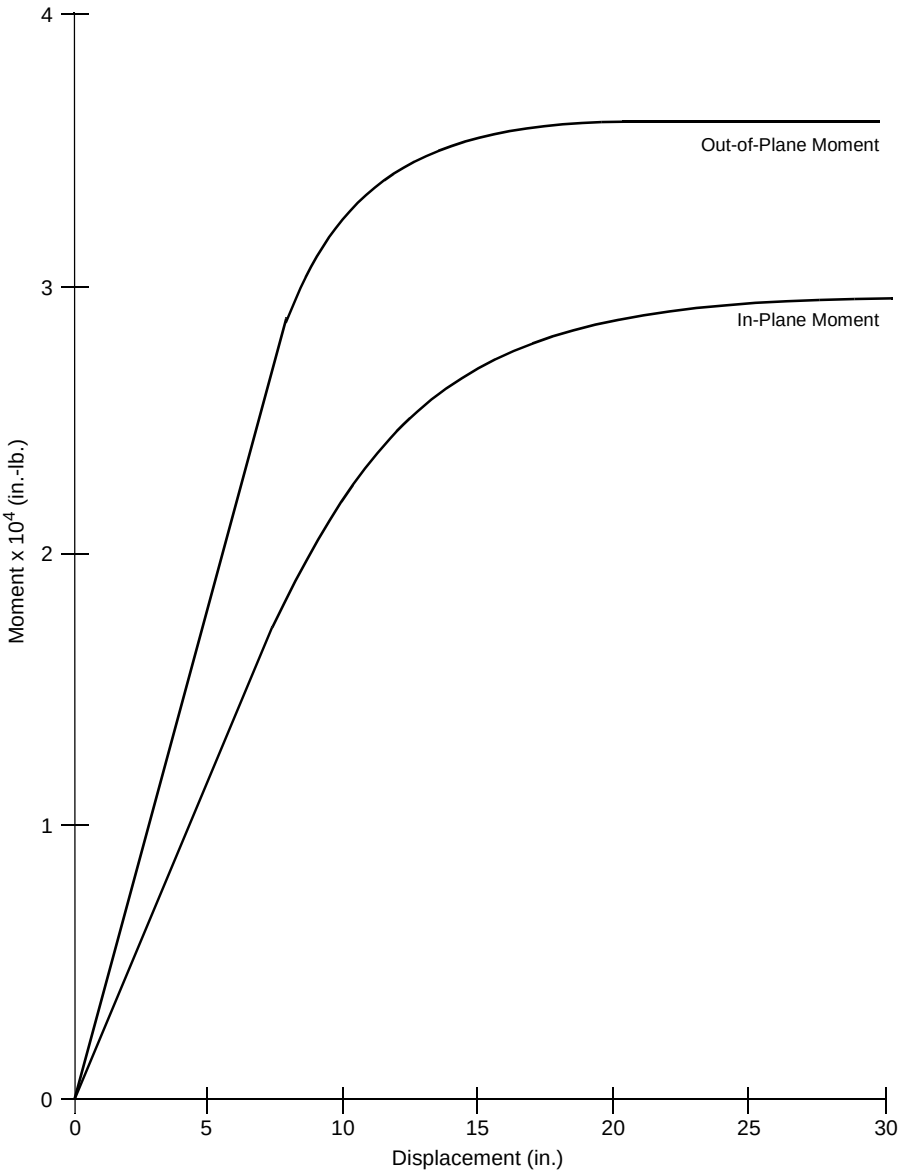

Figure 7.13-2 Load vs. Displacement

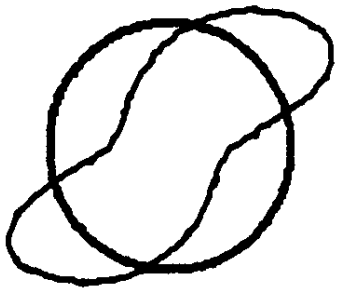

(a) Due to Out-of-Plane Moment

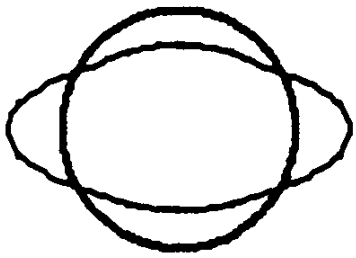

(b) Due to In-Plane Moment

Figure 7.13-3 Ovalization Behavior Due to Out-of-Plane and In-Plane Moments

7.14 Viscoelastic Analysis of an Externally Reinforced Thick-Walled Cylinder under Internal Pressure

A very long thick-walled cylinder (Figure 7.14-1) with an internal radius of 2 inches and an external radius of 4 inches is subjected to an internal pressure of 10 psi. The material is assumed to be isotropic and to be strictly elastic in dilatational response, having a constant bulk modulus of 10^5 psi. The time-dependent viscoelastic shear response is assumed to be represented by a simple Maxwell rheological model. A schematic diagram of such a model is shown in Figure 7.14-2. The constitutive representation in differential equation form can be expressed as:

$$A\frac{\partial S_{ij}}{\partial t} + BS_{ij} = \frac{\partial e_{ij}}{\partial t}$$

where S_{ij} is the deviatoric or shear component of stress and e_{ij} is the tensor component of the deviatoric or shear strain (that is, the engineering strain $\gamma_{ij} = 2\, e_{ij}$). The values of the coefficients A and B, which appear in the above expression, are those which were used by Lee et al. [1] and Zienkiewicz et al. [2] in their analyses of the same problem (i.e., $A = B = \frac{4}{3} \times 10^{-5}$).

A thin steel cylinder with an inner radius of 4 in. and thickness of 0.1212 in. is rigidly bonded to the outer surface of the viscoelastic cylinder. The Young's modulus for the steel casing is 30.0 x 10^6 and the Poisson's ratio is 0.3015. It is assumed that both cylinders are sufficiently long so that the deformation is considered to conform to the plane strain idealization with no axial motion.

We are interested in the time varying stresses within the inner viscoelastic cylinder. The numerical results are then compared to the closed form solution, which is readily obtained for this test case and developed in the following.

Constitutive Representation

The differential equation, which describes the shear response, can be re-expressed in the following form:

$$\frac{\partial s_{ij}}{\partial t}(\underset{\sim}{x}, t) + \frac{1}{\tau_1} S_{ij}(\underset{\sim}{x}, t) = G_1 \frac{\partial \gamma_{ij}}{\partial t}(\underset{\sim}{x}, t)$$

where the characteristic relaxation time, in this instance, is given by:

$$\tau_1 = \frac{A}{B} = 1$$

and the shear modulus amplitude is found to be:

$$G_1 = \frac{1}{2A} = 0.375 \times 10^5 \text{ psi}$$

In general, the expected form of the isotropic stress relaxation function in shear for the viscoelastic formulation is:

$$G(t) = G_\infty + \sum_{i=1}^{n} G_i \exp(-t/\tau_i)$$

where G_∞ is the final or steady state value of the shear modulus. For the simple Maxwell model under consideration, $G_\infty = 0$ and n = 1. Hence, $G(t) = G_1 \exp(-t/\tau_1) = 0.375 \times 10^5 \exp(-t)$.

Element

Element type 28 is an axisymmetric distorted quadrilateral element with six nodes and two degrees of freedom per node.

Model

Ten axisymmetric elements were used to represent the viscoelastic cylinder and one to represent the casing. The geometry of the cylinder and the obtained mesh are shown in Figure 7.14-3.

Geometry

No geometry input is necessary for this element.

ISOTROPIC/VISCELPROP

In this problem, the steel properties ($E = 30.0 \times 10^6$, $\nu = 0.3015$) are entered through the ISOTROPIC model definition option and the viscoelastic material properties are represented by the model definition options ISOTROPIC and VISCELPROP.

Both the Young's modulus (E) and the Poisson's ratio (ν) of the viscoelastic material are entered through the ISOTROPIC option. Recall that the expressions of shear modulus (G) and the bulk modulus (K) are:

$$G = \frac{E}{2(1+\nu)} \quad ; \quad K = \frac{E}{3(1-2\nu)}$$

By eliminating E, we obtain the expression of ν in terms of G and K as:

$$3(1-2\nu)K = 2(1+\nu)G$$

In the current problem, the bulk modulus K is equal to 10 and the shear modulus G is equal to $G(0) = 0.375 \times 10^5$. Thus, we obtain the values of $\nu = 0.333$ and $E = 1.0 \times 10^5$.

Rewrite the expression of time dependent shear relaxation modulus as:

$$G(t) = 0.375\, e^{-(t/1.0)}$$
$$= G_1 * e^{-(t/t_1)}$$

We have $G = 0.375$ and $\tau_1 = 1.0$ that are entered through the VISCELPROP option.

DIST LOADS

A 10 psi internal pressure is entered through DIST LOADS model definition option. An incremental load of 0.0 psi is entered after the END OPTION for ensuring a constant pressure during transient analysis.

TIME STEP/AUTO LOAD

A multi-step viscoelastic analysis is accomplished by including the TIME STEP/AUTO LOAD load incrementation block. In this analysis, a time step of 0.1 second is sufficiently small (that is, one-tenth of the relaxation time) to accurately determine the transient response. In addition, a total time span or period of 10.0 seconds (100 increments in AUTO LOAD option) is sufficient to reach approximately to the steady state condition. This analysis is performed with a constant time step. This is done for comparison of the numerical results with the closed form solution.

Results

Exact solutions of radially dependent stress distributions are plotted in Figure 7.14-4 and Figure 7.14-5. The numerical results are also shown in these figures. The agreement is excellent.

Figure 7.14-4 shows the radial compression stress at the outside (r = b), increasing gradually from about half the internal pressure to the full internal pressure for long durations of loading (compared with the relaxation time of the material in shear). This is associated with the relaxation of the shear strength of the cylinder material according to its Maxwell behavior (Figure 7.14-2), while constrained by the reinforcement. The shear strength relaxes to zero. In the limit, the viscoelastic material behaves as a liquid under uniform hydrostatic pressure ($\sigma_{rr} = \sigma\theta\theta = \sigma_{zz}$) of magnitude 10 psi, the internally applied value. The full internal pressure is finally transmitted to the reinforcement.

An analytical calculation of the circumferential stress in the casing accurately reflects the fact that this tension is directly proportional to the external radial compressive stress in the cylinder; that is,

$$\sigma^c_{\theta\theta} = \frac{-b}{t}\sigma_{rr}$$

Figure 7.14-5 shows that initial hoop tension occurs adjacent to the bore of the viscoelastic cylinder. The magnitude and sign of this stress depends on the stiffness of the reinforcement and the radius ratio, b/a. This circumferential tension changes to compression as the pressure is maintained, and the limit of uniform hydrostatic compression is reached when the shear strength has relaxed to zero.

It will be noted from the printout for this analysis that assembly of the overall stiffness matrix occurs only for the first three increments. Thereafter, only back-substitution is required to attain each incremental solution for this linear viscoelastic case. The effective incremental stress-strain matrix, $[G_{eff}]$, which is used to develop the overall stiffness matrix for the third and subsequent increments, was found to be:

$$[G_{eff}] = \left[[G_\infty] + \sum_{i=1}^{n} \frac{2\ \tau_i \beta_i(h_\varepsilon)[G_i]}{h} \right]$$

This form reflects the assumption of a linearly varying strain rate over each increment. However, the associated numerical procedure requires that the strain rates at the previous step are known. In the first viscoelastic step, this is not the case. In this increment, the assumption is made that the strain rate is constant. It can then be shown that the incremental stress for this first step is given by:

$$\Delta\sigma \Big|_{t=\Delta t} = \left[[G_\infty] + \sum_{i=1}^{n} \tau_1 [1 - \alpha_i(h_\varepsilon)][G_i] \right] \Delta\varepsilon \Big|_{t=\Delta t}$$

$$= -\sum_{i=1}^{n} [1 - \alpha_1(h_\varepsilon)]\sigma_i \Big|_{t=0^+}$$

where σ_i is the value of the state variable or stress supported by the i^{th} viscoelastic element in the generalized Maxwell model at the end of the instantaneous initial elastic step. It is given as:

$$(\sigma_i = G_\infty + G_i \cdot \varepsilon) \Big|_{t=0^+}$$

The increment in this variable for the first viscoelastic step is given as:

$$\Delta\sigma_i \Big|_{t=\Delta t} = -[1 - \alpha_i(h_\varepsilon)]\sigma_i \Big|_{t=0^+} + [1 - \alpha_i(h_\varepsilon)]G_i \frac{\Delta\varepsilon}{h} \Big|_{t=\Delta t}$$

In situations where there is a sudden and local sharp change in stress (for example, to an abrupt change in temperature in a thermo-rheologically simple solid), a few very small starting steps may be required. This minimizes the effect that any starting approximation error might have on the evaluation of the transient response and on the residual or steady state. For example, without such precautions, this type of error has been found to arise in the analysis of the tempering of thermo-rheologically simple glass sheets [3].

References

1. Lee, E. H., Radok, J. R. M., and Woodward, W. B., "Stress Analysis for Linear Viscoelastic Materials", *Trans. of the Society of Rheology*, Volume III, pp. 41-59 (1959).
2. Zienkiewicz, O. C., Watson, M. and King, I. P., "A Numerical Method of Visco-Elastic Stress Analysis", *Int. J. Mech. Sci*., Vol. 10, pp. 807-827 (1968).
3. Narayanaswamy, O. S. and Gardon, R., "Calculation of Residual Stresses in Glass", *Journal of the American Ceramic Society*, Volume 52, No. 10, pp. 554-558 (1969).

Parameters, Options, and Subroutines Summary

Example e7x14.dat:

Parameters	Model Definition Options	History Definition Options
ELEMENT	CONNECTIVITY	AUTO LOAD
END	CONTROL	CONTINUE
SIZING	COORDINATE	DIST LOADS
TITLE	DIST LOADS	TIME STEP
	END OPTION	
	FIXED DISP	
	ISOTROPIC	
	PRINT CHOICE	
	VISCELPROP	

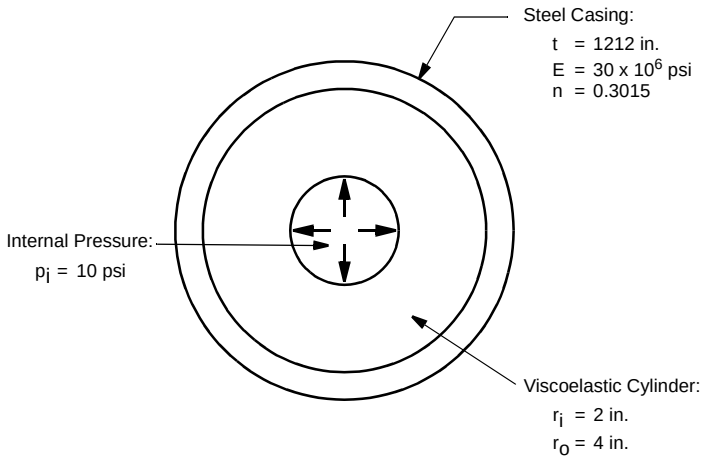

Figure 7.14-1 Long Thick-Walled Cylinder

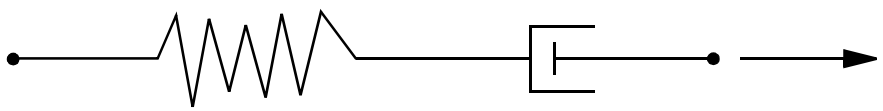

Figure 7.14-2 Simple Maxwell Model

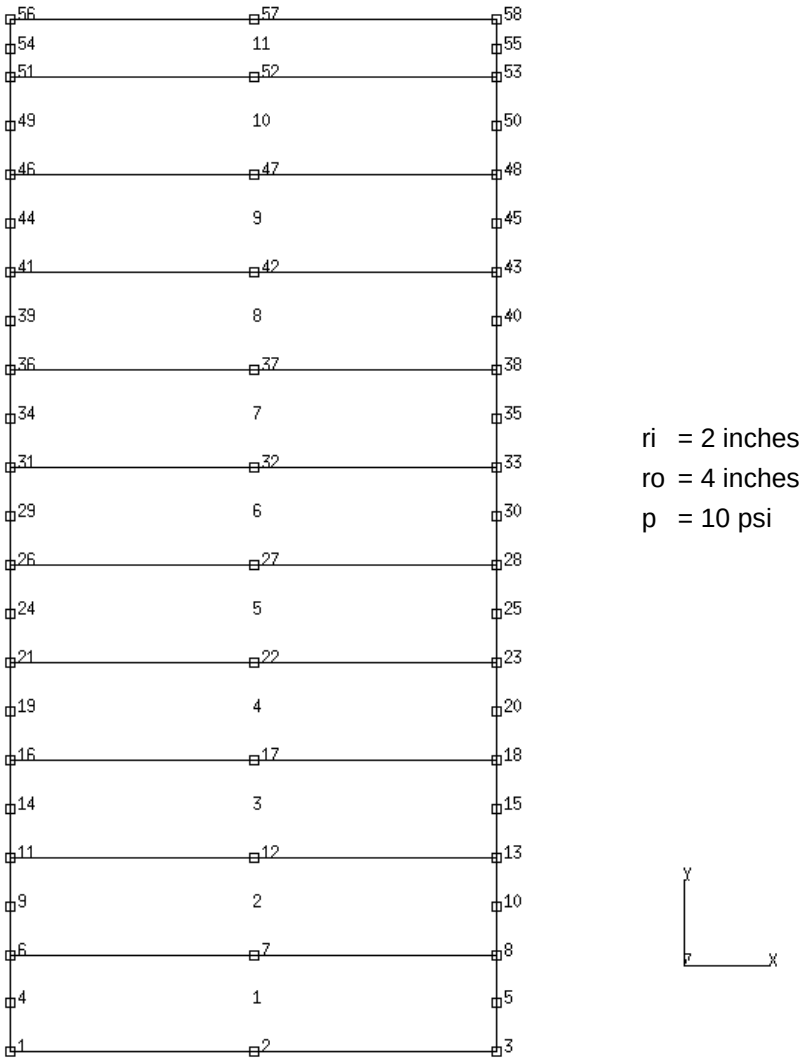

Figure 7.14-3 Finite Element Model

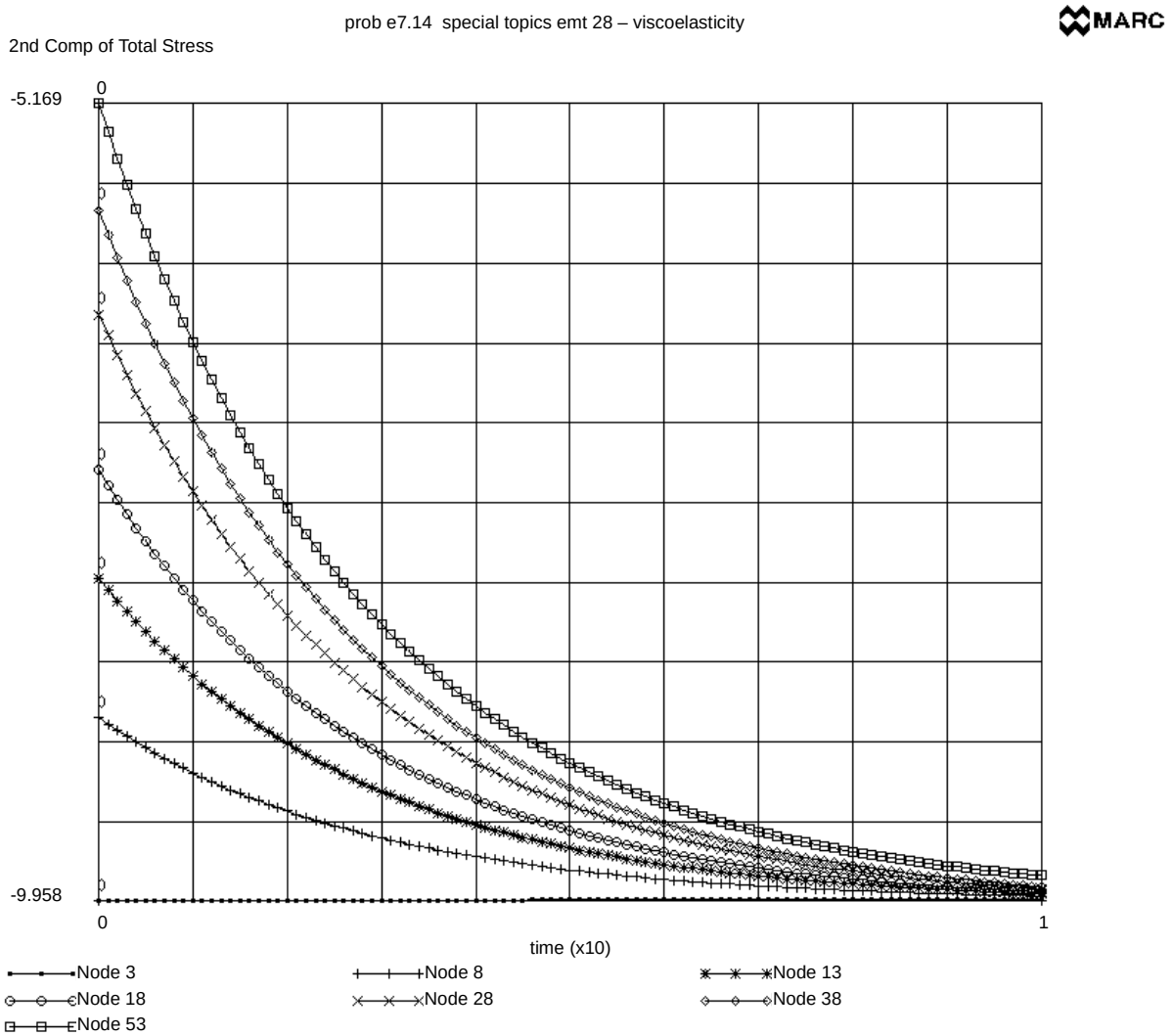

Figure 7.14-4 Radial Stress vs. Time

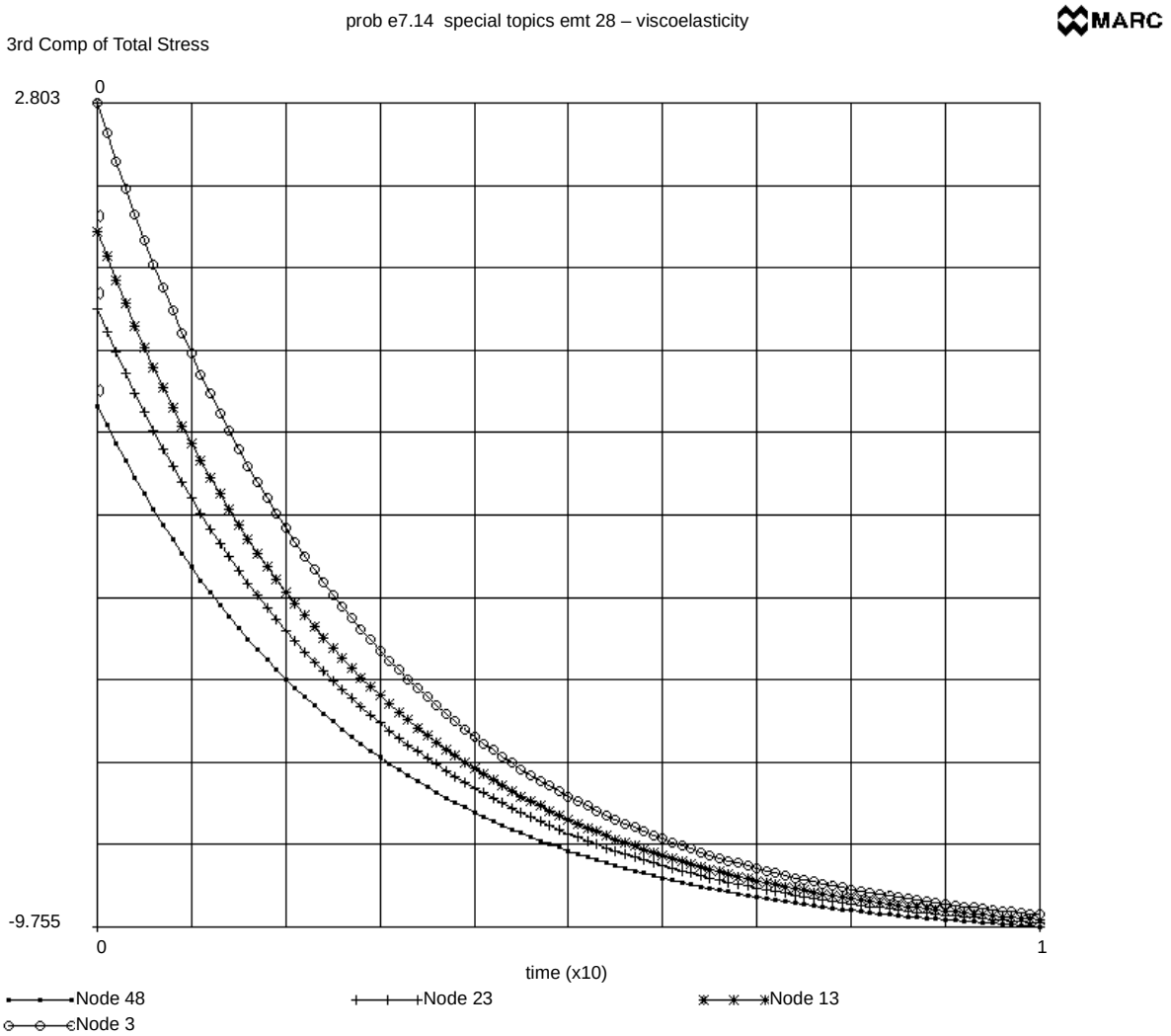

Figure 7.14-5 Hoop Stress vs. Time

7.15 Spiral Groove Thrust Bearing with Tilt

A spiral groove thrust bearing with tilt is analyzed to demonstrate the treatment of discontinuous film profiles as a result of the presence of grooves.

Element

Element type 37 is an arbitrary planar 3-noded triangular element chosen to model the lubricant.

Model

Problem details and the element mesh are shown in Figure 7.15-1. The dotted areas represent the lubricant grooves. The geometric specifications are as follows:

$h_2 = 30 \times 10^{-6}$ m

$h_3 = 15 \times 10^{-6}$ m

$h_0 = 96.774 \times 10^{-6}$ m

$r_1 = 75 \times 10^{-3}$ m

$r_2 = 150 \times 10^{-3}$ m

Due to the tilt of the longitudinal axis, the position with the smallest film thickness occurs on the axis X = 0 at the maximum Y-value. A total number of five spiral grooves has to be modeled. The required element mesh is generated by specifying a subset of nodal coordinates and elemental connectivities which subsequently are being used in user subroutines UFXORD and UFCONN to generate the complete mesh.

Thickness Field

The circumferential variation of the lubricant profile is specified per node in user subroutine UTHICK based on the nodal coordinates. In addition, user subroutine UGROOV is used to specify the contribution from the grooves to the total lubricant thickness.

Velocity Field

The relative velocity of the lubricant at the rotor surface, with respect to the grooved stationary part, is specified in user subroutine UVELOC. The angular velocity equals 100 rpm.

Material Properties

Viscosity of 0.020 N-sec/m^2 and density of 800 kg/m^3 are assumed.

Boundary Conditions

Atmospheric pressure is applied at the outer radius. It is assumed that a constant pressure occurs at the internal oil chamber. For this reason, all nodes on the inner radius are tied.

Results

Pressure distribution is calculated in increment 0. In addition, the resulting load-carrying capacity is determined by integrating the pressure distribution over the grooved surface. This results in a bearing force of:

$F_x = 0$ N

$F_y = 0$ N

$F_z = 23.714 \times 10^3$ N

The calculated bearing moment components with respect to the center of the thrust bearing are:

$M_x = 129.3$ Nm

$M_y = -70.6$ Nm

$M_z = 0.0$ Nm

Based on these results, the position of the resulting bearing force can be determined. If the coordinates of this point are denoted by (X_0,Y_0), it follows that:

$$X_0 = -\frac{M_y}{F_Z} = 2.997 \times 10^{-3}\text{m}$$

$$Y_0 = \frac{M_x}{F_z} = 5.4521 \times 10^{-3}\text{m}$$

The so-called attitude angle, which is the angle between the point (X_0,Y_0) and the Y-axis equals:

$$\arctan\frac{X_0}{Y_0} = \arctan\frac{M_y}{M_x} = 28.6 \text{ degrees}$$

Since the integration of the pressure distribution was only performed over the grooved surface, the contribution from the oil chamber has to be added. In addition, the contribution from the atmospheric pressure has to be subtracted.

A vector plot of the mass fluxes is shown in Figure 7.15-2. This yields for the actual vertical bearing force component:

$$F^*_z = F_z + \overline{Y}(r_1^2 P_{ch} - r_2^2 P_{at}) = 25.83\ 10^{-3}\ \text{N}$$

where $P_{ch} = \text{N/m}^2$.

Parameters, Options, and Subroutines Summary

Example e7x15.dat:

Parameters	Model Definition Options	History Definition Options
ELEMENT	CONNECTIVITY	AUTO LOAD
END	CONTROL	CONTINUE
SIZING	COORDINATE	DIST LOADS
TITLE	DIST LOADS	TIME STEP
	END OPTION	
	FIXED DISP	
	ISOTROPIC	
	PRINT CHOICE	
	VISCELPROP	

User subroutines in u7x15.f:

UFXORD
UFCONN
UTHICK
UVELOC
UGROOV

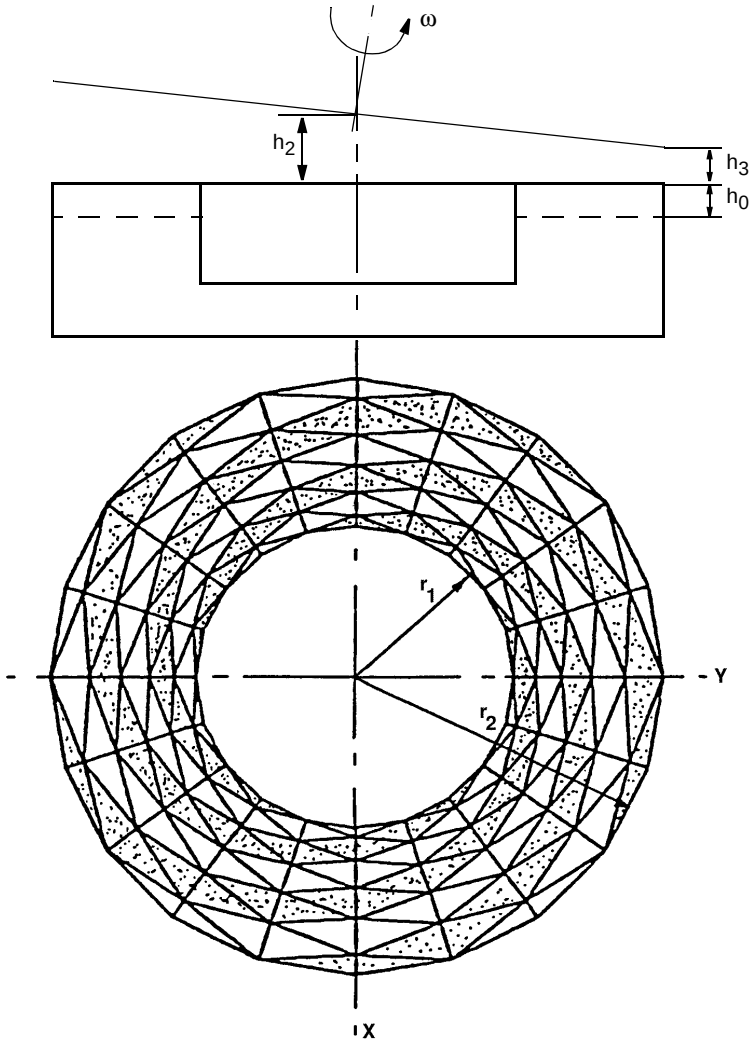

Figure 7.15-1 Spiral Groove Thrust Bearing with Tilt

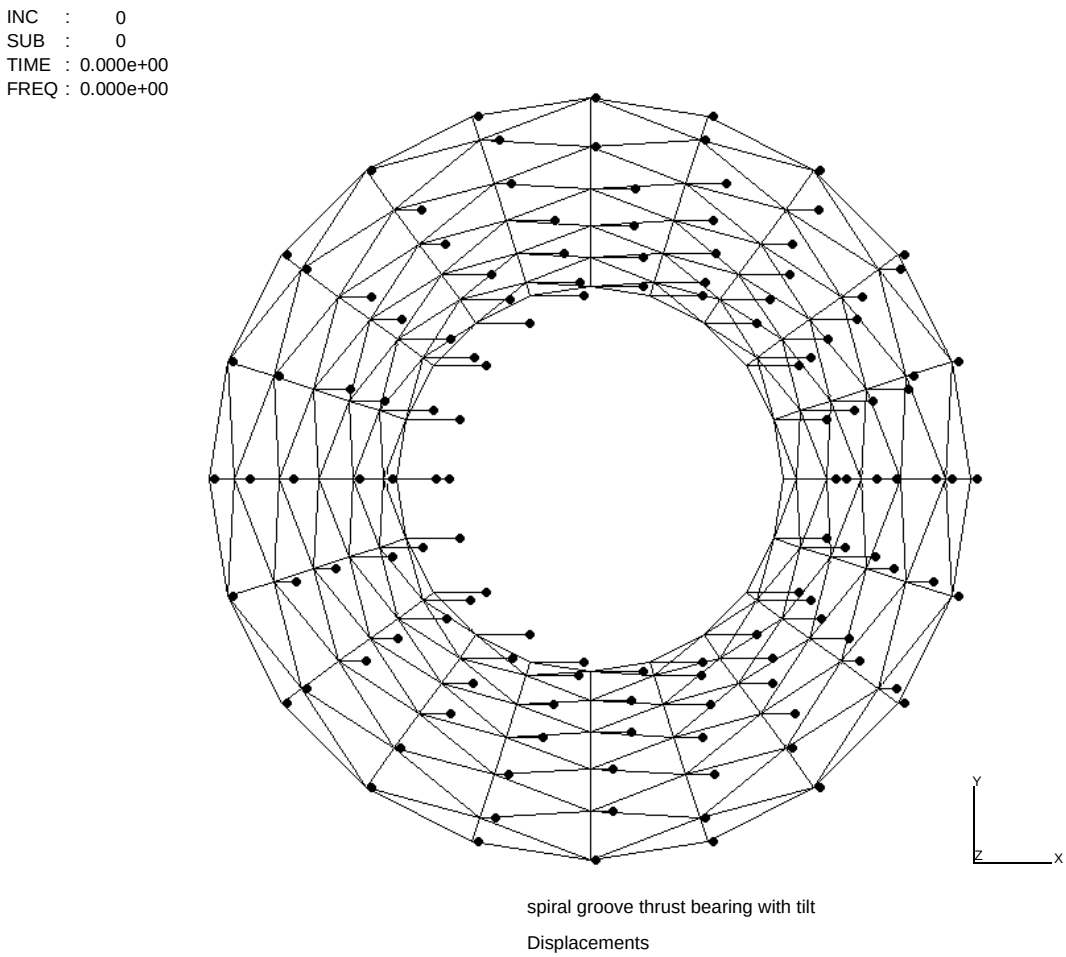

Figure 7.15-2 Vector Plot of Mass Flow

7.16 Hydrodynamic Journal Bearing of Finite Width

In this example, a journal bearing of finite width is analyzed. The load-carrying capacity as well as stiffness and damping properties are determined for a stationary bearing system. In addition, the procedure to be followed when analyzing the dynamic behavior of a nondeformable bearing system due to a change in the applied load vector is demonstrated.

Element

Element type 39, which is an arbitrary 4-node isoparametric quadrilateral element with bilinear pressure interpolation, is used to model the lubricant.

Model

The details of the journal bearing problem are given in Figure 7.16-1. In bearing analyses, the lubricant is modeled by means of planar finite elements. This is possible because it is assumed that the pressure does not vary over the lubricant thickness. Due to symmetry conditions, only half the bearing width needs to be modeled. The incremental mesh generators CONN GENER and NODE FILL are used to generate the element mesh.

Boundary Conditions

It is assumed that atmospheric pressure is acting on the end faces of the bearing system. The BC FILL option is used to generate these boundary conditions.

Tying

Tying was applied to the nodal pressures at both sides of the mesh to simulate the continuous pressure distribution in the circumferential direction.

Thickness Field

The variation of the lubricant thickness over the mesh due to the eccentric position of the rotor is specified in user subroutine UTHICK. This subroutine determines the nodal thickness values using the following expression:

$$h(\theta) = (20 - 10 \cos \theta)\ 10^{-6}\ \text{m}$$

Velocity Field

The relative velocity of the lubricant at the rotor surface, with respect to the stationary surface, is specified in the VELOCITY block. The angular velocity is 1250 rad/second.

Material Properties

All elements have lubricant properties as follows: viscosity of .015 N-sec/m^2 and density of 800 kg/m^3.

Load-Carrying Capacity

The pressure distribution for the given bearing system is calculated in increment 0. Because no external mass flux is prescribed, FLUXES need to be specified. The resulting pressure distribution is integrated to calculate the actual bearing force components. User subroutine UBEAR is included to specify at each node the physical orientation of the lubricant film. The following expressions are used:

$X = r \sin \theta$ $\quad n_X = -\cos \theta$

$Y = r \cos \theta$ $\quad n_Y = -\sin \theta$

$Z = -y$ $\quad n_Z = 0$

In addition, the resulting bearing moment components with respect to the origin of the global coordinate x, y, z system are calculated. Figure 7.16-2 shows a path plot of the calculated pressure distribution along the circumference.

The resulting bearing force yields:

$W_X = -1046$ N

$W_Y = -1814$ N

$W_Z = 0$

The resulting bearing moment yields:

$M_X =$ -6.846 Nm

$M_Y =$ 3.938 Nm

$M_Z = 0$

Because half of the structure was modeled, the components M_X and M_Y are not zero.

Damping and Stiffness Properties

The calculation of bearing characteristics (that is, damping and stiffness properties) is performed in subincrements based on a specified change in lubricant film thickness or thickness rate. This is achieved by activating the DAMPING COMPONENTS and the STIFFNS COMPONENTS options. The variation of the film thickness is again specified in user subroutine UTHICK. In total, four subincrements are specified. A displacement of the rotor center of 1.0×10^{-7}m in each global direction is given for both damping and stiffness properties.

The calculated properties are as follows:

Specified Thickness Rate	Damping Components
$\dot{h} = -1 \times 10^{-7} * \cos\theta$ m/s	$B_{XX} = -54.3 \times 10^{-3}$ N-sec/m $B_{YX} = -22.4 \times 10^{-3}$ N-sec/m
$\dot{h} = -1 \times 10^{-7} * \sin\theta$ m/s	$B_{XY} = -16.8 \times 10^{-3}$ N-sec/m $B_{YY} = -28.4 \times 10^{-3}$ N-sec/m

Stiffness

Specified Thickness Rate	Stiffness Components
$\Delta h = -1 \times 10^{-7} * \cos\theta$ m/s	$K_{XX} = -62.6$ N/m $K_{YX} = -84.1$ N/m
$\Delta h = -1 \times 10^{-7} * \sin\theta$ m/s	$K_{XY} = 119.8$ N/m $K_{YY=} 31.4$ N/m

Load-Carrying Capacity at New Rotor Position

Assume that the actual loading of the bearing system increases to the force F = (1408, 1390, 0). Since the resultant load-carrying capacity is not in equilibrium with this force, the rotor moves to a new position. Based on the calculated damping and stiffness properties, a new rotor position, which implies an incremental thickness change in a particular time period, can be estimated. This is done by investigating the mechanical equilibrium of the total system.

The force equilibrium conditions for a nondeformable bearing requires that:

$$F + W + \Delta W = 0$$

From this equation, the required correction for the load-carrying capacity can be calculated. This yields:

$$\Delta W = (-1362, 424, 0)$$

Any incremental change in position of the rotor center causes a change in the load-carrying capacity according to the following relation:

$$[B]\,\Delta\dot{u} + [K]\,\Delta u = \Delta W$$

where u is the incremental movement of the rotor center.

After substituting the previously calculated stiffness and damping properties, the above equation can be solved, which yields:

$$\Delta u = (-.450, -1.832, 0)\ 10^{-6}\ \text{m}$$

where a time increment of 10^{-3} seconds is assumed.

From the difference in magnitude of the damping and stiffness properties, it can be concluded that the initial response is dominated by the damping effects.

The above procedure is applied in increment 1. The incremental thickness change is defined in user subroutine UTHICK, based on the previous calculated bearing properties at the original rotor position. This change in film thickness is automatically added to the previous thickness field if the calculation of damping and/or stiffness properties is not activated.

According to the calculated pressure distribution for increment 2, this results in a bearing force of:

W_X = -1296 N

W_Y = -1513 N

W_Z = 0.0 N

Parameters, Options, and Subroutines Summary

Example e7x16.dat:

Parameters	Model Definition Options	History Definition Options
BEARING	BC FILL	CONTINUE
ELEMENT	CONN GENER	DAMPING COMPONENTS
END	CONNECTIVITY	STIFFNS COMPONENTS
SIZING	CONTROL	THICKNS CHANGE
TITLE	COORDINATE	
	END OPTION	
	FIXED PRESSURE	
	ISOTROPIC	
	NODE FILL	
	THICKNESS	
	TYING	
	VELOCITY	

User subroutines in u7x16.f:

UTHICK
UBEAR

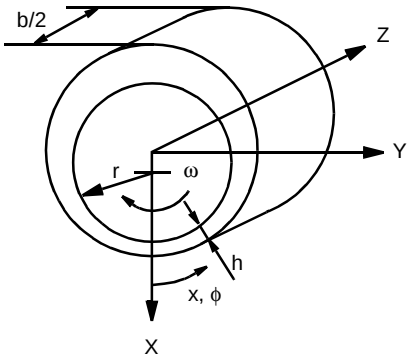

r = 20 mm
b = 10 mm
η = 0.015 N-sec/m2
h = (20 – 10cosθ) 10-6 m
ω = 1250 rad/sec

MARC

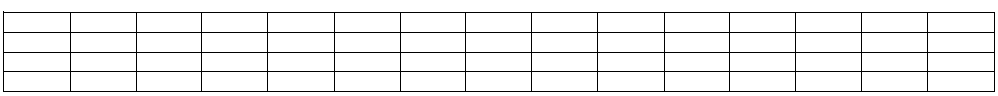

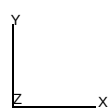

Figure 7.16-1 Journal Bearing of Finite Width

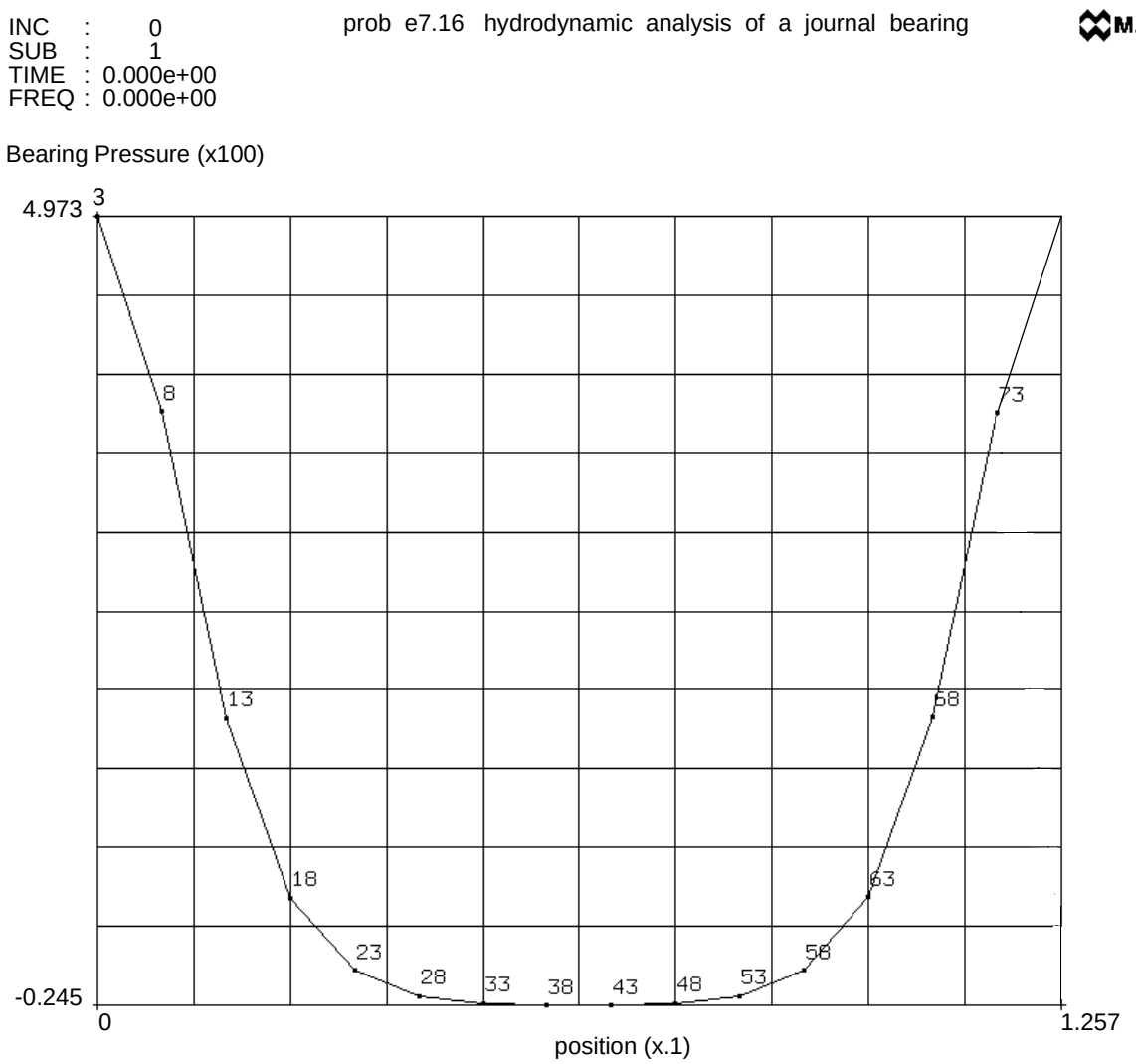

Figure 7.16-2 Path Plot of Pressure Distribution

7.17 Elastic-Plastic Finite Deformation of a Thick-Walled Cylinder

This problem demonstrates the rezoning technique for the elastic-plastic finite deformation of a thick cylinder. The cylinder is subjected to internal pressure which results in large elastic-plastic deformation, after which the load is removed leaving the structure in its permanent plastically deformed shape. Because of the amount of plastic deformation, the FINITE STRAIN option is used in conjunction with the UPDATED LAGRANGE option. Often, in this type of analysis, the mesh becomes seriously distorted, resulting in a low quality solution. This problem demonstrates the REZONING option to resolve this difficulty.

Model

The model consists of five axisymmetric type 10 elements and 12 nodes. The initial inner and outer radii are 1 and 2 m, respectively. The mesh is shown in Figure 7.17-1.

Material Properties

The elastic properties of the material are Young's modulus of 1000 N/m^2 and Poisson's ratio of 0.3. The material has an initial yield stress of 1 N/m^2 and strain hardens at a rate of 3 N/m^2.

Geometry

No thickness is associated with an axisymmetric element. The constant dilatation method is used for this element by indicating a 1. in the second field of this option.

Boundary Conditions

The thick cylinder is constrained to be under plane-strain conditions ($e_{zz} = 0$).

Loading

An incremental nodal load is prescribed to the nodes on the inner radius (nodes 1 and 2) through the FORCDT option. To determine the current applied pressure, this force needs to be divided by $2\pi R_{current}$. The prescribed load and resulting pressures are shown in Figure 7.17-2.

Controls

All calculations are saved on the restart file for every increment. The maximum number of increments allowed is 50. The maximum number of recycles was put to 10. This is because very large increments were chosen, and after a rezoning occurs the calculations are not in equilibrium. The PRINT CHOICE option is used to restrict the output to element 1.

Procedure

Using the first input, the analysis is completely carried out in 42 increments. The second input demonstrates the use of the REZONING option. The first analysis is restarted at the end of increment 10. The REAUTO option is used to prematurely discontinue the AUTO LOAD sequence that was defined previously in the first analysis.

The data after the END OPTION, beginning with REZONE and finishing with END REZONE, form one rezoning increment. In this analysis, the coordinates are redefined such that the new inner and outer radii are the same as the deformed radii at increment 10 of the previous analysis. The other points are located such that the new mesh would be regular.

At the conclusion of the rezoning increment, the analysis is continued to the same level of loading.

Results

Figure 7.17-3 shows the deformed mesh during different stages of the analysis. Clearly, the boundary of the deformed cylinder is virtually identical for both analyses.The pressure versus internal radius diagram is shown in Figure 7.17-4, together with the analytical solution for an equivalent rigid workhardening material. Excellent agreement is obtained, both between theory and finite element calculation and between the two analyses.

It should be commented that although rezoning was not necessary in this problem, it is extremely useful in many practical applications in the metal working area.

Parameters, Options, and Subroutines Summary

Example e7x17a.dat:

Parameters	Model Definition Options	History Definition Options
ALL POINTS	CONNECTIVITY	AUTO LOAD
ELEMENT	CONTROL	CONTINUE
END	COORDINATE	
FINITE	END OPTION	
LARGE DISP	FIXED DISP	
REZONE	FORCDT	
SIZING	GEOMETRY	
TITLE	ISOTROPIC	
UPDATE	POST	
	PRINT CHOICE	
	RESTART	
	WORK HARD	

Example e7x17b.dat:

Parameters	Model Definition Options	History Definition Options
ALL POINTS	CONNECTIVITY	AUTO LOAD
ELEMENT	CONTROL	CONTINUE
END	COORDINATE	
FINITE	END OPTION	
LARGE DISP	FIXED DISP	
REZONE	FORCDT	
SIZING	GEOMETRY	
TITLE	ISOTROPIC	
UPDATE	POST	
	PRINT CHOICE	
	REAUTO	
	RESTART	
	WORK HARD	

User subroutine in u7x17.f:

FORCDT

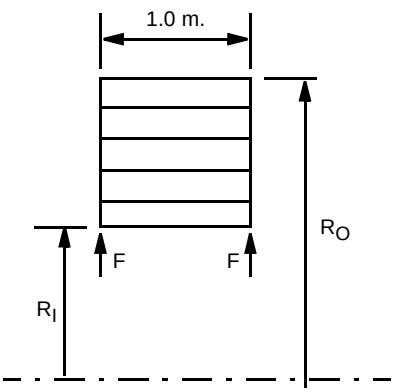

R_I = 1.0 m.
R_O = 2.0 m.
E = 1000 N/m^2
υ = 0.3
σy = 1.0 N/m^2
$\frac{\partial \bar{\sigma}_y}{\partial \varepsilon_p}$ = 3.0

Figure 7.17-1 Thick-Walled Cylinder

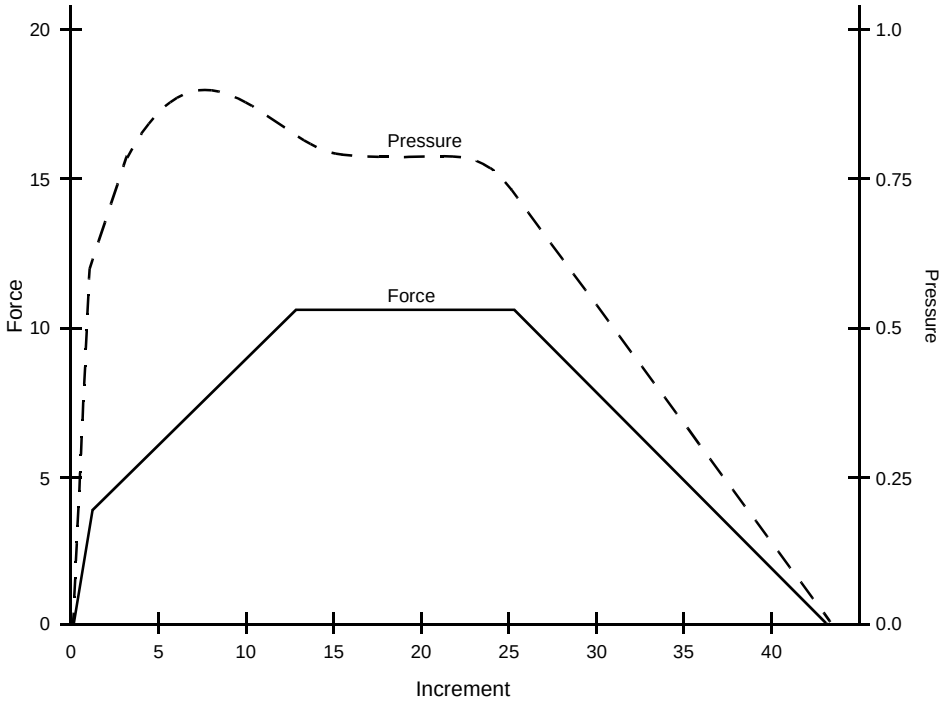

Figure 7.17-2 Applied Load History

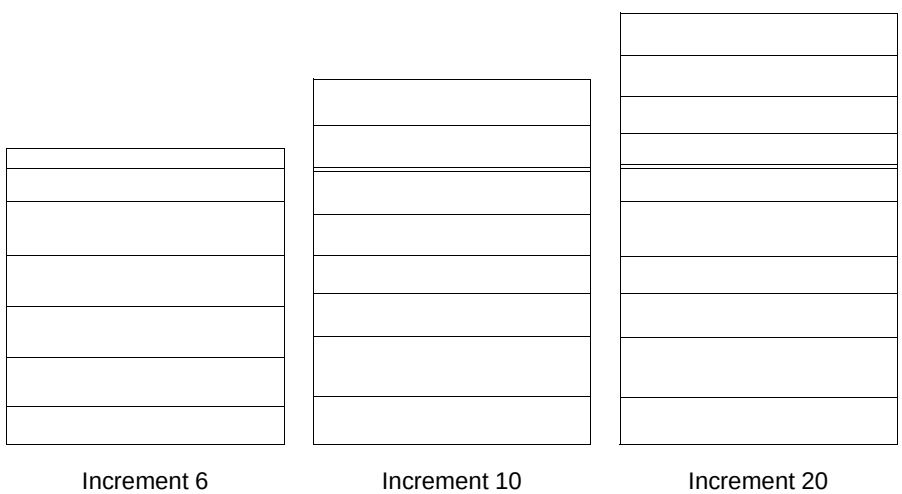

Figure 7.17-3 Deformed Meshes at Increments 6, 10, and 20

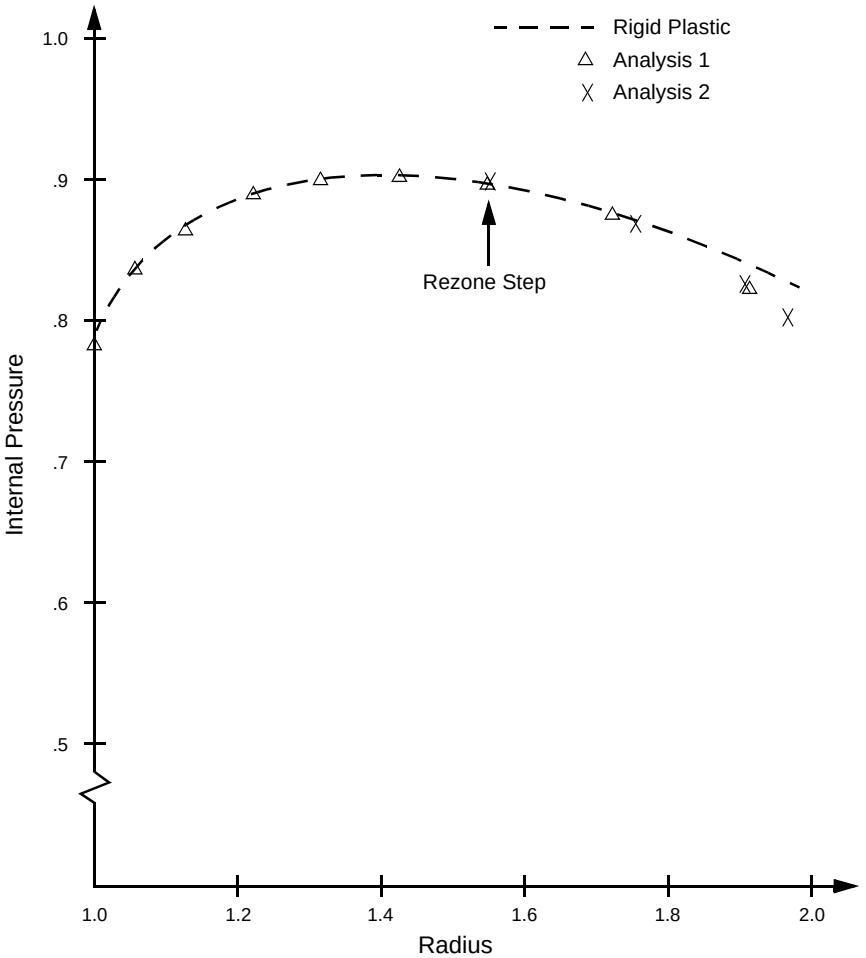

Figure 7.17-4 Internal Pressure vs. Inner Radius

7.18 Side Pressing of a Hollow Rubber Cylinder

The behavior of a thick, hollow, rubber cylinder, compressed between two rigid plates, is analyzed. The cylinder is long; hence, a condition of plane strain in the cross section is assumed. For reasons of symmetry, only one-quarter of the cylinder needs to be modeled. No friction is assumed between cylinder and plates. The VISCELMOONEY material behavior is used to represent the viscoelastic rubber. The LARGE DISPLACEMENT option is used.

Element

The quarter cylinder is modeled by using 8-node hybrid plane strain elements (MARC element type 32). This element can be used in conjunction with the Mooney material model. Element type 12 is used to model the contact conditions.

Model

Twelve elements are used for the mesh, with two elements specified over the thickness. The geometry of the cylinder and a mesh are shown in Figure 7.18-1.

Material Properties

The MOONEY model definition option is used to specify the rubber properties; the GAP DATA option is used for the input of the gap data. The GAP closure distance is defined as the relative distance before contact occurs, which in this problem equals the initial nodal distance between cylinder and plate. The instantaneous response of the rubber material (MOONEY) can be modeled as a Mooney-Rivlin material with $C_{10} = 8$ N/mm^2, $C_{01} = 2$ N/mm^2. The time dependent response (VISCELMOONEY) is modeled by a single exponential decay function, with a decay factor of 0.5 at infinite time and a relaxation time of 0.3 seconds.

Loading

The AUTO LOAD option is used to apply five displacement increments to the plate at time t = 0. The increment is equal to the one applied in the increment 0. Subsequently, 15 time-steps (AUTO LOAD) of 0.1 seconds (TIME STEP) are applied with zero displacement increments (DISP CHANGE). The applied displacement is reversed and five steps are carried out without change in time, followed by a relaxation period of two seconds applied in 20 increments.

Boundary Conditions

Boundary conditions are along the line r = 0 and z = 0 due to symmetry and to apply the prescribed motion of the plate.

Tying

The TYING option establishes the connections between the nodal degrees of freedom of the cylinder and that of the gaps. This is necessary as the degrees of freedom of these two elements are not the same.

Results

The cylinder diameter is reduced from 6 mm to 4 mm in five increments. The cylinder is in contact with the plate at four nodes (four gaps have been closed). The incremental displacements have become very small, and the equilibrium is satisfied with high accuracy. The incremental full Newton-Raphson method was used to solve the nonlinear system. The total force on the plate can either be calculated by summing up the gap forces, or can be directly obtained from the reaction force on node 75. In both cases, this leads to a total force F = 1.9098 N. A plot of the deformed cylinder is shown in Figure 7.18-2.

After relaxation for 1.5 seconds, the load is reduced by almost 50%, as predicted by the equation $F_t = F_o(1 - 0.5e^{-t/0.3})$. During that period, all properties are scaled down proportionally and the displacements do not change. The same is true for the second relaxation period.

Parameters, Options, and Subroutines Summary

Example e7x18.dat:

Parameters	Model Definition Options	History Definition Options
ELEMENT	CONNECTIVITY	AUTO LOAD
END	CONTROL	CONTINUE
LARGE DISP	COORDINATE	DISP CHANGE
SIZING	END OPTION	TIME STEP
TITLE	FIXED DISP	
	GAP DATA	
	MOONEY	
	POST	
	PRINT CHOICE	
	RESTART	
	TYING	
	VISCELMOON	

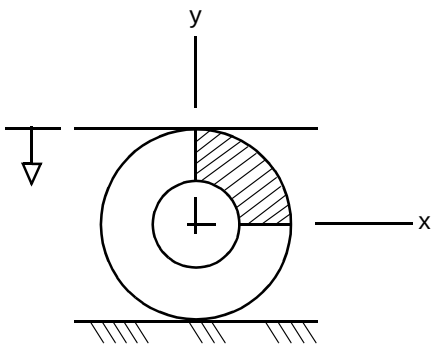

C_{10} = 8 N/mm^2
C_{01} = 2 N/mm^2
r_i = 2 mm
r_o = 3 mm

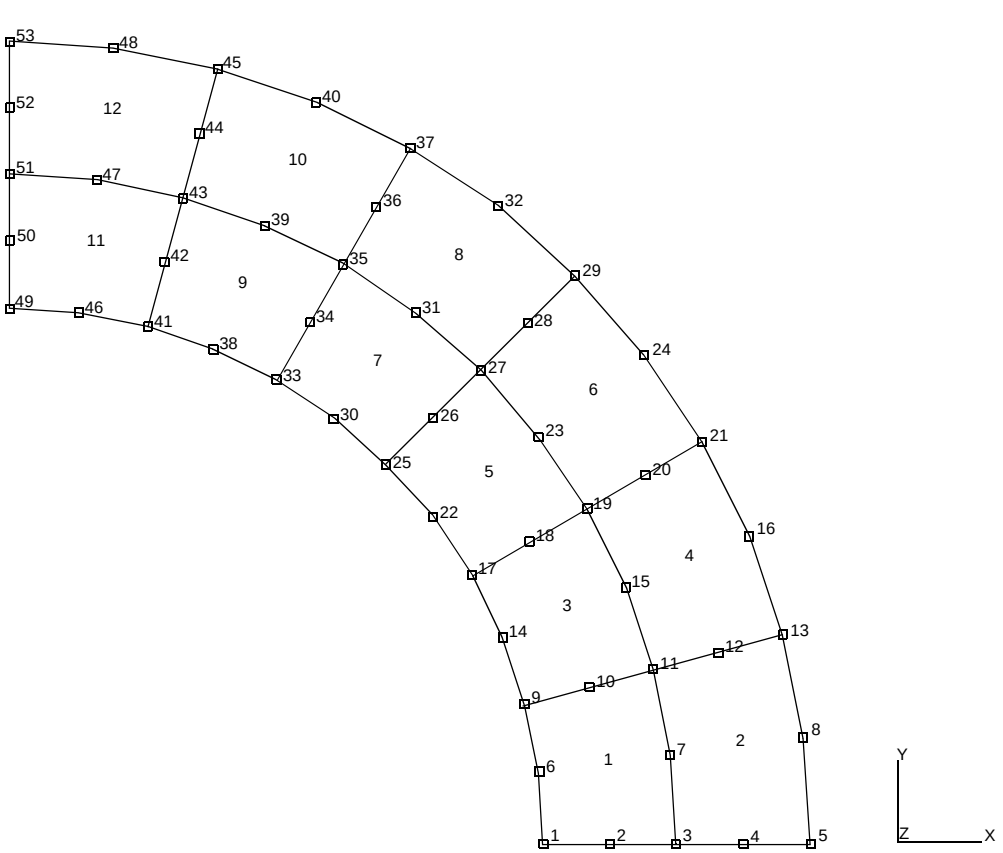

Figure 7.18-1 Rubber Cylinder and Mesh

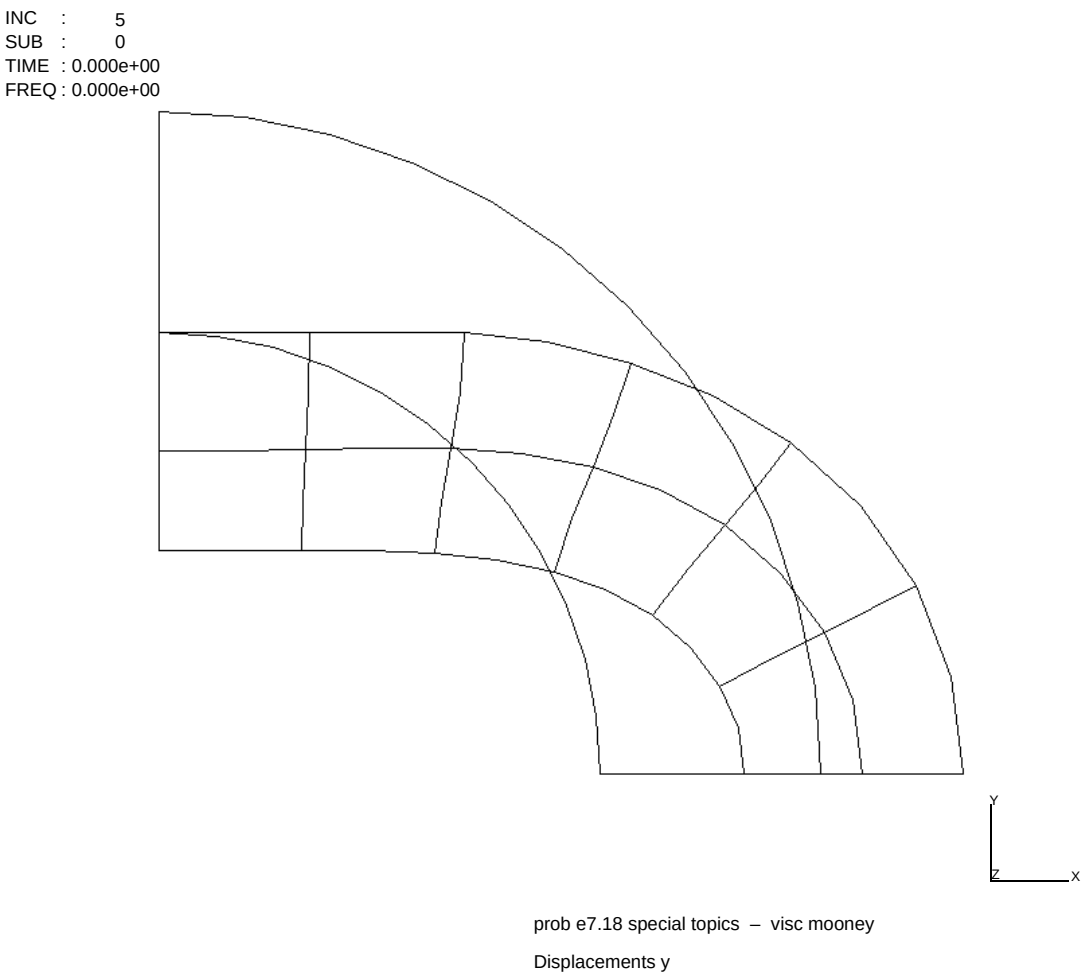

Figure 7.18-2 Deformed Mesh Plot

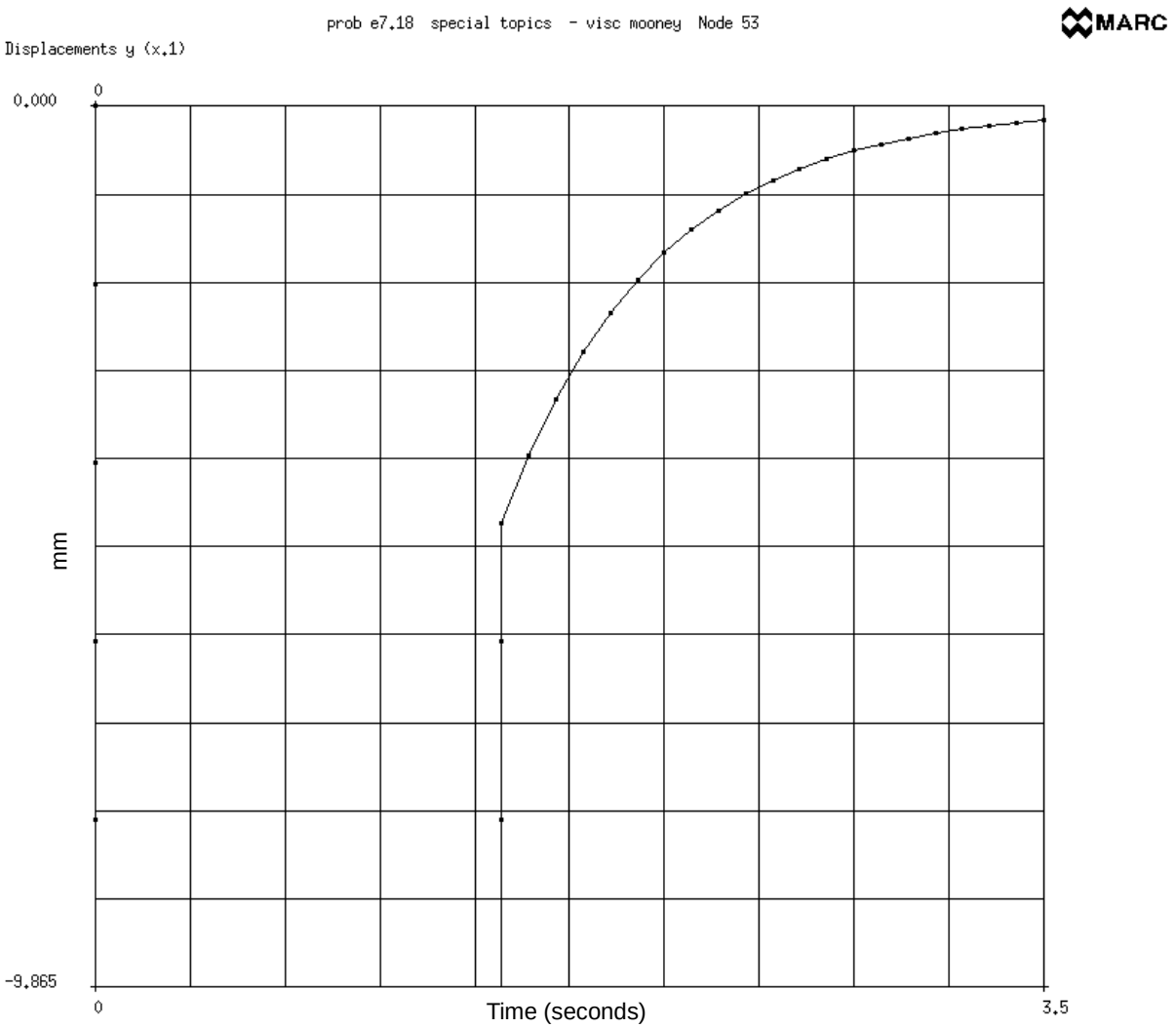

Figure 7.18-3 Displacement History of Node 53

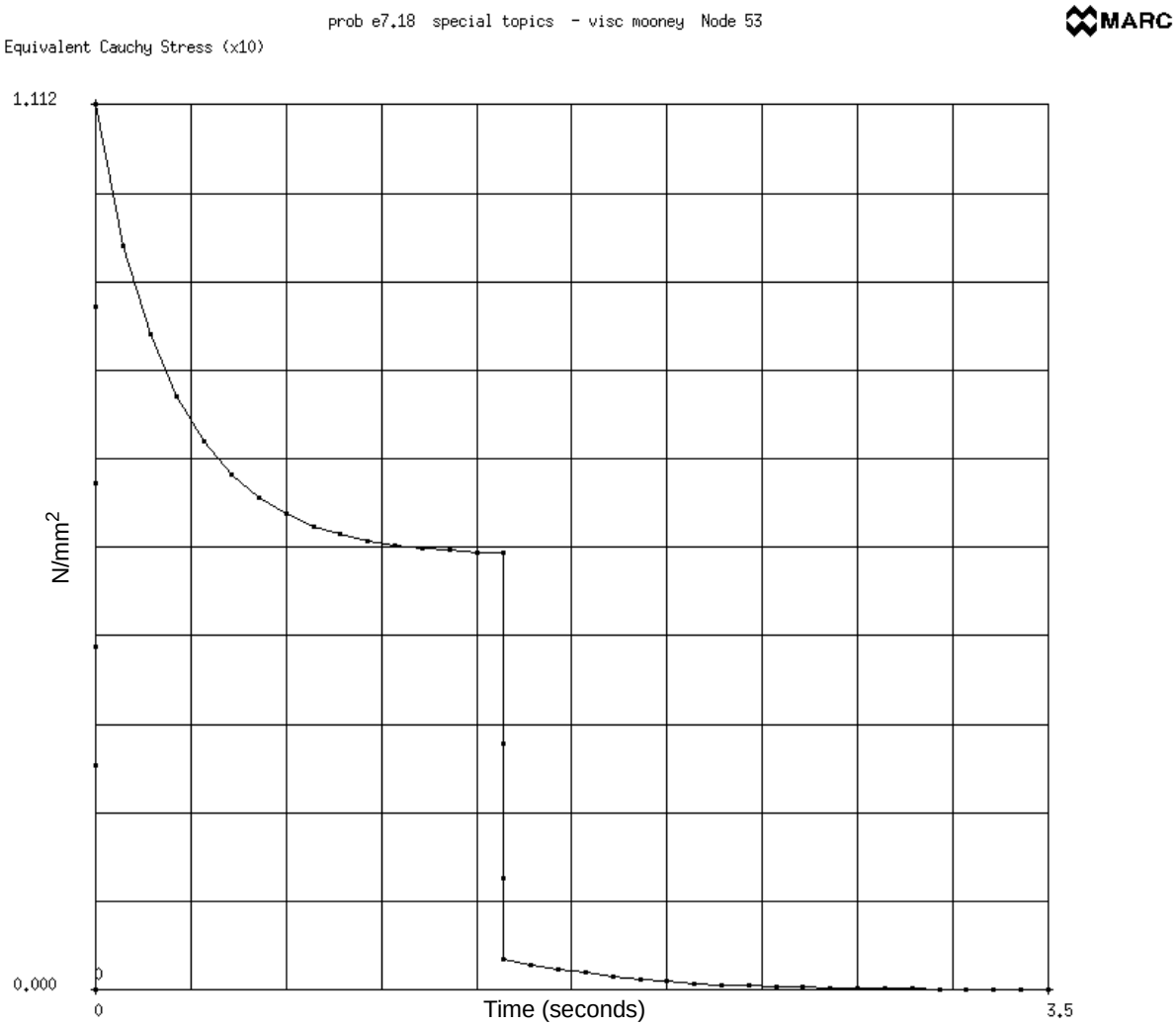

Figure 7.18-4 Stress Relaxation

7.19 Stretching of a Rubber Sheet with a Hole

This example demonstrates the use of the Mooney-Rivlin and Foam material model for a thin rubber sheet analysis with a hole.

This problem is modeled using the two techniques summarized below.

Data Set	Element Type(s)	Number of Elements	Number of Nodes	Differentiating Features
e7x19	26	80	277	Mooney Model
e7x19b	26	80	277	Foam Model

Model

A square sheet of 6.5 cm x 6.5 cm with a hole of radius 0.25 cm is to be analyzed. One quarter of the model is represented due to symmetry. The mesh shown in Figure 7.19-1 has 80 elements and 277 nodes. Element 26, the conventional displacement formulation 8-node quadrilateral, is used. When using the Mooney-Rivlin in compressible material mold, you normally use Herrmann elements. Because this is a plane-stress analysis, the use of Herrmann elements is not necessary. When using the Foam model, conventional elements should always be used. The thickness of the sheet is 0.079 which is entered through the GEOMETRY option.

Material Properties

The material is modeled using the general third-order deformation model with:

$C_{10} = 20.300\ N/cm^2$
$C_{01} = 5.810\ N/cm^2$
$C_{11} = 0.000\ N/cm^2$
$C_{20} = -0.720\ N/cm^2$
$C_{30} = 0.046\ N/cm^2$

for all elements. This data is entered through the MOONEY option.

The material of problem e7.19b is modeled using the three-term rubber-foam model:

Term	μ (N/cm)	α	β
1	1.48269	7.56498	-10.4156
2	-1.48269	-0.504321	-10.4155
3	¼0.0041819	12.1478	-5.67921

for all elements. This data is entered through the OGDEN option.

Boundary Conditions

The nodes along x = 0 (edge 1) are fixed in the x-direction. The nodes along y = 3.25 (edge 2) and along y = 0 (edge 4) are fixed in the y-direction. The nodes which are originally along x = 3.25 (edge 3) are all tied to node 277. This will allow you to keep this edge straight and easily calculate the total pulling force. The displacement of node 277 is first set to 0 in the x-direction and then changed through the DISP CHANGE option. The incremental displacement will be 0.325 cm/increment. A total of 10 increments are executed. Hence, the dimension in the x-direction doubles.

Results

For the Incompressible Model:

The deformed mesh is shown in Figure 7.19-2. The load-deflection curve for node 277 is shown in Figure 7.19-3. There is substantial thinning of the sheet.

For the Foam Model:

The deformed mesh is shown in Figure 7.19-4. The load deflection curve for node 277 is shown in Figure 7.19-4. Note that the deformation is significantly different near the hole.

Parameters, Options, and Subroutines Summary

Example e7x19.dat:

Parameters	Model Definition Options	History Definition Options
ELEMENT	CONNECTIVITY	AUTO LOAD
END	CONTROL	CONTINUE
SIZING	COORDINATES	DIST CHANGE
TITLE	END OPTION	
	DEFINE	
	FIXED DISP	
	GEOMETRY	
	MOONEY	
	POST	
	PRINT CHOICE	
	TYING	

Example e7x19b.dat:

Parameters	Model Definition Options	History Definition Options
ELEMENTS	CONNECTIVITY	AUTO LOAD
END	COORDINATE	CONTINUE
LARGE DISP	DEFINE	DIST CHANGE
SIZING	END OPTION	
TITLE	FIXED DISP	
	FOAM	
	GEOMETRY	
	POST	
	PRINT CHOICE	
	TYING	

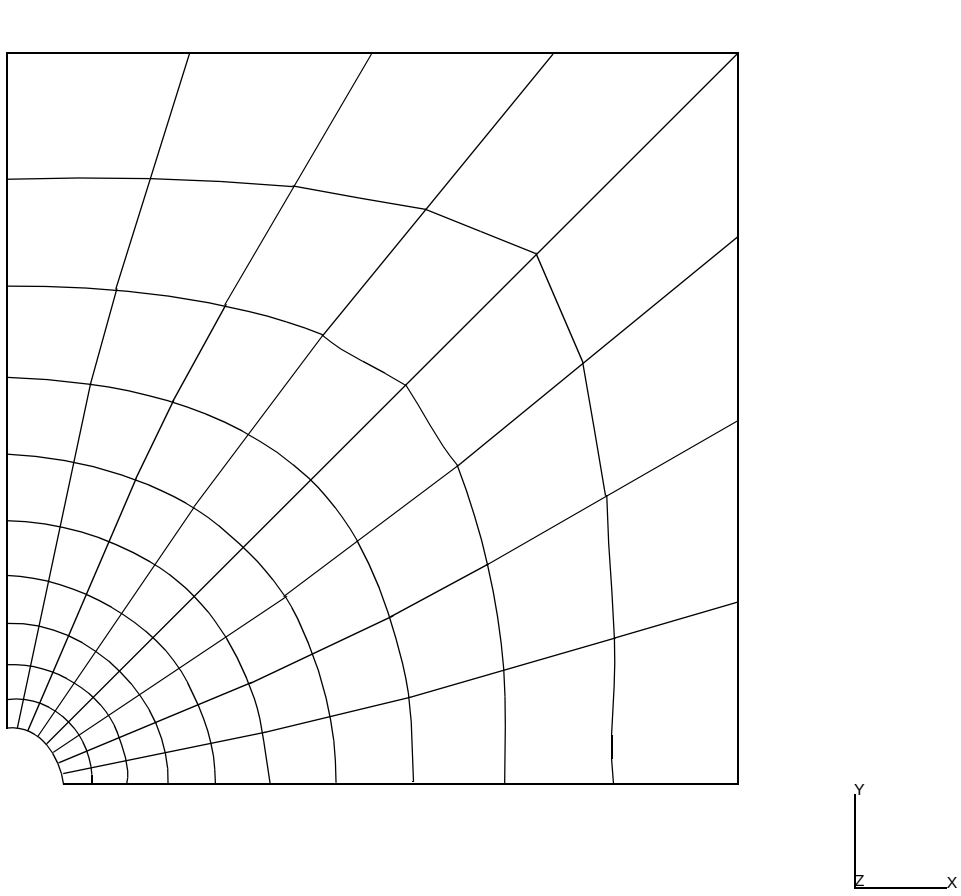

Figure 7.19-1 Finite Element Mesh

INC : 10
SUB : 0
TIME : 0.000e+00
FREQ : 0.000e+00

MARC

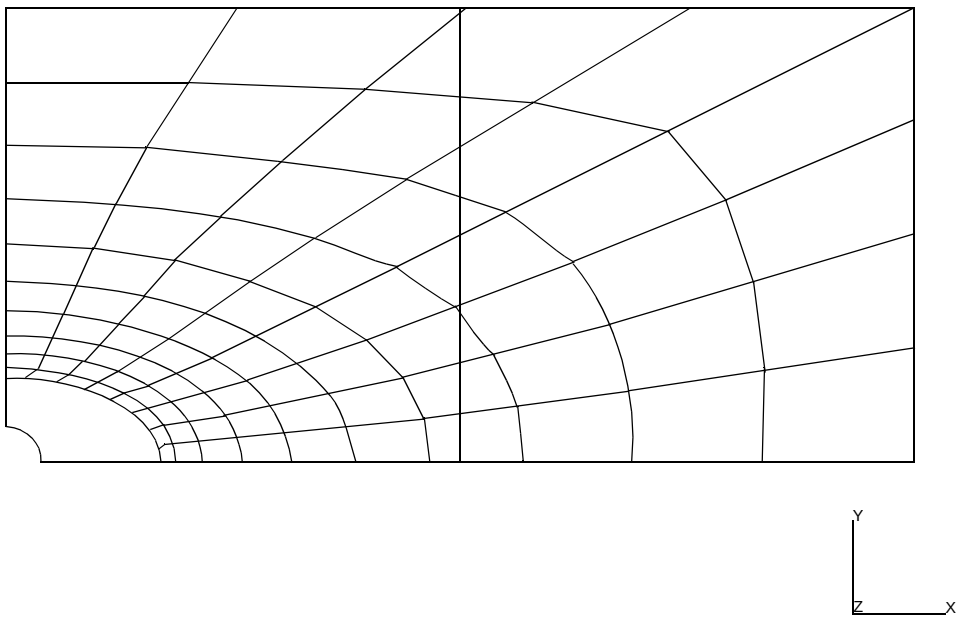

prob e7.19 plane stress rubber analysis – element 26
Displacement y

Figure 7.19-2 Incompressible Model Deformed Mesh

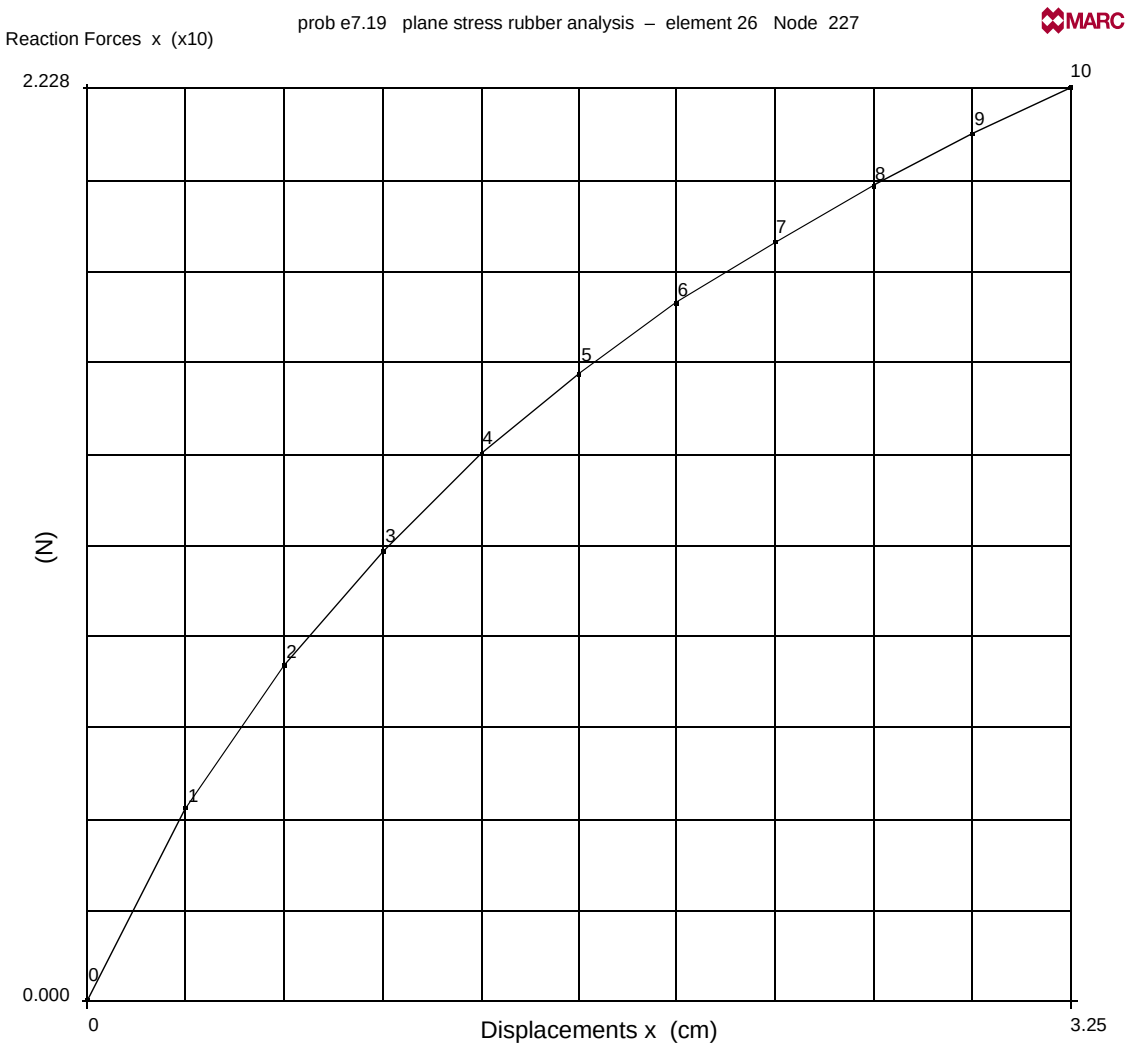

Figure 7.19-3 Incompressible Model Load Deflection Curve at Node 277

INC : 10
SUB : 0
TIME : 0.000e+00
FREQ : 0.000e+00

MARC

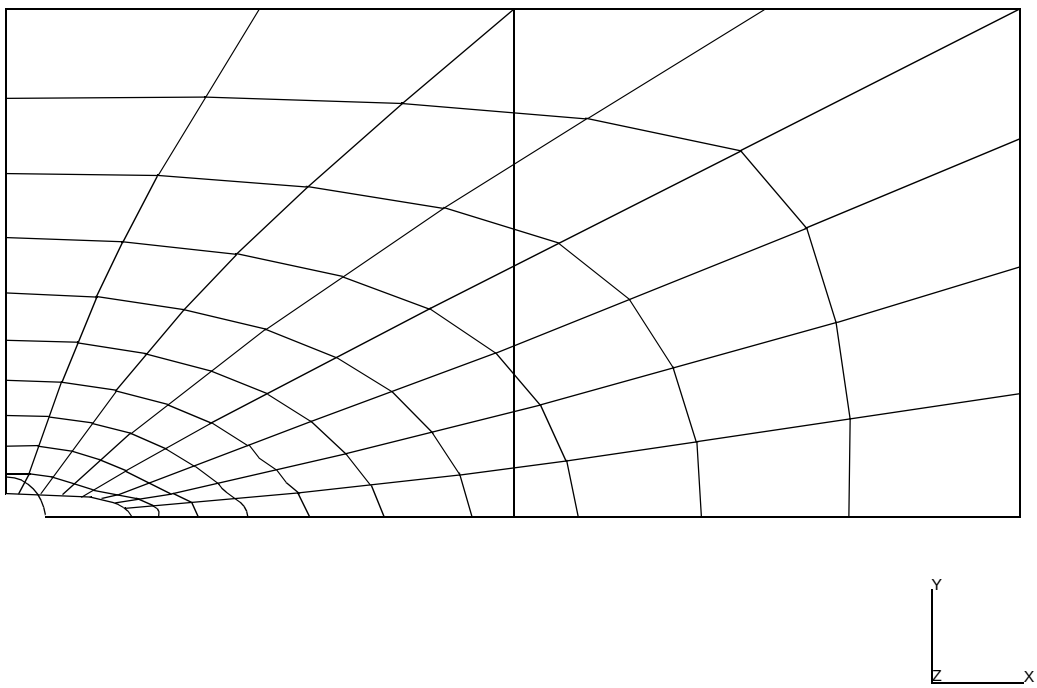

using foam model

Figure 7.19-4 Foam Model Deformed Mesh

INC : 10
SUB : 0
TIME : 0.000e+00
FREQ : 0.000e+00

MARC

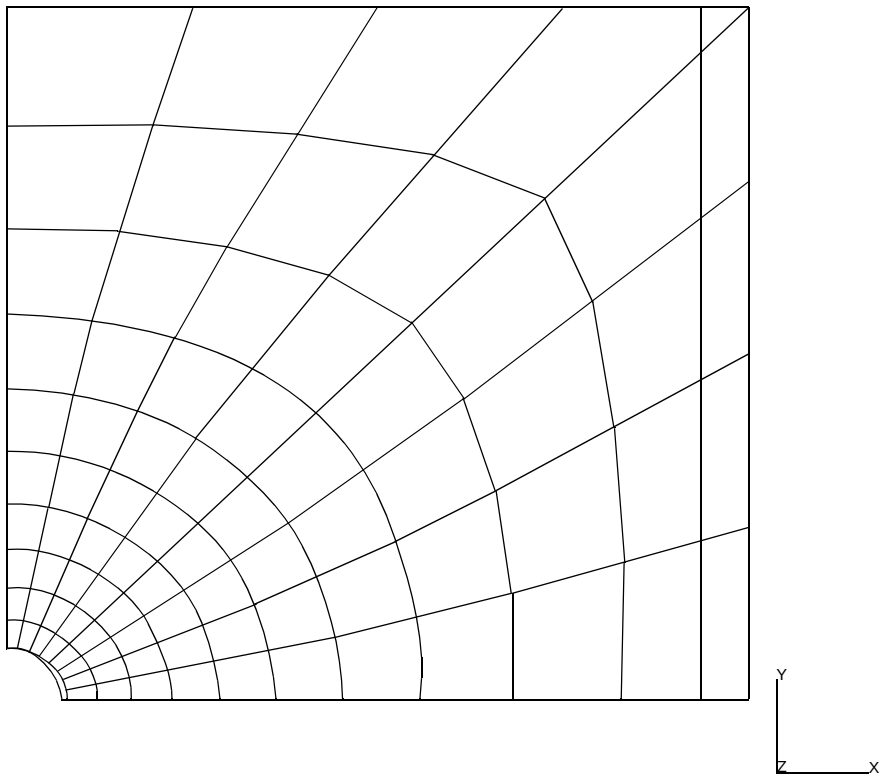

plate with hole using foam model

Figure 7.19-5 Foam Model Load Deflection Curve at Node 277

7.20 Compression of an O-Ring using Ogden Model

This example demonstrates the use of the Ogden rubber model for the high compression of an O-ring. The ring is compressed into a rigid channel. The second analysis is of the same problem, but the follower force stiffness is included. The third analysis uses a simpler mesh to begin with and then demonstrates the adaptive meshing capability. The last analysis demonstrates the use of conventional displacement based elements in an updated Lagrange framework of elasticity.

This problem is modeled using the four techniques summarized below.

Data Set	Element Type(s)	Number of Elements	Number of Nodes	Differentiating Features
e7x20	82	544	605	No Follower Force Stiffness
e7x20b	82	544	605	Follower Force Stiffness
e7x20c	82	29	40	Adaptive Meshing
e7x20d	10	544	605	Updated Lagrange, Follower Force Stiffness

Element

Library element 82, a 5-node axisymmetric element using the Herrmann formulation, is used for the first 3 data sets. In the first two analyses, there are 544 elements and 605 nodes as shown in Figure 7.20-1. Three rigid bodies are used to simulate the channel. The ring has a mean radius of 12 cm and the loading radius is 1.5 cm. In the third analysis, the coarse mesh shown in Figure 7.20-2 is used. This mesh begins with 29 elements and 40 nodes.

In the last analysis, the conventional displacement element type 10 is used. The incompressibility is treated using the same framework as the plasticity using F^eF^p formulation where the elemental pressure degrees-of-freedom are condensed out before element assembly. The output stresses is Cauchy by default while the output strain is the logarithmic or true strain in the current configuration.

The rigid surface at the outside radius is first moved inwards a distance of 0.5 cm in a period of 50 seconds. The surface is then frozen and an external pressure of 18.8 N/cm^2 is applied onto the left face during 47 increments. The FOLLOW FOR option is used to insure that the load is applied on the deformed geometry. In the second analysis, the follower force stiffness is included. This should improve the convergence behavior.

Material Properties

The O-ring can be described using the Ogden material model using a three term series. The stress-strain curve for this model is shown in Figure 7.20-3. The data was fit such that:

Term	μ (N/cm^2)	α
1	6.30	1.3
2	0.12	5.0
3	-0.10	-2.0

and the bulk modulus was 1.0E9 N/cm^2.

Contact/Boundary Conditions

All of the kinematic constraints are provided using rigid contact surfaces. Coulomb friction with a coefficient of friction of 0.1 is specified.

Controls

The full Newton-Raphson iterative method is used with a convergence tolerance of 10% on residuals requested. Because of the large compressive stresses that are generated, the solution of nonpositive definite systems is forced. Additionally, a flag is set that tells MARC to only use the deviatoric stresses in the initial stress stiffness matrix. While this can slow convergence, it tends to improve stability. The PRINT,5 option is used to obtain more information regarding the contact behavior. The NO PRINT option is used to suppress the printout.

Adaptive Meshing

In the third analysis, the adaptive meshing technique is demonstrated. The mean strain energy criteria is used with a factor of 0.9. The maximum number of subdivisions allowed is two. As the O-ring initially is round, this additional information is provided using the SURFACE option. A circle at origin (1.5, 12.0 cm) and a radius of 1.5 cm is defined. The ATTACH NODE option is used to associate the original nodes with this geometry.

Results

The deformed mesh at increments 10, 30, and 50 are shown in Figure 7.20-4 through Figure 7.20-6. One observes that at increment 50, the ring almost completely fills the corner regions. The mean second Piola-Kirchhoff stresses are shown in Figure 7.20-7. One should note that in all these plots, the free surface to which the pressure is applied remains almost perfectly circular. Finally, the contact forces are shown in Figure 7.20-8 for the total Lagrange formulation which, as expected, are identical to the ones obtained with the updated Lagrange formulation as shown in Figure 7.20-13.

The progression of meshes using the adaptive meshing is shown in Figure 7.20-9 through Figure 7.20-12. At the end of the analysis, the total number of elements is 104 and the number of nodes is 148.

Parameters, Options, and Subroutines Summary

Example e7x20.dat, e7x20b.dat, and e7x20d.dat:

Parameters	Model Definition Options	History Definition Options
ELEMENT	CONNECTIVITY	CONTINUE
END	CONTACT	DIST LOADS
FOLLOW FOR	CONTROL	MOTION CHANGE
LARGE DISP	COORDINATES	TIME STEP
PRINT	DEFINE	
SIZING	DIST LOADS	
TITLE	END OPTION	
	OGDEN	
	OPTIMIZE	
	POST	

Example e7x20c.dat:

Parameters	Model Definition Options	History Definition Options
ADAPTIVE	ADAPTIVE	AUTO LOAD
ELEMENT	ATTACH NODE	CONTINUE
END	CONNECTIVITY	DIST LOADS
FOLLOW FOR	CONTACT	MOTION CHANGE
LARGE DISP	CONTROL	TIME STEP
PRINT	COORDINATES	
SETNAME	DEFINE	
SIZING	DIST LOADS	
TITLE	END OPTION	
	OGDEN	
	OPTIMIZE	
	POST	

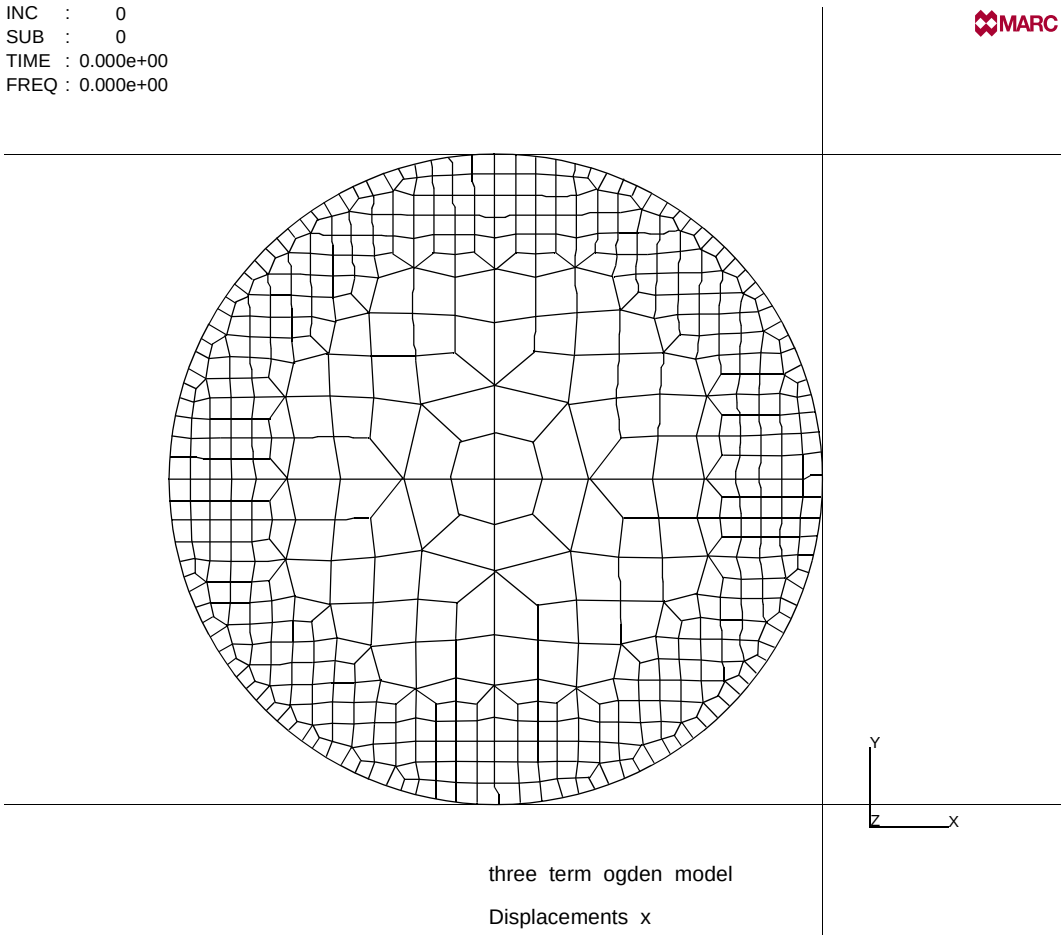

Figure 7.20-1 O-Ring Mesh

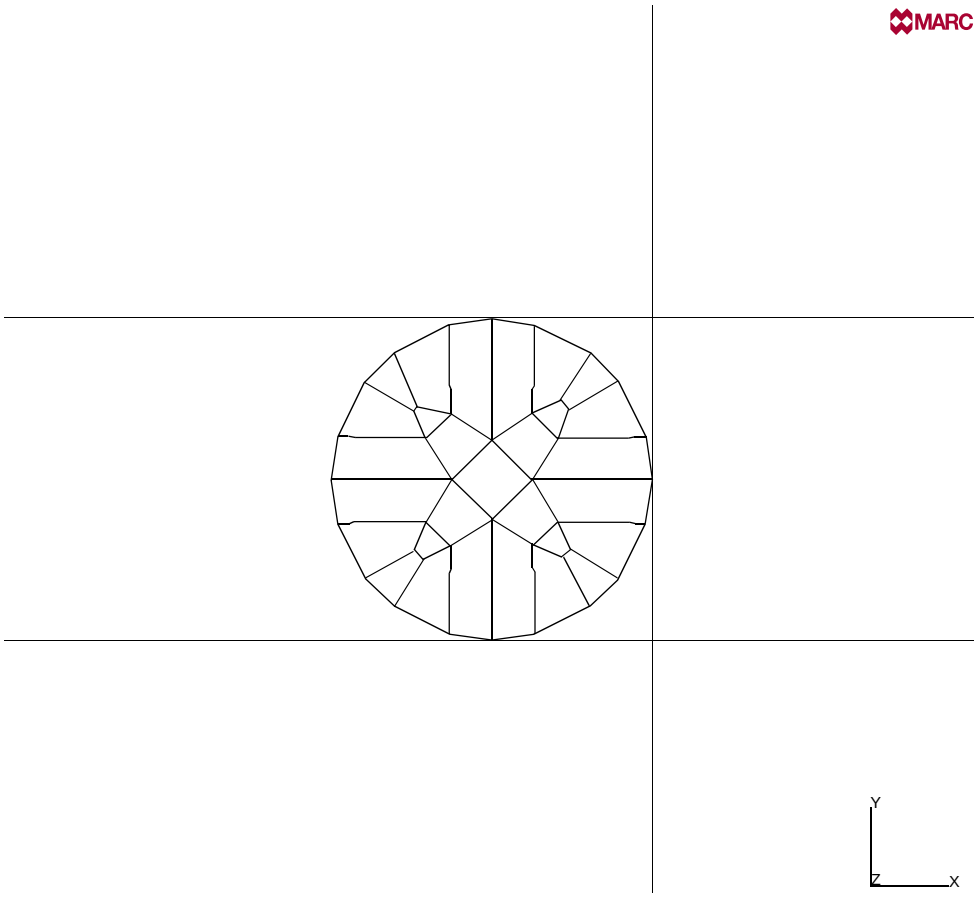

Figure 7.20-2 Coarse O-Ring Initial Mesh for Data Set e7x20c

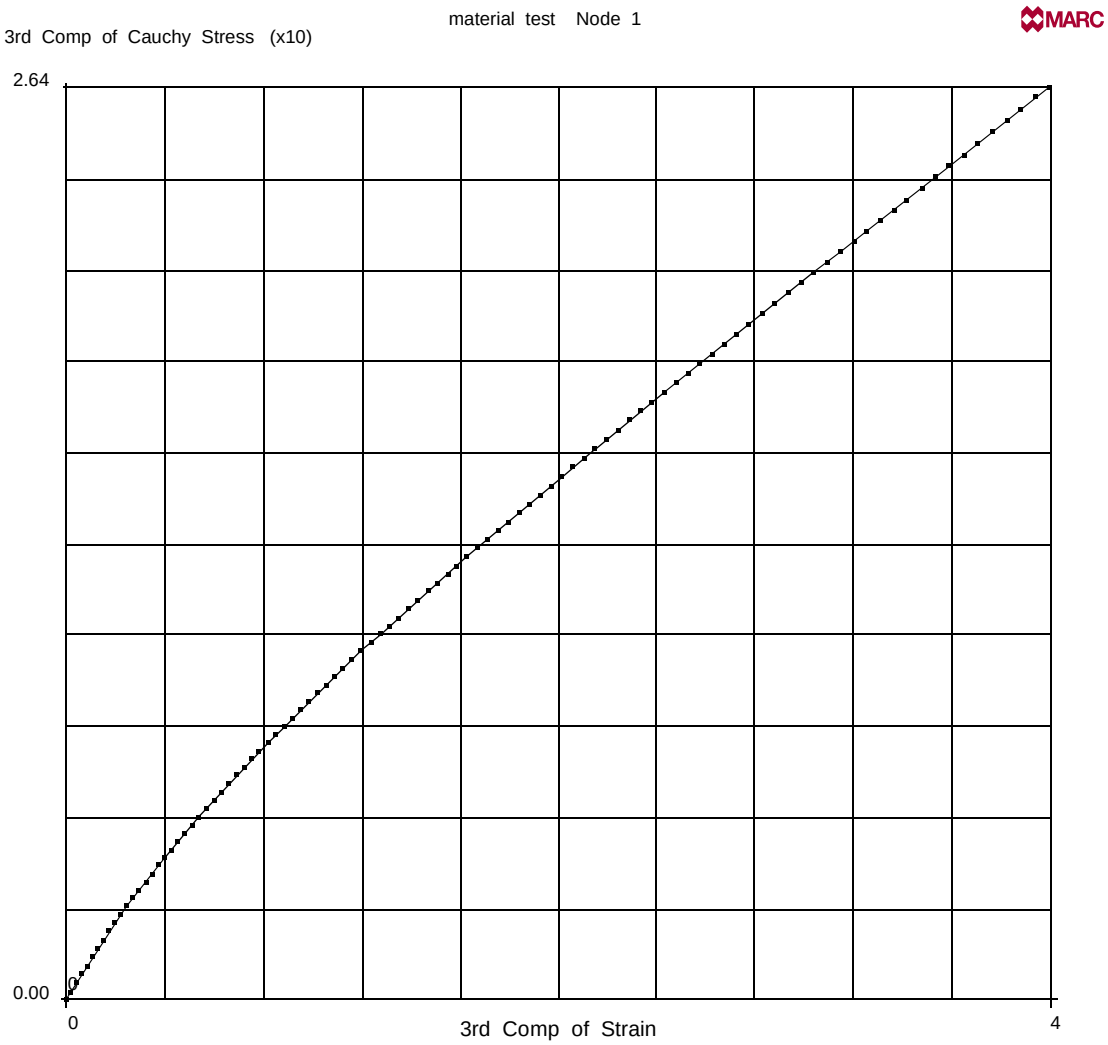

Figure 7.20-3 Stress-Strain Curve

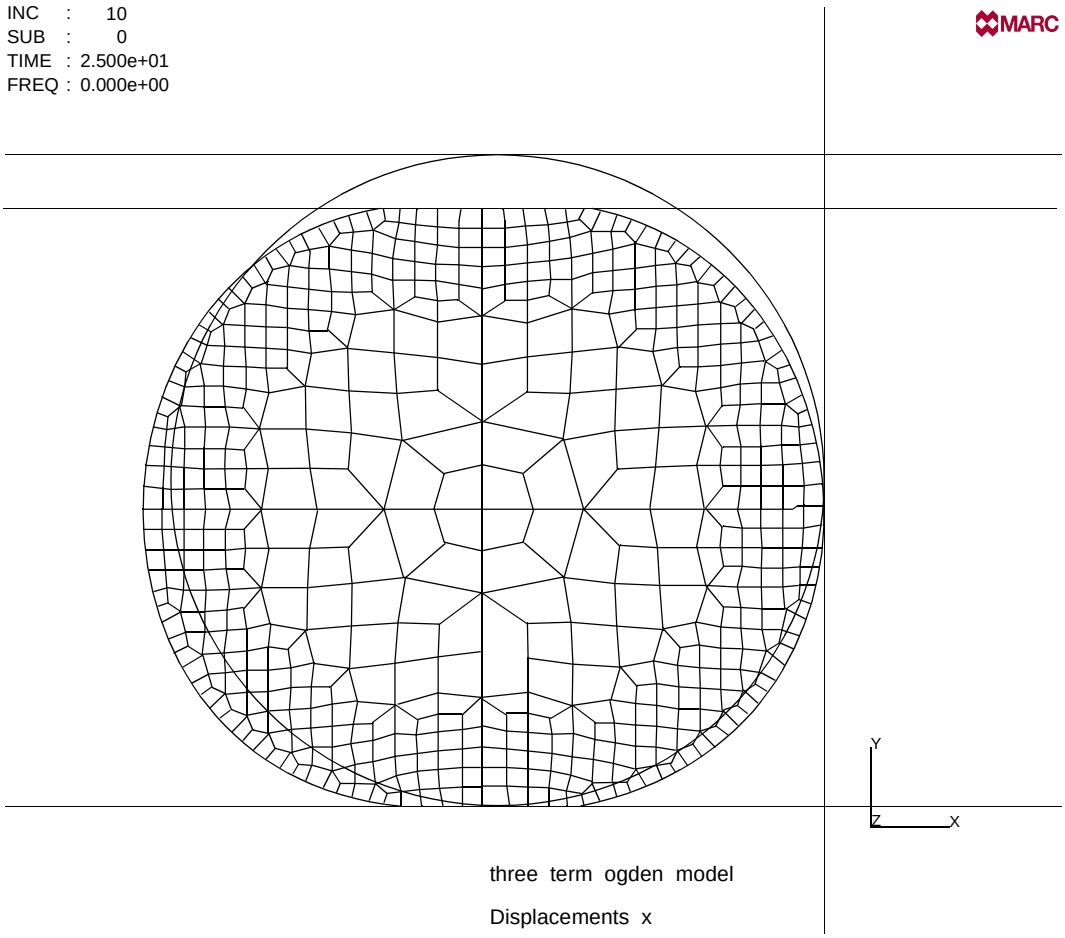

Figure 7.20-4 Deformed Mesh, Increment 10

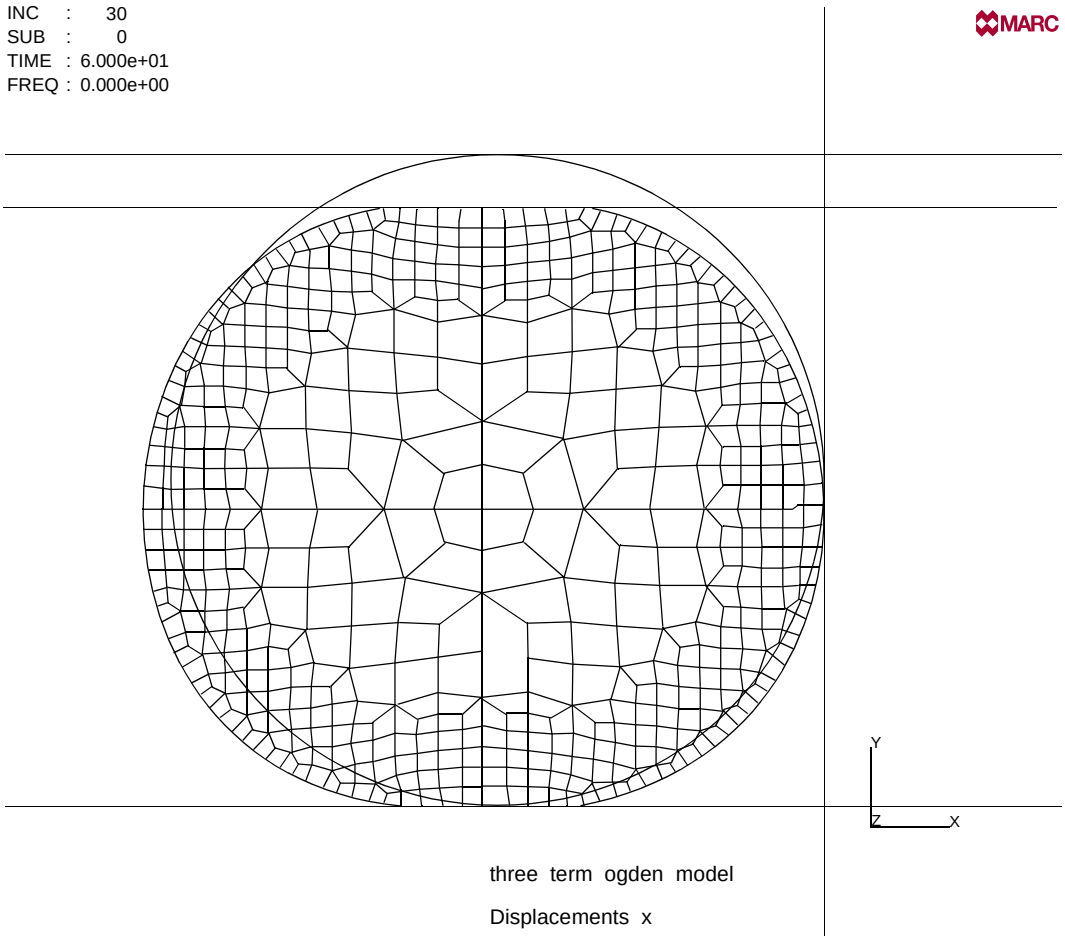

Figure 7.20-5 Deformed Mesh, Increment 30

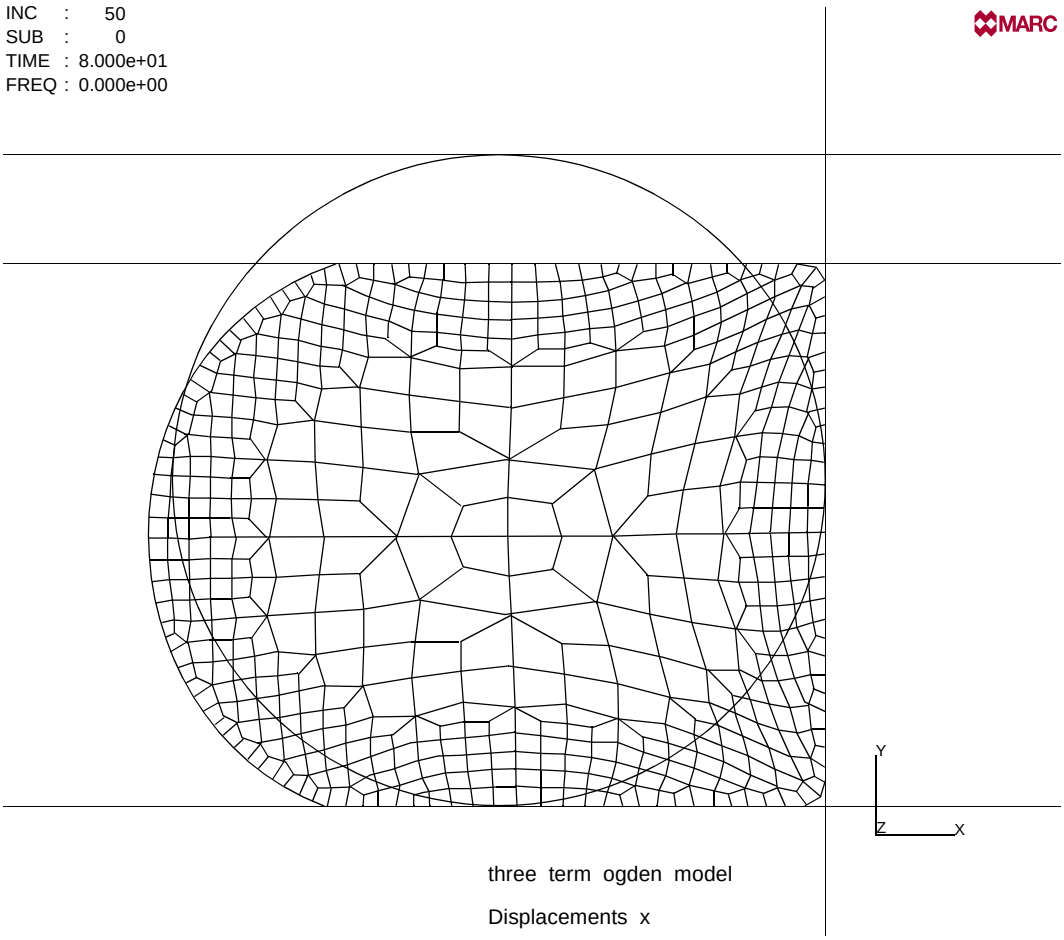

Figure 7.20-6 Deformed Mesh, Increment 50

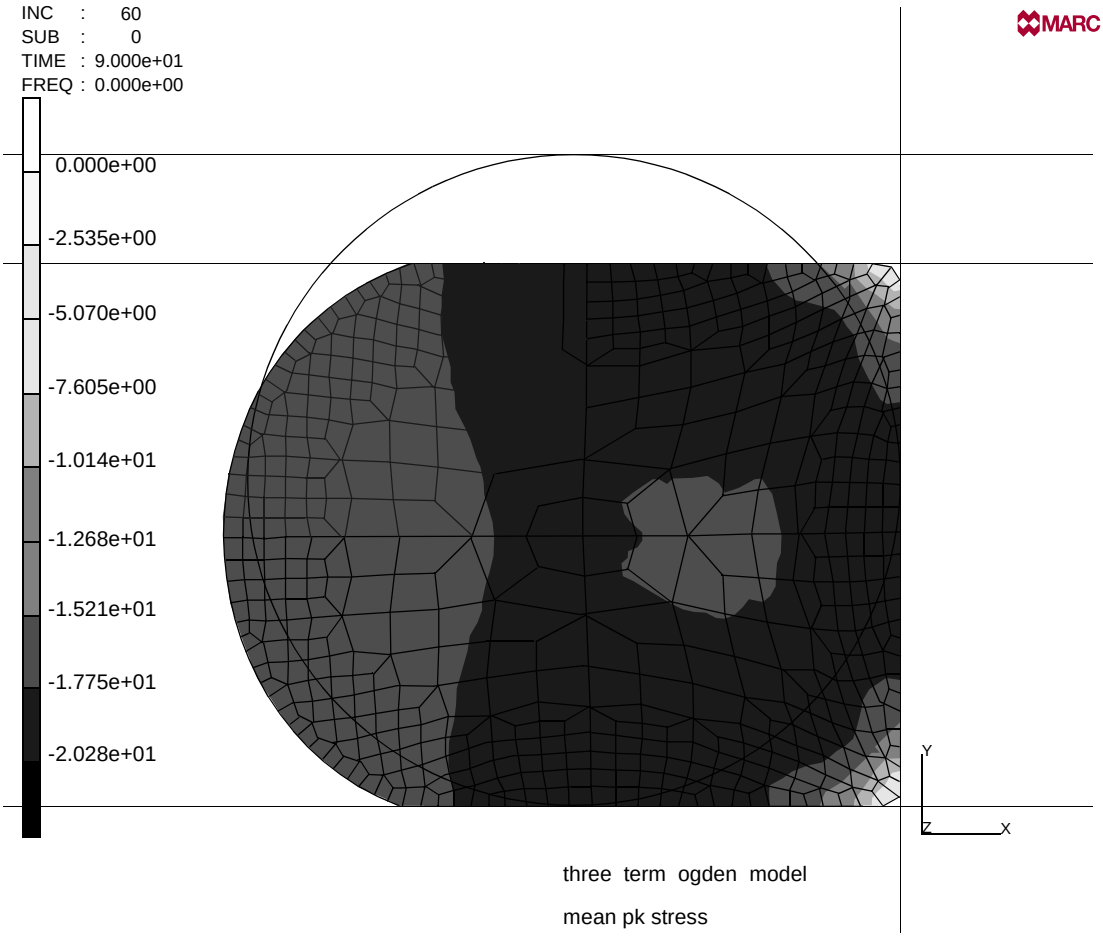

Figure 7.20-7 Mean Stress Distribution

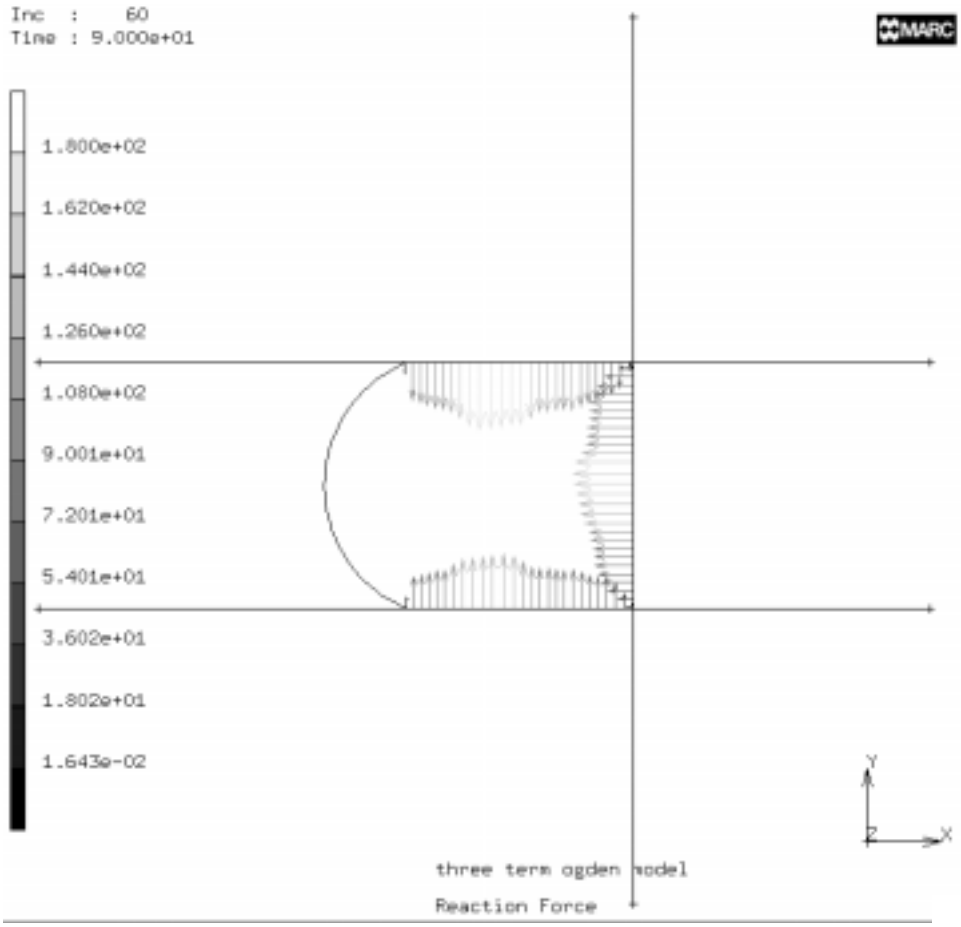

Figure 7.20-8 Contact Forces

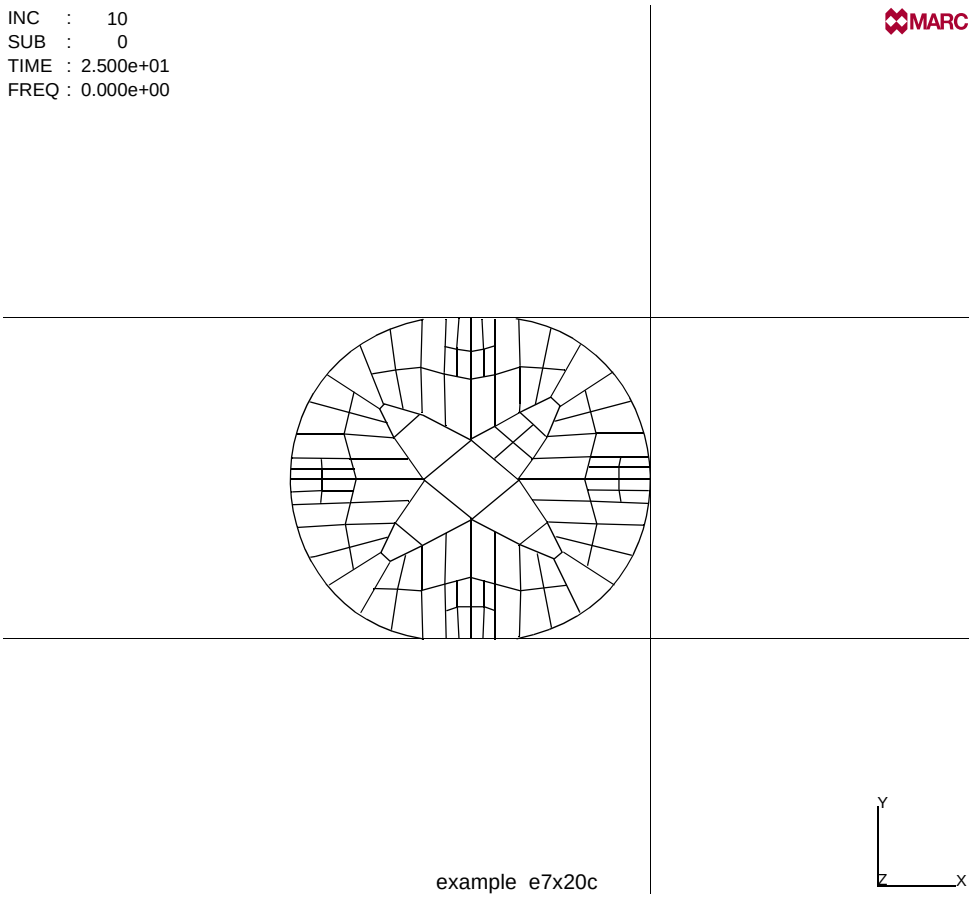

Figure 7.20-9 Adaptive Mesh at Increment 10

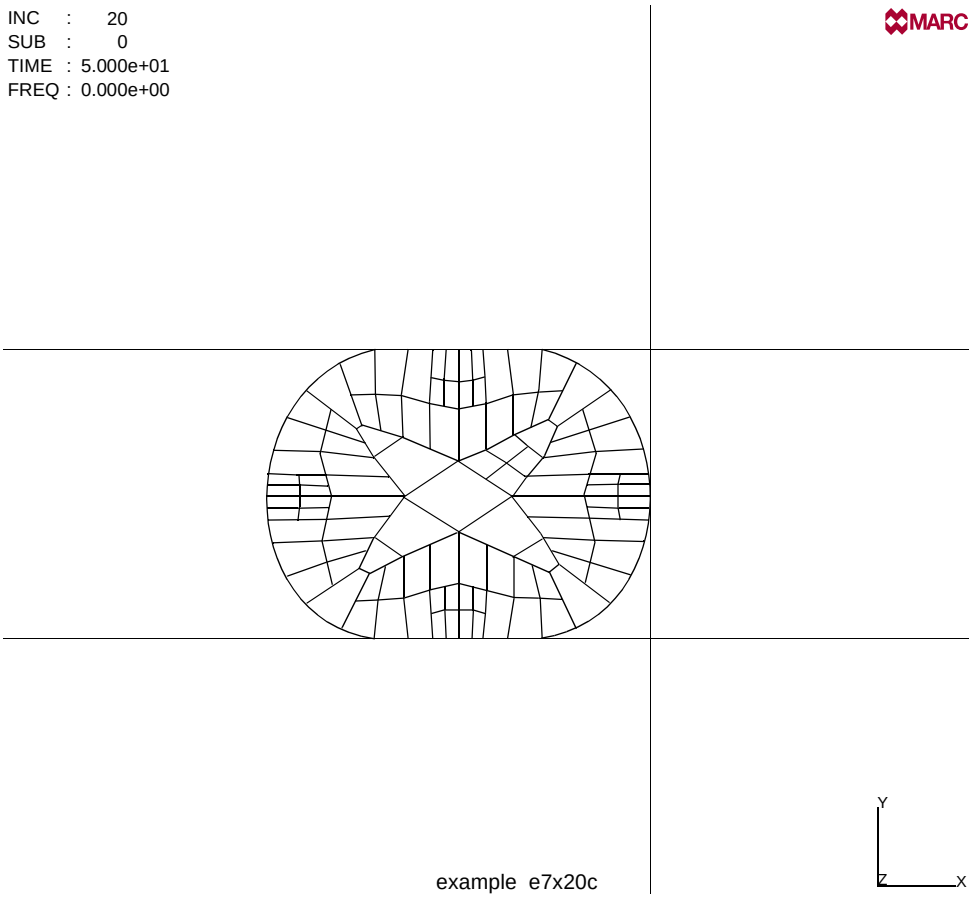

Figure 7.20-10 Adaptive Mesh at Increment 20

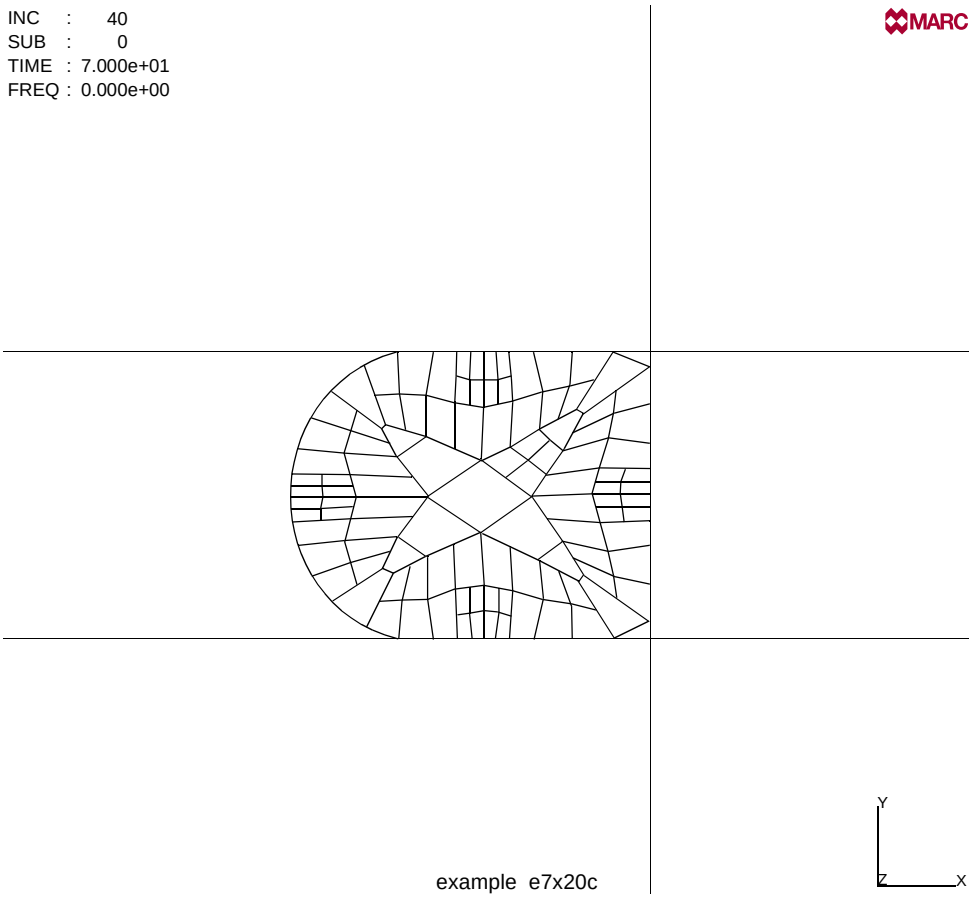

Figure 7.20-11 Adaptive Mesh at Increment 40

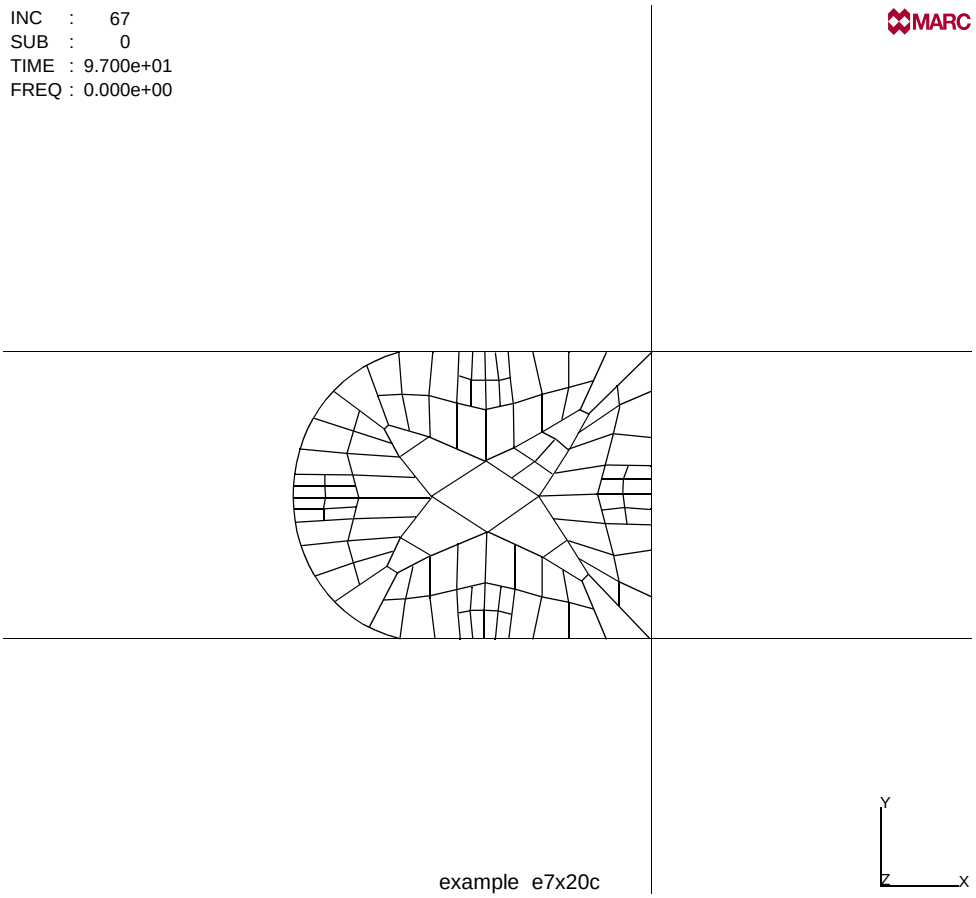

Figure 7.20-12 Adaptive Mesh at Increment 67

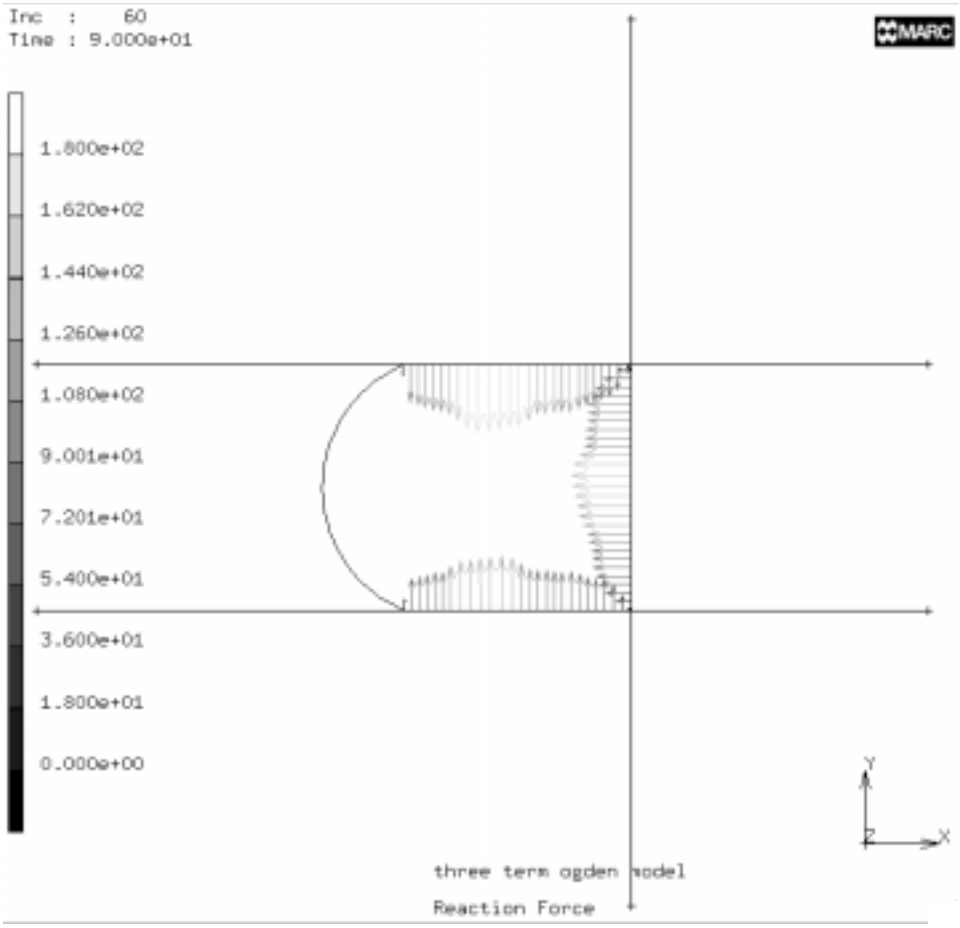

Figure 7.20-13 Contact Forces for the Updated Lagrange Formulation

7.21 Stretching of a Rubber Plate with Hole

This example demonstrates the use of the Ogden material model for a rubber sheet analysis.

Element

Element type 26 is an eight-node plane stress element. The plate is 10 cm x 10 cm, and the hole has a radius of 1. Due to symmetry, only one quarter of the model is used. The mesh is shown in Figure 7.21-1.

Loading

The x = 0 and y = 0 are symmetry planes. The line at x = 5 cm is being pulled with a uniform displacement of 2.5 cm over 5 increments through the DISP CHANGE and AUTO LOAD options.

Material Properties

The sheet is represented using the Ogden material model using a three-term series. The stress-strain curve for this model is shown in Figure 7.21-2. The data was fit such that:

Term	μ (N/cm^2)	α
1	19.7	1.3
2	0.038	5.0
3	-0.32	-2.0

The bulk modulus is 1 x 10^8 N/cm^2.

Geometry

The plate thickness is 1.0.

Controls

The full Newton-Raphson procedure is used with a convergence tolerance of one percent of residuals. Typically, one iteration was required to achieve convergence.

Results

The final deformed mesh is shown in Figure 7.21-3. The stress contours and the strain contours are shown in Figure 7.21-4 and Figure 7.21-5, respectively. One can observe that the strain was 250% in the vicinity of the hole.

Parameters, Options, and Subroutines Summary

Example e7x21.dat:

Parameters	Model Definition Options	History Definition Options
ELEMENT	CONNECTIVITY	AUTO LOAD
END	CONTROL	CONTINUE
LARGE DISP	COORDINATES	DISP CHANGE
SIZING	END OPTION	
TITLE	FIXED DISP	
	GEOMETRY	
	OGDEN	
	OPTIMIZE	
	POST	

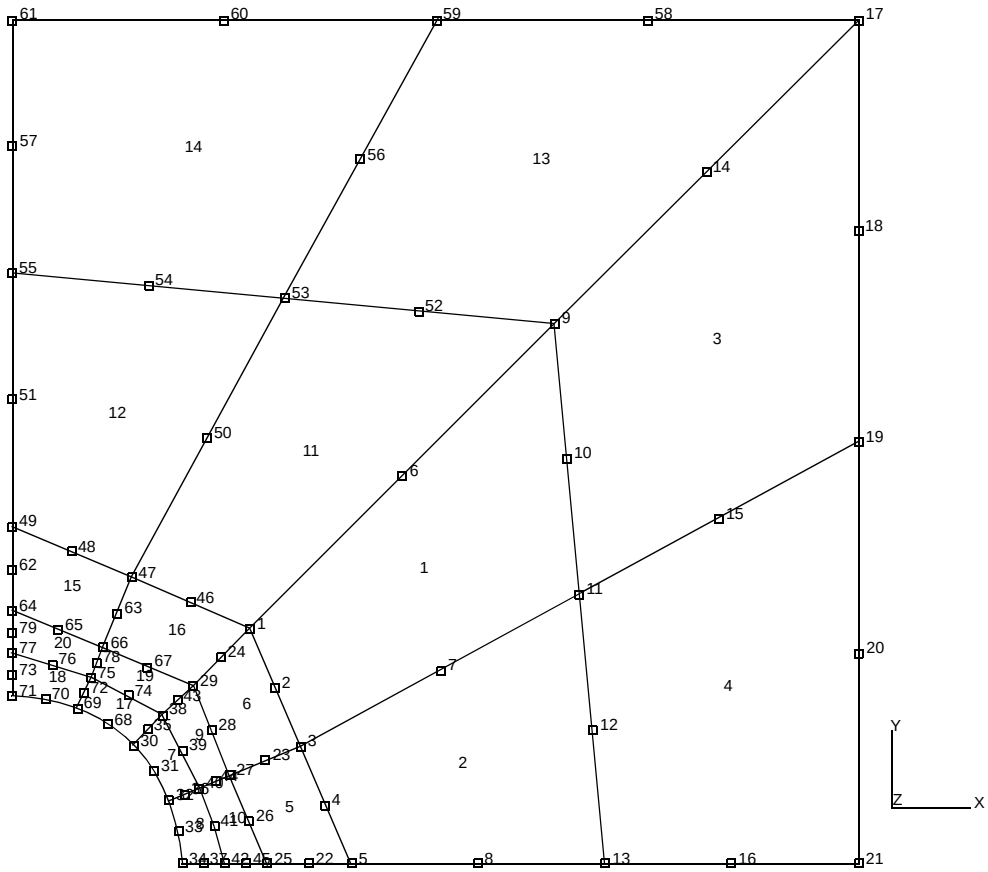

Figure 7.21-1 Finite Element Mesh

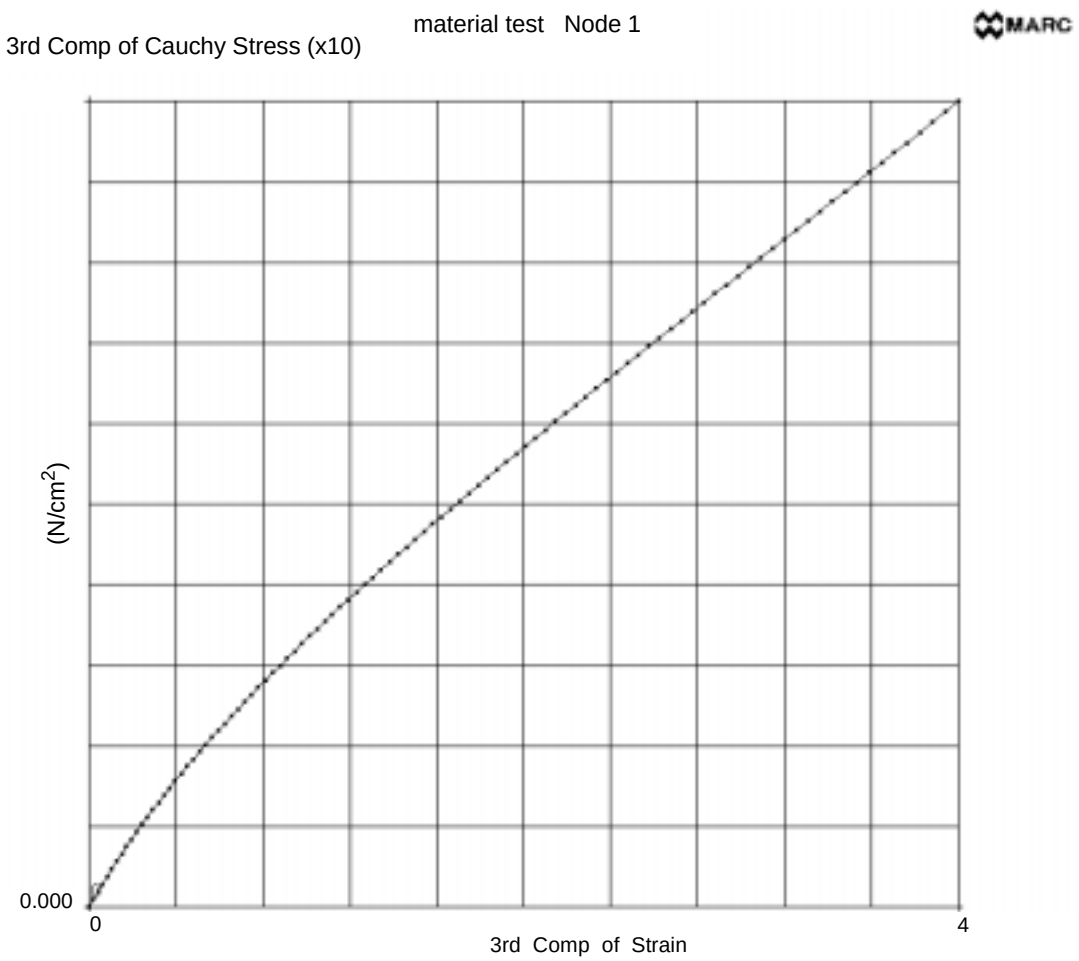

Figure 7.21-2 Stress-Strain Curve

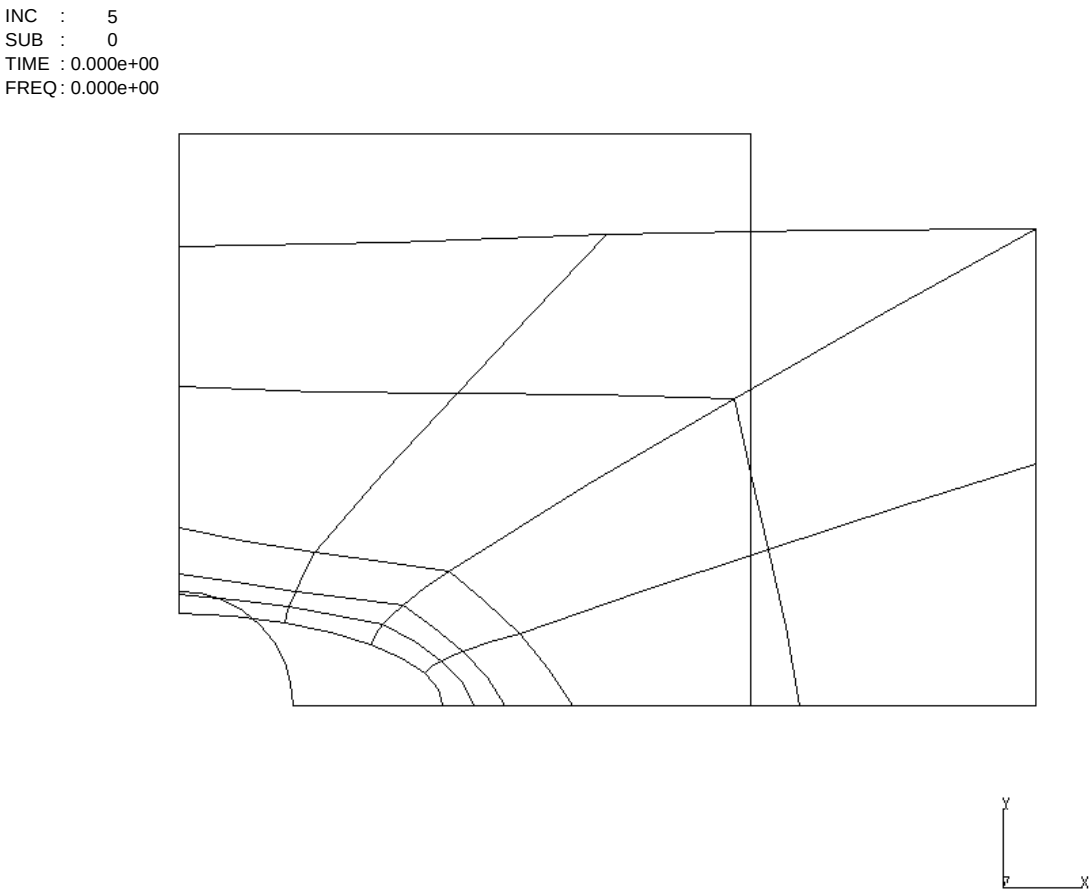

Figure 7.21-3 Deformed Mesh

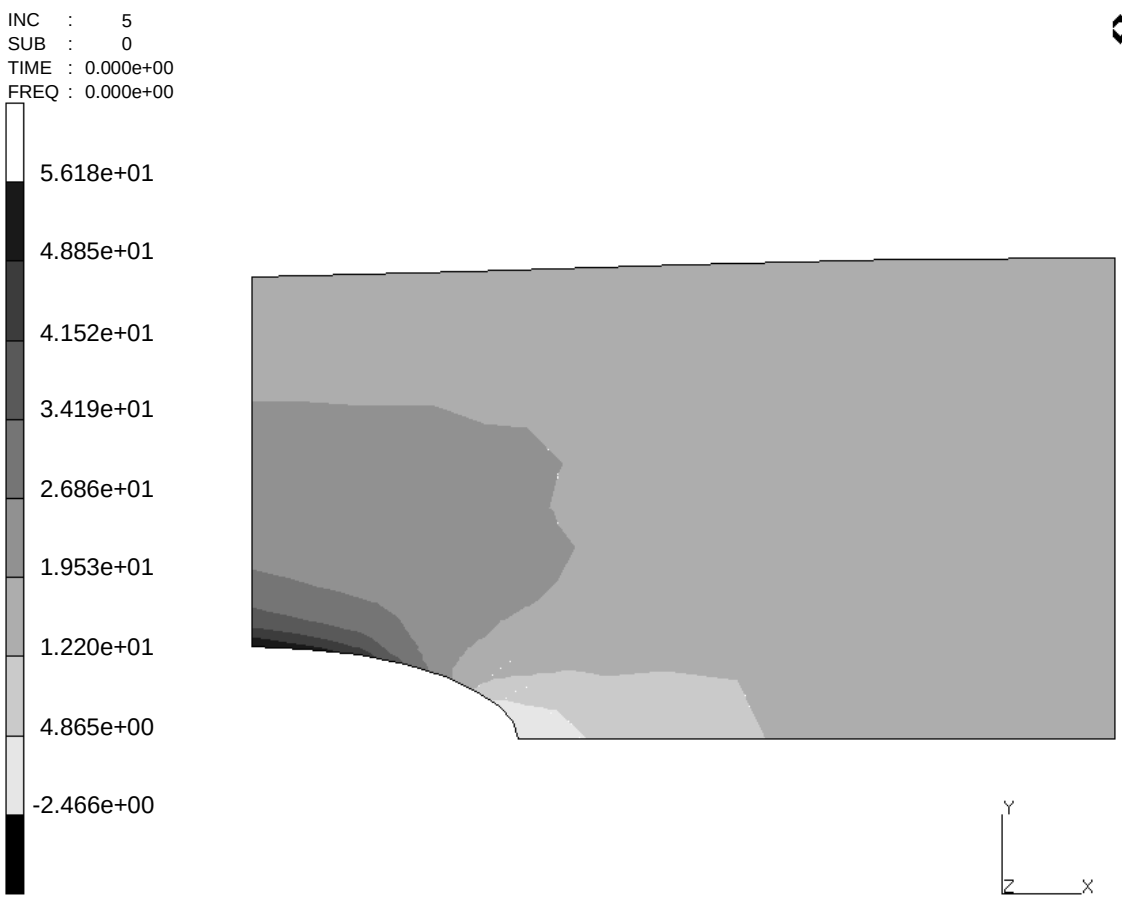

Figure 7.21-4 Stress Distribution

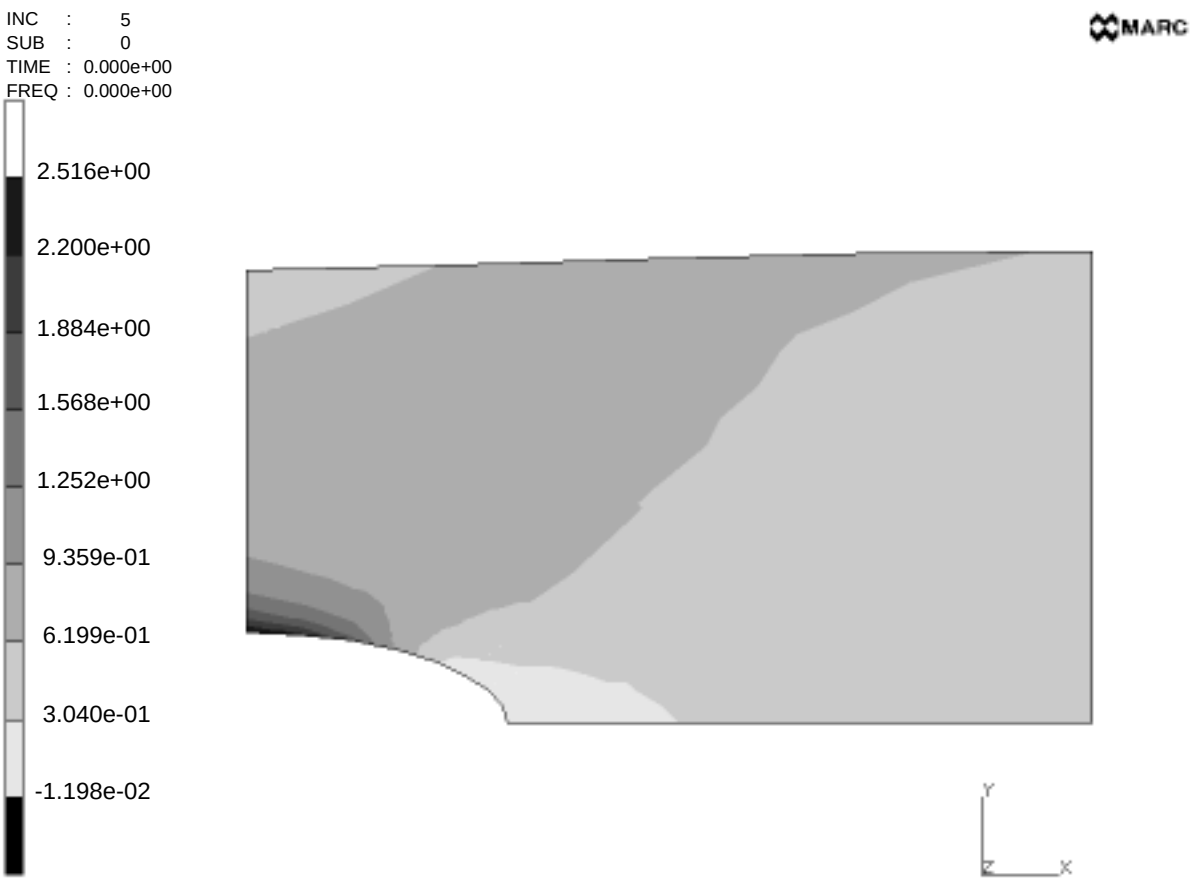

Figure 7.21-5 Strain Distribution

7.22 Loading of a Rubber Plate

This example illustrates the analysis of a rubber plate under cyclic loading. The analysis uses three different material models. The first analysis uses simply a three-term Ogden series; the second model incorporates damage; the third and most complex model incorporates both damage and viscoelasticity.

This problem is modeled using the three techniques summarized below.

Data Set	Element Type(s)	Number of Elements	Number of Nodes	Differentiating Features
e7x22a	75	25	36	Ogden
e7x22b	75	25	36	Ogden with damage
e7x22c	75	25	36	Ogden with visco and damage

Element

Element type 75 is a 4-node shell element used for this analysis. A 60 cm x 60 cm simply-supported plate is to be modeled. Because of symmetry, only one-quarter of the plate is represented using 25 elements as shown in Figure 7.22-1. The SHELL SECT option is used to prescribe three layers. This is adequate because it is a linear analysis. The thickness of 3 cm is specified in the GEOMETRY option.

Loading

The first and second models are rate insensitive. Two increments are taken to apply a distributed load of 0.004 on the complete plate followed by two increments to remove the load. In the third analysis, the initial load is also applied in two increments instantaneously; that is, the time step is zero. Hence, creep (viscoelasticity) does not occur. This is followed by a period of one second in which relaxation occurs in which no additional load is applied. Then, two increments follow during which the load is removed again and instantaneously followed by a final relaxation period of five seconds.

Material Properties

The rubber material is defined as a three-term Ogden series with a finite compressibility. The bulk modulus = 6000 N/cm^2 and the coefficients are:

Term	μ (N/cm^2)	α
1	6.300	1.3
2	0.012	5.0
3	-0.100	-2.0

The stress-strain law is shown in Figure 7.22-2.

The rubber damage model is used in the second and third analyses. Only deviatoric damage are considered with the damage rate being 0.050 and the maximum damage factor = 0.90. This is specified through the DAMAGE option.

The third model includes viscoelastic deviatoric behavior. Two terms are included in the Prony series to express the strain energy relaxation function:

Series	Multiplier	Relaxation Time (Seconds)
1	0.6	1.0
2	0.1	10.0

Notice that the total time of the analysis falls within the relaxation times specified.

Boundary Conditions

Displacements are prescribed such that nodes 1 to 6 and 1 to 31 by 6 have no normal displacement or rotations about the edge, and nodes 31 to 36 and 6 to 36 by 6 are symmetric boundary conditions. The in-plane rotation is constrained at all nodes.

Controls

The full Newton-Raphson method is used in this analysis. In those increments where the total applied load is nonzero, a five percent tolerance on residuals is required. When the applied load is zero, we would be attempting to measure residual/noise so the convergence is changed to displacement control. This is very important to insure efficient convergence to a meaningful accuracy.

Results

Figure 7.22-3 shows the displacement of the center node (36) as a function of the increment number for the first model. You can observe that the material goes back to the original configuration when the load has been removed. Displacement is of the order 10^{-6}. In Figure 7.22-4, one observes the displacement history when damage is included. Note that the maximum displacement is larger and the slope of the loading and unloading curve is substantially different. Upon unloading, there is a permanent deformation of the order 2.5×10^{-2}. Finally, Figure 7.22-5 shows the displacement history when both damage and viscoelasticity occur. You observe that there are four different regions: loading, creep, unloading and creep. Figure 7.22-6 is the same information but now plotted as a function of time.

Parameters, Options, and Subroutines Summary

Example e7x22a:

Parameters	Model Definition Options	History Definition Options
ELEMENT	CONNECTIVITY	AUTO LOAD
END	CONTROL	CONTINUE
LARGE DISP	COORDINATES	DIST LOADS
SHELL SEC	DIST LOADS	
SIZING	END OPTION	
TITLE	FIXED DISP	
	GEOMETRY	
	OGDEN	
	OPTIMIZE	
	POST	

Example e7x22b:

Parameters	Model Definition Options	History Definition Options
ELEMENT	CONNECTIVITY	AUTO LOAD
END	CONTROL	CONTINUE
LARGE DISP	COORDINATES	DIST LOADS
SHELL SECT	DAMAGE	
SIZING	DIST LOADS	
TITLE	END OPTION	
	FIXED DISP	
	GEOMETRY	
	OGDEN	
	OPTIMIZE	
	POST	

Example e7x22c:

Parameters	Model Definition Options	History Definition Options
ELEMENT	CONNECTIVITY	AUTO LOAD
END	CONTROL	CONTINUE
LARGE DISP	COORDINATES	DIST LOADS
SHELL SECT	DAMAGE	
SIZING	DIST LOADS	
TITLE	END OPTION	
	FIXED DISP	
	GEOMETRY	
	OGDEN	
	OPTIMIZE	
	POST	
	VISCELOGDEN	

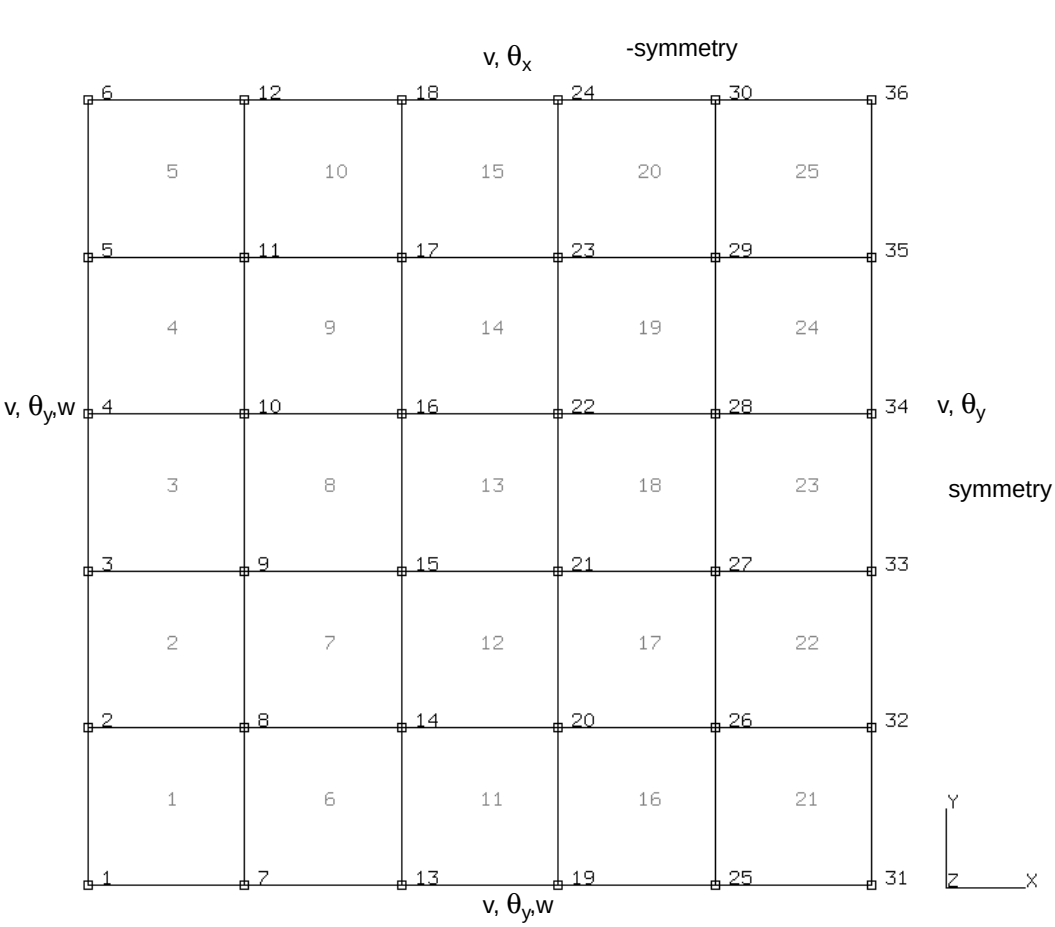

Figure 7.22-1 Finite Element Mesh

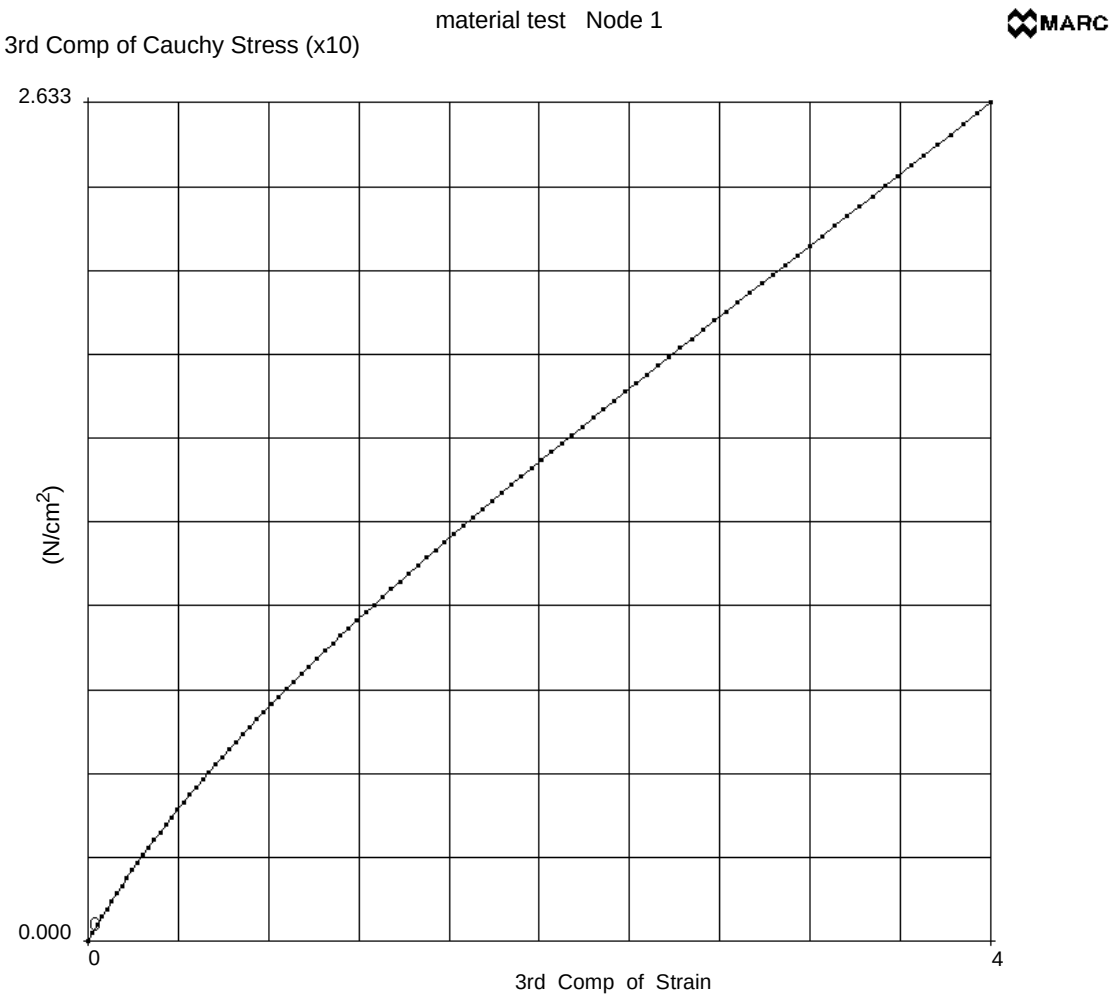

Figure 7.22-2 Stress-Strain Curve

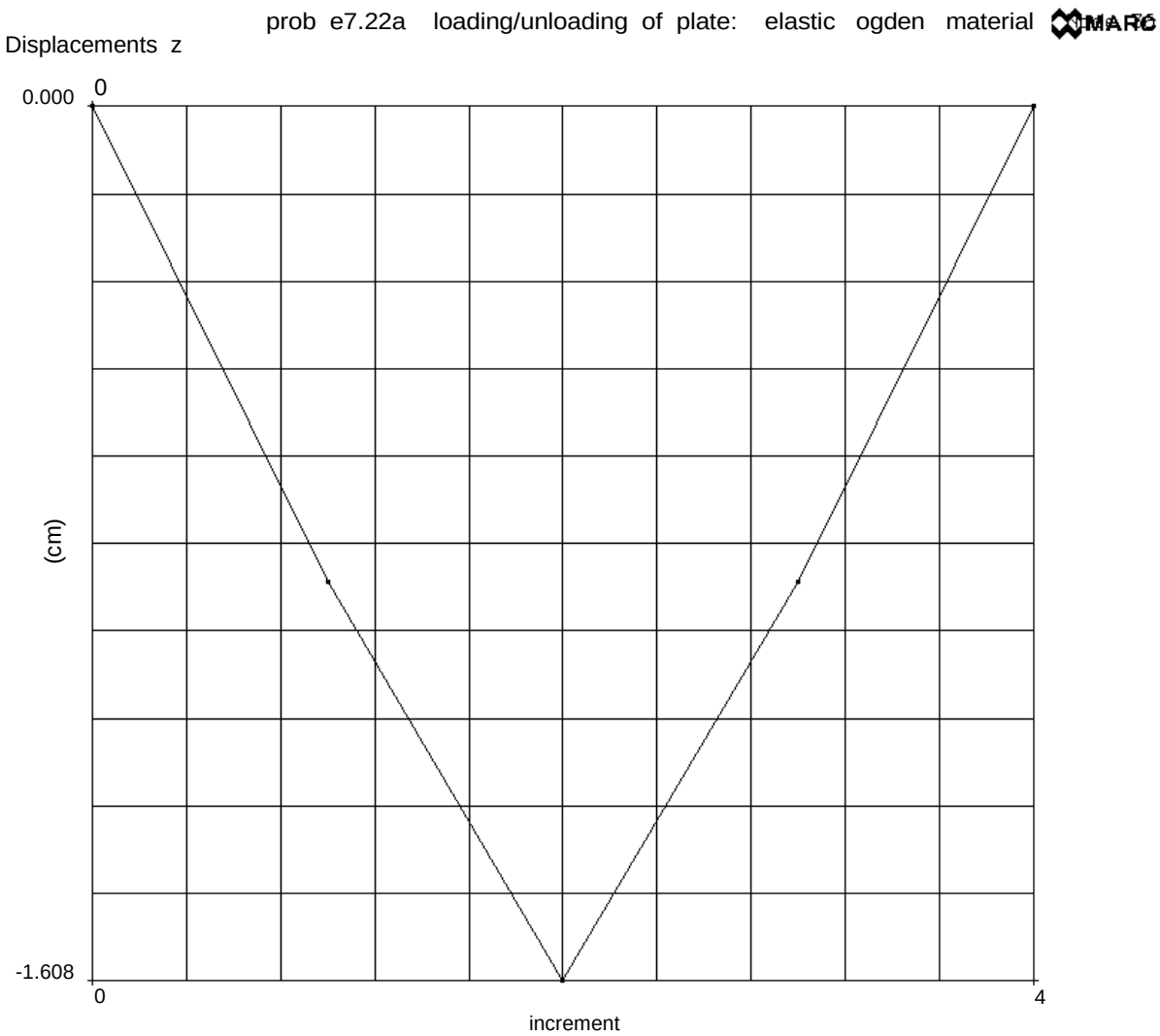

Figure 7.22-3 Displacement History of Center Node – Elastic Effects Only

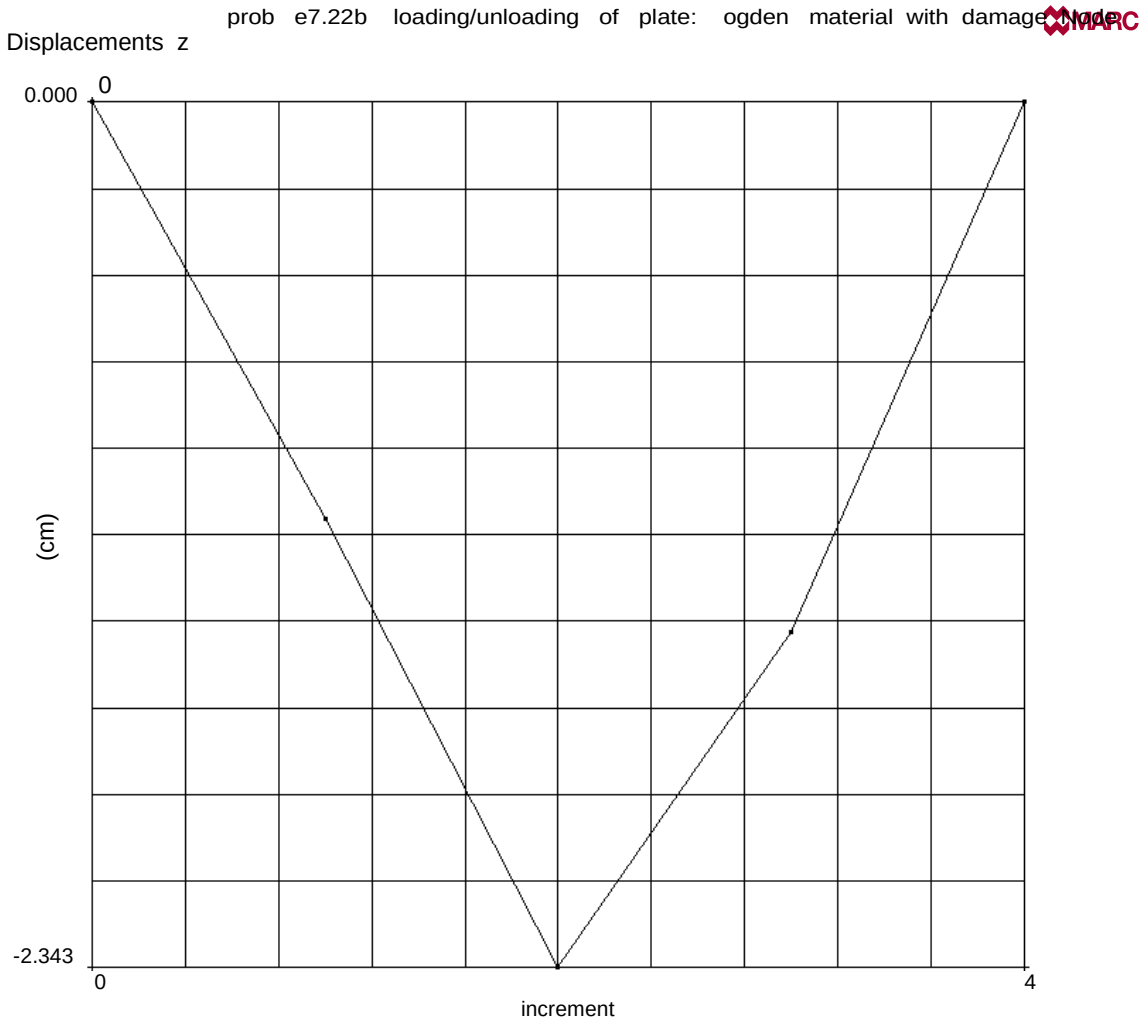

Figure 7.22-4 Displacement History of Center Node – Including Damage Effects

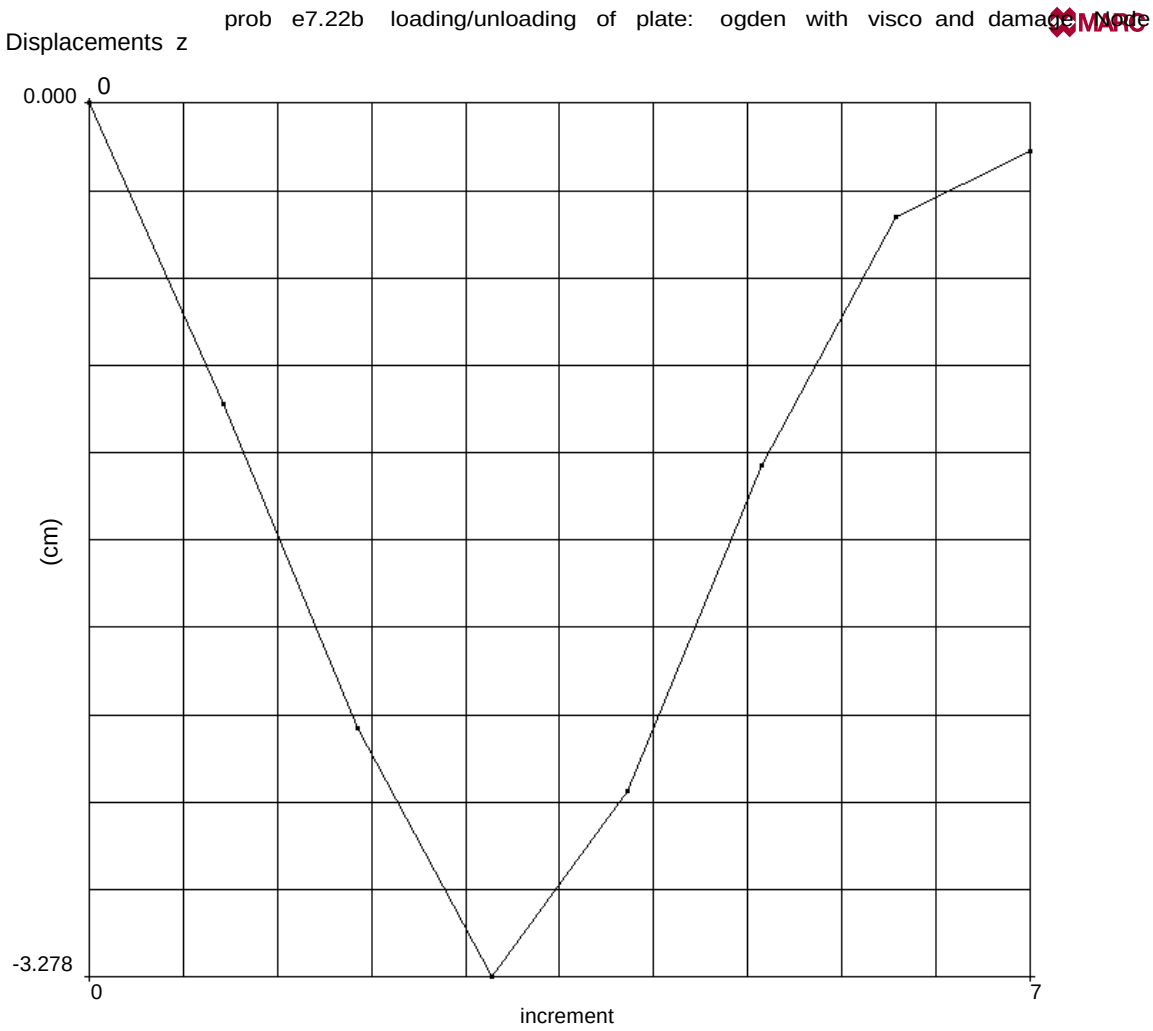

Figure 7.22-5 Displacement History of Center Node – Including Damage and Viscoelastic Effects

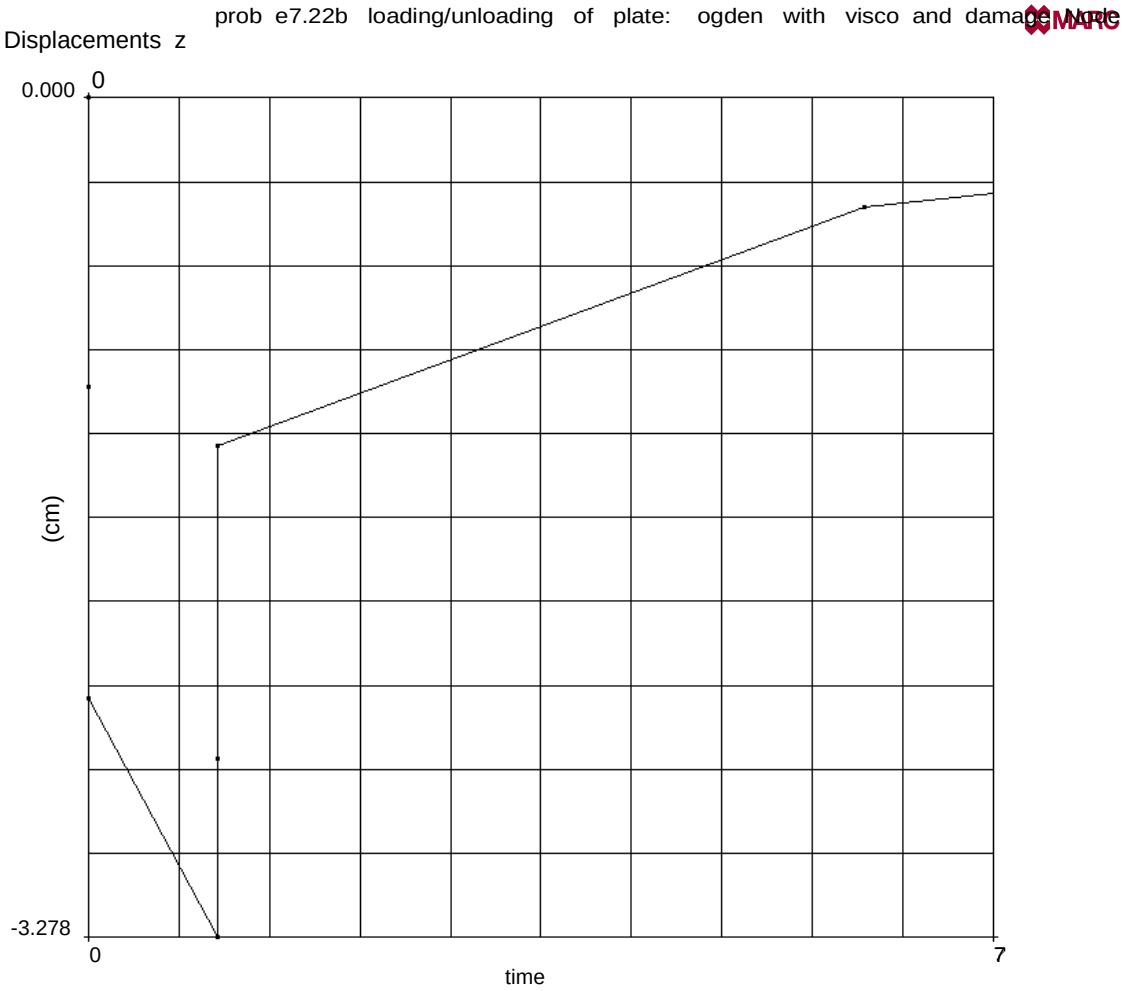

Figure 7.22-6 Displacement History as a Function of Time – Including Damage and Viscoelastic Effects

7.23 Compression of a Foam Tube

This example demonstrates the use of the generalized Ogden rubber foam model for the high compression of a tube.

Element

Library element 11, the plane strain, is used for this analysis. There are 140 elements and 175 nodes in the model as shown in Figure 7.23-1. Two rigid plates are moving toward the tube. The tube has an inner radius of 20 cm and an outer radius of 10 cm. Because of symmetry, only half of the tube of modeled.

Material Properties

The foam tube can be described using the foam material model using a two term series. The data was fixed such that:

Term	μ (N/cm)	α	β
1	0.0	2.0	-1.0
2	-32.0	-2.0	1.0

Contact/Boundary Conditions

All of the kinematic constrains are provided using rigid contact surfaces. The contact tolerance and the bias factor are set to 0.2 cm and 0.99 cm, respectively.

The rigid surface at the bottom and top move at a speed of 1.5 cm/second in a period of 8.15 seconds toward the tube.

Control

The full New-Raphson iterative method is used with a convergence tolerance of 1% on residuals requested.

Results

The deformed mesh at increments 10, 16, and 29 are shown in Figure 7.23-2 through Figure 7.23-4. The shear strain distribution is shown in Figure 7.23-5. Using Mentat, you can determine that the initial area is 469.90 cm^2 and the final area is 421.05 cm^2; hence, there is a 10% reduction in volume.

Parameters, Options, and Subroutines Summary

Example e7x23.dat:

Parameters	Model Definition Options	History Definition Options
ALL POINTS	CONNECTIVITY	AUTO LOAD
ELEMENTS	CONTACT	CONTINUE
END	CONTROL	TIME STEP
LARGE DISP	COORDINATE	
PRINT	DEFINE	
SETNAME	END OPTION	
SIZING	FIXED DISP	
TITLE	FOAM	
	NO PRINT	
	OPTIMIZE	
	POST	
	SOLVER	

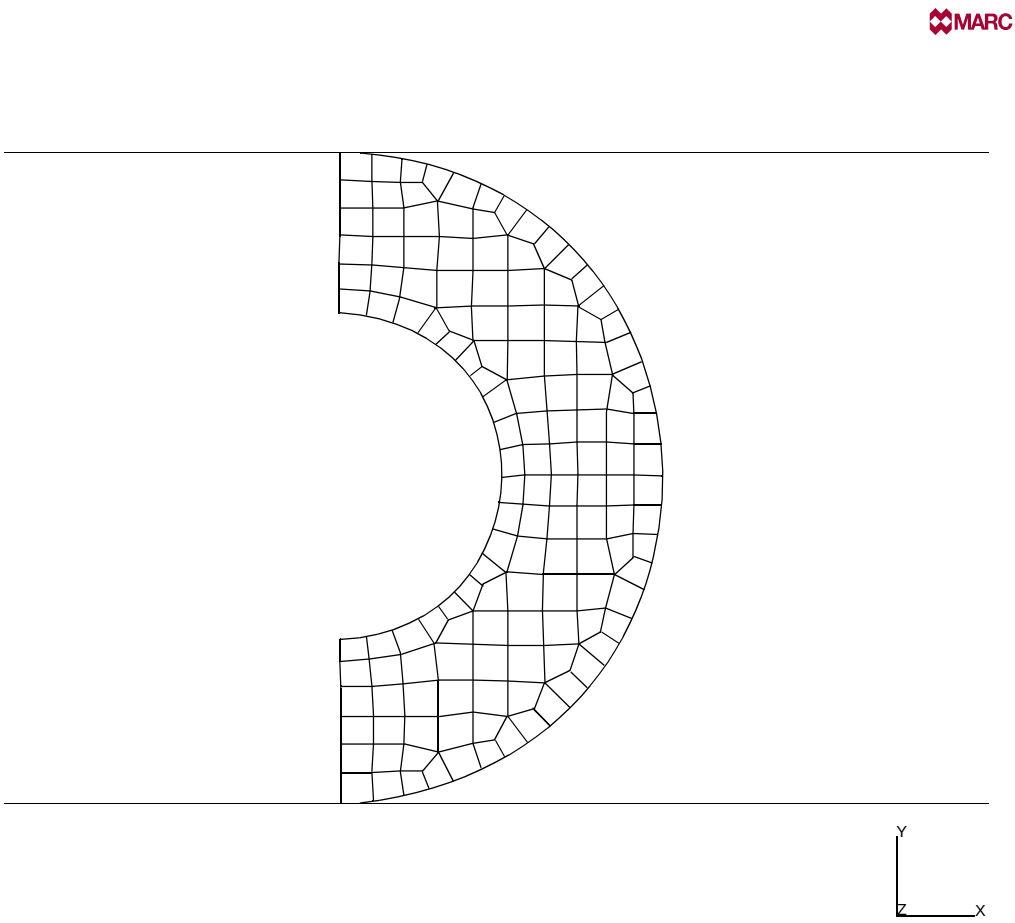

Figure 7.23-1 Finite Element Mesh of Tube

INC : 10
SUB : 0
TIME : 6.400e+00
FREQ : 0.000e+00

MARC

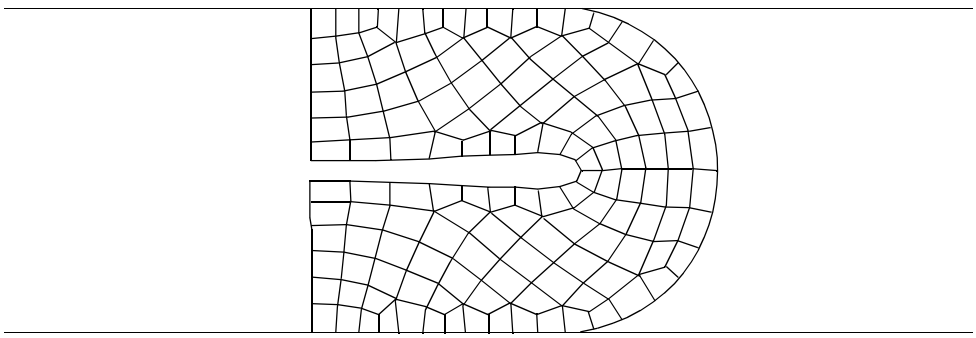

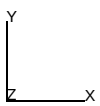

prob e7x23 compression of a foam tube

Figure 7.23-2 Deformed Mesh at Increment 10

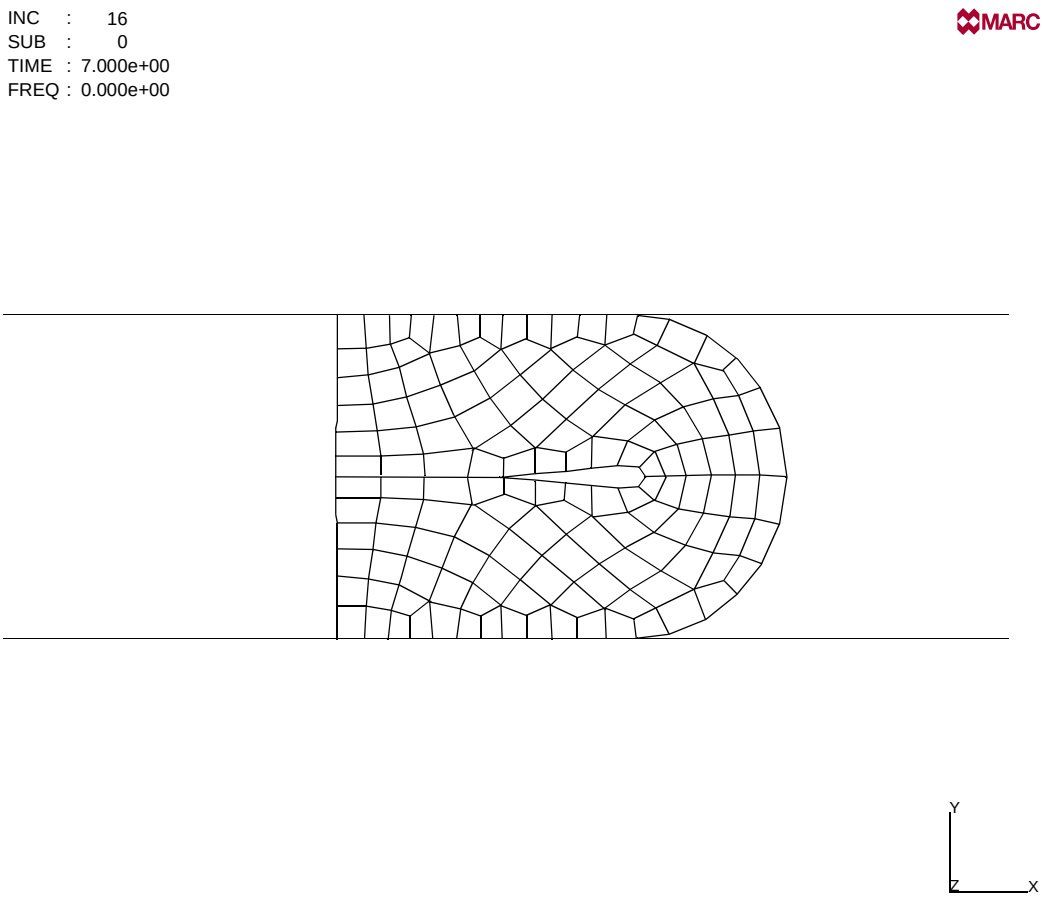

Figure 7.23-3 Deformed Mesh at Increment 16

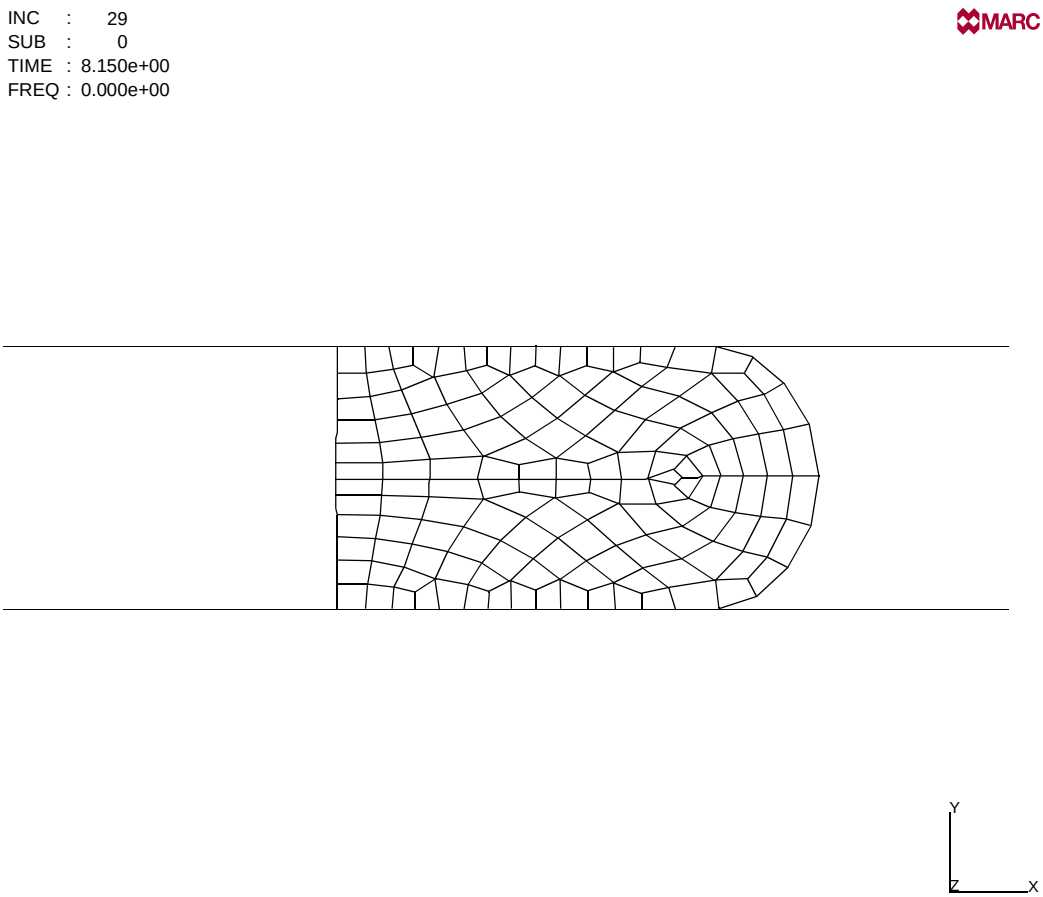

Figure 7.23-4 Deformed Mesh at Increment 29

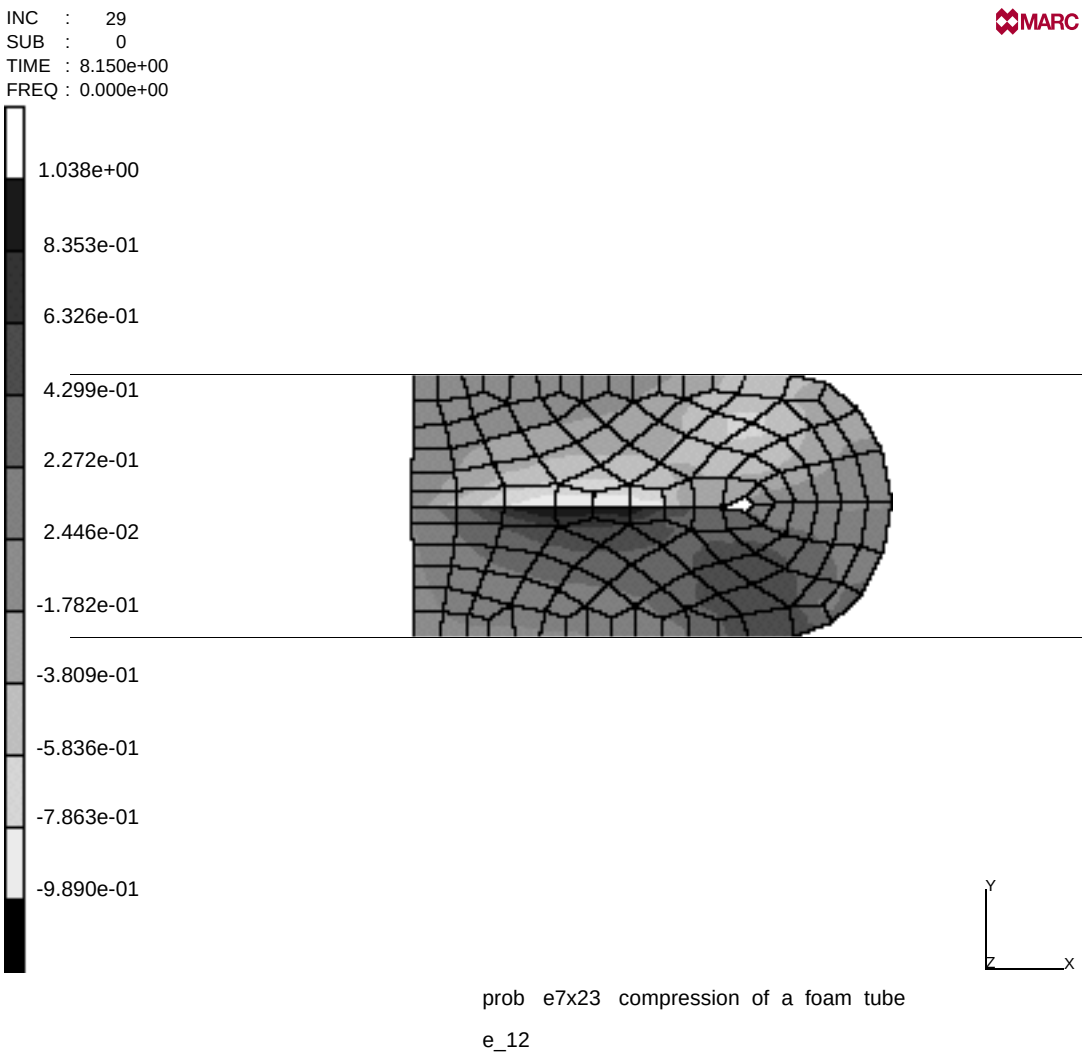

Figure 7.23-5 Shear Strain in Compressed Tube

7.24 Constitutive Law for a Composite Plate

This example provides an analytic qualification of the constitutive law existing in a composite laminated plate. The model is made of a single finite element.

Model

The plate is made of a single shell element (element 75 in MARC). The element has four nodes with bilinear interpolation of displacement and rotation components.

Material Properties

The plate is made of eight laminae of boron-epoxy set to produce an equilibrated and symmetric laminate with the angles:

/+45/-45/+45/-45/S

Each lamina in boron-epoxy has the following properties of orthotropic material:

E_{11} = 29.7 E6 psi
E_{22} = 2.97 E6 psi
ν_{12} = 0.33
G_{12} = 1. E psi

Geometry

The plate has total thickness THT = 0.4 inches. The thickness in every lamina is thus THL = 0.05 inches.

Orientation

The orientation of the lamina is given by assigning the reference axis E_1 to be side 1-2 of the element (see Figure 7.24-1) The angles assigned to the fibers imply rotations of +45° or -45° with respect to the normal E_3 to the plate. The rotation starts from E_1, positive if counterclockwise.

Boundary Conditions

The plate is loaded with a constant membrane strain in the x-direction. $\varepsilon_{mx} = 1$ is obtained by assigning to nodes 1 and 3 displacements $u_x = 2$, $u_y = 0$. While this would produce large strains, small strain theory is used here so you can easily compare the calculations with the analytical solution.

Results

By assigning a displacement $u_x = 2$ to a plate with H = B = 2 inches, you obtain for all laminae:

$\varepsilon_x = 1$
$\varepsilon_y = \gamma_{xy} = 0$

The strains and stresses in a lamina at +45° are computed as:

$$\varepsilon'_{45} = T_{45} \cdot \varepsilon = \begin{bmatrix} 0.5 & 0.5 & 0.5 \\ 0.5 & 0.5 & -0.5 \\ -1. & 1. & 0 \end{bmatrix} \cdot \begin{Bmatrix} 1 \\ 0 \\ 0 \end{Bmatrix} = \begin{Bmatrix} 0.5 \\ 0.5 \\ -1. \end{Bmatrix}$$

$$\sigma'_{45} = D \cdot \varepsilon'_{45} = 10^6 \begin{bmatrix} 30 & 1 & 0 \\ 1 & 3 & 0 \\ 0 & 0 & 1 \end{bmatrix} \cdot \begin{Bmatrix} 0.5 \\ 0.5 \\ -1. \end{Bmatrix} = 10^6 \begin{Bmatrix} 15.5 \\ 2. \\ -1. \end{Bmatrix}$$

Shear

The plate is loaded with membrane shear by assigning to nodes 2 and 3 the displacements $u_x = 0, u_y = 2$.

Results

By assigning displacements $u_x = 0$ and $u_y = 2$ to a plate with H = B = 2 inches, you obtain for all the laminae:

$\nu_{xy} = 1.$
$\varepsilon_y = \varepsilon_y = 0$

The strains and stresses in a laminae are computed as:

$$\varepsilon'_{45} = T_{45} \cdot \varepsilon = \begin{bmatrix} 0.5 & 0.5 & 0.5 \\ 0.5 & 0.5 & -0.5 \\ -1. & 1. & 0 \end{bmatrix} \cdot \begin{Bmatrix} 0 \\ 0 \\ 1 \end{Bmatrix} = \begin{Bmatrix} 0.5 \\ -0.5 \\ 0. \end{Bmatrix}$$

$$\sigma'_{45} = D \cdot \varepsilon'_{45} = 10^6 \begin{bmatrix} 30 & 1 & 0 \\ 1 & 3 & 0 \\ 0 & 0 & 1 \end{bmatrix} \cdot \begin{Bmatrix} 0.5 \\ -0.5 \\ 0. \end{Bmatrix} = 10^6 \begin{Bmatrix} 14.5 \\ -1. \\ 0. \end{Bmatrix}$$

Bending

The plate is loaded in bending by assigning to nodes 2 and 3 a rotation $\phi_y = 2$. You obtain a constant curvature $\chi_x = 1$.

Nodes 1 and 4 are clamped. Nodes 2 and 3 are free in the remaining degree of freedom.

Results

Assigning a rotation $\phi_y = 2$ to a plate with H = B = 2 inches, you obtain:

$\chi_x = 1.$
$\chi_y = \chi_y = 0$

The first lamina, at z = 0.175 from midspan, has $\varepsilon_x = z \cdot \chi_x = 0.175$ in local axes.

The strains and stresses in the first lamina at +45° are computed as:

$$\varepsilon'_{45} = T_{45} \cdot \varepsilon = \begin{bmatrix} 0.5 & 0.5 & 0.5 \\ 0.5 & 0.5 & -0.5 \\ -1. & 1. & 0 \end{bmatrix} \cdot \begin{Bmatrix} 0.175 \\ 0 \\ 0 \end{Bmatrix} = \begin{Bmatrix} 0.875 \\ -0.875 \\ 0.175 \end{Bmatrix}$$

$$\sigma'_{45} = D \cdot \varepsilon'_{45} = 10^6 \begin{bmatrix} 30 & 1 & 0 \\ 1 & 3 & 0 \\ 0 & 0 & 1 \end{bmatrix} \cdot \begin{Bmatrix} 0.875 \\ -0.875 \\ 0.175 \end{Bmatrix} = 10^6 \begin{Bmatrix} 2.175 \\ 0.35 \\ 0.175 \end{Bmatrix}$$

Parameters, Options, and Subroutines Summary

Example e7x24a.dat:

Parameters	Model Definition Options
ELEMENTS	COMPOSITE
END	CONNECTIVITY
SHELL SECT	COORDINATE
SIZING	END OPTION
TITLE	FIXED DISP
	ORIENTATION
	ORTHOTROPIC
	PRINT ELEMENT

Example e7x24b.dat:

Parameters	Model Definition Options
ELEMENTS	COMPOSITE
END	CONNECTIVITY
SHELL SECT	COORDINATE
SIZING	END OPTION
TITLE	FIXED DISP
	ORIENTATION
	ORTHOTROPIC
	PRINT ELEMENT

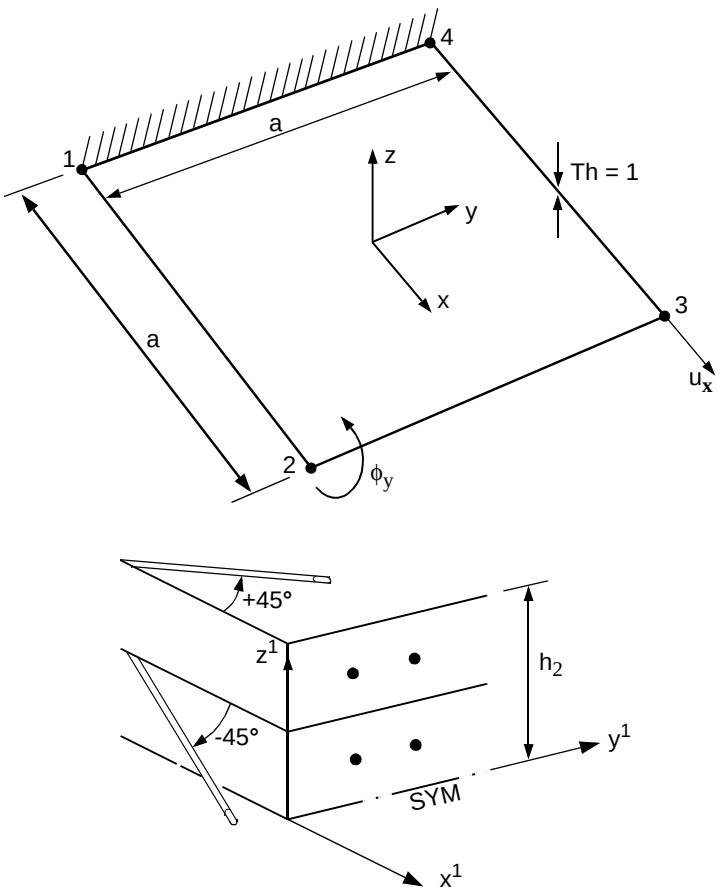

Figure 7.24-1 Geometry and Lamination of a Composite Plate

7.25 Progressive Failure of a Composite Strip

This problem tests the capability of MARC to performing progressive failure of composite structures. The test structure modeled here is a strip with a rectangular cross section clamped at both ends and loaded by concentrated forces at midspan.

The material is a laminate, with eight laminae alternating the fiber direction between 0° and 90°. The fiber failure stress in tension is taken here to be the same as in compression.

Under linear elastic behavior, the strip behaves like a beam clamped at both ends. The largest (bending) stresses occur at midspan and at the supports. The load is increased in 126 increments until the fibers are broken and only the matrix bears the load. Correspondingly, the deformed shape of the strip moves from that of a beam to a 3-hinged arch.

Model

Due to symmetry, only half of the strip is modeled. The FEM mesh includes 30 elements and 153 nodes. Element 22, (8-noded shell) is used. LARGE DISP and UPDATE are active for geometrically nonlinear analysis. The strip has length l = 200 mm, width b = 10mm, and thickness t = 1 mm. The mesh is shown in Figure 7.25-1.

Material Properties

The material is a laminated carbon-epoxy. Two outer skins, with a thickness of 0.25 mm, have the fibers in the longitudinal direction (global X axis). They confine a “core”, thick 0.5 mm, with fibers in the transverse direction. The laminae have 0.125 mm thickness. Therefore, eight laminae make up the strip.

$E_{11} = 2140000$ N/mm^2
$E_{22} = 9700$ N/mm^2
$\nu_{12} = 0.28$
$G_{12} = 5400$ N/mm^2
$G_{23} = 3600$ N/mm^2
$G_{31} = 5400$ N/mm^2

A lamina fails for maximum stress with the following limit values:

σ_1	= 1020	N/mm^2	in the direction of the fibers, tension or compression
σ_2	= 59	N/mm^2	in the direction orthogonal to the fibers, tension or compression
τ	= 95	N/mm^2	shear

Supports

Nodes 1, 2, and 3 at the strip end are clamped allowing for transverse dilation.

Nodes 151, 152, and 153 at midspan have symmetry conditions.

All midspan nodes undergo the same vertical deflection.

Loads

A concentrated load is applied at midspan. The magnitude is increased to p = 3000 N in 125 load increments.

Results

The time history of the tip deflection is shown in Figure 7.25-2. You can easily observe when plys failed in the system by the jump in the deflection. The first failure occurs in increment 10.

Figure 7.25-3 and Figure 7.25-4 show the time history of the stresses in layers 1 and 5. The final figure, Figure 7.25-5, shows the axial reaction force at the clamped end. Notice the sudden decrease in stress level. The strip deformation has already moved to that of a three-hinged arch.

Parameters, Options, and Subroutines Summary

Example e7x25.dat:

Parameters	Model Definition Options	History Definition Options
ELEMENTS	COMPOSITE	AUTO LOAD
END	CONNECTIVITY	CONTINUE
LARGE DISP	CONTROL	NO PRINT
SHELL SECT	COORDINATE	POINT LOAD
SIZING	END OPTION	POST INCREMENT
TITLE	FAIL DATA	PRINT ELEMENT
UPDATE	FIXED DISP	PROPORTIONAL INCREMENT
	ORIENTATION	
	ORTHOTROPIC	
	POST	
	TYING	

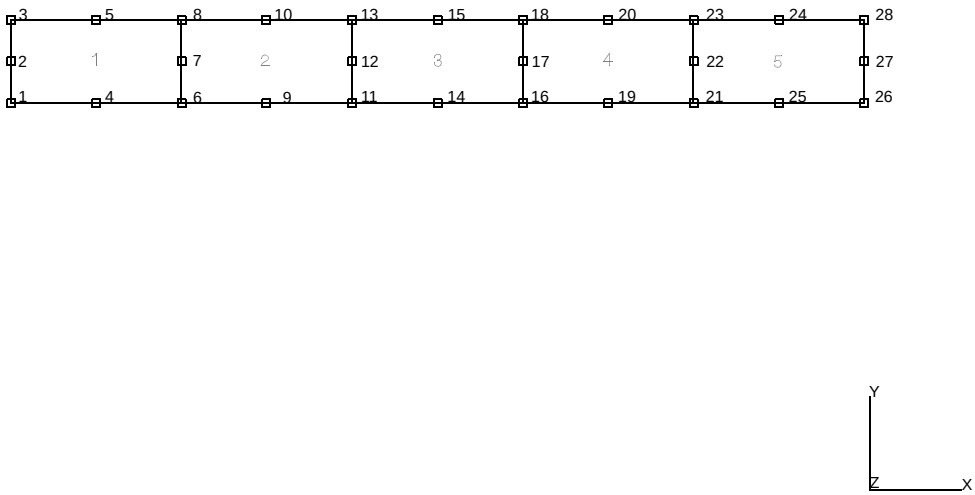

Figure 7.25-1 Finite Element Mesh of Strip

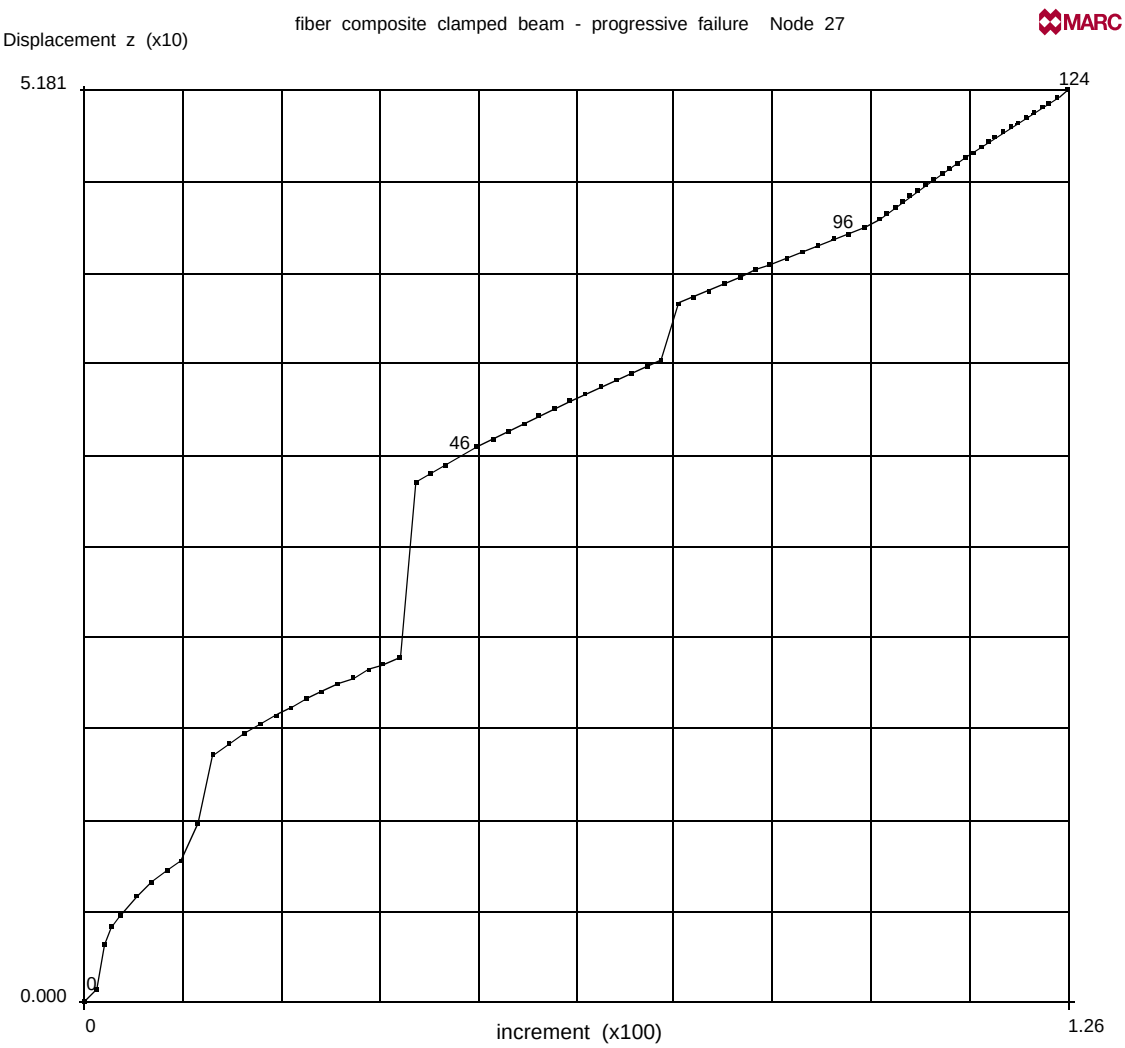

Figure 7.25-2 History of Deflection of the Tip

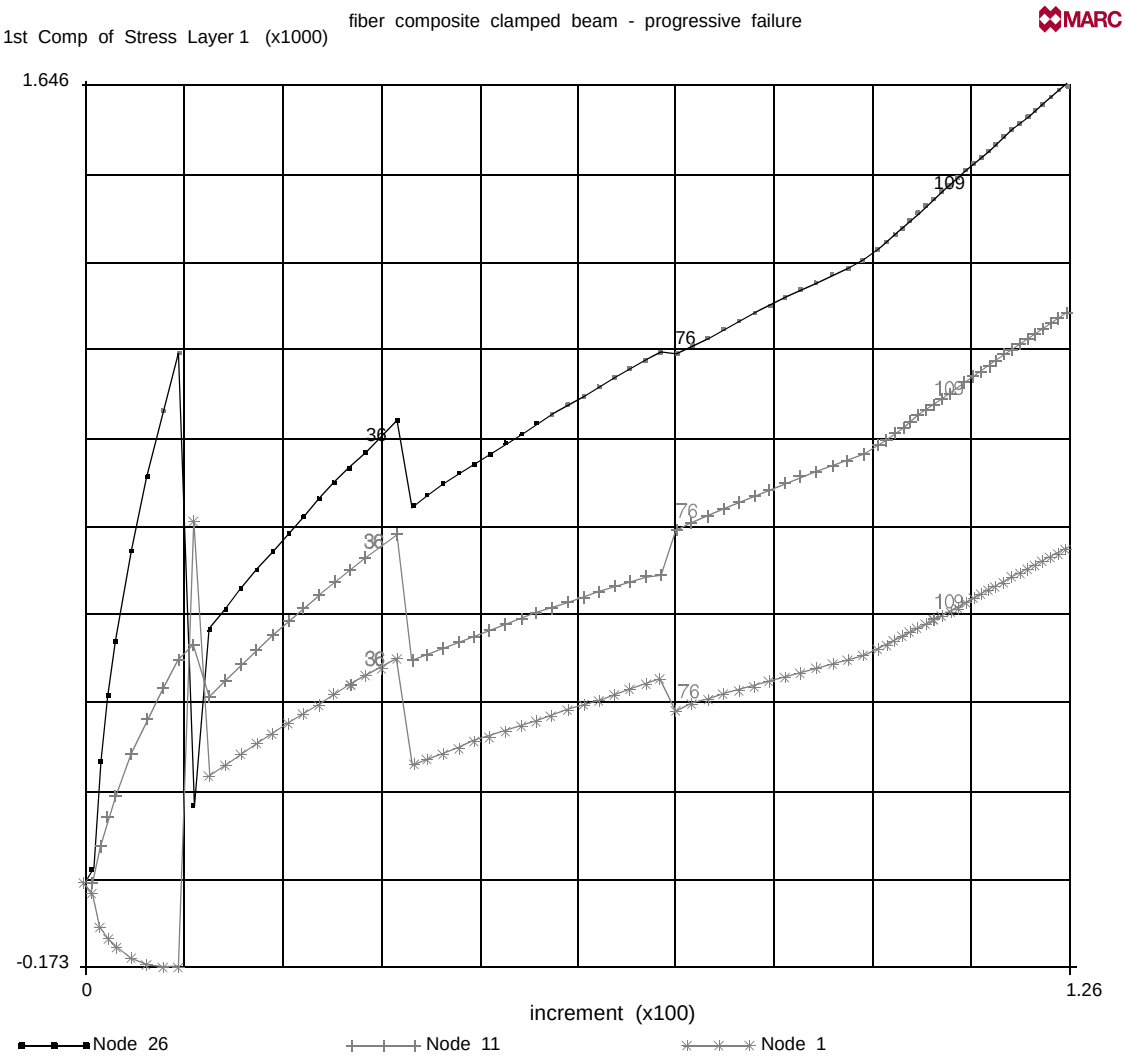

Figure 7.25-3 History of First Component of Stress in Layer 1

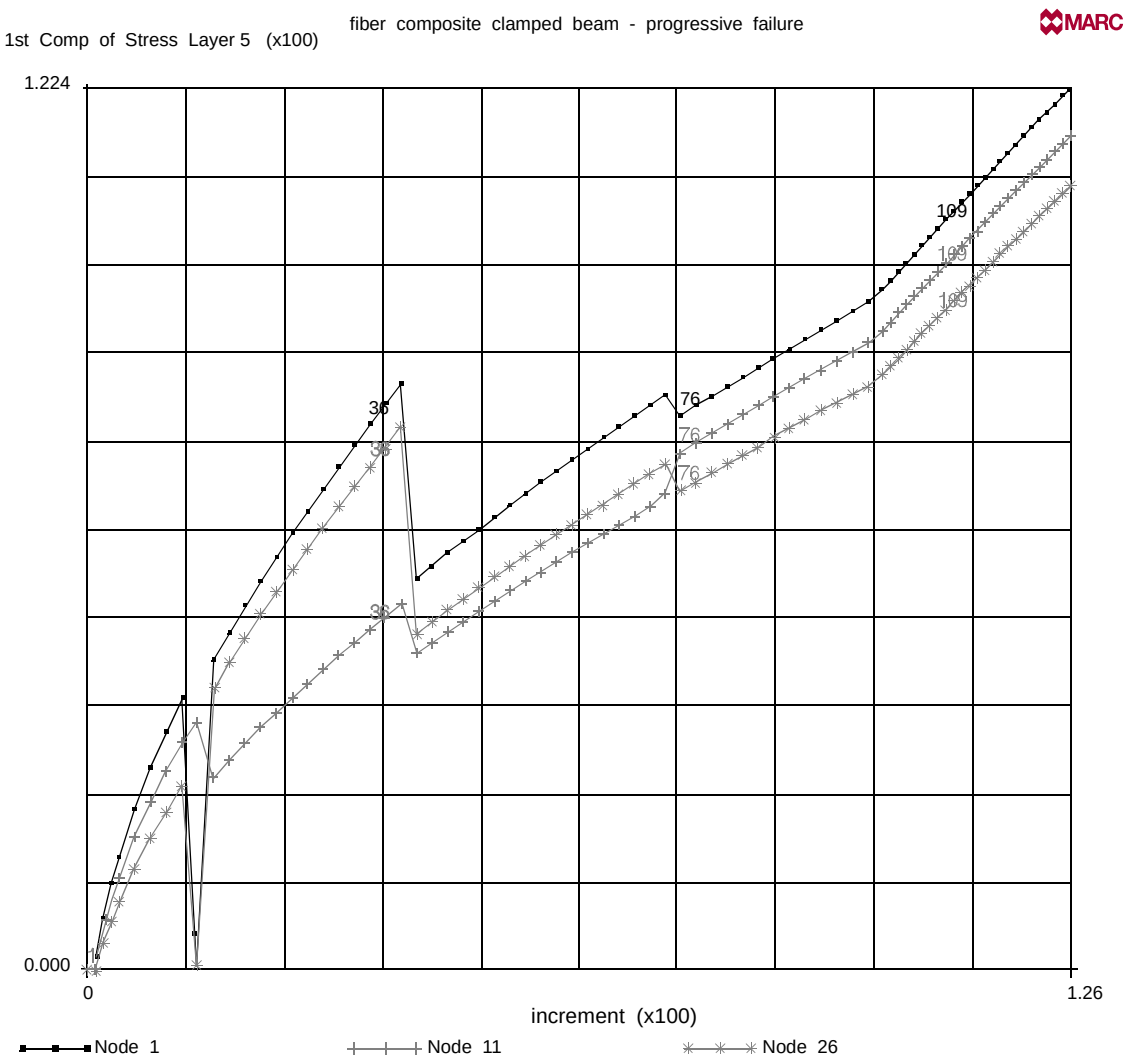

Figure 7.25-4 History of First Component of Stress in Layer 5

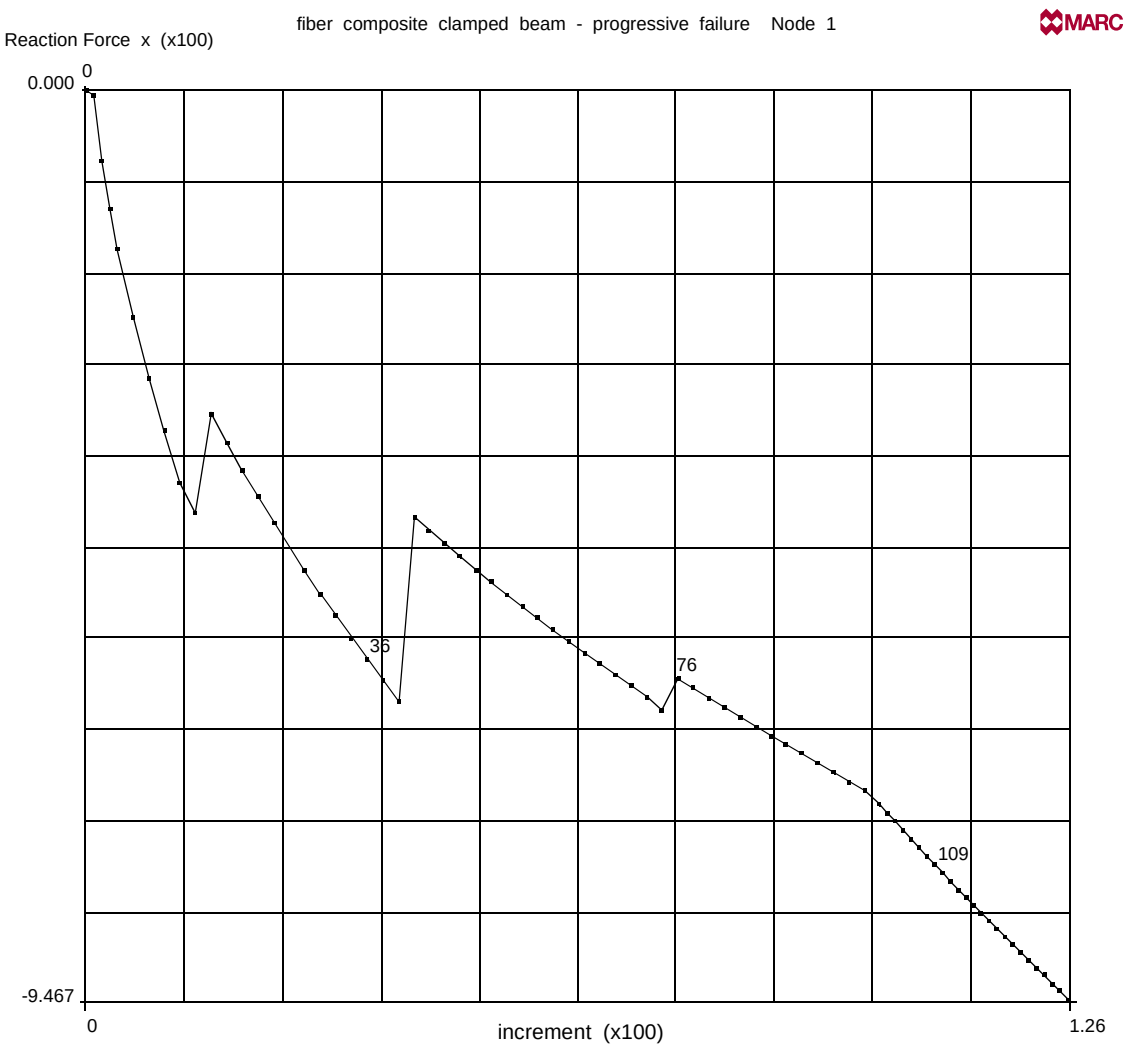

Figure 7.25-5 History of the Reaction Force at Clamped End

7.26 Pipe Collars in Contact

This problem demonstrates the plastic strain capability of the axisymmetric element 95 together with the non-axisymmetric gap element 97. Two pipes are connected under bending loads.

The quadrilateral element 95 represents the cross-section of a ring in the z,r symmetry plane at $\theta = 0°$. A pure axisymmetric deformation induces displacements u,v in the z,r plane. These remain constant for θ ranging from 0° to 360°. A flexural deformation in the z,r plane induces different displacements u,v at opposite sections, $\theta = 0°$ and $\theta = 180°$, along the ring. A twist in the ring induces a circumferential displacement w, equal at every θ, and assigned to the position $\theta = 90°$.

The gap element 97 works in the flexural mode. Extra degrees of freedom have been included to account for independent contact and friction between facing sides of element 95 (q = 0° - 180°). Motion can only occur in the z,r plane.

Element

In element 95, five degrees of freedom are associated with each node:

u,v displacements at 0° and 180°, respectively

w circumferential displacement at 90° angle

Element 95 is integrated numerically in the circumferential direction. The number of integration points (odd number) is given in the SHELL SECT parameter. The points are equidistant on the half circumference (see Figure 7.26-1 and Figure 7.26-2)

Here, nine integration points along the half circumference are chosen via the SHELL SECT parameter.

Element 97 is a 4-node gap and friction link with double contact and friction (0° - 180°). It is designed to be used with element type 95.

Model

The FEM model represents the longitudinal section of the pipe junction in the z,r plane. The mesh consists of 248 elements, type 95 and 9 elements type 97 for a total of 330 nodes. The mesh is shown in Figure 7.26-2.

Material Properties

The two pipes are made with the same material:

E	(Young modulus) =	2E5 N/mm^2
ν	(Poisson ratio) =	.3
σ_y	=	200. N/mm^2

A workhardening curve is assigned as follows:

σ [N/mm^2]	ε_p
200.	0
250.	.3
300.	.6

Loads

The bending load is applied as shown in Figure 7.26-1. The loads acts in the longitudinal direction (z-direction)

Results

The results produces by MARC for the pipe junction with gaps can be seen in the following figures.

Figure 7.26-3	The deformed section at 0°.
Figure 7.26-4 and Figure 7.26-5	The von Mises stress at 0° and 180° (layer 1 and 9, respectively)
Figure 7.26-6	The plastic strain at 0°. No plastic strain appears at 180°.

Note: Only the deformed shape at 0° can be visualized with the Mentat graphics program even if all the element variables can be visualized. The displacements and all the nodal quantities referring to 180° can be seen on the output file.

Parameters, Options, and Subroutines Summary

Example e7x26.dat:

Parameters	Model Definition Options	History Definition Options
ELEMENTS	CONNECTIVITY	CONTINUE
END	CONTROL	DIST LOADS
LARGE DISP	COORDINATES	
SHELL SECT	END OPTION	
SIZING	FIXED DISP	
TITLE	GAP DATA	
UPDATE	ISOTROPIC	
	OPTIMIZE	
	POST	

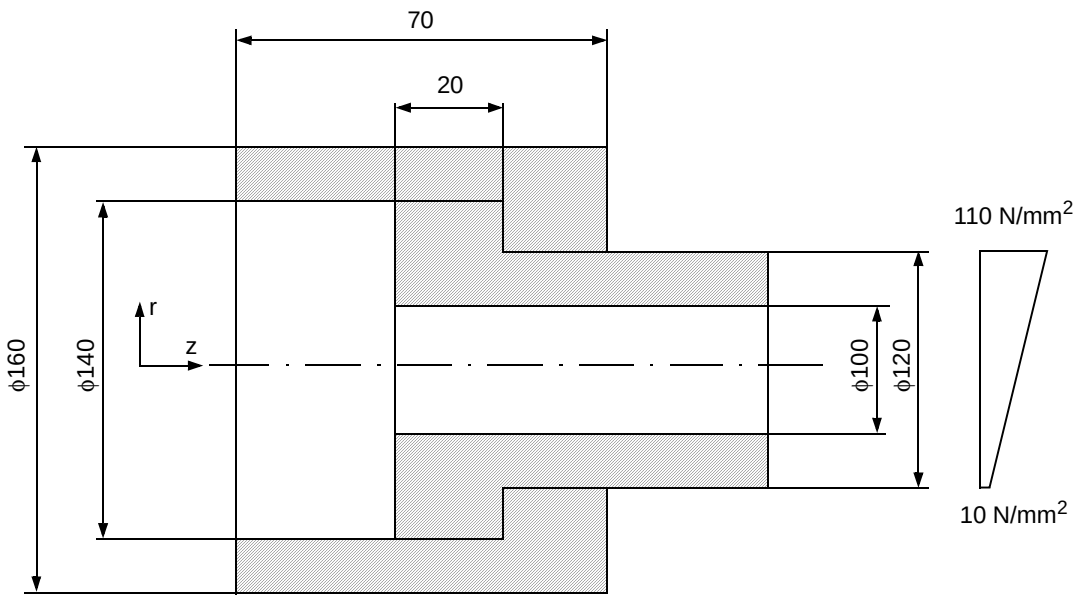

Figure 7.26-1 Geometric Dimension and Bending Loads

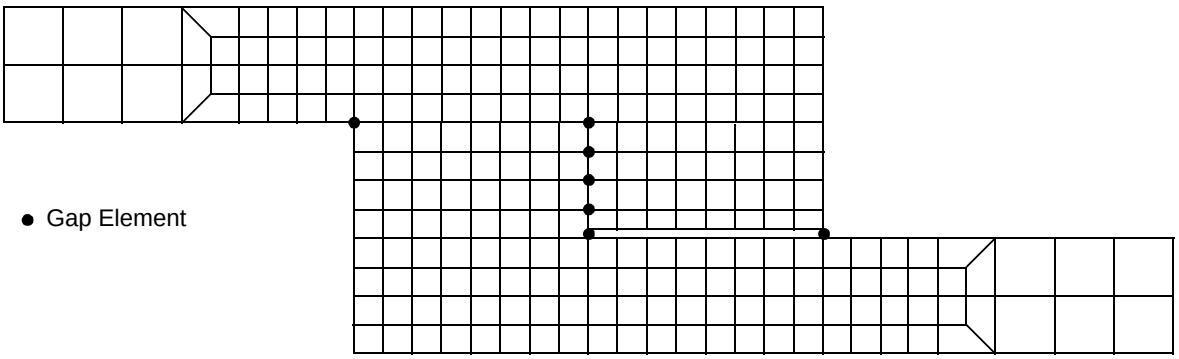

Figure 7.26-2 FEM Model

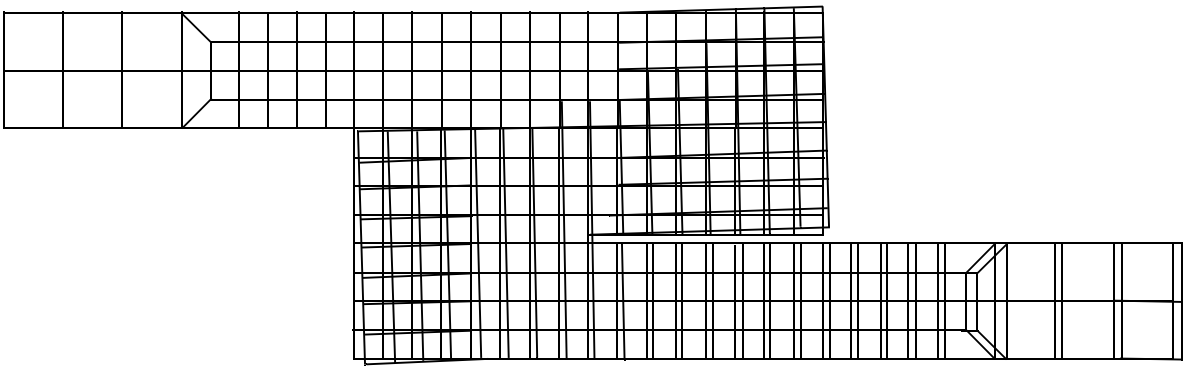

Figure 7.26-3 Deformed Shape at 0°

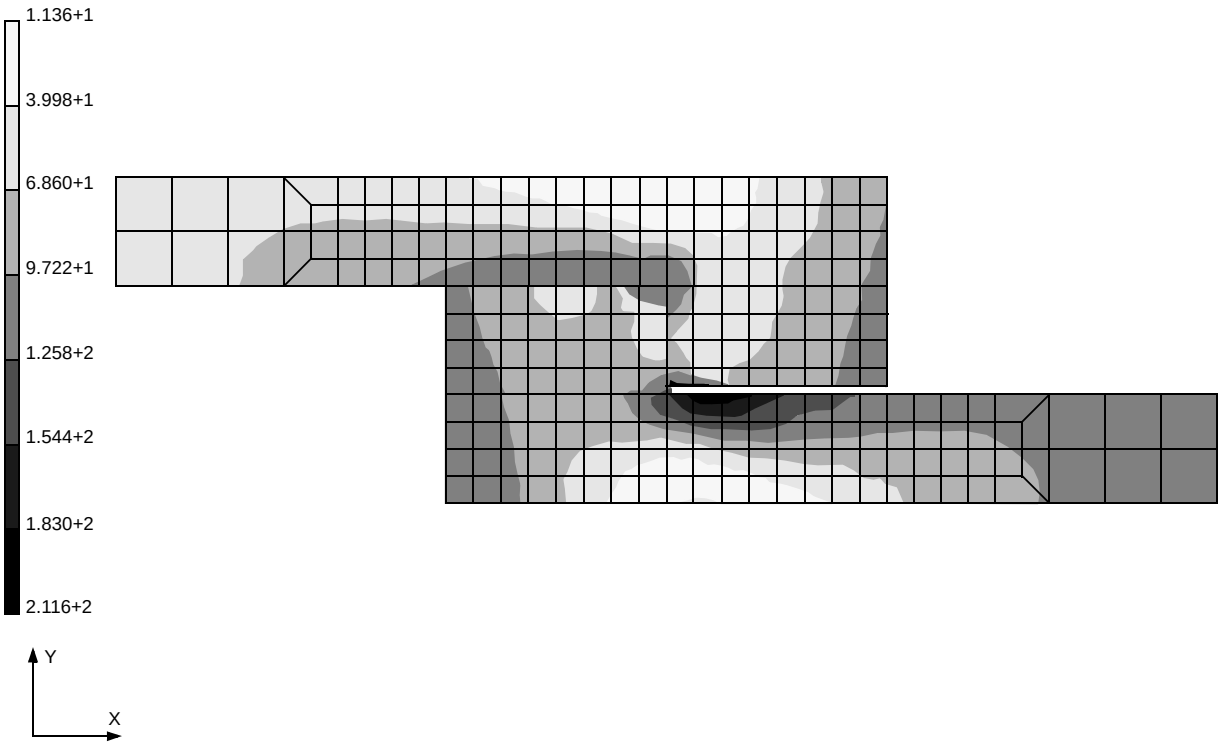

Figure 7.26-4 von Mises Stress Contour at 0°, Layer 1

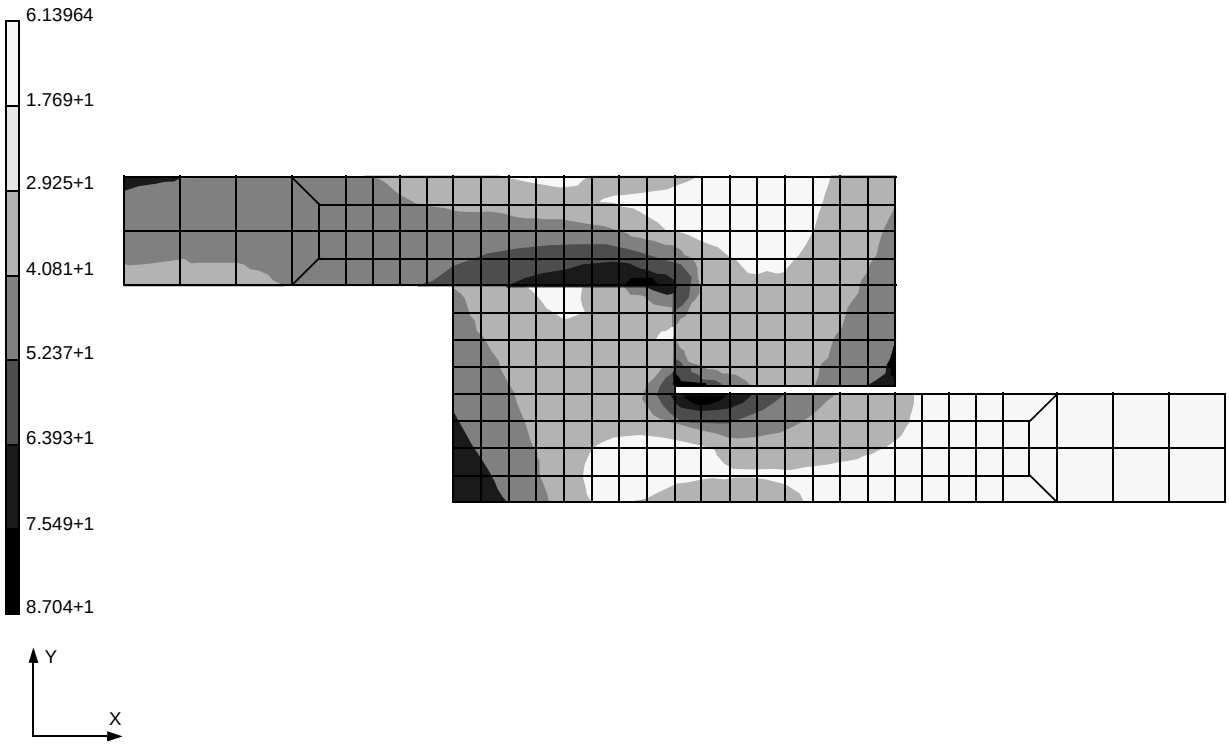

Figure 7.26-5 von Mises Stress Contour at 180°, Layer 9

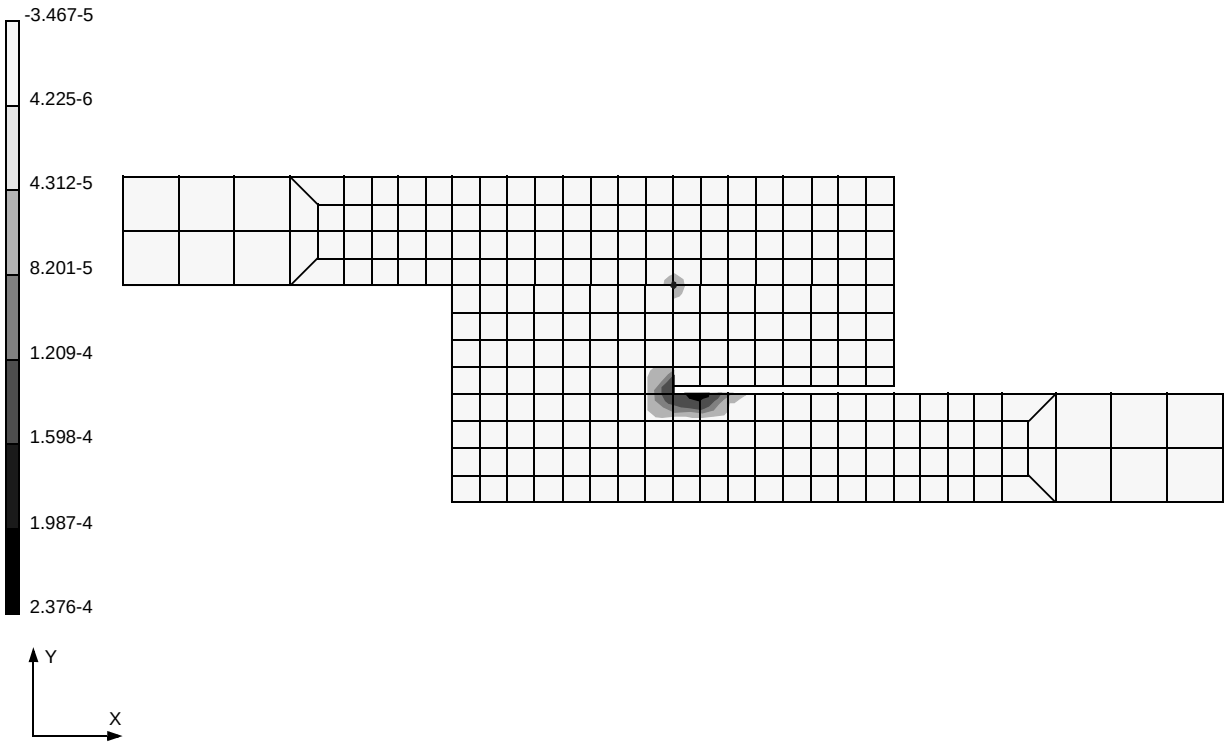

Figure 7.26-6 Plastic Strain Contour at 0°, Layer 1

7.27 Twist and Extension of Circular Bar of Variable Thickness at Large Strains

This problem illustrates the use of MARC element 67, higher order axisymmetric with twist element, for a large strain elastic analysis of a circular bar of variable thickness. The bar is subjected to both a twist moment and an axial force at the free end of the circular bar. The tying constraint option is used to insure that the cross section at the small end of the bar remains flat. The material is modeled using Ogden model. The ELASTICITY,2 option is used to activate the updated Lagrangian formulation.

Element

Element type 67, an 8-node axisymmetric element with twist, is used in this example.

Model

There are 12 elements, with a total of 53 nodes. Dimensions of the circular bar and the finite element mesh are shown in Figure 7.27-1.

Material Properties

Ogden material properties are given as:

$\mu_1 = 16$ lb/in^2, $\alpha_1 = 2$, $\mu_2 = -4$ lb/in^2, $\alpha_2 = -2$.

Boundary Conditions

Degrees of freedom u and w are 0 at the fixed end (nodes 1-5). Symmetry conditions are imposed at r = 0 (v = 0).

Loading

In each increment, a 10 pound point load in the positive x-direction and a 4 inch per pound torque is applied at node 49. Due to the applied tying, the point load is distributed over the whole cross section.

Tying

Tying type 1 is used at the free end to simulate a generalized plane-strain condition in the z-direction. The tied nodes are 50, 51, 52, and 53 and the retained node is 49.

Results

The deformed mesh and the distribution of Equivalent von Mises stress is depicted in Figure 7.27-2.

Parameters, Options, and Subroutines Summary

Example e7x27.dat:

Parameters	Model Definition Options	History Definition Options
ALIAS	CONNECTIVITY	AUTO LOAD
ELASTICITY	COORDINATE	CONTINUE
ELEMENTS	END OPTION	CONTROL
END	FIXED DISP	POINT LOAD
LARGE DISP	ISOTROPIC	
SIZING	OGDEN	
TITLE	POINT LOAD	
	POST	
	TYING	

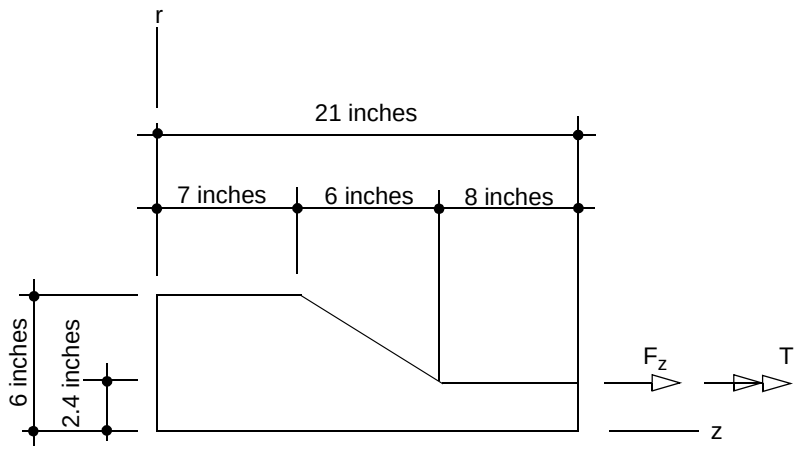

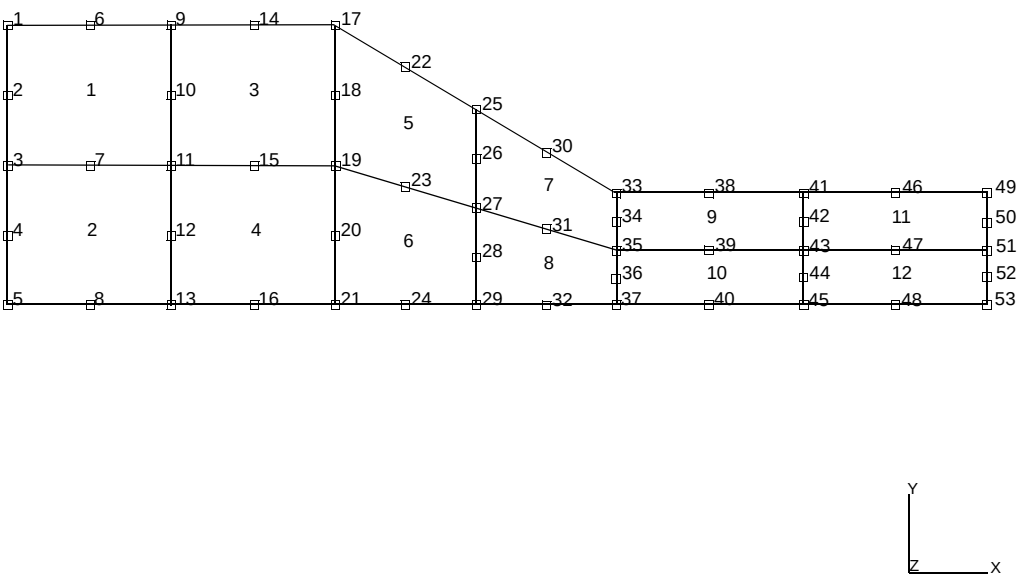

Figure 7.27-1 Circular Bar and Mesh

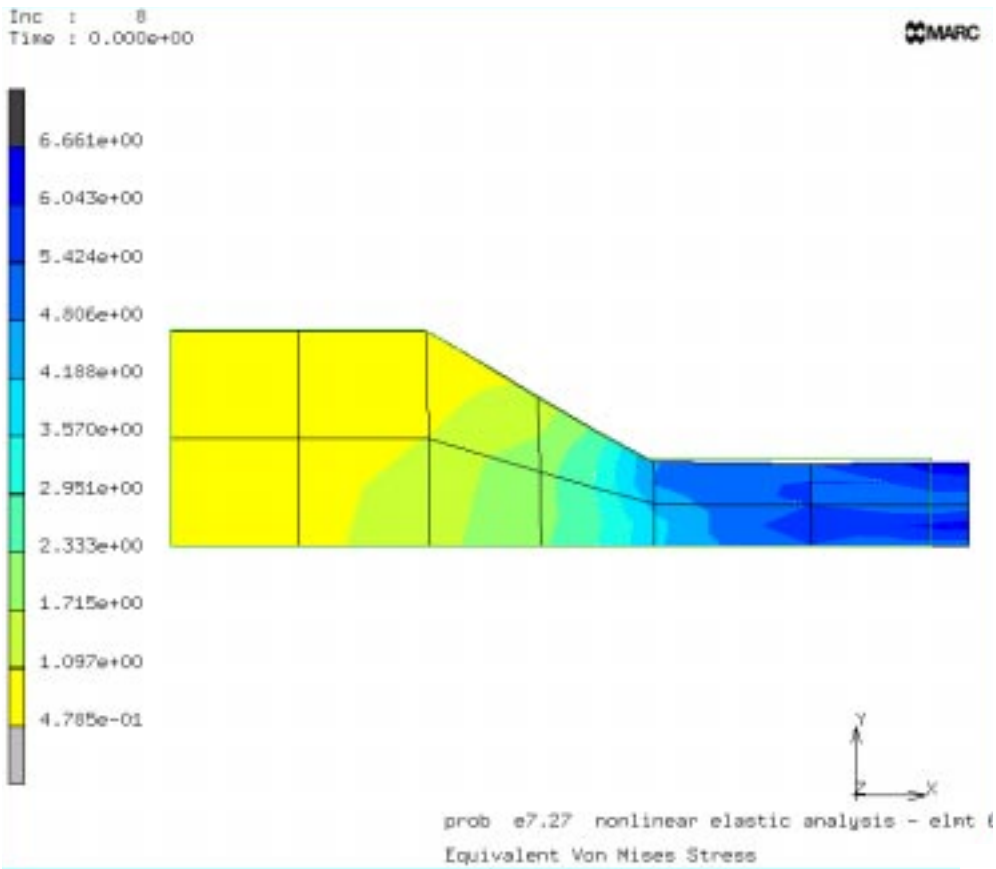

Figure 7.27-2 Deformed Mesh and Distribution of Equivalent von Mises Stress

7.28 Analysis of a Thick Rubber Cylinder under Internal Pressure

In this example, the deformation of a thick rubber cylinder under internal pressure is modeled.

This problem illustrates the use of MARC elements types 10, 28, 55, and 116 (4- and 8-node axisymmetric elements with only displacement degrees of freedom at nodes) for rubber materials. Option ELASTICITY,2 is invoked to activate MARC updated Lagrangian formulation. The rubber material is modeled with either the Ogden or Mooney material models.

Data Set	Element Type(s)	Number of Elements	Number of Nodes	Differentiating Features
e7x28a	10	4	20	Odgen
e7x28b	116	4	10	Mooney
e7x28c	28	4	23	Ogden
e7x28d	55	4	23	Ogden

Element

Library element 10 is a 4-node bilinear axisymmetric element with displacements in radial and axial directions as degrees of freedom. Library element 116 is a 4-node bilinear, reduced integration, axisymmetric element with displacements in radial and axial directions as degrees of freedom. Library element 28 is a 8-node axisymmetric element with displacements in radial and axial directions as degrees of freedom. Library element 55 is a 8-node, reduced integration, axisymmetric element with displacements in radial and axial directions as degrees of freedom.

Model

The cylinder has an internal radius of 1 mm and an external radius of 2 mm. Figure 7.28-1 shows the initial mesh for the data sets using 8-noded elements.

Material Properties

The Mooney material properties are given as:

$C_1 = 8$ N/mm^2, $C_2 = 2$ N/mm^2;

The Ogden material properties are given as:

$\mu_1 = 16$ N/mm^2, $\alpha_1 = 2$, $\mu_2 = 4$ N/mm^2, $\alpha_2 = -2$.

The bulk modulus is chosen as 200000 N/mm^2, resulting in the ratio of K/G being 10000. The material is therefore highly incompressible. Both materials are equivalent.

Loads

A uniformly distributed internal pressure of 11.5 N/mm^2 is applied on element number 1. This load is applied in increment zero. In MARC, increment zero is treated as linear. So an additional increment, with no additional load, is used to bring the solution to the correct nonlinear state.

Boundary Conditions

u = 0 on the planes z = 0 and z = 1.0 to simulate a plane strain condition.

Results

A. 8-Node Model (Element Type 28 and 55)

After the linear elastic step (increment 0), the radial displacements of the inside nodes for both elements 28 and 55 are 0.3833 mm.

They are the same as the analytical solution which predicts a radial displacement of 0.3833 mm.

After ten iterations, the radial displacement at the inside node is 1.0086 mm and the corresponding pressure can be computed from the following expression:

$$P = (C_1 + C_2)\left[\log\left(\frac{B^2a^2}{A^2(B^2 - A^2 + a^2)}\right) + \frac{(a^2 - A^2)(B^2 - A^2)}{a^2(B^2 - A^2 + a^2)}\right]$$

where A and B are the inner and outer radii of the cylinder in the undeformed state, “a” is the inner radius in the deformed state, and C_1 and C_2 are material constants.

The computed pressure of 11.5 N/mm^2 is in very good agreement with the prescribed value of 11.5 N/mm^2.

B. 4-Node Model (Element Type 10 and 116)

After the linear elastic step (increment 0), the radial displacements of the inside nodes (nodes 1 and 6) are 0.3817 mm (for element type 10) and 0.3834 mm (for element type 116) respectively.

Agreement with analytical solution of 0.3833 mm is good. After ten iterations, the radial displacement at inside node is 1.0068 mm, and the corresponding pressure is 11.5 N/mm^2 for element 10. For element 116, the displacement at the inside node is 1.0063 mm and the corresponding pressure is 11.5 N/mm^2. Agreement with prescribed value of 11.5 N/mm^2 is excellent.

Parameters, Options, and Subroutines Summary

Example e7x28a.dat:

Parameters	Model Definition Options	History Definition Options
ALIAS	CONNECTIVITY	CONTINUE
ELASTICITY	CONTROL	DIST LOAD
ELEMENTS	COORDINATES	
END	DIST LOAD	
FOLLOW FOR	END OPTION	
LARGE DISP	FIXED DISP	
SIZING	OGDEN	
TITLE	POST	

Example e7x28b.dat:

Parameters	Model Definition Options	History Definition Options
ALIAS	CONNECTIVITY	CONTINUE
ELASTICITY	CONTROL	DIST LOAD
ELEMENTS	COORDINATES	
END	DIST LOAD	
FOLLOW FOR	END OPTION	
LARGE DISP	FIXED DISP	
SIZING	MOONEY	
TITLE	POST	

Example e7x28c and e7x28d.dat:

Parameters	Model Definition Options	History Definition Options
ALIAS	CONNECTIVITY	CONTINUE
ELASTICITY	CONTROL	DIST LOAD
ELEMENTS	COORDINATES	
END	DIST LOAD	
FOLLOW FOR	END OPTION	
LARGE DISP	FIXED DISP	
SIZING	OGDEN	
TITLE	NODE FILL	
	POST	

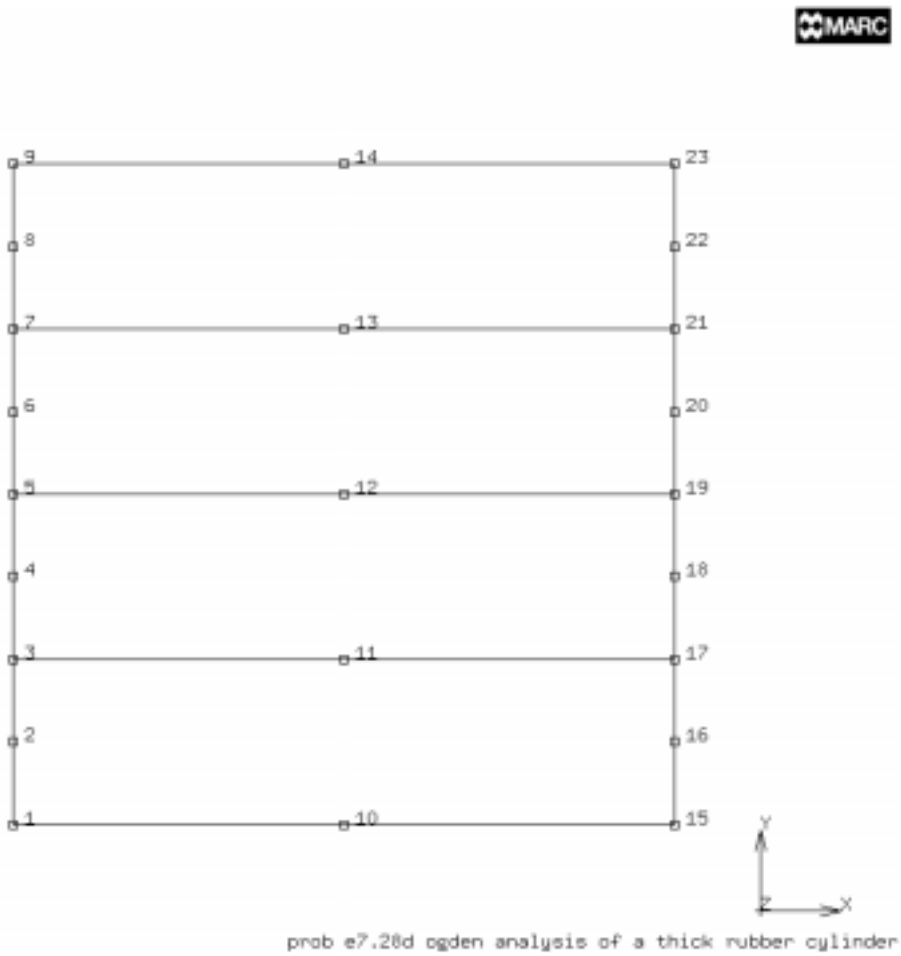

Figure 7.28-1 Cylinder Mesh (8-Node Model)

7.29 3D Analyses of a Plate with a Hole at Large Strains

This problem simulates the tensile loading of a plate with a hole at large strains. In e7x29a.dat, the HYPOELASTIC option and the user subroutine HYPELA2 are used to define constitutive behavior. Element type 7 is used and the material here is compressible. This job demonstrates the use of kinematics in defining user-defined material behavior. In e7x29b.dat, Element type 117 is used to model the plate (with the user-defined defaults file). The material in e7x29b.dat is modeled using Ogden model and is nearly incompressible.

This problem is modeled using the two techniques summarized below.

Data Set	Element Type(s)	Number of Elements	Number of Nodes	Differentiating Features
e7x29a	7	92	218	HYPOELASTIC HYPELA2
e7x29b	117	92	218	user default file

Element

Library element 7 is a 8-node trilinear brick element with global displacements as degrees of freedom. Library element 117 is a 8-node trilinear brick element with reduced integration and global displacements as degrees of freedom.

Model

Due to symmetry of the geometry and loading, a quarter of the actual model is simulated. The finite element model is made up of 92 elements and 218 nodes. The finite element mesh is shown in Figure 7.29-1.

Geometry

The model is assumed to be a square of side 2 mm from which a quarter of a circle of radius 0.6 mm has been cut out. The initial thickness is 0.2 mm.

Material Properties

In e7x29a.dat, a quadratic-logarithmic, nonlinear elastic model with the initial bulk modulus of 21666.67 N/mm^2 and the initial shear modulus of 10000.00 N/mm^2 is defined using the HYPOELASTIC option and the user subroutine HYPELA2. In e7x29b.dat, the Ogden parameters are given as μ_1=0.586 N/mm^2, α_1=2.0, μ_2=-0.354N/mm^2, and α_2=-2.0. The initial bulk modulus is 666666.667 N/mm^2.

Boundary Conditions and Loading

In addition to the boundary conditions due to symmetry, the third degree of freedom of the nodes located on the edges of the lower surface are fixed to avoid the rigid body motion in z-direction.

The loading is tensile. In e7x29a.dat, a uniform displacement of 1 mm is applied to one of the plate edges using 20 increments. The macroscopic total logarithmic strain is 40%. In e7x29b.dat, a uniform displacement of 2.5 mm is applied to one of the plate edges using 10 increments. The macroscopic total logarithmic strain is 81%.

Results

The distribution of equivalent von Mises stress and the deformed model for e7x29a.dat after 20 increments is shown in Figure 7.29-2. The distribution of equivalent von Mises stress and the deformed model for e7x29b.dat after 10 increments is shown in Figure 7.29-3.

Parameters, Options, and Subroutines Summary

Example e7x29a.dat:

Parameters	Model Definition Options	History Definition Options
ELEMENTS	CONNECTIVITY	AUTO LOAD
END	CONTROL	CONTINUE
LARGE DISP	COORDINATES	DISP CHANGE
PROCESS	END OPTION	
SETNAME	FIXED DISP	
SIZING	GEOMETRY	
TITLE	HYPOELASTIC	
UPDATE	OPTIMIZE	
	POST	

User Subroutine u7x29a.f

HYPELA2

Example e7x29b.dat:

Parameters	Model Definition Options	History Definition Options
ELEMENTS	CONNECTIVITY	AUTO LOAD
END	CONTROL	CONTINUE
SETNAME	COORDINATES	DISP CHANGE
SIZING	END OPTION	
TITLE	FIXED DISP	
	GEOMETRY	
	OGDEN	
	OPTIMIZE	
	POST	

User Defined Default Input e7x29_def.dat

Parameters	Model Definition Options
ALL POINTS	END OPTION
ELASTICITY	PARAMETER
END	
LARGE DISP	
PRINT	
PROCESS	

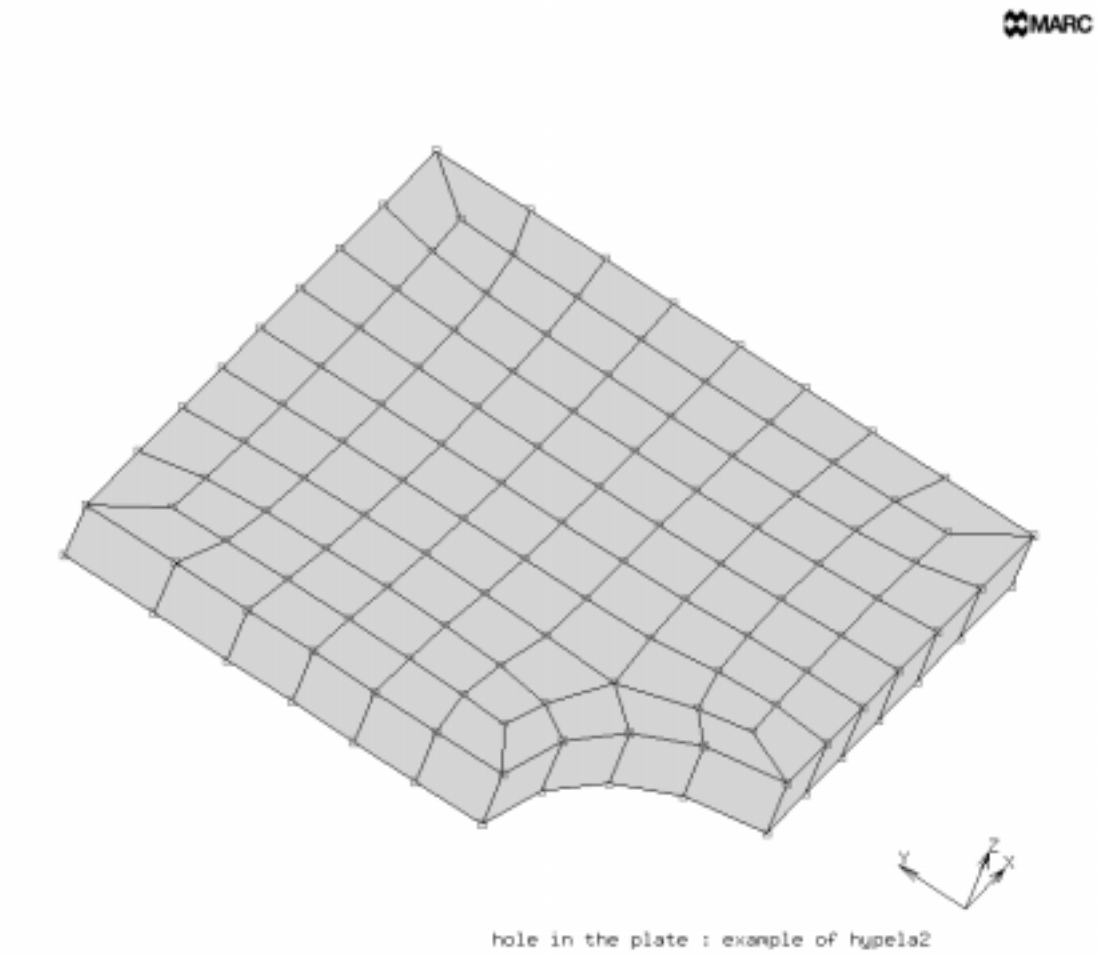

Figure 7.29-1 Initial Mesh

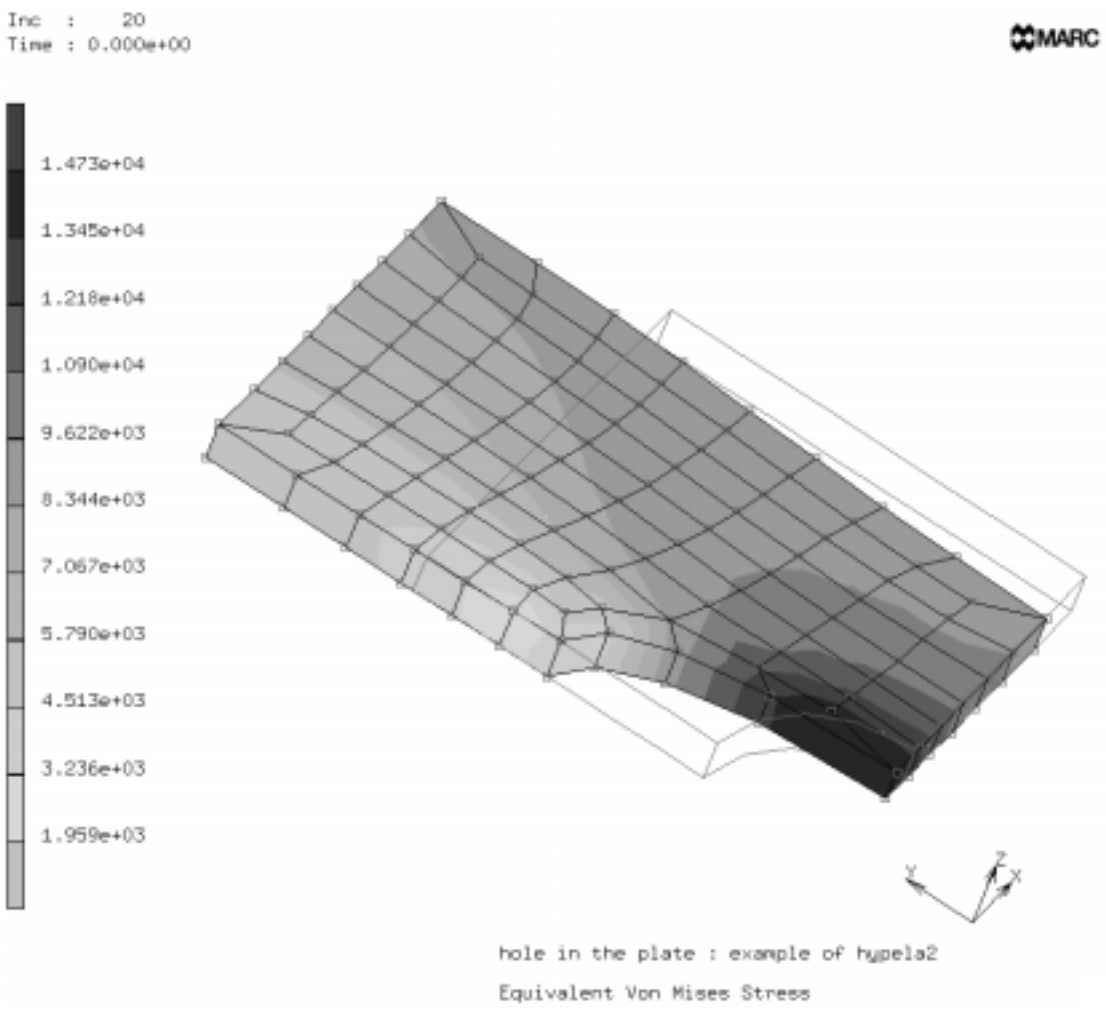

Figure 7.29-2 Deformed Model and Distribution of Equivalent von Mises Stress for e7x29a

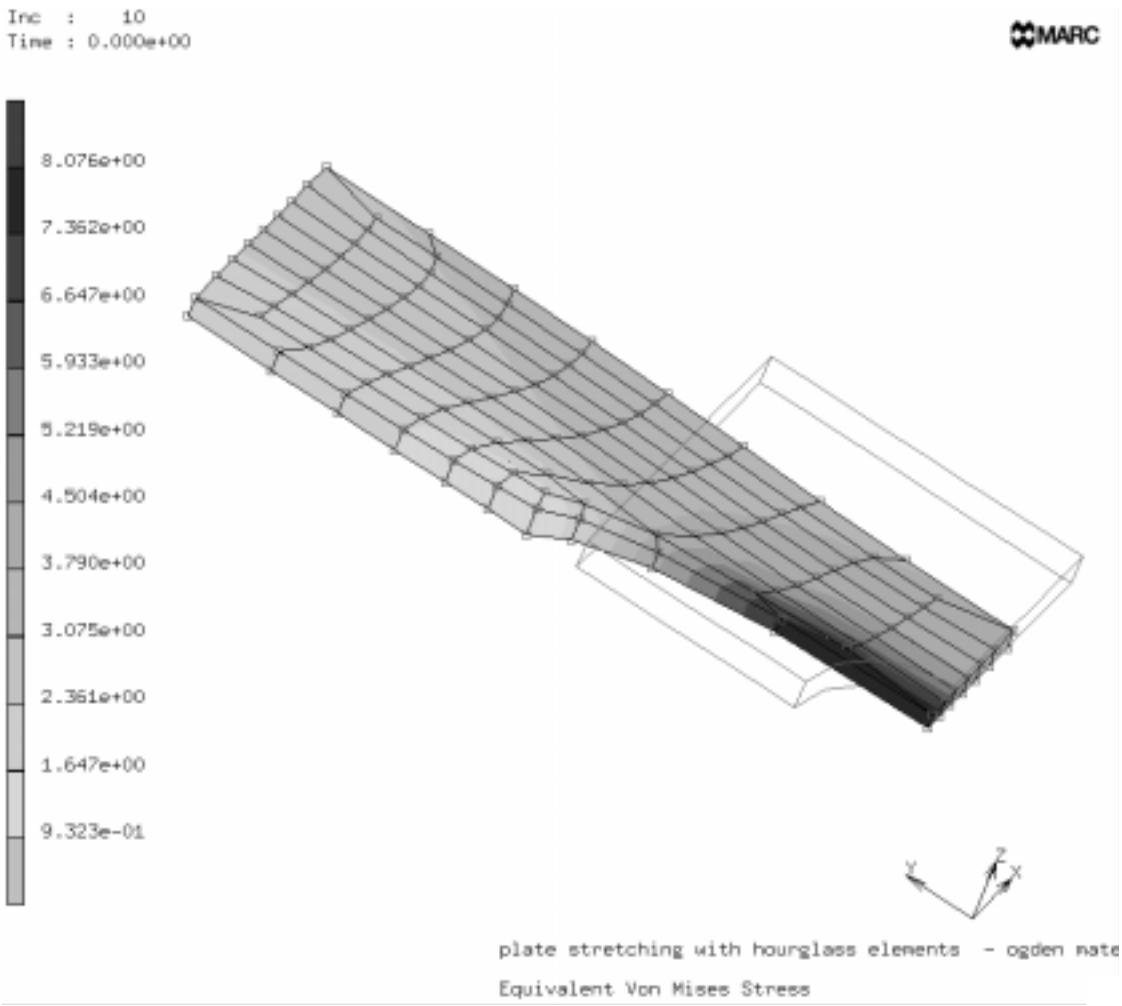

Figure 7.29-3 Deformed Model and Distribution of Equivalent von Mises Stress for e7x29b

7.30 Damage in Elastomeric Materials

Two phenomena observed in continuum damage have been evaluated in this example using continuous and discontinuous damage models. The discontinuous damage model essentially simulates the Mullins effect while the continuous damage model is able to capture the stiffness degradation (fatigue) due to cyclic loading.

This problem is modeled using the two techniques summarized below.

Data Set	Element Type(s)	Number of Elements	Number of Nodes	Differentiating Features
e7x30a	7	1	8	Discontinuous Damage Model
e7x30b	7	1	8	Continuous Damage Model

Model

A single element rubber cube, comprised of element 7, is subjected to tensile loading. The example is in itself very simple but demonstrates the two phenomena very effectively.

Material Properties

The material can be described using the Ogden material model using a three term series. The data was fit such that:

Term	μ (N/cm^2)	α
1	11.0	2.35
2	5.8e-4	7.03
3	0.73	1.28

and the bulk modulus was 1.0E9 N/cm^2.

The damage parameters for problem e7x30a.dat are:

	Discontinuous	Continuous
1st scale factor	0.4	0.0
1st relaxation factor	10.0	1.0
1st scale factor	0.1	0.0
2nd relaxation factor	100.0	1.0

The damage parameters for problem e7x30b.dat are:

	Discontinuous	Continuous
1st scale factor	0.0	0.40
1st relaxation factor	1.0	100.0
1st scale factor	0.0	0.1
2nd relaxation factor	1.0	100.0

Loads

The loading is applied as displacement boundary condition. The discontinuous damage is simulated by application of six loadcases while in the case of continuous damage, ten loadcases are applied. For the discontinuous damage, the applied loading increases with each set of tension and compression while for the continuous damage the applied loading is kept the same. The auto-increment option is used to apply the extension and compression in sets of 100 loading steps for each loadcase.

Results

It can be noticed from Figure 7.30-1 that the Mullin's effect is very well captured by the model, where three sets of loading and unloading show hysteresis, which increases in magnitude as the maximum applied strain in the model exceeds the previously applied level of strain. Also, once the material is reloaded past its previously applied maximum load, the loading continues on the previous loading path.

The progressive degradation of material stiffness with constant maximum applied strain level, namely fatigue, is simulated next. Figure 7.30-2 demonstrates that five sets of loading and unloading show hysteresis with a continuous loss of stiffness in the loading curve. The model implemented in MARC to simulate this behavior is due to C. Miehe.

Parameters, Options, and Subroutines Summary

Example e7x30a.dat and e7x30b.dat:

Parameters	Model Definition Options	History Definition Options
ELEMENT	CONNECTIVITY	AUTO INCREMENT
END	CONTACT	CONTINUE
ELASTICITY	CONTROL	DISP CHANGE
LARGE DISP	COORDINATES	CONTROL
PRINT	DEFINE	
SIZING	FIXED DISP	
TITLE	END OPTION	
	OGDEN	
	DAMAGE	
	POST	

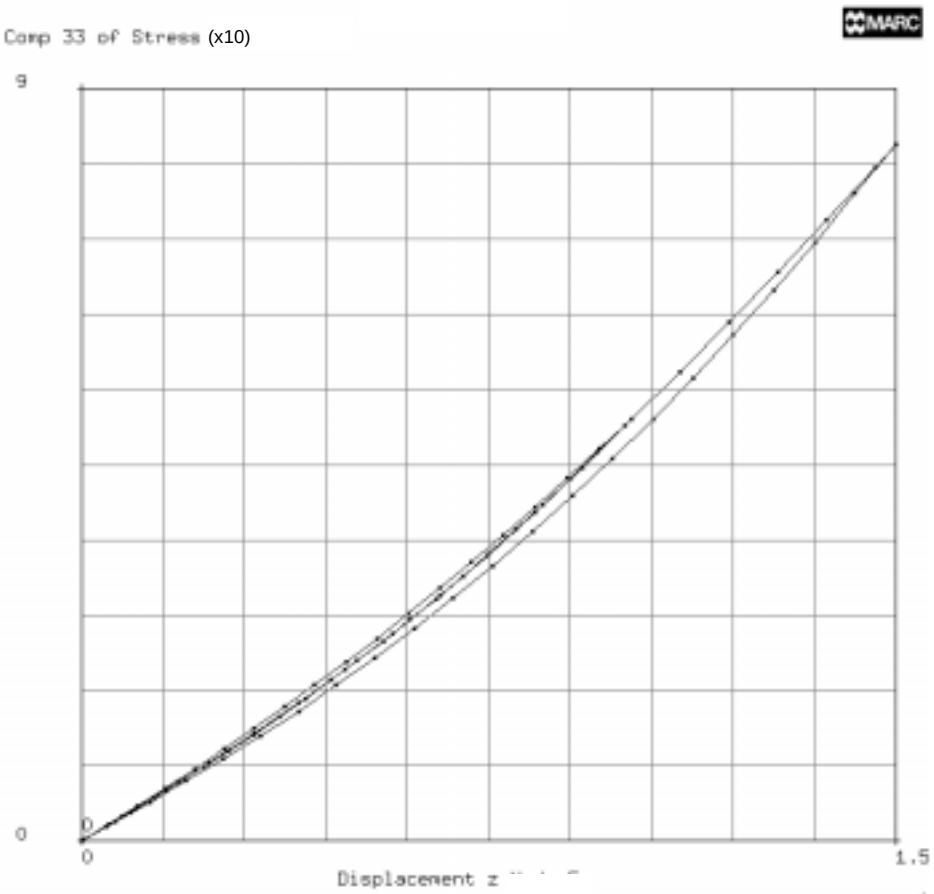

Figure 7.30-1 Discontinuous Damage

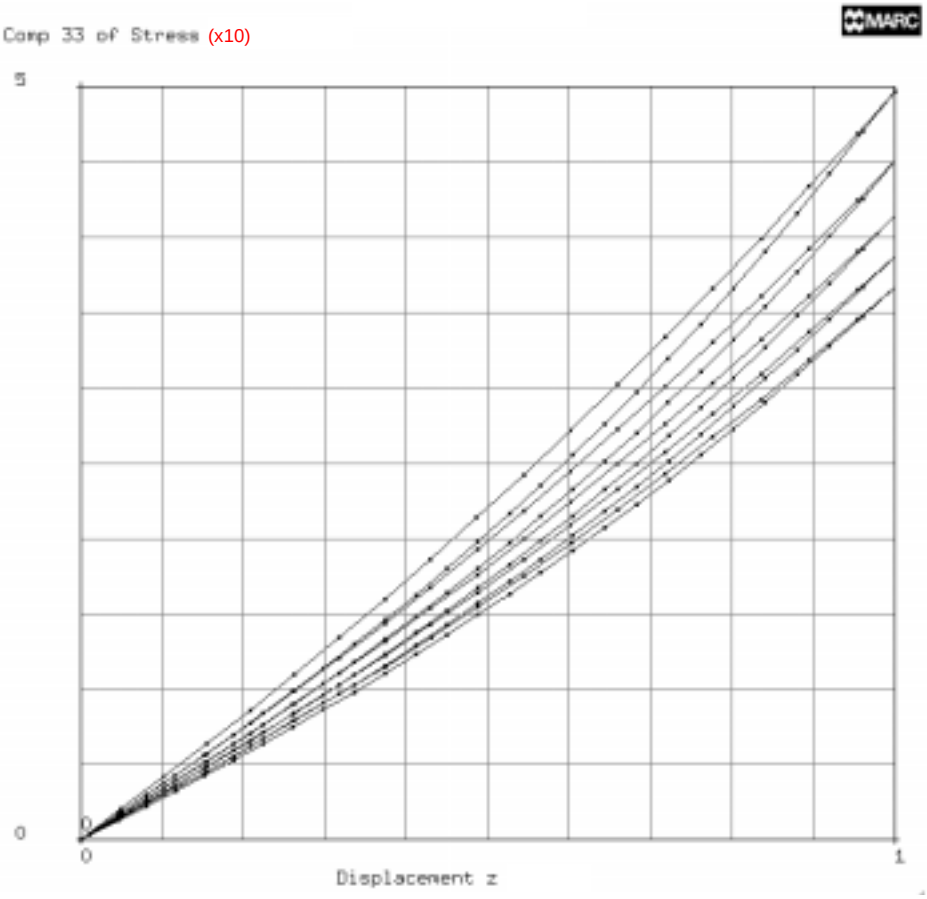

Figure 7.30-2 Continuous Damage

7.31 Rezoning in an Elastomeric Seal

This example demonstrates the capability of rezoning in an elastomeric seal. A rubber seal is being formed into its final shape by application of die pressure. Although the geometry itself is simple, the severely deformed configuration at an intermediate stage leads to a premature termination of the analysis due to excessive distortion in the elements. A new mesh via rezoning operation is clearly required for a successful completion of the analysis.

This problem is modeled using two data sets summarized below.

Data Set	Element Type(s)	Number of Elements	Number of Nodes	Differentiating Features
e7x31	11	382	433	Before Rezoning
e7x31b	11	633	692	After Rezoning

Model

The original model, i.e., before the rezoning step, consists of 382 4-node quadrilateral elements with 433 nodes. After the rezoning, the number of elements in the mesh increased to 633 while the number of nodes increased to 692. Displacement based plane strain element 11, is chosen to simulate the seal. For finite strain elasticity and plasticity material models, this element has special treatment for incompressibility.

Material Properties

The rubber seal can be described using the two term Ogden material model. The data was fit such that:

Term	μ (N/cm^2)	α
1	+0.324922	2.0
2	-0.568008	-2.0

and the bulk modulus was 8929.3 N/cm^2

Contact

The contact is modeled as frictionless and the contact bodies are modeled as NURBS. Default tolerances are taken in the run with the original mesh but in the run after the rezoning, the contact zone tolerance is increased to 0.007. The reason for this is that after the rezoning step,

there are some nodes that may be outside the default contact zone of 0.00680325. As a result, in the step after rezoning, there may be increment splitting which may sometimes lead to non-convergent solutions.

Results

The deformed meshes at increments 0, 7, 14, 15, and 29 are shown in Figure 7.31-1 to Figure 7.31-5. The sudden change in the mesh between the increments 14 and 15 reflects rezoning. Also, Figure 7.31-6 gives the plot of contact force distribution in the body.

When the analysis involves rezoning with updated Lagrange elasticity, the following items must be considered:

a. Drive down the residuals to a low value in the last one or two steps of the first analysis (before restart)

b. Take very small steps in the beginning of the second analysis (i.e. after restart)

Parameters, Options, and Subroutines Summary

Example e7x31a.dat:

Parameters	Model Definition Options	History Definition Options
ALIAS	CONNECTIVITY	AUTO LOAD
ELASTICITY	CONTACT	CONTINUE
ELEMENT	CONTACT TABLE	CONTROL
END	CONTROL	TIME STEP
LARGE DISP	COORDINATES	
PRINT	END OPTION	
REZONE	NO PRINT	
SIZING	OGDEN	
TITLE	POST	
	RESTART	

Example e7x31b.dat:

Parameters	Model Definition Options	History Definition Options
ALIAS	CONNECTIVITY	AUTO LOAD
ELASTICITY	CONNECTIVITY CHANGE	CONTINUE
ELEMENT	CONTACT	CONTROL
END	CONTACT CHANGE	TIME STEP
LARGE DISP	CONTACT TABLE	
PRINT	CONTROL RESTART	
REZONE	COORDINATE CHANGE	
SIZING	COORDINATES	
TITLE	END OPTION	
	END REZONE	
	NO PRINT	
	OGDEN	
	POST	
	REAUTO	
	RESTART	

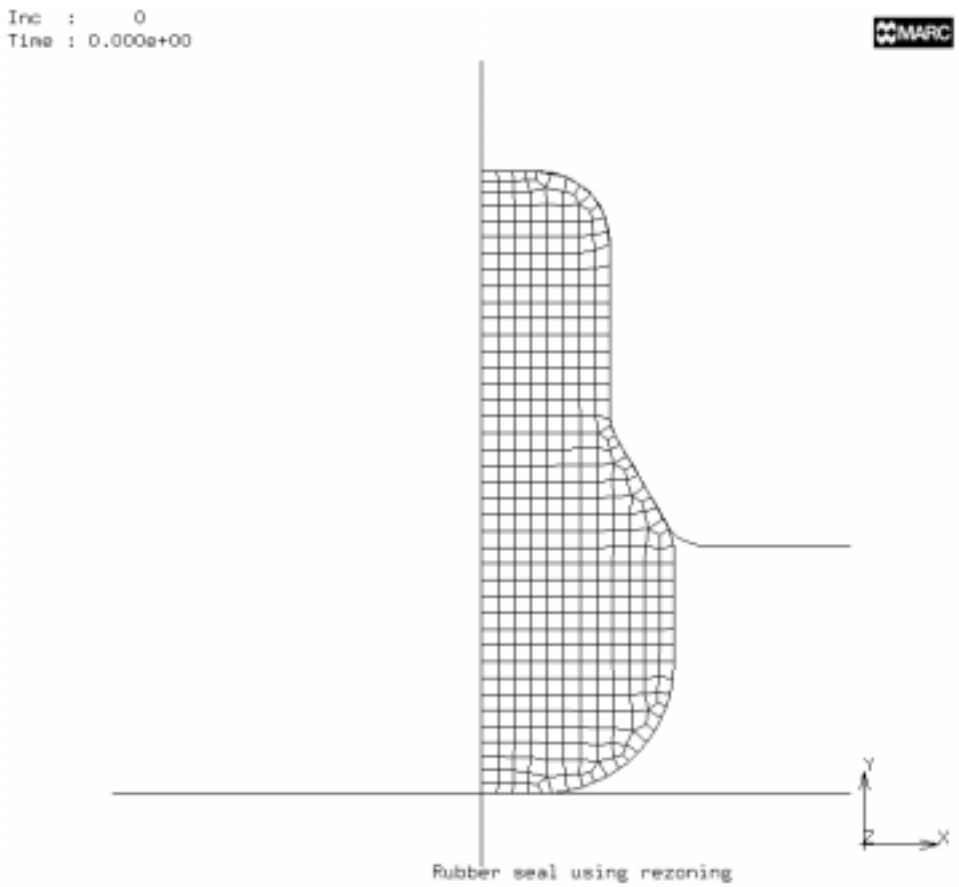

Figure 7.31-1 Deformed Mesh at Increment 0

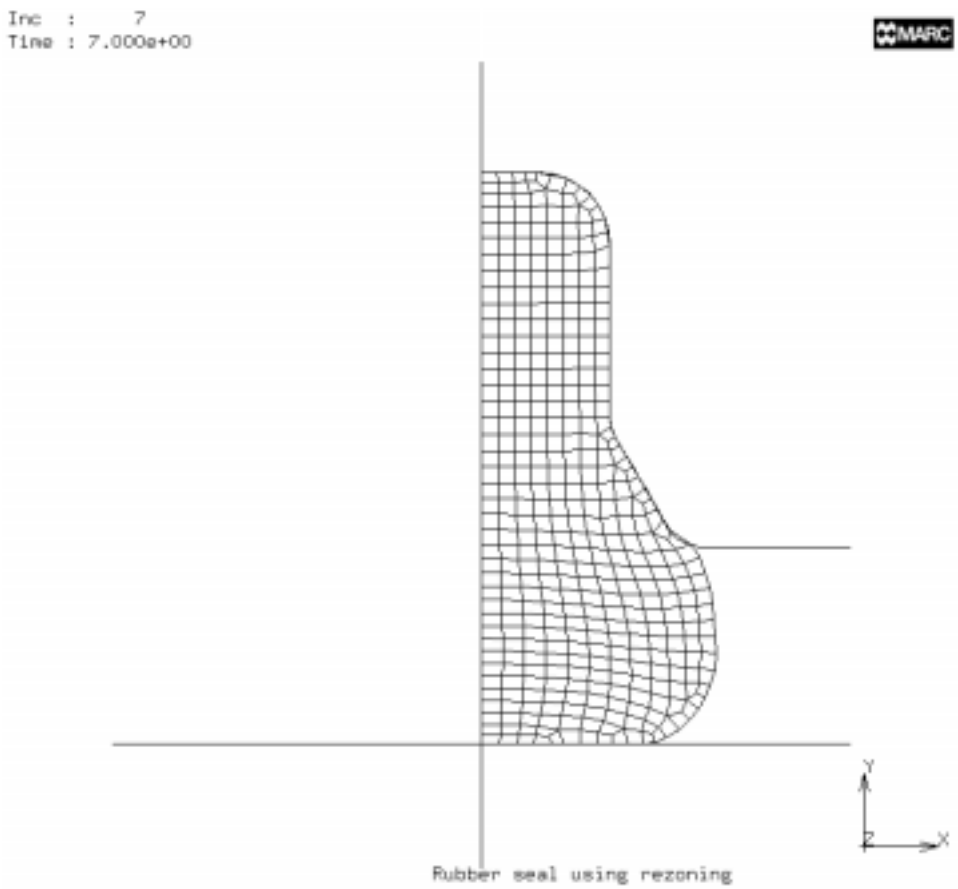

Figure 7.31-2 Deformed Mesh at Increment 7

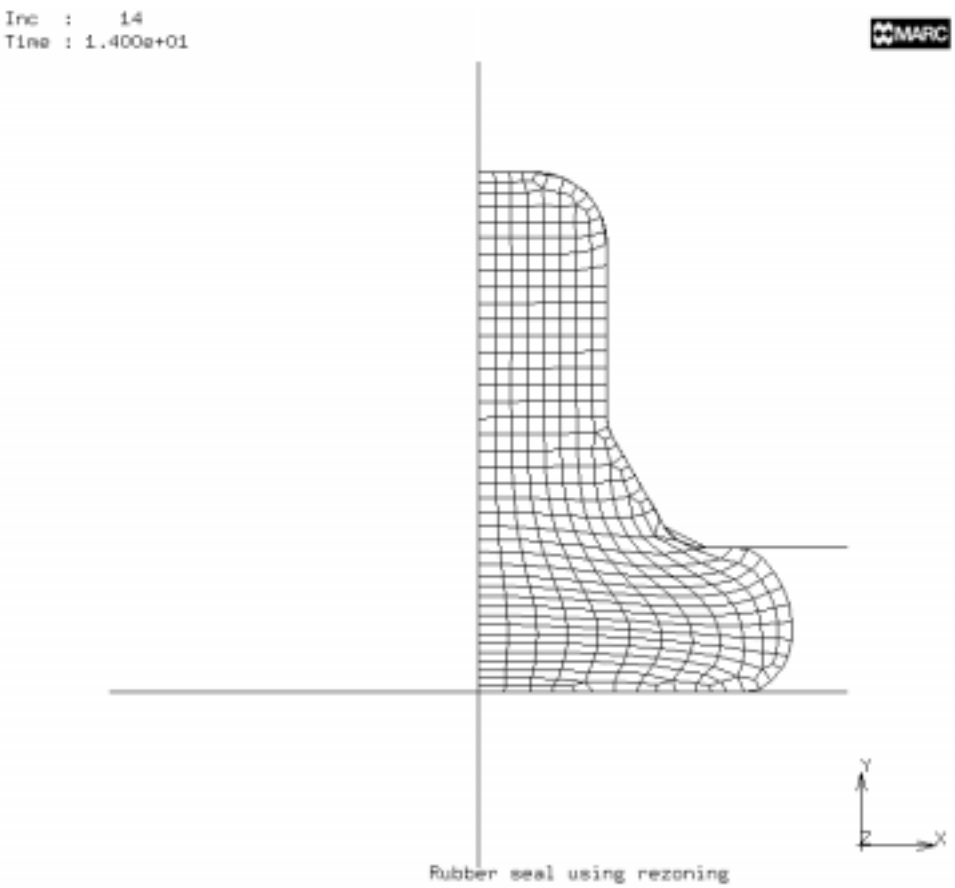

Figure 7.31-3 Deformed Mesh at Increment 14

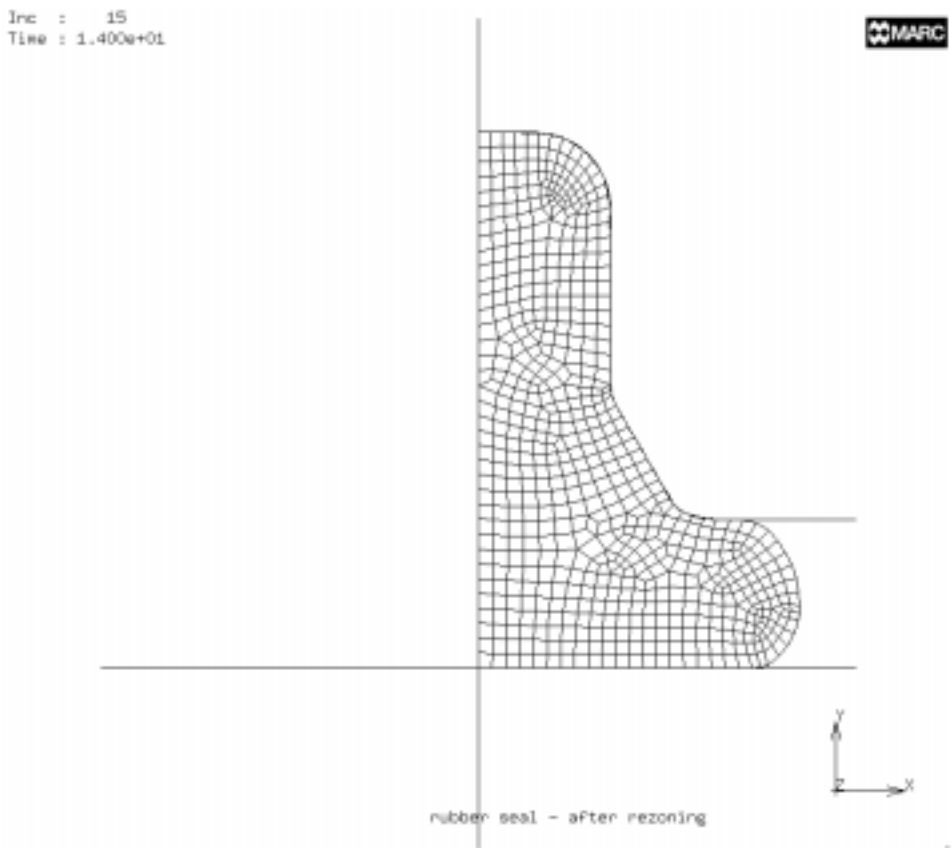

Figure 7.31-4 Deformed Mesh at Increment 15

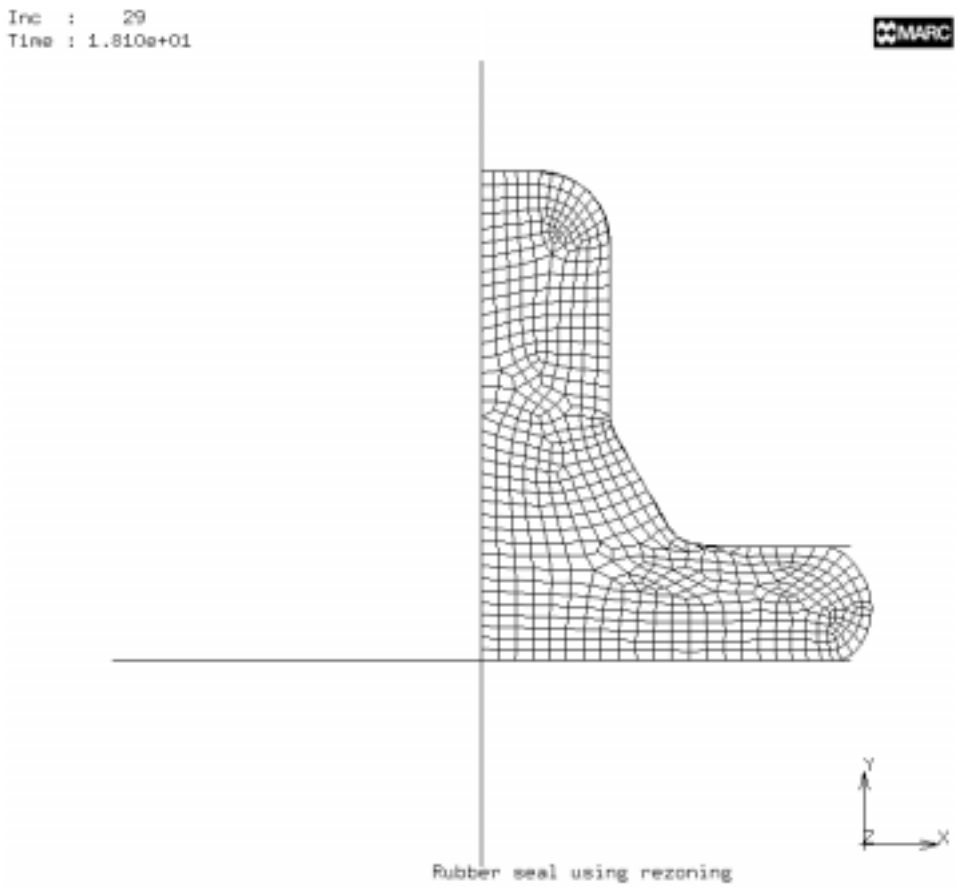

Figure 7.31-5 Deformed Mesh at Increment 29

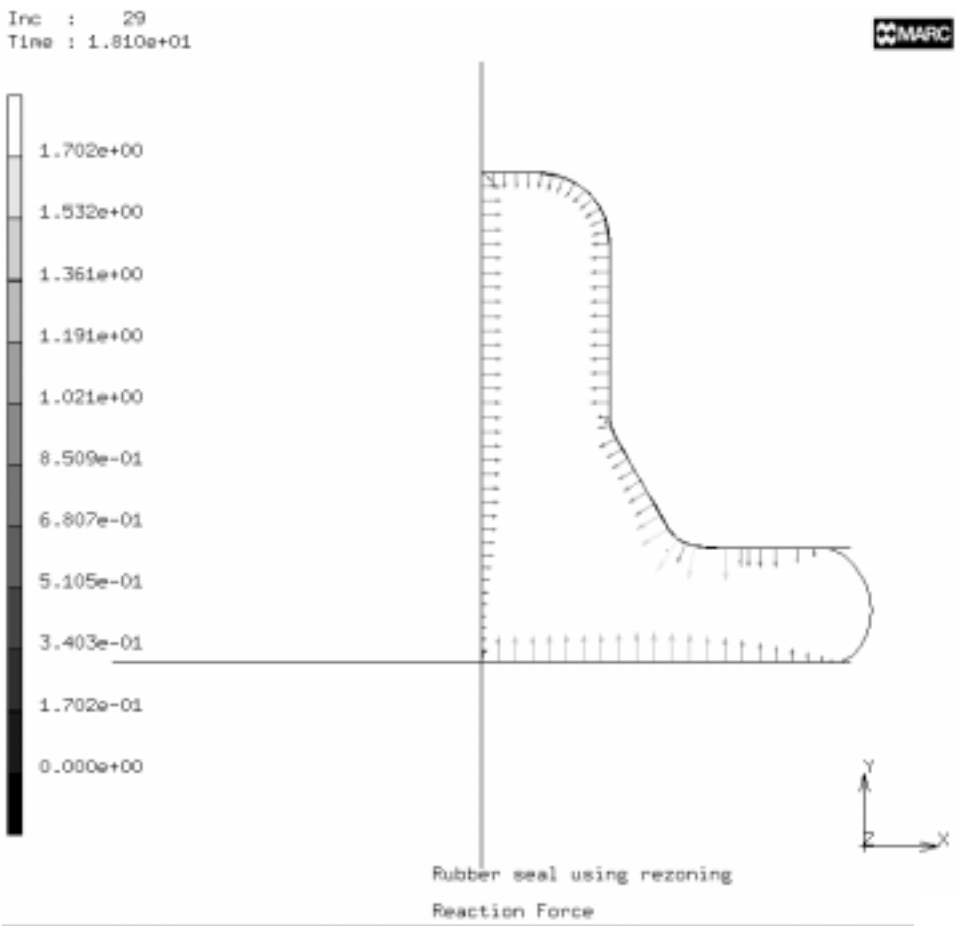

Figure 7.31-6 Contact Force Distribution

7.32 Structural Relaxation of a Glass Cube

Free structural relaxation of a glass cube subjected a cyclic temperature history, is simulated using Narayanaswamy model. This problem is modeled by means of element type 7.

The annealing of flat glass requires that the residual stresses be of an acceptable magnitude, while the specification for optical glass components usually includes a homogenous refractive index. The design of heat treated processes (for example, annealing) can be accomplished using the Narayanaswamy model. This allows you to study the time dependence of physical properties (for example, volumes) of glass subjected to a change in temperature.

The glass transition is a region of temperature in which molecular rearrangements occur on a scale of minutes or hours, so that the properties of a liquid change at a rate that is easily observed. Below the glass transition temperature, T_g, the material is extremely viscous and a solidus state exists. Above T_g the equilibrium structure is arrived at easily and the material is in liquidus state. Hence, the glass transition is revealed by a change in the temperature dependence of some property of a liquid during cooling. If a mechanical stress is applied to a liquid in the transition region, a time-dependent change in dimensions results due to the phenomenon of visco-elasticity.

If a liquid in the transition region is subjected to a sudden change in temperature, a time-dependent change in volume occurs. The latter process is called structural relaxation. Hence, structural relaxation governs the time-dependent response of a liquid to a change of temperature.

Element

Library element 7 is a 8-node trilinear brick element with global displacements as degrees of freedom.

Model

The side length of the glass cube is 2 mm. Because of the symmetry, only one eighth of the cube is modeled with one brick element.

Material Properties

The instantaneous moduli are given via ISOTROPIC option as: Young’s modulus is 5.58E4 N/mm^2; Poisson’s ratio is 0.0814. The time dependent values are entered using VISCEPROP option as:

Term No.	Shear Constant	Relaxation Time
1	1.08876E4	9.97000E-2
2	1.09134E4	9.40000E-3
3	3.97320E4	3.00000E-4

The solid and the liquid coefficients of the thermal expansion are chosen as 5.50E-7 and 1.93E-6, respectively. The weights and the reference relaxation times, used to define the response function, for each term in the series are input through SHIFT FUNCTION as:

Term No.	Weight	Reference Relaxation Time
1	1.0800E-1	1.4780E+0
2	4.4300E-1	3.2970E-1
3	1.6600E-1	1.2130E-1
4	1.6100E-1	4.4600E-2
5	4.6000E-2	1,6400E-2
6	7.6000E-2	3.7000E-3

Loads

An initial temperature of 6.20E2 is applied to the glass cube at increment 0. A cyclic temperature history is then applied: At first, the cube is gradually cooled down to 0.20E2 in 100 equal increments; Afterwards, it is heated up to the initial temperature at the equal incremental size.

Boundary Conditions

Boundary conditions are applied to the glass cube according to the symmetry.

Results

Suppose a glass is equilibrated at temperature T_1, and suddenly cooled to T_2 at t_0. The instantaneous change in volume is $\alpha_g(T_2 - T_1)$, followed by relaxation towards the equilibrium value $V(\infty,T_2)$. The total change in volume due to the temperature change is $\alpha_l(T_2 - T_1)$ as shown in Figure 7.32-1b. The rate of volume change depends on a characteristic time called the relaxation time.

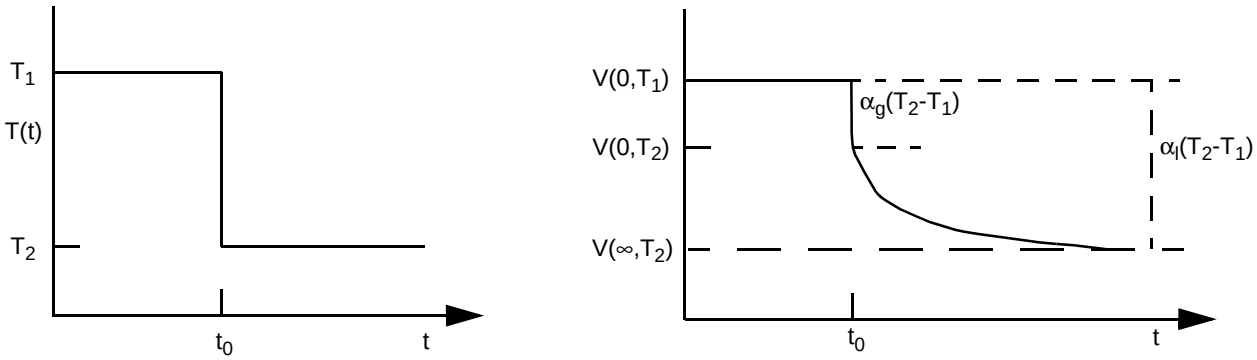

(a) Step Input for Temperature

(b) Volume Change as Function of Temperature

Figure 7.32-1 Structural Relaxation Phenomenon

The slope of dV/dT changes from the high value characteristic of the fluid α_l to the low characteristic of the glass α_g as shown in Figure 7.32-2. The glass transition temperature T_g is a point in the center of the transition region. The low-temperature slope α_g represents the change in volume V caused by vibration of the atoms in their potential wells. In the (glassy) temperature range, the atoms are frozen into a particular configuration. As the temperature T increases, the atoms acquire enough energy to break bonds and rearrange into new structures. That allows the volume to increase more rapidly, so $\alpha_l > \alpha_g$. The difference $\alpha = \alpha_l - \alpha_g$ represents the structural contribution to the volume.

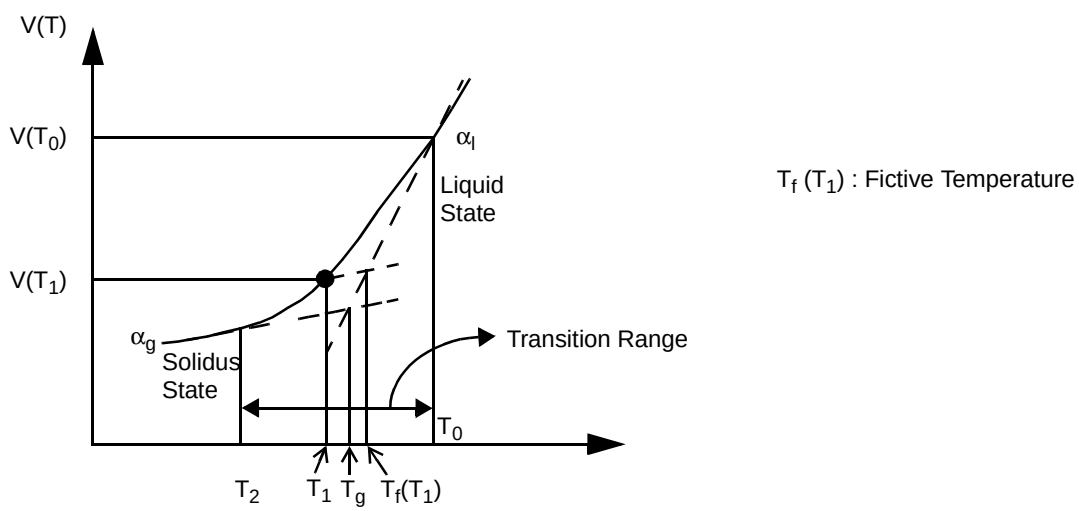

Figure 7.32-2 Property (Volume) – Temperature Plot

When a liquid is cooled and reheated, a hysteresis is observed.

The volume change of the glass cube with the change of the temperature 1 as calculated by MARC, is illustrated in Figure 7.32-3. The hysteresis shown in Figure 7.32-3 indicates the calculations are in a good qualitative agreement with experimental observations.

Parameters, Options, and Subroutines Summary

Example e7x32.dat:

Parameters	Model Definition Options	History Definition Options
ALL POINTS	CHANGE STATE	AUTO LOAD
ELEMENTS	CONNECTIVITY	CHANGE STATE
END	COORDINATES	CONTINUE
SETNAME	END OPTIONS	CONTROL
SIZING	FIXED DISP	TIME STEP
STATE VARS	ISOTROPIC	
TITLE	OPTIMIZE	
	PRINT CHOICE	
	POST	
	SHIFT FUNCTION	
	SOLVER	
	VISCEL EXP	
	VISCELPROP	
	$NO PRINT	

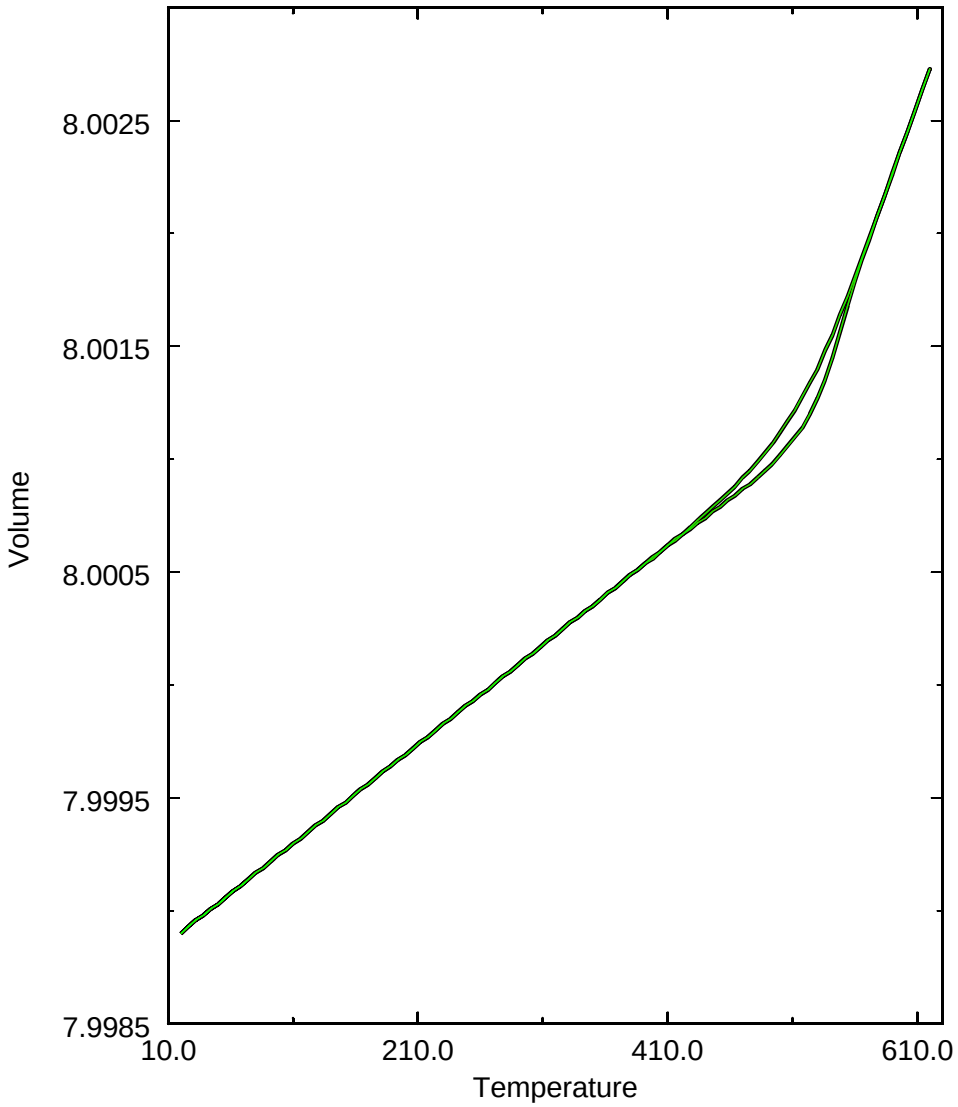

Figure 7.32-3 Volume Change during Cyclic Temperature History

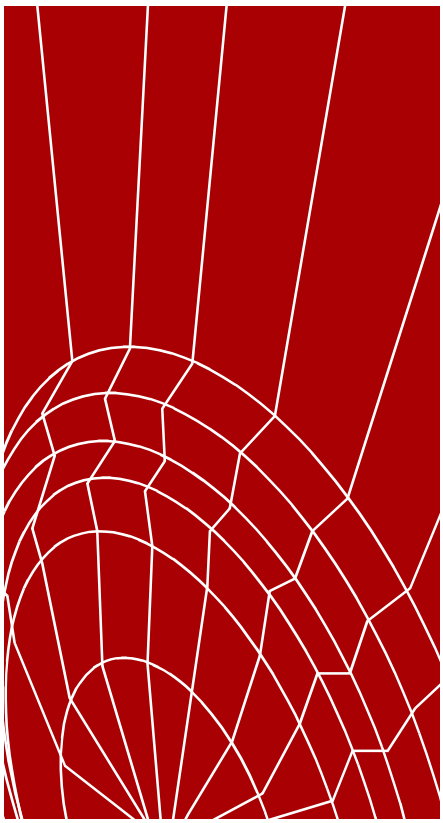

MARC Analysis Research Corporation

MARC®

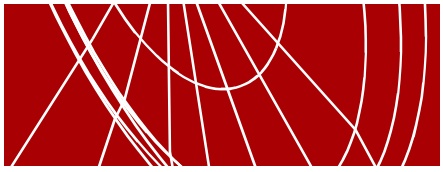

Volume E

Demonstration Problems

Version K7

Chapter 8
Advanced Topics

8 Advanced Topics Contents

Description	Problem
Plate with Circular Hole using Substructures	8.1
Double-Edge Notch Specimen using Substructures	8.2
End-Plate-Aperture Breakaway	8.3
Collapse of a Notched Concrete Beam	8.4
Cracking Behavior of a One-way Reinforced Concrete Slab using Shell Elements	8.5
Cracking Behavior of a One-way Reinforced Concrete Slab	8.6
Compression of a Block	8.7
Simply-supported Thick Plate under Uniform Pressure with Anisotropic Properties	8.8
Failure Criteria Calculation for Plane Stress Orthotropic Sheet	8.9
Beam Element 52 with Nonlinear Elastic Stress-Strain Relation	8.10
Element Deactivation/Activation and Error Estimate in the Analysis of a Plate with Hole	8.11
Forging of the Head of a Bolt	8.12
Coupled Analysis of Ring Compression	8.13
3D Contact with Various Rigid Surface Definitions	8.14
Double-Sided Contact	8.15
Demonstration of Springback	8.16
3D Extrusion Analysis with Coulomb Friction	8.17
3D Forming of a Circular Blank Using Shell or Membrane Elements and Coulomb Friction	8.18
3D Indentation and Rolling without Friction	8.19
2D Electrostatic Analysis of a Circular Region	8.20

Description	Problem
3D Electrostatic Analysis of a Circular Region	8.21
2D Magnetostatic Analysis of a Circular Region	8.22
3D Magnetostatic Analysis of a Coil	8.23
2D Nonlinear Magnetostatic Analysis	8.24
Acoustic Problem: Eigenvalue Analysis of a Circular Cavity	8.25
Acoustic Problem: Eigenvalue Analysis of a Rectangular Cavity	8.26
Progressive Failure of a Plate with a Hole	8.27
Linear Distribution of Dipoles	8.28
Magnetic Field around Two Wires carrying Opposite Currents	8.29
Harmonic Electromagnetic Analysis of a Wave Guide	8.30
Transient Electromagnetic Analysis around a Conducting Sphere	8.31
Cavity Resonator	8.32
Electromagnetic Analysis of an Infinite Wire	8.33
Triaxial Test on Normally Consolidated Weald Clay	8.34
Soil Analysis of an Embankment	8.35
Interference Fit of Two Cylinders	8.36
Interference Fit Analysis	8.37
Deep Drawing of a Box using NURB Surfaces	8.38
Contact of Two Beams using AUTO INCREMENT	8.39
Circular Disk under Point Loads Using Adaptive Meshing	8.40
Stress Singularity Analysis using Adaptive Meshing	8.41
Contact Analysis with Adaptive Meshing	8.42
Rubber Seal Analysis using Adaptive Meshing	8.43
Simplified Rolling Example with Adaptive Meshing	8.44
Use of the SPLINE Option for Deformable-Deformable Contact	8.45
Use of the EXCLUDE Option for Contact Analysis	8.46

Description	Problem
Simulation of Contact with Stick-Slip Friction	8.47
Simulation of Deformable-Deformable Contact with Stick-Slip Friction	8.48
Rolling of a Compressed Rubber Bushing with Stick-Slip Friction	8.49
Compression Test of Cylinder with Stick-Slip Friction	8.50
Modeling of a Spring	8.51
Deep Drawing of Sheet	8.52
Shell-Shell Contact and Separation	8.53
Self Contact of a Shell Structure	8.54
Deep Drawing of Copper Sheet	8.55
2D Contact Problem - Load Control and Velocity Control	8.56
The ADAPTIVE Capability with Shell Elements	8.57
Adaptive Meshing in Multiply Connected Shell Structures	8.58
Not Available	8.59
Simulation of Sheet Bending	8.60

8 Advanced Topics List of Figures

Figure		Page
8.1-1	Hole in Plate	8.1-4
8.1-2	Substructure 1,1	8.1-5
8.2-1	Double-Edge Notch Specimen.	8.2-4
8.2-2	Mesh for Double-Edge Notch Specimen Cross-Hatched Area Indicates Substructures	8.2-5
8.2-3	(A) Elements in Substructure 1-1	8.2-6
8.2-3	(B) Nodes in Substructure 1-1	8.2-7
8.2-4	(A) Elements at Highest Level.	8.2-8
8.2-4	(B) Nodes at Highest Level	8.2-9
8.2-5	Workhardening Slopes.	8.2-10
8.3-1	Geometry and Mesh of End Plate-Aperture	8.3-4
8.3-2	Transient Normal Force in Bolts	8.3-5
8.3-3	Transient Shear Force in Bolt	8.3-6
8.3-4	Radial Displacement at Outside Top (Node 46).	8.3-7
8.4-1	Geometry and Element Mesh	8.4-4
8.4-2	Element Numbering Detail of Mesh.	8.4-5
8.4-3	Node Numbering Detail of Mesh	8.4-6
8.4-4	Material Properties.	8.4-7
8.4-5	Comparison of Calculated and Experimental Load Deflection Curve Notched Beam Test.	8.4-7
8.5-1	Geometry of One-Way Reinforced Slab.	8.5-4
8.5-2	Element Mesh with Node Numbering	8.5-5
8.5-3	Element Mesh with Element Numbering	8.5-6
8.5-4	Load-Deflection Relationship for One-Way Reinforced Slab.	8.5-7

Figure **Page**

8.6-1 One-Way Reinforced Slab 8.6-4
8.6-2 Element Types used in Analysis 8.6-4
8.6-3 Node Numbering. 8.6-5
8.6-4 Element Numbering Concrete Elements. 8.6-6
8.6-5 Element Numbering Rebar Elements 8.6-7
8.6-6 Load/Deflection Relationship for One-Way Reinforced Slab 8.6-8

8.7-1 Mesh 8.7-5
8.7-2 Equivalent Stress, Increment 30 . . . . . 8.7-6
8.7-3 Temperature, Increment 30 . . . . . 8.7-7
8.7-4 Equivalent Stress, Increment 40 . . . . . 8.7-8
8.7-5 Temperature, Increment 40 . . . . . 8.7-9
8.7-6 Equivalent Stress, Increment 50 . . . . . 8.7-10
8.7-7 Temperature, Increment 50 . . . . . 8.7-11
8.7-8 Equivalent Stress, Increment 60 . . . . . 8.7-12
8.7-9 Temperature, Increment 60 . . . . . 8.7-13
8.7-10 Equivalent Stress, Increment 70 . . . . . 8.7-14
8.7-11 Temperature, Increment 70 . . . . . 8.7-15
8.7-12 Total Displacement, Increment 70. . . . . 8.7-16

8.8-1 Thick Plate Mesh 8.8-5
8.8-2 Anisotropic Behavior Stress Contours. 8.8-6
8.8-3 Isotropic Behavior Stress Contours 8.8-7

8.9-1 Orthotropic Square Plate. 8.9-4
8.9-2 Point Load (x 10^6) and Support 8.9-5

8.10-1 Cantilever Beam with Prescribed Tip Displacement 8.10-4

8.11-1 Mesh Layout for Plate with Hole 8.11-4

8.12-1 Model 8.12-8
8.12-2 Initial Mesh 8.12-9
8.12-3 Initial Mesh with Modified Rigid Body 3 for Adaptive Analysis 8.12-10
8.12-4 Rezoning Mesh 8.12-11
8.12-5 Equivalent Plastic Strain until Rezoning 8.12-12
8.12-6 Equivalent Mises Tensile Stress at Bolt Height = 22.68 . . . . . 8.12-13

Figure **Page**

8.12-7 Mean Normal Stress Until Rezoning 8.12-14
8.12-8 Final Equivalent Plastic Strain. 8.12-15
8.12-9 Final Equivalent von Mises Tensile Stress 8.12-16
8.12-10 Final Mean Normal Stress 8.12-17
8.12-11 Adapted Mesh at Increment 20 . . . . . 8.12-18
8.12-12 Adapted Mesh at Increment 40 . . . . . 8.12-19
8.12-13 Adapted Mesh at Increment 60 . . . . . 8.12-20
8.12-14 Equivalent Mises Tensile Stress at Bolt Height = 22.7 (F^eF^p) 8.12-21

8.13-1 Original Mesh 8.13-6
8.13-2 Deformed Mesh (50% Height Reduction). 8.13-7
8.13-3 Equivalent Plastic Strain. 8.13-8
8.13-4 Equivalent von Mises Tensile Stress 8.13-9
8.13-5 Total Nodal Temperature 8.13-10

8.14-1 Undeformed Block. 8.14-5
8.14-2 Block and Indentor. 8.14-6
8.14-3 Ruled Surface 8.14-7
8.14-3 Ruled Surface (Continued) 8.14-8
8.14-3 Ruled Surface (Continued) 8.14-9
8.14-4 Deformed Block 8.14-10

8.15-1 Mesh 8.15-6
8.15-2 Nodal Configuration, Element Type 11 . . . . . 8.15-7
8.15-3 Nodal Configuration, Element Type 27 . . . . . 8.15-8
8.15-4 Nodal Displacements at Increment 10, Element Type 11 . . . . . 8.15-9
8.15-5 Nodal Displacements at Increment 20, Element Type 11 . . . . . 8.15-10
8.15-6 Nodal Displacements at Increment 30, Element Type 11 . . . . . 8.15-11
8.15-7 Equivalent Plastic Strain at Increment 30, Element Type 11 . . . . . 8.15-12
8.15-8 Nodal Displacements at Increment 10, Element Type 27 . . . . . 8.15-13
8.15-9 Nodal Displacements at Increment 20, Element Type 27 . . . . . 8.15-14
8.15-10 Nodal Displacements at Increment 30, Element Type 27 . . . . . 8.15-15
8.15-11 Equivalent Plastic Strain at Increment 30, Element Type 27 . . . . . 8.15-16
8.15-12 Load History for Both Element Types. 8.15-17
8.15-13 Deformed Geometry at Increment 25 for Data Set e8x15d 8.15-18

Figure **Page**

8.15-14 Deformed Geometry at Increment 50 for Data Set e8x15d 8.15-19
8.15-15 Contours of Total Equivalent Plastic Strain on Final Geometry for Data Set e8x15d 8.15-20

8.16-1 Original Configuration. 8.16-4
8.16-2 Deformed Mesh 8.16-5
8.16-3 Equivalent Stress. 8.16-6
8.16-4 Initial and Deformed Geometry 53 Increments for Data Set e8x16b 8.16-7
8.16-5 Contours of Equivalent von Mises Stress at 53 Increments for Data Set e8x16b 8.16-8

8.17-1 Rigid Surfaces Defining Extrusion Die 8.17-4
8.17-2 Deformed Mesh, Increment 35 . . . . . 8.17-5
8.17-3 Deformed Mesh, Increment 35 . . . . . 8.17-6
8.17-4 Deformed Mesh, Increment 70 . . . . . 8.17-7
8.17-5 Deformed Mesh, Increment 70 . . . . . 8.17-8
8.17-6 Equivalent Plastic Strain, Increment 70 . . . . . 8.17-9
8.17-7 Equivalent Stress, Increment 70 . . . . . 8.17-10
8.17-8 Equivalent Plastic Strain at Increment 199 for Data Set e8x17b 8.17-11
8.17-9 Equivalent von Mises Effective Stress at Increment 199 for Data Set e8x17b . 8.17-12

8.18-1 Circular Blank Holder and Punch 8.18-6
8.18-2 Deformed Sheet at Increment 40 . . . . . 8.18-7
8.18-3 Plastic Strain at Increment 40 . . . . . 8.18-8
8.18-4 Equivalent Stress at Increment 40 . . . . . 8.18-9
8.18-5 Analytical Form of Rigid Contact Surfaces 8.18-10
8.18-6 Final Deformed Geometry for Data Set e8x18c 8.18-11
8.18-7 Final Deformed Geometry for Data Set e8x18d 8.18-12

8.19-1 Initial Geometry for both Data Sets 8.19-4
8.19-2 Deformed Mesh at Increment 12 for Data Set e8x19 . . . . . 8.19-5
8.19-3 Deformed Mesh at Increment 24 for Data Set e8x19 . . . . . 8.19-6
8.19-4 Deformed Mesh at Increment 36 for Data Set e8x19 . . . . . 8.19-7
8.19-5 Equivalent Total Plastic Strain at Increment 36 for Data Set e8x19 . . . . . 8.19-8
8.19-6 Equivalent Total Plastic Strain at Increment 164 for Data Set e8x19b 8.19-9
8.19-7 Equivalent von Mises Stress for Data Set e8x19 . . . . . 8.19-10
8.19-8 von Mises for Data Set e8x19b 8.19-11

Figure **Page**

8.20-1 Node Numbers in Circular Region 8.20-2
8.20-2 Element Numbers in Circular Region 8.20-3
8.20-3 Electric Potential Along Diameter 8.20-4
8.20-4 First Component of Electric Field 8.20-5

8.21-1 Node Numbers in Mesh 8.21-2
8.21-2 Element Numbers in Mesh 8.21-3
8.21-3 Scalar Potential Through Radius 8.21-4

8.22-1 Node Numbers in Circular Region 8.22-2
8.22-2 Element Numbers in Circular Region 8.22-3
8.22-3 Magnetic Scalar Potential along Radial Line 8.22-4
8.22-4 Magnetic Flux Distribution 8.22-5

8.23-1 Mesh and Applied Current 8.23-3
8.23-2 Third Component of Magnetic Flux along Radial Line 8.23-4
8.23-3 Magnetic Potential Vector 8.23-5

8.24-1 Mesh with Node Numbers 8.24-3
8.24-2 Mesh with Element Numbers 8.24-3
8.24-3 Magnetic Scalar Potential Linear Material Behavior 8.24-4
8.24-4 Magnetic Scalar Potential Nonlinear Material Behavior 8.24-5

8.25-1 Acoustic Cavity Mesh with Node Numbers 8.25-3
8.25-2 Acoustic Cavity Mesh with Element Numbers 8.25-4
8.25-3 Outline Plot Showing Internal Barrier 8.25-5
8.25-4 Second Mode 8.25-6
8.25-5 Third Mode 8.25-7
8.25-6 Fourth Mode 8.25-8
8.25-7 Fifth Mode 8.25-9
8.25-8 Sixth Mode 8.25-10
8.25-9 Acoustic Pressure at Time = 0.000001 . . . . . 8.25-11
8.25-10 Acoustic Pressure at Time = 0.005 . . . . . 8.25-12
8.25-11 Acoustic Pressure at Time = 0.01 . . . . . 8.25-13

Figure **Page**

8.26-1 Acoustic Cavity Mesh 8.26-3
8.26-2 Time History of Pressure Pulse 8.26-4

8.27-1 Finite Element Mesh – Nodes 8.27-4
8.27-2 Finite Element Mesh – Nodes 8.27-5
8.27-3 Failure Index, Increment 0. . . . . 8.27-6
8.27-4 Failure Index, Increment 5. . . . . 8.27-7
8.27-5 Failure Index – No Failure Allowed. 8.27-8
8.27-6 First Component of Stress in Preferred Direction 8.27-9
8.27-7 Second Component of Stress in the Preferred Direction 8.27-10

8.28-1 Finite Element Mesh with Dipole 8.28-3
8.28-2 Scalar Potential 8.28-4
8.28-3 Vector Plot of Electric Field. 8.28-5
8.28-4 Scalar Potential Distribution. 8.28-6

8.29-1 Finite Element Mesh and Parallel Wires 8.29-3
8.29-2 Magnetic Scalar Potential 8.29-4
8.29-3 Magnetic Flux Density. 8.29-5
8.29-4 Magnetic Flux Distribution 8.29-6

8.30-1 Finite Element Mesh with Node Numbers 8.30-3
8.30-2 Finite Element Mesh with Element Numbers 8.30-4
8.30-3 Third Component of Electric Field at 20 MHz 8.30-5

8.31-1 Finite Element Mesh. 8.31-3
8.31-2 Third Component of Magnetic Potential, Time = 2 Microseconds 8.31-4
8.31-3 Third Component of Magnetic Potential, Time = 25 Microseconds 8.31-5
8.31-4 Time History of Magnetic Potential 8.31-6
8.31-5 Current Density, Time = 25 Microseconds 8.31-7

8.32-1 Finite Element Mesh of Resonator 8.32-4

8.33-1 Sector of Circular Region 8.33-3
8.33-2 Third Component of Magnetic Potential using Harmonic Procedure 8.33-4
8.33-3 Time HIstory of Magnetic Potential of Node 1, Transient Procedure. 8.33-5

Figure **Page**

8.34-1 One-Element Model 8.34-3
8.34-2 Time History of Axial Stress 8.34-4
8.34-3 Time History of Void Ratio 8.34-5
8.34-4 Time History of Preconsolidation Pressure 8.34-6

8.35-1 Mesh of Embankment with Sets used for Material Definition and Initial Preconsolidation 8.35-4
8.35-2 Boundary Conditions 8.35-5
8.35-3 Contour of Settlement 8.35-6
8.35-4 Vertical Stresses 8.35-7
8.35-5 Mean Pressure in Soil 8.35-8
8.35-6 Void Ratio 8.35-9
8.35-7 Preconsolidation Pressure 8.35-10
8.35-8 Fluid Pore Pressure 8.35-11

8.36-1 Two Cylinders 8.36-3
8.36-2 Radial and Hoop Stresses through Radius 8.36-4

8.37-1 Finite Element Mesh with Symmetry Surfaces 8.37-3
8.37-2 Reaction and Contact (Interference) Forces 8.37-4

8.38-1 Plate with Rigid Surfaces 8.38-4
8.38-2 Male Punch Consisting of Seven NURBS 8.38-5
8.38-3 Blank Holder 8.38-6
8.38-4 Deformed Plate at Increment 20 . . . . . 8.38-7
8.38-5 Deformed Plate at Increment 50 . . . . . 8.38-8
8.38-6 Deformed Plate at Increment 80 . . . . . 8.38-9
8.38-7 Deformed Plate at Increment 110 . . . . . 8.38-10
8.38-8 Equivalent Stress at Midsurface at Increment 110 . . . . . 8.38-11
8.38-9 Equivalent Plastic Strain at Midsurface at Increment 110 . . . . . 8.38-12

8.39-1 Mesh of Two Beams 8.39-3
8.39-2 Initial Contact of Beams 8.39-4
8.39-3 Deformed Mesh at Increment 20 . . . . . 8.39-5
8.39-4 Deformed Mesh at Increment 30 . . . . . 8.39-6
8.39-5 Deformed Mesh at Increment 39 . . . . . 8.39-7
8.39-6 Load Deflection Curve 8.39-8

Figure **Page**

8.40-1 Original Mesh 8.40-3
8.40-2 First Adaptive Mesh 8.40-4
8.40-3 Second Adaptive Mesh 8.40-5
8.40-4 Third Adaptive Mesh 8.40-6
8.40-5 Fourth Adaptive Mesh 8.40-7

8.41-1 Original Finite Element Mesh 8.41-4
8.41-2 First Adaptive Mesh 8.41-5
8.41-3 Second Adaptive Mesh 8.41-6
8.41-4 Third Adaptive Meshing 8.41-7
8.41-5 Fourth Adaptive Mesh 8.41-8
8.41-6 Fifth Adaptive Mesh 8.41-9

8.42-1 Original Mesh 8.42-3
8.42-2 Deformed New Mesh at Increment 30 . . . . . 8.42-4
8.42-3 Deformed New Mesh at Increment 60 . . . . . 8.42-5
8.42-4 Deformed New Mesh at Increment 120 . . . . . 8.42-6
8.42-5 Deformed New Mesh at Increment 180 . . . . . 8.42-7

8.43-1 Close-up of Original Finite Element Mesh 8.43-5
8.43-2 Seal with Prescribed Boundary Conditions 8.43-6
8.43-3 Deformed Mesh showing New Elements 8.43-7
8.43-4 Deformed Mesh at Initial Contact 8.43-8
8.43-5 Adaptivity Due to Contact 8.43-9
8.43-6 Adaptivity Due to Contact (Updated Lagrange Formulation) 8.43-10

8.44-1 Original Finite Element Mesh for all 3 Data Sets 8.44-5
8.44-2 Adaptive Criteria Box for Data Set e8x44 and e8x44c 8.44-6
8.44-3 Deformed Mesh at Increment 48 for Data Set e8x44 . . . . . 8.44-7
8.44-4 Deformed Mesh at Increment 75 for Data Set e8x44 . . . . . 8.44-8
8.44-5 Deformed Mesh at Increment 100 for Data Set e8x44 . . . . . 8.44-9
8.44-6 Deformed Mesh at Increment 3 for Data Set e8x44b 8.44-10
8.44-7 Deformed Mesh at Increment 50 for Data Set e8x44b 8.44-11
8.44-8 Deformed Mesh at Increment 80 for Data Set e8x44b 8.44-12
8.44-9 Deformed Mesh at Increment 48 for Data Set e8x44c 8.44-13
8.44-10 Deformed Mesh at Increment 75 for Data Set e8x44c 8.44-14

Figure **Page**

8.44-11 Deformed Mesh at Increment 100 for Data Set e8x44c 8.44-15
8.44-12 Deformed Mesh at Increment 155 for Data Set e8x44c 8.44-16

8.45-1 Geometry for Problem 8.45 to show the SPLINE Option 8.45-3
8.45-2 Initial Model for this Example 8.45-4
8.45-3 Contours of Effective von Mises Stress 8.45-5

8.46-1 Initial Model 8.46-3
8.46-2 Final Deformed Shape after 10 Increments 8.46-4

8.47-1 Initial Model for Stick-Slip Problem 8.47-3
8.47-2 Distributed Load Boundary Conditions 8.47-3
8.47-3 Loading History for the Distributed Loads 8.47-4
8.47-4 First Slipping Motion (Increment 21) 8.47-5
8.47-5 First Slipping Motion (Increment 21) 8.47-6
8.47-6 Final Slip occurring in Increment 51 . . . . . 8.47-7
8.47-7 X Displacement History for Node 1 . . . . . 8.47-8

8.48-1 Initial Model for Stick-Slip Problem 8.48-3
8.48-2 Loading History - Y Axis is Load Per Unit Area divided by 10^6 . . . . . 8.48-3
8.48-3 First Slip occurs in Increment 13 . . . . . 8.48-4
8.48-4 Final Deformed Shape in Increment 20 . . . . . 8.48-5
8.48-5 History Plot of x Displacement for Node 51 . . . . . 8.48-6

8.49-1 Initial Model 8.49-3
8.49-2 Deformed Shape of Bushing at the End of Increment 25 . . . . . 8.49-4
8.49-3 Deformed Shape of Bushing at the End of Increment 27 . . . . . 8.49-5
8.49-4 Deformed Shape of Bushing at the End of Increment 40 . . . . . 8.49-6
8.49-5 Deformed Shape of Bushing at the End of Increment 51 . . . . . 8.49-7

8.50-1 Initial Model 8.50-3
8.50-2 Deformed Shape at End of 25 Increments 8.50-4
8.50-3 Deformed Shape at End of 50 Increments 8.50-5
8.50-4 Load Stroke Curve for the Deformation 8.50-6

8.51-1 Initial Model for Both Data Sets 8.51-4
8.51-2 Boundary Condition Definition for Both Data Sets 8.51-5

Figure **Page**

8.51-3 Deformed Shell Structure at Increment 5 for Data Set e8x51a 8.51-6
8.51-4 Deformed Shell Structure at Increment 10 for Data Set e8x51a 8.51-7
8.51-5 Deformed Shell Structure at Increment 20 for Data Set e8x51a 8.51-8
8.51-6 Deformed Shell Structure at Increment 25 for Data Set e8x51a 8.51-9
8.51-7 Deformed Shell Structure at Increment 5 for Data Set e8x51b 8.51-10
8.51-8 Deformed Shell Structure at Increment 10 for Data Set e8x51b 8.51-11
8.51-9 Deformed Shell Structure at Increment 20 for Data Set e8x51b 8.51-12
8.51-10 Deformed Shell Structure at Increment 25 for Data Set e8x51b 8.51-13

8.52-1 Initial Geometry - Only One Quarter is Modeled due to Symmetry 8.52-4
8.52-2 Deformed Geometry at the End of 10 Increments. 8.52-5
8.52-3 Deformed Geometry at the End of 20 Increments. 8.52-6
8.52-4 Deformed Geometry at the End of 30 Increments. 8.52-7
8.52-5 Effective Plastic Strain Distribution at the End of 30 Increments. 8.52-8

8.53-1 Initial Geometry for both Data Sets 8.53-3
8.53-2 End View of Original and Deformed Geometry after 14 Increments for Data Set e8x53a 8.53-4
8.53-3 Original and Deformed Geometry after 20 Increments for Data Set e8x53a . . 8.53-5
8.53-4 Original and Deformed Geometry after 14 Increments for Data Set e8x53b - End View 8.53-6
8.53-5 Original and Deformed Geometry after 20 Increments for Data Set e8x53b . . 8.53-7
8.53-6 History Plot of the Variation of the y Reaction Force at Node 405 for Data Set e8x53a 8.53-8
8.53-7 History Plot of the Variation of the y Reaction Force at Node 405 for Data Set e8x53b 8.53-9

8.54-1 Side View of Initial Geometry. 8.54-3
8.54-2 Initial Model of Structure 8.54-4
8.54-3 Deformed Shape of the Structure at Increment 5 . . . . . 8.54-5
8.54-4 Deformed Shape of the Structure at Increment 10. . . . . 8.54-6
8.54-5 Displacement x versus Reaction Force X for Node 26 . . . . . 8.54-7

8.55-1 Initial Model 8.55-4
8.55-2 Elements to which Clamp Down Pressure is Applied. 8.55-5
8.55-3 The Final Deformed Geometry for Data Set e8x55a 8.55-6
8.55-4 The Final Deformed Geometry for Data Set e8x55b 8.55-7

Figure **Page**

8.56-1 Initial Model for both Data Sets 8.56-3
8.56-2 The Final Deformed Shape for Data Set e8x56a 8.56-4
8.56-3 The Final Deformed Shape for Data Set e8x56b 8.56-5

8.57-1 Initial Model with Point Load applied on Node 1 . . . . . 8.57-3
8.57-2 Initial and Deformed Shape for Data Set e8x57a 8.57-4
8.57-3 Equivalent von Mises Stress for Data Set e8x57a 8.57-5
8.57-4 Equivalent von Mises Stress for Data Set e8x5c 8.57-6

8.58-1 Initial Model 8.58-2
8.58-2 Deformed Geometry with the Adapted Mesh 8.58-3

8.60-1 Initial Model 8.60-3
8.60-2 Deformed Geometry for Increment 25 . . . . . 8.60-4
8.60-3 Deformed Geometry for Increment 50 . . . . . 8.60-5
8.60-4 Deformed Geometry for Increment 100 . . . . . 8.60-6
8.60-5 Deformed Geometry for Increment 120 . . . . . 8.60-7
8.60-6 Deformed Geometry for Increment 130 . . . . . 8.60-8
8.60-7 Magnified View of Contours of Total Effective Plastic Strain for Increment 130 . . . . . 8.60-9

8 Advanced Topics List of Tables

Table		Page
8-1	Recent Analysis Capabilities in MARC	8-2
8.2-1	J-Integral Evaluation Results	8.2-3
8.9-1	Comparison of Results	8.9-3
8.10-1	Comparison of MARC Results vs. Analytical	8.10-3
8.11-1	σ_{yy} vs. Load Increment	8.11-3
8.28-1	Comparison of MARC Results	8.28-2
8.29-1	Comparison of MARC Results	8.29-2
8.30-1	Electric Field as a Function of Frequency	8.30-2
8.32-1	Electric Field as a Function of Frequency	8.32-2

8 Advanced Topics

This chapter demonstrates capabilities that have been added to MARC in the last few releases. These capabilities include substructures, cracking, composites, contact, electrostatics, magnetostatics, and acoustics capabilities among others. Discussions of these capabilities can be found in *MARC Volume A: Theory and User Information* and a summary of the various capabilities is given below:

Substructures

- Linear analysis
- Nonlinear analysis
- Cracking analysis

Thermal-mechanical coupled analysis

Composite analysis

- Failure criteria
- Progressive failure

Activate and deactivate

Contact analysis

- Two-dimensional
- Three-dimensional
- Springback
- Friction

Electrostatic analysis

Magnetostatic analysis

Acoustic analysis

Adaptive Meshing

- Linear analysis
- Nonlinear analysis

Compiled in this chapter are a number of solved problems. Table 8-1 shows the MARC elements and options used in these demonstration problems.

Table 8-1 Recent Analysis Capabilities in MARC

Problem Number	Element Type(s)	Parameters	Model Definition	History Definition	User Subroutines	Problem Description
8.1	26	ELASTIC SUBSTRUCT NEWDB SUPER	SUBSTRUCTURE DIST LOAD SUPERINPUT RESTART	BACK TO SUBS	SSTRAN	Hole in plate. Generate substructure (1-1) and 1-2). Combine substructures, perform analysis. Read RESTART tape, Go back to substructures to obtain results.
8.2	27	SUBSTRUCT NEWDB SUPER J-INT SCALE	SUBSTRUCTURE DIST LOADS SUPERINPUT J-INTEGRAL WORK HARD	AUTO LOAD PROPORTIONAL INC	WKSLP	Double-edge notch specimen using substructure. Elastic region away from the crack is treated as a substructure.
8.3	10 12	SUBSTRUCT NEWDB SUPER	SUBSTRUCTURE SUPERINPUT POINT LOADS GAP DATA	POINT LOADS AUTO LOAD BACK TO SUBS	—	End plate aperture breakaway problem. The rate is treated as a substructure leaving the contact elements to be at highest level.
8.4	26	—	ISOTROPIC CRACK DATA TYING	PROPORTIONAL INC AUTO LOAD	—	Collapse of a notched concrete beam.
8.5	75	PRINT	CONN GENER COMPOSITE ISOTROPIC ORTHOTROPIC	POINT LOADS AUTO INCREMENT	—	Cracking of a plate one-way reinforced using shell elements.
8.6	27 46	PRINT	CONN GENER NODE FILL CRACK DATA ISOTROPIC	POINT LOADS AUTO INCREMENT	REBAR	Cracking of a one-way reinforced plate using rebar elements.

Table 8-1 Recent Analysis Capabilities in MARC (Continued)

Problem Number	Element Type(s)	Parameters	Model Definition	History Definition	User Subroutines	Problem Description
8.7	11 12 39	FINITE UPDATE LARGE DISP COUPLE MESH PLOT	CONTROL FIXED DISP FIXED TEMP INITIAL TEMP ISOTROPIC GAP DATA CONVERT WORK HARD TEMP EFFECTS RESTART DIST FLUXES	TRANSIENT	—	Thermal-mechanically coupled analysis of the compression of a block.
8.8	21	—	ORTHOTROPIC DIST LOADS	—	HOOKLW ANELAS	Bending of a thick anisotropic plate.
8.9	3	—	DEFINE ORTHOTROPIC ORIENTATION FALL DATA PRINT ELEM	—	—	Failure criteria calculation of an orthotropic plate.
8.10	52	—	HYPOELASTIC	—	UBEAM	Nonlinear beam bending.
8.11	26	—	ERROR ESTIMATE	DEACTIVATE ACTIVATE	—	Example of Activate, Deactivate and error estimates.
8.12	10	PRINT,5 FINITE LARGE DISP UPDATE REZONING	WORK HARD CONTACT	AUTO LOAD TIME STEP REZONE CONTACT CHANGE ISOTROPIC CHANGE CONNECTIVITY CHANGE COORDINATE CHANGE END REZONE AUTO TIME	—	Forging of the head of a bolt.
8.13	10 116	PRINT,5 FINITE LARGE DISP UPDATE COUPLE	POST FIXED TEMP FIXED DISP TEMP EFFECTS WORK HARD DIST FLUXES CONTACT INITIAL TEMP CONVERT	TRANSIENT DISP CHANGE AUTO TIME	—	Coupled analysis of ring compression.

Table 8-1 Recent Analysis Capabilities in MARC (Continued)

Problem Number	Element Type(s)	Parameters	Model Definition	History Definition	User Subroutines	Problem Description
8.14	7	UPDATE FINITE LARGE DISP PRINT,5	—	AUTO LOAD TIME STEP	—	3D indentation problem demonstrating how rigid surfaces are defined.
8.15	11 27	UPDATE FINITE LARGE DISP PRINT,5	CONTACT CONTACT TABLE DEFINE RESTART LAST	AUTO LOAD TIME STEP	—	Double-sided contact between deformable bodies.
8.16	11	UPDATE FINITE LARGE DISP PRINT,5	SPRINGS CONTACT WORK HARD	AUTO LOAD TIME STEP RELEASE MOTION CHANGE	MOTION	Formation of a metal part and the examination of springback.
8.17	7	REZONING UPDATE FINITE LARGE DISP PRINT,8	CONTACT RESTART LAST	AUTO LOAD TIME STEP	—	Metal extrusion analysis using the CONTACT option. Coulomb friction.
8.18	75	SHELL SET,7 LARGE DISP UPDATE FINITE PRINT,8	CONTACT	AUTO LOAD TIME STEP MOTION CHANGE	WKSLP	Stretch forming of a circular sheet. Coulomb friction between sheet and punch.
8.19	7	UPDATE FINITE LARGE DISP PRINT,8 SIZING	CONTACT UMOTION	AUTO LOAD TIME STEP	MOTION	Three dimensional indentation rolling of elastic-perfectly plastic material.
8.20	39	SIZING ELECTRO	POINT CHARGE FIXED POTENTIAL	STEADY STATE	—	Point charge in a circular region.
8.21	43	SIZING ELECTRO	FIXED POTENTIAL POINT CHARGE	STEADY STATE	—	Point charge in a circular cylinder.
8.22	39	SIZING\ MAGNET	POINT CURRENT FIXED POTENTIAL	STEADY STATE	—	Point current in a circular region.
8.23	109	MAGNET	FIXED POTENTIAL POINT CURRENT	STEADY STATE	—	3D analysis of a magnetic field in a coil.
8.24	39	MAGNET	ISOTROPIC FIXED POTENTIAL POINT CURRENT B-H RELATION	STEADY STATE	—	2D nonlinear magnetostatic analysis.

Table 8-1 Recent Analysis Capabilities in MARC (Continued)

Problem Number	Element Type(s)	Parameters	Model Definition	History Definition	User Subroutines	Problem Description
8.25	39	ACOUSTIC PRINT,3	ISOTROPIC	DYNAMIC CHANGE	—	2D acoustic problem demonstrating the eigenvalue analysis in a circular cavity with barrier.
8.26	39	ACOUSTIC	ISOTROPIC FIXED PRESSURE	DYNAMIC CHANGE	FORCDT	2D acoustic problem demonstrating the eigenvalue analysis of a rectangular cavity.
8.27	26	INPUT TAPE	FIXED DISP ORTHOTROPIC	AUTO LOAD PROPORTIONAL CONTROL	—	Progressive failure of a plate with a hole.
8.28	41 103	ELECTRO	POINT CHARGE FIXED POTENTIAL	STEADY STATE	—	Linear distribution of dipoles.
8.29	41 103	MAGNET	POINT CHARGE FIXED POTENTIAL	STEADY STATE	—	Magnetic field around two wires carrying opposite currents.
8.30	111	EL-MA HARMONIC PRINT, 3	DIST CURRENT FIXED POTENTIAL	DIST CURRENT HARMONIC POINT CURRENT	—	Harmonic electromagnetic analysis of a waveguide.
8.31	112	EL-MA PRINT, 3	FIXED POTENTIAL	DYNAMIC CHANGE POTENTIAL CHANGE	—	Transient electromagnetic analysis around a conducting sphere.
8.32	113	EL-MA HARMONIC	FIXED POTENTIAL	DIST CURRENT HARMONIC	—	Calculate the resonance in a cavity.
8.33	111	EL-MA HARMONIC	FIXED POTENTIAL	POINT CURRENT CURRENT DYNAMIC CHANGE HARMONIC	—	Steady state analysis of an infinitely long wire using both harmonic and transient analysis.
8.34	28	PORE UPDATE ISTRESS	SOIL INITIAL PC INITIAL VOID INITIAL STRESS DIST LOADS	DIST LOADS TIME STEP DISP CHANGE AUTO LOAD	—	Drained triaxial test on normally consolidated clay.

Table 8-1 Recent Analysis Capabilities in MARC (Continued)

Problem Number	Element Type(s)	Parameters	Model Definition	History Definition	User Subroutines	Problem Description
8.35	32	PORE ISTRESS	SOIL SOLVER INITIAL PC INITIAL STRESS INITIAL VOID DIST LOADS DEFINE	DIST LOADS TIME STEP AUTO TIME CONTROL	—	Coupled pore-pressure calculation of stratified soil embankment.
8.36	116	PRINT, 5	SPRINGS CONTACT DEFINE	CONTACT TABLE AUTO LOAD TIME STEP	—	Interference fit of two cylinders.
8.37	11	PRINT, 8	CONTACT SPRINGS DEFINE	CONTACT TABLE AUTO LOAD TIME STEP	—	Interference fit between sectors of two cylinders. Demonstrates symmetry surfaces.
8.38	75	LARGE DISP UPDATE FINITE	CONTACT WORK HARD CONTACT TABLE	AUTO LOAD TIME STEP	—	Deep drawing of a box using rigid punch described as NURBS.
8.39	5	LARGE DISP	CONTACT POINT LOAD	AUTO INCREMENT POINT LOAD	—	Contact of two beams by a point load.
8.40	11	ADAPT ELASTIC	ADAPTIVE ATTACH NODES SURFACE POINT LOAD	—	—	Adaptive meshing of a disk subjected to point loads.
8.41	3	ADAPT ELASTIC	ADAPTIVE ERROR ESTIMATES	—	—	Adaptive meshing of a stress concentration.
8.42	11	ADAPT LARGE DISP FOLLOW FOR	CONTACT ATTACH NODE SURFACE DIST LOADS	MOTION CHANGE AUTO LOAD TIME STEP	—	Double-sided contact analysis with adaptive meshing.
8.43	119	LARGE DISP FOLLOW FOR ADAPT	ADAPTIVE MOONEY CONTACT	AUTO LOAD TIME STEP DISP CHANGE	—	Modeling a rubber seal with adaptive meshing.
8.44	11	UPDATE LARGE DISP FINITE ADAPT	WORK HARD ADAPTIVE CONTACT CONTACT TABLE	MOTION CHANGE TIME STEP AUTO LOAD	—	Rolling example with adaptive meshing.
8.45	11	EXTENDED	CHANGE STATE INITIAL STATE SPLINE CONTACT	AUTO LOAD TIME STEP MOTION CHANGE CHANGE STATE	—	Use of the SPLINE option for deformable-deformable contact.

Table 8-1 Recent Analysis Capabilities in MARC (Continued)

Problem Number	Element Type(s)	Parameters	Model Definition	History Definition	User Subroutines	Problem Description
8.46	3	EXTENDED DIST LOADS	CONTACT EXCLUDE FIXED DISP	AUTO LOAD DISP CHANGE DIST LOADS	—	Use of EXCLUDE option for contact analysis.
8.47	3	DIST LOADS	DIST LOADS FIXED DISP SPRINGS CONTACT	AUTO LOAD DIST LOADS TIME STEP	—	Simulation of contact with stick-slip friction.
8.48	3	LARGE DISP DIST LOADS	FIXED DISP SOLVER SPRINGS GEOMETRY	AUTO LOAD DISP CHANGE DIST LOADS TIME STEP	—	Simulation of deformable-deformable contact with stick-slip friction.
8.49	80	DIST LOADS LARGE DISP	CONTACT MOONEY	AUTO LOAD MOTION CHANGE TIME STEP	—	Rolling of a compressed rubber bushing with stick-slip friction.
8.50	10	UPDATE FINITE LARGE DISP	GEOMETRY WORK HARD	AUTO LOAD MOTION CHANGE TIME STEP	—	Compression test of cylinder with stick-slip friction.
8.51	139 75	FINITE LARGE DISP UPDATE SHELL SECT	CONTACT CONTACT TABLE FIXED DISP WORK HARD GEOMETRY	AUTO LOAD MOTION CHANGE TIME STEP	—	Modeling of a spring.
8.52	75	FINITE LARGE DISP UPDATE SHELL SECT	GEOMETRY CONTACT CONTACT TABLE WORK HARD	AUTO LOAD DISP CHANGE TIME STEP	—	Deep drawing of a sheet.
8.53	75 49	DIST LOADS LARGE DISP SHELL SECT	DIST LOADS GEOMETRY FIXED DISP	AUTO LOAD DIST LOADS DISP CHANGE TIME STEP	—	Shell-shell contact and separation.
8.54	75	LARGE DISP SHELL SECT UPDATE	CONTACT FIXED DISP	AUTO LOAD DISP CHANGE TIME STEP	—	Self contact of a shell structure.
8.55	75	FINITE LARGE DISP UPDATE SHELL SECT	CONTACT POINT LOAD WORK HARD	AUTO LEAD POINT LOAD TIME STEP	—	Deep drawing of copper sheet (velocity and load controlled dies.
8.56	10	FINITE LARGE DISP UPDATE	CONTACT WORK HARD	AUTO LOAD DISP CHANGE TIME STEP	—	2D contact problem (load and velocity controlled dies).

Table 8-1 Recent Analysis Capabilities in MARC (Continued)

Problem Number	Element Type(s)	Parameters	Model Definition	History Definition	User Subroutines	Problem Description
8.57	75 138 139 140	ADAPTIVE ELASTIC SHELL SECT	ADAPTIVE POINT LOAD	—	—	The adaptive capability with shell elements.
8.58	75	ADAPTIVE ELASTIC SHELL SECT	GEOMETRY DIST LOADS ADAPTIVE	—	—	Adaptive meshing in multiple connected shell structures.
8.59						Not Available at this Time.
8.60	11	PLASTICITY	CONTACT WORD HARD FIXED DISP	AUTO LOAD MOTION CHANGE TIME STEP	—	Simulation of sheet bending.

8.1 Plate with Circular Hole using Substructures

In this problem, the substructuring capability is demonstrated to solve an elastic problem of a square plate with a circular hole (see Figure 8.1-1). This example demonstrates the three aspects of using substructures:

1. Generate superelement
2. Combine superelements, obtaining results for external nodes
3. Obtain solution within the substructure.

Element

Element type 26 is an 8-node plane stress quadrilateral.

Model

Due to symmetry, only one quarter of the specimen is modeled. Because of symmetry about a 45° line, this quarter plate is modeled using two identical substructures.

Geometry

A unit thickness is used.

Boundary Conditions

Boundary conditions are used to enforce symmetry about the x-axis. When the 1,1 superelement is mirrored about the 45° line, this boundary condition will effectively be about the y-axis.

Material Properties

The material is elastic. Values for Young's modulus, Poisson's ratio are $30x10^6$ psi and 0.3, respectively.

DIST LOADS

A uniform pressure of 0 psi is applied to substructure 1,1. A uniform pressure of -1 psi is applied to substructure 1,2.

Substructure Procedure

In the first part of the first analysis, superelement level 1 number 1 is formed. On the SUBSTRUC parameter, it is requested that the substructure database be written to unit 31. Unit 16 is used to write the stiffness matrix. The NEWDB parameter indicates this is the first superelement created and, hence, the data base should be initialized. The SUBSTRUCTURE model definition option indicates which nodes are the external nodes. There are 11 external nodes.

In the second part of the first analysis, substructure level 1 number 1 is copied to substructure level 1 number 2. This is performed using the SUBSTRUC parameter. This new substructure is placed on unit 17. This substructure is given a different load factor than the previous one. When using substructures, the load can be modified using the AUTO LOAD option or the PROPORTIONAL increment option.

While forming substructures, multiple substructure formations can be performed during the same run. This is achieved by putting the MARC input "decks" back-to-back to create one large input.

In the second analysis, the two previous superelements are combined and the solution obtained for the external degrees-of-freedom. The SUPER parameter is used to indicate that superelements are used in this analysis. It also indicates the maximum number of nodes and degrees-of-freedom associated with a superelement. The SUPERINPUT model definition option is used to enter a correspondence table between previously defined external nodes and the nodes used in this analysis. In this problem, the externals lie along the 45° diagonal (see Figure 8.1-2). As there are no normal elements, there are no stresses or strains calculated here. A restart file is written. In addition, the calculated displacements are written back to the database.

User subroutine SSTRAN is used to reflect substructure level 1 number 2 by 90°. In the third analysis, the displacements calculated at the external nodes are used to calculate the internal degrees of freedom, the strains and the stresses. This is performed using the BACKTOSUBS option.

If desired, after the results are obtained in the subelement, plots could be obtained. In addition, if the POST option was used, the results would have been written for both substructures.

Parameters, Options, and Subroutines Summary

Example e8x1a.dat:

Parameters	Model Definition Options	History Definition Options
ELASTIC	CONNECTIVITY	CONTINUE
ELEMENT	COORDINATE	DIST LOADS
END	DIST LOADS	
MESH PLOT	END OPTION	
NEWDB	FIXED DISP	
SIZING	GEOMETRY	
SUBSTRUCTURE	ISOTROPIC	
TITLE	SUBSTRUCTURE	

Example e8x1b.dat:

Parameters	Model Definition Options
END	END OPTION
PRINT	RESTART
SIZING	SUPERINPUT
SUPER ELEMENT	
TITLE	

User subroutine in u8x1.f:

SSTRAN

Example e8x1c.dat:

Parameters	Model Definition Options	History Definition Options
END	END OPTION	BACKTOSUBS
MESH PLOT	RESTART	CONTINUE
PRINT	SUPERINPUT	
SIZING		
SUPER ELEMENT		
TITLE		

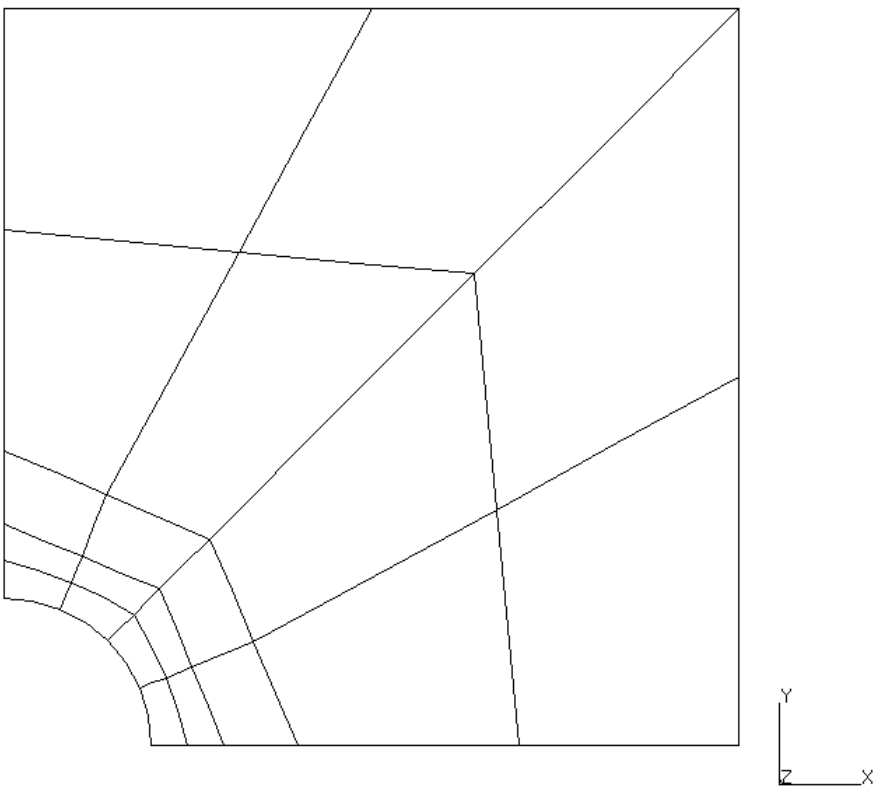

Figure 8.1-1 Hole in Plate

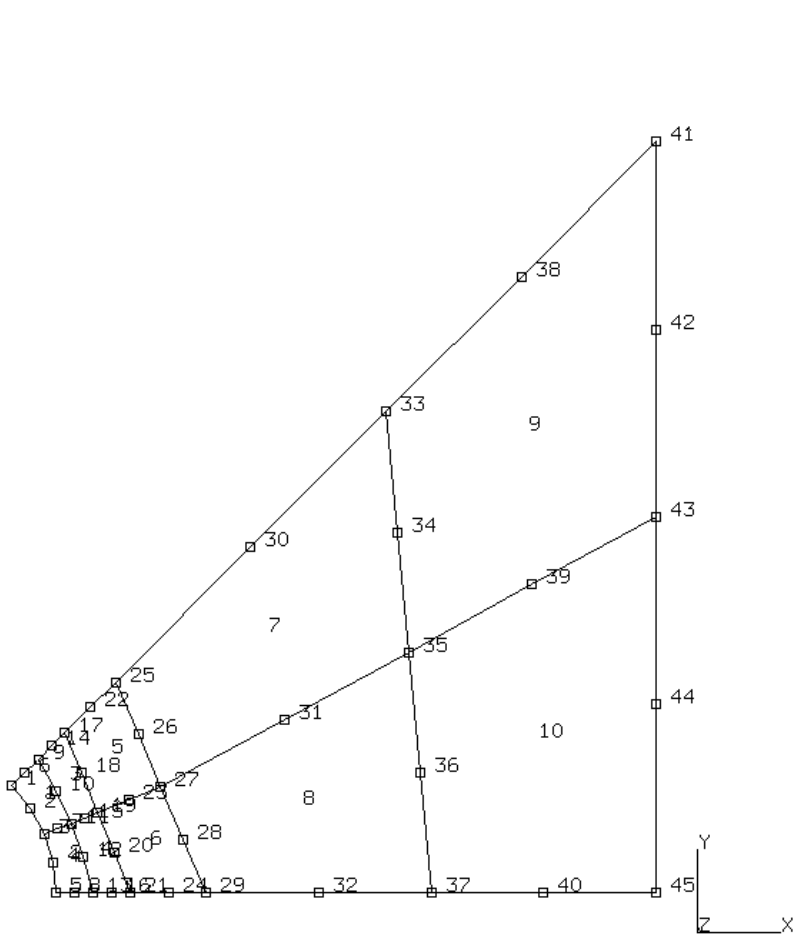

Figure 8.1-2 Substructure 1,1

8.2 Double-Edge Notch Specimen using Substructures

In this problem, the J-integral is evaluated for an elastic-plastic double-edge notch specimen under axial tension. The use of substructures for a nonlinear problem is demonstrated. Two different paths are used for the J-integral evaluation. The variation in the value of J between the two paths indicates the accuracy of the solution. This problem is identical to problem 3.8 with the exception that substructures are used. Substructures can be used in a nonlinear analysis as long as the area that is in the superelement remains linear elastic.

Element

Element type 27 is an eight-node plane strain quadrilateral.

Model

The full double-edge specimen with loading is shown in Figure 8.2-1. Due to symmetry, only one-quarter on the specimen is modeled. Figure 8.2-2 shows the mesh with 32 elements and 107 nodes.

Geometry

The option is not required for this element as a unit thickness is considered.

Boundary Conditions

Boundary conditions are used to enforce symmetry about the x- and y-axes.

Material Properties

The material is elastic-plastic with strain hardening. Values for Young's modulus, Poisson's ratio and yield stress used here are 30×10^6 psi, 0.3, and 50×10^3 psi, respectively.

Workhard

User subroutine WKSLP is used to input the workhardening slope. The workhardening curve is shown in Figure 8.2-5.

$$\bar{\sigma}(\bar{\varepsilon}^p) = \sigma_o(1 + E\bar{\varepsilon}^p/\sigma_o)^{0.2}$$

$$\frac{\partial\bar{\sigma}}{\partial\bar{\varepsilon}^p} = 0.2 \times E(1 + E\bar{\varepsilon}^p/\sigma_o)^{-0.8}$$

J-Integral

The J-integral is evaluated numerically by moving nodes within a certain ring of elements around the crack tip and measuring the change in strain energy. (This node movement represents a differential crack advance.) This mesh has two obvious "rings" of elements around the crack tip,

so that two evaluations of J are provided. A differential movement of 10^{-2} is used in all three evaluations. In problem 3.8, three paths were used. Because of the use of substructures, only two paths are possible at the highest level.

Loading

An initial uniform pressure of 100 psi is applied using the DIST LOAD option. The SCALE parameter is used to raise this pressure to a magnitude such that the highest stressed element (element 20 here) is at first yield. The pressure is scaled to 3,047 psi. The pressure is then incremented for five steps until the final pressure is 3,308 psi.

Substructure Technique

In performing a nonlinear analysis using substructures, it is important that the area included in the substructure remains elastic. In this analysis, the portion of Figure 8.2-2 that is cross-hatched is considered one substructure. Figure 8.2-2 and Figure 8.2-4 show the elements in the substructure and the highest level, respectively. It is far enough removed from the crack tip that plasticity is unlikely to occur there.

In the first part of the analysis, the superelement is created. It is written to the direct access database on unit 31. In this problem, no auxiliary sequential file is used. The SUBSTRUCTURE model definition option lists those nodes which are external. There are 17 external nodes along the thick line as shown. The distributed load is applied to the superelement. This is incremented in the second part. In the second part, the previously generated substructure is combined with the 16 elements nearest to the crack tip. The SUPER parameter indicates that file 31 is to be used; the number of super elements is 1 and there are 17 externals with two degrees of freedom. The SUPERINPUT model definition gives a correspondence table between the external node numbers and the node numbers used in this analysis. In this analysis, they are the same. After the END option is the load incrementation data. AUTO LOAD and/or PROPORTIONAL INC options can be used to modify loads in the SUBSTRUCTURE.

Results

MARC provides an output of the strain energy differences. This must be normalized by the crack opening area to obtain the value of J. Since this specimen is of unit thickness, the crack opening area is ¾1, where ¾1 is the differential crack motion. The mesh uses symmetry about the crack line, so that the strain energy change in the actual specimen is twice that printed out. These results are summarized in Table 8.2-1. It is clear that these results do demonstrate the path independence for the J-integral evaluation. Because of the use of substructures, this analysis was executed in 66% the time of problem 3.8. If the J-integrals are not evaluated, the run time is 50%. This shows the advantage of using substructures for locally nonlinear analysis.

Table 8.2-1 J-Integral Evaluation Results

	Move Tip Only	Move First Ring of Elements
Strain Energy Change for increment 0 (Δu)	6.23×10^{-2}	6.212×10^{-2}
J-Integral $\left(\frac{2\Delta u}{\Delta l}\right)$	12.46	12.424
Strain Energy Change for increment 1 (Δu)	6.869×10^{-2}	6.849×10^{-2}
J-Integral $\left(\frac{2\Delta u}{\Delta l}\right)$	13.738	13.698
Strain Energy Change for increment 2 (Δu)	7.539×10^{-2}	7.517×10^{-2}
J-Integral $\left(\frac{2\Delta u}{\Delta l}\right)$	15.078	15.034
Strain Energy Change for increment 3 (Δu)	8.241×10^{-2}	8.217×10^{-2}
J-Integral $\left(\frac{2\Delta u}{\Delta l}\right)$	16.482	16.434
Strain Energy Change for increment 4 (Δu)	8.974×10^{-2}	8.948×10^{-2}
J-Integral $\left(\frac{2\Delta u}{\Delta l}\right)$	17.948	17.896
Strain Energy Change for increment 5 (Δu)	9.738×10^{-2}	9.711×10^{-2}
J-Integral $\left(\frac{2\Delta u}{\Delta l}\right)$	19.476	19.422

Parameters, Options, and Subroutines Summary

Example e8x2.dat:

Parameters	Model Definition Options	History Definition Options
ELEMENT	CONNECTIVITY	AUTO LOAD
END	COORDINATE	BOUNDARY CHANGE
NEWDB	DIST LOADS	CONTINUE
SIZING	END OPTION	PROPORTIONAL INCREMENT
SUBSTRUCTURE	FIXED DISP	
TITLE	ISOTROPIC	

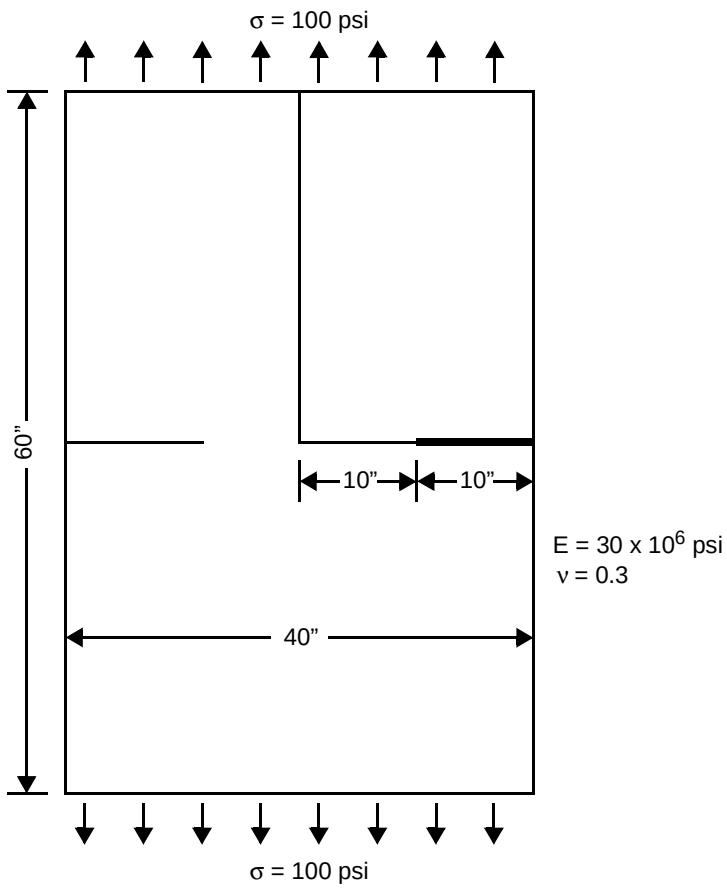

Figure 8.2-1 Double-Edge Notch Specimen

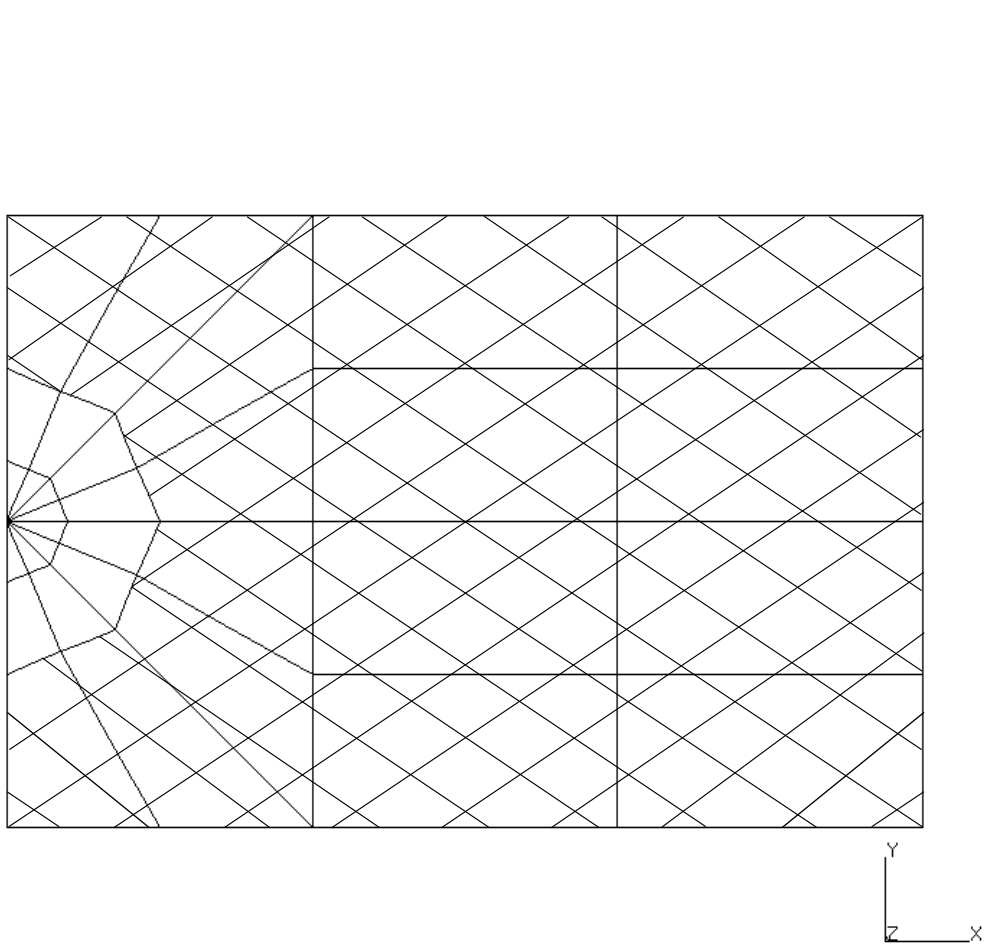

Figure 8.2-2 Mesh for Double-Edge Notch Specimen Cross-Hatched Area Indicates Substructures

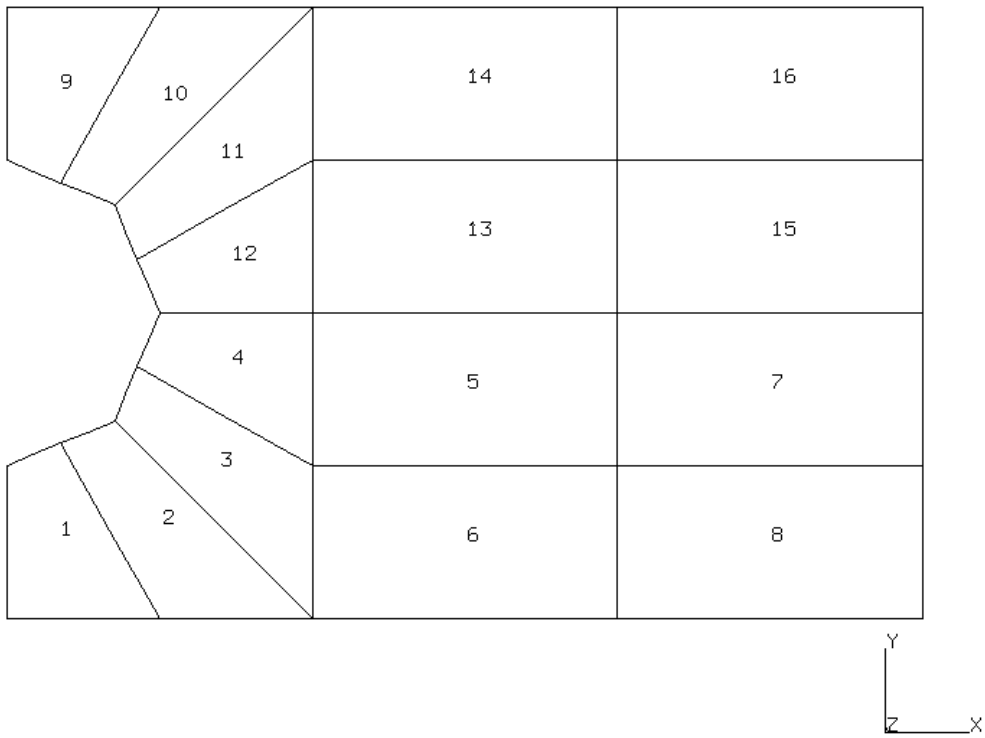

Figure 8.2-3 (A) Elements in Substructure 1-1

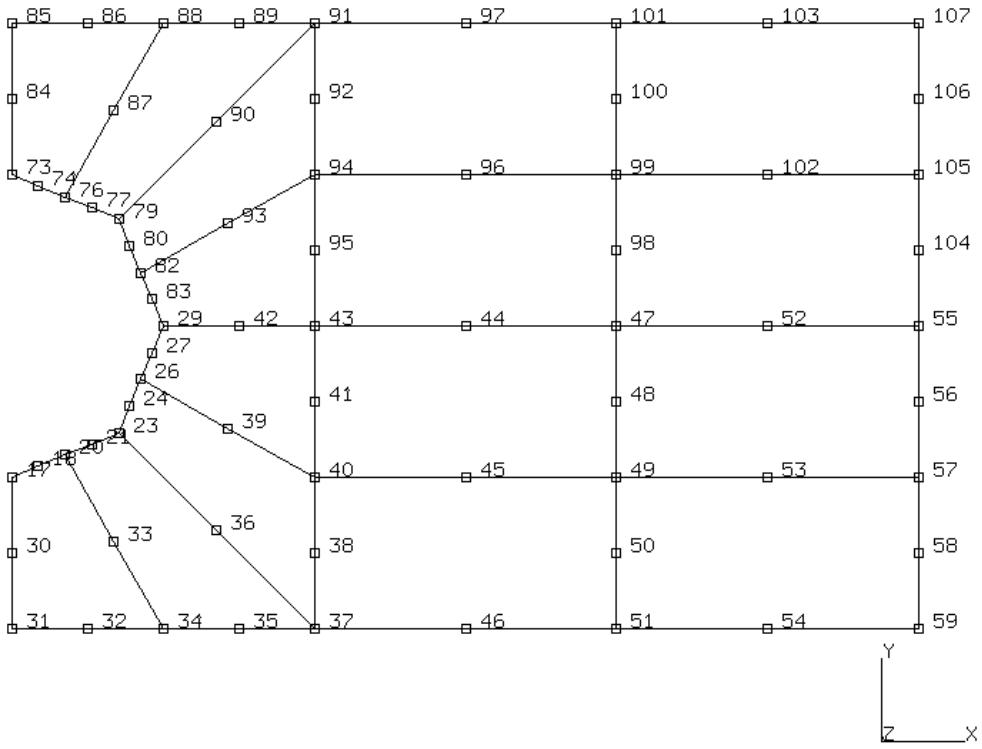

Figure 8.2-3 (B) Nodes in Substructure 1-1

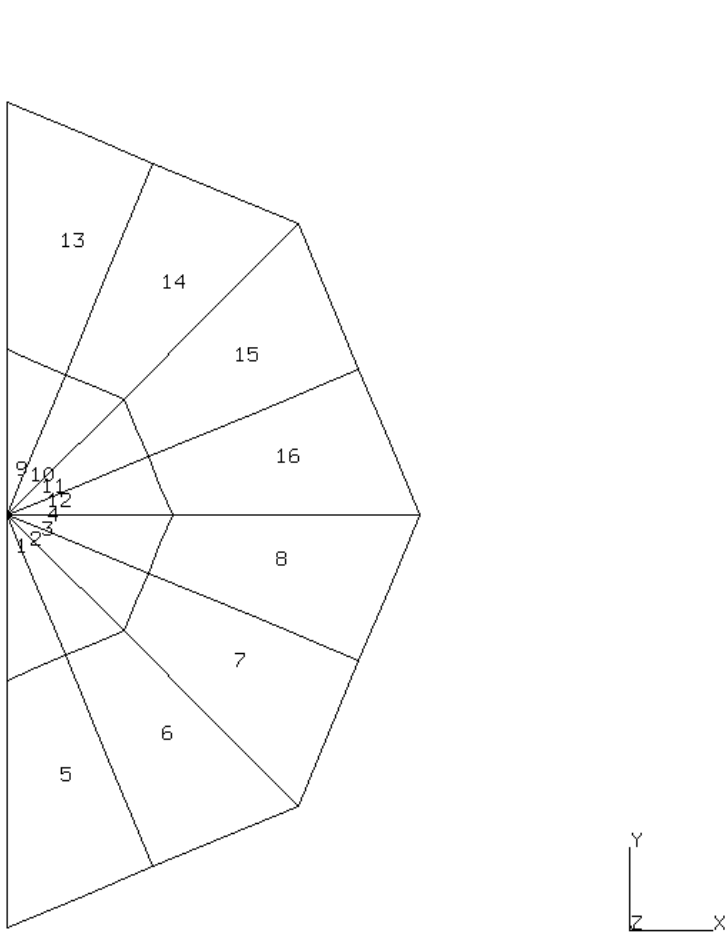

Figure 8.2-4 (A) Elements at Highest Level

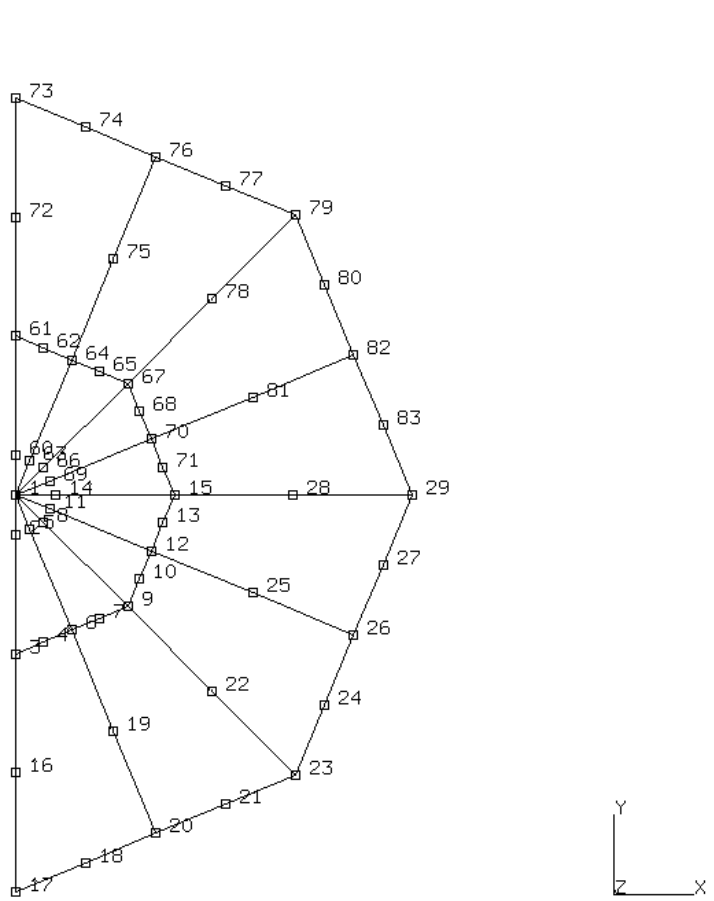

Figure 8.2-4 (B) Nodes at Highest Level

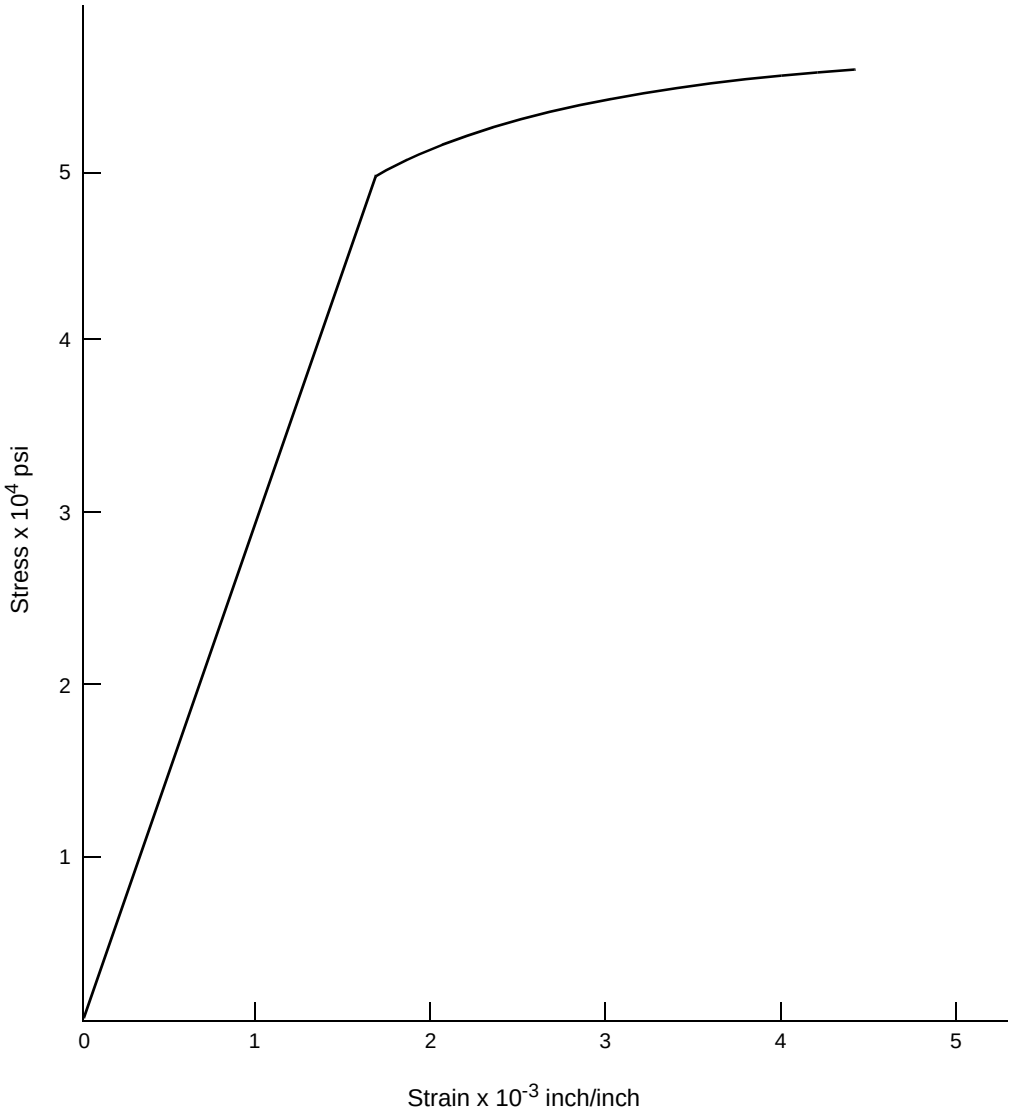

Figure 8.2-5 Workhardening Slopes

8.3 End-Plate-Aperture Breakaway

This example illustrates the use of substructures in an elastic contact problem. All of the elastic region is combined into one substructure. The gap elements which are inherently nonlinear are included in the highest level. This problem is identical to problem 7.2 with the exception that substructures are used.

This example illustrates the use of the gap and friction link, element type 12. This element allows surface friction effects to be modeled. This example is a simple model of a manhole cover in a pressure vessel. The axisymmetric mesh is shown in Figure 8.3-1. The objective of this analysis is to establish the response of the bolted joint between the manhole cover (elements 1-12) and the vessel (elements 13-27). The elements are combined into substructure level 1,1. The first bolts are tightened, and then the main vessel expands radially (as might occur due to thermal or internal pressure effects). You should be aware that this problem is presented only as a demonstration. The mesh is too coarse for accurate results.

Elements

Element 12 is a friction and gap element. It is based on the imposition of a gap closure constraint and/or a frictional constraint via Lagrange multipliers. The element has four nodes: nodes 1 and 4 are the end nodes of the link and each has two degrees of freedom (u, v,) in the global coordinate direction; node 2 gives the gap direction cosines (n_x, n_y) and has γ_n, the force in the gap direction, as its one degree of freedom; node 3 gives the friction direction cosines (t_{1_x}, t_{1_y}) and has γ_1, the frictional shear forces, and p, the net frictional slip, as its two degrees of freedom.

Model

Twenty-seven type 10 elements are used for the two discrete structures: the end cap and the aperture. These are then joined by four type 12 elements. There are 54 nodes.

Substructure Strategy

A substructure consisting of all of the axisymmetric elements is formed. The external nodes are those where the bolt load is applied (4,5,32,32), where the gap interfaces with the end cap and aperture (15 to 18 and 22 to 25) and where the radial load is applied (43 to 46). This is performed in the first part of the analysis.

In the second part of the analysis, the previously generated superelement is combined with the four gap elements.

Loading

The load history consists of applying bolt loads (that is, tightening down the bolts), then pulling out the outer perimeter of the main vessel model. Bolt loads are modeled here as point loads applied in opposite directions (self-equilibrating) on node pairs 4 and 32, 5 and 33. Since there is a possibility of gaps developing between the facing surfaces of the cover and vessel, the bolt load is initially applied as a small magnitude, then incremented up to the total value of 2000 lbs per bolt ring. This usually requires two runs of the problem: an initial run with a “small” load to see the pattern developing, from which some judgment can be made about the load steps which can be used to apply the total bolt force. In this actual run, the full bolt loads are applied in one increment.

The radial expansion of the main vessel is modeled as point loads on the outside circumference nodes (43 to 46). As there are no elements when performing the analysis, point loads rather than distributed loads are applied. Again, the purpose of the analysis is to watch the development of slippage between the main vessel and the cover plate, and the analyst cannot easily estimate the appropriate load increments to apply to model this nonlinearity. For this purpose, the RESTART option can be used effectively. A restart is written at the point where full bolt load is applied, and then a trial increment of pull-out force is applied. Based on the response to this (in the friction links), a reasonable size for the sequence of loading increments can be determined. This procedure is frequently necessary in such problems. For brevity, this example shows only the final load sequence obtained as a result of such trials.

Boundary Conditions

The nodes on the axis of symmetry are constrained radially, and the rigid body mode in the axial direction is suppressed at node 46.

Gap Data

In this example, a small negative closure distance of -.001 is given for the gaps. This indicates that the gaps are closed initially allowing an interference fit solution is to be obtained in increment 0. The coefficient of friction, μ, is input as 0.8.

Results

The results of the analysis are shown in Figure 8.3-2 through Figure 8.3-4. First of all, it is observed in Figure 8.3-2 that the link elements never go into tension.

In this case, the initial bolt load is carried quite uniformly (A in Figure 8.3-2), but as the pull-out increases, the inner two links take more of the stress and the outer link (element 31) sheds stress. The shear stress development is followed in Figure 8.3-3 – initially (bolt load only), all shear stresses are essentially zero. The two outer links slip first, but then the additional forces required to resist the pull develop in the inner two elements until the shear stress pattern follows the normal stress pattern, when the shear in the pair of links also slip ($\tau = \mu\sigma$). Figure 8.3-4 shows a plot of

the radial displacement of the outer perimeter against the pull-out force – notice the small loss of stiffness caused by slip developing, as the vessel model has to resist the extra force along without any further force transfer to the cover.

Convergence

Because the only ‘nodes’ in this structure are external nodes during the analysis phase, a different convergence path is followed than in problem 7.2. Displacement testing is automatically invoked by MARC. The gap forces at any increment are within one percent of those calculated in 7.2.

Computational Costs

Because of the use of substructures, this analysis was performed in 30% of the time of problem 7.2, which is a considerable computational savings.

Parameters, Options, and Subroutines Summary

Example e8x3.dat:

Parameters	Model Definition Options	History Definition Options
ELEMENT	CONNECTIVITY	AUTO LOAD
END	COORDINATE	BACKTOSUBS
NEWDB	END OPTION	CONTINUE
SIZING	FIXED DISP	CONTROL
SUBSTRUCTURE	ISOTROPIC	POINT LOAD
TITLE	SUBSTRUCTURE	

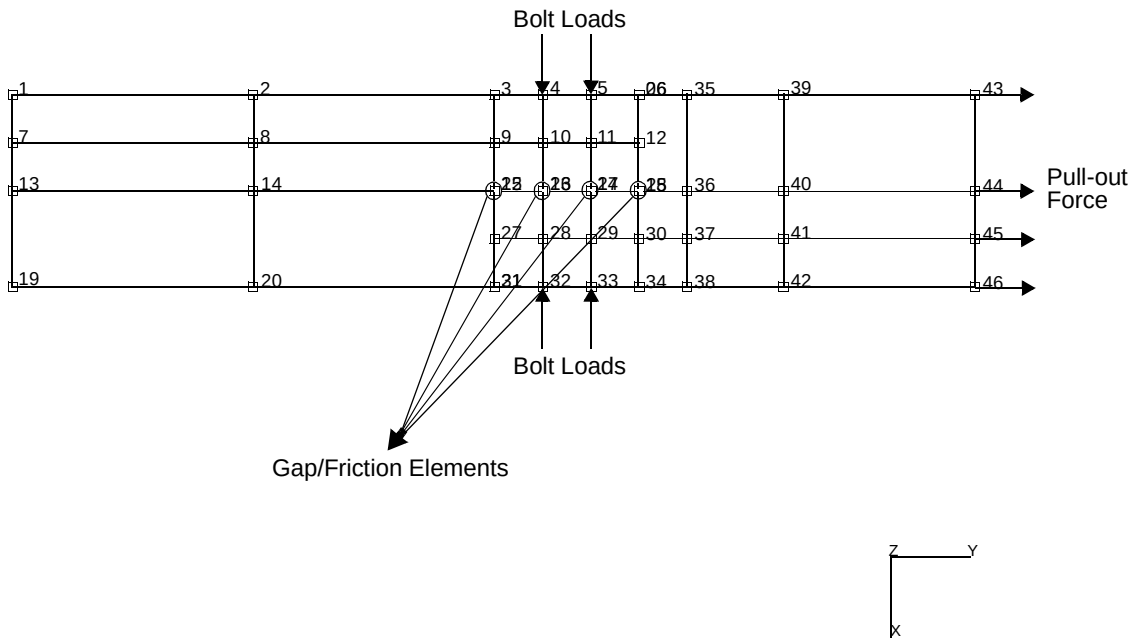

Figure 8.3-1 Geometry and Mesh of End Plate-Aperture

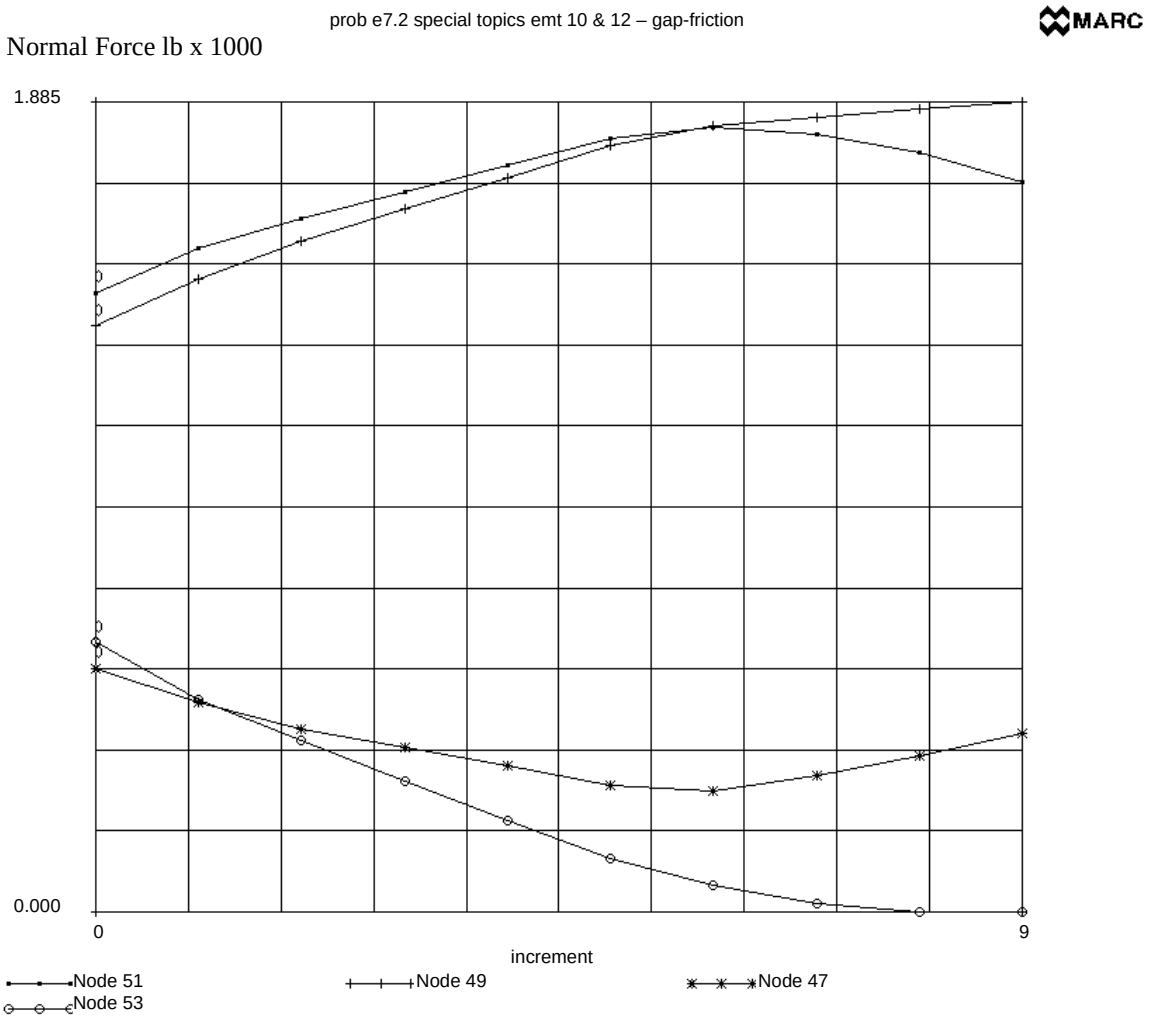

Figure 8.3-2 Transient Normal Force in Bolts

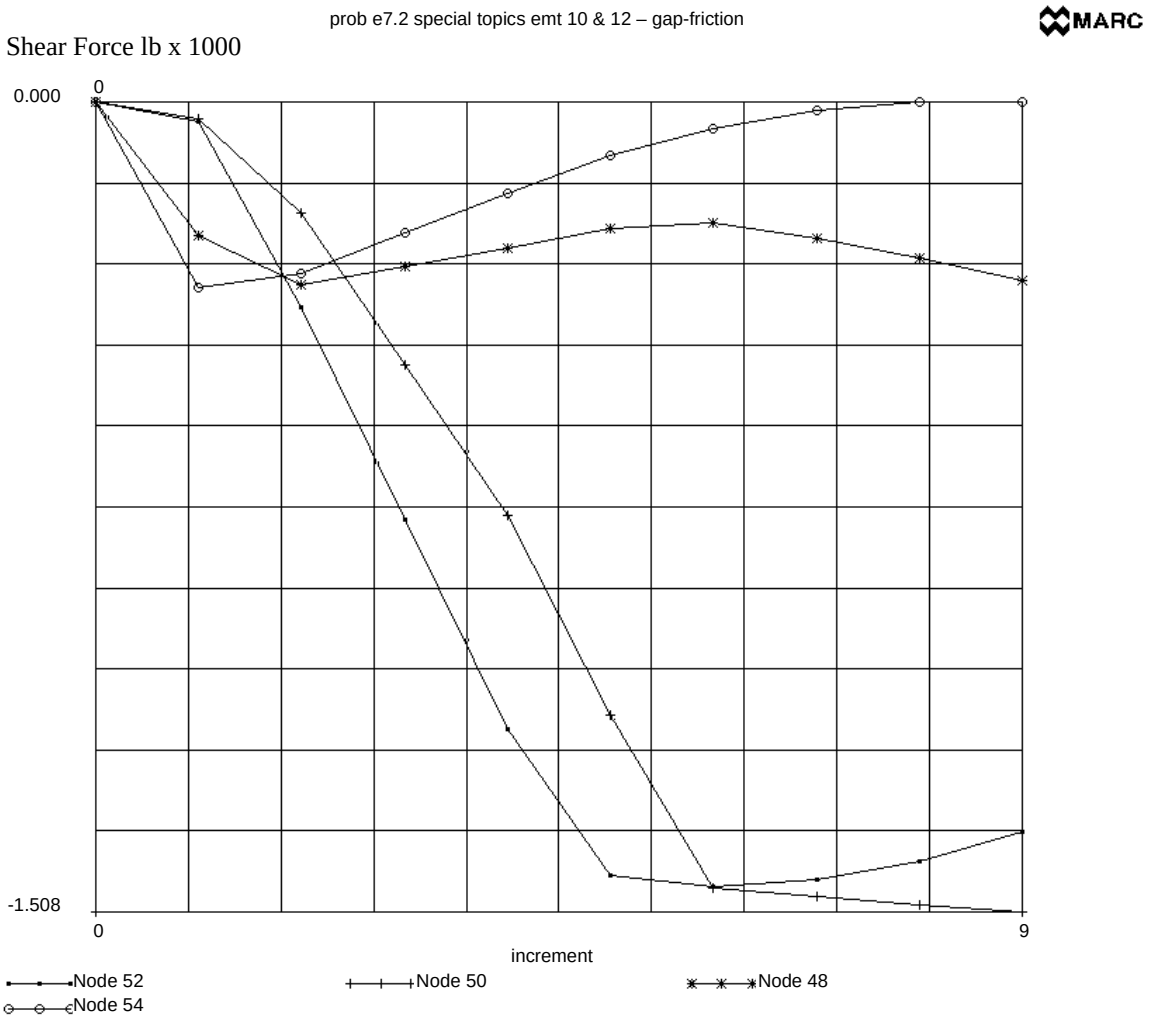

Figure 8.3-3 Transient Shear Force in Bolt

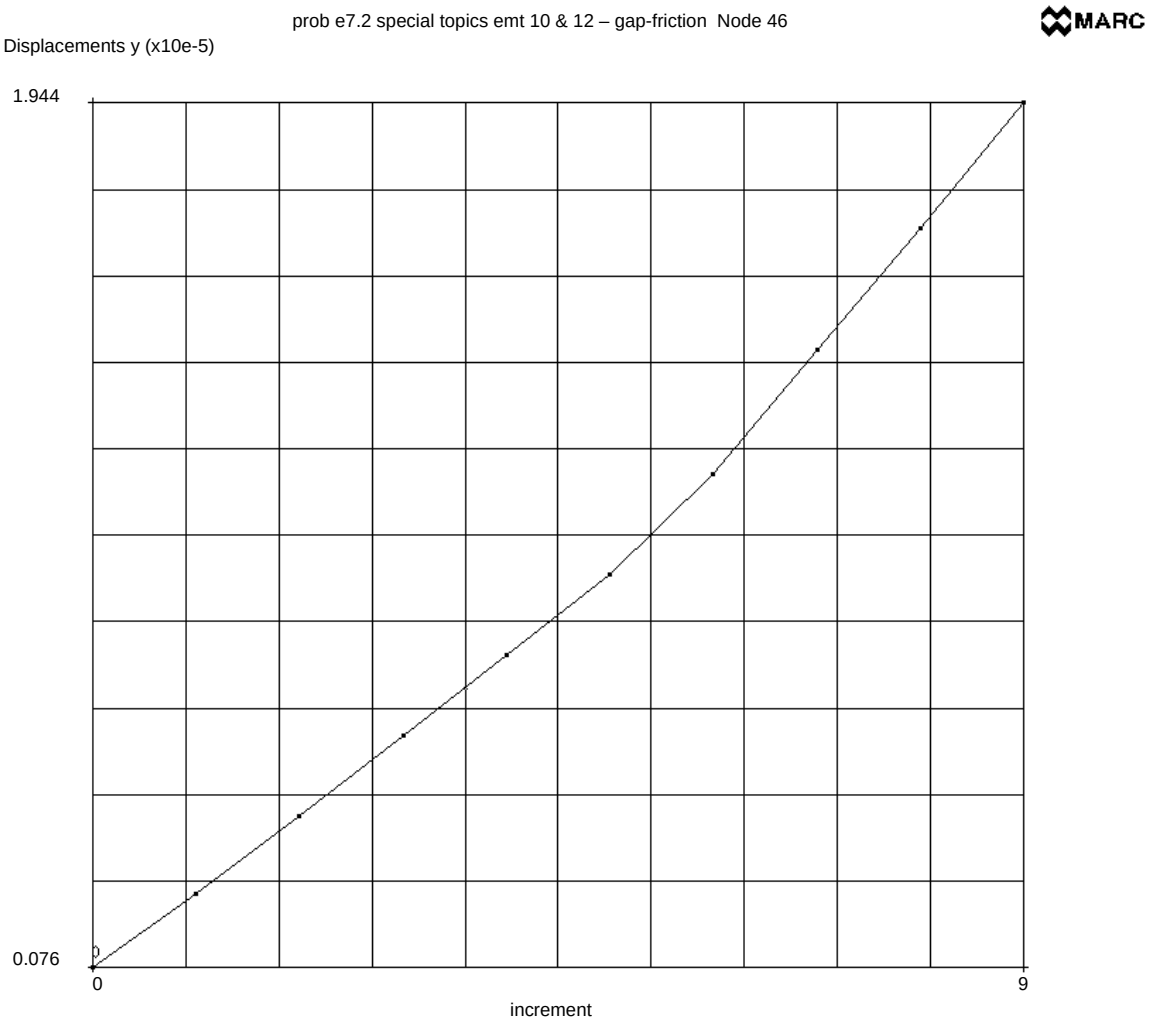

Figure 8.3-4 Radial Displacement at Outside Top (Node 46)

8.4 Collapse of a Notched Concrete Beam

A quasi static collapse analysis is carried out for a notched concrete beam. This analysis demonstrates the use of the cracking option for plane stress elements. An elastic tension softening material has been used in this analysis and the results obtained have been compared with experimental data (1).

Element

Element type 26 is an eight-node quadrilateral plane stress element with a nine point integration scheme.

Model

This notched beam (dimensions and element mesh in Figure 8.4-3) has been divided in 26 elements with a refinement near the notch. The beam is supported at its ends and loaded by a force applied just above the notch.

Tying

Tying type 32 is used to ensure a consistent displacement behavior near the mesh refinement. With this tying, the interior nodes of the elements of the refined side are coupled to the three retained nodes of the element on the coarse side. Eight tying equations of this type are needed.

Tying type 2 is needed to ensure equal displacements in the y-direction of the three nodes of the element above the notch on which the loads have to be applied.

Boundary Conditions

Simply supported and sliding conditions have been prescribed at the left and right bottom corners, respectively. At the midnode of the element above the notch, displacement increment in negative y-direction is prescribed. In the analysis, initially two displacement increments of -0.5 mm have been applied. With proportional increment, the displacement is scaled to 0.002 mm and 30 increments of this size have been applied.

Isotropic

An elastic isotropic material with Young's modulus E = 30000 N/mm^2 and a Poisson's ratio υ = 0.2 has been specified through the ISOTROPIC option. In addition, the cracking flag is turned on for material id 1.

Crack Data

In this block, the cracking data needs to be specified for each material group. The critical cracking stress is set to 3.33 N/mm^2. A linear tension softening behavior has been specified with a softening modulus E_s = 1790 N/mm^2 and is assumed to be independent of the element

size. The choice of a value of the tension softening modulus can be related to on the fracture energy G_f. Assuming that the micro-cracks are uniformly distributed over the specimen length l_s, the fracture energy is related to $G_f = l_s \int \sigma d\varepsilon^{cr}$, which results for a linear tension softening behavior in $G_f = \frac{1}{2} l_s \sigma_c \varepsilon_u$. For this particular analysis, it can be assumed that cracking only occurs in the elements just above the notch with a width h and in the energy expression, G_f can be expressed by $G_f = \frac{1}{2} h \sigma_c \varepsilon_u$. It is clear, that depending on the width of the notch, the value ε_u needs to be adapted and the tension softening modulus $E_s = \sigma_c/\varepsilon_u$ needs to be a function of the width of the notch.

The critical crushing strain is not set, and default a high value 10^{11} is used (crushing occurs at a critical value of the plastic strain and since no plasticity is allowed in the analysis, crushing does not occur). The shear retention factor is set to zero; hence, no shear stiffness is present at an integration point once a crack occurs.

Control

A maximum number of 32 loadsteps have been specified. In each step, maximal 5 iterations are allowed. The default full Newton-Raphson iterative technique has been used with tolerance checking on the residual forces (10% of the maximum reaction force).

Results

In increment 1, the first cracks initiate in the element just above the notch. At this increment, three recycles are needed to reach convergence. In the subsequent increments, no new cracks initiate and no recycles are needed. In increment 7, new cracks initiate with recycling followed by a number of steps with only back substitution. In subsequent increments, new cracks occur in increment 14, 20, 27 and 29. Cracks occur only in the elements above the notch (width 40 mm). The assumption needed in the choice of the tension softening modulus was correct. The calculated load-deflection curve is shown in Figure 8.4-5 and is compared with the experimental result (1). It is seen that the experimental result is overestimated. The reason for this overly stiff behavior can probably be found in the choice of the linear tension softening behavior.

Reference

1. Petersen, P. E., “Crack growth and development of fracture zones in plain concrete and similar materials,” Report TVM-1006, Lund Institute of Technology, Lund, Sweden, 1981.

Parameters, Options, and Subroutines Summary

Example e8x4.dat:

Parameters	Model Definition Options	History Definition Options
ELEMENT	CONNECTIVITY	AUTO LOAD
END	CONTROL	CONTINUE
PRINT	COORDINATE	PROPORTIONAL INCREMENT
SIZING	CRACK DATA	
TITLE	END OPTION	
	FIXED DISP	
	GEOMETRY	
	ISOTROPIC	
	POST	
	PRINT CHOICE	
	TYING	

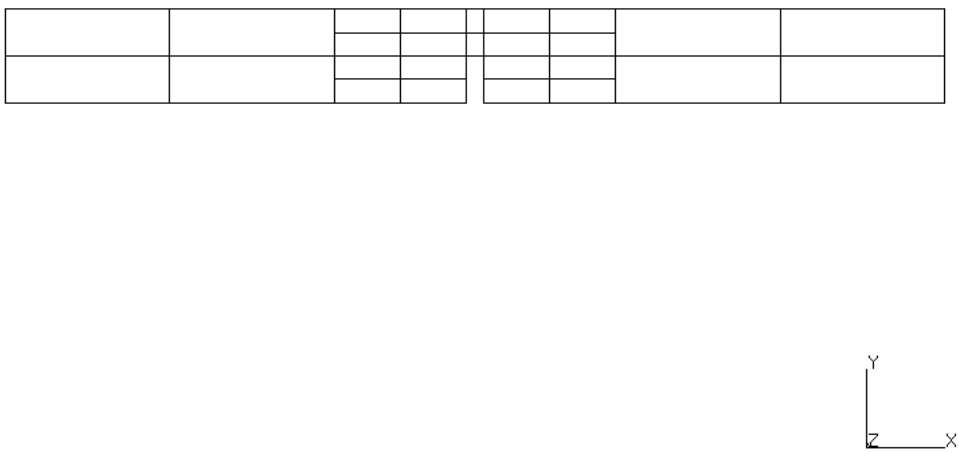

Figure 8.4-1 Geometry and Element Mesh

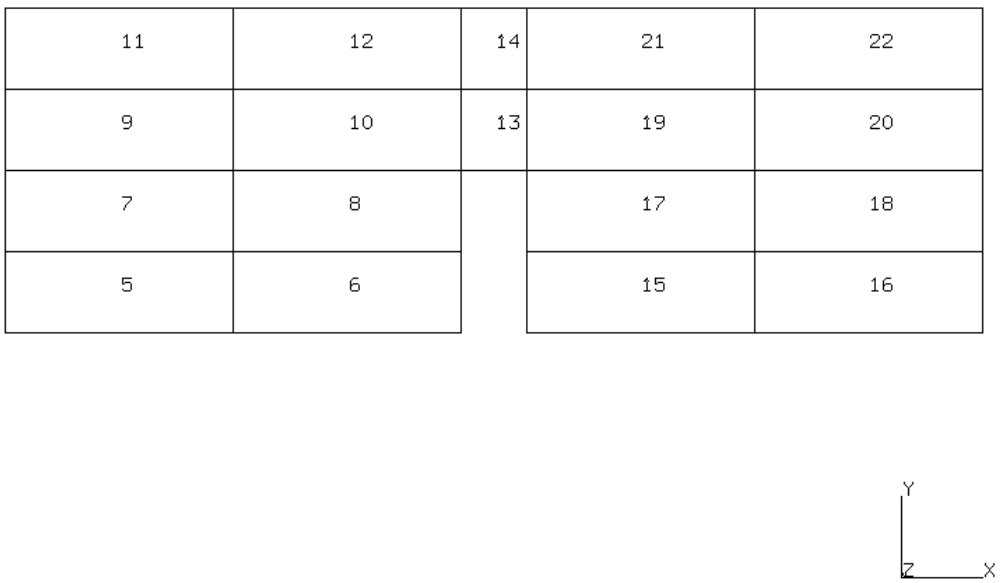

Figure 8.4-2 Element Numbering Detail of Mesh

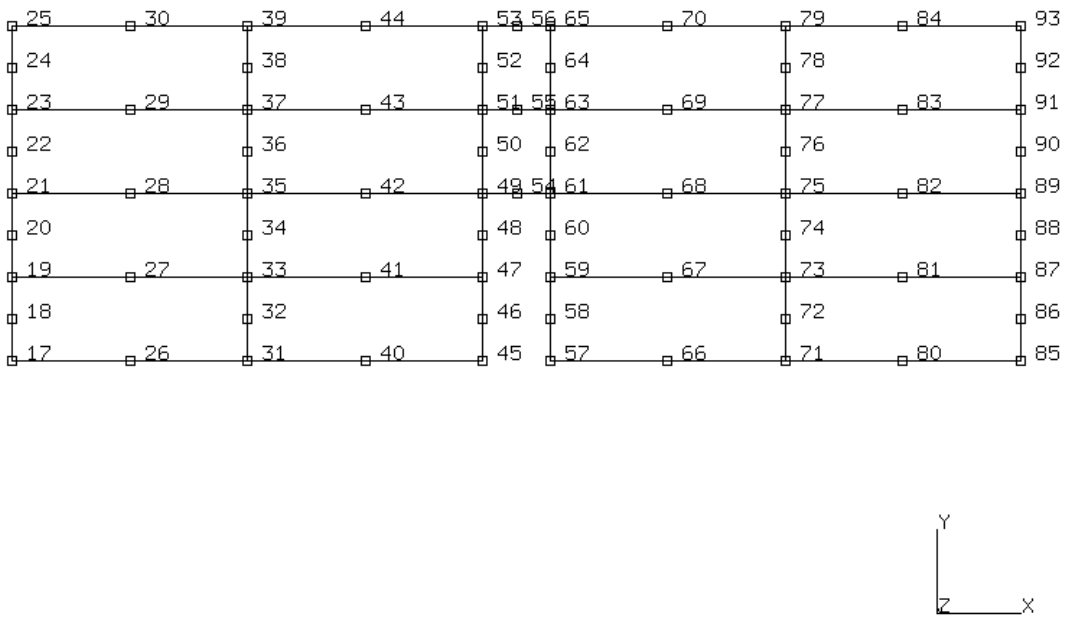

Figure 8.4-3 Node Numbering Detail of Mesh

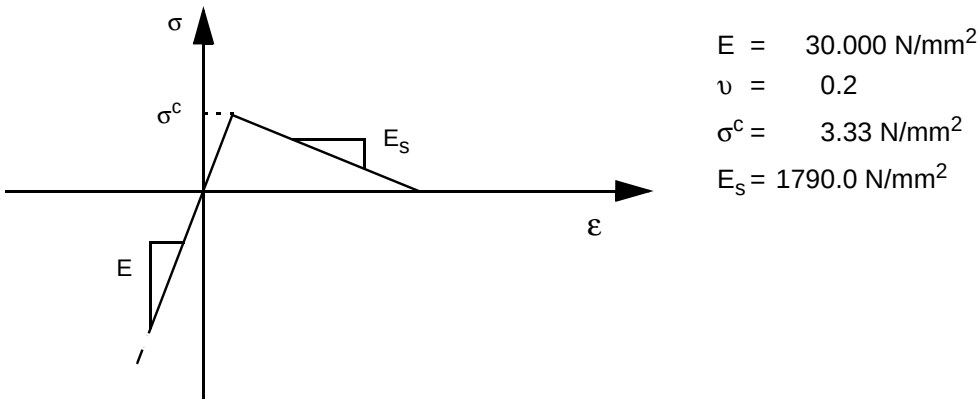

Figure 8.4-4 Material Properties

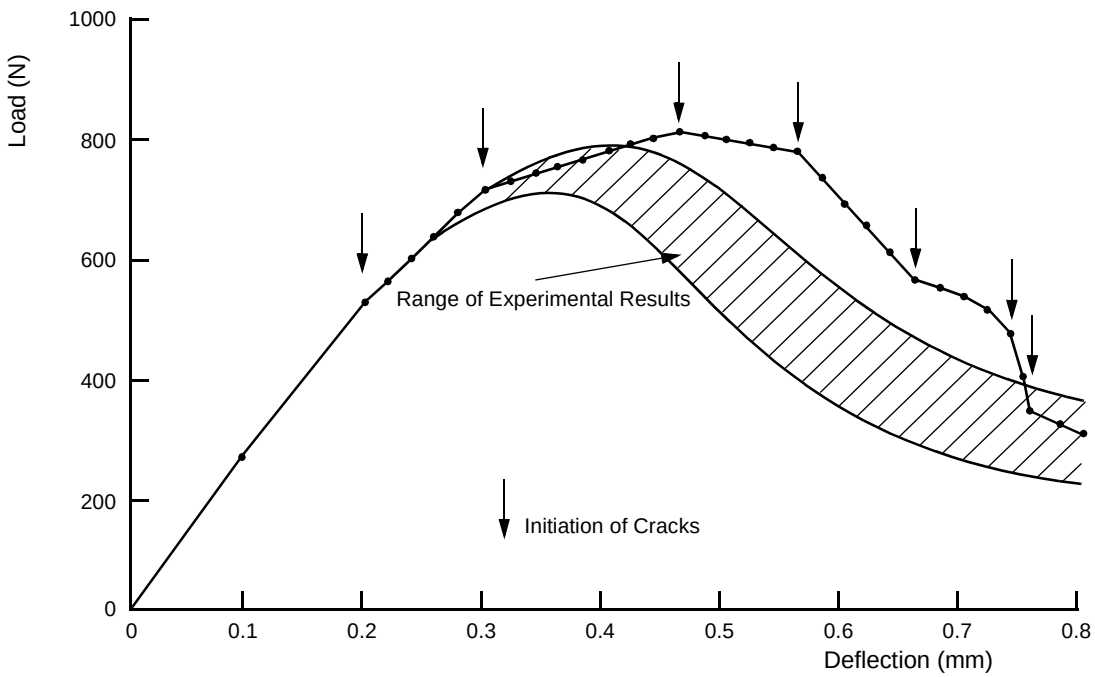

Figure 8.4-5 Comparison of Calculated and Experimental Load Deflection Curve Notched Beam Test

8.5 Cracking Behavior of a One-way Reinforced Concrete Slab using Shell Elements

This example demonstrates the analysis of a one-way reinforced concrete slab, which was tested by Jain and Kennedy [1] and material data for this problem can be found [2]. The slab is line supported at its ends (Figure 8.5-1) and loaded by a line load. The elastic cracking behavior with tension softening of the concrete and the elastic-plastic behavior of the steel reinforcement is demonstrated.

Element

Element type 75 is a 4-node thick shell element with six global degrees of freedom at each node.

Model

The slab, with dimensions shown in Figure 8.5-1, is divided into six shell elements. In these shell elements, integration of the material properties over the thickness is performed using nine layers; one layer represents the (smeared) steel reinforcement, while the other eight layers represent the concrete behavior. The mesh (Figure 8.5-2) is generated using the CONN GENER and NODE FILL option. Only one-half of the plate is modeled.

Material Properties

The concrete material is defined using the ISOTROPIC and the CRACK DATA options. First the ISOTROPIC option is defined to have a material ID of 1, and the cracking option is flagged. The properties are Young's modulus of 28960 N/mm^2, Poisson's ratio of 0.2 and initial yield stress of 31.6 N/mm^2. The CRACK DATA option indicates that the concrete has a ultimate stress of 2N/mm^2 and a shear retention of 0.5. In the first analysis, no tension softening is specified. In the second analysis, a tension softening of 3620 N/mm^2 is specified.

The steel reinforcement is modeled as a uniaxial material in a single layer of the shell element. This is done using the ORTHOTROPIC option, specifying an E_{xx} = 20,000 N/mm^2 and $E_{yy} = E_{zz} =$ 0.01 N/mm^2. The associated shear moduli are G_{xy} = 10,000 N/mm^2 and $G_{yz} = G_{zx} = G_{zx}$ = 0.005 N/mm^2. The steel has an initial yield stress of 221 N/mm^2.

COMPOSITE

The COMPOSITE option is used to indicate that there are nine layers of materials. The first six are of equal thickness of 5.166 mm each and are composed of material 1 (concrete). The seventh layer is the very thin steel layer, thickness of 0.272 mm and material ID = 2. Finally, layers 8 and 9 are concrete with a thickness of 3.364 mm.

Boundary Conditions

Symmetry conditions are specified on node 1 and 2 of the element mesh. On the line Y = 0, Z = 0, no translation in y-direction is allowed, and at nodes 13 and 14, a sliding support (no displacement in z-direction) is prescribed.

Control

On the control block, a maximum of 25 load steps is specified with a maximum of seven recycles per load increment. The default Newton-Raphson iterative procedure with testing on the relative residual forces (tolerance 10%) is used. The solution of nonpositive definite systems is forced by the PRINT,3 option.

Loading

On node 9 and 10, a point load with magnitude -1500 in z-direction is applied. This is the estimated maximum value of the collapse load. Via the AUTO INCREMENT option, the automatic load stepping procedure, using Riks algorithm, starts with 10% of the total load and a desired number of three recycles (must be smaller than the maximum number specified on the CONTROL block). The maximum numbers of steps in this load incrementation set is 20 and the maximum step size is 10% of the load.

Results

The calculated load center-deflection response is shown in Figure 8.5-4 for the run with and without tension softening. Without tension softening, an unstable behavior, present in the response, is caused by the loss of stiffness between reinforcement and concrete once a crack occurs. With tension softening, some artificial interaction is introduced and usually results in a more stable solution procedure. In the run with tension softening, fewer recycles are needed to reach convergence. Compared with the experimental result [1], [2], the effect of tension softening is clearly indicated. Best agreement is obtained with tension softening.

References

1. Jain, S.C. and Kennedy, J.B., “Yield criterion for reinforced concrete slabs,” *J. Struct. Div.*, Am. Soc. Civ. Engrs.,100,513, March 1974, pp. 631-644
2. Crisfield, M.A.“Variable step lengths for non-linear structural analysis,” Report 1049, Transport and Road Research Lab., Crowthorne, England, 1982.

Parameters, Options, and Subroutines Summary

Example e8x5a.dat:

Parameters	Model Definition Options	History Definition Options
ELEMENT	COMPOSITE	AUTO INCREMENT
END	CONN GENER	CONTINUE
PRINT	CONNECTIVITY	POINT LOAD
SIZING	CONTROL	
TITLE	COORDINATE	
	CRACK DATA	
	END OPTION	
	FIXED DISP	
	ISOTROPIC	
	NODE FILL	
	ORIENTATION	
	ORTHOTROPIC	
	POST	
	PRINT CHOICE	
	RESTART	

Example e8x5b.dat:

Parameters	Model Definition Options	History Definition Options
ELEMENT	COMPOSITE	AUTO INCREMENT
END	CONN GENER	CONTINUE
PRINT	CONNECTIVITY	POINT LOAD
SIZING	CONTROL	
TITLE	COORDINATE	
	CRACK DATA	
	END OPTION	
	FIXED DISP	
	ISOTROPIC	
	NODE FILL	
	ORIENTATION	
	ORTHOTROPIC	
	POST	
	PRINT CHOICE	
	RESTART	

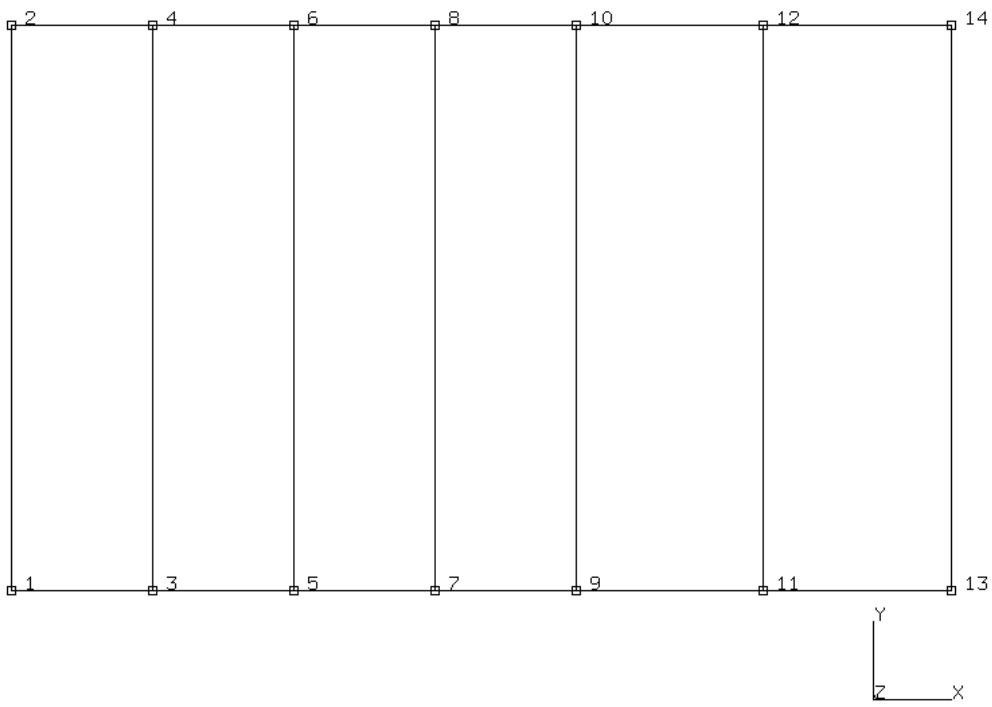

Figure 8.5-1 Geometry of One-Way Reinforced Slab

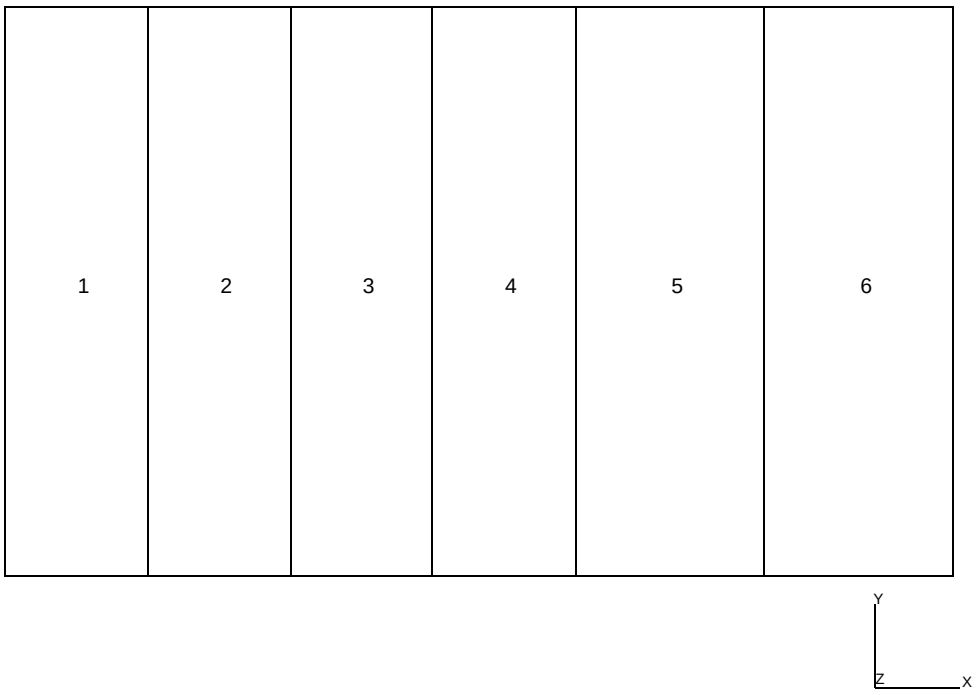

Figure 8.5-2 Element Mesh with Node Numbering

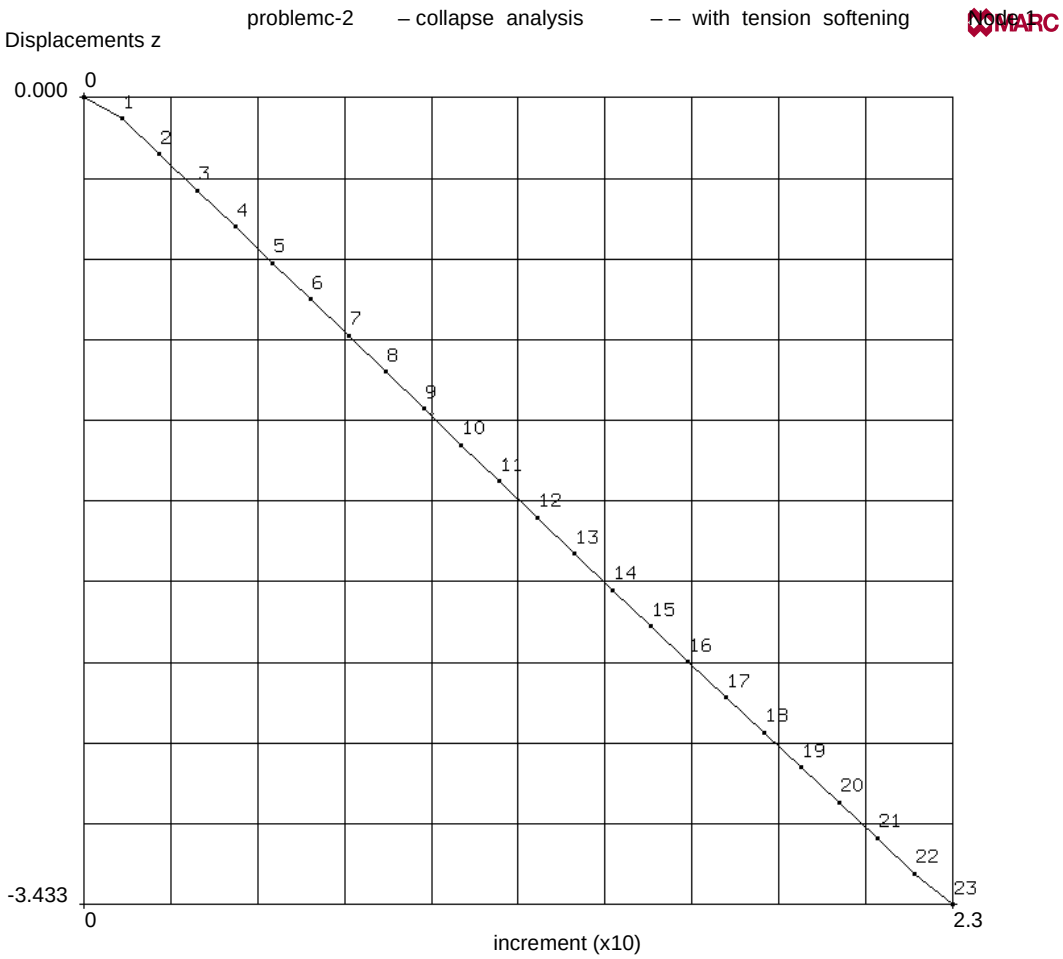

Figure 8.5-3 Element Mesh with Element Numbering

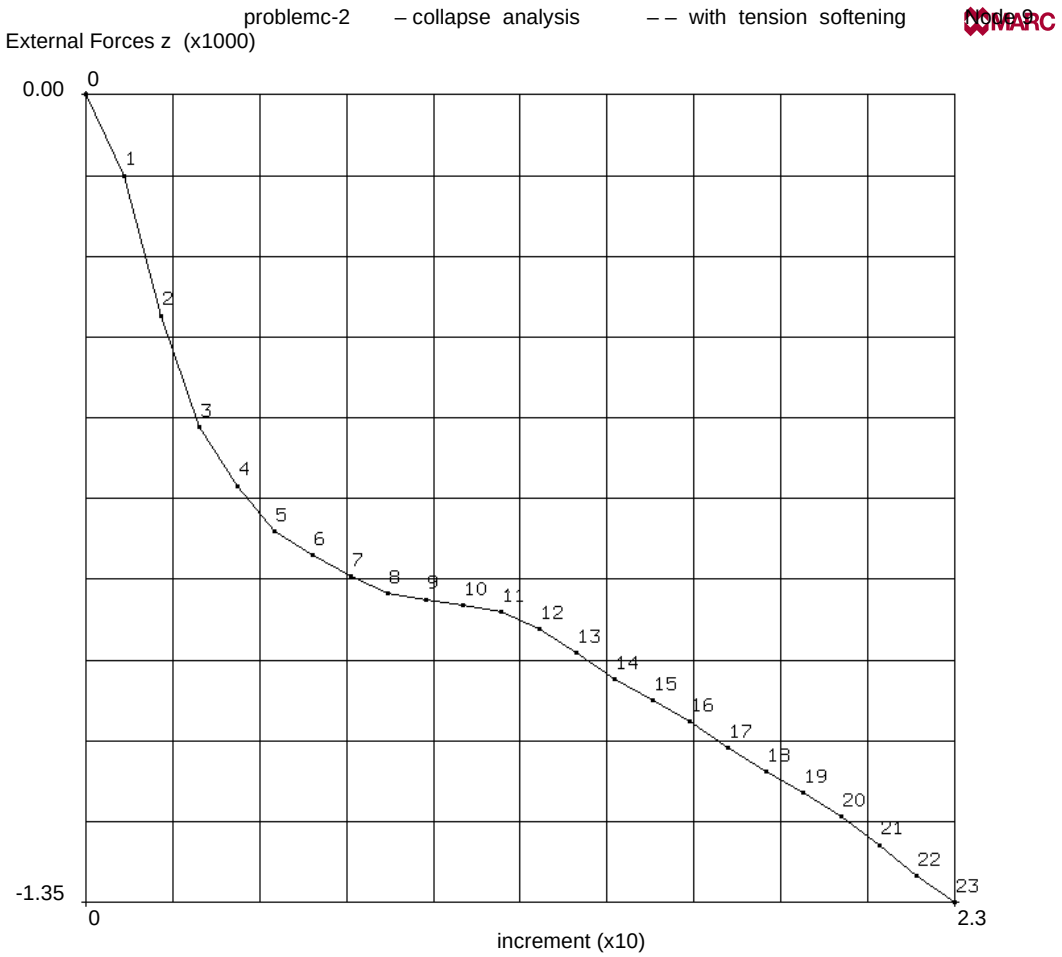

Figure 8.5-4 Load-Deflection Relationship for One-Way Reinforced Slab

8.6 Cracking Behavior of a One-way Reinforced Concrete Slab

This example is the same type of analysis as described in problem 8.5 (Figure 8.6-1). Instead of shell elements, however, continuum plane strain elements and rebar elements have been used, which is allowed since the problem is essentially two-dimensional. For the concrete, an elastic-cracking behavior with tension softening and shear retention is specified. In the rebar elements, an elastic-plastic behavior is possible.

Element

Element type 27 is an eight-node plane quadrilateral strain element with two degrees of freedom per node is used to model the concrete. This element is preferred over element 11 (four-node plane strain) since considerable shear is present in the beam. Element type 46 is an eight-node plane strain rebar element compatible with element 27 and is used to specify the reinforcement (Figure 8.6-2).

Model

The concrete is modeled with 10 plane strain elements (Figure 8.6-3 and Figure 8.6-4). At least two elements over the thickness are needed for accurate analysis of the bending of the beam. In each element, nine integration points are present, resulting in a six-point integration scheme over the thickness. Over the concrete elements below the neutral line (1 to 5), an overlay of rebar elements is used (elements 11 to 15). The position, thickness, and orientation of the reinforcement layers in this element needs to be specified via user subroutine REBAR.

The mesh is generated using the CONN GENER and NODE FILL option.

Material Properties

The elastic properties of the concrete (material identification number 1) is taken as:

Young's modulus	$E = 28{,}960\ N/mm^2$
Poisson's ratio	$\nu = 0.3$

The cracking flag is turned on for material number 1.

The following properties for the steel reinforcement (material identification number 2) is taken:

Young's modulus	$E = 200{,}000\ N/mm^2$
Poisson's ratio	$\nu = 0.2$
Yield stress	$\sigma_y = 221\ N/mm^2$

Crack Data

Only one set of cracking data needs to be specified since cracking is only possible in the concrete elements (specified via the ISOTROPIC option). The following values have been taken:

Critical cracking stress	$\sigma_c = 2$ N/mm^2
Tension softening modulus	$E = 3620$ N/mm^2
Shear retention factor	0.5

Boundary Conditions

Symmetry conditions are specified for nodes 1 to 5 and a sliding condition for node 41.

Control

On the CONTROL option, a maximum of 25 load steps is specified with a maximum of seven recycles per load increment. The default Newton-Raphson iterative procedure with testing on the relative residual forces (tolerance 10%) is used. The solution of nonpositive definite systems is forced by the PRINT,3 option.

Loading

On node 29, a point load with magnitude -1500 in y-direction is applied. This is the estimated maximum value of the collapse load. Via the AUTO INCREMENT option, the automatic load stepping algorithm, using the Riks algorithm, starts with 10% of the total load and a desired number of three recycles (must be smaller than the maximum number specified in the CONTROL option). The maximum numbers of steps in this load incrementation set is 20 and the maximum step size is 10% of the load.

Results

The calculated load-deflection response is shown in Figure 8.6-6 and compared with the experimental result. Compared with the results of tension softening using shell elements (problem 8.5), a nearly identical load-deflection curve is obtained. In the run with shell elements, no shear retention factor is used but sufficient shear stiffness is present even if large scale cracking occurs. In the run with plane strain elements, the absence of shear retention (meaning there is no shear stiffness if a crack occurs) results in an unstable behavior and very poor convergence. With shear retention, a stable behavior is obtained. The shear retention factor can be specified as a function of the crack length via user subroutine UCRACK.

Parameters, Options, and Subroutines Summary

Example e8x6.dat:

Parameters	Model Definition Options	History Definition Options
ELEMENT	CONN GENER	AUTO INCREMENT
END	CONNECTIVITY	CONTINUE
PRINT	COORDINATES	POINT LOAD
TITLE	CONTROL	
	CRACK DATA	
	END OPTION	
	FIXED DISP	
	GEOMETRY	
	ISOTROPIC	
	NODE FILL	
	POST	
	RESTART	

User subroutine in u8x6.f:

REBAR

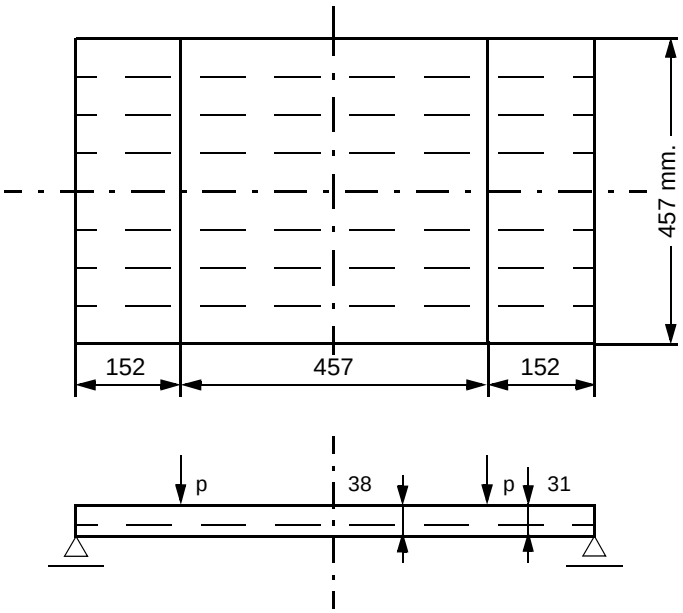

Figure 8.6-1 One-Way Reinforced Slab

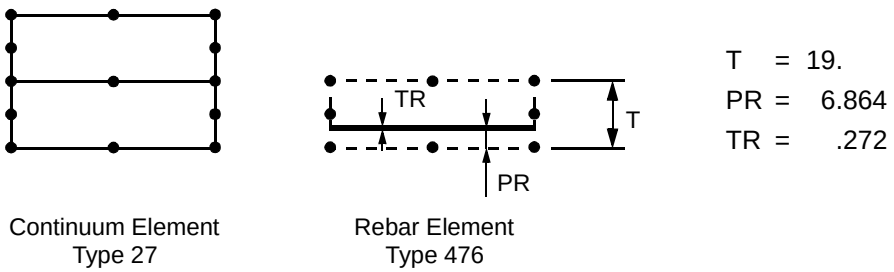

Figure 8.6-2 Element Types used in Analysis

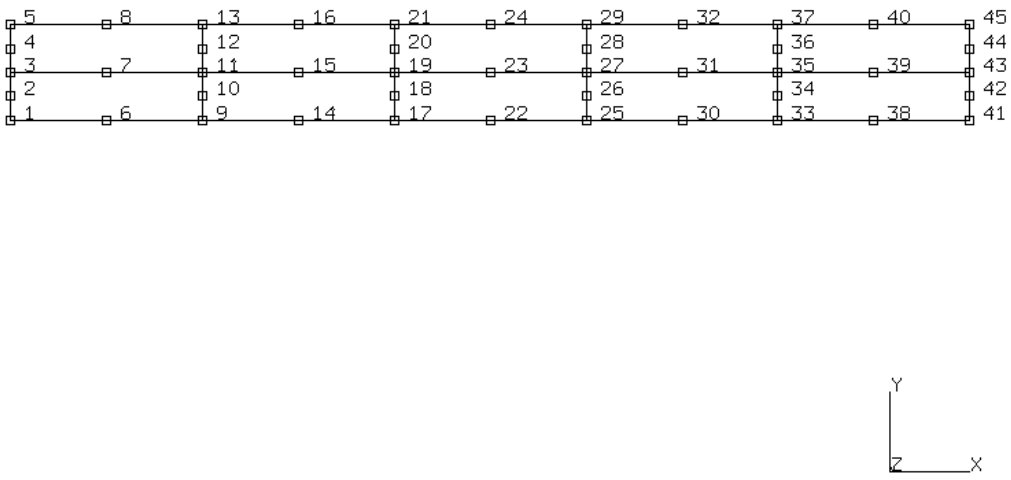

Figure 8.6-3 Node Numbering

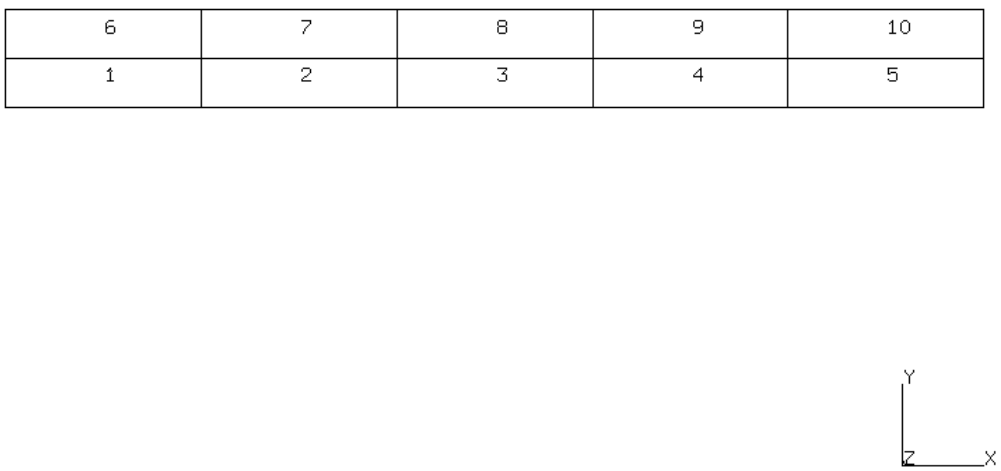

Figure 8.6-4 Element Numbering Concrete Elements

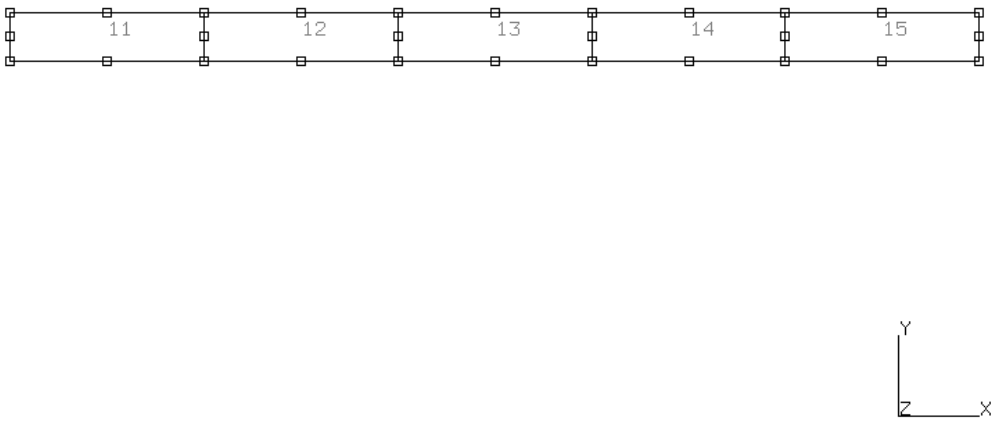

Figure 8.6-5 Element Numbering Rebar Elements

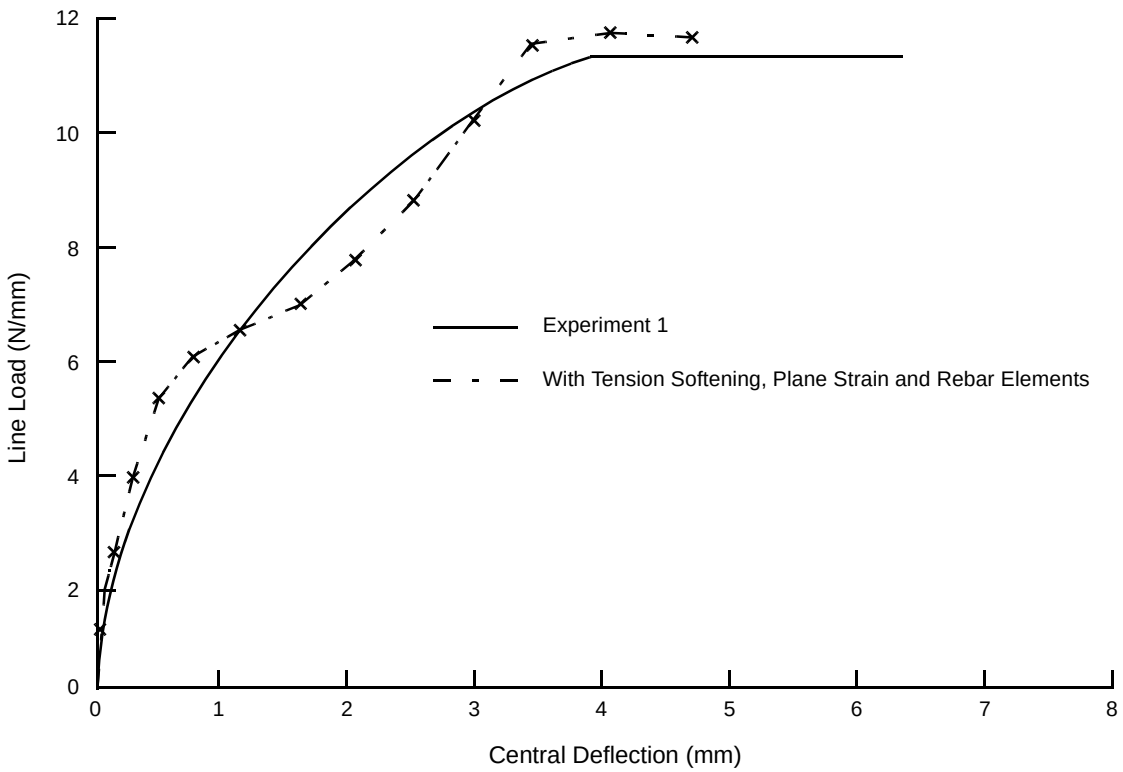

Figure 8.6-6 Load/Deflection Relationship for One-Way Reinforced Slab

8.7 Compression of a Block

This example demonstrates MARC's capability to perform a large deformation contact problem which incorporates thermal mechanical coupling. The block is considered an elastic-plastic deformable material, and both the deformations and temperatures are calculated. The platen is treated as a rigid region and only temperatures are calculated. Gap elements are used to insure that the contact condition is properly accounted for.

Coupling

There are four sources of coupling in this analysis:

1. As the temperature changes, thermal strains are developed; this is due to nonzero coefficient of thermal expansion.
2. As the temperature changes, the mechanical properties change because of the temperature-dependent elasticity.
3. As the geometry changes, the heat transfer problem changes.
4. As plastic work is performed, internal heat is generated.

Parameters

The UPDATE, FINITE, and LARGE DISP are included in the parameter section as this is a finite deformation analysis. The COUPLE option is used to indicate that a couple thermal-mechanical analysis is being performed.

Mesh Definition

Due to symmetry, only one quarter of the region is modeled. The mesh is shown in Figure 8.7-1. The deformable block is modeled using Element type 11 (4-node quadrilateral), while the platen is modeled with Element type 39 (4-node quadrilateral). In a coupled analysis, if the element type is a displacement element, a coupled (displacement-temperature) formulation will be used. If the element type is a thermal element, only a heat transfer analysis will be performed in that region; that is, rigid.

Two gap elements are used between the platen and the block. In a coupled analysis, when the gap elements are open, there is no load transmitted across the gap and the gap acts as a perfect insulator. When the gap closes, load is transmitted and the gap acts as a perfect conductor.

Geometry

A unit thickness is used. A '1' is placed in the second field which indicates that the constant dilatation formulation is used.

Boundary Conditions

Symmetry displacement boundary conditions are imposed on two surfaces. An applied displacement is used to model the plate. The intention is to compress the block to 60% of its original height. The displacement boundary conditions are entered via the FIXED DISP option. On the outside surface of the platen, the temperature is constrained to 70° by using the FIXED TEMP option. Because of an ambiguity in type, the BOUNDARY CONDITION option should not be used in a coupled analysis.

Initial Conditions

The block is given an initial temperature of 300°, and the platen an initial temperature of 70°.

Material Properties

The block is treated as an elastic plastic material with a Young's modulus of $1. \times 10^6$ psi, Poisson's ratio of 0.3, mass density of 0.1 lb/in^3, coefficient of thermal expansion of 1.3×10^{-5} in/in°F and a yield stress of 50,000 psi. The material is given an initial workhardening slope of 10,000 psi which reduces to 1000 psi at an equivalent plastic strain of 0.01.

The thermal properties are a conductivity of 21.6 in-lb/in°F and the specific heat of 2147 in-lb/lb°F. In the platen, no mechanical properties are given as it is rigid. The thermal properties are the same as the block. In a coupled analysis, the mass density must be entered on the first property.

Gap Data

For the two gap elements, the only property necessary is the closure distance. This is the original distance between the gap nodes attached to the block and the platen.

Temperature Effects

The elastic modulus is assumed to be a linear function of temperature such that:

$$E(T) = 1 \times 10^7 - (T - T_o) \times 1 \times 10^4,$$

where the reference temperature T_o is 0°F.

Distributed Flux

This distributed flux block is used to indicate that internal heat is generated due to plastic deformation.

Convert

This option is used to give the conversion factor between the mechanical energy and the thermal energy.

The internal volumetric flux per unit volume becomes:

$$f = c \cdot W^p$$

where W^P is the plastic strain energy density.

Control Options

The Cuthill-McKee optimizer is used to minimize the bandwidth. A formatted post file containing only nodal variables is written every ten increments. In a coupled analysis, the nodal variables are the total displacements, applied forces, reaction forces, temperatures, and applied flux. The restart file is written each increment. The PRINT CHOICE option is used to minimize the amount of output.

Two lines are used to enter the control tolerances. These are the default values.

Load Control

This problem is performed with a fixed time step, fixed increment size. This is specified with a time step of 1 second, and a total of 80 seconds is requested. As no proportional increment is used, each increment imposes a displacement of 0.2 inches.

In a coupled analysis, if an adaptive time-stepping is required, the AUTO TIME option should be invoked.

Results

Figure 8.7-2 through Figure 8.7-11 show the contour plots of the equivalent stress and the temperatures on the deformed body. The body folds over onto the platen at increment 45. The figures are shown until increment 70. At approximately increment 75 (depends on machine accuracy), the analysis stops because of very large distortion. A rezoning step should have been performed in increment 60.

The analysis shows in increment 30 that there is a small rigid region stress below yield under the platen, which remains for the entire analysis. The highest stress at increment 70 occurs where the material is folded over and is 10% above yield. This is an indication of the minimal amount of workhardening in the material. The final highest temperature of 340°F, an increment of 10°F above initial conditions, is due to the plastic deformation.

The printed results for a coupled analysis give the stress, total strain, plastic strain, thermal strain, and temperature for each integration point requested. In the platen (rigid region), only the temperatures are given. The nodal variables printed are the incremental and total displacements, temperatures, nodal forces and reaction forces.

Parameters, Options, and Subroutines Summary

Example e8x7.dat:

Parameters	Model Definition Options	History Definition Options
COUPLE	CONNECTIVITY	CONTINUE
ELEMENT	CONTROL	TRANSIENT
END	CONVERT	
FINITE	COORDINATE	
LARGE DISP	DIST FLUXES	
SIZING	END OPTION	
TITLE	FIXED DISP	
UPDATE	FIXED TEMPERATURE	
	GAP DATA	
	GEOMETRY	
	INITIAL TEMPERATURE	
	ISOTROPIC	
	POST	
	PRINT CHOICE	
	RESTART	
	TEMPERATURE EFFECTS	
	WORK HARD	

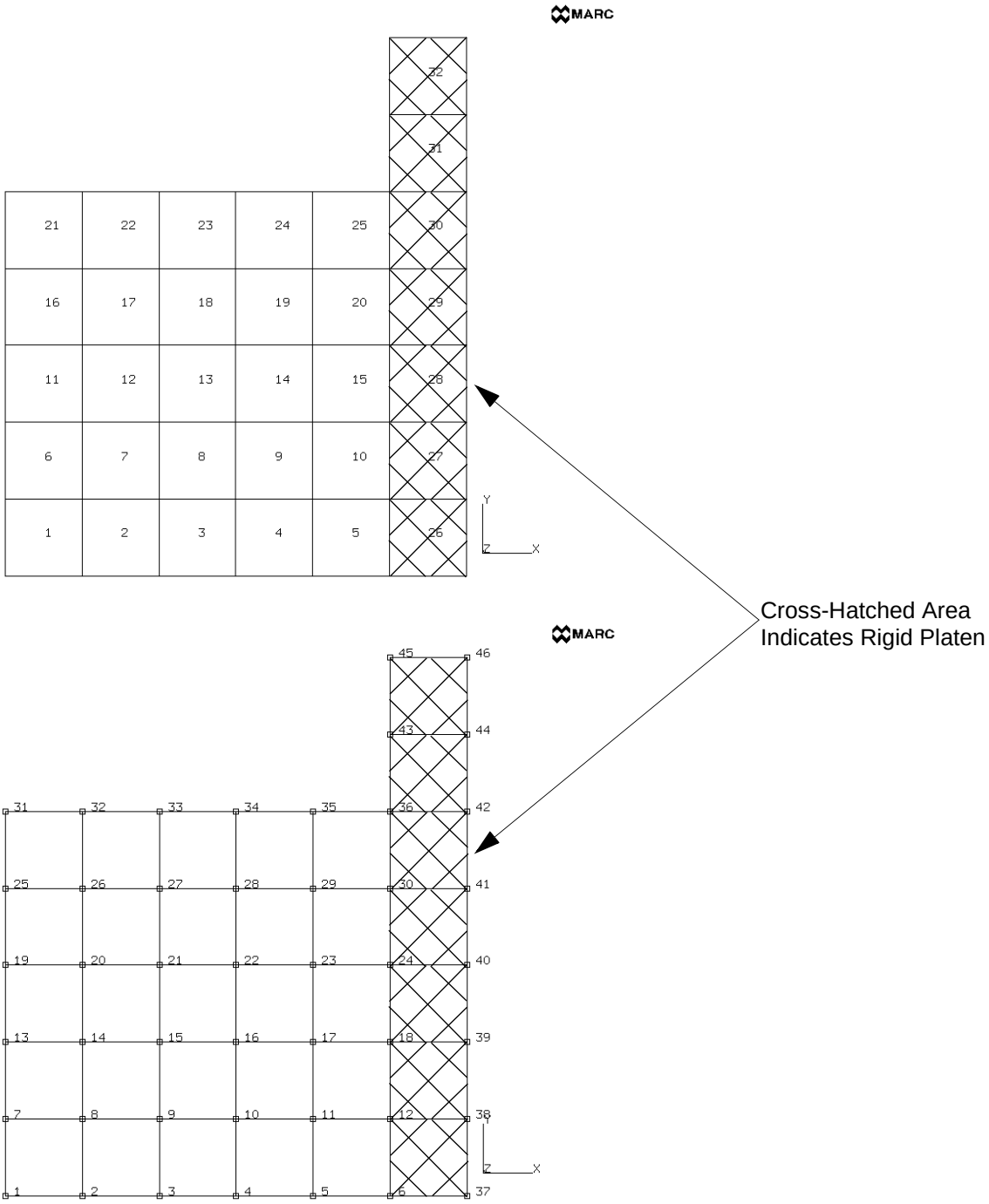

Figure 8.7-1 Mesh

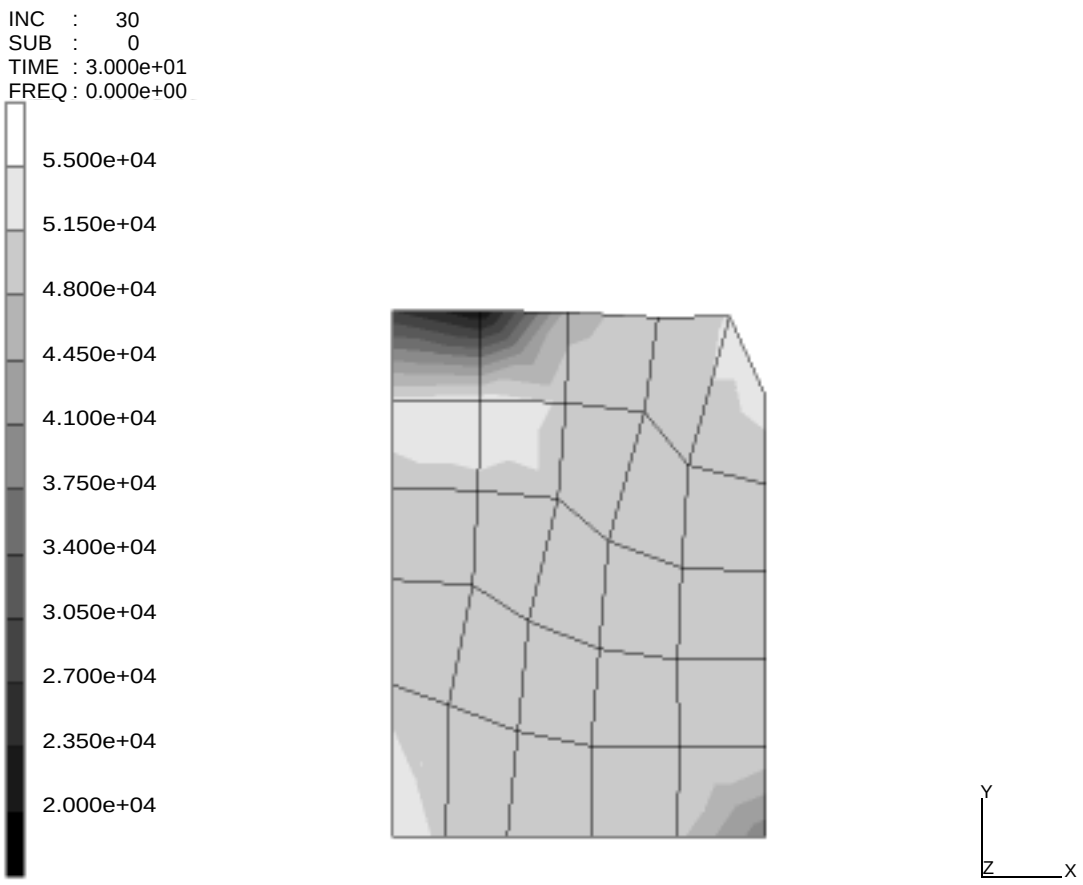

Figure 8.7-2 Equivalent Stress, Increment 30

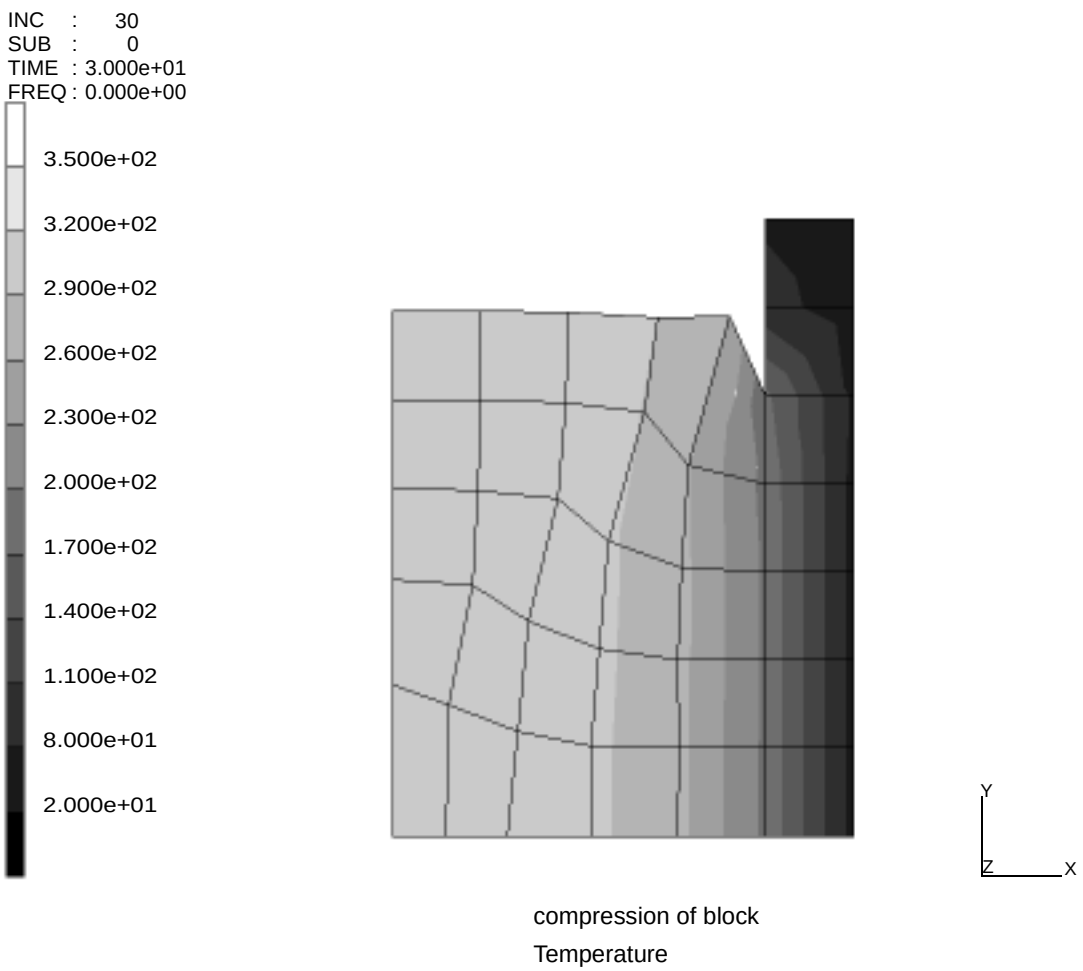

Figure 8.7-3 Temperature, Increment 30

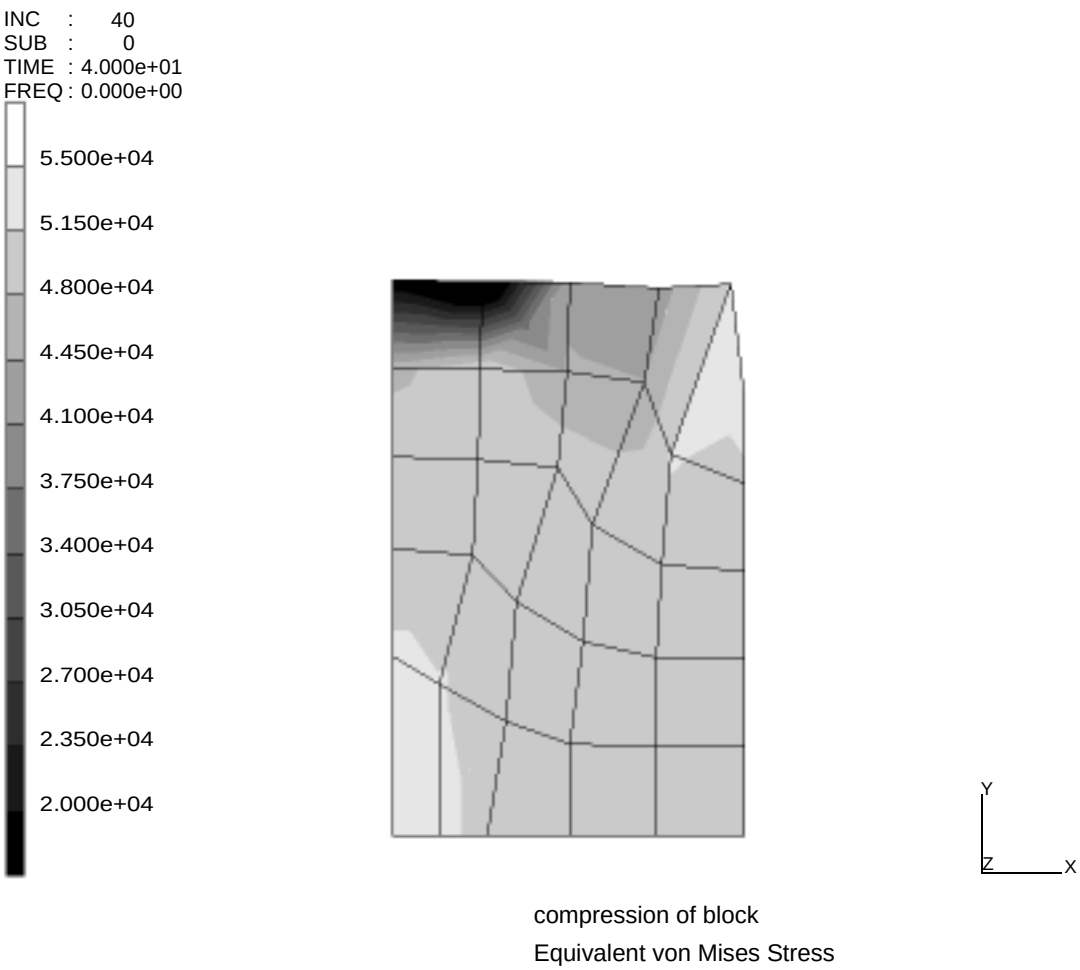

Figure 8.7-4 Equivalent Stress, Increment 40

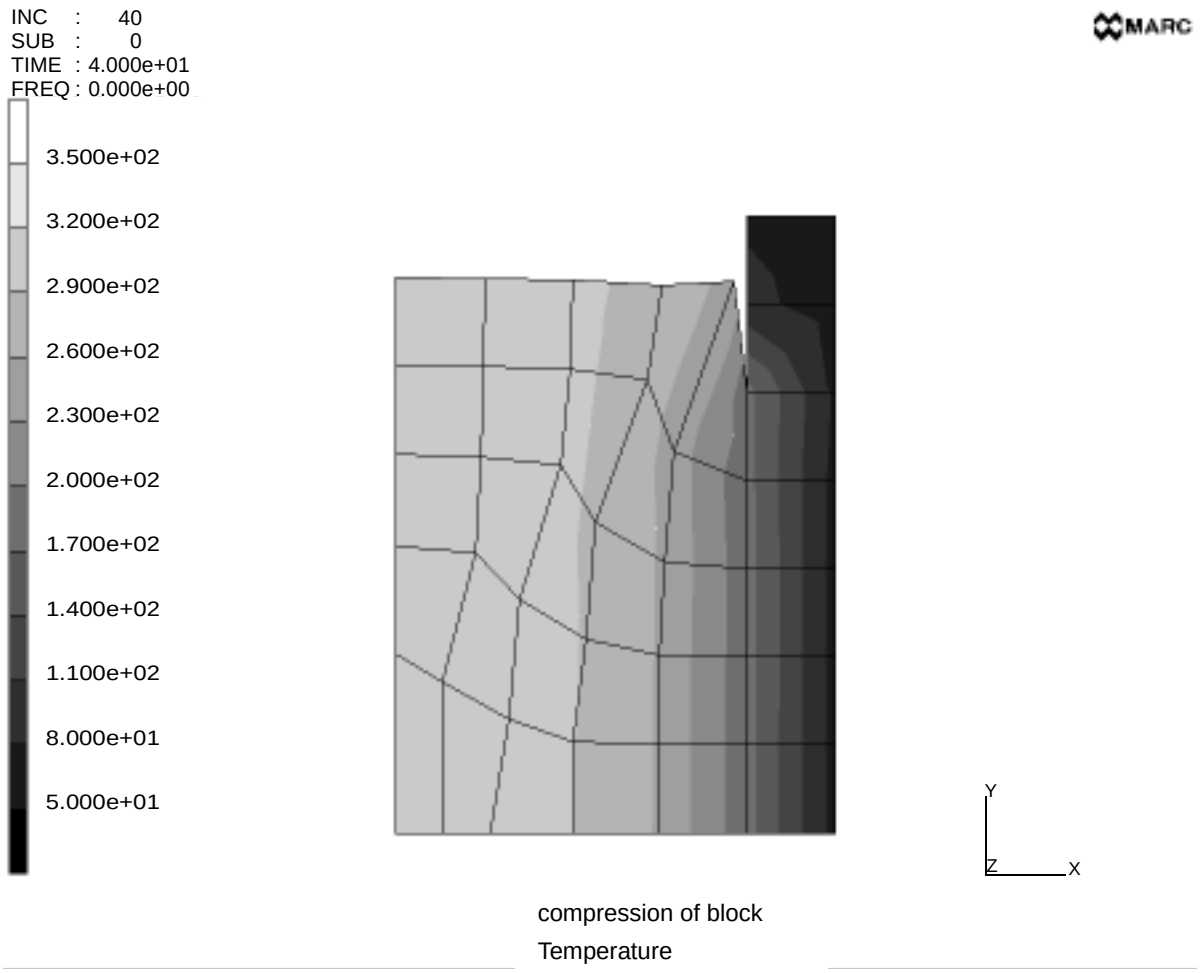

Figure 8.7-5 Temperature, Increment 40

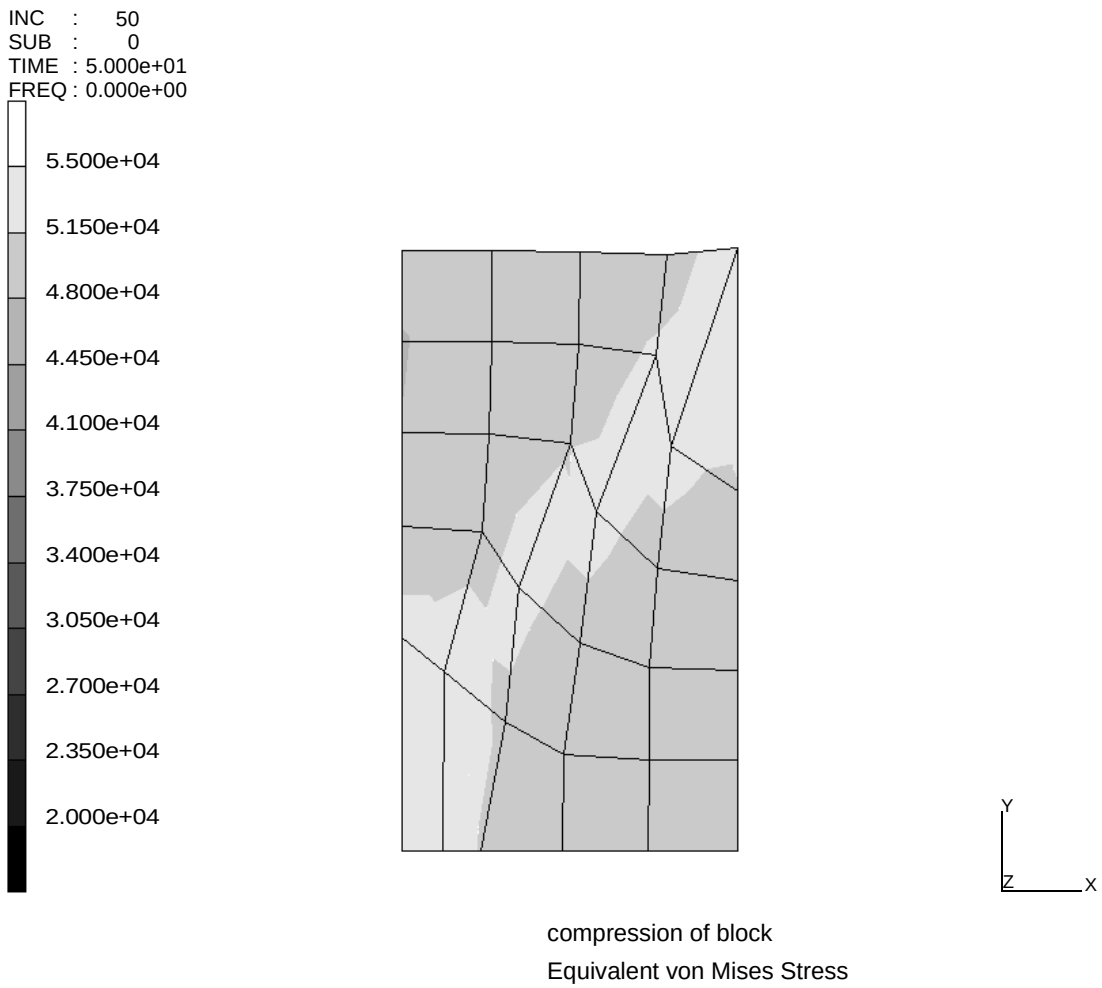

Figure 8.7-6 Equivalent Stress, Increment 50

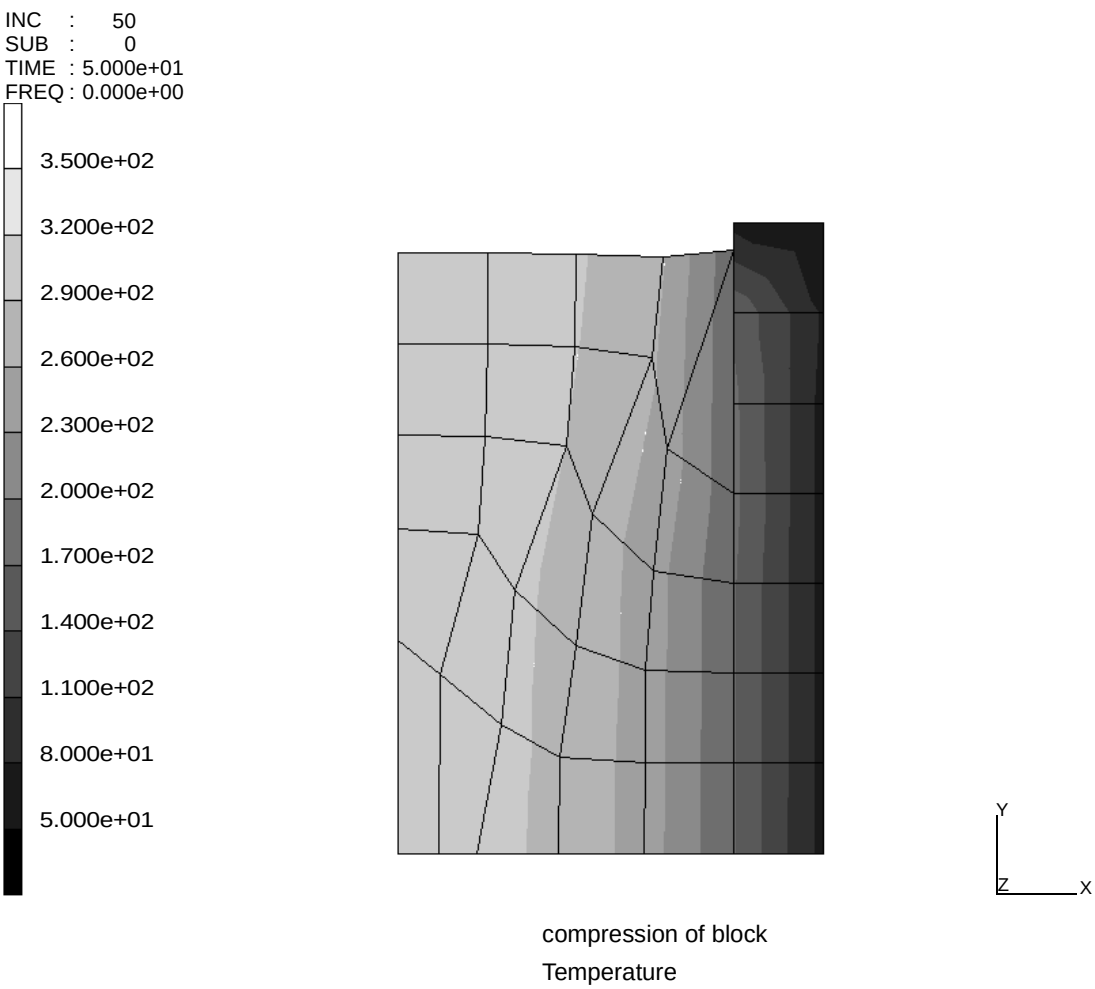

Figure 8.7-7 Temperature, Increment 50

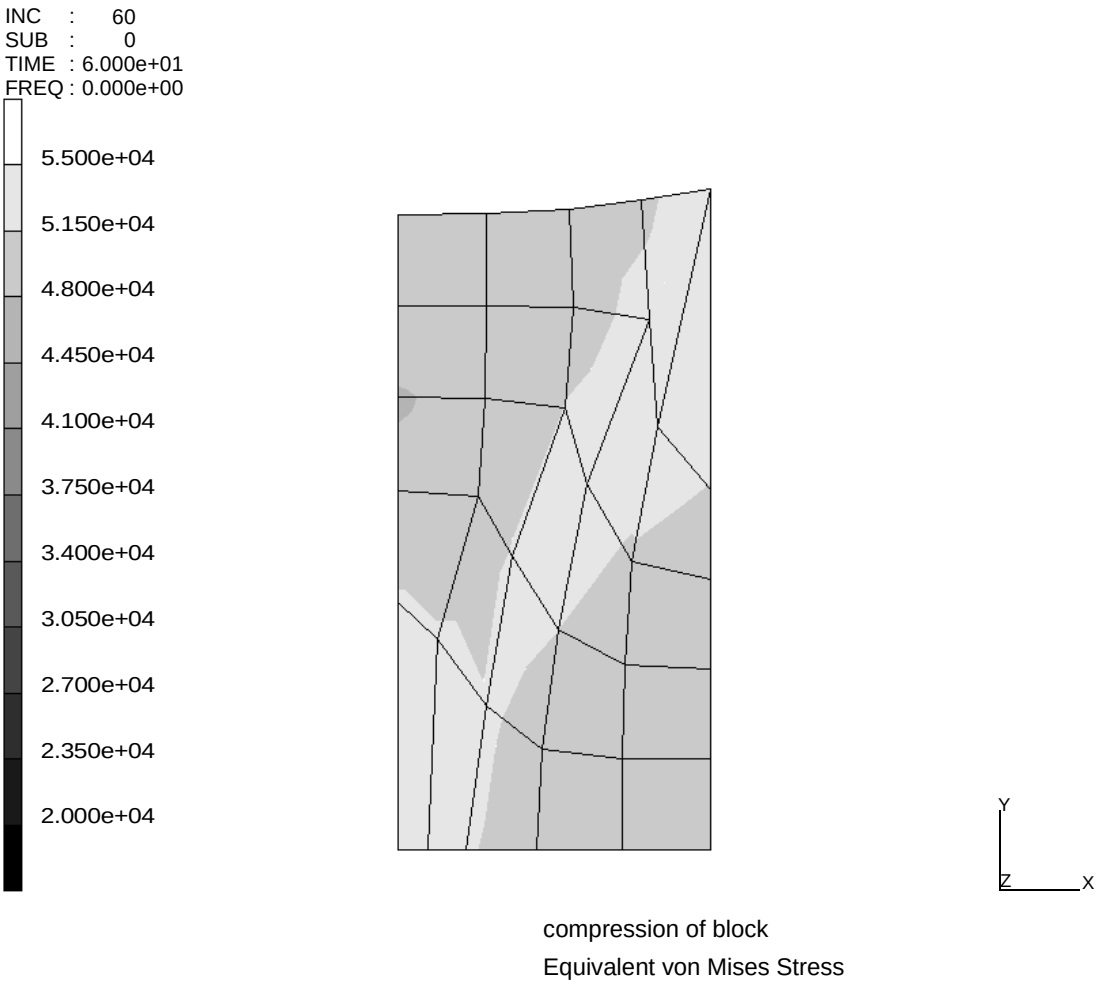

Figure 8.7-8 Equivalent Stress, Increment 60

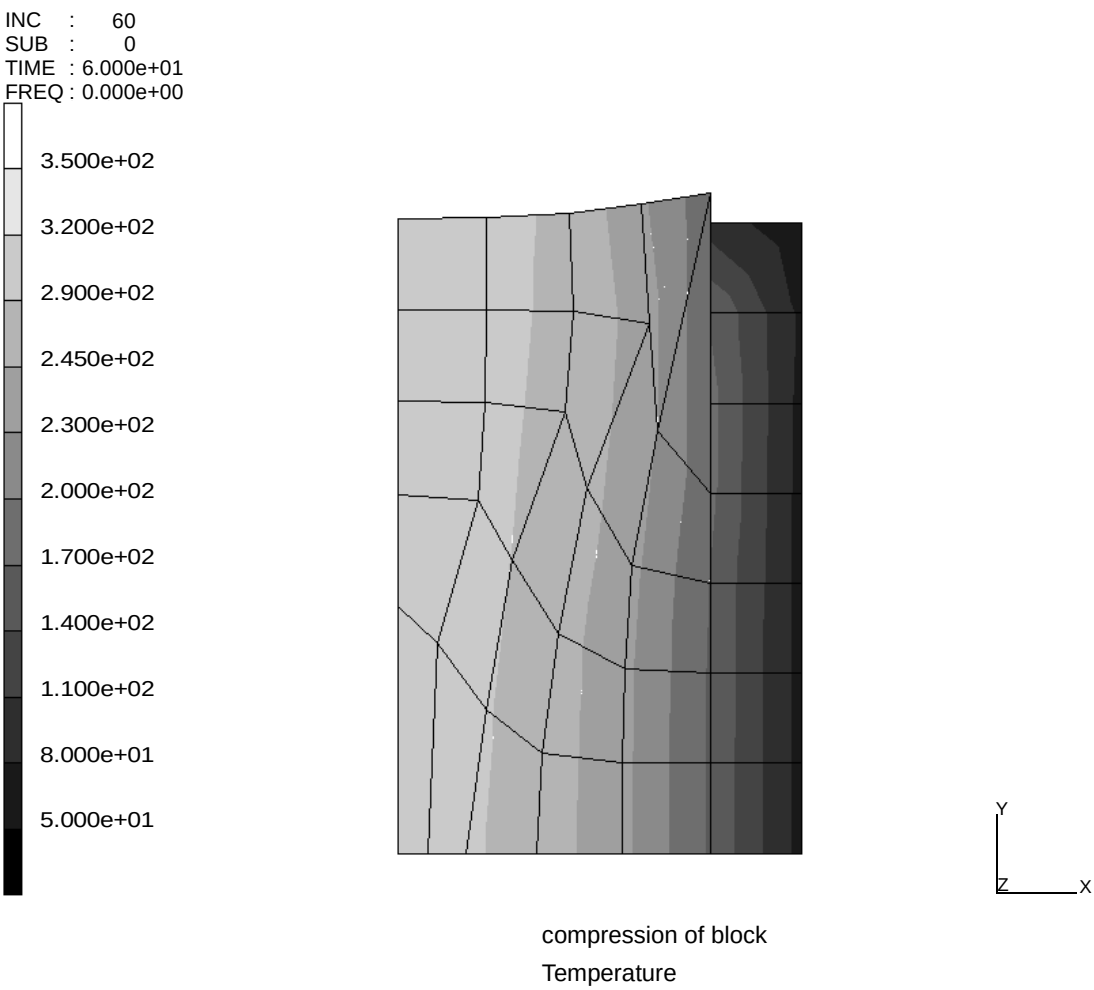

Figure 8.7-9 Temperature, Increment 60

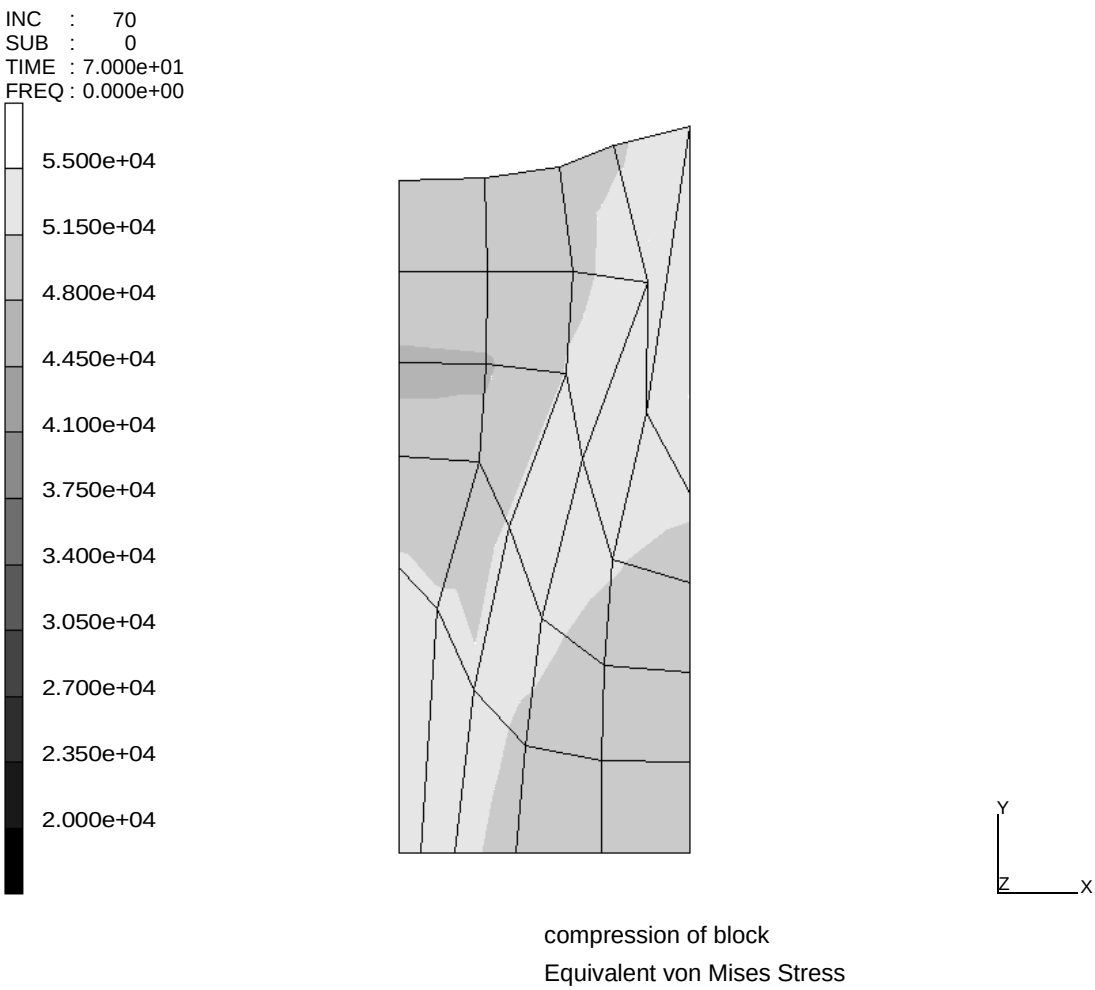

Figure 8.7-10 Equivalent Stress, Increment 70

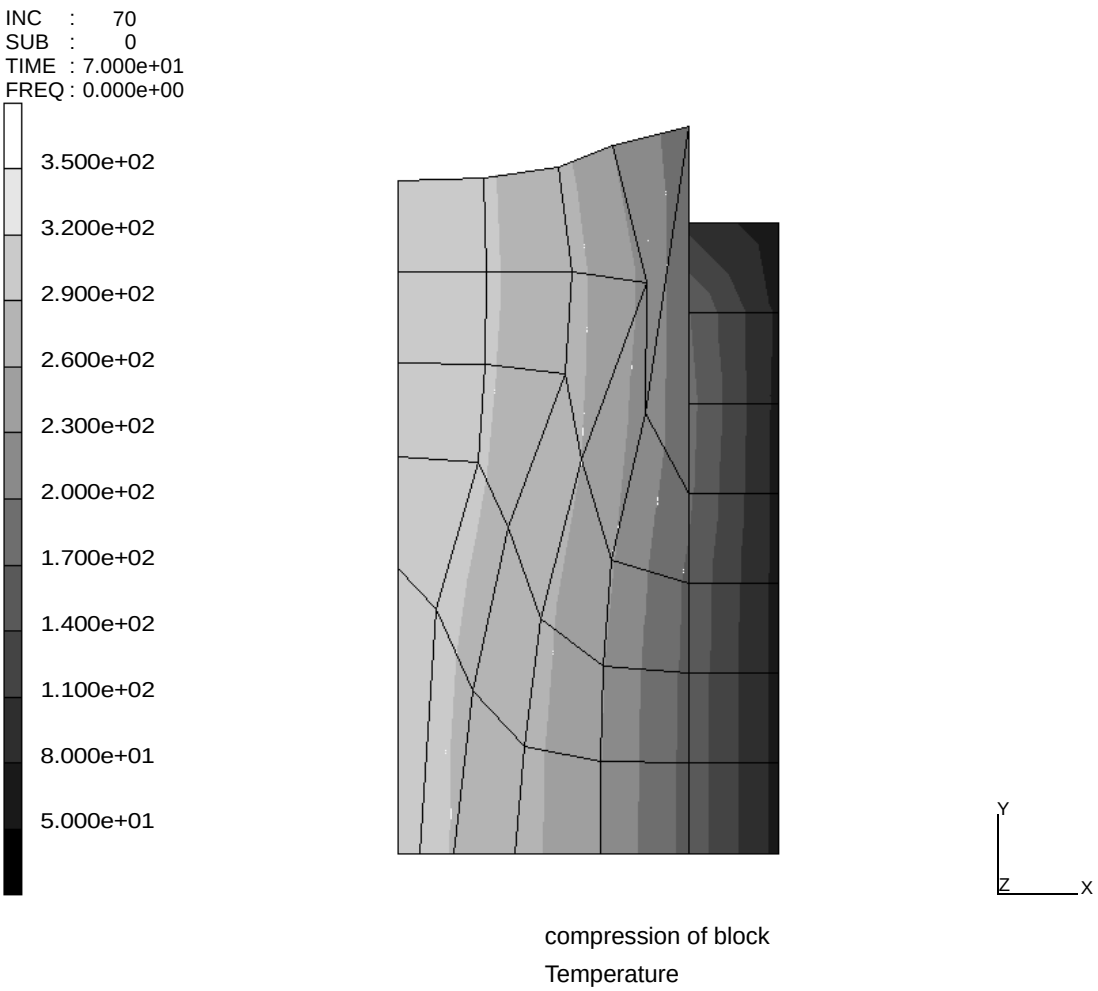

Figure 8.7-11 Temperature, Increment 70

Figure 8.7-12 Total Displacement, Increment 70

8.8 Simply-supported Thick Plate under Uniform Pressure with Anisotropic Properties

A thick plate, simply-supported around its perimeter, is analyzed with a pressure load normal to the plate surface. This problem demonstrates the use of various options for the input of anisotropic properties.

Element

Element type 21 is a 20-node isoparametric brick. There are three displaced degrees of freedom at each node; eight are corner nodes, 12 midside. Each edge of the brick can be parabolic; a curve is fitted through the midside node. Numerical integration is accomplished with 27 points using Gaussian quadrature. See *MARC Volume B: Element Library* for further details.

Model

Taking advantage of symmetry, only one-quarter of the plate is modeled. One element is used through the thickness; two in each direction in the plane of the plate. There are 51 nodes for a total of 153 degrees of freedom. See Figure 8.8-1.

Anisotropic Properties

Material properties in this problem are assumed to be anisotropic. The Young's moduli, Poisson's ratios, and shear moduli are:

$$E_x = 30 \times 10^6, \quad E_y = 20 \times 10^6, \quad E_z = 10 \times 10^6$$
$$\nu_{xy} = 0.3, \quad \nu_{yz} = 0.25, \quad \nu_{zx} = 0.2$$
$$G_{xy} = 10 \times 10^6, \quad G_{yz} = 5 \times 10^6, \quad G_{zx} = 1 \times 10^6$$

The preferred directions of the material are aligned with the global x- ,y-, z-axes, which are also the basis for the continuum element. Three input options are demonstrated in this example for the input of anisotropic properties. These options are: model definition block ORTHOTROPIC, user subroutine HOOKLW, and user subroutine ANELAS.

ORTHOTROPIC (Model Definition Block)

The anisotropic material properties can be directly entered through the model definition block ORTHOTROPIC. As shown in the input list e8.8A, this data block consists of seven lines. The keyword ORTHOTROPIC is on line series 1; the number of data sets is 1 on line series 2. On line series 3, the material identification number is entered as 1; on line series 4, 5, 6, the anisotropic properties (E_x, E_y, etc.) are sequentially entered. Finally, an element list (1 to 4) is entered on line series 7. In this example, the ORTHOTROPIC model definition block is used for entering the material data. The ORTHOTROPIC block can also be used for entering isotropic properties.

In such a case, the material constants must be set to the same constant:

$E_x = E_y = E_z$; $\nu_{xy} = \nu_{yz} = \nu_{zx}$, etc.

HOOKLW (User Subroutine)

The user subroutine HOOKLW allows for the input of stress-strain relation [B] at each integration point of an element. For MARC element 21 (20-node brick) used in this problem, the strain-stress relation $[B]^{-1}$ is expressed as:

$$\begin{Bmatrix} \varepsilon_{xx} \\ \varepsilon_{yy} \\ \varepsilon_{zz} \\ \gamma_{xy} \\ \gamma_{yz} \\ \gamma_{zx} \end{Bmatrix} = \begin{bmatrix} 1/E_{xx} & -\nu_{yx}/E_{yy} & -\nu_{zx}/E_{zz} & 0 & 0 & 0 \\ -\nu_{xy}/E_{xx} & 1/E_{yy} & -\nu_{zy}/E_{zz} & 0 & 0 & 0 \\ -\nu_{xz}/E_{xx} & -\nu_{yz}/E_{yy} & 1/E_{zz} & 0 & 0 & 0 \\ 0 & 0 & 0 & 1/G_{xy} & 0 & 0 \\ 0 & 0 & 0 & 0 & 1/G_{yz} & 0 \\ 0 & 0 & 0 & 0 & 0 & 1/G_{zx} \end{bmatrix} \begin{Bmatrix} \sigma_{xx} \\ \sigma_{yy} \\ \sigma_{zz} \\ \sigma_{xy} \\ \sigma_{yz} \\ \sigma_{zx} \end{Bmatrix}$$

or $\{\varepsilon\} = [B]^{-1} \{\sigma\}$.

As shown in the subroutine list HOOKLW, the matrix $[B]^{-1}$ is first evaluated directly from the anisotropic material data (E_x, E_y, E_z, ν_{xy}, ν_{yz}, ν_{zx}, G_{xy}, G_{yz}, and G_{zx}) and a MARC matrix inversion subroutine INVERT is called to invert the strain-stress matrix $[B]^{-1}$. The stress-strain matrix [B] is returned to MARC for the evaluation of element stiffness matrix. In order to activate the user subroutine HOOKLW, the model definition block ORTHOTROPIC must be used to indicate anisotropic material behavior as well as the use of HOOKLW user subroutine.

ANELAS (User Subroutine)

The user subroutine ANELAS allows for the input of anisotropy-to-isotropy ratios in the stress-strain relation at an integration point of an element. For MARC element 21 (20-node brick) used in this problem, the isotropic strain-stress relation is expressed as:

$$\begin{Bmatrix} \varepsilon_{xx} \\ \varepsilon_{yy} \\ \varepsilon_{zz} \\ \gamma_{xy} \\ \gamma_{yz} \\ \gamma_{zx} \end{Bmatrix} = \begin{bmatrix} 1/E & -\nu/E & -\nu/E & 0 & 0 & 0 \\ -\nu/E & 1/E & -\nu/E & 0 & 0 & 0 \\ -\nu/E & -\nu/E & 1/E & 0 & 0 & 0 \\ 0 & 0 & 0 & 1/G & 0 & 0 \\ 0 & 0 & 0 & 0 & 1/G & 0 \\ 0 & 0 & 0 & 0 & 0 & 1/G \end{bmatrix} \begin{Bmatrix} \sigma_{xx} \\ \sigma_{yy} \\ \sigma_{zz} \\ \sigma_{xy} \\ \sigma_{yz} \\ \sigma_{zx} \end{Bmatrix}$$

or $\{\varepsilon\} = [E]^{-1}\{\sigma\}$

and for anisotropic material as:

$$\begin{Bmatrix} \varepsilon_{xx} \\ \varepsilon_{yy} \\ \varepsilon_{zz} \\ \gamma_{xy} \\ \gamma_{yz} \\ \gamma_{zx} \end{Bmatrix} = \begin{bmatrix} 1/E_{xx} & -\nu_{yx}/E_{yy} & -\nu_{zx}/E_{zz} & 0 & 0 & 0 \\ -\nu_{xy}/E_{xx} & 1/E_{yy} & -\nu_{zy}/E_{zz} & 0 & 0 & 0 \\ -\nu_{xz}/E_{xx} & -\nu_{yz}/E_{yy} & 1/E_{zz} & 0 & 0 & 0 \\ 0 & 0 & 0 & 1/G_{xy} & 0 & 0 \\ 0 & 0 & 0 & 0 & 1/G_{yz} & 0 \\ 0 & 0 & 0 & 0 & 0 & 1/G_{zx} \end{bmatrix} \begin{Bmatrix} \sigma_{xx} \\ \sigma_{yy} \\ \sigma_{zz} \\ \sigma_{xy} \\ \sigma_{yz} \\ \sigma_{zx} \end{Bmatrix}$$

or $\{\varepsilon\} = [B]^{-1}\{\sigma\}$.

As shown in the subroutine list ANELAS, the matrices $[E]^{-1}$ and $[B]^{-1}$ are first evaluated from the isotropic material data (E and ν) and anisotropic material data (E_x, E_y, E_z, ν_{xy}, ν_{yz}, ν_{zx}, G_{xy}, G_{yz}, and G_{zx}). Then, the MARC matrix inversion subroutine INVERT is called to obtain the stress-strain relations [E] and [B] for isotropic and anisotropic properties, respectively. The anisotropy-to-isotropy ratios to be defined in the subroutine ANELAS are:

DRATS(I,J) = B(I,J)/E(I,J)
I,J = 1,...,3
DRATS(L,L) = B(L,L)/E(L,L)
L = 4,...,6

In order to activate the user subroutine ANELAS, the model definition block ORTHOTROPIC must be used to indicate anisotropic material behavior. In addition, the isotropic properties [$E_y = E_y = E_z = E$; $V_{xy} = V_{yz} = V_{zx} = \nu$; $G_{xy} = G_{zx} = G_{zx} = E/2(1+\nu)$] must also be entered through ORTHOTROPIC block.

Geometry

No geometry specification is used.

Loading

A uniform pressure of 1.00 psi is applied in the DIST LOADS block. Load type 4 is specified for uniform pressure on the 6-5-8-7 face of all four elements.

Boundary Conditions

On the symmetry planes, x = 30 and y = 30, in-plane movement is constrained. On the x = 30 plane, u = 0, and on the y = 30 plane, v = 0. On the plate edges, x = 0 and y = 0; the plate is simply supported, w = 0.

Results

A contour plot of the equivalent stress for all four elements is shown in Figure 8.8-3. A comparison of the contours (Figure 8.8-3 and Figure 8.8-3) between isotropic and anisotropic behavior clearly shows the effect of anisotropy on stress distributions.

Parameters, Options, and Subroutines Summary

Example e8x8a.dat:

Parameters	Model Definition Options
ELEMENT	CONNECTIVITY
END	COORDINATE
SIZING	DIST LOADS
TITLE	END OPTION
	FIXED DISP
	ORTHOTROPIC

Example e8x8b.dat:

Parameters	Model Definition Options
ELEMENT	CONNECTIVITY
END	COORDINATE
SIZING	DIST LOADS
TITLE	END OPTION
	FIXED DISP
	ORTHOTROPIC

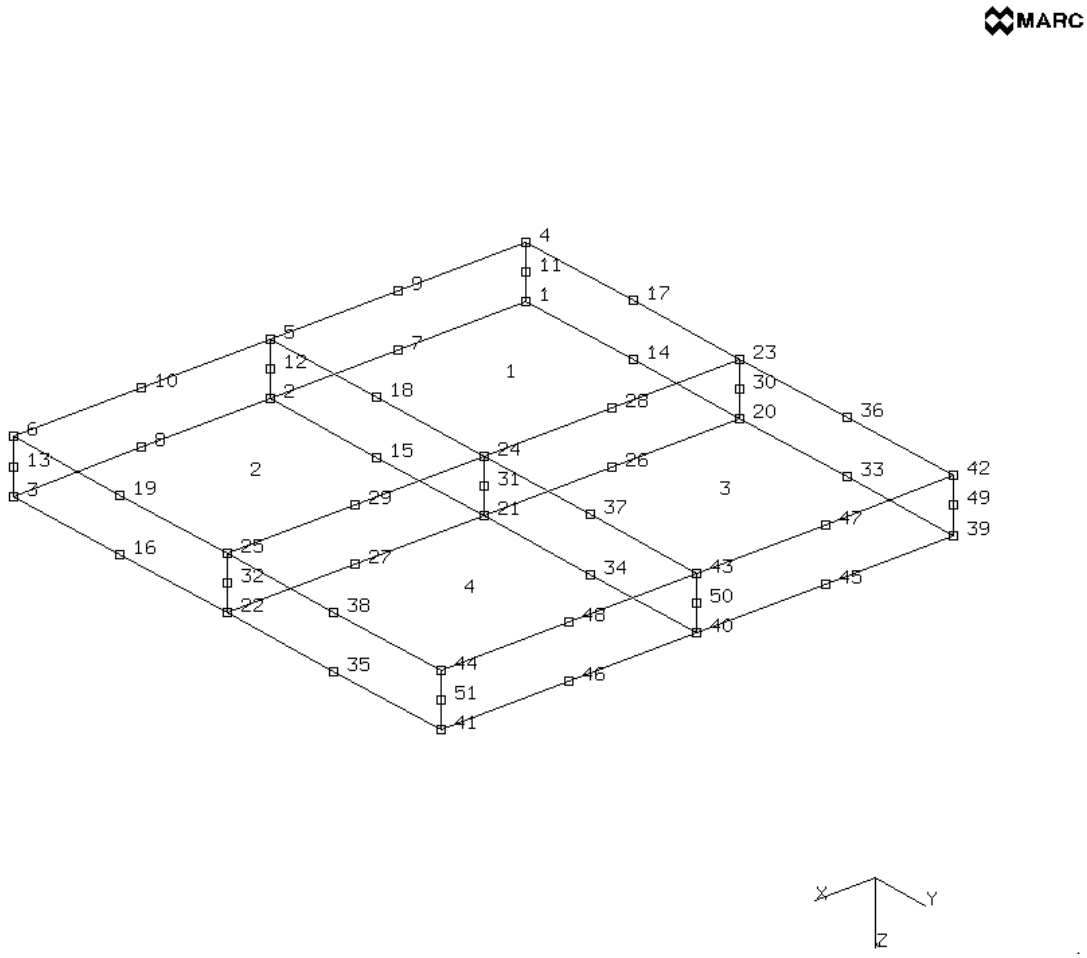

Figure 8.8-1 Thick Plate Mesh

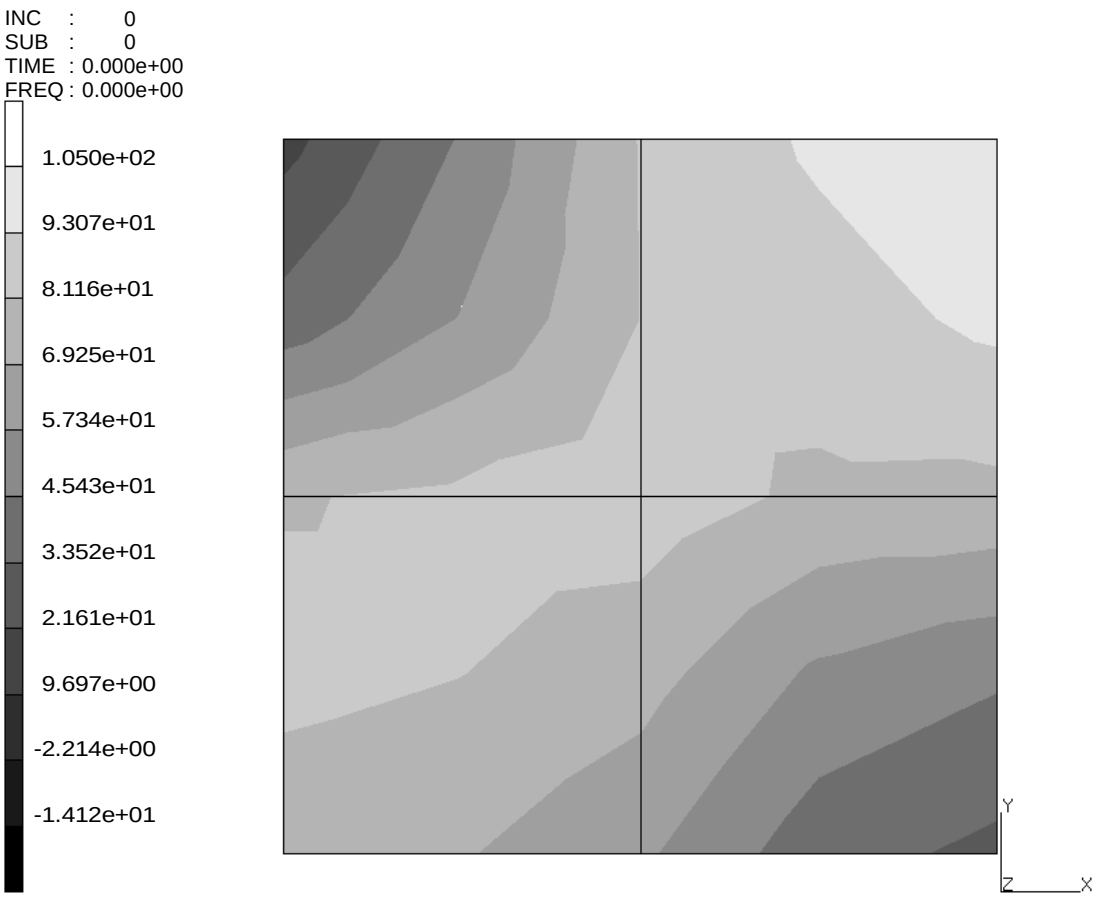

Figure 8.8-2 Anisotropic Behavior Stress Contours

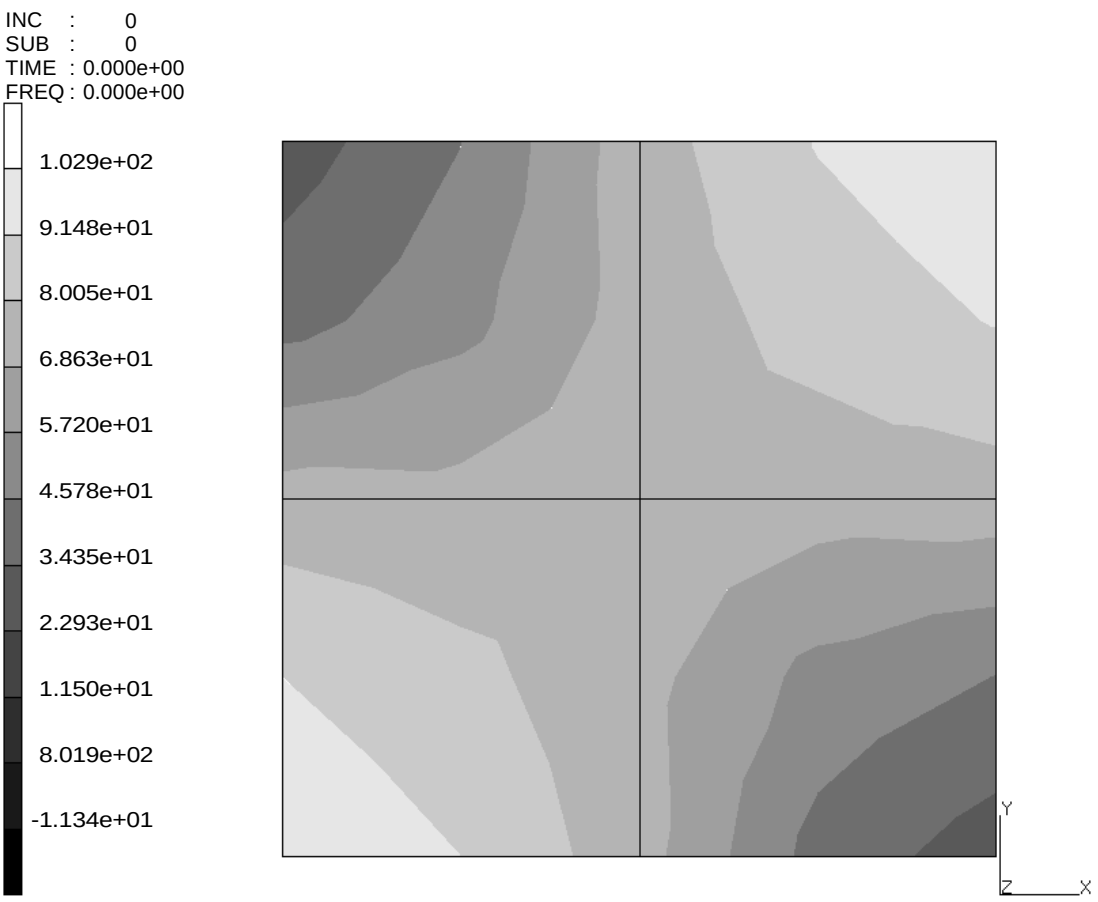

Figure 8.8-3 Isotropic Behavior Stress Contours

8.9 Failure Criteria Calculation for Plane Stress Orthotropic Sheet

This problem illustrates the use of the FAIL DATA model definition block to supply data used by MARC to calculate failure criteria based on the current state of stress in a material. In this problem, an orthotropic square plate is subjected to a biaxial state of stress. The resulting program calculated failure criteria is compared with a textbook solution of this problem.

Element

Element type 3, a two-dimensional plane stress quadrilateral is used to model the square plate. This element is a 4-node isoparametric arbitrary quadrilateral element with two translational (u,v) degrees-of-freedom at each node. See *MARC Volume B: Element Library* for a detailed discussion of this element.

Model

As shown in Figure 8.9-1, a square plate of 4 x 4 m^2 is subjected to a biaxial state of stress. The applied stresses are: σ_x = -3.5 x 10^6 N/m^2; σ_y = +7.0 x 10^6 N/m^2; and τ_{xy} = -1.4 x 10^6 N/m^2. The plate is assumed to be made of an orthotropic material with a preferred direction (LOCAL 1-DIRECTION) of 60 degrees from the global x-axis. Sixteen elements are used to model this plate. Both the element and the nodal numbers are purposely set to be nonconsecutive. For the purpose of preventing rigid body motion, roller and hinge supports are prescribed at one side of the plate. Set names are used for boundary nodes as well as elements in the mesh.

Orthotropic

The orthotropic material properties of the plate are:

E_{11} = 14.0E9, E_{22} = E_{33} = 3.5E9

ν_{12} = 0.4 ν_{23} = ν_{31} = 0.0

G_{12} = G_{23} = G_{31} = 4.2E9

Orientation

The preferred material direction (LOCAL 1-DIRECTION) of 60 degrees from the global x-axis, is entered through the PGLOBAL X option.

Fail Data

Five program calculated failure criteria provided in MARC are as follows:

1. maximum stress
2. maximum strain

3. Hill
4. Tsai-Wu
5. Hoffman

A user-defined criterion is also available through user subroutine UFAIL. The five preprogrammed criteria are valid only for states of plane stress, while user subroutine UFAIL can be used for a general 3D state of stress using the FAIL DATA block. You specify on a material basis your failure data. Up to three failure criteria can be calculated per material. Failure criterion output appears along with other element output. The failure data is given in the material principal coordinate system. These are the preferred coordinates in MARC and are specified by the ORIENTATION block.

Both the maximum stress (MX STRESS) and the Hill (HILL) failure criteria are requested in this analysis. The maximum stresses used for this criteria are:

MAX. X-TENSILE STRESS = 250.0E6

MAX. ABSOLUTE X-COMPRESSIVE STRESS = 0

MAX. Y-TENSILE STRESS = 0.5E6

MAX. ABSOLUTE Y-COMPRESSIVE STRESS = 10.0E6

MAX. ABSOLUTE SHEAR STRESS = 8.0E6

For Hill's criterion, a default failure index of 1.0 is used.

Fixed Disp

Roller supports (u = 0) are prescribed at nodes 2, 3, 4, 5 (LEFT EXCEPT 1); hinge (u = v = 0) support is prescribed at node 1, for the prevention of rigid body motion.

Point Load

Both the direct (σ_x,σ_y) and shear (τ_{xy}) stresses are represented by point loads acted at boundary nodal points. A distribution of the points loads is shown in Figure 8.9-2.

Nodal Thickness

In this problem, the plate thickness is specified in the NODAL THICKNESS block. A thickness of 1.0 is assumed for all nodal points in the mesh.

Results

In the reference, a solution to this problem is given. These results along with MARC output is summarized in Table 8.9-1. The comparison is favorable.

Table 8.9-1 Comparison of Results

Criterion	Reference	MARC
Max σ_2	1.26%*	1.3%
Max σ_2	68.0%	67.5%
Max τ_{12}	65.6%	65.6%
Hill	89.0%	88.6%

Note: * = 100% means failure occurs

References

Argarwal, B.D., and Broutman, L.J., *Analysis and Performance of Fiber Composites*, Wiley, 1980.

Parameters, Options, and Subroutines Summary

Example e8x9.dat:

Parameters	Model Definition Options
ELEMENT	CONNECTIVITY
END	COORDINATE
SIZING	DEFINE
TITLE	END OPTION
	FAIL DATA
	FIXED DISP
	NODAL THICKNESS
	ORIENTATION
	ORTHOTROPIC
	POINT LOAD
	POST
	PRINT ELEM

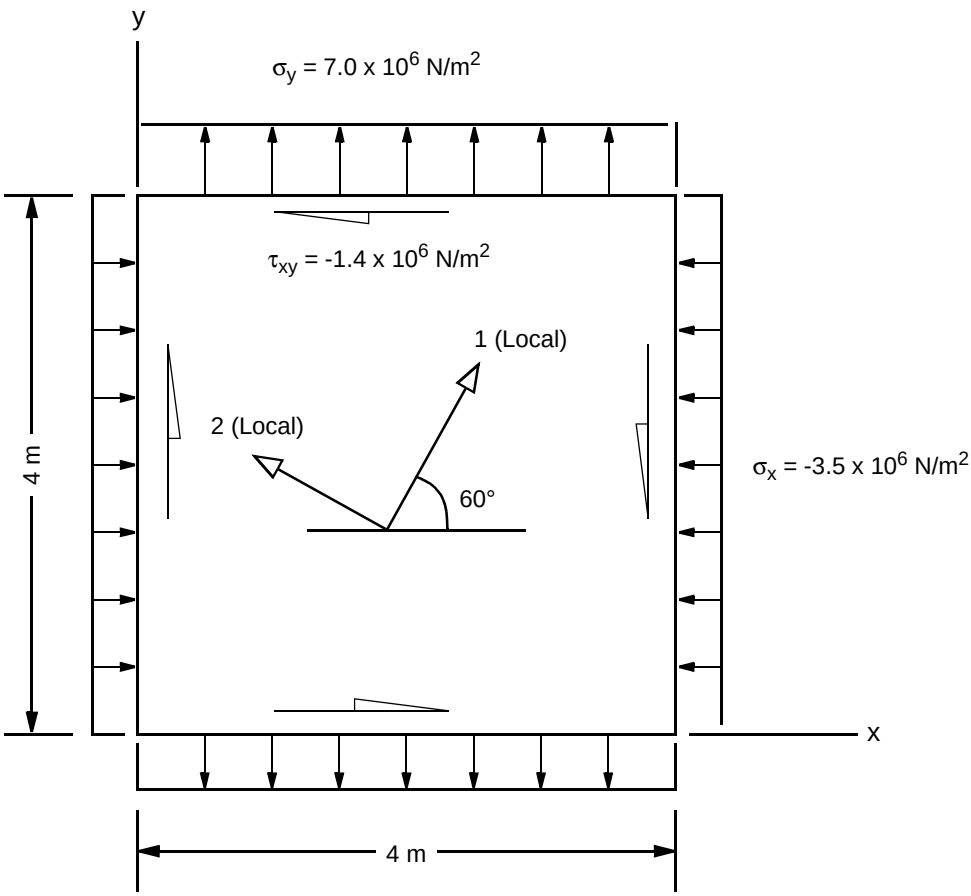

Figure 8.9-1 Orthotropic Square Plate

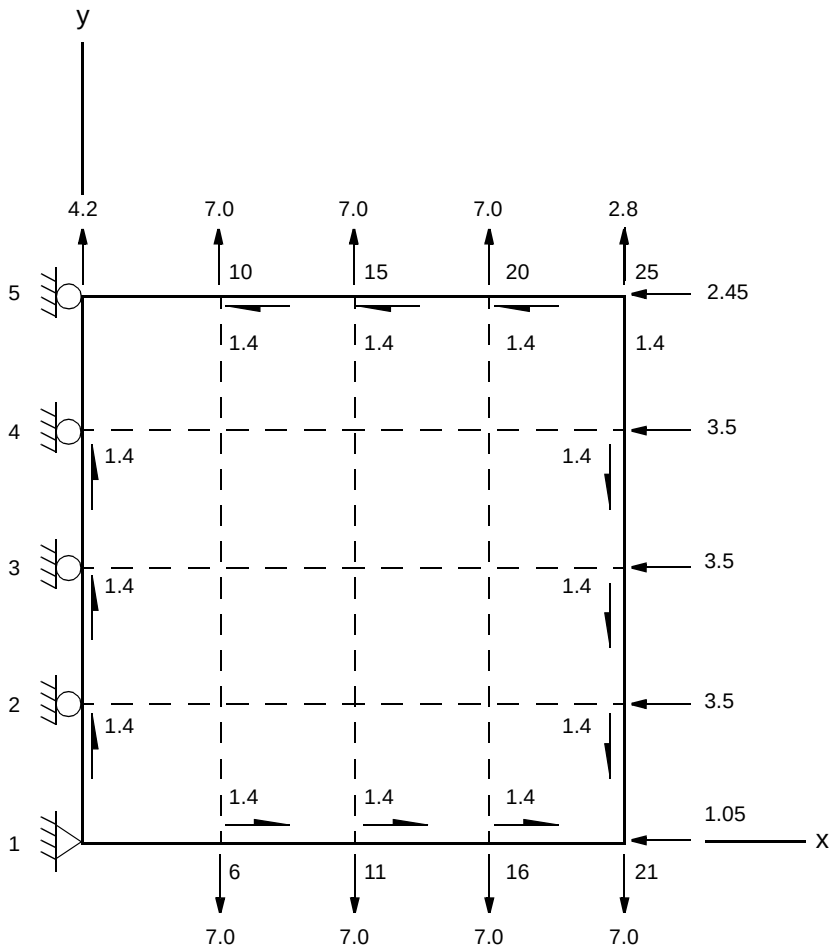

Figure 8.9-2 Point Load (x 10^6) and Support

8.10 Beam Element 52 with Nonlinear Elastic Stress-Strain Relation

As described in *MARC Volume B: Element Library*, the beam element 52 can be used for nonlinear elastic material. This problem demonstrates the use of model definition option HYPOELASTIC and user subroutine UBEAM for the nonlinear elastic behavior of a cantilever beam, modeled by element type 52, subjected to prescribed tip displacements.

Element

Element type 52 is a straight, Euler-Bernoulli beam in space with three translations and three rotations as degrees of freedom at each node of the element. The element is defined by nodal coordinates in global coordinate system and by section properties such as area, bending stiffnesses, as well as torsional stiffness. See *MARC Volume B: Element Library* for further detail.

Model

As shown in Figure 8.10-1, the cantilever beam is modeled by five beam elements with a fixed end at node 1, and prescribed displacements at node 6. The section and material properties are entered through GEOMETRY and HYPOELASTIC options; however, the user subroutine UBEAM is used for the description of nonlinear elastic stress-strain relation of the beam. The stress-strain relation is assumed to be dependent on strain quantities.

Geometry

A beam with a square cross section of length 0.2 inch is modeled. The area of the beam section is 0.04 in.^{2} and moments of inertia are $I_x = I_y = 0.000133333$ in.^{4}.

HYPOELASTIC

The HYPOELASTIC model definition option is used to indicate that all of the elements use this formulation. User subroutine UBEAM defines the material behavior.

The initial Young's modulus is 1,000,000 psi and the Poisson's ratio is 0.2, which are given in the user subroutine.

FIXED DISP and DISP CHANGE

All degrees of freedom at node 1 are fixed for the simulation of a fixed-end condition. A 0.2 incremental displacement is prescribed at node 6, for degrees of freedom 1, 4, 5, and 6 (axial displacement and rotations). The same incremental displacements are repeated for increments 1 through 3, using DISP CHANGE history definition option.

Nonlinear Stress-Strain Relation (User Subroutine UBEAM)

The generalized stress-generalized strain relation for element 52 can be expressed as follows:

$$\begin{Bmatrix} F \\ M_x \\ M_y \\ T \end{Bmatrix} = \begin{bmatrix} D_{11} & & & \\ & D_{22} & & \\ & & D_{33} & \\ & & & D_{44} \end{bmatrix} \begin{Bmatrix} \varepsilon \\ K_x \\ K_y \\ \theta \end{Bmatrix} \qquad \text{(EQ 1)}$$

where F, M_x, M_y, and T are axial force, bending and twist moments (generalized stress components); ε, K_x, K_y, and θ are axial stretch, curvatures and twist (generalized strain components), respectively.

For the purpose of demonstration, the terms D_{11}, D_{22}, D_{33}, and D_{44} in the stress-strain matrix are assumed to have the following dependence on strains:

$$\begin{aligned} D_{11} &= (EA)EXP(-C|\varepsilon|) \\ D_{22} &= (EA)EXP(-C|K_x|) \\ D_{33} &= (EA)EXP(-C|K_y|) \\ D_{44} &= (EA)EXP(-C|\theta|) \end{aligned} \qquad \text{(EQ 2)}$$

In EQ 2, E is the Young's modulus, A is the area, I_x, I_y are moments of inertia; $G = E/2(1+\nu)$ and $J = (I_x + I_y)$. The constant C is assumed to be 13.8.

The incremental generalized stress-generalized strain relation D(I,I), the incremental generalized stress DF(I), and the total generalized stress at the end of increment GS(I), I = 1,..., 4, are respectively computed in the subroutine and returned to MARC for further computations.

Results

Table 8.10-1 shows a comparison of MARC results with analytical solution computed from equations (EQ 1) and (EQ 2). The comparison is excellent.

Table 8.10-1 Comparison of MARC Results vs. Analytical

Tip Displacements (in.)	F (lb.)		M_x (in-lb.)		M_y (in-lb.)		T (in-lb.)	
	MARC	Analytical	MARC	Analytical	MARC	Analytical	MARC	Analytical
0.2	9.21275E2	9.2127E2	3.07901E0	3.0709E0	3.07091E0	3.0709E0	2.55909E0	2.5591E0
0.4	1.06093E3	1.0609E2	3.53644E0	3.5364E0	3.53644E0	3.5364E0	2.94703E0	2.9470E0
0.6	9.16324E2	9.1632E2	3.05442E0	3.0544E0	3.05458E0	3.0544E0	2.54533E0	2.5453E0
0.8	7.03489E2	7.0349E2	2.34496E0	2.3450E0	2.34494E0	2.3450E0	1.95413E0	1.9541E0

Parameters, Options, and Subroutines Summary

Example e8x10.dat:

Parameters

ELEMENT
END
SIZING
TITLE

Model Definition Options

CONNECTIVITY
CONTROL
COORDINATE
END OPTION
FIXED DISP
GEOMETRY
HYPOELASTIC

History Definition Options

CONTINUE
DISP CHANGE

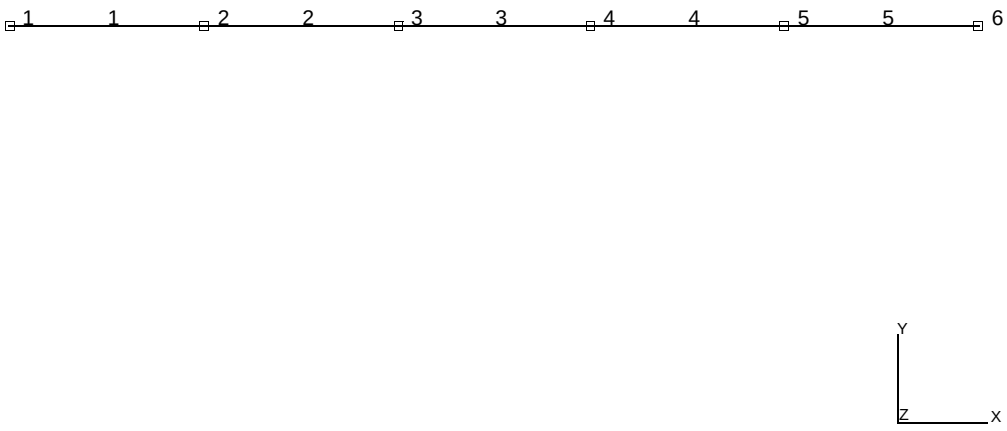

Figure 8.10-1 Cantilever Beam with Prescribed Tip Displacement

8.11 Element Deactivation/Activation and Error Estimate in the Analysis of a Plate with Hole

The problem of a plate with hole subjected to an in-plane tensile force (problem 2.9) is analyzed with the options DEACTIVATE, ACTIVATE, and ERROR ESTIMATE. These options allow for the deactivation or activation of elements during the analysis, and the estimation of errors on stress continuity and geometric measures (aspect and skew ratios).

During analysis, after the elements are deactivated, they retain the stress state in effect at the time of deactivation. At a later stage in the analysis, the elements can again be activated with the ACTIVATE history definition option. Elements which were deactivated before analysis have zero internal stress upon activation. Elements which were used earlier and deactivated during analysis have an internal stress which is equal to the state when they were deactivated.

The ERROR ESTIMATE option provides information regarding the error associated with the finite element discretization. There are two measures. The first evaluates the stress discontinuity between elements. A large value implies that the stresses gradients are not accurately represented in the finite element mesh.

The second error measure examines geometric distortion in the model. It first examines the aspect ratios and warpage of the elements and, in subsequent increments, measures how much these ratios change. This measure can be used to indicate the adequacy of the original mesh.

Element

Element type 26 is a second-order, isoparametric two-dimensional element for plane stress. There are eight nodes with two degrees of freedom at each node.

Model

The example uses a coarse mesh for demonstration purposes only. The mesh generated by MARC is shown in Figure 8.11-1.

Geometry

The plate thickness of one inch is entered in EGEOM1.

Property

Young's modulus is 30×10^6 psi, with Poisson's ratio as 0.3. These quantities are sufficient to define the material as isotropic linear-elastic.

Loading

To simulate a tension acting at infinity, a negative 1-psi load is applied to the top edge of the mesh.

FIXED DISP

The boundary conditions are determined by symmetry considerations. No displacement is permitted on the axis of symmetry perpendicular to the applied force direction. On the axis of symmetry parallel to the force direction, only parallel displacements are permitted.

Optimize

The Cuthill-McKee algorithm is chosen in this example. Ten iterations are sufficient to obtain a reasonably optimal bandwidth.

Error Estimates

Both the stress continuity and geometry measures are requested by inputting 1 , 1 , on the second card of this data block.

DEACTIVATE/ACTIVATE

After END OPTION, two DEACTIVATE increments and one ACTIVATE increment are provided for the deactivation of elements 7, 8, 17, 18 at the first increment; elements 9, 10, 19, 20 at the second increment; and the activation of all eight elements at the third increment.

Results

Table 8.11-1 shows σ_{yy} at element 8, integration point 6 and element 10, integration point 6, at increments 0 through 3. The effects of deactivation/activation of elements are clearly demonstrated. In addition, the stress discontinuity and geometry measures at increment 0 (ERROR ESTIMATE option) are as follows:

```
WORST ORIGINAL ASPECT RATIO IS 3.343 AT ELEMENT 1
WORST ORIGINAL WARPAGE RATIO IS 1.957 AT ELEMENT 3
WORST CURRENT ASPECT RATIO IS 3.343 AT ELEMENT 1
WORST CURRENT WARPAGE RATIO IS 1.957 AT ELEMENT 3
LARGEST CHANGE IN ASPECT RATIO IS 1.000 AT ELEMENT 7
LARGEST CHANGE IN WARPAGE RATIO IS 1.000 AT ELEMENT 8
                    GENERALIZED STRESSES
LARGEST NORMALIZED STRESS JUMP IS:
 0.11152E 02 AT NODE 17   COMPONENT 1    MEAN VALUE IS 0.28047E-02
LARGEST STRESS JUMP IS:
 0.23227E 00 AT NODE 76   COMPONENT 2    MEAN VALUE IS 0.23237E 01
```

Table 8.11-1 σ_{yy} vs. Load Increment

Inc. No.	EL 8, INT 6	EL 10, INT 6
0	2.62	1.89
1	2.62 (D)	6.24
2	2.62 (D)	6.24 (D)
3	2.88 (A)	5.68 (A)

Note: (D) – element DEACTIVATED

(A) – element ACTIVATED

Parameters, Options, and Subroutines Summary

Example e8x11.dat:

Parameters	Model Definition Options	History Definition Options
ELEMENT	CONNECTIVITY	ACTIVATE
END	COORDINATE	CONTINUE
SIZING	DIST LOADS	DEACTIVATE
TITLE	END OPTION	
	ERROR ESTIMATES	
	FIXED DISP	
	GEOMETRY	
	ISOTROPIC	
	PRINT NODE	

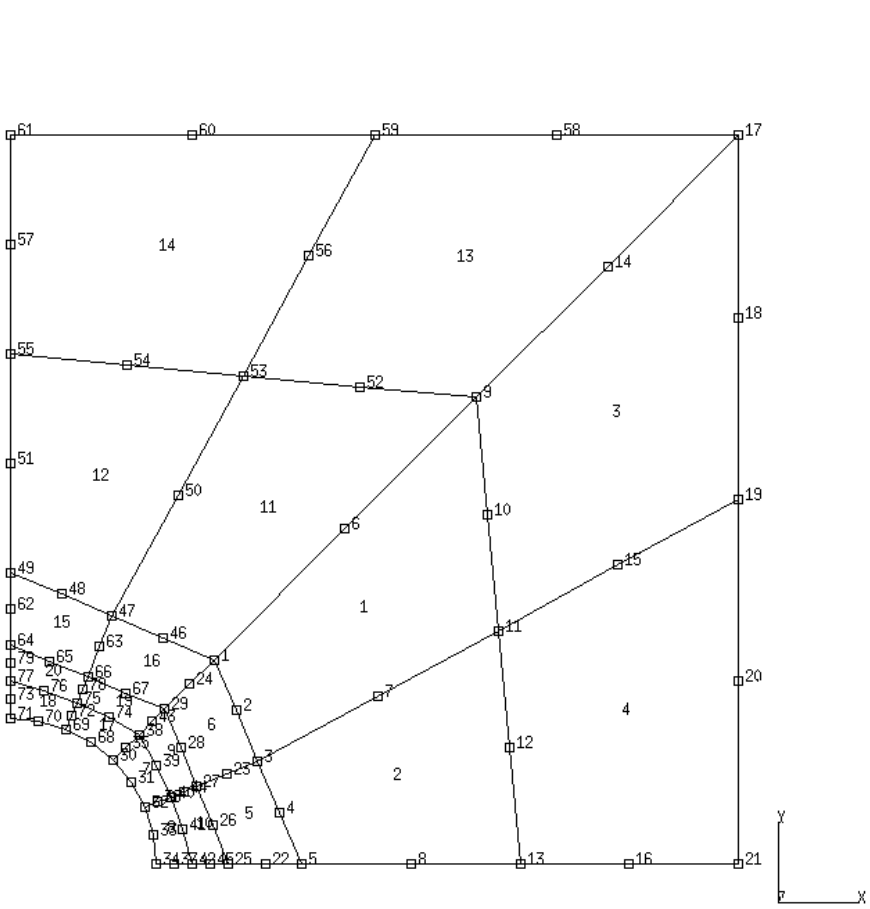

Figure 8.11-1 Mesh Layout for Plate with Hole

8.12 Forging of the Head of a Bolt

This example demonstrates the contact capability of MARC, using rigid surfaces for a simple forging analysis. An original cylindrical block is sitting in a surface with the shape of a cavity, and is deformed by another rigid surface which has the shape of the bolt head and moves at constant speed (Figure 8.12-2). The block is considered an elastic-plastic deformable material.

This problem is modeled using the six techniques summarized below.

Data Set	Element Type(s)	Number of Elements	Number of Nodes	Differentiating Features
e8x12	10	70	90	AUTO LOAD, REZONING
e8x12b	10	70	90	AUTO TIME
e8x12c	10	70	90	ADAPTIVE MESH, AUTO LOAD
e8x12d	10	70	90	AUTO STEP
e8x12e	10	70	90	F^eF^p, AUTO TIME
e8x12r	10	70	90	RESTART, REZONING

This analysis is done using three different approaches. In the first method (e8x12.dat), a fixed time step approach is used and the rezoning capability is used to improve the mesh when distortion occurs. In the second approach (e8x12b.dat), a variable time step approach is used by requesting the AUTO TIME option. In the third approach (e8x12c.dat), a fixed time step method is again used, but here the adaptive meshing capability is utilized. The restart capability is demonstrated based upon the first analysis (e8x12r.dat), which is typically used in rezoning analyses.

Parameters

The UPDATE, FINITE, and LARGE DISP options are included to trigger a finite deformation analysis for the first four analyses. Element 10, a 4-node bilinear axisymmetric element is used. The PRINT,5 block requests printed information on change in contact status of boundary nodes. In the first analysis, the SIZING parameter reserves space for 120 elements, 150 nodes, and 60 boundary conditions. The amounts are larger than the starting model which contains 70 elements and 90 nodes. This is done so that there is freedom to increase the size of the model later using the REZONING option. The REZONING parameter is included to indicate that this may be required.

In the second analysis, the same SIZING parameter is used even though rezoning is not performed. This results in an over allocation of memory, but is insignificant for this small problem.

In the third analysis, the number of elements and nodes is not specified on the SIZING parameter, but an upper bound is defined on the ADAPTIVE option. Here, the analysis initially starts with 70 elements and 90 nodes and re-allocates memory as the adaptive meshing process occurs. Two levels of refinement are allowed; so if all elements refine, the total would be 1120 which is less than the number specified on the ADAPTIVE parameter. Note that the SIZING option specifies an upper bound on the number of boundary conditions and distributed loads.

Mesh Definition

CONNECTIVITIES and COORDINATES were brought from a preprocessor. The mesh depicted in Figure 8.12-2 is quite regular over the rectangular block. Due to symmetry, only half of the cylinder needs to be modeled.

No gap elements are used in this problem, as the contact with the rigid surfaces are governed by the CONTACT option.

Geometry

A '1' is placed in the second field to indicate that the constant dilatation formulation is used for all of the analyses, except the analysis using F^eF^p. This is not necessary using the F^eF^p procedure as a mixed variational principal is automatically used.

Boundary Conditions

Symmetry displacement boundary conditions are applied to all nodes on the axis.

Material Properties

The bolt is treated as an elastic plastic material with a Young's modulus of 17,225., Poisson's ratio of 0.35, mass density of 1., and initial yield stress of 34.45. The material workhardens from the initial yield stress up to 150 at a strain of 400% according to the piecewise linear curve entered in WORK HARD DATA.

Control Options

A formatted post file is requested every twenty increments, as well a restart file. PRINT CHOICE is used to minimize the amount of output. In the third analysis, the print out is suppressed using the NO PRINT option. Convergence control is done by relative residuals, with a tolerance of 10%.

Contact

This option defines three bodies with no friction between them. The code is expected to determine by itself a contact tolerance. (See Figure 8.12-1.)

The first body is deformable and is made out of all the elements in the model.

The second body is the top rigid surface, defined by three sets of geometrical entities. It has a reference point along the axis, and is given a translational velocity of 1 parallel to the axis of symmetry. The first geometrical entity is a straight line, the second is a concave arc of a circle, and the third is another straight line. The last line was added so that the top node on the axis would not encounter the end of the rigid surface definition.

The third body is the bottom rigid surface, defined by one set of geometrical entities. It does not need a reference point and is not given any motion. The geometrical entities are three straight lines, defined by four points.

Note how the sequence of entering the geometrical data of the second and third bodies corresponds to following the profiles of such bodies in a counterclockwise direction.

Based upon information obtained in the first two analyses, a redesign of the third body was performed such that a circular fillet was placed between what was the second and third entities. This can be seen in Figure 8.12-3. The third body now consists of three entities:

First entity is a line segment with three points

Second entity is a circle using method 2 (starting point, end point, center, and radius)

Third entity is a straight line

Load Control

The first part of the analysis was performed with a fixed TIME STEP of 0.1 in a sequence of 100 increments.

As an alternative in the second input file (e8x12b), the AUTO TIME option was used to control the time step procedure. The initial time step was 0.1 second and a maximum of 150 steps were allowed to reach a total time of 10 seconds. Only 51 increments were necessary using this procedure.

In the third analysis (e8x12c), only 60 increments using a fixed TIME STEP of 0.2 were used.

In the fourth (e8x12d) and fifth (e8x12e) analyses, the AUTO STEP option is used. The period of 12 seconds was covered. The plasticity criteria was used to control the loading as shown below:

Allowable Plasticity Change	Range
1%	$0 < \varepsilon^p < 1\%$
1%	$1\% < \varepsilon^p < 10\%$
3%	$10\% < \varepsilon^p$

Rezoning

The next increment performs a rezoning operation. A new mesh is created with a preprocessor, which covers the profile of the previously deformed mesh (Figure 8.12-4). This mesh is defined by means of CONNECTIVITY CHANGE and COORDINATE CHANGE. Both the number of elements and the number of nodes are increased. The ISOTROPIC CHANGE option is also used to extend material properties to the new elements. Similarly, the CONTACT option is repeated to account for the new element definition of the deformable body; the contact tolerance is decreased because much thinner elements were created.

One increment of deformation, with a TIME STEP of 0.05, is then executed. At this point, it is necessary to include the DISPLACEMENT CHANGE to account for the new node numbers that are located along the axis of symmetry. An extra node at the convex corner of surface 3 is fixed. This is done to allow a very coarse mesh to represent a sharp corner without cutting it.

The rest of the deformation proceeded. Twenty increments with five steps of 0.04 are completed first, followed by seventy increments of time step 0.02. The reason for decreasing the time step is that as the deformation proceeds, the height of the bolt head becomes smaller and a constant movement of the second surface would produce larger and larger strains per increment.

Adaptive

In the third problem, the adaptive meshing technique is demonstrated. Such that the first 50 elements are enriched based upon the contact criteria. That is, if nodes associated with these elements come into contact, the element is refined. A limit of two levels of refinement is prescribed.

Results

Figure 8.12-5 through Figure 8.12-7, show the contour plots of the equivalent plastic strain, the equivalent von Mises stress, and the average stress in the deformed configuration before rezoning. The block completely fills the bottom surface and is folding into the top surface. The need to rezone stems from the fact that soon there will be too few nodes in the free surface that have to fit in the narrow gap between the two rigid bodies. The rezoning method allows us to represent the material flash. Comparison of Figure 8.12-6 with the results obtained using the F^eF^p method in Figure 8.12-14 indicate a very close agreement between the von Mises stresses obtained from the two theories as expected since the elasticity is small.

Virtually all the deformation takes place in the part of the block above the bottom surface.

Figure 8.12-8 through Figure 8.12-10 show the same contour plots in the final deformed configuration. At this stage, the full shape of the head of the bolt has been acquired by the original block and flash formed in the gap between surfaces. The strains are very concentrated in the part which folded on the bottom surface. The von Mises stress shows that the bottom cavity is elastic at the end of deformation.

The progression of the deformed adaptive mesh is shown in Figure 8.12-11 through Figure 8.12-13, for increments 20, 40, and 60, respectively. You can observe that, based upon the adaptive criteria, additional elements are formed as the workpiece comes into contact with the dies. At the end of the analysis, there are 187 elements and 250 nodes. Based upon this analysis, perhaps you would perform the analysis also with an adaptive criteria based upon strain energies or plastic strains.

The printed results of an analysis with the contact option include general information about rigid surfaces, such as the updated position of the reference point, the velocity of the surface, the loads on the surface, as well as the moment with respect to the reference point.

Parameters, Options, and Subroutines Summary

Example e8x12.dat:

Parameters	Model Definition Options	History Definition Options	Rezone Options
END	CONNECTIVITY	AUTO LOAD	CONNECTIVITY CHANGE
FINITE	CONTACT	CONTINUE	CONTACT CHANGE
LARGE DISP	CONTROL	DISPLACEMENT CHANGE	CONTINUE
PRINT	COORDINATES	TIME STEP	COORDINATE CHANGE
REZONE	END OPTION		END REZONE
SIZING	FIXED DISP		ISOTROPIC CHANGE
TITLE	GEOMETRY		REZONE
UPDATE	ISOTROPIC		
	POST		
	PRINT CHOICE		
	RESTART		
	WORK HARD		

Example e8x12b.dat:

Parameters	Model Definition Options	History Definition Options
END	CONNECTIVITY	AUTO TIME
FINITE	CONTACT	CONTINUE
LARGE DISP	CONTROL	
PRINT	COORDINATES	
SIZING	END OPTION	
TITLE	FIXED DISP	
UPDATE	GEOMETRY	
	ISOTROPIC	
	POST	
	PRINT CHOICE	
	WORK HARD	

Example e8x12c.dat:

Parameters	Model Definition Options	History Definition Options
ADAPTIVE	ADAPTIVE	AUTO LOAD
END	CONNECTIVITY	CONTINUE
FINITE	CONTACT	TIME STEP
LARGE DISP	CONTROL	
PRINT	COORDINATES	
TITLE	END OPTION	
UPDATE	FIXED DISP	
	GEOMETRY	
	ISOTROPIC	
	POST	
	PRINT CHOICE	
	WORK HARD	

Example e8x12d.dat:

Parameters	Model Definition Options	History Definition Options
END	CONNECTIVITY	AUTO STEP
FINITE	CONTACT	CONTINUE
LARGE DISP	CONTROL	
PRINT	COORDINATES	
TITLE	END OPTION	
UPDATE	FIXED DISP	
	GEOMETRY	
	ISOTROPIC	
	POST	
	PRINT CHOICE	
	WORK HARD	

Example e8x12e.dat:

Parameters	Model Definition Options	History Definition Options
END	CONNECTIVITY	AUTO STEP
PLASTICITY	CONTACT	CONTINUE
PRINT	CONTROL	
TITLE	COORDINATES	
	END OPTION	
	FIXED DISP	
	ISOTROPIC	
	POST	
	WORK HARD	

Example e8x12r.dat:

Parameters	Model Definition Options	History Definition Options	Rezone Options
END	CONNECTIVITY	CONTINUE	CONNECTIVITY CHANGE
FINITE	CONTACT	DISP CHANGE	CONTACT CHANGE
LARGE DISP	CONTROL		CONTINUE
PRINT	COORDINATE		COORDINATE CHANGE
REZONE	END OPTION		END REZONE
TITLE	FIXED DISP		ISOTROPIC CHANGE
UPDATE	GEOMETRY		
	ISOTROPIC		
	POST		
	PRINT CHOICE		
	RESTART		
	WORK HARD		

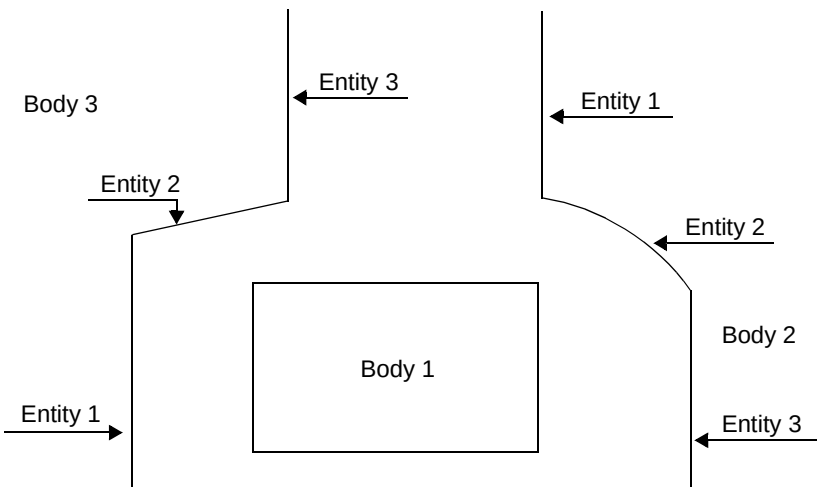

Figure 8.12-1 Model

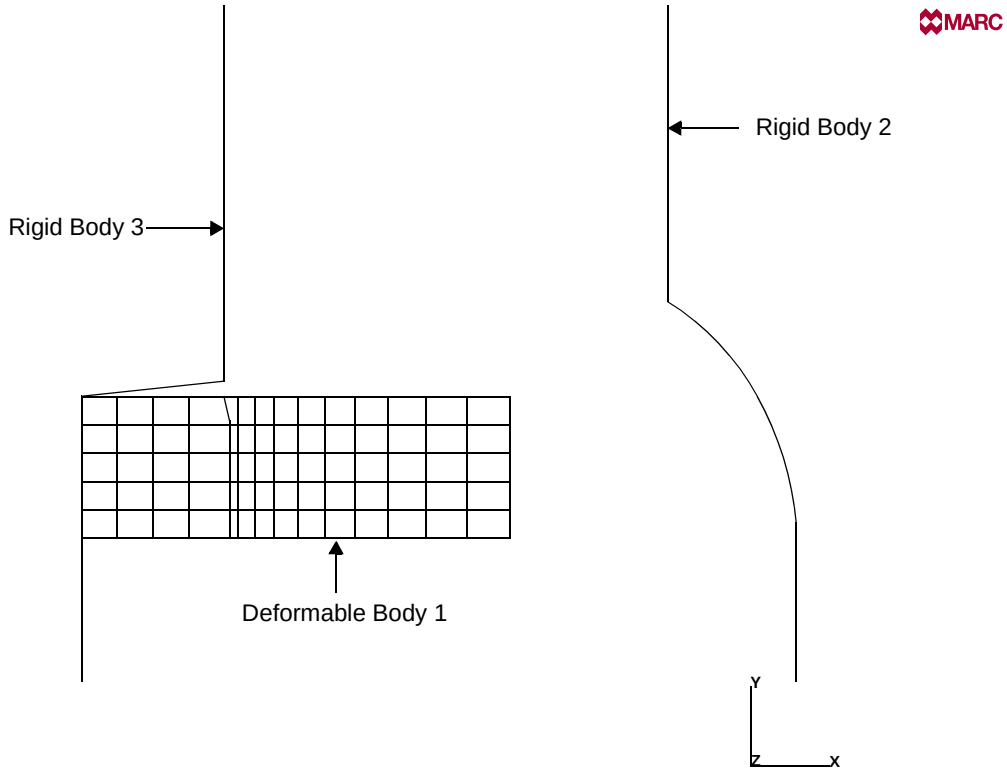

Figure 8.12-2 Initial Mesh

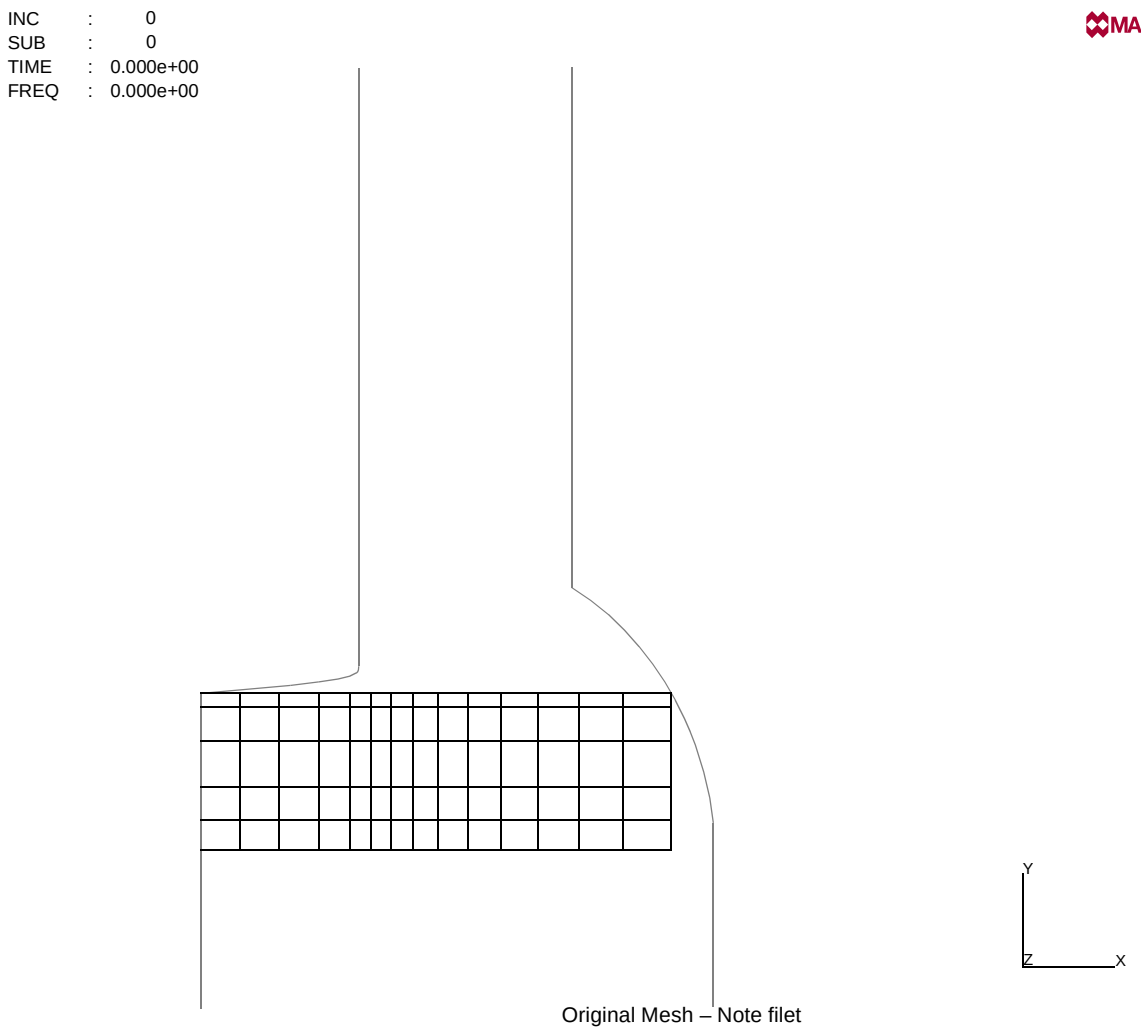

Figure 8.12-3 Initial Mesh with Modified Rigid Body 3 for Adaptive Analysis

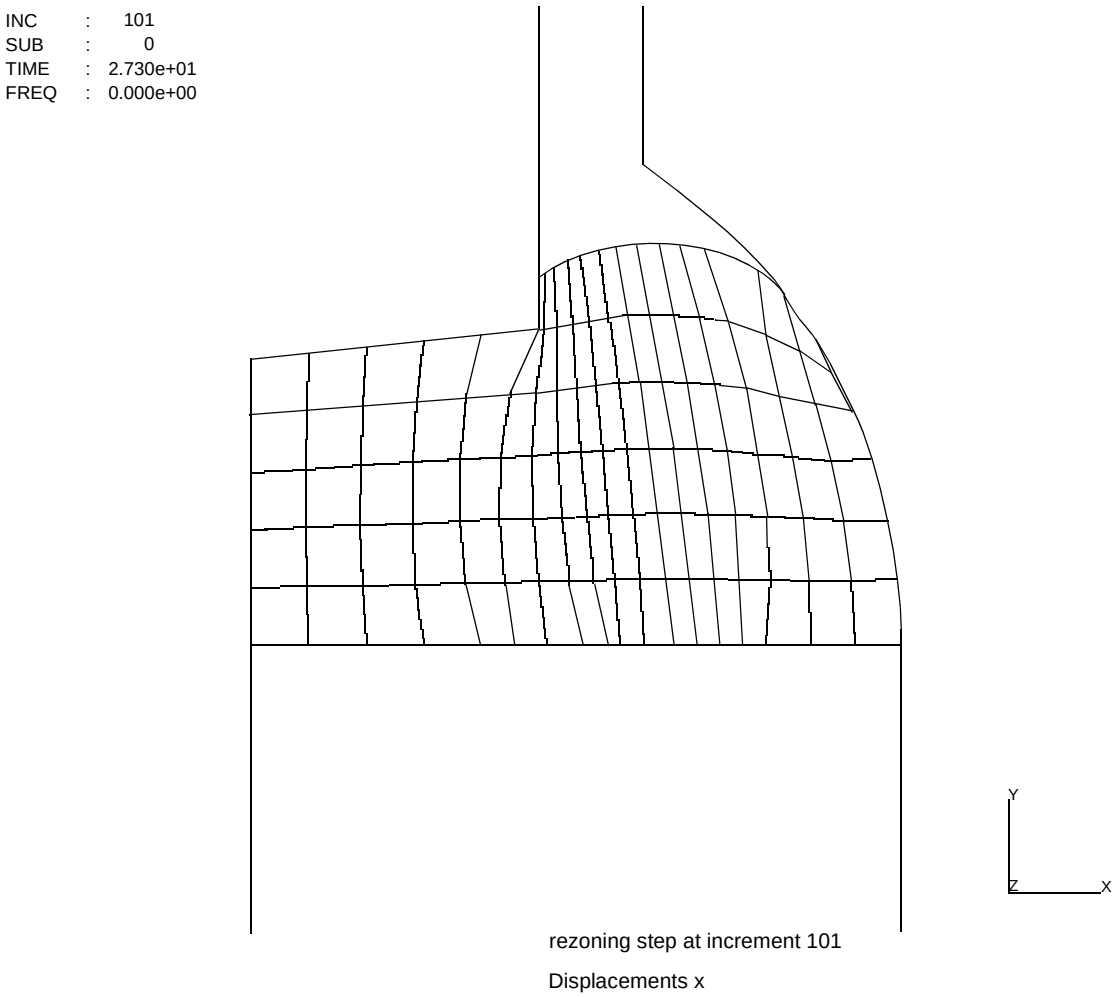

Figure 8.12-4 Rezoning Mesh

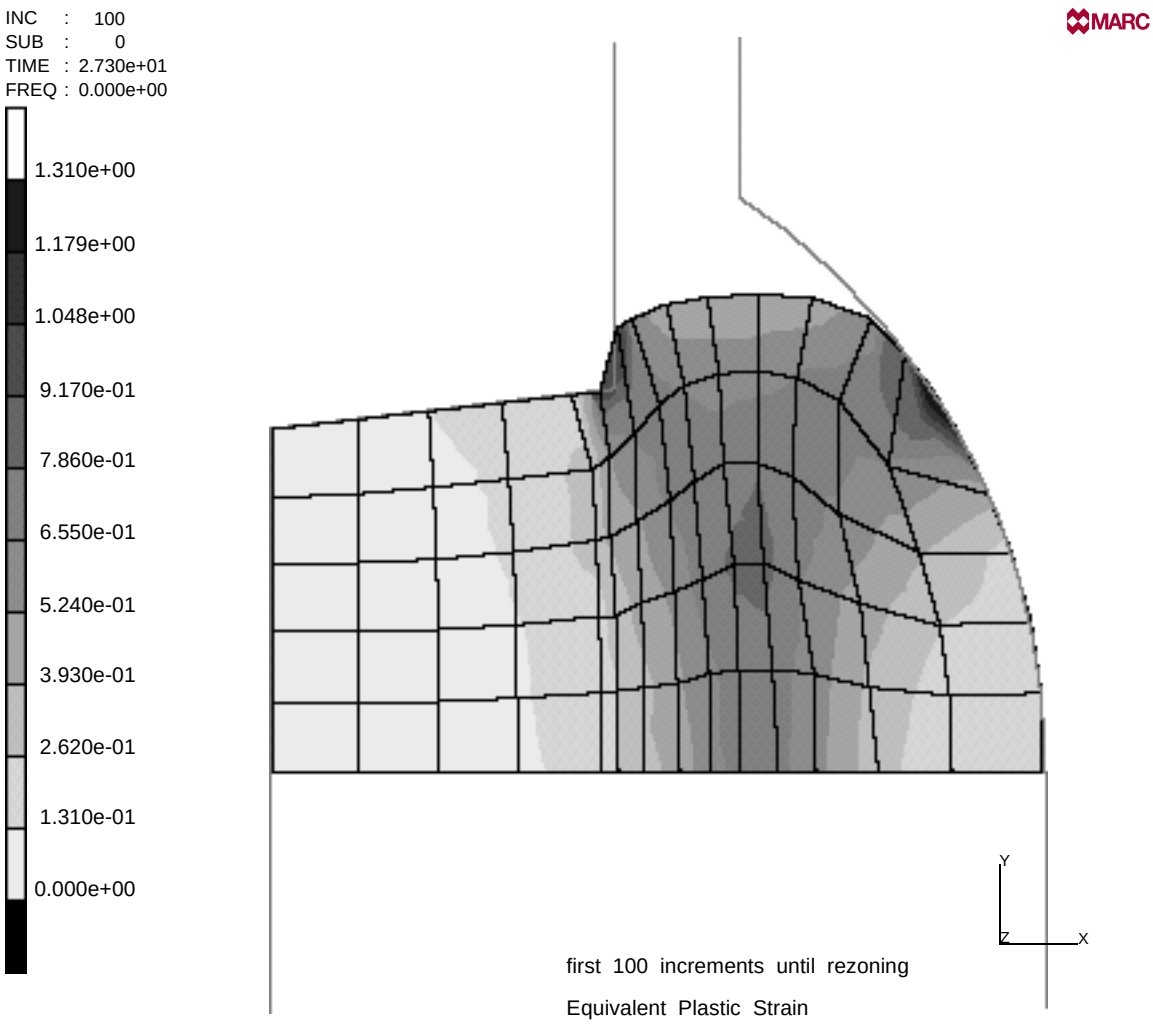

Figure 8.12-5 Equivalent Plastic Strain until Rezoning

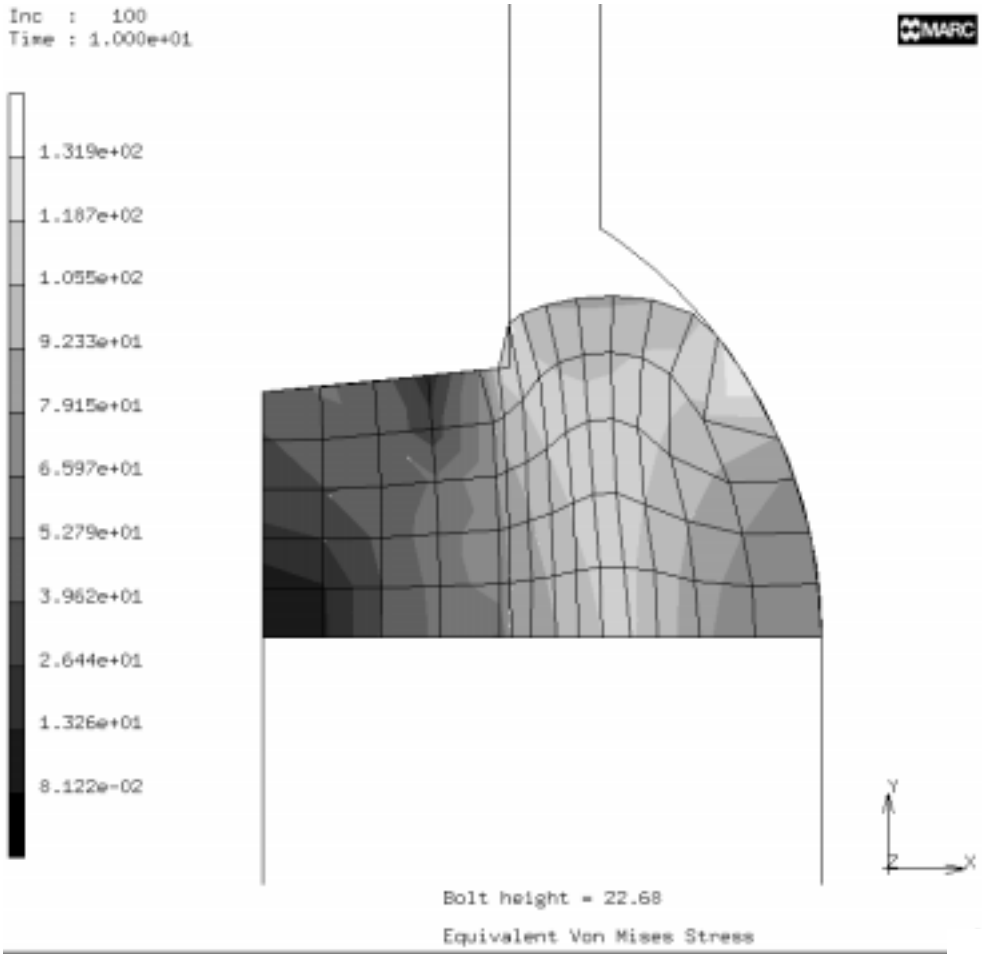

Figure 8.12-6 Equivalent Mises Tensile Stress at Bolt Height = 22.68

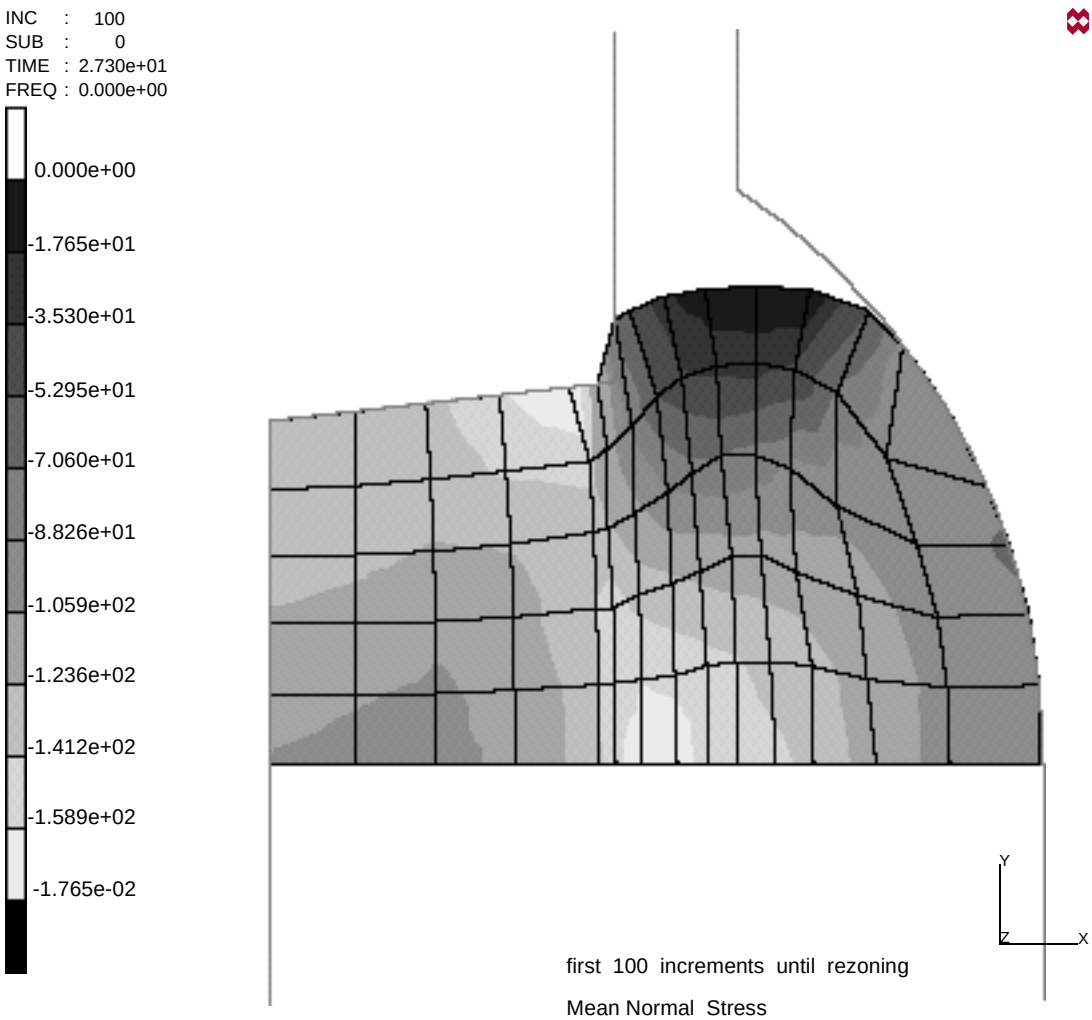

Figure 8.12-7 Mean Normal Stress Until Rezoning

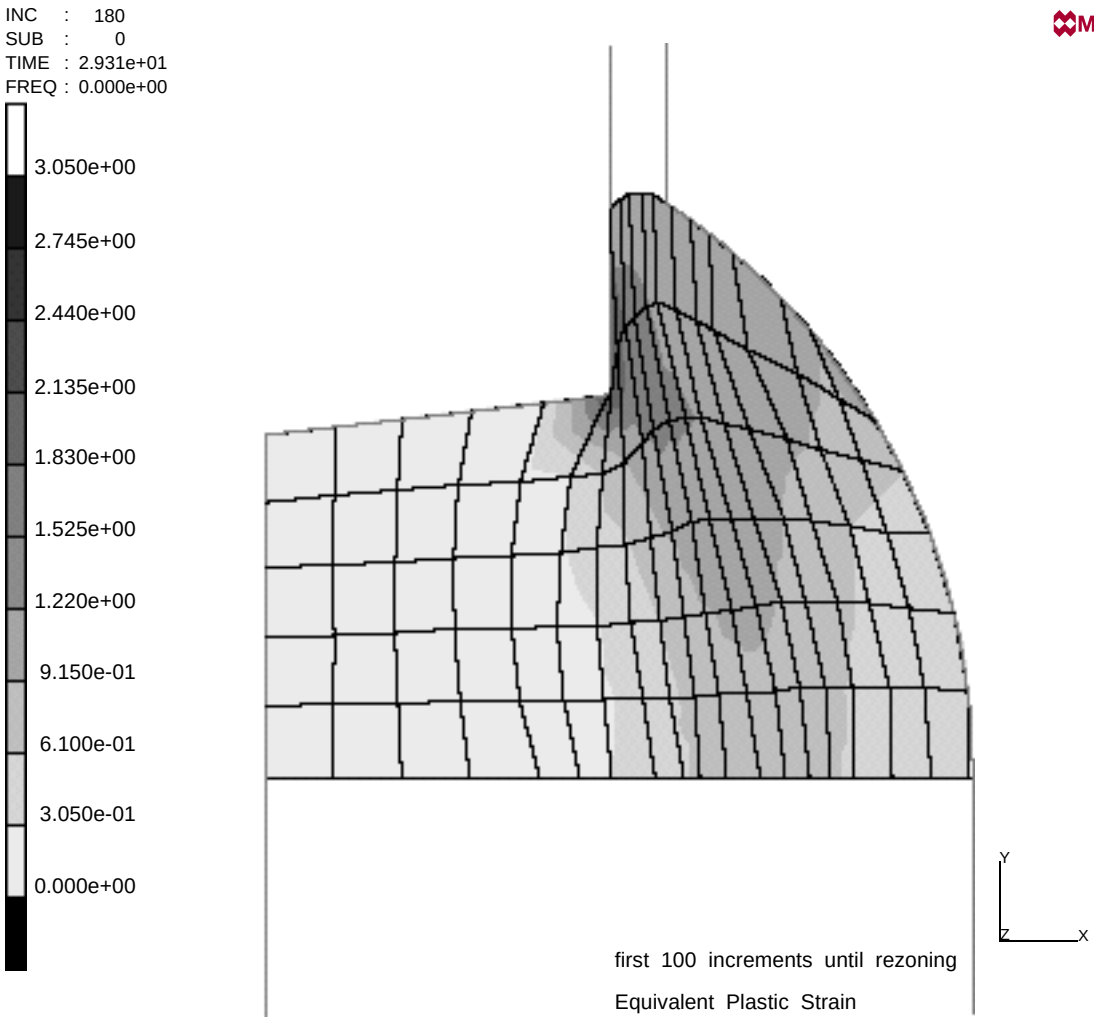

Figure 8.12-8 Final Equivalent Plastic Strain

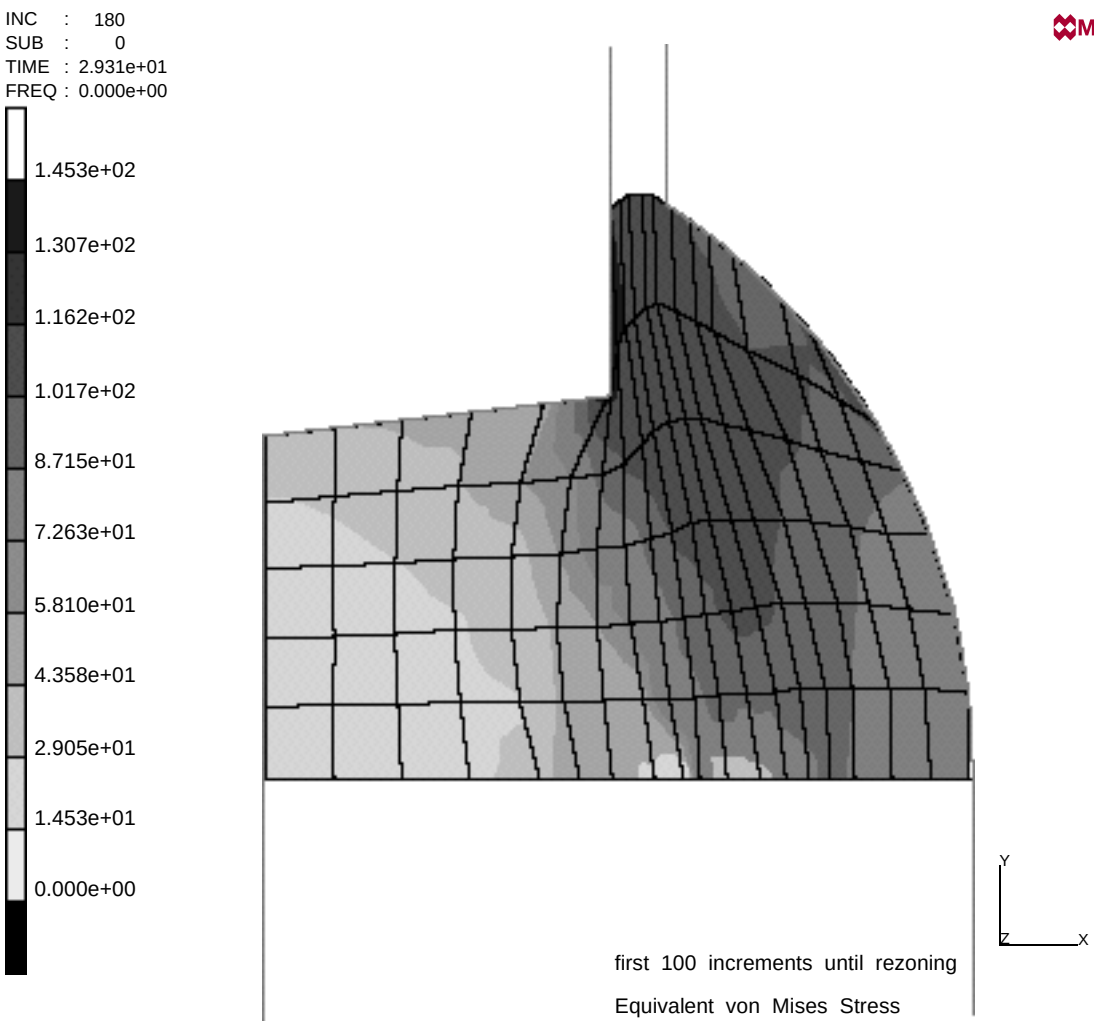

Figure 8.12-9 Final Equivalent von Mises Tensile Stress

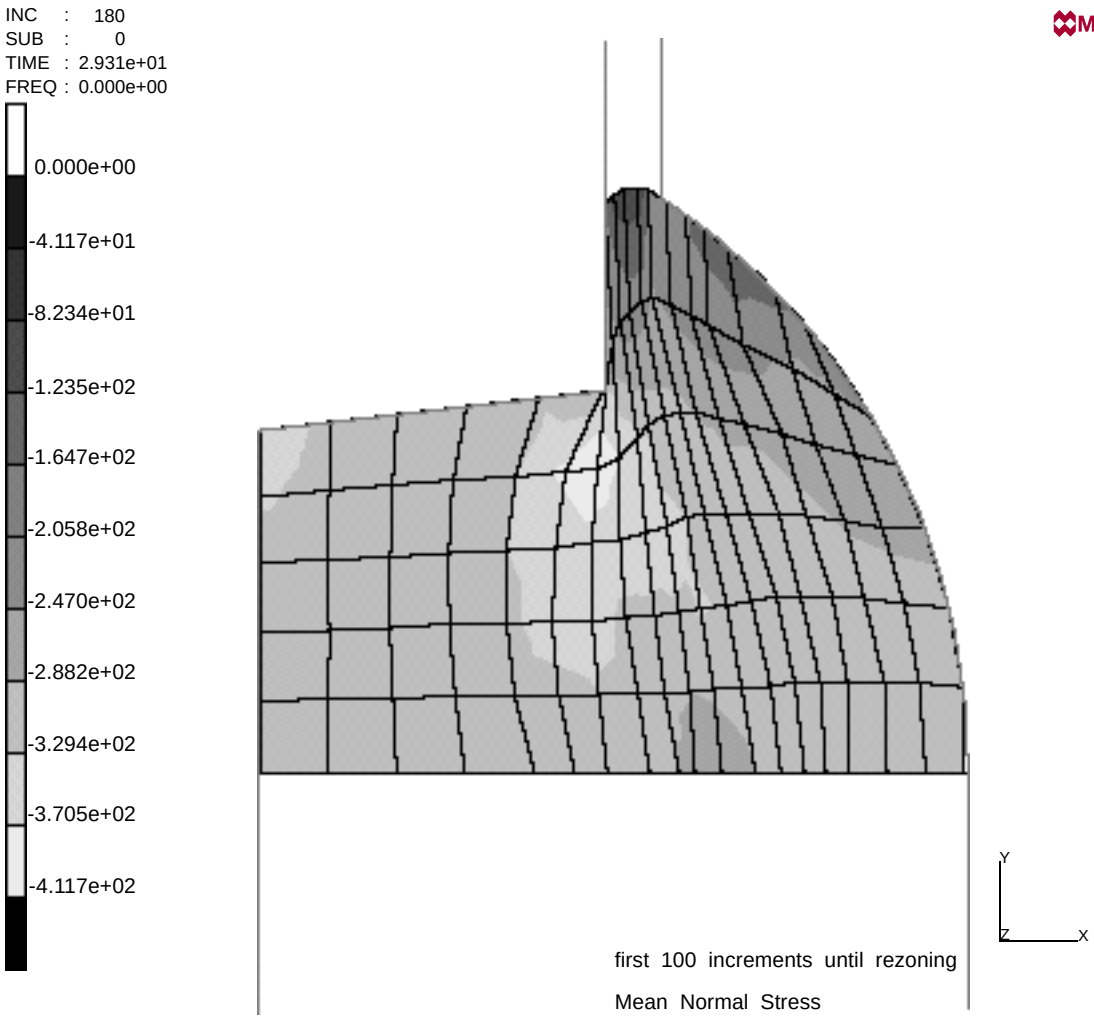

Figure 8.12-10 Final Mean Normal Stress

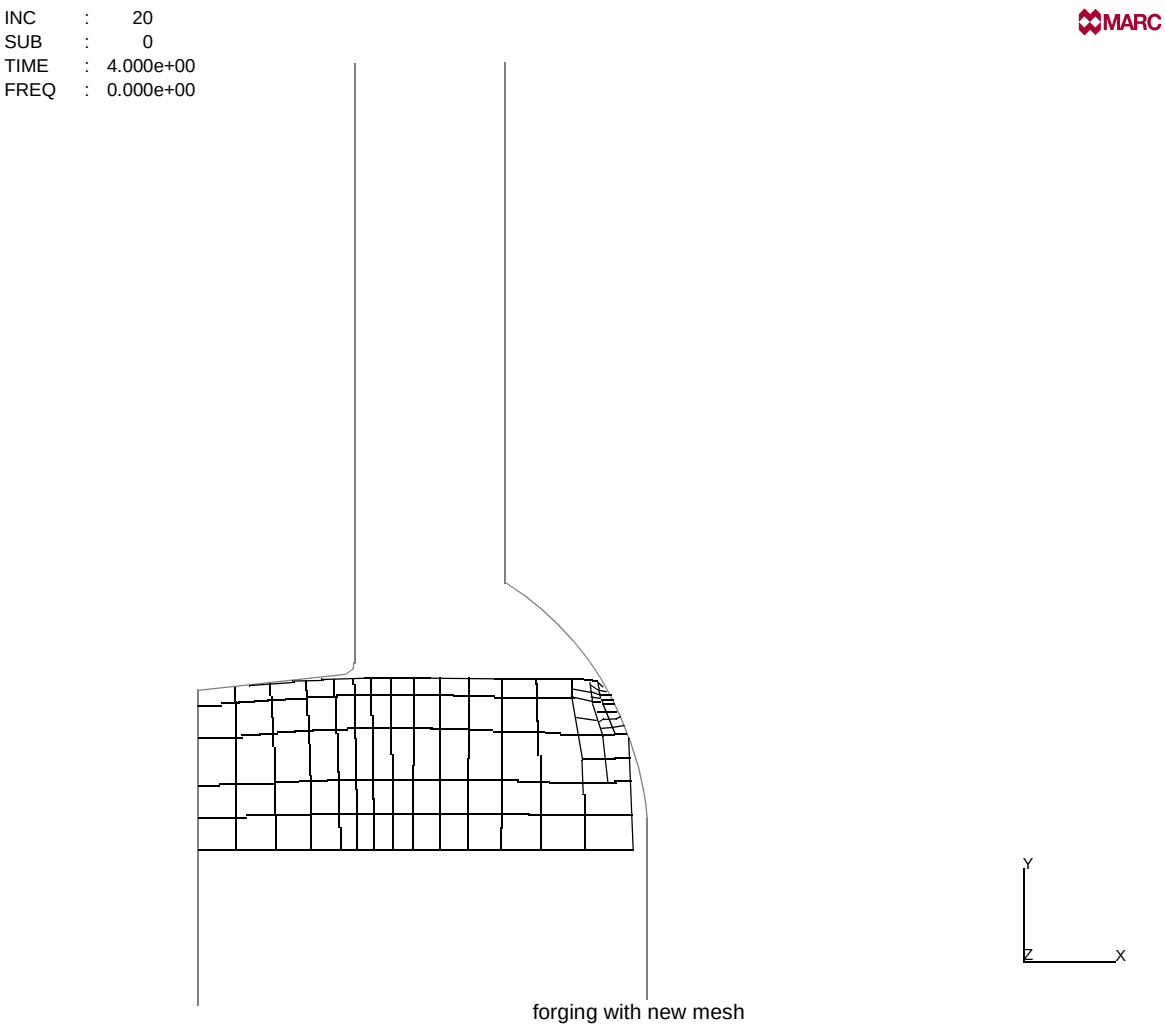

Figure 8.12-11 Adapted Mesh at Increment 20

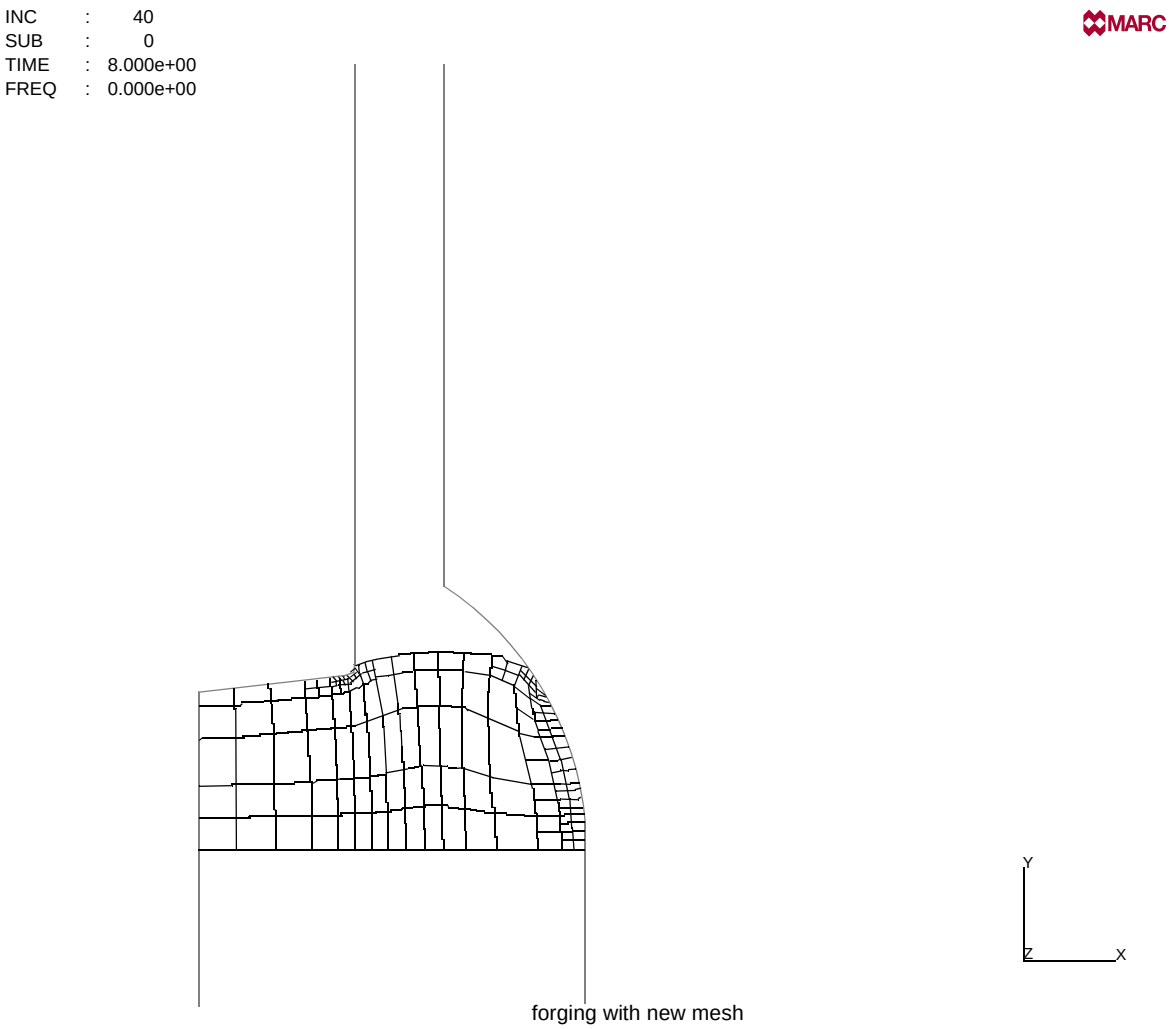

Figure 8.12-12 Adapted Mesh at Increment 40

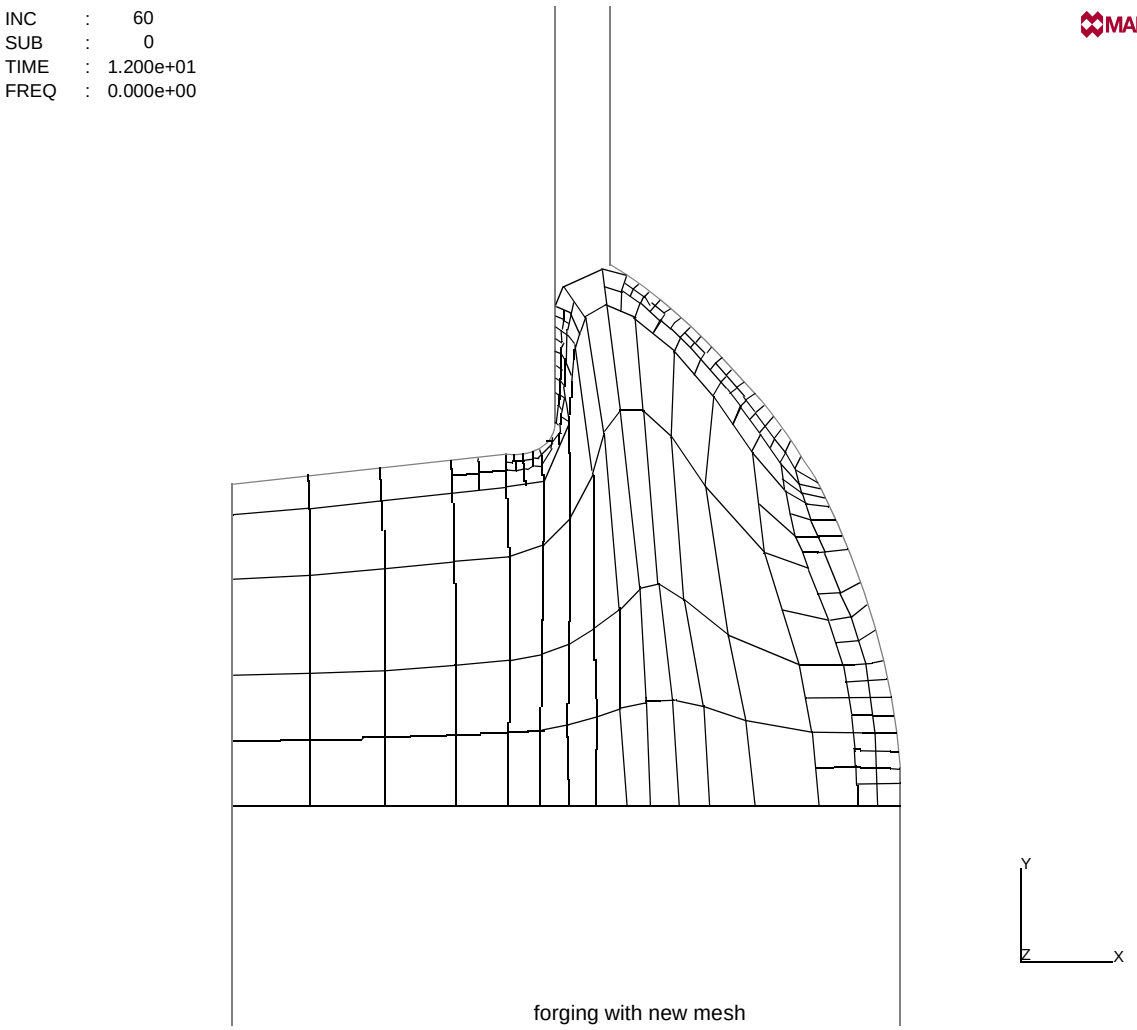

Figure 8.12-13 Adapted Mesh at Increment 60

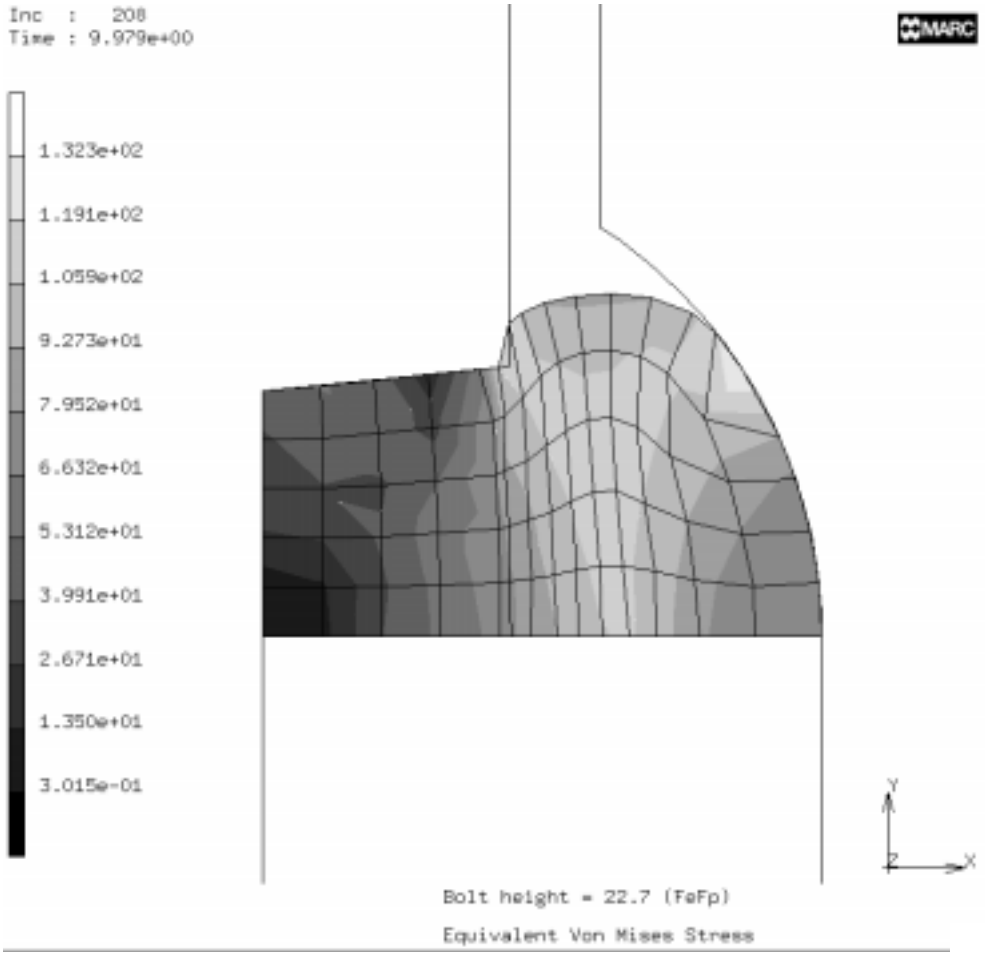

Figure 8.12-14 Equivalent Mises Tensile Stress at Bolt Height = 22.7 (F^eF^p)

8.13 Coupled Analysis of Ring Compression

This example demonstrates MARC's ability to perform a large deformation problem, incorporating thermal mechanical coupling and automated contact.

A ring of aluminum is deformed by a block of steel. Both have the capacity to deform, and possibly, slide between each other.

Coupling

There are several sources of coupling in this analysis.

1. As the temperature changes, thermal stresses are developed due to nonzero coefficient of thermal expansion.
2. As the temperature changes, the mechanical properties change. It happens in this case because of the temperature-dependent flow stress.
3. As the geometry changes, the heat transfer problem changes. This includes changes in the contacting interface.
4. As plastic work is performed, internal heat is generated.
5. As the bodies slide, friction generates heat.

Parameters

The UPDATE, FINITE, and LARGE DISP parameters indicate this is a finite deformation analysis.The COUPLE option is used to indicate that a coupled thermal-mechanical analysis is being performed. A four-node bilinear axisymmetric element is used. The PRINT,5 option requests additional information in the output regarding nodes acquiring or losing contact.

Mesh Definition

Mentat was used to determine the CONNECTIVITY and COORDINATES of the mesh. There are separate nodes along both sides of the contact interface so that sliding is possible. Due to symmetry, only one quarter of the region is modeled. The mesh is shown (with the units in mm) in Figure 8.13-1. In a coupled analysis, a displacement element automatically produces the coupled (displacement-temperature) formulation to be used.

This analysis is performed using both element type 10 and element type 116. Both elements are four-node axisymmetric elements. Element type 116 uses a single integration point and an hourglass stiffness stabilization procedure.

No gap elements are used. Free surfaces can have convection heat transfer to the environment. As soon as contact is detected, a contact thermal barrier, defined by means of a film coefficient, starts operating.

Geometry

A ‘1’ is placed in the second field to indicate that the constant dilatation formulation is used. This is not necessary for the analysis using element type 116.

Boundary Conditions

Symmetry displacement boundary conditions are imposed on the ring meridian plane and on the block axis. The block is moved down by application of displacement boundary conditions to the face opposite to the contact face. Space for such boundary conditions is reserved in the model definition section. The displacement boundary conditions are entered in the FIXED DISPLACEMENT option. On the outside surface of the block, the temperature is constrained to 20°C, to simulate a much larger size block. This is done with the FIXED TEMPERATURE option.

Control Options

A formatted post file containing stress components and effective plastic strain is written at the end of 50 increments. The NO PRINT option limits the amount of output to a minimum. Displacement control is used in the deformation part of the analysis with a relative error of 15%. As far as the heat transfer part of the analysis is concerned, a 10°C maximum error in temperature estimate is entered. Even if thermal material properties are not temperature-dependent, this provides a means of forcing recycling when heat transfer between two bodies produces large variations of temperature per increment.

Initial Conditions

The ring is given an initial temperature of 427°C, and the block is given an initial temperature of 20°C.

Material Properties

The ring is treated as an elastic-plastic material with a Young’s modulus of 1000 N/mm^2, a Poisson’s ratio of 0.33, a mass density of 1.0g/mm^3, a coefficient of thermal expansion of 1.3 x 10^{-5} mm/mm°C, and an initial yield stress of 3.4 N/mm^2, corresponding to a reference temperature of 200°C. The material workhardens from the initial yield stress to a yield stress of 5.78 N/mm^2 for strains above 70%, according to a piecewise linear function entered via WORK HARD DATA. The flow stress decreases with temperature increases at a rate of 0.007 N/mm^2 per degree. The thermal properties are conductivity of 242.0 N/s°C and specific heat of 2.4255 Nmm/g°C.

The block is treated as an elastic material with a Young’s modulus of 100,000 N/mm^2, a Poisson’s ratio of 0.33 and a mass density of 1 g/mm^3. The thermal properties are conductivity of 19.0 N/s°C and specific heat of 3.77 Nmm/g°C.

Distributed Flux

This distributed flux block is used to indicate that internal heat is generated due to plastic deformation.

Convert

The option is used to give the conversion factor between the mechanical energy and the thermal energy.

The internal volumetric flux per unit volume becomes:

$$\phi = cw^p$$

where w^p is the plastic strain energy density.

Contact

The CONTACT option declares that there are two bodies with adhesive friction between them. MARC calculates both the contact tolerance and the sticking tolerance.

The first body is deformable and is made of the elements of the ring. There is no need to specify any motion. The ring's free surfaces have convection heat transfer defined by a film coefficient of 0.01, and a sink temperature of 20°C. The second body is also deformable and made out of the elements of the block. A reference point and an axial velocity are given, although they are not used in the calculations; this is done as a reminder of what the imposed boundary conditions are simulating. A friction factor of 1.0 defines the interface friction conditions, based on the cohesive model. The block's free surfaces have convection heat transfer defined by a film coefficient of 0.01 N/s-mm°C, and a sink temperature of 20°C. The contact surfaces have a thermal barrier defined by a film coefficient of 35.

This ordering of the two bodies results in imposing the constraint so that the nodes of the ring do not penetrate the surface of the block. Friction and thermal barrier at the interface use data taken from the body defining the block.

Load Control

This problem is performed with a fixed time step and fixed increment size. It is specified with a time step of 0.0003 seconds with a total of 0.03 seconds requested. Each increment imposes a displacement of 0.045mm to the nodes of the block in the plane opposed to the contact surface. This displacement increment is declared in DISP CHANGE and not in the original boundary conditions because the CONTACT option always bypasses increment zero.

In a coupled analysis, if an adaptive time stepping is required, the AUTO TIME option should be invoked. This option is demonstrated in the second analysis. Using AUTO TIME, it is requested that a maximum of 100 increments be used. The analysis used only 26 increments as there are very few changes in the contact surface.

Results

Figure 8.13-2 shows the deformed body at the end of 100 increments compounding to 50% reduction in height of the ring. Due to the high friction, the ring folds several times into the block on both sides, and there is an increase of the outer diameter as well as a decrease of the inner diameter. It can be seen that the amount of interface sliding is very small, also due to the high friction. Elastic deformations on the block are not visible, therefore it looks like the block had a rigid body translation.

Figure 8.13-3 shows equivalent plastic strain contours produced on the ring. They range from small amounts in the middle of the contact area (neutral zone) and in the free surface, to very large amounts at the corners where folding took place, and in the center of the middle plane.

In Figure 8.13-4, the equivalent von Mises stresses give an idea of the stresses produced in the block, which are higher than in the ring. They increase from low values in the free standing areas towards the center. Local peaks in the friction shearing zones also appear.

The thermal part of the analysis produces the temperatures of Figure 8.13-5. The total time for the deformation is only 0.03 seconds. Therefore, all the effects are confined to the contact region. Aluminum's high temperature, low flow stress produces no noticeable heating due to plastic deformation. On the ring side, the temperature decreases about 75°C at the interface, while the block heats around 50°C. Steel's lower conductivity produces steeper temperature gradients.

Parameters, Options, and Subroutines Summary

Example e8x13.dat:

Parameters	Model Definition Options	History Definition Options
COUPLE	CONNECTIVITY	CONTINUE
ELEMENT	CONTACT	DISP CHANGE
END	CONTROL	TRANSIENT
FINITE	CONVERT	
LARGE DISP	COORDINATE	
PRINT	DIST FLUXES	
SIZING	END OPTION	
TITLE	FIXED DISP	
UPDATE	FIXED TEMPERATURE	
	GEOMETRY	
	INITIAL TEMPERATURE	
	ISOTROPIC	
	NO PRINT	
	POST	
	TEMPERATURE EFFECTS	
	WORK HARD	

Example e8x13b.dat:

Parameters	Model Definition Options
COUPLE	CONNECTIVITY
ELEMENT	CONTACT
END	CONTROL
FINITE	CONVERT
LARGE DISP	COORDINATE
PRINT	DIST FLUXES
SIZING	END OPTION
TITLE	FIXED DISP
UPDATE	FIXED TEMPERATURE
	GEOMETRY
	INITIAL TEMPERATURE
	ISOTROPIC
	NO PRINT
	POST
	TEMPERATURE EFFECTS
	WORK HARD

Example e8x13c.dat:

Parameters	Model Definition Options	History Definition Options
ALIAS	CONNECTIVITY	CONTINUE
COUPLE	CONTACT	DISP CHANGE
ELEMENT	CONTROL	TRANSIENT
END	CONVERT	
FINITE	COORDINATE	
LARGE DISP	DIST FLUXES	
PRINT	END OPTION	
SIZING	FIXED DISP	
TITLE	FIXED TEMPERATURE	
UPDATE	GEOMETRY	
	INITIAL TEMPERATURE	
	ISOTROPIC	
	NO PRINT	
	POST	
	TEMPERATURE EFFECTS	
	WORK HARD	

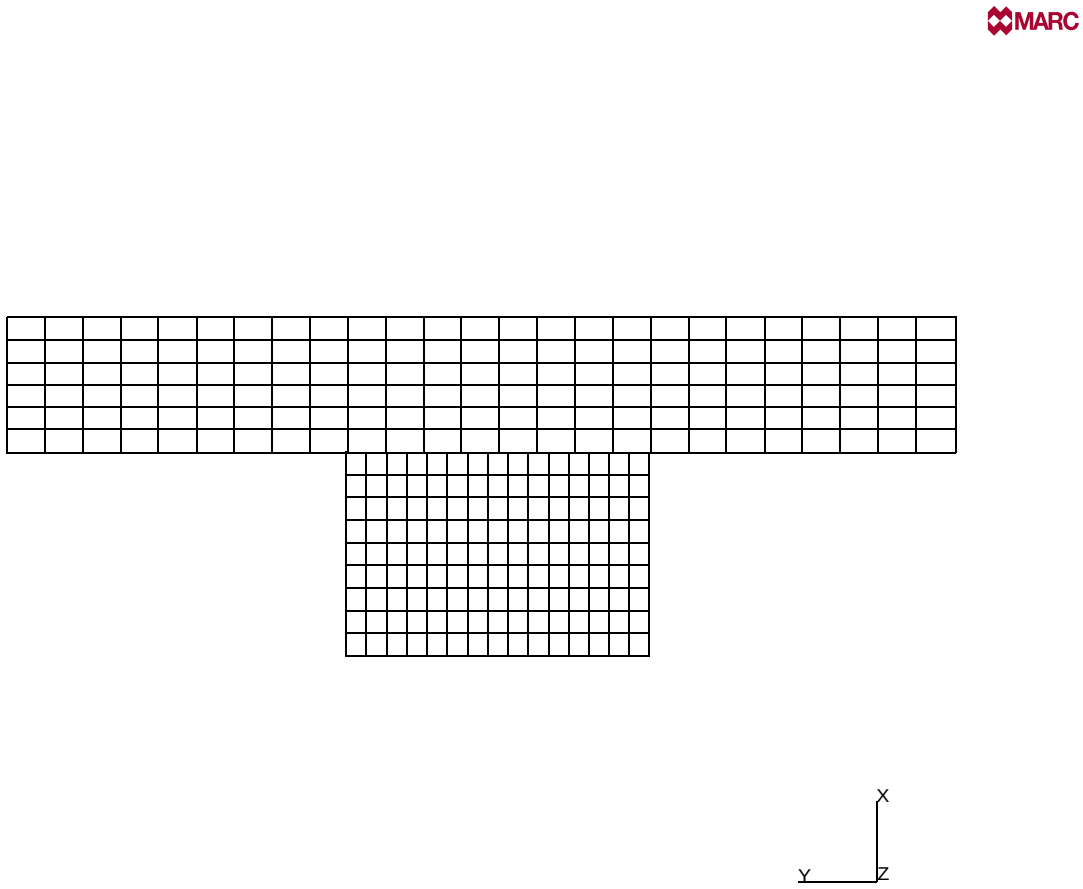

Figure 8.13-1 Original Mesh

INC : 100
SUB : 0
TIME : 3.000e-02
FREQ : 0.000e+00

MARC

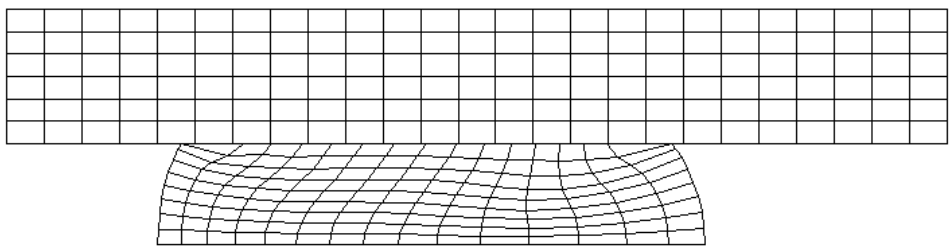

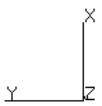

prob e8.13 coupled analysis of ring compression
Displacements x

Figure 8.13-2 Deformed Mesh (50% Height Reduction)

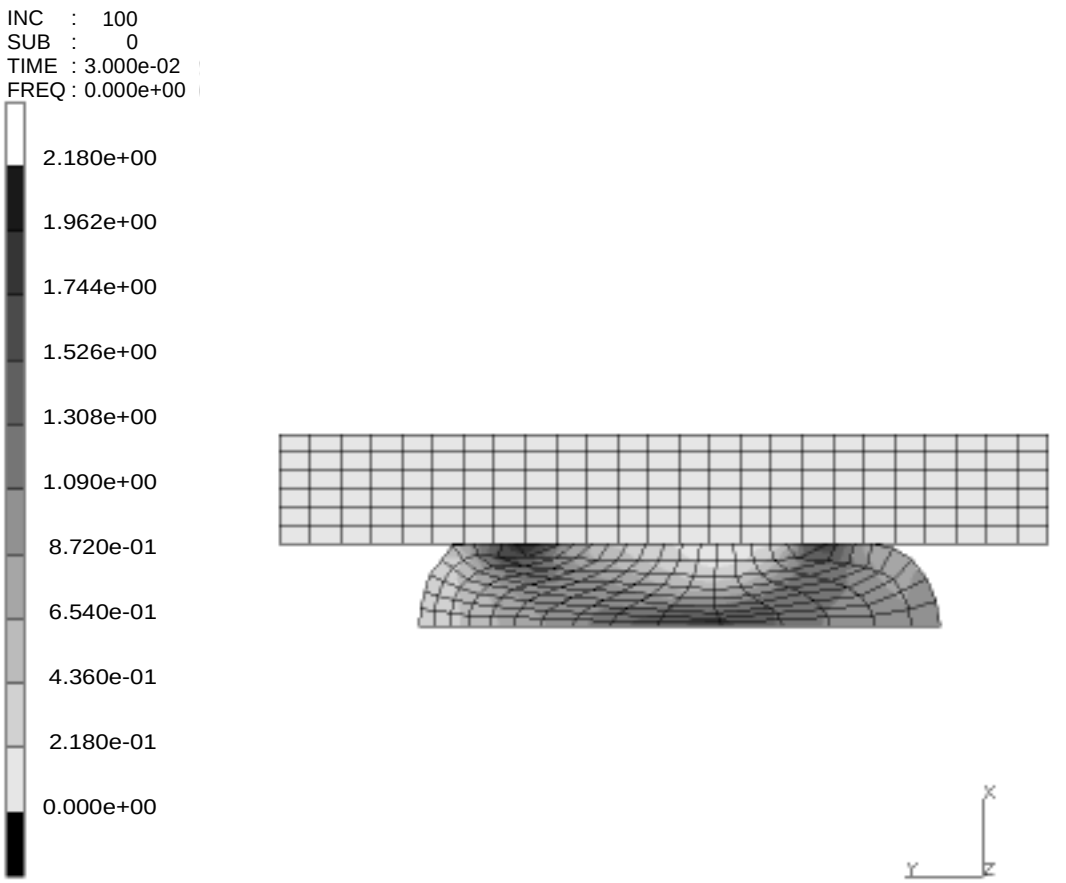

Figure 8.13-3 Equivalent Plastic Strain

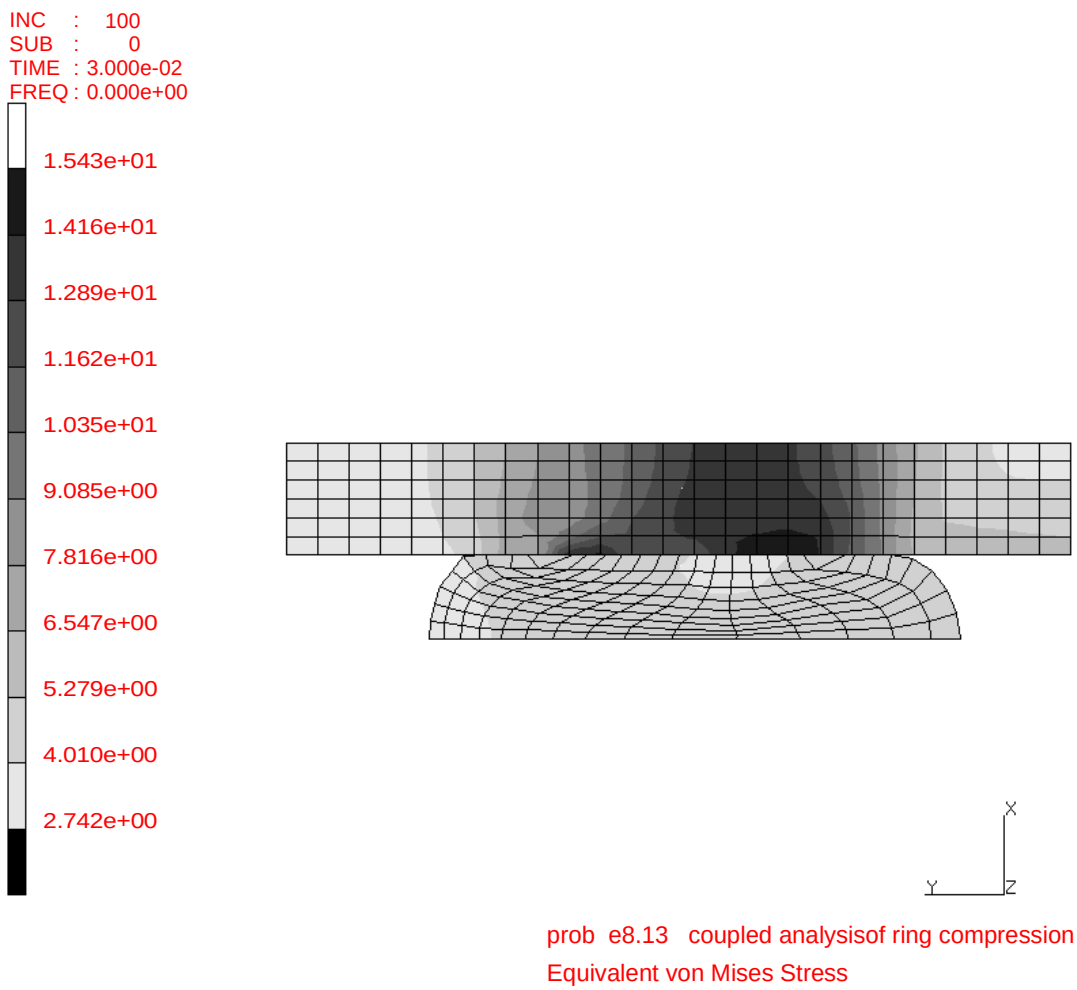

Figure 8.13-4 Equivalent von Mises Tensile Stress

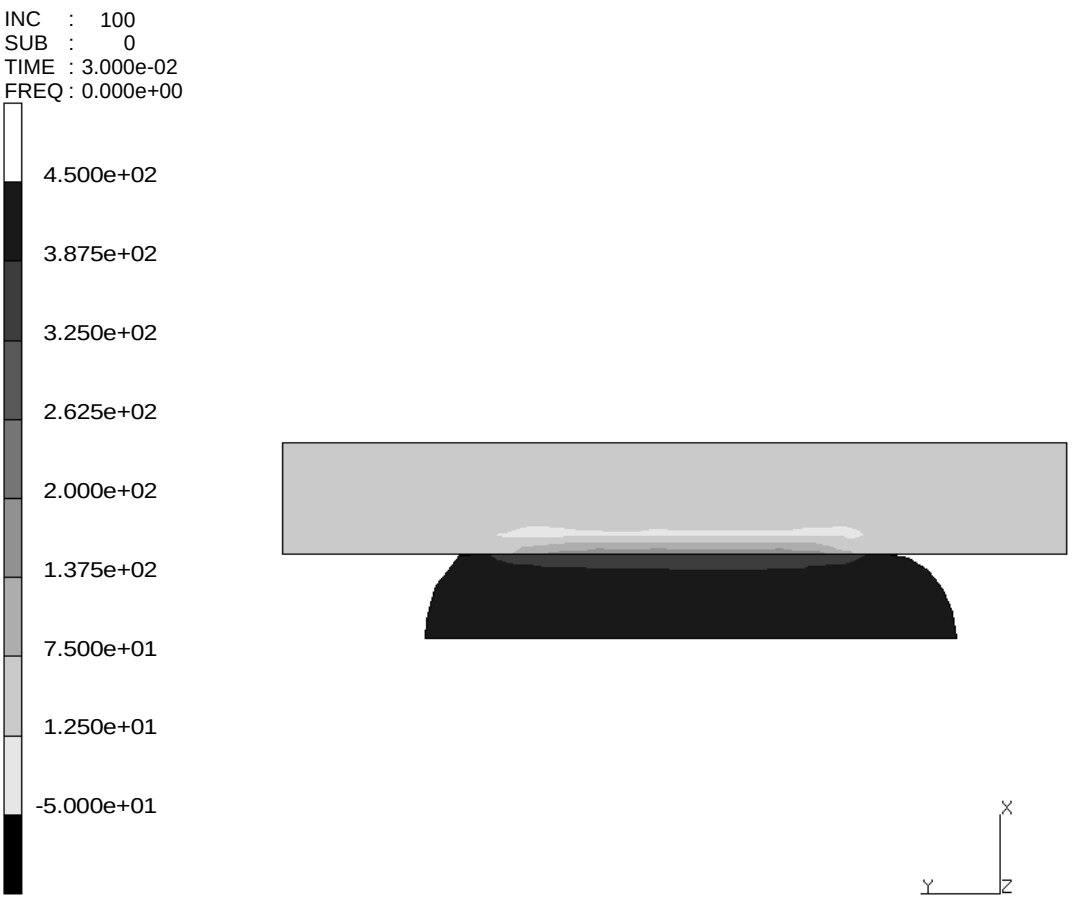

Figure 8.13-5 Total Nodal Temperature

8.14 3D Contact with Various Rigid Surface Definitions

This problem demonstrates MARC's ability to perform contact analysis between a deformable body and a rigid die described through various surface definitions. It also demonstrates MARC's ability to perform contact analysis between a flexible body and a rigid die described through the NURBS definition.

Parameters

The UPDATE, FINITE, and LARGE DISP parameters are included in the parameter section to indicate that this is a finite deformation analysis. The PRINT,5 option requests additional information in the output regarding nodes acquiring or losing contact.

Geometry

A '1' is placed in the second data field to indicate that the constant dilatation formulation is used. This is particularly useful for analysis of approximately incompressible materials and for structures in the fully plastic range.

Boundary Conditions

To prevent rigid body motions, several nodes are restrained from displacing in the global x-, y-, z-directions. These constraints are given through the FIXED DISP option.

POST/PRINT Control

It is requested that the E_{xx} strain (post code 1) be written onto a formatted post file. The NO PRINT option limits the amount of printed output to a minimum.

Control

A maximum of 200 increments is allowed, with no more than 20 recycles per increment. Displacement control is used, with a relative error of 10%. However, keep in mind that control parameters under the CONTACT option set generally govern the convergence of the problem.

Material Properties

The material for all elements is treated as an elastic-perfectly plastic material, with Young's modulus of 1.75E+07 psi, Poisson's ratio of .3, and an initial yield stress of 35,000 psi.

Contact

The CONTACT option declares that there are two bodies in contact with no friction between them. The distance tolerance is specified as 0.005 inches. The reaction and velocity tolerances is computed by MARC. A die velocity of -0.3 in/sec in the global z-direction constitutes the driving motion for this problem.

Load Control

This problem is loaded by the application of number of increments specified in the AUTO LOAD option of the prescribed die velocities in the CONTACT option. The load increment is applied once.

Die Surface Definitions

The only difference between problems e8x14a, b, c, d, and e is the type of surface defined for the rigid die. In data set 14a, it is a 3D ruled surface with straight line generators. In 14b, it is again a ruled surface with circular arc generators. In 14c, it is a surface of revolution. In 14d, it is a 4-node patch. Finally, in 14e, a 3D polysurface defines the rigid die.

In e8x14f, the second body is described by NURBS. The '1' in the fifth field (surface definition) indicates the analytical form of NURBS is used to implement contact conditions. If '0' is entered in the field, the surface is still divided into 4-node patches and uses the piecewise linear approach to do the analysis.

The NURBS is defined by 9 x 5 control points with four cubic degrees along the u- and v-directions. The surface is divided into 20 x 5 patches for visualization.

Results

Figure 8.14-2 shows the deformed body at the end of increment one with the deformation at the same scale as the coordinates.

Parameters, Options, and Subroutines Summary

Example e8x14a.dat:

Parameters	Model Definition Options	History Definition Options
ELEMENT	CONNECTIVITY	AUTO LOAD
END	CONTACT	CONTINUE
FINITE	CONTROL	TIME STEP
LARGE DISP	COORDINATE	
PRINT	END OPTION	
SIZING	FIXED DISP	
TITLE	GEOMETRY	
UPDATE	ISOTROPIC	
	NO PRINT	
	POST	

Example e8x14b.dat:

Parameters	Model Definition Options	History Definition Options
ELEMENT	CONNECTIVITY	AUTO LOAD
END	CONTACT	CONTINUE
FINITE	CONTROL	TIME STEP
LARGE DISP	COORDINATE	
PRINT	END OPTION	
SIZING	FIXED DISP	
TITLE	GEOMETRY	
UPDATE	ISOTROPIC	
	NO PRINT	
	POST	

Example e8x14c.dat:

Parameters	Model Definition Options	History Definition Options
ELEMENT	CONNECTIVITY	AUTO LOAD
END	CONTACT	CONTINUE
FINITE	CONTROL	TIME STEP
LARGE DISP	COORDINATE	
PRINT	END OPTION	
SIZING	FIXED DISP	
TITLE	GEOMETRY	
UPDATE	ISOTROPIC	
	NO PRINT	
	POST	

Example e8x14d.dat:

Parameters	Model Definition Options	History Definition Options
ELEMENT	CONNECTIVITY	AUTO LOAD
END	CONTACT	CONTINUE
FINITE	CONTROL	TIME STEP
LARGE DISP	COORDINATE	
PRINT	END OPTION	
SIZING	FIXED DISP	
TITLE	GEOMETRY	
UPDATE	ISOTROPIC	
	NO PRINT	
	POST	

Example e8x14e.dat:

Parameters	Model Definition Options	History Definition Options
ELEMENT	CONNECTIVITY	AUTO LOAD
END	CONTACT	CONTINUE
FINITE	CONTROL	TIME STEP
LARGE DISP	COORDINATE	
PRINT	END OPTION	
SIZING	FIXED DISP	
TITLE	GEOMETRY	
UPDATE	ISOTROPIC	
	NO PRINT	
	POST	

Example e8x14f.dat:

Parameters	Model Definition Options	History Definition Options
ELEMENTS	CONNECTIVITY	AUTO LOAD
END	CONTACT	CONTINUE
FINITE	CONTROL	TIME STEP
LARGE DISP	COORDINATE	
PRINT	END OPTION	
SIZING	FIXED DISP	
TITLE	GEOMETRY	
UPDATE	ISOTROPIC	
	NO PRINT	
	POST	

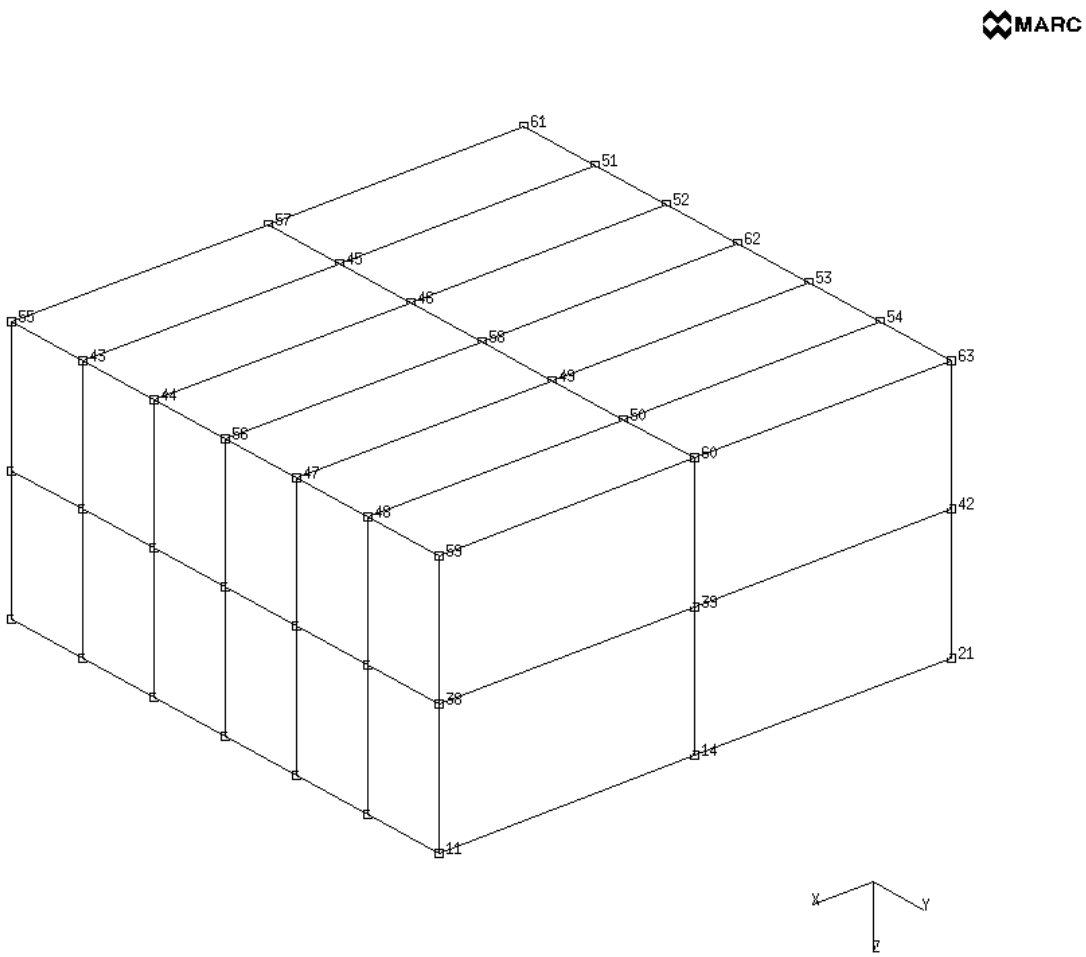

Figure 8.14-1 Undeformed Block

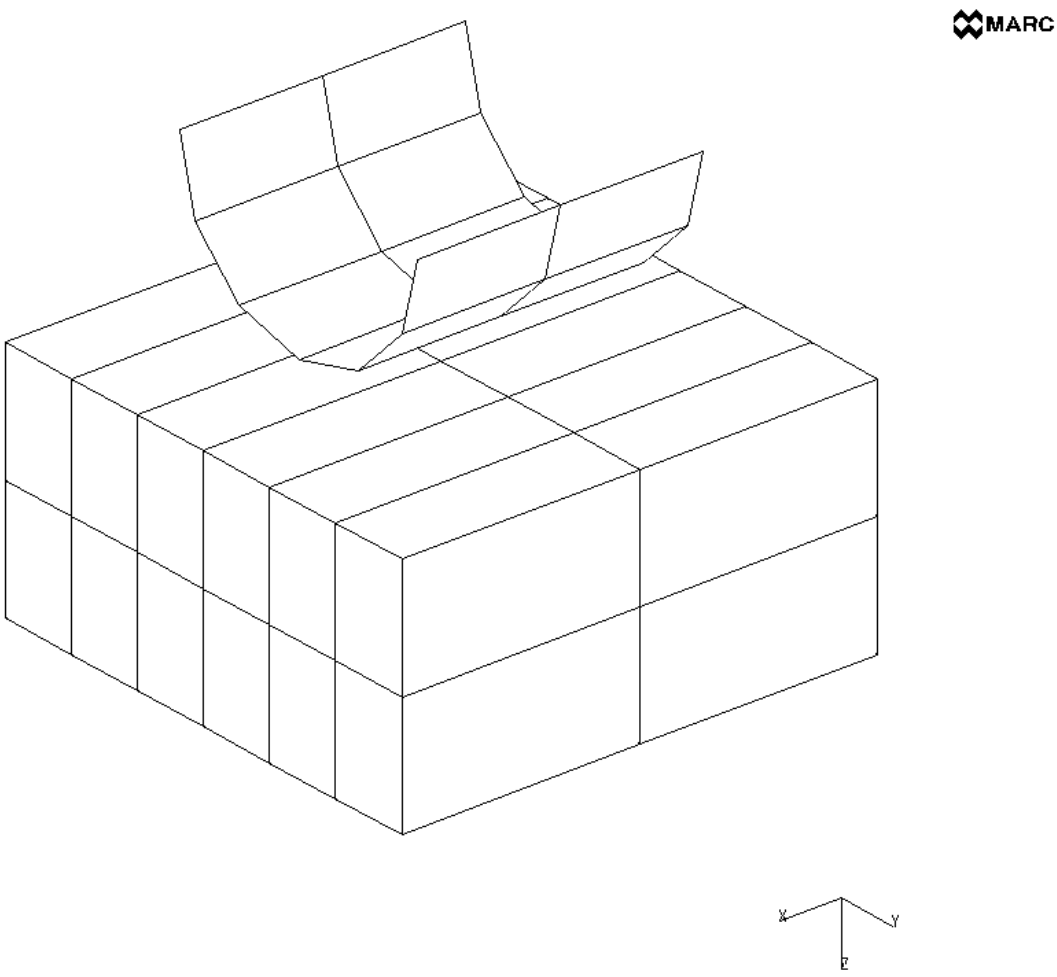

Figure 8.14-2 Block and Indentor

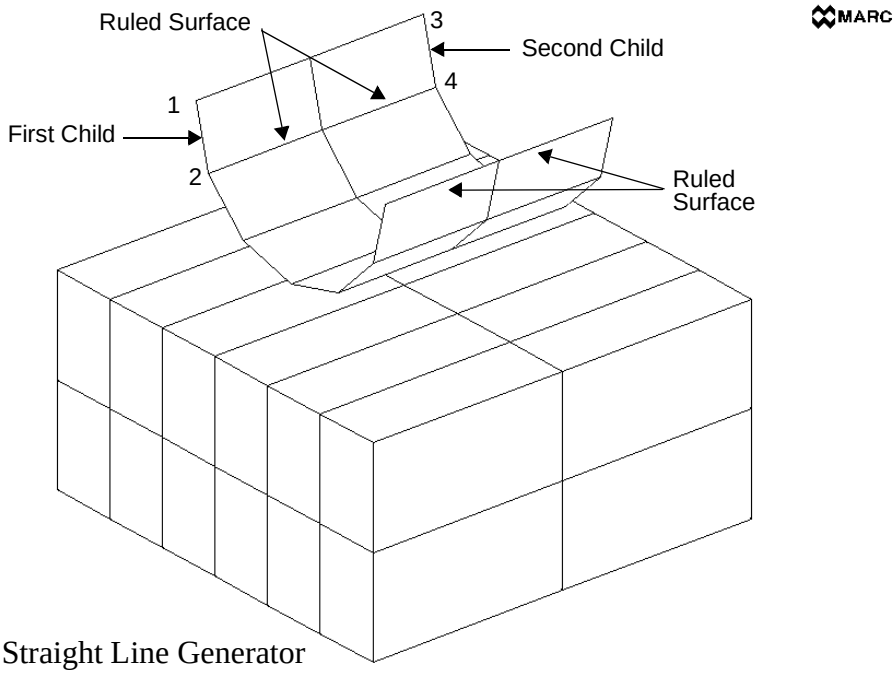

(a) Straight Line Generator

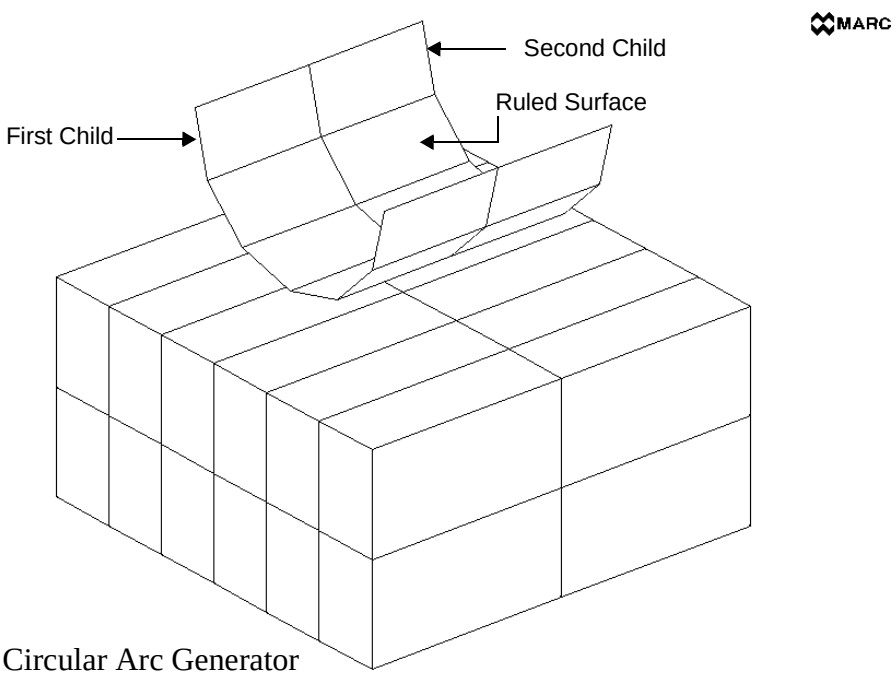

(b) Circular Arc Generator

Figure 8.14-3 Ruled Surface

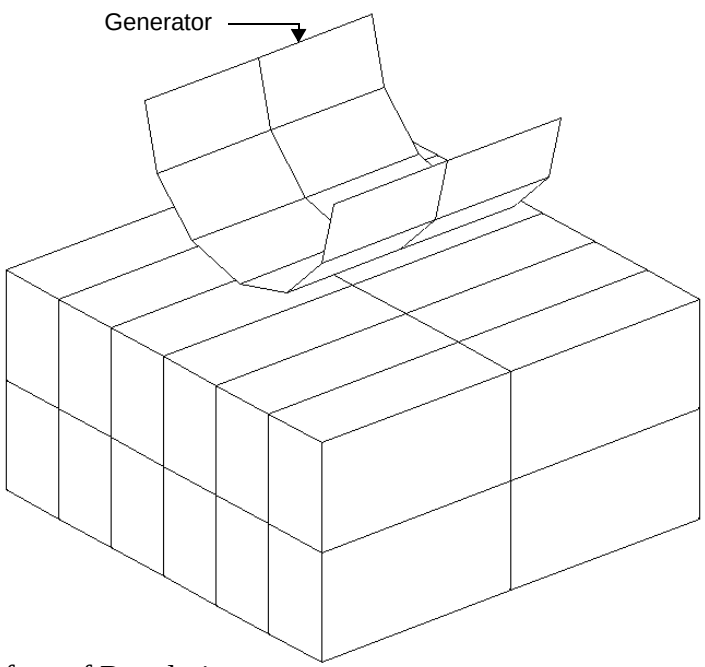

(c) Surface of Revolution

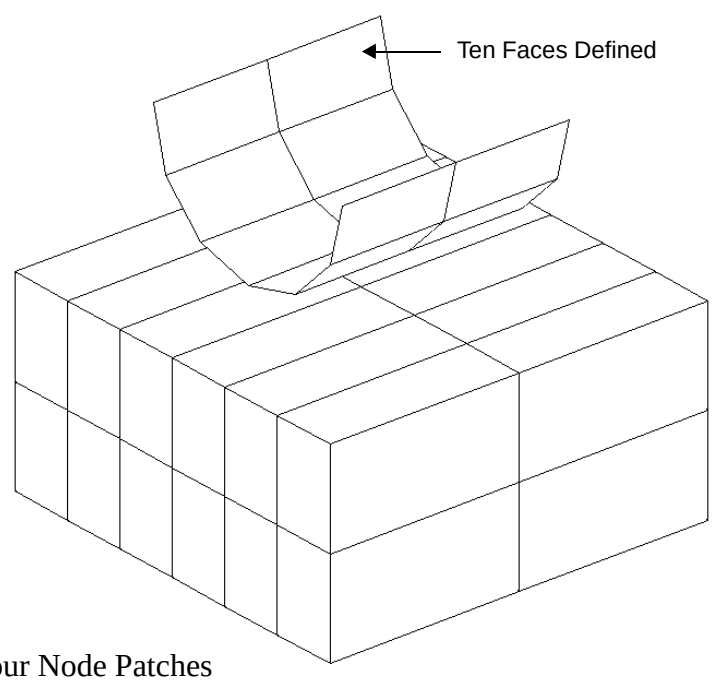

(d) Four Node Patches

Figure 8.14-3 Ruled Surface (Continued)

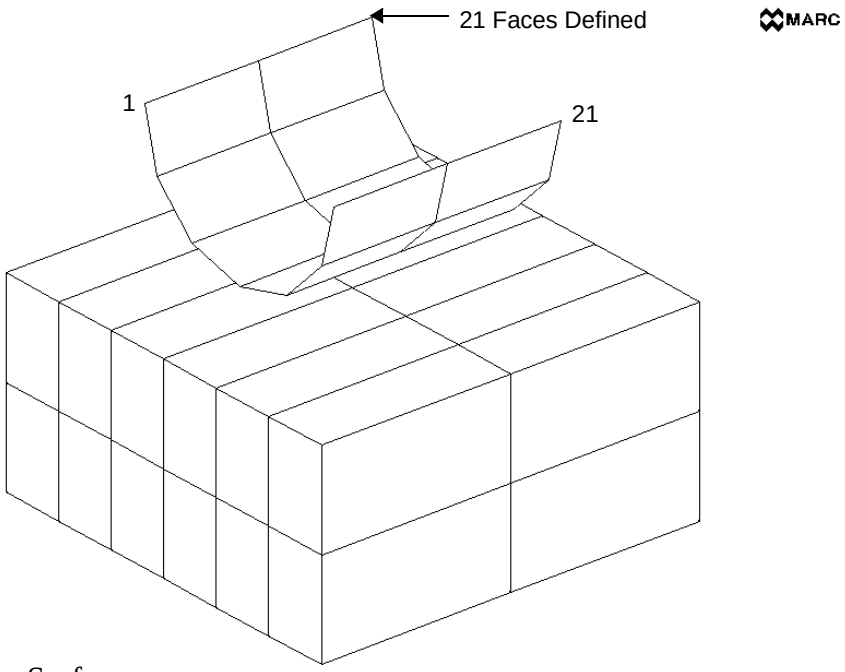

(d) Poly Surface

Figure 8.14-3 Ruled Surface (Continued)

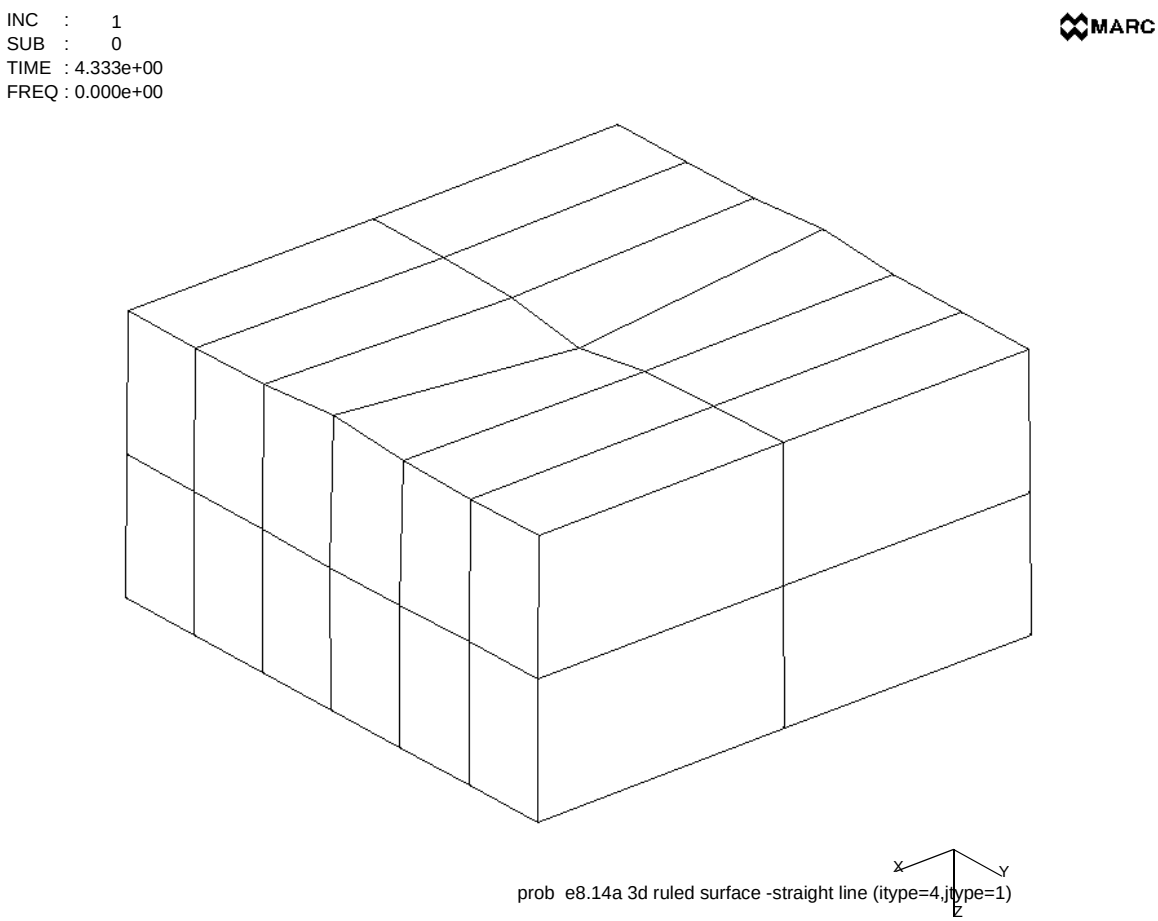

Figure 8.14-4 Deformed Block

8.15 Double-Sided Contact

This problem demonstrates MARC's ability to perform multibody contact, incorporating automated double-sided contact with friction between the contact surfaces for linear and parabolic elements. It is not necessary to assign either body as a master or slave.

This problem is modeled using the four techniques summarized below.

Data Set	Element Type(s)	Number of Elements	Number of Nodes	Differentiating Features
e8x15	11	120	158	Mean Normal Additive Decomposition Plasticity
e8x15b	27	120	434	Mean Normal Additive Decomposition Plasticity
e8x15c	11	120	158	Mean Normal Additive Decomposition Plasticity, No Increment Spliting
e8x15d	11	120	158	F^eF^p Plasticity, EXCLUDE option

Parameters

The UPDATE, FINITE, and LARGE DISP options are included in the parameter section to indicate that this is a finite deformation analysis for the first two analysis. The PLASTICITY option is used in the third analysis to indicate that the multiplicative decomposition procedure is used. The PRINT,5 option requests additional information in the output regarding nodes acquiring or losing contact.

Elements

Element types 11 and 27 are plane strain quadrilaterals with 4 and 8 nodes respectively.

Mesh Definition

Mentat is used to determine the CONNECTIVITY and COORDINATES of the mesh. The mesh is shown (with the units in inches) in Figure 8.15-1. In a contact analysis, double-sided contact is automatically checked during this deformation.

Geometry

A ‘1’ is placed in the second data field to indicate that the constant dilatation formulation is used when the additive decomposition procedure is used. This is particularly useful for analysis of approximately incompressible materials and for structures in the fully plastic range. This is not necessary when the multiplicative decomposition procedure is used. The ‘1.0’ placed in the first data field indicates the thickness of 1 inch.

Boundary Conditions

The nodes on the top surface (y = 3) are moved uniformly downward. The left (x = 0) and bottom (y = 0) side are constrained.

Material Properties

The material for all elements is treated as an elastic-plastic material, with Young’s modulus of 31.75E+06 psi, Poisson’s ratio of 0.268, a mass density of 7.4E-04 lbf-sec^2/in^4, a coefficient of thermal expansion of 5.13E-06 in/(in-deg F), corresponding reference temperature of 70°F, and an initial yield stress of 80,730 psi. The material work-hardens from the initial yield stress to a final yield stress of 162,747 psi at a strain of 1.0 in the WORK HARD DATA block.

Contact

The CONTACT option declares that there are two bodies in contact with adhesive friction between them. The relative ship velocity is defined as 0.01 in/second. The contact tolerance distance is 0.01 inches. The coefficient of friction associated with each body is 0.7. The reaction tolerance will be computed by the program.

The CONTACT TABLE is used to indicate that body 1 will potentially come in contact with body 2. Because the contact table is used, no contact between body 1 and itself or body 2 and itself is checked.

Load Control

This problem is loaded by the repeated application of the load increment created by the prescribed boundary conditions in the AUTO LOAD option. The load increment is applied 20 times. The TIME STEP option allows you to enter the time variable for static analysis. All contact analyses are time driven and require the definition of a time step. A formatted post file contains the equivalent plastic strain, the first two stress components, von Mises equivalent stress, and the mean normal stress. The NO PRINT option limits the amount of printed output to a minimum. Displacement control is used with a relative error of 20%. The RESTART LAST option is used to save the last increment of data if a later restart is required.

For data set e8x15d, the load incrementation is done using the AUTO STEP option. The initial time step is chosen to be 0.01 sec while the total time period is chosen to be 1 sec. The AUTO STEP option is chosen to control the maximum allowed effective plastic strain increment in each load increment. This is summarized in the table below:

Plastic Strain Range	Maximum Plastic Strain Increment
0.0 – 0.10	0.02
0.10 – 0.25	0.05
0.25 – 0.75	0.10
0.75 – 2.0	0.20

Results

Figure 8.15-1 shows the original mesh with the elements labeled of double-sided contact problem for both element types. Figure 8.15-2 and Figure 8.15-3, respectively, show the nodal labels for element types 11 and 27. Figure 8.15-4, Figure 8.15-5, and Figure 8.15-6 show the deformed body at the end of 10, 20 and 30 increments with the deformation at the same scale as the coordinates. Figure 8.15-8, Figure 8.15-9, and Figure 8.15-10 show the deformed body at the end of 10, 20 and 30 increments for element type 27. Due to the high level of friction, significant transverse deformation is shown along the contact surfaces. Figure 8.15-7 and Figure 8.15-11 show the equivalent plastic strain at the end of increment 30. The peak values of equivalent plastic strain are 137% and 151% for element types 11 and 27, respectively. The additional degrees of freedom in the model using element type 27 makes the structure more flexible. The larger plastic strain found for the higher degrees of freedom model is on the high side of convergence tolerance.

A user-written subroutine, IMPD, is used in conjunction with the UDUMP model definition option to sum the nodal loads across the y = 3 (top) surface and print the nodal load and displacement for each increment into the output file. This information is plotted and shown in Figure 8.15-12 for both element types. The overall force-displacement behavior of the two element types is in good agreement with all differences occurring in the early portion of the contact.

In the third analysis, a flag is set to indicate that increment splitting is not to be used. Also the CONTACT NODE option is used to only check contact for the corner nodes for the parabolic element, type 27.

For the fourth analysis (data set e8x15d), the deformed geometry at increments 25 and 50 are shown in Figure 8.15-13 and Figure 8.15-14 respectively. The final deformed shape after 53 increments is shown in Figure 8.15-15 with contours of total effective plastic strain superimposed.

Parameters, Options, and Subroutines Summary

Example e8x15.dat:

Parameters	Model Definition Options	History Definition Options
ELEMENT	CONNECTIVITY	AUTO LOAD
END	CONTACT	CONTINUE
FINITE	CONTACT TABLE	TIME STEP
LARGE DISP	CONTROL	
PRINT	COORDINATES	
SIZING	DEFINE	
TITLE	END OPTION	
UPDATE	FIXED DISP	
	GEOMETRY	
	ISOTROPIC	
	NO PRINT	
	POST	
	RESTART LAST	
	WORK HARD	

Example e8x15b.dat:

Parameters	Model Definition Options	History Definition Options
ELEMENT	CONNECTIVITY	AUTO LOAD
END	CONTACT	CONTINUE
FINITE	CONTACT TABLE	TIME STEP
LARGE DISP	CONTROL	
PRINT	COORDINATES	
SIZING	DEFINE	
TITLE	END OPTION	
UPDATE	FIXED DISP	
	GEOMETRY	
	ISOTROPIC	
	NO PRINT	
	POST	
	RESTART LAST	
	WORK HARD	

E8x15c.dat:

Parameters	Model Definition Options	History Definition Options
ELEMENT	CONNECTIVITY	AUTO LOAD
END	CONTACT	CONTINUE
FINITE	CONTACT NODE	TIME STEP
LARGE DISP	CONTACT TABLE	
PRINT	CONTROL	
SIZING	COORDINATES	
TITLE	DEFINE	
UPDATE	END OPTION	
	FIXED DISP	
	GEOMETRY	
	ISOTROPIC	
	NO PRINT	
	POST	
	RESTART LAST	
	WORK HARD	

Example e8x15d.dat:

Parameters	Model Definition Options	History Definition Options
ELEMENT	CONNECTIVITY	CONTINUE
END	CONTACT	AUTO STEP
PRINT	CONTACT TABLE	
SIZING	CONTROL	
TITLE	COORDINATES	
PLASTICITY	DEFINE	
	END OPTION	
	FIXED DISP	
	GEOMETRY	
	ISOTROPIC	
	NO PRINT	
	POST	
	RESTART LAST	
	WORK HARD	

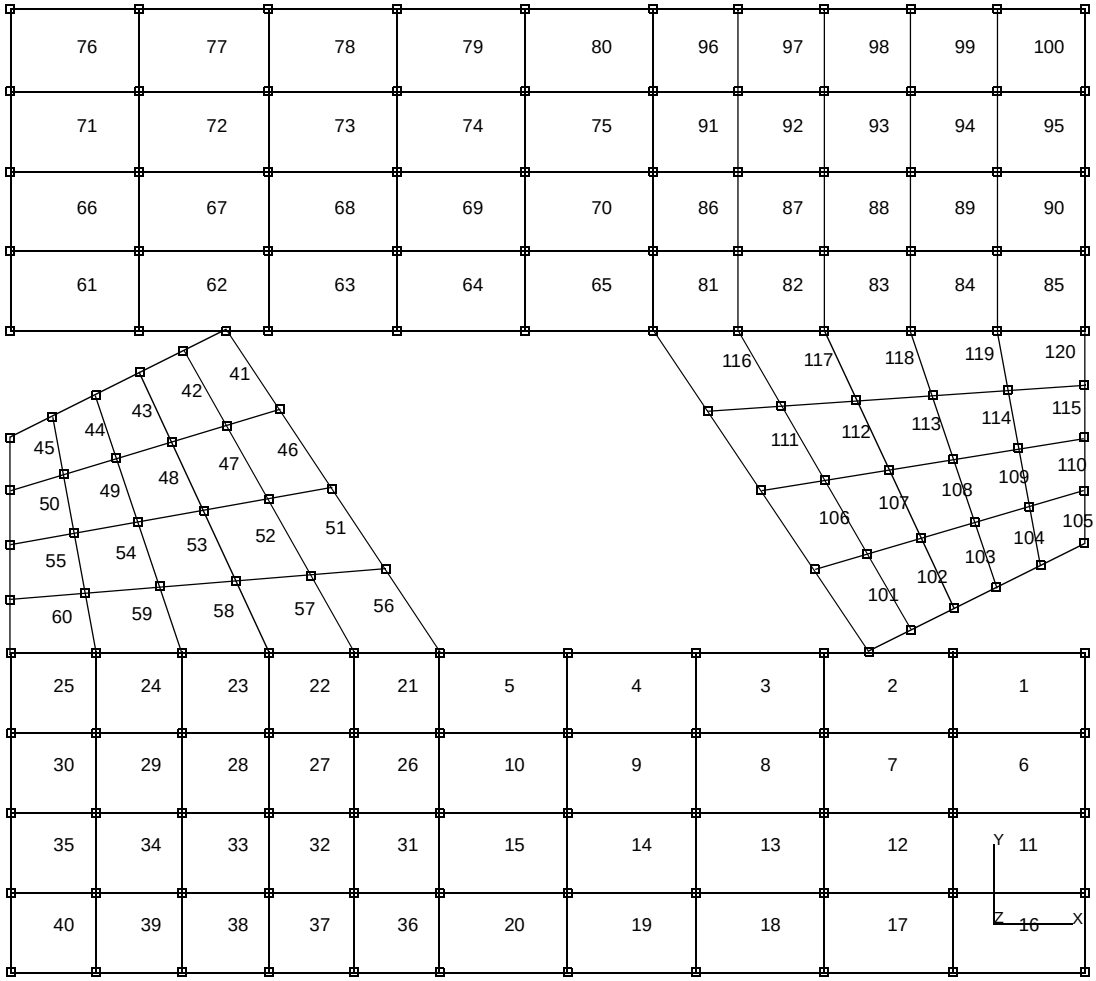

Figure 8.15-1 Mesh

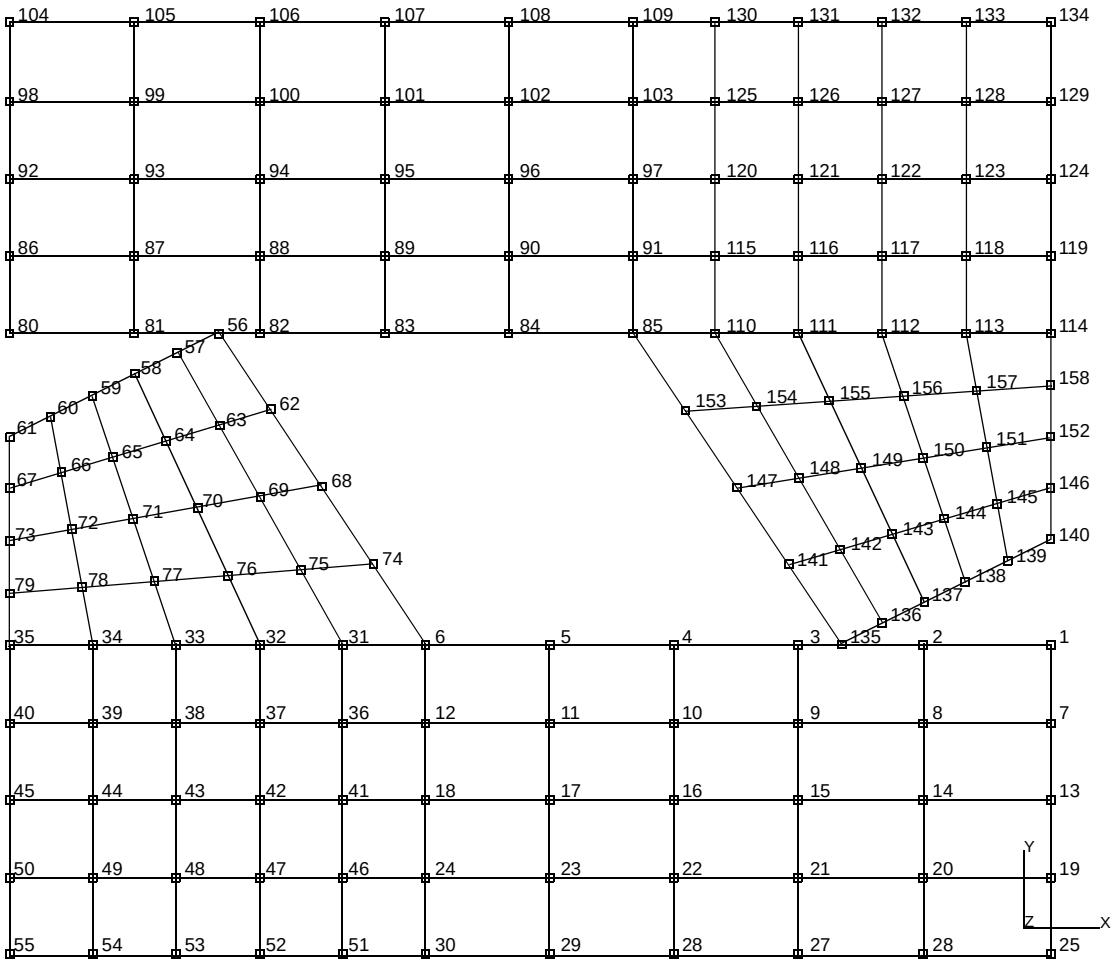

Figure 8.15-2 Nodal Configuration, Element Type 11

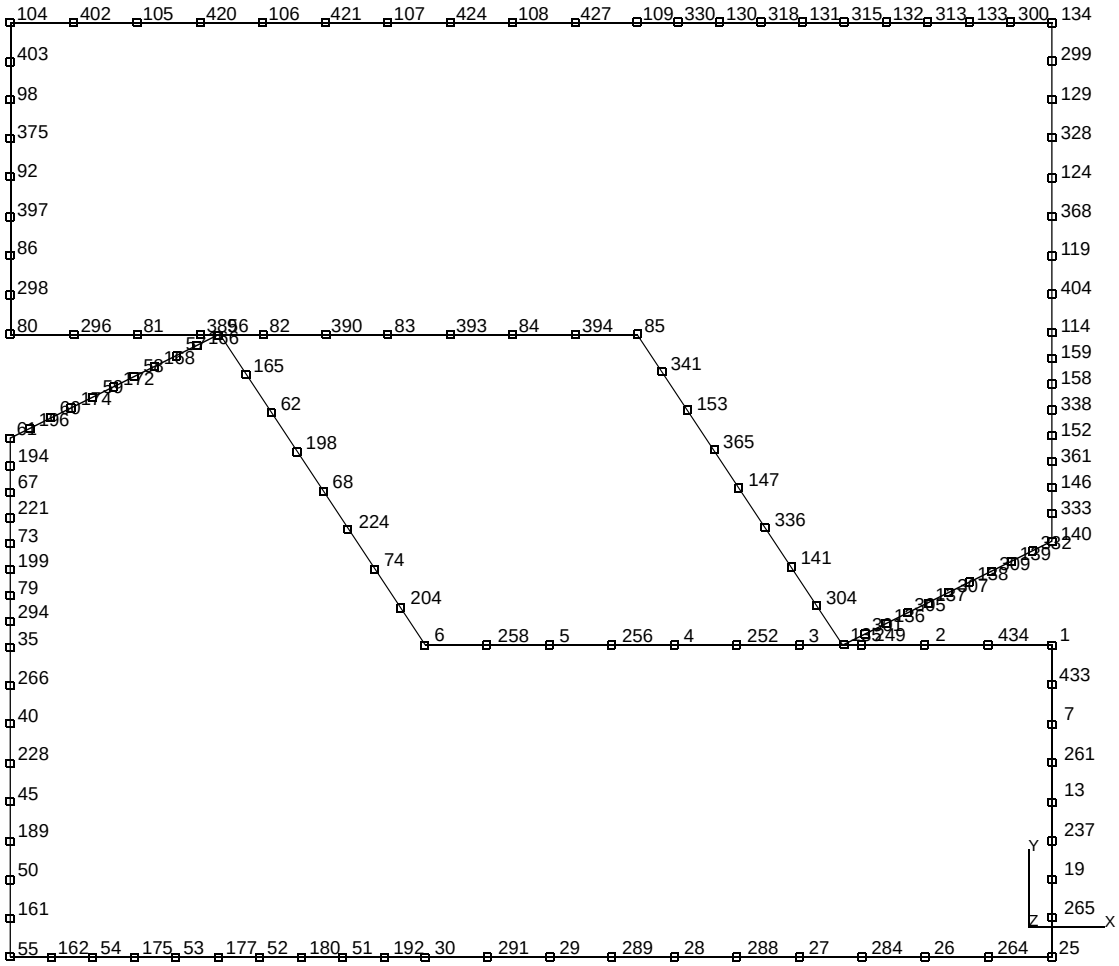

Figure 8.15-3 Nodal Configuration, Element Type 27

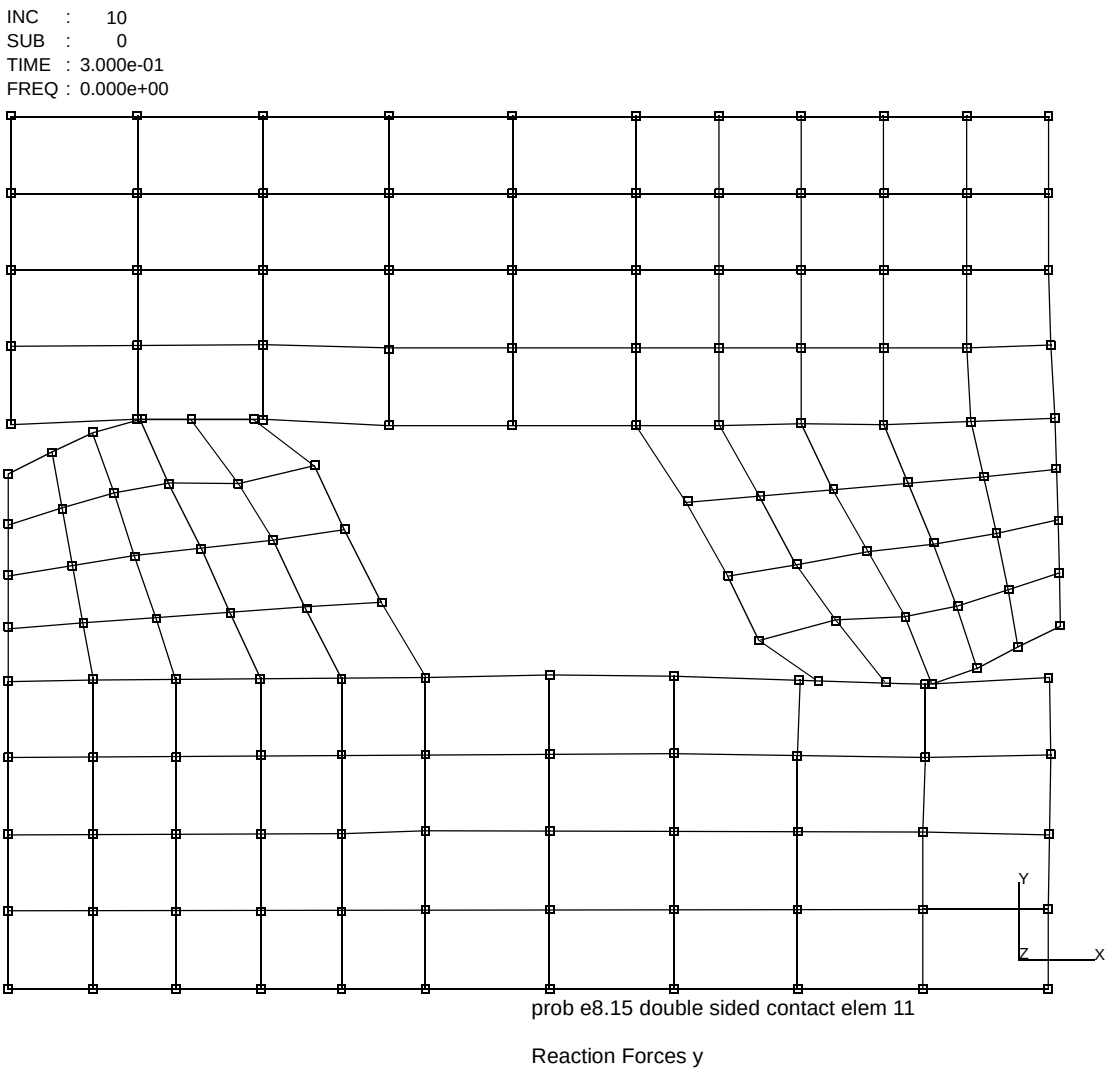

Figure 8.15-4 Nodal Displacements at Increment 10, Element Type 11

INC : 20
SUB : 0
TIME : 6.000e-01
FREQ : 0.000e+00

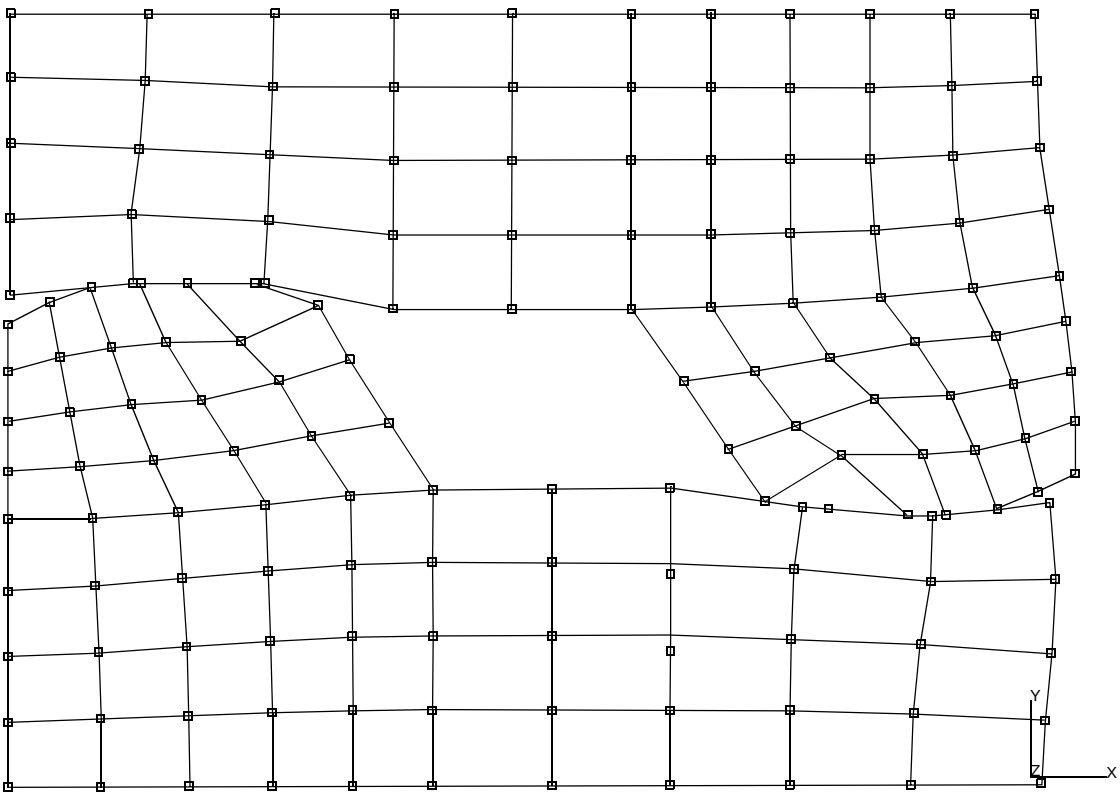

Figure 8.15-5 Nodal Displacements at Increment 20, Element Type 11

INC : 30
SUB : 0
TIME : 9.000e-01
FREQ : 0.000e+00

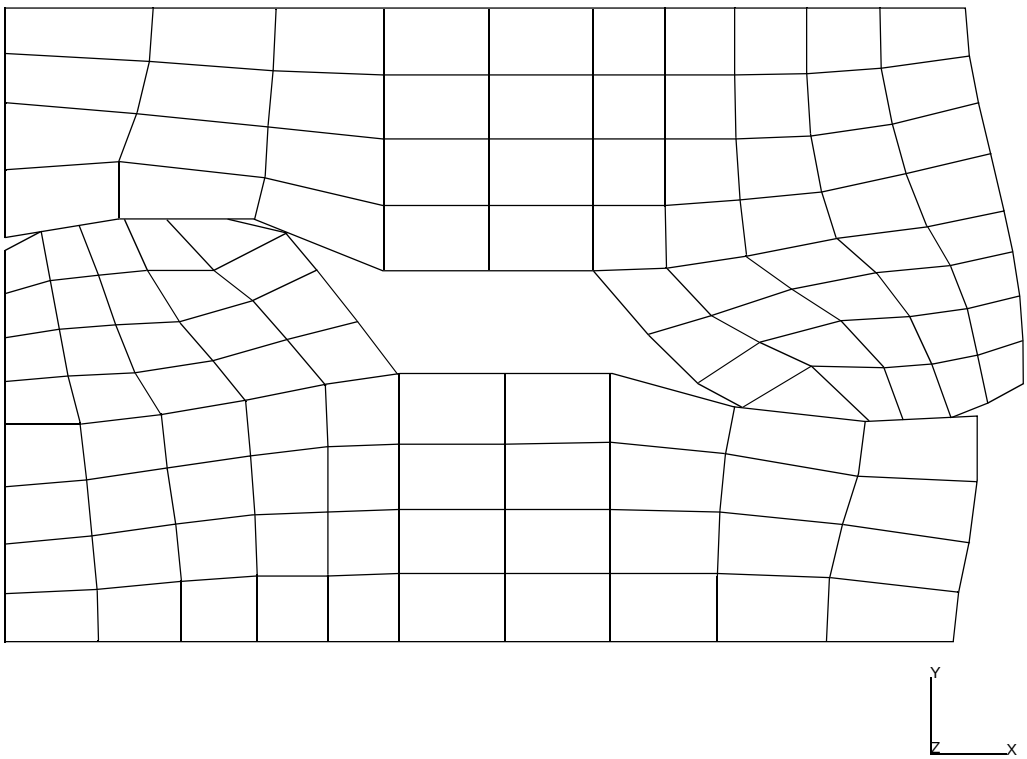

prob e8.15 double sided contact elem 11

Equivalent Plastic Strain

Figure 8.15-6 Nodal Displacements at Increment 30, Element Type 11

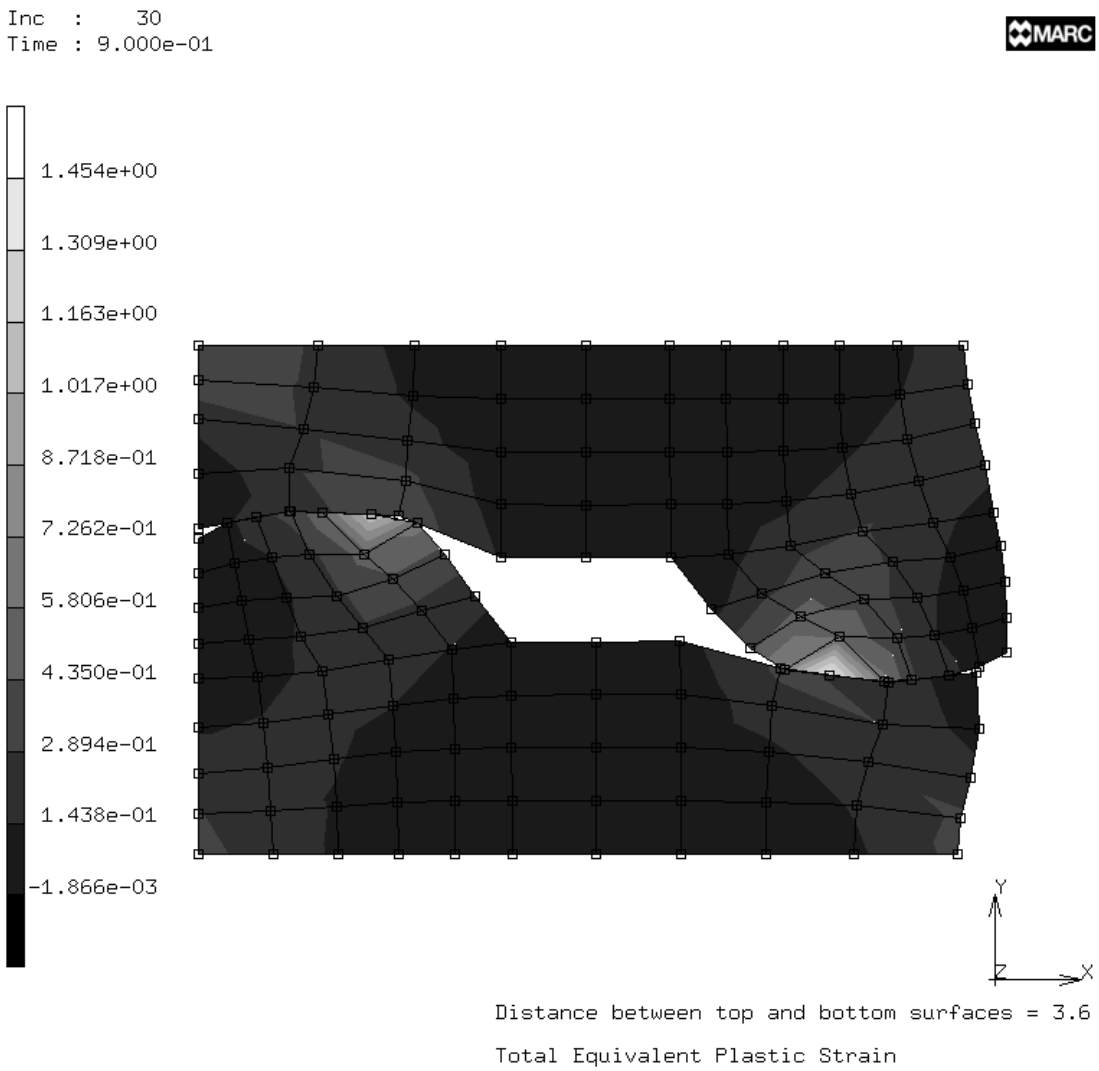

Figure 8.15-7 Equivalent Plastic Strain at Increment 30, Element Type 11

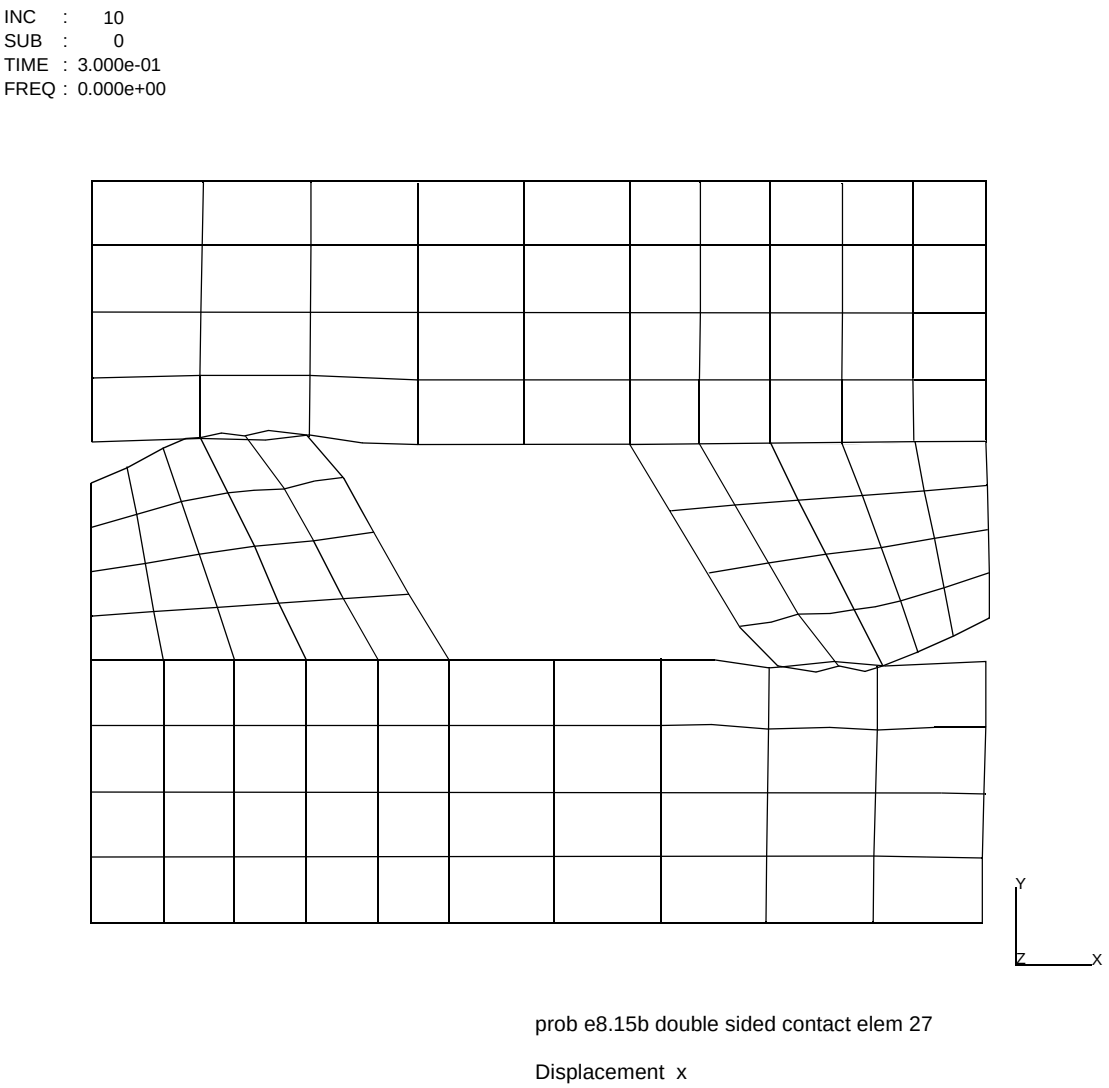

Figure 8.15-8 Nodal Displacements at Increment 10, Element Type 27

INC : 20
SUB : 0
TIME : 6.000e-01
FREQ : 0.000e+00

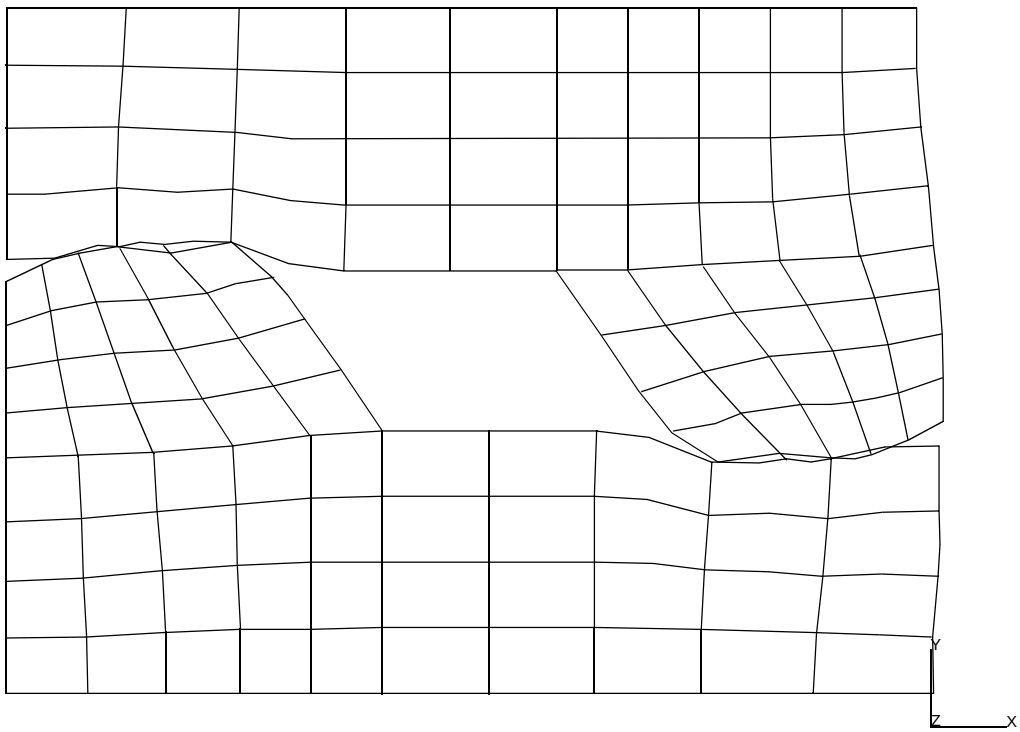

prob e8.15b double sided contact elem 27

Displacement x

Figure 8.15-9 Nodal Displacements at Increment 20, Element Type 27

INC : 30
SUB : 0
TIME : 9.000e-01
FREQ : 0.000e+00

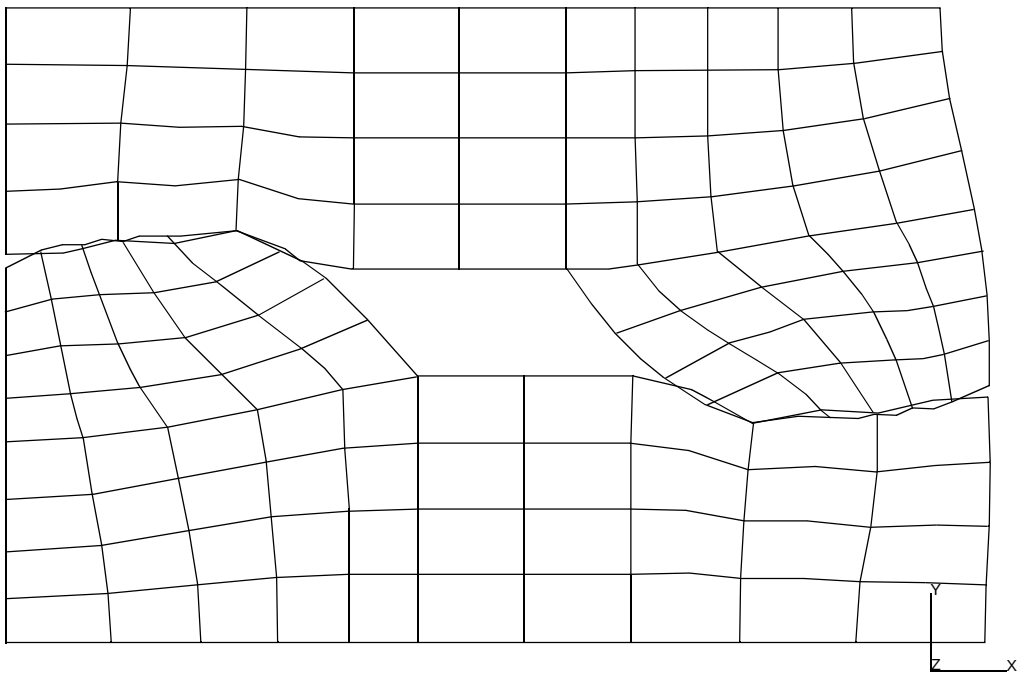

prob e8.15b double sided contact elem 27

Displacement x

Figure 8.15-10 Nodal Displacements at Increment 30, Element Type 27

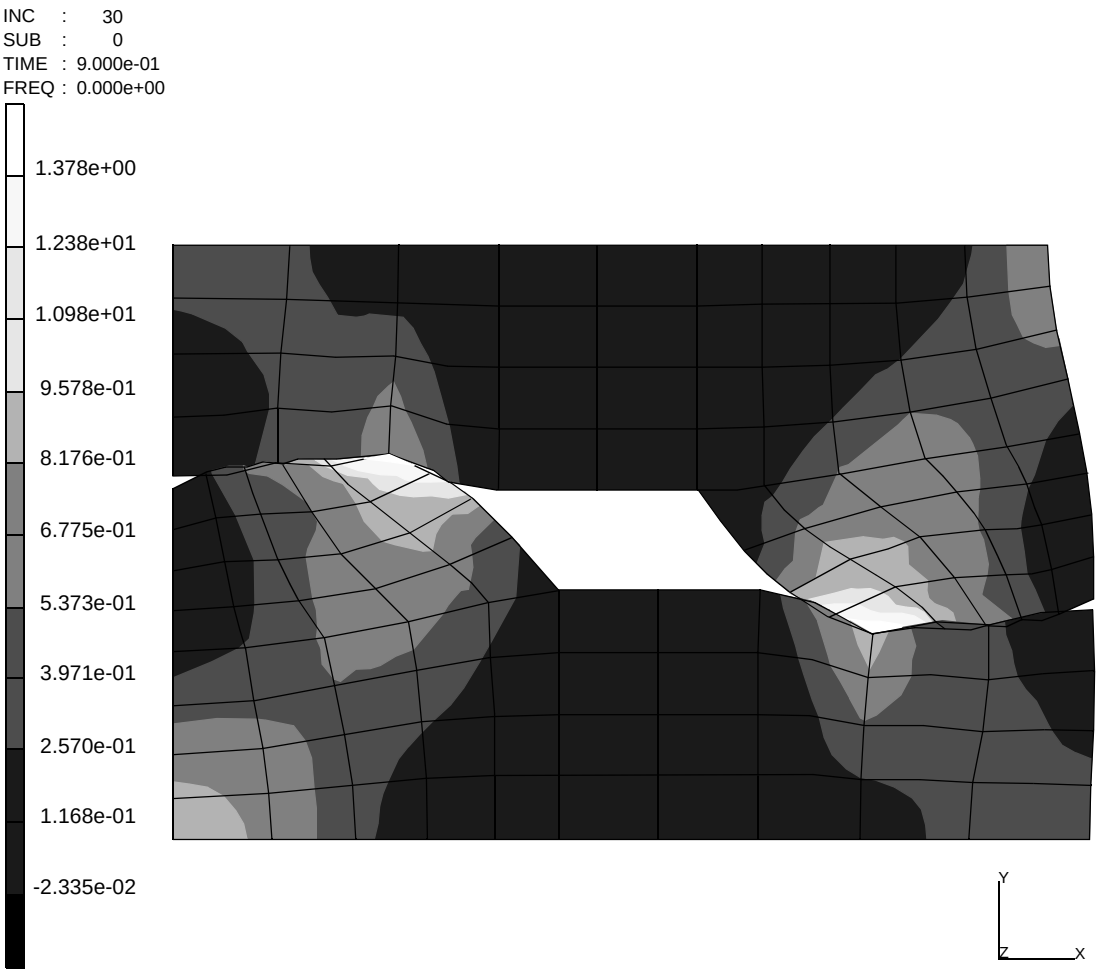

Figure 8.15-11 Equivalent Plastic Strain at Increment 30, Element Type 27

Disp (x-1e+0)	Load (x-1e+5)		Disp (x-1e+0)	Load (x-1e+5)	
	Type 11	Type 27		Type 11	Type 27
0.00000E+00	0.00000E+00	0.00000E+00	4.50000E-01	5.73937E+00	5.76850E+00
3.00000E-02	1.49358E+00	9.65015E-01	4.80000E-01	5.82146E+00	5.92706E+00
6.00000E-02	1.36351E+00	1.34468E+00	5.10000E-01	5.88858E+00	6.02711E+00
9.00000E-02	1.40418E+00	1.61070E+00	5.40000E-01	5.95362E+00	6.11778E+00
1.20000E-01	3.59213E+00	2.52490E+00	5.70000E-01	6.01384E+00	6.20322E+00
1.50000E-01	3.26189E+00	3.02085E+00	6.00000E-01	6.28412E+00	6.28309E+00
1.80000E-01	3.31538E+00	3.35550E+00	6.30000E-01	6.35279E+00	6.35828E+00
2.10000E-01	3.52452E+00	3.70196E+00	6.60000E-01	6.39055E+00	6.42653E+00
2.40000E-01	4.55123E+00	4.33235E+00	6.90000E-01	6.43786E+00	6.52579E+00
2.70000E-01	4.74629E+00	4.63125E+00	7.20000E-01	6.56095E+00	6.55766E+00
3.00000E-01	4.89159E+00	4.88421E+00	7.50000E-01	6.72437E+00	6.52325E+00
3.30000E-01	5.03333E+00	5.07415E+00	7.80000E-01	6.77405E+00	6.70139E+00
3.60000E-01	5.16167E+00	5.23750E+00	8.10000E-01	6.70833E+00	6.79742E+00
3.90000E-01	5.39677E+00	5.41752E+00	8.40000E-01	6.89754E+00	7.02602E+00
4.20000E-01	5.51851E+00	5.60917E+00	8.70000E-01	6.97591E+00	7.14885E+00
			9.00000E-01	7.01286E+00	7.24298E+00

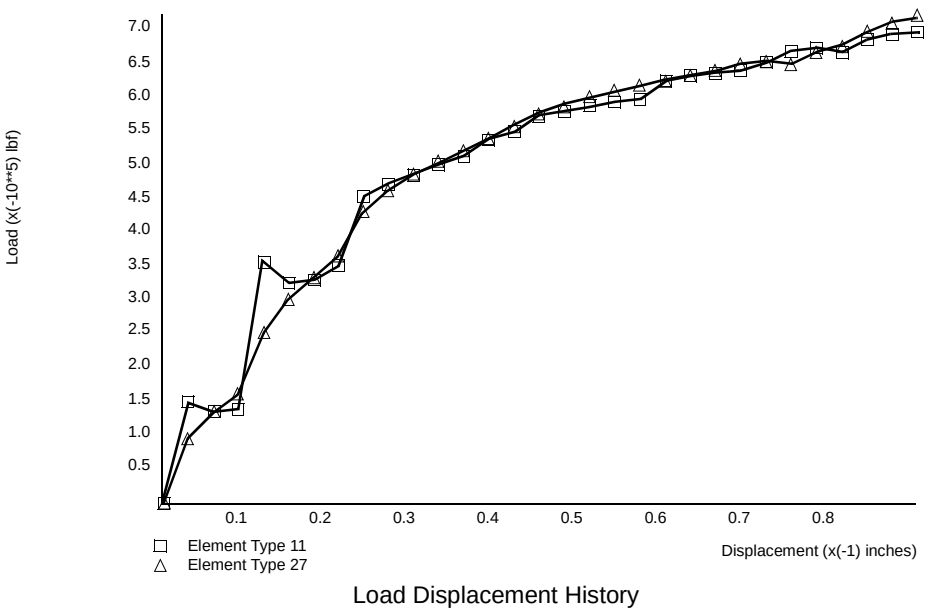

Figure 8.15-12 Load History for Both Element Types

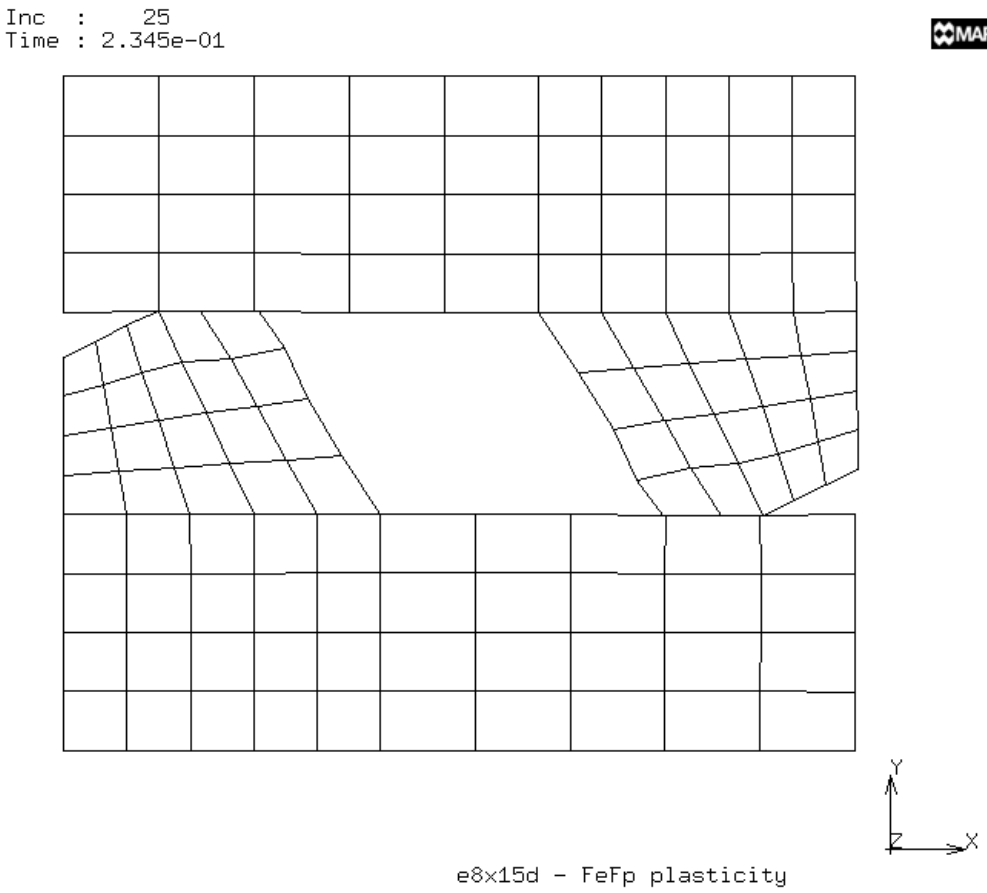

Figure 8.15-13 Deformed Geometry at Increment 25 for Data Set e8x15d

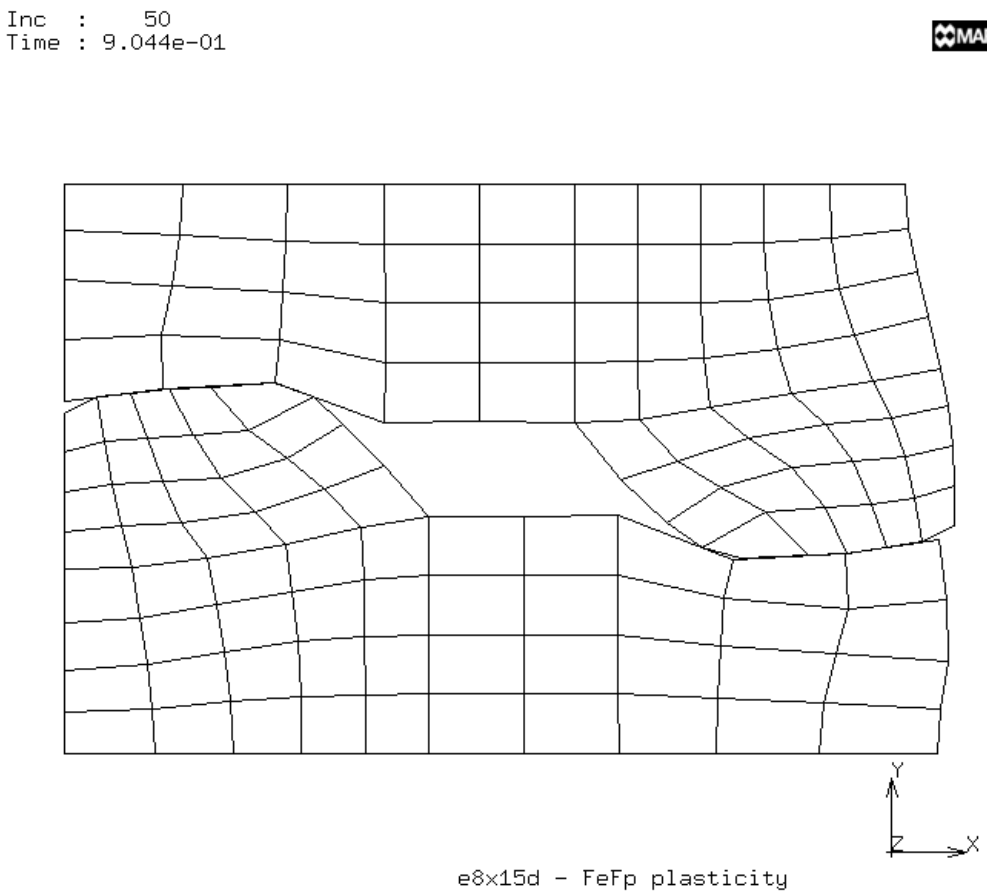

Figure 8.15-14 Deformed Geometry at Increment 50 for Data Set e8x15d

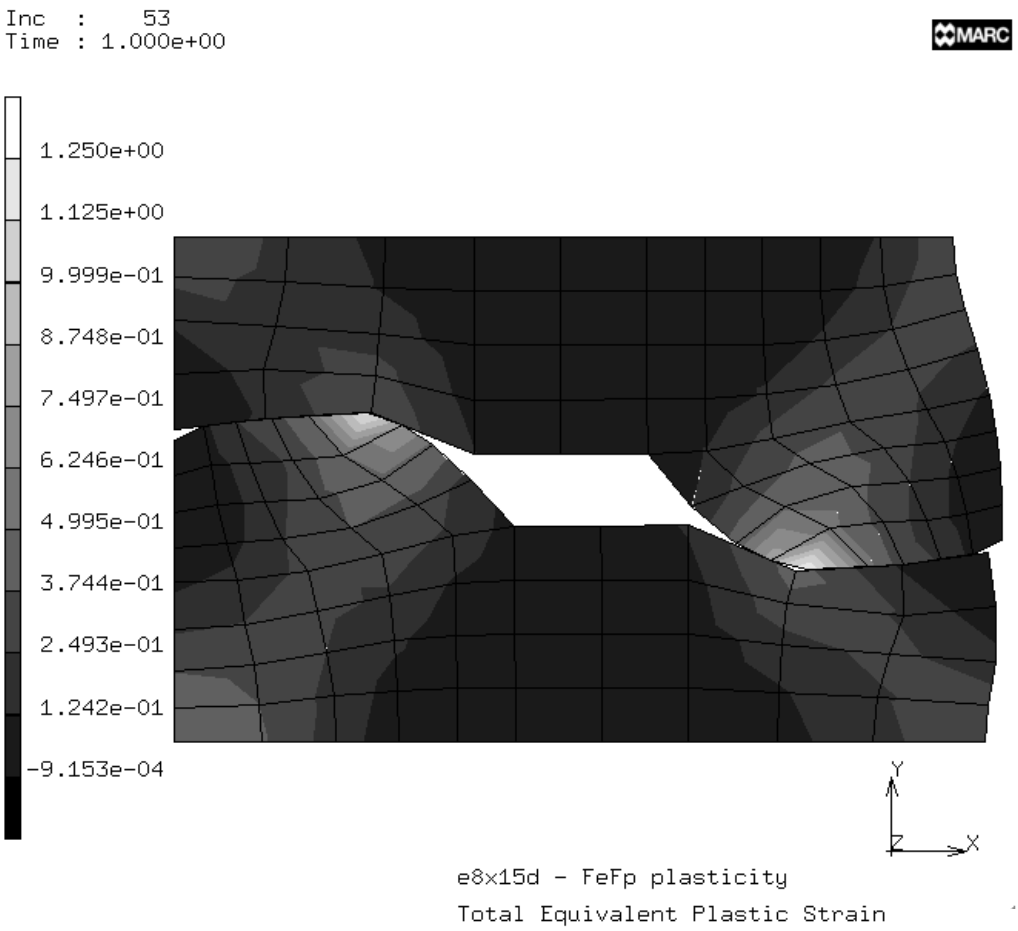

Figure 8.15-15 Contours of Total Equivalent Plastic Strain on Final Geometry for Data Set e8x15d

8.16 Demonstration of Springback

A metal part is formed and the springback is examined. A large strain elastic plastic analysis is performed.

This problem is modeled using the two data sets summarized below.

Data Set	Element Type(s)	Number of Elements	Number of Nodes	Differentiating Features
e8x16	11	147	178	Mean Normal Additive Decomposition Plasticity
e8x16b	11	147	178	Radial Return F^eF^p Plasticity

Model

The original part is shown in Figure 8.16-1 and is composed of 197 elements type 11 plane strain quadrilaterals. A rigid cylinder is used to deform the part.

Parameters

In the first analysis, the additive decomposition procedure is used. This is activated by using the LARGE DISP, FINITE, and UPDATE parameters.

In the second analysis, the multiplicative decomposition (F^eF^p) procedure is used. The PLASTICITY option is used. The PRINT, 5 option results in additional output regarding contact.

Geometry

The ‘1’ in the second field invokes the constant dilatation option. This gives improved behavior for nearly incompressible behavior that occurs during plastic deformation. The ‘1’ in the third field invokes the assumed strain formulation for element type 11. This gives improved behavior in bending which is the dominant mechanism in this problem. The geometry parameters are not necessary for the F^eF^p procedure.

Boundary Conditions

The left side is constrained in the first degree of freedom. A spring is used to constrain the motion in the y-degree of freedom, so there will not be any rigid body modes.

Material Properties

The part is made of aluminum with a Young's modulus of 10.6E+6 psi. The material strain hardens such that at 5.8% strain the flow stress will be 50,355 psi. It is important that the first stress in the WORK HARD DATA be the same as given through the ISOTROPIC option.

Contact

Two contact bodies are defined. The first is the deformable body, consisting of 147 elements. The second body is the rigid pin, defined as four circular arcs. Each arc is subdivided into ten segments. The circular pin has a velocity of 0.2 in/second.

Control

The full Newton-Raphson procedure is used in this analysis. Displacement control is requested with a tolerance of 2%. The Cuthill-McKee method is used to minimize the bandwidth. The post file frequency is specified through the POST and POST INCREM options. For data set e8x16, the post file was written at increments 0(default), 18 and 19. For data set e8x16b, the post file is written for every increment.

For data set e8x16, the AUTO LOAD and TIME STEP options are used to use 18 increments with a time step of 0.10 seconds. At this point, the pin is removed from the model allowing the workpiece to elastically springback. For data set e8x16b, the AUTO STEP option is used to impose the loading prior to springback.

Release

After the deformation, the rigid pin is removed from the hook and springback occurs. In the first analysis, this is done in one step by using the RELEASE and MOTION CHANGE options. The RELEASE option is used to ensure that all of the nodes separate from body 2, the rigid pin. In the second analysis, the rigid body is released, but the contact forces are gradually brought to zero over five increments. This is performed by using the RELEASE and AUTO LOAD options. This procedure is often advantageous as often the contact forces are quite large and cannot be redistributed in one increment. The MOTION CHANGE option is used to move the pin away from the body, so that it will not make any further contact.

Results

The deformed shape at increment 18 is shown in Figure 8.16-2. The stresses at this point are shown in Figure 8.16-3. After release of the pin, there is a slight amount of springback. Recall that the elastic strain is, at the most, 5.4 E4/10.6E6 = 0.5% which will limit the amount of springback.

For data set e8x16b, the deformed shape in increment 53 is shown in Figure 8.16-4. The contours of equivalent von Mises stress are shown in Figure 8.16-5 for increment 53.

Parameters, Options, and Subroutines Summary

Example e8x16.dat:

Parameters	Model Definition Options	History Definition Options
ELEMENT	CONNECTIVITY	AUTO LOAD
END	CONTACT	CONTINUE
FINITE	CONTROL	POST INCREMENT
LARGE DISP	COORDINATES	RELEASE
PRINT	END OPTION	TIME STEP
SIZING	FIXED DISP	
TITLE	GEOMETRY	
UPDATE	ISOTROPIC	
	OPTIMIZE	
	POST	
	PRINT CHOICE	
	WORK HARD	

Example e8x16b.dat:

Parameters	Model Definition Options	History Definition Options
ELEMENT	CONNECTIVITY	AUTO LOAD
END	CONTACT	AUTO STEP
FINITE	CONTROL	CONTINUE
LARGE DISP	COORDINATES	MOTION CHANGE
PRINT	END OPTION	POST INCREMENT
SIZING	FIXED DISP	RELEASE
TITLE	GEOMETRY	TIME STEP
UPDATE	ISOTROPIC	
	OPTIMIZE	
	POST	
	PRINT CHOICE	
	WORK HARD	

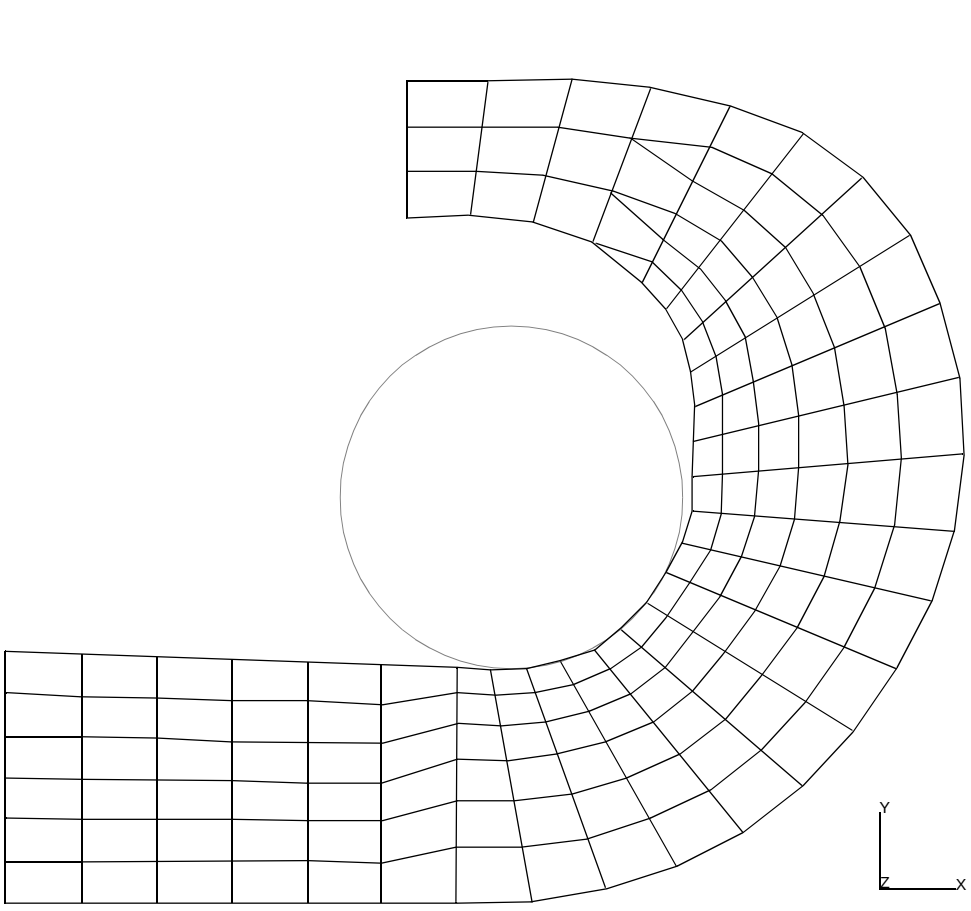

Figure 8.16-1 Original Configuration

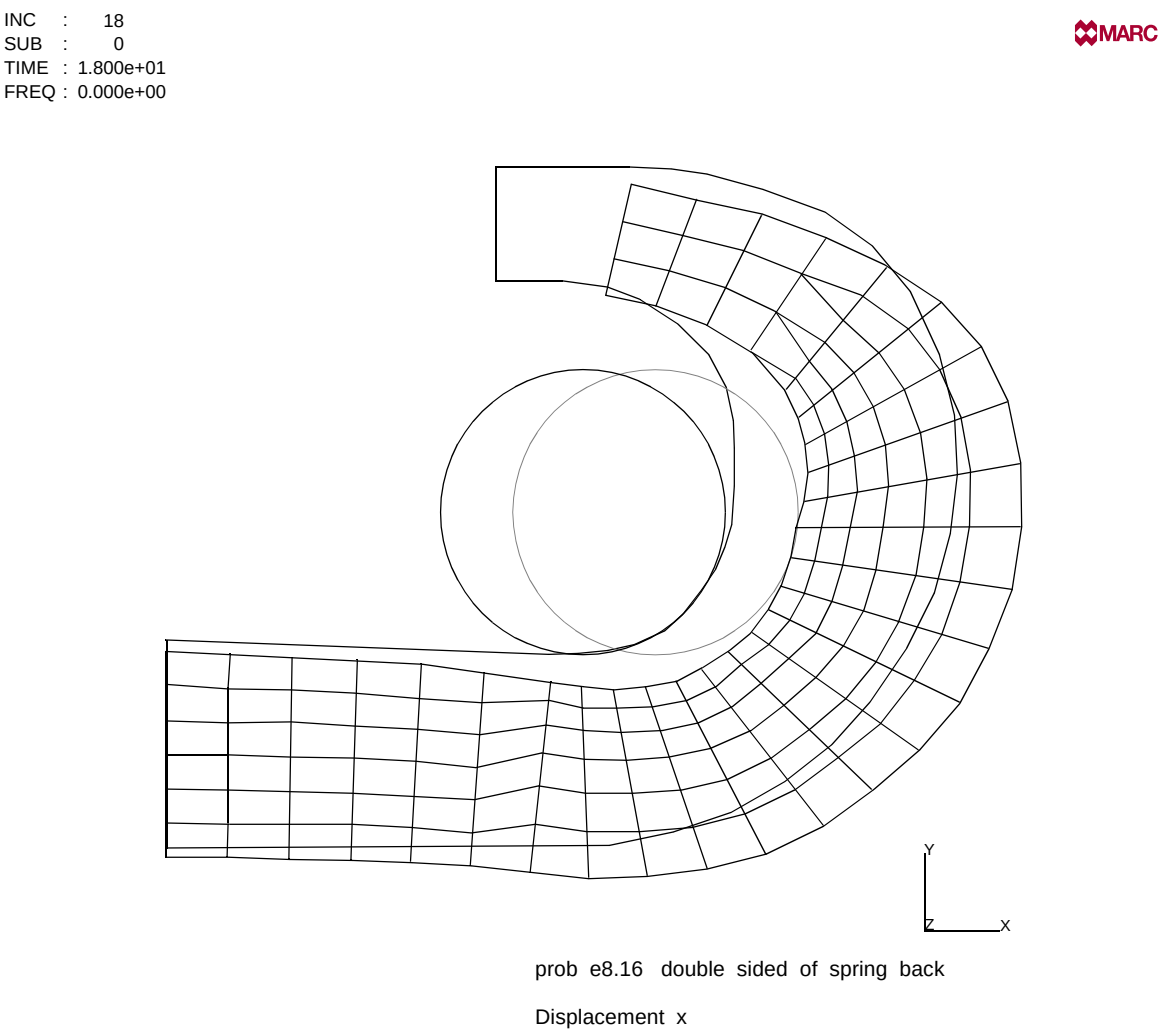

Figure 8.16-2 Deformed Mesh

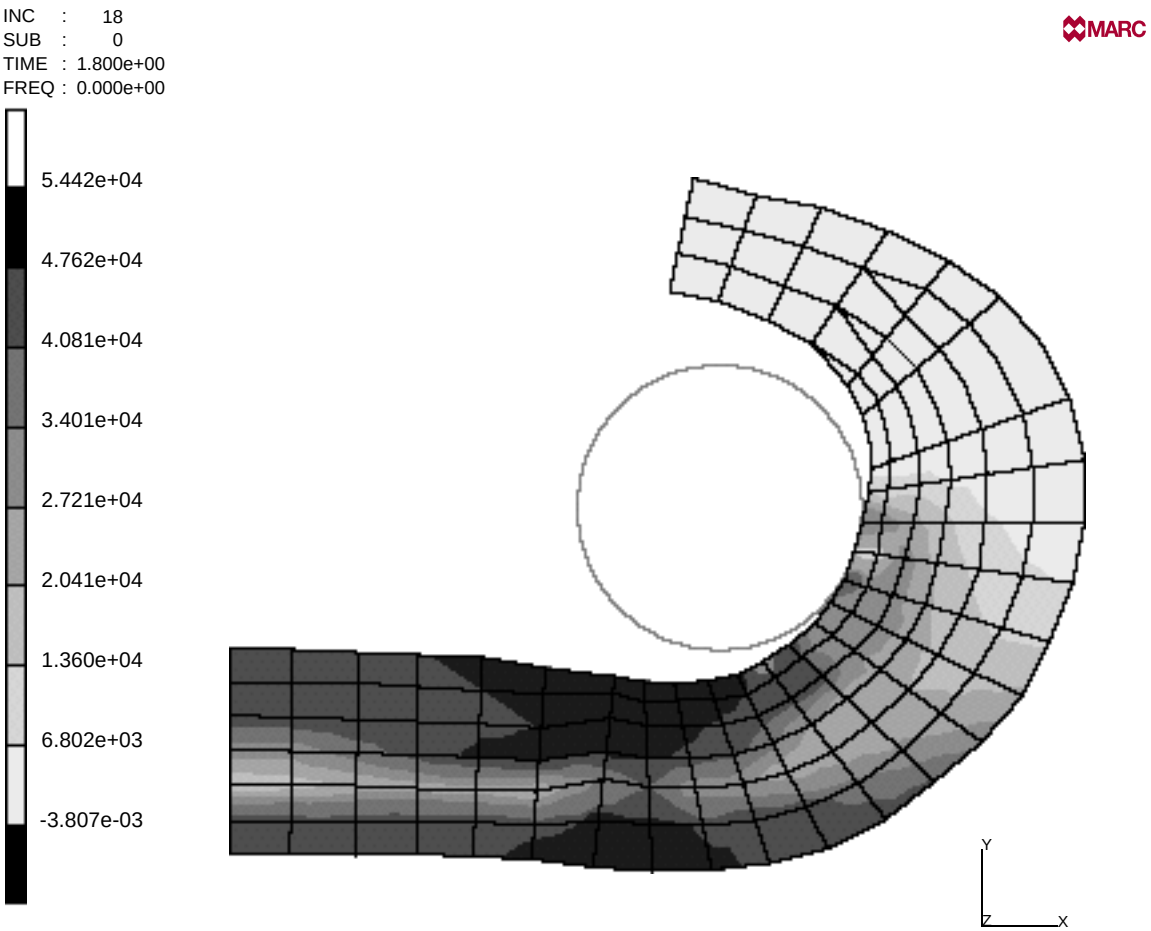

Figure 8.16-3 Equivalent Stress

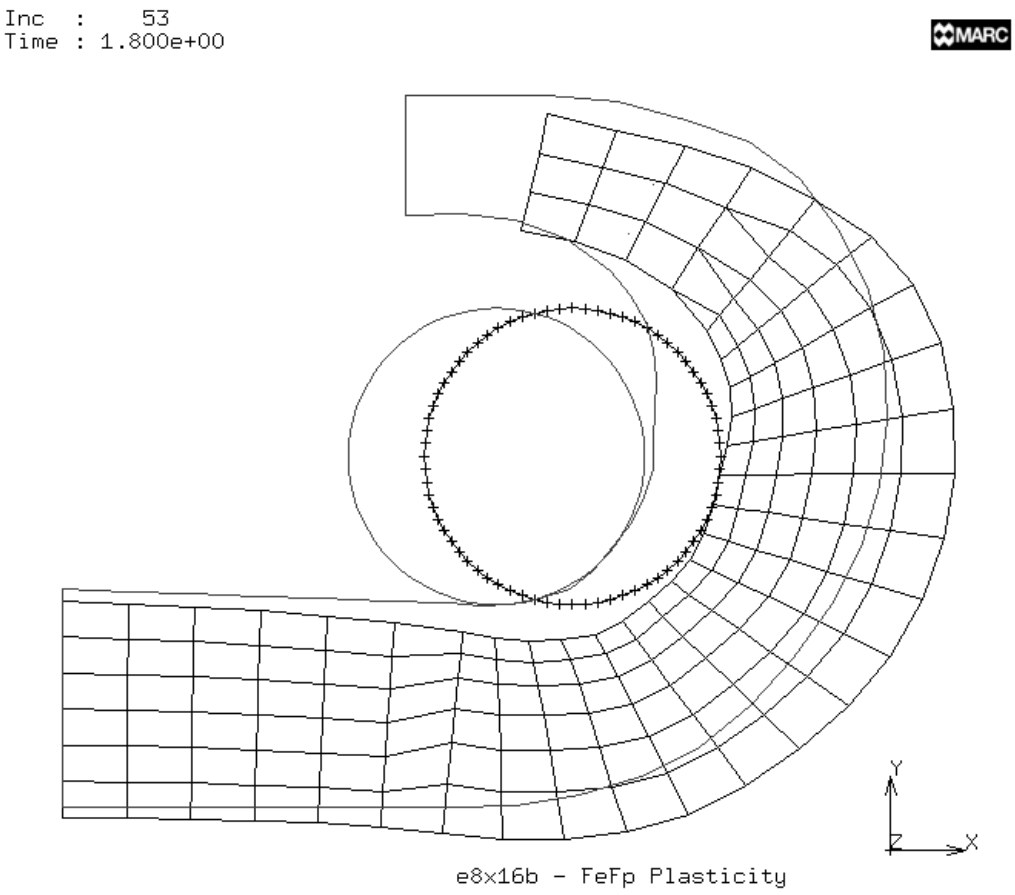

Figure 8.16-4 Initial and Deformed Geometry 53 Increments for Data Set e8x16b

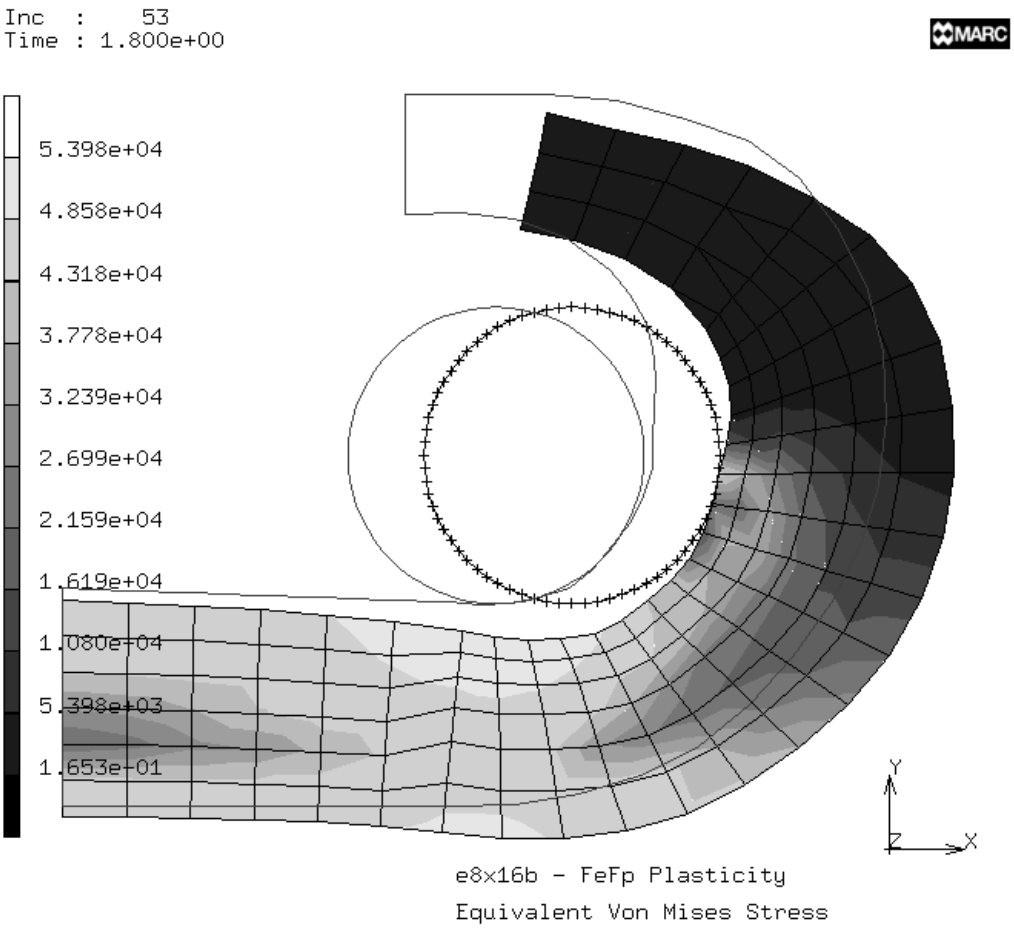

Figure 8.16-5 Contours of Equivalent von Mises Stress at 53 Increments for Data Set e8x16b

8.17 3D Extrusion Analysis with Coulomb Friction

This problem demonstrates MARC's ability to perform metal extrusion analysis using the CONTACT option. The analysis is complicated by the multiple intersecting contact surfaces.

This problem is modeled using the two data sets summarized below.

Data Set	Element Type(s)	Number of Elements	Number of Nodes	Differentiating Features
e8x17	7	16	45	Mean Normal Additive Decomposition Plasticity, CONSTANT DILATATION
e8x17b	7	16	45	Radial Return F^eF^p Plasticity

Parameters

In the first analysis, the UPDATE, FINITE, and LARGE DISP parameters are included in the parameter section to indicate this is a finite deformation analysis. The PRINT,8 option requests the output of additional information concerning contact. The REZONE parameter is included to allow the potential for future mesh rezoning to compensate for gross distortions in the original mesh.

In the second analysis, the PLASTICITY option is used to invoke the multiplicative decomposition (F^eF^p) procedure for finite strain plasticity.

Geometry

Element type 7, the eight-node brick element, is used in this analysis. For the first analysis, a '1' is placed in the second data field (EGEOM2) of the third data block of the GEOMETRY option to indicate that the constant dilatation formulation is used. This is done in recognition of the fact that metal extrusion results in large plastic deformations which are nearly incompressible. This is not necessary in the second analysis as the F^eF^p procedure used a mixed variational principal that accurately accounts for incompressibility.

Boundary Conditions

Appropriate nodal constraints are applied in the global X, Y directions to impose symmetry. The billet is extruded by having a constant velocity imposed.

POST/RESTART

The following variables are written to a formatted post file every 35 increments:

7} Equivalent plastic strain 17} Equivalent von Mises stress

The last converged increment is written to a restart file.

Control

A maximum of 200 increments are to be carried out, with no more than 20 recycles per increment. Displacement control is used, with a relative error of 10%.

Material Properties

The material for all elements is treated as an elastic-perfectly plastic material, with Young's modulus of 1.75E+07 psi, Poisson's ratio of 0.3, and an initial yield stress of 35,000 psi.

Contact

This option declares that there are three bodies in contact with Coulomb friction between them. In particular, the friction coefficient associated with each rigid die is 0.1. The relative slip velocity is 0.01 inch/second. The contact tolerance distance is 0.01 inches.

The three contact bodies are defined as follows:

Body 1: The deformable body consisting of 16 brick elements. Note that the velocity cannot be entered for a deformable body.

Body 2: A single plane is used to represent the ram and is given a velocity of -0.3 in/sec.

Body 3: Six planes are used to define the die.

Load Control

In the first analysis, the problem is loaded by the repeated application of the prescribed die velocities with the AUTO LOAD option. The load increment is applied 70 times. The TIME STEP option allows you to enter the time variable for static analysis should time dependent constitutive relations be used.

In the second analysis, the AUTO STEP option is used to adaptively change the time step.

Results

Figure 8.17-1 show the geometry configuration for the extrusion analysis. Figure 8.17-2 and Figure 8.17-3 shows the deformed body at the end of 35 increments with the deformation at the same scale as the coordinates. Due to the high level of friction, significant transverse deformation is shown along the contact surfaces.

Figure 8.17-4 and Figure 8.17-5 show the deformed body at the end of 70 increments.

Figure 8.17-6 shows the equivalent plastic strain contours on the deformed structure at increment 70 with the largest strain level at 0.705.

Figure 8.17-7 shows the equivalent von Mises stress contours on the deformed structure at increment 70 with peak values at 37,820 psi.

Figure 8.17-8 shows the contours of equivalent plastic strain at increment 199 for data set e8x17b.

Figure 8.17-9 shows the contours of von Mises effective stress at increment 199 for data set e8x17b.

The comparison of von Mises stresses and equivalent plastic strains show a very close agreement.

Parameters, Options, and Subroutines Summary

Example e8x17.dat:

Parameters	Model Definition Options	History Definition Options
ELEMENT	CONNECTIVITY	AUTO LOAD
END	CONTACT	CONTINUE
FINITE	CONTROL	TIME STEP
LARGE DISP	COORDINATE	
PRINT	END OPTION	
REZONE	FIXED DISP	
SIZING	GEOMETRY	
TITLE	ISOTROPIC	
UPDATE	POST	
	PRINT CHOICE	
	RESTART LAST	

Example e8x17b.dat:

Parameters	Model Definition Options	History Definition Options
ELEMENT	CONNECTIVITY	AUTO STEP
END	CONTACT	CONTINUE
FINITE	CONTROL	
LARGE DISP	COORDINATE	
PRINT	END OPTION	
REZONE	FIXED DISP	
SIZING	GEOMETRY	
TITLE	ISOTROPIC	
UPDATE	POST	
	PRINT CHOICE	
	RESTART LAST	

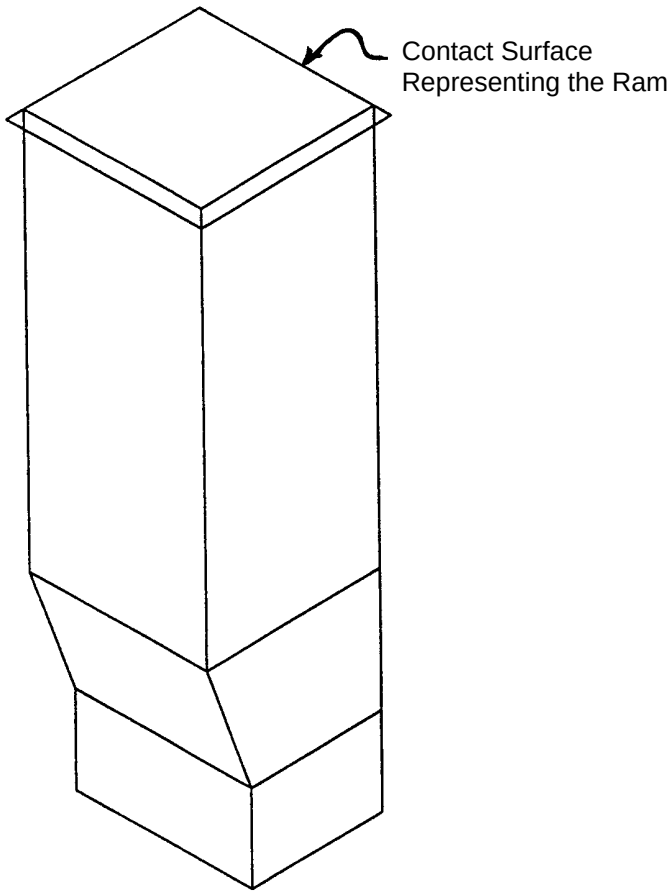

Figure 8.17-1 Rigid Surfaces Defining Extrusion Die

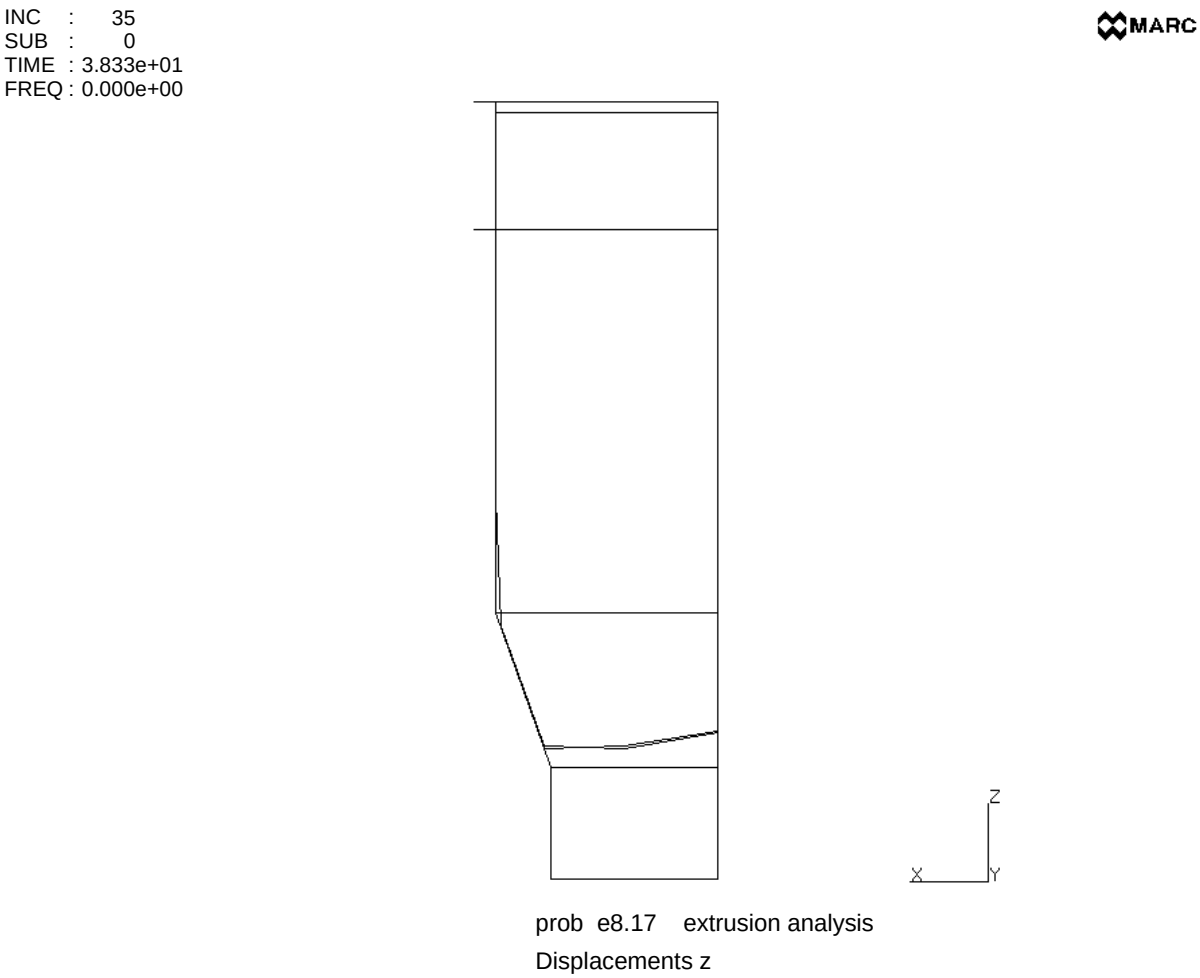

Figure 8.17-2 Deformed Mesh, Increment 35

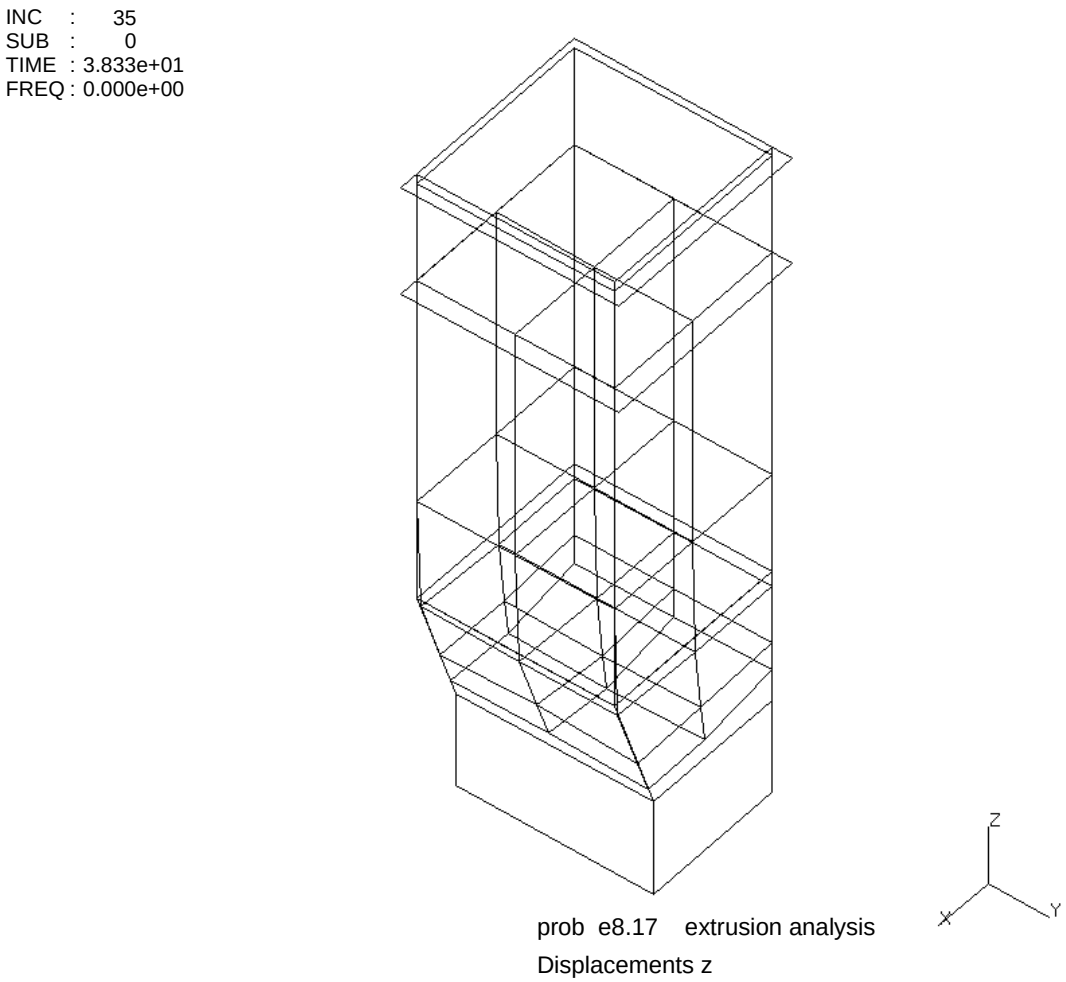

Figure 8.17-3 Deformed Mesh, Increment 35

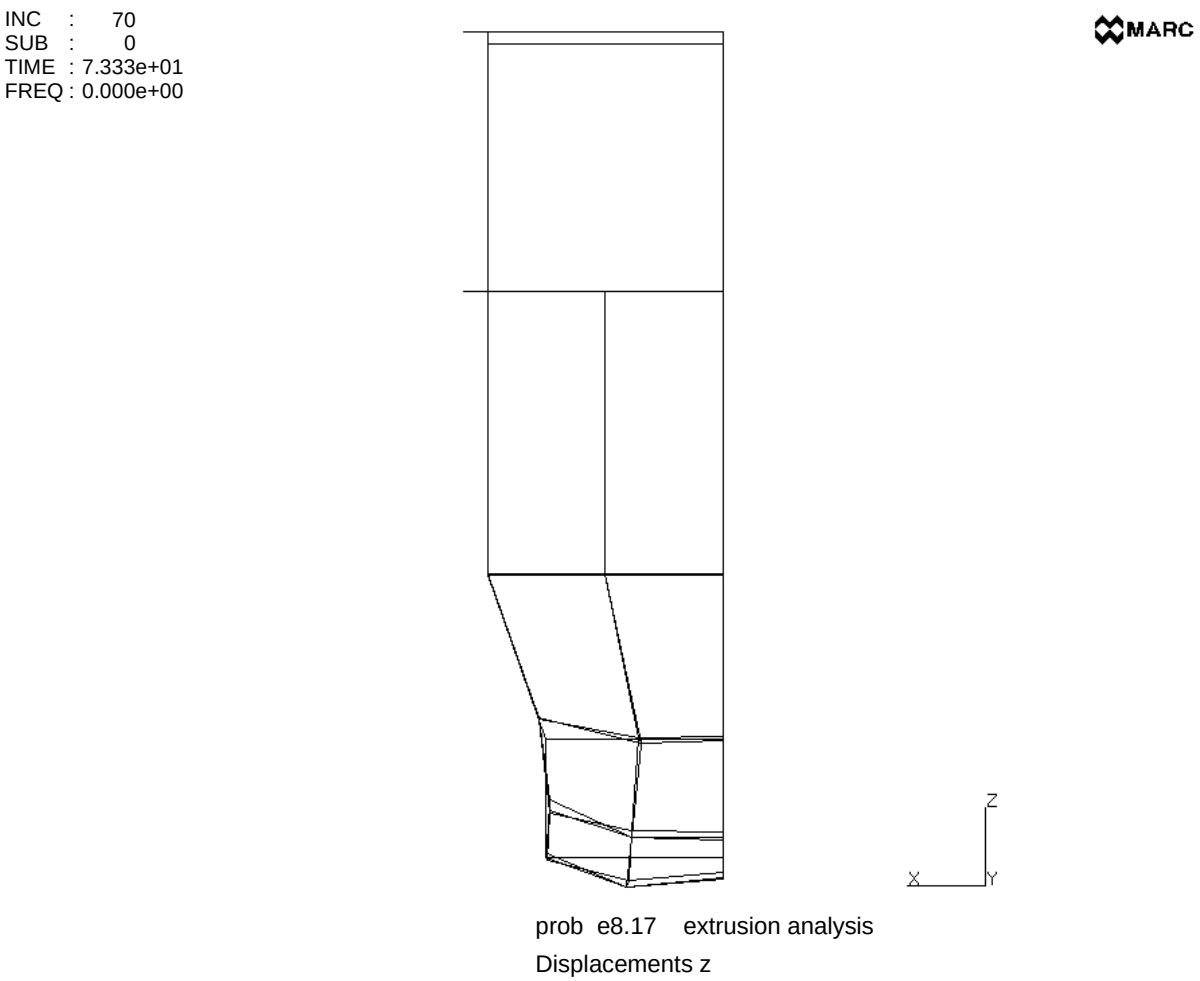

Figure 8.17-4 Deformed Mesh, Increment 70

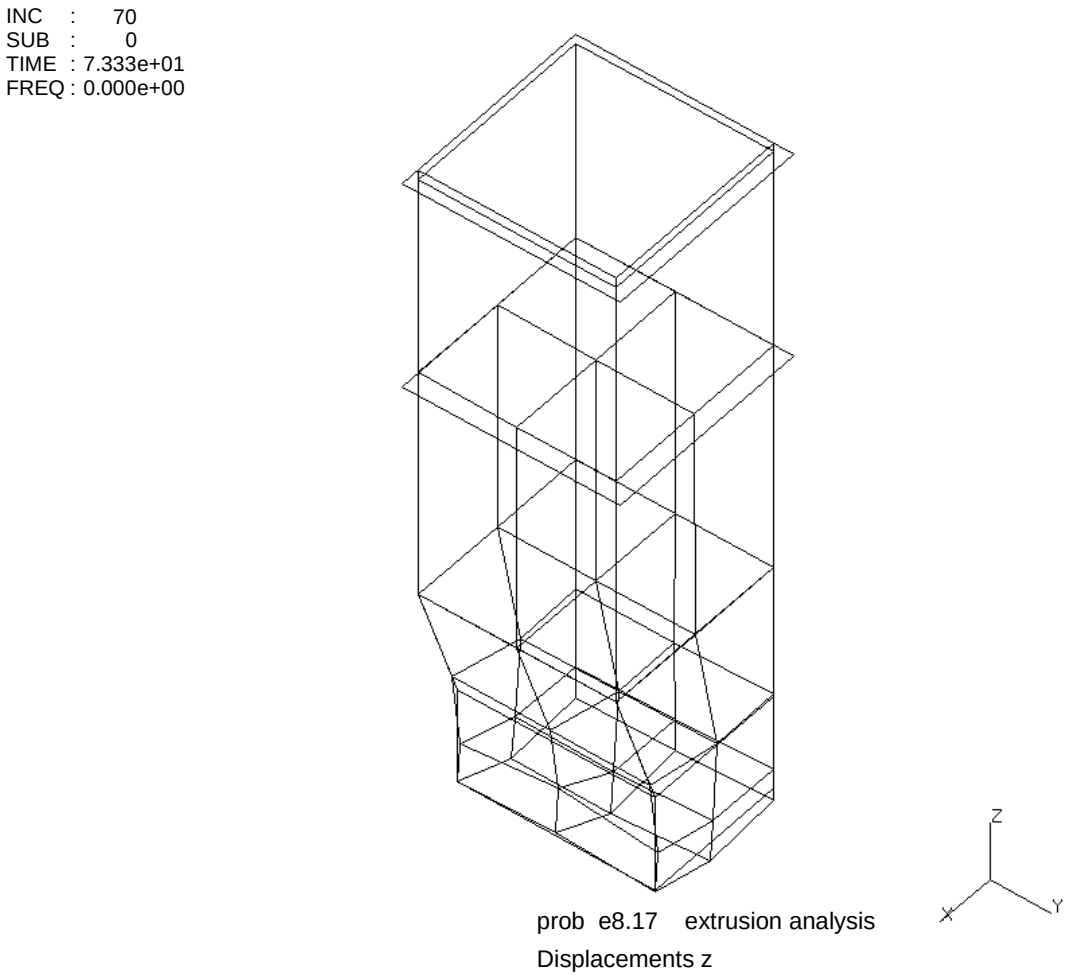

Figure 8.17-5 Deformed Mesh, Increment 70

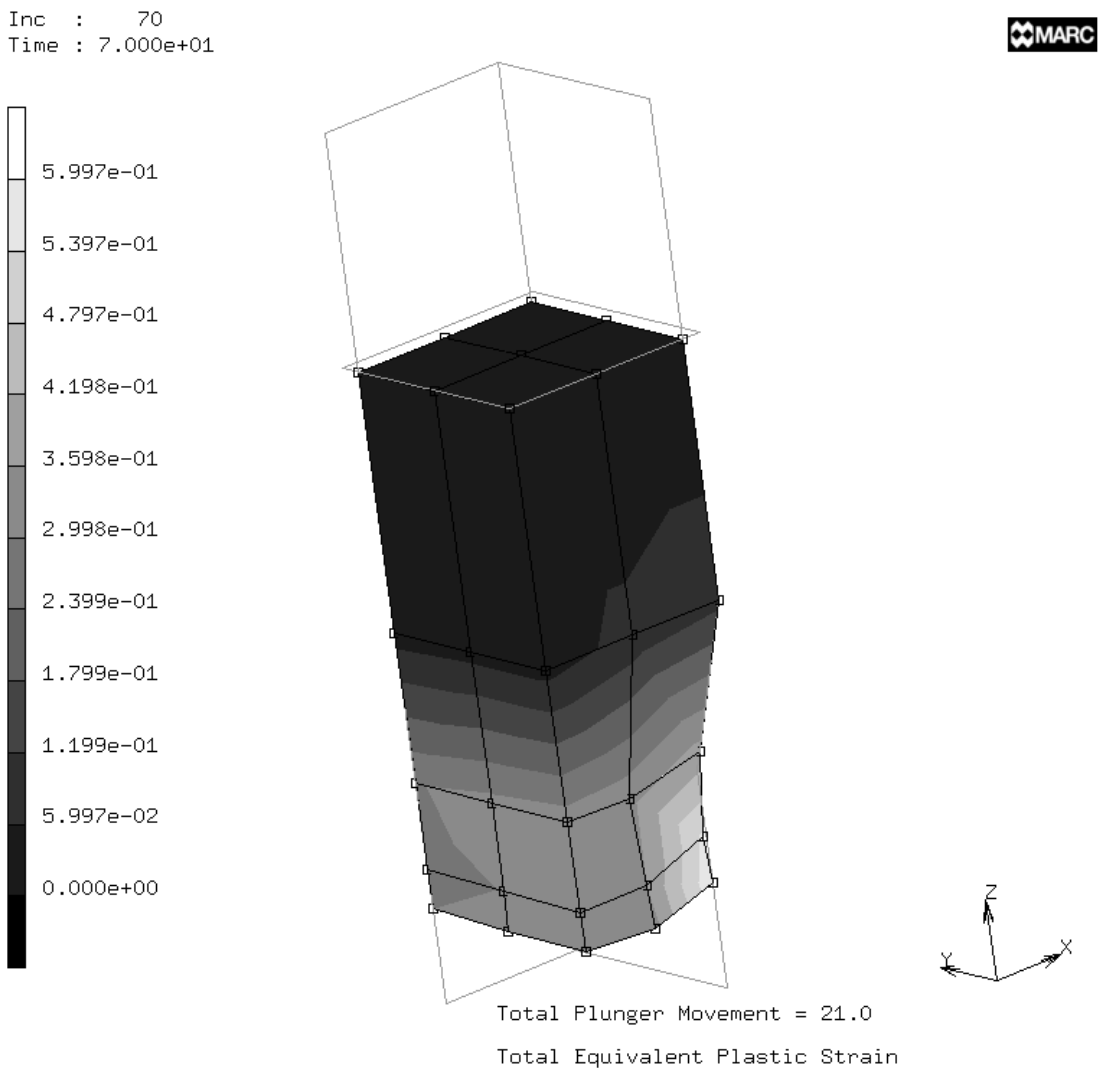

Figure 8.17-6 Equivalent Plastic Strain, Increment 70

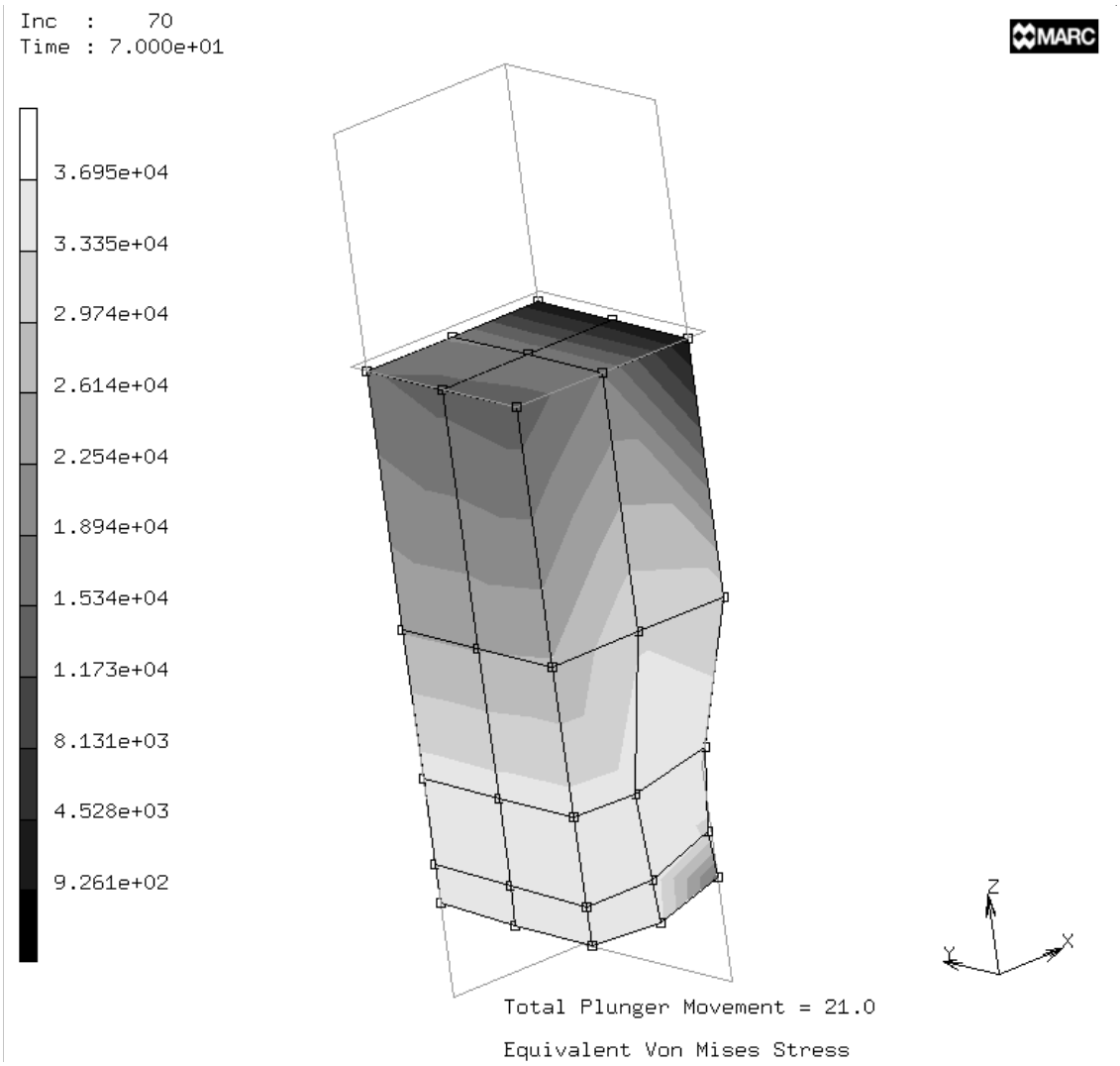

Figure 8.17-7 Equivalent Stress, Increment 70

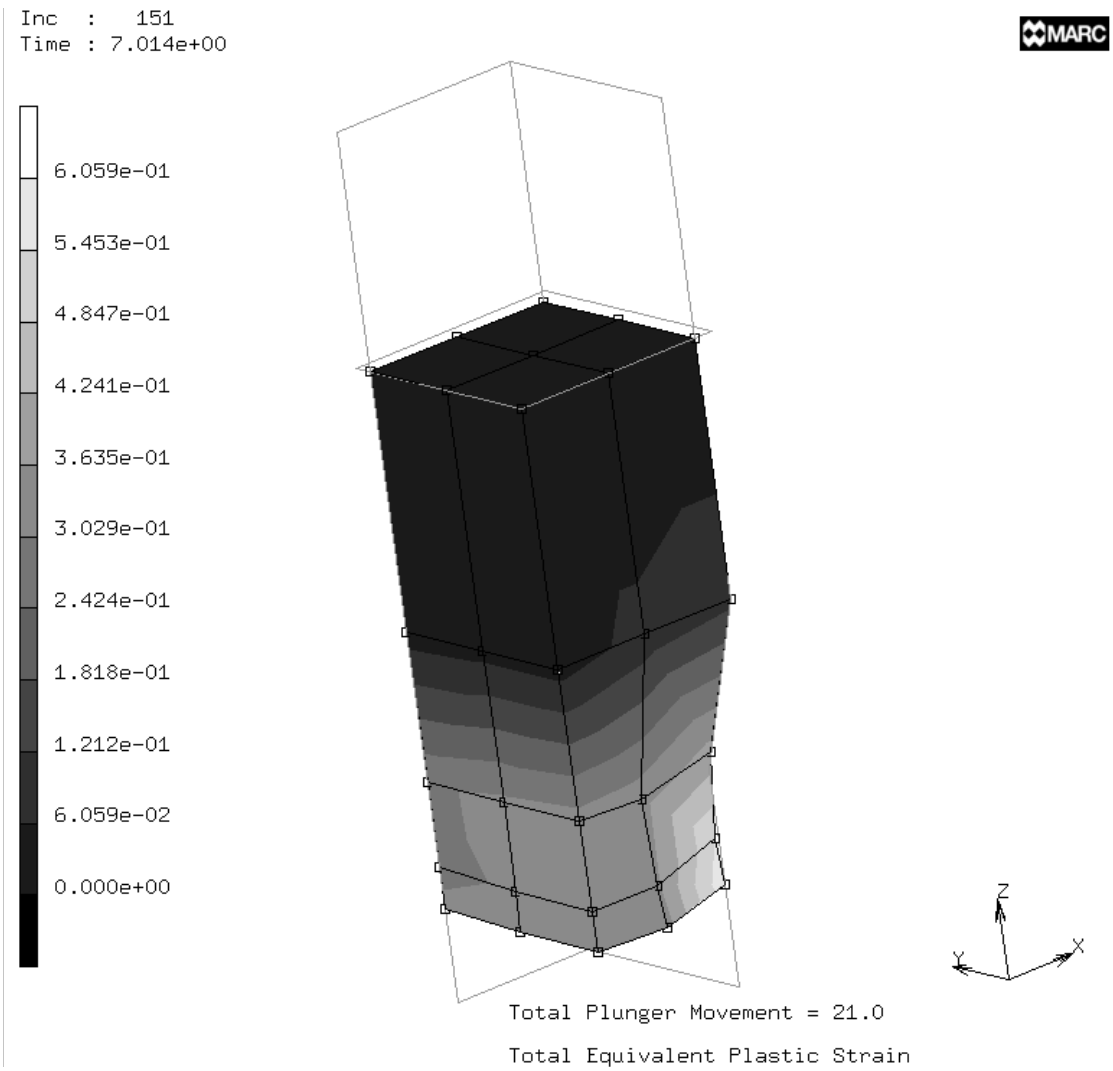

Figure 8.17-8 Equivalent Plastic Strain at Increment 199 for Data Set e8x17b

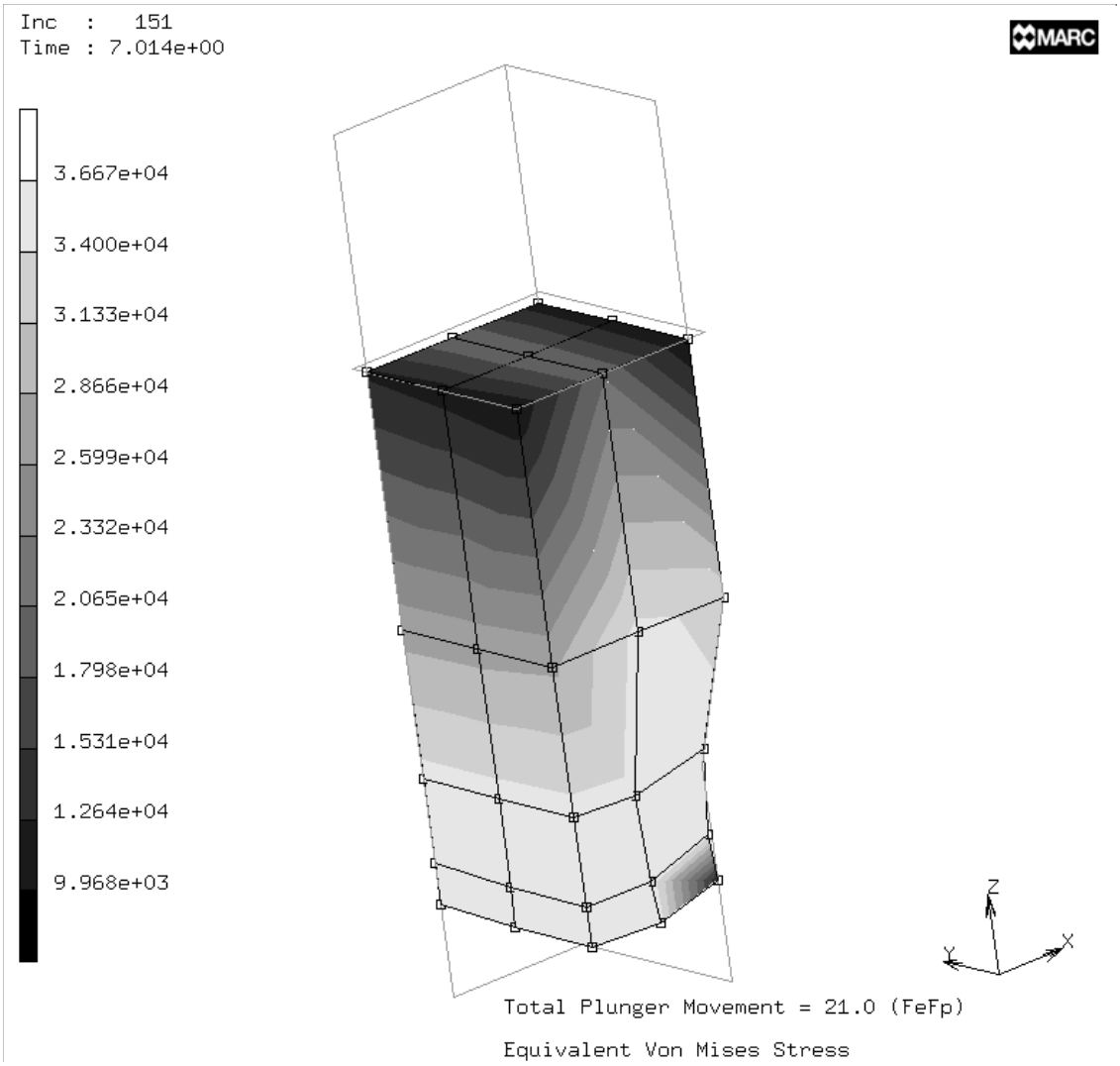

Figure 8.17-9 Equivalent von Mises Effective Stress at Increment 199 for Data Set e8x17b

8.18 3D Forming of a Circular Blank Using Shell or Membrane Elements and Coulomb Friction

This problem demonstrates MARC's ability to perform stretch forming by a spherical punch using the CONTACT option with shell or membrane elements.

This problem is modeled using the four techniques summarized below.

Data Set	Element Type(s)	Number of Elements	Number of Nodes	Differentiating Features
e8x18	75	112	127	Mean Normal Additive Decomposition Plasticity Piecewise Linear Representation of Rigid Surfaces
e8x18b	75	112	127	Mean Normal Additive Decomposition Plasticity with Analytical Representation for Rigid Surfaces
e8x18c	18	112	127	Multiplicative Decomposition F_eF_p Plasticity, Membrane Elements, Piecewise Linear Representation of Rigid Surfaces
e8x18d	75	112	127	Mean Normal Additive Decomposition Plasticity, Analytical Representation for Rigid Surfaces, AUTO STEP option controls loading

Parameters

Problems e8x18a, e8x18b, and e8x18d use the UPDATE, LARGE DISP, and FINITE parameters to indicate a finite deformation analysis. These three problems also use the 4-node thick shell element, element type 75. Seven layers are used through the shell thickness. Problem e8x18c uses element 18, a 4-node membrane element. Radial return multiplicative decomposition finite strain plasticity is used in problem e8x18c.

Geometry

A shell thickness of 1 cm is specified through the GEOMETRY option in the first field (EGEOM1).

Boundary Conditions

The first boundary condition is used to model the binding in the stretch forming process. The second and third boundary conditions are used to represent the symmetry conditions.

POST

The following variables are written to a formatted post file:

7} Equivalent plastic strain 17} Equivalent von Mises stress
20} Element thickness

Furthermore, the above three variables are also requested for all shell elements at layer number 4, which is the midsurface.

Control

A full Newton-Raphson iterative procedure is requested, along with the mean normal method approach to solve plasticity equations. Displacement control is used, with a relative error of 5%. Twenty-six load steps are prescribed, with a maximum of twenty recycles (iterations) per load step.

Material Properties

The material for all shell elements is treated as an elastic-plastic material, with Young's modulus of 690,040 lbf/cm^2, Poisson's ratio of 0.3, and an initial yield stress of 80.6 lbf/cm^2. The yield stress is given in the form of a power law and is defined through the WKSLP user subroutine. For membrane element problem e8x18c, a constant workhardening modulus of 100 ksi is used.

Contact

This option declares that there are three bodies in contact with Coulomb friction between them. A coefficient of friction of 0.3 is associated with each rigid die. The first body represents the workpiece. The second body is the lower die, defined as three surfaces of revolution. The first and third surfaces of revolution use a straight line as the generator, the second uses a circle as the generator. In examples e8x18and e8x18c, the third body (the punch) is defined as two surfaces of revolution. These surfaces are extended from -0.5 to 101.21 degrees. In examples e8x18b and e8x18d, the third body (the punch) is represented by a sphere. Its initial center is at 0, 0, 51.3 and the radius is 50. In problems e8x18 and e8x18c, the rigid surfaces are discretized into 4-node patches. This results in a piecewise-linear representation of the surface. In e8x18b and e8x18d, the analytical form is used. This results in a smooth representation of the surface. The relative slip velocity is specified as 0.01 cm/sec. The contact tolerance distance is 0.05 cm.

Load Control

This problem is displacement controlled with a velocity of 1 cm/sec applied in the negative z-direction with the AUTO LOAD option. The load increment is applied 40 times. The MOTION CHANGE option is illustrated to control the velocity of the rigid surfaces.

Results

Figure 8.18-2 shows the deformed body at the end of 40 increments with the deformation at the same scale as the coordinates. Due to the high level of friction, significant transverse deformation is shown along the contact surfaces.

Figure 8.18-3 shows the equivalent plastic strain contours on the deformed structure at increment 40, with the largest strain level at 60%.

Figure 8.18-4 shows the equivalent von Mises stress contours on the deformed structure at increment 40 with peak values at 527.4 lbf/cm^2.

Figure 8.18-5 shows the deformed body at the end of 40 increments. The computational performance and results are improved by using the analytical form.

Figure 8.18-6 shows the deformed geometry with contours of total effective plastic strain for data set e8x18c which uses membrane elements.

Figure 8.18-7 shows the final deformed geometry with contours of total effective plastic strain for data set e8x18d.

Parameters, Options, and Subroutines Summary

Example e8x18.dat:

Parameters	Model Definition Options	History Definition Options
ELEMENT	CONNECTIVITY	AUTO LOAD
END	CONTACT	CONTINUE
FINITE	CONTROL	MOTION CHANGE
LARGE DISP	COORDINATE	TIME STEP
PRINT	END OPTION	
SHELL SECT	FIXED DISP	
SIZING	GEOMETRY	
TITLE	ISOTROPIC	
UPDATE	POST	
	PRINT CHOICE	
	WORK HARD	

Example e8x18b.dat:

Parameters	Model Definition Options	History Definition Options
ELEMENTS	CONNECTIVITY	AUTO LOAD
END	CONTACT	CONTINUE
FINITE	CONTROL	MOTION CHANGE
LARGE DISP	COORDINATE	TIME STEP
PRINT	END OPTION	
SHELL SECT	FIXED DISP	
SIZING	GEOMETRY	
TITLE	ISOTROPIC	
UPDATE	POST	
	PRINT CHOICE	
	WORK HARD	

Example e8x18c.dat:

Parameters	Model Definition Options	History Definition Options
ELEMENTS	CONNECTIVITY	AUTO LOAD
END	CONTACT	CONTINUE
PLASTICITY	CONTROL	MOTION CHANGE
LARGE DISP	COORDINATE	TIME STEP
PRINT	END OPTION	
SIZING	FIXED DISP	
TITLE	GEOMETRY	
ALIAS	ISOTROPIC	
	POST	
	PRINT CHOICE	
	WORK HARD	

Example e8x18d.dat:

Parameters	Model Definition Options	History Definition Options
ELEMENTS	CONNECTIVITY	AUTO STEP
END	CONTACT	CONTINUE
FINITE	CONTROL	MOTION CHANGE
LARGE DISP	COORDINATE	TIME STEP
PRINT	END OPTION	
SHELL SECT	FIXED DISP	
SIZING	GEOMETRY	
TITLE	ISOTROPIC	
UPDATE	POST	
	PRINT CHOICE	
	WORK HARD	

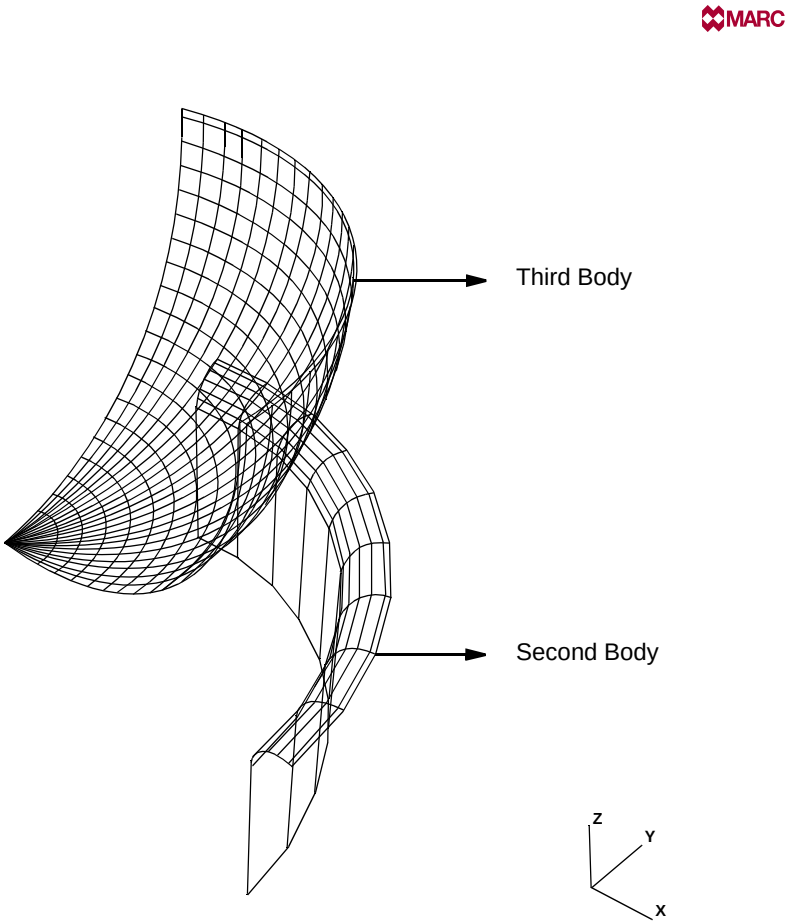

Figure 8.18-1 Circular Blank Holder and Punch

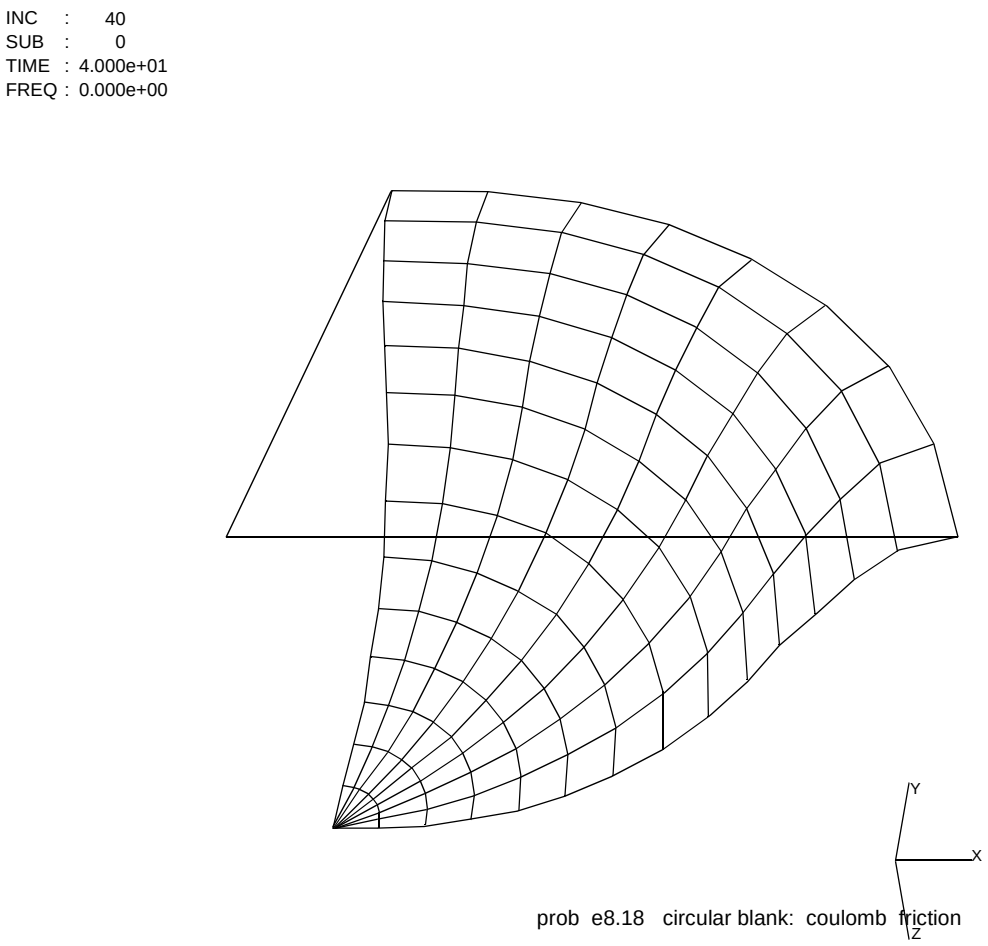

Figure 8.18-2 Deformed Sheet at Increment 40

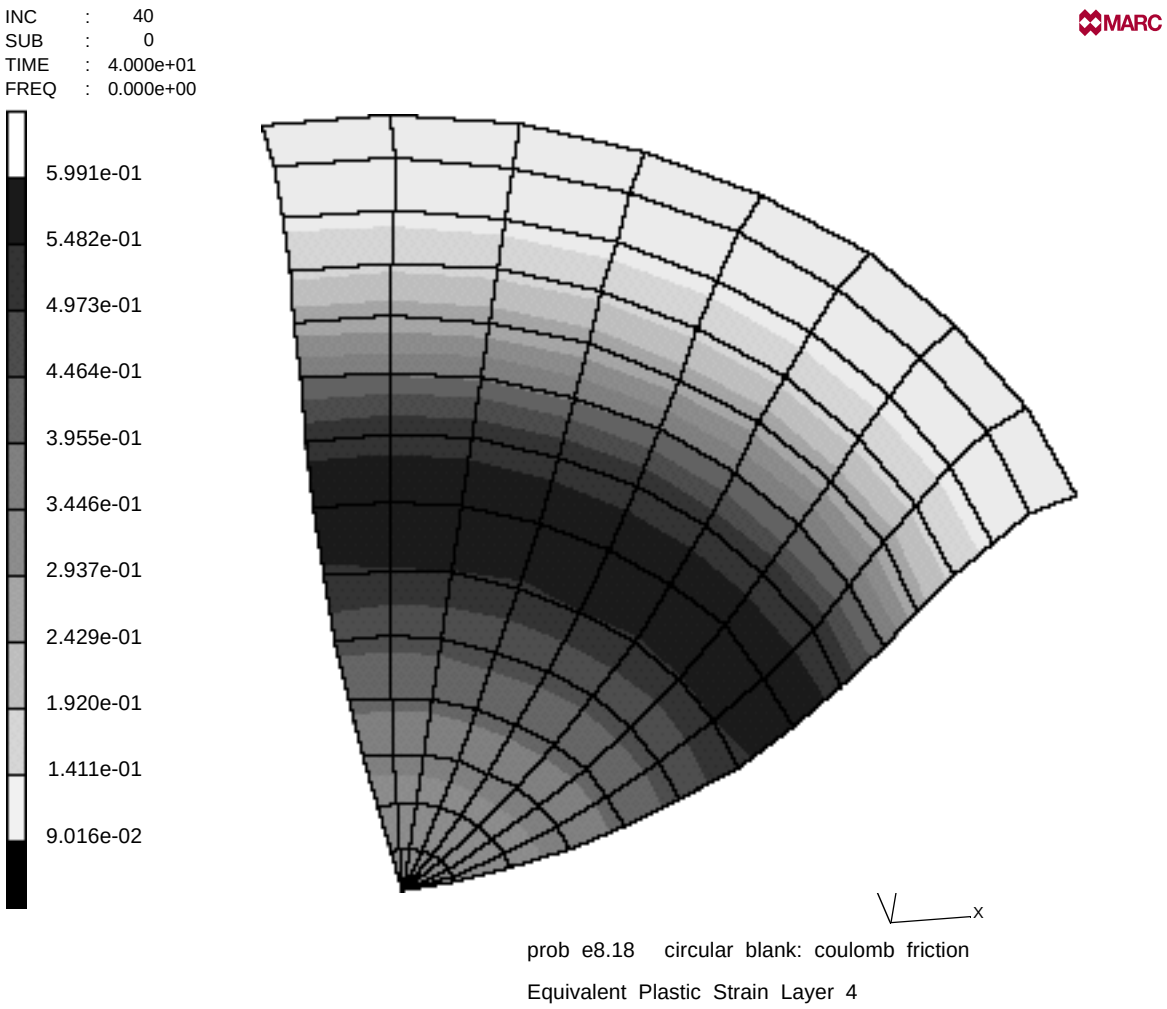

Figure 8.18-3 Plastic Strain at Increment 40

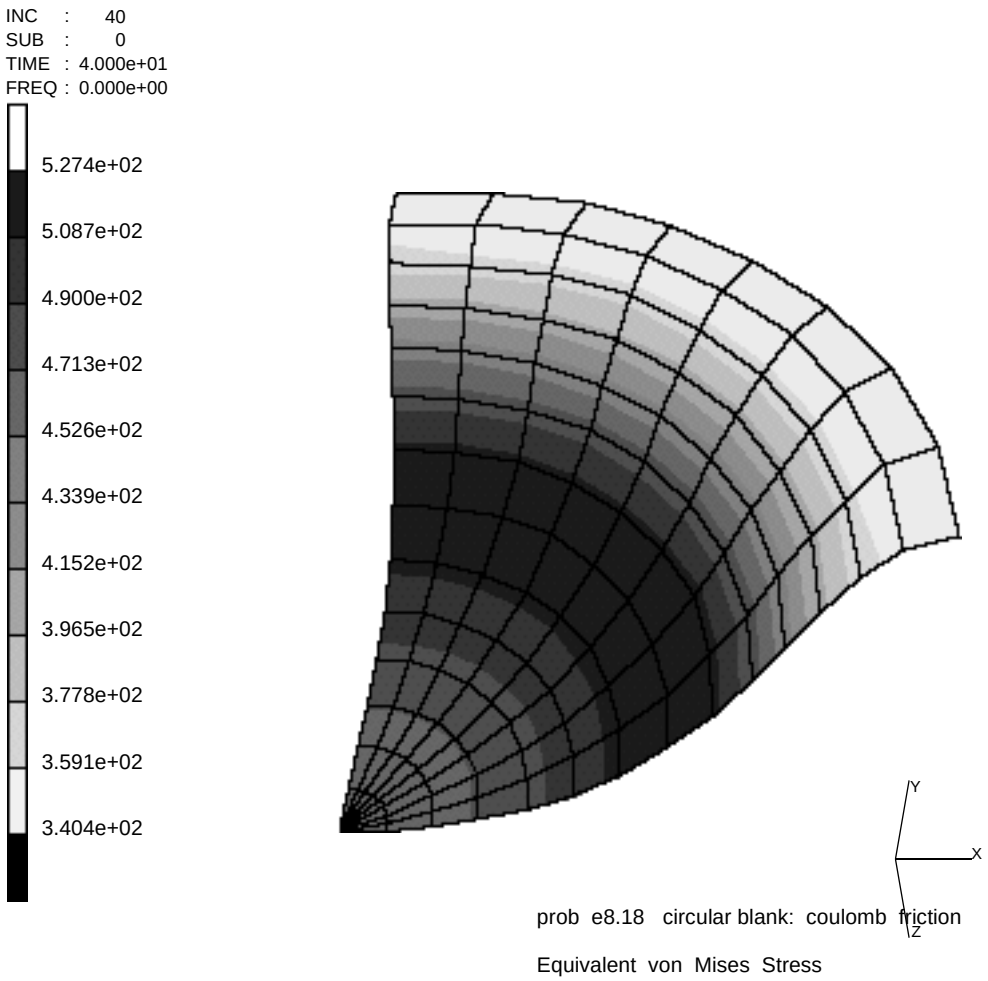

Figure 8.18-4 Equivalent Stress at Increment 40

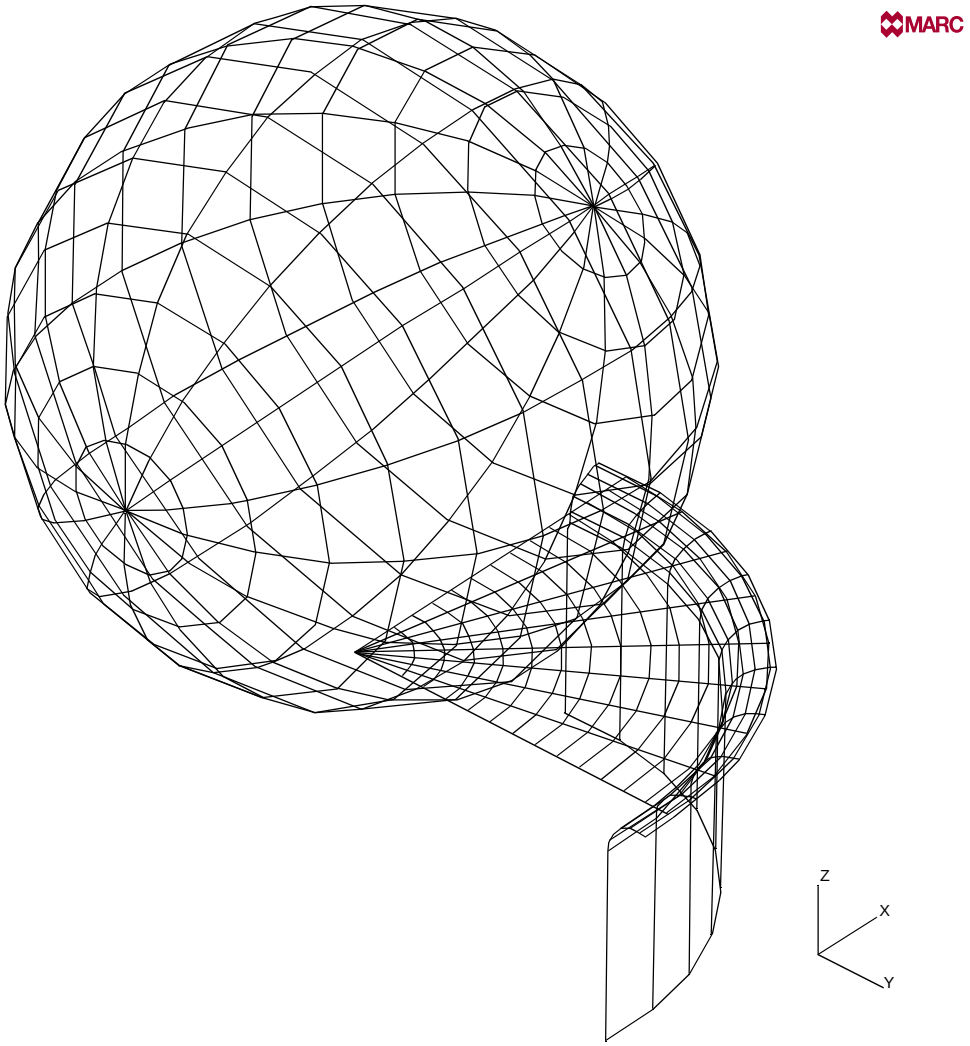

Figure 8.18-5 Analytical Form of Rigid Contact Surfaces

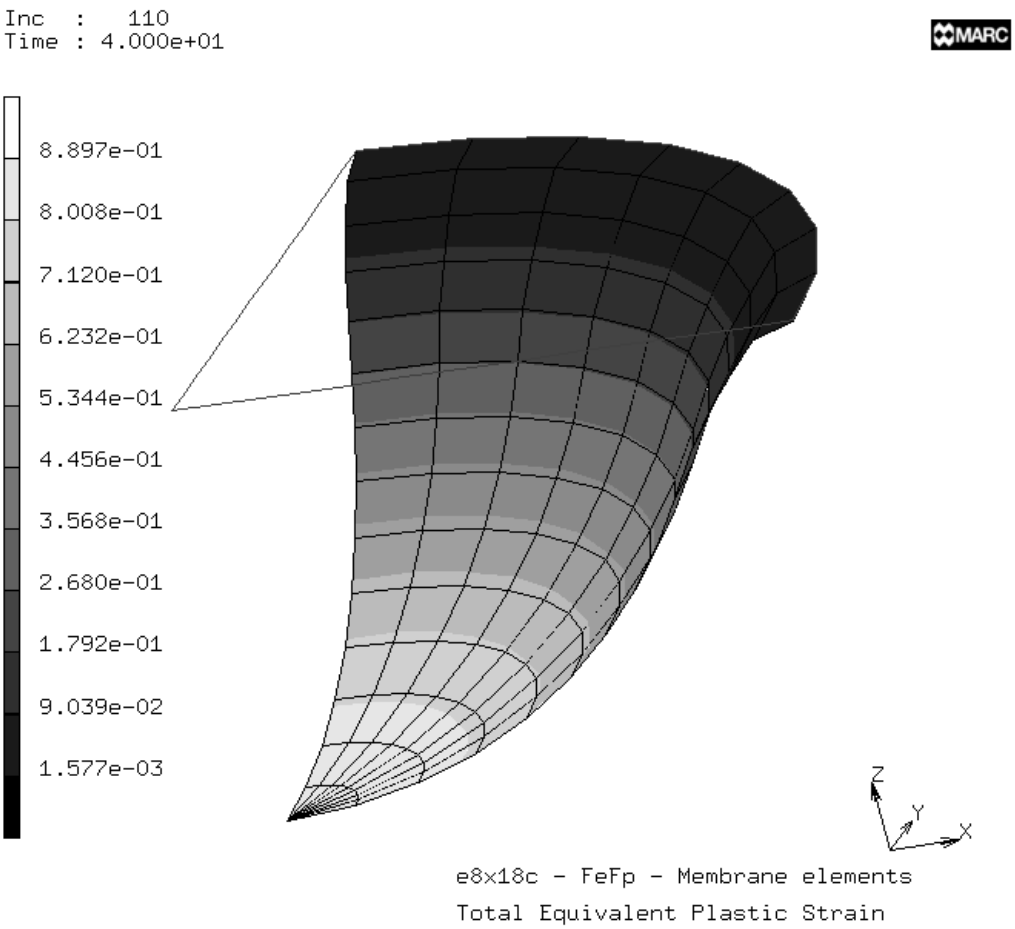

Figure 8.18-6 Final Deformed Geometry for Data Set e8x18c

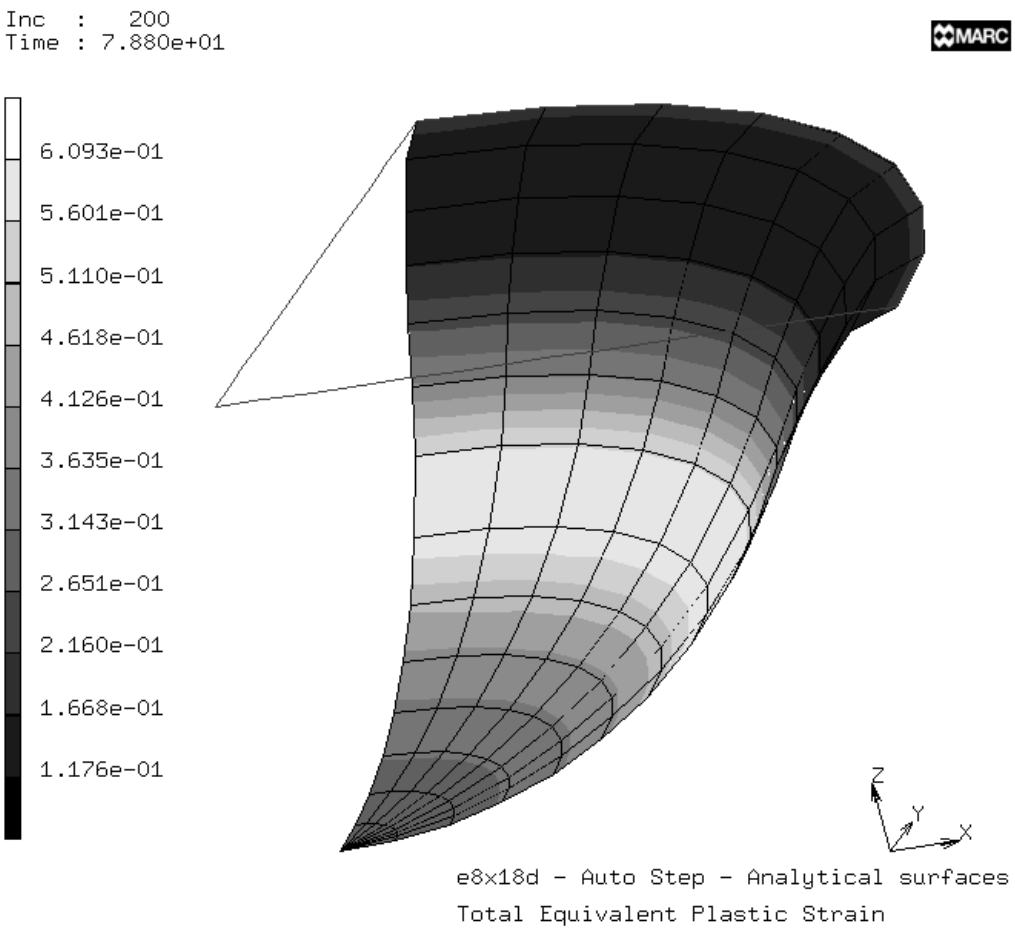

Figure 8.18-7 Final Deformed Geometry for Data Set e8x18d

8.19 3D Indentation and Rolling without Friction

This problem demonstrates the program's ability to perform metal forming analyses (for example, rolling) using the CONTACT option. Large plastic deformation is anticipated in this analysis.

This problem is modeled using the two techniques summarized below.

Data Set	Element Type(s)	Number of Elements	Number of Nodes	Differentiating Features
e8x19	7	128	225	Additive decomposition mean normal plasticity
e8x19b	7	128	225	Multiplicative decomposition (F^eF^p) radial return plasticity

Parameters

In the first analysis, the UPDATE, FINITE, and LARGE DISP parameters are used to indicate that the additive decomposition is to be used in the finite deformation analysis. In the second analysis, the PLASTICITY parameter is used to indicate that the multiplicative (F^eF^p) procedure is used. The PRINT,8 option requests the output of additional information regarding contact.

Geometry

The model consists of 128 brick elements, type 7. For the first analysis, a '1' is placed in the second data field (EGEOM2) to indicate that the constant dilatation formulation is used. This is done in recognition of the fact that metal extrusion results in large plastic deformations which are nearly incompressible.

Boundary Conditions

Appropriate nodal constraints are applied in the global X, Y directions. Since the geometry and loading are symmetric in the Z direction, no boundary conditions are applied in that direction. A contact surface is used to represent this symmetry surface.

POST/PRINT Control

The following variables are written to a formatted post file:

11 σ_{XX}
12 σ_{YY}
13 σ_{ZZ}
17 Mean normal stress
7 Equivalent total plastic strain.

These variables are written every 12th increment. The PRINT CHOICE option selects element number 1 as the only one which will have printed output (every 12th increment, like the post file). Such output will be for integration points 1 and 5 only.

Material Properties

The material for all elements is treated as an elastic-plastic material, with Young's modulus of 1.75E+07 psi, Poisson's ratio of 0.3, and an initial yield stress of 35,000 psi.

Contact

The first body is the deformable workpiece; the second is the rigid roller defined using the surface of revolution method. The radius is 10 inches. The third body is the symmetry surface. The contact tolerance distance is specified as 0.02 inches.

Load Control/Restart

Data sets e8x19 and e8x19b use the MOTION subroutine to specify the motion.

For data set e8x19, the rigid roll is pushed into the workpiece with a velocity of 0.25 in/sec for the first 25 increments. No motion is specified in the 26th increment. The total indentation is 6.25 inches. Following this, the roll is given an angular velocity of 0.05 radians/sec and a forward motion of 0.5 in/sec. A restart file is written at the end of increment 26.

For data set e8x19b, the rigid roll is pushed into the workpiece with a velocity of 0.25 in/sec for the first 110 increments. No motion is specified in the 111th increment. Following this, the roll is given an angular velocity of 0.05 radians/sec and a forward motion of 0.5 in/sec.

Since the problem involves large incremental changes of motion, many iterations may be required in each increment. A maximum of 20 recycles are chosen per increment. The convergence checking specifies a displacement increment relative norm with a tolerance of 0.10.

Results

Figure 8.19-1 shows the geometry configuration for this problem. The cylindrical rigid surface will be pushed into the deformable block that is resting on the flat rigid surface.

Figure 8.19-2, Figure 8.19-3, and Figure 8.19-4 show the deformed workpiece in increments 12, 24, and 36.

Figure 8.19-5 shows the equivalent total plastic strain for final deformed geometry for data set e8x19. Figure 8.19-6 shows the equivalent total plastic strain final deformed geometry for data set e8x19b. Figure 8.19-7 shows the von Mises for final deformed geometry for data set e8x19. Figure 8.19-8 shows the von Mises for final deformed geometry for data set e8x19b.

Parameters, Options, and Subroutines Summary

Example e8x19.dat:

Parameters	Model Definition Options	History Definition Options
ELEMENT	CONNECTIVITY	AUTO LOAD
END	CONTACT	CONTINUE
FINITE	CONTROL	TIME STEP
LARGE DISP	COORDINATE	
PRINT	END OPTION	
SIZING	FIXED DISP	
TITLE	GEOMETRY	
UPDATE	ISOTROPIC	
	POST	
	PRINT CHOICE	
	UDUMP	
	UMOTION	

Example e8x19b.dat:

Parameters	Model Definition Options	History Definition Options
ELEMENT	CONNECTIVITY	AUTO LOAD
END	CONTACT	CONTINUE
PLASTICITY	CONTROL	TIME STEP
PRINT	COORDINATE	
SIZING	END OPTION	
TITLE	FIXED DISP	
	GEOMETRY	
	ISOTROPIC	
	POST	
	PRINT CHOICE	
	UDUMP	
	UMOTION	

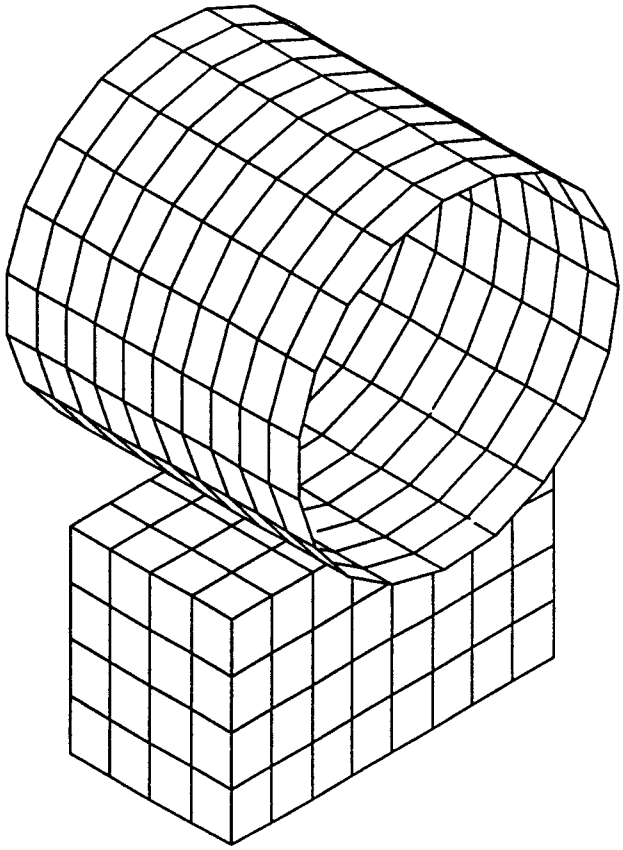

Figure 8.19-1 Initial Geometry for both Data Sets

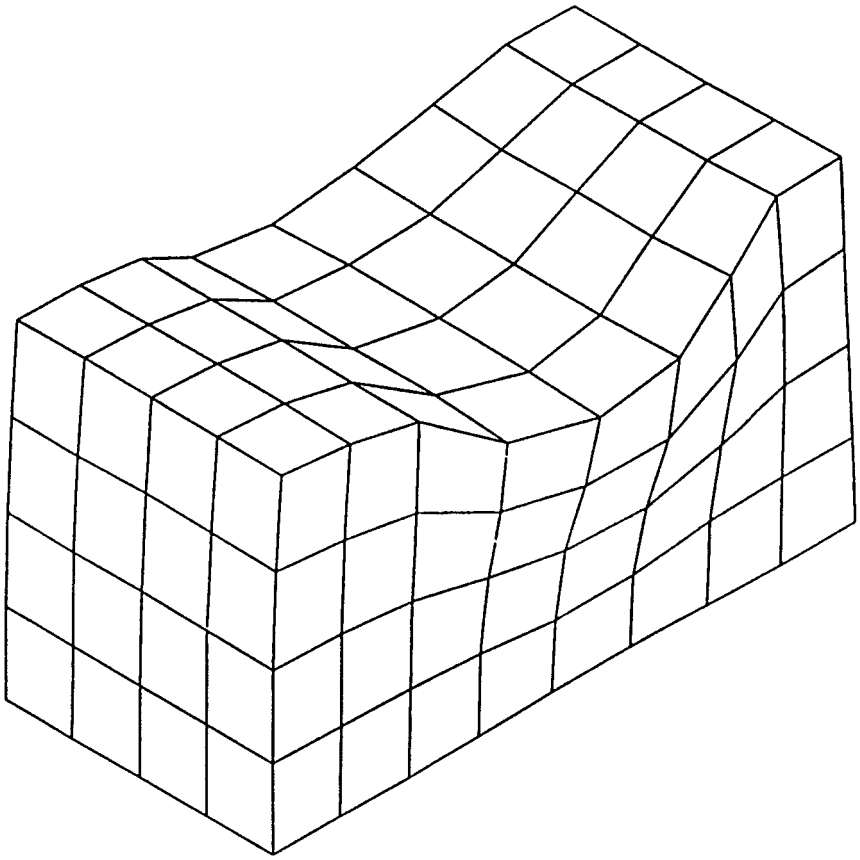

Figure 8.19-2 Deformed Mesh at Increment 12 for Data Set e8x19

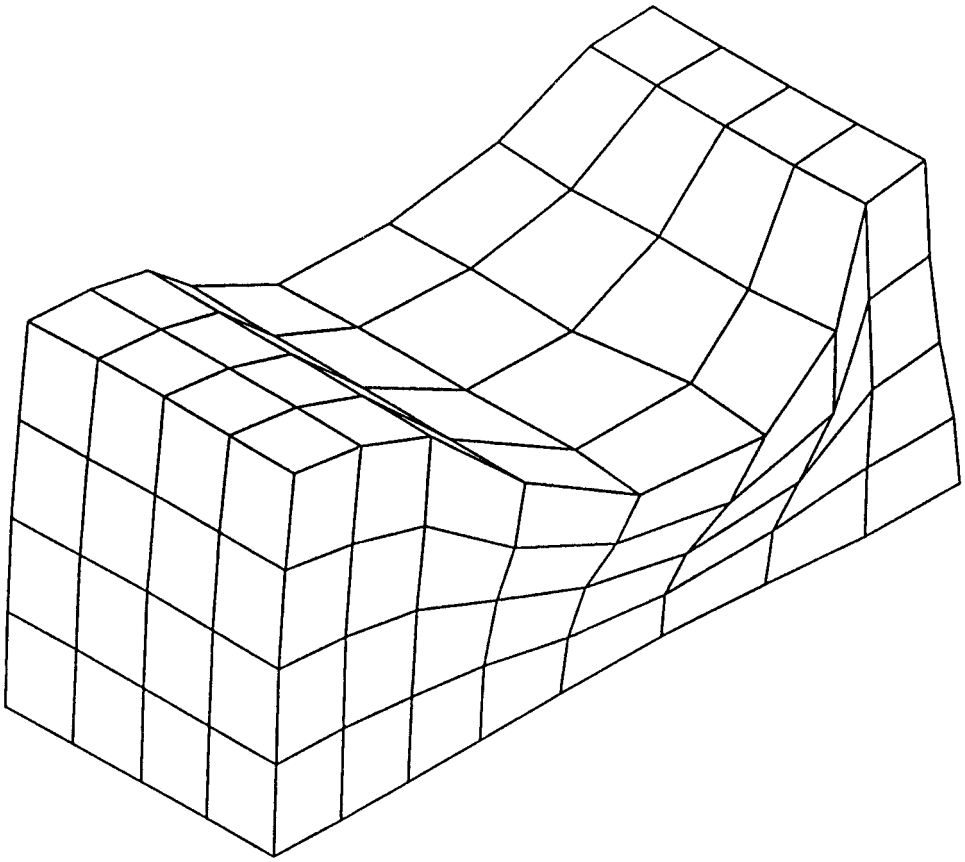

Figure 8.19-3 Deformed Mesh at Increment 24 for Data Set e8x19

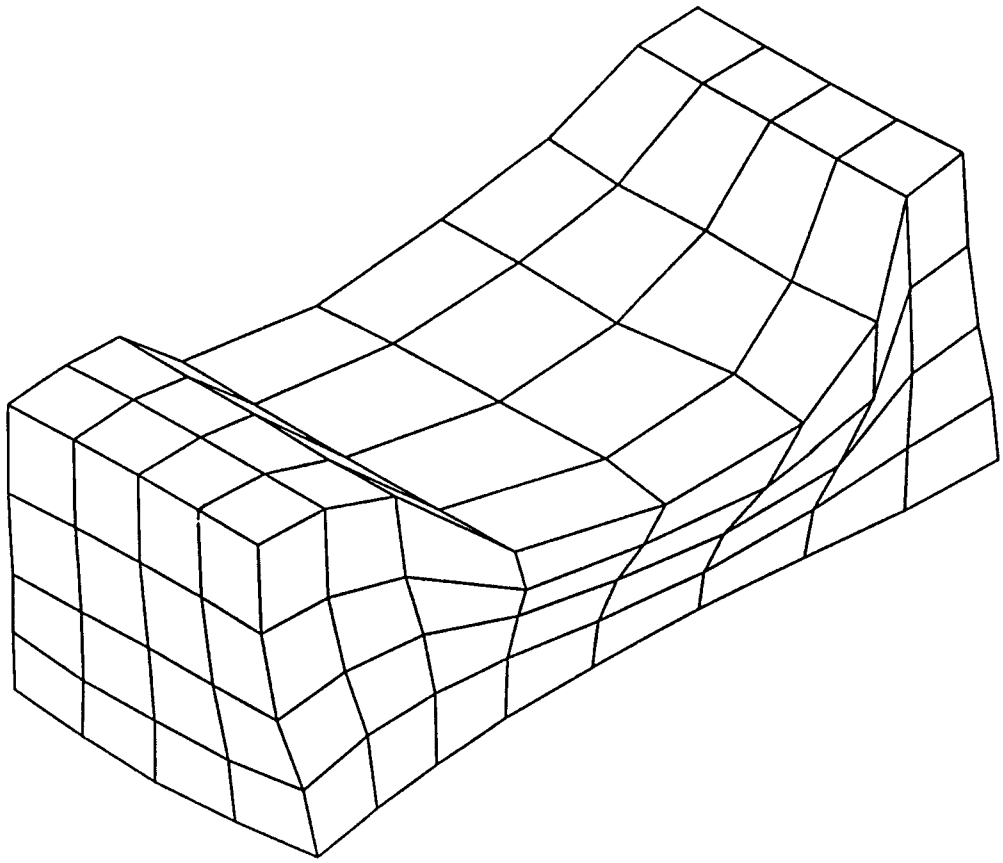

Figure 8.19-4 Deformed Mesh at Increment 36 for Data Set e8x19

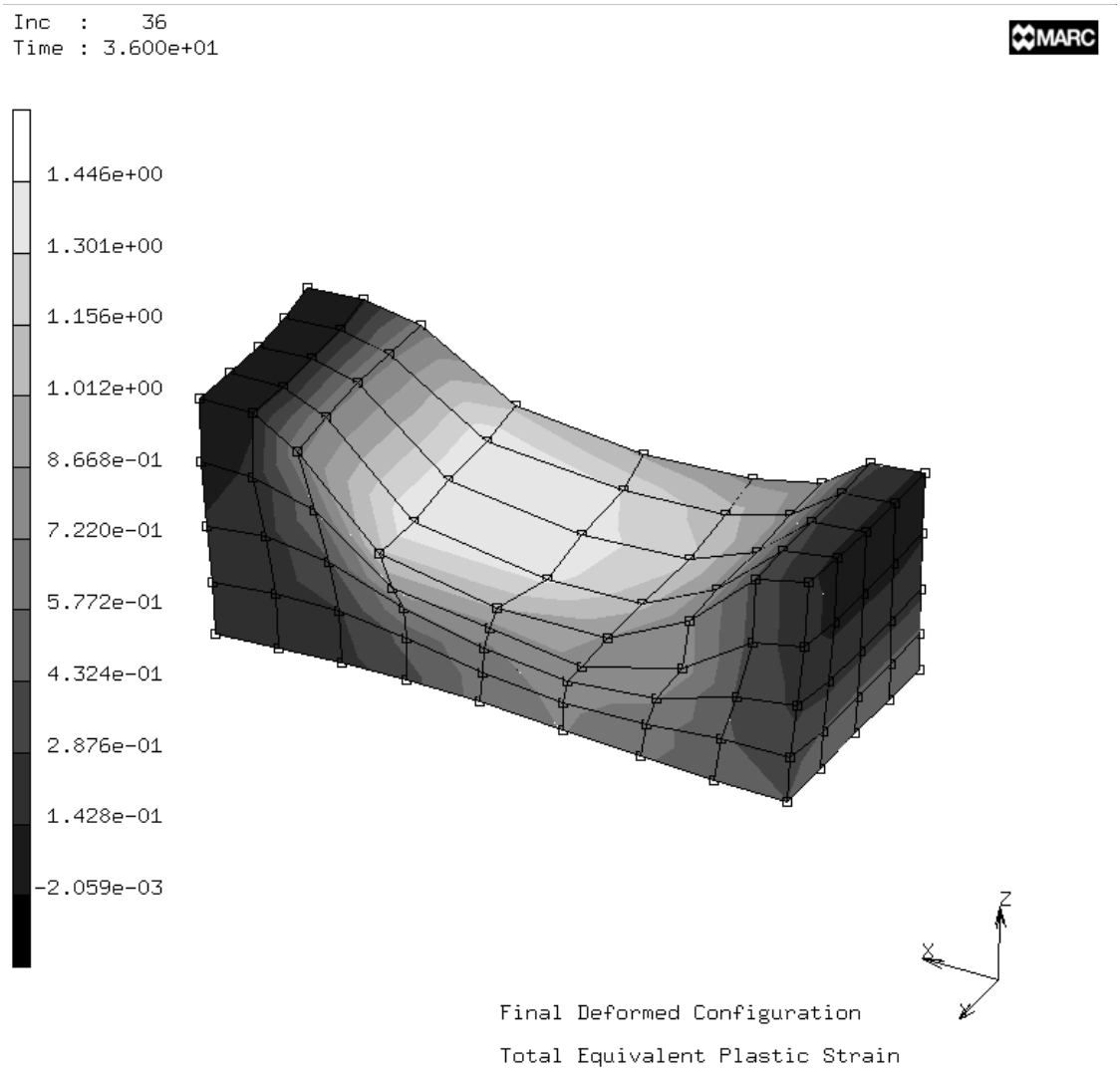

Figure 8.19-5 Equivalent Total Plastic Strain at Increment 36 for Data Set e8x19

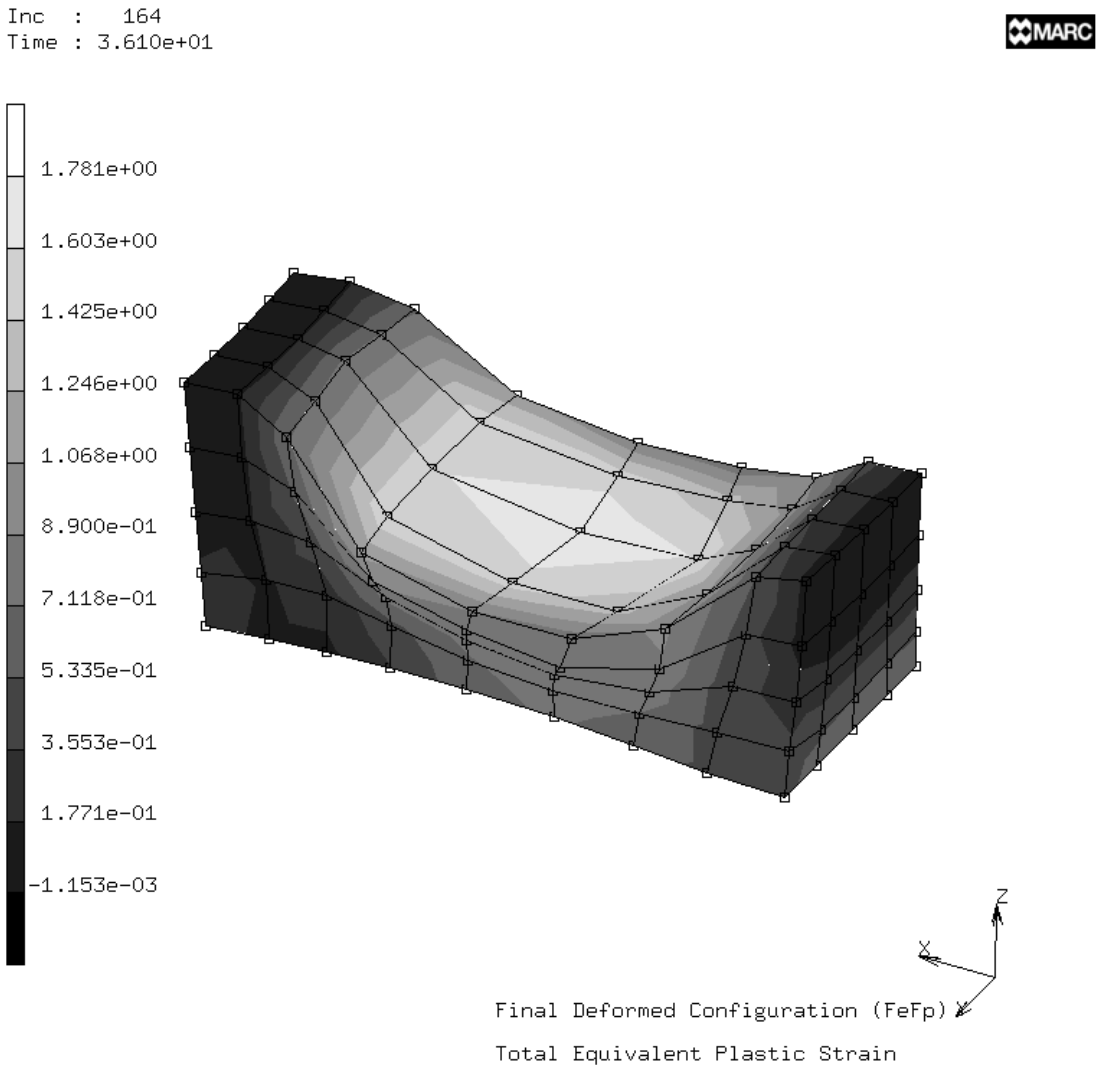

Figure 8.19-6 Equivalent Total Plastic Strain at Increment 164 for Data Set e8x19b

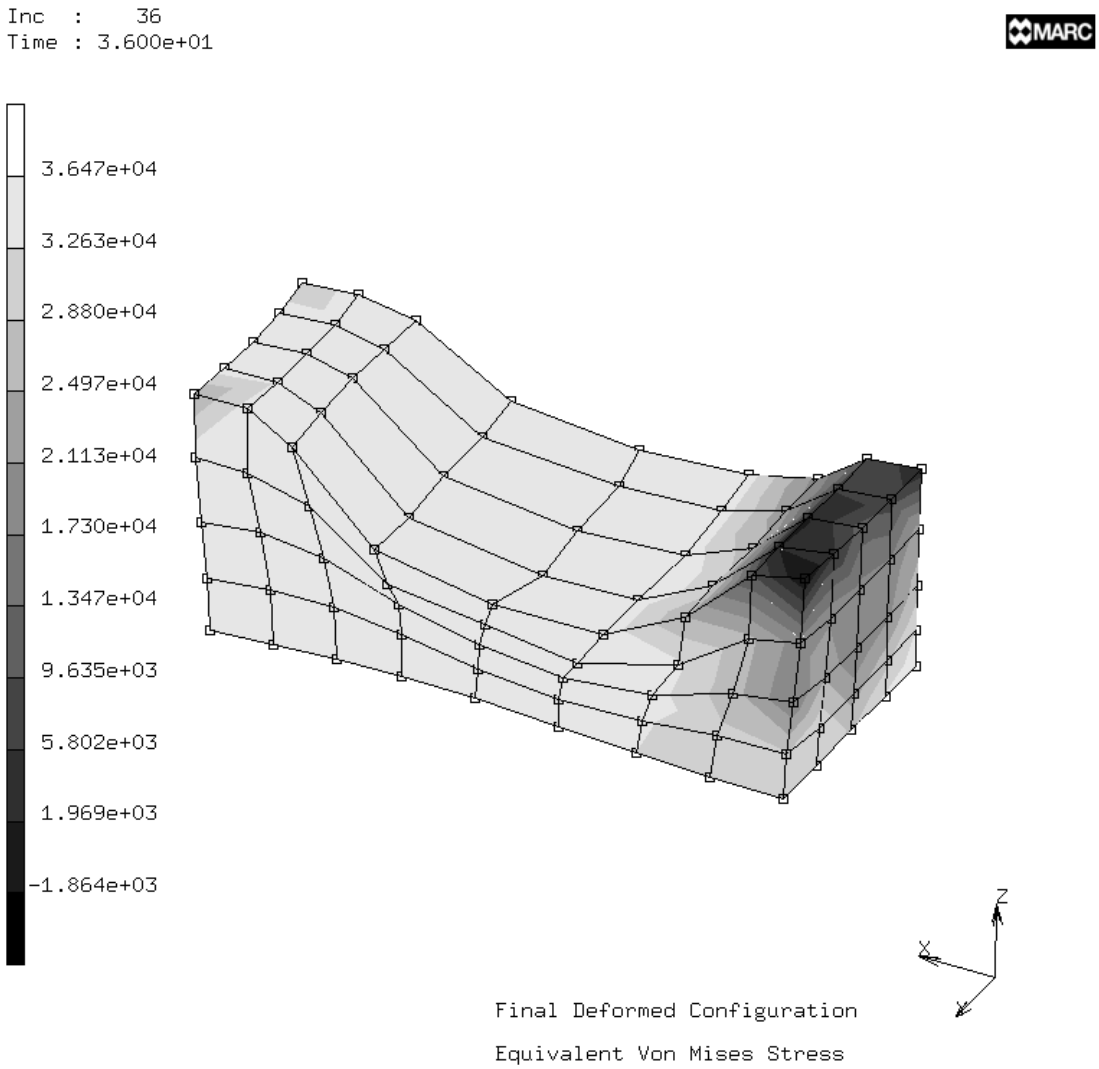

Figure 8.19-7 Equivalent von Mises Stress for Data Set e8x19

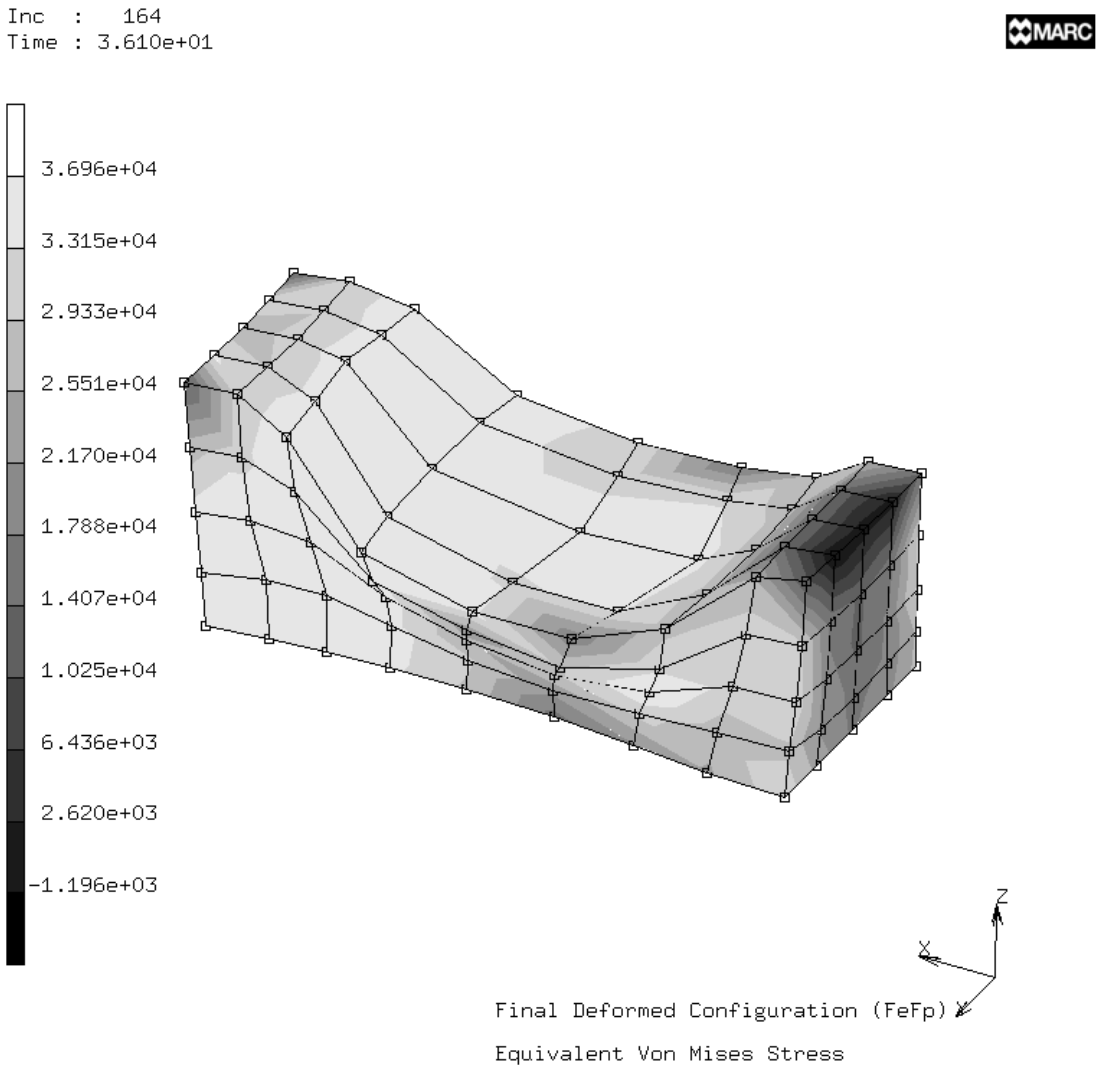

Figure 8.19-8 von Mises for Data Set e8x19b

8.20 2D Electrostatic Analysis of a Circular Region

This problem analyses a point charge in a circular region to demonstrate MARC's electrostatic analysis capability using a 2D element formulation. The electrostatic problem is governed by Poisson's equation for scalar potential, valid for heat transfer and electrostatic analyses among others. Using this duality, heat transfer elements (type 39) are used but all input and output is seen in terms of an electrical problem.

Parameters

The ELECTRO parameter is included to indicate an electrostatic analysis.

Mesh Definition

Half of the circle is modeled due to symmetry. The mesh has 100 elements and 111 nodes. Figure 8.20-1 shows the nodes, and Figure 8.20-2 shows the element configuration.

Boundary Conditions

A potential of zero volts is specified along the outer radius which is nodes 11 to 111 by 10 through the FIXED POTENTIAL option.

Material Properties

The permittivity of the medium is specified at 1.0 farad/cm in the ISOTRPOIC option.

Electrostatic Charge

A point charge of 1.0 Coulomb is applied at node 1 through the POINT CHARGE option.

POST

The following variables are requested to be written to both binary and formatted post files:

130 } Scalar potential 131,132 } Components of electric field vector
134,135 } Components of electric displacement vector

Control

The STEADY STATE option is used to initiate the analysis.

Results

Figure 8.20-3 shows the scalar potential (post code 130). Figure 8.20-4 and E8.20-5 show the first and second components of displacement the electric field (post codes 131,132). Figures E8.20-6 and E8.20-7 show the first and second components of electric displacements (post codes 134,135).

Parameters, Options, and Subroutines Summary

Example e8x20.dat:

Parameters	Model Definition Options	History Definition Options
ELECTROSTATIC	CONNECTIVITY	CONTINUE
ELEMENT	COORDINATE	STEADY STATE
END	END OPTION	
SIZING	FIXED POTENTIAL	
TITLE	ISOTROPIC	
	POINT CHARGE	
	POST	

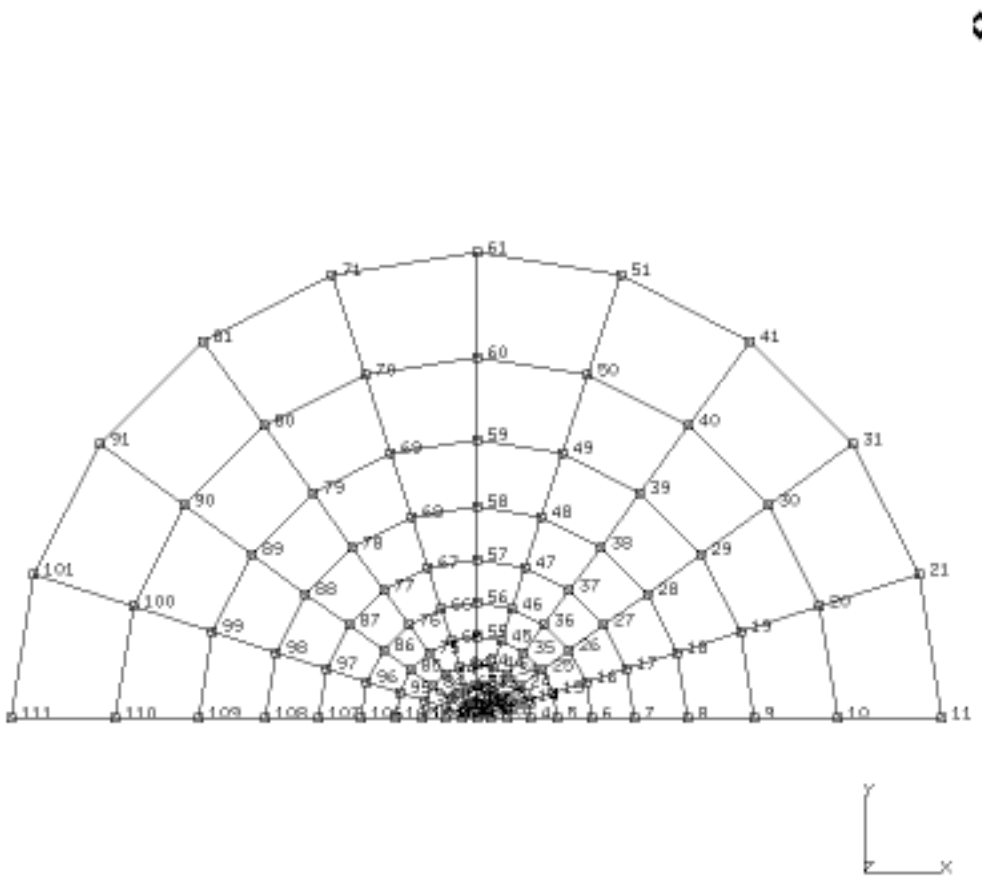

Figure 8.20-1 Node Numbers in Circular Region

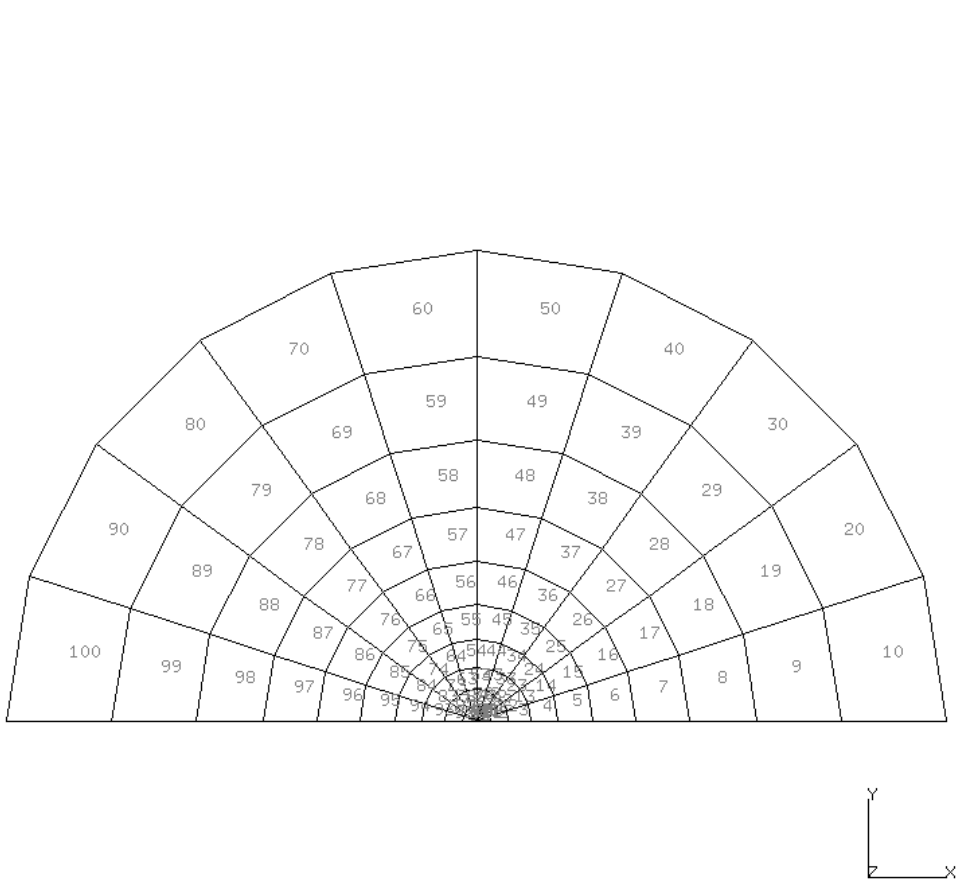

Figure 8.20-2 Element Numbers in Circular Region

INC : 1
SUB : 0
TIME : 0.000e+00
FREQ : 0.000e+00

prob e8.20 point charge on a circular region element 39

MARC

Electric Potential

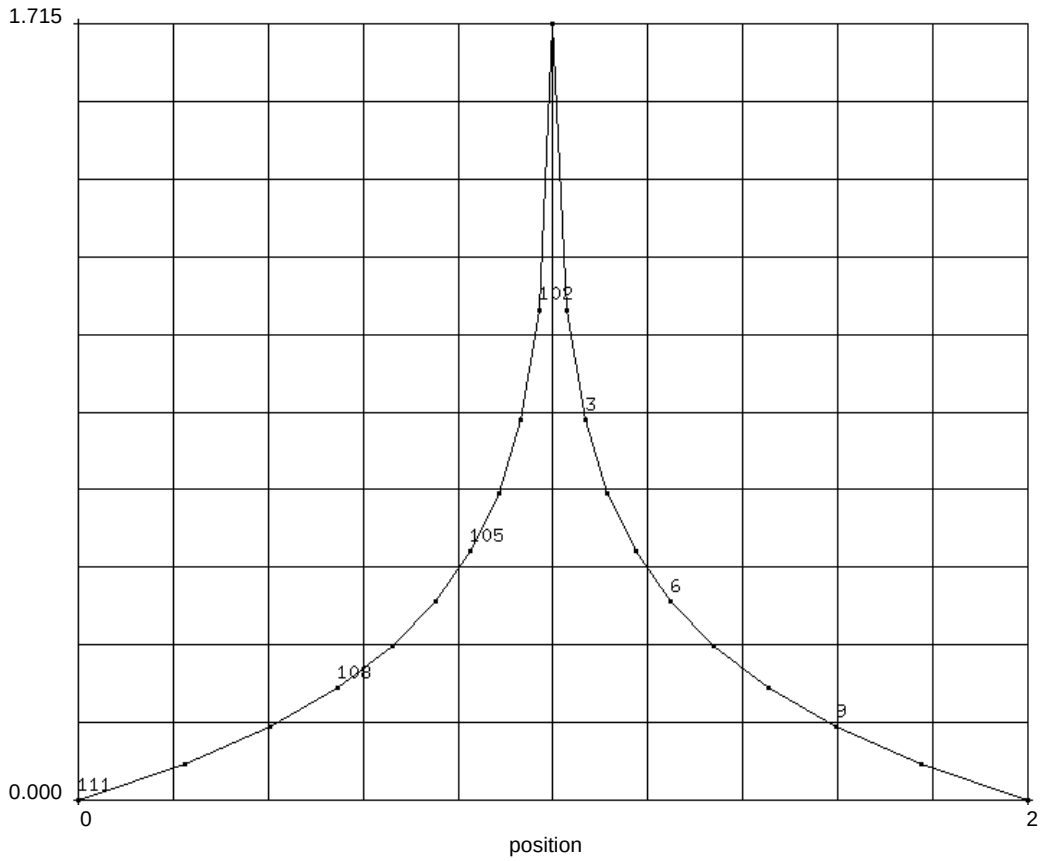

Figure 8.20-3 Electric Potential Along Diameter

INC : 1
SUB : 0
TIME : 0.000e+00
FREQ : 0.000e+00

prob e8.20 point charge on a circular region element 39

MARC

1st (Real) Comp of Electric Field (x10)

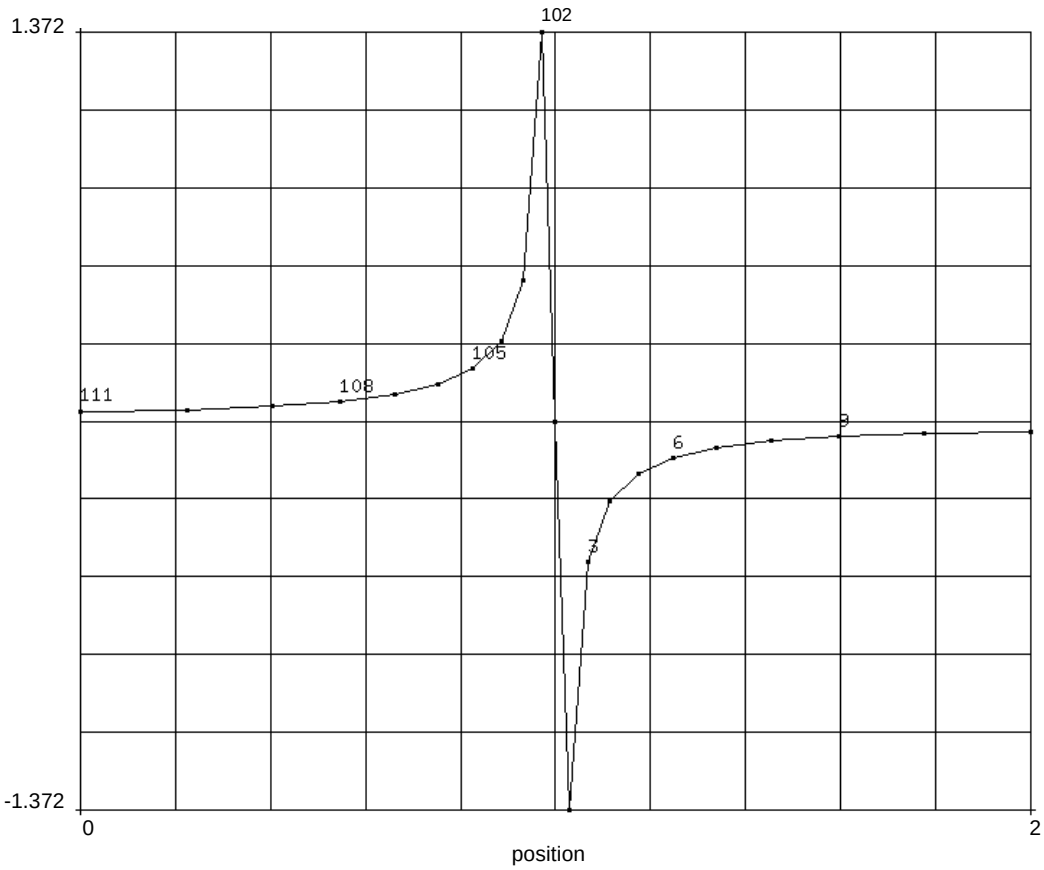

Figure 8.20-4 First Component of Electric Field

8.21 3D Electrostatic Analysis of a Circular Region

This problem analyses a point charge in a circular region to demonstrate MARC's electrostatic analysis capability using a 3D element formulation. The electrostatic problem is governed by Poisson's equation for scalar potential, valid for heat transfer and electrostatic analyses among others. Using this duality, eight-noded heat transfer elements (type 43) are used but all input and output is seen in terms of an electrical problem.

Parameters

The ELECTRO parameter is included to indicate an electrostatic analysis.

Mesh Definition

One half of the region is modeled due to symmetry. The model has 100 brick elements and 222 nodes. Figure 8.21-1 shows the mesh nodal points, and Figure 8.21-2 shows the element configuration.

Boundary Conditions

A potential of zero volts is specified along the outside radius at nodes 201 to 222.

Material Properties

The permittivity of the medium is specified at 1.0 farad/cm for all elements.

Electrostatic Charge

A point charge of 0.1 coulomb is applied at nodes 1 and 2.

POST

The following codes are requested to be output to both binary and formatted post files:

130 } Scalar potential 131-133 } Components of the electric field vector
134-136 } Components of the electric displacement vector

Control

The STEADY STATE option is used to initiate the analysis.

Results

Figure 8.21-3 shows the scalar potential (post code 130). As anticipated, the calculated potential is of the same magnitude as the two-dimensional problem E 8.20.

Parameters, Options, and Subroutines Summary

Example e8x21.dat:

Parameters	Model Definition Options	History Definition Options
ELECTROSTATIC	CONNECTIVITY	CONTINUE
ELEMENT	COORDINATE	STEADY STATE
END	END OPTION	
SIZING	FIXED POTENTIAL	
TITLE	ISOTROPIC	
	POINT CHARGE	
	POST	

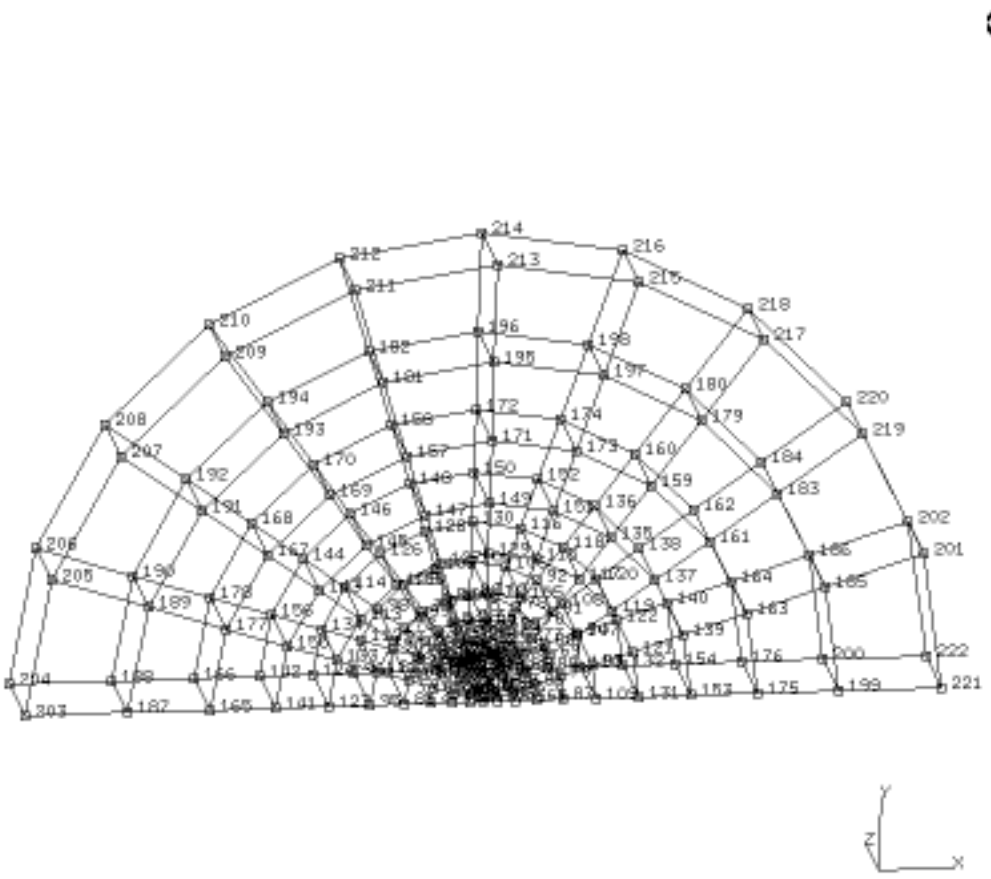

Figure 8.21-1 Node Numbers in Mesh

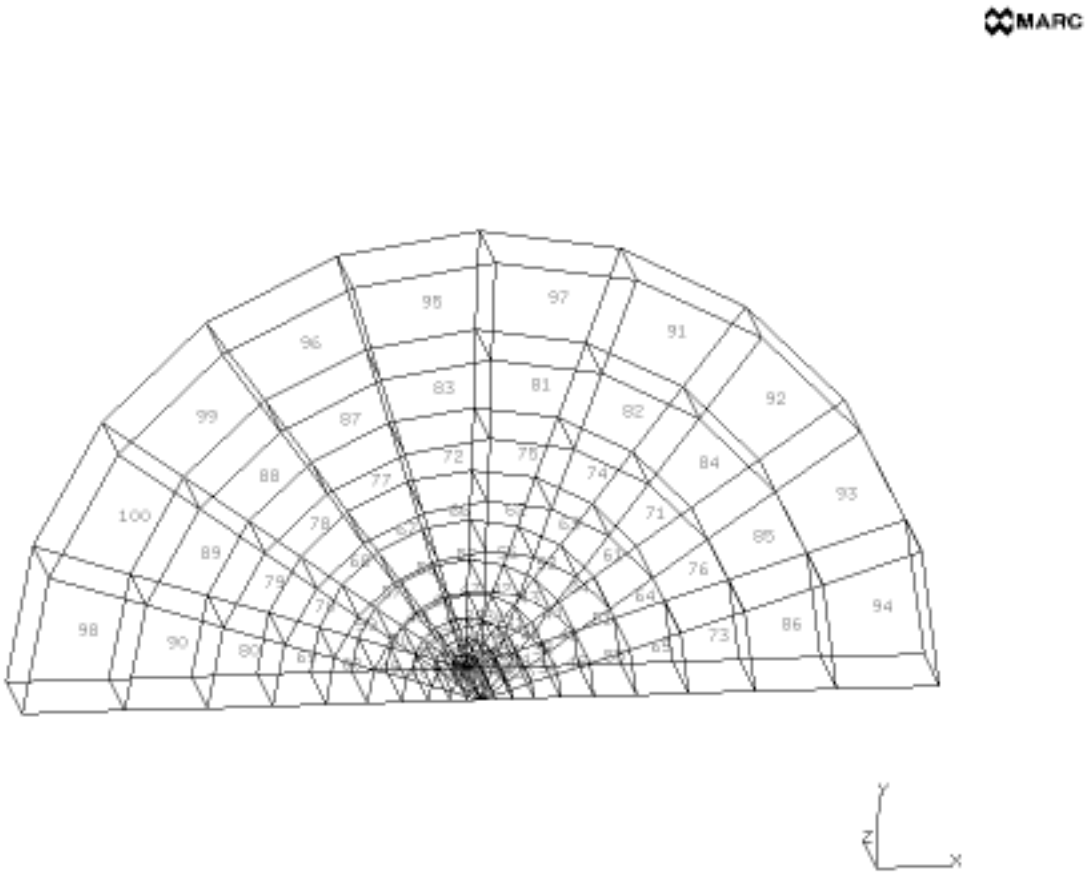

Figure 8.21-2 Element Numbers in Mesh

INC : 1
SUB : 0
TIME : 0.000e+00
FREQ : 0.000e+00

prob e8.21 point charge on a circular region element 43

MARC

Scalar Potential

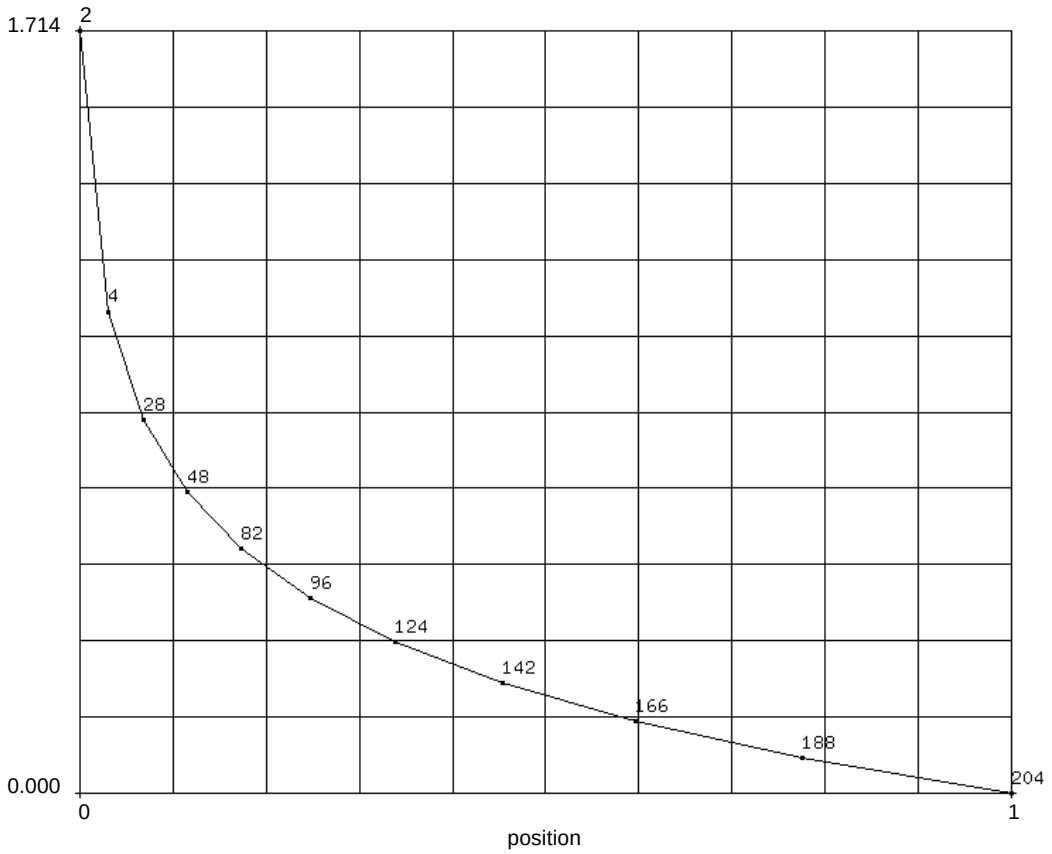

Figure 8.21-3 Scalar Potential Through Radius

8.22 2D Magnetostatic Analysis of a Circular Region

This problem shows MARC's magnetostatic analysis capability using a 2D element formulation. The two-dimensional magnetostatic problem is governed by Poisson's equation for scalar potential, valid for heat transfer, magnetostatic and electrostatic analyses among others. When using this duality, eight-noded heat transfer elements (type 39) are used, but all input and output is seen in terms of an electrical problem.

Parameters

The MAGNET parameter is included to indicate a magnetostatic analysis.

Mesh Definition

Half of the circular region is modeled due to symmetry. The mesh has 100 elements and 111 nodes. Figure 8.22-1 shows the nodal configuration of the mesh and Figure 8.22-2 shows the element configuration.

Boundary Conditions

A potential of zero volts is specified on the outside radius which is at nodes 11 to 111 by 10.

Material Properties

The magnetic permeability of the medium is specified at 1.0 Henry/cm for all elements.

Current

A point current of 1.0 amps is applied at node 1 through the POINT CURRENT option.

POST

The following variables are requested to be written to both a binary and a formatted post file:

140 } Scalar potential 141,142 } Components of magnetic flux
144,145} Components of magnetic density

Results

Figure 8.22-3 shows the scalar potential (POST code 140). Figure 8.22-4 shows the vector plot of the magnetic flux.

Parameters, Options, and Subroutines Summary

Example e8x22.dat:

Parameters	Model Definition Options	History Definition Options
ELEMENT	CONNECTIVITY	CONTINUE
END	COORDINATE	STEADY STATE
MAGNETOSTATIC	END OPTION	
SIZING	FIXED POTENTIAL	
TITLE	ISOTROPIC	
	POINT CURRENT	
	POST	

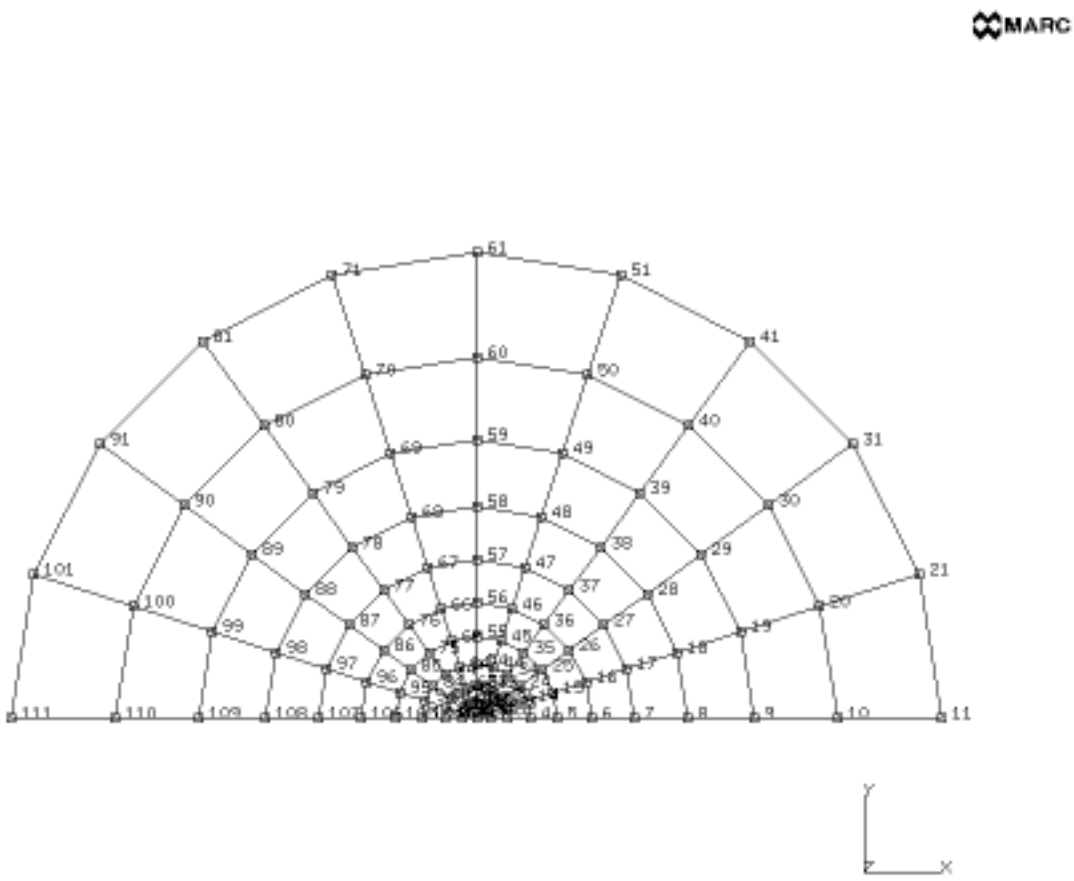

Figure 8.22-1 Node Numbers in Circular Region

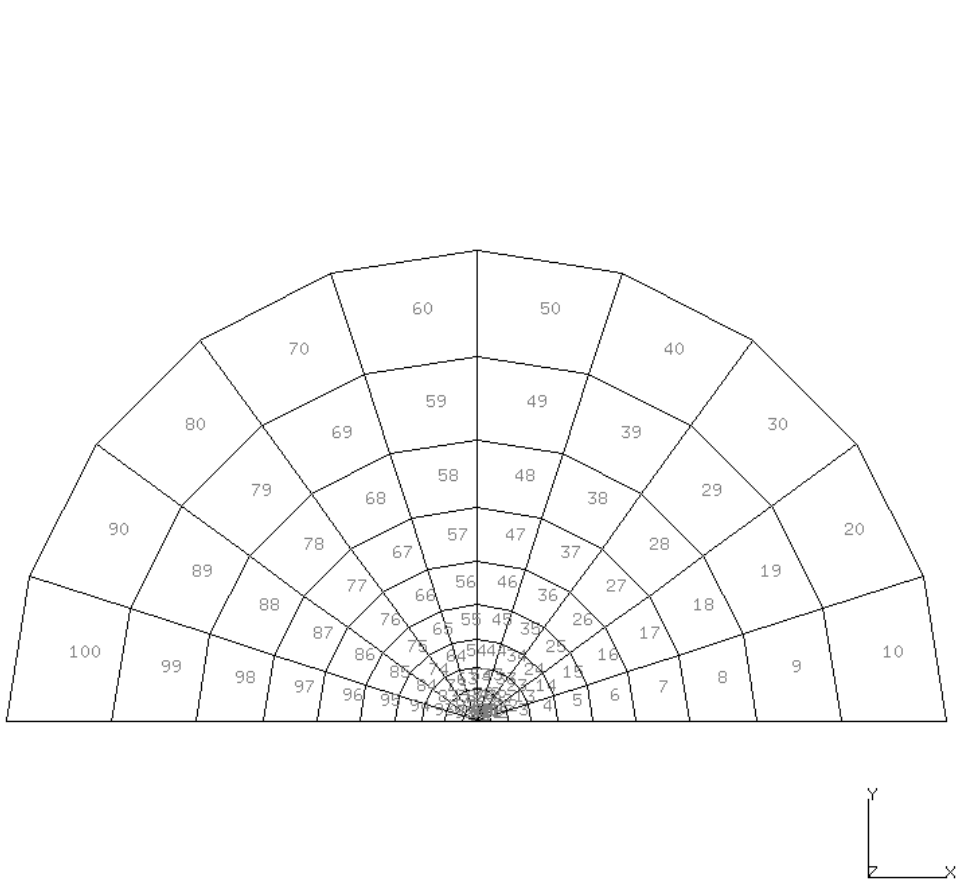

Figure 8.22-2 Element Numbers in Circular Region

INC : 1
SUB : 0
TIME : 0.000e+00
FREQ : 0.000e+00

prob e8.22 point current on a circular region element 39

MARC

Magnetic Potential

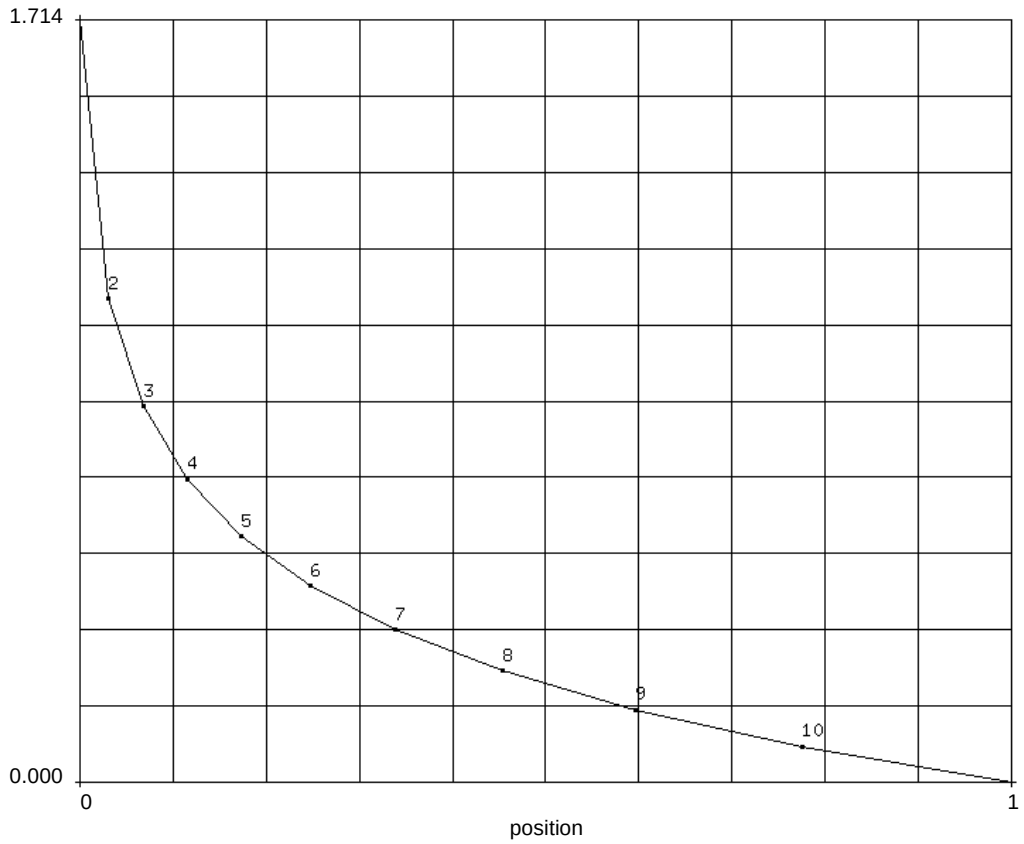

Figure 8.22-3 Magnetic Scalar Potential along Radial Line

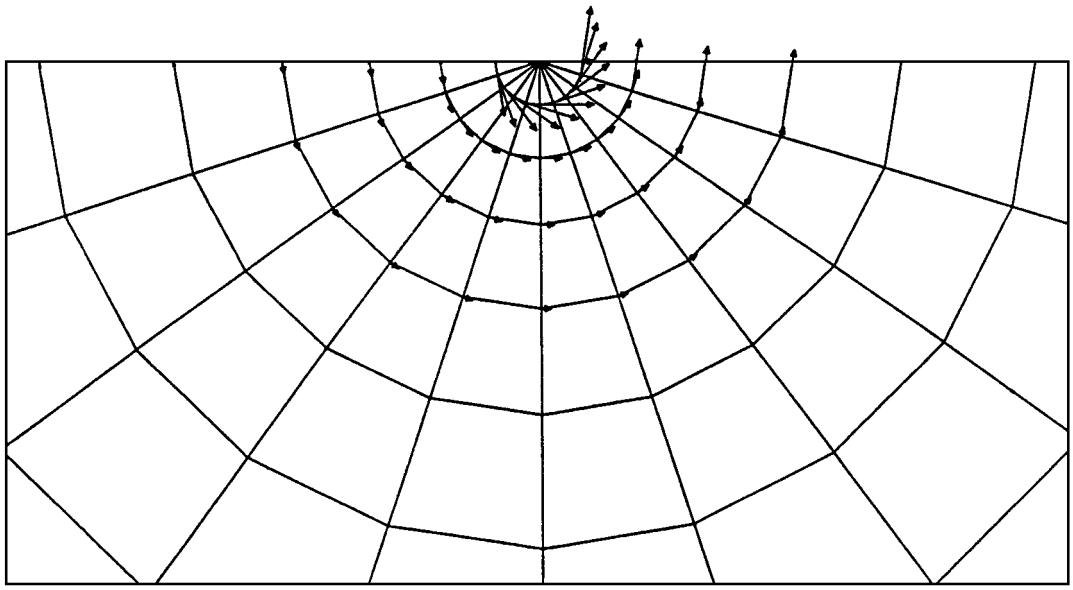

Figure 8.22-4 Magnetic Flux Distribution

8.23 3D Magnetostatic Analysis of a Coil

This problem shows magnetostatic analysis capability using a 3D element formulation in MARC. Since the potential to be solved is a new vector potential, the normal “heat transfer” approach cannot be used. Instead, an eight-noded magnetostatic element (type 109) is used for this analysis.

Parameters

The MAGNETO parameter is included to indicate a magnetostatic analysis.

Mesh Definition

One quarter of the coil is modeled using element type 109. The outside radius is 2.405 cm. Figure 8.23-1 shows the mesh and applied current.

Boundary Conditions

Along the y = 0 edge $A_1 = 0$. Along the x = 0 edge $A_2 = 0$. Along the outside radius $A_1 = A_2 = 0$. $A_3 = 0$ everywhere to simulate a two-dimensional problem.

Material Properties

The magnetic permeability of all elements is set to 1000.0 Henry/cm.

Currents

A current running in the circumferential direction at a radius of 1 cm is applied. The point currents ranging in value from -0.951 amps to +0.951 amps are applied at nodes 111 to 120.

POST

The following variables are written to both a binary and a formatted post file:

141-143 } Components of magnetic flux
144-146 } Components of magnetic intensity

Results

The third component of the magnetic flux is shown as a function of the radius in Figure 8.23-2. You can observe that a steep gradient occurs about the ring of nodes to which the current is applied. In addition, the total magnetization is zero, as:

$$\pi r_c^2 (338.5) + \pi(r_o^2 - r_c^2) (-42.32) = 2.7$$

where $r_c = 1$, and $r_o = 3$.

The vector potential A is shown in Figure 8.23-3.

Parameters, Options, and Subroutines Summary

Example e8x23.dat:

Parameters	Model Definition Options	History Definition Options
ELEMENT	CONNECTIVITY	CONTINUE
END	COORDINATE	STEADY STATE
MAGNETOSTATIC	END OPTION	
SIZING	FIXED POTENTIAL	
TITLE	ISOTROPIC	
	POINT CURRENT	
	POST	

Example e8x23b.dat:

Parameters	Model Definition Options	History Definition Options
ELEMENT	CONNECTIVITY	CONTINUE
END	COORDINATE	STEADY STATE
MAGNETOSTATIC	DEFINE	
SIZING	END OPTION	
TITLE	FIXED POTENTIAL	
	ISOTROPIC	
	POINT CURRENT	
	POST	

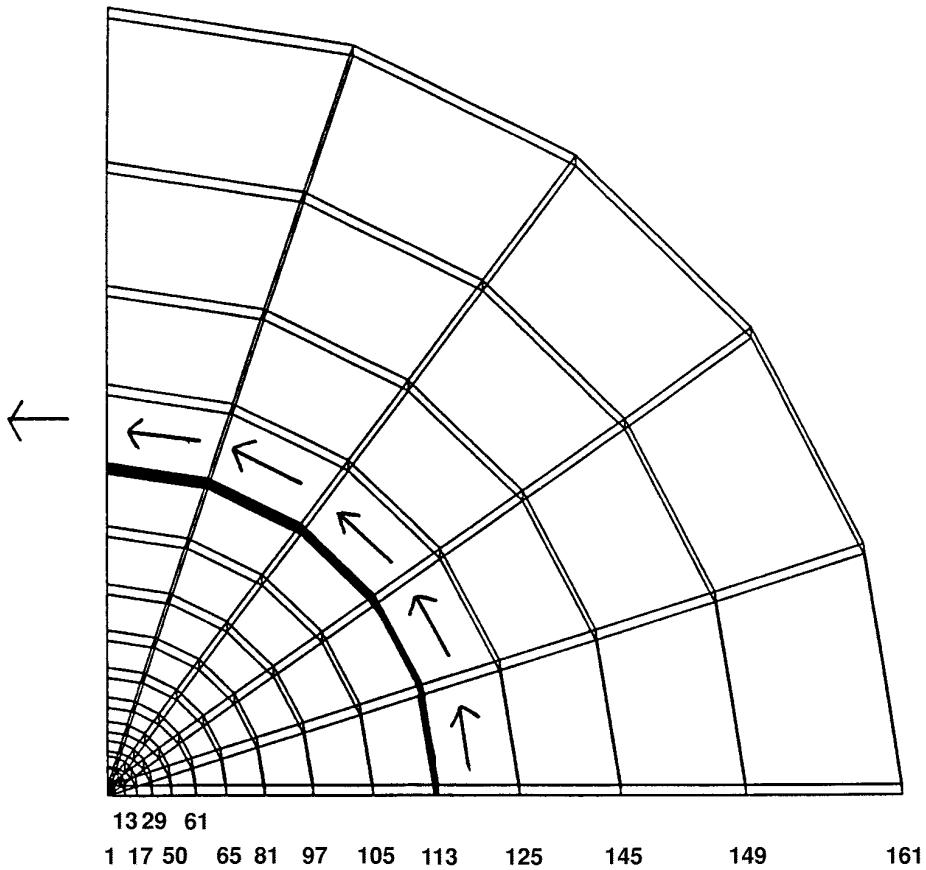

Figure 8.23-1 Mesh and Applied Current

INC : 1
SUB : 0
TIME : 0.000e+00
FREQ : 0.000e+00

prob e8.23 magnetostatic-analysis of coil

MARC

3rd (Real) Comp of Magnetic Flux (x100)

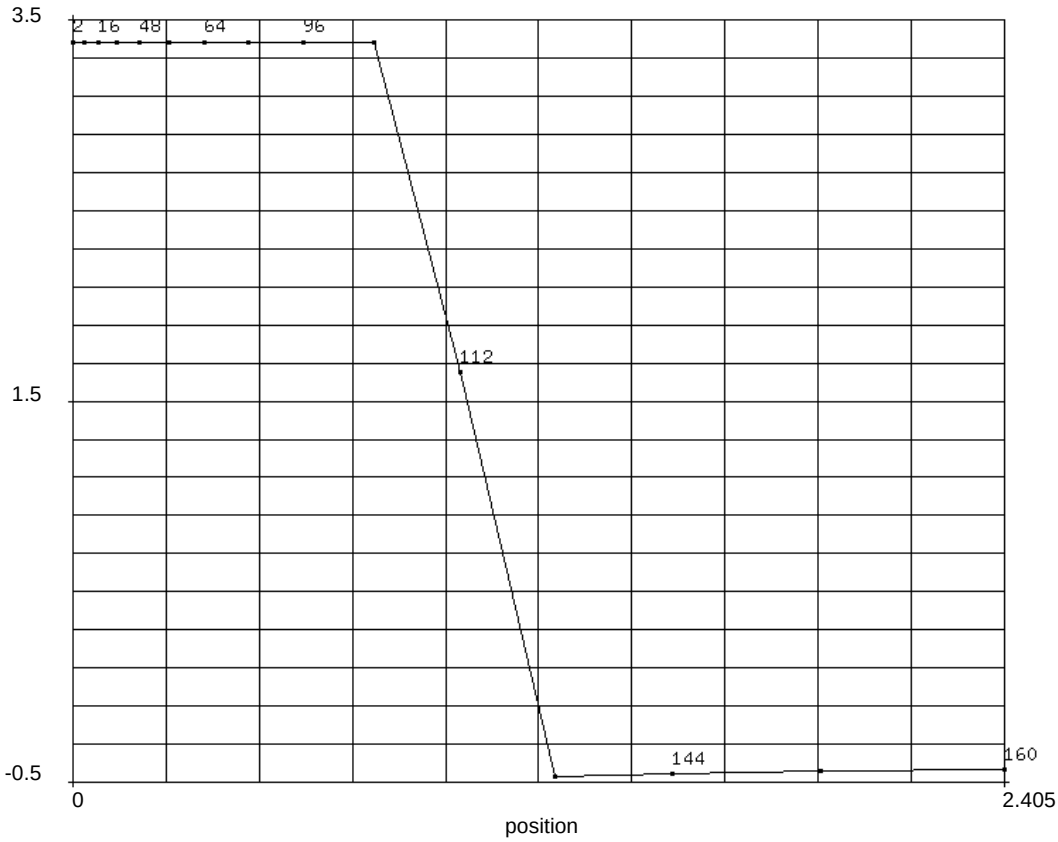

Figure 8.23-2 Third Component of Magnetic Flux along Radial Line

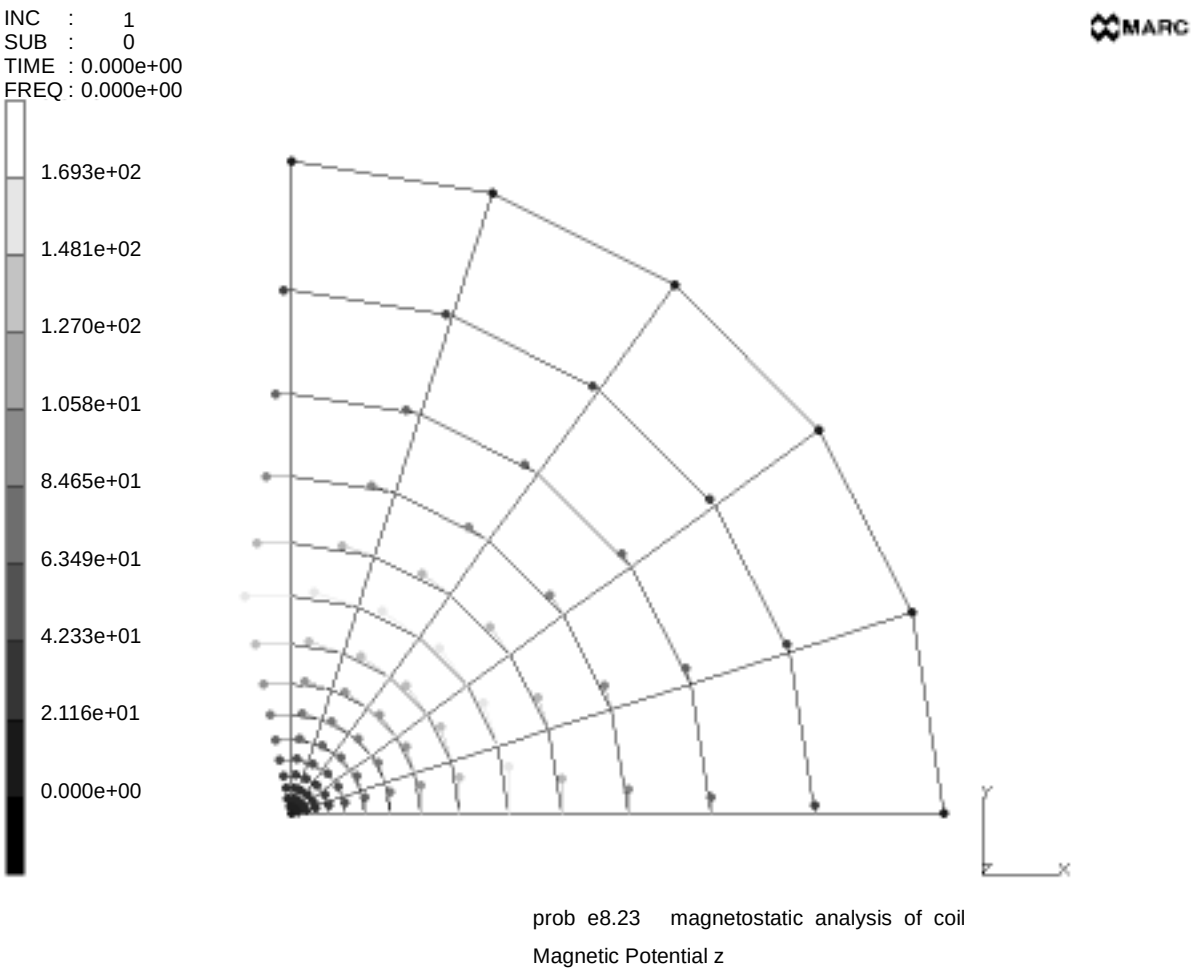

Figure 8.23-3 Magnetic Potential Vector

8.24 2D Nonlinear Magnetostatic Analysis

An infinite wire carries a current through a circular region.

This problem shows MARC's magnetostatic analysis capability using a 2D element formulation together with an orthotropic magnetic permeability that is a function of the magnetic flux density. The latter requires that a nonlinear problem be solved.

Parameters

The MAGNET parameter is included to indicate a magnetostatic analysis.

Mesh Definition

Only a section of the region is modeled due to symmetry. Element type 39, the 4-node heat transfer element, is used. Figure 8.24-1 shows the mesh nodal points, and Figure 8.24-2 shows the element configuration.

Boundary Conditions

A potential of zero volts is specified at nodes 20 and 21.

Material Properties

Use of the ORTHOTROPIC model definition option allows the input of the baseline magnetic permeabilities in the principal directions. These are set to 1000.0, 1200.0, and 1400.0 Henry/cm in the 1, 2, and 3 directions respectively. These permeabilities are functions of the magnetic flux density, the functionality being described through the B-H RELATION model definition option.

Current

A point current of 1.0 amps is applied at nodes 1.

POST

The following variables are written to a formatted post file:

140	} Scalar magnetic potential
141-142	} Components of magnetic flux
144-1465	} Components of magnetic intensity

Results

Figure 8.24-3 shows the scalar potential (post code 140) using linear material properties. Figure 8.24-4 shows the potential when the nonlinear material behavior is represented.

Parameters, Options, and Subroutines Summary

Example e8x24a.dat:

Parameters	Model Definition Options	History Definition Options
ELEMENT	CONNECTIVITY	CONTINUE
END	COORDINATE	STEADY STATE
MAGNETOSTATIC	END OPTION	
SIZING	FIXED POTENTIAL	
TITLE	ISOTROPIC	
	POINT CURRENT	
	POST	
	PRINT ELEM	

Example e8x24b.dat:

Parameters	Model Definition Options	History Definition Options
ELEMENT	B-H RELATION	CONTINUE
END	CONNECTIVITY	STEADY STATE
MAGNETOSTATIC	CONTROL	
SIZING	COORDINATE	
TITLE	END OPTION	
	FIXED POTENTIAL	
	ISOTROPIC	
	POINT CURRENT	
	POST	
	PRINT ELEM	

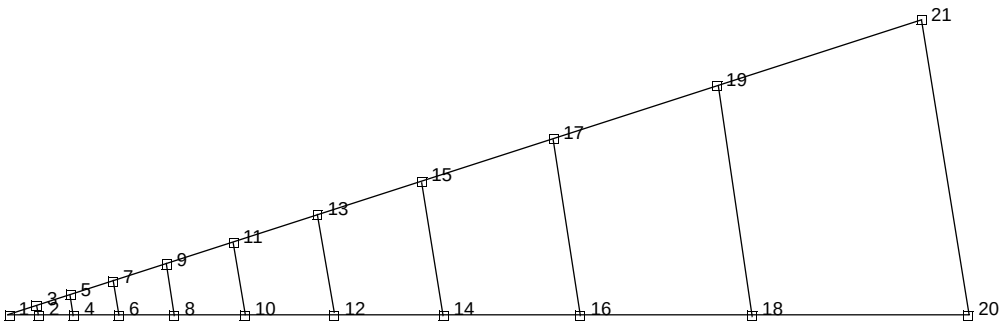

Figure 8.24-1 Mesh with Node Numbers

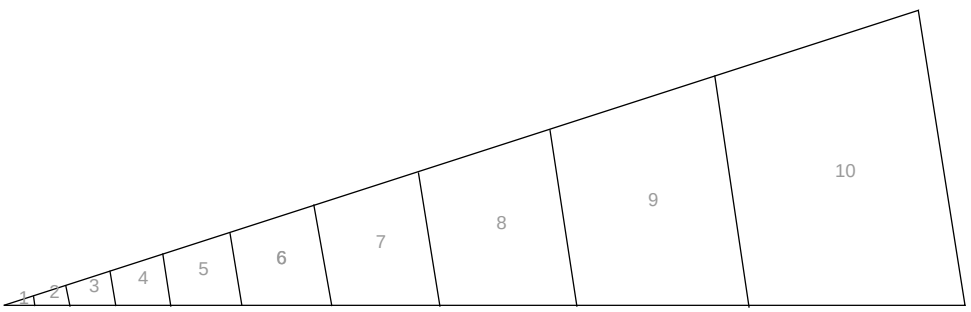

Figure 8.24-2 Mesh with Element Numbers

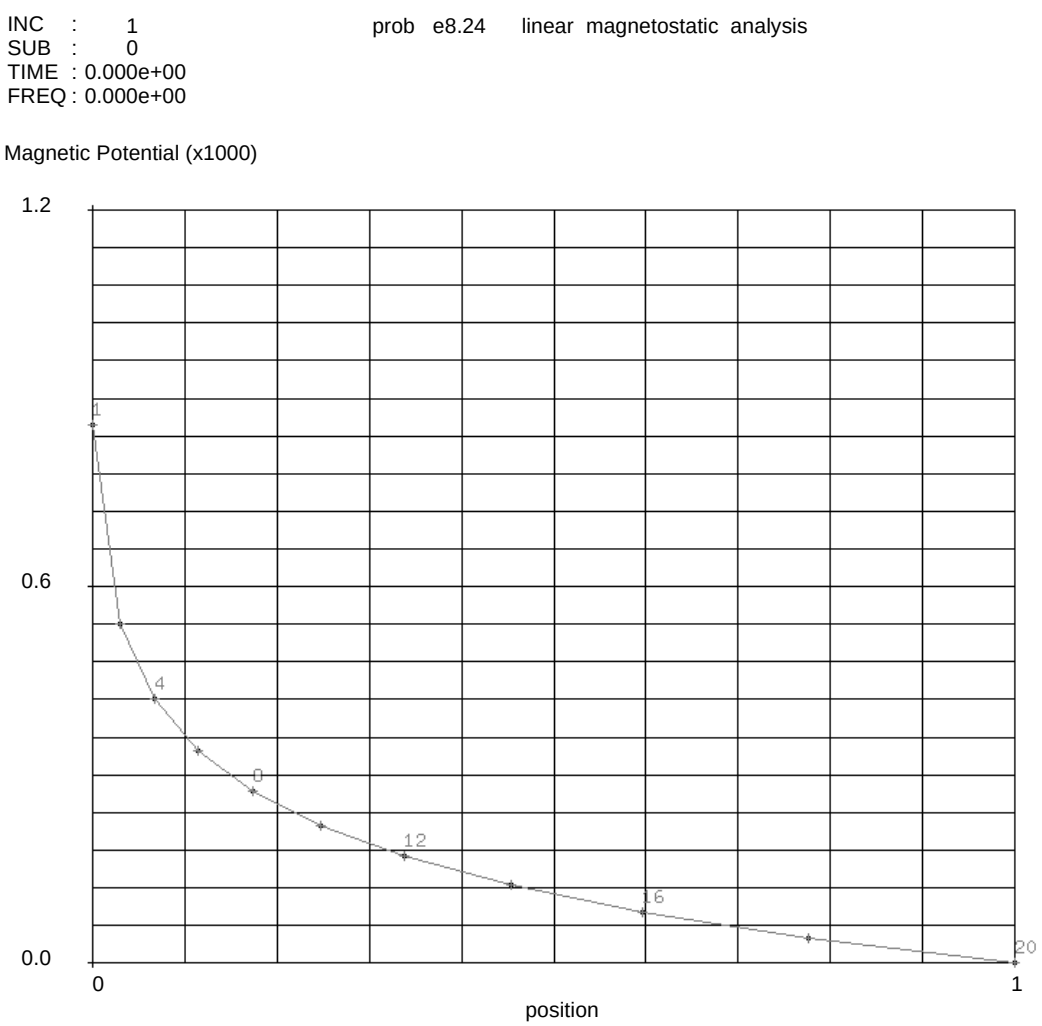

Figure 8.24-3 Magnetic Scalar Potential Linear Material Behavior

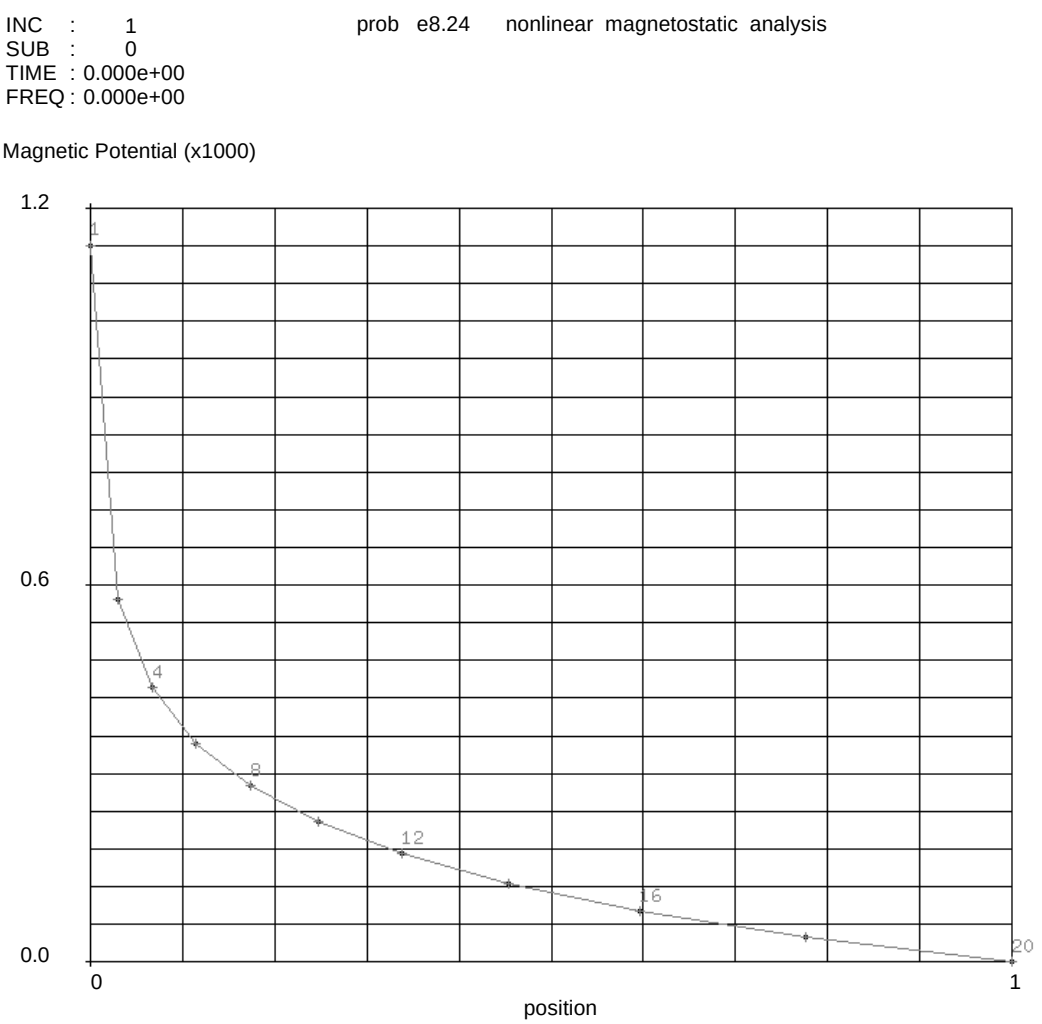

Figure 8.24-4 Magnetic Scalar Potential Nonlinear Material Behavior

8.25 Acoustic Problem: Eigenvalue Analysis of a Circular Cavity

This problem demonstrates the acoustic analysis capability using a 2D element formulation in MARC. MARC can be used to obtain the pressure distribution in a cavity with rigid reflecting boundaries. A transient analysis is then performed.

Parameters

The ACOUSTIC parameter is included to indicate an acoustic analysis. A maximum of six modes are to be used in the modal superposition. The Lanczos method is used for eigenvalue analysis, and resulting mode shapes are written onto the post file. PRINT, 3 is used to force the solution of a nonpositive definite stiffness matrix.

Elements/Mesh Definition

The input was originally created with element type 11. Using the ALIAS parameter, we can easily respecify them as element type 39. Figure 8.25-1 and Figure 8.25-2 show the node numbers and the elements in the cavity. The reflecting barrier is modeled by having a free surface. This can be seen in Figure 8.25-3 showing the double nodes. A refined mesh is used around the edges of the plate.

Boundary Conditions

No boundary conditions are applied. This will result in the first mode being the “rigid body” mode.

Material Properties

A bulk modulus of 139,000 psi and a material density of 1.2 lb/in^3 are specified through the ISOTROPIC model definition option.

Loading

An acoustic source pulse is applied in increment 1 with a time step of 0.000001. Ten increments are then performed with a time step of 0.001 at node 3. The DYNAMIC CHANGE option is used to define the time step.

Print Control

Print output of mode shapes and nodal reactions is requested through the use of a PRINT NODE option with MODE and REAC subparameters. All relevant element quantities are requested for elements 1 to 20 (at all four integration points) through the use of a PRINT ELEMENT option.

POST

The pressure (post code 120) and the first two components of the pressure gradient (post codes 121, 122) are written to a formatted post file. In addition, by providing a RECOVER option, the first two eigenvectors are also written to this file.

Results

Figure 8.25-4 through Figure 8.25-8 show the eigenmodes in the cavity. The frequencies are as follows:

Mode	Frequency (Hz)
1	0
2	653.7
3	978.1
4	1500
5	1638
6	1985

The pressure distribution in the transient analysis is shown in Figure 8.25-9 through Figure 8.25-11. You can observe the pressure pulse propagating through the cavity.

Parameters, Options, and Subroutines Summary

Example e8x25.dat:

Parameters	Model Definition Options	History Definition Options
ACOUSTIC	CONNECTIVITY	CONTINUE
ALIAS	COORDINATE	DYNAMIC CHANGE
ELEMENT	END OPTION	MODAL SHAPE
END	GEOMETRY	POINT SOURCE
PRINT	ISOTROPIC	RECOVER
SIZING	POST	
TITLE	PRINT ELEM	
	PRINT NODE	

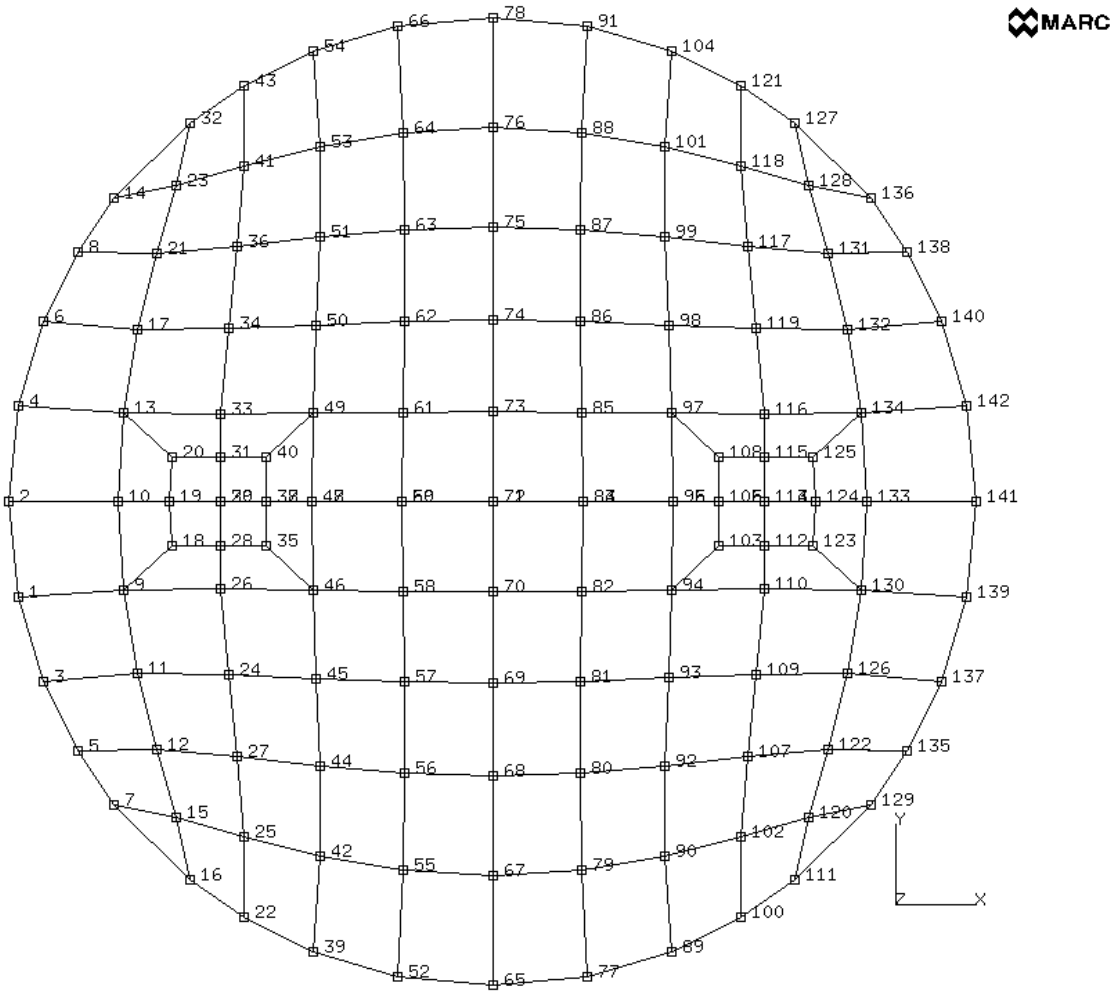

Figure 8.25-1 Acoustic Cavity Mesh with Node Numbers

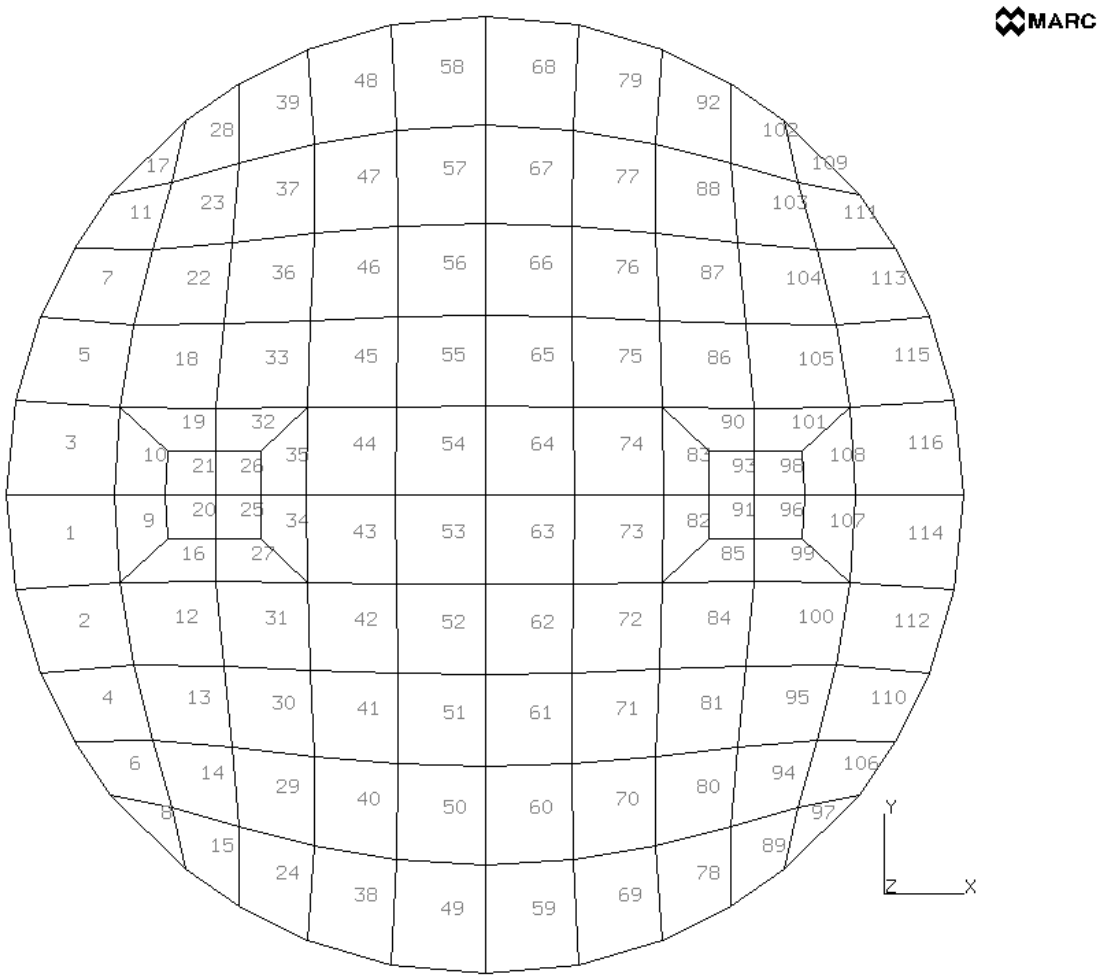

Figure 8.25-2 Acoustic Cavity Mesh with Element Numbers

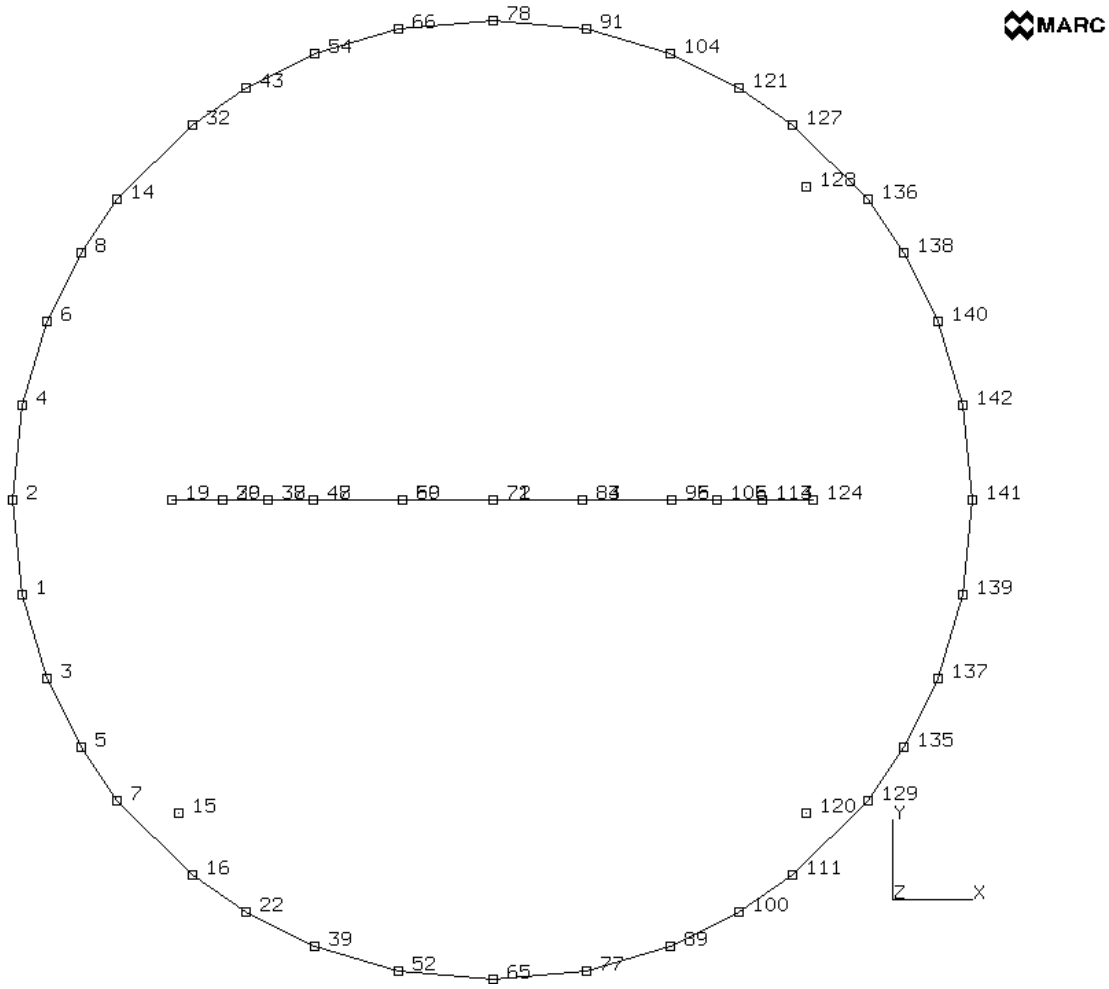

Figure 8.25-3 Outline Plot Showing Internal Barrier

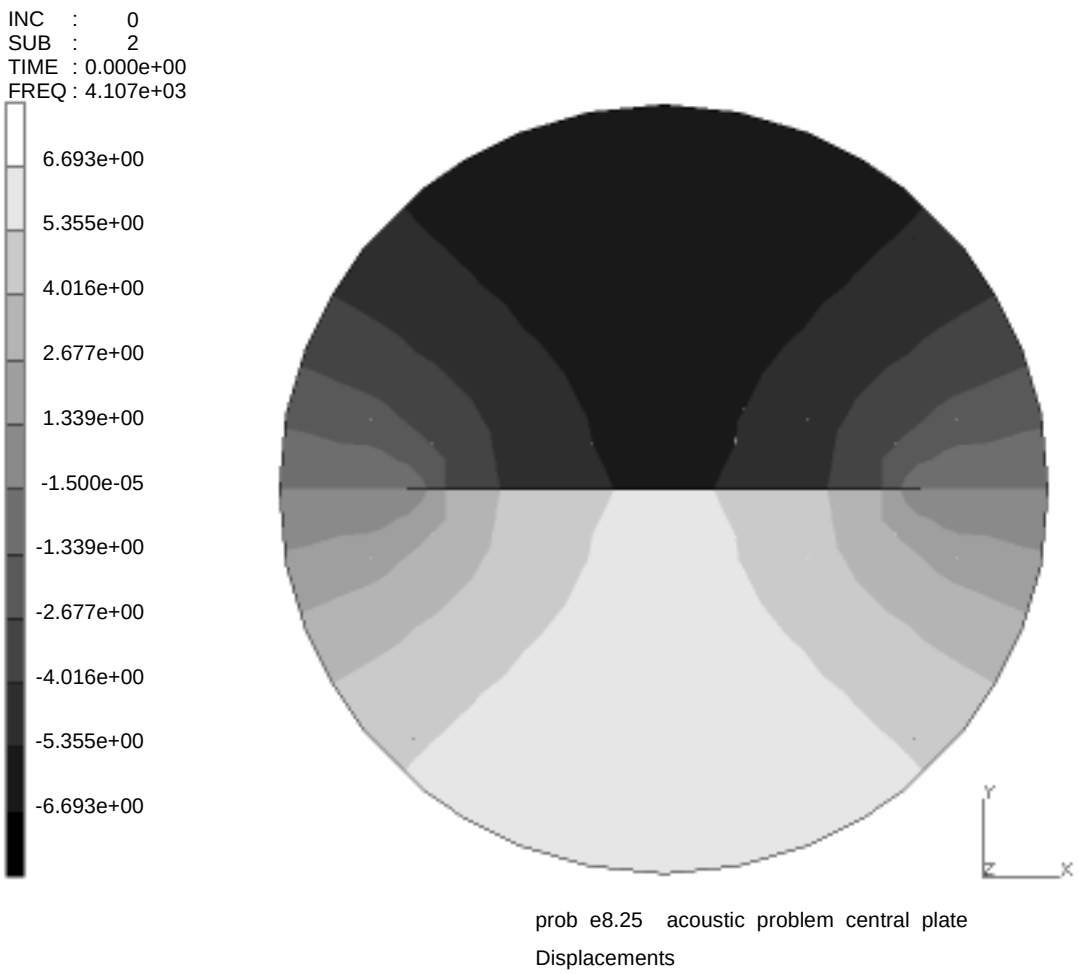

Figure 8.25-4 Second Mode

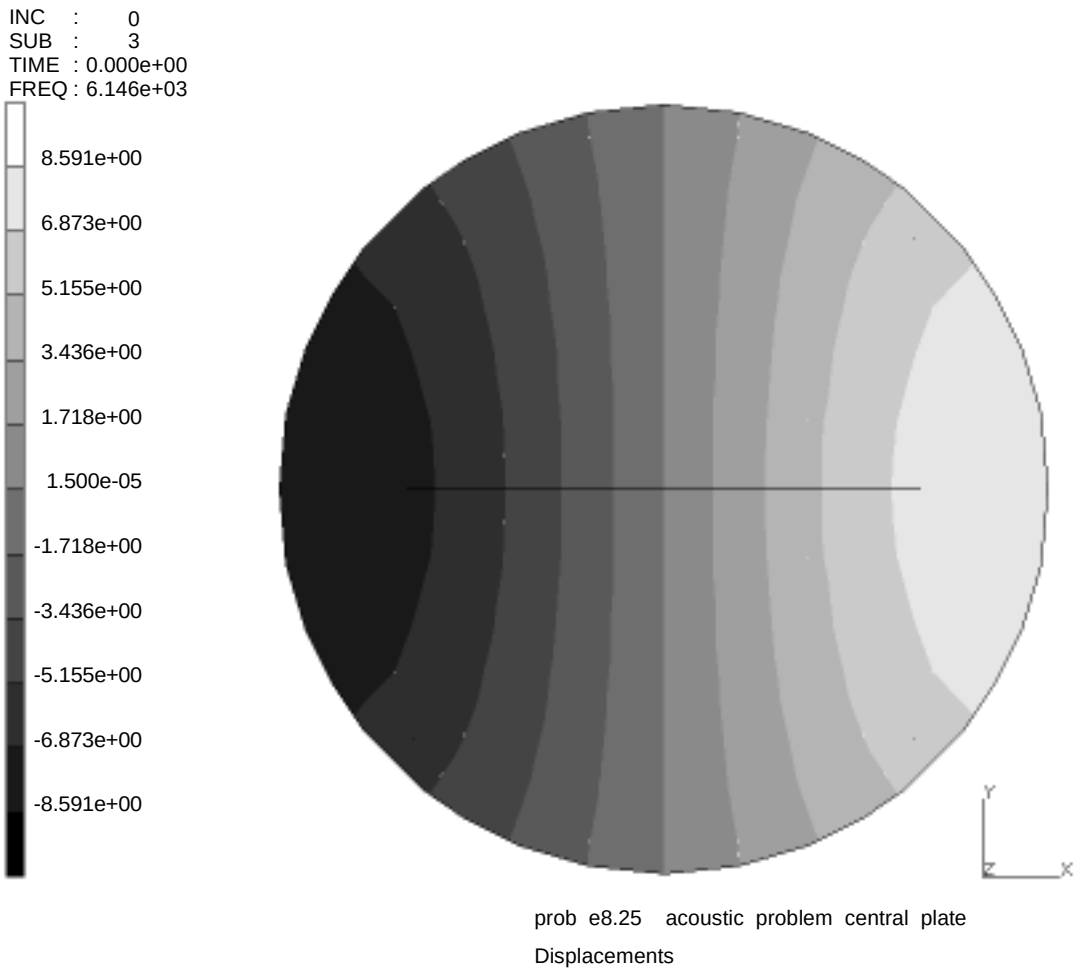

Figure 8.25-5 Third Mode

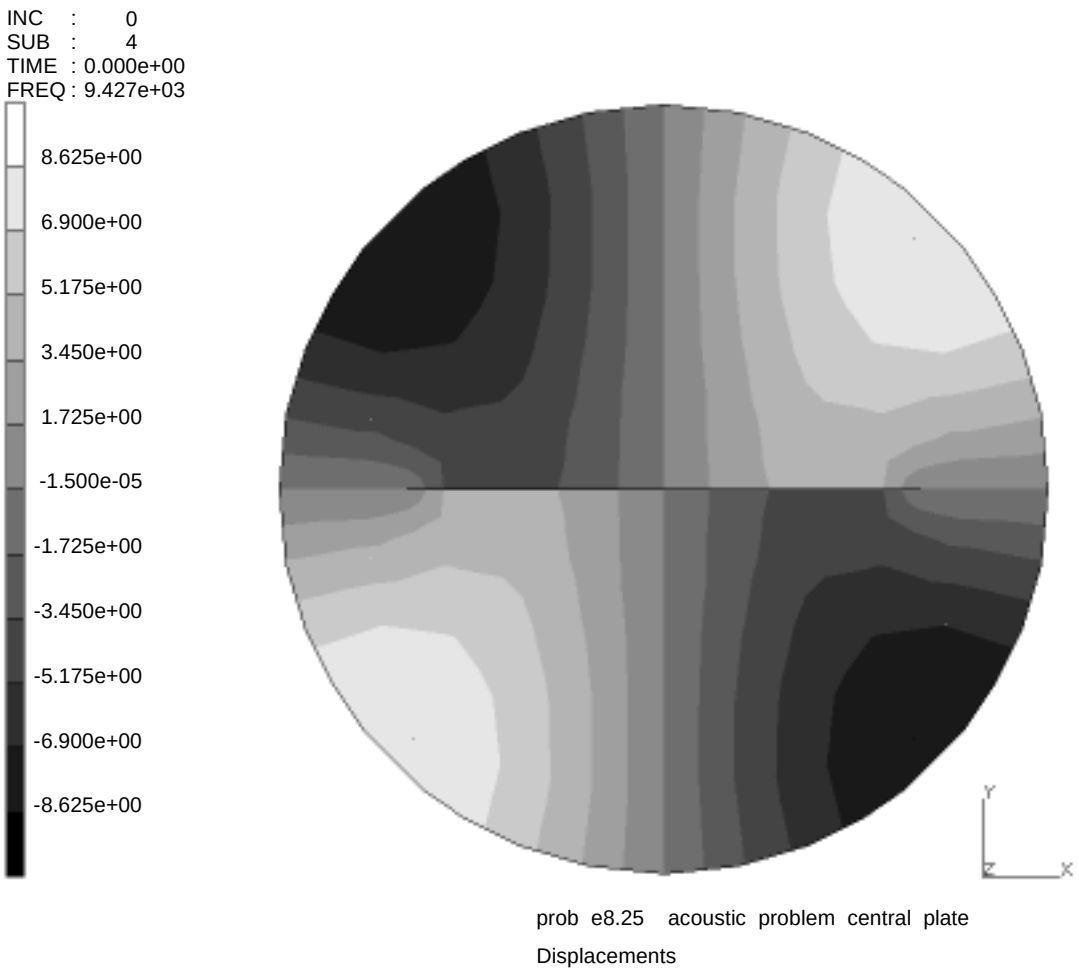

Figure 8.25-6 Fourth Mode

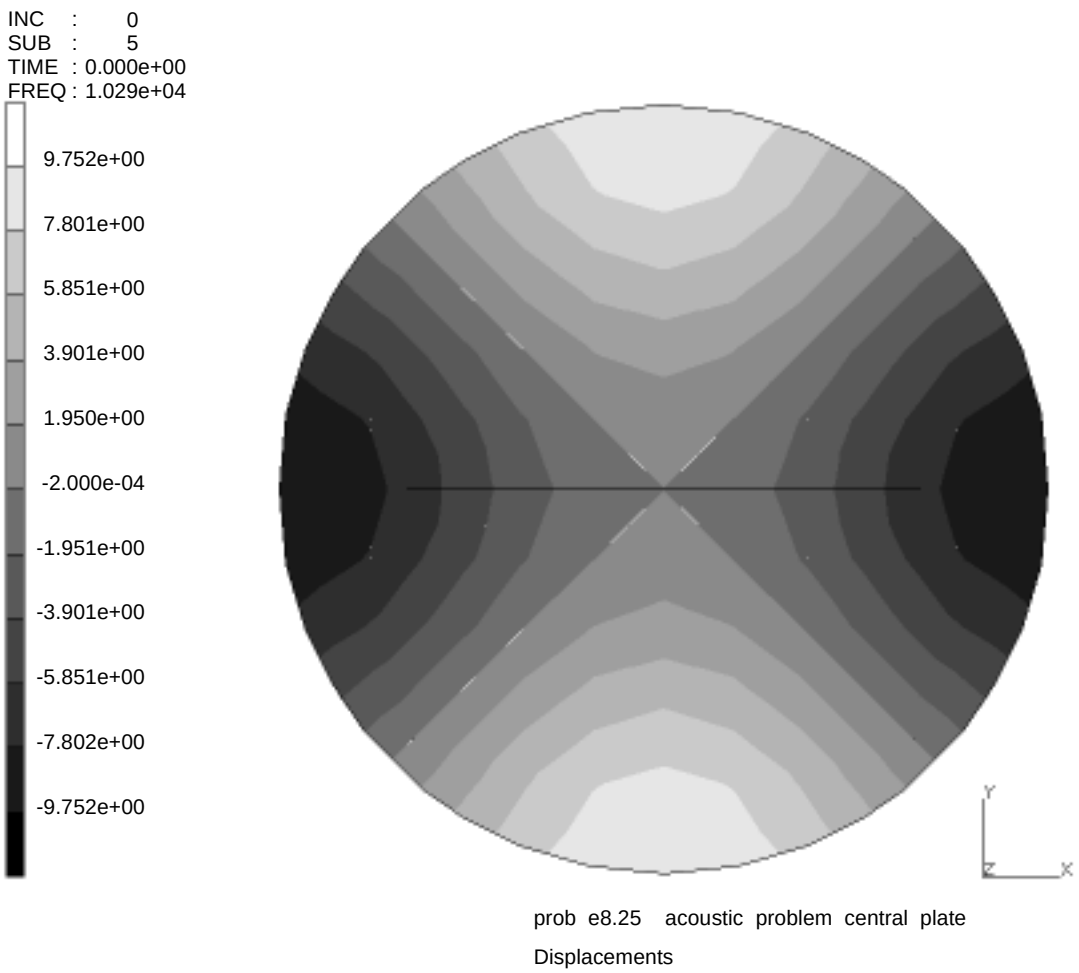

Figure 8.25-7 Fifth Mode

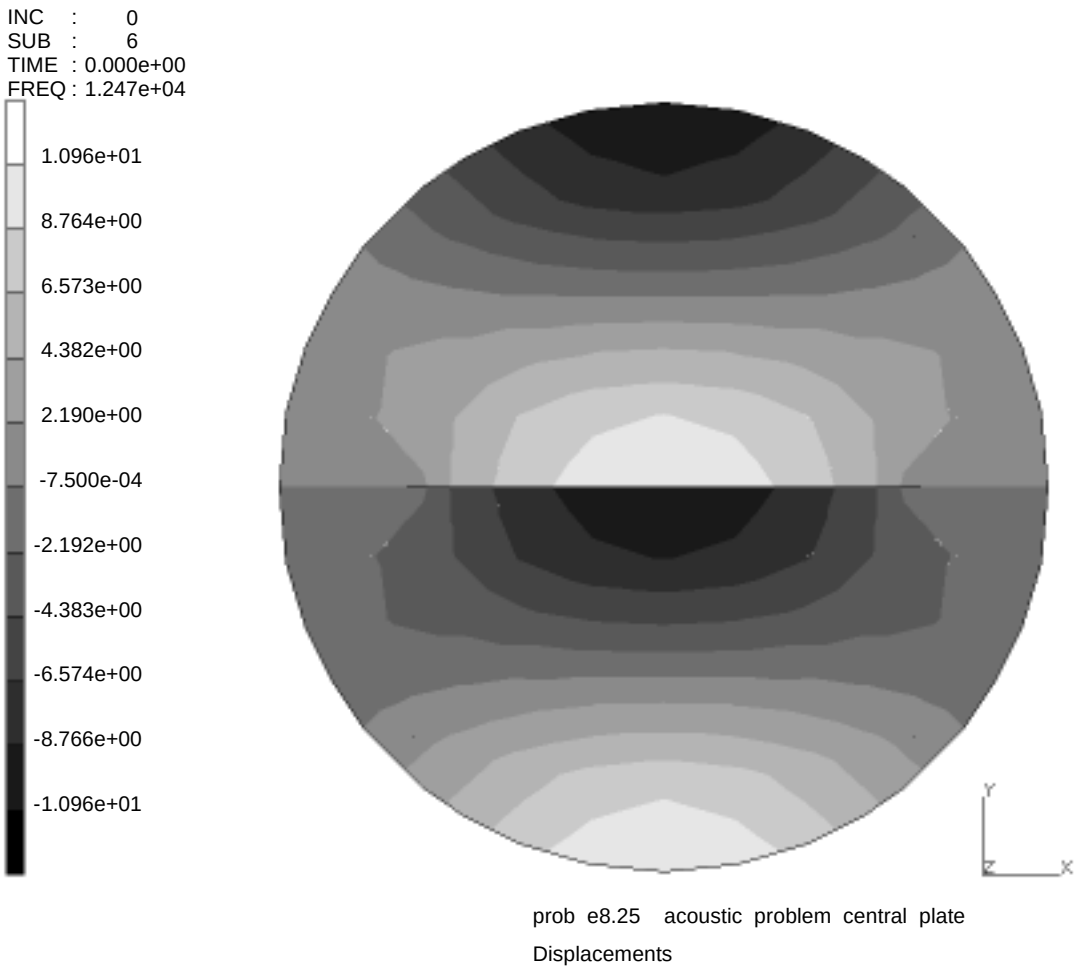

Figure 8.25-8 Sixth Mode

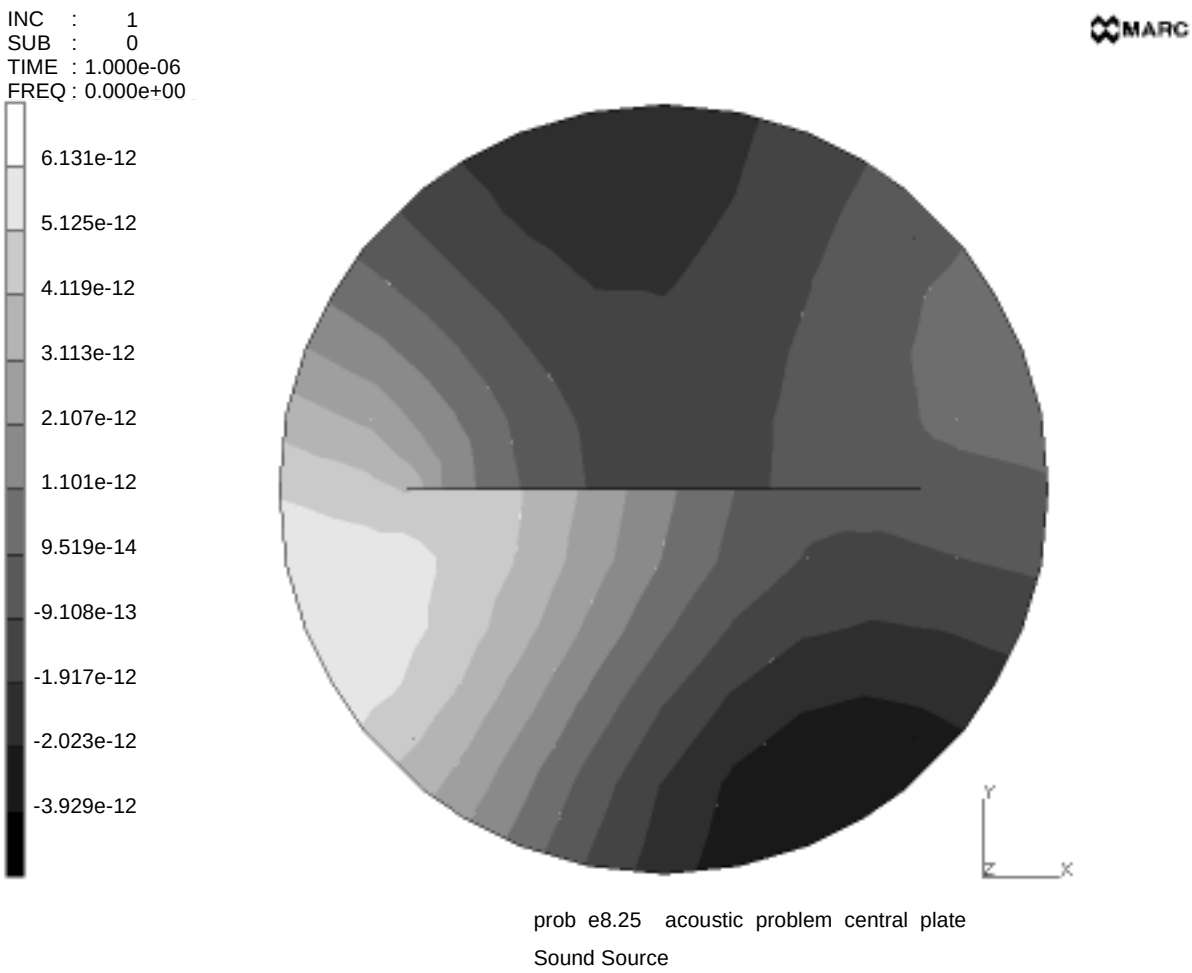

Figure 8.25-9 Acoustic Pressure at Time = 0.000001

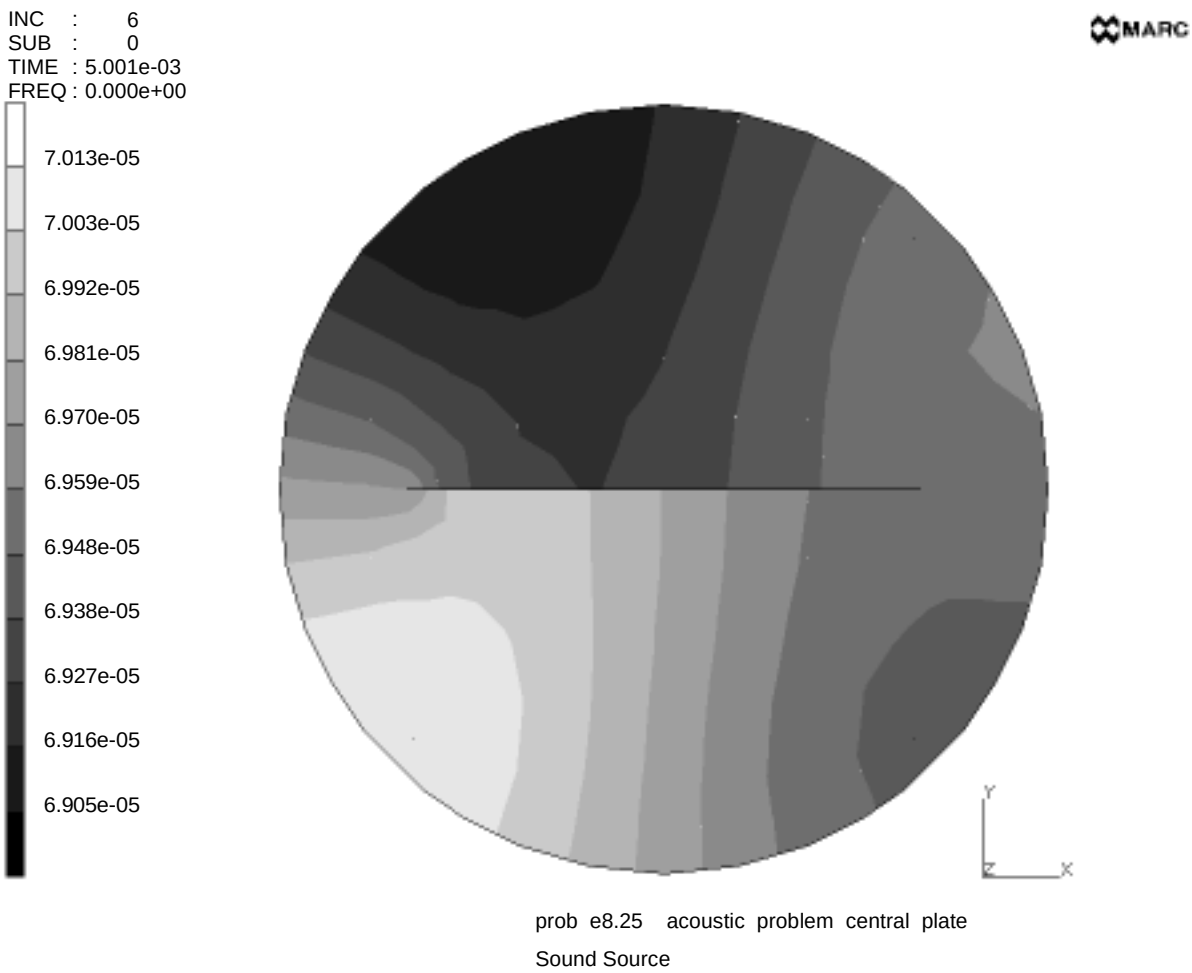

Figure 8.25-10 Acoustic Pressure at Time = 0.005

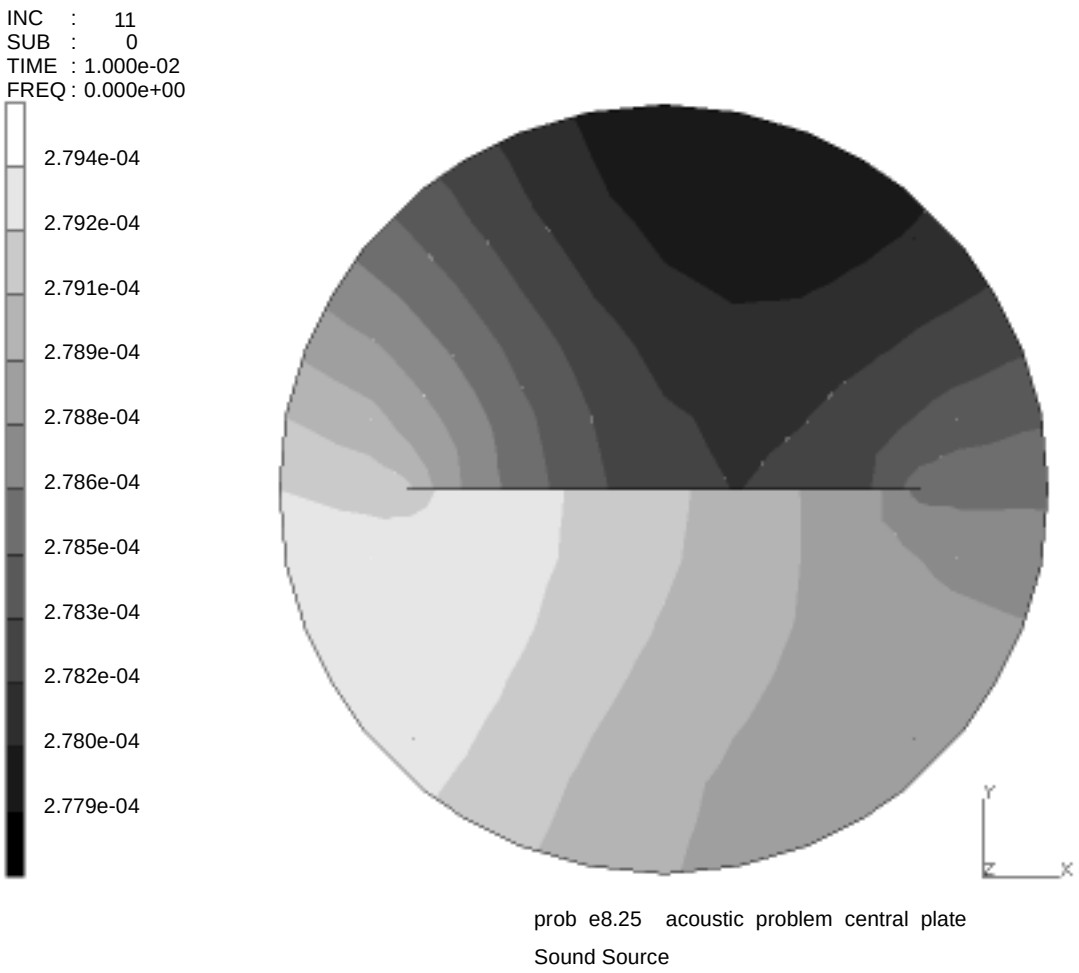

Figure 8.25-11 Acoustic Pressure at Time = 0.01

8.26 Acoustic Problem: Eigenvalue Analysis of a Rectangular Cavity

This problem shows MARC's acoustic analysis capability using a 2D element formulation. The acoustic pressure distribution in a rectangular cavity is to be calculated.

Parameters

The ACOUSTIC parameter is included to indicate an acoustic analysis. It further indicates that a maximum of five modes are to be used for modal superposition, that the eigenvalue problem is to be solved using the Lanczos formulation, and that the mode shapes are to be saved in the post file. PRINT, 3 is used to force the solution of a nonpositive definite stiffness matrix, which occurs due to the presence of a zero frequency (constant pressure) mode shape.

Boundary Conditions

A fixed pressure of zero psi is prescribed at nodes 1 and 2. The remaining edges have reflecting boundaries; no boundary conditions are required.

Material Properties

Through use of the ISOTROPIC option, the bulk modulus is given to be 139,000 psi, and the material density of 1.2 lbm/in^3.

Loads

A sinusoidal forcing function is defined using user subroutine FORCDT of magnitude sin (1074t) on the second edge of nodes 21 and 22. Note that FORCDT must apply incremental source quantities and not total source quantities.

Dynamics

A total of five mode shapes are to be extracted using the Lanczos eigensolver. The lowest frequency is specified to be -10 Hz, which ensures the capture of zero frequency modes. The DYNAMIC CHANGE option provides the following parameters that are necessary for the integration of the modal equations of motion:

Time step size = 0.0003 seconds Duration = 0.0091 seconds
Number of time steps = 30

Print Control/POST

Through the PRINT NODE option, it is requested that the both the mode shapes and the reactions/residual forces be output at each node. With a PRINT ELEMENT option, it is requested that all relevant quantities be output at integration points 1 to 4. The following variables are requested to be written to a formatted post tape:

120 } Pressure 121,122 } Components of pressure gradient

Results

Figure 8.26-1 shows the cavity with the node numbers.

The calculated eigenfrequencies are listed below:

Mode	Frequency (rad/time)
1	5.312 E2
2	1.619 E3
3	2.742 E3
4	3.932 E3
5	5.214 E3

Thus, the exitation frequency $\omega = 1074$ rad/second is in the range between the first and second mode of exitation.

The propagation of the acoustic wave in shown in Figure 8.26-2. The pressures are labeled “displacement” in this plot.

Parameters, Options, and Subroutines Summary

Example e8x26.dat:

Parameters	Model Definition Options	History Definition Options
ACOUSTIC	CONNECTIVITY	CONTINUE
ELEMENT	CONTROL	DYNAMIC CHANGE
END	COORDINATE	MODAL SHAPE
PRINT	DEFINE	
SIZING	END OPTION	
TITLE	FIXED PRESSURE	
	FORCDT	
	GEOMETRY	
	ISOTROPIC	
	POST	
	PRINT ELEM	
	PRINT NODE	

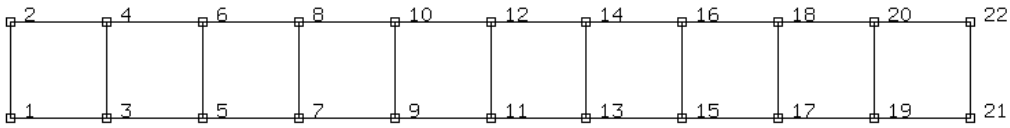

Figure 8.26-1 Acoustic Cavity Mesh

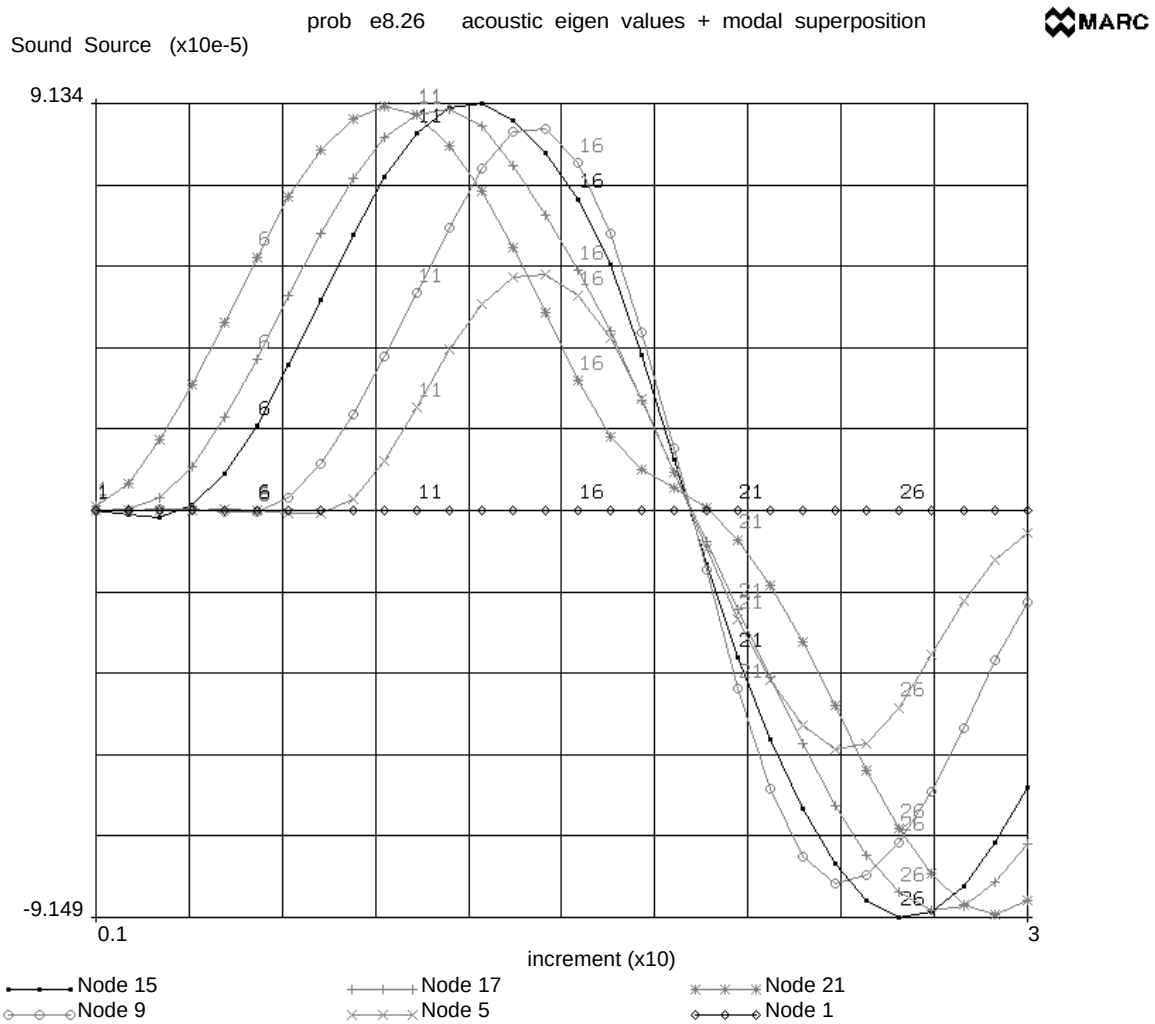

Figure 8.26-2 Time History of Pressure Pulse

8.27 Progressive Failure of a Plate with a Hole

This problem demonstrates the application of MARC's progressive failure modeling capability applied to a plane stress problem. A plate with a circular hole, made of an orthotropic material, is loaded until selective regions fail.

Parameters

The use of element 26 (8-noded plane stress quadrilateral) is specified through an ELEMENT parameter.

Mesh Definition

The square plate is 100 mm long. The radius of the hole is 10 mm. Only one-quarter of the plate is modeled due to symmetry. A thickness of 1 mm is provided through the first field in the GEOMETRY option (EGEOM1). Figure 8.27-1 shows the nodal configuration of the mesh and Figure 8.27-2 shows the element configuration.

Boundary Conditions

Constraints in the global X-, Y-directions are applied through the use of the FIXED DISP model definition option.

Material Properties

Use of the ORTHOTROPIC model definition option allows the input of directional moduli. The following values are specified:

```
E = 14.0 X 109 N/mm2    E = 3.50 X 109 N/mm2    G = 4.2 X 109 N/mm2
```

Poisson's ratio relating strains in the 1-2 directions is 0.4. The orthotropic axes are skewed with respect to the global X,Y by an angle of sixty degrees. To take this into account, an ORIENTATION option group is given defining the material axis base vectors to be a function of the intersection of the element tangent plane and the global ZX plane. The progressive failure option is invoked through the FAIL DATA model option, specifically by entering a '1' in the third field of the third record. Two failure criteria coexist: maximum stress (MX STRESS option) and Hill (HILL). For the both stress criteria, failure is predicated on the following stress levels:

σ_X (tension) = Sigma X (compression) = 250,000,000 N/mm^2
σ_Y (tension) = 500,000 N/mm^2
σ_Y (compression) = 10,000,000 N/mm^2
σ_{XY} = 8,000,000 N/mm^2

Failure occurs when the corresponding interaction equation (see *Volume A: User Information*) reaches or exceeds unity.

Loads

A distributed load of 300,000 N/mm^2 is applied on the 2-6-3 face of elements 13 and 14 during increment zero. Five load steps of 20% of the increment zero load are applied bringing the total distributed load magnitude to 600,000 N/mm^2. This is done through the use of the AUTO LOAD and PROPORTIONAL INC options.

Control

A maximum of ten load steps and four recycles per step is allowed through the CONTROL option. Furthermore, convergence is considered to be reached when the maximum residual force divided by the maximum reaction force falls below the value 0.1.

POST

A formatted post file is requested with the following variables:

code 94	Failure index
code 111	Direct stress 11 in preferred 1 direction
code 112	Direct stress 22 in preferred 2 direction
code 113	Shear stress 12

Results

Figure 8.27-3, Figure 8.27-4, and Figure 8.27-5 show the fourth failure index at increments 1, 3, and 5, respectively. The stresses in the preferred directions are shown in Figure 8.27-6 and Figure 8.27-7.

Parameters, Options, and Subroutines Summary

Example e8x27.dat:

Parameters	Model Definition Options	History Definition Options
ELEMENT	CONNECTIVITY	AUTO LOAD
END	CONTROL	CONTINUE
SIZING	COORDINATE	PROPORTIONAL INCREMENT
TITLE	DIST LOADS	
	END OPTION	
	FAIL DATA	
	FIXED DISP	
	GEOMETRY	
	ORIENTATION	
	ORTHOTROPIC	
	POST	
	PRINT ELEM	

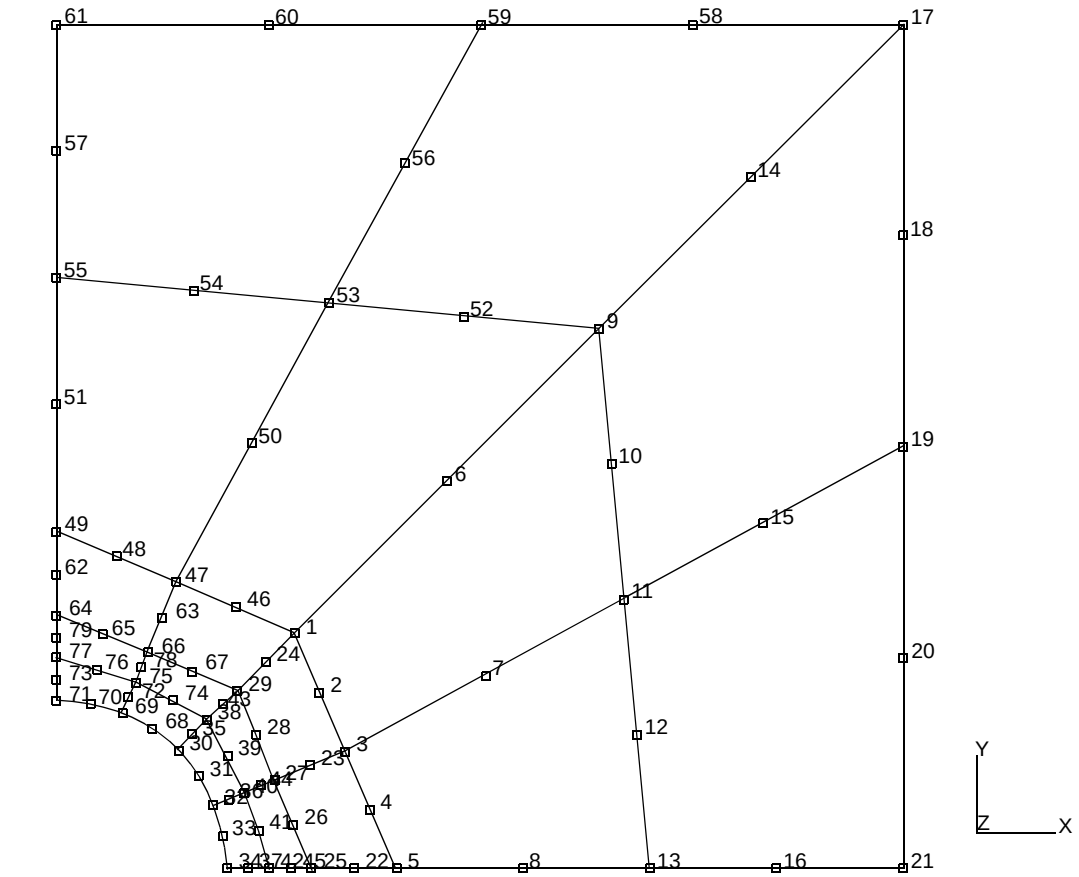

Figure 8.27-1 Finite Element Mesh – Nodes

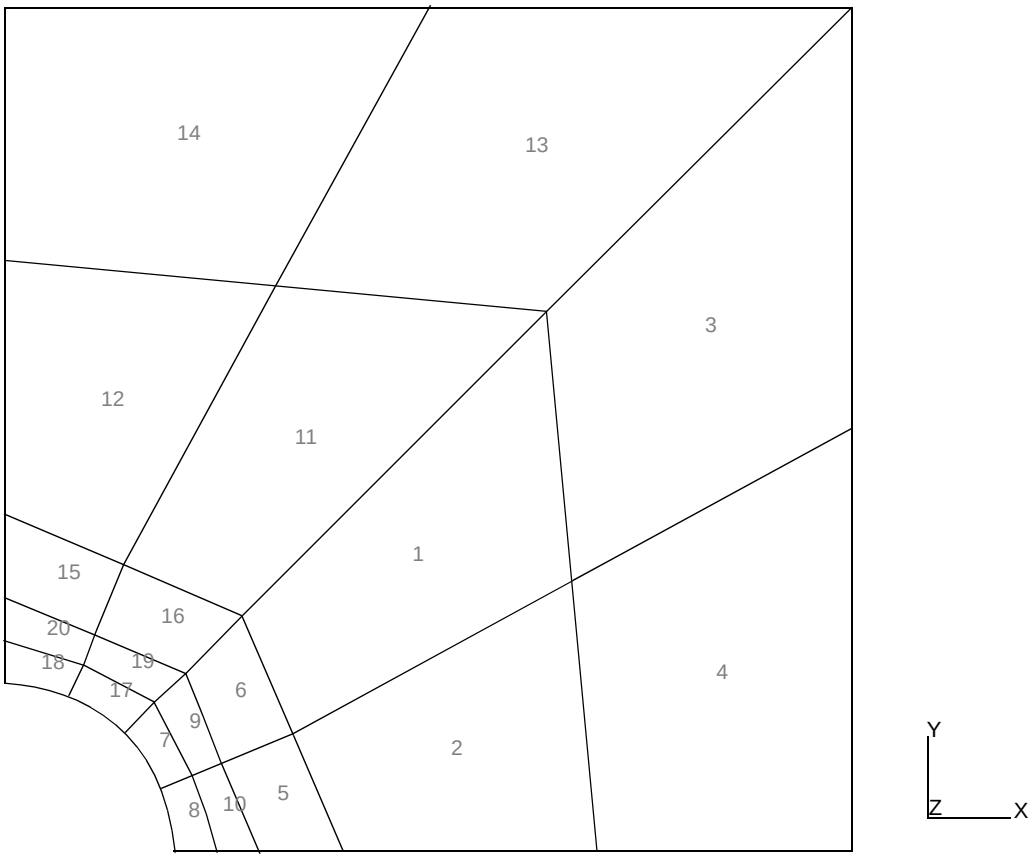

Figure 8.27-2 Finite Element Mesh – Nodes

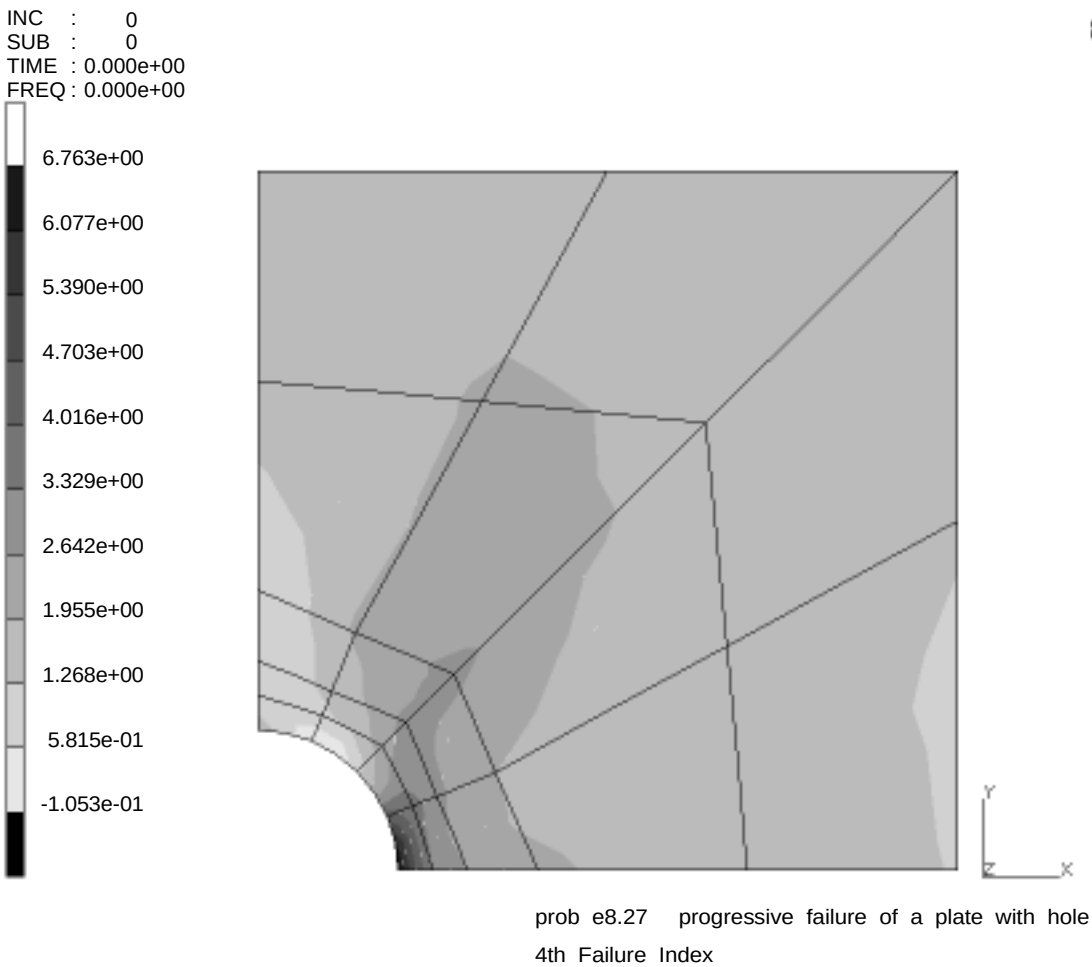

Figure 8.27-3 Failure Index, Increment 0

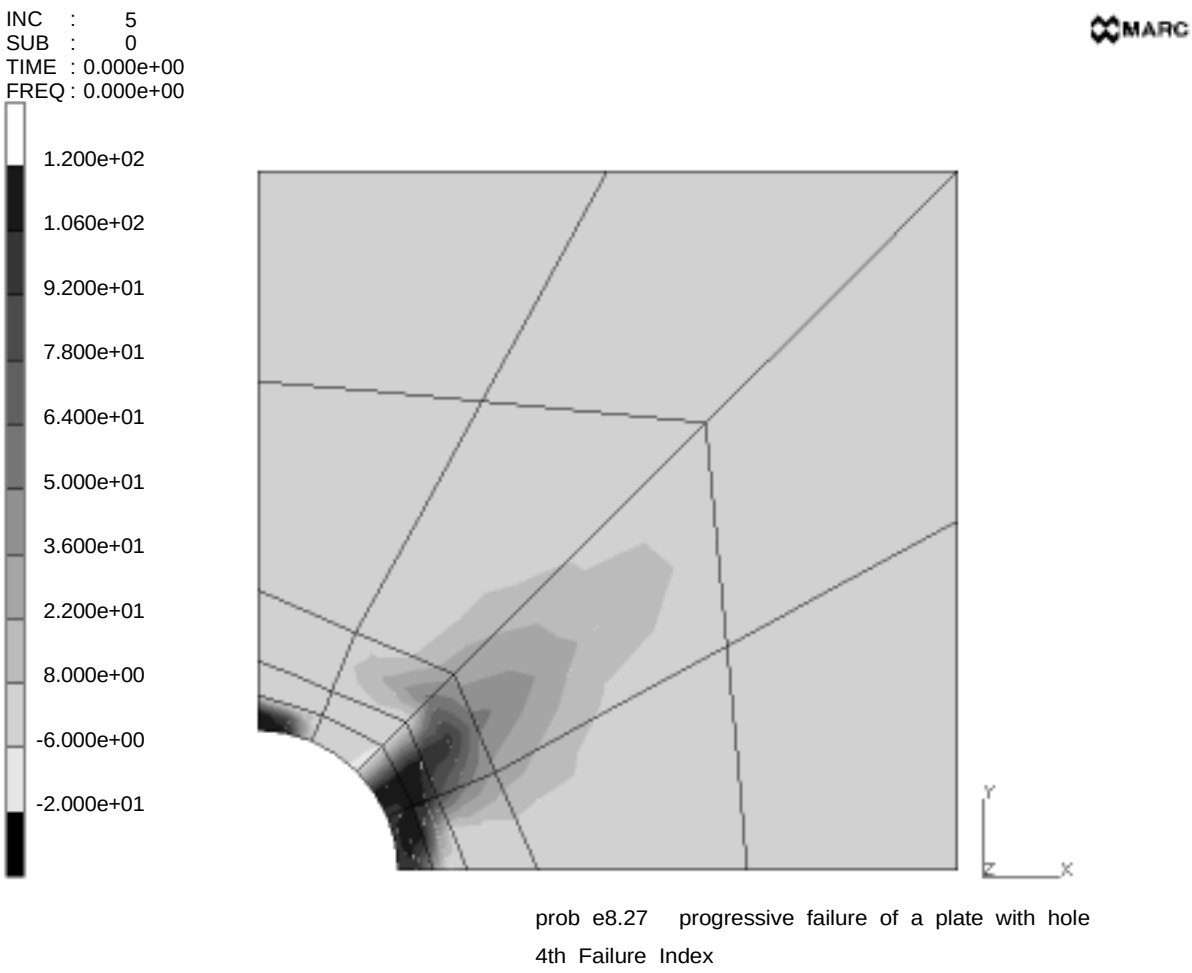

Figure 8.27-4 Failure Index, Increment 5

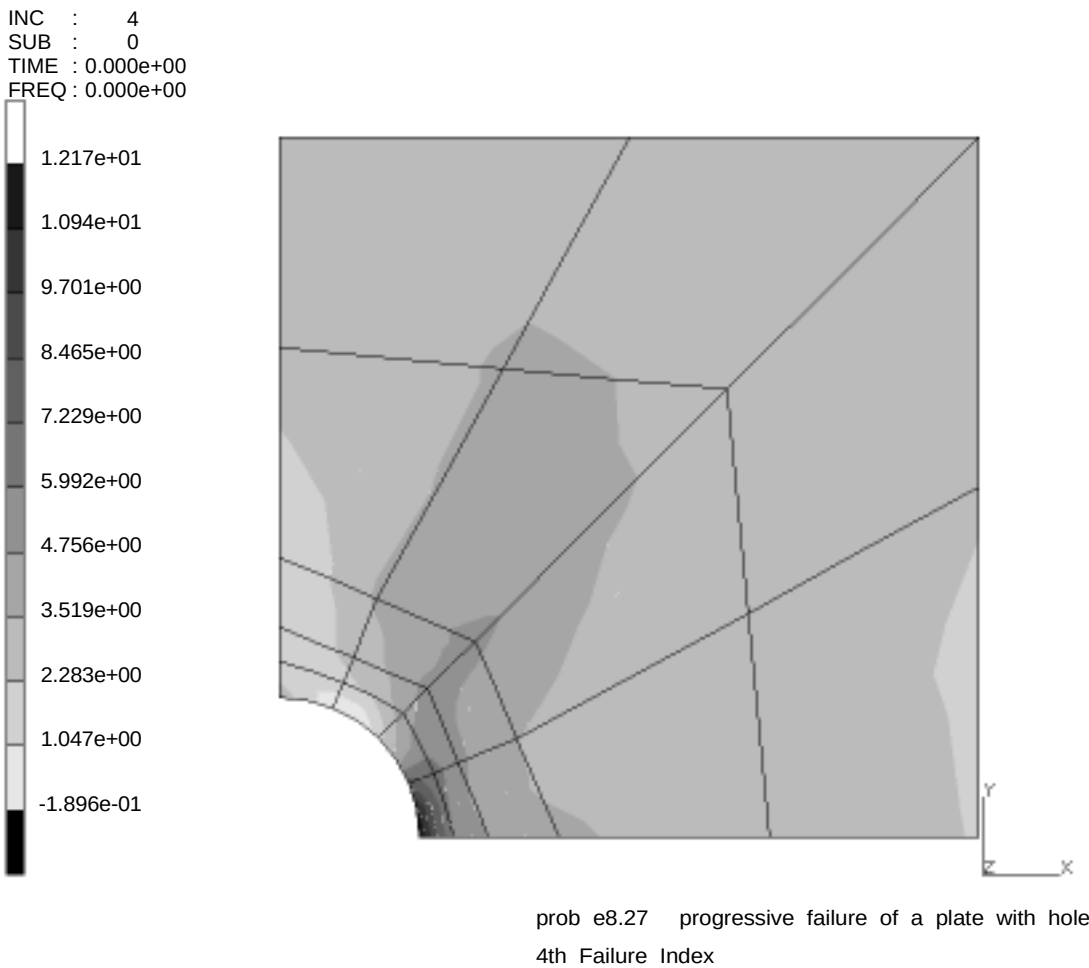

Figure 8.27-5 Failure Index – No Failure Allowed

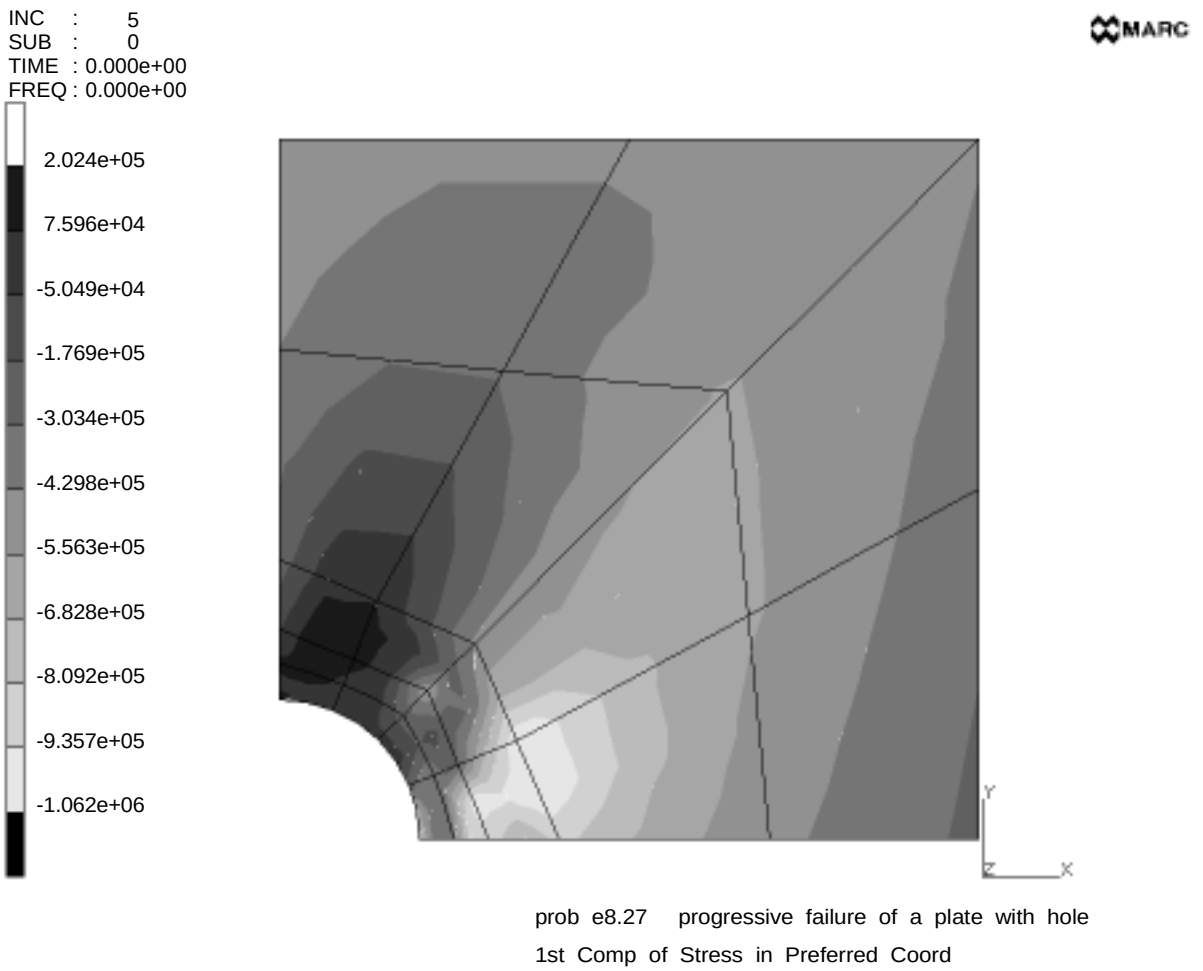

Figure 8.27-6 First Component of Stress in Preferred Direction

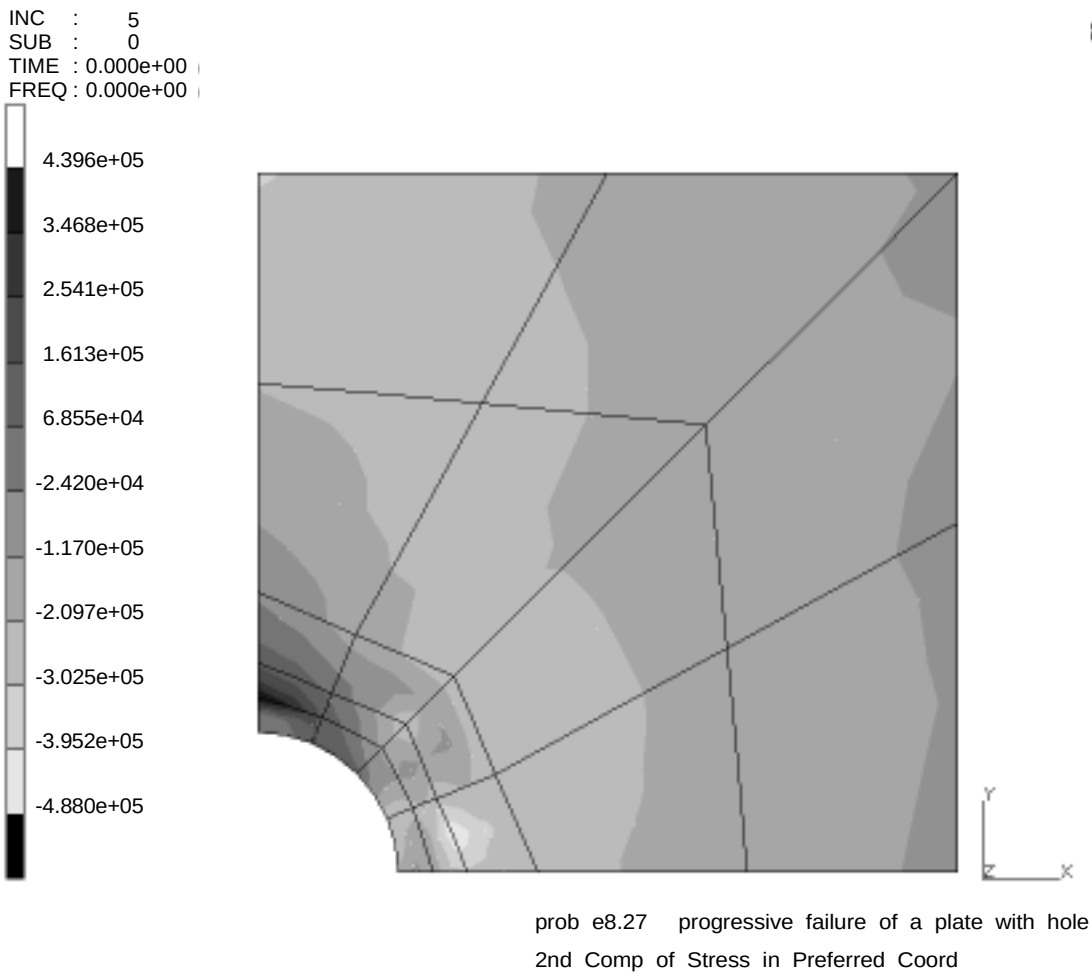

Figure 8.27-7 Second Component of Stress in the Preferred Direction

8.28 Linear Distribution of Dipoles

The problem presented here is the determination of the two-dimensional electric field generated in a vacuum around two wires with uniform electrostatic charge of opposite signs. The numerical results are compared with the analytic solution.

Parameters

The ELECTRO parameter is included to indicate that an electrostatic analysis is being performed.

Element

Elements type 41 and 103 are used.

Element 41 is a second-order planar isoparametric quadrilateral for “quasi-harmonic” field problems. Element type 103 is a nine-node semi-infinite element. In the first direction, special interpolation functions are used which can represent exponential decay.

Model

The mesh of the plane is shown in Figure 8.28-1. The outer ring is modeled with semi-infinite elements. The outer radius is 1.5 m.

Material Properties

The permittivity of the medium (vacuum) is 8.8×10^{-12} farad/m.

Point Charge

A linear distribution normal to the plane of 10^{-12} coulomb/m is prescribed with opposite signs at nodes 80 and 81 (X = 0, Y = ± 0.21621 m).

Fixed Potential

The potential is prescribed to be zero at the center of the plane.

Control

The STEADY STATE option initiates the analysis. A formatted post file is created.

Results

A contour plot of the electric potential is shown in Figure 8.28-2. A vector plot of the electric field is shown in Figure 8.28-3. An X-Y plot of the potential along the Y-axis is shown in Figure 8.28-4. Table 8.28-1 shows a comparison of the MARC results with the analytical solution.

Table 8.28-1 Comparison of MARC Results

Node	Y (m.)	Potential (Volt)		Error (%)
		MARC	Analytical	
8	0.07254	1.302	1.255	+ 3.7
36	0.14435	2.729	2.900	– 5.9
165	0.29150	3.257	3.432	– 5.1
320	0.48159	1.732	1.739	– 0.4
558	1.0	0.789	0.790	– 0.1

Parameters, Options, and Subroutines Summary

Example e8x28.dat:

Parameters	Model Definition Options	History Definition Options
ELECTROSTATIC	CONNECTIVITY	CONTINUE
ELEMENT	COORDINATE	STEADY STATE
END	DEFINE	
SIZING	END OPTION	
TITLE	FIXED POTENTIAL	
	ISOTROPIC	
	POINT CHARGE	
	POST	
	PRINT ELEM	

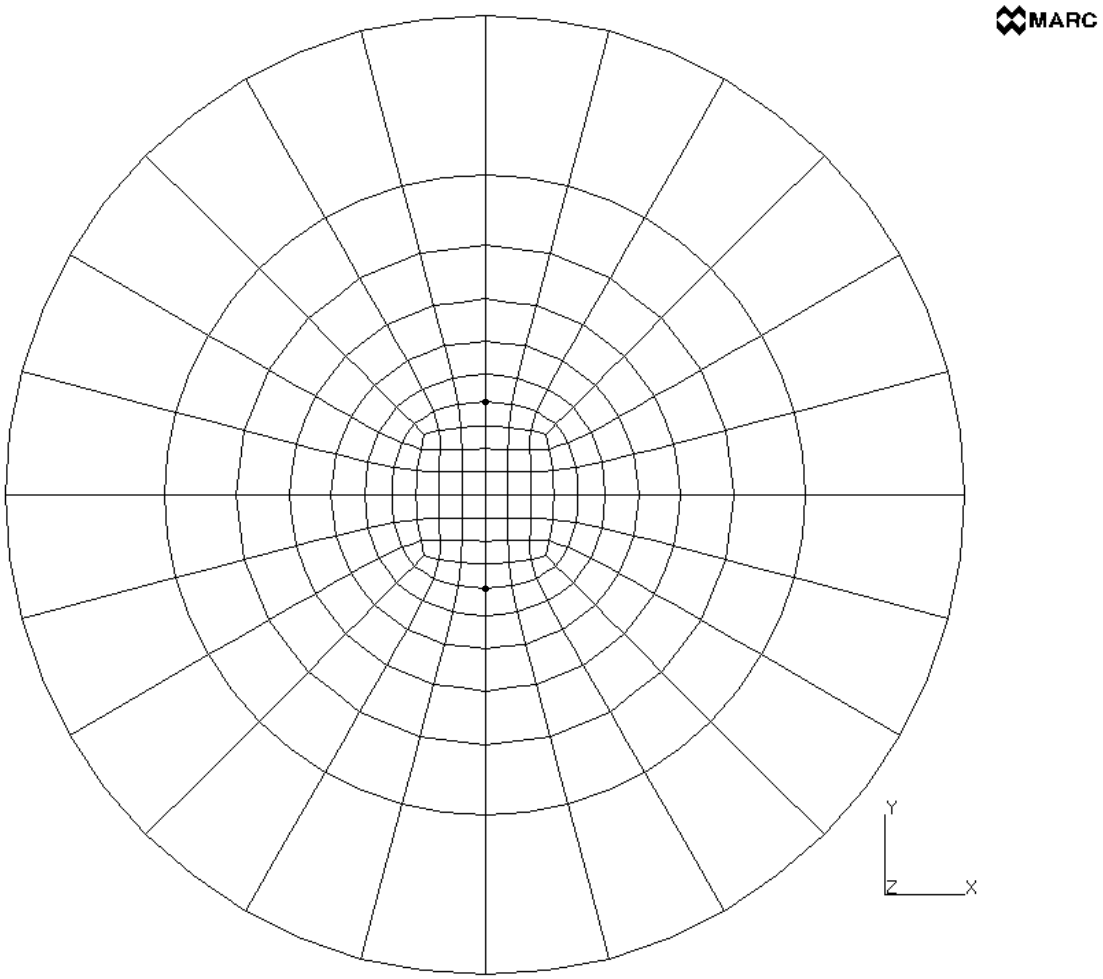

Figure 8.28-1 Finite Element Mesh with Dipole

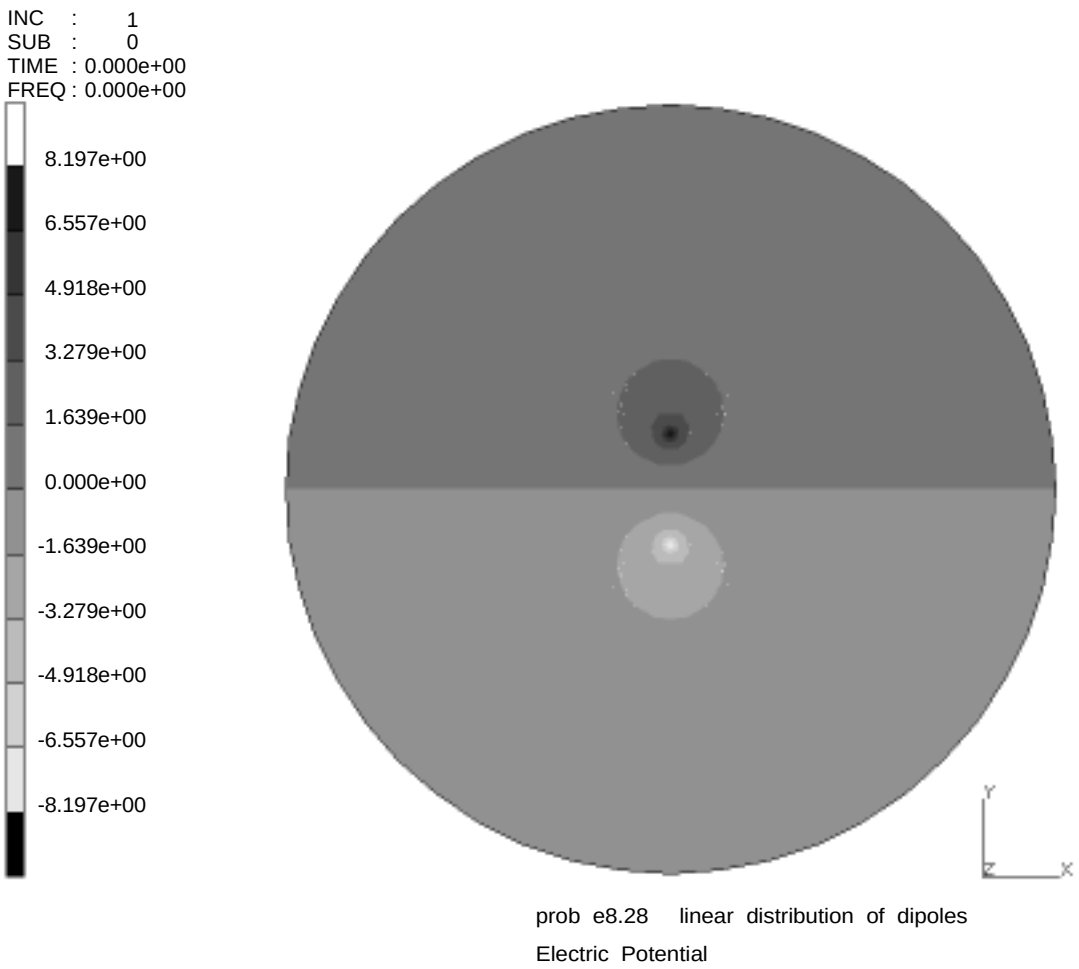

Figure 8.28-2 Scalar Potential

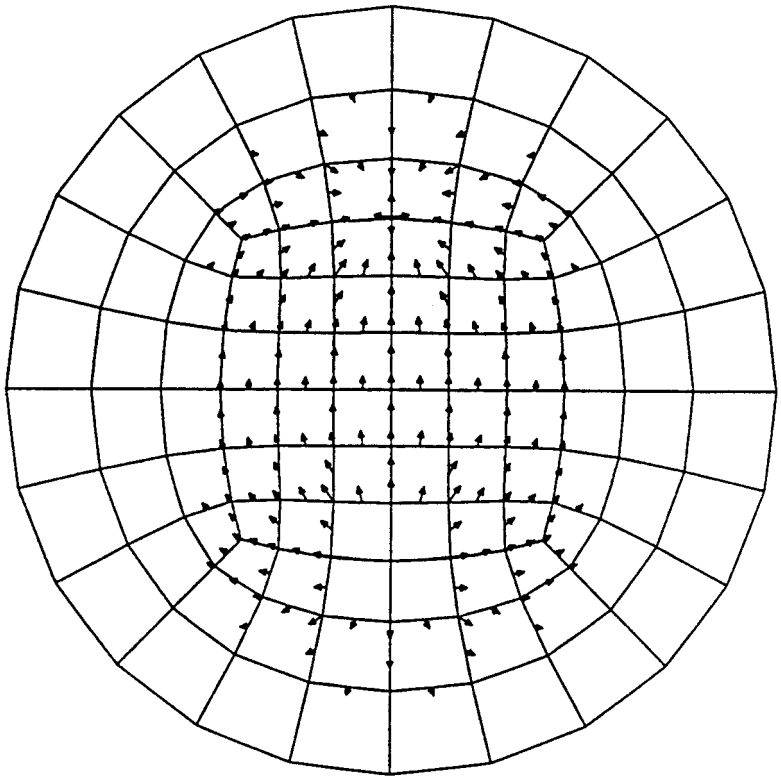

Figure 8.28-3 Vector Plot of Electric Field

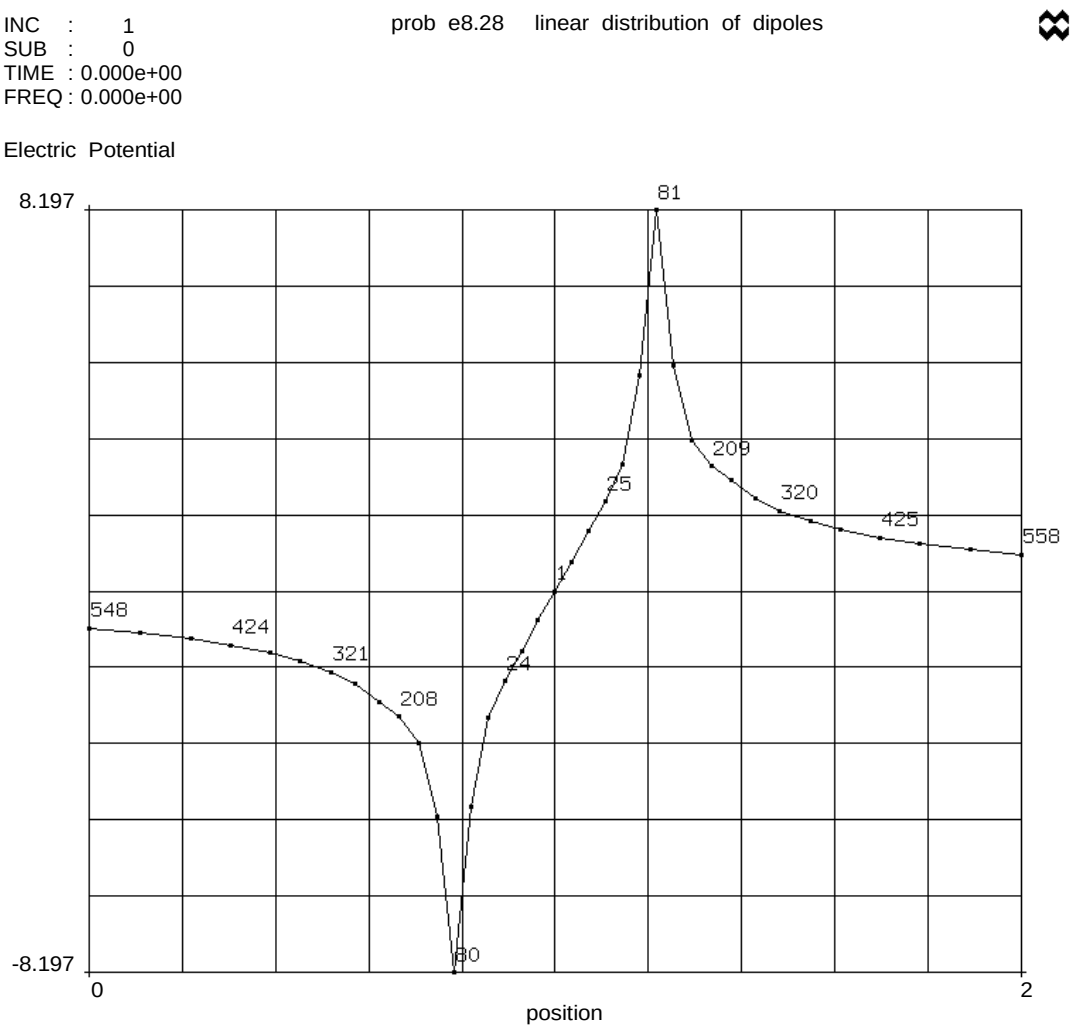

Figure 8.28-4 Scalar Potential Distribution

8.29 Magnetic Field around Two Wires carrying Opposite Currents

The problem presented here is the determination of the two-dimensional electric field generated in a vacuum around two wires carrying equal current of opposite signs. The numerical results are compared with the analytical solution.

Parameters

The MAGNETO parameter is included to indicate that a magnetostatic option is being performed.

Element

Elements type 41 and 103 are used.

Element 41 is a second-order planar isoparametric quadrilateral for “quasi-harmonic” field problems.

Element 103 is a nine-node planar semi-infinite quadrilateral for “quasi-harmonic” field problems.

Model

The mesh of the plane is shown in Figure 8.29-1. The outer ring is modeled with semi-infinite elements. The outer radius is 1.5 m.

Material Properties

The magnetic permeability of the medium (vacuum) is 1.26×10^{-6} henry/m.

Point Current

A point current of 10^{-6}amp running normal to the plane is prescribed with opposite signs at nodes 80 and 81 (X = 0, Y = ± 0.21621 m).

Fixed Potential

The potential is prescribed to be zero at the center of the plane.

Control

The STEADY STATE option initiates the analysis. A formatted post file is created.

Results

A contour plot of the scalar potential (only available for 2D magnetostatic) is shown in Figure 8.29-2. A vector plot of the magnetic flux density is shown in Figure 8.29-3. An X-Y plot of the potential along the Y-axis is shown in Figure 8.29-4. Table 8.29-1 shows a comparison of the MARC results with the analytical solution.

Table 8.29-1 Comparison of MARC Results

Node	X (m.)	Bx (weber/m^2)		Error (%)
		MARC	Analytical	
1	0.	1.855	1.855	+ 0.0
6	0.072534	1.674	1.667	+ 0.4
34	0.14434	1.288	1.283	+ 0.4
162	0.29149	0.664	0.658	+ 0.9
319	0.48158	0.316	0.311	+ 1.6
547	1.0	0.0832	0.0828	+ 0.5

Parameters, Options, and Subroutines Summary

Example e8x29.dat:

Parameters	Model Definition Options	History Definition Options
ELEMENT	CONNECTIVITY	CONTINUE
END	COORDINATE	STEADY STATE
MAGNETOSTATIC	DEFINE	
SIZING	END OPTION	
TITLE	FIXED POTENTIAL	
	ISOTROPIC	
	POINT CURRENT	
	POST	
	PRINT ELEM	

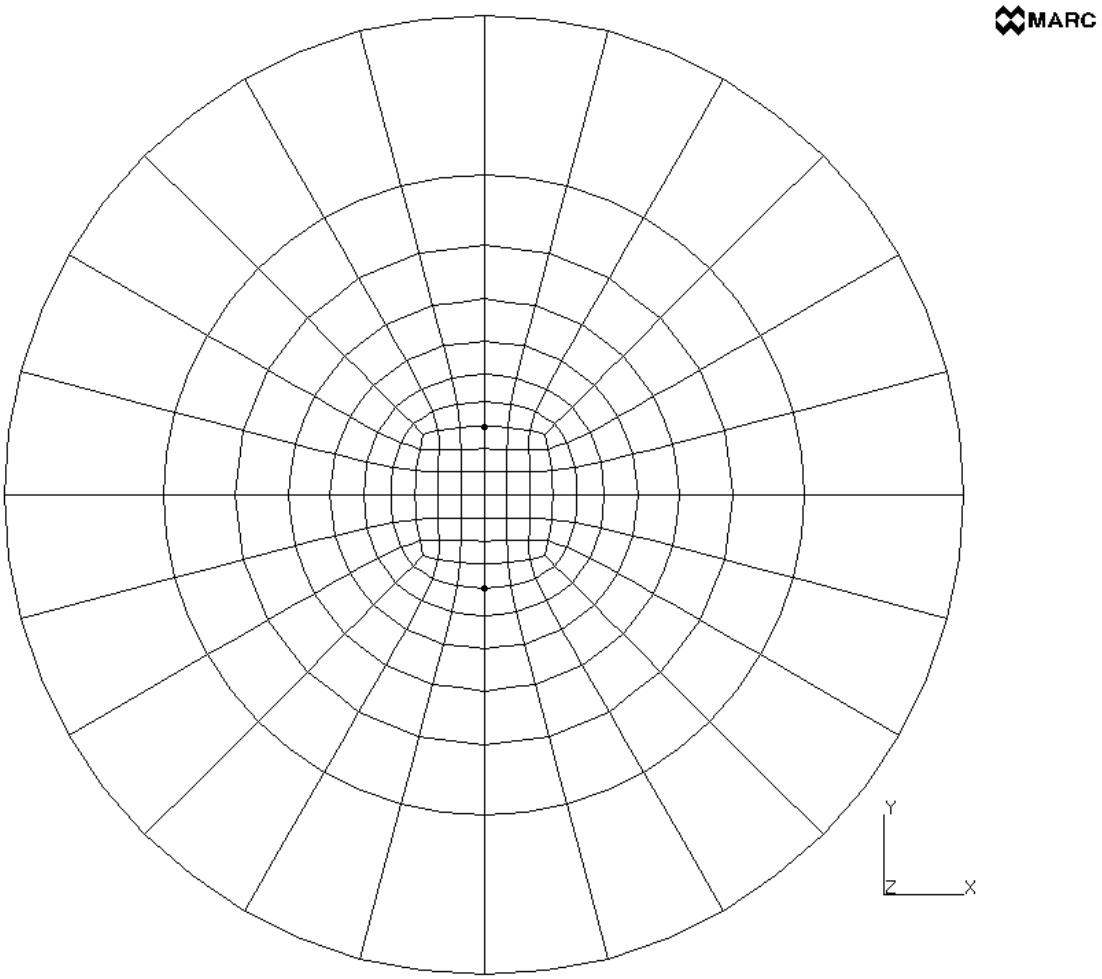

Figure 8.29-1 Finite Element Mesh and Parallel Wires

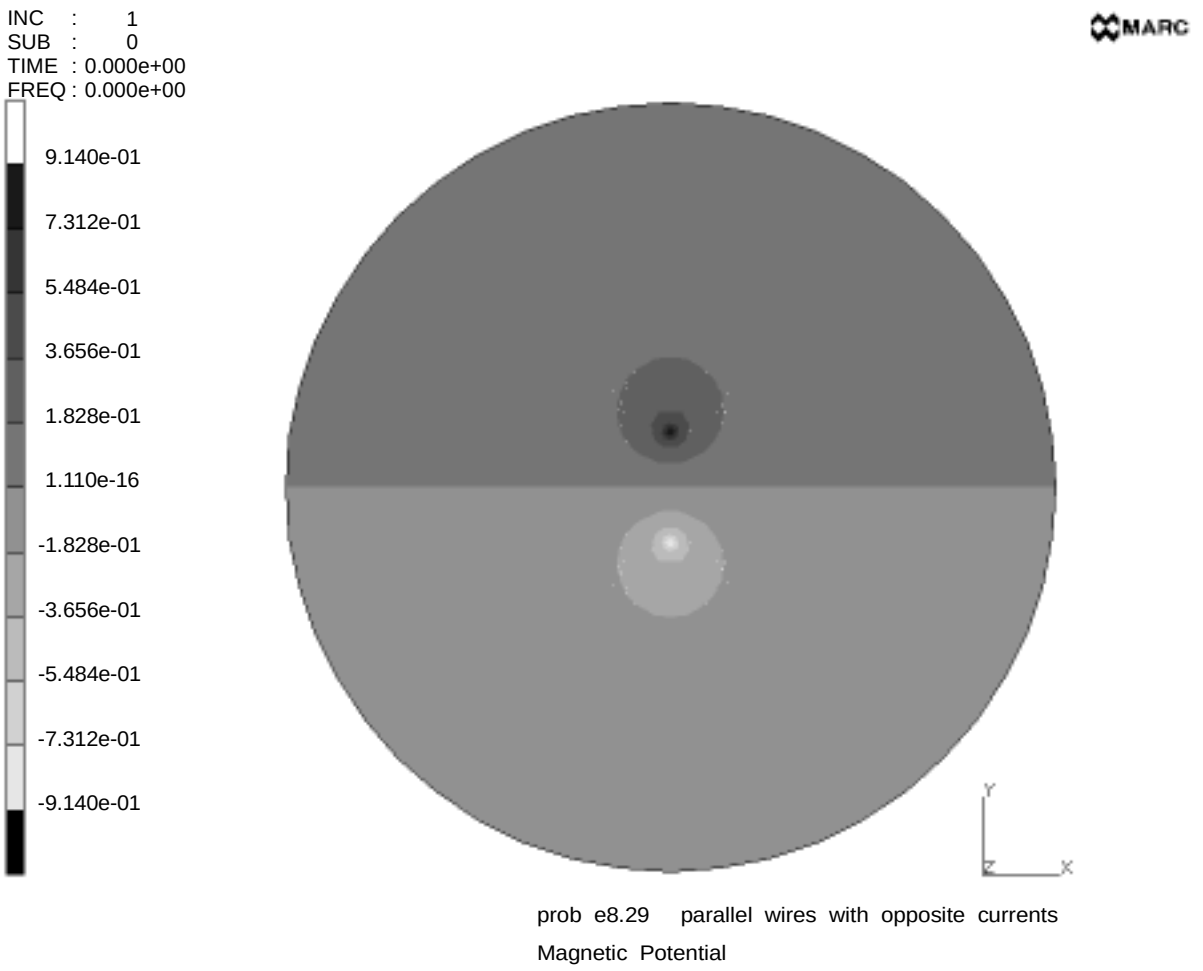

Figure 8.29-2 Magnetic Scalar Potential

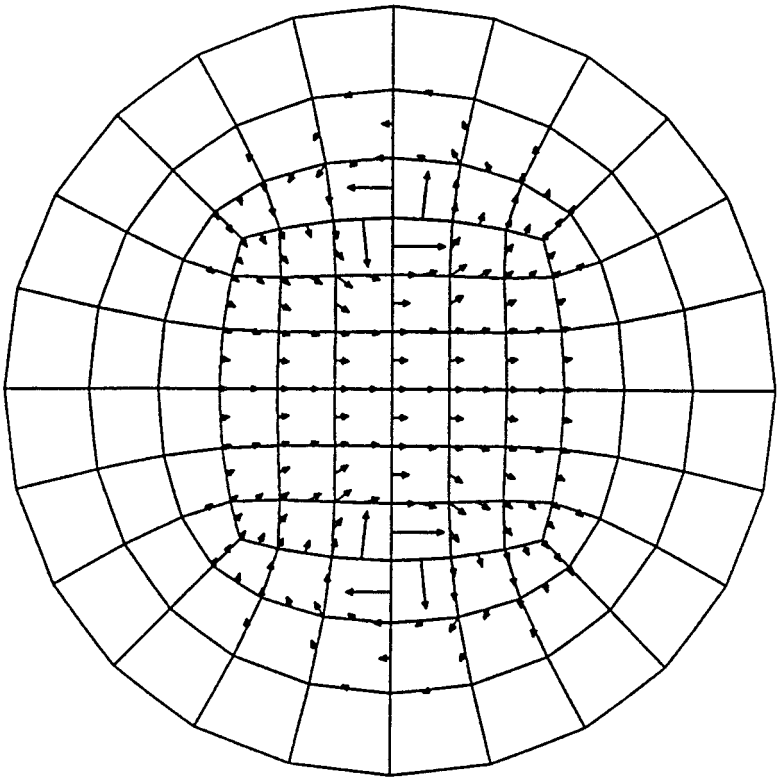

Figure 8.29-3 Magnetic Flux Density

INC : 1
SUB : 0
TIME : 0.000e+00
FREQ : 0.000e+00

prob e8.28 parallel wires with opposite currents

MARC

1st (Real) Comp of Magnetic Flux

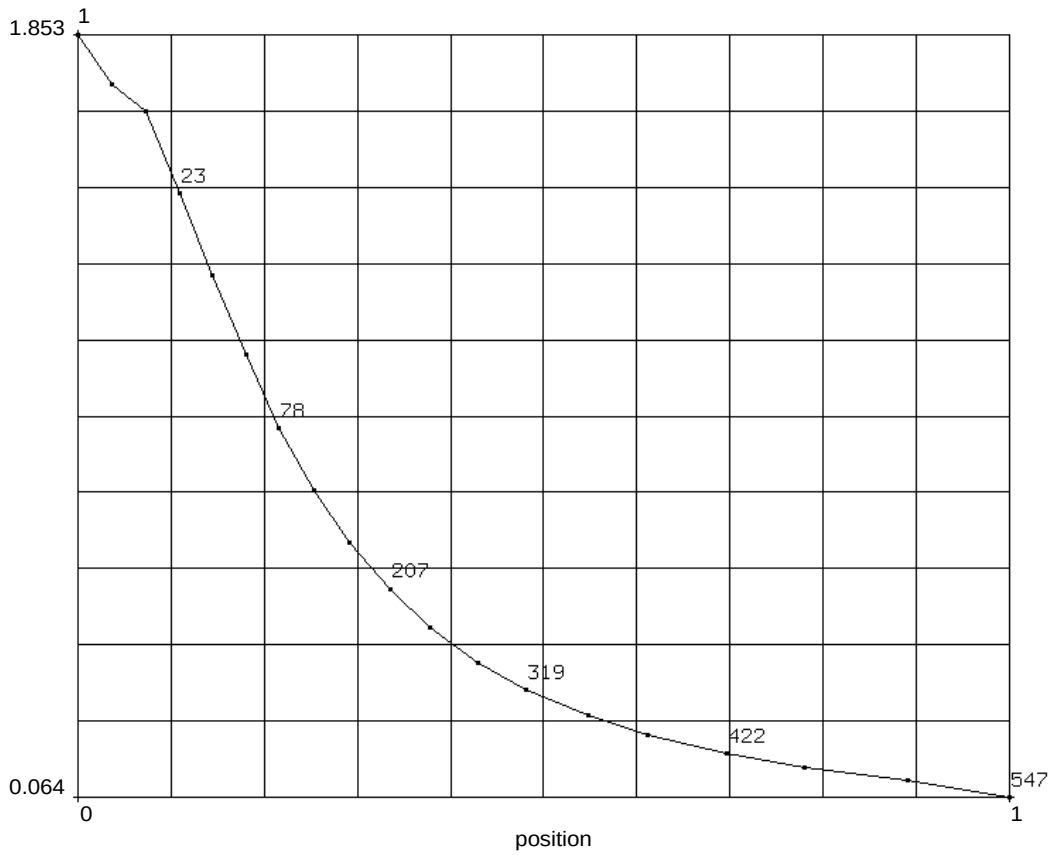

Figure 8.29-4 Magnetic Flux Distribution

8.30 Harmonic Electromagnetic Analysis of a Wave Guide

This problem demonstrates MARC's capability to perform electromagnetic analysis of a wave guide. The harmonic procedure is utilized in this problem.

Parameters

The EL-MA, 1 parameter is used to indicate that a harmonic electromagnetic analysis is to be performed. This always results in a complex formulation. The HARMONIC parameter is used to give an upper bound to the number of harmonic boundary conditions.

Element

Element 111 is used in this problem. This element is a four-node planar element for electromagnetic analysis. There are four degrees of freedom, the vector magnetic potential A, and the scalar electrical potential ϕ.

Model

The model, as shown in Figure 8.30-1, has a length of 1 m and a width of 0.5m. A wall is placed at 0.5 m which is 0.02 m thick (elements 33 to 36).

Loading

The outside periphery labeled "metal" is held at a fixed magnetic potential of zero. The corner, node 46, is given a fixed electrical potential of zero. A distributed current is applied to element one. The current is applied at a frequency between 200 MHz to 240 MHz in 2 MHz steps.

Material Properties

There are two materials in this analysis: the air and the wall. The material properties are:

	Permeability (henry/m)	Permittivity (farad/m)	Permeability of Air (henry/m)	Conductivity (s/m)
Air	1.2566×10^{-6}	8.854×10^{-12}	1.2566×10^{-6}	1000
Wall	1.2566×10^{-6}	8.854×10^{-12}	1.2566×10^{-6}	1×10^{-8}

Control

As this is a linear analysis, no controls are required.

Results

The third component of the electric field varies in magnitude from 0.989 to 0.831 over the frequency range requested. The user can also observe that there is no distribution on the right side of the wall in Figure 8.30-3. Note that the frequency is input in cycles/time, but Mentat reports the frequency in radians/time.

Table 8.30-1 Electric Field as a Function of Frequency

Subincrement	ω x MHz	E_3
1	200	9.892
5	210	9.512
10	220	9.076
15	230	8.679
20	240	8.314

Parameters, Options, and Subroutines Summary

Example e8x30.dat:

Parameters	Model Definition Options	History Definition Options
ELEMENT	CONNECTIVITY	CONTINUE
EL-MA	COORDINATE	DIST CURRENT
END	DEFINE	HARMONIC
PRINT	END OPTION	
SIZING	FIXED POTENTIAL	
TITLE	ISOTROPIC	
	OPTIMIZE	
	POST	

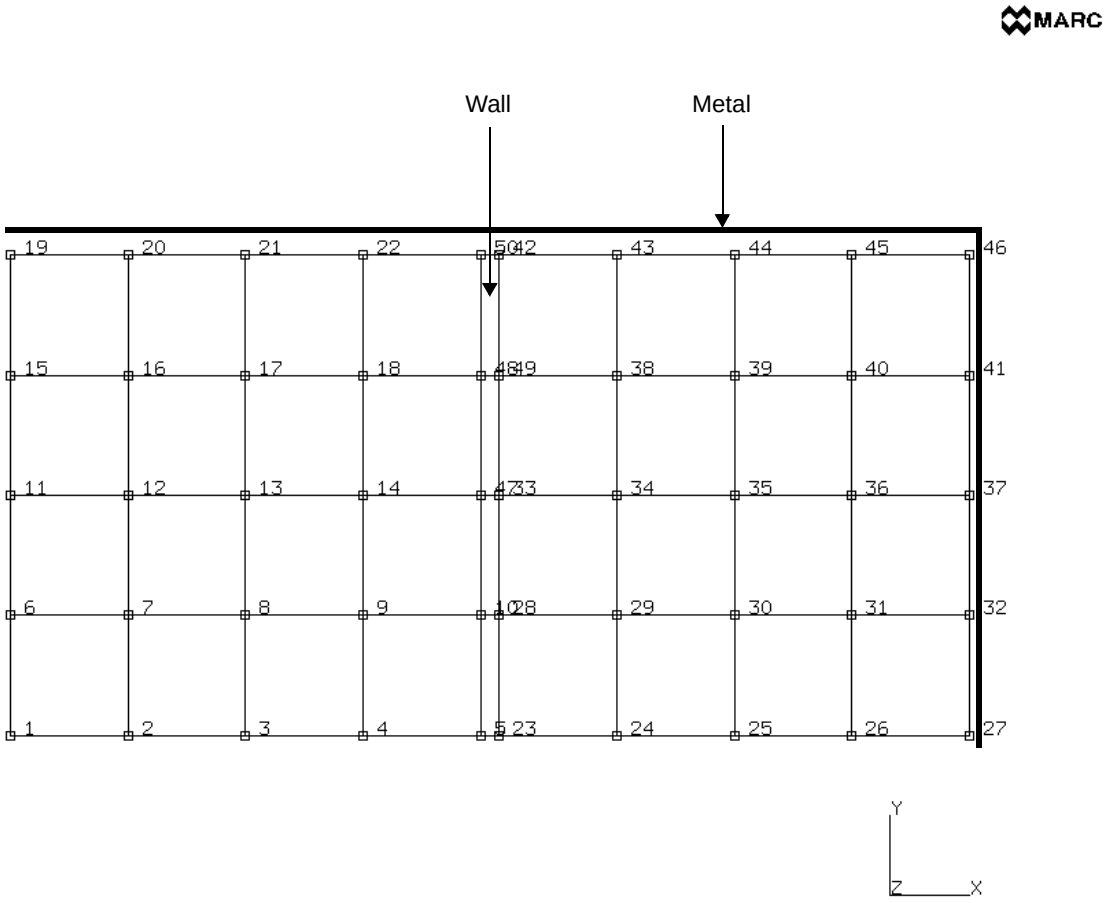

Figure 8.30-1 Finite Element Mesh with Node Numbers

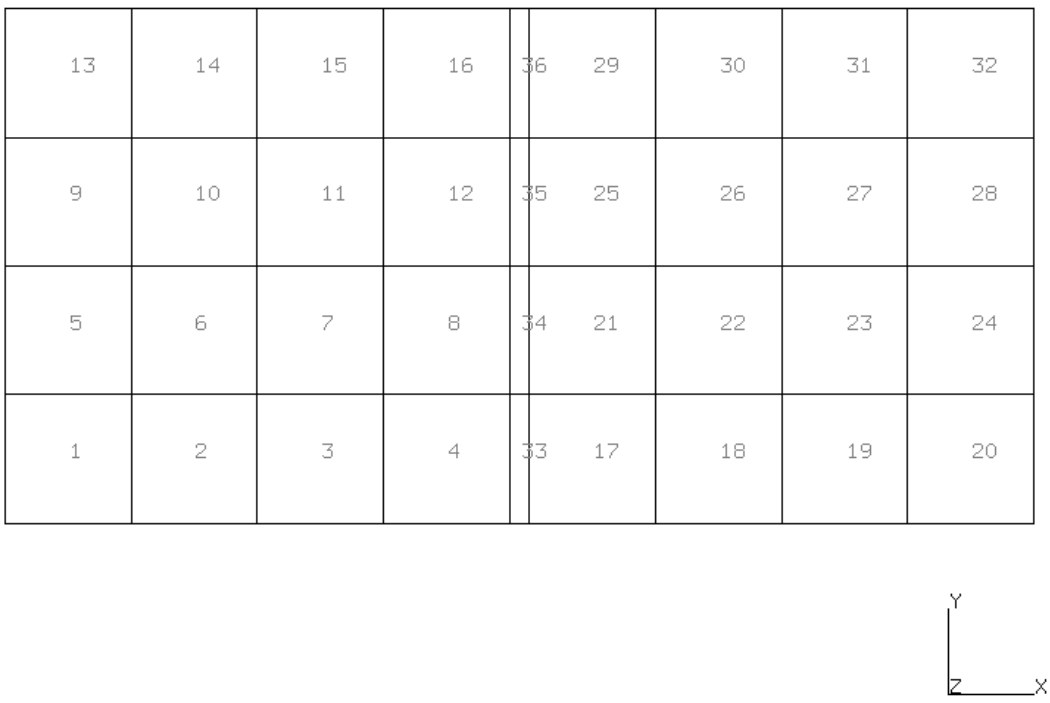

Figure 8.30-2 Finite Element Mesh with Element Numbers

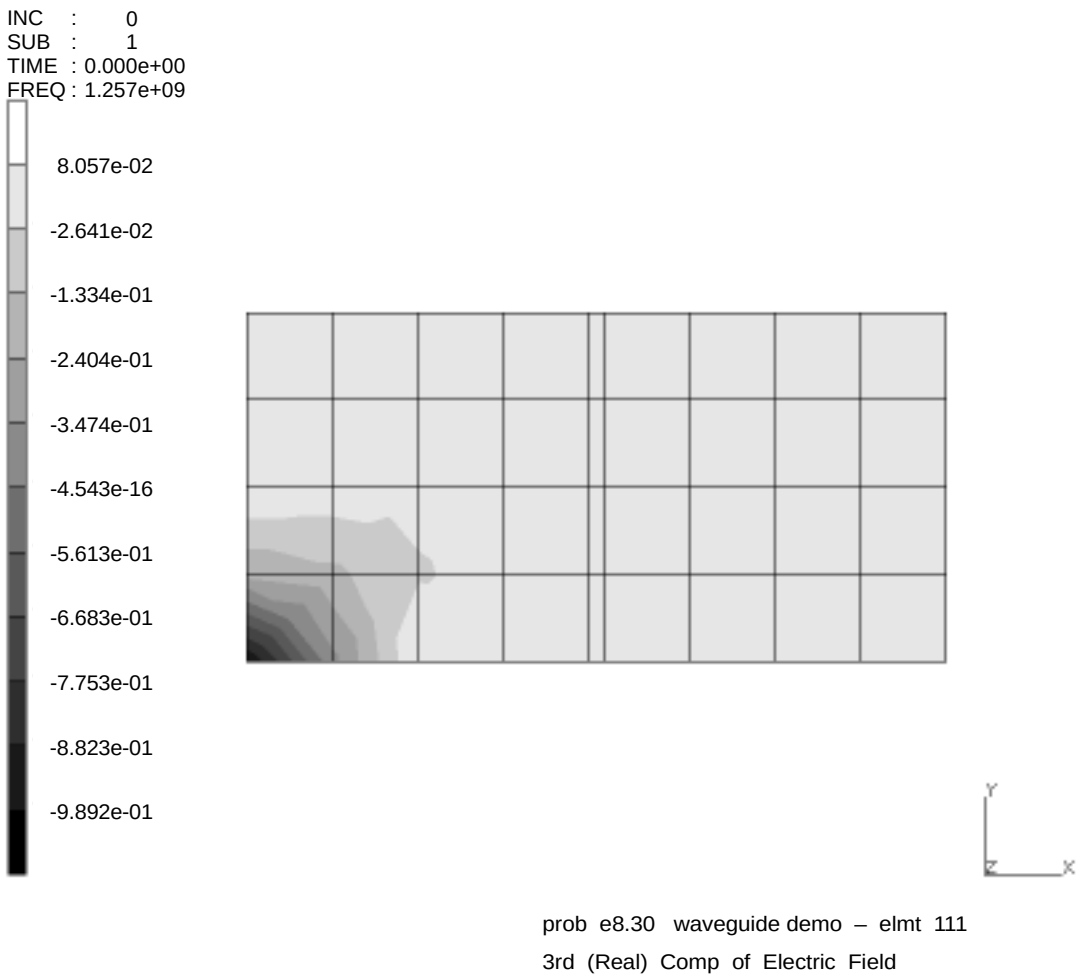

Figure 8.30-3 Third Component of Electric Field at 20 MHz

8.31 Transient Electromagnetic Analysis around a Conducting Sphere

This example demonstrates the transient electromagnetic analysis around a conducting sphere subjected to a planar pulse.

Parameters

The EL-MA,0 parameter is used to indicate that a transient electromagnetic analysis is to be performed.

Element

This model consists of 165 element type 112 as shown in Figure 8.31-1. Element type 112 is a four-node axisymmetric element for electromagnetic analysis. It has four degrees of freedom. The first three represent the magnetic vector potential. The last represents the scalar electrostatic potential. The spherical shell is elements 135-143 and 153. The inner radius is 5 cm and the outer radius is 5.5 cm.

Loading

The vertical symmetry line at z = 0 is constrained such that all components of A are zero. The nodes along z = 15 have $A_z = 0$. The nodes along r = 0 and r = 15 have A_x and A_z prescribed to be zero. The nodes along z = 15 have a ramp charge applied to the second component that varies from 0 to 25 x 10^{-6} coulomb over 25 microseconds. This data is entered using the DYNAMIC CHANGE and POTENTIAL CHANGE options.

Material Properties

There are two materials in this analysis: the air and the metal sphere. The material properties are as follows:

	Permeability (henry/m)	Permittivity (farad/m)	Permeability of Air (henry/m)	Conductivity (s/m)
Air	1.2566 x 10^{-6}	8.54 x 10^{-12}	1.2566 x 10^{-6}	5 x 10^{8}
Sphere	1.2566 x 10^{-6}	8.54 x 10^{-12}	1.2566 x 10^{-6}	0.0

These are specified through the ISOTROPIC option.

Control

The convergence tolerance requested is 10% on residuals. The POST option is used to save the magnetic flux for post processing. The DYNAMIC CHANGE option is used to specify a time period of 25 microseconds to be performed in 25 increments with a fixed time step of 1 microsecond.

Results

Figure 8.31-2 and Figure 8.31-3 show the propagation of the magnetic field with time. The time history of the magnetic field is shown in Figure 8.31-4. Finally, the current density is shown in Figure 8.31-5. As expected, most of the current is in the sphere and the magnetic field is virtually zero within the sphere.

Parameters, Options, and Subroutines Summary

Example e8x31.dat:

Parameters	Model Definition Options	History Definition Options
ELEMENT	CONNECTIVITY	CONTINUE
EL-MA	COORDINATE	DYNAMIC CHANGE
END	CONTROL	
PRINT	DEFINE	
SIZING	END OPTION	
TITLE	FIXED POTENTIAL	
	FORCDT	
	ISOTROPIC	
	OPTIMIZE	
	POST	

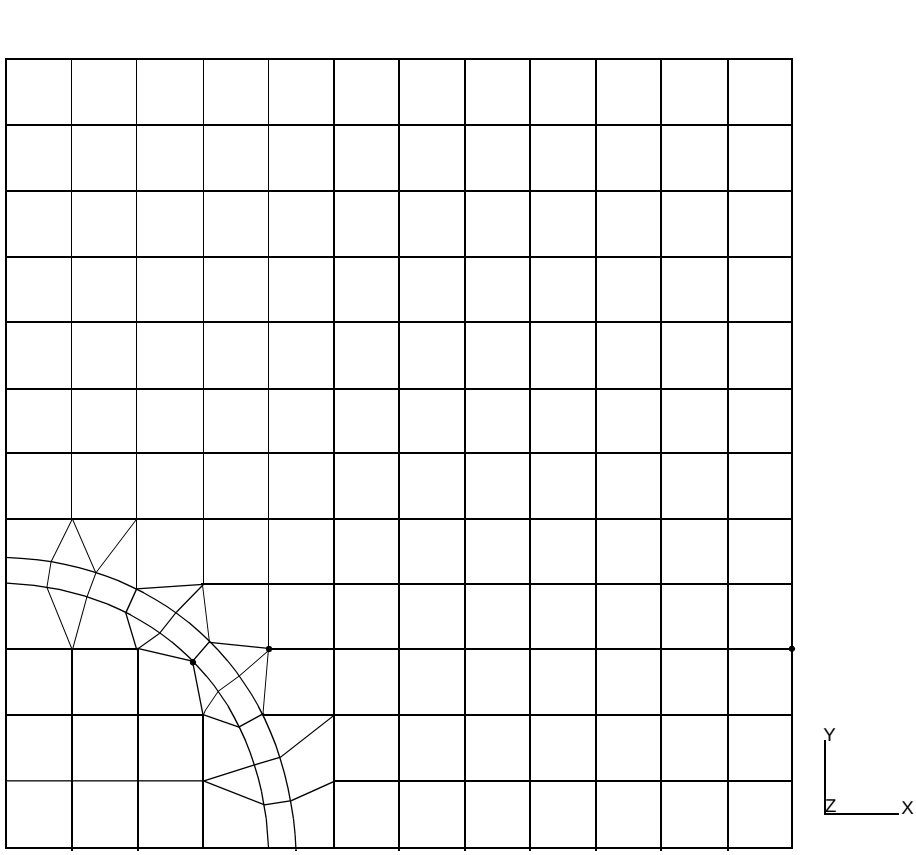

Figure 8.31-1 Finite Element Mesh

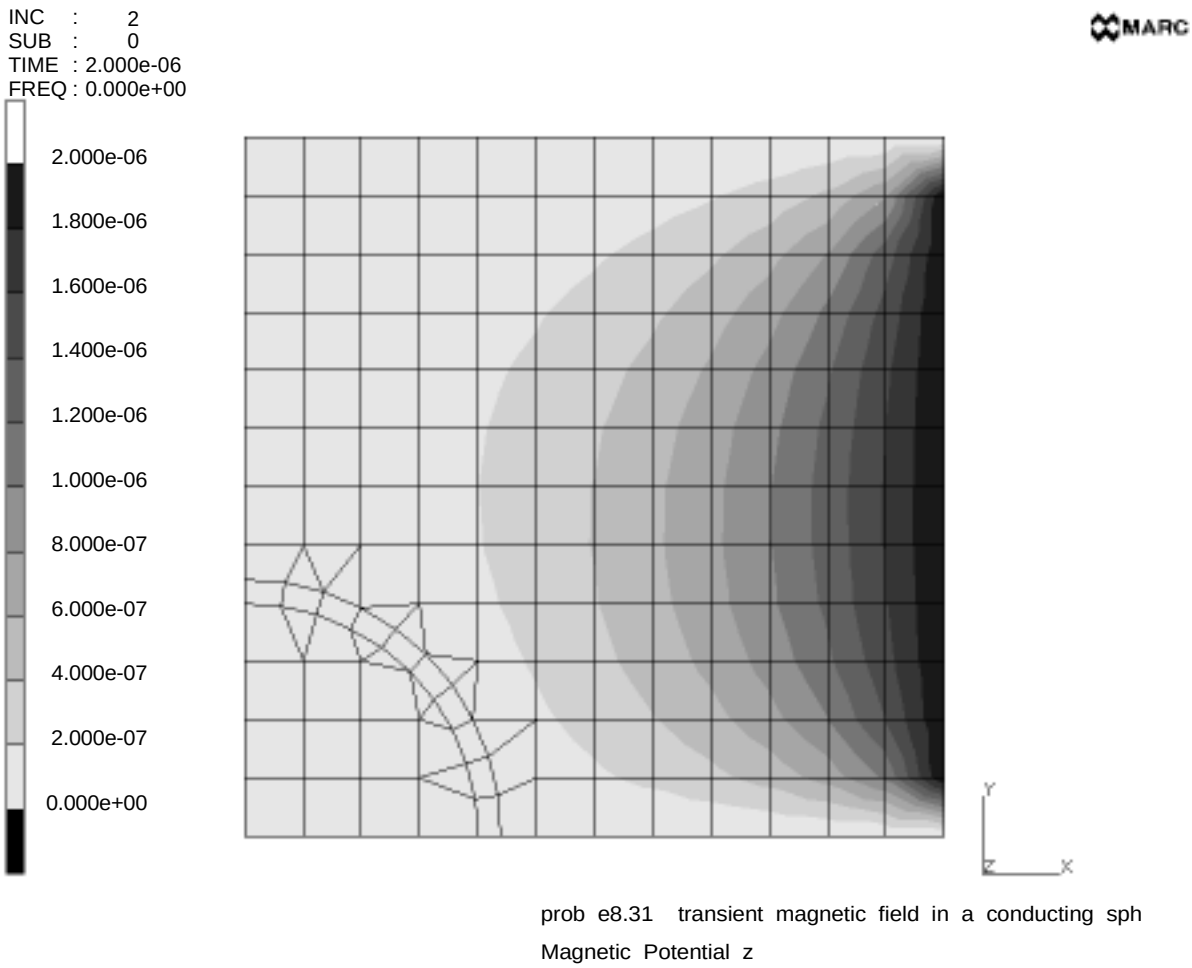

Figure 8.31-2 Third Component of Magnetic Potential, Time = 2 Microseconds

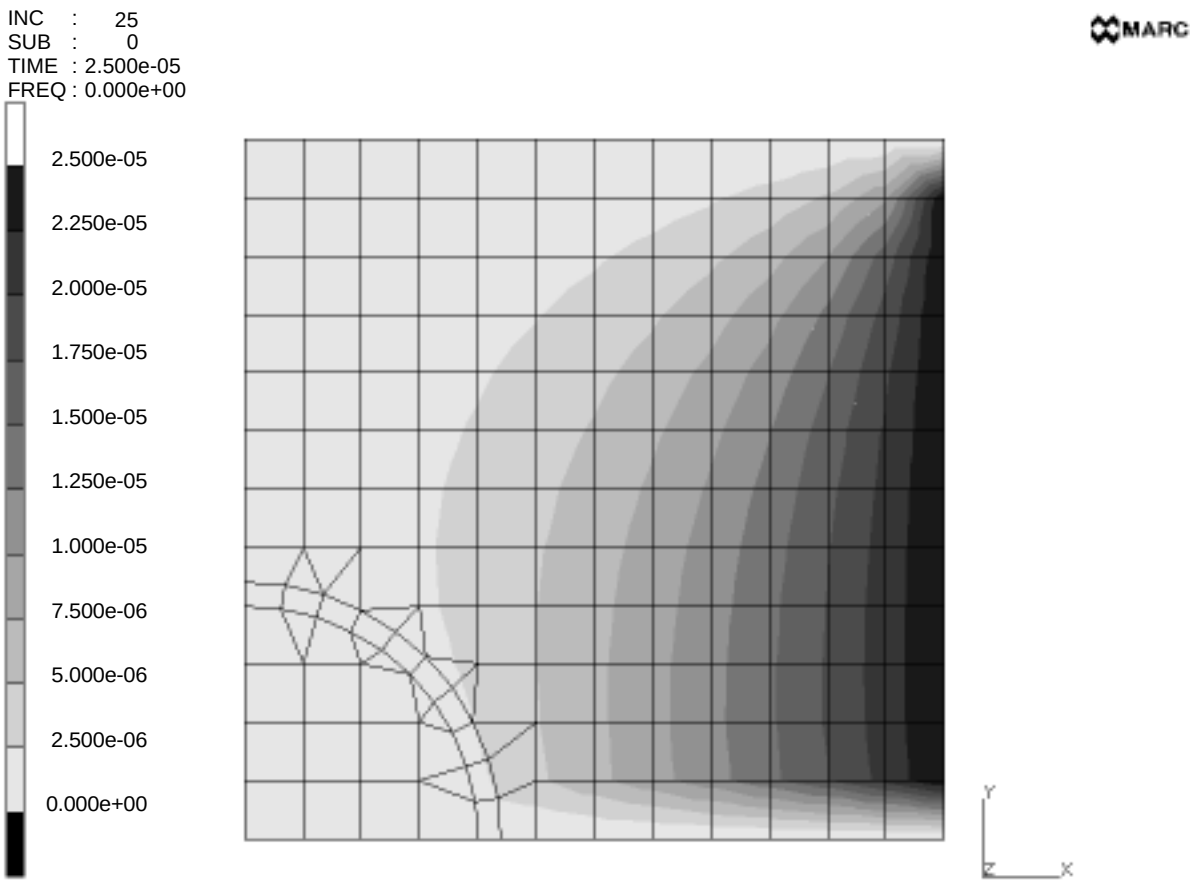

Figure 8.31-3 Third Component of Magnetic Potential, Time = 25 Microseconds

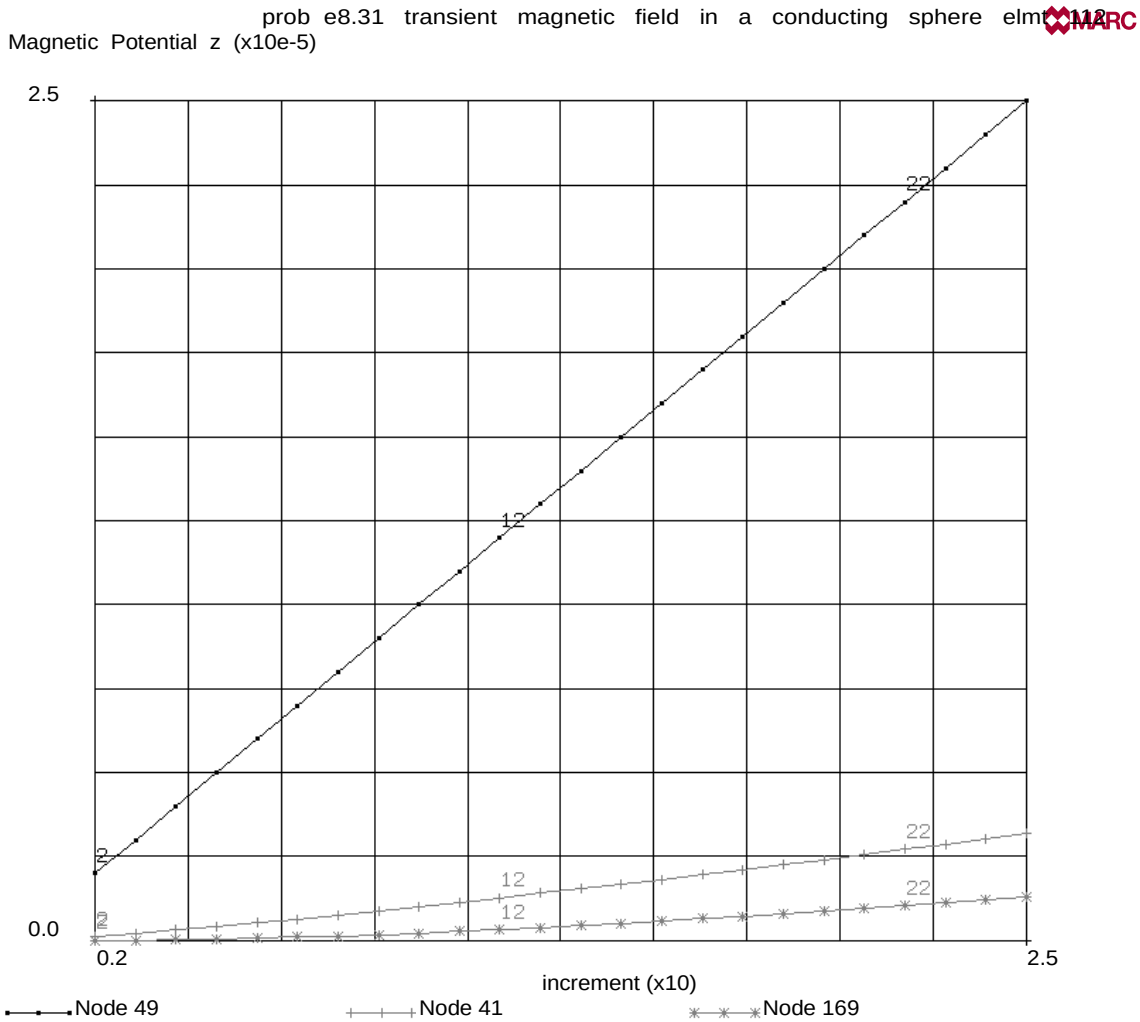

Figure 8.31-4 Time History of Magnetic Potential

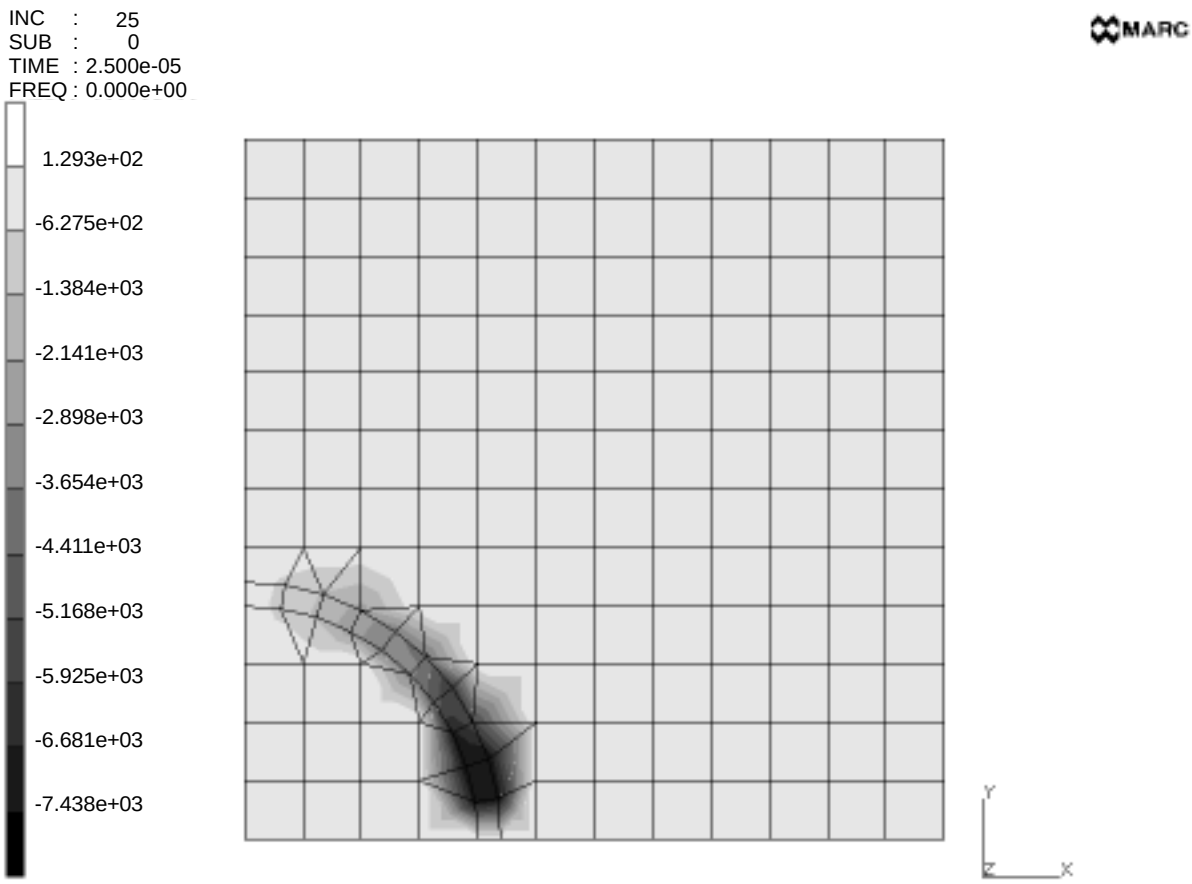

Figure 8.31-5 Current Density, Time = 25 Microseconds

8.32 Cavity Resonator

This problem demonstrates the use of the harmonic electromagnetic capability for a prismatic resonator.

Parameters

The EL-MA,1 parameter indicates that a harmonic electromagnetic analysis is to be performed. The HARMONIC option gives an upper bound to the number of harmonic boundary conditions.

Element

Element 113, an eight-node electromagnetic brick, is used in this example. The cavity is 0.5 x 0.25 x 1 meter long. The mesh of 12 elements is shown in Figure 8.32-1.

Loading

Along the surfaces x = 0 and x = 0.5 $A_y = A_z = 0.$

Along the surfaces y = 0 and y = 1.0 $A_x = A_z = 0.$

Along the surfaces z = 0 and z = 0.25 $A_x = A_y = 0.$

A current is placed on element 1. This is applied for a frequency range of 200 MHz to 250 MHz.

Material Properties

The material properties of the air in the cavity is permeability = 1.2566×10^{-6} henry/m, permittivity = 8.854×10^{-12} farad/m, and conductivity = 1×10^{-4} s/m.

Control

The POST option is used to save the electric field and magnetic flux (both real and imaginary components). As this is a linear problem, no additional controls are necessary. The PRINT option is used to force the solution of the nonpositive definite system.

Results

Table 8.32-1 gives the electric field as a function of frequency. The user observes that MARC indicates that the resonance occurs at 230 MHz.

Table 8.32-1 Electric Field as a Function of Frequency

Frequency (MHz)	$E_x \times 10^2$	$E_y \times 10^2$	$E_z \times 10^2$
200	-4.57	-3.42	-9.13
202	-4.38	-3.28	-8.76
204	2.43	1.82	4.87
206	5.45	4.09	10.90
208	-1.56	-1.17	-3.12
210	-14.52	-10.89	-2.90
212	-1.35	-1.02	-2.71
214	2.75	2.07	5.51
216	-5.14	-3.86	-10.29
218	-16.05	-12.04	-32.11
220	2.39	1.80	4.77
222	-0.32	-0.24	-0.60
224	-5.07	-3.80	-10.14
226	0.69	0.51	1.37
228	4.32	3.24	8.64
230	56.29	42.22	112.60
232	5.24	3.93	10.48
234	-0.82	0.61	-1.63
236	-16.15	-12.11	-32.30
238	-1.96	-1.47	-3.93
240	0.89	0.67	1.79
242	-1.15	0.86	-2.30
244	0.02	0.02	0.05
246	1.95	1.46	3.90
248	-4.14	-3.10	-8.27

Parameters, Options, and Subroutines Summary

Example e8x32.dat:

Parameters	Model Definition Options	History Definition Options
ELEMENT	CONNECTIVITY	CONTINUE
EL-MA	COORDINATE	DIST CURRENT
END	DEFINE	HARMONIC
HARMONIC	END OPTION	
PRINT,3	FIXED POTENTIAL	
SIZING	ISOTROPIC	
TITLE	OPTIMIZE	
	POST	

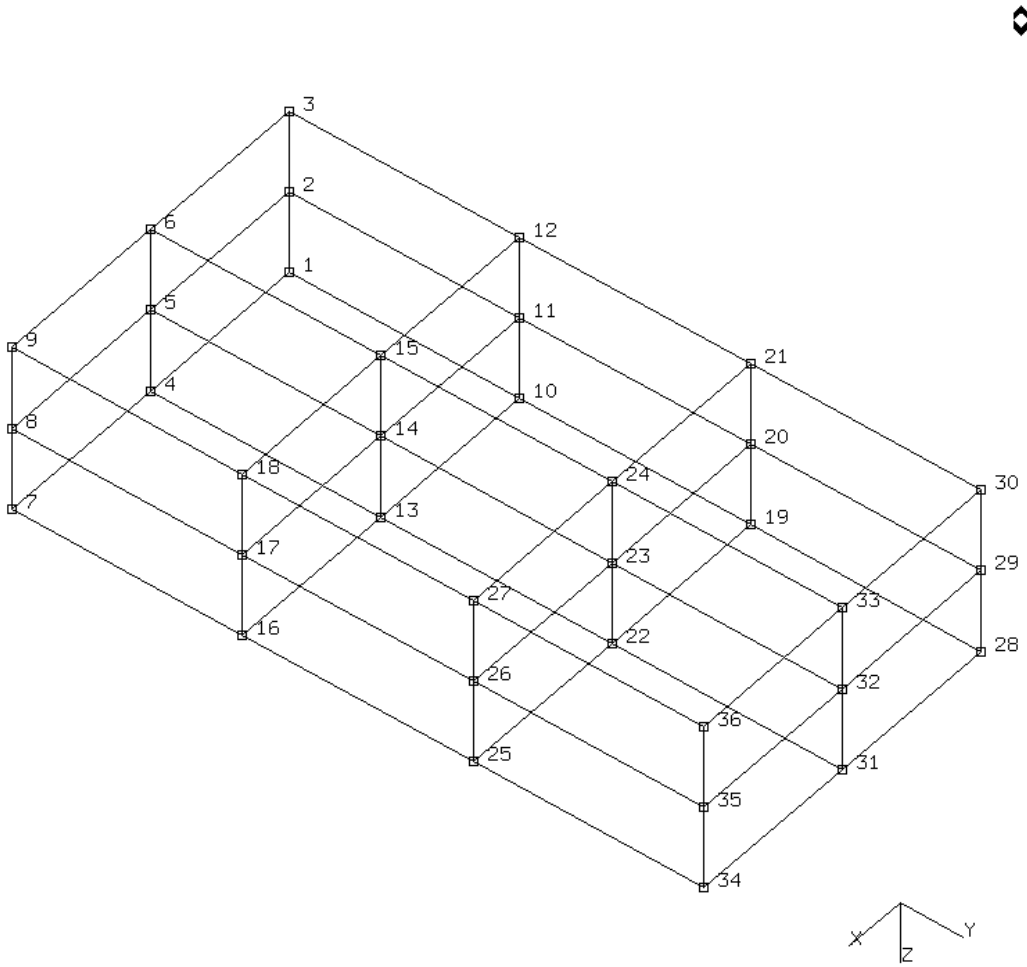

Figure 8.32-1 Finite Element Mesh of Resonator

8.33 Electromagnetic Analysis of an Infinite Wire

In this example, the harmonic and transient electromagnetic capabilities are used to predict the steady state magnetic field distribution due to a wire. This is the same as problem 8.24 where the MAGNETOSTATIC procedure is used.

Parameters

The EL-MA parameter option indicates that an electromagnetic analysis is being performed. The '0' option indicates a transient analysis while a '1' indicates a harmonic analysis.

Element

Element type 111, a four node planar electromagnetic element, is chosen. This element has the vector potential A and the scalar potential ϕ as its degrees of freedom.

Only a sector of a circular region is modeled as shown in Figure 8.33-1. The outer radius is 1 cm.

Loading

In both analyses, the magnetic potential and scalar at the outside radius is prescribed to be zero. A harmonic point charge of 0.05 amps is applied at node 1 at a frequency of 1×10^{-6} Hz in the harmonic analysis. In the transient analysis, a point charge of 0.05 amps is applied at node 1 during the first step of 0.01 seconds. This is then held constant for ten steps of 1×10^{6} second each. The load is applied using the POINT CURRENT-CHARGE option.

Material Properties

The magnetic permeability of 1000 henry/cm is entered through the ISOTROPIC option.

Results

When using the harmonic procedure, the z component of the magnetic potential is shown in Figure 8.33-2. It is virtually identical to Figure 8.24-3. When using the transient procedure, the solution oscillates about the correct solution. This is shown in Figure 8.33-3.

Parameters, Options, and Subroutines Summary

Example e8x33a.dat:

Parameters	Model Definition Options	History Definition Options
ELEMENT	CONNECTIVITY	CONTINUE
EL-MA	COORDINATE	HARMONIC
END	END OPTION	POINT CURRENT-CHARGE
HARMONIC	FIXED POTENTIAL	
SIZING	ISOTROPIC	
TITLE	POST	
	PRINT ELEMENT	

Example e8x33b.dat:

Parameters	Model Definition Options	History Definition Options
ELEMENT	CONNECTIVITY	CONTINUE
END	CONTROL	DYNAMIC CHANGE
PRINT	COORDINATE	POINT CURRENT-CHARGE
SIZING	END OPTION	
TITLE	FIXED POTENTIAL	
	ISOTROPIC	
	POST	
	PRINT ELEMENT	

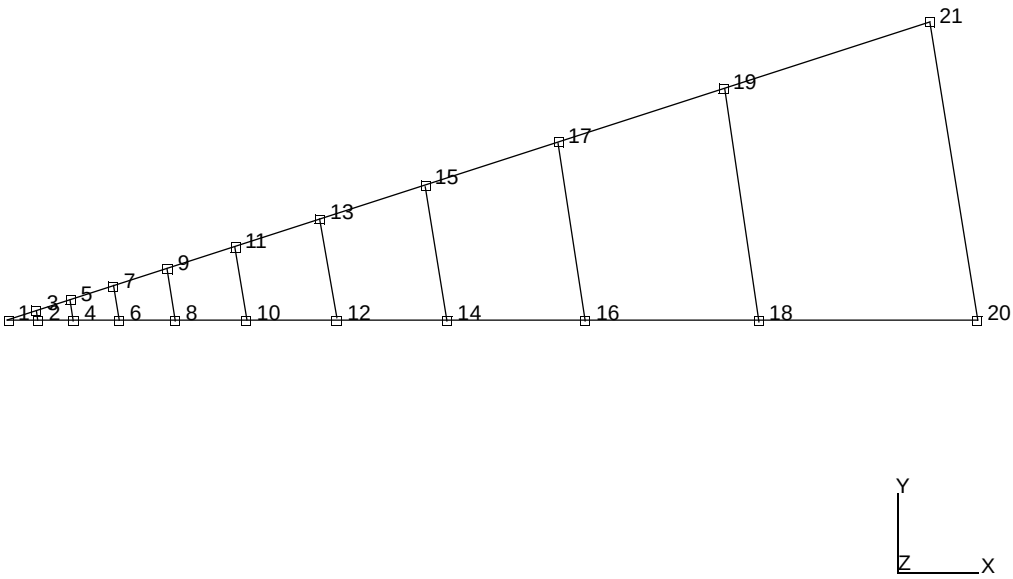

Figure 8.33-1 Sector of Circular Region

INC : 0
SUB : 1
TIME : 0.000e+00
FREQ : 6.283e-06

prob e8.33a mag2d test one (inf long filamentary current)

MARC

Displacements z (x100)

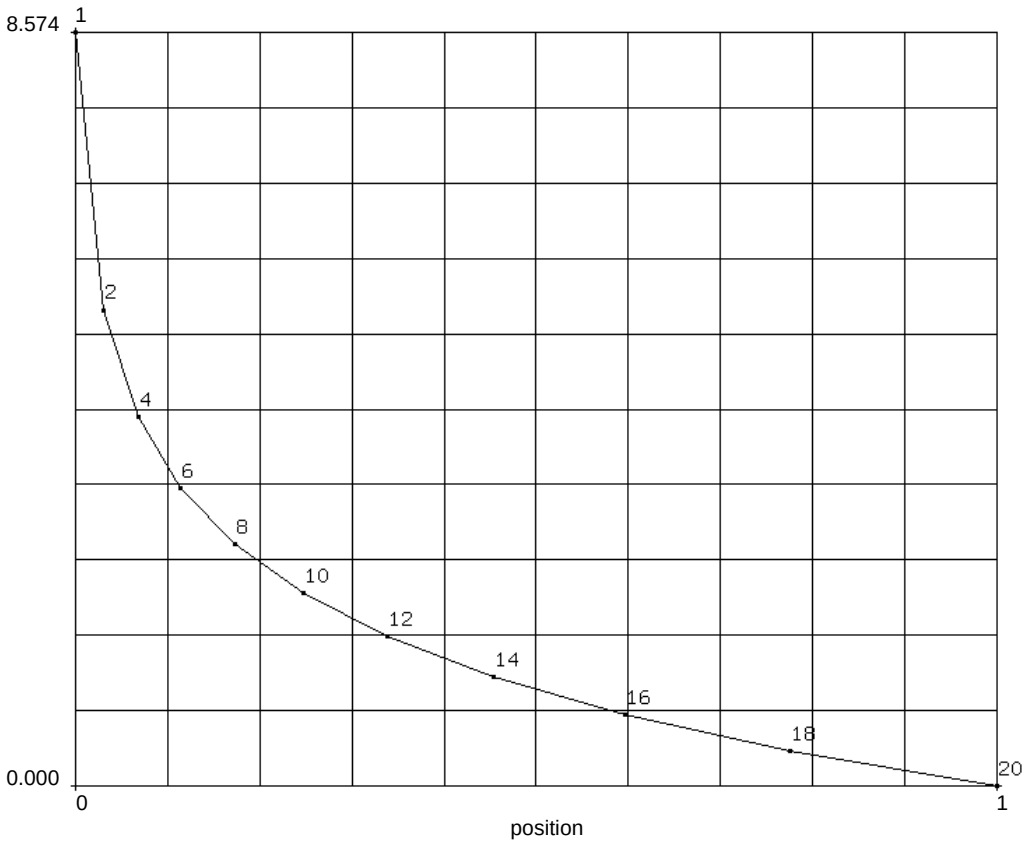

Figure 8.33-2 Third Component of Magnetic Potential using Harmonic Procedure

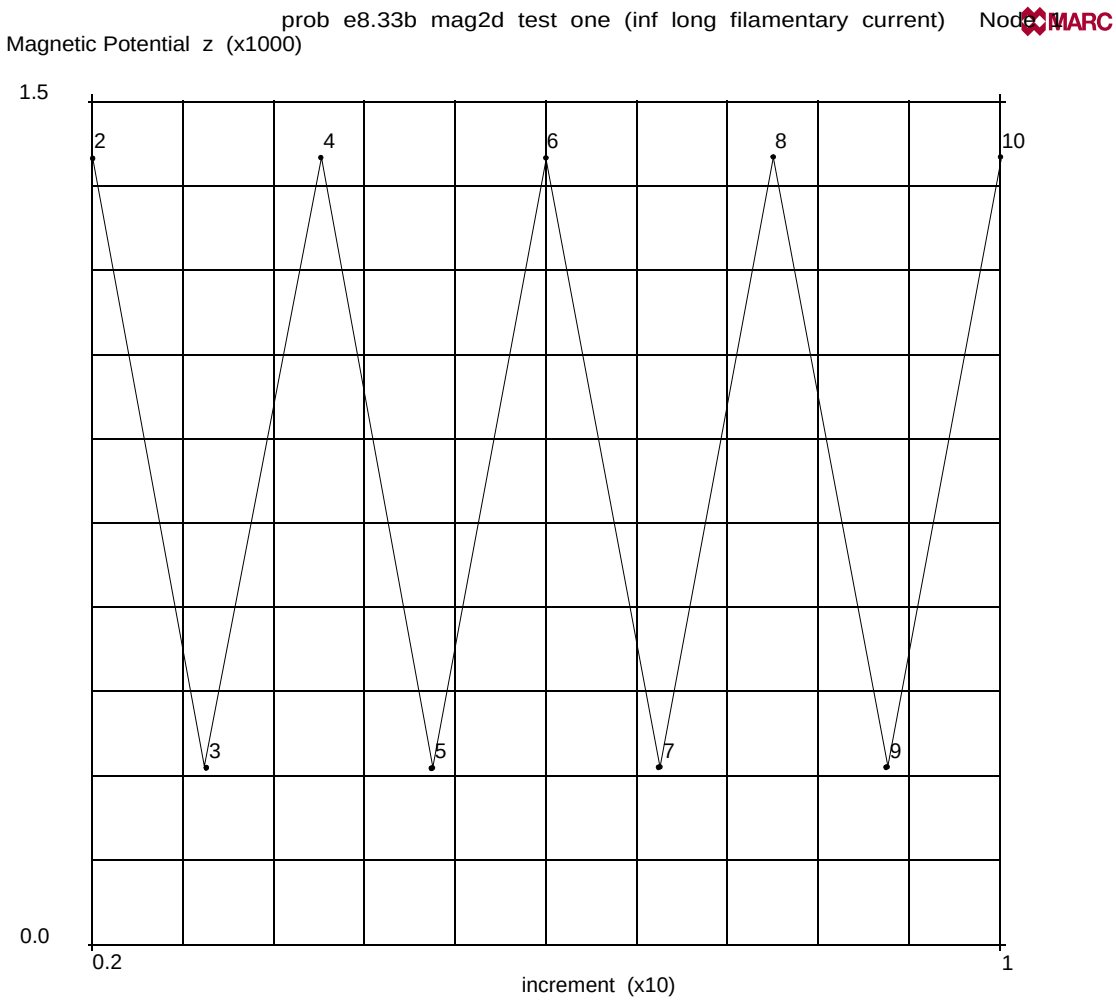

Figure 8.33-3 Time HIstory of Magnetic Potential of Node 1, Transient Procedure

8.34 Triaxial Test on Normally Consolidated Weald Clay

This problem demonstrates the uncoupled pore plasticity analysis of a homogeneous specimen. A drained triaxial test on a normally consolidated clay is simulated.

Parameters

The PORE, 0, 1 parameter indicates that a stress analysis is to be performed, but the fluid pore pressure is not calculated. The ISTRESS parameter indicates that an initial stress is defined as is usually the case in soil analysis. The UPDATE parameter indicates that the analysis is to perform the calculation using the current (deformed) geometric configuration. As the Cam-Clay soil model involves volumetric plastic behavior, a different procedure is used as compared to metal plasticity.

Model

A single axisymmetric element, type 28, is used in the analysis. The specimen is 4 inches long and has a radius of 0.75 inch as shown in Figure 8.34-1.

Material Properties

The Cam-Clay model is invoked using the SOIL model definition option. The material data is:

E	= 100 psi	Young's modulus
υ	= 0.4	Poisson's ratio
σ_y	= 200 psi	Yield stress
K_{Fluid}	= 100 psi	Bulk modulus of fluid
υ	= 0.3982	Dynamic viscosity of fluid
	= 0.0	Permeability of soil
λ	= 0.88	Virgin compression ratio
κ	= 0.031	Recompression ratio
M_{cs}	= 0.882	Slope of critical state line

In the Cam-Clay model, the Young's modulus and the Poisson's ratio are not actually used.

The initial void density, $e_0 = 0.7977$, is entered through the INITIAL VOID option. It is assumed to be homogeneous over all nine integration points.

Loading

The initial confining pressure is 30 psi. This is entered in two places. First, the INITIAL PC option is used to define the initial preconsolidation pressure to be 30 psi. The INIT STRESS is then used to enter the value of the initial stress to be -30 psi (remember that compressive stresses are negative).

In increment 0, no deformation occurs.

In increment 1, a pressure of 30 psi is applied on the outside radius and the right side. This is to ensure that equilibrium exists.

This is followed by an axial compression of 0.004 inch per increment for 200 increments. The total axial compression is then 0.8 or an engineering axial strain of about 20%. The time step is two seconds per increment.

Results

The time history of the axial stress is shown in Figure 8.34-2. The time history of the void ratio is shown in Figure 8.34-3. We can observe that the void ratio decreases from the original value of 0.7977 to 0.7202. The preconsolidation pressure history is shown in Figure 8.34-4. The value increases from 30 psi to 87.78 psi.

Parameters, Options, and Subroutines Summary

Example e8x34.dat:

Parameters	Model Definition Options	History Definition Options
ELEMENT	CONNECTIVITY	AUTO LOAD
END	CONTROL	CONTINUE
ISTRESS	COORDINATES	DISP CHANGE
PORE	DIST LOADS	DIST LOADS
SIZING	END OPTION	TIME STEP
TITLE	FIXED DISP	
UPDATE	INIT STRESS	
	INITIAL PC	
	INITIAL VOID	
	POST	
	SOIL	

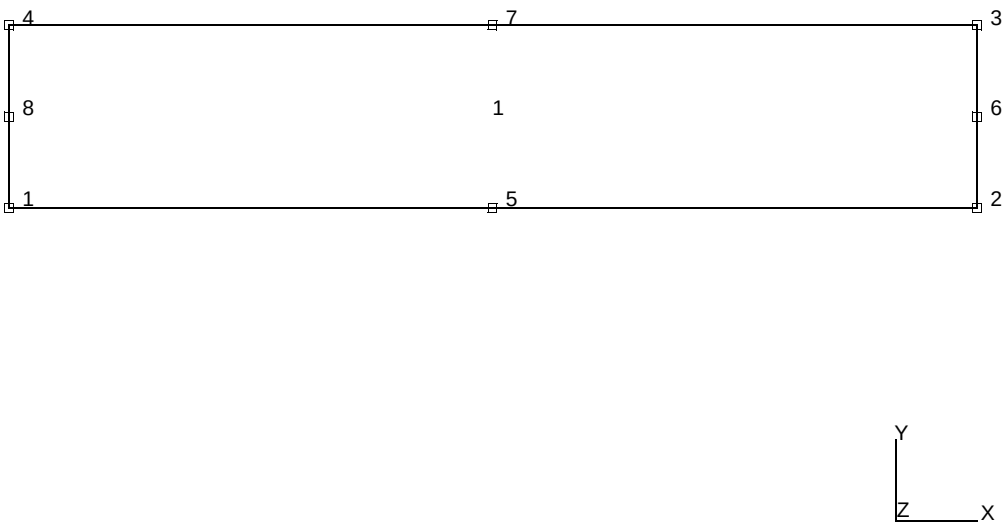

Figure 8.34-1 One-Element Model

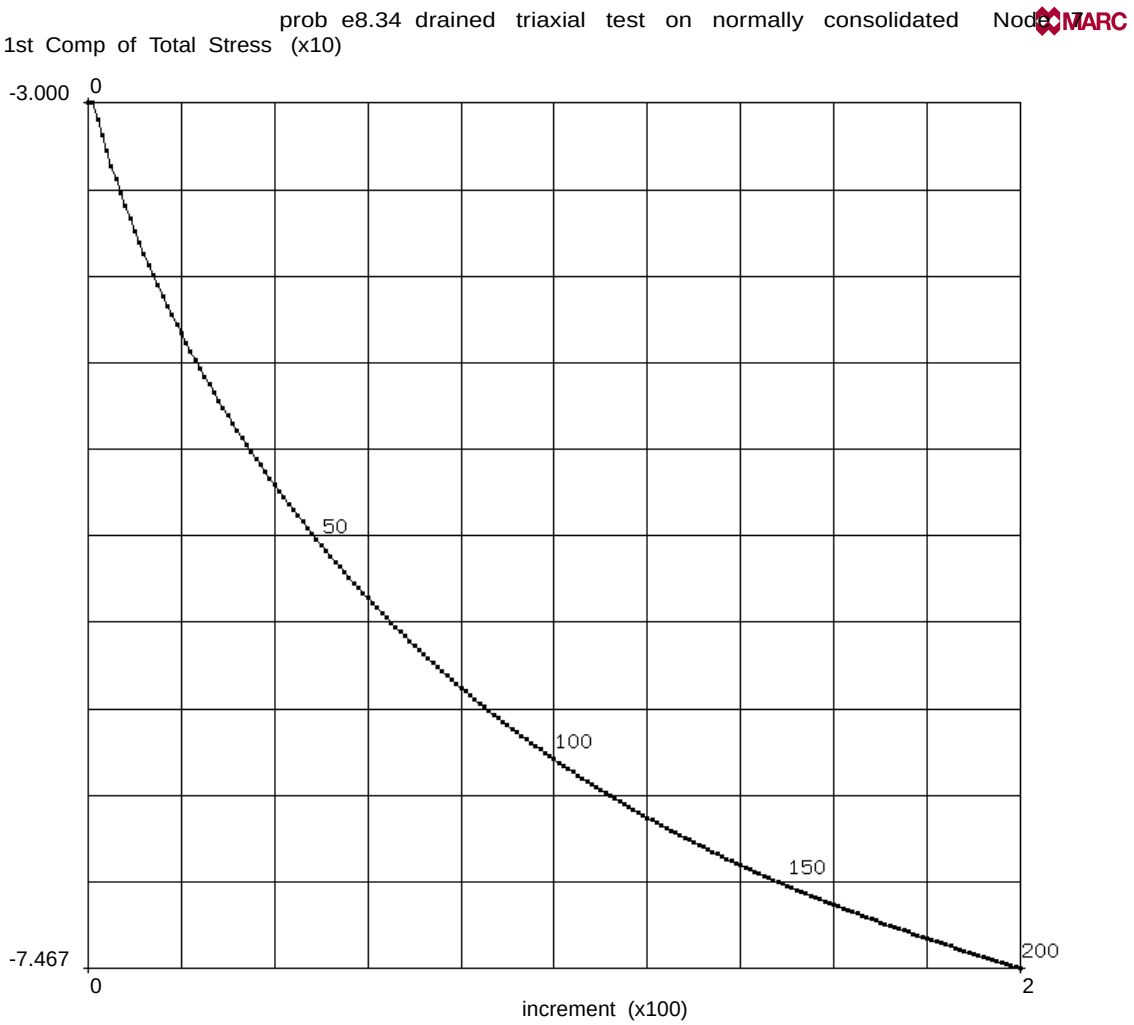

Figure 8.34-2 Time History of Axial Stress

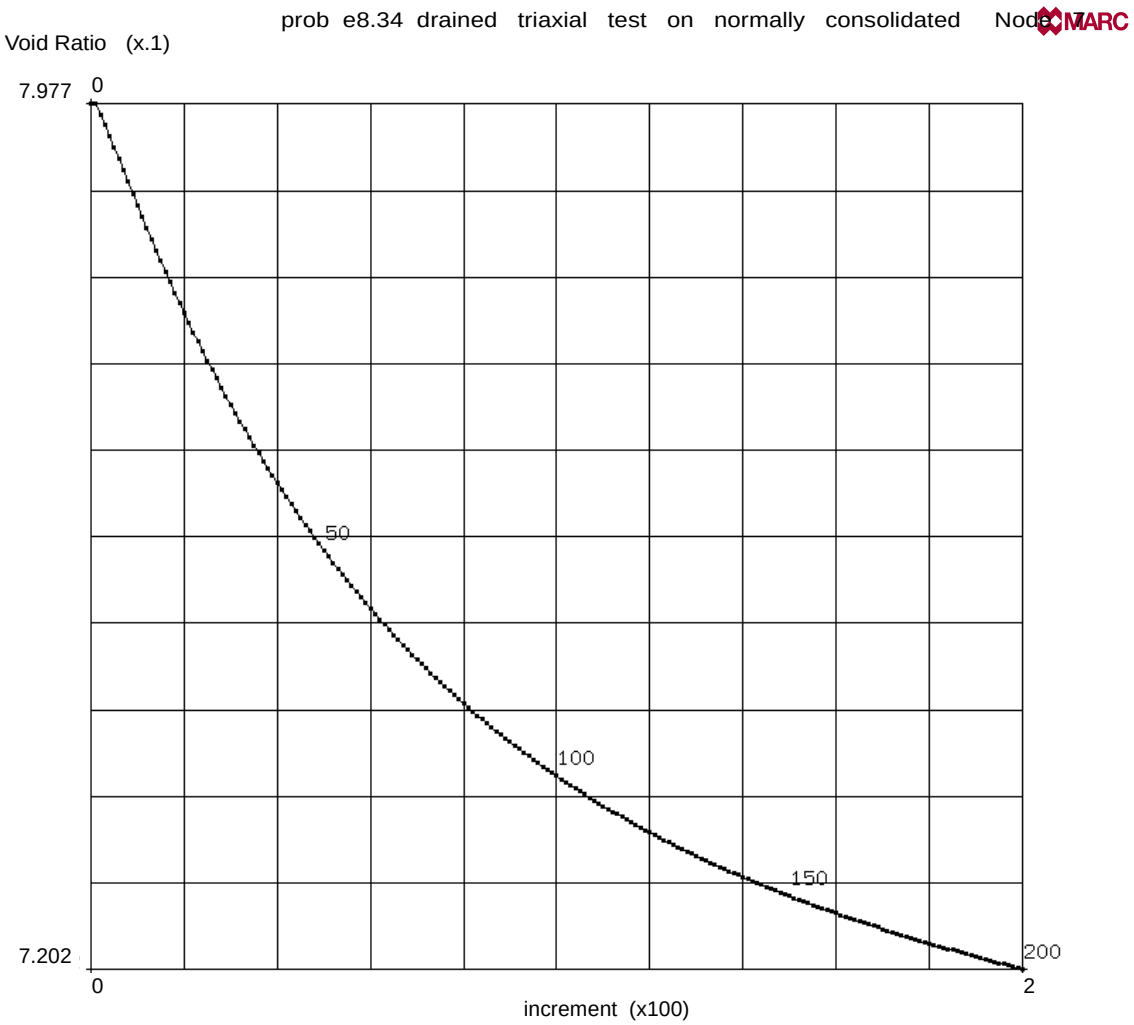

Figure 8.34-3 Time History of Void Ratio

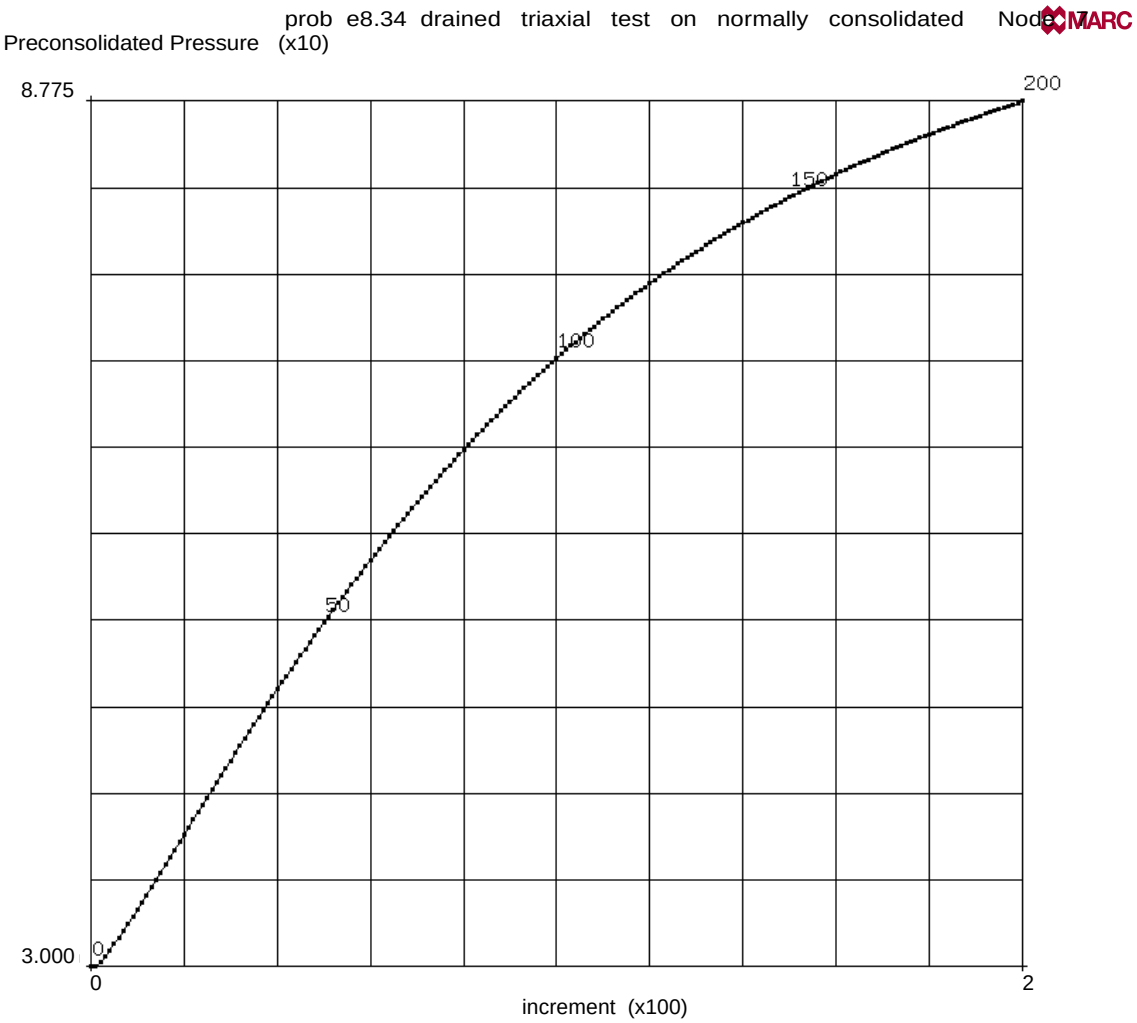

Figure 8.34-4 Time History of Preconsolidation Pressure

8.35 Soil Analysis of an Embankment

This problem demonstrates the use of MARC for a coupled pore pressure soil analysis. The I-95 embankment across the tidal marshes of Saugus, just north of Boston, is modeled under the conditions of plane strain. The original description was given by Wroth.

Parameters

The PORE, 2, 1 parameter indicates that a fully coupled pore pressure calculation is to be performed. The ISTRESS parameter indicates that an initial stress is applied in increment 0.

Model

Element type 32 is used in this analysis. This element is a Herrmann element which is normally used for incompressible material. When used in a pore pressure calculation, the fourth degree of freedom at the corner nodes is no longer the Lagrange multiplier, but instead the fluid pore pressure. The model consists of 126 elements and 427 nodes. The model consists of eight groups of elements that are used to define the different preconsolidation pressures. Three groups are used to define the material properties. These groups are shown in Figure 8.35-1.

Material Properties

The material properties are grouped into the fill, silt, and all of the rest (bbc). The properties are as follows:

	bbc	Silt	Fill
E (psi)	2.5×10^6	2.5×10^6	2.5×10^6
υ	0.4	0.4	0.4
ρ	0.000054	10.0	10.0
σ_y	0	0	0
K_{Fluid}	100	100	100
Dynamic viscosity of fluid – υ	0.1	0.1	0.1
Permeability	1	1	1
Virgin compression ratio – λ	0.147	0.147	0.147
Recompression ratio – κ	0.060	0.060	0.060
Slope of critical state line – M	1.05	1.05	1.05

This data is entered through the SOIL option.

When using the Cam-Clay model, Young's modulus, Poisson's ratio, and yield stress are ignored.

The initial preconsolidation is dependent on the depth. The values entered through the INITIAL PC option are as follows:

Region	Initial Preconsolidation (psi)
Fill	10
Silt	10,000
Layer 1	95
Layer 2	80
Layer 3	71
Layer 4	70
Layer 5	57
Layer 6	50

A small hydrostatic initial stress is entered for all elements as 1 psi. It is entered as a negative value to indicate compression. The Cam-Clay model does not behave well when the hydrostatic stress is zero or positive (tensile).

The initial void ratio is 0.74 for all elements. This is entered through the INITIAL VOID option.

Boundary Conditions

The boundary conditions consist of no motion in the x direction on the right and left side. No motion in the y direction along the bottom surface. And the pore pressure is zero along the top surface. This is shown in Figure 8.35-2.

In increment 0, only the initial stress is on the structure.

In increment 1, a pressure of 1 psi is placed along the complete top surface (fill). A very small time step of 1×10^{-20} seconds is chosen.

A uniform body force/area is then applied of magnitude 0.6 psi/in^2 per increment for 15 increments or a total of 9 psi/in^2. Each time step is 10000 seconds $\cong$ 2.78 hours.

This is followed by a distributed load of 0.5 psi/increment on the embankment and a load of 0.25 psi/increment on element 72. In the AUTO LOAD section, 290 increments are requested with each of a time step of 0.4138 seconds. Because the CONTROL option indicates 200 increments, this load sequence is not be completed.

Results

A contour plot of the vertical displacements on the superimposed deformed mesh is shown in Figure 8.35-3. The stress in the y-direction is given in Figure 8.35-4. The hydrostatic pressure is shown in Figure 8.35-5. The void ratio is shown in Figure 8.35-6. The preconsolidation stress is shown in Figure 8.35-7. The pore pressure is shown in Figure 8.35-8.

Parameters, Options, and Subroutines Summary

Example e8x34.dat:

Parameters	Model Definition Options	History Definition Options
ELEMENT	CONNECTIVITY	AUTO LOAD
END	CONTROL	CONTINUE
ISTRESS	COORDINATES	CONTROL
PORE	DEFINE	DIST LOAD
SIZING	DIST LOADS	TIME STEP
TITLE	FIXED DISP	
	INIT STRESS	
	INITIAL PC	
	INITIAL VOID	
	OPTIMIZE	
	POST	
	PRINT ELEM	
	PRINT NODE	
	RESTART	
	SOIL	
	SOLVER	

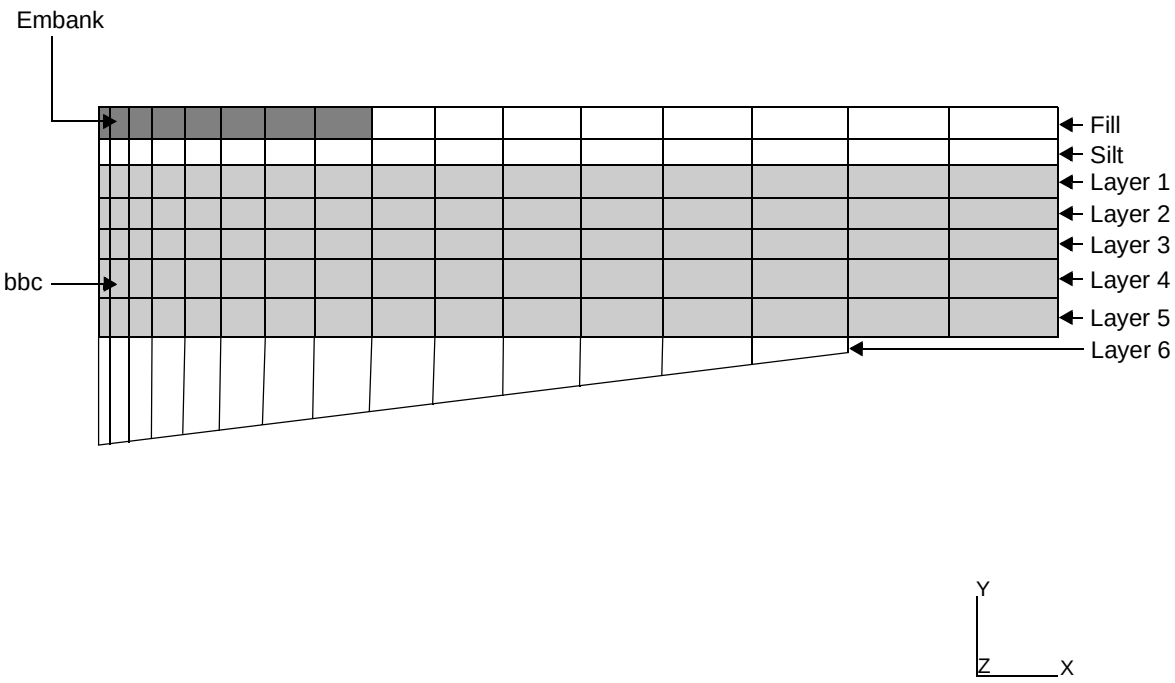

Figure 8.35-1 Mesh of Embankment with Sets used for Material Definition and Initial Preconsolidation

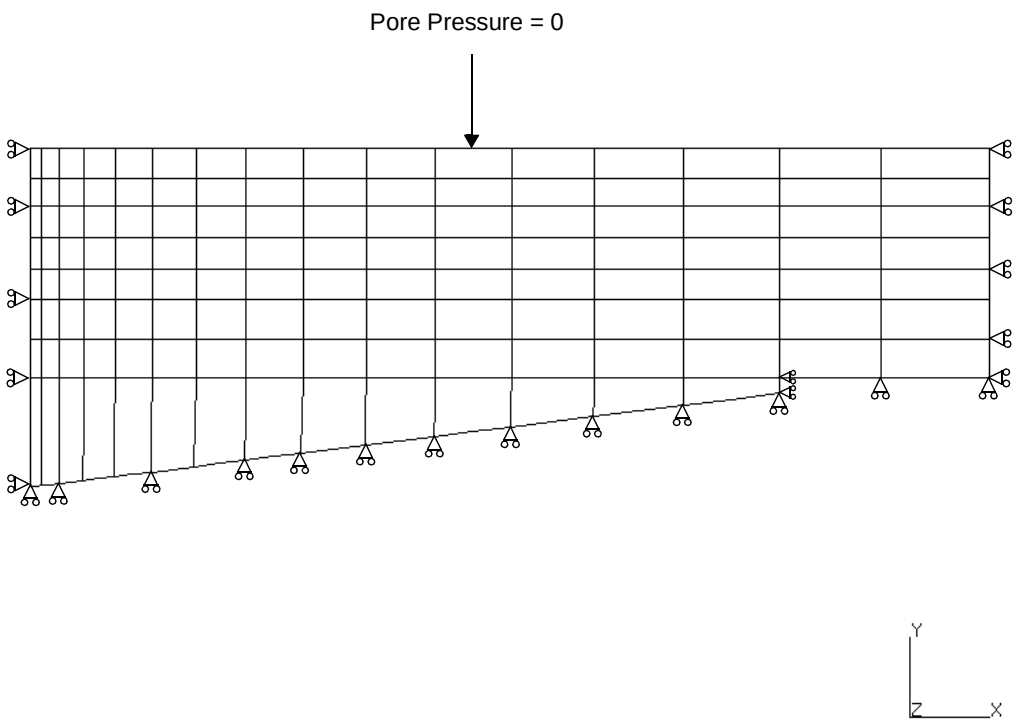

Figure 8.35-2 Boundary Conditions

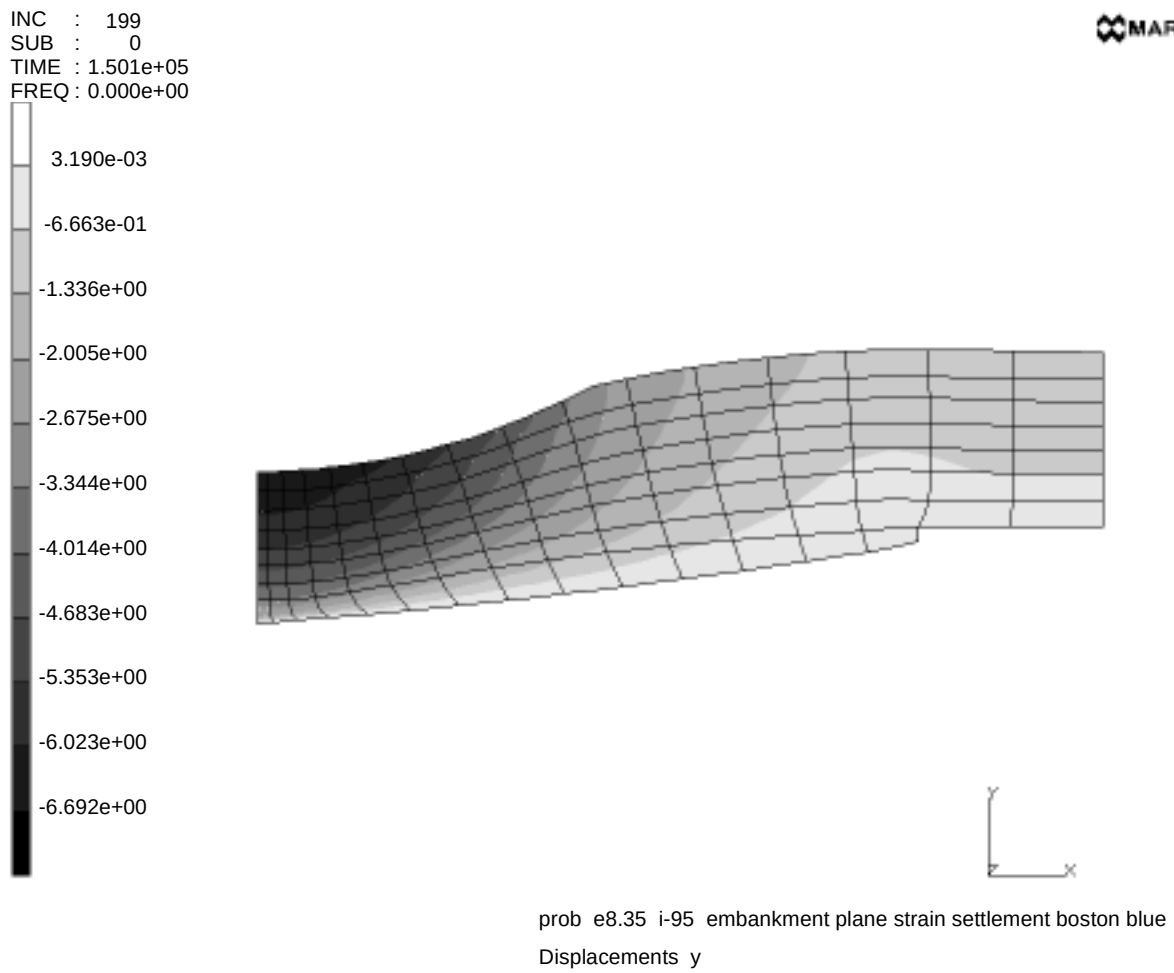

Figure 8.35-3 Contour of Settlement

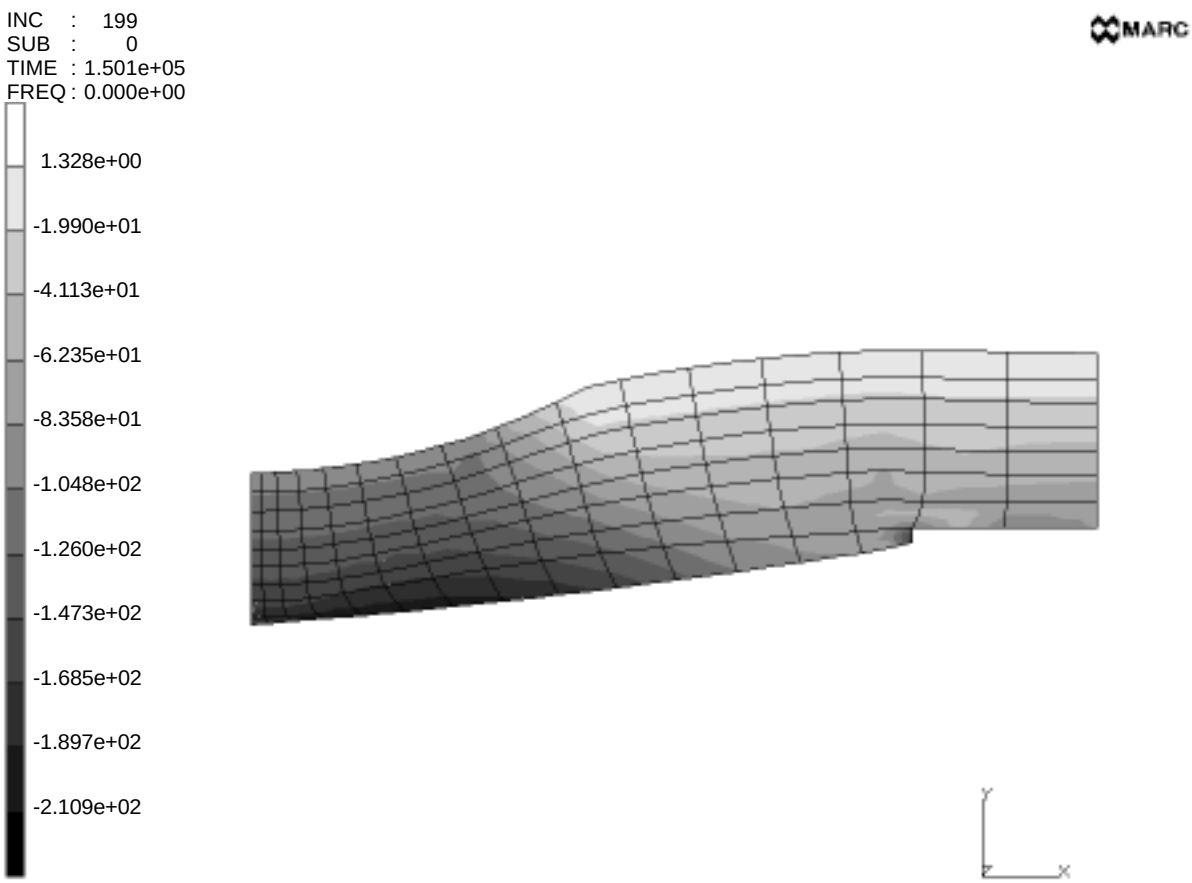

Figure 8.35-4 Vertical Stresses

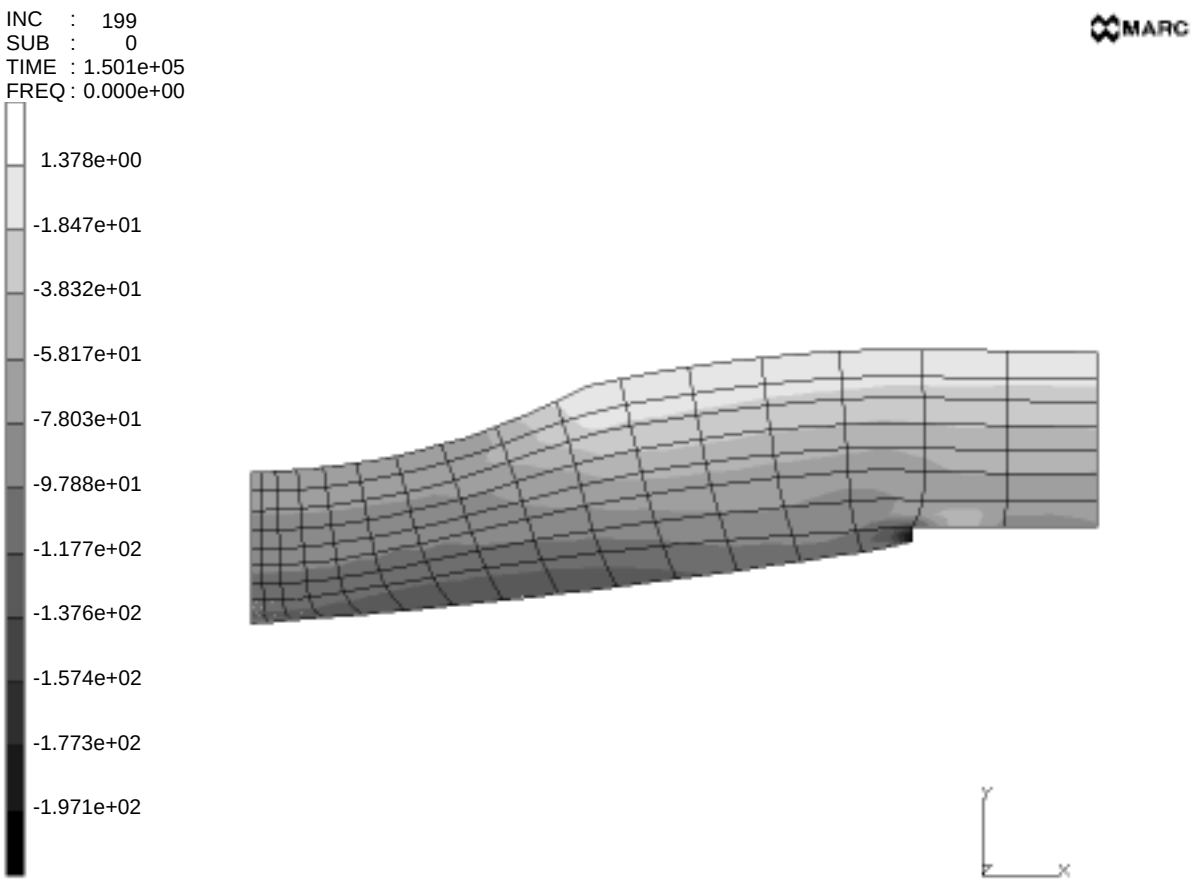

Figure 8.35-5 Mean Pressure in Soil

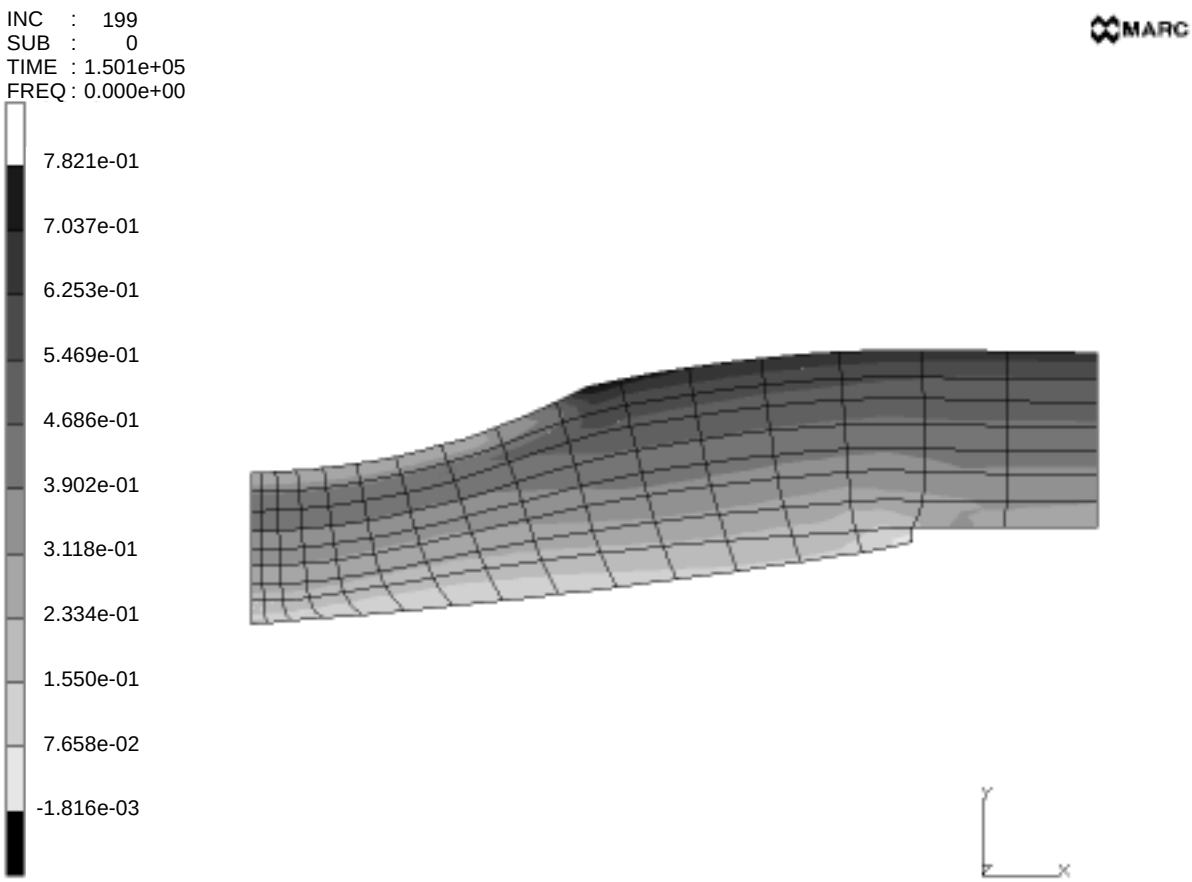

Figure 8.35-6 Void Ratio

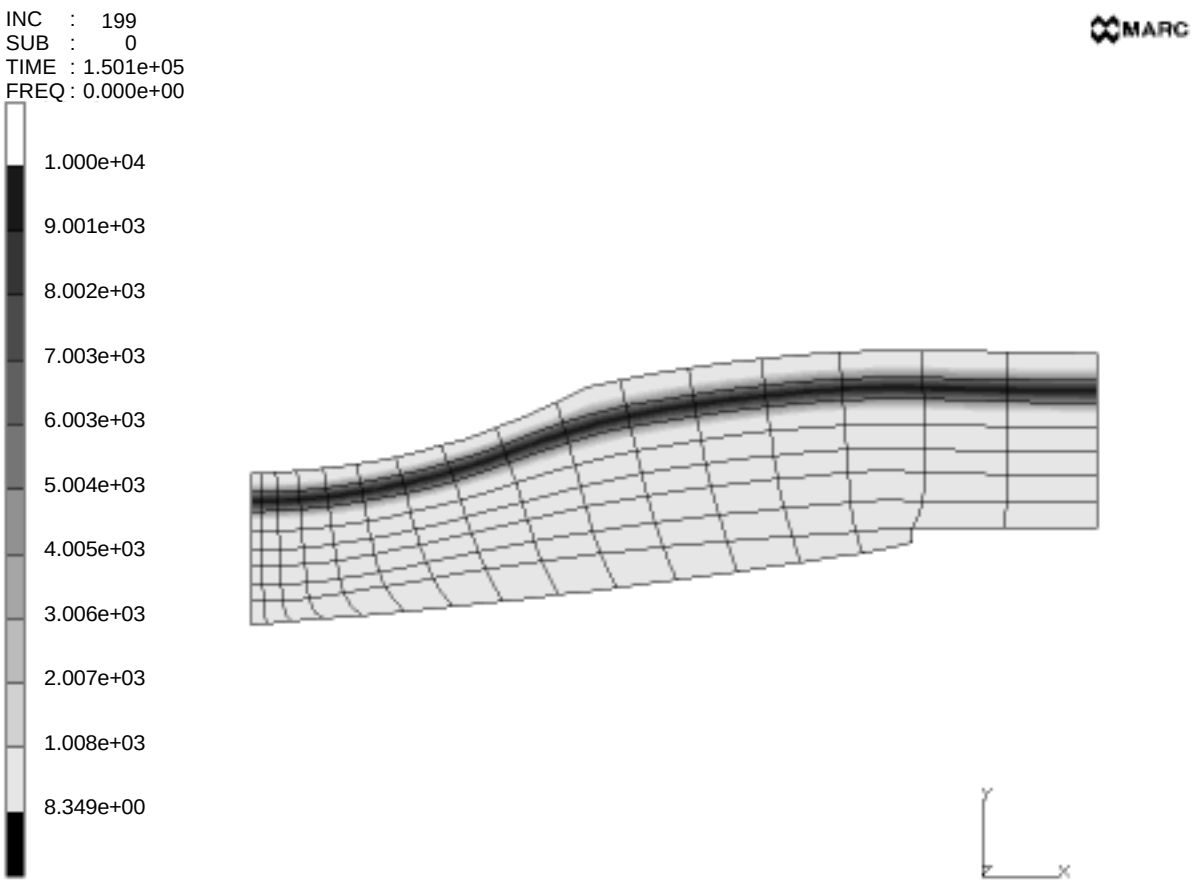

Figure 8.35-7 Preconsolidation Pressure

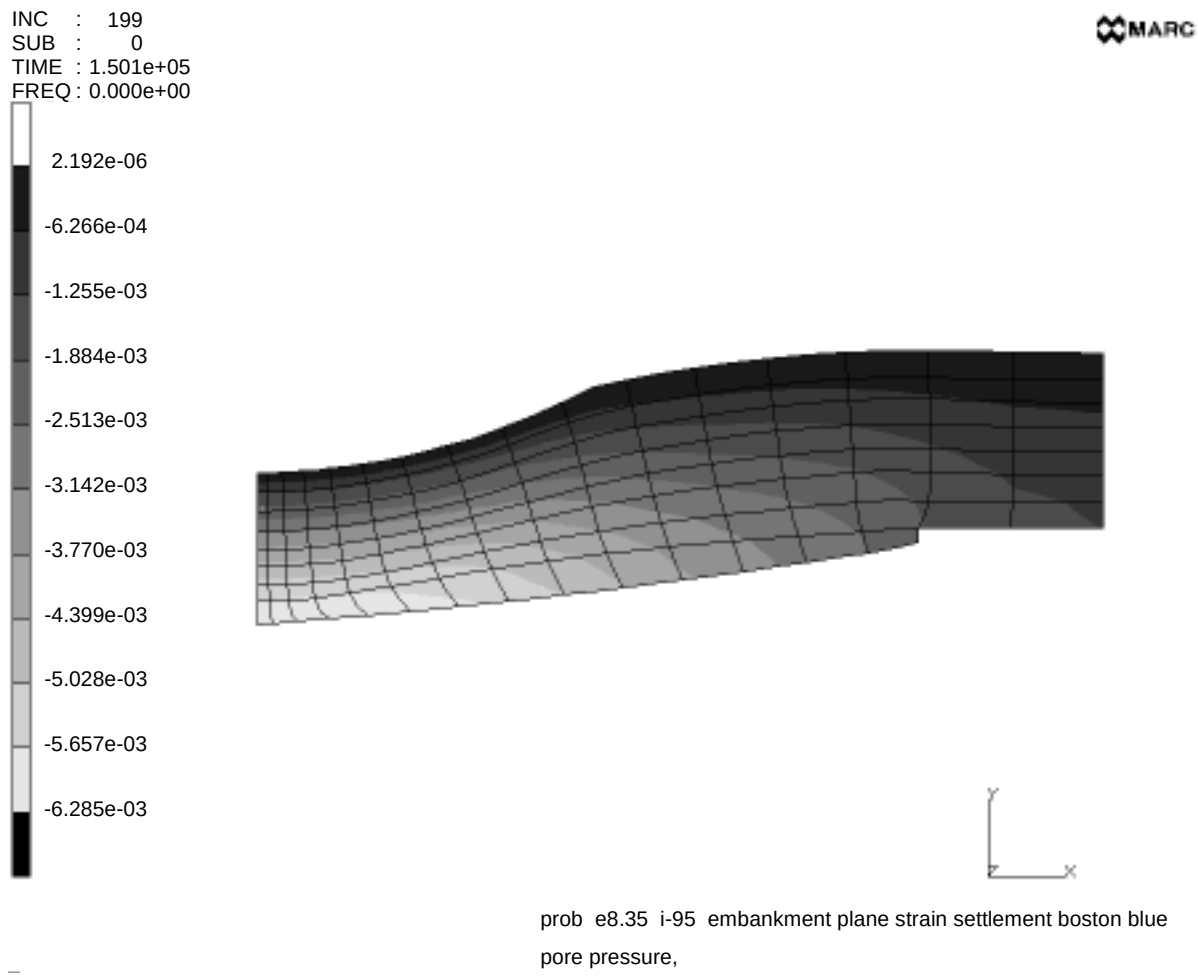

Figure 8.35-8 Fluid Pore Pressure

8.36 Interference Fit of Two Cylinders

This example demonstrates the interference fit capabilities and the use of symmetry planes in MARC. Two rings have an initial overclosure, and the resultant stress distribution is determined.

Element

Element type 116, a four node axisymmetric element with reduced integration and hourglass control, is used in this analysis. The mesh was originally defined using element type 10. The ALIAS option was used to switch it to type 116.

Loading

The line z = 0 is considered to be a symmetry boundary condition. A rigid surface (body 3) is defined and is given the characteristic of a symmetry plane. This means that the displacement of nodes initially in contact with this plane will be zero, and that the nodes cannot separate from this plane. No other loading or boundary condition is necessary.

The CONTACT option is used to specify that three bodies exist: inner cylinder, outer cylinder and the symmetry plane. There is no friction on any of the surfaces. A closure distance of 0.0001 is initially specified. This will be reset in the CONTACT TABLE option to be 0.0002.

The CONTACT TABLE option then specifies that body 1 and 2 have an interference distance of 0.001. It also specifies that body 1 and 2 are potentially in contact and that 1 and 2 are potentially in contact with 3. Note because of the geometries involved, this is more than a mere potential, but reality. The CONTACT TABLE option is a very powerful way to control the interaction between bodies. In this example, it was positioned in the LOAD INCREMENTATION block. This implies that this data can be changed during the incremental analysis.

Material Properties

The material is a high strength steel with Young's modulus = 30 x 10^6 psi, Poisson's ratio = 0.3, and the yield stress of 50,000 psi.

Control

The CONTROL option specifies that displacement control is being used with a tolerance of 10%. The convergence messages are written to the log file. A restart file and a post file is written for each increment. A single load step is performed with a time step of 0.03. The time step in this problem is totally arbitrary. A PRINT,5 option is included which generates additional messages in the output regarding contact.

Results

By examining the contact forces, you can calculate a total contact force of 44,177 pounds. This is available on the post file as the “EXTERNAL FORCES” and is given in the output.

Figure 8.36-2 shows the radial stress and the hoop stress as a function of the radius. Note that nodes 5 and 26 are the corresponding contact nodes between the inner and outer cylinder. You can easily observe that the inner cylinder has gone into compression (hoop stress) while the external cylinder has gone into tension. Also, observe the antisymmetries of the stress. Note that the radial stress should have gone to zero at nodes 1 and 30. The error is due to the extrapolation procedure employed.

Parameters, Options, and Subroutines Summary

Example e8x36.dat:

Parameters	Model Definition Options	History Definition Options
ALIAS	CONNECTIVITY	AUTO LOAD
ELEMENT	CONTACT	CONTACT TABLE
END	CONTROL	CONTINUE
PRINT	DEFINE	TIME STEP
SIZING	END OPTION	
TITLE	ISOTROPIC	
	POST	
	RESTART	

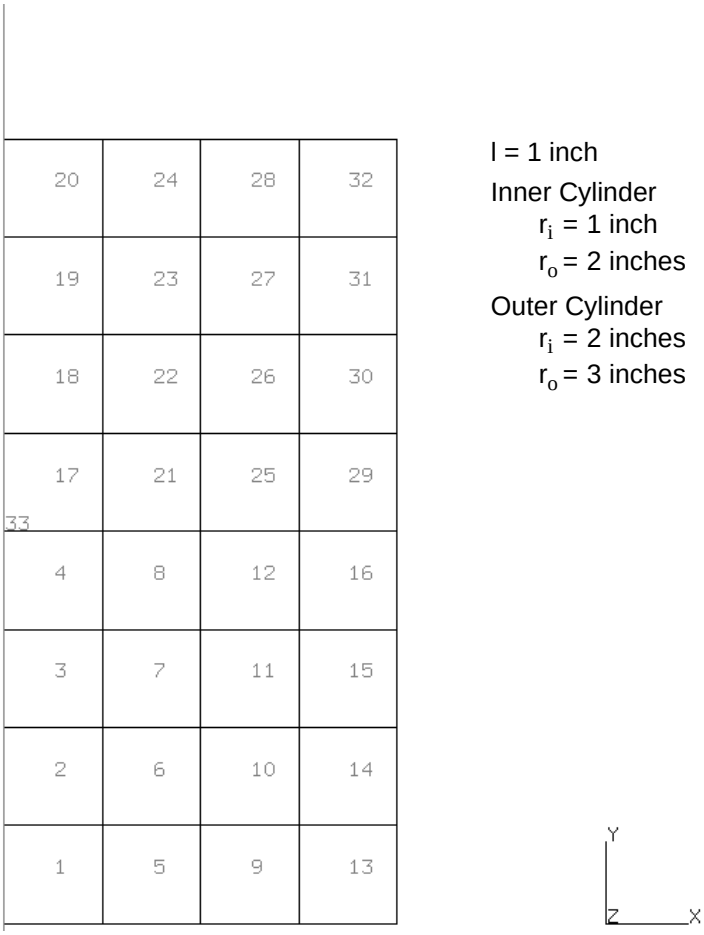

Figure 8.36-1 Two Cylinders

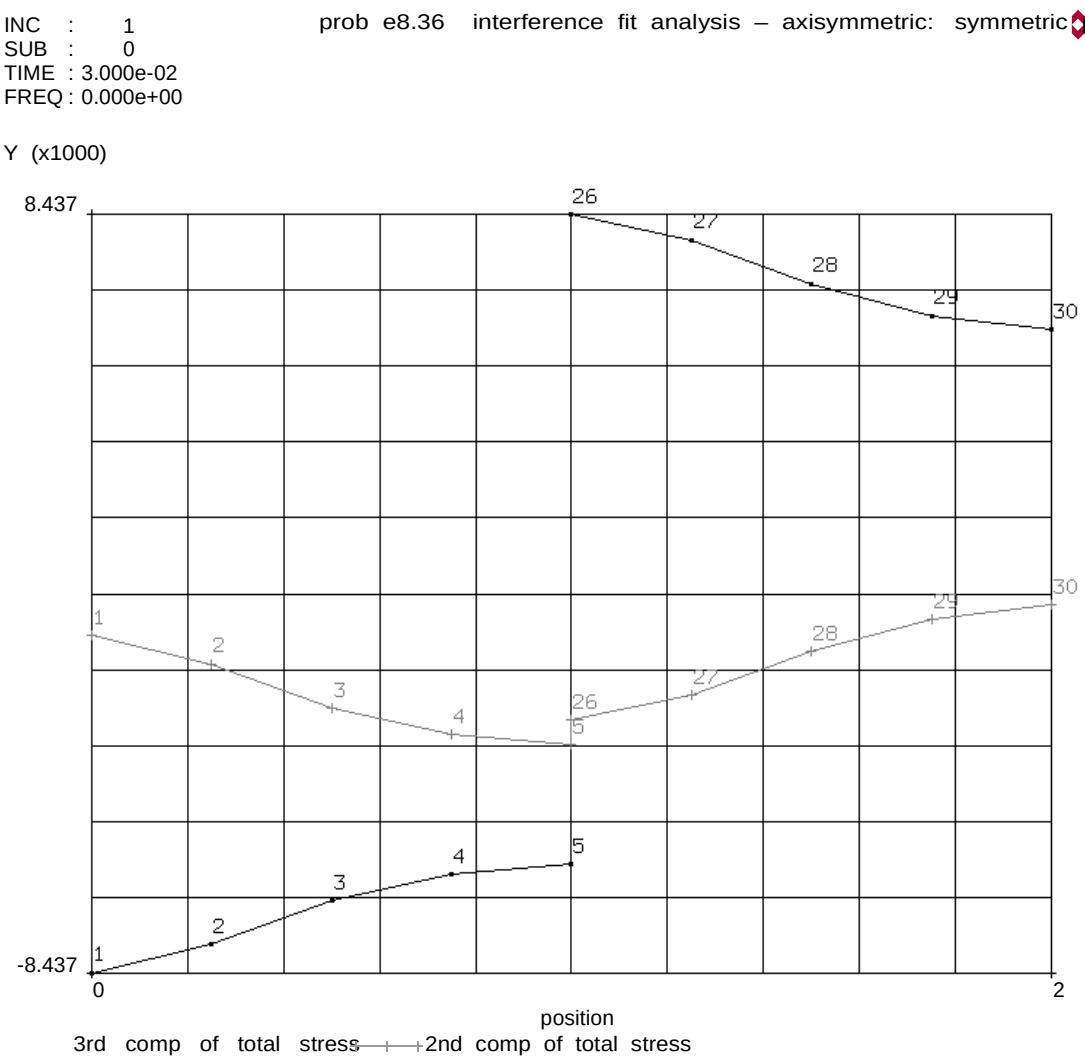

Figure 8.36-2 Radial and Hoop Stresses through Radius

8.37 Interference Fit Analysis

This example demonstrates the interference fit capabilities in MARC and the use of symmetry planes.

Element

Element type 11, a four node plane strain element, is used in this analysis. The model, as shown in Figure 8.37-1, consists of a 90° segment of two rings rotated by 45°. Ten elements (9° each) are used in the circumferential direction. The inner cylinder, with r_i = 1 inch and r_0 = 2 inches, has five elements through the radius. The outer cylinder, with r_i = 2 inches and r_o = 3 inches, has six elements. Two symmetry surfaces at 45° and 135° are used. To prevent any rigid body motion, a spring was placed between the two bodies. While this was not necessary in this problem, it is often a good idea.

Loading

The kinematic boundaries are specified using the symmetry surfaces. This problem is driven by the overclosure fit of 0.01 inch specified through the CONTACT TABLE option.

Material Properties

The material is a high strength steel with a Young's modulus of 30 x 10^6 psi, a Poisson's ratio of 0.3 and a yield stress of 50,000 psi. The material remains elastic in this analysis.

Contact

There are four bodies defined: the inner cylinder, outer cylinder, symmetry surface at θ = 135°, and symmetry surface at θ = 45°.

No friction exists on any surface. Note the flag set on the fourth data block to indicate that surface 3 and 4 are symmetry surfaces. The CONTACT TABLE option is used to indicate which bodies can potentially contact others and to specify the closure distance and the overclosure amount. The overclosure was set to 0.01 inch.

Control

Displacement control was used with a convergence tolerance of 10%. A post file was created using POST and the output was suppressed using NO PRINT. A single increment with a time step of 0.03 second was performed. In this rate independent problem, the time step is arbitrary. The OPTIMIZE option is used to reduce the bandwidth. This is very important in deformable-deformable contact problems.

The PRINT,8 option was used to obtain additional information regarding the contact conditions, such as when a node comes into contact and the displacements relative to rigid surfaces.

Results

The reaction and contact forces are shown in Figure 8.37-2. You can observe a nice uniform pattern along the contact surfaces. The stresses σ_{xx} and σ_{yy} are shown through the radius at $\theta = 90°$. These would be similar to the σ_{qq} and σ_{rr} components, respectively. Note that the stresses are an order of magnitude greater than in problem 8.36; but, on closer observation, the overclosure distance is also an order of magnitude larger. Note that accuracy could have been improved if the outer elements would have been offset relative to the inner elements by 4.5°. This would have resulted in a more accurate surface normal calculations.

Parameters, Options, and Subroutines Summary

Example e8x37.dat:

Parameters	Model Definition Options	History Definition Options
ELEMENT	CONNECTIVITY	AUTO LOAD
END	CONTACT	CONTACT TABLE
PRINT	CONTROL	CONTINUE
SIZING	COORDINATES	TIME STEP
TITLE	DEFINE	
	END OPTION	
	ISOTROPIC	
	NO PRINT	
	OPTIMIZE	
	POST	

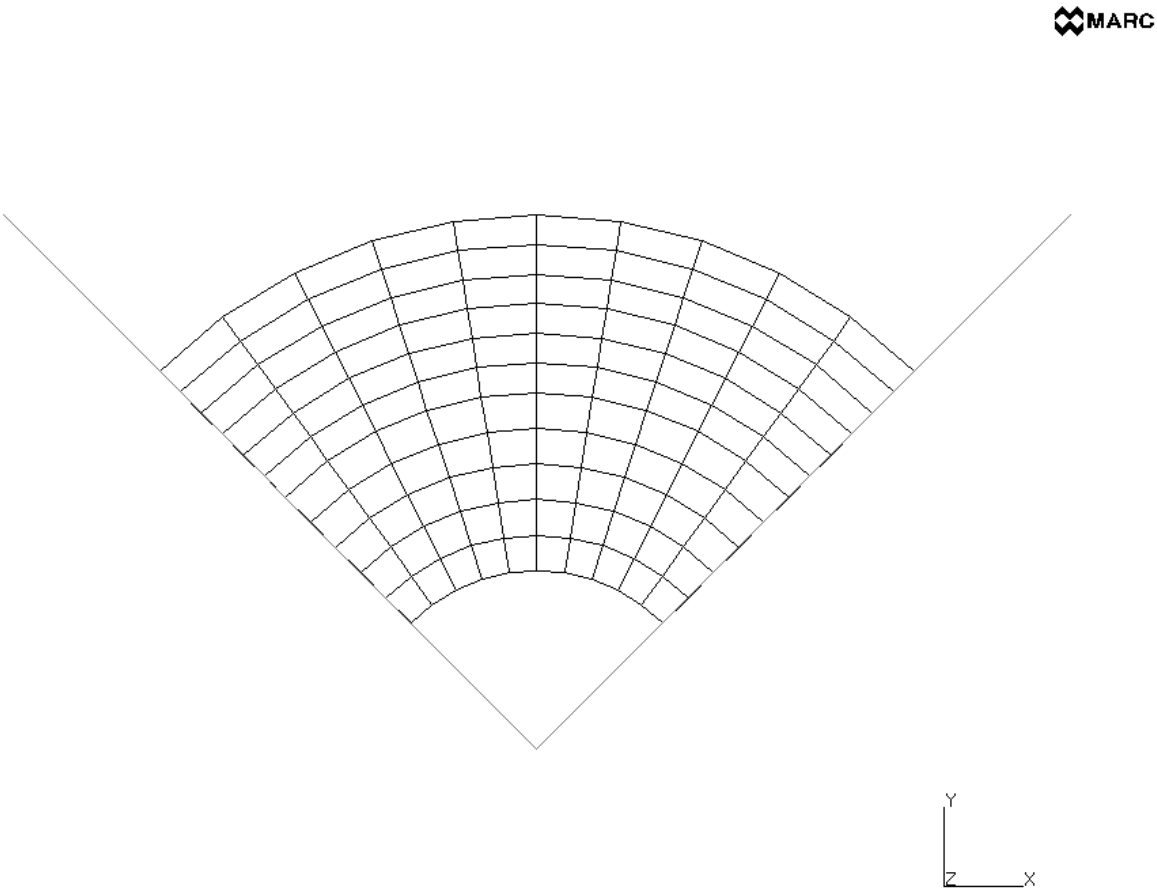

Figure 8.37-1 Finite Element Mesh with Symmetry Surfaces

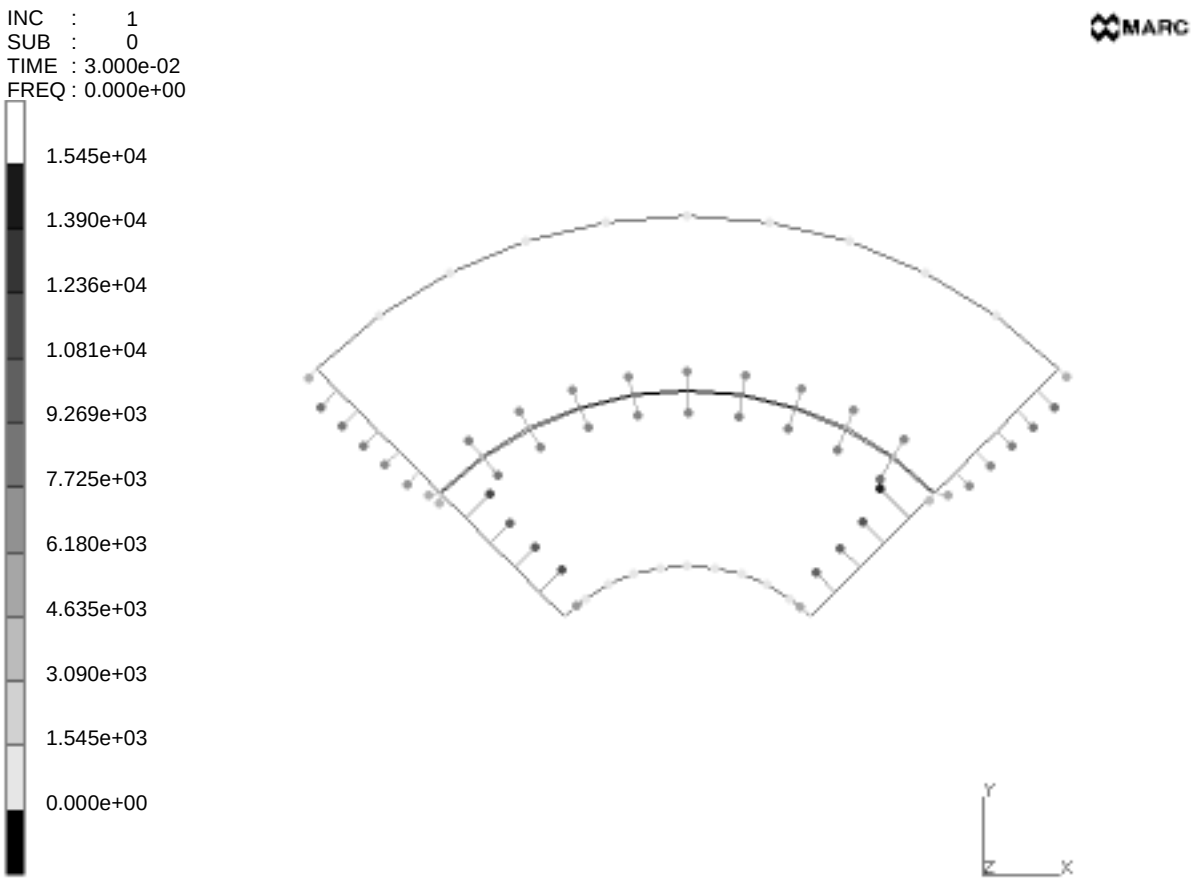

Figure 8.37-2 Reaction and Contact (Interference) Forces

8.38 Deep Drawing of a Box using NURB Surfaces

This example demonstrates the deep drawing of a box modeled with shell elements. The punch and holder are modeled with nurbs using the CONTACT option. The improvement in computational performance is demonstrated by the use of the sparse direct solver.

This problem is modeled using the four techniques summarized below.

Data Set	Element Type(s)	Number of Elements	Number of Nodes	Differentiating Features
e8x38a	75 or 139			
e8x38b				
e8x38c				
e8x38d				

Geometry

The sheet is made up of 636 element type 75 or element type 139 with dimensions of 225 cm by 220 cm. Element type 75 is a thick shell element which can also be used to simulate thin shells. Element type 139 is a thin shell element. The shell thickness (1.2 cm) is specified through the GEOMETRY option in the first field (EGEOM1).

Loading

The punch is given a constant velocity of 3 cm/second. The AUTO LOAD option with 112 step sizes is specified with each step size (0.25 seconds) specified through the TIME STEP option. The total motion is 84 cm.

Material Properties

The material is treated as elastic-plastic with a Young's modulus of 2.1e5 N/cm^2, a Poisson's ratio of 0.3, and an initial yield stress of 188.66 N/cm^2. The yield stress is given through the WORK HARD DATA model definition option.

Boundary Conditions

One-quarter of the geometry is used due to symmetry. The appropriate nodal constraints are applied in the global x,y directions to impose symmetry. The box is deep-drawn by a punch having a constant velocity of 3 cm/sec.

Contact

This option had three bodies. The first body is a rectangle of 626 shell elements. The second body is a rigid die which is made up of 7 different NURBS. The third body is the rigid holder which has two major parts – a flat holder and a curved shoulder with 12 NURBS to describe the complete shoulder. The workpiece is firmly held by the rigid dies with 0.02 contact tolerance and high separation force entered to simulate the condition. To avoid unnecessary self contact check, the contact table is used.

Control

Displacement control was used with a convergence tolerance of 10%. No more than 20 recycles per increment is specified.

Results

Three bodies are declared in e8x38a.dat with nonanalytical form for NURBS used for the analysis. All surface defined as NURBS are discretized into 4-node patches.

The difference in e8x38b.dat is that the rigid dies are using the analytical form of NURBS to implement contact conditions. Computational performance is improved 10% by use of the analytical NURBS when comparing CPU time for e8x38a.dat and e8x38b.dat. Because an exact representation of the surface is made, the results are better.

Four bodies are declared in e8x38c.dat with the shoulder in the third rigid die in e8x38b.dat becoming the fourth body.

Figure 8.38-1 shows the geometry configuration for the deep-drawing analysis. Figure 8.38-4 shows the 7 NURBS rigid punch. Figure 8.38-5 shows the 12 NURBS rigid holder. The deformation of the sheet is shown at increments 20, 50, 80, and 110 in Figure 8.38-4 through Figure 8.38-7. The equivalent stress is shown in Figure 8.38-8. The equivalent plastic strain is shown in Figure 8.38-9. You can observe that the maximum plastic strain is 70%.

Parameters, Options, and Subroutines Summary

Example e8x38a.dat, e8x38b.dat, e8x38c.dat, e8x38d.dat:

Parameters	Model Definition Options	History Definition Options
ELEMENTS	CONNECTIVITY	AUTO LOAD
END	CONTACT	CONTINUE
FINITE	CONTROL	TIME STEP
CONTACT TABLE	COORDINATES	
LARGE DISP	END OPTION	
PRINT	FIXED DISP	
SHELL SECT	GEOMETRY	
SIZING	ISOTROPIC	
TITLE	NO PRINT	
UPDATE	OPTIMIZE	
	POST	

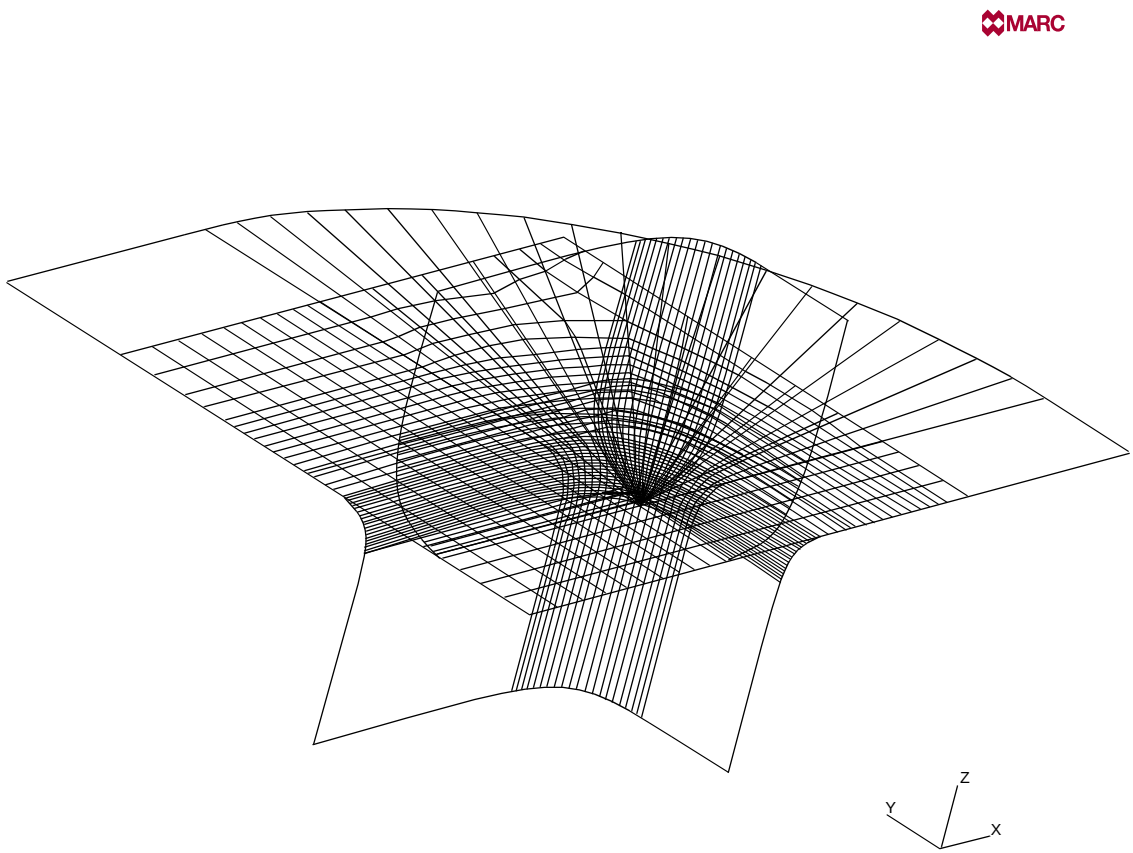

Figure 8.38-1 Plate with Rigid Surfaces

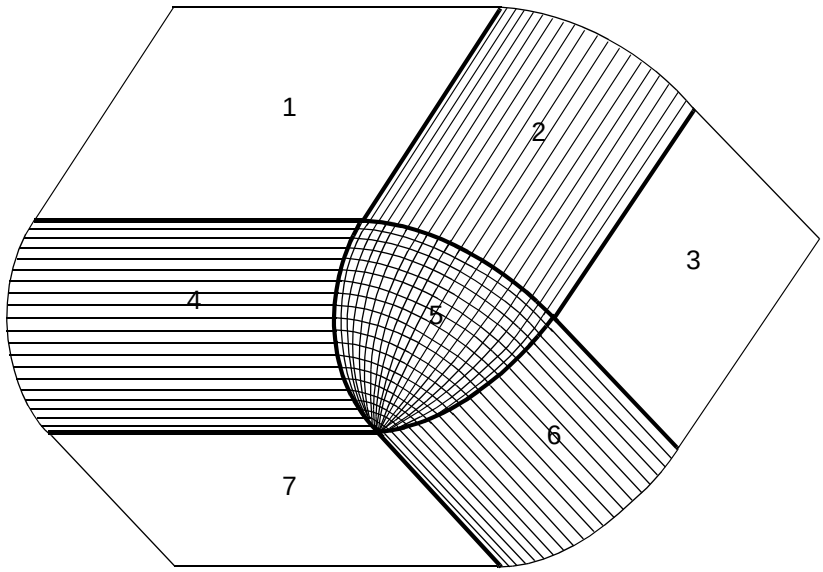

Figure 8.38-2 Male Punch Consisting of Seven NURBS

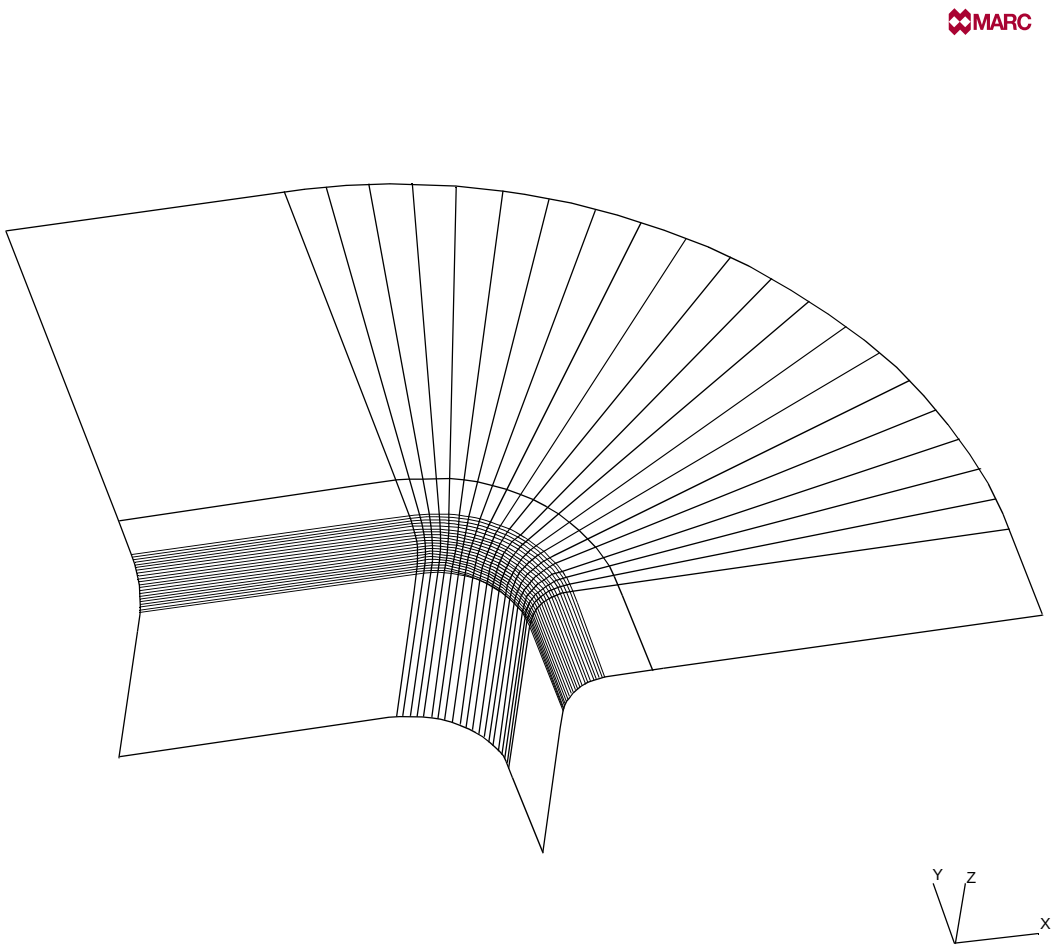

Figure 8.38-3 Blank Holder

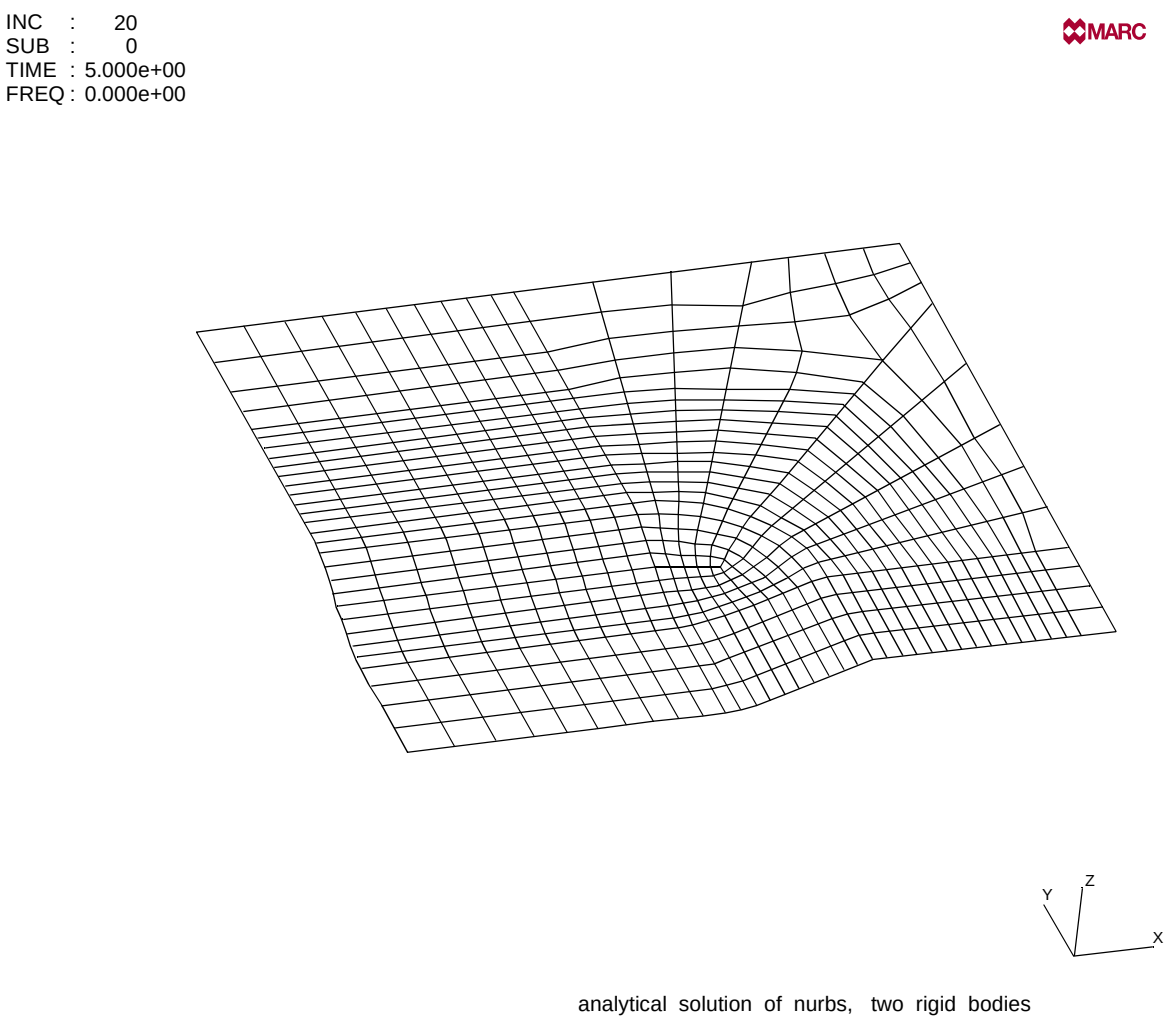

Figure 8.38-4 Deformed Plate at Increment 20

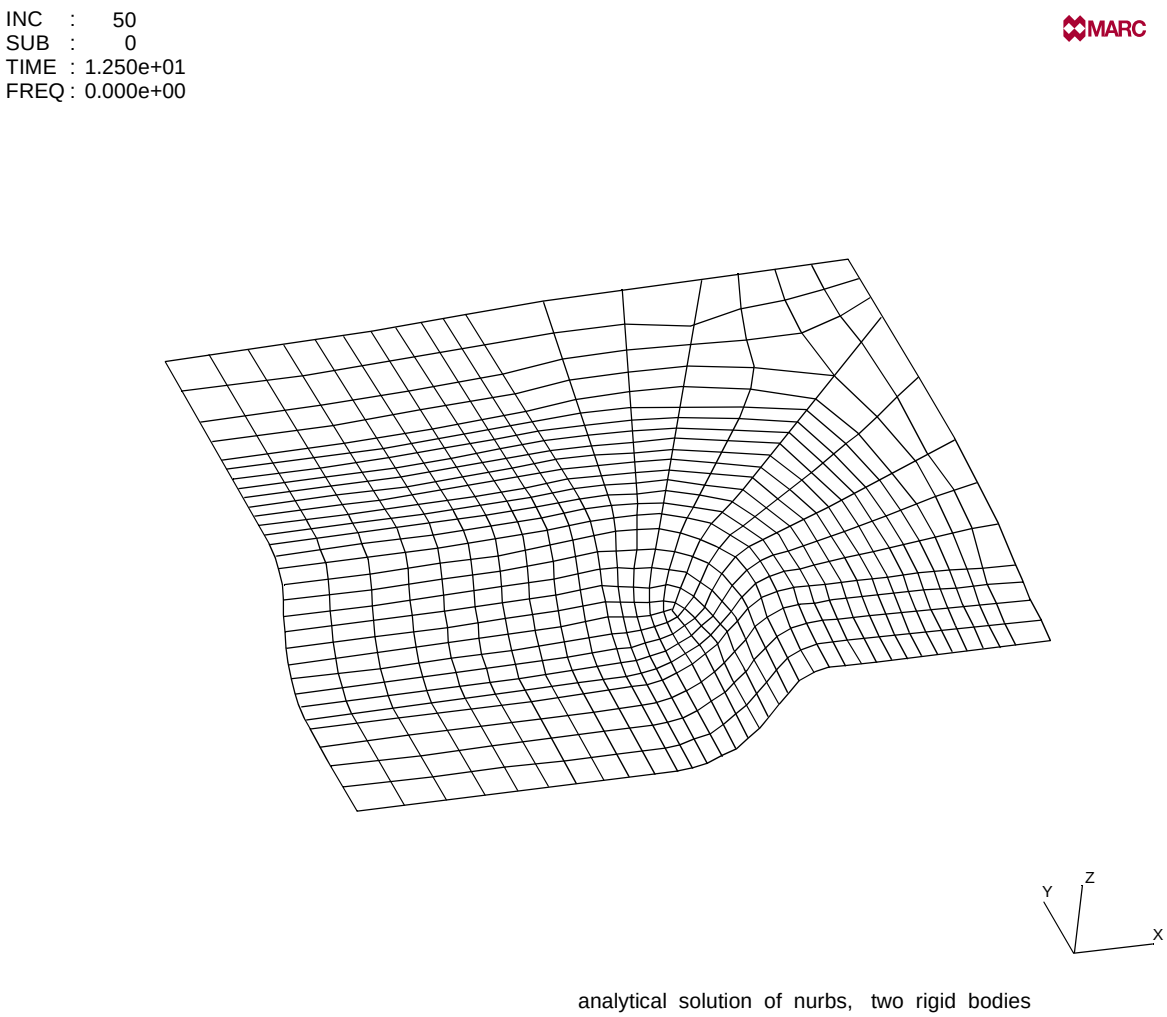

Figure 8.38-5 Deformed Plate at Increment 50

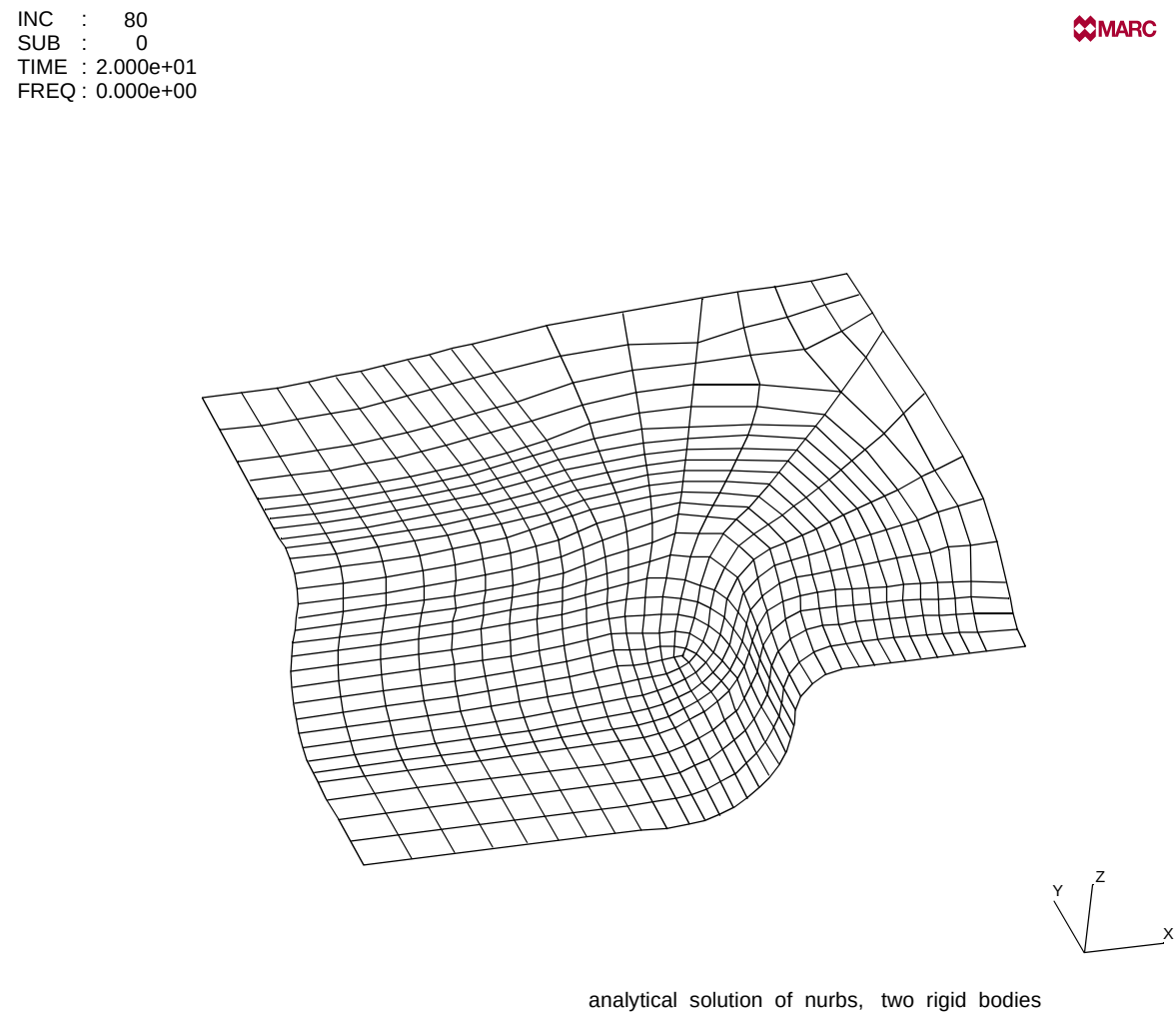

Figure 8.38-6 Deformed Plate at Increment 80

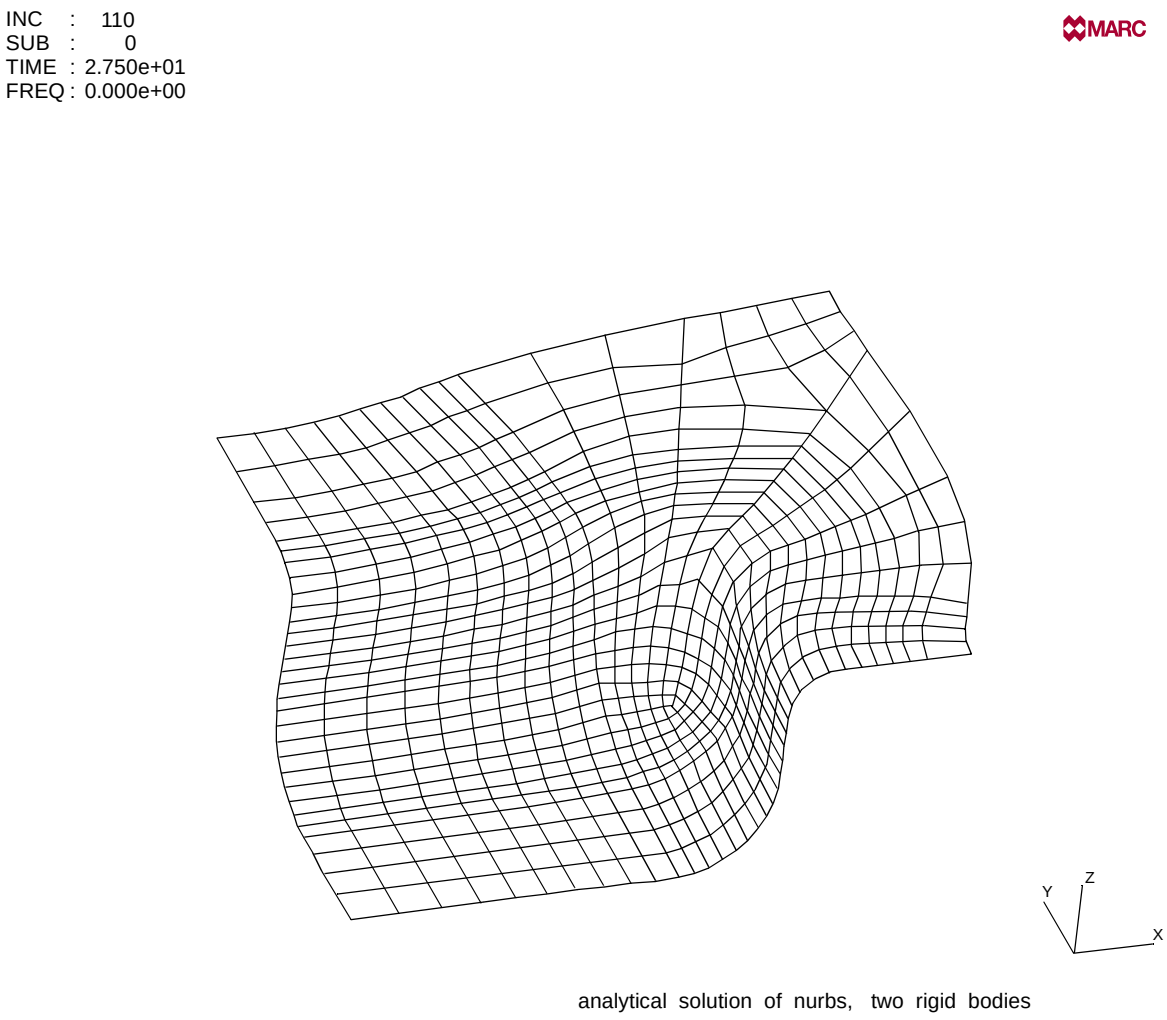

Figure 8.38-7 Deformed Plate at Increment 110

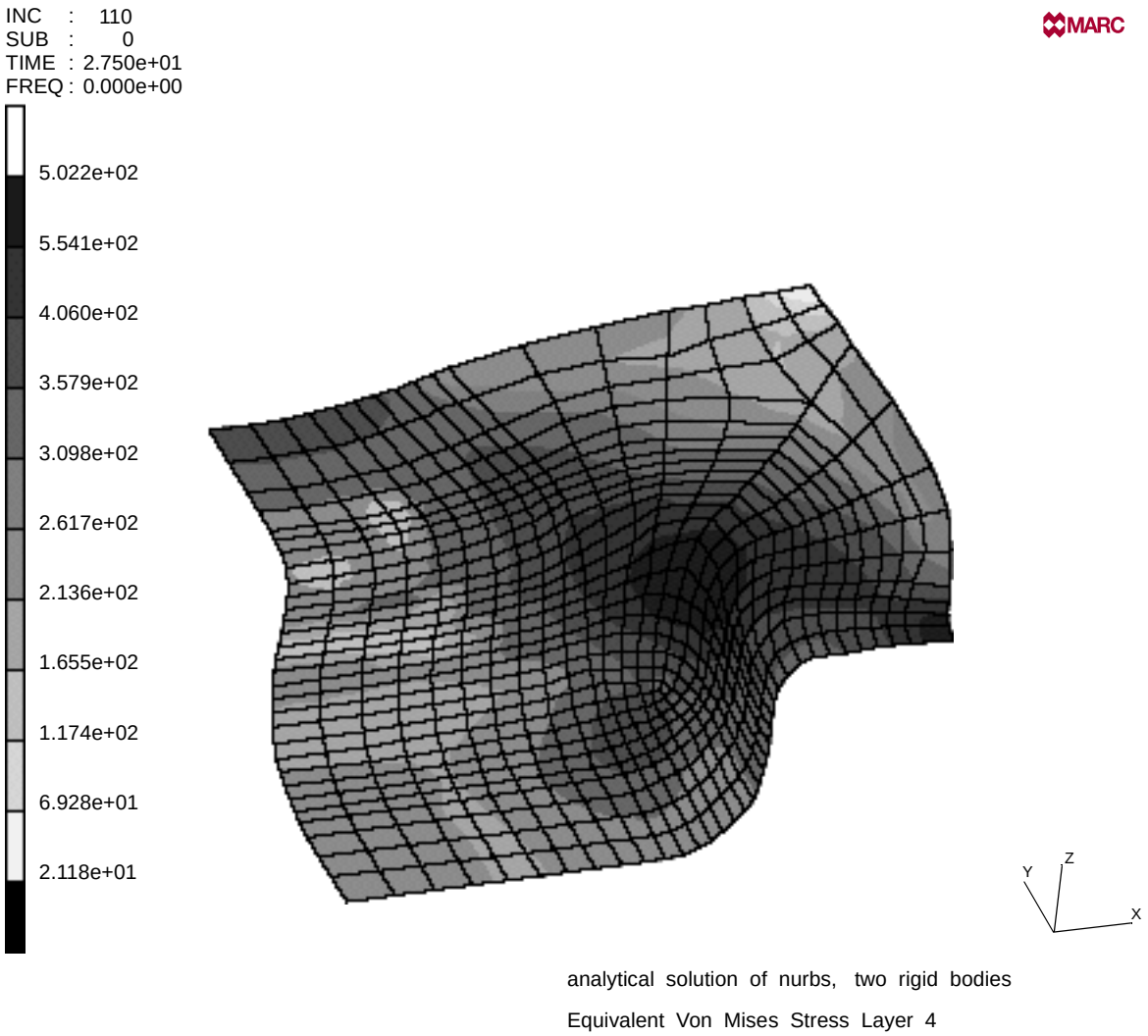

Figure 8.38-8 Equivalent Stress at Midsurface at Increment 110

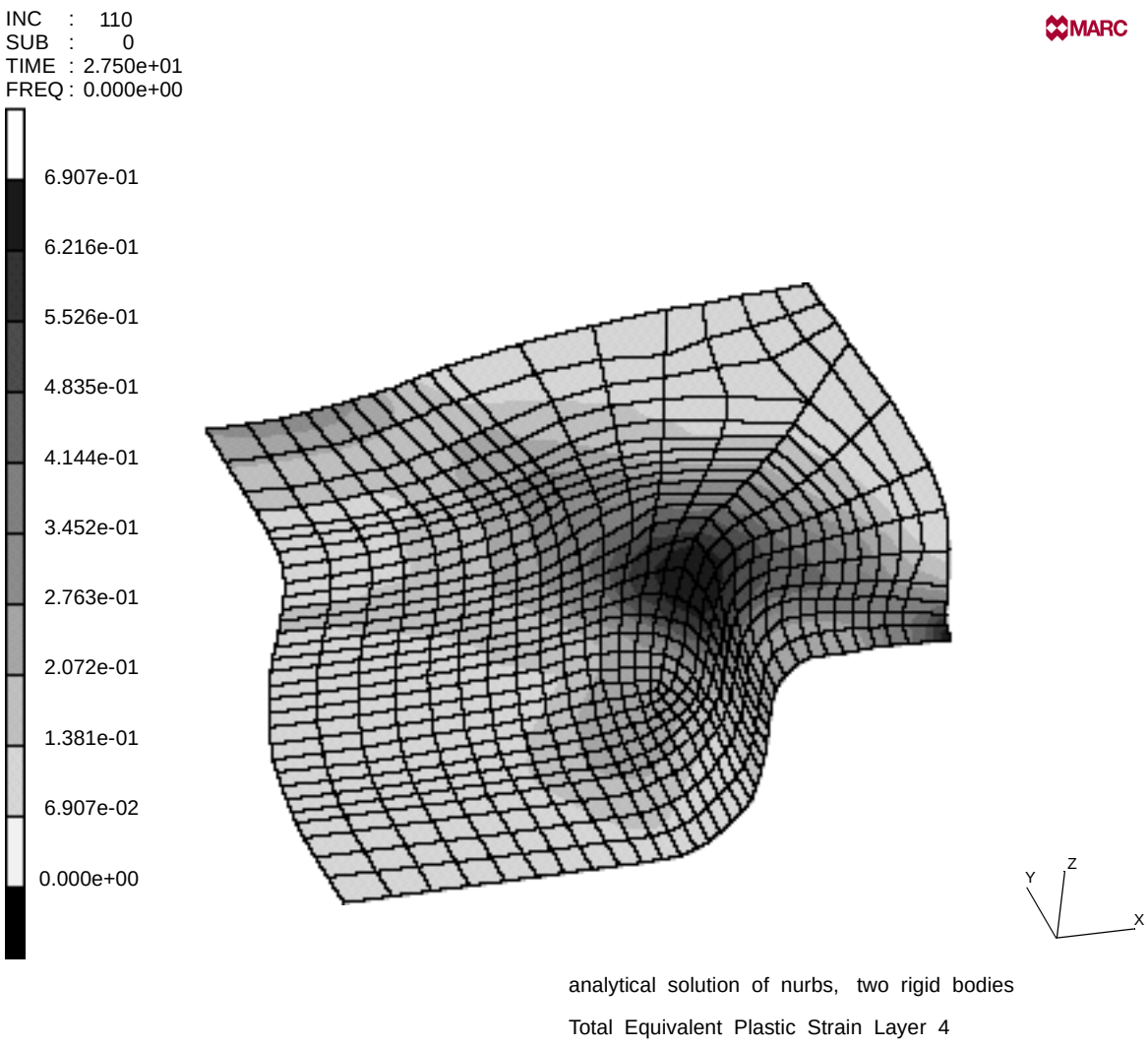

Figure 8.38-9 Equivalent Plastic Strain at Midsurface at Increment 110

8.39 Contact of Two Beams using AUTO INCREMENT

This problem demonstrates bringing two beams into contact as an example of large deflection which exhibits inelastic response. The AUTO INCREMENT option is used to control the magnitude of the load increment. A beam acted on by a point load eventually comes into contact with a second beam (Figure 8.39-1). The geometrically nonlinear problem is solved adaptively by the arc-length method. The procedure stops at the step before the upper beam slips from the lower beam (Figure 8.39-5).

Element

Element type 5 is 2-node rectangular-section beam-column with three global degrees of freedom per node.

Geometry

The beams are 80 inches in length with a distance of 20 inches separating the beams. The height of 2.5 is input in the first data field of GEOMETRY option. The cross-sectional area of 1 is input in the second data field (EGEOM2).

Material Properties

Linear elastic properties are specified in the ISOTROPIC option – Young's modulus = 1,000,000 psi and Poisson's ratio is 0.3333.

Boundary Conditions

Fully clamped conditions are applied to one end of each beam.

Geometric Nonlinearity

The LARGE DISP parameter indicates that geometric nonlinear analysis is to be performed.

Control

Residual-force control is used with a relative error of 10%. No more than 20 recycles per increment is specified.

Loading

The POINT LOAD option is used to enter the total applied load of 585 pounds at node 29 along the global Y-direction. The initial load is 1% of the total load in the first increment and subsequent loading is be adjusted adaptively based on arc-length method.

Contact

This option declares that there are two flexible bodies. Each is made of 20 beam elements. Contact tolerance distance is 0.01.

Results

The deformed beams are shown in Figure 8.39-2 through Figure 8.39-5. The load deflection curve is shown in Figure 8.39-6. When the beams contact, the distance between the contacting node and the warm segment is equal to half the thickness of the beam. After the beams contact, the upper beam comes into contact with the lower beam at point A. The effect of stiffening due to the additional stiffness of the lower beam is observed until point B, as the contact node, slips onto the lower beam. At that moment, the pure bending dominates the response and corresponds to another type of instability until point C, at which time the upper beam will slip away the lower beam.

Parameters, Options, and Subroutines Summary

Example e8x39.dat:

Parameters	Model Definition Options	History Definition Options
ELEMENTS	CONNECTIVITY	AUTO INCREMENT
END	CONTACT	CONTINUE
LARGE DISP	CONTROL	POINT LOAD
PRINT	COORDINATE	
SIZING	END OPTION	
TITLE	FIXED DISP	
	GEOMETRY	
	ISOTROPIC	
	POINT LOAD	
	POST	
	PRINT ELEMENT	
	PRINT NODE	

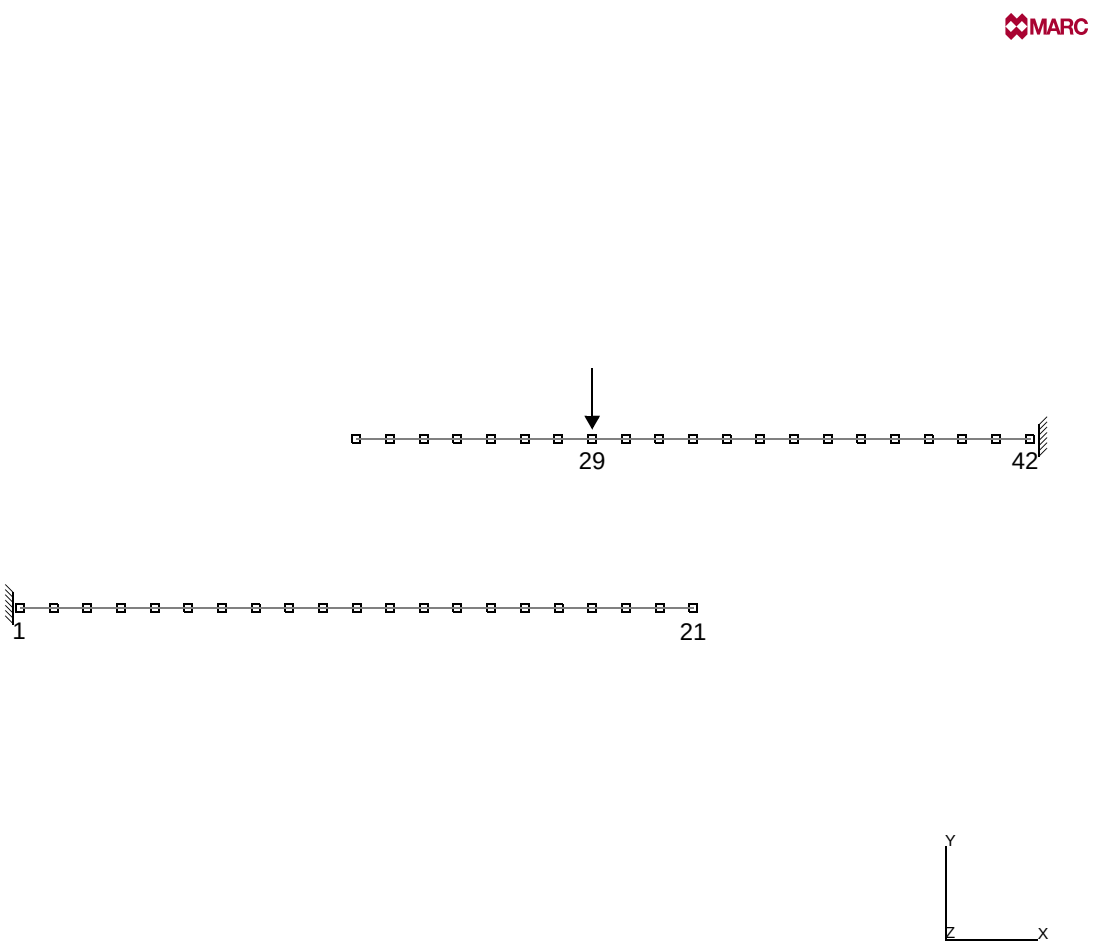

Figure 8.39-1 Mesh of Two Beams

Figure 8.39-2 Initial Contact of Beams

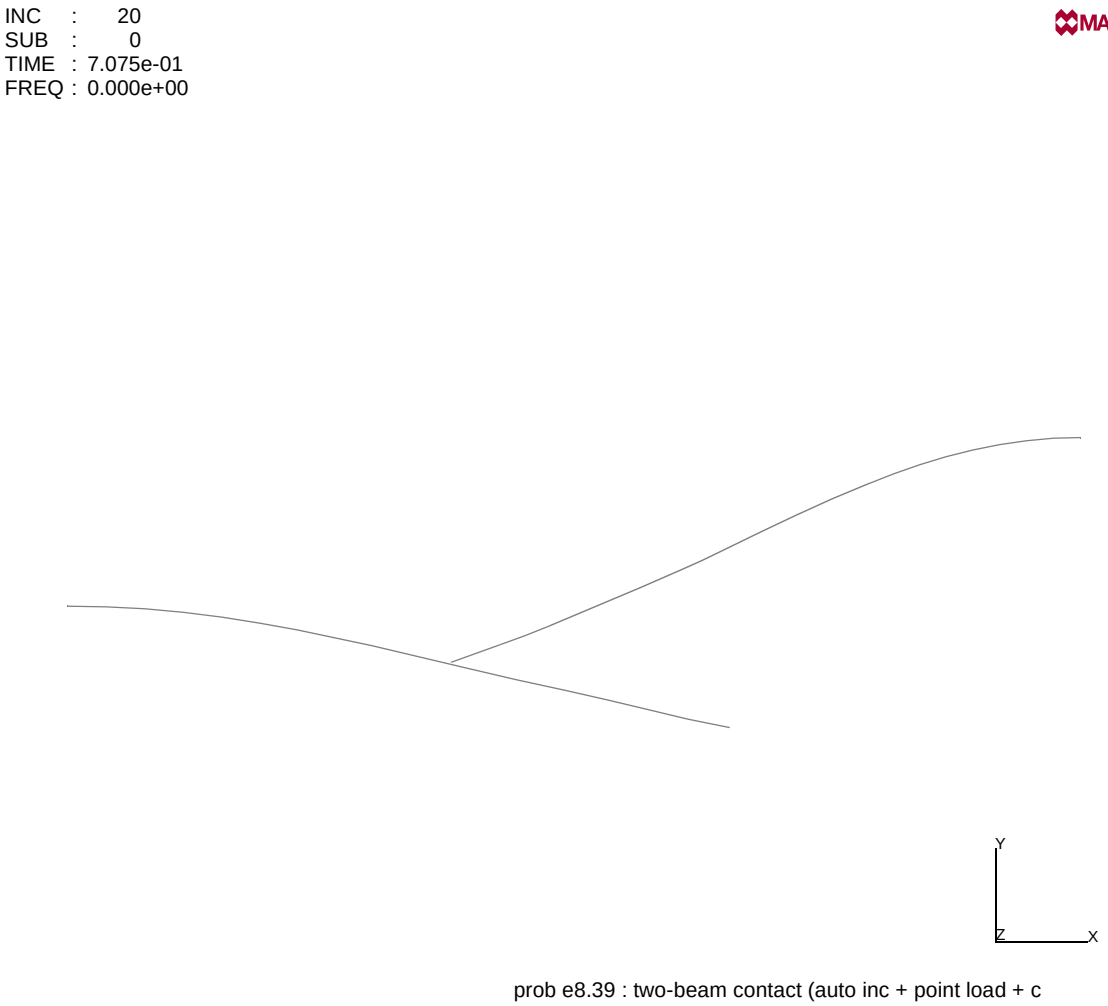

Figure 8.39-3 Deformed Mesh at Increment 20

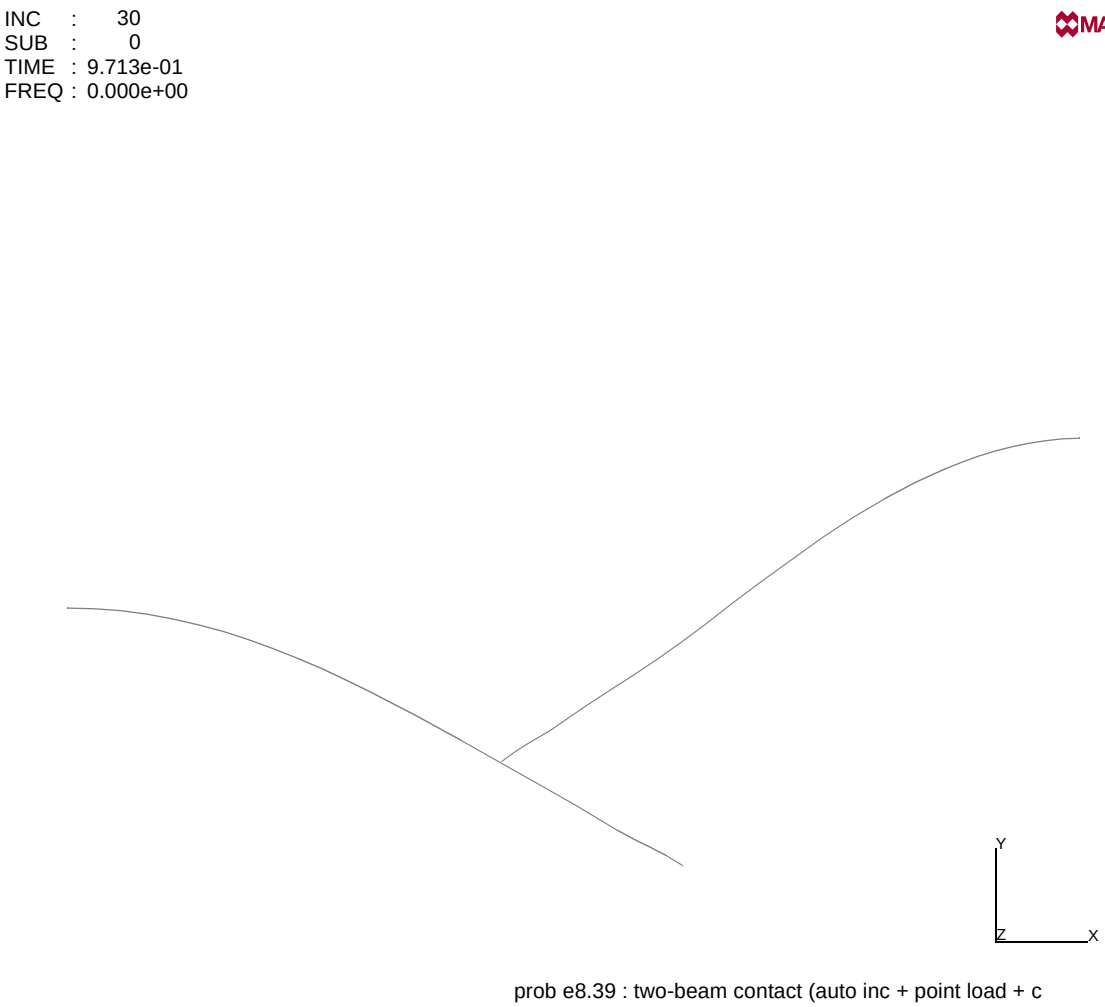

Figure 8.39-4 Deformed Mesh at Increment 30

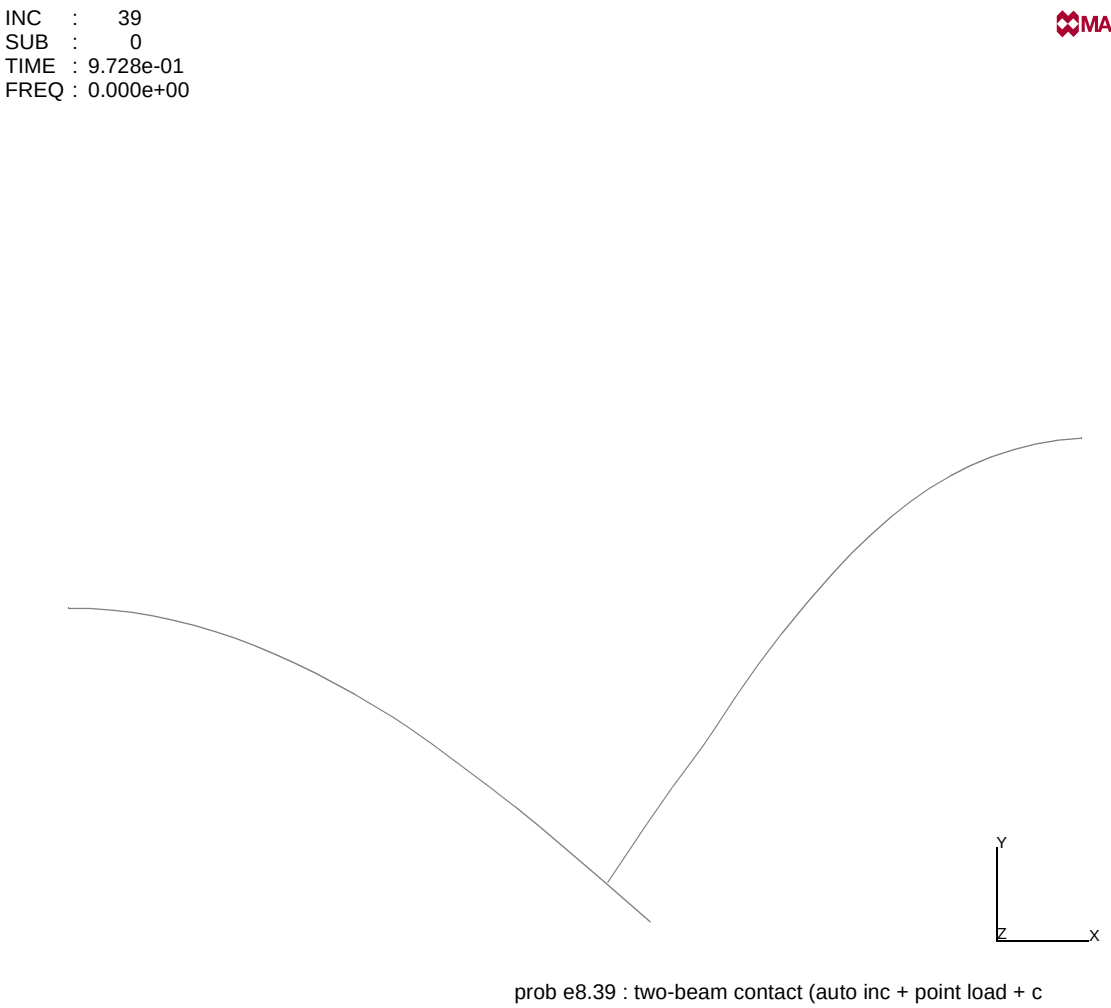

Figure 8.39-5 Deformed Mesh at Increment 39

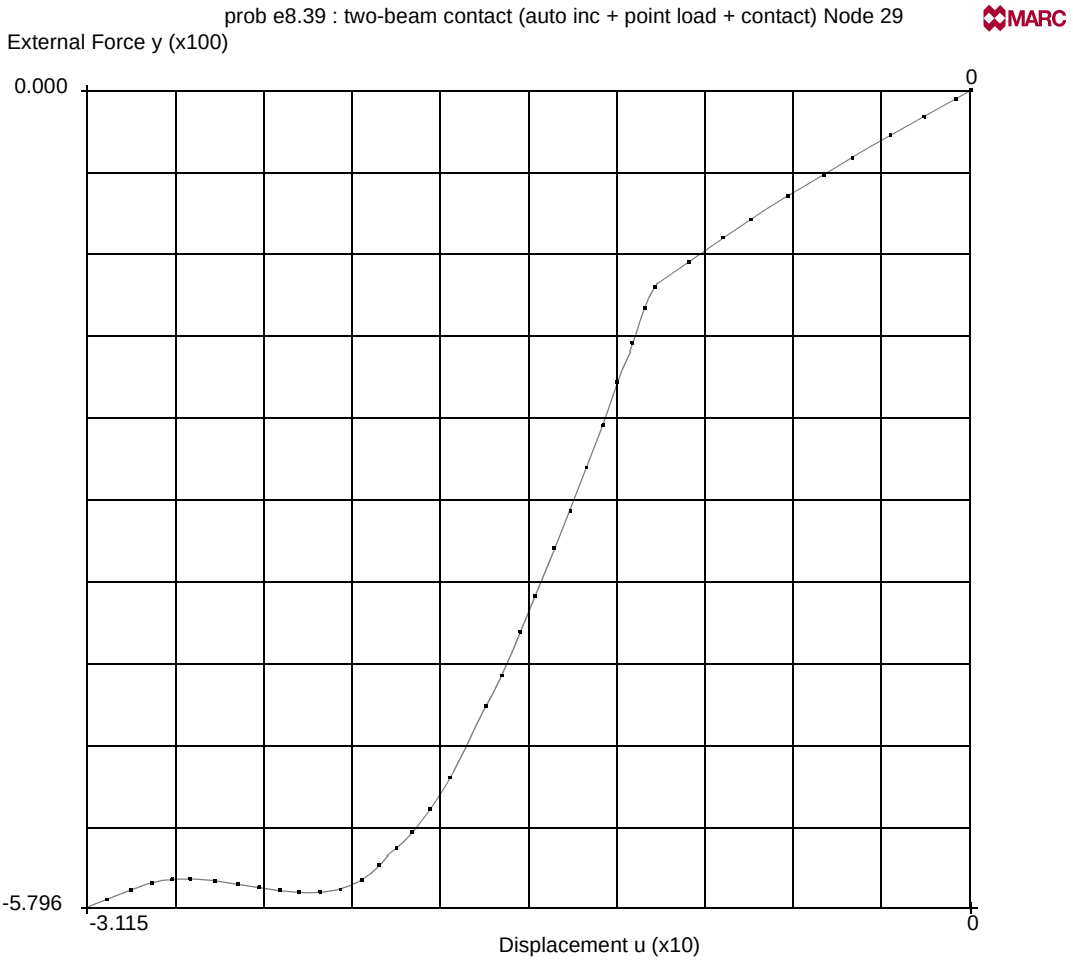

Figure 8.39-6 Load Deflection Curve

8.40 Circular Disk under Point Loads Using Adaptive Meshing

This problem illustrates the use of adaptive meshing for a simple geometry. A circular disk is crudely modeled, and MARC improves the finite element model.

Element

Element type 11, a 4-node linear isoparametric plane-strain element is used in the model.

Model

The original coarse mesh containing only four elements is shown in Figure 8.40-1. The disk has a radius of 1 mm and a unit thickness. The SURFACE option is used to define a circular curve which has this geometry. The ATTACH NODES option is used to specify that the boundary nodes are located on the curve. When new boundary nodes are created, they are automatically placed on the curve.

Geometry

No geometry is necessary as the default is used.

Material Properties

Young's modules is 2. 1x 10^5 N/mm^2, and Poisson's ratio is 0.3. As new elements are created, they are given these material properties.

Boundary Conditions

The bottom point, node 9, is constrained in both directions. The top point, node 1, is constrained in the x-direction to insure no rigid body motion. Additionally, it is given a point load of 0.1 N vertically.

Adaptive Meshing

The ADAPTIVE parameter is used to indicate the maximum number of elements and nodes allowed. The ELASTIC parameter is used to indicate that the analysis is to be repeated until the adaptive criteria is satisfied. Only the loads applied in increment 0 are considered.The ADAPTIVE model definition option is used to indicate that an element should be refined if the stress is greater than 75% of the maximum stress. A limit of 4 levels of subdivisions is allowed. In theory, the maximum number of elements would be 4 x 4^4 = 1024; this is less than given on the parameter.

Results

The progression of meshes is shown in Figure 8.40-2 through Figure 8.40-5. You can observe the concentration of elements in the vicinity of the point loads. Furthermore, the nodes on the boundary take on the shape of the circle. As the mesh is improved, the solution converges to the correct results. Looking at the maximum y displacement, you can observe that the original solution is substantially incorrect.

Level	Maximum Displacement $*10^{-6}$
0	.9070
1	.9054
2	1.067
3	1.331
4	1.548
5	1.549

Parameters, Options, and Subroutines Summary

Example e8x40.dat:

Parameters	Model Definition Options
ADAPTIVE	ADAPTIVE
ELASTIC	ATTACH NODE
ELEMENTS	CONNECTIVITY
END	COORDINATE
PRINT	END OPTION
SIZING	FIXED DISP
TITLE	ISOTROPIC
	NO PRINT
	POINT LOAD
	POST
	SOLVER
	SURFACE

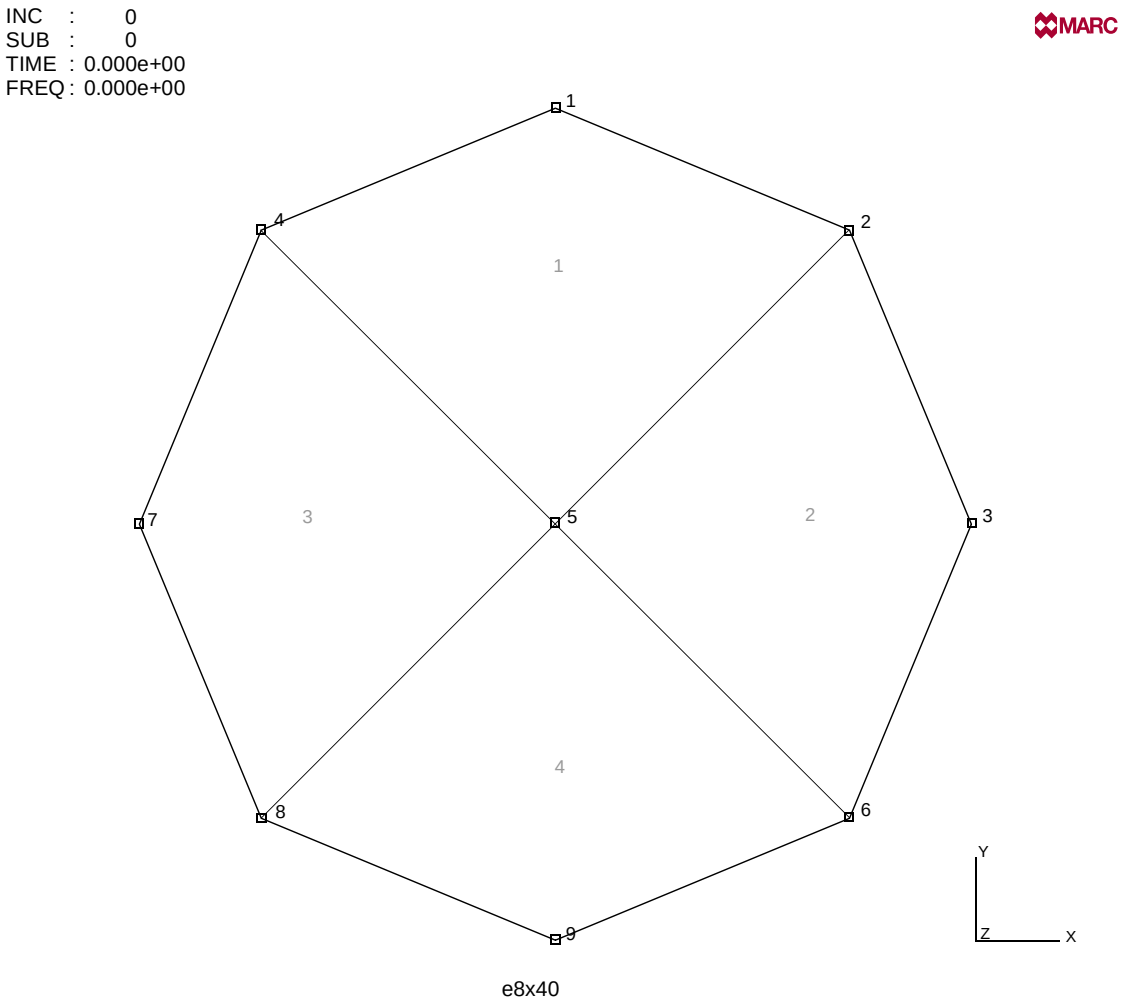

Figure 8.40-1 Original Mesh

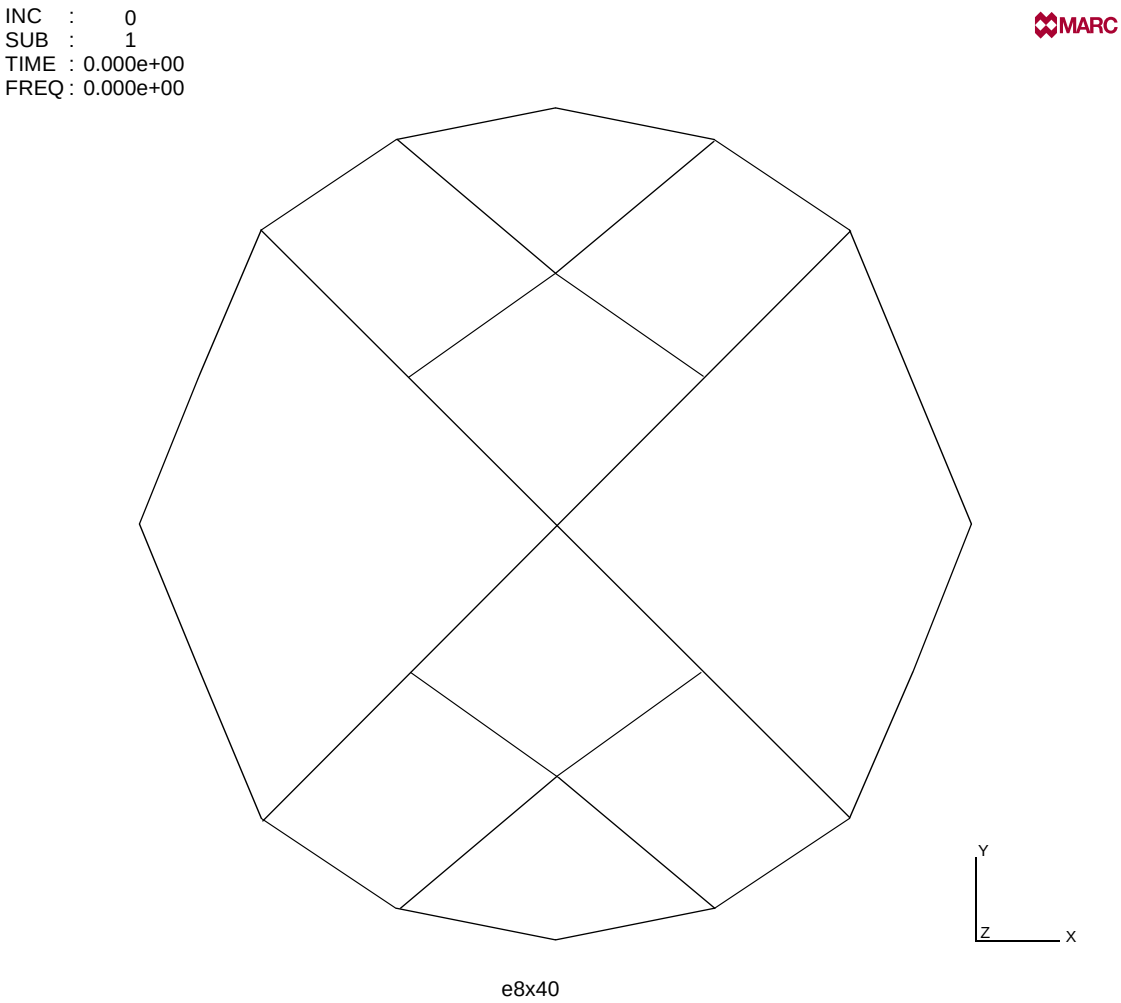

Figure 8.40-2 First Adaptive Mesh

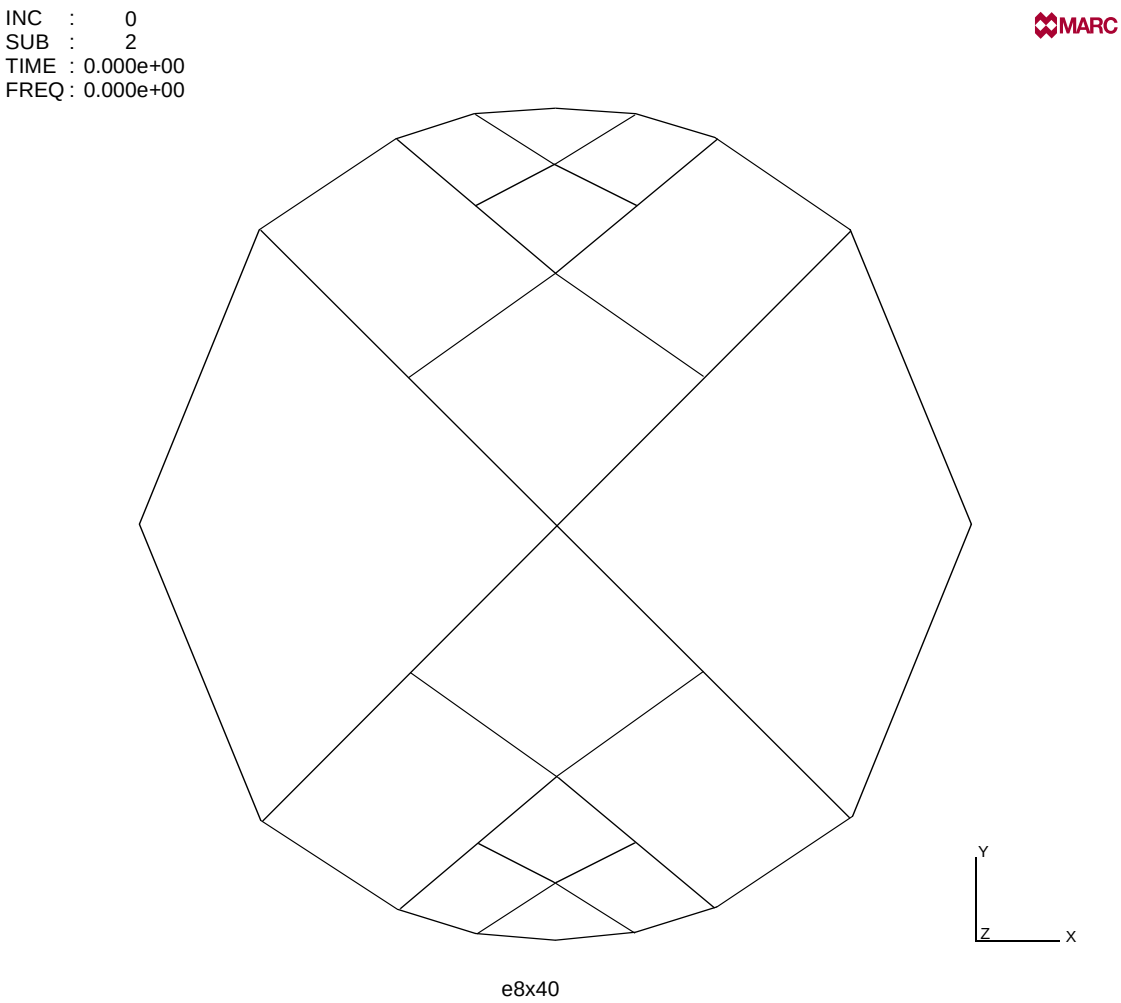

Figure 8.40-3 Second Adaptive Mesh

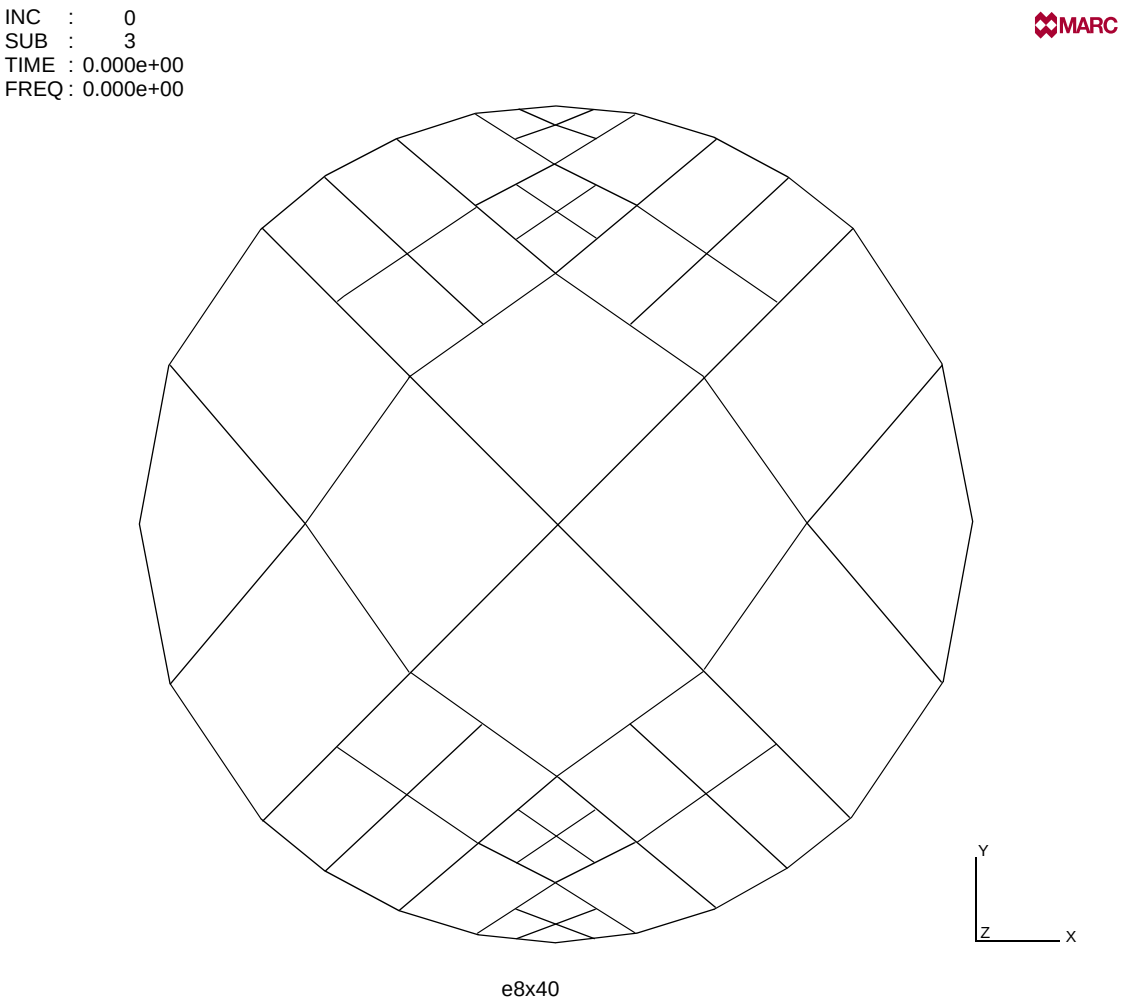

Figure 8.40-4 Third Adaptive Mesh

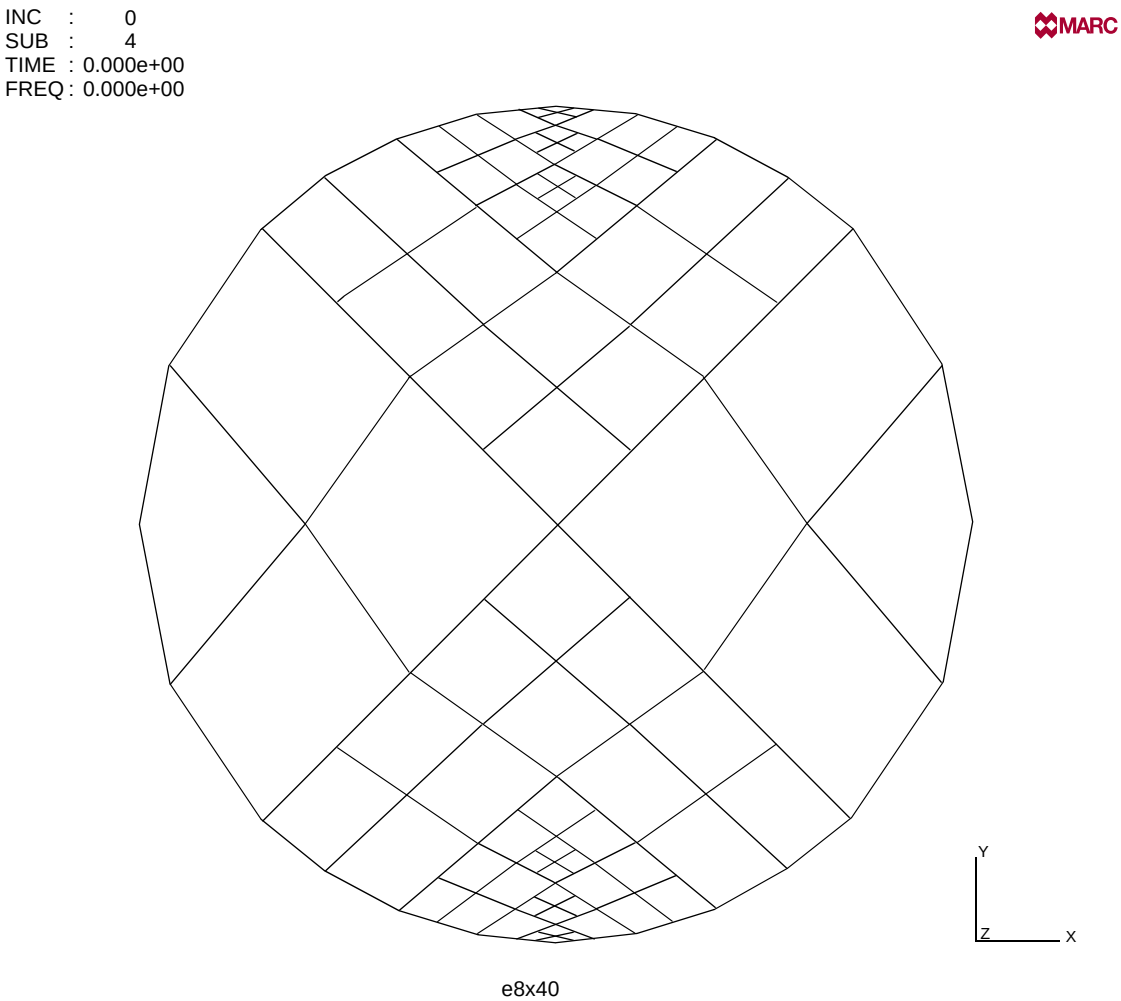

Figure 8.40-5 Fourth Adaptive Mesh

8.41 Stress Singularity Analysis using Adaptive Meshing

This problem demonstrates the use of adaptive meshing for the analysis of a stress singularity. The adaptive meshing increases the number of elements in the region of high stresses and/or high stress gradients.

Element

Element type 3, a 4-node plane-stress element, is used in this analysis.

Model

The plate is a square of dimensions of 100 inches with one-quarter cutout. The initial model, consisting of three elements and eight nodes is shown in Figure 8.41-1. A singular stress develops at node 5 because of the sharp corner.

Geometry

The plates are given a unit thickness.

Material Properties

The material is elastic with a Young's modulus of 30×10^6 psi and a Poisson's ratio of 0.3.

Boundary Conditions

Nodes 7 and 8 have constraints on y-motion while nodes 3 and 6 have constraints on x-motion. Nodes 1, 4, and 7 have a prescribed displacement in the negative x-direction of 0.01 inch. As new elements are created, displacement constraints are automatically generated as required.

Adaptive Meshing

The Zienkiewicz-Zhu error criteria is used with a very tight tolerance of 0.001. A limit of four levels of subdivisions is requested. In theory, the maximum number of elements that could exist at the end is $3 * 4^4 = 768$. The ELASTIC parameter is used to indicate that the analysis is to be repeated until the results satisfy the adaptive meshing error criteria. Additionally, the ERROR ESTIMATES option is used to evaluate the quality of the mesh.

Results

Figure 8.41-2 through Figure 8.41-6 show a progression of the created meshes. The stress at the corner node is shown below:

Iteration	σ_{xx} x 10^2 psi	σ_{xy} x 10^2 psi
0	2.33	3.469
1	2.376	4.825
2	2.892	6.535
3	3.229	9.615
4	4.271	13.56
5	4.498	14.80
6	4.583	14.56
7	4.577	14.53
8	4.583	14.53
9	4.583	14.54
10	4.583	14.54

Note that at higher iterations, the mesh refinement is propagating through the region. Because the number of levels is restricted to 4, the mesh is no longer being enriched at the corner. By iteration 7, the results do not substantially change. If the number of levels is allowed to increase, the solution will continue to change. The ERROR ESTIMATES option informs you that the aspect ratios and warpage is 1.0 and that the largest stress jump occurs at node 5.

Parameters, Options, and Subroutines Summary

Example e8x41.dat:

Parameters	Model Definition Options
ADAPTIVE	ADAPTIVE
ALL POINTS	CONNECTIVITY
ELASTIC	CONTROL
ELEMENTS	COORDINATE
END	END OPTION
PRINT	ERROR ESTIMATE
SIZING	FIXED DISP
TITLE	GEOMETRY
	ISOTROPIC
	POST

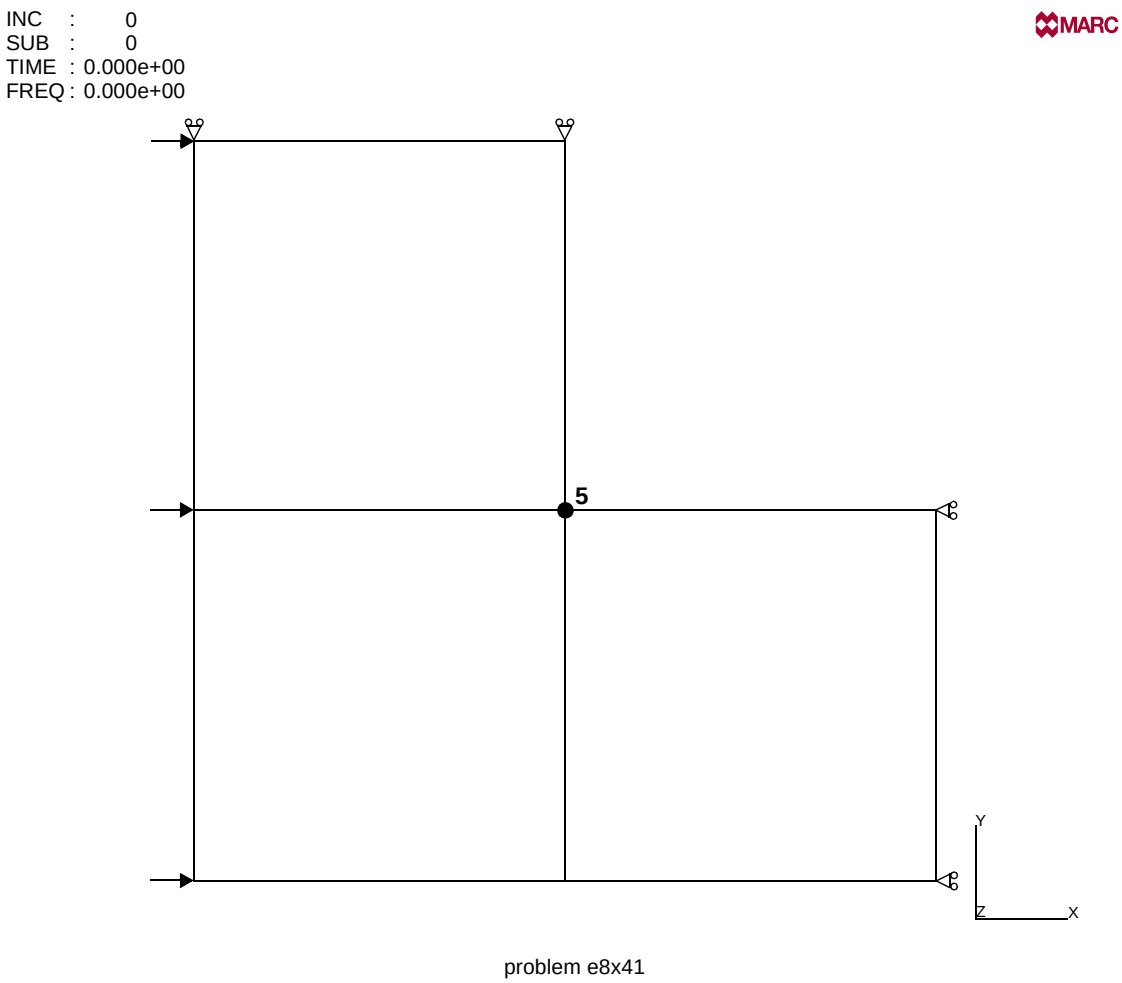

Figure 8.41-1 Original Finite Element Mesh

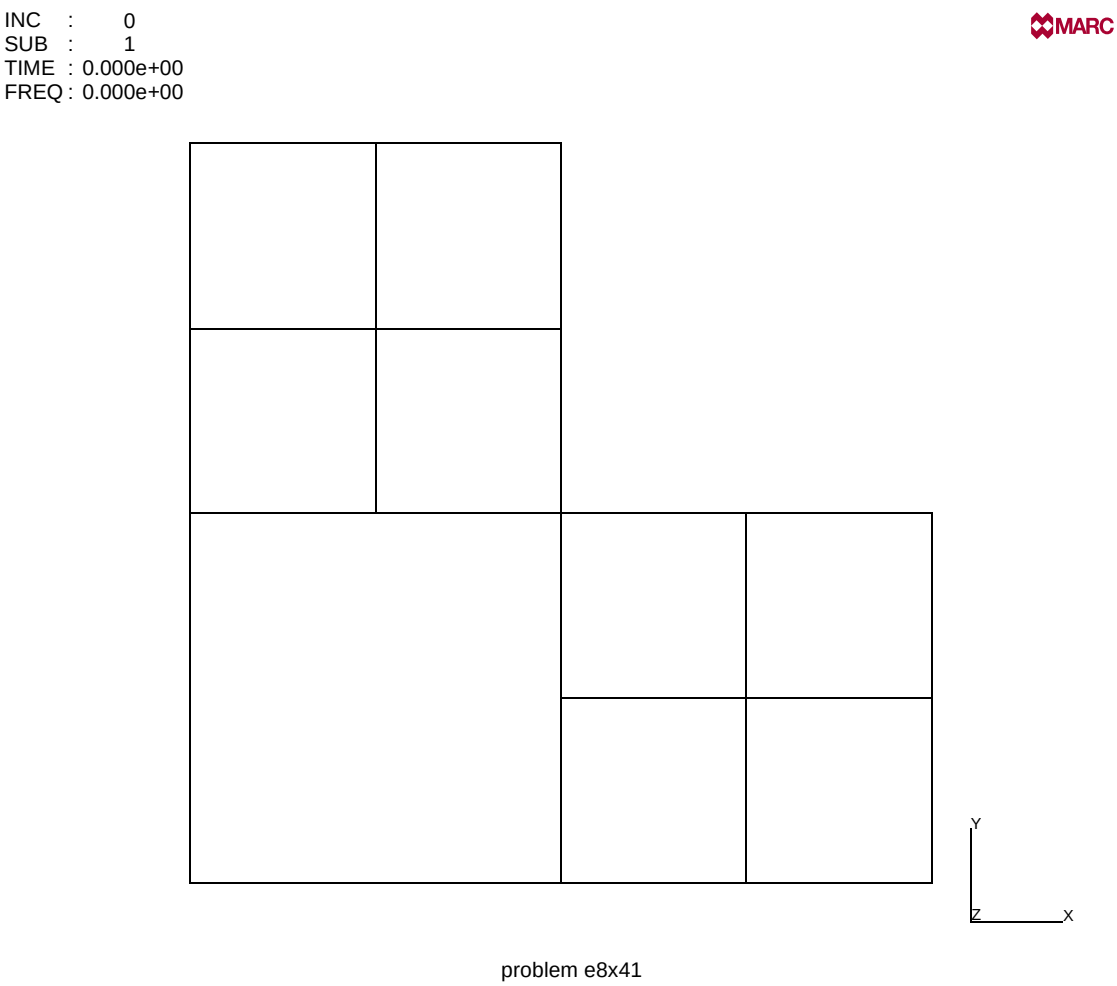

Figure 8.41-2 First Adaptive Mesh

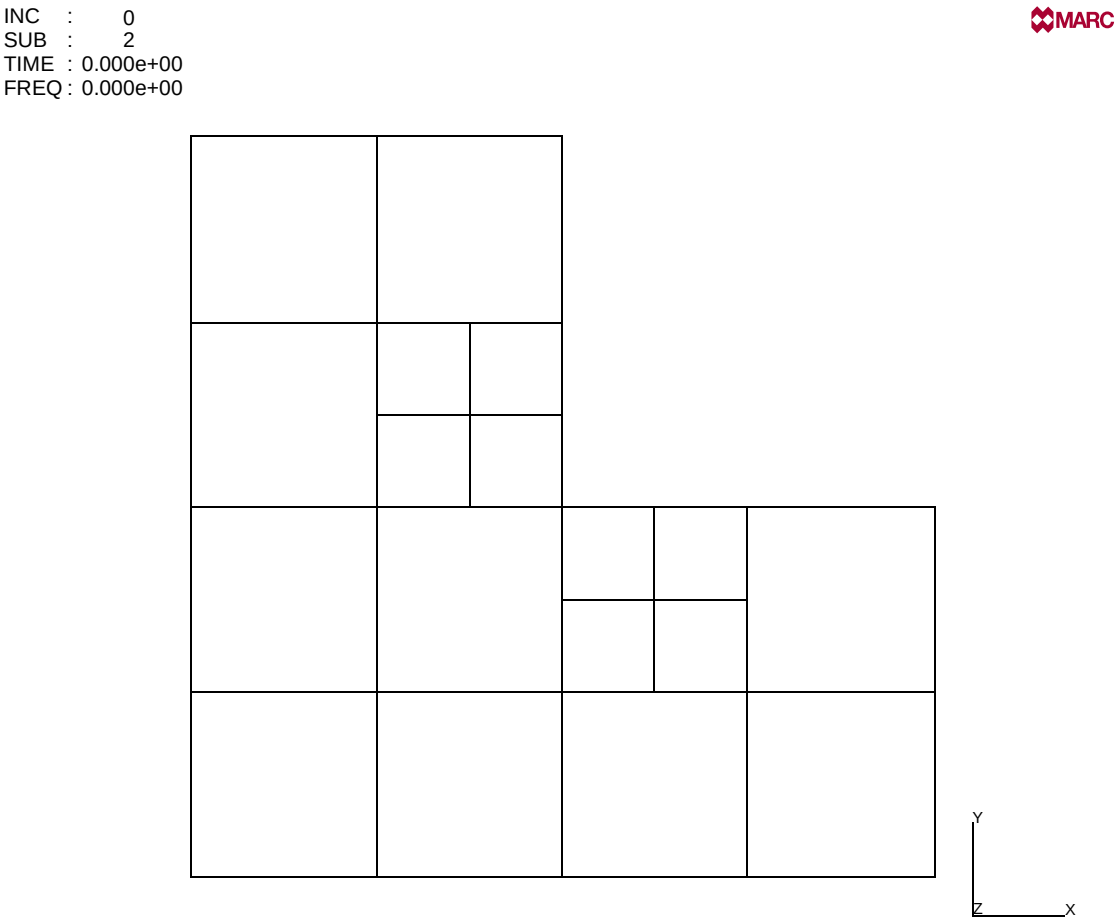

Figure 8.41-3 Second Adaptive Mesh

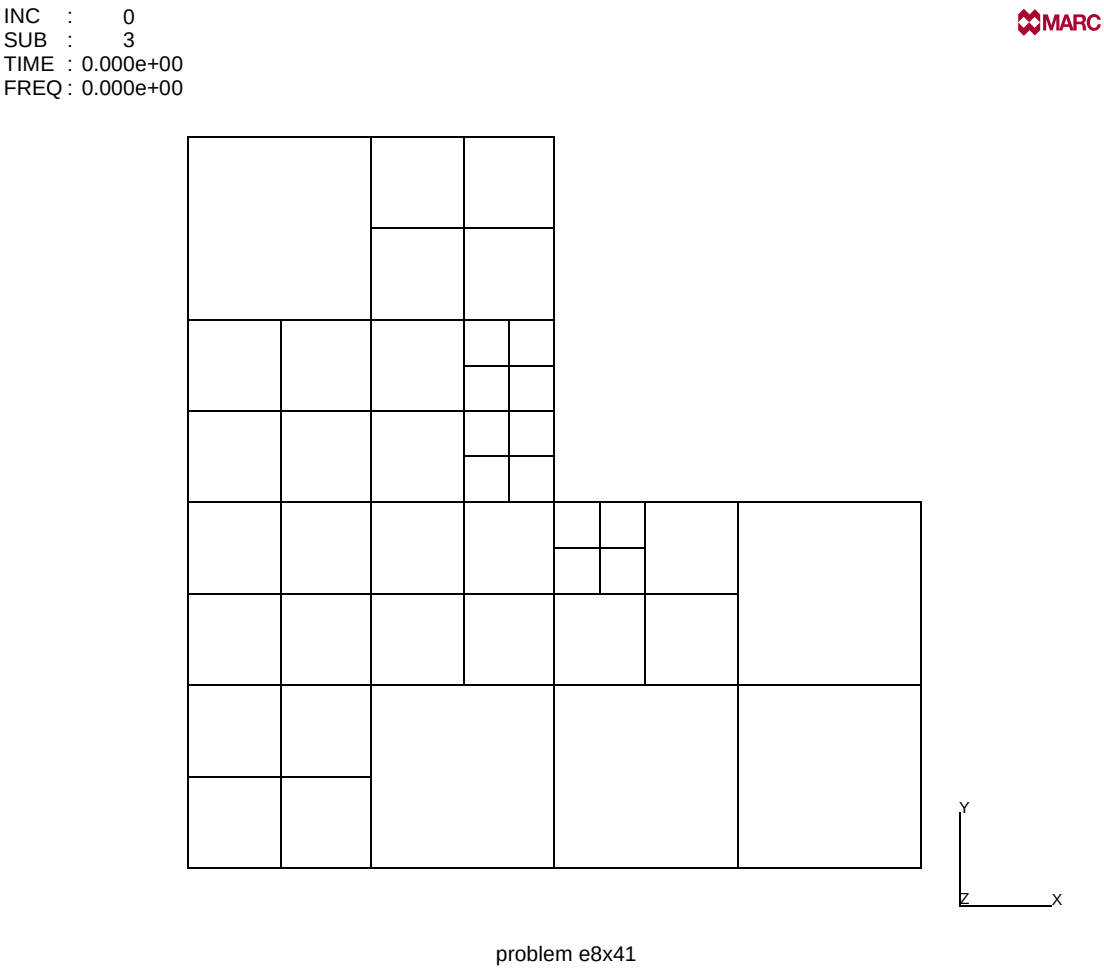

Figure 8.41-4 Third Adaptive Meshing

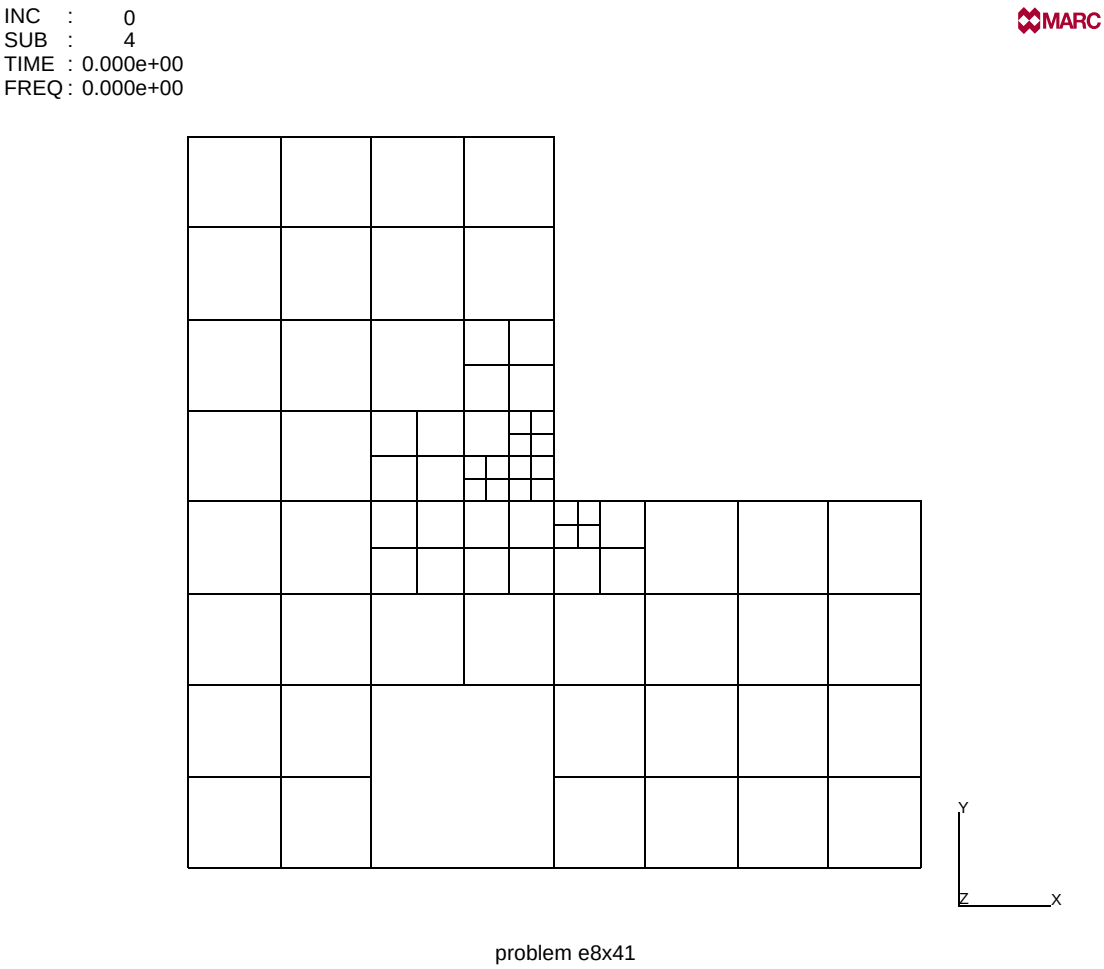

Figure 8.41-5 Fourth Adaptive Mesh

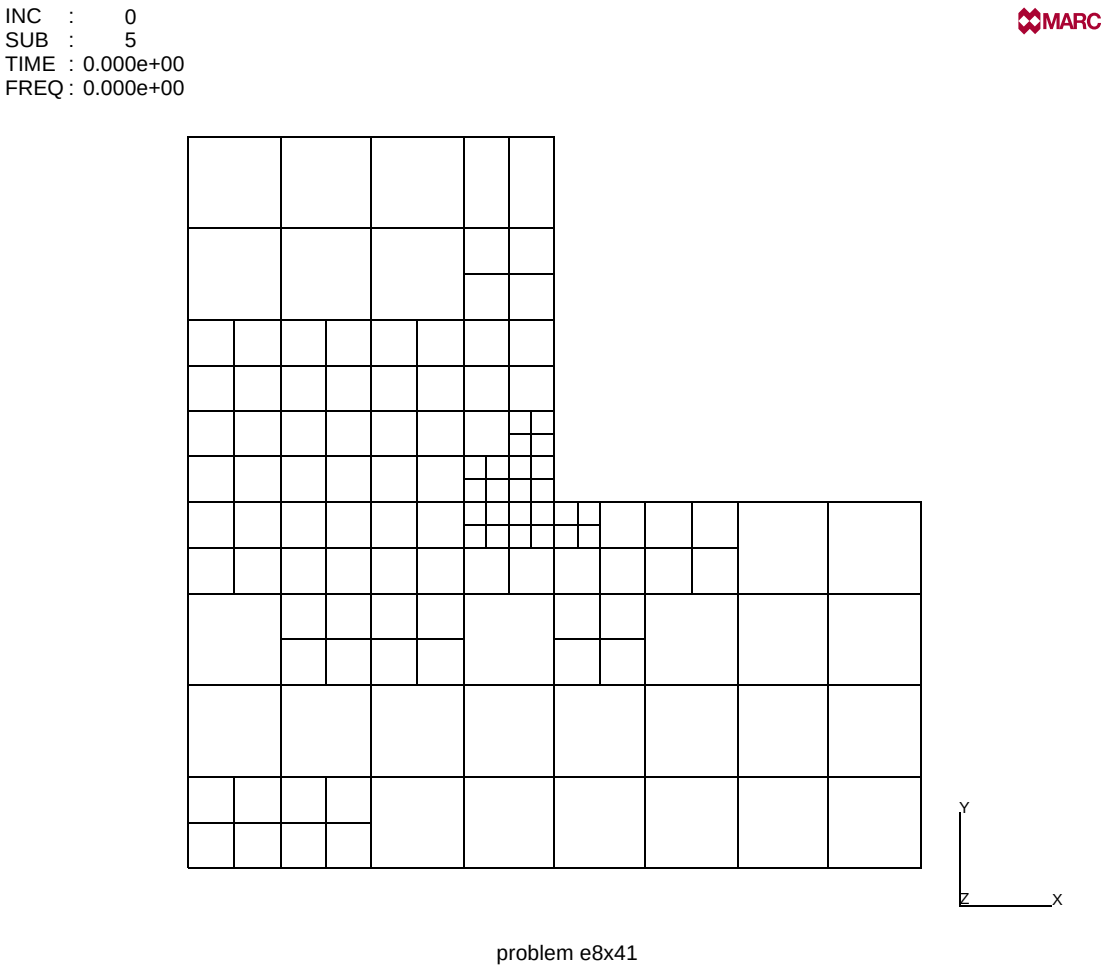

Figure 8.41-6 Fifth Adaptive Mesh

8.42 Contact Analysis with Adaptive Meshing

This problem demonstrates the capability of adaptive meshing analysis during a contact process. A rod is bent about a deformable roll by a rigid punch (Figure 8.42-1).

Geometry

The rod has a length of 0.28 m and a thickness of 0.02 m. The rigid roll has a radius of 0.31.

Material Properties

The material for all elements is treated as an elastic material with a Young's modulus of 1.5e7 N/m^2 and a Poisson's ratio 0.3.

Boundary Conditions

The upper end of the rod is firmly fixed. To avoid the rigid body mode, the center of the roller is fixed.

Control

Residual-force control is used with a relative error of 10%. A maximum of 15 iterations is used per load step.

Contact

This option declares three flexible bodies. The first is a one-layer rod and the second is a roller. The third body is a rigid punch moving with .005 cm/second along the global x-direction. Contact tolerance distance is 1.e-4 m. The ATTACH NODE option, in conjunction with the SURFACE option in an adaptive mesh analysis, allows new created nodes to attach to the surface. The surface the nodes are attached to is a circle with the center located at .037,2.6795 with a radius of .031. A list of nodes attached to this surface is the boundary nodes along the deformable roll.

Results

Initially, one element is placed through the thickness of the rod. As contact occurs between the punch and the rod, you can observe the mesh refinement. Similarly, where the rod contacts the deformable roll, both bodies show local mesh refinement. As the nonlinear process continues, adaptivity occurs when new regions come into contact. Finally, you can observe that the rod has been bent around and that the refinement has occurred on the rod through the thickness in the direction where contact has occurred. Two levels of refinement are allowed in this analysis. The deformed shape is shown in Figure 8.42-2 through Figure 8.42-5.

Parameters, Options, and Subroutines Summary

Example e8x42.dat:

Parameters	Model Definition Options	History Definition Options
ADAPTIVE	ADAPTIVE	AUTO LOAD
DIST LOADS	ATTACH NODE	CONTINUE
ELEMENTS	CONNECTIVITY	DIST LOADS
END	CONTACT	MOTION CHANGE
FOLLOW FOR	CONTROL	TIME STEP
LARGE DISP	COORDINATE	
PRINT	DEFINE	
SETNAME	DIST LOADS	
SIZING	END OPTION	
TITLE	FIXED DISP	
	GEOMETRY	
	ISOTROPIC	
	NO PRINT	
	OPTIMIZE	
	POINT LOAD	
	POST	
	RESTART	
	SOLVER	
	SURFACE	

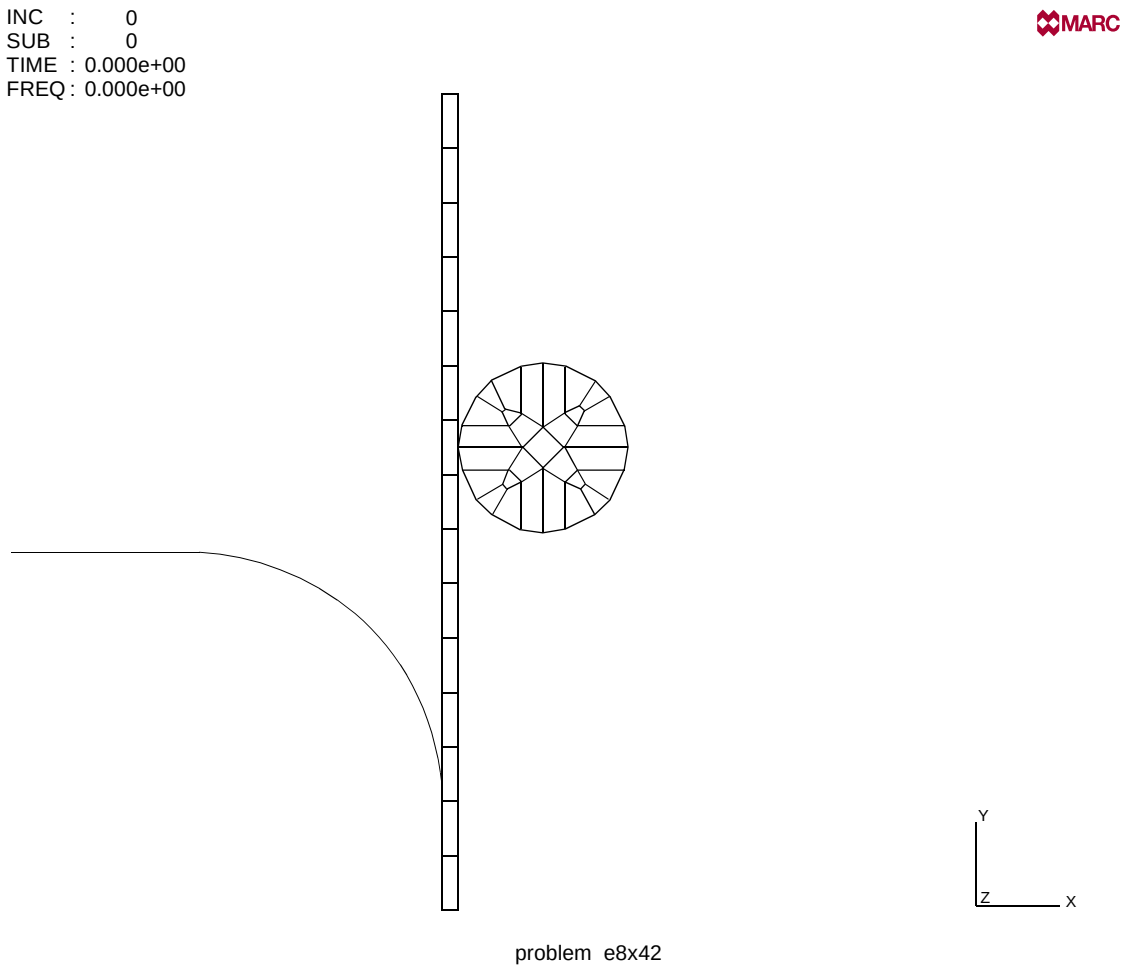

Figure 8.42-1 Original Mesh

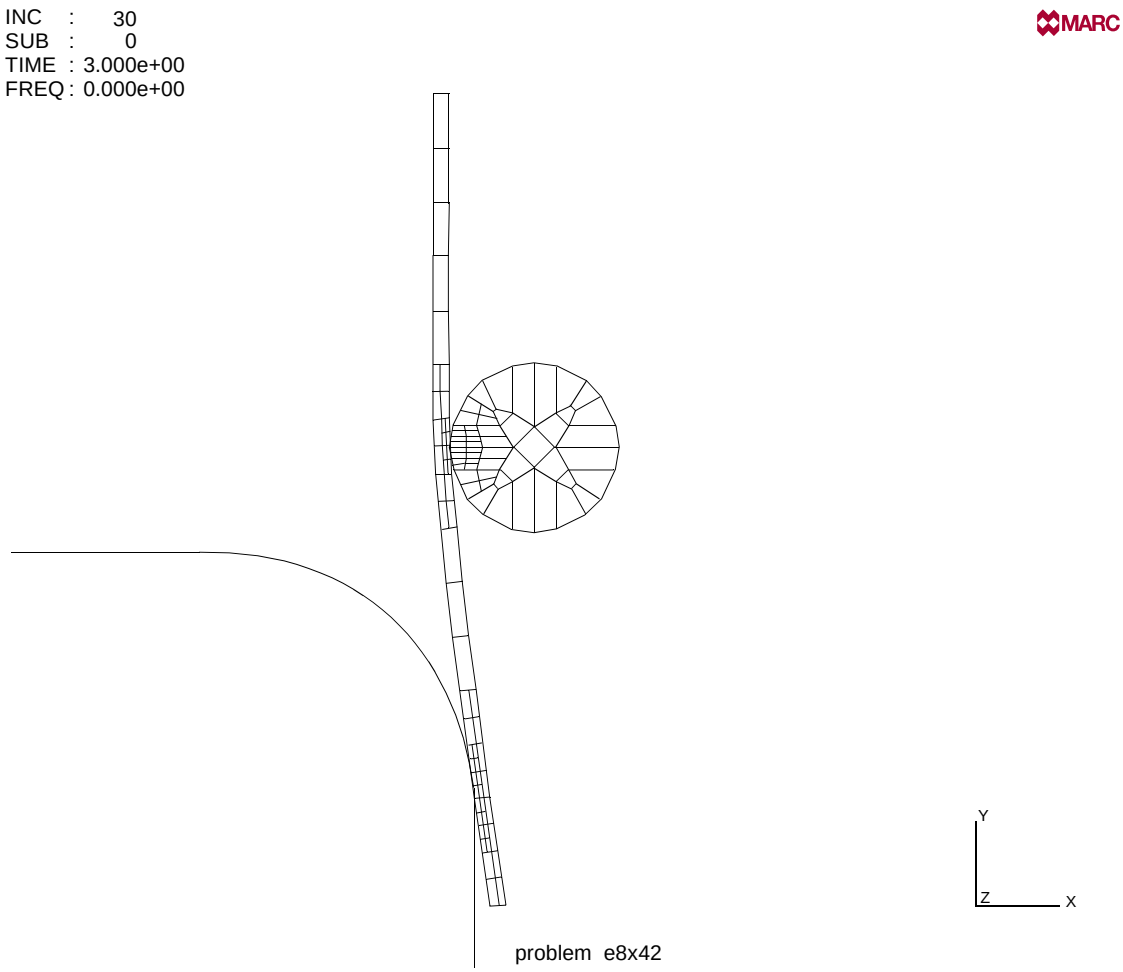

Figure 8.42-2 Deformed New Mesh at Increment 30

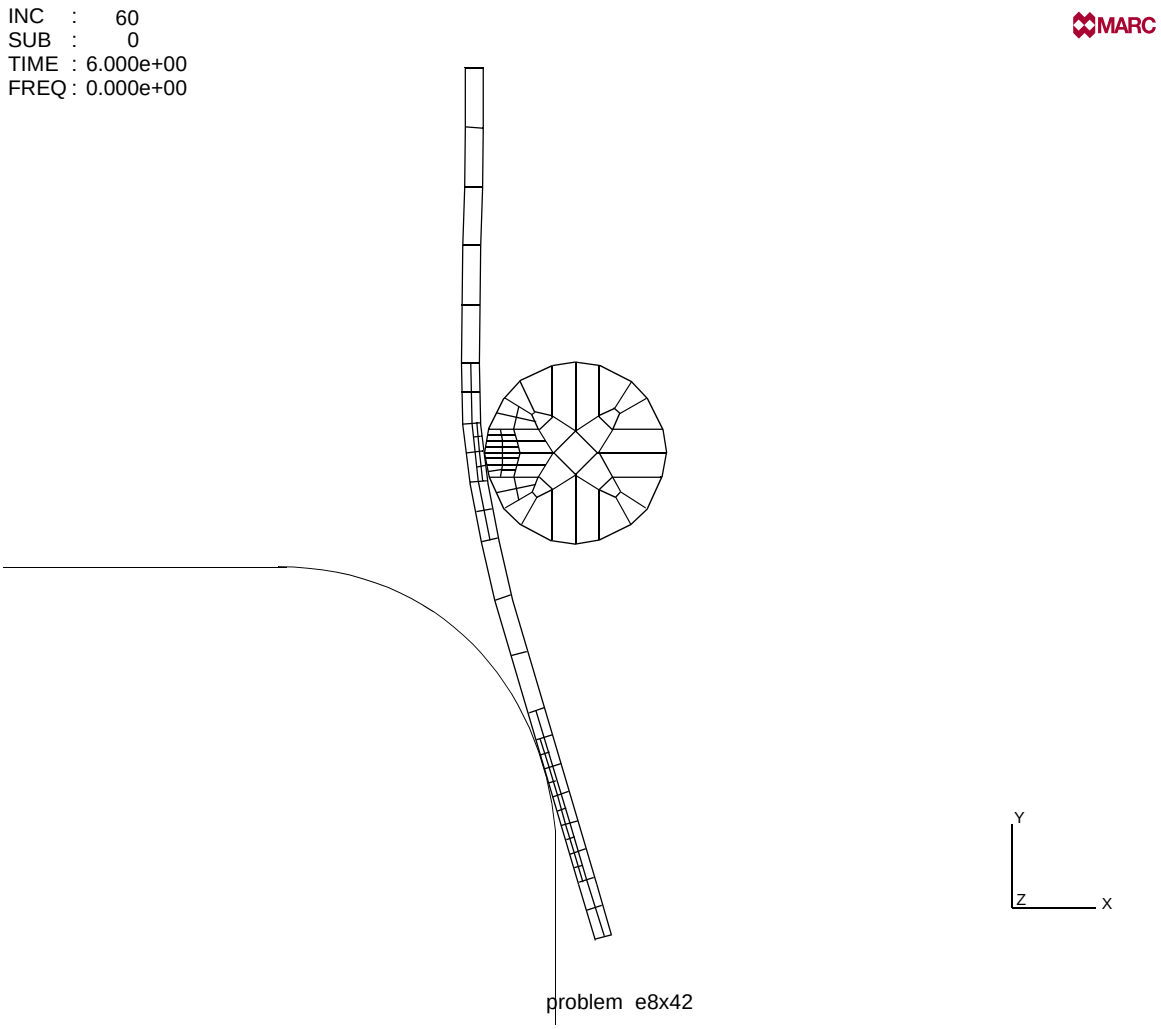

Figure 8.42-3 Deformed New Mesh at Increment 60

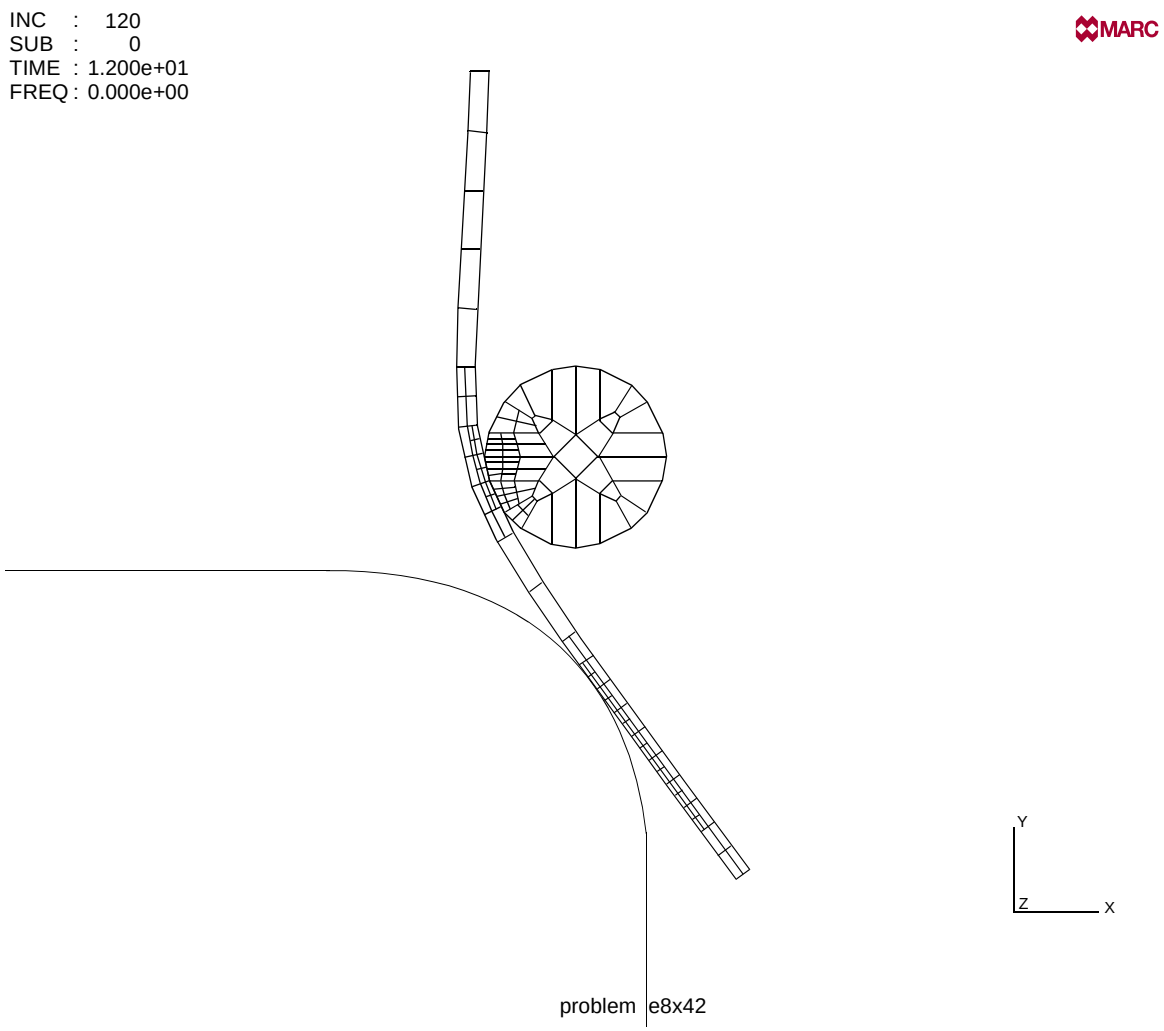

Figure 8.42-4 Deformed New Mesh at Increment 120

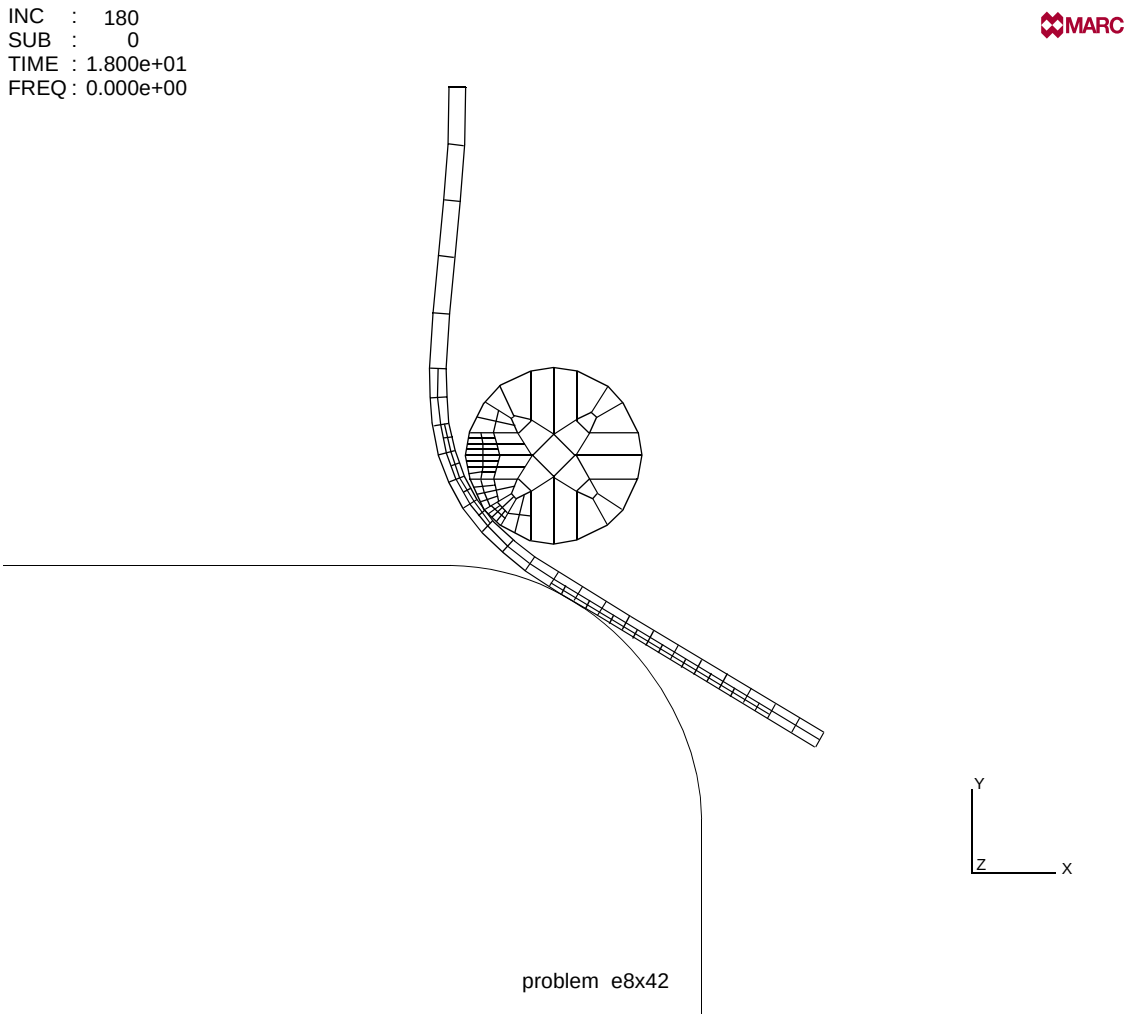

Figure 8.42-5 Deformed New Mesh at Increment 180

8.43 Rubber Seal Analysis using Adaptive Meshing

This problem demonstrates the use adaptive meshing in a nonlinear rubber analysis of a seal. In a nonlinear analysis, the mesh quality is checked at the end of each converged increment. If the mesh needs to be refined, this is performed before the beginning of the next increment. This model uses the Mooney material model. In the first analysis, the total Lagrange procedure is used. In the second and third analyses, the updated Lagrange procedure is used.

Hence, this problem is modeled using the three techniques summarized below.

Data Set	Element Type(s)	Number of Elements	Number of Nodes	Differentiating Features
e8x43	119	560	644	Total Lagrangian, reduced integration hourglass elements
e8x43b	10	560	644	Updated Lagrangian, full integration hourglass elements
e8x43c	116	560	644	Updated Lagrangian, reduced integration hourglass elements

Element

As the first analysis uses the total Lagrange approach, Herrmann elements are required. This example uses element type 119, a lower-order isoparametric axisymmetric element, using the modified Herrmann formulation. This element uses reduced integration with hourglass control. The four corner nodes have conventional displacement degrees of freedom with an additional degree of freedom representing the hydrostatic pressure. The original mesh was created using element type 82. The ALIAS option is used to convert element type 82 to element type 119.

In the second and third analyses, the updated Lagrange procedure is used and conventional displacement elements are used. Element type 10, a 4-node axisymmetric element, and element type 116, a 4-node axisymmetric reduced integration element, are used.

Model

The original model is shown in Figure 8.43-1 and consists of 560 elements and 644 nodes.

Material Properties

A two-term Mooney-Rivlin model is used with C_{10} = 0.3 N/cm^2 ; C_{01} = 0.04 N/cm^2.

Boundary Conditions

The region indicated in Figure 8.43-2 has prescribed displacement boundary conditions. In the first 8 increments, the tip of the seal is deflected 2 cm. In the next 12 increments, the tip is deflected an additional 3.0 cm. Additionally, a pressure load is placed on the region indicated which has a total magnitude of 0.25 N/cm^2. The AUTO LOAD option is used to specify that fixed increment sizes are to be used. The time step used by the contact procedure is 1 second.

Control

The PRINT, 5, 8 parameter is used to obtain additional information regarding the progress of contact. The Cuthill-McKee optimizer is used. The bandwidth is re-optimized when new elements are created due to the adaptive procedure or when self contact occurs in the seal. The CONTROL option specifies the maximum number of elements is 100 and the number of iterations is 10. Displacement convergence checking is used with a 10% tolerance. The initial stress stiffness terms are subjected to compressive behavior and neglecting these terms may prevent a nonpositive definite matrix from occurring.

Adaptive

Two adaptive criteria are used. The first indicates that elements should be refined when they come into contact. In this problem, the seal comes into self contact and elements on both surfaces are refined. The second criteria is based on the stress levels in the element. It implies subdivision of those elements whose stress is greater than 75% of maximum stress. This results in the subdivision of elements in the bend region.

Contact

There is one deformable body that can go into self contact. If contact occurs, the surfaces use a Coulomb friction with a coefficient of 0.3. To improve convergence, the body is not allowed to separate unless the force is greater than 100 N. Based on the size of the element, MARC chooses its own contact tolerance.

Results

Figure 8.43-3 shows the deformation after ten increments. The initial mesh refinement is due to the stress level. Figure 8.43-4 shows the deformation just as contact is to occur. The results at increment 19, Figure 8.43-5 for the total Lagrangian case and Figure 8.43-6 for the updated Lagrangian case, show that mesh refinement has occurred due to contact. Moreover, the deformations, as expected, are identical in the two cases. At the end of the analysis, the number of elements is 560 and the number of nodes is 716.

Parameters, Options, and Subroutines Summary

Example e8x43.dat:

Parameters	Model Definition Options	History Definition Options
ADAPTIVE	ADAPTIVE	AUTO LOAD
ALIAS	CONNECTIVITY	CONTINUE
DIST LOADS	CONTACT	CONTROL
ELEMENTS	COORDINATE	DISP CHANGE
END	DIST LOADS	DIST LOADS
FOLLOW FOR	END OPTION	TIME STEP
LARGE DISP	FIXED DISP	
PRINT	MOONEY	
SIZING	NO PRINT	
TITLE	OPTIMIZE	
	POINT LOAD	
	POST	

Example e8x43b.dat:

Parameters	Model Definition Options	History Definition Options
ADAPTIVE	ADAPTIVE	AUTO LOAD
ALIAS	CONNECTIVITY	CONTINUE
DIST LOADS	CONTACT	CONTROL
ELASTICITY	COORDINATE	DISP CHANGE
ELEMENTS	DIST LOADS	DIST LOADS
END	END OPTION	TIME STEP
FOLLOW FOR	FIXED DISP	
LARGE DISP	MOONEY	
PRINT	NO PRINT	
SIZING	OPTIMIZE	
TITLE	POINT LOAD	
	POST	

Example e8x43c.dat:

Parameters	Model Definition Options	History Definition Options
ADAPTIVE	ADAPTIVE	AUTO LOAD
ALIAS	CONNECTIVITY	CONTINUE
DIST LOADS	CONTACT	CONTROL
ELEMENTS	COORDINATE	DISP CHANGE
END	DIST LOADS	DIST LOADS
FOLLOW FOR	END OPTION	TIME STEP
LARGE DISP	FIXED DISP	
PRINT	MOONEY	
SIZING	NO PRINT	
TITLE	OPTIMIZE	
ELASTICITY	POINT LOAD	
	POST	

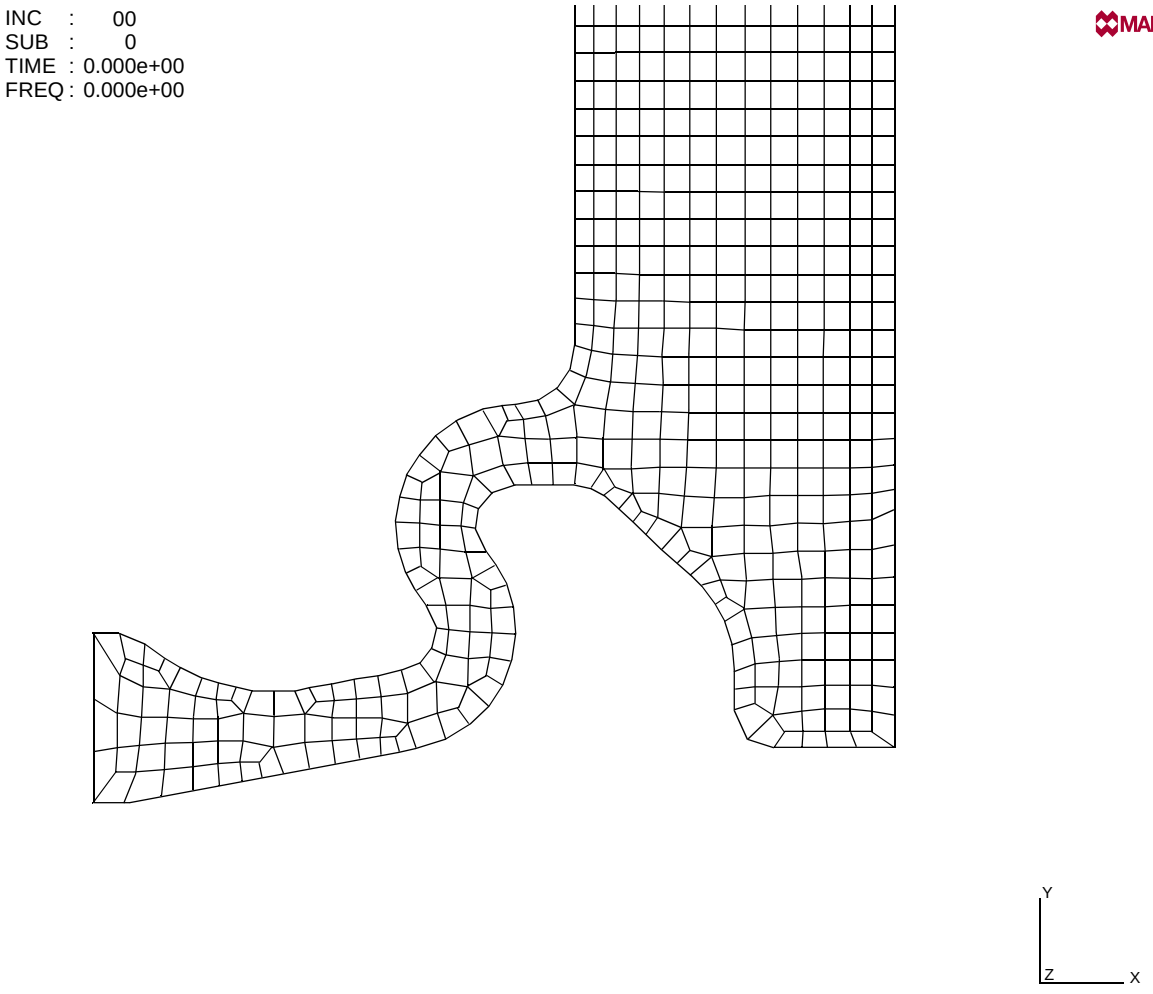

Figure 8.43-1 Close-up of Original Finite Element Mesh

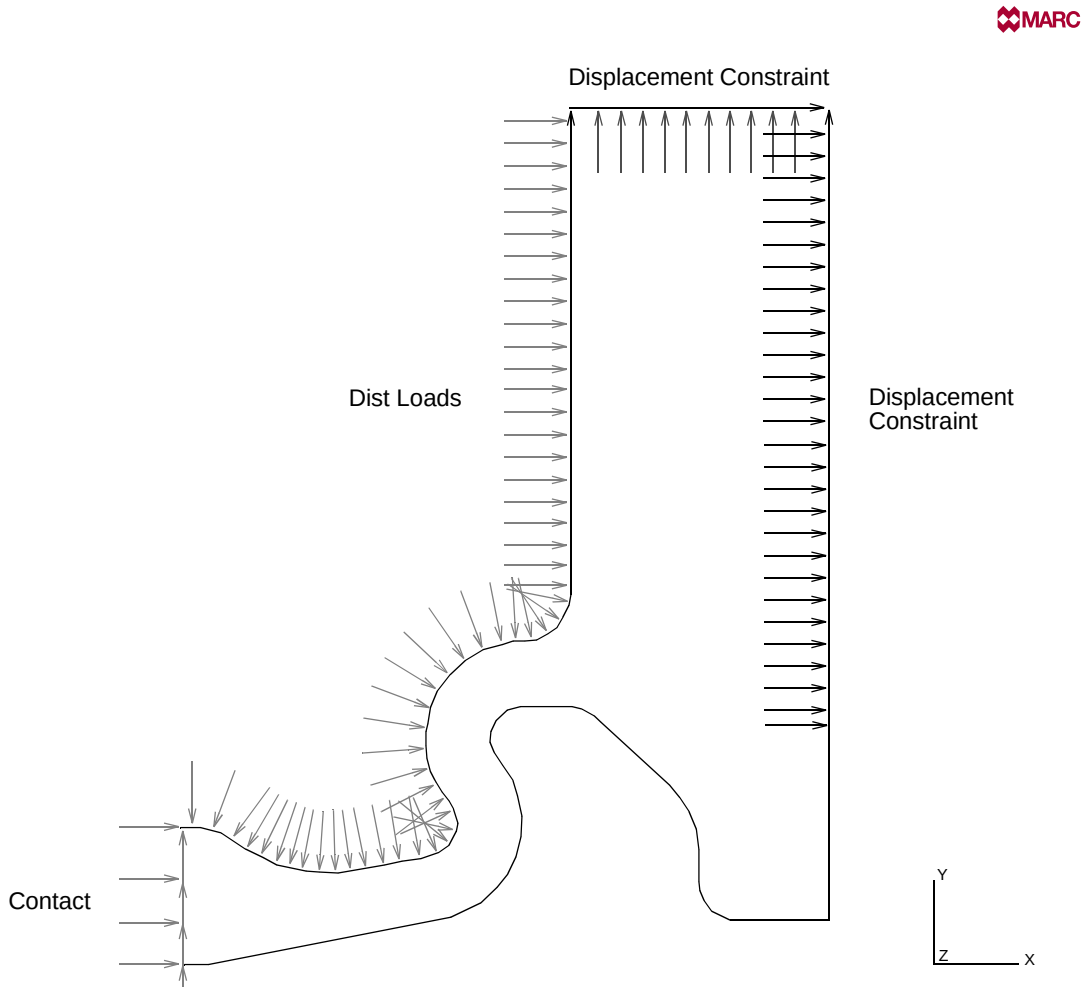

Figure 8.43-2 Seal with Prescribed Boundary Conditions

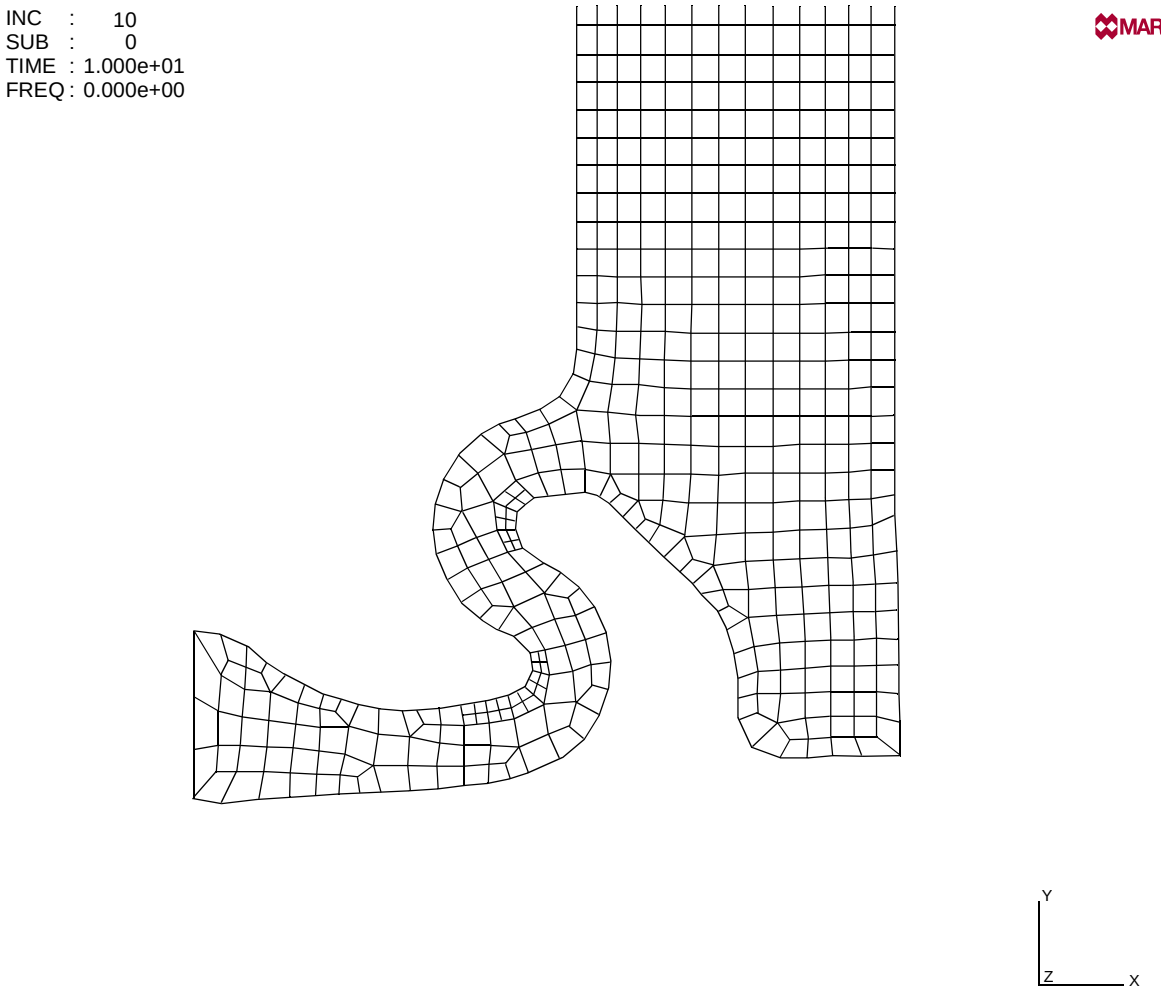

Figure 8.43-3 Deformed Mesh showing New Elements

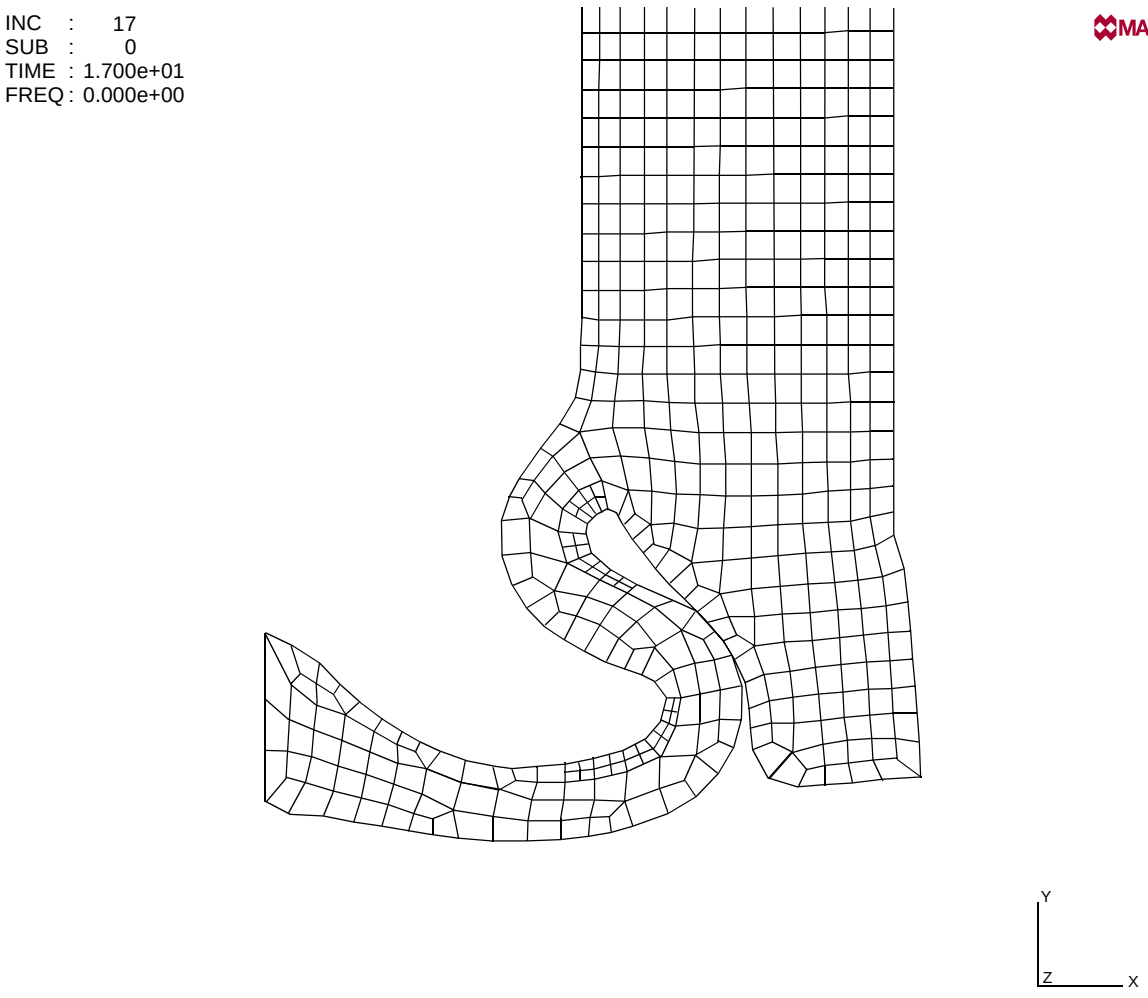

Figure 8.43-4 Deformed Mesh at Initial Contact

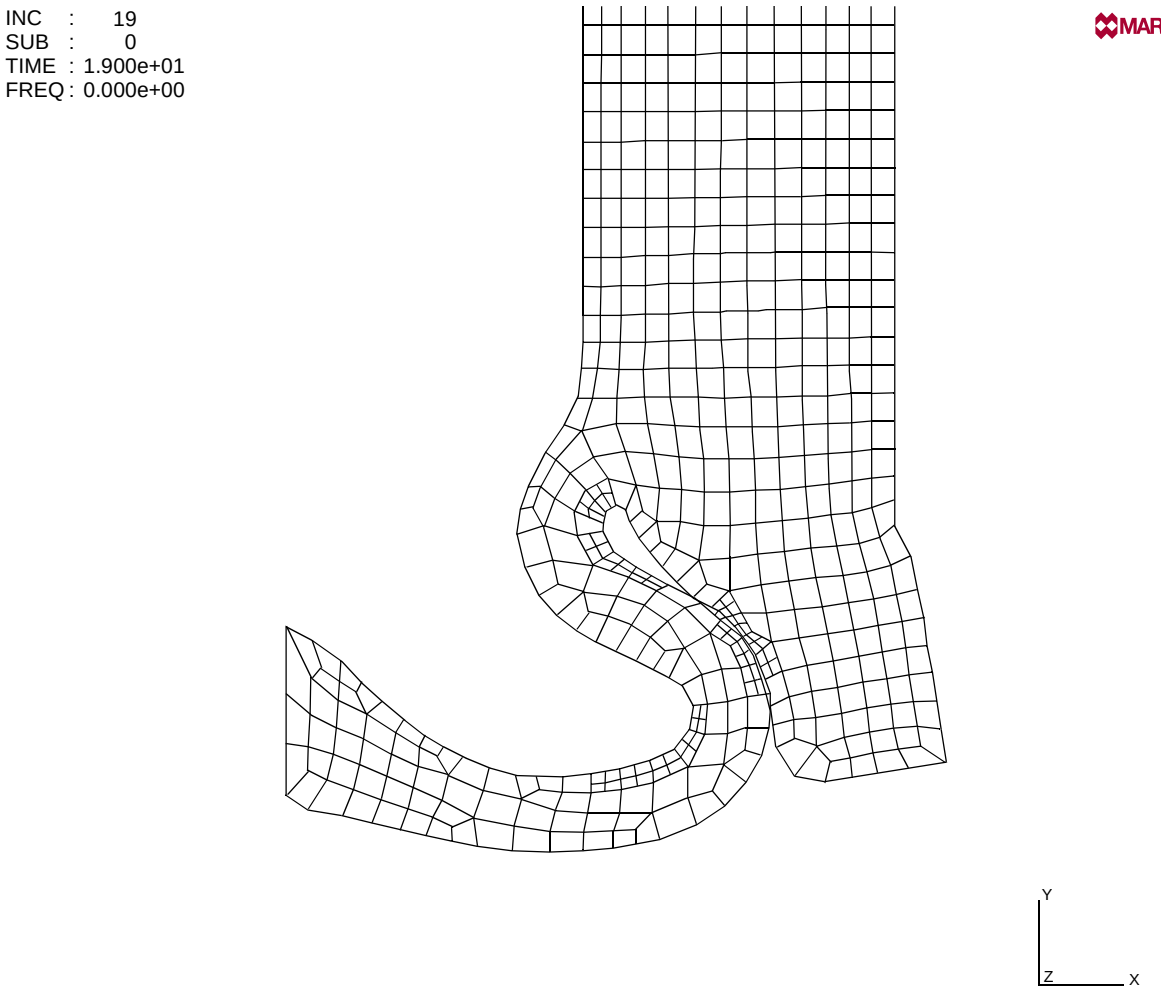

Figure 8.43-5 Adaptivity Due to Contact

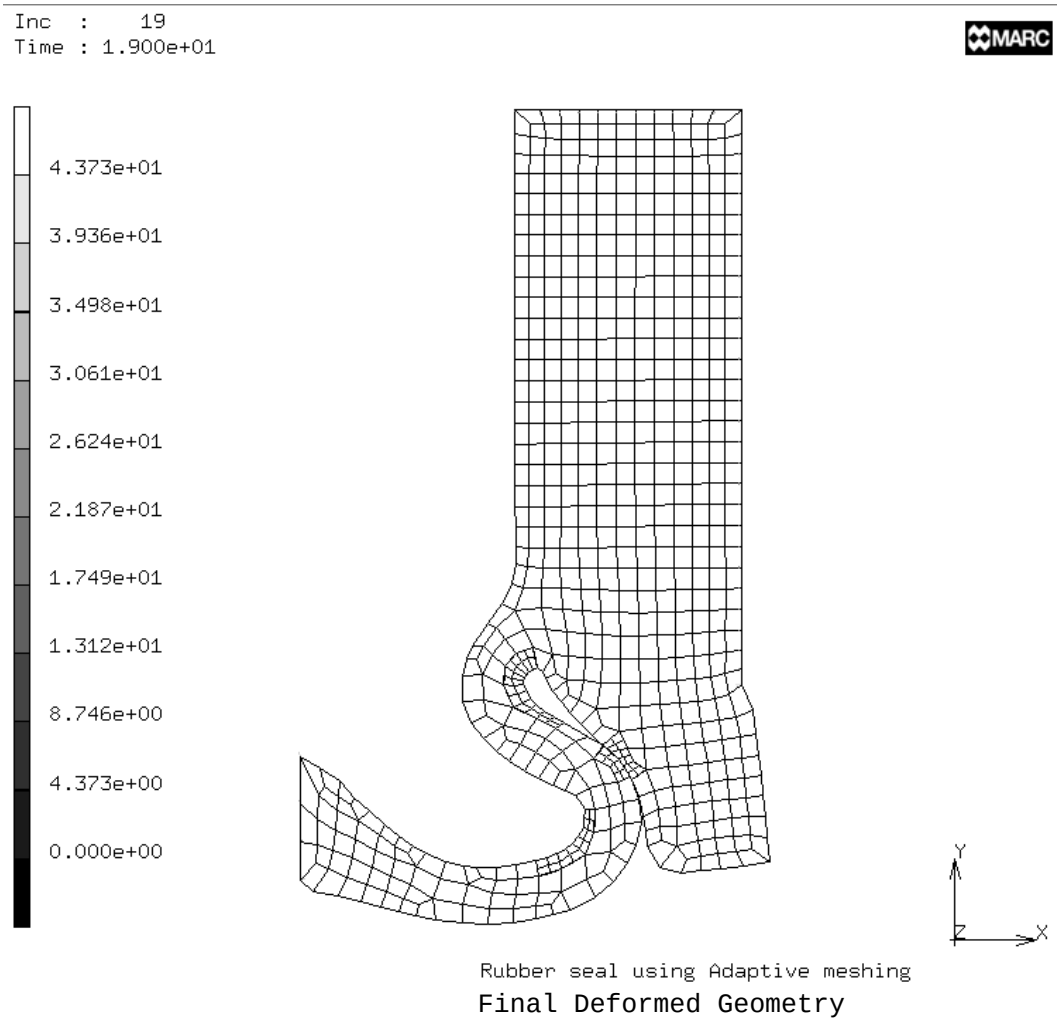

Figure 8.43-6 Adaptivity Due to Contact (Updated Lagrange Formulation)

8.44 Simplified Rolling Example with Adaptive Meshing

This problem demonstrates the use of adaptive meshing by simulating the rolling of sheet. The adaptive meshing capability in MARC allows you to selectively refine the mesh using various criteria. This example uses three different data sets (problems e8x44, e8x44b, and e8x44c). Each data set uses a different criterion for adaptive meshing. However, the maximum number of levels an element is adapted(subdivided) is set to 2 for all three data sets.

Data Set	Adaptive Meshing Criterion Used
e8x44	Subdivide an element if at least one of the nodes falls within the imaginary box: -3 < x <3 ; -100 < y < 100; -100 < z < 100
e8x44b	Subdivide an element if at least one of its nodes is in contact, or if it belongs to a segment that is contacted
e8x44c	Same as e8x44. In addition, if all nodes of an element leave the imaginary box, the already subdivided elements are merged together (unrefinement).

The initial model is the same for all three data sets.

Element

All three data sets use element 11, a 4-noded isoparametric plane strain element, to model the workpiece.

Model

The initial model for all three data sets is shown in Figure 8.44-1. The workpiece is 28 cm long and 1.025 cm thick. The roll radius is 64 cm and rotates at 1 radian/second. All three data sets employ 20 elements and 42 nodes to model the undeformed workpiece geometry. The number of nodes and elements change as the simulation proceeds due to the adaptive meshing processes of subdivision and merging.

Material Properties

The workpiece sheet is assumed to be made of high strength steel. The Young's modulus is 2.1×10^5 N/cm^2 and the Poisson's ratio is 0.30. The initial yield stress is 200 N/cm^2. The workhardening behavior is input using the WORK HARD DATA model definition option.

Geometry

The sheet is assumed to have a thickness of 1 unit. To model the incompressibility of the workpiece material, the constant dilatation option is chosen in the GEOMETRY model definition option.

Boundary Conditions

The model is assumed to be symmetric about the plane y = 0. Thus, all y displacements are set to zero on the surface y = 0.

Contact

There are three contact bodies in this model, the deformable workpiece (Body 1), the roller (Body 2), and the ram (Body 3) which pushes the workpiece into the roll gap. To enable efficient contact computations, the CONTACT TABLE option is used. This option details that Body 1 is allowed to contact only Body 2 and Body 3. This is because this problem will not realistically result in self contact of the deformable workpiece with itself.

Body 2 has its center of rotation at [-5.9,64.775]. It is modeled a circular arc with 60 divisions. A friction coefficient of 0.10 is chosen for this body. Friction forces are based on the nodal contact forces.

Body 3 is modeled as a single straight line segment.

History Definition

The motion of the workpiece through the roll gap is modeled by defining a velocity for the contact bodies using the MOTION CHANGE history definition option. The roll is subjected to a constant angular velocity while the ram pushes the workpiece into the roll gap.

In the first 15 increments, the roll is subjected to an angular velocity of 1 radian/second (approximately 57.3 degrees/second). To avoid any slipping between the workpiece and the roll at entry, the ram is given a linear velocity identical to the linear velocity at the tip of the roll ($v = r \omega$) of -64 cm/second.

At the end of 15 increments, the ram is removed from the system using the RELEASE option for Body 3. For all subsequent increments, the ram is given a positive velocity of 20 cm/second in the x direction and moves continuously opposite the direction of motion of the workpiece motion.

The CONTACT TABLE option is also redefined to exclude Body 3 from any further contact checking calculations. For the reminder of the simulation, the roll continues to rotate and the friction between the roll and workpiece draws the workpiece further into the roll gap.

For data sets e8x44 and e8x44c, 140 further increments are taken. For data set e8x44b, 80 further increments are employed.

Control

This analysis uses displacement control with a tolerance of 10%. A maximum of 25 iterations are chosen for each increment to converge.

Adaptive Meshing

The adaptive meshing procedure is used to create more elements in areas of high deformation. The three data sets employ different criteria. The imaginary box used for data sets e8x44 and e8x44c is indicated in Figure 8.44-2. This box encloses the roll gap region, which can be expected to be the area where the workpiece undergoes maximum deformation.

Results

For the data set e8x44, the deformed mesh at increments 48, 75 and 100 are shown in Figure 8.44-3 through Figure 8.44-5. Comparing Figure 8.44-1 and Figure 8.44-3, it can be seen that the adaptive process has created more elements by subdividing elements that entered the imaginary box specified. However, the subdivided elements have not been merged together after exiting the roll gap. This merging option is shown by the results of e8x44c.

Figure 8.44-6 through Figure 8.44-8 shows the results for data set e8x44b. The adaptive process is shown to create elements upon contact. Figure 8.44-6 shows the deformed and adapted mesh at increment 3. New elements have been created at both the ram and roll contact elements. Figure 8.44-7 shows the deformed mesh at increment 50. The elements subdivided at contact bodies are shown to be not merged together after exiting the contact bodies. Figure 8.44-8 shows the adapted mesh at increment 80 for data set e8x44b.

Figure 8.44-9 through Figure 8.44-12 shows the adaptive process with the option for elements to be merged (data set e8x44c). Figure 8.44-9 shows the adaptive process doing both the subdivision of elements inside the imaginary box and the merging of elements that have exited the imaginary box at increment 48. Figure 8.44-10 shows the deformed mesh at increment 75. Figure 8.44-11 shows the deformed mesh at increment 100. Finally, Figure 8.44-12 shows the final mesh at increment 155. Figure 8.44-9 may be contrasted against Figure 8.44-3. Figure 8.44-10 may be contrasted against Figure 8.44-4. Figure 8.44-11 may be contrasted against Figure 8.44-5.

Parameters, Options, and Subroutines Summary

Example e8x44.dat, e8x44b.dat, and e8x44c.dat:

Parameters	Model Definition Options	History Definition Options
ADAPTIVE	ADAPTIVE	AUTO LOAD
ELEMENTS	CONNECTIVITY	CONTACT TABLE
END	CONTACT	CONTINUE
FINITE	CONTACT TABLE	CONTROL
LARGE DISP	CONTROL	MOTION CHANGE
PRINT	COORDINATE	RELEASE
SIZING	END OPTION	TIME STEP
TITLE	FIXED DISP	
UPDATA	GEOMETRY	
	ISOTROPIC	
	NO PRINT	
	POST	
	RESTART	
	WORK HARD	

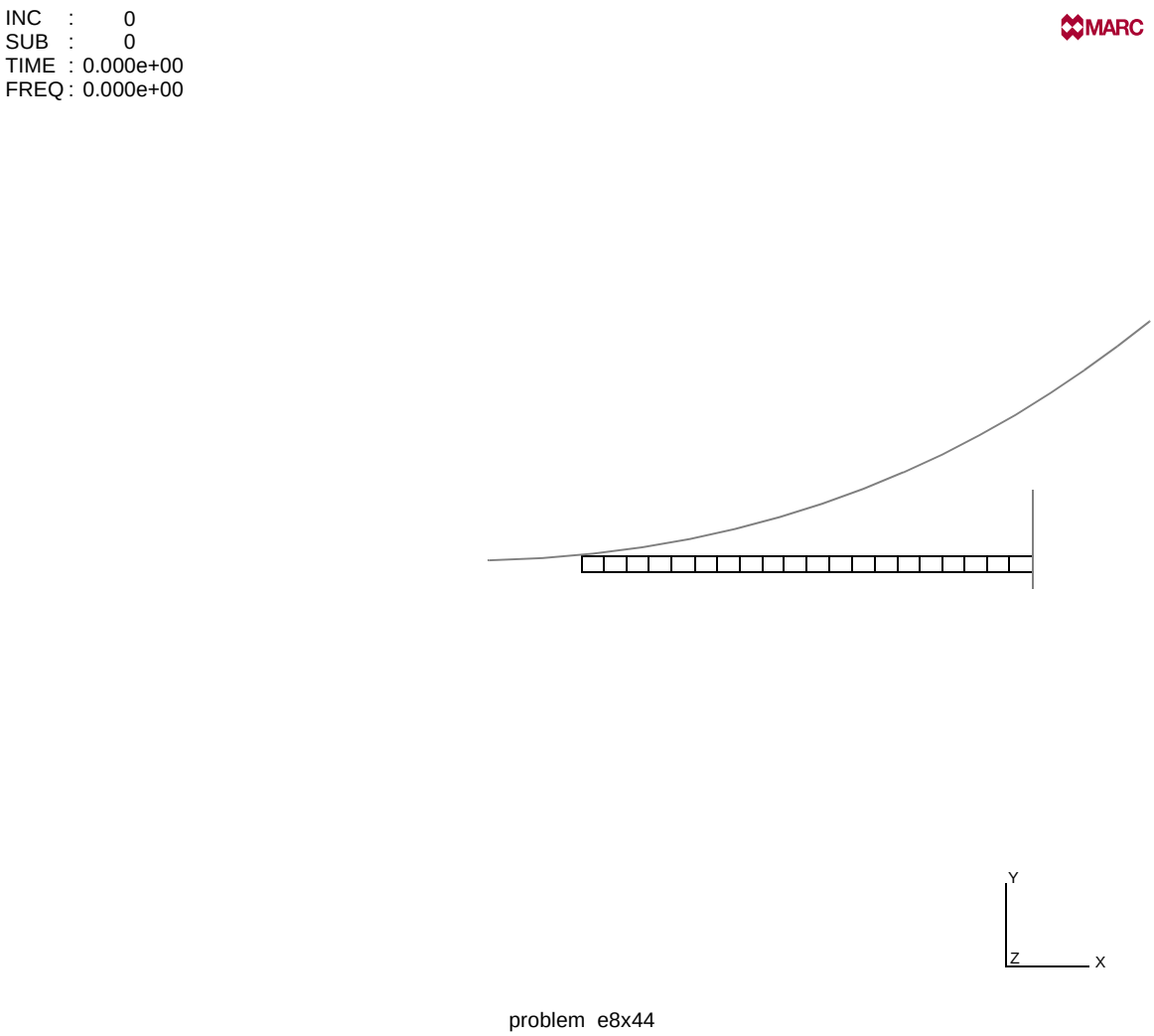

Figure 8.44-1 Original Finite Element Mesh for all 3 Data Sets

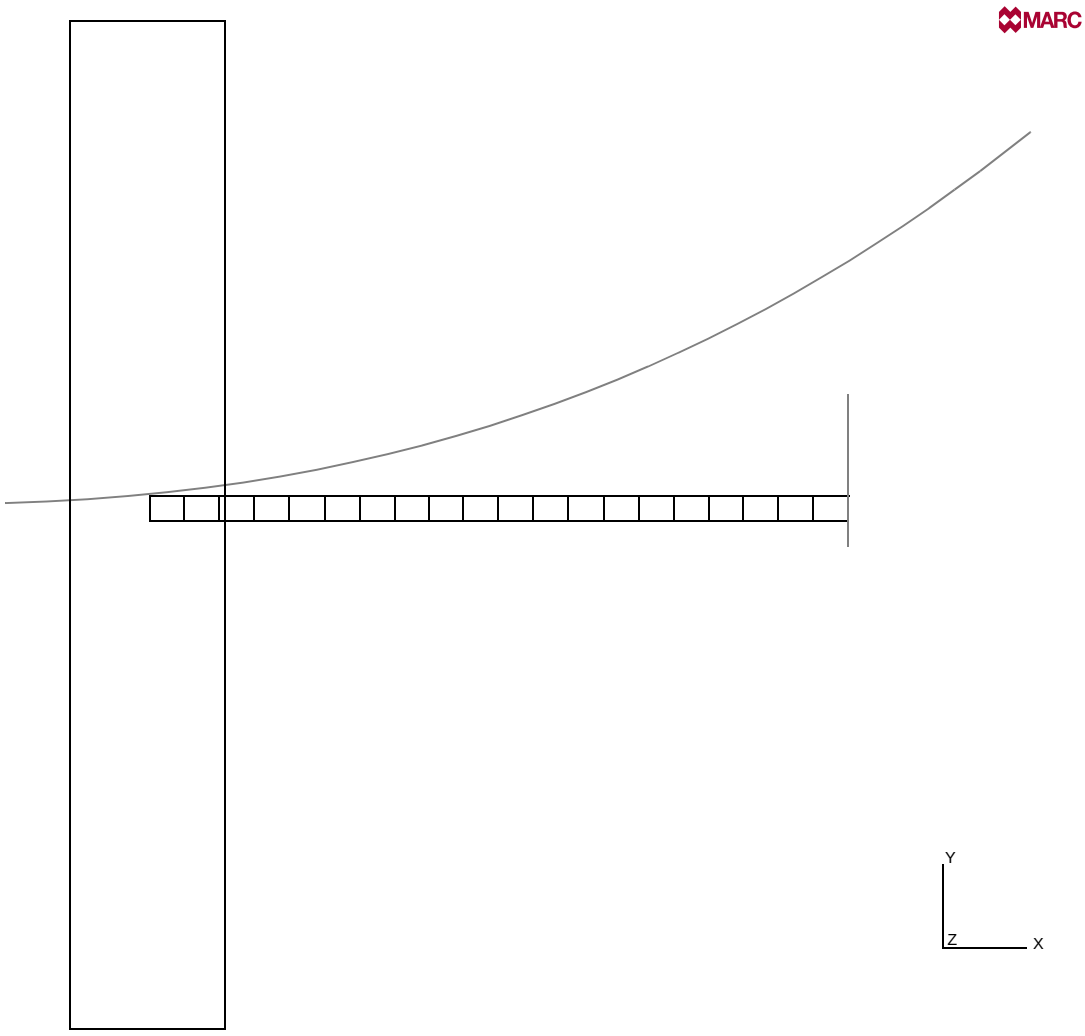

Figure 8.44-2 Adaptive Criteria Box for Data Set e8x44 and e8x44c

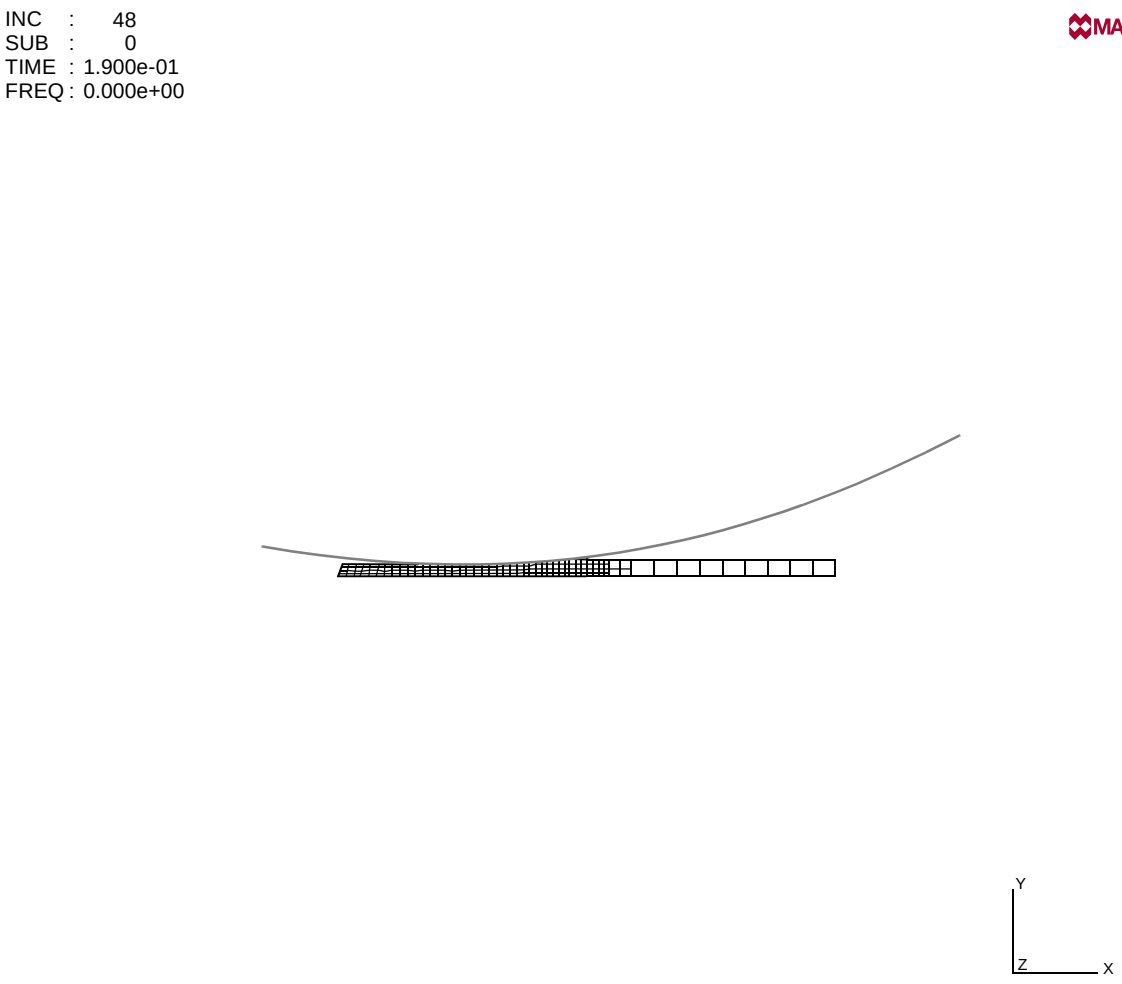

Figure 8.44-3 Deformed Mesh at Increment 48 for Data Set e8x44

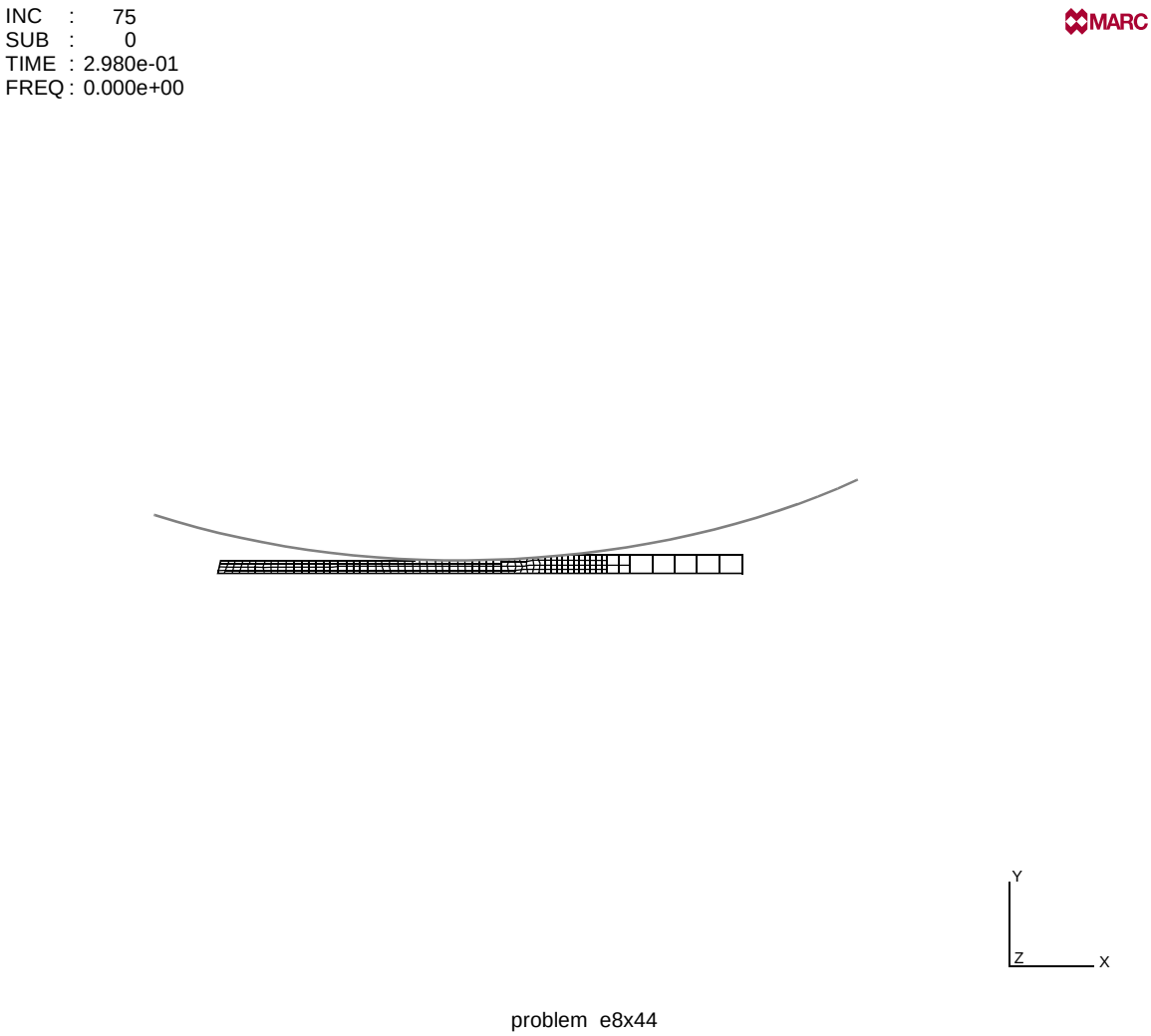

Figure 8.44-4 Deformed Mesh at Increment 75 for Data Set e8x44

INC : 100
SUB : 0
TIME : 3.980e-01
FREQ : 0.000e+00

MARC

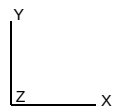

problem e8x44

Figure 8.44-5 Deformed Mesh at Increment 100 for Data Set e8x44

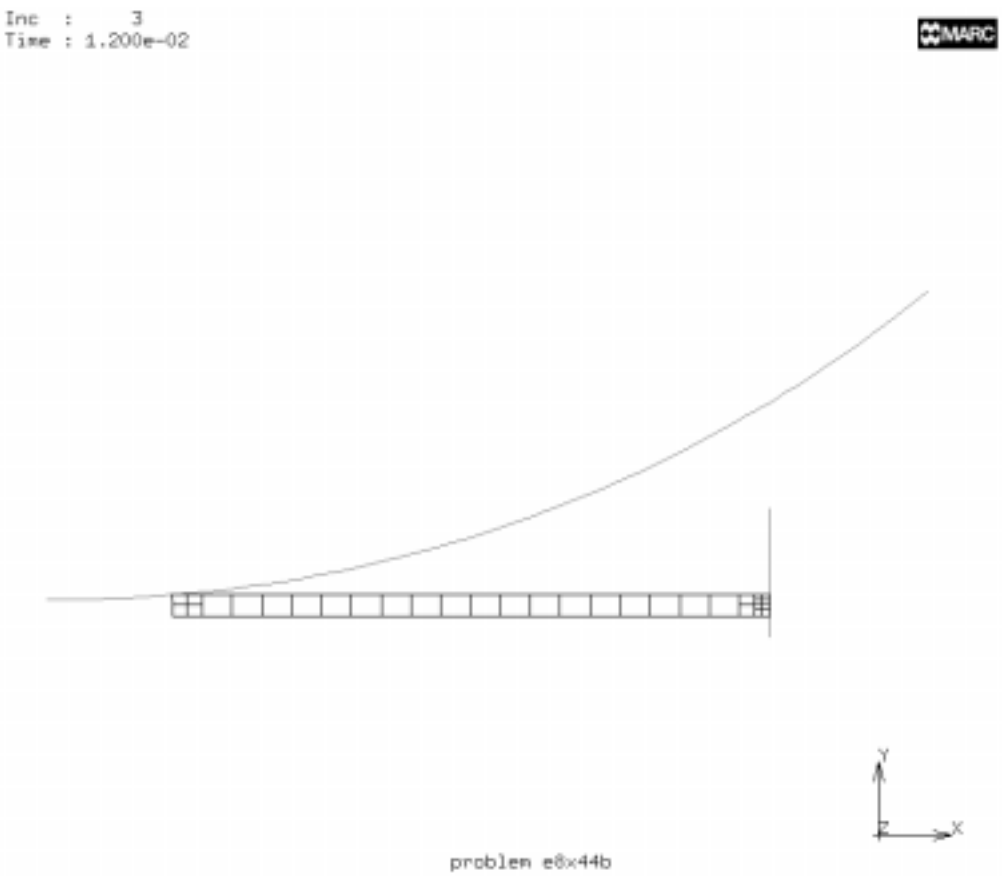

Figure 8.44-6 Deformed Mesh at Increment 3 for Data Set e8x44b

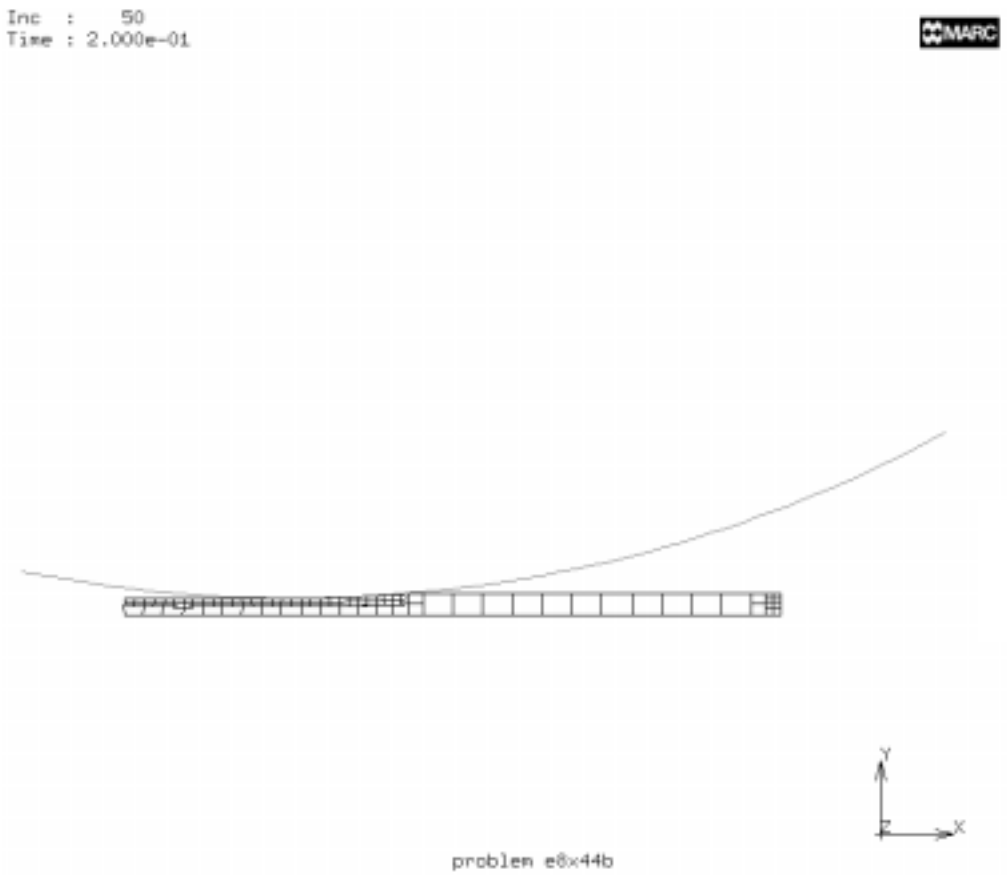

Figure 8.44-7 Deformed Mesh at Increment 50 for Data Set e8x44b

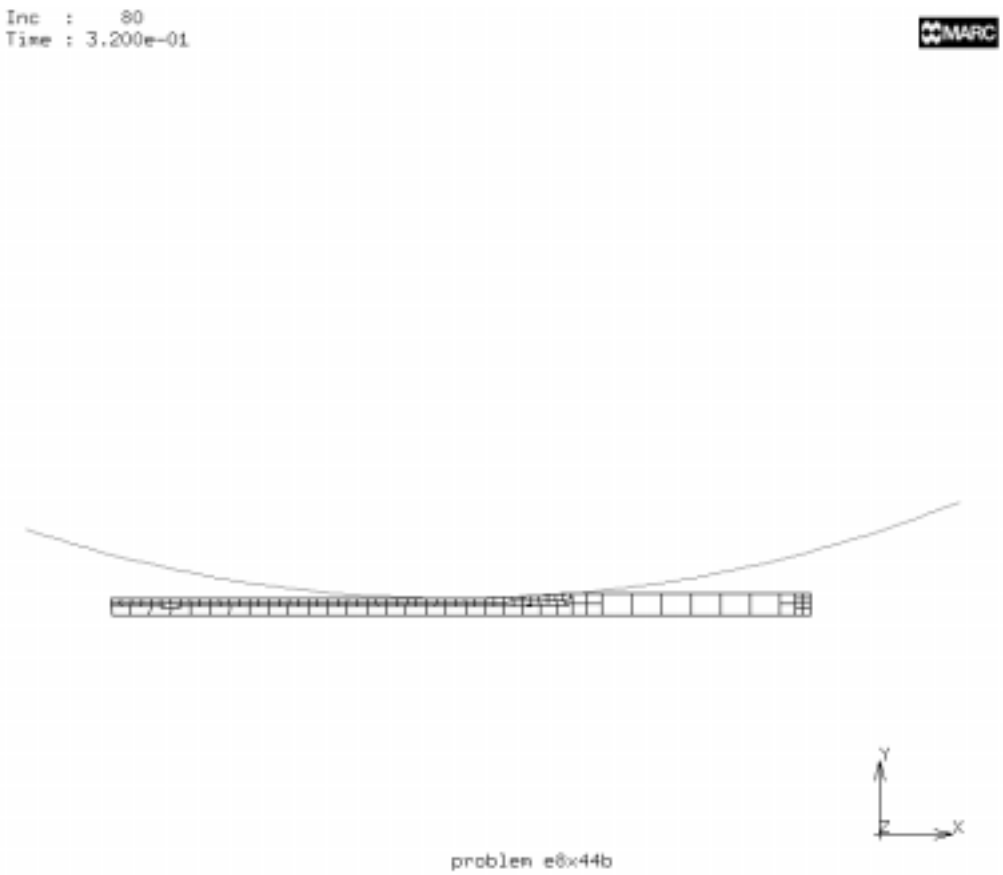

Figure 8.44-8 Deformed Mesh at Increment 80 for Data Set e8x44b

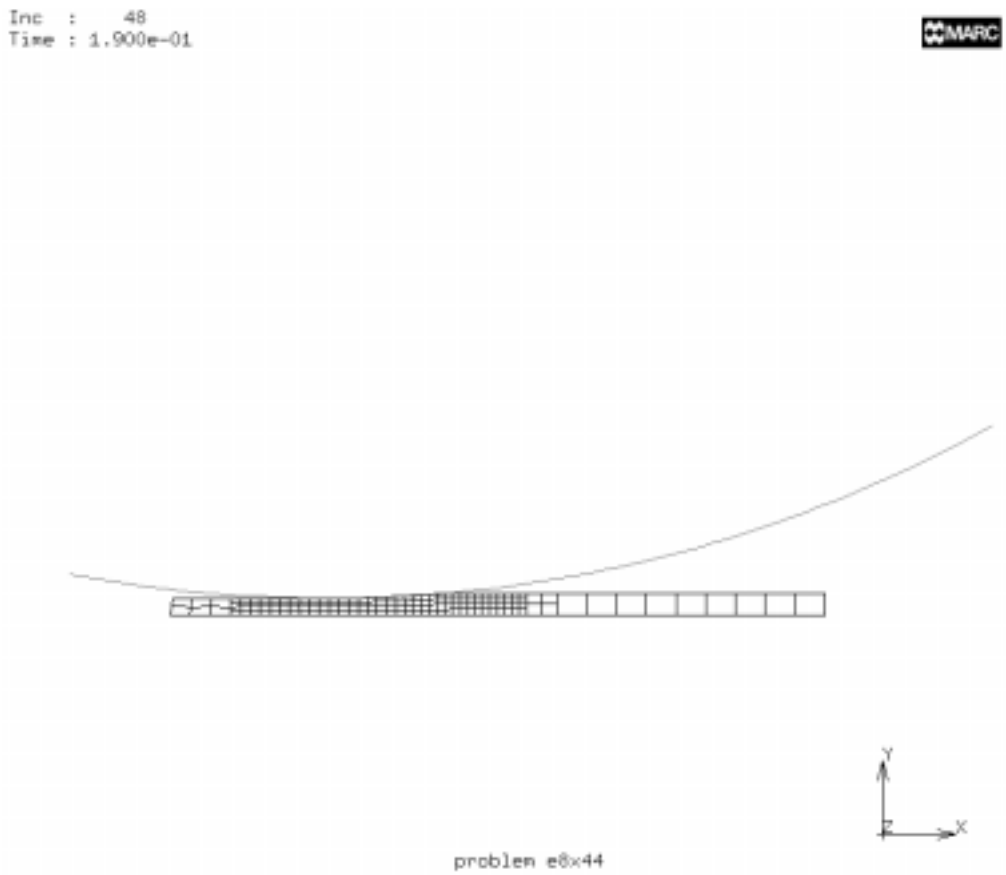

Figure 8.44-9 Deformed Mesh at Increment 48 for Data Set e8x44c

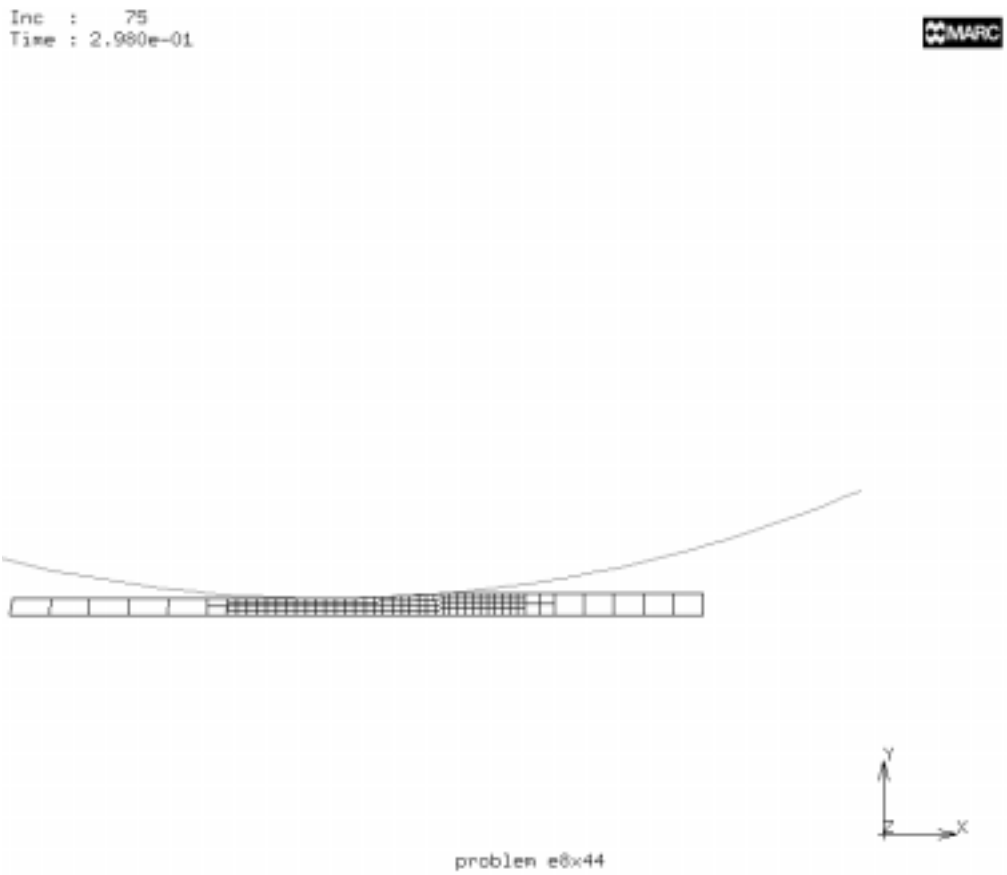

Figure 8.44-10 Deformed Mesh at Increment 75 for Data Set e8x44c

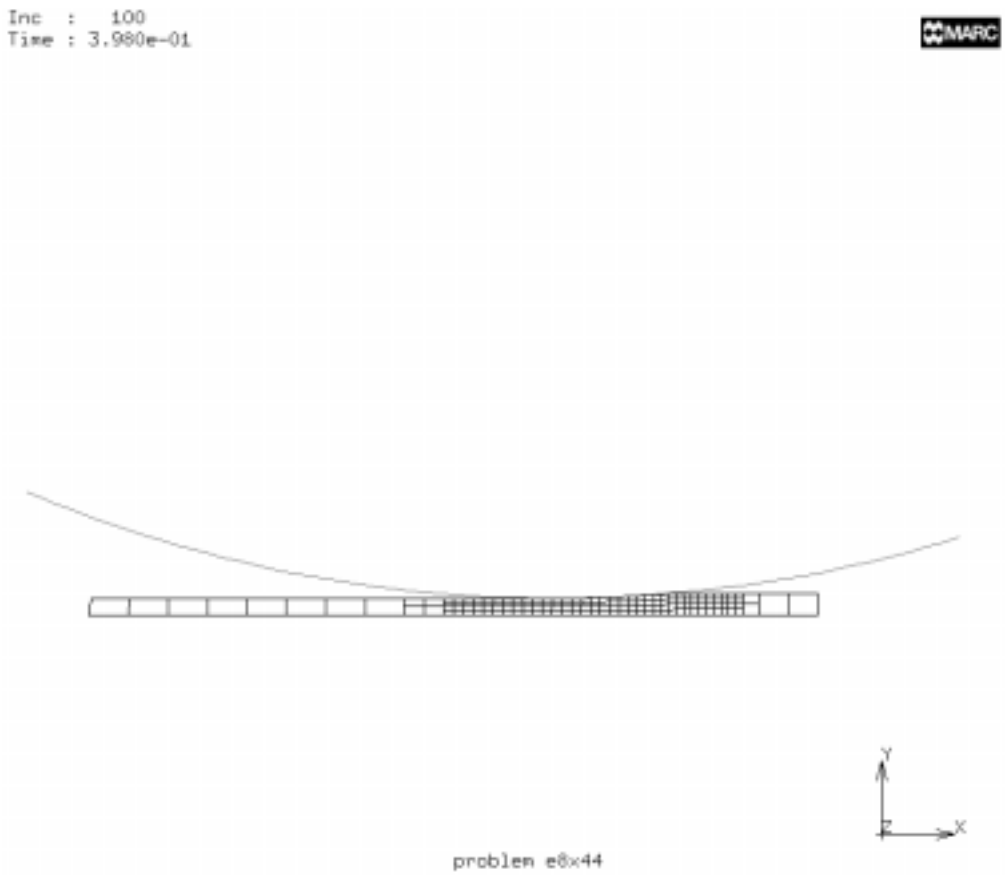

Figure 8.44-11 Deformed Mesh at Increment 100 for Data Set e8x44c

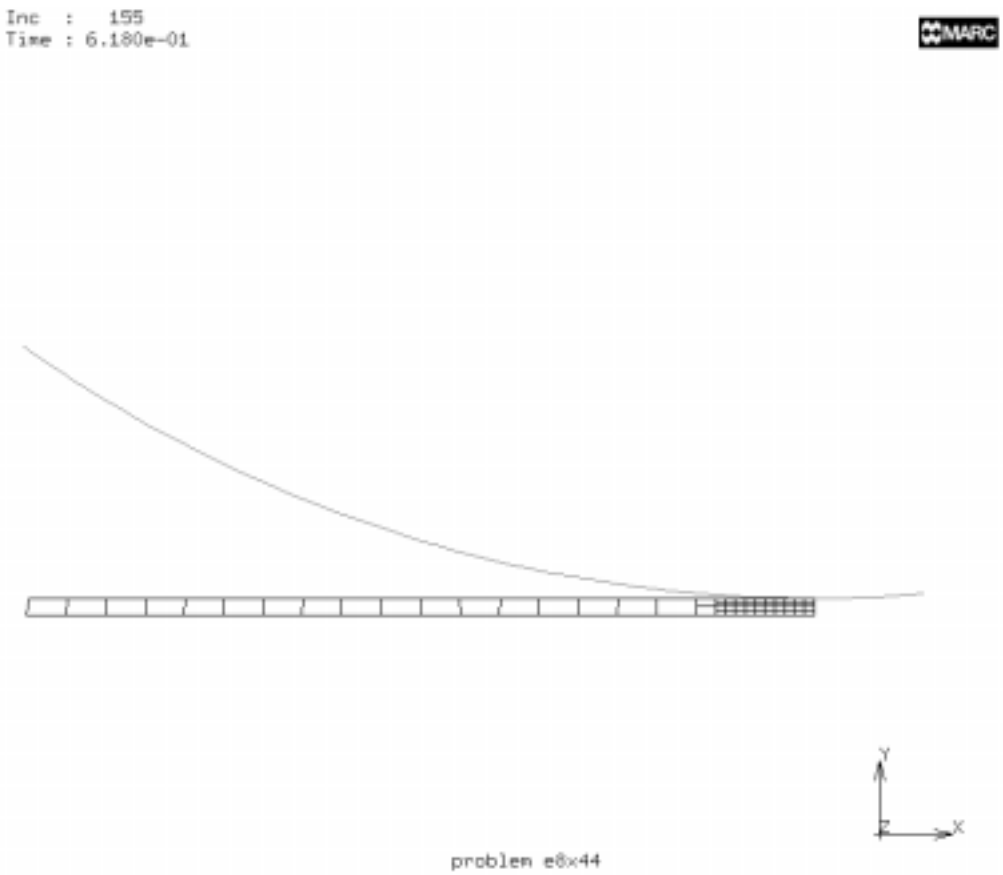

Figure 8.44-12 Deformed Mesh at Increment 155 for Data Set e8x44c

8.45 Use of the SPLINE Option for Deformable-Deformable Contact

This problem demonstrates the use of the SPLINE option in the simulation of problems involving deformable-to-deformable contact of bodies. In many cases, the accuracy of results in problems involving deformable-to-deformable contact depends on smoothness of the contact bodies can be defined, e.g. circular shafts. The SPLINE option can be used for 2D and 3D problems. This example illustrates a 2D plane strain case.

The geometry of the problem is shown in Figure 8.45-1. The model consists of two annular rings, each at a different temperature. The outer ring is hotter than the inner ring and gradually cools down to reach the temperature of the inner ring in five increments. The outer and inner rings are modeled as deformable bodies. The SPLINE option is applied to these two deformable bodies.

Element

Due to symmetry only a quarter of the rings are modeled using the isoparametric 4-noded element number 11. Elements 1 to 80 comprise the inner ring while elements 81 to 160 make up the outer ring. There are a total of 160 elements and 210 nodes in this model. The model is shown in Figure 8.45-2.

Material Properties

The deformable bodies have the same material properties. The Young's modulus is 2.1×10^6 GPa, and the Poisson's ratio is 0.33. The initial density is 1 Kg/m^3. The coefficient of thermal expansion in 10^{-4}/° C.

Boundary Conditions

Symmetry is enforced by the definition of rigid symmetry bodies along the x = 0 and y = 0 plane.

Initial State

The initial temperatures of the two bodies are defined using the INITIAL STATE option. The outer ring has an initial temperature of 200° C, while the inner ring has an initial temperature of 20° C.

Contact

There are four contact bodies defined in this problem. Contact body 1 is the outer ring. Contact body 2 is the inner ring. Both these contact bodies are deformable and the SPLINE option is used to represent their outer surfaces. Contact body 3 is the rigid symmetry surface defining x = 0.

Contact body 4 is the rigid symmetry surface defining y = 0. An analytical form of these rigid surfaces are used by the appropriate choice of the CONTACT option. There is no friction assumed in the model.

Spline

The SPLINE option is used for the deformable contact bodies 1 and 2. The SPLINE option enables an exact definition of the normal. But for some nodes, a unique normal does not exist. The outer ring (Contact body 1) has four nodes: 106, 126, 210, and 190 at which the normal is not defined. Similarly, the inner ring (Contact body 2) has four nodes: 1, 21, 105, and 85 at which the normal to the curve is not defined. Such nodes must be excluded from the definition of the SPLINE option. This is done using the appropriate choice in the SPLINE option.

Post

The post file has output written for the equivalent or von Mises stress.

History Definition

The initial temperature of the outer ring is 200° C. The initial temperature of the inner ring is 20° C. The outer ring is cooled to equal the temperature of the inner ring in five increments. Thus, each increment cools the outer ring by 36° C. The inner ring is maintained at a constant temperature during the simulation. As the outer ring cools, it contracts and presses inward radially on the inner ring. This is the mode of deformation for the problem. The CHANGE STATE option prescribes the temperature change for the outer ring.

Control

The residual tolerance is set to 0.01. Ten iterations are made for each increment.

Results

The use of the SPLINE option results in a good solution for the problem. Figure 8.45-3 shows contours of the equivalent von Mises stress. These contours are seen to be axisymmetric. Even if the nodes on the outside surface of the inner ring do not lie coincident with the nodes of the inside surfaces of the outer ring, the SPLINE option will ensure correct results at the contact surface. Not employing the SPLINE option in such cases, may result in inexact results in contact regions.

Parameters, Options, and Subroutines Summary

Example e8x45.dat:

Parameters	Model Definition Options	History Definition Options
ALL POINTS	CHANGE STATE	AUTO LOAD
ELEMENTS	CONNECTIVITY	CHANGE STATE
END	CONTACT	CONTINUE
EXTENDED	CONTROL	MOTION CHANGE
LARGE DISP	COORDINATES	TIME STEP
SETNAME	INITIAL STATE	
SIZING	OPTIMIZE	
TITLE	POST	
	SOLVER	
	SPLINE	

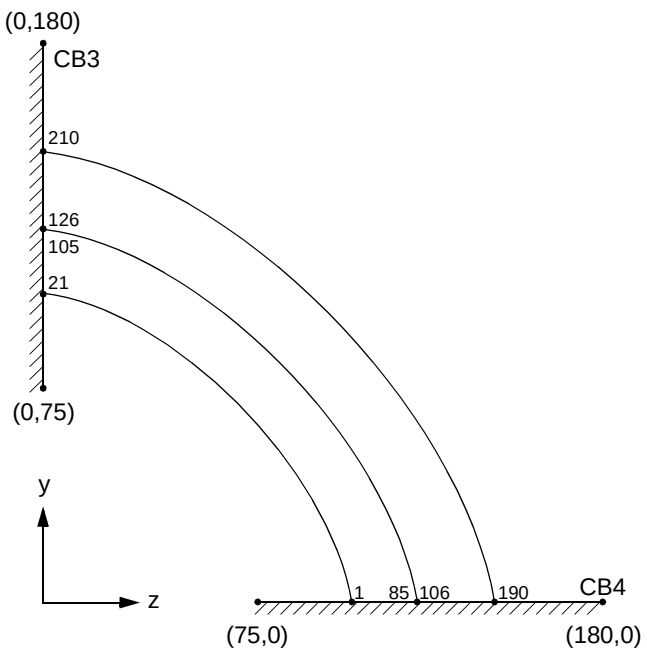

Figure 8.45-1 Geometry for Problem 8.45 to show the SPLINE Option

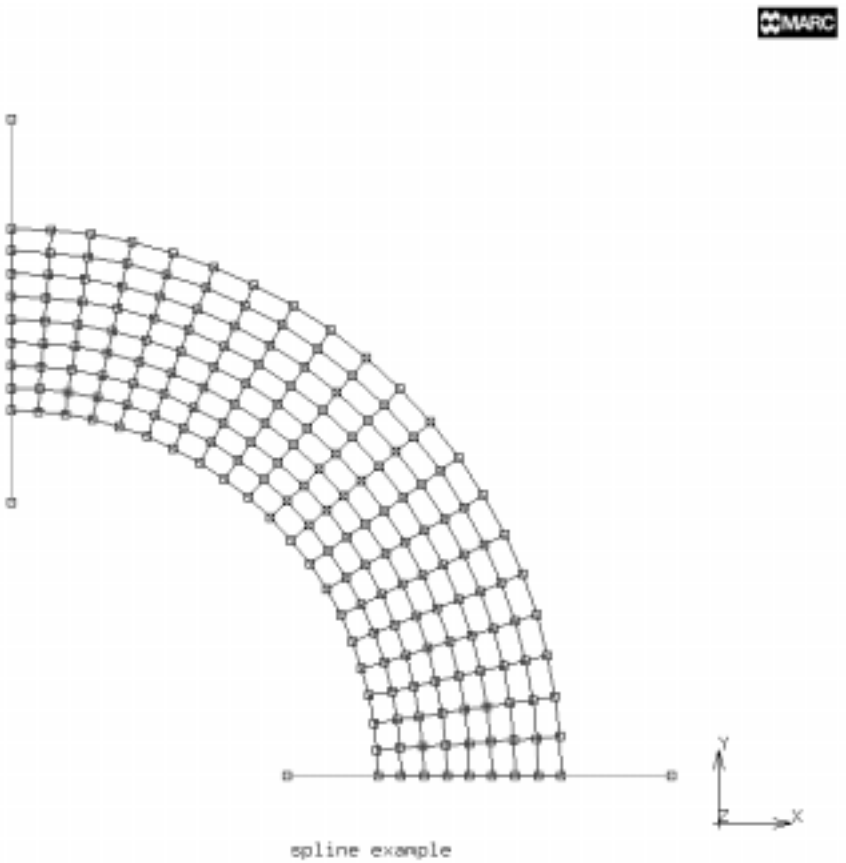

Figure 8.45-2 Initial Model for this Example

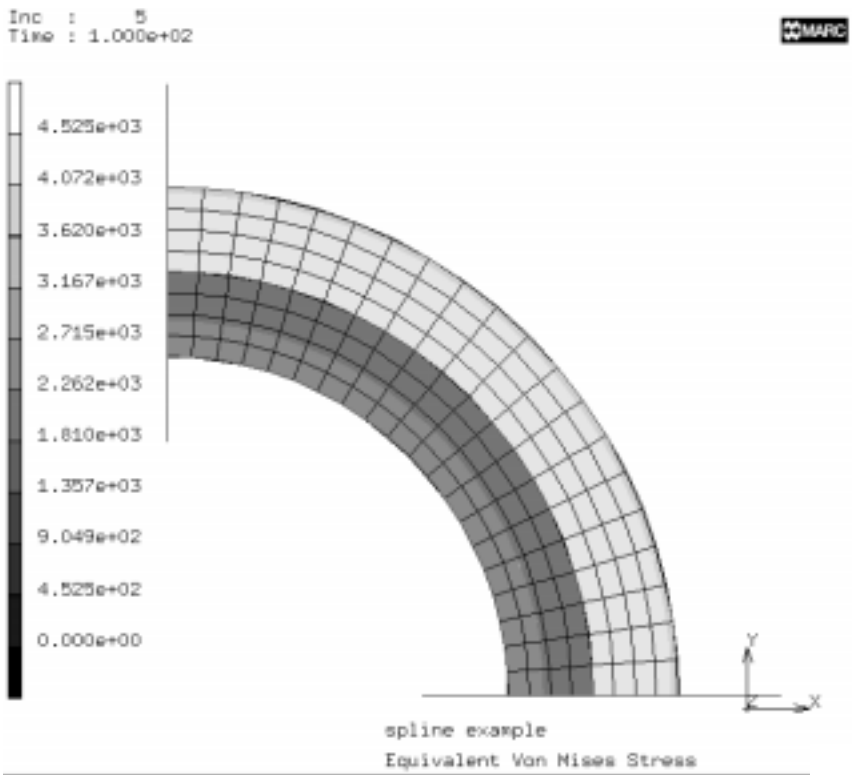

Figure 8.45-3 Contours of Effective von Mises Stress

8.46 Use of the EXCLUDE Option for Contact Analysis

This example shows the use of the EXCLUDE option for contact analysis. The EXCLUDE option is used in contact problems when you can, a priori, specify nodes which define certain segments that can be excluded from the contact calculations. This feature is especially helpful when there are sharp corners in a contact body or you want to restrict the motion of the body.

This example consists of three contact bodies. The initial model is shown in Figure 8.46-1. There are 12 elements and 27 nodes in the model. The elements associated with each contact body are given below.

Contact Body Number	Elements
1	1, 2, 3, 4
2	5, 6, 7, 8
3	9, 10, 11, 12

It can be seen that there are three segments here that can be excluded by you from the contact analysis. Each segment is defined by two nodes. Node 27 of Contact body 1 may slide along the segment defined by nodes 6 and 18 or along the segment defined by 6 and 19. However, it is physically unreasonable to expect that the node 27 may actually slide along the segment defined by nodes 6 and 19. Hence, you can EXCLUDE the segment defined by nodes 6 and 19 of Contact body 2. Similarly, once Contact body 1 slides down further, it would be better to exclude the segment defined by nodes 3 and 15 of Contact body 2, and the segment defined by nodes 25 and 26 of Contact body 3. Of course, if contact bodies 2 and 3 would be a single contact body, excluding the segments (3 & 5 or 25 & 26) would not be necessary.

Element

The 4-noded isoparametric plane stress quadrilateral element number 3 is used. There are 12 elements and 27 nodes in this model as shown by Figure 8.46-1.

Material Properties

All three contact bodies have identical isotropic material properties. The Young's modulus is 1×10^5 N/m^2. The Poisson's ratio is 0.30.

Boundary Conditions

To restrain the rigid body modes, nodes 1, 21, 24, 2, 16, and 5 are prescribed to have zero x and y displacements.

Contact

There is no friction used in this example. The CONTACT TABLE model definition option is used to expedite the CONTACT calculations.

Control

Ten iterations are chosen as a maximum for each increment. The residual tolerance is set to 0.10.

Loading

The loading consists of a distributed load on elements 3 and 4 pointing in the negative y direction. Displacements of 5.5×10^{-2} units are applied in each increment along the negative x direction on nodes 8 and 13 using the DISP CHANGE history definition option. A total of ten increments are applied using the AUTO LOAD history definition option.

Results

The final deformed shape configuration at the end of 10 increments is shown in Figure 8.46-2.

Parameters, Options, and Subroutines Summary

Example e8x46.dat:

Parameters	Model Definition Options	History Definition Options
ALL POINTS	CONNECTIVITY	AUTO LOAD
DIST LOADS	CONTACT	DISP CHANGE
ELEMENTS	CONTACT TABLE	DIST LOADS
EXTENDED	COORDINATES	TIME STEP
LARGE DISP	EXCLUDE	
PRINT	FIXED DISP	
SIZING	ISOTROPIC	
TITLE	OPTIMIZE	

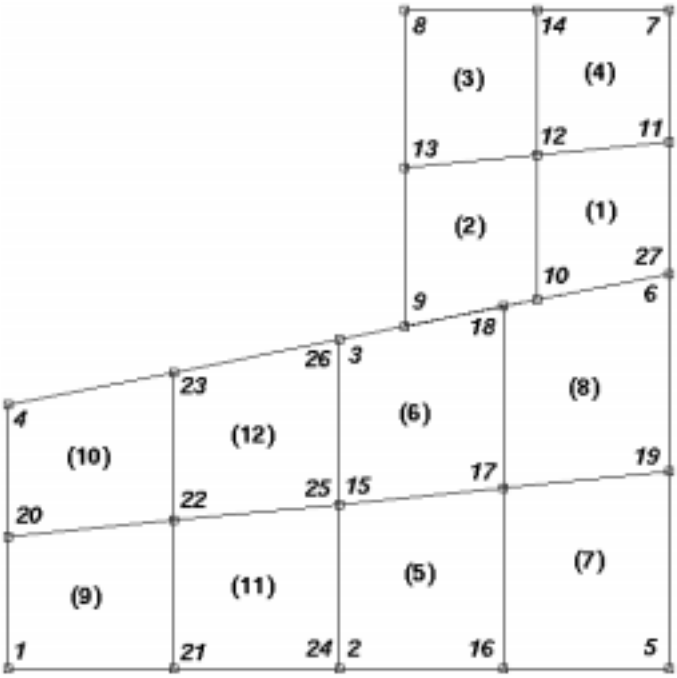

Figure 8.46-1 Initial Model

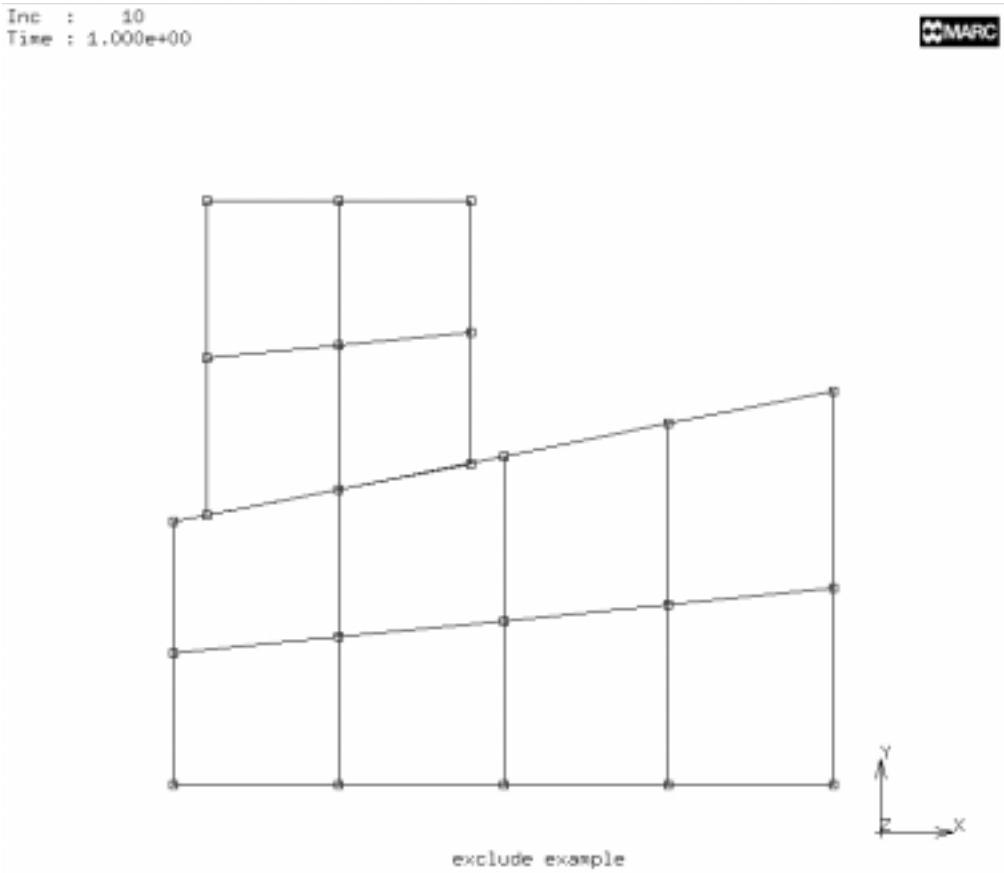

Figure 8.46-2 Final Deformed Shape after 10 Increments

8.47 Simulation of Contact with Stick-Slip Friction

This example illustrates the use of the stick-slip friction model. The model consists of a deformable body on a rigid surface. The deformable body is subjected to a normal distributed load that holds it down onto the rigid surface. A distributed shear load is applied in order to cause slip on the rigid surface. A spring restrains the deformable body and stores energy when slip occurs.

Model

The initial model is shown in Figure 8.47-1. There are 20 elements and 31 nodes in the model. The four noded plane stress isoparametric element number 3 is used to model the deformable workpiece. A spring connects node 1 on the deformable body with the detached node 31. The spring is linear with a unit stiffness.

Material Properties

The workpiece is assumed to be isotropic. The Young's modulus is 2.1×10^9 N/m^2, and the Poisson's ratio is 0.30. The spring is assumed to have a spring stiffness of 1.0 N/m.

Boundary Conditions

The detached node number 31 is restrained to have zero x and y displacements. Distributed loads are applied to the elements on the top surface of the deformable body (elements numbered 1, 5, 9, 13, 17) as shown in Figure 8.47-2. Both normal (P) and shear (τ) distributed loads are applied on these elements.

Contact

The stick-slip model is chosen in this problem. The slip to stick transition is assumed to be at a relative velocity of 1×10^{-6} m/s. A contact bias factor of 0.99 is used. The default values of 1.05 for the friction multiplier and 0.05 for the relative friction force tolerance are assumed. There are two contact bodies in the problem. A friction coefficient of 0.05 is assigned to the rigid contact body.

Control

The maximum allowed relative error in residual forces is chosen to be 0.10. A maximum of ten recycles are allowed for each increment.

History Definition

The distributed loads are given in Figure 8.47-3. The shear distributed load is gradually increased in the negative sense and then reversed in sense to become positive. The normal distributed load increases to 1.0 units in increment 1. It is held at that value until increment 50. It is reduced to 0.80 units in increment 51. The loading proceeds for a total of sixty increments.

Results

The shear load is not high enough to cause slipping until increment 20. However, it is increased to -0.30 units in the 21st increment. This causes the deformable body to slip along the positive x direction for the first time in increment 21. The deformed and initial positions of the deformable body are shown in Figure 8.47-4. There is no load incrementation until increment 31 when the distributed shear load is reset to zero. The restoring force in the spring is however insufficient to cause the deformable body to slip again. Hence, it continues to stick until increment 40. In increment 41, the shear load is ramped up to +1.1 units. This now causes the body to slip along the negative x direction as shown in Figure 8.47-5. In increment 51, the normal distributed load is decreased in magnitude to 0.80 units. This causes the deformable body to slip further, along the positive x direction as shown in Figure 8.47-6. The x displacement of node 1 is shown in Figure 8.47-7 for the entire loading history.

Parameters, Options, and Subroutines Summary

Example e8x47.dat:

Parameters	Model Definition Options	History Definition Options
ALL POINTS	CONNECTIVITY	AUTO LOAD
DIST LOADS	CONTACT	CONTINUE
ELEMENTS	CONTROL	DIST LOADS
END	COORDINATES	TIME STEP
SETNAME	DIST LOADS	
SIZING	FIXED DISP	
TITLE	ISOTROPIC	
	OPTIMIZE	
	POST	
	SOLVER	
	SPRINGS	

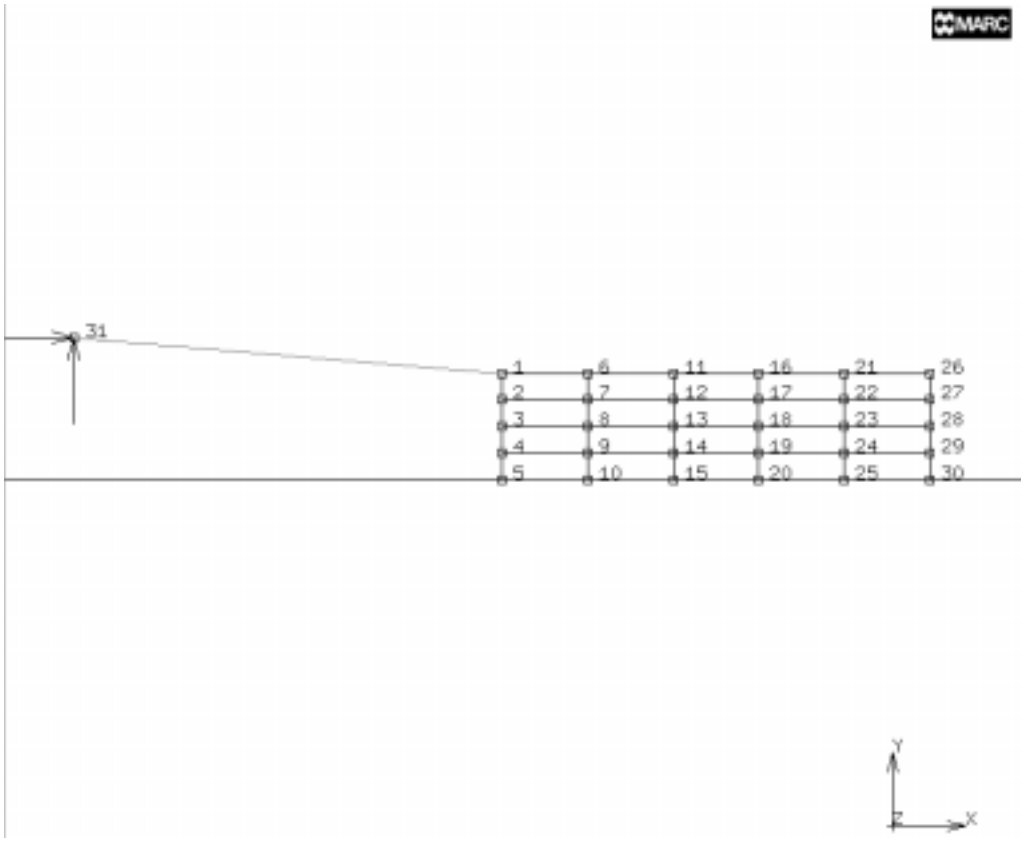

Figure 8.47-1 Initial Model for Stick-Slip Problem

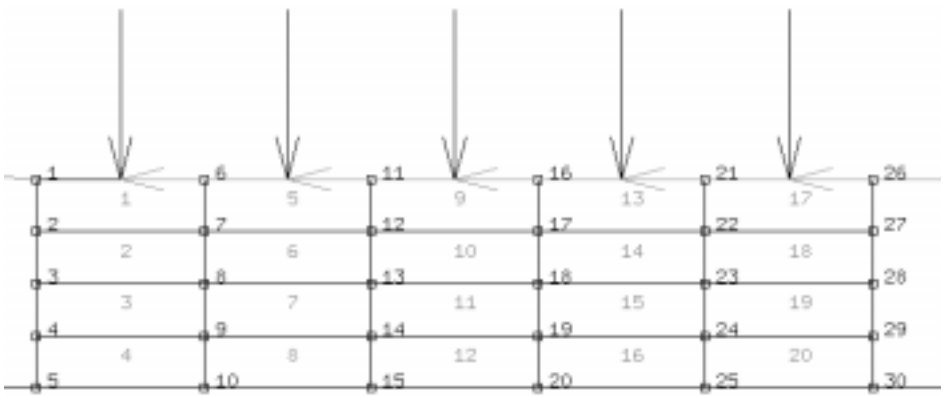

Figure 8.47-2 Distributed Load Boundary Conditions

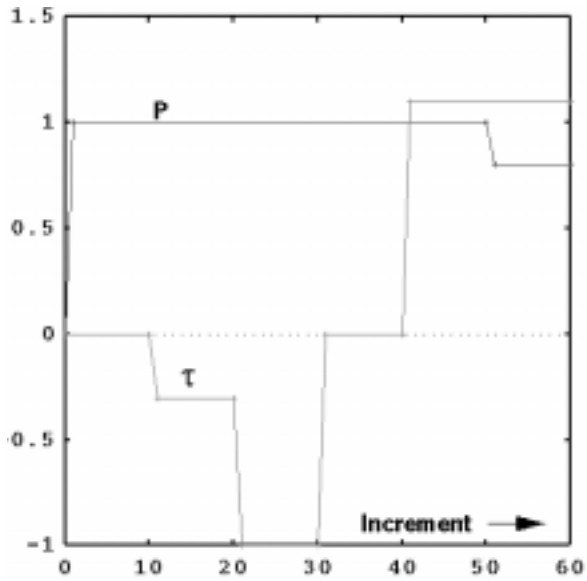

Figure 8.47-3 Loading History for the Distributed Loads

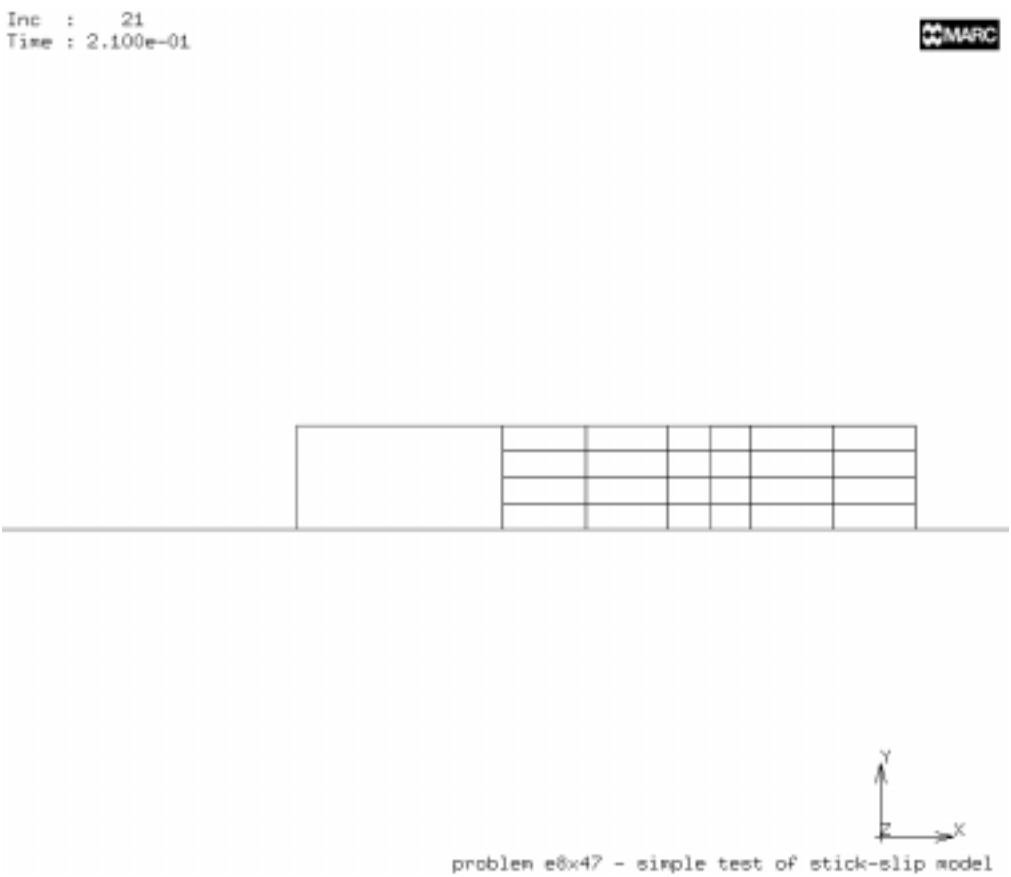

Figure 8.47-4 First Slipping Motion (Increment 21)

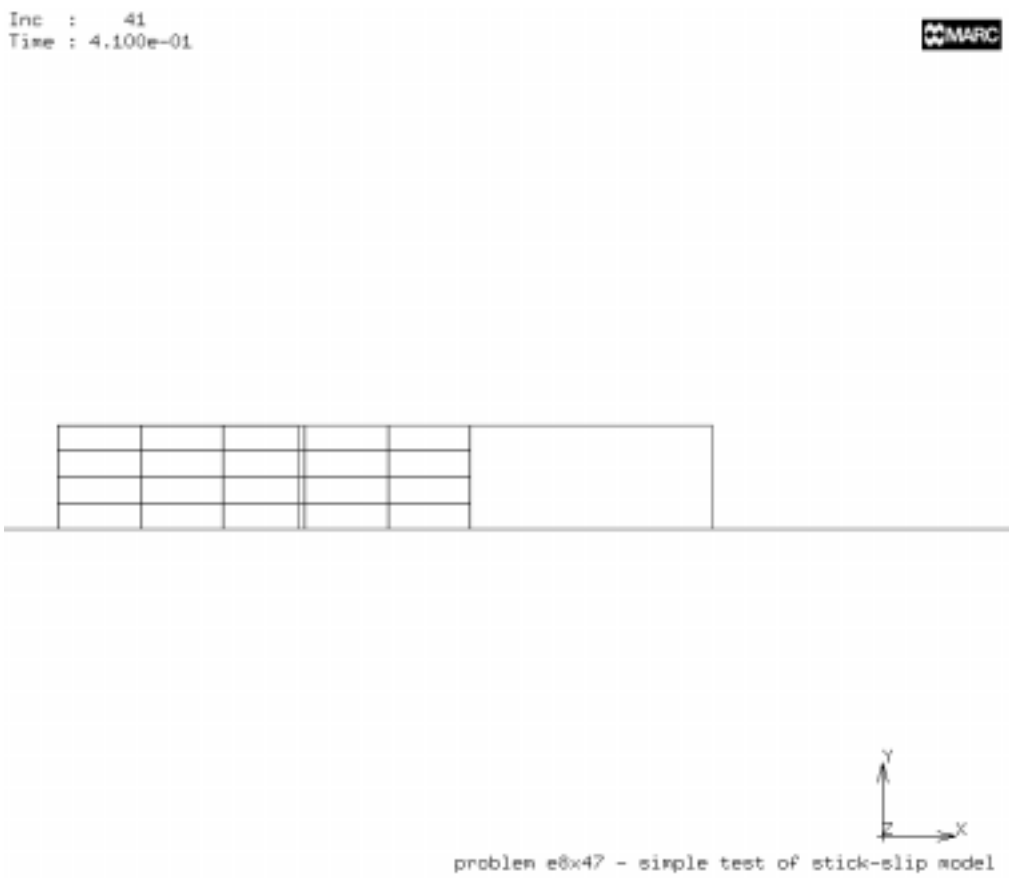

Figure 8.47-5 First Slipping Motion (Increment 21)

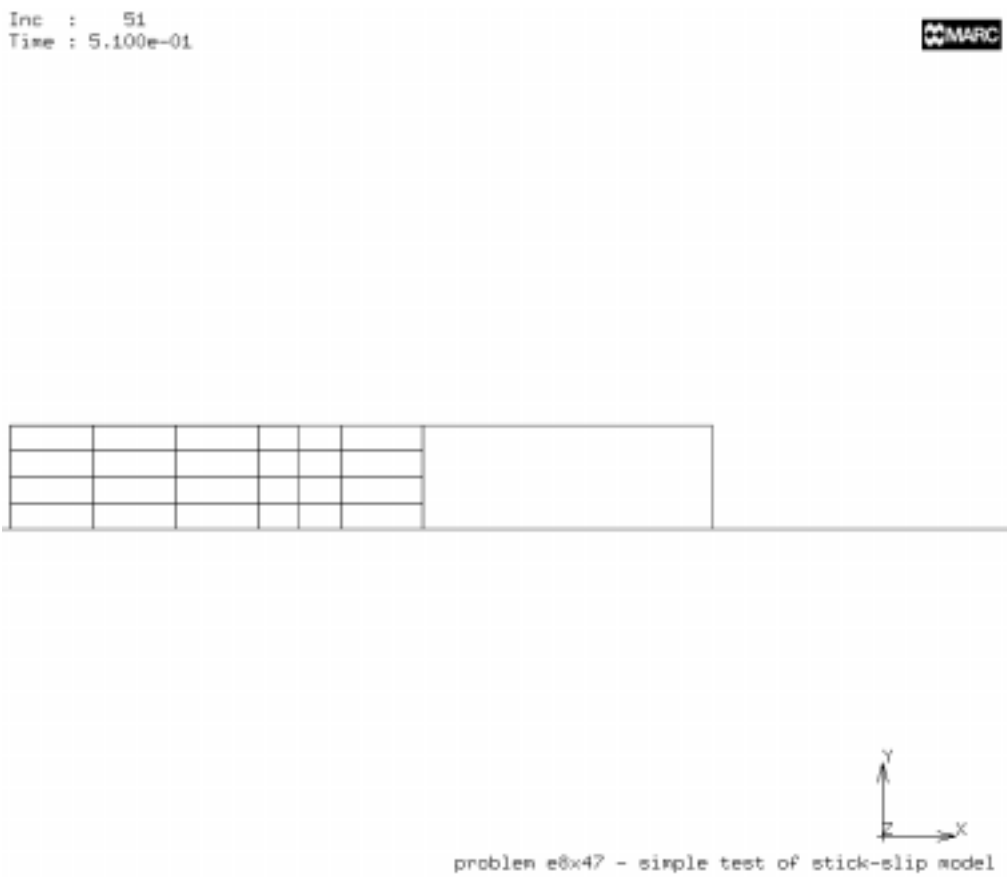

Figure 8.47-6 Final Slip occurring in Increment 51

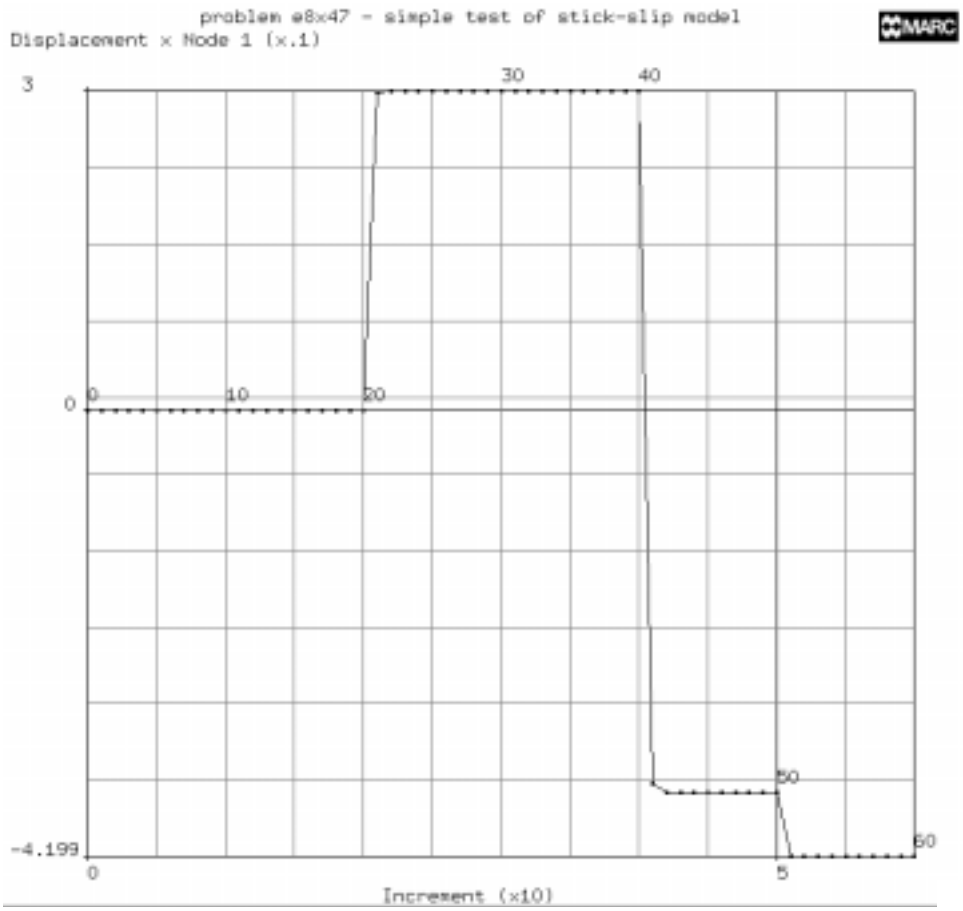

Figure 8.47-7 X Displacement History for Node 1

8.48 Simulation of Deformable-Deformable Contact with Stick-Slip Friction

This example illustrates the use of the stick-slip friction model in the simulation of the contact of two deformable bodies.

Model

The initial model is shown in Figure 8.48-1. There are 36 elements and 57 nodes in the model. The four noded plane stress isoparametric element number 3 is used to model the deformable workpiece. The body on top is contact body 1. The two nodes on the left most face of contact body 1 (nodes 51 and 46) are connected to detached nodes 57 and 56 by means of springs.

Material Properties

The two contact bodies are isotropic but have differing properties. The material properties are summarized below.

Contact Body	Comprised of Elements	E (N/m^2)	ν
1	33 to 36	3×10^9	0.30
2	1 to 32	2×10^{11}	0.30

Boundary Conditions

The detached nodes (nodes 56 and 57) are restrained to have zero x and y displacements. In addition, contact body 2 has its bottom surface fixed to have zero displacements. Thus, the x and y displacements are set to zero for nodes 1 to 9.

Contact

The stick-slip model is chosen in this problem. The slip to stick transition is assumed to be at a relative velocity of 1×10^{-5} units. A contact bias factor of 0.0 is used. The default values of 1.05 for the friction multiplier and 0.05 for the relative friction force tolerance are assumed. A friction co-efficient of 0.05 is used for contact body one and a friction co-efficient of 0.10 is used for the lower contact body.

Control

The maximum allowed relative change in displacement increments is chosen to be 0.05. A maximum of thirty recycles are allowed for each increment.

History Definition

There are a total of 20 increments in this problem. The loading consists of two distributed normal loads P_x and P_y, applied to contact body one as shown in Figure 8.47-1. The load P_y holds the upper contact body down on the lower contact body. P_y is ramped up to a value of 7.5×10^6 N/m^2 in 10 increments and is then maintained constant until the 20th increment. P_x is maintained at a value of zero until the 10th increment. Then it is ramped to a value of -15.0×10^6 N/m^2 in the 20th increment. The distributed load history is shown in Figure 8.48-2.

Results

P_x remains at a value of zero until increment 10. Hence, there is no slip possible. From increment 11, P_x is ramped up. The first slip occurs in increment 13. The deformed shape is shown in Figure 8.48-3. As P_x is ramped up further, contact body 1 continues to slip until the last increment (increment 20). The final deformed shape is shown in Figure 8.48-4.
Figure 8.48-5 shows the history plot of variation of x displacement at node 51 with increment number.

Parameters, Options, and Subroutines Summary

Example e8x48.dat:

Parameters	Model Definition Options	History Definition Options
ALL POINTS	CONNECTIVITY	AUTO LOAD
DIST LOADS	CONTACT	CONTINUE
ELEMENTS	CONTROL	DISP CHANGE
END	COORDINATES	DIST LOADS
LARGE DISP	FIXED DISP	TIME STEP
SIZING	GEOMETRY	
TITLE	ISOTROPIC	
	POST	
	SOLVER	
	SPRINGS	

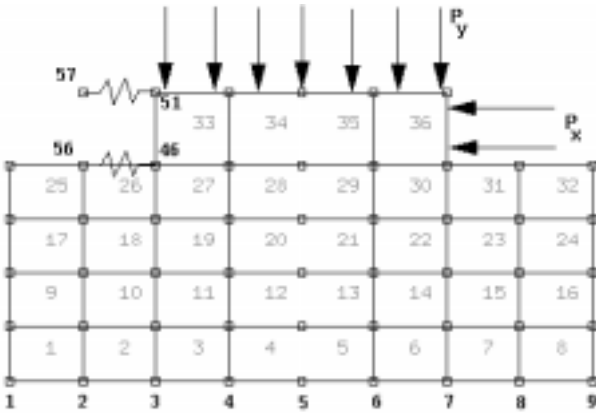

Figure 8.48-1 Initial Model for Stick-Slip Problem

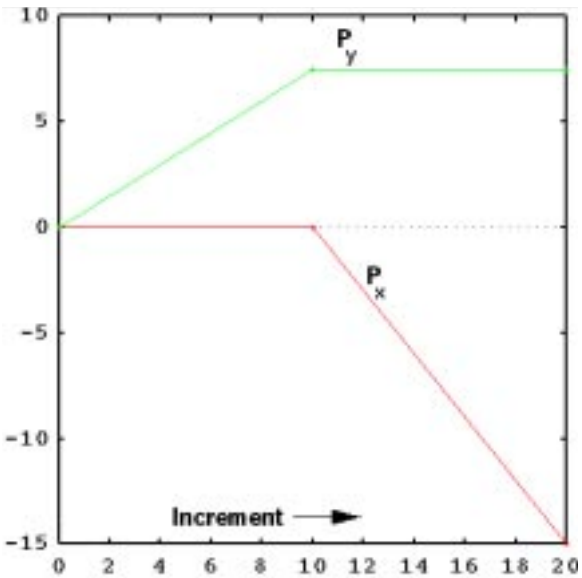

Figure 8.48-2 Loading History - Y Axis is Load Per Unit Area divided by 10^6

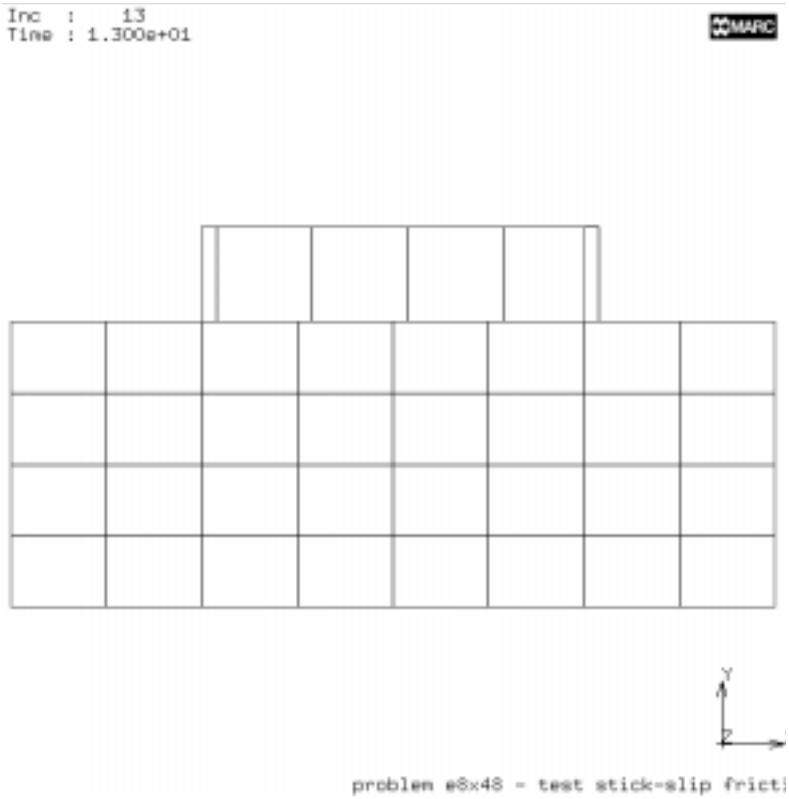

Figure 8.48-3 First Slip occurs in Increment 13

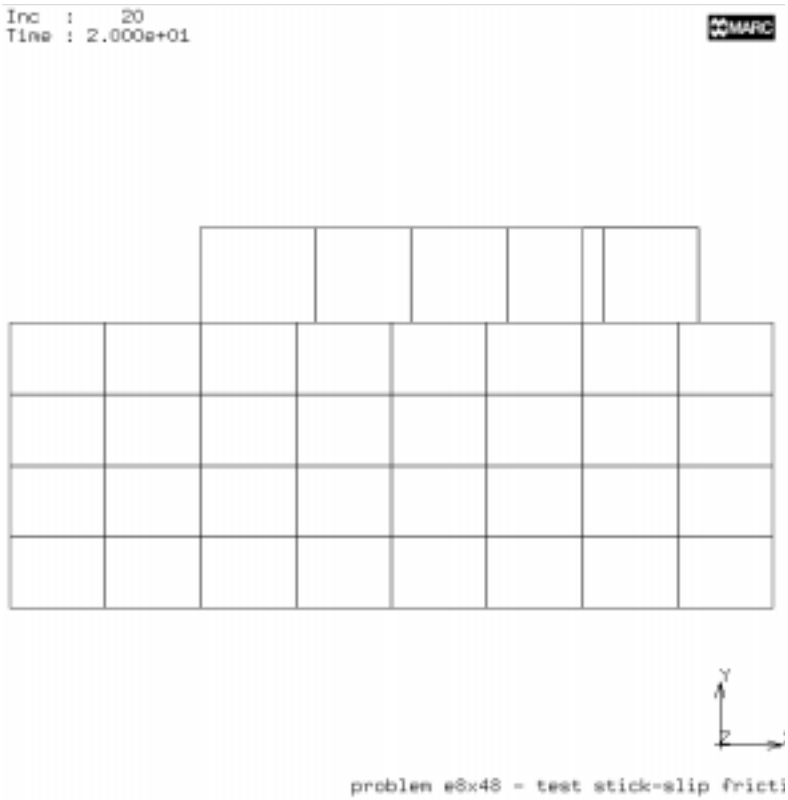

Figure 8.48-4 Final Deformed Shape in Increment 20

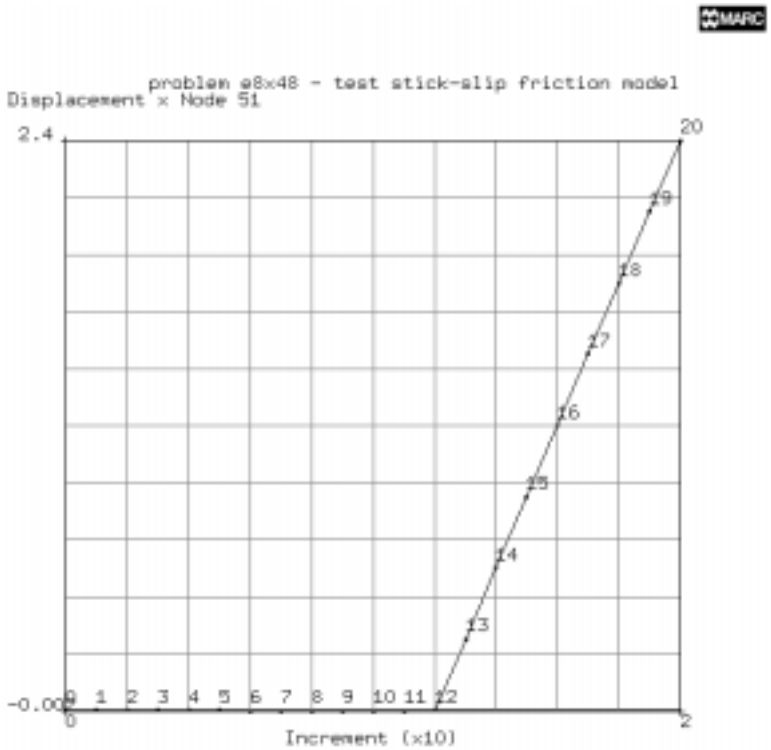

Figure 8.48-5 History Plot of x Displacement for Node 51

8.49 Rolling of a Compressed Rubber Bushing with Stick-Slip Friction

This example simulates the rolling of a rubber bushing with an off center compressed between two rigid surfaces. The rubber bushing material properties are assumed to approximate Mooney-Rivlin rubber material. The example shows large deformation behavior of rubber material along with contact simulated using the stick-slip algorithm.

Model

The initial model is shown in Figure 8.49-1. The bushing is modeled using element 80, which is a 4 noded isoparametric plane strain Herrmann element. The deformable bushing is modeled using 178 elements and 217 nodes. There are two rigid bodies in the model. The rigid body on top is contact body number 2. The bottom rigid body is contact body number 3. It is held fixed.

Material Properties

The deformable body is assumed to be made of Mooney-Rivlin material with constants given by C_{10} = 8 MPa and C_{01} = 2 MPa.

Boundary Conditions

Nodes 175 and 176 lie diametrically opposite on the equator of the off center hole in the bushing. Node 175 is constrained to have zero x displacement. Node 176 is constrained to have zero y displacement.

Contact

Contact is modeled with stick-slip friction. The default values of the stick-slip friction parameters are used. A value of 0.50 is used as a coefficient of friction for all contact bodies, The separation force is chosen to be 1 N.

Control

The maximum allowed relative error in residual forces is 0.01. A maximum of 10 recycles are chosen for each increment.

History Definition

The loading is imposed on contact body 2 using the MOTION CHANGE history definition option. Contact body 2 moves down and compresses the deformable bushing for 25 increments. Increments 26 and 27 involve a motion along the negative x direction in addition to compression of the cylinder. Subsequently, increments 28 to 51 involve the motion of contact body 2 along the negative x direction without any further displacement in the y direction.

Results

The deformed shape of the bushing in increment 25 is shown in Figure 8.49-2. It can be seen that more nodes have come into contact with the upper and lower contact bodies. The next two increments involve both x and y motion of the upper contact body. The friction between the contact bodies and the bushing enables the bushing to roll in response to the horizontal motion of contact body 2. The deformed shape of the bushing at the end of increment 27 is shown in Figure 8.49-3. Increments 28 through 51 involve further rotation of the bushing due to the translation of contact body 2 along the x direction. New nodes can be seen to come into contact with contact body two at the trailing edge of the bushing, while existing nodes at the periphery on the leading edge lose contact with contact body 2 as the rolling proceeds further. The deformed shapes of the bushing at the end of increments 40 and 51 are shown in Figure 8.49-4 and Figure 8.49-5 respectively.

Parameters, Options, and Subroutines Summary

Example e8x49.dat:

Parameters	Model Definition Options	History Definition Options
ALL POINTS	CONNECTIVITY	AUTO LOAD
DIST LOADS	CONTACT	CONTINUE
ELEMENTS	COORDINATES	MOTION CHANGE
END	FIXED DISP	TIME STEP
LARGE DISP	GEOMETRY	
SETNAME	MOONEY	
SIZING	OPTIMIZE	
TITLE	SOLVER	

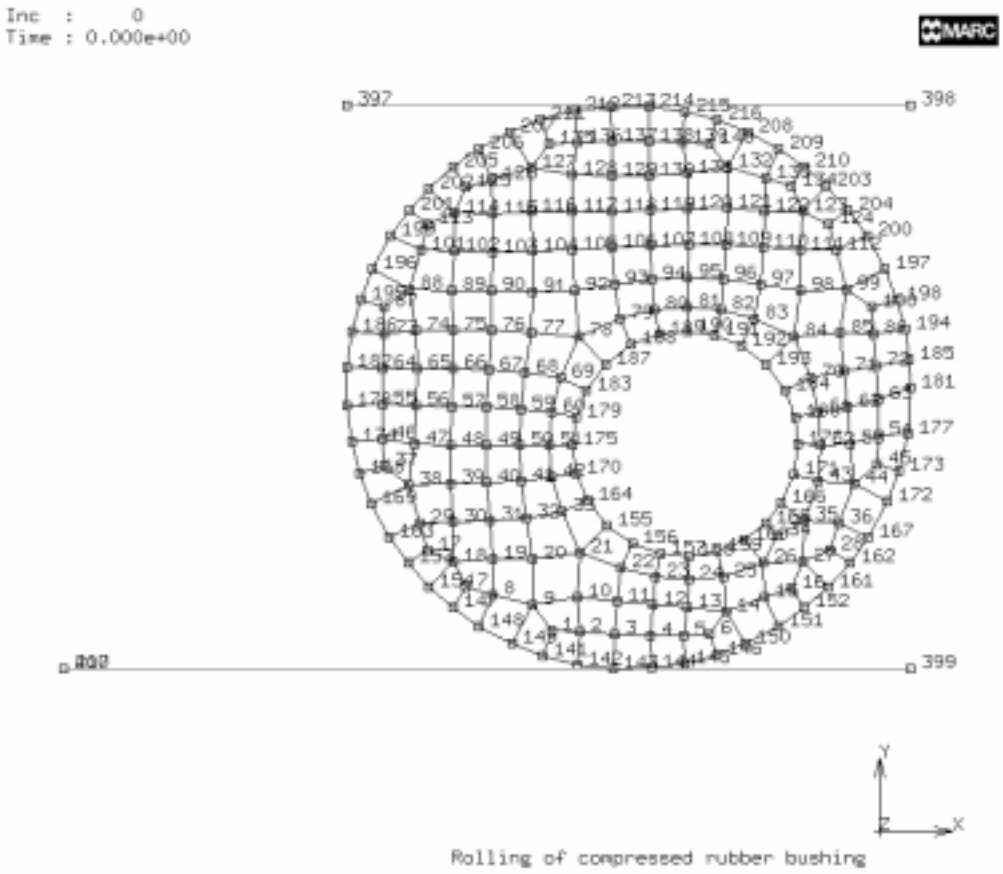

Figure 8.49-1 Initial Model

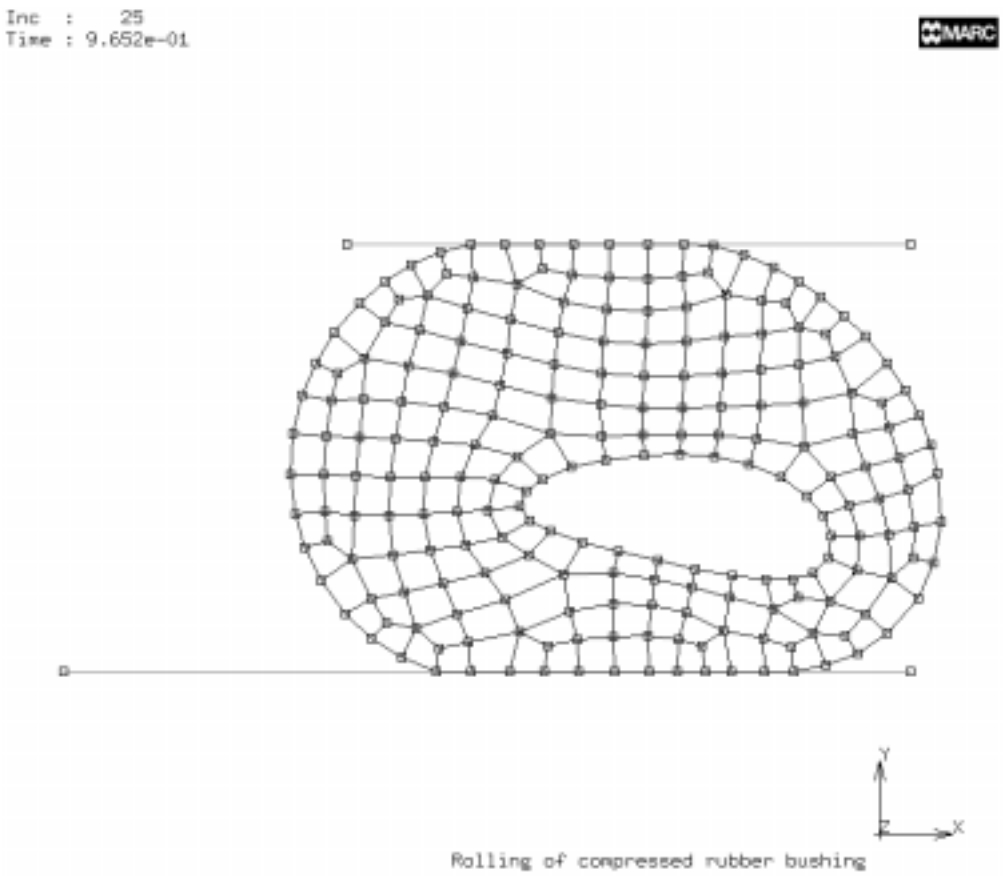

Figure 8.49-2 Deformed Shape of Bushing at the End of Increment 25

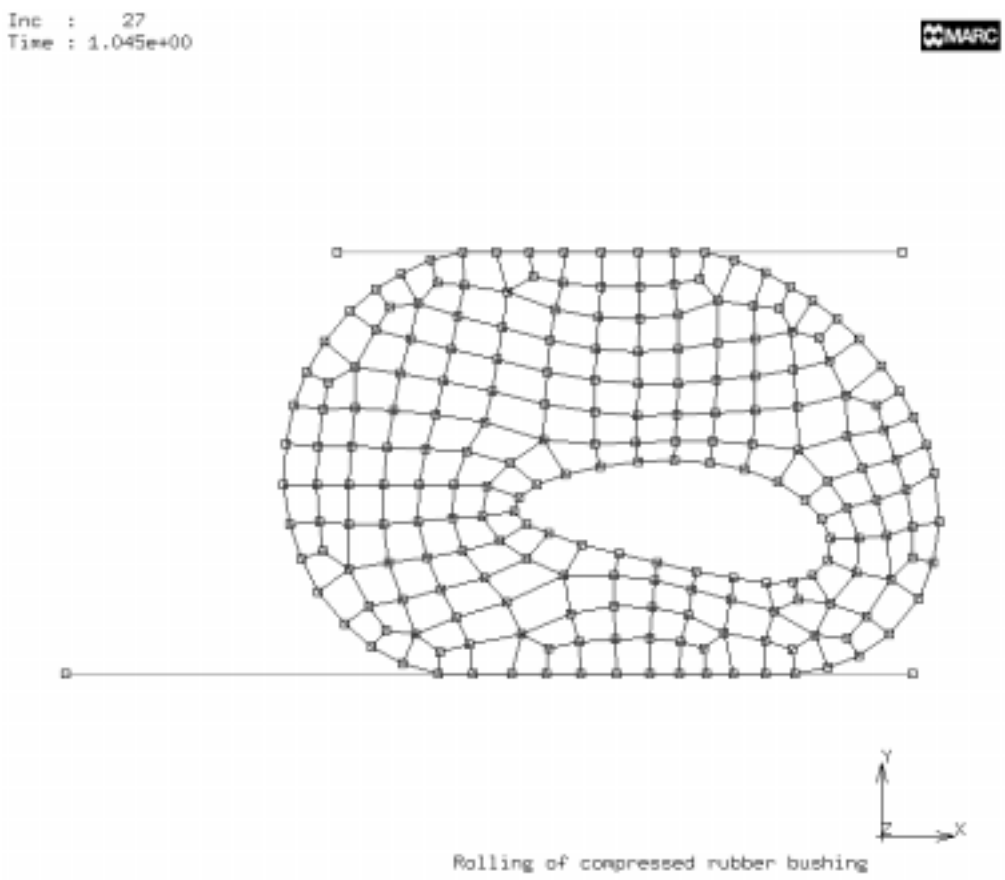

Figure 8.49-3 Deformed Shape of Bushing at the End of Increment 27

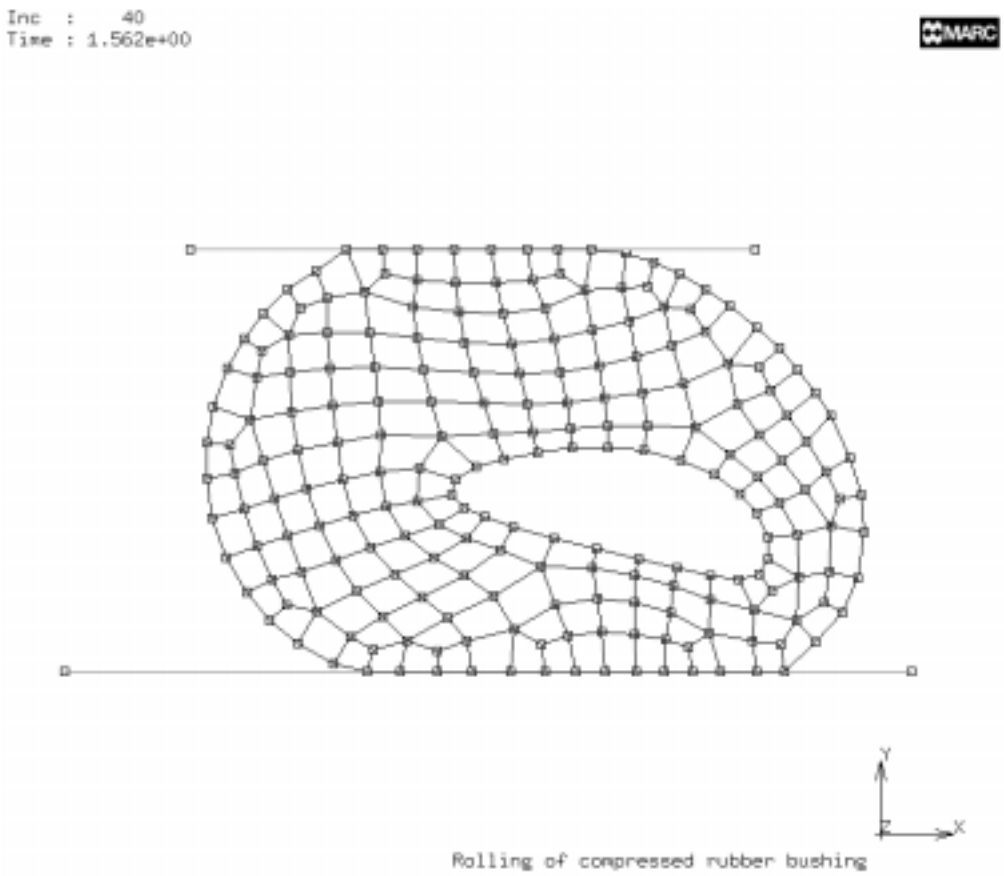

Figure 8.49-4 Deformed Shape of Bushing at the End of Increment 40

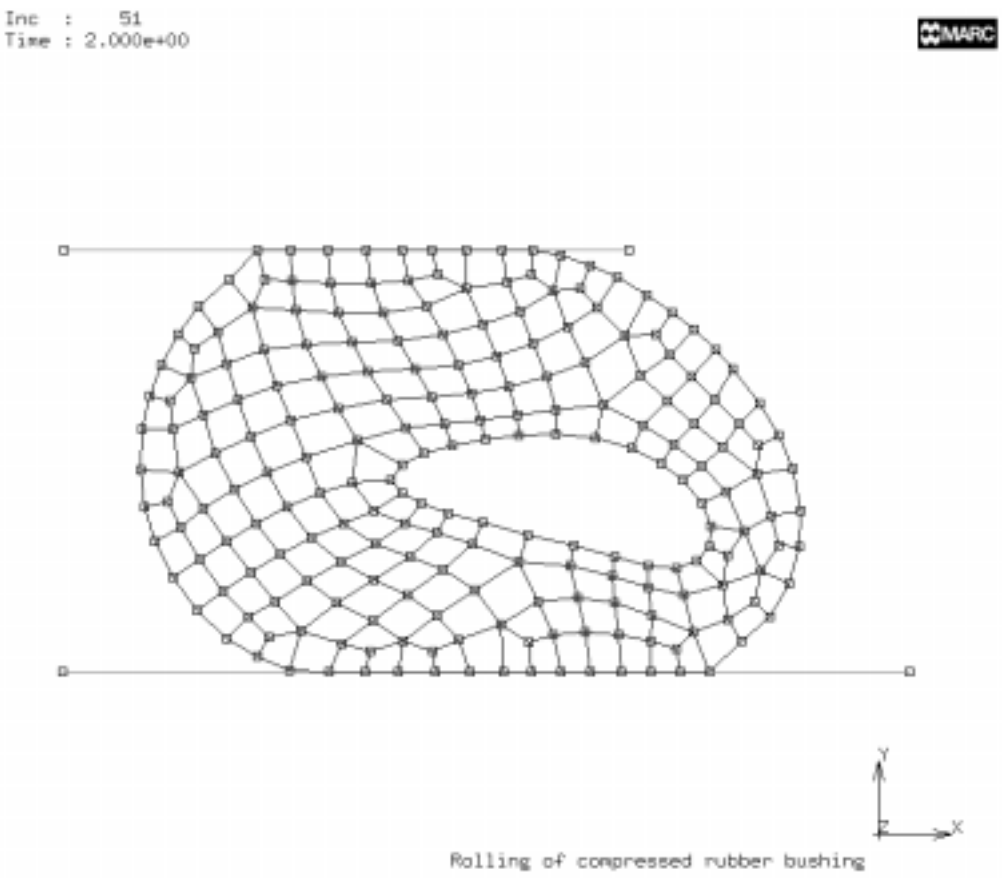

Figure 8.49-5 Deformed Shape of Bushing at the End of Increment 51

8.50 Compression Test of Cylinder with Stick-Slip Friction

This problem simulates the compression of an initially circular cylinder between rigid platens with stick-slip friction.

Model

The initial model is shown in Figure 8.50-1. The cylindrical billet is modeled using element number 10. Element 10 is an axisymmetric 4 noded isoparametric quadrilateral element. To model the billet, 160 elements and 187 nodes are used. The radial direction is along y while the axial direction is along x.

Material Properties

The billet is assumed to be made of an isotropic elastic plastic material. The Young's modulus is 5×10^3 Pa and the Poisson's ratio is assumed to be 0.30. The initial yield stress is taken to be 100 Pa. The workhardening data is input using the WORK HARD model definition block and is given below.

Plastic Strain	Flow Stress(Pa)
0.0	100.0
1.0	120.0
5.0	125.0

Contact

There are four contact bodies in the problem. The deformable billet is contact body 1. Contact body 2 is the fixed rigid platen and is the left most contact body in Figure 8.50-1. The moving rigid platen is contact body number 3 and is the right most contact body. Contact body 3 moves axially (along the negative x direction) at constant speed. Contact body 4 is the symmetry body represented by the line y = 0 in Figure 8.50-1. Stick-slip friction is used to model this problem, The slip to stick transition velocity is chosen as 10^{-6} m/s. A contact bias factor of 0.80 is used. A friction coefficient of 0.10 is assigned to contact bodies 2 and 3.

Control

The increments are controlled by a maximum allowed relative change in displacement increment of 0.01. A maximum of 10 recycles are allowed for each increment.

History Definition

The loading is accomplished by the motion of contact body 3 at a constant velocity. This is prescribed using the MOTION CHANGE option. A total of 50 increments are chosen.

Results

The deformed shape of the billet at the end of increment 25 is shown in Figure 8.50-2. The deformed shape of the billet at the end of increment 50 is shown in Figure 8.50-3. Figure 8.50-4 shows the load versus stroke profile for this example. The maximum load is seen to be 6.715×10^5 N.

Parameters, Options, and Subroutines Summary

Example e8x50.dat:

Parameters	Model Definition Options	History Definition Options
ELEMENTS	CONNECTIVITY	AUTO LOAD
END	COORDINATES	CONTINUE
FINITE	GEOMETRY	MOTION CHANGE
LARGE DISP	ISOTROPIC	TIME STEP
SIZING	OPTIMIZE	
TITLE	POST	
UPDATE	SOLVER	
	WORK HARD	

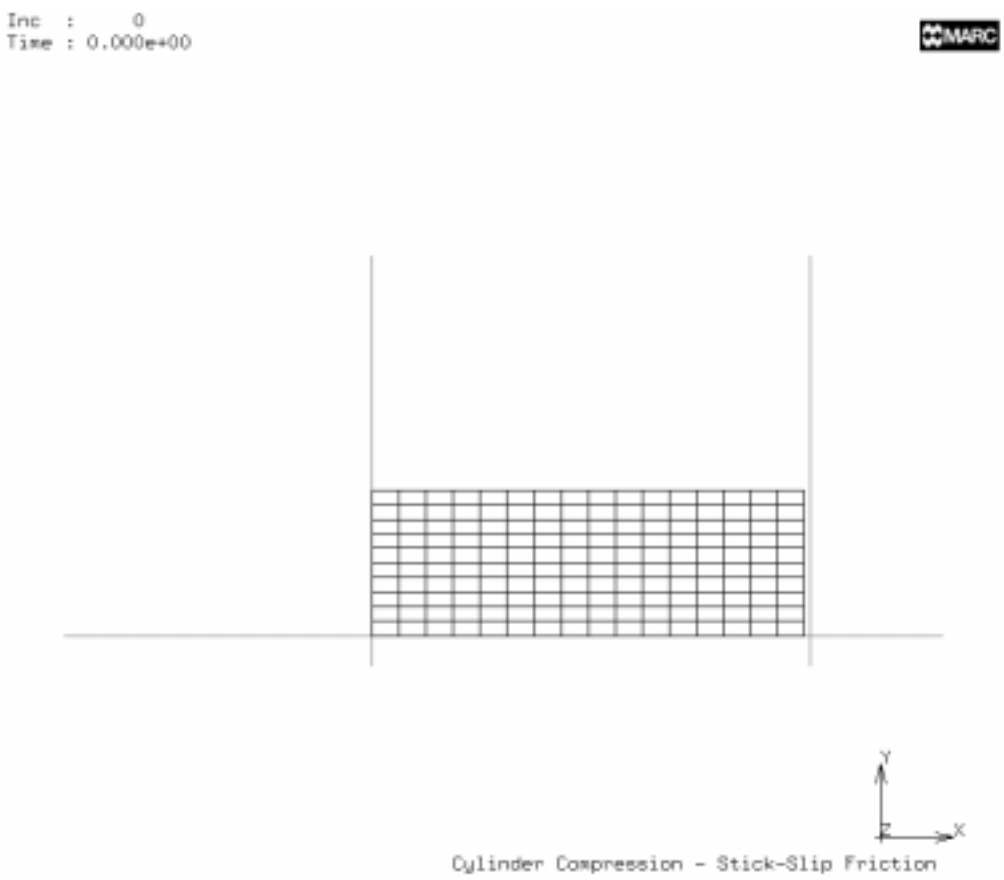

Figure 8.50-1 Initial Model

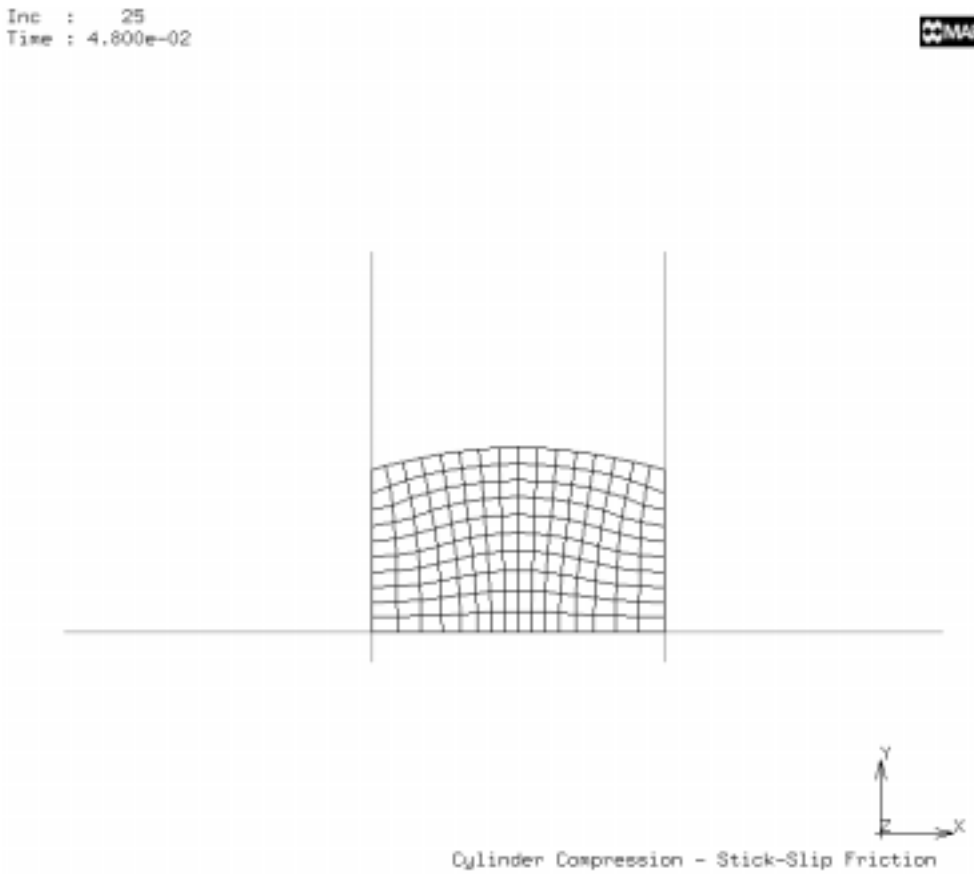

Figure 8.50-2 Deformed Shape at End of 25 Increments

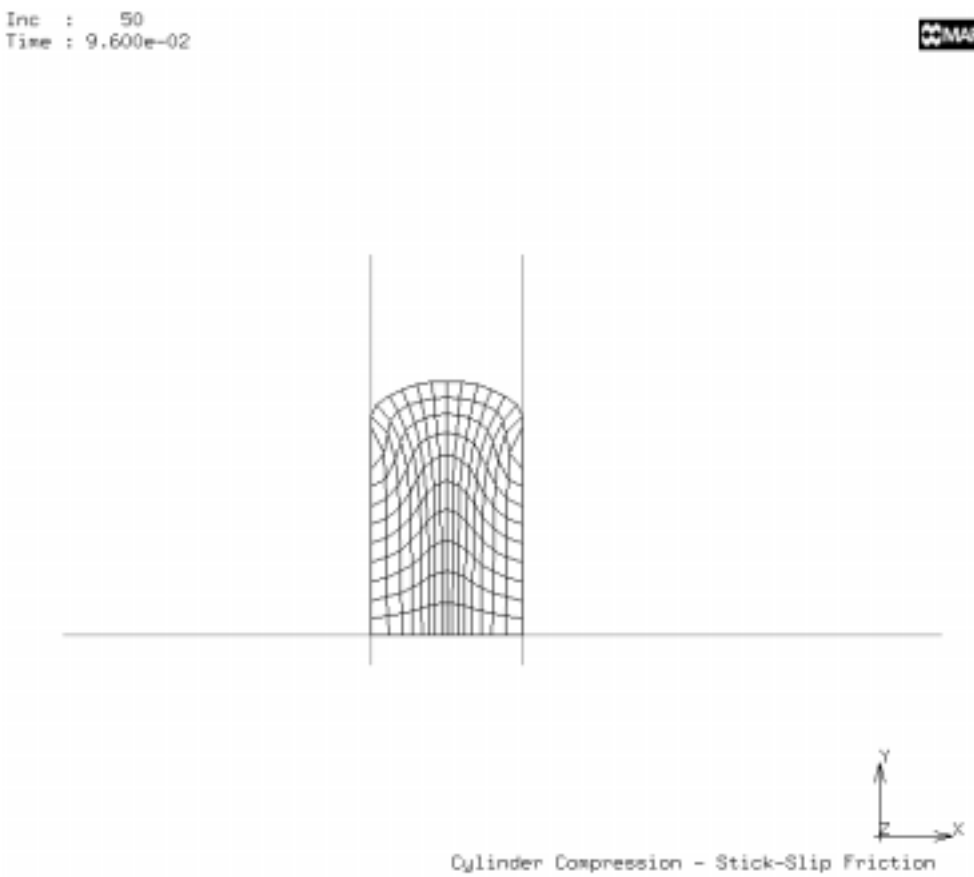

Figure 8.50-3 Deformed Shape at End of 50 Increments

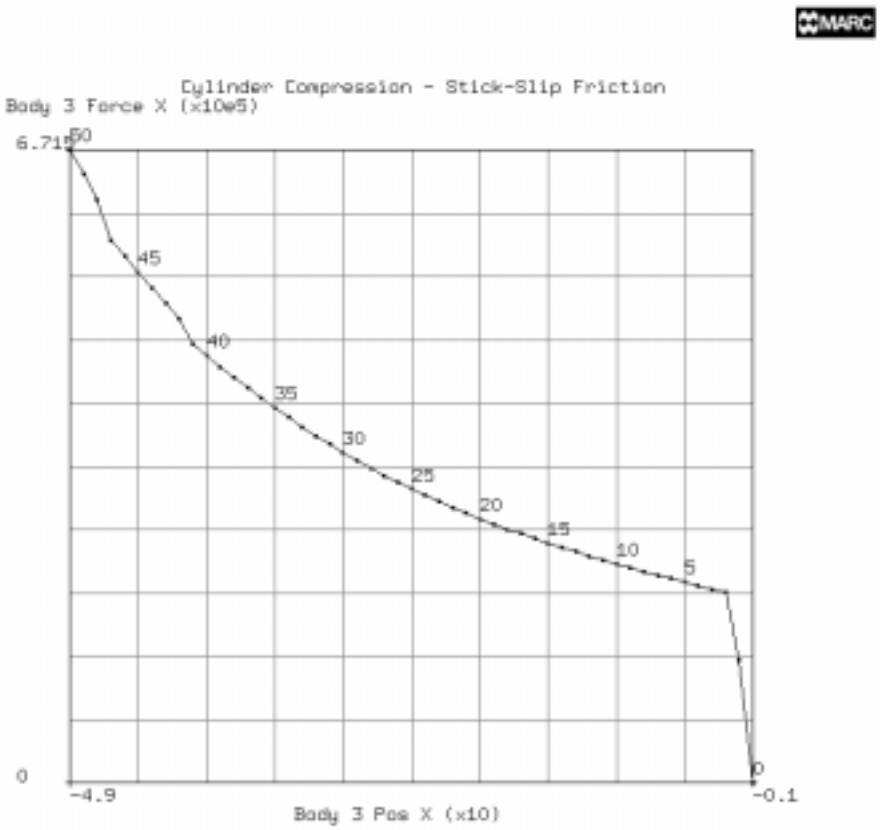

Figure 8.50-4 Load Stroke Curve for the Deformation

8.51 Modeling of a Spring

This example shows the shell contact capabilities MARC. A structure is a spring, made of shell elements is compressed between two rigid surfaces moving toward each other. Two cases are considered:

Data Set	Element Used
e8x51a	139
e8x51b	75

Model

The initial model is shown in Figure 8.51-1. The initial model is identical for both data sets with the exception of the element type used. There are 2790 4-node shell elements and 3354 nodes (Figure 8.51-2).

Element

Data set e8x51a uses element type 139. Element 139 is a 4-node bilinear thin shell element based on the discrete Kirchhoff theory. Element 75 is a 4-node bilinear thick shell element.

Material Properties

For both data sets, the shell elements are assumed to be modeled by a combined isotropic-kinematic workhardening behavior. The Young's modulus is 2.8×10^7 Pa and the Poisson's ratio is 0.30. The initial yield stress is 130×10^3 Pa. The workhardening data is input using the WORK HARD DATA option.

Boundary Conditions

The boundary conditions along the x-direction are imposed by the motion of the two contact bodies along the x-direction. The shell structure is restrained to have zero y and z displacements along the nodes 1, 2, 3, 4, 5, and 6 (edge AB in Figure 8.51-2) and along nodes 3349, 3350, 3351, 3352, 3353, and 3354 (edge CD in Figure 8.51-2).

Contact

The CONTACT option for the both data sets is identical except that in data set e8x51b (thick shell element 75) increment splitting is disallowed.

There are three contact bodies in this problem. There is no friction in the model. The distance below which a node is considered to touch a contact surface is assumed to be 10^{-3} m. The contact tolerance bias factor is assumed to be 0.90. Contact body 1 is a deformable body comprising all the elements in the model. Contact bodies 2 and 3 are rigid and each is made up of one four noded patch for contact definition. Contact body 2 is the planar surface defined by x = -1, while Contact body 3 is the planar surface defined by x = +1. The two rigid contact bodies compress the shell elements comprising the structure.

The CONTACT TABLE option is included to expedite the contact calculations. Contact body 1 is allowed to touch all the three contact bodies. Thus, self contact of the shell structure with itself is allowed. The two rigid bodies do not detect contact with each other.

History Definition

The MOTION CHANGE option specifies the motion of the rigid velocity controlled contact bodies. In increment zero, both contact bodies approach each other at constant velocity in order to just make contact with the shell structure. After increment zero, Contact body 2 is held stationary while Contact body 3 moves at constant speed in the -x-direction. There are a total of 25 increments of loading in this problem.

Results

For data set e8x51a, the deformed plots of the shell structure at increments 5, 10, 20, and 25 are shown in Figure 8.51-3 through Figure 8.51-6, respectively. For data set e8x51b, the deformed plots of the shell structure at increments 5, 10, 20, and 25 are shown in Figure 8.51-7 through Figure 8.51-10, respectively. On these deformed plots, the contours of the effective stress in layer 1 have been superimposed. It can be seen that both shell elements produce almost identical results. The comparison of x displacement for node 3351 is given below for the two data sets.

Increment Number	X Displacement at Node 3351	
	e8x51a	e8x51b
10	-0.3350	-0.3339
20	-0.3550	-0.3550

Parameters, Options, and Subroutines Summary

Example e8x51a.dat and e8x51b.dat:

Parameters	Model Definition Options	History Definition Options
ELEMENTS	CONNECTIVITY	AUTO LOAD
END	CONTACT	CONTINUE
FINITE	CONTACT TABLE	MOTION CHANGE
LARGE DISP	COORDINATES	TIME STEP
PRINT	FIXED DISP	
SETNAME	GEOMETRY	
SHELL SET	ISOTROPIC	
SIZING	SOLVER	
TITLE	WORK HARD	
UPDATE		

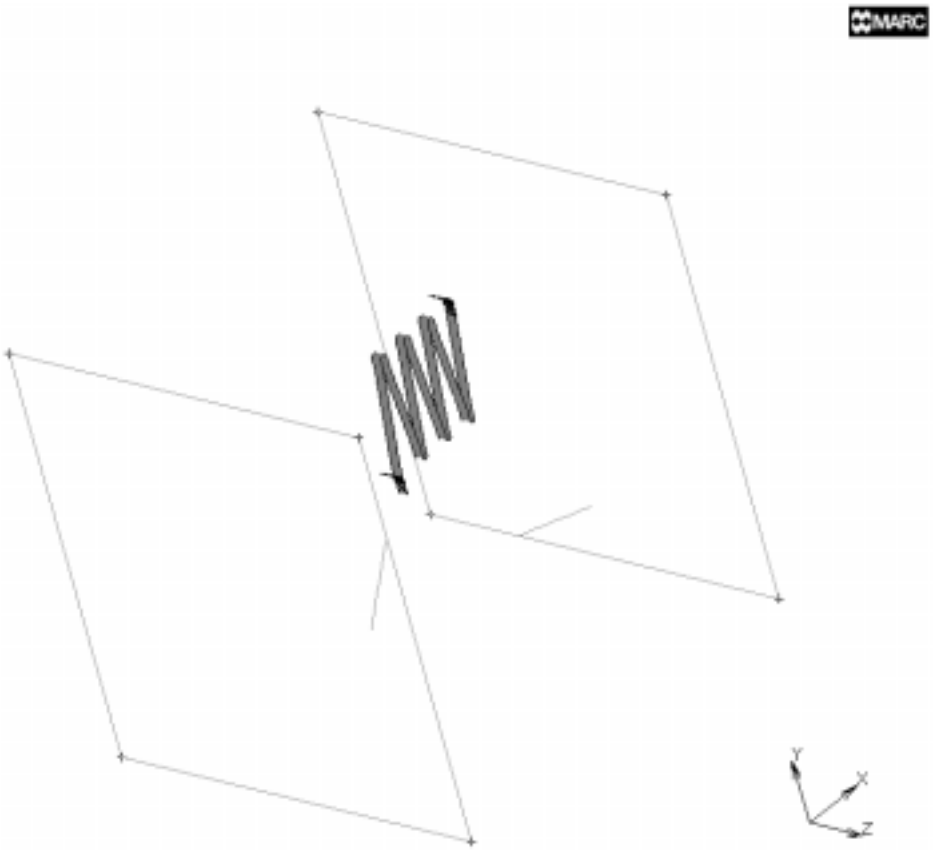

Figure 8.51-1 Initial Model for Both Data Sets

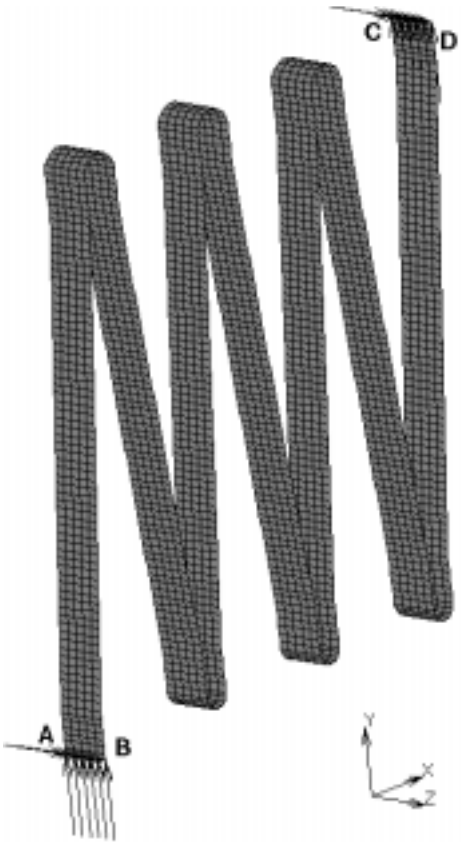

Figure 8.51-2 Boundary Condition Definition for Both Data Sets

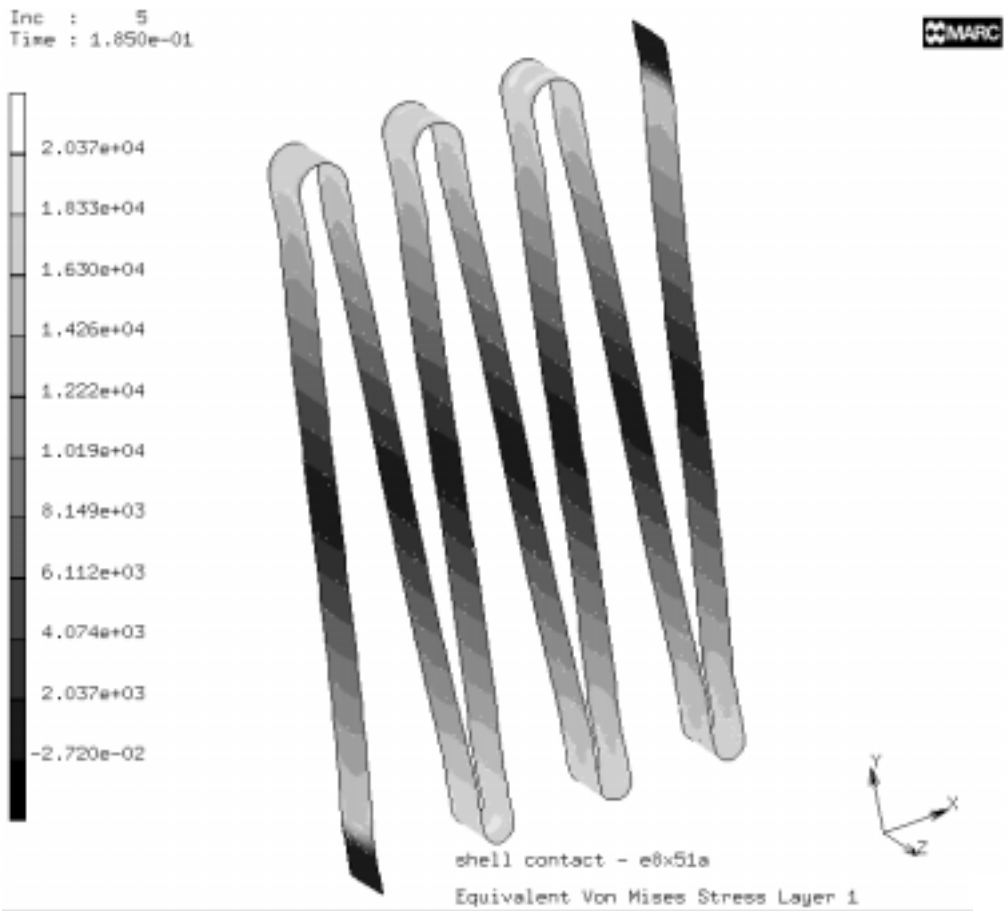

Figure 8.51-3 Deformed Shell Structure at Increment 5 for Data Set e8x51a

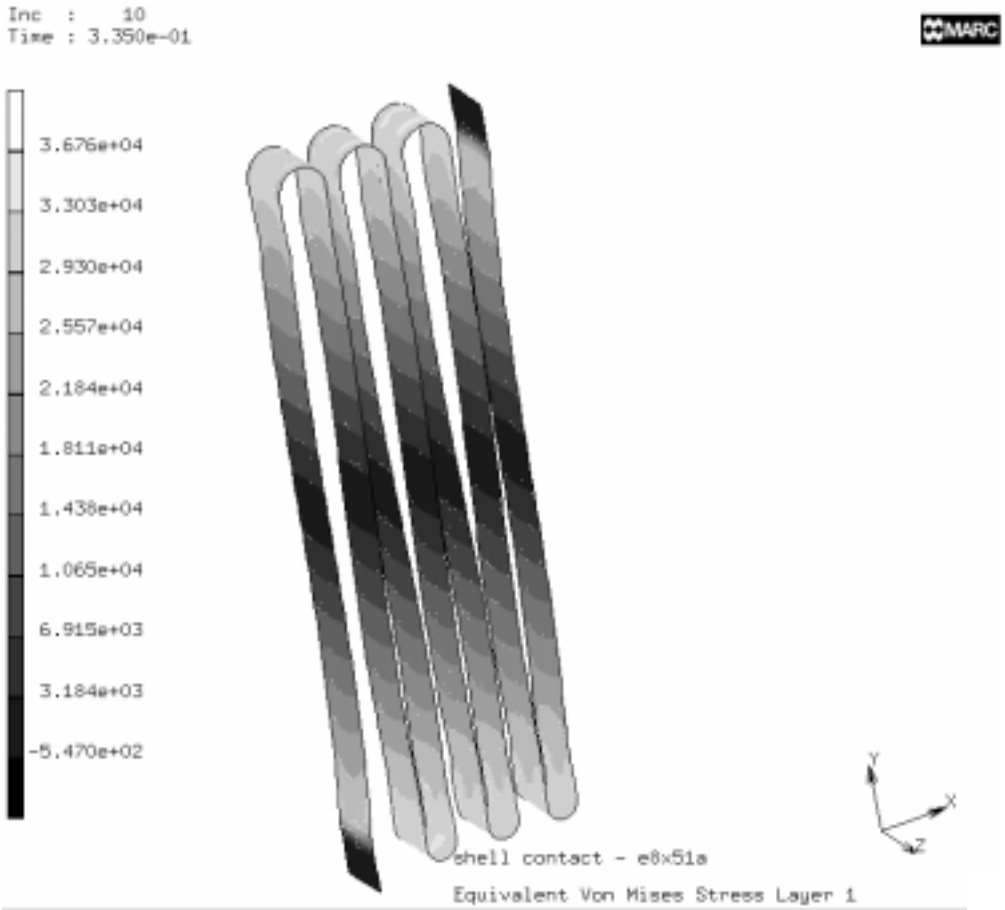

Figure 8.51-4 Deformed Shell Structure at Increment 10 for Data Set e8x51a

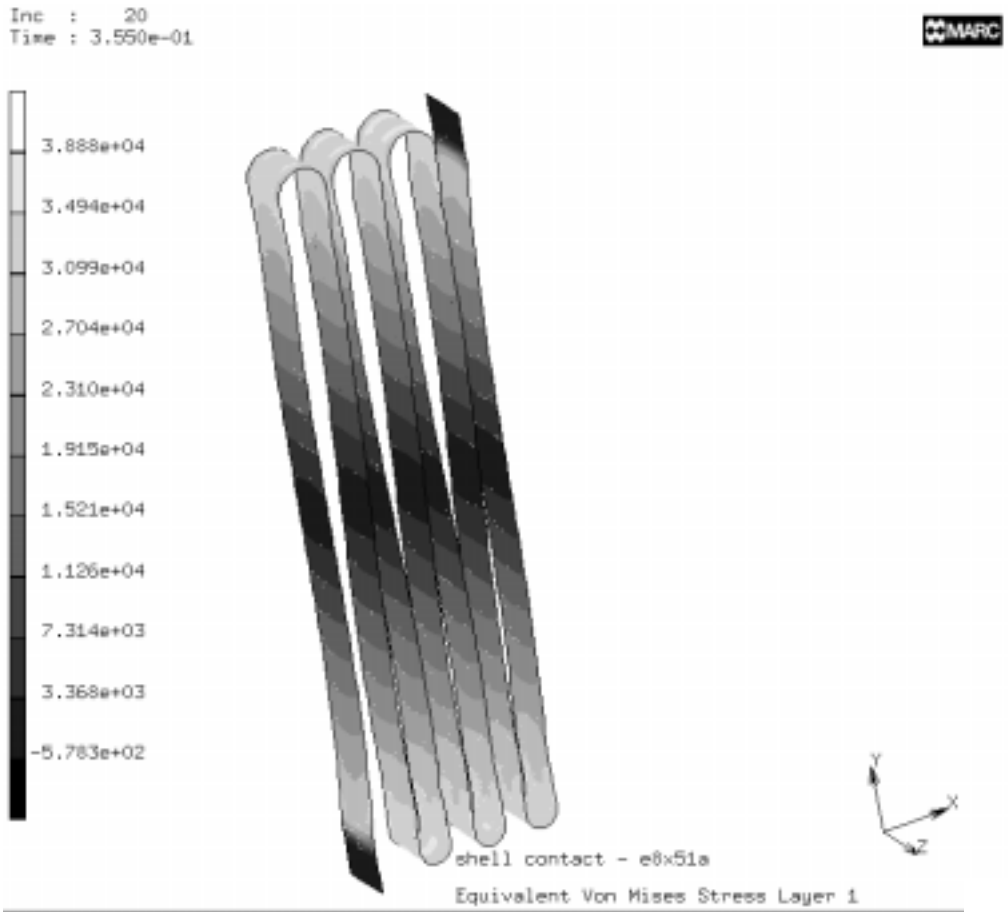

Figure 8.51-5 Deformed Shell Structure at Increment 20 for Data Set e8x51a

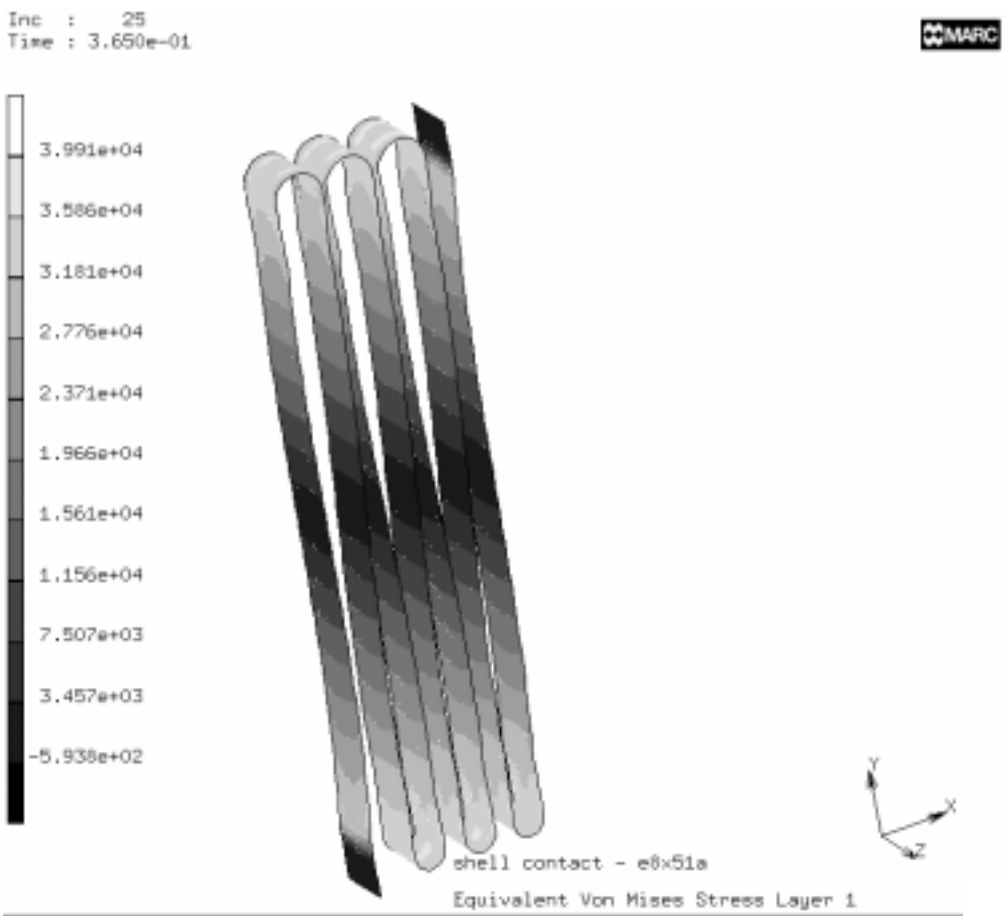

Figure 8.51-6 Deformed Shell Structure at Increment 25 for Data Set e8x51a

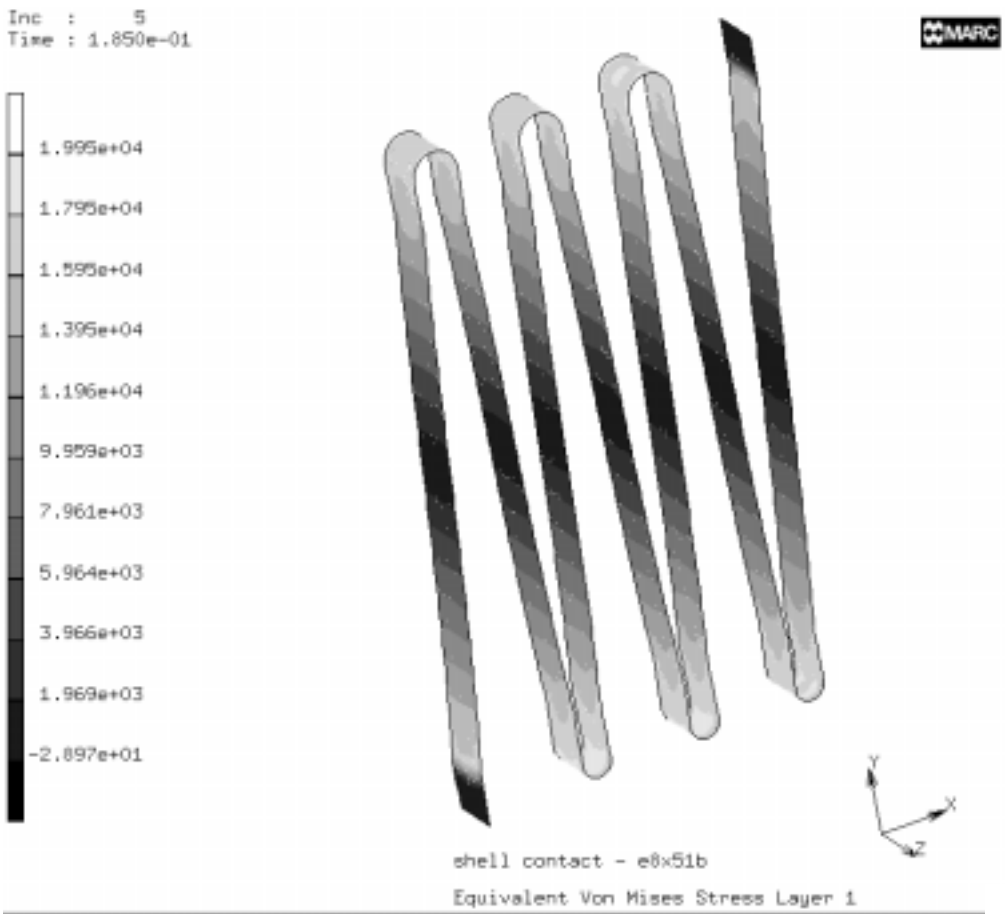

Figure 8.51-7 Deformed Shell Structure at Increment 5 for Data Set e8x51b

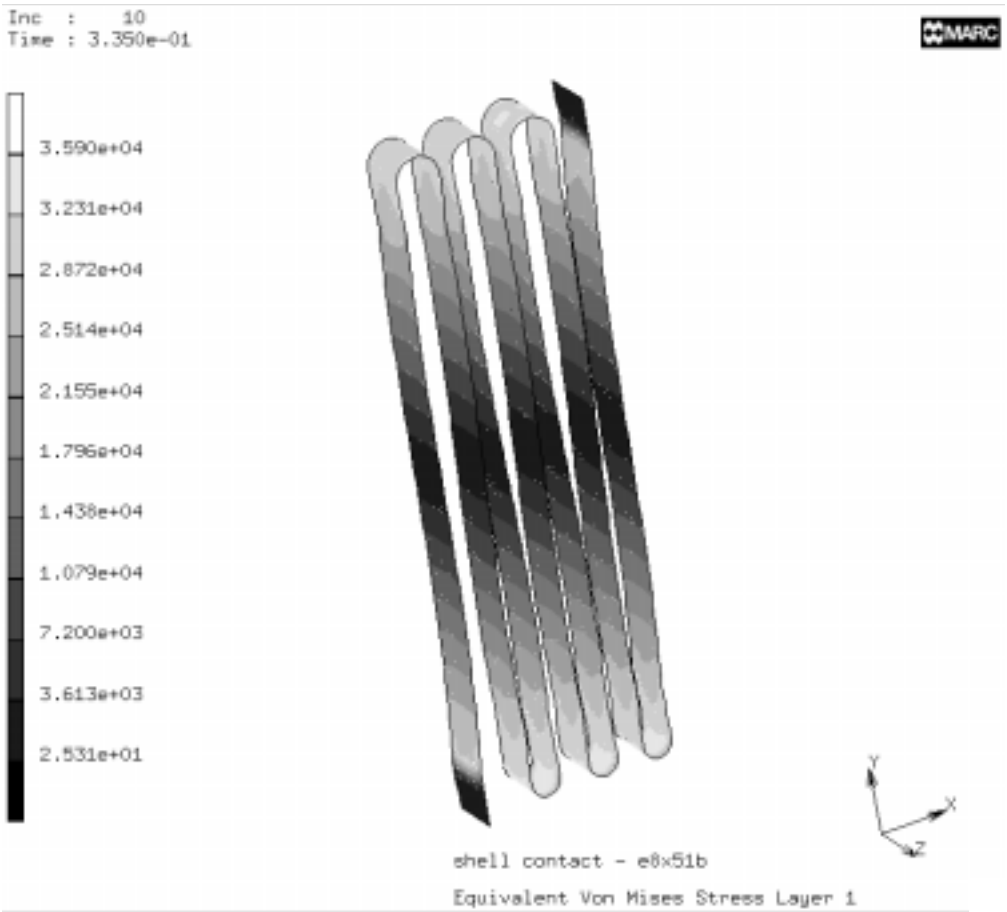

Figure 8.51-8 Deformed Shell Structure at Increment 10 for Data Set e8x51b

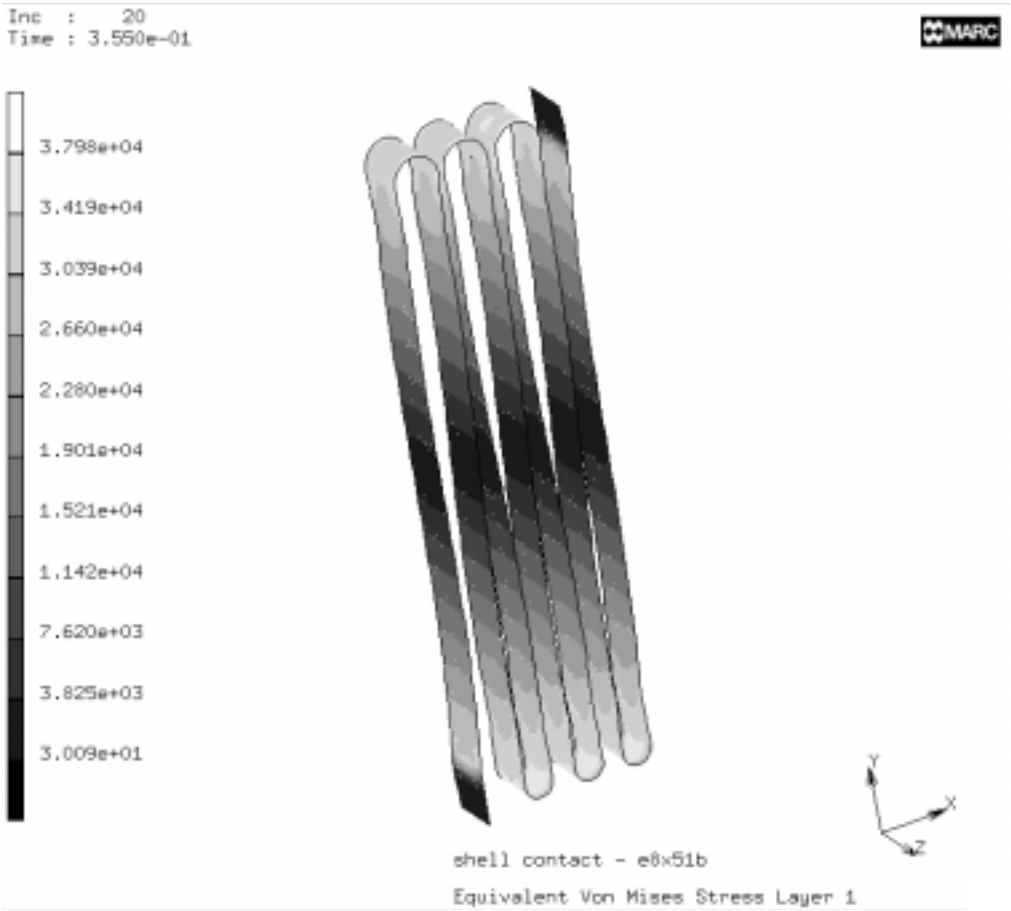

Figure 8.51-9 Deformed Shell Structure at Increment 20 for Data Set e8x51b

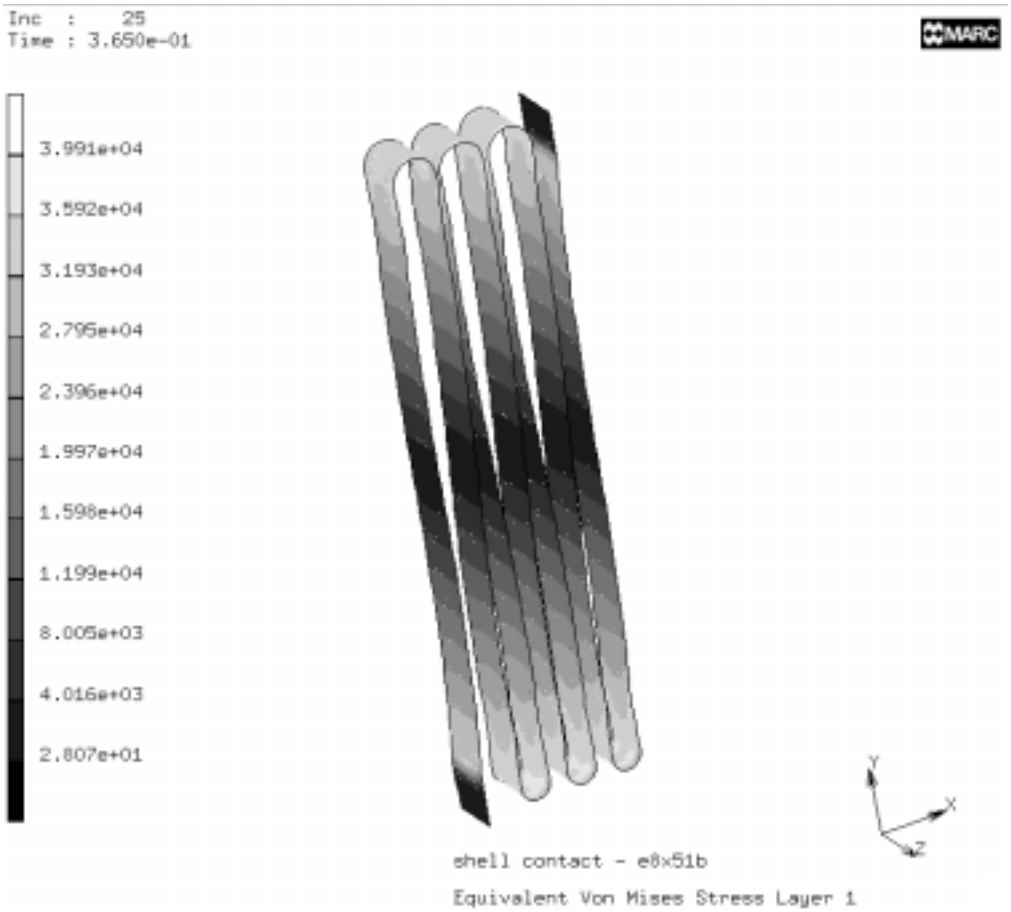

Figure 8.51-10 Deformed Shell Structure at Increment 25 for Data Set e8x51b

8.52 Deep Drawing of Sheet

This example shows the shell-shell contact capabilities. The example simulates the deep drawing of a sheet by a punch. The sheet is modeled using shell elements. The punch is also modeled using shell elements with stiffer material properties. Thus, the example shows a case of the contact of deformable-deformable shell-shell contact.

Model

The initial geometry for this problem is shown in Figure 8.52-1. Due to symmetry, only one quarter of this geometry is modeled. There are 792 elements and 848 nodes in the quarter model. Elements 1 to 360 comprise the sheet, while elements 361 to 792 constitute the punch. The deformable punch composed of stiffer shell elements stretches the sheet to form a cup.

Element

Both the sheet and punch are modeled using thick shell element number 75. Element 75 is a 4-node element.

Material Properties

Both the punch and the sheet are assumed to be modeled by an isotropic material. The material properties are:

Material	Young's Modulus (Pa)	Poisson's Ratio (Pa)	Initial Yield Stress
Sheet	6.90×10^{10}	0.30	1.59×10^{8}
Punch	1.38×10^{12}	0.30	1.00×10^{21}

The punch has a higher Young's modulus and an extremely high initial yield stress. Thus, the punch is stiffer than the sheet material. The workhardening behavior of the sheet material is input using the WORK HARD model definition option.

Boundary Conditions

The boundary conditions imposed are consistent with the four fold symmetry of the quarter model, about the z axis. Hence, the boundary conditions imposed are:

Sheet

On curve x = 0, $u_x = \theta_y = \theta_z = 0$.
On curve y = 0, $u_y = \theta_z = \theta_x = 0$.

On sheet circumference, $u_x = u_y = u_z = 0$
On sheet circumference, $\theta_x = \theta_y = \theta_z = 0$

Punch

On curve x = 0, $u_x = \theta_y = \theta_z = 0$.
On curve y = 0, $u_y = \theta_z = \theta_x = 0$.

Contact

There are two contact bodies in this simulation. Both contact bodies are deformable. Contact body 1 is the sheet and Contact body 2 is the punch. Coulomb friction is assumed with a coefficient of friction of 0.30. To prevent chattering, a node that contacts a contact body during an increment is prevented from separating during that increment. A contact bias factor of 0.99 is employed.

Control

The maximum allowed relative change in displacement increment is set to 0.05 and 20 recycles are chosen to the maximum for each increment.

History Definition

The deformable punch is moved downward by specifying a displacement increment along the negative z-direction on the nodes on the top circumference of the punch. The DISP CHANGE option is used. A total of 30 such increments are prescribed using the AUTO LOAD option.

Results

The deformed configuration for increments 10, 20, and 30 are shown in Figure 8.52-2, Figure 8.52-3, and Figure 8.52-4, respectively. The contours of effective plastic strain in the outer layer are plotted on the entire deformed geometry of the sheet in Figure 8.52-5.

Parameters, Options, and Subroutines Summary

Example e8x52.dat:

Parameters	Model Definition Options	History Definition Options
ELEMENTS	CONNECTIVITY	AUTO LOAD
END	CONTACT	CONTINUE
FINITE	CONTACT TABLE	DISP CHANGE
LARGE DISP	COORDINATES	TIME STEP
PRINT	FIXED DISP	
SETNAME	GEOMETRY	
SHELL SECTS	ISOTROPIC	
SIZING	OPTIMIZE	
TITLE	POST	
UPDATE	SOLVER	
	WORK HARD	

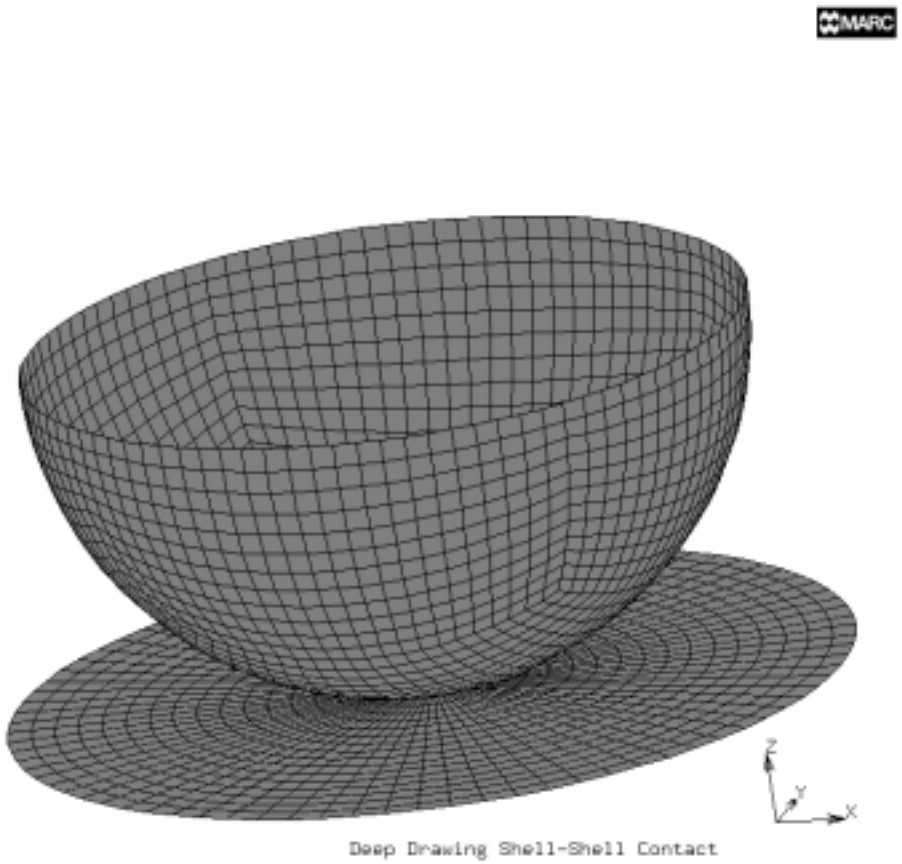

Figure 8.52-1 Initial Geometry - Only One Quarter is Modeled due to Symmetry

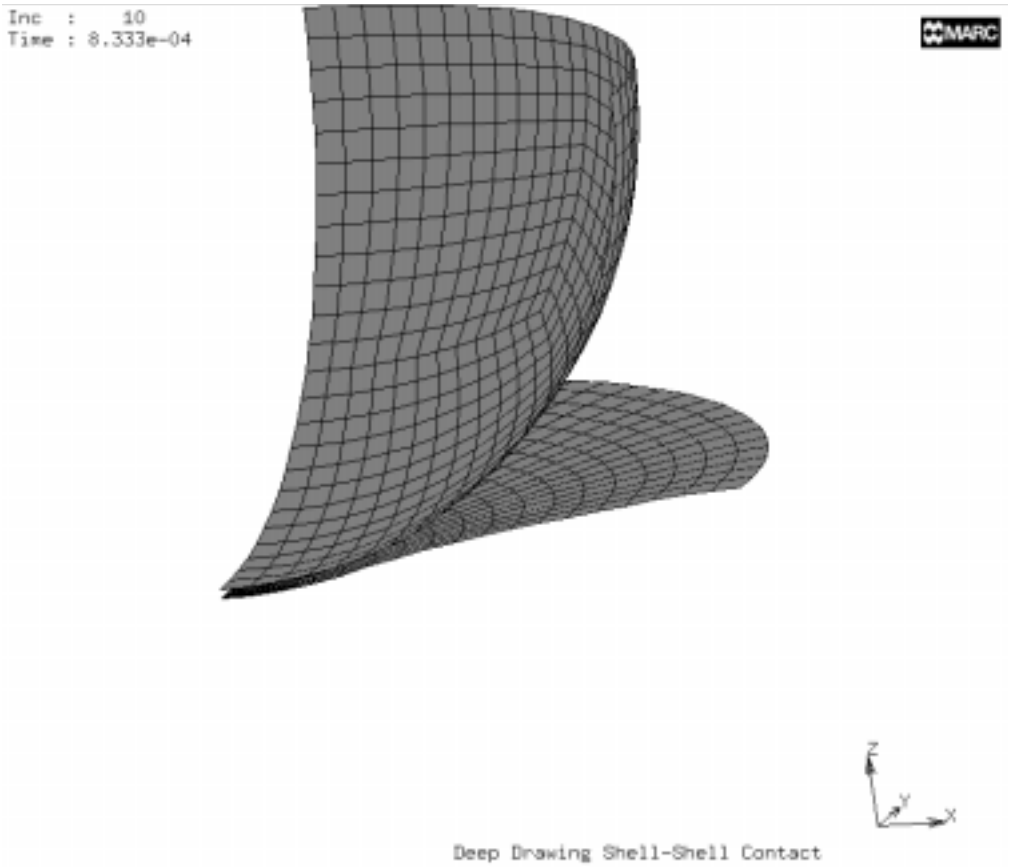

Figure 8.52-2 Deformed Geometry at the End of 10 Increments

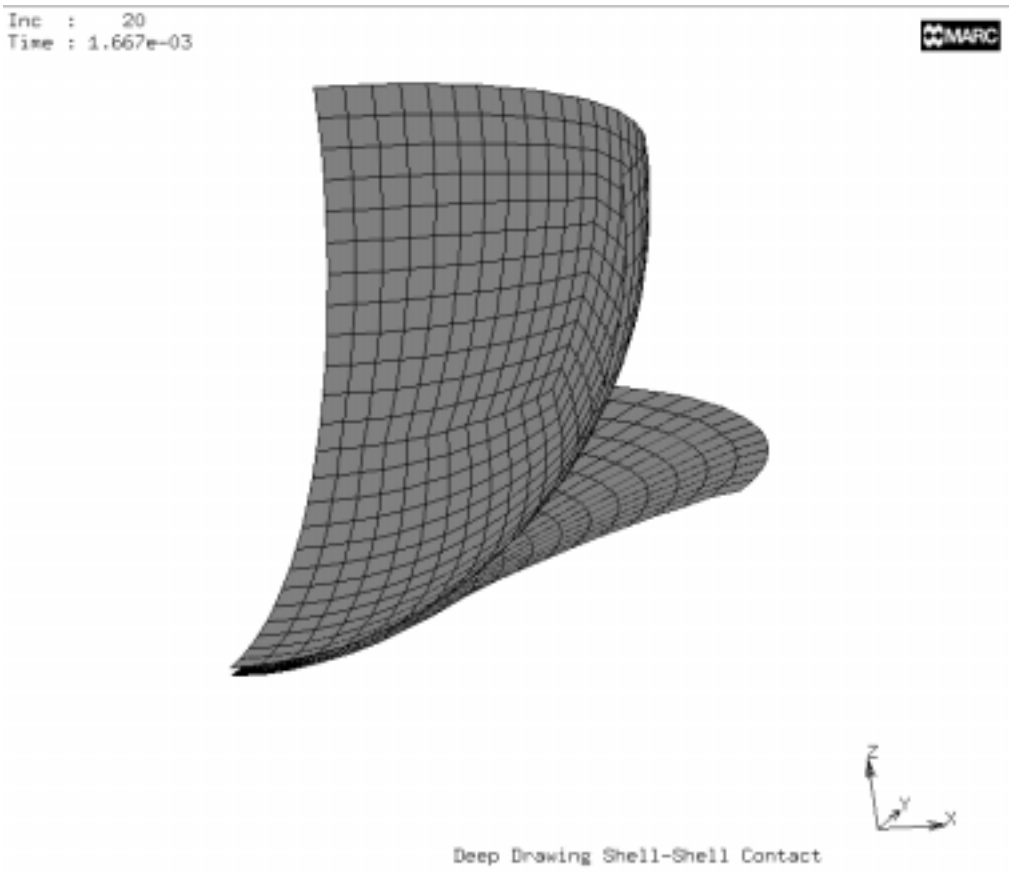

Figure 8.52-3 Deformed Geometry at the End of 20 Increments

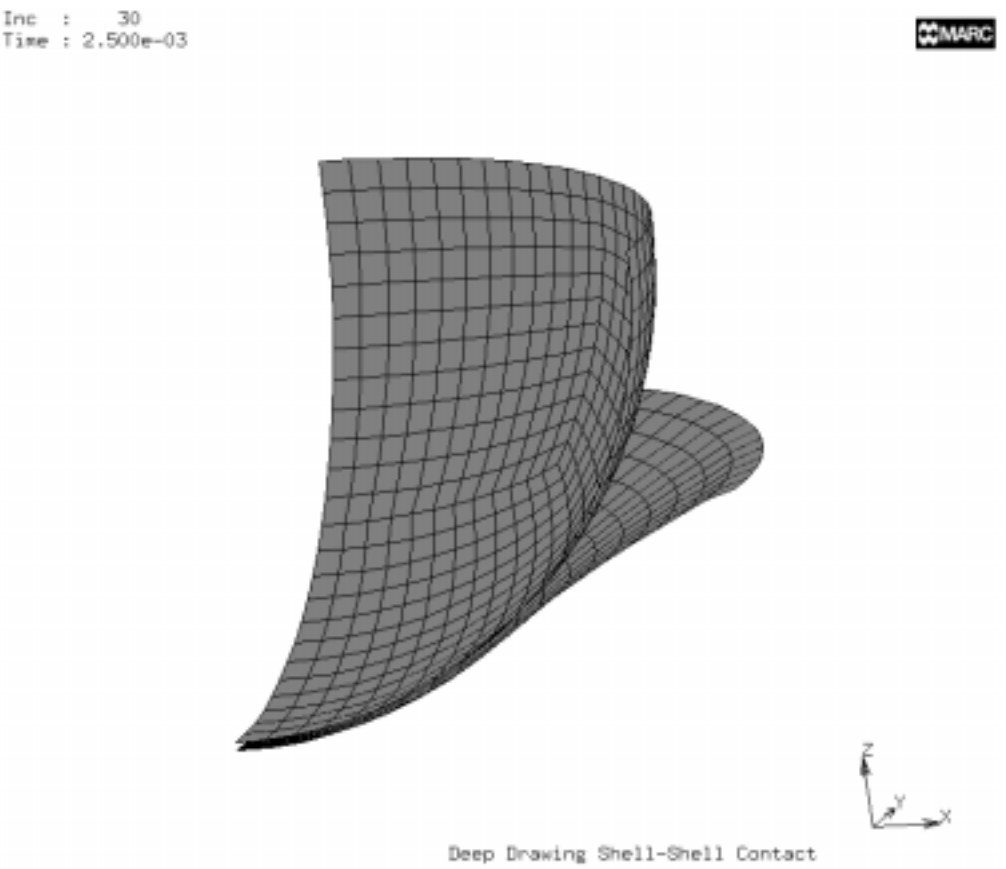

Figure 8.52-4 Deformed Geometry at the End of 30 Increments

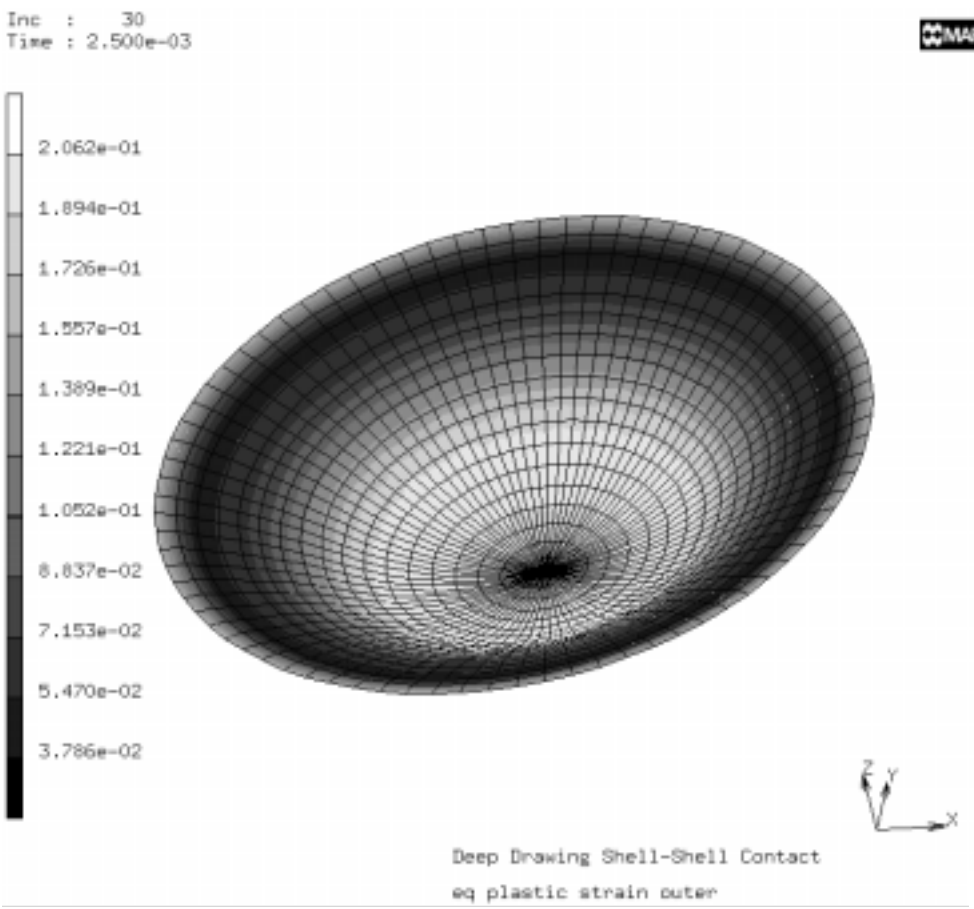

Figure 8.52-5 Effective Plastic Strain Distribution at the End of 30 Increments

8.53 Shell-Shell Contact and Separation

This example shows the simulation of shell-shell contact and separation. Two data sets are shown in this example.

Data Set	Element Used
e8x53a	75
e8x53b	49

Model

The initial model is shown in Figure 8.53-1. Data set e8x53a uses element type 75 which is a 4-node thick shell element. Data set e8x53b uses element type 49 which is a 6-node finite rotation thin shell element. Data set e8x53a uses 400 elements and 505 nodes. Data set e8x53b uses 800 elements and 1809 nodes

Material Properties

For both data sets, all materials are treated as isotropic elastic. The Young's modulus is 2.1×10^5 Pa and the Poisson's ratio is taken to be zero.

Boundary Conditions

The boundary conditions applied in the two cases are summarized below:

Data Set	Line AB	Curve AC	Line CD	Curve BD
e8x53a	$u_x=u_z=0$, $\theta_z=0$		$u_x=u_y=u_z=0$, $\theta_x=\theta_y=\theta_z=0$	
e8x53b	$u_x=u_z=0$, $\phi=0$	$\phi=0$	$u_x=u_y=u_z=0$, $\phi=0$	$\phi=0$

Geometry

The shell elements in the bottom flat portion of the shell structure have a thickness of 0.05 m while the remaining shell elements have a thickness of 0.03 m. This holds for both data sets.

Contact

There is just one contact body in this problem. No friction is assumed. The distance below which an element is considered touching a contact surface is set to 0.002 m.

Control

Ten recycles are set as a maximum for each increment. The maximum allowed relative error in residual forces is set to 0.01.

History Definition

The loading history is the same for both data sets. The loading is carried out by defining distributed pressure loads acting on the top face of the shell structure as shown in Figure 8.53-1. The pressure load is ramped up from 0.0 Pa to 0.25 Pa in 20 increments in a linear fashion. Following this, the pressure load is reduced to 0.0 Pa in a further 20 increments. There are a total of 40 increments in this problem.

Results

The top surface of the shell structure contacts the bottom surface of the shell structure at the end of 14 increments for both data sets. The end view of the deformed and initial geometry for data set e8x53a after 14 increments is shown in Figure 8.53-2. The initial and deformed geometry at the end of 20 increments is shown in Figure 8.53-3 for data set e8x53a. Figure 8.53-6 shows the variation of the y reaction force of node 405 (point D in Figure 8.53-1) with increment for data set e8x53a. The end view of the deformed and initial geometry for data set e8x53b after 14 increments is shown in Figure 8.53-4. The initial and deformed geometry at the end of 20 increments is shown in Figure 8.53-5 for data set e8x53b. Figure 8.53-7 shows the variation of the y reaction force of node 405 (point D in Figure 8.53-1) with increment for data set e8x53b. As expected, the triangular shell element 49 shows a stiffer behavior compared to the 4-node element 75. For both cases, the shell is found to completely springback to the original configuration after 40 increments when the applied distributed load returns to zero.

Parameters, Options, and Subroutines Summary

Example e8x53.dat:

Parameters	Model Definition Options	History Definition Options
ALL POINTS	CONNECTIVITY	AUTO LOAD
DIST LOADS	CONTACT	CONTINUE
ELEMENTS	COORDINATES	DISP CHANGE (for e8x53b only)
LARGE DISP	DIST LOADS	DIST LOADS
SETNAME	END OPTION	TIME STEP
SHELL SECT	FIXED DISP	
SIZING	GEOMETRY	
TITLE	ISOTROPIC	
	OPTIMIZE	
	SOLVER	

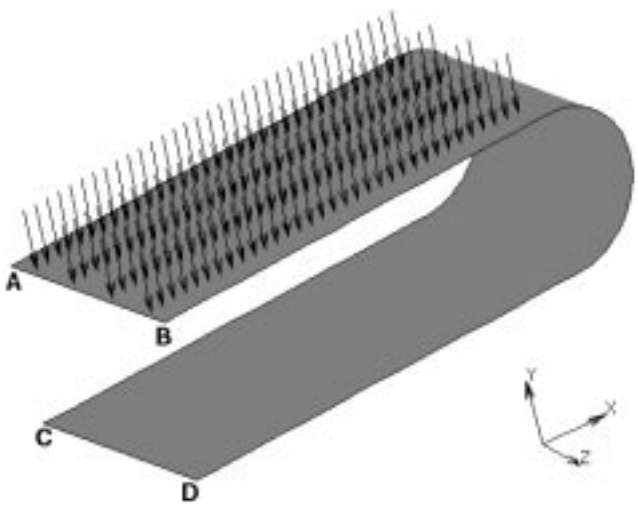

Figure 8.53-1 Initial Geometry for both Data Sets

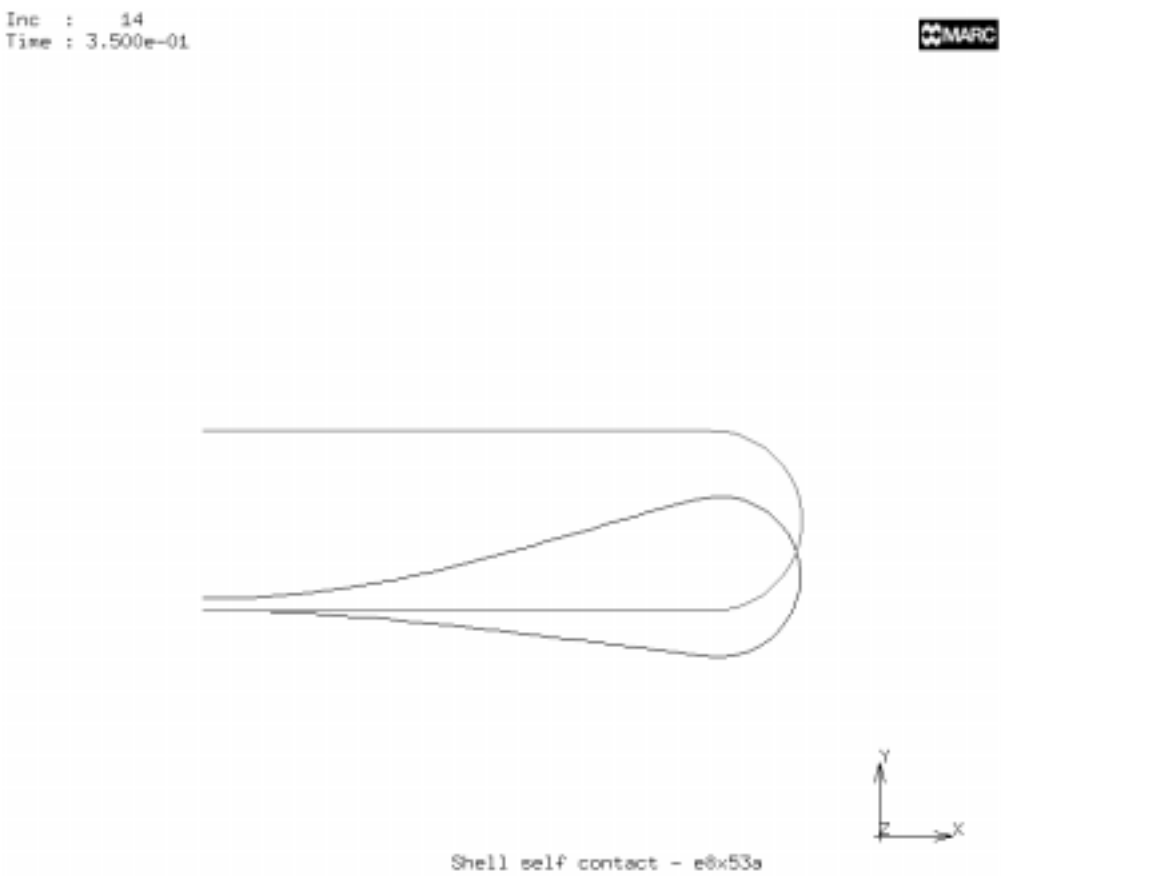

Figure 8.53-2 End View of Original and Deformed Geometry after 14 Increments for Data Set e8x53a

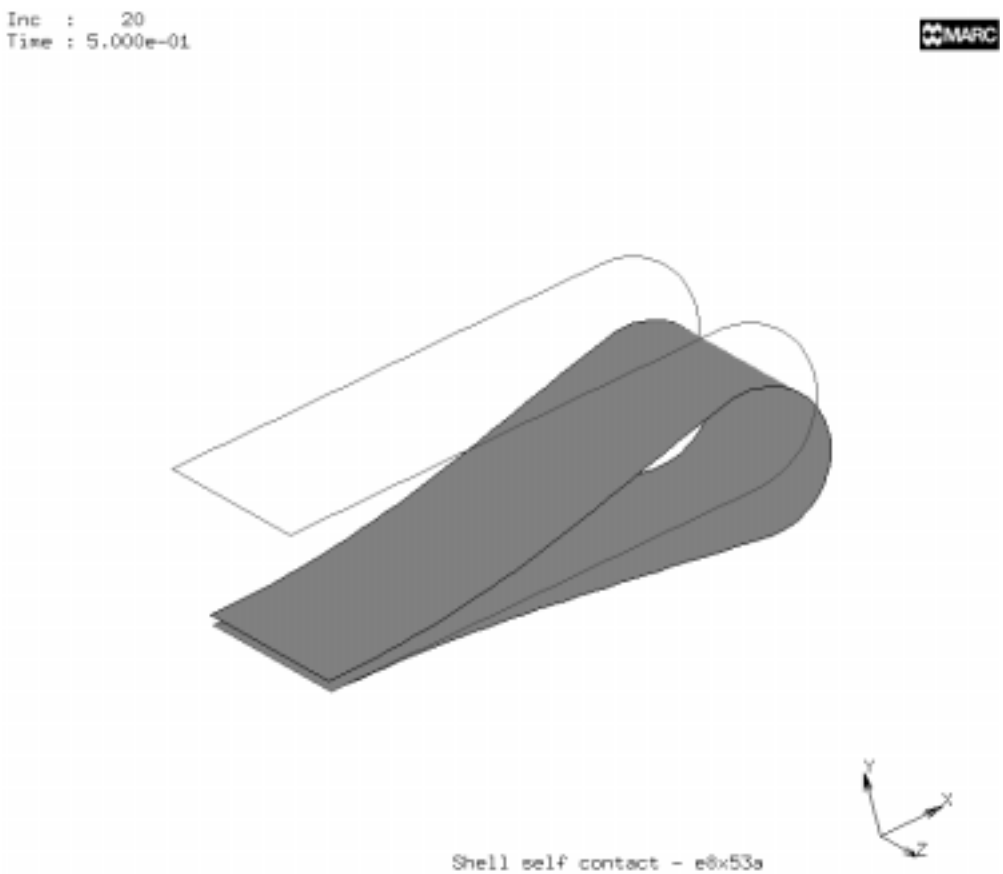

Figure 8.53-3 Original and Deformed Geometry after 20 Increments for Data Set e8x53a

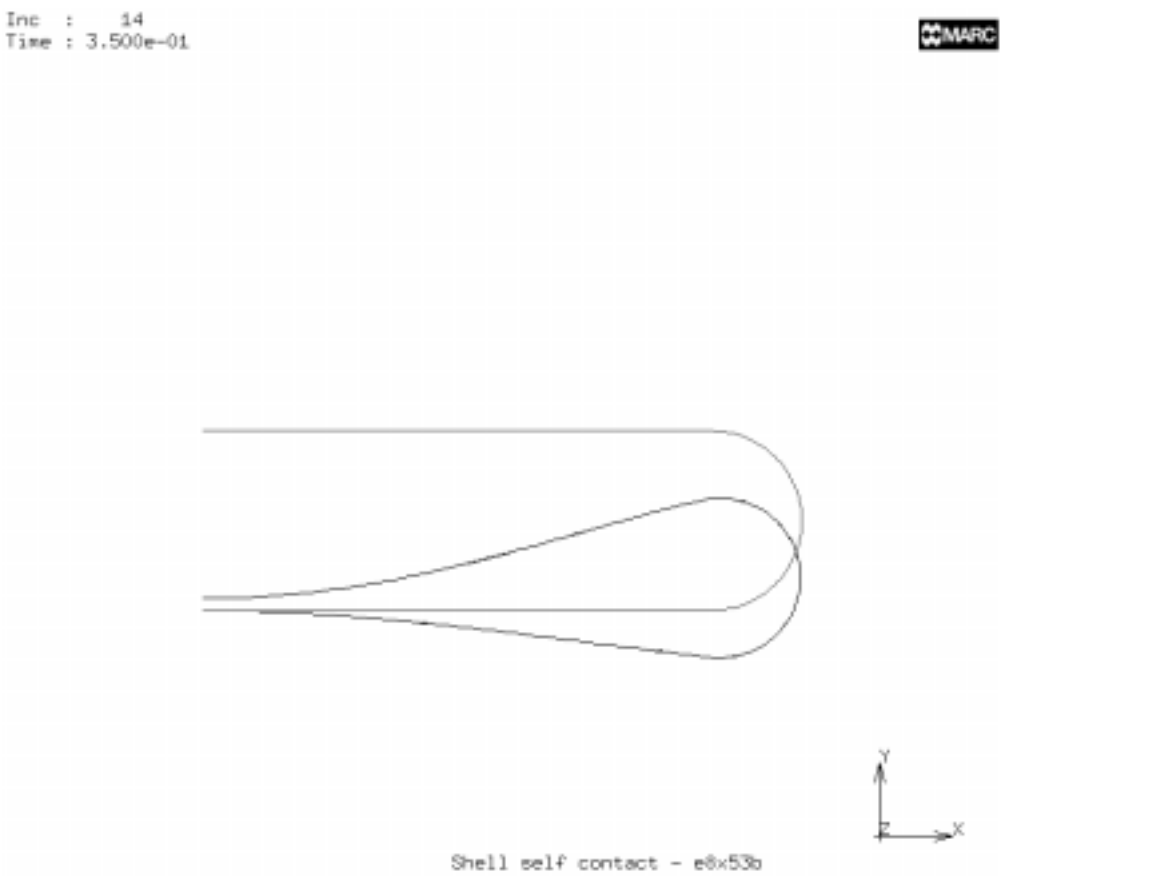

Figure 8.53-4 Original and Deformed Geometry after 14 Increments for Data Set e8x53b - End View

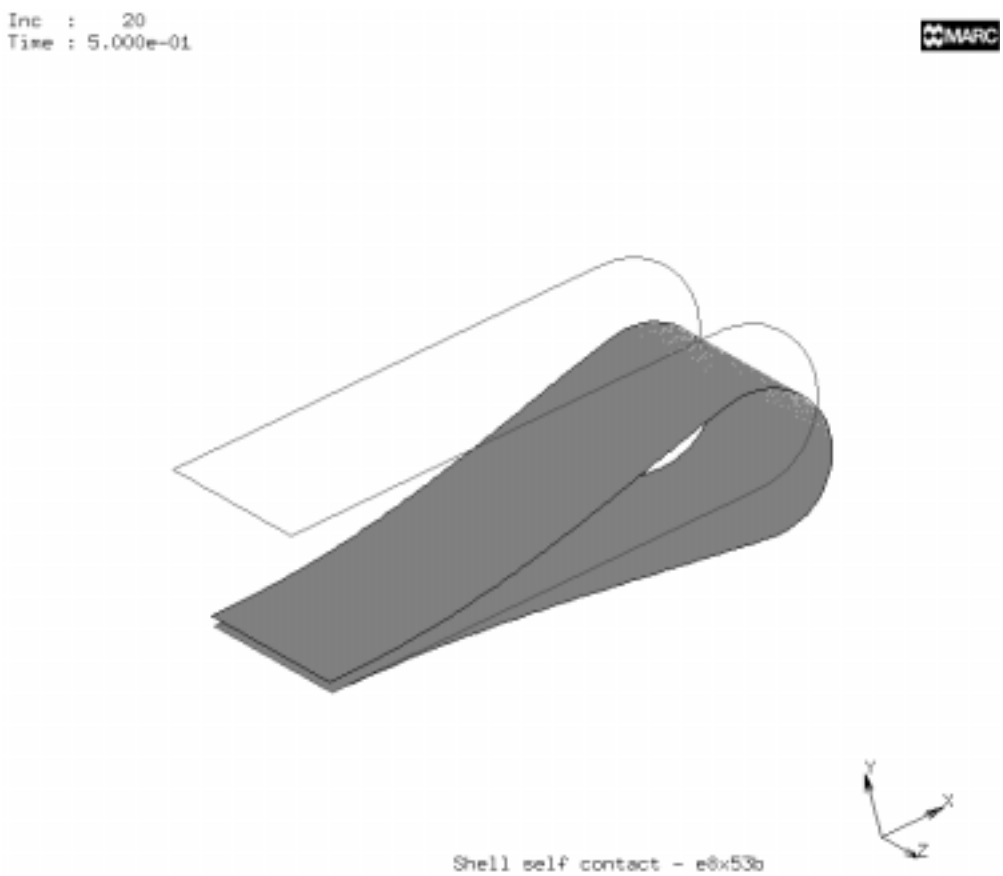

Figure 8.53-5 Original and Deformed Geometry after 20 Increments for Data Set e8x53b

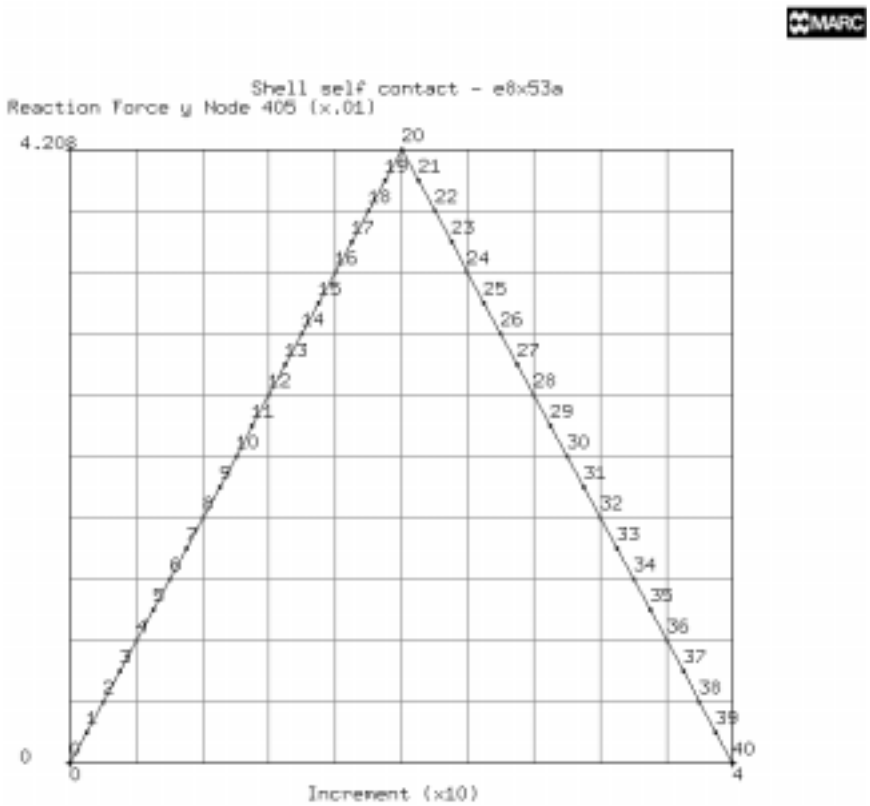

Figure 8.53-6 History Plot of the Variation of the y Reaction Force at Node 405 for Data Set e8x53a

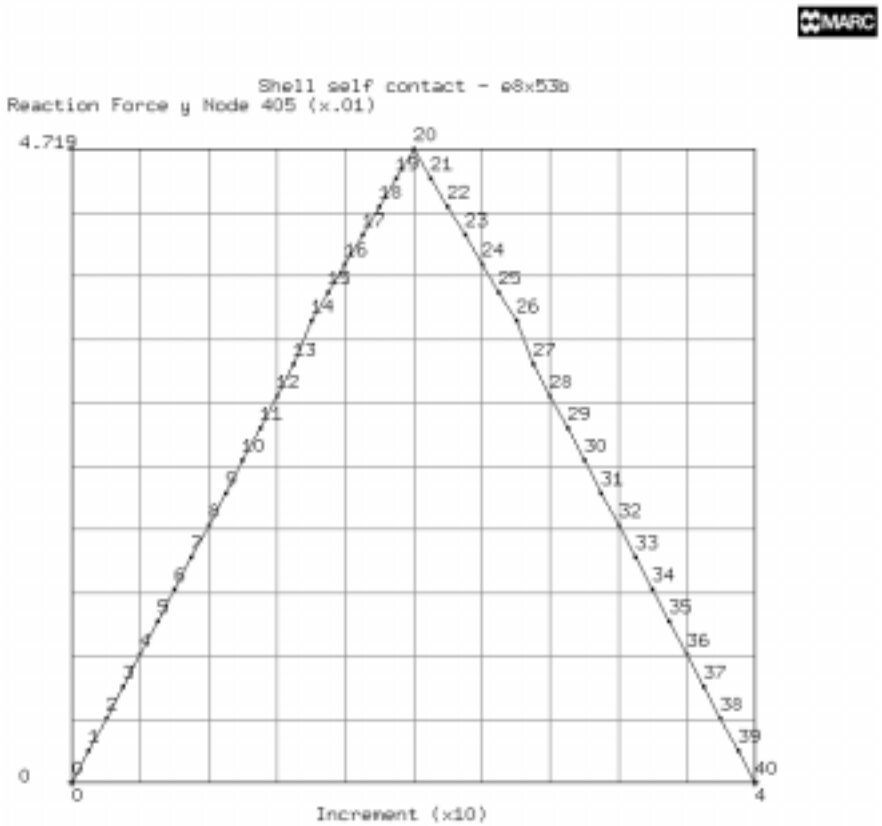

Figure 8.53-7 History Plot of the Variation of the y Reaction Force at Node 405 for Data Set e8x53b

8.54 Self Contact of a Shell Structure

This example shows the self contact of a shell structure. Even though there is little straining in this example, large displacements and finite rotations are involved which poses a numerical challenge to the computational algorithms in the code.

Model

The initial geometry of the model is shown in Figure 8.54-1 as a side view. The model is shown in Figure 8.54-2. There are 12 elements and 26 nodes in the problem. The 4-node thick shell element number 75 is used in the analysis.

Material Properties

The shell elements are assumed to be isotropic and elastic. The Young's modulus is 1.2×10^3 Pa and the Poisson's ratio is 0.295.

Boundary Conditions

The boundary conditions imposed on this problem are:

Nodes	Imposed Boundary Conditions
1, 2	$u_x=u_y=0$
1 to 26	$u_z=\theta_x=0$
25, 26	$u_y=0$

Contact

There is just one contact body here and self contact is allowed. No friction is assumed. The distance below which a node is assumed to be in contact is 0.02 m.

Geometry

The thickness of all elements is assumed to be 0.20 m.

Control

The maximum allowed error in residual forces is assumed to be 0.10. A maximum of 10 recycles is allowed per increment.

History Definition

The loading is imposed by x displacements at nodes 25 and 26. An incremental x displacement of 0.2m is imposed on nodes 25 and 26 in each increment. A total of 10 increments are applied.

Results

The deformed shape of the structure is shown in side view in Figure 8.54-3 for increment 5. The deformed shape of the structure is shown in side view in Figure 8.54-4 for increment 10. In both figures, the initial configuration is also plotted. The deformed and initial configurations show the large rotation involved in this shell-shell contact example. Figure 8.54-5 shows the variation of reaction force x versus x displacement for node 26.

Parameters, Options, and Subroutines Summary

Example e8x54.dat:

Parameters	Model Definition Options	History Definition Options
ELEMENTS	CONNECTIVITY	AUTO LOAD
END	CONTACT	CONTINUE
LARGE DISP	COORDINATES	DISP CHANGE
PRINT	END OPTION	TIME STEP
SETNAME	FIXED DISP	
SHELL SECT	GEOMETRY	
SIZING	ISOTROPIC	
TITLE	OPTIMIZE	
UPDATE	SOLVER	

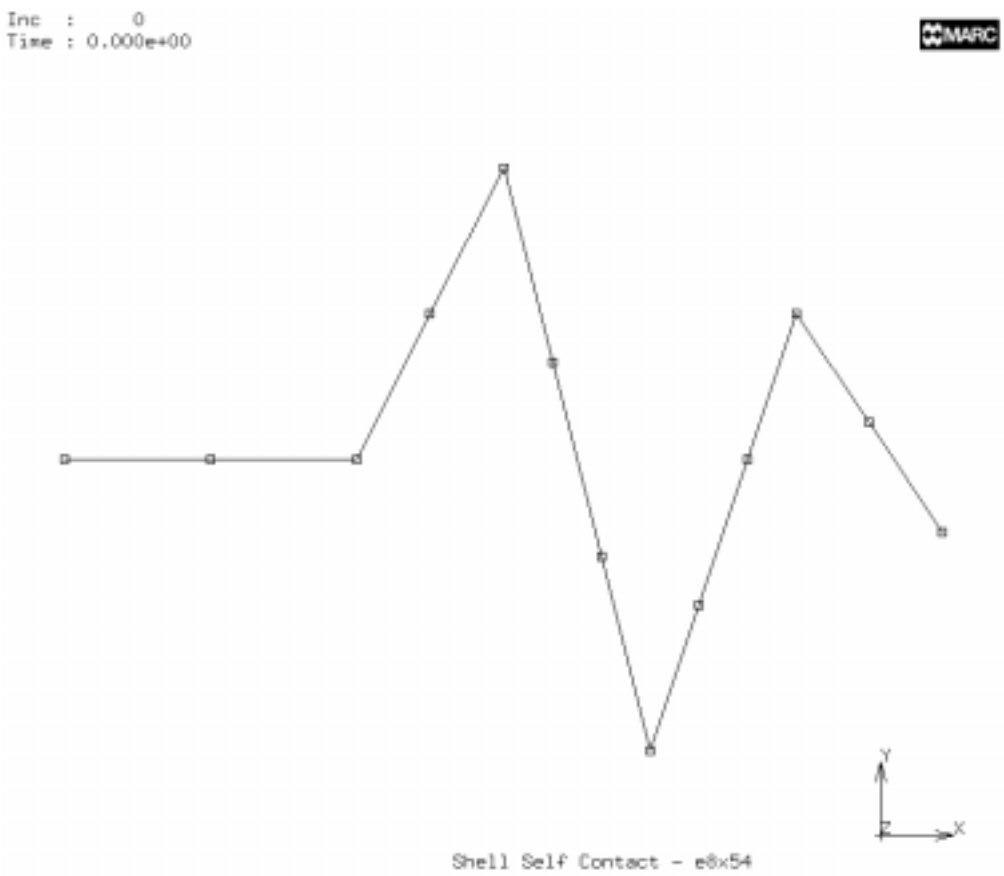

Figure 8.54-1 Side View of Initial Geometry

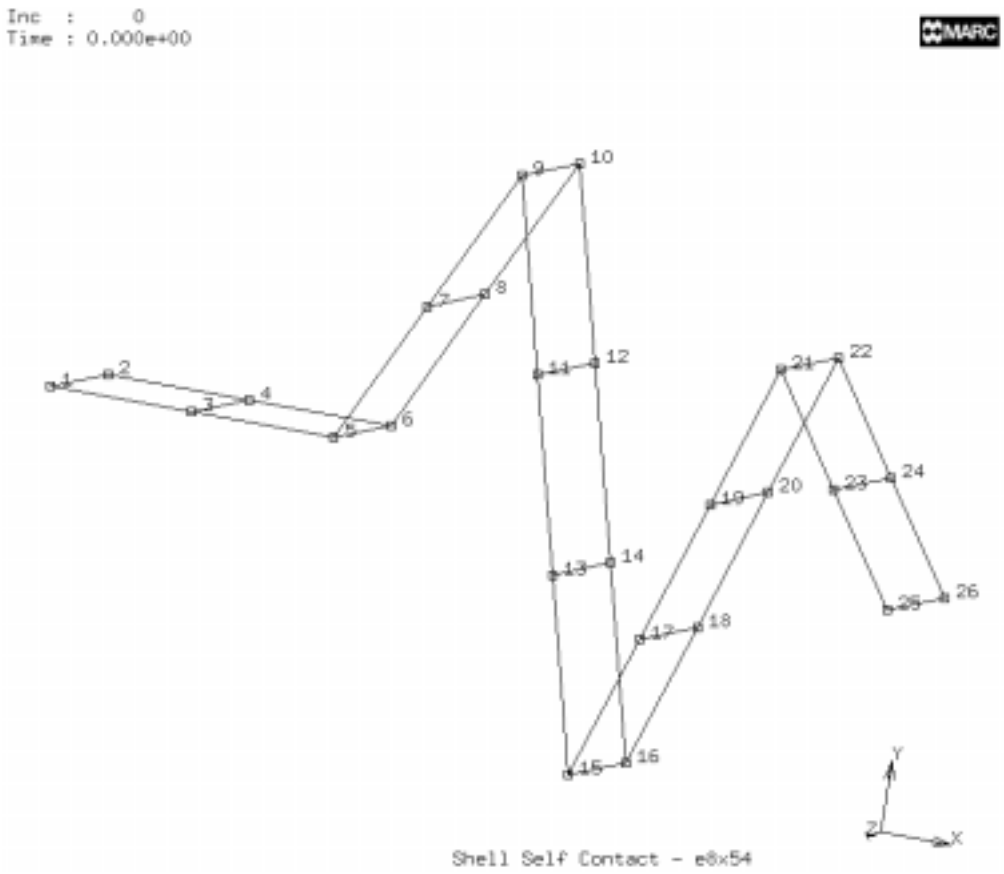

Figure 8.54-2 Initial Model of Structure

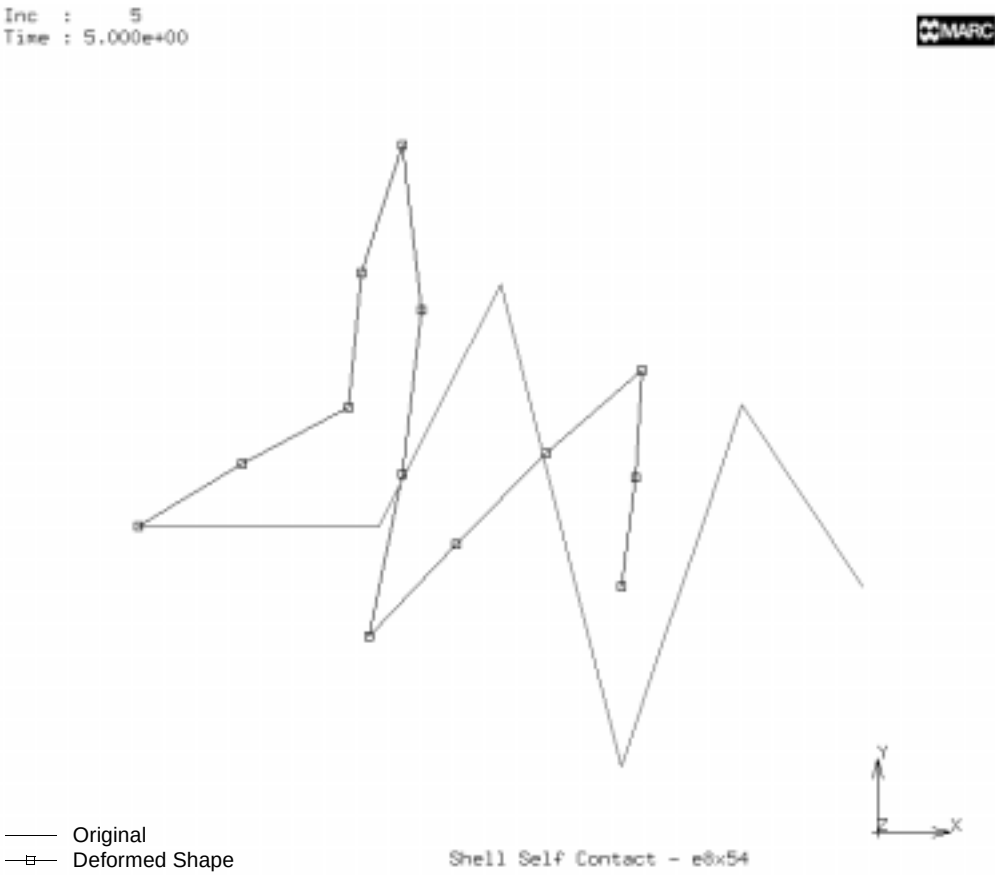

Figure 8.54-3 Deformed Shape of the Structure at Increment 5

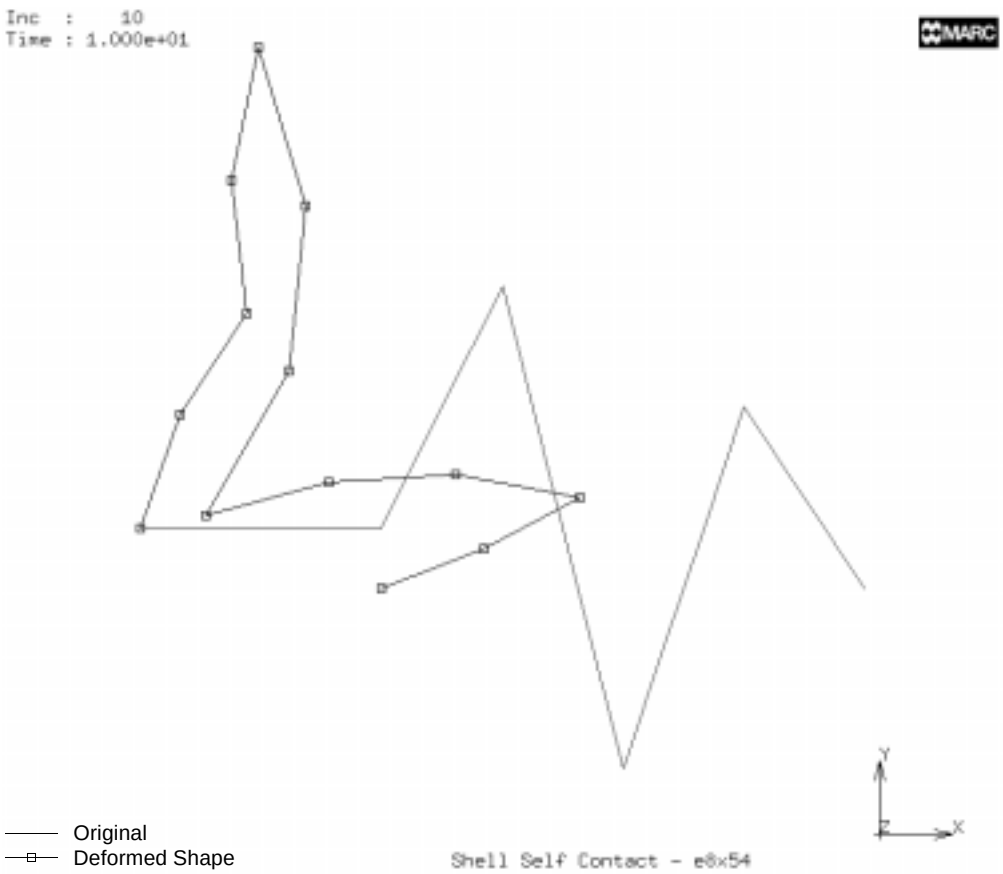

Figure 8.54-4 Deformed Shape of the Structure at Increment 10

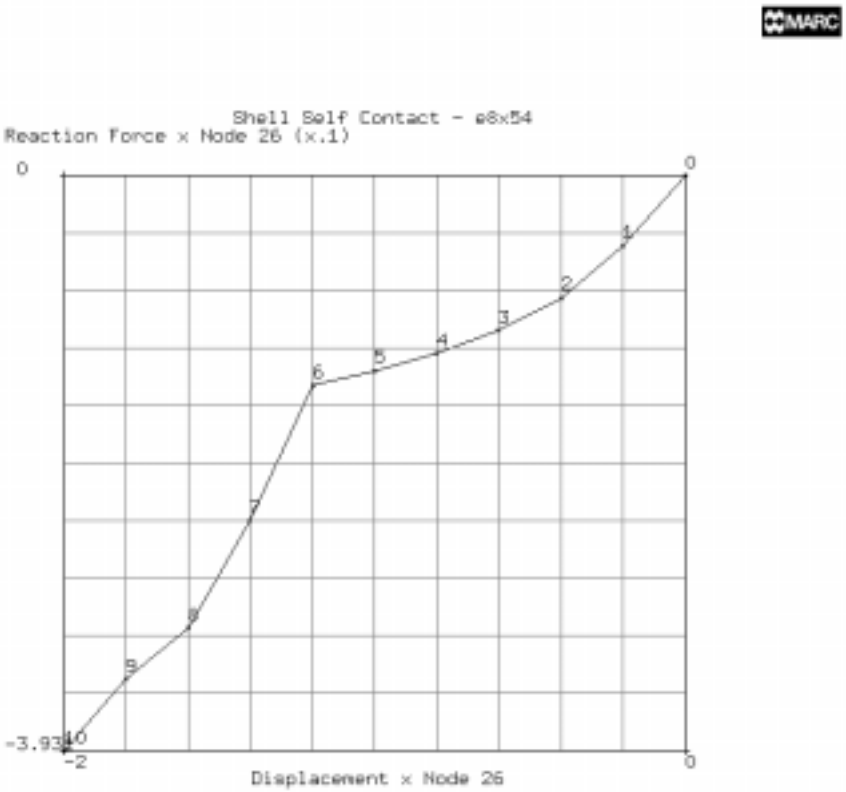

Figure 8.54-5 Displacement x versus Reaction Force X for Node 26

8.55 Deep Drawing of Copper Sheet

This example shows the deep drawing of a copper sheet. Shell elements are used to model the sheet. There are two data sets in this example. Data set e8x55a uses a velocity controlled punch. Data set e8x55b uses a load controlled punch. The effect of clamp down pressure is modeled using point loads.

Model

The initial model is shown in Figure 8.55-1. A 15° sector of the punch is used. The model consists of 79 elements and 121 nodes to model the sheet. There are four rigid bodies in the model, a punch, a lower die, and two symmetry bodies. In the case of data set e8x55b, an extra detached node (number 122) is associated with the rigid punch and a point load is applied to this node.

Element

The 4 noded thick shell element number 75 is used in this example to model the copper sheet.

Material Properties

The sheet is assumed to be isotropic with an elastic modulus of 17×10^6 psi and a Poisson's ratio of 0.33. The initial yield stress is assumed to be 1.08×10^4 psi. The workhardening characteristics of the sheet are given by the WORK HARD model definition option.

Boundary Conditions

The boundary conditions for this problem are imposed using the CONTACT option. Point loads are applied along the x direction on the nodes of elements 1 to 6 (Figure 8.55-2) to model the effect of the clamp down pressure to prevent wrinkling.

Contact

There are 5 contact bodies in this problem. Contact body 1 is the deformable body representing the sheet. Body 2 is a rigid body representing the punch. In the case of data set e8x55a, the punch is a velocity controlled body moving at a speed of 3.2 in/s along the +x direction. For data set e8x55b, the punch is load controlled. Contact body 3 represents the lower die. Contact bodies 4 and 5 represent the symmetry surfaces in the problem. Coulomb friction is used with a friction coefficient of 0.04. The distance below which a node is considered to be sticking to a contact surface is 8.75×10^{-4} in. A contact bias factor of 0.90 is used.

Control

The convergence control is displacement based. The maximum allowed relative change in displacement increment is 0.05.

History Definition

The effect of clamp down pressure is simulated by applying point loads to elements 1 to 6. In increment 1, the clamp down pressure is applied for both data sets. The clampdown pressure is unchanged for the entire simulation for both data sets. The clampdown pressure is detailed in the table below and is the same for both data sets.

Nodes	P_x (lb)
1, 3, 4, 6, 7, 9, 10, 12	2.6
2, 5, 8, 11	5.2

For data set e8x55a, the punch is moved along the +x direction at a speed of 3.2 in/s for a further 99 increments. For data set e8x55b, a load of 3.08 lbs per increment is applied along the x direction for 79 increments.

Results

The final deformed geometry is shown in Figure 8.55-3 for data set e8x55a. The contours of total effective plastic strain are superimposed. The final deformed geometry is shown in Figure 8.55-4 for data set e8x55b. The contours of total effective plastic strain are superimposed.

Parameters, Options, and Subroutines Summary

Example e8x55a.dat and e8x55b.dat:

Parameters	Model Definition Options	History Definition Options
ALL POINTS	CONNECTIVITY	AUTO LOAD
ELEMENTS	CONTACT	CONTINUE
END	CONTROL	POINT LOAD
FINITE	COORDINATES	TIME STEP
LARGE DISP	ISOTROPIC	
SHELL SECT	OPTIMIZE	
SIZING	POINT LOAD	
TITLE	WORK HARD	
UPDATE		

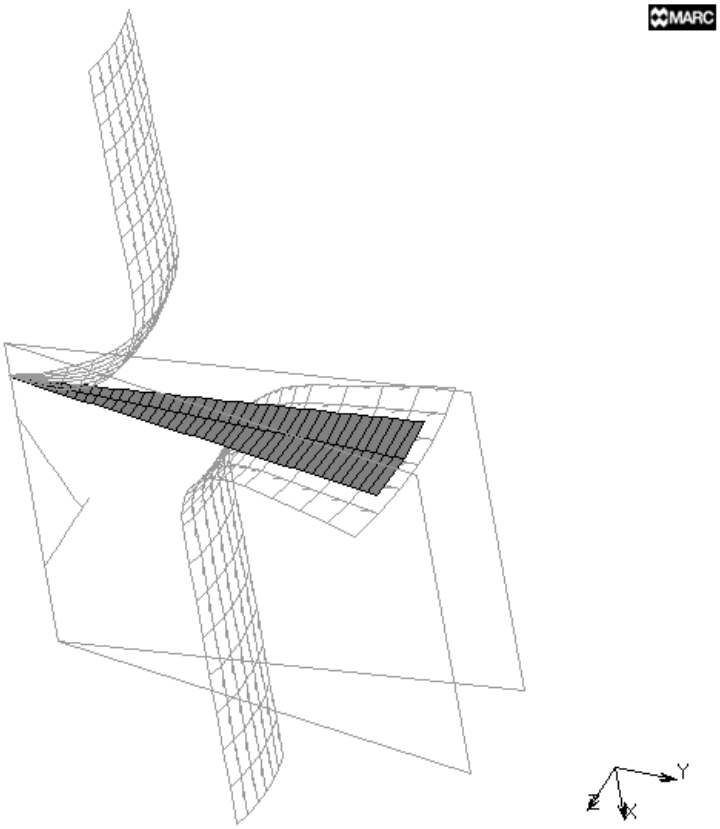

Figure 8.55-1 Initial Model

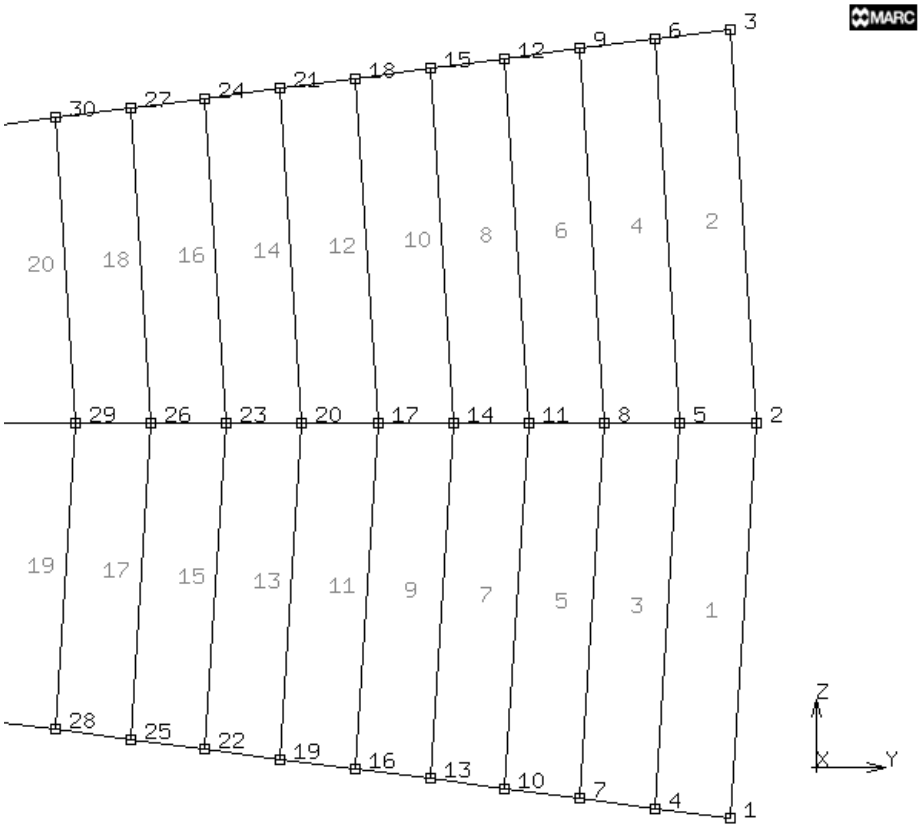

Figure 8.55-2 Elements to which Clamp Down Pressure is Applied

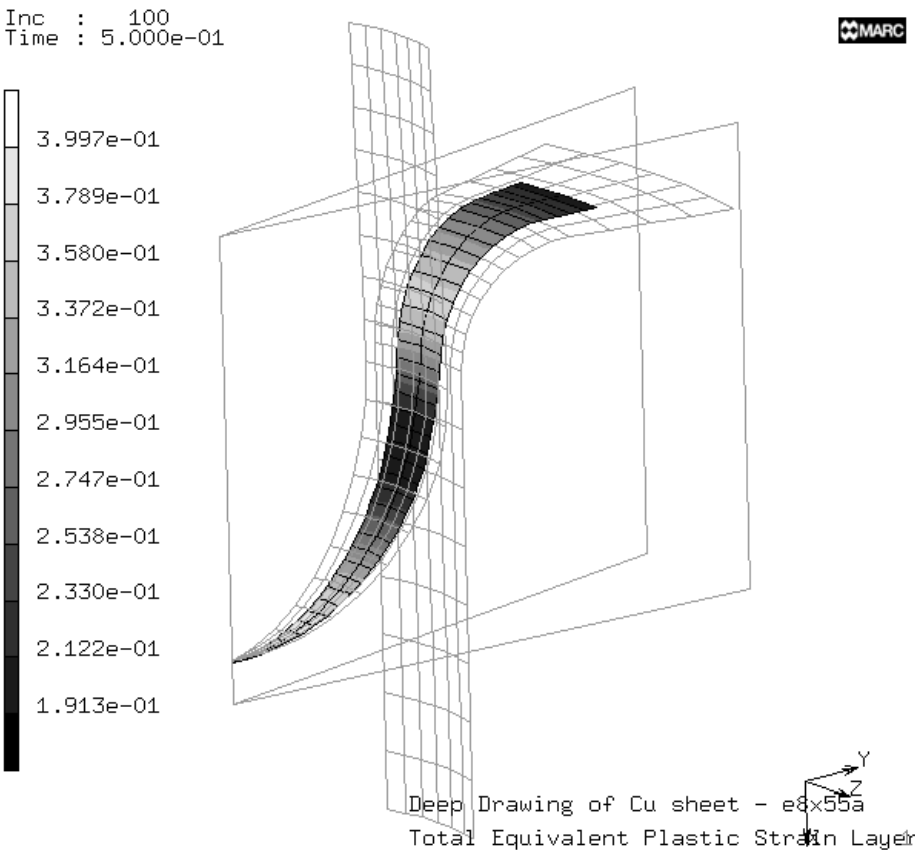

Figure 8.55-3 The Final Deformed Geometry for Data Set e8x55a

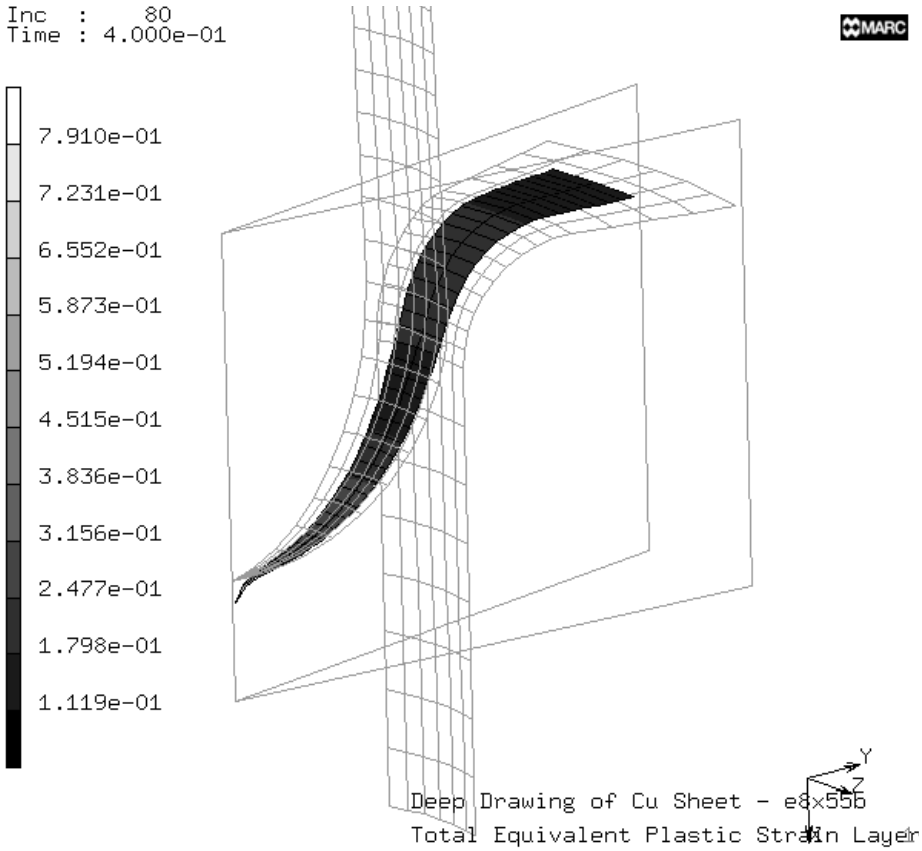

Figure 8.55-4 The Final Deformed Geometry for Data Set e8x55b

8.56 2D Contact Problem - Load Control and Velocity Control

This example shows the case of 2D contact. Two data sets are shown, one with load controlled contact bodies (e8x56a) and the other with velocity controlled contact bodies (e8x56b).

Model

The initial model is identical for both data sets and is shown in Figure 8.56-1. There are 320 elements and 405 nodes. An extra detached node (number 406) is added for data set e8x56b. This node is used to apply a point load to model the load controlled contact body in data set e8x56b.

Element

The axisymmetric 4-noded isoparametric element number 10 is used. The constant dilatation option is chosen.

Material Properties

The material properties are identical for both data sets. The Young's modulus is 3×10^7 psi and the Poisson's ratio is 0.70. The initial yield stress is 4×10^4 psi. The workhardening behavior is given using the WORK HARD model definition option.

Boundary Conditions

The nodes 1 to 5 are held to have zero x displacement. The boundary conditions along y are enforced by contact.

Contact

There are three contact bodies in this problem. Contact body 1 is the deformable body. Contact body 2 is the upper die and contact body 3 is the lower die. Contact body 2 is held stationary. Contact body 3 is velocity controlled for data set e8x56a. For data set e8x56b, contact body 3 is load controlled. A point load is applied along the +y direction to node 406 which is attached to contact body 3. Increment splitting is prevented for both data sets. The distance below which a node is considered to be sticking to a contact body is 0.001 in. The contact separation force is assumed to be 1×10^7 lb.

Control

Convergence control is displacement based. The maximum allowed relative change in displacement increment is set to 0.10.

History Definition

The loading is done using the CONTACT options. In data set e8x56a, the lower contact body (contact body 3) is velocity controlled. It is moved at a speed of 1 in/s along the +y direction. The first 18 increments are chosen with a time step of 0.1. Following this, 8 more increments are chosen with a time increment of 0.05.

For data set e8x56b, a point load of 1×10^5 lb is applied in every increment for the first 18 increments along the +y direction on node 406. Following this, load increments of 1×10^6 lb are applied for 24 more increments on node 406.

Results

The final deformed shape is shown in Figure 8.56-2 for data set e8x56a. The final deformed shape is shown in Figure 8.56-3 for data set e8x56b.

Parameters, Options, and Subroutines Summary

Example e8x56a.dat and e8x56b.dat:

Parameters	Model Definition Options	History Definition Options
ALL POINTS	CONNECTIVITY	AUTO LOAD
ELEMENTS	CONTACT	CONTINUE
END	CONTROL	DISP CHANGE
FINITE	COORDINATES	TIME STEP
LARGE DISP	FIXED DISP	
SIZING	ISOTROPIC	
TITLE	OPTIMIZE	
UPDATE	SOLVER	
	WORK HARD	

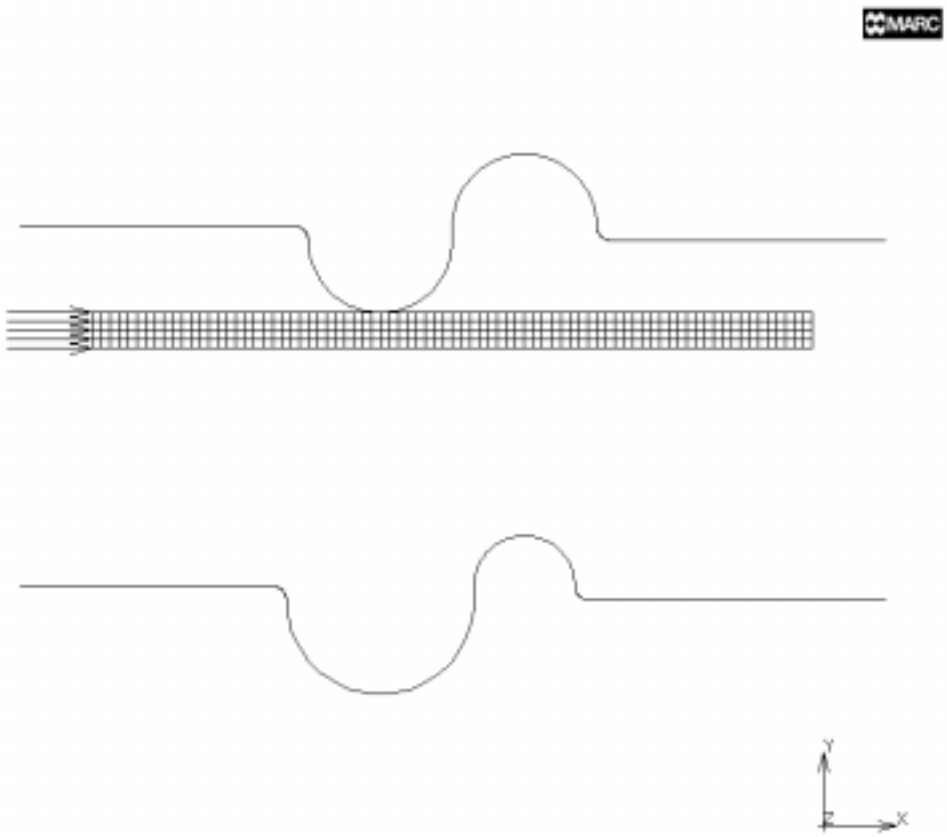

Figure 8.56-1 Initial Model for both Data Sets

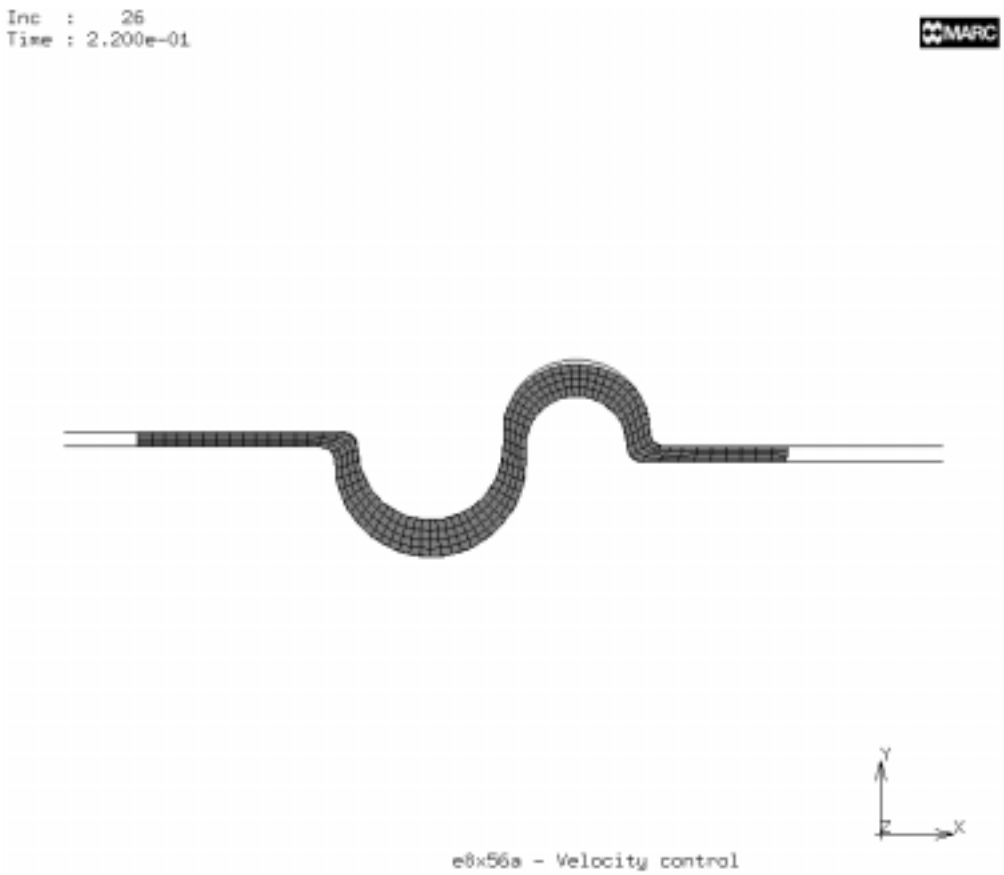

Figure 8.56-2 The Final Deformed Shape for Data Set e8x56a

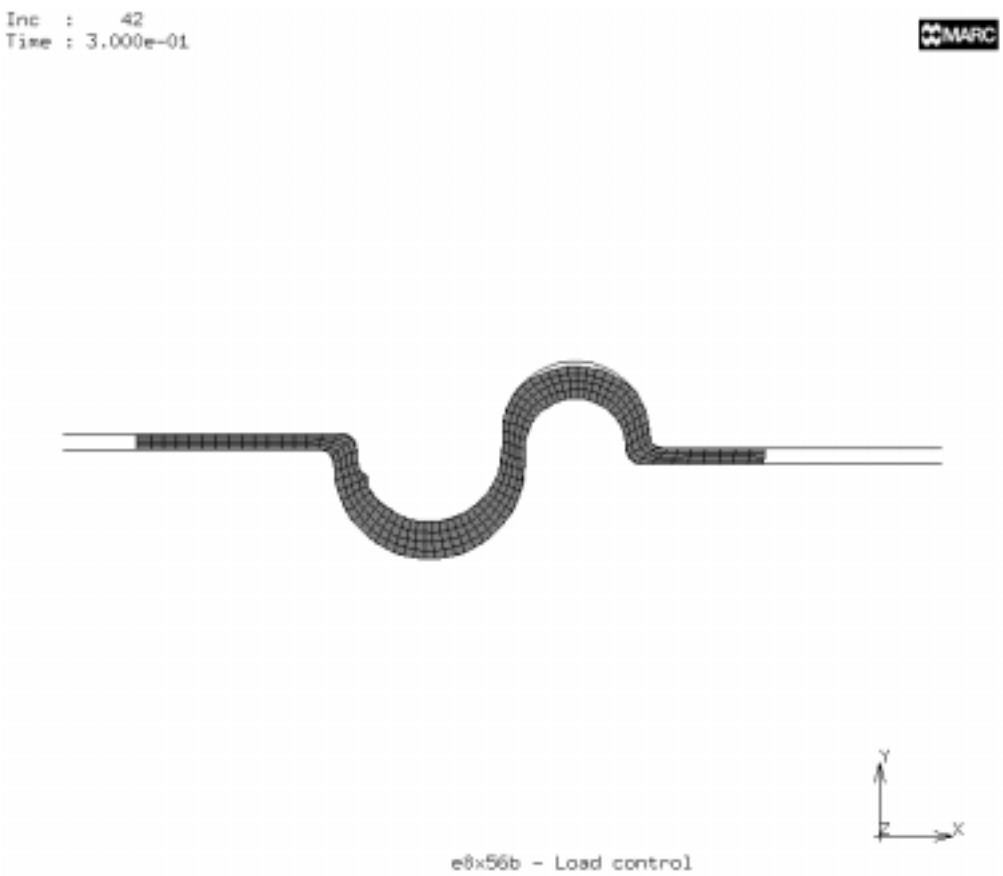

Figure 8.56-3 The Final Deformed Shape for Data Set e8x56b

8.57 The ADAPTIVE Capability with Shell Elements

This example shows the ADAPTIVE capability in conjunction with shell elements. The example consists of four data sets, as given below.

Data Set	Element Used
e8x57a	4-node thick shell element number 75
e8x57b	3-node thin shell element number 138
e8x57c	4-node thin shell element number 139
e8x57d	4-node reduced integration thick shell element number 140

In each of these data sets, the problem involves the deformation of the structure under a point load. The ADAPTIVE model definition choice uses the Zienkiewicz-Zhu stress error as the criterion.

Model

The model consists of one 4-node element for data sets e8x57a, e8x57c, and e8x57d. Data set e8x57b consists of two 3-node triangular elements. All four data sets comprise of 4 nodes. The 4 nodes form a square of side 0.5 units in the x-y plane.

Material Properties

All four data sets have identical material properties. The Young's modulus is assumed to be 1.092×10^7 psi and the Poisson's ratio is assumed to be 0.30.

Boundary Conditions

The boundary conditions are identical for all four data sets and are given below.

Boundary Condition	Nodes
$u_x = u_y = \theta_z = 0$	1, 2, 3, 4
$u_z = 0$	2, 3, 4
$\theta_y = 0$	1, 4
$\theta_x = 0$	1, 2
$P_z = 1$	1

Adaptive

The ADAPTIVE model definition card is used to indicate that element refinement must be performed. A maximum of eight level of refinement are chosen. The Zienkiewicz-Zhu stress error criterion is used to flag the ADAPTIVE capability.

History Definition

The loading is imposed by the help of the model definition card POINT LOAD. The problem is elastic and a single increment is sufficient to solve the problem. However, the ADAPTIVE criterion requires successive subincrements for the single increment. No history definition cards are necessary in this single increment problem.

Results

The initial and deformed shapes with the adapted elements are shown at the end of the final subincrement of increment zero for data set e8x57a in Figure 8.57-2. The deformed shape is similar for all four data sets. Data sets e8x57a and e8x57d use six adaptive subincrements while e8x57b and e8x57c need seven subincrements. Figure 8.57-3 and Figure 8.57-4 show contours of the equivalent von Mises stress for data sets e8x57a and e8x57c respectively. As expected, the maximum value of the von Mises equivalent stress is higher for the discrete Kirchhoff quadrilateral element 139 (e8x57c) than the thick shell element 75 (e8x57a).

Parameters, Options, and Subroutines Summary

Example e8x57.dat:

Parameters	Model Definition Options
ADAPTIVE	ADAPTIVE
ELASTIC	CONNECTIVITY
ELEMENTS	COORDINATES
END	END OPTION
SHELL SECT	FIXED DISP
SIZING	GEOMETRY
	ISOTROPIC
	OPTIMIZE
	POINT LOAD
	SOLVER

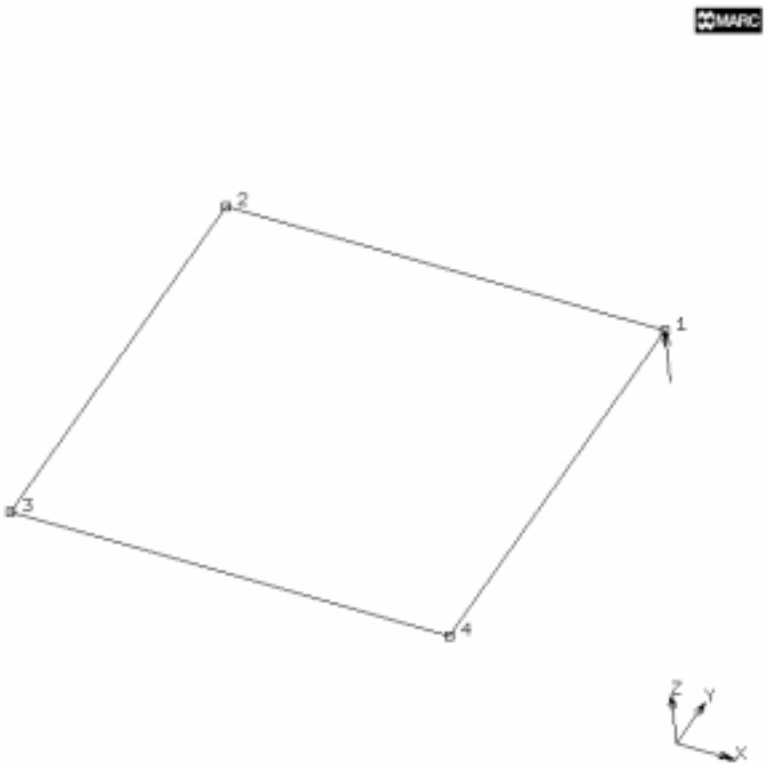

Figure 8.57-1 Initial Model with Point Load applied on Node 1

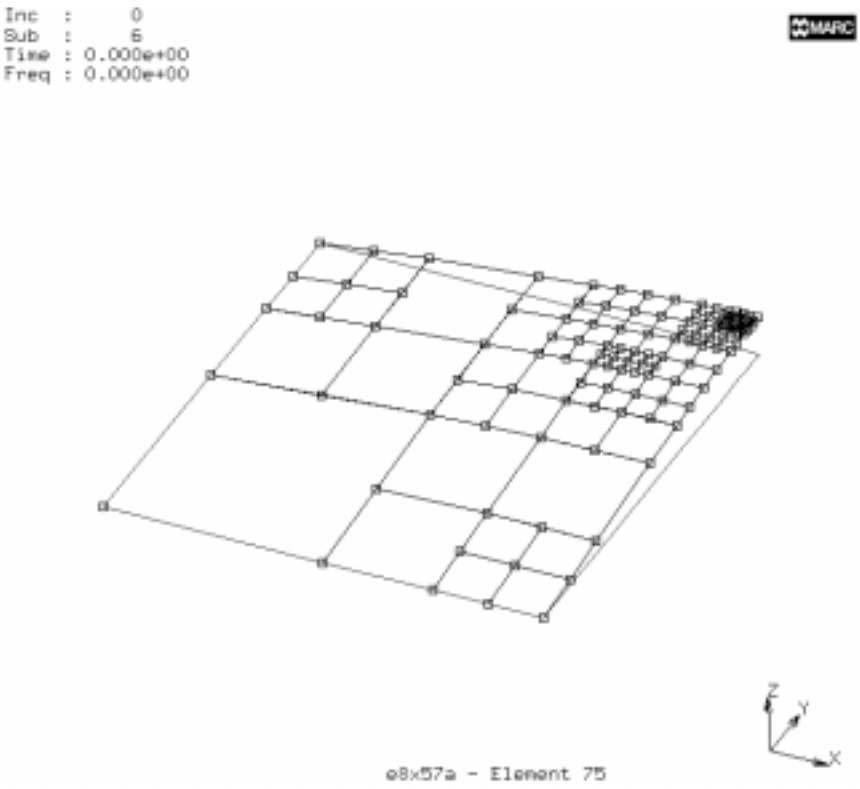

Figure 8.57-2 Initial and Deformed Shape for Data Set e8x57a

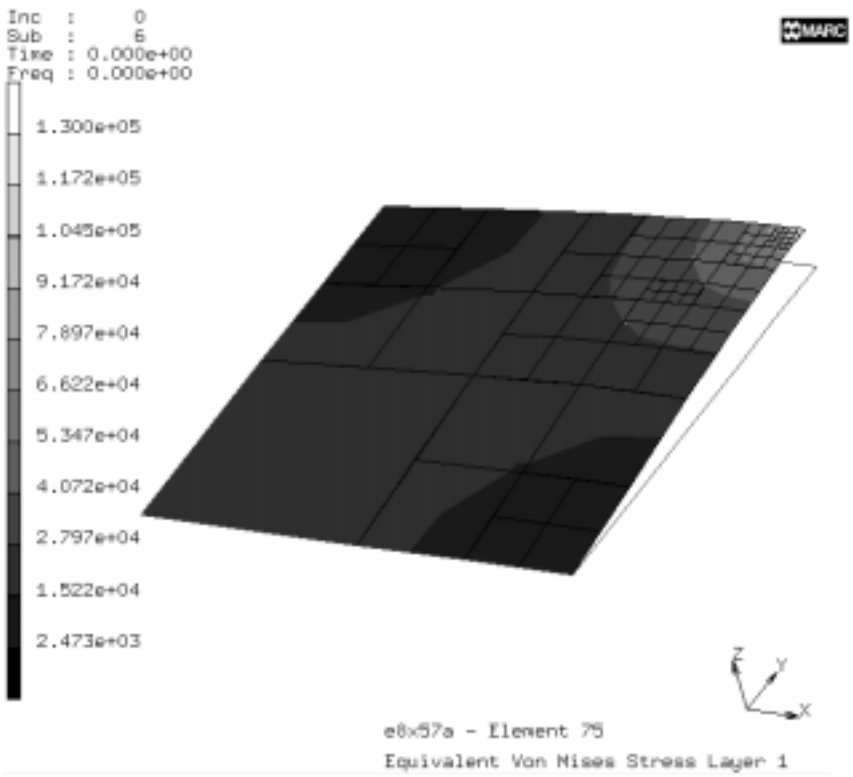

Figure 8.57-3 Equivalent von Mises Stress for Data Set e8x57a

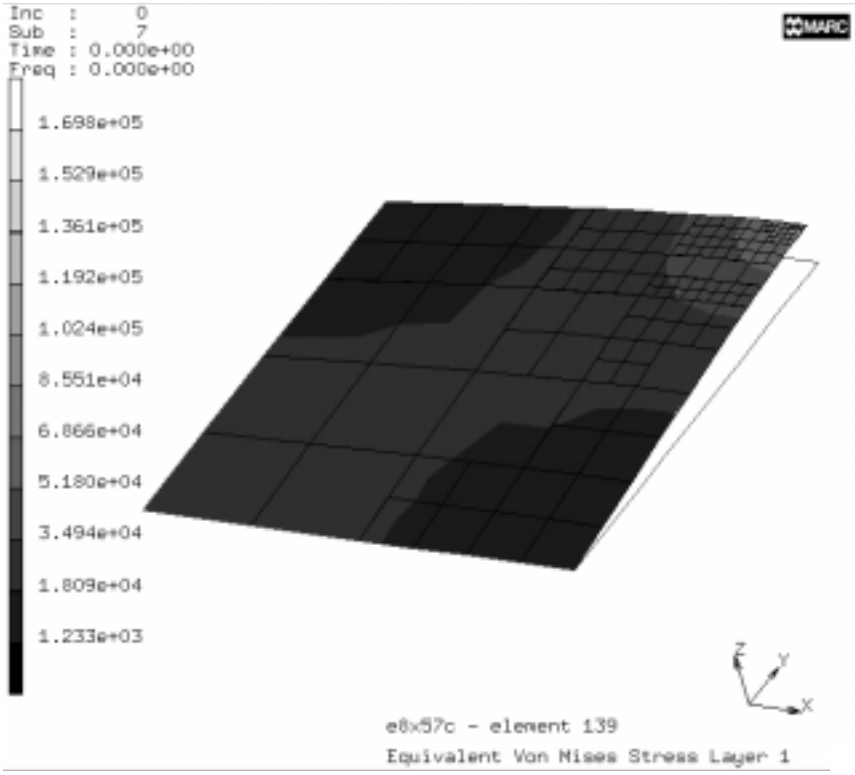

Figure 8.57-4 Equivalent von Mises Stress for Data Set e8x5c

8.58 Adaptive Meshing in Multiply Connected Shell Structures

This example shows the use of the ADAPTIVE criterion used at intersecting thin-walled structures.

Model

The model consists of three elements and 8-nodes. Element 75 which is a 4-node thick shell element is used. The initial model is shown in Figure 8.58-1.

Material Properties

All the three elements are linear elastic and have identical material properties with Young's modulus of 1.92×10^7 and a Poisson's ratio of 0.30.

Boundary Conditions

The nodal boundary conditions are summarized as follows.

Boundary Condition	Node Number
$u_x = u_y = u_z = 0$	1, 4, 5, 8
$\theta_x = \theta_y = \theta_z = 0$	1, 4, 5, 8

The loading is done by means of a face load (pressure) of $P_z = 0.01$ psi applied on elements 2 and 3.

Adaptive

The Zienkiewicz-Zhu stress error criterion is chosen with a maximum of eight levels of adaptation.

History Definition

The loading is accomplished in a single increment (increment zero) with the definition of the face loads on elements 2 and 3. No history definition cards are needed.

Results

A total of 9 subincrements are done in this example. The deformed geometry is shown in Figure 8.58-2. It can be seen that the subdivision takes place correctly at the areas of stress concentration, i.e. the intersection of the shell walls.

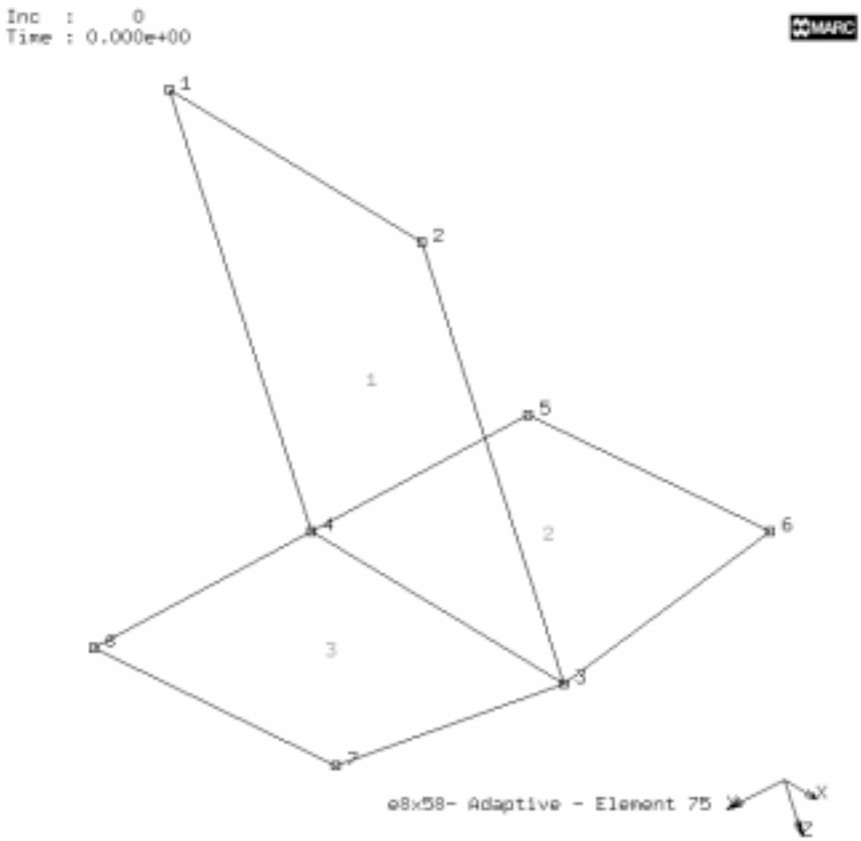

Figure 8.58-1 Initial Model

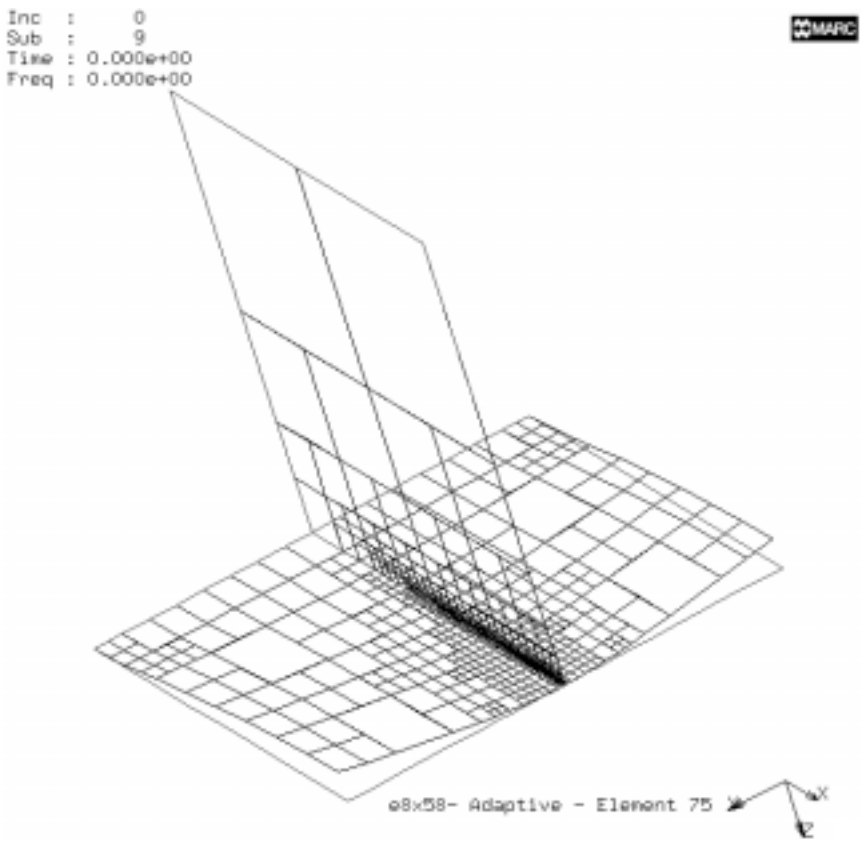

Figure 8.58-2 Deformed Geometry with the Adapted Mesh

8.59 Not Available

8.60 Simulation of Sheet Bending

This example shows a simulation of the sheet bending process. A sheet is bent by deforming it with a punch into a die. In the sheet forming terminology, it is also called air bending or v-bending. This example demonstrates the forming and springback of the sheet.

Model

The sheet is modeled with 300 elements and 366 nodes. The punch and die are modeled as rigid bodies. The initial model is shown in Figure 8.60-1.

Element

The 4-node isoparametric quadrilateral plane strain element number 11 is used with the constant dilatation option.

Material Properties

The sheet is assumed to be isotropic. The Young's modulus is 3×10^7 psi and the Poisson's ratio is 0.30. The initial yield stress is 5×10^4 psi. The workhardening behavior is input using the WORK HARD model definition option.

Boundary Conditions

The boundary conditions along the x direction are enforced by setting a zero x displacement boundary condition on all nodes at the center line of the sheet. The boundary conditions along the y direction are enforced through the contact option.

Contact

There are a total of three contact bodies in the problem. Contact body 1 is the deformable sheet. Body 2 is a velocity controlled rigid surface and models the punch. Body 3 is also a rigid surface and represents the lower die. Shear friction is assumed with a coefficient of 0.10. The relative velocity below which a node is assumed to be sticking to a contact surface is set to be 1×10^{-3} in/s. The nodal reaction force required to separate a contacting node from its contacted surface is assumed to be 1×10^{-2} lb.

Control

The convergence control is governed by a relative displacement increment norm. The maximum allowed relative change in displacement increment is set to 0.10.

History Definition

The loading is done by moving the punch (contact body 2) along the negative y direction with a speed of -5×10^{-3} in/s for 120 increments. At the end of 120 increments, the direction of motion of the punch is reversed by prescribing a speed of 5×10^{3} in/s along the positive y direction for a further 10 increments.

Results

The deformed shape is shown for increment 25 in Figure 8.60-2. The deformed shape is shown for increment 50 in Figure 8.60-3.The deformed shape is shown for increment 100 in Figure 8.60-4. At increment 118, the sheet contacts the flat portion of the lower die. For the next 2 increments, the sheet is driven into the lower die by the downward motion of the punch. The deformed shape is shown for increment 120 in Figure 8.60-5. For the next 10 increments, the punch moves upward and the sheet springs back. The final deformed configuration after springback is shown in Figure 8.60-6. A magnified view of contours of total effective plastic strain for increment 130 is shown in Figure 8.60-7.

Parameters, Options, and Subroutines Summary

Example e8x60.dat:

Parameters	Model Definition Options	History Definition Options
ALL POINTS	CONNECTIVITY	AUTO LOAD
ELEMENTS	CONTACT	CONTINUE
END	CONTROL	MOTION CHANGE
PLASTICITY	COORDINATES	TIME STEP
SETNAME	END OPTION	
SIZING	FIXED DISP	
TITLE	ISOTROPIC	
	SOLVER	
	WORK HARD	

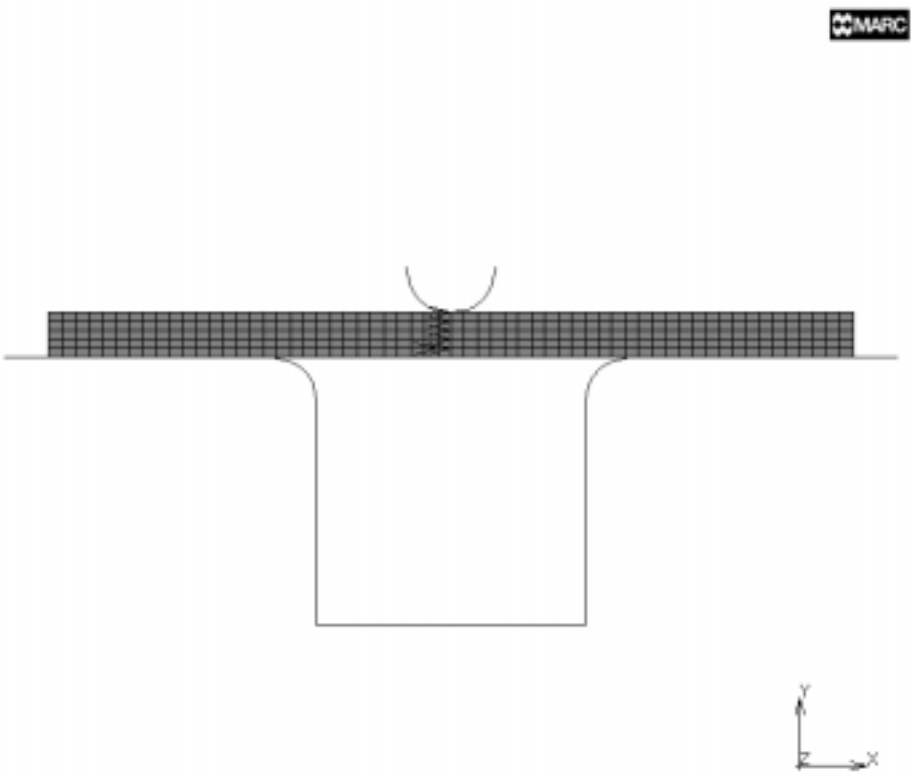

Figure 8.60-1 Initial Model

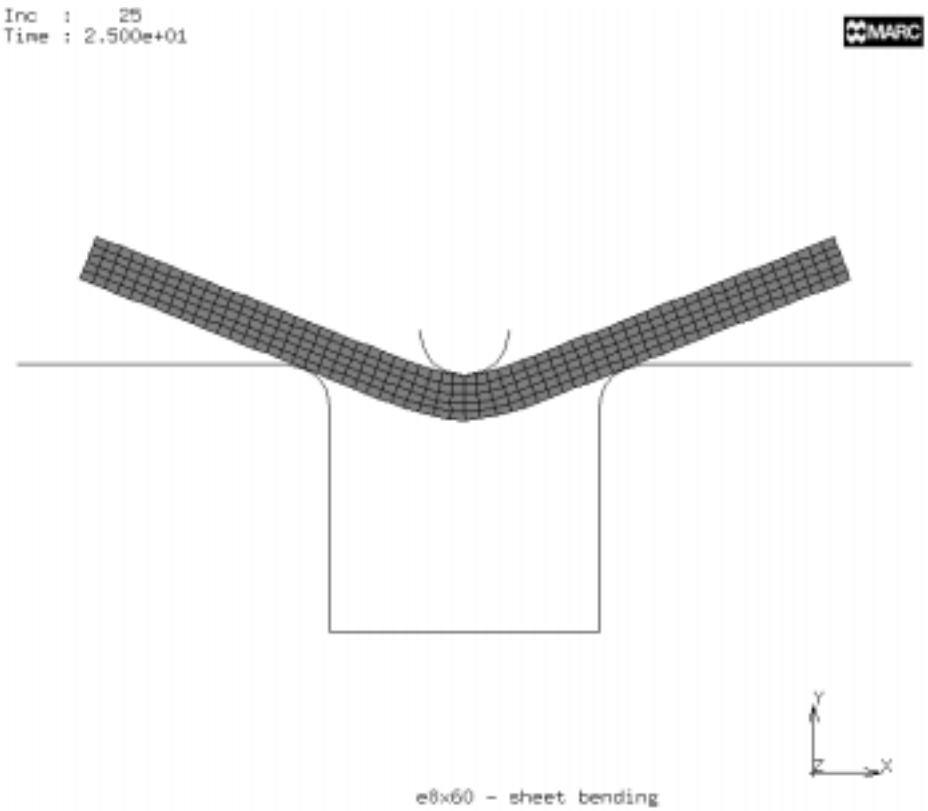

Figure 8.60-2 Deformed Geometry for Increment 25

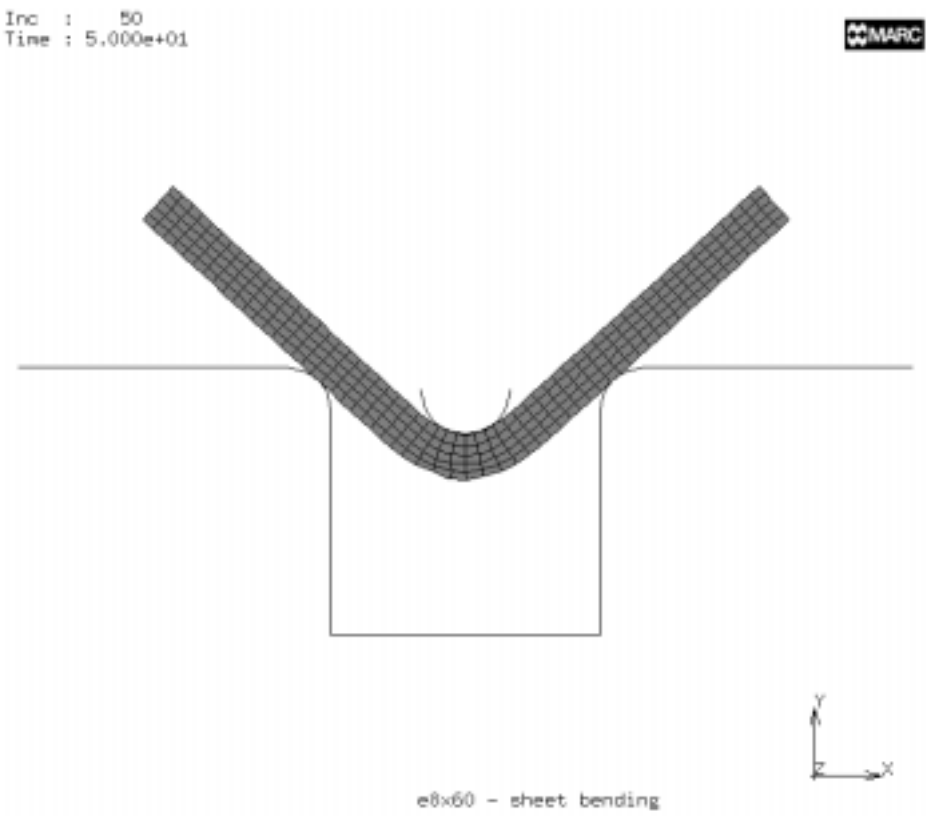

Figure 8.60-3 Deformed Geometry for Increment 50

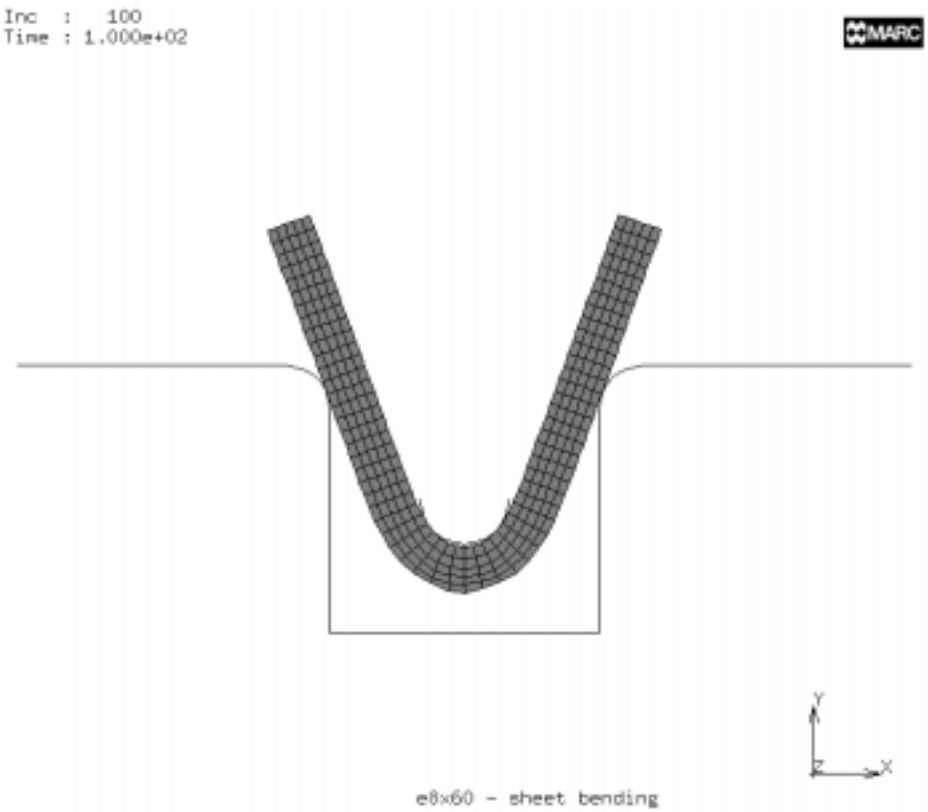

Figure 8.60-4 Deformed Geometry for Increment 100

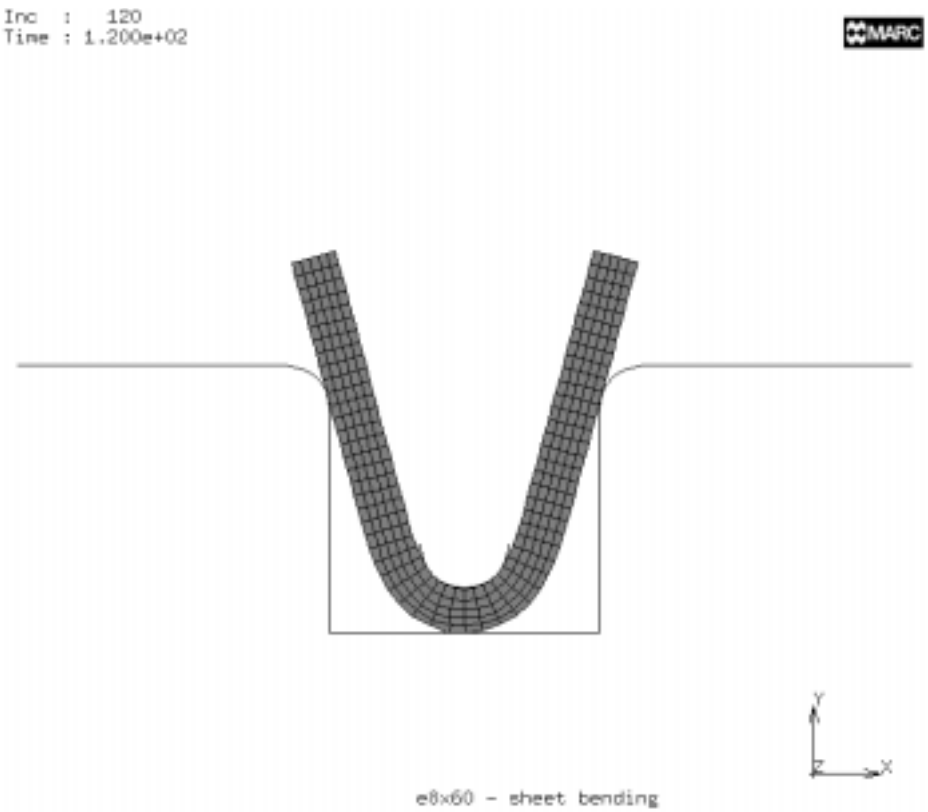

Figure 8.60-5 Deformed Geometry for Increment 120

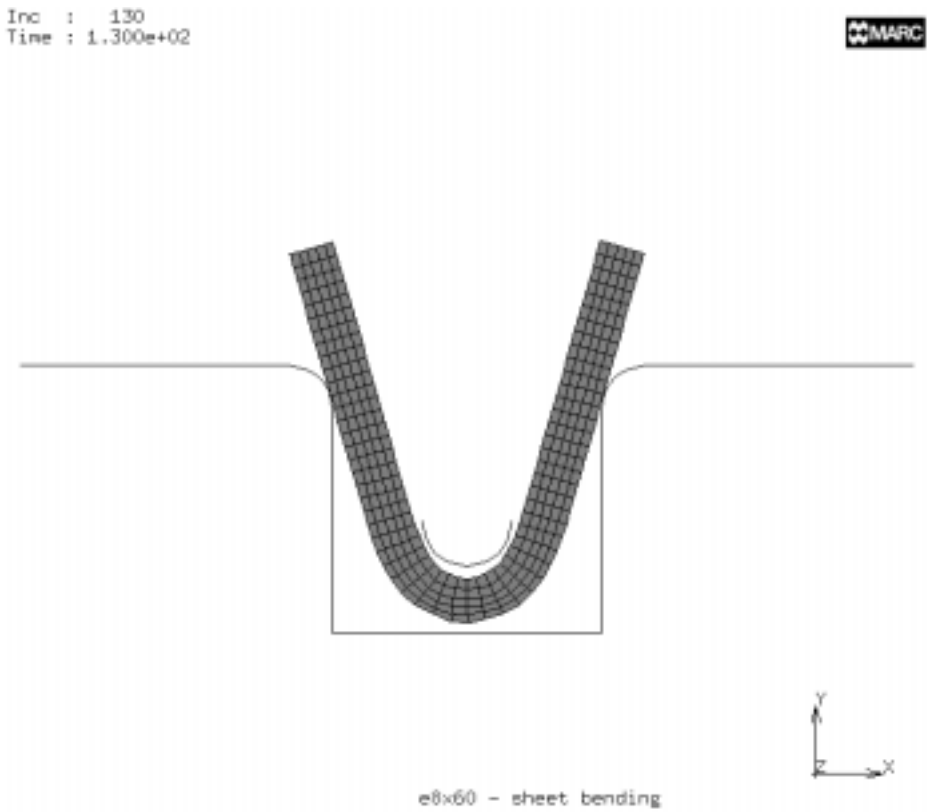

Figure 8.60-6 Deformed Geometry for Increment 130

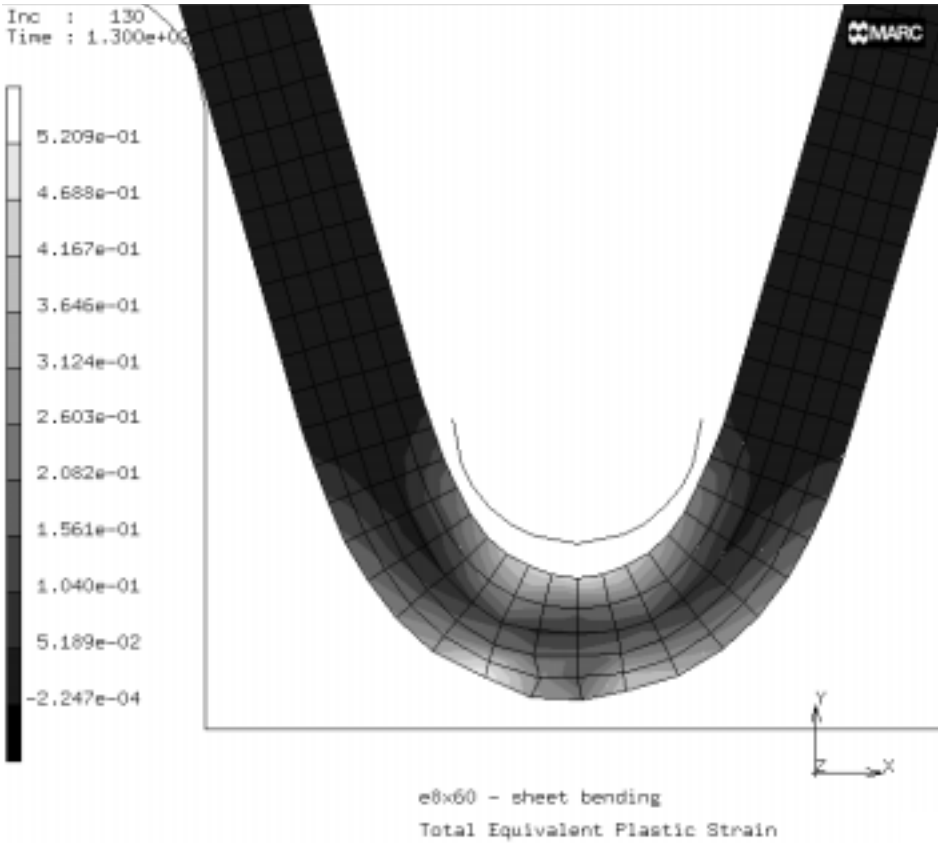

Figure 8.60-7 Magnified View of Contours of Total Effective Plastic Strain for Increment 130

MARC
Analysis
Research
Corporation

Document Title: **MARC® Volume E: Demonstration Problems, Part IV, K7**
Part Number: RF-3018-07.IV
Revision Date: June, 1998

UNITED STATES

CALIFORNIA - Palo Alto
MARC Corporate Headquarters
260 Sheridan Avenue, Suite 309
Palo Alto, CA 94306, USA
Tel: 1 650 329 6800
Fax: 1 650 323 5892
Email: support@marc.com

CALIFORNIA - San Diego
MARC Analysis Research Corp.
4330 LaJolla Village Drive, Suite 320
San Diego, CA 92122
Tel: 1 619 658 9588
Fax: 1 619 758 8710

CONNECTICUT - E. Berlin
MARC Analysis Research Corp.
1224 Mill Street
E. Berlin, CT 06023
Tel: 1 860 828 2055
Fax: 1 860 828 2031

MICHIGAN - Ann Arbor
MARC Analysis Research Corp.
24 Frank Lloyd Wright Drive
Ann Arbor, MI 48106-0523
Tel: 1 734 998 0540
Fax: 1 734 998 0542

EUROPE

CZECH REPUBLIC
MARC Overseas, Inc.
Podolska 50
147 00 Praha 4
Czech Republic
Tel: 420 (2) 6121 4123
420 (2) 6121 4111 x252
Fax: 420 (2) 6121 4123
Email: support@marc.cz

FRANCE
MARC France S.A.
Bercy Expo SR 6101A
40 Avenue des Terroirs de France
75611 Paris Cedex 12, France
Tel: 33 (1) 4474 1550
Fax: 33 (1) 4474 1554
Email: support@marc.fr

GERMANY - Munich
MARC Software Deutschland GmbH
Ismaninger Str. 9
85609 Aschheim (bie Munich)
Germany
Tel: 49 (89) 904 50 33
Fax: 49 (89) 903 06 76
Email: support@marc.de

GERMANY - Hannover
MARC Software Deutschland GmbH
Alte Dohrener Str. 66
D 30173 Hannover, Germany
Tel: 49 (511) 980 5182
Fax: 49 (511) 980 5187

ITALY
Espri-MARC s.r.l.
Viale Brigata Bisagno 2 / 10
16129 Genova, Italy
Tel: 39 (10) 585 949
Fax: 39 (10) 585 949
Email: espri.marc@interbusiness.it

THE NETHERLANDS
MARC Analysis Research Corporation
Dublinstraat 32
2713 HS Zoetermeer
The Netherlands
Tel: 31 (79) 3510 411
Fax: 31 (79) 3517 560
Email: support@marc.nl

UNITED KINGDOM
MARC UK Ltd.
11 Linford Forum, Rockingham Drive
Linford Wood
Milton Keynes, MK14 6LY
Tel: 44 (1908) 606 070
Fax: 44 (1908) 606 633
Email: support@marc.co.uk

PACIFIC RIM

CHINA
MARC Overseas, Inc.
Bright Chang An Building, Suite 321
7# Jian Guo Men Nei Street
Beijing, China 100 005
Tel: 86 (10) 6510 2056
86 (10) 6510 2057
86 (10) 6510 2058
Fax: 86 (10) 6510 2053
Email: marcbj@public.bta.net.cn

JAPAN - Nagoya
Nippon MARC Co., Ltd.
Nagoya Nishiki Daiichi Seimei Bldg.
2F, 6-5 Nishiki 1-chome
Naka-ku, Nagoya, Aichi 460-0003
Tel: 81 (52) 202 5661
Fax: 81 (52) 202 5665

JAPAN - Osaka
Nippon MARC Co., Ltd.
4F 2nd Kimi Building
2-11 Toyotucho Suita-shi
Osaka 564-0051
Tel: 81 (6) 385 1101
Fax: 81 (6) 385 4343

JAPAN - Tokyo
(Asian Operations Headquarters)
Nippon MARC Co., Ltd.
Shinjuku Daiichi Seimei Building
P.O. Box 5056
2-7-1 Nishi-Shinjuku, Shinjuku-ku
Tokyo 163-0704
Tel: 81 (3) 3345 0181
Fax: 81 (3) 3345 1529
Email: support@marc.co.jp

KOREA
Dong Kyung Bldg. 7FL
824-19 Yuksam-Dong
Kangnam-Ku, Seoul, Korea
Tel: 82 (2) 561 7543
Fax: 82 (2) 561 7767
Email: marck@unitel.co.kr

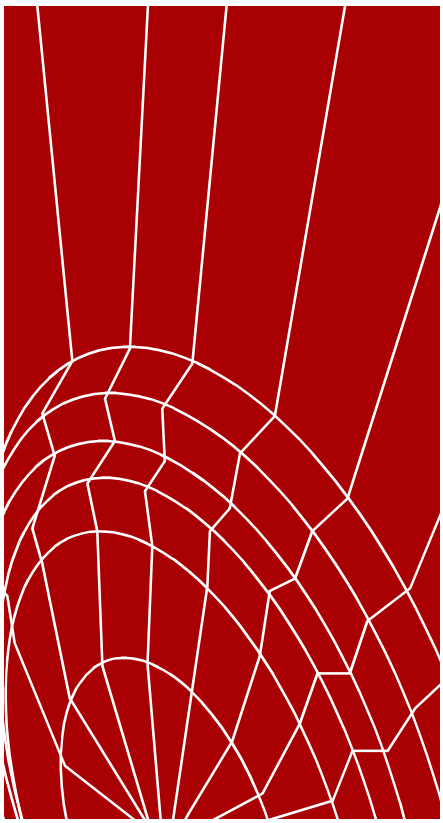

MARC Analysis Research Corporation

MARC®

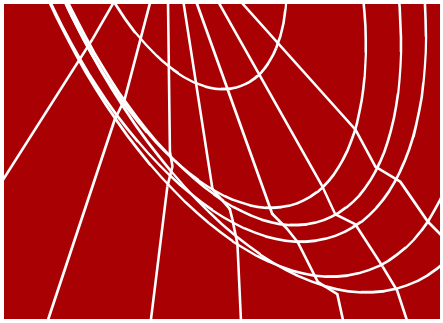

Volume E

Demonstration Problems

Version K7

MARC
Analysis
Research
Corporation

Copyright © 1998 MARC Analysis Research Corporation
Printed in U. S. A.
This notice shall be marked on any reproduction of this data, in whole or in part.

MARC Analysis Research Corporation
260 Sheridan Avenue, Suite 309
Palo Alto, CA 94306 USA

Phone: (650) 329-6800
FAX: (650) 323-5892

Document Title: **MARC® Volume E: Demonstration Problems, Part V, Version K7**
Part Number: RF-3018-07.V
Revision Date: June, 1998

Proprietary Notice

MARC Analysis Research Corporation reserves the right to make changes in specifications and other information contained in this document without prior notice.

ALTHOUGH DUE CARE HAS BEEN TAKEN TO PRESENT ACCURATE INFORMATION, MARC ANALYSIS RESEARCH CORPORATION DISCLAIMS ALL WARRANTIES WITH RESPECT TO THE CONTENTS OF THIS DOCUMENT (INCLUDING, WITHOUT LIMITATION, WARRANTIES OR MERCHANTABILITY AND FITNESS FOR A PARTICULAR PURPOSE) EITHER EXPRESSED OR IMPLIED. MARC ANALYSIS RESEARCH CORPORATION SHALL NOT BE LIABLE FOR DAMAGES RESULTING FROM ANY ERROR CONTAINED HEREIN, INCLUDING, BUT NOT LIMITED TO, FOR ANY SPECIAL, INCIDENTAL OR CONSEQUENTIAL DAMAGES ARISING OUT OF, OR IN CONNECTION WITH, THE USE OF THIS DOCUMENT.

This software product and its documentation set are copyrighted and all rights are reserved by MARC Analysis Research Corporation. Usage of this product is only allowed under the terms set forth in the MARC Analysis Research Corporation License Agreement. Any reproduction or distribution of this document, in whole or in part, without the prior written consent of MARC Analysis Research Corporation is prohibited.

Restricted Rights Notice

This computer software is commercial computer software submitted with “restricted rights.” Use, duplication, or disclosure by the government is subject to restrictions as set forth in subparagraph (c)(i)(ii) or the Rights in technical Data and Computer Software clause at DFARS 252.227-7013, NASA FAR Supp. Clause 1852.227-86, or FAR 52.227-19. Unpublished rights reserved under the Copyright Laws of the United States.

Trademarks

All products mentioned are the trademarks, service marks, or registered trademarks of their respective holders.

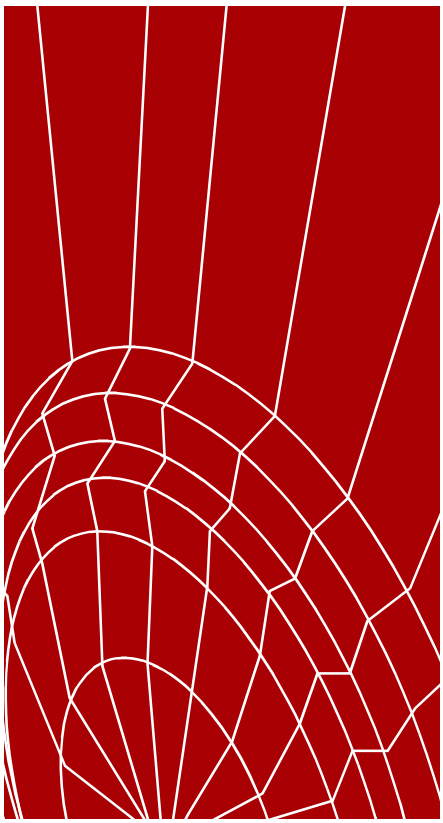

MARC Analysis Research Corporation

MARC®

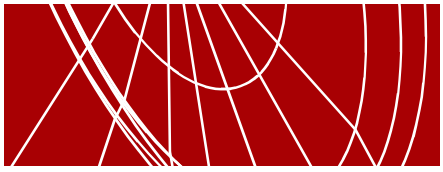

Volume E

Demonstration Problems

Version K7

Part V

- Fluids
- Design Sensitivity and Optimization

Part V

Volume E: Demonstration Problems

Chapter 9 **Fluids**

Chapter 10 **Design Sensitivity and Optimization**

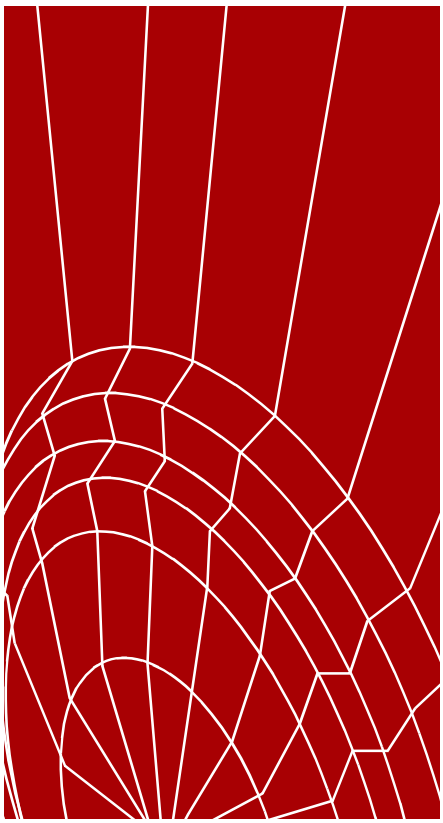

MARC Analysis Research Corporation

MARC®

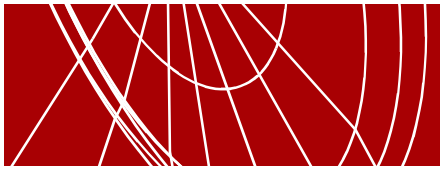

Volume E

Demonstration Problems

Version K7

Chapter 9
Fluids

9 Fluids Contents

Description	Problem
Planar Couette Flow	9.1
Poiseuille Flow	9.2
Fluid Squeezed Between Two Long Plates	9.3
Driven Cavity Flow	9.4
Flow Past a Circular Cylinder	9.5
Flow Over Electronic Chip	9.6
Natural Convection	9.7
Flow Around Tubes	9.8

9 Fluids List of Figures

Figure **Page**

9.1-1 Vector Plot of the Couette Flow Velocity Field, Discretized using Element Type 11 and the Mixed Method 9.1-3
9.1-2 Vector Plot of the Couette Flow Velocity Field, Discretized using Element Type 27 and the Mixed Method 9.1-4
9.1-3 Vector Plot of the Couette Flow Velocity Field, Discretized using Element Type 27 and the Penalty Method 9.1-5
9.1-4 Comparison of Computation and Analytical Results 9.1-6

9.2-1 Vector Plot of the Poiseuille Flow Velocity Field, Discretized using Element Type 10 and the Mixed Method 9.2-3
9.2-2 Vector Plot of the Poiseuille Flow Velocity Field, Discretized using Element Type 10 and the Mixed Method (Finer Mesh) 9.2-4
9.2-3 Vector Plot of the Poiseuille Flow Velocity Field, Discretized using Element Type 28 and the Mixed Method 9.2-5
9.2-4 Comparison of Computation and Analytical Results 9.2-6

9.3-1 Vector Plot of the Squeezed Fluid Velocity Field, Discretized using Element Type 11 and the Mixed Method 9.3-4
9.3-2 Vector Plot of the Squeezed Fluid Velocity Field, Discretized using Element Type 6 and the Mixed Method 9.3-5
9.3-3 Contour Plot of the Squeezed Fluid Pressure Field, Discretized using Element Type 11 and the Mixed Method 9.3-6
9.3-4 Contour Plot of the Squeezed Fluid Pressure Field, Discretized using Element Type 6 and the Mixed Method 9.3-7
9.3-5 Comparison of Fluid Velocity V_x Computation and Analytical Results at x=6 . . . . 9.3-8
9.3-6 Comparison of Fluid Velocity V_y Computation and Analytical Results at x=6 . . . . 9.3-9

9.4-1 Vector Plot of the Driven Cavity Flow Velocity Field, Discretized using Element Type 11 and the Mixed Method 9.4-3
9.4-2 Contour Plot of the Driven Cavity Flow Pressure Field, Discretized using Element Type 11 and the Mixed Method 9.4-4

Figure **Page**

9.5-1 Vector Plot of the Flow Over Cylinder Velocity Field, Discretized using Element Type 11 and the Mixed Method 9.5-4
9.5-2 Vector Plot of the Flow Over Cylinder Velocity Field, Discretized using Element Type 27 and the Mixed Method 9.5-5
9.5-3 Vector Plot of the Flow Over Cylinder Transient Velocity Field at the Tenth Increment, Discretized using Element Type 11 and the Mixed Method 9.5-6
9.5-4 Contour Plot of the Flow Over Cylinder Pressure Field, Discretized using Element Type 11 and the Mixed Method 9.5-7
9.5-5 Contour Plot of the Flow Over Cylinder Pressure Field, Discretized using Element Type 27 and the Mixed Method 9.5-8
9.5-6 Contour Plot of the Flow Over Cylinder Transient Pressure Field at the Tenth Increment, Discretized using Element Type 11 and the Mixed Method 9.5-9

9.6-1 Vector Plot of the Flow Over Multiple Steps Velocity Field, Discretized using Element Type 11 and the Mixed Method 9.6-3
9.6-2 Contour Plot of the Flow Over Multiple Steps Temperature Field, Discretized using Element Type 11 and the Mixed Method 9.6-4
9.6-3 Contour Plot of the Flow Over Multiple Steps Pressure Field, Discretized using Element Type 11 and the Mixed Method 9.6-5

9.7-1 Vector Plot of the Natural Convective Flow Velocity Field with Rayleigh Number = 1.0e+03, Discretized using Element Type 11 and the Penalty Method . 9.7-3
9.7-2 Vector Plot of the Natural Convective Flow Velocity Field with Rayleigh Number = 1.0e+04, Discretized using Element Type 11 and the Penalty Method . 9.7-4
9.7-3 Contour Plot of the Natural Convective Flow Temperature Field with Rayleigh Number = 1.0e+03, Discretized using Element Type 11 and the Penalty Method . 9.7-5
9.7-4 Contour Plot of the Natural Convective Flow Temperature Field with Rayleigh Number = 1.0e+04, Discretized using Element Type 11 and the Penalty Method . 9.7-6

9.8-1 Finite Element Mesh for the Flow Over Cylinders. 9.8-3
9.8-2 Contour Plot of the Flow Over Cylinders Velocity Field, Discretized using Element Type 11 and the Mixed Method 9.8-4
9.8-3 Contour Plot of the Flow Over Cylinders Pressure Field, Discretized using Element Type 11 and the Mixed Method 9.8-5

9 Fluids List of Tables

Table **Page**

9-1 Fluids Demonstration Problems 9-1

9.1-1 Comparison of Fluid Velocity Obtained from Finite Element Computation against Analytical Result 9.1-2

9.2-1 Comparison of Fluid Velocity Obtained from Finite Element Computation against Analytical Result 9.2-2

9.3-1 Comparison of Fluid Velocity X Obtained from Finite Element Computation against Analytical Result (at x=6) 9.3-2

9.3-2 Comparison of Fluid Velocity Y Obtained from Finite Element Computation against Analytical Result (at x=6) 9.3-2

9 Fluids

MARC provides a variety of analysis capabilities based on Navier-Stokes equations for viscous, incompressible fluid mechanic applications. A discussion on the use of fluid mechanics analysis can be found in *MARC Volume A: Theory and User Information*. The summary of the features is given below:

Selection of Element Topology:

- 2D triangular and quadrilateral
- Axisymmetric triangular and quadrilateral
- 3D tetrahedral and hexahedral

Choice of Element Formulation:

- Mixed method
- Penalty method

Selection of Material Behavior:

- Newtonian (linear) fluid material
- Non-Newtonian (shear-rate dependent viscosity) fluid material

Option for Multi-Physics Coupling:

- Fluid-Thermal
- Fluid-Solid
- Fluid-Solid-Thermal

Compiled in this chapter are a number of solved problems. Table 9-1 summarizes the element type and options used in these demonstration problems.

Table 9-1 Fluids Demonstration Problems

Problem Number	Element Type(s)	Parameters	Model Definition	History Definition	User Subroutines	Problem Description
9.1	11 27	DIST LOADS	DIST LOADS STEADY STATE	—	—	Planar Couette flow.
9.2	10 28	DIST LOADS	DIST LOADS STEADY STATE	–	—	Poiseuille flow.
9.3	11 6	—	STEADY STATE	—	—	Fluid squeezed between two plates.

Table 9-1 Fluids Demonstration Problems (Continued)

Problem Number	Element Type(s)	Parameters	Model Definition	History Definition	User Subroutines	Problem Description
9.4	11	—	STEADY STATE	—	—	Driven cavity flow.
9.5	11 27	—	INITIAL VEL	TRANSIENT NONAUTO	—	Flow past circular cylinder.
9.6	11	FLUID THERMAL	STEADY STATE	—	—	Flow over multiple steps in a channel.
9.7	11	DIST LOADS FLUID THERMAL	DIST LOADS STEADY STATE	—	—	Natural convection.
9.8	11	DIST LOADS	DIST LOADS STEADY STATE	—	—	Flow around tubes.

9.1 Planar Couette Flow

This is an example of simple shear flow of a viscous fluid between the parallel surfaces. A steady state analysis is performed. The results can be compared with the exact analytical solution.

This problem is modeled using three techniques summarized below:

Data Set	Element Type(s)	Number of Elements	Number of Nodes	Differentiating Features
e9x1a	11	24	35	Mixed method
e9x1b	27	6	29	Mixed method
e9x1c	27	6	29	Penalty method

Element

Element type 11 is a lower-order, 4-node, planar element using bilinear interpolation. Element 27 is a higher-order, 8-node, planar element using biquadratic interpolation functions.

When element types 11 and 27 are used in the mixed formulation, each node has two velocity degrees of freedom and one pressure degree of freedom.

When the penalty formulation is used, only the two velocity degrees of freedom are at each node. The penalty factor is entered via the PARAMETER model definition option.

Model

The two surfaces are 1.2 inches apart and the length is 2.0 inches. The meshes used are shown in Figures 9.1-1 through 9.1-3. Only the upper-half of the domain is discretized due to symmetry.

Boundary Conditions

It is assumed that parallel flow will develop; hence, along the inlet and outlet side the boundary conditions are $V_y = 0$. On the bottom surface, due to symmetry, $V_y = 0$. The top surface is considered to be moving with velocity $V_x = 1.0$. There is no relative velocity of the fluid and the surface. This is defined through the FIXED VELOCITY option.

Material

The material is a Newtonian fluid with a viscosity of 1.0 lbf. sec/square inch and a mass density of 1.0 lbs/cubic inch.

Results

The velocity profile is shown in Figure 9.1-1 through Figure 9.1-3 and is identical for all three element types used. Comparison of computation and analytical result is given in Table 9.1-1 and Figure 9.1-4.

Table 9.1-1 Comparison of Fluid Velocity Obtained from Finite Element Computation against Analytical Result

Vertical Distance	e9x1a	e9x1b	e9x1c	Analytical
0.000000e+00	1.000000e+01	1.000000e+01	1.000000e+01	1.000000e+01
1.000000e-01	9.750000e+00	9.750000e+00	9.749950e+00	9.750000e+00
2.000000e-01	9.000000e+00	9.000000e+00	9.000000e+00	9.000000e+00
3.000000e-01	7.750000e+00	7.750000e+00	7.749950e+00	7.750000e+00
4.000000e-01	6.000000e+00	6.000000e+00	6.000000e+00	6.000000e+00
5.000000e-01	3.750000e+00	3.750000e+00	3.749950e+00	3.750000e+00
6.000000e-01	1.000000e+00	1.000000e+00	1.000000e+00	1.000000e+00

Parameters, Options, and Subroutines Summary

Examples e9x1a.dat, e9x1b.dat, and e9x1c.dat:

Parameters	Model Definition Options
DIST LOADS	CONNECTIVITY
ELEMENTS	CONTINUE
END	COORDINATES
FLUID	CONTROL
SIZING	DIST LOADS
	END OPTION
	FIXED VELOCITY
	ISOTROPIC
	NO PRINT
	POST
	STEADY STATE

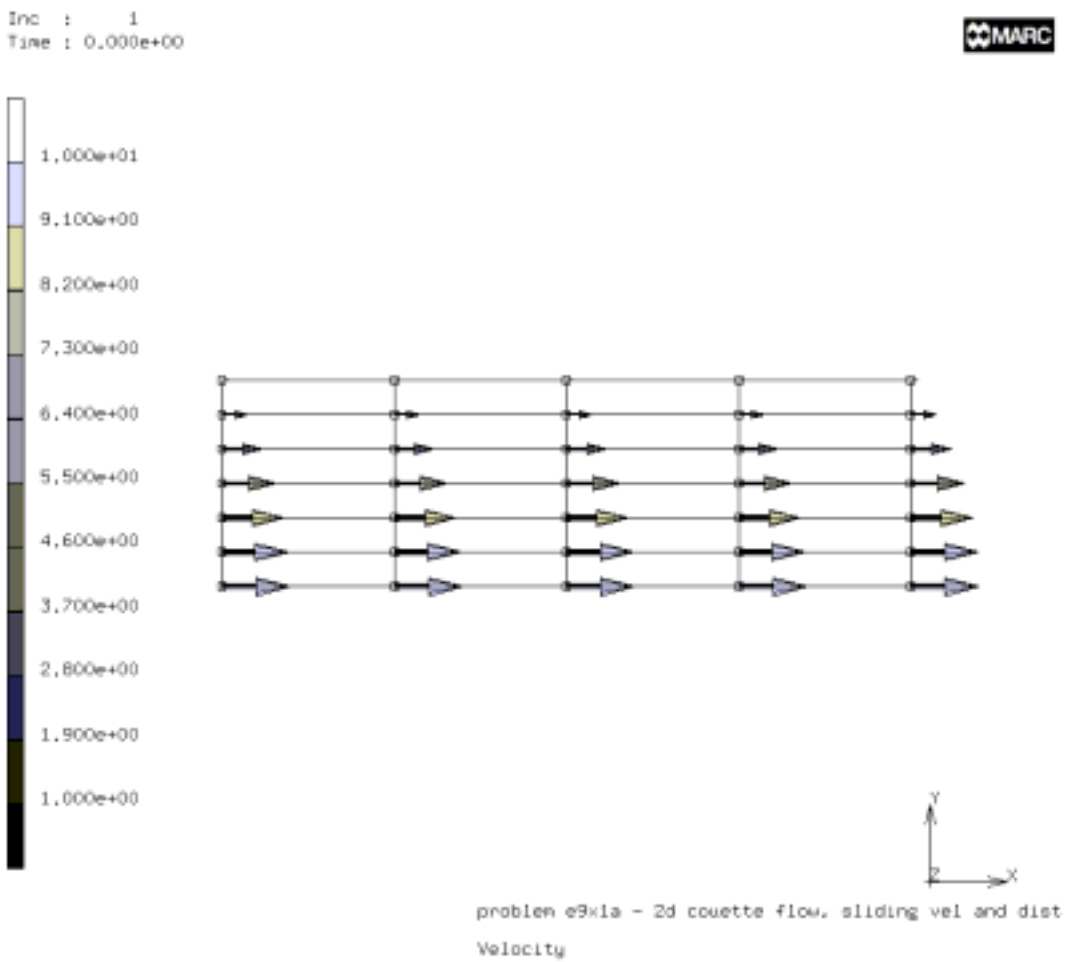

Figure 9.1-1 Vector Plot of the Couette Flow Velocity Field, Discretized using Element Type 11 and the Mixed Method

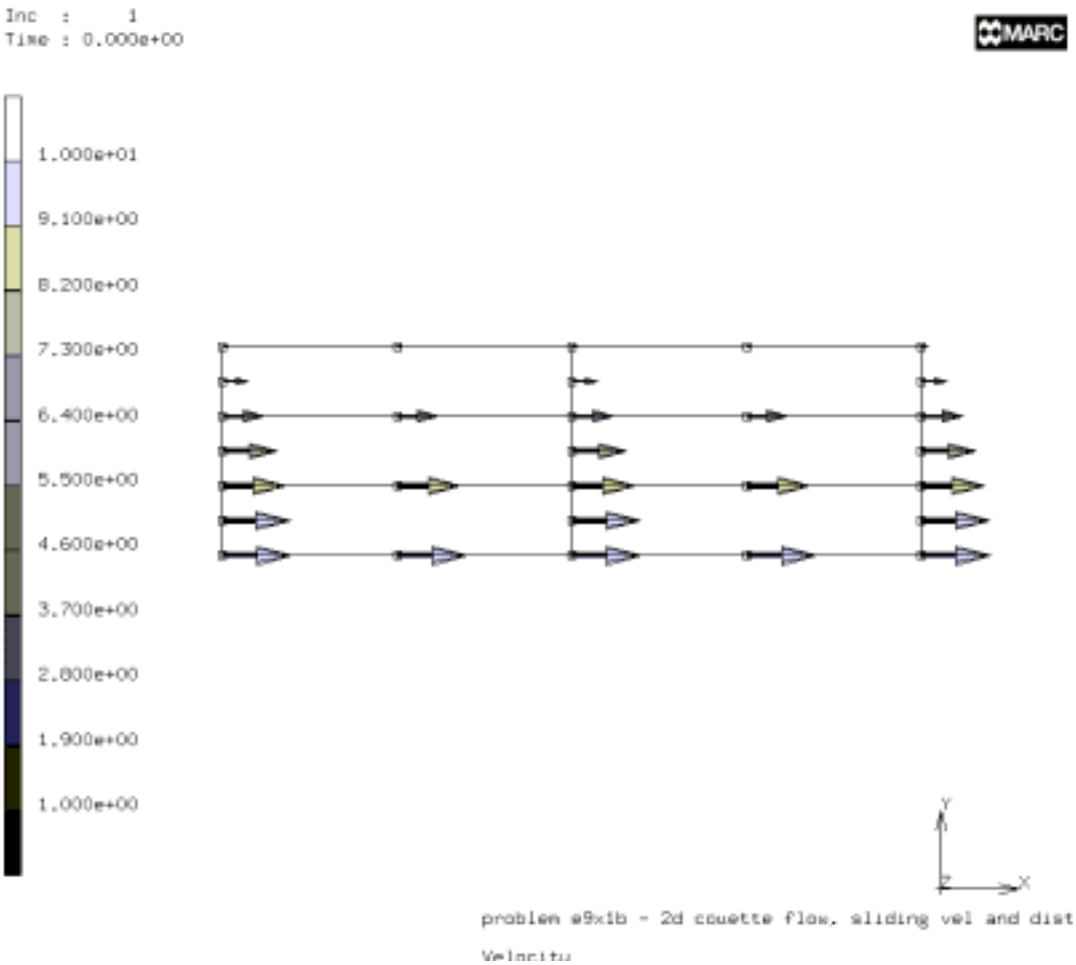

Figure 9.1-2 Vector Plot of the Couette Flow Velocity Field, Discretized using Element Type 27 and the Mixed Method

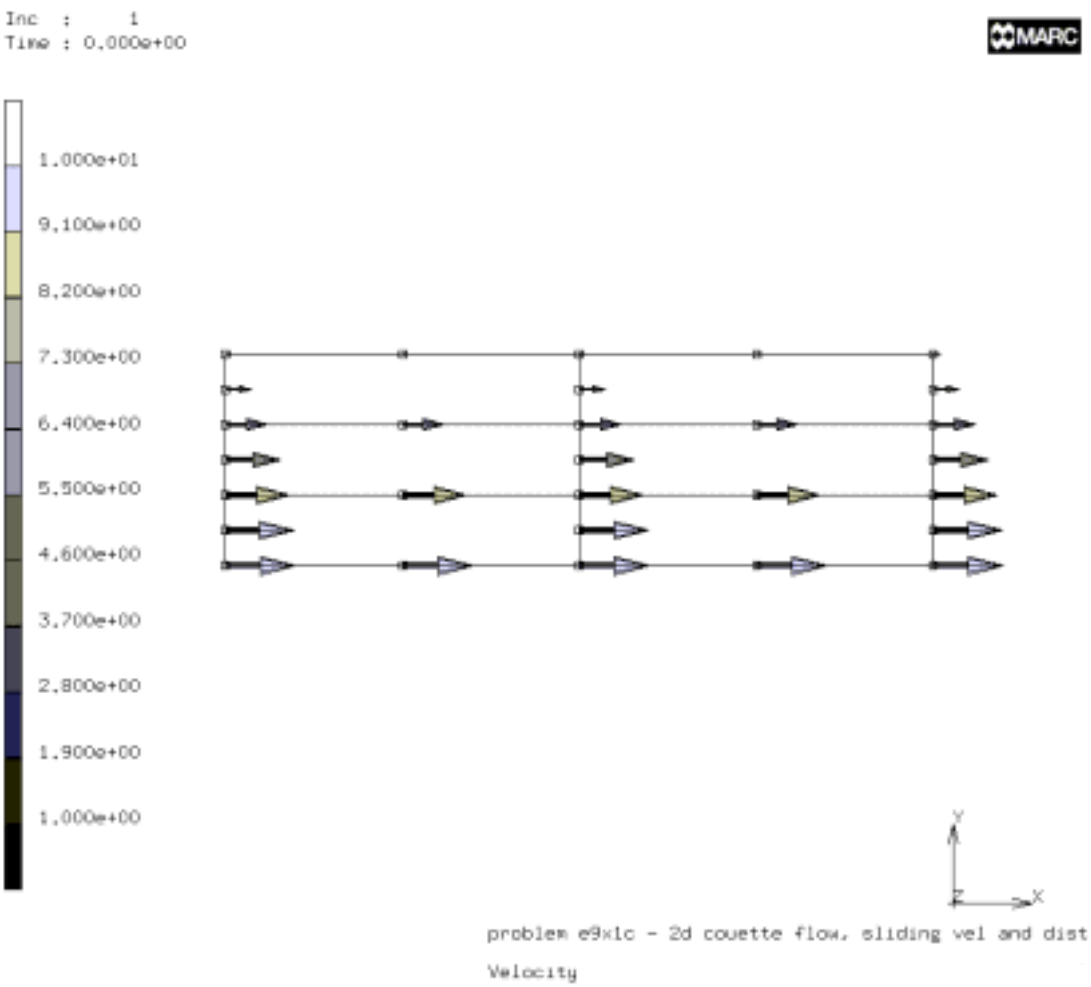

Figure 9.1-3 Vector Plot of the Couette Flow Velocity Field, Discretized using Element Type 27 and the Penalty Method

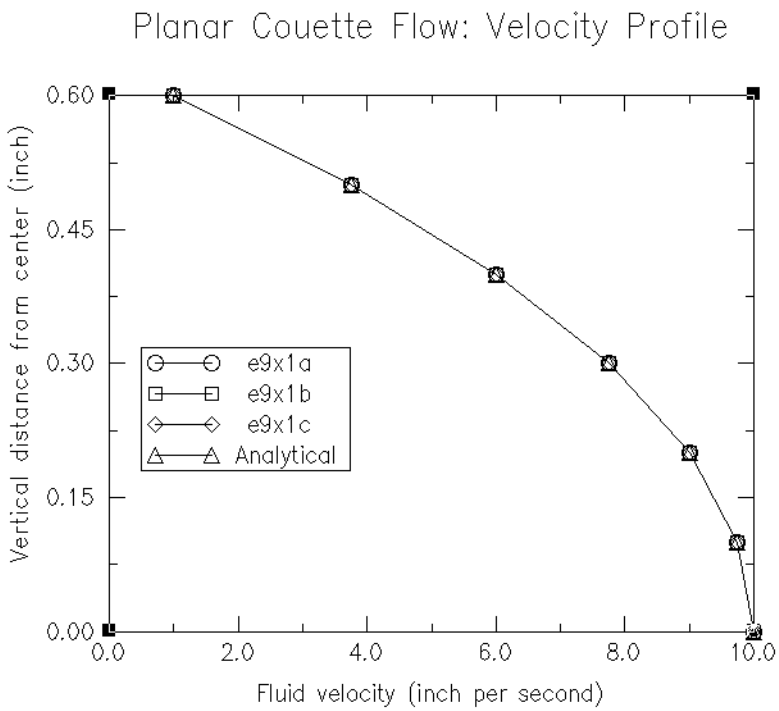

Figure 9.1-4 Comparison of Computation and Analytical Results

9.2 Poiseuille Flow

This problem demonstrates the steady state solution for a viscous fluid in a circular pipe. A pressure gradient is applied along the length of the pipe. The flow is assumed to be axisymmetric and, because the pipe is infinitely long, there will be no variation along the axis in steady state flow.

This problem is modeled using the three techniques summarized below:

Data Set	Element Type(s)	Number of Elements	Number of Nodes
e9x2a	10	24	35
e9x2b	10	48	63
e9x2c	28	24	93

Element

Element 10 is a 4-node, axisymmetric element using bilinear interpolation. Element 28 is an 8-node, axisymmetric element using biquadratic interpolation. The mixed formulation is used for all the above stated problems. Each node has two velocity degrees of freedom and a pressure degree of freedom.

Model

The radius of the pipe is 1.0 inch and the length is 3.0 inch. The finite element models are shown in Figures 9.2-1 through 9.2-3 for the different mesh density and/or element types.

Boundary Conditions

An axisymmetric analysis is performed; hence, along the line r = 0, the $V_r = 0$. At the outer radius is the rigid wall. No-slip boundary conditions require the fluid velocity on the wall to be equal to zero, so $V_r = V_z = 0$. The radial velocity is considered to be zero at the inlet (Z = 0) and outlet (Z = 3). A pressure gradient is applied by specifying a stress of 1 psi on the inlet surface.

Material

The fluid is Newtonian with a viscosity of 1.0 lbf/square inch and a mass density of 1.0 lb/cubic inch.

Results

The solution of this problem can be found in any text book on fluid mechanics. The steady state distribution of the axial velocity is:

$$V_z = -\frac{1}{4\mu}\frac{dp}{dz}(R^2 - r^2)$$

The MARC calculated solution for the different models is given in Figures 9.2-1 through 9.2-3. Comparison of computation and analytical result is given in Table 9.2-1 and Figure 9.2-4.

Table 9.2-1 Comparison of Fluid Velocity Obtained from Finite Element Computation against Analytical Result

Radical Distance	e9x2a	e9x2b	e9x2c	Analytical
0.000000e+00	8.719550e-02	8.454730e-02	8.333330e-02	8.333330e-02
1.625000e-01		8.161330e-02	8.113280e-02	8.113281e-02
3.250000e-01	7.545940e-02	7.476720e-02	7.453120e-02	7.453125e-02
4.625000e-01		6.565210e-02	6.550780e-02	6.550781e-02
6.000000e-01	5.363690e-02	5.340960e-02	5.333330e-02	5.333333e-02
7.125000e-01		4.107480e-02	4.102860e-02	4.102864e-02
8.250000e-01	2.669620e-02	2.663500e-02	2.661460e-02	2.661458e-02
9.125000e-01		1.395500e-02	1.394530e-02	1.394531e-02
1.000000e+00	1.338234e-11	6.111427e-12	1.440060e-12	0.000000e+00

Parameters, Options, and Subroutines Summary

Examples e9x2a.dat, e9x2b.dat, and e9x2c.dat:

Parameters	Model Definition Options
ELEMENTS	CONNECTIVITY
END	CONTINUE
FLUID	CONTROL
SIZING	COORDINATES
	DIST LOADS
	END OPTION
	FIXED VELOCITY
	ISOTROPIC
	POST
	PRINT ELEMENT
	STEADY STATE

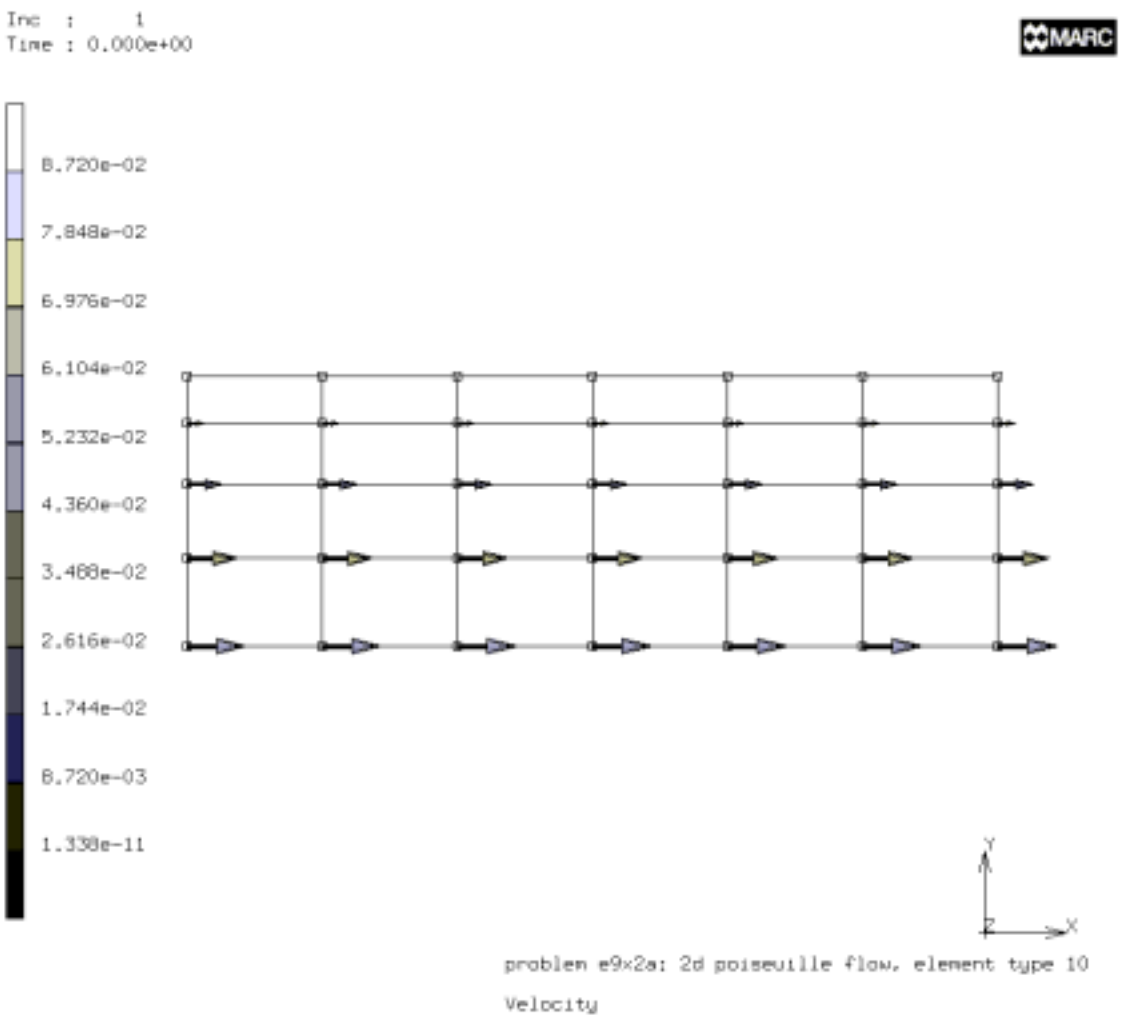

Figure 9.2-1 Vector Plot of the Poiseuille Flow Velocity Field, Discretized using Element Type 10 and the Mixed Method

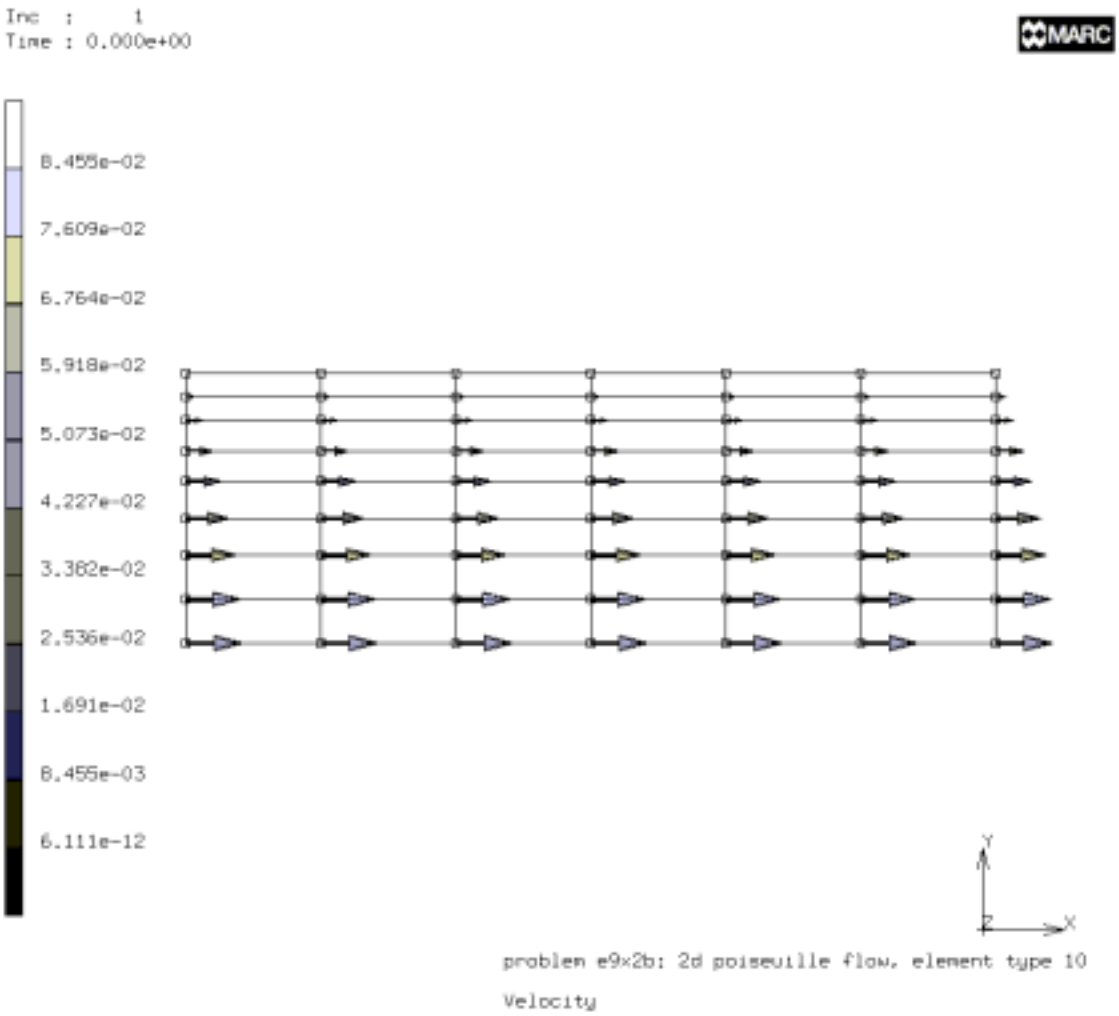

Figure 9.2-2 Vector Plot of the Poiseuille Flow Velocity Field, Discretized using Element Type 10 and the Mixed Method (Finer Mesh)

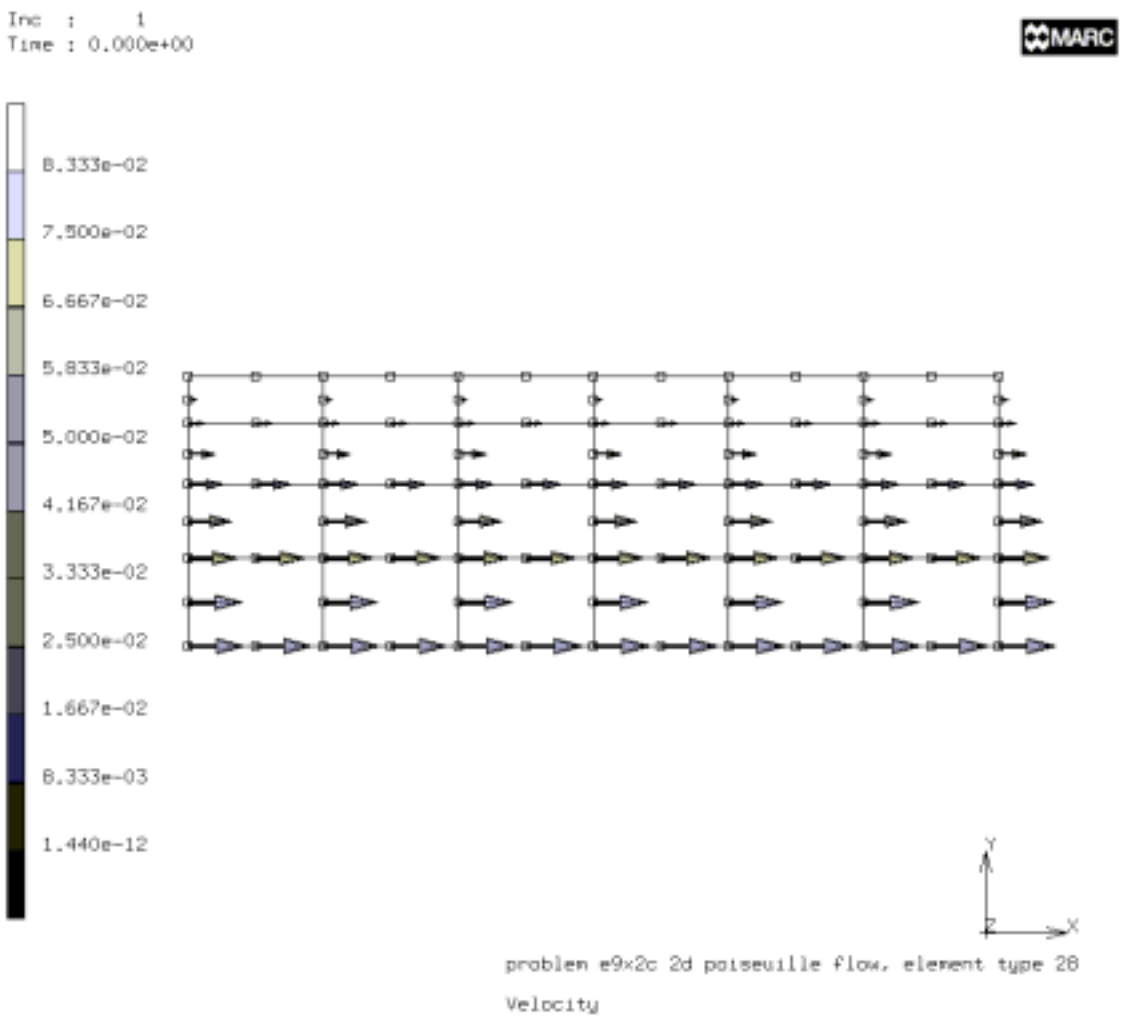

Figure 9.2-3 Vector Plot of the Poiseuille Flow Velocity Field, Discretized using Element Type 28 and the Mixed Method

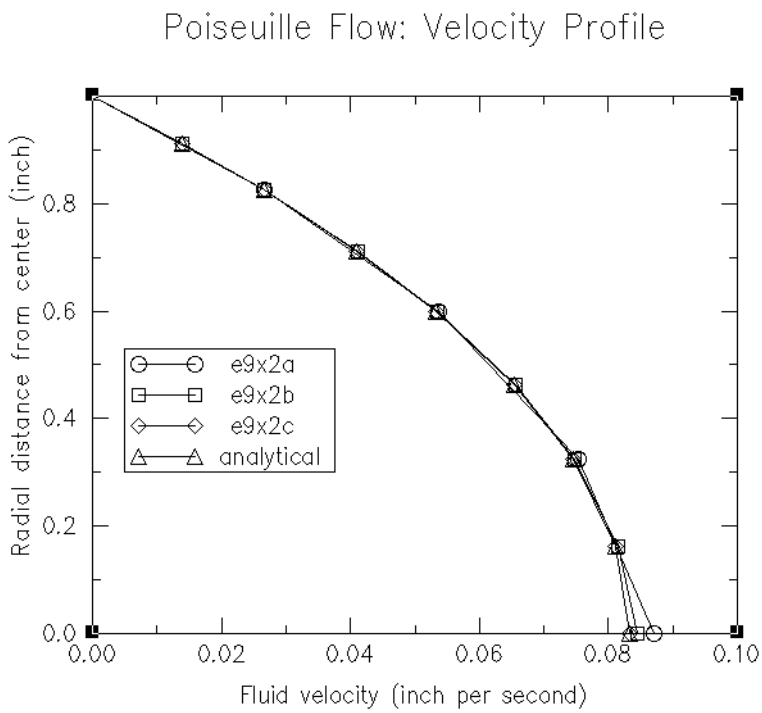

Figure 9.2-4 Comparison of Computation and Analytical Results

9.3 Fluid Squeezed Between Two Long Plates

This problem has an approximate analytical solution for viscous, incompressible fluids. The flow is generated by squeezing the fluid occupying the space in between two infinitely long, rigid plates. For this problem, the results obtained using steady state approximation, in combination with the mixed method, are presented.

This problem is modeled using the two techniques summarized below:

Data Set	Element Type(s)	Number of Elements	Number of Nodes
e9x3a	11	60	77
e9x3b	6	120	77

Element

Element type 11 is a lower-order, 4-node, bilinearly interpolated, planar element used in problem e9x3a to discretize the fluid domain. Three-noded triangular element of type 6 is used in problem e9x3b. Using the mixed method, each node has three degrees of freedom: two planar velocity components and a pressure.

Model

The six-by-two square inches of discretized fluid regions as shown in Figures 9.3-1 and 9.3-2 for problems e9x3a and e9x3b, respectively, represent a quadrant of the fluid domain obtained by considering symmetry with respect to both the x- and y-axis. The quadrilateral mesh has 60 elements, while the triangular mesh uses 120 elements. It is assumed here that the 1:3 aspect ratio chosen for the fluid domain is sufficient to accurately approximate the effects of infinitely long plates on the fluid.

Boundary Conditions

To model the squeezing effect from the top plate, the y component of fluid velocity along the top boundary is set to -1.0 inch per second; the x component is zero considering no-slip boundary condition. The left side of the domain is a symmetry line along the y-axis, so the velocity component along x-direction is set to zero. Also, the bottom side of the fluid domain is a symmetry line along the x-axis, hence the y-component of fluid velocity is given as zero.

Material

Newtonian fluid material with a viscosity of 1.0 lbf.sec/square inch and a mass density of 1.0E-06 pound per cubic inch is used to model this viscous flow.

Results

The vector plot of fluid velocity field is given in Figures 9.3-1 and 9.3-2, respectively, for problems e9x3a and e9x3b. The arrows representing velocity vectors are scaled according to their magnitues. The pressure distribution in the flow fields are given by the contour plots in Figures 9.3-3 and 9.3-4. Comparison of computation and analytical resut is given in Tables 9.3-1 and 9.3-2, and Figures 9.3-5 and 9.3-6.

Table 9.3-1 Comparison of Fluid Velocity X Obtained from Finite Element Computation against Analytical Result (at x=6)

Vertical Distance	e9x3a	e9x3b	Analytical
0.000000e+0	4.394480e+00	4.347870e+00	4.500000e+00
2.500000e-01	4.334840e+00	4.292710e+00	4.429688e+00
5.000000e-01	4.155030e+00	4.121650e+00	4.218750e+00
1.000000e+00	3.418850e+00	3.422630e+00	3.375000e+00
1.500000e+00	2.122560e+00	2.171330e+00	1.968750e+00
1.750000e+00	1.213830e+00	1.248630e+00	1.054688e+00
2.000000e+00	1.259060e-10	9.740150e-11	0.000000e+00

Table 9.3-2 Comparison of Fluid Velocity Y Obtained from Finite Element Computation against Analytical Result (at x=6)

Vertical Distance	e9x3a	e9x3b	Analytical
0.000000e+0	-3.249630e-11	-3.140290e-11	0.000000e+00
2.500000e-01	-1.570460e-01	-1.472210e-01	-1.865234e-01
5.000000e-01	-3.115110e-01	-2.918960e-01	-3.671875e-01
1.000000e+00	-6.053120e-01	-5.663410e-01	-6.875000e-01
1.500000e+00	-8.500980e-01	-8.076410e-01	-9.140625e-01
1.750000e+00	-9.561750e-01	-9.110980e-01	-9.775391e-01
2.000000e+00	-1.000000e+00	-1.000000e+00	-1.000000e+00

Parameters, Options, and Subroutines Summary

Examples e9x3a.dat and e9x3b.dat:

Parameters	Model Definition Options
ELEMENTS	CONNECTIVITY
END	CONTINUE
FLUID	CONTROL
SIZING	COORDINATES
	END OPTION
	FIXED VELOCITY
	ISOTROPIC
	POST
	PRINT ELEMENT
	STEADY STATE

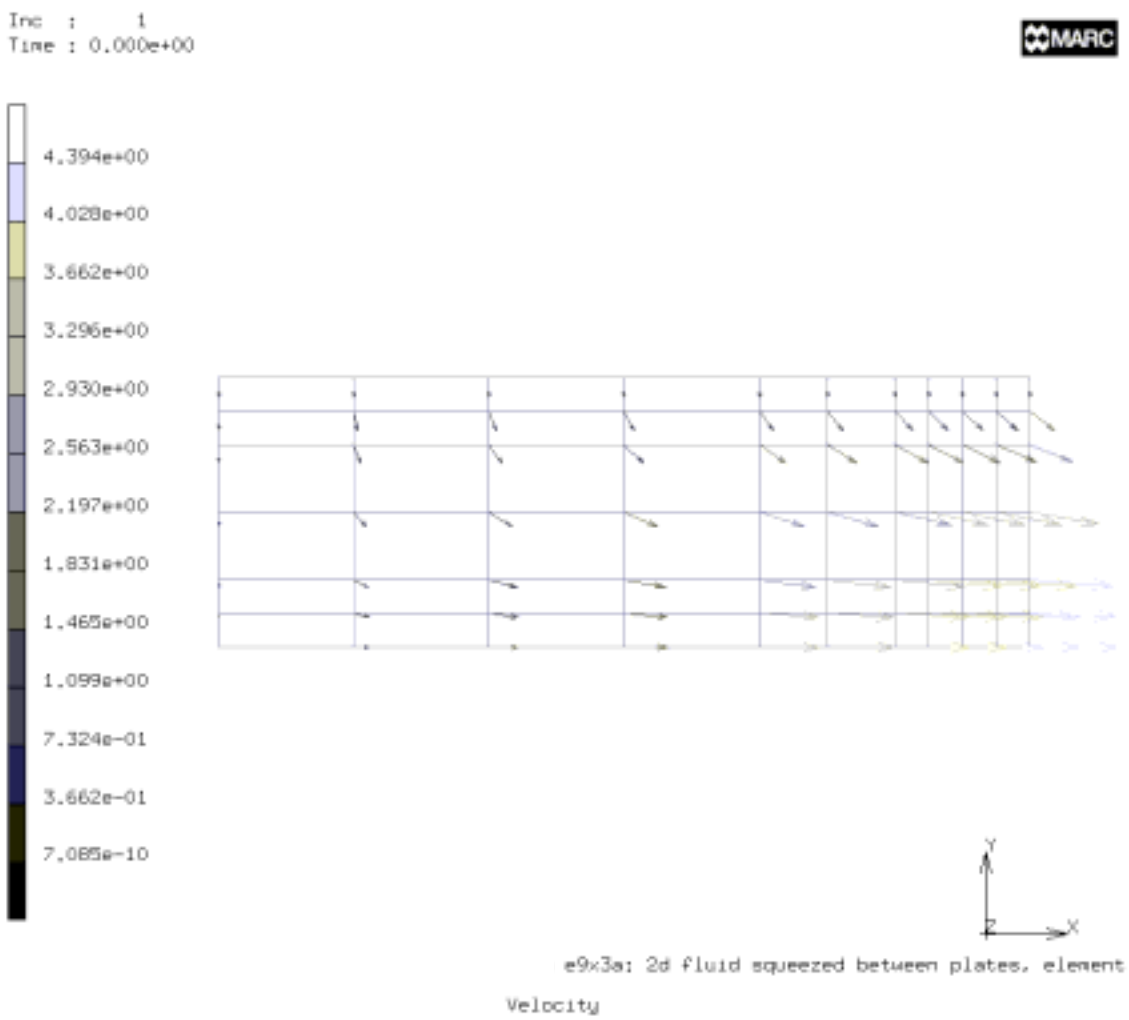

Figure 9.3-1 Vector Plot of the Squeezed Fluid Velocity Field, Discretized using Element Type 11 and the Mixed Method

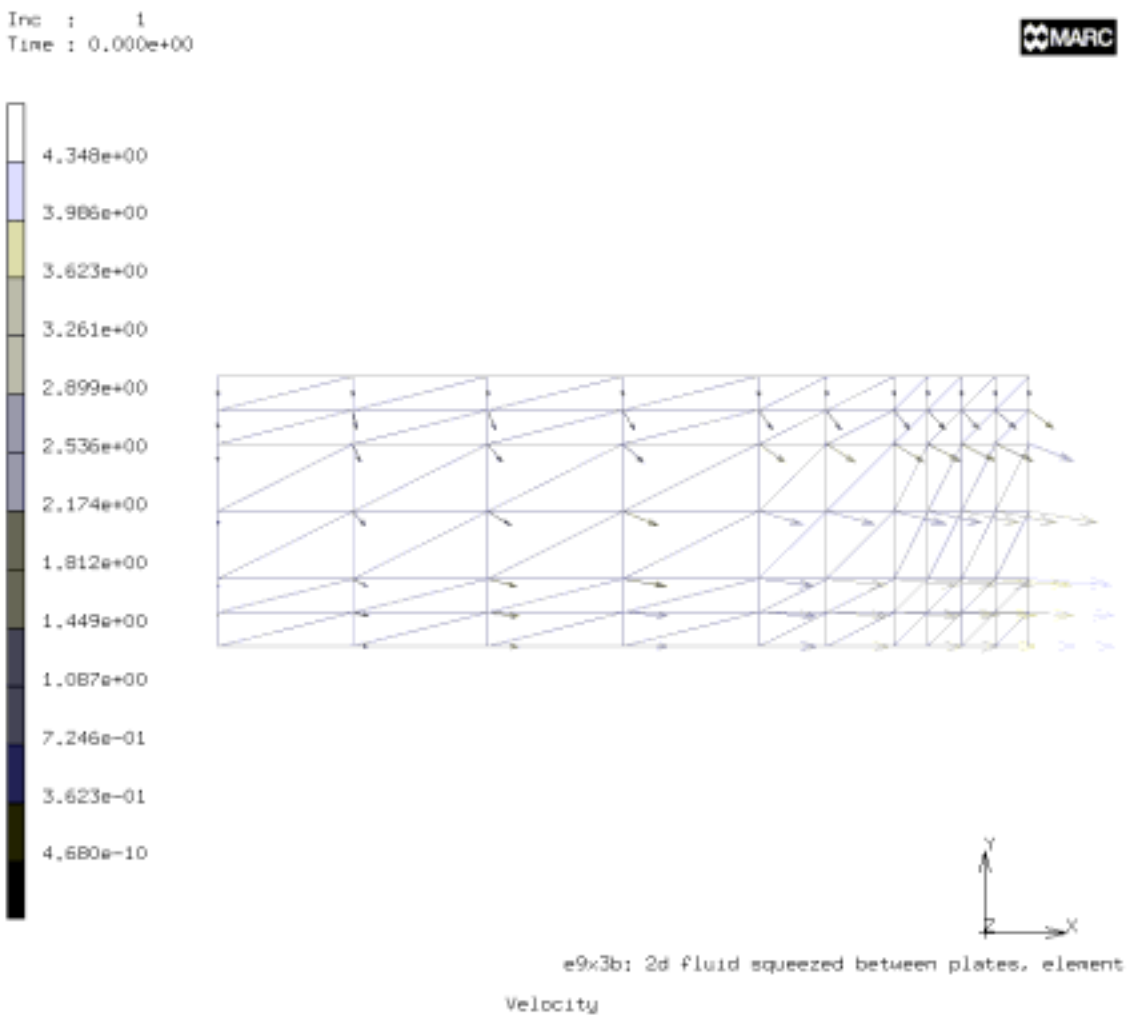

Figure 9.3-2 Vector Plot of the Squeezed Fluid Velocity Field, Discretized using Element Type 6 and the Mixed Method

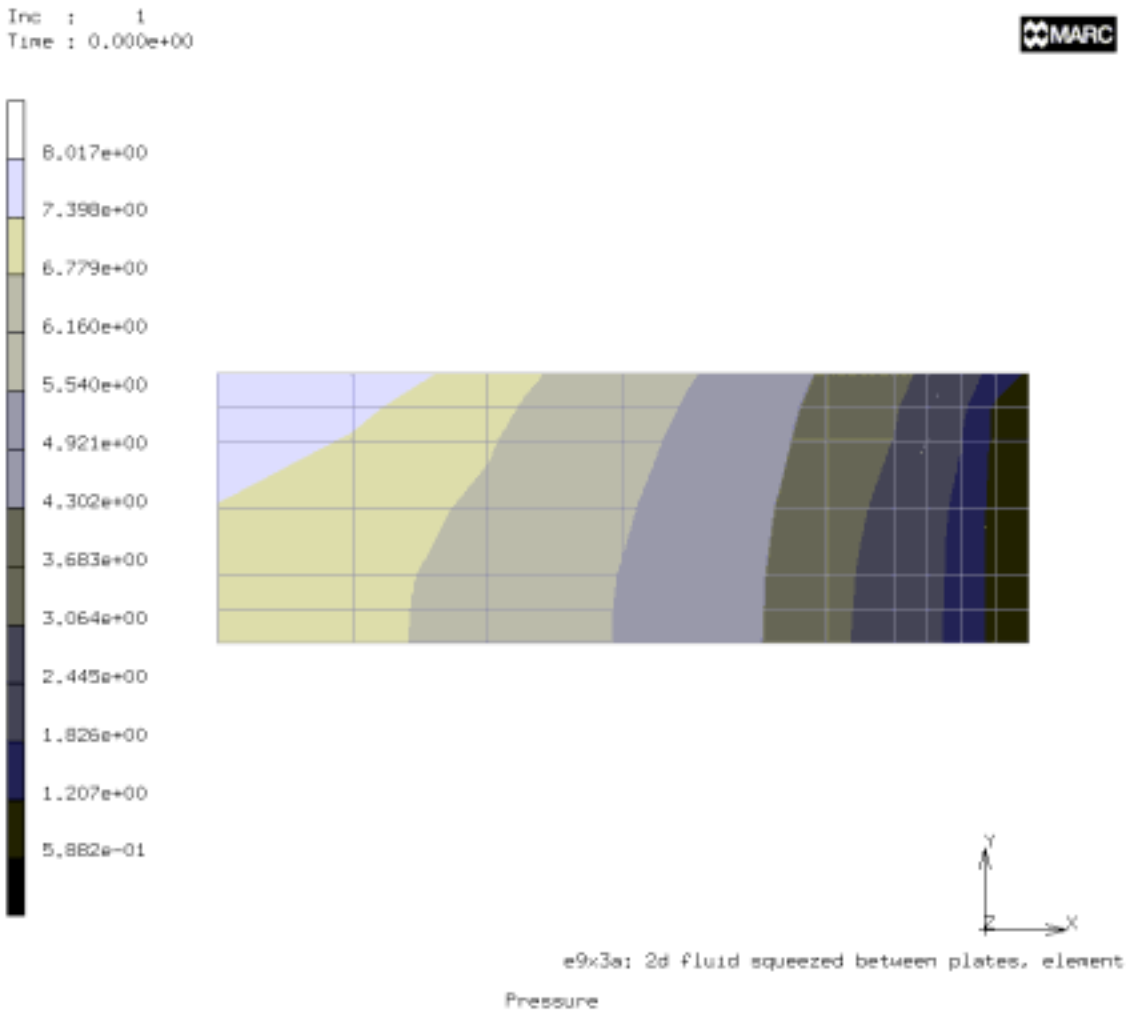

Figure 9.3-3 Contour Plot of the Squeezed Fluid Pressure Field, Discretized using Element Type 11 and the Mixed Method

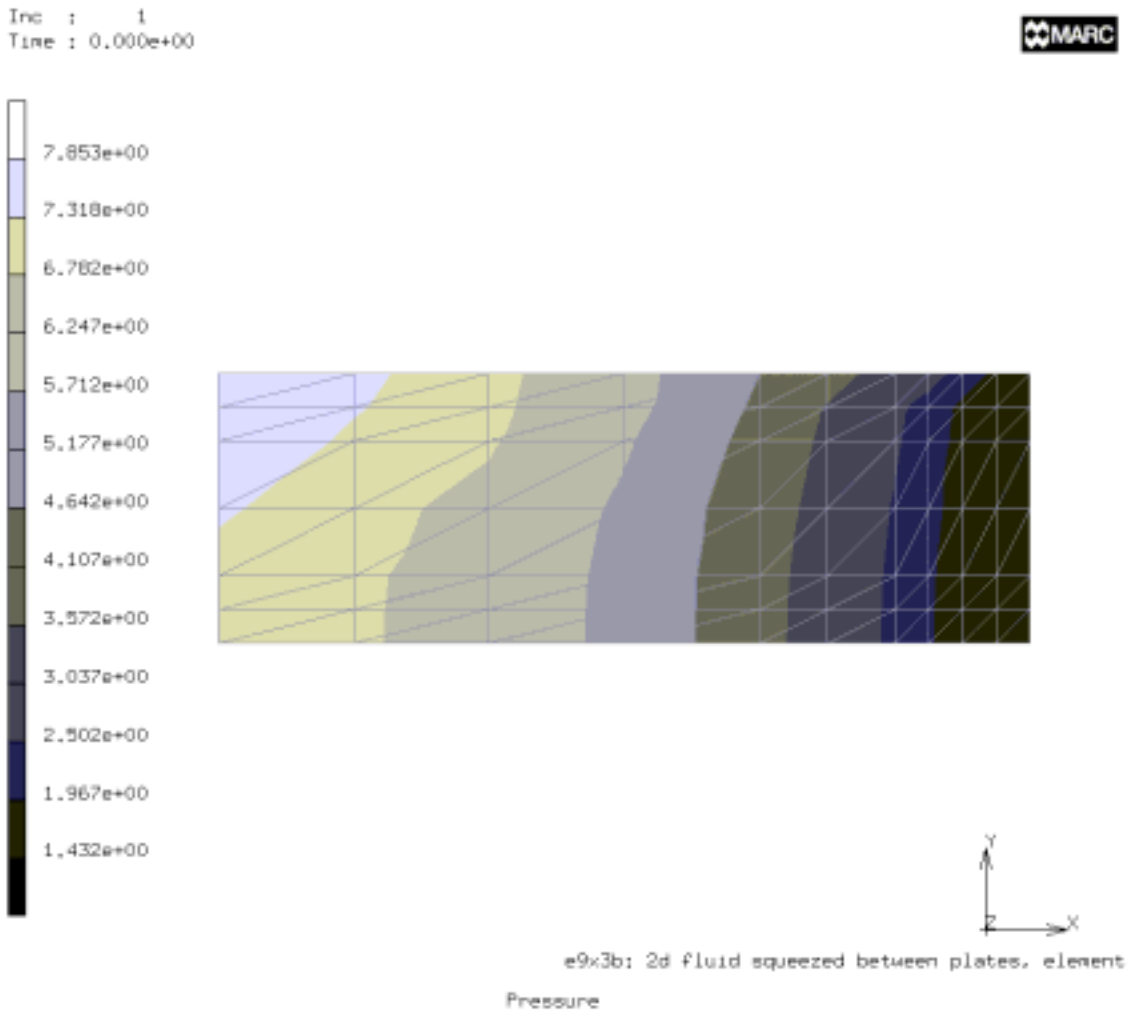

Figure 9.3-4 Contour Plot of the Squeezed Fluid Pressure Field, Discretized using Element Type 6 and the Mixed Method

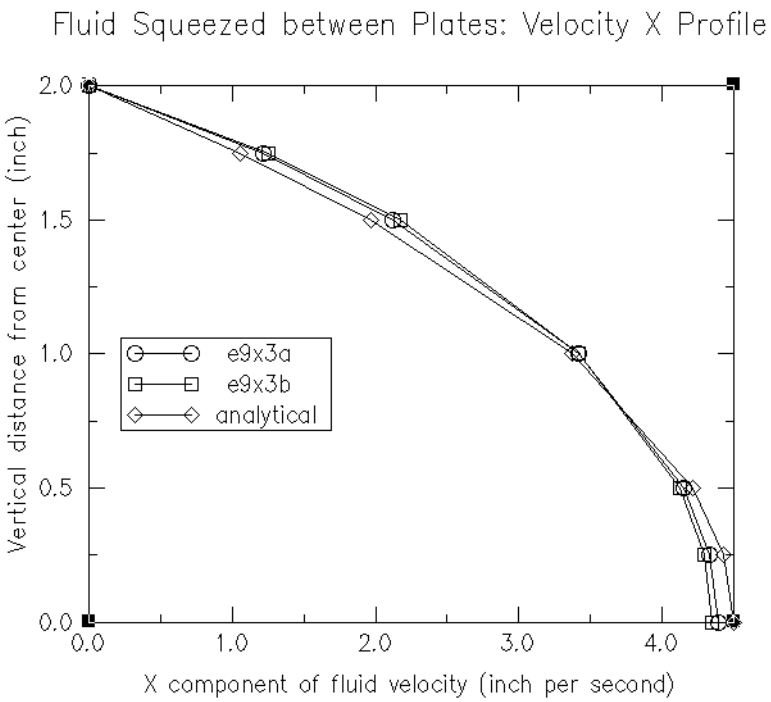

Figure 9.3-5 Comparison of Fluid Velocity V_x Computation and Analytical Results at x=6

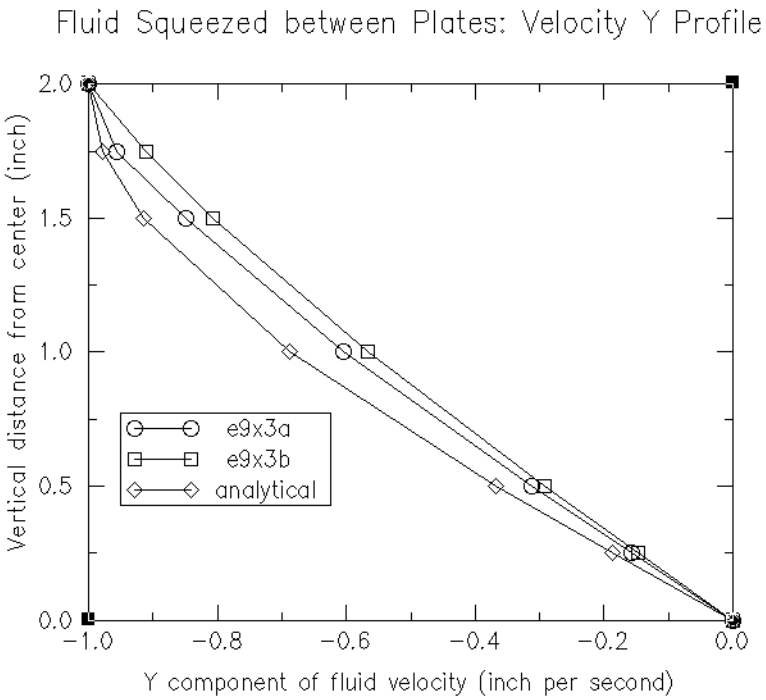

Figure 9.3-6 Comparison of Fluid Velocity V_y Computation and Analytical Results at x=6

9.4 Driven Cavity Flow

This is a commonly used problem to demonstrate a modeling of viscous, incompressible flow using Navier-Stokes equations. The flow is driven by a rigid lid sliding on top of the fluid filled cavity, which creates circulating flow in the fluid. For this problem, the result is obtained using steady state approximation in combination with the mixed method. Using the mixed method, Streamline Upwind Petrov-Galerkin (SUPG) and Pressure Stabilizing Petrov-Galerkin (PSPG) techniques are automatically invoked by MARC to prevent numerical instability, which is frequently observed as nonphysical wiggles in the flow field.

Element

Element type 11 is a lower-order, 4-node, bilinearly interpolated, planar element used in the problem to discretize the fluid domain. Using the mixed method, each node has three degrees of freedom: two planar velocity components and a pressure.

Model

The six-by-six square inches domain of the fluid is uniformly meshed as shown in Figure 9.4-1 using a total of 144 elements with 12-element discretization on each side.

Boundary Conditions

The fluid filled cavity is confined by rigid walls on its three sides; that is, left, right, and bottom. No-slip boundary condition requires that both components of the fluid velocity along the walls be set to zero. Flow in the cavity is driven by a rigid lid on top of the cavity, moving with a velocity of 1.0 inch per second along the negative x-direction. As such, the x components of the nodal velocities along the top of the cavity are assigned a value of -1.0 inch per second, and the corresponding y components are set to zero.

Material

Newtonian fluid material with a viscosity of 1.0 lbf.sec/square inch and a mass density of 1.0 pound per cubic inch is used to model this highly viscous flow. Reynolds number for this problem is less than 1.

Results

The vector plot of fluid velocity field is given in Figure 9.4-1 where the arrows are scaled according to their magnitudes. The circulating flow field as a result of the moving lid is shown. The pressure distribution in the flow field is given by the contour plot in Figure 9.4-2.

Parameters, Options, and Subroutines Summary

Example e9x4.dat:

Parameters	Model Definition Options
ELEMENTS	CONNECTIVITY
END	CONTINUE
FLUID	CONTROL
SIZING	COORDINATES
	END OPTION
	FIXED VELOCITY
	PRINT ELEMENT
	ISOTROPIC
	POST
	STEADY STATE

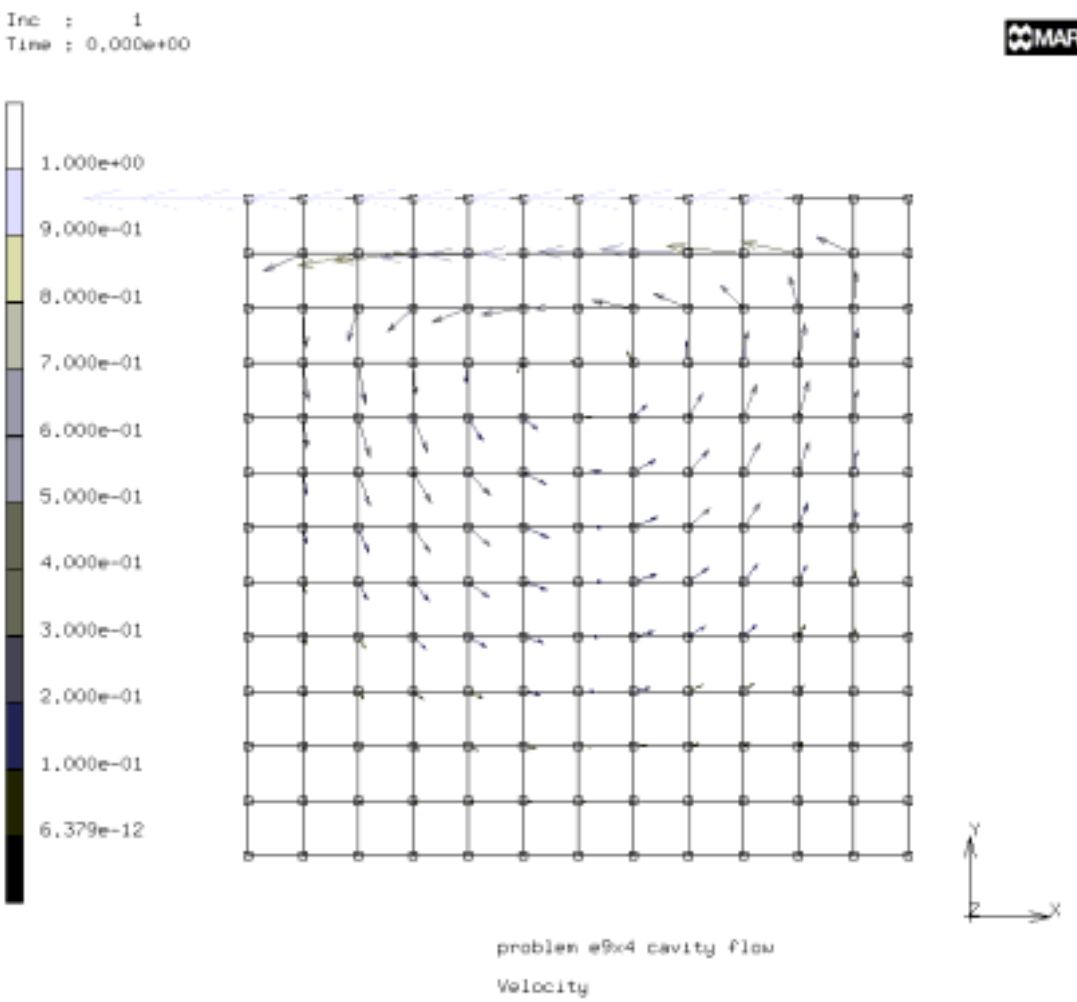

Figure 9.4-1 Vector Plot of the Driven Cavity Flow Velocity Field, Discretized using Element Type 11 and the Mixed Method

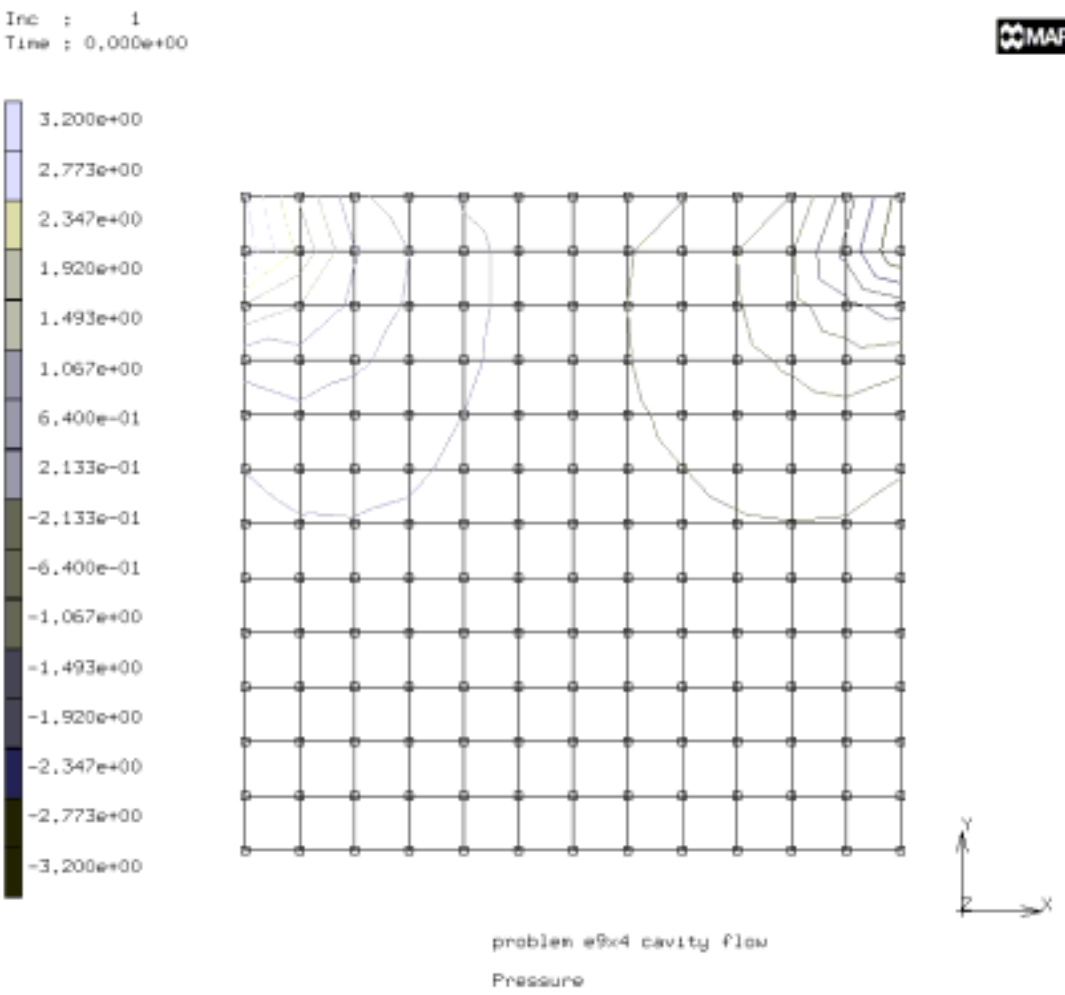

Figure 9.4-2 Contour Plot of the Driven Cavity Flow Pressure Field, Discretized using Element Type 11 and the Mixed Method

9.5 Flow Past a Circular Cylinder

This problem simulates the flow past a cylinder. This problem is performed as both a steady state analysis and transient analysis based on Navier-Stokes equations.

This problem is modeled using the five techniques summarized below.

Data Set	Element Type(s)	Number of Elements	Number of Nodes	Differentiating Features
e9x5a	11	440	483	Mixed method, steady state
e9x5b	11	440	483	Penalty method, steady state
e9x5c	27	440	1405	Mixed method, steady state
e9x5d	27	440	1405	Penalty method, steady state
e9x5e	11	440	483	Mixed method, transient method

Element

Element type 11 is a 4-node planar element using bilinear interpolation functions. Element type 27 is an 8-node planar element using biquadratic interpolation functions.

Model

A planar model of the flow is simulated. Because of symmetry conditions, only one half of the model is meshed. The cylinder has a radius of 1 inch. The channel is given a length of 5 inches in the upstream direction and a length of 10 inches in the downstream direction. The model is given a depth of 10 inches with the desire that this is enough to accurately capture the fluid behavior. The finite element mesh, consisting of 4-node elements, is shown in Figure 9.5-1. The 8-node element mesh is shown in Figure 9.5-2.

Boundary Conditions

Along the symmetry axis (Y = 0) $V_y = 0$. Along the upstream boundary condition, steady state fluid conditions are considered with $V_x = 1.0$ and $V_y = 0$ for problems e9x5a through e9x5e. Along the outlet downstream boundary, the fluid is considered traction free. At y = 5.0, the velocity is $V_x = 1$, $V_y = 0$.

Material

The fluid is treated as Newtonian with a viscosity of 1.0 lbf.sec/square inch and a mass density of 1.0 lb/cubic inch.

Numerical Procedure

In all of the analyses, the Newton Rapshon procedure is used to solve the nonlinear problem. In the transient analysis, a fixed time step procedure is used. Convergence is based upon the relative velocity criteria.

Results

The fluid flow has three different behaviors based upon the axial position. In the upstream area, the fluid flow is virtually parallel. In the region near the cylinder, three behaviors are observed. First, the fluid is deflected along the cylinder. Second, near the body, a boundary layer develops where the viscous behavior dominates. Third, as the cylinder acts to constrict the flow, the velocity in the region at X = 5 increases to satisfy incompressibility. At steady state, the Reynolds number is about 100.

Figures 9.5-4 and 9.5-5 show the pressure distribution in the fluid for problems e9x5a and e9x5c, respectively. Figure 9.5-6 shows the results for the transient analysis at the tenth increment. Figures 9.5-1 through 9.5-3 show the vector plots of the velocity for the analysis of problems e9x5a, e9x5c, and 39x5e, respectively.

Parameters, Options, and Subroutines Summary

Examples e9x5a.dat, e9x5b.dat, e9x5c.dat, and e9x5d.dat:

Parameters	Model Definition Options
ELEMENTS	CONNECTIVITY
END	COORDINATES
FLUID	CONTINUE
SIZING	CONTROL
	END OPTION
	FIXED VELOCITY
	ISOTROPIC
	POST
	PRINT ELEMENT
	STEADY STATE

Examples e9x5e.dat:

Parameters	Model Definition Options	History Definition Options
ELEMENTS	CONNECTIVITY	CONTINUE
END	CONTROL	TRANSIENT NON AUTO
FLUID	COORDINATES	
SIZING	END OPTION	
	FIXED VELOCITY	
	INITIAL VEL	
	ISOTROPIC	
	POST	
	PRINT ELEMENT	

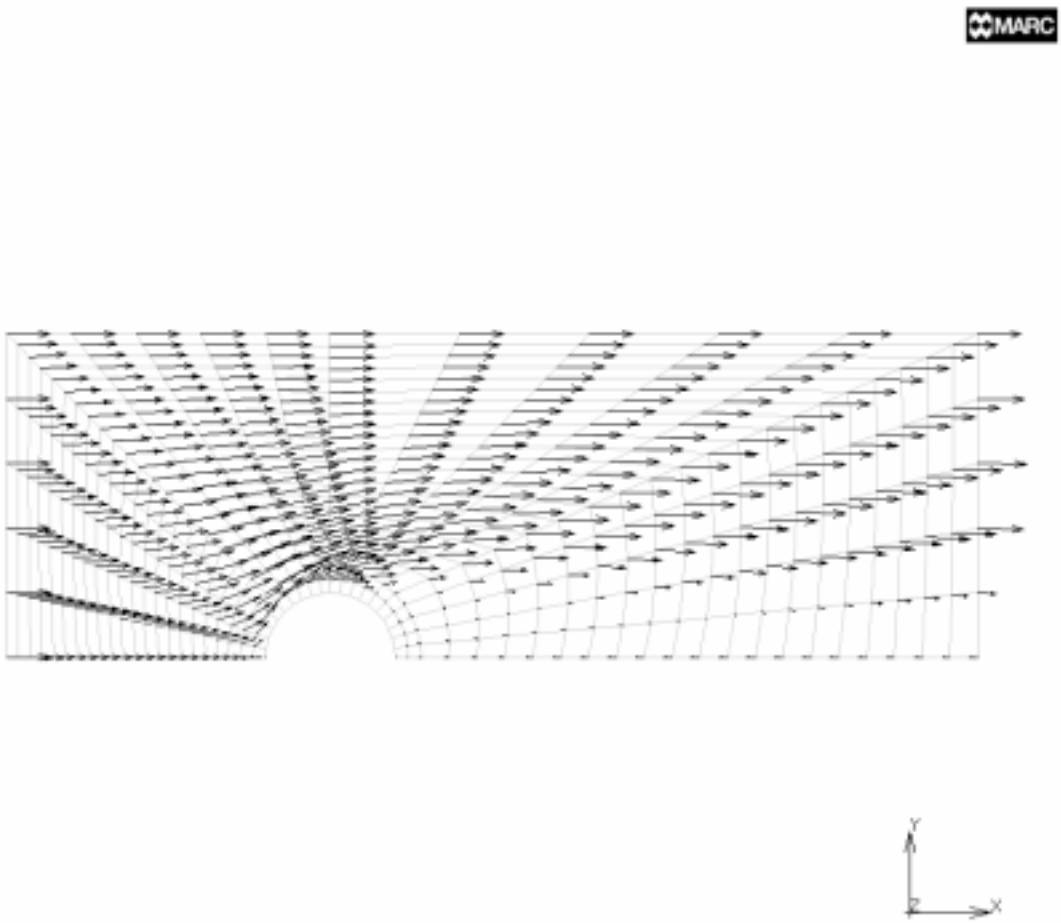

Figure 9.5-1 Vector Plot of the Flow Over Cylinder Velocity Field, Discretized using Element Type 11 and the Mixed Method

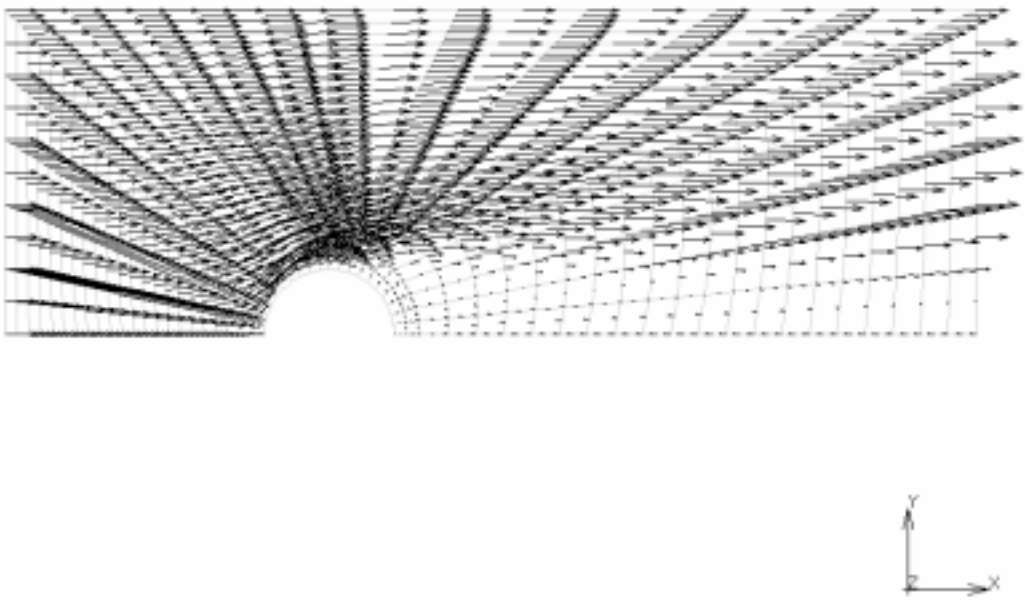

Figure 9.5-2 Vector Plot of the Flow Over Cylinder Velocity Field, Discretized using Element Type 27 and the Mixed Method

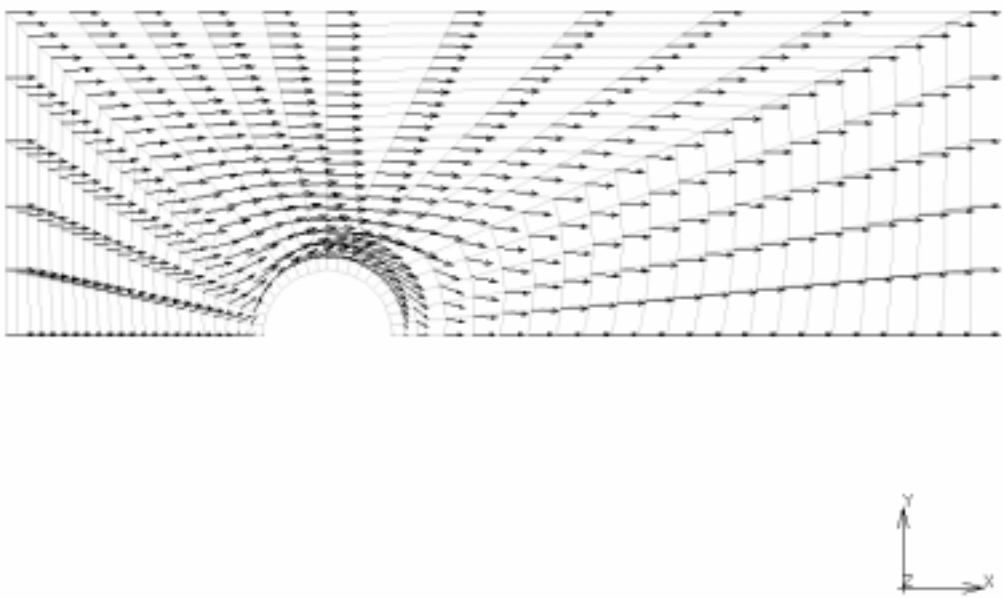

Figure 9.5-3 Vector Plot of the Flow Over Cylinder Transient Velocity Field at the Tenth Increment, Discretized using Element Type 11 and the Mixed Method

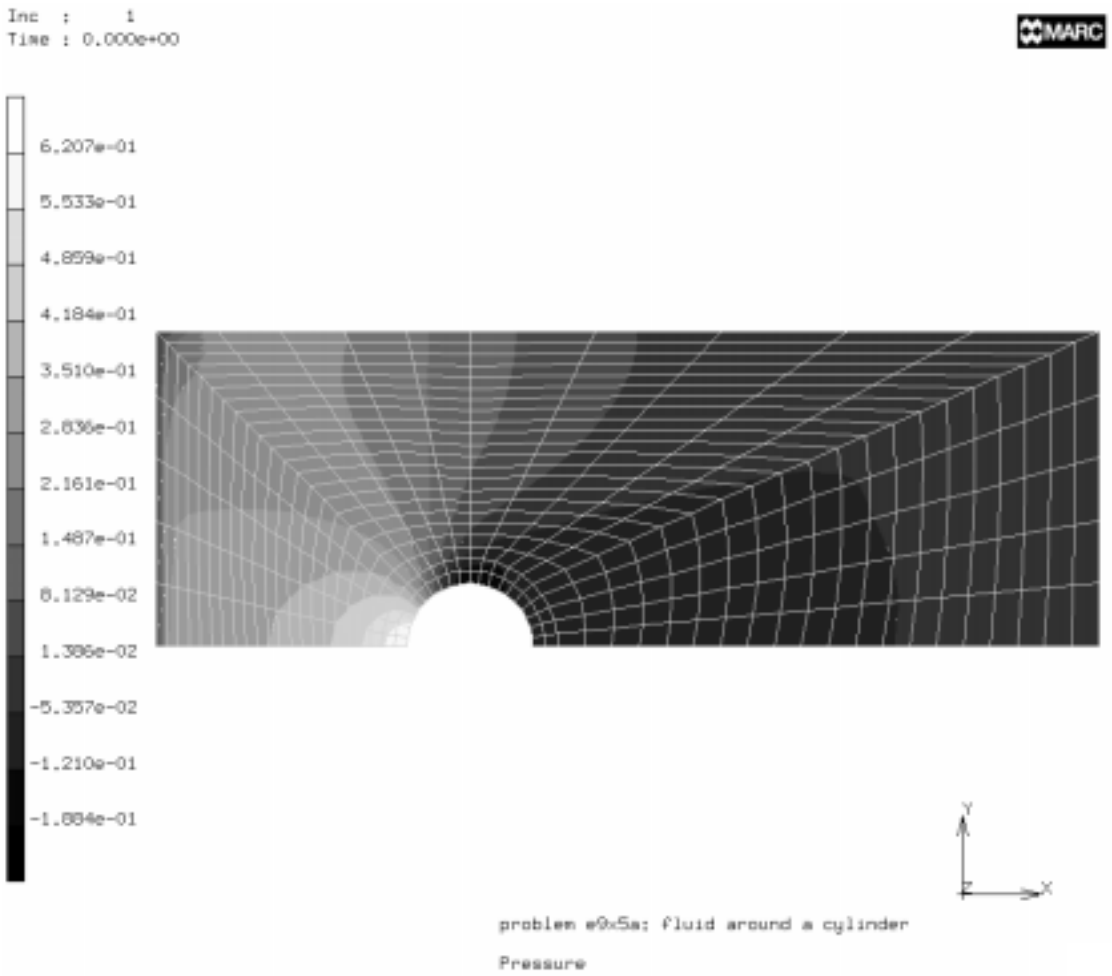

Figure 9.5-4 Contour Plot of the Flow Over Cylinder Pressure Field, Discretized using Element Type 11 and the Mixed Method

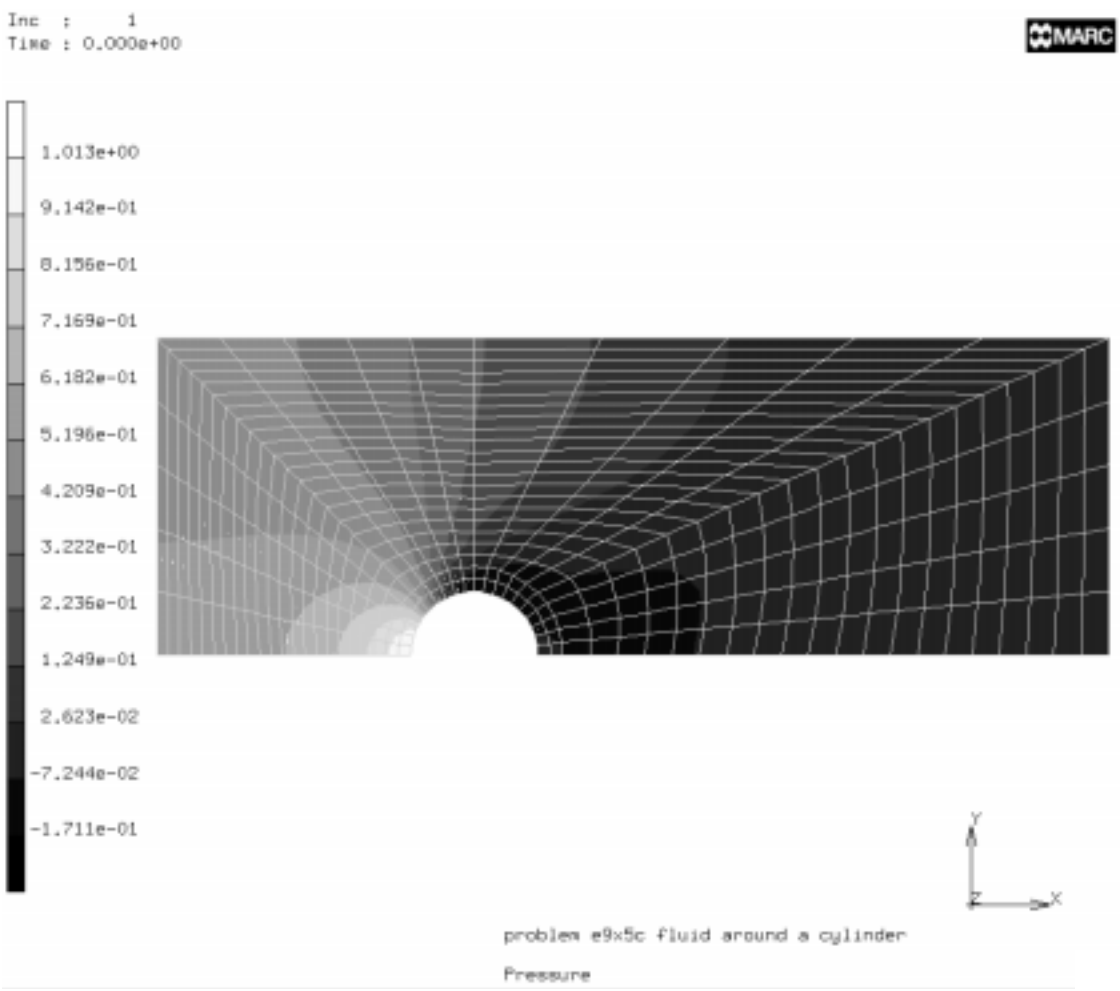

Figure 9.5-5 Contour Plot of the Flow Over Cylinder Pressure Field, Discretized using Element Type 27 and the Mixed Method

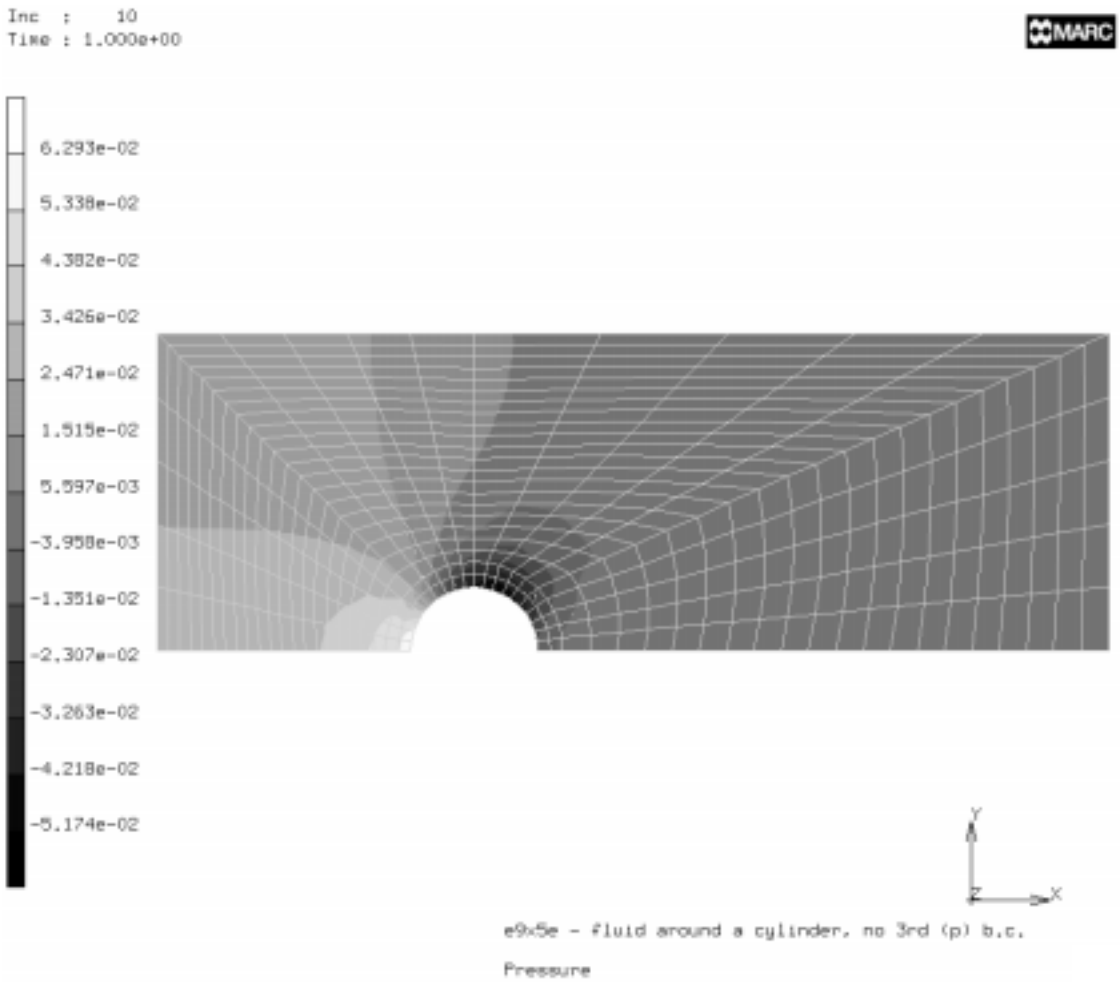

Figure 9.5-6 Contour Plot of the Flow Over Cylinder Transient Pressure Field at the Tenth Increment, Discretized using Element Type 11 and the Mixed Method

9.6 Flow Over Electronic Chip

This problem demonstrates coupled fluid-thermal behavior for the flow about electronic circuit chips. The flow is treated as two-dimensional and, in this example, the chips are considered to be at a constant temperature.

This problem is modeled using the two techniques summarized below.

Data Set	Element Type(s)	Number of Elements	Number of Nodes	Differentiating Features
e9x6a	11	311	370	Mixed method
e9x6b	11	311	370	Penalty method

Element

Element type 11, a 4-node isoparametric element, is used. For problem e9x6a, the mixed formulation procedure is used so the degrees of freedom are the velocities V_x, V_y, pressure, and the temperature. Problem e9x6b uses the penalty method which does not explicitly represent pressure as a nodal variable.

Model

The model is shown in Figure 9.6-1. The height of the channel is 1 inch and the chips have a dimension of 0.4 x 0.4 square inch and are separated by 1.0 inch. The amount of separation between the chips is significant as either a wake or recirculating flow can occur, depending on both the distance and the inlet velocity. The domain is discretized using 311 elements.

Boundary Conditions

The fluid enters the region at x = 0 with a velocity of V_x = 1.0 inch/second and V_y = 0. At the outflow section on the perimeter, the y-component of fluid velocity is set to zero. Other than the inlet and outlet sections, all velocity components are set to zero due to no-slip boundary conditions. Temperature along the perimeter of the domain are set to zero, except those nodes along the chips, which are set to 1°F.

Material

Newtonian fluid with a viscosity of 1.0 lbf.sec/square inch and a mass density of 1.0 lb/cubic inch is used to model the viscous flow. Thermal conductivity of the fluid is given as 0.0145 Btu/sec/in/°F.

Results

The vector plot of fluid velocity field for problem e9x6a is given in Figure 9.6-1 where the arrows are scaled according to their magnitude. The contour plots of temperature and pressure distributions are shown in Figures 9.6-2 and 9.6-3, respectively. Results obtained for problem e9.6b are indistinguishable from the above; therefore, they are not presented here.

Parameters, Options, and Subroutines Summary

Example e9x6a.dat and e9x6b.dat:

Parameters	Model Definition Options
ELEMENTS	CONNECTIVITY
END	CONTINUE
FLUID	CONTROL
SIZING	COORDINATES
	END OPTION
	FIXED VELOCITY
	ISOTROPIC
	POST
	PRINT ELEMENT
	STEADY STATE

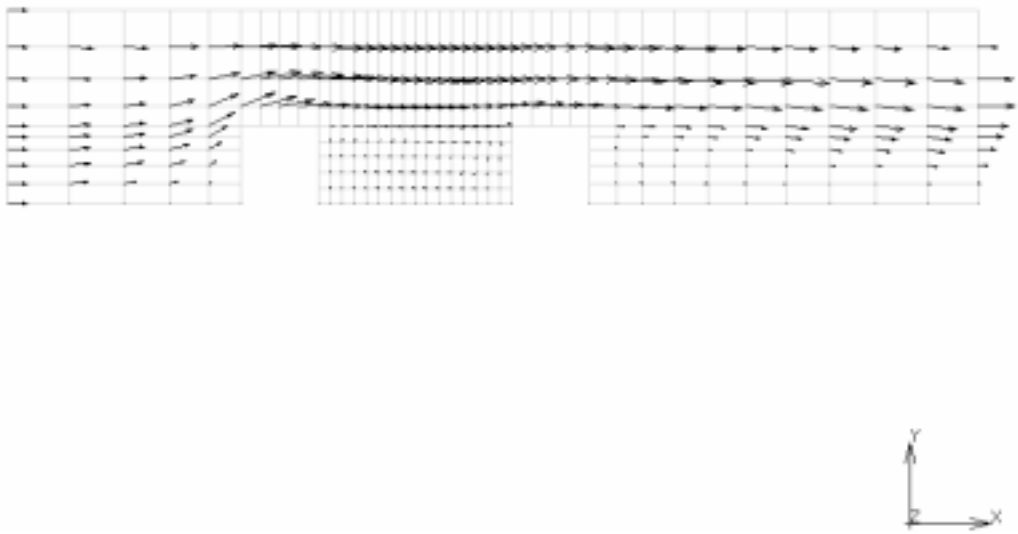

Figure 9.6-1 Vector Plot of the Flow Over Multiple Steps Velocity Field, Discretized using Element Type 11 and the Mixed Method

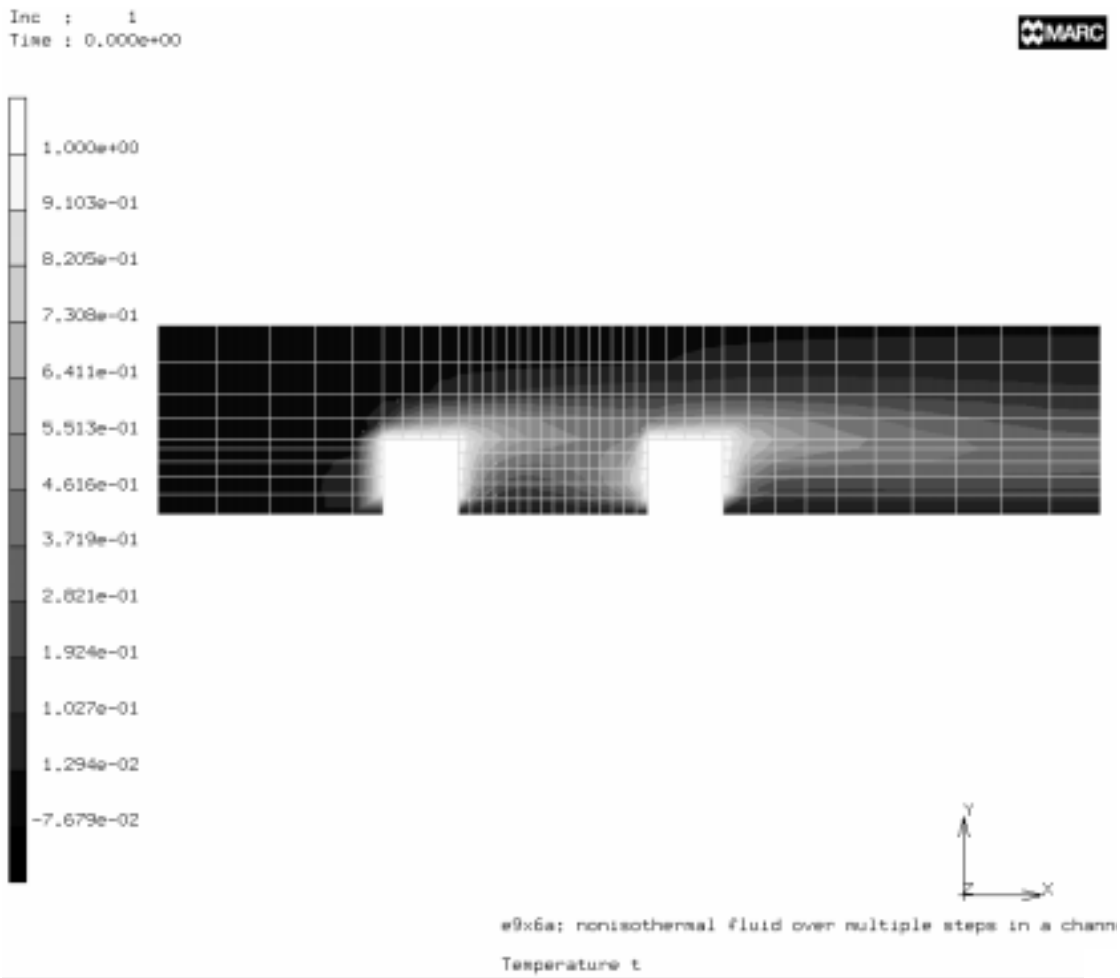

Figure 9.6-2 Contour Plot of the Flow Over Multiple Steps Temperature Field, Discretized using Element Type 11 and the Mixed Method

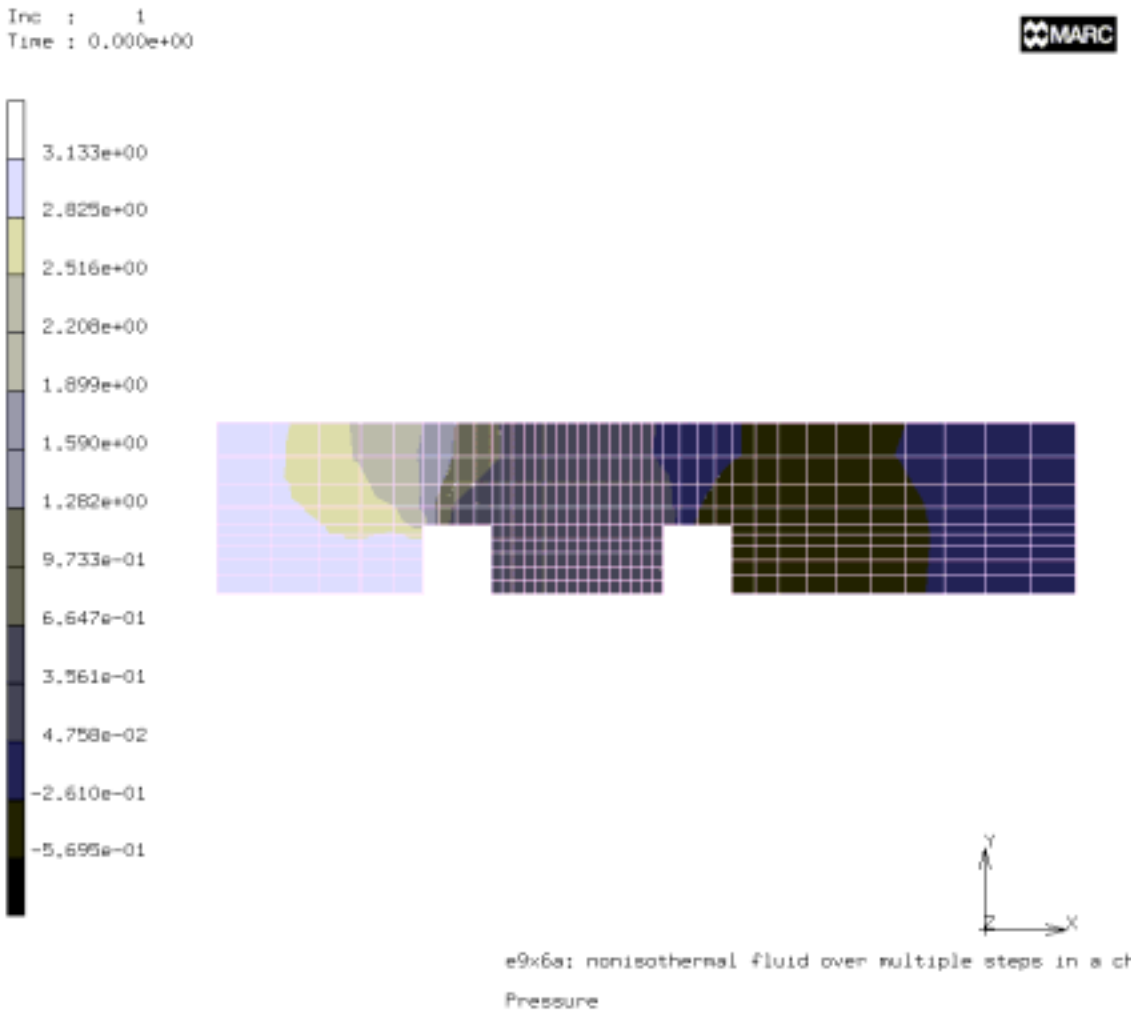

Figure 9.6-3 Contour Plot of the Flow Over Multiple Steps Pressure Field, Discretized using Element Type 11 and the Mixed Method

9.7 Natural Convection

A set of problems showing thermally induced fluid circulation in a cavity is presented to demonstrate buoyancy-driven, natural convection phenomena. This analysis feature is suitable for applications in electronic packaging and solidification process of metal castings, among others. Basically, the problems invoke coupling of heat transfer and fluid mechanics by way of density variation due to nonuniform temperature distribution. Boussinesq approximation is used by MARC to model this type of convective flows. Different levels of Rayleigh numbers are used in the following two cases to demonstrate MARC analysis capability.

This problem is modeled using the two techniques summarized below.

Data Set	Element Type(s)	Number of Elements	Number of Nodes	Differentiating Features
e9x7a	11	144	169	Coarser mesh
e9x7b	11	196	225	Finer mesh

Element

Element type 11 is a lower-order, 4-node, bilinearly interpolated, planar element used in this problem to discretize the fluid medium. Using the penalty method for fluid elements, and including the coupling with heat transfer, each node ends up with three degrees of freedom: two planar velocity components and a temperature.

Model

The one-by-one square inch domain of fluid is meshed as shown in Figures 9.7-1 and 9.7-2 for problems e9x7a and e9x7b, respectively. Problem e9x7a uses a total of 144 elements, with twelve-element discretization per side. On the other hand, problem e9x7b uses 14 element discretization per side, which results in a total of 196 elements. Graded meshes are used in both problems, with finer elements positioned closer to the perimeter of the fluid filled cavity to capture the steeper velocity gradient.

Load and Boundary Conditions

Gravity field oriented in the negative y direction is specified using load type 102. This is necessary in order to model buoyancy effects. The magnitude of gravity acceleration in this case is given by 1.0 force per unit mass. The fluid filled cavity is confined by rigid walls on all four sides. No-slip boundary conditions require that both components of fluid velocity along the walls be set to zero. Flow in the cavity is induced by the temperature difference between

the left-side and right-side walls. For both cases, the temperature of the left-side wall is set at 2.0°F., which is also the reference temperature for the problems. The temperature of the right-side wall is given at 3.0°F for both problems.

Material

Newtonian fluid material with a viscosity of 1.0 lbf.sec/square inch and a mass density of 1.0 lb/cubic inch is used to model incompressible, viscous flows in all three cases. Increasing values of volumetric expansion coefficients are used for the problems: 1.0E+03 and 1.0E+04 in/°F, which also represent the Rayleigh numbers for problems e9x7a and e9x7b, respectively. Fluid thermal conductivity of 1.0 Btu/sec/in/°F. is used in all cases.

Results

The vector plots of fluid velocity fields for problems e9x7a and e9x7b are given in Figures 9.7-1 and 9.7-2, respectively. The circulating flow fields, as shown by the arrows that are scaled according to their magnitudes, tend to reach an oval pattern as the Rayleigh number gets higher. The resulting temperature distributions in the fluids are given by the contour plots in Figures 9.7-3 and 9.7-4 for problems e9x7a and e9x7b, respectively. Higher Rayleigh numbers produce more significant effects of natural convection.

Parameters, Options, and Subroutines Summary

Examples e9x7a.dat and e9x7b.dat:

Parameters	Model Definition Options
DIST LOADS	CONNECTIVITY
ELEMENTS	COORDINATES
END	CONTINUE
FLUID	CONTROL
SIZING	DIST LOADS
	END OPTION
	FIXED VELOCITY
	ISOTROPIC
	PARAMETERS
	POST
	PRINT ELEMENT
	STEADY STATE

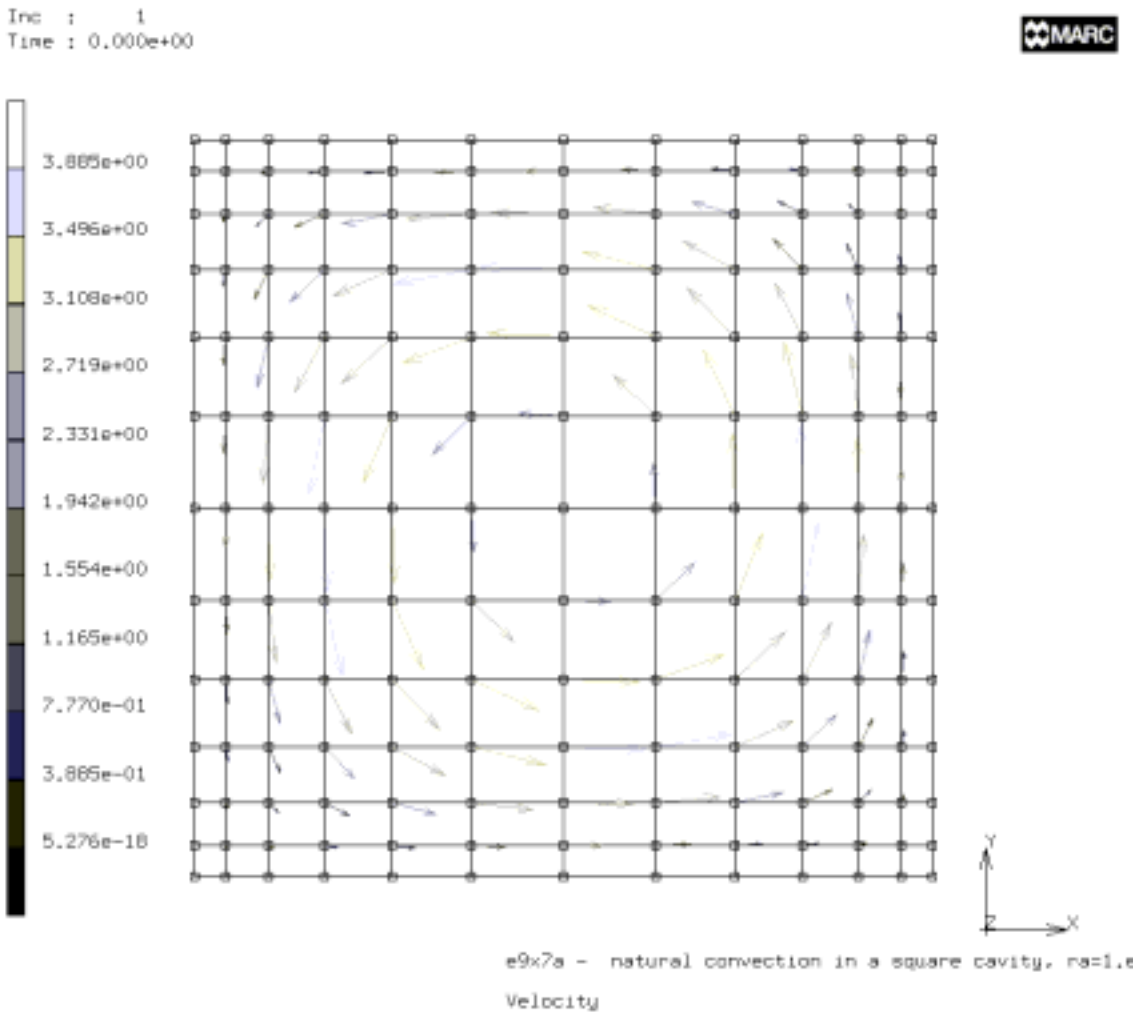

Figure 9.7-1 Vector Plot of the Natural Convective Flow Velocity Field with Rayleigh Number = 1.0e+03, Discretized using Element Type 11 and the Penalty Method

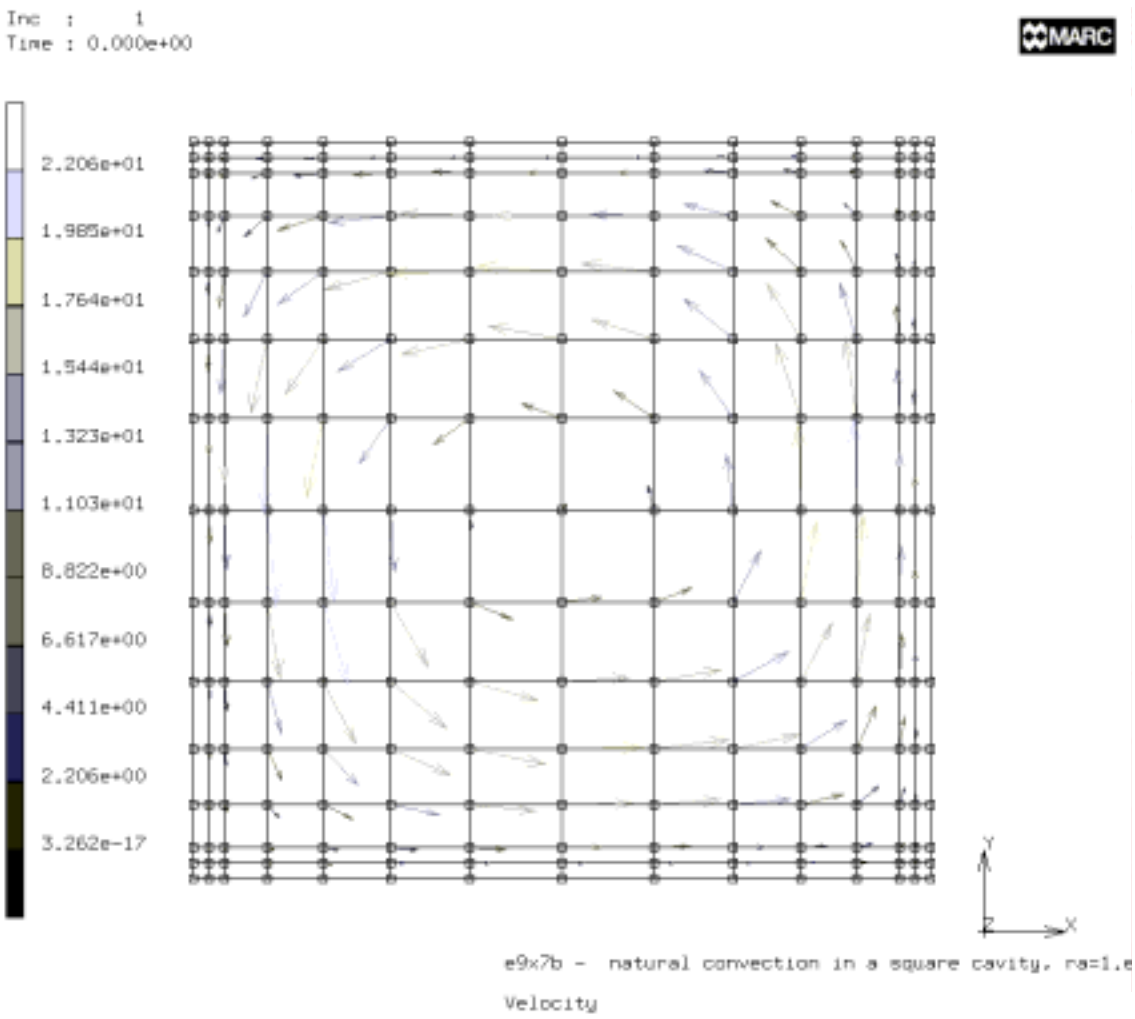

Figure 9.7-2 Vector Plot of the Natural Convective Flow Velocity Field with Rayleigh Number = 1.0e+04, Discretized using Element Type 11 and the Penalty Method

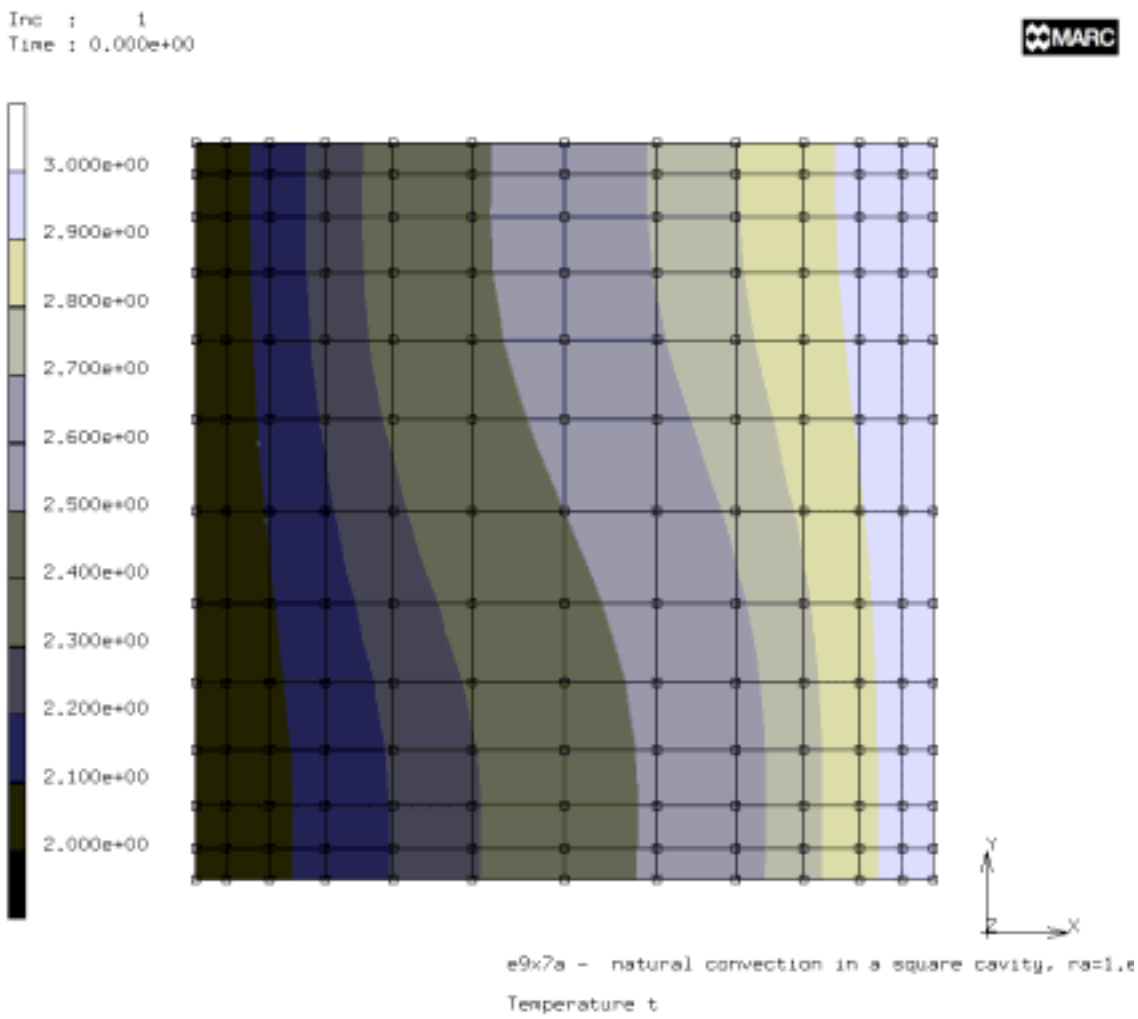

Figure 9.7-3 Contour Plot of the Natural Convective Flow Temperature Field with Rayleigh Number = 1.0e+03, Discretized using Element Type 11 and the Penalty Method

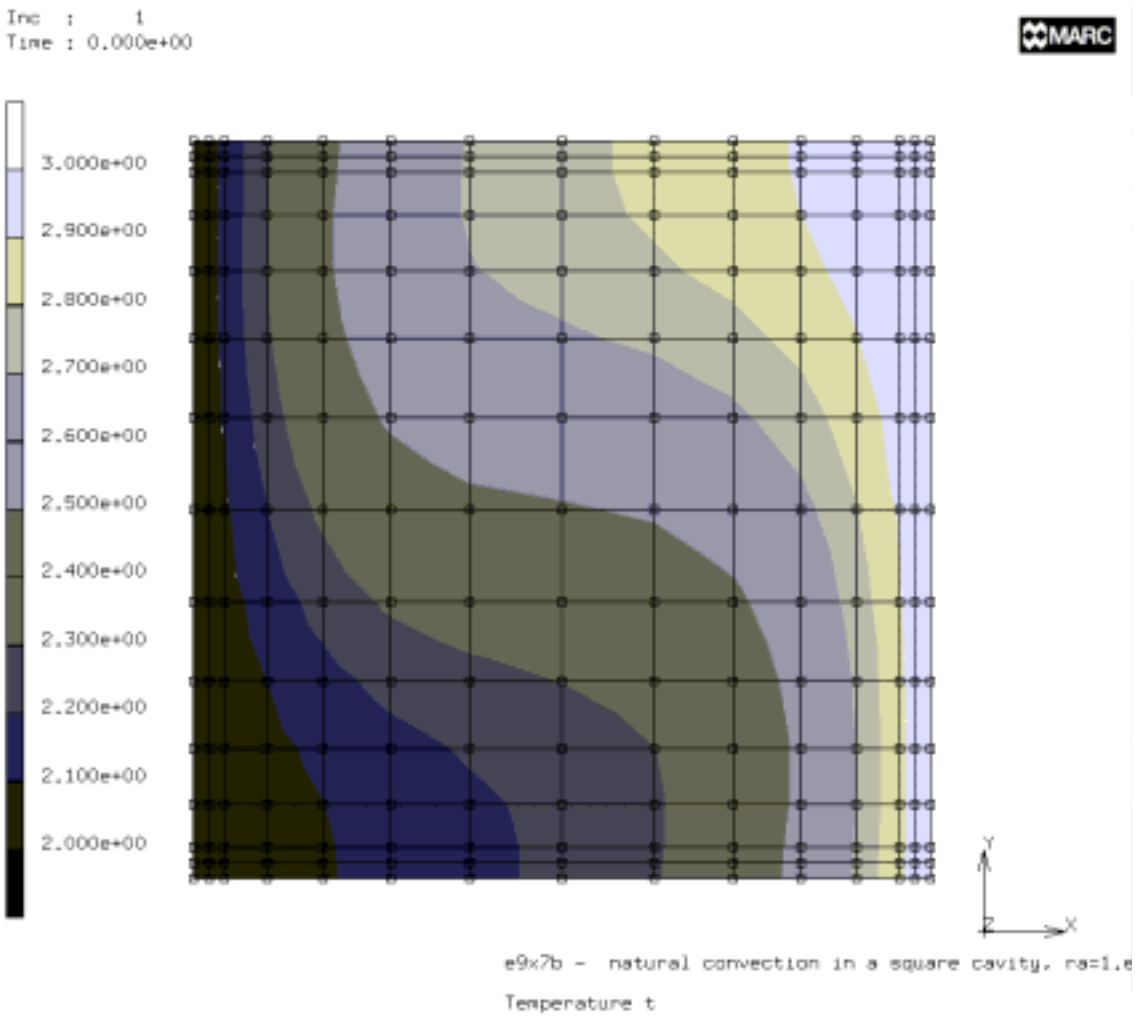

Figure 9.7-4 Contour Plot of the Natural Convective Flow Temperature Field with Rayleigh Number = 1.0e+04, Discretized using Element Type 11 and the Penalty Method

9.8 Flow Around Tubes

This problem demonstrates a modeling of viscous, incompressible flow around obstacles represented by a group of tubes. For this steady state approximation of isothermal flow using Navier-Stokes equations, the results obtained using the mixed method is presented.

Element

Element type 11 is a lower-order, 4-node, bilinearly interpolated, planar element used in this problem to discretize the fluid domain. Using the mixed method, each node has three degrees of freedom: two planar velocity components and a pressure.

Model

The rectangular eight-by-one square inches fluid domain is intersected by three rigid tubes crossing in the direction perpendicular to the domain. Each tube has a diameter of 1.0 inch. Only upper- or lower-half cross section of the tubes are cutting out the fluid domain. The finite element mesh is given in Figure 9.8-1, which consists of a total of 980 elements.

Boundary Conditions

All sections along the perimeter of the fluid domain, except for the openings for fluid inflow and outflow on the extreme left and right of the model, respectively, are considered rigid walls. No-slip boundary conditions along the walls requires that both components of fluid velocity along the sections be specified as zero. At the inflow section on the left, velocity of 1.0 inch per second is applied along the positive x-direction. The prescribed velocity pushes the fluid to flow through the obstacles created by the tubes. Velocity component at the y-direction is set to zero on both the inflow and the outflow sections along the perimeter.

Material

Newtonian fluid material with viscosity of 0.01 lbf.sec./square inch and a mass density of 1.0 lb/cubic inch is used to model the viscous flow. Reynolds number of this problem is 57.72.

Results

The contour plots of velocity (magnitude) and pressure distributions are given by Figures 9.8-2 and 9.8-3, respectively.

Parameters, Options, and Subroutines Summary

Examples e9x8.dat:

Parameters	Model Definition Options
DIST LOADS	CONNECTIVITY
ELEMENTS	COORDINATES
END	CONTINUE
FLUID	CONTROL
SIZING	END OPTION
	FIXED VELOCITY
	ISOTROPIC
	POST
	STEADY STATE

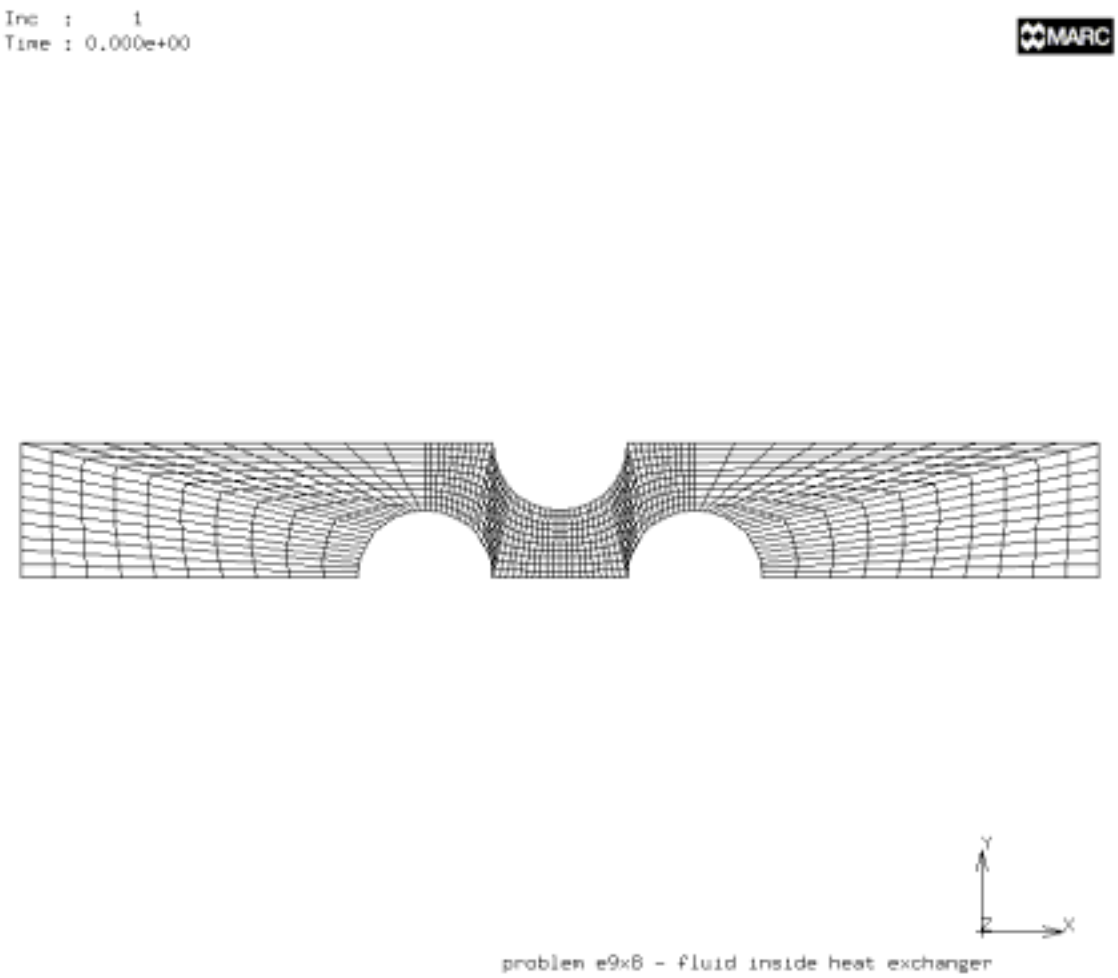

Figure 9.8-1 Finite Element Mesh for the Flow Over Cylinders

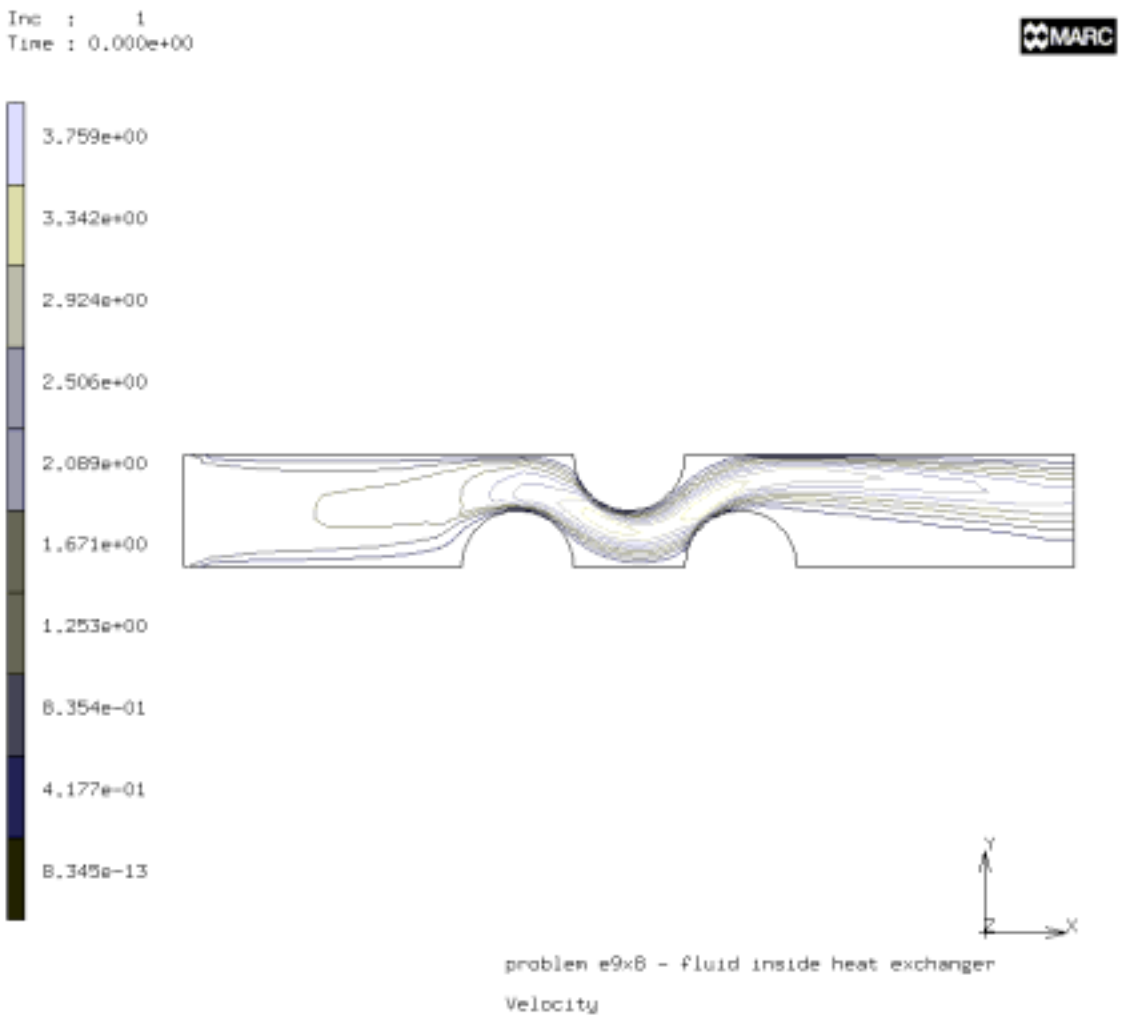

Figure 9.8-2 Contour Plot of the Flow Over Cylinders Velocity Field, Discretized using Element Type 11 and the Mixed Method

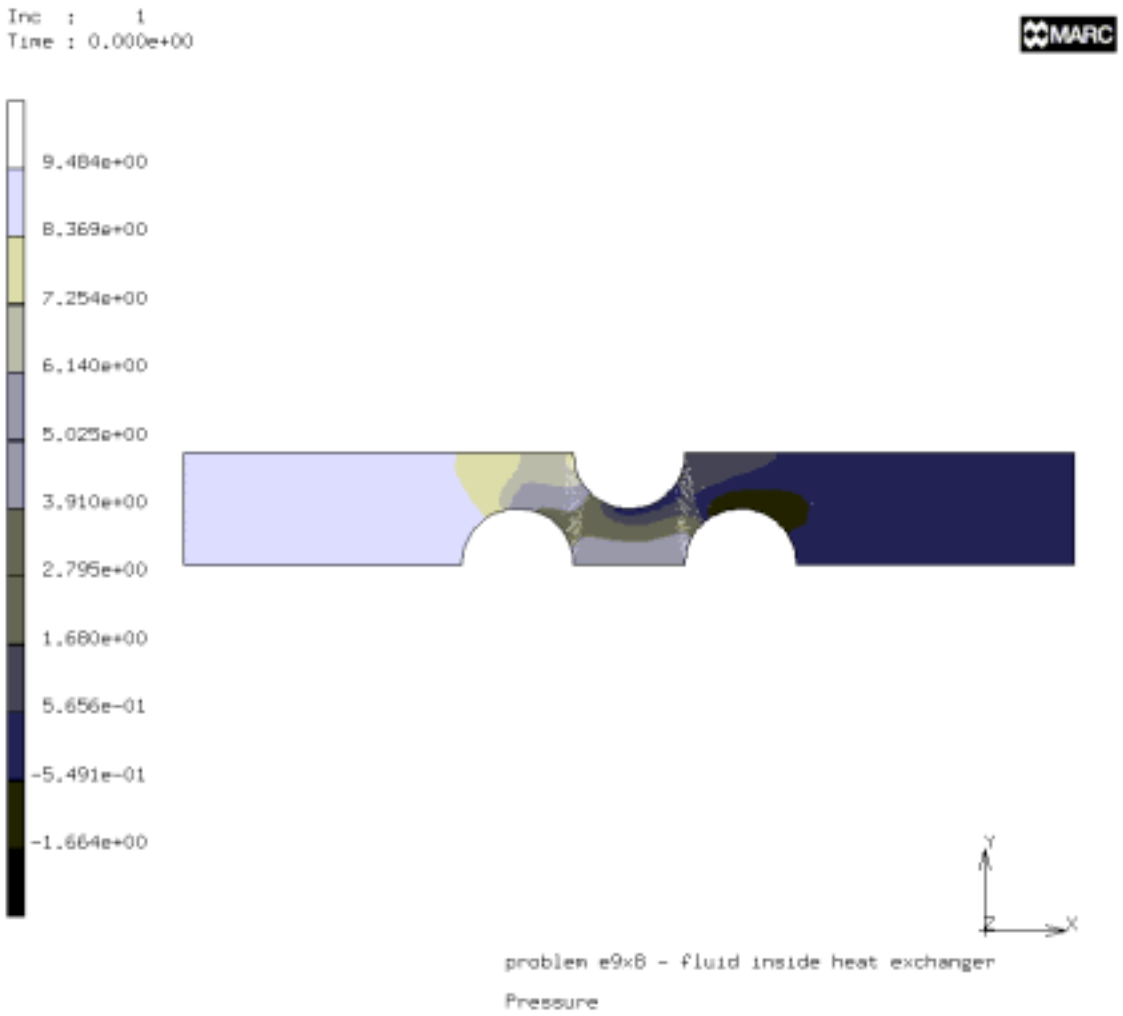

Figure 9.8-3 Contour Plot of the Flow Over Cylinders Pressure Field, Discretized using Element Type 11 and the Mixed Method

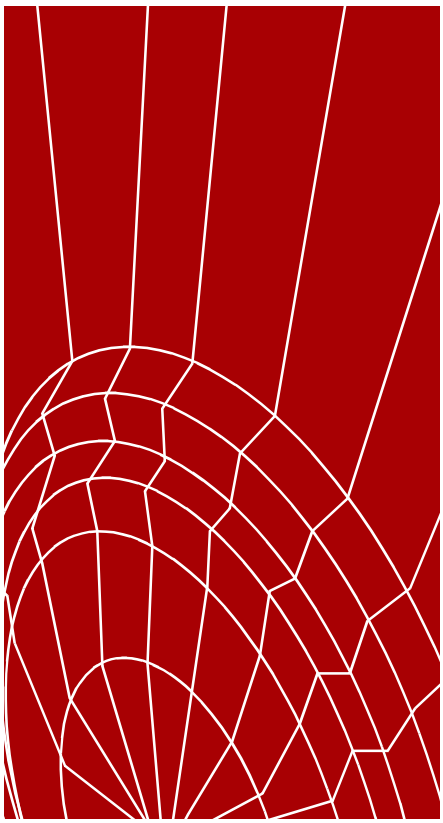

MARC Analysis Research Corporation

MARC®

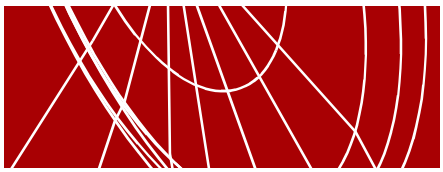

Volume E

Demonstration Problems

Version K7

Chapter 10
Design Sensitivity and Optimization

10 Design Sensitivity and Optimization Contents

Description	Problem
Design Sensitivity Analysis and Optimization of an Alternator Mount Frame using Element 52	10.1
Design Sensitivity Analysis and Optimization of a Plate with a Hole	10.2
Design Sensitivity Analysis and Optimization of a Simply-supported Thick Plate	10.3
Design Sensitivity Analysis and Optimization of a Shell Roof	10.4
Design Sensitivity Analysis and Optimization of a Composite Plate	10.5
Design Sensitivity Analysis and Optimization of a Ten-bar Truss	10.6
Design Sensitivity Analysis and Optimization of an Alternator Mount using Element 14	10.7

10 Design Sensitivity and Optimization List of Figures

Figure **Page**

10.1-1 Alternator Mount Frame Model using Element 52 . . . . . 10.1-4
10.1-2 Gradient of Maximum M_x (Element 2) with Respect to Design Variables, Load Case 2 . . . . . 10.1-5
10.1-3 Element Contributions to Response of Figure 10.1-2 . . . . . 10.1-6
10.1-4 History Plot of the Objective Function 10.1-7
10.1-5 Design Variables at Best Feasible Design (Cycle 2) 10.1-8

10.2-1 Finite Element Model of Quarter Plate with Hole (Element 26) 10.2-4
10.2-2 Gradient of Maximum von Mises Strain in Element 11, Load Case 2 . . . . . 10.2-5
10.2-3 Element Contributions to Response of Figure 10.2-2 . . . . . 10.2-6
10.2-4 History Plot of the Objective Function 10.2-7
10.2-5 Design Variables at Best Feasible Design (Cycle 9) 10.2-8

10.3-1 Finite Element Model of Quarter Thick Plate 10.3-4
10.3-2 Gradient of the First Eigenfrequency 10.3-5
10.3-3 Element Contributions to the First Eigenfrequency 10.3-6
10.3-4 History Plot of the Objective Function 10.3-7
10.3-5 History Plot of the Poisson's Ratio 10.3-8

10.4-1 Finite Element Model of the Shell Roof 10.4-4
10.4-2 Gradient of Difference Between First and Second Eigenfrequencies 10.4-5
10.4-3 Element Contributions to the Response of Figure 10.4-2 . . . . . 10.4-6
10.4-4 History Plot of the Objective Function 10.4-7
10.4-5 Design Variables at Best Feasible Design (Cycle 18) 10.4-8

10.5-1 Finite Element Model of Composite Plate 10.5-4
10.5-2 Gradient of Relative y-direction Translation Between Nodes 4 and 5 . . . . . 10.5-5
10.5-3 Element Contributions to Response of Figure 10.5-2 . . . . . 10.5-6
10.5-4 History Plot of the Objective Function 10.5-7
10.5-5 Design Variables at Best Feasible Design (Cycle 8) 10.5-8

Figure **Page**

10.6-1 Finite Element Model of Ten-bar Truss 10.6-4
10.6-2 Gradient of Axial Stress in Element 4 . . . . . 10.6-5
10.6-3 Element Contributions to Response of Figure 10.6-2. . . . . 10.6-6
10.6-4 History Plot of the Objective Function 10.6-7
10.6-5 Design Variables at Best Feasible Design (Cycle 50) 10.6-8

10.7-1 Alternator Mount Frame Model using Element 14. . . . . 10.7-4
10.7-2 Gradient of the First Eigenfrequency with Respect to Design Variables 10.7-5
10.7-3 Element Contributions to Response of Figure 10.7-2. . . . . 10.7-6
10.7-4 History Plot of the Objective Function 10.7-7
10.7-5 Design Variables at Best Design (Cycle 7) 10.7-8

10 Design Sensitivity and Optimization

Design sensitivity analysis and design optimization features have been available in MARC starting with Version K7.1. Substantial information about these features is now available in *MARC Volume A: Theory and User Information* and *MARC Volume C: Program Input*, as well as in the *MENTAT 3.1-MARC K7.1 New Features User Guide*, with supplemental material as it relates to various elements in *MARC Volume B: Element Library.*

Briefly summarized, the sensitivity analysis feature is useful in obtaining gradients of prescribed response quantities with respect to user-defined design variables, selectable from an available set. It is also useful in obtaining the finite element contributions to these prescribed response quantities. The sensitivity analysis feature is applicable to the fixed design submitted in a MARC data file.

The design optimization feature is useful in attempting to minimize a design objective, such as material mass, by variation of selected design variables, while adhering to limitations imposed on the response as well as on the values of the design variables. Since the design is going to change, the prescribed values of the design variables that appear in the MARC data file are replaced by those due to a varying design. Thus, for example, if a particular plate thickness is a design variable, then the value of that thickness given in the GEOMETRY option is no longer of interest (although a future algorithm may use it as a starting design). Instead, a series of values are generated for this thickness, and for any other design variables, based on their lower and upper bounds and on the flow of the design optimization algorithm.

The sensitivity analysis feature allows the plotting of the gradients and the element contributions, whereas the design optimization feature allows the generation of history plots for the changes in the objective function and in the design variables. It also allows the plotting of the design variable values at the end of any cycle of optimization. An important item to remember is that for sensitivity analysis, the sensitivity results are given as subincrements of the last increment, whereas for design optimization the optimization cycles are given as subincrements of the zeroth increment. For analysis purposes, the zeroth increment should be a dummy increment when design sensitivity analysis or design optimization is to be performed.

During design sensitivity analysis, any eigenfrequency analysis or applied load cases are given as increments 1 through, say, N. The N+1’th increment is that for which the M subincrements are sensitivity analysis results for M prescribed nontrivial response quantities. The results of K

cycles of design optimization are in the K subincrements of increment 0, the later increments being the results for the analysis of the best design obtained, for any prescribed eigenfrequency analysis and all applied load cases.

The results of both types of analyses are well documented numerically in the output files and you should refer to these as well as to the log file, in addition to the graphic representations obtainable via the interpretation of the post files through Mentat. An example of an important reason for this is that the graphic representations may show a small derivative to be insignificant in comparison to other derivatives, whereas that derivative may actually be quite important due to differences in the orders of magnitudes of the design variables.

The seven problems in this chapter treat different types of elements and response as well as different design variables and constraints. Thus, hopefully, they are a representative set in terms of the features offered to the user. Sensitivity analysis and design optimization are performed by means of different data files, which usually, but not always, differ only by the parameter data blocks "design sensitivity" and "design optimization". The design sensitivity data files are e10x1a.dat through e10x7a.dat, whereas the design optimization data files are e10x1b.dat through e10x7b.dat.

Table 10-1 summarizes the element type and options used in these demonstration problems.

Table 10-1 Design Sensitivity and Design Optimization Demonstration Problems

Problem Number	Element Type(s)	Parameters	Model Definition	History Definition	User Subroutines	Problem Description
10.1 (a)	52	DESIGN SENSITIVITY DYNAMIC	DESIGN DISPLACEMENT CONSTRAINTS DESIGN FREQUENCY CONSTRAINTS DESIGN OBJECTIVE DESIGN STRESS CONSTRAINTS DESIGN VARIABLES MASSES TYING	MODAL SHAPE POINT LOAD	—	Beam-column frame sensitivity analysis.
10.1 (b)	52	DESIGN OPTIMIZATION DYNAMIC	DESIGN DISPLACEMENT CONSTRAINTS DESIGN FREQUENCY CONSTRAINTS DESIGN OBJECTIVE DESIGN STRESS CONSTRAINTS DESIGN VARIABLES MASSES TYING	MODAL SHAPE POINT LOAD	—	Beam-column frame design optimization.
10.2 (a)	26	DESIGN SENSITIVITY	DESIGN OBJECTIVE DESIGN STRAIN CONSTRAINTS DESIGN VARIABLES	DIST LOADS POINT LOAD	—	Plane stress sensitivity analysis.
10.2 (b)	26	DESIGN OPTIMIZATION	DESIGN OBJECTIVE DESIGN STRAIN CONSTRAINTS DESIGN VARIABLES	DIST LOADS POINT LOAD	—	Plane stress design optimization.
10.3 (a)	21	DESIGN SENSITIVITY DYNAMIC	DESIGN DISPLACEMENT CONSTRAINTS DESIGN FREQUENCY CONSTRAINTS DESIGN OBJECTIVE DESIGN STRESS CONSTRAINTS DESIGN VARIABLES	DIST LOADS MODAL SHAPE	—	Thick plate (brick elements) design sensitivity.

Table 10-1 Design Sensitivity and Design Optimization Demonstration Problems (Continued)

Problem Number	Element Type(s)	Parameters	Model Definition	History Definition	User Subroutines	Problem Description
10.3 (b)	21	DESIGN OPTIMIZATION DYNAMIC	DESIGN DISPLACEMENT CONSTRAINTS DESIGN FREQUENCY CONSTRAINTS DESIGN OBJECTIVE DESIGN STRESS CONSTRAINTS DESIGN VARIABLES	DIST LOADS MODAL SHAPE	—	Thick plate (brick elements) design optimization.
10.4 (a)	75	DESIGN SENSITIVITY DYNAMIC SHELL SECT	DESIGN FREQUENCY CONSTRAINTS DESIGN OBJECTIVE DESIGN STRESS CONSTRAINTS DESIGN VARIABLES	MODAL SHAPE POINT LOAD	—	Shell roof design sensitivity.
10.4 (b)	75	DESIGN OPTIMIZATION DYNAMIC SHELL SECT	DESIGN FREQUENCY CONSTRAINTS DESIGN OBJECTIVE DESIGN STRESS CONSTRAINTS DESIGN VARIABLES	MODAL SHAPE POINT LOAD	—	Shell roof design optimization.
10.5 (a)	75	DESIGN SENSITIVITY DYNAMIC	COMPOSITE DESIGN DISPLACEMENTS CONSTRAINTS DESIGN OBJECTIVE DESIGN STRAIN CONSTRAINTS DESIGN STRESS CONSTRAINTS DESIGN VARIABLES ORIENTATION ORTHOTROPIC	POINT LOAD	—	Composite plate design sensitivity.

Table 10-1 Design Sensitivity and Design Optimization Demonstration Problems (Continued)

Problem Number	Element Type(s)	Parameters	Model Definition	History Definition	User Subroutines	Problem Description
10.5 (b)	75	DESIGN OPTIMIZATION DYNAMIC	COMPOSITE DESIGN DISPLACEMENTS CONSTRAINTS DESIGN OBJECTIVE DESIGN STRAIN CONSTRAINTS DESIGN STRESS CONSTRAINTS DESIGN VARIABLES ORIENTATION ORTHOTROPIC	POINT LOAD	—	Composite plate design optimization.
10.6 (a)	9	DESIGN SENSITIVITY	DESIGN OBJECTIVE DESIGN STRESS CONSTRAINTS DESIGN VARIABLES	POINT LOAD	—	Planar truss design sensitivity.
10.6 (b)	9	DESIGN OPTIMIZATION	DESIGN OBJECTIVE DESIGN STRESS CONSTRAINTS DESIGN VARIABLES	POINT LOAD	—	Planar truss design optimization.
10.7 (a)	14	DESIGN SENSITIVITY DYNAMIC	DESIGN DISPLACEMENTS CONSTRAINTS DESIGN FREQUENCY CONSTRAINTS DESIGN OBJECTIVE DESIGN STRESS CONSTRAINTS DESIGN VARIABLES MASSES TYING	MODAL SHAPE POINT LOAD	—	Beam-column frame sensitivity analysis.
10.7 (b)	14	DESIGN OPTIMIZATION DYNAMIC	DESIGN DISPLACEMENTS CONSTRAINTS DESIGN FREQUENCY CONSTRAINTS DESIGN OBJECTIVE DESIGN STRESS CONSTRAINTS DESIGN VARIABLES MASSES TYING	MODAL SHAPE POINT LOAD	—	Beam-column frame design optimization.

10.1 Design Sensitivity Analysis and Optimization of an Alternator Mount Frame using Element 52

A spatial frame representing the support of an alternator is considered. Design sensitivity and optimization of the system are performed with constraints on static response under two separate load cases and on eigenfrequencies.

Element

Element 52, a straight Euler-Bernoulli beam in space with linear elastic response, is used. The element has six coordinates per node: the first three are (x,y,z) global coordinates of the system, the other three are the global coordinates of a point in space which locates the local x-axis of the cross section.

Model

The 3D frame is modeled using 16 beam-column elements and 20 nodes. The columns are clamped at the base. The elements have arbitrary solid cross sections. Two masses are lumped in the middle of two horizontal beams at nodes 14 and 18 (Figure 10.1-1). Elements numbered 1 through 8 are the columns and the rest of the elements are the beams. The beam to column connections are obtained through tying of separately numbered nodes.

Geometry

The column elements are 250 cm long; the beam elements in the x-direction are 192.5 cm long and those in the z-direction are 157.5 cm. The column cross-sectional areas are 8625 cm whereas the beams have 6625 cm cross sections. I_{xx} and I_{yy} are the same for all elements: 9.5 x 10^6 and 4.0 x 10^6, respectively.

Element 52 computes the torsional stiffness of the section as:

$$K_t = \frac{E}{2(1+\nu)}(I_{xx} + I_{yy})$$

Then, in order to obtain the correct stiffness, an artificial Poisson's ratio ν^* is chosen to be used only for this purpose. See **Material Properties** below.

Material Properties

The material is assumed to be linearly elastic, homogeneous, and isotropic. Young's modulus is E = 2.5 x 10^8kg/cm sec^2 and the mass density is ρ = 2.55 10^{-3} kg/cm^3. The Poisson's ratio is an artificial one since it is used here to compute torsional stiffness only. The value of such an

artificial Poisson's ratio normally depends on the actual type of cross section used (see problem 6.10). However, currently MARC does not modify this ratio with changes in the cross section. The lumped masses are M = 19000 kg each.

Design Variables and Objective Function

For this problem, there are three design variables of the geometry type: the cross-sectional area A of the beam, the moment of inertia I_{xx} of the columns, and the moments of inertia I_{yy} of the beams in that order as variables 1, 2, and 3. The objective function for this problem is the total mass of the material used, which means that the design optimization procedure seeks to minimize the mass. The variables are linked over all beams or all columns, as applicable.

Design Constraints

The design constraints in this analysis includes stress constraints, displacement constraints, and frequency constraints. Stress constraints are imposed on generalized stresses in all of the elements. Displacement constraints consist of a limit on the translation along the first degree of freedom at node 15 under the first static load case, and a limit on the rotation about the first degree of freedom at node 19 under the second static load case. Frequency constraints are on the fundamental frequency and on the difference between the frequencies of the first two modes.

Results

The design sensitivity and design optimization cases are run as separate jobs, with the data files e10x1a.dat and e10x1b.dat, respectively. Figure 10.1-2 shows the gradient of the maximum second generalized stress (bending moment about x-axis) for element 2 under load case 2 (first static load case) with respect to all design variables. Figure 10.1-3 is a plot showing, on the finite element model, the element contributions to the response quantity in question.The gray scale being useless for frames, the unaveraged values are shown on the elements using an alphabetical scale. Figure 10.1-4 shows the change in the objective function with the optimization cycle in the form of a history plot. Figure 10.1-5 is a bar chart showing the values of the design variables at the best feasible (F) design obtained. Since the cross-sectional area value is several orders of magnitude smaller than the moments of inertia, a fitted plot shows the first variable value as the initial y-coordinate.

Parameters, Options. and Subroutines Summary

Listed below are the options used in example e10x1a.dat:

Parameters	Model Definition Options	History Definition Options
DESIGN SENSITIVITY	CONNECTIVITY	CONTINUE
DYNAMIC	COORDINATES	MODAL SHAPE
ELEMENTS	DESIGN DISPLACEMENT CONSTRAINTS	POINT LOAD
END	DESIGN FREQUENCY CONSTRAINTS	
SIZING	DESIGN OBJECTIVE	
TITLE	DESIGN STRESS CONSTRAINTS	
	DESIGN VARIABLES	
	END OPTION	
	FIXED DISP	
	GEOMETRY	
	ISOTROPIC	
	MASSES	
	POINT LOAD (dummy)	
	POST	
	TYING	

Listed below are the options used in example e10x1b.dat:

Parameters	Model Definition Options	History Definition Options
DESIGN OPTIMIZATION	CONNECTIVITY	CONTINUE
DYNAMIC	COORDINATES	MODAL SHAPE
ELEMENTS	DESIGN DISPLACEMENT CONSTRAINTS	POINT LOAD
END	DESIGN FREQUENCY CONSTRAINTS	
SIZING	DESIGN OBJECTIVE	
TITLE	DESIGN STRESS CONSTRAINTS	
	DESIGN VARIABLES	
	END OPTION	
	FIXED DISP	
	GEOMETRY	
	ISOTROPIC	
	MASSES	
	POINT LOAD (dummy)	
	POST	
	TYING	

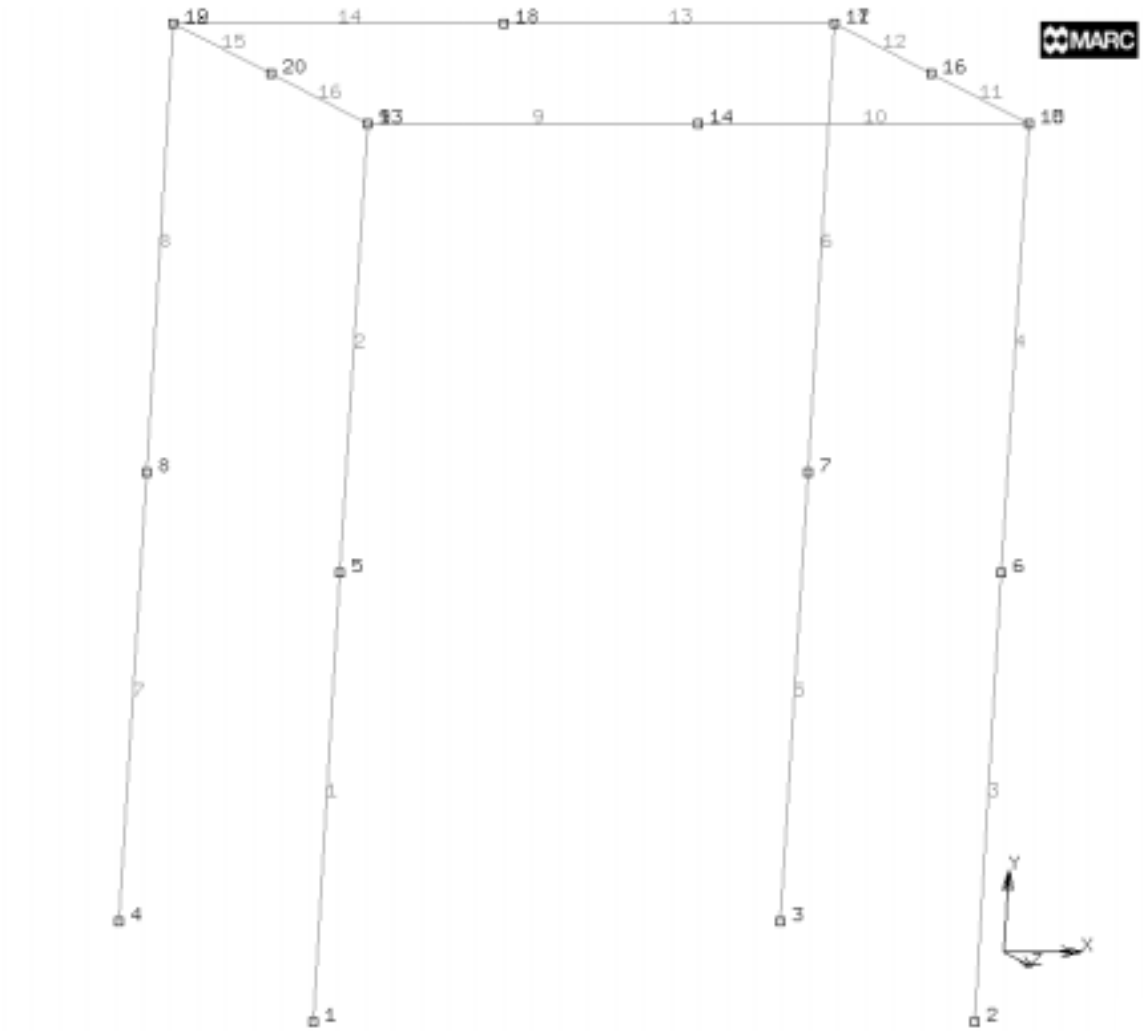

Figure 10.1-1 Alternator Mount Frame Model using Element 52

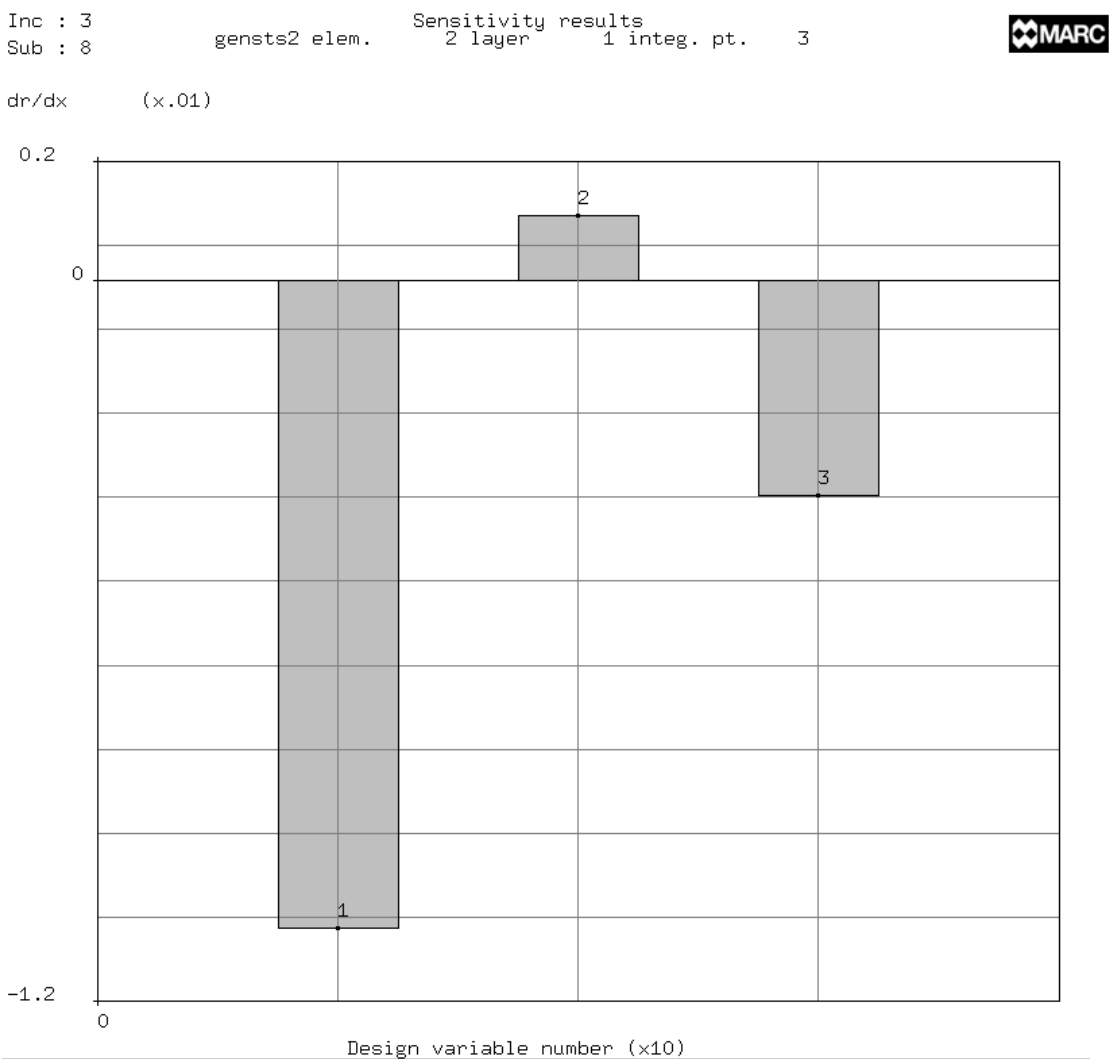

Figure 10.1-2 Gradient of Maximum M_x (Element 2) with Respect to Design Variables, Load Case 2

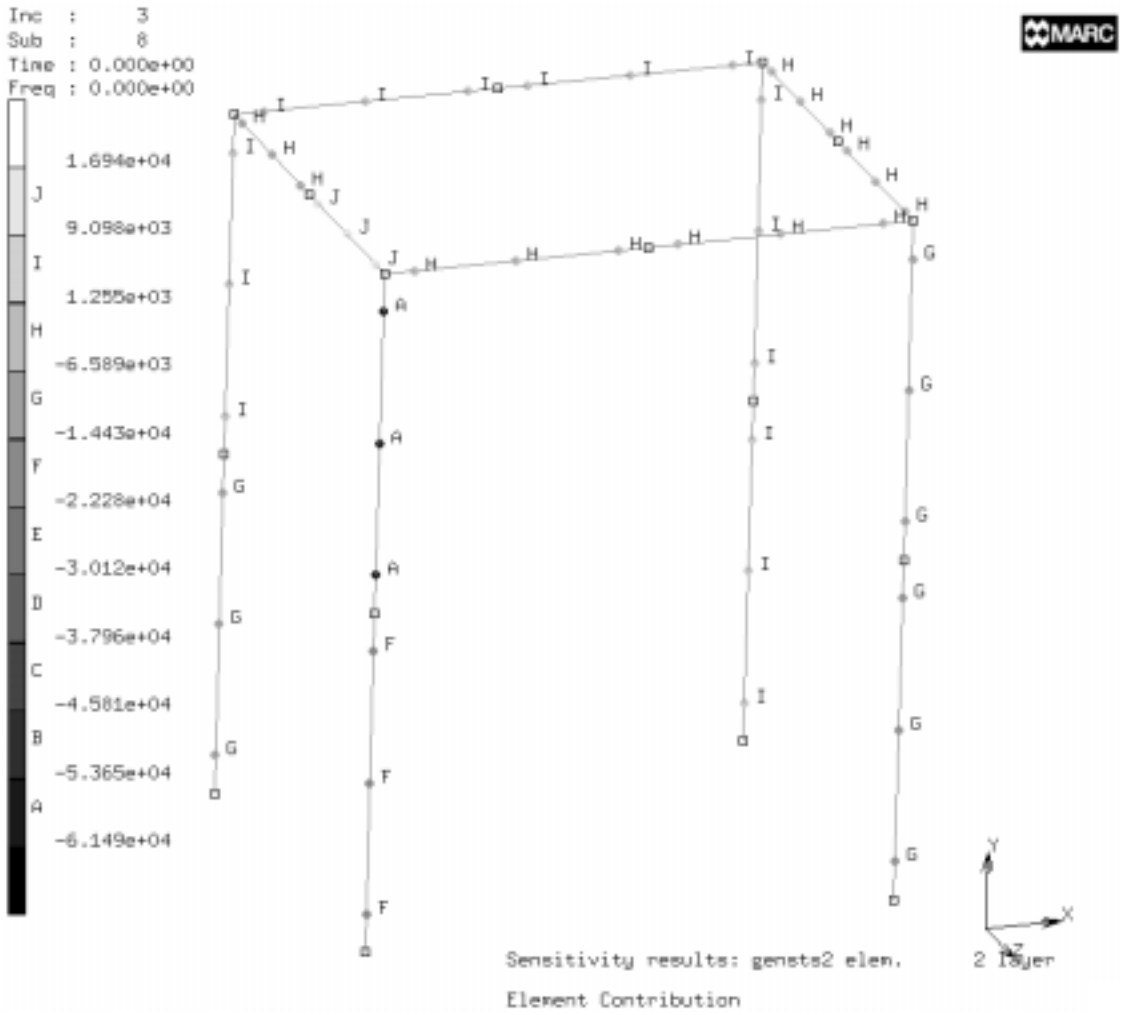

Figure 10.1-3 Element Contributions to Response of Figure 10.1-2

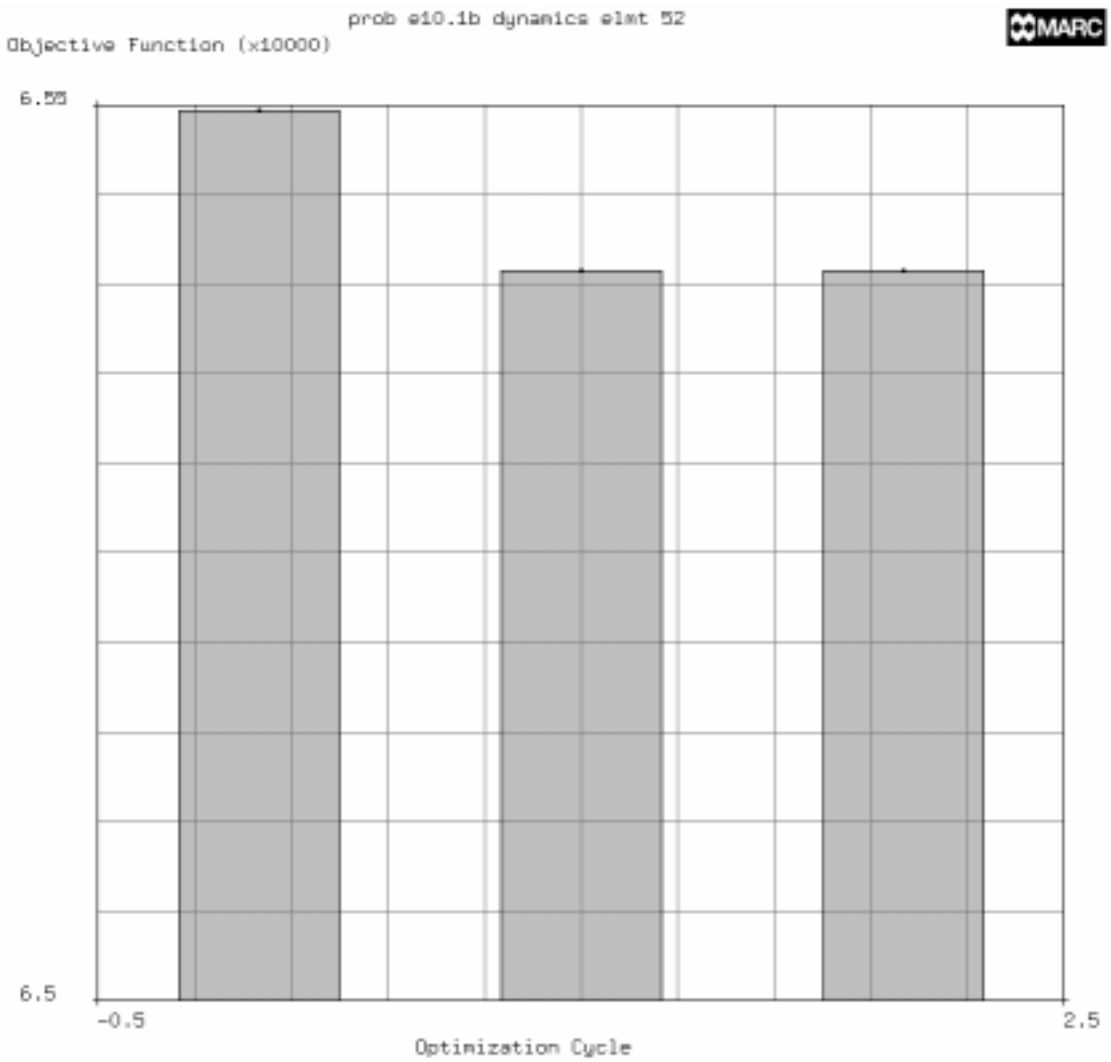

Figure 10.1-4 History Plot of the Objective Function

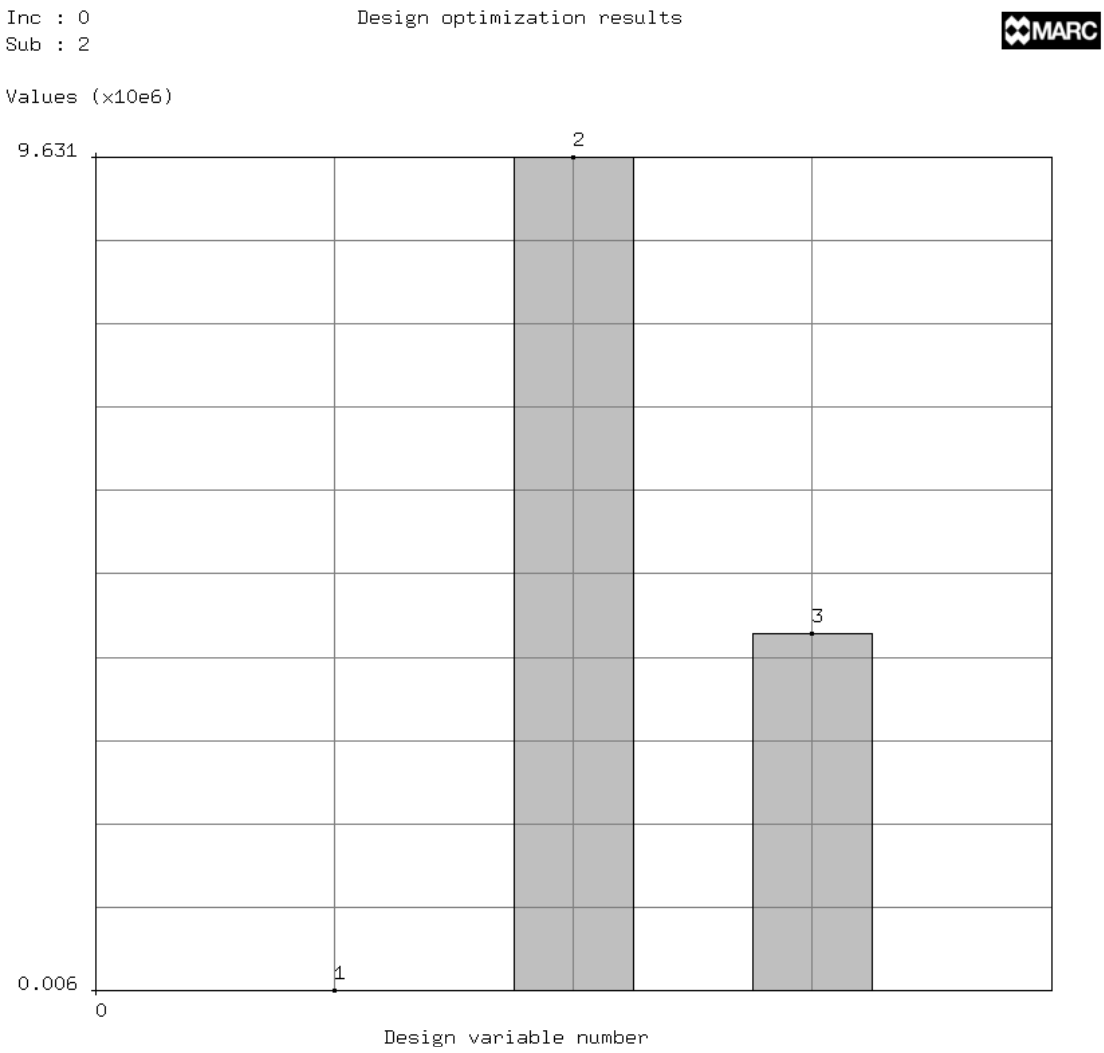

Figure 10.1-5 Design Variables at Best Feasible Design (Cycle 2)

10.2 Design Sensitivity Analysis and Optimization of a Plate with a Hole

The design sensitivity and design optimization features are applied to the problem of a square plate with a circular hole (Timoshenko and Goodier, *Theory of Elasticity*). The second order isoparametric plane stress element (type 26) is used.

Elements

Element type 26 is a second-order isoparametric plane stress element. It is an 8-noded quadrilateral.

Model

The dimensions of the plate are 10 inches square with a 2 inch radius central hole. Only one quarter of the plate is modeled due to symmetry conditions. The finite element mesh for this model is shown in Figure 10.2-1. The elements near the hole are smaller to capture the strain variation. There are 20 quadrilateral elements in the mesh.

Material Properties

The material for all of the elements is elastic and isotropic with a Young's modulus of 30.0E+06 psi and a Poisson's ratio (ν) of 0.3.

Geometry

The thicknesses prescribed for the purpose of sensitivity analysis are: 0.7 inch for elements 1 through 4 and 11 through 14; 1.0 inch for the rest.

Loads and Boundary Conditions

The structure is acted upon by two separate load cases. The first load case is a distributed load applied to the top edge of the quarter model. Point loads, acting horizontally along the nodes on the right edge of the mesh, represent the second load case. The boundary conditions are determined by the symmetry conditions and require that the nodes along $y = 0$ axis have no vertical displacement, and the nodes along the $x = 0$ axis have no horizontal displacement. The origin of the model is at the center of the hole.

Design Variables and Objective Function

There are three types of design variables employed: plate thickness (variables 1 and 2), Poisson's ratio (variable 3), and Young's modulus (variable 4). For the plate thickness, elements are linked in the same two groups as for the prescribed thicknesses. The first design variable links the 8 larger elements which are farther away from the hole, and the second design variable links the remaining

12 smaller elements. The objective function is the volume of the material. Therefore, the gradient of this function is to be obtained during sensitivity analysis. For design optimization, the total material volume is to be minimized.

Design Constraints

For this problem, only strain constraints are applied. These include the two independent normal strains, the in-plane shear strain, the von Mises strain, and the maximum absolute valued principal strain. These constrains are applied to the same element (number 11) for both load cases. For the first normal strain and the shear strain, the constraints are on the absolute value.

Results

The design sensitivity and design optimization cases are run as separate jobs, with the data files e10x2a.dat and e10x2b.dat, respectively. Figure 10.2-2 shows the gradient of the maximum von Mises strain over the integration points of element 11 under load case 2 with respect to all design variables. While the derivative with respect to the Young's modulus E is very small (-0.9×10^{-12}), and appears as zero in Figure 10.2-2, it should be kept in mind that E is many orders of magnitude greater than the other variables. Thus, the small derivative may not necessarily be considered trivial. Figure 10.2-3 is a contour plot showing, on the finite element model, the element contributions to the response quantity in question. Figure 10.2-4 shows the change in the objective function with the optimization cycle in the form of a history plot. It is noted that the best feasible (F) design is obtained at cycle 9. Figure 10.2-5 is a bar chart showing the values of the first three design variables at the best feasible design obtained. The value of E does not change from the starting vertex value of 3.1425×10^{8}, and, therefore, it is not plotted here so that the other three values can be seen.

Parameters, Options. and Subroutines Summary

Listed below are the options used in example e10x2a.dat:

Parameters	Model Definition Options	History Definition Options
DESIGN SENSITIVITY	CONNECTIVITY	CONTINUE
ELEMENTS	COORDINATES	DIST LOADS
END	DESIGN OBJECTIVE	POINT LOAD
SIZING	DESIGN STRAIN CONSTRAINTS	
TITLE	DESIGN VARIABLES	
	DIST LOADS (dummy)	
	END OPTION	
	FIXED DISP	
	GEOMETRY	
	ISOTROPIC	
	OPTIMIZE	
	POINT LOAD (dummy)	
	POST	

Listed below are the options used in example e10x2b.dat:

Parameter Options	Model Definition Options	History Definition Options
DESIGN OPTIMIZATION	CONNECTIVITY	CONTINUE
ELEMENTS	COORDINATES	DIST LOADS
END	DESIGN OBJECTIVE	POINT LOAD
SIZING	DESIGN STRAIN CONSTRAINTS	
TITLE	DESIGN VARIABLES	
	DIST LOADS (dummy)	
	END OPTION	
	FIXED DISP	
	GEOMETRY	
	ISOTROPIC	
	OPTIMIZE	
	POINT LOAD (dummy)	
	POST	

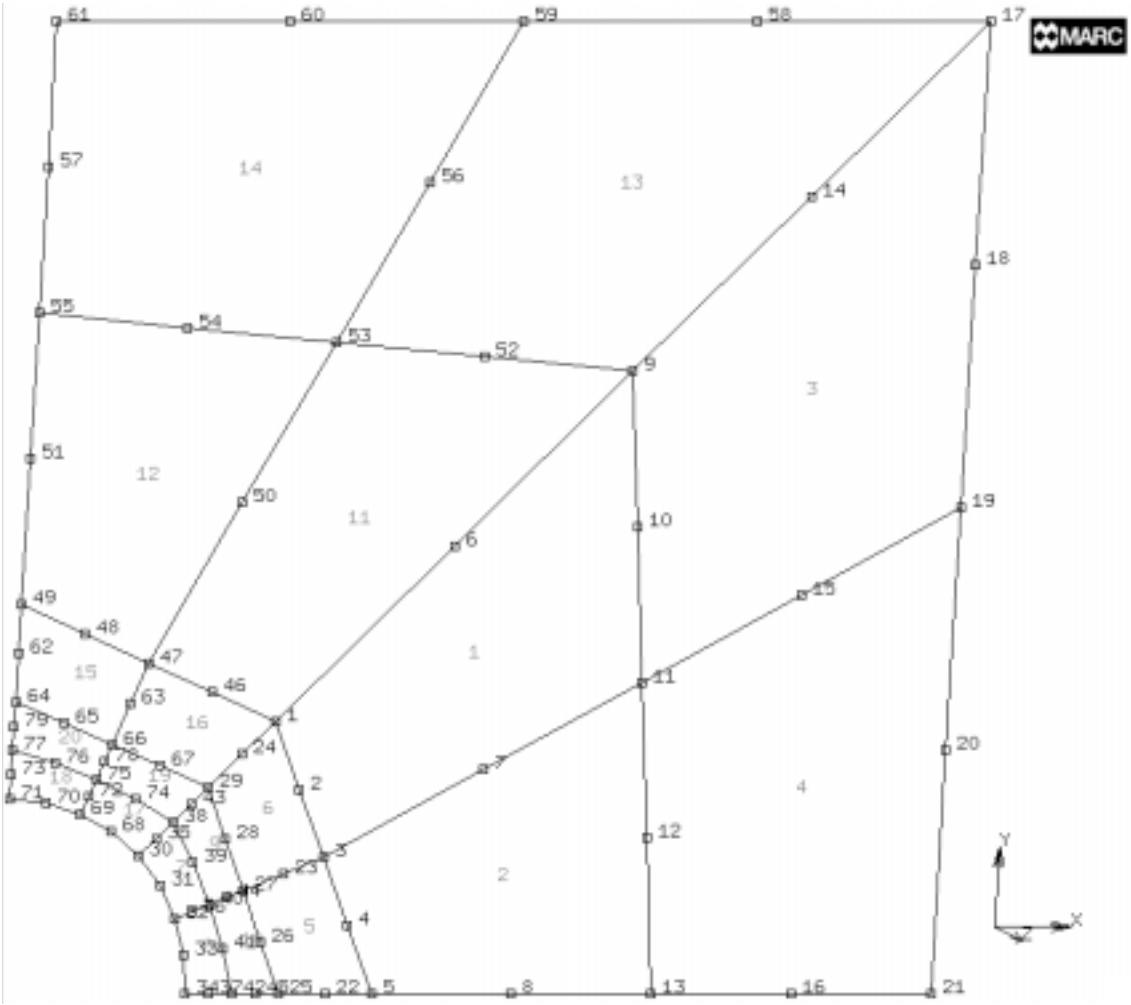

Figure 10.2-1 Finite Element Model of Quarter Plate with Hole (Element 26)

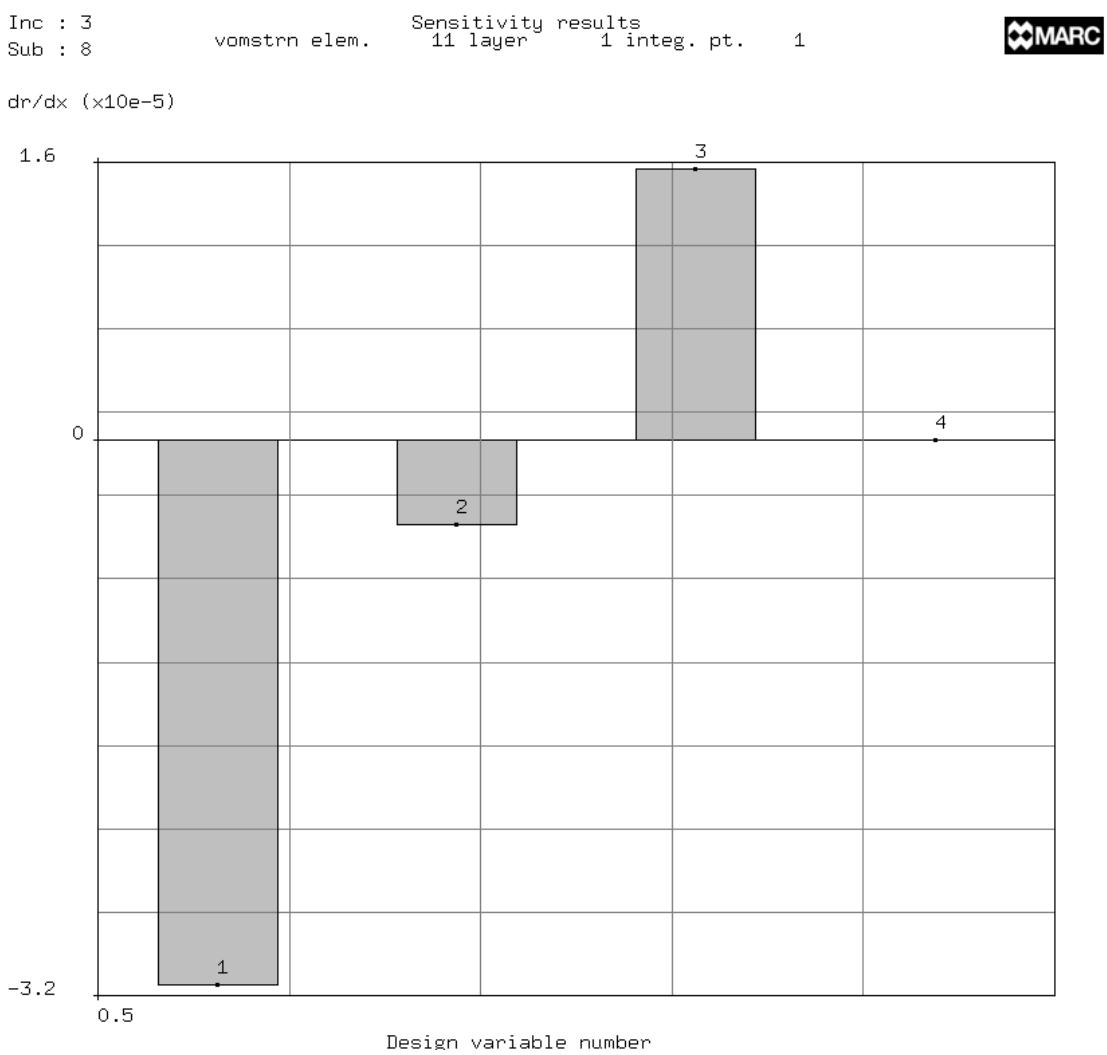

Figure 10.2-2 Gradient of Maximum von Mises Strain in Element 11, Load Case 2

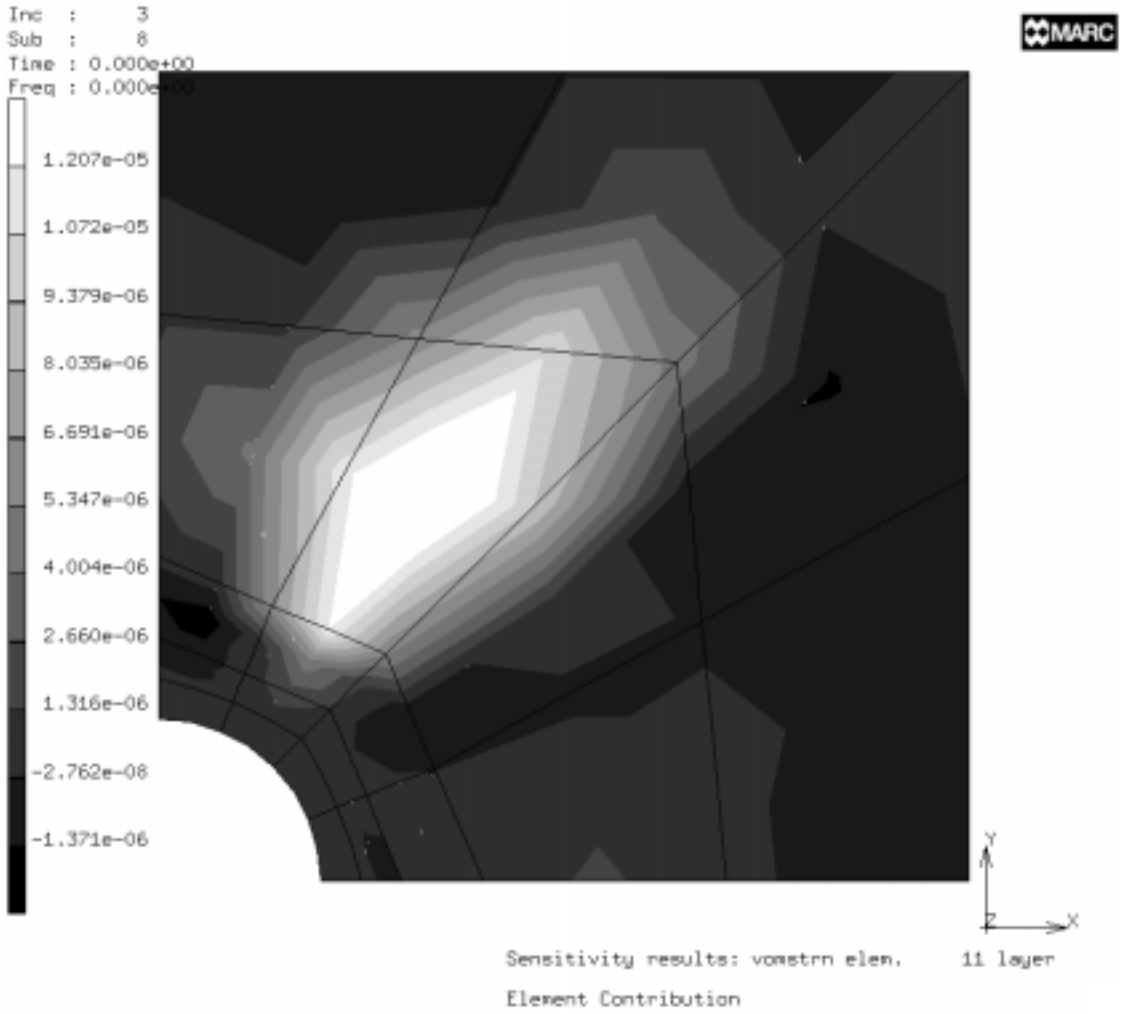

Figure 10.2-3 Element Contributions to Response of Figure 10.2-2

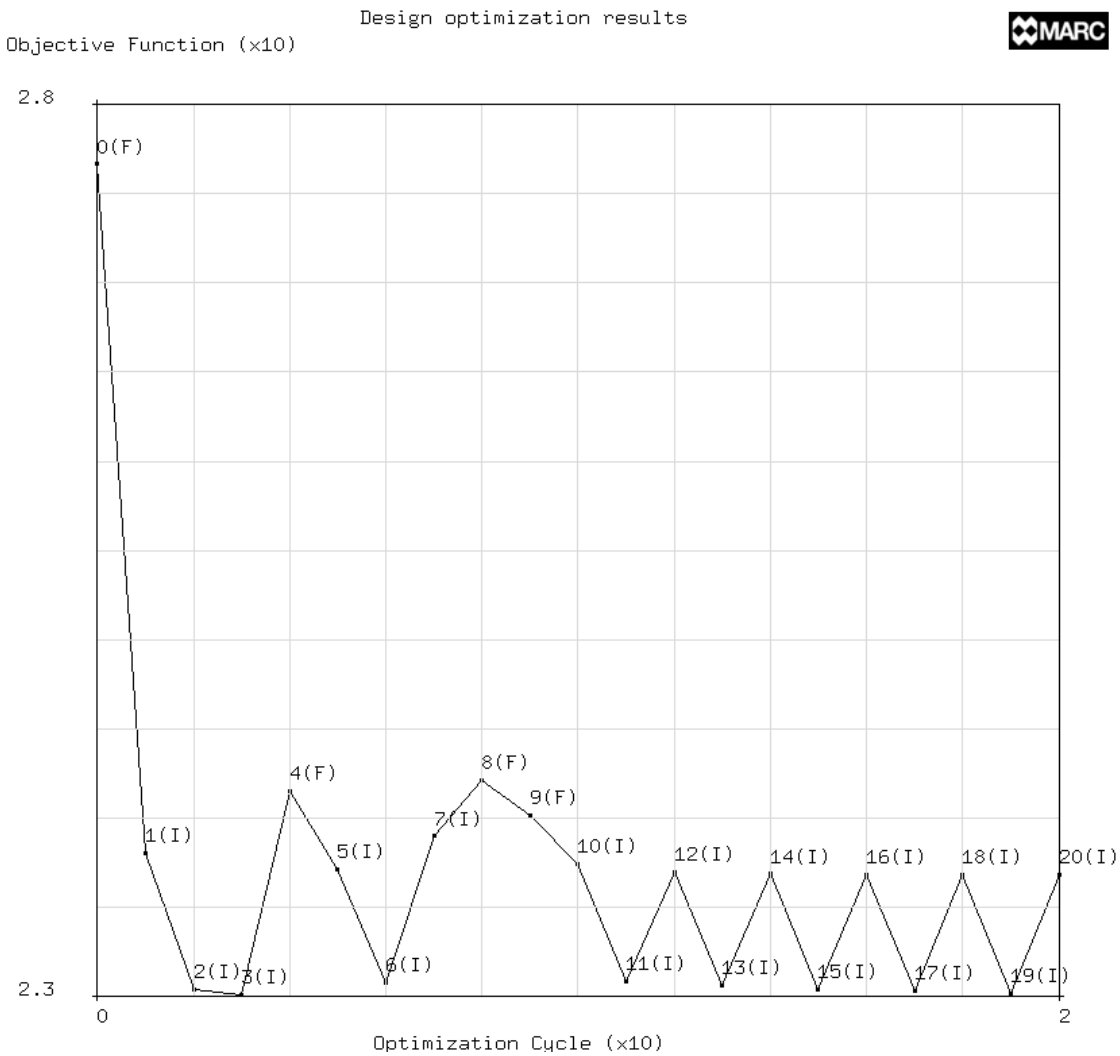

Figure 10.2-4 History Plot of the Objective Function

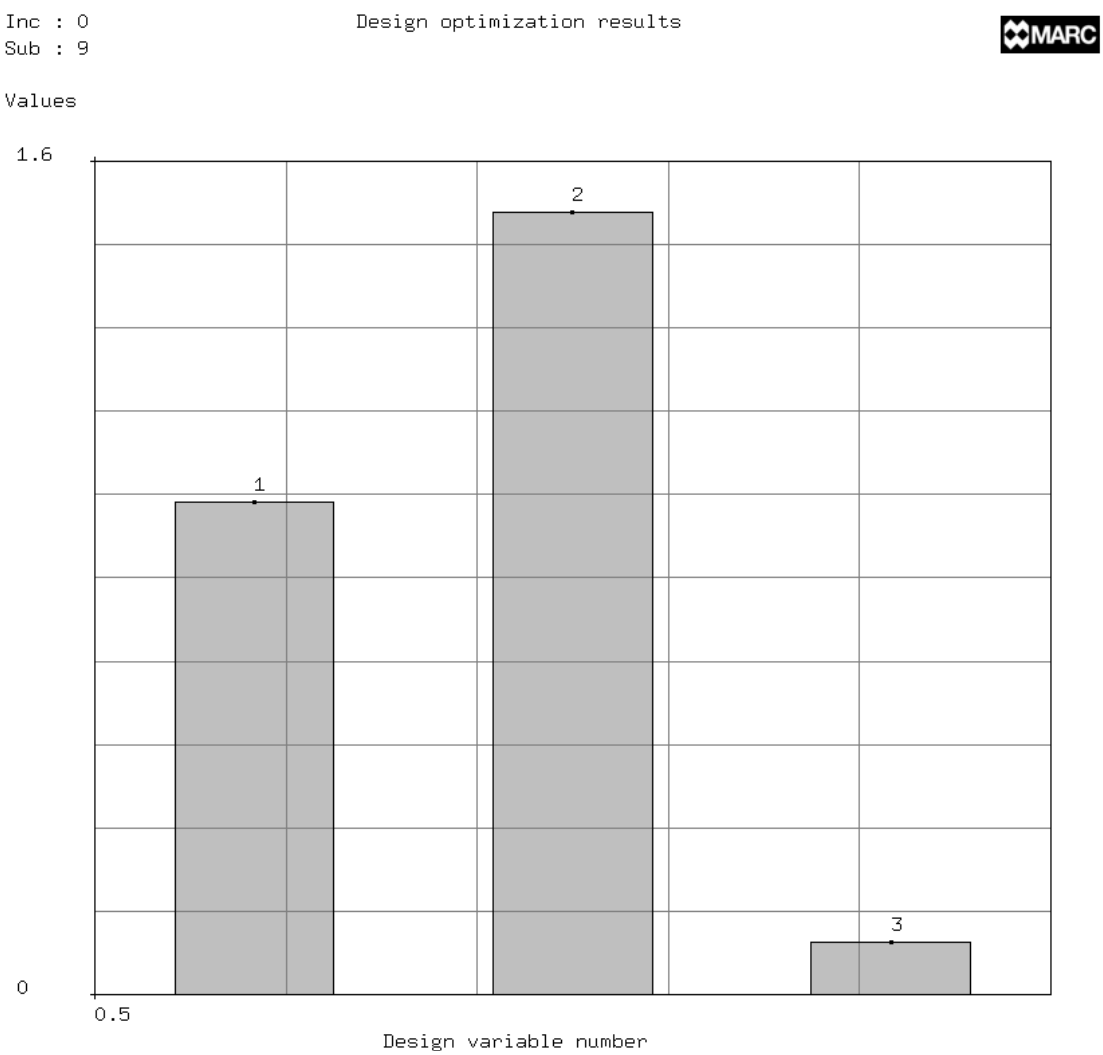

Figure 10.2-5 Design Variables at Best Feasible Design (Cycle 9)

10.3 Design Sensitivity Analysis and Optimization of a Simply-supported Thick Plate

With this problem, we examine the application of the design sensitivity and design optimization procedures for a simply supported thick plate, to be designed for free vibration characteristics and under uniformly distributed pressure.

Elements

Element type 21 is a 20-node isoparametric brick. Eight of the nodes are corner nodes, and twelve are midside nodes. There are three displacement degrees of freedom at each node. Each edge of the brick may be parabolic by means of a curve fitted through the midside node. Numerical integration is accomplished with 27 points using Gaussian quadrature. See Volume B for further details.

Model

Because of symmetry, only one-quarter of the plate is modeled (Figure 10.3-1). One element is used through the thickness, two in each direction in the plane of the plate for a total of four elements. There are 51 nodes and therefore a total of 153 degrees of freedom.

Geometry

No geometry data is used for this element.

Material Properties

The material is isotropic, however, element 4 has two-thirds the mass density of the others.

Loading

The first “load case” consists of an eigenvalue analysis imposed by the MODAL SHAPE data block. As the second load case, a uniform pressure is applied on element 4 by means of the DIST LOADS option. Load type 0 is specified for uniform pressure on the 1-2-3-4 face of element 4.

Boundary Conditions

On the plate edges (z = 0, y = 0, or x = 0, z = 0), the plate is simply supported (w = 0). On the symmetry planes (x = 30 or y = 30), in-plane movement is constrained. On the x = 30 plane, u = 0, and on the y = 30 plane, v = 0.

Design Variables and Objective Function

There are three design variables for this problem. The first is the Young’s modulus for material 1 (elements 1 to 3) with lower and upper limits of 1.8 x 10**7 and 3.0 x 10**7, respectively. The second and the third variables are the mass density and the Possion’s ratio, respectively, for the same material. The lower and upper bounds for both of these are 0.1 and 0.4. The

objective function for this problem is the total mass of the material used. Thus in design sensitivity analysis we obtain the gradient of the material mass with respect to the design variables. For design optimization, we seek to minimize the total material mass.

Design Constraints

Design constraints are on stress, displacement, and eigenfrequency response. Under the static load case, the maximum absolute valued principal stress and the fifth stress component (shear stress) are constrained for all elements. The translation in the first direction at node 15 is constrained in only one direction. We illustrate a pitfall with the second displacement constraint, which is a relative translation constraint between two nodes 15 and 16, along the second direction. In this case, the actual value is negative, but since absolute value was not specified, the constraint bounded from above becomes irrelevant.

Results

The design sensitivity and design optimization cases are run as separate jobs, with the data files e10x3a.dat and e10x3b.dat, respectively. Figure 10.3-2 shows the gradient of the first eigenfrequency with respect to the design variables. This is a case where the derivatives due to the three variables are all of substantially different orders of magnitude (6.4×10^{-7}; -33.0; 0.24). Thus, the first derivative is shown as 0 on the plot (although, it is important due to the magnitude of E) and the plot of the second is cut off at -1.0. Figure 10.3-3 is a contour plot showing, on the finite element model, the nodal averaged element contributions to the response quantity in question. Figure 10.3-4 shows the change in the objective function with the optimization cycle in the form of a history plot. The last cycle (cycle 7) is seen to give the best feasible (F) design. Figure 10.3-5 shows the change in the third design variable (Poisson’s ratio) during optimization.

Parameters, Options, and Subroutines Summary

Listed below are the options used in example e10x3a.dat:

Parameters	Model Definition Options	History Definition Options
DESIGN SENSITIVITY	CONNECTIVITY	CONTINUE
DYNAMIC	COORDINATES	DIST LOADS
ELEMENTS	DESIGN DISPLACEMENT CONSTRAINTS	MODAL SHAPE
END	DESIGN FREQUENCY CONSTRAINTS	
SIZING	DESIGN OBJECTIVE	
TITLE	DESIGN STRESS CONSTRAINTS	
	DESIGN VARIABLES	
	DIST LOADS (dummy)	
	END OPTION	
	FIXED DISP	
	ISOTROPIC	
	POST	

Listed below are the options used in example e10x3b.dat:

Parameters	Model Definition Options	History Definition Options
DESIGN OPTIMIZATION	CONNECTIVITY	CONTINUE
DYNAMIC	COORDINATES	DIST LOADS
ELEMENTS	DESIGN DISPLACEMENT CONSTRAINTS	MODAL SHAPE
END	DESIGN FREQUENCY CONSTRAINTS	
SIZING	DESIGN OBJECTIVE	
TITLE	DESIGN STRESS CONSTRAINTS	
	DESIGN VARIABLES	
	DIST LOADS (dummy)	
	END OPTION	
	FIXED DISP	
	ISOTROPIC	
	POST	

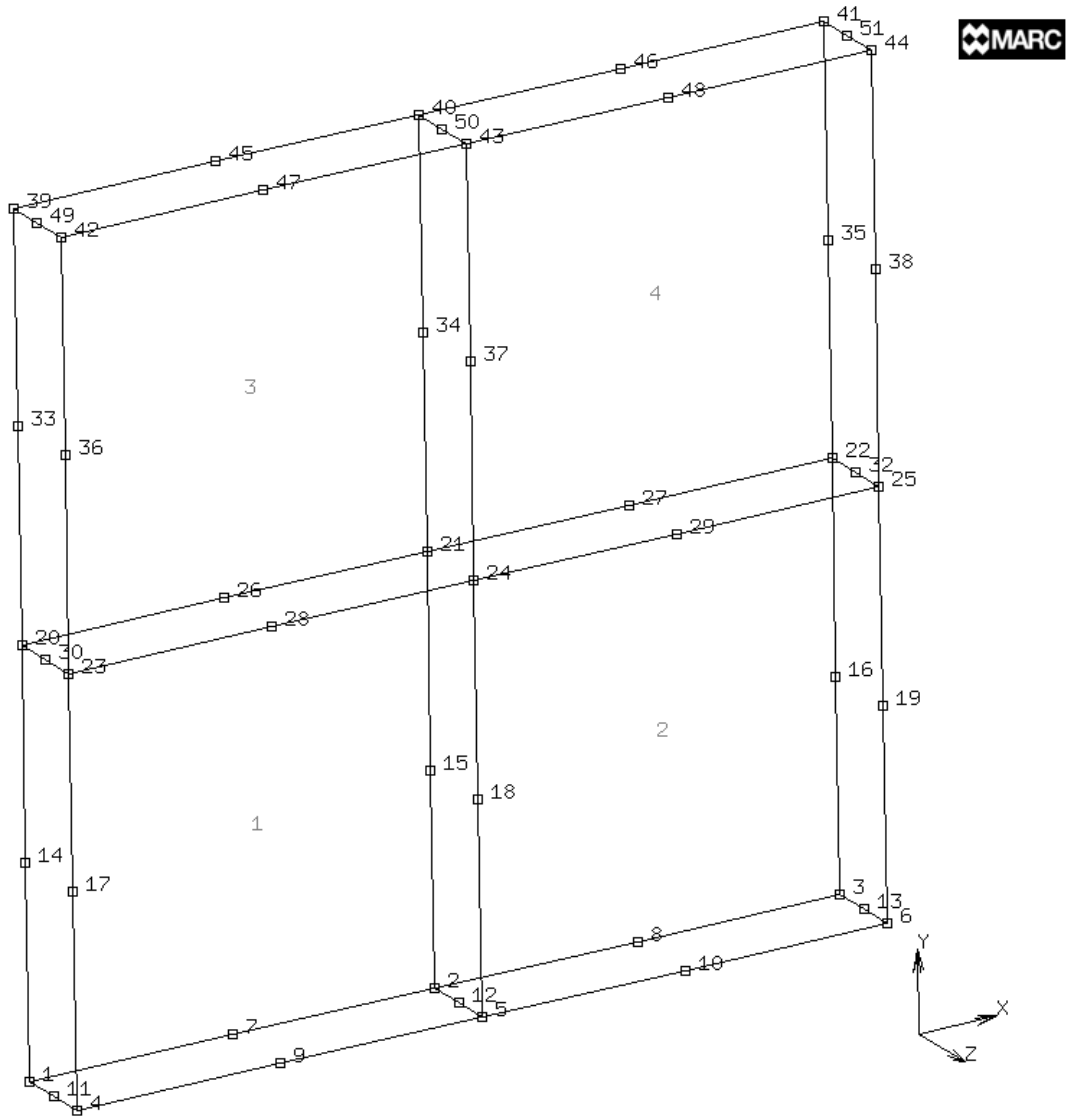

Figure 10.3-1 Finite Element Model of Quarter Thick Plate

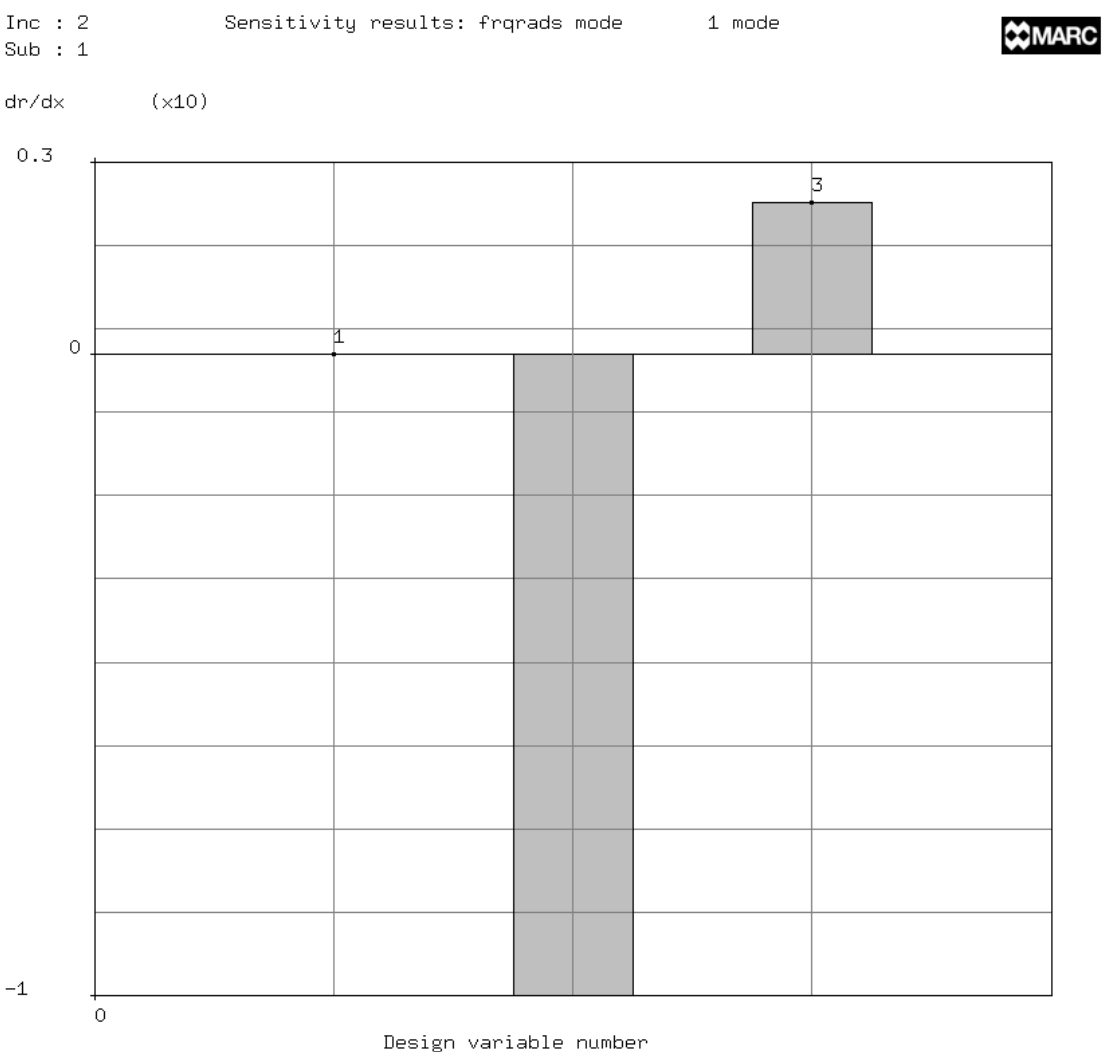

Figure 10.3-2 Gradient of the First Eigenfrequency

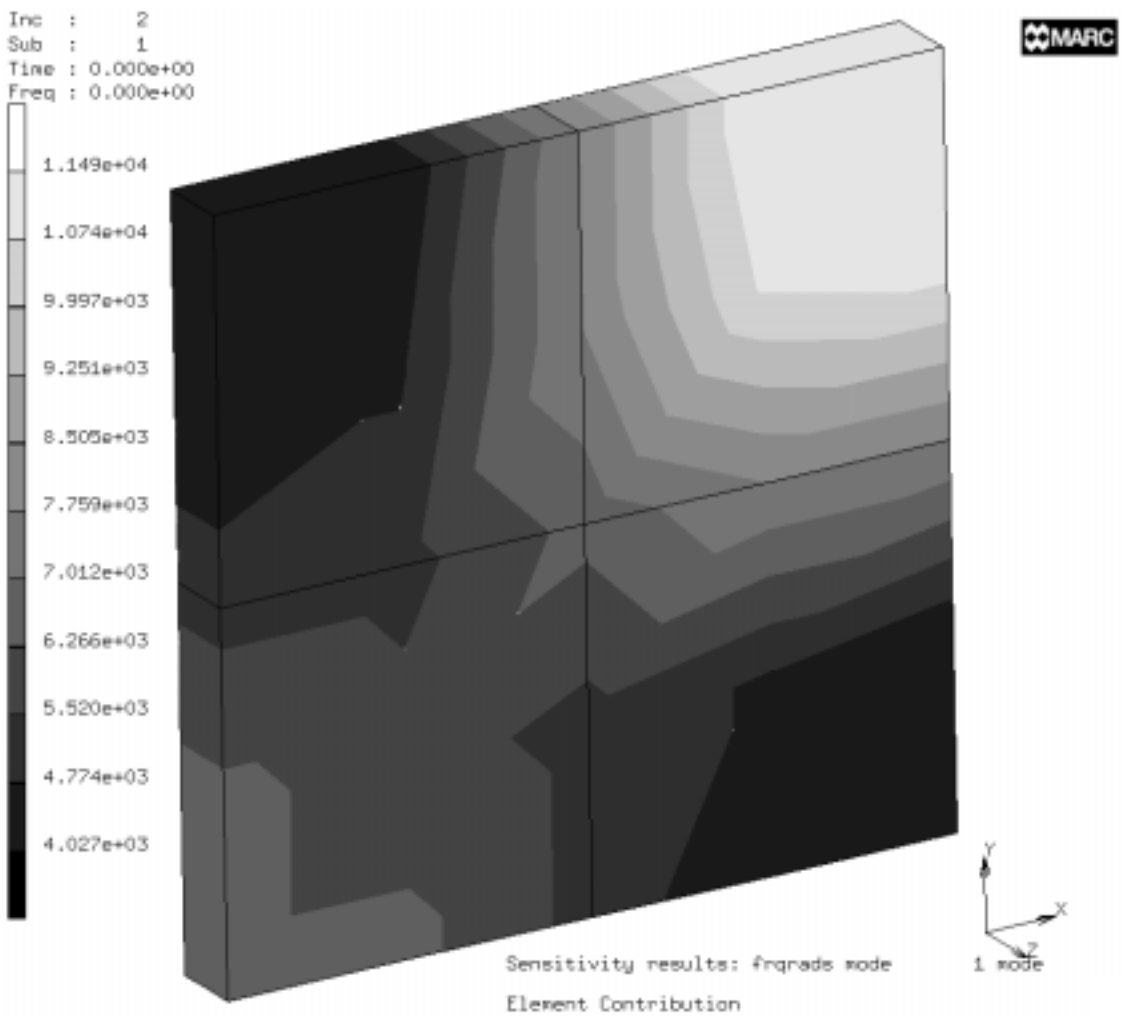

Figure 10.3-3 Element Contributions to the First Eigenfrequency

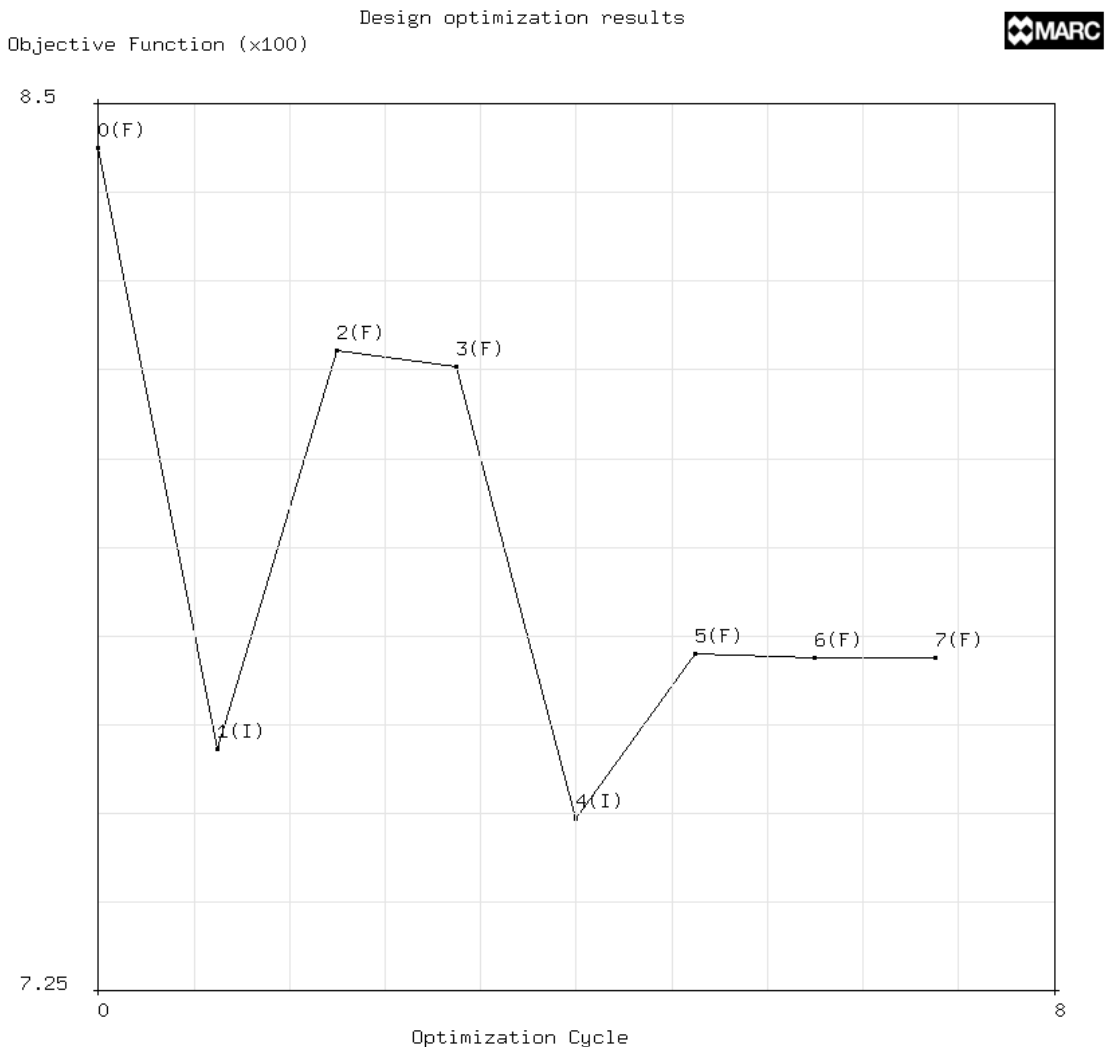

Figure 10.3-4 History Plot of the Objective Function

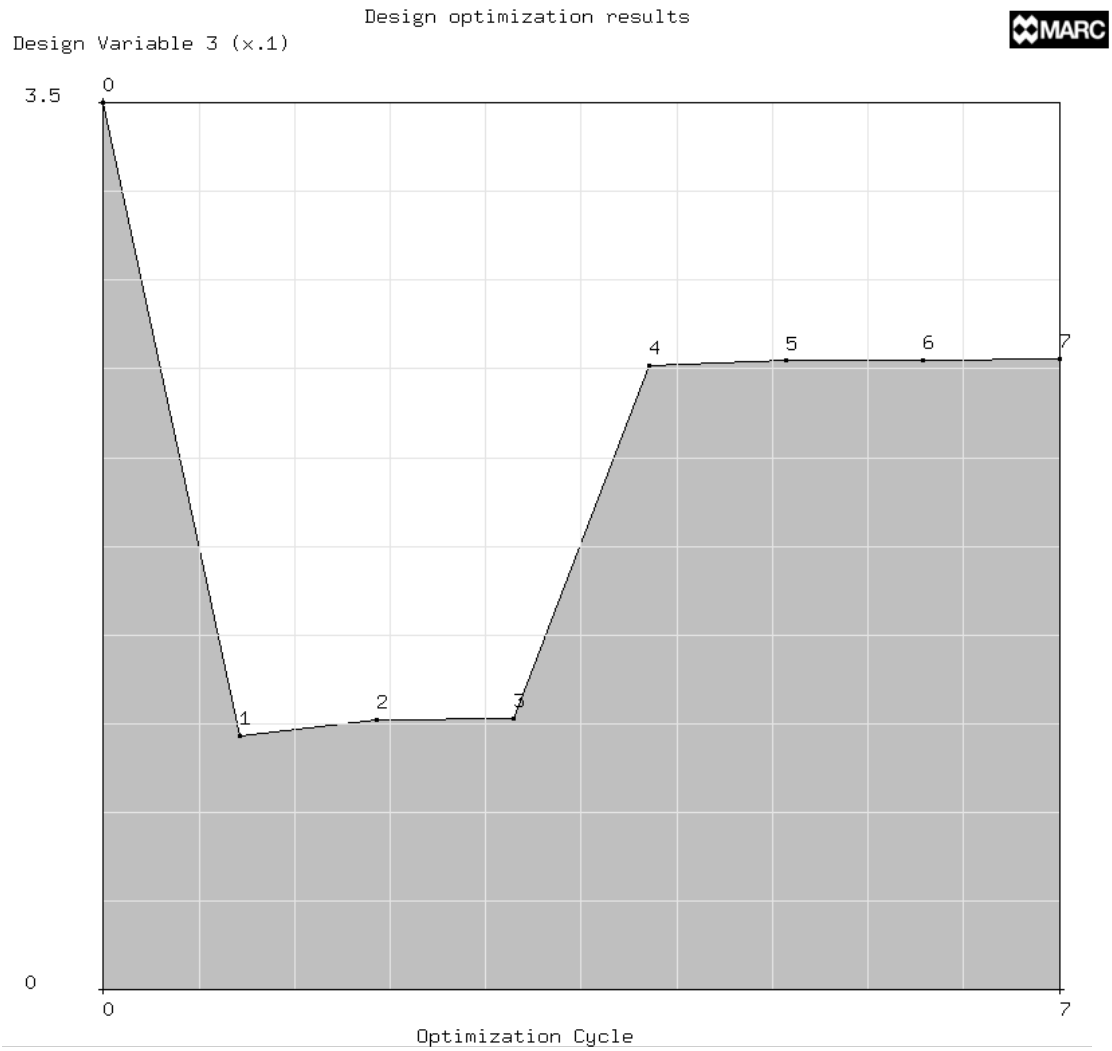

Figure 10.3-5 History Plot of the Poisson's Ratio

10.4 Design Sensitivity Analysis and Optimization of a Shell Roof

A shell type roof structure is considered for design sensitivity analysis and design optimization under the action of a static load case and for eigenfrequency response.

Elements

Element type 75 is a 4-node, thick-shell element with six global degrees of freedom per node.

Model

The finite element model is shown in Figure 10.4-1. The roof is modeled with 64 type 75 shell elements resulting in a total of 81 nodes.

Geometry

For sensitivity analysis purposes, a thickness of 0.01 is specified for elements from 1 through 54, and 0.015 is specified for elements from 55 through 64, using the GEOMETRY option.

Material Properties

The material is linearly elastic with a Young's modulus of 100,000 and a Poisson's ratio of 0.3.

Loading

The first load case consists of an eigenvalue analysis for free vibration. For the second, and static, load case, a point load and a moment resultant are applied at node 1 by means of the POINT LOAD option.

Boundary Conditions

Various boundary conditions are applied along the four edges.

Design Variables and Objective Function

The two of design variables for this problem are:

1. the thickness of elements 1 through 54
2. the thickness of elements 55 through 64

The objective function for the problem is the total mass of the material used, which means that we seek to minimize the mass by way of the design optimization procedure.

Design Constraints

The design constraints consist of stress constraints and frequency constraints. Stress constraints are imposed for certain elements on the generalized stresses and on stress components. Frequency constraints are on the fundamental frequency and on the difference between the frequencies of the first two modes.

Results

The design sensitivity and design optimization cases are run as separate jobs, with the data files e10x4a.dat and e10x4b.dat, respectively. Figure 10.4-2 shows the gradient of the difference between the first and second eigenfrequencies with respect to the two design variables. This difference is obviously governed by the first design variable; since the derivative due to the second variable is two orders of magnitude smaller, while the two variables are of the same order of magnitude. Figure 10.4-3 is a contour plot showing, on the finite element model, the element contributions to the response quantity in question. Figure 10.4-4 shows the change in the objective function with the optimization cycle in the form of a history plot. The best feasible (F) design is obtained at cycle 18. Figure 10.4-5 is a bar chart showing the values of the design variables at the best feasible design obtained.

Parameters, Options, and Subroutines Summary

Listed below are the options used in example e10x4a.dat:

Parameters	Model Definition Options	History Definition Options
ALL POINTS	CONNECTIVITY	CONTINUE
DESIGN SENSITIVITY	COORDINATES	MODAL SHAPE
DYNAMIC	DESIGN FREQUENCY CONTRAINTS	POINT LOAD
ELEMENTS	DESIGN OBJECTIVE	
END	DESIGN STRESS CONSTRAINTS	
SETNAME	DESIGN VARIABLES	
SHELL SECT	END OPTION	
SIZING	FIXED DISP	
TITLE	GEOMETRY	
	ISOTROPIC	
	OPTIMIZE	
	POINT LOAD (dummy)	
	POST	
	SOLVER	

Listed below are the options used in example e10x4b.dat:

Parameters	Model Definition Options	History Definition Options
ALL POINTS	CONNECTIVITY	CONTINUE
DESIGN OPTIMIZATION	COORDINATES	MODAL SHAPE
DYNAMIC	DESIGN FREQUENCY CONTRAINTS	POINT LOAD
ELEMENTS	DESIGN OBJECTIVE	
END	DESIGN STRESS CONSTRAINTS	
SETNAME	DESIGN VARIABLES	
SHELL SECT	END OPTION	
SIZING	FIXED DISP	
TITLE	GEOMETRY	
	ISOTROPIC	
	OPTIMIZE	
	POINT LOAD (dummy)	
	POST	
	SOLVER	

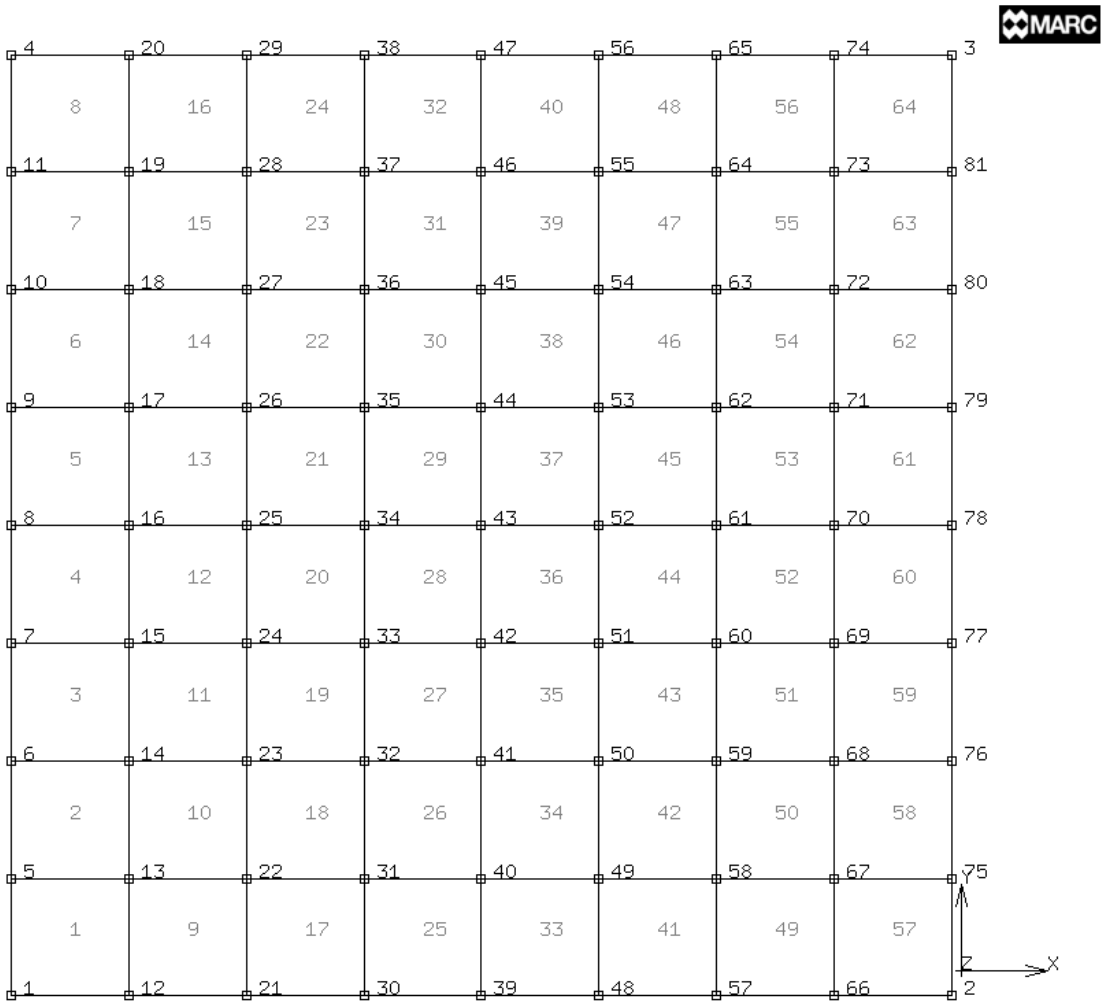

Figure 10.4-1 Finite Element Model of the Shell Roof

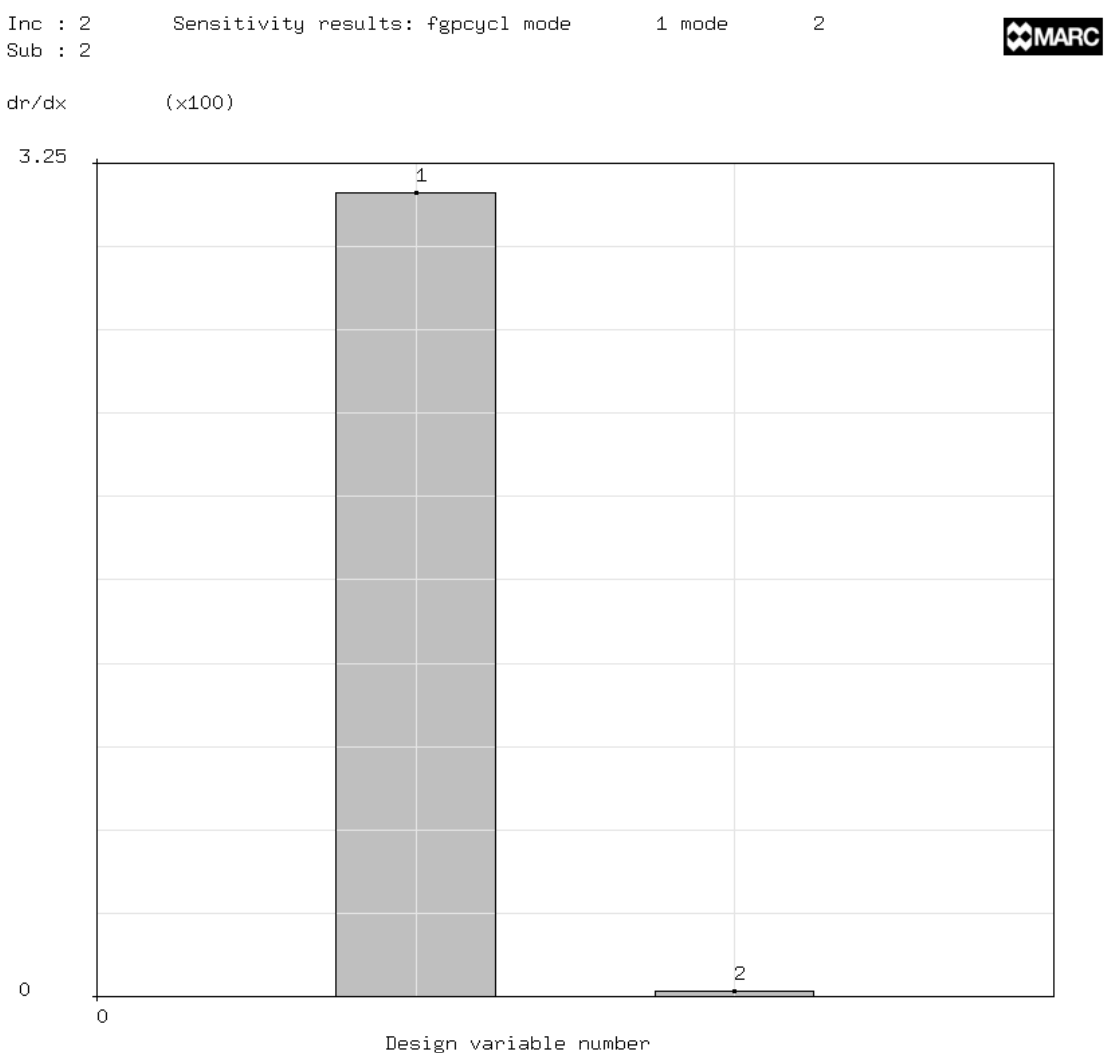

Figure 10.4-2 Gradient of Difference Between First and Second Eigenfrequencies

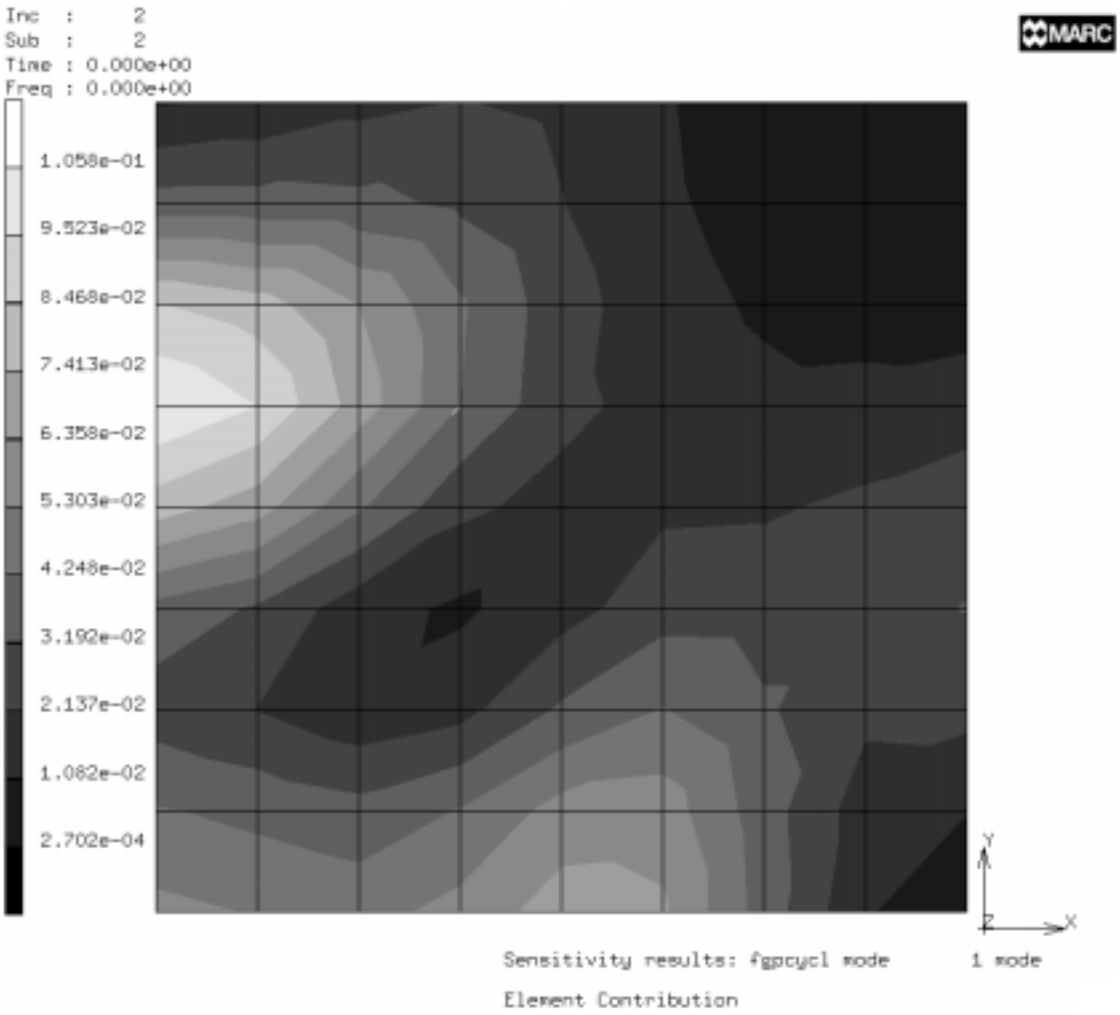

Figure 10.4-3 Element Contributions to the Response of Figure 10.4-2

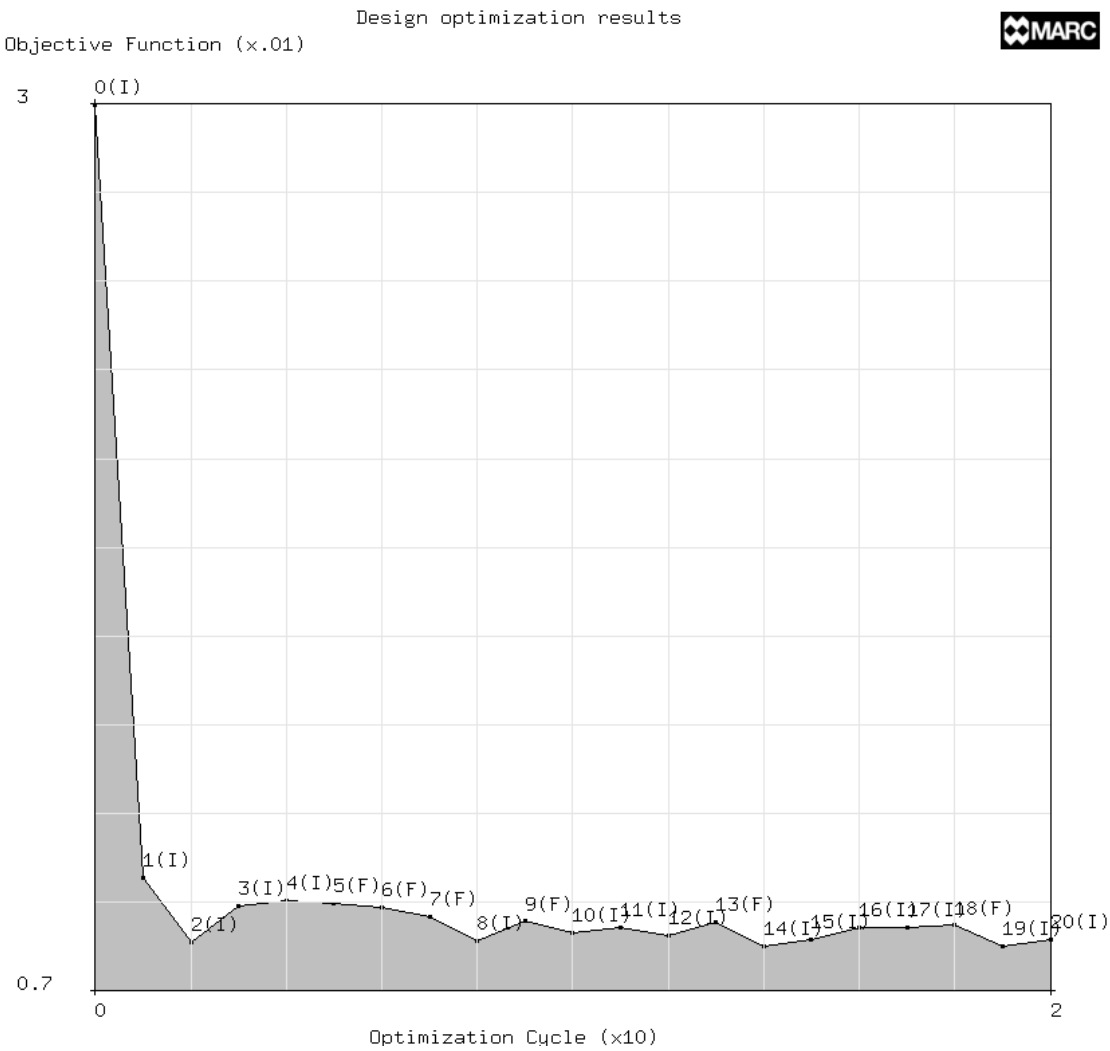

Figure 10.4-4 History Plot of the Objective Function

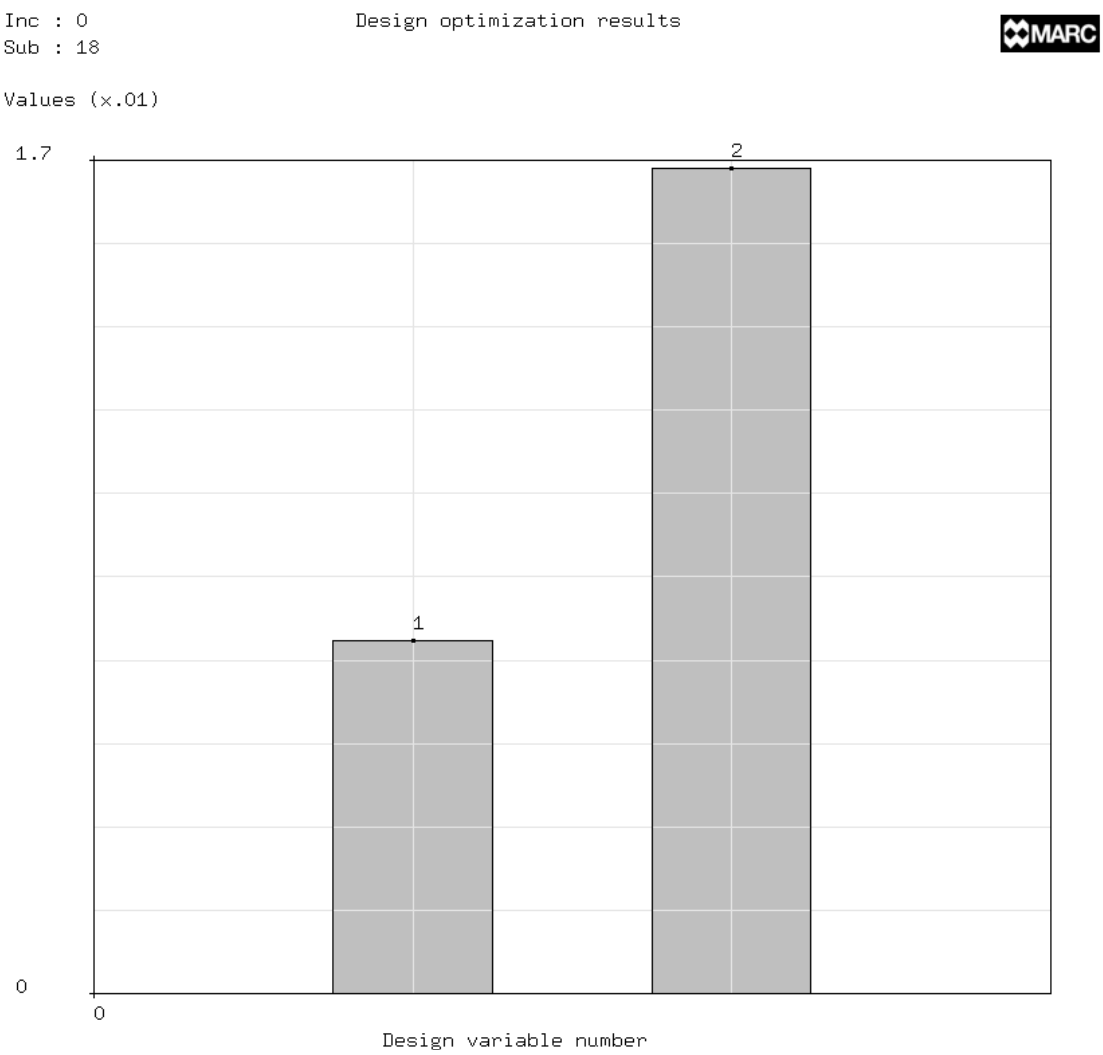

Figure 10.4-5 Design Variables at Best Feasible Design (Cycle 18)

10.5 Design Sensitivity Analysis and Optimization of a Composite Plate

This problem demonstrates the utilization of the design sensitivity and optimization procedures for a rectangular plate made up of multilayered composite material.

Element)

Element type 75 is a 4-node, thick-shell element with six global degrees of freedom per node.

Model

The model is shown in Figure 10.5-1. The plate is modeled with six type 75 elements and a total of 14 nodes.

Geometry

The elements are modeled as composites with nine layers. For sensitivity analysis, the prescribed layer thicknesses are 5.166 cm for layers 1 through 6, 0.272 cm for layer 7, and 3.364 cm for layers 8 and 9. The ply angle is zero degrees for all layers.

Material Properties

The composite elements contain two material types, one is an orthotropic material which is used for layer 7, and the other is an isotropic material used for the rest of the layers.

Loading and Boundary Conditions

The single load case consists of point loads of 350 applied through the POINT LOAD option to nodes 9 and 10 in the negative third direction. Various appropriate boundary conditions are applied.

Design Variables and Objective Function

The two types of design variables chosen are the ply angle and the layer thickness. The ply angle at layer 7 is the first design variable. The second and third design variables are the layer thicknesses linked over layers 1 through 6 and 8 and 9, respectively. The ply angle variable can change between 0.1 and 180 degrees. The lower and upper bounds for the layer thickness variables are 0.1 to 8.0 cm and 0.1 to 5.0 cm respectively.

The objective function for this problem is the total volume of the material used. For design sensitivity, we request the gradient of the total material volume. For design optimization, we seek to minimize the total material volume.

Design Constraints

Design constraints are imposed on stress, displacement, and strain response quantities. Stress constraints, which are on the von Mises stress, generalized stresses, and a normal stress component, are imposed for element 6 only. Displacement constraints consist of a bound on the translation in the second direction for node 6, and a limit on the relative translation in the second direction between nodes 4 and 5. The single strain constraint sets a limit on the magnitude of the second normal strain component.

Results

The design sensitivity and design optimization cases are run as separate jobs, with the data files e10x5a.dat and e10x5b.dat, respectively. For this particular case, the only difference between the two files is the parameter line specifying DESIGN SENSITIVITY or DESIGN OPTIMIZATION. Figure 10.5-2 shows the gradient of the relative y-direction translation between nodes 4 and 5 with respect to the design variables at the user prescribed design. Figure 10.5-3 is a contour plot showing, on the finite element model, the element contributions to the response quantity in question. Figure 10.5-4 shows the change in the objective function with the optimization cycle in the form of a history plot. The best feasible (F) design within twenty cycles is obtained at cycle 8. Figure 10.5-5 is a bar chart showing the values of the design variables at the best design obtained.

Parameters, Options, and Subroutines Summary

Listed below are the options used in example e10x5a.dat:

Parameter Options	Model Definition Options	History Definition Options
DESIGN SENSITIVITY	COMPOSITE	CONTINUE
DYNAMIC	CONN GENER	POINT LOAD
ELEMENTS	CONNECTIVITY	
END	COORDINATES	
PRINT	DESIGN DISPLACEMENTS	
SIZING	DESIGN OBJECTIVE	
TITLE	DESIGN STRAIN CONSTRAINTS	
	DESIGN STRESS CONSTRAINTS	
	DESIGN VARIABLES	
	END OPTION	
	FIXED DISP	
	ISOTROPIC	
	NODE FILL	
	ORIENTATION	
	ORTHOTROPIC	

Listed below are the options used in example e10x5b.dat:

Parameter Options	Model Definition Options	History Definition Options
DESIGN OPTIMIZATION	COMPOSITE	CONTINUE
DYNAMIC	CONN GENER	POINT LOAD
ELEMENTS	CONNECTIVITY	
END	COORDINATES	
PRINT	DESIGN DISPLACEMENTS CONSTRAINTS	
SIZING	DESIGN OBJECTIVE	
TITLE	DESIGN STRAIN CONSTRAINTS	
	DESIGN STRESS CONSTRAINTS	
	DESIGN VARIABLES	
	END OPTION	
	FIXED DISP	
	ISOTROPIC	
	NODE FILL	
	ORIENTATION	
	ORTHOTROPIC	

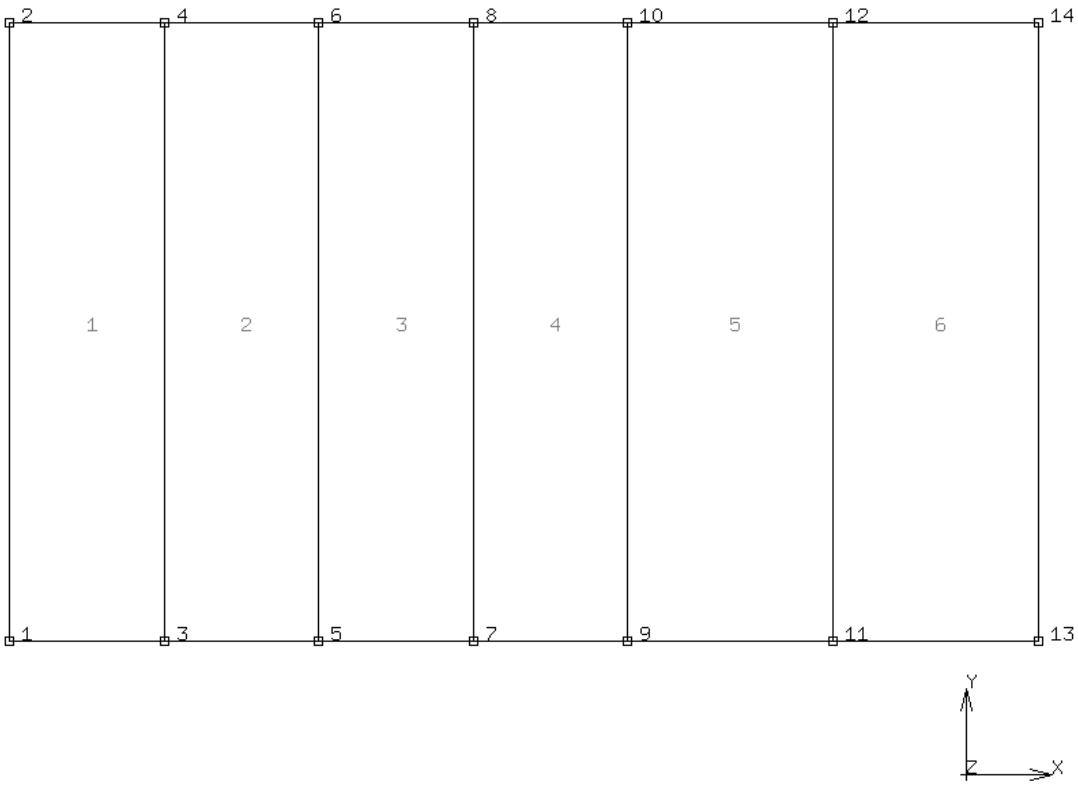

Figure 10.5-1 Finite Element Model of Composite Plate

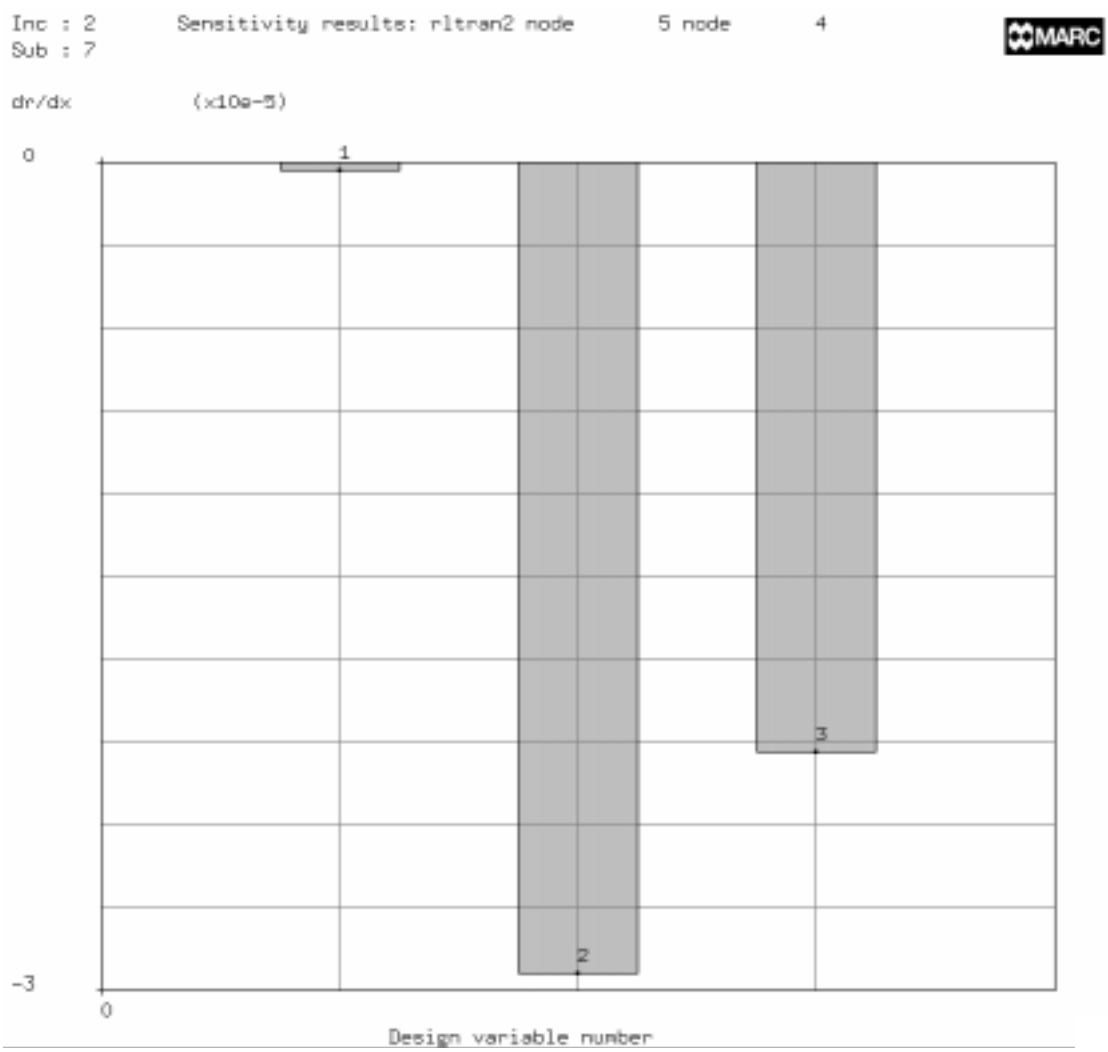

Figure 10.5-2 Gradient of Relative y-direction Translation Between Nodes 4 and 5

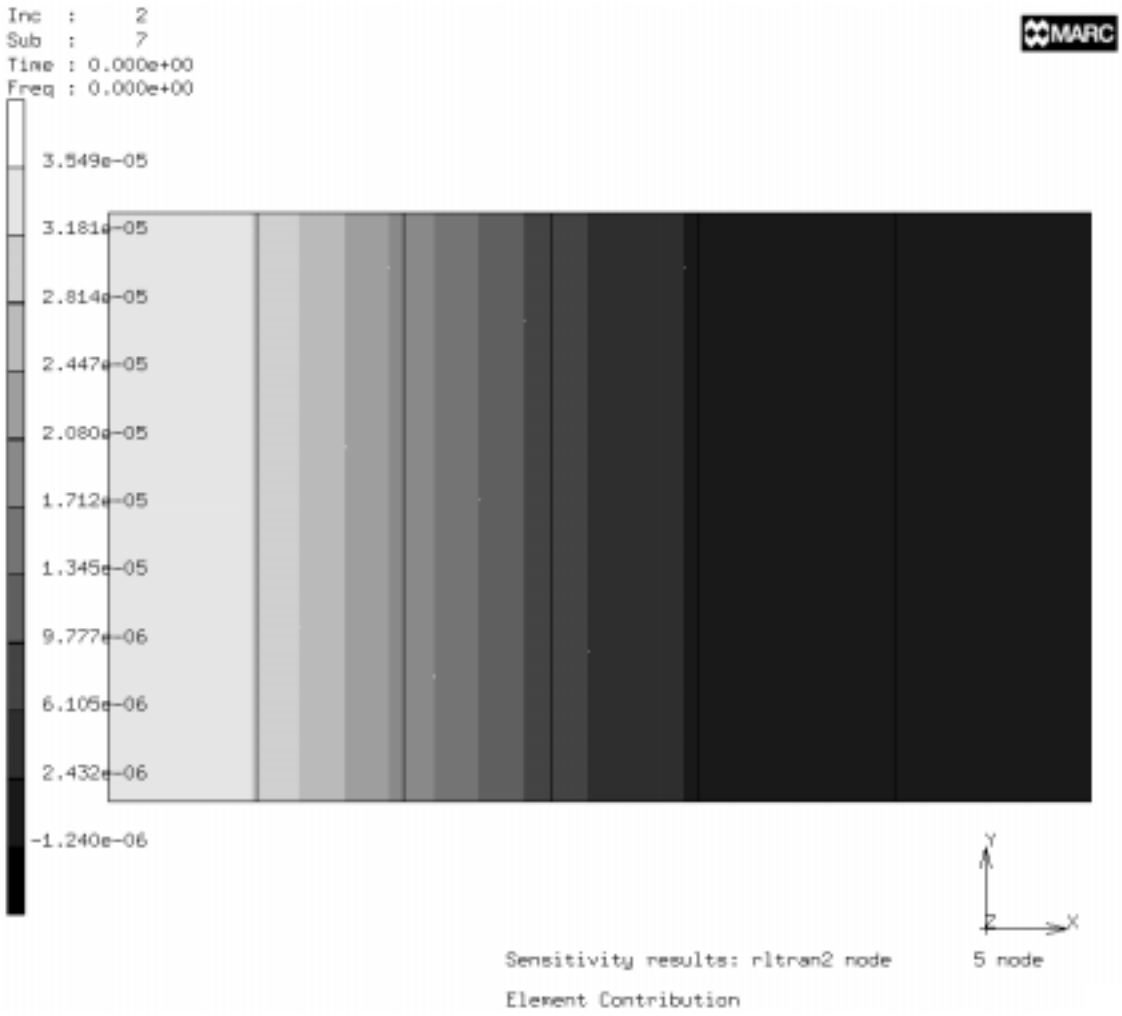

Figure 10.5-3 Element Contributions to Response of Figure 10.5-2

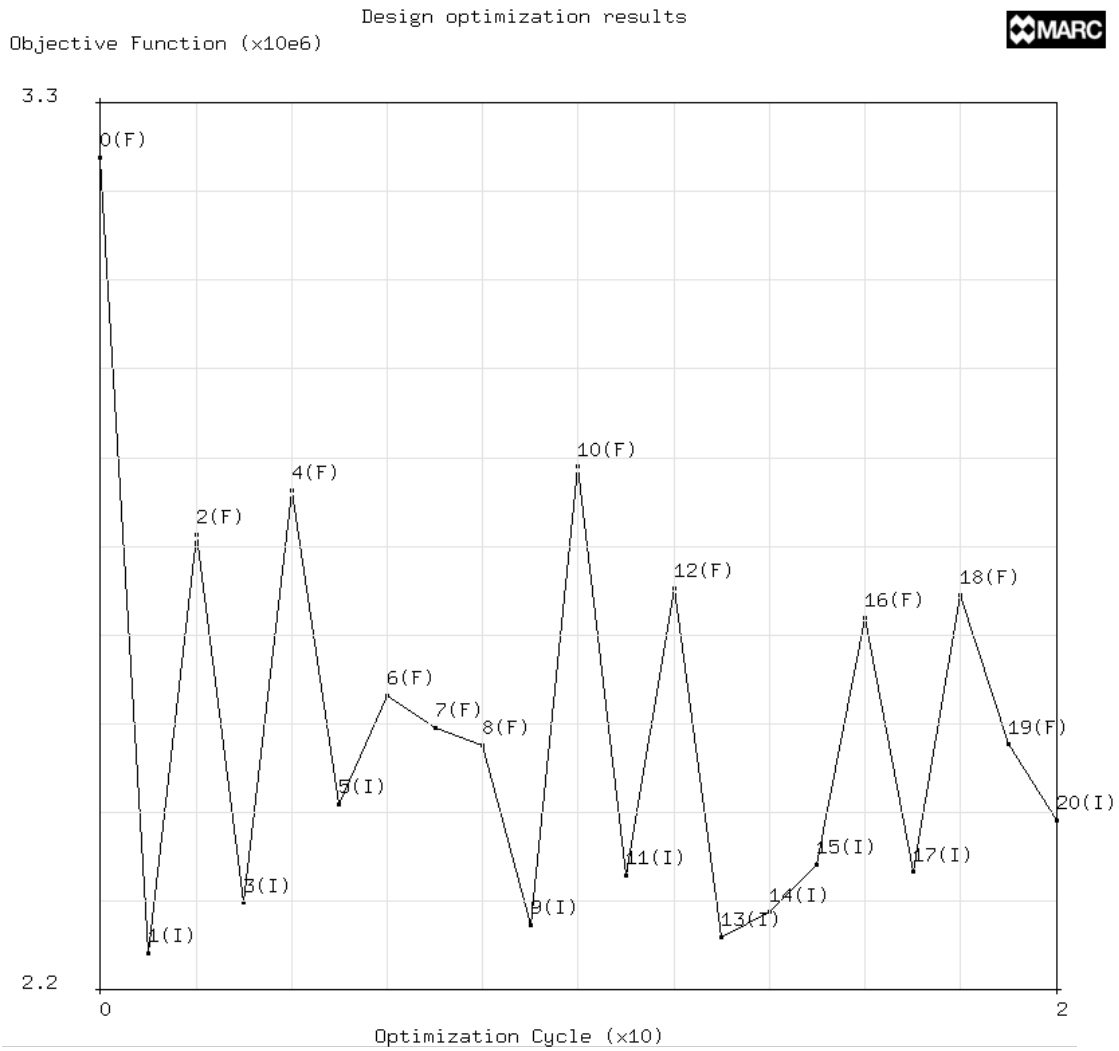

Figure 10.5-4 History Plot of the Objective Function

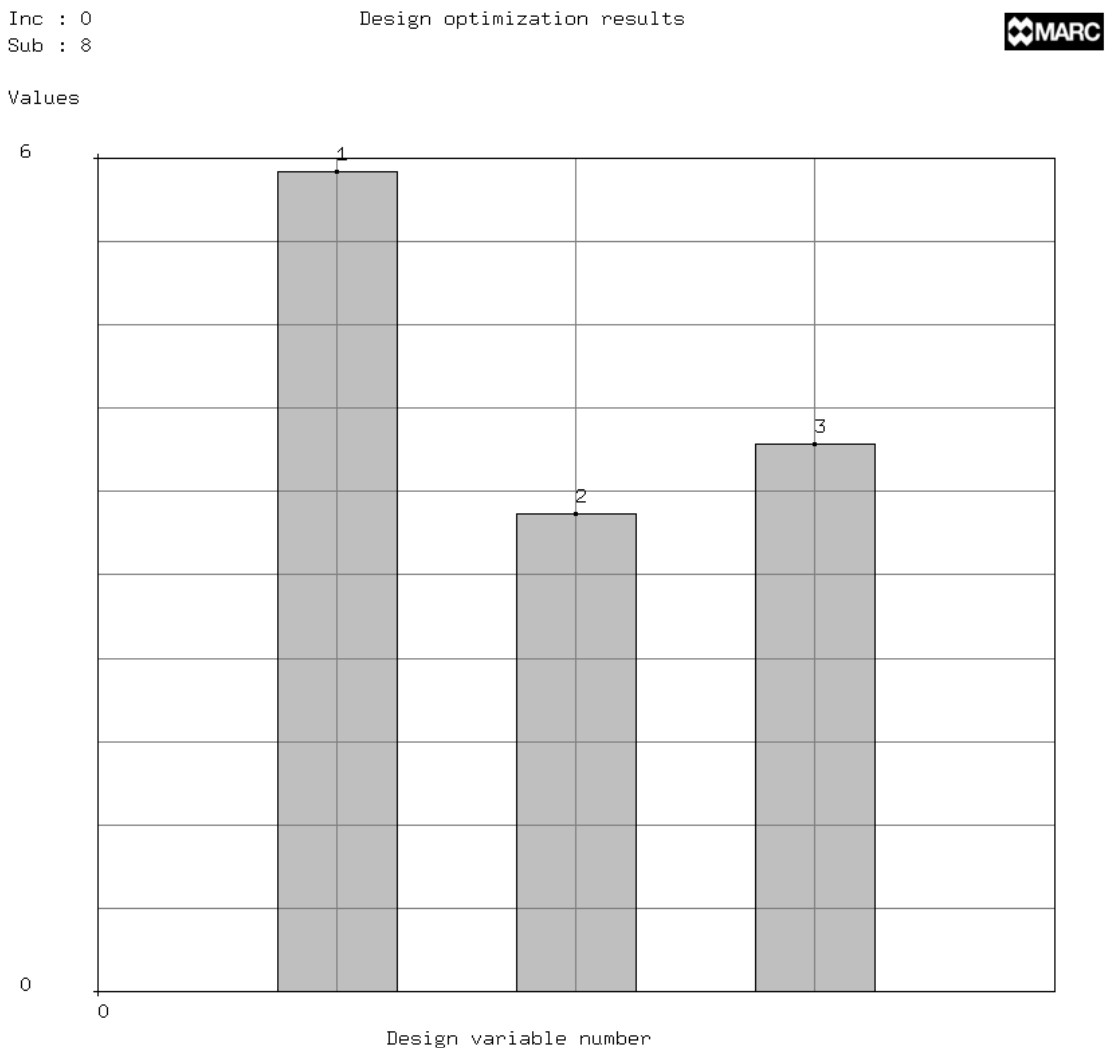

Figure 10.5-5 Design Variables at Best Feasible Design (Cycle 8)

10.6 Design Sensitivity Analysis and Optimization of a Ten-bar Truss

The cantilever ten-bar truss of Figure 10.6-1 is subjected to a single static load case. Design sensitivity analysis and design optimization are conducted with constraints on the stresses in the truss elements.

Elements

Element type 9 is a 2-node, 3D straight truss bar element with constant cross section and three degrees of freedom per node.

Model

The model is shown in Figure 10.6-1. It has a total of 10 axial bar elements and 6 nodes. The two nodes at the left end (nodes 2 and 4) are pinned to prevent any translation at these nodes. The total length of the cantilever is 20 units with a height of 10 units.

Geometry

The cross-sectional areas are five units each for purposes of design sensitivity analysis. The limits for design optimization are given with the DESIGN VARIABLES option.

Material Properties

The material is linearly elastic with a Young's modulus of 10,000 and a mass density of 1.0.

Loading

Point loads of 50 and 100 are applied to nodes 1 and 5, respectively, along the positive second degree of freedom (that is, upwards in Figure 10.6-1) through the POINT LOAD option.

Design Variables and Objective Function

For this problem, the only type of design variable is the cross-sectional areas. These design variables are unlinked over the elements, resulting in ten independent design variables, each corresponding to the cross-sectional area of a given truss element. Material mass is the prescribed objective function.

Design Constraints

The design constraints are on the axial stresses in the truss bars. The limit on the stresses is the same for both tension and compression, although MARC allows the specification of different limits.

Results

The design sensitivity and design optimization cases are run as separate jobs, with the data files e10x6a.dat and e10x6b.dat, respectively. Figure 10.6-2 shows the gradient of the axial stress in element 4 with respect to all ten design variables. Figure 10.6-3 shows the element contributions to the response quantity in question. Figure 10.6-4 shows the change in the objective function with the optimization cycle in the form of a history plot. Cycle 50 is seen to give the best feasible (F) design. Figure 10.6-5 is a bar chart showing the values of the design variables at the best feasible design obtained. It will be noted that the elements carrying the highest loads, elements 1 and 10, are the ones ending up with the largest cross-sectional areas in this stress-constrained problem.

Parameters, Options, and Subroutines Summary

Listed below are the options used in example e10x6a.dat:

Parameters	Model Definition Options	History Definition Options
ALL POINTS	CONNECTIVITY	CONTINUE
DESIGN SENSITIVITY	COORDINATES	POINT LOAD
ELEMENTS	DESIGN OBJECTIVE	
END	DESIGN STRESS CONSTRAINTS	
SETNAME	DESIGN VARIABLES	
SIZING	END OPTION	
TITLE	FIXED DISP	
	GEOMETRY	
	ISOTROPIC	
	NO PRINT	
	OPTIMIZE	
	POST	
	SOLVER	

Listed below are the options used in example e10x6b.dat:

Parameters	Model Definition Options	History Definition Options
ALL POINTS	CONNECTIVITY	CONTINUE
DESIGN OPTIMIZATION	COORDINATES	POINT LOAD
ELEMENTS	DESIGN OBJECTIVE	
END	DESIGN STRESS CONSTRAINTS	
SETNAME	DESIGN VARIABLES	
SIZING	END OPTION	
TITLE	FIXED DISP	
	GEOMETRY	
	ISOTROPIC	
	NO PRINT	
	OPTIMIZE	
	POST	
	SOLVER	

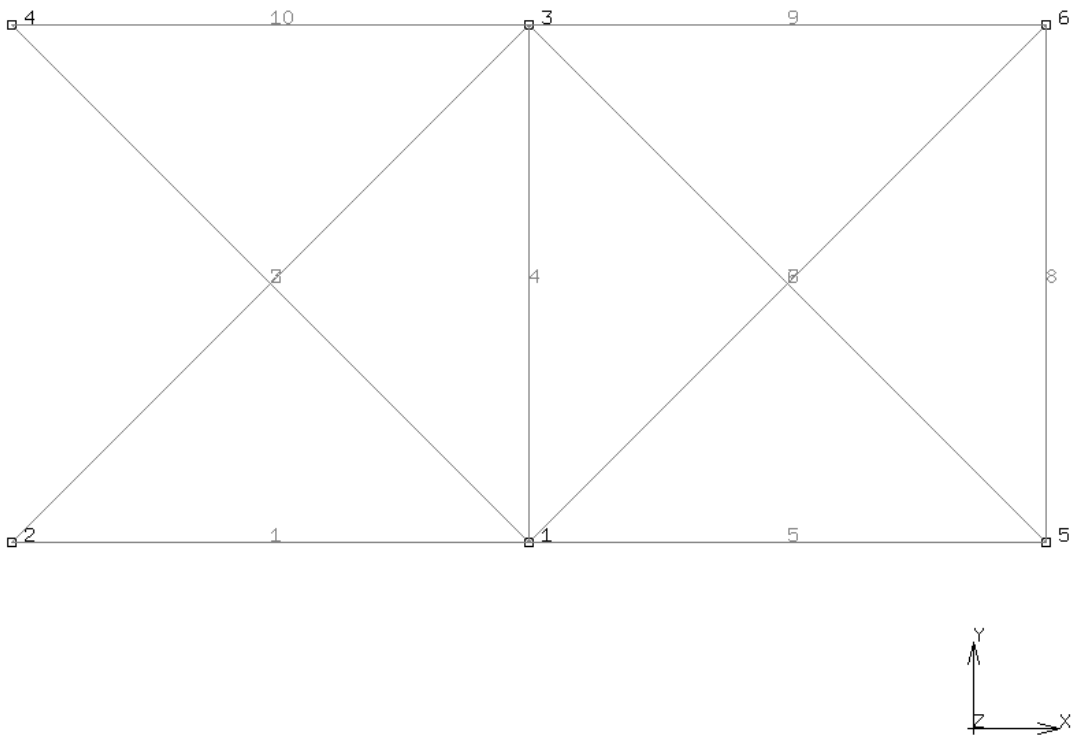

Figure 10.6-1 Finite Element Model of Ten-bar Truss

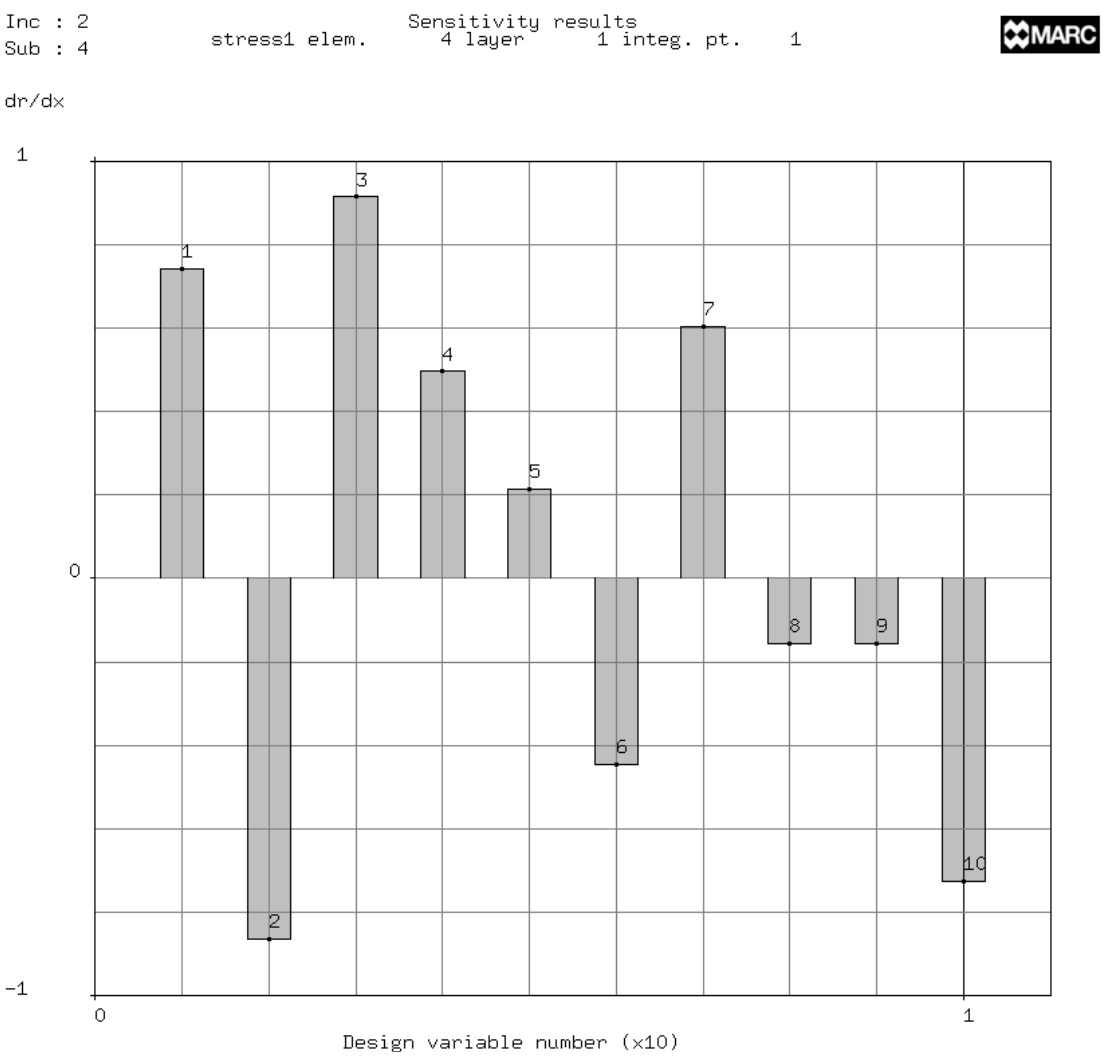

Figure 10.6-2 Gradient of Axial Stress in Element 4

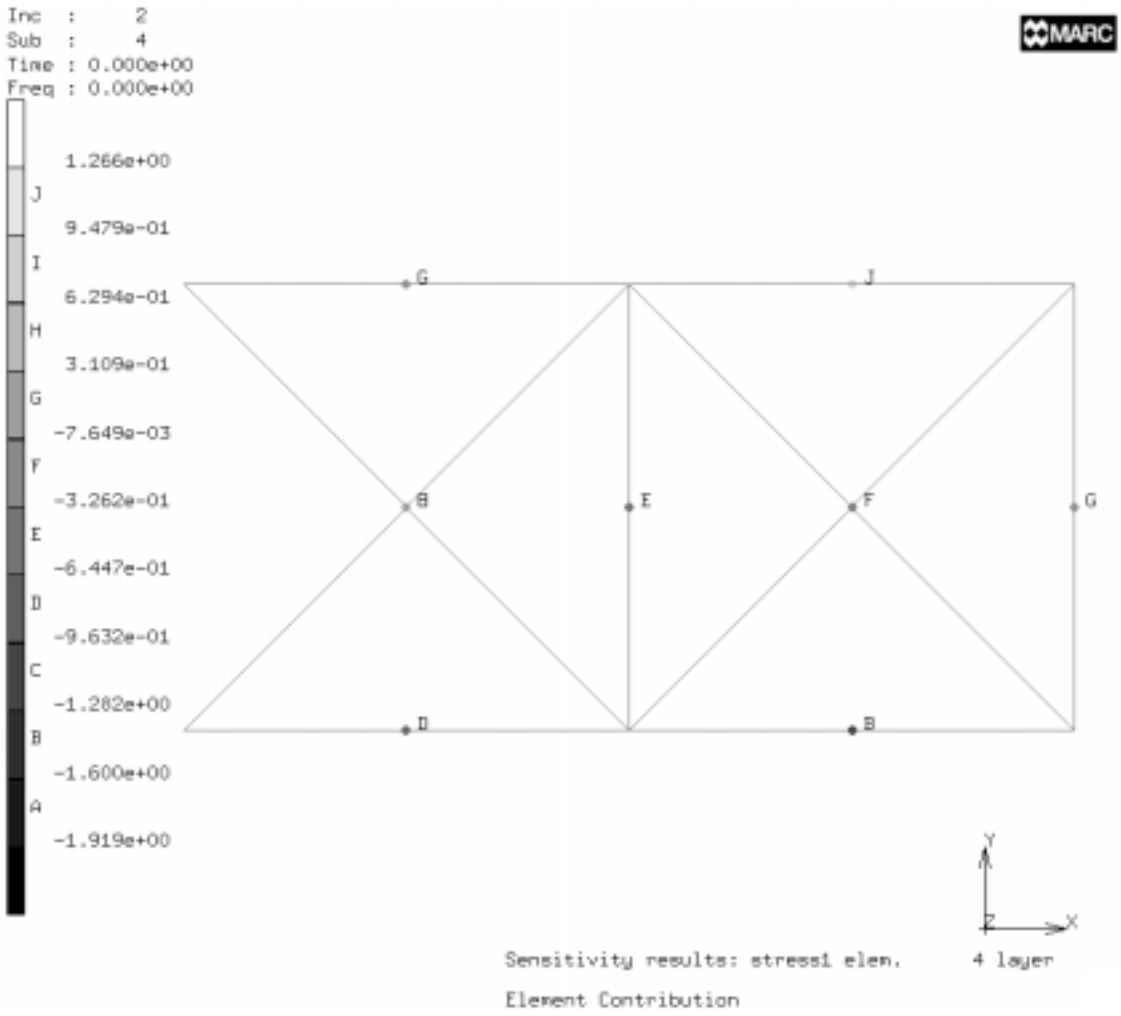

Figure 10.6-3 Element Contributions to Response of Figure 10.6-2

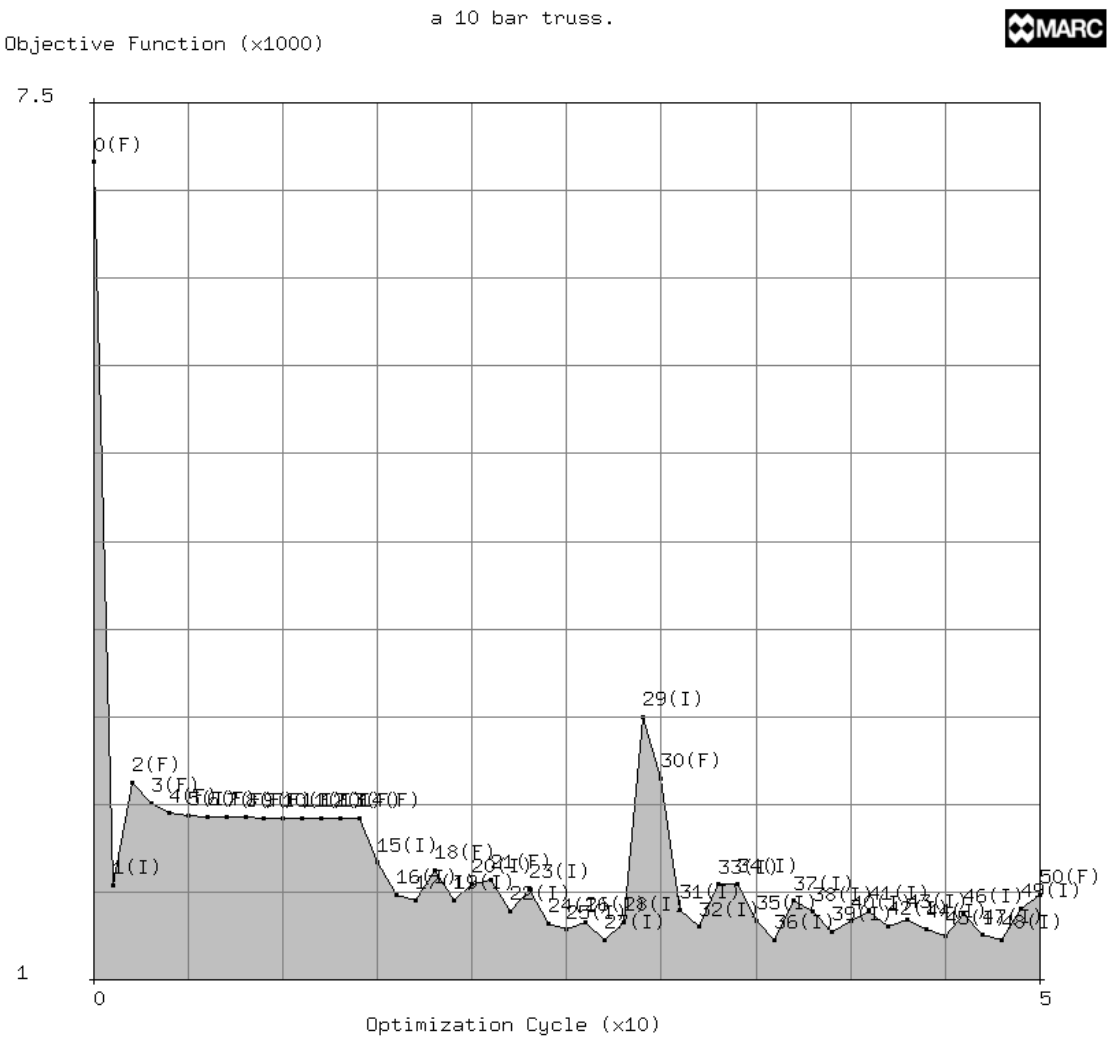

Figure 10.6-4 History Plot of the Objective Function

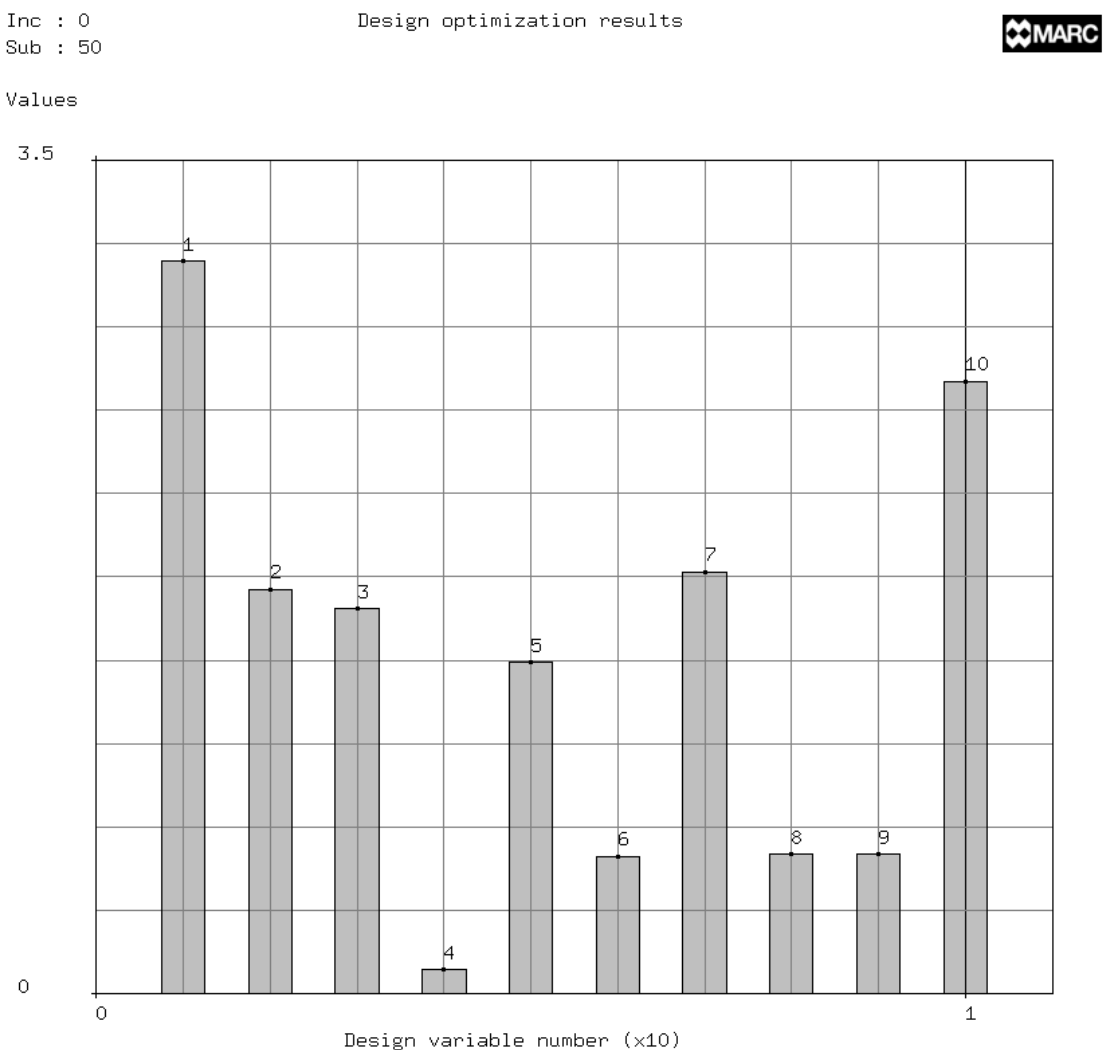

Figure 10.6-5 Design Variables at Best Feasible Design (Cycle 50)

10.7 Design Sensitivity Analysis and Optimization of an Alternator Mount using Element 14

This problem is geometrically similar to problem 10.1, except that the 3D frame model uses a different type of element which leads to a different choice of design variables. Differences also exist in material properties and, of course, in the geometry data.

Element)

The element used is type 14 with the default hollow circular section and two end nodes. The cross section of this element is defined by a wall-thickness and a mean radius.

Model

The 3D frame is modeled using 16 beam-column elements and 20 nodes. The columns are clamped at the base. The elements have arbitrary solid cross sections. Two masses are lumped in the middle of two horizontal beams at nodes 14 and 18 (Figure 10.7-1). Elements numbered 1 through 8 are the columns and the rest of the elements are the beams. All the elements have hollow circular cross sections. Column to beam connections are obtained through tying of separately numbered nodes.

Geometry

The geometry data consists of the wall-thickness and mean radius of the cross sections. For sensitivity analysis purposes, these are the same for all elements and are 0.1 and 10.0, respectively. For design optimization purposes, the lower- and upper-bounds are given by the DESIGN VARIABLES option.

Material Properties

The material is linearly elastic, homogeneous, and isotropic with a Young's modulus of 0.25×10^{9}, a Poisson's ratio of 0.349, and a mass density of 0.255×10^{-2}.

Loads

As in problem 10.1, there are three loadcases. The first consists of an eigenfrequency analysis. The second and third are static loadcases with point loads. All loadcases are the same as problem 10.1.

Design Variables and Objective Function

For elements 1 through 8 (the columns), the design variable is the wall-thickness linked over these elements (design variable 1). The lower- and upper-bounds for this first variable are 0.5 and 2.5, respectively. For elements 9 through 16 (the beams), the design variable is the mean radius of the cross section (design variable 2), again linked over the relevant elements. The lower- and upper-bounds for this second variable are 8.0 and 15.0, respectively.

The objective function for the problem is the total mass of the material used. Thus, sensitivity analysis obtains the gradient of this function and design optimization attempts to minimize it.

Design Constraints

The constraints are imposed on generalized stresses, a translation and a rotation, and eigenfrequencies. For demonstration purposes, all three generalized stress constraints are on element 13 for loadcase two, and the two displacement constraints are on nodes 15 and 19, respectively. The first eigenfrequency constraint is on the fundamental mode. The second eigenfrequency constraint is on the difference between the frequencies of the first and second modes of free vibration.

Results

The design sensitivity and design optimization cases are run as separate jobs, with the data files e10x7a.dat and e10x7b.dat, respectively. Figure 10.7-2 shows the gradient of the first eigenfrequency with respect to the two design variables. Figure 10.7-3 is an element values plot showing, on the finite element model, the element contributions to the response quantity in question. Figure 10.7-4 shows the change in the objective function with the optimization cycle in the form of a path plot. Figure 10.7-5 is a bar chart showing the values of the design variables at the best design obtained. It is noted that no feasible design is found for this problem. However, the normalized most critical value is -0.004 at the best design (cycle 7), indicating that this design is very close to being feasible. In comparison, the design at the starting vertex (cycle 0) had a most critical normalized constraint value of -0.175, indicating severe infeasibility.

Parameters, Options, and Subroutines Summary

Listed below are the options used in example e10x7a.dat:

Parameters	Model Definition Options	History Definition Options
DESIGN SENSITIVITY	CONNECTIVITY	CONTINUE
DYNAMIC	COORDINATES	MODAL SHAPE
ELEMENTS	DESIGN DISPLACEMENT CONSTRAINTS	POINT LOAD
END	DESIGN FREQUENCY CONSTRAINTS	
SIZING	DESIGN OBJECTIVE	
TITLE	DESIGN STRESS CONSTRAINTS	
	DESIGN VARIABLES	
	END OPTION	
	FIXED DISP	
	GEOMETRY	
	ISOTROPIC	
	MASSES	
	POINT LOAD (dummy)	
	POST	
	TYING	

Listed below are the options used in example e10x7b.dat:

Parameters	Model Definition Options	History Definition Options
DESIGN OPTIMIZATION	CONNECTIVITY	CONTINUE
DYNAMIC	COORDINATES	MODAL SHAPE
ELEMENTS	DESIGN DISPLACEMENT CONSTRAINTS	POINT LOAD
END	DESIGN FREQUENCY CONSTRAINTS	
SIZING	DESIGN OBJECTIVE	
TITLE	DESIGN STRESS CONSTRAINTS	
	DESIGN VARIABLES	
	END OPTION	
	FIXED DISP	
	GEOMETRY	
	ISOTROPIC	
	MASSES	
	POINT LOAD (dummy)	
	POST	
	TYING	

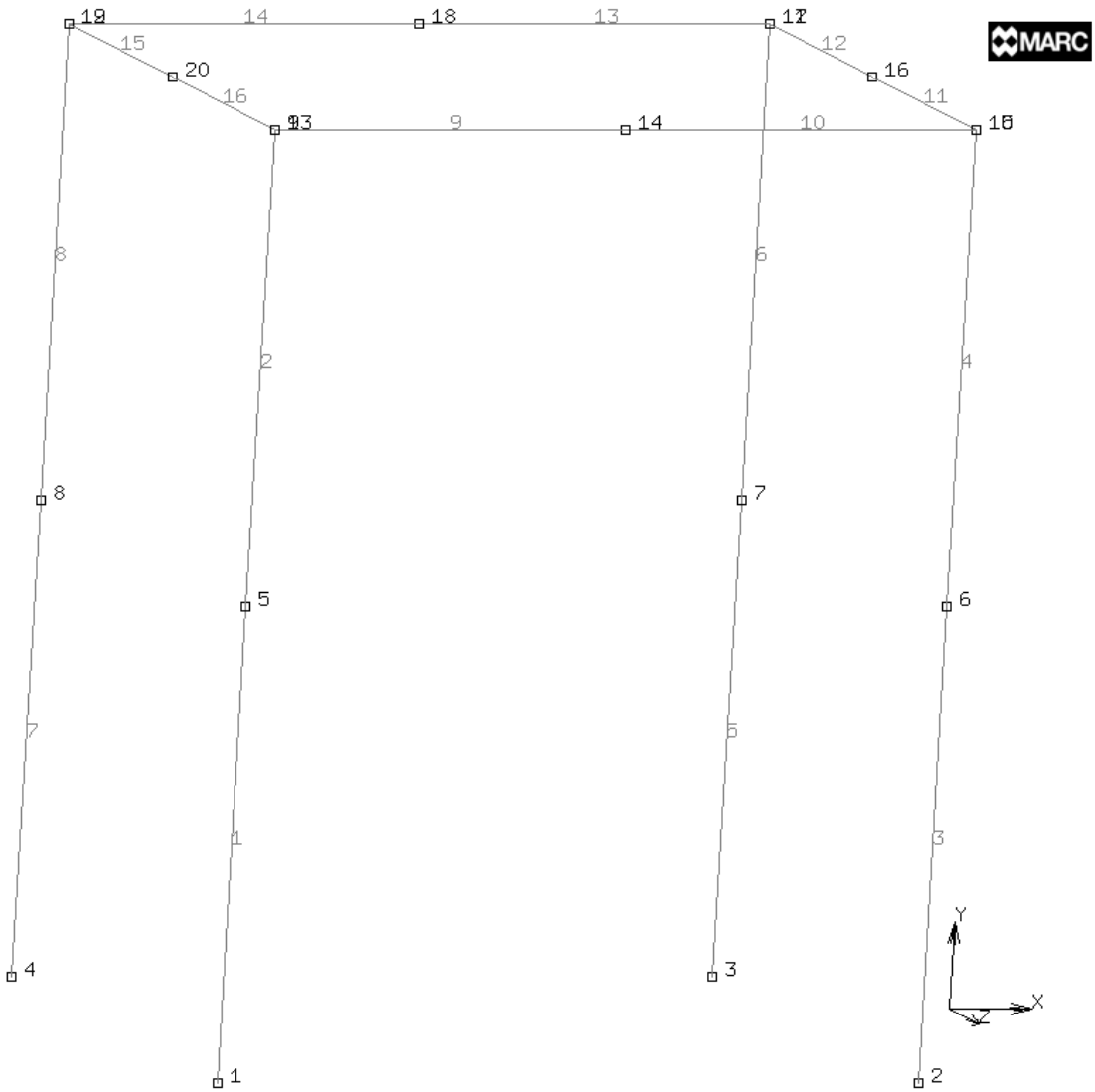

Figure 10.7-1 Alternator Mount Frame Model using Element 14

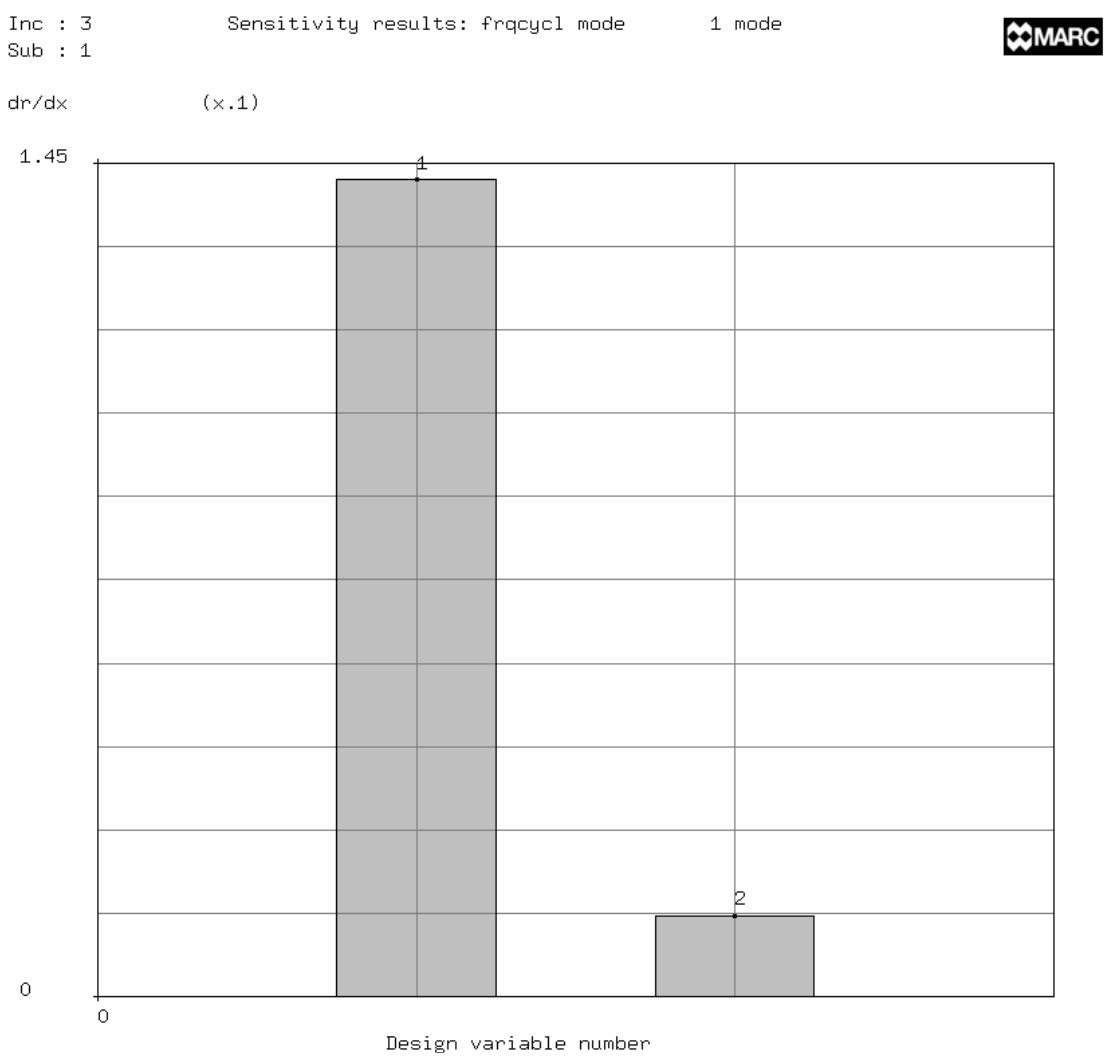

Figure 10.7-2 Gradient of the First Eigenfrequency with Respect to Design Variables

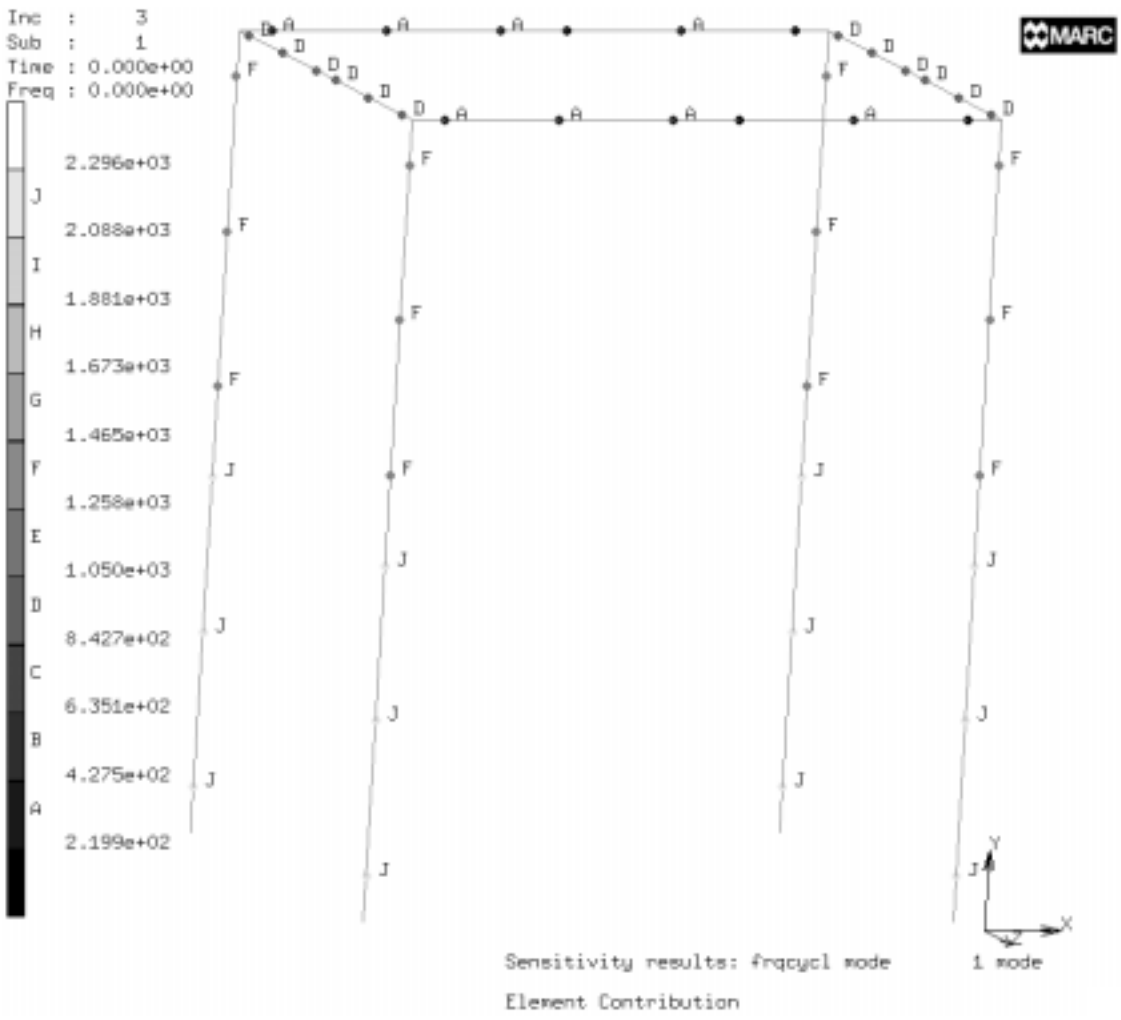

Figure 10.7-3 Element Contributions to Response of Figure 10.7-2

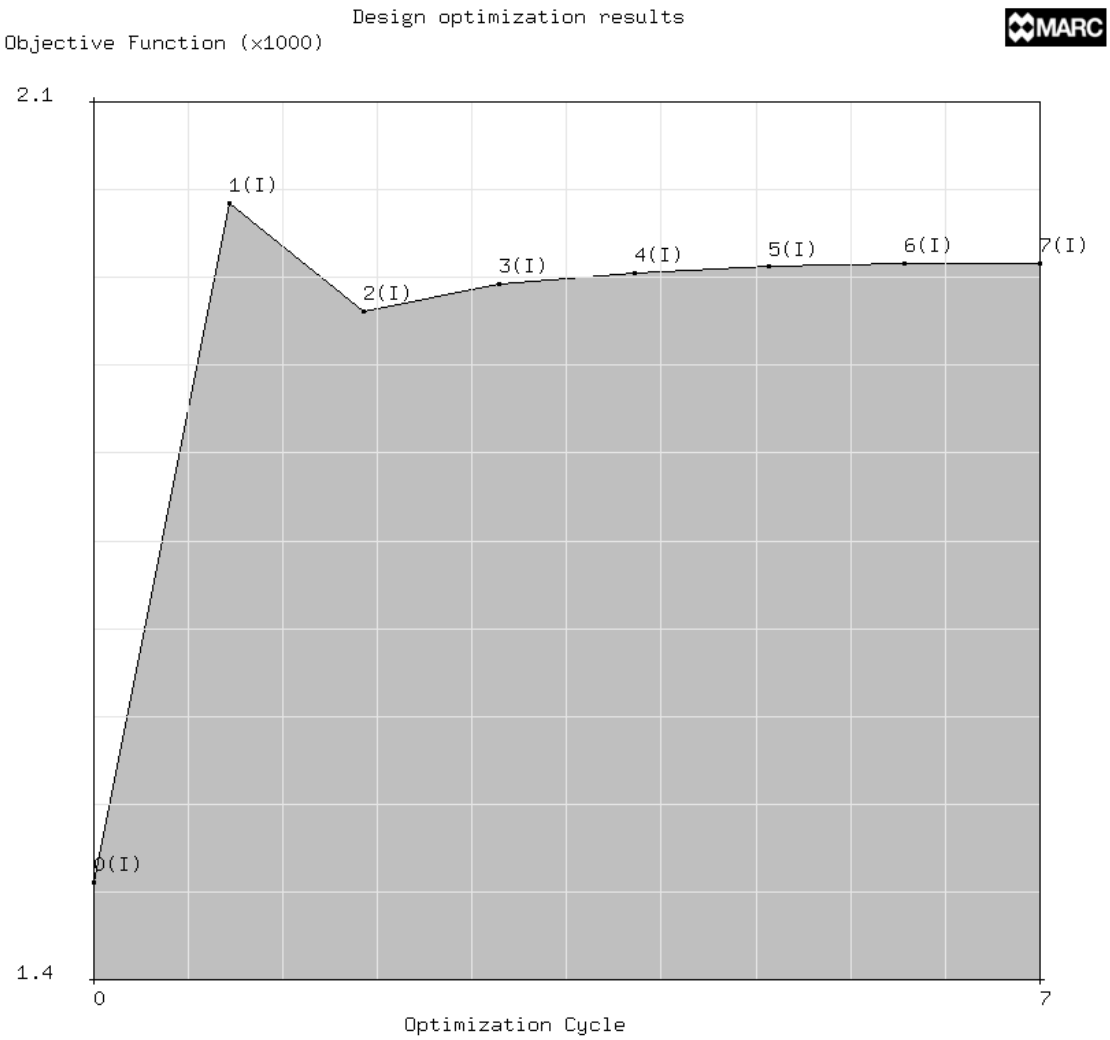

Figure 10.7-4 History Plot of the Objective Function

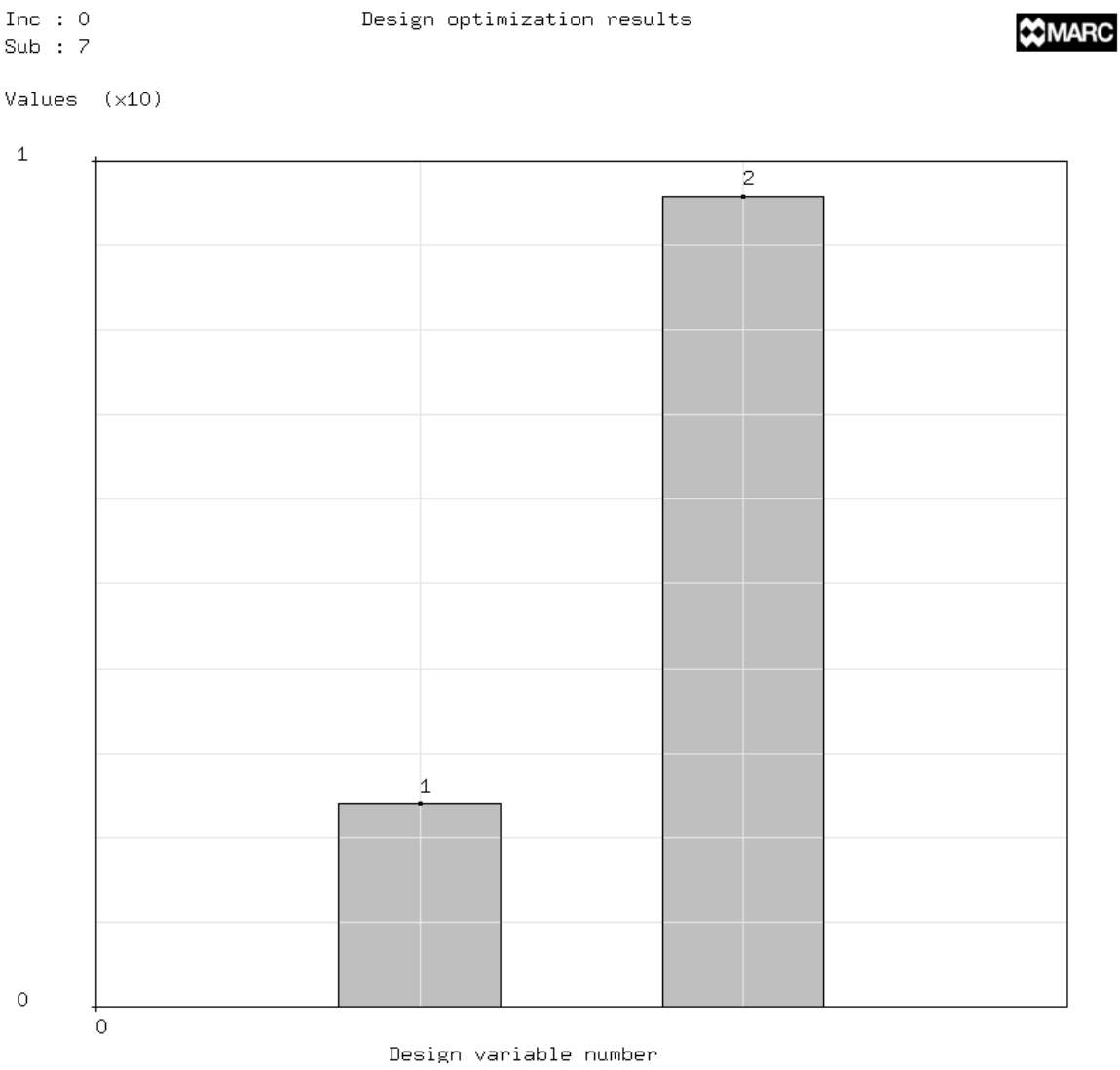

Figure 10.7-5 Design Variables at Best Design (Cycle 7)

MARC
Analysis
Research
Corporation

Document Title: **MARC® Volume E: Demonstration Problems, Part V, K7**
Part Number: RF-3018-07.V
Revision Date: June, 1998

UNITED STATES

CALIFORNIA - Palo Alto
MARC Corporate Headquarters
260 Sheridan Avenue, Suite 309
Palo Alto, CA 94306, USA
Tel: 1 650 329 6800
Fax: 1 650 323 5892
Email: support@marc.com

CALIFORNIA - San Diego
MARC Analysis Research Corp.
4330 LaJolla Village Drive, Suite 320
San Diego, CA 92122
Tel: 1 619 658 9588
Fax: 1 619 758 8710

CONNECTICUT - E. Berlin
MARC Analysis Research Corp.
1224 Mill Street
E. Berlin, CT 06023
Tel: 1 860 828 2055
Fax: 1 860 828 2031

MICHIGAN - Ann Arbor
MARC Analysis Research Corp.
24 Frank Lloyd Wright Drive
Ann Arbor, MI 48106-0523
Tel: 1 734 998 0540
Fax: 1 734 998 0542

EUROPE

CZECH REPUBLIC
MARC Overseas, Inc.
Podolska 50
147 00 Praha 4
Czech Republic
Tel: 420 (2) 6121 4123
420 (2) 6121 4111 x252
Fax: 420 (2) 6121 4123
Email: support@marc.cz

FRANCE
MARC France S.A.
Bercy Expo SR 6101A
40 Avenue des Terroirs de France
75611 Paris Cedex 12, France
Tel: 33 (1) 4474 1550
Fax: 33 (1) 4474 1554
Email: support@marc.fr

GERMANY - Munich
MARC Software Deutschland GmbH
Ismaninger Str. 9
85609 Aschheim (bie Munich)
Germany
Tel: 49 (89) 904 50 33
Fax: 49 (89) 903 06 76
Email: support@marc.de

GERMANY - Hannover
MARC Software Deutschland GmbH
Alte Dohrener Str. 66
D 30173 Hannover, Germany
Tel: 49 (511) 980 5182
Fax: 49 (511) 980 5187

ITALY
Espri-MARC s.r.l.
Viale Brigata Bisagno 2 / 10
16129 Genova, Italy
Tel: 39 (10) 585 949
Fax: 39 (10) 585 949
Email: espri.marc@interbusiness.it

THE NETHERLANDS
MARC Analysis Research Corporation
Dublinstraat 32
2713 HS Zoetermeer
The Netherlands
Tel: 31 (79) 3510 411
Fax: 31 (79) 3517 560
Email: support@marc.nl

UNITED KINGDOM
MARC UK Ltd.
11 Linford Forum, Rockingham Drive
Linford Wood
Milton Keynes, MK14 6LY
Tel: 44 (1908) 606 070
Fax: 44 (1908) 606 633
Email: support@marc.co.uk

PACIFIC RIM

CHINA
MARC Overseas, Inc.
Bright Chang An Building, Suite 321
7# Jian Guo Men Nei Street
Beijing, China 100 005
Tel: 86 (10) 6510 2056
86 (10) 6510 2057
86 (10) 6510 2058
Fax: 86 (10) 6510 2053
Email: marcbj@public.bta.net.cn

JAPAN - Nagoya
Nippon MARC Co., Ltd.
Nagoya Nishiki Daiichi Seimei Bldg.
2F, 6-5 Nishiki 1-chome
Naka-ku, Nagoya, Aichi 460-0003
Tel: 81 (52) 202 5661
Fax: 81 (52) 202 5665

JAPAN - Osaka
Nippon MARC Co., Ltd.
4F 2nd Kimi Building
2-11 Toyotucho Suita-shi
Osaka 564-0051
Tel: 81 (6) 385 1101
Fax: 81 (6) 385 4343

JAPAN - Tokyo
(Asian Operations Headquarters)
Nippon MARC Co., Ltd.
Shinjuku Daiichi Seimei Building
P.O. Box 5056
2-7-1 Nishi-Shinjuku, Shinjuku-ku
Tokyo 163-0704
Tel: 81 (3) 3345 0181
Fax: 81 (3) 3345 1529
Email: support@marc.co.jp

KOREA
Dong Kyung Bldg. 7FL
824-19 Yuksam-Dong
Kangnam-Ku, Seoul, Korea
Tel: 82 (2) 561 7543
Fax: 82 (2) 561 7767
Email: marck@unitel.co.kr